Scientific and Technical Aerospace Reports

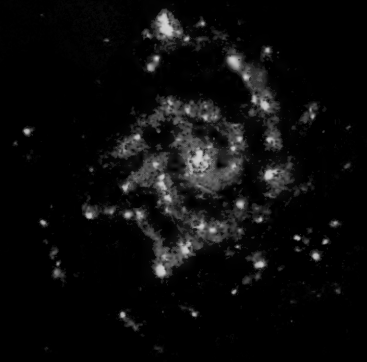

An Abstract Journal

Volume 32, Number 2
February 1994
N94-12788 to N94-14907

The NASA STI Program ... in Profile

Since its founding, NASA has been dedicated to the advancement of aeronautics and space science. The NASA Scientific and Technical Information (STI) Program plays a key part in helping NASA maintain this important role.

The NASA STI Program provides access to the NASA STI Database, the largest collection of aeronautical and space science STI in the world. The Program is also NASA's institutional mechanism for disseminating the results of its research and development activities.

Specialized services that help round out the Program's diverse offerings include creating custom thesauri, translating material to or from 34 foreign languages, building customized databases, organizing and publishing research results ... even providing videos.

For more information about the NASA STI Program, you can:

- **Phone** the NASA Access Help Desk at (301) 621-0390
- **Fax** your question to the NASA Access Help Desk at (301) 621-0134
- **E-mail** your question via the **Internet** to help@sti.nasa.gov
- **Write** to:

NASA Access Help Desk
NASA Center for AeroSpace Information
800 Elkridge Landing Road
Linthicum Heights, MD 21090-2934

Scientific and Technical Aerospace Reports

Scientific and Technical Aerospace Reports (STAR), is published each month as a major product of the International Aerospace Database, managed by the NASA Scientific and Technical Information (STI) Program.

Inside this issue you will find:

Front Matter
A typical citation and abstract sample explaining the standard format, which includes codes for ordering reports.

An Abstract Section
Citations and abstracts of reports and publications that provide comprehensive coverage of worldwide aerospace-related topics including aeronautics and space science technology. *STAR* lists published and publicly available reports entered into the NASA STI Database during the four weeks preceding publication of this issue. These citations and abstracts are listed by subject categories.

An Index Section
- Subject
- Personal author
- Corporate source
- Contract number
- Report number.

Appendix
A guide for ordering cited reports, registering with the NASA STI Program, and using the available products and services. Additionally, price schedules, phone numbers, and addresses are included in this information packed section.

NASA also sponsors companion journals, *International Aerospace Abstracts (IAA)*, and *NASA Open Volumes on Aerospace (NOVA)*. They list abstracts of the open literature on aerospace subjects available worldwide. IAA is available from the American Institute of Aeronautics and Astronautics (AIAA), and *NOVA* is for internal NASA use only, available from the NASA Center for AeroSpace Information (CASI).

Reports found in *STAR* are also available through the NASA online retrieval service, RECON, and the Aerospace Database through DIALOG.

The NASA STI Program gathers information through national and international agreements and exchanges and makes this information available to the NASA community and to the public in many forms through various outlets.

For additional information on the NASA STI Program, call the NASA Access Help Desk at (301) 621-0390, or write to:

NASA Center for AeroSpace Information
800 Elkridge Landing Road
Linthicum Heights, Maryland 21090-2934

US ISSN 0036-8741

This publication was prepared by the NASA Center for AeroSpace Information,
800 Elkridge Landing Road, Linthicum Heights, MD 21090-2934, (301) 621-0390.

Volume 32 Number 2 / February 1994

TABLE OF CONTENTS

AERONAUTICS For related information see also *Astronautics.*

01 AERONAUTICS (GENERAL) **499**

02 AERODYNAMICS **499**
Includes aerodynamics of bodies, combinations, wings, rotors, and control surfaces; and internal flow in ducts and turbomachinery. For related information see also 34 *Fluid Mechanics and Heat Transfer.*

03 AIR TRANSPORTATION AND SAFETY **510**
Includes passenger and cargo air transport operations; and aircraft accidents. For related information see also *16 Space Transportation* and *85 Urban Technology and Transportation.*

04 AIRCRAFT COMMUNICATIONS AND NAVIGATION **512**
Includes digital and voice communication with aircraft; air navigation systems (satellite and ground based); and air traffic control. For related information see also *17 Space Communications, Spacecraft Communications, Command and Tracking* and *32 Communications and Radar.*

05 AIRCRAFT DESIGN, TESTING AND PERFORMANCE **514**
Includes aircraft simulation technology. For related information see also *18 Spacecraft Design, Testing and Performance* and *39 Structural Mechanics.* For land transportation vehicles see *85 Urban Technology and Transportation.*

06 AIRCRAFT INSTRUMENTATION **516**
Includes cockpit and cabin display devices; and flight instruments. For related information see also *19 Spacecraft Instrumentation* and *35 Instrumentation and Photography.*

07 AIRCRAFT PROPULSION AND POWER **517**
Includes prime propulsion systems and systems components, e.g., gas turbine engines and compressors; and onboard auxiliary power plants for aircraft. For related information see also *20 Spacecraft Propulsion and Power, 28 Propellants and Fuels,* and *44 Energy Production and Conversion.*

08 AIRCRAFT STABILITY AND CONTROL **520**
Includes aircraft handling qualities; piloting; flight controls; and autopilots. For related information see also *05 Aircraft Design, Testing and Performance.*

09 RESEARCH AND SUPPORT FACILITIES (AIR) **527**
Includes airports, hangars and runways; aircraft repair and overhaul facilities; wind tunnels; shock tubes; and aircraft engine test stands. For related information see also *14 Ground Support Systems and Facilities (Space).*

ASTRONAUTICS For related information see also *Aeronautics.*

12 ASTRONAUTICS (GENERAL) **529**
For extraterrestrial exploration see *91 Lunar and Planetary Exploration.*

13 ASTRODYNAMICS **532**
Includes powered and free-flight trajectories; and orbital and launching dynamics.

14 GROUND SUPPORT SYSTEMS AND FACILITIES (SPACE) **532**
Includes launch complexes, research and production facilities; ground support equipment, e.g., mobile transporters; and simulators. For related information see also *09 Research and Support Facilities (Air).*

15 LAUNCH VEHICLES AND SPACE VEHICLES **533**
Includes boosters; operating problems of launch/space vehicle systems; and reusable vehicles. For related information see also *20 Spacecraft Propulsion and Power.*

16 SPACE TRANSPORTATION **533**
Includes passenger and cargo space transportation, e.g., shuttle operations; and space rescue techniques. For related information see also *03 Air Transportation and Safety* and *18 Spacecraft Design, Testing and Performance.* For space suits see *54 Man/System Technology and Life Support.*

17 SPACE COMMUNICATIONS, SPACECRAFT COMMUNICATIONS, COMMAND AND TRACKING **537**
Includes telemetry; space communications networks; astronavigation and guidance; and radio blackout. For related information see also *04 Aircraft Communications and Navigation* and *32 Communications and Radar.*

N.A.—No abstracts were assigned to this category for this issue.

18 SPACECRAFT DESIGN, TESTING AND PERFORMANCE **539**
Includes satellites; space platforms; space stations; spacecraft systems and components such as thermal and environmental controls; and attitude controls. For life support systems see *54 Man/System Technology and Life Support.* For related information see also *05 Aircraft Design, Testing and Performance*, *39 Structural Mechanics*, and *16 Space Transportation.*

19 SPACECRAFT INSTRUMENTATION **544**
For related information see also *06 Aircraft Instrumentation* and *35 Instrumentation and Photography.*

20 SPACECRAFT PROPULSION AND POWER **548**
Includes main propulsion systems and components, e.g., rocket engines; and spacecraft auxiliary power sources. For related information see also *07 Aircraft Propulsion and Power*, *28 Propellants and Fuels*, *44 Energy Production and Conversion*, and *15 Launch Vehicles and Space Vehicles.*

CHEMISTRY AND MATERIALS

23 CHEMISTRY AND MATERIALS (GENERAL) **554**

24 COMPOSITE MATERIALS **554**
Includes physical, chemical, and mechanical properties of laminates and other composite materials. For ceramic materials see *27 Nonmetallic Materials.*

25 INORGANIC AND PHYSICAL CHEMISTRY **561**
Includes chemical analysis, e.g., chromatography; combustion theory; electrochemistry; and photochemistry. For related information see also *77 Thermodynamics and Statistical Physics.*

26 METALLIC MATERIALS **567**
Includes physical, chemical, and mechanical properties of metals, e.g., corrosion; and metallurgy.

27 NONMETALLIC MATERIALS **575**
Includes physical, chemical, and mechanical properties of plastics, elastomers, lubricants, polymers, textiles, adhesives, and ceramic materials. For composite materials see *24 Composite Materials.*

28 PROPELLANTS AND FUELS **583**
Includes rocket propellants, igniters and oxidizers; their storage and handling procedures; and aircraft fuels. For related information see also *07 Aircraft Propulsion and Power*, *20 Spacecraft Propulsion and Power*, and *44 Energy Production and Conversion.*

29 MATERIALS PROCESSING **586**
Includes space-based development of products and processes for commercial application. For biological materials see *55 Space Biology:*

ENGINEERING For related information see also *Physics.*

31 ENGINEERING (GENERAL) **595**
Includes vacuum technology; control engineering; display engineering; cryogenics; and fire prevention.

32 COMMUNICATIONS AND RADAR **597**
Includes radar; land and global communications; communications theory; and optical communications. For related information see also *04 Aircraft Communications and Navigation* and *17 Space Communications, Spacecraft Communications, Command and Tracking.* For search and rescue see *03 Air Transportation and Safety,* and *16 Space Transportation.*

33 ELECTRONICS AND ELECTRICAL ENGINEERING **618**
Includes test equipment and maintainability; components, e.g., tunnel diodes and transistors; microminiaturization; and integrated circuitry. For related information see also *60 Computer Operations and Hardware* and *76 Solid-State Physics.*

34 FLUID MECHANICS AND HEAT TRANSFER **627**
Includes boundary layers; hydrodynamics; fluidics; mass transfer and ablation cooling. For related information see also *02 Aerodynamics* and *77 Thermodynamics and Statistical Physics.*

35 INSTRUMENTATION AND PHOTOGRAPHY **648**
Includes remote sensors; measuring instruments and gauges; detectors; cameras and photographic supplies; and holography. For aerial photography see *43 Earth Resources and Remote Sensing.* For related information see also *06 Aircraft Instrumentation* and *19 Spacecraft Instrumentation.*

36 LASERS AND MASERS **653**
Includes parametric amplifiers. For related information see also *76 Solid-State Physics.*

37 MECHANICAL ENGINEERING **660**
Includes auxiliary systems (nonpower); machine elements and processes; and mechanical equipment.

38 QUALITY ASSURANCE AND RELIABILITY **665**
Includes product sampling procedures and techniques; and quality control.

39 STRUCTURAL MECHANICS **669**
Includes structural element design and weight analysis; fatigue; and thermal stress. For applications see *05 Aircraft Design, Testing and Performance* and *18 Spacecraft Design, Testing and Performance.*

GEOSCIENCES For related information see also *Space Sciences.*

42 GEOSCIENCES (GENERAL) **683**

43 EARTH RESOURCES AND REMOTE SENSING **684**
Includes remote sensing of earth resources by aircraft and spacecraft; photogrammetry; and aerial photography. For instrumentation see *35 Instrumentation and Photography.*

44 ENERGY PRODUCTION AND CONVERSION **700**
Includes specific energy conversion systems, e.g., fuel cells; global sources of energy; geophysical conversion; and windpower. For related information see also *07 Aircraft Propulsion and Power, 20 Spacecraft Propulsion and Power,* and *28 Propellants and Fuels.*

45 ENVIRONMENT POLLUTION **705**
Includes atmospheric, noise, thermal, and water pollution.

46 GEOPHYSICS **711**
Includes aeronomy; upper and lower atmosphere studies; ionospheric and magnetospheric physics; and geomagnetism. For space radiation see *93 Space Radiation.*

47 METEOROLOGY AND CLIMATOLOGY **718**
Includes weather forecasting and modification.

48 OCEANOGRAPHY **725**
Includes biological, dynamic, and physical oceanography; and marine resources. For related information see also *43 Earth Resources and Remote Sensing.*

LIFE SCIENCES

51 LIFE SCIENCES (GENERAL) **727**

52 AEROSPACE MEDICINE **731**
Includes physiological factors; biological effects of radiation; and effects of weightlessness on man and animals.

53 BEHAVIORAL SCIENCES **734**
Includes psychological factors; individual and group behavior; crew training and evaluation; and psychiatric research.

54 MAN/SYSTEM TECHNOLOGY AND LIFE SUPPORT **736**
Includes human engineering; biotechnology; and space suits and protective clothing. For related information see also *16 Space Transportation.*

55 SPACE BIOLOGY **739**
Includes exobiology; planetary biology; and extraterrestrial life.

MATHEMATICAL AND COMPUTER SCIENCES

59 MATHEMATICAL AND COMPUTER SCIENCES (GENERAL) **739**

60 COMPUTER OPERATIONS AND HARDWARE **740**
Includes hardware for computer graphics, firmware, and data processing. For components see *33 Electronics and Electrical Engineering.*

61 COMPUTER PROGRAMMING AND SOFTWARE **742**
Includes computer programs, routines, algorithms, and specific applications, e.g., CAD/CAM.

62 COMPUTER SYSTEMS **758**
Includes computer networks and special application computer systems.

63 CYBERNETICS **761**
Includes feedback and control theory, artificial intelligence, robotics and expert systems. For related information see also *54 Man/System Technology and Life Support.*

64 NUMERICAL ANALYSIS **767**
Includes iteration, difference equations, and numerical approximation.

65 STATISTICS AND PROBABILITY **772**
Includes data sampling and smoothing; Monte Carlo method; and stochastic processes.

66 SYSTEMS ANALYSIS **774**
Includes mathematical modeling; network analysis; and operations research.

67 THEORETICAL MATHEMATICS **775**
Includes topology and number theory.

PHYSICS For related information see also *Engineering.*

70 PHYSICS (GENERAL) **775**
For precision time and time interval (PTTI) see *35 Instrumentation and Photography*; for geophysics, astrophysics or solar physics see *46 Geophysics, 90 Astrophysics*, or *92 Solar Physics.*

71 ACOUSTICS **776**
Includes sound generation, transmission, and attenuation. For noise pollution see *45 Environment Pollution.*

72 ATOMIC AND MOLECULAR PHYSICS **778**
Includes atomic structure, electron properties, and molecular spectra.

73 NUCLEAR AND HIGH-ENERGY PHYSICS **788**
Includes elementary and nuclear particles; and reactor theory. For space radiation see *93 Space Radiation.*

74 OPTICS **790**
Includes light phenomena and optical devices. For lasers see *36 Lasers and Masers.*

75 PLASMA PHYSICS **794**
Includes magnetohydrodynamics and plasma fusion. For ionospheric plasmas see *46 Geophysics.* For space plasmas see *90 Astrophysics.*

76 SOLID-STATE PHYSICS **803**
Includes superconductivity. For related information see also *33 Electronics and Electrical Engineering* and *36 Lasers and Masers.*

77 THERMODYNAMICS AND STATISTICAL PHYSICS **816**
Includes quantum mechanics; theoretical physics; and Bose and Fermi statistics. For related information see also *25 Inorganic and Physical Chemistry* and *34 Fluid Mechanics and Heat Transfer.*

SOCIAL SCIENCES

80 SOCIAL SCIENCES (GENERAL) **818**
Includes educational matters.

81 ADMINISTRATION AND MANAGEMENT **819**
Includes management planning and research.

82 DOCUMENTATION AND INFORMATION SCIENCE **820**
Includes information management; information storage and retrieval technology; technical writing; graphic arts; and micrography. For computer documentation see *61 Computer Programming and Software.*

83 ECONOMICS AND COST ANALYSIS ..... **N.A.**
Includes cost effectiveness studies.

84 LAW, POLITICAL SCIENCE AND SPACE POLICY **827**
Includes NASA appropriation hearings; aviation law; space law and policy; international law; international cooperation; and patent policy.

85 URBAN TECHNOLOGY AND TRANSPORTATION **828**
Includes applications of space technology to urban problems; technology transfer; technology assessment; and surface and mass transportation. For related information see *03 Air Transportation and Safety, 16 Space Transportation,* and *44 Energy Production and Conversion.*

SPACE SCIENCES For related information see also *Geosciences.*

88 SPACE SCIENCES (GENERAL) 828

89 ASTRONOMY 828
Includes radio, gamma-ray, and infrared astronomy; and astrometry.

90 ASTROPHYSICS 834
Includes cosmology; celestial mechanics; space plasmas; and interstellar and interplanetary gases and dust. For related information see also *75 Plasma Physics.*

91 LUNAR AND PLANETARY EXPLORATION 841
Includes planetology; and manned and unmanned flights. For spacecraft design or space stations see *18 Spacecraft Design, Testing and Performance.*

92 SOLAR PHYSICS 844
Includes solar activity, solar flares, solar radiation and sunspots. For related information see also *93 Space Radiation.*

93 SPACE RADIATION 846
Includes cosmic radiation; and inner and outer earth's radiation belts. For biological effects of radiation see *52 Aerospace Medicine.* For theory see *73 Nuclear and High-Energy Physics.*

GENERAL

Includes aeronautical, astronautical, and space science related histories, biographies, and pertinent reports too broad for categorization; histories or broad overviews of NASA programs.

99 GENERAL 849

SUBJECT INDEX I-1

PERSONAL AUTHOR INDEX I-147

CORPORATE SOURCE INDEX I-163

CONTRACT NUMBER INDEX I-187

REPORT NUMBER INDEX I-193

APPENDIX A-1

TYPICAL CITATION AND ABSTRACT

NASA SPONSORED

ON MICROFICHE

ACCESSION NUMBER → **N94-12270*#** United Technologies Corp., West Palm Beach, FL. ← CORPORATE SOURCE
Pratt and Whitney.

TITLE → **ADVANCED CONTROL FOR AIRBREATHING ENGINES, VOLUME 1: PRATT AND WHITNEY**

AUTHOR → J. A. Ralph Jul. 1993 83 p ← PUBLICATION DATE

CONTRACT OR GRANT → (Contract NAS3-25952; RTOP 505-62-61)

REPORT NUMBERS → (NASA-CR-189203; E-8006; NAS 1.26:189203) Avail: CASI HC A05/MF A01 ← AVAILABILITY SOURCE AND PRICE CODE

The application of advanced control concepts to air breathing engines may yield significant improvements in aircraft/engine performance and operability. Screening studies of advanced control concepts for air breathing engines were conducted by three major domestic aircraft engine manufacturers to determine the potential impact of concepts on turbine engine performance and operability. The purpose of the studies was to identify concepts which offered high potential yet may incur high research and development risk. A target suite of proposed advanced control concepts was formulated and evaluated in a two phase study to quantify each concept's impact on desired engine characteristics. To aid in the evaluation specific aircraft/engine combinations were considered: a Military High Performance Fighter mission, a High Speed Civil Transport mission, and a Civil Tiltrotor mission. Each of the advanced control concepts considered in the study are defined and described. The concept potential impact on engine performance was determined. Relevant figures of merit on which to evaluate the concepts are determined. Finally, the concepts are ranked with respect to the target aircraft/engine missions. A final report describing the screening studies was prepared by each engine manufacturer. Volume 1 of these reports describes the studies performed by Pratt & Whitney. Author (revised)

VOLUME 32 NUMBER 2 / February 1994

Scientific and Technical Aerospace Reports

A Monthly Publication of the National Aeronautics and Space Administration

01 AERONAUTICS (GENERAL)

N94-13108*# National Aeronautics and Space Administration. Lewis Research Center, Cleveland, OH.

AVERAGING TECHNIQUES FOR STEADY AND UNSTEADY CALCULATIONS OF A TRANSONIC FAN STAGE

M. L. Wyss (Cincinnati Univ., OH.), R. V. Chima, and D. L. Tweedt Jul. 1993 12 p Presented at the 24th AIAA Fluid Dynamics Conference, Orlando, FL, 6-9 Jul. 1993; sponsored by AIAA

(RTOP 535-05-10)

(NASA-TM-106231; E-7950; NAS 1.15:106231; AIAA Paper 93-3065)

Copyright Avail: CASI HC A03/MF A01

It is often desirable to characterize a turbomachinery flow field with a few lumped parameters such as total pressure ratio or stage efficiency. Various averaging schemes may be used to compute these parameters. The momentum, energy, and area averaging schemes are described and compared. The schemes were compared for two computed solutions of the midspan section of a transonic fan stage: a steady averaging-plane solution in which average rotor outflow conditions were used as stator inflow conditions, and an unsteady rotor-stator interaction solution. The solutions were computed on identical grids using similar Navier-Stokes codes and an algebraic turbulence model. The unsteady solution is described, some unsteady flow phenomena are discussed, and the steady pressure distributions are compared. Despite large unsteady pressure fluctuations on the stator surface, the steady pressure distribution matched the average unsteady distribution almost exactly. Stator wake profiles, stator loss coefficient, and stage efficiency were computed for the two solutions with the three averaging schemes and are compared. In general, the energy averaging scheme gave good agreement between the averaging-plane solution and the time-averaged unsteady solution, even though certain phenomena due to unsteady wake migration were neglected.

Author (revised)

N94-13520# Bombardier, Inc., Montreal (Quebec).

[ACTIVITIES OF BOMBARDIER, INC.] Annual Report, period ending 31 Jan. 1993

1993 57 p Original contains color illustrations

(ISBN-2-921393-11-5; CTN-93-60863) Copyright Avail: CASI HC A04/MF A01

Bombardier Inc. is a designer, manufacturer, and distributor of transportation equipment and other products and services related to its technology. Its corporate office is in Montreal, Quebec, and its production facilities are located in Canada, the United States, Mexico, Austria, Belgium, France, Finland, and the United Kingdom. Bombardier's Transportation Equipment Group manufactures railroad cars, locomotives, and related products and services. Its aerospace group includes Canadair, maker of the Canadair Regional Jet and the CL-415 amphibious aircraft; de Havilland Inc. (Canada), maker of the Dash-8 turboprop; Learjet Inc. (Wichita, Kansas), maker of the Learjet series of business aircraft; and Short Brothers (Northern Ireland), maker of military aircraft, components, and defense systems. Bombardier also has a consumer products group that makes snowmobiles, water craft and other items. In this 1992-93 annual report, highlights of activities and financial statements and summaries are presented. For 1992-93, Bombardier's income before taxes was $150.9 million on consolidated revenues of $4,448 million. Total aerospace sales were $2.2 billion, with a sales backlog of $3.3 billion.

CISTI

N94-13904# Technische Univ., Delft (Netherlands). Faculty of Aerospace Engineering.

THE DEVELOPMENT OF INSPECTION AND REPAIR METHODS FOR THE C-17 AFT CARGO DOOR Final Report

Robert Fredell Nov. 1992 54 p

(LR-704; ETN-93-94421) Avail: CASI HC A04/MF A01

The development of field level inspection and repair methods for the C-17 aft cargo door skins, constructed from ARALL 3, are reported. ARALL 3 is an advanced aramid/aluminum laminated sheet material with high strength and excellent fatigue resistance. The major areas of interest covered are: the effect of impact on the structural strength and durability; the effects of scratches on strength and durability; the limits of laminate workshop properties as they apply to repair; the most effective means of on-aircraft nondestructive inspection; and the development of acceptable practices for repair of damaged ARALL structures. The test program was focused on the following objectives: determining if the second cure cycle used in the manufacture of the door affects the fatigue and damage tolerance characteristics of the material; determining the effect of various levels of incidental damage on fatigue and residual strength properties of ARALL 3, and specifying what damage requires repair; and evaluating the structural effectiveness and ease of application of various concepts for base level repair of ARALL 3. The obtained results, conclusions, and recommendations are given.

ESA

02 AERODYNAMICS

Includes aerodynamics of bodies, combinations, wings, rotors, and control surfaces; and internal flow in ducts and turbomachinery.

For related information see also *34 Fluid Mechanics and Heat Transfer.*

N94-12852*# Institute for Computer Applications in Science and Engineering, Hampton, VA.

A COMPARISON OF TWO FORMULATIONS FOR HIGH-ORDER ACCURATE ESSENTIALLY NON-OSCILLATORY SCHEMES Final Report

Jay Casper (Vigyan Research Associates, Inc., Hampton, VA.), Chi-Wang Shu (Brown Univ., Providence, RI.), and H. L. Atkins (National Aeronautics and Space Administration. Langley Research Center, Hampton, VA.) Washington Jun. 1993 27 p Submitted for publication

(Contracts NAS1-19480; NAS1-19672; NAG1-1145; RTOP 505-90-52-01)

(NASA-CR-191476; NAS 1.26:191476; ICASE-93-27) Avail: CASI HC A03/MF A01

The finite-volume and finite-difference implementations of high-order accurate essentially non-oscillatory shock-capturing schemes are discussed and compared. Results obtained with fourth-order accurate algorithms based on both formulations are examined for accuracy, sensitivity to grid irregularities, resolution of waves that are oblique to the mesh, and computational efficiency. Some algorithm modifications that may be required for a given application are suggested. Conclusions that pertain to the relative merits of both formulations are drawn, and some circumstances for which each might be useful are noted.

Author (revised)

N94-12948# National Aerospace Lab., Tokyo (Japan). Aerodynamics Div.

NUMERICAL SIMULATION OF HYPERSONIC FLOW FOR THE DESIGN OF THE H-2 ORBITING PLANE (HOPE), PART 3 [HOPE NO GOKUCHOUONSOKURYUU SUUCHI SHIMYURESHON]

Yukimitsu Yamamoto Jul. 1992 97 p In JAPANESE Prepared in cooperation with NSDA, Tokyo, Japan
(NAL-TR-1168-Pt-3; JTN-93-80500-Pt-3) Avail: CASI HC A05/MF A02

Three-dimensional upwind flux-split Navier-Stokes codes are applied to examine hypersonic flow around HOPE-01 (H-2 Orbiting Plane) configurations. Numerical results are compared with experimental data from the National Aerospace Lab (NAL) hypersonic wind and shock tunnel. In order to enlarge the applicability of Computational Fluid Dynamics (CFD) for a more practical design purpose, the effects of rudder and elevon deflections were numerically investigated. In addition, to study the aerodynamic and aerothermodynamic environments at the high Mach numbers expected in the HOPE flight trajectory, computations were conducted using a Mach number of 12.0 and 15.0. Aerothermodynamic heating distributions were compared in detail with Calspan's shock tunnel data and fairly good quantitative agreements were obtained. Real gas effects were also analyzed using a chemical non-equilibrium Navier-Stokes code which was developed by combining finite-rate chemical reactions to the currently used perfect gas flux-split code. A fully implicit Alternative Directional Implicit (ADI) scheme is employed to avoid the stiffness problem occurring in the time integration process. Typical real gas effects on aerodynamic characteristics are revealed. This work was conducted as joint research of NAL and the National Space Development Agency (NASDA). Author (NASDA)

N94-12951# National Aerospace Lab., Tokyo (Japan). Dynamic Wind Tunnel Test Group.
IDENTIFYING THE NAL SPACEPLANE AERODYNAMIC MODEL USING DYNAMIC WIND TUNNEL TESTS [KEBURU SHIJI DOUTEKI FUUDOU SHIKEN NIYORU NAL SUPESUPUREN NO KUURIKI MODERU DOUTEI]
Masaaki Yanagihara Jul. 1992 45 p In JAPANESE
(NAL-TR-1171; JTN-93-80501) Avail: CASI HC A03/MF A01

An aerodynamic model identification technique utilized by the National Aerospace Laboratory (NAL) was applied to dynamic wind tunnel tests using a cable mounted model to extract aerodynamic parameters of the NAL Spaceplane. The estimated static parameters were evaluated by comparisons with static wind tunnel test results, whereas those for the dynamic parameters were evaluated by comparison with theoretically estimated values. In addition, mathematical flight simulations using both static and dynamic parameters were conducted for the total evaluation. The simulated results were subsequently compared with the wind tunnel test data, and satisfactory correlation was achieved, thereby, demonstrating the effectiveness of the dynamic tests. Author (NASDA)

N94-12989# Naval Surface Warfare Center, Dahlgren, VA.
IMPROVED AEROPREDICTION CODE. PART 1: SUMMARY OF NEW METHODS AND COMPARISON WITH EXPERIMENT
Frank G. Moore, Thomas C. Hymer, and Roy M. Mcinville May 1993 156 p
(AD-A266015; NSWCDD/TR-93/91) Avail: CASI HC A08/MF A02

A new and improved version of the Naval Surface Warfare Center, Dahlgren Division aeroprediction code (AP93) was developed. The new code contains new technology that allows planar aerodynamics of axisymmetric solid rocket-type weapons to be computed with engineering accurately over the entire Mach number range and for angles of attack to 30 deg. New technology developed and included in the AP93 includes: a new engineering method to compute aeroheating information at a high Mach number; extension of the second-order shock-expansion theory to include real-gas effects, including several new pressure prediction techniques; an improved body-alone nonlinear normal-force method; new methods for computing nonlinear aerodynamics of wing alone, wing body, and body wing due to angle of attack, and wing body due to control deflection; and a new base-drng database and improved empirical base-drag estimation technique. DTIC

N94-13076*# Tennessee Univ. Space Inst., Tullahoma. Center for Space Transportation and Applied Research.
A WALL INTERFERENCE ASSESSMENT/CORRECTION SYSTEM Semiannual Report No. 4, Jan. - Jun. 1993
Ching F. Lo 1993 45 p
(Grant NAG2-733)
(NASA-CR-194174; NAS 1.26:194174) Avail: CASI HC A03/MF A01

A Wall Signature method originally developed by Hackett was selected to be adapted for the Ames 12-ft Wind Tunnel Wall Interference Assessment/Correction (WIAC) System in the project. This method uses limited measurements of the static pressure at the wall, in conjunction with the solid wall boundary condition, to determine the strength and distribution of singularities representing the test article. The singularities are used in turn for estimating wall interference at the model location. The lifting interference will be treated separately by representing in a horseshoe vortex system for the model's lifting effects. The development and implementation of a working prototype will be completed, delivered, and documented with a software manual. The WIAC code will be validated by conducting numerically simulated experiments rather than actual wind tunnel experiments. The simulations will be used to generate both free-air and confined wind-tunnel flow fields for each of the test articles over a range of test configurations. Specifically, the pressure signature at the test section wall will be computed for the tunnel case to provide the simulated 'measured' data. These data will serve as the input for the WIAC method - Wall Signature method. The performance of the WIAC method then may be evaluated by comparing the corrected parameters with those for the free-air simulation. The following two additional tasks are included in the supplement No. 1 to the basic Grant. On-line wall interference calculation: The developed wall signature method (modified Hackett's method) for Ames 12-ft Tunnel will be the pre-computed coefficients which facilitate the on-line calculation of wall interference; and support system effects estimation: The effects on the wall pressure measurements due to the presence of the model support systems will be evaluated. Author (revised)

N94-13172*# National Aeronautics and Space Administration. Langley Research Center, Hampton, VA.
AERODYNAMICS OF A SPHERE AND AN OBLATE SPHEROID FOR MACH NUMBERS FROM 0.6 TO 10.5 INCLUDING SOME EFFECTS OF TEST CONDITIONS
M. Leroy Spearman and Dorothy O. Braswell Aug. 1993 26 p
(RTOP 505-69-20-01)
(NASA-TM-109016; NAS 1.15:109016) Avail: CASI HC A03/MF A01

Wind-tunnel tests were made for spheres of various sizes over a range of Mach numbers and Reynolds numbers. The results indicated some conditions where the drag was affected by changes in the afterbody pressure due to a shock reflection from the tunnel wall. This effect disappeared when the Mach number was increased for a given sphere size or when the sphere size was decreased for a given Mach number. Drag measurements and Schlieren photographs are presented that show the possibility of obtaining inaccurate data when tests are made with a sphere too large for the test section size and Mach number. Tests were also made of an oblate spheroid. The results indicated a region at high Mach numbers where inherent positive static stability might occur with the oblate-face forward. The drag results are compared with those for a sphere as well as those for various other shapes. The drag results for the oblate spheroid and the sphere are also compared with some calculated results. Author

N94-13180*# Georgia Inst. of Tech., Atlanta. School of Aerospace Engineering.
NUMERICAL STUDY OF THE EFFECTS OF ICING ON VISCOUS FLOW OVER WINGS Semiannual Progress Report, 1 Jan. - 30 Jun. 1993
L. N. Sankar Jul. 1993 38 p
(Grant NAG3-768)
(NASA-CR-193306; NAS 1.26:193306) Avail: CASI HC A03/MF A01

The progress made during the period 1 Jan. - 30 Jun. 1993 on the numerical study of the effects of icing on viscous flow over wings is summarized. The tasks performed were development of 3-D boundary layer methods for accurate estimates of the velocity field and surface heat transfer rates in the vicinity of the leading edge ice shape; studies of the effects of icing on 3-D highlift system performance; and continued improvement and validation of the 3-D Navier-Stokes solver. Results are discussed. CASI

N94-13198 Pennsylvania State Univ., University Park.
A TIME-ACCURATE NUMERICAL METHOD FOR CHEMICALLY REACTING FLOWS AT ALL MACH NUMBERS Ph.D. Thesis
James P. Withington 1992 223 p
Avail: Univ. Microfilms Order No. DA9311744

A time-accurate implicit scheme for solving chemically reacting flows

over a wide range of Mach numbers is developed and applied to selected problems of quasi one-dimensional and two-dimensional reacting flow. The motivation was to develop a unified solution algorithm capable of generating compressible flow solutions to flows that exhibit incompressible behavior in all or parts of the domain. The new formulation is based on the complete set of conservation laws, with a full account of finite-rate chemistry and thermodynamic and transport property variations with temperature and species concentration. To circumvent the computational difficulties at low Mach numbers common to typical schemes based on conservation law variables, the governing equations were modified by scaling the pressure term in the momentum equation and rederiving the conservative form of the governing equations from their non-conservative forms using a new equation of continuity based on a scaled pressure, rather than density. The result is that a well conditioned pseudo-time derivative vector replaces the original time derivative vector of conservation law quantities. Time-marching then evolves in a system of new dependent variables that include pressure rather than density. The advantage to this treatment is that numerically, pressure is much more sensitive to the flow solution than is the density. This is particularly true for low speed flows where density and temperature are nearly constant. The governing equations in the pseudo-time domain do not exhibit the stiffness and truncation error common in the standard density-based system. The equations are then solved using a dual time-stepping integration technique. While standard implicit schemes are implemented in pseudo-time, the converged solution represents a physically time-accurate solution at a particular physical time level. The technique is shown to be very robust, exhibiting convergence independent of Mach number for flows ranging from molecular diffusion velocity to supersonic speed. The equations cast in the new pseudo-time form behave similarly to density-based schemes in the moderate to high Mach number range, yet also offer the performance of low speed solvers for incompressible flows. Furthermore, it is able to achieve high-order temporal accuracy with only a fractional increase in computational cost due to the dual time-stepping procedure. The scheme is validated and capabilities of the algorithm are illustrated in its application to selected steady-state and transient flow problems including acoustic wave propagation, flame dynamics, and combustor flow fields of high contraction ratio. Finally, the scheme is applied to the study of combustion instabilities in a rocket combustion chamber. Dissert. Abstr.

N94-13260# Sandia National Labs., Albuquerque, NM.

PARACHUTE SYSTEM DESIGN, ANALYSIS, AND SIMULATION TOOL

W. D. Sundberg, D. D. McBride, K. W. Gwinn, D. E. Waye, and C. E. Hailey 1992 11 p Presented at the 12th Royal Aeronautical Society/AIAA Aerodynamic Decelerator Systems Technical Conference, London, England, 10 May 1993

(Contract DE-AC04-76DP-00789)

(DE93-013755; SAND-92-1888C; CONF-930580-3; AIAA Paper-93-1208) Avail: CASI HC A03/MF A01

For over twenty years designers at Sandia National Laboratories have developed various parachute simulation codes to model deployment, inflation, loading, trajectories, aircraft downwash, and line sail. In addition to these codes, material property data bases have been acquired. Recently we have initiated project to integrate these codes and data bases into a single software tool entitled SPARSYS (Sandia PARachute SYstem Simulation). We have constructed a graphical user interface as the driver and framework for SPARSYS. In this paper we present a status report on SPARSYS describing progress in developing and incorporating independent modules, in developing an integrated trajectory package, and in developing a materials data base including high-rate-of-strain data. DOE

N94-13266*# Stanford Univ., CA. Joint Inst. for Aeronautics and Acoustics.

THREE-DIMENSIONAL STRUCTURE OF STRAIGHT AND CURVED PLANE WAKES

James H. Weygandt and Rabindra D. Mehta Sep. 1993 339 p

(Contract NCC2-55)

(NASA-CR-194420; NAS 1.26:194420; JIAA-TR-110) Avail: CASI HC A15/MF A03

Although the plane wake is marked by the formation of strong spanwise vortices, the initially two-dimensional Karman-like vortices soon develop a three-dimensional structure in the form of secondary streamwise vortices. So far, this streamwise vortex structure has been studied mostly through flow visualization and at relatively low Reynolds numbers. The primary objective of the present program was to investigate the origin and evolution of the three-dimensional structure of straight and curved plane wakes at relatively high Reynolds numbers (Re(sub b) = 28,000) through detailed measurements of the mean and turbulent properties at several streamwise locations. The experiments were conducted in three phases. In the first phase, the development of a straight plane wake was investigated. In the second phase, the effects of imposed streamwise curvature on the wake development were examined. The streamwise curvature was of constant radius and very mild in terms of the curvature ratio (b/(square root of R) is less than 2 percent). In both the first and second phases, the role of initial conditions was examined in wakes generated from both untripped (laminar) and tripped (turbulent) initial boundary layers. In the third phase, the effects of injecting streamwise vorticity and the effects of increased Reynolds number on the tripped wake structure and development were investigated. Author (revised)

N94-13292*# Princeton Univ., NJ. Dept. of Mechanical and Aerospace Engineering.

EXPLORATORY STUDY OF IN-PLANE STREAMLINE CURVATURE EFFECTS ON A TURBULENT BOUNDARY LAYER AT A MACH NUMBER OF 3 Final Technical Report, 27 Jan. 1989 - 26 Jan. 1990

Seymour M. Bogdonoff May 1991 4 p

(Grant NAG1-961)

(NASA-CR-193673; NAS 1.26:193673) Avail: CASI HC A01/MF A01

This report on a program to study in-plane streamline curvature effects in a turbulent boundary layer at a Mach number of 3. The original proposal, for a 3-year program to explore in-plane streamline curvature effects on a supersonic turbulent boundary layer using three-dimensional pressure fields generated by fins and wall geometry, ended after one year. The purpose of these tests was to compare these streamline curvature effects to the more classical two-dimensional curvature generated by wall shape and imposed pressure gradients, previously considered primarily in a plane normal to the floor. The studies were carried out in the Mach number of 3, 8 x 8 inch High Reynolds Number Supersonic Tunnel. The usual surface visualization and mean wall static pressures were supplemented by the use of many small high frequency wall static pressure gauges (Kulites) to get some indication of the amplification of boundary layer disturbances by the in-plane streamline curvature caused by the three-dimensional pressure fields imposed on the boundary layer. Derived from text

N94-13340# National Aerospace Lab., Tokyo (Japan). Advanced Aircraft Research Group.

LOW-SPEED WIND TUNNEL TESTS ON FOUR TYPES OF JOINED-WING AIRCRAFT MODELS [HISHIGATA KETSUGOUYOKUKI 4 KEITAI NO TEISOKU FUUDOU JIKKEN]

Akihito Iwasaki, Toshimi Fujita, Hirotoshi Fujieda, and Naoto Takizawa Jul. 1992 24 p In JAPANESE

(NAL-TR-1167; JTN-93-80487) Avail: CASI HC A03/MF A01

Low-speed wind tunnel tests were conducted on four types of joined-wing aircraft models. Various ratios of horizontal tail to wing span were employed (40 percent, 60 percent, and 100 percent), and the leading-edge at the tip of horizontal tail was joined to the trailing-edge of the wing for three configurations. In addition, in one configuration, the tips of the horizontal tail and the wing were overlapped using the 100 percent ratio. The horizontal tail has minus 22 deg dihedral and minus 25 deg sweep angles (25 percent chord line). The main wing has respectively corresponding angles of 10 deg and 40 deg. The results indicated that the area and location of horizontal tail significantly effect the aerodynamic characteristics of the joined-wing aircraft. Author (NASDA)

N94-13341# National Aerospace Lab., Tokyo (Japan). Advanced Aircraft Research Group.

LOW-SPEED WIND TUNNEL TESTS ON A JOINED-WING AIRCRAFT MODEL WITH VARIOUS UPPER-FIN [HISHIGATA KETSUGOUYOKUKI (UEYOKU TSUKI) NO TEISOKU FUUDOU JIKKEN]

Akihito Iwasaki, Toshimi Fujita, Hirotoshi Fujieda, and Naoto Takizawa Jul. 1992 27 p In JAPANESE

(NAL-TR-1169; JTN-93-80488) Avail: CASI HC A03/MF A01

Low-speed wind tunnel tests were conducted on a joined-wing aircraft model with various upper-fins (small wing-like surface fitted on the wing or the horizontal tail). The upper-fin was used to enhance direct side-force

control capability. In this case, the upper-fin was equipped with a plain flap as a rudder. The effects of the upper-fin on the aerodynamic characteristics of a joined-wing aircraft are described. A 0.6 ratio of the rear to front wing span was selected as the best condition. Four different shaped upper-fins were installed at the three locations on each wing at 0.6 half span. Reynolds number based on the mean aerodynamic chord was from 6.5 to 6.7 x 10(exp 5). The angle of attack was varied from zero to 25 deg., and the side-slip angle from zero to 15 deg. The results indicated that the upper-fin acts like a 'boundary layer fence' and protects wing tip stall when the upper-fin is installed on the wing. On the other hand, the upper-fin produced local flow separation over the wing, and this flow separation caused asymmetric lateral and directional characteristics with side-slip angle. Author (NASDA)

N94-13342# National Aerospace Lab., Tokyo (Japan). Thermofluid Dynamics Div.

DEVELOPMENT OF A HIGH-SPEED MECHANICAL DRIVE SYSTEM FOR OSCILLATING AN ANNULAR BLADE ROW IN THE BENDING MODE [KOUSOKU KIKAISHIKI YOKUNETSU MAGE SHINDOU KASHIN SOUCHI TO SONO TOKUSEI]

Hideshi Oinuma and Hiroshi Kobayashi Jul. 1992 22 p In JAPANESE
(NAL-TR-1170; JTN-93-80489) Avail: CASI HC A03/MF A01

A novel high-speed mechanical drive system was developed which enables controlled-oscillations to be produced in an annular blade row in the bending mode, thus, allowing solutions to be obtained for cascade flutter in turbomachinery. This system makes possible to take unsteady aerodynamic force measurements in the National Aerospace Laboratory (NAL) Annular Cascade Test Facility at the realistic, reduced frequency level of supersonic flutter in turbomachinery. Blade row oscillation tests demonstrated that the presented system can controllably-oscillate, at up to 200 Hz, all 16 blades composing the annular blade row at a constant amplitude and interblade phase angles. Both aerodynamically unstable and stable conditions of the annular blade row can be controllably-oscillated while operating in a supersonic flow field. Author (NASDA)

N94-13345# National Aerospace Lab., Tokyo (Japan). Airframe Div.

ESTIMATION OF CRITICAL VALUES AND VIBRATION CHARACTERISTICS ON SUPERSONIC DELTA WINGS. PART 2: LOCALLY-STATIONARY TIME SERIES ANALYSIS OF NONSTATIONARY RANDOM RESPONSES [CHOUONSOKU DERUTAYOKU NO SHINDOU TOKUSEI TO ANTEIGENKAI NO SUITEI: HITEIJOUNA FUKISOKU OUTOU NO KYOKUSHO TEIJOU JIKEIRETSU KAISEKI]

Masakatsu Minegishi, Yasukatsu Andou, Yuuji Matsuzaki, Hiroshi Ejiri, Seizou Sakakibara, Junichi Noda, Kiyomichi Ishida, Hideo Sekine, Atsushi Tate, and Mitsunori Watanabe Sep. 1992 22 p In JAPANESE
(NAL-TR-1179; JTN-93-80492) Avail: CASI HC A03/MF A01

A locally-stationary time series analysis of nonstationary random responses in delta wings under supersonic conditions is presented. Since the partially supported cantilever delta wings failed during supersonic blowdown wind tunnel tests employing the injection and rejection systems, a safety device was introduced to prevent such failures. This enabled wing response data to be obtained from a test blow in which the dynamic pressure was increased at a constant speed with the Mach number being fixed. Estimated results indicated that the wing's critical values could be determined by applying the locally-stationary autoregressive process.
Author (NASDA)

N94-13369 Queens Univ., Kingston (Ontario). Dept. of Mechanical Engineering.

AN EXPERIMENTAL INVESTIGATION OF THE REDISTRIBUTION OF GAS STREAM TOTAL TEMPERATURE IN A HIGH TURNING ANGLE TRANSONIC PLANAR CASCADE Ph.D. Thesis

William Edward Carscallen Apr. 1990 170 p
(ISBN-0-315-60791-2; CTN-93-60734) Copyright Avail: Micromedia Ltd., Technical Information Centre, 165 Hotel de Ville, Place du Portage, Phase 2, Hull, Quebec J8X 3X2, Canada HC/MF

Early testing at the National Research Council of Canada's (NRC) Highly Loaded Turbine Test Rig revealed an apparent redistribution of the gas stream total temperature field as it passed through a transonic turbine nozzle. Furthermore, there appeared to be a change in area averaged total temperature across the nozzle row. In order to examine these observations, a transonic planar cascade of the exhauster type was constructed at NRC. Tests were carried out at pressure ratios giving nozzle isentropic exit Mach numbers ranging from low subsonic to low supersonic. Wedge probes were used to measure total temperature, total pressure, and flow angles downstream of the nozzle blades. Results of this detailed experimental investigation decisively indicated that the gas stream total temperature at the nozzle exit was highly redistributed. This total temperature separation or energy redistribution strongly depended on Mach number. A maximum temperature separation of 36.0 F occurred just prior to Mach number 1.0. The maximum negatively depressed values of the temperature change differ from those calculated by preliminary analysis and are not just a function of adiabatic wall temperature. An increase of area averaged temperature change was found and was attributed to heat transfer from the ambient surroundings to the planar cascade. Author (CISTI)

N94-13392# National Aerospace Lab., Tokyo (Japan). Flight Research Div.

ESTIMATION OF AIRCRAFT AERODYNAMIC DERIVATIVES WITH THE TOTAL LEAST SQUARES METHOD [TOTARUISUTO SUKUEA HOU WO MOCHIITA KOUKUUKI NO KUURIK I BIKEISUU NO SUITEI]

Kazuya Masui Apr. 1992 26 p In JAPANESE
(NAL-TR-1150; JTN-93-80483) Avail: CASI HC A03/MF A01

This report describes the Total Least Squares (TLS) Method which estimates unknown linear equation coefficients assuming that both the explanatory variables and the objective variable are affected by measurement errors. This method is one of the generalizations of the conventionally used Least Squares (LS) Method. The concept, algorithm, and characteristics of the TLS method are compared with those of the LS method. It is shown that the TLS method gives the unbiased coefficients and the correct standard deviations of them. In addition, an example of estimating aerodynamic derivatives from flight test data is presented.
Author (NASDA)

N94-13422*# MCAT Inst., San Jose, CA.

HIGH SPEED TRANSITION PREDICTION Final Report

Gediminis Gasperas Aug. 1993 20 p
(Contract NCC2-704)
(NASA-CR-194125; NAS 1.26:194125; MCAT-93-16) Avail: CASI HC A03/MF A01

The main objective of this work period was to develop, maintain and exercise state-of-the-art methods for transition prediction in supersonic flow fields. Basic state and stability codes, acquired during the last work period, were exercised and applied to calculate the properties of various flowfields. The development of a code for the prediction of transition location using a currently novel method (the PSE or Parabolized Stability Equation method), initiated during the last work period and continued during the present work period, was cancelled at mid-year for budgetary reasons. Other activities during this period included the presentation of a paper at the APS meeting in Tallahassee, Florida entitled 'Stability of Two-Dimensional Compressible Boundary Layers', as well as the initiation of a paper co-authored with H. Reed of the Arizona State University entitled 'Stability of Boundary Layers'.
Derived from text

N94-13454# National Aerospace Lab., Tokyo (Japan). Advanced Aircraft Research Group.

EXPERIMENTAL STUDIES OF VORTEX FLAPS AND VORTEX PLATES. PART 2: 1.15m SPAN 60 DEG DELTA WING

Kenichi Rinoie and John L. Stollery (Cranfield Inst. of Tech., Bedford, England.) Oct. 1992 39 p
(NAL-TR-1180T-Pt-2; JTN-93-80502-Pt-2) Avail: CASI HC A03/MF A01

Low-speed wind tunnel tests were carried out on several vortex flap and vortex plate configurations to assess their benefits. The force and surface pressure measurements were taken using a 1.15 m span, 60 deg delta wing model. Results indicate that the vortex flap deflection angle, which causes the flow to come almost smoothly onto the flap surface without any large separation, shows a much higher lift/drag ratio than the flap deflection angle which forms a leading-edge separation vortex over the flap surface. It was also found that there is no benefit in vortex flap deployment at incidences higher than the stall incidence. The performance of a vortex plate protruding from the leading-edge of the datum delta wing is shown to be comparable to that of the vortex flap. However, when the

vortex plate is used with the vortex flap deflected, these tests showed no benefits. Author (NASDA)

N94-13463*# Colorado Univ., Boulder. Dept. of Aerospace Engineering Sciences.

ANALYSIS OF THE HARRIER FOREBODY/INLET DESIGN USING COMPUTATIONAL TECHNIQUES Final Report, 1 Mar. 1991 - 31 Aug. 1993

Chuen-Yen Chow 1993 3 p

(Contract NCC2-714)

(NASA-CR-193616; NAS 1.26:193616) Avail: CASI HC A01/MF A01

Under the support of this Cooperative Agreement, computations of transonic flow past the complex forebody/inlet configuration of the AV-8B Harrier II have been performed. The actual aircraft configuration was measured and its surface and surrounding domain were defined using computational structured grids. The thin-layer Navier-Stokes equations were used to model the flow along with the Chimera embedded multi-grid technique. A fully conservative, alternating direction implicit (ADI), approximately-factored, partially flux-split algorithm was employed to perform the computation. An existing code was altered to conform with the needs of the study, and some special engine face boundary conditions were developed. The algorithm incorporated the Chimera technique and an algebraic turbulence model in order to deal with the embedded multi-grids and viscous governing equations. Comparison with experimental data has yielded good agreement for the simplifications incorporated into the analysis. The aim of the present research was to provide a methodology for the numerical solution of complex, combined external/internal flows. This is the first time-dependent Navier-Stokes solution for a geometry in which the fuselage and inlet share a wall. The results indicate the methodology used here is a viable tool for transonic aircraft modeling. Author

N94-13528# National Aerospace Lab., Amsterdam (Netherlands). Fluid Dynamics Div.

ON THE USE OF THE METHOD OF MATCHED ASYMPTOTIC EXPANSIONS IN PROPELLER AERODYNAMICS AND ACOUSTICS

H. H. Brouwer 9 Aug. 1991 52 p Submitted for publication

(NLR-TP-91307-U; ETN-93-94337) Avail: CASI HC A04/MF A01

The applicability of the method of matched asymptotic expansions to both propeller aerodynamics and acoustics is investigated. The method is applied to a propeller with blades of high aspect ratio, in a uniform axial flow. The first two terms of the inner expansion and the first three terms of the outer expansion are considered. The matching yields an expression for the spanwise distribution of the downwash velocity. However, recasting the analytical expressions into an integral equation, similar to Pradtl lifting line equation for wings, yields results for both aerodynamic and acoustic quantities, which agree well with experimental results. The method, thus, constitutes a practical analysis method for conventional propellers. ESA

N94-13530# National Aerospace Lab., Amsterdam (Netherlands). Informatics Div.

CLEBSCH VARIABLE MODEL FOR UNSTEADY, TRANSONIC FLOW; APPLICATION TO 2D AIRFOILS

J. Westland 11 Oct. 1991 85 p

(Contract NIVR-01904N)

(NLR-TP-91387-U; ETN-93-94339) Copyright Avail: CASI HC A05/MF A01

A three dimensional model is derived from the unsteady Euler equations, in which shock generated entropy and vorticity are modeled using a Clebsch variable. This flow model is an extension of full potential theory and is capable of describing unsteady, inviscid, transonic flow with strong shock waves. Its implementation in the existing computer code TULIPS for the calculation of unsteady, transonic flow around a two dimensional airfoil by means of full potential theory is described. Results obtained show good agreement with results obtained from codes based on the Euler equations. ESA

N94-13531# National Aerospace Lab., Amsterdam (Netherlands). Informatics/Fluid Dynamics Div.

A ROBUST QUASI-SIMULTANEOUS INTERACTION METHOD FOR A FULL POTENTIAL FLOW WITH A BOUNDARY LAYER WITH APPLICATION TO WING/BODY CONFIGURATIONS

A. J. VanderWees and J. VanMuijden 15 Oct. 1991 18 p Presented at the 5th Symposium on Numerical and Physical Aspects of Aerodynamical Flows, Long Beach, CA, 13-15 Jan. 1992

(Contract NIVR-01802N)

(NLR-TP-91397-U; ETN-93-94340) Avail: CASI HC A03/MF A01

A progress report on the system MATRICS (Multicomponent Aircraft Transonic Inviscid Computation System), for the calculation of the three dimensional inviscid transonic potential flow about wing/body configurations, is given. At present, work is in progress to extend MATRICS to take viscous effects into account through coupling with a boundary layer solver. This solver, MATRICS-5, is based on robust calculation methods for the boundary layer, the outer wing flow, and their interaction. MATRICS-5 is intended for (inverse) design purposes. The boundary layer and wake are based on an integral formulation of the unsteady first order boundary layer equations, the inviscid method is the existing MATRICS potential flow solver, and the interaction algorithm is of the quasisimultaneous type. ESA

N94-13555 Virginia Polytechnic Inst. and State Univ., Blacksburg.

A TECHNIQUE FOR DIRECT MEASUREMENT OF SKIN FRICTION IN SUPERSONIC COMBUSTION FLOW Ph.D. Thesis

Dianne Joan DeTurris 1992 162 p

Avail: Univ. Microfilms Order No. DA9310502

A technique has been developed to directly measure skin friction in the turbulent boundary layer of a three-dimensional supersonic combustion flow. A floating element cantilever beam configuration has been designed to detect two components of the small tangential shear forces created by the flow passing over the non-intrusive floating element. Although skin friction has been measured successfully in cold flow before, this gauge is uniquely designed for testing in high temperature, high heat flux environments. The application which specifically prompted the development of this technique was the propulsion system for the National Aero-Space Plane. An appreciable need exists to determine the skin friction inside the combustor of this scramjet engine, and the three-dimensional, supersonic, reacting flow field is difficult to predict numerically. Gauges were tested in a variety of supersonic combustion facilities, with each combustor requiring customization of the gauge design to the test conditions and geometry of the model wall. Maintaining constant temperature of the strain gages inside the sensor throughout the test cycle is of critical importance, due to their sensitivity to temperature changes. Over the course of the project, many parameters which may affect the measurement were identified and examined individually. Changes were adapted into the design when necessary, including tailoring the design to insure that the floating element temperature remains close to that of the surrounding wall. For this reason, a numerical heat transfer study was undertaken to check that the gauge could be adapted for new test conditions. The output from the gauge during supersonic combustion was found to be repeatable for the same nominal input conditions, and this repeatability was consistent from facility to facility. Results in two-dimensional, supersonic cold flow compare well with predicted flat plate values. Results indicate that C(sub f) is considerably higher in some cases than the corresponding value for a similar Reynolds number flow without combustion. The overall accuracy of the gauge is estimated to be +/- 10 percent. The gauge has made useful measurements in varying flow environments, and shown that its design is adaptable and durable. Author

N94-13556 Princeton Univ., NJ.

A THREE-DIMENSIONAL SUPERSONIC TURBULENT BOUNDARY LAYER GENERATED BY AN ISENTROPIC COMPRESSION Ph.D. Thesis

Wolfgang Konrad 1993 200 p

Avail: Univ. Microfilms Order No. DA9311224

An experimental study of a three-dimensional supersonic turbulent boundary layer generated by an isentropic compression is described. The incoming boundary layer was at Mach 2.9 and compressed by a 20 degree curved fin. The experimental data set comprises both mean and fluctuating data. Additionally, data from computations performed by Knight at Rutgers University were available for analysis. Surface flow visualizations, surface static pressures, flowfield surveys of Pitot pressure, yaw angle, and static pressure, and Preston tube measurements were included in the mean data. Hot-wire anemometry with normal and crossed-wires was used to obtain measurements of five of the six components of the Reynolds stress tensor ((-rho-bar)(v')(omego') being the only quantity not measured). The characteristics of the mean flowfield structure were revealed using both

the experimental and the computed mean data. Three different flow regimes were identified: the small crossflow region, the upstream convergence region, and the downstream convergence region. The features of each region were discussed in detail. The turbulence behavior was investigated at one location in each of these identified flow regimes. The mean flowfield behavior was used to explain the turbulence behavior and differences to two-dimensional flows in similar pressure gradients were pointed out. A comparison of the turbulence behavior to that in an adverse pressure gradient with identical initial conditions indicates that the Reynolds shear stress (-rho-bar)(u'v')-bar is significantly reduced due to three-dimensionality and streamline curvature. The results show for the first time in supersonic flow the stabilizing effect of in-plane curvature. Further comparisons with available turbulence data in a 10 degree sharp fin interaction showed a generally similar behavior which was attributed to similar mean flowfield structure. Dissert. Abstr.

N94-13607*# Virginia Polytechnic Inst. and State Univ., Blacksburg. Dept. of Aerospace and Ocean Engineering.

CALCULATION OF HYPERSONIC SHOCK STRUCTURE USING FLUX-SPLIT ALGORITHMS

W. M. Eppard and B. Grossman Jul. 1991 17 p

(Grant NAG1-776)

(NASA-CR-194296; NAS 1.26:194296; ICAM-91-07-04) Avail: CASI HC A03/MF A01

There exists an altitude regime in the atmosphere that is within the continuum domain, but wherein the conventional Navier-Stokes equations cease to be accurate. The altitude limits for this so called continuum transition regime depend on vehicle size and speed. Within this regime the thickness of the bow shock wave is no longer negligible when compared to the shock stand-off distance and the peak radiation intensity occurs within the shock wave structure itself. For this reason it is no longer valid to treat the shock wave as a discontinuous jump and it becomes necessary to compute through the shock wave itself. To accurately calculate hypersonic flowfields, the governing equations must be capable of yielding realistic profiles of flow variables throughout the structure of a hypersonic shock wave. The conventional form of the Navier-Stokes equations is restricted to flows with only small departures from translational equilibrium; it is for this reason they do not provide the capability to accurately predict hypersonic shock structure. Calculations in the continuum transition regime, therefore, require the use of governing equations other than Navier-Stokes. Several alternatives to Navier-Stokes are discussed; first for the case of a monatomic gas and then for the case of a diatomic gas where rotational energy must be included. Results are presented for normal shock calculations with argon and nitrogen. Author (revised)

N94-13621* National Aeronautics and Space Administration. Lewis Research Center, Cleveland, OH.

A FUTURE VIEW OF COMPUTATIONAL SCIENCE IN AIRCRAFT (Videotape)

Aug. 1989 Videotape: 9 min. 26 sec. playing time, in color, with sound

(NASA-TM-109284; NONP-VT-93-185300) Avail: CASI VHS A01/BETA A22

The accomplishments of LeRC in the field of computational fluid dynamics are presented. Author (revised)

N94-13632* National Aeronautics and Space Administration. Langley Research Center, Hampton, VA.

HL-20 PERSONNEL LAUNCH SYSTEM (Videotape)

Sep. 1990 Videotape: 5 min. 25 sec. playing time, in color, with sound

(NASA-TM-109292; NONP-VT-93-185307) Avail: CASI VHS A01/BETA A22

An overview of lifting body research to include LaRC's full scale engineering research model is presented. Author (revised)

N94-13705# Air Force Inst. of Tech., Wright-Patterson AFB, OH. School of Engineering.

A COMPARISON OF COMPUTATIONAL AND EXPERIMENTAL DATA FOR A SUBSCALE HIGH SPEED PROPULSIVE NOZZLE AT LOW MACH NUMBERS M.S. Thesis

Yonghee Hyun Jun. 1993 164 p

(AD-A266543; AFIT/GAE/ENY/93J-02) Avail: CASI HC A08/MF A02

This computational study of a hypersonic sub-scale nozzle/cowl configuration compares numerical solutions with experimental data for nozzle performance at off design conditions (subsonic through supersonic Mach numbers). A combination of Van Leer and Roe flux-splitting algorithms was used to solve the flow field. The explicit formulation assumed laminar planar flow and the perfect gas equation of state. A validation for the numerical algorithm was accomplished by comparing with experimental data for a variety of cases. Grid refinement, geometry, and operating conditions all influenced the comparison of the experimental and computational data. Generally, as the Mach number and nozzle pressure ratio increased, the consistency between the experimental results showed better agreement, although the computational investigation was performed on the basis of planar, laminar flow. For the different cowl configurations, the results for baseline and -5 degree cowl show a better agreement than the long and +5 degree cowl. DTIC

N94-13795# Army Research Lab., Aberdeen Proving Ground, MD.

A COMPUTATIONAL STUDY OF THE BASE REGION FLOW FIELD FOR THE M865 PROJECTILE Final Report, Nov. 1990 - Jun. 1991

Jubaraj Sahu Apr. 1993 33 p Supersedes BRL-IMR-955, Jan. 1991 Original contains color illustrations

(ARL-TR-109) Avail: CASI HC A03/MF A01

Recent firing tests for the M865 projectile have indicated that for reasons unknown, the tracer in the base cavity region does not remain visible during the entire flight. To assist in analyzing this problem, a computational study began to examine the base region flow field for this projectile including the base cavity. Flow computations for this projectile were performed at various supersonic Mach numbers, 2 less than M less than 5 and alpha = 0.0 degree using a time marching Navier-Stokes code. The computed results show sharp changes in the centerline pressure distributions in the base region near M = 3. This unexpected behavior may not be desirable and could be part of the problem. To minimize these pressure oscillations, several proposed configuration changes were made in the afterbody base cavity region and computations were performed for these modified configurations to analyze the effects on the flow field. One of these configurations with a new base cavity shape was found to improve the base region flow field. A modified version of this new base cavity was flight tested and the results revealed some improvement in the visibility of the tracer compared to the original configuration. Author (revised)

N94-14030*# MCAT Inst., San Jose, CA.

CNSFV CODE DEVELOPMENT, VIRTUAL ZONE NAVIER-STOKES COMPUTATIONS OF OSCILLATING CONTROL SURFACES AND COMPUTATIONAL SUPPORT OF THE LAMINAR FLOW SUPERSONIC WIND TUNNEL Final Report

Goetz H. Klopfer May 1993 30 p Original contains color illustrations

(Contract NCC2-616)

(NASA-CR-194259; NAS 1.26:194259; MCAT-93-14) Avail: CASI HC A03/MF A01; 2 functional color pages

The work performed during the past year on this cooperative agreement covered two major areas and two lesser ones. The two major items included further development and validation of the Compressible Navier-Stokes Finite Volume (CNSFV) code and providing computational support for the Laminar Flow Supersonic Wind Tunnel (LFSWT). The two lesser items involve a Navier-Stokes simulation of an oscillating control surface at transonic speeds and improving the basic algorithm used in the CNSFV code for faster convergence rates and more robustness. The work done in all four areas is in support of the High Speed Research Program at NASA Ames Research Center. Author (revised)

N94-14031# Institute for Aerospace Research, Ottawa (Ontario). Applied Aerodynamics Lab.

FLOW-FIELD INTERFERENCE PRODUCED BY AN ASYMMETRICAL SUPPORT STRUT

M. E. Beyers, H. J. Cai, and P. J. Penna Jan. 1993 45 p

(IAR-AN-75; NCR-32157; CTN-93-60735) Avail: CASI HC A03/MF A01

The interference flow field associated with an asymmetrical strut-mounted aircraft model was studied visually and through floor pressure measurements in a low-speed wind tunnel. The object of the investigation was to elucidate the unsteady interference phenomena which are expected to prevail in oscillatory tests. The conditions under which direct support interference and coupled support/wall interference could occur were explored qualitatively. Static support interference was found to be significant at

incidence angles below approximately 20 deg, and wall interference was found to be significant above this angle. Coupled support/wall interference is expected to be larger in pitch oscillation than in roll oscillation tests. This unsteady interference is expected to peak at intermediate incidence angles near 28 deg. These findings are generally applicable to test installations involving similarly sized models in closed, low-speed wind tunnels. Author (CISTI)

N94-14059# National Aerospace Lab., Tokyo (Japan). Advanced Aircraft Research Group.

EXPERIMENTAL STUDIES OF VORTEX FLAPS AND VORTEX PLATES. PART 1: 0.53 m SPAN 60 DEG DELTA WING

Kenichi Rinoie Mar. 1992 18 p

(DE93-767969; NAL-TR-1140T; JTN-93-80426) Avail: CASI HC A03/MF A01

Low-speed wind tunnel tests were conducted to investigate the flow around a leading-edge vortex flap at the maximum lift to drag (L/C) condition, and also to measure the performance of an inverted vortex flap and vortex plate. Associated force measurements and flow visualization tests were carried out on a 60 deg delta wing model. Results indicate that the maximum lift to drag ratio for any given flap deflection angle occurs when the flow smoothly comes onto the deflected vortex flap without forming a large leading-edge separation vortex on the flap surface. Use of a vortex plate was found to reduce the drag in comparison to the datum wing, a benefit due to some leading-edge suction acting on the forward facing region between the delta wing and the vortex plate. Author (NASDA)

N94-14061# National Aerospace Lab., Tokyo (Japan). Structural Mechanics Div.

NUMERICAL SIMULATION OF DYNAMIC STALL OF NACA0012 AIRFOIL OSCILLATING NEAR STATIC STALL ANGLE USING THE NAVIER-STOKES EQUATIONS

Kouji Isogai Mar. 1992 25 p Original contains color illustrations

(DE93-767970; NAL-TR-1141T; JTN-93-80427) Avail: CASI HC A03/MF A01

Numerical simulations were performed using the compressible Navier-Stokes equations to investigate the dynamic stall phenomena of the NACA0012 airfoil oscillating near the static stall angle. The Yee-Harten Total Variation Diminishing (TVD) scheme and the Baldwin-Lomax algebraic turbulence model were employed. The flow pattern, instantaneous pressure distribution, and behavior of the lift and pitching moment during dynamic stall were examined in detail. Computations showed that the major features of the dynamic stall phenomenon were qualitatively well reproduced, e.g., the formation of the leading-edge separation vortex and the behavior of the lift and pitching moment hysteresis loops. However, comparisons of the resultant pitching moment hysteresis loops with experimental data indicated that further research is necessary to obtain a rigorous quantitative prediction of the unsteady aerodynamic forces arising from the massively separated flows. Author (NASDA)

N94-14153# Von Karman Inst. for Fluid Dynamics, Rhode-Saint-Genese (Belgium).

METHODOLOGY OF HYPERSONIC TESTING

1993 339 p Presented at VKI/AEDC Special Course Lecture Series, Rhode Saint Genese, Belgium, 22-26 Feb. 1993

(VKI-LS-1993-03; D/1993/0238/409; ETN-93-94446) Copyright Avail: CASI HC A15/MF A03

An overview of the methods used in hypersonic testing and evaluation is presented and the principles behind those test techniques are explained. Topics covered include an introduction to hypersonic aerodynamics with descriptions of chemical and gas dynamic phenomena associated with hypersonic flight; categories and application of various hypersonic ground test facilities; characterization of facility flow fields; measurement techniques (both intrusive and non intrusive); hypersonic propulsion test principles and facilities; computational techniques and their integration into test programs; ground-test-to-flight data correlation methods; and test program planning. The Lecture Series begins at the introductory level and progressively increases in depth, culminating in a focus on special test and evaluation issues in hypersonics such as boundary layer transition, shock interactions, and electromagnetic wave testing. For individual titles, see N94-14154 through N94-14174.

N94-14154# Sverdrup Technology, Inc., Arnold AFS, TN.

HYPERSONIC OVERVIEW

Virgil K. Smith, III *In* VKI, Methodology of Hypersonic Testing 1993 23 p Prepared in cooperation with Arnold Engineering Development Center, Arnold AFS, TN (For primary document see N94-14153 02-02)

Copyright Avail: CASI HC A03/MF A03

An introduction to the field of hypersonic testing methodology is given by describing the traditional and future hypersonic system mission requirements. The terminology and phenomenology which is characteristic of hypersonic flow fields, including both the fluid mechanics and physical chemistry characteristics, are addressed. An overview of the hypersonic Test and Evaluation (T and E) requirements, which include the T and E challenges of future systems, the corresponding T and E facilities challenges and shortfalls, and the enabling methodologies and options is given. ESA

N94-14155# Calspan Corp., Arnold AFS, TN.

HYPERSONIC FLOW PHENOMENOLOGY

James R. Maus *In* VKI, Methodology of Hypersonic Testing 1993 15 p Prepared in cooperation with Arnold Engineering Development Center, Arnold AFS, TN (For primary document see N94-14153 02-02)

Copyright Avail: CASI HC A03/MF A03

A survey of some of the fundamental features of hypersonic flow is presented which introduces some of the purely fluid dynamic effects associated with high Mach numbers, as well as thermochemical effects inherent in high speed flows. Concepts such as Mach number independence and Newtonian theory are developed from simple gas dynamic relations. Boundary layer concepts are introduced, and the importance of the energy equation for predicting heating rates is discussed. The effect of entropy swallowing on the boundary layer development is addressed. Viscous interaction effects associated with the thick boundary layers of the high altitude flight regime are also introduced. Thermochemical effects arising due to elevated temperatures encountered in high speed flows are discussed. A method for calculating the equilibrium composition and thermodynamic properties of a reacting gas is described, and examples of the effects of chemical reactions on external and internal flows are presented. The phenomenological aspects of hypersonic flow are emphasized relying on a minimum of mathematical development. ESA

N94-14156# Tennessee Univ. Space Inst., Tullahoma. Dept. of Mechanical and Aerospace Engineering.

HYPERSONIC PROPULSION CHARACTERIZATION **c07**

Roger Crawford *In* VKI, Methodology of Hypersonic Testing 1993 10 p (For primary document see N94-14153 02-02)

Copyright Avail: CASI HC A02/MF A03

The propulsion cycle options for hypersonic vehicles are summarized including airbreathing, rocket and combinations. Each cycle is characterized by configuration, performance, efficiency and operating envelope. The major components of each propulsion system are identified and evaluated for influence on overall performance. Several combined cycle configurations offer the best propulsion characteristics for the various hypersonic missions from hypersonic transport to single stage to orbit. The unique experimental testing requirements for hypersonic propulsion systems present a significant challenge. ESA

N94-14157# Arnold Engineering Development Center, Arnold AFS, TN.

CHARACTERIZATION OF FLOW FIELDS IN HYPERSONIC GROUND TEST FACILITIES **c09**

Albert H. Boudreau *In* VKI, Methodology of Hypersonic Testing 1993 15 p Prepared in cooperation with Arnold Engineering Development Center, Arnold AFS, TN (For primary document see N94-14153 02-02)

Copyright Avail: CASI HC A03/MF A03

The fundamental differences between nonequilibrium encountered in flight and nonequilibrium phenomena encountered in ground test facilities are described. Focus is on facility induced non-equilibrium, describing the gross effects on bodies and the methods now available to characterize such flows. It shows that hypersonic test facilities are inherently difficult to characterize. In the past, many hypersonic facilities were reputed to produce test data of inferior quality when, in fact, it was poor characterization of the flow field principally at fault. With the renaissance in hypersonics at hand, experimentalists face new challenges in characterizing flow fields. The hypersonic test community has developed techniques to accurately

determine free stream conditions. These 'tools of characterization', are described and a standard by which all hypersonic wind tunnels should be compared is suggested. ESA

N94-14158# Calspan Corp., Arnold AFS, TN.
AERODYNAMIC AND AEROTHERMAL FACILITIES 1: HYPERSONIC WIND TUNNELS **c09**
A. Anderson and R. K. Matthews *In* VKI, Methodology of Hypersonic Testing 1993 13 p Prepared in cooperation with Arnold Engineering Development Center, Arnold AFS, TN (For primary document see N94-14153 02-02)
Copyright Avail: CASI HC A03/MF A03

An overview of hypersonic test facilities, which continue to play a major role in the development of hypersonic vehicles, is given. In the past, ground test facilities were often used to perform configuration parametric studies and/or to develop large data bases. Future testing will emphasize understanding of fluid physics and validation of codes. Computational Fluid Dynamics (CFD) has made great progress in the past two decades, but the marriage of CFD and ground testing is clearly a reality today, and will become even more important in the future as computational and experimental researchers learn how to work together. One of the challenges for the experimentalist is to develop and utilize facilities that simulate hypersonic flight, and to provide the required data precision to validate CFD codes. Fundamental considerations of facilities and simulation issues are reviewed. It is clear that no one facility will meet the wide variety of test objectives; therefore, the test facilities span a range of size, run time, complexity, and operating cost. Representative facilities are described, as well as their test capabilities and their shortfalls. ESA

N94-14159# Calspan Corp., Arnold AFS, TN.
AERODYNAMIC AND AEROTHERMAL FACILITIES 2. PART 1: SHORT-DURATION, HIGH-ENTHALPY FACILITIES **c09**
James R. Maus *In* VKI, Methodology of Hypersonic Testing 1993 15 p Prepared in cooperation with Arnold Engineering Development Center, Arnold AFS, TN (For primary document see N94-14153 02-02)
Copyright Avail: CASI HC A03/MF A03

Short duration facilities primarily used for aerodynamic or aerothermal testing are reviewed. Facilities which have useful run times ranging from a few hundred microseconds to a few hundred milliseconds are considered. The following types of facilities are addressed: arc heated hot shot tunnels, shock heated devices, compression heated wind tunnels, and aeroballistic ranges. Examples of both U.S. and European facilities are given. Principles of operation, facility performance, and strengths and weaknesses of the various types of facilities are emphasized. ESA

N94-14160# Tennessee Univ. Space Inst., Tullahoma. Dept. of Mechanical and Aerospace Engineering.
AERODYNAMIC AND AEROTHERMAL FACILITIES 2: CONTINUOUS FLOW HIGH ENTHALPY FACILITIES **c09**
Roger Crawford *In* VKI, Methodology of Hypersonic Testing 1993 32 p (For primary document see N94-14153 02-02)
Copyright Avail: CASI HC A03/MF A03

Facilities which provide the thermal equilibrium in structures and propulsion systems required for accurate evaluation of temperature and performance during hypersonic testing are considered. Combustion heated facilities and electric arc heated concepts are reviewed. Also the magnetohydrodynamic augmented arc heated facility performance is presented for very high Mach number simulation above 10. Propulsion system test and simulation requirements include: true enthalpy, correct entropy, free-stream total pressure and clean air for correct combustion kinetics. Exact simulation requires flight test, however each of the high enthalpy facilities reviewed meets most of the requirements for a range of Mach numbers. A set of overheads used in a lecture on arc heater types is annexed. ESA

N94-14161# Sverdrup Technology, Inc., Arnold AFS, TN.
AEROPROPULSION FACILITIES **c09**
Brian Wettlaufer *In* VKI, Methodology of Hypersonic Testing 1993 14 p Prepared in cooperation with Arnold Engineering Development Center, Arnold AFS, TN (For primary document see N94-14153 02-02)
Copyright Avail: CASI HC A03/MF A03

Test requirements of hypersonic propulsion systems and how they apply to the choice of ground test propulsion facilities are addressed. The ground test facilities required to support the development and evaluation testing of the propulsion systems must be capable of providing the correct test conditions for a sufficient period of time and be of adequate size to support full size test articles. Some required facility support systems for hypersonic propulsion testing are discussed and some facility shortfalls based on existing capabilities are identified. ESA

N94-14162# Calspan Corp., Arnold AFS, TN.
COMPUTATIONAL TECHNIQUES AND CAPABILITIES **c61**
James R. Maus (Arnold Engineering Development Center, Arnold AFS, TN.) *In* VKI, Methodology of Hypersonic Testing 1993 18 p Prepared in cooperation with Arnold Engineering Development Center, Arnold AFS, TN (For primary document see N94-14153 02-02)
Copyright Avail: CASI HC A03/MF A03

A review of numerical simulation techniques and capabilities, with emphasis on their relationship to the methodology of hypersonic testing, is presented. Flows in the continuum regime are dealt with exclusively and conservation principles and numerical techniques applicable to such flows are presented. The process of modeling complex physics and chemistry that must be included for a realistic treatment of high speed flow is discussed. Options with respect to formulation, discretization strategy, and numerics are presented. The application of some basic numerical algorithms to simplified model equations is undertaken to illustrate some features of the technique. The widening interface between Computational Fluid Dynamics (CFD) and ground testing is also addressed. The use of CFD in planning a ground test program, monitoring the experimental data, and evaluating the test results is discussed. Facility and instrumentation requirements to generate data useful for CFD code validation are indicated. ESA

N94-14163# Calspan Corp., Arnold AFS, TN.
TEST AND EVALUATION METHODS
R. K. Matthews (Arnold Engineering Development Center, Arnold AFS, TN.) and R. W. Rhudy (Arnold Engineering Development Center, Arnold AFS, TN.) *In* VKI, Methodology of Hypersonic Testing 1993 24 p Prepared in cooperation with Arnold Engineering Development Center, Arnold AFS, TN (For primary document see N94-14153 02-02)
Copyright Avail: CASI HC A03/MF A03

The procedures used in the continuous flow hypersonic tunnels of the AEDC for static stability, pressure, and heat transfer testing are described. Particular emphasis is on heat transfer techniques because of the importance of defining the thermal environment of hypersonic vehicles and because the static stability and pressure techniques are very similar to those used in subsonic and supersonic facilities. Aerothermal methodology includes thermal mapping, discrete gage techniques and gage calibration. Each specific test is described in terms of principle of operation, apparatus, data reduction, and illustrative data. ESA

N94-14164# Calspan Corp., Arnold AFS, TN.
MATERIALS/STRUCTURES TESTING **c39**
R. K. Matthews (Arnold Engineering Development Center, Arnold AFS, TN.) *In* VKI, Methodology of Hypersonic Testing 1993 12 p Prepared in cooperation with Arnold Engineering Development Center, Arnold AFS, TN (For primary document see N94-14153 02-02)
Copyright Avail: CASI HC A03/MF A03

An overview of the materials/structures test methodology used in the development of hypersonic vehicle components is presented. Focus is on aerothermal methodology and weather/erosion testing. For the latter, testing techniques which evaluate particle impact effects on vehicles operating at supersonic through hypersonic speeds in particle laden environments are described. Such facilities for increasing velocities are: wind tunnels/sleds; arc facilities; aeroballistic ranges. It is noted that it is of particular importance to demonstrate that flight components such as leading edges, cowl lips, and structural panels will survive the aerothermal flight environment. Specific components can experience very high heating rates and surface temperatures from 1100 to 1950 C. ESA

N94-14165# Sverdrup Technology, Inc., Arnold AFS, TN. Facility Enhancements.
AEROPROPULSION TEST AND EVALUATION METHODS **c07**
Brian Wettlaufer *In* VKI, Methodology of Hypersonic Testing 1993

18 p Prepared in cooperation with Arnold Engineering Development Center, Arnold AFS, TN (For primary document see N94-14153 02-02)
Copyright Avail: CASI HC A03/MF A03

Methods used for propulsion test and evaluation for both ground and flight testing, which are very important when the engine systems under consideration are supporting hypersonic vehicles, are considered. The propulsion systems of these vehicles are highly integrated within the airframe of the vehicle with many supporting systems being shared by both. To ground test an engine system such as this, it must first be separated from the vehicle. An approach to accomplish this through the use of reference planes is discussed. Both direct connect and free jet testing methods are discussed and some of the advantages, disadvantages, challenges, and issues associated with these testing techniques and approaches as they apply to hypersonic propulsion are addressed. ESA

N94-14166# Calspan Corp., Arnold AFS, TN.
HYPERSONIC FLOW FIELD MEASUREMENTS: INTRUSIVE
R. K. Matthews *In* VKI, Methodology of Hypersonic Testing 1993
13 p Prepared in cooperation with Arnold Engineering Development Center, Arnold AFS, TN (For primary document see N94-14153 02-02)
Copyright Avail: CASI HC A03/MF A03

'Intrusive' flow field measurements, ones that require a probe or other device to be inserted into the flow, are discussed. In general, these intrusive techniques are currently viewed as inferior to the more popular nonintrusive techniques. However, it should be remembered that in general these intrusive techniques have evolved over several decades while the flow field experience of nonintrusive techniques is relatively limited. Included in the intrusive classification are pitot tubes, total temperature probes, Mach/angularity probes, static pressure devices, hot wire anemometers, and flow visualization methods (vapor screen, and oil flow techniques). Each of these methods is considered. Within limits, each of these techniques can provide very useful data for the aerodynamicist. ESA

N94-14167# Calspan Corp., Arnold AFS, TN.
HYPERSONIC FLOW-FIELD MEASUREMENTS: NONINTRUSIVE
W. D. Williams *In* VKI, Methodology of Hypersonic Testing 1993
38 p Prepared in cooperation with Arnold Engineering Development Center, Arnold AFS, TN (For primary document see N94-14153 02-02)
Copyright Avail: CASI HC A03/MF A03

'Nonintrusive' techniques of hypersonic flow field measurement that are currently available, their basic principles, and advantages and disadvantages, are reviewed. An assessment of the state of applicability of the techniques is provided. The techniques include: Rayleigh scattering, particle scattering, laser and lamp absorption, line reversal, electron beam fluorescence, Raman scattering, holographic interferometry, and laser/laser tagging. A methodology for diagnostics selection and application is presented, and problem areas with possible solutions are examined. Numerous references of both a general nature for review of the fundamentals required for a better understanding of the measurement principles and a specific nature to show the level of advancement of the techniques are provided. ESA

N94-14168# Sverdrup Technology, Inc., Arnold AFS, TN.
HYPERSONIC FLIGHT TEST. PART 1: PROPULSION FLIGHT TESTING **c07**
Virgil K. Smith, III (Arnold Engineering Development Center, Arnold AFS, TN.) *In* VKI, Methodology of Hypersonic Testing 1993 10 p Prepared in cooperation with Arnold Engineering Development Center, Arnold AFS, TN (For primary document see N94-14153 02-02)
Copyright Avail: CASI HC A02/MF A03

The challenges of hypersonic system development, which require a combination of integrated ground testing, flight testing, and computational/simulation approaches, are considered. The role of flight testing in the triad of development approaches is addressed, and the reasons for hypersonic propulsion flight test is focused upon. Each reason is illustrated by specific mini-case studies, including the Lockheed X-7, North American X-15/Hypersonic Research Engine (HRE) combination, Russian Hypersonic Flying Laboratory (HFL), National Aeronautics and Space Administration (NASA) SR-71 External Burning Experiment, NASA Space Shuttle, and the German HYTEX Flying Prototype. Three types of hypersonic flight test systems are reviewed. The traditional and proposed propulsion flight test reasons and traditional/proposed approaches are reviewed. ESA

N94-14169# Calspan Corp., Arnold AFS, TN.
HYPERSONIC FLIGHT TESTING. PART 2: AEROTHERMAL FLIGHT TESTING **c07**
R. K. Matthews *In* VKI, Methodology of Hypersonic Testing 1993
6 p Prepared in cooperation with Arnold Engineering Development Center, Arnold AFS, TN (For primary document see N94-14153 02-02)
Copyright Avail: CASI HC A02/MF A03

Some of the fundamentals of hypersonic flight testing, which provides the only true environment to demonstrate that a vehicle has the material/structural integrity to survive hypersonic flight, are reviewed. An overview of aerothermal techniques is provided. Heat transfer gage measurements in particular are considered and some common problems encountered are discussed. ESA

N94-14170# Calspan Corp., Arnold AFS, TN.
EXTRAPOLATION OF GROUND TEST DATA TO FLIGHT
James R. Maus *In* VKI, Methodology of Hypersonic Testing 1993
16 p Prepared in cooperation with Arnold Engineering Development Center, Arnold AFS, TN (For primary document see N94-14153 02-02)
Copyright Avail: CASI HC A03/MF A03

The differences revealed by initial space flights between preflight aerodynamic predictions and actual flight data, were investigated. For the Space Shuttle these differences were notable for longitudinal trim during high speed reentry. To investigate these differences, several computer codes were applied to a modified Space Shuttle Orbiter to determine aerodynamic parameters over a wide range of conditions. Computations were carried out for wind tunnel conditions and flight conditions to assess Mach number, real gas, and viscous effects on the reentry aerodynamics of the orbiter. Based on the computational fluid dynamics results and a semiempirical analysis of viscous effects, an aerodynamic model for the orbiter was developed to extrapolate wind tunnel data for the Space Shuttle Orbiter to flight conditions. ESA

N94-14171# Calspan Corp., Arnold AFS, TN.
BOUNDARY-LAYER TRANSITION **c34**
R. K. Matthews *In* VKI, Methodology of Hypersonic Testing 1993
9 p Prepared in cooperation with Arnold Engineering Development Center, Arnold AFS, TN (For primary document see N94-14153 02-02)
Copyright Avail: CASI HC A02/MF A03

The prediction of the boundary layer transition Reynolds number for the design of hypersonic vehicles is considered. The boundary layer state (laminar or turbulent) that approaches the vehicle control surfaces can significantly affect the control surface effectiveness. In addition, the heating rates associated with turbulent boundary layers are often ten times higher than those of laminar boundary layers. Unfortunately, the methodology to predict transition has eluded the aerodynamicist for over three decades, and there are still many unanswered questions. Many parameters that affect transition are considered and numerous references for those who are interested in specializing in this topic are provided. It is emphasized that during wind tunnel testing it is very important to know the boundary layer state. Typically, heat transfer distributions can provide this information; however, it is often necessary to artificially trip the flow to induce a turbulent boundary layer. The methodology of using trip spheres is discussed, and illustrative data are presented. ESA

N94-14172# Sverdrup Technology, Inc., Arnold AFS, TN.
SHOCK/BOUNDARY-LAYER/SHOCK INTERACTIONS **c34**
Virgil K. Smith, III *In* VKI, Methodology of Hypersonic Testing 1993
10 p Prepared in cooperation with Arnold Engineering Development Center, Arnold AFS, TN (For primary document see N94-14153 02-02)
Copyright Avail: CASI HC A02/MF A03

The shock/shock interference phenomena and shock wave/boundary layer interactions in hypersonic flight are reviewed. The characteristic flow features are described, and the mechanisms for extremely high local heat transfer rates are emphasized. A classical example of interaction heating on the X-15 hypersonic vehicle is reviewed, and the damage caused by the unexpected aerodynamic heating is cited. These results serve as a strong reminder of the importance of shock impingement and interference heating cautions in hypersonic vehicle design, development, test, and evaluation. ESA

N94-14173# Calspan Corp., Arnold AFS, TN.
ELECTROMAGNETIC WAVE TEST **c32**
R. K. Matthews and S. A. Stepanek *In* VKI, Methodology of Hypersonic Testing 1993 7 p Prepared in cooperation with Arnold Engineering Development Center, Arnold AFS, TN (For primary document see N94-14153 02-02)
Copyright Avail: CASI HC A02/MF A03

Electromagnetic wave testing, which represents a relatively new test technique that involves the union of several disciplines (aerothermodynamics, electromagnetics, materials/structures, and advanced diagnostics) is introduced. The essence of this new technique deals with the transmission and possible distortion of electromagnetic waves (RF or IR) as they pass through the bow shock, flow field, and electromagnetic window of a missile flying at hypersonic speeds. Variations in gas density along the optical path can cause significant distortion of the electromagnetic waves and, therefore the missile seeker system may not effectively track the target. Two specific test techniques are described. The first example deals with the combining of a wind tunnel and an RF range while the second example discusses the complexities of evaluating IR seeker system performance. ESA

N94-14174# Tennessee Univ. Space Inst., Tullahoma. Dept. of Mechanical and Aerospace Engineering.
PROPULSION INTEGRATION **c07**
Roger Crawford *In* VKI, Methodology of Hypersonic Testing 1993 11 p (For primary document see N94-14153 02-02)
Copyright Avail: CASI HC A03/MF A03

The airframe-propulsion system integration of hypersonic vehicles is discussed considering the influences and problems of each of the contributing factors: inlet integration, combustion integration, nozzle integration, thermal management, and control system integration. It is noted that very high levels of efficiency in inlet, combustor and nozzle performance are required to assure net positive propulsive force in the integrated system. The higher the flight Mach number, the more difficult this integration task becomes. The inlet and nozzle integration requirements are evaluated for performance, stability and control influence on the flight vehicle. Combustor performance, fuel flow requirements and cooling loads are coupled by flight vehicle thermal management constraints. Low volumetric efficiency of the high energy density cryogenic fuels impacts the vehicle configuration due to the large fuel tank size. Thus the highly integrated hypersonic flight vehicle configuration is dominated by the propulsion system. ESA

N94-14208*# National Aeronautics and Space Administration. Lewis Research Center, Cleveland, OH.
MIXING NOISE REDUCTION FOR RECTANGULAR SUPERSONIC JETS BY NOZZLE SHAPING AND INDUCED SCREECH MIXING
Edward J. Rice and Ganesh Raman (Sverdrup Technology, Inc., Brook Park, OH.) Oct. 1993 12 p Proposed for presentation at the 15th AIAA Aeroacoustics Conference, Long Beach, CA, 25-27 Oct. 1993; sponsored by AIAA
(Contract NAS3-25266; RTOP 537-02-22)
(NASA-TM-106364; E-8165; NAS 1.15:106364; AIAA Paper 93-4322)
Avail: CASI HC A03/MF A01

Two methods of mixing noise modification were studied for supersonic jets flowing from rectangular nozzles with an aspect ratio of about five and a small dimension of about 1.4 cm. The first involves nozzle geometry variation using either single (unsymmetrical) or double bevelled (symmetrical) thirty degree cutbacks of the nozzle exit. Both converging (C) and converging-diverging (C-D) versions were tested. The double bevelled C-D nozzle produced a jet mixing noise reduction of about 4 dB compared to a standard rectangular C-D nozzle. In addition all bevelled nozzles produced an upstream shift in peak mixing noise which is conducive to improved attenuation when the nozzle is used in an acoustically treated duct. A large increase in high frequency noise also occurred near the plane of the nozzle exit. Because of near normal incidence, this noise can be easily attenuated with wall treatment. The second approach uses paddles inserted on the edge of the two sides of the jet to induce screech and greatly enhance the jet mixing. Although screech and mixing noise levels are increased, the enhanced mixing moves the source locations upstream and may make an enclosed system more amenable to noise reduction using wall acoustic treatment. Author

N94-14326*# Overset Methods, Inc., Vacaville, CA.
DOMAIN CONNECTIVITY AMONG SYSTEMS OF OVERSET GRIDS Progress Report
Robert L. Meakin 26 Jul. 1993 10 p
(Contract NCC2-783)
(NASA-CR-193390; NAS 1.26:193390) Avail: CASI HC A02/MF A01

This progress report describes research performed to achieve algorithmic improvements in the use of overset grids for the computation of unsteady flowfields about geometrically complex and moving component configurations. A hole-map computational method is detailed that reduces computational demand and corresponding demand on human resources. Results indicate that the method is both efficient and flexible for use in complex simulation cases. Tests were performed on shuttle orbiter/external tank, wing/store, and V-22 tilt-rotor configurations. The number of simulated points and the corresponding time on a SGI 4D-210 workstation are presented. CASI

N94-14538*# Georgia Inst. of Tech., Atlanta. School of Aerospace Engineering.
GUIDANCE LAW DEVELOPMENT FOR AEROASSISTED TRANSFER VEHICLES USING MATCHED ASYMPTOTIC EXPANSIONS Final Technical Report, 1 May 1990 - 1 Oct. 1993
Anthony J. Calise and Nahum Melamed Oct. 1993 100 p
(Grant NAG1-1139)
(NASA-CR-194523; NAS 1.26:194523) Avail: CASI HC A05/MF A02

This report addresses and clarifies a number of issues related to the Matched Asymptotic Expansion (MAE) analysis of skip trajectories, or any class of problems that give rise to inner layers that are not associated directly with satisfying boundary conditions. The procedure for matching inner and outer solutions, and using the composite solution to satisfy boundary conditions is developed and rigorously followed to obtain a set of algebraic equations for the problem of inclination change with minimum energy loss. A detailed evaluation of the zeroth order guidance algorithm for aeroassisted orbit transfer is performed. It is shown that by exploiting the structure of the MAE solution procedure, the original problem, which requires the solution of a set of 20 implicit algebraic equations, can be reduced to a problem of 6 implicit equations in 6 unknowns. A solution that is near optimal, requires a minimum of computation, and thus can be implemented in real time and on-board the vehicle, has been obtained. Guidance law implementation entails treating the current state as a new initial state and repetitively solving the zeroth order MAE problem to obtain the feedback controls. Finally, a general procedure is developed for constructing a MAE solution up to first order, of the Hamilton-Jacobi-Bellman equation based on the method of characteristics. The development is valid for a class of perturbation problems whose solution exhibits two-time-scale behavior. A regular expansion for problems of this type is shown to be inappropriate since it is not valid over a narrow range of the independent variable. That is, it is not uniformly valid. Of particular interest here is the manner in which matching and boundary conditions are enforced when the expansion is carried out to first order. Two cases are distinguished-one where the left boundary condition coincides with, or lies to the right of, the singular region, and another one where the left boundary condition lies to the left of the singular region. A simple example is used to illustrate the procedure where the obtained solution is uniformly valid to O(Epsilon(exp 2)). The potential application of this procedure to aeroassisted plane change is also described and partially evaluated. Author (revised)

N94-14541*# Eloret Corp., Sunnyvale, CA.
AN EXPERIMENTAL STUDY OF A TURBULENT BOUNDARY LAYER IN THE TRAILING EDGE REGION OF A CURCULATION-CONTROL AIRFOIL Progress Report, 1 Oct. 1992 - 30 Jun. 1993
Jeff Brown 12 Oct. 1993 6 p
(Contract NCC2-545)
(NASA-CR-194522; NAS 1.26:194522) Avail: CASI HC A02/MF A01

This report discusses progress made on NASA Cooperative Agreement NCC2-545, 'An Experimental Study of a Turbulent Boundary Layer in the Trailing-Edge Region of a Circulation-Control Airfoil,' during the period 1 Oct. 1992 - 30 Jun. 1993. The study, being conducted by Jeff Brown of the Eloret Institute, in conjunction with the Experimental Fluid Dynamics Branch at NASA Ames (Dennis Johnson, technical monitor), features 2-component laser Doppler velocimeter (LDV) measurements in the trailing edge and wake regions of a generic circulation-control airfoil model. The

final experimental phase of the study will be carried out in the Ames High Reynolds Number Channel II (HRC2) transonic blow-down facility. During the 9-month period covered by this report, important data were acquired using the near-wall laser Doppler velocimeter (LDV) whose development has been described in previous reports. These data point strongly to the viability of this new technique for measuring the full Reynolds Stress Tensor in 3D flows. Author (revised)

N94-14706# Royal Aerospace Establishment, Farnborough (England). Aerodynamics and Propulsion Dept.

INTRA-BLADE QUANTITATIVE TRANSONIC FLOW MEASUREMENTS AT THE DRA PYESTOCK ISENTROPIC LIGHT PISTON FACILITY USING PIV (PARTICLE IMAGE VELOCIMETRY)

K. S. Chana, I. W. Matthews, P. J. Bryanston-Cross (Warwick Univ., Coventry, England.), and M. Funes-Gallanzi (Warwick Univ., Coventry, England.) 15 Dec. 1992 16 p Presented at the 11th International Symposium on Measuring Techniques for Transonic and Supersonic Flows in Cascades and Turbomachines, Munich, Germany, 14-15 Sep. 1992 Original contains color illustrations

(RAE-TM-Aero/Prop-21; BR316329; ETN-93-94497) Copyright Avail: CASI HC A03/MF A01

Measurements made with the quantitative whole field flow visualization technique of Particle Image Velocimetry (PIV) in a transonic annular cascade are addressed. The measurements, which provided an instantaneous quantitative whole field visualization of unsteady region of flow, were compared with a full viscous prediction. The Isentropic Light Piston Facility used to make the measurements is described. The PIV techniques used are discussed along with the following: optical laser firing system; Nd/YAG pulse laser; diffraction limited optics; beam propagation optics; PIV optical probe design; imaging system; data processing; and preprocessing and data analysis. ESA

N94-14710# Messerschmitt-Boelkow-Blohm G.m.b.H., Munich (Germany). Military Aircraft Div.

SIMULATION OF HYPERSONIC, REACTING FLOW AROUND REENTRY BODIES: COMPARISONS OF NUMERICAL AND EXPERIMENTAL RESULTS

C. Mundt, R. R. Boyce (Australian National Univ., Canberra.), and E. H. Hirschel Sep. 1992 18 p Presented at DGLR-Jahrestagung 1992, Bremen, Germany, 29 Sep. - 2 Oct. 1992

(MBB-LME-211-S-PUB-507; DGLR-92-03-108; ETN-93-94196) Copyright Avail: CASI HC A03/MF A01

Results of an ongoing validation project for hypersonic flow prediction, which involved both numerical methods and experimental facilities, are presented. The flow was simulated numerically by solving the Euler and the second order boundary layer equations. For the description of the thermodynamic and chemical behavior of the test gases, different models were used depending on the state of the flow around the test body. The experimental facility used was the free piston hypervelocity shock tunnel T3, capable of simulating the real gas chemical effects encountered in reentry. Techniques to retrieve information about the flows range from surface measurements through bulk flow visualizations to single point optical flow diagnostics. The general strategy for the comparison is described and the results obtained for different parameters and different test gases are compared critically. A hyperboloid is chosen to be the test body. The results of the comparison provide confidence in both the numerical method and the modeling of high temperature physical and chemical effects. ESA

N94-14774# Duke Univ., Durham, NC.

NEW VORTEX DYNAMICS METHODS FOR ROTOR FREE WAKE ANALYSIS Final Report, 15 May 1988 - 14 May 1991

Donald B. Bliss May 1993 52 p

(Contract DAAL03-88-K-0062)

(AD-A266656; ARO-25747.1-EG) Avail: CASI HC A04/MF A01

This report summarizes recent work on rotorcraft aerodynamics involving novel methods for rotor free wake calculations. A new method called Analytical/Numerical Matching (ANM) was developed. ANM is a hybrid analytical and numerical method that achieves accurate results by combining a low resolution numerical solution with a high resolution analytical solution. Although originally developed for vortex dynamics, ANM has proven to be of a general nature. The application of ANM to the rotor wake problem provides accurate answers with a significant reduction in computation time. The use of ANM introduces the opportunity to develop new solution strategies, including Far-Field Linearization and Periodic Inversion. These methods afford the means to obtain accurate solutions Over the entire flight regime. Work involving applications of ANM has also led to a scheme that represents vortex filament dynamics by a hierarchy of nested problems of varying resolution joined by matching solutions. This approach, called ANM with Pyramiding (ANM/P), has reduced calculation times by more than a factor of twenty in some sample problems. DTIC

N94-14780*# National Aeronautics and Space Administration. Lewis Research Center, Cleveland, OH.

INTERACTION OF TWO GLANCING, CROSSING SHOCK WAVES WITH A TURBULENT BOUNDARY-LAYER AT VARIOUS MACH NUMBERS

Warren R. Hingst and Kevin E. Williams (Washington Univ., Seattle.) Sep. 1991 97 p

(RTOP 505-62-31)

(NASA-TM-103740; E-6566; NAS 1.15:103740) Avail: CASI HC A05/MF A02

A preliminary experimental investigation was conducted to study two crossing, glancing shock waves of equal strengths, interacting with the boundary-layer developed on a supersonic wind tunnel wall. This study was performed at several Mach numbers between 2.5 and 4.0. The shock waves were created by fins (shock generators), spanning the tunnel test section, that were set at angles varying from 4 to 12 degrees. The data acquired are wall static pressure measurements, and qualitative information in the form of oil flow and schlieren visualizations. The principle aim is two-fold. First, a fundamental understanding of the physics underlying this flow phenomena is desired. Also, a comprehensive data set is needed for computational fluid dynamic code validation. Results indicate that for small shock generator angles, the boundary-layer remains attached throughout the flow field. However, with increasing shock strengths (increasing generator angles), boundary layer separation does occur and becomes progressively more severe as the generator angles are increased further. The location of the separation, which starts well downstream of the shock crossing point, moves upstream as shock strengths are increased. At the highest generator angles, the separation appears to begin coincident with the generator leading edges and engulfs most of the area between the generators. This phenomena occurs very near the 'unstart' limit for the generators. The wall pressures at the lower generator angles are nominally consistent with the flow geometries (i.e. shock patterns) although significantly affected by the boundary-layer upstream influence. As separation occurs, the wall pressures exhibit a gradient that is mainly axial in direction in the vicinity of the separation. At the limiting conditions the wall pressure gradients are primarily in the axial direction throughout. Author (revised)

N94-14781# Flow Analysis, Inc., Brooklyn, NY.

FREE-WAKE COMPUTATION OF HELICOPTER ROTOR FLOWFIELD FOR GENERAL FLIGHT REGIMES Final Report, 1 Oct. 1989 - 30 Sep. 1992

Krishna Ramachandran, John Steinhoff, and Wenren Yonghu 30 Mar. 1993 79 p

(Contract DAAL03-89-C-0027)

(AD-A266692; ARO-25623.4-EG-S) Avail: CASI HC A05/MF A01

A CFD based computer code, HELIX 2 has been developed for computing helicopter rotor flowfield in hover and in forward flight. In order to predict the vibratory airloads in forward flight and the performance in hover the effect of shed wake has to be accurately accounted for. This has been accomplished by an unique vorticity embedding procedure. The wake is convected in a Lagrangian sense and does not suffer from numerical dissipation. The effect of this convected wake is included in the Eulerian using Clebsch representation. The unsteady full potential equation is solved in the Eulerian grid with the embedded vortical velocity accounting for the influence of wake. The wake evolves as a part of the solution. Dynamic grid modifications are performed at each time step to account for blade motion and deformation. These modifications are confined to regions near the blade using suitable blending functions. In addition a vorticity confinement method is developed which involves adding a term to the momentum conservation equation of fluid dynamics. This modification is very useful in the numerical solution of flow problems involving vortical regions. The Euler equations solved with this extra term can convect vortices without Numerical dissipation. DTIC

N94-14784# Auburn Univ., AL. Dept. of Mechanical Engineering.
A NEW TREATMENT OF PERIODIC SYSTEMS WITH APPLICATIONS TO HELICOPTER ROTOR BLADE DYNAMICS Final Report, 15 Sep. 1989 - 31 Mar. 1993
Subbash C. Sinha 28 May 1993 9 p
(Contract DAAL03-89-K-0172)
(AD-A266770; ARO-26061.15-EG) Avail: CASI HC A02/MF A01

A new solution technique for general periodic systems encountered in many mechanical systems including the helicopter rotor-blade dynamics has been developed. In this technique, the state transition matrices (STM) of periodic systems are obtained in terms of the shifted Chebyshev polynomials of first and second kind. Due to the excellent convergence properties of Chebyshev polynomials, the approach is found to be super efficient in terms of the CPU time with accuracy level comparable to any higher order numerical algorithms such as Runge-Kutta, Adams-Mouton, etc. The technique is suitable for both numerical and symbolic implementations. The method can be used in a variety of applications such as stability of linear and nonlinear periodic systems, response calculations of linear and nonlinear periodic systems, design of control systems for periodic systems, direct determination of periodic orbits of nonlinear systems and nonlinear analysis of periodic systems in stable, center and unstable manifolds. Case studies corresponding to each of these applications have been reported. Apart from the above mentioned utilities, the technique has resulted in a very practical procedure in obtaining the well-known Liapunov-Floquet (L-F) Transformation matrix which allows one to design a control system in the time-invariant domain. Currently, the research efforts are directed toward utilizing the L-F transformation matrix for various other problems such as order reduction, bifurcation analysis and nonlinear control design strategies for periodic systems. In the following, a short enumeration of the achievements of the project is presented.
DTIC

N94-14799# Rensselaer Polytechnic Inst., Troy, NY.
CENTER OF EXCELLENCE IN ROTARY WING TECHNOLOGY Final Report
O. Bauchau, Crespo M. daSilva, M. Darlow, P. Hajela, and E. Krempl 1 Apr. 1993 207 p
(Contract DAAL03-88-C-0004)
(AD-A266655; ARO-25462.13-EG-RW) Avail: CASI HC A10/MF A03

The activities of a Center of Excellence in Rotary Wing Technology at Rensselaer Polytechnic Institute under a second, continuation five year contract with the U.S. Army Research Office are reported here. The activities include the following: measures taken to revise and update comprehensive and in-depth curricula at advanced levels in rotorcraft technology; attract and retain outstanding young people in these programs; perform basic research at the leading edge of technology in structures, structural dynamics, unsteady aerodynamics, and aeroelasticity disciplines as applied to rotorcraft; and accomplishing technology transfer to the rotorcraft community beyond the Rensselaer campus. Descriptions, references, and statistics are provided to allow assessment of the extent to which these goals have been realized.
DTIC

N94-14800# Technische Univ., Berlin (Germany). Inst. fuer Luft- und Raumfahrt.
DEVELOPMENT OF EXPERIMENTAL DEMONSTRATION PROCESSES FOR LAMINAR-TURBULENT FLOW STATES AT WING PROFILES IN FREE FLIGHT Final Report [ENTWICKLUNG EXPERIMENTELLER NACHWEISVERFAHREN FUER LAMINAR-TURBULENTE STROEMUNGSZUSTAENDE AN TRAGFLUEGELPROLIFEN IM FREIFLUG. ABSCHLUSSBERICHT]
P. Mirow and W. Nitsche 1993 40 p In GERMAN Sponsored by BMFT
(ILR-Mitt-280(1993); ETN-93-94381) Avail: CASI HC A03/MF A01

Measurement techniques for industrial laminar wing experiments on a Grob 109B aircraft were developed and tested; two perturbation free surface measuring processes, piezoarray technique and CPM3 (Computational Preston tube Method), and an onboard supported data acquisition system are presented; CHM2 (Computational Hot-wire Method) was equally used for measuring wall shear stresses and torsional stress variations. CPM3 method was used for determination of local wall friction; power spectrum, time signals, and adaptation factors were obtained with piezoelectric foils, which proved to be very efficient for analysis of flow instabilities, but the method is found to be very expensive because of the necessity of multisensor arrays. It is concluded that a combination of both processes seems to be optimal for flight tests.
ESA

N94-14847*# National Aeronautics and Space Administration. Lewis Research Center, Cleveland, OH.
A NEW LAGRANGIAN METHOD FOR THREE-DIMENSIONAL STEADY SUPERSONIC FLOWS
Ching-Yuen Loh and Meng-Sing Liou Sep. 1993 39 p
(RTOP 505-62-52)
(NASA-TM-106068; E-7673; NAS 1.15:106068) Avail: CASI HC A03/MF A01

In this report, the new Lagrangian method introduced by Loh and Hui is extended for three-dimensional, steady supersonic flow computation. The derivation of the conservation form and the solution of the local Riemann solver using the Godunov and the high-resolution TVD (total variation diminished) scheme is presented. This new approach is accurate and robust, capable of handling complicated geometry and interactions between discontinuous waves. Test problems show that the extended Lagrangian method retains all the advantages of the two-dimensional method (e.g., crisp resolution of a slip-surface (contact discontinuity) and automatic grid generation). In this report, we also suggest a novel three dimensional Riemann problem in which interesting and intricate flow features are present.
Author

N94-14608# National Aeronautical Lab., Bangalore (India). Computational and Theoretical Fluid Dynamics Div.
A GRID GENERATION PACKAGE FOR HIGH ASPECT RATIO WINGS
J. S. Mathur and S. K. Chakrabartty *In its* Proceedings of the Fluid Dynamics Symposium in Honour of Professor R. Narasimha on his 60th Birthday Jul. 1993 p 115-121 (For primary document see N94-14598 02-34)
Avail: CASI HC A02/MF A03

N94-14609# National Aeronautical Lab., Bangalore (India). Computational and Theoretical Fluid Dynamics Div.
THE PHENOMENON OF VORTEX BREAKDOWN
Vidyadhar Y. Mudkavi *In its* Proceedings of the Fluid Dynamics Symposium in Honour of Professor R. Narasimha on his 60th Birthday Jul. 1993 p 123-135 (For primary document see N94-14598 02-34)
Avail: CASI HC A03/MF A03

N94-14612# National Aeronautical Lab., Bangalore (India). Computational and Theoretical Fluid Dynamics Div.
HYPERSONIC VISCOUS FLOW COMPUTATIONS
S. K. Saxena *In its* Proceedings of the Fluid Dynamics Symposium in Honour of Professor R. Narasimha on his 60th Birthday Jul. 1993 p 159-165 (For primary document see N94-14598 02-34)
(NAL Proj. CF-1-121)
Avail: CASI HC A02/MF A03

N94-14617# National Aeronautical Lab., Bangalore (India). Computational and Theoretical Fluid Dynamics Div.
PANEL CODES FOR AERODYNAMIC ANALYSIS AT NAL
S. Viswanathan, C. L. Narayana, V. Ramesh, S. S. Desai, and R. Rangarajan *In its* Proceedings of the Fluid Dynamics Symposium in Honour of Professor R. Narasimha on his 60th Birthday Jul. 1993 p 211-233 (For primary document see N94-14598 02-34)
Avail: CASI HC A03/MF A03

03 AIR TRANSPORTATION AND SAFETY

Includes passenger and cargo air transport operations; and aircraft accidents.

For related information see also *16 Space Transportation* and *85 Urban Technology and Transportation.*

N94-13247*# Ohio State Univ., Columbus. Dept. of Industrial and Systems Engineering.
COGNITIVE ENGINEERING IN AEROSPACE APPLICATION: PILOT INTERACTION WITH COCKPIT AUTOMATION

Nadine R. Sarter and David D. Woods Aug. 1993 71 p
(Contract NCC2-592)
(NASA-CR-177617; A-93108; NAS 1.26:177617) Avail: CASI HC A04/MF A01

Because of recent incidents involving glass-cockpit aircraft, there is growing concern with cockpit automation and its potential effects on pilot performance. However, little is known about the nature and causes of problems that arise in pilot-automation interaction. The results of two studies that provide converging, complementary data on pilots' difficulties with understanding and operating one of the core systems of cockpit automation, the Flight Management System (FMS) is reported. A survey asking pilots to describe specific incidents with the FMS and observations of pilots undergoing transition training to a glass cockpit aircraft served as vehicles to gather a corpus on the nature and variety of FMS-related problems. The results of both studies indicate that pilots become proficient in standard FMS operations through ground training and subsequent line experience. But even with considerable line experience, they still have difficulties tracking FMS status and behavior in certain flight contexts, and they show gaps in their understanding of the functional structure of the system. The results suggest that design-related factors such as opaque interfaces contribute to these difficulties which can affect pilots' situation awareness. The results of this research are relevant for both the design of cockpit automation and the development of training curricula specifically tailored to the needs of glass cockpits. Author (revised)

N94-13424*# Innovative Dynamics, Ithaca, NY.
SMART SKIN TECHNOLOGY DEVELOPMENT FOR MEASURING ICE ACCRETION, STALL, AND HIGH AOA AIRCRAFT PERFORMANCE. PART 1: CAPACITIVE ICE DETECTOR DEVELOPMENT Final Technical Report
Daniel A. Pruzan, Ateen A. Khatkhate, Joseph J. Gerardi, and Gail A. Hickman 23 Apr. 1993 86 p Revised
(Contract NAS3-25966; SBIR-03.01-0533)
(NASA-CR-194252; NAS 1.26:194252; Rept-93D-03-0423-Pt-1) Avail: CASI HC A05/MF A01

A reliable way to detect and measure ice accretion during flight is required to reduce the hazards of icing currently threatening present day aircraft. Many of the sensors used for this purpose are invasive (probe) sensors which must be placed in areas of the airframe where ice does not naturally form. Due to the difference in capture efficiency of the exposed surface, difficulties result in correlating the ice accretion on the probe to what is happening on a number of vastly different airfoil sections. Most flush mounted sensors in use must be integrated into the aircraft surface by cutting or drilling the aircraft surface. An alternate type of ice detector which is based on a NASA patent is currently being investigated at Innovative Dynamics, Inc. (IDI). Results of the investigation into the performance of different capacitive type sensor designs, both rigid as well as elastic, are presented. Author (revised)

N94-13534# Technische Univ., Delft (Netherlands). Faculty of Aerospace Engineering.
OPTIMAL LATERAL ESCAPE MANEUVERS FOR MICROBURST ENCOUNTERS DURING FINAL APPROACH
H. G. Visser Jul. 1992 44 p
(LR-691; ETN-93-94416) Avail: CASI HC A03/MF A01

The control and optimization of lateral escape trajectories in a microburst wind field for an aircraft on final approach is discussed. The performance index being minimized is the peak value of altitude drop. The characteristics of open loop extremal solutions for different locations of the microburst were calculated. If a sufficiently large bank angle limit is specified and the center of the microburst is not too far offset from the centerline extension of the approach runway, typically three trajectories can be found that satisfy the first order necessary conditions of optimality. The results bear out that trajectories that feature lateral maneuvering to turn the aircraft away from the microburst center, offer a significant improvement in the escape capability of the aircraft in comparison to a trajectory that passes through the center. In contrast to nonturning escape maneuvers, lateral escape maneuvers often exhibit an initial climb, rather than a descent. It is conjectured that this behavior is a result of optimal energy management. Efforts to develop a closed loop (feedback) guidance scheme that closely approximates the open loop trajectories are described. ESA

N94-13543 British Columbia Univ., Vancouver. Faculty of Commerce and Business Administration.
THE INTERNATIONAL REGULATION OF AIR TRANSPORT: CHANGING REGIMES AND PRICE EFFECTS Ph.D. Thesis
Martin Elliot Dresner Jul. 1989 340 p
(ISBN-0-315-55958-6; CTN-93-60728) Copyright Avail: Micromedia Ltd., Technical Information Centre, 165 Hotel de Ville, Place du Portage, Phase 2, Hull, Quebec J8X 3X2, Canada HC/MF

Regulatory changes in the international air transport industry are traced from World War II to the present. A modified version of hegemonic stability theory was formulated and applied to the industry to explain the developments. Additional domestic political and market structural variables were introduced to arrive at a more comprehensive model of regime change. The comprehensive model added significantly to the explanation of regime developments. Finally, the model was used to predict future developments in the industry. It was predicted that there was still political credit to be gained from air services liberalization in developed areas of the world and that regulations in these areas are likely to be liberalized. A model was also developed to explain price differences on international air routes. Major assumptions were that airlines competing on liberalized air routes engaged in Bertrand pricing behavior, while carriers on non-liberal routes colluded to set prices. Several empirical versions of the model were used to test for price effects that arose from liberal agreements. The liberal agreements were found to contribute to lower discount fares significantly but not necessarily to lower normal fares. The findings were consistent with the use of greater price discrimination under the liberal bilateral agreements. Author (CISTI)

N94-14008# Bundesanstalt fuer Flugsicherung, Frankfurt am Main (Germany).
[ACTIVITIES REPORT OF THE FEDERAL ADMINISTRATION FOR FLIGHT SAFETY (GERMANY)] Annual Report, 1991 [JAHRESBERICHT '91 DER BUNDESANSTALT FUER FLUGSICHERUNG]
1992 53 p In GERMAN
(ETN-93-94208) Copyright Avail: CASI HC A04/MF A01

Statistical information, technological advances and measures taken by German administration in the flight safety area are presented. The role of cooperation between transportation and defense departments was outlined. Air traffic service routes were created or modified in order to remedy to traffic increase. Standard flight safety processes were introduced at former East Germany airports. Safety management services for Netherlands, Belgium and Federal Republic of Germany decided the integration of their existing air traffic control system in a common project for optimization of radar information use, by means of radar data interchange network. Safety improvements, obtained with instrument and microwave ranging systems and modifications in information and data transfer facilities were reported. Design phase of a monopulse secondary radar subsystem in the framework of the radar modernization program was achieved by introducing critical design review concept. An integration test between sensor data processor and radar message conversion and distribution equipment was performed. Feasibility of a short term conflict alert system was examined and the American en route automated radar tracking system was chosen. A departure coordination system for reduction of coordination cost between toward and approach control and area control center workstations was implemented at the Frankfurt airport. A weather data and information visualization system with light waveguide transmission was implemented at new Munich airport. Statistical information about air traffic in Germany is given. ESA

N94-14186# Federal Aviation Administration, Atlantic City, NJ.
WIDEBODY CABIN WATER SPRAY OPTIMIZATION TESTS
Timothy R. Marker Aug. 1993 47 p Original contains color illustrations
(DOT/FAA/CT-TN93/29) Avail: CASI HC A03/MF A01

Nine full-scale tests were conducted in a modified DC-10 test article as part of an aircraft cabin water spray optimization study. The purpose of the study was to test several spray configurations by varying the orientation of the nozzles, the flow rate, and the quantity of water sprayed, while keeping the fire conditions constant, in an attempt to minimize the amount of water required to effectively suppress a postcrash aircraft fire and improve occupant survivability. The tests were used to validate optimization tests previously conducted in the narrowbody 707 test article. The initial test series employed a full-zone spray system, extending across the width of

the fuselage, consisting of 7 zones, each containing 12 nozzles. A thermocouple was centrally mounted at ceiling height in each of the 8 foot long zones, allowing for the activation of a particular zone when the temperature reached a pre-determined value. A second series of tests were run in which the original zones were divided in half, producing 5 zones on either side of the fuselage centerline for a total of 10. Each of the 10 zones contained 6 nozzles. The survival time was extended between 41 and 103 seconds, depending on zone configuration, discharge activation temperature, and cabin location. Author

N94-14292# Lawrence Livermore National Lab., CA.
A MODEL FOR FUEL FIRE DURATION AND APPLICATION TO THE B-1B BOMBER
D. E. Magnoli 15 Dec. 1992 67 p
(Contract W-7405-eng-48)
(DE93-013000; UCRL-ID-112576) Avail: CASI HC A04/MF A01 (US Sales Only)

A current national priority is ensuring that nuclear weapons remain safe (i.e., that they have a very low probability of plutonium dispersal) even when exposed to abnormal environments. In order to be able to quantify the probability of plutonium release, it is imperative to understand the abnormal environments to which weapons might be subjected. One type of abnormal environment arises from an accidental fuel fire. This report deals with the environment created by exposure to fire and represents an initial effort to quantify fire durations and to describe fire duration statistically. Section 1 of the report documents the model developed to describe the duration of fuel fires on aircraft, where the source of the fuel is leaking fuel tanks. Section 2 examines the question of spreading to determine under what conditions a fire due to a leak in one fuel tank will spread to another. A later report will describe a first-cut effort to correlate the fires examined here with a temperature distribution. DOE

N94-14744*# Decision Systems, Inc., Los Altos, CA.
THE INFLUENCE OF ATC MESSAGE LENGTH AND TIMING ON PILOT COMMUNICATION
Daniel Morrow and Michelle Rodvold (San Jose State Univ., CA.) Aug. 1993 24 p
(Contract NAS2-13210)
(NASA-CR-177621; A-93115; NAS 1.26:177621) Avail: CASI HC A03/MF A01

Pilot-controller communication is critical to safe and efficient flight. It is often a challenging component of piloting, which is reflected in the number of incidents and accidents involving miscommunication. Our previous field study identified communication problems that disrupt routine communication between pilots and controllers. The present part-task simulation study followed up the field results with a more controlled investigation of communication problems. Pilots flew a simulation in which they were frequently vectored by Air Traffic Control (ATC), requiring intensive communication with the controller. While flying, pilots also performed a secondary visual monitoring task. We examined the influence of message length (one message with four commands vs. two messages with two commands each) and noncommunication workload on communication accuracy and length. Longer ATC messages appeared to overload pilot working memory, resulting in more incorrect or partial readbacks, as well as more requests to repeat the message. The timing between the two short messages also influenced communication. The second message interfered with memory for or response to the first short message when it was delivered too soon after the first message. Performing the secondary monitoring task did not influence communication. Instead, communication reduced monitoring accuracy. Author

04 AIRCRAFT COMMUNICATIONS AND NAVIGATION

Includes digital and voice communication with aircraft; air navigation systems (satellite and ground based); and air traffic control.

For related information see also *17 Space Communications, Spacecraft Communications, Command and Tracking* and *Communications and Radar.*

N94-13082*# Ohio State Univ., Columbus. Dept. of Geodetic Science and Surveying.
INVESTIGATION FOR IMPROVING GLOBAL POSITIONING SYSTEM (GPS) ORBITS USING A DISCRETE SEQUENTIAL ESTIMATOR AND STOCHASTIC MODELS OF SELECTED PHYSICAL PROCESSES Annual Report
Clyde C. Goad and C. David Chadwell Aug. 1993 34 p
(Grant NAG5-2041; RF Proj. 760126/72687)
(NASA-CR-194167; NAS 1.26:194167) Avail: CASI HC A03/MF A01

GEODYNII is a conventional batch least-squares differential corrector computer program with deterministic models of the physical environment. Conventional algorithms were used to process differenced phase and pseudorange data to determine eight-day Global Positioning system (GPS) orbits with several meter accuracy. However, random physical processes drive the errors whose magnitudes prevent improving the GPS orbit accuracy. To improve the orbit accuracy, these random processes should be modeled stochastically. The conventional batch least-squares algorithm cannot accommodate stochastic models, only a stochastic estimation algorithm is suitable, such as a sequential filter/smoother. Also, GEODYNII cannot currently model the correlation among data values. Differenced pseudorange, and especially differenced phase, are precise data types that can be used to improve the GPS orbit precision. To overcome these limitations and improve the accuracy of GPS orbits computed using GEODYNII, we proposed to develop a sequential stochastic filter/smoother processor by using GEODYNII as a type of trajectory preprocessor. Our proposed processor is now completed. It contains a correlated double difference range processing capability, first order Gauss Markov models for the solar radiation pressure scale coefficient and y-bias acceleration, and a random walk model for the tropospheric refraction correction. The development approach was to interface the standard GEODYNII output files (measurement partials and variationals) with software modules containing the stochastic estimator, the stochastic models, and a double differenced phase range processing routine. Thus, no modifications to the original GEODYNII software were required. A schematic of the development is shown. The observational data are edited in the preprocessor and the data are passed to GEODYNII as one of its standard data types. A reference orbit is determined using GEODYNII as a batch least-squares processor and the GEODYNII measurement partial (FTN90) and variational (FTN80, V-matrix) files are generated. These two files along with a control statement file and a satellite identification and mass file are passed to the filter/smoother to estimate time-varying parameter states at each epoch, improved satellite initial elements, and improved estimates of constant parameters. Author (revised)

N94-13238*# Colorado Univ., Boulder. Center for Astrodynamics Research.
ERROR ANALYSIS OF REAL TIME AND POST PROCESSED OR BIT DETERMINATION OF GFO USING GPS TRACKING Final Report
William S. Schreiner 5 Oct. 1991 10 p
(Grant NGT-50623)
(NASA-CR-193646; NAS 1.26:193646; CU-1536481) Avail: CASI HC A02/MF A01

The goal of the Navy's GEOSAT Follow-On (GFO) mission is to map the topography of the world's oceans in both real time (operational) and post processed modes. Currently, the best candidate for supplying the required orbit accuracy is the Global Positioning System (GPS). The purpose of this fellowship was to determine the expected orbit accuracy for GFO in both the real time and post-processed modes when using GPS tracking. This report presents the work completed through the ending date of the fellowship. Derived from text

N94-13344# National Aerospace Lab., Tokyo (Japan). Navigation and Flight Experiment Team.

FLIGHT EVALUATIONS OF APPROACH/LANDING NAVIGATION SENSOR SYSTEMS: SUMMARY OF 1990 FLIGHT EXPERIMENTS [MLS TOU KOUHOUKEI HIKOU JIKKEN: HEIZEI 2 NENDO NO JIKKEN GAIYOU]

Kouichi Matsushima, Takatsugu Ono, Masaaki Murata, Yoshikazu Miyazawa, Yoshinori Okuno, Kazutoshi Ishikawa, Toshiharu Inagaki, Hirokimi Shinguu, and Tadao Uchida Jul. 1992 70 p In JAPANESE

(NAL-TR-1175; JTN-93-80491) Avail: CASI HC A04/MF A01

Flight experiments conducted at the Sendai airport (under a joint research project with National Aerospace Laboratory (NAL), National Space Development Agency (NASDA), and Electronic Navigation Research Institute (ENRI) in partial co-operation with Toshiba and NEC Corporations) were utilized to evaluate and establish new navigation sensor technologies which will play a key role in the unmanned spaceplane HOPE (H-2 Orbiting Plane) approach/landing (A/L) navigation system design. The Dornier-228-200 (Do-228), an experimental research aircraft of NAL, is used for the flight experiments. The navigation sensors tested include the Microwave Landing System (MLS), Global Positioning System (GPS), Inertial Navigation System (INS), and radio altimeter. The Differential GPS (DGPS) was also tested in both stand-alone and hybrid modes. The Do-228 is tracked during flight by a laser tracker, with subsequent data being used to provide a reference profile of the aircraft. Navigation accuracy is evaluated in the post-flight performance analysis as the difference between reference profile and navigation output from each navigation sensor or hybrid system. This comparison is made in the Runway Coordinate System (RCS), a reference navigation coordinate system which corresponds to the World Geodetic System 1984 (WGS84). The RCS was constructed using GPS interferometric positioning. In this report, emphasis is placed on describing the tested navigation sensors, data acquisition systems, ground guidance facilities, flight patterns, and analysis strategies. Some preliminary analysis results are also presented which evaluate the stand-alone performance of each navigation sensor as well as a hybrid GPS-INS system.

Author (NASDA)

N94-13346# National Aerospace Lab., Tokyo (Japan). Flight Research Div.

PERFORMANCE EVALUATION TESTS OF THE GPS/DGPS NAVIGATION SYSTEM INSTALLED IN THE NAL DORNIER 228: PRELIMINARY GROUND TEST RESULTS [JIKKENYOU KOUKUUKI DORUNIEKI NO GPS KOUHOU SOUCHI HYOUKA JIKKEN: CHIJOU KOTEITEN NIOKERU GPS/DGPS SOUKUI HYOUKA JIKKEN]

Takatsugu Ono and Kazutoshi Ishikawa Aug. 1992 19 p In JAPANESE

(NAL-TM-649; JTN-93-80493) Avail: CASI HC A03/MF A01

A real-time Differential Global Positioning System (DGPS), incorporating a ground-to-air data link system, was developed for the National Aerospace Laboratory (NAL) Dornier 228-200 flight research airplane. Preliminary ground tests were conducted to evaluate the system's position accuracy prior to flight testing. The onboard and ground GPS receivers used the same antenna in order to avoid unknown common errors (e.g., antenna system and tropospheric delays), and to enable comparison of the optimal case of differential operation. The GPS position accuracies of the stand-alone and differential modes are compared, with results showing that the differential mode improves position accuracy and eliminates Selective Availability (SA) errors. Author (NASDA)

N94-13457# National Aerospace Lab., Tokyo (Japan). STOL Research Aircraft Group.

FLIGHT PATH CONTROL FOR THE APPROACH AND LANDING OF THE QUIET STOL EXPERIMENTAL AIRCRAFT ASKA [TEISOUON STOL JIKKENKI ASKA NO KEIROKAKU SEIGYO TO CHAKURIKU SOUJUUSEI]

Noriaki Okada Nov. 1992 53 p In JAPANESE

(NAL-TR-1183; JTN-93-80505) Avail: CASI HC A04/MF A01

The Upper Surface Blowing STOL experimental aircraft, ASKA, operates well on the backside of the power required curve, so flight path control is accomplished with the throttle lever (thrust) during landing approaches. To compensate for the sluggish flight path response caused by engine lag, the Flight Path Control (FPC) law engages the Stability and Control Augmentation System (SCAS). Flight tests were conducted to evaluate flight path and airspeed response characteristics. This paper describes ASKA's flight path and airspeed response characteristics, as well as the principle involved in the design and construction of the FPC system.

Author (NASDA)

N94-13541 New Brunswick Univ., Fredericton. Dept. of Surveying Engineering.

GPS SATELLITE SKY DISTRIBUTION: IMPACT ON THE PROPAGATION OF SOME IMPORTANT ERRORS IN PRECISE RELATIVE POSITIONING Ph.D. Thesis

Rock Santerre Sep. 1989 221 p

(ISBN-0-315-51838-3; CTN-93-60726) Copyright Avail: Micromedia Ltd., Technical Information Centre, 165 Hotel de Ville, Place du Portage, Phase 2, Hull, Quebec J8X 3X2, Canada HC/MF

The impact of the Global Positioning System (GPS) satellite sky distribution on the propagation of some important errors in precise static relative positioning is investigated, for baselines shorter than about 100 km. The study uses an improved and expanded simulation technique in which the unknowns are the station coordinates, the relative receiver clock parameter, and the relative tropospheric zenith delay parameter. Biases analyzed are the relative tropospheric refraction, absolute ionospheric refraction, offset in horizontal coordinates of the fixed station, and offset in the height of the fixed station. The simulation results agree with those obtained from real GPS data processing with an associated error of about 25%. Orientation and shape of the confidence ellipsoid, and correlation among the selected unknowns, are used to monitor the behavior of the covariance matrix. Systematic errors introduced in the station network by the biases are represented as station coordinate discrepancies and affine transformation parameters. Numerical values of these parameters are presented for satellite configurations produced by both the prototype and the full GPS constellations. The magnitudes of the effects of the studied biases are up to 10 cm for baseline length independent errors and up to 10 ppM for baseline length dependent errors. Author (CISTI)

N94-13703# Wright Lab., Wright-Patterson AFB, OH.

EVALUATION OF INFRARED SENSORS FOR AUTONOMOUS LANDING GUIDANCE Final Report, 1 May - 30 Jun. 1992

Anthony E. Absi Apr. 1993 25 p

(AD-A266450; WL-TR-93-1054) Avail: CASI HC A03/MF A01

The objective of this program is to test sensors that could provide pilots with images of runway and landing zones under degraded weather conditions such as rain, snow, and fog. During these conditions pilots are unable to land aircraft by visual reference alone. Imaging RF and EO sensors may be able to provide a view of the runway or landing zone that is unaffected by degraded weather. Autonomous landing systems would allow operations at airfields not served by conventional ground-based radio landing aids and allow military operations at unprepared landing sites or drop zones. A test was conducted at Otis Air National Guard Base by Wright Laboratory personnel in June 1992 during heavy fog. Typical staring midwave infrared sensors were used to image a simulated runway (1500 foot asphalt pad) and grass background. The distance at which the pad could no longer be discerned was measured along with supporting meteorological and radiometric ground truth data. This report presents the results and compares them to standard infrared sensor performance prediction models. DTIC

N94-13957*# National Aeronautics and Space Administration. Ames Research Center, Moffett Field, CA.

HELICOPTER PRECISION APPROACH CAPABILITY USING THE GLOBAL POSITIONING SYSTEM Semiannual Progress Report, Jul. - Dec. 1992

David N. Kaufmann 31 Dec. 1992 60 p

(Contract NCC2-775)

(NASA-CR-194037; NAS 1.26:194037) Avail: CASI HC A04/MF A01

The period between 1 July and 31 December, 1992, was spent developing a research plan as well as a navigation system document and flight test plan to investigate helicopter precision approach capability using the Global Positioning System (GPS). In addition, all hardware and software required for the research was acquired, developed, installed, and verified on both the test aircraft and the ground-based reference station. Author (revised)

N94-14495*# San Jose State Univ., CA. Univ. Foundation.
OBSTACLE DETECTION BY RECOGNIZING BINARY EXPANSION PATTERNS Annual Progress Report
Yoram Baram (Israel Inst. of Tech., Haifa.) and Yair Barniv (National Aeronautics and Space Administration. Ames Research Center, Moffett Field, CA.) 20 Sep. 1993 15 p
(Contract NCC2-703)
(NASA-CR-194415; NAS 1.26:194415) Avail: CASI HC A03/MF A01

This paper describes a technique for obstacle detection, based on the expansion of the image-plane projection of a textured object, as its distance from the sensor decreases. Information is conveyed by vectors whose components represent first-order temporal and spatial derivatives of the image intensity, which are related to the time to collision through the local divergence. Such vectors may be characterized as patterns corresponding to 'safe' or 'dangerous' situations. We show that essential information is conveyed by single-bit vector components, representing the signs of the relevant derivatives. We use two recently developed, high capacity classifiers, employing neural learning techniques, to recognize the imminence of collision from such patterns. Author (revised)

N94-14563 Federal Aviation Administration, Cambridge, MA. National Transportation Systems Center.
DETERMINATION OF LORAN-C/GPS HUMAN FACTORS ISSUES Final Report, Aug. 1992 - Mar. 1993
R. J. Adams, C. A. Adams, D. Eldredge, and M. S. Huntley Apr. 1993 38 p Prepared in cooperation with Advanced Aviation Concepts, Jupiter, FL Limited Reproducibility: More than 20% of this document may be affected by microfiche quality
(PB93-199693; DOT-VNTSC-FAA-93-3; DOT/FAA/RD-93/4) Avail: CASI HC A03

The report identifies human factors issues and the problems that general aviation pilots have using Loran-C navigation systems in the National Airspace System (NAS). The issues discussed include system design, software logic, and handbook and training problems. Data was collected from group discussions with active pilots throughout the eastern United States and Canada during late 1991 and the first half of 1992. These discussions included air carrier, air taxi, corporate, business, and pleasure users of Loran-C and a limited number of GPS users. The purpose of the study was to anticipate the potential human factor problems that could be expected in the full integration of GPS into the NAS. NTIS

N94-14371*# Jet Propulsion Lab., California Inst. of Tech., Pasadena.
IMPROVED TREATMENT OF GLOBAL POSITIONING SYSTEM FORCE PARAMETERS IN PRECISE ORBIT DETERMINATION APPLICATIONS
Y. Vigue, S. M. Lichten, R. J. Muellerschoen, G. Blewitt, and M. B. Heflin *In its* The Telecommunications and Data Acquisition Report 15 Aug. 1993 p 14-20 (For primary document see N94-14369 02-32)
(RTOP 310-10-61-84-02)
Avail: CASI HC A02/MF A03

N94-14372*# Jet Propulsion Lab., California Inst. of Tech., Pasadena.
USE OF GLOBAL POSITIONING SYSTEM MEASUREMENTS TO DETERMINE GEOCENTRIC COORDINATES AND VARIATIONS IN EARTH ORIENTATION
R. P. Malla (Sterling Software, Inc., Pasadena, CA.), S.-C. Wu, and S. M. Lichten *In its* The Telecommunications and Data Acquisition Report 15 Aug. 1993 p 21-33 (For primary document see N94-14369 02-32)
(RTOP 310-10-61-84-02)
Avail: CASI HC A03/MF A03

05 AIRCRAFT DESIGN, TESTING AND PERFORMANCE

Includes aircraft simulation technology.

For related information see also *18 Spacecraft Design, Testing and Performance* and *39 Structural Mechanics*.For land transportation vehicles see *85 Urban Technology and Transportation.*

N94-12850*# National Aeronautics and Space Administration. Langley Research Center, Hampton, VA.
A METHOD OF PREDICTING QUASI-STEADY AERODYNAMICS FOR FLUTTER ANALYSIS OF HIGH SPEED VEHICLES USING STEADY CFD CALCULATIONS
Robert C. Scott and Anthony S. Pototzky (Lockheed Engineering and Sciences Co., Hampton, VA.) Jul. 1993 10 p Presented at the AIAA 34th Structures, Structural Dynamics, and Materials Conference, LaJolla, CA, 19-21 Apr. 1993 Previously announced in IAA as A93-33931
(RTOP 505-63-50-15)
(NASA-TM-109009; NAS 1.15:109009) Avail: CASI HC A02/MF A01

High speed linear aerodynamic theories like piston theory and Newtonian impact theory are relatively inexpensive to use for flutter analysis. These theories have limited areas of applicability depending on the configuration and the flow conditions. In addition, these theories lack the ability to capture viscous, shock, and real gas effects. CFD methods can model all of these effects accurately, but the unsteady calculations required for flutter are expensive and often impractical. This paper describes a method for using steady CFD calculations to approximate the generalized aerodynamic forces for a flutter analysis. Example two-and three-dimensional aerodynamic force calculations are provided. In addition, a flutter analysis of a NASP-type wing will be discussed. Author (revised)

N94-13338# National Aerospace Lab., Tokyo (Japan). Control Systems Div.
DEVELOPMENT OF AN ON-BOARD AIRCRAFT OPTICAL FIBER DATA BUS SYSTEM [KOUKUUKI TOUSAIGATA HIKARI DETABASU NO KAIHATSU]
Mitsuyoshi Mayanagi, Minoru Takizawa, Tadao Uchida, Toshiharu Inagaki, Kouki Hozumi, and Kazutoshi Ishikawa Jun. 1992 87 p In JAPANESE
(NAL-TR-1163; JTN-93-80485) Avail: CASI HC A05/MF A01

An optical fiber data bus system was developed to provide the necessary technological foundation to use on a Fly-By-Light (FBL) control system which will be required on future aircraft. This data bus system was designed and built in accordance with the protocol and system organization requirements set forth in MIL-STD-1553B (USAF). It is an on-board model comprised of a bus control unit, two remote terminal units, an optical transmission unit having three optical transmitters/receivers. an eight to eight star coupler, a pressurized bulkhead optical connector, and three sets of fiber optic cables. A single fiber optic cable is utilized as the data transmission medium, and it employs a newly developed electrically passive/transmitting eight to eight star coupler and a pressurized bulkhead optical connector for optical coupling. New serial bus control and message handling techniques were also developed for the data bus. In addition, an electrical transmission line is provided to back up the optical fiber transmission line, thereby, providing the necessary system reliability for testing the FBL control system. Performance evaluations of the optical fiber data bus were conducted by testing the optical transmission units, and by conducting environmental, laboratory, and flight test with results verifying suitable adaptability to the FBL control system. Author (NASDA)

N94-13459# National Aerospace Lab., Tokyo (Japan). Aerodynamics Div.
HYPERSONIC AERODYNAMIC CHARACTERISTICS OF SSTO-TYPE AEROSPACE PLANES. PART 1: THE NAL 0-th CONFIGURATION [SUPESUPUREN NO GOKUCHOUONSOKU KUURIKI TOKUSEI SHIKEN: DAI 0-JI KEIJOU]
Shigeya Watanabe, Kouichi Hozumi, Akira Yoshizawa, Tadao Koyama, and Shouichi Tsuda Dec. 1992 57 p In JAPANESE
(NAL-TR-1186; JTN-93-80507) Avail: CASI HC A04/MF A01

Tests to determine the aerodynamic characteristics of a horizontal takeoff, Single Stage To Orbit (SSTO) type aerospace plane (NAL 0-th configuration) were conducted at a Mach number of 7.1. Six components of force and

moment were measured in the blowdown-type 50 cm hypersonic wind tunnel at the National Aerospace Laboratory. Flow visualizations were also performed using the schlieren, surface oil flow, and vapor screen techniques. The force and moment test results showed that the configuration had a lift-to-drag ratio of 2.2 in the ascent flight condition and that Dutch-roll mode instability occurred due to directional instability. The focus of future aerodynamic configuration improvements are discussed in connection with these results. Author (NASDA)

N94-13606* National Aeronautics and Space Administration. Ames Research Center, Moffett Field, CA.

AIRBORNE ARCTIC STRATOSPHERIC EXPEDITION: OZONE (Videotape)

Dec. 1988 Videotape: 5 min. playing time, in color, with sound
(NASA-TM-109312; NONP-VT-93-185319) Avail: CASI VHS A01/BETA A22

This video shows the rollout of the ER-2 and DC-8 at Ames, takeoffs and landings, and operations aboard the DC-8 and ER-2 in Puntas Arenas, Chile. Animation of the north polar regions showing the ozone hole is also included. Author (revised)

N94-13618*# North Carolina State Univ., Raleigh. Mars Mission Research Center.

MULTIDISCIPLINARY DESIGN TECHNIQUES APPLIED TO CONCEPTUAL AEROSPACE VEHICLE DESIGN Ph.D. Thesis Final Technical Report

John Robert Olds and Gerald D. Walberg 1993 181 p
(Contract NCC1-168)
(NASA-CR-194409; NAS 1.26:194409) Avail: CASI HC A09/MF A02

Multidisciplinary design optimization (MDO) is an emerging discipline within aerospace engineering. Its goal is to bring structure and efficiency to the complex design process associated with advanced aerospace launch vehicles. Aerospace vehicles generally require input from a variety of traditional aerospace disciplines - aerodynamics, structures, performance, etc. As such, traditional optimization methods cannot always be applied. Several multidisciplinary techniques and methods were proposed as potentially applicable to this class of design problem. Among the candidate options are calculus-based (or gradient-based) optimization schemes and parametric schemes based on design of experiments theory. A brief overview of several applicable multidisciplinary design optimization methods is included. Methods from the calculus-based class and the parametric class are reviewed, but the research application reported focuses on methods from the parametric class. A vehicle of current interest was chosen as a test application for this research. The rocket-based combined-cycle (RBCC) single-stage-to-orbit (SSTO) launch vehicle combines elements of rocket and airbreathing propulsion in an attempt to produce an attractive option for launching medium sized payloads into low earth orbit. The RBCC SSTO presents a particularly difficult problem for traditional one-variable-at-a-time optimization methods because of the lack of an adequate experience base and the highly coupled nature of the design variables. MDO, however, with it's structured approach to design, is well suited to this problem. The result of the application of Taguchi methods, central composite designs, and response surface methods to the design optimization of the RBCC SSTO are presented. Attention is given to the aspect of Taguchi methods that attempts to locate a 'robust' design - that is, a design that is least sensitive to uncontrollable influences on the design. Near-optimum minimum dry weight solutions are determined for the vehicle. A summary and evaluation of the various parametric MDO methods employed in the research are included. Recommendations for additional research are provided. Author (revised)

N94-13687# Technische Univ., Delft (Netherlands). Faculty of Aerospace Engineering.

DEVELOPMENT AND APPLICATION OF A COMPREHENSIVE, DESIGN-SENSITIVE WEIGHT PREDICTION METHOD FOR WING STRUCTURES OF TRANSPORT CATEGORY AIRCRAFT

E. Torenbeek Sep. 1992 59 p
(LR-693; ETN-93-94417) Avail: CASI HC A04/MF A01

The development of an analytical empirical method to predict the structural weight of transport aircraft wings is described. The method is suitable for the preliminary design stage, when sensitivity studies are required of the effects of geometry and other variations on the design characteristics. The wing weight is computed as the sum of several functional components. The basic weight required to resist bending and shear loads is computed from integration of a spanwise material distribution. Weight penalties are derived for nonoptimum effects, including stiffness required to cope with aeroelastic effects. Methods for leading and trailing edge structures, including high lift devices and control surfaces are derived. Instead of using the suggested statistical data for mean stress levels, the user may input more accurate data, if available. The baseline is 1980+ technology. The method is applied to present day transport aircraft. For the cases considered the prediction error was below 4%. ESA

N94-13690# Aeronautical Research Inst. of Sweden, Stockholm. Structures Dept.

COMPUTATIONAL METHODS FOR RELIABLE FATIGUE AND DAMAGE TOLERANCE DIMENSIONING OF AIRCRAFT STRUCTURES

Boerje Andersson Feb. 1993 23 p Presented at the 5th Nordic Seminar on Computational Mechanics, Aalborg, Denmark, 5-6 Nov. 1992 Sponsored by Defence Material Administration, Stockholm, Sweden
(FFA-TN-1993-05; ETN-93-94489) Avail: CASI HC A03/MF A01

A computational procedure for reliable stress and linear elastic fracture mechanics analysis of aircraft components of high complexity is described. The numerical analysis is based on the h-p version of the finite element method. For analysis of stresses at fillets, a rational analysis procedure is developed. From one three dimensional fracture mechanics analysis, analytical formulae are obtained that accurately predict pointwise stresses as a function of geometry parameters, for example, the radius at a fillet. A model example is analyzed in order to demonstrate the simplicity, reliability, and accuracy obtainable with the suggested approach. Results from an analysis of an aircraft fuselage, using a model having two million degrees of freedom, exemplify the practical usefulness of the procedure when solving very complex aircraft design problems. ESA

N94-13839 Operational Research and Analysis Establishment, Ottawa (Ontario).

AN ANALYSIS OF HELICOPTER ATTRITION USING A LOW LEVEL COMBAT SIMULATION

P. J. Young and R. J. Hill Dec. 1992 66 p
(DSIS-93-00282; DLOR-RN-92-5; CTN-93-60797) Avail: CASI HC A04/MF A01

Low level combat simulations were applied to study the attrition of utility tactical transport helicopters (UTTH's) in their proposed roles as the Canadian Army's sole tactical aviation asset. A preliminary analysis is presented of the UTTH in the reconnaissance role only, using the HELSCAM combat simulator program. The effects of the flown nap-of-the-earth altitude and the physical signature of a reconnaissance helicopter on its survivability are examined. The scenarios were simulated with the UTTH at two altitudes: 2 m and 5 m. The observed loss rate at the higher altitude was more than double that at the lower altitude. In addition, the larger size of the UTTH compared to a conventional light observation helicopter operating at the same altitude, increased its loss rate by about 18 percent. The results suggest that the operational doctrine used for the UTTH can have a significant impact on its potential survivability and hence on its performance. Author (CISTI)

N94-13867 Operational Research and Analysis Establishment, Ottawa (Ontario).

HELSCAM V2.0: DEVELOPMENT AND APPLICATION GUIDE

P. J. Young Dec. 1992 128 p
(DSIS-93-00137; DLOR-RN-92-6; CTN-93-60805) Avail: CASI HC A07

The HELicopter SCenario Assessment Model (HELSCAM) was developed to study helicopter operations in support of the ground commander. The completed model comprised a simulation core, an event analyzer, and graphical facilities for route planning and scenario replay. The simulation core included sophisticated algorithms for movement, acquisition, and engagement processes. In the process of streamlining the model and generalizing its algorithms to model a wider variety of weapon systems, HELSCAM changed sufficiently to require a new development and application guide, which is presented. Major modifications to the simulation core of HELSCAM present in the new version 2.0 include addition of fixed wing systems, addition of a merged terrain base in the terrain data files, the modelling of delays imposed by weapon reloading, and revision of the line-of-sight algorithm. The guide includes an overview of HELSCAM system

hardware and software requirements, the simulation core, the analytical facility, and input definitions. An air raid scenario and its HELSCAM files are also included. CISTI

N94-13898# Institute for Aerospace Research, Ottawa (Ontario). Applied Aerodynamics Lab.
QUALITATIVE INVESTIGATION OF A GENERIC FIGHTER MODEL IN RADIO CONTROLLED GLIDING FLIGHT
P. J. Penna Jul. 1992 26 p
(LM-AA-003; CTN-93-60762) Avail: CASI HC A03/MF A01

A generic fighter model was flown in radio controlled gliding flight to investigate qualitatively some of its flight dynamic characteristics. Visual cues from the model's flight path, its motion about its center of gravity, and qualitative knowledge of the pilot's control inputs were used to infer certain dynamic characteristics. The observations showed that the model was statically stable in pitch with the center of gravity moved as far back as 23.3 percent of the mean aerodynamic chord of the wing. However, if the model was rotated rapidly in pitch, it had a tendency to pitch up into a deep stall. The model was found to be prone to entering a spin from a moderate stall. The spin is postulated to be caused by a separated-flow asymmetry at the nose ogive. Finally, the model's ailerons were found to provide acceptable roll control authority, but maximum aileron deflection caused visible adverse yaw. CISTI

N94-14104*# Iowa State Univ. of Science and Technology, Ames. Dept. of Aerospace Engineering and Engineering Mechanics.
TRAJECTORY OPTIMIZATION FOR THE NATIONAL AEROSPACE PLANE Semiannual Report, 13 Dec. 1992 - 12 Jun. 1993
Ping Lu Jul. 1993 14 p
(Grant NAG1-1255)
(NASA-CR-194146; NAS 1.26:194146) Avail: CASI HC A03/MF A01

During the past six months the research objectives outlined in the last semi-annual report were accomplished. Specifically, these are: three-dimensional (3-D) fuel-optimal ascent trajectory of the aerospace plane and the effects of thrust vectoring control (TVC) on the fuel consumption and trajectory shaping were investigated; the maximum abort landing area (footprint) was studied; preliminary assessment of simultaneous design of the ascent trajectory and the vehicle configuration for the aerospace plane was also conducted. The work accomplished in the reporting period is summarized. Author (revised)

N94-14106*# Texas A&M Univ., College Station. Aerospace Engineering Div.
FLIGHT VALIDATION OF A PULSED SMOKE FLOW VISUALIZATION SYSTEM Final Report
Donald T. Ward and Kenneth M. Dorsett Sep. 1993 44 p Sponsored by NASA. Washington
(Contract NCC2-742; RTOP 533-02-35)
(NASA-CR-186026; H-1914; NAS 1.26:186026) Avail: CASI HC A03/MF A01

A flow visualization scheme, designed to measure vortex fluid dynamics on research aircraft, was validated in flight. Strake vortex trajectories and axial core velocities were determined using pulsed smoke, high-speed video images, and semiautomated image edge detection hardware and software. Smoke was pulsed by using a fast-acting three-way valve. After being redesigned because of repeatedly jamming in flight, the valve shuttle operated flawlessly during the last two tests. A 25-percent scale, Gothic strake was used to generate vortex over the wing of a GA-7 Cougar and was operated at a local angle of attack of 22 degrees and Reynolds number of approximately 7.8 x 10(exp 5)/ft. Maximum axial velocities measured in the vortex core were between 1.75 and 1.95 times the freestream velocity. Analysis of the pulsed smoke system's affect on forebody vortices indicates that the system may reorient the forebody vortex system; however, blowing momentum coefficients normally used will have no appreciable affect on the leading-edge extension vortex system. It is recommended that a similar pulsed smoke system be installed on the F/A-18 High Angle Research Vehicle and that this approach be used to analyze vortex core dynamics during the remainder of its high-angle-of-attack research flights. Author (revised)

N94-14615# National Aeronautical Lab., Bangalore (India). Computational and Theoretical Fluid Dynamics Div.
SRISTI: THE NAL METHOD FOR THE DESIGN AND ANALYSIS OF NATURAL LAMINAR FLOW (NLF) AIRFOILS
K. R. Srilatha, G. S. Dwarakanath, and P. Ramamoorthy *In its* Proceedings of the Fluid Dynamics Symposium in Honour of Professor R. Narasimha on his 60th Birthday Jul. 1993 p 191-203 (For primary document see N94-14598 02-34)
Avail: CASI HC A03/MF A03

N94-14616# National Aeronautical Lab., Bangalore (India). Computational and Theoretical Fluid Dynamics Div.
VSAERO ANALYSIS OF A PIPER CUB AIRCRAFT
Ashok Srivastava, David Lednicer (Analytical Methods, Inc., Redmond, WA.), Ian Gilchrist (Analytical Methods, Inc., Redmond, WA.), and Jahan Saghafi (Analytical Methods, Inc., Redmond, WA.) *In its* Proceedings of the Fluid Dynamics Symposium in Honour of Professor R. Narasimha on his 60th Birthday Jul. 1993 p 205-210 Sponsored by Dept. of Science and Technology and Agency for International Development (For primary document see N94-14598 02-34)
Avail: CASI HC A02/MF A03

06 AIRCRAFT INSTRUMENTATION

Includes cockpit and cabin display devices; and flight instruments.

For related information see also *19 Spacecraft Instrumentation* and *35 Instrumentation and Photography.*

N94-12829*# Boeing Commercial Airplane Co., Seattle, WA.
FLIGHT CREW INTERFACE ASPECTS OF FORWARD-LOOKING AIRBORNE WINDSHEAR DETECTION SYSTEMS Final Report
Charles D. Anderson and David C. Carbaugh Jul. 1993 124 p Original contains color illustrations
(Contract NAS1-18027; RTOP 505-64-12-01)
(NASA-CR-191437; NAS 1.26:191437) Avail: CASI HC A06/MF A02; 11 functional color pages

The goal of this research effort was to conduct analyses and research which could provide guidelines for design of the crew interface of an integrated windshear system. Addressed were HF issues, crew/system requirements, candidate display formats, alerting criteria, and crew procedures. A survey identified five flight management issues as top priority: missed alert acceptability; avoidance distance needed; false alert acceptability; nuisance rate acceptability; and crew procedures. Results of a simulation study indicated that the warning time for a look-ahead alert needs to be between 11 and 36 seconds (target of 23 seconds) before the reactive system triggers in order to be effective. Pilots considered the standard go-around maneuver most appropriate for look-ahead alerts, and the escape maneuvers used did not require lateral turns. Prototype display formats were reviewed or developed for alerting the crew; providing guidance to avoid or escape windshear; and status displays to provide windshear situational awareness. The three alerting levels now in use were considered appropriate, with a fourth (time-critical) level as a possible addition, although many reviewers felt only two levels of alerting were needed. Another survey gathered expert opinion on what crew procedures and alerting criteria should be used for look-ahead, or integrated, windshear systems, with a wide diversity of opinion in these areas. Author

N94-13256*# National Aeronautics and Space Administration. Hugh L. Dryden Flight Research Facility, Edwards, CA.
PERSPECTIVE ON THE NATIONAL AERO-SPACE PLANE PROGRAM INSTRUMENTATION DEVELOPMENT
Rodney K. Bogue and Peter Erbland (Air Force Systems Command, Wright-Patterson AFB, OH.) May 1993 22 p Presented at the Aero Space Planes Conference, Orlando, FL, 1-3 Dec. 1992 Previously announced in IAA as A93-22356 Sponsored by NASA. Washington
(RTOP 763-21-41)
(NASA-TM-4505; H-1916; NAS 1.15:4505) Copyright Avail: CASI HC A03/MF A01

A review of the requirement for, and development of, advanced measurement technology for the National Aerospace Plane program is

presented. The objective is to discuss the technical need and the program commitment required to ensure that adequate and timely measurement capabilities are provided for ground and flight testing in the NASP program. The scope of the measurement problem is presented, the measurement process is described, how instrumentation technology development has been affected by NASP program evolution is examined, the national effort to define measurement requirements and assess the adequacy of current technology to support the NASP program is discussed, and the measurement requirements are summarized. The unique features of the NASP program that complicate the understanding of requirements and the development of viable solutions are illustrated. Author (revised)

N94-13451# National Aerospace Lab., Tokyo (Japan). Short Take-Off and Landing Research Aircraft Group.

POSITION ERROR DETERMINATION FOR THE SPEEDOMETER AND ALTIMETER OF THE NAL QSTOL EXPERIMENTAL AIRCRAFT ASKA [TEISOUON SHORT TAKE-OFF AND LANDING JIKKENKI ASUKA NO SOKUDOKEI OYOBI KOUDOKEI NO ICHI GOSA]

Kazuya Masui, Hamaki Inokuchi, and Kenji Yazawa Mar. 1992 69 p In JAPANESE

(NAL-TR-1144; JTN-93-80482) Avail: CASI HC A04/MF A01

The position error is reported for three different pitot-static systems used in the National Aerospace Laboratory (NAL) Quiet Short Take-Off and Landing (QSTOL) experimental aircraft, ASKA, being determined using only the static pressure error, and assuming that the total pressure error is negligible. It was found that a continuous reference altitude and a correction for pressure propagation lag, realized the determination of the position error during speed and altitude transition. The continuous reference altitude was obtained precisely by the combination of a radar altimeter and an aircraft tracking radar. The ground effect on the position error before touchdown is also reported. In addition, the position error in high angle of attack cases was discussed. The resultant position error correction was used for various analyses of flight test data. Furthermore, it was incorporated into the Digital Air Data Computer to indicate the calibrated airspeed and altitude to the pilots. Author (NASDA)

N94-13710*# National Aeronautics and Space Administration. Langley Research Center, Hampton, VA.

FUNCTIONAL CATEGORIES FOR FUTURE FLIGHT DECK DESIGNS

Terence S. Abbott Aug. 1993 15 p

(RTOP 505-64-53-02)

(NASA-TM-109005; NAS 1.15:109005) Avail: CASI HC A03/MF A01

With the addition of each new system on the flight deck, the danger of increasing overall operator workload while reducing crew understanding of critical mission information exists. The introduction of more powerful onboard computers, larger databases, and the increased use of electronic display media may lead to a situation of flight deck 'sophistication' at the expense of losses in flight crew capabilities and situational awareness. To counter this potentially negative impact of new technology, research activities are underway to reassess the flight deck design process. The fundamental premise of these activities is that a human-centered, systems-oriented approach to the development of advanced civil aircraft flight decks will be required for future designs to remain ergonomically sound and economically competitive. One of the initial steps in an integrated flight deck process is to define the primary flight deck functions needed to support the mission goals of the vehicle. This would allow the design team to evaluate candidate concepts in relation to their effectiveness in meeting the functional requirements. In addition, this would provide a framework to aid in categorizing and bookkeeping all of the activities that are required to be performed on the flight deck, not just activities of the crew or of a specific system. This could then allow for a better understanding and allocation of activities in the design, an understanding of the impact of a specific system on overall system performance, and an awareness of the total crew performance requirements for the design. One candidate set of functional categories that could be used to guide an advanced flight deck design are described. Author (revised)

N94-13791*# National Aeronautics and Space Administration. Hugh L. Dryden Flight Research Center, Edwards, CA.

RECENT FLIGHT-TEST RESULTS OF OPTICAL AIRDATA TECHNIQUES

Rodney K. Bogue Washington May 1993 22 p Presented at the SAE Aerotech 1992, Anaheim, CA, 5-8 Oct. 1992

(RTOP 505-68-50)

(NASA-TM-4504; H-1915; NAS 1.15:4504; SAE-92-1997) Avail: CASI HC A03/MF A01

Optical techniques for measuring airdata parameters were demonstrated with promising results on high performance fighter aircraft. These systems can measure the airspeed vector, and some are not as dependent on special in-flight calibration processes as current systems. Optical concepts for measuring freestream static temperature and density are feasible for in-flight applications. The best feature of these concepts is that the air data measurements are obtained nonintrusively, and for the most part well into the freestream region of the flow field about the aircraft. Current requirements for measuring air data at high angle of attack, and future need to measure the same information at hypersonic flight conditions place strains on existing techniques. Optical technology advances show outstanding potential for application in future programs and promise to make common use of optical concepts a reality. Results from several flight-test programs are summarized, and the technology advances required to make optical airdata techniques practical are identified.

Author (revised)

N94-13316*# Boeing Defense and Space Group, Philadelphia, PA.

HANDLING QUALITIES EFFECTS OF DISPLAY LATENCY

David W. King *In* NASA. Ames Research Center, Piloting Vertical Flight Aircraft: A Conference on Flying Qualities and Human Factors Jul. 1993 p 329-340 (For primary document see N94-13294 02-08)

Avail: CASI HC A03/MF A04

N94-13323*# National Aeronautics and Space Administration. Ames Research Center, Moffett Field, CA.

EVALUATION OF TWO COCKPIT DISPLAY CONCEPTS FOR CIVIL TILTROTOR INSTRUMENT OPERATIONS ON STEEP APPROACHES

William A. Decker, Richard S. Bray, Rickey C. Simmons, and George E. Tucker *In its* Piloting Vertical Flight Aircraft: A Conference on Flying Qualities and Human Factors Jul. 1993 p 433-452 (For primary document see N94-13294 02-08)

Avail: CASI HC A03/MF A04

07 AIRCRAFT PROPULSION AND POWER

Includes prime propulsion systems and systems components, e.g., gas turbine engines and compressors; and onboard auxilliary power plants for aircraft.

For related information see also *20 Spacecraft Propulsion and Power, 28 Propellants and Fuels,* and *44 Energy Production and Conversion.*

N94-13142*# National Aeronautics and Space Administration. Lewis Research Center, Cleveland, OH.

COMBUSTOR TECHNOLOGY FOR FUTURE SMALL GAS TURBINE AIRCRAFT

Valerie J. Lyons and Richard W. Niedzwiecki Aug. 1993 18 p Proposed for presentation at the Propulsion and Energetics Panel 82nd Meeting, Montreal, Ottawa, 4-8 Oct. 1993; sponsored by the Advisory Group for Aerospace Research and Development

(RTOP 535-05-10)

(NASA-TM-106312; E-8052; NAS 1.15:106312) Avail: CASI HC A03/MF A01

Future engine cycles proposed for advanced small gas turbine engines will increase the severity of the operating conditions of the combustor. These cycles call for increased overall engine pressure ratios which increase combustor inlet pressure and temperature. Further, the temperature rise through the combustor and the corresponding exit temperature also increase. Future combustor technology needs for small gas turbine engines is described. New fuel injectors with large turndown ratios which produce uniform circumferential and radial temperature patterns will be required. Uniform burning will be of greater importance because hot gas temperatures will approach turbine material limits. The higher combustion temperatures and increased radiation at high pressures will put a greater heat load on the combustor liners. At the same time, less cooling air will be available as more of the air will be used for combustion. Thus, improved cooling concepts and/or materials requiring little or no direct cooling will be required.

Although presently there are no requirements for emissions levels from small gas turbine engines, regulation is expected in the near future. This will require the development of low emission combustors. In particular, nitrogen oxides will increase substantially if new technologies limiting their formation are not evolved and implemented. For example, staged combustion employing lean, premixed/prevaporized, lean direct injection, or rich burn-quick quench-lean burn concepts could replace conventional single stage combustors. Author

N94-13143*# National Aeronautics and Space Administration. Lewis Research Center, Cleveland, OH.

ANALYSIS OF GAS TURBINE ENGINES USING WATER AND OXYGEN INJECTION TO ACHIEVE HIGH MACH NUMBERS AND HIGH THRUST

Hugh M. Henneberry (Analex Corp., Brook Park, OH.) and Christopher A. Snyder Jul. 1993 20 p

(RTOP 505-70-00)

(NASA-TM-106270; E-7998; NAS 1.15:106270) Avail: CASI HC A03/MF A01

An analysis of gas turbine engines using water and oxygen injection to enhance performance by increasing Mach number capability and by increasing thrust is described. The liquids are injected, either separately or together, into the subsonic diffuser ahead of the engine compressor. A turbojet engine and a mixed-flow turbofan engine (MFTF) are examined, and in pursuit of maximum thrust, both engines are fitted with afterburners. The results indicate that water injection alone can extend the performance envelope of both engine types by one and one-half Mach numbers at which point water-air ratios reach 17 or 18 percent and liquid specific impulse is reduced to some 390 to 470 seconds, a level about equal to the impulse of a high energy rocket engine. The envelope can be further extended, but only with increasing sacrifices in liquid specific impulse. Oxygen-airflow ratios as high as 15 percent were investigated for increasing thrust. Using 15 percent oxygen in combination with water injection at high supersonic Mach numbers resulted in thrust augmentation as high as 76 percent without any significant decrease in liquid specific impulse. The stoichiometric afterburner exit temperature increased with increasing oxygen flow, reaching 4822 deg R in the turbojet engine at a Mach number of 3.5. At the transonic Mach number of 0.95 where no water injection is needed, an oxygen-air ratio of 15 percent increased thrust by some 55 percent in both engines, along with a decrease in liquid specific impulse of 62 percent. Afterburner temperature was approximately 4700 deg R at this high thrust condition. Water and/or oxygen injection are simple and straightforward strategies to improve engine performance and they will add little to engine weight. However, if large Mach number and thrust increases are required, liquid flows become significant, so that operation at these conditions will necessarily be of short duration. Author (revised)

N94-13190*# National Aeronautics and Space Administration. Langley Research Center, Hampton, VA.

AN EXPERIMENTAL INVESTIGATION OF MIXING ENHANCEMENT IN A SIMULATED SCRAMJET COMBUSTOR BY USE OF SWIRLING JETS

M.S. Thesis

Donna Karen Kraus Aug. 1993 92 p Original contains color illustrations

(NASA-TM-109246; NAS 1.15:109246) Avail: CASI HC A05/MF A01; 4 functional color pages

It is desired to maintain supersonic flow through the combustor of supersonic airbreathing engines to reduce static temperatures and total pressure losses inherent in reducing flow to subsonic speeds. Due to the supersonic speeds through the combustor, mixing of the fuel and air must by rapid for complete combustion to occur within a reasonable streamwise distance. It was proposed that the addition of swirl to the fuel jet prior to injection might enhance the mixing of the fuel with the air. The effects of swirl on the mixing of a 30 deg wall jet into a Mach 2 flow were experimentally investigated. Swirl was introduced into the fuel stream by tangential injection into a cylindrical swirl chamber. The flow was then accelerated through a convergent-divergent nozzle with an area ratio of two, and supersonically injected into the Mach 2 flow such that the static pressure of the fuel matched the effective back pressure of the main flow. Two different cases with swirl and one without swirl were investigated, with both helium and air simulating the fuel. Rayleigh scattering was used to visualize the flow and seeding the fuel with water allowed it to be traced through the main flow. Using histograms of the pure molecular Rayleigh scattering images, the helium concentration in the jet-mixing region of the flow was monitored and found to decrease slightly with swirl, indicating better mixing. Thresholding the water-seeded images allowed the jet-mixing region to be isolated and showed a slight increase in this area with swirl. Penetration, however, was slightly less with swirl. Rescaling the data for equal mass flow rates allowed comparison for a scramjet application of a combustor with a single injector and the desire to fuel to a specified fuel-to-oxidant ratio. These results showed a substantial increase in the spreading area with swirl, an increase in the mixing occurring in this area, and slightly better penetration. Author (revised)

N94-13252# Federal Aviation Administration, Washington, DC.

AIRCRAFT ENGINE TYPE CERTIFICATION HANDBOOK: ADVISORY CIRCULAR

30 Jun. 1993 125 p Supersedes AC-33-2A

(AC-33-2B; ANE-110) Avail: CASI HC A06/MF A02

This advisory circular (AC) provides methods acceptable to the Administrator for showing compliance with the type certification requirements of aircraft engines in Part 33, inclusive through amendment 12, of the Federal Aviation Regulations (FAR). The procedures and guidance material provided in this AC may be used by an applicant seeking issuance of a type certificate, an amended type certificate, or a supplemental type certificate for the initial approval of a new type design, or a change in the type design. Consideration will be given to any other method of compliance the applicant elects to present. This information is not in itself mandatory, but serves as a guide to engine manufacturers, engine modifiers, and Federal Aviation Administration (FAA) engine type certification engineers. Individuals should be guided by the intent of the methods provided in this AC. Author

N94-13608* National Aeronautics and Space Administration. Ames Research Center, Moffett Field, CA.

ROTOR STATOR CGI (Videotape)

Apr. 1988 Videotape: 5 min. playing time, in color, with sound

(NASA-TM-109313; NONP-VT-93-185320) Avail: CASI VHS A01/BETA A22

This video contains computer graphics of numerous kinds of flow within jet engines. Analyses include pressure contours (shock waves), fluid pressures, etc. The video also contains dramatic views of jet engine manufacturing. Author (revised)

N94-13623* National Aeronautics and Space Administration. Lewis Research Center, Cleveland, OH.

FUTUREPATH 2 (Videotape)

Apr. 1989 Videotape: 28 min. 48 sec. playing time, in color, with sound

(NASA-TM-109285; NONP-VT-93-185301) Avail: CASI VHS A01/BETA A22

This covers advanced turboprop tests, the diesel engine as an aircraft propulsion system in helicopters, and the development of the Stirling engine as a space power system. Author

N94-14036*# National Aeronautics and Space Administration. Lewis Research Center, Cleveland, OH.

NOISE LEVELS FROM A MODEL TURBOFAN ENGINE WITH SIMULATED NOISE CONTROL MEASURES APPLIED

David G. Hall (Sverdrup Technology, Inc., Brook Park, OH.) and Richard P. Woodward Oct. 1993 15 p Proposed for presentation at the 15th AIAA Aeroacoustics Conference, Long Beach, CA, 25-27 Oct. 1993; sponsored by AIAA

(RTOP 535-03-10)

(NASA-TM-106318; E-8063; NAS 1.15:106318; AIAA Paper 93-4401)

Avail: CASI HC A03/MF A01

A study of estimated full-scale noise levels based on measured levels from the Advanced Ducted Propeller (ADP) sub-scale model is presented. Testing of this model was performed in the NASA Lewis Low Speed Anechoic Wind Tunnel at a simulated takeoff condition of Mach 0.2. Effective Perceived Noise Level (EPNL) estimates for the baseline configuration are documented, and also used as the control case in a study of the potential benefits of two categories of noise control. The effect of active noise control is evaluated by artificially removing various rotor-stator interaction tones. Passive noise control is simulated by applying a notch filter to the wind tunnel data. Cases with both techniques are included to evaluate

hybrid active-passive noise control. The results for EPNL values are approximate because the original source data was limited in bandwidth and in sideline angular coverage. The main emphasis is on comparisons between the baseline and configurations with simulated noise control measures. Author (revised)

N94-14448*# Wisconsin Univ., Madison. Engine Research Center.
THREE-DIMENSIONAL MODELING OF DIESEL ENGINE INTAKE FLOW, COMBUSTION AND EMISSIONS-2 Final Report
R. D. Reitz and C. J. Rutland Sep. 1993 64 p
(Contract NAG3-1087; DE-AI01-91CE-50306; RTOP 778-34-2A)
(NASA-CR-191189; E-8103; NAS 1.26:191189; DOE/NASA/1087-2)
Avail: CASI HC A04/MF A01

A three-dimensional computer code, KIVA, is being modified to include state-of-the-art submodels for diesel engine flow and combustion. Improved and/or new submodels which have already been implemented and previously reported are: wall heat transfer with unsteadiness and compressibility, laminar-turbulent characteristic time combustion with unburned HC and Zeldo'vich NO(x), and spray/wall impingement with rebounding and sliding drops. Progress on the implementation of improved spray drop drag and drop breakup models, the formulation and testing of a multistep kinetics ignition model, and preliminary soot modeling results are described. In addition, the use of a block structured version of KIVA to model the intake flow process is described. A grid generation scheme was developed for modeling realistic (complex) engine geometries, and computations were made of intake flow in the ports and combustion chamber of a two-intake-value engine. The research also involves the use of the code to assess the effects of subprocesses on diesel engine performance. The accuracy of the predictions is being tested by comparisons with engine experiments. To date, comparisons were made with measured engine cylinder pressure, temperature and heat flux data, and the model results are in good agreement with the experiments. Work is in progress that will allow validation of in-cylinder flow and soot formation predictions. An engine test facility is described that is being used to provide the needed validation data. Test results were obtained showing the effect of injection rate and split injections on engine performance and emissions. Author (revised)

N94-14450# National Aerospace Lab., Amsterdam (Netherlands). Structures and Materials Div.
PERFORMANCE OF GAS TURBINE COMPRESSOR CLEANERS [WASMIDDELEN VOOR GASTURBINES VALLEN VIES TEGEN]
H. J. Kolkman 23 Jul. 1991 15 p In DUTCH Submitted for publication
(NLR-TP-91291-U; ETN-93-94068) Avail: CASI HC A03/MF A01

The cleaning efficiency of compressor cleaners was studied. Recently developed cleaners are claimed to be ecologically sound. In addition, many new compressor cleaners contain a corrosion inhibitor. The cleaning efficiency of eight (old and new) compressor cleaners was determined by simulated compressor washing of compressor blades that had become foul in service. For the situation simulated, the cleaning efficiency of new, ecologically sound cleaners turned out to be poor as compared with old cleaners. ESA

N94-14841*# Jet Propulsion Lab., California Inst. of Tech., Pasadena.
AN IMPROVED APPROACH FOR FLIGHT READINESS CERTIFICATION: PROBABILISTIC MODELS FOR FLAW PROPAGATION AND TURBINE BLADE FAILURE. VOLUME 1: METHODOLOGY AND APPLICATIONS
N. R. Moore, D. H. Ebbeler, L. E. Newlin, S. Sutharshana, and M. Creager 30 Dec. 1992 200 p
(Contract NAS7-918; RTOP 553-02-01)
(NASA-CR-194496; JPL-Publ-92-32-Vol-1; NAS 1.26:194496) Avail: CASI HC A09/MF A03

An improved methodology for quantitatively evaluating failure risk of spaceflight systems to assess flight readiness and identify risk control measures is presented. This methodology, called Probabilistic Failure Assessment (PFA), combines operating experience from tests and flights with analytical modeling of failure phenomena to estimate failure risk. The PFA methodology is of particular value when information on which to base an assessment of failure risk, including test experience and knowledge of parameters used in analytical modeling, is expensive or difficult to acquire. The PFA methodology is a prescribed statistical structure in which analytical models that characterize failure phenomena are used conjointly with uncertainties about analysis parameters and/or modeling accuracy to estimate failure probability distributions for specific failure modes. These distributions can then be modified, by means of statistical procedures of the PFA methodology, to reflect any test or flight experience. State-of-the-art analytical models currently employed for designs failure prediction, or performance analysis are used in this methodology. The rationale for the statistical approach taken in the PFA methodology is discussed, the PFA methodology is described, and examples of its application to structural failure modes are presented. The engineering models and computer software used in fatigue crack growth and fatigue crack initiation applications are thoroughly documented. Author (revised)

N94-14842*# Jet Propulsion Lab., California Inst. of Tech., Pasadena.
AN IMPROVED APPROACH FOR FLIGHT READINESS CERTIFICATION: PROBABILISTIC MODELS FOR FLAW PROPAGATION AND TURBINE BLADE FAILURE. VOLUME 2: SOFTWARE DOCUMENTATION
N. R. Moore, D. H. Ebbeler, L. E. Newlin, S. Sutharshana, and M. Creager 30 Dec. 1992 507 p
(Contract NAS7-918; RTOP 553-02-01)
(NASA-CR-194497; JPL-Publ-92-32-Vol-2; NAS 1.26:194497) Avail: CASI HC A22/MF A04

An improved methodology for quantitatively evaluating failure risk of spaceflights systems to assess flight readiness and identify risk control measures is presented. This methodology, called Probabilistic Failure Assessment (PFA), combines operating experience from tests and flights with analytical modeling of failure phenomena to estimate failure risk. The PFA methodology is of particular value when information on which to base an assessment of failure risk, including test experience and knowledge of parameters used in analytical modeling, is expensive or difficult to acquire. The PFA methodology is a prescribed statistical structure in which analytical models that characterize failure phenomena are used conjointly with uncertainties about analysis parameters and/or modeling accuracy to estimate failure probability distributions for specific failure modes. These distributions can then be modified, by means of statistical procedures of the PFA methodology, to reflect any test or flight experience. State-of-the-art analytical models currently employed for design, failure prediction, or performance analysis are used in this methodology. The rationale for the statistical approach taken in the PFA methodology is discussed, the PFA methodology is described, and examples of its application to structural failure modes are presented. The engineering models and computer software used in fatigue crack growth and fatigue crack initiation applications are thoroughly documented. Author (revised)

N94-14855*# National Aeronautics and Space Administration. Hugh L. Dryden Flight Research Facility, Edwards, CA.
PERFORMANCE SEEKING CONTROL: PROGRAM OVERVIEW AND FUTURE DIRECTIONS
Glenn B. Gilyard and John S. Orme Aug. 1993 19 p Presented at the Guidance, Navigation, and Control Conference, Monterey, CA, 9-11 Aug. 1993; sponsored by AIAA See also A93-51360
(RTOP 533-02-39)
(NASA-TM-4531; H-1920; NAS 1.15:4531; AIAA Paper 93-3765)
Copyright Avail: CASI HC A03/MF A01

A flight test evaluation of the performance-seeking control (PSC) algorithm on the NASA F-15 highly integrated digital electronic control research aircraft was conducted for single-engine operation at subsonic and supersonic speeds. The model-based PSC system was developed with three optimization modes: minimum fuel flow at constant thrust, minimum turbine temperature at constant thrust, and maximum thrust at maximum dry and full afterburner throttle settings. Subsonic and supersonic flight testing were conducted at the NASA Dryden Flight Research Facility covering the three PSC optimization modes and over the full throttle range. Flight results show substantial benefits. In the maximum thrust mode, thrust increased up to 15 percent at subsonic and 10 percent at supersonic flight conditions. The minimum fan turbine inlet temperature mode reduced temperatures by more than 100 F at high altitudes. The minimum fuel flow mode results decreased fuel consumption up to 2 percent in the subsonic regime and almost 10 percent supersonically. These results demonstrate that PSC technology can benefit the next generation of fighter or transport aircraft. NASA Dryden is developing an adaptive aircraft performance technology system that is measurement based and uses feedback to ensure

optimality. This program will address the technical weaknesses identified in the PSC program and will increase performance gains. Author (revised)

N94-14156# Tennessee Univ. Space Inst., Tullahoma. Dept. of Mechanical and Aerospace Engineering.
HYPERSONIC PROPULSION CHARACTERIZATION
Roger Crawford *In* VKI, Methodology of Hypersonic Testing 1993 10 p (For primary document see N94-14153 02-02)
Copyright Avail: CASI HC A02/MF A03

N94-14165# Sverdrup Technology, Inc., Arnold AFS, TN. Facility Enhancements.
AEROPROPULSION TEST AND EVALUATION METHODS
Brian Wettlaufer *In* VKI, Methodology of Hypersonic Testing 1993 18 p Prepared in cooperation with Arnold Engineering Development Center, Arnold AFS, TN (For primary document see N94-14153 02-02)
Copyright Avail: CASI HC A03/MF A03

N94-14168# Sverdrup Technology, Inc., Arnold AFS, TN.
HYPERSONIC FLIGHT TEST. PART 1: PROPULSION FLIGHT TESTING
Virgil K. Smith, III (Arnold Engineering Development Center, Arnold AFS, TN.) *In* VKI, Methodology of Hypersonic Testing 1993 10 p Prepared in cooperation with Arnold Engineering Development Center, Arnold AFS, TN (For primary document see N94-14153 02-02)
Copyright Avail: CASI HC A02/MF A03

N94-14169# Calspan Corp., Arnold AFS, TN.
HYPERSONIC FLIGHT TESTING. PART 2: AEROTHERMAL FLIGHT TESTING
R. K. Matthews *In* VKI, Methodology of Hypersonic Testing 1993 6 p Prepared in cooperation with Arnold Engineering Development Center, Arnold AFS, TN (For primary document see N94-14153 02-02)
Copyright Avail: CASI HC A02/MF A03

N94-14174# Tennessee Univ. Space Inst., Tullahoma. Dept. of Mechanical and Aerospace Engineering.
PROPULSION INTEGRATION
Roger Crawford *In* VKI, Methodology of Hypersonic Testing 1993 11 p (For primary document see N94-14153 02-02)
Copyright Avail: CASI HC A03/MF A03

08 AIRCRAFT STABILITY AND CONTROL

Includes aircraft handling qualities; piloting; flight controls; and autopilots.

For related information see also *05 Aircraft Design, Testing and Performance.*

N94-12799*# MCAT Inst., San Jose, CA.
TURBULENCE MODELING OF FREE SHEAR LAYERS FOR HIGH-PERFORMANCE AIRCRAFT Progress Report
Douglas L. Sondak Aug. 1993 9 p
(Contract NCC2-663)
(NASA-CR-193659; NAS 1.26:193659; MCAT-93-15) Avail: CASI HC A02/MF A01

The High Performance Aircraft (HPA) Grand Challenge of the High Performance Computing and Communications (HPCC) program involves the computation of the flow over a high performance aircraft. A variety of free shear layers, including mixing layers over cavities, impinging jets, blown flaps, and exhaust plumes, may be encountered in such flowfields. Since these free shear layers are usually turbulent, appropriate turbulence models must be utilized in computations in order to accurately simulate these flow features. The HPCC program is relying heavily on parallel computers. A Navier-Stokes solver (POVERFLOW) utilizing the Baldwin-Lomax algebraic turbulence model was developed and tested on a 128-node Intel iPSC/860. Algebraic turbulence models run very fast, and give good results for many flowfields. For complex flowfields such as those mentioned above, however, they are often inadequate. It was therefore deemed that a two-equation turbulence model will be required for the HPA computations. The k-epsilon two-equation turbulence model was implemented on the Intel iPSC/860. Both the Chien low-Reynolds-number model and a generalized wall-function formulation were included. Author (revised)

N94-12820*# National Aeronautics and Space Administration. Ames Research Center, Moffett Field, CA.
KINEMATICS AND CONSTRAINTS ASSOCIATED WITH SWASHPLATE BLADE PITCH CONTROL
Jane A. Leyland Mar. 1993 35 p
(RTOP 505-61-51)
(NASA-TM-102265; A-90033; NAS 1.15:102265) Avail: CASI HC A03/MF A01

An important class of techniques to reduce helicopter vibration is based on using a Higher Harmonic controller to optimally define the Higher Harmonic blade pitch. These techniques typically require solution of a general optimization problem requiring the determination of a control vector which minimizes a performance index where functions of the control vector are subject to inequality constraints. Six possible constraint functions associated with swashplate blade pitch control were identified and defined. These functions constrain: (1) blade pitch Fourier Coefficients expressed in the Rotating System, (2) blade pitch Fourier Coefficients expressed in the Nonrotating System, (3) stroke of the individual actuators expressed in the Nonrotating System, (4) blade pitch expressed as a function of blade azimuth and actuator stroke, (5) time rate-of-change of the aforementioned parameters, and (6) required actuator power. The aforementioned constraints and the associated kinematics of swashplate blade pitch control by means of the strokes of the individual actuators are documented.
Author (revised)

N94-13254*# National Aeronautics and Space Administration. Hugh L. Dryden Flight Research Facility, Edwards, CA.
PRELIMINARY FLIGHT RESULTS OF A FLY-BY-THROTTLE EMERGENCY FLIGHT CONTROL SYSTEM ON AN F-15 AIRPLANE
Frank W. Burcham, Jr., Trindel A. Maine, C. Gordon Fullerton, and Edward A. Wells (McDonnell-Douglas Automation Co., Saint Louis, MO.) Washington Jun. 1993 19 p Presented at the 29th AIAA/SAE/ASME Joint Propulsion Conference, Monterey, CA, 28-30 Jun. 1993
(RTOP 533-02-34)
(NASA-TM-4503; H-1911; NAS 1.15:4503; AIAA Paper 93-1820)
Copyright Avail: CASI HC A03/MF A01

A multi-engine aircraft, with some or all of the flight control system inoperative, may use engine thrust for control. NASA Dryden has conducted a study of the capability and techniques for this emergency flight control method for the F-15 airplane. With an augmented control system, engine thrust, along with appropriate feedback parameters, is used to control flightpath and bank angle. Extensive simulation studies were followed by flight tests. The principles of throttles only control, the F-15 airplane, the augmented system, and the flight results including actual landings with throttles-only control are discussed. Author (revised)

N94-13255*# National Aeronautics and Space Administration. Hugh L. Dryden Flight Research Facility, Edwards, CA.
ACTUATOR AND AERODYNAMIC MODELING FOR HIGH-ANGLE-OF-ATTACK AEROSERVOELASTICITY
Martin J. Brenner Washington Jun. 1993 30 p Presented at the AIAA/ASME/ASCE/AHS/ASC Structures, Structural Dynamics and Materials Conference, LaJolla, CA, 19-22 Apr. 1993 Previously announced in IAA as A93-37433
(RTOP 533-02-35)
(NASA-TM-4493; H-1904; NAS 1.15:4493; AIAA Paper 93-1419)
Copyright Avail: CASI HC A03/MF A01

Accurate prediction of airframe/actuation coupling is required by the imposing demands of modern flight control systems. In particular, for agility enhancement at high angle of attack and low dynamic pressure, structural integration characteristics such as hinge moments, effective actuator stiffness, and airframe/control surface damping can have a significant effect on stability predictions. Actuator responses are customarily represented with low-order transfer functions matched to actuator test data, and control surface stiffness is often modeled as a linear spring. The inclusion of the physical properties of actuation and its installation on the airframe is therefore addressed using detailed actuator models which consider the physical, electrical, and mechanical elements of actuation. The aeroservoelastic analysis procedure is described in which the actuators are modeled as

detailed high-order transfer functions and as approximate low-order transfer functions. The impacts of unsteady aerodynamic modeling on aeroservoelastic stability are also investigated by varying the order of approximation, or number of aerodynamic lag states, in the analysis. Test data from a thrust-vectoring configuration of an F/A-18 aircraft are compared to predictions to determine the effects on accuracy as a function of modeling complexity. Author (revised)

N94-13294*# National Aeronautics and Space Administration. Ames Research Center, Moffett Field, CA.

PILOTING VERTICAL FLIGHT AIRCRAFT: A CONFERENCE ON FLYING QUALITIES AND HUMAN FACTORS

Christopher L. Blanken, ed. and Matthew S. Whalley, ed. (Army Aviation Systems Command, Moffett Field, CA.) Jul. 1993 488 p Workshop held at San Francisco, CA, 20-22 Jan. 1993

(RTOP 505-59-52)

(NASA-CP-3220; A-93074; NAS 1.55:3220) Avail: CASI HC A21/MF A04

This document contains papers from a specialists' meeting entitled 'Piloting Vertical Flight Aircraft: A Conference on Flying Qualities and Human Factors.' Vertical flight aircraft, including helicopters and a variety of Vertical Takeoff and Landing (VTOL) concepts, place unique requirements on human perception, control, and performance for the conduct of their design missions. The intent of this conference was to examine, for these vehicles, advances in: (1) design of flight control systems for ADS-33C standards; (2) assessment of human factors influences of cockpit displays and operational procedures; (3) development of VTOL design and operational criteria; and (4) development of theoretical methods or models for predicting pilot/vehicle performance and mission suitability. A secondary goal of the conference was to provide an initial venue for enhanced interaction between human factors and handling qualities specialists. For individual titles, see N94-13295 through N94-13325.

N94-13295*# National Research Council of Canada, Ottawa (Ontario). Flight Research Lab.

ADS-33C RELATED HANDLING QUALITIES RESEARCH PERFORMED USING THE NRC BELL 205 AIRBORNE SIMULATOR

J. Murray Morgan and Stewart W. Baillie *In* NASA. Ames Research Center, Piloting Vertical Flight Aircraft: A Conference on Flying Qualities and Human Factors Jul. 1993 p 3-15 (For primary document see N94-13294 02-08)

Avail: CASI HC A03/MF A04

Over 10 years ago a project was initiated by the U.S. Army AVSCOM to update the military helicopter flying qualities specification MIL-8501-A. While not yet complete, the project reached a major milestone in 1989 with the publication of an Airworthiness Design Standard, ADS-33C. The 8501 update project initially set out to identify critical gaps in the requisite data base and then proceeded to fill them using a variety of directed research studies. The magnitude of the task required that it become an international effort: appropriate research studies were conducted in Germany, the UK and Canada as well as in the USA. Canadian participation was supported by the Department of National Defence (DND) through the Chief of Research and Development. Both ground based and in-flight simulation were used to study the defined areas and the Canadian Bell 205-A1 variable stability helicopter was used extensively as one of the primary research tools available for this effort. This paper reviews the involvement of the Flight Research Laboratory of the National Research Council of Canada in the update project, it describes the various experiments conducted on the Airborne Simulator, it notes significant results obtained and describes ongoing research associated with the project. Author

N94-13296*# Naval Air Warfare Center, Warminster, PA. Aircraft Div.

MIL-H-8501B: APPLICATION TO SHIPBOARD TERMINAL OPERATIONS

A. N. Cappetta and J. B. Johns (Army Aviation Systems Command, Moffett Field, CA.) *In* NASA. Ames Research Center, Piloting Vertical Flight Aircraft: A Conference on Flying Qualities and Human Factors Jul. 1993 p 17-36 (For primary document see N94-13294 02-08)

Avail: CASI HC A03/MF A04

The philosophy and structure of the proposed U.S. Military Specification for Handling Qualities Requirements for Military Rotorcraft, MIL-H-8501B, are presented with emphasis on shipboard terminal operations. The impact of current and future naval operational requirements on the selection of appropriate combinations of basic vehicle dynamics and usable cue environments are identified. An example 'walk through' of MIL-H-8501B is conducted from task identification to determination of stability and control requirements. For selected basic vehicle dynamics, criteria as a function of input/response magnitude are presented. Additionally, rotorcraft design development implications are discussed. Author

N94-13297*# National Aeronautics and Space Administration. Ames Research Center, Moffett Field, CA.

DESIGN CRITERIA FOR INTEGRATED FLIGHT/PROPULSION CONTROL SYSTEMS FOR STOVL FIGHTER AIRCRAFT

James A. Franklin *In its* Piloting Vertical Flight Aircraft: A Conference on Flying Qualities and Human Factors Jul. 1993 p 37-5 (For primary document see N94-13294 02-08)

Avail: CASI HC A03/MF A04

As part of NASA's program to develop technology for short takeoff and vertical landing (STOVL) fighter aircraft, control system designs have been developed for a conceptual STOVL aircraft. This aircraft is representative of the class of mixed-flow remote-lift concepts that was identified as the preferred design approach by the US/UK STOVL Joint Assessment and Ranking Team. The control system designs have been evaluated throughout the powered-lift flight envelope on Ames Research Center's Vertical Motion Simulator. Items assessed in the control system evaluation were: maximum control power used in transition and vertical flight, control system dynamic response associated with thrust transfer for attitude control, thrust margin in the presence of ground effect and hot gas ingestion, and dynamic thrust response for the engine core. Effects of wind, turbulence, and ship airwake disturbances are incorporated in the evaluation. Results provide the basis for a reassessment of existing flying qualities design criteria applied to STOVL aircraft. Author

N94-13298*# Starmark Corp., Arlington, VA.

A PERSPECTIVE ON THE FAA APPROVAL PROCESS: INTEGRATING ROTORCRAFT DISPLAYS, CONTROLS AND WORKLOAD

David L. Green, Jake Hart (American Eurocopter Corp., Grand Prarie, TX.), and Peter Hwoschinsky (Federal Aviation Administration, Washington, DC.) *In* NASA. Ames Research Center, Piloting Vertical Flight Aircraft: A Conference on Flying Qualities and Human Factors Jul. 1993 p 59-68 (For primary document see N94-13294 02-08)

Avail: CASI HC A02/MF A04

The FAA is responsible for making the determination that a helicopter is safe for IFR operations in the National Airspace System (NAS). This involves objective and subjective evaluations of cockpit displays, flying qualities, procedures and human factors as they affect performance and workload. After all of the objective evaluations are completed, and all Federal Regulations have been met, FAA pilots make the final subjective judgement as to suitability for use by civil pilots in the NAS. The paper uses the flying qualities and pilot workload characteristics of a small helicopter to help examine the FAA pilot's involvement in this process. The result highlights the strengths of the process and its importance to the approval of new aircraft and equipments for civil IFR helicopter applications. The paper also identifies opportunities for improvement. Author

N94-13299*# Army Aviation Systems Command, Moffett Field, CA. Aeroflightdynamics Directorate.

SOME LESSONS LEARNED IN THREE YEARS WITH ADS-33C

David L. Key, Chris L. Blanken, and Roger H. Hoh (Hoh Aeronautics, Inc., Lomita, CA.) *In* NASA. Ames Research Center, Piloting Vertical Flight Aircraft: A Conference on Flying Qualities and Human Factors Jul. 1993 p 69-89 (For primary document see N94-13294 02-08)

Avail: CASI HC A03/MF A04

Three years of using the U.S. Army's rotorcraft handling qualities specification, Aeronautical Design Standard - 33, has shown it to be surprisingly robust. It appears to provide an excellent basis for design and for assessment, however, as the subtleties become more well understood, several areas needing refinement became apparent. Three responses to these needs have been documented in this paper: (1) The yaw-axis attitude quickness for hover target acquisition and tracking can be relaxed slightly. (2) Understanding and application of criteria for degraded visual environments needed elaboration. This and some guidelines for testing to obtain visual cue ratings have been documented. (3) The flight test maneuvers were an

innovation that turned out to be very valuable. Their extensive use has made it necessary to tighten definitions and testing guidance. This was accomplished for a good visual environment and is underway for degraded visual environments. Author

N94-13300*# Deutsche Forschungs- und Versuchsanstalt fuer Luft- und Raumfahrt, Brunswick (Germany). Institut feur Flugmechanik.

INVESTIGATION OF THE EFFECTS OF BANDWIDTH AND TIME DELAY ON HELICOPTER ROLL-AXIS HANDLING QUALITIES

Heinz-Juergen Pausder and Chris L. Blanken (Army Aviation Systems Command, Moffett Field, CA.) *In* NASA. Ames Research Center, Piloting Vertical Flight Aircraft: A Conference on Flying Qualities and Human Factors Jul. 1993 p 91-110 (For primary document see N94-13294 02-08)

Avail: CASI HC A03/MF A04

Several years of cooperative research conducted under the U.S./German Memorandum of Understanding (MOU) in helicopter flight control has recently resulted in a successful handling qualities study. The focus of this cooperative research has been the effects on handling qualities due to time delays in combination with a high bandwidth vehicle. The jointly performed study included the use of U.S. ground-based simulation and German in-flight simulation facilities. The NASA-Ames Vertical Motion Simulator (VMS) was used to develop a high bandwidth slalom tracking task which took into consideration the constraints of the facilities. The VMS was also used to define a range of the test parameters and to perform initial handling qualities evaluations. The flight tests were conducted using DLR's variable-stability BO 105 S3 Advanced Technology Testing Helicopter System (ATTHeS). Configurations included a rate command and an attitude command response system with added time delays up to 160 milliseconds over the baseline and bandwidth values between 1.5 and 4.5 rad/sec. Sixty-six evaluations were performed in about 25 hours of flight time during ten days of testing. The results indicate a need to more tightly constrain the allowable roll axis phase delay for the Level 1 and Level 2 requirements in the U.S. Army's specification for helicopter handling qualities, ADS-33C. Author

N94-13301*# Army Aviation Systems Command, Moffett Field, CA. Aeroflightdynamics Directorate.

A PILOTED SIMULATION INVESTIGATION OF THE NORMAL LOAD FACTOR AND LONGITUDINAL THRUST REQUIRED FOR AIR-TO-AIR ACQUISITION AND TRACKING

Matthew S. Whalley *In* NASA. Ames Research Center, Piloting Vertical Flight Aircraft: A Conference on Flying Qualities and Human Factors Jul. 1993 p 113-130 (For primary document see N94-13294 02-08)

Avail: CASI HC A03/MF A04

A piloted simulation study was performed by the U.S. Army Aeroflightdynamics Directorate to develop insight into the maneuverability requirements for aggressive helicopter maneuvering tasks such as air-to-air combat. Both a conventional helicopter and a helicopter with auxiliary thrust were examined. The aircraft parameters of interest were the normal and longitudinal load factor envelopes. Of particular interest were the mission performance and handling qualities tradeoffs with the parameters of interest. Two air-to-air acquisition and tracking tasks and a return-to-cover task were performed to assess mission performance. Results indicate that without auxiliary thrust, the ownship normal load factor capability needs to match that of the adversary in order to provide satisfactory handling qualities. Auxiliary thrust provides significant handling qualities advantages and can be substituted to some extent for normal load factor capability. Auxiliary thrust levels as low as 0.2 thrust/weight can provide significant handling qualities advantages. Author

N94-13302*# Eurocopter Deutschland G.m.b.H., Munich (Germany). Dept. Guidance and Control.

THE APPLICATION OF ACTIVE SIDE ARM CONTROLLERS IN HELICOPTERS

R. Knorr, C. Melz, A. Faulkner, and M. Obermayer *In* NASA. Ames Research Center, Piloting Vertical Flight Aircraft: A Conference on Flying Qualities and Human Factors Jul. 1993 p 131-140 (For primary document see N94-13294 02-08)

Avail: CASI HC A02/MF A04

Eurocopter Deutschland (ECD) started simulation trials to investigate the particular problems of Side Arm Controllers (SAC) applied to helicopters. Two simulation trials have been performed. In the first trial, the handling characteristics of a 'passive' SAC and the basic requirements for the application of an 'active' SAC were evaluated in pilot-in-the-loop simulations, performing the tasks in a realistic scenario representing typical phases of a transport mission. The second simulation trial investigated the general control characteristics of the 'active' in comparison to the 'passive' control principle. A description of the SACs developed by ECD and the principle of the 'passive' and 'active' control concept is given, as well as specific ratings for the investigated dynamic and ergonomic parameters effecting SAC characteristics. The experimental arrangements, as well as the trials procedures of both simulation phases, are described and the results achieved are discussed emphasizing the advantages of the 'active' as opposed to the 'passive' SAC concept. This also includes the presentation of some critical aspects still to be improved and proposals to solve them. Author (revised)

N94-13303*# Leicester Univ. (England). Dept. of Engineering.

ROTORCRAFT FLYING QUALITIES IMPROVEMENT USING ADVANCED CONTROL

D. Walker, I. Postlethwaite, J. Howitt (Defence Research Agency, Bedford, England.), and N. Foster *In* NASA. Ames Research Center, Piloting Vertical Flight Aircraft: A Conference on Flying Qualities and Human Factors Jul. 1993 p 141-155 (For primary document see N94-13294 02-08)

Avail: CASI HC A03/MF A04

We report on recent experience gained when a multivariable helicopter flight control law was tested on the Large Motion Simulator (LMS) at DRA Bedford. This was part of a study into the application of multivariable control theory to the design of full-authority flight control systems for high-performance helicopters. In this paper, we present some of the results that were obtained during the piloted simulation trial and from subsequent off-line simulation and analysis. The performance provided by the control law led to level 1 handling quality ratings for almost all of the mission task elements assessed, both during the real-time and off-line analysis. Author

N94-13304*# Defence Research Agency, Bedford (England).

THE IMPACT OF FLYING QUALITIES ON HELICOPTER OPERATIONAL AGILITY

Gareth D. Padfield, Nick Lappos (Sikorsky Aircraft, Stratford, CT.), and John Hodgkinson (McDonnell-Douglas Corp., Long Beach, CA.) *In* NASA. Ames Research Center, Piloting Vertical Flight Aircraft: A Conference on Flying Qualities and Human Factors Jul. 1993 p 157-170 (For primary document see N94-13294 02-08)

Avail: CASI HC A03/MF A04

Flying qualities standards are formally set to ensure safe flight and therefore reflect minimum, rather than optimum, requirements. Agility is a flying quality but relates to operations at high, if not maximum, performance. While the quality metrics and test procedures for flying, as covered for example in ADS33C, may provide an adequate structure to encompass agility, they do not currently address flight at high performance. This is also true in the fixed-wing world and a current concern in both communities is the absence of substantiated agility criteria and possible conflicts between flying qualities and high performance. AGARD is sponsoring a working group (WG19) title 'Operational Agility' that deals with these and a range of related issues. This paper is condensed from contributions by the three authors to WG19, relating to flying qualities. Novel perspectives on the subject are presented including the agility factor, that quantifies performance margins in flying qualities terms; a new parameter, based on maneuver acceleration is introduced as a potential candidate for defining upper limits to flying qualities. Finally, a probabilistic analysis of pilot handling qualities ratings is presented that suggests a powerful relationship between inherent airframe flying qualities and operational agility. Author

N94-13305*# McDonnell-Douglas Helicopter Co., Mesa, AZ.

A FOUR-AXIS HAND CONTROLLER FOR HELICOPTER FLIGHT CONTROL

Joe DeMaio *In* NASA. Ames Research Center, Piloting Vertical Flight Aircraft: A Conference on Flying Qualities and Human Factors Jul. 1993 p 171-175 (For primary document see N94-13294 02-08)

Avail: CASI HC A01/MF A04

A proof-of-concept hand controller for controlling lateral and longitudinal cyclic pitch, collective pitch and tail rotor thrust was developed. The purpose

of the work was to address problems of operator fatigue, poor proprioceptive feedback and cross-coupling of axes associated with many four-axis controller designs. The present design is an attempt to reduce cross-coupling to a level that can be controlled with breakout force, rather than to eliminate it entirely. The cascaded design placed lateral and longitudinal cyclic in their normal configuration. Tail rotor thrust was placed atop the cyclic controller. A left/right twisting motion with the wrist made the control input. The axis of rotation was canted outboard (clockwise) to minimize cross-coupling with the cyclic pitch axis. The collective control was a twist grip, like a motorcycle throttle. Measurement of the amount of cross-coupling involved in pure, single-axis inputs showed cross coupling under 10 percent of full deflection for all axes. This small amount of cross-coupling could be further reduced with better damping and force gradient control. Fatigue was not found to be a problem, and proprioceptive feedback was adequate for all flight tasks executed. Author

N94-13306*# Defence Research Agency, Bedford (England).
IN-FLIGHT SIMULATION OF HIGH AGILITY THROUGH ACTIVE CONTROL: TAMING COMPLEXITY BY DESIGN
Gareth D. Padfield and Roy Bradley (Caledonian Univ., Glasgow, Scotland.) *In* NASA. Ames Research Center, Piloting Vertical Flight Aircraft: A Conference on Flying Qualities and Human Factors Jul. 1993 p 177-195 (For primary document see N94-13294 02-08)
Avail: CASI HC A03/MF A04

The motivation for research into helicopter agility stems from the realization that marked improvements relative to current operational types are possible, yet there is a dearth of useful criteria for flying qualities at high performance levels. Several research laboratories are currently investing resources in developing second generation airborne rotorcraft simulators. The UK's focus has been the exploitation of agility through active control technology (ACT); this paper reviews the results of studies conducted to date. The conflict between safety and performance in flight research is highlighted and the various forms of safety net to protect against system failures are described. The role of the safety pilot, and the use of actuator and flight envelope limiting are discussed. It is argued that the deep complexity of a research ACT system can only be tamed through a requirement specification assembled using design principles and cast in an operational simulation form. Work along these lines conducted at DRA is described, including the use of the Jackson System Development method and associated Ada simulation. Author

N94-13307*# Canterbury Univ., Christchurch (New Zealand). Dept. of Psychology.
COMPATIBILITY OF INFORMATION AND MODE OF CONTROL: THE CASE FOR NATURAL CONTROL SYSTEMS
Dean H. Owen *In* NASA. Ames Research Center, Piloting Vertical Flight Aircraft: A Conference on Flying Qualities and Human Factors Jul. 1993 p 199-204 (For primary document see N94-13294 02-08)
Avail: CASI HC A02/MF A04

The operation of control systems has been determined largely by mechanical constraints. Compatibility with the characteristics of the operator is a secondary consideration, with the result that control may never be optimal, control workload may interfere with performance of secondary tasks, and learning may be more difficult and protracted than necessary. With the introduction of a computer in the control loop, the mode of operation can be adapted to the operator, rather than vice versa. The concept of natural control is introduced to describe a system that supports control of the information used by the operator in achieving an intended goal. As an example, control of speed during simulated approach to a pad by helicopter pilots is used to contrast path-speed control with direct control of global optical flow-pattern information. Differences are evidenced in the performance domains of control activity, speed, and global optical flow velocity. Derived from text

N94-13308*# Georgia Inst. of Tech., Atlanta. School of Aerospace Engineering and Aerospace Lab.
A MODEL FOR ROTORCRAFT FLYING QUALITIES STUDIES
Manoj Mittal and Mark F. Costello *In* NASA. Ames Research Center, Piloting Vertical Flight Aircraft: A Conference on Flying Qualities and Human Factors Jul. 1993 p 205-220 (For primary document see N94-13294 02-08)
Avail: CASI HC A03/MF A04

This paper outlines the development of a mathematical model that is expected to be useful for rotorcraft flying qualities research. A computer model is presented that can be applied to a range of different rotorcraft configurations. The algorithm computes vehicle trim and a linear state-space model of the aircraft. The trim algorithm uses non linear optimization theory to solve the nonlinear algebraic trim equations. The linear aircraft equations consist of an airframe model and a flight control system dynamic model. The airframe model includes coupled rotor and fuselage rigid body dynamics and aerodynamics. The aerodynamic model for the rotors utilizes blade element theory and a three state dynamic inflow model. Aerodynamics of the fuselage and fuselage empennages are included. The linear state-space description for the flight control system is developed using standard block diagram data. Author

N94-13309*# Starmark Corp., Arlington, VA.
INTERPRETED COOPER-HARPER FOR BROADER USE
David L. Green, Hal Andrews (Naval Air Systems Command, Washington, DC.), and Donald W. Gallagher (Federal Aviation Administration, Atlantic City, NJ.) *In* NASA. Ames Research Center, Piloting Vertical Flight Aircraft: A Conference on Flying Qualities and Human Factors Jul. 1993 p 221-234 (For primary document see N94-13294 02-08)
Avail: CASI HC A03/MF A04

The current aircraft assessment process typically makes extensive use of operational personnel during simulations and operational evaluations, with increased emphasis on evaluating the many pilot and/or operator/aircraft control loops. The need for a crew assessment in this broader arena has produced a variety of rating scales. The Cooper-Harper Rating Scale is frequently misused and routinely overlooked in the process, for these applications often extend the scale's use beyond its originally intended application. This paper agrees with the broader application of the Cooper-Harper Rating Scale and presents a concept for the development of a 'use unique' Interpreted Cooper-Harper Scale to help achieve this objective. This interpreted scale concept was conceived during efforts to support an FAA evaluation of a night vision enhancement system. It includes descriptive extensions, which are faithful to the intent of the current Cooper-Harper Scale and should provide the kind of detail that has historically been provided by trained test pilots in their explanatory comments. Author (revised)

N94-13310*# National Aeronautics and Space Administration. Ames Research Center, Moffett Field, CA.
IMPROVEMENTS IN HOVER DISPLAY DYNAMICS FOR A COMBAT HELICOPTER
Jeffrey A. Schroeder and Michelle M. Eshow (Army Aviation Systems Command, Moffett Field, CA.) *In its* Piloting Vertical Flight Aircraft: A Conference on Flying Qualities and Human Factors Jul. 1993 p 235-250 (For primary document see N94-13294 02-08)
Avail: CASI HC A03/MF A04

This paper describes a piloted simulation conducted on the NASA Ames Vertical Motion Simulator. The objective of the experiment was to investigate the handling qualities benefits attainable using new display law design methods for hover displays. The new display laws provide improved methods to specify the behavior of the display symbol that predicts the vehicle's ground velocity in the horizontal plane; it is the primary symbol that the pilot uses to control aircraft horizontal position. The display law design was applied to the Apache helmet-mounted display format, using the Apache vehicle dynamics to tailor the dynamics of the velocity predictor symbol. The representations of the Apache vehicle used in the display design process and in the simulation were derived from flight data. During the simulation, the new symbol dynamics were seen to improve the pilots' ability to maneuver about hover in poor visual cuing environments. The improvements were manifested in pilot handling qualities ratings and in measured task performance. The paper details the display design techniques, the experiment design and conduct, and the results. Author

N94-13311*# Glasgow Univ. (Scotland).
THE DEVELOPMENT AND POTENTIAL OF INVERSE SIMULATION FOR THE QUANTITATIVE ASSESSMENT OF HELICOPTER HANDLING QUALITIES
Roy Bradley and Douglas G. Thomson *In* NASA. Ames Research Center, Piloting Vertical Flight Aircraft: A Conference on Flying Qualities

and Human Factors Jul. 1993 p 251-263 (For primary document see N94-13294 02-08)
Avail: CASI HC A03/MF A04

In this paper it is proposed that inverse simulation can make a positive contribution to the study of handling qualities. It is shown that mathematical descriptions of the MTEs (Mission Task Elements) defined in ADS-33C may be used to drive an inverse simulation thereby generating, from an appropriate mathematical model, the controls and states of a subject helicopter flying it. By presenting the results of such simulations it is shown that, in the context of inverse simulation, the attitude quickness parameters given in ADS-33C are independent of vehicle configuration. An alternative quickness parameter, associated with the control displacements required to fly the MTE is proposed, and some preliminary results are presented. Author

N94-13312*# United Technologies Research Center, East Hartford, CT.
AN ANALYTIC MODELING AND SYSTEM IDENTIFICATION STUDY OF ROTOR/FUSELAGE DYNAMICS AT HOVER
Steven W. Hong and H. C. Curtiss, Jr. (Princeton Univ., NJ.) *In* NASA. Ames Research Center, Piloting Vertical Flight Aircraft: A Conference on Flying Qualities and Human Factors Jul. 1993 p 265-286 (For primary document see N94-13294 02-08)
Avail: CASI HC A03/MF A04

A combination of analytic modeling and system identification methods have been used to develop an improved dynamic model describing the response of articulated rotor helicopters to control inputs. A high-order linearized model of coupled rotor/body dynamics including flap and lag degrees of freedom and inflow dynamics with literal coefficients is compared to flight test data from single rotor helicopters in the near hover trim condition. The identification problem was formulated using the maximum likelihood function in the time domain. The dynamic model with literal coefficients was used to generate the model states, and the model was parametrized in terms of physical constants of the aircraft rather than the stability derivatives, resulting in a significant reduction in the number of quantities to be identified. The likelihood function was optimized using the genetic algorithm approach. This method proved highly effective in producing an estimated model from flight test data which included coupled fuselage/rotor dynamics. Using this approach it has been shown that blade flexibility is a significant contributing factor to the discrepancies between theory and experiment shown in previous studies. Addition of flexible modes, properly incorporating the constraint due to the lag dampers, results in excellent agreement between flight test and theory, especially in the high frequency range. Author

N94-13313*# National Aeronautics and Space Administration. Ames Research Center, Moffett Field, CA.
VISUAL CUEING AIDS FOR ROTORCRAFT LANDINGS
Walter W. Johnson and Anthony D. Andre *In its* Piloting Vertical Flight Aircraft: A Conference on Flying Qualities and Human Factors Jul. 1993 p 289-308 (For primary document see N94-13294 02-08)
Avail: CASI HC A03/MF A04

The present study used a rotorcraft simulator to examine descents-to-hover at landing pads with one of three approach lighting configurations. The impact of simulator platform motion upon descents to hover was also examined. The results showed that the configuration with the most useful optical information led to the slowest final approach speeds, and that pilots found this configuration, together with the presence of simulator platform motion, most desirable. The results also showed that platform motion led to higher rates of approach to the landing pad in some cases. Implications of the results for the design of vertiport approach paths are discussed. Author

N94-13314*# National Aeronautics and Space Administration. Ames Research Center, Moffett Field, CA.
VISUAL INFORMATION FOR JUDGING TEMPORAL RANGE **c53**
Mary K. Kaiser and Lyn Mowafy (Dayton Univ. Research Inst., Higley, AZ.) *In its* Piloting Vertical Flight Aircraft: A Conference on Flying Qualities and Human Factors Jul. 1993 p 309-313 (For primary document see N94-13294 02-08)
Avail: CASI HC A01/MF A04

Work in our laboratory suggests that pilots can extract temporal range information (i.e., the time to pass a given waypoint) directly from out-the-window motion information. This extraction does not require the use of velocity or distance, but rather operates solely on a 2-D motion cue. In this paper, we present the mathematical derivation of this information, psychophysical evidence of human observers' sensitivity, and possible advantages and limitations of basing vehicle control on this parameter. Author

N94-13315*# National Aeronautics and Space Administration. Ames Research Center, Moffett Field, CA.
VISUAL CUEING CONSIDERATIONS IN NAP-OF-THE-EARTH HELICOPTER FLIGHT HEAD-SLAVED HELMET-MOUNTED DISPLAYS **c54**
Arthur J. Grunwald and Silvia Kohn (Technion - Israel Inst. of Engineering, Haifa.) *In its* Piloting Vertical Flight Aircraft: A Conference on Flying Qualities and Human Factors Jul. 1993 p 315-327 (For primary document see N94-13294 02-08)
Avail: CASI HC A03/MF A04

The pilot's ability to derive Control-Oriented Visual Field Information from teleoperated Helmet-Mounted displays in Nap-of-the-Earth flight, is investigated. The visual field with these types of displays, commonly used in Apache and Cobra helicopter night operations, originates from a relatively narrow field-of-view Forward Looking Infrared Radiation Camera, gimbal-mounted at the nose of the aircraft and slaved to the pilot's line-of-sight, in order to obtain a wide-angle field-of-regard. Pilots have encountered considerable difficulties in controlling the aircraft by these devices. Experimental simulator results presented here indicate that part of these difficulties can be attributed to head/camera slaving system phase lags and errors. In the presence of voluntary head rotation, these slaving system imperfections are shown to impair the Control-Oriented Visual Field Information vital in vehicular control, such as the perception of the anticipated flight path or the vehicle yaw rate. Since, in the presence of slaving system imperfections, the pilot will tend to minimize head rotation, the full wide-angle field-of-regard of the line-of-sight slaved Helmet-Mounted Display, is not always fully utilized. Author (revised)

N94-13316*# Boeing Defense and Space Group, Philadelphia, PA.
HANDLING QUALITIES EFFECTS OF DISPLAY LATENCY **c06**
David W. King *In* NASA. Ames Research Center, Piloting Vertical Flight Aircraft: A Conference on Flying Qualities and Human Factors Jul. 1993 p 329-340 (For primary document see N94-13294 02-08)
Avail: CASI HC A03/MF A04

Display latency is the time delay between aircraft response and the corresponding response of the cockpit displays. Currently, there is no explicit specification for allowable display lags to ensure acceptable aircraft handling qualities in instrument flight conditions. This paper examines the handling qualities effects of display latency between 70 and 400 milliseconds for precision instrument flight tasks of the V-22 Tiltrotor aircraft. Display delay effects on the pilot control loop are analytically predicted through a second order pilot crossover model of the V-22 lateral axis, and handling qualities trends are evaluated through a series of fixed-base piloted simulation tests. The results show that the effects of display latency for flight path tracking tasks are driven by the stability characteristics of the attitude control loop. The data indicate that the loss of control damping due to latency can be simply predicted from knowledge of the aircraft's stability margins, control system lags, and required control bandwidths. Based on the relationship between attitude control damping and handling qualities ratings, latency design guidelines are presented. In addition, this paper presents a design philosophy, supported by simulation data, for using flight director display augmentation to suppress the effects of display latency for delays up to 300 milliseconds. Author

N94-13317*# Systems Technology, Inc., Hawthorne, CA.
EFFECTS OF SIMULATOR MOTION AND VISUAL CHARACTERISTICS ON ROTORCRAFT HANDLING QUALITIES EVALUATIONS
David G. Mitchell and Daniel C. Hart (Army Aviation Systems Command, Moffett Field, CA.) *In* NASA. Ames Research Center, Piloting Vertical Flight Aircraft: A Conference on Flying Qualities and Human Factors Jul. 1993 p 341-359 (For primary document see N94-13294 02-08)
Avail: CASI HC A03/MF A04

The pilot's perceptions of aircraft handling qualities are influenced by a combination of the aircraft dynamics, the task, and the environment under which the evaluation is performed. When the evaluation is performed

in a groundbased simulator, the characteristics of the simulation facility also come into play. Two studies were conducted on NASA Ames Research Center's Vertical Motion Simulator to determine the effects of simulator characteristics on perceived handling qualities. Most evaluations were conducted with a baseline set of rotorcraft dynamics, using a simple transfer-function model of an uncoupled helicopter, under different conditions of visual time delays and motion command washout filters. Differences in pilot opinion were found as the visual and motion parameters were changed, reflecting a change in the pilots' perceptions of handling qualities, rather than changes in the aircraft model itself. The results indicate a need for tailoring the motion washout dynamics to suit the task. Visual-delay data are inconclusive but suggest that it may be better to allow some time delay in the visual path to minimize the mismatch between visual and motion, rather than eliminate the visual delay entirely through lead compensation. Author

N94-13318*# Naval Air Warfare Center, Warminster, PA. Aircraft Div.
PRIMARY DISPLAY LATENCY CRITERIA BASED ON FLYING QUALITIES AND PERFORMANCE DATA
John D. Funk, Jr., Corin P. Beck, and John B. Johns (Army Aviation Systems Command, Moffett Field, CA.) *In* NASA. Ames Research Center, Piloting Vertical Flight Aircraft: A Conference on Flying Qualities and Human Factors Jul. 1993 p 361-374 (For primary document see N94-13294 02-08)
Avail: CASI HC A03/MF A04

With a pilots' increasing use of visual cue augmentation, much requiring extensive pre-processing, there is a need to establish criteria for new avionics/display design. The timeliness and synchronization of the augmented cues is vital to ensure the performance quality required for precision mission task elements (MTEs) where augmented cues are the primary source of information to the pilot. Processing delays incurred while transforming sensor-supplied flight information into visual cues are unavoidable. Relationships between maximum control system delays and associated flying qualities levels are documented in MIL-F-83300 and MIL-F-8785. While cues representing aircraft status may be just as vital to the pilot as prompt control response for operations in instrument meteorological conditions, presently, there are no specification requirements on avionics system latency. To produce data relating avionics system latency to degradations in flying qualities, the Navy conducted two simulation investigations. During the investigations, flying qualities and performance data were recorded as simulated avionics system latency was varied. Correlated results of the investigation indicates that there is a detrimental impact of latency on flying qualities. Analysis of these results and consideration of key factors influencing their application indicate that: (1) Task performance degrades and pilot workload increases as latency is increased. Inconsistency in task performance increases as latency increases. (2) Latency reduces the probability of achieving Level 1 handling qualities with avionics system latency as low as 70 ms. (3) The data suggest that the achievement of desired performance will be ensured only at display latency values below 120 ms. (4) These data also suggest that avoidance of inadequate performance will be ensured only at display latency values below 150 ms. Author

N94-13319*# Helikopter Service A/S, Oslo (Norway).
HUMAN FACTOR IMPLICATIONS OF THE EUROCOPTER AS332L-1 SUPER PUMA COCKPIT **c54**
R. Randall Padfield *In* NASA. Ames Research Center, Piloting Vertical Flight Aircraft: A Conference on Flying Qualities and Human Factors Jul. 1993 p 377-392 Presented at the 15th European Rotorcraft Forum, Amsterdam, The Netherlands, 12-15 Sep. 1989 Previously announced in AIAA as A91-45400 (For primary document see N94-13294 02-08)
Avail: CASI HC A03/MF A04

The purpose of this paper is to identify and describe some of the human factor problems which can occur in the cockpit of a modern civilian helicopter. After examining specific hardware and software problems in the cockpit design of the Eurocopter (Aerospatiale) AS332L-1 Super Puma, the author proposes several principles that can be used to avoid similar human factors problems in the design of future cockpits. These principles relate to the use and function of warning lights, the design of autopilots in two-pilot aircraft, and the labeling of switches and warning lights, specifically with respect to abbreviations and translations from languages other than English. In the final section of the paper, the author describes current trends in society which he suggests should be taken into consideration when designing future aircraft cockpits. Author

N94-13320*# National Aeronautics and Space Administration. Ames Research Center, Moffett Field, CA.
PILOTING CONSIDERATIONS FOR TERMINAL AREA OPERATIONS OF CIVIL TILTWING AND TILTROTOR AIRCRAFT
William S. Hindson, Gordon H. Hardy, George E. Tucker, and William A. Decker *In its* Piloting Vertical Flight Aircraft: A Conference on Flying Qualities and Human Factors Jul. 1993 p 393-410 (For primary document see N94-13294 02-08)
Avail: CASI HC A03/MF A04

The existing body of research to investigate airworthiness, performance, handling, and operational requirements for STOL and V/STOL aircraft was reviewed for its applicability to the tiltrotor and tiltwing design concepts. The objective of this study was to help determine the needs for developing civil certification criteria for these aircraft concepts. Piloting tasks that were considered included configuration and thrust vector management, glidepath control, deceleration to hover, and engine failure procedures. Flight control and cockpit display systems that have been found necessary to exploit the low-speed operating characteristics of these aircraft are described, and beneficial future developments are proposed. Author

N94-13321*# Sikorsky Aircraft, Stratford, CT.
DESIGN AND PILOT EVALUATION OF THE RAH-66 COMANCHE CORE AFCS
Donald L. Fogler, Jr. and James F. Keller (Boeing Defense and Space Group, Philadelphia, PA.) *In* NASA. Ames Research Center, Piloting Vertical Flight Aircraft: A Conference on Flying Qualities and Human Factors Jul. 1993 p 411-418 (For primary document see N94-13294 02-08)
Avail: CASI HC A02/MF A04

This paper addresses the design and pilot evaluation of the Core Automatic Flight Control System (AFCS) for the Reconnaissance/Attack Helicopter (RAH-66) Comanche. During the period from November 1991 through February 1992, the RAH-66 Comanche control laws were evaluated through a structured pilot acceptance test using a motion base simulator. Design requirements, descriptions of the control law design, and handling qualities data collected from ADS-33 maneuvers are presented. Author

N94-13322*# Sikorsky Aircraft, Stratford, CT.
DESIGN AND PILOT EVALUATION OF THE RAH-66 COMANCHE SELECTABLE CONTROL MODES
Phillip J. Gold and James B. Dryfoos (Boeing Defense and Space Group, Philadelphia, PA.) *In* NASA. Ames Research Center, Piloting Vertical Flight Aircraft: A Conference on Flying Qualities and Human Factors Jul. 1993 p 419-431 (For primary document see N94-13294 02-08)
Avail: CASI HC A03/MF A04

The RAH-66 Comanche helicopter has been designed to possess superior handling qualities over a wide range of flight conditions. The control laws have been tailored to satisfy the requirements of ADS-33C and the Weapon System Specification (WSS). This paper addresses the design of the Comanche Selectable Mode control laws (Velocity Stabilization/Hover Hold and Altitude Hold), which provide the additional stabilization and control augmentation needed when flying in a Degraded Visual Environment (DVE). An overview of the RAH-66 control laws is presented, including a detailed description of the Selectable Modes design. The primary focus of this paper is the results of piloted evaluation of these control laws in the Boeing motionbase simulator. These tests substantiate the detailed design of the Comanche Selectable Mode control laws. All tested DVE tasks (ADS-33C, sections 4.4 and 4.5) were rated Level 1. Other evaluation tasks confirmed the mission suitability of the control system. These control laws are ready for formal ADS-33C compliance testing in the Sikorsky Full Mission Simulator (FMS). Author

N94-13323*# National Aeronautics and Space Administration. Ames Research Center, Moffett Field, CA.
EVALUATION OF TWO COCKPIT DISPLAY CONCEPTS FOR CIVIL TILTROTOR INSTRUMENT OPERATIONS ON STEEP APPROACHES **c06**
William A. Decker, Richard S. Bray, Rickey C. Simmons, and George E.

Tucker *In its* Piloting Vertical Flight Aircraft: A Conference on Flying Qualities and Human Factors Jul. 1993 p 433-452 (For primary document see N94-13294 02-08)
Avail: CASI HC A03/MF A04

A piloted simulation experiment was conducted using the NASA Ames Research Center Vertical Motion Simulator to evaluate two cockpit display formats designed for manual control on steep instrument approaches for a civil transport tiltrotor aircraft. The first display included a four-cue (pitch, roll, power lever position, and nacelle angle movement prompt) flight director. The second display format provided instantaneous flight path angle information together with other symbols for terminal area guidance. Pilots evaluated these display formats for an instrument approach task which required a level flight conversion from airplane-mode flight to helicopter-mode flight while decelerating to the nominal approach airspeed. Pilots tracked glide slopes of 6, 9, 15 and 25 degrees, terminating in a hover for a vertical landing on a 150 feet square vertipad. Approaches were conducted with low visibility and ceilings and with crosswinds and turbulence, with all aircraft systems functioning normally and were carried through to a landing. Desired approach and tracking performance was achieved with generally satisfactory handling qualities using either display format on glide slopes up through 15 degrees. Evaluations with both display formats for a 25 degree glide slope revealed serious problems with glide slope tracking at low airspeeds in crosswinds and the loss of the intended landing spot from the cockpit field of view. Author

N94-13324*# Army Aviation Technical Test Center, Fort Rucker, AL.
FLIGHT TESTING AND FREQUENCY DOMAIN ANALYSIS FOR ROTORCRAFT HANDLING QUALITIES CHARACTERISTICS
Johnnie A. Ham, Charles K. Gardner, and Mark B. Tischler (Army Aviation Systems Command, Moffett Field, CA.) *In* NASA. Ames Research Center, Piloting Vertical Flight Aircraft: A Conference on Flying Qualities and Human Factors Jul. 1993 p 453-469 (For primary document see N94-13294 02-08)
Avail: CASI HC A03/MF A04

A demonstration of frequency domain flight testing techniques and analyses was performed on a U.S. Army OH-58D helicopter in support of the OH-58D Airworthiness and Flight Characteristics Evaluation and the Army's development and ongoing review of Aeronautical Design Standard 33C, Handling Qualities Requirements for Military Rotorcraft. Hover and forward flight (60 knots) tests were conducted in 1 flight hour by Army experimental test pilots. Further processing of the hover data generated a complete database of velocity, angular rate, and acceleration frequency responses to control inputs. A joint effort was then undertaken by the Airworthiness Qualification Test Directorate (AQTD) and the U.S. Army Aeroflightdynamics Directorate (AFDD) to derive handling qualities information from the frequency response database. A significant amount of information could be extracted from the frequency domain database using a variety of approaches. This report documents numerous results that have been obtained from the simple frequency domain tests; in many areas, these results provide more insight into the aircraft dynamics that affect handling qualities than to traditional flight tests. The handling qualities results include ADS-33C bandwidth and phase delay calculations, vibration spectral determinations, transfer function models to examine single axis results, and a six degree of freedom fully coupled state space model. The ability of this model to accurately predict aircraft responses was verified using data from pulse inputs. This report also documents the frequency-sweep flight test technique and data analysis used to support the tests. Author

N94-13325*# National Aeronautics and Space Administration. Ames Research Center, Moffett Field, CA.
PRELIMINARY DESIGN FEATURES OF THE RASCAL: A NASA /ARMY ROTORCRAFT IN-FLIGHT SIMULATOR **c09**
Edwin W. Aiken, Robert A. Jacobsen, Michelle M. Eshow (Army Aviation Systems Command, Moffett Field, CA.), William S. Hindson, and Douglas H. Doane *In its* Piloting Vertical Flight Aircraft: A Conference on Flying Qualities and Human Factors Jul. 1993 p 471-486 (For primary document see N94-13294 02-08)
Avail: CASI HC A03/MF A04

Salient design features of a new NASA/Army research rotorcraft - the Rotorcraft-Aircrew Systems Concepts Airborne Laboratory (RASCAL) - are described. Using a UH-60A Black Hawk helicopter as a baseline vehicle, the RASCAL will be a flying laboratory capable of supporting the research requirements of major NASA and Army guidance, control, and display research programs. The paper describes the research facility requirements of these programs together with other critical constraints on the design of the research system, including safety-of-flight. Research program schedules demand a phased development approach, wherein specific research capability milestones are met and flight research projects are flown throughout the complete development cycle of the RASCAL. This development approach is summarized, and selected features of the research system are described. The research system includes a full-authority, programmable, fault-tolerant/fail-safe, fly-by-wire flight control system and a real-time obstacle detection and avoidance system which will generate low-altitude guidance commands to the pilot on a wide field-of-view, color helmet-mounted display. Author

N94-13347# National Aerospace Lab., Tokyo (Japan). Aircraft Aerodynamics Div.
ROLLING MOMENT CONTROL IN THE NAL 10 cm X 10 cm MAGNETIC SUSPENSION AND BALANCE SYSTEM [KOUGIKEN 10 CM X 10 CM JIRYOKU SHIJU TENBIN SOUCHI YOKOYURE SEIGYO NITSUITE]
Hideo Sawada, Hisashi Suenaga, Takayuki Suzuki (Musashi Inst. of Tech., Tokyo, Japan.), and Nobukazu Ikeda (Musashi Inst. of Tech., Tokyo, Japan.) Jun. 1992 17 p In JAPANESE
(NAL-TR-1164; JTN-93-80494) Avail: CASI HC A03/MF A01

To have control the rolling moment acting on a model suspended in National Aerospace Laboratory (NAL) 10 cm x 10 cm Magnetic Suspension and Balance System (MSBS), two extra pairs of small magnets were attached perpendicular to the model axis at both the front and rear sides of it. Side force, yawing moment, and rolling moment acting on the model are controlled by the currents passing through the system's four side coils. Test results indicate the roll angle is suitably controlled using this method. An analytical approximation for estimating the rolling moment with the existing arrangement of magnetic moments and charges is described. This approximation correlates well with several experimental results. The NAL MSBS has the capability of controlling model motion with six degrees of freedom.
Author (NASDA)

N94-13469*# Texas A&M Univ., College Station. Dept. of Electrical Engineering.
KNOWLEDGE-BASED PROCESSING FOR AIRCRAFT FLIGHT CONTROL Final Report, period ending 17 Oct. 1991
John H. Painter 17 Oct. 1991 8 p
(Grant NAG1-1066)
(NASA-CR-194074; NAS 1.26:194074) Avail: CASI HC A02/MF A01

The purpose is to develop algorithms and architectures for embedding artificial intelligence in aircraft guidance and control systems. With the approach adopted, AI-computing is used to create an outer guidance loop for driving the usual aircraft autopilot. That is, a symbolic processor monitors the operation and performance of the aircraft. Then, based on rules and other stored knowledge, commands are automatically formulated for driving the autopilot so as to accomplish desired flight operations. The focus is on developing a software system which can respond to linguistic instructions, input in a standard format, so as to formulate a sequence of simple commands to the autopilot. The instructions might be a fairly complex flight clearance, input either manually or by data-link. Emphasis is on a software system which responds much like a pilot would, employing not only precise computations, but, also, knowledge which is less precise, but more like common-sense. The approach is based on prior work to develop a generic 'shell' architecture for an AI-processor, which may be tailored to many applications by describing the application in appropriate processor data bases (libraries). Such descriptions include numerical models of the aircraft and flight control system, as well as symbolic (linguistic) descriptions of flight operations, rules, and tactics. Author (revised)

N94-13859# Institute for Aerospace Research, Ottawa (Ontario). Applied Aerodynamics Lab.
MEASUREMENTS OF WING AND FIN BUFFETING ON THE STANDARD DYNAMICS MODEL
S. J. Zan May 1993 82 p
(IAR-AN-76; NRC-32158; CTN-93-60761) Avail: CASI HC A05/MF A01

A wind tunnel investigation was conducted on wing and fin buffeting

measured on the Standard Dynamics Model, a generic fighter aircraft configuration. Buffeting was investigated for three modes: the fin bending mode and the wing symmetric and antisymmetric bending modes. Tests were performed at four wind speeds corresponding to reduced frequencies ranging from 0.6 to 1.5 for the wings and 0.9 to 1.8 for the fin. The angle of attack ranged from zero to 53 deg and the sideslip angle ranged from minus 10 deg to plus 10 deg. The model was tested with and without strakes. The data are presented in terms of the buffet excitation parameter. It was found that the level of fin buffeting exceeded that of wing buffeting by an order of magnitude. This severe fin buffeting arises from the immersion of the fin in the swirling wake of the burst strake and/or forebody vortices. The fin buffet excitation peaked near an angle of attack corresponding to the onset of asymmetrical forebody flow. This excitation was sensitive to the presence of sideslip and to the value of the reduced frequency parameter. The magnitude of the parameter did not exceed 0.003, a limit that was achieved for cases where the excitation arose from the interaction of the strake and wing vortices or simply from separated flow unsteadiness over the wing. Author (CISTI)

N94-13906# Technische Univ., Delft (Netherlands). Faculty of Aerospace Engineering.
INVESTIGATION OF AN AEROELASTIC OSCILLATOR: ANALYSIS OF ONE-DEGREE-OF-FREEDOM GALLOPING WITH COMBINED TRANSLATIONAL AND TORSIONAL EFFECTS
B. W. vanOudheusden Dec. 1992 28 p
(LR-707; ETN-93-94424) Avail: CASI HC A03/MF A01

The investigation was carried out in the framework of a research project on aeroelastic oscillators. The results of literature investigations about the background and analysis of galloping and the construction of a test set up are summarized. Galloping is a type of flow induced vibration, which is caused by aerodynamic instability: the unsteady aerodynamic forces on the oscillating structure can amplify or sustain the vibration. The major assumptions underlying the theory with which galloping is described and an analysis of two types of one degree of freedom galloping are discussed. The purpose of the analysis is to give an insight into the relevant parameters of the phenomenon and the set up. ESA

N94-14322*# MCAT Inst., San Jose, CA.
NUMERICAL SIMULATION OF A POWERED-LIFT LANDING, TRACKING FLOW FEATURES USING OVERSET GRIDS, AND SIMULATION OF HIGH LIFT DEVICES ON A FIGHTER-LIFT-AND-CONTROL WING Final Report
Kalpana Chawla Aug. 1993 27 p Original contains color illustrations
(Contract NCC2-563)
(NASA-CR-194260; NAS 1.26:194260; MCAT-93-18) Avail: CASI HC A03/MF A01; 2 functional color pages

Attached as appendices to this report are documents describing work performed on the simulation of a landing powered-lift delta wing, the tracking of flow features using overset grids, and the simulation of flaps on the Wright Patterson Lab's fighter-lift-and-control (FLAC) wing. Numerical simulation of a powered-lift landing includes the computation of flow about a delta wing at four fixed heights as well as a simulated landing, in which the delta wing descends toward the ground. Comparison of computed and experimental lift coefficients indicates that the simulations capture the qualitative trends in lift-loss encountered by thrust-vectoring aircraft operating in ground effect. Power spectra of temporal variations of pressure indicate computed vortex shedding frequencies close to the jet exit are in the experimentally observed frequency range; the power spectra of pressure also provide insights into the mechanisms of lift oscillations. Also, a method for using overset grids to track dynamic flow features is described and the method is validated by tracking a moving shock and vortices shed behind a circular cylinder. Finally, Chimera gridding strategies were used to develop pressure coefficient contours for the FLAC wing for a Mach no. of 0.18 and Reynolds no. of 2.5 million. CASI

N94-14642*# National Aeronautics and Space Administration. Ames Research Center, Moffett Field, CA.
OPTIMIZATION-BASED CONTROLLER DESIGN FOR ROTORCRAFT
N.-K. Tsing (Maryland Univ., College Park.), M. K. H. Fan (Georgia Inst. of Tech., Atlanta.), J. Barlow (Maryland Univ., College Park.), A. L. Tits (Maryland Univ., College Park.), and M. B. Tischler *In* JPL, Proceedings of the Fifth NASA/NSF/DOD Workshop on Aerospace Computational Control 15 Feb. 1993 p 379-393 (For primary document see N94-14618 02-39)
Avail: CASI HC A03/MF A04

N94-14646*# National Aeronautics and Space Administration. Marshall Space Flight Center, Huntsville, AL.
CONTROL SYSTEM DESIGN FOR FLEXIBLE STRUCTURES USING DATA MODELS
R. Dennis Irwin (Ohio Univ., Athens.), W. Garth Frazier (Ohio Univ., Athens.), Jerrel R. Mitchell (Ohio Univ., Athens.), Enrique A. Medina (Ohio Univ., Athens.), and Angelia P. Bukley *In* JPL, Proceedings of the Fifth NASA/NSF/DOD Workshop on Aerospace Computational Control 15 Feb. 1993 p 463-477 (For primary document see N94-14618 02-39)
Avail: CASI HC A03/MF A04

N94-14650*# Phillips Lab., Edwards AFB, CA.
PACE: A TEST BED FOR THE DYNAMICS AND CONTROL OF FLEXIBLE MULTIBODY SYSTEMS
Moon K. Kwak, Monty J. Smith, and Alok Das *In* JPL, Proceedings of the Fifth NASA/NSF/DOD Workshop on Aerospace Computational Control 15 Feb. 1993 p 525-533 See also A93-34231 (For primary document see N94-14618 02-39)
Avail: CASI HC A02/MF A04

09 RESEARCH AND SUPPORT FACILITIES (AIR)

Includes airports, hangars and runways; aircraft repair and overhaul facilities; wind tunnels; shock tubes; and aircraft engine test stands.

For related information see also *14 Ground Support Systems and Facilities (Space).*

N94-12824*# Purdue Univ., West Lafayette, IN. School of Aeronautics and Astronautics.
METHOD OF CHARACTERISTICS DESIGN OF A SUPERSONIC WIND TUNNEL NOZZLE WITH SQUARE CROSS-SECTION, SUPPLEMENT 3 Status Report, 1 Sep. 1992 - 1 Jan. 1993
Steven P. Schneider 1993 41 p
(Grant NAG1-1133)
(NASA-CR-194359; NAS 1.26:194359) Avail: CASI HC A03/MF A01

Nozzle design codes developed earlier were modified and used in order to design a supersonic wind tunnel nozzle with square cross-sections. As part of the design process, a post-processing code that generates square nozzles from the output of the Sivells code was written. The method is based on the results of an axisymmetric method of characteristics code and an axisymmetric boundary layer code. These design codes are documented. Author (revised)

N94-13008*# National Aeronautics and Space Administration. Ames Research Center, Moffett Field, CA.
VERTICAL MOTION SIMULATOR FAMILIARIZATION GUIDE
George L. Danek May 1993 62 p
(RTOP 505-64-29)
(NASA-TM-103923; A-92031; NAS 1.15:103923) Avail: CASI HC A04/MF A01

The Vertical Motion Simulator Familiarization Guide provides a synoptic description of the Vertical Motion Simulator (VMS) and descriptions of the various simulation components and systems. The intended audience is the community of scientists and engineers who employ the VMS for research and development. The concept of a research simulator system is introduced and the building block nature of the VMS is emphasized. Individual sections describe all the hardware elements in terms of general properties and capabilities. Also included are an example of a typical VMS simulation which graphically illustrates the composition of the system and shows the signal flow among the elements and a glossary of specialized terms, abbreviations, and acronyms. Author

N94-13127*# Physical Sciences, Inc., Andover, MA.
PROPULSION SIMULATOR FOR MAGNETICALLY-SUSPENDED WIND TUNNEL MODELS Final Report
P. B. Joshi, M. R. Malonson, G. P. Sacco, C. L. Goldey, Keith Garbutt, and M. Goodyer Jan. 1992 166 p

(Contract NAS1-18845; SBIR-02.02-9030; RTOP 505-59-54-01)
(NASA-CR-189560; NAS 1.26:189560; PSI-2090/TR-1140) Avail: CASI HC A08/MF A02

In order to demonstrate the measurement of aerodynamic forces/moments, including the effects of exhaust jets in Magnetic Suspension and Balance System (MSBS) wind tunnels, two propulsion simulator models were developed at Physical Sciences Inc. (PSI). Both the small-scale model (1 in. diameter X 8 in. long) and the large-scale model (2.5 in. diameter X 15 in. long) employed compressed, liquefied carbon dioxide as a propellant. The small-scale simulator, made from a highly magnetizable iron alloy, was demonstrated in the 7 in. MSBS wind tunnel at the University of Southampton. It developed a maximum thrust of approximate 1.3 lbf with a 0.098 in. diameter nozzle and 0.7 lbf with a 0.295 in. diameter nozzle. The Southampton MSBS was able to control the simulator at angles-of attack up to 20 deg. The large-scale simulator was demonstrated to operate in both a steady-state and a pulse mode via a miniaturized solinoid valve. It developed a stable and repeatable thrust of 2.75 lbf over a period of 4s and a nozzle pressure ratio (NPR) of 5. Author (revised)

N94-13337# National Aerospace Lab., Tokyo (Japan). Control Systems Div.

CONTROL SYSTEM DESIGN OF A CABLE-MOUNTED MODEL USED FOR DYNAMIC WIND TUNNEL TESTING [KEBURU SHIJI DOUTEKI FUUDOU SHIKEN NO TAMENO MOKEI SEIGYOKEI SEKKEI]

Masaaki Yanagihara, Masahiko Nagayasu, Shuuichi Sasa, and Takashi Shimomura Jun. 1992 52 p In JAPANESE
(NAL-TR-1161; JTN-93-80484) Avail: CASI HC A04/MF A01

The control system of a cable-mounted aircraft model used for dynamic wind tunnel testing was designed using the root locus method. Computer simulations were initially performed to evaluate the designed control system, which was then applied to actual wind tunnel tests. Results confirmed the system's suitability, although the control gains required slight tuning. In addition, wind tunnel tests were conducted using the control system to identify the aerodynamic model of the cable-mounted model.
Author (NASDA)

N94-13498# National Aerospace Lab., Amsterdam (Netherlands). Flight Div.

FUTURE DEVELOPMENTS OF THE NLR RESEARCH FLIGHT SIMULATOR

C. J. Jansen 31 Mar. 1992 14 p Presented at the Aeronautical Students Association Simulation Symposium, Haarlem, Netherlands, 20 Mar. 1990
(NLR-TP-92143-U; ETN-93-94345) Avail: CASI HC A03/MF A01

The upgrading program of the flight simulator is overviewed. The period from some years ago, when the simulator had a relatively small motion system and limited vision of the outside world, till the end of 1994 is addressed. The following major improvements which have already been realized are described: the avionics system (this consists of an ARINC bus interface system to couple Electronic Flight Instrument System (EFIS) displays, a programmable EFIS, and a general purpose graphics station); a new fully hydrostatic 6 degrees of freedom motion system with high bandwidth (only 45 deg phase lag at 4 Hz for acceleration commands from the simulator computer); and a high bandwidth digital bus interface system. Upgrades foreseen for the coming two years are also described. These involve increasing the computational power; installation of an F-16 cockpit with g seat; and a visual system with an increased field of view, at least 150 deg horizontal by 60 deg vertical. ESA

N94-13544 Calgary Univ. (Alberta). Dept. of Civil Engineering.

AIRPORT TERMINALS: OPTIMUM CONFIGURATIONS AND GATE POSITION REQUIREMENT Ph.D. Thesis

J. M. S. J. Bandara Dec. 1989 325 p
(ISBN-0-315-61722-5; CTN-93-60729) Copyright Avail: Micromedia Ltd., Technical Information Centre, 165 Hotel de Ville, Place du Portage, Phase 2, Hull, Quebec J8X 3X2, Canada HC/MF

The level of service method and the minimum cost method are used to determine the number of gate positions required at an airport terminal. The former method is used to calculate the number of gate positions required to provide a given level of reliability. In the latter method, an optimum number of gate positions that will minimize the sum of the cost of gates and the cost of delay to aircraft is obtained. An approximate procedure to determine the deterministic delay to aircraft, based on the information regarding the peaking of the aircraft arrival rate and the number of peaks per day is presented. Closed-form solutions are obtained for the cases of one peak and several identical nonoverlapping peaks, respectively. Given the size of the terminal in terms of the number of aircraft gates, an analytic expression is obtained for the mean passenger walking distance. A continuum expression is used to model passenger walking within the piers or satellites. The optimum geometry in terms of the number of piers or satellites and their sizes is obtained by minimizing the mean walking distance for all the passengers. Statistical parameters suitable for choosing the best configuration for the terminal are suggested. A numerical example to illustrate the selection of the best terminal geometry is presented.
Author (CISTI)

N94-13588# Aeronautical Research Inst. of Sweden, Stockholm.

SIMULATOR STUDY OF UNCOUPLED CONTROL FUNCTIONS. USE OF MANUAL POINTING MODES WHEN AIMING AT GROUND TARGETS AND ONCOMING AIRBORNE TARGET

Aake Hyden and Gunnar Hovmark Oct. 1992 54 p
(Contracts FMV-Flyg-82450-87-348-24-001; FMV-Flyg-82450-88-341-73-0)
(FFA-TN-1992-18; ETN-93-94380) Avail: CASI HC A04/MF A01

A number of flight simulator tests were carried out to find whether manually controlled pointing in pitch and yaw would be valuable as a complement to an automatically controlled pointing mode. The results showed that a manual pointing mode will not give a general increase of the aircraft aiming capabilities. Most of the 19 pilots who tried the manual pointing modes in the simulator were quite positive in their opinions, but the aiming results and other results are only slightly better and sometimes not as good as the ones achieved with conventional control. The main advantage of pointing mode over conventional control was that a greater minimum distance to target could be achieved. The risk of confusing the controls, the often longer periods of straight flight paths, the pilots experiencing a higher workload and taking the left hand (and the control grip) away from other important tasks are factors that speak against manual pointing. ESA

N94-14876 Defence Research Agency, Bedford (England).

A GUIDE TO THE DRA 13 FT X 9 FT LOW SPEED WIND TUNNEL FACILITY

M. H. Hunter Apr. 1993 33 p Limited Reproducibility: More than 20% of this document may be affected by microfiche quality
(AD-A267739; DRA-TR-93014; DRIC-BR-318697) Avail: Issuing Activity (Defense Technical Information Center (DTIC))

This Technical Report is intended to provide a guide to the 13 ft. x 9 ft. Low Speed Wind Tunnel Facility. It details the model support and balance assemblies, provides an insight to the instrumentation and computing capabilities, and indicates the different flow visualization techniques available. A description of the tunnel and local facilities is included, along with contact numbers for customers' use. DTIC

N94-13325*# National Aeronautics and Space Administration. Ames Research Center, Moffett Field, CA.

PRELIMINARY DESIGN FEATURES OF THE RASCAL: A NASA /ARMY ROTORCRAFT IN-FLIGHT SIMULATOR

Edwin W. Aiken, Robert A. Jacobsen, Michelle M. Eshow (Army Aviation Systems Command, Moffett Field, CA.), William S. Hindson, and Douglas H. Doane *In its* Piloting Vertical Flight Aircraft: A Conference on Flying Qualities and Human Factors Jul. 1993 p 471-486 (For primary document see N94-13294 02-08)
Avail: CASI HC A03/MF A04

N94-14157# Arnold Engineering Development Center, Arnold AFS, TN.

CHARACTERIZATION OF FLOW FIELDS IN HYPERSONIC GROUND TEST FACILITIES

Albert H. Boudreau *In* VKI, Methodology of Hypersonic Testing 1993 15 p Prepared in cooperation with Arnold Engineering Development Center, Arnold AFS, TN (For primary document see N94-14153 02-02)
Copyright Avail: CASI HC A03/MF A03

N94-14158# Calspan Corp., Arnold AFS, TN.

AERODYNAMIC AND AEROTHERMAL FACILITIES 1: HYPERSONIC WIND TUNNELS

A. Anderson and R. K. Matthews *In* VKI, Methodology of Hypersonic Testing 1993 13 p Prepared in cooperation with Arnold Engineering Development Center, Arnold AFS, TN (For primary document see N94-14153 02-02)
Copyright Avail: CASI HC A03/MF A03

N94-14159# Calspan Corp., Arnold AFS, TN.
AERODYNAMIC AND AEROTHERMAL FACILITIES 2. PART 1: SHORT-DURATION, HIGH-ENTHALPY FACILITIES
James R. Maus *In* VKI, Methodology of Hypersonic Testing 1993 15 p Prepared in cooperation with Arnold Engineering Development Center, Arnold AFS, TN (For primary document see N94-14153 02-02)
Copyright Avail: CASI HC A03/MF A03

N94-14160# Tennessee Univ. Space Inst., Tullahoma. Dept. of Mechanical and Aerospace Engineering.
AERODYNAMIC AND AEROTHERMAL FACILITIES 2: CONTINUOUS FLOW HIGH ENTHALPY FACILITIES
Roger Crawford *In* VKI, Methodology of Hypersonic Testing 1993 32 p (For primary document see N94-14153 02-02)
Copyright Avail: CASI HC A03/MF A03

N94-14161# Sverdrup Technology, Inc., Arnold AFS, TN.
AEROPROPULSION FACILITIES
Brian Wettlaufer *In* VKI, Methodology of Hypersonic Testing 1993 14 p Prepared in cooperation with Arnold Engineering Development Center, Arnold AFS, TN (For primary document see N94-14153 02-02)
Copyright Avail: CASI HC A03/MF A03

12 ASTRONAUTICS (GENERAL)

For extraterrestrial exploration see *91 Lunar and Planetary Exploration.*

N94-13268# National Space Development Agency, Ibaraki (Japan).
THE SECOND WORKSHOP ON DEPLOYMENT AND ASSEMBLY EXPERIMENT OF LARGE SPACE STRUCTURE ON ORBIT [DAI 2 KAI KIDOUJOU NI OKERU OOGATA UCHUU KOUZOUBUTSU TENKAI KUMITATE JIKKEN NI KANSURU WAKU SHOPPU]
31 Mar. 1993 93 p In JAPANESE
(NASDA-CON-930003; JTN-93-80475) Avail: CASI HC A05/MF A01

The following topics were discussed: spacecraft structures, spacecraft components, structural design, large space structures, space erectable structures, expandable structures, inflatable structures, trusses, beams, hexa-link truss, helical truss beam, dynamic stability, structural stability, numerical analysis, antenna design, expandable type satellite antennas, modular mesh deployable antenna, orbital assembly, spacecraft construction materials, CFRP (Carbon Fiber Reinforced Plastics), polyimide matrix composite, thermal resistance, mechanical properties, spaceborne experiments, space technology experiments, radiation tolerance, space robots, remote manipulator systems, Japanese spacecraft, JEM (Japanese Experiment Module), and HOPE (H-2 Orbiting Plane). For individual titles, see N94-13269 through N94-13282.

N94-13269# Mitsubishi Electric Corp., Tokyo (Japan). Space Communications Research Div.
STRUCTURAL DESIGN OF HEXA-LINK TRUSS DEPLOYABLE ANTENNA [HEKISARINKU TORASU TENKAI ANTENA NO KOUZOU SEKKEI]
Takashi Ebisui, Teruki Okamoto, Yoshiyuki Ookawa, Kazuo Tanizawa, Masaki Tabata, and Hitoshi Taniai *In* NASDA, The Second Workshop on Deployment and Assembly Experiment of Large Space Structure on Orbit 31 Mar. 1993 p 1-6 In JAPANESE (For primary document see N94-13268 02-12)
Avail: CASI HC A02/MF A01

Structure of a 6 m deployable antenna mirror surface for communications satellite is designed paying attention to the following sections: the back structure section composed of 19 basic modules of hexagonal trapezoid shape, mirror mesh section composed of a cable net made from Al amide fiber with gold plated molybdenum mesh hung on it, and a deployment mechanism (sliding type and flexible type) of the deployable section for the offset parabolic antenna scale model of 6 m in aperture diameter. Deployment motion analysis was conducted with a hexagonal trapezoidal model of one module using the ADAMS (Automatic Dynamic Analysis of Mechanical System). Author (NASDA)

N94-13270# Mitsubishi Electric Corp., Tokyo (Japan). Space Communications Research Div.
THERMAL DISTORTION MEASUREMENT OF TETRUS TYPE THERMAL TEST MODEL OF LARGE DEPLOYABLE ANTENNA FOR MOBILE COMMUNICATIONS SATELLITE [IDOUTAI TSUUSHIN EISEIYOU OOGATA TENKAI ANTENA TETRUS GATA NETSU MODERU NO NETSUHIZUMI SOKUTEI] **c32**
Teruaki Orikasa, Teruki Okamoto, Kouichi Furukawa (Toshiba Corp., Kawasaki, Japan.), and Tatsuyoshi Aisaka (Toshiba Corp., Kawasaki, Japan.) *In* NASDA, The Second Workshop on Deployment and Assembly Experiment of Large Space Structure on Orbit 31 Mar. 1993 p 7-11 In JAPANESE (For primary document see N94-13268 02-12)
Avail: CASI HC A01/MF A01

A thermal test model using TETRUS (tetra trigonal prism truss) composed of three equilateral triangular cylindrical trusses was trial produced and evaluated for the effects caused by thermal environments on the mirror surface. The following topics related to the thermal environmental test are described: TETRUS, the thermal environment test model, the analysis on thermal distortion of the TETRUS, the process and the results of the thermal environmental test, the estimate analysis of electric property at the ambient temperature, and a high and a low temperature, the test configuration, the results of mirror surface accuracy measurements, and electric performance estimation analysis. Author (NASDA)

N94-13271# National Space Development Agency, Tokyo (Japan).
RESEARCH ON RADIATION RESISTANCE PROPERTIES OF STRUCTURAL MATERIALS FOR SPACE USE [UCHUUYOU KOUZOU ZAIRYOU NO TAIHOUSHASENSEI NO KENKYUU] **c24**
Kouzou Yudate, Yoshiki Morino, Tadao Seguchi (Japan Atomic Energy Research Inst., Tokyo.), Tsuneo Sasuga (Japan Atomic Energy Research Inst., Tokyo.), and Akira Udagawa (Japan Atomic Energy Research Inst., Tokyo.) *In its* The Second Workshop on Deployment and Assembly Experiment of Large Space Structure on Orbit 31 Mar. 1993 p 12-16 In JAPANESE (For primary document see N94-13268 02-12)
Avail: CASI HC A01/MF A01

This report describes the radiation effect to the CF (Carbon Fiber)/polyimide matrix composite material which will be used for the aerospace plane HOPE (H-2 Orbiting Plane) as a construction material. Results of the electron beam irradiation test, and characteristics measurement of the CF and polyimide composite material tests are described. The electron beam irradiation test was conducted using a 2 MeV electron beam and in a condition of 5 kGy/s in dose rate on the water cooling board at 40 cm below the acceleration tube. A three point bending test was conducted on each of the five samples of the CF/polyimide composite material and polyimide resin simplexes at a test speed of 5 mm/min at a span condition of 80 mm (span ratio 40 for composite material) and 32 mm (span ratio 16 for the resin simplexes). It was concluded that the polyimide resin shows a very high thermal resistance and cross links at a high dose rate of electron beam irradiation. The CF/polyimide composite material using this resin as the matrix show little characteristics change in the ambient temperature and is a material having a superior radiation resistant material. Author (NASDA)

N94-13272# Tsukuba Univ., Ibaraki (Japan). Inst. of Engineering Mechanics.
MEASURING METHODS FOR CFRP LAMINATES' BENDING AND TORSION RIGIDITIES CHARACTERISTICS [CFRP SEKISOUBAN NO MAGE/NEJIRI GOUSEI NO SOKUTEIHOU] **c24**
Tatsuzou Koga *In* NASDA, The Second Workshop on Deployment and Assembly Experiment of Large Space Structure on Orbit 31 Mar. 1993 p 17-20 In JAPANESE (For primary document see N94-13268 02-12)
Avail: CASI HC A01/MF A01

An overview of the experiment to assess the bending and torsion rigidities of orthotropic and aeolotropic plate is presented. The experiment consisted of statistical four point bending, and resonance experiments of rectangular plates by visualizing the deformation modes through a laser holography interference method are presented. The bending test method

of CFRP (Carbon Fiber Reinforced Plastics), pure bending deformation of orthotropic plates, and fringe patterns of pure bending deformation in bending and torsional modes are shown. Author (NASDA)

N94-13273# Tokyo Science Univ. (Japan).
PRESENT STATUS OF JEM UTILIZATION PROJECTS [JEM RIYOU KEIKAKU NO GENJOU] **c19**
Shigeo Kobayashi *In* NASDA, The Second Workshop on Deployment and Assembly Experiment of Large Space Structure on Orbit 31 Mar. 1993 p 21-28 In JAPANESE (For primary document see N94-13268 02-12)
Avail: CASI HC A02/MF A01

An overview of the revision of the space station program in the US including engineering change, the station assembly, and its utilization schedules are described. The following major items of the basic policy on the JEM (Japanese Experiment Module) utilization described in the report submitted by the space station subcommittee of the Space Development Commission are reviewed: (1) basic policy for establishing the utilization program; (2) basic policy for selecting the utilization themes; (3) each organization's role in establishing the utilization program; (4) basic policy for sharing the JEM utilization expenditures; (5) basic policy concerning common experiment equipment development and construction; and (6) basic concepts for the utilization promotion. The activities and their schedules after the AO (Announcement of Opportunity) are outlined.
Author (NASDA)

N94-13274# Nippon Telegraph and Telephone Public Corp., Yokosuka (Japan).
DEVELOPMENT OF MODULAR CABLE MESH DEPLOYABLE ANTENNA [MOJURUGATA KEBURU MESSHU TENKAI ANTENA NO KAIHATSU] **c32**
Akira Meguro, Jin Mitsugi, and Kazuhide Andou *In* NASDA, The Second Workshop on Deployment and Assembly Experiment of Large Space Structure on Orbit 31 Mar. 1993 p 29-35 In JAPANESE (For primary document see N94-13268 02-12)
Avail: CASI HC A02/MF A01

This report describes a concept and key technologies for the modular mesh deployable antenna. The antenna reflector composed of independently manufactured and tested modules is presented. Each module consists of a mesh surface, a cable network, and a deployable truss structure. The cable network comprises three kinds of cables, surface, tie, and back cables. Adjustment of tie cable lengths improves the surface accuracy. Synchronous deployment truss structures are considered as a supporting structure. Their design method, BBM's (Bread Board Model) and deployment analysis are also explained. Author (NASDA)

N94-13275# Kawasaki Heavy Industries Ltd., Kobe (Japan).
RESEARCH ON INFLATABLE STRUCTURE FOR SPACE USE [UCHUUYOU INFURETABURU KOUZOU NO KENKYUU] **c18**
Sumio Katou, Osamu Muragishi, Toyoyuki Oota, Michihiro Natori (Ministry of Education, Kanagawa, Japan.), Kouryou Miura (Ministry of Education, Kanagawa, Japan.), and Masamori Sakamaki (Ministry of Education, Kanagawa, Japan.) *In* NASDA, The Second Workshop on Deployment and Assembly Experiment of Large Space Structure on Orbit 31 Mar. 1993 p 36-42 In JAPANESE (For primary document see N94-13268 02-12)
Avail: CASI HC A02/MF A01

This report describes an overview of the trial manufacture and research related to the feasibility of the concepts of a reflector structure using inflatable elements, inflatable tube, and recommendations on experiments on the exposed facility of the JEM (Japanese Experiment Module). The expected roles of and basic structure concept concerning the configurations, dimensions, and film surface materials of the reflector are outlined. The results of the film pressure deformation test, film element hardening test, and film and supporting truss interface test are described. The strength, trial manufacture, and its results are outlined. The onboard JEM experiment concept concerning the research on the earth, preliminary experiment, and on-orbit experiment onboard JEM are introduced. Author (NASDA)

N94-13276# Ministry of Education, Kanagawa (Japan).
HELICAL TRUSS BEAM DEVELOPMENT FOR LARGE SPACE STRUCTURE [OOGATA UCHUU KOUZOUBUTSUYOU HERIKARUTORASU BIMU NO KAIHATSU NI TSUITE] **c18**
Michihiro Natori, Takayuki Kitamura (Japan Aircraft Mfg. Co. Ltd., Kanagawa.), Hideo Yanai (Japan Aircraft Mfg. Co. Ltd., Kanagawa.), and Yoshinari Takeuchi (Japan Aircraft Mfg. Co. Ltd., Kanagawa.) *In* NASDA, The Second Workshop on Deployment and Assembly Experiment of Large Space Structure on Orbit 31 Mar. 1993 p 43-46 In JAPANESE (For primary document see N94-13268 02-12)
Avail: CASI HC A01/MF A01

This report presents an overview of the development of helical truss beams for large space structures which has a high folding efficiency at launch, easily deployed, and has a high structural efficiency in space. The structure, folding and deployment systems, and merits and drawbacks of the helical truss beam are outlined. The trial manufacture of the one fifth scale model of the helical truss beams (basic frame work member size of 3 m in length and 30 mm in diameter), wire spring hinge for joints of frame work, and zip type latching mechanisms for the joints is explained. The results of the study using the trial manufactured units to verify the deployment and folding function and the folded configurations of the helical truss beams are also outlined. Author (NASDA)

N94-13277# Osaka Prefecture Univ., Sakai (Japan). Dept. of Aeronautical Engineering.
APPLICATION OF INTELLIGENTLY ADAPTABLE STRUCTURE AND ROBOT TO LARGE SPACE STRUCTURE [OOGATA UCHUU KOUZOUBUTSU NI TAISURU CHITEKI TEKIOU KOUZOUBUTSU TO ROBOTTO NO OUYOU] **c18**
Kei Senda and Yoshisada Murotsu *In* NASDA, The Second Workshop on Deployment and Assembly Experiment of Large Space Structure on Orbit 31 Mar. 1993 p 47-53 In JAPANESE (For primary document see N94-13268 02-12)
Avail: CASI HC A02/MF A01

The status of the research on applying intelligently a adaptable structure and robot to a large space structure is presented. The following items are described: (1) the selected research subjects; (2) the present status of the research on FFR (Free Flying Robot) including formulation concerning FFR, inertial parameter identification and manipulator orbit plan for controlling the attitude of rigid FFR, study on controlling of FFR with flexible manipulator applying virtual rigid manipulator concept, hardware experiments using a model with one or two of two link solid manipulator, and the one with a two link flexible manipulator; (3) the intelligently adaptable structure including actuator layout; (4) optimum attitude utilization as a docking mechanism; and (5) control of flexible space structure. Author (NASDA)

N94-13278# Mitsubishi Electric Corp., Tokyo (Japan). Space Communications Research Div.
TRIAL MANUFACTURE MODEL AND IN-SPACE VERIFICATION METHOD OF DEPLOYABLE ANTENNA [TENKAI ANTENA NO SHISAKU MODERU TO UCHUU JISSHOU HOUHOU] **c32**
Takashi Ebisui, Teruaki Orikasa, and Teruki Okamoto *In* NASDA, The Second Workshop on Deployment and Assembly Experiment of Large Space Structure on Orbit 31 Mar. 1993 p 54-58 In JAPANESE (For primary document see N94-13268 02-12)
Avail: CASI HC A01/MF A01

This report describes the 6m hexa-link truss type scale model (4 GHz band offset parabolic antenna with a 6m diameter aperture and a 6m focal length) and 2m TETRUS type scale model (12 GHz band offset parabolic antenna with a 1.7m diameter aperture and a 2.2m focal length). Each antenna has electrical and mechanical characteristics similar to those of the large truss-type mesh deployable antenna of the Geostationary Platform (GPF) mobile communication satellites. The antennas were chosen to satisfy the increasing communication demands and requirements for advanced and diversified communication. The microgravity performance verification of these scale models is discussed. Additionally, the following topics are discussed: examples of the structures of GPF-type mobile communication satellite, the hexa-link truss type scale model, and the TETRUS (Tetra Trigonal Prism Truss) type scale model; the orbit of the scale models; and their space verification. Author (NASDA)

N94-13279# National Space Development Agency, Tokyo (Japan).
A CONCEPT ON ON-ORBIT EXPERIMENTS OF DEPLOYABLE STRUCTURES UTILIZING JEM/HOPE [TENKAI KUMITATE KOUZOUBUTSU NO JEM/HOPE KIDOUJOU JISSHOU JIKKEN KOUSOU]
Shigeto Shibuta, Yoshiki Morino, and Hiroshi Saegusa *In its* The Second Workshop on Deployment and Assembly Experiment of Large Space Structure on Orbit 31 Mar. 1993 p 59-66 In JAPANESE (For primary document see N94-13268 02-12)
Avail: CASI HC A02/MF A01

The National Space Development Agency of Japan (NASDA) has been performing research and development in the area of deployable structures. The R&D effort has been designated as a key element for future large space structures. System design, component design, and preliminary simulation analysis were carried out. A study of the experimental scheme is the required next step. This report presents conceptual plans for on-orbit experiments that will utilize space vehicles or platforms such as JEM (Japanese Experiment Module)/HOPE (H-2 Orbiting Plane).
Author (NASDA)

N94-13280# Fuji Heavy Industries Ltd., Tokyo (Japan).
MOVEMENT OF DEPLOYABLE TRUSS [TENKAI TORASU NO UNDOU NI TSUITE] **c18**
Hiroshi Miura, Yoshiki Morino (National Space Development Agency, Tokyo, Japan.), and Shigeto Shibuta (National Space Development Agency, Tokyo, Japan.) *In* NASDA, The Second Workshop on Deployment and Assembly Experiment of Large Space Structure on Orbit 31 Mar. 1993 p 67-72 In JAPANESE (For primary document see N94-13268 02-12)
Avail: CASI HC A02/MF A01

The use of deployable trusses was analyzed, and related problems were examined. The basic deployment movement of the SHSF (Sliding Hinge Single Fold) was taken as the examination object, and the analysis results were studied. A pulley system which can cope with overloading and deviation from synchronization was adopted. Some trial models were manufactured. The behavior of the truss is controlled by three factors: (1) deployment pattern; (2) element characteristics (such as those of hinges); and (3) the environment of deployment. Only the structural elements which constitute the deployment section were subjected to the examination as it is not necessary to examine the overall SHSF when the frame members of the truss are rigid and in an ideal condition (such as frictionless). The basic concepts of the SHSF--sliding hinge movement via deployment angle, shape change in deployment, and the center of gravity position--and the results of vibration analysis of the SHSF are shown. Author (NASDA)

N94-13281# Nippon Electric Co. Ltd., Tokyo (Japan).
DEVELOPMENT AND APPLICATION OF ONE DIMENSIONAL DEPLOYABLE TRUSS [ICHIJIGEN TENKAIGATA TORASU NO KAIHATSU TO SONO OUYOU] **c18**
Hiroshi Irikado, Kouji Sekine, Yuuzou Shibayama, and Yoshiki Morino (National Space Development Agency, Tokyo, Japan.) *In* NASDA, The Second Workshop on Deployment and Assembly Experiment of Large Space Structure on Orbit 31 Mar. 1993 p 73-79 In JAPANESE (For primary document see N94-13268 02-12)
Avail: CASI HC A02/MF A01

This report describes the development of the SSDT (Sliding Strut Deployable Truss). The results of the truss structure vibration control experiment, wherein the piezoelectric actuators were built into the truss, are presented. The SSDT's characteristics, the design of the trial production model for its truss and driving mechanism sections, its operation function test results, vibration control of the truss structure, and the control test are outlined. The conceptual drawing, trial manufacture model configuration, truss section, sliding mechanism, driving mechanism, and deployment simulation of SSDT are shown. Author (NASDA)

N94-13282# Kawasaki Heavy Industries Ltd., Kagamihara (Japan).
STUDY OF A ONE-DIMENSIONAL DEPLOYABLE STRUCTURE EMPLOYING TELESCOPIC MEMBERS [TERESUKOPIKKU BUZAI O RIYOU SHITA ICHIJIGEN TENKAI TORASU KOUZOU NO KENTOU] **c18**
Osamu Muragishi, Sumio Katou, Yoshiki Morino (National Space Development Agency, Ibaraki, Japan.), and Shigeto Shibuta (National Space Development Agency, Ibaraki, Japan.) *In* NASDA, The Second Workshop on Deployment and Assembly Experiment of Large Space Structure on Orbit 31 Mar. 1993 p 80-85 In JAPANESE (For primary document see N94-13268 02-12)
Avail: CASI HC A02/MF A01

The basic concept of a deployable truss structure was studied. The truss structure introduced here is a one-dimensional box type which employs a simple folding mechanism using telescopic members for stowing. It is suitable for use in the main supporting structures of platform type spacecraft such as geostationary platforms. It is stowed compactly, deploys automatically, and has high rigidity in deployment. By mechanism analyses, the validity of deploying movement was confirmed and the deploying force was estimated. It was found that the deploying driving force could be very in zero gravity conditions. A functional model was fabricated to confirm the structural concept. Author (NASDA)

N94-13358 Massachusetts Inst. of Tech., Lexington. Lincoln Lab.
PROCEEDINGS OF THE 11TH SPACE SURVEILLANCE WORKSHOP, VOLUME 1 Project Report
R. W. Miller and R. Sridharan 1 Apr. 1993 238 p Workshop held in Lexington, MA, 30 Mar. - 1 Apr. 1993 Limited Reproducibility: More than 20% of this document may be affected by microfiche quality
(Contract F19628-90-C-0002)
(AD-A265120; STK-206-Vol-1; ESC-TR-93-207) Avail: CASI HC A11

This report of Proceedings of the 1993 Space Surveillance Workshop includes the following topics: the Maui space surveillance site infrared calibration sources; infrared detection of geosynchronous objects at AMOS; LWIR observations of geosynchronous satellites; LAGEOS-2 launch support navigation at JPL; space surveillance network sensor contribution analysis; NMD-GBR: new X-band sensors at sites in CONUS and USAKA for space surveillance; recent improvements at ALTAIR; enhancements to the ALCOR imaging radar; fiber optic phase control of the like Kickapoo NAVSPASUR transmitter; coherent data recording and signal processing capabilities at Ascension FPQ-15 radar for space surveillance applications; forecasting trans-ionospheric effects to improve space surveillance. DTIC

N94-13631* National Aeronautics and Space Administration. Lyndon B. Johnson Space Center, Houston, TX.
STS-32 MISSION HIGHLIGHTS RESOURCE TAPE (Videotape)
Mar. 1990 Videotape: 55 min. playing time, in color, with sound
(NASA-TM-109291; NONP-VT-93-185306) Avail: CASI VHS A01/BETA A22

Important visual events including launch, Syncom 4 deployment, LDEF retrieval, onboard crew activities, and landing are presented. Air-to-ground transmission between the crew and Mission Control is also included.
Author (revised)

N94-13640* National Aeronautics and Space Administration. Lyndon B. Johnson Space Center, Houston, TX.
STS-28 CREW PRESENTATION CLIP (Videotape)
Sep. 1989 Videotape: 23 min. 58 sec. playing time, in color, with sound
(NASA-TM-109298; NONP-VT-93-185313) Avail: CASI VHS A01/BETA A22

This Department of Defense space shuttle mission is shown during launch and landing. The video tape also includes scenes of the following: the crew working on the otolith Tilt Translation Reinterpretation Experiment, various views of the Earth, the crew during mealtime, and preparations for reentry. Author (revised)

N94-14080*# National Aeronautics and Space Administration, Washington, DC.
DISCOVERY MANAGEMENT WORKSHOP
25 May 1993 23 p Workshop held in San Juan, Puerto Rico, 13-15 Apr. 1993
(NASA-TM-108244; NAS 1.15:108244) Avail: CASI HC A03/MF A01

Two dozen participants assembled under the direction of the NASA Solar System Exploration Division (SEED) April 13-15, 1993. Participants supported the goals of cheaper and faster solar system exploration. The workshop concluded that the Discovery Program concept and goals are viable. Management concerns are articulated in the final report. Appendix A includes lists of participants in alphabetical order, by functional area, and by organization type. Appendix B includes the agenda for the meeting.
CASI

N94-14098# Science and Technology Agency, Tokyo (Japan).
ASIA-PACIFIC ISY CONFERENCE, VOLUME 1 [AJIA TAIHEIYOU KOKUSAI UCHUUNEN KAIGI]
31 Mar. 1993 256 p In ENGLISH and JAPANESE Conference held in Tokyo, Japan, 16 Nov. 1992 Prepared in cooperation with the Institute of Space and Astronautical Science, Kanagawa, Japan, NASDA, Tokyo, Japan; and Japan International Space Year Association, Tokyo, Japan Original contains color illustrations
(NASDA-CM-199-1; JTN-93-80453) Avail: CASI HC A12/MF A03

An overview of the proceedings of the Asia Pacific International Space Year Conference is presented. Comments, lectures in the opening ceremonies, and the keynote lectures and lectures in the following symposia on the theme of 'Mission to Planet Earth' (Session 1), 'Man in Space' (Session 2), 'Space Activities in the Asia Pacific Region' (Session 3), and 'Future Space Missions, Beyond the Horizon' (Session 4) are outlined. Dates, places and chair persons for the workshops (WS-A to O), and the exhibition and demonstrations are displayed. Author (NASDA)

N94-14273# Academia Sinica, Beijing (China). International Space Year China Preparatory Committee.
CHINA'S DEVOTION TO SPACE SCIENCE AND APPLICATIONS
Da-Heng Wang *In* Science and Technology Agency, Asia-Pacific ISY Conference, Volume 2 31 Mar. 1993 p 331-334 (For primary document see N94-14209 02-43)
Avail: CASI HC A01/MF A04

13 ASTRODYNAMICS

Includes powered and free-flight trajectories; and orbital and launching dynamics.

N94-13644# Mitsubishi Space Software Corp. (Japan).
ORBIT DETERMINATION ERROR ANALYSIS BASED ON THE REQUIREMENTS OF ADEOS MISSION [ADEOS MISSHON YOUKYUU NI MOTOZUKU KIDOU KETTEI GOSA KAISEKI]
Tokyo, Japan National Space Development Agency 31 Mar. 1993 18 p In JAPANESE
(NASDA-CNT-930008; JTN-93-80462) Avail: CASI HC A03/MF A01

A summary of the results of the atmospheric density error analysis and the study on the feasibility of orbit accuracy requirements corresponding to the observation system peculiar to the ILAS (Improved Limb Atmospheric Spectrometer) to be carried onboard the ADEOS (Advanced Earth Observing Satellite) is presented. The atmospheric drag coefficient which is deemed to cause the largest effects on orbit decision accuracy was investigated, and the results are shown. The orbit decision accuracy requirements for ILAS can be evaluated as the tangential altitude (an altitude defined by the perpendicular line from the earth center to the satellite-sun direction vector) error at the time of ILAS observation. The analysis was conducted according to the following procedures: (1) calculation of ADEOS orbit decision accuracy; and (2) conversion of the ADEOS orbit decision error covariance to the altitude error at the time of ILAS observation. Author (NASDA)

N94-14851*# George Washington Univ., Hampton, VA. Joint Inst. for Advancement of Flight Sciences.
OPTIMIZING INTERPLANETARY TRAJECTORIES WITH DEEP SPACE MANEUVERS M.S. Thesis
John Navagh Washington Sep. 1993 70 p
(Contract NCC1-104; RTOP 506-49-11-01)
(NASA-CR-4546; NAS 1.26:4546) Avail: CASI HC A04/MF A01

Analysis of interplanetary trajectories is a crucial area for both manned and unmanned missions of the Space Exploration Initiative. A deep space maneuver (DSM) can improve a trajectory in much the same way as a planetary swingby. However, instead of using a gravitational field to alter the trajectory, the on-board propulsion system of the spacecraft is used when the vehicle is not near a planet. The purpose is to develop an algorithm to determine where and when to use deep space maneuvers to reduce the cost of a trajectory. The approach taken to solve this problem uses primer vector theory in combination with a non-linear optimizing program to minimize Delta(V). A set of necessary conditions on the primer vector is shown to indicate whether a deep space maneuver will be beneficial. Deep space maneuvers are applied to a round trip mission to Mars to determine their effect on the launch opportunities. Other studies which were performed include cycler trajectories and Mars mission abort scenarios. It was found that the software developed was able to locate quickly DSM's which lower the total Delta(V) on these trajectories. Author (revised)

N94-14373*# Jet Propulsion Lab., California Inst. of Tech., Pasadena.
FAILURE MODES OF REDUCED-ORDER ORBIT DETERMINATION FILTERS AND THEIR REMEDIES
D. J. Scheeres *In its* The Telecommunications and Data Acquisition Report 15 Aug. 1993 p 34-42 (For primary document see N94-14369 02-32)
(RTOP 310-10-63-50-00)
Avail: CASI HC A02/MF A03

14 GROUND SUPPORT SYSTEMS AND FACILITIES (SPACE)

Includes launch complexes, research and production facilities; ground support equipment, e.g., mobile transporters; and simulators.

For related information see also *09 Research and Support Facilities (Air).*

N94-13796*# Jet Propulsion Lab., California Inst. of Tech., Pasadena.
SEQUENTIAL RANGING: HOW IT WORKS
Harold W. Baugh 15 Jun. 1993 24 p
(Contract NAS7-918)
(NASA-CR-194508; JPL-Publ-93-18; NAS 1.26:194508) Avail: CASI HC A03/MF A01

This publication is directed to the users of data from the Sequential Ranging Assembly (SRA), and to others who have a general interest in range measurements. It covers the hardware, the software, and the processes used in acquiring range data; it does not cover analytical aspects such as the theory of modulation, detection, noise spectral density, and other highly technical subjects. In other words, it covers how ranging is done, but not the details of why it works. The publication also includes an appendix that gives a brief discussion of PN ranging, a capability now under development. Author (revised)

N94-14068*# Eloret Corp., Sunnyvale, CA.
ADVANCED BALLISTIC RANGE TECHNOLOGY Periodic Research Report, 1 Feb. - 31 Oct. 1992
Leslie A. Yates 22 Jan. 1993 12 p
(Contract NCC2-583)
(NASA-CR-194396; NAS 1.26:194396) Avail: CASI HC A03/MF A01

Optical images, such as experimental interferograms, schlieren, and shadowgraphs, are routinely used to identify and locate features in experimental flow fields and for validating computational fluid dynamics (CFD) codes. Interferograms can also be used for comparing experimental and computed integrated densities. By constructing these optical images from flow-field simulations, one-to-one comparisons of computation and experiment are possible. During the period from February 1, 1992, to November 30, 1992, work has continued on the development of CISS (Constructed Interferograms, Schlieren, and Shadowgraphs), a code that constructs images from ideal- and real-gas flow-field simulations. In addition, research connected with the automated film-reading system and the proposed reactivation of the radiation facility has continued.
Derived from text

N94-14148*# McDonnell-Douglas Space Systems Co., Cocoa Beach, FL. Product Engineering and Definition.
PAYLOAD/GSE/DATA SYSTEM INTERFACE: USERS GUIDE FOR THE VPF (VERTICAL PROCESSING FACILITY)
28 Sep. 1993 88 p Revised
(Contract NAS10-11400)
(NASA-CR-194385; NAS 1.26:194385; KSC-DL-522-Rev-B) Avail: CASI HC A05/MF A01

Payload/GSE/data system interface users guide for the Vertical Processing Facility is presented. The purpose of the document is three fold. First, the simulated Payload and Ground Support Equipment (GSE)

Data System Interface, which is also known as the payload T-0 (T-Zero) System is described. This simulated system is located with the Cargo Integration Test Equipment (CITE) in the Vertical Processing Facility (VPF) that is located in the KSC Industrial Area. The actual Payload T-0 System consists of the Orbiter, Mobile Launch Platforms (MLPs), and Launch Complex (LC) 39A and B. This is referred to as the Pad Payload T-0 System (Refer to KSC-DL-116 for Pad Payload T-0 System description). Secondly, information is provided to the payload customer of differences between this simulated system and the actual system. Thirdly, a reference guide of the VPF Payload T-0 System for both KSC and payload customer personnel is provided. Author (revised)

N94-14540*# Eloret Corp., Sunnyvale, CA.
ADVANCED BALLISTIC RANGE TECHNOLOGY Report, 1 Nov. 1992 - 30 Jun. 1993
Leslie A. Yates 14 Oct. 1993 29 p
(Contract NCC2-583)
(NASA-CR-194530; NAS 1.26:194530) Avail: CASI HC A03/MF A01

Experimental interferograms, schlieren, and shadowgraphs are used for quantitative and qualitative flow-field studies. These images are created by passing light through a flow field, and the recorded intensity patterns are functions of the phase shift and angular deflection of the light. As part of the grant NCC2-583, techniques and software have been developed for obtaining phase shifts from finite-fringe interferograms and for constructing optical images from Computational Fluid Dynamics (CFD) solutions. During the period from 1 Nov. 1992 - 30 Jun. 1993, research efforts have been concentrated in improving these techniques. Author (revised)

N94-14735* National Aeronautics and Space Administration. Lyndon B. Johnson Space Center, Houston, TX.
STS-35 CREW TRASH COMPACTOR BRIEFING (Videotape)
May 1990 Videotape: 7 min. 50 sec. playing time, in color, with sound
(NASA-TM-109487; NONP-VT-93-190284) Avail: CASI VHS A01/BETA A22

Parker, Brand, and Gardner are shown in the CCT learning how to work the trash compactor on the middeck. Author

N94-14787* National Aeronautics and Space Administration. Lyndon B. Johnson Space Center, Houston, TX.
STS-35 INTEGRATED SIM IN SMS AND MOCR (Videotape)
May 1990 Videotape: 22 min. 10 sec. playing time, in color, with sound
(NASA-TM-109491; NONP-VT-93-190288) Avail: CASI VHS A01/BETA A22

A clip that intercuts between the MOCR and the SMS during an STS-35 sim is provided. Author (revised)

N94-14394*# Jet Propulsion Lab., California Inst. of Tech., Pasadena.
HARDWARE DESIGN FOR THE AUTONOMOUS VISIBILITY MONITORING (AVM) OBSERVATORY
K. Cowles *In its* The Telecommunications and Data Acquisition Report 15 Aug. 1993 p 295-301 (For primary document see N94-14369 02-32)
(RTOP 315-91-60-10-06)
Avail: CASI HC A03/MF A03

15 LAUNCH VEHICLES AND SPACE VEHICLES

Includes boosters; operating problems of launch/space vehicle systems; and reusable vehicles.

For related information see also *20 Spacecraft Propulsion and Power.*

N94-14824*# National Aeronautics and Space Administration. Marshall Space Flight Center, Huntsville, AL.
TERRESTRIAL ENVIRONMENT (CLIMATIC) CRITERIA GUIDELINES FOR USE IN AEROSPACE VEHICLE DEVELOPMENT, 1993 REVISION
D. L. Johnson, ed. Washington Aug. 1993 458 p Supersedes TM X-64589, TM X-64757, TM X-78118, and TM-82473
(NASA-TM-4511; M-723; NAS 1.15:4511) Avail: CASI HC A20/MF A04

Guidelines on terrestrial environment data specifically applicable in the development of design requirements/specifications for NASA aerospace vehicles and associated equipment development are provided. The primary geographic areas encompassed are the John F. Kennedy Space Center, FL; Vandenberg AFB, CA; Edwards AFB, CA; Michoud Assembly Facility, New Orleans, LA; John C. Stennis Space Center, MS; Lyndon B. Johnson Space Center, Houston, TX; and the White Sands Missile Range, NM. In addition, a section was included to provide information on the general distribution of natural environmental extremes in the conterminous United States that may be needed to specify design criteria in the transportation of space vehicle subsystems and components. A summary of climatic extremes for worldwide operational needs is also included. Although not considered as a specific vehicle design criterion, a section on atmospheric attenuation was added since sensors on certain Earth orbital experiment missions are influenced by the Earth's atmosphere. The latest available information on probable climatic extremes is presented and supersedes information presented in TM X-64589, TM X-64757, TM X-78118, and TM-82473. Information is included on atmospheric chemistry, seismic criteria, and on a mathematical model to predict atmospheric dispersion of aerospace engine exhaust cloud rise and growth. There is also a section on atmospheric cloud phenomena. The information is recommended for use in the development of aerospace vehicle and associated equipment design and operational criteria, unless otherwise stated in contract work specifications. The environmental data are primarily limited to information below 90 km. Author (revised)

16 SPACE TRANSPORTATION

Includes passenger and cargo space transportation, e.g., shuttle operations; and space rescue techniques.

For related information see also *03 Air Transportation and Safety* and *18 Spacecraft Design, Testing and Performance.* For space suits see *54 Man/System Technology and Life Support.*

N94-12806*# Rockwell International Corp., Canoga Park, CA. Rocketdyne Div.
STS-55 PAD ABORT: ENGINE 2011 OXIDIZER PREBURNER AUGMENTED SPARK IGNITER CHECK VALVE LEAK Final Report
22 Mar. 1993 132 p
(Contract NAS8-40000)
(NASA-CR-193830; NAS 1.26:193830; RSS-8898) Avail: CASI HC A07/MF A02

The STS-55 initial launch attempt of Columbia (OV102) was terminated on KSC launch pad A March 22, 1993 at 9:51 AM E.S.T. due to violation of an ME-3 (Engine 2011) Launch Commit Criteria (LCC) limit exceedance. The event description and timeline are summarized. Propellant loading was initiated on 22 March, 1993 at 1:15 AM EST. All SSME chill parameters and launch commit criteria (LCC) were nominal. At engine start plus 1.44 seconds, a Failure Identification (FID) was posted against Engine 2011 for exceeding the 50 psia Oxidizer Preburner (OPB) purge pressure redline. The engine was shut down at 1.50 seconds followed by Engines 2034 and 2030. All shut down sequences were nominal and the mission was safely aborted. The OPB purge pressure redline violation and the abort profile/overlay for all three engines are depicted. SSME Avionics hardware and software performed nominally during the incident. A review of vehicle data table (VDT) data and controller software logic revealed no failure indications other than the single FID 013-414, OPB purge pressure redline exceeded. Software logic was executed according to requirements and there was no anomalous controller software operation. Immediately following the abort, a Rocketdyne/NASA failure investigation team was assembled. The team successfully isolated the failure cause to the oxidizer preburner augmented spark igniter purge check valve not being fully closed due to contamination. The source of the contaminant was traced to a cut segment from a rubber O-ring which was used in a fine clean tool during valve production prior to 1992. The valve was apparently contaminated during its fabrication in 1985. The valve had performed acceptably on four previous flights of the engine, and SSME flight history shows 780 combined check valve flights without failure. The failure of an Engine 3 (SSME No. 2011) check valve to close was sensed by onboard engine instruments even though all other engine operations were normal. This resulted in an engine shutdown and safe sequential shutdown of all three engines prior to ignition of the solid boosters. Derived from text

N94-12810*# Chrysler Technologies Airborne Systems, Inc., New Orleans, LA. Data Management Systems.

RESULTS OF EXPERIMENTAL INVESTIGATIONS TO DETERMINE EXTERNAL TANK PROTUBERANCE LOADS USING A 0.03-SCALE MODEL OF THE SPACE SHUTTLE LAUNCH CONFIGURATION (MODEL 47-OTS) IN THE NASA/ARC UNITARY PLAN WIND TUNNEL, VOLUME 1

S. R. Houlihan (Rockwell International Corp., Los Angeles, CA.) Feb. 1992 414 p

(Contract NAS9-17840)

(NASA-CR-167690; NAS 1.26:167690; DMS-DR-2476-Vol-1) Avail: CASI HC A18/MF A04

Data were obtained on a 3-percent model of the Space Shuttle launch vehicle in the NASA/Ames Research Center 11x11-foot and 9x7-foot Unitary Plan Wind Tunnels. This test series has been identified as IA190A/B and was conducted from 7 Feb. 1980 to 19 Feb. 1980 (IA190A) and from 17 March 1980 to 19 March 1980 and from 8 May 1980 to 30 May 1980 (IA190B). The primary test objective was to obtain structural loads on the following external tank protuberances: (1) LO2 feedline, (2) GO2 pressure line, (3) LO2 antigeyser line, (4) GH2 pressure line, (5) LH2 tank cable tray, (6) LO2 tank cable tray, (7) Bipod, (8) ET/SRB cable tray, and (9) Crossbeam/Orbiter cable tray. To fulfill these objectives the following steps were taken: (1) Eight 3-component balances were used to measure forces on various sections of 1 thru 6 above. (2) 315 pressure orifices were distributed over all 9 above items. The LO2 feedline was instrumented with 96 pressure taps and was rotated to four positions to yield 384 pressure measurements. The LO2 antigeyser line was instrumented with 64 pressure taps and was rotated to two positions to yield 128 pressure measurements. (3) Three Chrysler miniature flow direction probes were mounted on a traversing mechanism on the tank upper surface centerline to obtain flow field data between the forward and aft attach structures. (4) Schlieren photographs and ultraviolet flow photographs were taken at all test conditions. Data from each of the four test phases are presented.

Author

N94-12900*# National Aeronautics and Space Administration. John F. Kennedy Space Center, Cocoa Beach, FL.

PROCEDURES FOR ANALYSIS OF DEBRIS RELATIVE TO SPACE SHUTTLE SYSTEMS Final Report, Jan. 1992 - Jul. 1993

Hae Soo Kim and Virginia J. Cummings May 1993 88 p Original contains color illustrations

(NASA-TM-109190; NAS 1.15:109190) Avail: CASI HC A05/MF A01; 8 functional color pages

Debris samples collected from various Space Shuttle systems have been submitted to the Microchemical Analysis Branch. This investigation was initiated to develop optimal techniques for the analysis of debris. Optical microscopy provides information about the morphology and size of crystallites, particle sizes, amorphous phases, glass phases, and poorly crystallized materials. Scanning electron microscopy with energy dispersive spectrometry is utilized for information on surface morphology and qualitative elemental content of debris. Analytical electron microscopy with wavelength dispersive spectrometry provides information on the quantitative elemental content of debris.

Author (revised)

N94-12965*# Chrysler Technologies Airborne Systems, Inc., New Orleans, LA. Data Management Services.

RESULTS OF WIND TUNNEL TESTS OF AN ASRM CONFIGURED 0.03 SCALE SPACE SHUTTLE INTEGRATED VEHICLE MODEL (47-OTS) IN THE AEDC 16-FOOT TRANSONIC WIND TUNNEL, VOLUME 2

J. Marroquin (Rockwell International Corp., Downey, CA.) and P. Lemoine (Rockwell International Corp., Downey, CA.) Oct. 1992 393 p Microfiche as supplement

(Contract NAS9-17840)

(NASA-CR-185697; NAS 1.26:185697; DMS-DR-2549-Vol-2) Avail: CASI HC A17/MF A04

An experimental Aerodynamic and Aero-Acoustic loads data base was obtained at transonic Mach numbers for the Space Shuttle Launch Vehicle configured with the ASRM Solid Rocket Boosters as an increment to the current flight configuration (RSRB). These data were obtained during transonic wind tunnel tests (IA 613A) conducted in the Arnold Engineering Development Center 16-Foot transonic propulsion wind tunnel from March 27, 1991 through April 12, 1991. This test is the first of a series of two tests covering the Mach range from 0.6 to 3.5. Steady state surface static and fluctuating pressure distributions over the Orbiter, External Tank and Solid Rocket Boosters of the Shuttle Integrated Vehicle were measured. Total Orbiter forces, Wing forces and Elevon hinge moments were directly measured as well from force balances. Two configurations of Solid Rocket Boosters were tested, the Redesigned Solid Rocket Booster (RSRB) and the Advanced Solid Rocket Motor (ASRM). The effects of the position (i.e., top, bottom, top and bottom) of the Integrated Electronics Assembly (IEA) box, mounted on the SRB attach ring, were obtained on the ASRM configured model. These data were obtained with and without Solid Plume Simulators which, when used, matched as close as possible the flight derived pressures on the Orbiter and External Tank base. Data were obtained at Mach numbers ranging from 0.6 to 1.55 at a Unit Reynolds Number of 2.5 million per foot through model angles of attack from -8 to +4 degrees at sideslip angles of 0, +4 and -4 degrees.

Author

N94-13028*# National Aeronautics and Space Administration. Lewis Research Center, Cleveland, OH.

TROPIX: A SOLAR ELECTRIC PROPULSION FLIGHT EXPERIMENT

J. Mark Hickman, G. Barry Hillard, and Steven R. Oleson (Sverdrup Technology, Inc., Brook Park, OH.) Sep. 1993 10 p Presented at the 23rd International Electric Propulsion Conference, Seattle, WA, 13-16 Sep. 1993; sponsored by AIAA, AIDAA, DGLR, and JSASS

(RTOP 920-20-08)

(NASA-TM-106297; E-8035; NAS 1.15:106297; IEPC-93-063) Avail: CASI HC A02/MF A01

The Transfer Orbit Plasma Interaction Experiment (TROPIX) is a proposed scientific experiment and flight demonstration of a solar electric propulsion vehicle. Its mission goals are to significantly increase our knowledge of Earth's magnetosphere and its associated plasma environment and to demonstrate an operational solar electric upper stage (SEUS) for small launch vehicles. The scientific investigations and flight demonstration technology experiments are uniquely interrelated because of the spacecraft's interaction with the surrounding environment. The data obtained will complement previous studies of the Earth's magnetosphere and space plasma environment by supplying the knowledge necessary to attain the strategic objectives of the NASA Office of Space Science. This first operational use of a primary ion propulsion vehicle, designed to withstand the harsh environments from low Earth orbit to geosynchronous Earth orbit, may lead to the development of a new class of electric propulsion upper stages or space-based transfer vehicles and may improve future spacecraft design and safety.

Author

N94-13191*# Chrysler Technologies Airborne Systems, Inc., New Orleans, LA. Data Management Services.

RESULTS OF WIND TUNNEL TESTS OF AN ASRM CONFIGURED 0.03 SCALE SPACE SHUTTLE INTEGRATED VEHICLE MODEL (47-OTS) IN THE AEDC 16-FOOT TRANSONIC WIND TUNNEL (IA613A), VOLUME 1

J. Marroquin (Rockwell International Corp., Downey, CA.) and P. Lemoine (Rockwell International Corp., Downey, CA.) Oct. 1992 998 p

(Contract NAS9-17840)

(NASA-CR-185696; NAS 1.26:185696; DMS-DR-2549-Vol-1) Avail: CASI HC A99/MF A10

An experimental Aerodynamic and Aero-Acoustic loads data base was obtained at transonic Mach numbers for the Space Shuttle Launch Vehicle configured with the ASRM Solid Rocket Boosters as an increment to the current flight configuration (RSRB). These data were obtained during transonic wind tunnel tests (IA 613A) conducted in the Arnold Engineering Development Center 16-Foot transonic propulsion wind tunnel from March 27, 1991 through April 12, 1991. This test is the first of a series of two tests covering the Mach range from 0.6 to 3.5. Steady state surface static and fluctuating pressure distributions over the Orbiter, External Tank and Solid Rocket Boosters of the Shuttle Integrated Vehicle were measured. Total Orbiter forces, Wing forces and Elevon hinge moments were directly measured as well from force balances. Two configurations of Solid Rocket Boosters were tested, the Redesigned Solid Rocket Booster (RSRB) and the Advanced Solid Rocket Motor (ASRM). The effects of the position (i.e. top, bottom, top and bottom) of the Integrated Electronics Assembly (IEA) box, mounted on the SRB attach ring, were obtained on the ASRM configured model. These data were obtained with and without Solid Plume Simulators which, when used, matched as close as possible the flight derived pressures on the Orbiter and External Tank base. Data were obtained at Mach

numbers ranging from 0.6 to 1.55 at a Unit Reynolds Number of 2.5 million per foot through model angles of attack from -8 to +4 degrees at sideslip angles of 0, +4 and -4 degrees. Author

N94-13599# Kawasaki Heavy Industries Ltd., Kobe (Japan).
HOPE REAL TIME FLIGHT OPERATIONS ANALYSES FOR RETURN TO EARTH PHASE, PART B [HOPE KIKAN KANSEI FEZU NO RIARU TAIMU UNYOU NO KAISEKI]
Tokyo, Japan National Space Development Agency 31 Mar. 1993 21 p In JAPANESE
(NASDA-CNT-930011; JTN-93-80465) Avail: CASI HC A03/MF A01

An overview of the results of the HOPE (H-2 Orbiting Plane) real time flight operation analyses in the return to earth phase is presented. The results of the analysis of the flight parameter real time estimation accuracy, including the following work items are outlined: (1) listing the data usable for the estimate; (2) study of the ground station and data relay satellite coverage; (3) HOPE return trajectory deviation limits; (4) listing the related ground stations and data relay satellite positions; (5) study of the methods for flight parameter real time estimation; (6) analysis of the flight parameter real time estimation accuracy; (7) study of the plane altitude estimation; (8) investigation and study of the reference materials related to the US Space Shuttle real time flight operation; and (9) formulating the estimate work plan. The results of the study of the flight path deviation limit were outlined. Author (NASDA)

N94-13600# Kawasaki Heavy Industries Ltd., Kobe (Japan).
HOPE CONCEPTUAL DESIGN IN FY 1991 [HEISEI 3 NENDO HOPE GAINEN SEKKEI]
Tokyo, Japan National Space Development Agency 31 Mar. 1993 198 p In JAPANESE
(NASDA-CNT-930017; JTN-93-80471) Avail: CASI HC A09/MF A03

A study on the system design and the technical problems of the HOPE (H-2 Orbiting Plane) subsystem, especially on tip fin feasibility study and trade-off of orbit injection system and major structural materials which is deemed to have great effects on establishing basic specifications of the airframe are conducted based on the results of studies conducted till last year. Reflecting the results of the above studies, the HOPE system study, study of overall operation concept, overall operation system and impact ellipse area, and development program were conducted. The items concerning the feasibility of the HOPE system was made clear and the accuracy of the study on those points was improved. Problems such as the lack of design data which is important for basic configuration establishment were pointed out, and the design theories were made clear. Author (NASDA)

N94-13638* National Aeronautics and Space Administration. Lyndon B. Johnson Space Center, Houston, TX.
LAUNCH, ENTRY, AND LANDING RESOURCE CLIP (Videotape)
Jan. 1989 Videotape: 9 min. 20 sec. playing time, in color, with sound
(NASA-TM-109297; NONP-VT-93-185312) Avail: CASI VHS A01/BETA A22

A video tape of scenes of the shuttle during launch is presented. The scenes were shot from various points of view. The following scenes are also included: SRB and ET separation, OMS burn, reentry glow, and landing at Edwards AFB, California. Author (revised)

N94-13641* National Aeronautics and Space Administration. Lyndon B. Johnson Space Center, Houston, TX.
STS-29 POST-INSERTION/DEORBIT PREP AND CREW BAILOUT (Videotape)
Jan. 1989 Videotape: 12 min. playing time, in color, with sound
(NASA-TM-109299; NONP-VT-93-185314) Avail: CASI VHS A01/BETA A22

Crew enters CCT after donning vests where they practice post insertion deorbit prepared for bailout procedure. Entire crew takes turns bailing out through the side hatch of the CCT. Author

N94-13645# Mitsubishi Heavy Industries Ltd., Tokyo (Japan).
HOPE REAL TIME FLIGHT OPERATIONS ANALYSES FOR RETURN TO EARTH PHASE, PART A [HOPE KIKAN KANSEI FEZU NO RIARU TAIMU UNYOU NO KAISEKI]
National Space Development Agency 31 Mar. 1993 17 p In JAPANESE
(NASDA-CNT-930010-Pt-A; JTN-93-80464) Avail: CASI HC A03/MF A01

The results of the HOPE (H-2 Orbiting Plane) real time flight operation analysis for return to earth phase are presented. The analyses of the flight parameter real time estimation accuracy was conducted (including definition of the estimate system operation, close examination of required function and programs, and study on the verification and experiment plans) and the following two items of the system verification and experiment are proposed: (1) utilization of the ETS-X (Engineering Test Satellite-X); and (2) utilization of mock-up landing experiment plane. The study on the limit of deviation from the flight path was conducted, and various factors to improve the flight path deviation are outlined. Author (NASDA)

N94-13656# Fuji Heavy Industries Ltd., Tokyo (Japan).
CONCEPTUAL DESIGN ON H-2 ORBITING PLANE (HOPE) [HEISEI 3 NENDO HOPE GAIKEN SEKKEI]
National Space Development Agency 31 Mar. 1993 53 p In JAPANESE
(NASDA-CNT-930018; JTN-93-80472) Avail: CASI HC A04/MF A01

An overview of the results of the studies on technical problems concerning the following subjects related to the HOPE (H-2 Orbiting Plane) is presented: (1) technical problems on system design, aerodynamic design, thermal structure design, thermal control system design, and guidance and control system design; (2) studies on designs for the system, aerodynamic characteristics, thermal structure, actuator system, thermal control system, payload support system, and guidance and control system; (3) studies on operational concepts and overall operation system; and (4) study of development program. Author (NASDA)

N94-13934*# Lockheed Engineering and Sciences Co., Houston, TX. Flight Evaluation and Engineering Office.
STS-53 SPACE SHUTTLE MISSION REPORT
Robert W. Fricke, Jr. Feb. 1993 39 p Sponsored by NASA. Johnson Space Center
(NASA-CR-193101; NAS 1.26:193101; NSTS-08281) Avail: CASI HC A03/MF A01

The STS-53 Space Shuttle Program Mission Report provides a summary of the Orbiter, External Tank (ET), Solid Rocket Booster/Redesigned Solid Rocket Motor (SRB/RSRM), and the Space Shuttle Main Engine (SSME) subsystems performance during the fifty-second flight of the Space Shuttle Program, and the fifteenth flight of the Orbiter vehicle Discovery (OV-103). In addition to the Orbiter, the flight vehicle consisted of an ET, which was designated as ET-49/LWT-42; three SSME's, which were serial numbers 2024, 2012, and 2017 in positions 1, 2, and 3, respectively; and two SRB's, which were designated BI-055. The lightweight RSRM's that were installed in each SRB were designated 360L028A for the left SRB, and 360L028B for the right SRB. The primary objective of this flight was to successfully deploy the Department of Defense 1 (DOD-1) payload. The secondary objectives of this flight were to perform the operations required by the Glow Experiment/Cryogenic Heat Pipe Experiment Payload (GCP); the Hand-Held, Earth-Oriented, Real-Time, Cooperative, User-Friendly, Location-Targeting and Environmental System (HERCULES); the Space Tissue Loss (STL); the Battlefield Laser Acquisition Sensor Test (BLAST); the Radiation Monitoring Equipment-III (RME-III); the Microcapsules in Space-1 (MIS-1); the Visual Function Tester-2 (VFT-2); the Cosmic Radiation Effects and Activation Monitor (CREAM); the Clouds Logic to Optimize Use of Defense Systems-1A (CLOUDS-1A); the Fluids Acquisition and Resupply Experiment (FARE); and the Orbital Debris Radar Calibration Spheres (ODERACS). In addition to presenting a summary of subsystem performance, this report also discusses each Orbiter, ET, SSME, SRB, and RSRM in-flight anomaly in the applicable section of the report. Listed in the discussion of each anomaly is the officially assigned tracking number as published by each Project Office in their respective Problem Tracking List. All times given in this report are in Greenwich mean time (G.m.t.) as well as mission elapsed time (MET). Author (revised)

N94-13935*# Lockheed Engineering and Sciences Co., Houston, TX. Flight Evaluation and Engineering Office.
STS-54 SPACE SHUTTLE MISSION REPORT
Robert W. Fricke, Jr. Mar. 1993 34 p Sponsored by NASA. Johnson

Space Center
(NASA-CR-194116; NAS 1.26:194116; NSTS-08282) Avail: CASI HC A03/MF A01

The STS-54 Space Shuttle Program Mission Report is a summary of the Orbiter, External Tank (ET), Solid Rocket Booster/Redesigned Solid Rocket Motor (SRB/RSRM), and the Space Shuttle Main Engine (SSME) subsystems performance during this fifty-third flight of the Space Shuttle Program, and the third flight of the Orbiter vehicle Endeavour (OV-105). In addition to the Orbiter, the flight vehicle consisted of an ET, which was designated ET-51; three SSME's, which were serial numbers 2019, 2033, and 2018 in positions 1, 2, and 3, respectively; and two retrievable and reusable SRB's which were designated BI-056. The lightweight RSRM's that were installed in each SRB were designated 360L029A for the left SRB, and 360L029B for the right SRB. The primary objectives of this flight were to perform the operations to deploy the Tracking and Data Relay Satellite-F/Inertial Upper Stage payload and to fulfill the requirements of the Diffuse X-Ray Spectrometer (DXS) payload. The secondary objective was to fly the Chromosome and Plant Cell Division in Space (CHROMEX), Commercial Generic Bioprocessing Apparatus (CGBA), Physiological and Anatomical Rodent Experiment (PARE), and the Solid Surface Combustion Experiment (SSCE). In addition to presenting a summary of subsystem performance, this report also discusses each Orbiter, ET, SSME, SRB, and RSRM in-flight anomaly in the applicable section of the report. The official tracking number for each in-flight anomaly, assigned by the cognizant project, is also shown. All times are given in Greenwich mean time (G.m.t.) and mission elapsed time (MET). Author (revised)

N94-14047*# Chrysler Technologies Airborne Systems, Inc., New Orleans, LA. Data Management Services.

RESULTS OF EXPERIMENTAL INVESTIGATIONS TO DETERMINE EXTERNAL TANK PROTUBERANCE LOADS USING A 0.03-SCALE MODEL OF THE SPACE SHUTTLE LAUNCH CONFIGURATION (MODEL 47-OTS) IN THE NASA/ARC UNITARY PLAN WIND TUNNEL, VOLUME 2

S. R. Houlihan (Rockwell International Corp., Los Angeles, CA.) Feb. 1992 80 p Microfiche as supplement
(Contract NAS9-17840)
(NASA-CR-167691; NAS 1.26:167691; DMS-DR-2476-Vol-2) Avail: CASI HC A05/MF A01

Data were obtained on a 3-percent model of the Space Shuttle launch vehicle in the NASA/Ames Research Center 11x11-foot and 9x7-foot Unitary Plan Wind Tunnels. This test series has been identified as IA19OA/B and was conducted from 7 Feb. 1980 to 19 Feb. 1980 (IA19OA) and from 17 March 1980 to 19 March 1980 and from 8 May 1980 to 30 May 1980 (IA19OB). The primary test objective was to obtain structural loads on the following external tank protuberances: (1) LO2 feedline; (2) GO2 pressure line; (3) LO2 antigeyser line; (4) GH2 pressure line; (5) LH2 tank cable tray; (6) LO2 tank cable tray; (7) Bipod; (8) ET/SRB cable tray; and (9) Crossbeam/Orbiter cable tray. To fulfill these objectives the following steps were taken: Eight 3-component balances were used to measure forces on various sections of 1 thru 6 above; 315 pressure orifices were distributed over all 9 above items. The LO2 feedline was instrumented with 96 pressure taps and was rotated to four positions to yield 384 pressure measurements. The LO2 antigeyser line was instrumented with 64 pressure taps and was rotated to two positions to yield 128 pressure measurements; Three Chrysler miniature flow direction probes were mounted on a traversing mechanism on the tank upper surface centerline to obtain flow field data between the forward and aft attach structures; and Schlieren photographs and ultraviolet flow photographs were taken at all test conditions. Data from each of the four test phases are presented. Author

N94-14099# Mitsubishi Heavy Industries Ltd., Tokyo (Japan).

THE CONCEPTUAL STUDY ON FUTURE SPACE TRANSPORTATION SYSTEMS. PART A: CONCEPTUAL STUDY OF FLYBACK BOOSTER [SHOURAIGATA ROKETTO NO KENKYUU: FURAIBAKKU BASUTA NO GAINEN KENTOU]

Tokyo, Japan National Space Development Agency 31 Mar. 1993 25 p
(NASDA-CNT-930013; JTN-93-80467) Avail: CASI HC A03/MF A01

The results of the study on a future space transportation system, a flyback booster, is presented. The initial sizing of the rocket was conducted, and the following guidelines concerning the selection of its configurations are presented: (1) the speed increment allotment for the booster is aimed at less than 3,000 m/s in an ideal velocity when the rocket is on the premise that the booster returning to the launch site; (2) to minimize the rocket size, upgrading the upper stage structural efficiency is effective in designing the flyback booster; and (3) assuming and comparing four kinds of returning systems, it is deemed most prosperous to return in ballistic flight by re-igniting the booster immediately after upper stage separation. A study was conducted on winged and flare type (non-winged) bodies as examples based on the initial sizing data, and it was concluded that both types are feasible within the category of the existing design and materials. Author (NASDA)

N94-14100# Mitsubishi Heavy Industries Ltd., Tokyo (Japan).

THE CONCEPT STUDY OF THE SPACE TRANSPORTATION SYSTEM HOPE IN FY 1991 [HEISEI 3 NENDO HOPE GAINEN SEKKEI]

Tokyo, Japan National Space Development Agency 31 Mar. 1993 102 p
(NASDA-CNT-930016; JTN-93-80470) Avail: CASI HC A06/MF A02

An system design was conducted on the HOPE (H-2 Orbiting Plane), focusing on the following technical problems which are deemed to have great effects on the specifications of the airframe: (1) the feasibility of the tip fin; (2) trade-off of main airframe structure materials; and (3) trade-off of the orbit injection systems. The feasibility of HOPE was confirmed. The following items of the system and each subsystem were straightend up: (1) detail of the design requirements and their feasibility; (2) standard specifications of the airframe and its alternatives; and (3) design studies. In a development concept study, it was confirmed that the HOPE first launch in FY (Fiscal Year) 2000 will be possible by advancing the development systematically. Author (NASDA)

N94-14310*# Tennessee Univ. Space Inst., Tullahoma. Center for Space Transportation and Applied Research.

AN INTEGRATED KNOWLEDGE SYSTEM FOR THE SPACE SHUTTLE HAZARDOUS GAS DETECTION SYSTEM Final Report, Jun. 1990 - Sep. 1993

Ching F. Lo, George Z. Shi, Carl Bangasser, Connie Fensky, Eric Cegielski, and Glenn Overbey 7 Oct. 1993 17 p
(Grant NAG8-835)
(NASA-CR-194533; NAS 1.26:194533) Avail: CASI HC A03/MF A01

A computer-based integrated Knowledge-Based System, the Intelligent Hypertext Manual (IHM), was developed for the Space Shuttle Hazardous Gas Detection System (HGDS) at NASA Marshall Space Flight Center (MSFC). The IHM stores HGDS related knowledge and presents it in an interactive and intuitive manner. This manual is a combination of hypertext and an expert system which store experts' knowledge and experience in hazardous gas detection and analysis. The IHM's purpose is to provide HGDS personnel with the capabilities of: locating applicable documentation related to procedures, constraints, and previous fault histories; assisting in the training of personnel; enhancing the interpretation of real time data; and recognizing and identifying possible faults in the Space Shuttle sub-systems related to hazardous gas detection. Author (revised)

N94-14323*# Rockwell International Corp., Downey, CA. Space Systems Div.

STRATEGIC AVIONICS TECHNOLOGY DEFINITION STUDIES. SUBTASK 3-1A: ELECTRICAL ACTUATION (ELA) SYSTEMS Final Report

Charles L. Pond, William A. McDermott, and Ben T. F. Lum 30 Sep. 1993 198 p
(Contract NAS9-18880)
(NASA-CR-194393; NAS 1.26:194393; SSD93D0505) Avail: CASI HC A09/MF A03

Electrical actuator (ELA) power efficiency and requirements are examined for space system application. Requirements for Space Shuttle effector systems are presented, along with preliminary ELA trades and selection to form a preliminary ELA system baseline. Power and energy requirements for this baseline ELA system are applicable to the Space Shuttle and similar space vehicles. CASI

N94-14734* National Aeronautics and Space Administration. Lyndon B. Johnson Space Center, Houston, TX.

STS-33 LAUNCH AND LANDING CLIP (Videotape Supplement)

Nov. 1989 Videotape: 20 min. playing time, in color, with sound
(NASA-TM-109468; NONP-VT-93-190265) Avail: CASI VHS A01/BETA A22

Launch (from engine gimbal to loss of sight) and landing of the Shuttle at Edwards AFB, California, from ground-based cameras is shown.
Author (revised)

N94-14736* National Aeronautics and Space Administration. Lyndon B. Johnson Space Center, Houston, TX.
STS-35 POST-FLIGHT PRESS CONFERENCE (Videotape)
May 1990 Videotape: 18 min. playing time, in color, with sound
(NASA-TM-109490; NONP-VT-93-190287) Avail: CASI VHS A01/BETA A22

The following contains footage selected and narrated by the crew. The footage covers the following areas: launch, work with the ASTRO-1 payload, onboard activities, and landing. Author (revised)

N94-14853*# National Aeronautics and Space Administration. Hugh L. Dryden Flight Research Facility, Edwards, CA.
THE DEVELOPMENT AND FLIGHT TEST OF A DEPLOYABLE PRECISION LANDING SYSTEM FOR SPACECRAFT RECOVERY
Alex G. Sim, James E. Murray, David C. Neufeld, and R. Dale Reed (PRC Kentron, Inc., Edwards, CA.) Sep. 1993 31 p
(RTOP 505-68-50)
(NASA-TM-4525; H-1933; NAS 1.15:4525) Avail: CASI HC A03/MF A01

A joint NASA Dryden Flight Research Facility and Johnson Space Center program was conducted to determine the feasibility of the autonomous recovery of a spacecraft using a ram-air parafoil system for the final stages of entry from space that included a precision landing. The feasibility of this system was studied using a flight model of a spacecraft in the generic shape of a flattened biconic which weighed approximately 150 lb and was flown under a commercially available, ram-air parachute. Key elements of the vehicle included the Global Positioning System guidance for navigation, flight control computer, ultrasonic sensing for terminal altitude, electronic compass, and onboard data recording. A flight test program was used to develop and refine the vehicle. This vehicle completed an autonomous flight from an altitude of 10,000 ft and a lateral offset of 1.7 miles which resulted in a precision flare and landing into the wind at a predetermined location. At times, the autonomous flight was conducted in the presence of winds approximately equal to vehicle airspeed. Several techniques for computing the winds postflight were evaluated. Future program objectives are also presented. Author (revised)

N94-14274# Science Univ. of Tokyo (Japan). Dept. of Mechanical Engineering.
SPACE TRANSPORTATION SYSTEMS AND SPACE ACTIVITIES IN THE 21ST CENTURY
Shigeo Kobayashi *In* Science and Technology Agency, Asia-Pacific ISY Conference, Volume 2 31 Mar. 1993 p 337-342 (For primary document see N94-14209 02-43)
Avail: CASI HC A02/MF A04

N94-14275# European Space Agency, Paris (France). Space Transportation Systems Directorate.
SPACE TRANSPORTATION SYSTEMS WITHIN ESA PROGRAMMES: CURRENT STATUS AND PERSPECTIVES
Maurice Delahais *In* Science and Technology Agency, Asia-Pacific ISY Conference, Volume 2 31 Mar. 1993 p 343-347 (For primary document see N94-14209 02-43)
Avail: CASI HC A01/MF A04

N94-14277# Tokyo Univ., Sagamihara (Japan). Inst. of Space and Astronautical Science.
RESEARCH AND DEVELOPMENT OF SPACE TRANSPORTATION SYSTEMS IN ISAS
Junjirou Onoda *In* Science and Technology Agency, Asia-Pacific ISY Conference, Volume 2 31 Mar. 1993 p 356-359 (For primary document see N94-14209 02-43)
Avail: CASI HC A01/MF A04

N94-14278# Science and Technology Agency, Tokyo (Japan). Research and Development Bureau.
CONTRIBUTIONS OF WINGED RE-ENTRY VEHICLE TO SPACE ACTIVITIES
Masaaki Yanagihara *In its* Asia-Pacific ISY Conference, Volume 2 31 Mar. 1993 p 360-363 (For primary document see N94-14209 02-43)
Avail: CASI HC A01/MF A04

N94-14279# Mitsubishi Research Inst., Inc., Tokyo (Japan).
MISSION SCENARIO OF HOPE
Yasushi Kawai and Kenji Takeuchi *In* Science and Technology Agency, Asia-Pacific ISY Conference, Volume 2 31 Mar. 1993 p 364-368 (For primary document see N94-14209 02-43)
Avail: CASI HC A01/MF A04

N94-14280# Tsukuba Space Center, Ibaragi (Japan).
THE STATUS OF THE HOPE CONCEPT STUDY
Jirou Kouchiyama and Akihiro Eguchi *In* Science and Technology Agency, Asia-Pacific ISY Conference, Volume 2 31 Mar. 1993 p 369-374 (For primary document see N94-14209 02-43)
Avail: CASI HC A02/MF A04

N94-14281# National Aerospace Lab., Tokyo (Japan).
SPACEPLANE PROGRAM AT NAL: SYSTEM CONCEPT AND RELATED TECHNOLOGY ISSUES
Masataka Maita *In* Science and Technology Agency, Asia-Pacific ISY Conference, Volume 2 31 Mar. 1993 p 375-378 (For primary document see N94-14209 02-43)
Avail: CASI HC A01/MF A04

17 SPACE COMM., SPACECRAFT COMM., COMMAND & TRACKING

Includes telemetry; space communications networks; astronavigation and guidance; and radio blackout.

For related information see also *04 Aircraft Communications and Navigation* and *32 Communications and Radar.*

N94-12809*# SRI International Corp., Menlo Park, CA.
TECHNICAL SUPPORT FOR DIGITAL SYSTEMS TECHNOLOGY DEVELOPMENT. TASK ORDER 1: ISP CONTENTION ANALYSIS AND CONTROL Final Report
Roy H. Stehle and Richard G. Ogier Jan. 1993 33 p
(Contract NAS3-25934; RTOP 690-60-21)
(NASA-CR-190758; E-7564; NAS 1.26:190758) Avail: CASI HC A03/MF A01

Alternatives for realizing a packet-based network switch for use on a frequency division multiple access/time division multiplexed (FDMA/TDM) geostationary communication satellite were investigated. Each of the eight downlink beams supports eight directed dwells. The design needed to accommodate multicast packets with very low probability of loss due to contention. Three switch architectures were designed and analyzed. An output-queued, shared bus system yielded a functionally simple system, utilizing a first-in, first-out (FIFO) memory per downlink dwell, but at the expense of a large total memory requirement. A shared memory architecture offered the most efficiency in memory requirements, requiring about half the memory of the shared bus design. The processing requirement for the shared-memory system adds system complexity that may offset the benefits of the smaller memory. An alternative design using a shared memory buffer per downlink beam decreases circuit complexity through a distributed design, and requires at most 1000 packets of memory more than the completely shared memory design. Modifications to the basic packet switch designs were proposed to accommodate circuit-switched traffic, which must be served on a periodic basis with minimal delay. Methods for dynamically controlling the downlink dwell lengths were developed and analyzed. These methods adapt quickly to changing traffic demands, and do not add significant complexity or cost to the satellite and ground station designs. Methods for reducing the memory requirement by not requiring the satellite to store full packets were also proposed and analyzed. In addition, optimal

packet and dwell lengths were computed as functions of memory size for the three switch architectures. Author (revised)

N94-13111*# National Aeronautics and Space Administration. Lewis Research Center, Cleveland, OH.

DESTINATION-DIRECTED, PACKET-SWITCHED ARCHITECTURE FOR A GEOSTATIONARY COMMUNICATIONS SATELLITE NETWORK

William D. Ivancic, Mary Jo Shalkhauser, Eric A. Bobinsky, Nitin J. Soni, Jorge A. Quintana, Heechul Kim, Paul Wager (Sverdrup Technology, Inc., Brook Park, OH.), and Mark Vanderaar (Sverdrup Technology, Inc., Brook Park, OH.) Washington Jul. 1993 19 p Presented at the World Space Congress, 43rd Congress of the International Astronautical Federation, Washington, DC, 28 Aug. - 5 Sep. 1992

(RTOP 506-72-21)

(NASA-TP-3379; E-7635; NAS 1.60:3379) Avail: CASI HC A03/MF A01

A major goal of the Digital Systems Technology Branch at the NASA Lewis Research Center is to identify and develop critical digital components and technologies that either enable new commercial missions or significantly enhance the performance, cost efficiency, and/or reliability of existing and planned space communications systems. NASA envisions a need for low-data-rate, interactive, direct-to-the-user communications services for data, voice, facsimile, and video conferencing. The network would provide enhanced very-small-aperture terminal (VSAT) communications services and be capable of handling data rates of 64 kbps through 2.048 Mbps in 64-kbps increments. Efforts have concentrated heavily on the space segment; however, the ground segment has been considered concurrently to ensure cost efficiency and realistic operational constraints. The focus of current space segment developments is a flexible, high-throughput, fault-tolerant onboard information-switching processor (ISP) for a geostationary satellite communications network. The Digital Systems Technology Branch is investigating both circuit and packet architectures for the ISP. Destination-directed, packet-switched architectures for geostationary communications satellites are addressed. Author (revised)

N94-13201*# National Aeronautics and Space Administration. Ames Research Center, Moffett Field, CA.

THERMAL EXPERT SYSTEM (TEXSYS): SYSTEMS AUTOMONY DEMONSTRATION PROJECT, VOLUME 1. OVERVIEW Final Report

B. J. Glass, ed. Oct. 1992 22 p

(RTOP 549-03-11)

(NASA-TM-102877; A-90319-Vol-1; NAS 1.26:102877) Avail: CASI HC A03/MF A01

The Systems Autonomy Demonstration Project (SADP) produced a knowledge-based real-time control system for control and fault detection, isolation, and recovery (FDIR) of a prototype two-phase Space Station Freedom external active thermal control system (EATCS). The Thermal Expert System (TEXSYS) was demonstrated in recent tests to be capable of reliable fault anticipation and detection, as well as ordinary control of the thermal bus. Performance requirements were addressed by adopting a hierarchical symbolic control approach-layering model-based expert system software on a conventional, numerical data acquisition and control system. The model-based reasoning capabilities of TEXSYS were shown to be advantageous over typical rule-based expert systems, particularly for detection of unforeseen faults and sensor failures. Volume 1 gives a project overview and testing highlights. Volume 2 provides detail on the EATCS test bed, test operations, and online test results. Appendix A is a test archive, while Appendix B is a compendium of design and user manuals for the TEXSYS software. Author (revised)

N94-13257*# Mitre Corp., Bedford, MA.

APPLICATION OF NEW ELECTRO-OPTIC TECHNOLOGY TO SPACE STATION FREEDOM DATA MANAGEMENT SYSTEM

C. R. Husbands and M. M. Girard Aug. 1993 75 p

(Contract NASw-4358)

(NASA-CR-177622; A-93117; NAS 1.26:177622) Avail: CASI HC A04/MF A01

A low risk design methodology to permit the local bus structures to support increased data carrying capacities and to speed messages and data flow between nodes or stations on the Space Station Freedom Data Management System in anticipation of growing requirements was evaluated and recommended. The recommended design employs a collateral fiber optic technique that follows a NATO avionic standard that is developed, tested, and available. Application of this process will permit a potential 25 fold increase in data transfer performance on the local wire bus network with a fiber optic network, maintaining the functionality of the low-speed bus and supporting all of the redundant transmission and fault detection capabilities designed into the existing system. The application of wavelength division multiplexing (WDM) technology to both the local data bus and global data bus segments of the Data Management System to support anticipated additional highspeed data transmission requirements was also examined. Techniques were examined to provide a dual wavelength implementation of the fiber optic collateral networks. This dual wavelength implementation would permit each local bus to support two simultaneous high-speed transfers on the same fiber optic bus structure and operate within the limits of the existing protocol standard. A second WDM study examined the use of spectral sliced technology to provide a fourfold increase in the Fiber Distributed Data Interface (FDDI) global bus networks without requiring modifications to the existing installed cable plant. Computer simulations presented indicated that this data rate improvement can be achieved with commercially available optical components. Author (revised)

N94-13918*# National Aeronautics and Space Administration. Lewis Research Center, Cleveland, OH.

SCAILET: AN INTELLIGENT ASSISTANT FOR SATELLITE GROUND TERMINAL OPERATIONS

A. K. Shahidi, J. A. Crapo, R. F. Schlegelmilch, R. C. Reinhart (Analex Corp., Brook Park, OH.), E. J. Petrik, J. L. Walters, and R. E. Jones May 1993 10 p Presented at the World Space Congress, Washington, DC, 28 Aug. - 5 Sep. 1993; sponsored by NASA, AIAA, and NAS Previously announced in IAA as A92-55855

(RTOP 506-72-1D)

(NASA-TM-105879; E-7302; NAS 1.15:105879) Avail: CASI HC A02/MF A01

NASA Lewis Research Center has applied artificial intelligence to an advanced ground terminal. This software application is being deployed as an experimenter interface to the link evaluation terminal (LET) and was named Space Communication Artificial Intelligence for the Link Evaluation Terminal (SCAILET). The high-burst-rate (HBR) LET provides 30-GHz-transmitting and 20-GHz-receiving, 220-Mbps capability for wide band communications technology experiments with the Advanced Communication Technology Satellite (ACTS). The HBR-LET terminal consists of seven major subsystems. A minicomputer controls and monitors these subsystems through an IEEE-488 or RS-232 protocol interface. Programming scripts (test procedures defined by design engineers) configure the HBR-LET and permit data acquisition. However, the scripts are difficult to use, require a steep learning curve, are cryptic, and are hard to maintain. This discourages experimenters from utilizing the full capabilities of the HBR-LET system. An intelligent assistant module was developed as part of the SCAILET software. The intelligent assistant addresses critical experimenter needs by solving and resolving problems that are encountered during the configuring of the HBR-LET system. The intelligent assistant is a graphical user interface with an expert system running in the background. In order to further assist and familiarize an experimenter, an on-line hypertext documentation module was developed and included in the SCAILET software. Author (revised)

N94-13989*# National Aeronautics and Space Administration. Ames Research Center, Moffett Field, CA.

THERMAL EXPERT SYSTEM (TEXSYS): SYSTEMS AUTONOMY DEMONSTRATION PROJECT, VOLUME 2. RESULTS Final Report

B. J. Glass, ed. Oct. 1992 123 p Contains microfiche as a supplement

(RTOP 549-03-11)

(NASA-TM-102877; A-90319-Vol-2; NAS 1.15:102877) Avail: CASI HC A06/MF A02

The Systems Autonomy Demonstration Project (SADP) produced a knowledge-based real-time control system for control and fault detection, isolation, and recovery (FDIR) of a prototype two-phase Space Station Freedom external active thermal control system (EATCS). The Thermal Expert System (TEXSYS) was demonstrated in recent tests to be capable of reliable fault anticipation and detection, as well as ordinary control of the thermal bus. Performance requirements were addressed by adopting a hierarchical symbolic control approach-layering model-based expert system software on a conventional, numerical data acquisition and control system. The model-based reasoning capabilities of TEXSYS were shown to be

advantageous over typical rule-based expert systems, particularly for detection of unforeseen faults and sensor failures. Volume 1 gives a project overview and testing highlights. Volume 2 provides detail on the EATCS testbed, test operations, and online test results. Appendix A is a test archive, while Appendix B is a compendium of design and user manuals for the TEXSYS software. Author

18 SPACECRAFT DESIGN, TESTING AND PERFORMANCE

Includes satellites; space platforms; space stations; spacecraft systems and components such as thermal and environmental controls; and attitude controls.

For life support systems see *54 Man/System Technology and Life Support.* For related information see also *05 Aircraft Design, Testing and Performance, 39 Structural Mechanics,* and *16 Space Transportation.*

N94-12790*# California Univ., Los Angeles. Flight Systems Research Lab.

NONLINEAR DAMPING MODEL FOR FLEXIBLE STRUCTURES Ph.D. Thesis

Weijian Zang Dec. 1990 178 p Sponsored by NASA. Dryden Flight Center

(Grant NsG-4015)

(NASA-CR-193711; NAS 1.26:193711; TR-1-FSRL-1990) Avail: CASI HC A09/MF A02

The study of nonlinear damping problem of flexible structures is addressed. Both passive and active damping, both finite dimensional and infinite dimensional models are studied. In the first part, the spectral density and the correlation function of a single DOF nonlinear damping model is investigated. A formula for the spectral density is established with O(Gamma(sub 2)) accuracy based upon Fokker-Planck technique and perturbation. The spectral density depends upon certain first order statistics which could be obtained if the stationary density is known. A method is proposed to find the approximate stationary density explicitly. In the second part, the spectral density of a multi-DOF nonlinear damping model is investigated. In the third part, energy type nonlinear damping model in an infinite dimensional setting is studied. Author (revised)

N94-12827*# Martin Marietta Corp., Denver, CO. Flight Systems.

CFM TECHNOLOGIES FOR SPACE TRANSPORTATION: MULTIPURPOSE HYDROGEN TESTBED SYSTEM DEFINITION AND TANK PROCUREMENT Final Report

E. C. Fox, E. R. Kiefel, G. L. McIntosh, J. B. Sharpe, D. R. Sheahan, and M. E. Wakefield Jul. 1993 93 p

(Contract NAS8-39201)

(NASA-CR-194355; NAS 1.26:194355) Avail: CASI HC A05/MF A01

The development of a test bed tank and system for evaluating cryogenic fluid management technologies in a simulated upper stage liquid hydrogen tank is covered. The tank is 10 ft long and is 10 ft in diameter, and is an ASME certified tank constructed of 5083 aluminum. The tank is insulated with a combination of sprayed on foam insulation, covered by 45 layers of double aluminized mylar separated by dacron net. The mylar is applied by a continuous wrap system adapted from commercial applications, and incorporates variable spacing between the mylar to provide more space between those layers having a high delta temperature, which minimizes heat leak. It also incorporates a unique venting system which uses fewer large holes in the mylar rather than the multitude of small holes used conventionally. This significantly reduces radiation heat transfer. The test bed consists of an existing vacuum chamber at MSFC, the test bed tank and its thermal control system, and a thermal shroud (which may be heated) surrounding the tank. Provisions are made in the tank and chamber for inclusion of a variety of cryogenic fluid management experiments. Author (revised)

N94-12909# Sandia National Labs., Albuquerque, NM.

EXPERIMENTAL TECHNIQUE TO SIMULATE ORBITAL-DEBRIS IMPACT ON SPACE SHIELDS AT IMPACT VELOCITIES OVER 10 km/s

L. C. Chhabildas and M. B. Boslough 1992 5 p Presented at the First European Conference on Space Debris, Darmstadt, Germany, 5-8 Apr. 1993

(Contract DE-AC04-76DP-00789)

(DE93-011619; SAND-92-2460C; CONF-9304135-1) Avail: CASI HC A01/MF A01

With the development of a new HyperVelocity Launcher, HVL, at Sandia, it is now possible to perform experiments over the velocity range of 7 to 12 km/s. This velocity range has not been previously accessible for gram-size plates. This meets the requisite mass-velocity criteria established for the orbital debris environment. In this paper, the technique employed to launch thin flier plates to velocities not previously accessible on a two-stage light-gas gun is reported. In particular, this technique has been used on a two-stage light-gas gun to launch nominally 0.5 to 1.0-mm thick aluminum, titanium, and magnesium flier plates intact to velocities up to 12.2 km/s. Since the mass-velocity capability of the newly developed HVL meets the average specifications of the space debris environment, it is expected to be a useful tool to evaluate the effects of debris impact on space structures and debris shields. Examples of a plate impact i.e., orbital debris impact on a thin Whipple shield are presented in this paper. DOE

N94-12943# National Aerospace Lab., Tokyo (Japan). Space Technology Research Group.

AN EXPERIMENTAL STUDY OF TETHER REEL SYSTEM: A LABORATORY MODEL

Shoichi Yoshimura and Osamu Okamoto Aug. 1992 18 p In ENGLISH and JAPANESE

(NAL-TR-1176T; JTN-93-80495) Avail: CASI HC A03/MF A01

A laboratory prototype model of a reel system has been made as the first step of an in-house hardware study of the tether system in space. The model consists of two main parts: a Reel Drum Driving (RDD) unit (25 kg weight) and a Power Supply/Signal Processing (PSSP) unit (32 kg). The tether (0.8 mm in diameter and 300 m long) consists of a Kevlar fiber core and a nylon fiber jacket. Following the preliminary functional test, a computer-controlled functional test has been carried out using a 32-bit personal computer as a control processor. The tests have shown that the stable operations of reel-out and reel-in are possible by tension control in both cases of a small tension (light end weight) and a high frequency input to the reel drum driving motor. Author (NASDA)

N94-12976*# George Washington Univ., Hampton, VA. Joint Inst. for Advancement of Flight Sciences.

SYSTEM IDENTIFICATION FOR SPACE STATION FREEDOM USING OBSERVER/KALMAN FILTER MARKOV PARAMETERS M.S. Thesis

Michael Papadopoulos and Robert H. Tolson Aug. 1993 122 p

(Grant NAG1-1416; RTOP 590-14-31-01)

(NASA-CR-191521; NAS 1.26:191521) Avail: CASI HC A06/MF A02

The Modal Identification Experiment (MIE) is a proposed experiment to define the dynamic characteristics of Space Station Freedom. Previous studies emphasized free-decay modal identification. The feasibility of using a forced response method (Observer/Kalman Filter Identification (OKID)) is addressed. The interest in using OKID is to determine the input mode shape matrix which can be used for controller design or control-structure interaction analysis, and investigate if forced response methods may aid in separating closely spaced modes. A model of the SC-7 configuration of Space Station Freedom was excited using simulated control system thrusters to obtain acceleration output. It is shown that an 'optimum' number of outputs exists for OKID. To recover global mode shapes, a modified method called Global-Local OKID was developed. This study shows that using data from a long forced response followed by free-decay leads to the 'best' modal identification. Twelve out of the thirteen target modes were identified for such an output. Author (revised)

N94-13006# Sandia National Labs., Albuquerque, NM.

COMPARISON OF ANALYTIC WHIPPLE BUMPER SHIELD BALLISTIC LIMITS WITH CTH SIMULATIONS

E. S. Hertel, Jr. May 1993 64 p

(Contract DE-AC04-76DP-00789)

(DE93-015126; SAND-92-0347) Avail: CASI HC A04/MF A01

A series of CTH simulations were conducted to assess the feasibility of using the hydrodynamic code for debris cloud formation and to predict any damage due to the subsequent loading on rear structures. Six axisymmetric simulations and one 3-dimensional simulation were conducted

for spherical projectiles impacting Whipple bumper shields. The projectile diameters were chosen to correlate with two well known analytic expressions for the ballistic limit of a Whipple bumper shield. It has been demonstrated that CTH can be used to simulate the debris cloud formation, the propagation of the debris across a void region, and the secondary impact of the debris against a structure. In addition, the results from the CTH simulations were compared to the analytic estimates of the ballistic limit. At impact velocities of 10 km/s or less, the CTH predicted ballistic limit lays between the two analytic estimates. However, for impact velocities greater than 10 km/s, CTH simulations predicted a ballistic limit larger than both analytical estimates. The differences at high velocities are not well understood. Structural failure at late times due to the time integrated loading of a very diffuse debris cloud has not been considered in the CTH model. In addition, the analytic predictions are extrapolated from relatively low velocity data and the extrapolation technique may not be valid. The discrepancy between the two techniques should be investigated further. DOE

N94-13016*# McDonnell-Douglas Corp., Huntington Beach, CA.
FEASIBILITY STUDY OF AN ORBITING LABORATORY FOR TESTING CSI TECHNOLOGY Final Report
Andrew S. Bicos and Gregory G. Loboda Aug. 1993 108 p
(Contract NAS1-18763; RTOP 585-03-11-08)
(NASA-CR-191524; NAS 1.26:191524; MDC-93H0100) Avail: CASI HC A06/MF A02

A concept for an orbiting laboratory for testing Controls-Structures Integration (CSI) technology is described. The CSI-Star concept reflects a lower cost, higher risk approach. The concept supports demonstration and validation testing for critical CSI technologies at a cost of $20M to $26M with a 1-year reliability of approximately 0.9. The Ball Aerospace QuickStar bus is the carrier for the CSI test article. QuickStar is launched as a secondary payload on the McDonnell Douglas Delta 2. The QuickStar/Delta 2 approach is flight proven. The CSI test article is a 20 foot, 1 Hz, truss beam which is deployed from the QuickStar bus. The test article is well instrumented for quality system identification. The laboratory provides three layers of active control consisting of global vibration suppression along the truss beam, vibration isolation between the beam and instrument platforms, and vibration compensation through the use of gimbaled platforms which point lasers relative to optical sensor targets. The configuration simulates the dynamics of multi-instrument science platforms such as those of the Earth Observation System (EOS) while maintaining strong ties to astrophysics missions such as the Optical Interferometer. Uplink/downlink services and a reprogrammable computer provide flexibility for long-term investigations by members of the CSI community (NASA, DoD, academia, and industry). CSI-Star fills the gap between short-term experiments, which have been conducted primarily on the Shuttle, and future science missions which require the technology. The on-orbit maturity of CSI technology must be established to obtain acceptance by project managers and to promote injection of the technology into future science missions. Author (revised)

N94-13109*# Michigan Univ., Ann Arbor. Dept. of Atmospheric, Oceanic, and Space Science.
PHOBOS/HARP POST LAUNCH SUPPORT Final Technical Report, May 1993
Andrew Nagy 25 Jun. 1993 3 p
(Grant NAGw-631)
(NASA-CR-193676; NAS 1.26:193676) Avail: CASI HC A01/MF A01

The activity under this grant concentrated on: (1) post-launch calibration of the HARP instrument; and (2) analysis and interpretation of the data from the HARP and other related instruments. The HARP was taken by scientists and engineers from the Hungarian Central Research Institute for Physics (CRIP) to NASA/MSFC for calibration in their plasma chamber, with partial support of this grant. This electron and ion calibration of the HARP, helped in transforming measured currents to actual flux values. The analysis and interpretation of the data, carried out jointly by our Russian and Hungarian colleagues and us, led to a number of journal publications and presentations at scientific meetings. Author (revised)

N94-13112*# Colorado Univ., Boulder. Dept. of Aerospace Sciences Engineering.
DYNAMICS OF ADAPTIVE STRUCTURES: DESIGN THROUGH SIMULATIONS
K. C. Park and S. Alexander 1993 5 p
(Grant NAG9-574)
(NASA-CR-193724; NAS 1.26:193724) Avail: CASI HC A01/MF A01

The use of a helical bi-morph actuator/sensor concept by mimicking the change of helical waveform in bacterial flagella is perhaps the first application of bacterial motions (living species) to longitudinal deployment of space structures. However, no dynamical considerations were analyzed to explain the waveform change mechanisms. The objective is to review various deployment concepts from the dynamics point of view and introduce the dynamical considerations from the outset as part of design considerations. Specifically, the impact of the incorporation of the combined static mechanisms and dynamic design considerations on the deployment performance during the reconfiguration stage is studied in terms of improved controllability, maneuvering duration, and joint singularity index. It is shown that intermediate configurations during articulations play an important role for improved joint mechanisms design and overall structural deployability. Derived from text

N94-13140*# Ithaco, Inc., Ithaca, NY.
LOW COST ATTITUDE CONTROL SYSTEM REACTION WHEEL DEVELOPMENT Final Report
William Bialke 8 Mar. 1991 100 p
(Contract NAS5-30307; SBIR-09.20-7640)
(NASA-CR-191332; NAS 1.26:191332; Rept-94044) Avail: CASI HC A06/MF A02

In order to satisfy a growing demand for low cost attitude control systems for small spacecraft, development of a low power and low cost Reaction Wheel Assembly was initiated. The details of the versatile design resulting from this effort are addressed. Tradeoff analyses for each of the major components are included, as well as test data from an engineering prototype of the hardware. Author (revised)

N94-13339# National Aerospace Lab., Tokyo (Japan). Space Technology Research Group.
TRANSMISSION ZEROS OF SPACECRAFT ATTITUDE CONTROL SYSTEM [JINKOU EISEI SHISEI SEIGYOKEI NO DENTATSU ZERO]
Takashi Kida and Isao Yamaguchi Jun. 1992 17 p In JAPANESE
(NAL-TR-1166; JTN-93-80486) Avail: CASI HC A03/MF A01

The importance of evaluating the control performance and the robust stability in the frequency-domain is being widely recognized. A pair of poles and zeros is a candidate characterizing the model of the control system when it is described in the transfer matrix form. This paper studies poles and zeros of a multi-input/multi-output spacecraft attitude control system. Some algebraic algorithms for obtaining them are derived, and their dynamical properties are clarified. The transmission zero, among many definitions of the multi-variable zeros, is considered. Author (NASDA)

N94-13398# Sandia National Labs., Albuquerque, NM.
SIMULATION OF ORBITAL DEBRIS IMPACTS ON BUMPER SHIELDS
E. S. Hertel, Jr. 1992 6 p Presented at the 1st European Conference on Space Debris, Darmstadt, Germany, 5-8 Apr. 1993
(Contract DE-AC04-76DP-00789)
(DE93-013773; SAND-92-2090C; CONF-9304135-2) Avail: CASI HC A02/MF A01

A series of numerical simulations were performed using CTH to predict secondary debris formation and rear structure damage for typical bumper shields under a variety of impact geometries The simulations span a range of velocities from approximately 3 to 12 km/s and are compared to the experiment data for the lower velocities (3 to 7 km/s). For one velocity (approximately 7 km/s), CTH was used to demonstrate the effects of bumper thickness on secondary debris formation and rear structure damage. CTH was also used to stimulate a 12 km/s impact of a sphere on a simple Whipple bumper shield, and this result will be compared to analytic damage predictions at that velocity. It has been found that CTH accurately predicts secondary debris propagation and rear damage for velocities throughout the experimentally accessible range. The CTH damage predictions at 12 km/s result in a higher ballistic limit than would be predicted from the analytic techniques. DOE

N94-13628* National Aeronautics and Space Administration. Langley Research Center, Hampton, VA.
SCOUT: THE UNSUNG HERO OF SPACE (Videotape)

Mar. 1991 Videotape: 30 min. playing time, in color and black and white, with sound
(NASA-TM-109289; NONP-VT-93-185304) Avail: CASI VHS A01/BETA A22

A history of the Scout program, managed by LaRC for 30 years, is presented. Author (revised)

N94-13634* National Aeronautics and Space Administration. Lyndon B. Johnson Space Center, Houston, TX.
STS-32 POST-FLIGHT PRESS CONFERENCE (Videotape)
Feb. 1990 Videotape: 19 min. 20 sec. playing time, in color, with sound
(NASA-TM-109294; NONP-VT-93-185309) Avail: CASI VHS A01/BETA A22

Video footage of the post-flight press conference of STS-32 is presented. The footage is narrated by the crew, and it covers the following topics: launch, deployment of Syncom IV-5, retrieval of the Long Duration Exposure Facility, in-orbit activities, and the landing. Author (revised)

N94-13637* National Aeronautics and Space Administration. Lyndon B. Johnson Space Center, Houston, TX.
HIGH VELOCITY GAS GUN (Videotape)
Oct. 1988 Videotape: 3 min. 30 sec. playing time, in color, with sound
(NASA-TM-109296; NONP-VT-93-185311) Avail: CASI VHS A01/BETA A22

A video tape related to orbital debris research is presented. The video tape covers the process of loading a High Velocity Gas Gun and firing it into a mounted metal plate. The process is then repeated in slow motion. Author (revised)

N94-13658# National Space Development Agency, Ibaraki (Japan). Thermal and Structural Engineering Lab.
THE STUDY ON LARGE SPACE STRUCTURE ASSEMBLY TECHNOLOGY: THE STUDY ON DEPLOYABLE TRUSS STRUCTURE, PART 1 Technical Progress Report [OOGATA KOUZOUBUTSU KUMITATE GIJUTSU NO KENKYUU: TENKAI KUMIATE KOUZOU NO KENKYUU]
31 Mar. 1993 88 p In JAPANESE
(NASDA-TMR-930002; TK-ST0213; JTN-93-80477) Avail: CASI HC A05/MF A01

An overview of the results of the study on large structure assembly technology is presented. The following aspects of the study are outlined: (1) placement and scope of the study; (2) study on large structure assembly technology, establishment of the dimensional requirements for the deployable structure, and extraction of critical elements in deployable structure system technology; (3) design study on critical elements, including study on the deployable structure systems, design study on one dimensional deployable truss structure and element technologies, and study on deployment simulation software and deployment test equipment; (4) planning of the trial production and test program; and (5) WBS (Work Breakdown Structure) for the deployable assembly structure study. Author (NASDA)

N94-13659# National Space Development Agency, Ibaraki (Japan). Thermal and Structural Engineering Lab.
THE STUDY ON LARGE SPACE STRUCTURE ASSEMBLY TECHNOLOGY: THE STUDY ON DEPLOYABLE TRUSS STRUCTURE, PART 2 AND 3 Technical Progress Report, FY 1990-1991 [OOGATA KOUZOUBUTSU KUMITATE GIJUTSU NO KENKYUU: TENKAI KUMITATE KOUZOU NO KENKYUU]
31 Mar. 1993 59 p In JAPANESE
(NASDA-TMR-930003-Pt-2-3; TK-ST0432; JTN-93-80478) Avail: CASI HC A04/MF A01

An overview of the results of the study on large structure assembly technology is presented. The following aspects of the study are outlined: (1) overall scheme of technology development for assembling and constructing large structure operated on orbit; (2) a brief description of the development from FY (Fiscal Year) 1998 through FY 1991; (3) design study on system and element technologies; (4) simulation analysis, including studies on the analytic software and mathematical model, and problems in analyzing technology; (5) ground test; (6) survey on the next generation structural materials; and (7) concept of on-orbit validation experiment. Author (NASDA)

N94-13660# National Space Development Agency, Ibaraki (Japan). Thermal and Structural Engineering Lab.
THE STUDY ON TEST OF DOCKING MECHANISM SYSTEM, PART 1 AND 2 Technical Progress Report, FY 1990-1991 [DOKKINGU KIKOU SHISUTEMU SHIKEN NO KENKYUU]
31 Mar. 1993 61 p In JAPANESE
(NASDA-TMR-930004-Pt-1-2; TK-ST0433; JTN-93-80479) Avail: CASI HC A04/MF A01

An overview of the study of docking mechanism system test is presented. The following aspects of the research and development are outlined: (1) overall scheme of the research and development; (2) research and development in each FY (Fiscal Year); (3) research and development in FY 1990, including total assembly of the docking mechanism system test model, test equipment, mechanism system test, and the results of the research and development; (4) research and development in FY 1991, including comparative evaluation of the system test and simulation analysis, and the conceptual design of the docking mechanism for the ETS-7 (Engineering Test Satellite-7); and (5) docking mechanism for ETS-7 composed of latching, umbilical connection, and separation mechanisms, and driving circuit section. Author (NASDA)

N94-13917*# National Aeronautics and Space Administration. Lewis Research Center, Cleveland, OH.
INTERACTIONS BETWEEN SPACECRAFT AND THEIR ENVIRONMENTS
Dale C. Ferguson Jan. 1993 12 p Presented at the 31st Aerospace Sciences Meeting, Reno, NV, 11-14 Jan. 1993; sponsored by AIAA Previously announced in IAA as A93-24801
(RTOP 506-41-52)
(NASA-TM-106115; E-7769; NAS 1.15:106115; AIAA Paper 93-0705)
Avail: CASI HC A03/MF A01

Spacecraft inevitably interact with their environments. Besides the interactions one immediately thinks of in space (zero-g, solar heating, atmospheric drag, expansion into vacuum conditions, etc.) other interactions are also important. Those of interest to spacecraft designers so far may be grouped under several headings; plasma interactions and spacecraft charging, impact of debris and micrometeoroids, chemical reactions with neutral species, radiation degradation, etc. Researchers have made great progress in defining and evaluating the interactions of spacecraft with their expected ambient environments near Earth and in interplanetary space. Some of these interactions are discussed with an eye toward expanding our knowledge into new environments, such as may be found at the moon and Mars, that will interact in new and different ways with exploring spacecraft and spacefarers. Author (revised)

N94-13955*# Texas A&M Univ., College Station. Research Foundation.
TECHNIQUES FOR ESTIMATING SPACE STATION AERODYNAMIC CHARACTERISTICS Final Technical Report, 1 Jul. 1989 - 31 Aug. 1992
Richard E. Thomas 1993 85 p
(Grant NAG9-386)
(NASA-CR-193394; NAS 1.26:193394) Avail: CASI HC A05/MF A01

A method was devised and calculations were performed to determine the effects of reflected molecules on the aerodynamic force and moment coefficients for a body in free molecule flow. A procedure was developed for determining the velocity and temperature distributions of molecules reflected from a surface of arbitrary momentum and energy accommodation. A system of equations, based on momentum and energy balances for the surface, incident, and reflected molecules, was solved by a numerical optimization technique. The minimization of a 'cost' function, developed from the set of equations, resulted in the determination of the defining properties of the flow reflected from the arbitrary surface. The properties used to define both the incident and reflected flows were: average temperature of the molecules in the flow, angle of the flow with respect to a vector normal to the surface, and the molecular speed ratio. The properties of the reflected flow were used to calculate the contribution of multiply reflected molecules to the force and moments on a test body in the flow. The test configuration consisted of two flat plates joined along one edge at a right angle to each other. When force and moment coefficients of this 90 deg concave wedge were compared to results that did not include multiple reflections, it was found that multiple reflections could nearly double lift and drag coefficients, with nearly a 50 percent increase in pitching moment for cases with specular or nearly specular accommodation. The cases of diffuse or nearly diffuse accommodation often had minor reductions

in axial and normal forces when multiple reflections were included. There were several cases of intermediate accommodation where the addition of multiple reflection effects more than tripled the lift coefficient over the convex technique. Author (revised)

N94-13988# Technische Univ., Delft (Netherlands). Faculty of Aerospace Engineering.

ALFIS: ASTRONOMICAL LOW FREQUENCY INTERFEROMETRY SATELLITES. A FEASIBILITY STUDY

M. P. Nieuwenhuizen, Richard Beenen, ed., and Wim Simons, ed. Sep. 1992 214 p

(LR-699; ETN-93-94011) Copyright Avail: CASI HC A10/MF A03

Several aspects of the project concerning the Astronomical Low Frequency Interferometric Satellites (ALFIS) is discussed. These satellites are directed towards imaging the entire sky at frequencies below 15 mHz, which are inaccessible from the ground due to ionospheric absorption and scattering. This frequency range covers the lowest energy region of the electromagnetic spectrum that is essentially unexplored by astronomy. The ALFIS instrumental concept is a single launch bus which places two free flying spacecraft into almost identical geostationary transfer orbits with a small inclination between them to provide for baseline components at right angles to the orbital plane. ALFIS is less ambitious and cheaper than previous proposals submitted to NASA. ESA

N94-14076*# Jet Propulsion Lab., California Inst. of Tech., Pasadena.

AN IMPROVED APPROACH FOR FLIGHT READINESS CERTIFICATION: METHODOLOGY FOR FAILURE RISK ASSESSMENT AND APPLICATION EXAMPLES, VOLUME 1

N. R. Moore, D. H. Ebbeler, L. E. Newlin, S. Sutharshana, and M. Creager 1 Jun. 1992 248 p

(Contract NAS7-918)

(NASA-CR-194498; JPL-Publ-92-15-Vol-1; NAS 1.26:194498) Avail: CASI HC A11/MF A03

An improved methodology for quantitatively evaluating failure risk of spaceflight systems to assess flight readiness and identify risk control measures is presented. This methodology, called Probabilistic Failure Assessment (PFA), combines operating experience from tests and flights with engineering analysis to estimate failure risk. The PFA methodology is of particular value when information on which to base an assessment of failure risk, including test experience and knowledge of parameters used in engineering analyses of failure phenomena, is expensive or difficult to acquire. The PFA methodology is a prescribed statistical structure in which engineering analysis models that characterize failure phenomena are used conjointly with uncertainties about analysis parameters and/or modeling accuracy to estimate failure probability distributions for specific failure modes. These distributions can then be modified, by means of statistical procedures of the PFA methodology, to reflect any test or flight experience. Conventional engineering analysis models currently employed for design of failure prediction are used in this methodology. The PFA methodology is described and examples of its application are presented. Conventional approaches to failure risk evaluation for spaceflight systems are discussed, and the rationale for the approach taken in the PFA methodology is presented. The statistical methods, engineering models, and computer software used in fatigue failure mode applications are thoroughly documented. Author (revised)

N94-14077*# Jet Propulsion Lab., California Inst. of Tech., Pasadena.

AN IMPROVED APPROACH FOR FLIGHT READINESS CERTIFICATION: METHODOLOGY FOR FAILURE RISK ASSESSMENT AND APPLICATION EXAMPLES. VOLUME 2: SOFTWARE DOCUMENTATION

N. R. Moore, D. H. Ebbeler, L. E. Newlin, S. Sutharshana, and M. Creager 1 Jun. 1992 361 p

(NASA-CR-194499; JPL-Publ-92-15-Vol-2; NAS 1.26:194499) Avail: CASI HC A16/MF A03

An improved methodology for quantitatively evaluating failure risk of spaceflight systems to assess flight readiness and identify risk control measures is presented. This methodology, called Probabilistic Failure Assessment (PFA), combines operating experience from tests and flights with engineering analysis to estimate failure risk. The PFA methodology is of particular value when information on which to base an assessment of failure risk, including test experience and knowledge of parameters used in engineering analyses of failure phenomena, is expensive or difficult to acquire. The PFA methodology is a prescribed statistical structure in which engineering analysis models that characterize failure phenomena are used conjointly with uncertainties about analysis parameters and/or modeling accuracy to estimate failure probability distributions for specific failure modes, These distributions can then be modified, by means of statistical procedures of the PFA methodology, to reflect any test or flight experience. Conventional engineering analysis models currently employed for design of failure prediction are used in this methodology. The PFA methodology is described and examples of its application are presented. Conventional approaches to failure risk evaluation for spaceflight systems are discussed, and the rationale for the approach taken in the PFA methodology is presented. The statistical methods, engineering models, and computer software used in fatigue failure mode applications are thoroughly documented. Author (revised)

N94-14078*# Jet Propulsion Lab., California Inst. of Tech., Pasadena.

AN IMPROVED APPROACH FOR FLIGHT READINESS CERTIFICATION: METHODOLOGY FOR FAILURE RISK ASSESSMENT AND APPLICATION EXAMPLES. VOLUME 3: STRUCTURE AND LISTING OF PROGRAMS

N. R. Moore, D. H. Ebbeler, L. E. Newlin, S. Sutharshana, and M. Creager 1 Jun. 1992 522 p

(NASA-CR-194500; JPL-Publ-92-15-Vol-3; NAS 1.26:194500) Avail: CASI HC A22/MF A04

An improved methodology for quantitatively evaluating failure risk of spaceflight systems to assess flight readiness and identify risk control measures is presented. This methodology, called Probabilistic Failure Assessment (PFA), combines operating experience from tests and flights with engineering analysis to estimate failure risk. The PFA methodology is of particular value when information on which to base an assessment of failure risk, including test experience and knowledge of parameters used in engineering analyses of failure phenomena, is expensive or difficult to acquire. The PFA methodology is a prescribed statistical structure in which engineering analysis models that characterize failure phenomena are used conjointly with uncertainties about analysis parameters and/or modeling accuracy to estimate failure probability distributions for specific failure modes. These distributions can then be modified, by means of statistical procedures of the PFA methodology, to reflect any test or flight experience. Conventional engineering analysis models currently employed for design of failure prediction are used in this methodology. The PFA methodology is described and examples of its application are presented. Conventional approaches to failure risk evaluation for spaceflight systems are discussed, and the rationale for the approach taken in the PFA methodology is presented. The statistical methods, engineering models, and computer software used in fatigue failure mode applications are thoroughly documented. Author (revised)

N94-14107# Norwegian Defence Research Establishment, Kjeller.

LABORATORY SIMULATION OF SPACECRAFT CHARGING IN THE PLASMA WAKE REGION

Jan Troeim and Roe Eirik 25 Jan. 1993 41 p Original contains color illustrations

(Contract ESTEC-7989/88/NL/PB(SC))

(FFI-93-7007; ETN-93-94454) Avail: CASI HC A03/MF A01

An investigation as to how insulated areas on the wake side of a larger spacecraft model embedded in a streaming plasma are charged when being exposed to beams of fast electrons is presented. It is relevant to differential charging on satellites in orbits crossing polar latitudes where they may be subjected to high energy electron precipitation. The measurements are performed in a medium size vacuum system (1 m diameter by 2 m) with thermal plasma generator and an electron accelerator. The velocity of the plasma stream can be varied to simulate the relative speed of a spacecraft moving through the ionosphere. The electron accelerator can operate at energies corresponding to typical auroral electron energies. Results of charging of different materials (Kapton in particular) as a function of plasma density and electron energy are presented. It is demonstrated how a charged area on the wake side of the spacecraft model modifies the plasma density structure downstream on the wake side of the model. ESA

N94-14112*# Committee on Earth Observations Satellites, London (England).

MINUTES OF THE SIXTH CEOS PLENARY MEETING

25 Mar. 1993 35 p Metting held in London, England, 9-11 Dec. 1992

(NASA-TM-108252; NAS 1.15:108252) Avail: CASI HC A03/MF A01

The Committee on Earth Observations Satellites (CEOS) minutes for the sixth plenary meeting held in London, December 9-11, 1992 are presented. Attending as prospective members were the Russian Space Agency (RSA), the Committee for Hydrometeorology and Environmental Monitoring of the Ministry for Ecology and Natural resources of the Russian Federation (ROSCOMGIDROMET), the Chinese Academy of Space Technology (CAST) and the National Remote Sensing Center of China (NRSCC). Actions taken at the meeting included membership issues, CEOS proposals, data policy, and working group reports. Data requirements of CEOS affiliates were also reported on. Additional summations and statements as well as lists of participants and future meetings are included. In general, topics covered related to remote sensing and global change. CASI

N94-14120*# Alabama Univ., Huntsville. Engineering Mechanics.
BALLIST: A COMPUTER PROGRAM TO EMPIRICALLY PREDICT THE BUMPER THICKNESS REQUIRED TO PREVENT PERFORATION OF THE SPACE STATION BY ORBITAL DEBRIS Final Report
William Keith Rule Dec. 1991 25 p
(Contract NAS8-38555)
(NASA-CR-193825; NAS 1.26:193825; BER-550-248) Avail: CASI HC A03/MF A01

A computer program called BALLIST that is intended to be a design tool for engineers is described. BALLIST empirically predicts the bumper thickness required to prevent perforation of the Space Station pressure wall by a projectile (such as orbital debris) as a function of the projectile's velocity. 'Ballistic' limit curves (bumper thickness vs. projectile velocity) are calculated and are displayed on the screen as well as being stored in an ASCII file. A Whipple style of spacecraft wall configuration is assumed. The predictions are based on a database of impact test results. NASA/Marshall Space Flight Center currently has the capability to generate such test results. Numerical simulation results of impact conditions that can not be tested (high velocities or large particles) can also be used for predictions. Author (revised)

N94-14352# European Space Agency, Paris (France).
ECS: EIGHTH YEAR IN ORBIT
D. W. Baston, P. Button, B. Demelenne, K. R. Derbyshire, P. J. Leggett, H. Meier, W. E. Neumann, E. Tilmans, R. Viddeleer, and W. R. Burke, ed. May 1992 34 p Original contains color illustrations
(ESA-BR-82; ISBN-92-9092-107-2; ETN-93-93947) Copyright Avail: CASI HC A03/MF A01

The experience gained with the European Communication System (ECS) satellites during the eight years of service in orbit is summarized. The performance of individual satellite systems is evaluated. They include reports on: thermal control, communications payload, number of operating hours, telemetry, tracking, command, solar arrays, batteries, attitude control, orbit control, and reaction control. In the reporting period, the ECS system accumulated a total of 292,618 channel hours. The total outage due to spurious switchoffs was 83 channel minutes, of which 69 channel minutes were due to a front-end failure in ECS-5. ESA

N94-14411* National Aeronautics and Space Administration, Washington, DC.
LARGE SPACE STRUCTURES AND SYSTEMS IN THE SPACE STATION ERA: A BIBLIOGRAPHY WITH INDEXES (SUPPLEMENT 05)
Mar. 1993 362 p
(NASA-SP-7085(05); NAS 1.21:7085(05)) Avail: CASI HC A16

Bibliographies and abstracts are listed for 1363 reports, articles, and other documents introduced into the NASA scientific and technical information system between January 1, 1991 and July 31, 1992. Topics covered include technology development and mission design according to system, interactive analysis and design, structural and thermal analysis and design, structural concepts and control systems, electronics, advanced materials, assembly concepts, propulsion and solar power satellite systems. Author

N94-14483*# Eagle Engineering, Inc., Houston, TX.
SECONDARY IMPACT HAZARD ASSESSMENT Final Report, 1 Jun. 1985 - 1 Jun. 1986
1 Jun. 1986 343 p
(NASA Order T-256M)
(NASA-CR-188261; NAS 1.26:188261; Rept-86-128) Avail: CASI HC A15/MF A03

A series of light gas gun shots (4 to 7 km/sec) were performed with 5 mg nylon and aluminum projectiles to determine the size, mass, velocity, and spatial distribution of spall and ejecta from a number of graphite/epoxy targets. Similar determinations were also performed on a few aluminum targets. Target thickness and material were chosen to be representative of proposed Space Station structure. The data from these shots and other information were used to predict the hazard to Space Station elements from secondary particles resulting from impacts of micrometeoroids and orbital debris on the Space Station. This hazard was quantified as an additional flux over and above the primary micrometeoroid and orbital debris flux that must be considered in the design process. In order to simplify the calculations, eject and spall mass were assumed to scale directly with the energy of the projectile. Other scaling systems may be closer to reality. The secondary particles considered are only those particles that may impact other structure immediately after the primary impact. The addition to the orbital debris problem from these primary impacts was not addressed. Data from this study should be fed into the orbital debris model to see if Space Station secondaries make a significant contribution to orbital debris. The hazard to a Space Station element from secondary particles above and beyond the micrometeoroid and orbital debris hazard is categorized in terms of two factors: (1) the 'view factor' of the element to other Space Station structure or the geometry of placement of the element, and (2) the sensitivity to damage, stated in terms of energy. Several example cases were chosen, the Space Station module windows, windows of a Shuttle docked to the Space Station, the habitat module walls, and the photovoltaic solar cell arrays. For the examples chosen the secondary flux contributed no more than 10 percent to the total flux (primary and secondary) above a given calculated critical energy. A key assumption in these calculations is that above a certain critical energy, significant damage will be done. This is not true for all structures. Double-walled, bumpered structures are an example for which damage may be reduced as energy goes up. The critical energy assumption is probably conservative, however, in terms of secondary damage. To understand why the secondary impacts seem to, in general, contribute less than 10 percent of the flux above a given critical energy, consider the case of a meteoroid impact of a given energy on a fixed, large surface. This impact results in a variety of secondary particles, all of which have much less energy than the original impact. Conservation of energy prohibits any other situation. Thus if damage is linked to a critical energy of a particle, the primary flux will always deliver particles of much greater energy. Even if all the secondary particles impacted other Space Station structures, none would have a kinetic energy more than a fraction of the primary impact energy. Author (revised)

N94-14683*# Virginia Polytechnic Inst. and State Univ., Blacksburg. Chemistry Dept.
SURFACE CHARACTERIZATION OF LDEF MATERIALS Final Technical Report, 18 Sep. 1990 - 1 Oct. 1993
J. P. Wightman and Holly Little Grammer Oct. 1993 249 p Original contains color illustrations
(Grant NAG1-1186)
(NASA-CR-194519; NAS 1.26:194519) Avail: CASI HC A11/MF A03; 8 functional color pages

The NASA Long Duration Exposure Facility (LDEF), a passive experimental satellite, was placed into low-Earth orbit by the Shuttle Challenger in Apr. 1984. The LDEF spent an unprecedented 69 months in space. The flight and recovery of the LDEF provided a wealth of information on the longterm space environmental effects of a variety of materials exposed to the low-Earth orbit environment. Surface characterization of LDEF materials included polymers, composites, thermal control paints, and aluminum. X-ray photoelectron spectroscopy (XPS), Auger electron spectroscopy (AES), scanning electron microscopy (SEM), and contact angle analysis were used to document changes in both the surface composition and surface chemistry of these materials. Detailed XPS analysis of the polymer systems, such as Kapton, polyimide polysiloxane copolymers, and fluorinated ethylene propylene thermal blankets on the backside of the LDEF revealed significant changes in both the surface composition and surface chemistry as a result of exposure to the low-Earth orbit environment. Polymer systems such as Kapton, polyimide polysiloxane copolymers, and

polysulfone showed a common trend of decreasing carbon content and increasing oxygen content with respect to the control sample. Carbon 1s curve fit XPS analysis of the composite samples, in conjunction with SEM photomicrographs, revealed significant ablation of the polymer matrix resin to expose the carbon fibers of the composite during exposure to the space environment. Surface characterization of anodized aluminum tray clamps, which were located at regular intervals over the entire LDEF frame, provided the first results to evaluate the extent of contamination with respect to position on the LDEF. The XPS results clearly showed that the amount and state of both silicon and fluorine contamination were directly dependent upon the position of the tray clamp on the LDEF.
Author (revised)

N94-14783*# National Aeronautics and Space Administration. Lewis Research Center, Cleveland, OH.
NASA IMAGES 8 (Videotape)
Feb. 1988 Videotape: 28 min. 7 sec. playing time, in color, with sound (NASA-TM-109416; NONP-VT-93-190213) Avail: CASI VHS A01/BETA A22

How various NASA satellites are used is illustrated. Satellites included are TIROS, ECHO, RELAY, HEAO, ERTS, LANDSAT, and ATS. CASI

N94-13275# Kawasaki Heavy Industries Ltd., Kobe (Japan).
RESEARCH ON INFLATABLE STRUCTURE FOR SPACE USE [UCHUUYOU INFURETABURU KOUZOU NO KENKYUU]
Sumio Katou, Osamu Muragishi, Toyoyuki Oota, Michihiro Natori (Ministry of Education, Kanagawa, Japan.), Kouryou Miura (Ministry of Education, Kanagawa, Japan.), and Masamori Sakamaki (Ministry of Education, Kanagawa, Japan.) *In* NASDA, The Second Workshop on Deployment and Assembly Experiment of Large Space Structure on Orbit 31 Mar. 1993 p 36-42 In JAPANESE (For primary document see N94-13268 02-12)
Avail: CASI HC A02/MF A01

N94-13276# Ministry of Education, Kanagawa (Japan).
HELICAL TRUSS BEAM DEVELOPMENT FOR LARGE SPACE STRUCTURE [OOGATA UCHUU KOUZOUBUTSUYOU HERIKARUTORASU BIMU NO KAIHATSU NI TSUITE]
Michihiro Natori, Takayuki Kitamura (Japan Aircraft Mfg. Co. Ltd., Kanagawa.), Hideo Yanai (Japan Aircraft Mfg. Co. Ltd., Kanagawa.), and Yoshinari Takeuchi (Japan Aircraft Mfg. Co. Ltd., Kanagawa.) *In* NASDA, The Second Workshop on Deployment and Assembly Experiment of Large Space Structure on Orbit 31 Mar. 1993 p 43-46 In JAPANESE (For primary document see N94-13268 02-12)
Avail: CASI HC A01/MF A01

N94-13277# Osaka Prefecture Univ., Sakai (Japan). Dept. of Aeronautical Engineering.
APPLICATION OF INTELLIGENTLY ADAPTABLE STRUCTURE AND ROBOT TO LARGE SPACE STRUCTURE [OOGATA UCHUU KOUZOUBUTSU NI TAISURU CHITEKI TEKIOU KOUZOUBUTSU TO ROBOTTO NO OUYOU]
Kei Senda and Yoshisada Murotsu *In* NASDA, The Second Workshop on Deployment and Assembly Experiment of Large Space Structure on Orbit 31 Mar. 1993 p 47-53 In JAPANESE (For primary document see N94-13268 02-12)
Avail: CASI HC A02/MF A01

N94-13280# Fuji Heavy Industries Ltd., Tokyo (Japan).
MOVEMENT OF DEPLOYABLE TRUSS [TENKAI TORASU NO UNDOU NI TSUITE]
Hiroshi Miura, Yoshiki Morino (National Space Development Agency, Tokyo, Japan.), and Shigeto Shibuta (National Space Development Agency, Tokyo, Japan.) *In* NASDA, The Second Workshop on Deployment and Assembly Experiment of Large Space Structure on Orbit 31 Mar. 1993 p 67-72 In JAPANESE (For primary document see N94-13268 02-12)
Avail: CASI HC A02/MF A01

N94-13281# Nippon Electric Co. Ltd., Tokyo (Japan).
DEVELOPMENT AND APPLICATION OF ONE DIMENSIONAL DEPLOYABLE TRUSS [ICHIJIGEN TENKAIGATA TORASU NO KAIHATSU TO SONO OUYOU]
Hiroshi Irikado, Kouji Sekine, Yuuzou Shibayama, and Yoshiki Morino (National Space Development Agency, Tokyo, Japan.) *In* NASDA, The Second Workshop on Deployment and Assembly Experiment of Large Space Structure on Orbit 31 Mar. 1993 p 73-79 In JAPANESE (For primary document see N94-13268 02-12)
Avail: CASI HC A02/MF A01

N94-13282# Kawasaki Heavy Industries Ltd., Kagamihara (Japan).
STUDY OF A ONE-DIMENSIONAL DEPLOYABLE STRUCTURE EMPLOYING TELESCOPIC MEMBERS [TERESUKOPIKKU BUZAI O RIYOU SHITA ICHIJIGEN TENKAI TORASU KOUZOU NO KENTOU]
Osamu Muragishi, Sumio Katou, Yoshiki Morino (National Space Development Agency, Ibaraki, Japan.), and Shigeto Shibuta (National Space Development Agency, Ibaraki, Japan.) *In* NASDA, The Second Workshop on Deployment and Assembly Experiment of Large Space Structure on Orbit 31 Mar. 1993 p 80-85 In JAPANESE (For primary document see N94-13268 02-12)
Avail: CASI HC A02/MF A01

N94-14640*# Boeing Defense and Space Group, Seattle, WA.
SPACE STATION COMMON BERTHING MECHANISM, A MULTI-BODY SIMULATION APPLICATION
Ian Searle *In* JPL, Proceedings of the Fifth NASA/NSF/DOD Workshop on Aerospace Computational Control 15 Feb. 1993 p 351-364 (For primary document see N94-14618 02-39)
Avail: CASI HC A03/MF A04

N94-14649*# TRW, Inc., Redondo Beach, CA. Space and Technology Group.
CONTROL STRUCTURAL INTERACTION TESTBED: A MODEL FOR MULTIPLE FLEXIBLE BODY VERIFICATION
M. A. Chory, A. L. Cohen, R. A. Manning, M. L. Narigon, and V. A. Spector *In* JPL, Proceedings of the Fifth NASA/NSF/DOD Workshop on Aerospace Computational Control 15 Feb. 1993 p 507-524 (For primary document see N94-14618 02-39)
Avail: CASI HC A03/MF A04

19 SPACECRAFT INSTRUMENTATION

For related information see also *06 Aircraft Instrumentation* and *35 Instrumentation and Photography.*

N94-13029# National Oceanic and Atmospheric Administration, Washington, DC. National Environmental Satellite, Data, and Information Service.
DEGRADATION OF THE VISIBLE AND NEAR-INFRARED CHANNELS OF THE ADVANCED VERY HIGH RESOLUTION RADIOMETER ON THE NOAA-9 SPACECRAFT: ASSESSMENT AND RECOMMENDATIONS FOR CORRECTIONS
C. R. NagarajaRao, ed. Jun. 1993 34 p
(NOAA-TR-NESDIS-70) Avail: CASI HC A03/MF A01

As part of the NOAA/NASA Advanced Very High Resolution Radiometer (AVHRR) Pathfinder Calibration Working Group activities, the in-orbit degradation of the AVHRR visible (channel 1: approximately 0.58-0.68 microns) and near-infrared (channel 2: approximately 0.72-1.05 microns) channels, which do not have any onboard calibration devices, was determined for the instrument on the NOAA-9 spacecraft, using the southeastern Libyan desert (21-23 degrees N latitude; 28-29 degrees E longitude) as a time-invariant calibration target. It was found from a statistical analysis of the relevant International Cloud Climatology Project (ISCCP) B3 data obtained over the calibration target that the gains (counts/(W/m(sup 2) microns sr)) in channels 1 and 2 of this instrument had degraded at the rate of 5.9 percent and 3.5 percent per year, respectively. To facilitate the computation of corrected radiances, the variation in time of the 'slope' - defined as the reciprocal of the 'gain' - in the two channels was determined by anchoring the relative variations of the gain to the 'absolute' calibrations based on congruent path aircraft/satellite measurements made over the White Sands area of New Mexico, U.S.A., during October/November 1986. Procedural details for obtaining the correct radiances from the measured signals in the two AVHRR channels, simple user-friendly formulae, and a look-up table are given. Author (revised)

N94-13067*# Smithsonian Astrophysical Observatory, Cambridge, MA.
PLANETARY SYSTEM DETECTION BY POINTS Semiannual Report Nos. 1-3 and Final Report, 15 Jun. 1988 - 31 Mar. 1990
Robert D. Reasenberg Sep. 1993 18 p
(Grant NAGw-1355)
(NASA-CR-194361; NAS 1.26:194361) Avail: CASI HC A03/MF A01

The final report and semiannual reports 1, 2, and 3 in response to the study of 'Planetary System Detection by POINTS' is presented. The grant covered the period from 15 Jun. 1988 through 31 Dec. 1989. The work during that period comprised the further development and refinement of the POINTS concept. The status of the POINTS development at the end of the Grant period was described by Reasenberg in a paper given at the JPL Workshop on Space Interferometry, 12-13 Mar. 1990, and distributed as CfA Preprint 3138. That paper, 'POINTS: a Small Astrometric Interferometer,' follows as Appendix-A. Our proposal P2276-7-09, dated July 1990, included a more detailed description of the state of the development of POINTS at the end of the tenure of Grant NAGW-1355. That proposal, which resulted in Grant NAGW-2497, is included by reference. Author (revised)

N94-13189*# Jet Propulsion Lab., California Inst. of Tech., Pasadena.
SPECTRAL ANALYSIS FOR AUTOMATED EXPLORATION AND SAMPLE ACQUISITION
Susan Eberlein and Gigi Yates 1 May 1992 19 p
(NASA-CR-194095; JPL-Publ-92-1; NAS 1.26:194095) Avail: CASI HC A03/MF A01

Future space exploration missions will rely heavily on the use of complex instrument data for determining the geologic, chemical, and elemental character of planetary surfaces. One important instrument is the imaging spectrometer, which collects complete images in multiple discrete wavelengths in the visible and infrared regions of the spectrum. Extensive computational effort is required to extract information from such high-dimensional data. A hierarchical classification scheme allows multispectral data to be analyzed for purposes of mineral classification while limiting the overall computational requirements. The hierarchical classifier exploits the tunability of a new type of imaging spectrometer which is based on an acousto-optic tunable filter. This spectrometer collects a complete image in each wavelength passband without spatial scanning. It may be programmed to scan through a range of wavelengths or to collect only specific bands for data analysis. Spectral classification activities employ artificial neural networks, trained to recognize a number of mineral classes. Analysis of the trained networks has proven useful in determining which subsets of spectral bands should be employed at each step of the hierarchical classifier. The network classifiers are capable of recognizing all mineral types which were included in the training set. In addition, the major components of many mineral mixtures can also be recognized. This capability may prove useful for a system designed to evaluate data in a strange environment where details of the mineral composition are not known in advance. Author

N94-13713*# National Aeronautics and Space Administration. Wallops Flight Facility, Wallops Island, VA.
NASA AIRBORNE SATELLITE INSTRUMENTATION CALIBRATOR (NASIC) TECHNICAL REFERENCE
John L. Ward and Gerry McIntire (Computer Sciences Corp., Wallops Island, VA.) Washington Jul. 1993 49 p
(NASA-RP-1315; Rept-93B00107; NAS 1.61:1315) Avail: CASI HC A03/MF A01

The NASA Satellite Instrumentation Calibrator (NASIC) is a visible and near-infrared spectrometer used to calibrate various satellite instruments by underflying those instruments in a NASA ER-2 aircraft. The calibration instrument's hardware and software are documented. The design, operation, and function of an Ebert-Fastie monochronomator, which by means of a moveable diffraction grating, becomes a visible and near-infrared spectrometer used to calibrate satellite-borne instruments by high altitude underflights in the NASA ER-2. Author (revised)

N94-13953*# Viking Instruments Corp., Reston, VA.
DEVELOPMENT OF AN ADVANCED SPACECRAFT TANDEM MASS SPECTROMETER Final Report
Russell C. Drew 31 Mar. 1992 196 p
(Contract NAS8-38422; SBIR-08.10-2214A)
(NASA-CR-194195; NAS 1.26:194195) Avail: CASI HC A09/MF A03

The purpose of this research was to apply current advanced technology in electronics and materials to the development of a miniaturized Tandem Mass Spectrometer that would have the potential for future development into a package suitable for spacecraft use. The mass spectrometer to be used as a basis for the tandem instrument would be a magnetic sector instrument, of Nier-Johnson configuration, as used on the Viking Mars Lander mission. This instrument configuration would then be matched with a suitable second stage MS to provide the benefits of tandem MS operation for rapid identification of unknown organic compounds. This tandem instrument is configured with a newly designed GC system to aid in separation of complex mixtures prior to MS analysis. A number of important results were achieved in the course of this project. Among them were the development of a miniaturized GC subsystem, with a unique desorber-injector, fully temperature feedback controlled oven with powered cooling for rapid reset to ambient conditions, a unique combination inlet system to the MS that provides for both membrane sampling and direct capillary column sample transfer, a compact and ruggedized alignment configuration for the MS, an improved ion source design for increased sensitivity, and a simple, rugged tandem MS configuration that is particularly adaptable to spacecraft use because of its low power and low vacuum pumping requirements. The potential applications of this research include use in manned spacecraft like the space station as a real-time detection and warning device for the presence of potentially harmful trace contaminants of the spacecraft atmosphere, use as an analytical device for evaluating samples collected on the Moon or a planetary surface, or even use in connection with monitoring potentially hazardous conditions that may exist in terrestrial locations such as launch pads, environmental test chambers or other sensitive areas. Commercial development of the technology could lead to a new family of environmental test instruments that would be small and portable, yet would give quick analyses of complex samples. Author

N94-14830*# Jet Propulsion Lab., California Inst. of Tech., Pasadena.
WORKSHOP PROCEEDINGS: OPTICAL SYSTEMS TECHNOLOGY FOR SPACE ASTROPHYSICS IN THE 21ST CENTURY, VOLUME 3
Juan A. Ayon, ed. 15 Aug. 1992 155 p Astrotech 21 Series 3: Integrated Technology Planning Workshop held in Pasadena, CA, 6-8 Mar. 1991 Original contains color illustrations
(NASA-CR-194102; JPL-Publ-91-24-Vol-3; NAS 1.26:194102) Avail: CASI HC A08/MF A02; 1 functional color page

A technology development program, Astrotech 21, is being proposed by NASA to enable the launching of the next generation of space astrophysical observatories during the years 1995-2015. Astrotech 21 is being planned and will ultimately be implemented jointly by the Astrophysics Division of the Office of Space Science and Applications and the Space Directorate of the Office of Aeronautics and Space Technology. A summary of the Astrotech 21 Optical Systems Technology Workshop is presented. The goal of the workshop was to identify areas of development within advanced optical systems that require technology advances in order to meet the science goals of the Astrotech 21 mission set, and to recommend a coherent development program to achieve the required capabilities. For individual titles, see N94-14831 through N94-14838.

N94-14831*# Jet Propulsion Lab., California Inst. of Tech., Pasadena.
EXECUTIVE SUMMARY
Juan A. Ayon *In its* Workshop Proceedings: Optical Systems Technology for Space Astrophysics in the 21st Century, Volume 3 15 Aug. 1992 p 1-7 (For primary document see N94-14830 02-19)
Avail: CASI HC A02/MF A02; 1 functional color page

The Astrotech 21 Optical Systems Technology Workshop was held in Pasadena, California on March 6-8, 1991. The purpose of the workshop was to examine the state of Optical Systems Technology at the National Aeronautics Space Administration (NASA), and in industry and academia, in view of the potential Astrophysics mission set currently being considered for the late 1990's through the first quarter of the 21st century. The principal result of the workshop is this publication, which contains an assessment of the current state of the technology, and specific technology advances in six critical areas of optics, all necessary for the mission set. The workshop was divided into six panels, each of about a dozen experts in specific fields, representing NASA, industry, and academia. In addition, each panel contained expertise that spanned the spectrum from x-ray to

submillimeter wavelengths. This executive summary contains the principal recommendations of each panel. The six technology panels and their chairs were: (1) Wavefront Sensing, Control, and Pointing, Thomas Pitts, Itek Optical Systems, A Division of Litton; (2) Fabrication, Roger Angel, Steward Observatory, University of Arizona; (3) Materials and Structures, Theodore Saito, Lawrence Livermore National Laboratory; (4) Optical Testing, James Wyant, WYKO Corporation; (5) Optical Systems Integrated Modeling, Robert R. Shannon, Optical Sciences Center, University of Arizona; and (6) Advanced Optical Instruments Technology, Michael Shao, Jet Propulsion Laboratory, California Institute of Technology. This Executive Summary contains the principal recommendations of each panel. Author

N94-14832*# Jet Propulsion Lab., California Inst. of Tech., Pasadena.
THE NEXT CENTURY ASTROPHYSICS PROGRAM
Paul N. Swanson *In its* Workshop Proceedings: Optical Systems Technology for Space Astrophysics in the 21st Century, Volume 3 15 Aug. 1992 p 11-23 (For primary document see N94-14830 02-19)
Avail: CASI HC A03/MF A02; 1 functional color page

The Astrophysics Division within the NASA Office of Space Science and Applications (OSSA) has defined a set of flagship and intermediate missions that are presently under study for possible launch during the next 20 years. These missions and tentative schedules, referred to as the Astrotech 21 Mission Set, are summarized. The missions are in three groups corresponding to the cognizant science branch within the Astrophysics Division. Phase C/D refers to the pre-launch construction and delivery of the spacecraft, and the Operations Phase refers to the period when the mission is active in space. Approximately 1.5 years before the start of Phase C/D, a non-advocate review (NAR) is held to ensure that the mission/system concept and the requisite technology are at an appropriate stage of readiness for full scale development to begin. Therefore, technology development is frozen (usually) as of the date of a successful NAR. An overview of the technology advances required for each of the three wavelength groups is provided in the following paragraphs, along with a brief description of the individual missions. Author (revised)

N94-14833*# Itek Corp., Lexington, MA.
WAVEFRONT SENSING, CONTROL, AND POINTING
Thomas Pitts, George Sevaston (Jet Propulsion Lab., California Inst. of Tech., Pasadena.), Michael Agronin (Jet Propulsion Lab., California Inst. of Tech., Pasadena.), Pierre Bely (Space Telescope Science Inst., Baltimore, MD.), Mark Colavita (Jet Propulsion Lab., California Inst. of Tech., Pasadena.), Mark Clampin (Johns Hopkins Univ., Baltimore, MD.), James Harvey (University of Central Florida, Orlando.), Paul Idell (Phillips Lab., Hanscom AFB, MA.), Dave Sandler (Thermo Electron Corp., Waltham, MA.), and Melville Ulmer (Northwestern Univ., Evanston, IL.) *In* JPL, Workshop Proceedings: Optical Systems Technology for Space Astrophysics in the 21st Century, Volume 3 15 Aug. 1992 p 29-57 (For primary document see N94-14830 02-19)
Avail: CASI HC A03/MF A02; 1 functional color page

A majority of future NASA astrophysics missions from orbiting interferometers to 16-m telescopes on the Moon have, as a common requirement, the need to bring light from a large entrance aperture to the focal plane in a way that preserves the spatial coherence properties of the starlight. Only by preserving the phase of the incoming wavefront, can many scientific observations be made, observations that range from measuring the red shift of quasi-stellar objects (QSO's) to detecting the IR emission of a planet in orbit around another star. New technologies for wavefront sensing, control, and pointing hold the key to advancing our observatories of the future from those already launched or currently under development. As the size of the optical system increases, either to increase the sensitivity or angular resolution of the instrument, traditional technologies for maintaining optical wavefront accuracy become prohibitively expensive or completely impractical. For space-based instruments, the low mass requirement and the large temperature excursions further challenge existing technologies. The Hubble Space Telescope (HST) is probably the last large space telescope to rely on passive means to keep its primary optics stable and the optical system aligned. One needs only look to the significant developments in wavefront sensing, control, and pointing that have occurred over the past several years to appreciate the potential of this technology for transforming the capability of future space observatories. Future developments in space-borne telescopes will be based in part on developments in ground-based systems. Telescopes with rigid primary mirrors much larger than 5 m in diameter are impractical because of gravity loading. New technologies are now being introduced, such as active optics, that address the scale problem and that allow very large telescopes to be built. One approach is a segmented design such as that being pioneered by the W.M. Keck telescope now under construction at the Mauna Kea Observatory. It consists of 36 hexagonal mirror segments, supported on a framework structure, which are positioned by actuators located between the structure and the mirrors. The figure of the telescope is initialized by making observations of a bright star using a Shack Hartmann sensor integrated with a white light interferometer. Then, using sensed data from the mirror edges to control these actuators, the figure of the mosaic of 36 segments is maintained as if it were a rigid primary mirror. Another active optics approach is the use of a thin meniscus mirror with actuators. This technique was demonstrated on the European Southern Observatory's New Technology Telescope (NTT) and is planned for use in the Very Large Telescope (consists of four 8-m apertures), which is now entering the design phase. Author (revised)

N94-14834*# National Aeronautics and Space Administration. Marshall Space Flight Center, Huntsville, AL.
FABRICATION
Roger Angel (Arizona Univ., Tucson.), Richard Helms (Jet Propulsion Lab., California Inst. of Tech., Pasadena.), Jim Bilbro, Norman Brown (Lawrence Livermore National Lab., CA.), Sverre Eng (Jet Propulsion Lab., California Inst. of Tech., Pasadena.), Steve Hinman (Eastman Kodak Co., Rochester, NY.), Greg Hull-Allen (United Technologies Optical Systems, Inc., Albuquerque, NM.), Stephen Jacobs (Rochester Univ., NY.), Robert Keim (Eastman Kodak Co., Rochester, NY.), and Melville Ulmer (Northwestern Univ., Evanston, IL.) et al *In* JPL, Workshop Proceedings: Optical Systems Technology for Space Astrophysics in the 21st Century, Volume 3 15 Aug. 1992 p 59-83 (For primary document see N94-14830 02-19)
Avail: CASI HC A03/MF A02; 1 functional color page

What aspects of optical fabrication technology need to be developed so as to facilitate existing planned missions, or enable new ones? Throughout the submillimeter to UV wavelengths, the common goal is to push technology to the limits to make the largest possible apertures that are diffraction limited. At any one wavelength, the accuracy of the surface must be better than lambda/30 (rms error). The wavelength range is huge, covering four orders of magnitude from 1 mm to 100 nm. At the longer wavelengths, diffraction limited surfaces can be shaped with relatively crude techniques. The challenge in their fabrication is to make as large as possible a reflector, given the weight and volume constraints of the launch vehicle. The limited cargo diameter of the shuttle has led in the past to emphasis on deployable or erectable concepts such as the Large Deployable Reflector (LDR), which was studied by NASA for a submillimeter astrophysics mission. Replication techniques that can be used to produce light, low-cost reflecting panels are of great interest for this class of mission. At shorter wavelengths, in the optical and ultraviolet, optical fabrication will tax to the limit the most refined polishing methods. Methods of mechanical and thermal stabilization of the substrate will be severely stressed. In the thermal infrared, the need for large aperture is tempered by the even stronger need to control the telescope's thermal emission by cooled or cryogenic operation. Thus, the SIRTF mirror at 1 meter is not large and does not require unusually high accuracy, but the fabrication process must produce a mirror that is the right shape at a temperature of 4 K. Future large cooled mirrors will present more severe problems, especially if they must also be accurate enough to work at optical wavelengths. At the very shortest wavelengths accessible to reflecting optics, in the x-ray domain, the very low count fluxes of high energy photons place a premium on the collecting area. It is not necessary to reach or even approach the diffraction limit, which would demand subnanometer fabrication and figure control. Replication techniques that produce large very lightweight surfaces are of interest for x-ray optics just as they are for the submillimeter region. Optical fabrication requirements are examined in more detail for missions in each of the three spectral regions of interest in astrophysics. Author (revised)

N94-14835*# National Aeronautics and Space Administration. Langley Research Center, Hampton, VA.
MATERIALS AND STRUCTURES
Theodore T. Saito (Lawrence Livermore National Lab., CA.), Sharon L. Langenbeck (Jet Propulsion Lab., California Inst. of Tech., Pasadena.),

Ghanim Al-Jamily (Barr Associates, Inc., Concord, MA.), Joe Arnold (United Technologies Optical Systems, Inc., Albuquerque, NM.), Troy Barbee (Lawrence Livermore National Lab., CA.), Dan Coulter (Jet Propulsion Lab., California Inst. of Tech., Pasadena.), Ben Dolgin (Jet Propulsion Lab., California Inst. of Tech., Pasadena.), Buck Fichter, Patricia George (Aerojet-General Corp., Azusa, CA.), and Paul Gorenstein (Harvard-Smithsonian Center for Astrophysics, Cambridge, MA.) et al *In* JPL, Workshop Proceedings: Optical Systems Technology for Space Astrophysics in the 21st Century, Volume 3 15 Aug. 1992 p 85-97 (For primary document see N94-14830 02-19)

Avail: CASI HC A03/MF A02; 1 functional color page

Materials and structures technology covers a wide range of technical areas. Some of the most pertinent issues for the Astrotech 21 missions include dimensionally stable structural materials, advanced composites, dielectric coatings, optical metallic coatings for low scattered light applications, low scattered light surfaces, deployable and inflatable structures (including optical), support structures in 0-g and 1-g environments, cryogenic optics, optical blacks, contamination hardened surfaces, radiation hardened glasses and crystals, mono-metallic telescopes and instruments, and materials characterization. Some specific examples include low coefficients of thermal expansion (CTE) structures (0.01 ppm/K), lightweight thermally stable mirror materials, thermally stable optical assemblies, high reliability/accuracy (1 micron) deployable structures, and characterization of nanometer level behavior of materials/structures for interferometry concepts. Large filled-aperture concepts will require materials with CTE's of 10(exp 9) at 80 K, anti-contamination coatings, deployable and erectable structures, composite materials with CTE's less than 0.01 ppm/K and thermal hysteresis, 0.001 ppm/K. Gravitational detection systems such as LAGOS will require rigid/deployable structures, dimensionally stable components, lightweight materials with low conductivity, and high stability optics. The Materials and Structures panel addressed these issues and the relevance of the Astrotech 21 mission requirements by dividing materials and structures technology into five categories. These categories, the necessary development, and applicable mission/program development phasing are summarized. For each of these areas, technology assessments were made and development plans were defined. Author (revised)

N94-14836*# National Aeronautics and Space Administration. Marshall Space Flight Center, Huntsville, AL.

OPTICAL TESTING

James Wyant (WYKO Corp., Tucson, AZ.), Eric Hochberg (Jet Propulsion Lab., California Inst. of Tech., Pasadena.), Robert Breault (Breault Research Organization, Tucson, AZ.), John Greivenkamp (Arizona Univ., Tucson.), Gary Hunt, Pete Mason (Jet Propulsion Lab., California Inst. of Tech., Pasadena.), James McGuire (Jet Propulsion Lab., California Inst. of Tech., Pasadena.), Aden Meinel (Jet Propulsion Lab., California Inst. of Tech., Pasadena.), Mike Morris (Rochester Univ., NY.), and Larry Scherr (Aerojet Electrosystems Co., Azusa, CA.) et al *In* JPL, Workshop Proceedings: Optical Systems Technology for Space Astrophysics in the 21st Century, Volume 3 15 Aug. 1992 p 99-121 (For primary document see N94-14830 02-19)

Avail: CASI HC A03/MF A02; 1 functional color page

Optical testing is one of the most vital elements in the process of preparing an optical instrument for launch. Without well understood, well controlled, and well documented test procedures, current and future mission goals will be jeopardized. We should keep in mind that the reason we test is to provide an opportunity to catch errors, oversights, and problems on the ground, where solutions are possible and difficulties can be rectified. Consequently, it is necessary to create tractable test procedures that truly provide a measure of the performance of all optical elements and systems under conditions which are close to those expected in space. Where testing is not feasible, accurate experiments are required in order to perfect models that can exactly predict the optical performance. As we stretch the boundaries of technology to perform more complex space and planetary investigations, we must expand the technology required to test the optical components and systems which we send into space. As we expand the observational wavelength ranges, so must we expand our range of optical sources and detectors. As we increase resolution and sensitivity, our understanding of optical surfaces to accommodate more stringent figure and scatter requirements must expand. Only with research and development in these areas can we hope to achieve success in the ever increasing demands made on optical testing by the highly sophisticated missions anticipated over the next two decades. Technology assessment and development plan for surface figure, surface roughness, alignment, image quality, radiometric quantities, and stray light measurement are presented. Author (revised)

N94-14837*# Arizona Univ., Tucson. Optical Sciences Center.

OPTICAL SYSTEMS INTEGRATED MODELING

Robert R. Shannon, Robert A. Laskin (Jet Propulsion Lab., California Inst. of Tech., Pasadena.), Si Brewer (Pagos Corp., Los Angeles, CA.), Chris Burrows (Space Telescope Science Inst., Baltimore, MD.), Harlan Epps (California Univ., Santa Cruz.), Garth Illingworth (California Univ., Santa Cruz.), Dietrich Korsch (Korsch Optics, Inc., Huntsville, AL.), B. Martin Levine (Jet Propulsion Lab., California Inst. of Tech., Pasadena.), Vini Mahajan (Aerospace Corp., El Segundo, CA.), and Chuck Rimmer (Optical Research Associates, Pasadena, CA.) et al *In* JPL, Workshop Proceedings: Optical Systems Technology for Space Astrophysics in the 21st Century, Volume 3 15 Aug. 1992 p 123-131 (For primary document see N94-14830 02-19)

Avail: CASI HC A02/MF A02; 1 functional color page

An integrated modeling capability that provides the tools by which entire optical systems and instruments can be simulated and optimized is a key technology development, applicable to all mission classes, especially astrophysics. Many of the future missions require optical systems that are physically much larger than anything flown before and yet must retain the characteristic sub-micron diffraction limited wavefront accuracy of their smaller precursors. It is no longer feasible to follow the path of 'cut and test' development; the sheer scale of these systems precludes many of the older techniques that rely upon ground evaluation of full size engineering units. The ability to accurately model (by computer) and optimize the entire flight system's integrated structural, thermal, and dynamic characteristics is essential. Two distinct integrated modeling capabilities are required. These are an initial design capability and a detailed design and optimization system. The content of an initial design package is shown. It would be a modular, workstation based code which allows preliminary integrated system analysis and trade studies to be carried out quickly by a single engineer or a small design team. A simple concept for a detailed design and optimization system is shown. This is a linkage of interface architecture that allows efficient interchange of information between existing large specialized optical, control, thermal, and structural design codes. The computing environment would be a network of large mainframe machines and its users would be project level design teams. More advanced concepts for detailed design systems would support interaction between modules and automated optimization of the entire system. Technology assessment and development plans for integrated package for initial design, interface development for detailed optimization, validation, and modeling research are presented. Author (revised)

N94-14838*# National Aeronautics and Space Administration. Marshall Space Flight Center, Huntsville, AL.

ADVANCED OPTICAL INSTRUMENTS TECHNOLOGY

Mike Shao (Jet Propulsion Lab., California Inst. of Tech., Pasadena.), Michael Chrisp (Jet Propulsion Lab., California Inst. of Tech., Pasadena.), Li-Jen Cheng (Jet Propulsion Lab., California Inst. of Tech., Pasadena.), Sverre Eng (Jet Propulsion Lab., California Inst. of Tech., Pasadena.), Thomas Glavich (Jet Propulsion Lab., California Inst. of Tech., Pasadena.), Larry Goad (Itek Corp., Lexington, MA.), Bill Jones, Philip Kaarat (Columbia Univ., New York, NY.), Max Nein, and William Robinson, uw319824 et al *In* JPL, Workshop Proceedings: Optical Systems Technology for Space Astrophysics in the 21st Century, Volume 3 15 Aug. 1992 p 133-148 (For primary document see N94-14830 02-19)

Avail: CASI HC A03/MF A02; 1 functional color page

The science objectives for proposed NASA missions for the next decades push the state of the art in sensitivity and spatial resolution over a wide range of wavelengths, including the x-ray to the submillimeter. While some of the proposed missions are larger and more sensitive versions of familiar concepts, such as the next generation space telescope, others use concepts, common on the Earth, but new to space, such as optical interferometry, in order to provide spatial resolutions impossible with other concepts. However, despite their architecture, the performance of all of the proposed missions depends critically on the back-end instruments that process the collected energy to produce scientifically interesting outputs.

The Advanced Optical Instruments Technology panel was chartered with defining technology development plans that would best improve optical instrument performance for future astrophysics missions. At this workshop the optical instrument was defined as the set of optical components that reimage the light from the telescope onto the detectors to provide information about the spatial, spectral, and polarization properties of the light. This definition was used to distinguish the optical instrument technology issues from those associated with the telescope, which were covered by a separate panel. The panel identified several areas for optical component technology development: diffraction gratings; tunable filters; interferometric beam combiners; optical materials; and fiber optics. The panel also determined that stray light suppression instruments, such as coronagraphs and nulling interferometers, were in need of general development to support future astrophysics needs. Author (revised)

N94-13273# Tokyo Science Univ. (Japan).
PRESENT STATUS OF JEM UTILIZATION PROJECTS [JEM RIYOU KEIKAKU NO GENJOU]
Shigeo Kobayashi *In* NASDA, The Second Workshop on Deployment and Assembly Experiment of Large Space Structure on Orbit 31 Mar. 1993 p 21-28 In JAPANESE (For primary document see N94-13268 02-12)
Avail: CASI HC A02/MF A01

N94-14214# Korea Aerospace Research Inst., Taejon (Republic of Korea). Dept. of Space Application Technology.
HIGH PERFORMANCE MULTI-MODE RADAR ALTIMETER FOR FUTURE SPACEBORNE APPLICATION
Yong-Hoon Kim *In* Science and Technology Agency, Asia-Pacific ISY Conference, Volume 2 31 Mar. 1993 p 39-44 (For primary document see N94-14209 02-43)
Avail: CASI HC A02/MF A04

20 SPACECRAFT PROPULSION AND POWER

Includes main propulsion systems and components, e.g., rocket engines; and spacecraft auxilliary power sources.

For related information see also *07 Aircraft Propulsion and Power, 28 Propellants and Fuels, 44 Energy Production and Conversion,* and *15 Launch Vehicles and Space Vehicles.*

N94-12807*# National Aeronautics and Space Administration. Lewis Research Center, Cleveland, OH.
SOLAR DYNAMIC POWER SYSTEM DEVELOPMENT FOR SPACE STATION FREEDOM
Jul. 1993 156 p Sponsored by NASA. Washington
(RTOP 474-52-10)
(NASA-RP-1310; E-7059; NAS 1.61:1310) Avail: CASI HC A08/MF A02

The development of a solar dynamic electric power generation system as part of the Space Station Freedom Program is documented. The solar dynamic power system includes a solar concentrator, which collects sunlight; a receiver, which accepts and stores the concentrated solar energy and transfers this energy to a gas; a Brayton turbine, alternator, and compressor unit, which generates electric power; and a radiator, which rejects waste heat. Solar dynamic systems have greater efficiency and lower maintenance costs than photovoltaic systems and are being considered for future growth of Space Station Freedom. Solar dynamic development managed by the NASA Lewis Research Center from 1986 to Feb. 1991 is covered. It summarizes technology and hardware development, describes 'lessons learned', and, through an extensive bibliography, serves as a source list of documents that provide details of the design and analytic results achieved. It was prepared by the staff of the Solar Dynamic Power System Branch at the NASA Lewis Research Center in Cleveland, Ohio. The report includes results from the prime contractor as well as from in-house efforts, university grants, and other contracts. Also included are the writers' opinions on the best way to proceed technically and programmatically with solar dynamic efforts in the future, on the basis of their experiences in this program. Author (revised)

N94-12870# EG and G Energy Measurements, Inc., Idaho Falls.
NUCLEAR PROPULSION SYSTEMS ENGINEERING
W. W. Madsen, J. E. Neuman, and D. H. VanHaften 1992 11 p Presented at the Nuclear Technologies for Space Exploration Conference, Jackson, WY, 16-19 Aug. 1992
(Contract DE-AC07-76ID-01570)
(DE93-010791; EGG-M-92502; CONF-920803-17) Avail: CASI HC A03/MF A01

The Nuclear Energy for Rocket Vehicle Application (NERVA) program of the 1960's and early 1970's was dramatically successful, with no major failures during the entire testing program. This success was due in large part to the successful development of a systems engineering process. Systems engineering, properly implemented, involves all aspects of the system design and operation, and leads to optimization of the entire system: cost, schedule, performance, safety, reliability, function, requirements, etc. The process must be incorporated from the very first and continued to project completion. This paper will discuss major aspects of the NERVA systems engineering effort and consider the implications for current nuclear propulsion efforts. DOE

N94-12911# Lawrence Livermore National Lab., CA.
REAL TIME RADIOGRAPHY OF TITAN 4 BOOSTER
M. LaChapell, D. Turner, K. Dolan, D. Perkins, and B. Costerus Apr. 1993 5 p
(Contract W-7405-eng-48)
(DE93-012450; UCRL-ID-113846) Avail: CASI HC A01/MF A01

Lawrence Livermore National Laboratory successfully completed a real-time radiography of the Titan 4 booster motor in February 1993. The success of this project depended on the quick response to Air Force criteria and securing a multi-disciplinary team addressing the numerous technical challenges. The team's challenges included the following: large area imager design and fabrication problems; vibrating mitigation obstacles; sound mitigation dilemmas; high levels of fail safe confidence; and operating a fragile, transportable x-ray linear accelerator. The data was viewed in real-time and stored utilizing standard video hardware. The data from the test is presently being analyzed. The multi-disciplinary team was presented with many serious technical challenges that needed to be addressed expeditiously. The purpose of this paper is to examine some of the technical issues and how they were executed. DOE

N94-12945# National Aerospace Lab., Kakuda (Japan). Research Center.
EFFECTS OF HYDROGEN ADDITION ON COMBUSTION PERFORMANCE OF A LOX/KEROSENE ROCKET [SUISO WO KONSHOU SHITA EKITAI SANSO-KEROSHIN ROKET TO NO NENSHOU TOKUSEI]
Fumiei Ono, Hiroshi Tamura, Akinaga Kumakawa, Hiroshi Sakamoto, Kazuo Sato, Masaki Sasaki, and Nobuyuki Yatsuyanagi Sep. 1992 18 p In JAPANESE
(NAL-TR-1177; JTN-93-80496) Avail: CASI HC A03/MF A01

The effect of the addition of hydrogen on the combustion performance of a LOX/kerosene rocket combustor was experimentally studied. Combustors with a seven kN thrust force at a nominal chamber pressure of 10 MPa were employed for the firing tests. Liquid Oxygen (LOX) and kerosene (RJ-1J) were used as the main propellants and gaseous hydrogen was added as auxiliary fuel. Two types of Fuel Oxidizer Fuel (FOF) triplet injectors (type A, type B) and one type of Oxidizer Fuel Oxidizer (OFO) triplet injector (type C) were used for main propellants injection. Hydrogen was added to each combustor either from a slit located on the chamber wall near the injector face (type A) or through the injector's porous face plate (type B, type C). The mass fraction of hydrogen to the total amount of fuel was varied from zero to 13 percent. Results indicated that such hydrogen to LOX/kerosene combustion does not improve combustor efficiency, e.g., when FOF injectors (type A, type B) were used and 10 percent hydrogen was added, combustion efficiency decreased by approximately two percent. In addition, when the OFO injector (type C) was used and hydrogen was added through the injector face, the combustion efficiency remained the same under all test conditions.. Author (NASDA)

N94-12981# Brookhaven National Lab., Upton, NY.
MCNP BENCHMARK ANALYSES OF CRITICAL EXPERIMENTS FOR THE SPACE NUCLEAR THERMAL PROPULSION PROGRAM
E. C. Selcow, R. J. Cerbone, H. Ludewig, S. F. Mughabghab, E. Schmidt, M. Todosow, E. J. Parma (Sandia National Labs., Albuquerque, NM.), R.

M. Ball (Babcock and Wilcox Co., Lynchburg, VA.), and G. S. Hoovler (Babcock and Wilcox Co., Lynchburg, VA.) 1993 6 p Presented at the 10th Symposium on Space Nuclear Power and Propulsion, Albuquerque, NM, 10-14 Jan. 1993

(Contract DE-AC02-76CH-00016)

(DE93-014046; BNL-48698; CONF-930103-38) Avail: CASI HC A02/MF A01 (US Sales Only)

Benchmark analyses have been performed of Particle Bed Reactor (PBR) critical experiments (CX) using the MCNP radiation transport code. The experiments have been conducted at the Sandia National Laboratory reactor facility in support of the Space Nuclear Thermal Propulsion (SNTP) program. The test reactor is a nineteen element water moderated and reflected thermal system. A series of integral experiments have been carried out to test the capabilities of the radiation transport codes to predict the performance of PBR systems. MCNP was selected as the preferred radiation analysis tool for the benchmark experiments. Comparison between experimental and calculational results indicate very good agreement. This paper describes the analyses of benchmark experiments designed to quantify the accuracy of the MCNP radiation transport code for predicting the performance characteristics of PBR reactors. DOE

N94-12996# EG and G Energy Measurements, Inc., Idaho Falls.

DESIGN, QUALIFICATION AND OPERATION OF NUCLEAR ROCKETS FOR SAFE MARS MISSIONS

D. Buden, W. W. Madsen, T. S. Olson, and L. R. Redd (Department of Energy, Idaho Falls, ID.) 1993 10 p Presented at the 10th Symposium on Space Nuclear Power and Propulsion, Albuquerque, NM, 10-14 Jan. 1993

(Contract DE-AC07-76ID-01570)

(DE93-010792; EGG-M-92569; CONF-930103-31) Avail: CASI HC A02/MF A01

Nuclear thermal propulsion modules planned for use on crew missions to Mars improve mission reliability and overall safety of the mission. This is greatly enhanced if the system specifications take into account safety from initiation of the design. For instance, the use of multiple engines in the propulsion module can lead to very high system safety and reliability. Operational safety enhancements may include the following: the use of multiple perigee burns, thus allowing time to ensure that all systems are functioning properly prior to departure from Earth orbit; the ability to perform all other parts of the mission in a degraded mode with little or no degradation of the mission; and the safe disposal of the nuclear propulsion module in a heliocentric orbit out of the ecliptic plane. The standards used to qualify nuclear rockets are one of the main cost drivers of the program. Concepts and systems that minimize cost and risk will rely on use of the element and component levels to demonstrate technology readiness and validation. Subsystem or systems testing then is only needed for verification of performance. Also, these will be the safest concepts because they will be more thoroughly understood, and the safety margins will be well established and confirmed by tests. DOE

N94-13034# Brookhaven National Lab., Upton, NY.

GENERATION OF NEUTRONIC THERMAL DATA IN SUPPORT OF SPACE NUCLEAR PROPULSION

S. Mughabghab, E. Schmidt, and H. Ludewig 1993 8 p Presented at the 10th Symposium on Space Nuclear Power and Propulsion, Albuquerque, NM, 10-14 Jan. 1993

(Contract DE-AC02-76CH-00016)

(DE93-013148; BNL-48540; CONF-930103-37) Avail: CASI HC A02/MF A01

The scattering kernel data for (sup 7)LiH have been generated for the first time in the temperature range 50-1000 K. This is based on a phonon distribution function derived from both experimental data and theoretical calculations. A detailed study of the variation of the moderator temperature coefficient alpha(sub m)(T) with temperature, T, is carried out for a typical space nuclear reactor of the particle bed type. It is established that the moderator temperature coefficient due to chemical binding effects follows the relationship alpha(sub m)(T) = C F(sub v)(H)(sup 1.6) where F(sub v)(H) is the volume fraction of bound solid hydrogen and C is a normalization constant which depends on the moderator capture thermal cross section. The value 1.65 is to be compared with 1.54 plus/minus 0.06 derived in a previous study where water scattering kernels are applied. For control and safety reasons, a minimization of this positive component temperature coefficient can be most effective by operating the moderator at high temperatures. Advantages of this approach are outlined. In addition, suggestions are made to render the overall temperature coefficient negative. DOE

N94-13055*# Jet Propulsion Lab., California Inst. of Tech., Pasadena.

ELECTRIC PROPULSION SYSTEM TECHNOLOGY Annual Report, 1990

John R. Brophy, Charles E. Garner, and Keith D. Goodfellow Dec. 1991 185 p

(NASA-CR-194100; JPL-Publ-91-16; NAS 1.26:194100) Avail: CASI HC A09/MF A02

The work performed on the Ion Propulsion System Technology Task in FY90 is described. The objectives of this work fall under two broad categories. The first of these deals with issues associated with the application of xenon ion thrusters for primary propulsion of planetary spacecraft, and the second with the investigation of technologies which will facilitate the development of larger, higher power ion thrusters to support more advanced mission applications. Most of the effort was devoted to investigation of the critical issues associated with the use of ion thrusters for planetary spacecraft. These issues may be succinctly referred to as life time, system integration, and throttling. Chief among these is the engine life time. If the engines do not have sufficient life to perform the missions of interest, then the other issues become unimportant. Ion engine life time was investigated through two experimental programs: an investigation into the reduction of ion engine internal sputter erosion through the addition of small quantities of nitrogen, and a long duration cathode life test. In addition, a literature review and analysis of accelerator grid erosion were performed. The nitrogen addition tests indicated that the addition of between 0.5 and 1.0 percent of nitrogen by mass to the xenon propellant results in a reduction in the sputter erosion of discharge chamber components by a factor of between 20 and 50, with negligible reduction in thruster performance. The long duration test of a 6.35-mm dia. xenon hollow cathode is still in progress, and has accumulated more than 4,000 hours of operation at an emission current of 25 A at the time of this writing. One of the major system integration issues concerns possible interactions of the ion thruster produced charge exchange plasma with the spacecraft. A computer model originally developed to describe the behavior of mercury ion thruster charge exchange plasmas was resurrected and modified for xenon propellant. This model enables one to calculate the flow direction and local density of the charge exchange plasma, and indicates the degree to which this plasma can flow upstream of the thruster exhaust plane. A continuing effort to investigate the most desirable throttling technique for noble gas ion thrusters concentrated this year on experimentally determining the fixed flow rate throttling range of a 30-cm dia. thruster with a two-grid accelerator system. These experiments demonstrated a throttling capability which covers a 2.8 to 1 variation in input power. This throttling range is 55 percent greater than expected, and is due to better accelerator system performance at low net-to-total voltage ratios than indicated in the literature. To facilitate the development of large, higher power ion thrusters several brief studies were performed. These include the development of a technique which simulates ion thruster operation without beam extraction, the development of an optical technique to measure ion thruster grid distortion due to thermal expansion, tests of a capacitance measurement technique to quantify the accelerator system grid separation, and the development of a segmented thruster geometry which enables near term development of ion thrusters at power levels greater than 100 kW. Finally, a paper detailing the benefits of electric propulsion for the Space Exploration Initiative was written.

Author (revised)

N94-13068*# Jet Propulsion Lab., California Inst. of Tech., Pasadena.

ELECTRIC PROPULSION SYSTEM TECHNOLOGY Annual Report, 1991

John R. Brophy, Charles E. Garner, Keith D. Goodfellow, Thomas J. Pivirotto, and James E. Polk Nov. 1992 153 p

(NASA-CR-194099; JPL-Publ-92-10; NAS 1.26:194099) Avail: CASI HC A08/MF A02

The work performed in fiscal year (FY) 1991 under the Propulsion Technology Program RTOP (Research and Technology Objectives and Plans) No. (55) 506-42-31 for Low-Thrust Primary and Auxiliary Propulsion technology development is described. The objectives of this work fall under two broad categories. The first of these deals with the development of ion engines for primary propulsion in support of solar system exploration. The second with the advancement of steady-state magnetoplasmadynamic (MPD)

thruster technology at 100 kW to multimegawatt input power levels. The major technology issues for ion propulsion are demonstration of adequate engine life at the 5 to 10 kW power level and scaling ion engines to power levels of tens to hundreds of kilowatts. Tests of a new technique in which the decelerator grid of a three-grid ion accelerator system is biased negative of neutralizer common potential in order to collect facility induced charge-exchange ions are described. These tests indicate that this SAND (Screen, Accelerator, Negative Decelerator) configuration may enable long duration ion engine endurance tests to be performed at vacuum chamber pressures an order of magnitude higher than previously possible. The corresponding reduction in pumping speed requirements enables endurance tests of 10 kW class ion engines to be performed within the resources of existing technology programs. The results of a successful 5,000-hr endurance of a xenon hollow cathode operating at an emission current of 25 A are described, as well as the initial tests of hollow cathodes operating on a mixture of argon and 3 percent nitrogen. Work performed on the development of carbon/carbon grids, a multi-orifice hollow cathode, and discharge chamber erosion reduction through the addition of nitrogen are also described. Critical applied-field MPD thruster technical issues remain to be resolved, including demonstration of reliable steady-state operation at input powers of hundreds to thousands of kilowatts, achievement of thruster efficiency and specific impulse levels required for missions of interest, and demonstration of adequate engine life at these input power, efficiency, and specific impulse levels. To address these issues we have designed, built, and tested a 100 kW class, radiation-cooled applied-field MPD thruster and a unique dual-beam thrust stand that enables separate measurements of the applied- and self-field thrust components. We have also initiated the development of cathode thermal and plasma sheath models that will eventually be used to guide the experimental program. In conjunction with the cathode modeling, a new cathode test facility is being constructed. This facility will support the study of cathode thermal behavior and erosion mechanisms, the diagnosis of the near-cathode plasma and the development and endurance testing of new, high-current cathode designs. To facilitate understanding of electrode surface phenomenon, we have implemented a telephoto technique to obtain photographs of the electrodes during engine operation. In order to reduce the background vacuum tank pressure during steady-state engine operation in order to obtain high fidelity anode thermal data, we have developed and are evaluating a gas-dynamic diffuser. A review of experience with alkali metal propellants for MPD thrusters led to the conclusion that alkali metals, particularly lithium, offer the potential for significant engine performance and lifetime improvements. These propellants are also condensible at room temperature, substantially reducing test facility pumping requirements. The most significant systems-level issue is the potential for spacecraft contamination. Subsequent experimental and theoretical efforts should be directed toward verifying the performance and lifetime gains and characterizing the thruster flow field to assess its impact on spacecraft surfaces. Consequently, we have begun the design and development of a new facility to study engine operation with alkali metal propellants. Author (revised)

N94-13147*# McDonnell-Douglas Corp., Huntington Beach, CA.
MIRROR FUSION PROPULSION SYSTEM: A PERFORMANCE COMPARISON WITH ALTERNATE PROPULSION SYSTEMS FOR THE MANNED MARS MISSION
Norman R. Schulze (National Aeronautics and Space Administration, Washington, DC.), Scott A. Carpenter (California Univ., Berkeley. Lawrence Berkeley Lab.), Marc E. Deveny, and T. OConnell (O'Connell, T., Placentia, CA.) Jun. 1993 20 p Presented at the 29th Joint Propulsion Conference and Exhibit, Monterey, CA, 28-30 Jun. 1993; sponsored by AIAA, SAE, ASME, and ASEE See also A93-49917 Sponsored by NASA, Washington
(NASA-TM-109248; NAS 1.15:109248; MDC-93H1355; AIAA Paper 93-2094) Copyright Avail: CASI HC A03/MF A01

The performance characteristics of several propulsion technologies applied to piloted Mars missions are compared. The characteristics that are compared are Initial Mass in Low Earth Orbit (IMLEO), mission flexibility, and flight times. The propulsion systems being compared are both demonstrated and envisioned: Chemical (or Cryogenic), Nuclear Thermal Rocket (NTR) solid core, NTR gas core, Nuclear Electric Propulsion (NEP), and a mirror fusion space propulsion system. The proposed magnetic mirror fusion reactor, known as the Mirror Fusion Propulsion System (MFPS), is described. The description is an overview of a design study that was conducted to convert a mirror reactor experiment at Lawrence Livermore National Lab (LLNL) into a viable space propulsion system. Design principles geared towards minimizing mass and maximizing power available for thrust are identified and applied to the LLNL reactor design, resulting in the MFPS. The MFPS' design evolution, reactor and fuel choices, and system configuration are described. Results of the performance comparison shows that the MFPS minimizes flight time to 60 to 90 days for flights to Mars while allowing continuous return-home capability while at Mars. Total MFPS IMLEO including propellant and payloads is kept to about 1,000 metric tons. Author

N94-13265*# National Aeronautics and Space Administration. Goddard Space Flight Center, Greenbelt, MD.
NASA HANDBOOK FOR NICKEL-HYDROGEN BATTERIES
James D. Dunlop, M. Rao Gopalakrishna, and Thomas Y. Yi Sep. 1993 362 p
(RTOP 730-00-00)
(NASA-RP-1314; Rept-93B00106; NAS 1.61:1314) Avail: CASI HC A16/MF A03

Nickel-hydrogen (NiH2) batteries are finding more applications in the aerospace energy storage. Since 1983, NiH2 batteries have become the primary energy storage system used for Geosynchronous-Orbit (GEO) Satellites. The first NASA application for NiH2 batteries was the Low Earth Orbit (LEO) Hubble Space Telescope Satellite launched in 1990. The handbook was prepared as a reference book to aid in the application of this technology. That is, to aid in the cell and battery design, procurement, testing, and handling of NiH2 batteries. The design of individual pressure vessel NiH2 cells is covered in Chapter I. LEO and GEO applications and their requirements are discussed in Chapter 2. The design of NiH2 batteries for both GEO and LEO applications is discussed in Chapter 3. Advanced design concepts such as the common pressure vessel and bipolar NiH2 batteries are described in Chapter 4. Performance data are presented in Chapter 5. Storage and handling of the NiH2 cells and batteries are discussed in Chapter 6. Standard test procedures are presented in Chapter 7. Cell and battery procurements are discussed in Chapter 8. Finally, safety procedures are discussed in Chapter 9. Author (revised)

N94-13351# EG and G Energy Measurements, Inc., Idaho Falls.
A MODULAR GAS-COOLED CERMET REACTOR SYSTEM FOR PLANETARY BASE POWER
S. N. Jahshan and J. A. Borkowski 16 Oct. 1992 8 p Presented at the 10th Symposium on Space Nuclear Power and Propulsion, Albuquerque, NM, 10-14 Jan. 1993
(Contract DE-AC07-76ID-01570)
(DE93-013672; EGG-M-92413; CONF-930103-33) Avail: CASI HC A02/MF A01 (US Sales Only)

Fission nuclear power is foreseen as the source for electricity in planetary colonization and exploration. This report discusses a six module, gas-cooled, cermet-fueled reactor which is proposed to meet the design objectives. The highly enriched core is compact and can operate at high temperatures for long periods of time. The helium coolant powers six modular Brayton cycles that compare favorably with the SP-100-based Brayton cycle. DOE

N94-13415*# Sverdrup Technology, Inc., Brook Park, OH. Lewis Research Center Group.
LOW POWER PULSED MPD THRUSTER SYSTEM ANALYSIS AND APPLICATIONS
Roger M. Myers, Matthew Domonkos (New Mexico Univ., Albuquerque.), and James H. Gilland Sep. 1993 28 p Presented at the 1993 Joint Propulsion Conference, Monterey, CA, 28 Jun. - 1 Jul. 1993; sponsored by AIAA, SAE, ASME, and ASEE
(Contract NAS3-25266; RTOP 506-42-31)
(NASA-CR-191187; AIAA Paper 93-2391; E-8099; NAS 1.26:191187)
Avail: CASI HC A03/MF A01

Pulsed magnetoplasmadynamic (MPD) thruster systems were analyzed for application to solar-electric orbit transfer vehicles at power levels ranging from 10 to 40 kW. Potential system level benefits of pulsed propulsion technology include ease of power scaling without thruster performance changes, improved transportability from low power flight experiments to operational systems, and reduced ground qualification costs. Required pulsed propulsion system components include a pulsed applied-field MPD thruster,

a pulse-forming network, a charge control unit, a cathode heater supply, and high speed valves. Mass estimates were obtained for each propulsion subsystem and spacecraft component using off-the-shelf technology whenever possible. Results indicate that for payloads of 1000 and 2000 kg pulsed MPD thrusters can reduce launch mass by between 1000 and 2500 kg over those achievable with hydrogen arcjets, which can be used to reduce launch vehicle class and the associated launch cost. While the achievable mass savings depends on the trip time allowed for the mission, cases are shown in which the launch vehicle required for a mission is decreased from an Atlas IIAS to an Atlas I or Delta 7920. Author

N94-13416*# Sverdrup Technology, Inc., Brook Park, OH.
ELECTROMAGNETIC PROPULSION FOR SPACECRAFT
Roger M. Myers Cleveland, OH NASA Sep. 1993 32 p Presented at the 1993 Aerospace Design Conference, Irvine, CA, 15-18 Feb. 1993 See also A93-30975
(Contract NAS3-25266; RTOP 506-42-31)
(NASA-CR-191186; E-8097; NAS 1.26:191186; AIAA Paper 93-1086)
Avail: CASI HC A03/MF A01

Three electromagnetic propulsion technologies, solid propellant pulsed plasma thrusters (PPT), magnetoplasmadynamic (MPD) thrusters, and pulsed inductive thrusters (PIT), were developed for application to auxiliary and primary spacecraft propulsion. Both the PPT and MPD thrusters were flown in space, though only PPT's were used on operational satellites. The performance of operational PPT's is quite poor, providing only approximately 8 percent efficiency at approximately 1000 s specific impulse. However, laboratory PPT's yielding 34 percent efficiency at 2000 s specific impulse were extensively tested, and peak performance levels of 53 percent efficiency at 5170 s specific impulse were demonstrated. MPD thrusters were flown as experiments on the Japanese MS-T4 spacecraft and the Space Shuttle and were qualified for a flight in 1994. The flight MPD thrusters were pulsed, with a peak performance of 22 percent efficiency at 2500 s specific impulse using ammonia propellant. Laboratory MPD thrusters were demonstrated with up to 70 percent efficiency and 700 s specific impulse using lithium propellant. While the PIT thruster has never been flown, recent performance measurements using ammonia and hydrazine propellants are extremely encouraging, reaching 50 percent efficiency for specific impulses between 4000 to 8000 s. The fundamental operating principles, performance measurements, and system level design for the three types of electromagnetic thrusters are reviewed, and available data on flight tests are discussed for the PPT and MPD thrusters. Author (revised)

N94-13417*# National Aeronautics and Space Administration. Marshall Space Flight Center, Huntsville, AL.
ELECTRICAL ACTUATION TECHNOLOGY BRIDGING
Monica Hammond, comp. and John Sharkey, comp. Washington May 1993 753 p Workshop held in Huntsville, AL, 29 Sep. - 1 Oct. 1992 Original contains color illustrations
(NASA-CP-3213; M-720; NAS 1.55:3213) Avail: CASI HC A99/MF A06; 15 functional color pages

This document contains the proceedings of the NASA Electrical Actuation Technology Bridging (ELA-TB) Workshop held in Huntsville, Alabama, September 29-October 1, 1992. The workshop was sponsored by the NASA Office of Space Systems Development and Marshall Space Flight Center (MSFC). The workshop addressed key technologies bridging the entire field of electrical actuation including systems methodology, control electronics, power source systems, reliability, maintainability, and vehicle health management with special emphasis on thrust vector control (TVC) applications on NASA launch vehicles. Speakers were drawn primarily from industry with participation from universities and government. In addition, prototype hardware demonstrations were held at the MSFC Propulsion Laboratory each afternoon. Splinter sessions held on the final day afforded the opportunity to discuss key issues and to provide overall recommendations. Presentations are included in this document. Author

N94-13430*# National Aeronautics and Space Administration. Lewis Research Center, Cleveland, OH.
RECENT TESTING OF 30 kW HYDROGEN ARCJET THRUSTERS
Thomas W. Haag Jun. 1993 18 p Presented at the 29th Joint Propulsion Conference and Exhibit, Monterey, CA, 28 Jun. - 1 Jul. 1993; cosponsored by AIAA, SAE, ASME, and ASEE
(RTOP 506-42-31)
(NASA-TM-106214; E-7923; NAS 1.15:106214; AIAA Paper 93-1902)
Avail: CASI HC A03/MF A01

NASA is conducting efforts to evaluate high-power hydrogen arcjets for orbit transfer propulsion applications. As part of this program, an attempt was made to reexamine both radiatively- and regeneratively-cooled, 30 kW thrusters first demonstrated by the Giannini Scientific Corp. in 1963. The arcjets were configured to force arc attachment upstream of the throat in a subsonic chamber region. While thruster currents were steady, the voltage traces exhibited sawtooth waveforms at frequencies on the order of 20 kHz. Voltage variations per cycle were typically between 100 and 310 volts, indicating major changes in the position of the arc attachment with time. When operated at their respective design points, the performance of both thrusters fell below the values listed in the 1960's development reports. The reason for the discrepancies is not currently understood and further investigations are in progress. However, the recently measured efficiencies were high compared to those obtained with constricted-arc designs at similar conditions, and further arcjet performance optimizations may be possible. Author

N94-13455# National Aerospace Lab., Tokyo (Japan). Aerodynamics Div.
ARC-HEATING TESTS OF THERMAL PROTECTION SYSTEM MATERIALS FOR THE H-2 ROCKET FAIRING [H-2 ROKETTO FEARINGU DANNETSUZAI NO AKU KANETSU SHIKEN]
Noriaki Hirabayashi, Takashi Matsuzaki, Yukio Fukushima (National Space Development Agency, Tokyo, Japan.), Tomihisa Nakamura (National Space Development Agency, Tokyo, Japan.), and Takeshi Fujita (National Space Development Agency, Tokyo, Japan.) Oct. 1992 24 p In JAPANESE
(NAL-TR-1181; JTN-93-80503) Avail: CASI HC A03/MF A01

Materials suitable for the Thermal Protection System (TPS) of the rocket fairing for the Japanese next generation launch vehicle named H-2 were tested using an arc-heated wind tunnel. The main constituents of the candidate materials were epoxy resin and silicon rubber. The heating rate was from 60 to 100 kW/(sq m) in accordance with the maximum heating rate of the nose region of an ascending H-2 rocket. Test results showed that polycondensed silicon rubber was the best candidate as the main component of the TPS, and also that a SiC coating was indispensable. In addition, based on results and a preliminary estimation of the skin temperatures of the fairing nose region, a SiC coating of about 2 mm in thickness is considered sufficient to achieve thermal protection capability. Author (NASDA)

N94-13514# Sandia National Labs., Albuquerque, NM.
PRELIMINARY NUCLEAR SAFETY ASSESSMENT OF THE NEPST (TOPAZ 2) SPACE REACTOR PROGRAM
A. C. Marshall 1993 8 p Presented at the 2nd Specialists Conference and Short Course on Thermionic Energy Conversion, Goteborg, Sweden, 3-7 May 1993
(Contract DE-AC04-76DP-00789)
(DE93-012853; SAND-93-1067C; CONF-9305179-1) Avail: CASI HC A02/MF A01

The United States (US) Strategic Defense Initiative Organization (SDIO) decided to investigate the possibility of launching a Russian Topaz 2 space nuclear power system. A preliminary nuclear safety assessment was conducted to determine whether or not a space mission could be conducted safely and within budget constraints. As part of this assessment, a safety policy and safety functional requirements were developed to guide both the safety assessment and future Topaz 2 activities. A review of the Russian flight safety program was conducted and documented. Our preliminary nuclear safety assessment included a number of deterministic analyses, such as the following: neutronic analysis of normal and accident configurations, an evaluation of temperature coefficients of reactivity, a reentry and disposal analysis, an analysis of postulated launch abort impact accidents, and an analysis of postulated propellant fire and explosion accidents. Based on the assessment to date, it appears that it will be possible to safely launch the Topaz 2 system in the US with a modification to preclude water flooded criticality. A full scale safety program is now underway. DOE

N94-13617* National Aeronautics and Space Administration. John C. Stennis Space Center, Bay Saint Louis, MS.
SSME TESTING AT STENNIS SPACE CENTER (Videotape)
Mar. 1989 Videotape: 9 min. 54 sec. playing time, in color, with sound
(NASA-TM-109310; NONP-VT-93-185327) Avail: CASI VHS A01/BETA A22

Different views of Space Shuttle Main Engine test firings on all three test stands including closeup of engine, day, and night firings are presented. Author (revised)

N94-13625* National Aeronautics and Space Administration. Lewis Research Center, Cleveland, OH.
LOW THRUST SPACE PROPULSION (Videotape)
Jul. 1987 Videotape: 6 min. 20 sec. playing time, in color, with sound
(NASA-TM-109286; NONP-VT-93-185302) Avail: CASI VHS A01/BETA A22

An overview of low rocket engine propulsion concepts for space missions is presented. Chemical and electrical rocket engines are shown. Animation illustrates propulsion applications. Author (revised)

N94-14013# EG and G Energy Measurements, Inc., Idaho Falls.
GAS CORE NUCLEAR THERMAL ROCKET ENGINE RESEARCH AND DEVELOPMENT IN THE FORMER USSR
M. W. Koehlinger, ed., R. G. Bennett, ed., and C. G. Motloch, ed. Sep. 1992 63 p
(Contract DE-AC07-76ID-01570)
(DE93-012165; EGG-NE-10391) Avail: CASI HC A04/MF A01

Beginning in 1957 and continuing into the mid 1970's, the USSR conducted an extensive investigation into the use of both solid and gas core nuclear thermal rocket engines for space missions. During this time the scientific and engineering problems associated with the development of a solid core engine were resolved. At the same time, research was undertaken on a gas core engine, and some of the basic engineering problems associated with the concept were investigated. At the conclusion of the program, the basic principles of the solid core concept were established. However, a prototype solid core engine was not built because no established mission required such an engine. For the gas core concept, some of the basic physical processes involved were studied both theoretically and experimentally. However, no simple method of conducting proof-of-principle tests in a neutron flux was devised. This report focuses primarily on the development of the gas core concept in the former USSR. A variety of gas core engine system parameters and designs are presented, along with a summary discussion of the basic physical principles and limitations involved in their design. The parallel development of the solid core concept is briefly described to provide an overall perspective of the magnitude of the nuclear thermal propulsion program and a technical comparison with the gas core concept. DOE

N94-14102*# National Aeronautics and Space Administration. Lewis Research Center, Cleveland, OH.
COMPUTER PROGRAM FOR THERMAL AND TRANSPORT PROPERTIES OF PARAHYDROGEN FROM 20 TO 10,000 K
James T. Walton Washington Aug. 1993 16 p
(RTOP 593-71-11)
(NASA-TP-3378; E-7594; NAS 1.60:3378) Avail: CASI HC A03/MF A01

A computer program was recently developed to provide thermal and transport properties for parahydrogen across a wide temperature and pressure range. The program, NBS+/-pH2, matches the most recent parahydrogen property data from the National Bureau of Standards up to 3000 K and property data from the NASA Lewis Research Center's Chemical Equilibrium Computer Program up to 10,000 K. The pressure range of NBS+/-pH2 is from 1 x 10(exp 4) to 1.6 x 10(exp 7) Pa. The program was developed to meet the need for accurate parahydrogen properties from liquid to dissociated conditions as required by propulsion simulation programs being developed under the Space Exploration Initiative. NBS+/-pH2 is a machine-independent, standard Fortran 77 program which provides density, thermal conductivity, viscosity, Prandtl number, entropy, specific heats, and speed of sound given pressure and either temperature or enthalpy. This program is described and a comparison to programs previously available is provided. Author (revised)

N94-14111# Brookhaven National Lab., Upton, NY.
NUCLEAR THERMAL PROPULSION ENGINE BASED ON PARTICLE BED REACTOR USING LIGHT WATER STEAM AS A PROPELLANT
J. R. Powell, H. Ludewig, and G. Maise 1993 6 p Presented at the 10th Symposium on Space Nuclear Power and Propulsion, Albuquerque, NM, 10-14 Jan. 1993
(Contract DE-AC02-76CH-00016)
(DE93-014336; BNL-48667; CONF-930103-40) Avail: CASI HC A02/MF A01 (US Sales Only)

In this paper the possibility of configuring a water cooled Nuclear Thermal Propulsion (NTP) rocket, based on a Particle Bed Reactor (PBR), is investigated. This rocket will be used to operate on water obtained from near earth objects. The conclusions reached in this paper indicate that it is possible to configure a PBR based NTP rocket to operate on water and meet the mission requirements envisioned for it. No insurmountable technology issues have been identified. DOE

N94-14309*# Tennessee Univ. Space Inst., Tullahoma. Center for Space Transportation and Applied Research.
IDENTIFICATION AND INTERPRETATION OF PATTERNS IN ROCKET ENGINE DATA Final Report, Jul. 1990 - Jul. 1993
C. F. Lo, K. Wu, and B. A. Whitehead 4 Oct. 1993 35 p
(Grant NAG8-166)
(NASA-CR-194534; NAS 1.26:194534) Avail: CASI HC A03/MF A01

A prototype software system was constructed to detect anomalous Space Shuttle Main Engine (SSME) behavior in the early stages of fault development significantly earlier than the indication provided by either redline detection mechanism or human expert analysis. The major task of the research project is to analyze ground test data, to identify patterns associated with the anomalous engine behavior, and to develop a pattern identification and detection system on the basis of this analysis. A prototype expert system which was developed on both PC and Symbolics 3670 lisp machine for detecting anomalies in turbopump vibration data was checked with data from ground tests 902-473, 902-501, 902-519, and 904-097 of the Space Shuttle Main Engine. The neural networks method was also applied to supplement the statistical method utilized in the prototype system to investigate the feasibility in detecting anomalies in turbopump vibration of SSME. In most cases the anomalies detected by the expert system agree with those reported by NASA. On the neural networks approach, the results are given the successful detection rate higher than 95 percent to identify either normal or abnormal running condition based on the experimental data as well as numerical simulation. Author (revised)

N94-14463*# National Aeronautics and Space Administration, Washington, DC.
THE PROBLEM OF TRAVELING IN OUTER SPACE: THE ROCKET MOTOR
Hermann Noordung Jun. 1993 218 p Transl. into ENGLISH of Das Problem der Befahrung des Weltraums: Der Raketen-Motor (Berlin, Germany, Richard Carl Schmidt and Co.), 1929 188 p Prepared by SCITRAN, Inc., Santa Barbara, CA
(Contract NASw-4693)
(NASA-TT-10002; NAS 1.77:10002) Avail: CASI HC A10/MF A03

This book is one of the first basic primers on space travel history. It covers the solar system and its related forces. It then discusses in some detail the problems associated with rockets and satellites. Several references are made to H. Oberth, considered by some to be the father of space travel. Author

N94-14491 Pennsylvania State Univ., University Park.
ANALYSIS OF REACTING FLOWFIELDS IN LOW-THRUST ROCKET ENGINES AND PLUMES Ph.D. Thesis
Jonathan Mitchell Weiss 1992 196 p
Avail: Univ. Microfilms Order No. DA9311743

The mixing and combustion processes in small gaseous hydrogen-oxygen thrusters and plumes are studied by means of a computational model developed as a general purpose analytic procedure for solving low speed, reacting, internal flowfields. The model includes the full Navier-Stokes equations coupled with species diffusion equations for a hydrogen-oxygen reaction kinetics system as well as the option to use either the k-Epsilon or q-Omega low Reynolds number, two-equation turbulence models. Solution of the governing equations is accomplished by a finite-volume formulation

with central-difference spatial discretizations and an explicit, four-stage, Runge Kutta time-integration procedure. The Runge-Kutta scheme appears to provide efficient convergence when applied to the calculation of turbulent, reacting flowfields in these small thrusters. Appropriate boundary conditions are developed to properly model propellant mass flowrates and regenerative wall cooling. The computational method is validated against measured engine performance parameters on a global level, as well as experimentally obtained exit plane and plume flowfield properties on a local level. The model does an excellent job of predicting the measured performance trends of an auxiliary thruster as a function of O/F ratio, although the performance levels are consistently underpredicted by approximately 4 percent. These differences arise because the extent to which the wall coolant layer and combustion gases mix and react is underpredicted. Predictions of velocity components, temperature and species number densities in the near-field plume regions of several low-thrust engines show reasonable agreement with experimental data obtained by two separate laser diagnostic techniques. Discrepancies between the predictions and measurements are primarily due to three-dimensional mixing processes which are not accounted for in the analysis. Both comparisons with experiment and the evident reason for errors in absolute levels of predicted quantities suggest the method should prove valuable for predicting parametric trends for design studies. In addition, issues such as numerical stability, robustness and computational efficiency are addressed. These include the evaluation of a numerically compatible two-equation turbulence model and the implementation of a time-derivative preconditioning method for convergence enhancement of low Mach number, chemically reacting flows. Author

N94-14682*# United Technologies Research Center, East Hartford, CT.
INVESTIGATION OF THE FEASIBILITY OF OPTICAL DIAGNOSTIC MEASUREMENTS AT THE EXIT OF THE SSME Final Report
John A. Shirley and Laurence R. Boedeker 1 Jul. 1993 47 p
(Contract NAS8-36861)
(NASA-CR-193832; NAS 1.26:193832; R93-957424-F) Avail: CASI HC A03/MF A01

Under Contract NAS8-36861 sponsored by NASA Marshall Space Flight Center, the United Technologies Research Center is conducting an investigation of the feasibility of remote optical diagnostics to measure temperature, species concentration and velocity at the exit of the Space Shuttle Main Engine (SSME). This is a two phase study consisting of a conceptual design phase followed by a laboratory experimental investigation. The first task of the conceptual design studies is to screen and evaluate the techniques which can be used for the measurements. The second task is to select the most promising technique or techniques, if as expected, more than one type of measurement must be used to measure all the flow variables of interest. The third task is to examine in detail analytically the capabilities and limitations of the selected technique(s). The results of this study are described in the section of this report entitled Conceptual Design Investigations. The conceptual design studies identified spontaneous Raman scattering and photodissociative flow-tagging for measurements respectively of gas temperature and major species concentration and for velocity. These techniques and others that were considered are described in the section describing the conceptual design. The objective of the second phase of investigations was to investigate experimentally the techniques identified in the first phase. The first task of the experimental feasibility study is to design and assemble laboratory scale experimental apparatus to evaluate the best approaches for SSME exit optical diagnostics for temperature, species concentrations and velocity, as selected in the Phase I conceptual design study. The second task is to evaluate performance, investigate limitations, and establish actual diagnostic capabilities, accuracies and precision for the selected optical systems. The third task is to evaluate design requirements and system trade-offs of conceptual instruments. Spontaneous Raman scattering excited by a KrF excimer laser pulse was investigated for SSME exit plane temperature and major species concentration measurements. The relative concentrations of molecular hydrogen and water vapor would be determined by measuring the integrated Q-branch scattering signals through narrow bandpass filters in front of photomultipliers. The temperature would be determined by comparing the signal from a single hydrogen rotational Raman line to the total hydrogen Q-branch signal. The rotational Raman line would be isolated by a monochromator and detected with a PMT. Derived from text

N94-14689# Los Alamos National Lab., NM.
PRIMARY AND SECONDARY ELECTRICAL SPACE POWER BASED ON ADVANCED PEM SYSTEMS
N. E. Vanderborgh, J. C. Hedstrom, K. R. Stroh, and J. R. Huff (Ballard Power Corp., Albuquerque, NM.) 1993 9 p Presented at the 4th Space Electrochemical Research and Technology Conference, Cleveland, OH, 14-15 Apr. 1993
(Contract W-7405-eng-36)
(DE93-012643; LA-UR-93-1305; CONF-9304142-1) Avail: CASI HC A02/MF A01

For new space ventures, power continues to be a pacing function for mission planning and experiment endurance. Although electrochemical power is a well demonstrated space power technology, current hardware limitations impact future mission viability. In order to document and augment electrochemical technology, a series of experiments for NASA LeRC are underway at the Los Alamos National Laboratory that define operational parameters on contemporary proton exchange membrane (PEM) hardware operating with hydrogen and oxygen reactants. Because of the high efficiency possible for water electrolysis, this hardware is also thought part of a secondary battery design built around stored reactants--the so-called regenerative fuel cell. An overview of stack testing at Los Alamos, and of analyses related to regenerative fuel cell systems are provided in this paper. Finally, this paper describes work looking at innovative concepts that remove complexity from stack hardware with the specific intent of higher system reliability. This new concept offers the potential for unprecedented electrochemical power system energy densities. DOE

N94-14725*# National Aeronautics and Space Administration. Lewis Research Center, Cleveland, OH.
PLASMA CONTACTOR TECHNOLOGY FOR SPACE STATION FREEDOM
Michael J. Patterson, John A. Hamley, Timothy Sarver-Verhey (Sverdrup Technology, Inc., Brook Park, OH.), George C. Soulas (Sverdrup Technology, Inc., Brook Park, OH.), James Parkes (Sverdrup Technology, Inc., Brook Park, OH.), Wayne L. Ohlinger (Georgia Tech Research Inst., Atlanta.), Michael S. Schaffner (Cleveland State Univ., OH.), and Amy Nelson (Purdue Univ., West Lafayette, IN.) Jun. 1993 23 p Presented at the 29th Joint Propulsion Conference and Exhibit, Monterey, CA, 28-30 Jun. 1993; sponsored by AIAA, SAE, ASME, and ASEE See also A93-50034
(RTOP 474-46-10)
(NASA-TM-106291; E-8028; NAS 1.15:106291; AIAA Paper 93-2228)
Avail: CASI HC A03/MF A01

Hollow cathode plasma contactors were baselined for Space Station Freedom (SSF) to control the electrical potentials of surfaces to eliminate/mitigate damaging interactions with the space environment. The system represents a dual-use technology which is a direct outgrowth of the NASA electric propulsion program and in particular the technology development effort on ion thruster systems. Specific efforts include optimizing the design and configuration of the contactor, validating its required lifetime, and characterizing the contactor plume and electromagnetic interference. The plasma contact or subsystems include the plasma contact or unit, a power electronics unit, and an expellant management unit. Under this program these will all be brought to breadboard and engineering model development status. New test facilities were developed, and existing facilities were augmented, to support characterizations and life testing of contactor components and systems. The magnitude, scope, and status of the plasma contactor hardware development program now underway and preliminary test results on system components are discussed. Author (revised)

N94-14726*# National Aeronautics and Space Administration. Lewis Research Center, Cleveland, OH.
DERATED ION THRUSTER DEVELOPMENT STATUS
Michael J. Patterson, Thomas W. Haag, and George J. Williams, Jr. (Princeton Univ., NJ.) Jun. 1993 16 p Presented at the 29th Joint Propulsion Conference and Exhibit, Monterey, CA, 28-30 Jun. 1993; sponsored by AIAA, SAE, ASME, and ASEE See also A93-50031
(RTOP 506-42-31)
(NASA-TM-106292; E-8029; NAS 1.15:106292; AIAA Paper 93-2225)
Avail: CASI HC A03/MF A01

A 30 cm diameter xenon ion thruster is under development at NASA to provide an ion propulsion option for auxiliary and primary propulsion on missions of national interest. Specific efforts include thruster design

optimizations, component life testing and validation, vibration testing, and performance characterizations. Under this program, the ion thruster will be brought to engineering model development status. The activities and preliminary test results to develop a 30 cm engineering model thruster are discussed. Author (revised)

N94-14771*# Thermacore, Inc., Lancaster, PA.
INSOLUBLE COATINGS FOR STIRLING ENGINE HEAT PIPE CONDENSER SURFACES Final Report
Peter M. Dussinger Sep. 1993 63 p
(Contract NAS3-26325; RTOP 324-01-00)
(NASA-CR-191188; E-8101; NAS 1.26:191188) Avail: CASI HC A04/MF A01

The work done by Thermacore, Inc., Lancaster, Pennsylvania, for the Phase 1, 1992 SBIR National Aeronautics and Space Administration Contract, 'Insoluble Coatings for Stirling Engine Heat Pipe Condenser Surfaces' is described. The work was performed between January 1992 and July 1992. Stirling heat engines are being developed for electrical power generation use on manned and unmanned earth orbital and planetary missions. Dish Stirling solar systems and nuclear reactor Stirling systems are two of the most promising applications of the Stirling engine electrical power generation technology. The sources of thermal energy used to drive the Stirling engine typically are non-uniform in temperature and heat flux. Liquid metal heat pipe receivers are used as thermal transformers and isothermalizers to deliver the thermal energy at a uniform high temperature to the heat input section of the Stirling engine. The use of a heat pipe receiver greatly enhances system efficiency and potential life span. One issue that is raised during the design phase of heat pipe receivers is the potential solubility corrosion of the Stirling engine heat input section by the liquid metal working fluid. This Phase 1 effort initiated a program to evaluate and demonstrate coatings, applied to nickel based Stirling engine heater head materials, that are practically 'insoluble' in sodium, potassium, and NaK. This program initiated a study of nickel aluminide as a coating and developed and demonstrated a heat pipe test vehicle that can be used to test candidate materials and coatings. Nickel 200 and nickel aluminide coated Nickel 200 were tested for 1000 hours at 800 C at a condensation heat flux of 25 W/sq cm. Subsequent analyses of the samples showed no visible sign of solubility corrosion of either coated or uncoated samples. The analysis technique, photomicrographs at 200X, has a resolution of better than 2.5 microns (.0001 in). The results indicate that the heat pipe environment is not directly comparable to liquid metal pumped loop data, that nickel aluminide is still a leading candidate for solubility corrosion protection, and that longer duration tests are required to reach a definitive conclusion whether coatings are required at all. Should further testing be required, the test vehicle and analytical tools were developed.
Author (revised)

N94-14806# Brookhaven National Lab., Upton, NY.
SPACE REACTOR FUEL ELEMENT TESTING IN UPGRADED TREAT
M. Todosow, P. Bezler, H. Ludewig, and W. Y. Kato 1993 6 p
Presented at the 10th Symposium on Space Nuclear Power and Propulsion, Albuquerque, NM, 10-14 Jan. 1993
(Contract DE-AC02-76CH-00016)
(DE93-012524; BNL-48700; CONF-930103-36) Avail: CASI HC A02/MF A01 (US Sales Only)

The testing of candidate fuel elements at prototypic operating conditions with respect to temperature, power density, hydrogen coolant flow rate, etc.; a crucial component in the development and qualification of nuclear rocket engines based on the Particle Bed Reactor (PBR); NERVA-derivative; and other concepts are discussed. Such testing may be performed at existing reactors, or at new facilities. A scoping study has been performed to assess the feasibility of testing PBR based fuel elements at the TREAT reactor. Initial results suggest that full-scale PBR elements could be tested at an average energy deposition of approximately 60-80 MW-s/L in the current TREAT reactor. If the TREAT reactor was upgraded to include fuel elements with a higher temperature limit, average energy deposition of approximately 100 MW/L may be achievable. DOE

N94-14907*# Thiokol Corp., Brigham City, UT. Space Operations.
TECHNICAL EVALUATION MOTOR NO. 10 (TEM-10) Final Report
Aug. 1993 130 p
(Contract NAS8-38100)
(NASA-CR-193846; NAS 1.26:193846; TWR-17674; Publ-940151) Avail: CASI HC A07/MF A02

Technical Evaluation Motor No. 10 (TEM-10) was static fired on 27 Apr. 1993 at the Thiokol Corporation full-scale motor static test bay, T-24. This final test report documents the procedures, performance, and results of the static test firing of TEM-10. All observations, discussions, conclusions, and recommendations contained are final. Included is a presentation and discussion of TEM-10 performance, anomalies, and test results in concurrence with the objectives outlined in CTP-0110, Revision D, Space Shuttle Technical Evaluation Motor No. 10 (TEM-10) Static Fire Test Plan.
Author (revised)

23 CHEMISTRY AND MATERIALS (GENERAL)

N94-14290# Los Alamos National Lab., NM.
SYNTHESIS OF ORGANIC LIGANDS FOR f-ELEMENT SEPARATIONS
R. T. Paine (New Mexico Univ., Albuquerque.) 1993 61 p
(Contract W-7405-eng-36)
(DE93-012915; LA-SUB-93-171) Avail: CASI HC A04/MF A01

The efficacy of CMP and CMPO (carbamoylmethylphosphonates, carbamoylmethylphosphine oxides) as extractants has stimulated interest in the design of new extractants, in particular, bifunctional and trifunctional ligands containing both P(double bond)O and N-O donors. 2,6-bis(diphenylphosphino) pyridine N,P,P-trioxide was selected as a target, with the bifunctional and trifunctional diphenylmethylphosphino analogs as alternate target ligands. The ligands were synthesized and characterized. Their coordination chemistry was studied using Pr, Tb, Yb, Th; a wider range of metal/ligand stoichiometries was found than is typically found for other ligands, and the ligands are sufficiently basic that, under some conditions, they displace nitrate ions from the inner coordination sphere, which is unusual for neutral donor ligands. For both 2:1 and 4:1 complexes, the ligand is bonded to the Ln(3) ions in a bidentate manner and in a tridentate manner for 1:1 and 2:1 complexes. These ligands may be unusually effective solvent extraction agents, and liquid-liquid extraction studies are in progress. DOE

24 COMPOSITE MATERIALS

Includes physical, chemical, and mechanical properties of laminates and other composite materials.

For ceramic materials see *27 Nonmetallic Materials.*

N94-12833*# Boeing Defense and Space Group, Seattle, WA.
RESIN TRANSFER MOLDING OF TEXTILE COMPOSITES Final Report, Jun. 1991 - Mar. 1993
Anthony Falcone, Harry Dursch, Karl Nelson, and William Avery Jul. 1993 139 p
(Contract NAS1-19247; RTOP 510-02-12-10)
(NASA-CR-191505; NAS 1.26:191505) Avail: CASI HC A07/MF A02

The design and manufacture of textile composite panels, tubes, and angle sections that were provided to NASA for testing and evaluation are documented. The textile preform designs and requirements were established by NASA in collaboration with Boeing and several vendors of textile reinforcements. The following four types of preform architectures were used: stitched uniweave, 2D-braids, 3D-braids, and interlock weaves. The preforms consisted primarily of Hercules AS4 carbon fiber; Shell RSL-1895 resin was introduced using a resin transfer molding process. All the finished parts were inspected using ultrasonics. Author (revised)

N94-12871*# National Aeronautics and Space Administration. Lewis Research Center, Cleveland, OH.
OHMIC HEATING OF COMPOSITE CANDIDATE GRAPHITE-FIBER/COATING COMBINATIONS
Phillip B. Abel Washington Jul. 1993 9 p
(RTOP 506-43-11)
(NASA-TM-4491; E-7689; NAS 1.15:4491) Avail: CASI HC A02/MF A01

Graphite fibers were heated in a vacuum to test the adhesion of deposited films at elevated temperatures. Copper-clad fibers and fibers with bilayer coatings were resistance heated by a direct-current power supply. Where possible, peak temperatures were measured with a long-focal-length optical pyrometer. Fiber surface wetting or nonwetting behavior could be clearly observed after this relatively quick and simple procedure. These results are discussed in the context of creating composites of graphite fibers in a copper matrix. Author (revised)

N94-13138*# National Aeronautics and Space Administration. Lewis Research Center, Cleveland, OH.

NDE OF TITANIUM ALLOY MMC RINGS FOR GAS TURBINE ENGINES

George Y. Baaklini, Larry D. Percival (Pratt and Whitney Aircraft, West Palm Beach, FL.), Robert N. Yancey (Advanced Research and Applications Corp., Dayton, OH.), and Harold E. Kautz Sep. 1993 14 p Proposed for presentation at the Tenth Biennial Conference on Reliability Stress Analysis and Failure Prevention, Albuquerque, NM, 19-22 Sep. 1993; sponsored by ASME

(RTOP 510-01-50)

(NASA-TM-106188; E-7892; NAS 1.15:106188) Avail: CASI HC A03/MF A01

Progress in the processing and fabrication of metal matrix composites (MMC's) requires appropriate mechanical and nondestructive testing methods. These methods are needed to characterize properties, assess integrity, and predict the life of engine components such as compressor rotors, blades, and vanes. Capabilities and limitations of several state-of-the-art nondestructive evaluation (NDE) technologies are investigated for characterizing titanium MMC rings for gas turbine engines. The use of NDE technologies such as x-ray computed tomography, radiography, and ultrasonics in identifying fabrication-related problems that caused defects in components is examined. Acousto-ultrasonics was explored to assess degradation of material mechanical properties by using stress wave factor and ultrasonic velocity measurements before and after the burst testing of the rings. Author (revised)

N94-13139*# Sverdrup Technology, Inc., Brook Park, OH.

AN ADVANCED TEST TECHNIQUE TO QUANTIFY THERMOMECHANICAL FATIGUE DAMAGE ACCUMULATION IN COMPOSITE MATERIALS Final Report

Michael G. Castelli Aug. 1993 9 p

(Contract NAS3-25266; RTOP 510-01-50)

(NASA-CR-191147; E-8068; NAS 1.26:191147) Avail: CASI HC A02/MF A01

A mechanical test technique was developed to assist in quantifying the accumulation of damage in composite materials during thermomechanical fatigue (TMF) cycling. This was accomplished by incorporating definitive elastic mechanical property measurements into an ongoing load-controlled TMF test without disturbing the test specimen or significantly altering the test conditions. The technique allows two fundamental composite properties consisting of the isothermal elastic static moduli and the macroscopic coefficient of thermal expansion (CTE) to be measured and collected as functions of the TMF cycles. The specific implementation was incorporated into the commonly employed idealized in-phase and out-of-phase TMF cycles. However, the techniques discussed could be easily implemented into any form of load-controlled TMF mission cycle. By quantifying the degradations of these properties, tremendous insights are gained concerning the progression of macroscopic composite damage and often times the progression of damage within a given constituent. This information should also be useful for the characterization and essential for the verification of analytical damage modeling methodologies. Several examples utilizing this test technique are given for three different fiber lay-ups of titanium metal matrix composites. Author

N94-13248# Argonne National Lab., IL. Materials and Components Technology Div.

MEASUREMENT OF RESIDUAL STRAIN IN COMPOSITES BY MEANS OF TIME-OF-FLIGHT NEUTRON DIFFRACTION

D. S. Kupperman, S. Majumdar, J. Richardson, and A. Saigal 1993 16 p Presented at the 1993 Annual Meeting of the American Crystallographic Association, Albuquerque, NM, 24-28 May 1993

(Contract W-31-109-eng-38)

(DE93-012939; ANL/MCT/CP-78715; CONF-9305188-1) Avail: CASI HC A03/MF A01

Neutron diffraction time-of-flight measurements using the Intense Pulsed Neutron Source at Argonne National Laboratory have been employed to study strain in various metal- and ceramic-matrix composites. For example, measurements carried out to 900 C on a composite composed of a titanium alloy matrix and silicon carbide fibers have been used to validate theoretical assumptions in the prediction of fabrication-induced residual stress. Sapphire reinforced nickel aluminide composites have also been studied. Studies of a high-temperature ceramic superconducting composite consisting of yttrium-barium-copper-oxide and silver with various volume fractions of silver have also been carried out. The results of these studies have provided information on the effect of Ag content on interface bonding. In addition, ceramic-matrix composites with randomly dispersed ceramic whiskers with varying fiber content have been investigated. DOE

N94-13267*# Bell Helicopter Co., Fort Worth, TX.

FLIGHT SERVICE EVALUATION OF COMPOSITE COMPONENTS ON THE BELL HELICOPTER MODEL 206L Final Report

Henry Wilson 1 Sep. 1993 129 p

(Contract NAS1-15279; RTOP 536-06-37-03)

(NASA-CR-191499; NAS 1.26:191499; Rept-699-099-359) Avail: CASI HC A07/MF A02

This is the final report on the advanced composite components which were placed in service on the 206L LongRanger helicopters in the continental United States, Canada, and Alaska. This report covers all test data which was gathered, as well as maintenance histories of the parts. The previous reports describe the fabrication, service experiences, and test data through 1986. This report contains information from these references, as well as data gathered after 1986. The status of the 40 sets of components is discussed. Each set consisted of a vertical fin, forward fairing, litter door, and baggage door. Almost 500,000 flight hours were accumulated on the 160 parts, with the high-time part accumulating 14,687 flight hours. Over 60 percent of the parts were destructively tested to measure strength and stiffness retention over the course of the program. The vertical fins had the greatest strength retention followed by the litter doors. The baggage doors had the poorest retention of strength. There was very little difference in property retention between the four primary operating regions: Northwest U.S., Southwest U.S., Gulf of Mexico Coastal Region, and the Northeast U.S. and Eastern Canada Region. The field problems have ranged from two lightning-struck fins to significant delaminations in the baggage doors. There was only one environmentally related field incident, in which the glass windows on the litter doors were found to loosen due to high temperatures experienced in the southwest region. Author (revised)

N94-13378*# Battelle Memorial Inst., Columbus, OH.

INELASTIC DEFORMATION MECHANISMS IN SCS-6/Ti 15-3 MMC LAMINA UNDER COMPRESSION

Golam M. Newaz and Bhaskar S. Majumdar Cleveland, OH NASA Sep. 1993 35 p

(Contract NAS3-26494; RTOP 510-01-50)

(NASA-CR-191170; E-8085; NAS 1.26:191170) Avail: CASI HC A03/MF A01

An investigation was undertaken to study the inelastic deformation mechanisms in (0)(sub 8) and (90)(sub 8) Ti 15-3/SCS-6 lamina subjected to pure compression. Monotonic tests were conducted at room temperature (RT), 538 C and 650 C. Results indicate that mechanical response and deformation characteristics were different in monotonic tension and compression loading whereas some of those differences could be attributed to residual stress effects. There were other differences because of changes in damage and failure modes. The inelastic deformation in the (0)(sub 8) lamina under compression was controlled primarily by matrix plasticity, although some evidence of fiber-matrix debonding was observed. Failure of the specimen in compression was due to fiber buckling in a macroscopic shear zone (the failure plane). The inelastic deformation mechanisms under compression in (90)(sub 8) lamina were controlled by radial fiber fracture, matrix plasticity, and fiber-matrix debonding. The radial fiber fracture was a new damage mode observed for MMC's. Constitutive response was predicted for both the (0)(sub 8) and (90)(sub 8) laminae, using AGLPLY, METCAN, and Battelle's Unit Cell FEA model. Results from the analyses were encouraging. Author (revised)

N94-13389# Lawrence Livermore National Lab., CA.
FRACTURE BEHAVIOR OF VANADIUM/VANADIUM SILICIDE IN-SITU COMPOSITES
M. J. Strum and G. A. Henshall 30 Nov. 1992 8 p Presented at the 16th Material Research Society International Symposium on the Scientific Basis for Nuclear Waste Management Fall Meeting, Boston, MA, 30 Nov. - 5 Dec. 1992
(Contract W-7405-eng-48)
(DE93-013422; UCRL-JC-112408; CONF-921101-119) Avail: CASI HC A02/MF A01

The fracture behavior of V-V(sub 3)Si in-situ composite alloys has been evaluated for intermetallic phase fractions of 30, 50, and 70 volume percent. In addition, the mechanical properties of the ductile constituent in these composites have been evaluated from two alloys containing silicon at its solubility-limit in vanadium at the eutectic temperature and at 1400 degrees C. The fracture toughness was found to increase monotonically with increasing volume fraction of ductile phase. Fractography has shown evidence of crack bridging by the vanadium solid solution phase and increased ductility within the composite relative to bulk measurements. The toughness results are compared with predictions based on an existing model of ductile-phase toughening using our measurements of component properties. DOE

N94-13557 Pennsylvania State Univ., University Park.
PROCESSING AND MECHANICAL PROPERTIES OF SILICON CARBIDE PLATELET REINFORCED ALUMINA COMPOSITES Ph.D. Thesis
Yeong-Shyung Chou 1992 223 p
Avail: Univ. Microfilms Order No. DA9311611

The processing and the mechanical properties of SiC-platelet/Al2O3 composites are examined. In the processing part, the goal is to identify the effect of forming methods on the microstructural evolution, in particular, the factors that influence preferred platelet orientation. Three forming techniques - slip casting, tape casting, and dry compaction - were employed to make the composites. Optical microscopy and an x-ray device, pole-figure goniometer, were used to analyze the degree of preferred orientation. Preferred orientation was studied on samples before and after hot-pressing. The effects of aspect ratio of platelets and of die pressure were also examined. The mechanical properties studied were Young's modulus, fracture toughness, and flexural strength. The effects of the platelet size and the microstructural anisotropy were examined. The optimum mechanical properties of the composites were a Young's modulus of 421 GPa, fracture toughness of 7.77 MPa(square root of m), and a flexural strength of 480 MPa. Based on the microstructural observations, a theoretical analysis on the toughening due to crack deflection in perfectly aligned disc composites was conducted. Toughening predictions of the initial tilt and the subsequent twist were calculated. The effect of the aspect ratio and the volume fraction of platelets were also considered. To test the model and to identify the predominant toughening mechanism, electron microscopy was first used to directly find the possible toughening mechanisms. Fracture toughness was measured with the bridge indentation method and compared with the theoretical predictions. R-curve behavior was measured to clarify the toughening contribution from bridging SiC platelets. In addition, fracture surface roughness was measured to provide a semi-quantitative assessment of the crack deflection process. From the combination of fracture surface roughness measurements, microstructural observation, comparison of experimental toughness with theoretical predictions, and measurements of R-curve behavior, it was concluded that crack deflection was the major toughening mechanism in the SiC-platelet/Al2O3 composites.
Dissert. Abstr.

N94-13558 Kansas State Univ., Manhattan.
NONLINEAR VIBRATIONS OF THICK COMPOSITE PLATES: HIGHER-ORDER SHEAR DEFORMATION PLATE THEORY Ph.D. Thesis
Hung-Yu Lu 1992 164 p
Avail: Univ. Microfilms Order No. DA9310835

The equations of motion and the associate boundary conditions for the nonlinear vibrations of a heterogeneous anisotropic thick annular plate are derived by using Hamilton's principle. The effects of shear deformation, rotatory inertia, inplane deformation and inplane inertia are all included to provide more accurate results for the design and analysis of annular plates. The shear deformation of the plate is assumed based on the higher-order shear deformation plate theory. Due to the complexity of the derived nonlinear coupled partial differential equations, a finite element method is used in the numerical analysis. The basic equation of motion in finite element formulation is obtained by using a variational approach. A numerical technique of using an incremental and iterative scheme is utilized for calculating frequency responses. The developed mathematical model is then applied to study axisymmetric nonlinear vibrations of various thick annular plates: homogeneous isotropic annular plates, homogeneous orthotropic annular plates, heterogeneous isotropic annular sandwich plates, and heterogeneous orthotropic annular sandwich plates. The numerical results for frequencies of each annular plate system are obtained. The effects of shear deformation and rotatory inertia are presented and discussed. The influence of lamination interchange of a heterogeneous annular sandwich plate is also demonstrated. Author

N94-13583# Pennsylvania Transportation Inst., University Park. Dept. of Engineering Science and Mechanics.
INHIBITING CORROSION IN Gr/Al AND Gr/Mg METAL MATRIX COMPOSITES USING NONEQUILIBRIUM ALLOYING TECHNIQUES Annual Report, 1 Apr. 1992 - 31 Mar. 1993
B. A. Shaw, W. C. Moshier, R. G. Wendt, P. L. Miller, and T. R. Schrecengost Jun. 1993 70 p
(Contract N00014-91-J-1196)
(AD-A266547) Avail: CASI HC A04/MF A01

Metal matrix composites (MMC's) have been heavily studied over the past thirty years. During that period, many proposals have been made to develop a matrix alloy that was compatible with the reinforcing phase. However, for one reason or another, the technology has continued to focus on conventional alloys and fabrication practices. Although tremendous advances have been made on composite materials, the basic technology remains similar to systems studied twenty years ago. This work represents the first new program where new alloys are being developed for graphite reinforced composites which are tailored to a novel processing technology for manufacturing corrosion resistant graphite reinforced composites.
DTIC

N94-13595 University of Southern Illinois, Carbondale.
DEVELOPMENT OF TIME-DEPENDENT ORTHOTROPIC CONSTITUTIVE LAW OF A THERMOPLASTIC COMPOSITE MATERIAL Ph.D. Thesis
Chien-Chain Lia 1992 133 p
Avail: Univ. Microfilms Order No. DA9312070

Thermoplastic composite materials have been receiving more usage in many industries over the past decade. However, the study of creep behavior of thermoplastic composites is not well understood. In this research, Graphite/PEEK thermoplastic composite material was used to develop the orthotropic creep compliance matrix (S(sub ij)(t,o)) and to investigate the long-term creep response. Short-term experiments were conducted to study feasibility of accelerated characterization (TSSP) of creep response for off-axis laminae. The fiber orientations studies for creep tests were 10, 15, 30, 45, 60, 75, and 90 degrees. Based on the short-term creep data of off-axis laminae, the time-dependent orthotropic constitutive law was established to model the non-linear viscoelastic behavior. Results of this research indicate that: (1) The accelerated characterization procedure could be performed using elevated stresses, and the Findley equation represented experimental creep data very accurately. (2) Excellent agreement was found between the experimental results and the predicted results based on the time-dependent orthotropic constitutive law for Graphite/PEEK thermoplastic composite. (3) In comparison with the shifted result from the master curve, the time dependent orthotropic constitutive theory could be more easily used to predict the long-term creep response for any stress level and fiber angle orientation. Dissert. Abstr.

N94-13663 Department of the Navy, Washington, DC.
MODIFIED CARBON FOR IMPROVED CORROSION RESISTANCE Patent Application
Alan S. Edelstein, inventor (to Navy), Richard K. Everett, inventor (to Navy), Patricia Tzaskoma, inventor (to Navy), and Benji Maruyama, inventor (to Navy) 15 Jan. 1993 15 p Limited Reproducibility: More than 20% of this document may be affected by microfiche quality
(AD-D015741; US-Patent-Appl-SN-004002; Navy-Case-74104) Avail: CASI HC A03

The present invention relates to reinforced composites and more particularly to composites reinforced by carbon or graphite that has been

treated to reduce corrosion between the reinforcement material and adjacent metals. Graphite or carbon particles with a graphitic skin are intercalculated with a compound including an oxidized form of a metal and then reduced in a hydrogen atmosphere. This process reduces the driving force for the galvanic reaction between the particles and active metals in aqueous environments. The particles may be present as a reinforcement for a metal matrix (e.g., graphite/aluminum metal matrix composites) or as a reinforcement for a non-metallic material (e.g., graphite/polyimide, graphite/polyester or graphite/cyanate composites). In the latter case, the composite is adjacent to a metal in a structure. By way of example, the graphite or carbon particle may be a fiber, the metal subject to attack may be aluminum or magnesium, and the intercalation compound may be NiCl2. DTIC

N94-13706# Air Force Inst. of Tech., Wright-Patterson AFB, OH. School of Engineering.

EXPERIMENTAL AND ANALYTICAL ANALYSIS OF THE RESPONSE OF A SMART BEAM TO RATE FEEDBACK M.S. Thesis

Terance J. Hoffman Jun. 1993 139 p

(AD-A266544; AFIT/GA/ENY/93J-01) Avail: CASI HC A07/MF A02

A smart beam with embedded sensors and actuators was analyzed and tested. The smart beam studied was constructed from graphite and epoxy with piezoceramic actuators and NiTiNOL sensors embedded. It was mounted vertically and subjected to transverse dynamic loading at the free end. Analytic expressions for the open loop and closed loop response (using strain rate feedback control) of the beam (including internal damping) to external forcing were derived in detail. Experimental testing of the beam, verified the accuracy of the predicted open loop response. DTIC

N94-13711*# National Aeronautics and Space Administration. Langley Research Center, Hampton, VA.

TESTING AND ANALYSIS OF CURVED FRAME SPECIMENS MADE FROM A LONG DISCONTINUOUS FIBER (LDF) MATERIAL

Dawn C. Jegley Aug. 1993 24 p

(RTOP 505-63-50-08)

(NASA-TM-109014; NAS 1.15:109014) Avail: CASI HC A03/MF A01

A long discontinuous fiber (LDF) material may be useful for constructing composite parts with complex curvature. Graphite-thermoplastic LDF curved frame specimens were studied to investigate the behavior of curved frame structures made from this material form. Experimental results for three curved frame specimens loaded in a four-point-bending configuration and finite-element predictions of strains and displacements are presented. Author

N94-13804# European Space Agency, Paris (France).

CHARACTERIZATION OF COMPOSITE MATERIALS FOR AEROSPACE STRUCTURES

Harald Twardy (Deutsche Forschungsanstalt fuer Luft- und Raumfahrt, Brunswick, Germany.), Holger Hanselka (Deutsche Forschungsanstalt fuer Luft- und Raumfahrt, Brunswick, Germany.), and Bernhard Beier (Deutsche Forschungsanstalt fuer Luft- und Raumfahrt, Brunswick, Germany.) Apr. 1993 20 p Transl. into ENGLISH of Charakterisierung von Verbundkunststoffen fuer Luft- und Raumfahrtstrukturen (Brunswick, Germany, DLR) Jul. 1990 p 1-25 Original language document announced as N91-23246

(ESA-TT-1260; DLR-MITT-90-15; ETN-93-94582) Avail: CASI HC A03/MF A01

Fiber reinforced polymers are applied as construction materials for astronautics and transatmospheric flight. They are submitted to a wide spectrum of environmental influences such as temperature, moisture, and radiation. These phenomena induce the variation of mechanical and physical properties of polymers. The reduced coefficients of elasticity, the thermal resistance to aging, and the viscoelastic behavior under the influence of elevated temperatures are investigated. ESA

N94-13866# Ecole Polytechnique, Montreal (Quebec).

MODELLING OF THE TEMPERATURE DISTRIBUTION IN A COPPER ROLL FOR THE DESIGN OF A SYSTEM OF COOLED ROLLS ADAPTED TO VERTICAL STRIP CASTING [MODELISATION DE LA DISTRIBUTION DE TEMPERATURE DANS UN ROULEAU DE CUIVRE POUR LA CONCEPTION D'UN SYSTEME DE ROULEAUX REFROIDIS ADAPTE A LA COULEE EN BANDE VERTICALE]

S. Turenne and M.-C. Heuzey Dec. 1992 28 p In FRENCH

(IMI-93RT-21200-1436-G; CNR-35325; CTN-93-60763) Avail: CASI HC A03/MF A01

In vertical strip casting of metal matrix composites, it is proposed to control the process with the help of a strategy yet to be defined. This strategy will be based on the acquisition of velocity signals from the rolls, on the load between the rolls, on the displacement of the mobile roll, and the temperatures at different locations. To facilitate control and the attaining of a steady state regime, it is necessary to design a cooling system for the rolls. A model was developed with the objective of evaluating the performance of such a system taking into account certain constraints. The rolls consist of a copper ring 2.54 cm thick in contact with a stainless steel core having cooling channels on its surface. All the model calculations are performed taking into consideration the A356 aluminum alloy used, whose lower melting point compared to the copper rolls imposes the object of limiting the temperature at the interface between the copper ring and the core. A polar coordinate system is used to model the two-dimensional geometry of the ring, employing a system of finite difference equations in which the temperature is determined at each node simultaneously. Results are presented which allow illustration of the temperature distribution in the copper ring over time. A FORTRAN program listing for calculating the temperature distribution is appended. CISTI

N94-13920*# General Electric Co., Cincinnati, OH. Aircraft Engines.

THERMAL SHOCK RESISTANCE OF CERAMIC MATRIX COMPOSITES Final Report

D. M. Carper and H. F. Nied (General Electric Co., Schenectady, NY.) Aug. 1993 50 p

(Contract NAS3-25640; RTOP 510-01-50)

(NASA-CR-189136; E-8070; NAS 1.26:189136) Avail: CASI HC A03/MF A01

The experimental and analytical investigation of the thermal shock phenomena in ceramic matrix composites is detailed. The composite systems examined were oxide-based, consisting of an aluminosilicate matrix with either polycrystalline aluminosilicate or single crystal alumina fiber reinforcement. The program was divided into three technical tasks; baseline mechanical properties, thermal shock modeling, and thermal shock testing. The analytical investigation focused on the development of simple expressions for transient thermal stresses induced during thermal shock. The effect of various material parameters, including thermal conductivity, elastic modulus, and thermal expansion, were examined analytically for their effect on thermal shock performance. Using a simple maximum stress criteria for each constituent, it was observed that fiber fracture would occur only at the most extreme thermal shock conditions and that matrix fracture, splitting parallel to the reinforcing fiber, was to be expected for most practical cases. Thermal shock resistance for the two material systems was determined experimentally by subjecting plates to sudden changes in temperature on one surface while maintaining the opposite surface at a constant temperature. This temperature change was varied in severity (magnitude) and in number of shocks applied to a given sample. The results showed that for the most severe conditions examined that only surface matrix fracture was present with no observable fiber fracture. The impact of this damage on material performance was limited to the matrix dominated properties only. Specifically, compression strength was observed to decrease by as much as 50 percent from the measured baseline. Author (revised)

N94-14042*# National Aeronautics and Space Administration. Lewis Research Center, Cleveland, OH.

OPTIMAL SYNTHESIS OF HOT COMPOSITE LAMINATES WITH INTERPHASE LAYERS

Christopher Rabzak (Sverdrup Technology, Inc., Brook Park, OH.), Dimitris A. Saravanos, and Christos C. Chamis Jun. 1993 22 p Presented at the Symposium on Functionally Graded, Advanced Composite Materials, Charlottesville, VA, 6-9 Jun. 1993; sponsored by SES, ASME and ASCE

(RTOP 510-01-50)

(NASA-TM-106326; E-8081; NAS 1.15:106326) Avail: CASI HC A03/MF A01

A method for the optimal grading of a single interphase layer in metal matrix composite laminates for the minimization of residual stresses is described. The capability to simultaneously tailor some fabrication parameters is also incorporated. Applications for unidirectional, cross-ply and

quasi-isotropic Graphite/Copper laminates are investigated to assess the potential of interphase layer in reducing matrix residual stresses in various laminate configurations. Simultaneous optimization of interphase and fabrication characteristics appears to be more effective in decreasing residual stresses. The results also indicate that the interphase layer is more effective in lowering residual stresses in unidirectional composites and selectively within individual plies of a laminate. Embedded interphase layers in all the plies did not produce a significant global reduction in residual stresses.
Author

N94-14050*# North Carolina Agricultural and Technical State Univ., Greensboro. Dept. of Mechanical Engineering.
GRAPHITE FIBER TEXTILE PREFORM/COPPER MATRIX COMPOSITES Semiannual Progress Report No. 1, 1 Jan. - 30 Jun. 1993
G. J. Filatovs 1993 8 p
(Grant NAG3-1432)
(NASA-CR-193797; NAS 1.26:193797) Avail: CASI HC A02/MF A01

This project has the objective of exploring the use of graphite fiber textile preform/copper matrix composites in spacecraft heat transmitting and radiating components. The preforms are to be fabricated by braiding of tows and when infiltrated with copper will result in a 3-D reinforced, near net shape composite with improved specific properties such as lower density and higher stiffness. It is anticipated that the use of textile technology will result in a more robust preform and consequently better final composite; it is hard to anticipate what performance tradeoffs will result, and these will be explored through testing and characterization. Author (revised)

N94-14105 Martec Ltd., Halifax (Nova Scotia).
DEVELOPMENT OF SOFTWARE FOR COMPOSITE MATERIALS ANALYSIS, PHASE 1, PART 1
J. C. Wallace and M. W. Chernuka Sep. 1990 44 p
(Contract DREA-W7707-0-0918/01-OSC)
(DSIS-93-00857-Pt-1-Phase-1; DREA-CR-90-442-Pt-1-Phase-1; CTN-93-60837) Avail: CASI HC A03

CMAPP (Composite Material Properties Prediction) is a menu-driven composite material analysis computer program capable of generating effective material properties for particulate, continuous fiber, and platelet composites. Constituent material properties can also be generated from composite properties. A collection of eight micromechanical material models has been incorporated into the CMAPP model library. A hierarchical arrangement of menus is used to guide the user through the process of defining various material parameters, entering all necessary material data, and storing or displaying the results. CMAPP will not only perform a single analysis, but will also perform analyses for a range of volume fractions. The latter option gives the user the ability to investigate the effect that a volume fraction change has on any desired material property. The program structure of CMAPP is described along with the various menus and menu options contained in the program. Data input and ouput options are noted, and the types of material models available in the program library are reviewed. Author (CISTI)

N94-14119# Los Alamos National Lab., NM.
MEASUREMENT OF STRAIN IN INDIVIDUAL PHASES OF COMPOSITES BEFORE, DURING, AND AFTER MECHANICAL LOADING
J. A. Goldstone, M. A.M. Bourke, Ning Shi, A. C. Lawson, and J. E. Allison (Ford Motor Co., Dearborn, MI.) 1993 10 p Presented at the 12th International Collaboration of Advanced Neutron Sources Meeting (ICANS), Abingdon, England, 24-28 May 1993
(Contract W-7405-eng-36)
(DE93-014585; LA-UR-93-1711; CONF-9305177-5) Avail: CASI HC A02/MF A01

At LANSCE, we have measured residual strains in a variety of metal-matrix systems using the Neutron Powder Diffractometer (NPD). In 1992, we developed a compact stress rig for in-situ strain measurement during applied loading. Comparison of experimental measurements made with the stress rig on aluminum titanium carbide with numerical predictions showed the importance of including initial thermal residual strains in the models. In Al/TiC, normal to the loading direction, the increase in the average matrix and reinforcement lattice strains was in a 'zigzag' manner. Finite element modeling indicated that this resulted from residual strains induced during cooling from fabrication temperatures. Data and modeling are presented.
DOE

N94-14121# Los Alamos National Lab., NM.
DYNAMIC MECHANICAL DEFORMATION OF A SiC(SUB p)/Al-Li (8090) COMPOSITE
R. U. Vaidya and A. K. Zurek 1993 5 p Presented at the 14th International Conference on High Pressure Science and Technology and 1993 Technical Meeting of the Topical Group on Shock Compression of Condensed Matter, Colorado Springs, CO, 28 Jun. - 3 Jul. 1993
(Contract W-7405-eng-36)
(DE93-014586; LA-UR-93-1710; CONF-9306167-2) Avail: CASI HC A01/MF A01

The deformation behavior in compression of a silicon carbide particle-reinforced aluminum-lithium (8090) matrix composite, at strain rates in the range of 10(exp -3) to 6500/s, was investigated and compared with that of unreinforced alloy samples. Dynamics strengthening in these composites was found to change depending on the direction of testing. These differences were attributed to differences in the orientation of the reinforcing particles. DOE

N94-14418# Michigan State Univ., East Lansing.
THEORETICAL STUDIES OF BREAKDOWN IN RANDOM MEDIA
P. M. Duxbury 1993 12 p
(Contract DE-FG02-90ER-45418)
(DE93-018107; DOE/ER-45418/3) Avail: CASI HC A03/MF A01

Failure initiates in local regions of a material microstructure which are either especially weak, or which carry an especially large field. The size and location of these weak or 'hotspots' depends on the microstructure and is especially sensitive to microstructural disorder. Using model random microstructures, we have developed analytic and numerical tools to predict where failure initiates, its initiation field, and how it propagates from the initiation sites. We have found it useful to divide the failure process into a nucleation stage, in which damage occurs quite randomly throughout the material, a localisation stage, where a critical crack nucleates, and a catastrophic failure stage during which an unstable crack propagates through the material. Results are being compared with experiments on: Highly porous materials (porous glass and porous gold); dielectric breakdown of metal loaded insulators (e.g. aluminum in poly-ethyelene) and; the critical current of superconductors containing cracks (Nb and Nb3Ge). This report summarizes our efforts in these areas. DOE

N94-14469# Los Alamos National Lab., NM.
THE STRUCTURE AND MECHANICAL PROPERTIES OF Ru-Cu AND Ru-Ti NANOLAYER COMPOSITES
H. Kung, M. Nastasi, T. R. Jervis, K. Hubbard, T. E. Mitchell, R. M. Messner (Minnesota Mining and Mfg. Co., Saint Paul.), and J. D. Embury (McMaster Univ., Hamilton, Ontario.) 1993 7 p Presented at the Spring Meeting of the MRS, San Francisco, CA, 12-16 Apr. 1993
(Contract W-7405-eng-36)
(DE93-014453; LA-UR-93-1927; CONF-930405-15) Avail: CASI HC A02/MF A01

Multilayers of Ru-Cu and Ru-Ti were prepared by electron beam evaporation technique. One set of composites has Ru thickness varying from 250 to 2500 Angstroms alternating with Cu or Ti of 15 Angstroms. The other set has 250 Angstroms of Ru and the Cu or Ti layer varies between 15 and 200 Angstroms. Nanoindentation measurements show that there is no significant change in hardness as either Ru or Cu/Ti thickness varies. However, the Ru-Cu multilayer has twice the hardness of the Ru-Ti system. The strengthening mechanism proposed by Koehler predicts that Ru-Ti composites would have a higher strength than Ru-Cu due to larger modulus difference between Ru and Ti. Discrepancy between prediction and experiment suggests that other strengthening mechanism(s) may be operating. Two models based on a 'shear' mechanism are proposed to explain the differences observed between these two systems. Effects of these mechanisms in controlling the deformation process in nanolayer composites are discussed. DOE

N94-14573# Joint Publications Research Service, Arlington, VA.
JPRS REPORT: SCIENCE AND TECHNOLOGY. CENTRAL EURASIA: MATERIALS SCIENCE
14 Sep. 1993 37 p Transl. into ENGLISH from various Russian articles (JPRS-UMS-93-006) Avail: CASI HC A03/MF A01

Translated articles cover the following topics: experimental investigation of the sensitivity of the mirror-shade method during testing of titanium

disks in gas turbine engines with focusing transducers; thermal expansion of composites reinforced with carbon fibers and fabrics; laser microgalvanics - new method for protecting metallic coatings from localized corrosion; and modern refractory casting alloys for gas turbine engine blades. CASI

N94-14574# Joint Publications Research Service, Arlington, VA.
JPRS REPORT: SCIENCE AND TECHNOLOGY. CENTRAL EURASIA: MATERIALS SCIENCE
21 Jun. 1993 17 p Transl. into ENGLISH from various Russian articles (JPRS-UMS-93-004) Avail: CASI HC A03/MF A01

Translated articles cover the following topics: an experimental investigation of effect of the factors existing in outer space on the durability of carbon fiber-reinforced plastics -- gas release from carbon fiber-reinforced plastics in the absence of protective coatings; an experimental investigation of effect of the factors existing in outer space on the durability of carbon fiber-reinforced plastics -- special features of gas release from metallized carbon fiber-reinforced plastic; and effect of metal + ceramic coatings on fatigue strength of heat-resistant Ni-alloys. CASI

N94-14575# Joint Publications Research Service, Arlington, VA.
JPRS REPORT: SCIENCE AND TECHNOLOGY. CENTRAL EURASIA: MATERIALS SCIENCE
6 Aug. 1993 32 p Transl. into ENGLISH from various Russian articles (JPRS-UMS-93-005) Avail: CASI HC A03/MF A01

Translated articles cover the following topics: behavior of composite materials under high stretching rates (cleavage); laser technology for imparting tribotechnical characteristics to friction surfaces; and structure and properties of coatings applied with a CO2 laser. CASI

N94-14690# Los Alamos National Lab., NM.
SMALL-ANGLE SCATTERING, CONTRAST VARIATION AND THE STUDY OF COMPLEX COMPOSITE MATERIALS: A STUDY OF THE STRUCTURE OF CARBON BLACK
R. P. Hjelm, Jr., P. A. Seeger, and W. A. Wampler (Sid Richardson Carbon Co., Forth Worth, TX.) 1993 19 p Presented at the American Chemical Society Meeting on Rubber Chemistry and Technology, Denver, CO, 18-22 May 1993
(Contract W-7405-eng-36)
(DE93-012707; LA-UR-93-1657; CONF-9305185-1) Avail: CASI HC A03/MF A01

Detailed studies are presented on the structure and aggregation of an experimental high surface area carbon black (HSA) using small-angle neutron scattering and the method of contrast variation. We find that the approximately 27 nm HSA particles form small, linear aggregates of average aggregation number 5 when suspended in cyclohexane. There is considerable density fluctuation in the interior of these particles with the denser regions being toward the outer part of the spherically-averaged structure. This information would not have been obtained from studies of carbon black without solvent. The results will be applied to similar scattering studies on solvent-swollen bound rubber gels made from HSA-polyisoprene. These result show, however, that the strong internal fluctuations of the carbon black will limit the information that can be obtained on the structure and conformation of the elastomer in the gel. There are additional limitation from compositional heterogeneity of the sample. DOE

N94-14715*# Texas A&M Univ., College Station. Aerospace Engineering Dept.
ANALYSIS OF NEW COMPOSITE ARCHITECTURES Interim Report, 1 Jul. 1992 - 30 Jun. 1993
John D. Whitcomb Oct. 1993 52 p
(Grant NAG3-1270)
(NASA-CR-194524; NAS 1.26:194524) Avail: CASI HC A04/MF A01

Presentations were made at two national conferences and one workshop. A paper titled 'Enhanced Direct Stiffness Method for Finite Element Analysis of Textile Composites' was presented at the 1992 ASME winter annual meeting in November 1992. A paper titled 'Global/Local Finite Element Analysis for Textile Composites' was presented at the 33rd SDM conference in April 1993. A paper titled 'Boundary Effects in Textile Composites' was presented at a workshop sponsored by NASA Langley Research Center in July, 1993. This paper was also presented at the Second U.S. National Congress on Computational Mechanics in August 1993. A copy of the first paper was included in last year's report. Copies of papers related to the other two talks are included. Details of the research can be found in the papers and theses. While we are encouraged by the results to date, our studies indicate that the current technique for interfacing of global and local models is not as accurate as we had hoped. The current technique involves exact displacement constraints. Because of the crudeness of the global model, this interfacing technique results in significant artifacts in the stress distributions near the global/local boundary. Of course, one could just include a larger region in the local model if there are sufficient computer resources. A high priority this year will be improving the global/local interfacing by using variations of mixed boundary constraints. This will result in some local violation of compatibility, but it might reduce the artifacts near the boundary. A variety of computer programs were developed. The primary programs will be documented during the third year and submitted to COSMIC. Author (revised)

N94-14719*# National Aeronautics and Space Administration. Lewis Research Center, Cleveland, OH.
ELASTIC-PLASTIC FINITE ELEMENT ANALYSES OF AN UNIDIRECTIONAL, 9 VOL PERCENT TUNGSTEN FIBER REINFORCED COPPER MATRIX COMPOSITE
Jose G. Sanfeliz Sep. 1993 21 p Original contains color illustrations
(RTOP 510-01-50)
(NASA-TM-106304; E-8045; NAS 1.15:106304) Avail: CASI HC A03/MF A01; 7 functional color pages

Micromechanical modeling via elastic-plastic finite element analyses were performed to investigate the effects that the residual stresses and the degree of matrix work hardening (i.e., cold-worked, annealed) have upon the behavior of a 9 vol percent, unidirectional W/Cu composite, undergoing tensile loading. The inclusion of the residual stress-containing state as well as the simulated matrix material conditions proved to be significant since the Cu matrix material exhibited plastic deformation, which affected the subsequent tensile response of the composite system. The stresses generated during cooldown to room temperature from the manufacturing temperature were more of a factor on the annealed-matrix composite, since they induced the softened matrix to plastically flow. This event limited the total load-carrying capacity of this matrix-dominated, ductile-ductile type material system. Plastic deformation of the hardened-matrix composite during the thermal cooldown stage was not considerable, therefore, the composite was able to sustain a higher stress before showing any appreciable matrix plasticity. The predicted room temperature, stress-strain response, and deformation stages under both material conditions represented upper and lower bounds characteristic of the composite's tensile behavior. The initial deformation stage for the hardened material condition showed negligible matrix plastic deformation while for the annealed state, its initial deformation stage showed extensive matrix plasticity. Both material conditions exhibited a final deformation stage where the fiber and matrix were straining plastically. The predicted stress-strain results were compared to the experimental, room temperature, tensile stress-strain curve generated from this particular composite system. The analyses indicated that the actual thermal-mechanical state of the composite's Cu matrix, represented by the experimental data, followed the annealed material condition. Author (revised)

N94-14769*# Cincinnati Univ., OH. Dept. of Materials Science and Engineering.
A STUDY OF FIBER VOLUME FRACTION EFFECTS IN NOTCHED UNIDIRECTIONAL SCS-6/Ti-15V-3Cr-3Al-3Sn COMPOSITE Ph.D. Thesis Final Report
Steven J. Covey Sep. 1993 226 p
(Grant NGT-40016; RTOP 510-01-50)
(NASA-CR-191165; E-8116; NAS 1.26:191165) Avail: CASI HC A11/MF A03

Notched unidirectional SCS-6/Ti-15-3 composite of three different fiber volume fractions (vf = 0.15, 0.37, and 0.41) was investigated for various room temperature microstructural and material properties including: fatigue crack initiation, fatigue crack growth, and fracture toughness. While the matrix hardness is similar for all fiber volume fractions, the fiber/matrix interfacial shear strength and matrix residual stress increases with fiber volume fraction. The composite fatigue crack initiation stress is shown to be matrix controlled and occurs when the net maximum matrix stress approaches the endurance limit stress of the matrix. A model is presented which includes residual stresses and presents the composite initiation stress

as a function of fiber volume fraction. This model predicts a maximum composite initiation stress at vf approximately 0.15 which agrees with the experimental data. The applied composite stress levels were increased as necessary for continued crack growth. The applied Delta(K) values at crack arrest increase with fiber volume fraction by an amount better approximated using an energy based formulation rather than when scaled linear with modulus. After crack arrest, the crack growth rate exponents for vf37 and vf41 were much lower and toughness much higher, when compared to the unreinforced matrix, because of the bridged region which parades with the propagating fatigue crack. However, the vf15 material exhibited a higher crack growth rate exponent and lower toughness than the unreinforced matrix because once the bridged fibers nearest the crack mouth broke, the stress redistribution broke all bridged fibers, leaving an unbridged crack. Degraded, unbridged behavior is modeled using the residual stress state in the matrix ahead of the crack tip. Plastic zone sizes were directly measured using a metallographic technique and allow prediction of an effective matrix stress intensity which agrees with the fiber pressure model if residual stresses are considered. The sophisticated macro/micro finite element models of the 0.15 and 0.37 fiber volume fractions presented show good agreement with experimental data and the fiber pressure model when an estimated effective fiber/matrix debond length is used. Author (revised)

N94-14794# University of Southern California, Los Angeles. Dept. of Chemistry.

OFFICE OF NAVAL RESEARCH/DARPA PUBLICATIONS: COMPOSITE MATERIALS WITH IMPROVED PROPERTIES IN COMPRESSION

William P. Weber 1993 27 p

(Contract N00014-89-J-1961)

(AD-A265509) Avail: CASI HC A03/MF A01

Dichloroketene, generated by the ultrasound-promoted dechlorination of trichloroacetylchlroide with zinc, has been added to the carbon-carbon double bond of poly (1,1-dimethyl-1-sila-cis-pent-3-ene)(poly-I). The molecular-weight distribution of the adduct polymer in which all of the carbon-carbon double bonds have reacted with dichloroketene, one dimethylsiylene). One hundred percent poly(I-Cl2C=C=O), has been characterized by bel permeation chromatography. The microstructure of the 100 percent poly(I-Cl2C=C=O) has been elucidated by H-1, C-13, and Si-29 nuclear magnetic resonance as well as by infrared spectroscopy. Similarly, a series of random copolymers have been prepared in which only some of the carbon-carbon double bonds of poly-I have reacted with dichloroketene. These have been characterized as above. The glass transition teperatures (T sub g) of these copolymers, as well as that of 100 percent poly(I-Cl2C=C=O), have been determined by differential scanning calorimetry. The T sub g values are found to increase linearly with the percentag of the carbon-carbon double bonds of poly-I that have reacted with dichloroketene. Author

N94-14815# Institut National des Sciences Appliquees de Lyon, Villeurbanne (France). Groupe d'Etudes de Metallurgie Physique et Physique des Materiaux.

STUDY OF DEFERRED ACOUSTIC EMISSION IN CARBON EPOXY COMPOSITES Ph.D. Thesis [ETUDE DE L'EMISSION ACOUSTIQUE DIFFEREE DANS LES COMPOSITES CARBONE-EPOXYDE DES MATERIAUX]

Nathalie Rochat-Retourne 1991 156 p In FRENCH Sponsored by Aerospatiale, France

(ISAL-91-0078; ETN-93-94357) Avail: CASI HC A08/MF A02

The state of damage of a composite is evaluated using the deferred acoustic emission technique. Deferred acoustic emission is the name given to the acoustic activity observed, under a constant charge, in material composites and carbon/matrix epoxy composite fibers. The mechanical behavior of the composites under constant charge is observed in order to model the phenomena which control deferred acoustic emission. The deferred acoustic emission is linked to the establishment of damage in the composite. Under a constant charge, the damage is governed by the evolution of the deformation of the composite linked to the rheology of the constitents. The method enables the evolution of the events to be monitored and the transition from a diffuse damage phase to a localized damage phase to be identified. ESA

N94-14822*# Sverdrup Technology, Inc., Brook Park, OH.

THERMOMECHANICAL AND ISOTHERMAL FATIGUE BEHAVIOR OF A (90)SUB 8 TITANIUM MATRIX COMPOSITE Final Report

Michael G. Castelli Oct. 1993 14 p Proposed for presentation at the Eighth Technical Conference on Composite Materials, Cleveland, OH, 19-21 Oct. 1993; sponsored by the American Society for Composites

(Contract NAS3-25266; RTOP 510-01-50)

(NASA-CR-191196; E-8156; NAS 1.26:191196) Avail: CASI HC A03/MF A01

An experimental investigation was conducted to analyze the fatigue damage mechanisms operative in a 35 fiber volume percent (90 deg) titanium matrix composite (TMC) under 427 C isothermal and thermomechanical loading conditions. The thermomechanical fatigue (TMF) tests were performed with a temperature cycle from 200 to 427 C under closely controlled conditions to define both the deformation and fatigue life behavior. Degradation of the TMC's isothermal elastic moduli and coefficient of thermal expansion were monitored throughout the TMF tests. The results indicated TMF life trends which contrasted those established in a comparable (0 deg) system, as TMF loading of the (90 deg) TMC was not found to be 'life-limiting' in comparison to maximum temperature isothermal conditions. In-phase lives were very similar to those established under 427 C isothermal conditions. High stress isothermal fatigue at 427 C produced increased strain ratchetting and stiffness degradation relative to TMF conditions. Out-of-phase loadings produced TMF lives approximately an order of magnitude greater than the lives determined under isothermal and in-phase conditions. Extensive fractography and metallography were also performed. Two key issues were identified and appeared to dominate the fatigue damage and life of the (90 deg) TMC, namely, the weak fiber/matrix interface and environmental attack of the fiber/matrix interface via the exposed (90 deg) fiber ends. Author (revised)

N94-14823*# National Aeronautics and Space Administration. Lewis Research Center, Cleveland, OH.

THERMOELASTIC RESPONSE OF METAL MATRIX COMPOSITES WITH LARGE-DIAMETER FIBERS SUBJECTED TO THERMAL GRADIENTS

Jacob Aboudi (Virginia Univ., Charlottesville.), Marek-Jerzy Pindera (Virginia Univ., Charlottesville.), and Steven M. Arnold Oct. 1993 76 p

(RTOP 510-01-50)

(NASA-TM-106344; E-8114; NAS 1.15:106344) Avail: CASI HC A05/MF A01

A new micromechanical theory is presented for the response of heterogeneous metal matrix composites subjected to thermal gradients. In contrast to existing micromechanical theories that utilize classical homogenization schemes in the course of calculating microscopic and macroscopic field quantities, in the present approach the actual microstructural details are explicitly coupled with the macrostructure of the composite. Examples are offered that illustrate limitations of the classical homogenization approach in predicting the response of thin-walled metal matrix composites with large-diameter fibers when subjected to thermal gradients. These examples include composites with a finite number of fibers in the thickness direction that may be uniformly or nonuniformly spaced, thus admitting so-called functionally gradient composites. The results illustrate that the classical approach of decoupling micromechanical and macromechanical analyses in the presence of a finite number of large-diameter fibers, finite dimensions of the composite, and temperature gradient may produce excessively conservative estimates for macroscopic field quantities, while both underestimating and overestimating the local fluctuations of the microscopic quantities in different regions of the composite. Also demonstrated is the usefulness of the present approach in generating favorable stress distributions in the presence of thermal gradients by appropriately tailoring the internal microstructure details of the composite. Author

N94-13271# National Space Development Agency, Tokyo (Japan).

RESEARCH ON RADIATION RESISTANCE PROPERTIES OF STRUCTURAL MATERIALS FOR SPACE USE [UCHUUYOU KOUZOU ZAIRYOU NO TAIHOUSHASENSEI NO KENKYUU]

Kouzou Yudate, Yoshiki Morino, Tadao Seguchi (Japan Atomic Energy Research Inst., Tokyo.), Tsuneo Sasuga (Japan Atomic Energy Research Inst., Tokyo.), and Akira Udagawa (Japan Atomic Energy Research Inst., Tokyo.) *In its* The Second Workshop on Deployment and Assembly

Experiment of Large Space Structure on Orbit 31 Mar. 1993 p 12-16 In JAPANESE (For primary document see N94-13268 02-12)
Avail: CASI HC A01/MF A01

N94-13272# Tsukuba Univ., Ibaraki (Japan). Inst. of Engineering Mechanics.
MEASURING METHODS FOR CFRP LAMINATES' BENDING AND TORSION RIGIDITIES CHARACTERISTICS [CFRP SEKISOUBAN NO MAGE/NEJIRI GOUSEI NO SOKUTEIHOU]
Tatsuzou Koga *In* NASDA, The Second Workshop on Deployment and Assembly Experiment of Large Space Structure on Orbit 31 Mar. 1993 p 17-20 In JAPANESE (For primary document see N94-13268 02-12)
Avail: CASI HC A01/MF A01

25 INORGANIC AND PHYSICAL CHEMISTRY

Includes chemical analysis, e.g., chromatography; combustion theory; electrochemistry; and photochemistry.

For related information see also *77 Thermodynamics and Statistical Physics.*.

N94-12819# Sandia National Labs., Albuquerque, NM.
COUPLED THERMAL RESPONSE OF OBJECTS AND PARTICIPATING MEDIA IN FIRES AND LARGE COMBUSTION SYSTEMS
L. A. Gritzo and V. F. Nicolette 1993 12 p Presented at the National Conference and Exposition on Heat Transfer, Atlanta, GA, 8-11 Aug. 1993
(Contract DE-AC04-76DP-00789)
(DE93-012848; SAND-93-0106C; CONF-930830-16) Avail: CASI HC A03/MF A01

When an object is subjected to the flow of combustion gas at a different temperature, the thermal responses of the object and the surrounding gas become coupled. The ability to model this interaction is of primary interest in the design of components which must withstand fire environments. One approach is to decouple the problem and treat the incident flux on the surface of the object as being emitted from a black-body at an approximate gas temperature. By neglecting the presence of the participating media, this technique overpredicts the heat fluxes initially acting on the object surface. The main goal of this work is to quantify the differences inherent in treating the combustion media as a blackbody as opposed to a gray gas. This objective is accomplished by solving the coupled participating media radiation and conduction heat transfer problem. A transient conduction analysis of a vertical flat plate was performed using a gray gas model to provide a radiation boundary condition. A 1-D finite difference algorithm was used to solve the conduction problem. The results are presented in terms of nondimensional parameters and include both average and local heat fluxes as a function of time. Early in the transient, a reduction in net heat fluxes of up to 65% was observed for the gray gas results as compared to the blackbody cases. This reduction in the initial net heat flux results in lower surface temperatures for the gray gas case. Due to the initially reduced surface temperatures, the gray gas net heat flux exceeds the net blackbody heat flux with increasing time. For radiation Blot numbers greater than 5, or values of the radiation parameter less than 10(sup -2). the differences inherent in treating the media as a gray gas are negligible and the blackbody assumption is valid. The results clearly indicate the importance of participating media treatment in the modeling of the thermal response of objects in fires and large combustion systems. DOE

N94-12830*# Auburn Univ., AL. Materials Engineering Program.
LIFETIME PREDICTION OF MATERIALS EXPOSED TO THE NATURAL SPACE ENVIRONMENT Final Report, 9 Apr. 1992 - 8 Apr. 1993
Ralph Zee 8 Apr. 1993 63 p
(Contract NAS8-39131)
(NASA-CR-193833; NAS 1.26:193833) Avail: CASI HC A04/MF A01

The goal of this study is to model the lifetime of different types of seal materials based on results obtained from accelerated experiments. A semi-mechanistic approach was taken. Thermal aging data were taken from the literature whereas experiments were conducted at Auburn under this contract for selected environments. The seal materials of interest are Silicone 383, Silicone 650, Viton 835, and Viton 747. The relevant conditions include thermal, oxygen, inert gas, vacuum, and gamma radiation. Compression set data available from NASA were used to examine the thermal effect. Experiments were conducted at Auburn University and at NASA to isolate the role of thermal, oxygen, inert gas, vacuum, gamma irradiation, and proton irradiation. A simple discrete stress relaxation method was developed to determine the relaxation response of the elastomers. Dynamic mechanical thermal analysis was also used to characterize the mechanical response of the specimens. These provide a more meaningful correlation between mechanisms and degradation. Author (revised)

N94-12841# Sandia National Labs., Albuquerque, NM.
PHOTOCATALYSIS FOR THE TREATMENT OF WASTE WATER: APPLICATIONS INVOLVING THE REMOVAL OF METALS
M. R. Prairie and B. M. Stange 1993 7 p Presented at the National Conference and Exposition on Heat Transfer, Atlanta, GA, 8-11 Aug. 1993
(Contract DE-AC04-76DP-00789)
(DE93-011669; SAND-93-0023C; CONF-930830-14) Avail: CASI HC A02/MF A01

This paper describes laboratory work investigating the applicability of solar-powered photocatalysis for the treatment of water contaminated with heavy metals and organics. It was found that Ag(I), Au(HI), Cr(VI), Hg(H), Pd(H), and PT(IV) are easily treated while Cd(U), Cu(II), and NI(II) are not. The importance of the entire photocatalytic redox cycle is demonstrated by showing that the rates of oxidation (of organics) and reduction (of metals) are intrinsically interrelated. Data are presented showing that photoefficiency decreases as light intensity increases in the range of 0 to 17 suns UV. This result suggests that one-sun systems are more efficient than those using concentrated solar radiation. Preliminary data are reported for three samples of actual waste: (1) gold mining leachate, (2) precious metals mining extract, and (3) photographic waste. In general, actual applications are less effective than predicted using laboratory data for clean systems. DOE

N94-12881# Lawrence Livermore National Lab., CA.
THE IMPORTANCE OF HARD CORE REPULSION IN MODELS OF ACTIVITY COEFFICIENTS IN AQUEOUS ELECTROLYTE SOLUTIONS: ILLUSTRATION IN THE CASE OF HYDRATION THEORY
T. J. Wolery and K. J. Jackson Jul. 1992 5 p Presented at the 7th Water-Rock Interaction Conference, Park City, UT, 9-23 Jul. 1992
(Contract W-7405-eng-48)
(DE93-012476; UCRL-JC-109948; CONF-920761-17) Avail: CASI HC A01/MF A01

Activity coefficients in aqueous electrolyte solutions are primarily affected by two kinds of phenomena. The standard Debye-Huckel equation represents only one of these--the long range electrical interactions. Of nearly equal importance is hard core (HC) repulsion, which is not electrical in nature. To a first-order approximation, HC repulsive effects are independent of the ionic strength depending instead on the sum of the solute molalities (Sigma(m)). Adding a term for HC repulsion to the standard Debye-Huckel model produces what we call a hybrid two-term model. In a previous work, we proposed a new method for making hydration corrections to the standard Debye-Huckel model. In the present work, we examine the effect of extending this model to include hard core repulsion. Although the activity coefficients of 1:1 electrolytes can be fit quite well by the model without a HC term the inclusion of such a term is critical to success in fitting the data for 2:1 and other higher-order electrolytes. DOE

N94-12910# Sandia National Labs., Albuquerque, NM.
MODELING IGNITION CHEMISTRY
M. L. Hobbs, M. R. Baer, and R. J. Gross 1993 10 p Presented at the 1993 Joint Army, Navy, NASA, Air Force Propulsion Systems Hazards Subcommittee Meeting, Ft. Lewis, 10-14 May 1993
(Contract DE-AC04-76DP-00789)
(DE93-012340; SAND-93-1069C; CONF-9305189-3) Avail: CASI HC A02/MF A01

An eXplosive CHEMical kinetics code (XCHEM) was developed to solve the reactive diffusion equations associated with thermal ignition of energetic material. This method-of-lines code uses stiff numerical methods and adaptive meshing. Solution accuracy is maintained between multilayered materials consisting of blends of reactive components and/or inert materials. Phase change and variable properties are included in one-dimensional slab, cylindrical, and spherical geometries. Temperature-dependent thermal properties were incorporated, and modification of thermal conductivities to

include decomposition effects are estimated using solid/gas volume fractions determined by species fractions. Gas transport properties are also included. Time varying temperature, heat flux, convective and thermal radiation boundary conditions, and layer to layer contact resistances are also implemented. The global kinetic mechanism, developed at Lawrence Livermore National Laboratory (LLNL), used to fit One-Dimensional Time to eXplosion (ODTX) data for the conventional energetic materials (HMX, RDX, TNT, and TATB) are presented as sample calculations representative of multistep chemistry. Calculated and measured ignition times for explosive mixtures of Comp B (RDX/TNT), Octol, (HMX/TNT), PBX 9404 (HMX/NC), and RX-26-AF (HMX/TATB) are compared. Geometry and size effects are accurately modeled, and calculations are compared to experiments with time varying boundary conditions. Finally, XCHEM calculations of initiation of an AN/oil/water emulsion, resistively heated, are compared to measurements. DOE

N94-13001# Delaware Univ., Newark.
LINEAR AND NONLINEAR SPECTROSCOPIC PROBING OF SOLUTE INTERACTIONS WITH CHEMICALLY MODIFIED SILICA SURFACE
1993 9 p
(Contract DE-FG02-91ER-14187)
(DE93-014648; DOE/ER-14187/1) Avail: CASI HC A02/MF A01

The objective of this project is to understand the surface science underlying liquid chromatographic separations enabling improvements in design of chromatographic stationary phases. Progress was made both in use of laser spectroscopy to probe chromatographic surfaces and in developing new stationary phases based on self-assembled monolayers. DOE

N94-13004# North Carolina State Univ., Raleigh. Dept. of Materials Science and Engineering.
INFRARED ABSORPTION SPECTROSCOPY AND CHEMICAL KINETICS OF FREE RADICALS
R. F. Curl and G. P. Glass Apr. 1993 5 p
(Contract DE-FG05-85ER-13439)
(DE93-015078; DOE/ER-13439/8) Avail: CASI HC A01/MF A01

During the last year, three projects were completed: a high resolution spectroscopic study of the CH stretch of HCCN, measurement of the rate constant of reaction between ethynyl (CCH) and H2 at 295-875 K, and measurement of recombination rate of propargyl (CH2CCH) at room temperature. DOE

N94-13045# Brookhaven National Lab., Upton, NY.
FIFTEENTH COMBUSTION RESEARCH CONFERENCE
1993 391 p Conference held at the Contractors' Meeting, Lake Harmony, PA, 2-4 Jun. 1993
(Contract DE-AC02-76CH-00016)
(DE93-015758; BNL-48923; CONF-9306172) Avail: CASI HC A17/MF A04

The BES research efforts cover chemical reaction theory, experimental dynamics and spectroscopy, thermodynamics of combustion intermediates, chemical kinetics, reaction mechanisms, combustion diagnostics, and fluid dynamics and chemically reacting flows. Ninety-eight papers and abstracts are included. Separate abstracts were prepared for the papers. DOE

N94-13048*# Alabama A & M Univ., Normal.
DETERMINATION OF TRACE ELEMENTS IN TRIGLYCINE SULFATE SOLUTIONS Final Technical Report
Shawky H. Tadros 31 Jul. 1993 14 p
(Grant NAG8-204)
(NASA-CR-193481; NAS 1.26:193481) Avail: CASI HC A03/MF A01

Ten elements were divided into 2 groups. The elements in the first group included iron, nickel, chromium, manganese, copper, and gold. The elements in the second group included zinc, cobalt, lead, cadmium, and gold. Five ppm of each element in each group was spiked in a 1 percent triglycine sulfate (TGS) solution. Glycine was removed with 1-naphthyl isocyanate in ether medium. The glycine derivative 1-naphthyl isocyanate glycine was removed by filtration, and the filtrates were analyzed for the different elements. Analysis of these elements was performed by using the 5100 Perkin-Elmer Atomic Absorption Spectrophotometer. The result of these experiments was the observation that there was a decrease in the concentration of chromium and gold, which was interpreted to be due to the chelation of these elements by the derivative 1-naphthyl isocyanate glycine. Further research is needed to determine the concentration of other elements in triglycine sulfate (TGS) solutions. These elements will include lithium, sodium, rubidium, magnesium, calcium, strontium, barium, aluminum, and silicon. These are the most likely elements to be found in the sulfuric acid used in manufacturing the TGS crystal. Moreover, we will extend our research to investigate the structural formula of the violet colored chelated compounds, which had been formed by interaction of the derivative 1-naphthyl isocyanate glycine with the different elements, such as gold, chromium. Author

N94-13085# Cambridge Univ. (England). Dept. of Engineering.
A COHERENT FLAME MODEL OF PREMIXED TURBULENT COMBUSTION IN A COUNTERFLOW GEOMETRY
A. S. Wu and K. N. C. Bray 26 Jan. 1993 34 p
(CUED/A-THERMO/TR.60) Avail: CASI HC A03/MF A01

Premixed combustion in turbulent counterflowing streams is studied theoretically by adopting a coherent flame model. With this model, a flame surface density Sigma-bar, described by a transport equation, is used to calculate the mean chemical reaction rate related to the distribution of a mean progress variable c-bar. The values of two model constants alpha and beta, connected to flame surface stretch and annihilation, are selected to match numerical solutions with experiments at different nozzle exit conditions giving various values of the mean progress variables at the stagnation point c-bar(0). It is found that two different regions exist in the counterflow field: an outer region, far from the stagnation point and without chemical reaction, and an inner sublayer, which is close to the stagnation point, which experiences a large bulk strain rate and is located in the combustion zone. In order to provide an appropriate theoretical description of the experimental conditions, the inner region is allowed to have a finite thickness, thus imposing a finite displacement on the outer solution, due to thermal expansion in the sublayer. A composite solution is obtained by matching the boundary conditions of the inner and outer solutions at the cold flame edge. The effective mean bulk strain rate is increased slightly by the displacement effect. Theoretical predictions are found to be in good agreement with the experimental data. Author (revised)

N94-13115*# Physical Sciences, Inc., Andover, MA.
NOVEL OXYGEN ATOM SOURCE FOR MATERIAL DEGRADATION STUDIES Final Report, 1 Mar. 1986 - 1 Sep. 1988
R. H. Krech and G. E. Caledonia Oct. 1988 104 p
(Contract NAS7-963; SBIR-04.14-9030)
(NASA-CR-191323; NAS 1.26:191323; PSI-1001/TR-871) Avail: CASI HC A06/MF A02

Physical Sciences Inc. (PSI) has developed a high flux pulsed source of energetic (8 km/s) atomic oxygen to bombard specimens in experiments on the aging and degradation of materials in a low earth orbit environment. The proof-of-concept of the PSI approach was demonstrated in a Phase 1 effort. In Phase 2 a large O-atom testing device (FAST-2) has been developed and characterized. Quantitative erosion testing of materials, components, and even small assemblies (such as solar cell arrays) can be performed with this source to determine which materials and/or components are most vulnerable to atomic oxygen degradation. The source is conservatively rated to irradiate a 100 sq cm area sample at greater than 10(exp 17) atoms/s, at a 10 Hz pulse rate. Samples can be exposed to an atomic oxygen fluence equivalent to the on-orbit ram direction exposure levels incident on Shuttle surfaces at 250 km during a week-long mission in a few hours. Author (revised)

N94-13222# Wisconsin Univ., Madison. Dept. of Chemistry.
INFRARED SPECTROSCOPY OF ORGANIC FREE RADICALS RELATED TO COMBUSTION PROCESSES
J. C. Weisshaar 25 Feb. 1993 5 p
(Contract DE-FG02-92ER-14306)
(DE93-017086; DOE/ER-14306/1) Avail: CASI HC A01/MF A01

We will explore a variant of resonant two-photon ionization (R2PI). Development of the IR + UV R2PI experiment is underway. We have used optical R2PI and pulsed field ionization detection to obtain vibrational spectra of the benzyl and phenylsilane cations. In benzyl, we have learned about the vibronic coupling in the mixed 1(sup 2)A(sub 2)-2(sup 2)B(sub 2) system near 450 nm by projecting the mixed states onto the manifold of cation vibrational states. In phenylsilane(sup +), we find that the sixfold

barrier to internal rotation of the silyl group is small (V(sub 6)= +19 /cm. We are beginning to understand the mechanisms of coupling of torsional states with vibrations, overall rotation, and other electronic states, and we are developing a model of internal rotation in aromatic compounds based on Weinhold's natural resonance theory. DOE

N94-13375# Wisconsin Univ., Madison.
EXPERIMENTAL AND KINETIC MODELING OF ACID/BASE AND REDOX REACTIONS OVER OXIDE CATALYSTS
1993 38 p
(Contract DE-FG02-84ER-13183)
(DE93-016203; DOE/ER-13183/8) Avail: CASI HC A03/MF A01

The research has involved the following: the characterization of catalyst acidity; D-2 NMR studies of Bronsted acid sites; and kinetic, calorimetric, and spectroscopic studies of methylamine synthesis and related reactions over acid catalysts. The approach of this work was to explore quantitative correlations between factors that control the generation, type, strength, and catalytic properties of acid sites on zeolite catalysts. Microcalorimetry, thermogravimetric analysis, IR spectroscopy, and NMR spectroscopy have provided information about the nature and strength of acid sites in zeolites. This was vital in understanding the catalytic cycles involved in methylamine synthesis and related reactions over zeolite catalysts. DOE

N94-13411# California Univ., Berkeley. Lawrence Berkeley Lab.
APPLICATION OF SYNCHROTRON RADIATION IN CHEMICAL DYNAMICS
P. Heimann, M. Koike, A. H. Kung, C. Y. Ng, M. G. White, and A. Wodtke May 1993 31 p Presented at the Application of Synchrotron Radiation and Chemical Dynamics Workshop Report, Oakland, CA, 3-5 Feb. 1993
(Contract DE-AC03-76SF-00098)
(DE93-015040; LBL-34131; CONF-9302107-Summ) Avail: CASI HC A03/MF A01

In Oct. 1992 funding was approved to begin construction of a beamline and two end stations to support chemical dynamics experiments at LBL's Advanced Light Source (ALS). This workshop was organized to develop specifications and plans and to select a working team to design and supervise the construction project. Target date for starting the experiments is Jan. 1995. Conclusions of the workshop and representative experiments proposed in earlier workshops to form the basis for beamline plans and end-station designs are summarized in this report. DOE

N94-13413# California Inst. of Tech., Pasadena. Dept. of Chemistry.
SURFACE SCIENCE INSTRUMENTATION FOR THE STUDY OF IMPORTANT CATALYTIC AND ELECTROCHEMICAL INTERFACES
1992 4 p
(Contract DE-FG05-90ER-75582)
(DE93-015068; DOE/ER-75582/T1) Avail: CASI HC A01/MF A01

The equipment combines several standard surface science probes (uv photoelectron spectra, thermal desorption, AES) with a state-of-the-art x-ray photoelectron spectrometer and integrates these in a custom design with a dry box and a custom-built electrochemical cell. Since the LEED chamber was remachined, the instrument has been performing satisfactorily. Various studies using the instrument were conducted in cooperation with other groups. Silicon surfaces were studied before and after use as a photoanode in a photoelectrochemical cell. DOE

N94-13458# National Aerospace Lab., Kakuda (Japan). Research Center.
CHEMICAL REACTIONS IN SCRAMJET ENGINES: REDUCED KINETIC MODELS FOR IGNITION, COMBUSTION AND NOZZLE FLOW [SUKURAMU JETTO NIOKERU KAGAKU HANNOU KANRYAKUKA HANNOUKEI NIYORU KOUSATSU]
Tooru Mitani Nov. 1992 32 p In JAPANESE
(NAL-TR-1184; JTN-93-80506) Avail: CASI HC A03/MF A01

Reduced kinetics for chemical reactions in scramjet engines were investigated. Ignition, combustion in combustors, and reactive flow in nozzles are described using a phase plane for radical concentrations. The effectiveness of radicals introduced to ignite premixtures was studied using analytical solutions representing time histories of three radical concentrations. The contribution of exothermicity to ignition delay and burning rate as well as inhibition caused by H2O were elucidated using simplified asymptotic analysis for H2/O2 systems. New reduced kinetic models for H2 combustion are proposed and compared with other models. Characteristics of ignition and flame-holding in scramjet combustors are discussed using the model derived here. Author (NASDA)

N94-13471# Japan Manned Space Systems Corp., Tokyo.
STUDY ON IMPROVEMENT OF FLAMMABILITY, ODOR AND OFFGASSING TESTS FOR MATERIALS [ANZENSEI JISSHOU SHIKEN NI KANSURU KENTOU]
Tokyo, Japan National Space Development Agency 31 Mar. 1993 88 p In JAPANESE
(NASDA-CNT-930009; JTN-93-80463) Avail: CASI HC A05/MF A01

A summary of the results of the studies on the following subjects is presented: (1) standard gases for offgassing tests in both statistical methods (including fixed vessel, non-fixed vessel, high-pressure vessel, and pressure ratio mixing methods) and dynamic methods (including flow rate ratio mixing, diffusion tube, and permeation tube methods); (2) studies on odor test equipment (including studies on equipment requirements, examination of the present status of the odor test equipment in Tsukuba Space Center, NASDA (National Space Development Agency of Japan) and proposals for test equipment improvement); (3) studies on gas generator container for producing odor test gases (including verification of the test vessel material, verification of the standard operation procedures, and generation of test gases); (4) studies on arc tracking test procedures (including the survey on the existing arc tracking test procedures, problems concerning the existing test procedures and proposal of the arc tracking test procedure (draft)); (5) studies on flammability test ignitor (including requirement specifications for the ignitor, NASA information concerning the ignitor, manufacturing conditions of ignitors, and survey on ignitor manufacturing equipment and units); and (6) preparation of the test procedures in English. Author (NASDA)

N94-13477# Washington Univ., Seattle. Dept. of Physics.
RECENT DEVELOPMENTS IN MULTIPLE-SCATTERING CALCULATIONS OF XAFS AND XANES
J. J. Rehr 1992 5 p Presented at the 7th International Conference on X Ray Absorption Fine Structure, Kobe, Japan, 23-29 Aug. 1992
(Contract DE-FG06-90ER-45415)
(DE93-010999; DOE/ER-45415/6; CONF-9208160-7) Avail: CASI HC A01/MF A01

Curved-wave multiple-scattering (MS) theory provides a unified treatment of XAFS, encompassing both EXAFS and XANES, as well as a formal equivalence between exact treatments and the (MS) expansion carried to all orders. Recent developments in the theory of XAFS are reviewed with an emphasis on progress in curved-wave MS calculations and on understanding the nature of MS contributions in EXAFS and XANES. In particular, a unified ab initio MS treatment of XAFS is discussed based on a scattering matrix formalism which has sufficient speed and accuracy to treat high-order MS in extended systems. Neither low-order MS nor full MS theories are fully satisfactory. Instead, sufficiently high-order MS appears to be necessary for the convergence of both EXAFS and XANES calculations. The approach also gives a MS interpretation of the sigma(*) shape-resonances observed in XANES. It is shown that these peaks result from coherent, high-order MS. A generalization of the Natoli rule correlating the resonance locations with bond length is obtained. DOE

N94-13478# Washington Univ., Seattle. Dept. of Physics.
MANY-BODY CORRECTIONS IN XAFS
J. J. Rehr 1992 5 p Presented at the International Workshop on Surface X Ray Absorption Fine Structure, Jaipur, India, Aug. 1992
(Contract DE-FG06-90ER-45415)
(DE93-011002; DOE/ER-45415/9; CONF-9208221-2) Avail: CASI HC A01/MF A01

The importance of many-body effects in the theory of XAFS is reviewed. The dominant effects are inelastic losses. Extrinsic losses refer to inelastic losses in the propagation of the photoelectron and are treated using a complex, energy-dependent self-energy. The real part of the self-energy yields an important energy-dependent shift in the phase of the XAFS oscillations, while the imaginary part contributes to the mean-free-path. Intrinsic losses refer to losses associated with the creation of the core-hole. They give rise to shake-up/shake-off contributions to the absorption spectra. These losses may be calculated in terms of a corehole Green's function.

Interference between these processes leads to dynamical corrections, which are important at low energies. DOE

N94-13487# Los Alamos National Lab., NM.
REDUCTION OF Pu(6) WITH HYDROGEN PEROXIDE: EFFECTS OF PLUTONIUM, PEROXIDE, AND IRON CONCENTRATIONS AND OF REACTION TIME
S. F. Marsh, E. A. Martinez, R. S. Day, and A. E. Nixon Jun. 1993 8 p
(Contract W-7405-eng-36)
(DE93-013598; LA-12554) Avail: CASI HC A02/MF A01 (US Sales Only)

The rate and extent of Pu(6) reduction in 7 M nitric acid were measured as a function of the concentration of plutonium, the relative concentrations of hydrogen peroxide and iron, and the reaction time. Plutonium concentrations of 2, 5, 15, 30, and 50 g/L were evaluated. At each plutonium concentration, the tested mole ratios of H2O2/Pu were 0, 2, 4, and 8, and the mole ratios of Fe/Pu were 0, 0.1, 0.3, and 0.5. Plutonium oxidation states were determined by absorption spectrophotometry before treatment and after reaction periods of 30 min, 2 h, and 6 h. High concentrations of plutonium promote the reduction of Pu(6) by peroxide. Iron hinders the reduction of Pu(6) at low concentrations of plutonium but promotes the reaction at higher plutonium concentrations. Although a significant portion of Pu(6) is often reduced completely to Pu(3) by peroxide in the absence of iron, Pu(3) is reoxidized to Pu(4) in nitric acid when iron is present. DOE

N94-13685 Alabama Univ., Huntsville.
NUMERICAL STUDIES OF SPRAY COMBUSTION IN LIQUID-FUELED ENGINES Ph.D. Thesis
Huan-Min Shang 1992 217 p
Avail: Univ. Microfilms Order No. DA9306600

A non-iterative numerical technique for computing time-dependent spray combustion flows has been developed and the numerical models are equipped with state-of-the-art sophisticated sub-physical models. The method is a fully interacting combination of Eulerian fluid and Lagrangian particle calculations. The interaction calculations between the two phases are formulated on a pressure-velocity coupling procedure based on the operator-splitting technique (PISO). This procedure eliminates the global iterations required in conventional Particle-Source-In-Cell (PSIC) procedure and, hence, is efficient for transient calculations. Particle motion is described on a Lagrangian coordinate for the present separated flow models. Particle dispersion by turbulent fluctuations is modeled by allowing particles to interact with a succession of eddies using a random-walk or Monte Carlo method and the related flow turbulence quantities are modeled through a two-equation k-Epsilon model. Parcel PDF model is used to improve computational efficiency of particle turbulent dispersion. Poly-disperse is achieved by using size distribution function through Monte Carlo technique or generated by breakup model. Droplet evaporation and heat transfer are calculated using Frossling correlation and Ranz-Marshall correlation respectively. The turbulence modulation effect caused by the two-way turbulence-particle interaction is also modeled based on the stochastic framework. Accurate calculation of droplet mass and heat transfer is achieved by automatic reductions in the timestep when the exchange rate becomes large. The variable thermophysical properties are obtained from JANAF data bank. A turbulent diffusion flame and single step chemical reaction model are used for spray combustion. Dense spray effects are taken into account by droplet breakup and collision models. Two breakup models including a Taylor analogy breakup (TAB) model and a wave instability model are incorporated and compared. The incorporated collision model stochastically calculates the outcome of every collision, either coalescence or grazing collision. Several particle dispersions in homogeneous and nearly-homogeneous turbulent flows are studied to calibrate the stochastic method for particle-turbulence interactions, and to evaluate the present parcel PDF model. The computations were performed for the solid particle dispersion in a nearly-homogeneous turbulent flow and a particle laden round jet within homogeneous turbulence. Non-evaporating transient and steady solid-cone sprays are used to test the models of dense spray effects including droplet breakup and collision/coalescence. Turbulence modulation effect and the efficiency of parcel PDF model for a dense spray case are tested at a steady solid-cone spray. A transient hollow cone spray presents the complicated two-phase interactions. Transient evaporating and burning sprays incorporating droplet breakup model, evaporation model and eddy-breakup combustion model demonstrate the sophisticated structures of such polydispersed spray combustion. The predictions show reasonable agreements with available experimental results and indicate that the present methodologies are accurate and efficient for simulation of spray combustion. Dissert. Abstr.

N94-13819 Alberta Univ., Edmonton. Faculty of Home Economics.
FLAMMABILITY OF CLOTHING, VOLUME 2 Final Project Report
E. M. Crown and J. D. Dale Jul. 1992 190 p
(DSIS-93-00036-Vol-2; CTN-93-60773) Avail: CASI HC A09

A bibliography is presented of research related to the flammability of clothing for military use. Articles are arranged in alphabetical order by author under keywords such as asbestos, body temperature measurement, breathing apparatus, comfort assessment, cooling systems, fibers, finishes, flammability, heat flux, insulative properties, protective clothing, thermal/heat stress, and thermal protection. CISTI

N94-13942 Defence Research Establishment, Ottawa (Ontario).
REVIEW OF TEST METHODS FOR MATERIAL FLAMMABILITY
J. J. Conn and G. A. Grant Mar. 1991 79 p
(DSIS-93-00480; CTN-93-60748) Avail: CASI HC A03

A general review of flammability and thermal protection is provided. The emphasis of this review is on the use of the many tests used to examine various aspects of flammability and on the limitations associated with the different methodologies. The study was done so that more refined test methods may be employed to evaluate the protection afforded under defined hazard conditions with varying fluences and fluxes of thermal radiation. Special attention is given to test methodologies employed to evaluate military equipment and materials to ascertain if the present methods are relevant to the actual hazard. The nature of skin burn injury is noted, factors involved in the determination of thermal protective performance are noted, and the characteristics of the sensors and the heat sources used in the various tests are detailed. CISTI

N94-13947*# Jet Propulsion Lab., California Inst. of Tech., Pasadena.
SURFACTANT STUDIES FOR BENCH-SCALE OPERATION Quarterly Technical Progress Report No. 2, 1 Oct. - 31 Dec. 1992
Gregory S. Hickey and Pramod K. Sharma 1 Mar. 1993 21 p
(Contract NAS7-918)
(NASA-CR-194511; JPL-Publ-93-7; NAS 1.26:194511) Avail: CASI HC A03/MF A01

A phase 2 study has been initiated to investigate surfactant-assisted coal liquefaction, with the objective of quantifying the enhancement in liquid yields and product quality. This report covers the second quarter of work. The major accomplishments were: completion of coal liquefaction autoclave reactor runs with Illinois number 6 coal at processing temperatures of 300, 325, and 350 C, and pressures of 1800 psig; analysis of the filter cake and the filtrate obtained from the treated slurry in each run; and correlation of the coal conversions and the liquid yield quality to the surfactant concentration. An increase in coal conversions and upgrading of the liquid product quality due to surfactant addition was observed for all runs. Author (revised)

N94-14025*# Alabama Univ., Huntsville. Dept. of Chemistry.
PARTIAL ANALYSIS OF LDEF EXPERIMENT A-0114 Final Report, 20 May 1985 - 19 Nov. 1991
John C. Gregory 1991 34 p
(Contract NAS8-36645)
(NASA-CR-193826; NAS 1.26:193826) Avail: CASI HC A03/MF A01

During the contract period, work concentrated on four main components. Data from the UAH silver pin hole camera was analyzed for determination of the mean Long Duration Exposure Facility (LDEF) satellite attitude and stability in orbit, to include pitch and yaw. Chemical testing performed on the AO-114 hot plate determined the form and locus of absorption of cosmogenic beryllium-7. Reaction rates of atomic oxygen with Kapton and other polymeric solids integrated over the whole LDEF orbital lifetime were analyzed. These rates were compared with the JSC estimated values for Space Station exposures. Metal and polymer films exposed on A0114 (C-9 and C-3 plates) were also analyzed. Author (revised)

N94-14194# Office National d'Etudes et de Recherches Aerospatiales, Paris (France). Direction de l'Energetique.
MODELING AND SIMULATION OF TRANSPORT AND COMBUSTION PHENOMENA IN A SUPERSONIC MIXING LAYER Ph.D. Thesis - Ecole Centrale de Paris [MODELISATION ET SIMULATION DES PHENOMENES DE TRANSPORT ET COMBUSTION DANS UNE COUCHE DE MELANGE SUPERSONIQUE]
Patrick Vuillermoz Nov. 1992 267 p In FRENCH Sponsored by SEP, Vernon, France, and Ministere de la Recherche et de l'Espace, Paris, France Original contains color illustrations
(ONERA-NT-1992-11; ETN-93-93970) Avail: CASI HC A12/MF A03

Numerical simulation and modeling of supersonic mixing layers are discussed. The theoretical background of compressible turbulence from a hydrodynamic point of view (Reynolds stress) as well as diffusive (turbulent mixing) and reactive turbulent combustion points of view are studied. The main experimental results and numerical studies in supersonic mixing are reviewed and the question of direct numerical simulation of turbulent mixing in nonsteady two dimensional and three dimensional mixing layers is addressed. These simulations are in agreement with experimental observations concerning the mixing regimes, the small scale structure in thin layers, and the effects of the convective Mach number. Before examining the effects of chemical reactions, the basic problem of one dimensional strained or unstrained diffusion flames are discussed as a benchmark for kinetics models and for the numerical codes. The theoretical analysis is carried out through a Crocco transformation that points out the inner structure of diffusion flames. These results were used for further numerical simulation of supersonic reactive mixing layers. The effect of the Damkoehler number in combustion regimes is studied. The simulations generated with reduced and with full chemistry are compared. A mixing enhancement technique is examined with simulations on a passively parallel computer. The results of the direct numerical simulations are used for modeling turbulent mixing and accounting for compressibility effects. ESA

N94-14346# EG and G Rocky Flats, Inc., Golden, CO.
HYDROGEN PEROXIDE SAFETY ISSUES
W. V. Conner 14 Apr. 1993 16 p
(Contract DE-AC34-90DP-62349)
(DE93-013895; RFP-4599) Avail: CASI HC A03/MF A01

A literature survey was conducted to review the safety issues involved in handling hydrogen peroxide solutions. Most of the information found in the literature is not directly applicable to conditions at the Rocky Flats Plant, but one report describes experimental work conducted previously at Rocky Flats to determine decomposition reaction-rate constants for hydrogen peroxide solutions. Data from this report were used to calculate decomposition half-life times for hydrogen peroxide in solutions containing several decomposition catalysts. The information developed from this survey indicates that hydrogen peroxide will undergo both homogeneous and heterogeneous decomposition. The rate of decomposition is affected by temperature and the presence of catalytic agents. Decomposition of hydrogen peroxide is catalyzed by alkalies, strong acids, platinum group and transition metals, and dissolved salts of transition metals. Depending upon conditions, the consequence of a hydrogen peroxide decomposition can range from slow evolution of oxygen gas to a vapor, phase detonation of hydrogen peroxide vapors. DOE

N94-14403# Minnesota Univ., Minneapolis.
HOMOGENEOUS-HETERGENEOUS COMBUSTION: THERMAL AND CHEMICAL COUPLING Annual Report
1993 6 p
(Contract DE-FG02-88ER-13878)
(DE93-016050; DOE/ER-13878/5) Avail: CASI HC A02/MF A01

Fundamental studies of reactions at low pressures and of boundary layers give microscopic information on homogeneous-heterogeneous reactions. Ignition and extinction studies over simple geometries give basic bifurcation behavior with which to characterize multiple steady states and their stabilities and (hopefully) to identify the types of behavior which may occur. Oxidation of methane, propane, and ammonia were studied; other fuels will be studied. Catalytic monoliths will be used. Modeling will be performed. DOE

N94-14465 Tel-Aviv Univ. (Israel). School of Physics and Astronomy.
LIQUID AND GAS EVANESCENT WAVE SPECTROSCOPY VIA TUNABLE LASERS AND SILVER HALIDE FIBERS M.S. Thesis
Avi Messica Jun. 1990 144 p In HEBREW
(ITN-93-85226) Copyright Avail: Issuing Activity (Tel-Aviv Univ., Exact Sciences Library, Ramat Aviv 69978, Israel)

Attenuated total reflection (ATR) spectroscopy depends on the existence of an evanescent, energy-non-transmitting field outside a totally internally reflecting waveguide. When the waveguide is immersed in a powder or liquid, attenuated total reflection (ATR) takes place at wavelengths corresponding to the energy bands of the powder or liquid. In ATR spectroscopy, the commonly used Fourier Transform Infrared Spectrometer (FTIR) can be replaced as an infrared (IR) source with a tunable IR laser, and expensive ZnSe or Ge prisms can be replaced as ATR elements with IR-transmitting fibers, which are inexpensive and easier to handle. In the present work, the ATR elements were AgCl(x)Br(1-x) fibers and semiconducting lead salts and CO2 lasers were used as tunable IR sources. Two different optical arrangements were used to demonstrate the practicability of recording ATR gas spectra. A three-dimensional theoretical model was developed to describe the ATR mechanism and the system was analysed. Potential applications of ATR spectroscopy of gases and liquids include measurements of solvent-solute concentrations and gas pressures, and control or study of chemical processes. The theoretical model can aid in designing the laser/fiber optical setup including the optimization of several controlled parameters. ISA

N94-14480*# Alabama Univ., Birmingham. Dept. of Materials Science and Engineering.
IMMISCIBLE PHASE INCORPORATION DURING DIRECTIONAL SOLIDIFICATION OF HYPERMONOTECTICS Final Report
J. Barry Andrews and Roger A. Merrick Aug. 1993 64 p
(Grant NAG8-768)
(NASA-CR-194412; NAS 1.26:194412) Avail: CASI HC A04/MF A01

Solidification processes in immiscible samples were investigated by directly observing the events taking place at the solid-liquid interface during directional solidification. Visualization of these events was made possible through the use of a transparent metal analog system and a temperature gradient stage assembly fitted to an optical microscope. The immiscible transparent analog system utilized was the succinonitrile-glycerol system. This system has been shown to exhibit the same morphological transitions as observed in metallic alloys of monotectic composition. Both monotectic and hypermonotectic composition samples were directionally solidified in order to gain an improved understanding of the manner in which the excess hypermonotectic liquid is incorporated into the solidifying structure. The processing conditions utilized prevented sedimentation of the excess hypermonotectic liquid by directionally solidifying the samples in very thin (13 microns), horizontally oriented cells. High thermal gradient to growth rate ratios (G/R) were used in an effort to prevent constitutional supercooling and the subsequent formation of L(sub 2) droplets in advance of the solidification front during the growth of fibrous composite structures. Results demonstrated that hypermonotectic composites could be produced in samples up to two weight percent off of the monotectic composition by using a G/R ratio greater than or equal to 4.6 x 10(exp 4) C(s)/mm(sup 2) to avoid constitutional supercooling. For hypermonotectic samples processed with G/R ratios below 4.6 x 10(exp 4) C(s)/mm(sup 2), constitutional supercooling occurred and resulted in slight interfacial instability. For these samples, two methods of incorporation of the hypermonotectic liquid were observed and are reported. The correlation between the phase spacing, lambda, and the growth rate, R, was examined and was found to obey a relationship generally associated with a diffusion controlled coupled growth process. For samples with compositions ranging from the monotectic composition up to 2 percent off of the monotectic composition, data indicated that the square of the phase spacing (lambda) varied linearly with the inverse of the growth rate (R). Author (revised)

N94-14525# Oak Ridge Y-12 Plant, TN.
DETERMINATION OF THE SURFACE CLEANLINESS OF METALS BY FT-IR SPECTROSCOPY
G. L. Powell and H. M. Meyer, III 16 Feb. 1993 4 p Presented at the DOE Compatibility, Aging and Service Life Conference, Aiken, SC, 20-22 Apr. 1993

(Contract DE-AC05-84OS-21400)
(DE93-013252; Y/DZ-990; CONF-9304103-6) Avail: CASI HC A01/MF A01

Remote-sensing 75 deg. specular (grazing angle with both s- and p-polarized light) reflectance mid-infrared spectroscopy has been used to inspect metal surfaces for contamination (i.e., cleanliness). This technique can analyze flat or convex surfaces with no restriction on the size of the specimen. Grazing angle specular reflectance off relatively flat metal objects is the most sensitive method of surface analysis with p-polarized light being absorbed by surface species and s-polarized light not absorbed by surface species. DOE

N94-14558 Tel-Aviv Univ. (Israel). School of Physics and Astronomy.
IONIC CONDUCTIVITY OF ALKALI HALIDES AND THEIR MIXTURES NEAR LIQUID-SOLID PHASE TRANSITION M.S. Thesis
Eli Shasha 2 Jun. 1992 46 p
(ITN-93-85222) Copyright Avail: Issuing Activity (Tel-Aviv Univ., Exact Sciences Library, Ramat Aviv 69978, Israel)

The starting point was the assumption that the distribution of the different ions among the lattice sites is random if two salts are soluble in the solid state. This randomness imposes disorder into the structure, possibly leading to a glassy state. Ionic conductivity measurements were carried out in mixed and pure salts, in order to detect possible signs of vitrification. An alternating current (AC) bridge was used to measure the modulus of impdedance and the angle between the real and imaginary components of conductivity. Measurements of conductivity were taken at different frequencies, so that we were able to observe different phases by measuring the conductivity modulus and frequency dispersion. It is shown that these characteristics behave differently in each phase. The motivation for measuring conductivity (the reciprocal of resistivity) comes from the obvious relation of this property to a coefficient of diffusion or a reciprocal viscosity. Both are known to change dramatically (by several orders of magnitude) at the freezing points of alkali halide salts. Thus the phase state could be detected by measurements of conductivity. The highest conductivity is expected in the liquid state, where it is governed by movement of free ions. A glass transition is an alternative to a crystallization. Thus, the conductivity was measured over a temperature interval containing both the liquid and solid states. We also performed a temperature cycling in order to observe the dynamics of the system. Author (ISA)

N94-14582# National Inst. of Standards and Technology, Gaithersburg, MD.
ULTRA-SOFT X RAY ABSORPTION SPECTROSCOPY: A BULK AND SURFACE PROBE OF MATERIALS
D. A. Fischer, G. E. Mitchell (Dow Chemical Co., Midland, MI.), B. M. Dekoven (Dow Chemical Co., Midland, MI.), A. T. Yeh (Michigan Univ., Ann Arbor.), J. L. Gland (Michigan Univ., Ann Arbor.), and Arnie R. Moodenbaugh (Brookhaven National Lab., Upton, NY.) 1993 6 p Presented at the Spring Meeting of the MRS, San Francisco, CA, 12-16 Apr. 1993
(Contract DE-AC02-76CH-00016)
(DE93-014325; BNL-48887; CONF-930405-12) Avail: CASI HC A02/MF A01

Direct comparisons between surface and bulk of diverse materials can be made by simultaneous electron yield (5 nm depth sensitivity) and fluorescence yield (200 nm) ultra soft x-ray absorption spectroscopy measurements utilizing a rapid sample interchange apparatus. For example the orientations of functional groups have been characterized at and near the surface of a series of model polymeric materials highlighting the chemical and molecular sensitivity of ultra-soft x-ray absorption spectroscopy. In addition we discuss a bulk sensitive use of fluorescence yield to non-destructively study a buried metal polymer interface. A second bulk sensitive example is the use of fluorescence yield oxygen K near edge x-ray spectroscopy as a method to determine the hole state density of high Tc materials. DOE

N94-14586# Syracuse Univ., NY.
UPGRADING OF RAW NATURAL GAS USING HIGH-PERFORMANCE POLYMER MEMBRANES
S. A. Stern, H. S. Meyer (Gas Research Inst., Chicago, IL.), V. K. Venkataraman (Department of Energy, Morgantown, WV.), and H. D. Shoemaker (Department of Energy, Morgantown, WV.) 1993 7 p Presented at the AFS Seminar and Expo Annual Meeting, Chicago, IL, 3-6 May 1993 Sponsored by Gas Research Inst., Chicago, IL, and DOE, Morgantowm, WV
(DE93-014041; DOE/METC-C/93/7068; CONF-9305166-2) Avail: CASI HC A02/MF A01

The separation of CO2 and H2S from raw natural gas is essential for enhancing the heating value of the gas and for providing environmental safety during nation and use. Membrane separation processes are particularly useful for this application because they are inherently energy-efficient. Membrane processes also offer other important advantages, such as ease of scale-up due to module design, good space and weight efficiency and great flexibility in handling variations in the flow rate, pressure and composition of the raw natural gas streams. In a coordinated effort, the Gas Research Institute and the Department of Energy, Morgantown Energy Technology Center are funding an extensive study at Syracuse University on the relationships between the chemical structure of various polymers and their permeability to different gases. Based on criteria derived from this study, novel fluorine-containing polyimides that exhibit very high CO2/CH4, selectivities as well as significant H2S/CH4, selectivities were synthesized. These 'dense' (homogeneous) membranes separated various mixtures of CO2/CH4, and H2S/CH4/CO2 at 35 C (95 F) and at pressures up to 10 atm (147 psi). The results of these measurements agree well with computer simulations. The CO2 content of CH4/CO2 mixtures containing as much as 40 mole percent CO2 can be reduced with the polyamide membranes to pipeline specifications (less than or equal to 2 mole percent CO2. To reduce the H2S content of H2S/CH4/CO2 mixtures to pipeline specifications (less than or equal to 4 ppM H2S), the membranes are best combined with conventional gas-absorption processes, such as a selective amine. Such 'hybrid' processes for the upgrading of natural gas can be more economical than conventional gas-absorption processes alone. DOE

N94-14694# Argonne National Lab., IL.
PROCUREMENT AND EXECUTION OF PCB ANALYSES: CUSTOMER-ANALYST INTERACTIONS
M. D. Erickson 1993 14 p Presented at the 5th International Conference for the Remediation of PCB Contamination, Houston, TX, 15-16 Mar. 1993
(Contract W-31-109-eng-38)
(DE93-009964; ANL/ER/CP-77861; CONF-9303123-1) Avail: CASI HC A03/MF A01

The practical application of PCB (polychlorinated biphenyl) analyses begins with a request for the analysis and concludes with provision of the requested analysis. The key to successful execution of this iteration is timely, professional communication between the requester and the analyst. Often PCB analyses are not satisfactorily executed, either because the requester failed to give adequate instructions or because the analyst simply 'did what he/she was told.' The request for and conduct of a PCB analysis represents a contract for the procurement of a product (information about the sample); if both parties recognize and abide by this contractual relationship, the process generally proceeds smoothly. Requesters may be corporate purchasing agents working from a scope of work, a sample management office, a field team leader, a project manager, a physician's office, or the analyst himself. The analyst with whom the requester communicates may be a laboratory supervisor, a sample-receiving department, a salesperson for the laboratory, or the analyst himself. The analyst conducting the analysis is often a team, with custody of the sample being passed from sample receiving to the extraction laboratory, to the cleanup laboratory, to the gas chromatography (GC) laboratory, to the data reduction person, to the package preparation person, to the quality control (QC) department for verification, and finally, to shipping. Where a team of analysts is involved, the requester needs a central point of contact to minimize confusion and frustration. For the requester-analyst interface to work smoothly, it must function as if it is a one-to-one interaction. This article addresses the pitfalls of the requester-analyst interaction and provides suggestions for improving the quality of the analytical product through the requester-analyst interface. DOE

N94-14869# Los Alamos National Lab., NM.
COMPARATIVE IGNITION OF HEXANE AND OCTANE ISOMERS IN A SHOCK TUBE
A. Burcat (Technion - Israel Inst. of Tech., Haifa.), W. J. Pitz, and C. K. Westbrook Feb. 1993 23 p Presented at the 18th International

Conference on Shock Waves and Shock Tubes, Sendai, Japan, 21-26 Jul. 1992
(Contract W-7405-eng-48)
(DE93-016535; UCRL-JC-112692; CONF-9207205-1) Avail: CASI HC A03/MF A01

Ignition delay times of hexane isomers are investigated behind shock waves. Initial concentrations of fuel oxygen and argon and the post shock temperature were varied systematically in order to establish the influence of these parameters on the ignition delay time. The fuels used were n-octane, 2-methylpentane, and 3-methylpentane. The temperature range of the experiments was 1100-1700 K and the initial pressures were 55-200 torr. These experiments are compared with a similar set of experiments performed on octane isomers (n-octane; 2,2,4-trimethylpentane and 2,3,4-trimethylpentane), and the reaction mechanism developed for them. DOE

N94-14884 Joint Inst. for Nuclear Research, Dubna (USSR). Lab. of Nuclear Problems.
FINE-POWDER Al2O3 AND SiO2 FOR PREPARATION OF MULTIELEMENT STANDARDS FOR RARE-EARTH ELEMENTS ANALYSIS
V. M. Nazarov, V. P. Chinaeva, M. V. Frontasyeva, S. Parry, B. A. Bennet, Sen Pal Chen, and Chel Zu Li 1991 8 p Limited Reproducibility: More than 20% of this document may be affected by microfiche quality
(DE93-625118; JINR-E-14-91-398) Avail: CASI HC A02 (US Sales Only)

The present paper based on the experimental results contains the discussions and suggestions on the possible use of the fine-powder Al2O3 and SiO2 as multielement standards for neutron activation analysis with original content of microimpurities up to 40 elements. DOE

N94-14764*# Stanford Univ., CA. Center for Turbulence Research.
THE EVOLUTION EQUATION FOR THE FLAME SURFACE DENSITY IN TURBULENT PREMIXED COMBUSTION
A. Trouve and T. Poinsot (Institut de Mecanique des Fluides de Toulouse, France.) *In its* Studying Turbulence Using Numerical Simulation Databases. 4: Proceedings of the 1992 Summer Program Nov. 1992 p 325-343 (For primary document see N94-14745 02-34)
Avail: CASI HC A03/MF A04; 3 functional color pages

N94-14765*# Ecole Centrale de Lyon (France).
NUMERICAL SIMULATIONS OF TURBULENT PREMIXED H2/O2/N2 FLAMES WITH COMPLEX CHEMISTRY
M. Baum, T. J. Poinsot (Institut de Mecanique des Fluides de Toulouse, France.), and D. C. Haworth (General Motors Corp., Warren, MI.) *In* Stanford Univ., Studying Turbulence Using Numerical Simulation Databases. 4: Proceedings of the 1992 Summer Program Nov. 1992 p 345-366 Original contains color illustrations (For primary document see N94-14745 02-34)
Avail: CASI HC A03/MF A04; 3 functional color pages

N94-14766*# Sandia National Labs., Albuquerque, NM. Combustion Research Facility.
EFFECT OF FINITE-RATE CHEMISTRY AND UNEQUAL SCHMIDT NUMBERS ON TURBULENT NON-PREMIXED FLAMES MODELED WITH SINGLE-STEP CHEMISTRY
J. H. Chen, S. Mahalingam (Colorado Univ., Boulder.), I. K. Puri (Illinois Univ., Chicago.), and L. Vervisch (Stanford Univ., CA.) *In* Stanford Univ., Studying Turbulence Using Numerical Simulation Databases. 4: Proceedings of the 1992 Summer Program Nov. 1992 p 367-387 Sponsored in part by DOE (For primary document see N94-14745 02-34)
Avail: CASI HC A03/MF A04; 3 functional color pages

N94-14767*# Sandia National Labs., Albuquerque, NM. Combustion Research Facility.
STRUCTURE OF TURBULENT NON-PREMIXED FLAMES MODELED WITH TWO-STEP CHEMISTRY
J. H. Chen, S. Mahalingam (Colorado Univ., Boulder.), I. K. Puri (Illinois Univ., Chicago.), and L. Vervisch (Stanford Univ., CA.) *In* Stanford Univ., Studying Turbulence Using Numerical Simulation Databases. 4: Proceedings of the 1992 Summer Program Nov. 1992 p 389-402 Sponsored in part by DOE (For primary document see N94-14745 02-34)
Avail: CASI HC A03/MF A04; 3 functional color pages

26 METALLIC MATERIALS

Includes physical, chemical, and mechanical properties of metals, e.g., corrosion; and metallurgy.

N94-12825*# Arizona Univ., Tucson. Coll. of Engineering and Mines.
THERMOSOLUTAL CONVECTION AND MACROSEGREGATION IN DENDRITIC ALLOYS Final Technical Report
David R. Poirier and J. C. Heinrich Sep. 1993 52 p
(Grant NAG3-1060)
(NASA-CR-194039; NAS 1.26:194039) Avail: CASI HC A04/MF A01

A mathematical model of solidification, that simulates the formation of channel segregates or freckles, is presented. The model simulates the entire solidification process, starting with the initial melt to the solidified cast, and the resulting segregation is predicted. Emphasis is given to the initial transient, when the dendritic zone begins to develop and the conditions for the possible nucleation of channels are established. The mechanisms that lead to the creation and eventual growth or termination of channels are explained in detail and illustrated by several numerical examples. A finite element model is used for the simulations. It uses a single system of equations to deal with the all-liquid region, the dendritic region, and the all-solid region. The dendritic region is treated as an anisotropic porous medium. The algorithm uses the bilinear isoparametric element, with a penalty function approximation and a Petrov-Galerkin formulation. The major task was to develop the solidification model. In addition, other tasks that were performed in conjunction with the modeling of dendritic solidification are briefly described. Author (revised)

N94-12834# Purdue Univ., West Lafayette, IN. Dept. of Chemistry.
ANCHORING STRATEGIES FOR BIMETALLIC SPECIES IN ZEOLITES
T. Bein Mar. 1993 7 p
(Contract DE-FG02-92ER-14281)
(DE93-015622; DOE/ER-14281/1) Avail: CASI HC A02/MF A01

We explore a new approach by introducing heterobinuclear organometallic compounds for linking catalytic functions to zeolite frameworks. With two different metals present, the complexes are being anchored to the support via one oxophilic metal, ligand exchange and catalytic reactions may proceed at the second metal center. Anchoring chemistry, thermal stability and reactivity of Me3SnMn(CO)5 in zeolite NaY and acid forms of zeolite Y was studied with X-ray absorption spectroscopy (Sn, Mn edge EXAFS) and in-situ FTIR/TPD-MS techniques. Subsequently, the tin-cobalt complex Me3SnCo(CO)4 has been a focus of detailed synthetic and spectroscopic studies. The reactivity of tricarbonyl (cyclopentadienyl) (trimethylstannyl) molybdenum in new mesoporous hosts has been explored. A recent development is the design of vanadium oxo species in different micro- and mesoporous hosts. These are of great interest for the selective reduction of nitrogen oxides by ammonia, and selective oxidation of different hydrocarbons, such as xylenes, olefines and alkanes. Combination analytical techniques used to probe local structural changes at the molecular level, include EXAFS (Extended X-Ray Absorption Fine Structure) spectroscopy utilizing synchrotron radiation, in situ FT-IR coupled to thermodesorption/MS, UV-NIR, and CCD Raman. DOE

N94-12836# Virginia Commonwealth Univ., Richmond.
STRUCTURE STABILITY AND SPECTROSCOPY OF METAL CLUSTERS
1993 15 p
(Contract DE-FG05-87ER-45316)
(DE93-016142; DOE/ER-45316/T1) Avail: CASI HC A03/MF A01

Theory based on self-consistent field-linear combinations of atomic orbitals-molecular orbital theory was applied to clusters. Four areas were covered: electronic structure, equilibrium geometries, and stability of charged clusters, interaction of metal clusters with H and halogen atoms, thermal stability of isolated clusters, and stability and optical properties of hetero-atomic clusters. DOE

N94-12899# Lawrence Livermore National Lab., CA.
EFFECT OF PRESSURE ON ORDER AND STABILITY IN ALLOYS: THE CASE OF Al-Ge
P. E. A. Turchi, M. Sluiter, and G. M. Stocks (Oak Ridge National Lab., TN.) 1 Dec. 1992 8 p Presented at the 16th Material Research Society International Symposium on the Scientific Basis for Nuclear Waste Management Fall Meeting, Boston, MA, 30 Nov. - 5 Dec. 1992

(Contracts W-7405-eng-48; DE-AC05-84OR-21400)
(DE93-013842; UCRL-JC-110687; CONF-921101-115) Avail: CASI HC A02/MF A01

A parameter-free approach to phase stability in substitutional alloys is applied to the influence of pressure on order-disorder phenomena in Al-Ge. The methodology is based upon an application of the Generalized Perturbation Method to the Korringa-Kohn-Rostoker scattering formulation of the Coherent Potential Approximation. For fcc-based Al-Ge alloys, it is shown that the tendency towards phase separation at normal pressure originates from a structural difference between the pure species. By applying pressure, the structural energy difference is reduced, and a significant increase in the tendency towards order, especially for Al-rich alloys, is theoretically observed, leading, as an example, to the possible observation of a DO(sub 22) ordered state around 25 at. %. The electronic origin of the ordering tendencies induced by pressure is discussed and the theoretical predictions are related to experimental facts. DOE

N94-12977# Sandia National Labs., Albuquerque, NM.
MULTIPHASE EQUATION OF STATE FOR IRON
G. I. Kerley Feb. 1993 64 p
(Contract DE-AC04-76DP-00789)
(DE93-013956; SAND-93-0027) Avail: CASI HC A04/MF A01

The PANDA code is used to build a multiphase equation of state (EOS) table for iron. Separate EOS tables were first constructed for each of the individual phases. The phase diagram and multiphase EOS were then determined from the Helmholtz free energies. The model includes four solid phases (alpha, gamma, delta, and epsilon) and a fluid phase (including the liquid, vapor, and supercritical regions). The model gives good agreement with experimental thermophysical data, static compression data, phase boundaries, and shock-wave measurements. Contributions from thermal electronic excitation, computed from a quantum-statistical-mechanical model, were found to be very important. This EOS covers a wide range of densities (0-1000 g/cm(sup 3)) and temperatures (0-1.2 x 10(sup 7) K). It is also applicable to RHA steel. The new EOS is used in hydrocode simulations of plate impact experiments, a nylon ball impact on steel, and the shaped charge perforation of an RHA plate. The new EOS table can be accessed through the SNL-SESAME library as material number 2150. DOE

N94-12993# Aluminum Co. of America, Alcoa Center, PA.
ROLE OF MICROSTRUCTURE ON FATIGUE DURABILITY OF ALUMINUM AIRCRAFT ALLOYS
J. R. Brockenbrough, R. J. Bucci, A. J. Hinkle, J. Liu, and P. E. Magnusen 15 Apr. 1993 131 p
(Contract F33615-92-C-5915)
(AD-A265627) Avail: CASI HC A07/MF A02

The goal of this program is to affect change in metallic aircraft life assessment methodology through quantitative understanding of how material microstructure impacts fatigue durability performance. Various studies have shown that most metal cracking problems encountered in service involve fatigue. Further studies have shown that metallurgical discontinuities and/or manufacturing imperfections often tend to exacerbate such problems by causing cracks to occur sooner than expected. This program concentrates on the initiation and early growth stage of fatigue cracks where the majority of structural life is spent. The program has two general objectives: (1) quantifying the effect of aluminum alloy microstructure on early stage fatigue damage evolution and growth, and (2) establishing an analytical framework to quantify structural component life benefits attainable through modification of intrinsic material microstructure. The modeling approach taken couples quantitative characterizations of representative material microstructures with concepts of probabilistic fracture mechanics. DTIC

N94-12998# Oak Ridge National Lab., TN.
HIGH-TEMPERATURE CORROSION AND PROTECTION OF MATERIALS
P. F. Tortorelli 19 Jun. 1992 13 p
(Contract DE-AC05-84OR-21400)
(DE93-011072; ORNL/FTR-4283) Avail: CASI HC A03/MF A01 (US Sales Only)

Two papers were presented by P.F. Tortorelli at the Third International Symposium on High-Temperature Corrosion and Protection of Materials in Les Embiez, France. Substantial interest was shown in current ORNL research on iron aluminides, Cr-Nb alloys, and mechanical properties of oxide scales. At least two other organizations are actively pursuing applications for iron aluminides. A good mix of basic and applied research papers contributed to the value of the symposium. Dr. Tortorelli also visited Harwell Laboratory and Cranfield Institute of Technology in the United Kingdom (UK). At Harwell, he discussed experimental procedures for very-high-temperature oxidation and innovative methods of corrosion analysis. During his visit to Cranfield, he was briefed on the modeling of erosion and corrosion processes and had discussions related to the mechanical properties of oxide scales. Efforts in corrosion, erosion, and coatings at Cranfield are extensive and impressive. DOE

N94-13000# Ames Lab., IA.
GAS ATOMIZED Er3Ni POWDER FOR CRYOCOOLER APPLICATIONS
I. E. Anderson, M. G. Osborne, H. Takeya, and K. A. Gschneidner, Jr. 1992 14 p Presented at the 7th International Cryocooler Conference, Santa Fe, NM, 15-19 Nov. 1992
(Contract W-7405-eng-82)
(DE93-011564; IS-M-746; CONF-921130-2) Avail: CASI HC A03/MF A01

A high pressure gas atomization (HPGA) approach was developed to produce uniform spherical powders of high purity Er3Ni and 3 batches of about 1.3 kg each were prepared. Average yield of high quality spherical powders between 0.15 and 0.35mm was about 16% of the initial atomizer charge weight. Microstructural analysis of sectioned powder samples revealed single phase particles with some internal cracking but no evidence of an oxidized surface shell. Chemical analysis and x-ray diffraction measurements verified that single phase particles of the stoichiometric composition had been generated. Vacuum fusion measurements indicated that the powder contained 2600 ppM oxygen. The heat capacity of a hot pressed, partially sintered Er3Ni powder sample was measured from 2 to 80K; results indicated a maximum heat capacity of 0.43 J/cu cm K at 7K and the peak appears to be about 0.04 J/cu cm K higher and narrower than reported by Sahashi. The Sahashi heat capacity peak has two maxima, suggesting the two phases in their material. Our Er3Ni powder has a larger heat capacity than Pb over the entire range of temperatures up to about 25K which should permit a lower final temperature for a cryocooler stage composed of this material. DOE

N94-13035# Pacific Northwest Lab., Richland, WA.
INTERFACIAL PRECIPITATION, SEGREGATION AND DEFORMATION IN ALLOY 600: IMPLICATIONS ON PRIMARY-SIDE IGSCC
S. M. Bruemmer Apr. 1993 7 p Presented at the Alloy 600 Experts Meeting, Warrenton, VA, 5-9 Apr. 1993
(Contract DE-AC06-76RL-01830)
(DE93-013161; PNL-SA-22257; CONF-9304146-1) Avail: CASI HC A02/MF A01

A great many unknowns still exist concerning the mechanisms controlling intergranular stress corrosion cracking (IGSCC) of alloy 600 in high-temperature, deaerated water environments. Any proposed mechanism must involve the microstructure, microchemistry and mechanical properties of grain boundary regions. To facilitate basic understanding, specific aspects of alloy 600 metallurgy are reviewed and discussed. Interfacial carbide precipitation, chromium depletion, impurity segregation and local deformation characteristics are examined and related to IGSCC behavior. Purpose of this paper is to provide information, and prompt discussion, on these various issues for the EPRI Alloy 600 Experts Meeting. DOE

N94-13036# Lawrence Livermore National Lab., CA.
THE X RAY DICHROISM EXPERIMENTS USING CIRCULAR POLARIZATION
J. G. Tobin, G. D. Waddill, P. A. Sterne, T. Gouder, A. Jankowski, D. P. Pappas, and D. J. Webb Aug. 1992 2 p Presented at the Advanced Light Source Users Meeting, Berkeley, CA, 27-28 Aug. 1992
(Contract W-7405-eng-48)
(DE93-013195; UCRL-JC-111973; CONF-9208225-1) Avail: CASI HC A01/MF A01

We report giant circular dichroism in the near-edge core-level x-ray absorption of a near-monolayer metal film. We have performed magnetic circular dichroism experiments on Fe/Cu(001), using both core-level photoemission and near-edge absorption fine structure, as well as photoemission of the exchange split 3s states. Coverage and temperature

dependences were investigated. A simple, one electron picture supported by supercell calculations has worked well to explain normalized branching ratio measurements. DOE

N94-13050# Johns Hopkins Univ., Baltimore, MD.
EFFECT OF MICROSTRUCTURE ON PASSIVE FILM FORMATION AND BREAKDOWN ON Al ALLOYS Final Report, 15 Dec. 1988 - 14 Dec. 1992
J. Kruger, J. W. Wagner, R. S. Lillard, and C. C. Streinz 31 May 1993 28 p
(Contract N00014-89-J-1180)
(AD-A265339) Avail: CASI HC A03/MF A01

Two in situ techniques, dynamic imaging microellipsometry (DIM) and local impedance spectroscopy (LEIS), were developed and applied to a study of the effect of microstructure on passive film formation and breakdown on Al-Ta alloys. DIM acquires ellipsometric data (thickness and optical constants of the films on surfaces) at a spatial resolution of ca. 20 micrometers using a radiometric full-field imaging approach. LEIS is an electrochemical impedance technique that generates local a.c. impedance data by measuring a.c. solution current densities very near the microstructural features of an electrode surface. The DIM technique was used to look at passive film formation in the Al3Ta precipitate, the dealloyed zone adjacent to the precipitate, and the solid solution phase that is present in Al-Ta alloys. The DIM technique observed different film thicknesses and optical constants for the films that form on these phases at potentials in the passive regions. The LEIS technique was used to study the precipitate and the region surrounding it under conditions where passive film breakdown occurs. Using these techniques, insight was obtained into the passive film formation and breakdown processes that control localized corrosion. DTIC

N94-13137# Lawrence Livermore National Lab., CA.
ELECTRONIC STRUCTURE AND PHASE STABILITY PROPERTIES IN TERNARY SUBSTITUTIONAL ALLOYS
A. J. S. Traiber, M. Sluiter, P. E. A. Turchi, and S. M. Allen (Massachusetts Inst. of Tech., Cambridge.) 1 Dec. 1992 8 p Presented at the 16th Material Research Society International Symposium on the Scientific Basis for Nuclear Waste Management Fall Meeting, Boston, MA, 30 Nov. - 5 Dec. 1992
(Contract W-7405-eng-48)
(DE93-013848; UCRL-JC-111000; CONF-921101-122) Avail: CASI HC A02/MF A01

Electronic structure and stability properties of ternary-metal alloys are examined using an extension of the Coherent Potential Approximation -Generalized Perturbation Method approach within the Tight-Binding description of the chemically random alloy. In particular, we report on calculations of density of states, mixing energies and effective cluster interactions which build up the ordering energy. The study focuses on the Ti-V-Fe system and its binary components. DOE

N94-13221# Brookhaven National Lab., Upton, NY.
STRIPPING EFFICIENCIES FOR 277 MeV/amu GOLD BEAM ON COPPER FOILS
T. Roser 1993 3 p Presented at the International Particle Accelerator Conference, Washington, DC, 17-20 May 1993
(Contract DE-AC02-76CH-00016)
(DE93-014306; BNL-48218; CONF-930511-129) Avail: CASI HC A01/MF A01

Stripping efficiencies were measured for 277 MeV/amu Au(sub 33+) ions with Copper foils ranging in thickness from 25 to 100 microns. The charge state distribution was analyzed using the beam line magnets of the transfer line between the AGS Booster and the AGS at Brookhaven. The relative charge state abundances were analyzed to find the optimum foil thicknesses for fully stripped Au(sup 79+) and Helium-like Au(sup 77+). It was also possible to extract electron stripping and pick-up cross sections. DOE

N94-13227# International Centre for Theoretical Physics, Trieste (Italy).
INCOMPLETE MELTING OF THE Au(100) SURFACE
G. Bilalbegovic and E. Tosatti Jan. 1993 36 p
(DE93-623192; IC-93/7) Avail: CASI HC A03/MF A01 (US Sales Only)

We study the high-temperature disordering of the reconstructed Au(100) surface by molecular dynamics simulation using a many-body interatomic potential. We find that the surface deconstructs at 0.8T(sub m) in good agreement with experimental data, but proper surface melting does not occur close to the bulk melting point. Instead there is an in-plane disordering of the two topmost layers. The thickness of the disordered region remains constant with increasing temperature, indicating blocked, or incomplete, melting of the (100) crystalline substrate. An analysis of the structure reveals that crystalline and disordered islands coexist on two first surface layers for temperature between deconstruction and bulk melting. DOE

N94-13242# Oak Ridge National Lab., TN.
THE CORROSION BEHAVIOR OF 8001 Al UNDER HEAT-TRANSFER CONDITIONS IN AN AQUEOUS LOOP SYSTEM
R. E. Pawel, D. K. Felde, M. T. McFee, and J. A. Clinard Apr. 1993 135 p
(Contract DE-AC05-84OR-21400)
(DE93-013450; ORNL/NPR-92/65) Avail: CASI HC A07/MF A02 (US Sales Only)

Specimens of 8001 aluminum were exposed to flowing water under heat-transfer conditions relevant to the proposed New Production Reactor-heavy-water reactor (NPR-HWR) in a Corrosion Test Loop System. The growth of oxide films on the reacting surfaces was characterized by temperature measurements on the specimen during the course of the experiments and by post-test examinations and analyses of the specimens. For all tests, the major reaction product was boehmite (Al2O3(center dot)H2O) with, in many instances, a thin, iron-rich outer layer that formed as a consequence of aqueous mass transport from the cooler stainless steel sections of the loop. In a series of five tests, each up to eight weeks in duration, the measured film growth rates were shown to be sensitive to both thermal-hydraulic and chemical variables and were compared to the predictions of existing data correlations. DOE

N94-13360 Academy of Sciences of the Ukraine, Kharkov.
ABOUT THE INFLUENCE OF INERT GAS ION IMPLANTATION ON METAL CORROSION STABILITY
V. G. Artyukh, V. A. Belous, and L. P. Rekova 1991 38 p In RUSSIAN Limited Reproducibility: More than 20% of this document may be affected by microfiche quality
(DE93-620574; INIS-mf-13456) Avail: CASI HC A03 (US Sales Only)

The results of review were systematized on main factors which presumably have an influence on metal corrosion stability: appearance of surface films, changes of surface topography, radiation damages in metal surface layer, presence of implanted inert gas atoms. It was shown that the observed effects depend in a complicated manner on the considered factors and experimental conditions of ion implantation and corrosion testing. DOE

N94-13367 Montreal Univ. (Quebec). Dept. de Genie Metallurgique.
PREPARATION AND CHARACTERIZATION OF RAPIDLY SOLIDIFIED Al-Li ALLOYS Ph.D. Thesis [ELABORATION ET CARACTERISATION D'ALLIAGES AL-LI SOLIDIFIES RAPIDEMENT]
Mohamed Hajjaji Jun. 1990 296 p In FRENCH
(ISBN-0-315-58948-5; CTN-93-60855) Copyright Avail: Micromedia Ltd., Technical Information Centre, 165 Hotel de Ville, Place du Portage, Phase 2, Hull, Quebec J8X 3X2, Canada HC/MF

A study was conducted to study the effects of rapid solidification processing by free-jet chill-block melt spinning (FJCBMS) on the microstructure and precipitation characteristics of Al-Li ribbons containing up to 10 weight percent Li for various wheel speeds and preparation atmospheres. Ribbons were prepared in a specially constructed melt spin apparatus to control the major extrinsic parameters that affect ribbon morphology, topography, and microstructure as well as to provide an inert atmosphere for alloying. The preparation atmosphere has a marked effect on the volatilization of Li during processing, the wetting of the liquid Al-Li alloy on the chill block, and the formation of the Li2O and Li2CO3 contaminants. A relationship was found between the ribbon thickness and the wheel velocity which is independent of Li concentration and solidification mechanism. Changes in Li content also have a marked effect on the solidification mechanisms. For ribbons containing up to 1.79 percent Li, solidification occurs under the melt puddle and the ribbon microstructure consists mainly of columnar grains without Al3Li precipitation. Ribbons with over 3 percent Li solidify away from the effects of the puddle and their

microstructure exhibits featureless and segregated zones. Two distinct mechanisms of Al3Li precipitation occur for the 1.79 percent Li ribbon at aging temperatures of 66, 75, and 200 C. Author (CISTI)

N94-13374# Georgia Inst. of Tech., Atlanta. School of Physics.
FIRST-PRINCIPLES STUDIES OF PHASE STABILITY AND THE STRUCTURAL AND DYNAMICAL PROPERTIES OF HYDROGEN-METAL SYSTEMS
M. Y. Chou May 1993 12 p
(Contract DE-FG05-90ER-45431)
(DE93-016129; DOE/ER-45431/3) Avail: CASI HC A03/MF A01

First-principles calculations were performed for the hydrogen-yttrium system using the pseudopotential method within the local density functional approximation (LDA). We have studied the nature of hydrogen pairing in the solid solution phase ((alpha)-YH(x)) and identified the connection with electronic structure. The vibrational spectra, diffusion barrier, and migration path were also investigated. We have also studied the binding characteristics for different interstitial sites and the (420)-plane ordering of octahedral hydrogen in (beta)YH(2+x) within the lattice gas model. Temperature-composition phase diagram was calculated by cluster variational method with the multibody interactions extracted from total energies of related ordered structures. Moreover, the discovery of Peierls distortions in YH3 explained the unusual hydrogen displacements found in neutron diffraction and the possibility of an excitonic insulating ground state was speculated. Several new improvements in the calculational techniques have also been developed: separable nonlocal pseudopotentials, a scheme to calculate the full phonon spectrum, and distance dependent tight-binding parameters. The Ru(0001)-H system was also studied. DOE

N94-13460# National Aerospace Lab., Kakuda (Japan). Research Center.
TENSILE PROPERTIES OF LE-7 ENGINE MATERIAL WITH WELDED JOINT Report No. 1 [LE-7 YOU ZAIRYOU YOUSETSU TSUGITE NO HIPPARI TOKUSEI]
Tomoyuki Hashimoto, Yoshiaki Watanabe, and Mitsumasa Sakamoto Dec. 1992 15 p In JAPANESE
(NAL-TR-1188; JTN-93-80508) Avail: CASI HC A03/MF A01

The LE-7 engine which will be used as the first stage main engine for the H-2 rocket has been under development in Japan. This engine has many welded joints that have developed a variety of problems. Therefore, tensile properties and microstructures of Inconel-718 test specimens with welded joints were investigated at various temperatures in high pressure hydrogen and helium environments to study the fundamental characteristics of the welded joints. The results indicated that the ductility of the welded joints was less than that of the parent metal and that the deterioration of ductility was due to the dendrite structure of the Ni3Nb phase.
Author (NASDA)

N94-13497# National Aerospace Lab., Amsterdam (Netherlands). Structures and Materials Div.
MODERN ALUMINIUM SHEET ALLOYS FOR AEROSPACE APPLICATIONS
R. J. H. Wanhill, L. Schra, and W. G. T. tHart 20 Feb. 1992 11 p Presented at the Third International Conference on Aluminum Alloys, Trondheim, Norway, 22-27 Jun. 1992 Sponsored by Netherlands Agency for Aerospace Programs, Delft, and EEC
(NLR-TP-92057-U; ETN-93-94344) Avail: CASI HC A03/MF A01

Several aluminum sheet alloys which have emerged as candidates for replacing the industry standard damage tolerant AlCuMg alloy 2024-T3 in aircraft structures are considered. These alloys include the AlLiCuMgZr (Al-Li) alloys 2091-T84 and 8090-T81, and the AlMgSiCu alloy 6013-T6. These alloys are compared with respect to mechanical properties, fracture toughness and crack resistance, fatigue crack growth under constant amplitude and flight simulation loading, and corrosion and stress corrosion resistances. The practical significance of the results is discussed, and the current status and prospects are indicated. ESA

N94-13512# Los Alamos National Lab., NM.
EXCIMER LASER SURFACE PROCESSING OF TITANIUM
T. R. Jervis, K. M. Hubbard, T. G. Zocco, L. Foster, M. Nastasi, and J. R. Tesmer 1993 26 p Presented at the Annual Meeting of the Minerals, Metals and Materials Society, Denver, CO, 22 Feb. 1993
(Contract W-7405-eng-36)
(DE93-012633; LA-UR-93-1142; CONF-9302103-2) Avail: CASI HC A03/MF A01

We have examined the effect of laser surface processing of Ti alloys using pulsed excimer laser light at 248 nm. Thermal transformations of the surface are accomplished by the heating of the surface and rapid cooling. Alloying and formation of compounds can be obtained by melting and mixing surface layers into the material and by gas alloying. Multiple melting-resolidification cycles result in the inter-diffusion of surface layers in the liquid state and the diffusion of gas species into the material. The effect of alloying from both solid and gas sources and the effects of thermal transformations on the microstructure and surface hardness properties of these alloys will be examined. DOE

N94-13532# National Aerospace Lab., Amsterdam (Netherlands). Materials Dept.
THE ASCOR TEST: A SIMPLE AUTOMATED METHOD FOR STRESS CORROSION TESTING OF ALUMINIUM ALLOYS
L. Schra and F. F. Groep (National Aerospace Lab., Emmeloord, Netherlands.) 7 Nov. 1991 22 p Submitted for publication
(NLR-TP-91438-U; ETN-93-94341) Avail: CASI HC A03/MF A01

A simple automated stress corrosion testing method called the ASCOR (Automated Stress COrrosion Ring) test was developed to test aluminum alloys according to the ASTM specification G44. The method involves testing cylindrical or sheet specimens in a loading ring provided with strain gauges to measure the load. Initiation of a stress corrosion crack results in a small load decrease. During the test, the load is measured periodically and stored in a data acquisition system controlled by a personal computer. A specific load decrease is used as the criterion for stress corrosion crack initiation. The main advantages of the method are that a large number of specimens can be tested simultaneously in a climate chamber, and that stress corrosion cracking initiation lives can be determined according to a clearly defined criterion without time consuming and subjective inspections, and without disturbing the test procedure. ESA

N94-13616* National Aeronautics and Space Administration. Marshall Space Flight Center, Huntsville, AL.
MID-DECK EXPERIMENTS, STS-26 (Videotape)
Sep. 1988 Videotape: 3 min. 37 sec. playing time, in color, with sound
(NASA-TM-109308; NONP-VT-93-185326) Avail: CASI VHS A01/BETA A22

Phase partitioning, ISO electric focusing, automated directional solidification furnace, mesoscale experiment, and others are explained.
Author (revised)

N94-13666 National Physical Lab., Teddington (England). Materials Metrology Div.
UK INTERLABORATORY TENSILE TESTS ON Al ALLOY/SiC PARTICULATE METAL MATRIX COMPOSITES
B. Roebuck, L. N. McCartney, P. M. Cooper, E. G. Bennett, J. D. Lord, and L. P. Orkney Dec. 1992 115 p Original contains color illustrations
(NPL-DMM(A)-77; ETN-93-94460) Copyright Avail: National Physical Laboratory, Teddington, Middlesex TW11 0LW, United Kingdom HC

The results of comparisons of the application of tensile test methods for metals to SiC particulate reinforced aluminum alloy Metal Matrix Composites (MMC) are presented. For the first phase a material blended from powders was extruded and machined into rectangular specimens for test by about thirty organizations. For the second phase a commercial material was used and machined into both rectangular and round specimens for test by essentially the same organizations as in the first phase. The major factors which contribute to uncertainties in the measurement of tensile properties of MMC are identified. Recommendations for the further work required in order for an agreed tensile test method for particulate reinforced MMC to be developed are made. ESA

N94-13670 Idaho Univ., Moscow.
FATIGUE CRACK INITIATION AND PROPAGATION IN ALUMINUM ALLOYS 8090 AND 2124 IN HYDROGENOUS ATMOSPHERES Ph.D. Thesis
Orval H. Hilliard 1992 235 p
Avail: Univ. Microfilms Order No. DA9312470

An Al-Li-Cu-Mg-Zr alloy, 8090-T8 (short transverse orientation), was evaluated with corrosion fatigue tests. This material was compared with 2124-T851 in dry helium and hydrogen-bearing atmospheres of dry hydrogen and water vapor saturated helium. The microstructures of both alloys were characterized using microscopy with image analysis. The monotonic mechanical properties were determined by tensile testing. Both 8090-T8 and 2124-T851, in short transverse orientation, suffered loss of ductility from the presence of large precipitate particles. This was more severe for 8090-T8. Fatigue crack initiation specimens were evaluated using replicas and SEM examination. Atmosphere and stress amplitude were variables. The environments were dry helium, dry hydrogen, and saturated helium at ambient temperatures. The response of the alloys to these environments was evaluated by qualitative observation of slip bands, surface crack count, and number of cycles to failure. Low cycle corrosion fatigue tests provided data for evaluating strain hardening characteristics and determining the fatigue strength, ductility, and cyclic strength constants. Fatigue performance in inert and hydrogen-bearing environments was compared over a range of strain amplitudes. The variation of fatigue ductility coefficients and exponents with environment aggressiveness clearly shows effects by environment on strain controlled fatigue behavior, e.g. the fatigue ductility exponents changed by 50 percent or more between dry and saturated helium. Load controlled fatigue under fully reversed loading, in dry helium, hydrogen, or saturated helium, provided S/N plots to illustrate the effects of aggressive environments. The presence of water vapor decreased the fatigue life of 8090-T8 by an order of magnitude at low stress amplitudes. The fatigue life of 2124-T851 decreased in dry hydrogen, but was unaffected in saturated helium. At high stress amplitudes, 2124-T851 is superior to 8090-T8 in all tested environments. At low stress amplitudes, 8090-T8 is superior in dry environments. In saturated helium, 2124-T851 is superior at all stress amplitudes. A model was proposed to rationalize the observed effects of the aggressive hydrogenous atmosphere. This model suggests that particle matrix decohesion is enhanced in the aggressive environments. If this is true, then particle-matrix decohesion would occur at smaller particles than in inert atmospheres. Decohesion would continue to occur at large particles. Dissert. Abstr.

N94-13697# Aluminum Co. of America, Alcoa Center, PA.
ROLE OF MICROSTRUCTURE ON FATIGUE DURABILITY OF ALUMINUM AIRCRAFT ALLOYS Interim Status Report
9 Mar. 1993 26 p
(Contract N00014-91-C-0128)
(AD-A266350) Avail: CASI HC A03/MF A01

Alcoa historical 7050 fatigue test data has been assembled and reviewed. The range of microstructures examined in the program has been expanded from two in the contract proposal to five. In addition to the old and new quality thick plate, the program includes low porosity thick plate, low particle thick plate, and thin plate. These materials provide a range of microstructures/fatigue failure modes to help understand and model early stage fatigue damage. Though the scope of the program has expanded, the total program cost to the Navy has not changed. The fatigue test data on additional microstructural variants of 7050 have been assembled. Fractography of failed coupon specimens has been completed. The microstructural features controlling fatigue initiation have been identified. Samples of old and new quality plate have been supplied to the UCLA team in support of their ONR program. DTIC

N94-13715*# National Aeronautics and Space Administration. Marshall Space Flight Center, Huntsville, AL.
MICROSTRUCTURAL EVOLUTION OF NARloy-Z AT ELEVATED TEMPERATURES
J. Singh, G. Jerman, B. N. Bhat, and R. Poorman Sep. 1993 29 p
(NASA-TM-108419; NAS 1.15:108419) Avail: CASI HC A03/MF A01

Microstructural evolution was studied in samples of wrought and vacuum plasma sprayed (VPS) NARloy-Z exposed to temperatures up to 970 C (1,780 F) for up to 60 h. Samples were heated in a vacuum furnace, followed by rapid quenching in helium (He) gas at a cooling rate of 166 C (300 F) per second. Microstructural analyses were conducted using optical microscopy, scanning electron microscopy (SEM), and electron probe microanalysis (EPMA). In both the wrought and VPS conditions, precipitates rich in silver (Ag) and zirconium (Zr) were present in the matrix and at the grain boundaries even after long exposure to elevated temperatures. Islands rich in oxygen (O2) and Zr were also observed, as well as incipient melting at the grain boundary triple points. Results indicated that the alloy cannot be homogenized by heat treatment at elevated temperatures. Author (revised)

N94-13840 Carleton Univ., Ottawa (Ontario). Dept. of Mechanical and Aeronautical Engineering.
THE MICROSTRUCTURAL RESPONSE OF NEAR GAMMA-TiAl+W TO HEAT TREATMENT
J. Beddoes, L. Zhao (Institute for Aerospace Research, Ottawa, Ontario.), and W. Wallace (Institute for Aerospace Research, Ottawa, Ontario.) 1992 5 p Sponsored by Dept. of National Defence
(DSIS-93-00237; CTN-93-60799) Avail: CASI HC A01

The phase transformations and kinetics of the grain coarsening reaction occurring during heat treatment in the alpha+gamma and alpha phase fields were investigated for powder metallurgically (PM) produced near gamma-TiAl+W alloy. This alloy was chosen because the W addition promotes the formation of third phase W-rich beta. As well, a fine initial microstructure exists due to the inherent rapid solidification of PM processing. Potentially, these factors can alter the transformation and grain growth kinetics. Two series of heat treatments were undertaken: two hours at temperatures ranging from 1250 C to 1400 C, and treatment at 1400 C for times ranging from 10 to 240 minutes. Heat treatment in the single phase region was found to cause rapid transformation of gamma to alpha in under 10 minutes. The grain growth kinetics at 1400 C for TiAl+W are slower than for other near gamma-TiAl alloys. The dependence of grain size D on heat treatment time t can be described by the equation D=70.3t raised to the 0.29 power. Heat treatment for over three hours at 1400 C produces a grain size of about 300 microns. During heat treatment in the alpha+gamma region, alpha plates develop on the (111) planes. Author (CISTI)

N94-13891*# Vanderbilt Univ., Nashville, TN. Center for Microgravity Research and Applications.
THE INFLUENCE OF A MICROGRAVITY ENVIRONMENT ON THE DENDRITIC MORPHOLOGY DURING DIRECTIONAL SOLIDIFICATION OF HYPOEUTECTIC Al-Si ALLOYS Final Technical Report, 1 May 1991 - 30 Apr. 1992
Richard N. Grugel 1993 7 p
(Grant NAGw-2540)
(NASA-CR-194139; NAS 1.26:194139) Avail: CASI HC A02/MF A01

NASA grant NAGW-2540 provided the opportunity to evaluate and extend ongoing studies of directionally solidified Al-Si alloys. Microstructural development was further characterized in terms of solidification processing parameters; novel relationships between processing and development of dendrite trunk diameters and tertiary dendrite arm spacings were found. This has resulted in three publications (one in print, one in press, and one in review). Microstructural development under conditions of controlled acceleration during directional solidification has been investigated; this has culminated in a Master's degree and will be submitted for publication. The above work not only contributes to our understanding of solidification phenomena but also defines the processing parameters for a successful microgravity experiment while providing a data base to which mu g samples can be unequivocally compared and evaluated. Derived from text

N94-13977# Utah Univ., Salt Lake City. Dept. of Chemistry.
THERMOCHEMISTRY OF TRANSITION METAL CLUSTERS
P. B. Armentrout 1993 4 p
(Contract DE-FG02-91ER-14193)
(DE93-016201; DOE/ER-14193/5) Avail: CASI HC A01/MF A01

The objective is to obtain thermodynamic properties of transition metal ion clusters, their binding energies to ligands, and their reactions, using a mass spectrometer and a photodissociation spectrometer. In addition to metal cluster ions, atomic metal ions with up to 4 H2O molecules or He or Ar atoms as ligands have been generated. DOE

N94-14021# Oak Ridge National Lab., TN.
FATIGUE DESIGN CURVES FOR 6061-T6 ALUMINUM
G. T. Yahr 1993 14 p Presented at the Pressure Vessel and Piping Conference, Denver, CO, 25-29 Jul. 1993
(Contract DE-AC05-84OR-21400)
(DE93-011849; CONF-930702-14) Avail: CASI HC A03/MF A01

A request has been made to the ASME Boiler and Pressure Vessel

Committee that 6061-T6 aluminum be approved for use in the construction of Class 1 welded nuclear vessels so it can be used for the pressure vessel of the Advanced Neutron Source research reactor. Fatigue design curves with and without mean stress effects have been proposed. A knock-down factor of two is applied to the design curve for evaluation of welds. The basis of the curves is explained. The fatigue design curves are compared to fatigue data from base metal and weldments. DOE

N94-14058# Pacific Northwest Lab., Richland, WA.
RADIATION HARDENING AND RADIATION-INDUCED CHROMIUM DEPLETION EFFECTS ON INTERGRANULAR STRESS CORROSION CRACKING OF AUSTENITIC STAINLESS STEELS
S. M. Bruemmer and E. P. Simonen Mar. 1993 14 p Presented at the NACE Annual Corrosion Conference and Materials Performance and Corrosion Show, New Orleans, LA, 7-12 Mar. 1993
(Contract DE-AC06-76RL-01830)
(DE93-011602; PNL-SA-21491; CONF-930318-9) Avail: CASI HC A03/MF A01

Available data on neutron-irradiated materials have been analyzed, and correlations were developed between fluence, yield strength, grain boundary chromium concentration, and cracking susceptibility in high-temperature water environments. Large heat-to-heat differences in critical fluence (0.2 to 2.5 n/sq cm) for IGSCC are documented. In many cases, this variability is consistent with yield strength differences among irradiated materials. IGSCC correlated better to yield strength than to fluence for most heats suggesting the possible role of radiation-induced hardening (and microstructure) in cracking. However, isolated heats reveal a wide range of yield strengths from 450 to 800 MPa necessary to promote IGSCC which cannot be understood by strength effects alone. Grain boundary Cr depletion explain differences in IGSCC susceptibility for irradiated stainless steels. Cr contents versus SCC shows that all materials showing IG cracking have some grain boundary depletion (greater than or equal to 2%). Grain boundary Cr concentrations for cracking (below approximately 16 wt %) are in good agreement with similar SCC tests on unirradiated 304 SS with controlled depletion profiles. Heats that prompt variability in the yield strength correlation are accounted for by differences in their interfacial Cr contents. Certain stainless steels are more resistant to cracking even though they have significant radiation-induced Cr depletion. It is proposed that Cr depletion is required for IASCC, but observed susceptibility is modified by other microchemical and microstructural components. DOE

N94-14123*# Wisconsin Univ., Madison. Dept. of Materials Science and Engineering.
CONTAINERLESS PROCESSING OF UNDERCOOLED MELTS Final Report, 1 Mar. 1989 - 28 Feb. 1993
J. H. Perepezko 1993 28 p
(Grant NAG8-771)
(NASA-CR-194350; NAS 1.26:194350) Avail: CASI HC A03/MF A01

The investigation focused on the control of microstructural evolution in Mn-Al, Fe-Ni, Ni-V, and Au-Pb-Sb alloys through the high undercooling levels provided by containerless processing, and provided fundamental new information on the control of nucleation. Solidification analysis was conducted by means of thermal analysis, x-ray diffraction, and metallographic characterization on samples processed in a laboratory scale drop tube system. The Mn-Al alloy system offers a useful model system with the capability of phase separation on an individual particle basis, thus permitting a more complete understanding of the operative kinetics and the key containerless processing variables. This system provided the opportunity of analyzing the nucleation rate as a function of processing conditions and allowed for the quantitative assessment of the relevant processing parameters. These factors are essential in the development of a containerless processing model which has a predictive capability. Similarly, Ni-V is a model system that was used to study duplex partitionless solidification, which is a structure possible only in high under cooling solidification processes. Nucleation kinetics for the competing bcc and fcc phases were studied to determine how this structure can develop and the conditions under which it may occur. The Fe-Ni alloy system was studied to identify microstructural transitions with controlled variations in sample size and composition during containerless solidification. This work was forwarded to develop a microstructure map which delineates regimes of structural evolution and provides a unified analysis of experimental observations. The Au-Pb-Sb system was investigated to characterize the thermodynamic properties of the undercooled liquid phase and to characterize the glass transition under a variety of processing conditions. By analyzing key containerless processing parameters in a ground based drop tube study, a carefully designed flight experiment may be planned to utilize the extended duration microgravity conditions of orbiting spacecraft. Author (revised)

N94-14133*# Stanford Univ., CA.
LIQUID METAL DROP EJECTION Final Report
B. T. Khuri-Yakub Aug. 1993 3 p
(Grant NAG3-1253)
(NASA-CR-193718; NAS 1.26:193718) Avail: CASI HC A01/MF A01

The aim of this project was to demonstrate the possibility of ejecting liquid metals using drop on demand printing technology. The plan was to make transducers for operation in the 100 MHz frequency range and to use these transducers to demonstrate the ability to eject drops of liquid metals such as gallium. Two transducers were made by indium bonding piezoelectric lithium niobate to quartz buffer rods. The lithium niobate plates were thinned by mechanical polishing to a thickness of 37 microns for operation at 100 MHz. Hemispherical lenses were polished in the opposite ends of the buffer rods. The lenses, which focus the sound waves in the liquid metal, had an F-number equals 1. A mechanical housing was made to hold the transducers and to allow precise control over the liquid level above the lens. We started by demonstrating the ability to eject drops of water on demand. The drops of water had a diameter of 15 microns which corresponds to the wavelength of the sound wave in the water. A videotape of this ejection was made. We then used a mixture of Gallium and Indium (used to lower the melting temperature of the Gallium) to demonstrate the ejection of liquid metal drops. This proved to be difficult because of the oxide skin which forms on the surface of the liquid. In some instances, we were able to eject metal drops, however, this was not consistent and reproducible. An experiment was set up at NASA-Lewis to stabilize the process of drop on demand liquid metal ejection. The object was to place the transducer and liquid metal in a vacuum station so that no oxide would form on the surface. We were successful in demonstrating that liquid metals could be ejected on demand and that this technology could be used for making sheet metal in space. Author (revised)

N94-14184# Pacific Northwest Lab., Richland, WA.
REVERSE MICELLE SYNTHESIS OF NANOSCALE METAL CONTAINING CATALYSTS
J. G. Darab, J. L. Fulton, and J. C. Linehan Mar. 1993 8 p Presented at the 205th American Chemical Society National Meeting, Denver, CO, 28 Mar. - 2 Apr. 1993
(Contract DE-AC06-76RL-01830)
(DE93-012869; PNL-SA-21663; CONF-930304-19) Avail: CASI HC A02/MF A01

The need for morphological control during the synthesis of catalyst precursor powders is generally accepted to be important. In the liquefaction of coal, for example, iron-bearing catalyst precursor particles containing individual crystallites with diameters in the 1-100 nanometer range are believed to achieve good dispersion throughout the coal-solvent slurry during liquefaction 2 runs and to undergo chemical transformations to catalytically active iron sulfide phases. The production of the nanoscale powders described here employs the confining spherical microdomains comprising the aqueous phase of a modified reverse micelle (MRM) microemulsion system as nanoscale reaction vessels in which polymerization, electrochemical reduction, and precipitation of solvated salts can occur. The goal is to take advantage of the confining nature of micelles to kinetically hinder transformation processes which readily occur in bulk aqueous solution in order to control the morphology and phase of the resulting powder. We have prepared a variety of metal, alloy, and metal- and mixed metal-oxide nanoscale powders from appropriate MRM systems. Examples of nanoscale powders produced include Co, Mo-Co, Ni3Fe, Ni, and various oxides and oxyhydroxides of iron. Here, we discuss the preparation and characterization of nickel metal (with a nickel oxide surface layer) and iron oxyhydroxide MRM nanoscale powders. We have used extended x-ray absorption fine structure (EXAFS) spectroscopy to study the chemical polymerization process in situ, x-ray diffraction (XRD), scanning and transmission electron microcroscopies (SEM and TEM), elemental

analysis, and structural modelling to characterize the nanoscale powders produced. The catalytic activity of these powders is currently being studied. DOE

N94-14316# Mound Lab., Miamisburg, OH.
ESTIMATION OF STRAIN IN 1-kW PRIMARY CONTAINMENT VESSELS BY MICROSTRUCTURAL EXAMINATION
P. M. Schleitweiler and C. W. Merten 19 Apr. 1993 50 p
(Contract DE-AC04-88DP-43495)
(DE93-013053; MLM-3767) Avail: CASI HC A03/MF A01

Weld sections were analyzed and strain estimated in five 1-kW primary containment vessels submitted to the EG&G Mound Physical Metallurgy Group for evaluation. Four of the vessels had been subjected to compression testing, and one was untested. Metallographic sectioning was done on regions of greatest deformation and on weld areas. Strain was estimated by measuring the grain deformation with a line intercept method. DOE

N94-14364# Westinghouse Hanford Co., Richland, WA.
BAKEOUT: A COMPUTER PROGRAM FOR PREDICTING DIFFUSIVE OUTGASSING FROM STAINLESS STEEL
M. P. Weis Dec. 1992 11 p Presented at the Pressure Vessels and Piping Conference, Denver, CO, 25-29 Jul. 1993
(Contract DE-AC06-87RL-10930)
(DE93-012613; WHC-SA-1361; CONF-930702-24) Avail: CASI HC A03/MF A01

The outgassing load from a leak-tight and well-baked vacuum vessel is frequently dominated by the diffusive outgassing of hydrogen gas from the materials of which the vessel is constructed. Stainless steel, in particular, can be a major source of hydrogen. The diffusive transport of gas through materials is governed by the second order partial differential equation, D (partial derivative)(sup 2)C/(partial derivative)X(sup 2) = (partial derivative)C/(partial derivative)t, known as Fick's Law. Two alternate solutions to this equation give exact numerical answers of the diffusive outgassing rate versus time. A simplified approximation of each solution allows prediction of both the short-term and the long-term behavior. BAKEOUT, a computer program based on Fick's Law, was developed to predict an elevated temperature step function of time (that is, a bakeout) that will achieve a desired hydrogen diffusive outgassing rate from a stainless steel vessel under vacuum. This paper presents the mathematical development of the computer program and an example case. DOE

N94-14402# Purdue Univ., West Lafayette, IN.
CATALYTIC ARENE HYDROGENATION USING EARLY TRANSITION METAL HYDRIDE COMPOUNDS
I. P. Rothwell 15 Mar. 1993 4 p
(Contract DE-FG02-92ER-14280)
(DE93-015500; DOE/ER-14280/1) Avail: CASI HC A01/MF A01

Progress was achieved in four areas: development of surface supported Group 5 metal organometallic compounds for catalytic arene hydrogenation, isolation and reactivity of possible intermediates in catalytic arene hydrogenation, synthesis and characterization of new d(sup 0)-metal hydride compounds, and stoichiometric reactivity of d(sup 0) metal hydride, aryloxide compounds. DOE

N94-14474# California Univ., Berkeley. Lawrence Berkeley Lab.
MICROSTRUCTURAL INFLUENCES ON THE MECHANICAL PROPERTIES OF SOLDER
J. W. Morris, Jr., J. L. F. Goldstein, and Z. Mei Apr. 1993 48 p Presented at the 3rd International Workshop on Materials and Mechanics Issues of Solder Alloy Applications, Sante Fe, NM, 9-11 Sep. 1993
(Contract DE-AC03-76SF-00098)
(DE93-015044; LBL-34012; CONF-9209360-1) Avail: CASI HC A03/MF A01

Intent of this book is to review analytic methods for predicting behavior of solder joints, based on continuum mechanics. The solder is treated as a continuous, homogeneous body, or composite of such bodies, whose mechanical behavior is uniform and governed by simple constitutive equations. The microstructure of a solder joint influences its mechanical properties in three ways: it governs deformation and failure; common solders deform inhomogeneously; and common solders are microstructurally unstable. The variety of microstructures often found in solder joints are briefly reviewed, and some of the ways are discussed in which the microstructure influences the common types of high-temperature mechanical behavior. DOE

N94-14537# Oak Ridge National Lab., TN.
HEAVY SECTION STEEL IRRADIATION EXPERIMENT
M. T. Hurst 1993 10 p Presented at the Intelligent User's Association Meeting, Greenville, SC, 2-5 Mar. 1993
(Contract DE-AC05-84OR-21400)
(DE93-015517; CONF-9303188-1) Avail: CASI HC A02/MF A01

This experiment in University of Michigan's Phoenix Ford Reactor is designed to test various materials used in reactor pressure vessel construction. Tests are performed with specimens maintained at a constant temperature and pressure in a high neutron flux close to the reactor core. The metallurgical test specimens are sandwiched between two steel plates, and each plate contains nine independently controllable electrical heaters. DOE

N94-14700# Oak Ridge National Lab., TN.
INVESTIGATIONS OF LOW-TEMPERATURE NEUTRON EMBRITTLEMENT OF FERRITIC STEELS
K. Farrell, S. T. Mahmood, R. E. Stoller, and L. K. Mansur 1992 28 p Presented at the 20th Water Reactor Safety Information Meeting, Bethesda, MD, 21-23 Oct. 1992
(Contract DE-AC05-84OR-21400)
(DE93-015460; CONF-921007-32) Avail: CASI HC A03/MF A01

Investigations were made into reasons for accelerated embrittlement of surveillance specimens of ferritic steels irradiated at 50 C at the High Flux Isotope Reactor (HFIR) pressure vessel. Major suspects for the precocious embrittlement were a highly thermalized neutron spectrum, a low displacement rate, and the impurities boron and copper. None of these were found guilty. A dosimetry measurement shows that the spectrum at a major surveillance site is not thermalized. A new model of matrix hardening due to point defect clusters indicates little effect of displacement rate at low irradiation temperature. Boron levels are measured at 1 wt ppM or less, inadequate for embrittlement. Copper at 0.3 wt percent and nickel at 0.7 wt percent are shown to promote radiation strengthening in iron binary alloys irradiated at 50 to 60 C, but no dependence on copper and nickel was found in steels with 0.05 to 0.22 percent Cu and 0.07 to 3.3 percent Ni. It is argued that copper impurity is not responsible for the accelerated embrittlement of the HFIR surveillance specimens. The dosimetry experiment has revealed the possibility that the fast fluence for the surveillance specimens may be underestimated because the stainless steel monitors in the surveillance packages do not record an unexpected component of neutrons in the spectrum at energies just below their measurement thresholds of 2 to 3 MeV. DOE

N94-14779# Wisconsin Univ., Madison. Dept. of Chemical Engineering.
REACTOR STUDIES OF METAL IONS ASSOCIATED WITH CHROMATOGRAPHIC SILICA Final Report
Stanley H. Langer 20 Apr. 1993 5 p
(Contract DAAL03-90-G-0123)
(AD-A266675; ARO-27600.9-CH) Avail: CASI HC A01/MF A01

Chromatographic effects from transition metal ion association with the silica used as packing materials in high-performance liquid chromatography were emphasized with special attention given to their catalytic properties and methods for studying them. Retention changes for selected solutes resulting from silica modification were also studied. For rate process analysis, a statistical method based on the first moment of the overall elution profile was developed for first-order type chemical reactions under special conditions. This approach alleviated difficulties in resolving and analyzing reactant and product overlap, and it also facilitated the study of features associated with catalysis such as adsorption. With this approach as a start and hydroquinone oxidation as a probe reaction, significant progress was made toward developing a stable, reproducible, iron(3) ion-modified silica stationary phase with considerable catalytic activity. DTIC

N94-14786# Carnegie-Mellon Univ., Pittsburgh, PA. Dept. of Materials Science and Engineering.
AN INVESTIGATION OF THE ROLE OF SECOND PHASE PARTICLES IN THE DESIGN OF ULTRA HIGH STRENGTH STEELS OF IMPROVED TOUGHNESS Final Report, 1 Oct. 1989 - 31 Dec. 1992

Warren M. Garrison, Jr. 14 May 1993 34 p
(Contract DAAL03-89-K-0175)
(AD-A266774; ARO-27407.1-MS) Avail: CASI HC A03/MF A01

The influence of inclusion distributions and fine scale microstructure on the fracture toughness and fracture processes of ultra high strength steels have been investigated. The inclusion distributions vary in the sulfide type. The sulfide types considered were MnS, CrS, La2O2S, and Ti2CS. The MnS and CrS particles are smaller and more closely spaced than particles of La2O2S. Resistance to void nucleation is the same if the sulfur is gettered as CrS, MnS, or La2O2S. The particles of Ti2CS are smaller and much more resistant to void nucleation than the other sulfide types. The fine scale microstructures were those obtained for the as-quenched, tempered at 425 C and tempered at 510 C conditions for HY180 and AF1410 steels. The topics addressed are as follows: (1) effect of fine scale microstructure and inclusion distributions on blunting behavior, (2) the role of inclusion spacing at constant inclusion volume fraction on fracture toughness of three fine scale microstructures for HY 180 steel, (3) effect of gettering sulfur as Ti2CS on the fracture toughness of three fine scale microstructures of HY180 steel, (4) morphology of Ti2CS particles, (5) effect of gettering sulfur as Ti2CS on the fracture toughness of AF1410 steel tempered at 510 C, and (6) conclusions regarding improving toughness by gettering sulfur as Ti2CS. DTIC

N94-14793 Lawrence Livermore National Lab., CA.
STATICS AND KINETICS OF PHASE TRANSFORMATIONS IN bcc Fe-Cr
L. Reinhard 17 Nov. 1992 5 p Presented at the NATO Advanced Study Institute on Statics and Dynamics of Alloy Phase Transformations, Rhodes, Greece, 21 Jun. - 3 Jul. 1992 Limited Reproducibility: More than 20% of this document may be affected by microfiche quality
(Contract W-7405-eng-48)
(DE93-013839; UCRL-JC-112060; CONF-9206202-7) Avail: CASI HC A01

The Fe-Cr phase diagram exhibits a bcc solid solution (alpha-Fe-Cr) in a wide concentration range at high temperatures. This paper presents applications of the Monte Carlo method in the framework of the three-dimensional Ising model to the problem of phase separation in alpha-Fe-Cr and compare the simulation results with experiment. DOE

N94-14795 California Univ., Berkeley. Lawrence Berkeley Lab.
THE EFFECT OF CRYSTAL TILT ON HIGH RESOLUTION MICROGRAPHS OF SMALL METAL PARTICLES
J. O. Malm (Lund Univ., Sweden.) and M. A. OKeefe Jan. 1993 2 p Presented at the Conference on Electron Microscopy, Lund, Sweden, 9-11 Jun. 1993 Limited Reproducibility: More than 20% of this document may be affected by microfiche quality
(Contract DE-AC03-76SF-00098)
(DE93-013915; LBL-33753; CONF-9306164-1) Avail: CASI HC A01

The structure of small (1.5-5 nm) metal particles has been studied by high resolution transmission electron microscopy. For particles of this size, it is not possible to use tilting techniques (selected area diffraction), which means that the microscopist has to rely on the image when deciding in which direction the particle is viewed. This work points out some of the problems of intuitive determination of the viewing direction. DOE

N94-14814# Institut National des Sciences Appliquees de Lyon, Villeurbanne (France). Groupe d'Etudes de Metallurgie Physique et Physique des Materiaux.
MICROSTRUCTURAL ORIGINS AND MODELING OF INTERGRANULAR CRACK INITIATION IN AN Al-Li-Cu-Mg-(Zr) ALLOY Ph.D. Thesis [ORIGINES MICROSTRUCTURALES ET MODELISATION DE L'AMORCAGE DES FISSURES INTERGRANULAIRES D'UN ALLIAGE AL-LI-CU-MG-(ZR)]
Catherine Bourges-Verdu 1991 239 p In FRENCH Sponsored by Centre de Recherche de Pechiney, France
(ISAL-91-0012; ETN-93-94356) Avail: CASI HC A11/MF A03

Microscopic mechanisms of intergranular fracture of Al-Li-Cu-Mg-(Zr) alloys are studied and modeled. An original experimental method was used to show that this fracture is linked to plastic deformation of the alloy. Only a single family of slip planes was observed due to the marked crystallographic texture and due to the shearing of the Al3Si precipitates. The intergranular fracture resulted principally because of the interaction with the joint grains, rectilinear and sinuous shears. The intergranular precipitation of the quasicrystalline phase T2 and the presence of a zone without Al3Li precipitates favors the initiation of intergranular cracks because of the incompatibility of plastic deformation between the T2 phase and the matrix. ESA

N94-14821 GKSS-Forschungszentrum Geesthacht (Germany). Materials Research Inst.
INFLUENCE OF HEAT TREATMENT ON MICROSTRUCTURE OF Ti-35wt Al PREPARED BY ELEMENTAL POWDER METALLURGY
G.-X. Wang and M. Dahms 1992 10 p Repr. from Scripta Metallurgica et Materialia, Elmsford, NY, Pergamon Press, v. 26, no. 5, 1992 p 712-722
(GKSS/92/E/27; ETN-93-94610) Copyright Avail: Issuring Activity (GKSS-Forschungszentrum Geesthacht G.M.B.H., D-W-2054, Geesthacht, Germany)

The hardness of the Ti-35 wt. percent Al alloy, as an indicator for mechanical properties under unidirectional loading, is investigated as a function of the microstructure obtained. The influence of heat treatment on the alloy's microstructure is analyzed. Titanium aluminide alloys based on the intermetallic compound gamma-TiAl are potential materials for high performance airframe and gas turbines. The powder mixture was pressed at room temperature and after canning in Ti tubes the samples were hot isostatically pressed. The results of the microstructure analysis showed that: the element distribution after hot isostatically pressing treatment was very homogeneous with Ti content varying from 42 to 68 atoms; four different structures can be observed; the lamellar volume fraction is strongly dependent on heat treatment. The results of microhardness tests are shown. ESA

N94-14828# Royal Aerospace Establishment, Farnborough (England).
THE GROWTH OF SHORT FATIGUE CRACKS IN AN ALUMINIUM ALLOY
R. Cook 24 Nov. 1992 50 p
(RAE-TR-92063; RAE-Mat/Str-363; ICAF-1867; BR315742; ETN-93-94500) Copyright Avail: CASI HC A03/MF A01

Fatigue tests were carried out to establish the effects of various constant amplitude and standardized variable amplitude loading sequences on the growth of short and long crack in 2024-T3 aluminum alloy. In most cases, the growth rates of short cracks were greater than those of long cracks for the same nominal stress intensity factor ranges, and short cracks grew at stress intensity factor ranges below the long crack threshold values. The experimental crack growth results are discussed and compared with predictions based on the FASTRAN crack closure model of Newman. Experimental work which represented the United Kingdom contribution to the core program of the AGARD cooperative program on short crack growth behavior is included. ESA

N94-14850*# Analytical Services and Materials, Inc., Hampton, VA.
EFFECT OF THERMAL PROCESSING PRACTICES ON THE PROPERTIES OF SUPERPLASTIC Al-Li ALLOYS Final Report
Stephen J. Hales and Henry E. Lippard (Northwestern Univ., Evanston, IL.) Washington Sep. 1993 63 p
(Contract NAS1-19399; RTOP 505-63-50-03)
(NASA-CR-4548; NAS 1.26:4548) Avail: CASI HC A04/MF A01

The effect of thermal processing on the mechanical properties of superplastically formed structural components fabricated from three aluminum-lithium alloys was evaluated. The starting materials consisted of 8090, 2090, and X2095 (Weldalite(TM) 049), in the form of commercial-grade superplastic sheet. The experimental test matrix was designed to assess the impact on mechanical properties of eliminating solution heat treatment and/or cold water quenching from post-forming thermal processing. The extensive hardness and tensile property data compiled are presented as a function of aging temperature, superplastic strain and temper/quench rate for each alloy. The tensile properties of the materials following superplastic forming in two T5-type tempers are compared with the baseline T6 temper. The implications for simplifying thermal processing without degradation in properties are discussed on the basis of the results. Author (revised)

N94-14873# North Carolina State Univ., Raleigh. Dept. of Nuclear Engineering.
A STUDY OF HYDROGEN EFFECTS ON FRACTURE BEHAVIOR OF RADIOACTIVE WASTE STORAGE TANKS

K. L. Murty and T. S. Elleman 1993 11 p
(Contract DE-FG05-92ER-75784)
(DE93-018171; DOE/ER-75784/1) Avail: CASI HC A03/MF A01

Since the high-level radioactive waste at Savannah River and Hanford may have to occupy steel tanks for many years before processing, research was directed toward examination of hydrogen effects in carbon steels and identification of radiation-enhanced hydrogen uptake in steels. Results to date are too preliminary for any conclusions to be made; however, experimental methods for measuring hydrogen gradients appear to be satisfactory. DOE

N94-14878# Army Research Lab., Watertown, MA.
YIELD PROPERTIES OF TUNGSTEN AND TUNGSTEN HEAVY ALLOYS
Kenneth F. Ryan and Robert J. Dowding Jun. 1993 13 p
(AD-A266833; ARL-TR-143) Avail: CASI HC A03/MF A01

This report describes the progress made in dynamic thermo-mechanical investigations, using the Gleeble 1500, of the yield properties of tungsten heavy alloys. This study describes properties of tungsten heavy alloy at elevated temperatures and strain rates, that can be useful in the modeling of long rod kinetic energy penetrator behavior. DTIC

27 NONMETALLIC MATERIALS

Includes physical, chemical, and mechanical properties of plastics, elastomers, lubricants, polymers, textiles, adhesives, and ceramic materials.

For composite materials see *24 Composite Materials*.

N94-12789*# Auburn Univ., AL. Dept. of Chemistry.
ANALYSIS OF SAMPLES OF REFLECTOR MATERIALS WHICH ARE MULTICOATED AND METAL SAMPLES WITH OXIDE COATINGS WHICH HAVE BEEN EXPOSED THE SPACE ENVIRONMENT IN LDEF TESTING Final Report
W. C. Neely 30 Sep. 1992 2 p
(Grant NAG1-1313)
(NASA-CR-193647; NAS 1.26:193647) Avail: CASI HC A01/MF A01

The use of low angle x-ray diffraction (XRD), x-ray photoelectron spectrometry (XPS), and Auger spectrometry have been tested as suitable methods for analysis of thin oxide films on metal substrates exposed to the space environment during Long Duration Exposure Facility (LDEF) testing. No significant changes in the composition of silicon monoxide overcoats on aluminum surfaces was found. XPS and Auger testing appear to be more suitable for ultrathin films than XRD. Author (revised)

N94-12792*# Boeing Defense and Space Group, Seattle, WA. Research and Engineering.
SYSTEM INTEGRATION AND DEMONSTRATION OF ADHESIVE BONDED HIGH TEMPERATURE ALUMINUM ALLOYS FOR AEROSPACE STRUCTURE, PHASE 2 Final Report
Anthony Falcone and John H. Laakso Jul. 1993 108 p
(Contract NAS1-18560; RTOP 505-63-20-01)
(NASA-CR-191459; NAS 1.26:191459; D658-10313-1) Avail: CASI HC A06/MF A02

Adhesive bonding materials and processes were evaluated for assembly of future high-temperature aluminum alloy structural components such as may be used in high-speed civil transport aircraft and space launch vehicles. A number of candidate high-temperature adhesives were selected and screening tests were conducted using single lap shear specimens. The selected adhesives were then used to bond sandwich (titanium core) test specimens, adhesive toughness test specimens, and isothermally aged lap shear specimens. Moderate-to-high lap shear strengths were obtained from bonded high-temperature aluminum and silicon carbide particulate-reinforced (SiC(sub p)) aluminum specimens. Shear strengths typically exceeded 3500 to 4000 lb/in(sup 2) and flatwise tensile strengths exceeded 750 lb/in(sup 2) even at elevated temperatures (300 F) using a bismaleimide adhesive. All faceskin-to-core bonds displayed excellent tear strength. The existing production phosphoric acid anodize surface preparation process developed at Boeing was used, and gave good performance with all of the aluminum and silicon carbide particulate-reinforced aluminum alloys investigated. The results of this program support using bonded assemblies of high-temperature aluminum components in applications where bonding is often used (e.g., secondary structures and tear stoppers). Author (revised)

N94-12812 Technion Research and Development Foundation Ltd., Haifa (Israel).
ELECTROPHORETIC AND ELECTROLYTIC DEPOSITION OF CERAMIC PARTICLES ON POROUS SUBSTRATES Final Report, 1 Mar. 1988 - 30 Nov. 1992
L. Gal-Or, S. Haber, and S. Liubovich 30 Sep. 1992 278 p Limited Reproducibility: More than 20% of this document may be affected by microfiche quality
(Grant AF-AFOSR-0474-89)
(AD-A265141; AFOSR-93-0344TR) Avail: CASI HC A13

Electrophoretic deposition of ceramic particles and their penetration into the pores of graphite and a 2D C-C composite were demonstrated and studied theoretically and experimentally for colloidal SiO2, SiC, Si3N4, Al2TiOs and HfTiO4. The effect of deposition parameters (field intensity, particle concentration, and ratio of dielectric constant/viscosity of fluid) on the amount of induced material was experimentally studied. Penetration depth of particles as function of the above parameters was analyzed theoretically. Penetration is enhanced by large Peclet numbers and is higher in aqueous suspensions, while coating morphology is better in propanol suspensions. Optimal conditions for coverage and penetration in a two-stage process were determined. Subsequent deposition of two layers was demonstrated and studied for Si3N4 on Al2TiO5 and SiC on a glass ceramic. Single (Si3Ni4, Al2TiO5, and HfTiO4) and multilayer (Si3N4 on Al2TiO5, and Si3N4 on fused SiO2) coatings were deposited, sintered in a N2 atmosphere, and their phase composition and morphology studied. Oxidation resistance of coated specimens was studied at 830 C in continuous and intermittent exposures. Graphite exhaust nozzles were coated and tested in an air breathing engine simulation. Very efficient protection was achieved. Electrolytic deposition of ZrO2, Al2O3, and Al2O3+ZrO2 was achieved from aqueous solutions of ZrO(NO3)2 and Al(NO3)3. The deposition kinetics and microstructure of the deposits were studied. The initial amorphous deposits transformed into crystalline phases with monocrystalline dimensions after heat treatment. DTIC

N94-12842*# National Aeronautics and Space Administration. Lewis Research Center, Cleveland, OH.
A VACUUM FOUR-BALL TRIBOMETER TO EVALUATE LIQUID LUBRICANTS FOR SPACE APPLICATIONS
Masabumi Masuko (Tokyo Inst. of Tech., Japan.), William R. Jones, Jr., Ralph Jansen, Ben Ebihara, Stephen V. Pepper, and Larry S. Helmick (Cedarville Coll., OH.) Jul. 1993 11 p Proposed for presentation at the STLE Annual Meeting, Pittsburgh, PA, 2-5 May 1994; sponsored by Society of Tribologists and Lubrication Engineers
(RTOP 505-33-13)
(NASA-TM-106264; E-7991; NAS 1.15:106264) Avail: CASI HC A03/MF A01

The design and operation of a vacuum tribometer, based on the four-ball configuration, is described. This tribometer evaluates the tribological characteristics of liquid lubricants for space applications. Operating conditions include: room temperature, loads to approximately 1000N, speeds to approximately 500 rpm, and pressures of approximately 10(exp -6)Pa. Tests can also be run at atmospheric pressure with air or nitrogen. Some typical test results are included. Author (revised)

N94-12861# North Carolina State Univ., Raleigh.
THEORETICAL TREATMENT OF THE BULK AND SURFACE PROPERTIES OF FLUIDS CONTAINING LONG, FLEXIBLE MOLECULES
1993 5 p
(Contract DE-FG05-91ER-14181)
(DE93-015560; DOE/ER-14181/1) Avail: CASI HC A01/MF A01

The purpose is to develop an equation of state for predicting the thermodynamic properties of fluids containing chain-like molecules ranging from alkanes to polymers. Foundation of this work is the Generalized Flory Dimer (GFD) theory. GFD is extended to square-well chain mixtures. The second virial coefficient has been evaluated for hard-chain and square-well chain fluids using a Monte Carlo approach. The polymer RISM theory was used to determine the segment-segment radial distribution function for hard chain fluids. Monte Carlo simulations are being performed of the self-diffusion

coefficient, shear and longitudinalviscosities, and thermal conductivity for hard chain fluids. DOE

N94-12866# Sandia National Labs., Albuquerque, NM.
AMORPHOUS SOL-GEL INSULATING FILMS
C. J. Brinker (New Mexico Univ., Albuquerque.), W. L. Warren, M. N. Logan, and C. S. Ashley 1993 12 p Presented at the 16th Material Research Society International Symposium on the Scientific Basis for Nuclear Waste Management Fall Meeting, Boston, MA, 30 Nov. - 5 Dec. 1992
(Contract DE-AC04-76DP-00789)
(DE93-012859; SAND-93-0582C; CONF-921101-114) Avail: CASI HC A03/MF A01

The porosity of sol-gel thin films may be tailored for specific applications through control of the size and structure of inorganic polymers within the coating sol, the extent of polymer reaction and interpenetration during film formation, and the magnitude of the capillary pressure exerted during the final stage of drying. By maximizing the capillary pressure and avoiding excessive condensation, dense insulating films may be prepared as passivation layers on silicon substrates. Such films can exhibit excellent dielectric integrity, viz., low interface trap densities and insulating properties approaching those of thermally grown SiO2. Alternatively, through exploitation of the scaling relationship of mass and density of fractal objects, silica films can be prepared that show a variation in porosity (7-29 percent) and refractive index (1.42-1.31) desired for applications in sensors, membranes, and photonics. DOE

N94-12867 Academy of Sciences of the Ukraine, Kharkov. Fiziko-Tekhnicheskij Inst.
DEPOSITION OF CRYSTALLINE BORON THICK LAYERS FROM GAS PHASE [OSAZHDENIE TOLSTYKH SLOEV KRISTALLICHESKOGO BORA IZ GAZOVOJ FAZY]
A. P. Patokin, V. V. Sagalovich, and V. L. Khrebtov 1992 11 p In RUSSIAN Limited Reproducibility: More than 20% of this document may be affected by microfiche quality
(DE93-620499; KFTI-92-35) Avail: CASI HC A03 (US Sales Only)

Properties of boron obtained by its trichloride reduction in hydrogen were studied with the help of electron microscopy, X-ray spectroscopy, spectroscopy and metallography methods. It was shown that in the 1080 - 1250 C temperature range layers of high-dense crystalline boron of tetragonal modification are deposited. Twins are the main type of structural defects in boron. The average coefficient of boron thermal expansion is 8.5 x 0(sup -6) deg(sup -1) and anisotropy degree is 0.01. DOE

N94-12885# Lawrence Livermore National Lab., CA.
RECOVERY OF MATERIALS IMPACTED AT HIGH VELOCITY
W. J. Nellis and A. J. Gratz Dec. 1992 11 p Presented at the Hypervelocity Impact Symposium, Austin, TX, 17-20 Nov. 1992
(Contract W-7405-eng-48)
(DE93-014150; UCRL-JC-110081; CONF-921162-16) Avail: CASI HC A03/MF A01

Hypervelocity impact can produce unique effects in materials including crystal structures, microstructures, and properties. Examples include impact-driven shock waves to synthesize novel materials--1 mm and 1 micron thin--shocked to pressures up to 100 GPa (1 Mbar), preferential crystallographic alignment achieved by taking into account the shape and size of powder particles, and high-pressure phase transitions quenched in geological materials. Thin specimens are used to achieve the highest quench rates. Methods are described which show that the experiments can be performed by precooling or preheating specimens in the range -170 to +1000 C. Calculational results for the quartz experiments show the importance of computational simulations to determine the pressure history in the specimen. DOE

N94-12912# Sandia National Labs., Albuquerque, NM.
CORRELATIONS OF THE GROWTH, STRUCTURE, AND STRESS WITH THE ADHESION OF DIAMOND FILMS ON TUNGSTEN
M. Alam (New Mexico Inst. of Mining and Technology, Socorro.), D. E. Peebles, D. R. Tallant, and J. A. Ohlhausen 1993 17 p Presented at the International Conference on Metallurgical Coatings and Thin Films, San Diego, CA, 19-23 Apr. 1993
(Contract DE-AC04-76DP-00789)
(DE93-012855; SAND-93-0826C; CONF-930419-1) Avail: CASI HC A03/MF A01

Diamond films were deposited on tungsten substrates by a filament-assisted chemical vapor deposition process as a function of seven different processing parameters. The effect of variations in measured film characteristics such as growth rate, texture, diamond-to-nondiamond carbon Raman band intensity ratio and strain on the adhesion between the diamond film/tungsten substrate pairs as measured by a tensile pull method were investigated. The measured adhesion values do not correlate with any of the measured film characteristics mentioned above. The problem arises because of the non-reproducibility of the adhesion test results, due to the non-uniformity of film thickness, surface preparation and structural homogeneity across the full area of the substrate. DOE

N94-12916# Los Alamos National Lab., NM.
CERAMIC MATRIX COMPOSITES BY MICROWAVE ASSISTED CVI
R. P. Currier and D. J. Devlin 1993 11 p Presented at the 95th Annual Meeting of the Americdan Ceramic Society, Cincinnati, OH, 18-22 Apr. 1993
(Contract W-7405-eng-36)
(DE93-012640; LA-UR-93-1322; CONF-930438-14) Avail: CASI HC A03/MF A01

Chemical vapor infiltration (CVI) processes for producing continuously reinforced ceramic composites are reviewed. The potential advantages of microwave assisted CVI are noted. Recent numerical studies of microwave assisted CVI are then reviewed. These studies predict inverted thermal gradients in fibrous ceramic preforms subjected to microwave radiation and suggest processing strategies for achieving uniformly dense composites. Comparisons are made to experimental results obtained using silicon based composite systems. The importance of microwave-material interactions is stressed. In particular, emphasis is placed on the role played by the relative ability of fiber and matrix to dissipate microwave energy. Results suggest that microwave induced inverted gradients can in fact be exploited using the CVI technique to promote inside-out densification. DOE

N94-12932 Army Research Lab., Watertown, MA.
MODELING THE IMPACT BEHAVIOR OF AD85 CERAMIC UNDER MULTI-AXIAL LOADING Final Report
A. M. Rajendran May 1993 45 p Limited Reproducibility: More than 20% of this document may be affected by microfiche quality
(AD-A265877; ARL-TR-137) Avail: CASI HC A03

This report presents an advanced constitutive model to describe the complex behavior of ceramic materials under impact loading conditions. The governing equations utilize a set of microphysically based constitutive relationships to model deformation and damage processes in a ceramic. The total strain is decomposed into elastic, plastic, and microcracking components. The model parameters for the AD85 ceramic were determined using the data from split Hopkinson bar (SHB) and bar-on-bar experiments under uniaxial stress state and plate impact experiment under uniaxial strain state. To further validate the generality of the model parameters, modeling of a diagnostic ballistic experiment in which a steel projectile impacted an AD85 ceramic front-faced thick aluminum plate was considered. In this experiment, stress histories were measured in the target by embedded manganin and carbon stress gauges. The results from the numerical simulations of the ballistic experiment, using a shock wave propagation based finite element code, successfully matched the measured stress history. Author (DTIC)

N94-12939# Lawrence Livermore National Lab., CA.
PROJECT PROPOSAL FOR PARTIAL COMPUTATIONAL PHYSICS SUPPORT FOR SURVIVABILITY OF COATINGS PROGRAM
C. E. Rhoades, Jr. Mar. 1993 10 p
(Contract W-7405-eng-48)
(DE93-013788; UCRL-ID-113715) Avail: CASI HC A02/MF A01

Currently, the Survivability of Coatings (SOC) program uses the XRT computer code to calculate the effects of X-rays of various spectra on mirrors consisting of one or more optical coatings of specified thicknesses over various substrates. The following physical processes are modeled by XRT in one spatial dimension: (1) X-ray deposition and transport, (2) electron production, deposition and transport, (3) thermal conduction and transport, and (4) resulting static and dynamic stress and deformation. In general, the numerical techniques used in XRT are deterministic ones: X-ray transport

is handled by multigroup discrete ordinates, electron transport is performed by the method of characteristics applied to a two term spherical harmonics expansion approximation (PI) of the Spencer-Lewis transport equations, and thermal transport is done by a simple Richardson extrapolation of a backward Euler solution to the heat conduction equation. XRT has been used for both preshot and postshot analyses of samples for both aboveground tests (AGT) and underground tests (UGT). Agreement of analyses with experiment has been reasonably good. However, several samples predicted not to fail did appear to be damaged in a recent UGT. In addition, at least one sample predicted to fail did not. Preliminary analysis of the experimental samples on the recent AGT performed at Maxwell Laboratories in San Diego for the SOC program shows similar difficulties. DOE

N94-12985# University of Southern Mississippi, Hattiesburg. Dept. of Polymer Science.

CHARACTERIZATION OF 1:1 RANDOM COPOLYMERS OBTAINED FROM 6-, 7-, 11-, AND 12-CARBON AMINO ACIDS Technical Report, 1 Jun. 1992 - 31 May 1993

C. G. Johnson and Lon J. Mathias 7 Jun. 1993 27 p

(Contract N00014-89-J-1225)

(AD-A265827; TR-55) Avail: CASI HC A03/MF A01

Copolymers were prepared from the title amino acids by melt condensation under dry nitrogen. The resulting copolymers were characterized by solution and solid-state NMR, FTIR, DSC, and WAXD. Solution NMR spectra (at 75.5 MHz) showed multiple peaks with almost equal intensities in the carbonyl region (indicating random copolymer formation) with no evidence of end-group peaks (confirming high molecular weight). Solid-state C-13 (at 100.6 MHz) and N-15 (at 20.3 MHz) spectra of most solution cast films contained peaks consistent with the gamma-form crystallites (delta(sub N-15) ca 89) being the predominant ordered phase. Only nylon 6-co-7 formed almost exclusive alpha-form on soiution casting (delta(sub N-15) 84.5). Nylon 7-co-11 formed the alpha-form almost exclusively from the melt but gave a combination of alpha- and gamma-phases (delta(sub N-15) 84.5 and 88.7) on solution casting. The copolymers possessed 3-component C-13 T(sub 1) values ranging from 21 to 97 s for the slowest-relaxing component, indicating less-ordered domains than for the homopolymers. DTIC

N94-12986# University of Southern Mississippi, Hattiesburg. Dept. of Polymer Science.

UNEXPECTEDLY RAPID HYDROSILATION POLYMERIZATION OF THE DIALLYL DERIVATIVE OF BISPHENOL A AND 2,6-DIALLYLPHENOL Technical Report, 1 Jun. 1992 - 31 May 1993

Lon J. Mathias and Charles M. Lewis 7 Jun. 1993 14 p

(Contract N00014-89-J-1225)

(AD-A265832; TR-51) Avail: CASI HC A03/MF A01

Several members of a novel family of reactive oligomers and polymers have been synthesized using the hydrosilation polyaddition of 1,1,3,3-tetramethyldisiloxane and 1,1,3,3,5,5-hexa-methyltrisiloxane with the 2,2'-diallyl derivative of bisphenol A (BPA) or 2,6-diallylphenol. Polymerization occurred much faster than that observed for any other hydrosilation reaction of which we are aware: while a typical hydrosilation takes minutes to hours to complete with catalytic amounts of various platinum catalysts, and most unprotected functional groups inhibit the addition, reactions of 2-allylphenol moieties occur virtually instantaneously. In fact, reactions of the diallyl monomers listed must be cooled to prevent explosive loss of reagents from the reaction vessel; even then, thermal loss of the silane monomers can disrupt stoichiometric balance. With cooling, good yields of polymers were obtained which possess excellent solubility in virtually all organic solvents and intrinsic viscosity values of 0.21-0.23 dL/g. DTIC

N94-13032# Argonne National Lab., IL. Materials and Components Technology Div.

DEVELOPMENT OF NONDESTRUCTIVE EVALUATION METHODS AND PREDICTION OF EFFECTS OF FLAWS ON THE FRACTURE BEHAVIOR OF STRUCTURAL CERAMICS

W. A. Ellingson, J. P. Singh, D. L. Holloway, S. L. Dieckman, D. Singh, and E. A. Sivers Mar. 1993 12 p Presented at the 7th Annual Conference on Fossil Energy Materials, Oak Ridge, TN, 11-13 May 1993

(Contract W-31-109-eng-38)

(DE93-012942; ANL/MCT/CP-79029; CONF-9305135-3) Avail: CASI HC A03/MF A01

Work emphasized continuous-fiber ceramic matrix composites (CFCC's) with 2-D lay-ups composed of chemical-vapor-infiltrated (CVI) SiC/SiC materials, mostly made of Nicalon plain weave with 16 x 16 tows/in. One sample examined comprised a 3-D SiC/SiC braid made by Techniweave. Using a new 1024 x 1024 x 14 bit detector, images from 3-D X-ray CT data with pixel sizes of less than 140 microns and 2-D fast-Fourier transform (FFT) image processing, we have shown that fiber orientations can be measured to plusminus 2-1/2 deg. 3-D FFT analysis was used to determine 3-D braid/weave fiber spacing. Multinuclear (H-1, C-13, and SI-29) NMR spectroscopy, is being studied. Surface chemistry of fibers and chemistry of interfacial regions in composites are being studied. We are also conducting initial studies to investigate the bulk composition of matrix materials (alpha, beta, amorphous phase, silica, and oxynitride concentration) and surface chemistry of Si3N4 and SiC fibers. Fracture mechanics work to correlate with NDE data focused on strength distribution of as-fabricated Nicalon fibers obtained from bundle tests. Strength distribution of fractured Nicalon fibers in composites was assessed from fracture mirror radii. SEM was used to determine distribution of fiber pullout length distribution for fibers in composites, for their strength distribution. From the strength distribution plots, scale parameters were determined to be 3.45 GPa for as-fabricated fibers and 1.31 GPa for fibers in processed composites. However, the Weibull moduli for the two distributions were similar. Reduction in strength of the fibers in processed composites is believed to be due to surface flaws and defects. Effects of fiber misorientation on mechanical properties of NDE-tested CVI continuous-fiber composites are currently being investigated. DOE

N94-13070# Pittsburgh Univ., PA.

COMPUTER SIMULATIONS FOR THE ADSORPTION OF POLYMERS ONTO SURFACES

A. C. Balazs 1993 13 p

(Contract DE-FG02-90ER-45438)

(DE93-016667; DOE/ER-45438/3) Avail: CASI HC A03/MF A01

Polymer-surface interactions are important in every stage of oil and coal production, production of new energy-efficient composite materials, and in medicine. Therefore, it is important to isolate the factors that influence the interfacial activity of polymer chains. We developed theoretical models and computer simulations to determine effects of polymer architecture, solvent quality, and surface morphology on properties of chains at penetrable and impenetrable interfaces. DOE

N94-13072# Cornell Univ., Ithaca, NY. Dept. of Chemistry.

SYNTHESIS AND PROPERTIES OF NOVEL CLUSTER PHASES

F. DiSalvo 15 Jan. 1993 6 p

(Contract DE-FG02-87ER-45298)

(DE93-017056; DOE/ER-45298/9) Avail: CASI HC A02/MF A01

The research was in the area of solid cluster compounds containing metal clusters. Two classes of materials were studied: those based on solutions formed by dissolving LiMo3Se3 in polar solvents, and those based on M6X8 clusters. The cluster phases were synthesized and their properties examined. Nb6I11 and Mo6X8 were also studied. DOE

N94-13089*# Yale Univ., New Haven, CT. High Temperature Chemical Reaction Engineering Lab.

RESEARCH ON CHEMICAL VAPOR DEPOSITION PROCESSES FOR ADVANCED CERAMIC COATINGS Final Technical Report, 1 Mar. 1988 - 1 Nov. 1992

Daniel E. Rosner Jan. 1993 24 p

(Grant NAG3-884)

(NASA-CR-193613; NAS 1.26:193613) Avail: CASI HC A03/MF A01

Our interdisciplinary background and fundamentally-oriented studies of the laws governing multi-component chemical vapor deposition (VD), particle deposition (PD), and their interactions, put the Yale University HTCRE Laboratory in a unique position to significantly advance the 'state-of-the-art' of chemical vapor deposition (CVD) R&D. With NASA-Lewis RC financial support, we initiated a program in March of 1988 that has led to the advances described in this report (Section 2) in predicting chemical vapor transport in high temperature systems relevant to the fabrication of refractory ceramic coatings for turbine engine components. This Final Report covers our principal results and activities for the total NASA grant of $190,000.

over the 4.67 year period: 1 March 1988-1 November 1992. Since our methods and the technical details are contained in the publications listed (9 Abstracts are given as Appendices) our emphasis here is on broad conclusions/implications and administrative data, including personnel, talks, interactions with industry, and some known applications of our work.
Author (revised)

N94-13118# Allied-Signal Aerospace Co., Kansas City, MO.
DRY FILM LUBRICANT EVALUATION
R. M. Bryan Apr. 1993 15 p
(Contract DE-AC04-76DP-00613)
(DE93-013114; KCP-613-5044) Avail: CASI HC A03/MF A01

The lubrication characteristics of a modified tungsten disulfide (WS2) were compared to the existing dry film lubricant, a molybdenum disulfide (MoS2). WS2 was verified as meeting all Environment, Safety, and Health (ES&H) requirements for a replacement dry film lubricant. However, in life and wear characteristics, the present lubricant outperformed the WS2. Two studies to determine if welding could be performed through the WS2 coating indicated functionally strong welds, but evaluation showed cracks which would not meet weld requirements. Bearing tests comparing WS2, a low molecular weight tetrafluoroethylene (TFE), and unlubricated bearings indicated that WS2 bearing torque was 70 percent higher than TFE. DOE

N94-13246*# University of North Texas, Denton. Dept. of Physics.
SCANNING TUNNELING MICROSCOPY STUDIES OF DIAMOND FILMS AND OPTOELECTRONIC MATERIALS Progress Report, 1 Dec. 1992 - 1 Oct. 1993
Jose M. Perez 1993 20 p Original contains color illustrations
(Grant NAG1-1468)
(NASA-CR-194363; NAS 1.26:194363) Avail: CASI HC A03/MF A01; 3 functional color pages

In this report, we report on progress achieved from 12/1/92 to 10/1/93 under the grant entitled 'Scanning Tunneling Microscopy Studies of Diamond Films and Optoelectronic Materials'. We have set-up a chemical vapor deposition (CVD) diamond film growth system and a Raman spectroscopy system to study the nucleation and growth of diamond films with atomic resolution using scanning tunneling microscopy (STM). A unique feature of the diamond film growth system is that diamond films can be transferred directly to the ultrahigh vacuum (UHV) chamber of a scanning tunneling microscope without contaminating the films by exposure to air. The University of North Texas (UNT) provided $20,000 this year as matching funds for the NASA grant to purchase the diamond growth system. In addition, UNT provided a Coherent Innova 90S Argon ion laser, a Spex 1404 double spectrometer, and a Newport optical table costing $90,000 to set-up the Raman spectroscopy system. The CVD diamond growth system and Raman spectroscopy system will be used to grow and characterize diamond films with atomic resolution using STM as described in our proposal. One full-time graduate student and one full-time undergraduate student are supported under this grant. In addition, several graduate and undergraduate students were supported during the summer to assist in setting-up the diamond growth and Raman spectroscopy systems. We have obtained research results concerning STM of the structural and electronic properties of CVD grown diamond films, and STM and scanning tunneling spectroscopy of carbon nanotubes. In collaboration with the transmission electron microscopy (TEM) group at UNT, we have also obtained results concerning the optoelectronic material siloxene. These results were published in refereed scientific journals, submitted for publication, and presented as invited and contributed talks at scientific conferences. Derived from text

N94-13408# Arizona State Univ., Tempe.
SURFACES AND INTERFACES OF CERAMICS AND METALS
1992 16 p
(Contract DE-FG02-86ER-45228)
(DE93-014959; DOE/ER-45228/65) Avail: CASI HC A03/MF A01

Structures of surfaces of several ceramic oxides were studied by use of reflection electron microscopy (REM) and associated techniques. High-temperature annealing in air or oxygen gives smooth, flat crystal faces in most cases, including the (111) MgO surface, previously thought to be facetted. Stability of the (111) MgO surface is shown to be due to a surface superlattice reconstruction. Surface superlattices, stable in air, have also been shown to exist on sapphire and rutile crystal faces. The segregation of Ca to the surface of MgO has been studied using reflection electron energy loss techniques. Initial studies of Cu-Au alloy crystal surfaces, necessarily carried out in ultra-high vacuum, have been made using RHEED and Auger electron spectroscopy. Clean alloy surfaces show surface reconstructions associated with the segregation of Au atoms at the surface. High-temperature annealing results in the segregation of sulfur to the surface and the formation of a variety of surface superlattice structures. Structures of solid-solid interfaces have been studied using a wide variety of electron-optical techniques including nanodiffraction and electron holography. In particular, the interfaces in semiconductor multiple quantum well structures and also multilayer structures of Si and Co have been studied. DOE

N94-13431*# McDonnell-Douglas Corp., Saint Louis, MO.
HIGH TEMPERATURE ELECTROMAGNETIC CHARACTERIZATION OF THERMAL PROTECTION SYSTEM TILE MATERIALS Final Report
Garrett G. Heil Sep. 1993 138 p
(Contract NAS1-18763; RTOP 592-01-11-12)
(NASA-CR-189687; NAS 1.26:189687; MDC-92B0034) Avail: CASI HC A07/MF A02

This study investigated the impact of elevated temperatures on the electromagnetic performance of the LI-2200 thermal protection system. A 15-kilowatt CO2 laser was used to heat an LI-2200 specimen to 3000 F while electromagnetic measurements were performed over the frequency range of l9 to 21 GHz. The electromagnetic measurement system consisted of two Dual-Lens Spot-Focusing (DLSF) antennas, a sample support structure, and an HP-8510B vector network analyzer. Calibration of the electromagnetic system was accomplished with a Transmission-Reflection-Line (TRL) procedure and was verified with measurements on a two-layer specimen of known properties. The results of testing indicated that the LI-2200 system's electromagnetic performance is slightly temperature dependent at temperatures up to 3000 F.
Derived from text

N94-13468# Polish Academy of Sciences, Warsaw. Inst. of Fundamental Technological Research.
THERMODIFFUSION IN HETEROGENEOUS ELASTIC SOLIDS AND HOMOGENIZATION
A. Galka, J. J. Telega, and R. Wojnar 1993 77 p
(Rept-14/1993) Avail: CASI HC A05/MF A01

Overall behavior of microheterogeneous elastic solids in which thermodiffusion occurs is studied by using homogenization methods. Heterogeneities are characterized by a small positive parameter epsilon. The material coefficients of the coupled system of linear equations describing thermodiffusion depend on epsilon. In the periodic case, when heterogeneities are distributed periodically, the homogenization is performed by applying the method of two-scale asymptotic expansions. The convergence and corrector theorems are formulated for a nonperiodic microstructure. It is shown that the initial conditions for the temperature and chemical potential of the homogenized system are changed in comparison with the primal one provided that the initial conditions for the latter system are nonhomogenous. For a layered composite with periodically distributed layers analytical formulas are derived for all the effective material coefficients. Particular cases are studied by exploiting some available experimental data. The analysis itself and homogenization problem are preceded by an overview of the results concerning thermal problems in microheterogeneous solids and composites. Author (revised)

N94-13493# Westinghouse Savannah River Co., Aiken, SC.
CANONICAL CORRELATION OF WASTE GLASS COMPOSITIONS AND DURABILITY, INCLUDING pH
D. Oeksoy, L. D. Pye (Alfred Univ., NY.), D. F. Bickford, and W. G. Ramsey 1993 16 p Presented at the 95th Annual Meeting of the American Ceramic Society, Cincinnati, OH, 18-22 Apr. 1993
(Contract DE-AC09-89SR-18035)
(DE93-012754; WSRC-MS-93-222; CONF-930438-8) Avail: CASI HC A03/MF A01

Control of waste glass durability is a major concern in the immobilization of radioactive and mixed wastes. Leaching rate in standardized laboratory tests is being used as a demonstration of consistency of the response of waste glasses in the final disposal environment. The leaching of silicate and borosilicate glasses containing alkali or alkaline earth elements is known to be autocatalytic, in that the initial ion exchange of alkali in the glass for hydrogen ions in water results in the formation of OH and

increases the pH of the leachate. The increased pH then increases the rate of silicate network attack, accelerating the leaching effect. In well formulated glasses this effect reaches a thermodynamic equilibrium when leachate saturation of a critical species, such as silica, or a dynamic equilibrium is reached when the pH shift caused by incremental leaching has negligible effect on pH. This report analyzes results of a seven leach test on waste glasses. DOE

N94-13584# Stanford Univ., CA. Dept. of Chemical Engineering.
POLING OF THIN POLYMER FILMS IN ELECTRO OPTIC APPLICATIONS Final Report, 1 Apr. 1990 - 30 Mar. 1993
Gerald G. Fuller 8 Jun. 1993 2 p
(Contract DAAL03-90-G-0081)
(AD-A266562; ARO-26883.2-MS) Avail: CASI HC A01/MF A01

Many polymeric glasses must be orientationally ordered for the materials to exhibit useful characteristics. The objective of this work was to understand the dynamics of the orientation and relaxation processes and to relate these behaviors to the structural characteristics of the polymeric material. In this study we considered materials suitable for nonlinear optical applications. In particular, thin polymer films, either doped with nonlinear optical chromophores or films with the chromophores covalently bonded to side groups were studied. Orientation of these chromophores was achieved by the birefringence resulting from chromophore concentration, spacer length, and molecular dominant factor determining the steady state and transient behaviors. The relationship between monomer and polymer structure and the resulting effect on the orientation dynamics is discussed. Qualitative agreement with theoretical predictions was obtained for the simpler guest/host system, but the model was shown to be inadequate to explain the behaviors of the more complex systems studied. The results reported here have provided valuable insight into the molecular processes that occur during the chromophore orientation and relaxation and the effects of structural characteristics of the polymers on these mechanisms. DTIC

N94-13783# Rutherford Appleton Lab., Chilton (England). ISIS Science Div.
THE USE OF POLARISED NEUTRON REFLECTION FOR UNIQUE DENSITY PROFILE DETERMINATION IN THIN FILMS
J. Penfold, J. R. P. Webster, D. G. Bucknall, and D. S. Sivia Mar. 1993 13 p
(PB93-187136; RAL-93-011) Avail: CASI HC A03/MF A01

A recent paper by Sivia et al showed that theoretically the use of polarized neutrons and a magnetized substrate to determine uniquely a density profile from neutron reflectometry data. Presented are preliminary results of the technique applied to a polymer film on a magnetized nickel substrate. Author (revised)

N94-13888# Sandia National Labs., Albuquerque, NM.
PROBLEMS AND OPPORTUNITIES IN MICROWAVE JOINING OF CERAMICS
R. E. Loehman 1993 13 p Presented at the 95th Annual Meeting of the American Ceramic Society, Cincinnati, OH, 18-22 Apr. 1993
(Contract DE-AC04-76DP-00789)
(DE93-014998; SAND-93-1068C; CONF-930438-23) Avail: CASI HC A03/MF A01

This document briefly reviews ceramic joining and considers some aspects relevant to heating using microwave energy. It is concluded that the general applicability of microwave heating for ceramic joining has yet to be demonstrated. There are particular applications, such as joining of SiC to itself, that may hold promise. However, more work needs to be done. DOE

N94-13903# Aerospace Corp., El Segundo, CA. Mechanics and Materials Technology Center.
APPLICATIONS OF SURFACE SCIENCE TO SOLID LUBRICANTS
Stephen V. Didziulis and Paul D. Fleischauer 15 Mar. 1993 55 p
(Contract F04701-88-C-0089)
(SMC-TR-93-24; TR-93(3935)-4; AD-A267563) Avail: CASI HC A04/MF A01

Solid lubricants fill a very important niche in the world of tribology by providing low-friction surfaces under harsh operating conditions, such as high or very low temperature and high vacuum. The successful use of solid lubricants in most applications relies on controlling the chemical interactions occurring at several interfaces, and the use of surface science techniques to study and understand these chemical interactions has become increasingly more important in recent years. In this report, the surface properties of molybdenum disulfide (MoS2), the most widely used solid lubricant for space applications, are studied with a variety of techniques. The techniques discussed are: valence band photoelectron spectroscopy (PES) to determine electronic structure properties; scanning tunneling and atomic force microscopies to examine surface structure; high-resolution electron energy loss spectroscopy to determine surface phonon properties; core level PES with synchrotron radiation to study metal/MoS2 interfacial chemistry; core level x-ray photoelectron spectroscopy to study steel and ceramic substrate chemistry; and extended x-ray absorption fine structure, electron microscopies, and x-ray diffraction to study film structure. In addition, theoretical and tribological studies of MoS2 are discussed. The goal of this work is to develop a fundamental understanding of the electronic structure and reactivity of MoS2 as determined by these surface science techniques, and to relate this fundamental understanding to the performance of MoS2 as a solid lubricant. Author (revised)

N94-13964*# Southwest Texas State Univ., San Marcos. Dept. of Chemistry.
HIGHLY FLUORINATED POLYMERS Semiannual Status Report, 1 Jan. - 1 Jul. 1993
Patrick E. Cassidy 1993 11 p
(Grant NAG1-631)
(NASA-CR-194147; NAS 1.26:194147) Avail: CASI HC A03/MF A01

The topics covered include the following: highly fluorinated polyesters; N-alkylated polyamides; highly fluorinated polyethers; and silicon-containing fluoropolymers. Derived from text

N94-13974# Argonne National Lab., IL.
WEAR-MECHANISM MODELLING
M. F. Ashby Mar. 1993 8 p Prepared in cooperation with Cambridge Univ., England
(Contract W-31-109-eng-38)
(DE93-012311; ANL/OTM/CR-3) Avail: CASI HC A02/MF A01

The goals of the program are to calculate the surface temperatures in dry sliding, develop a soft wear tester for ceramics, survey the wear mechanisms in brittle solids, and couple the temperature calculations with models to give wear maps for brittle solids. DOE

N94-13978# State Univ. of New York, Stony Brook. Dept. of Chemistry.
PHASE TRANSITION IN POLYMER BLENDS AND STRUCTURE OF IONOMERS AND COPOLYMERS
1993 9 p
(Contract DE-FG02-86ER-45237)
(DE93-016256; DOE/ER-45237/7) Avail: CASI HC A02/MF A01

The main thrust of the program in the past 3 years are summarized: SAXS instrumentation development; structure and dynamics of macro- and supra-molecules; phase transitions in polymer blends and solutions; structure of ionomers; and fractals and anisotropic systems. DOE

N94-14007# Fraunhofer Inst. fuer Werkstoffmechanik, Freiburg (Germany).
A PROCESS FOR EVALUATION OF MECHANICAL BEHAVIOR OF SURFACE FILMS Thesis - Freiburg Univ. [EIN VERFAHREN ZUR BEWERTUNG DES MECHANISCHEN VERHALTENS VON RANDSCHICHTEN]
J. M. Olaf Mar. 1992 100 p In GERMAN
(Contracts DFG-So-104/9-1; DFG-So-104/9-2)
(W-1/92; ETN-93-94206) Avail: CASI HC A05/MF A02

Vickers hardness measurement with the finite element method is simulated. Calculations were performed for homogeneous specimen materials and for film systems from core material and surface film. Three dimensional and two dimensional models with finite elements of indentation processes on the basis of different test body models were realized for calculation of mechanical reaction of laminate systems to external loading due to sharp test bodies. Strains and stresses at impact location, indentation depth in the specimen surface and material hardness as a function of applied force were calculated. Numerical results for elastic materials were estimated by comparison with analytical solutions. Simulation results for elastic-plastic materials were compared with experimental data. Relative influence of test

machine and specimen parameters was discussed. Friction influence in contact area between specimen and test body for sharp and round bodies was simulated. Material effects on indentation behavior was examined by variation of specimen parameters. ESA

N94-14124# Lawrence Livermore National Lab., CA.
LASER-DAMAGE SUSCEPTIBILITY OF NODULAR DEFECTS IN DIELECTRIC MIRROR COATINGS: AFM MEASUREMENTS AND ELECTRIC-FIELD MODELING
M. R. Kozlowski, J. F. DeFord, and M. C. Staggs 15 Apr. 1993 6 p Presented at the 2nd International Conference on Laser Ablation, Knoxville, TN, 19-22 Apr. 1993
(Contract W-7405-eng-48)
(DE93-014655; UCRL-JC-112981; CONF-9304144-1) Avail: CASI HC A02/MF A01

Atomic force microscopy (AFM) and electromagnetic field modeling were used to study the influence of nodular coating defects on laser-induced damage of multilayer dielectric coatings. In studies of HfO2/SiO2 mirrors with 1.06 microns illumination, AFM results showed that nodular defects with high dome heights (greater than 0.6 microns) were most susceptible to laser damage. Crater defects, formed by nodules ejected from the coating prior to illumination, were not damaged when illuminated over the same range of fluences. A finite-difference time-domain electromagnetic modeling code was used to study the influence of 3-D nodule defects on the E-field distribution within the interference coating. The modeling results show that E-field enhancements as large as a factor of 4 can be present at the defects. Crater defects, however, result in minimal enhancement of the E-fields within the coating. These modeling results are consistent with the AFM experimental data, indicating that E-field enhancement is a contributing mechanism in defect-dominated laser damage of optical coatings. DOE

N94-14126# Army Research Lab., Watertown, MA.
SYNTHETIC LUBRICANTS AND HIGH-PERFORMANCE FUNCTIONAL FLUIDS: PHOSPHAZENES Final Report
Robert E. Singler and Mary Jo Bieberich (Naval Surface Warfare Center, Annapolis, MD.) Jan. 1993 18 p Repr. from Synthetic Lubricants and High Performance Functional Fluids: Phosphazenes, Chapter 10, 1992 p 215-228
(ARL-TR-45) Avail: CASI HC A03/MF A01

The synthesis, properties, and development of phosphazene fluids are reviewed, with an emphasis on military applications. Most of their search and development of phosphazene fluids has centered on the alkoxy- and aryloxycyclophosphazenes for fire-resistant, compression-ignition-resistant hydraulic fluids to meet requirements for MIL-H-19457. Related developments include applications such as high temperature lubricants for aircraft gas turbine engines, lubricity additives, applications in the electronic industry, fire-resistant additives, vacuum pump oil, and electrorheological fluids. Chemical compositions, physical properties, lubricity data, and toxicity information are given, along with projected costs for high volume use applications. Currently, some phosphazene fluids are commercially available in small quantities. Author

N94-14142# Brookhaven National Lab., Upton, NY.
SPIN POLARIZED PHOTOEMISSION STUDIES OF INTERFACIAL AND THIN FILM MAGNETISM
P. D. Johnson, N. B. Brookes, Y. Chang, and K. Garrison 1993 10 p Presented at the Spring Meeting of the Materials Research Society, San Francisco, CA, 12-16 Apr. 1993
(Contract DE-AC02-76CH-00016)
(DE93-014326; BNL-48953; CONF-930405-13) Avail: CASI HC A02/MF A01

Spin polarized photoemission is used to study the electronic structure of noble metals deposited on ferromagnetic substrates. Studies of Ag deposited on an Fe(001) substrate reveal a series of minority spin interface or quantum well states with binding energies dependent on the thickness of the silver. Similar behavior is observed for Cu films deposited on a fct Co(001) substrate. Tight-binding modeling reproduces many of the observations and shows that hybridization of the sp-bands with the noble metal d-bands cannot be ignored. DOE

N94-14179# Los Alamos National Lab., NM.
SCHEMES FOR THE USE OF CONDUCTING POLYMERS AS ACTIVE MATERIALS IN ELECTROCHEMICAL SUPERCAPACITORS
A. Rudge, J. Davey, S. Gottesfeld, and J. P. Ferraris 1993 13 p Presented at the 183rd Electrochemical Society Meeting, Honolulu, HI, 16-21 May 1993
(Contract W-7405-eng-36)
(DE93-012713; LA-UR-93-1618; CONF-930571-14) Avail: CASI HC A03/MF A01

The development of a novel conducting polymer based system for use in electrochemical capacitors is described. This system utilizes a new conducting polymer, poly-3-(4-fluorophenyl)-thiophene (PFPT), that can be reversibly n- and p-doped to high charge density. The electrochemical n-dopability of this material can be further improved by cycling in an acetonitrile solution that contains a new electrolyte, tetramethylammonium trifluoromethanesulfonate (Me4NCF3SO3). We discuss these improvements in n-dopability in terms of potential electronic and steric influences. We believe that the substituent fluorophenyl group does not communicate with the polythiophene backbone through resonance, and conclude that the ability to n-dope PFPT to high charge density may occur as a result of electron transfer reactions from the conducting polymer backbone into the substituent. This new system for electrochemical capacitors provides the best achievable performance from conducting polymers and generates high energy and power densities that are comparable with noble metal oxide systems, potentially at a fraction of the cost. DOE

N94-14297# Pacific Northwest Lab., Richland, WA.
SEQUESTERING CARBON DIOXIDE IN INDUSTRIAL POLYMERS: BUILDING MATERIALS FOR THE 21ST CENTURY
P. M. Molton and D. A. Nelson Jun. 1993 25 p
(Contract DE-AC06-76RL-01830)
(DE93-016087; PNL-SA-22528) Avail: CASI HC A03/MF A01

This study was undertaken to determine the possibility of developing beneficial uses for carbon dioxide as a key component for a large-volume building product. Such a use may provide an alternative to storing the gas in oceanic sinks or clathrates as a way to slow the rate of global warming. The authors investigated the concept that carbon dioxide might be used with other chemicals to make carbon-dioxide-based polymers which would be lightweight, strong, and economical alternatives to some types of wood and silica-based building materials. As a construction-grade material, carbon dioxide would be fixed in a solid, useful form where it would not contribute to global warming. With the probable imposition of a fuel carbon tax in industrialized countries, this alternative would allow beneficial use of the carbon dioxide and could remove it from the tax basis if legislation were structured appropriately. Hence, there would be an economic driver towards the use of carbon-dioxide-based polymers which would enhance their future applications. Information was obtained through literature searches and personal contacts on carbon dioxide polymers which showed that the concept (1) is technically feasible, (2) is economically defensible, and (3) has an existing industrial infrastructure which could logically develop it. The technology exists for production of building materials which are strong enough for use by industry and which contain up to 90% by weight of carbon dioxide, both chemically and physically bound. A significant side-benefit of using this material would be that it is self-extinguishing in case of fire. This report is the first stage in the investigation. Further work being proposed will provide details on costs, specific applications and volumes, and potential impacts of this technology. DOE

N94-14311# Lawrence Livermore National Lab., CA.
MACHINING ASPECTS OF NICKEL-PHOSPHORUS COATINGS
J. W. Dini Jul. 1992 6 p Presented at the Minerals, Metals, and Materials Society/American Society for Metals Materials Week 1992, Chicago, IL, 2-5 Nov. 1992
(Contract W-7405-eng-48)
(DE93-013037; UCRL-JC-110996; CONF-9211117-7) Avail: CASI HC A02/MF A01

Nickel-phosphorus coatings with greater than 10% phosphorus have been widely used for diamond turning applications such as fabrication of large optics and other high precision parts. This paper discusses the importance of phosphorus content of the alloy on wear of the diamond tool and provides some speculation on the role of phosphorus on machining characteristics. DOE

N94-14319# Lawrence Livermore National Lab., CA.
FORMATION OF TEXTURED YBCO FILMS BY LASER ABLATION
A. F. Jankowski and B. L. Olsen Nov. 1992 12 p Presented at the 16th Material Research Society International Symposium on the Scientific Basis for Nuclear Waste Management Fall Meeting, Boston, MA, 30 Nov. - 5 Dec. 1992
(Contract W-7405-eng-48)
(DE93-013131; UCRL-JC-111025; CONF-921101-118) Avail: CASI HC A03/MF A01

Yttrium-Barium-Cooper-Oxide (YBCO) thin films are prepared using laser ablation. The (100) orientation of the 0.2-0.3 micron thin film is controlled using both substrate temperature and deposited buffer layers for epitaxial growth. Highly textured films are prepared with a c-axis preferred orientation using substrates of SrTiO3 (100) and MgO (100) at a temperature of 780 C whereas a,b-axis films result if a 100nm buffer of Praseodymium- Barium-Copper- Oxide is first deposited at 700 C. The use of a 15nm buffer layer of SrTiO3 on MgO (100) produces films with superconducting transitions equivalent to those YBCO films deposited directly on SrTiO3 (100) substrates. DOE

N94-14327# Los Alamos National Lab., NM.
MICROWAVE HYBRID HEATING OF ALUMINA FILAMENTS
G. J. Vogt and W. P. Unruh 1993 14 p Presented at the 95th Annual Meeting of the American Ceramic Society, Cincinnati, OH, 18-22 Apr. 1993
(Contract W-7405-eng-36)
(DE93-012642; LA-UR-93-1306; CONF-930438-9) Avail: CASI HC A03/MF A01

Low loss oxide ceramics filaments are not readily heated to sintering temperatures (greater than 900 C) by direct microwave heating at 2.45 GHz. Use of high power levels typically yields thermal runaway with catastrophic melting. In other studies, hybrid, or indirect, heating has been successfully applied to processing bulk oxide ceramics. In this work, commercial alumina-based filaments have been indirectly heated to 700 - 900 C through a lossy carbon coating on the filament tow. Specific filaments can reach higher temperatures by direct coupling after preheating with a lossy coating. The results of microwave hybrid heating in a single mode TE(sub 102) cavity will be described for commercial alumina-based filaments. DOE

N94-14337# Nebraska Univ., Lincoln. Dept. of Electrical Engineering.
STUDY OF NOVEL CONDUCTIVE PAINTS FOR SOLAR CELL ELECTROMAGNETIC FIELDS
R. J. Soukup and N. J. Ianno 1993 6 p
(Contract DE-FG01-92CE-15974)
(DE93-015088; DOE/CE-15974/T4) Avail: CASI HC A02/MF A01

Progress in adhesion and electric resistivity studies on paints for use as solar cell contacts is reviewed. Some results on resistivity vs. baking temperature for some paints are shown. DOE

N94-14340# Los Alamos National Lab., NM.
MICROWAVE SINTERING OF LARGE ALUMINA BODIES
R. D. Blake and J. D. Katz 1993 9 p Presented at the 95th Annual Meeting of the American Ceramic Society, Cincinnati, OH, 18-22 Apr. 1993
(Contract W-7405-eng-36)
(DE93-012752; LA-UR-93-1456; CONF-930438-6) Avail: CASI HC A02/MF A01

The application of microwaves as an energy source for materials processing of large alumina bodies at elevated temperatures has been limited to date. Most work has concerned itself with small laboratory samples. The nonuniformity of the microwave field within a cavity subjects large alumina bodies to areas of concentrated energy, resulting in uneven heating and subsequent cracking. Smaller bodies are not significantly affected by field nonuniformity due to their smaller mass. This work will demonstrate a method for microwave sintering of large alumina bodies while maintaining their structural integrity. Several alumina configurations were successfully sintered using a method which creates an artificial field or environment within the microwave cavity. DOE

N94-14343# Westinghouse Savannah River Co., Aiken, SC.
RELATIONSHIP BETWEEN BOROSILICATE GLASS COMPOSITION, STRUCTURE, AND DURABILITY TEST RESPONSE (SRS)
W. G. Ramsey, C. M. Jantzen, and T. D. Taylor (Clemson Univ., SC.) 1992 11 p Presenting at the 95th Annual Meeting of the American Ceramic Society, Cincinnati, OH, 18-22 Apr. 1993
(Contract DE-AC09-89SR-18035)
(DE93-013578; WSRC-MS-92-485; CONF-930438-19) Avail: CASI HC A03/MF A01

The chemical durability of 30 glasses from the Na2O * B2O3 * SiO2 * Al2O3* Fe2O3 * CaO system was examined. Two standard leach tests, MCC-1P and PCT, were performed in unbuffered, deionized water. PCT tests were performed for durations up to twenty-four weeks to obtain glass dissolution rate data. Short-term MCC-1P test leachate solutions are determined by the glass composition. Long-term glass dissolution rates, however, are dependent on glass structure in addition to glass composition. The applicability of the free energy of hydration and other dissolution and durability models to this system is discussed. DOE

N94-14400# California Univ., Berkeley. Lawrence Berkeley Lab.
PORE-SIZE-DISTRIBUTION OF CATIONIC POLYACRYLAMIDE HYDROGELS
M. Kremer and J. M. Prausnitz Jun. 1992 80 p
(Contract DE-AC03-76SF-00098)
(DE93-015218; LBL-32845) Avail: CASI HC A05/MF A01

The pore size distribution of a AAm/MAPTAC (acrylamide copolymerized with (3-methacrylamidopropyl) trimethylammonium chloride) hydrogel was investigated using Kuga's mixed-solute-exclusion method, taking into account the wall effect. A Brownian-motion model is also used. Results show the feasibility of determining pore-size distribution of porous materials using the mixed-solute-exclusion method in conjunction with solution of the Fredholm equation; good agreement was obtained with experiment, even for bimodal pore structures. However, different pore size distributions were calculated for the two different probe-solutes (Dextran and poly(ethylene glycol/oxide)). Future work is outlined. DOE

N94-14421 National Lab. for High Energy Physics, Ibaraki (Japan).
WORKSHOP ON FORMATION OF SUPERMOLECULAR STRUCTURES IN COMPOSITE FLUID: PHASE RULE AND DYNAMICS
Fumihiko Tanaka, ed., Takao Ohta, ed., and Hironobu Ikeda, ed. Oct. 1992 85 p Workshop held in Tsukuba, Japan, 2-3 Jul. 1992 Limited Reproducibility: More than 20% of this document may be affected by microfiche quality
(DE93-782887; KEK-PROC-92-10; CONF-9207190) Avail: CASI HC A05/MF A01

This is the report of the workshop held at the National Laboratory for High Energy Physics on 2-3 Jul. 1992. This workshop was planned as a part of the research project on the utilization of booster neutrons in this Laboratory, and is one of the attempts to apply the technique of neutron scattering with wide visual field. Composite liquid means the solution that has the capability of forming the structure in 10-1000 nm and contains polymers, liquid crystals, micelles, or films inside. The hierarchy of the concept of supermolecules, the flexibility of the form of particles, multiple composition mixture system, and so on are the subjects in this field. In the workshop of this time, the themes were limited to three phenomena, that is, the formation of networks, microscopic phase separation and mesophase, and solvation and the formation of micelles. The measurement of neutron scattering by label method offers a powerful means hereafter for elucidating the structure and the dynamics of supermolecular liquid. DOE

N94-14432# Lawrence Livermore National Lab., CA.
MODELING SURFACE AREA TO VOLUME EFFECTS ON BOROSILICATE GLASS DISSOLUTION
W. L. Bourcier, W. L. Ebert (Argonne National Lab., IL.), and X. Feng (Argonne National Lab., IL.) Nov. 1992 8 p Presented at the 16th Material Research Society International Symposium on the Scientific Basis for Nuclear Waste Management, Boston, MA, 30 Nov. - 5 Dec. 1992
(Contracts W-7405-eng-48; W-31-109-eng-38)
(DE93-011891; UCRL-JC-112832; CONF-921101-111) Avail: CASI HC A02/MF A01

We simulated the reaction of SRL-131 glass with equilibrated J-13 water in order to investigate the effects of surface area to volume ratio (SA/V) on glass dissolution. We show that glass-fluid ion exchange causes solution pH to rise to progressively higher values as SA/V increases.

Because the ion exchange is rapid relative to the duration of the glass dissolution experiment, the pH effect does not scale with (SA/V)*time. Experiments compared at the same (SA/V)*time value have different pHs, with higher pHs at higher SA/V ratios. Both experimental data and our simulation results show similar trends of increasing reaction rate as a function of SA/V ratio when scaled to (SA/V)*time. Glasses which react in systems of differing SA/V ratio follow different reaction paths and high SA/V ratios cannot be used to generate data which accurately scales to long time periods unless the ion exchange effect is taken into account. We suggest some simple test designs which enable more reliable high. DOE

N94-14436# Los Alamos National Lab., NM.
NONLINEAR WAVE PREDICTIONS IN CERAMICS
D. A. Mandell 1993 6 p Presented at the International Union of Theoretical and Applied Mechanics Symposium, Victoria, Canada, 15-20 Aug. 1993
(Contract W-7405-eng-36)
(DE93-016516; LA-UR-93-2437; CONF-9308130-1) Avail: CASI HC A02/MF A01

Accurate numerical prediction of nonlinear waves in metals and ceramics is important in the design of many products including aerospace structures, automobile engines, and other devices. The material strength and fracture of ceramics must be predicted in order to achieve optimum designs. As part of a project to develop a reliable, robust, design computer program, a number of material strength and fracture models have been implemented into the MESA-2D hydrocode and the predictions from the code have been compared to data. MESA-2D is an explicit, finite-difference Eulerian code with hydrodynamics, high explosives, material strength, fracture, and a number of equation of state models. The interface velocity as a function of time between an alumina target and a lithium fluorids window, impacted by an alumina disk at velocities between 544 m/s and 2329 m/s, was predicted by using the Steinberg ceramic material strength model and a maximum tensile fracture model. These one-dimensional flyer plate experiments were conducted at Sandia National Laboratories using Coors AD 995 alumina. DOE

N94-14511# Sandia National Labs., Albuquerque, NM.
PORTABLE ACOUSTIC WAVE SENSOR SYSTEMS FOR REAL-TIME MONITORING OF VOLATILE ORGANIC COMPOUNDS
R. W. Cernosek, G. C. Frye, and D. W. Gilbert 1993 8 p Presented at the Conference on Physics Computing, Albuquerque, NM, 31 May - 4 Jun. 1993
(Contract DE-AC04-76DP-00789)
(DE93-013753; SAND-93-0100C; CONF-930557-1) Avail: CASI HC A02/MF A01

Portable acoustic wave sensor (PAWS) systems are being developed for real-time, on-line and in situ monitoring of volatile organic compounds (VOCs). These systems are built around surface acoustic wave (SAW) devices coated with viscoelastic polymers. Two independent responses of the SAW sensor, wave velocity and attenuation, are measured to provide information about the chemical species sorbed by the coating. Sensing is rapid and reversible, and coatings can be optimized for particular chemical selectivity and sensitivity. The complete PAWS system consists of two SAW devices (a sensor and a reference), RF oscillator electronics to drive the devices, digital interface/communications electronics, gas handling hardware to sample the environment, and a notebook computer to control the hardware and display responses in real-time. These systems have been demonstrated for on-line monitoring of exhaust stack vapors in environmentally conscious manufacturing (ECM) applications, for real-time documentation of off-gas contaminants from vacuum extraction processes at DOE remediation sites, and for down-hole sensing of volatile organics in vadose zone (above the groundwater level) monitoring wells. DOE

N94-14513# Nagoya Univ. (Japan).
HOW TO READ A PHASE EQUILIBRIUM DIAGRAM FOR HIGH-TEMPERATURE CERAMICS MATERIAL AS MAIN OBJECT
A. Yamaguchi 30 Aug. 1992 132 p In JAPANESE
(DE93-512333; ETDE/JP-mf-93512333) Avail: CASI HC A07/MF A02

A book on how to read a phase equilibrium diagram of high-temperature ceramic material is discussed. The book comprises three sections: fundamentals, applications, and conclusions and exercise. The fundamentals section details phase rules, equilibrium condition in binary and tertiary phase components and O-N system phase, and existence phases of molten compounds (coincidence and decomposition). The applications section describes how to read equilibrium diagrams for six phases including CaO-Al2O3-SiO2 system phases, and ten items including Al2O3-SiO2 system refractories and alkalis as well as sintering auxiliaries. The conclusions and exercise include seven precautionary items important for reading phase diagrams, the relation between Alkemade lines and boundary lines, identification of coincidence and decomposition in molten compounds, and how to distinguish characteristic curves and points. The 20 system phase diagrams in Phase Diagrams for Ceramists, published by American Ceramics Society Institutes, are used for the exercise. DOE

N94-14531# Oak Ridge National Lab., TN.
STRUCTURAL CHANGE OF GRAPHITE DURING ELECTRON IRRADIATION
J. Koike and D. F. Pedraza 1992 6 p Presented at the 16th Material Research Society International Symposium on the Scientific Basis for Nuclear Waste Management Fall Meeting, Boston, MA, 30 Nov. - 5 Dec. 1992
(Contract DE-AC05-84OR-21400)
(DE93-015961; CONF-921101-134) Avail: CASI HC A02/MF A01

Highly oriented pyrolytic graphite was irradiated at room temperature with 300-keV electrons. High resolution transmission electron microscopy and electron energy loss spectroscopy were employed to study the structure of electron-irradiated graphite. Results consistently indicated absence of long-range order periodicity in the basal plane, and loose retention of the c-axis periodicity. Structure was modeled based on a mixture of sixfold and non-sixfold atom rings. Formation of non-sixfold atom rings was related to the observed buckling and discontinuity of the original graphite basal plane. DOE

N94-14539*# Old Dominion Univ., Norfolk, VA. Dept. of Civil Engineering.
POLYMER INFILTRATION STUDIES Quarterly Progress Report, 1 Jul. - 30 Sep. 1993
Joseph M. Marchello Sep. 1993 27 p
(Grant NAG1-1067)
(NASA-CR-194521; NAS 1.26:194521) Avail: CASI HC A03/MF A01

During the past three months, significant progress has been made on the preparation of carbon fiber composites using advanced polymer resins. The results are set forth in recent reports and publications, and will be presented at forthcoming national and international meetings. Current and ongoing research activities reported herein include: textile composites from powder-coated towpreg; role of surface coating in braiding; prepregger hot sled operation; ribbonizing powder-impregenated towpreg; textile composites from powder-coated towpreg; role of bulk factor powder curtain prepreg process advanced tow placement (ATP) open-section part warpage control. During the coming months research will be directed toward further development of the new powder curtain prepregging method and on ways to customize dry powder towpreg for textile and robotic applications in aircraft part fabrication. Studies of multi-tow powder prepregging and ribbon preparation will be conducted in conjunction with continued development of prepregging technology and the various aspects of composite part fabrication using customized towpreg. Also, during the period ahead work will continue on the analysis of the performance of the new solution prepregger. Author (revised)

N94-14543*# Case Western Reserve Univ., Cleveland, OH.
PROCESSING AND TESTING OF HIGH TOUGHNESS SILICON NITRIDE CERAMICS Final Report
Veena Tikare, William A. Sanders (Analex Corp., Brook Park, OH.), and Sung R. Choi (Cleveland State Univ., OH.) Sep. 1993 11 p Proposed for presentation at the Pacific Rim Meeting of the American Ceramic Society, Honolulu, HI, 7-10 Nov. 1993; sponsored by the American Ceramic Society
(Contract NAS3-133; RTOP 505-63-5A)
(NASA-CR-191190; E-8120; NAS 1.26:191190) Avail: CASI HC A03/MF A01

High toughness silicon nitride ceramics were processed with the addition of small quantities of beta-Si3N4 whiskers in a commercially available alpha-Si3N4 powder. These whiskers grew preferentially during sintering resulting in large, elongated beta-grains, which acted to toughen the matrix

by crack deflection and grain pullout. The fracture toughness of these samples seeded with beta-Si3N4 whiskers ranged from 8.7 to 9.5 MPa m(exp 0.5) depending on the sintering additives. Author (revised)

N94-14693# Lawrence Livermore National Lab., CA.
ION ASSISTED SPUTTER DEPOSITION OF Mo-Si MULTILAYERS
S. P. Vernon (Vernon Applied Physics, Torrance, CA.), D. G. Stearns, and R. S. Rosen Nov. 1992 20 p Presented at the Soft X Ray Projection Lithography Topical Meeting, Monterey, CA, 6-8 Apr. 1992
(Contract W-7405-eng-48)
(DE93-013830; UCRL-JC-109359-Rev-1; CONF-9204120-9-Rev-1) Avail: CASI HC A03/MF A01

X-ray multilayer (ML) structures fabricated utilizing magnetron sputter deposition exhibit a degradation instructural quality with increased deposition pressure. The observed change in morphology is attributed to a reduced mobility of surface adatoms which inhibits the formation of smooth, continuous layers. The application of a negative substrate bias produces ion bombardment of the growing film surface by sputtering gas ions extracted from the plasma and allows direct control of the energy density supplied to the film surface during thin film growth. The technique supplements the energy lost to thermalization in high pressure deposition and permits the fabrication of high quality ML structures at elevated processing pressures. A three fold improvement in the soft x-ray normal incidence reflectance (NIR) at 130 (Angstrom) results for substrate bias voltages of order (approximately) -150V for Mo-Si MLs deposited at 10 mTorr Ar. DOE

N94-14801 Trane Co., LaCrosse, WI.
COMPATIBILITY OF REFRIGERANTS AND LUBRICANTS WITH MOTOR MATERIALS
R. Doerr, S. Kujak, and T. Waite Jan. 1993 56 p Prepared for Air-Conditioning and Refrigeration Technology Inst., Inc., Arlington, VA Limited Reproducibility: More than 20% of this document may be affected by microfiche quality
(Contract DE-FG02-91CE-23810)
(DE93-014768; DOE/CE-23810/8C) Avail: CASI HC A04

Equipment manufacturers are challenged to replace CFC-based refrigerants and their lubricants with environmentally acceptable alternatives. Information on the compatibility of motor materials with these alternative refrigerants and lubricants is a basic requirement for reliable performance. This report presents compatibility data for 24 commercially used motor materials exposed to 17 refrigerant/lubricant combinations. This compatibility data will enable the phase out of CFC's to continue at its current fast pace and insure the continued reliable performance of refrigerant-based equipment. DOE

N94-14845*# National Aeronautics and Space Administration. Lewis Research Center, Cleveland, OH.
THERMAL HISTORY EFFECTS ON ELECTRICAL RELAXATION AND CONDUCTIVITY FOR POTASSIUM SILICATE GLASS WITH LOW ALKALI CONCENTRATIONS
Paul W. Angel, Raiford E. Hann, and Alfred R. Cooper (Case Western Reserve Univ., Cleveland, OH.) Aug. 1993 21 p
(RTOP 505-62-70)
(NASA-TM-106324; E-8077; NAS 1.15:106324) Avail: CASI HC A03/MF A01

Electrical response measurements from 10 Hz to 100 kHz between 120 and 540 C were made on potassium-silicate glasses with alkali oxide contents of 2, 3, 5 and 10 mol percent. Low alkali content glasses were chosen in order to try to reduce the Coulombic interactions between alkali ions to the point that frozen structural effects from the glass could be observed. Conductivity and electrical relaxation responses for both annealed and quenched glasses of the same composition were compared. Lower DC conductivity (sigma(sub DC)) activation energies were measured for the quenched compared to the annealed glasses. The two glasses with the lowest alkali contents exhibited a non-Arrhenius concave up curvature in the log(sigma(sub DC)) against 1/T plots, which decreased upon quenching. A sharp decrease in sigma(sub DC) was observed for glasses containing K2O concentrations of 5 mol percent or less. The log modulus loss peak (M") maximum frequency plots against 1/T all showed Arrhenius behavior for both annealed and quenched samples. The activation energies for these plots closely agreed with the sigma(sub DC) activation energies. A sharp increase in activation energy was observed for both series as the potassium oxide concentration decreased. Changes in the electrical response are attributed to structural effects due to different alkali concentrations. Differences between the annealed and quenched response are linked to a change in the distribution of activation energies (DAE). Author (revised)

28 PROPELLANTS AND FUELS

Includes rocket propellants, igniters, and oxidizers; their storage and handling procedures; and aircraft fuels.

For related information see also *07 Aircraft Propulsion and Power, 20 Spacecraft Propulsion and Power,* and *44 Energy Production and Conversion.*

N94-12921# Los Alamos National Lab., NM.
EQUATION OF STATE FOR DETONATION PRODUCTS
W. C. Davis 1993 19 p Presented at the 10th Detonation Symposium, Boston, MA, 12-16 Jul. 1993
(Contract W-7405-eng-36)
(DE93-012671; LA-UR-93-1421; CONF-930713-8) Avail: CASI HC A03/MF A01

An equation of state for detonation products, with the usual form p = p(v,E), is proposed. It allows independent calibration of the adiabatic gamma and the Grueneisen gamma, and it gives them forms in agreement with recent theoretical studies. The equation of state is given by p = E/v(k - 1 + F(v)(1 + b(1 - E/E(exp s)(v))) where F(v) drops from a finite value at small v to zero at large v, b is a constant, and E(exp s)(v) is the specific internal energy on the principal isentrope. Its relationship to the polytropic gas equation of state p = (E/v)(gamma - 1) is easily seen, and it reduces to this form at large volume. DOE

N94-12987# Army Research Lab., Aberdeen Proving Ground, MD.
FLAMESPREADING IN GRANULAR SOLID PROPELLANT: DESIGN OF AN EXPERIMENT Final Report, Jan. 1991 - Oct. 1992
Douglas E. Kooker, Lang-Mann Chang, and Stephen L. Howard Jun. 1993 38 p
(AD-A266009; Rept-1L161102AH43) Avail: CASI HC A03/MF A01

When flamespreading in a gun system is rapid and reproducible, there is little incentive to improve our fundamental understanding of the ignition and flamespreading process. However, low-vulnerability (LOVA) propellants which are deliberately difficult to ignite can sometimes lead to anomalous ignition and flamespreading behavior. The present investigation is an attempt to study the fundamental behavior in a packed bed of granular gun propellant with a laboratory simulator. The apparatus consists of a hollow cylindrical pipe divided into two chambers. A small quantity of ball powder is burned in the igniter chamber sealed by a diaphragm and multiple-nozzle plate from the flow chamber which contains the sample granular solid propellant. Once the diaphragm bursts, combustion gases initially confined in the igniter chamber are driven through the nozzle plate forming a hot-gas planar wave which then propagates through the flow chamber. Behavior of this apparatus is discussed along with experimental pressure time-histories when the chamber is empty and filled with inert granular propellant. Results from a theoretical model help interpret some of the behavior. DTIC

N94-13002# Oak Ridge National Lab., TN.
CONVERSION OF LIGHT HYDROCARBON GASES TO METAL CARBIDES FOR PRODUCTION OF LIQUID FUELS AND CHEMICALS
A. F. Diaz, A. J. Modestino, J. B. Howard, and W. A. Peters Apr. 1993 6 p
(Contract DE-AC22-92PC-92111)
(DE93-014962; DOE/PC-92111/T2; FE-MIT-92111-2) Avail: CASI HC A02/MF A01

Work on this project will be performed according to two tasks. Task 1 is entitled 'Industrial Chemistry and Applied Kinetics of Light Hydrocarbon Gas Conversion to Metal Carbides H2 and CO.' We are building a laboratory-scale electric arc discharge reactor, in which to assess the technical feasibility of producing Mg2C3, H2, and CO from methane and MgO. We will also do experimental runs with CaO as well as mixtures of CaO and MgO and measure conversions of methane, CaO and/or MgO, and yields of Mg2C3, and/or CaC2, H2, and CO to identify the operating conditions of interest for implementing these reactions on a commercial scale. Reaction conditions and parameters will be chosen based on the

previous work at MIT with CaO and CH and on results of thermodynamic and thermochemical kinetics calculations. Task 2 is entitled 'Mechanistic Foundations for Converting Light Hydrocarbon Gases to Metal Carbides, H2, and CO.' We will evaluate the technical feasibility of carrying out methane reactions with CaO and MgO by thermal (e.g. 1500-2000 C) rather than under plasma conditions by performing experiments with the use of electrical screen heaters, heated tubular reactors, or other suitable apparatus. Extents and global rates of methane conversion, and yields as well as global production rates of CaC2, Mg2C3, H2, and CO will be measured upon subjecting mixtures of methane and CaO and/or MgO to high temperatures and controlled residence times. We will conduct hypothesis-testing of possible mechanistic pathways with selected experiments and perform reaction modeling to better understand the underlying chemical and physical processes that could influence process scale-up possibilities. DOE

N94-13099# Los Alamos National Lab., NM.
SYNTHESIS AND CHARACTERIZATION OF 1,4-DINITROGLYCOLURIL (DINGU)
J. A. Sanchez, M. M. Stinecipher, and L. A. Stretz Jun. 1993 11 p
(Contract W-7405-eng-36)
(DE93-014111; LA-12455-MS) Avail: CASI HC A03/MF A01 (US Sales Only)

The synthesis and properties of 1,4-dinitroglycoluril (DINGU) have been studied. Isomers formed during the DINGU synthesis reaction were identified. The synthesis reaction was scaled up and reaction conditions optimized to produce the maximum yield of DINGU. This study evaluated DINGU as an energy contributing material in cast and plastic-bonded explosive formulations. Plastic coating of DINGU into a plastic-bonded explosive using several binders was also investigated. Testing indicated that DINGU has lower than expected explosive performance both as a pure material and when formulated in a plastic-bonded explosive. DOE

N94-13491# Los Alamos National Lab., NM.
DESTRUCTION OF WASTE ENERGETIC MATERIALS USING BASE HYDROLYSIS
T. M. Benziger, G. A. Buntain, J. A. Sanchez, and T. Spontarelli 1993 10 p Presented at the 12th Annual International Symposium on Thermal Treatment Technologies-Incineration Conference, Knoxville, TN, 3-7 May 1993
(Contract W-7405-eng-48)
(DE93-012738; LA-UR-93-1527; CONF-930572-3) Avail: CASI HC A02/MF A01

In dismantling weapons for stockpile reduction, environmentally acceptable degradation of the associated high explosive (HE) waste to non-energetic forms is a critical objective. Base hydrolysis appears to be a simple, inexpensive method for converting propellants, explosives, and pyrotechnics (PEP's) into non-energetic materials that can be released directly or, if necessary, treated further. We have demonstrated that many PEP's can be hydrolyzed with aqueous sodium hydroxide or ammonia at temperatures ranging from 60 to 150 C. Hydrolysis experiments have been performed on pure compounds as well as DOE and DoD formulations, such as plastic-bonded explosive (PBX) 9404, tritonal, and rocket motor propellant. Small particle size of the energetic material is desirable, but not necessary. We have decomposed molding powder, pressed charges up to two pounds in weight, and partially exposed, metal-encased pieces. The products formed are dependent on the starting material composition, but usually consist of organic and inorganic salts, e.g., sodium formate, acetate, nitrite, and nitrate. The major gaseous product from the base hydrolysis of PEP's is nitrous oxide. The time required for complete destruction varies with the material being hydrolyzed and is dependent on solubility and mass transfer. Hydrolysis rates can be increased by particle size reduction, efficient stirring, and addition of organic solvent to the alkaline solution. Rate enhancement by ultrasonic agitation is a possibility that we have just begun to study. DOE

N94-13560 Pennsylvania State Univ., University Park.
COMBUSTION-INDUCED CRACK/DEBOND PROPAGATION IN SOLID PROPELLANTS Ph.D. Thesis
Seng-Rung Wu 1992 154 p
Avail: Univ. Microfilms Order No. DA9311746

In a solid-rocket motor, combustion-induced crack/debond propagation could cause chamber over-pressurization and failure of a mission. To explore this malfunction of solid-rocket motors, experimental studies and theoretical simulations were conducted. The test samples under investigation were AP/PBAN/Al and polyester-based high-elongation metalized propellants with EPDM insulators and Kevlar/epoxy cases. Crack/debond samples were installed in a windowed test chamber and rapidly pressurized in a combustion environment. The effects of chamber pressurization rate and sample's boundary condition on the development of crack/debond propagations were studied. Three distinct modes of crack propagation (stationary, propagation, and bifurcated cracks) were observed for AP/PBAN/Al propellants, according to various chamber pressurization rates. For polyester-based high-elongation propellants, the crack propagation included propagation, zigzag, mixed, and branched modes; different types of crack propagation modes were observed from the opposite surfaces of the recovered samples. Crack speeds related to chamber pressurization rates were obtained in a correlation form. Debond propagation in a burning metalized propellant grain with a composite case was also studied. In general, the debond took place along the bondline with no branchings. The empirical correlations relating debond propagation speeds V(sub d) to chamber pressurization rates delta(p)/delta(t) were obtained in a power-law form (V(sub d) equals A(delta(p)/delta(t))(exp n)). It was found that the exponent n depends on debond geometries; however, the preexponent A is a function of material properties and sample geometries. In the theoretical approach, the mechanisms responsible for crack initiation and bifurcation were examined. A finite-difference scheme for combustion formulation in a propagating debond cavity was coupled with a finite-element analysis for propellant structural deformation and fracture. Case expansion responsible for the debond propagation was simulated. Results for the debond model include solving combustion processes in a debond flaw; calculating pressure-driven structural deformation; and simulating combustion-induced debond propagation in a motor analog. The theoretical simulation was in good agreement with experimental observations, ensuring the applicability of this model to predict a flawed solid rocket motor.
Author

N94-14089# Midwest Research Inst., Golden, CO. National Renewable Energy Lab.
STATUS AND FUTURE OPPORTUNITIES FOR CONVERSION OF SYNTHESIS GAS TO LIQUID ENERGY FUELS Final Report
G. Mills May 1993 187 p Prepared in cooperation with Delaware Univ., Newark, DE
(Contract DE-AC02-83CH-10093)
(DE93-010025; NREL/TP-421-5150) Avail: CASI HC A09/MF A02

The manufacture of liquid energy fuels from syngas (a mixture of H2 and CO, usually containing CO2) is of growing importance and enormous potential for the following reasons: (1) Abundant U.S. supplies of coal, gas, and biomass can be used to provide the needed syngas. (2) The liquid fuels produced, oxygenates or hydrocarbons, can help lessen environmental pollution. Indeed, oxygenates are required to a significant extent by the Clean Air Act Amendments (CAAA) of 1990. (3) Such liquid synfuels make possible high engine efficiencies because they have high octane or cetane ratings. (4) There is new, significantly improved technology for converting syngas to liquid fuels and promising opportunities for further improvements. This is the subject of this report. The purpose of this report is to provide an account and evaluative assessment of advances in the technology for producing liquid energy fuels from syngas and to suggest opportunities for future research deemed promising for practical processes. Much of the improved technology for selective synthesis of desired fuels from syngas has resulted from advances in catalytic chemistry. However, novel process engineering has been particularly important recently, utilizing known catalysts in new configurations to create new catalytic processes. This report is an update of the 1988 study Catalysts for Fuels from Syngas: New Directions for Research, which is included as Appendix A. Technology for manufacture of syngas is not part of this study. The manufacture of liquid synfuels is capital intensive. Thus, in evaluating advances in fuels technology, the focus is on the potential for improved economics, particularly on lowering plant investment costs. A second important criteria is the potential for environmental benefits. The discussion is concerned with two types of hydrocarbon fuels and three types of oxygenate fuels that can be synthesized from syngas. Seven alternative reaction pathways are involved. DOE

N94-14145# Army Research Lab., Aberdeen Proving Ground, MD.
CLOSED-CHAMBER ANALYSIS OF M5 PROPELLANT LOT RAD-64597 Final Report, Nov. 1992 - Feb. 1993
William F. Oberle Jun. 1993 137 p
(AD-A266321; ARL-MR-83) Avail: CASI HC A07/MF A02

The Advanced Propulsion Technology Branch (APTB) of the Propulsion and Flight Division (PFD) is currently engaged in the investigation of both liquid and solid propellant electrothermal-chemical (ETC) propulsion concepts. A major goal of this technology investigation is to demonstrate that ETC propulsion offers performance advantages (increase muzzle kinetic energy) in comparison to conventional solid propellant performance. To experimentally quantify differences in performance between ETC and conventional solid propellant technologies requires optimization of the propelling charges. For solid propellant ETC (SPETC) such an optimization requires an accurate knowledge of the burning characteristics (linear burn rate) of the propellant. For the APTB experimental program, one of the baseline solid propellants will be M5, lot RAD-64597. DTIC

N94-14180# Los Alamos National Lab., NM.
A STUDY OF THE ROLE OF HOMOGENEOUS PROCESS IN HETEROGENEOUS HIGH EXPLOSIVES
P. K. Tang 1993 8 p Presented at the 10th Detonation Symposium, Boston, MA, 12-16 Jul. 1993
(Contract W-7405-eng-36)
(DE93-012733; LA-UR-93-1557; CONF-930713-10) Avail: CASI HC A02/MF A01

In a new hydrodynamic formulation of shock-induced chemical reaction, we can show formally that the presence of certain homogenous reaction characteristics is becoming more evident as shock pressure increase even in heterogeneous high explosives. The homogeneous reaction pathway includes nonequilibrium excitation and deactivation stages prior to chemical reaction. The excitation process leads to an intermediate state at higher energy level than the equilibrium state, and as a result, the effective activation energy appears to be lower than the value based on thermal experiments. As the pressure goes up higher, the homogeneous reaction can even surpass the heterogeneous process and becomes the dominant mechanism. DOE

N94-14454# Midwest Research Inst., Golden, CO. National Renewable Energy Lab.
BIOFUELS FOR TRANSPORTATION: THE ROAD FROM RESEARCH TO THE MARKETPLACE
Mar. 1993 6 p
(Contract DE-AC02-83CH-10093)
(DE93-000091; NREL/SP-420-5439) Avail: CASI HC A02/MF A01

This brief document describes research sponsored by the National Renewable Energy Laboratory (NREL) in support of producing and processing biomass for automotive fuel production. An overview of feedstocks, pretreatment, bioconversion, product recovery, and ethanol and co-products is given. DOE

N94-14490 Pennsylvania State Univ., University Park.
NUMERICAL SIMULATION OF VELOCITY-COUPLED COMBUSTION RESPONSE OF SOLID ROCKET PROPELLANTS Ph.D. Thesis
I-Shih Tseng 1992 157 p
Avail: Univ. Microfilms Order No. DA9311736

A numerical analysis has been conducted to study solid-propellant rocket motor internal flowfields under both steady and oscillatory conditions. The formulation is based on the time-dependent Navier-Stokes equations for compressible flows, with consideration of finite-rate chemical kinetics and variable properties. Turbulence closure is achieved using a modified k-Epsilon two-equation model and a two-layer model. Both models take into account the wall-injection effect arising from the surface combustion of propellants. The analysis consists of two parts: cold-flow simulation of unsteady motions in a porous chamber, and investigation of combustion of homogeneous propellants. A time-accurate finite-difference program based on the four-stage Runge-Kutta scheme, and a finite-volume program based on the dual time-stepping integration technique, were used for the cold-flow and reacting-flow simulations, respectively. The results from cold-flow simulation indicate that while the acoustic pressure field remains one-dimensional, the acoustic velocity exhibits a more complicated oscillation behavior than a plane wave. The flow-turning loss of the acoustic field is as important as the viscous loss which occurs within the acoustic boundary layer. From the reacting-flow simulation, it was found that the strong temperature gradient within the flame zones has an effect on the distribution of acoustic velocity. The interactions between acoustic waves and gas phase chemical reactions are also demonstrated by the large amplitude of temperature fluctuations when the characteristic time scales of these two mechanisms are closely matched. Author

N94-14507 Tel-Aviv Univ. (Israel). School of Applied Mathematics.
THE MOTION OF A CONICAL SHAPED LINER DRIVEN BY EXPLOSIVE LOAD M.S. Thesis
Ido Holzmann Oct. 1991 84 p In HEBREW
(ITN-93-85215) Copyright Avail: Issuing Activity (Tel-Aviv Univ., Exact Sciences Library, Ramat Aviv 69978, Israel)

The metallic jet formed by the detonation of a cylindrical explosive charge with a metal-lined cavity at one end comprises the following: a single, massive high-velocity tip particle, weighing 1-5 g and travelling at 7-10 km/sec; a jet with a velocity gradient from the tip velocity at the front to 0.5-1 km/sec at the rear end; and a slug, containing most of the liner mass, travelling at 0.5-1 km/sec. The jet eventually breaks up and its penetration is proportional to its length and depends strongly on the time to breakup and the number of fragments. Existing one-dimensional mathematical models of the jet formation process are strongly dependent on the basic assumptions made about the collapse process, so that each fits only a small range of charge designs. In the present work, a 2-dimensional numerical model was developed for calculating the pressure function; it enables the simple one-dimensional jet formation model to be combined with an accurate numerical solution of the collapse process. Shell grids are used to model the liner and the charge confinement; mass points are driven by the pressure of the detonation products acting on the area between the mass points and the velocity directions are calculated from the angles between the mass points. At the collision point, a non-steady state model due to Pugh, Eichelberger and Rostoker (the PER model) is used to determine the jet and slug masses and velocities. ISA

N94-14535# Los Alamos National Lab., NM.
REVIEW OF NUCLEAR THERMAL PROPULSION CARBIDE REACTOR FUEL CORROSION AND EXHIBIT
D. Pellacio, M. S. El-Genk, and D. P. Butt 1993 15 p Presented at the Joint AIAA/SAE/ASME Propulsion Conference, Monterey, CA, 28-30 Jun. 1993
(Contract W-7405-eng-36)
(DE93-016605; LA-UR-93-2174; CONF-930633-1) Avail: CASI HC A03/MF A01

Uranium carbide forms complete, nearly ideal solid solutions with the refractory compounds ZrC, NbC, HfC, and TaC. These compounds have very high melting points. By incorporating uranium carbide into a solid solution, a very high melting point nuclear fuel is attained. In the present study, the thermodynamics of refractory carbide fuels as it relates to vaporization or corrosion behavior is experimentally examined. The vaporization behavior of refractory carbide fuels is modeled, based on the equilibrium partial pressures of important vapor species. DOE

N94-14829 Weizmann Inst. of Science, Rehovoth (Israel).
THE 4TH INTERNATIONAL SYMPOSIUM ON ANALYSIS AND DETECTION OF EXPLOSIVES
Sep. 1992 70 p Symposium held in Jerusalem, Israel, 7-10 Sep. 1992
Limited Reproducibility: More than 20% of this document may be affected by microfiche quality
(DE93-620280; INIS-mf-13494; CONF-9209325) Avail: CASI HC A04 (US Sales Only)

From among the presentations given at the 4th International Symposium on Analysis and Detection of Explosives (7-10 Sep. 1992, Jerusalem, Israel), three were considered to be in INIS scope and separately indexed. DOE

29 MATERIALS PROCESSING

Includes space-based development of products and processes for commercial applications.

For biological materials see *55 Space Biology*.

N94-12805*# Intersonics, Inc., Northbrook, IL.
STABILIZED ELECTROMAGNETIC LEVITATOR Final Report, Jun. 1991 - Aug. 1993
T. J. Danley, C. D. Anderson, D. R. Merkley, P. C. Nordine, C. A. Rey, and M. M. Zatarski 31 Aug. 1993 64 p
(Contract NAS8-38958)
(NASA-CR-194261; NAS 1.26:194261) Avail: CASI HC A04/MF A01

The purpose of the Stabilized Electromagnetic Levitator (SEL) Phase 2 project was to develop electromagnetic (EM) positioning and heating instrumentation for containerless experimentation with specific application to low-gravity operation. The three major areas of effort were to optimize the technology in a single-axis system, characterize operation with typical materials, and develop a multi-axis positioner. The major design goals were to: control heating and positioning functions independently; use high EM frequencies to enable processing of smaller, more resistive specimens; control EM stirring in molten materials for improved quiescence; provide power sufficient for melting and low gravity positioning of metals and alloys; and maintain optical access for diagnostics. Both the single-axis and three-axis instruments were shown to be feasible for low-gravity containerless experimentation. The high operating frequencies of the SEL technology make it applicable to a much larger range of materials than are conventional, lower frequency, single-axis EM positioners. Separate control of heating and positioning functions was demonstrated for the single axis device. The three-axis instrument had the ability to control fluid motions in melts and may be applied to achieve, for the first time, a high degree of quiescence in liquid specimens that are EM positioned and heated in low-gravity. Author (revised)

N94-13732*# National Aeronautics and Space Administration. Marshall Space Flight Center, Huntsville, AL.
SPACELAB J EXPERIMENT DESCRIPTIONS
Teresa Y. Miller, ed. Washington Aug. 1993 246 p
(NASA-TM-4517; M-725; NAS 1.15:4517) Avail: CASI HC A11/MF A03

Brief descriptions of the experiment investigations for the Spacelab J Mission which was launched from the Kennedy Space Center aboard the Endeavour in Sept. 1992 are presented. Experiments cover the following: semiconductor crystals; single crystals; superconducting composite materials; crystal growth; bubble behavior in weightlessness; microgravity environment; health monitoring of Payload Specialists; cultured plant cells; effect of low gravity on calcium metabolism and bone formation; and circadian rhythm. For individual titles, see N94-13733 through N94-13775.

N94-13733*# Nippon Telegraph and Telephone Public Corp., Tokyo (Japan). Basic Research Labs.
GROWTH EXPERIMENT OF NARROW BAND-GAP SEMICONDUCTOR PbSnTe SINGLE CRYSTALS IN SPACE (M-1)
Tomoaki Yamada *In* NASA. Marshall Space Flight Center, Spacelab J Experiment Descriptions Aug. 1993 p 3-7 (For primary document see N94-13732 02-29)
Avail: CASI HC A01/MF A03

An experiment on crystal growth of Pb(1-x)Sn(x)Te in microgravity is planned. This material is an alloy of the compound semiconductors PbTe and SnTe. It is a promising material for infrared diode lasers and detectors in the wavelength region between 6 and 30 micron. Since the electrical properties of Pb(1-x)Sn(x)Te depend greatly on the Pb/Sn ratio and crystalline defects as well as impurity concentration, homogeneous, defect-free, high-quality crystals are anticipated. Although many growth methods, such as the pulling method, the Bridgman method, the vapor growth method, etc., have been applied to the growth of Pb(1-x)Sn(x)Te, large, homogeneous, low-defect-density crystals have not yet been grown on Earth. The unsuccessful results were caused by buoyancy-driven convection in the fluids induced by the specific gravity difference between heated and cooled fluids on Earth. A crystal is grown by cooling the melt from one end of the ampoule. In crystal growth from the melt, about 30 percent of the SnTe in the melt is rejected at the solid-liquid interface during solidification. On Earth, the rejected SnTe is completely mixed with the remaining melt by convection in the melt. Therefore, SnTe concentration in the melt, and accordingly in the crystal, increases as the crystal grows. In the microgravity environment, buoyancy-driven convection is suppressed because the specific gravity difference is negligible. In that case, the rejected SnTe remains at the solid-liquid interface and its concentration increases only at the interface. If the growth rate is higher than the PbTe-SnTe interdiffusion rate, the amount of SnTe which diffuses from the interface into the melt increases as SnTe piles up at the interface, and finally it balances the amount of rejected SnTe during solidification, resulting in steady-state SnTe transportation at the interface. By using this principle, compositionally homogeneous crystals can be grown. Furthermore, low-defect-density crystals will be grown in microgravity, because convection causes crystalline defects by mising hot and cold fluids and generating temperature fluctuations in them. Author (revised)

N94-13734*# Institute of Physical and Chemical Research, Saitama (Japan).
GROWTH OF PbSnTe SINGLE CRYSTAL BY TRAVELING-ZONE METHOD IN LOW GRAVITY (M-2)
Y. Segawa *In* NASA. Marshall Space Flight Center, Spacelab J Experiment Descriptions Aug. 1993 p 9-13 (For primary document see N94-13732 02-29)
Avail: CASI HC A01/MF A03

The single-crystal lead tin telluride (PbSnTe) semiconductor is most promising as a laser radiation element and infrared detecting element in the far infrared region. However, it is very difficult to grow a large single crystal with a homogeneous composition on Earth because the elements have a very strong tendency to separate from each other in the molten phase due to differences in their specific gravities and melting points. The purpose of the experiment is to grow a single crystal of PbSnTe by a traveling zone method in microgravity, and to study the spatial fluctuation of the composition and the electrical properties of the crystal.
Author (revised)

N94-13735*# National Research Inst. for Metals, Tokyo (Japan).
GROWTH OF SEMICONDUCTOR COMPOUND SINGLE CRYSTAL InSb BY FLOATING ZONE METHOD (M-3)
I. Nakatani *In* NASA. Marshall Space Flight Center, Spacelab J Experiment Descriptions Aug. 1993 p 15-19 (For primary document see N94-13732 02-29)
Avail: CASI HC A01/MF A03

Floating zone methods have potential applications in growing single high-quality semi-conductor crystals. In this method, melts can be sustained without containers and, therefore, are free from contamination from the containers. The main objective of this project is to use the Image Furnace to study a large diameter, (20 mm) single crystal of InSb under microgravity conditions. The behavior of the liquid column is recorded on the VTR tapes and is compared with what is expected theoretically. The single crystal grown in space is characterized by comparing it with single crystals grown on the ground with respect to crystallographic and electronic properties. The goal of this project is to confirm the effects of the microgravity on the single crystals. Author (revised)

N94-13736*# National Research Inst. for Metals, Tsukuba (Japan).
CASTING OF SUPERCONDUCTING COMPOSITE MATERIALS (M-4)
Kazumasa Togano *In* NASA. Marshall Space Flight Center, Spacelab J Experiment Descriptions Aug. 1993 p 21-25 (For primary document see N94-13732 02-29)
Avail: CASI HC A01/MF A03

An aluminum-lead-bismuth alloy is a flexible alloy and is promising for easily workable embedded-type, filament-dispersed superconducting wire material. It is difficult to produce homogeneous ingots of this material because it is easily separated into elements when melted on Earth due to the large specific gravity differences. In this experiment, a homogeneous alloy will first be produced in molten state in microgravity. It will then be returned to Earth and processed into a wire or tape form. It will then be dispersed as the second phase in micro texture form into the primary phase of aluminum. Superconducting wire material with high-critical-magnetic-field characteristics will be produced. The texture of the material will be observed, and its performance will be evaluated. In addition to the above alloy, a four-element alloy will be produced from silver, a rare Earth element, barium, and copper. The alloys will be oxidized

and drawn into wire after being returned to Earth. The materials are expected to be forerunners in obtaining superconducting wire materials from oxide superconductors. Author

N94-13737*# National Research Inst. for Metals, Tokyo (Japan).
FORMATION OF DEOXIDIZATION PRODUCTS IN IRON INGOT BY THE ADDITION OF Al, Si, AND/OR Mn (M-5)
Akira Fukazawa *In* NASA. Marshall Space Flight Center, Spacelab J Experiment Descriptions Aug. 1993 p 27-30 (For primary document see N94-13732 02-29)
Avail: CASI HC A01/MF A03

The objective of this work is to examine the morphology, composition, and distribution of deoxidation products in iron and iron-10 percent Ni alloy ingots. The deoxidation agents Si, Mn, Al, and their mixtures are selected to investigate the formation mechanism of the deoxidation products and to compare the differences of oxide formation among these agents in microgravity. After the experiment in space, the tested specimens are going to be analyzed by the use of the latest physical and/or chemical analytical equipment, and the information obtained will be a great help for the comprehension of the formation of oxide inclusion in steel for practical purposes, and also for the study of the solidification mechanism theory in the theoretical field. Author

N94-13738*# National Research Inst. for Metals, Tokyo (Japan).
PREPARATION OF PARTICLE-DISPERSION ALLOYS (M-6)
Yuji Muramatsu *In* NASA. Marshall Space Flight Center, Spacelab J Experiment Descriptions Aug. 1993 p 31-35 (For primary document see N94-13732 02-29)
Avail: CASI HC A01/MF A03

A particle dispersion alloy is one type of metal-ceramic composite material, and is used as heat resistance material, wear resistance material, and electrical material. This material consists of a metal matrix and dispersed particles, and for its unique structure it has both tenacity as a metal and hardness as a ceramic. Its properties improve when the particles become finer and disperse more uniformly. Most of the particle dispersion alloys are produced by the powder metallurgical process. This process is favorable for uniform dispersion of particles, but it consists of complicated techniques such as mechanical alloying and hot extrusion, and has the following drawbacks: (1) it is difficult to fabricate large-sized products; (2) the amount of particles is limited to a few percent; and (3) the process is complicated and expensive. To overcome these drawbacks, recently special attention has been paid to conventional melting process. However, under terrestrial conditions, dispersions separate immediately due to the different specific gravities of the metal matrix and the particles and thermal convection effects. The microgravity environment is, therefore, considered to be an attractive place for fabricating the dispersion alloy. This space experiment is carried out to clarify the influence of microgravity on the properties of the particle dispersion alloy and to obtain a deeper understanding of the experiment under the microgravity environment. Author

N94-13739*# National Research Inst. for Metals, Tokyo (Japan).
DIFFUSION IN LIQUID STATE AND SOLIDIFICATION OF BINARY SYSTEM (M-7)
T. Dan *In* NASA. Marshall Space Flight Center, Spacelab J Experiment Descriptions Aug. 1993 p 37-39 (For primary document see N94-13732 02-29)
Avail: CASI HC A01/MF A03

Diffusion is one of the most fundamental physical phenomena. It relates to the manufacturing of almost all materials. Therefore, the precise knowledge of diffusivities of relevant materials is necessary for the optimization of these processes. On the other hand, such knowledge is indispensable to understanding the diffusion mechanism and structure of liquid metal in the field of physical metallurgy. Many diffusion experiments on solid metal were undertaken and a lot of data were accumulated. But on liquid metals there are few measurements because of experimental difficulties, such as thermal convection, induced by very slight temperature gradients in the specimen. Under microgravity conditions, the movement of liquid metal due to density differences and thermal convection must be suppressed markedly. Therefore, the transportation process will be controlled only by the diffusion of constituent atoms. These conditions offer the optimum environments for the diffusion experiment. The experiments are briefly described. Diffusion couples are prepared by attaching end to end two rods of different pure metals using hot press equipment. These couples are inserted into a graphite crucible and then doubly enclosed by two silica ampoules, respectively. The specimen is inserted into a tantalum cartridge, which is welded in a vacuum using an electron-beam apparatus. These cartridges are charged in the continuous heating furnace in space and held at a given temperature for a predetermined time and then solidified. The concentration distribution of elements in these specimens will be measured along the rod axis by means of an electron probe microanalyzer. The counterdiffusivity of the liquid metal binary system is determined on the basis of the compensated concentration distribution profile for thermal contraction. Author (revised)

N94-13740*# Kyoto Univ. (Japan).
HIGH TEMPERATURE BEHAVIOR OF GLASS (M-8)
Naohiro Soga *In* NASA. Marshall Space Flight Center, Spacelab J Experiment Descriptions Aug. 1993 p 41-44 (For primary document see N94-13732 02-29)
Avail: CASI HC A01/MF A03

The twofold purpose of this experiment is to obtain data on the occurrence of flow in a viscous glass sphere in microgravity, and to confirm data obtained on Earth for volume-temperature relationships of glass. To do this, a cubic sample of glass laced with gold particles will be heated in the IMF. The sample's properties will be measured at high temperature, and the volume of the sample varied to measure the expansion coefficient. Movement of the gold particles, if any, will determine flow within the sample. The apparatus for this experiment is schematically shown and the photographs of the image furnace with samples before and after melting, respectively. In this apparatus, shape and size of the sample are observed by video camera and recorded by video recorder. The recorded images of the sample are schematically shown. Symbols A, B, and C denote low, intermediate, and high temperatures, respectively. From these images, the volume of the sample is estimated and the temperature dependence of the volume, is obtained. If there is agreement between the data collected in this experiment and data obtained on Earth, it would tend to verify Earth-collected data. Author (revised)

N94-13741*# Tokyo Univ. (Japan).
GROWTH OF Si SPHERICAL CRYSTALS AND THE SURFACE OXIDATION (M-9)
Tatau Nishinaga *In* NASA. Marshall Space Flight Center, Spacelab J Experiment Descriptions Aug. 1993 p 45-49 (For primary document see N94-13732 02-29)
Avail: CASI HC A01/MF A03

Nearly 90 percent of semiconductor devices are produced with Si single crystals as the starting materials. For instance, the integrated circuits (IC), which are used in almost all electronic equipments such as TV, tape recorders, audio amplifiers, etc., are made after various processings of Si single crystal wafers. In these wafers, the same controlled amounts of impurities are added and the uniformities in their distributions are extremely important. Growth under microgravity makes it possible to eliminate the buoyancy-driven convection in the melt, which is one of the main origins of convections which results in non-uniformity of the impurity. Another source of convection is known as Marangoni convection which is driven on the free surface when a temperature gradient occurs. One of the merits of microgravity experimentation is that the detailed study of this convection becomes possible. Another important advantage of microgravity is that growth of crystals without a crucible is possible. This makes it possible to study melt growth without the strain which is usually introduced on the ground. Nevertheless, we should repeat and analyze many growth experiments in space to get reliable results. However, since in the FMPT, the time for the experiment is limited, we plan to carry out two kinds of very simple and basic experiments as the first step for the semiconductor growth experiment. In the first experiment, we use single crystal Si sphere as the starting material and as shown, this sphere is heated in the furnace at a slightly higher temperature than the melting point. After the melting front moves nearly half way to its center, the temperature is decreased to stop the melting and to start the growth from the seed for which we use the unmelted solid party of the sphere. The sphere is centered by quartz protuberances inside of the quartz crucible. There exists the possibility of temperature fluctuations being introduced when the molten sphere occasionally touches the protuberances. The total time needed for the melting and the growth processes is estimated to be 30 minutes. Infrared

emission from the sphere is monitored in order to prevent the accidental loss of the central solid core. The schematical illustration of the second experient is shown. A single crystal, Si rod is used as the starting material. In the first stage, the rod is melted from one end to obtain a liquid sphere. In the second stage, the single crystal is grown by decreasing the temperature from the unmelted part of the rod which is used as the seed. The second experient somewhat resembles the Czochralski method used on the ground; however, in the space experiment, no crucible is employed and the temperature uniformity is much superior. In both experiments, phosphorous is doped to allow observation of the change in the shape of the liquid solid interface during crystal growth and the impurity striations, if any. Author (revised)

N94-13742*# Tokyo Inst. of Tech. (Japan). Dept. of Metallurgical Engineering.

STUDY ON SOLIDIFICATION OF IMMISIBLE ALLOYS (M-10)

Akihiko Kamio *In* NASA. Marshall Space Flight Center, Spacelab J Experiment Descriptions Aug. 1993 p 51-60 (For primary document see N94-13732 02-29)

Avail: CASI HC A02/MF A03

Alloying of immiscible alloys under microgravity is of interest in metallurgical processes. Several experiments investigating the alloying of immiscible alloys, such as Al-In, Al-Bi, Zn-Bi, and Zn-Pb, were done in space. Homogeneous distribution of small L2 particles in the matrix, such as an emulsion structure, was expected in the space-solidifed alloys. However, the alloys demonstrated an extremely segregated structure. To date insufficient information was obtained to explain these unexpected results. Our experiment was proposed to clarify the solidification manner of immiscible alloys and to obtain fundamental information concerning structural control of the alloys. In space, density differences between the two liquids separated in immiscible regions can be neglected, so that no sedimentation of L(sub 2) phase will take place. When the growth of the alloys is interrupted and this status is frozen by an adequate rapid cooling procedure, it will provide much information concerning decomposing homogeneous liquid and the interaction between the monotectic growth front morphology and the distribution of L(sub 2) phase. It is anticipated that the results will be useful for elucidating the monotectic solidification manner and it will be instructive to explain the segregated structures obtained in the past space experiments. Author (revised)

N94-13743*# Tokyo Inst. of Tech. (Japan). Dept. of Metallurgical Engineering.

FABRICATION OF VERY-LOW-DENSITY, HIGH-STIFFNESS CARBON FIBER/ALUMINUM HYBRIDIZED COMPOSITE WITH ULTRA-LOW DENSITY AND HIGH STIFFNESS (M-11)

Tomoo Suzuki *In* NASA. Marshall Space Flight Center, Spacelab J Experiment Descriptions Aug. 1993 p 61-67 (For primary document see N94-13732 02-29)

Avail: CASI HC A02/MF A03

Fabrication of a composite material with ultra-low density and high stiffness in microgravity is the objective of the investigation. The composite structure to be obtained is a random three-dimensional array of high modulus, short carbon fibers bonded at contact points by an aluminum alloy coated on the fibers. The material is highly porous and thus has a very low density. The motivation toward the investigation, simulation experiments, choice of the component materials, and on-flight experiment during ballistic trajectory of a NASDA rocket, are described. Author (revised)

N94-13744*# Tokyo Univ. (Japan).

STUDY ON THE MECHANISM OF LIQUID PHASE SINTERING (M-12)

S. Kohara *In* NASA. Marshall Space Flight Center, Spacelab J Experiment Descriptions Aug. 1993 p 69-74 (For primary document see N94-13732 02-29)

Avail: CASI HC A02/MF A03

The objectives were to (1) obtain the data representing the growth rate of solid particles in a liquid matrix without the effect of gravity; and (2) reveal the growth behavior of solid particles during liquid phase sintering using the data obtained. Nickel and tungsten are used as the constituent materials in liquid phase sintering. The properties of the constituent metals are given. When a compact of the mixture of tungsten and nickel powders is heated and kept at 1550 C, nickel melts down but tungsten stays solid. As the density of tungsten is much greater than that of nickel, the sedimentation of tungsten particles occurs in the experiment on Earth. The difference between the experiments on Earth and in space is illustrated. The tungsten particles sink to the bottom and are brought into contact with each other. The resulting pressure at the contact point causes the accelerated dissolution of tungsten. Consequently, flat surfaces are formed at the contact sites. As a result of dissolution and reprecipitation of tungsten, the shape of particles changes to a polygon. This phenomenon is called 'flattening.' An example of flattening of tungsten particles is shown. Thus, the data obtained by the experiment on Earth may not represent the exact growth behavior of the solid particles in a liquid matrix. If the experiments were done in a microgravity environment, the data corresponding to the theoretical growth behavior of solid particles could be achieved. Derived from text

N94-13745*# Osaka Univ., Toyonaka (Japan).

FABRICATION OF Si-As-Te TERNARY AMORPHOUS SEMICONDUCTOR IN THE MICROGRAVITY ENVIRONMENT (M-13)

Yoshihiro Hamakawa *In* NASA. Marshall Space Flight Center, Spacelab J Experiment Descriptions Aug. 1993 p 75-78 (For primary document see N94-13732 02-29)

Avail: CASI HC A01/MF A03

Ternary chalcogenide Si-As-Te system is an interesting semiconductor from the aspect of both basic physics and technological applications. Since a Si-As-Te system consists of a IV-III-II hedral bonding network, it has a very large glass forming region with a wide physical constant controllability. For example, its energy gap can be controlled in a range from 0.6 eV to 2.5 eV, which corresponds to the classical semiconductor Ge (0.66 eV), Si (1.10 eV), GaAs (1.43 eV), and GaP (2.25 eV). This fact indicates that it would be a suitable system to investigate the compositional dependence of the atomic and electronic properties in the random network of solids. In spite of these significant advantages in the Si-As-Te amorphous system, a big barrier impending the wide utilization of this material is the huge difficulty encountered in the material preparation which results from large differences in the weight density, melting point, and vapor pressure of individual elements used for the alloying composition. The objective of the FMPT/M13 experiment is to fabricate homogeneous multi-component amorphous semiconductors in the microgravity environment of space, and to make a series of comparative characterizations of the amorphous structures and their basic physical constants on the materials prepared both in space and in normal terrestrial gravity. Author (revised)

N94-13746*# Nagoya Univ. (Japan). Faculty of Science.

GAS-EVAPORATION IN LOW-GRAVITY FIELD (COGELATION MECHANISM OF METAL VAPORS) (M-14)

N. Wada *In* NASA. Marshall Space Flight Center, Spacelab J Experiment Descriptions Aug. 1993 p 79-82 (For primary document see N94-13732 02-29)

Avail: CASI HC A01/MF A03

When metal and alloy compounds are heated and vaporized in a rare gas such as helium, argon, or xenon, the vaporized substances diffused in the rare gas are supersaturated resulting in a smoke of fine particles of the material congealing as snow or fog. The gas vaporizing method is a fine particle generation method. Though the method has a variety of applications, the material vapor flow is disturbed by gravitational convection on Earth. The inability to elucidate the fine particle generation mechanism results in an obstruction to improving the method to mass production levels. As no convection occurs in microgravity in space, the fine particle generation mechanism influenced only by diffusion can be investigated. Investigators expect that excellent particles with homogeneous diameter distribution can be obtained. Experiment data and facts will assist in improving efficiency, quality, and scale or production processes including element processes such as vaporization, diffusion, and condensation. The objective of this experiment is to obtain important information related to the mechanism of particle formation in the gas atmosphere (smoke particles) and the production of submicron powders of extremely uniform size. Author (revised)

N94-13747*# National Aerospace Lab., Tokyo (Japan).

DROP DYNAMICS IN SPACE AND INTERFERENCE WITH ACOUSTIC FIELD (M-15)

Tatsuo Yamanaka *In* NASA. Marshall Space Flight Center, Spacelab J

Experiment Descriptions Aug. 1993 p 83-85 (For primary document see N94-13732 02-29)
Avail: CASI HC A01/MF A03

The objective of the experiment is to study contactless positioning of liquid drops, excitation of capillary waves on the surface of acoustically levitated liquid drops, and deformation of liquid drops by means of acoustic radiation pressure. Contactless positioning technologies are very important in space materials processing because the melt is processed without contacting the wall of a crucible which can easily contaminate the melt specifically for high melting temperatures and chemically reactive materials. Among the contactless positioning technologies, an acoustic technology is especially important for materials unsusceptible to electromagnetic fields such as glasses and ceramics. The shape of a levitated liquid drop in the weightless condition is determined by its surface tension and the internal and external pressure distribution. If the surface temperature is constant and there exist neither internal nor external pressure perturbations, the levitated liquid drop forms a shape of perfect sphere. If temperature gradients on the surface and internal or external pressure perturbations exist, the liquid drop forms various modes of shapes with proper vibrations. A rotating liquid drop was specifically studied not only as a classical problem of theoretical mechanics to describe the shapes of the planets of the solar system, as well as their arrangement, but it is also more a contemporary problem of modern non-linear mechanics. In the experiment, we are expecting to observe various shapes of a liquid drop such as cocoon, tri-lobed, tetropod, multi-lobed, and doughnut. Author (revised)

N94-13748*# National Aerospace Lab., Tokyo (Japan).
STUDY OF BUBBLE BEHAVIOR IN WEIGHTLESSNESS (EFFECTS OF THERMAL GRADIENT AND ACOUSTIC STATIONARY WAVE) (M-16)
H. Azuma *In* NASA. Marshall Space Flight Center, Spacelab J Experiment Descriptions Aug. 1993 p 87-88 (For primary document see N94-13732 02-29)
Avail: CASI HC A01/MF A03

The aim of this experiment is to understand how bubbles behave in a thermal gradient and acoustic stationary wave under microgravity. In microgravity, bubble or bubbles in a liquid will not rise upward as they do on Earth but will rest where they are formed because there exists no gravity-induced buoyancy. We are interested in how bubbles move and in the mechanisms which support the movement. We will try two ways to make bubbles migrate. The first experiment concerns behavior of bubbles in a thermal gradient. It is well known than an effect of surface tension which is masked by gravity on the ground becomes dominant in microgravity. The surface tension on the side of the bubble at a lower temperature is stronger than at a higher temperature. The bubble migrates toward the higher temperature side due to the surface tension difference. The migration speed depends on the so-called Marangoni number, which is a function of the temperature difference, the bubble diameter, liquid viscosity, and thermal diffusivity. At present, some experimental data about migration speeds in liquids with very small Marangoni numbers were obtained in space experiments, but cases of large Marangoni number are rarely obtained. In our experiment a couple of bubbles are to be injected into a cell filled with silicon oil, and the temperature gradient is to be made gradually in the cell by a heater and a cooler. We will be able to determine migration speeds in a very wide range of Marangoni numbers, as well as study interactions between the bubbles. We will observe bubble movements affected by hydrodynamical and thermal interactions, the two kinds of interactions which occur simultaneously. These observation data will be useful for analyzing the interactions as well as understanding the behavior of particles or drops in materials processing. The second experiment concerns bubble movement in an acoustic stationary wave. It is known that a bubble in a stationary wave moves toward the node or the loop according to whether its diameter is larger or smaller than that of the main resonant radius. In our experiment fine bubbles will be observed to move according to an acoustic field formed in a cylindrical cell. The existence of bubbles varies the acoustic speed, and the interactive force between bubbles will make the bubble behavior collective and complicated. This experiment will be very useful to development of bubble removable technology as well as to the understanding of bubble behavior.
Author (revised)

N94-13749*# Government Industrial Research Inst., Osaka (Japan).
PREPARATION OF OPTICAL MATERIALS USED IN NON-VISIBLE REGION (M-17)
J. Hayakawa *In* NASA. Marshall Space Flight Center, Spacelab J Experiment Descriptions Aug. 1993 p 89-93 (For primary document see N94-13732 02-29)
Avail: CASI HC A01/MF A03

The purpose of the experiment was the following: development of containerless glass melting technique; fabrication of high purity glass; and development of acoustic levitation technique. For the space experiment, glass 65CaO-25Ga2O3-10GeO2 was selected out of various types of glasses. The expected results are: ultra-high purity glass and manipulation by acoustics. Derived from text

N94-13750*# Ishikawajima-Harima Heavy Industries Co. Ltd., Tokyo (Japan).
MARANGONI EFFECT INDUCED CONVECTION IN MATERIAL PROCESSING UNDER MICROGRAVITY (M-18)
S. Enya *In* NASA. Marshall Space Flight Center, Spacelab J Experiment Descriptions Aug. 1993 p 95-100 (For primary document see N94-13732 02-29)
Avail: CASI HC A02/MF A03

On the ground the upper layer of the liquid in a vessel heated from below becomes hotter than the lower layer. This well-known phenomenon results from buoyancy-induced convection. Though this means that the buoyancy-induced convection is not dominant under microgravity conditions in space, another convection called Marangoni convection may possibly occur. This convection results from an intermolecular force which acts on a free surface, that is surface tension. Since it is stronger at lower temperatures, the liquid surface near the heated wall is pulled to the cooled side as shown. This surface movement causes the inner convection. Marangoni convection, however, may be negligible on the Earth, for the molecular force is generally smaller than buoyancy. Various tests on material processing were recently conducted in space and some high quality crystals free from buoyancy convection were obtained. But, at the same time, others proved to be less uniform than expected in the components' distribution. This nonuniformity seems to be mainly caused by Marangoni convection. It is, therefore, very important to know how to control the convection by studying its characteristics, but the problem is that on the ground it is impossible to carry out the experiment without gravity. That is what a space experiment aboard the space shuttle is planned as the First Material Processing Tests (FMPT) of Japan. The experiment on Marangoni flow visualization is being performed in order to investigate the characteristics of convection in uni-dimensional melt growth under microgravity conditions.
Author

N94-13751*# Chiba Inst. of Tech., Narashino (Japan).
SOLIDIFICATION OF EUTECTIC SYSTEM ALLOYS IN SPACE (M-19)
Atsumi Ohno *In* NASA. Marshall Space Flight Center, Spacelab J Experiment Descriptions Aug. 1993 p 101-105 (For primary document see N94-13732 02-29)
Avail: CASI HC A01/MF A03

It is well known that in the liquid state eutectic alloys are theoretically homogeneous under 1 g conditions. However, the homogeneous solidified structure of this alloy is not obtained because thermal convection and non-equilibrium solidification occur. The present investigators have clarified the solidification mechanisms of the eutectic system alloys under 1 g conditions by using the in situ observation method; in particular, the primary crystals of the eutectic system alloys never nucleated in the liquid, but instead did so on the mold wall, and the crystals separated from the mold wall by fluid motion caused by thermal convection. They also found that the equiaxed eutectic grains (eutectic cells) are formed on the primary crystals. In this case, the leading phase of the eutectic must agree with the phase of the primary crystals. In space, no thermal convection occurs so that primary crystals should not move from the mold wall and should not appear inside the solidified structure. Therefore no equiaxed eutectic grains will be formed under microgravity conditions. Past space experiments concerning eutectic alloys were classified into two types of experiments: one with respect to the solidification mechanisms of the eutectic alloys and the other to the unidirectional solidification of this alloy. The former type of experiment has the problem that the solidified structures between microgravity and 1 g conditions show little difference. This is why the flight

samples were prepared by the ordinary cast techniques on Earth. Therefore it is impossible to ascertain whether or not the nucleation and growth of primary crystals in the melt occur and if primary crystals influence the formation of the equiaxed eutectic grains. In this experiment, hypo- and hyper-eutectic aluminum copper alloys which are near eutectic point are used. The chemical compositions of the samples are Al-32.4mass%Cu (Hypo-eutectic) and Al-33.5mass%Cu (hyper-eutectic). Long rods for the samples are cast by the Ohno Continuous Casting Process and they show the unidirectionally solidified structure. Each flight and ground sample was made of these same rods. The dimensions of all samples are 4.5 mm in diameter and 23.5 mm in length. Each sample is put in a graphite capsule and then vacuum sealed in a double silica ampoule. Then the ampoule is put in the tantalum cartridge and sealed by electron beam welding. For onbard experiments, a Continuous Heating Furnance (CHF) will be used for melting and solidifying samples under microgravity conditions. Six flight samples will be used. Four samples are hypo-eutectic and two are hyper-eutectic alloys. The surface of the two hypo-eutectic alloy samples are covered with aluminum oxide film to prevent Marangoni convection expected under microgravity conditions. Each sample will be heated to 700 C and held at that temperature for 5 min. After that the samples will be allowed to cool to 500 C in the furnace and they will be taken out of the furnace for He gas cooling. The heating and cooling diagrams for the flight experiments are shown. After collecting the flight samples, the solidified structures of the samples will be examined and the mechanisms of eutectic solidification under microgravity conditions will be determined. It is likely that successful flight experiment results will lead to production of high quality eutectic alloys and eutectic composite materials in space.

Author (revised)

N94-13752*# National Inst. for Research in Inorganic Materials, Tokyo (Japan).

GROWTH OF SAMARSKITE CRYSTAL UNDER MICROGRAVITY CONDITIONS (M-20)

S. Takekawa *In* NASA. Marshall Space Flight Center, Spacelab J Experiment Descriptions Aug. 1993 p 107-111 (For primary document see N94-13732 02-29)

Avail: CASI HC A01/MF A03

The purpose of the experiment was to grow single crystals of samarskite under microgravity conditions by the traveling solvent float zone (TSFZ) method, and to study the phase relations in the samarskite-related systems involving liquid phases by the slow cooling float zone (SCFZ) method. Samarskite is one of the minerals in a metamict state and is composed of Ca, Fe, Y, U, Th, Nb, Ta, O, etc. Alpha-particles radiating from uranium and/or thorium in the samarskite itself has destroyed its original structure without damaging its chemical composition and its external form. Consequently its structure was converted into a vitreous structure.

Derived from text

N94-13753*# Agency of Industrial Science and Technology, Tsukuba (Japan). Electrotechnical Lab.

GROWTH EXPERIMENT OF ORGANIC METAL CRYSTAL IN LOW GRAVITY (M-21)

Hiroyuki Anzai *In* NASA. Marshall Space Flight Center, Spacelab J Experiment Descriptions Aug. 1993 p 113-116 (For primary document see N94-13732 02-29)

Avail: CASI HC A01/MF A03

The purpose of this experiment is to grow large, high-quality single crystals of the organic metal (TMTTF-TCNQ) by the diffusion method without thermal fluctuation due to convection and gravitational sedimentation, and to evaluate the difference in properties between such crystals grown in low gravity and the ones obtained on Earth. The expected results may fix several physical properties of TMTTF-TCNQ, lead to the discovery of new phenomena, and enable us to analyze diffusion processes in a precise way. The result will contribute to the development of research on organic metals and, generally, on crystal growth.

Author

N94-13754*# Sumitomo Electric Industries Ltd., Osaka (Japan).

CRYSTAL GROWTH OF COMPOUND SEMICONDUCTORS IN A LOW-GRAVITY ENVIRONMENT (InGaAs CRYSTALS) (M-22)

Masami Tatsumi *In* NASA. Marshall Space Flight Center, Spacelab J Experiment Descriptions Aug. 1993 p 117-120 (For primary document see N94-13732 02-29)

Avail: CASI HC A01/MF A03

Compound semiconductor crystals, such as gallium arsenide and indium phosphide crystals, have many interesting properties that silicon crystals lack, and they are expected to be used as materials for optic and/or electro-optic integrated devices. Generally speaking, alloy semiconductors, which consist of more than three elements, demonstrate new functions. For example, values of important parameters, such as lattice constant and emission wavelength, can be chosen independently. However, as it is easy for macroscopic and/or microscopic fluctuations of composition to occur in alloy semiconductor crystals, it is difficult to obtain crystals having homogeneous properties. Macroscopic change of composition in a crystal is caused by the segregation phenomenon. This phenomenon is due to a continuous change in the concentration of constituent elements at the solid-liquid interfacing during solidification. On Earth, attempts were made to obtain a crystal with homogeneous composition by maintaining a constant melt composition near the solid-liquid interface, through suppression of the convection flow of the melt by applying a magnetic field. However, the attempt was not completely successful. Convective flow does not occur in microgravity because the gravity in space is from four to six orders of magnitude less than that on Earth. In such a case, mass transfer in the melt is dominated by the diffusion phenomenon. So, if crystal growth is carried out at a rate that is higher than the rate of mass transfer due to this phenomenon, it is expected that crystals having a homogeneous composition will be obtained. In addition, it is also possible that microscopic composition fluctuations (striation) may disappear because microscopic fluctuations diminish in the absence of convection. We are going to grow a bulk-indium gallium arsenide (InGaAs) crystal using the gradient heating furnace (GHF) in the first material processing test (FMPT). The structure of the sample is shown where InGaAs polycrystals in a crucible are doubly sealed in two quartz tubes for safety. The GHF consists of two zones, namely, high temperature and low temperature zones, which results in a large temperature gradient at the interface. Crystal growth is performed by moving the furnace (i.e. the temperature profile) from the left to right at a definite rate. Thus, we will grow crystals both on Earth and in space under the same conditions. As previously described, it is possible to obtain good quality crystals which are homogeneous in composition both macroscopically and microscopically due to the lack of convection in space. We are planning to study the effects of convection on crystal growth from a melt by comparing and characterizing the properties of crystals grown on Earth with those grown in space.

Author (revised)

N94-13755*# National Aeronautics and Space Administration. Lewis Research Center, Cleveland, OH.

MICROGRAVITY ACCELERATION MEASUREMENT ENVIRONMENT CHARACTERIZATION

Richard DeLombard *In* NASA. Marshall Space Flight Center, Spacelab J Experiment Descriptions Aug. 1993 p 121-127 (For primary document see N94-13732 02-29)

Avail: CASI HC A02/MF A03

The Space Acceleration Measurement System (SAMS) is a general-purpose instrumentation system designed to measure the accelerations onboard the shuttle Orbiter and shuttle/Spacelab vehicles. These measurements are used to support microgravity experiments and investigations into the microgravity environment of the vehicle. Acceleration measurement can be made at locations remote from the SAMS main instrumentation unit by the use of up to three remote triaxial sensor heads. The SAMS was developed by NASA's Lewis Research Center (LeRC) in support of NASA's microgravity science programs. In the past, numerous acceleration measurement systems have flown on various space missions. These systems were tailored to measure accelerations for a narrow set of requirements and were limited in bandwidth, dynamic range, and recording capability. In addition, these systems were mission-peculiar and not easily modified for other applications or missions. The result has been an inability to accurately assess the expected microgravity environment prior to a mission for a particular experiment and/or location. The prime science objective for SAMS on the SL-J mission will be to measure the accelerations experienced by a multitude of experiments in the two racks of the Japanese First Materials Processing Test (FMPT). The FMPT consists of a variety of materials science and life science experiments contained in racks no. 7 and no. 10. The SAMS data will be made available to the FMPT principal

investigators after the mission for their analysis with the FMPT data. A secondary science objective for SAMS will be the characterization of the acceleration environment of the Spacelab module. This will include an analysis of the acceleration transfer function of the Spacelab module which will utilize the FMPT acceleration measurement along with measurements at the rack no. 9 structure. Another analytical effort to be undertaken is a general characterization of the acceleration environment of the Spacelab as an orbiting laboratory. These analysis efforts will be in conjunction with similar measurements and analyses on other SAMS Spacelab missions.

Author

N94-13756*# Alabama Univ., Birmingham.

PROTEIN CRYSTAL GROWTH

Charles E. Bugg *In* NASA. Marshall Space Flight Center, Spacelab J Experiment Descriptions Aug. 1993 p 129-135 (For primary document see N94-13732 02-29)

Avail: CASI HC A02/MF A03

Proteins account for 50% or more of the dry weight of most living systems and play a crucial role in virtually all biological processes. Since the specific functions of essentially all biological molecules are determined by their three-dimensional structures, it is obvious that a detailed understanding of the structural makeup of a protein is essential to any systematic research pertaining to it. At the present time, protein crystallography has no substitute, it is the only technique available for elucidating the atomic arrangements within complicated biological molecules. Most macromolecules are extremely difficult to crystallize, and many otherwise exciting and promising projects have terminated at the crystal growth stage. There is a pressing need to better understand protein crystal growth, and to develop new techniques that can be used to enhance the size and quality of protein crystals. There are several aspects of microgravity that might be exploited to enhance protein crystal growth. The major factor that might be expected to alter crystal growth processes in space is the elimination of density-driven convective flow. Another factor that can be readily controlled in the absence of gravity is the sedimentation of growing crystal in a gravitational field. Another potential advantage of microgravity for protein crystal growth is the option of doing containerless crystal growth. One can readily understand why the microgravity environment established by Earth-orbiting vehicles is perceived to offer unique opportunities for the protein crystallographer. The near term objectives of the Protein Crystal Growth in a Microgravity Environment (PCG/ME) project is to continue to improve the techniques, procedures, and hardware systems used to grow protein crystals in Earth orbit. Derived from text

N94-13757*# National Space Development Agency, Tokyo (Japan).

HEALTH MONITORING OF JAPANESE PAYLOAD SPECIALIST: AUTONOMIC NERVOUS AND CARDIOVASCULAR RESPONSES UNDER REDUCED GRAVITY CONDITION (L-0) **c52**

Chiharu Sekiguchi *In* NASA. Marshall Space Flight Center, Spacelab J Experiment Descriptions Aug. 1993 p 139-144 (For primary document see N94-13732 02-29)

Avail: CASI HC A02/MF A03

In addition to health monitoring of the Japanese Payload Specialists (PS) during the flight, this investigation also focuses on the changes of cardiovascular hemodynamics during flight which will be conducted under the science collaboration with the Lower Body Negative Pressure (LBNP) Experiment of NASA. For the Japanese, this is an opportunity to examine firsthand the effects of microgravity of human physiology. We are particularly interested in the adaption process and how it relates to space motion sickness and cardiovascular deconditioning. By comparing data from our own experiment to data collected by others, we hope to understand the processes involved and find ways to avoid these problems for future Japanese astronauts onboard Space Station Freedom and other Japanese space ventures. The primary objective of this experiment is to monitor the health condition of Japanese Payload Specialists to maintain a good health status during and after space flight. The second purpose is to investigate the autonomic nervous system's response to space motion sickness. To achieve this, the function of the autonomic nervous system will be monitored using non-invasive techniques. Data obtained will be employed to evaluate the role of autonomic nervous system in space motion sickness and to predict susceptibility to space motion sickness. The third objective is evaluation of the adaption process of the cardiovascular system to microgravity. By observation of the hemodynamics using an echocardiogram we will gain insight on cardiovasc[illegible]tioning. The last objective is to create a data base for use in the health care of Japanese astronauts by obtaining control data in experiment L-O in the SL-J mission.

Author (revised)

N94-13758*# Nagoya Univ. (Japan).

ENDOCRINE AND METABOLIC CHANGES IN PAYLOAD SPECIALIST (L-1) **c52**

Nobuo Matsui *In* NASA. Marshall Space Flight Center, Spacelab J Experiment Descriptions Aug. 1993 p 145-149 (For primary document see N94-13732 02-29)

Avail: CASI HC A01/MF A03

The endocrine system plays an important role in the adaptation to unusual environments by secreting hormones to control metabolism. Since human beings have long evolved on the surface of the Earth under a gravity environment, the weightless environment must be quite unusual for them. The purpose of this experiment is to study the mechanisms of human adaptation to a weightless environment from endocrine and metabolic changes. Our study plan is focused on four major physiological changes which were reported during past space flights or which may be expected to occur under that condition: (1) hormone and metabolic changes associated with fluid shift; (2) bone demineralization and muscle atrophy; (3) altered circadian rhythm; and (4) stress reaction during space flight.

Derived from text

N94-13759*# Nagoya Univ. (Japan). Research Inst. of Environmental Medicine.

NEUROPHYSIOLOGICAL STUDY ON VISUO-VESTIBULAR CONTROL OF POSTURE AND MOVEMENT IN FISH DURING ADAPTATION TO WEIGHTLESSNESS **c52**

Shigeo Mori *In* NASA. Marshall Space Flight Center, Spacelab J Experiment Descriptions Aug. 1993 p 151-153 (For primary document see N94-13732 02-29)

Avail: CASI HC A01/MF A03

We can stand upright and walk smoothly without paying any particular attention to it. This is because we have established in ourselves an integration center that controls our body subconsciously in response to input from eyes, muscles, joints, foot soles, and also from the gravity sensor in the inner ear (the otolith organ). It has been shown that the cerebellum plays an important role for the establishment of the integration center and that the control pattern is comparable to that of a highly sophisticated computer system. The programming for the control, however, may well be acquired for the 1-g ground condition and does not cover the 0-g in space. Although each of the above organs function as it does on the ground, the signal pattern sent to the center must be different under 0-g and, in addition, complementary signals from the otolith organ are missing, leading to confusion in the integration center and causing a variety of symptoms similar to those of car-sickness or sea-sickness. After exposure to microgravity an immediate process of re-programming will begin and be completed in 2-4 days. There is strong supporting evidence for this sensory conflict theory as an explanation for space motion sickness (SMS) episodes. Fish were selected as test organisms for this investigation because they swim around freely in three dimensions and have well-developed organs for vision and gravity detection. They also have an innate nature to orient their back toward a light source. Actually, on the ground, the fish tilts its vertical axis toward the light when illuminated laterally, and the tilt angle is a function of the intensity of light and the magnitude of gravity, while its posture is completely light-dependent in the low-gravity environment produced by aircraft parabolic flight or when the otolith organs are removed. This implies that fish posture is entirely under visual and otolithic control. In this case, the cerebellum will also contribute to the control. In the space shuttle experiment, two fish (one with otolith-removed and the other with intact otoliths) are onboard for 7 days. The arrangement of the experiment is shown. Lamps illuminate each fish alternately from different directions at a duration of 20 seconds for 10 minutes totally, twice a day. The video images and the brain waves from the cerebellum are analyzed later. If the sensory conflict theory is acceptable, then the confusion at the onset and the following recovery process will be manifested both in the light-dependent behavior and also in the cerebellar activity. In addition, there should be some variation in response between the two fish. Even if the results are positive in the present fish experiment, they would not be extensive enough to allow us to understand the complete mechanisms of

SMS. However, what is currently needed is a collection of evidence based on animal experiments on which to base future investigations. Countermeasures for SMS are mandatory since SMS-induced vomiting occurring within a space suit could be fatal for a crew member during extravehicular activities. We expect that countermeasures will be developed before the space station era starts, and that the results of these studies will be applied to improving human welfare. Author (revised)

N94-13760*# Osaka Univ. (Japan). Medical School.
SEPARATION OF BIOGENIC MATERIALS BY ELECTROPHORESIS UNDER ZERO GRAVITY (L-3) **c51**
Masao Kuroda *In* NASA. Marshall Space Flight Center, Spacelab J Experiment Descriptions Aug. 1993 p 155-160 (For primary document see N94-13732 02-29)
Avail: CASI HC A02/MF A03

Electrophoresis separates electrically charged materials by imposing a voltage between electrodes. Though free-flow electrophoresis is used without carriers such as colloids to separate and purify biogenic materials including biogenic cells and proteins in blood, its resolving power and separation efficiency is very low on Earth due to sedimentation, flotation, and thermal convection caused by the specific gravity differences between separated materials and buffer solutions. The objective of this experiment is to make a comparative study of various electrophoresis conditions on the ground and in zero-gravity in order to ultimately develop a method for separating various important 'vial' components which are difficult to separate on the ground. Author (revised)

N94-13761*# Nagoya Univ. (Japan).
COMPARATIVE MEASUREMENT OF VISUAL STABILITY IN EARTH AND COSMIC SPACE (L-4) **c52**
Kazugo Koga *In* NASA. Marshall Space Flight Center, Spacelab J Experiment Descriptions Aug. 1993 p 161-163 (For primary document see N94-13732 02-29)
Avail: CASI HC A01/MF A03

The frequency and the intensity of space motion sickness was reviewed and investigated. Unusual induced-gravity situations, such as rotation, linear acceleration, parallel swinging etc. were investigated as well. Visually-induced motion sensation or distorted perception were evaluated with respect to visual stability by many investigators. These studies are all concerned with the effect of gravity and the induction of motion sickness through human visual perception. Direct investigation under the microgravity situation, such as parabolic flight, Skylab, and Spacelab, was carried out. These studies focused on how human visual stability is established through various sensory afferents in specific gravity conditions. Results from these investigations indicate that sensory mismatch probably plays an important role in space motion sickness. The interaction of visual, vestibular, and somatosensory perception is smoothly coordinated under normal gravitational conditions on the Earth in our daily life. When the cooperation is destroyed or a mismatch occurs among them, motion sickness may develop not only on the Earth but also in microgravity. The latter case may be the cause of space motion sickness or space adaption syndrome. How human beings obtain visual stability even with posture changes on the ground was investigated. Visual stability can be categorized as static or dynamic. Static visual stability is concerned with orientation and dynamic stability is concerned with object motion perception. The perception of visual stability is modified by many other sensations, such as somatosensory, vestibular, and muscle tension. We will mainly focus on modifications by vestibular inputs to visual perception produced by eye movements in microgravity. The Vestibular-Oscular Reflex (VOR) is a well-known characteristic which results from the relationship between eye mobility and vestibular afferent inputs. Eye movements also modify dynamic visual perception, such as perceived object motion velocity. The VOR is constantly simulated under 1-g conditions on Earth. In fact, human beings have been habituated and 'programmed' for orientation (visual stability) in their everyday, 1-g environment. When humans are exposed to a different gravity situation, this programmed behavior must change; that is, it is reprogrammed. This is called habituation or familiarization. We hope to examine how object motion perception is perturbed and subsequently adapted in the microgravity environment. This experiment is focused on the cooperation of visual, vestibular, and somatosensory perception coordination and how it is changed or reduced in space compared to 1-g environment. We will obtain information on the coordination between eye movement and neck muscle activity by using EOG and EMG. We will also collect data from Payload Specialists using a self-diagnostic questionnaire concerned with perceptual abnormality. When each sensory input function and its integration in the higher nervous system are well-characterized, then more effective techniques to control SAS may be developed. Author (revised)

N94-13762*# Fuji Oil Co. Ltd., Tsukuba (Japan). Research and Development Center.
CRYSTAL GROWTH OF ENZYMES IN LOW GRAVITY (L-5)
Yuhei Morita *In* NASA. Marshall Space Flight Center, Spacelab J Experiment Descriptions Aug. 1993 p 165-170 (For primary document see N94-13732 02-29)
Avail: CASI HC A02/MF A03

Recent developments in protein engineering have expanded the possibilities of studies of enzymes and other proteins. Now such studies are not limited to the elucidation of the relationship between the structure and function of the protein. They also aim at the production of proteins with new and practical functions, based on results obtained during investigation of structure and function. For continuing research in this field, investigation of the tertiary structure of proteins is important. X-ray diffraction of single crystals of protein is usually used for this purpose. The main difficulty is the preparation of the crystals. The theme of the research is to prepare such crystals at very low gravity, with the main purpose being to obtain large single crystals of proteins suitable for x-ray diffraction studies. Author (revised)

N94-13763*# Tokyo Medical and Dental Univ. (Japan).
STUDIES ON THE EFFECTS OF MICROGRAVITY ON THE ULTRASTRUCTURE AND FUNCTIONS OF CULTURED MAMMALIAN CELLS (L-6) **c51**
Atsushige Sato *In* NASA. Marshall Space Flight Center, Spacelab J Experiment Descriptions Aug. 1993 p 171-172 (For primary document see N94-13732 02-29)
Avail: CASI HC A01/MF A03

The human body consists of 10(exp 13) cells. Understanding the mechanisms by which the cells sense and respond to microgravity is very important as the basis for space biology. The cells were originally isolated aseptically from mammalian bodies and cultured in vitro. A set of cell culture vessels was developed to be applied to three kinds of space flight experiments. Experiment 1 is to practice the cell culture technique in a space laboratory and obtain favorable growth of the cells. Aseptic handling in tryspin treatment and medium renewal will be tested. The cells, following space flight, will be returned to the ground and cultured continuously to investigate the effects of space flight on the cellular characteristics. Experiment 2 is to examine the cytoskeletal structure of the cells under microgravity conditions. The cytoskeletal structure plays essential roles in the morphological construction, movements, axonal transport, and differentiation of the cells. The cells fixed during space flight will be returned and the cytoskeleton and ultrastructure observed using electron microscopy and fluorescence microscopy. Experiment 3 is to study the cellular productivity of valuable substances. The waste medium harvested during space flight are returned and quantitated for the cellular products. The effects of microgravity on mammalian cells will be clarified from the various aspects. Author (revised)

N94-13764*# State Univ. of New York, Stony Brook.
GRAVITY, CHROMOSOMES, AND ORGANIZED DEVELOPMENT IN ASEPTICALLY CULTURED PLANT CELLS **c51**
Abraham D. Krikorian *In* NASA. Marshall Space Flight Center, Spacelab J Experiment Descriptions Aug. 1993 p 173-176 (For primary document see N94-13732 02-29)
Avail: CASI HC A01/MF A03

The objectives of the PCR experiment are: to test the hypothesis that microgravity will in fact affect the pattern and developmental progression of embryogenically competent plant cells from one well-defined, critical stage to another; to determine the effects of microgravity in growth and differentiation of embryogenic carrot cells grown in cell culture; to determine whether microgravity or the space environment fosters an instability of the differentiated state; and to determine whether mitosis and chromosome behavior are adversely affected by microgravity. The methods employed will consist of the following: special embryogenically competent carrot cell cultures will be grown in cell culture chambers provided by NASDA; four

cell culture chambers will be used to grow cells in liquid medium; two dishes (plant cell culture dishes) will be used to grow cells on a semi-solid agar support; progression to later embryonic stages will be induced in space via crew intervention and by media manipulation in the case of liquid grown cell cultures; progression to later stages in case of semi-solid cultures will not need crew intervention; embryo stages will be fixed at a specific interval (day 6) in flight only in the case of liquid-grown cultures; and some living cells and somatic embryos will be returned for continued post-flight development and 'grown-out.' These will derive from the semi-solid grown cultures. Author (revised)

N94-13765*# Showa Univ., Tokyo (Japan).
EFFECT OF LOW GRAVITY ON CALCIUM METABOLISM AND BONE FORMATION (L-7) **c52**
Tatsuo Suda *In* NASA. Marshall Space Flight Center, Spacelab J Experiment Descriptions Aug. 1993 p 177-178 (For primary document see N94-13732 02-29)
Avail: CASI HC A01/MF A03

Recently, attention has been focused on the disorders of bone and calcium metabolism during space flight. The skeletal system has evolved on the Earth under 1-g. Space flights under low gravity appear to cause substantial changes in bone and calcium homeostasis of the animals adapted to 1-g. A space experiment for the First Materials Processing Test (FMPT) was proposed to examine the effects of low gravity on calcium metabolism and bone formation using chick embryos loaded in a space shuttle. This space experiment was proposed based on the following two experimental findings. First, it has been reported that bone density decreases significantly during prolonged space flight. The data obtained from the US Skylab and the U.S.S.R. Salyut-6 cosmonauts have also documented that the degree of bone loss is related to the duration of space flight. Second, the US-Soviet joints space experiment demonstrated that the decrease in bone density under low gravity appears to be due to the decrease in bone formation rather than the increase in bone resorption. The purpose of our space experiment is, therefore, to investigate further the mechanisms of bone growth under low gravity using fertilized chick embryos. Author (revised)

N94-13766*# Kyoto Univ. (Japan). Radiation Biology Center.
GENETIC EFFECTS OF HZE AND COSMIC RADIATION (L-9) **c51**
Mituo Ikenaga *In* NASA. Marshall Space Flight Center, Spacelab J Experiment Descriptions Aug. 1993 p 181-184 (For primary document see N94-13732 02-29)
Avail: CASI HC A01/MF A03

The purpose of our experiment is to detect mutations in Drosophila possibly induced by space radiation during the SL-J mission, so that we will be able to obtain basic information about 'the genetic (mutational) risk of space radiation' which can be used to estimate human risk of cancer induction by space flight. As an example of somatic mutation, we will analyze morphological changes in hair growing on the surface of the wing of an adult fly. A piece of wing consists of about 30 thousand wing cells and in the wild type Drosophila a long single piece of hair is growing on the surface of each wing cell. When Drosophila is exposed to radiation as its early stage of development, such as embryonic stage or larval (maggot) stage, some mutations will appear in the wing hair of the adult fly with a certain low frequency, depending on the radiation dose. Among the mutations, the most frequent one is a change in the number of hairs per cell, that is, usually three or more hairs are coming out from a single wing cell. In the actual SL-J flight, we will install thousands of Drosophila larvae (maggots) into the Space Shuttle Discovery and expose them to space radiation during the 7-day mission. Immediately after the re-entry to the ground, these larvae are expected to develop (emerge) into adult flies. Then the wings will be fixed by ethylalcohol and permanent samples will be prepared. Finally, we will analyze the wing samples microscopically in order to detect mutations. Author (revised)

N94-13767*# National Aerospace Lab., Tokyo (Japan).
MANUAL CONTROL IN SPACE RESEARCH ON PERCEPTUAL-MOTOR FUNCTIONS UNDER ZERO GRAVITY CONDITIONS (L-10) **c54**
Akira Tada *In* NASA. Marshall Space Flight Center, Spacelab J Experiment Descriptions Aug. 1993 p 185-187 (For primary document see N94-13732 02-29)
Avail: CASI HC A01/MF A03

Are human abilities to control vehicles and other machines the same in space as those on Earth? The L-10 Manual Control Experiment of the First Materials Processing Tests (FMPT) started from this question. Suppose a pilot has the task to align the head of a space vehicle toward a target. His actions are to look at the target, to determine the vehicle movement, and to operate the manipulator. If the activity of the nervous system were the same as on Earth, the movements, of the eye and hand would become excessive because the muscles do not have to oppose gravity. The timing and amount of movement must be arranged for appropriate actions. The sensation of motion would also be affected by the loss of gravity because the mechanism of the otolith, the major acceleration sensor, depends on gravity. The possible instability of the sensation of direction may cause mistakes in the direction of control of manipulator movement. Thus, the experimental data can be used for designing man-machine systems in space, as well as for investigation of physiological mechanisms. In this experiment, the direction of vehicle heading is expressed by a light spot on an array of light emitting diodes and the manipulator is of a finger stick type. As the light spot moves up and down, the Japanese Payload Specialist, and the subject, must move the manipulator forward and backward to keep the movement of the light spot within the neighborhood of the central point of the display. The position of the light spot is computed in such a manner that when the stick is kept at the neutral position, a motion whose acceleration is proportional to the angle of deflection is added to the movement of the light spot. The Operator Describing Function, which is an expression of human control characteristics, can be calculated from 2 minutes of raw data of the light spot position and stick deflection. The 2 minutes of operation is called a run, and 8 runs with resting periods composes a session. The on-orbit experiment will be conducted on the second, fourth, and seventh days. One session of experiment of each of these days is conducted following the L-4 experiment, which uses the same apparatus. The Payload Specialist, aided by a Mission Specialist, will take our apparatus from a rack container, set up the apparatus, attach electrodes for measurements of eye movement and muscle activity, conduct the L-4 Visual Stability Experiment, conduct one session of the manual control experiment, and then dissemble and stow the apparatus. In addition to the flight experiment, pre-flight and post-flight experiments will be conducted. The data of three sessions on orbit will reflect adaption of physiological systems to microgravity. The data of post-flight experiments, on the other hand, will reflect re-adaptation of physiological systems to the gravity condition on the ground. Control data collected with and without psychological tension will be scheduled just prior to and long before launch. Author (revised)

N94-13768*# National Space Development Agency, Tokyo (Japan).
STUDY ON THE BIOLOGICAL EFFECT OF COSMIC RADIATION AND THE DEVELOPMENT OF RADIATION PROTECTION TECHNOLOGY (L-11) **c52**
Shunji Nagaoka *In* NASA. Marshall Space Flight Center, Spacelab J Experiment Descriptions Aug. 1993 p 189-196 (For primary document see N94-13732 02-29)
Avail: CASI HC A02/MF A03

NASDA is now participating in a series of flight experiments on Spacelab missions. The first experiment was carried out on the first International Microgravity Laboratory Mission (IML-1) January 1992, and the second experiment will be conducted on the Spacelab-J Mission, First Materials Processing Test (FMPT). The equipment or Radiation Monitoring Container Devices (RMCD) includes passive dosimeter systems and biological specimens. The experiments using this hardware are designed by NASDA to measure and investigate the radiation levels inside spacecraft like space shuttle and to look at the basic effects of the space environment from the aspect of radiation biology. The data gathered will be analyzed to understand the details of biological effects as well as the physical nature of space radiation registered in the sensitive Solid-State Track Detectors (SSTD). Author (revised)

N94-13769*# Shizuoka Univ. (Japan).
A CIRCADIAN RHYTHM OF CONIDIATION IN NEUROSPORA CRASSA (L-12) **c51**
Yashuhiro Miyoshi *In* NASA. Marshall Space Flight Center, Spacelab J Experiment Descriptions Aug. 1993 p 197-200 (For primary document see N94-13732 02-29)
Avail: CASI HC A01/MF A03

Two fungi growth chambers containing six growth tubes each are

used in this experiment. One chamber is for the space experiment; the other is for the simultaneous ground control experiment. The hyphae of Neurospora crassa band A mutant are inoculated at one end of each tube. Both the chambers are kept at 3 C plus or minus 1.5 C to stop hyphae growth until the Spacelab is activated. After the activation, each chamber is transferred simultaneously to the Spacelab and a phytotron in KSC and kept in continuous light at the same temperature. After about 24 hours of light exposure, each chamber is inserted into a growth chamber bag to keep it in constant darkness. The circadian rhythm of conidiation is initiated by this light to dark transition. After the dark incubation for 5 days at room temperature, both the growth chambers are kept at 3 C plus or minus 1.5 C to stop growth of the hyphae. After the space shuttle lands, both conidiation patterns are compared and analyzed. It has been known that numerous physiological phenomena show circadian rhythms. They are characterized by the fact that the oscillation can persist under constant conditions of light and temperature. Therefore, it has been accepted by most investigators that the generation mechanism of the circadian rhythm is endogeneous. However, one cannot reject the possibility that these rhythms are caused by some geophysical exogeneous factor having a 24-hour period, such as atmospheric pressure, gravity, or electromagnetic radiation. We use Neurospora crassa band A mutual which shows an obvious circadian rhythm in its spore-forming (conidiation) on the ground, and we intend to attempt the conidation of this mutant in the Spacelab where 24-hour periodicity is severely attenuated and to elucidate the effect of the geophysical exogeneous factor in the generation mechanism of the circadian rhythm. Author (revised)

N94-13770*# National Aeronautics and Space Administration. Ames Research Center, Moffett Field, CA.

AMPHIBIAN FERTILIZATION AND DEVELOPMENT IN MICROGRAVITY **c51**

Kenneth A. Souza *In* NASA. Marshall Space Flight Center, Spacelab J Experiment Descriptions Aug. 1993 p 201-207 (For primary document see N94-13732 02-29)

Avail: CASI HC A02/MF A03

During the year before launch, female frogs will be tested every 3 months for the quantity and quality of eggs produced. Two weeks or more prior to launch, male and female frogs will be transported to the John F. Kennedy Space Center (KSC). During the few weeks before launch, groups will be periodically tested for egg quality to assure that the frogs have adapted to the KSC laboratory environment. About 27 hours before launch, four females will be placed in a damp foam-lined box, called the Adult Frog Box (AFB), through which 100 cc/min of air wil be circulated. The AFB will be lowered into the Spacelab and loaded into the Frog Environmental Unit (FEU) during the final pre-launch preparations. A sperm suspension, for use in flight to fertilize the eggs, will also be prepared and loaded during the pre-launch period. The sperm suspension, together with a kit of syringes containing Human Chorionic Gonadotropin (HCG), will be stored in a refrigerator aboard the shuttle until needed in flight. On the first day of flight, the AFB will be transferred from the FEU to the General Purpose Work Station (GPWS), which is a type of glove box specially designed to allow the crew to use chemicals and biological materials during the flight without contaminating the shuttle/Spacelab environment. Inside the GPWS the four adult frogs will be injected with the HCG hormone and returned to the FEU. Approximately 16 hours after injection, ovulation should have taken place and 15 to 20 eggs from each frog will be placed on each of two egg baskets and covered with sperm for 10 minutes. The egg baskets are inserted into acrylic egg chambers and 50 ml of 'pond water' (20 percent strength Modified Ringers solution (is added. One of the chambers from each frog will be placed on a centrifuge within the FEU and rotated to simulate normal terrestrial gravity (1 g). The remaining chambers are incubated under microgravity conditions within the FEU. Forty minutes after fertilization, the four chambers exposed to 1 g will be removed and observed within the GPWS using a dissecting microscope and camera system. On the basis of egg rotation and egg appearance, the 'best' and 'second best' frogs will be selected to contribute additional eggs. Using the two best frogs, 22 egg chambers will be loaded with eggs and fertilized. Eleven chambers wil be incubated at microgravity and eleven will be incubated on the centrifuge. At various times during the flight, chambers will be removed from the FEU and transferred to the GPWS where a formaldehyde-based fixative will be injected in order to preserve important developmental stages for in depth study following the flight. Five of the 22 chambers plus the eight fertilization test chambers will be returned to Earth with live tadpoles. The swimming behavior of these free swimming tadpoles will be examined within several hours of landing and some will be fixed for a detailed analysis of their inner ear, the otolity, the animals 'balance system.' Lychakov and Vinikov reported an increase in otolith size in tadpoles that developed (but were not fertilized) in space. Live tadpoles from the SL-J flight will be raised through metamorphsis for studies of maturation including an analysis of the effects of space flight on their ability to produce normal progency. Following the flight, the fixed embryos will be serially sectioned and stained using procedures that were developed for this experiment. The embroys fixed at the 2-4 cell stage will be examined for the distribution of cytoplasmic contents, including the various classes of yolk platelets, and the location and shape of the cleavage furrows. The gastrulae will be assessed for the normality of the complex cellular rearrangements that constitute blastopore formation and involution, i.e., the differentiation of the embryo into its specialized body parts. Using a new procedure, the gastrulae will be bleached which will enable the initial sperm entry point (SEP) to be located. The correlation between the SEP and the dorsal lip of the blastopore will be determined. Under normal terrestrial conditions it was shown that the SEP typically is located on the side of the egg opposite the future dorsal side of the embryo. The neurulae will be examined for the normality and completeness of the neural plate and archenteron expansion. The tadpole stages will be used to study the allometry and morphology of the various organ systems. Author (revised)

N94-13771*# Baylor Coll. of Medicine, Houston, TX. Dept. of Medicine.

MAGNETIC RESONANCE IMAGING AFTER EXPOSURE TO MICROGRAVITY **c52**

Adrian LeBlanc *In* NASA. Marshall Space Flight Center, Spacelab J Experiment Descriptions Aug. 1993 p 209-211 (For primary document see N94-13732 02-29)

Avail: CASI HC A01/MF A03

A number of physiological changes were demonstrated in bone, muscle, and blood from exposure of humans and animals to microgravity. Determining mechanisms and the development of effective countermeasures for long-duration space missions is an important NASA goal. Historically, NASA has had to rely on tape measures, x-ray, and metabolic balance studies with collection of excreta and blood specimens to obtain this information. The development of magnetic resonance imaging (MRI) offers the possibility of greatly extending these early studies in ways not previously possible; MRI is also non-invasive and safe; i.e., no radiation exposure. MRI provides both superb anatomical images for volume measurements of individual structures and quantification of chemical/physical changes induced in the examined tissues. This investigation will apply MRI technology to measure muscle, intervertebral disc, and bone marrow changes resulting from exposure to microgravity. Author (revised)

N94-13772*# National Aeronautics and Space Administration. Lyndon B. Johnson Space Center, Houston, TX.

COUNTERMEASURE FOR REDUCING POST-FLIGHT ORTHOSTATIC INTOLERANCE: LOWER BODY NEGATIVE PRESSURE (LBNP) EXPERIMENT E140 **c52**

John B. Charles *In* NASA. Marshall Space Flight Center, Spacelab J Experiment Descriptions Aug. 1993 p 213-222 (For primary document see N94-13732 02-29)

Avail: CASI HC A02/MF A03

Investigators have shown that after 1-2 weeks of bed rest ingestion of 1000 ml of a salt water solution during 4 hours of continuous exposure to 30 mm Hg of lower body negative pressure will protect plasma volume and orthostatic function for up to 24 hours. We hypothesize that a similar countermeasure will reduce the effects of fluid loss induced by headward fluid shift during space flight. The objective of this flight experiment is to evaluate the efficacy of the proposed countermeasure in reversing these effects on the cardiovascular system. Lower Body Negative Pressure (LBNP) involves exposing the legs and lower abdomen to reduced air pressure. The LBNP device is an air-tight chamber that seals the subject's waist to enclose the lower body. As used in this experiment, LBNP provides both the candidate treatment as well as the means of assessing the effectiveness of the treatment. Author (revised)

N94-13773*# Saint Louis Univ., MO. School of Medicine.
BONE CULTURE RESEARCH **c52**
Nicola C. Partridge *In* NASA. Marshall Space Flight Center, Spacelab J Experiment Descriptions Aug. 1993 p 223-226 (For primary document see N94-13732 02-29)
Avail: CASI HC A01/MF A03

The experiments described are aimed at exploring PTH regulation of production of collagenase and protein inhibitors of collagenase (tissue inhibitors of metalloproteases, TIMP-1 and -2) by osteoblast-like osteosarcoma cells under conditions of weightlessness. The results of this work will contribute to information as to whether a microgravity environment alters the functions and responsiveness of the osteoblast. The objectives of the Bone Culture Research (BCR) experiment are: to observe the effects of microgravity on the morphology, rate of proliferation, and behavior of the osteoblastic cells, UMR 106-01; to determine whether microgravy affects the hormonal sensitivity of osteroblastic cells; and to measure the secretion of collagenase and its inhibitors into the medium under conditions of microgravity. The methods employed will consist of the following: the osteoblast-like cells, UMR-106-01, will be cultured in four NASDA cell culture chambers; two chambers will be subjected to microgravity on SL-J; two chambers will remain on the ground at KSC as ground controls but subjected to an identical set of culture conditions as on the shuttle; media will be changed four times; twice the cells will receive the hormone parathyroid hormone-related protein (PTHrP) and media collected; cells will be photographed under conditions of microgravity; and media and photographs will be analyzed upon return to determine whether functions of the cells changed. Author (revised)

N94-13774*# National Aeronautics and Space Administration. Lyndon B. Johnson Space Center, Houston, TX.
AUTOGENIC FEEDBACK TRAINING EXPERIMENT: A PREVENTATIVE METHOD FOR SPACE MOTION SICKNESS **c52**
Patricia S. Cowings *In* NASA. Marshall Space Flight Center, Spacelab J Experiment Descriptions Aug. 1993 p 227-248 (For primary document see N94-13732 02-29)
Avail: CASI HC A03/MF A03

Space motion sickness is a disorder which produces symptoms similar to those of motion sickness on Earth. This syndrome has affected approximately 50 percent of all astronauts and cosmonauts exposed to microgravity in space, but it differs from what is commonly known as motion sickness in a number of critical ways. There is currently no ground-based method for predicting susceptibility to motion sickness in space. Antimotion sickness drugs have had limited success in preventing or counteracting symptoms in space, and frequently caused debilitating side effects. The objectives were: (1) to evaluate the effectiveness of Autogenic-Feedback Training as a countermeasure for space motion sickness; (2) to compare physiological data and in-flight symptom reports to ground-based motion sickness data; and (3) to predict susceptibility to space motion sickness based on pre-flight data of each treatment group crew member. Author (revised)

N94-13775*# National Aeronautics and Space Administration. Lyndon B. Johnson Space Center, Houston, TX.
IN-FLIGHT DEMONSTRATION OF THE SPACE STATION FREEDOM HEALTH MAINTENANCE FACILITY FLUID THERAPY SYSTEM (E300/E05) **c54**
Charles W. Lloyd *In* NASA. Marshall Space Flight Center, Spacelab J Experiment Descriptions Aug. 1993 p 249-257 (For primary document see N94-13732 02-29)
Avail: CASI HC A02/MF A03

The Space Station Freedom (SSF) Health Maintenance Facility (HMF) will provide medical care for crew members for up to 10 days. An integral part of the required medical care consists of providing intravenous infusion of fluids, electrolyte solutions, and nutrients to sustain an ill or injured crew member. In terrestrial health care facilities, intravenous solutions are normally stored in large quantities. However, due to the station's weight and volume constraints, an adequate supply of the required solutions cannot be carried onboard SSF. By formulating medical fluids onboard from concentrates and station water as needed, the Fluid Therapy System (FTS) eliminates weight and volume concerns regarding intravenous fluids. The first full-system demonstration of FTS is continuous microgravity will be conducted in Spacelab-Japan (SL-J). The FTS evaluation consists of two functional objectives and an in-flight demonstration of intravenous administration of fluids. The first is to make and store sterile water and IV solutions onboard the spacecraft. If intravenous fluids are to be produced in SSF, successful sterilization of water and reconstituting of IV solutions must be achieved. The second objective is to repeat the verification of the FTS infusion pump, which had been performed in Spacelab Life Sciences - 1 (SLS-1). during SLS-1, the FTS IV pump was operated in continuous microgravity for the first time. The pump functioned successfully, and valuable knowledge on its performance in continuous microgravity was obtained. Finally, the technique of starting an IF in microgravity will be demonstrated. The IV technique requires modifications in microgravity, such as use of restraints for equipment and crew members involved. Author (revised)

N94-14026*# Pennsylvania State Univ., State College. Applied Research Lab.
THE FEASIBILITY OF PRODUCING ALUMINUM-LITHIUM STRUCTURES FOR CRYOGENIC TANKAGE APPLICATIONS BY LASER BEAM WELDING
R. P. Martukanitz and K. G. Lysher Apr. 1993 74 p Prepared in cooperation with the Space and Naval Warfare Systems Command, Washington, DC
(NASA Order L-4409-D; RTOP 505-63-50-03)
(NASA-CR-191527; NAS 1.26:191527; TM-93-067) Avail: CASI HC A04/MF A01

Aluminum-lithium alloys exhibit high strength, high elastic modulus, and low density as well as excellent cryogenic mechanical properties making them ideal material candidates for cryogenic tanks. NASA has proposed the use of 'built-up' structure for panels fabricated into cryogenic tanks replacing current conventional machining. Superplastically formed stiffeners would be joined to sheet (tank skin) that had been roll formed to the radius of the tank in order to produce panels. Aluminum-lithium alloys of interest for producing the built-up structure include alloy 2095-T6 stiffeners to 2095-T8 sheet and alloy 8090-T6 stiffeners to 2090-T83 sheet. Laser welding, with comparable joint properties, offers the following advantages over conventional welding: higher production rates, minimal degradation within the heat affected zones, and full process automation. This study established process parameters for laser beam welding, mechanical property determinations, metallographic characterization, and fabrication of prototype panels. Tensile tests representing partial penetration of the skin alloys provided joint efficiencies between 65 and 77 percent, depending upon alloy and degree of penetration. Results of tension shear tests of lap welds indicated that the combination of 2095-T6 to 2090-T8 exhibited significantly higher weld shear strength at the interface in comparison to welds of 8090-T6 to 2090-T83. The increased shear strength associated with 2095 is believed to be due to the alloy's ability to precipitation strengthening (naturally age) after welding. Author (revised)

31 ENGINEERING (GENERAL)

Includes vacuum technology; control engineering; display engineering; cryogenics; and fire prevention.

N94-13021# Air-Conditioning and Refrigeration Technology Inst., Inc., Arlington, VA.
ARTI REFRIGERANT DATABASE
J. M. Cain 30 Apr. 1993 121 p
(Contract DE-FG02-91CE-23810)
(DE93-014774; DOE/CE-23810/11D) Avail: CASI HC A06/MF A02

The Refrigerant Database consolidates and facilitates access to information to assist industry in developing equipment using alternative refrigerants. The underlying purpose is to accelerate the phase out of chemical compounds of environmental concern. The database provides bibliographic citations and abstracts for publications that may be useful in the research and design of air-conditioning and refrigeration equipment. The complete documents are not included. The database identifies sources of specific information on R-32, R-123, R-124, R-125, R-134, R-134a, R-141b, R-142b, R-143a, R-152a, R-245ca, R-290 (propane), R-717 (ammonia), ethers, and others as well as azeotropic and zeotropic blends of these fluids. It addresses lubricants including alkylbenzene, polyalkylene glycol, ester, and other synthetics as well as mineral oils. It also references documents addressing compatibility of refrigerants and lubricants with metals,

plastics, elastomers, motor insulation, and other materials used in refrigerant circuits. Incomplete citations or abstracts are provided for some documents to accelerate availability of the information and will be completed or replaced in future updates. DOE

N94-13141*# SatCon Technology Corp., Cambridge, MA.
A SUPERCONDUCTING LARGE-ANGLE MAGNETIC SUSPENSION Final Report
James R. Downer, George V. Anastas, Jr., Dariusz A. Bushko, Frederick J. Flynn, James H. Goldie, Vijay Gondhalekar, Timothy J. Hawkey, Richard L. Hockney, and Richard P. Torti Dec. 1992 328 p
(Contract NAS1-18853; SBIR-09.01-0540A; RTOP 324-02-01)
(NASA-CR-189735; NAS 1.26:189735) Avail: CASI HC A15/MF A03

SatCon Technology Corporation has completed a Small Business Innovation Research (SBIR) Phase 2 program to develop a Superconducting Large-Angle Magnetic Suspension (LAMS) for the NASA Langley Research Center. The Superconducting LAMS was a hardware demonstration of the control technology required to develop an advanced momentum exchange effector. The Phase 2 research was directed toward the demonstration for the key technology required for the advanced concept CMG, the controller. The Phase 2 hardware consists of a superconducting solenoid ('source coils') suspended within an array of nonsuperconducting coils ('control coils'), a five-degree-of-freedom positioning sensing system, switching power amplifiers, and a digital control system. The results demonstrated the feasibility of suspending the source coil. Gimballing (pointing the axis of the source coil) was demonstrated over a limited range. With further development of the rotation sensing system, enhanced angular freedom should be possible. Author (revised)

N94-13407# Iowa State Univ. of Science and Technology, Ames. Dept. of Mechanical Engineering.
MISCIBILITY OF LUBRICANTS WITH REFRIGERANTS, PHASE 1
M. B. Pate, S. C. Zoz, and L. J. Berkenbosch Oct. 1992 58 p Prepared for Air-Conditioning and Refrigeration Technology Inst., Inc., Arlington, VA
(Contract DE-FG02-91CE-23810)
(DE93-014766-Phase-1; DOE/CE-23810/6) Avail: CASI HC A04/MF A01

Miscibility data have been obtained for a variety of non-CFC refrigerants and their potential lubricants. Ten different refrigerants and seven different lubricants were investigated. Experiments are being performed in two phases: phase 1, reported herein, focuses on performing screening tests for miscibility; and phase 2 consists of developing miscibility plots. The miscibility tests are being performed in a test facility consisting of a series of miniature test cells submerged in a constant temperature bath. The bath temperature can be precisely controlled over a temperature range of -50 to 90 C (-58 to 194 F). The test cells are constructed to allow for complete visibility of lubricant-refrigerant mixtures under all test conditions. DOE

N94-13684# National Research Council of Canada, Ottawa (Ontario). Industrial Materials Inst.
EFFECT OF STABILIZATION ON THE RECYCLING OF POLYOLEFINS IN BLOW MOULDING
L. Pecora and R. W. DiRaddo Mar. 1993 41 p
(IMI-93RT-42400-1477-G; CTN-93-60820) Avail: CASI HC A03/MF A01

Extrusion blow molding experiments were conducted on two polyolefins to demonstrate two classes of degradation that occurs during the recycling or reprocessing of polymers. The two main degradation reactions that reduce product performance are chain scission and crosslinking. Polyethylene undergoes both chain scission and crosslinking, while polypropylene undergoes only chain scission. The degradation reactions cause a shift in the molecular weight distribution of the material in question. This material property shift generally affects parison swell and sag. The changes in parison formation behavior manifest themselves in the final blow molded part. The use of appropriate stabilizers can minimize these changes and render the final part acceptable. Also, the use of stabilization can allow an increase in the amount of recycled feedstock in the final product.
Author (CISTI)

N94-13790*# National Aeronautics and Space Administration. Ames Research Center, Moffett Field, CA.
DYNAMIC FORMS. PART 1: FUNCTIONS
George Meyer and G. Allan Smith Aug. 1993 86 p
(RTOP 505-64-52)
(NASA-TP-3397; A-93078; NAS 1.60:3397) Avail: CASI HC A05/MF A01

The formalism of dynamic forms is developed as a means for organizing and systematizing the design control systems. The formalism allows the designer to easily compute derivatives to various orders of large composite functions that occur in flight-control design. Such functions involve many function-of-a-function calls that may be nested to many levels. The component functions may be multiaxis, nonlinear, and they may include rotation transformations. A dynamic form is defined as a variable together with its time derivatives up to some fixed but arbitrary order. The variable may be a scalar, a vector, a matrix, a direction cosine matrix, Euler angles, or Euler parameters. Algorithms for standard elementary functions and operations of scalar dynamic forms are developed first. Then vector and matrix operations and transformations between parameterization of rotations are developed in the next level in the hierarchy. Commonly occurring algorithms in control-system design, including inversion of pure feedback systems, are developed in the third level. A large-angle, three-axis attitude servo and other examples are included to illustrate the effectiveness of the developed formalism. All algorithms were implemented in FORTRAN code. Practical experience shows that the proposed formalism may significantly improve the productivity of the design and coding process.
Author (revised)

N94-13798*# Michigan Univ., Ann Arbor. Dept. of Mechanical Engineering.
APPLICATION OF SYMBOLIC AND ALGEBRAIC MANIPULATION SOFTWARE IN SOLVING APPLIED MECHANICS PROBLEMS
Wen-Lang Tsai and Noboru Kikuchi Aug. 1993 164 p Sponsored by NASA. Washington
(Contract NCA2-136)
(NASA-CR-4544; A-93112; NAS 1.26:4544) Avail: CASI HC A08/MF A02

As its name implies, symbolic and algebraic manipulation is an operational tool which not only can retain symbols throughout computations but also can express results in terms of symbols. This report starts with a history of symbolic and algebraic manipulators and a review of the literatures. With the help of selected examples, the capabilities of symbolic and algebraic manipulators are demonstrated. These applications to problems of applied mechanics are then presented. They are the application of automatic formulation to applied mechanics problems, application to a materially nonlinear problem (rigid-plastic ring compression) by finite element method (FEM) and application to plate problems by FEM. The advantages and difficulties, contributions, education, and perspectives of symbolic and algebraic manipulation are discussed. It is well known that there exist some fundamental difficulties in symbolic and algebraic manipulation, such as internal swelling and mathematical limitation. A remedy for these difficulties is proposed, and the three applications mentioned are solved successfully. For example, the closed from solution of stiffness matrix of four-node isoparametrical quadrilateral element for 2-D elasticity problem was not available before. Due to the work presented, the automatic construction of it becomes feasible. In addition, a new advantage of the application of symbolic and algebraic manipulation found is believed to be crucial in improving the efficiency of program execution in the future. This will substantially shorten the response time of a system. It is very significant for certain systems, such as missile and high speed aircraft systems, in which time plays an important role. Author (revised)

N94-13889# Sandia National Labs., Albuquerque, NM.
A PERSPECTIVE ON AVS IN AN ENGINEERING SCIENCES ENVIRONMENT
M. W. Glass 1993 10 p Presented at the Application Visualization System (AVS) 1993 Users Group Meeting, Orlando, FL, 24-26 May 1993
(Contract DE-AC04-76DP-00789)
(DE93-015011; SAND-93-1002C; CONF-9305168-3) Avail: CASI HC A02/MF A01

At Sandia National Laboratories, the Engineering Sciences Center has made a commitment to integrate the Application Visualization System (AVS) into our computing environment as the primary tool for scientific visualization. AVS will be used on an everyday basis by a broad spectrum of users ranging from the occasional computer user to AVS module developers.

Additionally, AVS will be used to visualize structured grid, unstructured grid, gridless, 1D, 2D, 3D, steady-state, transient, computational, and experimental data. The following is one user's perspective on how AVS meets this task. Several examples of how AVS is currently being utilized will be given along with some future directions. DOE

N94-14055# Technical Research Centre of Finland, Espoo. Building Lab.

TRANSITION OF BUILDING ENERGY CONSUMPTION USING MULTI-INPUT, SINGLE-OUTPUT DYNAMIC MODEL

Jouko Pakanen Oct. 1992 46 p Sponsored by Ministry of Trade and Industry, Finland

(VTT-PUBS-116; ISBN-9-51-384234-7; ETN-93-94485) Avail: CASI HC A03/MF A01

A new method based upon online measurements of weather and other characteristic data is proposed. The method is capable of being used with building automation systems for failure detection. The method uses a multi input, single output dynamic model to predict the power fluctuation of the building. The model parameters are identified recursively by measuring the actual power, outdoor temperature, solar radiation, wind velocity, and indoor temperatures. The stochastic variations in power caused by occupants, equipment, and lights, can be included in the model. Measurements are taken once every half hour and are used to update the model parameters by a recursive extended least square algorithm. The identified model can be used to detect failures of equipment and systems. Verification of the method was accomplished using real weather data and the TARP computer program for the simulation of a town house and measurements collected from a real test building. ESA

N94-14070# National Research Council of Canada, Ottawa (Ontario). Industrial Materials Inst.

AN EXPERIMENTAL STUDY ON THE EFFECT OF DIE GEOMETRY ON SWELL AND SAG IN THE PARISON EXTRUSION STAGE

L. Pecora and R. W. DiRaddo 15 Jan. 1993 34 p

(IMI-93RT-42400-1476-G; NRC-35347; CTN-93-60819) Avail: CASI HC A03/MF A01

Extrusion blow molding is the process of choice for production of many hollow parts. The process involves extrusion of a molten parison and inflation of the parison into the final part, whereupon the part is cooled and ejected. The ability to predict parison behavior is important as the parison dimensions govern the shape and thickness distribution of the final product. The effect of die geometry on parison swell and sag was studied in experiments employing three diverging dies of 3.5 cm diameter. Three mandrel angles were studied, being 25, 30, and 40 deg from the vertical. For each die angle, six gaps ranging from 0.3 to 2.0 mm were studied. The material used was a blow molding high density polyethylene grade. Preliminary results were obtained showing that the sag increases and the swell decreases as the die gap is increased. Swell was found to increase as die angle increased. The parison swell depends directly on the shear and extensional components in the die. The extensional component has a stronger effect than shear for a given level of stress. Author (CISTI)

N94-14410*# National Aeronautics and Space Administration, Washington, DC.

NASA METROLOGY AND CALIBRATION, 1993

1993 608 p Proceedings of the Sixteenth Annual Workshop held in Rockville, MD, 20-22 Apr. 1993

(NASA-TM-109280; NAS 1.15:109280) Avail: CASI HC A99/MF A06

Th sixteenth annual workshop of NASA's Metrology and Calibration Working Group was held April 20-22, 1993. The goals of the Working Group are to provide Agencywide standardization of individual metrology programs, where appropriate; to promote cooperation and exchange of information within NASA, with other Government agencies, and with industry; to serve as the primary Agency interface with the National Institute of Standards and Technology; and to encourage formal quality control techniques such as Measurement Assurance Programs. These proceedings contain unedited reports and presentations from the workshop and are provided for information only. Derived from text

N94-14592# Los Alamos National Lab., NM.

A RECUPERATIVE SUPERFLUID STIRLING REFRIGERATOR

J. G. Brisson and G. W. Swift 1993 6 p Presented at the International Cryogenic Engineering Conference and International Cryogenic Materials Conference, Albuquerque, NM, 12-16 Jul. 1993

(Contract W-7405-eng-36)

(DE93-016521; LA-UR-93-2415; CONF-930703-2) Avail: CASI HC A02/MF A01

A superfluid Stirling refrigerator has been built with a counterflow heat exchanger serving as a recuperative regenerator. It has achieved temperatures of 296 mK with a 4% He-3 - He-4 mixture. Cooling power versus temperature and speed is presented for a 6.6% mixture. DOE

N94-14808# Technische Univ., Eindhoven (Netherlands). Facultaet Bouwkunde.

FLEXIBILITY AND COSTS IN THE DESIGN PROCESS: A DECISION SUPPORT MODEL Ph.D. Thesis [FLEXIBILITEIT EN KOSTEN IN HET ONTERWERPPROCES: EEN BESLUITVORMINGONDERSTEUNEND MODEL]

Matthijs Prins 1992 166 p In DUTCH Sponsored by Netherlands Technology Foundation

(ISBN-9-06-814522-3; ETN-93-94047) Copyright Avail: CASI HC A08/MF A02

A decision support system was developed to increase flexibility and reduce costs in the design process of buildings. The most important terminology is presented as a set of building blocks to support the theory. Quality control is becoming increasingly more important in view of decreasing quantitative demands, increasing qualitative demands for differentiation in buildings, and shrinking financial means. Several terms related to the time dimension of buildings are discussed. Buildings are described in terms of systems (consisting of individual elements) and building oriented flexibility models. A financial economic calculating model for buildings is presented. The process model implements the flexibility model and the calculation method in a decision support system. Suggestions for further research are given. ESA

N94-14877# Aerospace Corp., El Segundo, CA. Engineering and Technology Group.

DOUBLE INLET PULSE TUBE CRYOCOOLER THEORY

Harold Mirels 2 Feb. 1993 27 p

(AD-A266832; ATR-93(8399)-2) Avail: CASI HC A03/MF A01

An analytical model has been developed for the performance of a double inlet pulse tube cryocooler employing a stepped piston compressor. Numerical results are presented as a function of the area ratio of the stepped piston. The double inlet pulse tube cryocooler is shown to have more refrigeration power than the corresponding single inlet device. However, the increased refrigeration power is achieved at the cost of reduced thermal efficiency. DTIC

32 COMMUNICATIONS AND RADAR

Includes radar; land and global communications; communications theory; and optical communications.

For related information see also *04 Aircraft Communications and Navigation* and *17 Space Communications, Spacecraft Communications, Command and Tracking.* For search and rescue see *03 Air Transportation and Safety,* and *16 Space Transportation.*

N94-12804*# National Aeronautics and Space Administration. Langley Research Center, Hampton, VA.

THE MRIS FEASIBILITY STUDY

Robert T. Neece, Aubrey E. Cross (Research Triangle Inst., Hampton, VA.), and James H. Schrader (Research Triangle Inst., Hampton, VA.) Jun. 1993 72 p

(RTOP 505-64-12-04)

(NASA-TM-107763; NAS 1.15:107763) Avail: CASI HC A04/MF A01

The Microwave Reflectometer Ionization Sensor (MRIS) is an instrument being developed for use in detecting and ranging of electron density layers in the reentry plasma of a space transfer vehicle. The rationale for the selection of the Double Sideband Suppressed Carrier (DSBSC) system used in the feasibility study for the MRIS is presented. A 25 GHz single-oscillator system and a 220 GHz double-oscillator system are described. The 25 GHz system was constructed and tested in the laboratory

and test results are presented. As developed, the system employs a sideband spacing of 160 MHz. Based on an estimated electromagnetic wave velocity in the plasma, a round-trip phase shift measurement accuracy of +/- 7.6 degrees was required for the desired +/- 1/2 cm distance measurement accuracy. The interaction of parallel ground and reflecting planes produces interference that prevents the basic DSBSC system from meeting the accuracy goal so a frequency modulation was added to the system to allow averaging of the measured phase deviation. With an FM deviation of +/- 1 GHz, laboratory measurements were made for distances from 5 to 61 cm tip free space. Accounting for the plasma velocity factor, 82 percent of the data were equal to or better than the desired accuracy. Based on this measured result a sideband spacing to 250 MHz could be expected to yield data approximately 96 percent within the accuracy goal.
Author (revised)

N94-12811*# National Aeronautics and Space Administration. Langley Research Center, Hampton, VA.
THE 24 GHz MEASUREMENTS OF 2.2 LAMBDA CONICAL HORN ANTENNAS ILLUMINATING A CONDUCTING SHEET
A. E. Cross (Research Triangle Inst., Hampton, VA.), R. E. Marshall (Research Triangle Inst., Hampton, VA.), C. P. Hearn, and R. T. Neece Jun. 1993 66 p
(RTOP 505-64-12-04)
(NASA-TM-109002; NAS 1.15:109002) Avail: CASI HC A04/MF A01

Monostatic reflection-coefficient magnitude, absolute value of Gamma, measurements occurring between a radiating horn and a metal reflecting plate are presented for a family of three 2.2 lambda diameter conical horn antennas. The three horns have different aperture phase deviations: 6 deg, 22.5 deg, and 125 deg. Measurements of the magnitude of absolute value of Gamma as a function of horn-plate separation (d) extend from an effective antenna aperture short (d = O) to beyond the far-field boundary (d = 2D(sup 2)/lambda, where D is the antenna diameter). Measurement data are presented with various physical environments for each of the horns. Measured scalar data are compared with theoretical data from two models, a numerical model for a circular waveguide aperture in a ground plane and a scalar diffraction theory model. This work was conducted in support of the development effort for a spaceborne multifrequency microwave reflectometer designed to accurately determine the distance from a space vehicle's surface to a reflecting plasma boundary. The metal reflecting plate was used to simulate the RF reflectivity of a critically dense plasma. The resulting configuration, a ground plane mounted aperture facing a reflecting plane in close proximity, produces a strong interaction between the ground plane and the reflecting plate, especially at integral half-wavelength separations. The transition coefficient is characterized by large amplitude variations. Author (revised)

N94-12920*# Georgia Inst. of Tech., Atlanta. School of Electrical Engineering.
RECURSIVE TIME-VARYING FILTER BANKS FOR SUBBAND IMAGE CODING
Mark J. T. Smith and Wilson C. Chung 1992 20 p
(Grants NAG5-2187; NSF MIP-91-16113)
(NASA-CR-193726; NAS 1.26:193726) Avail: CASI HC A03/MF A01

Filter banks and wavelet decompositions that employ recursive filters have been considered previously and are recognized for their efficiency in partitioning the frequency spectrum. This paper presents an analysis of a new infinite impulse response (IIR) filter bank in which these computationally efficient filters may be changed adaptively in response to the input. The filter bank is presented and discussed in the context of finite-support signals with the intended application in subband image coding. In the absence of quantization errors, exact reconstruction can be achieved and by the proper choice of an adaptation scheme, it is shown that IIR time-varying filter banks can yield improvement over conventional ones.
Author (revised)

N94-12925 British Broadcasting Corp., Kingswood (England). Research Dept.
DIGITAL SOUND: THE SELECTION OF CRITICAL PROGRAMME MATERIAL AND PREPARATION OF RECORDINGS FOR CCIR TESTS ON LOW BIT-RATE CODECS
N. H. C. Gilchrist 1993 13 p
(BBC-RD-1993/1) Avail: Issuing Activity

A draft of a new recommendation on low bit-rate digital audio coding for broadcasting is in preparation within CCIR Study Group 10. As part of this work, subjective tests are being conducted to determine the preferred coding systems to be used in the various applications, and at which bit rates they should be used. The BBC has been contributing to the work by conducting preliminary listening tests to select critical program material, and by preparing recordings using this material for use by the CCIR's testing centers. Derived from text

N94-12926 British Broadcasting Corp., Kingswood (England). Research Dept.
DIGITAL SOUND: SUBJECTIVE TESTS ON COMMENTARY-QUALITY CODECS
N. H. C. Gilchrist and A. J. Oxenham 1993 16 p
(BBC-RD-1993/2) Avail: Issuing Activity

Subjective tests have been carried out on five commentary-quality audio codecs on behalf of CCIR Task Group 10/2. All codecs operated at a bit rate of 60 kbit/s per mono signal, and were tested in both mono and stereo configurations. Significant differences in performance were found. All codecs introduced some impairment on the most critical program items.
Derived from text

N94-13090*# Jet Propulsion Lab., California Inst. of Tech., Pasadena.
ENVIRONMENTAL PROJECTS. VOLUME 15: ENVIRONMENTAL ASSESSMENT: PROPOSED 1-MEGAWATT RADAR TRANSMITTER AT THE MARS SITE
15 Oct. 1992 112 p
(Contract NAS7-918)
(NASA-CR-194098; JPL-Publ-87-4-Vol-15; NAS 1.26:194098) Avail: CASI HC A06/MF A02

The Goldstone Deep Space Communications Complex (GDSCC), located in the Mojave Desert about 64.5 km (40 mi) north of Barstow, California. and about 258 km (160 mi) northeast of Pasadena, California, is part of the National Aeronautics and Space Administration's (NASA's) Deep Space Network (DSN), one of the world's larger and more sensitive scientific telecommunications and radio navigation networks. The Goldstone Complex is managed, technically directed, and operated for NASA by the Jet Propulsion Laboratory (JPL) of the California Institute of Technology in Pasadena, California. Activities at the GDSCC support the operation of six parabolic dish antennas located at five separate sites called Deep Space Stations (DSS's). Four sites, named Echo, Mars, Uranus, and Apollo, are operational for space missions, while the remaining Venus Site is devoted to research and development activities. The Mars Site at the GDSCC contains two antennas: the Uranus antenna (DSS 15, 34 m) and the Mars antenna (DSS 14, 70 m). This present volume deals solely with the DSS-14 Mars antenna. The Mars antenna not only can act as a sensitive receiver to detect signals from spacecraft, but it also can be used in radar astronomy as a powerful transmitter to send out signals to probe the solar system. At present, the Mars antenna operates as a continuous-wave microwave system at a frequency of 8.51 GHz at a power level of 0.5 MW. JPL has plans to upgrade the Mars antenna to a power level of 1 MW. Because of the anticipated increase in the ambient levels of radio frequency radiation (RFR), JPL retained Battelle Pacific Northwest Laboratories (BPNL), Richland, Washington, to conduct an environmental assessment with respect to this increased RFR. This present volume is a JPL-expanded version of the BPNL report titled Environmental Assessment of the Goldstone Solar System Radar, which was submitted to JPL in Nov. 1991. This BPNL report concluded that the operation of the upgraded Mars antenna at the GDSCC, with its increased potential electromagnetic radiation hazards and interferences, would have no significantly adverse biological, physical, or socioeconomic effects on the environment. Thus, a Finding of No Significant Impact (FONSI) is appropriate in accordance with local, State, Federal, and NASA environmental rules and regulations. Author (revised)

N94-13195 Tel-Aviv Univ. (Israel). Dept. of Computer Science.
ON THE END-TO-END COMMUNICATION PROBLEM IN UNRELIABLE NETWORKS M.S. Thesis
Adi Rosen Jun. 1990 33 p
(ITN-93-85188) Copyright Avail: Issuing Activity (Tel Aviv Univ., Exact Sciences Library, Ramat Aviv 69978, Israel)

Several protocols are presented to solve the end-to-end communication problem across an unreliable network. A protocol solving the problem is to

transmit from a sender to a receiver a sequence of data items input to the sender in an on-line manner. The difficulty in solving the problem in unreliable networks lies in the fact that one cannot rely on any specific path between the sender and the receiver to be operational. This work is centered around a simple method to deliver tokens between two communicating parties in an unreliable network. The token delivery protocol, called SLIDE, guarantees that, at any time, the network holds, at most, a bounded number of tokens and that no token is lost. When the network is full, the sender is prohibited from inputting more tokens until the receiver removes some. However, tokens are output at the receiver by the SLIDE, not necessarily in the same order in which they were input (i.e., the SLIDE is non-FIFO (first-in, first-out)). Basing ourselves on these properties of the SLIDE, we present a sequence of three end-to-end protocols. The first protocol is very simple, and its bit communication complexity per data item is O(n(exp 2)mD) bits, where n and m are the total number of nodes and links in the network, respectively, and D is the size in bits of the data item. However, it is data dependent, that is, the content of the data items is used by the protocol. The second protocol obtains the same bit communication complexity, but uses colors on the tokens to remove the data dependency of our first protocol. For large data items (D = Omega(nm logn)), where the performances of the first two algorithms degrade, we develop a third algorithm whose communication complexity is linear, O(nD) bits, per data item. This protocol combines techniques of the two first algorithms with the Information Dispersal Algorithm of Rabin. By collecting many data itsm of smaller size into one item of at least Omega(nm log n) bits, a linear (O(nD)) amortized bit communication complexity protocol can be obtained. Author (ISA)

N94-13196 Tel-Aviv Univ. (Israel). Dept. of Electronic Communications, Control and Computer Systems.

LOWER BOUNDS ON TIME OF ARRIVAL ESTIMATION OF PULSE COMPRESSION WAVEFORMS M.S. Thesis

Israel Ben-Ivri Apr. 1990 237 p In HEBREW

(ITN-93-85189) Copyright Avail: Issuing Activity (Tel-Aviv Univ., Exact Sciences Library, Ramat Aviv 69978, Israel)

The Weiss-Weinstein Lower Bound (WWLB), the Bellini-Tartara Lower Bound (BTLB), and the Kotelnikov inequality were applied to analysis of the attainable error in estimating the time of arrival (TOA) of a known (deterministic) signal embedded in additive Gaussian noise. The main advantage of the above bounds over the commonly used Cramer-Rao Lower Bound (CRLB) is that they can be applied to analysis of the estimation error over a wide range of signal to noise ratios (SNR), including threshold effects and ambiguity phenomena. The results of the above analysis were applied to TOA estimation using linear FM (frequency modulation) and Barker-13, which are typical pulse compression waveforms used in radar systems. For each signal, the estimation errors were evaluated for sampling and estimation of a baseband signal and of a bandpass signal. For baseband signals, the SNR domain comprises three regions: the local error domain in which the mean standard error (MSE) is described by the CRLB or an alternative; a threshold effect region where the MSE increases sharply; and a noise-dominated region. In the case of bandpass signals, two distinct threshold phenomena divide the SNR domain into five distinct regions: a Cramer-Rao region in which the MSE converges to CRLB; a region of transition from ambiguous estimation to local error estimation; an ambiguity dominated region in which an estimate can be obtained by using the envelope of the received signal; a threshold effect region in which there is a sharp increase in the MSE; and a noise dominated region in which the signal observations are essentially useless to estimation. Closed form analytical expressions for the threshold points SNR as functions of signal bandwidth, center frequency, and a-priori parameter domain, are obtained. We also derive lower bounds on the probability of occurrence of large estimation errors in the system. Comparison with the maximum likelihood (ML) estimator (that is the matched filter) reveals that the lower bounds are tight for a wide range of SNR conditions, and that the matched filter is near optimal above the threshold. Author (ISA)

N94-13236*# Michigan Univ., Ann Arbor. Dept. of Electrical Engineering and Computer Science.

A HYBRID FINITE ELEMENT-BOUNDARY INTEGRAL FOR THE ANALYSIS OF CAVITY-BACKED ANTENNAS OF ARBITRARY SHAPE

Jian Gong, John L. Volakis, A. C. Woo, and H. T. G. Wang Aug. 1993 36 p

(Contract NCA2-653)

(NASA-CR-193719; NAS 1.26:193719; UMICH-028918-5-T) Avail: CASI HC A03/MF A01

This is the final report on this project which was concerned with the analysis of cavity-backed antennas and more specifically spiral antennas. The project was a continuation of a previous analysis, which employed rectangular brick elements, and was, thus, restricted to planar rectangular patch antennas. A total of five reports were submitted under this project and we expect that at least four journal papers will result from the research described in these reports. The abstracts of the four previous reports are included. The first of the reports (028918-1-T) is over 75 pages and describes the general formulation using tetrahedral elements and the computer program. Report 028918-2-T was written after the completion of the computer program and reviews the capability of the analysis and associated software for planar circular rectangular patches and for a rectangular planar spiral. Measurements were also done at the University of Michigan and at Mission Research Corp. for the purpose of validating the software. We are pleased to acknowledge a partial support from Mission Research Corp. in carrying out the work described in this report. The third report (028918-3-T) describes the formulation and partial validation (using 2D data) for patch antennas on a circular platform. The 3D validation and development of the formulation for patch antennas on circular platforms is still in progress. The fourth report (028918-4-T) is basically an invited journal paper which will appear in the 'J. Electromagnetic Waves and Applications' in early 1994. It describes the application of the finite element method in electromagnetics and is primarily based on our work here at U-M. This final report describes the culmination of our efforts in characterizing complex cavity-backed antennas on planar platforms. The report describes for the first time the analysis of non-planar spirals and non-rectangular slot antennas as well as traditional planar patch antennas. The comparisons between measurements and calculations are truly impressive. Another unique aspect of this work is the incorporation of the FFT as part of the BiCG solver by overlaying a structured triangular mesh over the unstructured mesh. The implementation of this BiCG-FFT solution algorithm is important in minimizing the CPU and storage requirements. This final report will be submitted for publication in a refereed journal. Derived from text

N94-13237 Tel-Aviv Univ. (Israel). Dept. of Electrical Engineering and Electronics.

INDUCED VOLTAGES AT AIR GAPS DUE TO ELECTROMAGNETIC FIELD CAUSED BY DIRECT AND INDIRECT LIGHTNING STROKES M.S. Thesis

David Berla Dec. 1991 116 p In HEBREW

(ITN-93-85203) Copyright Avail: Issuing Activity (Tel-Aviv Univ., Exact Sciences Library, Ramat Aviv 69978, Israel)

During the last two decades there has been great development in power systems, electronic devices, and circuits, which are all sensitive to overvoltages caused by switching, induction, or atmospheric phenomena. In the present work, the induced voltages in a given configuration, due to direct and indirect lightning strokes were studied, from the point of view of the design requirements for economically and electrically optimal protective elements and devices. An approximate method is presented for calculating induced voltages, based on the electromagnetic field concept and using a system of compensating currents (CC). In the first part of the thesis, the basic equations of induced electric field strength components, due to current or charge waves, are introduced. These waves have a step-function character, and the mechanism of compensating currents, and their influence on the electromagnetic field are discussed. The second part of the thesis deals with the calculation of the induced voltages at air gaps in two geometrical models. The calculations are based on primary vectors describing the changes of the induced voltages at the air gap, due to the current on the main conductor and the compensating currents at the conducting loop and their mutual interactions. The main aim of this work was to develop a method, suitable for use with a personal computer, for calculating the induced voltage at an air gap, in a given geometrical model. Author (ISA)

N94-13264*# Chicago Univ., IL. Dept. of Electrical Engineering and Computer Science.

COMPUTER CODE FOR SCATTERING FROM IMPEDANCE BODIES OF REVOLUTION. PART 3: SURFACE IMPEDANCE WITH s AND PHI VARIATION. ANALYTICAL AND NUMERICAL RESULTS

Piergiorgio L. E. Uslenghi, Sharad R. Laxpati, and Stephen F. Kawalko

Jun. 1993 89 p
(Grants NAG2-544; NSF ECS-93-0000N)
(NASA-CR-193396; NAS 1.26:193396; EML-93-6-1) Avail: CASI HC A05/MF A01

The third phase of the development of the computer codes for scattering by coated bodies that has been part of an ongoing effort in the Electromagnetics Laboratory of the Electrical Engineering and Computer Science Department at the University of Illinois at Chicago is described. The work reported discusses the analytical and numerical results for the scattering of an obliquely incident plane wave by impedance bodies of revolution with phi variation of the surface impedance. Integral equation formulation of the problem is considered. All three types of integral equations, electric field, magnetic field, and combined field, are considered. These equations are solved numerically via the method of moments with parametric elements. Both TE and TM polarization of the incident plane wave are considered. The surface impedance is allowed to vary along both the profile of the scatterer and in the phi direction. Computer code developed for this purpose determines the electric surface current as well as the bistatic radar cross section. The results obtained with this code were validated by comparing the results with available results for specific scatterers such as the perfectly conducting sphere. Results for the cone-sphere and cone-cylinder-sphere for the case of an axially incident plane were validated by comparing the results with the results with those obtained in the first phase of this project. Results for body of revolution scatterers with an abrupt change in the surface impedance along both the profile of the scatterer and the phi direction are presented. Author (revised)

N94-13466*# Georgia Inst. of Tech., Atlanta. School of Electrical Engineering.
EXACT RECONSTRUCTION ANALYSIS/SYNTHESIS FILTER BANKS WITH TIME-VARYING FILTERS
J. L. Arrowood, Jr. and M. J. T. Smith 1993 4 p
(Grants NAG5-2187; NSF MIP-91-16113)
(NASA-CR-193725; NAS 1.26:193725) Avail: CASI HC A01/MF A01

This paper examines some of the analysis/synthesis issues associated with FIR time-varying filter banks where the filter bank coefficients are allowed to change in response to the input signal. Several issues are identified as being important in order to realize performance gains from time-varying filter banks in image coding applications. These issues relate to the behavior of the filters as transition from one set of filter banks to another occurs. Lattice structure formulations for the time varying filter bank problem are introduced and discussed in terms of their properties and transition characteristics. Author (revised)

N94-13488 Carleton Univ., Ottawa (Ontario). Dept. of Electronics.
FINE TIME UPLINK SYNCHRONIZATION FOR FREQUENCY-HOPPED SPREAD SPECTRUM SATELLITE COMMUNICATION SYSTEM M.S. Thesis
Rolands Eriks Ezers Aug. 1989 132 p
(ISBN-0-315-54370-1; CTN-93-60722) Copyright Avail: Issuing Activity (Micromedia Ltd., Technical Information Centre, 165 Hotel de Ville, Place du Portage, Phase 2, Hull, Quebec J8X 3X2, Canada HC)

A fine time uplink synchronization scheme for a frequency hopped spread spectrum satellite communication system has been implemented in a hardware based laboratory experiment. The experiment is implemented using an analog surface acoustic wave spectrum analyzer. The synchronization scheme employed is the two-tone method. Measurements are taken using the two-tone method with and without bias reduction. Experimental results taken using the method without bias reduction lead to an inconsistent estimator for the actual timing error. The method with bias reduction produces a consistent estimator for the actual timing error. The experimental results from the method with bias reduction have been compared with simulated results generated from theory. The two results agree very well. Thus, the two-tone method is a viable method for fine time uplink synchronization. Author (CISTI)

N94-13489 Carleton Univ., Ottawa (Ontario). Dept. of Electronics.
A COMBINED ANALOGUE AND DIGITAL PULSE COMPRESSION SYSTEM USING LARGE TIME BANDWIDTH PRODUCT SIGNALS FOR USE IN SYNTHETIC APERTURE RADAR M.S. Thesis
Pushkar E. Godbole 5 Jul. 1989 148 p
(ISBN-0-315-54373-6; CTN-93-60723) Copyright Avail: Issuing Activity (Micromedia Ltd., Technical Information Centre, 165 Hotel de Ville, Place du Portage, Phase 2, Hull, Quebec J8X 3X2, Canada HC)

Pulse compression, widely used in modern radar systems, has the advantage in that it allows the use of long duration low-power pulses which facilitate low-power transmission. A synthetic aperture radar (SAR) pulse compression system able to compress very large time bandwidth product signals while still retaining high dynamic range capability and flexibility would be very advantageous. The possibility of implementing the compression in two stages is investigated, in which the first stage compression processing is done by an analog device followed by digital techniques in the second stage. Various signal coding methods were evaluated to determine those most suitable to the two-stage process, and various means of implementing the second stage were compared. A two-stage pulse compression system was then designed and built to generate arbitrarily coded expanded pulses with bandwidths in excess of 200 MHz. Its performance was evaluated in the presence of tone, noise, and jamming. It was shown that the two-stage pulse compression system exhibited greater resistance to quantizer saturation than a comparable digital system. The processing effort required to implement the compression using a digital adaptive matched filter was found to be slightly less than double that of a basic pulse compression system. Author (CISTI)

N94-13537 Tel-Aviv Univ. (Israel). Dept. of Electrical Engineering - Systems.
CONSTANT FALSE ALARM RATE (CFAR) DETECTION IN WEIBULL CLUTTER M.S. Thesis
Rafi Ravid Sep. 1990 93 p
(ITN-93-85190) Copyright Avail: Issuing Activity (Tel-Aviv Univ., Exact Sciences Library, Ramat Aviv 69978, Israel)

A constant false alarm rate (CFAR) detector maintains a constant false alarm probability in the face of changes of the properties of the cause of the false alarms. False alarms in radar systems arise from receiver noise or clutter; clutter is considered. The CFAR processor maintains a constant false alarm rate by estimating the clutter level in a set of reference cells in the vicinity of the cell under test (CUT) and deciding on the basis of this information whether the CUT contains clutter or a target. Among the distribution functions which were fitted to the radar clutter were the Rayleigh distribution, the log-normal distribution, and the K distribution. The Weibull distribution was chosen, which has the cumulative distribution function: $F(x) = 1 - \exp(-(x/b)(\exp c))$ in which b is the scale parameter which controls the mean level of the variate, and c is the shape parameter which controls the skewness of the distribution. The Weibull distribution was found to describe land and sea clutter, especially for small resolution cell sizes and low depression angles. For the special case of $c = 2$, the Weibull distribution reduces to the Rayleigh distribution, which can be shown to be the distribution of a large number of scatterers of similar size. For c less than 2, the tail of the distribution becomes larger. Various CFAR algorithms which could be applied to the problem are discussed; various treatments using order-statistics (OS) CFAR processing were used. ISA

N94-13538 Tel-Aviv Univ. (Israel). Dept. of Electronics, Communications Control and Computer Systems.
CANCELLATION OF MULTIPATH FOR MONOPULSE RADARS M.S. Thesis
Yuval Yehudar Jun. 1990 60 p
(ITN-93-85191) Copyright Avail: Issuing Activity (Tel-Aviv Univ., Exact Sciences Library, Ramat Aviv 69978, Israel)

When radar is operated in tracking mode, loss of track caused by multipath can be easily avoided, but it is difficult to reduce the tracking error to the limits required for certain applications. Signal processing algorithms developed for phased array radars cannot be directly applied to monopulse radars, which have insufficient sensors to dissociate the multiple returns. Monopulse tracker operation and the multipath phenomenon are discussed, and some methods of dealing with it are summarized. A model is developed to represent the various problem parameters as simply as possible and a solution is based on the application to a monopulse radar of an algorithm used in phased arrays, in order to improve monopulse accuracy in the presence of multipath. A Maximum Likelihood Estimation (MLE) technique is suggested, in which sufficient independent data to resolve the estimation problem are obtained by sampling for longer periods, so allowing the relative phase between the direct and the indirect returns

to vary significantly. A comparative performance evaluation is presented and it is shown that use of the MLE technique can give an improvement by two orders of magnitude in the root-mean-square (RMS) error, compared with the usual processing technique, provided that phase coherence can be maintained over the data sampling time interval. Author (ISA)

N94-13566 Tel-Aviv Univ. (Israel). Dept. of Electronic Engineering - Systems.

BOUNDS ON TIME DELAY ESTIMATION GIVEN UNKNOWN SIGNAL SPECTRAL PARAMETERS M.S. Thesis

Shalom Tsruya Apr. 1991 164 p In HEBREW

(ITN-93-85194) Copyright Avail: Issuing Activity (Tel-Aviv Univ., Exact Sciences Library, Ramat Aviv 69978, Israel)

The bounds on the time delay estimation error variance are well understood for the case of a Gaussian, stationary, flat-spectrum-source signal with known spectral density. This work presents a bound on time delay estimation error variance for the case of an arbitrary unknown spectrum. The bound presented in this work is based on the Barankin bound on the multi-dimensional parameter estimation problem. The Barankin bound has been used with some success to overcome the ambiguity problem. The source signal is modeled as a linear combination of flat spectrum signals with different unknown spectral levels. In this work we derived an expression for a lower bound on the time delay estimation error of a signal with N unknown spectral parameters (spectral levels). This is one of the few times that the Barankin bound multi-dimensional version has been applied to a practical problem. The threshold phenomenon in the Barankin bound for unknown parameters was considered in this work. The results are: 1. Generally, the estimation performance depends on the knowledge of the source spectral parameters. However, in most practical cases the degration in the performance of the time delay estimation as a result of the unknown spectral parameters is neglected. For large M (number of sensors) and small ratio, w(sub c) to w, we received significant degradation. 2. The achievable estimation performance depends strongly on the shape of the source spectrum. 3. Generally, the point at which the threshold occurs depends on knowledge of the source spectral parameters. In most practical cases the threshold location is insensitive to prior knowledge of the source spectra parameters. Author (ISA)

N94-13567 Tel-Aviv Univ. (Israel). Dept. of Electrical Engineering - Systems.

SIGNAL DESIGN FOR DATA COMMUNICATION THROUGH RAPIDLY VARYING LINEAR CHANNELS M.S. Thesis

Boaz Rippin Jan. 1992 94 p

(ITN-93-85195) Copyright Avail: Isuing Activity (Tel-Aviv Univ., Exact Sciences Library, Ramat Aviv 69978, Israel)

We consider the problem of data communication through an unknown rapidly varying linear channel, such as in mobile communication or underwater acoustic telemetry. The use of training sequences to identify the channel response at each transmission period may be impractical, owing to the fast varying nature of the channel. Therefore, as an alternative solution, we propose to use a signal design strategy in which we restrict the transmitted data stream to specific sequences. A generalized likelihood ratio test for detecting the transmitted sequence is developed, and the probability of detection is analysed. A bound on the detection performance is also developed. Based on that, we propose optimal and sub-optimal signal design strategies, one class of which consists of a new concept of all-pole, or autoregressive modulation of the data bits. Author (ISA)

N94-13650 California Univ., Los Angeles.

THE PROPAGATION CHARACTERISTICS AND INSTABILITY PROPERTIES OF LOW-FREQUENCY ELECTROMAGNETIC WAVES IN THE IO PLASMA TORUS Ph.D. Thesis

Yi Mei 1992 304 p

Avail: Univ. Microfilms Order No. DA9310866

We explore the propagation characteristics and instability properties of low frequency electromagnetic waves in the Io plasma torus using a wave ray tracing technique HOTRAY. We evaluate the convective growth of ion cyclotron waves for each propagating frequency band below the gyrofrequency of protons f(sub H+) in the entire Io torus. We build up an analytical diffusive equilibrium density model (under some reasonable assumptions) which extrapolates the equatorial plasma conditions based on the in situ Voyager data analysis to high latitude regions along the field lines. This 2-D (in a meridian plane) analytical density model for Io plasma torus can be very useful for other computer simulation studies of the Io torus. The method to obtain this approximate analytical solution can be generalized to other multiple species plasma, e.g., the diffusive equilibrium distribution of ions in planetary ionosphere. A survey of wave excitation and propagation throughout the torus is presented and the sensitivities of the waves to the plasma parameters have been tested. The spatial regions for wave growth or damping are shown in a meridian plane for 6 is less than or equal to L is less than or equal to 10. The multispecies plasma in the torus limits L-mode wave propagation to several district bands in frequency. The top band waves with frequencies f(sub O+2) is less than f is less than f(sub H+) (approximately 10 Hz) are studied and compared with the previous works done by Thorne and Moses. Waves in this band may grow at intermediate latitude near L equivalent to 8, and the overall amplification is extremely sensitive to plasma parameters. The other bands with frequencies f less than f(sub O+) are examined here for the first time. Some of those waves (f equivalent to 0.5 Hz) can be very unstable near the equator at L equivalent to 7 - 10; this result is relatively independent of the plasma conditions. We have made predictions of possible unstable waves encountered by the ULYSSES spacecraft during its passage through Io torus high latitude regions on February, 1992. Dissert. Abstr.

N94-13661 California Univ., Berkeley.

ELECTRON BEAM PROBE MEASUREMENTS OF ELECTRIC FIELDS IN rf DISCHARGES Ph.D. Thesis

Arthur Hideyuki Sato 1992 221 p

Avail: Univ. Microfilms Order No. DA9305062

An electron beam diagnostic has been developed to measure small electric fields (less than 20 V/cm) in low pressure capacitive rf discharges. The electron beam diagnostic is described, and data are presented showing the existence of transient double layers at the sheath boundary, and evidence for a negative bulk plasma resistance. The electric field measurements motivated more careful measurements of the discharge current waveforms. The current waveforms together with the electric field measurements, provide evidence for negative bulk plasma resistance. The current measurements, in turn, allowed comparison between experimental discharge impedance data and results from a global discharge model. A modified version of the work of Misium et al. is presented. This includes a reformulation of the secondary electron contribution to the electron power balance, and incorporation of electrode asymmetry. The results of this model are compared to experimental results obtained from current and voltage measurements. The model predictions of current amplitude and phase shift at the first harmonic fit the experimental results surprisingly well for realistic values of the secondary emission coefficient. In particular, it is also shown how an additional electron energy deposition mechanism can result in a more linear current (I) to voltage (V) amplitude relation. Alternate explanations for a linear I-V dependence are discussed. A two-coupled-sheath model is presented that qualitatively describes current conduction through asymmetric discharges. Some results of this model are: (1) The time-averaged sheath voltages are somewhat insensitive to the shape of the current waveform, and hence much of what is known about the sheath voltage ratios remains true. (2) At moderate area ratios (less than 10) the current waveforms can maintain top-bottom symmetry if the driving voltage is allowed to distort slightly, and the external circuit prevents free circulation of the higher harmonic components of the current. The current waveforms will be skewed, distinguishing them from current waveforms of a symmetric discharge. (3) At higher area ratios (greater than 10) the top-bottom symmetry of the current waveform is difficult to preserve since the system is so close to being a single sheath. In this case, the conduction current spike remains prominent since it cannot be suppressed by distortions of the sheath voltage. Dissert. Abstr.

N94-13696# Sandia National Labs., Albuquerque, NM.

LOCALLY NON-UNIFORM FINITE-DIFFERENCE TIME DOMAIN WITH APPLICATION TO STEALTH, CROSSTALK, AND NARROW APERTURES

D. J. Riley Apr. 1993 104 p

(Contract DE-AC04-76DP-00789)

(DE93-013958; SAND-93-0735) Avail: CASI HC A06/MF A02

A technique to integrate a dense, locally non-uniform mesh into finite-difference time-domain (FDTD) codes is presented. The method is designed for the full-wave analysis of multi-material layers that are physically

thin, but perhaps electrically thick. Such layers are often used for the purpose of suppressing electromagnetic reflections from conducting surfaces. Throughout the non-uniform local mesh, average values for the conductivity and permittivity are used, where as variations in permeability are accommodated by splitting H-field line integrals and enforcing continuity of the normal B field. A unique interpolation scheme provides accuracy and late-time stability for mesh discontinuities as large as 1000 to 1. Application is made to resistive sheets, the absorbing Salisbury screen, crosstalk on printed circuit boards, and apertures that are narrow both in width and depth with regard to a uniform cell. Where appropriate, comparisons are made with the MoM code CARLOS and transmission-line theory. The hybrid mesh formulation has been highly optimized for both vector and parallel-processing on Cray Y-MP architectures. DOE

N94-13720*# Michigan Univ., Ann Arbor. Dept. of Electrical Engineering and Computer Science.

SCATTERING BY A GROOVE IN AN IMPEDANCE PLANE

Sunil Bindiganavale and John L. Volakis Sep. 1993 21 p

(Grant NAG1-1478)

(NASA-CR-193362; NAS 1.26:193362; UMA-030601-2-T) Avail: CASI HC A03/MF A01

An analysis of two-dimensional scattering from a narrow groove in an impedance plane is presented. The groove is represented by a impedance surface and the problem reduces to that of scattering from an impedance strip in an otherwise uniform impedance plane. On the basis of this model, appropriate integral equations are constructed using a form of the impedance plane Green's functions involving rapidly convergent integrals. The integral equations are solved by introducing a single basis representation of the equivalent current on the narrow impedance insert. Both transverse electric (TE) and transverse magnetic (TM) polarizations are treated. The resulting solution is validated by comparison with results from the standard boundary integral method (BIM) and a high frequency solution. It is found that the presented solution for narrow impedance inserts can be used in conjunction with the high frequency solution for the characterization of impedance inserts of any given width. Author (revised)

N94-13799*# Arizona State Univ., Tempe. Telecommunication Research Center.

ANTENNA PATTERN CONTROL USING IMPEDANCE SURFACES Final Report, 16 Sep. 1990 - 15 Sep. 1993

Constantine A. Balanis, Kefeng Liu, and Panayiotis A. Tirkas 15 Sep. 1993 122 p

(Grant NAG1-1183)

(NASA-CR-194517; NAS 1.26:194517; TRC-CAB-9308) Avail: CASI HC A06/MF A02

During the period of this research project, a comprehensive study of pyramidal horn antennas was conducted. Full-wave analytical and numerical techniques were developed to analyze horn antennas with or without impedance surfaces. Based on these full-wave analytic techniques, research was conducted on the use of impedance surfaces on the walls of the horn antennas to control the antenna radiation patterns without a substantial loss of antenna gain. It was found that the use of impedance surfaces could modify the antenna radiation patterns. In addition to the analytical and numerical models, experimental models were also constructed and they were used to validate the predictions. Excellent agreement between theoretical predictions and the measured data was obtained for pyramidal horns with perfectly conducting surfaces. Very good comparisons between numerical and experimental models were also obtained for horns with impedance surfaces. Author (revised)

N94-13801 University of Western Ontario, London. Faculty of Engineering Science.

METEOR FORWARD SCATTER STUDIES Final Report

A. R. Webster, J. Jones, and K. A. Ellis Apr. 1992 28 p

(DSIS-93-00382; CTN-93-60759) Avail: CASI HC A03

A meteor forward-scatter system was operated between sites located near Ottawa and London, Ontario to conduct studies on the occurrence of meteors which would be useful to the prediction of the performance of a forward scatter link. These included the rate of incoming meteors suitable for reflection and their radiant distributions, which will allow such predictions to be made. The system was put into operation in late Feb. 1991 and results covering the Mar.-Dec. 1991 period are presented, representing a total of about 80,000 individual meteor echoes. Graphs are included showing the diurnal and seasonal variations in meteor echoes and the radiant point of individual echoes from the measured angles of arrival. CISTI

N94-13802# Saskatchewan Univ., Saskatoon. Plasma Physics Lab.

SCATTERING OF REFLECTOMETER SIGNALS FROM RIPPLED SURFACES

G. D. Conway Jun. 1993 18 p

(PPL-138; CTN-93-60760) Avail: CASI HC A03/MF A01

Transverse coherent density fluctuations at the plasma cutoff layer are modeled by a rippled conducting surface. Two simulations are presented which give the reflectometer back-scattered power as functions of ripple wavelength, amplitude, and phase. Results from an experimental simulation of the STOR-M tokamak geometry and a numerical simulation using the Helmholtz integral and a paraxial Gaussian probe beam, agree in showing three ripple wavelength (L) sensitivity regions defined by beam radius (w) and reflectometer probe wavelength (lambda). Short wavelengths (L/lambda much less than 2w/lambda) experience large Bragg scattering. Long wavelengths (L/lambda much greater than 10w/lambda) experience no scattering. Intermediate wavelengths experience complex scattering with strong modulation of reflected power at twice ripple frequency. CISTI

N94-13810*# Jet Propulsion Lab., California Inst. of Tech., Pasadena.

USING A FOCAL-PLANE ARRAY TO ESTIMATE ANTENNA POINTING ERRORS

S. Zohar and V. A. Vilnrotter 25 Oct. 1991 84 p

(Contract NAS7-918)

(NASA-CR-194502; JPL-Publ-91-45; NAS 1.26:194502) Avail: CASI HC A05/MF A01

The use of extra collecting horns in the focal plane of an antenna as a means of determining the Direction of Arrival (DOA) of the signal impinging on it, provided it is within the antenna beam, is considered. Our analysis yields a relatively simple algorithm to extract the DOA from the horns' outputs. An algorithm which, in effect, measures the thermal noise of the horns' signals and determines its effect on the uncertainty of the extracted DOA parameters is developed. Both algorithms were implemented in software and tested in simulated data. Based on these tests, it is concluded that this is a viable approach to the DOA determination. Though the results obtained are of general applicability, the particular motivation for the present work is their application to the pointing of a mechanically deformed antenna. It is anticipated that the pointing algorithm developed for a deformed antenna could be obtained as a small perturbation of the algorithm developed for an undeformed antenna. In this context, it should be pointed out that, with a deformed antenna, the array of horns and its associated circuitry constitute the main part of the deformation-compensation system. In this case, the pointing system proposed may be viewed as an additional task carried out by the deformation-compensation hardware. Author (revised)

N94-13813*# Jet Propulsion Lab., California Inst. of Tech., Pasadena.

SUBMILLIMETER, MILLIMETER, AND MICROWAVE SPECTRAL LINE CATALOGUE, REVISION 3

H. M. Pickett, R. L. Poynter, and E. A. Cohen 1 Jun. 1992 224 p

(Contract NAS7-918)

(NASA-CR-194501; JPL-Publ-80-23-Rev-3; NAS 1.26:194501) Avail: CASI HC A10/MF A03

A computer-accessible catalog of submillimeter, millimeter, and microwave spectral lines in the frequency range between 0 and 10,000 GHz (i.e., wavelengths longer than 30 micrometers) is described. The catalog can be used as a planning or as an aid in the identification and analysis of observed spectral lines. The information listed for each spectral line includes the frequency and its estimated error, the intensity, the lower state energy, and the quantum number assignment. This edition of the catalog has information on 206 atomic and molecular species and includes a total of 630,924 lines. The catalog was constructed by using theoretical least square fits of published spectral lines to accepted molecular models. The associated predictions and their estimated errors are based upon the resultant fitted parameters and their covariances. Future versions of this catalog will add more atoms and molecules and update the present listings as new data appear. The catalog is available as a magnetic data tape recorded in card images, with one card image per spectral line, from the National Space Science Data Center, located at Goddard Space Flight Center. Author (revised)

N94-13818 Defence Research Establishment, Ottawa (Ontario). Communications Electronics Warfare Section.

KALMAN FILTER BASED ARCHITECTURES FOR INTERFERENCE EXCISION

Brian Kozminchuk Dec. 1991 37 p

(DSIS-93-00034; DREO-RN-1118; CTN-93-60772; AD-A259650) Avail: CASI HC A03

A novel Kalman filtering approach is presented for the suppression of narrowband interference from direct sequence spread spectrum communications systems. The algorithm is based on the digital phase-locked loop Kalman filter. Because the interference is assumed to be much stronger than either the signal or the noise, the Kalman filter locks onto a function related to the interference. The net result is an estimate of the phase of the interference and its amplitude. The algorithm is characterized through computer simulation for the case of narrowband Gaussian noise interference. Examples of the phase- and envelope-tracking capabilities of the algorithm are presented, followed by bit error rate curves for interference bandwidths ranging from 0.5 to 5.0 percent of the chip rate of the spread spectrum signal. Three adaptive architectures are then described. The first is suitable for constant envelope interference; the second is a more general structure; and the third incorporates a decision feedback structure accompanied with a training sequence. Author (CISTI)

N94-13829# Defence Research Establishment, Ottawa (Ontario). Communications Electronic Warfare Section.

A REVIEW OF ROBUST DETECTION

Eric April Oct. 1992 27 p

(DSIS-93-00400; DREO-TN-92-13; CTN-93-60749) Avail: CASI HC A03

A comprehensive survey is presented of the most important results published to date on robust detection. A robust detector is one for which good performance is obtained under nominal conditions while an acceptable level of performance is maintained for deviations of the observation statistics, within some allowable uncertainty class. The basic principles of robust detection are given and it is seen that the uncertainty model plays an important role in the derivation of the optimum scheme. For an eta contamination model, a censored version of the likelihood ratio constitutes the desired robust detector. The fundamental robust detection systems for various signal conditions are discussed and the asymptotic minimax robust detection approach is introduced in order to solve the problem for weak signals and large sample sizes. Some of the latest major contributions include results for dependent noise, asymmetric distributed noise, and adaptive robust detectors. Some concerns relating to the derivation of robust detection structures for continuous time processes are noted. Finally, recent topics such as the potential benefits of using the large deviations approach for robust detection are considered. Author (CISTI)

N94-13832# Defence Research Establishment, Ottawa (Ontario). Surface Radar Section.

MUSIC AND MAXIMUM LIKELIHOOD USING A REFINED PROPAGATION MODEL: PERFORMANCE COMPARISON FOR RADAR LOW-ANGLE TRACKING

Eloi Bosse, Ross M. Turner, and Daniel Brookes (Advanced Information Technologies Corp., Nepean, Ontario.) Jan. 1992 48 p

(DREO-RN-1122; CTN-93-60766) Avail: CASI HC A03/MF A01

The performance of the MUSIC (multiple signal classification) algorithm and many other superresolution methods degrades severely with the highly correlated multipath signals encountered in radar low-angle tracking. This deficiency is overcome by deriving new versions of the MUSIC and maximum likelihood algorithms, which use a search vector based on a model of the specular multipath. The performance of these two approaches is then compared with that of the MUSIC algorithm using spatial smoothing. Monte Carlo simulations and experiments at X-band indicate that the use of a specular model combined with an array radar having frequency agility gives much more accurate tracking than do the conventional approaches. The experiments were conducted at a site on the shore of the North Sea, using corner reflectors mounted on poles inserted in the sea bed. Sea conditions varied from sea state one to five. Author (CISTI)

N94-13837# Defence Research Establishment, Ottawa (Ontario). Radar ESM Section.

THE DREO ELINT BROWSER UTILITY (DEBU) REFERENCE MANUAL

Barbara Ford and David Jones (Prior Data Sciences Ltd.) Apr. 1992 70 p

(DSIS-92-03900; DREO-RN-1130; CTN-93-60795) Avail: CASI HC A04/MF A01

An electronic intelligent database browsing tool called DEBU has been developed that allows databases such as ELP, Kilting, EWIR, and AFEWC to be reviewed and analyzed from a user-friendly environment on a personal computer. DEBU's basic function is to allow users to examine the contents of user-selected subfiles of user-selected emitters of user-selected databases. DEBU augments this functionality with support for selecting (filtering) and combining subsets of emitters by user-selected attributes such as name, parameter type, or parameter value. DEBU provides facilities for examining histograms and x-y plots of selected parameters, for doing ambiguity analysis and mode level analysis, and for generating and printing a variety of reports. A manual is provided for users of DEBU, including descriptions and illustrations of menus and windows. Author (CISTI)

N94-13838# Defence Research Establishment, Ottawa (Ontario). Radar ESM Section.

DIGITAL QUADRATURE DEMODULATION FOR RADAR ESM APPLICATIONS

Robert Inkol and Ron Saper May 1992 60 p

(DREO-TN-92-10; CTN-93-60796; AD-A260166) Avail: CASI HC A04/MF A01

The feasibility of using digital techniques for coherent demodulation of wideband signals was investigated for application in radar electronic support measures systems. Several different design approaches and analysis methods were considered: a medium bandwidth design with simple Hilbert transformer, a medium bandwidth design with zero direct current offset, and a wide bandwidth matched response design with zero direct current offset. It was found that the processing requirements to achieve good accuracy for pulse and other wideband signals can be minimized through appropriate choice of intermediate frequency, the use of half-band finite impulse response filters, and the application of decimation. This suggests that an application specific integrated circuit implementation of a digital coherent demodulator should have potential cost and performance advantages over existing analog approaches. CISTI

N94-13841 University of Western Ontario, London. Faculty of Engineering Science.

A STUDY OF METEOR SCATTER COMMUNICATIONS Final Report

A. R. Webster and J. Jones Apr. 1991 20 p

(Contract DSS-36001-9-3601-01-SS)

(DSIS-93-00151; CTN-93-60800) Avail: CASI HC A03

Communications over 500-2000 km by means of forward scatter from meteor trains is of increased interest due to improvements in both the available technology and the coding schemes and protocols. Studies were conducted to improve the knowledge of background statistics such as meteor rates and duration times. The primary objective was to develop a system capable of measuring accurately the direction of the echoes obtained from meteor forward scatter on a path of medium length. The distribution in amplitude and duration of echoes was also felt to be of importance and echo sampling methods and rates were to be consistent with this. The basic technique used involves phase measurements of the signals received on spaced antennas. Field experiments were conducted using a transmitter frequency of 48.7 MHz and two orthogonal receiving arrays, with transmitter and receiver located respectively in Ottawa and London, Ontario. Around 500 meteor echoes per day have been recorded since start of data collection in February 1991. The characteristics of representative echoes are illustrated. Two basic kinds of echoes were observed, a classic underdense echo where the radio wave penetrates the column of ionization left by the passage of the meteoroid and the overdense case with the echo persisting until the electron density falls to levels which allow penetration.

Author (CISTI)

N94-13843 McMaster Univ., Hamilton (Ontario). Communications Research Lab.

PORTABLE MULTIPATH MEASUREMENT SYSTEM Final Report, Jun. 1990 - May 1991

L. Lai, T. Lo, A. Chan, and J. Litva Jul. 1991 87 p

(Contract DSS-W7714-0-9383-01-SS)

(DSIS-93-00177; CRL-233; CTN-93-60802) Avail: CASI HC A05

A portable very high frequency (VHF) multipath measurement system

(PMMS) has been developed for use in performing field measurements and establishing a statistical data base for characterizing the propagation environment pertinent to VHF radio direction finding (DF). The problems related to radio DF which are to be investigated include the following: multipath effects due to assorted types of terrain, mutual coupling effects of the DF antenna array, analysis of the PMMS measurement data, and the construction of a multipath scattering model. The development of the digital DF system is described and simulation results are presented which will be used to support forthcoming VHF multipath studies. The calibration procedure for the PMMS system, the estimation of angle of arrival using a circular antenna array, the multipath model which simulates electromagnetic scattering from a rough surface, and radio wave propagation in forest environments are also described. CISTI

N94-13869 Applied Silicon, Inc., Ottawa (Ontario).
ADAPTIVE SIGNAL PROCESSING TESTBED Final Report
Hugh A. Parliament 10 Sep. 1991 15 p
(Contract DREO-W7714-0-9504)
(DSIS-93-00258; CTN-93-60807) Avail: CASI HC A03

The design and implementation of a system for the acquisition, processing, and analysis of signal data is described. The initial application for the system is the development and analysis of algorithms for excision of interfering tones from direct sequence spread spectrum communication systems. The system is called the Adaptive Signal Processing Testbed (ASPT) and is an integrated hardware and software system built around the TMS320C30 chip. The hardware consists of a radio frequency data source, digital receiver, and an adaptive signal processor implemented on a Sun workstation. The software components of the ASPT consists of a number of packages including the Sun driver package; UNIX programs that support software development on the TMS320C30 boards; UNIX programs that provide the control, user interaction, and display capabilities for the data acquisition, processing, and analysis components of the ASPT; and programs that perform the ASPT functions including data acquisition, despreading, and adaptive filtering. The performance of the ASPT system is evaluated by comparing actual data rates against their desired values. A number of system limitations are identified and recommendations are made for improvements. CISTI

N94-13870 Applied Silicon, Inc., Ottawa (Ontario).
ADAPTIVE SIGNAL PROCESSING TESTBED: SOFTWARE DESIGN SPECIFICATION
Hugh A. Parliament Jun. 1990 82 p
(Contract DREO-W7714-0-9504)
(DSIS-93-00259; CTN-93-60808) Avail: CASI HC A05/MF A01

The Adaptive Signal Processing Testbed is a system for the analysis and characterization of adaptive filtering algorithms used for the excision of interfering tones from direct sequence spread spectrum communications systems. The design specification for the software to be developed for this testbed is described. The testbed system is divided into a number of subsystems and the required software for each subsystem is presented. The control and data flow between the subsystem as well as a modular breakdown of the software is provided. The online component of the host software provides all the control, monitoring, and storage functions for the embedded software system that resides on the bus in the host computer, a Sun workstation. The online component consists of five separate modules: user interface, graphical display, central processing, data storage, and development. The offline, or post-processing, component of the host software provides sophisticated statistical and spectral analysis of the data stored on disk. An interactive environment is provided for the user to develop customized analysis methods. CISTI

N94-13899# Oak Ridge National Lab., TN.
CURRENT DISTRIBUTION TOMOGRAPHY FOR DETERMINATION OF INTERNAL CURRENT DENSITY DISTRIBUTIONS
P. C. Gailey 1993 9 p Presented at the Applied Computational Electromagnetic Society (ACES) Meeting, Monterey, CA, 24 Mar. 1993
(Contract DE-AC05-84OR-21400)
(DE93-015463; CONF-9303182-1) Avail: CASI HC A02/MF A01

A method is presented for the determination of current densities inside a cylindrical object using measurements of the magnetic fields outside the object. The cross section of the object is discretized with the current assumed constant over each defined region. Magnetic fields outside the object are related to the internal current densities through a geometry matrix which can be inverted to yield a solution for the current densities in terms of the measured fields. The primary limitation of this technique results from singularities in the geometry matrix that arise due to cylindrical symmetry of the problem. Methods for circumventing the singularities to obtain information about the distribution of current densities are discussed. This process of current distribution tomography is designed to determine internal body current densities using measurements of the external magnetic field distribution. It is non-invasive, and relatively simple to implement. Although related to a more general study of magnetic imaging which has been used to investigate endogenous currents in the brain and other parts of the body, it is restricted to currents either applied directly or induced by exposure to an external field. The research is related to public concern about the possibility of health effects resulting from exposure to power frequency electric and magnetic fields. DOE

N94-13909*# Technology Group, Los Angeles, CA.
TRELLIS CODING WITH CONTINUOUS PHASE MODULATION (CPM) FOR SATELLITE-BASED LAND-MOBILE COMMUNICATIONS Final Report, 7 May 1987 - 7 Aug. 1989
Sep. 1989 297 p
(Contract NAS7-1003; SBIR-14.05-6455)
(NASA-CR-191325; NAS 1.26:191325) Avail: CASI HC A13/MF A03

This volume of the final report summarizes the results of our studies on the satellite-based mobile communications project. It includes: a detailed analysis, design, and simulations of trellis coded, full/partial response CPM signals with/without interleaving over various Rician fading channels; analysis and simulation of computational cutoff rates for coherent, noncoherent, and differential detection of CPM signals; optimization of the complete transmission system; analysis and simulation of power spectrum of the CPM signals; design and development of a class of Doppler frequency shift estimators; design and development of a symbol timing recovery circuit; and breadboard implementation of the transmission system. Studies prove the suitability of the CPM system for mobile communications.
Author (revised)

N94-13916*# National Aeronautics and Space Administration. Langley Research Center, Hampton, VA.
ANALYSIS OF MICROSTRIP PATCH ANTENNAS WITH NONZERO SURFACE RESISTANCE
David G. Shively and M. C. Bailey Washington Aug. 1993 18 p Sponsored in part by Army Communications Electronics Command, Fort Monmouth, NJ
(RTOP 505-64-20-54)
(NASA-TP-3362; CECOM-TR-93-E-2; L-17219; NAS 1.60:3362) Avail: CASI HC A03/MF A01

The scattering properties of a microstrip patch antenna with nonzero surface impedance are examined. The electric field integral equation for a current element on a grounded dielectric slab is developed for a rectangular geometry by using Galerkin's technique with subdomain piecewise linear basis functions. The integral equation includes a resistive boundary condition on the surface of the patch. The incident field on the patch is expressed as a function of incidence angle. The resulting system of equations is then solved for the unknown current modes on the patch, and the radar cross section is calculated for a given scattering angle. Theoretical results in the form of radar cross section as a function of frequency are compared with results measured at the NASA Langley Research Center. Author

N94-13939# Applied Silicon, Inc., Ottawa (Ontario).
ADVANCED COMMUNICATIONS ESM SYSTEM (ACES) TESTBED: INTEGRATION STUDY
Rick E. Ingram and Hugh A. Parliament 14 Jul. 1992 62 p
(DSIS-93-00345; CTN-93-60744) Avail: CASI HC A04

The Advanced Communications Electronic Support Measures (ESM) System (ACES) testbed is being developed to provide a research environment to explore new techniques in a variety of ESM-related functions. ACES receives radio signals from the outside world, performs signal of interest detection and analysis, and provides results in the form of audio signals, data for post-processing, or sensory input data to the Data Fusion and Correlation Techniques Testbed. The components of the ACES testbed are detailed: a wide-band signal source based on a digital receiver; a wide-band analysis subsystem to analyze the input from the signal source;

a narrow band signal extractor which reduces the bandwidth of the wide-band data; a narrow band analysis subsystem; the ACES system controller; and a real-time data storage subsystem. The current status of each component is given along with options and suggestions for those components not yet specified. The proposed strategy for ACES integration and interfaces between the various components are described. The interfacing requirements can be satisfied by developing three custom microprocessor boards. An interim solution for system integration that provides a limited set of functions for a fixed application is also proposed. A task-by-task breakdown, time schedule, and cost summary for the integration plan is included. CISTI

N94-13941 Defence Research Establishment, Ottawa (Ontario). Communications and Navigation Section.
SIMULATION OF DOWNLINK SYNCHRONIZATION FOR A FREQUENCY-HOPPED SATELLITE COMMUNICATION SYSTEM
Lyle Wagner Apr. 1992 37 p
(DSIS-93-00477; DREO-TN-92-9; CTN-93-60745; AD-A259606) Avail: CASI HC A03

Frequency hopped spread spectrum satellite communication systems provide robust communications resilient to many types and levels of jamming. Unfortunately, this increase in resilience is offset by an increase in complexity while establishing the communication link, termed synchronization. A two-step downlink synchronization method is examined, involving the transmission by satellite of synchronization hops that are modulated with a synchronization code and are received by the ground terminal where the two-step algorithm is implemented. The first step is the envelope detection of the sync hops, coarse time synchronization. When the terminal is confident that the coarse synchronization process is complete, the second step (fine time synchronization) is activated. This involves correlating a downlink sync hop with an internally generated reference sync hop to obtain an accurate time estimate. Additionally, a prediction of the frequency offset can be made to fine-tune the local oscillator. Computer simulations were made of the synchronization process using synchronization codes of varying lengths to verify the algorithm. These simulations demonstrate that the proposed algorithm is capable of operating under severe jamming conditions and is compatible with the corresponding communication link. Author (CISTI)

N94-13946*# Jet Propulsion Lab., California Inst. of Tech., Pasadena.
STOCHASTIC PERFORMANCE MODELING AND EVALUATION OF OBSTACLE DETECTABILITY WITH IMAGING RANGE SENSORS
Larry Matthies and Pierrick Grandjean 15 Mar. 1993 23 p
(Contract NAS7-918)
(NASA-CR-194510; JPL-Publ-93-11; NAS 1.26:194510) Avail: CASI HC A03/MF A01

Statistical modeling and evaluation of the performance of obstacle detection systems for Unmanned Ground Vehicles (UGVs) is essential for the design, evaluation, and comparison of sensor systems. In this report, we address this issue for imaging range sensors by dividing the evaluation problem into two levels: quality of the range data itself and quality of the obstacle detection algorithms applied to the range data. We review existing models of the quality of range data from stereo vision and AM-CW LADAR, then use these to derive a new model for the quality of a simple obstacle detection algorithm. This model predicts the probability of detecting obstacles and the probability of false alarms, as a function of the size and distance of the obstacle, the resolution of the sensor, and the level of noise in the range data. We evaluate these models experimentally using range data from stereo image pairs of a gravel road with known obstacles at several distances. The results show that the approach is a promising tool for predicting and evaluating the performance of obstacle detection with imaging range sensors. Author (revised)

N94-13950# Centre National d'Etudes Spatiales, Toulouse (France).
CHARACTERISTICS OF THE AMATEUR RADIO MEANS OF THE ARSENE SATELLITE [CARACTERISTIQUES DES MOYENS DE TRAFIC RADIOAMATEUR DU SATELLITE ARSENE]
Andre Cuisin Nov. 1992 41 p In FRENCH
(CNES-NT-131; ETN-93-93978) Copyright Avail: CASI HC A03/MF A01

The Arsene (Ariane amateur radio satellite for space education) satellite is designed to provide amateur radio telecommunications services. Its equatorial orbit (20,000/36,000 km/0 deg) provides some 50 hours of continuous visibility by a radioamateur station. This radioamateur network will transmit in Packet AX25, SSB, and TTY modes and will provide voice transmission. In addition to the usual Very High Frequencies (VHF) and Ultra High Frequencies (VHF), an S-band spacecraft/ground link are included. Packet and S-band Arsene telemetry reception will enable users to monitor spacecraft behavior in orbit. Accessible to universities, colleges of further education, and technical colleges, these facilities will contribute to the teaching of space related subjects. ESA

N94-13968# Norwegian Defence Research Establishment, Kjeller.
MEASUREMENT OF WAVE PROPAGATION FOR VHF/UHF AND A COMPARISON BETWEEN MEASURED AND PREDICTED VALUES [MAALING AV BOELGEPROPAGASJON FOR VHF/UHF SAMT SAMMENLIGNING MED PREDIKTERTE VERDIER]
Bjoern Askeland 14 Aug. 1992 31 p In NORWEGIAN
(FFI/RAPPORT-92/7024; ETN-93-93973) Avail: CASI HC A03/MF A01

Transmission loss measurements for the frequencies 39.0, 58.0, and 348.0 MHz at 41 different locations are presented. A broad band chirp signal was used to dissolve multipath propagation. A comparison between predicted values and measured values is presented. ESA

N94-14015 Applied Silicon, Inc., Ottawa (Ontario).
ADAPTIVE SIGNAL PROCESSING TESTBED: VME-BASED DSP BOARD MARKET SURVEY
Rick E. Ingram Apr. 1992 19 p
(Contract DREO-W7714-0-9504)
(DSIS-93-00274; CTN-93-60812) Avail: CASI HC A03

The Adaptive Signal Processing Testbed (ASPT) is a real-time multiprocessor system utilizing digital signal processor technology on VMEbus based printed circuit boards installed on a Sun workstation. The ASPT has specific requirements, particularly as regards to the signal excision application, with respect to interfacing with current and planned data generation equipment, processing of the data, storage to disk of final and intermediate results, and the development tools for applications development and integration into the overall EW/COM computing environment. A prototype ASPT was implemented using three VME-C-30 boards from Applied Silicon. Experience gained during the prototype development led to the conclusions that interprocessor communications capability is the most significant contributor to overall ASPT performance. In addition, the host involvement should be minimized. Boards using different processors were evaluated with respect to the ASPT system requirements, pricing, and availability. Specific recommendations based on various priorities are made as well as recommendations concerning the integration and interaction of various tools developed during the prototype implementation. Author (CISTI)

N94-14033# Defence Research Establishment, Ottawa (Ontario). Communications Electronic Warfare Section.
ENVELOPE AND INSTANTANEOUS FREQUENCY ESTIMATION OF NARROWBAND MODULATED SIGNALS
Rene Lamontagne Dec. 1991 53 p
(DREO-TN-92-3; CTN-93-60736) Avail: CASI HC A04/MF A01

Generally, the transmission of a message signal in the radio frequency spectrum is accomplished by modulating the phase (corresponding to the instantaneous frequency) and amplitude of a carrier. The signal envelope and instantaneous frequency constitute, therefore, useful features to characterize the different modulation types. These two features are thus often used in an automatic modulation recognition system. The implementation of a digital algorithm for signal envelope and instantaneous frequency estimation is discussed. The modulation types involved are amplitude modulation, frequency modulation (FM), single sideband suppressed carrier, on-off keying or amplitude shift keying, frequency shift keying, and binary phase shift keying. The outputs of the envelope detector and frequency discriminator are presented for two types of signal: noisy (signal to noise ratio (SNR) of 25 dB) and very noisy (SNR = 5 dB). Also discussed are the following: the advantages of a median filter over a standard lowpass filter, the use of Lagrange's formula to estimate derivatives of discrete signals, and the effect of the noise at the outputs of the envelope detector and frequency discriminator. It appears that the output of the FM discriminator contains numerous click-noise spikes when the signal is very noisy, and it is difficult to distinguish among the modulation types. Author (CISTI)

N94-14037 Applied Silicon, Inc., Ottawa (Ontario).
ADAPTIVE SIGNAL PROCESSING TESTBED SIGNAL EXCISION SOFTWARE: USER'S MANUAL
Hugh A. Parliament May 1992 25 p
(Contract DREO-W7714-0-9504)
(DSIS-93-00260; CTN-93-60809) Avail: CASI HC A03

The Adaptive Signal Processing Testbed (ASPT) signal excision software is a set of programs that provide real-time processing functions for the excision of interfering tones from a live spread-spectrum signal as well as off-line functions for the analysis of the effectiveness of the excision technique. The processing functions provided by the ASPT signal excision software are real-time adaptive filtering of live data, storage to disk, and file sorting and conversion. The main off-line analysis function is bit error determination. The purpose of the software is to measure the effectiveness of an adaptive filtering algorithm to suppress interfering or jamming signals in a spread spectrum signal environment. A user manual for the software is provided, containing information on the different software components available to perform signal excision experiments: the real-time excision software, excision host program, file processing utilities, and despreading and bit error rate determination software. In addition, information is presented describing the excision algorithm implemented, the real-time processing framework, the steps required to add algorithms to the system, the processing functions used in despreading, and description of command sequences for post-run analysis of the data. CISTI

N94-14038 Applied Silicon, Inc., Ottawa (Ontario).
ADAPTIVE SIGNAL PROCESSING TESTBED APPLICATION SOFTWARE: USER'S MANUAL
Hugh A. Parliament May 1992 20 p
(Contract DREO-W7714-0-9504)
(DSIS-93-00261; CTN-93-60810) Avail: CASI HC A03

The Adaptive Signal Processing Testbed (ASPT) application software is a set of programs that provide general data acquisition and minimal processing functions on live digital data. The data are obtained from a digital input interface whose data source is the DAR4000 digital quadrature receiver that receives a phase shift keying signal at 21.4 MHz intermediate frequency. The data acquisition software is used to acquire raw unprocessed data from the DAR4000 and store it on disk in the Sun workstation based ASPT. File processing utilities are available to convert the stored files for analysis. The data evaluation software is used for the following functions: acquisition of data from the DAR4000, conversion to IEEE format, and storage to disk; acquisition of data from the DAR4000, power spectrum estimation, and on-line plotting on the graphics screen; and processing of disk file data, power spectrum estimation, and display and/or storage to disk in the new format. A user's guide is provided that describes the acquisition and evaluation programs along with how to acquire, evaluate, and use the data. CISTI

N94-14054 Defence Research Establishment, Ottawa (Ontario). Communications Electronic Warfare Section.
A COMPARISON OF RECURSIVE LEAST SQUARES AND KALMAN FILTERING EXCISORS FOR SWEPT TONE INTERFERENCE
Brian Kozminchuk Oct. 1992 26 p
(DSIS-93-00362; DREO-TN-92-14; CTN-93-60758; AD-A259913) Avail: CASI HC A03

A Kalman filtering approach is presented which is used for filtering narrow band interference out of direct sequence spread spectrum signals. The approach is based on the digital phase-locked loop Kalman filter and is close to optimum insofar as demodulating a frequency modulated type of interferer. Because the interference is assumed to be much stronger than either the signal or the noise, the Kalman filter locks onto the interference and produces estimates of its phase and envelope. The algorithm is compared, through computer simulation, with the recursive least squares lattice algorithm for the case of a swept tone interferer. Examples of the phase- and envelope- tracking capabilities of the algorithm are presented, followed by bit error rate curves for the case of an interferer of bandwidth equal to 20 percent of the chip rate of the spread spectrum signal. The results show that with proper selection of the Kalman filter parameters, the Kalman filter excisor can outperform the recursive least squares algorithm by 2 dB. It is suggested that performance could perhaps be improved further by using a higher order Kalman filter to remove the residual phase-tracking error produced by the second order Kalman filter. Author (CISTI)

N94-14062# Defence Research Establishment, Ottawa (Ontario). Airborne Radar Section.
TESTING VARIOUS TIME-FREQUENCY DISTRIBUTION TECHNIQUES
Robert Klepko and Khanh N. Tran (Ottawa Univ., Ontario.) Nov. 1992 55 p
(DREO-TN-92-17; CTN-93-60738) Avail: CASI HC A04/MF A01

Two time-frequency distributions (TFD's), the Choi-Williams and the Wigner-Ville, are described and tested to illustrate how each technique can resolve stationary and nonstationary signals in both time and frequency domains. The results were compared to those obtained with the standard method used for spectral analysis, short-time discrete Fourier transformation. The tests were performed with discrete simulated sinusoidal signals as well as real signals representing the temporal radar backscatter collected from a synthetic aperture radar. The general properties of the backscatter are the fading in and out of narrowband signals and shifting of signal frequency through time as a result of scatterer motion. Using a TFD allows analysis of the Doppler frequency history of the scatterers located on a target of interest. The major conclusion from the tests performed with real signals is that the Choi-Williams distribution is preferred over both the Wigner-Ville distribution and discrete Fourier transformation as a result of improved signal to noise ratios in the spectral domain. Subroutines used to compute the various distributions are appended. Author (CISTI)

N94-14063# Defence Research Establishment, Ottawa (Ontario). Communications and Navigation Section.
MULTIPLE-SYMBOL DIFFERENTIAL DETECTION OF DPSK WITH FREQUENCY OFFSET
Martin Turgeon Dec. 1991 49 p
(DREO-TN-92-5; CTN-93-60739) Avail: CASI HC A03/MF A01

A ground terminal (GT) simulator for an extremely high frequency satellite communications system is being developed. The GT demodulator uses multiple symbol differential detection of differential phase-shift keying (MSDPSK), a demodulation technique which estimates the phase reference of a differential phase shift keying (DPSK) modulated, burst signal over a sequence of N symbols. The bit error rate (BER) performance is investigated and the simulation results are presented. The BER performance of MSDPSK is shown to approach that of coherently detected DPSK for large values of N. The effects of frequency offset are also examined. For a specific amount of frequency uncertainty, there is an optimum sequence size N that yields the best BER performance. For example, given a burst size of 13 bits and a frequency offset up to one fiftieth of the bit rate, the optimum sequence size is in the range of three to five bits.
Author (CISTI)

N94-14064# Defence Research Establishment, Ottawa (Ontario). Radar ESM Section.
I/Q DEMODULATION OF RADAR SIGNALS WITH CALIBRATION AND FILTERING
Jim P. Y. Lee Dec. 1991 67 p
(DREO-RN-1119; CTN-93-60740; AD-A260153) Avail: CASI HC A04/MF A01

A simple in-phase quadrature (I/Q) demodulator architecture which can measure the amplitude, phase, and instantaneous frequency of radar signals is examined. This architecture has the potential for radar electronic support measure applications where wide instantaneous bandwidth and simple algorithms for extracting the modulation characteristics of radar signals are required. This I/Q architecture can meet the requirement by splitting an incoming signal into its in-phase and quadrature components using analog hardware. However, in practice, there are amplitude and phase imbalances between the two components and direct current offsets, which can introduce large systematic errors in the measurements. Novel techniques are presented which can greatly reduce the systematic errors and improve the accuracy of the measurement. A time domain analysis of the systematic errors is given. A calibration technique which can be used to correct for the imbalances and offsets is discussed. The effect of noise on the accuracy of the measurement is also examined. Finally, a post-processing technique employing moving averages is presented. The technique is shown to be effective for improving the output signal to noise ratio and reducing systematic errors. Author (CISTI)

N94-14065 Applied Silicon, Inc., Ottawa (Ontario).
EWTEST SIGNAL EXCISION TESTBED: SYSTEM EVALUATION
Rick E. Ingram Jan. 1992 11 p
(DSIS-93-00346; CTN-93-60752) Avail: CASI HC A03

A digital signal processing testbed is being developed to provide a platform for the development of spread spectrum signal excision algorithms. The testbed performs real-time acquisition and signal excision on the acquired data. It also provides a post-processing capability for algorithm evaluation. The system is to be implemented using the VMEC30 boards from Applied Silicon, installed in a Sun workstation. The proposed design of the real-time portion of the system is analyzed with respect to general system structure, host/VMEC30 communications, inter-VMEC30 communications, and task distribution. Specific recommendations are made for overcoming the observed limitations of the system, as well as recommendations regarding testbed extensibility and future enhancements.
Author (CISTI)

N94-14066 Applied Silicon, Inc., Ottawa (Ontario).
DSP SOFTWARE DEVELOPMENT ENVIRONMENTS FOR THE ADAPTIVE SIGNAL PROCESSING TESTBED
Hugh A. Parliament Mar. 1992 15 p
(DSIS-93-00347; CTN-93-60753) Avail: CASI HC A03

Three digital signal processing (DSP) software development environments are examined for the Adaptive Signal Processing Testbed. The Texas Instruments Debugger/Simulator, the SPOX DSP Operating System with debugger, and the COMDISCO Signal Processing Worksystem are compared with respect to their capabilities for debugging, prototyping, and simulation, DSP libraries, ease of porting to the VMEC30 board, standalone capabilities, automatic code generation, and price. The COMDISCO Signal Processing Worksystem is recommended as the development environment of choice due to its powerful capabilities, its flexibility in operating with or without the VMEC30, and its expandability to other DSP hardware architectures.
Author (CISTI)

N94-14204 Defence Research Establishment Valcartier (Quebec).
BRIDGING THE GAP BETWEEN THE RAYLEIGH AND THOMSON LIMITS FOR VARIOUS CONVEX BODIES
G. R. Fournier and B. T. N. Evans Jan. 1993 31 p
(DSIS-93-00613; DREV-R-4692-93; CTN-93-60843) Avail: CASI HC A03

If a particle is geometrically and optically small enough, approximate formulae usually called the Rayleigh approximation can be found for the extinction and scattering efficiencies as well as the phase function of these particles. If the particle is still geometrically small but optically very large, the Thomson approximation results. Often, however, a geometrically small particle may be neither optically small nor very large, creating a gap. A transform of Mie coefficients and their series expansion is demonstrated that bridges this gap for spheres and infinite cylinders. This transform generalizes, in an approximate form, to other convex bodies when a Rayleigh or Thomson-like series can be obtained. The results of a comparison between the newly obtained series and the exact codes for spheres and spheroids is also presented. This research will aid in the design and performance analysis of potential new obscurants using high refractivity materials. The electromagnetic extinction through rain, smoke, or other nonspherical atmospheric aerosols can also be evaluated by this approach, an essential first step in the evaluation of the performance of all electro-optical systems.
Author (CISTI)

N94-14291# Oak Ridge National Lab., TN.
ELECTRICAL CHARACTERIZATION OF THE JET A(SUB 2) ANTENNA: COMPARISON OF MODEL WITH MEASUREMENTS WADE, T.
P. M. Ryan, R. H. Goulding, V. Bhatnagar, A. Kaye, and T. Wade 1993 5 p Presented at the 10th Topical Conference on Radio Frequency Power in Plasmas, Boston, MA, 1-3 Apr. 1993
(Contract DE-AC05-84OR-21400)
(DE93-012964; CONF-9304112-8) Avail: CASI HC A01/MF A01

The JET experiment is replacing its previous (A1) antennas with upgraded designs (A2) for its upcoming 'pumped diverter' operation. These antennas are more directional than the previous two-strap A1 antennas when operated as a phased array. The frequency range is 23 to 57 MHz. A full-scale low power 'flat' mockup was tested at JET; strap lengths were adjusted to give balanced operation with resonance at 42 MHz. A second mockup module, differing only slightly from the original, was subsequently fabricated and both modules were sent to ORNL for additional measurements and to test the operation of the power compensator circuit. There are benefits to using a transmission line model to characterize coupled antenna systems, primarily in the ease of incorporating the antennas into the overall analysis of the transmission, tuning, and matching system. The characteristics of the array under arbitrary phasing are also needed for the design, analysis, and control of the power compensator. There are aspects of the JET A2 antenna geometry that differ considerably from previously modeled cases. Each transmission line feeds two poloidally-stacked straps connected in parallel. The parallel straps present different electrical loads at the match point due to geometrical differences. Currents in one section of the strap influence other sections of the same strap as well as in neighboring straps due to internal inductive coupling. The lengths of the inner and outer straps differ; moreover, the inner straps are fed from ports located behind the outer straps, resulting in increased coupling between the inner and outer straps due to the long feed lines and in greater disparity between the electrical loads presented at the inner and outer feed ports. The present effort is to determine whether a more general coupled transmission line model can characterize the array response with sufficient accuracy for the purpose of design and analysis.
DOE

N94-14369*# Jet Propulsion Lab., California Inst. of Tech., Pasadena.
THE TELECOMMUNICATIONS AND DATA ACQUISITION REPORT
Progress Report, Apr. - Jun. 1993
Edward C. Posner, ed. 15 Aug. 1993 358 p
(NASA-CR-194388; TDA-PR-42-114; NAS 1.26:194388) Avail: CASI HC A16/MF A03

Reports on developments in programs managed by JPL's Office of Telecommunications and Data Acquisition (TDA) are provided. In space communications, radio navigation, radio science, and ground-based radio and radar astronomy, it reports on activities of the Deep Space Network (DSN) in planning, supporting research and technology, implementation, and operations. Also included are standards activity at JPL for space data and information systems and reimbursable DSN work performed for other agencies through NASA. For individual titles, see N94-14370 through N94-14398.

N94-14370*# Jet Propulsion Lab., California Inst. of Tech., Pasadena.
RADIO METRIC ERRORS DUE TO MISMATCH AND OFFSET BETWEEN A DSN ANTENNA BEAM AND THE BEAM OF A TROPOSPHERE CALIBRATION INSTRUMENT
R. P. Linfield and J. Z. Wilcox *In its* The Telecommunications and Data Acquisition Report 15 Aug. 1993 p 1-13 (For primary document see N94-14369 02-32)
(RTOP 310-10-60-93-01)
Avail: CASI HC A03/MF A03

Two components of the error of a troposphere calibration measurement were quantified by theoretical calculations. The first component is a beam mismatch error, which occurs when the calibration instrument senses a conical volume different from the cylindrical volume sampled by a Deep Space Network (DSN) antenna. The second component is a beam offset error, which occurs if the calibration instrument is not mounted on the axis of the DSN antenna. These two error sources were calculated for both delay (e.g., VLBI) and delay rate (e.g., Doppler) measurements. The beam mismatch error for both delay and delay rate drops rapidly as the beamwidth of the troposphere calibration instrument (e.g., a water vapor radiometer or an infrared Fourier transform spectrometer) is reduced. At a 10-deg elevation angle, the instantaneous beam mismatch error is 1.0 mm for a 6-deg beamwidth and 0.09 mm for a 0.5-deg beam (these are the full angular widths of a circular beam with uniform gain out to a sharp cutoff). Time averaging for 60-100 sec will reduce these errors by factors of 1.2-2.2. At a 20-deg elevation angle, the lower limit for current Doppler observations, the beam-mismatch delay rate error is an Allan standard deviation over 100 sec of 1.1 x 10(exp -14) with a 4-deg beam and 1.3 x 10(exp -l5) for a 0.5-deg beam. A 50-m beam offset would result in a fairly modest (compared to other expected error sources) delay error (less than or equal to 0.3 mm for 60-sec integrations at any elevation angle is greater than or equal to 6 deg). However, the same offset would cause a large error in delay rate measurements (e.g., an Allan standard deviation of 1.2 x 10(exp -14) over 100 sec at a 20-deg elevation angle), which would dominate over other known error sources if the beamwidth is 2 deg or smaller. An on-axis location is essential for accurate troposphere calibration of delay

rate measurements. A half-power beamwidth (for a beam with a tapered gain profile) of 1.2 deg or smaller is desired for calibration of all types of radio metrics. A water-vapor radiometer calibration beam of this size with very low sidelobes would require a clear aperture antenna with a diameter of at least 1.5 m if the primary water vapor sensing channel were in the 20-22 GHz range. Author (revised)

N94-14371*# Jet Propulsion Lab., California Inst. of Tech., Pasadena.
IMPROVED TREATMENT OF GLOBAL POSITIONING SYSTEM FORCE PARAMETERS IN PRECISE ORBIT DETERMINATION APPLICATIONS **c04**

Y. Vigue, S. M. Lichten, R. J. Muellerschoen, G. Blewitt, and M. B. Heflin *In its* The Telecommunications and Data Acquisition Report 15 Aug. 1993 p 14-20 (For primary document see N94-14369 02-32)
(RTOP 310-10-61-84-02)
Avail: CASI HC A02/MF A03

Data collected from a worldwide 1992 experiment were processed at JPL to determine precise orbits for the satellites of the Global Positioning System (GPS). A filtering technique was tested to improve modeling of solar-radiation pressure force parameters for GPS satellites. The new approach improves orbit quality for eclipsing satellites by a factor of two, with typical results in the 25- to 50-cm range. The resultant GPS-based estimates for geocentric coordinates of the tracking sites, which include the three DSN sites, are accurate to 2 to 8 cm, roughly equivalent to 3 to 10 nrad of angular measure. Author (revised)

N94-14372*# Jet Propulsion Lab., California Inst. of Tech., Pasadena.
USE OF GLOBAL POSITIONING SYSTEM MEASUREMENTS TO DETERMINE GEOCENTRIC COORDINATES AND VARIATIONS IN EARTH ORIENTATION **c04**

R. P. Malla (Sterling Software, Inc., Pasadena, CA.), S.-C. Wu, and S. M. Lichten *In its* The Telecommunications and Data Acquisition Report 15 Aug. 1993 p 21-33 (For primary document see N94-14369 02-32)
(RTOP 310-10-61-84-02)
Avail: CASI HC A03/MF A03

Geocentric tracking station coordinates and short-period Earth-orientation variations can be measured with Global Positioning System (GPS) measurements. Unless calibrated, geocentric coordinate errors and changes in Earth orientation can lead to significant deep-space tracking errors. Ground-based GPS estimates of daily and subdaily changes in Earth orientation presently show centimeter-level precision. Comparison between GPS-estimated Earth-rotation variations, which are the differences between Universal Time 1 and Universal Coordinated Time (UT1-UTC), and those calculated from ocean tide models suggests that observed subdaily variations in Earth rotation are dominated by oceanic tidal effects. Preliminary GPS estimates for the geocenter location (from a 3-week experiment) agree with independent satellite laser-ranging estimates to better than 10 cm. Covariance analysis predicts that temporal resolution of GPS estimates for Earth orientation and geocenter improves significantly when data collected from low Earth-orbiting satellites as well as from ground sites are combined. The low Earth GPS tracking data enhance the accuracy and resolution for measuring high-frequency global geodynamical signals over time scales of less than 1 day. Author

N94-14373*# Jet Propulsion Lab., California Inst. of Tech., Pasadena.
FAILURE MODES OF REDUCED-ORDER ORBIT DETERMINATION FILTERS AND THEIR REMEDIES **c13**

D. J. Scheeres *In its* The Telecommunications and Data Acquisition Report 15 Aug. 1993 p 34-42 (For primary document see N94-14369 02-32)
(RTOP 310-10-63-50-00)
Avail: CASI HC A02/MF A03

Ways in which failure can occur in reduced-order, orbit determination filter, error covariance calculations are discussed. In the context of this article, reduced-order filters denote nonoptimal filters which include fixed levels of uncertainty in some parameters of the measurement models or in the spacecraft dynamical model which are not explicitly estimated in the filter equations. Failure is defined as an increase in the orbit determination covariance with the addition of data or as an unreasonable growth in the covariance with time, i.e., nonasymptotic behavior of the covariance. Some simple, known cases of failure are discussed along with their traditional remedies. In addition, more modern remedies are discussed which are currently under development at the Jet Propulsion Laboratory. The article first describes the known problems of reduced-order filters when they are employed for orbit determination, and their traditional remedies. Then, having defined these, the relevancy and desirability of the more modern remedies are made apparent. Author (revised)

N94-14374*# Jet Propulsion Lab., California Inst. of Tech., Pasadena.
CAMMATIC: AN APPROACH TO IMPROVE DSS 13 ANTENNA GRAVITY-LOADING PERFORMANCE

R. Levy and D. Strain (Planning Research Corp., Pasadena, CA.) *In its* The Telecommunications and Data Acquisition Report 15 Aug. 1993 p 43-50 (For primary document see N94-14369 02-32)
(RTOP 310-20-65-86-04)
Avail: CASI HC A02/MF A03

Corrective actuator forces are applied to the DSS 13 antenna structure to improve its accuracy. These forces are calibrated according to the antenna elevation requirements. The calibration is derived from accurate field measurements and is not subject to the errors that result from computer modeling. A successful demonstration provided significant antenna surface improvement. An improvement of 0.6 to 1 dB is predicted. Author (revised)

N94-14375*# Jet Propulsion Lab., California Inst. of Tech., Pasadena.
A CRYOGENIC SEVEN-ELEMENT HEMT FRONT END FOR DSS 13

J. Bowen and D. Neff *In its* The Telecommunications and Data Acquisition Report 15 Aug. 1993 p 51-60 (For primary document see N94-14369 02-32)
(RTOP 310-20-66-91-02)
Avail: CASI HC A02/MF A03

A cryogenically cooled Ka-band (33.6-GHz), seven-element front-end array for the DSN was built and tested. This system uses seven high electron mobility transistor (HEMT) low-noise amplifiers cooled by a two-stage closed-cycle refrigerator. All system components from the polarizers to the output isolators are cooled to a physical temperature between 18 and 35 K. The noise temperatures of the individual elements range from 64 to 84 K over a 2.75-GHz bandwidth. Author

N94-14376*# Jet Propulsion Lab., California Inst. of Tech., Pasadena.
INSERTION LOSS AND NOISE-TEMPERATURE CONTRIBUTION OF HIGH-TEMPERATURE SUPERCONDUCTING BANDPASS FILTERS CENTERED AT 2.3 AND 8.45 GHz **c33**

J. L. Prater and J. J. Bautista *In its* The Telecommunications and Data Acquisition Report 15 Aug. 1993 p 61-67 (For primary document see N94-14369 02-32)
(RTOP 310-20-66-92-01)
Avail: CASI HC A02/MF A03

Two superconducting Tl-Ca-Cu-Ba-O bandpass filters were fabricated for JPL by Superconductor Technologies Incorporated, Santa Barbara, California. The filters were designed to operate at 2.3 GHz (S-band) with a 0.5-dB bandwidth of 60 MHz and at 8.45 GHz (X-band) with a 0.5-dB bandwidth of 150 MHz. The structure selected for both filters incorporates half-wavelength thin-film resonators in a stripline configuration. The S-band filter uses an edge-coupled interdigital design and the X-band filter uses an end-coupled design. The insertion loss and the noise-temperature contribution were measured at 12 K for both filters. Author (revised)

N94-14377*# Jet Propulsion Lab., California Inst. of Tech., Pasadena.
CODING PERFORMANCE OF THE PROBE-ORBITER-EARTH COMMUNICATION LINK

D. Divsalar, S. Dolinar, and F. Pollara *In its* The Telecommunications and Data Acquisition Report 15 Aug. 1993 p 68-83 (For primary document see N94-14369 02-32)
(RTOP 310-30-71-83-04)
Avail: CASI HC A03/MF A03

The coding performance of the Probe-Orbiter-Earth communication link is analyzed and compared for several cases. It is assumed that the coding system consists of a convolutional code at the Probe, a quantizer and another convolutional code at the Orbiter, and two cascaded Viterbi decoders or a combined decoder on the ground. Author

N94-14378*# Johns Hopkins Univ., Baltimore, MD.
EXPLOITING THE CANNIBALISTIC TRAITS OF REED-SOLOMON CODES
O. Collins *In* JPL, The Telecommunications and Data Acquisition Report 15 Aug. 1993 p 84-89 Prepared for Jet Propulsion Lab., California Inst. of Tech., Pasadena (For primary document see N94-14369 02-32)
(RTOP 310-30-71-83-02)
Avail: CASI HC A02/MF A03

In Reed-Solomon codes and all other maximum distance separable codes, there is an intrinsic relationship between the size of the symbols in a codeword and the length of the codeword. Increasing the number of symbols in a codeword to improve the efficiency of the coding system thus requires using a larger set of symbols. However, long Reed-Solomon codes are difficult to implement and many communications or storage systems cannot easily accommodate an increased symbol size, e.g., M-ary frequency shift keying (FSK) and photon-counting pulse-position modulation demand a fixed symbol size. A technique for sharing redundancy among many different Reed-Solomon codewords to achieve the efficiency attainable in long Reed-Solomon codes without increasing the symbol size is described. Techniques both for calculating the performance of these new codes and for determining their encoder and decoder complexities is presented. These complexities are usually found to be substantially lower than conventional Reed-Solomon codes of similar performance. Author (revised)

N94-14379*# Jet Propulsion Lab., California Inst. of Tech., Pasadena.
ESTIMATING THE SIZE OF HUFFMAN CODE PREAMBLES
R. J. McEliece and T. H. Palmatier (California Inst. of Tech., Pasadena.) *In its* The Telecommunications and Data Acquisition Report 15 Aug. 1993 p 90-95 (For primary document see N94-14369 02-32)
(RTOP 310-30-71-83-02)
Avail: CASI HC A02/MF A03

Data compression via block-adaptive Huffman coding is considered. The compressor consecutively processes blocks of N data symbols, estimates source statistics by computing the relative frequencies of each source symbol in the block, and then synthesizes a Huffman code based on these estimates. In order to let the decompressor know which Huffman code is being used, the compressor must begin the transmission of each compressed block with a short preamble or header file. This file is an encoding of the list n = (n(sub 1), n(sub 2)....,n(sub m)), where n(sub i) is the length of the Hufffman codeword associated with the ith source symbol. A simple method of doing this encoding is to individually encode each n(sub i) into a fixed-length binary word of length log(sub 2)l, where l is an a priori upper bound on the codeword length. This method produces a maximum preamble length of mlog(sub 2)l bits. The object is to show that, in most cases, no substantially shorter header of any kind is possible.
Author (revised)

N94-14380*# Jet Propulsion Lab., California Inst. of Tech., Pasadena.
ENHANCED DECODING FOR THE GALILEO S-BAND MISSION
S. Dolinar and M. Belongie *In its* The Telecommunications and Data Acquisition Report 15 Aug. 1993 p 96-111 (For primary document see N94-14369 02-32)
(RTOP 314-30-61-02-07)
Avail: CASI HC A03/MF A03

A coding system under consideration for the Galileo S-band low-gain antenna mission is a concatenated system using a variable redundancy Reed-Solomon outer code and a (14,1/4) convolutional inner code. The 8-bit Reed-Solomon symbols are interleaved to depth 8, and the eight 255-symbol codewords in each interleaved block have redundancies 64, 20, 20, 20, 64, 20, 20, and 20, respectively (or equivalently, the codewords have 191, 235, 235, 235, 191, 235, 235, and 235 8-bit information symbols, respectively). This concatenated code is to be decoded by an enhanced decoder that utilizes a maximum likelihood (Viterbi) convolutional decoder; a Reed Solomon decoder capable of processing erasures; an algorithm for declaring erasures in undecoded codewords based on known erroneous symbols in neighboring decodable words; a second Viterbi decoding operation (redecoding) constrained to follow only paths consistent with the known symbols from previously decodable Reed-Solomon codewords; and a second Reed-Solomon decoding operation using the output from the Viterbi redecoder and additional erasure declarations to the extent possible. It is estimated that this code and decoder can achieve a decoded bit error rate of 1 x 10(exp 7) at a concatenated code signal-to-noise ratio of 0.76 dB. By comparison, a threshold of 1.17 dB is required for a baseline coding system consisting of the same (14,1/4) convolutional code, a (255,223) Reed-Solomon code with constant redundancy 32 also interleaved to depth 8, a one-pass Viterbi decoder, and a Reed Solomon decoder incapable of declaring or utilizing erasures. The relative gain of the enhanced system is thus 0.41 dB. It is predicted from analysis based on an assumption of infinite interleaving that the coding gain could be further improved by approximately 0.2 dB if four stages of Viterbi decoding and four levels of Reed-Solomon redundancy are permitted. Confirmation of this effect and specification of the optimum four-level redundancy profile for depth-8 interleaving is currently being done. Author (revised)

N94-14381*# Jet Propulsion Lab., California Inst. of Tech., Pasadena.
STABILITY MEASUREMENTS OF THE RADIO SCIENCE SYSTEM AT THE 34-m HIGH-EFFICIENCY ANTENNAS
T. T. Pham, J. C. Breidenthal, T. K. Peng, S. F. Abbate, and S. T. Rockwell *In its* The Telecommunications and Data Acquisition Report 15 Aug. 1993 p 112-139 (For primary document see N94-14369 02-32)
(RTOP 314-40-41-11-06)
Avail: CASI HC A03/MF A03

From 1991 to 1993 the fractional frequency stability of the operational Radio Science System was measured at DSS's 15, 45, and 65. These stations are designed to have the most stable uplink and downlink equipment in the Deep Space Network (DSN). Some measurements were performed when the antenna was moving and the frequency was ramped. The stability, including contributions of all elements in the station except for the antenna and the hydrogen maser, was measured to be 0.3 to 1.3 x 10(exp -15) when the frequency was fixed, and 0.6 to 6.0 x 10(exp -15) when the frequency was ramped (sample interval, 1000 sec). Only one measurement out of fifteen exceeded specification. In all other cases, when previous measurements on the antenna and the hydrogen maser were added, a total system stability requirement of 5.0 x 10(exp -15) as met. In addition, ambient temperature was found to cause phase variation in the measurements at a rate of 5.5 deg of phase per deg C. Author (revised)

N94-14382*# Jet Propulsion Lab., California Inst. of Tech., Pasadena.
PERFORMANCE RESULTS OF A DIGITAL TEST SIGNAL GENERATOR **c33**
B. O. Gutierrez-Luaces, M. Marina, and B. Parham (OAO Corp., Los Angeles, CA.) *In its* The Telecommunications and Data Acquisition Report 15 Aug. 1993 p 140-153 (For primary document see N94-14369 02-32)
(RTOP 314-40-41-11-06)
Avail: CASI HC A03/MF A03

Performance results of a digital test signal-generator hardware-demonstration unit are reported. Capabilities available include baseband and intermediate frequency (IF) spectrum generation, for which test results are provided. Repeatability in the setting of a given signal-to-noise ratio (SNR) when a baseband or an IF spectrum is being generated ranges from 0.01 dB at high SNR's or high data rates to 0.3 dB at low data rates or low SNR's. Baseband symbol SNR and carrier SNR (Pc/No) accuracies of 0.1 dB were verified with the built-in statistics circuitry. At low SNR's that accuracy remains to be fully verified. These results were confirmed with measurements from a demodulator synchronizer assembly for the baseband spectrum generation, and with a digital receiver (Pioneer 10 receiver) for the IF spectrum generation. Author

N94-14383*# Jet Propulsion Lab., California Inst. of Tech., Pasadena.
FORMAL FUNCTIONAL TEST DESIGNS WITH A TEST REPRESENTATION LANGUAGE
J. M. Hops *In its* The Telecommunications and Data Acquisition Report 15 Aug. 1993 p 154-169 (For primary document see N94-14369 02-32)
(RTOP 314-40-41-21-03)
Avail: CASI HC A03/MF A03

The application of the category-partition method to the test design phase of hardware, software, or system test development is discussed. The method provides a formal framework for reducing the total number of possible test cases to a minimum logical subset for effective testing. An automatic tool and a formal language were developed to implement the method and produce the specification of test cases. Author (revised)

N94-14384*# Jet Propulsion Lab., California Inst. of Tech., Pasadena.
PC4CAST: A TOOL FOR DSN LOAD FORECASTING AND CAPACITY PLANNING
S. J. Loyola *In its* The Telecommunications and Data Acquisition Report 15 Aug. 1993 p 170-184 (For primary document see N94-14369 02-32)
(RTOP 315-90-22-70-19)
Avail: CASI HC A03/MF A03

Effectively planning the use and evolution of the Deep Space Network (DSN) is a complex problem involving many parameters. The tool that models many of these complexities, yet requires simple structured inputs and provides concise easy-to-understand metrics to aid in the planning process is discussed. The tool, PC4CAST, is used for both load forecasting (predicting how well planned that DSN resources meet expected demand) and as a decision support tool in the capacity-planning process (determining the relative benefits of capacity expansion options). It is now in use in the TDA Planning Office, has been used in numerous studies, and is also being used by the JPL Multimission Operations System Office (MOSO) as an integral part of Resource Allocation Team activities. Experience using the tool has helped to identify additional requirements that will further improve the planning process, which can be met by future PC4CAST versions. Author

N94-14385*# Jet Propulsion Lab., California Inst. of Tech., Pasadena.
ASYNCHRONOUS TRANSFER MODE LINK PERFORMANCE OVER GROUND NETWORKS
E. T. Chow and R. W. Markley *In its* The Telecommunications and Data Acquisition Report 15 Aug. 1993 p 185-191 (For primary document see N94-14369 02-32)
(RTOP 316-30-19-41-04)
Avail: CASI HC A02/MF A03

The results of an experiment to determine the feasibility of using asynchronous transfer mode (ATM) technology to support advanced spacecraft missions that require high-rate ground communications and, in particular, full-motion video are reported. Potential nodes in such a ground network include Deep Space Network (DSN) antenna stations, the Jet Propulsion Laboratory, and a set of national and international end users. The experiment simulated a lunar microrover, lunar lander, the DSN ground communications system, and distributed science users. The users were equipped with video-capable workstations. A key feature was an optical fiber link between two high-performance workstations equipped with ATM interfaces. Video was also transmitted through JPL's institutional network to a user 8 km from the experiment. Variations in video depending on the networks and computers were observed, the results are reported.
Author (revised)

N94-14386*# Jet Propulsion Lab., California Inst. of Tech., Pasadena.
AN OVERVIEW OF THE GALILEO OPTICAL EXPERIMENT (GOPEX)
K. E. Wilson and J. R. Lesh *In its* The Telecommunications and Data Acquisition Report 15 Aug. 1993 p 192-204 (For primary document see N94-14369 02-32)
(RTOP 315-91-60-10-03)
Avail: CASI HC A03/MF A03

Uplink optical communication to a deep-space vehicle was demonstrated. In the Galileo Optical Experiment (GOPEX), optical transmissions were beamed to the Galileo spacecraft by Earth-based transmitters at the Table Mountain Facility (TMF), California, and Starfire Optical Range (SOR), New Mexico. The demonstration took place over an eight-day period (9 Dec. through 16 Dec. 1992) as Galileo receded from Earth on its way to Jupiter, and covered ranges from 1-6 million km. At 6 million km (15 times the Earth-Moon distance), the laser beam transmitted from TMF eight days after Earth flyby covered the longest known range for transmission and detection. Author (revised)

N94-14387*# Jet Propulsion Lab., California Inst. of Tech., Pasadena.
CALIBRATION OF THE RECEIVER CHANNEL FOR THE GOPEX PRECURSOR EXPERIMENTS
A. Biswas *In its* The Telecommunications and Data Acquisition Report 15 Aug. 1993 p 205-212 (For primary document see N94-14369 02-32)
(RTOP 315-91-60-10-03)
Avail: CASI HC A02/MF A03

Calibration measurements for the cooled (253 K) photomultiplier tube (PMT) detector, used on the receiver channel of the transmit/receive (T/R) switch for GOPEX, were conducted in the laboratory. A pulsed frequency-doubled neodymium:yttrium-aluminum-garnet (Nd:YAG) laser was used to direct 532-mn light on the PMT. By monitoring the energy per pulse of the light incident on the PMT, the minimum number of photons detected could be determined. These results agreed with the photon flux back-calculated from the PMT output waveform. Approximately 700 incident photons arriving during a temporal pulse width of approximately 65 nsec were detected with a signal-to-noise ratio (SNR) of approximately 1. Other receiver channel characteristics, such as PMT dark currents, optical transmission, and interference filter sensitivity to angle of light incidence, were also measured. Author (revised)

N94-14388*# Jet Propulsion Lab., California Inst. of Tech., Pasadena.
DATA ANALYSIS FOR GOPEX IMAGE FRAMES
B. M. Levine, K. S. Shaik, and T.-Y. Yan *In its* The Telecommunications and Data Acquisition Report 15 Aug. 1993 p 213-229 (For primary document see N94-14369 02-32)
(RTOP 315-91-60-10-03)
Avail: CASI HC A03/MF A03

The data analysis based on the image frames received at the Solid State Imaging (SSI) camera of the Galileo Optical Experiment (GOPEX) demonstration conducted between 9-16 Dec. 1992 is described. Laser uplink was successfully established between the ground and the Galileo spacecraft during its second Earth-gravity-assist phase in December 1992. SSI camera frames were acquired which contained images of detected laser pulses transmitted from the Table Mountain Facility (TMF), Wrightwood, California, and the Starfire Optical Range (SOR), Albuquerque, New Mexico. Laser pulse data were processed using standard image-processing techniques at the Multimission Image Processing Laboratory (MIPL) for preliminary pulse identification and to produce public release images. Subsequent image analysis corrected for background noise to measure received pulse intensities. Data were plotted to obtain histograms on a daily basis and were then compared with theoretical results derived from applicable weak-turbulence and strong-turbulence considerations. Processing steps are described and the theories are compared with the experimental results. Quantitative agreement was found in both turbulence regimes, and better agreement would have been found, given more received laser pulses. Future experiments should consider methods to reliably measure low-intensity pulses, and through experimental planning to geometrically locate pulse positions with greater certainty. Author (revised)

N94-14389*# Jet Propulsion Lab., California Inst. of Tech., Pasadena.
TELESCOPE POINTING FOR GOPEX
W. M. Owen, Jr. *In its* The Telecommunications and Data Acquisition Report 15 Aug. 1993 p 230-235 (For primary document see N94-14369 02-32)
(RTOP 315-91-60-10-03)
Avail: CASI HC A02/MF A03

In order for photons emitted by the GOPEX lasers to be detected by Galileo's camera, the telescopes at Table Mountain Observatory and Starfire Optical Range had to be pointed in the right direction within a tolerance less than the beam divergence. At both sites nearby stars were used as pointing references. The technical challenge was to ensure that the transmission direction and the star positions were specified in exactly the same coordinate system; given this assurance, neither the uncertainty in the star catalog positions nor the difficulty in offset pointing was expected to exceed the pointing error budget. The correctness of the pointing scheme was verified by the success of GOPEX. Author

N94-14390*# Jet Propulsion Lab., California Inst. of Tech., Pasadena.
GALILEO OPTICAL EXPERIMENT (GOPEX) OPTICAL TRAIN: DESIGN AND VALIDATION AT THE TABLE MOUNTAIN FACILITY
J. Yu and M. Shao *In its* The Telecommunications and Data Acquisition Report 15 Aug. 1993 p 236-247 (For primary document see N94-14369 02-32)
(RTOP 315-91-60-10-03)
Avail: CASI HC A03/MF A03

The Galileo Optical Experiment (GOPEX) has demonstrated the first laser communications uplink to a deep space vehicle. The optical design and validation tests performed at the Table Mountain Facility (TMF)

transmitter site are described. The system used a 0.6-m telescope and an optical system at coude focus to produce the uplink beam. The optical system used a pulsed neodymium:yttrium-aluminum-garnet (Nd:Yag) laser and beam diverger optics to produce the required optical output. In order to validate the optical design, a number of uplinks were performed on Earth-orbiting satellites (e.g., Lageos 1 and 2). Author (revised)

N94-14391*# Jet Propulsion Lab., California Inst. of Tech., Pasadena.
GOPEX LASER TRANSMISSION AND MONITORING SYSTEMS c36
G. Okamoto and K. Masters *In its* The Telecommunications and Data Acquisition Report 15 Aug. 1993 p 248-254 (For primary document see N94-14369 02-32)
(RTOP 315-91-60-10-03)
Avail: CASI HC A02/MF A03

The laser transmission and monitoring system for the Galileo Optical Experiment (GOPEX) at the Table Mountain Facility (TMF) in Wrightwood, California is described. The transmission system configuration and the data measurement techniques are described. The calibration procedure and the data analysis algorithm are also discussed. The mean and standard deviation of the laser energy transmitted each day of GOPEX show that the laser transmission system performed well and within the limit established in conjunction with the Galileo Project for experiment concurrence.
Author (revised)

N94-14392*# Phillips Lab., Kirtland AFB, NM. Starfire Optical Range.
GOPEX AT THE STARFIRE OPTICAL RANGE
R. Q. Fugate *In* JPL, The Telecommunications and Data Acquisition Report 15 Aug. 1993 p 255-279 (For primary document see N94-14369 02-32)
(RTOP 315-91-60-10-03)
Avail: CASI HC A03/MF A03

The Starfire Optical Range successfully conducted laser upink experiments to the Galileo spacecraft during the early morning hours of December 9, 10, 11, and 12, 1992, when the spacecraft was at ranges between 700,000 and 3 million km from Earth. Analysts at JPL have reported as many as 79 pulse detections by the spacecraft. The best weather conditions occurred on the second night when 37 pulses were detected with as many as five on one frame. Signal levels at the spacecraft generally agree with predictions. Author

N94-14393*# Jet Propulsion Lab., California Inst. of Tech., Pasadena.
PRELIMINARY DESIGN AND IMPLEMENTATION OF THE BASELINE DIGITAL BASEBAND ARCHITECTURE FOR ADVANCED DEEP SPACE TRANSPONDERS
T. M. Nguyen and H.-G. Yeh *In its* The Telecommunications and Data Acquisition Report 15 Aug. 1993 p 280-294 (For primary document see N94-14369 02-32)
(RTOP 315-91-10-13-08)
Avail: CASI HC A03/MF A03

The baseline design and implementation of the digital baseband architecture for advanced deep space transponders is investigated and identified. Trade studies on the selection of the number of bits for the analog-to-digital converter (ADC) and optimum sampling schemes are presented. In addition, the proposed optimum sampling scheme is analyzed in detail. Descriptions of possible implementations for the digital baseband (or digital front end) and digital phase-locked loop (DPLL) for carrier tracking are also described. Author (revised)

N94-14394*# Jet Propulsion Lab., California Inst. of Tech., Pasadena.
HARDWARE DESIGN FOR THE AUTONOMOUS VISIBILITY MONITORING (AVM) OBSERVATORY c14
K. Cowles *In its* The Telecommunications and Data Acquisition Report 15 Aug. 1993 p 295-301 (For primary document see N94-14369 02-32)
(RTOP 315-91-60-10-06)
Avail: CASI HC A03/MF A03

The hardware for the three Autonomous Visibility Monitoring (AVM) observatories was redesigned. Changes in hardware design include electronics components, weather sensors, and the telescope drive system. Operation of the new hardware is discussed, as well as some of its features. The redesign will allow reliable automated operation.
Author (revised)

N94-14395*# Jet Propulsion Lab., California Inst. of Tech., Pasadena.
LAYOUT AND CABLING CONSIDERATIONS FOR A LARGE COMMUNICATIONS ANTENNA ARRAY
R. T. Logan, Jr. *In its* The Telecommunications and Data Acquisition Report 15 Aug. 1993 p 302-310 (For primary document see N94-14369 02-32)
(RTOP 315-91-60-10-07)
Avail: CASI HC A02/MF A03

Layout considerations for a large deep space communications antenna array are discussed. A fractal geometry for the antenna layout is described that provides optimal packing of antenna elements, efficient cable routing, and logical division of the array into identical sub-arrays. Author (revised)

N94-14396*# Jet Propulsion Lab., California Inst. of Tech., Pasadena.
AN INITIAL STUDY OF USING THE 34-m ANTENNA FOR LUNAR MISSION SUPPORT
A. Cha and P. Cramer *In its* The Telecommunications and Data Acquisition Report 15 Aug. 1993 p 311-315 (For primary document see N94-14369 02-32)
(RTOP 316-30-19-41-05)
Avail: CASI HC A01/MF A03

As a part of the long-range planning of future Mars and lunar missions, a feasibility study was made of a 34-m antenna system with differentially pointed multiple beams. The performance loss mechanisms of the differentially pointed multiple-beam systems were identified and quantified. Techniques that can significantly improve the multiple-beam system performance are identified. The goal is to determine the feasibility of using the 34-m antenna to support widely separated elements associated with lunar missions. Author (revised)

N94-14397*# Jet Propulsion Lab., California Inst. of Tech., Pasadena.
HRMS SKY SURVEY WIDEBAND FEED SYSTEM DESIGN FOR DSS 24 BEAM WAVEGUIDE ANTENNA
P. H. Stanton, P. R. Lee, and H. F. Reilly *In its* The Telecommunications and Data Acquisition Report 15 Aug. 1993 p 316-326 (For primary document see N94-14369 02-32)
(RTOP 314-30-69-40-06)
Avail: CASI HC A03/MF A03

The High-Resolution Microwave Survey (HRMS) Sky Survey project will be implemented on the DSS 24 beam waveguide (BWG) antenna over the frequency range of 2.86 to 10 GHz. Two wideband, ring-loaded, corrugated feed horns were designed to cover this range. The horns match the frequency-dependent gain requirements for the DSS 24 BWG system. The performance of the feed horns and the calculated system performance of DSS 24 are presented. Author

N94-14398*# Jet Propulsion Lab., California Inst. of Tech., Pasadena.
THE FLIGHT PERFORMANCE OF THE GALILEO ORBITER USO
D. D. Morabito, T. P. Krisher, and S. W. Asmar *In its* The Telecommunications and Data Acquisition Report 15 Aug. 1993 p 327-345 (For primary document see N94-14369 02-32)
(RTOP 314-40-31-30-26; RTOP 889-54-62-01-00)
Avail: CASI HC A03/MF A03

Results are presented from an analysis of radio metric data received by the DSN stations from the Galileo spacecraft using an Ultrastable Oscillator (USO) as a signal source. These results allow the health and performance of the Galileo USO to be evaluated, and are used to calibrate this Radio Science instrument and the data acquired for Radio Science experiments such as the Red-shift Observation, Solar Conjunction, and Jovian occultations. Estimates for the USO-referenced spacecraft-transmitted frequency and frequency stability were made for 82 data acquisition passes conducted between launch (October 1989) and November 1991. Analyses of the spacecraft-transmitted frequencies show that the USO is behaving as expected. The USO was powered off and then back on in August 1991 with no adverse effect on its performance. The frequency stabilities measured by Allan deviation are consistent with expected values due to thermal wideband noise and the USO itself at the appropriate time intervals. The Galileo USO appears to be healthy and functioning normally in a reasonable manner. Author (revised)

N94-14501*# Virginia Polytechnic Inst. and State Univ., Blacksburg. Dept. of Electrical Engineering.

FEASIBILITY STUDY OF A SYNTHESIS PROCEDURE FOR ARRAY FEEDS TO IMPROVE RADIATION PERFORMANCE OF LARGE DISTORTED REFLECTOR ANTENNAS Semiannual Status Report

W. L. Stutzman, K. Takamizawa, P. Werntz, J. LaPean, and B. Shen Oct. 1993 13 p

(Grant NAG1-859)

(NASA-CR-194491; NAS 1.26:194491; SATCOM-93-15) Avail: CASI HC A03/MF A01

The manpower on this effort was reduced during this reporting period. Activity in the past six months is summarized. The Type 1 antenna is complete and documentation is in final phases. The Type 2 antenna design is complete and a journal article was prepared and was accepted for publication in EEE Transactions on Antennas and Propagation. The spherical antenna configurations are complete and a journal article will appear in the June 1993 issue of EEE Transactions on Antennas and Propagation. In addition, a patent for the spherical antenna is being pursued. The final current activity is that of optimization techniques and they are approaching completion as well. The Tri-Reflector synthesis code (TSAP) was put into user friendly format. A user's guide (Report 93-13) was written and distributed to LaRC. Work continues on EASY7. EASY7 is a user friendly code used to create an input file to GRASP7. Author (revised)

N94-14512# Sandia National Labs., Albuquerque, NM.

IONOSPHERIC EFFECTS ON A WIDE-BANDWIDTH, POLARIMETRIC, SPACE-BASED, SYNTHETIC-APERTURE RADAR

B. C. Brock Jan. 1993 67 p

(Contract DE-AC04-76DP-00789)

(DE93-015084; SAND-92-1967) Avail: CASI HC A04/MF A01

The earth's ionosphere consists of an ionized plasma which will interact with any electromagnetic wave propagating through it. The interaction is particularly strong at vhf and uhf frequencies but decreases for higher microwave frequencies. These interaction effects and their relationship to the operation of a wide-bandwidth, synthetic-aperture, space-based radar are examined. Emphasis is placed on the dispersion effects and the polarimetric effects. Results show that high-resolution (wide-bandwidth) and high-quality coherent polarimetrics will be very difficult to achieve below 1 GHz. DOE

N94-14542*# National Aeronautics and Space Administration. Lewis Research Center, Cleveland, OH.

TRANSFORM CODING FOR SPACE APPLICATIONS

Daniel Glover Oct. 1993 11 p Proposed for presentation at the Computing in Aerospace 9 Conference, San Diego, CA, 19-21 Oct. 1993; sponsored by AIAA

(RTOP 144-10-10)

(NASA-TM-106362; E-8160; NAS 1.15:106362; AIAA Paper 93-4670)

Avail: CASI HC A03/MF A01

Data compression coding requirements for aerospace applications differ somewhat from the compression requirements for entertainment systems. On the one hand, entertainment applications are bit rate driven with the goal of getting the best quality possible with a given bandwidth. Science applications are quality driven with the goal of getting the lowest bit rate for a given level of reconstruction quality. In the past, the required quality level has been nothing less than perfect allowing only the use of lossless compression methods (if that). With the advent of better, faster, cheaper missions, an opportunity has arisen for lossy data compression methods to find a use in science applications as requirements for perfect quality reconstruction runs into cost constraints. This paper presents a review of the data compression problem from the space application perspective. Transform coding techniques are described and some simple, integer transforms are presented. The application of these transforms to space-based data compression problems is discussed. Integer transforms have an advantage over conventional transforms in computational complexity. Space applications are different from broadcast or entertainment in that it is desirable to have a simple encoder (in space) and tolerate a more complicated decoder (on the ground) rather than vice versa. Energy compaction with new transforms are compared with the Walsh-Hadamard (WHT), Discrete Cosine (DCT), and Integer Cosine (ICT) transforms. Author

N94-14654*# Jet Propulsion Lab., California Inst. of Tech., Pasadena.

PROCEEDINGS OF THE SEVENTEENTH NASA PROPAGATION EXPERIMENTERS MEETING (NAPEX 17) AND THE ADVANCED COMMUNICATIONS TECHNOLOGY SATELLITE (ACTS) PROPAGATION STUDIES MINIWORKSHOP

Faramaz Davarian, ed. 1 Aug. 1993 329 p Meeting held in Pasadena, CA, 14-15 Jun. 1993

(Contract NAS7-918)

(NASA-CR-194096; JPL-Publ-93-21; NAS 1.26:194096) Avail: CASI HC A15/MF A03

The NASA Propagation Experimenters Meeting (NAPEX) is convened annually to discuss studies made on radio wave propagation by investors from domestic and international organizations. NAPEX 17 was held on 15 June 1993. The meeting was organized into two technical sessions. The first session was dedicated to slant path propagation studies and experiments. The second session focused on propagation studies for mobile and personal communications. Preceding NAPEX 17, the Advanced Communications Technology Satellite (ACTS) Propagation Studies Miniworkshop was held on 14 June 1993 to review ACTS propagation activities with emphasis on ACTS experiments status and data collection, processing, and exchange. For individual titles, see N94-14655 through N94-14678.

N94-14655*# Jet Propulsion Lab., California Inst. of Tech., Pasadena.

OPENING REMARKS: CURRENT AND FUTURE ACTIVITIES

Faramaz Davarian *In its* Proceedings of the Seventeenth NASA Propagation Experimenters Meeting (NAPEX 17) and the Advanced Communications Technology Satellite (ACTS) Propagation Studies Miniworkshop 1 Aug. 1993 p 1-11 (For primary document see N94-14654 02-32)

Avail: CASI HC A03/MF A03

It is our custom to present the Propagation Program's recent accomplishments and future plans at the onset of a NAPEX meeting. A summary is presented. The data analysis phase of the U.S. Olympus Campaign is nearing its end. The final report will be published by Virginia Tech by midsummer 1993. The report will comprise measurement analysis for 12 months. It will include monthly and annual attenuation statistics and statistics on scintillation effects. A number of prediction models will be presented. The ACTS propagation experiment preparations are moving forward as expected. The mobile/personal channel characterization efforts continued during the last year. Data collected by the University of Texas in 1992 are being analyzed and will become available by September 1993. We have recently started a study to characterize LEO mobile/personal channels. Topics such as indoor reception, tree shadowing, blockage, and delay spread will be investigated. These results will become available in one to two years from now. We have also collected Ka-band mobile data using Olympus 20 GHz beacon transmissions. The University of Texas has already collected five years of low-elevation angle, 11GHz propagation data. The work on database for propagation models has progressed very well. The first release is ready, and the participants of this meeting will receive a copy of the software. We had an active year where CCIR is concerned. An input document on land mobile satellite system (LMSS) propagation models was submitted to the U.S. national committee and was approved and sent to Geneva. Author (revised)

N94-14656*# Jet Propulsion Lab., California Inst. of Tech., Pasadena.

NEW CHALLENGES IN PROPAGATION RESEARCH IN THE US

Faramaz Davarian *In its* Proceedings of the Seventeenth NASA Propagation Experimenters Meeting (NAPEX 17) and the Advanced Communications Technology Satellite (ACTS) Propagati on Studies Miniworkshop 1 Aug. 1993 p 13-24 (For primary document see N94-14654 02-32)

Avail: CASI HC A03/MF A03

Earth/space propagation research in the U.S. is tied to new developments in satellite communications. In spite of the fiber optics competition for trunked point-to-point communications, a host of emerging services are discovering the great potential of satellites for wireless communications. The application of satellites for radio communications appears to grow with a rapid pace in the areas of thin-route and mobile/personal communications. An important factor influencing the future of satellite communications is the congestion of the spectral slots at Ku- and lower bands. This heavy usage of the spectrum gives rise to conflicts among the users and consequently forces regulatory organizations to relocate frequency assignments, a decision that, for obvious reasons, is unpopular

with the relocated service. Because of this frequency shortage, frequencies in Ka- and higher spectral bands are currently viewed as good candidates for Earth/space communications in the future. Therefore, new challenges in propagation research in the U.S. include the characterization of mobile/personal links and the investigation of higher bands for satellite communications. The plans and the challenges of the propagation research in the U.S. are briefly reviewed. Author (revised)

N94-14657*# Atlantic Research Corp., Landover, MD. Professional Services Group.

USER NEEDS FOR PROPAGATION DATA

Thomas M. Sullivan *In* JPL, Proceedings of the Seventeenth NASA Propagation Experimenters Meeting (NAPEX 17) and the Advanced Communications Technology Satellite (ACTS) Propagation Studies Miniworkshop 1 Aug. 1993 p 27-30 (For primary document see N94-14654 02-32)

Avail: CASI HC A01/MF A03

New and refined models of radio signal propagation phenomena are needed to support studies of evolving satellite services and systems. Taking an engineering perspective, applications for propagation measurements and models in the context of various types of analyses that are of ongoing interest are reviewed. Problems that were encountered in the signal propagation aspects of these analyses are reviewed, and potential solutions to these problems are discussed. The focus is on propagation measurements and models needed to support design and performance analyses of systems in the Mobile-Satellite Service (MSS) operating in the 1-3 GHz range. These systems may use geostationary or non-geostationary satellites and Frequency Division Multiple Access (FDMA), Time Division Multiple Access Digital (TDMA), or Code Division Multiple Access (CDMA) techniques. Many of the propagation issues raised in relation to MSS are also pertinent to other services such as broadcasting-satellite (sound) at 2310-2360 MHz. In particular, services involving mobile terminals or terminals with low gain antennas are of concern. Author (revised)

N94-14658*# Virginia Polytechnic Inst. and State Univ., Blacksburg. Satellite Communications Group.

STATISTICAL RESULTS FROM THE VIRGINIA TECH PROPAGATION EXPERIMENT USING THE OLYMPUS 12, 20, AND 30 GHz SATELLITE BEACONS

Warren L. Stutzman, A. Safaai-Jazi, Timothy Pratt, B. Nelson, J. Laster, and H. Ajaz *In* JPL, Proceedings of the Seventeenth NASA Propagation Experimenters Meeting (NAPEX 17) and the Advanced Communications Technology Satellite (ACTS) Propagation Studies Miniworkshop 1 Aug. 1993 p 33-45 (For primary document see N94-14654 02-32)

Avail: CASI HC A03/MF A03

Virginia Tech has performed a comprehensive propagation experiment using the Olympus satellite beacons at 12.5, 19.77, and 29.66 GHz (which we refer to as 12, 20, and 30 GHz). Four receive terminals were designed and constructed, one terminal at each frequency plus a portable one with 20 and 30 GHz receivers for microscale and scintillation studies. Total power radiometers were included in each terminal in order to set the clear air reference level for each beacon and also to predict path attenuation. More details on the equipment and the experiment design are found elsewhere. Statistical results for one year of data collection were analyzed. In addition, the following studies were performed: a microdiversity experiment in which two closely spaced 20 GHz receivers were used; a comparison of total power and Dicke switched radiometer measurements, frequency scaling of scintillations, and adaptive power control algorithm development. Statistical results are reported. Author (revised)

N94-14659*# Virginia Polytechnic Inst. and State Univ., Blacksburg. Satellite Communication Group.

RESULTS FROM A STUDY OF SCINTILLATION BEHAVIOR AT 12, 20, AND 30 GHz USING THE RESULTS FROM THE VIRGINIA TECH OLYMPUS RECEIVERS

Timothy Pratt and F. Haidara *In* JPL, Proceedings of the Seventeenth NASA Propagation Experimenters Meeting (NAPEX 17) and the Advanced Communications Technology Satellite (ACTS) Propagation Studies Miniworkshop 1 Aug. 1993 p 47-58 (For primary document see N94-14654 02-32)

Avail: CASI HC A03/MF A03

Tropospheric scintillations are rapid fluctuations of signal caused by multiple scattering from the small scale turbulent refractive index inhomogeneities in the troposphere. They can strongly impair satellite communications links operating at frequency above 10 GHz. The VA Tech OLYMPUS propagation experiment which includes 12, 20, and 30 GHz beacon receivers at an elevation angle of 14 degrees provides us with valuable multifrequency scintillation data. A long term analysis of tropospheric scintillation results from the VA Tech OLYMPUS experiment is presented. It includes statistics of both the scintillation intensity and the attenuation relative to clear air as well as seasonal, diurnal and meteorological trends. A comparison with the Consultative Committee for International Radio (CCIR) predictive model for scintillation fading is presented. Author (revised)

N94-14660*# National Oceanic and Atmospheric Administration, Boulder, CO. Wave Propagation Lab.

RADIOMETRIC OBSERVATIONS OF ATMOSPHERIC ATTENUATION AT 20.6 AND 31.65 GHz: THE WAVE PROPAGATION LABORATORY DATA BASE

Mark D. Jacobson, J. B. Snider, and E. R. Westwater *In* JPL, Proceedings of the Seventeenth NASA Propagation Experimenters Meeting (NAPEX 17) and the Advanced Communications Technology Satellite (ACTS) Propagation Studies Miniworkshop 1 Aug. 1993 p 61-79 (For primary document see N94-14654 02-32)

Avail: CASI HC A03/MF A03

The National Oceanic and Atmospheric Administration (NOAA) Wave Propagation Laboratory (WPL) presently operates five dual-channel microwave radiometers, one triple-channel microwave radiometer, and one six-channel microwave radiometer. The dual-channel radiometers operate at frequencies of 20.6 or 23.87 GHz and 31.4 or 31.65 GHz. The triple-channel radiometer operates at 20.6, 31.65, and 90.0 GHz. The six-channel radiometer operates at frequencies of 20.6, 31.65, 52.85, 53.85, 55.45, and 58.8 GHz. Recent brightness temperature measurements and attenuation values from some of the above radiometers are presented. These radiometric measurements, taken in different locations throughout the world, have given WPL a diverse set of measurements under a variety of atmospheric conditions. We propose to do a more complete attenuation analysis on these measurements in the future. In addition, a new spinning reflector was installed recently for the dual-channel radiometer at the Platteville, Colorado site. This reflector will extend our measurement capabilities during precipating conditions. Locating the three-channel and portable dual-channel radiometers at or near Greeley, Colorado to support the Advanced Communications Technology Satellite (ACTS) program is discussed. Author (revised)

N94-14661*# Texas Univ., Austin. Electrical Engineering Research Lab.

LONG DURATION MEASUREMENTS OF FADING ON A LOW ELEVATION ANGLE, 11-GHz SATELLITE PATH

Wolfhard J. Vogel and Geoffrey W. Torrence *In* JPL, Proceedings of the Seventeenth NASA Propagation Experimenters Meeting (NAPEX 17) and the Advanced Communications Technology Satellite (ACTS) Propagation Studies Miniworkshop 1 Aug. 1993 p 81-85 (For primary document see N94-14654 02-32)

Avail: CASI HC A01/MF A03

Some rainfall rate and beacon fade results from the first 5 years of continuous observations of an 11.2 GHz satellite beacon with a 5.8 degree elevation angle in Austin, Texas are presented and compared to Consultative Committee for International Radio (CCIR) predictions. Author (revised)

N94-14662*# Texas Univ., Austin. Electrical Engineering Research Lab.

LARGE-SCALE RAINFALL DIVERSITY FOR ACTS

H. P. Lin and Wolfhard J. Vogel *In* JPL, Proceedings of the Seventeenth NASA Propagation Experimenters Meeting (NAPEX 17) and the Advanced Communications Technology Satellite (ACTS) Propagation Studies Miniworkshop 1 Aug. 1993 p 87-91 (For primary document see N94-14654 02-32)

Avail: CASI HC A01/MF A03

From the NOAA 15 minute precipitation file for the US, data were selected for a set of 23 stations spanning a 5 year period. The selection covers the spot beam locations for ACTS and the propagation experiment sites. There is a 2 percent probability of having any simultaneous rain at 3 or more stations, but this reduces to less than 0.001 percent at a rainfall rate of 40 mm/hr. Author (revised)

N94-14663*# Johns Hopkins Univ., Laurel, MD. Applied Physics Lab.
RAIN RATE DURATION STATISTICS DERIVED FROM THE MID-ATLANTIC COAST RAIN GAUGE NETWORK **c47**
Julius Goldhirsh *In* JPL, Proceedings of the Seventeenth NASA Propagation Experimenters Meeting (NAPEX 17) and the Advanced Communications Technology Satellite (ACTS) Propagation Studies Miniworkshop 1 Aug. 1993 p 93-103 (For primary document see N94-14654 02-32)
(Contract N00039-91-C-0001)
Avail: CASI HC A03/MF A03

A rain gauge network comprised of 10 tipping bucket rain gauges located in the Mid-Atlantic coast of the United States has been in continuous operation since June 1, 1986. Rain rate distributions and estimated slant path fade distributions at 20 GHz and 30 GHz covering the first five year period were derived from the gauge network measurements, and these results were described by Goldhirsh. In this effort, rain rate time duration statistics are presented. The rain duration statistics are of interest for better understanding the physical nature of precipitation and to present a data base which may be used by modelers to convert to slant path fade duration statistics. Such statistics are important for better assessing optimal coding procedures over defined bandwidths. Author (revised)

N94-14664*# Oklahoma Univ., Norman.
RAIN-RATE DATA BASE DEVELOPMENT AND RAIN-RATE CLIMATE ANALYSIS **c47**
Robert K. Crane *In* JPL, Proceedings of the Seventeenth NASA Propagation Experimenters Meeting (NAPEX 17) and the Advanced Communications Technology Satellite (ACTS) Propagation Studies Miniworkshop 1 Aug. 1993 p 105-128 (For primary document see N94-14654 02-32)
Avail: CASI HC A03/MF A03

The single-year rain-rate distribution data available within the archives of Consultative Committee for International Radio (CCIR) Study Group 5 were compiled into a data base for use in rain-rate climate modeling and for the preparation of predictions of attenuation statistics. The four year set of tip-time sequences provided by J. Goldhirsh for locations near Wallops Island were processed to compile monthly and annual distributions of rain rate and of event durations for intervals above and below preset thresholds. A four-year data set of tropical rain-rate tip-time sequences were acquired from the NASA TRMM program for 30 gauges near Darwin, Australia. They were also processed for inclusion in the CCIR data base and the expanded data base for monthly observations at the University of Oklahoma. The empirical rain-rate distributions (edfs) accepted for inclusion in the CCIR data base were used to estimate parameters for several rain-rate distribution models: the lognormal model, the Crane two-component model, and the three parameter model proposed by Moupfuma. The intent of this segment of the study is to obtain a limited set of parameters that can be mapped globally for use in rain attenuation predictions. If the form of the distribution can be established, then perhaps available climatological data can be used to estimate the parameters rather than requiring years of rain-rate observations to set the parameters. The two-component model provided the best fit to the Wallops Island data but the Moupfuma model provided the best fit to the Darwin data. Author (revised)

N94-14665*# Jet Propulsion Lab., California Inst. of Tech., Pasadena.
A DATABASE FOR PROPAGATION MODELS
Anil V. Kantak, Krisjani Suwitra, and Choung Le *In its* Proceedings of the Seventeenth NASA Propagation Experimenters Meeting (NAPEX 17) and the Advanced Communications Technology Satellite (ACTS) Propagation Studies Miniworkshop 1 Aug. 1993 p 129-141 (For primary document see N94-14654 02-32)
Avail: CASI HC A03/MF A03

The NASA Propagation Program supports academic research that models various propagation phenomena in the space research frequency bands. NASA supports such research via school and institutions prominent in the field. The products of such efforts are particularly useful for researchers in the field of propagation phenomena and telecommunications systems engineers. The systems engineer usually needs a few propagation parameter values for a system design. Published literature on the subject, such as the Cunsultative Committee for International Radio (CCIR) publications, may help somewhat, but often times, the parameter values given in such publications use a particular set of conditions which may not quite include the requirements of the system design. The systems engineer must resort to programming the propagation phenomena model of interest and to obtain the parameter values to be used in the project. Furthermore, the researcher in the propagation field must then program the propagation models either to substantiate the model or to generate a new model. The researcher or the systems engineer must either be a skillful computer programmer or hire a programmer, which of course increases the cost of the effort. An increase in cost due to the inevitable programming effort may seem particularly inappropriate if the data generated by the experiment is to be used to substantiate the already well-established models, or a slight variation thereof. To help researchers and the systems engineers, it was recommended by the participants of NASA Propagation Experimenters (NAPEX) 15 held in London, Ontario, Canada on 28-29 June 1991, that propagation software should be constructed which will contain models and prediction methods of most propagation phenomenon. Moreover, the software should be flexible enough for the user to make slight changes to the models without expending a substantial effort in programming.
Author (revised)

N94-14666*# Jet Propulsion Lab., California Inst. of Tech., Pasadena.
CONTRIBUTION TOWARDS A DRAFT REVISION OF RECOMMENDATIONS 681: PROPAGATION DATA REQUIRED FOR THE DESIGN OF EARTH-SPACE LAND MOBILE TELECOMMUNICATIONS SYSTEMS
Faramaz Davarian and Dennis Bishop *In its* Proceedings of the Seventeenth NASA Propagation Experimenters Meeting (NAPEX 17) and the Advanced Communications Technology Satellite (ACTS) Propagation Studies Miniworkshop 1 Aug. 1993 p 145-157 (For primary document see N94-14654 02-32)
Avail: CASI HC A03/MF A03

Propagation models that can be used for the design of earth-space land mobile-satellite telecommunications systems are presented. These models include: empirical roadside shadowing, attenuation frequency scaling, fade and non-fade duration distribution, multipath in a mountain environment, and multipath in a roadside tree environment. Propagation data from helicopter-mobile and satellite-mobile measurements in Australia and the United States were used to develop the models. Author

N94-14667*# Jet Propulsion Lab., California Inst. of Tech., Pasadena.
PROPAGATION ISSUES FOR EMERGING MOBILE AND PORTABLE COMMUNICATIONS: A SYSTEMS PERSPECTIVE
Nasser Golshan *In its* Proceedings of the Seventeenth NASA Propagation Experimenters Meeting (NAPEX 17) and the Advanced Communications Technology Satellite (ACTS) Propagation Studies Miniworkshop 1 Aug. 1993 p 159-169 (For primary document see N94-14654 02-32)
Avail: CASI HC A03/MF A03

The viewpoint of a system engineer regarding the format of propagation information and models suitable for the design of mobile and portable satellite communications systems for the following services: audio broadcast, two way voice, and packet data is presented. Topics covered include: propagation impairments for portable indoor reception in satellite communications systems; propagation impairments and mitigation techniques for mobile satellite communications systems; characterization of mobile satellite communications channels in the presence of roadside blockage when interleaving and FEC coding are implemented; characterization of short-term mobile satellite signal variations; and characterization of long-term signal variations. Author (revised)

N94-14668*# American Mobile Satellite Corp., Washington, DC.
PROPAGATION CONSIDERATIONS IN THE AMERICAN MOBILE SATELLITE SYSTEM DESIGN
Charles Kittiver and Charles E. Sigler, Jr. *In* JPL, Proceedings of the Seventeenth NASA Propagation Experimenters Meeting (NAPEX 17) and the Advanced Communications Technology Satellite (ACTS) Propagation Studies Miniworkshop 1 Aug. 1993 p 171-181 (For primary document see N94-14654 02-32)
Avail: CASI HC A03/MF A03

An overview of the American Mobile Satellite Corporation (AMSC) mobile satellite services (MSS) system with special emphasis given to the propagation issues that were considered in the design is presented. The aspects of the voice codec design that effect system performance in a shadowed environment are discussed. The strategies for overcoming

Ku-Band rain fades in the uplink and downlink paths of the gateway station are presented. A land mobile propagation study that has both measurement and simulation activities is described. Author (revised)

N94-14669*# European Space Agency. European Space Research and Technology Center, ESTEC, Noordwijk (Netherlands).
CHARACTERISATION OF THE LMS PROPAGATION CHANNEL AT L- AND S-BANDS: NARROWBAND EXPERIMENTAL DATA AND CHANNEL MODELLING
Mario Sforza and Sergio Buonomo *In* JPL, Proceedings of the Seventeenth NASA Propagation Experimenters Meeting (NAPEX 17) and the Advanced Communications Technology Satellite (ACTS) Propagation Studies Miniworkshop 1 Aug. 1993 p 183-192 (For primary document see N94-14654 02-32)
Avail: CASI HC A02/MF A03

During the period 1983-1992 the European Space Agency (ESA) carried out several experimental campaigns to investigate the propagation impairments of the Land Mobile Satellite (LMS) communication channel. A substantial amount of data covering quite a large range of elevation angles, environments, and frequencies was obtained. Results from the data analyses are currently used for system planning and design applications within the framework of the future ESA LMS projects. This comprehensive experimental data base is presently utilized also for channel modeling purposes and preliminary results are given. Cumulative Distribution Functions (PDF) and Duration of Fades (DoF) statistics at different elevation angles and environments were also included. Author (revised)

N94-14670*# Surrey Univ., Guildford (England). Centre for Satellite Engineering Research.
RESULTS OF MULTIBAND (L, S, Ku BAND) PROPAGATION MEASUREMENTS AND MODEL FOR HIGH ELEVATION ANGLE LAND MOBILE SATELLITE CHANNEL
M. A. N. Parks, G. Butt, Barry G. Evans, and M. Richharia (International Maritime Satellite Organization, London, England.) *In* JPL, Proceedings of the Seventeenth NASA Propagation Experimenters Meeting (NAPEX 17) and the Advanced Communications Technology Satellite (ACTS) Propagation Studies Miniworkshop 1 Aug. 1993 p 193-202 (For primary document see N94-14654 02-32)
Avail: CASI HC A02/MF A03

Signal propagation in the land mobile satellite (LMS) service is an important consideration due to its critical impact on the overall economic and commercial viability of the system. At frequencies allocated for LMS systems, shadowing of the line-of-sight (LOS) signal as well as multipath propagation phenomena can severely impair the link availability. In particular, as most of the studies have shown, the shadowing of LOS signal causes long and deep fades in a variety of mobile environments due to the inherent nature of the channel between the satellite and a mobile. Roadside obstacles, such as buildings, trees, utility poles etc., in the immediate vicinity of a mobile and the surrounding terrain are major sources of signal shadowing in LMS links. Therefore, a proper knowledge of link degradation is essential for cost-effective planning of a satellite based mobile communication system. The results of a propagation campaign undertaken to characterize the fading nature of LMS channel at high elevation angles is presented. It was envisaged that one of the most important physical variables contributing to the amount of LOS signal shadowing is the elevation angle of the satellite. At higher elevation angles to the satellite, less obstructions in the direct satellite-to-mobile path would therefore amount to statistically better link availability. Narrowband channel measurements were carried out at three RF frequencies corresponding to L (1.3 GHz), S (2.32/2.45 GHz), and Ku (10.4 GHz) bands. The campaign itself was divided into two phases to observe the effects of seasonal variation of foliage on the roadside trees. Phase measurements were carried out in September 1991 and in April 1992. Some important aspects from the statistical analysis of the propagation data are presented.
Author (revised)

N94-14671*# Colorado Univ., Boulder. Dept. of Electrical and Computer Engineering.
EFFECTS OF THE EQUATORIAL IONOSPHERE ON L-BAND EARTH-SPACE TRANSMISSIONS
Ernest K. Smith and Warren L. Flock *In* JPL, Proceedings of the Seventeenth NASA Propagation Experimenters Meeting (NAPEX 17) and the Advanced Communications Technology Satellite (ACTS) Propagation Studies Miniworkshop 1 Aug. 1993 p 203-218 (For primary document see N94-14654 02-32)
Avail: CASI HC A03/MF A03

Ionosphere scintillation can effect satellite telecommunication up to Ku-band. Nighttime scintillation can be attributed to large-scale inhomogeneity in the F-region of the ionosphere predominantly between heights of 200 and 600 km. Daytime scintillation has been attributed to sporadic E. It can be thought of as occurring in three belts: equatorial, high-latitude, and mid-latitude, in order of severity. Equatorial scintillation occurs between magnetic latitudes +/- 25 degrees, peaking near +/- 10 degrees. It commonly starts abruptly near 2000 local time and dies out shortly after midnight. There is a strong solar cycle dependence and a seasonal preference for the equinoxes, particularly the vernal one. Equatorial scintillation occurs more frequently on magnetically quiet than on magnetically disturbed days in most longitudes. At the peak of the sunspot cycle scintillation depths as great as 20 dB were observed at L-band.
Author (revised)

N94-14672*# Texas Univ., Austin. Electrical Engineering Research Lab.
TREE ATTENUATION AT 20 GHz: FOLIAGE EFFECTS
Wolfhard J. Vogel and Julius Goldhirsh (Johns Hopkins Univ., Laurel, MD.) *In* JPL, Proceedings of the Seventeenth NASA Propagation Experimenters Meeting (NAPEX 17) and the Advanced Communications Technology Satellite (ACTS) Propagation Studies Miniworkshop 1 Aug. 1993 p 219-223 (For primary document see N94-14654 02-32)
(Contracts JPL-956520; N00039-91-C-0001)
Avail: CASI HC A01/MF A03

Static tree attenuation measurements at 20 GHz (K-Band) on a 30 deg slant path through a mature Pecan tree with and without leaves showed median fades exceeding approximately 23 dB and 7 dB, respectively. The corresponding 1% probability fades were 43 dB and 25 dB. Previous 1.6 GHz (L-Band) measurements for the bare tree case showed fades larger than those at K-Band by 3.4 dB for the median and smaller by approximately 7 dB at the 1% probability. While the presence of foliage had only a small effect on fading at L-Band (approximately 1 dB additional for the median to 1% probability range), the attenuation increase was significant at K-Band, where it increased by about 17 dB over the same probability range.
Author (revised)

N94-14673*# National Aeronautics and Space Administration. Lewis Research Center, Cleveland, OH.
ADVANCED COMMUNICATIONS TECHNOLOGY SATELLITE (ACTS) PROGRAM: ACTS PROJECT UPDATE
Robert Bauer *In* JPL, Proceedings of the Seventeenth NASA Propagation Experimenters Meeting (NAPEX 17) and the Advanced Communications Technology Satellite (ACTS) Propagation Studies Miniworkshop 1 Aug. 1993 p 227-242 (For primary document see N94-14654 02-32)
Avail: CASI HC A03/MF A03

The Advanced Communications Technology Satellite (ACTS) Program status is reported. Project status, experiments program status, and Earth station status are described. CASI

N94-14674*# Virginia Polytechnic Inst. and State Univ., Blacksburg. Satellite Communications Group.
THE ACTS PROPAGATION TERMINAL DELIVERY AND SUPPORT
Warren L. Stutzman *In* JPL, Proceedings of the Seventeenth NASA Propagation Experimenters Meeting (NAPEX 17) and the Advanced Communications Technology Satellite (ACTS) Propagation Studies Miniworkshop 1 Aug. 1993 p 247-265 (For primary document see N94-14654 02-32)
Avail: CASI HC A03/MF A03

Viewgraphs on the Advanced Communications Technology Satellite (ACTS) propagation terminal delivery and support are included. Topics covered include: the ACTS propagation terminal (APT) development program; terminal overview; physical units; test results; status of terminals and schedule; shipping cartons; and site support. CASI

N94-14675*# Virginia Polytechnic Inst. and State Univ., Blacksburg. Satellite Communications Group.
DATA COLLECTION WITH THE ACTS PROPAGATION TERMINAL
Will Remaklus *In* JPL, Proceedings of the Seventeenth NASA Propagation

Experimenters Meeting (NAPEX 17) and the Advanced Communications Technology Satellite (ACTS) Propagation Studies Miniworkshop 1 Aug. 1993 p 267-274 (For primary document see N94-14654 02-32)
Avail: CASI HC A02/MF A03

Viewgraphs on data collection with the ACTS propagation terminal are included. Topics covered include: DACS system overview; DACS board; APT data collection computer; APT software downloading; data storage for APT; and ACTS propagation experiment data flow. CASI

N94-14676*# Virginia Polytechnic Inst. and State Univ., Blacksburg. Satellite Communications Group.
PREPROCESSING DATA COLLECTED WITH THE ACTS PROPAGATION TERMINAL
Doug Gaff *In* JPL, Proceedings of the Seventeenth NASA Propagation Experimenters Meeting (NAPEX 17) and the Advanced Communications Technology Satellite (ACTS) Propagation Studies Miniworkshop 1 Aug. 1993 p 275-288 (For primary document see N94-14654 02-32)
Avail: CASI HC A03/MF A03

Viewgraphs on preprocessing data collected with the ACTS propagation terminal are presented. The steps in ACTS data preprocessing are reviewed. CASI

N94-14677*# Texas Univ., Austin. Electrical Engineering Research Lab.
ACTS DATA CENTER Status Report
Ali Syed and Wolfhard J. Vogel *In* JPL, Proceedings of the Seventeenth NASA Propagation Experimenters Meeting (NAPEX 17) and the Advanced Communications Technology Satellite (ACTS) Propagation Studies Miniworkshop 1 Aug. 1993 p 289-295 (For primary document see N94-14654 02-32)
Avail: CASI HC A02/MF A03

Viewgraphs on ACTS Data Center status report are included. Topics covered include: ACTS Data Center Functions; data flow overview; PPD flow; RAW data flow; data compression; PPD distribution; RAW Data Archival; PPD Audit; and data analysis. CASI

N94-14678*# Colorado State Univ., Fort Collins. Dept. of Electrical Engineering.
ACTS PROPAGATION EXPERIMENT DISCUSSION: Ka-BAND PROPAGATION MEASUREMENTS USING THE ACTS PROPAGATION TERMINAL AND THE CSU-CHILL AND SPACE COMMUNICATIONS TECHNOLOGY CENTER FLORIDA PROPAGATION PROGRAM
V. N. Bringi, V. Chandrasekar, Eugene A. Mueller, Joseph Turk, John Beaver, Henry F. Helmken (Florida Atlantic Univ., Boca Raton.), and Rudy Henning (University of South Florida, Tampa.) *In* JPL, Proceedings of the Seventeenth NASA Propagation Experimenters Meeting (NAPEX 17) and the Advanced Communications Technology Satellite (ACTS) Propagation Studies Miniworkshop 1 Aug. 1993 p 307-320 (For primary document see N94-14654 02-32)
Avail: CASI HC A03/MF A03

Papers on Ka-band propagation measurements using the ACTS propagation terminal and the Colorado State University CHILL multiparameter radar and on Space Communications Technology Center Florida Propagation Program are discussed. Topics covered include: microwave radiative transfer and propagation models; NASA propagation terminal status; ACTS channel characteristics; FAU receive only terminal; FAU terminal status; and propagation testbed. CASI

N94-14717# Laboratoire d'Automatique et d'Analyse des Systemes, Toulouse (France). Groupe Circuits et Composants Micro-Ondes.
ELECTRICAL NOISE IN MICROWAVE FIELD EFFECT AND BIPOLAR TRANSISTORS Ph.D. Thesis - Toulouse Univ. [BRUIT DE FOND DANS LES TRANSISTORS A EFFET DE CHAMP ET BIPOLAIRES POUR MICRO-ONDES]
Robert Plana 1993 208 p In FRENCH
(LAAS-93042; ETN-93-94366) Avail: CASI HC A10/MF A03

Electrical noise in microwave field effect transistors (MESFET, HEMT and pseudomorphic HEMT) and in Heterojunction Bipolar Transistors (HBT) is investigated. The excess noise in the low frequency range which can limit or degrade the performance of nonlinear microwave circuits such as oscillators or mixers is described. The noise in the microwave range which takes a prominent place in the performance of linear microwave applications (amplifiers, active filters, etc.) is considered. A theoretical background on the excess noise sources in active microwave devices is given. Results of low fequency noise measurements versus frequency, geometrical features, bias and temperature performed on Field Effect Transistor (FET) and Heterojunction Bipolar Transistor (HBT) are presented. This study allowed the possible sources of excess noise to be understood and the corner noise frequency of these devices to be determined. Microwave noise on GaAs FET and HBT is also investigated. Noise measurements versus bias in GaAs FET confirmed the higher capabilities of pseudomorphic High Electron Mobility Transistor (HEMT) than HEMT for low noise amplification. Concerning the noise potentialities of HBT, a minimum figure smaller than 3 dB at 20 GHz on GaInP/GaAs structure was observed which is considered to be the lowest noise figure observed on bipolar devices at K band. ESA

N94-14724# Technische Univ., Berlin (Germany). Fachbereich Elektrotechnik.
SPEAKER INDEPENDENT RECOGNITION OF ISOLATED WORDS USING VECTOR QUANTIZATION AND NEURAL NETWORKS Ph.D. Thesis [SPRECHERUNABHAENGIGE ERKENNUNG VON ISOLIERT GESPROCHENEN EINZELWOERTERN UNTER VERWENDUNG DER VEKTORQUANTISIERUNG UND VON NEURONALEN NETZEN]
Ming Zhu 1992 112 p In GERMAN
(ETN-93-94390) Avail: CASI HC A06/MF A02

A modular test model for isolated word recognition with restricted vocabulary is developed and an effective and compact parameter representation of speech signal is realized for extraction of robust speech features. Standard processes, mathematical methods and algorithms for speech recognition and coding, such as vector quantization, dynamic programming and time warping, hidden Markov models and Viterbi algorithm, are presented. An experimental system for speech signal preprocessing, which combines modules of mel-scale cepstral coefficients, trace segmentation and dynamic time normalization, is described. Implementation possibilities of neuronal networks were discussed with focus on multilayer perceptrons because of its learning capabilities. ESA

N94-14742 British Broadcasting Corp., Kingswood (England). Research Dept.
COVERAGE ASPECTS OF A SINGLE FREQUENCY NETWORK DESIGNED FOR DIGITAL AUDIO BROADCASTING
C. P. Bell and W. F. Williams 1993 14 p Original contains color illustrations
(BBC-RD-1993/3) Copyright Avail: Issuing Activity (BBC, Kingswood, England)

Since the early 1960s, the VHF/FM pilot tone system has been used by broadcasters to supply high quality stereophonic programs to listeners equipped with fixed receivers and modest gain directional antennas mounted externally at a height of about ten meters above ground levels. More recently, with the advent of improved radio receivers and digital technology in the reproduction industry, the broadcasters' target audience has changed and listeners now expect high fidelity reception, comparable to CD quality, on their portable and mobile receivers. In many areas, the demand for high quality can be supplied using the existing VHF/FM networks. There are, however, areas where good portable and mobile reception cannot be obtained, due to shadowing and multipath. This report discusses the coded orthogonal frequency division multiplex (COFDM) channel coding and modulation system developed within the Eureka 147 digital audio broadcasting (DAB) project, which is able to overcome the problems of multipath. Indeed, it can make use of multipath signals. This fact leads to the concept of a Single Frequency Network (SFN) where a single DAB COFDM frequency block can be used to supply five or six programs to a whole country. The derivation of minimum required field strength levels for DAB COFDM signals, and the allowances required for high percentage location coverage, necessary for digital systems, are presented together with a spectrum efficiency comparison between SFN and VHF/FM networks. Theoretical lattice planning, using the CCIR Rec. 370 prediction method, is used initially to illustrate the SFN concept and suggest required effective radiated powers. The results of SFN coverage studies for the UK, using existing broadcast transmitter sites and utilizing both the Rec. 370 and the BBC terrain data based prediction methods, are given. In addition, a possible four frequency block SFN plan for Europe is discussed. The Report concludes that, in comparison, networks using the Eureka 147 DAB system exhibit a

distinct spectrum and power advantage over conventional FM networks.
Author (revised)

N94-14743*# Georgia Inst. of Tech., Atlanta.
H2S DATA REDUCTION
David DeBoer 7 Jul. 1993 6 p
(Grant NAGw-533)
(NASA-CR-193389; NAS 1.26:193389) Avail: CASI HC A02/MF A01

Calculating microwave opacity from a weakly absorbing gas mixture using a resonator requires measuring the quality factor of that resonator which necessitates accurately determining the center frequency (f(sub O)) and the half power bandwidth (Delta-f) of a noisy resonant line. The center frequency can be determined very accurately and varies very little over many measurements (a few kHz at GHz frequencies or a few hundredths of a percent). The greater source of error in estimating the Q of a resonator come from the bandwidth measurements. The half power bandwidth is determined essentially by eye-fitting a curve over a noisy resonant line and measuring with a spectrum analyzer. Author (revised)

N94-14817# Technische Univ., Berlin (Germany). Fachbereich Elektrotechnik.
OPTIMIZATION OF A SUBBAND CODING FOR HIGH DEFINITION TELEVISION WITH MOTION CONTROLLED THREE DIMENSIONAL FREQUENCY BAND DECOMPOSITION Ph.D. Thesis [OPTIMIERUNG EINER TEILBAND-CODIERUNG FUER HDTV MIT BEWEGUNGSGESTEUERTER DREIDIMENSIONALER FREQUENZGANGZERLEGUNG]
Guenter Schamel 1992 114 p In GERMAN
(Contract BMFT-412-7491-K-0275-5)
(ETN-93-94396) Avail: CASI HC A06/MF A02

A subband coding is designed with space-time frequency spectrum decomposition. Digitalized television signals and general discrete three dimensional signals are described and spectrum and spectral recurrences in space-time frequency area were calculated. A three dimensional subscanning with a time periodicity of four half images was carried out in motion controlled decomposition so that the time redundancy parts of a television signal are taken into account; varied possibilities of filtration were estimated with this scanning sampling and analyzed in terms of advantages and disadvantages for coding. Computerized simulations of very critical television and high definition television image sequences were carried out so that statistical parameters in subbands could be measured and the effectiveness of source coding processes was established with dependence on filter properties. An empirical method was chosen for subband coding and the influence of coding errors on the reconstructed image was examined with simulation. Perturbation spectrum was evaluated with frequency response of synthesis filter. A concept for data reduction of the components of high definition television signals such as luminance signal and two color difference signals is presented. It is established that three dimensional decomposition with motion controlled analysis and synthesis filtration allows higher reductions to be obtained than with purely spatial decomposition. ESA

N94-14819 GKSS-Forschungszentrum Geesthacht (Germany). Inst. fuer Physik.
SIGNAL AND REFERENCE WAVELENGTHS FOR THE ELIMINATION OF SO2 CROSS SENSITIVITY IN REMOTE MEASUREMENTS OF TROPOSPHERIC OZONE WITH LIDAR [MESS UND VERGLEICHSWELLENLAENGEN ZUR ELIMINATION VON SO2-QUEREMPFINDLICHKEITEN BEI DER LIDAR FERNMESSUNG TROPOSPHAERISCHEN OZONS]
Claus Weitkamp, Olaf Thomsen, and Peter Bisling (Spindler und Hoyer G.m.b.H. und Co., Goettingen, Germany.) 2 Aug. 1992 7 p In GERMAN
(GKSS/92/E/24; ETN-93-94608) Avail: Issuing Activity
(GKSS-Forschungszentrum Geesthacht G.M.B.H., D-W-2054, Geesthacht, Germany)

The role of sulfur dioxide in lidar remote measurement of ozone is investigated. Measurements of tropospheric ozone with ultraviolet differential absorption lidar are found to be perturbed by sulfur dioxide unless lidar signal and reference wavelengths are chosen so that the differential SO2 absorption cross section is zero. Measurements of SO2 cross sections were performed between 265 and 298 nm with a resolution inferior to 3 micrometers, wavelengthh uncertainty lower than 4 picometers and cross section error lower than 3 percent. 13 pairs of wavelengths between 277.6 and 289.6 nm, with ozone cross section differences between 2 and 20 by 10 (exp -23)sq m, are proposed for which SO2 cross sections are minimum or equal. ESA

N94-14820 GKSS-Forschungszentrum Geesthacht (Germany).
THE MOBILE LIDAR SYSTEM ARGOS FOR SPATIAL RESOLUTION REMOTE MEASURING OF GASEOUS AIR POLLUTANTS [DAS MOBILE LIDARSYSTEM ARGOS ZUR ORTSAUFGELOESTEN FERNMESSUNG GASFOERMIGER LUFTSCHADSTOFFE]
Claus Weitkamp, Uta-Barbara Goers, Juergen Glauer, Wilhelm Lahmann, Peter Bisling, Sundolf Koehler, and Walfried Michaelis 1992 12 p Reprint from Verein Deutscher Ingenieure Tagungsbericht, Duesseldorf, Germany, 1992 p 105-114 In GERMAN Presented at Umwelt-Messtechnik Congress, Germany, 26-28 Feb. 1992
(GKSS/92/E/26; ETN-93-94609) Copyright Avail: Issuing Activity
(GKSS-Forschungszentrum Geesthacht G.M.B.H., D-W-2054, Geesthacht, Germany)

A remote measuring system, which is based on the principle of differential absorption and diffusion lidar, is developed for detection of nitrogen dioxide, sulfur dioxide, and ozone. The ARGOS (Advanced Remote Gaseous Oxides Sensor) system uses differential absorption of light with different wavelengths; for that two short light pulses from pumped dye lasers are simultaneously sent in the atmosphere. A three component Doppler sodar is used for measuring wind direction and velocity. The system allows atmosphere backscattering coefficient to be estimated as a measure for spray and dust concentration in the air. Curves of SO2 distribution in an industrial area and horizontal profile of ozone concentration are presented as examples. ESA

N94-14883 Academy of Sciences of the Ukraine, Kharkov. Fiziko-Tekhnicheskij Inst.
ON TRANSPORT OF ENERGY, MOMENTUM, ORBITAL ANGULAR MOMENTUM AND SELF-ANGULAR MOMENTUM OF ELECTROMAGNETIC WAVE IN DISPERSAL MEDIA
Yu. A. Kurochkin and K. N. Stepanov 1992 20 p Limited Reproducibility: More than 20% of this document may be affected by microfiche quality
(DE93-624179; KFTI-92-50) Avail: CASI HC A03 (US Sales Only)

The transport equations for energy, momentum, orbital angular momentum and self-angular momentum of the electromagnetic wave packet propagating in the weakly absorbing homogeneous stationary anisotropic and gyrotropic medium with temporal and spacial dispersion have been obtained. These equations contain terms up to second order expansion in series for values lambda/L and Omega/omega (here lambda and omega are the wave length and wave frequency, L and i/Omega-the characteristic length and time of the wave amplitude change). It has been shown that the self-angular momentum (spin) conservation law is true only for transversal waves with circular polarization. Expressions for spin density, its flux, and power losses have been determined. DOE

N94-14892 Joint Inst. for Nuclear Research, Dubna (USSR). Lab. of High Energy.
THE ELECTRIC FIELD OF A CURRENT-CARRYING CONDUCTOR
V. N. Streltsov 1991 4 p Limited Reproducibility: More than 20% of this document may be affected by microfiche quality
(DE93-626637; JINR-D-2-91-499) Avail: CASI HC A01 (US Sales Only)

A subject concerning the relativistic invariance of the Gauss theorem is discussed. The appearance of the electric field around the neutral conductor after excitation of the current in it doesn't signify the change of its charge. DOE

N94-13270# Mitsubishi Electric Corp., Tokyo (Japan). Space Communications Research Div.
THERMAL DISTORTION MEASUREMENT OF TETRUS TYPE THERMAL TEST MODEL OF LARGE DEPLOYABLE ANTENNA FOR MOBILE COMMUNICATIONS SATELLITE [IDOUTAI TSUUSHIN EISEIYOU OOGATA TENKAI ANTENA TETRUS GATA NETSU MODERU NO NETSUHIZUMI SOKUTEI]
Teruaki Orikasa, Teruki Okamoto, Kouichi Furukawa (Toshiba Corp., Kawasaki, Japan.), and Tatsuyoshi Aisaka (Toshiba Corp., Kawasaki, Japan.) *In* NASDA, The Second Workshop on Deployment and Assembly

Experiment of Large Space Structure on Orbit 31 Mar. 1993 p 7-11 In JAPANESE (For primary document see N94-13268 02-12)
Avail: CASI HC A01/MF A01

N94-13274# Nippon Telegraph and Telephone Public Corp., Yokosuka (Japan).
DEVELOPMENT OF MODULAR CABLE MESH DEPLOYABLE ANTENNA [MOJURUGATA KEBURU MESSHU TENKAI ANTENA NO KAIHATSU]
Akira Meguro, Jin Mitsugi, and Kazuhide Andou *In* NASDA, The Second Workshop on Deployment and Assembly Experiment of Large Space Structure on Orbit 31 Mar. 1993 p 29-35 In JAPANESE (For primary document see N94-13268 02-12)
Avail: CASI HC A02/MF A01

N94-13278# Mitsubishi Electric Corp., Tokyo (Japan). Space Communications Research Div.
TRIAL MANUFACTURE MODEL AND IN-SPACE VERIFICATION METHOD OF DEPLOYABLE ANTENNA [TENKAI ANTENA NO SHISAKU MODERU TO UCHUU JISSHOU HOUHOU]
Takashi Ebisui, Teruaki Orikasa, and Teruki Okamoto *In* NASDA, The Second Workshop on Deployment and Assembly Experiment of Large Space Structure on Orbit 31 Mar. 1993 p 54-58 In JAPANESE (For primary document see N94-13268 02-12)
Avail: CASI HC A01/MF A01

N94-13440# University of Electro-Communications, Tokyo (Japan).
ANALYSIS OF FUNDAMENTAL FREQUENCY PATTERN IN SPEECH
Takeshi Okudera and Yoshimitsu Takasawa *In its* Bulletin of the University of Electro-Communications, Volume 6, No. 1, Serial No. 11 Jun. 1993 p 69-78 In JAPANESE (For primary document see N94-13432 02-61)
Avail: CASI HC A02/MF A02

N94-13441# University of Electro-Communications, Tokyo (Japan).
RECONSIDERATION OF THE AUTONOMOUS VIEW OF LANGUAGE
Eijiro Tsuboi *In its* Bulletin of the University of Electro-Communications, Volume 6, No. 1, Serial No. 11 Jun. 1993 p 79-96 In JAPANESE (For primary document see N94-13432 02-61)
Avail: CASI HC A03/MF A02

N94-14173# Calspan Corp., Arnold AFS, TN.
ELECTROMAGNETIC WAVE TEST
R. K. Matthews and S. A. Stepanek *In* VKI, Methodology of Hypersonic Testing 1993 7 p Prepared in cooperation with Arnold Engineering Development Center, Arnold AFS, TN (For primary document see N94-14153 02-02)
Copyright Avail: CASI HC A02/MF A03

N94-14282# Ministry of Posts and Telecommunications, Beijing (China). Directorate General of Telecommunications.
THE DEVELOPMENTS OF SATELLITE COMMUNICATIONS OF CHINA
Shen Liu *In* Science and Technology Agency, Asia-Pacific ISY Conference, Volume 2 31 Mar. 1993 p 381-384 (For primary document see N94-14209 02-43)
Avail: CASI HC A01/MF A04

N94-14284# Ministry of Posts and Telecommunications, Tokyo (Japan). Space Communication Research Office.
JOINT EXPERIMENTS USING ETS-5
Mutsumi Nakata *In* Science and Technology Agency, Asia-Pacific ISY Conference, Volume 2 31 Mar. 1993 p 389-392 (For primary document see N94-14209 02-43)
Avail: CASI HC A01/MF A04

N94-14285# Ministry of Posts and Telecommunications, Tokyo (Japan). Communications Research Lab.
SPACE COMMUNICATIONS TECHNOLOGY RESEARCH IN CRL
Takashi Iida *In* Science and Technology Agency, Asia-Pacific ISY Conference, Volume 2 31 Mar. 1993 p 393-396 (For primary document see N94-14209 02-43)
Avail: CASI HC A01/MF A04

N94-14286# Nippon Telegraph and Telephone Public Corp., Yokosuka (Japan). Satellite Communication Systems Lab.
NTT'S ACTIVITIES IN SATELLITE COMMUNICATIONS TECHNOLOGY DEVELOPMENT
Shuuichi Samejima *In* Science and Technology Agency, Asia-Pacific ISY Conference, Volume 2 31 Mar. 1993 p 397-400 (For primary document see N94-14209 02-43)
Avail: CASI HC A01/MF A04

N94-14287# Kokusai Denshin Denwa Co. Ltd., Saitama (Japan). Research and Development Labs.
FUTURE OUTLOOK ON INTERNATIONAL SATELLITE COMMUNICATIONS IN ASIA PACIFIC REGION
Yasuhiko Itou *In* Science and Technology Agency, Asia-Pacific ISY Conference, Volume 2 31 Mar. 1993 p 401-404 (For primary document see N94-14209 02-43)
Avail: CASI HC A01/MF A04

N94-14288# Japan Broadcasting Corp., Tokyo. Radio Engineering Research Div.
TECHNOLOGICAL DEVELOPMENT FOR BROADCASTING SATELLITES IN NHK LABORATORIES
Youji Morishita *In* Science and Technology Agency, Asia-Pacific ISY Conference, Volume 2 31 Mar. 1993 p 405-408 (For primary document see N94-14209 02-43)
Avail: CASI HC A01/MF A04

33 ELECTRONICS AND ELECTRICAL ENGINEERING

Includes test equipment and maintainability; components, e.g., tunnel diodes and transistors; microminiaturization; and integrated circuitry.

For related information see also *60 Computer Operations and Hardware* and *76 Solid-State Physics.*

N94-12821# Sandia National Labs., Albuquerque, NM.
DESIGN AND TESTING OF PLANAR MAGNETIC MICROMOTORS FABRICATED BY DEEP X RAY LITHOGRAPHY AND ELECTROPLATING
H. Guckel (Wisconsin Univ., Madison.), T. R. Christenson (Wisconsin Univ., Madison.), K. J. Skrobis (Wisconsin Univ., Madison.), J. Klein (Wisconsin Univ., Madison.), and M. Karnowsky 1993 5 p Presented at the 7th International Conference on Solid State Sensors and Actuators, Japan, 13-15 May 1993
(Contract DE-AC04-76DP-00789)
(DE93-012856; SAND-93-1006C; CONF-9305186-1) Avail: CASI HC A01/MF A01

The successful design and testing of a three-phase planar integrated magnetic micromotor is presented. Fabrication is based on a modified deep X-ray lithography and electroplating or LIGA process. Maximum rotational speeds of 33,000 rpm are obtained in air with a rotor diameter of 285 microns and do not change when operated in vacuum. Real time rotor response is operated with an integrated shaft encoder. Long lifetime is evidenced by testing to over 5(10)(sup 7) rotation cycles without changes in performance. Projected speeds of the present motor configuration am in the vicinity of 100 krpm and are limited by torque ripple. Higher speeds, which are attractive for sensor applications. require constant torque characteristic excitation as is evidenced by ultracentrifuge and gyroscope design. Further understanding of electroplated magnetic material properties will drive these performance improvements. DOE

N94-12856 Academy of Sciences of the Ukraine, Kharkov. Fiziko-Tekhnicheskij Inst.
NON-LINEAR EFFECTS IN VORTEX VISCOUS FLOW IN SUPERCONDUCTORS-ROLE OF FINITE HEAT REMOVAL VELOCITY [NELINEJNYE EHFFEKTY V VYAZKOM TECHENII VIKHREJ V SVERKHPROVODNIKAKH - ROL' KONECHNOJ SKOROSTI TEPLOO TVODA]
A. I. Bezuglyj and V. A. Shklovskij 1991 8 p In RUSSIAN Limited

Reproducibility: More than 20% of this document may be affected by microfiche quality
(DE93-621785; KFTI-91-31) Avail: CASI HC A02 (US Sales Only)

The role of finite heat removal velocity in experiments on non-linear effects in vortex viscous flow in superconducting films near critical temperature was investigated. It was shown that the account of thermal effects permits to explain the experimentally observed dependence of electron energy relaxation time and current break-down in voltage-current characteristic from magnetic field value. DOE

N94-12891# International Centre for Theoretical Physics, Trieste (Italy).
A METHOD FOR DETERMINATION OF THE SUPERFICIAL CHARGE DENSITY
F. Vila Oct. 1992 14 p
(DE93-622896; IC-92/319) Avail: CASI HC A01/MF A01 (US Sales Only)

In this article is presented a new method for determining superficial charge density in nonconducting materials which is based in the combination of laboratory calibrated experiments in conducting surfaces with theoretical calculations for nonconducting surfaces. DOE

N94-12892# Westinghouse Electric Corp., Pittsburgh, PA.
PROCESSING, FABRICATION AND DEMONSTRATION OF HTS INTEGRATED MICROWAVE CIRCUITS Status Report No. 7, 25 Jan. - 25 Apr. 1993
G. R. Wagner 25 Apr. 1993 18 p
(Contract N00014-91-C-0112)
(AD-A265789) Avail: CASI HC A03/MF A01

A description of progress is presented for these tasks: comparative technology assessment, integrated subsystem specifications, functional component and subsystem design, fabrication, and testing, PVD multilayer film fabrication, MOCVD multilayer film fabrication, and rf characterization of film properties. CASI

N94-12897*# Georgia Inst. of Tech., Atlanta. School of Electrical Engineering.
SPATIALLY-VARYING IIR FILTER BANKS FOR IMAGE CODING
Wilson C. Chung and Mark J. T. Smith 1992 4 p
(Grants NAG5-2187; NSF MIP-91-16113)
(NASA-CR-193727; NAS 1.26:193727) Avail: CASI HC A01/MF A01

This paper reports on the application of spatially variant infinite impulse response (IIR) filter banks to subband image coding. The new filter bank is based on computationally efficient recursive polyphase decompositions that dynamically change in response to the input signal. In the absence of quantization, reconstruction can be made exact. However, by proper choice of an adaptation scheme, we show that subband image coding based on time varying filter banks can yield improvement over the use of conventional filter banks. Author (revised)

N94-12942# Sandia National Labs., Albuquerque, NM.
1/f NOISE AND OXIDE TRAPS IN MOSFETs
D. M. Fleetwood, T. L. Meisenheimer, and J. H. Scofield (Oberlin Coll., OH.) 1993 8 p Presented at the 12th International Conference on Noise in Physical Systems and 1/f Fluctuations, Saint Louis, MO, 16-20 Aug. 1993
(Contract DE-AC04-76DP-00789)
(DE93-007581; SAND-93-0037C; CONF-930866-1) Avail: CASI HC A02/MF A01

MOSFET's historically have exhibited large 1/f noise magnitudes because of carrier-defect interactions that cause the number of channel carriers and their mobility to fluctuate. Uncertainty in the type and location of defects that lead to the observed noise have made it difficult to optimize MOSFET processing to reduce the level of 1/f noise. This has limited one's options when designing devices or circuits (high-precision analog electronics, preamplifiers, etc.) for low-noise applications at frequencies below (approximately)10-100 kHz. We have performed detailed comparisons of the low-frequency 1/f noise of MOSFET's manufactured with radiation-hardened and non-radiation-hardened processing. We find that the same techniques which reduce the amount of MOSFET radiation-induced oxide-trap charge can also proportionally reduce the magnitude of the low-frequency 1/f noise of both unirradiated and irradiated devices. MOSFET's built in radiation-hardened device technologies show noise levels up to a factor of 10 or more lower than standard commercial MOSFET's of comparable dimensions, and our quietest MOSFET's show noise magnitudes that approach the low noise levels of JFETS. DOE

N94-12967# Research Triangle Inst., Research Triangle Park, NC. Center for Systems Engineering.
CHIP-LEVEL TESTABILITY REQUIREMENTS GUIDELINES
James W. Watterson, Mark Royals, and Nick Kanapoulis Nov. 1992 165 p
(Contract F30602-90-D-0097)
(AD-A262583; RTI/4968/01F; RL-TR-92-309) Avail: CASI HC A08/MF A02

Guidelines and rationale that will assist system developers in specifying consistent, necessary, and achievable chip-level testability requirements are provided. A bottom-up design procedure is recommended that emphasizes the importance of chip testability estimation and built-in-test evaluation during chip design to minimize system life-cycle cost. A comprehensive set of cost-related testability attributes was developed, which address test generation, test application, and fault isolation and repair. This set of attributes was then prioritized on the basis of usefulness and estimation cost. A set of chip-level design-for-testability and built-in-test techniques were selected from open literature sources. Preliminary analyses of eleven of the more promising techniques considered nine criteria in the areas of: impact on testability, cost, and applicability to standard design practices. Three of the techniques were subjected to in-depth analyses that included the results of case studies. The techniques considered in the in-depth studies were: Circular Built-In-Self-Test, LSSD On-Chip Self-Test (LOCST), and CrossCheck. DTIC

N94-12994# Lawrence Livermore National Lab., CA.
METAL-SEMICONDUCTOR, COMPOSITE RADIATION DETECTORS
W. J. Orvis, J. H. Yee, and D. Fuess Dec. 1992 23 p
(Contract W-7405-eng-48)
(DE93-013313; UCRL-ID-112587) Avail: CASI HC A03/MF A01

In 1989, two researchers published a design for an increased efficiency x-ray detector. The design increased the efficiency of a semiconductor detector by interspersing layers of high-z metal within it. Semiconductors such as silicon make good, high-resolution radiation detectors, but they have low efficiency because they are low-z materials ($z = 14$). High-z metals, on the other hand, are good absorbers of high-energy photons. By interspersing high-z metal layers with semiconductor layers, the researchers combined the high absorption efficiency of the high-z metals with the good detection capabilities of a semiconductor. This project is an attempt to use the same design to produce a high-efficiency, room temperature gamma ray detector. By their nature, gamma rays require thicker metal layers to efficiently absorb them. These thicker layers change the behavior of the detector by reducing the resolution, compared to a solid state detector, and shifting the photopeak by a predictable amount. During the last year, the authors have procured and tested a commercial device with operating characteristics similar to those of a single layer of the composite device. They have modeled the radiation transport in a multi-layered device, to verify the initial calculations of layer thickness and composition. They have modeled the electrostatic field in different device designs to locate and remove high-field regions that can cause device breakdown. They have fabricated 14 single layer prototypes. DOE

N94-13026*# California Univ., Los Angeles. Dept. of Electrical Engineering.
ANALYSIS AND CHARACTERIZATIONS OF PLANAR TRANSMISSION STRUCTURES AND COMPONENTS FOR SUPERCONDUCTING AND MONOLITHIC INTEGRATED CIRCUITS Final Technical Report, 1 Jan. - 31 Dec. 1991
Tatsuo Itoh 16 Mar. 1992 4 p
(Contract NCC3-192)
(NASA-CR-193675; NAS 1.26:193675) Avail: CASI HC A01/MF A01

The research effort was continued to design and characterize superconducting transmission line structures. The research during this period was concentrated on the implementation of a superconductor into coplanar waveguide structures. First, the superconducting coplanar waveguide was examined, and compared with a superconducting microstrip line in terms of loss characteristics and their design aspects. Then, the research was carried on the design and characterization of the coplanar waveguide family

in the packaging environment. The transition between the coaxial line to the conductor backed coplanar waveguide was also designed for the measurement of the superconducting conductor backed coplanar waveguide. Author (revised)

N94-13031# Los Alamos National Lab., NM.
METAL OXIDE VARISTOR FEASIBILITY STUDY
L. M. Levinson and H. A. Comanzo 1993 34 p
(Contract W-7405-eng-36)
(DE93-012921; LA-SUB-93-168) Avail: CASI HC A03/MF A01

We have successfully fabricated varistor material meeting the initial voltage stabilization specifications for the Dual Axis Radiographic Hydratest (DARHT) facility. A time dependent voltage droop ('overshoot') has been identified as a potential issue and some promising avenues to reduce the overshoot are outlined. In particular, preliminary tests using series capacitance gives an overshoot of a few percent. These data, coupled with our previous experience on low-overshoot varistor formulations, lead to the conclusion that specially tailored varistor material might be suitable for the DARHT application. DOE

N94-13040# Army Armament Research, Development and Engineering Center, Picatinny Arsenal, NJ.
SOLDERABILITY OF SURFACE MOUNT DEVICES
Nanette S. Holder Jun. 1993 14 p
(AD-A265751; ARFSD-TR-93001) Avail: CASI HC A03/MF A01

As electronic products become much smaller, a limiting factor in the reduction of product size has been the size of the electronic components which make up the product. The leads of the current electronic components are inserted onto a printed circuit board through holes. Due to the use of wire leads, it becomes more difficult to decrease the size of the components. A new method was created to mount components directly to the surface of the printed circuit board. This new technique is surface mount technology. A concern over the use of this is experienced by the military. Since the leads are not inserted through the board and crimped before soldering as conventional components are mounted, there is some regard as to whether the components can be mounted securely to the board. Due to the high forces that many munitions experience when dispensed, it is imperative that the electronic components be soldered to the circuits boards so they will not slip out of place or fall from the board. The military also requires many munitions to lie dormant in storage warehouses for up to 20 years. When the munition is needed, it must perform reliably. Little work has been done to study the effects of this long-term storage on these surface mount devices, particularly on the ability of different soldering techniques used to attach surface mount components to printed circuit boards to withstand damaging effects of long-term storage. DTIC

N94-13094# Allied-Signal Aerospace Co., Kansas City, MO.
RIGID-FLEXIBLE PRINTED WIRING BOARDS
E. V. Sydow May 1993 52 p
(Contract DE-AC04-76DP-00613)
(DE93-013938; KCP-613-5043) Avail: CASI HC A04/MF A01

Rigid-flexible printed wiring board materials, fabrication processes, product requirements, and reliability were established. Considerable effort was spent testing plated-through holes, analyzing plated-through hole failure mechanisms, and then incorporating materials, processes, and product requirements to provide adequate control and reduce failures. The principal processes developed were tooling concepts, process sequence, lamination, drilling, plasma etchback, copper electroplating, and solder coating. Product requirements and reliability were established with thermal shock, thermal stress, innerlayer adhesion, and fold flexibility tests. Plated-through hole failure mechanisms were analyzed with thermal mechanical and finite element analyses. DOE

N94-13106*# Varian Associates, Palo Alto, CA. Microwave Tube Div.
A MILLIMETER-WAVE TUNNELADDER TWT Final Report, Oct. 1982 - Jan. 1986
D. Wilson Oct. 1988 54 p
(Contract NAS3-23347; RTOP 506-61-42)
(NASA-CR-182183; NAS 1.26:182183) Avail: CASI HC A04/MF A01

A millimeter-wave traveling wave tube (TWT) was developed using a dispersive, high-impedance forward wave interaction structure based on a ladder, with non-space-harmonic interaction, for a tube with high gain per inch and high efficiency. The 'TunneLadder' interaction structure combines ladder properties modified to accommodate Pierce gun beam optics in a radially magnetized PM focusing structure. The development involved the fabrication of chemically milled, shaped ladders diffusion brazed to diamond cubes which are in turn active diffusion brazed to each ridge of a doubly ridged waveguide. Cold-test data, representing the (omega)(beta) and and impedance characteristics of the modified ladder circuit, were used in small and large-signal computer programs to predict TWT gain and efficiency. The structural design emphasizes ruggedness and reliability. Actual data from tested tubes verify the predicted performance while providing broader bandwidth than expected. Author (revised)

N94-13110*# National Aeronautics and Space Administration. Lewis Research Center, Cleveland, OH.
LOW-CURRENT TRAVELING WAVE TUBE FOR USE IN THE MICROWAVE POWER MODULE
Raymond W. Palmer, Peter Ramins, Dale A. Force, James A. Dayton, Ben T. Ebihara, and Robert P. Gruber Washington Jul. 1993 15 p
(RTOP 506-72-00)
(NASA-TP-3344; E-7329; NAS 1.60:3344) Avail: CASI HC A03/MF A01

The results of a traveling-wave-tube/multistage depressed-collector (TWT-MDC) design study in support of the Advanced Research Projects Agency/Department of Defense (ARPA/DOD) Microwave Power Module (MPM) Program are described. The study stressed the possible application of dynamic and other tapers to the RF output circuit of the MPM traveling wave tube as a means of increasing the RF and overall efficiencies and reducing the required beam current (perveance). The results indicate that a highly efficient, modified dynamic velocity taper (DVT) circuit can be designed for the broadband MPM application. The combination of reduced cathode current (lower perveance) and increased RF efficiency leads to (1) a substantially higher overall efficiency and reduction in the prime power to the MPM, and (2) substantially reduced levels of MDC and MPM heat dissipation, which simplify the cooling problems. However, the selected TWT circuit parameters need to be validated by cold test measurements on actual circuits. Author (revised)

N94-13125*# Irvine Sensors Corp., Costa Mesa, CA.
HYMOSS SIGNAL PROCESSING FOR PUSHBROOM SPECTRAL IMAGING Final Technical Report
David E. Ludwig 11 Jun. 1991 91 p
(Contract NAS7-1065; SBIR-08.01-8211)
(NASA-CR-191341; NAS 1.26:191341; ISC158-ICN-FR/91-001) Avail: CASI HC A05/MF A01

The objective of the Pushbroom Spectral Imaging Program was to develop on-focal plane electronics which compensate for detector array non-uniformities. The approach taken was to implement a simple two point calibration algorithm on focal plane which allows for offset and linear gain correction. The key on focal plane features which made this technique feasible was the use of a high quality transimpedance amplifier (TIA) and an analog-to-digital converter for each detector channel. Gain compensation is accomplished by varying the feedback capacitance of the integrate and dump TIA. Offset correction is performed by storing offsets in a special on focal plane offset register and digitally subtracting the offsets from the readout data during the multiplexing operation. A custom integrated circuit was designed, fabricated, and tested on this program which proved that nonuniformity compensated, analog-to-digital converting circuits may be used to read out infrared detectors. Irvine Sensors Corporation (ISC) successfully demonstrated the following innovative on-focal-plane functions that allow for correction of detector non-uniformities. Most of the circuit functions demonstrated on this program are finding their way onto future IC's because of their impact on reduced downstream processing, increased focal plane performance, simplified focal plane control, reduced number of dewar connections, as well as the noise immunity of a digital interface dewar. The potential commercial applications for this integrated circuit are primarily in imaging systems. These imaging systems may be used for: security monitoring systems, manufacturing process monitoring, robotics, and for spectral imaging when used in analytical instrumentation. Author (revised)

N94-13134*# National Aeronautics and Space Administration. Lewis Research Center, Cleveland, OH.
SCREENING OF SOLAR CELLS
J. Appelbaum, A. Chait, and D. A. Thompson (Akron Univ., OH.) Jul.

1993 13 p
(Contract NCC3-104; RTOP 506-41-11)
(NASA-TM-106298; E-7987; NAS 1.15:106298) Avail: CASI HC A03/MF A01

Because solar cells in a production batch are not identical, screening is performed to obtain similar cells for aggregation into arrays. A common technique for screening is based on a single operating point of the I-V characteristic of the cell, usually the maximum power point. As a result, inferior cell matching may occur at the actual operating points. Screening solar cells based on the entire I-V characteristic will inherently result in more similar cells in the array. An array consisting of more similar cells is likely to have better overall characteristics and more predictable performance. Solar cell screening methods and cell ranking are discussed. The concept of a mean cell is defined as a cell 'best' representing all the cells in the production batch. The screening and ranking of all cells are performed with respect to the mean cell. The comparative results of different screening methods are illustrated on a batch of 50 silicon cells of the Space Station Freedom. Author (revised)

N94-13186*# Alabama Univ., Huntsville. Research Inst.
ADVANCED ELECTRIC MOTOR TECHNOLOGY FLUX MAPPING Final Report, 10 Apr. 1992 - 1993
George B. Doane, III, Warren Campbell, and Garvin Dean 8 Mar. 1993 158 p
(Contract NAS8-38609)
(NASA-CR-193824; NAS 1.26:193824; UAH-5-32903) Avail: CASI HC A08/MF A02

Design of electric motors which fulfill the needs of Thrust Vector Control (TVC) actuators used in large rocket propelled launch vehicles is covered. To accomplish this end the methodology of design is laid out in some detail. In addition a point design of a motor to fulfill the requirements of a certain actuator specified by MSFC is accomplished and reported upon. In the course of this design great stress has been placed on ridding the actuator of internally generated heat. To conduct the heat out of the motor use is made of the unique properties of the in house MSFC designed driving electronics. This property is that as along as they are operated in a quasi-linear mode the electronics nullify the effects of armature inductance as far as the phase of the armature current versus the rotor position is concerned. Actually the additional inductance due to the extended end turns in this design is of benefit because in the shorted armature failure mode the armature current in the fault (caused by the rotor flux sweeping past the armature) is diminished at a given rotor speed when compared to a more conventional motor with lower inductance. The magnetic circuit is analyzed using electromagnetic finite element methods. Author (revised)

N94-13194*# National Aeronautics and Space Administration. Lewis Research Center, Cleveland, OH.
A PHOTOVOLTAIC CATENARY-TENT ARRAY FOR THE MARTIAN SURFACE
M. Crutchik (Tel-Aviv Univ., Israel.), Anthony J. Colozza (Sverdrup Technology, Inc., Brook Park, OH.), and J. Appelbaum Aug. 1993 18 p
(Contract NAS3-25266; NAGw-2022; RTOP 506-41-11)
(NASA-TM-106306; E-8047; NAS 1.15:106306) Avail: CASI HC A03/MF A01

To provide electrical power during an exploration mission to Mars, a deployable tent-shaped structure with a flexible photovoltaic (PV) blanket is proposed. The array is designed with a self-deploying mechanism utilizing pressurized gas expansion. The structural design for the array uses a combination of cables, beams, and columns to support and deploy the PV blanket. Under the force of gravity a cable carrying a uniform load will take the shape of a catenary curve. A catenary-tent collector is self shadowing which must be taken into account in the solar radiation calculation. The shape and the area of the shadow on the array was calculated and used in the determination of the global radiation on the array. The PV blanket shape and structure dimension were optimized to achieve a configuration which maximizes the specific power (W/kg). The optimization was performed for four types of PV blankets (Si, GaAs/Ge, GaAs CLEFT, and amorphous Si) and four types of structure materials (Carbon composite, Aramid Fiber composite, Aluminum, and Magnesium). The results show that the catenary shape of the PV blanket, which produces the highest specific power, corresponds to zero end angle at the base with respect to the horizontal. The tent angle is determined by the combined effect of the array structure specific mass and the PV blanket output power. The combination of carbon composite structural material and GaAs CLEFT solar cells produce the highest specific power. The study was carried out for two sites on Mars corresponding to the Viking Lander locations. The designs were also compared for summer, winter, and yearly operation. Author (revised)

N94-13224# Gosudarstvennyi Komitet po Ispolzovaniyu Atomnoi Energii, Moscow (USSR).
ON A NONMINIMAL GAUGE INTERACTION OF A SCALAR FIELD IN D=2+1 CHERN-SIMONS-MAXWELL THEORY
S. M. Latinskij and D. P. Sorokin 1991 6 p
(DE93-621380; KFTI-91-12) Avail: CASI HC A01/MF A01 (US Sales Only)

The consequences of spontaneous symmetry breaking are considered in a model, describing nonminimal gauge interaction of a scalar field (analogous to that of spin-1/2 particle with anomalous magnetic momentum). It is shown that the gauge field Chern-Simons term can be generated as a result of symmetry breaking if it was not initially present in the action and, at the same time, the Maxwell term can be canceled by symmetry breaking corrections. DOE

N94-13333 Queens Univ., Kingston (Ontario). Dept. of Electrical Engineering.
DESIGN AUTOMATION TOOLS FOR TESTABLE VLSI CIRCUITS Ph.D. Thesis
Saman M. I. Adham Kingston, Ontario Queen's Univ. 1991 257 p
(ISBN-0-315-61461-7; CTN-93-60718) Copyright Avail: Micromedia Ltd., Technical Information Centre, 165 Hotel de Ville, Place du Portage, Phase 2, Hull, Quebec J8X 3X2, Canada HC

A very large scale integration (VLSI) circuit is assumed to contain a number of modules such as random logic circuits and read-only memories. By modifying the subcircuits locally, via selecting a design for testability (DFT) scheme, and monitoring the whole test globally the VLSI circuit is made testable. Following this framework, two problems are recognized: selection of the proper DFT technique to optimize the testability aspects of the macro cell, and modification of the macro cell to conform with the chosen DFT scheme. A generalized selection methodology has been developed to solve the selection problem employing an optimization technique and a satisfaction procedure to arrive at a solution that meets the user constraints. A knowledge based system that implements the selection mechanism has been developed to choose a built-in self-test (BIST) technique for random logic circuits. Modifying a circuit to comply with a given DFT scheme has also been studied for two DFT techniques and a number of tools have been developed. A new scan design methodology has been introduced which has simple design rules and employs two area efficient memory elements as internal storage. A comprehensive design tool has been developed to check circuits for design rule violations, check and correct scan design rule violations, and synthesize the scan path. Author (CISTI)

N94-13336*# Hughes Aircraft Co., Torrance, CA. Gallium Arsenide Operations.
MMIC PACKAGING TECHNOLOGY DEVELOPMENT Final Technical Report, Nov. 1989 - Mar. 1993
K. Li and S. Yuan 15 Mar. 1993 62 p
(Contract NAS3-25864)
(NASA-CR-194183; NAS 1.26:194183; W-4G157) Avail: CASI HC A04/MF A01

Packaging technology for microwave and millimeter-wave monolithic integrated circuits (MMIC's) was developed. Two packaging approaches were investigated for RF performance and mechanical integrity. One is a packaging approach using quartz (fused silica) material and a glass sealing process. The other is a packaging approach using ceramic (92 percent Alumina) material and a co-firing process. Test results indicate both packaging approaches provide wide frequency band and low insertion loss. The quartz package-breadboard components exhibited operating frequency up to 35 GHz, with insertion loss less than 1.30 dB at 35 GHz. Quartz packages were designed and fabricated to investigate reproducibility. Findings from sample fabrication indicate that metallization and glass sealing process for quartz packages requires substantial improvement before reproducibility can be established. Ceramic packages were designed and

fabricated for proof-of-concept in support of MMIC packaging technology development. The ceramic packages exhibited operating frequency up to 36 GHz, with insertion loss less than 1.7 dB at 36 GHz. These proof-of-concept MMIC packages not only show low insertion loss and wide frequency band but also demonstrated the hermetic-seal capability and the mechanical strength for many MMIC applications. Current co-fired ceramic process permits cost effectiveness and timely insertion of MMIC's technology. Author (revised)

N94-13425# Society of Non-Traditional Technology, Tokyo (Japan).
STUDY ON SUPERCONDUCTING BASIC TECHNOLOGY FOR SPACE APPLICATION, PART 1 [UCHUUYOU CHOUDENDOU YOUSO GIJUTSU NO KENKYUU]
Tokyo, Japan National Space Development Agency 31 Mar. 1993 157 p In JAPANESE Original contains color illustrations
(NASDA-CNT-930015-Pt-1; JTN-93-80469-Pt-1) Avail: CASI HC A08/MF A02

Feasibility studies on application of superconductivity to the space technology have been made for three years, since FY (Fiscal Year) 1988. In FY 1991, three basic technology, i.e., SIS (Superconductor Insulator Superconductor) mixer, microwave circuit element and superconductive magnetic bearing, are selected as potential technology in the space, and the following further studies were performed: (1) a review of current R & D (Research and Development) status on the technology; (2) a survey on potential use in the space; (3) a survey on the required features of the technology in space use; and (4) a preliminary design study of the devices and/or systems used by the technology, applicable on a satellite. Review works have also made on the current status of R and D programs of superconductive material processing test in the micro gravity environment, and ASTROMAG (Particle Astrophysics Magnet Facility) project.
Author (NASDA)

N94-13552# Centre National d'Etudes Spatiales, Toulouse (France).
POWER CONVERTERS FOR THE 120 V BUS SUPPLY CONTROL [CONVERTISSEURS DE PUISSANCE POUR LA REGULATION DE BARRE D'ALIMENTATION 120 V]
Christian Elisabelar Mar. 1993 52 p In FRENCH
(CNES-NT-134; ETN-93-94411) Copyright Avail: CASI HC A04/MF A01

Power converters for the 120 V bus supply control in such projects as Columbus and Hermes are addressed. Because of the power levels involved and the existing state of the art, several converter modules need to be connected in parallel to supply a single bus. To simplify the study, the power of each converter is set at around 1 kW. Many converter structures which satisfy requirement specifications and several solutions, with or without galvanic insulation, are proposed. The choice and sizing of the converter structure are considered. Stress factors and available technology are selection criteria in determining the most suitable structures. The dimensions of each structure, taking into account the rules of space design enable efficiency to be analytically estimated and it is subsequently verified experimentally. The converter command and its functional performance are then addressed. Numerical simulations with SUCCESS software are run to observe the actual operation of the power part of the converter and to develop the command law with its regulation parameters. The converter is simulated in its entirety and different transients are studied like load variation, no load operating point, short circuit. The response time, stability and behavior under disturbed conditions are thus known. A comparison of the various structures studied enabled the optimal converter to be chosen for some 120 V regulated bus applications. ESA

N94-13776# Microelectronics Center of North Carolina, Research Triangle Park.
FIELD EMITTER ARRAY RF AMPLIFIER DEVELOPMENT PROJECT. PHASE 1: CATHODE TECHNOLOGY DEVELOPMENT Quarterly Progress Report No. 6, 1 Jan. - 31 Mar. 1993
Bertram Hui 31 May 1993 39 p
(Contract MDA972-91-C-0028)
(AD-A266346) Avail: CASI HC A03/MF A01

Process in research and development continues at all sites. MCNC's program continues at full speed with smooth transition of project personnel. Electrical testing of field emitter arrays fabricated at MCNC continues at all sites. Effects of anode proximity on emission current capture are being investigated. Two new processes for gate opening alignment are under development. Both eliminate the necessity of retaining the nitride caps on the field emitter tips through the entire processing sequence. One requires alignment during an additional photolithography step, the other is self-aligning. Refinements in processing continue. Better control of the anisotropic silicon etch for tip formation has been achieved. In-house chem-mechanical polishing is still under investigation as a method for wafer planarization. Other materials are being evaluated for use as the insulating layer between substrate and gate. Better methods for depositing evaporated oxides are being sought, and the oxides as deposited are being characterized. Vacuum bonder and test system is operational. The bonding chamber has been outfitted for DC testing to improve test throughput, with electrical feedthroughs rated for 700 V at 10 A. Failure analysis of field emitter arrays from two lots was completed. Five mechanisms in two classes were identified as contributors to device failures: those mechanisms that destroyed working emitters, and those that prevented emitters from working. In anticipation of continued ARPA funding for the field emitter amplifier project, revised budgetary and scheduling information was prepared. Design of the process and reticle set for the next generation of devices has already begun. DTIC

N94-13786*# TRW Systems Group, Redondo Beach, CA. Space and Technology Group.
OPERATION OF HIGH POWER CONVERTERS IN PARALLEL Final Report
D. K. Decker and L. Y. Inouye Mar. 1993 7 p
(Contract NAS3-25093; RTOP 474-42-10)
(NASA-CR-191096; E-7685; NAS 1.26:191096) Avail: CASI HC A02/MF A01

High power converters that are used in space power subsystems are limited in power handling capability due to component and thermal limitations. For applications, such as Space Station Freedom, where multi-kilowatts of power must be delivered to user loads, parallel operation of converters becomes an attractive option when considering overall power subsystem topologies. TRW developed three different unequal power sharing approaches for parallel operation of converters. These approaches, known as droop, master-slave, and proportional adjustment, are discussed and test results are presented. Author (revised)

N94-13797*# Lockheed Engineering and Sciences Co., Hampton, VA.
SIMULATOR FOR HETEROGENEOUS DATAFLOW ARCHITECTURES Report, 1 Jun. 1991 - 31 Aug. 1992
Mahyar R. Malekpour Sep. 1993 56 p
(Contract NAS1-19000; RTOP 586-03-11-31)
(NASA-CR-191545; NAS 1.26:191545) Avail: CASI HC A04/MF A01

A new simulator is developed to simulate the execution of an algorithm graph in accordance with the Algorithm to Architecture Mapping Model (ATAMM) rules. ATAMM is a Petri Net model which describes the periodic execution of large-grained, data-independent dataflow graphs and which provides predictable steady state time-optimized performance. This simulator extends the ATAMM simulation capability from a heterogenous set of resources, or functional units, to a more general heterogenous architecture. Simulation test cases show that the simulator accurately executes the ATAMM rules for both a heterogenous architecture and a homogenous architecture, which is the special case for only one processor type. The simulator forms one tool in an ATAMM Integrated Environment which contains other tools for graph entry, graph modification for performance optimization, and playback of simulations for analysis. Author

N94-13811*# Jet Propulsion Lab., California Inst. of Tech., Pasadena.
COMMUNICATIONS AND CONTROL FOR ELECTRIC POWER SYSTEMS Report, 1990
H. Kirkham, A. Goettsche, D. Niebur, H. Friend, and A. Johnston 15 Jan. 1991 105 p
(Contract NAS7-918)
(NASA-CR-194503; JPL-Publ-91-44; NAS 1.26:194503) Avail: CASI HC A06/MF A02

The first section of the report describes the AbNET system, a hardware and software communications system designed for distribution automation (it can also find application in substation monitoring and control). The topology of the power system fixes the topology of the communications network, which can therefore be expected to include a larger number of

branch points, tap points, and interconnections. These features make this communications network unlike any other. The network operating software has to solve the problem of communicating to all the nodes of a very complex network in as reliable a way as possible even if the network is damaged, and it has to do so with minimum transmission delays and at minimum cost. The design of the operating protocols is described within the framework of the seven-layer Open System Interconnection hierarchy of the International Standards Organization. Section 2 of the report describes the development and testing of a high voltage sensor based on an electro-optic polymer. The theory of operation is reviewed. Bulk fabrication of the polymer is discussed, as well as results of testing of the electro-optic coefficient of the material. Fabrication of a complete prototype sensor suitable for use in the range 1-20 kV is described. The electro-optic polymer is shown to be an important material for fiber optic sensing applications. Appendix A is theoretical support for this work. The third section of the report presents the application of an artificial neural network, Kohonen's self-organizing feature map, for the classification of power system states. This classifier maps vectors of an N-dimensional space to a 2-dimensional neural net in a nonlinear way preserving the topological order of the input vectors. These mappings are studied using a nonlinear power system model. Author (revised)

N94-13834 McMaster Univ., Hamilton (Ontario). Accelerator Lab.
SINGLE EVENT UPSET (SEU) TESTING OF SEMICONDUCTOR COMPONENTS AT THE MCMASTER ACCELERATOR LABORATORY
J. A. Davies, F. J. D. Almeida, D. Comedi, and J. W. Stark Mar. 1991 32 p
(DSIS-93-00071; CTN-93-60775) Avail: CASI HC A03

Single event upsets (SEU) occur when a single ionizing particle such as a cosmic ray passes through a microelectronic device, causing a random change in the logic state of a bistable circuit. The SEU phenomenon is of great interest since it is a source of errors and failures, notably on spaceborne microelectronic chips. A Van de Graaff accelerator was used to simulate the cosmic ray heavy ion linear energy transfer (LET) distribution found in earth orbit, and accelerator experiments were conducted in a dedicated facility for SEU testing of microelectronic devices. The first set of experiments set out to compare data obtained by two different SEU memory tester systems, and a second set attempted to compare data obtained using ions of different species and energy but the same LET, and to determine the accuracy of the concept of a constant SEU cross-section for a given LET. Observation of a fluence dependent SEU cross section and transient behavior led to a third set of experiments, designed to allow observation in more detail of the dynamics of these newly observed phenomena. The charge collection efficiency of detectors to high LET ions was also measured. CISTI

N94-13846# National Defence Headquarters, Ottawa (Ontario).
ELECTROCHEMICAL NOISE IN LITHIUM PRIMARY CELLS
George J. Donaldson, Wing S. Nip (Farrington Lockwood Co. Ltd., Kanata, Ontario.), Timothy J. Patraboy (Farrington Lockwood Co. Ltd., Kanata, Ontario.), James S. Anderson (Farrington Lockwood Co. Ltd., Kanata, Ontario.), and Michael D. Farrington (Farrington Lockwood Co. Ltd., Kanata, Ontario.) 1991 22 p
(DSIS-93-00236; CTN-93-60780) Avail: CASI HC A03/MF A01

Electrochemical noise is interpreted as the occurrence of microscopic fluctuations of the potential of an electrochemical cell. A study was conducted on a number of commercial lithium cells to evaluate the practicality of electrochemical noise measurement as a diagnostic tool for performance and/or safety. The survey was limited to the following lithium based systems: sulfur dioxide, thionyl chloride, and manganese dioxide. The cells were subjected to a program of storage, environmental, and discharge conditions and then examined to determine whether there was any detectable effect on the electrochemical noise characteristics. While the study was of limited scope, it was nevertheless established that all cells exhibited some measurable electrochemical noise under certain conditions. The characteristics of the noise and its magnitude were influenced by many factors. The occurrence of observable noise above the instrumental background was generally associated with cells which had been discharged to between 80 and 100 percent of their nominal capacity. Most of the noise of interest was found at frequencies below 100 Hz. Author (CISTI)

N94-13871*# National Aeronautics and Space Administration. Goddard Space Flight Center, Greenbelt, MD.
MONGOOSE ASIC MICROCONTROLLER PROGRAMMING GUIDE
Brian S. Smith Washington Sep. 1993 33 p
(NASA-RP-1319; Rept-93E02366; NAS 1.61:1319) Avail: CASI HC A03/MF A01

The 'Mongoose' ASIC microcontroller is a radiation-hard implementation of the R3000 microprocessor. This document describes the internals of the microcontroller in a level of detail necessary for someone implementing a software design. Author

N94-13878*# National Aeronautics and Space Administration. Goddard Space Flight Center, Greenbelt, MD.
PHASE ALIGNER FOR THE ELECTRONICALLY SCANNED THINNED ARRAY RADIOMETER (ESTAR) INSTRUMENT
William A. Chren, Jr. and Brian G. Zomberg Washington Sep. 1993 16 p
(NASA-TM-4518; Rept-93E02368; NAS 1.15:4518) Avail: CASI HC A03/MF A01

A prototype Phase Aligner (PA) or the Electronically Scanned Thinned Array Radiometer instrument has been designed and tested. Implemented in a single Xilinx XC3042PC84-125 Field Programmable Gate Array (FPGA), it is a dual-port register file which allows independent storage and phase coherent retrieval of antenna array data by the Central Processing Unit (CPU). It has dimensions of 4 x 20 bits and can be used at clock frequencies as high as 25 MHz. The ESTAR is a passive synthetic-aperture radiometer designed to sense soil moisture and ocean salinity at L-band. Author

N94-13892# Sandia National Labs., Albuquerque, NM.
DEVELOPMENT OF UHF SPARK-SWITCHED L-C OSCILLATORS
L. F. Rinehart, J. F. Aurand, J. M. Lundstrom, C. A. Frost, M. T. Buttram, P. E. Patterson, and W. R. Crowe 1993 4 p Presented at the 9th IEEE Pulsed Power Conference, Albuquerque, NM, 21-23 Jun. 1993
(Contract DE-AC04-76DP-00789)
(DE93-015019; SAND-93-1280C; CONF-930616-2) Avail: CASI HC A01/MF A01

Spark switched L-C Oscillator (LCO) transmitters have operated in the Low, Medium, and High Frequency Bands (10's of kHz to 10's of MHz) throughout the history of radio. In the 1970's they were pushed into the VHF Band by Moran, et al. By applying ultra-fast gas switching techniques and by overcoming spark gap losses, the authors have operated LCO transmitters in the UHF (300 MHz to 3 GHz) region. Repetition rates greater than 1 kHz with peak voltages greater than 100 kV have been achieved. UHF oscillators are inherently small because of the low inductance and capacitance required to generate ultra-high frequencies. This size constraint forces the device to operate at very high voltage in order to store enough energy to drive the antenna in spite of series switch losses and parallel corona and stray capacity losses. The spark gap must close in a time short compared to one half an R-F cycle for efficient switching; this equates to a few hundred picoseconds at UHF. The LCO output is a damped sinusoid of a few cycles duration. While the fractional bandwidth (3-dB bandwidth divided by the center frequency) can be 10% to 80% depending on the Q, it is much smaller than the bandwidth of UWB impulse sources (100% bandwidth with multioctave coverage). Compared to UWB, the narrower bandwidth permits the use of higher gain antennas which can efficiently increase the effective radiated power (ERP) over a given frequency range. The authors have constructed L-C Oscillators with center frequencies of 450 MHz up to 800 MHz. The Q of these oscillators varies from 6 to 8 for the 450 MHz device, down to 1 to 2 for the 800 MHz unit. Q is increased when a resonant antenna or antenna-reflector combination is added. Prototypes with simple fat-dipole antennas and small parabolic reflectors (8 inches x 20 inches) have radiated normalized electric field strengths of 30 kV/m at 1 meter (measured in far-field and extrapolated back to 1 meter). DOE

N94-13925# Argonne National Lab., IL.
THE DE HAAS-VAN ALPHEN STUDIES AND FERMI SURFACE PROPERTIES OF ORGANIC SUPERCONDUCTORS (ET)2X
J. Wosnitza (Karlsruhe Univ., Germany.), G. W. Crabtree, J. M. Williams, H. H. Wang, K. D. Carlson, and U. Geiser Apr. 1993 5 p Presented at the 1992 International Conference on Science and Technology of Synthetic Metals (ICSM), Goeteborg, Sweden, 12-18 Aug. 1992

(Contract W-31-109-eng-38)
(DE93-015157; ANL/MSD/CP-79640; CONF-9208132-13) Avail: CASI HC A01/MF A01

The de Haas-van Alphen (dHvA) measurements of organic superconductors (ET)2X, where ET stands for bis(ethylene) dithiotetrathiafulvalene (or BEDT-TTF) and X = IBr2, (NH4)Hg(SCN4) and Cu(NCS2) are reported. The strong two-dimensionality of the Fermi surface (FS) is clearly seen by the perfect 1/cos((Theta))-behavior of the dHvA frequency. The distinctive kind of beating and the angular dependence of the dHvA signal in (beta)-(ET)2IBr2 gives clear evidence for a lightly corrugated structure of the FS. Due to the nearly cylinder-shape of the FS the bare band structure effective mass, m(sub b), also shows a 1/cos((Theta))-dependence which is responsible for spin splitting zeros at certain angles. At these points, where the fundamental amplitude of the dHvA signal is vanishing, m(sub b) could exactly be determined and by comparison with the independently measured cyclotron effective mass the electron-phonon coupling constant could be estimated. DOE

N94-13928# Allied-Signal Aerospace Co., Kansas City, MO.
MINIATURE MECHANISM ASSEMBLY
R. L. Stubenhofer May 1993 12 p
(Contract DE-AC04-76DP-00613)
(DE93-015595; KCP-613-5078) Avail: CASI HC A03/MF A01

Miniature assembly operations were reviewed to provide candidates for improvements to part handling, assembly, fixturing, equipment setup, and work verification. Four areas of emphasis were chosen -- two specific products and two generic processes. The work done in conjunction with this project resulted in improvements to flowtimes and yields. Groundwork for further improvements in miniature assembly operations is now in place. DOE

N94-13937# Allied-Signal Aerospace Co., Kansas City, MO. Technical Communications.
ALTERNATE CLEANING METHODS FOR LCCAS Final Report
B. E. Adams Apr. 1993 36 p
(Contract DE-AC04-76DP-00613)
(KCP-613-5045) Avail: CASI HC A03/MF A01

The purpose of this project was to evaluate DI water followed by isopropyl alcohol (IPA) cleaning and no cleaning of leadless chip carriers (LCCs). Both environmentally safe methods were to be tested against the current chlorofluorocarbon (CFC) material cleaning baseline. Several experiments were run to compare production and electrical yields of LCCs cleaned by all three methods. The critical process steps most affected by cleaning were wire bonding, sealing, particle induced noise detection (PIND), moisture content, and electrical. Yields for the experimental lots cleaned by CFC, DI water plus IPA, and no cleaning were 56, 72, and 75 percent, respectively. The overall results indicated that vapor degreasing/ultrasonic cleaning in CFCs could be replaced by the aqueous method. No cleaning could also be considered if an effective dry method of particle removal could be developed. Author (revised)

N94-13948*# Jet Propulsion Lab., California Inst. of Tech., Pasadena.
COMMUNICATIONS AND CONTROL FOR ELECTRIC POWER SYSTEMS: POWER FLOW CLASSIFICATION FOR STATIC SECURITY ASSESSMENT
D. Niebur and A. Germond Feb. 1993 25 p
(Contract NAS7-918)
(NASA-CR-194512; JPL-Publ-93-6; NAS 1.26:194512) Avail: CASI HC A03/MF A01

This report investigates the classification of power system states using an artificial neural network model, Kohonen's self-organizing feature map. The ultimate goal of this classification is to assess power system static security in real-time. Kohonen's self-organizing feature map is an unsupervised neural network which maps N-dimensional input vectors to an array of M neurons. After learning, the synaptic weight vectors exhibit a topological organization which represents the relationship between the vectors of the training set. This learning is unsupervised, which means that the number and size of the classes are not specified beforehand. In the application developed in this report, the input vectors used as the training set are generated by off-line load-flow simulations. The learning algorithm and the results of the organization are discussed. Author (revised)

N94-13951# Centre National d'Etudes Spatiales, Toulouse (France).
STUDY OF THE INTERMATEABILITY OF CANNON AND SOURIAU SUBMINIATURE CONNECTORS [ETUDE DE L'INTERMARIABILITE DES CONNECTEURS SUBMINIATURES DE MARQUES CANNON ET SOURIAU]
Serge Clement Nov. 1992 71 p In FRENCH
(CNES-NT-132; ETN-93-93979) Copyright Avail: CASI HC A04/MF A01

A method to verify the intermateability of connectors which have different origins and common specifications is provided. These connectors are designed for space applications and are known as Sub D connectors. These Sub D connectors investigated are specified under the American military standard MIL-C 24308. The evaluation of the connectors was carried out under three steps involving dimensional control, technological analysis, and a validation phase. The purpose of the dimensional control was to check the physical functionality of coupling these two different connectors. The technological analysis aimed at stressing and understanding possible performance differences between both connectors. The validation consisted of tests to evaluate the performance of two coupled connectors. ESA

N94-13998# Technische Univ., Berlin (Germany). Fachbereich Elektrotechnik.
MUTUAL INDUCTANCE BETWEEN PARTIALLY WOUND TORI AND A BIFILAR CONDUCTOR Ph.D. Thesis [GEGENINDUKTIVATAET ZWISCHEN TEILWEISE BEWICKELTEM RINGKERN UND EINER DOPPELLEITUNG]
Kanaga Sabapathy Mylvaganam 1992 126 p In GERMAN
(ETN-93-94388) Avail: CASI HC A07/MF A02

The solution of the three dimensional magnetostatic problem in cylindrical and toroidal coordinates is used to develop analytic expressions for the mutual inductance between bifilar current carrying conductors and partially wound tori of rectangular and circular cross sections. The double series containing associated Legendre functions obtained for the mutual inductance in the case of toroid with circular cross section was evaluated for certain dimensions of the toroid, after introducing a gemetrical factor dependent only on the dimensions of the toroid. To solve Laplace equations using only cylindrical coordinates, the rectangular toroid was viewed as one element of an infinite number of tori located symmetrically to the axis rotation and placed parallel to the flat surfaces of the original toroid. The mutual inductance in the case of the toroid with the rectangular cross-section was calculated using matrix formulation of the solution to the potential problem and the double series obtained for the mutual inductance was evaluated for the rectangular toroid dimensioned in such a way that both types of tori have the same average diameter and cross sectional area. To check the results from the two boundary value problems involving circular and rectangular tori, various special configurations of the rectangular toroid in the field of the bifilar lines were studied. The first configuration was that of an infinitely long toroid, on the surface of which the magnetic field was calculated and compared with the values obtained from the general solution. For two tori with almost equal cross sections the induced voltages in the windings were measured and calculated, whereby the results are found totally well within the experimental errors. For rough estimation of the induced voltage, some approximate expressions were given and numerically and experimentally verified. ESA

N94-14012# Argonne National Lab., IL.
BATTERY TESTING AT ARGONNE NATIONAL LABORATORY
W. H. DeLuca, K. R. Gillie, J. E. Kulaga, J. A. Smaga, A. F. Tummillo, and C. E. Webster 25 Mar. 1993 23 p Presented at the Interagency Advanced Power Working and Group Meeting, White Oak, MD, 25 Mar. 1993
(Contract W-31-109-eng-38)
(DE93-011761; ANL/CMT/CP-79338; CONF-9303137-1) Avail: CASI HC A03/MF A01

Argonne National Laboratory's Analysis & Diagnostic Laboratory (ADL) tests advanced batteries under simulated electric and hybrid vehicle operating conditions. The ADL facilities also include a post-test analysis laboratory to determine, in a protected atmosphere if needed, component compositional changes and failure mechanisms. The ADL provides a common basis for battery performance characterization and life evaluations with unbiased application of tests and analyses. The battery evaluations and post-test examinations help identify factors that limit system performance and life

and the most-promising R&D approaches for overcoming these limitations. Since 1991, performance characterizations and/or life evaluations have been conducted on eight battery technologies: Na/S, Li/S, Zn/Br, Ni/MH, Ni/Zn, Ni/Cd, Ni/Fe, and lead-acid. These evaluations were performed for the Department of Energy's. Office of Transportation Technologies, Electric and Hybrid Propulsion Division (DOE/OTT/EHP), and Electric Power Research Institute (EPRI) Transportation Program. The results obtained are discussed. DOE

N94-14096# Helsinki Univ. of Technology, Espoo (Finland). Radio Lab.
MEASUREMENT ELECTRONICS OF INDUSTRIAL MICROWAVE RESONATOR SENSORS Ph.D. Thesis
Pertti V. Vainikainen Nov. 1991 32 p Sponsored by Academy of Finland; Technology Development Center of Finland; Raute Oy; Imatran Voima Oy; Ivoinfra Oy; and Jenny and Antii Wihuri Foundation
(TKK-S-RAD-S194; TKK-DISS-794; ISBN-951-22-0722-2; ETN-93-93473)
Avail: CASI HC A03/MF A01

The measurement methods of the properties of high frequency electromagnetic resonators used as industrial sensors are described. A short overview of the utilization of microwaves in industrial measurements is given and a theoretical analysis of the aspects affecting the performance of the measurement methods is presented. Several practical realizations of the measurement electronics of different types of resonator sensors are described. ESA

N94-14138# Centre National d'Etudes Spatiales, Toulouse (France).
MULTI-OUTPUT FLYBACK CONVERTER WITH ULTRAFAST CURRENT PROTECTION [CONVERTISSEUR FLYBACK A SORTIES MULTIPLES AVEC PROTECTION DE COURANT ULTRA RAPIDE]
Alphonse Barnaba Nov. 1992 21 p In FRENCH
(CNES-NT-133; ETN-93-93980) Copyright Avail: CASI HC A03/MF A01

The static regulations of a flyback converter with mono- and multioutputs are studied. The implementation of ultra far current protection and the analysis of the mutual inductance decoupling between outputs are discussed. Three breadboard model converters were investigated: a 'heavy' mode flyback converter, a 'light' mode flyback converter, and a miniwatt flyback converter. The experiments with the 'heavy' and 'light' breadboard models were performed with their own servomechanisms. An efficiency greater than 80% with an output less than 1 W was obtained for the miniwatt model converter. Such converters are often used for tensions inferior to 50 W. ESA

N94-14324*# Clemson Univ., SC. Dept. of Ceramic Engineering.
SUPERCONDUCTIVITY DEVICES: COMMERCIAL USE OF SPACE Annual Report, 3 Jul. 1992 - 2 Jul. 1993
Gene Haertling, Eugene Furman, Chi-Shiung Hsi, and Guang Li 6 Sep. 1993 197 p
(Grant NAG1-1301)
(NASA-CR-194163; NAS 1.26:194163) Avail: CASI HC A09/MF A03

The processing and screen printing of the superconducting BSCCO and 123 YBCO materials on substrates is described. The resulting superconducting properties and the use of these materials as possible electrode materials for ferroelectrics at 77 K are evaluated. Also, work performed in the development of solid-state electromechanical actuators is reported. Specific details include the fabrication and processing of high strain PBZT and PLZT electrostrictive materials, the development of PSZT and PMN-based ceramics, and the testing and evaluation of these electrostrictive materials. Finally, the results of studies on a new processing technology for preparing piezoelectric and electrostrictive ceramic materials are summarized. The process involves a high temperature chemical reduction which leads to an internal pre-stressing of the oxide wafer. These reduced and internally biased oxide wafers (RAINBOW) can produce bending-mode actuator devices which possess a factor of ten more displacement and load bearing capacity than present-day benders. CASI

N94-14325*# Idaho Univ., Moscow.
NASA SPACE ENGINEERING RESEARCH CENTER FOR VLSI SYSTEMS DESIGN Annual Report
Jan. 1991 80 p
(Grant NAGw-1406)
(NASA-CR-194035; NAS 1.26:194035) Avail: CASI HC A05/MF A01

This annual review reports the center's activities and findings on very large scale integration (VLSI) systems design for 1990, including project status, financial support, publications, the NASA Space Engineering Research Center (SERC) Symposium on VLSI Design, research results, and outreach programs. Processor chips completed or under development are listed. Research results summarized include a design technique to harden complementary metal oxide semiconductors (CMOS) memory circuits against single event upset (SEU); improved circuit design procedures; and advances in computer aided design (CAD), communications, computer architectures, and reliability design. Also described is a high school teacher program that exposes teachers to the fundamentals of digital logic design. CASI

N94-14336 California Univ., Berkeley. Lawrence Berkeley Lab.
ELECTRONIC SCHEMATICS FOR THE DONNER 600 CRYSTAL TOMOGRAPH
R. H. Huesman, S. E. Derenzo, W. W. Moses, J. L. Cahoon, A. B. Geyer, B. T. Turko, D. C. Uber, M. Colina, M. H. Ho, and T. F. Budinger Sep. 1992 58 p Limited Reproducibility: More than 20% of this document may be affected by poor print
(Contract DE-AC03-76SF-00098)
(DE93-015277; LBL-29628) Avail: Issuing Activity (Department of Energy (DOE))

This report provides a collection of electronic schematics detailing the layout and wiring of the Donner 600 Crystal Tomograph. DOE

N94-14427# Lawrence Livermore National Lab., CA.
AN ULTRA-COMPACT PROCESSOR MODULE BASED ON THE R3000
D. J. Mullenhoff, J. L. Kaschmitter, J. C. Lyke (Phillips Lab., Kirtland AFB, NM.), and G. A. Forman (General Electric Co., Schenectady, NY.) 14 Aug. 1992 4 p Presented at the GOMAC 1992 Government Manufacturing and Applications Conference, Las Vegas, NV, 9-12 Nov. 1992
(Contract W-7405-eng-48)
(DE93-012549; UCRL-JC-110031; CONF-9211106-2) Avail: CASI HC A01/MF A01

Viable high density packaging is of critical importance for future military systems, particularly space borne systems which require minimum weight and size and high mechanical integrity. A leading, emerging technology for high density packaging is multi-chip modules (MCM). During the 1980's, a number of different MCM technologies have emerged. In support of Strategic Defense Initiative Organization (SDIO) programs, Lawrence Livermore National Laboratory (LLNL) has developed, utilized, and evaluated several different MCM technologies. Prior LLNL efforts include modules developed in 1986, using hybrid wafer scale packaging, which are still operational in an Air Force satellite mission. More recent efforts have included very high density cache memory modules, developed using laser pantography. As part of the demonstration effort, LLNL and Phillips Laboratory began collaborating in 1990 in the Phase 3 Multi-Chip Module (MCM) technology demonstration project. The goal of this program was to demonstrate the feasibility of General Electric's (GE) High Density Interconnect (HDI) MCM technology. The design chosen for this demonstration was the processor core for a MIPS R3000 based reduced instruction set computer (RISC), which has been described previously. It consists of the R3000 microprocessor, R3010 floating point coprocessor and 128 Kbytes of cache memory. DOE

N94-14522# Lawrence Livermore National Lab., CA.
INDEPENDENT ADJUSTMENT OF THE HIGHER ORDER FREQUENCY DEPENDENT PHASE IN CHIRPED PULSE AMPLIFICATION SYSTEMS
W. E. White, F. G. Patterson, R. Combs, L. Seppala, D. F. Price, R. L. Shepherd, and D. H. Reitze 14 Apr. 1993 3 p Presented at the 5th Short Wavelength: Physics With Intense Laser Pulses, San Diego, CA, 29-31 Mar. 1993
(Contract W-7405-eng-48)
(DE93-017106; UCRL-JC-113601; CONF-9303119-4) Avail: CASI HC A01/MF A01

We have developed a system that allows compensation of higher order phase terms that limit chirped pulse amplification systems. Results indicate phase can be compensated by a properly adjusted air-spaced doublet within the stretcher. DOE

N94-14533# Allied-Signal Aerospace Co., Kansas City, MO.
MICROWAVE INTERCONNECTION

P. E. Fry Jun. 1993 23 p
(Contract DE-AC04-76DP-00613)
(DE93-016580; KCP-613-5110) Avail: CASI HC A03/MF A01

A limited evaluation was made of two commonly found microwave interconnections: microstrip-to-microstrip and coaxial-to-microstrip. The evaluation attempted to select the interconnection technique which worked best for the particular interface type. Short ribbon wires worked best for the microstrip-to-microstrip interconnection. A published method of compensating the microstrip conductor had the best performance for the coaxial-to-microstrip interconnection. The work was conducted under the Microwave Technology Process Capability Assurance Program at Allied-Signal Inc., Kansas City Division. DOE

N94-14686 Bureau of Mines, Norris, TN.
EARLY DETECTION OF INSULATION FAILURE IN ELECTRIC MOTORS Report of Investigations, 1993
G. T. Homce 1993 26 p Limited Reproducibility: More than 20% of this document may be affected by microfiche quality
(PB93-198208; BU-RI-9450) Avail: CASI HC A03

A system capable of monitoring mine electrical power systems and detecting impending component failure could significantly improve power system safety and reduce unscheduled equipment downtime. Such monitoring would require a method of evaluating electrical parameters, calculated from terminal values, for indications of component deterioration. The U.S. Bureau of Mines has targeted electrical failure of squirrel cage induction motors and examined the use of mathematical models to aid in the evaluation. The initial stage of the work is complete and has produced polynomial networks called adaptive learning networks (ALN's) that can detect and quantify winding insulation leakage simulated on laboratory motors. In the modeling process, empirical data from laboratory motors were used to select the electrical parameters most significant for assessing motor conditions, and mathematical expressions relating these parameters to simulated deterioration were formed. NTIS

N94-14698# Laboratoire d'Automatique et d'Analyse des Systemes, Toulouse (France).
A HIGH VOLTAGE DIELECTRICALLY ISOLATED SMART POWER TECHNOLOGY BASED ON SILICON DIRECT BONDING Ph.D. Thesis - Inst. National des Sciences Appliquees, Toulouse [FILIERE TECHNOLOGIQUE DE PUISSANCE INTELLIGENTE HAUTE TENSION A ISOLATION DIELECTRIQUE BASEE SUR LA SOUDURE DIRECTE SUR SILICIUM]
Veronique Macary 1992 183 p In FRENCH Sponsored in part by Ministere de la Recherche et de la Technologie, Paris, France
(LAAS-92492; ETN-93-94360) Avail: CASI HC A09/MF A02

The feasibility of a dielectrically isolated technology based on the silicon direct bonding technique, for high voltage smart power applications in the 1000 to 1550 V/1 to 20 A range, where a vertical power switch is necessary, is investigated and demonstrated. Static and dynamic isolation of the low voltage circuitry integrated beside the vertical power transistor is the main concern of this family of circuits. The dielectric isolation offers better protection to the low voltage part than does the junction isolation, because of the elimination of the parasitic bipolar transistor inherent to the latter isolation technique. Silicon direct bonding provides a cost effective way to obtain a buried oxide isolation layer. In addition, the application requires a Si/Si bonded area in the active region of the vertical power switch. Strong influence of the prebonding cleaning in the electrical characteristics of the Si/Si interface is pointed out, and presence of crystalline defects is assumed to be at the origin of electrical failures. The main problems of silicon direct bonding process compatibility with standard processes were overcome, and a complete process flow, including the simultaneous integration of a vertical power bipolar transistor together with a bipolar control circuitry, was validated. Using a peripheral biased ring is shown to provide an easy way to optimize high voltage termination for the smart power circuit, while adding a non-additional technological step. This technique was studied by dimensional electrical simulations (BIDIM2 software), as well as analytically computed. ESA

N94-14711# Laboratoire d'Automatique et d'Analyse des Systemes, Toulouse (France). Composants Integres de Puissance.
DESIGN AND OPTIMIZATION OF HIGH VOLTAGE LATERAL DMOS DEVICES USING RESURF TECHNOLOGY Ph.D. Thesis - Toulouse Univ. [CONCEPTION ET OPTIMISATION DES COMPOSANTS DMOS LATERAUX HAUTE TENSION EN TECHNOLOGIE RESURF]
Mohamed El Amine Bouanane 1992 161 p In FRENCH
(LAAS-92511; ETN-93-94361) Avail: CASI HC A08/MF A02

One of the most promising solutions of the fabrication of switches for high voltage integrated circuits, Metal Oxide Semiconductor, the Lateral Double diffused Metal Oxide Semiconductor transistor (LDMOS) using the RESURF technique is discussed. This device is compatible with the low voltage circuits (CMOS or bipolar or BiCMOS); furthermore the LDMOS RESURF is easy to process, shows a high voltage handling capability and a good isolation. However, two major problems arise when optimizing this device: high on resistance value, and severe sensitivity of the breakdown voltage on technological parameters. To bypass these drawbacks the use of the following is used: shallow implantation to increase the concentration of the drift area between the channel and the drain; semiresistive layer, like SIPOS, deposited on the oxide between the gate and the drain. Numerical analysis shows that the use of both surface doping and the SIPOS technique will greatly improve the on resistance (between 40 and 60 of the On resistance value of the classic LDMOS RESURF). Moreover, an optimum breakdown voltage value can be reached for geometrical and physical parameters compatible with real technological tolerances. Geometrical parameters (channel drain distance, epi thickness and oxide thickness) and physical ones (epi doping, concentration and junction depth of surface doping) are optimized to obtain a breakdown voltage around 400 V. For the validation purpose of these rules, diodes and RESURF transistors using a surface doping technique and a SIPOS layer are fabricated. ESA

N94-14713# Laboratoire d'Automatique et d'Analyse des Systemes, Toulouse (France).
THERMAL DESIGN OF HYBRID CIRCUITS: TOOLS AND METHODOLOGY Ph.D. Thesis - Inst. National des Sciences Appliquees, Toulouse [METHODOLOGIE DE LA CONCEPTION THERMIQUE DES CIRCUITS ELECTRONIQUES HYBRIDES ET PROBLEMES CONNEXES]
Patrick Tounsi 1992 158 p In FRENCH
(LAAS-92515; ETN-93-94363) Avail: CASI HC A08/MF A02

The theoretical basis and the software computer implementation of new tools, intended for solving three dimensional static or dynamic conductive heat transfer problems in multilayered medias, are considered. These tools are particularly well adapted for thermal analysis of hybrid power circuits. Methodology of thermal design with the help of these tools is proposed. A comparison with experimental results is done and a way to solve electrothermal problems is outlined. ESA

N94-14730*# National Aeronautics and Space Administration. Lewis Research Center, Cleveland, OH.
SOLAR RADIATION ON MARS: STATIONARY PHOTOVOLTAIC ARRAY
J. Appelbaum, I. Sherman (Tel-Aviv Univ., Israel.), and G. A. Landis (Sverdrup Technology, Inc., Brook Park, OH.) Oct. 1993 21 p
(Contract NAS3-25266; NAGw-2022; RTOP 506-41-11)
(NASA-TM-106321; E-8071; NAS 1.15:106321) Avail: CASI HC A03/MF A01

Solar energy is likely to be an important power source for surface-based operation on Mars. Photovoltaic cells offer many advantages. In this article we have presented analytical expressions and solar radiation data for stationary flat surfaces (horizontal and inclined) as a function of latitude, season and atmospheric dust load (optical depth). The diffuse component of the solar radiation on Mars can be significant, thus greatly affecting the optimal inclination angle of the photovoltaic surface. Author

N94-14805# Los Alamos National Lab., NM.
OPTICAL DEGRADATION ISSUES FOR XUV PROJECTION LITHOGRAPHY SYSTEMS
B. E. Newnam 1992 9 p Presented at the Symposium on Optical Materials for High-Power Lasers, Boulder, CO, 28-30 Oct. 1992
(Contract W-7405-eng-36)
(DE93-012658; LA-UR-93-1212; CONF-921047-3) Avail: CASI HC A02/MF A01

We review the degradation susceptibility of the various optical components proposed for use in XUV projection lithography systems at 13-20 nm. Contamination by laser plasma target debris and carbonaceous films are two primary hazards that must be essentially nullified. Pertinent experimental results of a number of researchers illustrate the present status. DOE

N94-14812# Istituto Elettrotecnico Nazionale (Galileo Ferraris), Turin (Itlay).
[ACTIVITIES REPORT OF THE NATIONAL ELECTROTECHNICAL INSTITUTE GALILEO FERRARIS] Annual Report, 1991 [ISTITUTO ELETTROTECNICO NAZIONALE GALILEO FERRARIS, RAPPORTO ANNUALE 1991]
May 1992 208 p In ENGLISH and ITALIAN
(ETN-93-94224) Avail: CASI HC A10/MF A03

Progress in the scientific and technical activities in the following areas are described: time, frequency and electromagnetic metrology; electrical metrology; photometry; acoustics; materials; electromechanics; systems engineering; research carried out by the study center for television. The main scientific areas covered concern: metrology, regarding time and frequency; electromagnetic, photometric and acoustic quantities, with research carried out in primary measurement standards and the determination of fundamental physical constants; matter physics with the study of magnetic materials, amorphous thin film semiconductors and high critical temperature superconductors, and with the evaluation of magnetic, electrical, radiometric, photometric and acoustic properties of materials for specific applications; electrical equipment, with researchers and experimental activity aiming at improving characteristics, reliability and safety of electrical devices and plants; and techniques for information processing, with the development of techniques for image understanding and researchers on reliability of complex systems. A description of the calibration service in Italy is also given. ESA

N94-14870# Lawrence Livermore National Lab., CA.
ELECTROCHEMICAL PLANARIZATION FOR MICROELECTRONIC CIRCUITS
R. J. Contolini, S. T. Mayer, and A. F. Bernhardt 25 Mar. 1993 4 p Presented at the National Center for Advanced Information Components Manufacturing (NCAICM) Workshop, Albuquerque, NM, 30-31 Mar. 1993
(Contract W-7405-eng-48)
(DE93-017214; UCRL-JC-113618; CONF-9303198-1) Avail: CASI HC A01/MF A01

The need for flatter and smoother surfaces (planarization) in microelectronic circuits increases as the number of metal levels in ultra large scale integrated (ULSI) circuits increases. At Lawrence Livermore National Laboratory, the authors have developed an electrochemical planarization process that fills vias and trenches with metal (without voids) and subsequently planarizes the surface. Use is made of plasma-enhanced chemical vapor deposition (PECVD) of SiO2 for the dielectric layers and electroplated copper for the metalization. This report describes the advantages of this process over existing techniques, possibilities for collaboration, and previous technology transfer. DOE

N94-14885 Joint Inst. for Nuclear Research, Dubna (USSR). Lab. of High Energy.
A HIGH-PRECISION DIRECT CURRENT MEASURING DEVICE OVER A KILOAMPERE RANGE
M. A. Voevodin, Yu. V. Gusakov, N. A. Korukov, Sh. Z. Sajfulin, and I. N. Yalovoj 1991 4 p Limited Reproducibility: More than 20% of this document may be affected by microfiche quality
(DE93-626409; JINR-R-13-91-424) Avail: Issuing Activity (Department of Energy (DOE)) (US Sales Only)

In power supply systems, a need arises for wide-band loading currents monitors with a not galvanic contact from a control circuit. The measuring device is a reaction self-regulation circuit with a compensation of the value of the measured parameter. The measuring device may find extensive application in measurements of supply currents magnets and accelerator lenses. DOE

N94-13433# University of Electro-Communications, Tokyo (Japan).
FABRICATION OF AlGaAs/GaAs-LIGHT-EMITTING DEVICES BY SELECTIVE MOCVD USING DIALKYLMETALCHLORIDE
Koichi Yamaguchi, Shigeki Kishida, and Kotaro Okamoto *In its* Bulletin of the University of Electro-Communications, Volume 6, No. 1, Serial No. 11 Jun. 1993 p 1-8 In JAPANESE (For primary document see N94-13432 02-61)
Avail: CASI HC A02/MF A02

N94-13434# University of Electro-Communications, Tokyo (Japan).
STUDENT'S WORKS AND POWER SUPPLIES IN ELECTRONIC CIRCUIT LABORATORY
Kiyoomi Tanaka, Takashi Warashina, and Yoshihiko Hayakawa *In its* Bulletin of the University of Electro-Communications, Volume 6, No. 1, Serial No. 11 Jun. 1993 p 9-19 In JAPANESE (For primary document see N94-13432 02-61)
Avail: CASI HC A03/MF A02

N94-14376*# Jet Propulsion Lab., California Inst. of Tech., Pasadena.
INSERTION LOSS AND NOISE-TEMPERATURE CONTRIBUTION OF HIGH-TEMPERATURE SUPERCONDUCTING BANDPASS FILTERS CENTERED AT 2.3 AND 8.45 GHz
J. L. Prater and J. J. Bautista *In its* The Telecommunications and Data Acquisition Report 15 Aug. 1993 p 61-67 (For primary document see N94-14369 02-32)
(RTOP 310-20-66-92-01)
Avail: CASI HC A02/MF A03

N94-14382*# Jet Propulsion Lab., California Inst. of Tech., Pasadena.
PERFORMANCE RESULTS OF A DIGITAL TEST SIGNAL GENERATOR
B. O. Gutierrez-Luaces, M. Marina, and B. Parham (OAO Corp., Los Angeles, CA.) *In its* The Telecommunications and Data Acquisition Report 15 Aug. 1993 p 140-153 (For primary document see N94-14369 02-32)
(RTOP 314-40-41-11-06)
Avail: CASI HC A03/MF A03

34 FLUID MECHANICS AND HEAT TRANSFER

Includes boundary layers; hydrodynamics; fluidics; mass transfer; and ablation cooling.

For related information see also *02 Aerodynamics* and *77 Thermodynamics and Statistical Physics.*

N94-12803*# Computational Fluid Dynamics Research Corp., Huntsville, AL. Research and Development Services and Software.
A COMPUTER MODEL FOR LIQUID JET ATOMIZATION IN ROCKET THRUST CHAMBERS Final Report, 22 May 1989 - 21 Nov. 1991
M. G. Giridharan, J. G. Lee, A. Krishnan, H. Q. Yang, E. Ibrahim, S. Chuech, and A. J. Przekwas 31 Dec. 1991 143 p Original contains color illustrations
(Contract NAS8-38425; SBIR-11.04-6576C)
(NASA-CR-194194; NAS 1.26:194194; CFDRC-4041/1) Avail: CASI HC A07/MF A02; 5 functional color pages

The process of atomization has been used as an efficient means of burning liquid fuels in rocket engines, gas turbine engines, internal combustion engines, and industrial furnaces. Despite its widespread application, this complex hydrodynamic phenomenon has not been well understood, and predictive models for this process are still in their infancy. The difficulty in simulating the atomization process arises from the relatively large number of parameters that influence it, including the details of the injector geometry, liquid and gas turbulence, and the operating conditions. In this study, numerical models are developed from first principles, to quantify factors influencing atomization. For example, the surface wave dynamics theory is used for modeling the primary atomization and the droplet energy conservation principle is applied for modeling the secondary atomization. The use of empirical correlations has been minimized by shifting the analyses to fundamental levels. During applications of these models, parametric studies are performed to understand and correlate the influence of relevant parameters on the atomization process. The predictions of these models are compared with existing experimental data. The main tasks of this study were the following: development of a primary atomization model; development of a secondary atomization model; development of a

model for impinging jets; development of a model for swirling jets; and coupling of the primary atomization model with a CFD code.

Derived from text

N94-12884# Sandia National Labs., Albuquerque, NM.

HIGH-FLUX TESTING OF HEAT PIPES FOR POINT-FOCUS SOLAR COLLECTOR SYSTEMS

D. R. Adkins 1993 7 p Presented at the National Conference and Exposition on Heat Transfer, Atlanta, GA, 8-11 Aug. 1993 -11 Aug. 1993

(Contract DE-AC04-76DP-00789)

(DE93-011581; SAND-92-2346C; CONF-930830-13) Avail: CASI HC A02/MF A01

The Department of Energy is currently funding the development of a power conversion system that uses a parabolic-dish collector to direct solar energy onto a 25-kWe Stirling engine/generator system. As part of this program, heat-pipe solar receivers are being developed to transfer 65 kW of thermal energy from the focus of the concentrator to the heater-tubes of the engine. These receivers operate at temperatures up to 800 C and with peak flux loads approaching 100 W/cm(sup 2). Designing a wick structure that can withstand these operating conditions has been a major part of the heat-pipe receiver development activities. Recently, bench-scale tests were performed on two advanced artery structures that are candidates for full-scale receivers. The arteries were able to lift sodium over 40 cm to cool a 30-cm(sup 2) patch on the bench-scale receiver's surface. Peak flux levels of approximately 80 W/cm(sup 2) were applied to the receiver surface. DOE

N94-12888*# Institute for Computer Applications in Science and Engineering, Hampton, VA.

MODULATIONAL STABILITY OF PERIODIC SOLUTIONS OF THE KURAMOTO-SIVASKINSKY EQUATION Final Report

Demetrios T. Papageorgiou, George C. Papanicolaou (New York Univ., New York.), and Yiorgos S. Smyrlis (Manchester Univ., England.) Washington Jul. 1993 31 p Submitted for publication

(Contracts NAS1-19480; NAS1-18605; F49620-92-J-0023; NSF DMS-90-03227; NATO-CRG-920097; RTOP 505-90-52-01)

(NASA-CR-191502; NAS 1.26:191502; ICASE-93-44) Avail: CASI HC A03/MF A01

We study the long-wave, modulational, stability of steady periodic solutions of the Kuramoto-Sivashinsky equation. The analysis is fully nonlinear at first, and can in principle be carried out to all orders in the small parameter, which is the ratio of the spatial period to a characteristic length of the envelope perturbations. In the linearized regime, we recover a high-order version of the results of Frisch, She, and Thual, which shows that the periodic waves are much more stable than previously expected.

Author (revised)

N94-12959*# Hawaii Univ., Honolulu. Inst. for Astronomy.

STUDIES OF GAS IN COOLING FLOW CLUSTERS Final Report, 1 Nov. 1989 - 31 Oct. 1991

Esther M. Hu and Lennox L. Cowie 31 Oct. 1991 3 p

(Grant NAG5-1257)

(NASA-CR-193597; NAS 1.26:193597) Avail: CASI HC A01/MF A01

This report describes studies of cooling flows in rich clusters of galaxies, found to be sources of strong, extended X-ray emission seen by the EINSTEIN satellite. Two complementary lines of investigation were pursued: (1) studies of the dust content of the cluster gas using multi-wavelength data from archival records of the IUE and IRAS satellites in combination with previously obtained optical, and (2) coronal line spectroscopic studies of the bright emission systems. Derived from text

N94-12961# Massachusetts Inst. of Tech., Cambridge. Dept. of Chemical Engineering.

ON THE MOTION THROUGH A VISCOUS FLUID OF A SPHERICAL PARTICLE TOUCHING A PLANE WALL: SLIP BOUNDARY CONDITIONS

A. M. J. Davis, M. T. Kezirian, and H. Brenner 1992 7 p Presented at the 3rd International Symposium on Current Problems in Rheology, Biorheology and Biomechanics, Moscow, Russia, 1-5 Sep. 1992

(Contract DE-FG02-88ER-13896)

(DE93-012540; CONF-9209344-1) Avail: CASI HC A02/MF A01

Understanding the hydrodynamic forces acting upon immersed particles touching surfaces is of central importance in clean room technology and a variety of rheological and biological applications. This paper addresses the translation and rotation of a sphere translating and rotating parallel to a nearby plane wall bounding an otherwise quiescent semi-infinite viscous fluid, while allowing for slip on the wall and/or the sphere. The motivation for disregarding the classical, no-slip boundary condition on solid surfaces arises from an embarrassing discrepancy between theoretical and observed predictions of the translational velocity of a sphere 'rolling' under the influence of gravity down an inclined plane bounding an effectively semi-infinite viscous fluid. According to theory the force and torque on a translating and/or rotating sphere moving parallel to the plane wall become logarithmically infinite with the gap width as the gap between the sphere and well goes to zero. As such, the theoretical conclusion is that the sphere cannot translate down the plane, despite the gravity force that acts to animate it. Experiments, however, reveal that the sphere does, in fact, roll down the plane--at a reproducible mean terminal velocity. In the noninertial, small Reynolds number limit, the experimentally observed drag coefficient was found to be about 8.9 times that given by Stokes law for the unbounded case. This suggests a conventional hydrodynamic wall effect, rather than the logarithmically singular behavior predicted by the theory. It was in an attempt to resolve this glaring contradiction that we have elected here to examine the possible effects of slip. DOE

N94-12966# Instituto de Pesquisas Espaciais, Sao Jose dos Campos (Brazil).

STUDY OF POSSIBLE MECHANISMS OF INSTABILITY DUE TO HEAT TRANSFER M.S. Thesis [ESTUDO DE POSSIVEIS MECANISMOS DE INSTABILIDADE DEVIDA A TROCAS DE CALOR]

Inocencio GomesdaRocha Sep. 1992 73 p In PORTUGESE

(INPE-5448-TDI/494) Avail: CASI HC A04/MF A01

Possible mechanism causing instabilities in heat generating flows was analyzed, focusing heat-exchanges between an incompressible fluid and the tube walls. Heat transport and temperature profiles were therefore studied in a unidimensional laminar flow occurring in a thin-walled tube without radiative exchanges (thereby leading to different results from those experimentally obtained); a sinusoidal speed field was imposed, there being regions with and without heat-generation of reactive origin within the tube. The resulting coupled equations were solved by up wind finite differences. Values of sinusoidal oscillations in temperature and speed were typical of existing Helmholtz combustors. By adopting a 30-600 Hz oscillating frequency range, and a 0.0028-0.28 Mach range in the fluid speed (the fluid being nitrogen, with properties similar to those of products from combustion of hydrocarbon with air), with an induction time varying from 0.02 to 0.05 sec., no thermal instability in the flow was observed. Author

N94-12968*# National Aeronautics and Space Administration. Lewis Research Center, Cleveland, OH.

AN ANALYTICAL INVESTIGATION OF TRANSIENT EFFECTS ON REWETTING OF HEATED THIN FLAT PLATES

J. A. Platt Aug. 1993 11 p Presented at the Fundamentals of Heat Transfer in a Microgravity Environment, ASME 1993 Winter Annual Meeting, New Orleans, LA, 28 Nov. - 3 Dec. 1993; sponsored by ASME

(RTOP 674-24-05)

(NASA-TM-106120; E-7779; NAS 1.15:106120) Avail: CASI HC A03/MF A01

The rewetting of a hot surface is a problem of prime importance in the microgravity application of heat pipe technology, where rewetting controls the time before operations can be re-established following depriming of a heat pipe. Rewetting is also important in the nuclear industry (in predicting behavior during loss-of-coolant accidents), as well as in the chemical and petrochemical industries. Recently Chan and Zhang have presented a closed-form solution for the determination of the rewetting speed of a liquid film flowing over a finite (but long) hot plate subject to uniform heating. Unfortunately, their physically unreasonable initial conditions preclude a meaningful analysis of start-up transient behavior. A new nondimensionalization and closed-form solution for an infinitely-long, uniformly-heated plate is presented. Realistic initial conditions (step change in temperature across the wetting front) and boundary conditions (no spatial temperature gradients infinitely far from the wetting front) are employed. The effects of parametric variation on the resulting simpler closed-form solution are presented and compared with the predictions of a 'quasi-steady' model. The time to reach steady-state rewetting is found to be a strong

function of the initial dry-region plate temperature. For heated plates it is found that in most cases the effect of the transient response terms cannot be neglected, even for large times. Author (revised)

N94-13007*# San Diego State Univ., CA. Dept. of Aerospace Engineering.
INTEGRATION OF VISCOUS EFFECTS INTO INVISCID COMPUTATIONAL METHODS Final Report
Joseph Katz Aug. 1990 4 p
(Contract NCC2-458)
(NASA-CR-193677; NAS 1.26:193677; SDSU-CEP-524067) Avail: CASI HC A01/MF A01

A variety of practical fluid dynamic problems related to the low-speed, high Reynolds number flow over aircraft and ground vehicles fall in a category where some simplified mathematical models become applicable. This provides the fluid dynamicists with a more economical computational tool, compared to the alternative solution of the Navier Stokes equations. The objective was to provide a brief survey of some of the viscous boundary layer solution methods and to propose a method for coupling between the inviscid outer flow and the viscous boundary layer solutions. Results of this survey and details of the viscous/inviscid flow coupling efforts are presented. Author (revised)

N94-13027*# National Aeronautics and Space Administration. Lewis Research Center, Cleveland, OH.
TWO-DIMENSIONAL NAVIER-STOKES HEAT TRANSFER ANALYSIS FOR ROUGH TURBINE BLADES
R. J. Boyle and K. C. Civinskas Jun. 1991 13 p Presented at the 27th Joint Propulsion Conference and Exhibit, Sacramento, CA, 24-27 Jun. 1991; sponsored by AIAA, SAE, and ASME Previously announced in IAA as A91-45790 Prepared in cooperation with ARL, Cleveland, OH
(RTOP 505-62-52)
(NASA-TM-106008; E-7755; NAS 1.15:106008; ARL-MR-14; AIAA Paper 91-2129) Avail: CASI HC A03/MF A01

A quasi-three-dimensional thin-layer Navier-Stokes analysis was used to predict heat transfer to rough surfaces. Comparisons are made between predicted and experimental heat transfer for turbine blades and flat plates of known roughness. The effect of surface roughness on heat transfer was modeled using a mixing length approach. The effect of near-wall grid spacing and convergence criteria on the accuracy of the heat transfer predictions are examined. An eddy viscosity mixing length model having an inner and outer layer was used. A discussion of the appropriate model for the crossover between the inner and outer layers is included. The analytic results are compared with experimental data for both flat plates and turbine blade geometries. Comparisons between predicted and experimental heat transfer showed that a modeling roughness effects using a modified mixing length approach results in good predictions of the trends in heat transfer due to roughness. Author

N94-13064*# Analytical Services and Materials, Inc., Hampton, VA.
LARGE-EDDY SIMULATION OF LAMINAR-TURBULENT BREAKDOWN AT HIGH SPEEDS WITH DYNAMIC SUBGRID-SCALE MODELING
Nabil M. El-Hady Washington NASA Aug. 1993 60 p
(Contract NAS1-19320; RTOP 505-59-50-01)
(NASA-CR-4533; NAS 1.15:4533) Avail: CASI HC A04/MF A01

The laminar-turbulent breakdown of a boundary-layer flow along a hollow cylinder at Mach 4.5 is investigated with large-eddy simulation. The subgrid scales are modeled dynamically, where the model coefficients are determined from the local resolved field. The behavior of the dynamic-model coefficients is investigated through both an a priori test with direct numerical simulation data for the same case and a complete large-eddy simulation. Both formulations proposed by Germano et al. and Lilly are used for the determination of unique coefficients for the dynamic model and their results are compared and assessed. The behavior and the energy cascade of the subgrid-scale field structure are investigated at various stages of the transition process. The investigations are able to duplicate a high-speed transition phenomenon observed in experiments and explained only recently by the direct numerical simulations of Pruett and Zang, which is the appearance of 'rope-like' waves. The nonlinear evolution and breakdown of the laminar boundary layer and the structure of the flow field during the transition process were also investigated. Author (revised)

N94-13066*# High Technology Corp., Hampton, VA.
TRANSITION PREDICTION AND CONTROL IN SUBSONIC FLOW OVER A HUMP
Jamal A. Masad and Venkit Iyer (Vigyan Research Associates, Inc., Hampton, VA.) Washington NASA Sep. 1993 57 p
(Contracts NAS1-19299; NAS1-19672; RTOP 537-03-23-03)
(NASA-CR-4543; NAS 1.26:4543) Avail: CASI HC A04/MF A01

The influence of a surface roughness element in the form of a two-dimensional hump on the transition location in a two-dimensional subsonic flow with a free-stream Mach number up to 0.8 is evaluated. Linear stability theory, coupled with the N-factor transition criterion, is used in the evaluation. The mean flow over the hump is calculated by solving the interacting boundary-layer equations; the viscous-inviscid coupling is taken into consideration, and the flow is solved within the separation bubble. The effects of hump height, length, location, and shape; unit Reynolds number; free-stream Mach number, continuous suction level; location of a suction strip; continuous cooling level; and location of a heating strip on the transition location are evaluated. The N-factor criterion predictions agree well with the experimental correlation of Fage; in addition, the N-factor criterion is more general and powerful than experimental correlations. The theoretically predicted effects of the hump's parameters and flow conditions on transition location are consistent and in agreement with both wind-tunnel and flight observations. Author

N94-13073*# Vigyan Research Associates, Inc., Hampton, VA.
THREE-DIMENSIONAL BOUNDARY-LAYER PROGRAM (BL3D) FOR SWEPT SUBSONIC OR SUPERSONIC WINGS WITH APPLICATION TO LAMINAR FLOW CONTROL
Venkit Iyer Washington NASA Aug. 1993 133 p
(Contract NAS1-19672; RTOP 537-03-23-03)
(NASA-CR-4531; NAS 1.26:4531) Avail: CASI HC A07/MF A02

The theory, formulation, and solution of three-dimensional, compressible attached laminar flows, applied to swept wings in subsonic or supersonic flow are discussed. Several new features and modifications to an earlier general procedure described in NASA CR 4269, Jan. 1990 are incorporated. Details of interfacing the boundary-layer computation with solution of the inviscid Euler equations are discussed. A description of the computer program, complete with user's manual and example cases, is also included. Comparison of solutions with Navier-Stokes computations with or without boundary-layer suction is given. Output of solution profiles and derivatives required in boundary-layer stability analysis is provided. Author (revised)

N94-13074*# Institute for Computer Applications in Science and Engineering, Hampton, VA.
SURROGATES FOR NUMERICAL SIMULATIONS; OPTIMIZATION OF EDDY-PROMOTER HEAT EXCHANGERS Final Report
Anthony T. Patera (Massachusetts Inst. of Tech., Cambridge.) and Anthony Patera (Massachusetts Inst. of Tech., Cambridge.) Washington NASA Aug. 1993 56 p Submitted for publication
(Contracts NAS1-19480; N00014-91-J-1889; N00014-90-J-4124; N00014-89-J-1610; RTOP 505-90-52-01)
(NASA-CR-191510; NAS 1.26:191510; ICASE-93-50) Avail: CASI HC A04/MF A01

Although the advent of fast and inexpensive parallel computers has rendered numerous previously intractable calculations feasible, many numerical simulations remain too resource-intensive to be directly inserted in engineering optimization efforts. An attractive alternative to direct insertion considers models for computational systems: the expensive simulation is evoked only to construct and validate a simplified, input-output model; this simplified input-output model then serves as a simulation surrogate in subsequent engineering optimization studies. A simple 'Bayesian-validated' statistical framework for the construction, validation, and purposive application of static computer simulation surrogates is presented. As an example, dissipation-transport optimization of laminar-flow eddy-promoter heat exchangers are considered: parallel spectral element Navier-Stokes calculations serve to construct and validate surrogates for the flowrate and Nusselt number; these surrogates then represent the originating Navier-Stokes equations in the ensuing design process. Author (revised)

N94-13075*# Institute for Computer Applications in Science and Engineering, Hampton, VA.

THE THREE-DIMENSIONAL FLOW PAST A RAPIDLY ROTATING CIRCULAR CYLINDER

James P. Denier (New South Wales Univ., Sydney, Australia.) and Peter W. Duck (Manchester Univ., England.) Washington Aug. 1993 19 p (Contract NAS1-19480; RTOP 505-90-52-01)

(NASA-CR-191512; ICASE-93-52; NAS 1.26:191512) Avail: CASI HC A03/MF A01

The high Reynolds number (Re) flow past a rapidly rotating circular cylinder is investigated. The rotation rate of the cylinder is allowed to vary (slightly) along the axis of the cylinder, thereby provoking three-dimensional flow disturbances, which are shown to involve relatively massive (O(Re)) velocity perturbations to the flow away from the cylinder surface. Additionally, three integral conditions, analogous to the single condition determined in two dimensions by Batchelor, are derived, based on the condition of periodicity in the azimuthal direction. Author (revised)

N94-13078*# California Polytechnic State Univ., San Luis Obispo. Dept. of Mechanical Engineering.

EVALUATION OF DUAL FLOW THRUST VECTOR NOZZLES WITH EXHAUST STREAM IMPINGEMENT Semiannual Progress Report, Jun. - Dec. 1992

Thomas W. Carpenter, Sean Dobbins, and Steven Vaccarezza 1992 51 p

(Grant NAG2-778)

(NASA-CR-193392; NAS 1.26:193392) Avail: CASI HC A04/MF A01

To supplement previous work performed by NASA, a cold-jet facility was established at the California Polytechnic State University, San Luis Obispo campus. The purpose of this facility is to continue the studies of cold flow multiaxis thrust vectoring conducted at the NASA Langley Research Center. A single nozzle test apparatus was completed and is presently operational. Included are the results of the single flow test envelope that was requested by NASA personnel. Details about the test apparatus are included in the Cal Poly Semi-Annual Progress report. Author (revised)

N94-13114*# Institute for Computer Applications in Science and Engineering, Hampton, VA.

PINCHING SOLUTIONS OF SLENDER CYLINDRICAL JETS Final Report

Demetrios T. Papageorgiou (New Jersey Inst. of Tech., Newark.) and Oscar Orellana (Universidad Tecnica Federico Santa Maria, Valparaiso, Chile.) Washington NASA Jun. 1993 29 p Submitted for publication

(Contracts NAS1-19480; NAS1-18605; RTOP 505-90-52-01; FNDCT-246/91)

(NASA-CR-191482; NAS 1.26:191482; ICASE-93-32) Avail: CASI HC A03/MF A01

Simplified equations for slender jets are derived for a circular jet of one fluid flowing into an ambient second fluid, the flow being confined in a circular tank. Inviscid flows are studied which include both surface tension effects and Kelvin-Helmholtz instability. For slender jets a coupled nonlinear system of equations is found for the jet shape and the axial velocity jump across it. The equations can break down after a finite time and similarity solutions are constructed, and studied analytically and numerically. The break-ups found pertain to the jet pinching after a finite time, without violation of the slender jet ansatz. The system is conservative and admissible singular solutions are those which conserve the total energy, mass, and momentum. Such solutions are constructed analytically and numerically, and in the case of vortex sheets with no surface tension certain solutions are given in closed form. Author (revised)

N94-13117# European Space Agency, Paris (France).

FUNDAMENTAL STUDY OF SHOCK WAVE/TURBULENT BOUNDARY LAYER INTERACTIONS WITH PASSIVE CONTROL IN TRANSONIC FLOWS

Reynald Bur (Office National d'Etudes et de Recherches Aerospatiales, Paris, France.) May 1993 270 p Transl. into ENGLISH of Etude fondamentale sure le controle passif de l'interaction onde de choc/couche limite turbulente en ecoulement transsonique (Paris, France, ONERA), 1991 p 1-238 Original language document announced as N92-19932

(ESA-TT-1278; ONERA-NT-1991-9; ETN-93-94583) Avail: CASI HC A12/MF A03

The techniques for controlling shock wave/turbulent boundary layer interaction are reviewed. A passive control device makes it possible to improve the performance of airfoils at transonic velocities. An interaction subjected to passive control was performed in a transonic channel. The flow is described by means of Schlieren visualization, measurements of pressure on the walls of the duct and two dimensional laser velocimetry. A momentum balance carried out in the control region made it possible to infer configurations for which the friction drag is reduced by comparison with the reference case without control. The theoretical study is based on a boundary layer type approach using the first order Prandtl equations. Experimental results obtained for the reference case and a case with control are compared. ESA

N94-13128*# Institute for Computer Applications in Science and Engineering, Hampton, VA.

THE EFFECT OF CROSSFLOW ON TAYLOR VORTICES: A MODEL PROBLEM Final Report

S. R. Otto and Andrew P. Bassom (Exeter Univ., England.) Washington Jun. 1993 21 p Submitted for publication

(Contract NAS1-19480; RTOP 505-90-52-01)

(NASA-CR-191487; NAS 1.26:191487; ICASE-93-33) Avail: CASI HC A03/MF A01

A number of practically relevant problems involving the impulsive motion or the rapid rotation of bodies immersed in fluid are susceptible to vortex-like instability modes. Depending upon the configuration of any particular problem the stability properties of any high-wavenumber vortices can take on one of two distinct forms. One of these is akin to the structure of Gortler vortices in boundary layer flows while the other is similar to the situation for classical Taylor vortices. Both the Gortler and Taylor problems have been extensively studied when crossflow effects are excluded from the underlying base flows. Recently, studies were made concerning the influence of crossflow on Gortler modes and a linearized stability analysis is used to examine crossflow properties for the Taylor mode. This work allows us to identify the most unstable vortex as the crossflow component increases and it is shown how, like the Gortler case, only a very small crossflow component is required in order to completely stabilize the flow. Our investigation forms the basis for an extension to the nonlinear problem and is of potential applicability to a range of pertinent flows.

Author (revised)

N94-13133*# Institute for Computer Applications in Science and Engineering, Hampton, VA.

INTERACTING SCALES AND ENERGY TRANSFER IN ISOTROPIC TURBULENCE Final Report

Ye Zhou (National Aeronautics and Space Administration. Langley Research Center, Hampton, VA.) Washington Jun. 1993 37 p Submitted for publication

(Contract NAS1-19480; RTOP 505-90-52-01)

(NASA-CR-191477; NAS 1.26:191477; ICASE-93-28) Avail: CASI HC A03/MF A01

The dependence of the energy transfer process on the disparity of the interacting scales is investigated in the inertial and far-dissipation ranges of isotropic turbulence. The strategy for generating the simulated flow fields and the choice of a disparity parameter to characterize the scaling of the interactions is discussed. The inertial range is found to be dominated by relatively local interactions, in agreement with the Kolmogorov assumption. The far-dissipation is found to be dominated by relatively non-local interactions, supporting the classical notion that the far-dissipation range is slaved to the Kolmogorov scales. The measured energy transfer is compared with the classical models of Heisenberg, Obukhov, and the more detailed analysis of Tennekes and Lumley. The energy transfer statistics measured in the numerically simulated flows are found to be nearly self-similar for wave numbers in the inertial range. Using the self-similar form measured within the limited scale range of the simulation, an 'ideal' energy transfer function and the corresponding energy flux rate for an inertial range of infinite extent are constructed. From this flux rate, the Kolmogorov constant is calculated to be 1.5, in excellent agreement with experiments.

Author (revised)

N94-13197 Tel-Aviv Univ. (Israel). Dept. of Fluid Mechanics and Heat Transfer.

THE TRANSIENT BEHAVIOR OF A BOUNDARY LAYER EXPOSED TO UNIFORM SUCTION M.S. Thesis

Tomer Bachar Mar. 1992 119 p In HEBREW
(ITN-93-85205) Copyright Avail: Issuing Activity (Tel-Aviv Univ., Exact Sciences Library, Ramat Aviv 69978, Israel)

An experimental investigation in a low-turbulence wind tunnel was performed to study the influence of uniform suction on laminar and turbulent boundary layers. A zero-pressure-gradient boundary layer was developed over a flat plate with a porous section, across which the suction system maintained a uniform suction, which could be switched on and off abruptly. Throughout the experiments, a constant freestream was maintained. The basic boundary layer was either laminar Blasius-like or fully turbulent. The latter mode was achieved by using distributed roughness to trip the flow. The controlled suction rates varied between 0 and 0.45%. The influence of the suction on the streamwise velocity distributions was investigated along the line of symmetry of the flat plate, in steady-state and transient flows. This was done by measuring the longitudinal velocity component with a hot wire. The influence of suction on the boundary layer was found to be negligible upstream of the porous plate; it modified the velocity profile to an asymptotic profile over the porous region, and shifted the virtual origin of the boundary layer downstream from the porous plate. These sections were separated by transition zones, in which the flow adapted to the approaching condition. The length of each interface zone depended on the suction rate. An exponential temporal function was found to be a good approximation to the boundary layer response to sudden changes in suction. The power of the function depended on the flow characteristics and the suction rate. The relative impact of suction is stronger for the laminar boundary layer, while the turbulent boundary layer responds faster to a sudden suction. Author (ISA)

N94-13244# California Univ., Berkeley. Lawrence Berkeley Lab.
CAPILLARY SURFACES IN A WEDGE: DIFFERING CONTACT ANGLES
P. Concus and R. Finn (Stanford Univ., CA.) Apr. 1993 12 p Presented at the International Symposium on Microgravity Science and Application, Beijing, China, 10-13 May 1993
(Contract DE-AC03-76SF-00098)
(DE93-013903; LBL-33995; CONF-9305197-1) Avail: CASI HC A03/MF A01

The possible zero-gravity equilibrium configurations of capillary surfaces u(x,y) in cylindrical containers whose sections are (wedge) domains with corners are investigated mathematically, for the case in which the contact angles on the two sides of the wedge may differ. In such a situation the behavior can depart in significant qualitative ways from that for which the contact angles on the two sides are the same. Conditions are described under which such qualitative changes must occur. Numerically computed surfaces are depicted to indicate the behavior. DOE

N94-13249# Lawrence Livermore National Lab., CA.
NUMERICAL SIMULATIONS AND EXPERIMENTS ON PHYSICS OF HIGH MACH NUMBER SHOCKWAVE: TURBULENT FLOW INTERACTIONS
A. C. Buckingham and J. Grun Dec. 1992 10 p Presented at the 4th International Workshop on the Physics of Compressible Turbulent Mixing, Cambridge, England, 29 Mar. - 1 Apr. 1993
(Contract W-7405-eng-48)
(DE93-013424; UCRL-JC-112287; CONF-9303126-3) Avail: CASI HC A02/MF A01

When a shock moves into and interacts with an existing turbulent field, a substantial enhancement of the after-shock turbulent intensity and a simultaneous distortion and realignment of the tensor stress rate field and associated tensor stress field results. Component mixing, advective transport, and diffusion, as well as associated momentum and energy dissipation, are intensified over their pre-shocked levels. A combination of low preshocked turbulent intensity and strong shocks (e.g. shock Mach numbers substantially greater than one) produces the most pronounced interactive change in the turbulence level. In contrast, when a weak shock (Mach number only slightly greater than one) moves through relatively intense upstream turbulence, the turbulence change is modest, but the dynamical distortion and erratic motion of the shock front is much more pronounced. It is a commonly held view that if the interactive shock Mach number is in the hypersonic range (shock Mach numbers equal to or greater than about 6), rapid reinforcement of shock strength at the front by non-linear pressure field interactions and consequent self-healing of shock front geometric irregularity would act to suppress front distortion and also suppress the influence of the shock interactions on the surrounding turbulence. In the present work, recent experiments, numerical large eddy simulations (LES), and analysis are presented which contradict this notion. This work suggests that pronounced shock front distortion and substantial interactive modification of the turbulence persists even for shocks propagating at shock Mach numbers well in excess of 100. DOE

N94-13250# Lawrence Livermore National Lab., CA.
SUB-GRID SCALE MODELING FOR LARGE EDDY SIMULATIONS IN ANALYSIS OF SHOCK-TURBULENCE INTERACTIONS
A. C. Buckingham and J. Grun (Naval Research Lab., Washington, DC.) Dec. 1992 16 p Presented at the 8th International Conference on Numerical Methods in Laminar and Trubulent Flow, Swansea, England, 18-23 Jul. 1993
(Contract W-7405-eng-48)
(DE93-013425; UCRL-JC-112286; CONF-930785-1) Avail: CASI HC A03/MF A01

We continue to study the influence of dynamic shock wave interactions on turbulence. The interactions may significantly increase turbulent energy and Reynolds stress. Strong support for tensor amplification is supplied by the sharp, transiently distorted strain field in the immediate neighborhood of the shock. Beyond this, there develops a gradual decay to a new, more modestly amplified state relative to the pre-shocked level. Practical interest is centered on the significantly altered, albeit shock localized, post-shock turbulent kinetic energy, eddy transport, eddy component mixing and diffusion, wall shear, and heat transfer. In the shock interaction and post-shock region, compressible two dimensional large eddy simulations (LES) are applied. A compressibility modified Smagorinsky model is adapted to represent the non-resolved sub-grid scales. Favre mass-weighted average space and time discretized compressible Navier-Stokes equations are used to represent the explicitly resolved grid scale motions. Predicted amplification levels, modal energy partition, shock translational to turbulence kinetic energy transfer, and viscoelastic response of turbulence to shock interaction are examined in comparison with available experimental evidence. A two-band dynamic eddy viscosity model representing the unresolved subgrid scale field is a possible replacement for the Smagorinsky model. Improvement is sought for predictions in the near wall region, under the influence of stochastic subgrid scale backscatter, and in the neighborhood of the shock. Wall-bounded supersonic compression corner flow experiments and hypersonic cylindrical shock wave turbulence interaction experiments are used as trial cases for test and comparison of the two classes of subgrid scale models. DOE

N94-13365# Instituto de Pesquisas Espaciais, Sao Jose dos Campos (Brazil).
EXPERIMENTAL DETERMINATION OF DROPLETS LOCAL MEAN DIAMETER OF A SPRAG FROM IMPINGING JETS Thesis [DETERMINACAO EXPERIMENTAL DO DIAMETRO MEDIO LOCAL DAS GOTAS DE UM SPRAY DE UM INJETOR DO TIPO JATOS COLIDENTES]
Luiz Carlos deQueiroz May 1992 64 p In PORTUGESE
(INPE-5469-TDI/500) Avail: CASI HC A04/MF A01

Reviews of the light scattering theory and of the droplet size distribution modeling from impinging jets by Couto et al are presented. A technique based on the light diffractive scattering was used to determine the Sauter mean diameter of drops in water sprays. Spray produced by impinging jets with the following total impinging angles: 60 deg, 70 deg, and 90 deg. The experimental results obtained showed a agreement to the theoretical diameters. Author (revised)

N94-13385*# National Aeronautics and Space Administration. Lewis Research Center, Cleveland, OH.
A MULTIPLE-SCALE TURBULENCE MODEL FOR INCOMPRESSIBLE FLOW
B. S. Duncan (Sverdrup Technology, Inc., Brook Park, OH.), W. W. Liou, and T. H. Shih Jan. 1993 14 p Presented at the 31st Aerospace Sciences Meeting and Exhibit, Reno, NV, 11-14 Jan. 1993; sponsored by AIAA See also A93-24228
(RTOP 505-62-40)
(NASA-TM-106113; ICOMP-93-11; CMOTT-93-3; E-7765; NAS 1.15:106113) Avail: CASI HC A03/MF A01

A multiple-scale eddy viscosity model is described. This model splits

the energy spectrum into a high wave number regime and a low wave number regime. Dividing the energy spectrum into multiple regimes simplistically emulates the cascade of energy through the turbulence spectrum. The constraints on the model coefficients are determined by examining decaying turbulence and homogeneous turbulence. A direct link between the partitioned energies and the energy transfer process is established through the coefficients. This new model was calibrated and tested for boundary-free turbulent shear flows. Calculations of mean and turbulent properties show good agreement with experimental data for two mixing layers, a plane jet and a round jet. Author (revised)

N94-13397# Sandia National Labs., Albuquerque, NM.
A MULTIPHASE MODEL FOR SHOCK-INDUCED FLOW IN LOW DENSITY FOAM
M. R. Baer 1993 6 p Presented at the 19th International Symposium on Shock Waves, Marseille, France, 26-30 Jul. 1993
(Contract DE-AC04-76DP-00789)
(DE93-013767; SAND-93-0725C; CONF-930788-1) Avail: CASI HC A02/MF A01

A multiphase mixture model is applied to describe shocked-induced flow in deformable low-density foam. This model includes interphase drag and heat transfer and all phases are treated as compressible. Volume fraction is represented as an independent kinematic variable, and the entropy inequality suggests a thermodynamically-admissable evolutionary equation to describe rate-dependent compaction. This multiphase model has been applied to shock tube experiments in the study of normal shock impingement on a wall-supported low density porous layer. Numerical solution of the multiphase flow equations employs a high resolution adaptive finite element method which accurately resolves contact surfaces and shock interactions. Additional studies are presented in an investigation of the effect of initial gas pressure in the foam layer, the shock interaction on multiple layers of foam, and the shock-induced flow in an unsupported foam layer. DOE

N94-13467*# National Aeronautics and Space Administration. Langley Research Center, Hampton, VA.
A PRIORI ERROR ESTIMATES FOR AN hp-VERSION OF THE DISCONTINUOUS GALERKIN METHOD FOR HYPERBOLIC CONSERVATION LAWS
Kim S. Bey and J. Tinsley Oden (Texas Univ., Austin.) Jun. 1993 27 p
(RTOP 505-43-31)
(NASA-TM-108993; NAS 1.15:108993) Avail: CASI HC A03/MF A01

A priori error estimates are derived for hp-versions of the finite element method for discontinuous Galerkin approximations of a model class of linear, scalar, first-order hyperbolic conservation laws. These estimates are derived in a mesh dependent norm in which the coefficients depend upon both the local mesh size h(sub K) and a number p(sub k) which can be identified with the spectral order of the local approximations over each element. Author

N94-13474 McGill Univ., Montreal (Quebec). Dept. of Mechanical Engineering.
FULLY DEVELOPED TURBULENT FLOW IN RECTANGULAR INTERRUPTED-PLATE DUCTS Ph.D. Thesis
Robert Kevin McBrien Nov. 1989 448 p
(ISBN-0-315-63594-0; CTN-93-60731) Copyright Avail: Issuing Activity (Micromedia Ltd., Technical Information Centre, 165 Hotel de Ville, Place du Portage, Phase 2, Hull, Quebec J8X 3X2, Canada HC)

Rectangular flow passages with interrupted surface configurations are often found in heat transfer equipment such as compact heat exchanger cores widely used in automobiles, spacecraft, aircraft, and the power and process industries. Experimental and numerical investigations of turbulent spatially periodic fully developed flows in straight ducts of rectangular cross section with interrupted plate inserts are presented. A computer code, based on a finite volume method and incorporating a low Reynolds number turbulence model, was developed, tested, and used in the investigation. The experimental work was aimed at obtaining accurate and complete data that would allow fair evaluation of the numerical model and lead to an enhanced understanding of spatially periodic fully developed turbulent flows. Such flows in three different interrupted plate ducts were investigated. The results presented include module friction factor versus Reynolds number plots, plate surface streamline photographs, and plots of intramodular time-mean wall static pressure distributions. The details and implications of these results are discussed. CISTI

N94-13509 International Centre for Theoretical Physics, Trieste (Italy).
HEAT FLOWS AND HARMONIC MAPS WITH A FREE BOUNDARY
Jiayu Li Jan. 1993 12 p Limited Reproducibility: More than 20% of this document may be affected by microfiche quality
(DE93-622856; IC-93/3) Avail: CASI HC A03 (US Sales Only)

In this paper we prove the existence of the heat flow of a harmonic map with a free boundary and the convergence of the heat flow to a harmonic map. DOE

N94-13511 International Centre for Theoretical Physics, Trieste (Italy).
ON THE THEORY OF THE DECAYING DEVELOPED TURBULENCE WITH SPONTANEOUS PARITY VIOLATION
L. T. Adzhemyan (Saint Petersburg Technical Univ., Russia.), M. Hnatich, D. Horvath (Slovak Academy of Sciences, Kosice, Czechoslovakia.), and M. Stehlik (Slovak Academy of Sciences, Kosice, Czechoslovakia.) Jan. 1993 10 p Limited Reproducibility: More than 20% of this document may be affected by microfiche quality
(DE93-623190; IC-93/17) Avail: CASI HC A02 (US Sales Only)

The statistical approach of maximal randomness of the velocity field is extended for the case of decaying turbulence with spontaneous parity violation. The set of self-consistent equations in one-loop approximation is obtained. It is without the infrared and ultraviolet divergences and has a scaling solution which leads to Kolmogorov spectrum in inertial range of wave numbers K and gives the well-known time-dependence laws for integral turbulence scale r(sub c)(t) approx t(sup 2/5) and turbulent energy per mass e(t) approx t(sup -6/5). The set of equations for scaling functions of energy and helicity spectral density, depending only on dimensionless parameter kr(sub c), is presented. DOE

N94-13533# National Aerospace Lab., Amsterdam (Netherlands). Space Div.
THERMAL GRAVITATIONAL MODELLING AND SCALING OF TWO-PHASE HEAT TRANSPORT SYSTEMS: SIMILARITY CONSIDERATIONS AND USEFUL EQUATIONS PREDICTIONS VERSUS EXPERIMENTAL RESULTS
A. A. M. Delil 30 Dec. 1991 26 p Presented at 1st European Symposium on Fluids in Space, Ajaccio, France, 18-22 Nov. 1991
(NLR-TP-91477-U; ETN-93-94343) Avail: CASI HC A03/MF A01

A review on various aspects of thermal gravitational scaling of spacecraft two phase heat transport systems is presented. Supporting similarity considerations, based on dimension analysis, and useful equations and correlations are given. The assessment of the applicability (validity and restrictions) of the modeling and scaling approach is supported by a comparison of two phase flow pressure drops measured under low gravity conditions and modeling predictions. Terrestrial scaling experiments with an ammonia test rig are identified for the support of the development of the ESA capillary pumped two phase ammonia experiment in Get Away Special G-557 and the development of the mechanically pumped ESA R114 Two Phase Heat Transport System (TPHTS). ESA

N94-13535# Stockholm Univ. (Sweden). Dept. of Meteorology.
A HIGH-RESOLUTION LAX-FRIEDRICHS SCHEME FOR HYPERBOLIC CONSERVATION LAWS WITH SOURCE TERMS: APPLICATION TO SHALLOW WATER EQUATIONS
Gerhard Erbes 25 Mar. 1992 51 p
(DM-62; ETN-93-94487) Avail: CASI HC A04/MF A01

A recently developed high resolution, non oscillatory staggered method, based upon the Lax-Friedrichs scheme, for hyperbolic conservation laws, is considered. The staggered method is extended to include source terms, and it is also shown how to implement multiple dimensions. The advantage of using a staggered method is that Riemann problems no longer need to be solved. Numerical experiments are performed with the shallow water equations for which the staggered method yields sharp nonoscillatory shocks while retaining a high accuracy in regions where the flow is smooth. The accuracy obtained with the staggered method is significantly higher than in conventional finite difference schemes used in the field of meteorology. ESA

N94-13553 Iowa State Univ. of Science and Technology, Ames.
EFFECTS OF SURFACE THERMAL FORCING ON STRATIFIED FLOW PAST AN ISOLATED OBSTACLE Ph.D. Thesis
Jon Reisner 1992 104 p
Avail: Univ. Microfilms Order No. DA9311529

The present study investigates basic aspects of the flow of a density-stratified fluid past three-dimensional obstacles for Froude number is approximately O(1) and isolated surface thermal forcing representative of diurnally varying mesoscale flows past mountainous islands such as Hawaii. In order to minimize parameter space, we have excluded the effects of friction, rotation, nonuniform ambient flow, and the complexities of realistic surface boundary layer and terrain. Through simple scaling arguments, we deduce that the parameter eta* controls thermally forced flows for a given Froude number, and we provide crude estimates of a flow response for a range of eta*. The principal question addressed is for what values of eta* will a transition occur from the low-Froude-number flow regime, characterized by the stagnation and splitting of the lower upwind flow, to the regime in which flow passes over rather than around the obstacle. We show that the linear theory captures such a tendency consistently with simple scaling arguments. To provide quantitative measures of flow variability with the Froude number and eta*, we employ an efficient isentropic numerical code and summarize the results of numerous simulations in the form of a regime diagram. The principal result is a simple criterion for the transition of a heated flow from the blocked to unblocked flow regime. We illustrate the relevance of the idealized study to natural flows with an example of applications to a flow past the Hawaiian Archipelago. Author

N94-13559 Texas Univ., Austin.
HIGH FREESTREAM TURBULENCE EFFECTS ON THE TRANSPORT OF HEAT AND MOMENTUM Ph.D. Thesis
Karen Ann Thole 1992 279 p
Avail: Univ. Microfilms Order No. DA9309297

Understanding high freestream turbulence effects on the transport of heat and momentum is needed for better predictive schemes. This dissertation presents the effects of very high freestream turbulence levels, between Tu equals 10 percent and 20 percent, on surface heat transfer and skin friction in terms of the turbulent transport of heat and momentum. Both the velocity and thermal fields are quantified for a boundary layer influenced by high freestream turbulence and are compared to a boundary layer with negligible freestream turbulence. In addition to quantifying the mean and rms values of temperature and velocity, the turbulent heat flux profiles are quantified through simultaneous temperature/velocity measurements. Spectra and length scales for both temperature and velocity are also quantified in the freestream and throughout the boundary layer. The results of this study indicate that scaling the heat transfer en-ancement is best accomplished using St' which uses the maximum rms streamwise velocity as the velocity scale in the Stanton number. Similarly, scaling the skin friction enhancement is best accomplished using Cf' which also uses the maximum rms streamwise velocity as the velocity in the skin friction coefficient. In the case of St', a constant value occurs for all turbulence levels and was found to be independent of turbulent length scales and momentum Reynolds numbers. Cf' remains constant for turbulence levels less than 15 percent, but then decreases as the turbulence levels increase. When using the other scaling parameters that depend on turbulence level and length scale, more consistent trends were found for the integral length scale rather than the dissipation length scale. The present data indicate that a highly turbulent freestream does not enhance the skin friction as much as the heat transfer. However, the turbulent transport of momentum does scale with the surface shear stress and the turbulent transport of heat does scale with the surface heat flux. Thus, these turbulent transport mechanisms are similarly affected by the high freestream turbulence. The reduced shear stress enhancement is attributed to large-scale, inactive motions from the highly turbulent freestream which penetrate into the turbulent boundary layer, displace the active motions, and reduce the average shear stress. These actions result in reduced correlation of the turbulent fluctuations which counter-balances the enhancement effect of increased turbulence levels so that there is no net increase in wall shear. However, these inactive motions have less effect on the normal heat flux. Therefore, heat transfer continues to be enhanced as turbulence levels increase.
Author

N94-13569 Pennsylvania State Univ., University Park.
NUMERICAL SIMULATIONS OF UNSTEADY FLOWS IN TURBOMACHINES Ph.D. Thesis
Daniel Joseph Dorney 1992 314 p
Avail: Univ. Microfilms Order No. DA9311624

The performance of axial and centrifugal turbomachines is significantly affected by the presence of unsteady and viscous flow mechanisms. Most contemporary design systems, however, use steady or linearized unsteady inviscid flow analyses to generate new blade shapes. In an effort to increase the understanding of unsteady viscous flows in turbomachinery blade rows, and to determine the limitations of linearized inviscid flow analyses, a two-part investigation was conducted. In the first portion of this investigation, a nonlinear viscous flow analysis was developed for the prediction of unsteady flows in two dimensional axial turbomachinery blade rows. The boundary conditions were formulated to allow the specification of vortical, entropic and acoustic excitations at the inlet, and acoustic excitations at exit, of a cascade. Numerical simulations were performed for flat plate and compressor exit guide vane cascades, and the predicted results were compared with solutions from classical linearized theory and linearized inviscid flow analysis. The unsteady pressure fields predicted with the current analysis showed close agreement with the linearized solutions for low to moderate temporal frequency vortical and acoustic excitations. As the temporal frequency of the excitations was increased, nonlinear effects caused discrepancies to develop between the linearized and Navier-Stokes solution sets. The inclusion of viscosity had a significant impact on the unsteady vorticity field, but only a minimal effect on the unsteady pressure field. In the second part of this investigation, a quasi-three-dimensional Navier-Stokes analysis was modified and applied to flows in centrifugal turbomachinery blade rows. Inviscid and viscous flow simulations were performed for a centrifugal impeller at three operating conditions. By comparing the predicted and experimental circumferential distributions of the relative frame velocity and flow angle downstream of the impeller, it was hypothesized that in the experiments the end secondary flows energize the impeller suction surface boundary making the local flow behave like an inviscid fluid. The performance curve generated from the viscous calculations showed close agreement with the experimental data. Author

N94-13572 Virginia Polytechnic Inst. and State Univ., Blacksburg.
TOPICS ON SPATIALLY HIGH-ORDER ACCURATE METHODS AND PRE-CONDITIONING FOR THE NAVIER-STOKES EQUATIONS WITH FINITE-RATE CHEMISTRY Ph.D. Thesis
Andrew Grady Godfrey 1992 237 p
Avail: Univ. Microfilms Order No. DA9311573

This dissertation discusses two aspects of computational fluid dynamics: high-order spatial accuracy and convergence-rate acceleration through system preconditioning. Concerning high-order accuracy, the computational qualities of various spatial methods for the finite-volume solution of the Euler equations are presented. The two-dimensional essentially non-oscillatory (ENO), k-exact, and dimensionally split ENO reconstruction operators are discussed and compared in terms of reconstruction and solution accuracy and computational cost. Standard variable extrapolation methods are included for completeness. Inherent steady-state convergence difficulties are demonstrated for adaptive-stencil algorithms. Methods for reconstruction error analysis are presented and an exact solution to the heat equation is used as an example. Numerical experiments presented include the Ringleb flow for numerical accuracy and a shock-reflection problem. A vortex-shock interaction demonstrates the ability of the ENO scheme to excel in capturing unsteady high-frequency flow physics. Concerning convergence-rate acceleration, characteristic-wave preconditioning is extended to include generalized finite-rate chemistry with non-equilibrium thermodynamics. Additionally, the proper preconditioning for the one-dimensional Navier-Stokes equations is presented. Eigenvalue stiffness is resolved and convergence-rate acceleration is demonstrated over the entire Mach-number range from the incompressible to the hypersonic. Specific benefits are realized at low and transonic flow speeds. The extended preconditioning matrix accounts for thermal and chemical non-equilibrium and its implementation is explained for both explicit and implicit time marching. The effects of high-order spatial accuracy and various flux splittings are investigated. Numerical analysis reveals the possible theoretical improvements from using preconditioning at all Mach numbers. Numerical results confirm the expectations from the analysis. The

preconditioning matrix is applied with dual time stepping to obtain arbitrarily high-order accurate temporal solutions within an implicit formulation. Representative test cases include flows with previously troublesome embedded high-condition-number regions. Author

N94-13574 Pennsylvania State Univ., University Park.
AN EXPERIMENTAL INVESTIGATION OF SHOCK WAVE/VORTEX INTERACTION Ph.D. Thesis
Louis Nicholas Cattafesta, III 1992 279 p
Avail: Univ. Microfilms Order No. DA9311604

Although shock wave/vortex interaction is a basic and important fluid dynamics problem, very little research has been conducted on this topic. Therefore, a detailed experimental study of the interaction between a supersonic streamwise turbulent vortex and a shock wave has been carried out at the Penn State Gas Dynamics Laboratory. A vortex is produced by replaceable swirl vanes located upstream of the throat of various converging-diverging nozzles. The supersonic vortex is then injected into either a coflowing supersonic stream or ambient air. The structure of the isolated vortex is investigated in a supersonic wind tunnel using miniature, fast-response, five-hole and total temperature probes and in a free jet using Laser Doppler Velocimetry. The cases tested have unit Reynolds numbers in excess of 25 million per meter, axial Mach numbers ranging from 2.5 to 4.0, and peak tangential Mach numbers from 0 (i.e. a pure jet) to about 0.7. The results show that the typical supersonic wake-like vortex consists of a non-isentropic, rotational core, where the reduced circulation distribution is self-similar, and an outer isentropic, irrotational region. The vortex core is also a region of significant turbulent fluctuations. Radial profiles of turbulent kinetic energy and axial-tangential Reynolds stress are presented. The interactions between the vortex and both oblique and normal shock waves are investigated using nonintrusive optical diagnostics (i.e. schlieren, Planar Laser Scattering, and Laser Doppler Velocimetry). Of the various types, two Mach 2.5 overexpanded-nozzle Mach-disc interactions are examined in detail. Below a certain vortex strength, a 'weak' interaction exists in which the normal shock is perturbed locally into an unsteady 'bubble' shock near the vortex axis, but vortex breakdown (i.e. a stagnation point) does not occur. For stronger vortices, a random unsteady 'strong' interaction results that causes vortex breakdown. The vortex core reforms downstream of the rear stagnation point, and the reduced circulation distribution once again becomes self-similar in this region. A new model of this interaction is proposed. Finally, a curve defining the approximate limits of supersonic vortex breakdown is presented. Author

N94-13598 Ecole Polytechnique, Montreal (Quebec).
PASSAGE-AVERAGED APPROXIMATION OF TURBOMACHINERY FLOWS USING VORTICITY-POTENTIAL METHOD Ph.D. Thesis
Xudong Zhang 1991 206 p
(ISBN-0-315-72716-0) Avail: Univ. Microfilms Order No. DANN72716

A physical and mathematical model based on a passage-averaged vorticity-potential formulation for the simulation of flows in a rotor-stator stage of a turbomachine is presented. The passage-averaged governing equations were developed by taking into account the viscous effects through the three-dimensional Navier-Stokes equations applied to flows within blade rows. An implicit three-dimensional algorithm was also developed for solving, within the blade passages, the three-dimensional Navier-Stokes equations in terms of vorticity, scalar and vector potentials. This algorithm is coupled with the passage-averaged governing equations to form a closed set of equations describing rotor-stator flow interactions. Validation of the numerical algorithms is primarily performed on a number of test problems, including the developing flows in a channel rotating annulus, straight and curved ducts. A more realistic test computation for an impeller with planar blades completes the validation. The numerical results are compared with available analytical solutions and experimental data. Dissert. Abstr.

N94-13630 Pennsylvania State Univ., University Park.
NUMERICAL SIMULATION OF STEADY THREE-DIMENSIONAL FLOWS IN AXIAL TURBOMACHINERY BLADEROWS Ph.D. Thesis
Anton Herman Basson 1992 275 p
Avail: Univ. Microfilms Order No. DA9311593

The formulation for and application of a numerical model for low Mach number steady three-dimensional flows in axial turbomachinery blade rows is presented. The formulation considered here includes an efficient grid generation scheme (particularly suited to computational grids for the analysis of turbulent turbomachinery flows) and a semi-implicit, pressure-based computational fluid dynamics scheme that directly includes artificial dissipation, applicable to viscous and inviscid flows. The grid generation technique uses a combination of algebraic and elliptic methods, in conjunction with the Minimal Residual Method, to economically generate smooth structured grids. For typical H-grids in turbomachinery bladerows, when compared to a purely elliptic grid generation scheme, the presented grid generation scheme produces grids with much improved smoothness near the leading and trailing edges, allows the use of small near wall grid spacing required by low Reynolds number turbulence models, and maintains orthogonality of the grid near the solid boundaries even for high flow angle cascades. A specialized embedded H-grid for application particularly to tip clearance flows is presented. This topology smoothly discretizes the domain without modifying the tip shape, while requiring only minor modifications to H-grid flow solvers. Better quantitative modeling of the tip clearance vortex structure than that obtained with a pinched tip approximation is demonstrated. The formulation of artificial dissipation terms for a semi-implicit, pressure-based (SIMPLE type) flow solver, is presented. It is applied to both the Euler and the Navier-Stokes equations, expressed in generalized coordinates using a non-staggered grid. This formulation is compared to some SIMPLE and time marching formulations, revealing the artificial dissipation inherent in some commonly used semi-implicit formulations. The effect of the amount of dissipation on the accuracy of the solution and the convergence rate is quantitatively demonstrated for a number of flow cases. The ability of the formulation to model complex steady turbomachinery flows is demonstrated, e.g. for pressure driven secondary flows, turbine nozzle wakes, turbulent boundary layers. The formulation's modeling of blade surface heat transfer is assessed. The numerical model is used to investigate the structure of phenomena associated with tip clearance flows in a turbine nozzle. Author

N94-13635 Mississippi State Univ., State College.
A SOLUTION ALGORITHM FOR THE PREDICTION OF COMPRESSIBLE LAMINAR AND TURBULENT SHEAR FLOWS Ph.D. Thesis
Murali Beddhu 1992 124 p
Avail: Univ. Microfilms Order No. DA9312038

An implicit, finite volume code was developed for solving the complete set of three dimensional compressible Navier-Stokes equations for both laminar and turbulent cases to study separated flows with or without turbulence. For turbulent flows, mass weighted averaged equations for the mean flow along with a two equation (kappa-epsilon) closure are used. The governing equations are cast in general, time dependent curvilinear coordinates. First, the mean flow equations are solved using a fractional time stepping algorithm and then the equations for kappa and epsilon are solved separately using a modified two pass scheme at each time step. The fractional time stepping algorithm solves the convective and pressure terms only during the first fraction of the time step and then corrects this field in the second fraction by solving the viscous and turbulent terms. Integration through the first fraction of the time step is performed by an implicit Euler code that uses modified two pass scheme with Roe's flux difference splitting on the right hand side and flux vector splitting on the left hand side. Integration through the second fraction of the time step is performed using the Thomas algorithm, after casting the governing equations to yield a tridiagonal system. Numerous results for a wide range of Reynolds numbers and Mach numbers and with different geometries were obtained to test the validity of the code. Laminar channel flow at M(sub infinity) = 0.3 and Re(sub infinity) = 300 with both adiabatic wall and constant wall temperatures were obtained. Solutions for the channel flow and for the flow over an impulsively started flat plate at various wall temperatures agree very well with exact analytical solutions. Separated flow over a backward facing step at M(sub infinity) = 0.3 and Re(sub infinity) = 300 agrees well with experiments. Laminar flow over a waisted (contoured) axisymmetric body at M(sub infinity) = 1.39 and Re(sub infinity) = 5.04 x 10(exp 6) and over a bump on the floor of a wind tunnel at M(sub infinity) = 0.14 and Re(sub infinity) = 10800 are also presented and compared with other experiments and computations. Turbulent solutions obtained for a channel flow at M(sub infinity) = 0.3 and Re = 1.0xe(sup 6) were shown to agree well with other numerical results. These solutions are obtained using the kappa-epsilon equations with a modified near wall effect term in the epsilon equation. Dissert. Abstr.

N94-13652 Texas Univ., Austin.
EXPERIMENTAL MEASUREMENT OF LOCAL HEAT TRANSFER COEFFICIENTS OVER DISCRETE ROUGHENED PLATES USING INFRARED THERMOGRAPHY Ph.D. Thesis
David Alfredo Aliaga 1992 268 p
Avail: Univ. Microfilms Order No. DA9309114

Convective heat transfer over ribbed surfaces is a very complex process that requires detailed measurements for further understanding. Recent developments in infrared detector designs, optical attachments and computer and video capabilities have produced accurate infrared thermography systems with the spatial resolution required to obtain local heat transfer measurements on surfaces of complex geometry. Thus infrared thermography represents an attractive alternative to existing methods for heat transfer measurements (i.e. thermocouples, naphthalene sublimation, or liquid crystal measurements). The present investigation describes a new experimental method which uses infrared thermography in a subsonic wind tunnel to obtain detailed temperature measurements over ribbed plates with constant heat flux. The infrared system used in this study incorporated an infrared detector with a closed cycle microcooler which permitted the infrared camera to be positioned at arbitrary viewing angles. This flexibility permitted direct observations of the ribbed surface without the use of reflective optics that would have increased the inaccuracy of the procedure. Reference thermocouples placed at strategic locations over the ribbed plates were used to correct temperature readings of the infrared system in order to minimize measurement errors. Three ribbed plates were tested. Plates A and B had ribs of square cross section. The rib spacing (pitch) on plate A was designed so that regions of separation and reattachment would occur on the plate between ribs whereas plate B was designed to produce only regions of separation and recirculation. Plate C was constructed as an improved version of plate A and included trapezoidal ribs. The rib height and pitch on plate C was the same as on plate A. The trapezoidal shape of the rib for plate C was designed to minimize the recirculation regions in the front and back of the ribs while allowing reattachment at the base surface of the plate. Local heat transfer coefficients surrounding the ribs are presented and comparisons between plates are drawn. It is shown that the new method of heat transfer measurement is able to detect numerous small scale features of the complex flow field and consequent heat transfer distribution around ribs of arbitrary shape. Dissert. Abstr.

N94-13662 Toronto Univ. (Ontario).
FLOW LIMITATION AND FLUTTER IN MEMBRANE WALLED COLLAPSIBLE TUBES: A MODEL FOR EXPIRATORY WHEEZING Ph.D. Thesis
Colin Walsh 1992 291 p
(ISBN-0-315-73875-8) Avail: Univ. Microfilms Order No. DANN73875

During forced expiration from a full lung, the flow are limits due to collapse of the central airways. This is accompanied by audible wheezes, which are attributed to flow-induced oscillation of the collapsed airway wall. Mechanical and theoretical models of such physiological phenomena are referred to as 'collapsible tubes'. Most studies consider flow in rubber tubes where the collapse is complex. Thus, corresponding one dimensional (1-D) nonlinear theories rely on ad hoc structural models. The central airways have stiff anterior and lateral walls and a compliant posterior membrane suggesting simplified models. Experiments use a rectangular trough closed by a latex sheet. The oscillations involve three modes: weak low and intermediate frequency modes and a strong high frequency one. There is nonlinear interaction between the low and high frequency modes and the intermediate and high frequency ones are insensitive to the downstream flow properties. An axisymmetric annular geometry retains important experimental features and simplifies the current analysis. The nonlinear equations assume a shallowness condition and it is shown that normal inertia is negligible while axial inertia remains significant for the conditions in our experiments. Thus, the pressure drop across the wall is a static function of the local wall geometry: a generalized tube law. Numerical solutions display flutter for which axial tension is strongly stabilizing. The energy transfer from the mean flow depends on both the wall inertia and on variations in the axial tension due to variations in the axial stretch, mediated by compound wall curvature. Nonlinear effects modify the flutter, but the available mechanisms are normally unable to limit the growth. However, stable large amplitude oscillations can occur, and spectral analysis reveals three modes that have the qualitative properties of the experimental ones. However, there is extra harmonic structure and the intermediate frequency mode continues to grow disrupting any large amplitude oscillations that do develop. No other 1-D unsteady formulation considers wall inertia, compound curvature, or axial motion. Further, the qualitative agreement between the new experimental and numerical results suggests that these features may be significant and that the annular geometry is a useful model for studying the stability collapsible tube flows. Dissert. Abstr.

N94-13676*# Brown Univ., Providence, RI. Div. of Engineering.
STUDIES OF TURBULENT SHEAR FLOWS AND THEIR CONTROL Final Report, 22 Feb. 1989 - 17 Oct. 1992
Joseph T. C. Liu 17 Oct. 1992 5 p
(Grant NAG3-1016)
(NASA-CR-194114; NAS 1.26:194114) Avail: CASI HC A01/MF A01

The intent of the original proposal and the work carried out under the grant was to explore the instabilities of turbulent free shear flows of an incompressible fluid. The purpose for doing so was that coherent instabilities are susceptible to control via upstream forcing and because at sufficient finite amplitudes, the coherent modes enter into nonlinear interactions with the mean motion and thus, through such nonlinear interactions, the control of mixing and of mean flow spreading can be effected through the control of the coherent structures. Derived from text

N94-13683 McGill Univ., Montreal (Quebec).
A CONTROL VOLUME FINITE ELEMENT METHOD FOR THREE-DIMENSIONAL, INCOMPRESSIBLE, VISCOUS FLUID FLOW Ph.D. Thesis
Helmut John Saabas 1991 442 p
(ISBN-0-315-72019-0) Avail: Univ. Microfilms Order No. DANN72019

An equal-order co-located Control Volume Finite Element Method (CVFEM) for the prediction of multidimensional, incompressible, viscous fluid flow problems were formulated. CVFEM's provide the geometric flexibility traditionally associated with finite element methods. In addition, their control volume based formulation facilitates physically meaningful interpretation of the resulting discretization equations. In the proposed CVFEM, the calculation domain is divided into three-node triangular and four-node tetrahedral finite elements in two and three-dimensions, respectively. Each element is further subdivided in such a way that upon assembly of all elements, complete control volumes are formed about each node in the calculation domain. Interpolation functions for the dependent variables are prescribed in a manner that is consistent with the physical process they are intended to approximate. In this context, three different interpolation schemes of the convective flux across control volume surfaces are investigated, one of which guarantees positive contributions to the coefficients in the algebraic discretization equations. Appropriate conservation laws are imposed on the control volumes associated with the nodes. The resulting sets of integral conservation equations are then approximated by algebraic discretization equations, using the previously-mentioned interpolation functions. These nonlinear, coupled, algebraic equations are solved by a sequential solution procedure which incorporates Picard iterations. The proposed method was implemented into computer programs, and used to solve several test problems. These include convection-diffusion problems, and laminar and turbulent flow problems, in both two- and three-dimensions. The results demonstrate the ability of the proposed CVFEM to accurately solve the mathematical model used. Lastly, the CVFEM was used to predict flows similar to those found in film cooled gas turbine aerofoils. A complementary experimental program was designed and set up to investigate such flows. The numerical predictions were compared to the experimental observations of mean velocities, normal turbulent stresses, and one component of the turbulent shear stress. These comparisons indicated that the high Reynolds number Kappa-Epsilon turbulence model used is unable to capture certain features of the flow. It appears as if a low-Reynolds number turbulence model, with appropriate modifications to account for streamline curvature and non-isotropy of the turbulence in the vicinity of the walls, would be better suited to the prediction of such flows. This new model can be easily incorporated into the CVFEM proposed. Dissert. Abstr.

N94-13699# Houston Univ., TX. Dept. of Chemical Engineering.
STUDIES OF MOMENTUM AND ENERGY TRANSFER ACROSS WAVY GAS-LIQUID INTERFACES Final Report
A. E. Dukler 1 Jun. 1993 67 p

(Contract N00014-90-J-1090)
(AD-A266432) Avail: CASI HC A04/MF A01

Two phase gas-liquid flow and its associated interfaces exist in a wide variety of situations of importance to the Navy and this has prompted the study of the basic flow mechanics which underlie this complex process. The existence of wind-wave interactions over large bodies of water have long been recognized as a special case of two phase flow where the presence of the deformable interface plays a complex role in the generation of waves due to the action of the wind. Less well recognized, but of great importance, are situations of two phase flow which are found in component of power systems such as condensers, boiler refrigeration loops, and cryogen lines. Here the characteristics of two phase flow are critical to the reliable design and safe operation of such systems. DTIC

N94-13718*# National Aeronautics and Space Administration. Langley Research Center, Hampton, VA.
DEVELOPMENT OF A RECURSION RNG-BASED TURBULENCE MODEL
Ye Zhou, George Vahala, and S. Thangam Washington Aug. 1993 31 p Submitted for publication
(Contract NAS1-19480; RTOP 505-90-52-01)
(NASA-CR-191511; ICASE-93-51; NAS 1.26:191511) Avail: CASI HC A03/MF A01

Reynolds stress closure models based on the recursion renormalization group theory are developed for the prediction of turbulent separated flows. The proposed model uses a finite wavenumber truncation scheme to account for the spectral distribution of energy. In particular, the model incorporates effects of both local and nonlocal interactions. The nonlocal interactions are shown to yield a contribution identical to that from the epsilon-renormalization group (RNG), while the local interactions introduce higher order dispersive effects. A formal analysis of the model is presented and its ability to accurately predict separated flows is analyzed from a combined theoretical and computational stand point. Turbulent flow past a backward facing step is chosen as a test case and the results obtained based on detailed computations demonstrate that the proposed recursion -RNG model with finite cut-off wavenumber can yield very good predictions for the backstep problem. Author (revised)

N94-13724*# Institute for Computer Applications in Science and Engineering, Hampton, VA.
EVOLUTION OF DISTURBANCES IN STAGNATION POINT FLOW Final Report
William O. Criminale (Washington Univ., Seattle.), Thomas L. Jackson (National Aeronautics and Space Administration. Langley Research Center, Hampton, VA.), and D. Glenn Lasseigne (Old Dominion Univ., Norfolk, VA.) Washington Aug. 1993 25 p Submitted for publication
(Contract NAS1-19480; AF-AFOSR-0180-91; RTOP 505-90-52-01)
(NASA-CR-191516; NAS 1.26:191516; ICASE-93-56) Avail: CASI HC A03/MF A01

The evolution of three-dimensional disturbances in an incompressible three-dimensional stagnation-point flow in an inviscid fluid is investigated. Since it is not possible to apply classical normal mode analysis to the disturbance equations for the fully three-dimensional stagnation-point flow to obtain solutions, an initial-value problem is solved instead. The evolution of the disturbances provide the necessary information to determine stability and indeed the complete transient as well. It is found that when considering the disturbance energy, the planar stagnation-point flow, which is independent of one of the transverse coordinates, represents a neutrally stable flow whereas the fully three-dimensional flow is either stable or unstable, depending on whether the flow is away from or towards the stagnation point in the transverse direction that is neglected in the planar stagnation point. Author (revised)

N94-13730# McDonnell-Douglas Missile Systems Co., Saint Louis, MO.
HIGH FLUX HEAT EXCHANGER Interim Report, 1 Oct. 1990 - 29 Oct. 1991
Edward M. Flynn and Michael J. Mackowski Jan. 1993 49 p
(Contract F33615-90-C-2054)
(AD-A266341; WL-TR-93-2027) Avail: CASI HC A03/MF A01

This interim report documents the results of the first two phases of a four-phase program to develop a high flux heat exchanger for cooling future high performance aircraft electronics. Phase 1 defines future needs for high flux heat removal in advanced military electronics systems. The results are sorted by broad application categories: (1) commercial digital systems, (2) military data processors, (3) power processors, and (4) radar and optical systems. For applications expected to be fielded in five to ten years, the outlook is for steady state flux levels of 30-50 W/sq cm for digital processors and several hundred W/sq cm for power control applications. In Phase 1, a trade study was conducted on emerging cooling technologies which could remove a steady state chip heat flux of 100 W/sq cm while holding chip junction temperature to 90 C. Constraints imposed on heat exchanger design, in order to reflect operation in a fighter aircraft environment, included a practical lower limit on coolant supply temperature, the preference for a nontoxic, nonflammable, and nonfreezing coolant, the need to minimize weight and volume, and operation in an accelerating environment. The trade study recommended the Compact High Intensity Cooler (CHIC) for design, fabrication, and test in the final two phases of this program. DTIC

N94-13780# Air Force Inst. of Tech., Wright-Patterson AFB, OH. School of Engineering.
EXPERIMENTAL INVESTIGATION OF THE EFFECTS OF BLOWING RATIO PARAMETER ON HEAT TRANSFER TO A FILM-COOLED FLAT PLATE M.S. Thesis
Marco R. Valencia Jun. 1993 182 p
(AD-A266599; AFIT/GAE/ENY/93J-01) Avail: CASI HC A09/MF A02

The effects of blowing ratio on film cooling effectiveness were investigated. Two round-nosed test plates were used, one made of aluminum and the second of corian (low thermal conductivity). Injection at 35 degrees in the downstream direction was studied. Helium was mixed with air to produce a density ratio (coolant to mainstream) of 1.6 and 2.0, while the blowing ratio varied from 0.3 to 2.2. Surface temperature was measured by thin film gages located up to a nondimensional downstream distance X/D of 30. Two injection regimes, weak and strong, were found. In the weak regime, film cooling reduced gage heat flux at all thin film gage locations, however, film cooling was more effective for X/D less than 10. In the strong regime, the effectiveness of film cooling for X/D less than 10 was greatly reduced. Maximum film cooling effectiveness occurred between the weak and strong regime at a blowing ratio of 1.0. Changing the density ratio from 1.6 to 2.0 varied the measured gage heat flux less than 5 percent. Gage heat flux was correlated by the velocity ratio scaling parameter (X/D)VR to the -4/3 in both injection regimes. Gage heat flux with no film cooling, assuming a turbulence level of 10 percent, deviated less than 8 percent from theoretical results using the corian plate and less than 10 percent using the aluminum plate. DTIC

N94-13785*# Institute for Computer Applications in Science and Engineering, Hampton, VA.
ON THE SECONDARY INSTABILITY OF THE MOST DANGEROUS GOERTLER VORTEX Final Report
S. R. Otto and James P. Denier (New South Wales Univ., Kensington, Australia.) Washington Jul. 1993 14 p
(Contract NAS1-19480; RTOP 505-90-52-01)
(NASA-CR-191504; ICASE-93-46; NAS 1.26:191504) Avail: CASI HC A03/MF A01

Recent studies have demonstrated the most unstable Goertler vortex mode is found in flows, both two and three-dimensional, with regions of (moderately) large body curvature and these modes reside within a thin layer situated at the base of the conventional boundary layer. Further work concerning the nonlinear development of the most dangerous mode demonstrates that the flow results in a self induced flow reversal. However, prior to the point at which flow reversal is encountered, the total streamwise velocity profile is found to be highly inflectional in nature. Previous work then suggests that the nonlinear vortex state will become unstable to secondary, inviscid, Rayleigh wave instabilities prior to the point of flow reversal. Our concern is with the secondary instability of the nonlinear vortex states, which result from the streamwise evolution of the most unstable Goertler vortex mode, with the aim of determining whether such modes can induce a transition to a fully turbulent state before separation is encountered. Author (revised)

N94-13817*# Institute for Computer Applications in Science and Engineering, Hampton, VA.
STABILITY OF OSCILLATORY TWO PHASE COUETTE FLOW Final Report

Adrian V. Coward (Manchester Univ., England.) and Demetrios T. Papageorgiou (New Jersey Inst. of Tech., Newark.) Jul. 1993 29 p Submitted for publication
(Contract NAS1-19480; RTOP 505-90-52-01)
(NASA-CR-191501; ICASE-93-43; NAS 1.26:191501) Avail: CASI HC A03/MF A01

We investigate the stability of two phase Couette flow of different liquids bounded between plane parallel plates. One of the plates has a time dependent velocity in its own plane, which is composed of a constant steady part and a time harmonic component. In the absence of time harmonic modulations, the flow can be unstable to an interfacial instability if the viscosities are different and the more viscous fluid occupies the thinner of the two layers. Using Floquet theory, we show analytically in the limit of long waves, that time periodic modulations in the basic flow can have a significant influence on flow stability. In particular, flows which are otherwise unstable for extensive ranges of viscosity ratios, can be stabilized completely by the inclusion of background modulations, a finding that can have useful consequences in many practical applications. Author (revised)

N94-13827*# Nevada Univ., Reno. Engineering Research and Development Center.
NUMERICAL INVESTIGATIONS IN THREE-DIMENSIONAL INTERNAL FLOWS Semiannual Status Report, 1 Jan. - 30 Jun. 1993
William C. Rose 1993 31 p
(Contract NCC2-507)
(NASA-CR-194143; NAS 1.26:194143) Avail: CASI HC A03/MF A01

In the present reporting period, the 3D STUFF code was used to solve the underbody flow for the waverider configuration vehicle. In order to start the space-marched version of the code, the time-marched version (TUFF) was used to solve the forward portion of the underside of the forebody flowfield. A grid was generated which went from the tip of the nose to the location of the cowl lip. This includes all of the inlet ramp system. Previous indications were that three-dimensional effects could be expected on the ramps of such an aircraft. For purposes of the present study, no sidewalls were assumed. The sidewalls were eliminated to simplify the calculations and to show the potential effects of three-dimensional flow in the absence of a full sidewall. Further, this flow was also analyzed using the newly released OVERFLOW code and comparisons between the two codes were made. In addition to these 3D calculations, 2D calculations using the OVERFLOW code were also obtained for the Mach 5 inlet model in this reporting period. Comparisons between the experimental data, previous computational fluid dynamics (CFD) results and those from OVERFLOW were made. Author (revised)

N94-13862# National Research Council of Canada, Ottawa (Ontario). Cold Regions Engineering.
POTENTIAL FLOW IN IN-LINE AND STAGGERED TUBE BANKS
S. B. Beale Feb. 1993 54 p
(IME-CRE-TR-006; NRC-36183; CTN-93-60836) Avail: CASI HC A04/MF A01

An analytical solution for the potential flow in in-line and staggered banks of tubes is derived using complex variable theory. The complex potential is written as a power series in terms of displacement. Series coefficients are provided for in-line square, rotated square, and equilateral triangle tube banks with pitch to diameter ratios in the range of 1.05:1 to 100:1. Contour plots of velocity potential, streamlines, and pressure, together with graphs of velocity and pressure around the cylinder diameter and across the minimum cross section, are illustrated for typical tube bank arrangements. A listing of the computer program that generates tables of coefficients as well as pressure and velocity data is appended. CISTI

N94-13959*# Alabama Univ., Huntsville. Dept. of Mechanical and Aerospace Engineering.
SLOSHING DYNAMICS ON ROTATING HELIUM DEWAR TANK Final Report
R. J. Hung Sep. 1993 66 p
(Grant NAG8-129)
(NASA-CR-194403; NAS 1.26:194403) Avail: CASI HC A04/MF A01

The generalized mathematical formulation of sloshing dynamics for partially filled liquid of cryogenic superfluid helium II in dewar containers driven by both the gravity gradient and jitter accelerations applicable to scientific spacecraft which is eligible to carry out spinning motion and/or slew motion for the purpose to perform scientific observation during the normal spacecraft operation are investigated. An example is given with Gravity Probe-B (GP-B) spacecraft which is responsible for the sloshing dynamics. The jitter accelerations include slew motion, spinning motion, atmospheric drag on the spacecraft, spacecraft attitude motions arising from machinery vibrations, thruster firing, pointing control of spacecraft, crew motion, etc. Explicit mathematical expressions to cover these forces acting on the spacecraft fluid systems are derived. The numerical computation of sloshing dynamics were based on the non-inertia frame spacecraft bound coordinate, and solve time dependent, three-dimensional formulations of partial differential equations subject to initial and boundary conditions. The explicit mathematical expressions of boundary conditions to cover capillary force effect on the liquid vapor interface in microgravity environments are also derived. The formulations of fluid moment and angular moment fluctuations in fluid profiles induced by the sloshing dynamics, together with fluid stress and moment fluctuations exerted on the spacecraft dewar containers were derived. Results were widely published in the open journals. Author (revised)

N94-14040# Norwegian Defence Research Establishment, Kjeller.
THE SPECTRAL VISCOSITY METHOD APPLIED TO SIMULATION OF WAVES IN A STRATIFIED ATMOSPHERE
Oeyvind Andreassen, Ivar Lie, and Carl Erik Wasberg 15 Dec. 1992 45 p
(FFI-92/7047; ETN-93-94452) Avail: CASI HC A03/MF A01

A spectral collocation method is used to solve an atmospheric gravity wave simulation problem. It is modeled by the nonlinear, inviscid, two dimensional Euler equations including gravity. The nonlinear transfer of energy to higher frequencies destroys the long time calculations if no method is applied for this purpose. Implementation aspects, effects on the resulting system of ordinary differential equations, tuning of parameters, and evaluation of results are discussed. An implementation that works well for larger simulations is found. Guidelines for the application of the method are given. ESA

N94-14045# Deutsche Forschungsanstalt fuer Luft- und Raumfahrt, Cologne (Germany). Abt. Aerothermodynamik und Verbrennung.
TURBULENT PARTICLE DISPERSION IN CONFINED SWIRLING FLOWS Ph.D. Thesis - Ruhr Univ. [TURBULENTE PARTIKELDISPERSION IN EINGESCHLOSSENEN DRALLSTROEMUNGEN]
Erich Walter Bluemcke Apr. 1992 181 p In GERMAN Original contains color illustrations
(DLR-FB-92-32; ETN-93-93962) Avail: CASI HC A09/MF A02

Turbulent particle dispersion, a dominant transport phenomena in gas turbine combustion chambers, is investigated by numerical simulations. A physical model is evaluated using results from a model experiment. Besides averaged transport parameters the instantaneous transport phenomena are analyzed for monosized droplets in swirling flows relevant for gas turbine combustion chambers. A good agreement between measured and calculated data can be stated. A parameter variation evidences the impact of the detailed description of the characteristics of gas turbulence. A simulation procedure is established for promotion in solving the engineering problem of the design of gas turbine combustion chambers. ESA

N94-14053# California Univ., Berkeley. Lawrence Berkeley Lab.
THE METHOD OF LAPLACE TRANSFORM MULTIQUADRICS (LTMQ) FOR THE SOLUTION OF THE GROUNDWATER FLOW EQUATION
G. J. Moridis and E. Kansa (California Univ., Livermore. Lawrence Livermore Lab.) Jun. 1992 7 p Presented at the 7th International Association for Mathematics and Computers in Simulation Conference on Computer Methods for Partial Differential Equations, New Brunswick, NJ, 22-24 Jun. 1993
(Contract DE-AC03-76SF-00098)
(DE93-010408; LBL-32529; CONF-9306153-1) Avail: CASI HC A02/MF A01

This paper presents a new numerical method, the Laplace Transform MultiQuadrics (LTMQ) method, developed for the solution of the diffusion-type parabolic Partial Differential Equation (PDE) of fluid flow through porous media. LTMQ combines a MultiQuadrics (MQ) approximation scheme with a Laplace transform formulation. The use of MQ in the spatial approximations allows the accurate description of problems in complex porous media with a very limited number of nodes. The Laplace transform

formulation eliminates the need for time discretization, thus allowing an unlimited time step size without any loss of accuracy. LTMQ is tested against results from three test problems of groundwater flow obtained from a standard Finite Difference (FD) model, as well as from analytical solutions. An excellent agreement between the LTMQ and the analytical and FD solutions is observed, while significant reductions in computer execution times may be achieved. DOE

N94-14086*# California Polytechnic State Univ., San Luis Obispo. Dept. of Mechanical Engineering.
DESIGN AND EVALUATION OF SINGLE AND DUAL FLOW THRUST VECTOR NOZZLES WITH POST EXIT VANES Semiannual Progress Report, Jun. - Dec. 1992
Thomas W. Carpenter, Stephen E. Vaccarezza, and Sean Dobbins 1992 35 p Original contains color illustrations
(Contract NCC2-748)
(NASA-CR-193393; NAS 1.26:193393) Avail: CASI HC A03/MF A01; 12 functional color pages

This Thrust Vectored Research project required that a 1/24 scale model of the F/A-18 High Alpha Research Vehicle, (HARV), propulsion system be constructed on the university campus. This propulsion system was designed for cold flow testing on a multicomponent test rig. Forces and moments were measured to study nozzle performance parameters. The flow visualization technique of color Schlieren photography was performed to investigate the flow phenomena at the nozzle exit. The flow interactions that were identified consisted of vane nozzleing between the outer and lower vanes and vane tip interference. The thrust vectoring system consisted of three asymmetrically spaced vanes installed circumferentially on a maximum afterburner nozzle. The performance of the nozzle was investigated with the outer and lower vanes equally deflected, (-10 deg is less than delta(sub v) is less than 25 deg), and with the upper vane fully retracted, (delta(sub v) equals -10 deg). The nozzle pressure ratio ranged from 4 to 6. The results indicated that a vane nozzleing effect developed at nozzle pressure ratios of 4 and 6 when the outer and lower vanes were deflected far enough into the flow field such that the increase in vane area accelerated the flow past the vanes causing distorted shock waves. This accelerated flow was a result of a pressure differential existing between the inside surface of the vane and the ambient pressure. The stagnation pressure that developed along the inside surface of the vane accelerated the flow past the vanes causing it to equalize with ambient pressure, thus providing distorted shock waves. A tip interference was present at the trailing edge of the upper vane as a result of low nozzle pressure, NPR 4, with high vane deflection, delta(sub v) equals 25 degrees, and also with a high nozzle pressure, NPR 6, and low vane deflections, delta(sub v) equals 15 degrees. Author (revised)

N94-14188# Deutsche Forschungsanstalt fuer Luft- und Raumfahrt, Goettingen (Germany). Gruppe Instationaere Aerodynamik.
FULL RIEMANN SOLUTION OF THE ONE- AND TWO-DIMENSIONAL EULER EQUATIONS Ph.D. Thesis - Tech. Univ. Munich [VOLLSTAENDIGE RIEMANNLOESUNG DER EIN- UND ZWEIDIMENSIONALEN EULER-GLEICHUNGEN]
Wolfgang Wegner Nov. 1992 142 p In GERMAN
(DLR-FB-92-34; ETN-93-93963) Avail: CASI HC A07/MF A02

The complete solution in closed form of the Riemann problem in gas dynamics is reported: physical discontinuities are taken into account, and the complete solution is not constructed iteratively. Starting with the compatibility equations, validity is illustrated by the so called complementary wave model. The full Riemann solution is further applied to a different method for the numerical solution of the one and two dimensional Euler equations. The numerical solutions are analyzed and compared with the presently used methods based on approximated Riemann solutions. ESA

N94-14308*# Pennsylvania State Univ., University Park. Propulsion Engineering Research Center.
DROPLET-TURBULENCE INTERACTIONS IN SPRAYS EXPOSED TO SUPERCRITICAL ENVIRONMENTAL CONDITIONS Final Report
Domenic A. Santavicca Sep. 1993 27 p
(Grant NAG8-160)
(NASA-CR-194408; NAS 1.26:194408) Avail: CASI HC A03/MF A01

The goal of this research was to experimentally characterize the behavior of droplets in vaporizing sprays under conditions typical of those encountered in high pressure combustion systems such as liquid fueled rocket engines. Of particular interest are measurements of droplet drag and lift, droplet dispersion, droplet heating, and droplet vaporization under both subcritical and supercritical conditions. A summary of the major accomplishments achieved during the period from June 1990 through June 1993, a brief description and status report on five research areas, which were directly or indirectly supported by this grant, and a list of publications and personnel associated with this research is included. Author (revised)

N94-14318# Lawrence Livermore National Lab., CA.
THE ACCURACY OF APPROXIMATING RADIATIVE HEAT TRANSFER USING A TEMPERATURE DEPENDENT THERMAL CONDUCTIVITY
J. R. Creighton 11 Feb. 1993 25 p
(Contract W-7405-eng-48)
(DE93-013105; UCRL-ID-113019) Avail: CASI HC A03/MF A01

Radiative heat transfer across the gap between two coaxial cylinders can be approximated using an equivalent thermal conductivity that is a cubic polynomial in the temperatures T(sub 1) and T(sub 2) of the two surfaces (T(sub 1) greater than T(sub 2)). It is convenient to write the polynomial in terms of the average temperature, yielding T(sub avg(exp 3)) multiplied by an expression in T(sub avg)/T(sub 1). This expression has a value close to unity when the temperature difference is small and approaches 2 as the lower temperature approaches zero. The approximation is valid if the temperature of each surface is uniform. Numerical calculations showed that it is also reasonably accurate when the temperature varies with height on the cooler surface. An electrical circuit analogy shows that this should be generally true, but that the approximation may be poor when the hotter surface temperature is not uniform. The appendix shows the derivation of the view factors used in the radiative heat transport calculations. DOE

N94-14351# Louisiana State Univ., Baton Rouge.
BOAST 2 FOR THE IBM 3090 AND RISC 6000
P. Hebert, A. T. Bourgoyne, Jr., and J. Tyler May 1993 150 p
(Contract DE-FG07-89ID-12842)
(DE93-000138; DOE/ID-12842/2) Avail: CASI HC A07/MF A02

BOAST 2 simulates isothermal, darcy flow in three dimensions. It assumes that reservoir liquids can be described in three fluid phases (oil, gas, and water) of constant composition, with physical properties that depend on pressure, only. These reservoir fluid approximations are acceptable for a large percentage of the world's oil and gas reservoirs. Consequently, BOAST 2 has a wide range of applicability. BOAST 2 can simulate oil and/or gas recovery by fluid expansion, displacement, gravity drainage, and capillary imhibition mechanisms. Typical field production problems that BOAST 2 can handle include primary depletion studies, pressure maintenance by water and/or gas injection, and evaluation of secondary recovery waterflooding and displacement operations. Technically, BOAST 2 is a finite, implicit pressure, explicit saturation (IMPES) numerical simulator. It applies both direct and iterative solution techniques for solving systems of algebraic equations. The well model allows specification of rate or pressure constraints on well performance, and the user is free to add or to recomplete wells during the simulation. In addition, the user can define multiple rock and PVT regions and can choose from three aquifer models. BOAST 2 also provides flexible initialization, a bubble-point tracking scheme, automatic time-step control, and a material balance check on solution stability. The user controls output, which includes a run summary and line-printer plots of fieldwide performance. DOE

N94-14356*# Fluent, Inc., Lebanon, NH.
MULTIGRID SOLUTION OF INTERNAL FLOWS USING UNSTRUCTURED SOLUTION ADAPTIVE MESHES Final Report
Wayne A. Smith and Kenneth R. Blake Nov. 1992 37 p
(Contract NAS3-25785; SBIR-01.01-3800)
(NASA-CR-194233; NAS 1.26:194233; TN-035) Avail: CASI HC A03/MF A01

This is the final report of the NASA Lewis SBIR Phase 2 Contract Number NAS3-25785, Multigrid Solution of Internal Flows Using Unstructured Solution Adaptive Meshes. The objective of this project, as described in the Statement of Work, is to develop and deliver to NASA a general three-dimensional Navier-Stokes code using unstructured solution-adaptive meshes for accuracy and multigrid techniques for convergence acceleration. The code will primarily be applied, but not necessarily limited, to high speed internal flows in turbomachinery. Derived from text

N94-14434# Lawrence Livermore National Lab., CA.
AN ADAPTIVE PROJECTION METHOD FOR THE INCOMPRESSIBLE EULER EQUATIONS
A. S. Almgren, J. B. Bell, L. H. Howell, and P. Colella (California Univ., Berkeley.) Jun. 1993 10 p Presented at the 11th International Computational Fluid Dynamics Conference, 28th Thermophysics Conference and 23rd Fluid Dynamics, Plasma Dynamics and Laser Conference, Orlando, FL, 5-7 Jul. 1993
(Contracts W-7405-eng-48; DE-FG03-92ER-25140)
(DE93-016428; UCRL-JC-113853; CONF-930714-2) Avail: CASI HC A02/MF A01

We present a method for solving the time-dependent incompressible Euler equations on an adaptive grid. The method is based on a projection formulation in which we first solve convection equations to predict intermediate velocities, and then project these velocities onto a space of approximately divergence-free vector fields. Our treatment of the convection step uses a specialized second-order upwind method for differencing the nonlinear convection terms that provides a robust treatment of these terms suitable for inviscid flow. Our approach to adaptive refinement uses a nested hierarchy of grids with simultaneous refinement of the grids in both space and time. The integration algorithm on the grid hierarchy is a recursive procedure in which a coarse grid is advanced; fine grids are advanced multiple steps to reach the same time as the coarse grid and the grids are then synchronized. We will describe the integration algorithm in detail, with emphasis on the projection used to enforce the incompressibility constraint. Numerical examples are presented to demonstrate the convergence properties of the method and to illustrate the behavior of the method at the interface between coarse and fine grids. An additional example demonstrates the performance of the method on a more realistic problem. DOE

N94-14443# Deutsche Forschungsanstalt fuer Luft- und Raumfahrt, Oberpfaffenhofen (Germany). Inst. fuer Physik der Atmosphaere.
TURBULENT DIFFUSION IN HOMOGENEOUS SHEAR FLOW WITH STABLE DENSITY STRATIFICATION Ph.D. Thesis - Tech. Univ. Munich [TURBULENTE DIFFUSION IN EINER HOMOGENEN SCHERSTROEMUNG MIT STABILER DICHTESCHICHTUNG]
Hans-Jakob Kaltenbach Aug. 1992 157 p In GERMAN
(DLR-FB-92-26; ETN-93-9395763) Avail: CASI HC A08/MF A02

The mixing properties of homogeneous turbulent flows, which are influenced by stable density stratification and mean shear, are investigated using direct numerical simulation and large eddy simulation. The dependency of the components of the turbulence diffusivity tensor on the value of the Gradient Richardson number is demonstrated. Stable stratification reduces the vertical transport of species stronger than the horizontal transport. In cases with strong background stratification the Froude number plays an important role besides the Richardson number. Little different is found between direct simulation and large eddy simulation results. Both types of simulations are concluded to refer to the same order of magnitude of the Reynolds number. The results are sensitive to the value of the Prandtl number in cases with Richardson number greater than 0.25. ESA

N94-14464 National Physical Lab., Teddington (England). Materials Metrology Div.
A CONDUCTION MODEL FOR THE VACUUM ARC REMELTING PROCESS
D. H. Ferriss Apr. 1993 18 p
(NPL-DMM(A)-98; ETN-93-94606) Copyright Avail: Issuing Activity (National Physical Laboratory, Teddington, Middlesex TW11 0LW, United Kingdom)

Equations describing the time dependent heat transfer by conduction during the vacuum arc remelting process are presented. The model is assumed axisymmetric and allows for latent heat effects using a simple enthalpy formulation. Boundary conditions allow for various modes of surface heat transfer including the combination of radiation effects and heat transfer coefficients. Scaling of the equations identifies various non dimensional parameters characterizing the problem solution. The results of a specimen calculation are presented. ESA

N94-14503 Tel-Aviv Univ. (Israel). School of Physics and Astronomy.
COLLISIONS AND SEPARATIONS IN 2D HYDRODYNAMICAL CODE M.S. Thesis
Shimon Asida Jun. 1991 106 p In HEBREW
(ITN-93-85225) Copyright Avail: Issuing Activity (Tel-Aviv Univ., Exact Sciences Library, Ramat Aviv 69978, Israel)

Hydrodynamic problems involving the collision or separation of zones of different materials include the following types: armor penetration by a jet formed in the explosion of a shaped charge or by a kinetic projectile, and instabilities in cosmic jets. Calculations of hydrodynamic processes are based on numerical simulations which solve the differential equations by means of difference equations. A special grid is defined and the physical system is advanced via finite steps in time; in a Eulerian treatment, the grid is stationary in space whereas in a Lagrangian treatment it moves together with the fluid. In Lagrangian methods, the grid is defined on the fluid and the boundaries between materials are formed by the edges of computational cells, so that the shape of the grid depends on the shape of the boundary. Where there is a strong flow, the cells distort and the grid must be frequently redefined to enable the calculation to continue. Boundary collisions cause difficulty in defining a grid. In Eulerian methods, where the computational grid is defined over all the space through which the materials flow, it is necessary to use cells with non-homogeneous contents to follow the boundaries; such calculations are more complicated and less accurate. The aim of the present work was to develop a Lagrangian method for treating such collisions. The code, based on an existing 2D Lagrangian code with the addition of a new collision mechanism, uses a mixed computational grid, comprising squares and triangles, with which it is possible to describe systems. ISA

N94-14598# National Aeronautical Lab., Bangalore (India). Computational and Theoretical Fluid Dynamics Div.
PROCEEDINGS OF THE FLUID DYNAMICS SYMPOSIUM IN HONOUR OF PROFESSOR R. NARASIMHA ON HIS 60TH BIRTHDAY
S. K. Chakrabartty, ed., S. S. Desai, ed., S. Majumdar, ed., D. K. Prabhu, ed., S. K. Saxena, ed., and P. N. Shankar, ed. Jul. 1993 212 p Symposium held in Bangalore, India, 9 Jul. 1993 Original contains color illustrations
(NAL Proj. CF-0-900)
(NAL-SP-9315) Avail: CASI HC A10/MF A03

This special report contains 19 papers presented at a symposium held in honor of Prof. R. Narasimha, Director of the National Aerospace Laboratories in Bangalore, India. The papers address research in the development of computational methods for the analysis and modeling of fluid dynamic phenomena. For individual titles, see N94-14599 through N94-14617.

N94-14599# National Aeronautical Lab., Bangalore (India). Computational and Theoretical Fluid Dymanics Div.
A VERTEX-BASED FINITE-VOLUME ALGORITHM FOR THE NAVIER-STOKES EQUATIONS
S. K. Chakrabartty and K. Dhanalakshmi *In its* Proceedings of the Fluid Dynamics Symposium in Honour of Professor R. Narasimha on his 60th Birthday Jul. 1993 p 1-7 (For primary document see N94-14598 02-34)
Avail: CASI HC A02/MF A03

A vertex-based, finite-volume algorithm has been developed to solve the Reynolds-averaged Navier-Stokes equations without thin-layer approximation. An explicit, five-stage Runge-Kutta, time-stepping scheme has been used for time integration along with different acceleration techniques to reach the steady state. A code employing multi-block grid structure has been developed. This code can accept any type of grid topology. As test cases, the turbulent flow past RAE-2822 and NACA-0012 airfoils, and the laminar flow past a cropped delta wing at ten degrees angle of attack have been computed and the results compared with available numerical and experimental results. The Baldwin-Lomax turbulence model has been used in the case of turbulent flows. Author

N94-14600# National Aeronautical Lab., Bangalore (India). Computational and Theoretical Fluid Dynamics Div.
DEVELOPMENT OF FULL-POTENTIAL CODES IN THE DECADE 1983-1993
S. S. Desai and R. Rangarajan *In its* Proceedings of the Fluid Dynamics Symposium in Honour of Professor R. Narasimha on his 60th Birthday Jul. 1993 p 9-23 (For primary document see N94-14598 02-34)
Avail: CASI HC A03/MF A03

Computational expedience and adequate predictive accuracy for certain engineering applications, make the transonic full-potential formulation a useful application tool for the design and analysis of aerospace configurations in the transonic flow regime. A summary is presented of the work done in the development of full potential codes during the decade 1983-1993 at the National Aeronautical Laboratory, Bangalore. Author

N94-14601# National Aeronautical Lab., Bangalore (India). Computational and Theoretical Fluid Dynamics Div.

THE STRUCTURE OF LAMINAR FLOW IN A THREE-DIMENSIONAL DRIVEN CAVITY

M. D. Deshpande and P. N. Shankar *In its* Proceedings of the Fluid Dynamics Symposium in Honour of Professor R. Narasimha on his 60th Birthday Jul. 1993 p 25-36 (For primary document see N94-14598 02-34)

Avail: CASI HC A02/MF A03

We present some details of the steady laminar flow fields that are generated in a fluid filled cavity by the motion of one of the faces. The flow fields have been obtained by the numerical solution of the Navier-Stokes equations in the Reynolds number range 0 less than Re less than or equal to 1000. The streamline patterns clearly indicate the very complicated nature of the eddy structures and their dependence on Reynolds number. Further work is currently in progress to extend the computations to higher Reynolds numbers in order that transition and turbulence in the cavity may be studied. Author (revised)

N94-14602# National Aeronautical Lab., Bangalore (India). Computational and Theoretical Fluid Dynamics Div.

A VORTEX METHOD FOR VISCOUS UNSTEADY FLOWS

P. K. Dutta *In its* Proceedings of the Fluid Dynamics Symposium in Honour of Professor R. Narasimha on his 60th Birthday Jul. 1993 p 37-50 (For primary document see N94-14598 02-34)

Avail: CASI HC A03/MF A03

A simple method is presented for the creation of vorticity from a solid boundary in the form of discrete vortex blobs. These vortices have uniform-vorticity cores and are released from a number of points distributed around the body surface at a small distance away from the surface. Their strengths are obtained by satisfying the no-slip condition at the midpoints of the corresponding vortex sheets. The dynamics of these vortices is then considered by including the effect of viscous diffusion by random walk approach. The method is applied to the starting flow past a circular cylinder. A detailed parametric study shows that viscosity has the most significant effect on the computed results and, in order to obtain meaningful results, it must be reduced suitably to compensate for the artificial viscosity arising from numerical integration of equations of motion of the discrete vortices. Results are obtained for three typical Reynolds numbers of 9500, 3000 and 550, and are found to be in very good agreement with experimental measurements for the centerline velocity distribution. In particular, the case of Re = 550 illustrates the usefulness of the present model even at low Reynolds numbers. The vortex patterns, velocity vectors and particle path lines also conform to the experimental flow visualization pictures. Though the method is developed for a simple configuration like a circular cylinder, it can be easily extended to any general body shape. Author

N94-14603# National Aeronautical Lab., Bangalore (India). Computational and Theoretical Fluid Dynamics Div.

AN IMPLICIT FINITE VOLUME NODAL POINT SCHEME FOR THE SOLUTION OF TWO-DIMENSIONAL COMPRESSIBLE NAVIER-STOKES EQUATIONS

Vimala Dutta *In its* Proceedings of the Fluid Dynamics Symposium in Honour of Professor R. Narasimha on his 60th Birthday Jul. 1993 p 51-59 (For primary document see N94-14598 02-34)

Avail: CASI HC A02/MF A03

An implicit finite volume nodal point scheme has been developed for solving the two-dimensional compressible Navier-Stokes equations. The numerical scheme is evolved by efficiently combining the basic ideas of the implicit finite-difference scheme of Beam and Warming (1978) with those of nodal point schemes due to Hall (1985) and Ni (1982). The 2-D Navier-Stokes solver is implemented for steady, laminar/turbulent flows past airfoils by using C-type grids. Turbulence closure is achieved by employing the algebraic eddy-viscosity model of Baldwin and Lomax (1978). Results are presented for the NACA-0012 and RAE-2822 airfoil sections. Comparison of the aerodynamic coefficients with experimental results for the different test cases presented here establishes the validity and efficiency of the method. Author

N94-14604# National Aeronautical Lab., Bangalore (India). Computational and Theoretical Fluid Dynamics Div.

WALL INTERFERENCE STUDIES: REVISITED

R. Gopinath *In its* Proceedings of the Fluid Dynamics Symposium in Honour of Professor R. Narasimha on his 60th Birthday Jul. 1993 p 61-68 (For primary document see N94-14598 02-34)

Avail: CASI HC A02/MF A03

A brief review is made of the methods currently available for assessing and correcting the data for effects due to wall interference. Computational simulation of ventilated walls has been described. The DLR panel code available in the division is being modified to handle flow past a model with sting and support strut in a wind tunnel whose walls could be either solid, or, ventilated, or, open-jet. The effect of sting, strut, and walls on the model data is under study. Author

N94-14605# National Aeronautical Lab., Bangalore (India). Computational and Theoretical Fluid Dynamics Div.

STABILITY OF SPATIALLY DEVELOPING BOUNDARY LAYERS

Rama Govindarajan *In its* Proceedings of the Fluid Dynamics Symposium in Honour of Professor R. Narasimha on his 60th Birthday Jul. 1993 p 69-76 (For primary document see N94-14598 02-34)

Avail: CASI HC A02/MF A03

A new formulation of the stability of boundary-layer flows in pressure gradients is presented, taking into account the spatial development of the flow. The formulation assumes that disturbance wavelength and eigenfunction vary downstream no more rapidly than the boundary-layer thickness, and includes all terms of O(1) and O(R(exp -1)) in the boundary-layer Reynolds number R. Although containing the Orr-Sommerfeld operator, the present approach does not yield the Orr-Sommerfeld equation in any rational limit. In Blasius flow, the present stability equation is consistent with that of Bertolotti et al. (1992) to terms of O(R(exp -1)). For the Falkner-Skan similarity solutions neutral boundaries are computed without the necessity of having to march in space. Results show that the effects of spatial growth are striking in flows subjected to adverse pressure gradients.

Author (revised)

N94-14606# National Aeronautical Lab., Bangalore (India). Computational and Theoretical Fluid Dynamics Div.

NAVIER-STOKES SIMULATION OF TRANSONIC VORTEX FLOW OVER A DELTA WING

Anand Kumar *In its* Proceedings of the Fluid Dynamics Symposium in Honour of Professor R. Narasimha on his 60th Birthday Jul. 1993 p 77-89 (For primary document see N94-14598 02-34)

Avail: CASI HC A03/MF A03

An explicit multi-stage Runge-Kutta time-stepping scheme with cell-centered finite volume spatial discretization is employed to solve three-dimensional, compressible Navier-Stokes equations. A novel variation for computation of viscous fluxes is used. Convergence to steady state is expedited through acceleration techniques. The vortex flow over a 65 degree cropped rounded leading edge delta wing is computed, and the results are compared with experimental data and Euler solution. Author

N94-14607# National Aeronautical Lab., Bangalore (India). Computational and Theoretical Fluid Dynamics Div.

A FINITE VOLUME METHOD FOR COMPUTATION OF VISCOUS FLOW IN COMPLEX CONFIGURATIONS

Sekhar Majumdar *In its* Proceedings of the Fluid Dynamics Symposium in Honour of Professor R. Narasimha on his 60th Birthday Jul. 1993 p 91-114 (For primary document see N94-14598 02-34)

Avail: CASI HC A03/MF A03

A calculation procedure is presented for computation of steady, recirculating viscous flows in complex configurations. The algorithm has been developed for non-orthogonal coordinate systems using collocated variable arrangement. In order to handle both incompressible and compressible flows, pressure has been selected as a primary dependent variable in preference to density. The pressure field is evaluated using the pressure-velocity correction strategy of the SIMPLE algorithm, suitably modified for collocated variable arrangement. The capability of the

three-dimensional version of the algorithm has been demonstrated for prediction of two incompressible laminar flow situations with complex geometry. Author

N94-14608# National Aeronautical Lab., Bangalore (India). Computational and Theoretical Fluid Dynamics Div.

A GRID GENERATION PACKAGE FOR HIGH ASPECT RATIO WINGS **c02**

J. S. Mathur and S. K. Chakrabartty *In its* Proceedings of the Fluid Dynamics Symposium in Honour of Professor R. Narasimha on his 60th Birthday Jul. 1993 p 115-121 (For primary document see N94-14598 02-34)

Avail: CASI HC A02/MF A03

A grid generation package has been developed to generate a quasi-three-dimensional grid of either O-H or C-H topology. Grid stacking has been implemented here to use two dimensional grid generation routines at different span stations, and then stack these together to get a three-dimensional grid. An algebraic grid generation routine for C-type grid with all the flexibilities of grid stretching and an elliptic grid generation routine with control functions for O-type grid have been used to generate two-dimensional grids. To demonstrate the method, a sample grid generated for the ONERA-M6 wing has been presented here. Author

N94-14609# National Aeronautical Lab., Bangalore (India). Computational and Theoretical Fluid Dynamics Div.

THE PHENOMENON OF VORTEX BREAKDOWN **c02**

Vidyadhar Y. Mudkavi *In its* Proceedings of the Fluid Dynamics Symposium in Honour of Professor R. Narasimha on his 60th Birthday Jul. 1993 p 123-135 (For primary document see N94-14598 02-34)

Avail: CASI HC A03/MF A03

Vortex breakdown is an abrupt change of flow structure that occurs in swirling flows. More than 3 decades of research in this area has not shed light upon this very basic fluid dynamical phenomenon. The mechanism that leads to vortex breakdown is very poorly understood despite numerous theoretical and experimental investigations. There is still a need for a coherent theory. In this paper these issues are considered in the form of a review of current literature on the phenomenon of vortex breakdown. Some existing criteria to predict the breakdown are presented. Author

N94-14610# National Aeronautical Lab., Bangalore (India). Computational and Theoretical Fluid Dynamics Div.

COMPUTATION OF NONEQUILIBRIUM FLOWS USING PNS EQUATIONS

Dinesh K. Prabhu *In its* Proceedings of the Fluid Dynamics Symposium in Honour of Professor R. Narasimha on his 60th Birthday Jul. 1993 p 137-151 (For primary document see N94-14598 02-34)

Avail: CASI HC A03/MF A03

The laminar, hypersonic flow of five-species (N2, O2, NO, N, O) nonequilibrium air over a 10 degree axisymmetric cone is computed using a non-iterative, implicit finite-difference scheme. The numerical algorithm is based on central differencing of the inviscid and viscous fluxes. Two gas models are considered in this study - one in which the constituent species are both calorically and thermally perfect and the other in which the constituent species are only thermally perfect. The effects of the two gas models and the types of wall boundary conditions on the computed solution are studied and discussed. Author (revised)

N94-14611# National Aeronautical Lab., Bangalore (India). Computational and Theoretical Fluid Dynamics Div.

DEVELOPMENT OF PC-BASED AERONAUTICAL SOFTWARE (AEROWARE) **c61**

Premalatha Ramamoorthy and P. Ramamoorthy *In its* Proceedings of the Fluid Dynamics Symposium in Honour of Professor R. Narasimha on his 60th Birthday Jul. 1993 p 153-158 (For primary document see N94-14598 02-34)

Avail: CASI HC A02/MF A03

The development of a software package called 'AEROWARE' (AEROnautical softWARE) is described. The organization of the first version of the package, including user interface utilities, is explained. The hardware and software resources needed for the development, are briefly discussed. Recommendations are made for future versions of the package. Author

N94-14612# National Aeronautical Lab., Bangalore (India). Computational and Theoretical Fluid Dynamics Div.

HYPERSONIC VISCOUS FLOW COMPUTATIONS **c02**

S. K. Saxena *In its* Proceedings of the Fluid Dynamics Symposium in Honour of Professor R. Narasimha on his 60th Birthday Jul. 1993 p 159-165 (For primary document see N94-14598 02-34)

(NAL Proj. CF-1-121)

Avail: CASI HC A02/MF A03

A brief description of the work currently underway on hypersonic viscous flow computations, based on the solution of thin-layer Navier-Stokes equations employing upwind TVD schemes, is presented. Both van Leer and Roe schemes are considered. Some representative computational results presented indicate that these schemes are quite robust and can provide sharp description of the shocks. The importance of parallel computing on machines like Flosolver and the use of implicit techniques to accelerate the computations is emphasized. The future direction of hypersonic research is indicated. Author

N94-14613# National Aeronautical Lab., Bangalore (India). Computational and Theoretical Fluid Dynamics Div.

DEVELOPMENT OF A GENERAL PURPOSE MULTIGRID ACCELERATED NAVIER-STOKES SOLVER

J. P. Singh, D. Schwamborn (Deutsche Forschungsanstalt fuer Luft- und Raumfahrt, Goettingen, Germany.), and C. Kloppmann (Deutsche Forschungsanstalt fuer Luft- und Raumfahrt, Goettingen, Germany.) *In its* Proceedings of the Fluid Dynamics Symposium in Honour of Professor R. Narasimha on his 60th Birthday Jul. 1993 p 167-179 (For primary document see N94-14598 02-34)

Avail: CASI HC A03/MF A03

The present work describes the development of a fairly general purpose 2-D multigrid accelerated Reynolds-averaged Navier-Stokes solver. For turbulent flows the eddy viscosity is computed using the Baldwin-Lomax model. The code has been successfully used to compute a variety of flows like near-incompressible flows, subsonic flows, flows with massive separation around stall, flow past laminar flow airfoils with long laminar runs, transonic flows with moderate and strong shock, and at supersonic speeds. Results are in good agreement. This shows the robustness and wide applicability of the code. The convergence history in almost all these cases presents a fairly smooth curve with a steep drop to low residue levels. The present level of success in the computation of supersonic flows leads us to expect that this work is directly extendible to hypersonic flows without dissociation effects. Author

N94-14614# National Aeronautical Lab., Bangalore (India). Computational and Theoretical Fluid Dynamics Div.

DEVELOPMENT OF PARALLEL PROCESSING AT NAL: A RETROSPECT **c62**

U. N. Sinha, V. R. Sarasamma, S. Rajalakshmy, C. R. Sreenivasan, and G. S. Dwarakanath *In its* Proceedings of the Fluid Dynamics Symposium in Honour of Professor R. Narasimha on his 60th Birthday Jul. 1993 p 181-190 (For primary document see N94-14598 02-34)

Avail: CASI HC A02/MF A03

The present report describes the design and development of the Flosolver series of parallel computers at NAL. Built with the specific aim of providing the much-needed computing power for complex aerospace problems, the Flosolver series has evolved from Flosolver Mk1 with four processing elements based on the 16-bit Intel 8086/8087 CISC processor, to the the latest version, Flosolver Mk3 with 7 processing elements based on the 32-bit Intel i860 RISC processor. Starting with a discussion of the strategies adopted in the design of these machines, the paper also discusses the various phases in the development and fabrication of the system software, and the application codes currently operational on them. Author

N94-14615# National Aeronautical Lab., Bangalore (India). Computational and Theoretical Fluid Dynamics Div.

SRISTI: THE NAL METHOD FOR THE DESIGN AND ANALYSIS OF NATURAL LAMINAR FLOW (NLF) AIRFOILS **c05**

K. R. Srilatha, G. S. Dwarakanath, and P. Ramamoorthy *In its* Proceedings of the Fluid Dynamics Symposium in Honour of Professor R. Narasimha on his 60th Birthday Jul. 1993 p 191-203 (For primary document see N94-14598 02-34)

Avail: CASI HC A03/MF A03

A software package (called SRISTI) for the design and analysis of NLF airfoils is described. As an illustration, an NLF airfoil for NAL's Light Transport Aircraft has been designed using this package. Its aerodynamic characteristics have been extensively compared with GAW-2 airfoil and also with wind tunnel experiments. Author

N94-14616# National Aeronautical Lab., Bangalore (India). Computational and Theoretical Fluid Dynamics Div.

VSAERO ANALYSIS OF A PIPER CUB AIRCRAFT **c05**

Ashok Srivastava, David Lednicer (Analytical Methods, Inc., Redmond, WA.), Ian Gilchrist (Analytical Methods, Inc., Redmond, WA.), and Jahan Saghafi (Analytical Methods, Inc., Redmond, WA.) *In its* Proceedings of the Fluid Dynamics Symposium in Honour of Professor R. Narasimha on his 60th Birthday Jul. 1993 p 205-210 Sponsored by Dept. of Science and Technology and Agency for International Development (For primary document see N94-14598 02-34)

Avail: CASI HC A02/MF A03

A Piper Cub aircraft configuration has been analyzed using the VSAERO code and the aerodynamic characteristics have been obtained at two incidences. Detailed pressure distributions have been computed along wing-body-tail sections. A comparison of lift characteristics with flight data shows reasonable agreement. Author

N94-14617# National Aeronautical Lab., Bangalore (India). Computational and Theoretical Fluid Dynamics Div.

PANEL CODES FOR AERODYNAMIC ANALYSIS AT NAL **c02**

S. Viswanathan, C. L. Narayana, V. Ramesh, S. S. Desai, and R. Rangarajan *In its* Proceedings of the Fluid Dynamics Symposium in Honour of Professor R. Narasimha on his 60th Birthday Jul. 1993 p 211-233 (For primary document see N94-14598 02-34)

Avail: CASI HC A03/MF A03

The National Aerospace Laboratories' (NAL's) panel code capability buildup has been highlighted and several interesting applications are discussed to bring out the utility of panel methods in aerospace research and development. Author

N94-14708# Kernforschungszentrum G.m.b.H., Karlsruhe (Germany). Projekt Nukleare Sicherheitsforschung.

REVIEW OF MATHEMATICAL AND PHYSICAL BASIS OF TWO-PHASE FLOW MODELING

M. Bottoni (Argonne National Lab., IL.) and W. Sengpiel Aug. 1992 165 p

(KfK-4759; ETN-93-94189) Copyright Avail: CASI HC A08/MF A02

Starting from a continuum mechanical approach a detailed overview of the deduction of conservation equations for the analytical description of two phase flows by means of an adequate averaging process resulting in a two fluid model and a homogeneous mixture model is given. The mathematical process of averaging leads to macroscopic formulations of stress terms and interfacial interactions terms. These terms depend on microscopic variables and thus give some helpful insight into the physical processes which have to be described by constitutive relations. ESA

N94-14722*# National Aeronautics and Space Administration. Lewis Research Center, Cleveland, OH.

NUMERICAL STUDY OF SHOCK-INDUCED COMBUSTION IN METHANE-AIR MIXTURES

Shaye Yungster and Martin J. Rabinowitz Jun. 1993 15 p Presented at the 29th Joint Propulsion Conference and Exhibit, Monterey, CA, 28-30 Jun. 1993; sponsored by AIAA, SAE, ASME, and ASEE See also A93-49783

(Contract NCC3-233; RTOP 505-90-5K)

(NASA-TM-106354; ICOMP-93-32; E-8138; NAS 1.15:106354; AIAA Paper 93-1917) Avail: CASI HC A03/MF A01

The shock-induced combustion of methane-air mixtures in hypersonic flows is investigated using a new reaction mechanism consisting of 19 reacting species and 52 elementary reactions. This reduced model is derived from a full kinetic mechanism via the Detailed Reduction technique. Zero-dimensional computations of several shock-tube experiments are presented first. The reaction mechanism is then combined with a fully implicit Navier-Stokes computational fluid dynamics (CFD) code to conduct numerical simulations of two-dimensional and axisymmetric shock-induced combustion experiments of stoichiometric methane-air mixtures at a Mach number of M = 6.61. Applications to the ram accelerator concept are also presented. Author (revised)

N94-14728*# National Aeronautics and Space Administration. Lewis Research Center, Cleveland, OH.

DEVELOPMENT OF AN EXPLICIT MULTIBLOCK/MULTIGRID FLOW SOLVER FOR VISCOUS FLOWS IN COMPLEX GEOMETRIES

E. Steinthorsson, M. S. Liou, and L. A. Povinelli Jun. 1993 17 p Presented at the 29th Joint Propulsion Conference and Exhibit, Monterey, CA, 28-30 Jun. 1993; sponsored by AIAA, SAE, ASME, and ASEE See also A93-50148

(Contract NCC3-233; RTOP 505-62-27)

(NASA-TM-106356; E-8140; ICOMP-93-34; NAS 1.15:106356; AIAA Paper 93-2380) Avail: CASI HC A03/MF A01

A new computer program is being developed for doing accurate simulations of compressible viscous flows in complex geometries. The code employs the full compressible Navier-Stokes equations. The eddy viscosity model of Baldwin and Lomax is used to model the effects of turbulence on the flow. A cell centered finite volume discretization is used for all terms in the governing equations. The Advection Upwind Splitting Method (AUSM) is used to compute the inviscid fluxes, while central differencing is used for the diffusive fluxes. A four-stage Runge-Kutta time integration scheme is used to march solutions to steady state, while convergence is enhanced by a multigrid scheme, local time-stepping, and implicit residual smoothing. To enable simulations of flows in complex geometries, the code uses composite structured grid systems where all grid lines are continuous at block boundaries (multiblock grids). Example results shown are a flow in a linear cascade, a flow around a circular pin extending between the main walls in a high aspect-ratio channel, and a flow of air in a radial turbine coolant passage. Author (revised)

N94-14729*# National Aeronautics and Space Administration. Lewis Research Center, Cleveland, OH.

LINEAR INSTABILITY OF CURVED FREE SHEAR LAYERS

William W. Liou Jul. 1993 18 p Presented at the 3rd Shear Flow Control Conference, Orlando, FL, 6-9 Jul. 1993; sponsored by AIAA See also A93-46797

(Contract NCC3-233; RTOP 505-90-5K)

(NASA-TM-106290; ICOMP-93-28; E-8027; NAS 1.15:106290; CMOTT-93-11; AIAA Paper 93-03252) Avail: CASI HC A03/MF A01

The linear inviscid hydrodynamic stability of slightly curved free mixing layers is studied in this paper. The disturbance equation is solved numerically using a shooting technique. Two mean velocity profiles that represent stably and unstably curved free mixing layers are considered. Results are shown for cases of five curvature Richardson numbers. The stability characteristics of the shear layer are found to vary significantly with the introduction of the curvature effects. The results also indicate that, in a manner similar to the Goertler vortices observed in a boundary layer along a concave wall, instability modes of spatially developing streamwise vortex pairs may appear in centrifugally unstable curved mixing layers. Author (revised)

N94-14732*# National Aeronautics and Space Administration. Lewis Research Center, Cleveland, OH.

A STUDY OF THIN LIQUID SHEET FLOWS

Donald L. Chubb, Frederick D. Calfo, Marc W. McConley (Princeton Univ., NJ.), Matthew S. McMaster (Toledo Univ., OH.), and Abdollah A. Afjeh (Toledo Univ., OH.) Aug. 1993 28 p

(RTOP 506-41-11)

(NASA-TM-106323; E-7854-1; NAS 1.15:106323) Avail: CASI HC A03/MF A01

This study was a theoretical and experimental investigation of thin liquid sheet flows in vacuum. A sheet flow created by a narrow slit of width, W, coalesces to a point at a distance, L, as a result of surface tension forces acting at the sheet edges. As the flow coalesces, the fluid accumulates in the sheet edges. The observed triangular shape of the sheet agrees with the calculated triangular result. Experimental results for L/W as a function of Weber number, We, agree with the calculated result, L/W = the sq. root of 8We. The edge cross sectional shape is found to oscillate from elliptic to 'cigar' like to 'peanut' like and then back to elliptic in the flow direction. A theoretical one-dimensional model was developed that yielded

only elliptic solutions for the edge cross section. At the points where the elliptic shapes occur, there is agreement between theory and experiment.
Author (revised)

N94-14741*# Remtech, Inc., Huntsville, AL.
LOW ALTITUDE PLUME IMPINGEMENT HANDBOOK
Sheldon D. Smith 9 Aug. 1991 56 p Prepared in cooperation with SECA, Inc., Huntsville, AL
(Contract NAS8-38423; NASA Order 1504; NASA Order 1575; NASA Order 1633; NASA Order 1688; NASA Order 1808; SBIR-02.08-8581A)
(NASA-CR-194193; NAS 1.26:194193; SECA-TR-91-8) Avail: CASI HC A04/MF A01

Plume Impingement modeling is required whenever an object immersed in a rocket exhaust plume must survive or remain undamaged within specified limits, due to thermal and pressure environments induced by the plume. At high altitudes inviscid plume models, Monte Carlo techniques along with the Plume Impingement Program can be used to predict reasonably accurate environments since there are usually no strong flowfield/body interactions or atmospheric effects. However, at low altitudes there is plume-atmospheric mixing and potential large flowfield perturbations due to plume-structure interaction. If the impinged surface is large relative to the flowfield and the flowfield is supersonic, the shock near the surface can stand off the surface several exit radii. This results in an effective total pressure that is higher than that which exists in the free plume at the surface. Additionally, in two phase plumes, there can be strong particle-gas interaction in the flowfield immediately ahead of the surface. To date there have been three levels of sophistication that have been used for low altitude plume induced environment predictions. Level 1 calculations rely on empirical characterizations of the flowfield and relatively simple impingement modeling. An example of this technique is described by Piesik. A Level 2 approach consists of characterizing the viscous plume using the SPF/2 code or RAMP2/LAMP and using the Plume Impingement Program to predict the environments. A Level 3 analysis would consist of using a Navier-Stokes code such as the FDNS code to model the flowfield and structure during a single calculation. To date, Level 1 and Level 2 type analyses have been primarily used to perform environment calculations. The recent advances in CFD modeling and computer resources allow Level 2 type analysis to be used for final design studies. Following some background on low altitude impingement, Level 1, 2, and 3 type analysis will be described. Author (revised)

N94-14745*# Stanford Univ., CA. Center for Turbulence Research.
STUDYING TURBULENCE USING NUMERICAL SIMULATION DATABASES. 4: PROCEEDINGS OF THE 1992 SUMMER PROGRAM
Debra Spinks, comp. Nov. 1992 421 p Program held in Stanford, CA, 13 Jul. - 7 Aug. 1992 Original contains color illustrations
(Contract NCC2-460)
(NASA-CR-194556; NAS 1.26:194556) Avail: CASI HC A18/MF A04; 3 functional color pages

Papers are presented under the following subject areas: small scales; turbulence physics; compressible flow and modeling; and reacting flows and combustion. For individual titles, see N94-14746 through N94-14768.

N94-14746*# Minnesota Univ., Minneapolis. Dept. of Aerospace Engineering and Mechanics.
A SMALL-SCALE TURBULENCE MODEL
T. S. Lundgren *In* Stanford Univ., Studying Turbulence Using Numerical Simulation Databases. 4: Proceedings of the 1992 Summer Program Nov. 1992 p 5-20 (For primary document see N94-14745 02-34)
Avail: CASI HC A03/MF A04; 3 functional color pages

A model for the small-scale structure of turbulence is reformulated in such a way that it may be conveniently computed. The model is an ensemble of randomly oriented structured two dimensional vortices stretched by an axially symmetric strain flow. The energy spectrum of the resulting flow may be expressed as a time integral involving only the enstrophy spectrum of the time evolving two-dimensional cross section flow, which may be obtained numerically. Examples are given in which a k(exp -5/3) spectrum is obtained by this method without using large wave number asymptotic analysis. The k(exp -5/3) inertial range spectrum is shown to be related to the existence of a self-similar enstrophy preserving range in the two-dimensional enstrophy spectrum. The results are insensitive to time dependence of the strain-rate, including even intermittent on-or-off strains. Author (revised)

N94-14747*# National Aeronautics and Space Administration. Ames Research Center, Moffett Field, CA.
THE STRUCTURE OF INTENSE VORTICITY IN HOMOGENEOUS ISOTROPIC TURBULENCE
J. Jimenez (Stanford Univ., CA.), A. A. Wray, P. G. Saffman (California Inst. of Tech., Pasadena.), and R. S. Rogallo *In* Stanford Univ., Studying Turbulence Using Numerical Simulation Databases. 4: Proceedings of the 1992 Summer Program Nov. 1992 p 21-45 (For primary document see N94-14745 02-34)
Avail: CASI HC A03/MF A04; 3 functional color pages

The structure of the intense vorticity regions is studied in numerically simulated homogeneous, isotropic, equilibrium turbulent flow fields at four different Reynolds numbers in the range Re(sub lambda) = 36-171. In accordance with previous investigators, this vorticity is found to be organized in coherent, cylindrical or ribbon-like, vortices ('worms'). A statistical study suggests that they are just especially intense features of the background, O(omega'), vorticity. Their radii scale with the Kolmogorov microscale and their lengths with the integral scale of the flow. An interesting observation is that the Reynolds number based on the circulation of the intense vortices, gamma/nu, increases monotonically with Re(sub lambda), raising the question of the stability of the structures in the limit of Re(sub lambda) approaching infinity. One and two-dimensional statistics of vorticity and strain are presented; they are non-gaussian, and the behavior of their tails depends strongly on the Reynolds number. There is no evidence of convergence to a limiting distribution in our range of Re(sub lambda), even though the energy spectra and the energy dissipation rate show good asymptotic properties in the higher Reynolds number cases. Evidence is presented to show that worms are natural features of the flow and that they do not depend on the particular forcing scheme. Author (revised)

N94-14748*# Johns Hopkins Univ., Baltimore, MD.
ON THE LOCAL NATURE OF THE ENERGY CASCADE
C. Meneveau, T. S. Lund (Stanford Univ., CA.), and J. Chasnov (Stanford Univ., CA.) *In* Stanford Univ., Studying Turbulence Using Numerical Simulation Databases. 4: Proceedings of the 1992 Summer Program Nov. 1992 p 47-59 (For primary document see N94-14745 02-34)
(Contract N00014-92-J-1109; NSF CTS-91-13048)
Avail: CASI HC A03/MF A04; 3 functional color pages

The local nature of the energy cascade in space and time is studied using direct numerical simulation of decaying and forced isotropic turbulence. To examine the concept that large scales evolve into smaller ones, we compute the Lagrangian correlation coefficient between local kinetic energy at different scales. This correlation is found to peak at a Lagrangian time-delay that increases with scale separation. The results show that, on average, the flow of energy to smaller scales is predominantly local in physical space and that the view of eddies decaying into smaller ones while transferring their kinetic energy appears to be, on average, quite realistic. To examine the spectral characteristics of the cascade under unsteady conditions, a pulse of large-scale energy is added to the large-eddy simulation of forced isotropic turbulence. As time progresses, the evolution of this pulse through bands of increasing wavenumbers is studied.
Author (revised)

N94-14749*# Johns Hopkins Univ., Baltimore, MD.
SEARCH FOR SUBGRID SCALE PARAMETERIZATION BY PROJECTION PURSUIT REGRESSION
C. Meneveau, T. S. Lund (Stanford Univ., CA.), and Parviz Moin (Stanford Univ., CA.) *In* Stanford Univ., Studying Turbulence Using Numerical Simulation Databases. 4: Proceedings of the 1992 Summer Program Nov. 1992 p 61-81 (For primary document see N94-14745 02-34)
(Contract N00014-92-J-1109; NSF CTS-91-13048)
Avail: CASI HC A03/MF A04; 3 functional color pages

The dependence of subgrid-scale stresses on variables of the resolved field is studied using direct numerical simulations of isotropic turbulence, homogeneous shear flow, and channel flow. The projection pursuit algorithm, a promising new regression tool for high-dimensional data, is used to systematically search through a large collection of resolved variables, such as components of the strain rate, vorticity, velocity gradients at neighboring grid points, etc. For the case of isotropic turbulence, the search algorithm

recovers the linear dependence on the rate of strain (which is necessary to transfer energy to subgrid scales) but is unable to determine any other more complex relationship. For shear flows, however, new systematic relations beyond eddy viscosity are found. For the homogeneous shear flow, the results suggest that products of the mean rotation rate tensor with both the fluctuating strain rate and fluctuating rotation rate tensors are important quantities in parameterizing the subgrid-scale stresses. A model incorporating these terms is proposed. When evaluated with direct numerical simulation data, this model significantly increases the correlation between the modeled and exact stresses, as compared with the Smagorinsky model. In the case of channel flow, the stresses are found to correlate with products of the fluctuating strain and rotation rate tensors. The mean rates of rotation or strain do not appear to be important in this case, and the model determined for homogeneous shear flow does not perform well when tested with channel flow data. Many questions remain about the physical mechanisms underlying these findings, about possible Reynolds number dependence, and, given the low level of correlations, about their impact on modeling. Nevertheless, demonstration of the existence of causal relations between sgs stresses and large-scale characteristics of turbulent shear flows, in addition to those necessary for energy transfer, provides important insight into the relation between scales in turbulent flows.

Author (revised)

N94-14750*# National Aeronautics and Space Administration. Ames Research Center, Moffett Field, CA.

TRIAD INTERACTIONS IN THE DISSIPATION RANGE

S. Kida (Kyoto Univ., Japan.), Robert H. Kraichnan (Kraichnan, Robert H., Los Alamos, NM.), R. S. Rogallo, F. Waleffe (Stanford Univ., CA.), and Y. Zhou (Stanford Univ., CA.) *In* Stanford Univ., Studying Turbulence Using Numerical Simulation Databases. 4: Proceedings of the 1992 Summer Program Nov. 1992 p 83-99 (For primary document see N94-14745 02-34)

Avail: CASI HC A03/MF A04; 3 functional color pages

Nonlocality of the triad interactions in the dissipation range of developed turbulence is investigated by numerical simulation and the quasi-normal theories. It is found that the energy transfer is dominated by nonlocal triad interactions over the wavenumber range 0.1 is less than k/k(sub d) is less than 4, where k(sub d) is the Kolmogorov wave number. The nonlocality of the interaction has a close relation with the power of an algebraic prefactor of the exponential decay of the energy spectrum in the far-dissipation range. Author (revised)

N94-14751*# Commonwealth Scientific and Industrial Research Organization, Highett (Australia).

A STUDY OF THE FINE SCALE MOTIONS OF INCOMPRESSIBLE TIME-DEVELOPING MIXING LAYERS

J. Soria, M. S. Chong (Melbourne Univ., Parkville, Australia.), R. Sondergaard (Stanford Univ., CA.), A. E. Perry (California Inst. of Tech., Pasadena.), and B. J. Cantwell (Stanford Univ., CA.) *In* Stanford Univ., Studying Turbulence Using Numerical Simulation Databases. 4: Proceedings of the 1992 Summer Program Nov. 1992 p 101-121 (For primary document see N94-14745 02-34)

Avail: CASI HC A03/MF A04; 3 functional color pages

This work is an extension of a project conducted at the previous CTR summer program and was reported by Chen et al. (1990). In that program, the geometry and topology of the dissipating motions in a variety of shear flows was examined. All data was produced by direct numerical simulations (DNS). The partial derivatives of the velocity field were determined at every grid point in the flow and various invariants and related quantities were computed from the velocity gradient tensor. Motions characterized by high rates of kinetic energy dissipation and high enstrophy were of particular interest. Scatter diagrams of the invariants were mapped out and interesting and unexpected patterns were seen. Each type of shear layer produced its own characteristic scatter plot. In the present project, attention is focused on the incompressible plane mixing layer, and the scatter diagrams are replaced with more useful joint probability density contours. Comparison of the topology of the dissipating motions of flows at different Reynolds numbers are made. Also, plane mixing layers at the same Reynolds number but with different initial conditions are compared. Author

N94-14752*# National Aeronautics and Space Administration. Ames Research Center, Moffett Field, CA.

ISOTROPY OF SMALL SCALE TURBULENCE

R. A. Antonia (Newcastle Univ., Australia.) and J. Kim *In* Stanford Univ., Studying Turbulence Using Numerical Simulation Databases. 4: Proceedings of the 1992 Summer Program Nov. 1992 p 123-136 (For primary document see N94-14745 02-34)

Avail: CASI HC A03/MF A04; 3 functional color pages

The degree to which local isotropy is satisfied has been examined using direct numerical simulations for a fully developed channel flow. Attention is mainly given to the high wavenumber part of vorticity and temperature derivative spectra. The ratio of these spectra and their isotropic values depends on the particular quantity considered, the departure from isotropy being more pronounced for the temperature derivative than for the vorticity. When the Kolmogorov-normalized wavenumber is sufficiently large, isotropy is satisfied provided the (Kolmogorov-normalized) mean strain rate is sufficiently small. This result appears to be independent of the quantity considered and of the Reynolds number. Author

N94-14753*# Tel-Aviv Univ. (Israel).

LES VERSUS DNS: A COMPARATIVE STUDY

L. Shtilman and J. R. Chasnov (Stanford Univ., CA.) *In* Stanford Univ., Studying Turbulence Using Numerical Simulation Databases. 4: Proceedings of the 1992 Summer Program Nov. 1992 p 137-143 (For primary document see N94-14745 02-34)

Avail: CASI HC A02/MF A04; 3 functional color pages

We have performed Direct Numerical Simulations (DNS) and Large Eddy Simulations (LES) of forced isotropic turbulence at moderate Reynolds numbers. The subgrid scale model used in the LES is based on an eddy viscosity which adjusts instantaneously the energy spectrum of the LES to that of the DNS. The statistics of the large scales of the DNS (filtered DNS field or fDNS) are compared to that of the LES. We present results for the transfer spectra, the skewness and flatness factors of the velocity components, the PDF's of the angle between the vorticity and the eigenvectors of the rate of strain, and that between the vorticity and the vorticity stretching tensor. The above LES statistics are found to be in good agreement with those measured in the fDNS field. We further observe that in all the numerical measurements, the trend was for the LES field to be more gaussian than the fDNS field. Future research on this point is planned. Author

N94-14754*# Aeronautical Research Labs., Melbourne (Australia). Air Operations Div.

BEHAVIOR OF STREAMWISE RIB VORTICES IN A THREE-DIMENSIONAL MIXING LAYER

J. M. Lopez and C. J. Bulbeck *In* Stanford Univ., Studying Turbulence Using Numerical Simulation Databases. 4: Proceedings of the 1992 Summer Program Nov. 1992 p 147-164 (For primary document see N94-14745 02-34)

Avail: CASI HC A03/MF A04; 3 functional color pages

The structure and behavior of a streamwise rib vortex in a direct numerical simulation of a time-developing three-dimensional incompressible plane mixing layer is examined. Where the rib vortex is being stretched, the vorticity vector is primarily directed in the vortex axial direction and the radial and azimuthal velocity distribution is similar to that of a Burger's vortex. In the region where the vortex stretching is negative, there is a change in the local topology of the vortex. The axial flow is decelerated and a negative azimuthal component of vorticity is induced. These features are characteristic of vortex breakdown. The temporal evolution of the rib vortex is similar to the evolution of an axisymmetric vortex in the early stages of vortex breakdown. The effect of vortex breakdown on other parts of the flow is, however, not as significant as the interaction between the rib vortex and other vortices. Author

N94-14755*# Rome Univ. (Italy).

DIRECT SIMULATION OF POLYMER DRAG REDUCTION IN FREE SHEAR FLOWS AND VORTEX DIPOLES

P. Orlandi, G. M. Homsy (Stanford Univ., CA.), and J. Azaiez (Stanford Univ., CA.) *In* Stanford Univ., Studying Turbulence Using Numerical Simulation Databases. 4: Proceedings of the 1992 Summer Program Nov. 1992 p 165-174 (For primary document see N94-14745 02-34)

Avail: CASI HC A02/MF A04; 3 functional color pages

One of the most efficient techniques for drag reduction is the injection of polymers near a wall which can achieve a reduction in drag up to 80 percent. Several experimental observations tend to indicate that polymers modify the turbulence structures within the buffer layer and show that the changes consist of a weakening of the strength of the streamwise vortices. In this paper, we investigate the effects of viscoelasticity on two different types of flows: the vortex dipole impinging walls to model streamwise vortices in a turbulent boundary layer and the mixing layer that represents free shear flows. For this purpose, we examined three different rheological models: the Oldroyd-B model, the Jeffrey's corotational model, and the FENE-P model. Author

N94-14756*# General Motors Corp., Warren, MI. Research and Environmental Staff.

ESTIMATION OF THE VORTEX LENGTH SCALE AND INTENSITY FROM TWO-DIMENSIONAL SAMPLES

D. L. Reuss and W. P. Cheng *In* Stanford Univ., Studying Turbulence Using Numerical Simulation Databases. 4: Proceedings of the 1992 Summer Program Nov. 1992 p 175-195 Original contains color illustrations (For primary document see N94-14745 02-34)

Avail: CASI HC A03/MF A04; 3 functional color pages

A method is proposed for estimating flow features that influence flame wrinkling in reciprocating internal combustion engines, where traditional statistical measures of turbulence are suspect. Candidate methods were tested in a computed channel flow where traditional turbulence measures are valid and performance can be rationally evaluated. Two concepts are tested. First, spatial filtering is applied to the two-dimensional velocity distribution and found to reveal structures corresponding to the vorticity field. Decreasing the spatial-frequency cutoff of the filter locally changes the character and size of the flow structures that are revealed by the filter. Second, vortex length scale and intensity is estimated by computing the ensemble-average velocity distribution conditionally sampled on the vorticity peaks. The resulting conditionally sampled 'average vortex' has a peak velocity less than half the rms velocity and a size approximately equal to the two-point-correlation integral-length scale. Author

N94-14757*# National Aeronautics and Space Administration. Ames Research Center, Moffett Field, CA.

RAPID DISTORTION ANALYSIS AND DIRECT SIMULATION OF COMPRESSIBLE HOMOGENEOUS TURBULENCE AT FINITE MACH NUMBER

C. Cambon (Ecole Centrale de Lyon, France.), G. N. Coleman (Stanford Univ., CA.), and N. N. Mansour *In* Stanford Univ., Studying Turbulence Using Numerical Simulation Databases. 4: Proceedings of the 1992 Summer Program Nov. 1992 p 199-230 (For primary document see N94-14745 02-34)

Avail: CASI HC A03/MF A04; 3 functional color pages

The effect of rapid mean compression on compressible turbulence at a range of turbulent Mach numbers is investigated. Rapid distortion theory (RDT) and direct numerical simulation results for the case of axial (one-dimensional) compression are used to illustrate the existence of two distinct rapid compression regimes. These regimes are set by the relationships between the timescales of the mean distortion, the turbulence, and the speed of sound. A general RDT formulation is developed and is proposed as a means of improving turbulence models for compressible flows. Author

N94-14758*# Purdue Univ., West Lafayette, IN.

INVESTIGATION OF THE DILATATIONAL DISSIPATION IN COMPRESSIBLE HOMOGENEOUS SHEAR FLOW

G. A. Blaisdell and O. Zeman (Stanford Univ., CA.) *In* Stanford Univ., Studying Turbulence Using Numerical Simulation Databases. 4: Proceedings of the 1992 Summer Program Nov. 1992 p 231-245 (For primary document see N94-14745 02-34)

Avail: CASI HC A03/MF A04; 3 functional color pages

The dilatational dissipation rate within compressible homogeneous turbulent shear flow is studied using data from direct numerical simulations. It is found that the dilatational dissipation rate is mainly associated with large scale acoustic waves. Eddy shocklets are observed; however, they have little contribution to the average dissipation rate. A mechanism for the generation of eddy shocklets is shown to be the focusing of acoustic waves. Turbulence models for the dilatational dissipation rate are compared with data from the simulations. It is found that the formulation of Zeman used by Viegas & Rubesin to calculate a compressible mixing layer agrees well with the numerical simulation results for turbulent Mach numbers less than 0.3. However, it is also found that, for the Mach number range occurring in mixing layers, the model does not accurately represent the theory upon which it is based. Author (revised)

N94-14759*# Institut National des Sciences Appliquees, Routen (France).

RESPONSE OF A SUPERSONIC BOUNDARY LAYER TO A COMPRESSION CORNER

D. Vandromme and O. Zeman (Stanford Univ., CA.) *In* Stanford Univ., Studying Turbulence Using Numerical Simulation Databases. 4: Proceedings of the 1992 Summer Program Nov. 1992 p 247-258 (For primary document see N94-14745 02-34)

Avail: CASI HC A03/MF A04; 3 functional color pages

On the basis of direct numerical simulations of rapidly compressed turbulence, Zeman and Coleman have developed a model to represent rapid directional compression contribution to the pressure dilatation term in the turbulent kinetic energy equation. The model has been implemented in the CFD code for simulation of supersonic compression corner flow with an extended separated region. The computational results have shown a significant improvement with respect to the baseline solution given by the standard k- epsilon turbulence model which does not contain any compressibility corrections. Author (revised)

N94-14760*# California Univ., Irvine.

VORTEX-INDUCED DISTURBANCE FIELD IN A COMPRESSIBLE SHEAR LAYER

D. Papamoschou and S. K. Lele (Stanford Univ., CA.) *In* Stanford Univ., Studying Turbulence Using Numerical Simulation Databases. 4: Proceedings of the 1992 Summer Program Nov. 1992 p 259-276 (For primary document see N94-14745 02-34)

Avail: CASI HC A03/MF A04; 3 functional color pages

The disturbance field induced by a small isolated vortex in a compressible shear layer is studied using direct simulation in a convected frame. The convective Mach number, M(sub c), is varied from 0.1 to 1.25. The vorticity perturbation is rapidly sheared by the mean velocity gradient. The resulting disturbance pressure field is observed to decrease both in magnitude and extent with increasing M(sub c), becoming a narrow transverse zone for M(sub c) greater than 0.8. A similar trend is seen for the perturbation velocity magnitude and for the Reynolds shear stress. By varying the vortex size, we verified that the decrease in perturbation levels is due to the mean-flow Mach number and not the Mach number across the vortex. At high M(sub c), the vortex still communicates with the edges of the shear layer, although communication in the mean-flow direction is strongly inhibited. The growth rate of perturbation kinetic energy declines with M(sub c) primarily due to the reduction in shear stress. For M(sub c) greater than or equal to 0.6, the pressure dilatation also contributes to the decrease of growth rates. Calculation of the perturbation field induced by a vortex doublet revealed the same trends as in the single-vortex case, illustrating the insensitivity of the Mach-number effect to the specific form of initial conditions. Author (revised)

N94-14761*# Cambridge Univ. (England).

EVOLUTION OF THE SHOCK FRONT AND TURBULENCE STRUCTURES IN THE SHOCK/TURBULENCE INTERACTION

N. Kevlahan, K. Mahesh (Stanford Univ., CA.), and S. Lee (Stanford Univ., CA.) *In* Stanford Univ., Studying Turbulence Using Numerical Simulation Databases. 4: Proceedings of the 1992 Summer Program Nov. 1992 p 277-292 (For primary document see N94-14745 02-34)

Avail: CASI HC A03/MF A04; 3 functional color pages

The interaction of a weak shock front with isotropic turbulence has been investigated using Direct Numerical Simulation (DNS). Two problems were considered: the ability of the field equation (the equation for a propagating surface) to model the shock; and a quantitative study of the evolution of turbulence structure using the database generated by Lee et al. Field equation model predictions for front shape have been compared with DNS results; good agreement is found for shock wave interaction with 2D turbulence and for a single steady vorticity wave. In the interaction of 3D isotropic turbulence with a normal shock, strong alignment of vorticity with the intermediate eigenvector of the rate of strain tensor (S(sup *)(sub

ij) = S(sub ij) - (1/3)(delta(sub ij))(S(sub kk))) is seen to develop upstream of the shock and to be further amplified on passage through the shock. Vorticity tends to align at 90 deg to the largest eigenvector, but there is no preferred alignment with the smallest eigenvector. Upstream of the shock, the alignments continue to develop even after the velocity derivative skewness saturates. There is a significant tendency, which increases with time throughout the computational domain, for velocity to align with vorticity. The alignment between velocity and vorticity is strongest in eddy regions and weakest in convergence regions. Author (revised)

N94-14762*# National Aeronautics and Space Administration. Lewis Research Center, Cleveland, OH.

A TRANSPORT EQUATION FOR EDDY VISCOSITY

P. A. Durbin (Stanford Univ., CA.) and Z. Yang *In* Stanford Univ., Studying Turbulence Using Numerical Simulation Databases. 4: Proceedings of the 1992 Summer Program Nov. 1992 p 293-303 (For primary document see N94-14745 02-34)

Avail: CASI HC A03/MF A04; 3 functional color pages

A transport equation for eddy viscosity is proposed for wall bounded turbulent flows. The proposed model reduces to a quasi-homogeneous form far from surfaces. Near to a surface, the nonhomogeneous effect of the wall is modeled by an elliptic relaxation model. All the model terms are expressed in local variables and are coordinate independent; the model is intended to be used in complex flows. Turbulent channel flow and turbulent boundary layer flows with/without pressure gradient are calculated using the present model. Comparisons between model calculations and direct numerical simulation or experimental data show good agreement. Author

N94-14763*# Institut de Mecanique des Fluides de Toulouse (France).

DNS AND MODELING OF THE INTERACTION BETWEEN TURBULENT PREMIXED FLAMES AND WALLS

T. J. Poinsot and D. C. Haworth (General Motors Corp., Warren, MI.) *In* Stanford Univ., Studying Turbulence Using Numerical Simulation Databases. 4: Proceedings of the 1992 Summer Program Nov. 1992 p 307-323 (For primary document see N94-14745 02-34)

Avail: CASI HC A03/MF A04; 3 functional color pages

The interaction between turbulent premixed flames and walls is studied using a two-dimensional full Navier-Stokes solver with simple chemistry. The effects of wall distance on the local and global flame structure are investigated. Quenching distances and maximum wall heat fluxes during quenching are computed in laminar cases and are found to be comparable to experimental and analytical results. For turbulent cases, it is shown that quenching distances and maximum heat fluxes remain of the same order as for laminar flames. Based on simulation results, a 'law-of-the-wall' model is derived to describe the interaction between a turbulent premixed flame and a wall. This model is constructed to provide reasonable behavior of flame surface density near a wall under the assumption that flame-wall interaction takes place at scales smaller than the computational mesh. It can be implemented in conjunction with any of several recent flamelet models based on a modeled surface density equation, with no additional constraints on mesh size or time step. Author

N94-14764*# Stanford Univ., CA. Center for Turbulence Research.

THE EVOLUTION EQUATION FOR THE FLAME SURFACE DENSITY IN TURBULENT PREMIXED COMBUSTION **c25**

A. Trouve and T. Poinsot (Institut de Mecanique des Fluides de Toulouse, France.) *In its* Studying Turbulence Using Numerical Simulation Databases. 4: Proceedings of the 1992 Summer Program Nov. 1992 p 325-343 (For primary document see N94-14745 02-34)

Avail: CASI HC A03/MF A04; 3 functional color pages

One central ingredient in flamelet models for turbulent premixed combustion is the flame surface density. This quantity conveys most of the effects of the turbulence on the rate of energy release and is obtained via a modeled transport equation, called the Sigma-equation. Past theoretical work has produced a rigorous approach that leads to an exact, but unclosed, formulation for the turbulent Sigma-equation. In this exact Sigma-equation, it appears that the dynamical properties of the flame surface density are determined by a single parameter, namely the turbulent flame stretch. Unfortunately, the flame surface density and the turbulent flame stretch are not available from experiments and, in the absence of experimental data, little is known on the validity of the closure assumptions used in current flamelet models. Direct Numerical Simulation (DNS) is the obvious, complementary approach to get basic information on these fundamental quantities. Three-dimensional DNS of premixed flames in isotropic turbulent flow is used to estimate the different terms appearing in the Sigma-equation. A new methodology is proposed to provide the source and sink terms for the flame surface density, resolved both temporally and spatially throughout the turbulent flame brush. Using this methodology, the effects of the Lewis number on the rate of production of flame surface area are described in great detail and meaningful comparisons with flamelet models can be performed. The analysis reveals in particular the tendency of the models to overpredict flame surface dissipation as well as their inability to reproduce variations due to thermo-diffusive phenomena. Thanks to the detailed information produced by a DNS-based analysis, this type of comparison not only underscores the shortcomings of current models but also suggests ways to improve them. Author (revised)

N94-14765*# Ecole Centrale de Lyon (France).

NUMERICAL SIMULATIONS OF TURBULENT PREMIXED H2/O2/N2 FLAMES WITH COMPLEX CHEMISTRY **c25**

M. Baum, T. J. Poinsot (Institut de Mecanique des Fluides de Toulouse, France.), and D. C. Haworth (General Motors Corp., Warren, MI.) *In* Stanford Univ., Studying Turbulence Using Numerical Simulation Databases. 4: Proceedings of the 1992 Summer Program Nov. 1992 p 345-366 Original contains color illustrations (For primary document see N94-14745 02-34)

Avail: CASI HC A03/MF A04; 3 functional color pages

Premixed stoichiometric H2/O2/N2 flames propagating in two-dimensional turbulence were studied using direct numerical simulation (simulations in which all fluid and thermochemical scales are fully resolved) including realistic chemical kinetics and molecular transport. Results are compared with earlier zero-chemistry (flame sheet) and one-step chemistry simulations. Consistent with the simpler models, the turbulent flame with realistic chemistry aligns preferentially with extensive strain rates in the tangent plane and flame curvature probability density functions are close to symmetric with near-zero means. By contrast to simple-chemistry results with non-unity Lewis numbers (ratio of thermal to species diffusivity), local flame structure does not correlate with curvature but rather with tangential strain rate. Turbulent straining results in substantial thinning of the flame relative to the steady unstrained laminar case. Heat release and H2O2 contours remain thin and connected ('flamelet-like') while species including H-atom and OH are more diffuse. Peak OH concentration occurs well behind the peak heat-release zone. The feasibility of incorporating realistic chemistry into full turbulence simulations to address issues such as pollutant formation in hydrocarbon-air flames is suggested. Author (revised)

N94-14766*# Sandia National Labs., Albuquerque, NM. Combustion Research Facility.

EFFECT OF FINITE-RATE CHEMISTRY AND UNEQUAL SCHMIDT NUMBERS ON TURBULENT NON-PREMIXED FLAMES MODELED WITH SINGLE-STEP CHEMISTRY **c25**

J. H. Chen, S. Mahalingam (Colorado Univ., Boulder.), I. K. Puri (Illinois Univ., Chicago.), and L. Vervisch (Stanford Univ., CA.) *In* Stanford Univ., Studying Turbulence Using Numerical Simulation Databases. 4: Proceedings of the 1992 Summer Program Nov. 1992 p 367-387 Sponsored in part by DOE (For primary document see N94-14745 02-34)

Avail: CASI HC A03/MF A04; 3 functional color pages

The interaction between a quasi-laminar flame and a turbulent flowfield is investigated through direct numerical simulations (DNS) of reacting flow in two- and three-dimensional domains. Effects due to finite-rate chemistry are studied using a single step global reaction A (fuel) + B (oxidizer) yields P (product), and by varying a global Damkoehler number, as a result of which the turbulence-chemistry interaction in the flame is found to generate a wide variety of conditions, ranging from near-equilibrium to near-extinction. Differential diffusion effects are studied by changing the Schmidt number of one reactive species to one-half. It is observed that laminar flamelet response is followed within the turbulent flowfield, except in regions where transient effects seem to dominate. Author (revised)

N94-14767*# Sandia National Labs., Albuquerque, NM. Combustion Research Facility.

STRUCTURE OF TURBULENT NON-PREMIXED FLAMES MODELED WITH TWO-STEP CHEMISTRY **c25**

J. H. Chen, S. Mahalingam (Colorado Univ., Boulder.), I. K. Puri (Illinois Univ., Chicago.), and L. Vervisch (Stanford Univ., CA.) *In* Stanford Univ., Studying Turbulence Using Numerical Simulation Databases. 4: Proceedings of the 1992 Summer Program Nov. 1992 p 389-402 Sponsored in part by DOE (For primary document see N94-14745 02-34)
Avail: CASI HC A03/MF A04; 3 functional color pages

Direct numerical simulations of turbulent diffusion flames modeled with finite-rate, two-step chemistry, A + B yields I, A + I yields P, were carried out. A detailed analysis of the turbulent flame structure reveals the complex nature of the penetration of various reactive species across two reaction zones in mixture fraction space. Due to this two zone structure, these flames were found to be robust, resisting extinction over the parameter ranges investigated. As in single-step computations, mixture fraction dissipation rate and the mixture fraction were found to be statistically correlated. Simulations involving unequal molecular diffusivities suggest that the small scale mixing process and, hence, the turbulent flame structure is sensitive to the Schmidt number. Author (revised)

N94-14768*# National Aeronautics and Space Administration. Ames Research Center, Moffett Field, CA.
STOCHASTIC MODELING OF TURBULENT REACTING FLOWS
R. O. Fox (Kansas State Univ., Manhattan.), J. C. Hill (Iowa State Univ. of Science and Technology, Ames.), F. Gao (Stanford Univ., CA.), R. D. Moser, and M. M. Rogers *In* Stanford Univ., Studying Turbulence Using Numerical Simulation Databases. 4: Proceedings of the 1992 Summer Program Nov. 1992 p 403-424 (For primary document see N94-14745 02-34)
(Grant NSF CTS-91-58124)
Avail: CASI HC A03/MF A04; 3 functional color pages

Direct numerical simulations of a single-step irreversible chemical reaction with non-premixed reactants in forced isotropic turbulence at R(sub lambda) = 63, Da = 4.0, and Sc = 0.7 were made using 128 Fourier modes to obtain joint probability density functions (pdfs) and other statistical information to parameterize and test a Fokker-Planck turbulent mixing model. Preliminary results indicate that the modeled gradient stretching term for an inert scalar is independent of the initial conditions of the scalar field. The conditional pdf of scalar gradient magnitudes is found to be a function of the scalar until the reaction is largely completed. Alignment of concentration gradients with local strain rate and other features of the flow were also investigated. Author (revised)

N94-14816# Technische Univ., Berlin (Germany). Fachbereich Mathematik.
CONTRIBUTIONS TO NUMERICAL SOLUTION OF NAVIER-STOKES EQUATIONS IN TWO AND THREE DIMENSIONAL FLOWS Ph.D. Thesis [BEITRAEGE ZUR NUMERISCHEN LOESUNG DER NAVIER-STOKES-GLEICHUNGEN IN ZWEI UND DREI RAUMDIMENSIONEN]
Lutz Welchlin 1992 165 p In GERMAN
(ETN-93-94395) Avail: CASI HC A08/MF A02

A method for solving Navier-Stokes continuity and energy equations with reduced computation time and memory allocation is presented. A three dimensional stream function formulation with four partial differential equations was given and reduced to a two dimensional form. Two particular cases were considered such as Benard problem and low Prandtl fluids. The Newton chord process was used for numerical solution of the two dimensional formulation. A partial linear differential equation system as a block three diagonal system and an eigenvalue problem in a Banach space were obtained. A local and global continuity method was used for discretization. Results obtained for free and Marangoni convection are presented, which show the importance of boundary condition choice.
ESA

N94-14849*# Institute for Computer Applications in Science and Engineering, Hampton, VA.
ANALYTICAL DESCRIPTION OF THE BREAKUP OF LIQUID JETS IN AIR Final Report
Demetrios T. Papageorgiou (New Jersey Inst. of Tech., Newark.) Jul. 1993 30 p Submitted for publication
(Contract NAS1-19480; RTOP 505-90-52-01)
(NASA-CR-191503; NAS 1.26:191503; ICASE-93-45) Avail: CASI HC A03/MF A01

A viscous or inviscid cylindrical jet with surface tension in a vacuum tends to pinch due to the mechanism of capillary instability. Similarity solutions are constructed which describe this phenomenon as a critical time is encountered, for two physically distinct cases: inviscid jets governed by the Euler equations and highly viscous jets governed by the Stokes equations. In both cases the only assumption imposed is that at the time of pinching the jet shape has a radial length scale which is smaller than the axial length scale. For the inviscid case, we show that our solution corresponds exactly to one member of the one-parameter family of solutions obtained from slender jet theories and the shape of the jet is locally concave at breakup. For highly viscous jets our theory predicts local shapes which are monotonic increasing or decreasing indicating the formation of a mother drop connected to the jet by a thin fluid tube. This qualitative behavior is in complete agreement with both direct numerical simulations and experimental observations. Author (revised)

N94-14895# Lawrence Livermore National Lab., CA.
TOWARD A QUASI-LINEAR CLOSURE FOR COMPRESSIBLE TURBULENCE
J. A. H. Futterman and W. P. Dannevik Mar. 1993 23 p Presented at the 4th International Workshop on the Physics of Compressible Turbulent Mixing, Cambridge, England, 29 Mar. - 1 Apr. 1993
(Contract W-7405-eng-48)
(DE93-017185; UCRL-JC-112562; CONF-9303126-6) Avail: CASI HC A03/MF A01

The authors are developing a quasilinear closure model for compressible turbulence based on a transformation of the averaged Navier-Stokes equations into a form that is at most quadratically nonlinear in the mean and fluctuating variables. Following the transformation, they discard third-order cumulants, in hope of arriving at a one-point closure model without adjustable parameters which will be applicable to systems undergoing rapid deformation, such as imploding Inertial Confinement Fusion capsules. This paper reports current progress. DOE

N94-14906*# Scientific Research Associates, Inc., Glastonbury, CT.
SIMULATION OF PREBURNER SPRAYS, VOLUME 1 Final Report
May 1993 5 p Prepared in cooperation with Imperial Coll. of Science and Technology, London, England
(Contract NAS8-38872)
(NASA-CR-193844; NAS 1.26:193844; SRA-R93-9083-F-Vol-1) Avail: CASI HC A01/MF A01

Under the present contract a study was made on the characteristics of the sprays of coaxial injectors with particular emphasis on those aspects relevant to the performance of rocket engines. The technical effort was performed primarily by Imperial College of Science and Technology and the details of this effort are contained in the accompanying technical report by Hardalupas and Whitelaw, which forms Vol. 2 of the report. The role of Scientific Research Associates was review of material, initial direction of the technical effort and review of all reports. The study considered characteristics of sprays under a variety of conditions. Control of these sprays is important as the spray details can control both rocket combustion stability and efficiency. Imperial College considered the following: first, measurement of the size and rate of spread of the sprays produced by single coaxial airblast nozzles with axial gaseous stream. The local size, velocity and flux characteristics for a wide range of gas and liquid flowrates were measured and the results were correlated with the conditions of the spray at the nozzle exit. Second, examination of the effect of the geometry of single coaxial airblast atomizers on spray characteristics. The gas and liquid tube diameters were varied over a range of values, the liquid tube recess was varied and the shape of the exit of the gaseous jet was varied from straight to converging. Third, quantification of the effect of swirl in the gaseous stream on the spray characteristics produced by single coaxial airblast nozzles. Fourth, quantification of the effect of reatomization by impingement of the spray on a flat disc positioned around 200 mm from the nozzle exit. This models spray impingement on the turbopump dome during the startup process of the preburner of the Space Shuttle Main Engine (SSME). Fifth, study of the interaction between multiple sprays without and with swirl in their gaseous stream. The spray characteristics of single nozzles were compared with that of three identical nozzles with their axis at a small distance from each other. This study simulates the sprays in the preburner of the SSME, where there are around 260 elements on the faceplate of the combustion chamber. And lastly, design an

experimental facility to study the characteristics of sprays at high pressure conditions and at supercritical pressure and temperature for the gas but supercritical pressure and subcritical temperature for the liquid.
Author (revised)

N94-14171# Calspan Corp., Arnold AFS, TN.
BOUNDARY-LAYER TRANSITION
R. K. Matthews *In* VKI, Methodology of Hypersonic Testing 1993 9 p Prepared in cooperation with Arnold Engineering Development Center, Arnold AFS, TN (For primary document see N94-14153 02-02)
Copyright Avail: CASI HC A02/MF A03

N94-14172# Sverdrup Technology, Inc., Arnold AFS, TN.
SHOCK/BOUNDARY-LAYER/SHOCK INTERACTIONS
Virgil K. Smith, III *In* VKI, Methodology of Hypersonic Testing 1993 10 p Prepared in cooperation with Arnold Engineering Development Center, Arnold AFS, TN (For primary document see N94-14153 02-02)
Copyright Avail: CASI HC A02/MF A03

35 INSTRUMENTATION AND PHOTOGRAPHY

Includes remote sensors; measuring instruments and gages; detectors; cameras and photographic supplies; and holography.

For aerial photography see *43 Earth Resources and Remote Sensing*. For related information see also *06 Aircraft Instrumentation*, and *19 Spacecraft Instrumentation*.

N94-12874*# National Aeronautics and Space Administration. Lewis Research Center, Cleveland, OH.
STRAIN SENSING TECHNOLOGY FOR HIGH TEMPERATURE APPLICATIONS
W. Dan Williams Washington Aug. 1993 11 p Presented at the AIAA 4th International Aerospace Planes Conference, Orlando, FL, 1-4 Dec. 1992
(RTOP 505-62-50)
(NASA-TM-4498; E-7650; NAS 1.26:4498) Avail: CASI HC A03/MF A01

This review discusses the status of strain sensing technology for high temperature applications. Technologies covered are those supported by NASA such as required for applications in hypersonic vehicles and engines, advanced subsonic engines, as well as material and structure development. The applications may be at temperatures of 540 C (1000 F) to temperatures in excess of 1400 C (2500 F). The most promising technologies at present are the resistance strain gage and remote sensing schemes. Resistance strain gages discussed include the BCL gage, the LaRC compensated gage, and the PdCr gage. Remote sensing schemes such as laser based speckle strain measurement, phase-shifting interferometry, and x-ray extensometry are discussed. Present status and limitations of these technologies are presented. Author (revised)

N94-13044# Sandia National Labs., Albuquerque, NM.
HIGH SPATIAL RESOLUTION X RAY MICROANALYSIS: COMPARISON OF EXPERIMENT AND INCOHERENT SCATTERING CALCULATIONS
J. R. Michael and A. D. Romig, Jr. 1993 2 p Presented at the Annual Meeting of the Electron Microscopy Society of America, Cincinnati, OH, 1-6 Aug. 1993
(Contract DE-AC04-76DP-00789)
(DE93-011685; SAND-93-0812C; CONF-930822-1) Avail: CASI HC A01/MF A01

The capability of the incoherent scattering model (Monte Carlo simulations) to describe recent experimental measurements from embedded particles is demonstrated. DOE

N94-13135*# National Aeronautics and Space Administration. Lewis Research Center, Cleveland, OH.
A SURVEY AND ANALYSIS OF EXPERIMENTAL HYDROGEN SENSORS
Gary W. Hunter Oct. 1992 16 p
(RTOP 590-21-11)
(NASA-TM-106300; E-8040; NAS 1.15:106300) Avail: CASI HC A03/MF A01

In order to ascertain the applicability of hydrogen sensors to aerospace applications, a survey was conducted of promising experimental point-contact hydrogen sensors and their operation was analyzed. The techniques discussed are metal-oxide-semiconductor or MOS based sensors, catalytic resistor sensors, acoustic wave detectors, and pyroelectric detectors. All of these sensors depend on the interaction of hydrogen with Pd or a Pd-alloy. It is concluded that no single technique will meet the needs of aerospace applications but a combination of approaches is necessary. The most promising combination is an MOS based sensor with a catalytic resistor.
Author (revised)

N94-13176*# Daedalus Enterprises, Inc., Ann Arbor, MI.
DEVELOPMENT OF A PORTABLE MULTISPECTRAL THERMAL INFRARED CAMERA Final Report
Frederick G. Osterwisch 30 May 1991 24 p
(Contract NAS7-1063; SBIR-08.06-5649)
(NASA-CR-191340; NAS 1.26:191340) Avail: CASI HC A03/MF A01

The purpose of this research and development effort was to design and build a prototype instrument designated the 'Thermal Infrared Multispectral Camera' (TIRC). The Phase 2 effort was a continuation of the Phase 1 feasibility study and preliminary design for such an instrument. The completed instrument designated AA465 has application in the field of geologic remote sensing and exploration. The AA465 Thermal Infrared Camera (TIRC) System is a field-portable multispectral thermal infrared camera operating over the 8.0 - 13.0 micron wavelength range. Its primary function is to acquire two-dimensional thermal infrared images of user-selected scenes. Thermal infrared energy emitted by the scene is collected, dispersed into ten 0.5 micron wide channels, and then measured and recorded by the AA465 System. This multispectral information is presented in real time on a color display to be used by the operator to identify spectral and spatial variations in the scenes emissivity and/or irradiance. This fundamental instrument capability has a wide variety of commercial and research applications. While ideally suited for two-man operation in the field, the AA465 System can be transported and operated effectively by a single user. Functionally, the instrument operates as if it were a single exposure camera. System measurement sensitivity requirements dictate relatively long (several minutes) instrument exposure times. As such, the instrument is not suited for recording time-variant information. The AA465 was fabricated, assembled, tested, and documented during this Phase 2 work period. The detailed design and fabrication of the instrument was performed during the period of June 1989 to July 1990. The software development effort and instrument integration/test extended from July 1990 to February 1991. Software development included an operator interface/menu structure, instrument internal control functions, DSP image processing code, and a display algorithm coding program. The instrument was delivered to NASA in March 1991. Potential commercial and research uses for this instrument are in its primary application as a field geologists exploration tool. Other applications have been suggested but not investigated in depth. These are measurements of process control in commercial materials processing and quality control functions which require information on surface heterogeneity. Derived from text

N94-13326*# Alabama Univ., Huntsville. Center for Microgravity and Materials Research.
TEMPERATURE DEPENDENCE OF DIFFUSIVITIES, PRELIMINARY DEFINITION PHASE Final Report, 3 Feb. - 31 Jul. 1993
Franz Rosenberger, R. Michael Banish, and Arunan Nadarajah 1993 9 p
(Contract NAS8-39716)
(NASA-CR-192613; NAS 1.26:192613) Avail: CASI HC A02/MF A01

During the six months definition phase of the instrument development program, research personnel at the Center for Microgravity and Materials Research of the University of Alabama in Huntsville (UAH) were to furnish all of the necessary labor, services, materials, and facilities necessary to provide science requirement definition, initiate hardware development activities, requirements and timetable for integration and experimental accommodation of the GAS payload into the Shuttle cargo bay and an updated ground-based research flight program proposal consistent with the NRA selection letter. These activities were to be accomplished in parallel and consistent with the necessary research and development work toward the accomplishment of the overall objectives of the selected proposal.
Author (revised)

N94-13343# National Aerospace Lab., Tokyo (Japan). Control Systems Div.

CALCULATION OF THE REQUIRED SENSOR ACCURACY TO OBTAIN A SPECIFIED STATE ESTIMATION ACCURACY [SHITEISARETA JOUTAI SUITEI SEIDO JITSUGEN NO TAMENO SENSA YOUKYUU SEIDO NO DOUSHUTSU]

Shuuichi Sasa and Masahiko Nagayasu Jul. 1992 8 p In JAPANESE
(NAL-TR-1173; JTN-93-80490) Avail: CASI HC A02/MF A01

For the design of sensor systems for flight test data acquisition, the determination of necessary accuracy of the sensors is important. In this report, one method is presented to calculate the sensor accuracy to obtain a specified state estimation accuracy by a Kalman filter. This is an inverse problem of a state estimation problem in which observation sensor or input sensor accuracy is obtained by an optimization method. The Gauss-Newton method is applied in the iterative optimization calculation, and the basic performance is presented by numerical example using 3rd order linear system model. Author (NASDA)

N94-13366# Instituto de Pesquisas Espaciais, Sao Jose dos Campos (Brazil).

ATTITUDE DETERMINATION OF STRATOSPHERIC BALLOONS USING KALMAN FILTERS M.S. Thesis [DETERMINACAO DE ATITUDE DE BALOES ESTRATOSFERICOS UTILIZANDO FILTROS DE KALMAN]

Luiz deSiqueiraMartinsFilho Dec. 1992 120 p In PORTUGESE
(INPE-5498-TDI/513) Avail: CASI HC A06/MF A02

The application of state estimation, via extended Kalman filter, in attitude determination of a balloon borne telescope was studied. This astrophysical experiment - the MASCO project requires a pointing accuracy with maximum error of 20 arcmin in the stabilization phase. The attitude determination uses three gyroscope axis, a two axis sun sensor and a three axis magnetometer. The cinematic model of the gyroscope substitutes the telescope motion dynamic model in the Kalman filter and the attitude description is performed using quaternions. A second configuration of estimation uses constant Kalman gain for calculus simplification and processing time reduction. The two configurations are analyzed and compared through digital computer simulations. Author (revised)

N94-13395# Sandia National Labs., Albuquerque, NM.

ISOLATION OF A PIEZORESISTIVE ACCELEROMETER USED IN HIGH ACCELERATION TESTS

V. I. Bateman, F. A. Brown, and N. T. Davie 1992 20 p Presented at the 17th Transducer Workshop, San Diego, CA, 22-24 Jun. 1993
(Contract DE-AC04-76DP-00789)
(DE93-013764; SAND-92-2712C; CONF-9306170-1) Avail: CASI HC A03/MF A01

Both uniaxial and triaxial shock isolation techniques for a piezoresistive accelerometer have been developed for pyroshock and impact tests. The uniaxial shock isolation technique has demonstrated acceptable characteristics for a temperature range of -50 to +186 F and a frequency bandwidth of DC to 10 kHz. The triaxial shock isolation technique has demonstrated acceptable results for a temperature range of -50 to 70 F and a frequency bandwidth of DC to 10 kHz. These temperature ranges, that are beyond the accelerometer manufacturer's operational limits of -30 and +150 F, required the calibration of accelerometers at high shock levels and at the temperature extremes of -50 and +160 F. The purposes of these calibrations were to insure that the accelerometers operated at the field test temperatures and to provide an accelerometer sensitivity at each test temperature. Since there is no NIST-traceable (National Institute of Standards and Technology traceable) calibration capability at shock levels of 5,000 - 15,000 g for the temperature extremes of -50 and +160 F, a method for calibrating and certifying the Hopkinson bar with a transfer standard was developed. Time domain and frequency domain results are given that characterize the Hopkinson bar. The NIST-traceable accuracy for the standard accelerometer in shock is +-5%. The Hopkinson bar has been certified by the Sandia Secondary Standards Division with an uncertainty of 6%. DOE

N94-13410# Varian Associates, Palo Alto, CA.

LONG-PULSE OPERATION OF A GYROTRON WITH BEAM/RF SEPARATION

K. Felch, T. S. Chu, J. Feinstein, H. Huey, H. Jory, J. Neilson, and R. Schumacher Sep. 1992 3 p Prepared for Lawrence Livermore National Lab., CA
(Contract W-7405-eng-48)
(DE93-015007; UCRL-CR-111879) Avail: CASI HC A01/MF A01

Varian is carrying out the development of high-power, cw gyrotrons at frequencies ranging from 85-140 GHz. An experimental tube employing a TE(sub 22,2,1)-mode cavity and utilizing an output coupling concept where the collection of the spent electron beam is separated from the outgoing microwave power has been designed and constructed. In initial tests on the tube, output powers of 450-500 kW have been obtained for pulse durations out to 2.5 seconds, in the desired TE(sub 22,2,1) mode at a frequency of 110 GHz. Electron cyclotron resonance heating (ECRH) requirements for planned magnetic fusion experiments such as the International Thermonuclear Experimental Reactor (ITER) will require millimeter-wave sources capable of output powers of at least 1 MW cw at frequencies in the range, 100-200 GHz. Initial megawatt-level development work at Varian resulted in a gyrotron design that was tested to output powers of 1 MW for short pulses (approximately 1 ms) and 400 kW for 0.5-s pulses at a frequency of 140 GHz. Output powers up to 1 MW have been achieved for short pulses (1 ms). Future tests on this and subsequent experimental tubes will be aimed at achieving 1 MW power levels under long-pulse and ultimately, cw conditions. DOE

N94-13456# National Aerospace Lab., Tokyo (Japan). Control Systems Div.

KALMAN FILTER INPUT ESTIMATION [KARUMAN FIRUTA NIYORU NYUURYOKU SUITEI]

Shuuichi Sasa and Masahiko Nagayasu Nov. 1992 7 p In JAPANESE
(NAL-TR-1182; JTN-93-80504) Avail: CASI HC A02/MF A01

As system output includes information concerning system input, it seems possible that system output can be used to estimate noisy system input. For Single Input Single Output (SISO) systems, the problem of input estimation using a Kalman filter is examined. Since the problem is different from an ordinary Kalman filter problem, it is first modified to an ordinary Kalman filter problem, and the input estimation accuracy is then calculated from the measurement accuracy through the Riccati equation. The input accuracy for an integrator system is analyzed, and a sinusoidal input is estimated using the simulated output of an integrator system.
Author (NASDA)

N94-13464*# Cornell Univ., Ithaca, NY.

ROVER IMAGING SYSTEM FOR THE MARS ROVER/SAMPLE RETURN MISSION Final Report

28 Feb. 1993 4 p Sponsored by Langley Research Center
(NASA-CR-193413; NAS 1.26:193413) Avail: CASI HC A01/MF A01

In the past year, the conceptual design of a panoramic imager for the Mars Environmental Survey (MESUR) Pathfinder was finished. A prototype camera was built and its performace in the laboratory was tested. The performance of this camera was excellent. Based on this work, we have recently proposed a small, lightweight, rugged, and highly capable Mars Surface Imager (MSI) instrument for the MESUR Pathfinder mission. A key aspect of our approach to optimization of the MSI design is that we treat image gathering, coding, and restoration as a whole, rather than as separate and independent tasks. Our approach leads to higher image quality, especially in the representation of fine detail with good contrast and clarity, without increasing either the complexity of the camera or the amount of data transmission. We have made significant progress over the past year in both the overall MSI system design and in the detailed design of the MSI optics. We have taken a simple panoramic camera and have upgraded it substantially to become a prototype of the MSI flight instrument. The most recent version of the camera utilizes miniature wide-angle optics that image directly onto a 3-color, 2096-element CCD line array. There are several data-taking modes, providing resolution as high as 0.3 mrad/pixel. Analysis tasks that were performed or that are underway with the test data from the prototype camera include the following: construction of 3-D models of imaged scenes from stereo data, first for controlled scenes and later for field scenes; and checks on geometric fidelity, including alignment errors, mast vibration, and oscillation in the drive system. We have outlined a number of tasks planned for Fiscal Year '93 in order to prepare us for submission of a flight instrument proposal for MESUR Pathfinder.
Author (revised)

N94-13527# National Aerospace Lab., Amsterdam (Netherlands). Flight Div.

PHOTOGRAMMETRIC METHODS FOR TRAJECTORY MEASUREMENTS

A. J. L. Willekens 15 Apr. 1991 33 p Presented at the SFTE 4th European Mini Symposium, Rome, Italy, 1991

(NLR-TP-91166-U; ETN-93-94336) Avail: CASI HC A03/MF A01

A photogrammetric method for trajectory measurements in flight testing at short range is discussed. A theoretical overview of the method used is given, this being a combination of a camera and equipment on board of the aircraft like Global Positioning System (GPS) or inertial navigation system and a baro-altimeter. On the ground a minimum of equipment is required: only surveyed ground control points are needed. The accuracy further depends strongly on the method used, so different methods are discussed. Operational aspects also are important for the selected method. The resulting method is relatively simple, quite accurate, and can be used under many different conditions. The practical aspects are discussed in chronological order. This illustrates how the method evolved from a simple camera and equally simple calculations to the equipment nowadays. The manual work involved decreased with each amelioration. Some operational aspects of the new system are discussed. Based on today's system, some remarks of future evolutions can be made. Here is the question whether and where can the Charge Coupled Device (CCD) (video) camera replace the film used today. This question has more than only technical relevance: operational issues are equally important. ESA

N94-13665# Norwegian Defence Research Establishment, Kjeller.

SUPPRESSION OF BRIGHT OBJECTS USING A SPATIAL LIGHT MODULATOR WHEN IMAGING WITH CCD- AND IMAGE INTENSIFIED CAMERAS [UNDERTRYCKING AV OBJEKTER MED HOEY LUMINANS VED HJELP AV EN ROMLIG LYSMODULATION UNDER AVBILDNING MED CCD- OG LYSFORSTERKNINGSKAMERA]

Torbjoern Groeder 28 Jan. 1993 143 p In NORWEGIAN Original contains color illustrations

(FFI-93/7008; ETN-93-94455) Avail: CASI HC A07/MF A02

The operation of CCD (Charge Coupled Devices) and intensified cameras is described with emphasis on the problems caused by local overexposure of the image sensor. In trying to reduce the amount of blooming in the image, a transmissive graphic Liquid Crystal Display (LCD) operating as a spatial light modulator was placed in front of the cameras, and the transmission of the display elements was dynamically controlled in real time from a Personal Computer (PC). By activating the LCD elements in front of strongly illuminated areas of the image sensor, improvement of the image quality was demonstrated. Various types of LCDs were studied in trying to learn which ones would be best suited for this particular application, and this work may suggest a new application area for LCD's. ESA

N94-13814*# Eloret Corp., Sunnyvale, CA.

IMAGES CONSTRUCTED FROM COMPUTED FLOW FIELDS

Leslie A. Yates [1992] 17 p

(Contract NCC2-583)

(NASA-CR-194397; NAS 1.26:194397) Avail: CASI HC A03/MF A01

A method for constructing interferograms, schlieren, and shadowgraphs from ideal- and real-gas, two- and three-dimensional computed flow fields is described. The computational grids can be structured or unstructured, and multiple grids are an option. The constructed images are compared to experimental images for several types of flow, including a ramp, a blunt-body, a nozzle, and a reacting flow. The constructed images simulate the features observed in the experimental images. They are sensitive to errors in the flow-field solutions and can be used to identify solution errors. In addition, techniques for obtaining phase shifts from experimental finite-fringe interferograms and for removing experimentally induced phase-shift errors are discussed. Both the constructed images and calculated phase shifts can be used for validation of computational fluid dynamics (CFD) codes. Author

N94-13815*# Eloret Corp., Sunnyvale, CA.

DEVELOPMENT OF AN AUTOMATED FILM-READING SYSTEM FOR BALLISTIC RANGES

Leslie A. Yates [1992] 13 p

(Contract NCC2-583)

(NASA-CR-194398; NAS 1.26:194398) Avail: CASI HC A03/MF A01

Software for an automated film-reading system that uses personal computers and digitized shadowgraphs is described. The software identifies pixels associated with fiducial-line and model images, and least-squares procedures are used to calculate the positions and orientations of the images. Automated position and orientation readings for sphere and cone models are compared to those obtained using a manual film reader. When facility calibration errors are removed from these readings, the accuracy of the automated readings is better than the pixel resolution, and it is equal to, or better than, the manual readings. The effects of film-reading and facility-calibration errors on calculated aerodynamic coefficients is discussed. Author

N94-13876*# National Aeronautics and Space Administration. Lewis Research Center, Cleveland, OH.

TOMOGRAPHIC METHODS IN FLOW DIAGNOSTICS

Arthur J. Decker Sep. 1993 19 p Presented at the Summer School on Optical Diagnostics for Flow Processes, Roskilde, Denmark, 26 Sep. - 2 Oct. 1993; cosponsored by Danish Research Academy and The European Community Programme on Human Capital and Mobility

(RTOP 505-62-50)

(NASA-TM-106330; E-8091; NAS 1.15:106330) Avail: CASI HC A03/MF A01

This report presents a viewpoint of tomography that should be well adapted to currently available optical measurement technology as well as the needs of computational and experimental fluid dynamists. The goals in mind are to record data with the fastest optical array sensors; process the data with the fastest parallel processing technology available for small computers; and generate results for both experimental and theoretical data. An in-depth example treats interferometric data as it might be recorded in an aeronautics test facility, but the results are applicable whenever fluid properties are to be measured or applied from projections of those properties. The paper discusses both computed and neural net calibration tomography. The report also contains an overview of key definitions and computational methods, key references, computational problems such as ill-posedness, artifacts, missing data, and some possible and current research topics. Author (revised)

N94-14009# Office National d'Etudes et de Recherches Aerospatiales, Paris (France).

HIGH FRAME RATE THERMAL IMAGER FOR HYPERSONIC WIND TUNNEL APPLICATIONS Ph.D. Thesis - Paris-Sud Univ. [CAMERA INFRAROUGE A FREQUENCE IMAGE ELEVEE POUR APPLICATIONS EN SOUFFLERIE HYPERSONIQUE]

Stephane Barbe Nov. 1992 185 p In FRENCH Original contains color illustrations

(ONERA-NT-1992-12; ETN-93-93971) Avail: CASI HC A09/MF A02

Infrared thermography is used to derive heat transfer coefficients from thermal mappings of wind tunnel models. Due to the short duration of the runs in hypersonic F4 facilities, a high frame rate infrared camera is needed to record the thermal variations of the model. In accordance with F4 wind tunnel specifications, a 400 Hz frame rate thermal imager was developed. An HgCdTe 64 by 64 focal plane array in the 3 to 5 micrometers spectral band is used. The complete set of hardware devices and software is described. The F4 wind tunnel infrared background variation is estimated, in order to evaluate photometric measurement errors. After photometric and spatial criteria analysis, an experimental setup is used to measure camera sensitivity and to test the fixed pattern correction for different sets of parameter values. The minimum resolved temperature difference is less than 0.1K for 50K temperature range with 300K background. To check that the instrument works properly at the 400 Hz frame rate, a frame sequence of a fast thermal event is shown. The camera was then tested in the F4 wind tunnel. ESA

N94-14029*# Georgia Tech Research Inst., Atlanta. School of Electrical and Computer Engineering.

AN ACOUSTIC CHARGE TRANSPORT IMAGER FOR HIGH DEFINITION TELEVISION APPLICATIONS Semiannual Status Report, 1 Apr. - 30 Sep. 1993

William D. Hunt, Kevin F. Brennan, and Christopher J. Summers 30 Sep. 1993 85 p

(Grant NAGw-2753)

(NASA-CR-194518; NAS 1.26:194518; E21-687; E21-H83) Avail: CASI HC A05/MF A01

This report covers: (1) invention of a new, ultra-low noise, low operating voltage APD which is expected to offer far better performance than the existing volume doped APD device; (2) performance of a comprehensive series of experiments on the acoustic and piezoelectric properties of ZnO films sputtered on GaAs which can possibly lead to a decrease in the required rf drive power for ACT devices by 15dB; (3) development of an advanced, hydrodynamic, macroscopic simulator used for evaluating the performance of ACT and CTD devices and aiding in the development of the next generation of devices; (4) experimental development of CTD devices which utilize a p-doped top barrier demonstrating charge storage capacity and low leakage currents; (5) refinements in materials growth techniques and in situ controls to lower surface defect densities to record levels as well as increase material uniformity and quality. Author (revised)

N94-14044# Deutsche Forschungsanstalt fuer Luft- und Raumfahrt, Oberpfaffenhofen (Germany). Abt. Prozessortechnik.

A WIDGET BASED OPERATIONS SIMULATOR FOR A PLANETARY CAMERA: A MODEL FOR THE HIGH RESOLUTION STEREO CAMERA ON MARS 94

Bernd Aberle, Jens Henkner, Gottfried Schwarz, and Desiree Zalme Aug. 1992 111 p Original contains color illustrations

(DLR-FB-92-30; ETN-93-93961) Avail: CASI HC A06/MF A02

The use of a common workstation and its associated software tools for the support of a planetary camera experiment for the efficient analysis and visualization of the expected Mars surface coverage together with the display of key imaging parameters is reported. As a concrete example, the imaging environment and operations of the High Resolution Stereo Camera (HRSC) is simulated. During the Mars 94 mission, this instrument will record selected image strips of the Martian surface. ESA

N94-14046# Oak Ridge National Lab., TN.

CAMERA CALIBRATION IN A HAZARDOUS ENVIRONMENT PERFORMED IN SITU WITH AUTOMATED ANALYSIS AND VERIFICATION

F. W. DePiero and R. L. Kress 1993 8 p Presented at the 5th Topical Meeting on Robotics and Remote Systems, Knoxville, TN, 26-29 Apr. 1993

(Contract DE-AC05-84OR-21400)

(DE93-010274; CONF-930403-39) Avail: CASI HC A02/MF A01

Camera calibration using the method of Two Planes is discussed. An implementation of the technique is described that may be performed in situ, e.g., in a hazardous or contaminated environment, thus eliminating the need for decontamination of camera systems before recalibration. Companion analysis techniques used for verifying the correctness of the calibration are presented. DOE

N94-14149# Cologne Univ. (Germany). Inst. fuer Geophysik und Meteorologie.

A CALIBRATION PROCEDURE FOR RADIATION BUDGET RADIOMETERS AND ITS INFLUENCE ON INTERPRETATION OF MEASURED VALUES [EIN EICHVERFAHREN FUER STRAHLUNGSBILANZRADIOMETER UND SEIN EINFLUSS AUF DIE INTERPRETATION DER MESSWERTE]

Johannes Mueller 1991 129 p In GERMAN

(Contract BMFT-01-QS-88168)

(Mitt-82; ETN-93-94382) Avail: CASI HC A07/MF A02

A procedure for the calibration of the spectral broadband satelliteborne radiometer 'ScaRaB' (Scanner for Radiation Budget) is developed. The calibration was divided into a preflight ground calibration and an onboard calibration. The onboard calibration was repeated five times per orbit. During the presentation of the calibration process, the influence of the properties of calibration sources on the results of the measurements was analyzed. A procedure was developed to minimize the necessary corrections on the measurements by the choice of sources. The calibration sources were investigated, and the achievable accuracies were evaluated. The spectral qualities of the ground calibration sources determine the conversion of the filtered radiances into unfiltered radiances. A black body source and a calibrated solar diffusor were supposed to be sufficient for the ground calibration. A black body simulator, a calibration lamp, and a solar diffusor were the designated onboard sources. They are revised critically with respect to homogeneity, isotropy, and spectral emission. The black body simulators fulfill these requirements well. The isotropy of the lamp sources was tolerable, but should be improved in future. The onboard solar diffusors are not sufficient in their present design. An alternative concept of solar diffusors is presented. ESA

N94-14416# Lawrence Livermore National Lab., CA.

IMAGING FOURIER TRANSFORM SPECTROMETER

C. L. Bennett, M. R. Carter, D. J. Fields, and J. Hernandez 14 Apr. 1993 11 p Presented at the Society of Photo-Optical Instrumentation Engineers OE/Aerospace Science and Sensing Meeting, Orlando, FL, 11-16 Apr. 1993

(Contract W-7405-eng-48)

(DE93-017193; UCRL-JC-113273; CONF-930445-18) Avail: CASI HC A03/MF A01

The operating principles of an Imaging Fourier Transform Spectrometer (IFTS) are discussed. The advantages and disadvantages of such instruments with respect to alternative imaging spectrometers are discussed. The primary advantages of the IFTS are the capacity to acquire more than an order of magnitude more spectral channels than alternative systems with more than an order of magnitude greater etendue than for alternative systems. The primary disadvantage of IFTS, or FTS in general, is the sensitivity to temporal fluctuations, either random or periodic. Data from the IRIFTS prototype instrument, sensitive in the infrared (IR), are presented having a spectral sensitivity of 0.01 absorbance units, a spectral resolution of 6 cm(exp -1) over the range 0 to 7899 cm(exp -1), and a spatial resolution of 2.5 mr. DOE

N94-14447*# MetroLaser, Irvine, CA.

TWO COLOR HOLOGRAPHIC INTERFEROMETRY FOR MICROGRAVITY APPLICATION Technical Report No. 5, 1 Apr. - 1 Oct. 1993

James D. Trolinger Oct. 1993 19 p

(Contract NAS8-39402)

(NASA-CR-194424; NAS 1.26:194424; DCN-1-2-ES-44818) Avail: CASI HC A03/MF A01

Holographic interferometry is a primary candidate for the measurement of temperature and concentration in various crystal growth experiments destined for space. The method measures refractive index changes in the experiment test cell. A refractive index change can be caused by concentration changes, temperature changes, or a combination of temperature and concentration changes. If the refractive index changes are caused by temperature and concentration changes occurring simultaneously in the experiment test cell, the contributions by the two effects cannot be separated by conventional measurement methods. By using two wavelengths, two independent interferograms can be produced from the reconstruction of the hologram. The two interferograms will be different due to dispersion properties of fluid materials. These differences provide the additional information that allows the separation of simultaneously occurring temperature and concentration gradients. There is no other technique available that can provide this type of information. The primary objectives of this effort are to experimentally verify the mathematical theory of two color holographic interferometry and to determine the practical value of this technique for space application. To achieve these objectives, the accuracy and sensitivity of the technique must be determined for geometry's and materials that are relevant to the Materials Processing in the Space program of NASA. This will be achieved through the use of a specially designed two-color holographic interferometry breadboard optical system. In addition to experiments to achieve the primary goals, the breadboard will also provide inputs to the design of an optimum space flight system. Author

N94-14452# Fermi National Accelerator Lab., Batavia, IL.

HIGH COUNTING RATE RESISTIVE-PLATE CHAMBER

V. Peskov, D. F. Anderson, and S. Kwan May 1993 14 p

(Contract DE-AC02-76CH-03000)

(DE93-014928; FNAL-TM-1838) Avail: CASI HC A03/MF A01

Parallel-plate avalanche chambers (PPAC) are widely used in physics experiments because they are fast (less than 1 ns) and have very simple construction: just two parallel metallic plates or mesh electrodes. Depending on the applied voltage they may work either in spark mode or avalanche mode. The advantage of the spark mode of operation is a large signal amplitude from the chamber, the disadvantage is that there is a large

dead time (msec) for the entire chamber after an event. The main advantage of the avalanche mode is high rate capability 10(exp 5) counts/mm(sup 2). A resistive-plate chamber (RPC) is similar to the PPAC in construction except that one or both of the electrodes are made from high resistivity (greater than 10(exp 10) Omega(cm) materials. In practice RPC's are usually used in the spark mode. Resistive electrodes are charged by sparks, locally reducing the actual electric field in the gap. The size of the charged surface is about 10 mm(sup 2), leaving the rest of the detector unaffected. Therefore, the rate capability of such detectors in the spark mode is considerably higher than conventional spark counters. Among the different glasses tested the best results were obtained with electron type conductive glasses, which obey Ohm's law. Most of the work with such glasses was done with high pressure parallel-plate chambers (10 atm) for time-of-flight measurements. Resistive glasses have been expensive and produced only in small quantities. Now resistive glasses are commercially available, although they are still expensive in small scale production. From the positive experience of different groups working with the resistive glasses, it was decided to review the old idea to use this glass for the RPC. This work has investigated the possibility of using the RPC at 1 atm and in the avalanche mode. This has several advantages: simplicity of construction, high rate capability, low voltage operation, and the ability to work with non-flammable gases. DOE

N94-14497*# Thiokol Corp., Brigham City, UT. Space Operations.
QUALIFICATION TEST OF THE ROSS DOUBLE PLANETARY MIXER Final Report
Kurt F. Lueders Jul. 1993 24 p
(Contract NAS8-38100)
(NASA-CR-192600; NAS 1.26:192600; TWR-50222) Avail: CASI HC A03/MF A01

This test report describes the qualification test of the Ross Double Planetary Mixer used to mix room temperature vulcanized (RTV) silicone (Dow Corning 90-006-2) for the redesigned solid rocket motor (RSRM) nozzle joints. Testing was completed 18 June 1993 in the M-113A Nozzle Fabrication Facility at Thiokol Corporation, Space Operations, Brigham City, Utah. The Ross mixer provides better mixing and better control on temperature and humidity, resulting in better quality RTV and a longer usable pot life. The test began on 3 May 1993 and was stopped due to operator error during the tensile strength and elongation testing. Specimens were ruined without gathering any useful data. A 'no test' was declared, the problem was remedied, and the test was re-run with MSFC approval. The test was run and all pass/fail criteria were met, most with a considerable margin. The Ross Double Planetary Mixer met all certification objectives and is recommended for immediate use for mixing RTV silicone for RSRM nozzle joints. Author (revised)

N94-14534# Allied-Signal Aerospace Co., Kansas City, MO.
MOISTURE METER EVALUATION
R. A. Metzler Jun. 1993 36 p
(Contract DE-AC04-76DP-00613)
(DE93-016581; KCP-613-5081) Avail: CASI HC A03/MF A01

This report documents the details of the correlation and bake-out studies performed on five moisture meters. The meters used were as follows: three resistance type, one dielectric type (capacitance), and one dielectric type (power loss). Also included is the sequence of events requiring the study, results from a statistical review of the data, and some general information regarding moisture meters and moisture content of redwood obtained from the meter manufacturers and personnel at the USDA Forest Products Laboratories. DOE

N94-14578# Sandia National Labs., Albuquerque, NM.
CALIBRATION OF A MAGNETIC INDUCTION SYSTEM FOR MEASUREMENT OF HYPERVELOCITIES
S. P. Breeze Mar. 1993 17 p
(Contract DE-AC04-76DP-00789)
(DE93-013949; SAND-92-2816) Avail: CASI HC A03/MF A01 (US Sales Only)

A device to measure the velocity and to determine the character of a material launched in a flight tube during the execution of an experiment has been constructed. This measurement device provides a self generating signal, is nonintrusive, compact, and accurate. The signals are reproducible, and it is relatively inexpensive to procure. The MAgnetic Velocity Induction System (MAVIS) has been the technique used to measure projectile velocities in the two-stage light gas gun at Sandia for many years. Several experiments were conducted to study the MAVIS data signatures produced by various metal projectiles at velocities raging from 0.8 km/sec to nearly 7.0 km/sec, as well as fragmented metal projectiles, and a highly conductive carbon plasma. This report deals with the results of those calibration experiments. The data signature study may be used as an aid in the interpretation of the other test data records. DOE

N94-14684*# National Center for Atmospheric Research, Boulder, CO. High Altitude Observatory.
VACUUM ULTRAVIOLET INSTRUMENTATION FOR SOLAR IRRADIANCE AND THERMOSPHERIC AIRGLOW Semiannual Report, FY 1993
Thomas N. Woods, Gary J. Rottman, Scott M. Bailey (Colorado Univ., Boulder.), and Stanley C. Solomon (Colorado Univ., Boulder.) 25 Aug. 1993 21 p
(Grant NAG5-676)
(NASA-CR-194525; NAS 1.26:194525) Avail: CASI HC A03/MF A01

A NASA sounding rocket experiment was developed to study the solar extreme ultraviolet (EUV) spectral irradiance and its effect on the upper atmosphere. Both the solar flux and the terrestrial molecular nitrogen via the Lyman-Birge-Hopfield bands in the far ultraviolet (FUV) were measured remotely from a sounding rocket on October 27, 1992. The rocket experiment also includes EUV instruments from Boston University (Supriya Chakrabarti), but only the National Center for Atmospheric Research (NCAR)/University of Colorado (CU) four solar instruments and one airglow instrument are discussed here. The primary solar EUV instrument is a 1/4 meter Rowland circle EUV spectrograph which has flown on three rockets since 1988 measuring the solar spectral irradiance from 30 to 110 nm with 0.2 nm resolution. Another solar irradiance instrument is an array of six silicon XUV photodiodes, each having different metallic filters coated directly on the photodiodes. This photodiode system provides a spectral coverage from 0.1 to 80 nm with about 15 nm resolution. The other solar irradiance instrument is a silicon avalanche photodiode coupled with pulse height analyzer electronics. This avalanche photodiode package measures the XUV photon energy providing a solar spectrum from 50 to 12,400 eV (25 to 0.1 nm) with an energy resolution of about 50 eV. The fourth solar instrument is an XUV imager that images the sun at 17.5 nm with a spatial resolution of 20 arc-seconds. The airglow spectrograph measures the terrestrial FUV airglow emissions along the horizon from 125 to 160 nm with 0.2 nm spectral resolution. The photon-counting CODACON detectors are used for three of these instruments and consist of coded arrays of anodes behind microchannel plates. The one-dimensional and two-dimensional CODACON detectors were developed at CU by Dr. George Lawrence. The pre-flight and post-flight photometric calibrations were performed at our calibration laboratory and at the Synchrotron Ultraviolet Radiation Facility (SURF) at the National Institute of Standards and Technology (NIST) in Gaithersburg, Maryland. Author

N94-14687# National Inst. of Standards and Technology, Boulder, CO. Electronics and Electrical Engineering Lab.
SHIELDED OPEN-CIRCUITED SAMPLE HOLDERS FOR DIELECTRIC AND MAGNETIC MEASUREMENTS OF LIQUIDS AND POWDERS
J. Baker-Jarvis, M. D. Janezic, and R. B. Stafford (Virginia Polytechnic Inst. and State Univ., Blacksburg.) Mar. 1993 33 p
(PB93-198851; NISTIR-5001) Avail: CASI HC A03/MF A01

The report overviews shielded open-circuit measurements and presents a comprehensive uncertainty analysis. The authors use a dominant-mode scattering formulation to develop an expression for the reflection coefficient in terms of bead and sample parameters. The formulation developed here eliminates the transformation through the various sections of the sample holder. The authors also extend the formulation to include magnetic measurements. The uncertainty analysis indicates a decrease in relative uncertainty with increasing sample length and with increasing frequency. The real part of the permittivity at low frequencies is very sensitive to the measured phase of the reflection coefficient and the sample length. The imaginary part of the permittivity of low-loss materials is not extremely sensitive to the sample length. For high-loss materials both the real and the imaginary parts of the permittivity are sensitive to the sample lengths. NTIS

N94-14701# Royal Aerospace Establishment, Farnborough (England). Aerodynamics and Propulsion Dept.
OPTICAL FIBRE FABRY-PEROT INTERFEROMETERS FOR CALORIMETRIC HEAT TRANSFER GAUGES
K. S. Chana (Heriot-Watt Univ., Edinburgh, Scotland.), S. R. Kidd (Heriot-Watt Univ., Edinburgh, Scotland.), I. W. Matthews (Heriot-Watt Univ., Edinburgh, Scotland.), J. S. Barton, and J. D. C. Jones 15 Dec. 1992 15 p Presented at the 11th International Symposium on Measuring Techniques for Transonic and Supersonic Flows in Cascades and Turbomachines, Munich, Germany, 14-15 Sep. 1992 Sponsored in part by Ministry of Defence, London, England
(RAE-TM-Aero/Prop-20; BR316596; ETN-93-94496) Copyright Avail: CASI HC A03/MF A01

A heat flux measurement system comprising a laser diode, a single mode optical fiber interferometer, and a passive optical fiber component is described. The system was designed for use in transient flow wind tunnels and has a resolution of 1 kW/sq m, a dynamic range of 20 MW/sq m, and a bandwidth greater than 100 kHz. Heat flux measurements were made with the system on the endwall of a cascade of stator blades. ESA

N94-14772 Lawrence Livermore National Lab., CA.
IMAGE RECONSTRUCTION FOR X RAY HOLOGRAPHIC MICROSCOPY
J. Brase, T. Yorkey, and J. Trebes Sep. 1992 11 p Presented at the Society of Photo-Optical Instrumentation Engineers (SPIE) International Symposium on Optical Applied Science and Engineering, San Diego, CA, 19-24 Jul. 1992 Limited Reproducibility: More than 20% of this document may be affected by microfiche quality
(Contract W-7405-eng-48)
(DE93-013094; UCRL-JC-111495; CONF-920792-56) Avail: CASI HC A03

This paper gives a basic overview of holography as applied to x-ray microscopy. Topics discussed include Fourier transform holography, phase recovery from a hologram, reconstruction of scattered fields, and the use of straight ray approximations. Three dimensional spatial resolution below 100 nm is possible. DOE

N94-14782# Defence Research Establishment, Ottawa (Ontario).
PERFORMANCE EVALUATION OF THE HONEYWELL GG1308 MINIATURE RING LASER GYROSCOPE
M. F. Vinnins and L. D. Gallop Jan. 1993 49 p
(AD-A266694; DREO-1166) Avail: CASI HC A03/MF A01

This report describes the results of the performance evaluation of a Honeywell GG1308 miniature Ring Laser Gyroscope (RLG). The tests include turn-on and cold start, bias drift, scale factor, scale factor linearity, thermal transients, and effects of dither compensation. The gyroscope demonstrated excellent high-rate performance although significant scale factor deviations were noted during temperature variations. Instrument design characteristics and areas of potential future investigation are also discussed. DTIC

N94-14792 Lawrence Livermore National Lab., CA.
A FAST FRAME RATE 512 X 512 CCD DIGITAL CAMERA SYSTEM
A. Conder, R. Mitchell, and H. Schulte Jan. 1993 9 p Presented at the IS and T/SPIE Symposium on Electronic Imaging Science and Technology, San Jose, CA, 31 Jan. - 5 Feb. 1993 Limited Reproducibility: More than 20% of this document may be affected by microfiche quality
(Contract W-7405-eng-48)
(DE93-013048; UCRL-JC-112602; CONF-930163-2) Avail: CASI HC A02

This paper details the performance and shows images obtained from a 512 x 512 CCD camera capable of recording 400 digitized frames per second. A brief description of the data acquisition hardware and image analysis software is also included. DOE

N94-14827# Royal Aerospace Establishment, Farnborough (England). Aerodynamics and Propulsion Dept.
THE 3D PNEUMATIC AND 2D DYNAMIC PROBES: THEIR DEVELOPMENT AND SUBSEQUENT USE IN A TRANSONIC FAN
M. A. Cherrett, J. D. Bryce, and H. P. Hodson (Cambridge Univ., England.) 22 Dec. 1992 18 p Presented at the 11th International Symposium on Measuring Techniques for Transonic and Supersonic Flows in Cascades and Turbomachines, Munich, Germany, 14-15 Sep. 1992 Sponsored by Ministry of Defence, London, England, and Dept. of Trade and Industry, London, England
(RAE-TM-Aero/Prop-22; BR315905; ETN-93-94498) Copyright Avail: CASI HC A03/MF A01

Three different three dimensional (3D) pneumatic probes--a four hole wedge probe, a stem pyramid probe, and a sting pyramid probe--were built and calibrated in detail, along with two dynamic yawmeters and a geometrically identical pneumatic yawmeter. The aerodynamic performance of the probes are discussed, and detailed steady state flow field measurements taken with the probes at stator exit in a transonic fan are compared. ESA

N94-14858# Sandia National Labs., Albuquerque, NM.
IMAGE MOTION PHOTOGRAPHY
A. A. Sehmer Apr. 1993 14 p
(Contract DE-AC04-76DP-00789)
(DE93-013962; SAND-93-0645) Avail: CASI HC A03/MF A01 (US Sales Only)

Streak cameras operating in the image motion mode are widely used in the photo instrumentation field to measure the velocities of high-velocity projectiles. The larger format cameras are also capable of producing detailed photographs of high-velocity projectiles with virtually no image blur. Although the images produced by these cameras appear to be ordinary photographs, there are major differences that must be understood before any data reduction is undertaken. This report addresses the theory of operating streak cameras in the image motion mode, and the precautions that must be taken during image analysis. DOE

36 LASERS AND MASERS

Includes parametric amplifiers.
For related information see also *76 Solid-State Physics.*

N94-12857 Melbourne Univ., Parkville (Australia). School of Physics.
CONFOCAL PROFILOMETER WITH NANOMETRIC VERTICAL RESOLUTION
D. J. Butler, A. Horsfall, M. Hrynevych, P. D. Kearney, and K. A. Nugent 1992 15 p Limited Reproducibility: More than 20% of this document may be affected by microfiche quality
(DE93-622698; UM-P-92/51) Avail: CASI HC A03 (US Sales Only)

An optical system is described which is based on the method of Kobayashi et al. The instrument is capable of simultaneous confocal imaging and profilometry with nanometric (nm) vertical resolution. The profile is independent of the reflectivity of the sample and is obtained by raster-scanning the sample without active feedback. It is shown that the vertical resolution of this technique may be extended down to 1 nm and have recorded images with a resolution of better than 3 nm. The concept and design is considerably simpler than most optical profilometers and may represent the most affordable method of profilometry with nanometric resolution available. DOE

N94-12898# Lawrence Livermore National Lab., CA.
RECENT RESULTS FROM MATERIAL PROCESSING STUDIES ON NEW GENERATION LASERS
D. D. Kautz, E. P. Dragon, M. E. Werve, and R. S. Hargrove Dec. 1993 10 p Presented at the 5th International Conference on Welding and Melting by Electron and Laser Beams, La Baule, France, 14-18 Jun. 1993
(Contract W-7405-eng-48)
(DE93-013841; UCRL-JC-109388; CONF-930658-1) Avail: CASI HC A02/MF A01

High power and radiance dye lasers developed at Lawrence Livermore National Laboratory show promise for material processing tasks. Evaluations using welding heat flow models suggests significant increases in precision and speed are expected. We started processing studies to determine the viability of these lasers for cutting and drilling. Titanium and stainless steel alloys were chosen as materials for the preliminary studies. Results show that cuts and holes with extremely fine features can be made with dye and copper-vapor lasers. High radiance beams produce low distortion and small heat affected zones. We have accomplished very high aspect ratios and micron scale kerfs and holes in both stainless steel and titanium alloys. DOE

N94-12962# Lawrence Livermore National Lab., CA.
THREE DIMENSIONAL TIME-DEPENDENT HYDRODYNAMIC AND PROPAGATION MODELING OF X RAY LASER EMISSION
R. P. Ratowsky, M. D. Feit, R. A. London, R. S. Walling, G. M. Shimkaveg, A. L. Osterheld, M. R. Carter, and R. S. Craxton Jun. 1992 5 p Presented at the 3rd International Colloquium on X Ray Lasers, Schliersee, Germany, 18-22 May 1992
(Contract W-7405-eng-48)
(DE93-012575; UCRL-JC-110000; CONF-920523-12) Avail: CASI HC A01/MF A01

We have carried out three dimensional time-dependent calculations of x-ray emission in exploding, foil-line, focus-produced plasmas relevant to neon-like yttrium experiments at the Lawrence Livermore National Laboratory (LLNL). Hydrodynamic simulations using LASNEX and a simple gain profile based on XRASER are input into CASER, which solves the radiation transport equation along three dimensional ray orbits. Experimental observables such as farfield patterns and x-ray signal vs. laser length are then computed and compared with experiment. Similar two dimensional calculations have also been performed using the wave optics code WAVE to calculate coherence and confirm the accuracy of the ray optics treatment. We have found good agreement between both experiment and simulation and between the ray and wave optics codes. DOE

N94-12963# Lawrence Livermore National Lab., CA.
EVOLUTION OF HIGH-REPETITION-RATE INDUCTION ACCELERATORS THROUGH ADVANCEMENTS IN SWITCHING
H. C. Kirbie, G. J. Caporaso, M. A. Newton, and S. S. Yu 20 Aug. 1992 7 p Presented at the 16th International LINAC Conference, Ottawa, Ontario, 23-28 Aug. 1992
(Contract W-7405-eng-48)
(DE93-012599; UCRL-JC-110213; CONF-9208109-88) Avail: CASI HC A02/MF A01

Future applications of linear and recirculating induction accelerators include microwave sources for plasma heating and linear colliders, industrial manufacturing processes, and heavy ion fusion. These applications require pulsed sources capable of sustained operation at high pulse-repetition rates. Powering these new accelerators places severe switching demands on the source, demands that often can not be met withcommercially-available technology. Consequently, several new accelerator switching schemes have been developed at Lawrence Livermore National Laboratory (LLNL). Our transition from spark-gap technology to magnetic switching has merged the formerly independent roles of source and cell into a single system and reshaped our design methods to emphasize high efficiency. Treatment of the accelerator as a system has also enabled us to optimize new accelerator designs based on cost considerations. Presently, we are developing a technology for driving a heavy-ion induction recirculator at pulse rates exceeding 100 kHz. In this case, the switching method is all solid state and the source and cell have evolved into a unified device. DOE

N94-13013# Texas Univ., Austin. Dept. of Physics.
KINETIC STUDIES FOLLOWING STATE-SELECTIVE LASER EXCITATION
J. W. Keto Oct. 1992 44 p
(Contracts DE-FG05-84ER-13191; DE-FG03-93ER-14348)
(DE93-012970; DOE/ER-13191/13) Avail: CASI HC A03/MF A01

Measurements of state-to-state deactivation cross sections and radiative lifetimes were made for Xe*(6p,6p',7p) and Kr*(5p) states in xenon and krypton buffer gases. These results are relevant to kinetic models of both excimer lasers and the infrared xenon laser. Attempts were made to continue studies of two-photon laser assisted collisions in the reaction Xe + Cl2 + (Dirac h)(omega) yields (Xe(+)(circ)Cl2(-)) yields XeCl*(high v) + Cl. These experiments along with studies of the XeCl*(B, C, and D) branching fractions are reported along with studies of the two-photon spectroscopy of Cl2. In addition, significant progress was made in the study of the spectroscopy of small molecules and excimers formed in supersonic beams. Although emphasis is on xenon excimers excited in two-photon transitions, larger rare gas clusters were measured. Splitting between the 2s and 2p excitons is not explainable by currently accepted models for excitons in liquid xenon. Finally, work to obtain fluorescent spectra of xenon excimers in supersonic jets is described. DOE

N94-13022# Michigan State Univ., East Lansing. Dept. of Chemistry.
DIRECT PROBING OF CHROMATOGRAPHY COLUMNS BY LASER-INDUCED FLUORESCENCE
V. L. McGuffin Dec. 1992 25 p
(Contract DE-FG02-89ER-14056)
(DE93-015208; DOE/ER-14056/14) Avail: CASI HC A03/MF A01

This report summarizes the progress and accomplishments of this research project from 1 Sep. 1989 to 28 Feb. 1993. During this period, we have accomplished all of the primary scientific objectives of the research proposal: (1) constructed and evaluated a laser-induced fluorescence detection system that allows direct examination of the chromatographic column, (2) examined nonequilibrium processes that occur upon solute injection and elution, (3) examined solute retention in liquid chromatography as a function of temperature and pressure, (4) examined solute zone dispersion in liquid chromatography as a function of temperature and pressure, and (5) developed appropriate theoretical models to describe these phenomena. In each of these studies, substantial knowledge has been gained of the fundamental processes that are responsible for chromatographic separations. In addition to these primary research objectives, we have made significant progress in three related areas: (1) examined pyrene as a fluorescent polarity probe in supercritical fluids and liquids as a function of temperature and pressure, (2) developed methods for the class-selective identification of polynuclear aromatic hydrocarbons in coal-derived fluids by microcolumn liquid chromatography with fluorescence quenching detection, and (3) developed methods for the determination of saturated and unsaturated (including omega-3) fatty acids in fish oil extracts by microcolumn liquid chromatography with laser-induced fluorescence detection. In these studies, the advanced separation and detection techniques developed in our laboratory are applied to practical problems of environmental and biomedical significance. DOE

N94-13058# Maryland Univ., College Park.
MICROWAVE GENERATION FOR MAGNETIC FUSION ENERGY APPLICATIONS
T. M. Antonsen, Jr., W. W. Destler, V. L. Granatstein, and B. Levush Feb. 1993 36 p
(Contract DE-FG05-87ER-52147)
(DE93-013864; DOE/ER-52147/6) Avail: CASI HC A03/MF A01

This work strives to develop high average power FEL's at voltages below I MV allowing for smaller and less costly power supplies. To achieve operation of an FEL with 100 GHZ (approx It) f (approx It) 150 GHz and with relatively modest voltage, we have been investigating the use of small period ((lambda)(sub (omega)) (approximately) 1 cm) planar wiggler magnets together with sheet electron beams. The sheet beam geometry allows for an FEL interaction region in the form of a narrow slit with high wiggler field at the center plane where the electrons are concentrated. The total current and power may then be increased without making current density excessive by increasing the wide dimension of the sheet beam. Sheet beam FEL design parameters for both a Proof-of-Principle (PoP) FEL experiment, which is current in progress, and an ITER relevant FEL design are shown. A central issue in the sheet beam FEL concept is propagation of the beam through the interaction region without excessive interception by the walls. In section 2 below we describe a successful experimental demonstration of sheet beam propagation through a 56 period uniform wiggler. Cold testing and initial hot test operation of the (PoP) FEL amplifier are also described. Finally, we present a theoretical investigation of the bandwidth of an FEL amplifier with a tapered wiggler operating in saturation is described. DOE

N94-13091*# Schwartz Electro-Optics, Inc., Orlando, FL.
NOVEL Co:MgF2 LIDAR FOR AEROSOL PROFILER Final Report
M. A. Acharekar Sep. 1993 44 p Original contains color illustrations
(Contract NAS1-19300)
(NASA-CR-191525; NAS 1.26:191525) Avail: CASI HC A03/MF A01; 2 functional color pages

Lidars are of great interest because of their unique capabilities in remote sensing applications in sounding of the atmosphere, meteorology, and climatology. In this small business innovative research (SBIR) phase II program, laser sources including Co:MgF2, CTH:YAG, CTH:YSGG, CT:YAG, and Er:Glass were evaluated. Modulator of fused silica and TeO2 materials with Brewster's angle end faces were used with these lasers as acousto-optical (AO) Q-switches. A higher hold-oif energy and hence a

higher Q-switched energy was obtained by using a high power RF driver. The report provides performance characteristics of these lasers. The tunable (1.75-2.50 microns) Co:MgF2 laser damaged the TeO2 Q-switch cell. However, the CTH:YAG laser operating at 2.09 microns provided output energy of over 300 mJ/p in 50 ns pulse width using the fused silica Q-switch. This Q-switched CTH:YAG laser was used in a breadboard vertical aerosol profiler. A 40 cm diameter telescope, InSb and InGaAs detectors were used in the receiver. The data obtained using this lidar is provided in the report. The data shows that the eye safe lidar using CTH:YAG laser for the vertical aerosol density and range measurements is the viable approach. Author (revised)

N94-13145# Lawrence Livermore National Lab., CA.
PREDICTED PERFORMANCE OF A DC BEAM DRIVEN FEM OSCILLATOR DESIGNED FOR FUSION APPLICATIONS AT 200-250 GHz
M. Caplan, R. W. B. Best, A. G. A. Verhoeven, M. J. VanderWiel, W. H. Urbanus, V. L. Bratman, and G. G. Denisov 21 Aug. 1992 22 p Presented at the 14th International Free Electron Laser Conference, Kobe, Japan, 23-28 Aug. 1992
(Contract W-7405-eng-48)
(DE93-013414; UCRL-JC-111690; CONF-9208142-22) Avail: CASI HC A03/MF A01

A Free Electron Laser (FEL) using a DC beam with a depressed collector is being developed at the FOM Institute (Netherlands) for plasma heating. The FEL will be capable of producing 1 MW CW output over an adjustable tuning range of 200-250 GHz. The basic design parameters for the electron beam, undulator, and waveguide circuit are determined using a 3D non-wiggle averaged waveguide mode particle interaction code including AC space charge effects. Novel features of the design include using a step tapered two section wiggler to achieve both the high gain (10) and the required efficiency (approximately 5%) as well as a rectangular corrugated HE(sub 11) waveguide circuit to handle the high average power requirements. Results are presented on FEM performance including dependence on beam emittance, percent feedback, and operating frequency. DOE

N94-13243# Lawrence Livermore National Lab., CA.
ABSORPTION AND DAMAGE THRESHOLDS OF LOW DEFECT DENSITY HAFNIA DEPOSITED WITH ACTIVATED OXYGEN
R. Chow, S. Falabella, G. E. Loomis, F. Rainer, C. J. Stolz, and M. R. Kozlowski Oct. 1992 16 p Presented at the Laser-Induced Damage in Optical Materials, Boulder, CO, 28-30 Oct. 1992
(Contract W-7405-eng-48)
(DE93-013853; UCRL-JC-111458; CONF-9210356-1) Avail: CASI HC A03/MF A01

Motivation for this work included observations of a correlation between increasing laser damage thresholds and both decreasing nodular-defect density and absorption of coatings. We reduced the nodular-defect densities by a factor of over 4x in hafnia coatings deposited by reactive e-beam evaporation from a Hf target source. In order to increase the metal oxidation kinetics at the coated surface, Hf was e-beam deposited reactively with oxygen activated by a (mu)-wave discharge. The effect of using activated oxygen during the evaporation of a hafnia target source was also evaluated. A series of hafnia layers were made with various conditions; we alternated between two (mu)-wave configurations, hafnium and hafnia targets and two reactive oxygen pressures. Laser damage thresholds (1064 nm -10 ns pulses), absorption (at 511 nm) and nodular-defect densities from these coatings are reported. The damage threshold correlated inversely with the coating absorption. DOE

N94-13258# Lawrence Livermore National Lab., CA.
IMAGING MICROSCOPY WITH X RAY LASERS AT LAWRENCE LIVERMORE NATIONAL LABORATORY
L. B. DaSilva, J. E. Trebes, S. Mrowka, B. J. MacGowan, J. A. Koch, D. L. Matthews, T. W. Barbee, Jr., R. Balhorn, J. Gray, and E. Andersen et al 28 Jul. 1992 8 p Presented at the Society of Photo-Optical Instrumentation Engineers International Symposium on Optical Applied Science and Engineering, San Diego, CA, 19-24 Jul. 1992
(Contract W-7405-eng-48)
(DE93-013419; UCRL-JC-111801; CONF-920792-59) Avail: CASI HC A02/MF A01

Imaging microscopy with short pulse (200 ps) x-ray lasers offers the opportunity of high resolution three-dimensional imaging of specimens in an aqueous environment without the blurring effects associated with natural motion. As a first step towards this goal we have performed imaging experiments which clearly resolved 500 A features on a gold test pattern. In addition, we have taken images of dried biological specimens as a basis for comparison in future wet specimen imaging. Results of these experiments will be described. We also discuss some of the alignment problems involved in doing x-ray microscopy with low rep rate systems where in situ focusing of the imaging optics is not practical as single shot exposures can alter the specimen. DOE

N94-13259# Lawrence Livermore National Lab., CA.
THE X RAY LASERS AS SOURCES FOR X RAY MICROSCOPY
B. J. MacGowan Jul. 1992 12 p Presented at the Society of Photo-Optical Instrumentation Engineers International Symposium on Optical Applied Science and Engineering, San Diego, CA, 19-24 Jul. 1992
(Contract W-7405-eng-48)
(DE93-013420; UCRL-JC-111802; CONF-920792-60) Avail: CASI HC A03/MF A01

Laboratory x-ray lasers are currently being developed by researchers worldwide as potential sources for x-ray imaging and other applications. Laser action has been demonstrated at wavelengths as short as 35.6 A, and there is a large effort underway to enhance the coherent power output of the Ni-like Ta x-ray laser at 44.83 A as a source for x-ray imaging of live cells. Part of this effort is dedicated to producing a more affordable, compact laser to pump the x-ray laser in order to increase the accessibility of x-ray laser sources. DOE

N94-13261# Sandia National Labs., Albuquerque, NM.
NON-SCANNED LADAR IMAGING AND APPLICATIONS
John P. Anthes, Phil Garcia, Joe T. Pierce, and Paul V. Dressendorfer 1992 12 p Presented at the Society of Photo-Optical Instrumentation Engineers OE/Aerospace Science and Sensing Meeting, Orlando, FL, 11-16 Apr. 1993
(Contract DE-AC04-76DP-00789)
(DE93-013772; SAND-92-2210C; CONF-930445-14) Avail: CASI HC A03/MF A01 (US Sales Only)

A scannerless LAser Detection And Ranging (LADAR) system is presently under development for applications at Sandia National Laboratories. This LADAR design eliminates the need for a mechanical laser beam scanner which is often the system component that limits the use of laser radars for many applications. Range to the target scene is determined in this approach by measuring the phase shift of the intensity modulation on the received optical return compared to the reference. The approach used in this LADAR is unique because the method used to detect this phase shift is an array of time integrating detectors that also records the image of the target scene. An analytical model will be presented that describes the LADAR system performance. Applications of this LADAR system will also be reviewed. The applications include terminal guidance of advanced conventional munitions, perimeter surveillance of secure facilities, mapping potholes/cracks in the US highway system for improved maintenance scheduling, active collision avoidance of commercial/private vehicles, robotic vision integrated into advanced manufacturing concepts, and a novel airborne multi-sensor system containing LADAR, SAR, and LIDAR to locate and measure the thickness of ocean oil spills. DOE

N94-13387# Naval Research Lab., Washington, DC. Computational Physics and Fluids Dynamics Div.
SHOCK-FREE ACCELERATION OF LASER DRIVEN TARGETS
10 Dec. 1992 15 p
(Contract DE-AI03-79DP-40092)
(DE93-008050; NRL/MR-6440-92-7170) Avail: CASI HC A03/MF A01 (US Sales Only)

The ability of recently developed laser smoothing techniques to produce uniform ablation pressures is strongly contingent on the degree of thermal smoothing. Thermal smoothing is not effective at reducing residual laser nonuniformities during the start up phase of a shaped, reactor-like laser pulse. The impact of the first shock can be diminished by adiabatically compressing the target with a temporally long, slowly rising laser pulse. This Memorandum Report discusses an elastic-plastic laser-matter-interaction model and shows that a shock-free, induced spatial incoherence-smoothed

laser pulse can accelerate a target to nearly the conditions required for uniform implosion. Author

N94-13420*# American Univ., Washington, DC.
SOLID STATE LASER SYSTEMS FOR SPACE APPLICATION Semiannual Report No. 4
Richard B. Kay 1 Sep. 1993 7 p
(Grant NAG5-1319)
(NASA-CR-194133; NAS 1.26:194133) Avail: CASI HC A02/MF A01

Work on the development of an interferometric system for the purpose of absolute length determination commenced in January of this year. Our goal is to develop a system capable of measurements on the order of one meter with an accuracy of 1 part in 10 or greater. A modified Michelson bread board with stabilized laser diode source was assembled. Some preliminary measurements began using the tunable Santek laser in an FM modulation scheme. During this same period a literature search yielded a paper by Suematsu and Takeda which discusses a promising fourier transform technique for real time data analysis. We are in the process of evaluating this technique while we continue to change and upgrade the system configuration. Author (revised)

N94-13481# Lawrence Livermore National Lab., CA.
DESIGN AND PERFORMANCE OF AN AUTOMATED VIDEO-BASED LASER BEAM ALIGNMENT SYSTEM
W. J. Rundle (Martin Marietta Energy Systems, Inc., Livermore, CA.), M. W. Kartz (KMI Energy, Livermore, CA.), E. S. Bliss, R. E. English, Jr., R. L. Peterson, G. R. Thompson, and D. M. Uhlich 14 Jul. 1992 14 p Presented at the Society of Photo-Optical Instrumentation Engineers International Symposium on Optical Applied Science and Engineering, San Diego, CA, 19-24 Jul. 1992
(Contract W-7405-eng-48)
(DE93-012571; UCRL-JC-109276; CONF-920792-57) Avail: CASI HC A03/MF A01

This paper describes the design and performance of an automated, closed-loop, laser beam alignment system. Its function is to sense a beam alignment error in a laser beam transport system and automatically steer mirrors preceding the sensor location as required to maintain beam alignment. The laser beam is sampled by an optomechanical package which uses video cameras to sense pointing and centering errors. The camera outputs are fed to an image processing module, which includes video digitizers and uses image storage and software to sense the centroid of the image. Signals are sent through a VMEbus to an 'optical device controller' (ODC), which drives stepper-motor actuators on mirror mounts preceding the beam-sampling location to return the beam alignment to the prescribed condition. Photodiodes are also used to extend the control bandwidth beyond that which is achievable with video cameras. This system has been operated at LLNL in the Atomic Vapor Laser Isotope Separation (AVLIS) program to maintain the alignment of copper and dye laser beams, the latter to within +/- 2 micro-r in pointing and less than 1 mm in centering. The optomechanical design of the instrumented package, which includes lens, mirror, and video mounts in a rigid housing, the automated control system architecture, and the performance of this equipment is described. DOE

N94-13522 Alberta Univ., Edmonton. Dept. of Electrical Engineering.
CHARACTERISTICS OF SEMICONDUCTOR LASERS WITH OPTICAL FEEDBACK Ph.D. Thesis
Jann Oluf Binder 1989 221 p
(ISBN-0-315-55435-5; CTN-93-60721) Copyright Avail: Micromedia Ltd., Technical Information Centre, 165 Hotel de Ville, Place du Portage, Phase 2, Hull, Quebec J8X 3X2, Canada HC/MF

Discrete optical and fiber optic components were used along with a semiconductor diode to create both Fabry-Perot and ring-type external cavity lasers. The number of external cavity modes (ECM's) and the distribution of power in those modes in the weak optical feedback domain were studied. In the ECM, oscillation with minimum linewidth was observed and agreed with a frequency fluctuation model. The upper limit of stable operation in the weak feedback domain and the tradeoff between minimum linewidth and minimum number of ECM's is discussed. An optimized fiber-ring feedback assembly was observed to reduce the linewidth drastically and provide over 20 dB of suppression of ECM side modes. In the strong optical feedback domain, large changes in the carrier density and changes in the gain and resonance frequency of the cavity occurring due to injection of light were analyzed. A model is presented for the experimentally observed bistability and tuning range of an external grating laser, the effect of residual reflectivity on tuning characteristics, and the change of threshold current with resonator loss. The light versus current characteristic and spectral properties of a unidirectional semiconductor optical fiber ring laser were also investigated. Author (CISTI)

N94-13571 Tel-Aviv Univ. (Israel). Biomedical Engineering Program.
LASER CO2 BEAM TRANSMISSION THROUGH HOLLOW METALLIC WAVEGUIDE COATED BY A THIN INTERNAL DIELECTRIC LAYER M.S. Thesis
Thierry Boutboul Apr. 1991 164 p In HEBREW
(ITN-93-85201) Copyright Avail: Issuing Activity (Tel-Aviv Univ., Exact Sciences Library, Ramat Aviv 69978, Israel)

The CO2 laser, which is the most commonly used laser in medicine, is usually restricted to external use, owing to the lack of a waveguide suitable for transmitting its radiation. It has been proposed to solve this problem by using a hollow metallic waveguide with an internal dielectric coating, since air is a quasi-transparent medium for radiation of wavelength 10.6 micron. The potential contribution of a dielectric layer has been proved both experimentally and theoretically. A theoretical model was developed, based on wave theory and Maxwell's equations, to compute laser beam transmission through a waveguide of this type. Based on knowledge of the waveguide inlet fields, it was possible to compute the radiation power density at each point on the waveguide outlet plane. The model uses the fact that the tangential field components on the metallic boundary cancel, in order to develop the longitudinal components into a Fourier-Bessel series when all the computations were done on the Laplace plane. The transverse components could be expressed as a function of the longitudinal components on the Laplace plane. Laplace inverse transform computation enabled the transverse components on the real plane and the power density at each point at the outlet to be computed. The theoretical model was applied to a silver waveguide with a thin coating of silver iodide, taking account of the transition region between the different materials. ISA

N94-13573 California Univ., Los Angeles.
HORIZONTAL-CAVITY SURFACE-EMITTING LASERS, SUPERLUMINESCENT LEDs, AND AMPLIFIERS, AND PARABOLIC GAIN UNSTABLE RESONATOR SEMICONDUCTOR LASERS Ph.D. Thesis
Dennis Patrick Bowler 1992 234 p
Avail: Univ. Microfilms Order No. DA9310956

Two separate but related problems are addressed in this dissertation. The first is concerned with the transverse mode of folded-cavity devices (e.g. HC SELs, SLEDs, amplifiers) containing an intracavity 45 degree mirror. These devices are conducive to large scale cost effective fabrication and high power operation. The second problem is lateral mode control of broad area lasers using gain tailored unstable resonators. A beam propagation model for folded-cavity devices is presented which includes Fresnel reflections from multilayer thin-films, angular errors in the 45 degree micromirror, the dependence on the horizontal reflector separation, Fresnel beam propagation, and waveguide coupling losses of the reflected field. There is excellent agreement with experimental data for horizontal-cavity surface-emitting lasers (HC SELs) when scattering losses are included. Folded-end mirror performance can be improved by tilting the micromirror slightly toward normal incidence. Superluminescent light emitting diodes (SLEDs) and optical amplifiers are analyzed. Antireflection substrate coatings can improve performance significantly. Half-symmetric parabolic gain unstable resonator semiconductor lasers (URSLs) with Hermite-Gaussian lateral eigenmodes promise high power diffraction limited performance. Devices employing half-tone (HT) and lens-train (LT) electrode patterns are analyzed and fabricated. The HT electrode pattern promises better performance as compared to the LT approach. Although, the LT design which is more tolerant of processing variations, performed better than the HT approach, in this research. The parabolic gain URSLs appear to have significantly better lateral mode control under continuous wave (cw) operation than comparable rectangular stripe devices. A single lateral mode output of one watt cw was achieved with a LT parabolic gain URSL. Author

N94-13624 Clarkson Univ., Potsdam, NY.
THEORETICAL INVESTIGATION OF SCATTERING BY HOMOGENEOUS OR COATED DIELECTRIC SPHERES ILLUMINATED WITH A STEADY STATE OR PULSED LASER BEAM Ph.D. Thesis
Elsayed Esam M. Khaled 1993 170 p
Avail: Univ. Microfilms Order No. DA9311980

A method of calculating the internal and scattered electric fields of a sphere illuminated with a Gaussian beam is presented. The vector nature of the beam is considered. The beam can be located arbitrarily with respect to the object. The method uses the angular spectrum of plane waves technique and the T-matrix method. This combination is used to investigate the scattering behavior of homogeneous and coated spheres. The electric energy in a lossless or lossy homogeneous spherical particle illuminated with a plane wave or a Gaussian beam is investigated. The amount of energy coupling into the particle for different beam illuminations is also investigated. Modes having high-Q morphology dependent resonances (MDR) can dominate the internal energy distribution in lossless or lossy spheres even when they are excited many line widths from the resonant location. This dominance of the high-Q mode increases when the beam is shifted farther away from the sphere. The effects of the absorption on the dominance of the internal fields by a high-Q mode decreases as the beam is shifted farther away from the particle. Although the coupled energy decreases as the beam is shifted farther from the sphere, most of that energy is in the lowest-order mode. Internal and scattered time-dependent intensities are calculated for a homogeneous dielectric sphere illuminated with a pulsed Gaussian beam. The center frequency of the pulse spectrum is chosen to be on, near, or far away from a morphology-dependent resonance of the sphere. The center of the beam is positioned inside, on the edge, or outside the sphere. Two different decay rates in the internal and scattered time dependent intensity are observed: a decay rate that depends on the incident pulse spectrum and a rate which depends on the line shape of the resonant mode of the sphere. The intensity of scattered fields by a coated sphere illuminated with an on- or off-axis Gaussian beam is calculated. As the beam is shifted farther away from the surface of the sphere, the higher-Q morphology dependent resonances become increasingly important in the backscatter spectra, and the angular scattering intensity becomes smoother. As the beam is moved farther away from the sphere, the effect of the core on the scattering intensity decreases. When the incident Gaussian beam is focused outside of a particle with a relatively small core, the scattering spectra and angular scattering patterns become similar to those of a homogeneous sphere having the refractive index of the coat. Author

N94-13812*# Jet Propulsion Lab., California Inst. of Tech., Pasadena.
SINGLE EVENT EFFECTS AND LASER SIMULATION STUDIES
Q. Kim, H. Schwartz, K. McCarty, J. Coss, and C. Barnes 15 Aug. 1993 24 p
(Contract NAS7-918)
(NASA-CR-194506; JPL-Publ-93-23; NAS 1.26:194506) Avail: CASI HC A03/MF A01

The single event upset (SEU) linear energy transfer threshold (LETTH) of radiation hardened 64K Static Random Access Memories (SRAM's) was measured with a picosecond pulsed dye laser system. These results were compared with standard heavy ion accelerator (Brookhaven National Laboratory (BNL)) measurements of the same SRAM's. With heavy ions, the LETTH of the Honeywell HC6364 was 27 MeV-sq cm/mg at 125 C compared with a value of 24 MeV-sq cm/mg obtained with the laser. In the case of the second type of 64K SRAM, the IBM640ICRH no upsets were observed at 125 C with the highest LET ions used at BNL. In contrast, the pulsed dye laser tests indicated a value of 90 MeV-sq cm/mg at room temperature for the SEU-hardened IBM SRAM. No latchups or multiple SEU's were observed on any of the SRAM's even under worst case conditions. The results of this study suggest that the laser can be used as an inexpensive laboratory SEU prescreen tool in certain cases.
Author (revised)

N94-13882# Lawrence Livermore National Lab., CA.
DESIGN AND PERFORMANCE OF THE TERAWATT Cr:LiSrAlF6 LASER SYSTEM
T. Ditmire, H. Nguyen, S. Herman, and M. D. Perry 28 Jan. 1993 22 p
(Contract W-7405-eng-48)
(DE93-014678; UCRL-ID-113182) Avail: CASI HC A03/MF A01

The authors have developed a compact, flashlamp-pumped Cr:LiSrAlF6 laser system capable of producing peak powers in excess of one terawatt. The chirped pulse amplification approach has been optimized for amplification of femtosecond pulses in Cr:LiSrAlF6. The system includes a Cr:LiSAF regenerative amplifier followed by a Cr:LiSAF power amplifier chain. The regenerative amplifier produces 12 mJ pulses at a 5 Hz repetition rate which are further amplified to energies above 300 mJ at a 0.5 Hz repetition rate. Recompression results in a pulse energy of 150 mJ and pulse duration of under 135 fsec.
DOE

N94-13970# Norwegian Defence Research Establishment, Kjeller.
NUMERICAL SIMULATIONS OF Nd:YAG LASER AMPLIFIERS
Halvor Ajer, Stig Landroe, and Knut Stenersen 12 Oct. 1992 45 p
(FFI/RAPPORT-92/7028; ETN-93-93974) Avail: CASI HC A03/MF A01

Numerical simulations of Nd:YAG amplifiers are presented. The simulations are based on a rate equation model which correctly accounts for the lower laser level decay rate. A model for single pass amplification of fluence (energy per area) for arbitrary temporal behavior of the input pulse is developed. By use of reasonable approximations, this model is applicable to double pass amplification of Q switched pulses. The coupled differential equations of the system are solved numerically by using the programs SIMNON and MATLAB. General examples of amplification of fluence are first presented, including investigation of the influence of the lower level lifetime. Amplification of a Gaussian transverse fluence distribution incident on an amplifier rod with uniform gain is then presented. A diode laser pumped rod amplifier is simulated (single and double pass) assuming a Gaussian input distribution; diffraction effects are addressed for this example.
ESA

N94-13976# Lawrence Livermore National Lab., CA.
OSCILLATOR-AMPLIFIER EXPERIMENTS IN NEON-LIKE YTTRIUM
G. M. Shimkaveg, M. R. Carter, R. S. Walling, J. M. Ticehurst, R. R London, and R. E. Stewart 24 Jul. 1992 8 p Presented at the 3rd International Colloquium on X Ray Lasers, Schliersee, Germany, 18-22 May 1992
(Contract W-7405-eng-48)
(DE93-012577; UCRL-JC-111233; CONF-920523-13) Avail: CASI HC A02/MF A01

We present the first results from spatially and temporally separated x-ray lasing plasmas. The plasmas were shot sequentially with the emission of the first directed into the second.
DOE

N94-13996# Technische Univ., Berlin (Germany). Fachbereich Physik.
CONSTRUCTION AND TEST OF A FACILITY FOR PHOTON-STIMULATED FIELD DESCRIPTION USING EXCIMER LASER AND TIME OF FLIGHT Ph.D. Thesis [AUFBAU UND TEST EINER ANORDNUNG ZUR PHOTONENSTIMULIERTEN FELDDESORPTION MITTELS EXCIMERLASER UND FLUGZEITMASSENSPEKTROMETRIE]
Sun-Dal Song 1992 108 p In GERMAN
(ETN-93-94386) Avail: CASI HC A06/MF A02

A facility for examination of solid bodies surface, based on photon desorption and ionization in the electric field, is developed. A pulse excimer laser with raman shifter and vacuum monochromator was used as radiation source in order to bring different light wavelengths, such as Stokes and anti Stokes lines, with high intensity to a field emitter point. Desorpted species were detected using time of flight mass spectrometry with a transient recorder, which allows ion spectrum to be recorded independently of ion number; emitter surface structure was simultaneously observed in atomic resolution with a field ion microscope. Several absorbates such as NO, He, and H2 were examined on tungsten at 80K, with several wavelengths and field intensities to establish apparatus functionality. The influence of NO gas pressure and photon energy on mass spectrum was studied.
ESA

N94-14067 National Optics Inst., Ste-Foy (Quebec).
STUDY OF SPECKLE REDUCTION WHEN USING A CO2 WAVEGUIDE LASER CLOSE TO ITS THRESHOLD STATE
Michel Morin, Bruno Labranche, and Pierre Bernard Dec. 1992 41 p
(Contract DSS-W7702-1-R289-01-XSG)
(DSIS-93-00250; DRES-CR-4-93; INO-92-5102; CTN-93-60803) Avail: CASI HC A03

Experiments were conducted with a CO2 metallic waveguide laser to determine whether the coherence of the laser, a source of interest for

active infrared imaging systems, can be reduced by near-threshold operation. The study also evaluated the impact of such a procedure on the other laser properties and the speckle contrast reduction from this coherence decrease. Analysis indicates that coherence reduction through near-threshold operation is not a viable approach with the type of laser used. The strength of the spontaneous emission is insufficient and non-radiative processes quench the population inversion without allowing any significant extraction of energy through radiation. Experimentally, attempts to operate the laser at output powers below 0.4 W led to extinction of the beam, with no measurable radiative power coming out of the waveguide. Procedures for generation and detection of speckle patterns on a depolished aluminum plate with a CO2 laser were established and verified. All measurements were found to be consistent with theory. No contrast reduction was observed, which could be linked to a degradation of the coherence of the laser.
Author (CISTI)

N94-14114# Lawrence Livermore National Lab., CA.
THE INTERACTION OF INTENSE FEMTOSECOND LASER PULSES WITH SOLID TARGETS
D. E. Klem, C. Darrow, S. Lane, and M. D. Perry 30 Dec. 1992 4 p Presented at the 5th Short Wavelength: Physics With Intense Laser Pulses, San Diego, CA, 29-31 Mar. 1993
(Contract W-7405-eng-48)
(DE93-014415; UCRL-JC-112630; CONF-9303119-3) Avail: CASI HC A01/MF A01

The absorption of 800 fsec Nd-glass laser pulses obliquely incident on solid targets is measured at intensities up to 10(exp 18) W/sq cm. The associated production of hard x-rays is also measured. DOE

N94-14152# Lawrence Livermore National Lab., CA.
THE LIVERMORE X RAY LASER PROGRAM
D. L. Matthews 20 Aug. 1992 7 p Presented at the 3rd International Colloquium on XRay Lasers, Schliersee, Germany, 18-22 May 1992
(Contract W-7405-eng-48)
(DE93-014118; UCRL-JC-110706; CONF-920523-14) Avail: CASI HC A02/MF A01

I will report on the status of x-ray laser development and applications at Livermore. I will review some of our recent results and comment on where our future research is headed including plans for developing a compact x-ray laser users facility. Finally, I will briefly summarize the results of an X-ray Laser Applications Workshop that was held in San Francisco in Jan. 1992. DOE

N94-14175# Lawrence Livermore National Lab., CA.
SELENIUM X RAY LASER LINE PROFILE MEASUREMENTS
J. A. Koch, B. J. MacGowan, L. DaSilva, D. L. Matthews, S. Mrowka, J. H. Underwood, and P. J. Batson Jul. 1992 8 p Presented at the 3rd International Colloquium on X Ray Lasers, Schliersee, Germany, 18-22 May 1992
(Contracts W-7405-eng-48; DE-AC03-76SF-00098)
(DE93-012580; UCRL-JC-110974; CONF-920523-10) Avail: CASI HC A02/MF A01

We discuss our recent measurements of the spectral width of the 206.38 A laser in Ne-like Se. These measurements were performed over a wide range of amplifier length and indicate an intrinsic line width of 50 mA FWHM (full-width at half-maximum), show gain narrowing to 10 mA in intermediate length amplifiers, and show no significant re-broadening in long, saturated amplifiers. We briefly discuss the experiments and interpretations. DOE

N94-14414# California Univ., Berkeley. Lawrence Berkeley Lab.
MULTI-BUNCH BEAM-BREAK-UP STUDIES FOR A SWFEL/TBA
J. S. Kim, H. Henke, A. M. Sessler, and D. H. Whittum May 1993 3 p Presented at the International Particle Accelerator Conference, Washington, DC, 17-20 May 1993
(Contract DE-AC03-76SF-00098)
(DE93-016973; LBL-33255; CONF-930511-234) Avail: CASI HC A01/MF A01

A set of parameters minimizing BBU is obtained for a high current, low energy 'drive beam' in a standing wave, free electron laser/two-beam acceleration (FEL/TBA). A large reduction in the transverse wake function is obtained by making the cavity-iris junction gradual by means of a cone. BBU is examined under various BBU reduction schemes. DOE

N94-14415# Pacific Northwest Lab., Richland, WA.
UV AND IR LASER ABLATION FOR INDUCTIVELY COUPLED PLASMA MASS SPECTROMETRY
M. R. Smith, D. W. Koppenaal, and O. T. Farmer Jun. 1993 7 p Presented at the 2nd International Conference on Laser Ablation: Mechanisms and Applications, Knoxville, TN, 19-22 Apr. 1993
(Contract DE-AC06-76RL-01830)
(DE93-017124; PNL-SA-22070; CONF-9304144-9) Avail: CASI HC A02/MF A01

Laser ablation particle plume compositions are characterized using inductively coupled plasma/mass spectrometry (ICP/MS). This study evaluates the mass response characteristics peculiar to ICP/MS detection as a function of laser fluence and frequency. Evaluation of the ICP/MS mass response allows deductions to be made concerning how representative the laser ablation produced particle plume composition is relative to the targeted sample. Using a black glass standard, elemental fractionation was observed, primarily for alkalis and other volatile elements. The extent of elemental fractionation between the target sample and the sampled plume varied significantly as a function of laser fluences and IR and UV laser frequency. DOE

N94-14437# Lawrence Livermore National Lab., CA.
LASER BEAM CONTROL AND DIAGNOSTIC SYSTEMS FOR THE COPPER-PUMPED DYE LASER SYSTEM AT LAWRENCE LIVERMORE NATIONAL LABORATORY
E. S. Bliss, R. L. Peterson, J. T. Salmon, and R. A. Thomas Nov. 1992 17 p Presented at the OE/LASE 1993 International Society for Optical Engineering Conference, Los Angeles, CA, 16-23 Jan. 1993
(Contract W-7405-eng-48)
(DE93-016529; UCRL-JC-112671; CONF-930159-41) Avail: CASI HC A03/MF A01

The laser system described in the previous paper is used for experiments in which success requires tight tolerances on beam position, direction, and wavefront. Indeed, the optimum performance of the laser itself depends on careful delivery of copper laser light to the dye amplifiers, precise propagation of dye laser beams through restricted amplifier apertures, and accurate monitoring of laser power at key locations. This paper describes the alignment systems, wavefront correction systems, and laser diagnostics systems which ensure that the control requirements of both the laser and associated experiments are met. Because laser isotope separation processes utilize more than one wavelength, these systems monitor and control multiple wavelengths simultaneously. DOE

N94-14442# Lawrence Livermore National Lab., CA.
MICROCHANNEL COOLED HEATSINKS FOR HIGH AVERAGE POWER LASER DIODE ARRAYS
W. J. Bennett, B. L. Freitas, D. Ciarlo, R. Beach, S. Sutton, M. Emanuel, and R. Solarz 15 Jan. 1993 12 p Presented at the OE/LASE 1993: International Society for Optical Engineering (SPIE) Conference, Los Angeles, CA, 16-23 Jan. 1993
(Contract W-7405-eng-48)
(DE93-016533; UCRL-JC-112678; CONF-930159-42) Avail: CASI HC A03/MF A01

Detailed performance results for an efficient and low impedance laser diode array heatsink are presented. High duty factor and even CW operation of fully filled laser diode arrays at high stacking densities are enabled at high average power. Low thermal impedance is achieved using a liquid coolant and laminar flow through microchannels. The microchannels are fabricated in silicon using an anisotropic chemical etching process. A modular rack-and-stack architecture is adopted for heat sink design, allowing arbitrarily large two-dimensional arrays to be fabricated and easily maintained. The excellent thermal control of the microchannel heatsinks is ideally suited to pump army requirements for a high average power crystalline laser because of the stringent temperature demands that are required to efficiently couple diode light to several-nanometer-wide absorption features characteristic of lasing ions in crystals. DOE

N94-14520# California Univ., Berkeley. Lawrence Berkeley Lab.
THE STANDING WAVE FEL/TBA: REALISTIC CAVITY GEOMETRY AND ENERGY EXTRACTION
Jin-Soo Kim, A. M. Sessler, W. M. Sharp, and H. Henke May 1993 3 p Presented at the International Particle Accelerator Conference, Washington, DC, 17-20 May 1993
(Contract DE-AC03-76SF-00098)
(DE93-016972; LBL-33257; CONF-930511-223) Avail: CASI HC A01/MF A01

A set of parameters for standing wave free electron laser two beam accelerators (SWFEL/TBA) is evaluated for realistic cavity geometry taking into account beam-break-up and the sensitivity of output power to imperfections. Also given is a power extraction system using cavity coupled wave guides. DOE

N94-14547 Tel-Aviv Univ. (Israel).
ADIABATIC AND NON ADIABATIC EFFECTS IN FREE ELECTRON LASER (FEL) NON LINEAR INTERACTIONS Ph.D. Thesis
Zvi Sheena Aug. 1990 167 p
(ITN-93-85224) Copyright Avail: Issuing Activity (Tel-Aviv Univ., Exact Sciences Library, Ramat Aviv 69978, Israel)

This work describes the theoretical and experimental research performed in order to study adiabatic and non-adiabatic effects in FEL interactions in the non-linear regime. The research was based on a scheme in which a non-relativistic electron beam interacts with the ponderomotive field (beat wave) resulting from two counter-propagating TEA CO2 laser beams operating at different frequencies in a simulated Compton scattering scheme. A mathematical model was built and then used to study and to develop several adiabatic and non-adiabatic interaction schemes. A final scheme that can simulate both types of interaction was chosen. In this scheme the electron beam can interact adiabatically with the ponderomotive wave using a circular or a slanted entry path to cause the electrons to be trapped by the wave and to travel at its phase velocity along a linear path, to produce what is called a phase area displacement type of interaction, in which the electrons follow open trajectories in the phase-space diagram. The electron beam can also interact non-adiabatically with the ponderomotive wave, using an abrupt shift in the energy of the electrons to produce efficient trapping. An experimental setup that physically simulates these interaction schemes was constructed. Using this setup, experiments were conducted to investigate the energy exchange relationships between the electrons and the ponderomotive wave. The experimental results revealed that efficient electron trapping can be obtained using an abrupt shift in their energy in order to bring them into resonance with the ponderomotive wave. Author (ISA)

N94-14572# Brookhaven National Lab., Upton, NY.
WAKE-FIELD AND SPACE CHARGE EFFECTS ON HIGH BRIGHTNESS BEAMS CALCULATIONS AND MEASURED RESULTS FOR THE LASER DRIVEN PHOTOELECTRONS AT BNL-ATF
Z. Parsa May 1993 53 p Presented at the Accelerator Physics and Modeling, Upton, NY, 17 Sep. 1991
(Contract DE-AC02-76CH-00016)
(DE93-015787; BNL-48958; CAP-95-ATF-93C; CONF-9109349-2) Avail: CASI HC A04/MF A01

We discuss the formalism used to study the effects of the interactions between the highly charged particles and the fields in the accelerating structure, including space charge and wake fields. Some of our calculations and numerical simulation results obtained for the Brookhaven National Laboratory (BNL) high-brightness photoelectron beam at the Accelerator Test Facility (ATF) and the measured data at ATF are also included. DOE

N94-14576*# City Coll. of the City Univ. of New York, NY. Dept. of Physics.
TETRAVALENT CHROMIUM (Cr(4+)) AS LASER-ACTIVE ION FOR TUNABLE SOLID-STATE LASERS Semiannual Progress Report, 31 Mar. - 31 Oct. 1992
A. Seas, V. Petricevic, and Robert R. Alfano 1992 9 p
(Grant NAG1-1346)
(NASA-CR-194527; NAS 1.26:194527) Avail: CASI HC A02/MF A01

Generation of femtosecond pulses from a continuous-wave mode-locked chromium-doped forsterite (Cr(4+):Mg2SiO4) laser has been accomplished. The forsterite laser was actively mode-locked using an acousto-optic modulator operating at 78 MHz with two Brewster high-dispersion glass prisms for intra-cavity chirp compensation. Transform-limited sub-100-fs pulses were routinely generated in the TEM(sub 00) mode with 85 mW of continuous power (with 1 percent output coupler), tunable over 1230-1280 nm. The shortest pulses of 60-fs pulsewidth were measured. Derived from text

N94-14594# Lawrence Livermore National Lab., CA.
HIGH-ORDER HARMONIC GENERATION WITH SHORT-PULSE LASERS
K. J. Schafer, J. L. Krause, and K. C. Kulander Dec. 1992 9 p Presented at the OE/LASE 1993: International Society for Optical Engineering (SPIE) Conference, Los Angeles, CA, 16-23 Jan. 1993
(Contract W-7405-eng-48)
(DE93-016532; UCRL-JC-112624; CONF-930159-43) Avail: CASI HC A02/MF A01

Recent progress in the understanding of high-order harmonic conversion from atoms and ions exposed to high-intensity, short-pulse optical lasers is reviewed. We find that ions can produce harmonics comparable in strength to those obtained from neutral atoms, and that the emission extends to much higher order. Simple scaling laws for the strength of the harmonic emission and the maximum observable harmonic are suggested. These results imply that the photoemission observed in recent experiments in helium and neon contains contributions from ions as well as neutrals. DOE

N94-14595# Lawrence Livermore National Lab., CA.
EXPERIMENTAL MEASUREMENTS OF SELENIUM X-RAY LASER SPECTRAL LINE PROFILES
J. A. Koch, B. J. MacGowan, L. B. DaSilva, D. L. Matthews, R. A. London, R. W. Lee, S. Mrowka, J. H. Underwood (California Univ., Berkeley. Lawrence Berkeley Lab.), and P. J. Batson (California Univ., Berkeley. Lawrence Berkeley Lab.) 1 Mar. 1993 8 p Presented at the 1992 International Conference on Lasers, Houston, TX, 7-11 Dec. 1992
(Contracts W-7405-eng-48; DE-AC03-76SF-00098)
(DE93-016543; UCRL-JC-113290; CONF-921256-5) Avail: CASI HC A02/MF A01

The authors discuss their recent measurements of the spectral width of the 206.38 Angstrom x-ray laser transition in Ne-like Se. These measurements used a high-resolution grating spectrometer and were performed over a wide range of laser amplifier lengths. The data have enabled them to extrapolate the intrinsic line width and to observe the effects of gain-narrowing and saturation on the line profile. They find an intrinsic width which is 1.4 times the Doppler width, they observe gain-narrowing in intermediate length amplifiers, and they observe no re-broadening in long, saturated amplifiers. These results suggest that collisional line-broadening has a significant effect on the line profile and saturation behavior of this laser. DOE

N94-14681# Aerospace Corp., El Segundo, CA. Engineering and Technology Group.
AlGaAs DIODE LASER BLUE SHIFT RESULTING FROM FAST NEUTRON IRRADIATION
J. C. Camparo, S. B. Delcamp, and R. P. Frueholz 10 Nov. 1992 36 p
(Contract F04701-88-C-0089)
(AD-A266642; TR-0091(6925-13)-2; SMC-TR-93-27) Avail: CASI HC A03/MF A01

Six TJS (transverse junction stripe) AlGaAs diode lasers were exposed to fast neutrons with fluences ranging from 2 x 10(exp 12) to 3 x 10(exp 13) n/sq cm, and their tuning, gain, and dispersion curves were measured. The tuning and gain curves of four lasers showed blue shifts of several meV at neutron fluences as low as 2 x 10(exp 12) n/sq cm, the other two lasers never showed this blue shift. In addition, the lasers that displayed a blue shift also showed an increase in their threshold currents. None of the lasers exhibited any change in their dispersion curves. To explain the blue shift, it is hypothesized that neutron irradiation reduces the efficiency for lasing in the bandtail states of these devices, forcing lasing action to occur between states with greater energy separation. A model in which the reduced efficiency takes the form of a decrease in the transition matrix element is found to yield blue shifts of the correct order of magnitude. Though bandtail effects may also explain the difference in radiation sensitivity

among the TJS lasers, at present the reason why only four of the six lasers blue shifted after neutron irradiation is not well understood. DTIC

N94-14863# Oak Ridge National Lab., TN.
LASER LITHOGRAPHY BY PHOTON SCANNING TUNNELING MICROSCOPY
I. Lee, R. J. Warmack, and T. L. Ferrell 1993 6 p Presented at the 2nd International Conference on Laser Ablation: Mechanisms and Applications, Knoxville, TN, 19-22 Apr. 1993
(Contract DE-AC05-84OR-21400)
(DE93-015962; CONF-9304144-8) Avail: CASI HC A02/MF A01

We have investigated the possibility of using a photon scanning tunneling microscope (PSTM) for laser lithography. A contrast enhancement material (CEM) is coated onto a sample slide and coupled to the prism of a PSTM. The CEM becomes transparent above a laser (HeCd at a wavelength of 442 nm) intensity threshold attained due to the proximity of the probe tip. The same surface can then be inspected using the given experimental configuration by replacing the HeCd laser line with a non-exposing 633-nm HeNe laser line. Direct patterns can be produced by varying the exposure time and the shape of the probe tip. DOE

N94-14888# Lawrence Livermore National Lab., CA.
OPTIMIZATION STUDY OF X RAY LASER COHERENCE IN Ni-LIKE Ta
P. Amendt, R. A. London, and M. Strauss (Israel Atomic Energy Commission, Beersheba.) Jun. 1993 6 p Presented at the 3rd International Colloquium on X Ray Lasers, Schliersee, Germany, 18-22 May 1992
(Contract W-7405-eng-48)
(DE93-016419; UCRL-JC-110084; CONF-920523-16) Avail: CASI HC A02/MF A01

By separately employing a wave optics treatment based on a modal expansion of the laser electric field and ray optics methods, criteria are proposed which serve to optimize transverse coherence. Refraction is shown to increase the saturation gain-length of the laser, thereby enabling a higher coherent energy output. Under optimum conditions the calculated output for a single stage Ni-like Ta x-ray laser of nearly one mJ in 100 psec from a single stage Ni-like Ta x-ray laser may be satisfactory for 300 A resolution holographic imaging of biological specimens. DOE

N94-14904*# Sirius Group, Peabody, MA.
LASER POWER BEAMING SYSTEM ANALYSES Final Report
Glenn W. Zeiders, Jr. 25 Aug. 1993 15 p
(NASA Order H-20780-D)
(NASA-CR-193840; NAS 1.26:193840; NASA-93-01) Avail: CASI HC A03/MF A01

The successful demonstration of the PAMELA adaptive optics hardware and the fabrication of the BTOS truss structure were identified by the program office as the two most critical elements of the NASA power beaming program, so it was these that received attention during this program. Much of the effort was expended in direct program support at MSFC, but detailed technical analyses of the AMP deterministic control scheme and the BTOS truss structure (both the JPL design and a spherical one) were prepared and are attached, and recommendations are given.
Author (revised)

N94-14391*# Jet Propulsion Lab., California Inst. of Tech., Pasadena.
GOPEX LASER TRANSMISSION AND MONITORING SYSTEMS
G. Okamoto and K. Masters *In its* The Telecommunications and Data Acquisition Report 15 Aug. 1993 p 248-254 (For primary document see N94-14369 02-32)
(RTOP 315-91-60-10-03)
Avail: CASI HC A02/MF A03

37 MECHANICAL ENGINEERING

Includes auxiliary systems (nonpower); machine elements and processes; and mechanical equipment.

N94-12791*# Rotordynamics-Seal Research, Inc., Simi Valley, CA.
CRYOGENIC FLUID FILM BEARING TESTER DEVELOPMENT STUDY Final Report, 16 Apr. - 16 Jun. 1993
Joseph K. Scharrer, ed., Brian T. Murphy, and Lawrence A. Hawkins 13 Jun. 1993 109 p
(NASA Order H-19675-D)
(NASA-CR-192586; NAS 1.26:192586; RSR-C002-93) Avail: CASI HC A06/MF A02

Conceptual designs were developed for the determination of rotordynamic coefficients of cryogenic fluid film bearings. The designs encompassed the use of magnetic and conventional excitation sources as well as the use of magnetic bearings as support bearings. Test article configurations reviewed included overhung, floating housing, and fixed housing. Uncertainty and forced response analyses were performed to assess quality of data and suitability of each for testing a variety of fluid film bearing designs. Development cost and schedule estimates were developed for each design. Facility requirements were reviewed and compared with existing MSFC capability. The recommended configuration consisted of a fixed test article housing centrally located between two magnetic bearings. The magnetic bearings would also serve as the excitation source. Author

N94-12802*# NASTEC, Inc., Cleveland, OH.
ROLLER-GEAR DRIVES FOR ROBOTIC MANIPULATORS DESIGN, FABRICATION AND TEST Final Report
William J. Anderson and William Shipitalo Sep. 1991 250 p Original contains color illustrations
(Contract NAS3-25803; SBIR-05.03-1391A)
(NASA-CR-194248; NAS 1.26:194248) Avail: CASI HC A11/MF A03; 4 functional color pages

Two single axis planetary roller-gear drives and a two axis roller-gear drive with dual inputs were designed for use as robotic transmissions. Each of the single axis drives is a two planet row, four planet arrangement with spur gears and compressively loaded cylindrical rollers acting in parallel. The two axis drive employs bevel gears and cone rollers acting in parallel. The rollers serve a dual function: they remove backlash from the system, and they transmit torque when the gears are not fully engaged.
Derived from text

N94-12851# Brookhaven National Lab., Upton, NY.
LOW PRESSURE STORAGE OF NATURAL GAS ON ACTIVATED CARBON
J. Wegrzyn, H. Wiesmann, and T. Lee 1992 11 p Presented at the 1992 Annual Automotive Technology Development Contractors' Coordination Meeting (ATD/CCM), Dearborn, MI, 2-5 Nov. 1992
(Contract DE-AC02-76CH-00016)
(DE93-014053; BNL-48685; CONF-9211240-1) Avail: CASI HC A03/MF A01

The introduction of natural gas to the transportation energy sector offers the possibility of displacing imported oil with an indigenous fuel. The barrier to the acceptance of natural gas vehicles (NGV) is the limited driving range due to the technical difficulties of on-board storage of a gaseous fuel. In spite of this barrier, compressed natural gas (CNG) vehicles are today being successfully introduced into the market place. The purpose of this work is to demonstrate an adsorbent natural gas (ANG) storage system as a viable alternative to CNG storage. It can be argued that low pressure ANG has reached near parity with CNG, since the storage capacity of CNG (2400 psi) is rated at 190 V/V, while low pressure ANG (500 psi) has reached storage capacities of 180 V/V in the laboratory. A program, which extends laboratory results to a full-scale vehicle test, is necessary before ANG technology will receive widespread acceptance. The objective of this program is to field test a 150 V/V ANG vehicle in FY 1994. As a start towards this goal, carbon adsorbents have been screened by Brookhaven for their potential use in a natural gas storage system. This paper reports on one such carbon, trade name Maxsorb, manufactured by Kansai Coke under an Amoco license. DOE

N94-12988# Texas A&M Univ., College Station. Turbomachinery Labs.
ROTORDYNAMIC AND LEAKAGE CHARACTERISTICS OF A 4-STAGE BRUSH SEAL Final Report, 30 Oct. 1988 - 30 Aug. 1992
K. J. Conner and D. W. Childs Dec. 1992 147 p
(Contract F33615-88-C-2908)
(AD-A266012; WL-TR-92-2125) Avail: CASI HC A07/MF A02

Experimental results are presented for the direct and cross-coupled stiffness and damping coefficients as well as the leakage performance for a 4-stage brush seal. Variable test parameters include the inlet pressure, pressure ratio, shaft speed, fluid prerotation, and seal spacing. Direct

damping is shown to increase with running speed; otherwise, the rotordynamic coefficients are relatively insensitive to changes in the test parameters. Cross-coupled stiffness is generally unchanged by increasing the inlet tangential velocity to the seals, suggesting that the brush seal is not affected by inlet swirl. Direct stiffness is shown to increase with frequency; however, the magnitudes of direct stiffness are always positive. Cross-coupled stiffness increases slightly with frequency; yet not as drastically as direct stiffness. Comparisons of test results for the 4-stage brush seal with an 8-cavity labyrinth showed superior rotordynamics performance for the brush seal; viz., large values for direct stiffness and lower values for the (destabilizing) cross-coupled stiffness coefficient. The damping for brush seals is smaller, but comparable to labyrinth seals. The whirl-frequency ratio is always smaller for the brush seal. DTIC

N94-13122# Aerospace Corp., El Segundo, CA. Engineering and Technology Group.
SURFACE ANALYSIS OF BEARINGS
M. R. Hilton and S. V. Didziulis 31 Mar. 1993 29 p
(Contract F04701-88-C-0089)
(AD-A266800; TR-93(3935)-1; SMC-TR-93-26) Avail: CASI HC A03/MF A01

The report reviews the techniques used to conduct a failure analysis of precision bearings. The review is arranged in a manner consistent with the sequence of bearing disassembly. The information to be gained by and the limitations of each technique are identified, and appropriate examples of fluid- and solid-lubricated systems are presented. The techniques used for lubricant analysis and micro-examination are reviewed, but particular emphasis is given to their integration with surface analysis. DTIC

N94-13129*# Meridian Corp., Alexandria, VA.
FORCE REFLECTING HAND CONTROLLER FOR MANIPULATOR TELEOPERATION Final Technical Report, Jul. 1989 - Jul. 1991
Mark D. Bryfogle 31 Dec. 1991 115 p
(Contract NAS7-1069; SBIR-05.01-3600)
(NASA-CR-191345; NAS 1.26:191345) Avail: CASI HC A06/MF A02

A force reflecting hand controller based upon a six degree of freedom fully parallel mechanism, often termed a Stewart Platform, has been designed, constructed, and tested as an integrated system with a slave robot manipulator test bed. A force reflecting hand controller comprises a kinesthetic device capable of transmitting position and orientation commands to a slave robot manipulator while simultaneously representing the environmental interaction forces of the slave manipulator back to the operator through actuators driving the hand controller mechanism. The Stewart Platform was chosen as a novel approach to improve force reflecting teleoperation because of its inherently high ratio of load generation capability to system mass content and the correspondingly high dynamic bandwidth. An additional novelty of the program was to implement closed loop force and torque control about the hand controller mechanism by equipping the handgrip with a six degree of freedom force and torque measuring cell. The mechanical, electrical, computer, and control systems are discussed and system tests are presented. Author (revised)

N94-13285 Bechtel Corp., Vernon, CA.
COMPENDIUM OF EXECUTIVE SUMMARIES FROM THE MAGLEV SYSTEM CONCEPT DEFINITION Final Report, Nov. 1991 - Sep. 1992
Mar. 1993 124 p Sponsored by Federal Railroad Administration, Washington, DC, and Corps. of Engineers, Washington, DC Prepared in cooperation with Foster-Miller, Inc., Waltham, MA, and Gruman Aerospace Corp., Betpage, NY Limited Reproducibility: More than 20% of this document may be affected by microfiche quality
(PB93-154938/GAR; DOT/FRA/NMI-93/02) Avail: CASI HC A06

The Executive Summaries from the four System Concept Definition (SCD) studies awarded under the National Maglev Initiative are included. These summaries present the technical feasibility, performance, capital, operating, and maintenance costs for a maglev system that would be available by the year 2000. Performance on a hypothetical route, provided to test these concepts in order for the NMI to make performance and cost comparisons, is briefly discussed. This compendium constitutes the principle publication of those SCD reports on technical matters.
Author (revised)

N94-13445*# Maryland Univ., College Park. Inst. for Systems Research.
FLEX-GEAR ELECTRICAL POWER TRANSMISSION Final Report, 15 Jul. 1992 - 15 Sep. 1993
John Vranish and Jonathan Peritt 15 Sep. 1993 133 p
(Grant NAG5-2004)
(NASA-CR-194422; NAS 1.26:194422) Avail: CASI HC A07/MF A02

This study was conducted to develop an alternative way of transferring electricity across a continuously rotating joint, with little wear and the potential for low electrical noise. The problems with wires, slip rings, electromagnetic couplings, and recently invented roll-rings are discussed. Flex-gears, an improvement of roll-rings, are described. An entire class of flexgear devices is developed. Finally, the preferred flex-gear device is optimized for maximum electrical contact and analyzed for average mechanical power loss and maximum stress. For a device diameter of six inches, the preferred device is predicted to have a total electrical contact area of 0.066 square inches. In the preferred device, a small amount of internal sliding produces a 0.003 inch-pound torque that resists the motion of the device. Author (revised)

N94-13521 Concordia Univ., Montreal (Quebec). Dept. of Mechanical Engineering.
TECHNIQUES FOR IMPROVING THE PERFORMANCE OF A SIMPLIFIED ELECTRONIC FUEL CONTROLLER WITH INCREMENTAL ACTUATION FOR SMALL GAS TURBINE ENGINES Ph.D. Thesis
Antanios Ioannou Georgantas Apr. 1990 273 p
(ISBN-0-315-56062-2; CTN-93-60719) Copyright Avail: Micromedia Ltd., Technical Information Centre, 165 Hotel de Ville, Place du Portage, Phase 2, Hull, Quebec J8X 3X2, Canada HC/MF

Concepts are introduced which improve the performance of an inexpensive electronic fuel control unit for small gas turbine engines suitable for use in small aircraft and helicopters. A conventional hydromechanical fuel control unit is modified and adapted for digital electronic control. The conversion involves the replacement of the pneumatic computing and actuating mechanism with digital computation and incremental electronic actuation of a flow metering valve. A mathematical model of the unit is developed, implemented, and validated. The model is used for simulation and study of the system dynamics. Some new methods are applied in the design and development of a digital controller. An optimization scheme for tuning the controller is formulated and implemented experimentally. As a next step toward improvement of the simple electronic fuel controller, a concept of two electronic actuators, one operating the metering valve and the other a bypass valve, is introduced and investigated. Higher flexibility and faster transient response, as compared to the conventional system and the single actuator unit, are demonstrated. The possibility of a backup scheme in case of failure of one of two actuating mechanisms is also discussed. Author (CISTI)

N94-13575 Minnesota Univ., Minneapolis.
GENERALIZED IMPEDANCE CONTROL OF A REDUNDANT MANIPULATOR Ph.D. Thesis
Michael Peter Hennessey 1993 242 p
Avail: Univ. Microfilms Order No. DA9312488

In this thesis, we consider the general problem of impedance control of an n degree-of-freedom (dof) serial link manipulator with emphasis on the redundant manipulator case. Other approaches in the literature insist upon keeping the number of impedance dofs less than or equal to the number of manipulator dofs with a clear partitioning of se lf motion and desired end effect or motion. Our approach does not possess these limitations and is based on, and even encourages, the imposition of multiple conflicting impedance objectives (including distributed impedances). These desired impedances can be either 'fictitious' or actual, 'link' or 'joint' based, and can be customized to a particular application of interest. Impedance interpolation is the key vehicle for resolving the multiple (and likely conflicting) impedance objectives to produce a blended or compromise solution. We show (using singular value decomposition) that provided that a sufficient number (or distribution) and type of impedance dofs are specified (e.g. is greater than or equal to n for the discrete case), a stable control law solution will always exist. Furthermore, singularity robustness of the control law solution can be increased by judiciously adding impedance dofs to the problem. The resultant local dynamics are studied and shown to be conditionally stable and can always be made unconditionally stable by introducing sufficiently high joint impedances. Experimental aspects of

Generalized Impedance Control are studied for the case of interpolated stiffness control of a 3 dof serial link manipulator. In addition, a computationally efficient approach to solving the inverse kinematics problem for an n degree-of-freedom (dof) serial link manipulator is presented; regardless of the manipulator's kinematic configuration or whether it is redundant or nonredundant. The method referred to as the 'multiplexed joint' method is based on individually moving joints in such a manner as to minimize the weighted norm of the resultant linearized location error transformation. A higher level joint scheduling algorithm controls which joints are to be moved. The simplest form of this joint scheduling algorithm would be to cyclicly sequence through all of the joints--hence the analogy to the multiplex or operation. Simulation results are presented for the case of a 3 dof planar redundant manipulator. Author

N94-13597 McGill Univ., Montreal (Quebec).
DYNAMICS AND DESIGN OF NONHOLONOMIC ROBOTIC MECHANICAL SYSTEMS Ph.D. Thesis
Subir Kumar Saha 1991 202 p
(ISBN-0-315-72009-3) Avail: Univ. Microfilms Order No. DANN72009

An approach in formulating kinematic constraints and a methodology for the dynamic modeling of mechanical systems with nonholonomic couplings are presented. The method presented is based on the natural orthogonal complement (NOC) of the kinematic constraint matrix associated with the linear homogeneous form of the kinematic constraints. The method of the NOC is used to model mechanical systems consisting of multiple-loop kinematic chains with nonholonomic constraints. Moreover, the method of the NOC, when coupled with an optimization technique, can be used for the feedforward control of redundantly actuated systems, as shown. The method of the NOC is first discussed in detail with the aid of an example of a two-wheeled mechanical system. Then, nonholonomic robotic mechanical systems, for example, automatic guided vehicles (AGV's), are analyzed for simulation purposes. As a result, general purpose software is developed for the kinematic and dynamic analyses of three-degree-of-freedom (3-DOF) AGV's. These AGV's use omnidirectional wheels which, in contrast to conventional wheels, e.g., the wheels in an automobile, result in 3-DOF motion of the vehicle. Isotropic designs of 3-DOF AGV's for direct kinematics are proposed, which should enhance the control of the vehicle. With advanced computer graphics, a common trend is to use motion animation in assessing the time response of the systems under study. This brought about issues of algorithmic complexity that are inherent to motion animation. These issues are addressed with an example involving the attitude representation of a rigid body and the choice of a suitable coordinate frame in representing the dynamic equations of motion. Dissert. Abstr.

N94-13604* National Aeronautics and Space Administration. Goddard Space Flight Center, Greenbelt, MD.
GODDARD SPACE FLIGHT CENTER ROBOTICS DEMO (Videotape)
Nov. 1988 Videotape: 15 min. playing time, in color, with sound
(NASA-TM-109302; NONP-VT-93-185317) Avail: CASI VHS A01/BETA A22

Documentary footage of a fascinating look at Goddard Space Flight Center's Robotic Capability during a demonstration by Goddard robotics engineers is presented. Author

N94-13642 Pennsylvania State Univ., University Park.
ROBUST SYNTHESIS OF DISCRETE-TIME MULTIVARIABLE CONTROL SYSTEMS WITH INDUCED DELAYS Ph.D. Thesis
Hong Shen 1992 142 p
Avail: Univ. Microfilms Order No. DA9311722

In many real-time distributed control systems such as those for advanced aircraft, spacecraft, and autonomous manufacturing plants, the sensor and control signals within a feedback loop are subjected to delays induced by multiplexed data communication networks. From this perspective, algorithms for synthesizing multivariable discrete-time control systems with induced delays were formulated by stochastic and deterministic approaches. In the stochastic approach, a linear quadratic stochastic regulator was proposed to account for the randomly varying distributed delays in the closed loop system, which was then improved by a stochastic estimator for output feedback control. In the deterministic approach, a multi-step delay compensator was proposed, assuming that the sensor, controller, and actuator have a constant and identical sampling period T, and the randomly varying delays in the closed loop system are bounded. Focus is on improvement of performance and stability robustness of the multi-step delay compensator. The specifications for performance and stability robustness are expressed as matrix-valued functions of frequency. Three algorithms are proposed to minimize the H2-norm of the sensitivity error matrix. The third algorithm, which is an extension of the standard loop transfer recovery (LTR) procedure from one-step prediction to the general case of the p-step prediction (p is greater than or equal to 1), is found to be most suitable among the proposed three algorithms from the perspectives of performance, stability robustness, and computational simplicity. It is shown that the concept of the steady-state minimum-variance filter gain as the H2-minimal solution of the difference between the target sensitivity matrix and the actual sensitivity matrix for one-step prediction does hold for p-step prediction (p is greater than 1). Therefore, the proposed multi-step delay compensator can be used with the synthesized observer gain and adjusted controller gain to mitigate the detrimental effects of the induced delays, and maintain the performance and stability robustness of the closed loop control system. The efficacy of the control synthesis procedure for delay compensation is demonstrated via simulation experiments using the flight dynamic model of an advanced aircraft. Dissert. Abstr.

N94-13794# Army Research Lab., Watertown, MA.
THE EFFECT OF TIN COATINGS ON THE ROLLING CONTACT FATIQUE BEHAVIOR OF M50 BEARING STEEL Final Report
R. M. Middleton, P. J. Huang, M. G. H. Wells, and R. A. Kant (Naval Research Lab., Washington, DC.) Dec. 1992 44 p
(ARL-TR-40) Avail: CASI HC A03/MF A01

There is a continuing requirement for improved bearing performance for both commercial and military applications. Service temperatures are increasing steadily due to increased power requirements and corrosion of components remains a major concern as well, particularly for bearings in military systems. A number of different coatings were applied to VIM-VAR M50 bearing steel to improve both corrosion resistance and rolling contact fatigue behavior. This report deals specifically with coatings produced by the ion beam assisted deposition (IBAD) of TiN, details of the coating process, and test results obtained. The rolling contact fatigue performance of IBAD TiN coated M50 samples demonstrated increased lifetime performance and durability for a 1 micrometer thick coating. Preliminary data on corrosion properties is also presented. Author (revised)

N94-13800*# Texas A&M Univ., College Station. Dept. of Mechanical Engineering.
EVALUATION OF THE SHUTTLE REMOTE MANIPULATOR Final Report
Louis J. Everett and R. C. Redfield 23 Sep. 1993 17 p
(Grant NAG9-450)
(NASA-CR-194351; NAS 1.26:194351) Avail: CASI HC A03/MF A01

The objective initially proposed was to analyze shuttle remote manipulator (SRM) performance data collected during a Shuttle Flight. The data was to consist of video TRAC data collected via a video recorder. Unfortunately, the flight never collected the data due to higher priority experiments superseding it. As a result, the research team at Texas A&M was directed to work on several other pressing issues regarding the TRAC sensor. All but one of these issues were reported earlier in the form of periodic status reports. In fulfillment of the grant conditions, the last issue investigated is being reported as the final report. Ordinarily, a TRAC sensor determines the orientation of an object by analyzing the image reflected from a mirror target. The concern addressed is to develop a method for using the TRAC sensor when the target does not reflect a usable image. Author (revised)

N94-13808 National Physical Lab., Teddington (England). Materials Metrology Div.
THE DESIGN OF CHAIN LINKS AND SLINGS
T. A. E. Gorley Mar. 1993 21 p
(NPL-DMM(A)-94; ETN-93-94542) Copyright Avail: National Physical Laboratory, Teddington, Middlesex, TW11 0LW, United Kingdom HC

The technical items that have been submitted to the various British, International, and European committees that have been drafting standards for chains and for slings of all materials during the last twenty five years are summarized. Discussions are now taking place to draft European standards within the CEN organization. ESA

N94-13874 Southampton Univ. (England). Inst. of Sound and Vibration Research.

PISTON ENGINE INTAKE AND EXHAUST SYSTEM DESIGN

P. O. A. L. Davies Jul. 1993 58 p Limited Reproducibility: More than 20% of this document may be affected by microfiche quality

(ISVR-TR-222) Copyright Avail: Issuing Activity

The aim of intake and exhaust system design is to control the transfer of acoustic energy from the sources and its emission by the system with minimal loss of engine performance. A rational design process depends on the adoption of a design methodology based on predictive modeling of acoustic behavior. Virtually any system geometry can be modeled by breaking it down to a sequence of simple elements or chambers. An initial design layout is then produced with simple parametric models of individual element behavior. This design is then refined to prototype level by systematic modification of detail using realistic assessments of system performance in its operational environment. Following prototype validation by practical testing, further necessary development is again assisted by predictive modeling. The application of appropriate procedures is illustrated by a series of practical examples. These concern improvements in interior noise by control of intake noise, of vehicle performance by reducing flow losses, of the environment by control of exhaust emissions, and lastly with the control of flow noise. The report concludes with a brief outline of current and new developments involving integrated design procedures.

Author (revised)

N94-13975# Lawrence Livermore National Lab., CA.

SOME ASPECTS OF SHEET FORMING SIMULATION USING EXPLICIT FINITE ELEMENT TECHNIQUES

R. G. Whirley, B. E. Engelmann, and R. W. Logan 28 Jul. 1992 9 p Presented at the Winter Annual Meeting of the ASME, Anaheim, CA, 8-13 Nov. 1992

(Contract W-7405-eng-48)

(DE93-012479; UCRL-JC-111227; CONF-921110-49) Avail: CASI HC A02/MF A01

This paper discusses some aspects of the application of the explicit nonlinear finite element code DYNA3D to the numerical simulation of sheet forming processes. Although DYNA3D is intrinsically a code for transient dynamic response, it has been successfully applied to the quasistatic sheet forming problem by slow application of the loads. Although somewhat nontraditional, this approach has proven very robust in application to large-scale problems. This paper discusses the components of a successful sheet forming analysis, including constitutive modeling, contact definition, guidelines for load application, and some suggestions for solution evaluation. Further, this paper illustrates the use of DYNA3D to compute the Limiting Draw Ratio as a function of material anisotropy and compares the computed results for 3-D forming problems with experimental data. DOE

N94-14113# Mason and Hanger-Silas Mason Co., Inc., Amarillo, TX.

COMPATIBILITY TESTING OF VACUUM SEAL MATERIALS

P. A. Foster and W. A. Rodin May 1993 30 p

(Contract DE-AC04-91AL-65030)

(DE93-014366; MHSMP-93-08) Avail: CASI HC A03/MF A01

Small scale materials compatibility testing was conducted for three elastomers considered for use as vacuum seal materials: Adiprene MOCA-cured; Adiprene Cyanacured; and Sylgard silastic rubber. The tests were conducted using orthogonal array designed experiments for each of the elastomers placed in contact with three materials commonly used during weapon disassembly operations: Duxseal, Sylgard 186 grease, and 2-propyl alcohol. The test results indicated that only the 2-propyl alcohol had a significant effect on the elastomer hardness and physical properties. The alcohol had the largest effect on the two Adiprene materials, and the silastic rubber was the least affected. DOE

N94-14134*# Alabama Univ., Tuscaloosa. Bureau of Engineering Research.

DESIGN AND APPLICATION OF ELECTROMECHANICAL ACTUATORS FOR DEEP SPACE MISSIONS Annual Report, 16 Aug. 1992 - 15 Aug. 1993

Tim A. Haskew and John Wander Sep. 1993 72 p

(Grant NAG8-240)

(NASA-CR-194145; NAS 1.26:194145; BER-597-163) Avail: CASI HC A04/MF A01

The annual report Design and Application of Electromechanical Actuators for Deep Space Missions is presented. The reporting period is 16 Aug. 1992 to 15 Aug. 1993. However, the primary focus will be work performed since submission of our semi-annual progress report in Feb. 1993. Substantial progress was made. We currently feel confident in providing guidelines for motor and control strategy selection in electromechanical actuators to be used in thrust vector control (TVC) applications. A small portion was presented in the semi-annual report. At this point, we have implemented highly detailed simulations of various motor/drive systems. The primary motor candidates were the brushless dc machine, permanent magnet synchronous machine, and the induction machine. The primary control implementations were pulse width modulation and hysteresis current control. Each of the two control strategies were applied to each of the three motor choices. With either pulse width modulation or hysteresis current control, the induction machine was always vector controlled. A standard test position command sequence for system performance evaluation is defined. Currently, we are gathering all of the necessary data for formal presentation of the results. Briefly stated for TVC application, we feel that the brushless dc machine operating under PWM current control is the best option. Substantial details on the topic, with supporting simulation results, will be provided later, in the form of a technical paper prepared for submission and also in the next progress report with more detail than allowed for paper publication. Author (revised)

N94-14147# New Brunswick Univ., Fredericton. Dept. of Mechanical Engineering.

MACHINERY DYNAMICS ACTIVITIES IN CANADIAN INDUSTRIES

Robert J. Rogers and Paul Y. Kim (National Research Council of Canada, Vancouver, British Columbia.) May 1992 39 p

(IME-MET-TR-006; CTN-93-60781) Avail: CASI HC A03/MF A01

Results are presented from a survey of Canadian industries to determine their activities related to machinery dynamics. Responses were obtained from industries in the categories of electric utilities, consultants, petrochemicals, research laboratories, aircraft related, and machinery manufacturers. The permanent manpower allocated for tasks such as monitoring machinery vibration, balancing, fault diagnosis, or rotor dynamic analysis has increased significantly in the past five years. A list of individuals who can be contacted to exchange information is included. The use of various instruments is also documented. Small computers and microprocessor based instruments are widely used to record and process vibration data. A wide variety of standards and guides are used for allowable vibration severity and residual imbalance. Some data were obtained for typical normal, alarm, and shutdown vibration values for twenty categories of equipment. The median cost of setting up a vibration program was generally one percent of the total cost of plant and machinery. Fifteen research projects in machinery dynamics are tabulated. Author (CISTI)

N94-14195# National Research Council of Canada, Ottawa (Ontario). Advanced Manufacturing Technology.

CANADIAN TARGET ASSEMBLY (CTA) TO AIRBORNE SUPPORT EQUIPMENT (ASE) VIBRATION TEST REPORT [RAPPORT D'ESSAI DE VIBRATION DE L'ARTICULATION A ROTULE ENTRE LE MODULE CIBLE CANADIEN (MCC) ET LE MATERIEL DE SOUTIEN AEROPORTE]

J. E. Ross Dec. 1992 52 p

(IME-AMT-TR-001; NRC-33592; CTN-93-60859) Avail: CASI HC A04/MF A01

The full flight vibration load testing of the Canadian Target Assembly (CTA) to Airborne Support Equipment (ASE) ball and socket joint (CABS) is documented. The CTA is an optical target that was flown on the Shuttle orbiter, and required a very low friction release latch system. A description is presented of the test hardware and procedures. Results are presented for the numerous tests carried out to assess the performance of combinations of power level, pre-load, lubricant, contact pad material, ball material, and trunnion material. CISTI

N94-14445*# McGill Mfg. Co., Valparaiso, IN.

COMPUTER PROGRAM FOR ANALYSIS OF HIGH SPEED, SINGLE ROW, ANGULAR CONTACT, SPHERICAL ROLLER BEARING, SASHBEAN. VOLUME 1: USER'S GUIDE Final Report

Arun K. Aggarwal Sep. 1993 68 p Prepared for Sikorsky Aircraft, Stratford, CT

(Contract NAS3-25423; RTOP 505-63-36; DA Proj. 1L1-62211-A-47-A)
(NASA-CR-191183; E-8089-Vol-1; NAS 1.26:191183; ARL-CR-82-Vol-1)
Avail: CASI HC A04/MF A01

The computer program SASHBEAN (Sikorsky Aircraft Spherical Roller High Speed Bearing Analysis) analyzes and predicts the operating characteristics of a Single Row, Angular Contact, Spherical Roller Bearing (SRACSRB). The program runs on an IBM or IBM compatible personal computer, and for a given set of input data analyzes the bearing design for it's ring deflections (axial and radial), roller deflections, contact areas and stresses, induced axial thrust, rolling element and cage rotation speeds, lubrication parameters, fatigue lives, and amount of heat generated in the bearing. The dynamic loading of rollers due to centrifugal forces and gyroscopic moments, which becomes quite significant at high speeds, is fully considered in this analysis. For a known application and it's parameters, the program is also capable of performing steady-state and time-transient thermal analyses of the bearing system. The steady-state analysis capability allows the user to estimate the expected steady-state temperature map in and around the bearing under normal operating conditions. On the other hand, the transient analysis feature provides the user a means to simulate the 'lost lubricant' condition and predict a time-temperature history of various critical points in the system. The bearing's 'time-to-failure' estimate may also be made from this (transient) analysis by considering the bearing as failed when a certain temperature limit is reached in the bearing components. The program is fully interactive and allows the user to get started and access most of its features with a minimal of training. For the most part, the program is menu driven, and adequate help messages were provided to guide a new user through various menu options and data input screens. All input data, both for mechanical and thermal analyses, are read through graphical input screens, thereby eliminating any need of a separate text editor/word processor to edit/create data files. Provision is also available to select and view the contents of output files on the monitor screen if no paper printouts are required. A separate volume (Volume-2) of this documentation describes, in detail, the underlying mathematical formulations, assumptions, and solution algorithms of this program. Author (revised)

N94-14446*# McGill Mfg. Co., Valparaiso, IN.
COMPUTER PROGRAM FOR ANALYSIS OF HIGH SPEED, SINGLE ROW, ANGULAR CONTACT, SPHERICAL ROLLER BEARING, SASHBEAN. VOLUME 2: MATHEMATICAL FORMULATION AND ANALYSIS Final Report
Arun K. Aggarwal Sep. 1993 50 p Prepared for Sikorsky Aircraft, Stratford, CT
(Contract NAS3-25423; RTOP 505-63-36; DA Proj. 1L1-62211-A-47-A)
(NASA-CR-191182; E-8088-Vol-2; NAS 1.26:191182; ARL-CR-81-Vol-2)
Avail: CASI HC A03/MF A01

Spherical roller bearings have typically been used in applications with speeds limited to about 5000 rpm and loads limited for operation at less than about 0.25 million DN. However, spherical roller bearings are now being designed for high load and high speed applications including aerospace applications. A computer program, SASHBEAN, was developed to provide an analytical tool to design, analyze, and predict the performance of high speed, single row, angular contact (including zero contact angle), spherical roller bearings. The material presented is the mathematical formulation and analytical methods used to develop computer program SASHBEAN. For a given set of operating conditions, the program calculates the bearings ring deflections (axial and radial), roller deflections, contact areas stresses, depth and magnitude of maximum shear stresses, axial thrust, rolling element and cage rotational speeds, lubrication parameters, fatigue lives, and rates of heat generation. Centrifugal forces and gyroscopic moments are fully considered. The program is also capable of performing steady-state and time-transient thermal analyses of the bearing system. Author (revised)

N94-14457# Los Alamos National Lab., NM.
MACHINING AND GRINDING: HIGH RATE DEFORMATION IN PRACTICE
P. S. Follansbee 1993 5 p Presented at the 1993 ASPE Spring Topical Meeting, Tucson, AZ, 13-15 Apr. 1993
(Contract W-7405-eng-36)
(DE93-010718; LA-UR-93-791; CONF-9304106-1) Avail: CASI HC A01/MF A01

Machining and grinding are well-established material-working operations involving highly non-uniform deformation and failure processes. A typical machining operation is characterized by uncertain boundary conditions (e.g., surface interactions), three-dimensional stress states, large strains, high strain rates, non-uniform temperatures, highly localized deformations, and failure by both nominally ductile and brittle mechanisms. While machining and grinding are thought to be dominated by empiricism, even a cursory inspection leads one to the conclusion that this results more from necessity arising out of the complicated and highly interdisciplinary nature of the processes than from the lack thereof. With these conditions in mind, the purpose of this paper is to outline the current understanding of strain rate effects in metals. DOE

N94-14565# EG and G Rocky Flats, Inc., Golden, CO.
WELDING TECHNOLOGIES AS APPLIED TO NUCLEAR MANUFACTURING
J. R. Roper 23 Oct. 1992 22 p
(Contract DE-AC34-90DP-62349)
(DE93-010924; DOE/FTR-93010924) Avail: CASI HC A03/MF A01 (US Sales Only)

This is the trip report of John R. Roper, who traveled to England 25 Sep. through 8 Oct. 1992. Dr. Roper attended the US/UK JOWOG 22-D Joining Technical Exchange meeting and gave a presentation on Welding Finite Element Analysis and the Precision Joining Center at the Atomic Weapons Establishment in Aldermaston, United Kingdom. Dr. Roper also toured the Welding Institute in Abington, UK and discussed technology exchange of weld thermal and mechanical material responses. DOE

N94-14727*# National Aeronautics and Space Administration. Lewis Research Center, Cleveland, OH.
A HOT DYNAMIC SEAL RIG FOR MEASURING HYPERSONIC ENGINE SEAL DURABILITY AND FLOW PERFORMANCE
Jeffrey H. Miller (Sverdrup Technology, Inc., Brook Park, OH.), Bruce M. Steinetz, Paul J. Sirocky (Sverdrup Technology, Inc., Brook Park, OH.), and Lawrence A. Kren (Case Western Reserve Univ., Cleveland, OH.) Apr. 1993 11 p Presented at the 34th Structures, Structural Dynamics, and Materials Conference, La Jolla, CA, 19-21 Apr. 1993; sponsored by AIAA, ASME, AHS, and ASC See also A93-33916
(RTOP 763-22-41)
(NASA-TM-106294; E-8031; NAS 1.15:106294; AIAA Paper 93-1346)
Avail: CASI HC A03/MF A01

A test fixture for measuring the dynamic performance of candidate high-temperature engine seal concepts was installed at NASA Lewis Research Center. The test fixture was designed to evaluate seal concepts under development for advanced hypersonic engines, such as those being considered for the National Aerospace Plane (NASP). The fixture can measure dynamic seal leakage performance from room temperature up to 840 C (1550 F) and air pressure differentials up to 690 kPa (100 psi). Performance of the seals can be measured while sealing against flat or distorted walls. In the fixture two seals are preloaded against the sides of a 30 cm (1 ft) long saber that slides transverse to the axis of the seals, simulating the scrubbing motion anticipated in these engines. The capabilities of this test fixture along with preliminary data showing the dependence of seal leakage performance on high temperature cycling are addressed. Author (revised)

N94-14848*# Mississippi State Univ., Mississippi State. Engineering for Research Center.
THE DEVELOPMENT OF A SCALABLE PARALLEL 3-D CFD ALGORITHM FOR TURBOMACHINERY M.S. Thesis Final Report
Edward Allen Luke Jul. 1993 83 p
(Grant NAG3-1073)
(NASA-CR-193604; NAS 1.26:193604) Avail: CASI HC A05/MF A01

Two algorithms capable of computing a transonic 3-D inviscid flow field about rotating machines are considered for parallel implementation. During the study of these algorithms, a significant new method of measuring the performance of parallel algorithms is developed. The theory that supports this new method creates an empirical definition of scalable parallel algorithms that is used to produce quantifiable evidence that a scalable parallel application was developed. The implementation of the parallel application and an automated domain decomposition tool are also discussed. Author (revised)

N94-14901# Columbia Univ., New York, NY.
THE FURTHER DEVELOPMENT AND REFINEMENT OF AN EXPERT-SYSTEMS APPROACH TO THE CREATIVE DESIGN OF MECHANISMS AND MECHANICAL SYSTEMS Final Report, 1 Jun. 1990 - 30 May 1993
Ferdinand Freudenstein and David Hoeltzel Jun. 1993 17 p
(Contract DAAL03-90-G-0130)
(AD-A266812; ARO-26995.3-EG) Avail: CASI HC A03/MF A01

The research has been concerned with a comprehensive analysis of robotic end effectors including frictional energy dissipation and rigid-body as well as flexible elements. The design analysis involves a set of nonlinear simultaneous equations for quantifying such phenomena as preloads, internal forces, frictional drag, kinematic and dynamic performance and optimization criteria, energy losses and efficiency. The analysis facilitates the optimization of robotic systems in the design stage. A new concept, which we may call a cylindrical actuator, was developed in the course of the research (and communicated to the U.S. Army Research Office (ARO)) and may have significant applications, both in robotics, as well as in other areas of mechanical design. Author (revised)

38 QUALITY ASSURANCE AND RELIABILITY

Includes product sampling procedures and techniques; and quality control.

N94-12941# Instituto de Pesquisas Espaciais, Sao Jose dos Campos (Brazil).
VISART: ARTIFICIAL VISION FOR INDUSTRIAL USE. A COMPREHENSIVE SYSTEM Ph.D. Thesis [VISART - VISAO ARTIFICIAL PARA USO INDUSTRIAL: UM SISTEMA ABRANGENTE]
Sdnei deBritoAlves Feb. 1992 185 p In PORTUGESE
(INPE-5379-TDI/474) Avail: CASI HC A09/MF A02

A thorough description of a Computer Vision System applied to inspection activities is presented, all of the life-cycle stages of this system being dealt with in detail. It was conceived, designed, and implemented within the scope of an applied research, entitled (VISART) Artificial Vision for Industrial Use: A Comprehensive System. During the effort employed in the development of this work, significant contributions were incorporated to the state-of-the-art in processing of binary images. The VISART system includes resources, concepts, and inovations not yet seen in similar systems. A new terminology with technical terms nearer to those used by engineers and technicians, in industrial environments, is proposed and it might contribute for acceptance and dissemination of Vision Systems in these environments. Concepts of Group Technology have been associated to Vision Systems and they might contribute for a greater integration of the industrial process automation. A special data structure was conceived for image data storage, allowing to reduce the processing time of algorithms of industrial part features-extraction. A library with a considerable number of feature extraction algorithms, used for recognition, acceptance or rejection of industrial products under inspection, was conceived and implemented. New algorithms can be appended to this library by the user, without the necessity of reprogramming the modules of the VISART system. Within this respect lies one of the main comprisement features of VISART. It has a graphic editor which makes possible to use it in activities such as teaching and formation of skilled personnel in the area of vision. At first, this facility exempts the use of sensors, making it more economic for use in these activities. All in all, this research work is a pioneer in Brazil, and its divulgation must contribute significantly for the dissemination and growth of the computer vision area applied to inspection, in the country. Author (revised)

N94-13042# Kansas Univ., Lawrence. Center for Research.
AUTOMATED CRACK IDENTIFICATION FOR CEMENT PASTE Final Report, 4 Jun. 1990 - 13 Apr. 1993
Kirk W. Ketcham, Francisco A. Romero, David Darwin, Shanglong Gong, and Mohamed N. Abou-Zeid Apr. 1993 77 p
(Grant AF-AFOSR-0296-89)
(AD-A265753; SM-34; AFOSR-93-0385TR) Avail: CASI HC A05/MF A01

The development of an automated procedure for the identification of microcracks in cementitious materials is described. The degree and nature of microcracking is measured using backscattered electron images obtained with an integrated scanning electron microscope/image analysis system. Multiple images for specimens are analyzed using a computer program developed to identify and measure microcracks within the individual phases of cement paste. The procedure is developed to assist in the determination of the roles played by individual phases in cement paste in the formation and propagation of microcracks. Procedures for specimen testing, preparation, imaging, and crack analysis are described, along with a description of the development of the analysis program. The analysis capabilities of the program are demonstrated. The gray level of epoxy-filled cracks in polished cement paste specimens is affected by the atomic number density of underlying and adjacent phases. As a result, cracks cannot be identified based on gray level alone. Epoxy-filled cracks in polished cement paste specimens can be identified of geometric requirements; combined procedures that establish the floor of a crack, minimum gradient and gray level adjacent to cracks, and minimum differences in gray level between the floor of a crack and adjacent solid phases provide a reproducible and consistent technique for crack identification in cement paste. DTIC

N94-13056*# National Aeronautics and Space Administration. Lewis Research Center, Cleveland, OH.
QUANTITATIVE MAPPING OF PORE FRACTION VARIATIONS IN SILICON NITRIDE USING AN ULTRASONIC CONTACT SCAN TECHNIQUE
Don J. Roth, James D. Kiser, Suzanne M. Swickard, Steven A. Szatmary (Cleveland State Univ., OH.), and David P. Kerwin (Cleveland State Univ., OH.) Washington Aug. 1993 36 p
(RTOP 506-43-11)
(NASA-TP-3377; E-7558; NAS 1.60:3377) Avail: CASI HC A03/MF A01

An ultrasonic scan procedure using the pulse-echo contact configuration was employed to obtain maps of pore fraction variations in sintered silicon nitride samples in terms of ultrasonic material properties. Ultrasonic velocity, attenuation coefficient, and reflection coefficient images were obtained simultaneously over a broad band of frequencies (e.g., 30 to 110 MHz) by using spectroscopic analysis. Liquid and membrane (dry) coupling techniques and longitudinal and shear-wave energies were used. The major results include the following: Ultrasonic velocity (longitudinal and shear wave) images revealed and correlated with the extent of average through-thickness pore fraction variations in the silicon nitride disks. Attenuation coefficient images revealed pore fraction nonuniformity due to the scattering that occurred at boundaries between regions of high and low pore fraction. Velocity and attenuation coefficient images were each nearly identical for machined and polished disks, making the method readily applicable to machined materials. Velocity images were similar for wet and membrane coupling. Maps of apparent Poisson's ratio constructed from longitudinal and shear-wave velocities quantified Poisson's ratio variations across a silicon nitride disk. Thermal wave images of a disk indicated transient thermal behavior variations that correlated with observed variations in pore fraction and velocity and attenuation coefficients. Author

N94-13148*# Jet Propulsion Lab., California Inst. of Tech., Pasadena.
NINTH ANNUAL NASA/CONTRACTORS CONFERENCE ON QUALITY AND PRODUCTIVITY. WORLD CLASS EXCELLENCE: THE JOURNEY CONTINUES. KEYNOTE PRESENTATIONS
Geoffrey B. Templeton, ed. (National Aeronautics and Space Administration, Washington, DC.) 1992 43 p Conference held in Pasadena, CA, 20-21 Oct. 1992
(NASA-CR-194513; NAS 1.26:194513) Avail: CASI HC A03/MF A01

This coference provided an excellent forum for the members of the NASA community to share their experience and expertise in an effort to continuously improve the quality of the US space program. The topics covered include the following: NASA's approach to continual improvement; commitment to total quality; total quality at AlliedSignal Aerospace; organizational TQM; recognition of the 1992 Low Trophy Finalists; announcement of the 1992 Low Trophy Recipients; and the changing face of aerospace contracting. Derived from text

N94-13153*# Jet Propulsion Lab., California Inst. of Tech., Pasadena.
NINTH ANNUAL NASA/CONTRACTORS CONFERENCE ON QUALITY AND PRODUCTIVITY. WORLD CLASS EXCELLENCE: THE JOURNEY CONTINUES. CONFERENCE PRESENTATIONS

Geoffrey B. Templeton, ed. (National Aeronautics and Space Administration, Washington, DC.) and Lynne M. Stewart, ed. (National Aeronautics and Space Administration, Washington, DC.) 1992 375 p Conference held in Pasadena, CA, 20-21 Oct. 1992
(NASA-CR-194514; NAS 1.26:194514) Avail: CASI HC A16/MF A03

The topics covered include the following: The George M. Low Trophy; total quality assessment and measurement; using award criteria to improve organizational effectiveness; results--keeping an eye on the bottom line; capturing customer satisfaction; moving from management to leadership; leadership versus management; transforming the management team; leadership success stories; success stories in the quest for excellence; small business successes; education success stories; government success stories; tools and techniques for total quality management (TQM) integration; planning and organizing for TQM integration; successful stories for implementing system level TQM/CI tools; assessing TQM results; establishing an environment for continuous improvement at NASA; empowerment; synergism of partnering; and partnerships in education. For individual titles, see N94-13154 through N94-13169.

N94-13154*# American Productivity and Air Quality Center, Houston, TX.
MEASURING QUALITY PROGRESS
Larry D. Lambert *In* JPL, Ninth Annual NASA/Contractors Conference on Qualtiy and Productivity. World Class Excellence: The Journey Continues. Conference Presentations 1992 21 p (For primary document see N94-13153 02-38)
Avail: CASI HC A03/MF A03

The study by the American Productivity & Quality Center (APQC) was commissioned by Loral Space Information Systems, Inc. and the National Aeronautics and Space Administration (NASA) to evaluate internal assessment systems. APQC benchmarked approaches to the internal assessment of quality management systems in three phases. The first phase included work conducted for the International Benchmarking Clearinghouse (IBC) and consisted of an in-depth analysis of the 1991 Malcolm Baldrige National Quality Award criteria. The second phase was also performed for the IBC and compared the 1991 award criteria among the following quality awards: Deming Prize, Malcolm Baldrige National Quality Award, The President's Award for Quality and Productivity Improvement, The NASA Excellence Award (The George M. Lowe Trophy) for Quality and Productivity Improvement and the Shigeo Shingo Award for Excellence in Manufacturing. The third phase compared the internal implementation approaches of 23 companies selected from American industry for their recognized, formal assessment systems. Derived from text

N94-13155*# National Aeronautics and Space Administration. Lyndon B. Johnson Space Center, Houston, TX.
DEFINING THE PERFORMANCE GAP: CONDUCTING A SELF-ASSESSMENT
Susan A. Braymer, David L. Stoner (Loral Space Information Systems, Houston, TX.), and William C. Powell (Spectra Research Systems, Inc., Houston, TX.) *In* JPL, Ninth Annual NASA/Contractors Conference on Quality and Productivity. World Class Excellence; The Journey Continues. Conference Presentations 1992 8 p (For primary document see N94-13153 02-38)
Avail: CASI HC A02/MF A03

This paper presents two different approaches to performing self-assessments of continuous improvement activities. Case Study 1 describes the activities performed by JSC to assess the implementation of continuous improvement efforts at the NASA Center. The JSC approach included surveys administered to randomly selected NASA personnel and personal interviews with NASA and contractor management personnel. Case Study 2 describes the continuous improvement survey performed by the JSC Safety, Reliability, and Quality Assurance (SR&QA) organization. This survey consisted of a short questionnaire (50 questions) administered to all NASA and contractor SR&QA personnel. The questionnaire is based on the eight categories of the President's Award for Quality and Productivity Improvement. It is designed to objectively determine placement on the TQ benchmark and identify a roadmap for improvement. Derived from text

N94-13156*# Sirota and Alper Associates, Inc., Bethesda, MD.
WHAT'S THE BOTTOM LINE PAYBACK FOR TQM?
Brian Usilaner *In* JPL, Ninth Annual NASA/Contractors Conference on Quality and Productivity. World Class Excellence; The Journey Continues. Conference Presentations 1992 17 p (For primary document see N94-13153 02-38)
Avail: CASI HC A03/MF A03

The purpose of this article is to explore in detail TQM's impact on improving organization performance and how effective TQM strategies are designed and implemented. Both of these issues are addressed primarily by a discussion of a recent study of TQM efforts conducted by the U.S. General Accounting Office (GAO). The GAO study examines the impact of formal TQM improvement strategies on the performance of selected U.S. companies. The study grew out of a concern by a number of U.S. Congressmen that little is known about the impact of various quality-related efforts many companies have adopted to remain viable and profitable in an increasingly competitive world marketplace. Specifically, the study addresses: what has been the performance impact of adopting TQM improvement strategies, how has improved quality been achieved, and what lessons may be applicable to U.S. companies in general. A number of other studies are also used to expand upon the GAO data.
Derived from text

N94-13157*# Paramax Systems Corp., Houston, TX. Space Systems.
PARTNERSHIP WITH THE CUSTOMER
Gregory S. Trachta *In* JPL, Ninth Annual NASA/Contractors Conference on Quality and Productivity. World Class Excellence: The Journey Continues. Conference Presentations 1992 8 p (For primary document see N94-13153 02-38)
Avail: CASI HC A02/MF A03

This discussion will recount some historical observations about establishing partnerships with the customer. It suggests that such partnerships are established as the natural evolutionary product of a continuous improvement culture. Those are warm, ethereal terms about a topic that some people think already suffers from an excess of hot air. We will focus on some real-world activities and workplace artifacts to show there are substantive concepts behind the TQM buzzwords.
Derived from text

N94-13158*# National Aeronautics and Space Administration. Lyndon B. Johnson Space Center, Houston, TX.
STRATEGIC PLANNING AS A FOCUS FOR CONTINUOUS IMPROVEMENT. A CASE STUDY
John W. ONeill and Lyn Gordon-Winkler *In* JPL, Ninth Annual NASA/Contractors Conference on Quality and Productivity. World Class Excellence: The Journey Continues. Conference Presentations 1992 12 p (For primary document see N94-13153 02-38)
Avail: CASI HC A03/MF A03

What do most of the successful people and organizations in our world have in common? Instead of worrying about the future, they work to create it. They have a plan, or a vision of what they want to accomplish and they focus their efforts on success. Strategic planning has been described as a disciplined, ongoing process to produce fundamental decisions and actions that shape what an organization is, what it does, and how it will respond to a changing environment. This case study discussion will evaluate the relationship between strategic planning and Total Quality Management (TQM), or continuous improvement, through the experience of the NASA Johnson Space Center in developing a strategy for the future. That experience clearly illustrates the value of strategic planning in setting the framework and establishing the overall thrust of continuous improvement initiatives. Equally significant, the fundamentals of a quality culture such as strong customer and supplier partnerships, participative involvement, open communications, and ownership were essential in overcoming the challenges inherent in the planning process. A reinforced management commitment to the quality culture was a clear, long-term benefit. Derived from text

N94-13159*# Allied-Signal Aerospace Canada, Toronto (Ontario).
THE POWER OF CROSS-FUNCTIONAL TEAMS IN DRIVING TOTAL QUALITY
Tim M. McClung and Tom J. McMaster *In* JPL, Ninth Annual NASA/Contractors Conference on Quality and Productivity. World Class Excellence: The Journey Continues. Conference Presentations 1992 21 p (For primary document see N94-13153 02-38)
Avail: CASI HC A03/MF A03

Garrett Canada, a Division of Allied-Signal Aerospace Canada, has

been a member of the Canadian aerospace industry for 40 years. Although Garrett Canada has always been a profitable division with a solid market share, the changing and turbulent business environment and globalization of the aerospace industry has created new demands and challenges. The marketplace is demanding faster introduction of new products, as well as shorter leadtimes for repairs and spares. It was recognized that reducing cycle times for new products and for ongoing production would not only satisfy our customers, it would also enhance our business performance through reduced inventories, lower past due, and more responsiveness to change. It was evident that drastic function changes were required if we were to maintain our position as a premier aerospace supplier. The challenge was to convert a stable, somewhat slow-paced work environment with strong functional boundaries into a boundaryless world class team functioning in a total quality environment and focused on customer satisfaction. Complete and uncompromised customer satisfaction has become our driving force, with Total Quality being our engine to continuously improve our processes and increase our speed. The way in which this transition has been brought about is the subject of this presentation. Author (revised)

N94-13160*# TRW Space Technology Labs., Redondo Beach, CA. Federal Systems Div.

SPACECRAFT COst REduction TEAM (SCORE): TQM/CI ON A MASSIVE SCALE

Jerry D. Bullard *In* JPL, Ninth Annual NASA/Contractors Conference on Quality and Productivity. World Class Excellence: The Journey Continues. Conference Presentations 1992 10 p (For primary document see N94-13153 02-38)

Avail: CASI HC A02/MF A03

The business of building satellites and space systems has matured. Few missions require, or can afford, excellent performance at any price. The new paradigm is doing more with less, providing quality systems at lower cost--in other words, doing our job 'Faster-Better-Cheaper.' The TRW Spacecraft COst REduction (SCORE) initiative was launched in 1990 by Daniel S. Goldin, then general manager of TRW's Space & Technology Group. The SCORE mission is to apply continuous improvement (CI) techniques to effect major reductions in the cost (our primary goal) and span time (as a corollary) required for the production of spacecraft. SCORE is a multi-year initiative that is having a profound effect on both the procedural and the cultural aspects of how we do business. The objectives of this initiative are being realized. The focus of this paper is not on the results of SCORE per se, but rather on the things we have leaned about how to do continuous improvement on a massive scale, with multilevel (hierarchical) CI teams. The following sections summarize the chronology of the SCORE initiative, from team formation to development of the year-end report for 1991. Lessons learned, the core of this presentation, are discussed--with particular focus on the unique aspects of SCORE. The SCORE initiative is continuing and, as a part of our evolving culture, will never end. It has resulted in profound insights into the way we do work and (the topic at hand) how to do CI for large and complex multidisciplinary development activities. Author (revised)

N94-13161*# Sterling Software, Inc., Palo Alto, CA.

OBJECT-ORIENTED PRODUCTIVITY METRICS

John L. Connell and Nancy Eller *In* JPL, Ninth Annual NASA/Contractors Conference on Quality and Productivity. World Class Excellence: The Journey Continues. Conference Presentations 1992 8 p (For primary document see N94-13153 02-38)

Avail: CASI HC A02/MF A03

Software productivity metrics are useful for sizing and costing proposed software and for measuring development productivity. Estimating and measuring source lines of code (SLOC) has proven to be a bad idea because it encourages writing more lines of code and using lower level languages. Function Point Analysis is an improved software metric system, but it is not compatible with newer rapid prototyping and object-oriented approaches to software development. A process is presented here for counting object-oriented effort points, based on a preliminary object-oriented analysis. It is proposed that this approach is compatible with object-oriented analysis, design, programming, and rapid prototyping. Statistics gathered on actual projects are presented to validate the approach.

Author (revised)

N94-13162*# Kinlaw Associates, Norfolk, VA.

KENNEDY SPACE CENTER'S NASA/CONTRACTOR TEAM-CENTERED TOTAL QUALITY MANAGEMENT SEMINAR: RESULTS, METHODS, AND LESSONS LEARNED

Dennis C. Kinlaw and Jeannette Eads (Edgerton, Germeshausen and Grier, Inc., Cocoa Beach, FL.) *In* JPL, Ninth Annual NASA/Contractors Conference on Quality and Productivity. World Class Excellence: The Journey Continues. Conference Presentations 1992 12 p (For primary document see N94-13153 02-38)

Avail: CASI HC A03/MF A03

It is apparent to everyone associated with the Nation's aeronautics and space programs that the challenge of continuous improvement can be reasonably addressed only if NASA and its contractors act together in a fully integrated and cooperative manner that transcends the traditional boundaries of proprietary interest. It is, however, one thing to assent to the need for such integration and cooperation; it is quite another thing to undertake the hard tasks of turning such a need into action. Whatever else total quality management is, it is fundamentally a team-centered and team-driven process of continuous improvement. The introduction of total quality management at KSC, therefore, has given the Center a special opportunity to translate the need for closer integration and cooperation among all its organizations into specific initiatives. One such initiative that NASA and its contractors have undertaken at KSC is a NASA/Contractor team-centered Total Quality Management Seminar. It is this seminar which is the subject of this paper. The specific purposes of this paper are to describe the following: Background, development, and evolution of Kennedy Space Center's Total Quality Management Seminar; Special characteristics of the seminar; Content of the seminar; Meaning and utility of a team-centered design for TQM training; Results of the seminar; Use that one KSC contractor, EG&G Florida, Inc. has made of the seminar in its Total Quality Management initiative; and Lessons learned.

Author (revised)

N94-13163*# National Aeronautics and Space Administration. John C. Stennis Space Center, Bay Saint Louis, MS.

HERE'S THE BEEF: A CASE STUDY IN ORGANIZATIONAL TRANSFORMATION

William F. Huseonica and Marco J. Giardino *In* JPL, Ninth Annual NASA/Contractors Conference on Quality and Productivity. World Class Excellence: The Journey Continues. Conference Presentations 1992 4 p (For primary document see N94-13153 02-38)

Avail: CASI HC A01/MF A03

The Science and Technology Lab (STL) is tasked with the design, development, and application of the science and engineering services. Formed in the early 1970's STL adhered to many traditional attitudes including barriers to communication, excessive management control, parochial strategies, unclear measures of success, lack of customer focus, underutilization of people, and excessive administrative burdens on scientists and engineers. The challenge for the STL was to maximize customer satisfaction through the effective and efficient application of the notable skills and talents of the STL's workforce. In this way, the Lab would begin its exciting journey toward becoming world class. A discussion of this on-going transformation is presented. Author (revised)

N94-13164*# National Aeronautics and Space Administration, Washington, DC.

BUILDING A QUALITY CULTURE IN THE OFFICE OF SPACE FLIGHT: APPROACH, LESSONS LEARNED AND IMPLICATIONS FOR THE FUTURE

C. Shannon Roberts *In* JPL, Ninth Annual NASA/Contractors Conference on Quality and Productivity. World Class Excellence: The Journey Continues. Conference Presentations 1992 14 p (For primary document see N94-13153 02-38)

Avail: CASI HC A03/MF A03

The purpose of this paper is to describe the approach and lessons learned by the Office of Space Flight (OSF), National Aeronautics and Space Administration (NASA), in its introduction of quality. In particular, the experience of OSF Headquarters is discussed as an example of an organization within NASA that is considering both the business and human elements of the change and the opportunities the quality focus presents to improve continuously. It is hoped that the insights shared will be of use to those embarking upon similar cultural changes. The paper is presented in

the following parts: the leadership challenge; background; context of the approach to quality; initial steps; current initiatives; lessons learned; and implications for the future. Author (revised)

N94-13165*# National Aeronautics and Space Administration. Lyndon B. Johnson Space Center, Houston, TX.

NASA JOHNSON SPACE CENTER: TOTAL QUALITY PARTNERSHIP

Charlie Harlan and Alfred A. Boyd (Loral Space Information Systems, Houston, TX.) *In* JPL, Ninth Annual NASA/Contractors Conference on Quality and Productivity. World Class Excellence: The Journey Continues. Conference Presentations 1992 16 p (For primary document see N94-13153 02-38)

Avail: CASI HC A03/MF A03

The development of and benefits realized from a joint NASA, support contractor continuous improvement process at the Johnson Space Center (JSC) is traced. The joint effort described is the Safety, Reliability, and Quality Assurance Directorate relationship with its three support contractors which began in early 1990. The Continuous Improvement effort started in early 1990 with an initiative to document and simplify numerous engineering change evaluation processes. This effort quickly grew in scope and intensity to include process improvement teams, improvement methodologies, awareness, and training. By early 1991, the support contractor had teams in place and functioning, program goals established and a cultural change effort underway. In mid-l991 it became apparent that a major redirection was needed to counter a growing sense of frustration and dissatisfaction from teams and managers. Sources of frustration were isolated to insufficient joint participation on teams, and to a poorly defined vision. Over the next year, the effort was transformed to a truly joint process. The presentation covers the steps taken to define vision, values, goals, and priorities and to form a joint Steering Committee and joint process improvement teams. The most recent assessment against the President's award criteria is presented as a summary of progress. Small, but important improvement results have already demonstrated the value of the joint effort.

Author (revised)

N94-13166*# National Aeronautics and Space Administration. Lyndon B. Johnson Space Center, Houston, TX.

SHARED VISIONS: PARTNERSHIP OF ROCKWELL INTERNATIONAL AND NASA COST EFFECTIVENESS ENHANCEMENTS (CEE) FOR THE SPACE SHUTTLE SYSTEM INTEGRATION PROGRAM

Bohdan I. Bejmuk (Rockwell International Corp., Huntsville, AL.) and Larry Williams *In* JPL, Ninth Annual NASA/Contractors Conference on Quality and Productivity. World Class Excellence: The Journey Continues. Conference Presentations 1992 9 p (For primary document see N94-13153 02-38)

Avail: CASI HC A02/MF A03

As a result of limited resources and tight fiscal constraints over the past several years, the defense and aerospace industries have experienced a downturn in business activity. The impact of fewer contracts being awarded has placed a greater emphasis for effectiveness and efficiency on industry contractors. It is clear that a reallocation of resources is required for America to continue to lead the world in space and technology. The key to technological and economic survival is the transforming of existing programs, such as the Space Shuttle Program, into more cost efficient programs so as to divert the savings to other NASA programs. The partnership between Rockwell International and NASA and their joint improvement efforts that resulted in significant streamlining and cost reduction measures to Rockwell International Space System Division's work on the Space Shuttle System Integration Contract is described. This work was a result of an established Cost Effectiveness Enhancement (CEE) Team formed initially in Fiscal Year 1991, and more recently expanded to a larger scale CEE Initiative in 1992. By working closely with the customer in agreeing to contract content, obtaining management endorsement and commitment, and involving the employees in total quality management (TQM) and continuous improvement 'teams,' the initial annual cost reduction target was exceeded significantly. The CEE Initiative helped reduce the cost of the Shuttle Systems Integration contract while establishing a stronger program based upon customer needs, teamwork, quality enhancements, and cost effectiveness. This was accomplished by systematically analyzing, challenging, and changing the established processes, practices, and systems. This examination, in nature, was work intensive due to the depth and breadth of the activity. The CEE Initiative has provided opportunities to make a difference in the way Rockwell and NASA work together - to update the methods and processes of the organizations. The future success of NASA space programs and Rockwell hinges upon the ability to adopt new, more efficient and effective work processes. Efficiency, proficiency, cost effectiveness, and teamwork are a necessity for economic survival. Continuous improvement initiatives like the CEE are, and will continue to be, vehicles by which the road can be traveled with a vision to the future.

Author (revised)

N94-13167*# TRW Electronic Systems Group, Redondo Beach, CA. Measurement and Computer Resource Center.

TEAMWORK FOR OVERSIGHT OF PROCESSES AND SYSTEMS (TOPS). IMPLEMENTATION GUIDE FOR TOPS VERSION 2.0, 10 AUGUST 1992

Albert A. Strand and Darryl J. Jackson *In* JPL, Ninth Annual NASA/Contractors Conference on Quality and Productivity. World Class Excellence: The Journey Continues. Conference Presentations 1992 31 p (For primary document see N94-13153 02-38)

Avail: CASI HC A03/MF A03

As the nation redefines priorities to deal with a rapidly changing world order, both government and industry require new approaches for oversight of management systems, particularly for high technology products. Declining defense budgets will lead to significant reductions in government contract management personnel. Concurrently, defense contractors are reducing administrative and overhead staffing to control costs. These combined pressures require bold approaches for the oversight of management systems. In the Spring of 1991, the DPRO and TRW created a Process Action Team (PAT) to jointly prepare a Performance Based Management (PBM) system titled Teamwork for Oversight of Processes and Systems (TOPS). The primary goal is implementation of a performance based management system based on objective data to review critical TRW processes with an emphasis on continuous improvement. The processes are: Finance and Business Systems, Engineering and Manufacturing Systems, Quality Assurance, and Software Systems. The team established a number of goals: delivery of quality products to contractual terms and conditions; ensure that TRW management systems meet government guidance and good business practices; use of objective data to measure critical processes; elimination of wasteful/duplicative reviews and audits; emphasis on teamwork--all efforts must be perceived to add value by both sides and decisions are made by consensus; and synergy and the creation of a strong working trust between TRW and the DPRO. TOPS permits the adjustment of oversight resources when conditions change or when TRW systems performance indicate either an increase or decrease in surveillance is appropriate. Monthly Contractor Performance Assessments (CPA) are derived from a summary of supporting system level and process-level ratings obtained from objective process-level data. Tiered, objective, data-driven metrics are highly successful in achieving a cooperative and effective method of measuring performance. The teamwork-based culture developed by TOPS proved an unequaled success in removing adversarial relationships and creating an atmosphere of continuous improvement in quality processes at TRW. The new working relationship does not decrease the responsibility or authority of the DPRO to ensure contract compliance and it permits both parties to work more effectively to improve total quality and reduce cost. By emphasizing teamwork in developing a stronger approach to efficient management of the defense industrial base TOPS is a singular success. Author (revised)

N94-13168*# National Aeronautics and Space Administration. Goddard Space Flight Center, Greenbelt, MD.

NASA/CONTRACTOR PARTNERSHIP ON THE SECOND TDRSS GROUND TERMINAL PROGRAM: BREAKING BARRIERS

Paul G. Tierney (General Electric Co., Philadelphia, PA.) *In* JPL, Ninth Annual NASA/Contractors Conference on Quality and Productivity. World Class Excellence: The Journey Continues. Conference Presentations 1992 5 p (For primary document see N94-13153 02-38)

Avail: CASI HC A01/MF A03

The Second Tracking and Data Relay Satellite System (TDRSS) Ground Terminal (STGT) Program from its technical and programmatic backgrounds is introduced and then several techniques to enhance communication and empower the NASA Contractor team are described. A major factor in our success was an approach used to shorten the time span of the Critical

Design Review phase. This approach is described. The relationships involving NASA's O&M contractor are discussed. A set of lessons learned is included. Author (revised)

N94-13169*# National Aeronautics and Space Administration. Goddard Space Flight Center, Greenbelt, MD.
GOVERNMENT/CONTRACTOR PARTNERSHIPS FOR CONTINUOUS IMPROVEMENT. A GODDARD SPACE FLIGHT CENTER EXAMPLE
Richard C. Tagler *In* JPL, Ninth Annual NASA/Contractors Conference on Quality and Productivity. World Class Excellence: The Journey Continues. Conference Presentations 1992 8 p (For primary document see N94-13153 02-38)
Avail: CASI HC A02/MF A03

The efforts of a government organization and its major contractors to foster a continuous improvement environment which transcends the traditional government/contractor relationship is discussed. This relationship is aimed at communication, partnership, and trust - creating benefits for all involved. Author (revised)

N94-13396*# National Aeronautics and Space Administration, Washington, DC.
GEORGE M. LOW TROPHY: NASA'S QUALITY AND EXCELLENCE AWARD. 1992 RECIPIENTS: HONEYWELL CLEARWATER, IBM HOUSTON
1992 26 p
(NASA-TM-109265; NAS 1.15:109265) Avail: CASI HC A03/MF A01

The George M. Low Trophy is awarded to current NASA contractors, subcontractors, and suppliers in the aerospace industry who have demonstrated sustained excellence and outstanding achievements in quality and productivity for three or more years. The objectives of the award are to increase public awareness of the importance of quality and productivity to the Nation's aerospace program and industry in general; encourage domestic business to continue efforts to enhance quality, increase productivity, and thereby strengthen competitiveness; and provide the means for sharing the successful methods and techniques used by the applicants with other American enterprises. Information is given on candidate eligibility for large businesses, the selection process, the nomination letter, and the application report. The 1992 highlights and recipients are included. CASI

N94-13857# Materials Research Labs., Ascot Vale (Australia). Materials Div.
STRUCTURAL INVESTIGATION OF A DAMAGED GRP/FOAM SANDWICH COMPOSITE USING X RAY COMPUTED TOMOGRAPHY
B. Suendermann, J. R. Davis (Monash Univ., Melbourne, Australia.), P. Lambrineas, P. Wells (Monash Univ., Melbourne, Australia.), K. R. Thomson (Melbourne Univ., Parkville, Australia.), R. L. Woodward, G. T. Egglestone, and K. Challis [1993] 10 p
Avail: CASI HC A02/MF A01

Glass-reinforced plastic (GRP)/foam sandwich construction is a method of obtaining stiff lightweight composite structures. These composites find Naval applications in superstructures and in the hulls of vessels requiring a low magnetic signature. The application of such composites requires that they can be inspected by nondestructive testing (NDT) techniques for flaws in manufacturing or for service induced damage, including internal damage from the passage of explosion induced shocks. An investigation of the degree to which x ray computed tomography (CT) can be used to characterize such features, using a composite which contains a number of artifacts of manufacturing, as well as deliberately induced flaws and shock damage is described. Author (revised)

N94-14101*# Applied Research, Inc., Huntsville, AL.
ENHANCED NDE SYSTEMS Final Report
28 Jul. 1993 24 p
(Contract NAS8-39394)
(NASA-CR-192603; NAS 1.26:192603) Avail: CASI HC A03/MF A01

The goal of this contractual effort was to evaluate the Langley narrow-band ultrasonic debond detection method for a factory use configuration. Successful accomplishment requires establishing the robustness of the method, and enhancing it if necessary. It is also desirable to strive for simplicity of implementation, such as attachment to in-place scanning devices planned for nondestructive evaluation (NDE) measurements. The contract was established with three phases for the ultrasonic work: (1) establish the method and robustness of the ultrasonic method; (2) follow up on any questions which arise with respect to the method or its implementation and produce a Phase A design; and (3) fabricate and test the Phase A design. This is a report on Phase 1. Derived from text

N94-14143# Los Alamos National Lab., NM.
COMPUTATIONAL PROBLEMS WITH THE BINOMIAL FAILURE RATE MODEL AND INCOMPLETE COMMON CAUSE FAILURE RELIABILITY DATA
P. H. Kvam 1993 6 p Presented at the Interface Computing Science and Statistics, San Diego, CA, 14-17 Apr. 1993
(Contract W-7405-eng-36)
(DE93-014346; LA-UR-93-1980; CONF-9304154-1) Avail: CASI HC A02/MF A01

In estimating the reliability of a system of components, it is ordinarily assumed that the component lifetimes are independently distributed. This assumption usually alleviates the difficulty of analyzing complex systems, but it is seldom true that the failure of one component in an interactive system has no effect on the lifetimes of the other components. Often, two or more components will fail simultaneously due to a common cause event. Such an incident is called a common cause failure (CCF) and is now recognized as an important contribution to system failure in various applications of reliability. We examine current methods for reliability estimation of system and component lifetimes using estimators derived from the binomial failure rate model. Computational problems require a new approach, like iterative solutions via the EM algorithm. DOE

N94-14321*# National Aeronautics and Space Administration. Lyndon B. Johnson Space Center, Houston, TX.
THE EIGHTH ANNUAL NASA/CONTRACTORS CONFERENCE AND 1991 NATIONAL SYMPOSIUM ON QUALITY AND PRODUCTIVITY: EXTENDING THE BOUNDARIES OF TOTAL QUALITY MANAGEMENT Summary Report
Geoffrey B. Templeton, ed. (National Aeronautics and Space Administration, Washington, DC.), Lynne M. Stewart, ed. (National Aeronautics and Space Administration, Washington, DC.), and William T. Still, ed. Apr. 1992 281 p
(NASA-TM-109276; NAS 1.15:109276) Avail: CASI HC A13/MF A03

The Eighth Annual NASA/Contractors Conference and 1991 National Symposium on Quality and Productivity provided a forum to exchange knowledge and experiences in these areas of continuous improvement. The more than 1,100 attendees from government, industry, academia, community groups, and the international arena had a chance to learn about methods, tools, and strategies for excellence and to discuss continuous improvement strategies, successes, and failures. This event, linked via satellite to concurrent conferences hosted by the NASA Goddard Space Flight Center in Greenbelt, Maryland, and Martin Marietta Astronautics Group in Denver, Colorado, also explored extending the boundaries of Total Quality Management to include partnerships for quality within communities and encouraged examination, evaluation, and change to incorporate the principles of continuous improvement. Derived from text

39 STRUCTURAL MECHANICS

Includes structural element design and weight analysis; fatigue; and thermal stress.

For applications see *05 Aircraft Design, Testing and Performance* and *18 Spacecraft Design, Testing and Performance.*

N94-12831*# National Aeronautics and Space Administration. Marshall Space Flight Center, Huntsville, AL.
STRUCTURAL DESIGN/MARGIN ASSESSMENT
R. S. Ryan Washington Sep. 1993 80 p
(NASA-TP-3410; M-730; NAS 1.60:3410) Avail: CASI HC A05/MF A01

Determining structural design inputs and the structural margins following design completion is one of the major activities in space exploration. The end result is a statement of these margins as stability, safety factors on ultimate and yield stresses, fracture limits (fracture control), fatigue lifetime, reuse criteria, operational criteria and procedures, stability factors, deflections, clearance, handling criteria, etc. The process is normally called

a load cycle and is time consuming, very complex, and involves much more than structures. The key to successful structural design is the proper implementation of the process. It depends on many factors: leadership and management of the process, adequate analysis and testing tools, data basing, communications, people skills, and training. This process and the various factors involved are discussed. Author (revised)

N94-12872*# National Aeronautics and Space Administration. Lewis Research Center, Cleveland, OH.
ON CURVE VEERING AND FLUTTER OF ROTATING BLADES
Dare Afolabi (Purdue Univ., Indianapolis, IN.) and Oral Mehmed Aug. 1993 22 p
(Contract NCC3-233; RTOP 505-90-5K)
(NASA-TM-106282; ICOMP-93-27; E-8020; NAS 1.15:106282) Avail: CASI HC A03/MF A01

The eigenvalues of rotating blades usually change with rotation speed according to the Stodola-Southwell criterion. Under certain circumstances, the loci of eigenvalues belonging to two distinct modes of vibration approach each other very closely, and it may appear as if the loci cross each other. However, our study indicates that the observable frequency loci of an undamped rotating blade do not cross, but must either repel each other (leading to 'curve veering'), or attract each other (leading to 'frequency coalescence'). Our results are reached by using standard arguments from algebraic geometry--the theory of algebraic curves and catastrophe theory. We conclude that it is important to resolve an apparent crossing of eigenvalue loci into either a frequency coalescence or a curve veering, because frequency coalescence is dangerous since it leads to flutter, whereas curve veering does not precipitate flutter and is, therefore, harmless with respect to elastic stability. Author (revised)

N94-12887# Los Alamos National Lab., NM.
MICROMECHANICAL STRENGTH EFFECTS IN SHOCK COMPRESSION OF SOLIDS
J. N. Johnson 1993 5 p Presented at the Joint AIRAPT/APS Meeting, Colorado Springs, CO, 28 Jun. - 3 Jul. 1993
(Contract W-7405-eng-36)
(DE93-014425; LA-UR-93-1670; CONF-9306167-4) Avail: CASI HC A01/MF A01

Time-resolved shock-wave measurements and post-shock recovery have long been used for inferring the underlaying micromechanics controlling high-rate deformation of solids; this requires considerable subjective interpretation. In spite of this, progress has been made in experimentation and theoretical interpretation of the shock-compression/release cycle and some of the results are reviewed here for weak shocks. This cycle involves the elements of the elastic precursor, plastic loading wave, pulse duration, release wave, and post-mortem examination. Those topics are examined with emphasis on the second and fourth elements. The Cu and Ta results show how shock data can be used to determine the transition from deformation mechanism of thermal activation to that of dislocation drag. Release-wave studies indicate that the leading observable release disturbance in fcc metals may not be propagating with the ideal longitudinal elastic-wave speed. DOE

N94-12908# Sandia National Labs., Albuquerque, NM.
THE 3-D MASSIVELY PARALLEL IMPACT SIMULATIONS USING PCTH
H. E. Fang and A. C. Robinson 1992 6 p Presented at the SCSC 1993 Summer Computer Simulation Conference, Boston, MA, 19-21 Jul. 1993
(Contract DE-AC04-76DP-00789)
(DE93-011593; SAND-92-2845C; CONF-930765-2) Avail: CASI HC A02/MF A01

Simulations of hypervelocity impact problems are performed frequently by government laboratories and contractors for armor/anti-armor applications. These simulations need to deal with shock wave physics phenomena, large material deformation, motion of debris particles, and complex geometries. As a result, memory and processing time requirements are large for detailed, three-dimensional calculations. The large massively parallel supercomputing systems of the future will provide the power necessary to greatly reduce simulation times currently required by shared-memory, vector supercomputers. This paper gives an introduction to PCTH, a next-generation shock wave physics code which is being built at Sandia National Laboratories for massively parallel supercomputers, and demonstrates that massively parallel hydrocodes, such as PCTH, can provide highly-detailed, three-dimensional simulations of armor/anti-armor systems. DOE

N94-12927 Aeronautical Research Labs., Melbourne (Australia).
A BENCHMARK BENDING TEST OF A THICK SPECIMEN, PART 1: EXPERIMENTS Research Report No. 6
J. M. Finney and E. Kowal Jun. 1993 45 p
(ARL-RR-6-Pt-1; AR-008-363) Copyright Avail: Issuing Activity

An experiment has been undertaken to provide benchmark data for validating methods of calculating the plastic behavior of metals. In this experiment a 30 mm square-test-section specimen of 7050-T7451 aluminum alloy has been loaded in four-point bending, and the surface distortions of all four faces have been measured with the aid of a square grid pattern imposed on the surfaces before deformation. This part of the report describes the experimental details and gives the results of the material property tests, thus, providing sufficient information for the prediction of surface displacements. Part II of the report gives the measured displacements with which predictions may be compared. Derived from text

N94-12928 Aeronautical Research Labs., Melbourne (Australia). Dept. of Defence.
A BENCHMARK BENDING TEST OF A THICK SPECIMEN. PART 2: SURFACE DISPLACEMENT MEASUREMENTS Research Report No. 6
J. M. Finney and E. Kowal Jun. 1993 150 p Original contains color illustrations
(ARL-RR-6-Pt-2; AR-008-364) Copyright Avail: Issuing Activity

An experiment has been undertaken to provide benchmark data for validating methods of calculating the plastic behavior of metals. In this experiment, a 30 mm square-test-section specimen of 7050-T7451 aluminum alloy has been loaded in four-point bending, and the surface distortions of all four faces have been measured with the aid of a square grid pattern imposed on the surfaces before deformation. Part 1 of the report describes the experimental details and gives the results of the material property tests, thus, providing sufficient information for the prediction of surface displacements. This part of the report gives the displacements measured and describes the various manipulation and averaging procedures used with the data to put them in a form suitable for comparison with predictions. Author (revised)

N94-13053*# National Aeronautics and Space Administration. Lewis Research Center, Cleveland, OH.
MICROMECHANICAL MODELING OF LAMINATED COMPOSITES WITH INTERFACES AND WOVEN COMPOSITES USING THE BOUNDARY ELEMENT METHOD
Robert K. Goldberg and Dale A. Hopkins Oct. 1993 12 p Proposed for presentation at the Eighth American Society for Composites Technical Conference on Composite Materials, Cleveland, OH, 19-21 Oct. 1993
(RTOP 510-01-50)
(NASA-TM-106280; E-8019; NAS 1.15:106280) Avail: CASI HC A03/MF A01

The boundary element method is utilized to analyze the effects of fiber/matrix interfaces on the micromechanical behavior of laminated composites as well as the elastic behavior of woven composites. Effective composite properties are computed for laminated SiC/RBSN and SiC/Ti-15-3 composites, as well as a woven SiC/SiC composite. The properties calculated using the computerized tool BEST-CMS match the experimental results well. Author

N94-13063*# Virginia Polytechnic Inst. and State Univ., Blacksburg. Dept. of Engineering Science and Mechanics.
DESIGN AND APPLICATION OF A QUASISTATIC CRUSH TEST FIXTURE FOR INVESTIGATING SCALE EFFECTS IN ENERGY ABSORBING COMPOSITE PLATES M.S. Thesis
J. Andre Lavoie and John Morton Washington Jul. 1993 65 p
(Grant NAG1-343; RTOP 505-63-50-09)
(NASA-CR-4526; NAS 1.26:4526) Avail: CASI HC A04/MF A01

A crush test fixture for measuring energy absorption of flat plate specimens from an earlier study was redesigned to eliminate the problem of binding of the load transfer platen with the guide posts. Further modifications were to increase the stroke, and combine the two scaled text fixtures into one. This new crush text fixture was shown to produce

load-displacement histories exhibiting well developed sustained crushing loads over long strokes. An experimental study was conducted on two material systems: AS4/3502 graphite/epoxy, and a hybrid AS4-Kevlar/3502 composite. The effect of geometric scaling of specimen size, the effect of ply level and sublaminate-level scaling of the stacking sequence of the full scale specimens, and the effect of trigger mechanism on the energy absorption capability were investigated. The new crush test fixture and flat plate specimens produced peak and sustained crushing loads that were lower than obtained with the old crush text fixture. The trigger mechanism used influenced the specific sustained crushing stress (SSCS). The results indicated that to avoid any reduction in the SSCS when scaling from the 1/2 scale to full scale specimen size, the sublaminate-level scaling approach should be used, in agreement with experiments on tubes. The use of Kevlar in place of the graphite 45 deg plies was not as effective a means for supporting and containing the 0 deg graphite plies for rushing of flat plates and resulted in a drop in the SSCS. This result did not correlate with that obtained for tubes. Author (revised)

N94-13124*# Engineering Mechanics Association, Inc., Torrance, CA.
METHODS FOR EVALUATING THE PREDICTIVE ACCURACY OF STRUCTURAL DYNAMIC MODELS Final Report, Jul. 1989 - Dec. 1991
Timothy K. Hasselman and Jon D. Chrostowski Dec. 1991 306 p
(Contract NAS7-1064; SBIR-04.10-2551)
(NASA-CR-191337; NAS 1.26:191337; EMA-TR-91-1152) Avail: CASI HC A14/MF A03

Modeling uncertainty is defined in terms of the difference between predicted and measured eigenvalues and eigenvectors. Data compiled from 22 sets of analysis/test results was used to create statistical databases for large truss-type space structures and both pretest and posttest models of conventional satellite-type space structures. Modeling uncertainty is propagated through the model to produce intervals of uncertainty on frequency response functions, both amplitude and phase. This methodology was used successfully to evaluate the predictive accuracy of several structures, including the NASA CSI Evolutionary Structure tested at Langley Research Center. Test measurements for this structure were within + one-sigma intervals of predicted accuracy for the most part, demonstrating the validity of the methodology and computer code. Author (revised)

N94-13179*# Eloret Corp., Sunnyvale, CA.
SIMULATION STUDIES FOR SURFACES AND MATERIALS STRENGTH Semiannual Progress Report, 1 Nov. 1992 - 30 Apr. 1993
Timur Halicioglu 1993 47 p
(Contract NCC2-297)
(NASA-CR-193305; NAS 1.26:193305) Avail: CASI HC A03/MF A01

During this period investigations were carried out in three areas. Optimum energies and structures were estimated for single step ledges formed in the (111) surface of diamond. Binding energies of carbon atoms adsorbed on a (2x1) reconstructed Si(100) surface were calculated as a function of sub-monolayer coverages. Calculations were conducted to analyze the strain dependence of the binding energy of a carbon atom deposited on a (2x1) dimerized Si(100) surface. Results are discussed. CASI

N94-13379*# National Aeronautics and Space Administration. Lewis Research Center, Cleveland, OH.
A PROBABILISTIC METHOD FOR THE BUCKLING ASSESSMENT OF STIFFENED COMPOSITE SHELLS
Michael C. Shiao (Sverdrup Technology, Inc., Brook Park, OH.), Galib H. Abumeri (Sverdrup Technology, Inc., Brook Park, OH.), Surendra N. Singhal (Sverdrup Technology, Inc., Brook Park, OH.), and Christos C. Chamis Jul. 1993 16 p Presented at the Ninth International Conference on Composite Materials, Madrid, Spain, 12-16 Jul. 1993
(RTOP 510-02-12)
(NASA-TM-106286; E-8024; NAS 1.15:106286) Avail: CASI HC A03/MF A01

A method is described to computationally simulate probabilistic buckling behavior of multilayered composite shells. The simulation accounts for all naturally-occurring uncertainties including those in constituent (fiber/matrix) material properties, fabrication variables, and structure geometry. The method is demonstrated for probabilistically assessing the buckling survivability of a specific case of a stiffened composite cylindrical shell with and without cutouts. The sensitivities of various uncertain variables on the buckling survivability are evaluated at specified reliability. The results show that the buckling survivability for a shell without cutouts depends primarily on shell skin related uncertainties. However, stringer related uncertainties become important for a shell with cutouts. Author (revised)

N94-13501# Societe Europeenne de Propulsion, Vernon (France). Div. Grosse Propulsion a Liquides.
RESIDUAL CONTACT RESTRAINTS IN CRYOGENICS [CONTRAINTES RESIDUELLES DE CONTACT EN AMBIANCE CRYOTECHNIQUE]
J. F. Cretegny and J. M. deMonicault 1992 22 p In FRENCH Presented at Colloque Contraintes Residuelles, Luso-Bucaco, Portugal, 28-30 Apr. 1992
(ETN-93-94375) Avail: CASI HC A03/MF A01

The use of residual stress measurements to evaluate the state of cryogenic turbomachines, whose surfaces are worn by the working conductions in dry contact, is addressed. Their contribution to the understanding of the reasons of possible ruptures is considered. It is stated that residual stress measurements should be used as a complementary tool rather than as input data for models. It is shown, thanks to two examples concerning the ball bearings and splines of the liquid hydrogen turbopump of the Vulcain engine, what can be expected from such techniques. Total exploitation of the results has still to be done, but preliminary results are quite encouraging. ESA

N94-13565 Institute for Aerospace Research, Ottawa (Ontario). Structures and Materials Lab.
SHEAR BUCKLING OF FIBER METAL LAMINATES: COMPARISON BETWEEN ORTHOTROPIC AND ANISOTROPIC PLATE MODELS USING FINITE ELEMENT METHOD
S. Krishnakumar Jul. 1993 44 p
(LTR-ST-1934; CTN-93-60861) Avail: Issuing Activity (Micromedia Ltd., Technical Information Centre, 165 Hotel de Ville, Place du Portage, Phase 2, Hull, Quebec J8X 3X2, Canada HC)

The finite element method is used to compare the results provided by two approaches for the simulation of shear buckling of anisotropic fiber metal laminates, ARALL and GLARE. Two different load cases are studied: uniform shear stresses along the boundary, as is usually employed in theoretical analyses; and shear displacement along one edge of a plate, as is normally the case under test conditions. The orthotropic approximation yields solutions that are independent of the sign of the applied stresses and have only a mild variation with changes in the orientation of the reinforcing fibers. The influence of anisotropy is much larger in the case of applied shear displacement than in the uniform stress case, for all laminates except the pseudo-isotropic GLARE3 material. A reversal of the applied load direction can alter the buckling strength by a factor of 2.5 for this load condition. In unidirectional laminates subjected to in-plane shear displacement, the orthotropic model overestimates the buckling load by about 55 percent in some cases, and underestimates it by nearly 40 percent in others. In the case of GLARE3, the difference between the anisotropic solution and the orthotropic model is less than 2 percent.
Author (CISTI)

N94-13579# Army Armament Research, Development and Engineering Center, Watervliet, NY. Benet Lab.
AUTOFRETTAGE: STRESS DISTRIBUTION UNDER LOAD AND RETAINED STRESSES AFTER DEPRESSURIZATION. A MODIFIED PLANE-STRAIN CASE Final Technical Report
Boaz Avitzur Apr. 1993 63 p
(AD-A266320; ARCCB-TR-93015) Avail: CASI HC A04/MF A01

There is a long-standing interest in developing a capability to predict the distribution of retained stresses in thick-walled pressure vessels after the removal of an internal pressure--post autofrettage. The key to such a prediction is in the capacity to compute the stress distribution in a vessel while under externally imposed stress sufficient enough to cause at least partial plastic deformation. A good approximation of the stress distribution was developed by Mises in his 1913 plane-stress solution. The fact that such vessels are not representative of the plane-stress condition not withstanding, Mises recognized that his solution was mathematically restricted to a limited range of vessels' wall ratios. More recently, Avitzur offered a solution similar to that of Mises, but for a plane-strain condition. Depending on the material's Poisson's factor, Avitzur's solution is also mathematically applicable for a limited range of vessels' wall ratios only. The wall ratio, beyond which Avitzur's solution in plane-strain is not applicable, is a few

times larger than that which limits Mises' solution in plane-stress. This work introduces a modification to Avitzur's solution in plane-strain, which makes its applicability unlimited. DTIC

N94-13593 Texas Univ., Austin.
INVESTIGATION OF CRITERIA FOR DUCTILE FRACTURE UNDER FULLY-PLASTIC CONDITIONS Ph.D. Thesis
Robert Joseph Dexter 1992 387 p
Avail: Univ. Microfilms Order No. DA9309149

Under fully-plastic conditions, a plot of the J integral vs. crack extension (J-R curve) and other essentially equivalent approaches are excessively dependent on test specimen geometry and cannot be reliably used to predict tearing in full-scale members. Two alternative approaches were developed and tested in this research. Critical strain values (just prior to fracture) were estimated from large-deformation finite-element simulations of tensile tests. There was less than 12 percent variation in the critical strain values obtained from flat, round, and notched tensile specimens of a clean low-carbon pipeline steel. Application of the critical strain to tearing experiments required an accurate estimate of the three-dimensional strain field at a distance less than two millimeters from the crack tip and such a large-deformation analysis was impractical at this time. The three-dimensional strain field at a distance less than two millimeters from the crack tip and such a large deformation analysis was impractical at this time. The incremental generalization of the J integral (T*) was modified to calculate the energy dissipation rate in a small box including several layers of elements surrounding the crack tip. Because this modified T* parameter is calculated from the stresses and strains outside this box, this approach can be used with a small-strain two-dimensional analysis. The modified T* integral as well as the conventional J integral were calculated from such a small-strain simulation of tearing tests of two geometries for two pipeline steels. The calculated J-R curves were very close to the measured J-R curves and the slopes of these curves varied between specimens by more than 72 percent. A plot of the modified T* integral vs. crack extension was essentially constant with crack extension. The mean steady-state values varied between specimens by less than 45 percent, i.e. the modified T* integral during crack propagation was relatively independent of specimen geometry. Dissert. Abstr.

N94-13594 Illinois Inst. of Tech., Chicago.
A STOCHASTIC MODEL FOR BEHAVIOR ANALYSIS OF FIBER-REINFORCED QUASI-BRITTLE MATERIALS Ph.D. Thesis
Artur Stanislaw Kurzydlo 1992 205 p
Avail: Univ. Microfilms Order No. DA9311941

Short fiber reinforced composites are established as a class of materials today. Modeling of such heterogeneous materials is still in the development stage. A proposed model which combines stochastic concepts with micromechanical approach is designed to predict the behavior of such materials. It is based on stochastic models for material behavior and combines the classical theory of deformation with a statistical treatment of imperfect materials. The model uses the principle of superposition of strain rates as a basis. Therefore such deformations as microcracking, plastic flow, thermoelastic behavior, and growth, coalescence and nucleation of voids, and crack-fiber interaction as well as most other kinds of inelastic behavior can be incorporated in the model. The stochastic material theory is expanded to predict a variety of uncertain material behavior. In the new model, such characteristics as random positions of fibers in the matrix, interactions between random cracks and fibers, change in the overall material behavior due to the changes in the structure of fibers and cracks during a loading process, deformation due to microcracking are treated by analyzing the 'open' and 'closed' cracks and considering the shearing of closed cracks. In this model, cracks are assumed to be circular (penny-shaped), and of random orientations and size, described by a probability density function. Available analytical solutions for the opening cracks and for the stability of penny-shaped cracks (both for tension and shear) are combined and included in the model to account for any arbitrary state of stress. Plastic flow is characterized by a kinematic-hardening model; and large deformations are accounted for through the polar decomposition theorem by separating them each into a stretch and a rotation component. Distinction between the fixed and rotating reference frames (which is crucial for isotropic materials) is also made; and elastic modulus is taken as a variable to account for the microcracking behavior. Dissert. Abstr.

N94-13596 Illinois Univ., Chicago.
FINITE ELEMENT ANALYSIS OF COMPOSITE PLATES BY USE OF MODIFIED COMPLEMENTARY ENERGY PRINCIPLE Ph.D. Thesis
Payman Afshari 1992 179 p
Avail: Univ. Microfilms Order No. DA9310117

Multilayered composite plates are of interest for a variety of structural application in such industries as automotive and aerospace where high strength to weight ratios are desirable. A composite plate can be distinguished from their single layered isotropic counterpart in that the transverse shear deformation plays a significant role in the structural behavior of the plate. This effect is present even for geometrically thin composite plate. The inclusion of transverse shear deformation, the extension-bending, twisting-extension and twisting-bending coupling effects that exist due to the different orthotropic material properties of each layer, requires a more sophisticated approach. A series of plate elements are formulated based on a variational principle, namely, Modified Complementary Energy. Mindlin thin plate theory is selected to govern the general characteristics and behavior of this type of structure. Transverse shear deformation is included in the formulation. A series of in-plane strain functions are assumed, from which the corresponding stresses for each lamina are determined. By satisfying the equilibrium equations, the transverse stresses are calculated. These elements are invariant and do not exhibit any shear locking in the thin plate limit. Also, no shear correction factor is included in the development of the formulation or the computer code. A FORTRAN code, CPLATE, is developed. Eight node isoparametric elements are utilized to describe the displacement field. Each node has five degrees of freedom, which are three displacements and two independent cross-sectional rotations. To identify the scope of application and limitations of these elements, several example problems are selected to cover a variety of geometrical and material properties. The outcome of the displacement and vibration analyses shows excellent agreement between the exact elasticity solutions and current formulation. Also, the predicted transverse shear stress profile and magnitude, using the present formulation, matched with those of the exact elasticity and high order plate theories, in the thin to moderately thick plate limit. Dissert. Abstr.

N94-13669 Clarkson Univ., Potsdam, NY.
BOUNDARY FORMULATIONS FOR NONLINEAR DESIGN SENSITIVITY ANALYSIS Ph.D. Thesis
Hua Wang 1993 200 p
Avail: Univ. Microfilms Order No. DA9308244

This dissertation describes an investigation into the prospect of generating efficient and accurate boundary formulations for shape design sensitivity analysis (DSA) for nonlinear thermal and nonlinear structural problems. Theoretical formulations of DSA for thermal conduction problems with temperature dependent conductivity, temperature dependent convection, and radiation boundary conditions are developed. The temperature dependent conductivity problem is treated via a Kirchhoff transformation. Implicit differentiation of the discretized boundary integral equations governing the conduction of heat in solid objects subjected to nonlinear boundary conditions is shown to generate an accurate and economical approach for the computation of shape sensitivities for this class of problems. The computer algorithmic details for BEA and DSA for nonlinear thermal problems are presented and examined. Several iterative strategies are presented for the solution of the resulting sets of nonlinear equations and the computational performances are examined. Boundary formulations for shape DSA for solid mechanics problems exhibiting small strain elastoplastic behavior is also investigated. The theoretical formulation accounts for elastoplastic effects by the utilization of particular integrals. The computer algorithmic details for BEA and DSA for these nonlinear structural problems are developed and examined. An iterative strategie is presented for the solution of the resulting sets of nonlinear equations and the computational performances are examined. This particular integral approach to DSA for elastoplastic problems allots for the computation of response sensitivity without the need for domain discretization. Multi-zone modeling and zone condensation techniques are employed in the nonlinear thermal problems to improve the computational efficiency of nonlinear DSA for boundary element analysis (BEA) models with partial geometric sensitivity to design variables. It is demonstrated that the technique provides substantive computational economies in this process for models with either localized nonlinear boundary conditions or regions of geometric insensitivity to design

variables. A series of nonlinear thermal and structural examples that have analytical solutions are presented to quantify the accuracy of the formulations developed. Exact analytical expressions for shape sensitivities associated with these problems are developed and are compared with the sensitivities computed using the boundary element formulation. Dissert. Abstr.

N94-13673*# Structural Analysis Technology, Inc., Santa Clara, CA.
AN EXPERT SYSTEM FOR INTEGRATED STRUCTURAL ANALYSIS AND DESIGN OPTIMIZATION FOR AEROSPACE STRUCTURES Final Technical Report
Apr. 1992 70 p
(Contract NAS3-25642; SBIR-04.04-1319)
(NASA-CR-194225; NAS 1.26:194225; SAT-380.02) Avail: CASI HC A04/MF A01

The results of a research study on the development of an expert system for integrated structural analysis and design optimization is presented. An Object Representation Language (ORL) was developed first in conjunction with a rule-based system. This ORL/AI shell was then used to develop expert systems to provide assistance with a variety of structural analysis and design optimization tasks, in conjunction with procedural modules for finite element structural analysis and design optimization. The main goal of the research study was to provide expertise, judgment, and reasoning capabilities in the aerospace structural design process. This will allow engineers performing structural analysis and design, even without extensive experience in the field, to develop error-free, efficient and reliable structural designs very rapidly and cost-effectively. This would not only improve the productivity of design engineers and analysts, but also significantly reduce time to completion of structural design. An extensive literature survey in the field of structural analysis, design optimization, artificial intelligence, and database management systems and their application to the structural design process was first performed. A feasibility study was then performed, and the architecture and the conceptual design for the integrated 'intelligent' structural analysis and design optimization software was then developed. An Object Representation Language (ORL), in conjunction with a rule-based system, was then developed using C++. Such an approach would improve the expressiveness for knowledge representation (especially for structural analysis and design applications), provide ability to build very large and practical expert systems, and provide an efficient way for storing knowledge. Functional specifications for the expert systems were then developed. The ORL/AI shell was then used to develop a variety of modules of expert systems for a variety of modeling, finite element analysis, and design optimization tasks in the integrated aerospace structural design process. These expert systems were developed to work in conjunction with procedural finite element structural analysis and design optimization modules (developed in-house at SAT, Inc.). The complete software, AutoDesign, so developed, can be used for integrated 'intelligent' structural analysis and design optimization. The software was beta-tested at a variety of companies, used by a range of engineers with different levels of background and expertise. Based on the feedback obtained by such users, conclusions were developed and are provided. Author (revised)

N94-13689# Aeronautical Research Inst. of Sweden, Stockholm.
AN 8-NODE AXISYMMETRIC ACOUSTIC FINITE ELEMENT FOR NON-AXISYMMETRIC FLUID-STRUCTURE INTERACTION ANALYSIS
Magnus Alvelid Jan. 1993 62 p Sponsored in part by Swedish National Board for Industrial and Technical Development
(Contract ESTEC-9307/91/NL/PP(SC))
(FFA-TN-1993-03; ETN-93-94488) Avail: CASI HC A04/MF A01

Two acoustic elements were developed for use in calculations of axisymmetric geometries subject to nonaxisymmetric loading. One of the elements is an 8 noded continuum fluid element and the other is a corresponding 6 noded coupling element, needed in fluid structure interaction problems. The elements were incorporated into the ASKA Harmonic System (HS) which is a subsystem within the ASKA code. The concept in ASKA-HS relies on Fourier decomposition of the loading and displacement/pressure field. If the loading may be described with only a few terms, in the Fourier decomposition of the variation in the circumferential direction, the analysis method described requires considerably fewer degrees of freedom compared to a full three dimensional (3D) analysis for reaching the same accuracy. The elements were verified against corresponding 3D analyses for one uncoupled and one coupled problem. ESA

N94-13726# Technische Univ., Delft (Netherlands). Faculty of Aerospace Engineering.
SOME COMPUTATIONAL TOOLS FOR THE ANALYSIS OF THROUGH CRACKS IN STIFFENED FUSELAGE SHELLS
C. C. Rankin (Lockheed Missiles and Space Co., Palo Alto, CA.), F. A. Brogan (Lockheed Missiles and Space Co., Palo Alto, CA.), and E. Riks Oct. 1992 24 p Original contains color illustrations
(LR-701; ETN-93-94419) Avail: CASI HC A03/MF A01

A method for computing the energy release rate for cracks of varying length in a typical stiffened metallic fuselage under general loading conditions is presented. Reliable analytical methods that predict the structural integrity and residual strength of aircraft fuselage structures containing cracks are needed to help to understand the behavior of pressurized stiffened shells with damage, to determine the safe life of such a shell. The models used in the simulation are derived from an extensive analysis of a fuselage barrel section subjected to operational flight loads. Energy release rates are computed as a function of the length of the crack, its location, and the crack propagation mode. ESA

N94-13777# Army Armament Research, Development and Engineering Center, Watervliet, NY. Benet Lab.
THERMAL GRADIENT-INDUCED DEFLECTION OF A THICK-WALLED CYLINDER WITH BENDING RESIDUAL STRESSES Final Report
John H. Underwood and G. P. OHara Apr. 1993 21 p
(AD-A266347; ARCCB-TR-93017) Avail: CASI HC A03/MF A01

The interaction of a thermal gradient with bending residual stresses in a thick-walled cylinder is investigated using experimental measurements from prior work, mechanics analysis, and finite element stress analysis. A temperature gradient is applied to a cylinder containing residual stresses due to plastic bending resulting in transient elastic relaxation of the nonaxisymmetric residual stresses and bending of the cylinder. Analysis of the well-known similar problem in a rectangular bar is done first using solid mechanics solutions of ideal cases. Finite element calculations are made of the residual stresses following plastic bending of a thick-walled cylinder, the effects of a temperature distribution, and the resultant changes in stresses and strains and the associated tube bending. Results from the two approaches for a 200 C temperature gradient show a maximum angular displacement of 0.004 to 0.008 deg/m and the displacement returning to zero as the thermal gradient diminishes with time. DTIC

N94-13778# Princeton Univ., NJ. Dept. of Civil Engineering and Operations Research.
MICROMECHANICAL DAMAGE THEORIES FOR BRITTLE SOLIDS WITH INTERACTING MICROCRACKS Final Report, 1 Sep. 1990 - 31 Aug. 1992
Jiann-Wen Ju 15 Mar. 1993 153 p
(Grant AF-AFOSR-0336-90)
(AD-A266348; AFOSR-93-0434TR) Avail: CASI HC A08/MF A02

Two-dimensional and three-dimensional statistical micromechanical damage models with randomly located interacting microcracks are presented to investigate the overall nonlinear mechanical responses of microcrack-weakened brittle solids. The macroscopic stress-strain relations of elastic solids with interacting micro-cracks are micromechanically derived by taking the ensemble average over all possible realizations. Several different approximate analytical solutions of a two-crack interaction model are introduced to account for micro-crack interaction among many randomly oriented and distributed microcracks. The overall elastic damage compliances of microcrack-weakened brittle solids are also derived by further taking the volume average of the ensemble-averaged stress-strain relations over the entire material mesostructural domain. Some special examples are investigated by using the proposed framework. At variance with existing phenomenological damage models, the proposed framework does not employ any fitted 'material parameters.' 'Cleavage 1' microcrack growth and 'evolutionary damage models' within the proposed context are also presented. DTIC

N94-13787# Technische Univ., Delft (Netherlands). Faculty of Aerospace Engineering.
ON THE ORTHOTROPICITY ASSUMPTION AND DISCONTINUITY CONDITIONS OF CONICAL SHELLS
Guo Qi Zhang, Menahem Baruch, and Johann Arbocz Jun. 1992 14 p
(LR-703; ETN-93-94420) Avail: CASI HC A03/MF A01

The existence or nonexistence of the classical orthotropicity assumption for conical shells is examined. It is shown that an orthotropic shell with constant stiffness coefficients can not be achieved by using manufacturing techniques of composite materials. An approximation of such a shell can be obtained by using a special kind of stiffness. For the case of axially loaded orthotropic conical shells, buckling loads lower than the ones published in the literature are obtained. The discontinuous transition from conical to cylindrical shells for a case of classical boundary conditions is reexamined. ESA

N94-13803# Technische Univ., Delft (Netherlands). Faculty of Aerospace Engineering.

FATIGUE AND RESIDUAL STRENGTH CHARACTERISTICS OF FIBER METAL LAMINATES SUBJECTED TO INCIDENTAL DAMAGE

Robert Fredell, Ad Vlot, and Marc Verbruggen (Structural Laminates Co., Alcoa Center, PA.) Dec. 1992 23 p Presented at 1992 USAF Aircraft Structural Integrity Program Conference, San Antonio, TX, 1-3 Dec. 1992
(LR-708; ETN-93-94425) Avail: CASI HC A03/MF A01

The fatigue and residual strength characteristics of the fiber metal laminates GLARE and ARALL, following damage typically encountered in the service environment, were investigated. Comparative impact tests showed a gereral trend of increasing impact resistance from carbon thermoplastic composites (poorest) to ARALL, monolithic aluminum 2024-T3, and GLARE 3 (best). Fatigue and residual strength tests carried out on impact and scratch damaged fiber metal laminates demonstrated the excellent tolerance of laminates to in-service damage. The extremely slow crack growth characteristics of laminates were not deteriorated by scratches. Impacts which caused perforations in GLARE and ARALL continued to exhibit the extremely slow fatigue crack growth for which the laminates are known. Repair criteria based on the blunt notch strength of the laminates have been proposed for in-service damage to riveted fiber metal laminate structures. Techniques used for the repair of aluminium structures can apply to laminates. ESA

N94-13833 Defence Research Establishment Atlantic, Dartmouth (Nova Scotia).

TORSION PROBLEM OF ELASTOSTATICS: AN APPLICATION OF BOUNDARY ELEMENT METHOD AND RELATION WITH CONFORMAL MAPPING

Thomas S. Z. Hu Sep. 1992 32 p
(DSIS-92-03794; DREA-TM-92-218; CTN-93-60769) Avail: CASI HC A03

The boundary integral equation method can be applied to the solution of many types of partial differential equations which arise in mathematical physics. The governing equations of the torsion problem in elastostatics can be simplified to either Laplace's equation or Poisson's equation, and the boundary integral techniques developed for solving potential flow can be applied. The boundary integral formulation of Laplace's equation and its discretization are presented. The physical meaning of such equations is demonstrated through the application of the boundary element method to the torsion problem. The inaccuracy of the solutions at the corners of the domain is studied via the theory of conformal mapping. The method of conformal transformation is shown to be a useful tool in dealing with numerical difficulties. Author (CISTI)

N94-13861# Institute for Aerospace Research, Ottawa (Ontario). Structures and Materials Lab.

REVIEW OF CANADIAN AERONAUTICAL FATIGUE WORK, 1991-1993

D. L. Simpson, comp. 10 May 1993 95 p Presented at the 23rd Conference of the International Committee on Aeronautical Fatigue
(LTR-ST-1932; CJ5-07; CTN-93-60835) Avail: CASI HC A05/MF A01

Detailed reviews are presented of research into aeronautical fatigue conducted by private companies, universities, and government research institutions in Canada over the 1991-1993 period. Research projects are described in the areas of full-scale tests of aircraft and components, loads monitoring and measurement, fracture mechanics and crack propagation, composite materials and structures, and the fatigue and damage tolerance of gas turbine engines. CISTI

N94-13873*# Northwestern Univ., Evanston, IL.

VARIATIONAL APPROACH TO PROBABILISTIC FINITE ELEMENTS Final Report

T. Belytschko, W. K. Liu, A. Mani, and G. Besterfield Aug. 1991 177 p
(Grant NAG3-535; RTOP 505-63-5B)
(NASA-CR-187179; NAS 1.26:187179) Avail: CASI HC A09/MF A02

Probabilistic finite element methods (PFEM), synthesizing the power of finite element methods with second-moment techniques, are formulated for various classes of problems in structural and solid mechanics. Time-invariant random materials, geometric properties and loads are incorporated in terms of their fundamental statistics viz. second-moments. Analogous to the discretization of the displacement field in finite element methods, the random fields are also discretized. Preserving the conceptual simplicity, the response moments are calculated with minimal computations. By incorporating certain computational techniques, these methods are shown to be capable of handling large systems with many sources of uncertainties. By construction, these methods are applicable when the scale of randomness is not very large and when the probabilistic density functions have decaying tails. The accuracy and efficiency of these methods, along with their limitations, are demonstrated by various applications. Results obtained are compared with those of Monte Carlo simulation and it is shown that good accuracy can be obtained for both linear and nonlinear problems. The methods are amenable to implementation in deterministic FEM based computer codes. Author

N94-13887# Technical Research Centre of Finland, Espoo. Production Engineering Lab.

CONTRIBUTION TO COMPARISON OF METHODS FOR DETERMINING WELDING PROCEDURES FOR THE AVOIDANCE OF HYDROGEN CRACKING

Risto A. Karppi and Pekka Nevasmaa Aug. 1992 52 p
(VTT-PUBS-107; IIW-IX-1673-92; ISBN-9-51-384225-8; ETN-93-94481)
Copyright Avail: CASI HC A04/MF A01

The method named VTT/OU (acronym for the Technical Center of Finland (VTT) and the Osaka University (OU)) is described. The VTT/OU method is based on the comparison of two values of the stress field parameter sigma(sub I) at the crack initiation area. The required value of sigma(sub I) is assessed by the restraint of the structure and the joint geometry. The attainable level of sigma(sub I) is determined by the steel composition, conditions were determined by the VTT/OU method in terms of minimum arc energy without preheat, and minimum preheat for three arc energies: 1,2, and 3 kJ/mm. As parameters, the hydrogen level, joint type (butt and fillet) and plate thickness were varied. The VTT/OU method was shown to take a somewhat different stand from the others on the importance of crack controlling factors. The joint geometry, especially with butt joints, is regarded as an essential factor affecting the level of precautions necessary. The VTT/OU method considers the use of low hydrogen electrodes and hydrogen removal by preheating above 100C more effective. For the fillet welds, the VTT/OU method is found to agree very well with CTS test results. ESA

N94-13905# Technische Univ., Delft (Netherlands). Faculty of Aerospace Engineering.

THE NUMERICAL SIMULATION OF THE COLLAPSE PROCESS OF AXIALLY COMPRESSED CYLINDRICAL SHELLS WITH MEASURED IMPERFECTIONS

E. Riks, C. C. Rankin, and F. A. Brogan 1992 10 p Original contains color illustrations
(LR-705; ETN-93-94422) Avail: CASI HC A02/MF A01

A numerical computation of the collapse process of a cylindrical shell under prescribed edge displacement is discussed. The shell chosen for the computational experiment was manufactured, measured, and tested some twenty years ago. The purpose of the study is to compute the static, pre-collapse loading path and the subsequent snap (dynamic process) to the post buckling state. The test specimen is an integrally machined stringer stiffened cylindrical shell. The wave pattern in the pre-collapse state was observed to be dominated by a mode of one half wave in the axial direction and 9 waves in the circumferential direction. In the post buckling state after the snap, one half wave in the axial direction and ten full waves in the circumferential direction were observed. The simplifications applied in the model concern the adaptation of symmetry in the imperfection pattern and deformation after the load is applied. ESA

N94-13907# Allied-Signal Aerospace Co., Kansas City, MO. Technical Communications.

DEVELOPMENT OF TEST TECHNIQUES TO SIMULATE HIGH-FREQUENCY MECHANICAL SHOCK ON WEAPON COMPONENTS Final Report

Larry F. Thorne, John E. Britt, and Robert D. Jump Feb. 1993 29 p Original contains color illustrations

(Contract DE-AC04-76DP-00613)

(KCP-613-4998) Avail: CASI HC A03/MF A01

A test capability has been developed to subject components to high-level pyro-shock testing. Oscillatory-type shock pulses can be produced that simulate structural responses. The project culminated in the design and fabrication of an airgun facility. The airgun fires 3-inch-diameter projectiles weighing up to 40 pounds into large aluminum fixture plates. The plates are designed to resonate at a predetermined frequency and produce oscillatory acceleration-time waveforms which are transmitted to mounted samples. Shock response spectra (SRS) calculated from these waveforms verify compliance with the shock requirements. Author

N94-13919*# National Aeronautics and Space Administration. Lewis Research Center, Cleveland, OH.

ELASTIC-PLASTIC MIXED-ITERATIVE FINITE ELEMENT ANALYSIS: IMPLEMENTATION AND PERFORMANCE ASSESSMENT

Edhi Sutjahjo (Sverdrup Technology, Inc., Brook Park, OH.) and Christos C. Chamis May 1993 39 p

(RTOP 505-63-53)

(NASA-TM-106164; E-7864; NAS 1.15:106164) Avail: CASI HC A03/MF A01

An elastic-plastic algorithm based on Von Mises and associative flow criteria is implemented in MHOST-a mixed iterative finite element analysis computer program developed by NASA Lewis Research Center. The performance of the resulting elastic-plastic mixed-iterative analysis is examined through a set of convergence studies. Membrane and bending behaviors of 4-node quadrilateral shell finite elements are tested for elastic-plastic performance. Generally, the membrane results are excellent, indicating the implementation of elastic-plastic mixed-iterative analysis is appropriate. Author

N94-13929# Technische Univ., Delft (Netherlands). Faculty of Aerospace Engineering.

A SURVEY OF CRACK PATH STABILITY CRITERIA AND THEIR APPLICATION TO CRACK FLAPPING PHENOMENA IN STIFFENED STRUCTURES

K. J. J. M. Zaal Sep. 1992 153 p

(LR-681; ETN-93-94005) Avail: CASI HC A08/MF A02

In unstiffened and stiffened cylindrical shells, longitudinal cracks are known to flap. Above a certain length, the cracks no longer propagate in the longitudinal direction but turn towards a circumferentially oriented direction. In a pressurized fuselage, this type of U shaped crack could enable a controlled decompression in case of accidental damage or rapid growth of a fatigue crack. Both the T stress criterion of Cotterell and Rice and the criterion of Finnie and Saith can predict the directional stability of the path a crack is following. The predictions of both criteria to experimental results of Swift are compared. The crack path stability criterion of Finnie and Saith seems to emerge as the best available crack path stability criterion. The criterion is material dependent. In combination with a geometrical nonlinear finite element analysis, it may be the first candidate for someone studying directional stability of cracks. ESA

N94-13931# Technische Univ., Delft (Netherlands). Faculty of Aerospace Engineering.

COMPRESSIVE BUCKLING OF CURVED, ANISOTROPIC PANELS STIFFENED IN TWO DIRECTIONS. PART 1: DERIVATION OF THE GOVERNING EQUATIONS

J. L. Verolme Aug. 1992 44 p

(LR-694; ETN-93-94006) Avail: CASI HC A03/MF A01

A designer's tool for calculating the compressive buckling of aircraft fuselage panels is described. The technique applied is an extension of the adjacent equilibrium criterion from which information about the initial postbuckling behavior is obtained. The basic equations, on which most of the modules of the tool are based, are derived using the energy method. Stability equations in the out of plane coordinate and Airy's stress function, together with jump and boundary conditions, are obtained. The assumptions made are listed. The physical behavior of fuselage panels in compression is treated. ESA

N94-13933# Technische Univ., Delft (Netherlands). Faculty of Aerospace Engineering.

FATIGUE PREDICTIONS AND SCATTER

J. Schijve Aug. 1992 25 p Presented at Euromech Colloquium 297, Corsica, France, 1-4 Sep. 1992

(LR-696; ETN-93-94008) Avail: CASI HC A03/MF A01

Experience with scatter in fatigue properties is illustrated with an attempt to trace the origins of scatter. Most experience with scatter is born in the laboratory. This experience should be evaluated to see the relevance for practical problems. Statistical descriptions of fatigue properties and possible goals to have such descriptions are summarized. Observations of scatter as observed in laboratory tests are presented. Comments on statistical distribution functions, scatter under variable amplitude loading, and scatter in service are given. ESA

N94-13945# Carleton Univ., Ottawa (Ontario).

AN EXPERIMENTAL INVESTIGATION INTO THE DAMAGE RESISTANCE AND COMPRESSION-AFTER-IMPACT STRENGTH OF T800H/3900-2

H. Vietinghoff, C. Poon (Institute for Aerospace Research, Ottawa, Ontario.), P. V. Straznicky, and R. Gould (Institute for Aerospace Research, Ottawa, Ontario.) Jan. 1993 93 p Original contains color illustrations

(LTR-ST-1909; CTN-93-60764) Avail: CASI HC A05/MF A01

An experimental investigation was conducted into impact behavior of a Toray T800H/3900-2 material system, a system representative of the most recent generation of toughened graphite-epoxy composites selected for use in several new airframes. In the investigation, test specimens featuring quasi-isotropic and midplane symmetric layup with 24 plies were fabricated and impacted at five different impact energy levels, resulting in damage ranging from barely visible to severe. Damage was characterized using nondestructive and destructive inspection, including ultrasound and x-ray techniques, and the specimens were then compressively loaded to failure. The carefully controlled set of experiments resulted in a detailed three dimensional characterization of the damage induced in the selected laminate layup for a range of impact energies. Compression after impact testing resulted in a correlation of impact energy and damage area with residual compressive strength. The results will be used to calibrate and test the analytical prediction methods being developed as part of a project on impact resistance and tolerance of composite materials, and as reference data on the material system. Author (CISTI)

N94-13986# Technische Univ., Delft (Netherlands). Structures and Material Lab.

MSD IN FUSELAGE LAP JOINTS: REQUIREMENTS FOR INSPECTION INTERVALS FOR TYPICAL FUSELAGE LAP JOINT PANELS WITH MULTIPLE SITE DAMAGE M.S. Thesis

G. P. Wit Jul. 1992 160 p

(LR-697; ETN-93-94009) Avail: CASI HC A08/MF A02

Inspection of failed aircraft structures and fractography on fatigue specimens showed that after a high number of flights, cracks can appear simultaneously in riveted lap joints. When these crack tips approach each other, a mutual interaction causes an unexpected fast crack growth and new coalescence of cracks. The term Multiple Site Damage (MSD) is used when the mutual interaction of two or more damages is noticeable. A model to predict the fatigue life of a riveted lap joint and the minimum necessary inspection interval for safe aircraft operation is presented. The program was developed to simulate the fatigue process and aircraft inspection. Input for this analysis are scatter data for initiation, the stress distribution between frames and the geometry of the structure. Methods that can be used to avoid accidents due to MSD are reviewed. A test program to support the analysis is described. ESA

N94-14035# Institute for Aerospace Research, Ottawa (Ontario). Structures and Materials Lab.

FINITE ELEMENT CALCULATION OF STRESS-INTENSITY FACTORS FOR THRU-THICKNESS CRACKS IN DEN SPECIMENS

W. Beres and A. K. Koul Nov. 1992 35 p

(LTR-ST-1905; CTN-93-60765) Avail: CASI HC A03/MF A01

The accepted techniques for stress intensity factor (SIF) extraction from finite element method (FEM) calculation results are reviewed. Results are then summarized for through-thickness cracks emanating from a semicircular notch surface of double edge notch (DEN) specimens of two different geometries corresponding to AGARD and Institute of Aerospace Research dimensions. The AGARD specimen has a notch radius to specimen width ratio (R/W) of 1/16 and the other has a R/W of 1/8. Two-dimensional FEM models were run on NISA 2/DISPLAY 2 and ABAQUS FEM software packages to calculate SIF's. Results based on the models of Yamamoto (1974), Schijve (1982), Newman (1990), and Kujawski (1991) are compared and the effect of R/W on the SIF of small through-thickness cracks in DEN specimens are assessed. Among all empirical models analyzed, Kujawski's predictions provide the best fit with the FEM results. Yamamoto's model provides the best fit for crack lengths in the 0.8 to 1.0 mm range. Relative to a single crack in only one notch of the DEN specimen, the presence of two cracks (one at each notch root) does not significantly influence the SIF values. A change in R/W significantly influences the SIF values: above a crack length of 0.3 mm, an increase of R/W from 1/16 to 1/8 increases the SIF by about 28 percent. Below this length the percentage difference in SIF is lower. Author (CISTI)

N94-14041*# National Aeronautics and Space Administration. Lewis Research Center, Cleveland, OH.

HIERARCHICAL NONLINEAR BEHAVIOR OF HOT COMPOSITE STRUCTURES

P. L. N. Murthy, C. C. Chamis, and S. N. Singhal (Sverdrup Technology, Inc., Brook Park, OH.) Jun. 1993 20 p Presented at the First Joint SES, ASME, and ASCE Meeting, Charlottesville, VA, 7-9 Jun. 1993
(RTOP 505-63-5B)
(NASA-TM-106229; E-7947; NAS 1.15:106229) Avail: CASI HC A03/MF A01

Hierarchical computational procedures are described to simulate the multiple scale thermal/mechanical behavior of high temperature metal matrix composites (HT-MMC) in the following three broad areas: (1) behavior of HT-MMC's from micromechanics to laminate via METCAN (Metal Matrix Composite Analyzer), (2) tailoring of HT-MMC behavior for optimum specific performance via MMLT (Metal Matrix Laminate Tailoring), and (3) HT-MMC structural response for hot structural components via HITCAN (High Temperature Composite Analyzer). Representative results from each area are presented to illustrate the effectiveness of computational simulation procedures and accompanying computer codes. The sample case results show that METCAN can be used to simulate material behavior such as the entire creep span; MMLT can be used to concurrently tailor the fabrication process and the interphase layer for optimum performance such as minimum residual stresses; and HITCAN can be used to predict the structural behavior such as the deformed shape due to component fabrication. These codes constitute virtual portable desk-top test laboratories for characterizing HT-MMC laminates, tailoring the fabrication process, and qualifying structural components made from them. Author

N94-14408*# Virginia Polytechnic Inst., Blacksburg. Dept. of Engineering Science and Mechanics.

PROBABILISTIC MICROMECHANICS FOR HIGH-TEMPERATURE COMPOSITES Final Report

J. N. Reddy Sep. 1993 45 p
(Grant NAG3-933; RTOP 510-01-50)
(NASA-CR-191150; E-8113; NAS 1.26:191150) Avail: CASI HC A03/MF A01

The three-year program of research had the following technical objectives: the development of probabilistic methods for micromechanics-based constitutive and failure models, application of the probabilistic methodology in the evaluation of various composite materials and simulation of expected uncertainties in unidirectional fiber composite properties, and influence of the uncertainties in composite properties on the structural response. The first year of research was devoted to the development of probabilistic methodology for micromechanics models. The second year of research focused on the evaluation of the Chamis-Hopkins constitutive model and Aboudi constitutive model using the methodology developed in the first year of research. The third year of research was devoted to the development of probabilistic finite element analysis procedures for laminated composite plate and shell structures. Author

N94-14456# Sandia National Labs., Albuquerque, NM.

PREDICTING THE VIBRATIONS OF A SPINNING INFLATED MEMBRANE

D. J. Segalman and A. Slavin 1993 14 p Presented at the Conference on Vibration and Noise, Albuquerque, NM, 20-22 Sep. 1993
(Contract DE-AC04-76DP-00789)
(DE93-010690; SAND-92-2240C; CONF-9309116-2) Avail: CASI HC A03/MF A01

The primary difficulty of computing the vibration of spinning inflated membranes arises from the low natural frequencies of such systems. When such systems are rotated near their own natural frequencies the dynamics equations must account for higher order kinematics than is necessary for more rigid structures. These complications results from the membrane loads that develop within the bodies in reaction to the accelerations of the overall body. When second order kinematics act against these membrane loads, the resulting energies become of the same order as the potential and kinetic energies of the vibrations that would be calculated by first order kinematics. These complications apply to the problem addressed here. We consider a spin-stabilized, inflated membrane, spinning around its minor axis. This structure is very flexible and somewhat viscoelastic, so vibrations excited by the overall motion of the structure will dissipate energy of the system, thus, reducing the kinetic energy. A reduction in kinetic energy consistent with a conservation of angular momentum results in coning and, eventually, tumbling. Here we must address the excitation of vibration by the rigid-body motion and then we must address the retarding effect of the energy dissipation on the rigid-body motion. DOE

N94-14530# Oak Ridge National Lab., TN.

SOME FREQUENCY AND DAMPING MEASUREMENTS OF LAMINATED BERYLLIUM BEAMS

J. Andriulli and L. C. Rogers 1993 7 p Presented at the Damping 1993, San Francisco, CA, 24-26 Feb. 1993
(Contract DE-AC05-84OR-21400)
(DE93-015909; CONF-9302129-1) Avail: CASI HC A02/MF A01

A quantum leap in vibration performance of beryllium structure has been experimentally investigated. Laminations, segmentation, and sandwich syntactic foam core have been demonstrated to have both high specific flexural structural stiffness and high damping for reduced vibratory response. Acquisition cost, weight, machinability, and environmental benefits are also expected. Applications to the structure of optical and inertial navigation equipment would lead to reductions in jitter levels and other vibratory response measures. DOE

N94-14585# Brookhaven National Lab., Upton, NY.

DYNAMIC SOIL PRESSURES ON RIGID CYLINDRICAL VAULTS

A. S. Veletsos (Rice Univ., Houston, TX.) and A. H. Younan (Rice Univ., Houston, TX.) Feb. 1993 57 p
(Contract DE-AC02-76CH-00016)
(DE93-013930; BNL-52372) Avail: CASI HC A04/MF A01

A critical evaluation is made of the dynamic pressures and the associated forces induced by ground shaking on an upright, circular, rigid vault that is embedded in a uniform viscoelastic stratum of constant thickness and infinite extent in the horizontal plane. Both the vault and the stratum are presumed to be supported on a non- deformable base undergoing a space-invariant, uniform horizontal motion. The effects of both harmonic and earthquake-induced excitations are examined. Simple approximate expressions for the responses of the system are formulated, and comprehensive numerical data are presented which elucidate the underlying response mechanisms and the effects and relative importance of the various parameters involved. The parameters investigated include the height to radius ratio for the vault, the conditions at the vault-medium interface, and the material properties of the stratum. In addition to valuable insights into the response of the particular system being examined, the results presented provide a conceptual framework for the analysis and interpretation of solutions for more involved systems as well. DOE

N94-14591# Los Alamos National Lab., NM.

DIFFERENTIAL SENSITIVITY THEORY APPLIED TO THE MESA CODE FOR HIGH PRESSURE INTERACTIONS

P. J. Maudlin, R. J. Henninger, and E. N. Harstad 1993 13 p Presented at the 14th International Conference on High Pressure Science and Technology and 1993 Technical Meeting of the Topical Group on Shock

Compression of Condensed Matter, Colorado Springs, CO, 28 Jun. - 3 Jul. 1993
(Contract W-7405-eng-36)
(DE93-016460; LA-UR-93-2323; CONF-9306167-5) Avail: CASI HC A03/MF A01

A technique called Differential Sensitivity Theory (DST) is applied to the system of equations solved by the MESA hydrocode. DST uses adjoint techniques to determine exact sensitivity derivatives, i.e., if R is a calculational result of interest (response R) and alpha(sub i) is a calculational input (parameter alpha(sub i)), then (partial derivative)R/(partial derivative)alpha(sub i) is defined as the sensitivity. The advantage of using DST is that for an n-parameter problem all n sensitivities can be obtained by integrating the solutions from only two calculations, a MESA calculation and its corresponding adjoint calculation using an Adjoint Continuum Mechanics code (ACM). This work describes the derivation and solution of the appropriate set of adjoint and sensitivity equations for the purpose of computing sensitivities for high-rate two-dimensional, multi-component, high deformation problems. As an example, results are presented for a flyer plate problem. DOE

N94-14618*# Jet Propulsion Lab., California Inst. of Tech., Pasadena.
PROCEEDINGS OF THE FIFTH NASA/NSF/DOD WORKSHOP ON AEROSPACE COMPUTATIONAL CONTROL
M. Wette, ed. and G. K. Man, ed. 15 Feb. 1993 554 p Workshop held in Santa Barbara, CA; cosponsored by NSF and DOD
(NASA-CR-194515; JPL-Publ-93-02; NAS 1.26:194515) Avail: CASI HC A24/MF A04

The Fifth Annual Workshop on Aerospace Computational Control was one in a series of workshops sponsored by NASA, NSF, and the DOD. The purpose of these workshops is to address computational issues in the analysis, design, and testing of flexible multibody control systems for aerospace applications. The intention in holding these workshops is to bring together users, researchers, and developers of computational tools in aerospace systems (spacecraft, space robotics, aerospace transportation vehicles, etc.) for the purpose of exchanging ideas on the state of the art in computational tools and techniques. For individual titles, see N94-14619 through N94-14652.

N94-14619*# Victoria Univ. (British Columbia). Dept. of Mechanical Engineering.
GEOMETRIC STIFFENING IN MULTIBODY DYNAMICS FORMULATIONS
Inna Sharf *In* JPL, Proceedings of the Fifth NASA/NSF/DOD Workshop on Aerospace Computational Control 15 Feb. 1993 p 1-24 Sponsored by Natural Sciences and Engineering Research Council (For primary document see N94-14618 02-39)
Avail: CASI HC A03/MF A04

In this paper we discuss the issue of geometric stiffening as it arises in the context of multibody dynamics. This topic has been treated in a number of previous publications in this journal and appears to be a debated subject. The controversy revolves primarily around the 'correct' methodology for incorporating the stiffening effect into dynamics formulations. The main goal of this work is to present the different approaches that have been developed for this problem through an in-depth review of several publications dealing with this subject. This is done with the goal of contributing to a precise understanding of the existing methodologies for modelling the stiffening effects in multibody systems. Thus, in presenting the material we attempt to illuminate the key characteristics of the various methods as well as show how they relate to each other. In addition, we offer a number of novel insights and clarifying interpretations of these schemes. The paper is completed with a general classification and comparison of the different approaches. Author (revised)

N94-14620*# Photon Research Associates, Inc., Cambridge, MA. Dynamics and Control Div.
STRESS STIFFENING AND APPROXIMATE EQUATIONS IN FLEXIBLE MULTIBODY DYNAMICS
Carlos E. Padilla and Andreas H. vonFlotow (Massachusetts Inst. of Tech., Cambridge.) *In* JPL, Proceedings of the Fifth NASA/NSF/DOD Workshop on Aerospace Computational Control 15 Feb. 1993 p 25-35 See also A92-55169 (For primary document see N94-14618 02-39)
Avail: CASI HC A03/MF A04

A useful model for open chains of flexible bodies undergoing large rigid body motions, but small elastic deformations, is one in which the equations of motion are linearized in the small elastic deformations and deformation rates. For slow rigid body motions, the correctly linearized, or consistent, set of equations can be compared to prematurely linearized, or inconsistent, equations and to 'oversimplified,' or ruthless, equations through the use of open loop dynamic simulations. It has been shown that the inconsistent model should never be used, while the ruthless model should be used whenever possible. The consistent and inconsistent models differ by stress stiffening terms. These are due to zeroth-order stresses effecting virtual work via nonlinear strain-displacement terms. In this paper we examine in detail the nature of these stress stiffening terms and conclude that they are significant only when the associated zeroth-order stresses approach 'buckling' stresses. Finally it is emphasized that when the stress stiffening terms are negligible the ruthlessly linearized equations should be used. Author (revised)

N94-14621*# National Aeronautics and Space Administration. Langley Research Center, Hampton, VA.
SOME EXPERIENCES WITH KRYLOV VECTORS AND LANCZOS VECTORS
Roy R. Craig, Jr. (Texas Univ., Austin.), Tzu-Jeng Su, and Hyoung M. Kim (McDonnell-Douglas Space Systems Co., Houston, TX.) *In* JPL, Proceedings of the Fifth NASA/NSF/DOD Workshop on Aerospace Computational Control 15 Feb. 1993 p 37-53 (For primary document see N94-14618 02-39)
(Grant NAG9-357)
Avail: CASI HC A03/MF A04

This paper illustrates the use of Krylov vectors and Lanczos vectors for reduced-order modeling in structural dynamics and for control of flexible structures. Krylov vectors and Lanczos vectors are defined and illustrated, and several applications that have been under study at The University of Texas at Austin are reviewed: model reduction for undamped structural dynamics systems, component mode synthesis using Krylov vectors, model reduction of damped structural dynamics systems, and one-sided and two-sided unsymmetric block-Lanczos model-reduction algorithms. Author

N94-14622*# Jet Propulsion Lab., California Inst. of Tech., Pasadena.
A COMPONENT MODES PROJECTION AND ASSEMBLY MODEL REDUCTION METHODOLOGY FOR ARTICULATED, MULTI-FLEXIBLE BODY STRUCTURES
Allan Y. Lee and Walter S. Tsuha *In its* Proceedings of the Fifth NASA/NSF/DOD Workshop on Aerospace Computational Control 15 Feb. 1993 p 55-75 See also A92-55168 (For primary document see N94-14618 02-39)
Avail: CASI HC A03/MF A04

A two-stage model reduction methodology, combining the classical Component Mode Synthesis (CMS) method and the newly developed Enhanced Projection and Assembly (EP&A) method, is proposed in this research. The first stage of this methodology, called the COmponent Modes Projection and Assembly model REduction (COMPARE) method, involves the generation of CMS mode sets, such as the MacNeal-Rubin mode sets. These mode sets are then used to reduce the order of each component model in the Rayleigh-Ritz sense. The resultant component models are then combined to generate reduced-order system models at various system configurations. A composite mode set which retains important system modes at all system configurations is then selected from these reduced-order system models. In the second stage, the EP&A model reduction method is employed to reduce further the order of the system model generated in the first stage. The effectiveness of the COMPARE methodology has been successfully demonstrated on a high-order, finite-element model of the cruise-configured Galileo spacecraft. Author

N94-14623*# Draper (Charles Stark) Lab., Inc., Cambridge, MA.
APPLICATIONS OF COMPUTER ALGEBRA TO DISTRIBUTED PARAMETER SYSTEMS
Joel A. Storch *In* JPL, Proceedings of the Fifth NASA/NSF/DOD Workshop on Aerospace Computational Control 15 Feb. 1993 p 77-90 (For primary document see N94-14618 02-39)
Avail: CASI HC A03/MF A04

In the analysis of vibrations of continuous elastic systems, one often encounters complicated transcendental equations with roots directly related to the system's natural frequencies. Typically, these equations contain system

parameters whose values must be specified before a numerical solution can be obtained. The present paper presents a method whereby the fundamental frequency can be obtained in analytical form to any desired degree of accuracy. The method is based upon truncation of rapidly converging series involving inverse powers of the system natural frequencies. A straightforward method to developing these series and summing them in closed form is presented. It is demonstrated how Computer Algebra can be exploited to perform the intricate analytical procedures which otherwise would render the technique difficult to apply in practice. We illustrate the method by developing two analytical approximations to the fundamental frequency of a vibrating cantilever carrying a rigid tip body. The results are compared to the numerical solution of the exact (transcendental) frequency equation over a range of system parameters. Author

N94-14624*# California Univ., Santa Barbara. Dept. of Mechanical Engineering.

INVERSE DYNAMICS: SIMULTANEOUS TRAJECTORY TRACKING AND VIBRATION REDUCTION WITH DISTRIBUTED ACTUATORS

Santosh Devasia and Eduardo Bayo *In* JPL, Proceedings of the Fifth NASA/NSF/DOD Workshop on Aerospace Computational Control 15 Feb. 1993 p 91-103 (For primary document see N94-14618 02-39) (Contract F49620-91-C-0095)

Avail: CASI HC A03/MF A04

This paper addresses the problem of inverse dynamics for articulated flexible structures with both lumped and distributed actuators. This problem arises, for example, in the combined vibration minimization and trajectory control of space robots and structures. A new inverse dynamics scheme for computing the nominal lumped and distributed inputs for tracking a prescribed trajectory is given. Author

N94-14625*# Victoria Univ. (British Columbia). Dept. of Mechanical Engineering.

MODELLING ROBOTIC SYSTEMS WITH DADS **c61**

L. W. Churchill and I. Sharf *In* JPL, Proceedings of the Fifth NASA/NSF/DOD Workshop on Aerospace Computational Control 15 Feb. 1993 p 105-116 (For primary document see N94-14618 02-39)

Avail: CASI HC A03/MF A04

With the appearance of general off-the-shelf software packages for the simulation of mechanical systems, modelling and simulation of mechanisms has become an easier task. The authors have recently used one such package, DADS, to model the dynamics of rigid and flexible-link robotic manipulators. In this paper, we present this overview of our learning experiences with DADS, in the hope that it will shorten the learning process for others interested in this software. Author (revised)

N94-14626*# DYNACS Engineering Co., Inc., Houston, TX.

COMPUTATIONAL CONTROLS WORKSTATION: ALGORITHMS AND HARDWARE **c60**

R. Venugopal and M. Kumar *In* JPL, Proceedings of the Fifth NASA/NSF/DOD Workshop on Aerospace Computational Control 15 Feb. 1993 p 117-123 (For primary document see N94-14618 02-39)

Avail: CASI HC A02/MF A04

The Computational Controls Workstation provides an integrated environment for the modeling, simulation, and analysis of Space Station dynamics and control. Using highly efficient computational algorithms combined with a fast parallel processing architecture, the workstation makes real-time simulation of flexible body models of the Space Station possible. A consistent, user-friendly interface and state-of-the-art post-processing options are combined with powerful analysis tools and model databases to provide users with a complete environment for Space Station dynamics and control analysis. The software tools available include a solid modeler, graphical data entry tool, O(n) algorithm-based multi-flexible body simulation, and 2D/3D post-processors. This paper describes the architecture of the workstation while a companion paper describes performance and user perspectives. Author

N94-14627*# Jet Propulsion Lab., California Inst. of Tech., Pasadena.

CAESY: A SOFTWARE TOOL FOR COMPUTER-AIDED ENGINEERING **c61**

Matt Wette *In its* Proceedings of the Fifth NASA/NSF/DOD Workshop on Aerospace Computational Control 15 Feb. 1993 p 125-130 (For primary document see N94-14618 02-39)

Avail: CASI HC A02/MF A04

A new software tool, Caesy, is described. This tool provides a strongly typed programming environment for research in the development of algorithms and software for computer-aided control system design. A description of the user language and its implementation as they currently stand are presented along with a description of work in progress and areas of future work. Author

N94-14628*# National Aeronautics and Space Administration. Goddard Space Flight Center, Greenbelt, MD.

ASTEC AND MODEL: CONTROLS SOFTWARE DEVELOPMENT AT GODDARD SPACE FLIGHT CENTER **c61**

John P. Downing, Frank H. Bauer, and Jeffrey L. Surber (Fairchild Space Co., Germantown, MD.) *In* JPL, Proceedings of the Fifth NASA/NSF/DOD Workshop on Aerospace Computational Control 15 Feb. 1993 p 131-141 (For primary document see N94-14618 02-39)

Avail: CASI HC A03/MF A04

The ASTEC (Analysis and Simulation Tools for Engineering Controls) software is under development at the Goddard Space Flight Center (GSFC). The design goal is to provide a wide selection of controls analysis tools at the personal computer level, as well as the capability to upload compute-intensive jobs to a mainframe or supercomputer. In the last three years the ASTEC (Analysis and Simulation Tools for Engineering Controls) software has been under development. ASTEC is meant to be an integrated collection of controls analysis tools for use at the desktop level. MODEL (Multi-Optimal Differential Equation Language) is a translator that converts programs written in the MODEL language to FORTRAN. An upgraded version of the MODEL program will be merged into ASTEC. MODEL has not been modified since 1981 and has not kept with changes in computers or user interface techniques. This paper describes the changes made to MODEL in order to make it useful in the 90's and how it relates to ASTEC. Author (revised)

N94-14629*# Boeing Defense and Space Group, Seattle, WA.

ANIMATION OF MULTI-FLEXIBLE BODY SYSTEMS AND ITS USE IN CONTROL SYSTEM DESIGN **c61**

Carl Juengst and Ron Stahlberg (Iowa Univ., Iowa City.) *In* JPL, Proceedings of the Fifth NASA/NSF/DOD Workshop on Aerospace Computational Control 15 Feb. 1993 p 143-151 (For primary document see N94-14618 02-39)

Avail: CASI HC A02/MF A04

Animation can greatly assist the structural dynamicist and control system analyst with better understanding of how multi-flexible body systems behave. For multi-flexible body systems, the structural characteristics (mode frequencies, mode shapes, and damping) change, sometimes dramatically with large angles of rotation between bodies. With computer animation, the analyst can visualize these changes and how the system responds to active control forces and torques. A characterization of the type of system we wish to animate is presented. The lack of clear understanding of the above effects was a key element leading to the development of a multi-flexible body animation software package. The resulting animation software is described in some detail here, followed by its application to the control system analyst. Other applications of this software can be determined on an individual need basis. A number of software products are currently available that make the high-speed rendering of rigid body mechanical system simulation possible. However, such options are not available for use in rendering flexible body mechanical system simulations. The desire for a high-speed flexible body visualization tool led to the development of the Flexible Or Rigid Mechanical System (FORMS) software. This software was developed at the Center for Simulation and Design Optimization of Mechanical Systems at the University of Iowa. FORMS provides interactive high-speed rendering of flexible and/or rigid body mechanical system simulations, and combines geometry and motion information to produce animated output. FORMS is designed to be both portable and flexible, and supports a number of different user interfaces and graphical display devices. Additional features have been added to FORMS that allow special visualization results related to the nature of the flexible body geometric representations. Author (revised)

N94-14630*# Air Force Academy, CO.
THE USE OF LINKED LISTS IN THE SIMULATION OF CONTROLLER-STRUCTURE INTERACTION **c61**
Ralph Quan *In* JPL, Proceedings of the Fifth NASA/NSF/DOD Workshop on Aerospace Computational Control 15 Feb. 1993 p 153-166 See also A93-44533 (For primary document see N94-14618 02-39)
Avail: CASI HC A03/MF A04

An algorithm for the computer simulation of large space structures under active control is considered. Linked lists are used in a matrix data structure to implement the trapezoidal rule on the system differential equations. The use of the trapezoidal rule ensures that the numerical stability is equivalent to the system stability, which is essential for this type of simulation. The sparsity of the system matrices is exploited by the linked lists, and the algorithm efficiently steps through the lists in an orderly fashion. Results of simulations on a NASA large space structure experiment are reported. Author

N94-14631*# Jet Propulsion Lab., California Inst. of Tech., Pasadena.
SPATIAL OPERATOR ALGEBRA FOR FLEXIBLE MULTIBODY DYNAMICS **c61**
A. Jain and G. Rodriguez *In its* Proceedings of the Fifth NASA/NSF/DOD Workshop on Aerospace Computational Control 15 Feb. 1993 p 167-183 (For primary document see N94-14618 02-39)
Avail: CASI HC A03/MF A04

This paper presents an approach to modeling the dynamics of flexible multibody systems such as flexible spacecraft and limber space robotic systems. A large number of degrees of freedom and complex dynamic interactions are typical in these systems. This paper uses spatial operators to develop efficient recursive algorithms for the dynamics of these systems. This approach very efficiently manages complexity by means of a hierarchy of mathematical operations. Author

N94-14632*# Texas A&M Univ., College Station. Center for Mechanics and Control.
NONRECURSIVE FORMULATIONS OF MULTIBODY DYNAMICS AND CONCURRENT MULTIPROCESSING
Andrew J. Kurdila and Ramesh Menon *In* JPL, Proceedings of the Fifth NASA/NSF/DOD Workshop on Aerospace Computational Control 15 Feb. 1993 p 185-204 (For primary document see N94-14618 02-39)
Avail: CASI HC A03/MF A04

Since the late 1980's, research in recursive formulations of multibody dynamics has flourished. Historically, much of this research can be traced to applications of low dimensionality in mechanism and vehicle dynamics. Indeed, there is little doubt that recursive order N methods are the method of choice for this class of systems. This approach has the advantage that a minimal number of coordinates are utilized, parallelism can be induced for certain system topologies, and the method is of order N computational cost for systems of N rigid bodies. Despite the fact that many authors have dismissed redundant coordinate formulations as being of order N(exp 3), and hence less attractive than recursive formulations, we present recent research that demonstrates that at least three distinct classes of redundant, nonrecursive multibody formulations consistently achieve order N computational cost for systems of rigid and/or flexible bodies. These formulations are as follows: (1) the preconditioned range space formulation; (2) penalty methods; and (3) augmented Lagrangian methods for nonlinear multibody dynamics. The first method can be traced to its foundation in equality constrained quadratic optimization, while the last two methods have been studied extensively in the context of coercive variational boundary value problems in computational mechanics. Until recently, however, they have not been investigated in the context of multibody simulation, and present theoretical questions unique to nonlinear dynamics. All of these nonrecursive methods have additional advantages with respect to recursive order N methods: (1) the formalisms retain the highly desirable order N computational cost; (2) the techniques are amenable to concurrent simulation strategies; (3) the approaches do not depend upon system topology to induce concurrency; and (4) the methods can be derived to balance the computational load automatically on concurrent multiprocessors. In addition to the presentation of the fundamental formulations, this paper presents new theoretical results regarding the rate of convergence of order N constraint stabilization schemes associated with the newly introduced class of methods. Author (revised)

N94-14633*# California Univ., Santa Barbara. Dept. of Mechanical Engineering.
NON-RECURSIVE AUGMENTED LAGRANGIAN ALGORITHMS FOR THE FORWARD AND INVERSE DYNAMICS OF CONSTRAINED FLEXIBLE MULTIBODIES
Eduardo Bayo and Ragnar Ledesma *In* JPL, Proceedings of the Fifth NASA/NSF/DOD Workshop on Aerospace Computational Control 15 Feb. 1993 p 205-219 Sponsored in part by TRW, Inc. (For primary document see N94-14618 02-39)
(Contract F49620-91-C-0095)
Avail: CASI HC A03/MF A04

A technique is presented for solving the inverse dynamics of flexible planar multibody systems. This technique yields the non-causal joint efforts (inverse dynamics) as well as the internal states (inverse kinematics) that produce a prescribed nominal trajectory of the end effector. A non-recursive global Lagrangian approach is used in formulating the equations for motion as well as in solving the inverse dynamics equations. Contrary to the recursive method previously presented, the proposed method solves the inverse problem in a systematic and direct manner for both open-chain as well as closed-chain configurations. Numerical simulation shows that the proposed procedure provides an excellent tracking of the desired end effector trajectory. Author

N94-14634*# Toronto Univ. (Ontario). Inst. for Aerospace Studies.
A NEURAL-NETWORK APPROACH TO ROBOTIC CONTROL **c63**
D. P. W. Graham and G. M. T. DEleuterio *In* JPL, Proceedings of the Fifth NASA/NSF/DOD Workshop on Aerospace Computational Control 15 Feb. 1993 p 221-236 Sponsored by Natural Science and Engineering Research Council; Inst. for Robotics and Intelligent Systems; Inst. for Space and Terrestrial Science (For primary document see N94-14618 02-39)
Avail: CASI HC A03/MF A04

An artificial neural-network paradigm for the control of robotic systems is presented. The approach is based on the Cerebellar Model Articulation Controller created by James Albus and incorporates several extensions. First, recognizing the essential structure of multibody equations of motion, two parallel modules are used that directly reflect the dynamical characteristics of multibody systems. Second, the architecture of the proposed network is imbued with a self-organizational capability which improves efficiency and accuracy. Also, the networks can be arranged in hierarchical fashion with each subsequent network providing finer and finer resolution. Author

N94-14635*# Illinois Univ., Chicago. Dept. of Mechanical Engineering.
COMPUTATIONAL STRATEGIES IN THE DYNAMIC SIMULATION OF CONSTRAINED FLEXIBLE MBS
F. M. L. Amirouche and M. Xie *In* JPL, Proceedings of the Fifth NASA/NSF/DOD Workshop on Aerospace Computational Control 15 Feb. 1993 p 237-241 (For primary document see N94-14618 02-39)
Avail: CASI HC A01/MF A04

This research focuses on the computational dynamics of flexible constrained multibody systems. At first a recursive mapping formulation of the kinematical expressions in a minimum dimension as well as the matrix representation of the equations of motion are presented. The method employs Kane's equation, FEM, and concepts of continuum mechanics. The generalized active forces are extended to include the effects of high temperature conditions, such as creep, thermal stress, and elastic-plastic deformation. The time variant constraint relations for rolling/contact conditions between two flexible bodies are also studied. The constraints for validation of MBS simulation of gear meshing contact using a modified Timoshenko beam theory are also presented. The last part deals with minimization of vibration/deformation of the elastic beam in multibody systems making use of time variant boundary conditions. The above methodologies and computational procedures developed are being implemented in a program called DYAMUS. Author (revised)

N94-14636*# Jet Propulsion Lab., California Inst. of Tech., Pasadena.
PARALLEL O(LOG n) ALGORITHMS FOR OPEN- AND CLOSED-CHAIN RIGID MULTIBODY SYSTEMS BASED ON A NEW MASS MATRIX FACTORIZATION TECHNIQUE **c61**
Amir Fijany *In its* Proceedings of the Fifth NASA/NSF/DOD Workshop on Aerospace Computational Control 15 Feb. 1993 p 243-266 (For

primary document see N94-14618 02-39)
Avail: CASI HC A03/MF A04

In this paper, parallel O(log n) algorithms for computation of rigid multibody dynamics are developed. These parallel algorithms are derived by parallelization of new O(n) algorithms for the problem. The underlying feature of these O(n) algorithms is a drastically different strategy for decomposition of interbody force which leads to a new factorization of the mass matrix (M). Specifically, it is shown that a factorization of the inverse of the mass matrix in the form of the Schur Complement is derived as M(exp -1) = C - B(exp *)A(exp -1)B, wherein matrices C, A, and B are block tridiagonal matrices. The new O(n) algorithm is then derived as a recursive implementation of this factorization of M(exp -1). For the closed-chain systems, similar factorizations and O(n) algorithms for computation of Operational Space Mass Matrix lambda and its inverse lambda(exp -1) are also derived. It is shown that these O(n) algorithms are strictly parallel, that is, they are less efficient than other algorithms for serial computation of the problem. But, to our knowledge, they are the only known algorithms that can be parallelized and that lead to both time- and processor-optimal parallel algorithms for the problem, i.e., parallel O(log n) algorithms with O(n) processors. The developed parallel algorithms, in addition to their theoretical significance, are also practical from an implementation point of view due to their simple architectural requirements. Author

N94-14637*# Ohio State Univ., Columbus. Dept. of Electrical Engineering.
PARALLEL METHODS FOR DYNAMIC SIMULATION OF MULTIPLE MANIPULATOR SYSTEMS **c62**
Scott McMillan, P. Sadayappan, and David E. Orin *In* JPL, Proceedings of the Fifth NASA/NSF/DOD Workshop on Aerospace Computational Control 15 Feb. 1993 p 267-281 (For primary document see N94-14618 02-39)
Avail: CASI HC A03/MF A04

In this paper, efficient dynamic simulation algorithms for a system of m manipulators, cooperating to manipulate a large load, are developed; their performance, using two possible forms of parallelism on a general-purpose parallel computer, is investigated. One form, temporal parallelism, is obtained with the use of parallel numerical integration methods. A speedup of 3.78 on four processors of CRAY Y-MP8 was achieved with a parallel four-point block predictor-corrector method for the simulation of a four manipulator system. These multi-point methods suffer from reduced accuracy, and when comparing these runs with a serial integration method, the speedup can be as low as 1.83 for simulations with the same accuracy. To regain the performance lost due to accuracy problems, a second form of parallelism is employed. Spatial parallelism allows most of the dynamics of each manipulator chain to be computed simultaneously. Used exclusively in the four processor case, this form of parallelism in conjunction with a serial integration method results in a speedup of 3.1 on four processors over the best serial method. In cases where there are either more processors available or fewer chains in the system, the multi-point parallel integration methods are still advantageous despite the reduced accuracy because both forms of parallelism can then combine to generate more parallel tasks and achieve greater effective speedups. This paper also includes results for these cases. Author (revised)

N94-14638*# Jet Propulsion Lab., California Inst. of Tech., Pasadena.
REAL-TIME DYNAMICS SIMULATION OF THE CASSINI SPACECRAFT USING DARTS. PART 1: FUNCTIONAL CAPABILITIES AND THE SPATIAL ALGEBRA ALGORITHM **c61**
A. Jain and G. K. Man *In its* Proceedings of the Fifth NASA/NSF/DOD Workshop on Aerospace Computational Control 15 Feb. 1993 p 297-306 (For primary document see N94-14618 02-39)
Avail: CASI HC A02/MF A04

This paper describes the Dynamics Algorithms for Real-Time Simulation (DARTS) real-time hardware-in-the-loop dynamics simulator for the National Aeronautics and Space Administration's Cassini spacecraft. The spacecraft model consists of a central flexible body with a number of articulated rigid-body appendages. The demanding performance requirements from the spacecraft control system require the use of a high fidelity simulator for control system design and testing. The DARTS algorithm provides a new algorithmic and hardware approach to the solution of this hardware-in-the-loop simulation problem. It is based upon the efficient spatial algebra dynamics for flexible multibody systems. A parallel and vectorized version of this algorithm is implemented on a low-cost, multiprocessor computer to meet the simulation timing requirements. Author (revised)

N94-14639*# Jet Propulsion Lab., California Inst. of Tech., Pasadena.
REAL-TIME DYNAMIC SIMULATION OF THE CASSINI SPACECRAFT USING DARTS. PART 2: PARALLEL/VECTORIZED REAL-TIME IMPLEMENTATION **c61**
A. Fijany, J. A. Roberts, A. Jain, and G. K. Man *In its* Proceedings of the Fifth NASA/NSF/DOD Workshop on Aerospace Computational Control 15 Feb. 1993 p 307-326 (For primary document see N94-14618 02-39)
Avail: CASI HC A03/MF A04

Part 1 of this paper presented the requirements for the real-time simulation of Cassini spacecraft along with some discussion of the DARTS algorithm. Here, in Part 2 we discuss the development and implementation of parallel/vectorized DARTS algorithm and architecture for real-time simulation. Development of the fast algorithms and architecture for real-time hardware-in-the-loop simulation of spacecraft dynamics is motivated by the fact that it represents a hard real-time problem, in the sense that the correctness of the simulation depends on both the numerical accuracy and the exact timing of the computation. For a given model fidelity, the computation should be computed within a predefined time period. Further reduction in computation time allows increasing the fidelity of the model (i.e., inclusion of more flexible modes) and the integration routine. Author

N94-14640*# Boeing Defense and Space Group, Seattle, WA.
SPACE STATION COMMON BERTHING MECHANISM, A MULTI-BODY SIMULATION APPLICATION **c18**
Ian Searle *In* JPL, Proceedings of the Fifth NASA/NSF/DOD Workshop on Aerospace Computational Control 15 Feb. 1993 p 351-364 (For primary document see N94-14618 02-39)
Avail: CASI HC A03/MF A04

This paper discusses an application of multi-body dynamic analysis conducted at the Boeing Company in connection with the Space Station (SS) Common Berthing Mechanism (CBM). After introducing the hardware and analytical objectives we will focus on some of the day-to-day computational issues associated with this type of analysis. Author

N94-14641*# Jet Propulsion Lab., California Inst. of Tech., Pasadena.
SIMULATION OF LINEAR MECHANICAL SYSTEMS **c61**
S. W. Sirlin *In its* Proceedings of the Fifth NASA/NSF/DOD Workshop on Aerospace Computational Control 15 Feb. 1993 p 365-377 (For primary document see N94-14618 02-39)
Avail: CASI HC A03/MF A04

A dynamics and controls analyst is typically presented with a structural dynamics model and must perform various input/output tests and design control laws. The required time/frequency simulations need to be done many times as models change and control designs evolve. This paper examines some simple ways that open and closed loop frequency and time domain simulations can be done using the special structure of the system equations usually available. Routines were developed to run under Pro-Matlab in a mixture of the Pro-Matlab interpreter and FORTRAN (using the .mex facility). These routines are often orders of magnitude faster than trying the typical 'brute force' approach of using built-in Pro-Matlab routines such as bode. This makes the analyst's job easier since not only does an individual run take less time, but much larger models can be attacked, often allowing the whole model reduction step to be eliminated. Author

N94-14642*# National Aeronautics and Space Administration. Ames Research Center, Moffett Field, CA.
OPTIMIZATION-BASED CONTROLLER DESIGN FOR ROTORCRAFT **c08**
N.-K. Tsing (Maryland Univ., College Park.), M. K. H. Fan (Georgia Inst. of Tech., Atlanta.), J. Barlow (Maryland Univ., College Park.), A. L. Tits (Maryland Univ., College Park.), and M. B. Tischler *In* JPL, Proceedings of the Fifth NASA/NSF/DOD Workshop on Aerospace Computational Control 15 Feb. 1993 p 379-393 (For primary document see N94-14618 02-39)
Avail: CASI HC A03/MF A04

An optimization-based methodology for linear control system design is outlined by considering the design of a controller for a UH-60 rotorcraft in hover. A wide range of design specifications is taken into account: internal

stability, decoupling between longitudinal and lateral motions, handling qualities, and rejection of windgusts. These specifications are investigated while taking into account physical limitations in the swashplate displacements and rates of displacement. The methodology crucially relies on user-machine interaction for tradeoff exploration. Author (revised)

N94-14643*# California Univ., Los Angeles. Dept. of Chemical Engineering.

ON l(1): OPTIMAL DECENTRALIZED PERFORMANCE c63

Dennis Sourlas and Vasilios Manousiouthakis *In* JPL, Proceedings of the Fifth NASA/NSF/DOD Workshop on Aerospace Computational Control 15 Feb. 1993 p 395-411 (For primary document see N94-14618 02-39)

Avail: CASI HC A03/MF A04

In this paper, the Manousiouthakis parametrization of all decentralized stabilizing controllers is employed in mathematically formulating the l(sup 1) optimal decentralized controller synthesis problem. The resulting optimization problem is infinite dimensional and therefore not directly amenable to computations. It is shown that finite dimensional optimization problems that have value arbitrarily close to the infinite dimensional one can be constructed. Based on this result, an algorithm that solves the l(sup 1) decentralized performance problems is presented. A global optimization approach to the solution of the infinite dimensional approximating problems is also discussed. Author (revised)

N94-14644*# California Univ., Santa Barbara. Dept. of Electrical and Computer Engineering.

A RATIONAL INTERPOLATION METHOD TO COMPUTE FREQUENCY RESPONSE

Charles Kenney, Stephen Stubberud, and Alan J. Laub *In* JPL, Proceedings of the Fifth NASA/NSF/DOD Workshop on Aerospace Computational Control 15 Feb. 1993 p 413-425 (For primary document see N94-14618 02-39)

(Grant AF-AFOSR-0240-91)

Avail: CASI HC A03/MF A04

A rational interpolation method for approximating a frequency response is presented. The method is based on a product formulation of finite differences, thereby avoiding the numerical problems incurred by near-equal-valued subtraction. Also, resonant pole and zero cancellation schemes are developed that increase the accuracy and efficiency of the interpolation method. Selection techniques of interpolation points are also discussed. Author

N94-14645*# Purdue Univ., West Lafayette, IN. Space Systems Control Lab.

AN APPLICATION OF THE IMC SOFTWARE TO CONTROLLER DESIGN FOR THE JPL LSCL EXPERIMENT FACILITY c61

Guoming Zhu and Robert E. Skelton *In* JPL, Proceedings of the Fifth NASA/NSF/DOD Workshop on Aerospace Computational Control 15 Feb. 1993 p 427-462 (For primary document see N94-14618 02-39)

Avail: CASI HC A03/MF A04

A software package which Integrates Model reduction and Controller design (The IMC software) is applied to design controllers for the JPL Large Spacecraft Control Laboratory Experiment Facility. Modal Cost Analysis is used for the model reduction, and various Output Covariance Constraints are guaranteed by the controller design. The main motivation is to find the controller with the 'best' performance with respect to output variances. Indeed it is shown that by iterating on the reduced order design model, the controller designed does have better performance than that obtained with the first model reduction. Author

N94-14646*# National Aeronautics and Space Administration. Marshall Space Flight Center, Huntsville, AL.

CONTROL SYSTEM DESIGN FOR FLEXIBLE STRUCTURES USING DATA MODELS c08

R. Dennis Irwin (Ohio Univ., Athens.), W. Garth Frazier (Ohio Univ., Athens.), Jerrel R. Mitchell (Ohio Univ., Athens.), Enrique A. Medina (Ohio Univ., Athens.), and Angelia P. Bukley *In* JPL, Proceedings of the Fifth NASA/NSF/DOD Workshop on Aerospace Computational Control 15 Feb. 1993 p 463-477 (For primary document see N94-14618 02-39)

Avail: CASI HC A03/MF A04

The dynamics and control of flexible aerospace structures exercises many of the engineering disciplines. In recent years there has been considerable research in the developing and tailoring of control system design techniques for these structures. This problem involves designing a control system for a multi-input, multi-output (MIMO) system that satisfies various performance criteria, such as vibration suppression, disturbance and noise rejection, attitude control and slewing control. Considerable progress has been made and demonstrated in control system design techniques for these structures. The key to designing control systems for these structures that meet stringent performance requirements is an accurate model. It has become apparent that theoretically and finite-element generated models do not provide the needed accuracy; almost all successful demonstrations of control system design techniques have involved using test results for fine-tuning a model or for extracting a model using system ID techniques. This paper describes past and ongoing efforts at Ohio University and NASA MSFC to design controllers using 'data models.' The basic philosophy of this approach is to start with a stabilizing controller and frequency response data that describes the plant; then, iteratively vary the free parameters of the controller so that performance measures become closer to satisfying design specifications. The frequency response data can be either experimentally derived or analytically derived. One 'design-with-data' algorithm presented in this paper is called the Compensator Improvement Program (CIP). The current CIP designs controllers for MIMO systems so that classical gain, phase, and attenuation margins are achieved. The center-piece of the CIP algorithm is the constraint improvement technique which is used to calculate a parameter change vector that guarantees an improvement in all unsatisfied, feasible performance metrics from iteration to iteration. The paper also presents a recently demonstrated CIP-type algorithm, called the Model and Data Oriented Computer-Aided Design System (MADCADS), developed for achieving H(sub infinity) type design specifications using data models. Control system design for the NASA/MSFC Single Structure Control Facility are demonstrated for both CIP and MADCADS. Advantages of design-with-data algorithms over techniques that require analytical plant models are also presented. Author (revised)

N94-14647*# Jet Propulsion Lab., California Inst. of Tech., Pasadena.

COMPUTATIONAL ISSUES IN OPTIMAL TUNING AND PLACEMENT OF PASSIVE DAMPERS

C. C. Chu and M. H. Milman *In its* Proceedings of the Fifth NASA/NSF/DOD Workshop on Aerospace Computational Control 15 Feb. 1993 p 479-490 (For primary document see N94-14618 02-39)

Avail: CASI HC A03/MF A04

The effectiveness of viscous elements in introducing damping in a structure is a function of several variables including their number, their location in the structure, and their physical properties. In this paper, the optimal damper placement and tuning problem is posed to optimize these variables. Both discrete and continuous optimization problems are formulated and solved corresponding, respectively, to the problems of placement of passive elements and to the tuning of their parameters. The paper particularly emphasizes the critical computational issues resulting from the optimization formulations. Numerical results involving a lightly damped testbed structure are presented. Author (revised)

N94-14648*# National Aeronautics and Space Administration. Lyndon B. Johnson Space Center, Houston, TX.

COMPUTATIONAL CONTROL WORKSTATION: USERS' PERSPECTIVES c54

Carlos M. Roithmayr, Timothy M. Straube (Colorado Univ., Boulder.), and Jeffrey S. Tave (Lockheed Engineering and Sciences Co., Houston, TX.) *In* JPL, Proceedings of the Fifth NASA/NSF/DOD Workshop on Aerospace Computational Control 15 Feb. 1993 p 491-505 (For primary document see N94-14618 02-39)

Avail: CASI HC A03/MF A04

A Workstation has been designed and constructed for rapidly simulating motions of rigid and elastic multibody systems. We examine the Workstation from the point of view of analysts who use the machine in an industrial setting. Two aspects of the device distinguish it from other simulation programs. First, one uses a series of windows and menus on a computer terminal, together with a keyboard and mouse, to provide a mathematical and geometrical description of the system under consideration. The second hallmark is a facility for animating simulation results. An assessment of the amount of effort required to numerically describe a system to the Workstation is made by comparing the process to that used with other multibody

software. The apparatus for displaying results as a motion picture is critiqued as well. In an effort to establish confidence in the algorithms that derive, encode, and solve equations of motion, simulation results from the Workstation are compared to answers obtained with other multibody programs. Our study includes measurements of computational speed.
Author

N94-14649*# TRW, Inc., Redondo Beach, CA. Space and Technology Group.
CONTROL STRUCTURAL INTERACTION TESTBED: A MODEL FOR MULTIPLE FLEXIBLE BODY VERIFICATION **c18**
M. A. Chory, A. L. Cohen, R. A. Manning, M. L. Narigon, and V. A. Spector *In* JPL, Proceedings of the Fifth NASA/NSF/DOD Workshop on Aerospace Computational Control 15 Feb. 1993 p 507-524 (For primary document see N94-14618 02-39)
Avail: CASI HC A03/MF A04

Conventional end-to-end ground tests for verification of control system performance become increasingly complicated with the development of large, multiple flexible body spacecraft structures. The expense of accurately reproducing the on-orbit dynamic environment and the attendant difficulties in reducing and accounting for ground test effects limits the value of these tests. TRW has developed a building block approach whereby a combination of analysis, simulation, and test has replaced end-to-end performance verification by ground test. Tests are performed at the component, subsystem, and system level on engineering testbeds. These tests are aimed at authenticating models to be used in end-to-end performance verification simulations: component and subassembly engineering tests and analyses establish models and critical parameters, unit level engineering and acceptance tests refine models, and subsystem level tests confirm the models' overall behavior. The Precision Control of Agile Spacecraft (PCAS) project has developed a control structural interaction testbed with a multibody flexible structure to investigate new methods of precision control. This testbed is a model for TRW's approach to verifying control system performance. This approach has several advantages: (1) no allocation for test measurement errors is required, increasing flight hardware design allocations; (2) the approach permits greater latitude in investigating off-nominal conditions and parametric sensitivities; and (3) the simulation approach is cost effective, because the investment is in understanding the root behavior of the flight hardware and not in the ground test equipment and environment. Author (revised)

N94-14650*# Phillips Lab., Edwards AFB, CA.
PACE: A TEST BED FOR THE DYNAMICS AND CONTROL OF FLEXIBLE MULTIBODY SYSTEMS **c08**
Moon K. Kwak, Monty J. Smith, and Alok Das *In* JPL, Proceedings of the Fifth NASA/NSF/DOD Workshop on Aerospace Computational Control 15 Feb. 1993 p 525-533 See also A93-34231 (For primary document see N94-14618 02-39)
Avail: CASI HC A02/MF A04

The Phillips Laboratory at Edwards AFB has constructed a test bed for the validation and comparison of modeling and control theories for the dynamics and control of flexible multibody systems. This project is called the Planar Articulating Controls Experiment (PACE). This paper presents the experimental apparatus for PACE and the problem formulation. An in-depth analysis on DC motor dynamics was also performed. Author

N94-14651*# Computer Motion, Inc., Goleta, CA.
DESIGN AND CONTROL OF A MACRO-MICRO ROBOT FOR PRECISE FORCE APPLICATIONS **c63**
Yulun Wang, Amante Mangaser, Keith Laby, Steve Jordan, and Jeff Wilson *In* JPL, Proceedings of the Fifth NASA/NSF/DOD Workshop on Aerospace Computational Control 15 Feb. 1993 p 535-552 Sponsored in part by NSF (For primary document see N94-14618 02-39)
Avail: CASI HC A03/MF A04

Creating a robot which can delicately interact with its environment has been the goal of much research. Primarily two difficulties have made this goal hard to attain. The execution of control strategies which enable precise force manipulations are difficult to implement in real time because such algorithms have been too computationally complex for available controllers. Also, a robot mechanism which can quickly and precisely execute a force command is difficult to design. Actuation joints must be sufficiently stiff, frictionless, and lightweight so that desired torques can be accurately applied. This paper describes a robotic system which is capable of delicate manipulations. A modular high-performance multiprocessor control system was designed to provide sufficient compute power for executing advanced control methods. An 8 degree of freedom macro-micro mechanism was constructed to enable accurate tip forces. Control algorithms based on the impedance control method were derived, coded, and load balanced for maximum execution speed on the multiprocessor system. Delicate force tasks such as polishing, finishing, cleaning, and deburring, are the target applications of the robot. Author

N94-14652*# National Aeronautics and Space Administration. Marshall Space Flight Center, Huntsville, AL.
A PROGRAM FOR THE INVESTIGATION OF THE MULTIBODY MODELING, VERIFICATION, AND CONTROL LABORATORY **c61**
Patrick A. Tobbe (Logicon Control Dynamics Co., Huntsville, AL.), Paul M. Christian (DYNACS Engineering Co., Inc., Huntsville, AL.), John M. Rakoczy, and Marlon L. Bulter *In* JPL, Proceedings of the Fifth NASA/NSF/DOD Workshop on Aerospace Computational Control 15 Feb. 1993 p 553-567 (For primary document see N94-14618 02-39)
Avail: CASI HC A03/MF A04

The Multibody Modeling, Verification, and Control (MMVC) Laboratory is under development at NASA MSFC in Huntsville, Alabama. The laboratory will provide a facility in which dynamic tests and analyses of multibody flexible structures representative of future space systems can be conducted. The purpose of the tests are to acquire dynamic measurements of the flexible structures undergoing large angle motions and use the data to validate the multibody modeling code, TREETOPS, developed under sponsorship of NASA. Advanced control systems design and system identification methodologies will also be implemented in the MMVC laboratory. This paper describes the ground test facility, the real-time control system, and the experiments. A top-level description of the TREETOPS code is also included along with the validation plan for the MMVC program. Dynamic test results from component testing are also presented and discussed. A detailed discussion of the test articles, which manifest the properties of large flexible space structures, is included along with a discussion of the various candidate control methodologies to be applied in the laboratory. Author (revised)

N94-14653# Imatran Voima Oy, Helsinki (Finland).
EFFECT OF SIZE, SHAPE, AND END CONDITION OF TEST SPECIMEN ON COMPRESSIVE STRENGTH OF HIGH-STRENGTH CONCRETE
A. Ipatti 1992 50 p
(DE93-500412; IVO-A-10/92) Avail: CASI HC A03/MF A01

Compressive testing of high-strength concrete is a critical issue on which no consensus has yet been reached. Among the many factors that are under discussion are the size, shape, and end condition of test specimens for high-strength concrete. The experimental program described herein was designed primarily to investigate the effects and the possible interactions of the above-mentioned factors on compressive strength of high-strength concrete. Three levels of specimen sizes, three methods of specimen capping (mould surface, sulphur capping, grinding), and four grades of concrete strengths were selected. A 3 x 3 x 4 factorial experimental design was adopted with two replicates (each an average of three specimens), giving a total of 72 test values (216 specimens). The strictest possible precautions were taken to ensure that all other factors which would conceivably effect the compressive strength were held constant. The statistical methods utilized included analyses of variance, linear regressions, and pairwise comparisons of factor main effects. DOE

N94-14692*# Technische Univ., Delft (Netherlands). Faculty of Aerospace Engineering.
THE EFFECT OF INITIAL IMPERFECTIONS ON SHELL STABILITY: AN UPDATED REVIEW
J. Arbocz Sep. 1992 193 p
(Grant NAGW-2317)
(LR-695; ISBN-9-06-275814-2; ETN-93-94007) Copyright Avail: CASI HC A09/MF A03

The development of the Delft Interactive Shell Design Code (DISDECO) is described. The purpose is to make the accumulated theoretical, numerical, and practical knowledge of the last years readily accessible to users interested in the analysis of buckling sensitive structures. With this open ended, hierarchical, interactive computer code, the user can access

workstation programs of increasing complexity. As a first update of DISDECO, the computational modules of the initial level were modified so as to handle combined loads consisting of axial compression, internal and external pressure, and clockwise or counter clockwise torque. The applied load is assumed to have a uniform spatial distribution and is divided into a fixed and a variable part. The magnitude of the variable part is allowed to vary in proportion to a load parameter Lambda. This leads to an eigenvalue problem for the critical lambda sub C. ESA

N94-14776*# National Aeronautics and Space Administration. Lewis Research Center, Cleveland, OH.
BUCKLING ANALYSIS OF LAMINATED THIN SHELLS IN A HOT ENVIRONMENT
Pascal K. Gotsis and James D. Guptil Sep. 1993 22 p
(RTOP 537-04-20)
(NASA-TM-106302; E-8043; NAS 1.15:106302) Avail: CASI HC A03/MF A01

Results are presented of parametric studies to assess the effects of various parameters on the buckling behavior of angle-ply, laminated thin shells in a hot environment. These results were obtained by using a three-dimensional finite element analysis. An angle-ply, laminated thin shell with fiber orientation of (theta/-theta)(sub 2) was subjected to compressive mechanical loads. The laminated thin shell had a cylindrical geometry. The laminate contained T300 graphite fibers embedded in an intermediate-modulus, high-strength (IMHS) matrix. The fiber volume fraction was 55 percent and the moisture content was 2 percent. The residual stresses induced into the laminate structure during the curing were taken into account. Parametric studies were performed to examine the effect on the critical buckling load of the following parameters: cylinder length and thickness, internal hydrostatic pressure, different ply thicknesses, different temperature profiles through the thickness of the structure, and different lay up configurations and fiber volume fractions. In conjunction with these parameters the ply orientation was varied from 0 deg to 90 deg. Seven ply angles were examined: 0 deg, 15 deg, 30 deg, 45 deg, 60 deg, 75 deg, and 90 deg. The results show that the ply angle theta and the laminate thickness had significant effects on the critical buckling load. The fiber volume fraction, the fiber orientations, and the internal hydrostatic pressure had important effects on the critical buckling load. The cylinder length had a moderate influence on the buckling load. The thin shell with (theta/-theta)(sub 2) or (theta/-theta)(sub s) angle-ply laminate had better buckling-load performance than the thin shell with (theta)(sub 4) angle-ply laminate. The temperature profiles through the laminate thickness and various laminates with the different ply thicknesses has insignificant effects on the buckling behavior of the thin shells. Author (revised)

N94-14818# Royal Aerospace Establishment, Farnborough (England).
A COMPUTER PROGRAM TO CALCULATE GROWTH RATES FOR CRACKS AT NOTCHES IN REGIONS OF RESIDUAL STRESS
R. Cook, S. Dorey, and D. P. Rooke 24 Nov. 1992 57 p
(RAE-TM-Mat/Str-1207; ICAF-1866; BR316512; ETN-93-94501) Copyright Avail: CASI HC A04/MF A01

A computer program which can be used to predict the growth rates of fatigue cracks emanating from notches and growing through residual stress fields is described. The residual stress distributions, alternating loading conditions and specimen geometry must be specified by the user. The program uses a Green's function technique to calculate the stress intensity factor due to the applied and residual stresses for any crack length. The calculated stress intensity factor can be corrected to account for the exact crack shape, if it is known. The crack growth rate is obtained from a data base of experimentally determined crack growth data as a function of stress intensity factor, for a number of different materials. ESA

N94-14902# Naval Civil Engineering Lab., Port Hueneme, CA.
NONLINEAR WAVE FORCES ON LARGE OCEAN STRUCTURES Final Report, Oct. 1991 - Sep. 1992
Erick T. Huang Apr. 1993 53 p
(DA Proj. R00-0-NO)
(AD-A266820; NCEL-TN-1857) Avail: CASI HC A04/MF A01

This study explores the significance of second-order wave excitations on a large pontoon and tests the feasibility of reducing a nonlinear free surface problem by perturbation expansions. A simulation model has been developed based on the perturbation expansion technique to estimate the wave forces. The model uses a versatile finite element procedure for the solution of the reduced linear boundary value problems. This procedure achieves a fair compromise between computation costs and physical details by using a combination of 2D and 3D elements. A simple hydraulic model test was conducted to observe the wave forces imposed on a rectangle box by Cnoidal waves in shallow water. The test measurements are consistent with the numerical predictions by the simulation model. This result shows favorable support to the perturbation approach for estimating the nonlinear wave forces on shallow draft vessels. However, more sophisticated model tests are required for a full justification. Both theoretical and experimental results show profound second-order forces that could substantially impact the design of ocean facilities. DTIC

N94-14164# Calspan Corp., Arnold AFS, TN.
MATERIALS/STRUCTURES TESTING
R. K. Matthews (Arnold Engineering Development Center, Arnold AFS, TN.) *In* VKI, Methodology of Hypersonic Testing 1993 12 p
Prepared in cooperation with Arnold Engineering Development Center, Arnold AFS, TN (For primary document see N94-14153 02-02)
Copyright Avail: CASI HC A03/MF A03

42 GEOSCIENCES (GENERAL)

N94-14484*# Alabama Univ., Huntsville. Dept. of Computer Science.
EARTH SCIENCE AND APPLICATION Final Report, 15 Jan. - 14 Jul. 1992
Danny Hardin, Helen Conover, and Sara J. Graves 14 Jul. 1992 8 p
(Contract NAS8-36955)
(NASA-CR-184381; NAS 1.26:184381; UAH-5) Avail: CASI HC A02/MF A01

The University of Alabama in Huntsville (UAH) has completed the research proposed. The major tasks under this contract were: (1) research into visualization of scientific data sets (browse); (2) studies of standard data formatting procedures; and (3) investigations of approaches for submission of scientific data sets for archival. Summaries of each activity are presented along with travel reports and conclusions and recommendations.
Author (revised)

N94-14500*# Maryland Univ., College Park. Center for Ocean-Land-Atmosphere Interactions.
INTEGRATION OF SPACE AND IN-SITU OBSERVATIONS TO STUDY ATMOSPHERE, OCEAN AND LAND PROCESSES Final Technical Report, 1 Sep. 1987 - 31 Aug. 1992
J. Shukla and J. L. Kinter, III 1992 11 p
(Grant NAGw-1166)
(NASA-CR-194495; NAS 1.26:194495) Avail: CASI HC A03/MF A01

A research investigation was conducted into the possibility of using atmospheric observations made in the past from both terrestrial and space-based platforms to create a global, coherent four dimensional analysis for the purpose of studying atmospheric, oceanic, and land surface processes relevant to climate simulation, monitoring, and change. This investigation consisted of the following tasks: (1) a mature global data assimilation system was obtained from the National Meteorological Center and modified for use on a Cray X-MP computer system; (2) atmospheric observations for the period 20 Nov. 1982 through 1 Mar. 1983, including rawinsonde soundings, aircraft-based measurements, pilot balloons, and temperature soundings from polar orbiting satellites were obtained from several sources; and (3) the global data assimilation system was used to reassimilate the atmospheric observations to produce a new atmospheric analysis which was then compared with the contemporaneous analysis. The global hydrologic cycle, including fluxes between the atmosphere and both the land and ocean surfaces, was estimated. The flux of water from the ocean surface into the atmosphere, its transport in the form of latent heat to remote regions, and its return to the surface in the form of precipitation were estimated globally. In addition, several regional budgets for selected tropical oceanic and extratropical continental areas were also done.
Author (revised)

43 EARTH RESOURCES AND REMOTE SENSING

Includes remote sensing of earth resources by aircraft and spacecraft; photogrammetry; and aerial photography.

For instrumentation see *35 Instrumentation and Photography.*

N94-13123# Beleidscommissie Remote Sensing, Delft (Netherlands).
PREPARATIONS FOR AND FIRST RESULTS OF THE CALIBRATION AND INTERPRETATION OF ERS-1 SAR IMAGERY OVER LAND
A. C. vandenBroek (Physics and Electronics Lab. TNO, The Hague, Netherlands.) and J. S. Groot (Physics and Electronics Lab. TNO, The Hague, Netherlands.) Aug. 1992 23 p
(BCRS-92-13; ISBN-90-5411-056-2; ETN-93-93755) Avail: CASI HC A03/MF A01

Preparatory and calibration work done for this project whose objectives were the calibration of the ERS-1 Synthetic Aperture Radar (SAR) data by the use of homogeneous distributed targets, identification, and (possibly) monitoring of agricultural crops in SAR images are reported. The project history and the first quality analysis of ERS-1 SAR data are discussed. The current project status of the AO-NL3 experiment is summarized. Some conclusions are drawn. ESA

N94-13331# Instituto de Pesquisas Espaciais, Sao Jose dos Campos (Brazil).
DENDROMETRIC VARIABLES ESTIMATION IN HOMOGENEOUS FORESTS USING LANDSAT TM DATA M.S. Thesis, 1991 [ESTIMATIVA DE VARIAVEIS DENDROMETRICAS EM FLORESTAS HOMOGENEAS A PARTIR DE DADOS LANDSAT TM]
Marcos Leandro Kazmierczak Jan. 1992 211 p In PORTUGESE Original contains color illustrations
(INPE-5455-TDI/497) Avail: CASI HC A10/MF A03

The obtainment of information inherent to growing and productivity is fundamental for forest activities planning, due to the long periods of time involved between implementation and final cut. Considering the fact that the obtainment of this information through traditional forest inventory represents a very high cost, a methodology associating field and orbital data was developed to generate prognosis equations. The study area defined for this work was the Passo Fundo National Forest (RS), in areas with 'Araucaria angustifolia' and 'Pinus.' The inventory of natural sites regarding types of soil rended as a base for the forest inventory, supplying stratified information, which were then correlated with orbital data. The approach applied presented some promising results on the estimate of general dendrometric variables from spectral data measured by the TM (Thematic Mapper) sensor, on board the Landsat-5 satellite. The quadratic function (Y = a+bX+cX(exp 2)) seemed the function that best adjusts the data into two studied species and the TM5 spectral response (1.55 to 1.75 m) seemed the isolated band to constitute the best independent variable. The quantification of some variables of interest could be done within acceptable error levels, as in the case of basal area in Pinus (8.16 percent). The dominant height and the basal area variables for Araucaria and the annual medium increment in volume, medium height, basal area and age for Pinus could be estimated with an accuracy between 84 and 92 percent, allowing the obtainment of preliminary information more rapidly and with lower costs. Author (revised)

N94-13364# Instituto de Pesquisas Espaciais, Sao Jose dos Campos (Brazil).
EVALUATION OF BETA-SPLINE INTERPOLATION IN DIGITAL TERRAIN MODELS Thesis [AVALIACAO DO INTERPOLADAR BETA-SPLINE EM MODELOS DIGITAIS DE ELEVACAO]
Carlos Eduardo Nery Jun. 1992 68 p In PORTUGESE
(INPE-5475-TDI/506) Avail: CASI HC A04/MF A01

The objective is to study the beta-Spline interpolator and evaluate its capability to generate Digitals Elevation Models. The study area is localized in the periphery of the city of Belo Horizonte, the principal district of the state of Minas Gerais. This place was chosen because it had digital format datas, and this made the ground survey more simple. In the beginning, the software was developed in PC computers but then it was necessary to work with VAX computer. Then two kinds of languages were used: C language (for PC's) and FORTRAN languages (for VAX). The results were evaluated applying the STATGRAPHICS software, and are graphically presented to be possible a visual analysis between the real model and the interpolated model generating a difference model. Author (revised)

N94-13368 New Brunswick Univ., Fredericton. Dept. of Surveying Engineering.
J2000.0 MODELLING OF GEOAIM IN THE ANALYSIS OF VLBI DATA FROM THE NASA CRUSTAL DYNAMICS PROJECT M.S. Thesis
Xin Tan Jul. 1990 167 p
(ISBN-0-315-59463-2; CTN-93-60857) Copyright Avail: Micromedia Ltd., Technical Information Centre, 165 Hotel de Ville, Place du Portage, Phase 2, Hull, Quebec J8X 3X2, Canada HC/MF

GEOAIM (GEOdetic Analysis of Interferometric Measurements) is a very long baseline interferometry (VLBI) data analysis program created in 1979 and updated several times since. The latest revision, called GEOAIM-2000, was developed to replace the old time reference epoch B1950.0 definitions and constants with the ones of J2000.0. Sixteen subprograms in the software package were amended and some other options were added to make GEOAIM-2000 more flexible in the analysis of VLBI data sets. A new ionospheric correction program was developed to enable freeing of data from ionospheric delay before GEOAIM-2000 processing. Some results are presented from using GEOAIM-2000 to process eight data sets collected under NASA's Crustal Dynamics Project 1984-85 at seven VLBI stations in North America. The processing results of six baselines and the positions of seven stations from GEOAIM-2000 processing indicate that cm-level repeatability in baseline length and tens of cm level repeatability in the relative position of stations was achieved. Comparison of the precession results from GEOAIM-2000 and its previous version shows that the accuracy of the model was increased by more than two orders of magnitude. Comparison of these results with those from NASA Goddard Space Flight Center show a few tens of cm of difference in values. Author (CISTI)

N94-13377# Instituto de Pesquisas Espaciais, Sao Jose dos Campos (Brazil).
SPECTRAL REFLECTANCE OF SOILS FROM SAO PAULO STATE [COMPORTAMENTO ESPECTRAL DE SOLOS DO ESTRADO DE SAO PAULO]
Jose Carlos Neves Epiphanio, Antonio Roberto Formaggio, Marcio deMorissonValeriano, and Joao Bertoldo deOliveira Jun. 1992 145 p In PORTUGESE Sponsored by Fundacao de Amparo a Pesquisa do Estado de Sao Paulo Original contains color illustrations
(INPE-5424-PRP/172) Avail: CASI HC A07/MF A02

Comprehension of the spectral reflectance of soils is required for effective use of remote sensing products. The absence of studies concerned to spectral reflectance of the soils from the tropical region in the 400 to 2500 nm spectral range is the main motivation of this research. The aim is the obtention of the bidirectional reflectance factor of 111 selected soil samples, grouped in 14 soil classes, taken from 54 sites (Sao Paulo State, Brazil). Each soil sample is associated to a set of physical and chemical analyses data. Part of these sites are characterized in published descriptive reports on soil surveys. The dependence between these and the spectral data were discussed. IRIS spectroradiometer, which can operate in the 400 to 2500 nm region of the electromagnetic spectrum, was used for the bidirectional reflectance factor measurements. It was also made a colorimetric analysis, which resulted in bright and saturation values, as well as in the dominant wavelength and in the tricromacity coordinates of the soil samples colors. Besides the analyses of the physical and chemical properties, a trial about moisture effects on the reflectance of selected soil samples was conducted. Additionally, colored photographs of samples are presented to allow observation of their superficial conditions. Author

N94-13426# Instituto de Pesquisas Espaciais, Sao Jose dos Campos (Brazil).
REMOTE SENSING OF AQUATIC SYSTEM Report No. 1, May 1989 - Jun. 1990 [SENSORIAMENTO REMOTO DE SISTEMAS AQUATICOS]
Evlyn Marcia LeaodeMoraesNovo and Claudia Zuccari Fern Braga May 1991 85 p In PORTUGESE
(INPE-5271-PRP/159) Avail: CASI HC A05/MF A01

This is the first technical report of the 'Remote Sensing of the Aquatic Systems' Project sent to the 'Fundasao de Amparo a Pesquisa do Estado de Sao Paulo' describing the activities performed between May 1989 and

June 1990. The methodology and technical aspects are discussed. They also present a bibliographic review on the subject and the discussion of the preliminary results. Author (revised)

N94-13475 Waterloo Univ. (Ontario).
NET RADIATION MAPPING OF MOUNTAINOUS TERRAIN USING LANDSAT-5 THEMATIC MAPPER IMAGERY AND DIGITAL TERRAIN DATA Ph.D. Thesis
Claude R. Duguay 1990 309 p
(ISBN-0-315-57755-X; CTN-93-60732) Copyright Avail: Issuing Activity (Micromedia Ltd., Technical Information Centre, 165 Hotel de Ville, Place du Portage, Phase 2, Hull, Quebec J8X 3X2, Canada HC)

A method for mapping the spatial distribution of surface net radiation in mountainous terrain using Landsat 5 Thematic Mapper (TM) imagery and digital terrain data is presented. Digital terrain data were used for image registration, atmospheric corrections in satellite imagery, and together with a two-stream radiation transfer model for the computation of shortwave and longwave irradiance. The visible, near infrared and mid-infrared reflectance derived from Landsat TM were combined into a measure of albedo using a weighted average scheme. Landsat TM thermal Band 6 was utilized in the determination of surface thermal excitance. Predicted values of shortwave and longwave irradiance, as well as of surface albedo and thermal excitance, were evaluated against field measurements. The proposed method using Landsat-5 TM imagery and digital terrain data yielded data in good agreement with data obtained using traditional field instruments. Maps of surface albedo, thermal excitance, and net radiation were produced to examine the spatial distribution of these parameters along a transect in the Colorado Front Range. Implications of this work for the modeling of daily net shortwave radiation in the alpine tundra are discussed. Diurnal variations of net shortwave radiation for selected cover types in the study area are summarized in graphical form. Author (CISTI)

N94-13523 Carleton Univ., Ottawa (Ontario). Dept. of Earth Sciences.
A KNOWLEDGE-BASED MODEL FOR THE INTEGRATION OF REMOTE SENSING INTO A MINERAL EXPLORATION PROGRAM Ph.D. Thesis
John Keith Hornsby Apr. 1990 328 p
(ISBN-0-315-58982-5; CTN-93-60730) Copyright Avail: Micromedia Ltd., Technical Information Centre, 165 Hotel de Ville, Place du Portage, Phase 2, Hull, Quebec J8X 3X2, Canada HC/MF

A study was conducted to research, develop, and demonstrate a knowledge based model for the application of remote sensing to mineral exploration in the Canadian environment. This environment is characterized by the cover of vegetation and various depths of overburden separating the bedrock geology of interest from the sensor. The study area chosen to test the model is situated in the Grenville province in Ontario, where exploration and mining activities have taken place for Au, Pb, and Zn associated with metavolcanics and overlying carbonates. The remote sensing exploration model is hierarchical, progressing through reconnaissance and detailed exploration levels with associated stages to achieve the goal of targeting sites of high mineral potential. The model focuses on obtaining evidence to support a working model of mineralization. The strategic approach developed is based on the concept of geobotany, in that vegetation will reflect in some degree the underlying geology. A methodology has been developed to identify anomalous areas in the remote sensing data using a geobotanical strategy. Data processing procedures were determined and geobotanical relationships identified. A methodology was developed to integrate geophysical, geobotanical, and geochemnical anomalies to produce mineral potential maps. Author (CISTI)

N94-13542 McGill Univ., Montreal (Quebec). Geophysics Lab.
APPLICATION OF TRANSIENT AIRBORNE ELECTROMAGNETIC AND GROUND RESISTIVITY METHODS TO GEOLOGICAL MAPPING IN TROPICAL TERRAINS Ph.D. Thesis
Justus Obiko Barongo May 1989 228 p
(ISBN-0-315-57172-1; CTN-93-60727) Copyright Avail: Micromedia Ltd., Technical Information Centre, 165 Hotel de Ville, Place du Portage, Phase 2, Hull, Quebec J8X 3X2, Canada HC/MF

The feasibility of using ground resistivity and time domain airborne electromagnetic (AEM) methods in geological mapping in tropical terrains is investigated. The investigation is based on evaluation of the linear inverse theory in the determination of physical parameters of the weathered layer necessary for interpretation of underlying lithology. Inversion of ground resistivity sounding data from the greenstone belt in western Kenya yields conductivities and thicknesses consistent with geology. A similar inversion of modelled time domain airborne electromagnetic data shows that conductivity, thickness, and depth to the top of the conductive weathered layer can be uniquely determined if its response does not suffer the thin sheet response problem. The results further show that this problem can be quite common in tropical regions since much of the weathered layer has low conductivity and thickness and, consequently, the response is weak. In this situation, conductivity and thickness are correlated and conductivity thickness product is better determined than these two parameters independently. By virtue of the weak time domain AEM response of the weathered layer, much of the response remains buried in noise. A method for reducing some of this noise before carrying out the inversion is presented. Author (CISTI)

N94-13592 Oregon State Univ., Corvallis.
ANALYTICAL FRAMEWORK FOR MODELING SCALE-RELATED VARIABILITIES IN REMOTE SENSING Ph.D. Thesis
Chaur-Fong Chen 1992 126 p
Avail. Univ. Microfilms Order No. DA9311051

A general analytical framework was established to investigate the scale-related variabilities in remote sensing. The variabilities were studied first by investigating canopy structure, canopy interaction with light, relation between spectral reflectance and plant phenological parameters. The variabilities simulated by the plant model were compared with the actual spectral data acquired by ground spectroradiometer and satellite sensors. The theoretical relation between orthogonal based transform and Kahunen-Loeve transform was investigated in the vector space. The role of spectral indices in identifying the status of phenological parameters was briefly studied. The radio metric corrections of the remotely sensed data were carefully controlled to avoid the unwanted noise introduced by typical resampling/correction procedures from commercial operation. The nonlinearity and sensor response corrections were applied to the spectral data as necessary. Variability analysis was conducted to illustrate the complexities of spectral variability embedded in the remotely sensed data. The information extraction in spatial frequency domain was investigated with emphasis in Fourier domain feature extraction. The Radon transform was introduced as the potential tool to enhance the spatial information of the Fourier transformed image. The adequacy of entropy and fractal dimension as image information measures was proved. A functional link between entropy and fractal dimension was established. The image information content was extracted using various first and second order statistics, entropy, and fractal dimension. Results were presented for different remote sensors based on the full image information content and specific agricultural ground features. The quality of spatial resampling algorithms was tested by investigating the capability to maintain image information in the resampled image. Finally, two applications utilizing this analytical framework were presented to show its potential in land-use classification and multiscale data fusion. Dissert. Abstr.

N94-13610# Instituto de Pesquisas Espaciais, Sao Jose dos Campos (Brazil).
OPERATIONAL TEST OF THE AIRBORNE DATA ACQUISITION SYSTEM: SADA, THE BARA BONITA EXPERIMENT [TESTE OPERACIONAL DO SISTEMA DE AQUISICAO DE DADOS AEROTRANPORTADO - SADA O EXPERIMENTO BARRA BONITA]
Carlos Alberto Steffen, Fabio Furlan Gama, and Evlyn M. L. M. Novo Oct. 1992 22 p In PORTUGESE Original contains color illustrations
(INPE-5451-NTC/305) Avail: CASI HC A03/MF A01

The nature of the spectral interaction between radiant energy and the Earth's surface components is very important for the development of Remote Sensing techniques. One of the most effective ways to understand those interactions is through the measurement and analysis of the spectral reflectance of those components. The use of field ground reflectance data for the calibration of satellite imagery can be more accurate if the measurements are done using a radiometer whose field of view has similar dimensions to that of the satellite imaging system. Many modern spectral radiometers, based upon CCD technology, have made the field reflectance measurements easier owing to their portability, speed of data acquisition and reliability. To take advantage of these new capabilities and to fulfill the geometric and spectral requirements of the ground data, the Laboratory for Radiometry of the National Institute of Space Research (INPE/BRAZIL),

developed the Airborne Data Acquisition System (SADA), that uses two SPECTRON SE590 radiometers and an helicopter as its operational platform. The SADA system is able to collect ground reflectance spectra at high sampling rates and over extensive or inaccessible targets such as water bodies and forests. The first operational test of the system was carried out on the Barra Bonita reservoir at the Sao Paulo State. In this experiment the SADA was used for the measurement of the bidirectional spectral reflectance factors of the different water masses of the reservoir. The results of this test showed that the system has an excellent operational flight performance and is very effective for the quick collection of field reflectance data over this kind of target. Author (revised)

N94-13729# Instituto de Pesquisas Espaciais, Sao Jose dos Campos (Brazil).
SATELLITE IMAGERY AND EXOGENOUS DATA INTEGRATION BY NEURAL NETWORK IN AUTOMATION LAND-COVER CLASSIFICATION
Maria Suelena S. Barros 1993 10 p Presented at the International Society for Optical Engineering - SPIE, Washington, DC, Jul. 1992
(INPE-5480-PRE/1778) Avail: CASI HC A02/MF A01

Certainly data integration for land-cover classification requires a non-linear system to associate satellite imagery with exogenous imagery. In this study we present some results of a Neural Network based methodology to provide land-cover classifications. Two approaches are investigated: (1) The Monolithic integration: all required registered images are the inputs of only one Back-Error Propagation (BEP) network. The network is trained on purpose to get the final classification. (2) The class-distributed integration: for each class a specific network learns from all satellite imageries its class characteristics. In both approaches, topographic mapping is taken into account as exogenous data. Author (revised)

N94-13789# Instituto de Pesquisas Espaciais, Sao Jose dos Campos (Brazil).
NONLINEAR ASPECTS OF DATA INTEGRATION FOR LAND-COVER CLASSIFICATION IN A NEURAL NETWORK ENVIRONMENT
Maria Suelena S. Barros and Valter Rodrigues 1993 17 p Presented at the 29th Plenary Meeting of the Committee on Space Research - COSPAR/The World Congress, Washington, DC, 1992
(INPE-5479-PRE/1778) Avail: CASI HC A03/MF A01

Some results of exploring nonlinear aspects of a neural network methodology to provide land-cover in satellite imagery are presented. All required images are used in a Back-Error Propagation (BEP) network which is a nonlinear data integrator for spatial patterns classification. The network is trained to give the basic categories: grass, moisted soil, bare soil, forest, water and built-up areas. The results of a partial classification are used in a posterior analysis which is done to get the final classification in more detailed classes of land use. The performance results show how powerful a neural-network based methodology is for satellite imagery integration and classification. Author (revised)

N94-13872*# Jet Propulsion Lab., California Inst. of Tech., Pasadena.
THEORY OF POST-BLOCK 2 VLBI OBSERVABLE EXTRACTION
Stephen T. Lowe 15 Jul. 1992 131 p
(NASA-CR-194543; JPL-Publ-92-7; NAS 1.26:194543) Avail: CASI HC A07/MF A02

The algorithms used in the post-Block II fringe-fitting software called 'Fit' are described. The steps needed to derive the very long baseline interferometry (VLBI) charged-particle corrected group delay, phase delay rate, and phase delay (the latter without resolving cycle ambiguities) are presented beginning with the set of complex fringe phasors as a function of observation frequency and time. The set of complex phasors is obtained from the JPL/CIT Block II correlator. The output of Fit is the set of charged-particle corrected observables (along with ancillary information) in a form amenable to the software program 'Modest.' Author (revised)

N94-13994# Institut Royal Meteorologique de Belgique, Brussels.
POTENTIAL EVAPOTRANSPIRATION IN BELGIUM: SPATIAL AND TEMPORAL VARIABILITY [L'EVAPOTRANSPIRATION POTENTIELLE EN BELGIQUE: VARIABILITE SPATIALE ET TEMPORELLE]
F. Gellens-Meullenberghs and D. Gellens 1992 45 p In FRENCH
(Publ-Ser-A-130; ETN-93-94222) Avail: CASI HC A03/MF A01

A brief reminder of a method, based on the Penman formula, to assess the free water evaporation and evapotranspiration of natural surfaces, is presented. The monthly and annual means of the evaporation from a sheet of surface water and the potential evapotranspiration from grass, leaves and conifers estimated on a 20 years period at 13 stations throughout Belgium are presented. Tables and maps which describes their spatial and temporal variability and are commented upon. ESA

N94-14056# Sandia National Labs., Albuquerque, NM.
FEATURE DISCOVERY ON SEGMENTED OBJECTS IN SAR IMAGERY USING SELF-ORGANIZING NEURAL NETWORKS
R. J. Fogler, M. W. Koch, M. M. Moya, and D. R. Hush 1992 12 p Presented at the Society of Photo-Optical Instrumentation Engineers OE/Aerospace Science and Sensing Meeting, Orlando, FL, 11-16 Apr. 1993
(Contract DE-AC04-76DP-00789)
(DE93-010685; SAND-92-2086C; CONF-930445-1) Avail: CASI HC A03/MF A01

In this paper we investigate the applicability of the feature extraction mechanisms found in the neurophysiology of mammals to the problem of object recognition in synthetic aperture radar imagery. Our approach is to present multiple views of objects to be recognized to a two-stage self-organizing neural network architecture. The first stage, a two-layer Neocognitron, performs feature extraction in each layer. The resulting feature vectors are presented to the second stage, an ART-2A classifier, self-organizing neural network which clusters the features into multiple object categories. The feature extraction operators resulting from the self-organization process are compared to the feature extraction mechanisms found in the neurophysiology of vision. In a previous paper, the Neocognitron was trained on raw SAR imagery. The architecture was able to recognize a simulated vehicle at arbitrary azimuthal orientations at a single depression angle while rejecting clutter as well as other vehicles. Feature extraction on raw imagery yielded features that were robust but very difficult to interpret. In this paper we report the results of some new experiments in which the self-organization process is applied separately to shadow and bright returns from objects to be recognized. Feature extraction on shadow returns yield oriented contrast edge operators suggestive of bipartite simple cells observed in the striate cortex of mammals. Feature extraction on the specularity patterns in bright returns yield a collection of operators resembling a two-dimensional Haar basis set. We compare the performance of the earlier two-stage neural network trained on raw imagery with a modified network using the new feature set. DOE

N94-14073# Beleidscommissie Remote Sensing, Delft (Netherlands).
[ACTIVITIES REPORT OF THE NETHERLANDS REMOTE SENSING BOARD] Annual Report, 1991 [BELEIDSCOMMISSIE REMOTE SENSING, JAARVERSLAG 1991]
1992 138 p In DUTCH Original contains color illustrations
(ETN-93-93880) Avail: CASI HC A07/MF A02

Remote sensing techniques were used for meteorological and oceanographic studies, mainly based on satellite data. Aerial multiband SAR (Synthetic Aperture Radar) techniques were used for sea bottom mapping. Satellite observations were combined with in situ measurements and a temperature model for a three dimensional temperature field of seas. Remote sensing techniques were used for the operational management and morphodynamic studies of the Wadden sea. Satellite data were used to establish land use data bases. Tropospheric trace gases were analyzed in the framework of climatological and environmental studies. Meteosat measurements were used to establish mesoscale energy balances of Egypt and Bostwana. Several technological developments were performed. ESA

N94-14081*# Washington Univ., Seattle. Dept. of Atmospheric Sciences.
OPTICAL PROPERTIES OF CO2 ICE AND CO2 SNOW IN THE ULTRAVIOLET, VISIBLE, AND INFRARED Final Report, 1 Jun. 1989 - 30 Nov. 1992
Stephen Warren 31 Aug. 1993 8 p
(Grant NAGw-1734)
(NASA-CR-194110; NAS 1.26:194110) Avail: CASI HC A02/MF A01

The project was to measure the optical constants of CO2 ice in the spectral regions of weak absorption. Many previous measurements had been made by others in the strong absorption bands, but the weak regions had been poorly measured or not measured at all. In these regions the emissivity of CO2 frost and CO2 clouds is quite sensitive to particle sizes

and to the value of the absorption coefficient, so the new measurements will have applications to energy budget and remote sensing of the Martian surface and atmosphere. During the time period covered by this grant, a method was developed for growing clear crystals of CO2, 4 cm in length. An apparatus was constructed for accurate measurement of spectral transmission through these crystals, for wavelengths 0.18-3.8 micrometers, covering the near-ultraviolet, visible, and near-infrared regions, bounded by the strong ultraviolet absorption and the 4.3-micrometer band. Our new best estimate of the spectral absorption coefficient (expressed as imaginary refractive index) is shown. It is a composite result of many measurements on dozens of crystals. Now that we have a good dataset for the shortwave absorption spectrum, the focus of the research has moved to the thermal infrared, for which a Fourier Transform interferometer has been adapted for use with C02-ice crystals. Derived from text

N94-14082# Instituto de Pesquisas Espaciais, Sao Jose dos Campos (Brazil).
INTELLIGENT ENVIRONMENT FOR INTERPRETATION TASKS OF REMOTELY SENSED IMAGES
Carlos Alberto deOliveira 1993 9 p Presented at the 17th Congress ISPRS, Washington, DC, 2-14 Aug. 1992
(INPE-5466-PRE/1774) Avail: CASI HC A02/MF A01

Digital image interpretation tasks in Remote Sensing applications have been exhaustively studied. Achievements in the area have used deterministic and statistical algorithms. Usually these algorithms only base their decisions on spatial data furnished as representative of patterns (classes). This paper presents a study on the use of Artificial Intelligence (AI) Techniques for interpretation purposes. The following topics are covered in the paper: representation of the knowledge involved in interpretation tasks (local and spatial ones), development or an intelligent interface (for Brazilian users) for interactive classification tasks and educational purposes in Remote Sensing, and the use of the PROLOG language as the principal tool for implementing the inference rules. As a preliminary result a prototype has been tested translating Natural Language queries (in Portuguese) into a Geometric representation language. Author

N94-14091# National Space Development Agency, Saitama (Japan).
EARTH OBSERVATION CENTER ANNUAL REPORT ON RESEARCH AND DEVELOPMENT, FISCAL YEAR 1992 [HEISEI 4 NENDO CHIKYUU KANSOKU SENTA SEIKA HOUKOK USHO]
15 Mar. 1993 247 p In JAPANESE Original contains color illustrations
(EOC-92-01-0007; JTN-93-80452) Avail: CASI HC A11/MF A03

The following topics were discussed: Japanese spacecraft, satellite design, JERS-1 (Japanese Earth Resources Satellite-1), ERS-1, ADEOS (Advanced Earth Observing Satellite), remote sensors, SAR (Synthetic Aperture Radar), OPS (Optical Sensor), radiometers, scatterometers, sensor calibration, instrument compensation, data reduction, data acquisition, data recording, image analysis, image processing, data system, forest management, land management, sea ice observation, mission planning, and ocean temperature. For individual titles, see N94-14092 through N94-14094.

N94-14092# National Space Development Agency, Saitama (Japan).
CALIBRATION AND IN-HOUSE VALIDATION RESULTS OF JERS-1 DATA [JERS-1 DETA KOUSEI TO NAIBU KENSHOU KEKKA]
Takashi Moriyama, Masanobu Shimada, Masao Nakai, and Yumi Kasai *In its* Earth Observation Center Annual Report on Research and Development, Fiscal Year 1992 15 Mar. 1993 p 1-163 In JAPANESE Original contains color illustrations (For primary document see N94-14091 02-43)
Avail: CASI HC A07/MF A03

The purposes of system validation, forms of implementation, sensors subjected to the validation, present status of operation of JERS-1, calibration and validation of the SAR and OPS, examples of calibrated data application, and the outline of NASDA (National Space Development Agency of Japan)-NASA joint research are described. Topics discussed include: image data obtained from satellite-borne sensors; geophysical value measurement accuracy; conversion to various physical values necessary for global environment monitoring; NASDA in-house validation; joint research with overseas research institutes; Announcement of Opportunity (AO) validation based on public recruitment; the Synthetic Aperture Radar (SAR) and Optical Sensors (OPSs) for the JERS-1 (Japanese Earth Resources Satellite-1); and sensors for the ERS-1. This report is represented in viewgraphs only. Author (NASDA)

N94-14093# National Space Development Agency, Saitama (Japan).
EARTH OBSERVATION EXPERIMENT DATA ANALYSIS [CHIKYUU KANSOKU JIKKEN DETA KAISEKI]
Hiroyuki Koguma, Takashi Moriyama, Yukihiro Nakaya, and Hironori Maejima *In its* Earth Observation Center Annual Report on Research and Development, Fiscal Year 1992 15 Mar. 1993 p 165-230 In JAPANESE Original contains color illustrations (For primary document see N94-14091 02-43)
Avail: CASI HC A04/MF A03

An overview of earth observation experiments and their data analysis, experimenting with and data analysis of the observation experiments on Kushiro marshland and those for the Sea of Kumano, and plans for FY 1993 observation experiments are outlined. Topics discussed include: sites of observation; characteristics of the conditions and observation spectrums of airborne Multi-Spectral Scanner (MSS); on-ground data acquisition equipment and units; observation experiments by the Marine Observation Satellite-1 (MOS-1) Visible and Thermal Infrared Radiometer (VTIR); and airborne MSS and Advanced Experimental Bottom Temperature (AXBT) systems. This report is represented in viewgraphs only. Author (NASDA)

N94-14094# National Space Development Agency, Saitama (Japan).
ADEOS PROJECT [ADEOS PUROJEKUTO NI TSUITE]
Isao Nakanishi, Shinichi Suzuki, and Takashi Moriyama *In its* Earth Observation Center Annual Report on Research and Development, Fiscal Year 1992 15 Mar. 1993 p 231-287 In JAPANESE Original contains color illustrations (For primary document see N94-14091 02-43)
Avail: CASI HC A04/MF A03

An overview of Advanced Earth Observing Satellite (ADEOS), equipment development and operation plan, data products, and validation plan related to ADEOS are outlined. Topics discussed include: the purpose of ADEOS program; data related to ADEOS; sensors carried onboard ADEOS; core sensors; Ocean Color and Temperature Sensor (OCTS); Advanced Visible and Near-Infrared Radiometer (AVNIR); Announcement of Opportunity (AO) of sensors; Interferometric Monitor for Greenhouse Gases (IMG); Improved Limb Atmospheric Spectrometer (ILAS); Retroreflector In Space (RIS); NASA Scatterometer (NSCAT); and Total Ozone Mapping Spectrometer (TOMS). This report is represented in viewgraphs only. Author (NASDA)

N94-14127# Beleidscommissie Remote Sensing, Delft (Netherlands).
INTEGRATION OF REMOTELY SENSED DATA AND CADASTRAL OWNERSHIP BOUNDARIES FOR LAND INVENTORY PURPOSES
Lucas L. F. Janssen (Wageningen Agricultural Univ., Netherlands.) and Dennis M. Keeman (Wageningen Agricultural Univ., Netherlands.) Aug. 1992 43 p Sponsored by Beleidscommissie Remote Sensing, Delft, Netherlands Original contains color illustrations
(BCRS Proj. 3.1/TO-01)
(BCRS-92-16; ISBN-9-05-411057-0; ETN-93-93758) Avail: CASI HC A03/MF A01

The objectives of this study were to assess: the possibilities of using cadastral ownership boundaries to extract land cover data from satellite images by means of the object classification; the accuracy of the cadastral land use and remote sensing derived land cover data; and the use of satellite remote sensing for updating the cadastral land use data. For this purpose the digital cadastal boundaries and a Spot and Thematic Mapper image were required for the Lunteren area (The Netherlands). The Lunteren area is a rural area of 3600 ha, consisting of 2110 cadastral parcels. Both satellite images were used for a multitemporal object classification which resulted in one land cover label per cadastral parcel. The underlying assumption of the object classification is that one object (one cadastral parcel) has one land cover type. The multitemporal classification was realized by means of a look up table. The classification results were compared with observations from a field survey in which 289 cadastral parcels were visited. The selection of these parcels was based on a number of criteria to enable comparison between the land use data as stored at the Cadaster (in AKR, an information system that stores administrative information for each cadastral parcel), and the land cover derived from remote sensing. ESA

N94-14131# Instituto de Pesquisas Espaciais, Sao Jose dos Campos (Brazil).
MULTISENSOR REMOTE SENSING DATA AND GIS TECHNIQUES FOR MONITORING PRESERVATION AREAS: A CASE STUDY
Yosio Edemir Shimabukuro, David Chung Liang Lee, and Joao RobertodosSantos Jun. 1991 14 p Presented at the 24th International Symposium on Remote Sensing of Environment, Rio de Janeiro, Brazil, 27-31 May 1991 Previously announced in IAA as A92-41028
(INPE-5317-PRE/1714) Avail: CASI HC A03/MF A01

The objective is to present the capability of remote sensing and GIS techniques for detecting and monitoring the anthropic alterations (mainly, fire action) which sometimes occur in preservation areas. For example, in the Brazil Central region occupied by savanna ('cerrado'), the vegetation burning procedure is commonly employed in the process of implantation and management of cattle raising and agricultural activities. During this annual burning process, fires even reach the environmental protection areas such as National Parks. The Emas National Park, located in South-western of Goias State, Brazil, between 52 deg 40 min W to 53 deg IO min W and 17 deg 50 min S to 18 deg 25 min S, was selected as the study area. This National Park had its area frequently burned in the dry season, as well as in August, 1988. In this investigation, the TM/Landsat data from 29 July 1988 (before the fire) and 14 August 1988 (after the fire) and AVHRR/NOAA data obtained in this period covered by TM images were used for monitoring the biomass burning. The TM images were registered to a topographic map in order to build a database including information such as drainage, roads, elevation and vegetation type for this National Park. Pixels classified as burned areas using band 3 (3.55 um to 3.93 um) of AVHRR images were overlayed on the map derived from the database. The SITIM (Image Processing System) and SGI (Geographic Information System) developed by INPE were utilized in this research. The integration of elevation, TM multitemporal data and information extracted from AVHRR images is a valuable tool for the managers to detect and evaluate the damage occurred as well as to monitor the regeneration process of land cover. Author (revised)

N94-14135# Deutsche Forschungsanstalt fuer Luft- und Raumfahrt, Oberpfaffenhofen (Germany). Hauptabt. Angewandte Datentechnik.
AN ALGORITHM FOR THE REMOTE SENSING OF FOG USING SATELLITE-DATA AND ADDITIONAL INFORMATION [EIN ALGORITHMUS ZUR NEBELFERNERKUNDUNG AUS SATELLITENDATEN UND ZUSATZINFORMATIONEN]
Stephan Schaedlich Aug. 1992 85 p In GERMAN
(DLR-FB-92-23; ETN-93-93740) Avail: CASI HC A05/MF A01

The development of an algorithm for the detection of fog during daytime using NOAA-AVHRR (Advanced Very High Resolution Radiometer) data is described. APOLLO programs are applied to perform cloud detection, cloud classification, and cloud analysis using AVHRR data. Both for the development and the verification, additional information is integrated (synopdata, digital elevation model). The fog detection will be carried out in two steps: after the separation of fog or low stratus from other clouds, land, and ocean, an attempt is made to separate fog from low stratus. The statistical verification with synopdata shows that fog and low stratus are well detected only at radiation weather conditions. The described automatic method for the determination of the cloud top heights of fog and low stratus does not work at all times. ESA

N94-14151# Department of Energy, Morgantown, WV. Energy Technology Center.
OVERVIEW: GAS HYDRATE GEOLOGY AND GEOGRAPHY
R. D. Malone 1993 9 p Presented at the International Conference on Natural Gas Hydrates, New Paltz, NY, 20-24 Jun. 1993
(DE93-014043; DOE/METC-C/93/7069; CONF-930687-2) Avail: CASI HC A02/MF A01

Several geological factors which are directly responsible for the presence or absence of gas hydrates have been reviewed. The factors are as follows: tectonic position of the region; sedimentary environments; structural deformation; shale diapirism; hydrocarbon generation and migration; thermal regime in the hydrate formation zone (HFZ); pressure conditions; and hydrocarbon gas supply to the HFZ. Work on gas hydrate formation in the geological environment has made significant advances, but there is still much to be learned. Work is continuing in the deeper offshore areas through the Ocean Drilling Program, Government Agencies, and Industry. The pressure/temperature conditions necessary for formation have been identified for various compositions of natural gas through laboratory investigations, and conditions for formation are being advanced through drilling in areas where gas hydrates exist. DOE

N94-14209# Science and Technology Agency, Tokyo (Japan).
ASIA-PACIFIC ISY CONFERENCE, VOLUME 2 [AJIA TAIHEIYOU KOKUSAI UCHUUNEN KAIGI]
31 Mar. 1993 396 p Conference held in Tokyo, Japan, 16-20 Nov. 1992 Prepared in cooperation with Tokyo Univ., Sagamihara, Japan; NASDA, Tokyo, Japan; and International Space Year Association, Tokyo, Japan
(NASDA-CM-199-Vol-2; JTN-93-80454) Avail: CASI HC A17/MF A04

The following topics were discussed: remote sensing, satellite observation, satellite imagery, satellite sounding, image processing, image analysis, data reduction, ocean observation, sea surface temperature, ocean current, ice mapping, vegetative index, forest management, land management, change detection, pollution monitoring, environmental monitoring, atmospheric sounding, hydrological cycle, ozone depletion, atmospheric effects, satellite communication, communication networks, mobile communication, satellite design, spacecraft design, aerospace planes, space transportation system, japanese spacecrafts, space programs, remote sensors, spaceborne radars, infrared radiometers, infrared spectrometers, synthetic aperture radar, and TRMM (Tropical Rainfall Measuring Mission) project. For individual titles, see N94-14210 through N94-14288.

N94-14210# European Space Agency. European Space Research and Technology Center, ESTEC, Noordwijk (Netherlands).
RESULTS FROM ERS-1 AND JERS-1 SAR CALIBRATION EXPERIMENTS AND DATA ANALYSIS
Y.-L. Desnos and M. Loiselet *In* Science and Technology Agency, Asia-Pacific ISY Conference, Volume 2 31 Mar. 1993 p 23-26 (For primary document see N94-14209 02-43)
Avail: CASI HC A01/MF A04

With the successful launches and operations of ERS-1 and JERS-1 (Japanese Earth Resources Satellite-1) SAR (Synthetic Aperture Radar), a new era of continuous spaceborne remote sensing of the earth is now open and the synergy provided by the different frequencies of the SAR instruments is fully available. This report summarizes the work performed using ERS-1 data, which started in July 1991 during the ERS-1 commissioning phase and was followed by some additional work performed during the operational phase of the satellite. This work got a natural extension with the experiments we have set up for the JERS-1 system verification program starting in July 1992 and extending to 1993. A preliminary overview of this is presented. Author (NASDA)

N94-14211# Geological Survey of Japan, Ibaraki.
GEOLOGIC APPLICATION OF JERS-1 SAR DATA
Yasushi Yamaguchi *In* Science and Technology Agency, Asia-Pacific ISY Conference, Volume 2 31 Mar. 1993 p 27-30 (For primary document see N94-14209 02-43)
Avail: CASI HC A01/MF A04

An overview of the preliminary investigation on the Synthetic Aperture Radar (SAR) images of the Japanese Earth Resources Satellite-1 (JERS-1) mainly for geologic applications is presented. Comparing SAR images acquired by JERS-1 and the ERS-1, the JERS-1 SAR image with a larger off-nadir angle is more useful for geologic interpretation than the ERS-1 SAR image, indicating regional geologic structures such as synclines and anticlines which are important for basic geologic researches and for petroleum exploration. It is concluded that it might be difficult to directly obtain information on rock and soil under tree cover using L-band SAR due to backscattering from vegetation canopy, and the JERS-1 SAR images of L-band exhibit a better capability of discriminating vegetation types, particularly between forests and grasslands than the C-band ERS-1 and X-band airborne SAR images. Author (NASDA)

N94-14212# Ministry of Posts and Telecommunications, Tokyo (Japan). Communications Research Lab.
ARTIFICIAL OIL POLLUTION DETECTION AND WAVE OBSERVATION IN THE SEA ADJACENT TO JAPAN BY ERS-1 SAR
Kenichi Okamoto, Harunobu Masuko, Kenji Nakamura, Masanobu Shimada (National Space Development Agency, Saitama, Japan.), Masao Nakai

(National Space Development Agency, Saitama, Japan.), and Akira Shibata (Meteorological Research Inst., Tsukuba, Japan.) *In* Science and Technology Agency, Asia-Pacific ISY Conference, Volume 2 31 Mar. 1993 p 31-34 (For primary document see N94-14209 02-43)
Avail: CASI HC A01/MF A04

On November 10 and 13, 1991, an experiment was performed to detect an artificial oil pollution and ocean waves by the C-band SAR (Synthetic Aperture Radar) of ERS-1. Artificial oil slick was made by spilling oleyl alcohol from a small vessel in the Pacific Ocean about 100 km off the Coast of Omaezaki, Shizuoka Prefecture, Japan. Sea truth data were gathered from the research vessel 'Keifu-maru' of JMA (Japan Meteorological Agency) and from a small vessel. Synchronous observation by X-band, VV (Vertical Transmission/Vertical Reception Mode) polarization airborne real aperture SLAR (Side-Looking Airborne Radar) of CRL (Communications Research Laboratory) was made together with the observation by SAR. The SAR images were produced by NASDA. In the SAR image, it was found clearly the artificial oil polluted area which looks dark by the damping of the capillary wave on November 10, 1991. The decrement of the scattering cross section was about 2.5 dB at the maximum. Author (NASDA)

N94-14213*# Jet Propulsion Lab., California Inst. of Tech., Pasadena.
AN EXACT PROCESSING ALGORITHM FOR WIDE BEAM SPACEBORNE SAR DATA
Michael Y. Jin *In* Science and Technology Agency, Asia-Pacific ISY Conference, Volume 2 31 Mar. 1993 p 35-38 Sponsored by NASA, Washington (For primary document see N94-14209 02-43)
Avail: CASI HC A01/MF A04

Signal processing algorithms for a spaceborne SAR (Synthetic Aperture Radar) system were based on the approximation that the phase history of a point-target is a second order polynomial. For a wide beam or a spotlight mode spaceborne SAR systems, this assumption cannot be applied. This report gives the derivation for the spectrum of a wide beam point-target response and describes a processing algorithm based on this spectrum. Author (NASDA)

N94-14214# Korea Aerospace Research Inst., Taejon (Republic of Korea). Dept. of Space Application Technology.
HIGH PERFORMANCE MULTI-MODE RADAR ALTIMETER FOR FUTURE SPACEBORNE APPLICATION c19
Yong-Hoon Kim *In* Science and Technology Agency, Asia-Pacific ISY Conference, Volume 2 31 Mar. 1993 p 39-44 (For primary document see N94-14209 02-43)
Avail: CASI HC A02/MF A04

The new generation of spaceborne radar altimeter will have to provided with several operating modes in order to cope with the various mission requirements such as land topography mapping in high or moderate resolution, wide swath imaging, and possibly rain rate measurement. A system concept of novel high performance radar altimeter to meet that requirements as well as the land and flight experiment results obtained with the first demonstration prototype are described. The advantages of this type altimeter are high measurement accuracy and flexible for the various operation mode. Author (NASDA)

N94-14215# National Space Development Agency, Tokyo (Japan).
SENSOR OPERATION OF ADVANCED EARTH OBSERVING SATELLITE (ADEOS)
Nobuo Iwasaki *In* Science and Technology Agency, Asia-Pacific ISY Conference, Volume 2 31 Mar. 1993 p 47-50 (For primary document see N94-14209 02-43)
Avail: CASI HC A01/MF A04

An overview of the concept of communication systems, sensor operation ground systems, operation for the Advanced Earth Observing Satellite (ADEOS), and ADEOS spacecraft and ground system is presented. Communication system for sensor data transmission (including Direct Transmission (DT), Inter-orbit Communication Subsystem (IOCS), and Mission Data Recorders (MDR's)), and ground data system to acquire, process, and distribute the data (including data receiving and recording subsystem, data processing, calibration and validation, product generation and inspection and evaluation subsystem, and mission operation management and information retrieval subsystem) are outlined. The communication system; sensor operation pattern and operation requirements; data transmission; and data and information flow for ADEOS are outlined. Author (NASDA)

N94-14216# Saga Univ. (Japan). Dept. of Information Science.
METHODS FOR CALIBRATION/VALIDATION OF AVNIR
Kouhei Arai *In* Science and Technology Agency, Asia-Pacific ISY Conference, Volume 2 31 Mar. 1993 p 51-54 (For primary document see N94-14209 02-43)
Avail: CASI HC A01/MF A04

An overview of the investigation on user requirements (inoperations such as disaster prevention; basic research such as land use, agricultural use, etc.; and in methodologies) is presented for working group activities on 12 themes, concerning a calibration and validation management plan in two categories: (1) radiometric and geometric peformances for the Advanced Visible and Near Infrared Radiometer (AVNIR) to be carried onboard the Advanced Earth Observing Satellite (ADEOS), and in-flight test site calibration methods for the ADEOS. Pre-launch and in-flight calibration accuracies are discussed. Author (NASDA)

N94-14217# National Inst. for Resources and Environment, Ibaraki (Japan).
IMG: INTERFEROMETRIC MONITOR FOR GREENHOUSE GASES c45
R. Imasu, T. Ogawa (Tokyo Univ., Japan.), H. Shimoda (Tokai Univ., Tokyo, Japan.), and H. Kobayashi (Central Research Inst. of Electric Power Industry, Tokyo, Japan.) *In* Science and Technology Agency, Asia-Pacific ISY Conference, Volume 2 31 Mar. 1993 p 55-58 (For primary document see N94-14209 02-43)
Avail: CASI HC A01/MF A04

The instrumentation for, data processing and analysis of, and expected results of the Interferometric Monitor for Greenhouse Effect Gases (IMG) such as CO2, CH4, N2O, and chlorofluorocarbons (CFC) to be carried onboard the Advanced Earth Observing Satellite (ADEOS), are outlined. The structure of the major optical component of the IMG Michelson interferometer is shown in a picture of its Breadboard Model (BBM), and the detectability of changes in greenhouse gas concentration by the IMG and an example of spectral irradiance observed by the IMG BBM are shown. Methods applied to its data processing and analysis are discussed. The expected results of IMG are discussed, and altitude-wise resolution functions for the measurements of temperature and water vapor for U.S. Standard Atmosphere, an altitude-wise resolution, and an example of retrieved concentration of CH4 are shown. Author (NASDA)

N94-14218# National Inst. for Environmental Studies, Tsukuba (Japan).
SPECTROSCOPIC METHOD AND DATA REDUCTION ALGORITHM FOR LASER LONG-PATH ABSORPTION MEASUREMENTS USING RIS
Nobuo Sugimoto, Atsushi Minato, and Yasuhiro Sasano *In* Science and Technology Agency, Asia-Pacific ISY Conference, Volume 2 31 Mar. 1993 p 59-62 (For primary document see N94-14209 02-43)
Avail: CASI HC A01/MF A04

The measurement and data reduction method of the ground system for the experiment on earth-satellite-earth laser long-path absorption of atmospheric trace species with the Retroreflector In-Space (RIS), which is to be carried onboard the Advanced Earth Observing Satellite (ADEOS), is presented. The ground system for the RIS experiment, atmospheric transmission spectrum and laser lines for measurement of ozone and CFCl2, target molecules and CO2 laser lines, simulated return signal in the ozone measurement at a laser energy of 100 mJ/pulse and a laser beam divergence of 0.1 mr, and ozone profile retrieved from the simulated signal are shown. Author (NASDA)

N94-14219# Kanazawa Inst. of Tech. (Japan).
IMAGE PROCESSING AND ANALYSIS OF AIRBORNE POLDER DATA
Y. Kawata, M. Takizawa, and T. Kusaka *In* Science and Technology Agency, Asia-Pacific ISY Conference, Volume 2 31 Mar. 1993 p 63-66 (For primary document see N94-14209 02-43)
Avail: CASI HC A01/MF A04

An overview of data processing and data analysis of the airborne version of the Polarization and Directionality of Earth Reflectances (POLDER) is presented. Processing and analyzing airborne POLDER data over the sea and the land, measured polarization data contains more optical information on atmospheric particles than on the sea or ground objects. Comparison between the data obtained over the Mediterranean sea and models is shown. Author (NASDA)

N94-14220# National Inst. for Environmental Studies, Tsukuba (Japan).
OVERVIEW OF THE ILAS OPERATIONAL DATA PROCESSING SYSTEM
T. Yokota, T. Nakajima (Tokyo Univ., Japan.), M. Suzuki, S. Mukai (Kinki Univ., Osaka, Japan.), and Y. Sasano *In* Science and Technology Agency, Asia-Pacific ISY Conference, Volume 2 31 Mar. 1993 p 67-70 (For primary document see N94-14209 02-43)
Avail: CASI HC A01/MF A04

An overview of operational data processing system designed for processing the data obtained by the Improved Limb Atmospheric Spectrometer (ILAS), which is one of the Announcement of Opportunity (AO) sensors provided by the Japanese Environment Agency and scheduled to be launched onboard the Advanced Earth Observing Satellite (ADEOS), is presented. The measurement region, measurement targets, instrument specification, data retrieval algorithms, measured data, and operational data processing system for ILAS are outlined. Solar occultation geometry, ILAS observation latitudes after launch, an overview of ILAS, characteristics of ILAS instrument, and ILAS operational data processing system are shown.
Author (NASDA)

N94-14221*# National Aeronautics and Space Administration, Washington, DC.
TRMM SYSTEM OVERVIEW AND STATUS IN THE UNITED STATES
John S. Theon *In* Science and Technology Agency, Asia-Pacific ISY Conference, Volume 2 31 Mar. 1993 p 73-75 (For primary document see N94-14209 02-43)
Avail: CASI HC A01/MF A04

An overview of the mission development status of the Tropical Rainfall Measuring Mission (TRMM) in the U.S. is presented. The mission objectives (including the approach for addressing the problems involved in the mission which were facilitated through ground-based radar data, precipitation data acquired in a variety of field experiments including rain gage networks and satellite observations, and modeling to advance understanding of the rainfall and cloud processes); NASA research announcement of TRMM; algorithm development to incorporate the information available from the multiple sensors on TRMM, including Precipitation Radar (PR) and TRMM Microwave Imager (TMI); and the NASA TRMM Office and its activities are outlined. Two instruments related to the rain measuring objectives of TRMM added at the request of NASA, the Clouds and Earth's Radiant Energy System (CERES), and the Lightning Imaging Sensor (LIS) are also outlined.
Author (NASDA)

N94-14222# National Space Development Agency, Tokyo (Japan). Earth Observation Satellite Group.
TRMM PROJECT IN JAPAN: OVERVIEW AND STATUS
Hideo Takamatsu *In* Science and Technology Agency, Asia-Pacific ISY Conference, Volume 2 31 Mar. 1993 p 76-79 (For primary document see N94-14209 02-43)
Avail: CASI HC A01/MF A04

This report describes the TRMM (Tropical Rainfall Measuring Mission) related activities in Japan. Japan's contributions to the TRMM project include development of PR (Precipitation Radar), launching the satellite into orbit, as well as data processing and distribution. PR is the main sensor of the TRMM and will be the first spaceborne rain radar. Also, TRMM is the first foreign user satellite launched by a Japanese launch vehicle. This requires many works to coordinate the interface between the satellite and H-2 launch vehicle as well as Tanegashima launch facilities. Author (NASDA)

N94-14223*# National Aeronautics and Space Administration. Langley Research Center, Hampton, VA.
CLOUDS AND THE EARTH'S RADIANT ENERGY SYSTEM (CERES) ON THE TROPICAL RAINFALL MEASURING MISSION (TRMM) **c47**
Stephen L. Carman (TRW Space Technology Labs., Redondo Beach, CA.) and Leonard P. Kopia *In* Science and Technology Agency, Asia-Pacific ISY Conference, Volume 2 31 Mar. 1993 p 80-83 (For primary document see N94-14209 02-43)
Avail: CASI HC A01/MF A04

An overview of the Clouds and the Earth's Radiant Energy System (CERES) on the Tropical Rainfall Measuring Mission (TRMM), a joint U.S.-Japan mission, is presented. The structure and functions of the CERES instrument, which is a three-channel radiometer like the Earth Radiation Budget Experiment (ERBE) scanner, and the absolute radiometric calibration facility with a shortwave reference source and longwave calibration blackbodies which provide longwave calibration tracable to International Temperature Scale (ITS-90) are outlined. The CERES instrument with covers open, CERES sensor assembly, and CERES radiometric calibration chamber are shown.
Author (NASDA)

N94-14224# Ministry of Posts and Telecommunications, Tokyo (Japan). Communications Research Lab.
TRMM PRECIPITATION RADAR ALGORITHM **c61**
Kenichi Okamoto *In* Science and Technology Agency, Asia-Pacific ISY Conference, Volume 2 31 Mar. 1993 p 84-87 (For primary document see N94-14209 02-43)
Avail: CASI HC A01/MF A04

The TRMM (Tropical Rainfall Measuring Mission) PR (Precipitation Radar) algorithms have been studied by the TRMM PR team. The radar products are classified and are shown according to the processing levels. The general processing structure suggests a primary division of radar algorithms into either deterministic or statistical techniques. The deterministic methods can be divided into backscattering and attenuation methods. Some candidate rain rate retrieval algorithms are introduced with their merits and demerits. The TRMM standard radar algorithms are also introduced according to the processing levels.
Author (NASDA)

N94-14225# Tokyo Univ. (Japan). Center for Climate System Research.
ESTIMATE OF SAMPLING ERRORS OF TRMM RAINFALL OBSERVATION BY USING RADAR-AMeDAS COMPOSITE DATA **c47**
Akimasa Sumi, Riko Oki, and aikan Oki *In* Science and Technology Agency, Asia-Pacific ISY Conference, Volume 2 31 Mar. 1993 p 88-91 (For primary document see N94-14209 02-43)
Avail: CASI HC A01/MF A04

Errors of rainfall estimates due to TRMM (Tropical Rainfall Measuring Mission) satellite is estimated by using radar-AMeDAS (Automated Meteorological Data Acquisition System) composite rainfall data around Japan, which is a radar-rainfall estimate validated by dense surface rain-gauge network (AMeDAS). In this study, sampling errors of a monthly rainfall estimate due to TRMM radar measurement are estimated over the TRMM domain (500 km by 500 km) for two years, and it is concluded that the sampling error around Japan is about 20 percent, which is relatively larger than the previous studies.
Author (NASDA)

N94-14226# Ministry of Posts and Telecommunications, Tokyo (Japan). Communications Research Lab.
MULTIPARAMETER AIRBORNE RAIN RADAR DEVELOPMENT FOR TRMM VALIDATION AND TRMM-FOLLOW-ON STUDY **c47**
Hiroshi Kumagai, Kenichi Okamoto, Kenji Nakamura (Ministry of Posts and Telecommunications, Ibaraki, Japan.), Hiroshi Hanado (Ministry of Posts and Telecommunications, Ibaraki, Japan.), and Hiroaki Horie (Ministry of Posts and Telecommunications, Ibaraki, Japan.) *In* Science and Technology Agency, Asia-Pacific ISY Conference, Volume 2 31 Mar. 1993 p 92-95 (For primary document see N94-14209 02-43)
Avail: CASI HC A01/MF A04

The overall feature of the new multiparameter airborne radar developed in the Communications Research Laboratory (CRL) is to provide the useful data for the TRMM (Tropical Rainfall Measuring Mission) algorithm development during pre-launch period and TRMM validation experiments in the mission period. Both coherent radar system and full polarimetric capability, which are newly installed, will allow the microphysics in the precipitation to be extracted in great detail, which contributes the accurate rain retrieval in TRMM through both the development of algorithms and refined precipitation model. The experiments using these capabilities will provide an opportunity to test candidate techniques for future rain radar missions. The system parameters, the block diagram, and signal to noise ratio per pulse of multiparameter airborne radar are shown.
Author (NASDA)

N94-14227*# National Aeronautics and Space Administration, Washington, DC.
SPACE MEASUREMENTS FOR DETERMINING THE EARTH'S ENERGY AND WATER CYCLES
James C. Dodge *In* Science and Technology Agency, Asia-Pacific ISY Conference, Volume 2 31 Mar. 1993 p 96-99 (For primary document see N94-14209 02-43)
Avail: CASI HC A01/MF A04

This report describes the increasing number of space data sets which are becoming available from current satellite sensors and which may be used to study the earth's global energy and water cycles. An attempt will be made to point out those aspects of each cycle which can be measured well globally and those components which still have large uncertainties. In the process of explaining the cycles, consideration will be given to the flux data from the Earth Radiation Budget Experiment (ERBE); the cloud observations from the global set of satellites participation in the International Satellite Cloud Climatology Project (ISCCP); the water vapor, precipitation, and cloud liquid water observations from the passive microwave radiometer named the Special Sensor Microwave Imager (SSM/I); and sea-surface temperatures from the Advanced Very High Resolution Radiometer (AVHRR). Some of these data are currently available through NOAA/NESDIS (National Environmental Satellite, Data, and Information Service) and/or NASA Distributed Active Archive Centers (DAAC's) or in CD-ROM data sets. Others will soon be available as part of the on-going NASA/NOAA Pathfinder Data Set Program. The report will conclude with a description of the additional value which will be obtained from the Tropical Rainfall Measuring Mission (TRMM) and Earth Observation Satellite (EOS) data in terms of attempting to understand the global cycles as well as trying to detect significant changes or trends over longer periods. Author (NASDA)

N94-14228*# National Aeronautics and Space Administration, Washington, DC.

FUTURE TRMM FOLLOW-ON MISSION

Nobuyoshi Fugono (Ministry of Posts and Telecommunications, Tokyo, Japan.) and John S. Theon *In* Science and Technology Agency, Asia-Pacific ISY Conference, Volume 2 31 Mar. 1993 p 100-103 (For primary document see N94-14209 02-43)

Avail: CASI HC A01/MF A04

The basic concept of the TRMM (Tropical Rainfall Measuring Mission) follow-on mission to be developed aiming at its launch in 2000 for the data continuation from TRMM is discussed. The basic instruments and radar are rain radar, microwave radiometer, visible and infrared radiometer, CERES (Clouds and Earth's Radiation Energy System) following those for TRMM, upgraded rain radar, and other new instruments if satellite bus limitations and also time and budget allow. The conceivable instruments for the TRMM follow-on mission are: (1) cloud radar; (2) microwave sounder for water vapor and temperature profiling; (3) water vapor LIDAR (Laser Infrared Radar); and (4) wind LIDAR, but only microwave sounder and cloud lidar may remain due to the tight time schedule. Power consumption and weight of radar and the orbit and concept of radar for TRMM follow-on mission are shown. Author (NASDA)

N94-14229# Tokyo Univ. (Japan). Center for Climate System Research.

REMOTE SENSING OF LOW LEVEL CLOUD OPTICAL CHARACTERISTICS

Teruyuki Nakajima and Tadahiro Hayasaka (Tohoku Univ., Sendai, Japan.) *In* Science and Technology Agency, Asia-Pacific ISY Conference, Volume 2 31 Mar. 1993 p 107-110 (For primary document see N94-14209 02-43)

Avail: CASI HC A01/MF A04

Remote sensing of cloud microphysics is studied making use of spectral solar reflection data. Statistics of retrieved cloud microphysical quantities is further used to evaluate climatic impact of cloud field change in the course of anthropogenic contamination of atmosphere. Case studies of marine stratocumulus clouds, modulated by ship-emitted Cloud Condensation Nuclei (CCN), and cumulus clouds over Amazon area, modulated by forest fire, showed different response of clouds to CCN injection. This difference comes from the difference in CCN concentration in the ambient atmosphere and drizzle particle concentration in clouds. Author (NASDA)

N94-14230# Tokyo Univ. (Japan). Center for Climate System Research.

THE EFFECTS OF ANTHROPOGENIC AEROSOLS ON OPTICAL THICKNESS AND PARTICLE SIZE OF CLOUDS. PART 1: RETRIEVAL ALGORITHM **c45**

Zhao Fengsheng and Teruyuki Nakajima *In* Science and Technology Agency, Asia-Pacific ISY Conference, Volume 2 31 Mar. 1993 p 111-116 (For primary document see N94-14209 02-43)

Avail: CASI HC A02/MF A04

The radiative calculation and its application of the effects of anthropogenic aerosols on optical thickness and particle size of clouds are outlined. An algorithm for retrieval of the optical thickness and microphysics of aerosol clouds from the AVHRR (Advanced Very High Resolution Radiometer) image was developed. Application of this algorithm to the area nearby the Chinese east coast shows that the results of retrieved optical thickness and microphysics of aerosols and clouds are quite reasonable. Sensitivity to optical thickness and exponent of Junge size distribution, contour of the standard deviation, and example of retrieved cloud optical thickness, effective radius, and geometric standard deviation are shown. Author (NASDA)

N94-14231# National Oceanic and Atmospheric Administration, Washington, DC. National Environmental Satellite, Data, and Information Service.

CLIMATE PRODUCTS FROM NOAA OPERATIONAL SATELLITES **c47**

P. Krishna Rao and A. Gruber *In* Science and Technology Agency, Asia-Pacific ISY Conference, Volume 2 31 Mar. 1993 p 117-120 (For primary document see N94-14209 02-43)

Avail: CASI HC A01/MF A04

Significance of space-based observation in observing and understanding the nature of climate and global change is discussed. Although the current satellites are primarily designed for weather observation, the satellite measurements contain considerable information on climate and global change parameters. Information is available on sea surface temperature, sea ice, vegetation index, planetary radiation budget, clouds, ozone, aerosols, snow cover, and surface temperature. Examples of satellite derived products are as follows: (1) total cloud amount derived from operational geostationary satellites; (2) average snow cover over the Northern Hemisphere obtained from the NOAA polar orbiter satellite visible channel data; (3) the influence of the Mt. Pinatubo aerosols obtained by comparing satellite derived Sea Surface Temperature (SST) anomaly distribution with the ship data; (4) total ozone distribution over the South Pole; and (5) the total ozone amount over the Southern Hemisphere. Author (NASDA)

N94-14232# Institute of Disaster and Earth Sciences, Ibaraki (Japan).

SEASONAL CHANGE OF THE LAND-SURFACE TEMPERATURE OVER ASIAN CONTINENT DERIVED FROM GAC DATA ON NOAA-11 AVHRR **c47**

Kazurou Nakane *In* Science and Technology Agency, Asia-Pacific ISY Conference, Volume 2 31 Mar. 1993 p 122-125 (For primary document see N94-14209 02-43)

Avail: CASI HC A01/MF A04

Seasonal change of monthly mean air temperature over the Asian Continent, which are derived from the regional image data extracted from NOAA-11 AVHRR (Advanced Very High Resolution Radiometer) GAC (Global Area Coverage) data using the new regression equation are presented. The regression equation consists of three explanatory variables, which are the data of the split window channels and a cosine of the zenith distance. This regression equation is applicable through a year, and the multiple correlation coefficients of the derived regression equations were almost more than 0.9. The standard deviation errors were within 2 C.

Author (NASDA)

N94-14233# National Oceanic and Atmospheric Administration, Washington, DC. Satellite Research Lab.

EARTH RADIATION BUDGET, CLOUD, AND AEROSOL PARAMETERS DERIVED FROM AVHRR AND TOVS MEASUREMENTS **c47**

Herbert Jacobowitz and Larry L. Stowe *In* Science and Technology Agency, Asia-Pacific ISY Conference, Volume 2 31 Mar. 1993 p 126-129 (For primary document see N94-14209 02-43)

Avail: CASI HC A01/MF A04

Since 1974, the Earth's Radiation Budget (ERB) has been estimated almost continually from the NOAA polar satellites. The current capabilities with the Advanced Very High Resolution Radiometer (AVHRR) and future use of multichannel TIROS Operational Vertical Sounder (TOVS) observations are discussed. Two separate studies to develop a cloud monitoring capability, one using the AVHRR and the other using the TOVS, are briefly discussed. Over the last few years, the aerosol optical thickness has been monitored using AVHRR observations. The dramatic spreading of the aerosols from the Mt. Pinatubo volcano as it eventually encircled the globe is demonstrated. Author (NASDA)

N94-14234# National Oceanic and Atmospheric Administration, Washington, DC. Satellite Research Lab.

THE DEVELOPMENT AND IMPLEMENTATION OF AN INTERACTIVE RETRIEVAL/ANALYSIS/FORECAST ALGORITHM **c61**

Henry E. Fleming, Mitchell D. Goldberg, Wayman E. Baker, John C. Derber, and Bert B. Katz (General Sciences Corp., Washington, DC.) *In* Science and Technology Agency, Asia-Pacific ISY Conference, Volume 2 31 Mar. 1993 p 130-133 (For primary document see N94-14209 02-43)

Avail: CASI HC A01/MF A04

A new retrieval system for deriving temperature and moisture profiles from TIROS-N TOVS (TIROS Operational Vertical Sounder) measurements has been developed. This system, unlike the current operational library search approach, uses the six-hour forecast from the NMC (National Meteorological Center's) Medium Range Forecast Model for constructing the retrieval algorithm's initial (first) guess. The system is interactive because the satellite-retrieved parameters, in addition to conventional in situ data, are analyzed to produce initial conditions for the subsequent forecast by NMC's GDAS (Global Data Assimilation System), and that forecast is used as the initial guess for the subsequent temperature/moisture retrievals. The system is expected to become operational as part of NMC's GDAS in 1993. Author (NASDA)

N94-14235# China Centre for Resources Satellite Data and Application, Beijing.

THE REMARKABLE ACHIEVEMENT OF CHINA SATELLITE APPLICATION

Mei-Rong Wu *In* Science and Technology Agency, Asia-Pacific ISY Conference, Volume 2 31 Mar. 1993 p 137-140 (For primary document see N94-14209 02-43)

Avail: CASI HC A01/MF A04

In this report, a brief survey of satellite applications in China is presented. It covers the main fields of satellite application such as telecommunications, earth-observation remote-sensing techniques, meteorological forecasting, and microgravity experiments. A list of 29 launches using home-made satellites and ground equipment can be drawn, including six earth-stationary-orbit communications satellites, 13 low-orbit recoverable remote-sensing satellites, two polar-orbit meteorological satellites, and 12 science-and-technological test satellites. Multiple purpose and typical examples are given showing good social and economic benefits attained. In China, since the successful launch of DFH-1 dated April 24, 1970, 33 launches have been made whereby 33 self-developed satellites, one COMSAT (Communications Satellite Corp., CS) Asia-1, one AUSSAT (Australian Satellite) (CS (Communication Satellite)) and two S & T (Science and Technology) test satellites (one for Pakistan, another for Sweden) were sent into appropriate orbits. Author (NASDA)

N94-14236# United Nations Educational, Scientific and Cultural Organization, Paris (France). Div. of Earth Sciences.

SATELLITE TECHNOLOGY FOR ENVIRONMENTAL MONITORING IN DEVELOPING COUNTRIES **c45**

Kumon Tokumaru and Felix Kogan (National Oceanic and Atmospheric Administration, Washington, DC.) *In* Science and Technology Agency, Asia-Pacific ISY Conference, Volume 2 31 Mar. 1993 p 141-144 (For primary document see N94-14209 02-43)

Avail: CASI HC A01/MF A04

The background, organization, preliminary analysis of some of the results of the workshop 'National Satellite Data Center (SDC): Infrastructure for remote sensing application', including necessary actions for operational use of remote sensing data, such as universal data catalog, selecting complete country coverage data, data management at national level, network creation at national, and international-level implementation of national SDC project are described. VCI (Vegetation Condition Index) and its use for drought monitoring (an example of operational technique), VCI's principles and its validations, and VCI's conclusions and appeal for international cooperation are outlined. Author (NASDA)

N94-14237# Indonesian National Inst. of Aeronautics and Space, Jakarta. Ground Segment and Aerospace Mission Center.

SOME POTENTIALS OF THE INDONESIAN REGION FOR EARTH OBSERVATION

J. H. Soenarjo *In* Science and Technology Agency, Asia-Pacific ISY Conference, Volume 2 31 Mar. 1993 p 145-148 (For primary document see N94-14209 02-43)

Avail: CASI HC A01/MF A04

In the effort to increase concern about the planet earth, space science and technology is obviously a good way to benefit mankind. The increasing use of space applications and space research need the support of space technology development, potential locations for earth observation, and international cooperation. Indonesia has been using space technology to sustain national development programs and has been developing infrastructures to carry out space activities. The Indonesian territory lies in the equatorial region which provides some unique atmospheric phenomena, and is abundant of natural resources. Space activities and several international cooperations in Indonesia are described and potential locations of the Indonesian region for earth observation are explained. Author (NASDA)

N94-14238# Tokyo Univ. (Japan). International Center for Disaster-Mitigation Engineering.

APPLICATION OF SATELLITE REMOTE SENSING TECHNOLOGY IN DISASTER MITIGATION: A CASE STUDY OF BANGLADESH

M. A. H. Pramanik *In* Science and Technology Agency, Asia-Pacific ISY Conference, Volume 2 31 Mar. 1993 p 149-153 (For primary document see N94-14209 02-43)

Avail: CASI HC A01/MF A04

An overview of the following physiographic, morphological, and other conditions which make Bangladesh vulnerable to disasters like floods, droughts, windstorms, and others are outlined: (1) flat topography; (2) rapid run-off and drainage congestion; and (3) enormous discharge of river-water heavily laden with sediments (funnel-shaped and shallow northern Bay of Bengal). Disasters forecasting, warning systems, and use of RS-GIS (Integrated Remote Sensing and Geographic Information System) are covered. Related Bangladesh organizations (such as BMD (Bangladesh Meteorological Department), SPARRSO (Bangladesh Space Research and Remote Sensing Organization), CPP (Cyclone Preparedness Programme), MORR (Ministry of Relief and Rehabilitation), BWDB (Bangladesh Water Development Board), and the Department of Environment are also outlined. Author (NASDA)

N94-14239# Bangladesh Univ. of Engineering and Technology, Dhaka. Inst. of Flood Control and Drainage Research.

INTEGRATION OF REMOTE SENSING AND MATHEMATICAL MODELLING IN DISASTER MITIGATION

Mohammad Rezaur Rahman *In* Science and Technology Agency, Asia-Pacific ISY Conference, Volume 2 31 Mar. 1993 p 154-157 (For primary document see N94-14209 02-43)

Avail: CASI HC A01/MF A04

Bangladesh is predominantly an agricultural country. Frequently occurring disasters such as floods and cyclones wreak havoc on its agriculture. The disasters can be mitigated considerably if the agricultural plots can be replanted quickly. However, when a disaster strikes, the communication link is usually in disarray and as a result it is often difficult to make a satisfactory estimation of the extent and severity of damage. Moreover, due to the severe limitation of resources, it is usually not possible for the government to cover the entire damaged area. The government needs to make an unpleasant decision regarding which areas to cover and which not to, in order to maximize the return on the agricultural rehabilitation effort. Remote sensing and mathematical modeling can play a useful role in helping decision makers to make timely and sufficiently accurate decisions in this regard. Author (NASDA)

N94-14240# Malayan Centre for Remote Sensing, Kuala-Lampur.

SOIL EROSION MAPPING USING REMOTE SENSING AND GIS TECHNIQUES

Nik Nasruddin Mahmood *In* Science and Technology Agency, Asia-Pacific ISY Conference, Volume 2 31 Mar. 1993 p 158-163 (For primary document see N94-14209 02-43)

Avail: CASI HC A02/MF A04

An overview of the soil erosion assessment of land development project areas using remote sensing and GIS (Geographical Information System) techniques, adopting USLE (Universal Soil Loss Equation) of Wischmeiser and Smith with minor modification in estimating some of the relevant parameters, is presented. Both the current soil erosion susceptibility and

the future potential soil erosion susceptibility maps of the Upper King Valley, Selanger, Malaysia, which is currently experiencing dynamic development, were generated and are shown. Author (NASDA)

N94-14241# Asian Inst. of Tech., Bangkok (Thailand). Div. of Computer Science.

DETECTING LAND COVER CHANGES IN CHIANG-MAI AREA IN THAILAND

T. Hosomura and P. K. M. M. Pallewatta *In* Science and Technology Agency, Asia-Pacific ISY Conference, Volume 2 31 Mar. 1993 p 164-172 (For primary document see N94-14209 02-43)

Avail: CASI HC A02/MF A04

Remote sensing techniques can be effectively used as a tool to monitor land cover change. Global coverage, high spatial resolution, and high revisit capabilities of modern remote sensing satellites provide large amounts of data daily. Land cover changes in Chiang-Mai area in Thailand are analyzed. The study has been carried out using two multitemporal images of MOS-1 (Marine Observation Satellite-1) MESSR (Multispectral Electronic Self-Scanning Radiometer) data. The analysis is done using difference images and classification results. The classification has been carried out using a neural network classifier, whose structure has been obtained by using a special technique developed. Author (NASDA)

N94-14242# National Inst. of Agro-Environmental Science, Ibaraki (Japan).

LAND EVALUATION FOR AGRICULTURAL PRODUCTIVITY IN NORTH-EAST THAILAND USING LANDSAT TM DATA AND GEOGRAPHIC INFORMATION

Tsuyoshi Akiyama, Genya Saitou, Yasuharu Yamada, Pongpit Piyapongse (Ministry of Agriculture and Cooperatives, Bangkok, Thailand.), and Ekkanit Hansakdi (Ministry of Agriculture and Cooperatives, Bangkok, Thailand.) *In* Science and Technology Agency, Asia-Pacific ISY Conference, Volume 2 31 Mar. 1993 p 173-176 (For primary document see N94-14209 02-43)

Avail: CASI HC A01/MF A04

A method for land use classification suitable for tropical areas with distinct rainy and dry seasons is presented that uses LANDSAT TM (Thematic Mapper) data, geographic information (including soil type and fertilization information), ground truth data, vegetation indices (calculated from the CCT (Computer Compatible Tape) values at TM band 3 and 4), vegetation cover rate, and soil organic matter content derived from the TM band 3 values. The classification results are considered to agree well with the ground truth data, and the trend of land productivity coincided with yield data. The procedure for constructing a productivity map for paddy and upland crop fields is shown. Author (NASDA)

N94-14243# Chiba Univ. (Japan). Remote Sensing and Image Research Center.

EFFECTS OF TYPHOON ON TOMS DATA **c47**

Nobuo Takeuchi, Fumihiko Hiruma, and Kiyoshi Tsuchiya (Teikyo Univ., Utsunomiya, Japan.) *In* Science and Technology Agency, Asia-Pacific ISY Conference, Volume 2 31 Mar. 1993 p 177-180 (For primary document see N94-14209 02-43)

Avail: CASI HC A01/MF A04

Ozone distribution around typhoons in the area bounded by the latitude and longitude lines 18 N/55 N, 105 E/160 E was studied in the typhoon seasons (July to October) during the period 1979 through 1989. Based on the analysis of TOMS (Total Ozone Mapping Spectrometer) data, the signature (pattern of the ozone concentration) is classified as follows: (1) CD (Central Dense)-type--larger ozone concentration in the center surrounded by less concentrated area in the shape of moat around a castle; (2) N-type--similar to CD-type, however, lacking the central part; and (3) S (Spiral)-type--ozone concentration is in the form of spiral converging into the center. Statistical results of the analysis, such as the numbers of ozone signature in the subject study period and tendency or strengthening and weakening the typhoon are outlined. Author (NASDA)

N94-14244# Institute of Disaster and Earth Sciences, Tsukuba (Japan).

SATELLITE REMOTE SENSING FOR DISASTER MITIGATION

Shinkichi Kishi *In* Science and Technology Agency, Asia-Pacific ISY Conference, Volume 2 31 Mar. 1993 p 181-184 (For primary document see N94-14209 02-43)

Avail: CASI HC A01/MF A04

Several examples of detection of the disaster-stricken areas mainly from Landsat data are shown, and based on these examples, a consideration to characterize the future space technological capabilities to the observation monitoring is presented. It has been made clear by the actual examples that the satellite remote sensing will be very useful technology in the operational activities of disaster management in this decade. Resolution and spectral bands of TM (Thematic Mapper) data are actually practical in detection and mapping of the distribution of the regions stricken by the disaster such as flood and volcanic eruption. To realize the administrative use in disaster management of satellite remote sensing, it is necessary to increase the frequency of observation as well as increasing data distribution. Author (NASDA)

N94-14245# Nippon Electric Co. Ltd., Yokohama (Japan). Space Systems Development Div.

A CONCEPT FOR THE WORLD ENVIRONMENT AND DISASTER OBSERVATION SYSTEM

Takaji Kuroda and Shinkichi Koizumi *In* Science and Technology Agency, Asia-Pacific ISY Conference, Volume 2 31 Mar. 1993 p 185-188 (For primary document see N94-14209 02-43)

Avail: CASI HC A01/MF A04

An ideal system to observe the earth's environment and to monitor disaster status using satellites is described. Three possible concepts of a satellite system for continuous and frequent observation of the earth environment and disasters are as follows: (1) a system consisting of geostationary earth observation satellites similar to the current geostationary meteorological satellite system under the World Meteorological Organization; (2) a system based on agreement whereby the countries currently undertaking earth observation; and (3) a completely new international earth observation system. The system configuration of the WEDOS (World Environment Disaster Observation System) and its data-relay-satellite system and ground system composed of MMC (Mission Management Center), SCS (Satellite Control Station), MGS (Master Ground Station), and LUS (Local User Station) are outlined. It can be concluded that the WEDOS system would be an ideal system for a satellite earth observation system on a global scale, and would enable the realization of continuous observation of the earth's environment and disasters. Author (NASDA)

N94-14246# Byelorussian Scientific and Technical Centre of Environment Remote Diagnostics, Minsk.

STUDY OF THE CONSEQUENCES OF THE CHERNOBYL ACCIDENT AND TECHNOGENIC ACTIVITY IN THE REPUBLIC BELARUS USING AEROSPACE METHODS **c45**

Alexander Kovalyov *In* Science and Technology Agency, Asia-Pacific ISY Conference, Volume 2 31 Mar. 1993 p 189-192 (For primary document see N94-14209 02-43)

Avail: CASI HC A01/MF A04

Maps of radionuclide distribution on the territory of the Republic of Belarus are made using the data of aerial gamma-spectrometry and ground sampling, taking into account radionuclide deposition. The influence of natural and technogenic Potassium-40 on the radiation situation is investigated; a prognosis of radionuclide migration for the next thirty years is made. Using the data of complex aerospace and ground experiments, 12 types of ecological maps of the scale 1:50,000 are made for the districts with intense technogenic stress. Scientific approaches are developed and the first stage of the Belarussian National Ecogeoinformation System is implemented. A helicopter laboratory created in Belarus and equipped with the devices for ultraviolet, visible, infrared, and microwave ranges of spectrum is described, as well as mobile ecological and radiation laboratories. Author (NASDA)

N94-14247# Chinese Academy of Space Technology, Beijing.

A TENTATIVE PLAN ON CHINA AND ASIAN-PACIFIC SATELLITE SYSTEM FOR DISASTER REDUCTION

Guo-Fu Zhang and Shang-Min Zheng *In* Science and Technology Agency, Asia-Pacific ISY Conference, Volume 2 31 Mar. 1993 p 193-198 (For primary document see N94-14209 02-43)

Avail: CASI HC A02/MF A04

China's satellite system for disaster reduction and its implementation, consisting of a space monitoring system of natural disasters and a ground

application system for natural disaster information acquisition and processing is proposed. The main tasks of the system are as follows: (1) to carry out 24 hour, all-weather monitoring of major natural disasters, such as rain storm, flood, drought, forest fire, etc.; (2) to improve the forecast of major natural disasters and the assessment of their effects, thus, providing a scientific basis for decisions on disaster prevention, fighting, and relief works; (3) to assure unimpeded disaster information transmission channels and command channels; (4) to increase capabilities for rapid response to sudden disaster; and (5) to raise the effectiveness of the same. The system would create necessary conditions for China and Asian-Pacific region to participate in international cooperations for utilizing international earth environment and disaster monitoring systems, and for further increasing capabilities of disaster reduction. Author (NASDA)

N94-14248# Deutsche Versuchsanstalt fuer Luft- und Raumfahrt, Oberpfaffenhofen (Germany).

EARTH OBSERVATION FROM LOW-INCLINATION ORBIT AS A NECESSARY COMPLEMENT TO POLAR MISSIONS

Werner Kirchhof, Dieter Beran, and Torsten Esdar (Dornier System G.m.b.H., Friedrichshafen, Germany.) *In* Science and Technology Agency, Asia-Pacific ISY Conference, Volume 2 31 Mar. 1993 p 199-203 (For primary document see N94-14209 02-43)

Avail: CASI HC A01/MF A04

Earth observation on near-polar orbits provides a coverage of nearly the complete globe. By using low-inclination orbits, dominant dynamic processes in the tropics and subtropics can be monitored with high coverage performance. The effects of orbit inclination, altitude and sensor field of view on local observation time, revisit frequency, and illumination conditions are illustrated. These elements describe the capabilities for the measurement of dynamic processes, diurnal cycles, seasonal and interannual variations, and for the forecast or observation of catastrophic events as a necessary complement to polar missions. Time and illumination dependent measurement needs are listed. Author (NASDA)

N94-14249# Ludwig-Maximilians-Univ., Munich (Germany). Dept. for General and Applied Geology.

DEVELOPMENT OF A REMOTE SENSING GEOGRAPHIC INFORMATION SYSTEM FOR LAND COVER CHANGES AND ASSESSMENT OF RISK DUE TO NATURAL AND MAN MADE HAZARDS COVERING THE AREA OF THE INNER DELTA OF THE YELLOW RIVER **c82**

A. Hirscheider, J. Bodechtel, C. Yuan, m1459168, W. Zhang (Ministry of Geology and Mineral Resources, Beijing, China.), T. Zhang (Geology Science Inst., Henan, China.), T. Chen (Geology Science Inst., Henan, China.), and W. Mauser *In* Science and Technology Agency, Asia-Pacific ISY Conference, Volume 2 31 Mar. 1993 p 204-207 (For primary document see N94-14209 02-43)

Avail: CASI HC A01/MF A04

An overview of a pilot project, a subproject of the ISY (International Space Year) Global Land Cover Change Project, on the application of remote sensing data and techniques as well as the development of a concept for a GIS (Geographic Information System) for land cover changes and the assessment of the susceptibility of the environment to natural and man-made hazards is presented. Thematic and technical background, scenario, structure of the data base, and combination of input data to thematic maps are outlined. Structure scheme of the information contents within the source data base and overall scheme on the output products based on the information of the source data base are shown.

Author (NASDA)

N94-14250# Freie Univ., Berlin (Germany). Inst. for Meteorology.

THE ROLE OF THE DYNAMICS FOR THE DEVIATION OF THE TOTAL OZONE FROM THE LONG-TERM MEAN AT THE EDGE OF THE POLAR VORTEX **c45**

Karin Petzoldt *In* Science and Technology Agency, Asia-Pacific ISY Conference, Volume 2 31 Mar. 1993 p 211-214 Sponsored by BMFT (For primary document see N94-14209 02-43)

Avail: CASI HC A01/MF A04

Dynamic effects causing extremely low ozone columns in winter during 14 years of the TOMS (Total Ozone Mapping Spectrometers) were investigated to separate them from the ozone variations measured during the EASOE (European Arctic Stratospheric Ozone Experiment), the aim of which is to measure chemical tracers responsible for possible ozone destruction at high altitudes. The unusual low ozone columns over Europe during the EASOE winter 1991 and 1992 were generated dynamically by a tropospheric blocking and strong wave activity in the middle stratosphere. The adiabatically cooling produced an elevated tropopause at the edge of the stratospheric vortex over Europe. Ozone was lifted by the adiabatic ascent and transported to higher levels. For all cases of the period 1979 to 92 when TOMS observed total values below 225 DU over Europe, a similar dynamical situation was present with temperatures at the tropopause below -70 C together with 30 hPa temperatures below -82 C.

Author (NASDA)

N94-14251# Natural Environmental Research Council, Swindon (England).

THE EUROPEAN ARCTIC OZONE EXPERIMENT: AN INVESTIGATION OF NORTHERN HEMISPHERE OZONE DEPLETION **c45**

Richard A. Cox *In* Science and Technology Agency, Asia-Pacific ISY Conference, Volume 2 31 Mar. 1993 p 215-219 (For primary document see N94-14209 02-43)

Avail: CASI HC A01/MF A04

Over the past year, new data has been gathered relating to ozone depletion over the Northern Hemisphere. A major contribution to these data has come from the European Arctic Stratospheric Ozone Experiment (EASOE), a campaign built around measurements from aircraft, balloons, and remote sensing from the ground, conducted throughout the winter of 1991/92. This paper provides a description of the activities, a summary of some of the results, and an update on the situation regarding ozone depletion in the Northern Hemisphere. Author (NASDA)

N94-14252*# National Aeronautics and Space Administration. Langley Research Center, Hampton, VA.

SPACE-BASED ACTIVITIES: SAM 2 AND SAGE 2

Lamont R. Poole *In* Science and Technology Agency, Asia-Pacific ISY Conference, Volume 2 31 Mar. 1993 p 220-223 (For primary document see N94-14209 02-43)

Avail: CASI HC A01/MF A04

Long-term stratospheric observations have been made by the orbiting solar occultation instruments, SAM 2 (Stratospheric Aerosol Measurement 2) and SAGE 2 (Stratospheric Aerosol and Gas Experiment 2). SAM 2 (1978-present) has provided 1 km vertical resolution data on aerosol extinction in the polar regions which show the effects of volcanic eruptions on stratospheric aerosol loading as well as the seasonal formation of Polar Stratospheric Clouds (PSC's). SAGE 2 (1984-present) measures ozone, water vapor, and NO2 profiles in addition to multi-wavelength aerosol extinction. These illustrate, for example, seasonal changes in aerosol characteristics and the spatial and vertical extent of the chemically perturbed region over Antarctica in spring. This report describes the two satellite experiments and discusses important results regarding polar stratospheric ozone depletion. Author (NASDA)

N94-14253# Institute of Atmospheric Physics, Beijing (China).

NEW EVIDENCES SUPPORTED THE WEI HYPOTHESIS ABOUT THE FORMATION OF THE ANTARCTIC OZONE HOLE **c45**

Ding-Wen Wei *In* Science and Technology Agency, Asia-Pacific ISY Conference, Volume 2 31 Mar. 1993 p 224-228 (For primary document see N94-14209 02-43)

Avail: CASI HC A01/MF A04

Based on a great number of data analysis, a new hypothesis on the formation of the Antarctic ozone hole by the end of 1988 has been presented. This is basically an 'electrochemistry-dynamics' model, and it is related to the solar charged particles emission in the 11 year solar cycle and the Antarctic vortex. For short, some scientists call it the Wei hypothesis. In this report, some new evidences such as the trends of upper layer ozone and the Antarctic observations that support it are presented.

Author (NASDA)

N94-14254# Forest Research Inst., Helsinki (Finland).

MULTI-SOURCE NATIONAL FOREST INVENTORY OF FINLAND

Erkki Tomppo *In* Science and Technology Agency, Asia-Pacific ISY Conference, Volume 2 31 Mar. 1993 p 231-235 (For primary document see N94-14209 02-43)

Avail: CASI HC A01/MF A04

A new forest inventory system developed by the Finnish Forest Research Institute using satellite image data, digital map data, and other geographical data is outlined. Image analysis methods have been chosen so that estimates of all variables of the inventory can be computed for each pixel to produce thematic maps and statistics for large and small areas. The results are compared with the estimate of an in-situ forest inventory and, for large areas, with estimates based on field sample plots of the NFI (National Forest Inventory). The most feasible satellite image data are Landsat TM (Thematic Mapper), SPOT, and MOS-1 (Marine Observation Satellite-1) images. The method of image interpretation and examples of large area results, including possible ways to judge the goodness of estimates by comparing them with those based on field measurements or with characteristics of in-situ inventory data measured for forest management planning purposes are discussed. The utilization of the inventory results is creating new cooperation between practical forestry and forest research.

Author (NASDA)

N94-14255# Tokyo Univ. (Japan). Inst. of Industrial Science.

GLOBAL ASSESSMENT OF HUMAN ACTIVITIES

Yoshiaki Honda and Shunji Murai *In* Science and Technology Agency, Asia-Pacific ISY Conference, Volume 2 31 Mar. 1993 p 236-239 (For primary document see N94-14209 02-43)

Avail: CASI HC A01/MF A04

A world vegetation map has been produced with the use of NOAA GVI (Global Vegetation Index) data. The actual vegetation map shows disturbed or changed land use as a result of human activities. A potential vegetation map through the use of climate data has been produced. This shows the virgin status of vegetation as generated from only climate conditions without disturbances due to human activities. The difference between the actual and potential vegetation tells about the impact of human activities. CO2 fixation change from that difference was estimated. It is of urgent importance to moderate deforestation and to promote reforestation to prevent global warming due to the increase of CO2 in the atmosphere. Therefore, global map for forest conservation/reforestation was generated with the use evaluating land condition such as vegetation and soil. Author (NASDA)

N94-14256# Swedish Space Corp., Solna.

THE SWEDISH ISY CONTRIBUTION

A. Rosenqvist and H. Oesterlund *In* Science and Technology Agency, Asia-Pacific ISY Conference, Volume 2 31 Mar. 1993 p 240-243 (For primary document see N94-14209 02-43)

Avail: CASI HC A01/MF A04

The Swedish contribution in the celebration of the ISY (International Space Year) has materialized in an active participation in the world forest watch project of the earth science and technology panel but also in the training in the remote sensing applications program within the education and applications panel. The Swedish world forest watch contributions have been formed under the theme of remote sensing for forest management. The projects comprise a wide range of forest and forestry remote sensing applications using different technical approaches. Author (NASDA)

N94-14257# Tokyo Univ. (Japan). Inst. of Industrial Science.

VEGETATION MAPPING OF INDO-CHINA PENINSULA USING MOS-1 MESSR AND NOAA AVHRR

Masataka Takagi, Shunji Murai, and Yoshiaki Honda *In* Science and Technology Agency, Asia-Pacific ISY Conference, Volume 2 31 Mar. 1993 p 244-247 (For primary document see N94-14209 02-43)

Avail: CASI HC A01/MF A04

In the Indo-China Peninsula, the ecosystem is changed by commercial logging or shifting cultivation. In order to watch a current environmental condition, a vegetation map of the Indo-China Peninsula is generated using the MOS-1 (Marine Observation Satellite-1) MESSR (Multispectral Electronic Self-Scanning Radiometer) and NOAA AVHRR (Advanced Very High Resolution Radiometer). A total of 405 scenes of MOS-1 MESSR data were selected for the vegetation mapping in order to cover the whole Indo-China Peninsula. These images were synthesized to generate a mosaic image. Most scenes of MOS-1 data were received in different seasons. Therefore, a radiometric correction system for the mosaic image was developed by using a cloud-free mosaic of NOAA AVHRR data with a wide coverage and multitemporal data. This system was very helpful in applying high resolution satellite data to a wide area. A vegetation map was generated from the radiometrically corrected mosaic images with NVI (Normalized Vegetation Index) value. Vegetation distributions of four countries (Thailand, Cambodia, Laos, Vietnam) were compared with land use data made by the FAO (Food and Agriculture Organization). In Cambodia, the vegetation area is much less than the statistics of the FAO.

Author (NASDA)

N94-14258# Ghent Univ. (Belgium). Lab. of Remote Sensing and Forest Management.

REMOTE SENSING FOR MONITORING TROPICAL MOIST FORESTS IN THE INDO-CHINESE REGION

Robert deWulf, Roland Goossens, and Bruno Verbist *In* Science and Technology Agency, Asia-Pacific ISY Conference, Volume 2 31 Mar. 1993 p 248-251 (For primary document see N94-14209 02-43)

Avail: CASI HC A01/MF A04

A summary of results obtained in a number of projects completed or in execution, on monitoring of moist tropical forests in the Indo-Chinese region in cooperation with WWF (World Wide Fund for Nature International), and with the Joint Research Center of the European Community is presented. The choice of sensor, channel selection, and classification strategy for and the accuracy of tropical forest classification are described. Examples of monitoring deforestation (forest cover change between 1973 and 1988 from archives of LANDSAT/MSS (Multi Spectral Scanner) and recent LANDSAT/TM (Thematic Mapper)) and major constraints for applications (such as the difficulties in obtaining sufficient and reliable field data) are outlined. Author (NASDA)

N94-14259# National Inst. of Agro-Environmental Science, Ibaraki (Japan).

ESTIMATION OF VEGETATION DAMAGE DUE TO ASH FALL IN MT. PINATUBO AREA USING MOS-1 DATA

Genya Saitou, Arlene M. Evangelista (Soil Research and Development Center, Quezon City, Philippines.), and John A. Grace *In* Science and Technology Agency, Asia-Pacific ISY Conference, Volume 2 31 Mar. 1993 p 252-255 (For primary document see N94-14209 02-43)

Avail: CASI HC A01/MF A04

An overview of the monitoring of the northern part of Luzon Island in the Philippines and estimation of vegetation damages caused by the ash falling from Mt. Pinatubo using the MOS-1 (Marine Observation Satellite-1)/MESSR (Multispectral Electronic Self-Scanning Radiometer) before and after the Mt. Pinatubo eruption is presented. In the multi-temporal analysis, the data acquired on both pre- and post-eruption were used for evaluating the extent of volcanic ash damage. Formulas used for analyses, such as radiometric correction of sun elevation, vegetation indices, and determination of the extent of damage are described. The application of satellite image analysis to natural disaster damage evaluation of ash damaged (90 to 100 percent of vegetation degraded) had attained as much as 200,000 ha in analyzing the data of three weeks after the eruption. This value decreased to about 40,000 ha, but the total of more than 30 percent damaged area still remained more than 200,000 ha at the time of four months after eruption. Author (NASDA)

N94-14260# Bangladesh Space Research and Remote Sensing Organization, Dhaka.

MANGROVE AFFORESTATION MONITORING USING REMOTE SENSING

A. K. M. Fariduddin Bhuiyan and M. Jinnahtul Islam *In* Science and Technology Agency, Asia-Pacific ISY Conference, Volume 2 31 Mar. 1993 p 256-265 (For primary document see N94-14209 02-43)

Avail: CASI HC A02/MF A04

An overview of the mangrove afforestation monitoring conducted by the SPARRSO (Bangladesh Space Research and Remote Sensing Organization) using satellite remote sensing data is presented. The first five year program of afforestation to construct forest protection belt under the World Bank's financial assistance to protect life and property from the ravages of cyclones and storm surges were implemented by the Bangladesh Forest Department during the project period of 1980 to 1985. Several other projects of the mangrove afforestation project were the stabilization of the newly accredited lands by plantations and conservation of the stabilized lands from erosion and acceleration of the process of further land accretion in the Bay of Bengal. The ultimate objectives is to reclaim agricultural land within the zone of plantation areas, increase production of fuel wood and timber for industrial and constructional uses, increase the

total forest area and improve the socio-economic condition of the coastal population, and coastal plantation monitoring and mapping using satellite remote sensing data are outlined. Author (NASDA)

N94-14261# Tsukuba Space Center, Ibaragi (Japan).
OUTLINE OF ISY SEA SURFACE TEMPERATURE DATA SETS **c48**
Korehiro Maeda and Hironori Maejima (National Space Development Agency, Ohashi, Japan.) *In* Science and Technology Agency, Asia-Pacific ISY Conference, Volume 2 31 Mar. 1993 p 269-273 (For primary document see N94-14209 02-43)
Avail: CASI HC A01/MF A04

Mission to Planet Earth is the main theme of International Space Year (ISY). The National Space Development Agency of Japan (NASDA) is responsible for the data sets concerning Sea Surface Temperature (SST) and Polar Ice Extent (PIE) important for global warming as a part of Earth Science and Technology (ES and T) which is one of the panels of experts for the Space Agency Forum for ISY (SAFISY). NASDA has developed various data sets using Marine Observation Satellite-1 (MOS-1)/MOS-1b and other satellite data for the aforementioned items. In this report, an outline of SST data set using MOS-1/1b data and other satellite data is presented. Author (NASDA)

N94-14262# Remote Sensing Technology Center, Tokyo (Japan).
INTEGRATION OF SST DATA SETS USING MOS-1 SATELLITE DATA: FOR VALIDATION AND MONITORING **c48**
Shouji Takeuchi, Yasunori Nakayama, and Tsuyoshi Tomita *In* Science and Technology Agency, Asia-Pacific ISY Conference, Volume 2 31 Mar. 1993 p 274-277 Sponsored by NASDA (For primary document see N94-14209 02-43)
Avail: CASI HC A01/MF A04

The configuration of the integrated SST (Sea Surface Temperature) data set derived from the MOS-1 (Marine Observation Satellite-1)/VTIR (Visible and Thermal Infrared Radiometer) combined with those by other MOS-1 sensors, such as MSR (Microwave Scanning Radiometer) and MESSR (Multispectral Electronic Self-Scanning Radiometer) and derived from the NOAA/AVHRR (Advanced Very High Resolution Radiometer) and sea truth data by several ocean data buoys is outlined. The results of preliminary validation using the data set are also outlined. The regional SST data set around Japan acquired by VTIR and by the combination of VTIR and AVHRR is outlined. Results of regression analysis for the MOS-1/VTIR data set and that for the VTIR and MSR combined data set are presented. The relation between SST estimate errors and the number of days from launch of the MOS-1 is shown. Author (NASDA)

N94-14263# Commonwealth Scientific and Industrial Research Organization, Mordialoc (Australia). Atmospheric Research Div.
GEOPHYSICAL VALIDATION OF ATSR SEA SURFACE TEMPERATURES **c48**
I. J. Barton, D. T. Llewellyn-Jones (Rutherford Appleton Lab., Chilton, England.), A. J. Prata, and R. P. Cechet *In* Science and Technology Agency, Asia-Pacific ISY Conference, Volume 2 31 Mar. 1993 p 278-281 (For primary document see N94-14209 02-43)
Avail: CASI HC A01/MF A04

The Along Track Scanning Radiometer (ATSR), which was launched on the ERS-1 in 1991, is supplying global Sea Surface Temperature (SST) measurements which are useful for climate research applications. To ensure that the radiometer is able to supply highly accurate estimates of SST, several cruises have been undertaken in Australian waters during which ship based measurements have been compared to those from space. A summary of this intercomparison is given along with a case study of comparisons between the ship measurements and those made using data from the Advanced Very High Resolution Radiometer (AVHRR) on the NOAA-11 meteorological satellite. Author (NASDA)

N94-14264# Iwate Univ., Morioka (Japan). Dept. of Computer and Information Science.
ACCURACY VALIDATION TEST OF ESTIMATED SEA SURFACE TEMPERATURE BY SATELLITE DATA **c48**
Sumio Tanba, Takashi Souma, Isao Yoshida, Takashi Watanabe, and Ryuuzou Yokoyama *In* Science and Technology Agency, Asia-Pacific ISY Conference, Volume 2 31 Mar. 1993 p 282-285 (For primary document see N94-14209 02-43)
Avail: CASI HC A01/MF A04

By using the sea truth data of MBAMMBS (Mutsu Bay Automatic Marine Monitoring Buoy System), the accuracy of the SST (Sea Surface Temperature) estimated by the NOAA-11/AVHRR (Advanced Very High Resolution Radiometer) data was evaluated. An SST estimation function was calculated by the regression analysis based on the SWM (Split Window Method), and it provided the standard error of 0.70 C. Some match-ups were found to be exposed to strong SSE (Sea Surface Effect): that means the large temperature difference between the sea skin for the satellite detection and the 1 m depth of the buoy detection. By removing those match-ups, a regression function, whose coefficients are almost equal to those in the regression function by NOAA-9/AVHRR in Mutsu Bay, with the standard error of 0.36 C is obtained. Author (NASDA)

N94-14265# Iwate Univ., Morioka (Japan). Dept. of Computer Science.
SEA SURFACE EFFECT ON THE SEA SURFACE TEMPERATURE ESTIMATION BY SATELLITE DATA **c48**
Ryuuzou Yokoyama, Sumio Tanba, and Takashi Souma *In* Science and Technology Agency, Asia-Pacific ISY Conference, Volume 2 31 Mar. 1993 p 286-289 (For primary document see N94-14209 02-43)
Avail: CASI HC A01/MF A04

By using a Sea Surface Temperature Profiler Buoy (SSTPB), the behavior of the vertical temperature profile was observed in Mutsu Bay. In the midday under clear and calm condition in summer, there occurred a large temperature difference, of at most 5 C, between the sea skin and the 1 m depth. The difference suddenly disappeared when it began to blow more than 5 m/s. The sea surface effect must be a dominant error factor in the Sea Surface Temperature (SST) estimation by satellite data other than the atmospheric effect. Author (NASDA)

N94-14266# Maritime Safety Agency, Tokyo (Japan). Hydrographic Dept.
ON THE SEA TRUTH DATA OF THE KUROSHIO MEANDER AND COLD EDDY MOVEMENT **c48**
Masataka Hishida and Yutaka Michida *In* Science and Technology Agency, Asia-Pacific ISY Conference, Volume 2 31 Mar. 1993 p 290-298 (For primary document see N94-14209 02-43)
Avail: CASI HC A02/MF A04

An overview of observed phenomena of the KLM (Kuroshio Large Meander), relationship of sea level difference in the Tokara Strait where the ocean condition is strongly affected by that in the ECS (East China Sea), and formation of TCW (Tanegashima Cold Water) and KLM are presented. A new schematic representation of the ocean current system in the ECS obtained by compiling the knowledge derived from satellite IR (Infrared) image data provided by the MOS-1 (Marine Observation Satellite-1) and NOAA is proposed. The quick bulletin about the ocean condition named 'Kaiyou Sokuhou', and trajectories of surface drifters, an oceanographic atlas of the Japan-China Joint Research Program on the Kuroshio (JRK), and many other references are also proposed. The SST (Sea Surface Temperature) image in spring is useful to analyze the Kuroshio meander because TCW formation occurs, and this phenomenon will trigger the formation of the KLM. SST images from satellite show many changes of time dependent eddy movements. The satellite image data suggest that new physical ocean process or theory has to be considered.
Author (NASDA)

N94-14267# Tohoku Regional Fisheries Research Lab., Miyagi (Japan).
TRACKING OF CHANGE OF A WARM-CORE RING STRUCTURE **c48**
Denzou Inagake and Akira Tomosada *In* Science and Technology Agency, Asia-Pacific ISY Conference, Volume 2 31 Mar. 1993 p 299-302 (For primary document see N94-14209 02-43)
Avail: CASI HC A01/MF A04

A warm streamer, which was observed by a hydrographic survey onboard the research vessel Soyo Maru from May 20 to 22 in 1989, was tracked by MOS-1 (Marine Observation Satellite-1) VTIR (Visible and Thermal Infrared Radiometer) images and NOAA-10/AVHRR (Advanced Very High Resolution Radiometer) images from February to August in 1989. These images presented a generation of the streamer, spiraling warm water into the Kuroshio warm core ring, and development of the ring. The warm streamer around the Kuroshio warm core ring had a structure beyond 500 m in depth with a geostrophic current structure. Also, another warm streamer

was observed in the warm core ring. It can be considered that the inner streamer was taken into the warm core ring several weeks before and that the spiraling outer warm band was a new warmstreamer around the Kuroshio warm core ring. Author (NASDA)

N94-14268# National Space Development Agency, Ohashi (Japan). Earth Observation Center.

OUTLINE OF ISY KUROSHIO OBSERVATION EXPERIMENT **c48**

Hironori Maejima, Hiroaki Ochiai (Toba Merchant Marine Coll., Japan.), and Hideo Tameishi (Japan Fisheries Information Service Center, Tokyo.) *In* Science and Technology Agency, Asia-Pacific ISY Conference, Volume 2 31 Mar. 1993 p 303-306 Prepared in cooperation with Tokyo Univ., Japan; Nakanihon Air Service Co. Ltd., Aichi, Japan; and Remote Sensing Technology Center, Tokyo, Japan (For primary document see N94-14209 02-43)

Avail: CASI HC A01/MF A04

An overview of the ISY (International Space Year) Kuroshio observation experiment conducted in Kumanonada using the data by the MOS-1 (Marine Observation Satellite-1) observation, the AXBT (Airborne Expendable Bathy Thermography), and vessel observation is presented. The observation area; the AXBT configuration; the airborne MSS (Multi Spectral Scanner) characteristics; and the data obtained by the MOS-1/VTIR (Visible and Thermal Infrared Radiometer), airborne MSS, and 3-D (Dimensional) sea temperature profile image from AXBT data are shown. Author (NASDA)

N94-14269# Saga Univ. (Japan). Dept. of Information Science.

A METHOD FOR ESTIMATION OF PARTIAL CLOUD COVER WITHIN A PIXEL AND ITS EFFECT **c47**

Kouhei Arai *In* Science and Technology Agency, Asia-Pacific ISY Conference, Volume 2 31 Mar. 1993 p 307-310 (For primary document see N94-14209 02-43)

Avail: CASI HC A01/MF A04

The topics covered include the following: sea surface temperature estimation of the pixel suffered from partial cloud cover, methods for estimating partial cloud cover within a pixel, and experiments with simulated data. Author (NASDA)

N94-14270# Japan Fisheries Information Service Center, Tokyo.

WARM STREAMERS EXTENDED FROM WARM CORE RINGS (WCR'S) AND THEIR ROLE ON FISH MIGRATION AND FISHING GROUND FORMATION **c48**

Hideo Tameishi and Takeshige Sugimoto (Tokyo Univ., Japan.) *In* Science and Technology Agency, Asia-Pacific ISY Conference, Volume 2 31 Mar. 1993 p 311-316 (For primary document see N94-14209 02-43)

Avail: CASI HC A02/MF A04

It is recognized that the Warm Streamers (WS's) often branch out toward the north or northwest from Warm Core Rings (WCR's), in satellite thermal imageries. They become migrating paths toward the North and from offshore to nearshore. In this study, the relationship between these fine structures and fishing grounds, were investigated, using NOAA/AVHRR (Advanced Very High Resolution Radiometer) data with assistance of aircraft data and fisheries information. The obtained results are as follows: (1) NOAA/AVHRR imageries with spatial resolution of 1.1 km represent the structures of the WS's of about 10 km in width around the WCR's well; (2) by using the simultaneous aircraft data, many sardine's schools are recognized at the head of WS, in which coastal region sardine's fishing grounds are often formed; (3) it seems that WS is useful for the transfer of schools toward the coast; and (4) schools of sardine, mackerel, and other species make zonation across the front of WCR's. Author (NASDA)

N94-14271# Meteorological Research Inst., Tsukuba (Japan).

ATMOSPHERIC CORRECTION FOR SEA SURFACE TEMPERATURE BY APPLICATION OF MICROWAVE DUAL-CHANNEL TECHNIQUE TO VTIR DATA **c48**

Youzou Takayama *In* Science and Technology Agency, Asia-Pacific ISY Conference, Volume 2 31 Mar. 1993 p 317-320 (For primary document see N94-14209 02-43)

Avail: CASI HC A01/MF A04

Atmospheric correction for estimating sea surface temperature (SST) from VTIR data by using the IR split-window technique (11 and 12 microns) and dual-frequency microwave channels (23.8 and 31.4 GHz) are presented. Both methods have the same capability for correcting the water-vapor absorption effect to estimate SST. However, the microwave dual-frequency method bring better SST estimation than the split-window technique for VTIR data. The simulation study shows that this better estimation of SST by the microwave dual-frequency is due to a better signal-to-noise ratio for correction of atmospheric absorption than the split-window technique, in the case of VTIR observation. By using the different radiation characteristics between infrared and microwave channels, it is feasible to improve the accuracy in estimating the SST in the case of the existing dense stratospheric aerosol. Author (NASDA)

N94-14272# Remote Sensing Applications Centre, Jakarta (Indonesia). National Inst. of Aeronautics and Space.

SOME THOUGHTS ON THE SPACE PROGRAMS IN THE ASIA PACIFIC REGIONS

Bambang Hidayat *In* Science and Technology Agency, Asia-Pacific ISY Conference, Volume 2 31 Mar. 1993 p 323-330 Prepared in cooperation with Observatorium Bosscha, Bandung, Indonesia (For primary document see N94-14209 02-43)

Avail: CASI HC A02/MF A04

The prospective activities for the study of global change and related problems are summarized. It is suggested that institutionalization would be more beneficial than a mere organization. The emphasis should be given to the way of how to do rather than what to do. Author (NASDA)

N94-14273# Academia Sinica, Beijing (China). International Space Year China Preparatory Committee.

CHINA'S DEVOTION TO SPACE SCIENCE AND APPLICATIONS **c12**

Da-Heng Wang *In* Science and Technology Agency, Asia-Pacific ISY Conference, Volume 2 31 Mar. 1993 p 331-334 (For primary document see N94-14209 02-43)

Avail: CASI HC A01/MF A04

An overview of China's space science and its application activities are described. The following topics are included: meteorological satellite launching and satellite meteorology; remote sensing applications (such as the CLSPN (Chinese Land-Sea Satellite Positioning Network), mapping, the GIST (Geographical Information System Tool Kit), land use, and land cover monitoring, deforestation and afforestation monitoring, and natural disaster (flooding and forest fire) monitoring and evaluation); space science research programs (such as ionospheric studies, theoretical studies of solar wind Alfven wave, magnetic storm studies, etc.); microgravity experiments (including solidification and recrystalization of semiconductor materials during space flight); and space environment tests (bio-mutational effects on various vegetable seeds and grained exposed to the space environment) using retrievable satellites. Author (NASDA)

N94-14274# Science Univ. of Tokyo (Japan). Dept. of Mechanical Engineering.

SPACE TRANSPORTATION SYSTEMS AND SPACE ACTIVITIES IN THE 21ST CENTURY **c16**

Shigeo Kobayashi *In* Science and Technology Agency, Asia-Pacific ISY Conference, Volume 2 31 Mar. 1993 p 337-342 (For primary document see N94-14209 02-43)

Avail: CASI HC A02/MF A04

An overview of the space activities, the demands for space transportation, the future space transportation systems, and the scenario of future space transportation system in Japan expected in the 21st century are outlined. The following topics are covered: the architecture of space activities in which Japan will actively participate showing the summary of the report of the Committee on the Long-term Policy for the Space Development in Japan; the earth and low earth orbit; low earth orbit and geostationary orbit; the moon base and planets; partially or fully reusable manned or unmanned winged vehicles; expendable or reusable orbit transfer vehicles; and expendable or reusable cost-effective cargo launching vehicles; and the HOPE (H-2 Orbiting Plane). Author (NASDA)

N94-14275# European Space Agency, Paris (France). Space Transportation Systems Directorate.

SPACE TRANSPORTATION SYSTEMS WITHIN ESA PROGRAMMES: CURRENT STATUS AND PERSPECTIVES **c16**

Maurice Delahais *In* Science and Technology Agency, Asia-Pacific ISY Conference, Volume 2 31 Mar. 1993 p 343-347 (For primary document

see N94-14209 02-43)
Avail: CASI HC A01/MF A04

An overview of the space transportation aspects of the ESA (European Space Agency) programs as they result from history, present status, and decisions taken at the ministerial level conference in Granada, Spain is presented. The new factors taken into consideration for the long term plan proposed in Munich, Germany, the three strategic options for the reorientation of the ESA long term plan, and the essential elements of space transportation in the Granada long term plan in three areas of space activities, scientific, and commercial launches with expendable launch vehicles, manned flight and in-orbit infrastructure, and future transportation systems are outlined. The new ESA long term plan, in the field of space transportation systems, constitutes a reorientation of the initial program contemplated in previous councils at ministerial level. It aims at balancing the new economic situation with the new avenues of cooperation, and the outcome will be a new implementation of the space transportation systems policy.

Author (NASDA)

N94-14276*# National Aeronautics and Space Administration, Washington, DC.

MY EXPERIENCES IN MANNED SPACE FLIGHT **c99**

Michel Weeks *In* Science and Technology Agency, Asia-Pacific ISY Conference, Volume 2 31 Mar. 1993 p 348-355 (For primary document see N94-14209 02-43)
Avail: CASI HC A02/MF A04

An outline of the last thirty four years of manned space flights; the Mercury and Vostok history; Mercury capsule and its launch of the Atlas-Mercury; Gemini and its launch vehicle; USSR SL-4 with a Soyuz; early US history of Mercury, Gemini, and Apollo; Aerospace Corp. of US Air Force (USAF); activities of the LLVPG (Large Launch Vehicle Planning Group) and MOL (Manned Orbiting Laboratory); Space Shuttle Program; USSR manned space flight activities; summary of US space flight; NASP (National Aero-space Plane) concept; and the lessons of history are outlined and some possible conclusions on a strong space program by the CIS (Commonwealth of Independent States), ESA (European Space Agency), Japan and the US are outlined. Author (NASDA)

N94-14277# Tokyo Univ., Sagamihara (Japan). Inst. of Space and Astronautical Science.

RESEARCH AND DEVELOPMENT OF SPACE TRANSPORTATION SYSTEMS IN ISAS **c16**

Junjirou Onoda *In* Science and Technology Agency, Asia-Pacific ISY Conference, Volume 2 31 Mar. 1993 p 356-359 (For primary document see N94-14209 02-43)
Avail: CASI HC A01/MF A04

An overview of the research and development activities in the ISAS (the Institute of Space and Astronautical Science) focusing on the Mu-5 launch vehicle, the winged space vehicle, and the ATR (Air Turbo Ramjet) engine is presented. The design guidelines, characteristics, dimensions, and subsystems, such as rocket motor, nose fairing, and attitude control subsystem of the Mu-5 launch vehicle, one of the versions of Mu series rocket, which is capable of launching 1.8 tons of payload into LEO (Low Earth Orbit) are outlined. The research and development activities on winged space vehicle called the HIMES (Highly Maneuverable Experimental Space) Vehicle and the ATR propulsion system are outlined. Author (NASDA)

N94-14278# Science and Technology Agency, Tokyo (Japan). Research and Development Bureau.

CONTRIBUTIONS OF WINGED RE-ENTRY VEHICLE TO SPACE ACTIVITIES **c16**

Masaaki Yanagihara *In its* Asia-Pacific ISY Conference, Volume 2 31 Mar. 1993 p 360-363 (For primary document see N94-14209 02-43)
Avail: CASI HC A01/MF A04

An overview of some results of the space infrastructure study based on the fundamental policy of Japan's space development decided by the SAC (Space Activities Commission) is presented. Three phases of the life cycle of space segment, five kinds of systems composing space infrastructure, an example of a space infrastructure with a central system called LASER (Low Earth Orbit Advanced Station Equipped with Robot), reusable space transportation systems such as space plane, the ultimate manned space transportation system, and the unmanned space transportation system HOPE (H-2 Orbiting Plane) launched by the H-2 launch vehicle under development by the NASDA (National Space Development Agency of Japan) are outlined. Author (NASDA)

N94-14279# Mitsubishi Research Inst., Inc., Tokyo (Japan).

MISSION SCENARIO OF HOPE **c16**

Yasushi Kawai and Kenji Takeuchi *In* Science and Technology Agency, Asia-Pacific ISY Conference, Volume 2 31 Mar. 1993 p 364-368 (For primary document see N94-14209 02-43)
Avail: CASI HC A01/MF A04

An overview of the study for analyzing the HOPE (H-2 Orbiting Plane) utilization, which will be launched by the H-2 launch vehicle by the end of the 1990's, and the HOPE contributions to the progress in science and technology is presented. A questionnaire was sent out for potential user organizations of the HOPE, namely, universities, national laboratories, foundations, and private enterprises. Also, other methods such as cross impact matrix method, are being used to clarify the relation between the manufacture of high quality glass under microgravity and the technological development. Author (NASDA)

N94-14280# Tsukuba Space Center, Ibaragi (Japan).

THE STATUS OF THE HOPE CONCEPT STUDY **c16**

Jirou Kouchiyama and Akihiro Eguchi *In* Science and Technology Agency, Asia-Pacific ISY Conference, Volume 2 31 Mar. 1993 p 369-374 (For primary document see N94-14209 02-43)
Avail: CASI HC A02/MF A04

National Space Development Agency of Japan (NASDA) has been studying an unmanned winged vehicle called the H-2 Orbiting Plane (HOPE). The HOPE will be launched by H-2 launch vehicle or H-2 derivative launch vehicle, and injected into low orbit. After a few days stay in space for access to the space station, HOPE will de-orbit and go back to a named landing site automatically. The concept of the 10-ton class vehicle launched by H-2 launch vehicle was prepared in 1988. However, its payload capability is not enough for the practical use of the space station expected at the beginning of the 21st century. Therefore, the concept of 20-ton class vehicle launched by the Solid Rocket Booster (SRB)-added H-2 launch vehicle without the second stage (Liquid Engine-5A (LE-5A) engine) was studied in 1989. This vehicle will be injected into low orbit by its own propulsion system. Its payload capability was estimated at 3 tons. In the study from 1990 to 1991, it was revealed that the reduction of the HOPE weight is the most important problem. At present, the shapes of the main wing, the orbital injection systems (reusable engine or expendable one), and the materials of the main structure (carbon/polyimide) are being studied to reduce the weight. Author (NASDA)

N94-14281# National Aerospace Lab., Tokyo (Japan).

SPACEPLANE PROGRAM AT NAL: SYSTEM CONCEPT AND RELATED TECHNOLOGY ISSUES **c16**

Masataka Maita *In* Science and Technology Agency, Asia-Pacific ISY Conference, Volume 2 31 Mar. 1993 p 375-378 (For primary document see N94-14209 02-43)
Avail: CASI HC A01/MF A04

An overview of the space plane program planned by the NAL (National Aerospace Laboratory) is presented. The tentative base line mission requirements such as space transportation to and from LEO (Low Earth Orbit); short term experimental laboratory orbit for earth observation; microgravity; servicing to platforms, maintenance, and repair; space passenger tour through orbital and sub-orbital flight; etc. are outlined. The characteristics of the SSTO (Single Stage to Orbit) vehicle concept are summarized as follows: (1) integration of SCRAMJET (Supersonic Combustion Ramjet) engine and LACE (Liquid Air Cycle Engine); (2) fueling with slush hydrogen with fuel weight fraction of less than 70 percent; and (3) total gross weight of 350 tons with the structural weight reduction by 20 percent of the curreni technological potential. Author (NASDA)

N94-14282# Ministry of Posts and Telecommunications, Beijing (China). Directorate General of Telecommunications.

THE DEVELOPMENTS OF SATELLITE COMMUNICATIONS OF CHINA **c32**

Shen Liu *In* Science and Technology Agency, Asia-Pacific ISY Conference, Volume 2 31 Mar. 1993 p 381-384 (For primary document see

N94-14209 02-43)
Avail: CASI HC A01/MF A04

Present status of satellite communication system development in China is introduced. An overview of the space segment arrangements of international or regional satellites for domestic satellite telecommunication, trunk routes, provincial and regional satellite links, VSAT (Very Small Aperture Terminal) applications for data transmissions, and international satellite communications is presented. Author (NASDA)

N94-14283# Ministry of Communications, Anyang (Republic of Korea). Radio Wave Div.

THE CURRENT SITUATION, TRENDS, INTERNATIONAL COOPERATION OF SPACE COMMUNICATION TECHNOLOGICAL DEVELOPMENT IN THE REPUBLIC OF KOREA **c84**

Moo-Gon Pyun and Jai-Rim Yuk *In* Science and Technology Agency, Asia-Pacific ISY Conference, Volume 2 31 Mar. 1993 p 385-388 (For primary document see N94-14209 02-43)
Avail: CASI HC A01/MF A04

Trends of Korean space communication technology are reviewed. The following topics are discussed with respect to the KOREASAT satellite: the characteristics of the satellite services to be provided; major characteristics of the satellite (including its dimensions, modes of operations, and beam coverage); and the ground segment to keep up control and management (including the tracking telemetry and command station, satellite control center and network control center, and ground communication station composed of various functional divisions such as gateway station, VSAT (Very Small Aperture Terminal), and mobile station). Author (NASDA)

N94-14284# Ministry of Posts and Telecommunications, Tokyo (Japan). Space Communication Research Office.

JOINT EXPERIMENTS USING ETS-5 **c32**

Mutsumi Nakata *In* Science and Technology Agency, Asia-Pacific ISY Conference, Volume 2 31 Mar. 1993 p 389-392 (For primary document see N94-14209 02-43)
Avail: CASI HC A01/MF A04

An overview of the PARTNERS (Pan-Pacific Regional Telecommunications Network Research Satellite) project, which is the post-mission utilization of the ETS-5 (Engineering Test Satellite-5) is presented. The project was registered at SAFISY (Space Agency Forum for International Space Year) and includes the following experiments: (1) research on radio propagation characteristics in satellite links in Pan-Pacific region; (2) joint study on development of rural satellite network using simple mobile station; (3) experiments on telecommunication using personal computers for academic network; (4) experiments on remote education and training through satellite networks; (5) experiments on remote medicine; (6) experiments on the operation of medical information data base; (7) experiments on transmission of the earth observation data; and (8) demonstration of real time transmission of Asia-Pacific ISY (International Space Year) Conference. The experiment systems consisting of space segment (ETS-5) and simple and low cost ground system composed of 1.2 m aperture parabolic antenna, TV (Television) conference system, and terminal equipment are outlined. Author (NASDA)

N94-14285# Ministry of Posts and Telecommunications, Tokyo (Japan). Communications Research Lab.

SPACE COMMUNICATIONS TECHNOLOGY RESEARCH IN CRL **c32**

Takashi Iida *In* Science and Technology Agency, Asia-Pacific ISY Conference, Volume 2 31 Mar. 1993 p 393-396 (For primary document see N94-14209 02-43)
Avail: CASI HC A01/MF A04

This report overviews the current research of space communications technology in Communications Research Laboratory (CRL), Ministry of Posts, and Telecommunications. The Engineering Test Satellite-5 (ETS-5) project has been conducted these five years for mobile communications development. The international cooperations using ETS-5 has been performed. It describes the project of Communications and Broadcasting Engineering Test Satellite (COMETS) to be launched in 1997 for experiments of advanced mobile satellite communication and advanced broadcasting. It also mentions the project of Engineering Test Satellite-6 (ETS-6), to be launched in 1994, in which the CRL's missions of ETS-6 are the inter-satellite communication of S-band, millimeter-wave, and optical. Finally, this report describes the technologies of large antenna assembly experiment, small satellite communications, and cluster satellite briefly. Author (NASDA)

N94-14286# Nippon Telegraph and Telephone Public Corp., Yokosuka (Japan). Satellite Communication Systems Lab.

NTT'S ACTIVITIES IN SATELLITE COMMUNICATIONS TECHNOLOGY DEVELOPMENT **c32**

Shuuichi Samejima *In* Science and Technology Agency, Asia-Pacific ISY Conference, Volume 2 31 Mar. 1993 p 397-400 (For primary document see N94-14209 02-43)
Avail: CASI HC A01/MF A04

An overview of the recently developed ISDN (Integrated Services Digital Network) and its future expansion and technology development in mobile satellite communications by NTT (Nippon Telegraph and Telephone Corp.) is presented. A TDMA (Time Division Multiple Access) system developed for narrow band ISDN through satellite connection to meet the communication demand in the area where the terrestrial facilities are not equipped, and the concept of broad band ISDN undergoing development to offer more sophisticated service in the future are described. The frequency band, multibeam technology, services, orbits of the satellite used, and future prospects related to mobile satellite communication are outlined. Author (NASDA)

N94-14287# Kokusai Denshin Denwa Co. Ltd., Saitama (Japan). Research and Development Labs.

FUTURE OUTLOOK ON INTERNATIONAL SATELLITE COMMUNICATIONS IN ASIA PACIFIC REGION **c32**

Yasuhiko Itou *In* Science and Technology Agency, Asia-Pacific ISY Conference, Volume 2 31 Mar. 1993 p 401-404 (For primary document see N94-14209 02-43)
Avail: CASI HC A01/MF A04

An overview of the present status and a future trend of the international satellite communication in the Asia Pacific region is presented. The measures to solve the problems of the low penetration of the VSAT (Very Small Aperture Terminal) for international communication; the lack of standardization between different countries; regulatory difficulties and the lack of suitable satellite systems, including CCIR (Comite Consultatif International des Radio-communications) recommendations; and possibility of digital video transmission for SNG (Satellite News Gathering) are discussed. The present status and new technologies of, and satellite orbits (LEO (Low Earth Orbit)), ICO (Intermediate Circular Orbit), and GEO (Geostationary Earth Orbit)) for marine, mobile, and personal communication by hand-carried equipment are outlined. Author (NASDA)

N94-14288# Japan Broadcasting Corp., Tokyo. Radio Engineering Research Div.

TECHNOLOGICAL DEVELOPMENT FOR BROADCASTING SATELLITES IN NHK LABORATORIES **c32**

Youji Morishita *In* Science and Technology Agency, Asia-Pacific ISY Conference, Volume 2 31 Mar. 1993 p 405-408 (For primary document see N94-14209 02-43)
Avail: CASI HC A01/MF A04

An overview of the development results by the NHK (Nippon Hoso Kyokai) of 12 GHz TWT (Traveling Wave Tubes), onboard antennas (shaped reflector antennas), and multiplexers (12 GHz eight channel 200 W multiplexers) for the future DBS (Direct Broadcasting Satellite) is presented. An overview of the system studies concerning 21 GHz global broadcasting satellite systems expected for HDTV (High Definition Television) broadcasting or ISDB (Integrated Service Digital Broadcasting) is also presented. The bipolar radiation pattern of the antenna and the block diagram of the variable EIRP (Equivalent Isotropically Radiated Power) are shown. Author (NASDA)

N94-14353# European Space Agency. ESRIN, Frascati (Italy).

ERS-1 SYSTEM

Pam Vass, ed. (Earth Observation Sciences Ltd., Guildford, England.) and Bruce Battrick, ed. Sep. 1992 76 p Original contains color illustrations
(ESA-SP-1146; ISBN-92-9092-021-1; ETN-93-93948) Copyright Avail: CASI HC A05/MF A01

The European Remote Sensing-1 (ERS-1) objectives and mission program are summarized. Information on the satellite, its instruments, the ground

facilities, and services from a data user's point of view is given. The ERS-1 satellite carries a set of active microwave sensors, supported by: an active microwave instrument, a radar altimeter, a scanning radiometer, a range-rate equipment, and laser-retro-reflectors. The ERS-1 was designed to acquire data from oceans, ice, and meteorology. The high resolution imaging capability can collect information on land areas and coastal zones. ESA

N94-14428# Deutsche Forschungsanstalt fuer Luft- und Raumfahrt, Oberpfaffenhofen (Germany). Abt. fuer Fernerkundung.
SUPERVISED CLASSIFICATION OF REMOTELY SENSED IMAGES [UEBERWACHTE KLASSIFIKATION VON FERNERKUNDUNGSAUFNAHMEN]
Helmut Schumacher Oct. 1992 213 p In GERMAN Original contains color illustrations
(DLR-FB-92-07; ETN-93-93954) Avail: CASI HC A10/MF A03

The analysis and enhancement of the methods employed in supervised classification in remote sensing is addressed. An implementation of the maximum likelihood method on the basis of a per class principal component transformation is suggested. This efficient implementation is also robust in the case of ill conditioned covariance matrices. A generalization of the maximum likelihood method is proposed which can be used for highly correlated (multi-collinear) features of high dimension. It is also suggested to allow class specific selections of features. This makes it possible to discard features showing non-normal distribution on a class by class basis. These generalizations require a normalization of distance measures across all feature spaces (possibly of different dimension). As a tool for this normalization, the paradigm of fuzzy set theory is suggested: distance measures are mapped into grades of memberships to individual classes. This leads to fuzzy classification methods: a vector of memberships to the various classes is assigned to each pixel. Besides the possibility of using different features and different classificators within a single classification run, a new approach to multitemporal classification is emerging. A method for implementing a geocoded thematic database is discussed and a method for detecting and resolving mixed pixels is proposed. A context sensitive reclassification method is presented which is particularly useful in the case of sensor data of high spatial resolution. The effectiveness of this method is demonstrated for synthetic data as well as thematic mapper data. A comparison with probabilistic relaxation method and classification after segmentation shows that the new method is a significant improvement in utilizing context in reclassification. ESA

N94-14544# Beleidscommissie Remote Sensing, Delft (Netherlands). Programmabureau.
THE NATIONAL REMOTE SENSING PROGRAM (NRSP-2 1991 - 2000): THE 1992 ANNUAL PLAN OF THE NETHERLANDS REMOTE SENSING BOARD [NATIONAAL REMOTE SENSING PROGRAMMA (NRSP-2 1991 - 2000): BCRS JAARPLAN 1992]
Oct. 1992 33 p In DUTCH
(BCRS-92-22; ISBN-9-05-411066-X; ETN-93-94092) Avail: CASI HC A03/MF A01

The NRSP-2 program for 1992 has two focal points: stimulation of operational applications of remote sensing in governmental departments; promotion of collaboration in the Netherlands in the fields of background research, technological developments, and the establishment of a permanent infrastructure for remote sensing. The priorities for the period 1991-1995 are: implementation of operational remote sensing applications for users; development of commercial remote sensing products for service departments; study of climate changes and environment using data from ESA Earth observation satellite systems; and development of remote sensing forestry and environmental applications in the framework of cooperation with developing countries. ESA

N94-14566# Lawrence Livermore National Lab., CA.
COMPUTER VISION AND SENSOR FUSION FOR DETECTING BURIED OBJECTS
G. A. Clark, J. E. Hernandez, S. K. Sengupta, R. J. Sherwood, P. C. Schaich, M. R. Buhl, R. J. Kane, and N. K. DelGrande Oct. 1992 7 p Presented at the 26th Annual Asilomar Conference on Signals, Systems, and Computers, Pacific Grove, CA, 25-30 Oct. 1992
(Contract W-7405-eng-48)
(DE93-012605; UCRL-JC-112103; CONF-9210231-4) Avail: CASI HC A02/MF A01

Given multiple images of the surface of the earth from dual-band infrared sensors, our system fuses information from the sensors to reduce the effects of clutter and improve the ability to detect buried or surface target sites. Supervised learning pattern classifiers (including neural networks) are used. We present results of experiments to detect buried land mines from real data and evaluate the usefulness of fusing information from multiple sensor types. The novelty of the work lies mostly in the combination of the algorithms and their application to the very important and currently unsolved problem of detecting buried land mines from an airborne standoff platform. DOE

N94-14810# Winand Staring Centre, Wageningen (Netherlands).
OBTAINING DIGITAL REGIONAL PLANNING INFORMATION FROM AERIAL PICTURES [VERKRIJGEN VAN DIGITALE RUIMTELIJKE INFORMATIE UIT LUCHTFOTO'S]
B. J. vanBleek and P. G. Lentjes 1992 58 p In DUTCH
(Rept-228; ETN-93-94093) Copyright Avail: CASI HC A04/MF A01

The use of aerial photography for digital regional planning information and the role of scanning therein was investigated. Digitizing the information from aerial pictures allows a vector inventory to be obtained. Digitation can be performed by single picture mapping or stereomapping. For digitation from a screen the aerial picture has first to be scanned. Scanned aerial pictures can be used for digital terrain models, digital orthophotos, visual support of other digital regional planning information, and digitation of vector information. Aerial pictures can be used for orientation in the field, geometric information, thematic information, and geographic information systems. The combination of geometric and thematic information provides an object oriented terrain description. ESA

44 ENERGY PRODUCTION AND CONVERSION

Includes specific energy conversion systems, e.g., fuel cells; global sources of energy; geophysical conversion; and windpower.

For related information see also *07 Aircraft Propulsion and Power, 20 Spacecraft Propulsion and Power,* and *28 Propellants and Fuels.*

N94-12822# Japan Solar Energy Society, Tokyo.
THE 1992 JSEE/JWEA JOINT CONFERENCE
3 Dec. 1992 305 p In JAPANESE Conference held in Osaka, Japan, 3-4 Dec. 1992 Prepared in cooperation with Japan Wind Energy Association, Tokyo
(DE93-793955; CONF-921276) Avail: CASI HC A14/MF A03

The proceedings of the conference include the results of research and development of the photovoltaic power generation system, the wind power generation and biomass. As for the photovoltaic power generation system, reports are made on the following: power generation efficiency of the system, output characteristics of solar cell module, interconnected power system, optical properties of solar cells, solar cell array, development of intermittent flow redox batteries to be used for the photovoltaic power generation system. As to solar radiation utilization, studies on the following are made public: an optical/thermal hybrid heat collector which is designed to obtain light and heat at the same time using a solar cell as a heat collecting board, solar car, a silica gel layer used in a solar thermal utilization direct regenerating type adsorption tank, a solar greenhouse, a solar refrigerating system, solar pond, a solar energy ground thermal storage system, a solar-cell blade wind turbine as a composite system, photovoltaic-thermo composite pannels, solar house, passive solar heating. A small wind turbine generation system for mountainous regions is described. As biomass, production of tall-golden-rod is reported. DOE

N94-12868# Midwest Research Inst., Golden, CO.
PHOTOVOLTAIC SUBCONTRACT PROGRAM
Mar. 1993 319 p
(Contract DE-AC02-83CH-10093)
(DE93-000092; NREL/TP-410-5335) Avail: CASI HC A14/MF A03

This report summarizes the FY-92 progress of the subcontracted photovoltaic (PV) research and development (R&D) performed under the Photovoltaic Advanced Research and Development Project at the National

Renewable Energy Laboratory (NREL)--formerly the Solar Energy Research Institute (SERI). The mission of the national PV program is to develop PV technology for large-scale generation of economically competitive electric power in the United States. The technical sections of the report cover the main areas of the subcontract program: the Crystalline Materials and Advanced Concepts project, the Polycrystalline Thin Films project, Amorphous Silicon Research project, the Photovoltaic Manufacturing Technology (PVMaT) project, PV Module and System Performance and Engineering project, and the PV Analysis and Applications Development project. Technical summaries of each of the subcontracted programs provide a discussion of approaches, major accomplishments in FY-92, and future research directions. DOE

N94-12902# Midwest Research Inst., Golden, CO. National Renewable Energy Lab.
PHOTOVOLTAICS: CONTRACT LISTS, FISCAL YEAR 1992
Mar. 1993 112 p
(Contract DE-AC02-83CH-10093)
(DE93-000093; DOE/CH-10093/210) Avail: CASI HC A06/MF A02

US DOE's Photovoltaics Program has helped photovoltaic technologies evolve from materials and concepts in laboratories to competitive products rolling off automated assembly lines. The program is working to expand industrial capacity while continuing basic and applied technology R and D. This document is a tabulation of photovoltaics R and D that were begun, continued, or completed during this period. National laboratories or industrial, academic, and nonprofit research institutions perform the R and D activities. The document is organized first by directing organization, then by project title and individual task. Each listing provides the name of contractor, period of performance, funding, objectives, accomplishments, and FY 1993 milestones. An index of contractors is included. DOE

N94-12913# Abacus Technology Corp., Chevy Chase, MD.
TECHNOLOGY ASSESSMENTS OF ADVANCED ENERGY STORAGE SYSTEMS FOR ELECTRIC AND HYBRID VEHICLES
30 Apr. 1993 117 p
(Contract DE-AC01-91CE-50337)
(DE93-014395; DOE/CE-50337/T1) Avail: CASI HC A06/MF A02

Flywheels, hydropneumatic accumulators (in vehicles with a hydrostatic powertrain), and superconducting magnets were assessed as candidate technologies for recovering braking energy and averaging power demands in electric and hybrid vehicles. The technologies were also assessed for their suitability for fulfilling the entire energy storage requirement in vehicles. The scope of the technology assessments included the current state-of-the-art and developments anticipated within the next few years in the US and abroad. Key individuals and companies currently working on each technology contributed technical information to the study. Some of these individuals and companies are nearing the pre-production prototype stage with systems suitable for automobiles. Several have constructed systems using similar technology for other applications, including satellites and industrial equipment. DOE

N94-12914# Midwest Research Inst., Golden, CO. National Renewable Energy Lab.
PHOTOVOLTAICS: PROGRAM OVERVIEW, FISCAL YEAR 1992
Mar. 1993 39 p
(Contract DE-AC02-83CH-10093)
(DE93-000055; DOE/CH-10093/190) Avail: CASI HC A03/MF A01

The U.S. DOE's Photovoltaics program has helped photovoltaic technologies evolve from materials and concepts in the laboratories to competitive products rolling off automated assembly lines. This document is divided into the following sections: 1992 PV program accomplishments, expanding markets for photovoltaic systems, developing today's systems with utilities and industry, working with industry to advance the technology, cooperative research to improve materials and devices, selected achievements in cooperative R and D, and PV program services. DOE

N94-13093# Energy Research Corp., Danbury, CT.
CARBONATE FUEL CELL ENDURANCE: HARDWARE CORROSION AND ELECTROLYTE MANAGEMENT STATUS
C. Yuh, R. Johnsen, M. Farooque, and H. Maru 1993 15 p Presented at the 183rd Electrochemical Society Meeting, Honolulu, HI, 16-21 May 1993
(Contract DE-AC21-90MC-27168)
(DE93-013800; DOE/MC-27168/93/C0188; CONF-930571-13) Avail: CASI HC A03/MF A01

Endurance tests of carbonate fuel cell stacks (up to 10,000 hours) have shown that hardware corrosion and electrolyte losses can be reasonably controlled by proper material selection and cell design. Corrosion of stainless steel current collector hardware, nickel clad bipolar plate and aluminized wet seal show rates within acceptable limits. Electrolyte loss rate to current collector surface has been minimized by reducing exposed current collector surface area. Electrolyte evaporation loss appears tolerable. Electrolyte redistribution has been restrained by proper design of manifold seals. DOE

N94-13187*# Jet Propulsion Lab., California Inst. of Tech., Pasadena.
SURFACTANT STUDIES FOR BENCH-SCALE OPERATION Quarterly Technical Progress Report No. 1, 1 Jul. - 30 Sep. 1992
Gregory S. Hickey and Pramod K. Sharma 30 Dec. 1992 13 p
(Contract DE-AI21-92PC-92150)
(NASA-CR-194097; JPL-Publ-92-30; NAS 1.26:194097) Avail: CASI HC A03/MF A01

A phase 2 study was initiated to investigate surfactant-assisted coal liquefaction, with the objective of quantifying the enhancement in liquid yields and product quality. This publication covers the first quarter of work. The major accomplishments were: the refurbishment of the high-pressure, high-temperature reactor autoclave, the completion of four coal liquefaction runs with Pittsburgh #8 coal, two each with and without sodium lignosulfonate surfactant, and the development of an analysis scheme for the product liquid filtrate and filter cake. Initial results at low reactor temperatures show that the addition of the surfactant produces an improvement in conversion yields and an increase in lighter boiling point fractions for the filtrate. Author (revised)

N94-13214# New Energy and Industrial Technology Development Organization, Tokyo (Japan).
PROMOTION OF GEOTHERMAL ENERGY DEVELOPMENT IN 1991 Survey Report No. 30
Jan. 1993 31 p In JAPANESE
(DE93-799057; ETDE/JP-MF-93799057) Avail: CASI HC A03/MF A01

The paper investigates how hot springs are affected by drilling of environmental survey wells and blowout/injection of geothermal fluids which are incidental to the geothermal energy development in the Hakkoda west area. The hot springs in the survey are classified as follows: Sukayu hot springs; acidity-containing Al-Ca-SO4 spring, Jogakura No. 2 spring, Na-HCO3(center dot)Cl(center dot)SO4 type simple spring, Jogakura No.3 spring; alcaline/Na-HCO3 type simple spring, Kansuizawa hot spring; and Na-HCO3, Cl spring. As compared with the environmental survey in fiscal 1989 before blowout, the hot springs except the Jogakura No. 3 spring were relatively smaller in variations and brought almost stabilized results. Moreover, large variations in each survey item relating to the Jogakura No. 3 spring agreed with those at the time of stopping pumping facilities due to reduction in output of hot water, and it is hard to think that it was caused by drilling of geothermal exploratory wells. Accordingly, there are no observed effects of drilling for geothermal exploration on the neighboring hot springs. For geothermal survey, however, it is desirable to investigate hydrologic structures and then to take measures such as injection of all geothermal water into the depth of the underground. DOE

N94-13215# New Energy and Industrial Technology Development Organization, Tokyo (Japan).
PROMOTION OF GEOTHERMAL ENERGY DEVELOPMENT IN 1991 Survey Report No. 31
Jan. 1993 37 p In JAPANESE
(DE93-799058; ETDE/JP-MF-93799058) Avail: CASI HC A03/MF A01

The paper investigates hot springs in fumarolic gas in the Iwatesan west area and evaluates effects of regional development on the neighboring environment. Details of each spring--PH, total evaporation residue, and spring quality--are as follows: 7.8, 2190mg/l, and Ca(center dot)Mg-HCO3(center dot)SO4 spring for Water well No. 18; 7.4, 1285mg/l, and Na-HCO3(center dot) Cl spring for Genbu hot spring; 7.6, 471mg/l, and Na(center dot)Ca-HCO3 type simple spring for Nukumori hot spring; and 2.9, 461mg/l, and acidity-Ca-SO4 type simple spring for Matsukawa hot spring. Variations are smaller than those in fiscal 1989. Only the

Matsukawa hot spring has a large variation in its output of hot water, but a coefficient of its correlation with precipitation is 0.38. When installing a geothermal power plant, it is necessary to investigate the injection of geothermal water into the ground, hydrologic structures, etc. and to give careful consideration to the effect of the development on the sources of the hot spring. DOE

N94-13380# M-C Power Corp., Burr Ridge, IL.
MOLTEN CARBONATE FUEL CELL PRODUCT DEVELOPMENT TEST ENVIRONMENTAL ASSESSMENT/PROTECTION PLAN
Nov. 1992 13 p
(Contract DE-FC21-92MC-28065)
(DE93-000288; DOE/MC-28065/3371) Avail: CASI HC A03/MF A01

The objective of proposed action is to conduct a 250-kW product development test of M-C Power Corporation's molten carbonate fuel cell concept, at the Kaiser Permanente San Diego Medical Center. A review of the environmental impact of this test indicates the following: no impact on solid waste disposal, water quality, noise levels, floodplains, wetlands, ecology, historic areas, or socioeconomic resources. Impacts on air quality are expected to be positive. DOE

N94-13381# Midwest Research Inst., Golden, CO. National Renewable Energy Lab.
REFLECTIVE COATINGS FOR SOLAR APPLICATIONS
G. Jorgensen May 1993 9 p Presented at the 36th Annual Society of Vacuum Coaters Technical Conference, Dallas, TX, 27-29 Apr. 1993
(Contract DE-AC02-83CH-10093)
(DE93-010026; NREL/TP-471-5536; CONF-9304149-1) Avail: CASI HC A02/MF A01

Many applications of solar energy require large mirrors to provide high levels of concentrated sunlight. The success of such conversion systems hinges on the optical durability and economic viability of the reflector materials. A major effort at the National Renewable Energy Laboratory (NREL) has been to improve the existing reflector materials technology and to identify candidates that retain optical performance and durability criteria and offer potential for reduced cost. To attain the goals, it is desirable to maintain and increase the involvement of industrial organizations in reflective materials R&D related to the conversion of solar resources to useful energy. Toward this end, NREL has recently initiated several collaborative efforts with industry to develop advanced reflector materials. DOE

N94-13386# Midwest Research Inst., Golden, CO. National Renewable Energy Lab.
LOW TEMPERATURE METAL-ORGANIC CHEMICAL VAPOR DEPOSITION GROWTH PROCESSES FOR HIGH EFFICIENCY SOLAR CELLS Ph.D. Thesis, 1988 Final Technical Report, 1 Sep. 1985 - 30 Nov. 1989
Qisheng Chen and P. D. Dapkus (California Univ., Los Angeles.) Feb. 1993 288 p
(Contracts DE-AC02-83CH-10093; N00014-89-J-1229)
(DE92-010562; NREL-TP-451-4853) Avail: CASI HC A13/MF A03

This report describes the results of a program to develop a more complete understanding of the physical and chemical processes involved in low-temperature growth of III-V compounds by metal-organic chemical vapor deposition (MOCVD) and to develop a low-temperature process that is suitable for the growth of high-efficiency solar cells. The program was structured to develop a better understanding of the chemical reactions involved in MOCVD growth, to develop a model of the processes occurring in the gas phase, to understand the physical kinetics and reactions operative on the surface of the growing crystal, and to develop an understanding of the means by which these processes may be altered to reduce the temperature of growth and the utilization of toxic hydrides. The basic approach was to develop the required information about the chemical and physical kinetics operative in the gas phase and on the surface by the direct physical measurement of the processes whenever possible. The program included five tasks: (1) MOCVD growth process characterization; (2) photoenhanced MOCVD studies; (3) materials characterization; (4) device fabrication and characterization; and (5) photovoltaic training. Most of the goals of the program were met and significant progress was made in defining an approach that would allow both high throughput and high uniformity growth of compound semiconductors at low temperatures. The technical activity was focused on determining the rates of thermal decomposition of trimethyl gallium, exploring alternate arsenic sources for use MOCVD, and empirical studies of atomic layer epitaxy as an approach. Author

N94-13402# Los Alamos National Lab., NM.
ELECTROCATALYSIS ISSUES IN POLYMER ELECTROLYTE FUEL CELLS
M. S. Wilson, C. R. Derouin, J. A. Valerio, and S. Gottesfeld 1993 7 p Presented at the 28th Intersociety Energy Conversion Engineering Conference, Atlanta, GA, 8-13 Aug. 1993
(Contract W-7405-eng-36)
(DE93-014450; LA-UR-93-1689; CONF-930804-2) Avail: CASI HC A02/MF A01

Various electrocatalysis issues of importance to low platinum loading polymer electrolyte fuel cells (PEFCs) are discussed. Thin film catalyst layer assemblies are used to investigate the effects of CO and CO2 on the anode as well as efforts to restore performance by oxygen bleeding into the anode feedstream. These electrodes behave differently than ionomer-impregnated E-TEK electrodes because of the extra, exposed Pt in the latter case. The tolerance of Pt-Ru alloy thin film anodes to CO and CO2 are also evaluated. Thin film electrodes are also used to study Pt particle growth in aged electrodes as well as particle size effects on specific activity. DOE

N94-13403# Los Alamos National Lab., NM.
HOT DRY ROCK ENERGY Annual Report, Fiscal Year 1992
W. W. Winchester, ed. Apr. 1993 80 p
(Contract W-7405-eng-36)
(DE93-014452; LA-UR-93-1678) Avail: CASI HC A05/MF A01

Hot Dry Rock technology took a giant leap forward this year as the long-awaited long-term flow test (LTFT) of the Phase 2 HDR reservoir at Fenton Hill got underway. Energy was produced on a twenty-four hour a day basis for a continuous period of nearly four months of steady-state testing. Hot water was brought to the surface at 90-100 gallons per minute (gpm) with temperatures of 180 C (356 F) and higher. During that time, the HDR plant achieved an on-line record of 98.8%. Surface temperature measurements and temperature logging deep within the wellbore confirmed that no decline in the average temperature of fluid produced from the reservoir occurred. Tracer experiments indicated that flow paths within the reservoir were undergoing continuous change during the test. Remarkably, it appeared that longer flow paths carried a larger proportion of the flow as the test proceeded, while more direct fluid pathways disappeared or carried a significantly reduced flow. In sum, access to hot rock appeared to improve over the span of the test. Water losses during the test averaged 10-12% and showed a slow long-term decline. These results confirmed what had been previously discovered in static pressurization testing: water consumption declines significantly during extended operation of an HDR reservoir. In combination with a recent demonstration by the Japanese that water losses can be greatly reduced by the proper placement of multiple production wells, the recent results at Fenton Hill have effectively demonstrated that excessive water consumption should not be an issue for a properly engineered HDR facility at a well chosen site. DOE

N94-13570 Tel-Aviv Univ. (Israel). Dept. of Electrical Engineering - Systems.
FIELD OF SOLAR COLLECTORS: EFFECT OF SHADOWING ON THE OPTIMAL FIELD DESIGN M.S. Thesis
Marcos Crutchik Jan. 1992 216 p
(ITN-93-85197) Copyright Avail: Issuing Activity (Tel-Aviv Univ., Exact Sciences Library, Ramat Aviv 69978, Israel)

For a field of solar energy collectors, the effects on energy output of mutual and self-shading of the collectors are analyzed, in relation to the physical parameters of the field. Among the parameters considered are the spacing between the collectors, the tilt and azimuth angles of the collectors and the slope and orientation of the field. The self-shading of convex and concave collectors and the special case of the new catenary-tent collector, conceived for eventual use on non-terrestrial planets are also considered. The results of the shading analysis are used to determine the optimal deployment of an arbitrarily oriented and sloped field of stationary collectors. The optimization criteria considered were: maximum energy output; minimum plant cost and minimum produced energy cost. The deployment

parameters considered for each of these criteria were number and spacing of rows and tilt angle of the collectors. For the first criterion a fixed field area was considered; for the other two, both fixed and unlimited land dimensions were considered. In every case, yearly average and worst month (January) insolation figures were considered. The optimizations based on maximum energy output or minimum energy cost led to higher initial plant costs, owing to the larger number of rows required, but led to lower costs of produced energy. The solution which minimized the plant cost led to the highest cost of produced energy. A sensitivity analysis covering all the parameters showed that variations in the individual collector parameters (collector height, length and efficiency) have the most effect on the optimal solution. ISA

N94-13639 Wayne State Univ., Detroit, MI.
THE 1.00 MeV PROTON RADIATION RESISTANCE STUDIES OF AMORPHOUS SILICON-BASED ALLOY SOLAR CELLS Ph.D. Thesis
Salman Saib Abdulaziz 1992 230 p
Avail: Univ. Microfilms Order No. DA9310613

Amorphous silicon based (a-Si) alloy solar cells have been proposed as candidates for space applications. However, before space-born applications of a-Si cells can take place, the influence of the harsh space environment on the cells operating characteristics needs to be determined. The focus of this work is to investigate and model the effects of 1.00 MeV proton irradiation in the fluence range 10(exp I4) to 10(exp I5) cm(exp -2) and their annealing in the temperature range 0 to 200 C on the current density-voltage (J-V) and quantum efficiency (QE) characteristics of a-Si solar cells. 1.00 MeV protons degrade the J-V characteristics of a-Si cells. Single-junction a-Si:H cells show higher radiation resistance than either single-junction a-Si(sub x)Ge(sub I-x):H or dual-junction a-Si:H cells. The J(sub SC) is related to the fluence and electron drift-length/i-layer thickness ratio. The FF and eta/eta(sub O) are modeled as a function of fluence. Our experimental results were generally found to be in harmony with our simple models. Significant annealing of the J-V characteristics were observed at temperatures of 0 C and 22 C. A one-hour anneal at 200 C restored the J-V characteristics of the a-Si cells to their virgin values. Using first-order kinetics, the annealing of Jsc, FF and Eta/Eta(sub O) were modeled as a function of fast and slow annealing defects, and good agreement was found. The 1.00 MeV protons degraded the QE in a non-uniform fashion. The peak of the QE shifted toward the blue end of the spectrum. The QE of the a-Si cells was modeled as a function of thickness and electron drift-length. The experimental data were found to be in acceptable agreement with our simple model. The J(sub SC) was calculated from the convolution of the QE and AM1.5G spectrum. An average error of 45.3 percent (QE measured without light bias), and 6.8 percent (light biased QE) was observed between the calculated and measured J(sub SC). The J(sub SC) under AM0 illumination was calculated from the measured J(sub SC) under AM1.5G illumination . Author

N94-13691# Westinghouse Savannah River Co., Aiken, SC.
MATERIALS COMPATIBILITY OF HYDRIDE STORAGE MATERIALS WITH AUSTENITIC STAINLESS STEELS
E. A. Clark 21 Sep. 1992 26 p
(Contract DE-AC09-89SR-18035)
(DE93-013688; WSRC-TR-92-438) Avail: CASI HC A03/MF A01

This task evaluated the materials compatibility of LaNi(5-x)Al(x) (x= 0.3, 0.75) hydrides and palladium coated kieselguhr with austenitic stainless steel in hydrogen and tritium process environments. Based on observations of retired prototype hydride storage beds and materials exposure testing samples designed for this study, no materials compatibility problem was indicated. Scanning electron microscopy observations of features on stainless steel surfaces after exposure to hydrides are also commonly found on as-received materials before hydriding. These features are caused by either normal heat treating and acid cleaning of stainless steel or reflect the final machining operation. DOE

N94-13693# Energy Research Corp., Danbury, CT.
PERFORMANCE EFFECTS OF COAL-DERIVED CONTAMINANTS ON THE CARBONATE FUEL CELL
A. Pigeaud and G. Wilemski (Physical Sciences, Inc., Andover, MA.) 1993 20 p Presented at the 3rd International Symposium on Carbonate Fuel Cell Technology, Honolulu, HI, 16-21 May 1993
(Contract DE-AC21-90MC-27168)
(DE93-013801; DOE/MC-27168/93/C0189; CONF-9305101-1) Avail: CASI HC A03/MF A01

Coal-derived contaminant studies have been pursued at ERC since the early 1980's when the pace of carbonate fuel cell development began to markedly increase. Initial work was concerned with performance effects on laboratory and bench-scale carbonate fuel cells primarily due to sulfur compounds. Results have now also been obtained with respect to nine additional coal-gas contaminants, including volatile trace metal species. Thermochemical calculations, out-of-cell experiments, and cell performance as well as endurance tests have recently been conducted which have involved the following species: NH3, H2S (COS), HCl, AsH3(As2(v)), Zn(v), Pb(v), Cd(v), H2Se, Hg(v), Sn(v). Employing thermochemically calculated results, thermogravimetric (TGA) and pre-, and post-test analytical data as well as fuel cell performance observations, it has been shown that there are four main mechanisms of contaminant interaction with the carbonate fuel cell. These have been formulated into performance models for six significant contaminant species, thus providing long-term endurance estimations. DOE

N94-13886# Sandia National Labs., Albuquerque, NM.
EMITTER WRAP-THROUGH SOLAR CELL
J. M. Gee, W. K. Schubert, and P. A. Basore 1992 6 p Presented at the 23rd Institute of Electrical and Electronics Engineers (IEEE) Photovoltaic Specialists Conference, Louisville, KY, 10-14 May 1993
(Contract DE-AC04-76DP-00789)
(DE93-014996; SAND-92-2872C; CONF-930540-3) Avail: CASI HC A02/MF A01

The authors present a new cell concept (Emitter Wrap-Through or EWT) for a back-contact cell. The cell has laser-drilled vias to wrap the emitter on the front surface to contacts on the back surface and uses a potentially low-cost process sequence. Modeling calculations show that efficiencies of 18 and 21% are possible with large-area solar-grade multi- and monocrystalline silicon EWT cells, respectively. DOE

N94-13940*# Jet Propulsion Lab., California Inst. of Tech., Pasadena.
THE LARGE AREA PULSED SOLAR SIMULATOR (LAPSS)
R. L. Mueller 15 Aug. 1993 12 p
(Contract NAS7-918)
(NASA-CR-194507; JPL-Publ-93-22; NAS 1.26:194507) Avail: CASI HC A03/MF A01

A Large Area Pulsed Solar Simulator (LAPSS) has been installed at JPL. It is primarily intended to be used to illuminate and measure the electrical performance of photovoltaic devices. The simulator, originally manufactured by Spectrolab, Sylmar, California, occupies an area measuring about 3 meters wide by 12 meters long. The data acquisition and data processing subsystems have been modernized. Tests on the LAPSS performance resulted in better than +/- 2 percent uniformity of irradiance at the test plane and better than +/- 0.3 percent measurement repeatability after warm-up. Glass absorption filters are used to reduce the level of ultraviolet light emitted from the xenon flash lamps. This provides a close match to standard airmass zero and airmass 1.5 spectral irradiance distributions. The 2 millisecond light pulse prevents heating of the device under test, resulting in more reliable temperature measurements. Overall, excellent electrical performance measurements have been made of many different types and sizes of photovoltaic devices. Author (revised)

N94-13997# Technische Univ., Berlin (Germany). Fachbereich fuer Elektrotecknik.
NUMERICAL SIMULATION AND ANALYSIS OF ELECTRICAL AND OPTICAL PROPERTIES OF Al(x)Ga(1-x)As / GaAs Ph.D. Thesis [NUMERISCHE SIMULATION UND ANALYSE DER ELEKTRISCHEN UND OPTISCHEN EIGENSCHAFTEN VON ALXGA(1-X)AS/GAAS-SOLARZELLEN]
Heinz Eschrich 1992 123 p In GERMAN
(ETN-93-94387) Avail: CASI HC A06/MF A02

A numerical algorithm for description of gallium arsenide solar cells behavior with photovoltaic active window layer is developed. A partial nonlinear differential equation system, based on current, balance and Poisson equations, was solved using finite difference method. Spatial distributions of charge carrier concentration and potential were calculated using a recursive and iterative solution algorithm. Reflexion losses at all phase

boundaries were determined using a matrix method. Solution algorithm was tested considering results of an analytical model of a solar cell with abrupt pn transition. From results of analytic optimization calculations, an improved structure was obtained, with a thinner emitter of 820 nm. The influence of surface and boundary recombination, diffusion length and cell geometry on spectral internal quantum efficiency was simulated. ESA

N94-14109# Midwest Research Inst., Golden, CO. National Renewable Energy Lab.

CONTINUOUS ROLL-TO-ROLL a-Si PHOTOVOLTAIC MANUFACTURING TECHNOLOGY

M. Izu Apr. 1993 52 p Prepared in cooperation with Energy Conversion Devices, Inc., Troy, MI

(Contract DE-AC02-83CH-10093)

(DE93-010006; NREL/TP-411-5453) Avail: CASI HC A04/MF A01

This report describes work performed by ECD to accomplish the following goals: to advance its roll-to-roll, triple-junction photovoltaic manufacturing technologies; to reduce the module production costs; to increase the stabilized module performance; and to expand the commercial capacity utilizing ECD technology. The 3-year goal is to develop advanced large-scale manufacturing technology incorporating ECD's earlier research advances with the capability of producing modules with stable 11% efficiency at a cost of approximately $1/W(sub p). Major efforts during Phase 1 are as follows: (1) the optimization of the high-performance back-reflector system, (2) the optimization of a-Si-Ge narrow band-gap solar cell, and (3) the optimization of the stable efficiency of the module. The goal is to achieve a stable 8% efficient 0.3-m (times) 1.2-m (1-ft (times) 4-ft) module. Also, the efforts include work on a proprietary, high-deposition-rate, microwave plasma, CVD manufacturing technology and on the investigation of material cost reduction. DOE

N94-14110# Midwest Research Inst., Golden, CO. National Renewable Energy Lab.

OPTIMIZATION OF TRANSPARENT AND REFLECTING ELECTRODES FOR AMORPHOUS SILICON SOLAR CELLS

R. G. Gordon Apr. 1993 101 p Prepared in cooperation with Energy Conversion Devices, Inc., Troy, MI

(Contract DE-AC02-83CH-10093)

(DE93-010009; NREL/TP-411-5456) Avail: CASI HC A06/MF A02

This report describes work to improve the performance of solar cells by improving the electrical and optical properties of their transparent conducting oxide (TCO) layers. Boron-doped zinc-oxide films were deposited by atmospheric pressure chemical vapor deposition in a laminar-flow reactor from diethyl zinc, tert-butanol, and diborane in the temperature range between 300 C and 420 C. When the deposition temperature was above 320 C, both doped and undoped films have highly oriented crystallites with their c-axes perpendicular to the substrate plane. Films deposited from 0.07% diethyl zinc and 2.4% tert-butanol have electron densities between 3.5 x 10(exp 20)/cu cm and 5.5 x 10(exp 20)/cu cm, conductivities between 250/Omega and 2500/Omega and mobilities between 2.5 sq cm/V-s and 35.0 sq cm/V-s, depending on dopant concentration, film thickness, and deposition temperature. Optical measurements show that the maximum infrared reflectance of the doped films is close to 90%, compared to about 20% for undoped films. Film visible absorption and film conductivity were found to increase with film thickness. The ratio of conductivity to visible absorption coefficient for doped films was between 0.1 Omega and 1.1/Omega. The band gap of the film changes from 3.3 eV to 3.7 eV when the film is doped with 0.012% diborane. DOE

N94-14333# California Univ., Berkeley. Lawrence Berkeley Lab.

SIMULATING THE DAYLIGHT PERFORMANCE OF FENESTRATION SYSTEMS AND SPACES OF ARBITRARY COMPLEXITY: THE IDC METHOD

K. Papamichael and L. Beltran Apr. 1993 5 p Presented at the 3rd International Conference of the International Building Performance Simulation Association, Adelaide, Australia, 16-18 Aug. 1993

(Contract DE-AC03-76SF-00098)

(DE93-015177; LBL-33945; CONF-9308111-1) Avail: CASI HC A01/MF A01

A new method to simulate the daylight performance of fenestration systems and spaces is presented. This new method, named IDC (Integration of Directional Coefficients), allows the simulation of the daylight performance of fenestration systems and spaces of arbitrary complexity, under any sun, sky, and ground conditions. The IDC method is based on the combination of scale model photometry and computer-based simulation. Physical scale models are used to experimentally determine a comprehensive set of 'directional illuminance coefficients' at reference points of interest, which are then used in analytical, computer-based routines, to determine daylight factors or actual daylight illuminance values under any sun, sky, and ground conditions. The main advantage of the IDC method is its applicability to any optically complex environment. Moreover, the computer-based analytical routines are fast enough to allow for hourly simulation of the daylight performance over the course of an entire year. However, the method requires appropriate experimental facilities for the determination of the Directional Coefficients. The IDC method has been implemented and used successfully in inter-validation procedures with various daylight simulation computer programs. Currently, it is used to simulate the daylight performance of fenestration systems that incorporate optically complex components, such as Venetian blinds, optically treated light shelves and light pipes. DOE

N94-14350# Midwest Research Inst., Golden, CO.

PHOTOVOLTAIC ADVANCED RESEARCH AND DEVELOPMENT PROJECT: SOLAR RADIATION RESEARCH Annual Report, 1 Oct. 1990 - 30 Sep. 1991

R. Hulstrom, T. Cannon, T. Stoffel, and C. Riordan Oct. 1992 17 p

(Contract DE-AC02-83CH-10093)

(DE92-016430; NREL/TP-411-5013) Avail: CASI HC A03/MF A01

This report is a summary of 1991's research activities and results under the Solar Radiation Research task of the Photovoltaic (PV) Advanced Research and Development project at the National Renewable Energy Laboratory (NREL). This task directly supports the characterization, testing, and design of PV cells modules, and systems. The development of a scientific and engineering understanding of incident (i.e., available to PV devices) solar irradiance and the appropriate instrumentation systems and measurement methods are the activities and results of this project. Activities described in this report include the completion of the Atmospheric Optical Calibration Systems (AOCS) and the comparison of instrumentation systems that collect site-specific measurements of solar irradiance for the purpose of PV system feasibility studies and/or design. DOE

N94-14355# Department of Energy, Morgantown, WV. Energy Technology Center.

STATUS OF SOFC DEVELOPMENT IN USA

D. T. Hooie 1993 5 p Presented at the 3rd International Symposium on Carbonate Fuel Cell Technology, Honolulu, HI, 16-21 May 1993

(DE93-015568; DOE/METC-C/93/7083; CONF-9305101-3) Avail: CASI HC A01/MF A01

Solid oxide fuel cells represent a highly efficient power generation/cogeneration source in the United States and worldwide. Currently, the US is a leader in this technology in the tubular, monolithic, and planar solid oxide fuel cell areas. In addition, research is being conducted in intermediate temperature solid oxide fuel cells. An overview of the status of these technologies, research, and critical issues is presented. DOE

N94-14422# Midwest Research Inst., Golden, CO.

NREL SOLAR RADIATION RESOURCE ASSESSMENT PROJECT: STATUS AND OUTLOOK

D. Renne, E. Maxwell, T. Stoffel, B. Marion, M. Rymes, S. Wilcox, D. Myers, C. Riordan, E. Hammond, and T. Ismailidis Jun. 1993 71 p

(Contract DE-AC02-83CH-10093)

(DE93-010034; NREL/TP-463-5428) Avail: CASI HC A04/MF A01

This annual report discusses the activities and accomplishments of the Solar Radiation Resource Assessment Project during FY-92 (1 Oct. to 30 Sep. 1992). Managed by the Analytic Studies Division of the National Renewable Energy Laboratory, this project is the major activity of the US Department of Energy's Resource Assessment Program. DOE

N94-14423# Midwest Research Inst., Golden, CO.

INFLOW CHARACTERISTICS ASSOCIATED WITH HIGH-BLADE-LOADING EVENTS IN A WIND FARM

N. D. Kelley Jul. 1993 12 p Presented at the 25th IEA Experts Meeting: Increased Loads in Wind Power Stations, Wind Farms, Gothenburg,

Sweden, 3-4 May 1993
(Contract DE-AC02-83CH-10093)
(DE93-010042; NREL/TP-442-5623; CONF-9305243-1) Avail: CASI HC A03/MF A01

The stochastic characteristics of the turbulent inflow have been shown to be of major significance in the accumulation of fatigue in wind turbines. Because most of the wind turbine installations in the U.S. have taken place in multi-turbine or windfarm configurations, the fatigue damage associated with the higher turbulence levels within such arrangements must be taken into account when making estimates of component service lifetimes. The simultaneous monitoring of two adjacent wind turbines over a wide range of turbulent inflow conditions has given the authors more confidence in describing the structural load distributions that can be expected in such an environment. The adjacent testing of the two turbines allowed the authors to postulate that observed similarities in the response dynamics and load distributions could be considered quasi-universal, while the dissimilarities could be considered to result from the differing design of the rotors. The format has also allowed them to begin to define appropriate statistical load distribution models for many of the critical components in which fatigue is a major driver of the design. In addition to the adjacent turbine measurements, they also briefly discuss load distributions measured on a teetered-hub turbine. DOE

N94-14430*# Dynamic Systems Research and Training Corp., Huntsville, AL.
EXPERIMENTAL INSTRUMENTATION SYSTEM FOR THE PHASED ARRAY MIRROR EXTENDIBLE LARGE APERTURE (PAMELA) TEST PROGRAM Final Report, 10 May - 30 Sep. 1993
William H. Boykin, Jr. 30 Sep. 1993 19 p
(Contract NAS8-39218)
(NASA-CR-194421; NAS 1.26:194421; TR-HSV-93-0002) Avail: CASI HC A03/MF A01

Adaptive optics are used in telescopes for both viewing objects with minimum distortion and for transmitting laser beams with minimum beam divergence and dance. In order to test concepts on a smaller scale, NASA MSFC is in the process of setting up an adaptive optics test facility with precision (fraction of wavelengths) measurement equipment. The initial system under test is the adaptive optical telescope called PAMELA (Phased Array Mirror Extendible Large Aperture). Goals of this test are: assessment of test hardware specifications for PAMELA application and the determination of the sensitivities of instruments for measuring PAMELA (and other adaptive optical telescopes) imperfections; evaluation of the PAMELA system integration effort and test progress and recommended actions to enhance these activities; and development of concepts and prototypes of experimental apparatuses for PAMELA. Derived from text

N94-14504# Colorado State Univ., Fort Collins. Solar Energy Applications Lab.
COLORADO STATE UNIVERSITY PROGRAM FOR DEVELOPING, TESTING, EVALUATING, AND OPTIMIZING SOLAR HEATING AND COOLING SYSTEMS
Jun. 1993 11 p
(Contract DE-FG02-86SF-16306)
(DE93-016018; DOE/SF-16306/36) Avail: CASI HC A03/MF A01

Results of heat loss tests for the Integral Collector Storage Unit are shown. Work on unique solar system components is summarized briefly. DOE

N94-14510# Lawrence Livermore National Lab., CA.
BIOMIMETIC METHANE OXIDATION
B. E. Watkins, M. W. Droege, R. T. Taylor, and J. H. Satcher 12 Jun. 1992 8 p Presented at the International Gas Research Conference, Orlando, FL, 16-19 Nov. 1992
(Contract W-7405-eng-48)
(DE93-013196; UCRL-JC-110675; CONF-921152-14) Avail: CASI HC A02/MF A01

Methane monooxygenase (MMO) is an enzyme found in methanotrophs that catalyses the selective oxidation of methane to methanol. MMO is protein complex one component of which is a binuclear metal center containing oxygenase. We have completed one round of a design/synthesis/evaluation cycle in the development of coordination complexes that mimic the structure/function of the MMO active site. One of these, a binuclear, coordinately-asymmetric copper complex, is capable of oxidizing cyclohexane to a mixture of cyclohexanol and cyclohexanone in the presence of hydrogen peroxide. DOE

N94-14679# New Energy and Industrial Technology Development Organization, Tokyo (Japan).
PROMOTION OF GEOTHERMAL ENERGY DEVELOPMENT IN 1991 Survey Report No. 38
Jan. 1993 211 p In JAPANESE
(DE93-799061; ETDE/JP-MF-93799061) Avail: CASI HC A10/MF A03

The paper evaluates effects of geothermal energy exploration activities on the environment in the Mt. Aso west area. At survey points, H2S and SO2 are detected. Hg is 0.002-0.038 micro-g/cu m. Quality of river water is pure at each point. Most of the survey area is occupied by substitutional community like grassland, afforestation, etc. For geothermal development, it is necessary to pay attention to the protection of regions where natural vegitation is distributed and to make the deforestation area necessary and minimum. If the geothermal power plant is installed, it contributes further to the region in terms of employment and finance based on the development of the local industry. It is estimated that the five hot springs are formed by the heating of ground water, which originates as rain water, or by heating of the meteoric water which permeates the underground. For development, it is necessary to take measures to inject the output of the geothermal water into the deep underground. DOE

N94-14861# Sandia National Labs., Albuquerque, NM.
MULTICRYSTALLINE SILICON SOLAR CELLS: GETTERING OPTIMIZATION AND CHARACTERIZATION
W. K. Schubert 1993 6 p Presented at the 23rd Institute of Electrical and Electronics Engineers (IEEE) Photovoltaic Specialists Conference, Louisville, KY, 10-14 May 1993
(Contract DE-AC04-76DP-00789)
(DE93-015001; SAND-92-2868C; CONF-930540-7) Avail: CASI HC A02/MF A01

Three multicrystalline silicon materials were used in preliminary experiments in preparation for a planned comprehensive gettering study on several industrial solar cell materials. Two processes commonly used to upgrade material quality were investigated: phosphorus gettering and aluminum-alloying. Microwave-detected photoconductance decay measurements of minority carrier lifetime and detailed analyses of full solar cells were used to determine the response to the gettering processes. Lateral nonuniformities were shown to be significant in these multicrystalline materials. Identification of the nature of the nonuniformities is important in developing an understanding of gettering effects. DOE

45 ENVIRONMENT POLLUTION

Includes atmospheric, noise, thermal, and water pollution.

N94-12869# Brookhaven National Lab., Upton, NY.
GATHERING AND EXCHANGE INFORMATION ON ATMOSPHERIC CHEMISTRY AND POLLUTED ATMOSPHERES
L. Newman 30 Oct. 1992 12 p
(Contract DE-AC02-76CH-00016)
(DE93-009940; BNL-70246) Avail: CASI HC A03/MF A01 (US Sales Only)

Detailed examination and information was obtained concerning the Netherlands Energy Research Foundation designed Wet Annular Denuder that is used for the determination of ammonia, nitric acid, and sulfur dioxide. We are now actively considering whether to borrow and or purchase an instrument for use in our field campaigns. If done, it will be the first such instrument deployed in the U.S. Highlights from the 4 German institutes visited include information on the following topics: sophisticated deployment of OH measuring capabilities involving lasers--including laser induced fluorescence, long path UV, and differential optical absorption; tunable diode lasers utilized to measure a variety of substances; field investigations directed at elucidating cloud processes and reactions in ground based fogs; and extensive use of spectroscopy to measure elemental and gaseous pollutants. DOE

N94-12904# Department of Energy, New York, NY. Environmental Measurements Lab.
PROJECT AIRSTREAM: TRACE GAS Final Report
R. Leifer Dec. 1992 164 p
(DE93-008849; EML-549) Avail: CASI HC A08/MF A02

The results of 10 years of sampling for trace gases in the upper troposphere and lower stratosphere are presented. These samples were collected under the auspices of the Atomic Energy Commission (AEC), the Energy Research and Development Administration (ERDA), and the Department of Energy (DOE). Almost 1000 whole air samples were collected during the years 1973 to 1983 under Project AIRSTREAM. Project AIRSTREAM was part of the Environmental Measurements Laboratory's (EML, at that time called the Health and Safety Laboratory/HASL) research effort to investigate the impact of the injection of radionuclides and stable compounds into the stratosphere. One or more of the following compounds were analyzed: CCl3F, CCl2F2, CCl4, N2O, SF6, CO2, CH4, CH3CCl3, and COS. Details of the Project's quality assurance program are discussed. Also included in the report are two-dimensional plots of the concentration of CCl3F and a complete tabulation of the data. DOE

N94-12905# Pacific Northwest Lab., Richland, WA.
SOIL EROSION RATES CAUSED BY WIND AND SALTATING SAND STRESSES IN A WIND TUNNEL
M. W. Ligotke Feb. 1993 83 p
(Contract DE-AC06-76RL-01830)
(DE93-009154; PNL-8478) Avail: CASI HC A05/MF A01

Wind erosion tests were performed in a wind tunnel in support of the development of long-term protective barriers to cap stabilized waste sites at the Hanford Site. Controlled wind and saltating sand erosive stresses were applied to physical models of barrier surface layers to simulate worst-case eolian erosive stresses. The goal of these tests was to provide information useful to the design and evaluation of the surface layer composition of an arid-region waste site barrier concept that incorporates a deep fine-soil reservoir. A surface layer composition is needed that will form an armor resistant to eolian erosion during periods of extreme dry climatic conditions, especially when such conditions result in the elimination or reduction of vegetation by water deprivation or wildfire. Because of the life span required of Hanford waste barriers, it is important that additional work follow these wind tunnel studies. A modeling effort is planned to aid the interpretation of test results with respect to the suitability of pea gravel to protect the finite-soil reservoir during long periods of climatic stress. It is additionally recommended that wind tunnel tests be continued and field data be obtained at prototype or actual barrier sites. Results wig contribute to barrier design efforts and provide confidence in the design of long-term waste site caps for and regions. DOE

N94-12937# Pacific Northwest Lab., Richland, WA.
A REVIEW OF THE GLOBAL EMISSIONS, TRANSPORT, AND EFFECTS OF HEAVY METALS IN THE ENVIRONMENT
J. R. Friedman, W. B. Ashton, and R. D. Rapoport May 1993 38 p
(Contract DE-AC06-76RL-01830)
(DE93-013507; PNL-SA-22394) Avail: CASI HC A03/MF A01

The purpose of this report is to describe the current state of knowledge regarding the sources and quantities of heavy metal emissions, their transport and fate, their potential health and environmental effects, and strategies to control them. The approach is to review the literature on this topic and to consult with experts in the field. Ongoing research activities and research needs are discussed. DOE

N94-13054# Brookhaven National Lab., Upton, NY.
THE NORTH ATLANTIC REGIONAL EXPERIMENT (NARE)
P. Daum 22 Mar. 1993 4 p
(Contract DE-AC02-76CH-00016)
(DE93-010126; BNL-70309) Avail: CASI HC A01/MF A01 (US Sales Only)

A planning meeting for the North Atlantic Regional Experiment (NARE) summer 1993 field intensive was attended. The meeting was held at the University of East Anglia, Norwich, England from January 26--29, 1993. The meeting was organized by Stuart Penkett, and was attended by scientists from both North America and Europe. The summer intensive will be conducted during the month of August. Participating North American scientists will focus efforts on measurements along the northeastern coast of the US and in Nova Scotia. They will also support surface measurements in the Azores, Iceland, and in Bermuda. At least three instrumented aircraft will contribute to the North American effort. European activities will focus on the British Meteorological Office C-130 aircraft. The Europeans will also activate a number of existing sites to measure ozone concentration profiles. The coordination between measurements conducted on either side of the Atlantic will not be close because of the lack of meteorological data in the mid-Atlantic which would allow prediction of transoceanic transport. DOE

N94-13079# New York Univ., New York. Dept. of Applied Science.
THE ROLE OF CLOUDS AND OCEANS IN GLOBAL GREENHOUSE WARMING
M. I. Hoffert Dec. 1992 21 p
(Contract DE-FG02-90ER-61014)
(DE93-016206; DOE/ER-61014/3) Avail: CASI HC A03/MF A01

During the past three years we have conducted several studies using models and a combination of satellite data, in situ meteorological and oceanic data, and paleoclimate reconstructions, under the DoE program, 'Quantifying the Link Between Change in Radiative Balance and Atmospheric Temperature.' Our goals were to investigate the effects of global cloudiness variations on global climate and their implications for cloud feedback and continue development and application of NYU transient climate/ocean models, with emphasis on coupled effects of greenhouse warming and feedbacks by both the clouds and oceans. Our original research plan emphasized the use of cloud, surface temperature, and ocean data sets interpreted by focused climate/ocean models to develop a cloud radiative forcing scenario for the past 100 years and to assess the transient climate response; to narrow key uncertainties in the system; and to identify those aspects of the climate system most likely to be affected by greenhouse warming over short, medium, and long time scales. DOE

N94-13095# Lawrence Livermore National Lab., CA.
THE FOOTPRINT AREA INFLUENCING A HIGH-VOLUME AIR SAMPLER
J. Shinn and F. Gouveia Oct. 1992 6 p
(Contract W-7405-eng-48)
(DE93-013947; UCRL-ID-112181) Avail: CASI HC A02/MF A01

A recent question posed by air sampling analysts is how to calculate the source area that contributes to the collection of material by a high-volume (HV) air sampler. In micrometeorology studies theoretical and numerical approaches have been used to determine the 'footprint' of an atmospheric flux from the ground that influences a sensor at any given height. Over the course of a few days or more, the influence of atmospheric stability on a high volume air sampler run can be neglected. For surfaces that have dense vegetative cover, the boundary layer is displaced upward by the vegetation height and the roughness is proportional to the vegetation height. It can be concluded that for typical surface conditions, the HV air sampler is 90% influenced by material flux from the surface less than 145-175 m upwind. For rougher surfaces, the upwind bounded distances are shorter. There may be some very specialized cases (e.g., empty parking lots) where the upwind bounded distances are much greater. DOE

N94-13170*# Georgia Inst. of Tech., Atlanta. School of Earth and Atmospheric Sciences.
DIAGNOSTIC STUDIES OF THE HxOy-NxOy-O3 PHOTOCHEMICAL SYSTEM USING DATA FROM NASA GTE FIELD EXPEDITIONS Final Report, 1 Jul. 1987 - 31 Jul. 1990
W. L. Chameides 7 Sep. 1990 6 p
(Grant NAG1-786)
(NASA-CR-193672; NAS 1.26:193672) Avail: CASI HC A02/MF A01

The research effort supported in part by the subject grant focused on three related topics. Our major effort was concentrated on the analysis of data gathered during GTE field expeditions. Ancillary efforts were directed at: the development and application of a Global Chemical Transport Model for the study of the atmospheric reactive nitrogen budget; the development and application of a one-dimensional, time dependent cloud model for the study of the impact of in-cloud aqueous phase chemistry on the atmospheric sulfur budget; and mechanistic studies of the chemical processes involved in dry deposition of ozone to vegetative surfaces. In the sections below, we briefly summarize the central conclusions of each of these efforts. These discussions are followed by a listing of the papers completed during

the granting period and the graduate students supported by funds from the grant. Reprints and preprints of all papers completed with support from the grant are attached as appendices. Author (revised)

N94-13218# National Fertilizer Development Center, Muscle Shoals, AL.
ENVIRONMENTAL AWARENESS
1992 38 p
(DE93-014192; TVA/NFERC-92/6; TVA-Bull-Y-228) Avail: CASI HC A03/MF A01

This brochure is intended to provide guidance on environmental regulations to National Fertilizer and Environmental Research Center (NFERC) employees. Topics covered include the following: handling of hazardous materials, disposal of hazardous wastes, spill prevention and remediation, pcb contamination, pesticide use, asbestos remediation, solid waste disposal, and environmental laws. Safety aspects are emphasized. DOE

N94-13330# Instituto de Pesquisas Espaciais, Sao Jose dos Campos (Brazil).
MODELING OF BIOSPHERE-ATMOSPHERE INTERACTION FOR FOREST AND PASTURELAND IN THE AMAZON M.S. Thesis [MODELAGEM DA INTERACAO BIOSFERA-ATMOSFERA PARA AREAS DE FLORESTA E DE PASTAGEM NA AMAZONIA]
Humberto RibeirodaRocha May 1992 145 p In PORTUGESE
(INPE-5454-TDI/496) Avail: CASI HC A07/MF A02

Along the lines of the most recent studies of deforestation in the Amazon and its impact on the climate change, such as the decrease of the local evaporation (Wright et al., 1992), and the reduction of 20 percent in the regional rainfall (Nobre et al., 1991), the biosphere model SiB is calibrated for an Amazonian pastureland, and the bearing of surface vegetation in the boundary layer structure and in the development of convection in the atmospheric column is analyzed. A one-dimensional model is used to study the interaction of vegetation-atmosphere, having 18 layers in the vertical and parameterizations of surface, turbulent vertical diffusion, short and long waves radiation, deep and shallow convection, and large scale precipitation. A comparison is made between a control model (Ctr1D), which surface parameterization is based on the similarity laws of Monin and Obukhov (1954) and Penman-Monteith concept of evaporation, coupled to a 1st order turbulent closure model in the boundary layer, with a biosphere-coupled model (SiB1D), having SiB model at the surface and a 2nd order turbulent closure scheme (Mellor and Yamada, 1982). The 24 hours simulations of SiB1D appear to show more realistic sensible and latent heat fluxes at the surface, when admissing either forest or pastureland at the Amazon and comparing with observations. In addition, the numerical solution of SiB1D is more effective in suppressing some previous oscillations found in the Ctr1D model. Simulations of SiB1D model showed the convection in the atmospheric column to be stronger upon the forest either than the pasture, leading to an increase in the precipitation from 25 to 50 percent. The resulting effects are of heating the middle troposphere up to 2.5 K, and the moistening of the boundary layer up to 2.0 g/kg, both larger upon the forest. Author (revised)

N94-13383# Argonne National Lab., IL. Environmental Assessment and Information Sciences Div.
AQUIS: A PC-BASED SOURCE INFORMATION MANAGER
A. E. Smith, C. C. Huber, J. Tschanz, and S. J. Ryckman, Jr. 1993 10 p Presented at the 86th Annual Meeting and Exhibition of the Air and Waste Management Association, Denver, CO, 13-18 Jun. 1993
(Contract W-31-109-eng-38)
(DE93-012893; ANL/EAIS/CP-78850; CONF-930647-3) Avail: CASI HC A02/MF A01

The Air Quality Utility Information System (AQUIS) was developed to calculate emissions and track them along with related information about sources, stacks, controls, and permits. The system runs on IBM-compatible personal computers with dBASE IV and tracks more than 1,200 data items distributed among various source categories. AQUIS is currently operating at 11 US Air Force facilities, which have up to 1,000 sources, and two headquarters. The system provides a flexible reporting capability that permits users who are unfamiliar with database structure to design and prepare reports containing user-specified information. In addition to the criteria pollutants, AQUIS calculates compound-specific emissions and allows users to enter their own emission estimates. DOE

N94-13384# Oak Ridge National Lab., TN.
OCEAN UPTAKE OF CARBON DIOXIDE
Tsung-Hung Peng and Taro Takahashi 1993 44 p Presented at the National Conference and Exposition on Heat Transfer, Atlanta, GA, 8-11 Aug. 1993
(Contract DE-AC05-84OR-21400)
(DE93-012967; CONF-930830-17) Avail: CASI HC A03/MF A01

Factors controlling the capacity of the ocean for taking up anthropogenic C02 include carbon chemistry, distribution of alkalinity, pCO2 and total concentration of dissolved C02, sea-air pCO2 difference, gas exchange rate across the sea-air interface, biological carbon pump, ocean water circulation and mixing, and dissolution of carbonate in deep sea sediments. A general review of these processes is given and models of ocean-atmosphere system based on our understanding of these regulating processes are used to estimate the magnitude of C02 uptake by the ocean. We conclude that the ocean can absorb up to 35 percent of the fossil fuel emission. Direct measurements show that 55 percent of C02 from fossil fuel burning remains in the atmosphere. The remaining 10 percent is not accounted for by atmospheric increases and ocean uptake. In addition, it is estimated that an amount equivalent to 30 percent of recent annual fossil fuel emissions is released into the atmosphere as a result of deforestation and farming. To balance global carbon budget, a sizable carbon sink besides the ocean is needed. Storage of carbon in terrestrial biosphere as a result of C02 fertilization is a potential candidate for such missing carbon sinks. DOE

N94-13390# Allied-Signal Aerospace Co., Kansas City, MO.
POLLUTION PREVENTION THROUGH TOTAL QUALITY
D. L. Stoltz, M. G. Byrant, D. M. Eggers, R. W. Gough, and W. H. Schlosberg May 1993 16 p Presented at the 9th Waste Minimization and Pollution Prevention Conference, San Francisco, CA, 13-15 Apr. 1993
(Contract DE-AC04-76DP-00613)
(DE93-013814; KCP-613-5138; CONF-930483-7) Avail: CASI HC A03/MF A01

Application of Total Quality to AlliedSignal Inc., Kansas City Division's (KCD) Pollution Prevention Program has created a dynamic and focused effort to significantly reduce process inefficiencies and waste generation. KCD is demonstrating TQ's usefulness by empowering associates and obtaining their buy-in and ownership of pollution prevention principles. Specific pollution prevention working groups include: (1) establishing a comprehensive recycling process; (2) capitalizing on Environmentally Conscious Manufacturing (ECM) expertise; and (3) encouraging the internal implementation of ECM. TQ produces the performance results that promote and sustain plant-wide pollution prevention goals and activities. KCD uses AlliedSignall's nine step 'Process Improvement Problem/Solving Model' (Appendix A). Although this program only formally began within the past year, many of the tools have been used over the last eight years to achieve pollution prevention objectives. This paper focuses on the new attitude and gives examples of how each of the nine steps is being used in the KCD Pollution Prevention Program. This paper describes each step of the process and provides specific pollution prevention examples. DOE

N94-13486# Oak Ridge National Lab., TN.
FOREST MANAGEMENT FOR FIXING AND SEQUESTERING CARBON
G. Marland, V. Dale, R. Graham, R. Luxmoore, S. Marland, S. McLaughlin, R. Norby, W. M. Post, T. Tschaplinski, and J. Tuskan et al 1993 5 p Presented at the 2nd US/Japan Workshop on Global Change Research: Environmental Response Technologies, Honolulu, HI, 1-3 Feb. 1993
(Contract DE-AC05-84OR-21400)
(DE93-013520; CONF-930285-1) Avail: CASI HC A01/MF A01

The concept of planting trees as part of a strategy to confront the possibility of global climate change is now widely accepted. As trees grow they remove CO2 from the atmosphere and thus slow the atmospheric build-up of CO2, an important greenhouse gas. Within the global-climate-change context, there are two fundamental problems with managing trees to store carbon. First, the magnitude of fossil-fuel related emissions of CO2 is so large, 6 billion metric tons of carbon per year that it takes very large areas of tree planting to make a significant impact. Second, as trees mature their rate of growth, and hence rate of net carbon uptake, declines. The large demand on land area suggests that there is a limit to the fraction of total CO2 emissions that we might reasonably expect to offset with growing trees. The ultimate maturation of

forests suggests that there is a limit on the length of time over which offsets are feasible and that we need to ask what to do as the rate of C uptake declines. Acknowledging that the availability of land will constrain the ability of tree planting to offset industrial emissions of CO2, we consider how the land which is available can be used most effectively. This report speculates on how much land might be available for a forest management strategy motivated (at least partially) by concerns about climate change, but our principal focus is on how a given land area can be best used to minimize net emissions of CO2 and how much might be achieved on a unit of land. We do not suggest that carbon management should be the principal criteria for land management, but we discuss the implications if it were. Confronting global and local changes in climate will be one of many objectives in land management and we explore for the most effective strategy for pursuing this objective. DOE

N94-13495# Argonne National Lab., IL. Environmental Assessment and Information Sciences Div.

AN EXAMINATION OF UTILITY EMISSIONS CONTRIBUTIONS TO ELEVATED OZONE CONCENTRATIONS IN THE CHICAGO AREA

M. E. Fernau, K. A. Guziel, and D. W. South 1993 11 p Presented at the 86th Annual Meeting and Exhibition of the Air and Waste Management Association, Denver, CO, 13-18 Jun. 1993

(Contract W-31-109-eng-38)

(DE93-012852; ANL/EAIS/CP-78927; CONF-930647-2) Avail: CASI HC A03/MF A01

In order to reduce the pollutant load to the atmosphere and subsequent damaging effects, Titles 1 and 4 of the Clean Air Act Amendments of 1990 (CAAA's) require reductions in emissions of sulfur dioxide (SO2), nitrogen oxides (NO(x)), and volatile organic compounds (VOC's). Title 4 is aimed at reducing acidic deposition and requires utilities to reduce SO(2) and NO(x) emissions to specified levels. As a consequence of this, many utilities will have to install SO2 and NO(x) control technologies. Title 1 is concerned with bringing regions into compliance with the National Ambient Air Quality Standards (NAAQS) for the criteria pollutants, among which is ozone (O3). The NAAQS for O3 is 120 ppb (parts per billion by volume) hourly average concentration, not to be exceeded four times in three years. O3 is a secondary pollutant formed in the atmosphere when NO(x) and VOC's react together in the presence of sunlight. Utilities are a significant source of NO(x) and an unimportant source of VOC's. In the past, O3 control strategy has focused on reducing VOC emissions because of the possibility that reducing NO(x) actually might make O3 concentrations higher. However, this approach has not worked, perhaps because of underestimation of natural and manmade VOC emissions and transport of O3 from other regions. Computer modeling has shown that for many highly polluted areas massive NO(x) reductions may be necessary in addition to or in place of VOC controls. Utilities are a potential source of these NO(x) reductions. DOE

N94-13602* National Aeronautics and Space Administration. Goddard Space Flight Center, Greenbelt, MD.

ARCTIC OZONE EXPEDITION (Videotape)

Feb. 1989 Videotape: 18 min. 14 sec. playing time, in color, with sound

(NASA-TM-109301; NONP-VT-93-185316) Avail: CASI VHS A01/BETA A22

Documenting the expedition of scientists to the uppermost reaches of the North Pole, this tape shows what is involved in collecting this valuable climatic data. Author

N94-13667 National Physical Lab., Teddington (England). Materials Metrology Div.

STABILITY OF REFERENCE MASSES 1: EVIDENCE FOR POSIIBLE VARIATIONS IN THE MASS OF REFERENCE KILOGRAMS ARISING FROM MERCURY CONTAMINATION

P. J. Cumpson and M. P. Seah Jan. 1993 16 p

(NPL-DMM(A)-86; ETN-93-94461) Copyright Avail: National Physical Laboratory, Teddington, Middlesex TW11 OLW, United Kingdom HC

Samples of Pt/10 percent Ir were studied by X-ray Photoelectron Spectroscopy (XPS) to assess environmental contamination of reference kilogram masses. Samples were sputtered clean and distributed to four places where reference kilograms are kept. All four specimens showed carbon and oxygen contamination. All four specimens additionally showed mercury contamination, with levels that varied from venue to venue. Of all metals, mercury has the highest vapor pressure, is commonly used in laboratories, and reacts with platinum; in hindsight the results are not surprising. The worst venue, wherein the reference kilogram had an effective mass increase of 0.26 micrograms of mercury/day, was the case enclosing the UK primary balance. The mercury is not removed by washing or by scrubbing with a chamois leather soaked in ethanol and ether. The mercury level is therefore probably stable after a period following manufacture, unless the mass is exposed to a venue with a higher mercury level. It is recommended that in relation to Pt or Pt/Ir masses all equipment containing mercury be removed from weighing laboratories, venues be monitored for mercury by XPS, and further work be done to determine whether best mass stability would be achieved by controlled mercury saturation after the reference mass is made, or by storage in a rigorously contaminant free environment. ESA

N94-13821# Norwegian Defence Research Establishment, Kjeller.

ESTIMATION OF THE CONCENTRATION VERSUS THE TIME PROFILE OF ZINC CHLORIDE PARTICLES IN SMOKE CLOUDS GENERATED BY THE RAUFOSS A/S INSTANTANEOUS SMOKE RA-90 AND DM-45 HC SMOKE GENERATOR

Jan H. Blanch 10 Feb. 1993 12 p

(FFI-93/6001; ETN-93-94453) Avail: CASI HC A03/MF A01

Possible hazards that may arise from the outdoor use of two smoke generating devices, specifically the DM-45 HC smoke generator and the recently developed RA-90 instantaneous smoke concept, are investigated. To accomplish such a task, it is necessary to know the concentration versus time profiles of the most hazardous compound in the smoke clouds generated by these devices. The concentration of zinc chloride in clouds generated by RA-90 and DM-45 in two typical weather situations is estimated. The DM-45 HC smoke generator produces smoke with markedly higher maximum concentrations of zinc chloride particles than the RA-90 instantaneous smoke concept. The maximum time personnel may be exposed to the highest zinc chloride concentrations is also markedly longer for the DM-45. ESA

N94-13880 National Physical Lab., Teddington (England). Radiation Science and Acoustics Div.

ENVIRONMENTAL RADIOACTIVITY INTERCOMPARISON 1992

S. M. Jerome, M. J. Woods, S. E. M. Lucas, and A. C. Hooley Jan. 1993 42 p

(NPL-RSA(EXT)-37; ETN-93-94464) Copyright Avail: National Physical Laboratory, Teddington, Middlesex TW11 0LW, United Kingdom HC

An account of the third in the series of environmental radioactivity measurement intercomparison exercises is given. Two sets of samples were prepared, one containing alpha emitters and one containing beta and beta/gamma emitters. The participants fell into three groups: the nuclear industry and the statutory monitoring organizations, organizations with a secondary interest in the nuclear industry (such as water companies) and contract laboratories. The results for this exercise are reported. In general, the results are satisfactory and the level of performance is comparable to previous years. ESA

N94-13910# Pacific Northwest Lab., Richland, WA.

SPATIAL AND TEMPORAL VARIABILITY OF PRECIPITATION AND CHEMISTRY: CASE STUDIES FROM THE FRONTAL BOUNDARY STUDY

M. T. Dana Jan. 1993 7 p Presented at the 73rd American Meteorological Society Annual Meeting, Anaheim, CA, 17-22 Jan. 1993

(Contract DE-AC06-76RL-01830)

(DE93-007883; PNL-SA-21492; CONF-930133-10) Avail: CASI HC A02/MF A01

Regional and larger-scale models of pollutant transport and deposition generally, by practical necessity, must be limited in output of precipitation rate and chemical composition to values for selected time intervals representing areas on the order of 10(exp 4) sq km. Naturally, it is of some concern that these values be reasonably representative of natural variations both in time and space. This question may be approached through field studies involving detailed spatial (using a network of samplers on the model grid scale) and temporal (using sequential sampling) measurements. This paper presents an initial analysis, using simple statistical concepts, of data bases from such a field study, the Frontal Boundary Study (FBS). DOE

N94-13911# Pacific Northwest Lab., Richland, WA.
BINARY HOMOGENEOUS NUCLEATION: TEMPERATURE AND RELATIVE HUMIDITY FLUCTUATIONS AND NON-LINEARITY
R. C. Easter and L. K. Peters (Kentucky Univ., Lexington.) Jan. 1993 9 p Presented at the 73rd American Meteorological Society Annual Meeting, Anaheim, CA, 17-22 Jan. 1993
(Contract DE-AC06-76RL-01830)
(DE93-007884; PNL-SA-21486; CONF-930133-9) Avail: CASI HC A02/MF A01

This report discusses binary homogeneous nucleation involving H2SO4 and water vapor, which is thought to be the primary mechanism for new particle formation in the marine boundary layer. The temperature, relative humidity, and partial pressure of H2SO4 vapor are the most important parameters in fixing the binary homogeneous nucleation rate in the H2SO4/H2O system. The combination of thermodynamic calculations and laboratory experiments indicates that this rate varies roughly as the tenth power of the saturation ratio of H2SO4 vapor. Furthermore, the vapor pressure of H2SO4 is a function of temperature, and similar dependencies of the binary homogeneous nucleation rate on relative humidity can be noted as well. These factors thus introduce strong non-linearities into the system, and fluctuations of temperature, relative humidity, and H2SO4 vapor concentrations about mean values may strongly influence the nucleation rate measured in the atmosphere. DOE

N94-14020# Los Alamos National Lab., NM.
QUALITY ASSURANCE FOR ENVIRONMENTAL CHEMISTRY, 1991, VOLUME 1
M. A. Gautier, E. S. Gladney, E. A. Jones, N. L. Koski, B. T. OMalley, G. H. Brooks, and W. D. Moss Dec. 1992 149 p
(Contract W-7405-eng-36)
(DE93-011791; LA-12436-MS-Vol-1) Avail: CASI HC A07/MF A02

This report documents the continuing quality assurance efforts of the Environmental Chemistry Group (EM-9) at the Los Alamos National Laboratory. The philosophy, methodology, computing resources, and laboratory information management system used by the quality assurance program to encompass the diversity of the analytical chemistry practiced by the group are described. Included in the report are all quality assurance reference materials used, along with their certified or consensus concentrations, and all analytical chemistry quality assurance measurements made by EM-9 during 1991. DOE

N94-14022# Lawrence Livermore National Lab., CA.
THE ROLE OF HUMAN ACTIVITY AND LAND USE CHANGE IN ATMOSPHERIC CHEMISTRY AND AIR QUALITY
J. E. Penner Jul. 1992 45 p Presented at the SNOWMASS Meeting, Denver, CO, 21 Jul. - 10 Aug. 1991
(Contract W-7405-eng-48)
(DE93-011871; UCRL-JC-110922; CONF-9107235-1) Avail: CASI HC A03/MF A01

In the this paper, I review the importance of several fossil fuel combustion byproducts in terms of atmospheric chemistry, air quality, and climate. I then review current estimates of the sources for each specie, deriving the fraction of each source that is due to specific land use practices or land cover categories. Understanding the current trends of those species with known increasing abundances and projecting increases into the future is possible if the estimated sources from human activity and land use change can be projected and if the known atmospheric sinks and the interactions in atmospheric chemistry and climate change are appropriately taken into account. Regional trends in the short-lived species can be projected as well, assuming the estimated sources and sinks are correct. However, significant uncertainties continue to surround the estimated budgets for most of these species. Uncertainties and the estimated ranges in different source strength estimates for each are also discussed. DOE

N94-14087# Midwest Research Inst., Golden, CO. National Renewable Energy Lab.
BIODIESEL/AQUATIC SPECIES PROJECT REPORT, FY 1992
L. Brown, E. Jarvis, T. Dunahay, P. Roessler, K. Zeiler, and S. Sprague (Department of Energy, Washington, DC.) May 1993 33 p
(Contract DE-AC02-83CH-10093)
(DE93-010024; NREL/TP-422-5259) Avail: CASI HC A03/MF A01

The primary goal of the Biodiesel/Aquatic Species Project is to develop the technology for growing microalgae as a renewable biomass feedstock for the production of a diesel fuel substitute (biodiesel), thereby reducing the need for imported petroleum. Microalgae are of interest as a feedstock because of their high growth rates and tolerance to varying environmental conditions, and because the oils (lipids) they produce can be extracted and converted to substitute petroleum fuels such as biodiesel. Microalgae can be grown in arid and semi-arid regions with poor soil quality, and saline water from aquifers or the ocean can be used for growing microalgae. Biodiesel is an extremely attractive candidate to fulfill the need for a diesel fuel substitute. Biodiesel is a cleaner fuel than petroleum diesel; it is virtually free of sulfur, and emissions of hydrocarbons, carbon monoxide, and particulates during combustion are significantly reduced in comparison to emissions from petroleum diesel. Biodiesel provides essentially the same energy content and power output as petroleum-based diesel fuel. DOE

N94-14095 Commonwealth Scientific and Industrial Research Organization, Sydney (Australia). Div. of Atmospheric Research.
SYNTHESIS INVERSION OF ATMOSPHERIC CO2 USING THE GISS TRACER TRANSPORT MODEL
I. G. Enting, C. M. Trudinger, R. J. Francey, and H. Granek 1993 47 p
(CSIRO-TP-29; ISBN-0-643-05251-8) Copyright Avail: Issuing Activity

The atmospheric CO2 budget for the period around 1986-1987 is estimated using a Bayesian synthesis analysis. The source strengths of a set of industrial, biotic, and ocean processes are estimated by matching observed concentrations to modeled concentrations calculated using the GISS three-dimensional tracer transport model. The Bayesian synthesis uses prior estimates of these process strengths to stabilize what is otherwise an ill-conditioned inversion. The analysis gives preliminary estimates of the ranges of uncertainty arising from the inversion. The inversion uses observations of the concentration and delta(13)C of atmospheric CO2. The ability to estimate uncertainties makes it possible to compare the relative importance of various data items in reducing these uncertainties. The main result is that global totals of oceanic versus biotic exchange are determined primarily by the combined global budgets for CO2 and (13)CO2. The atmospheric transport model constrains the regional sources and sinks but these constraints make only a small contribution to reducing the uncertainty in the global budget. Our best estimate of the global net air-sea carbon flux is 1.4 +/- 1.0 Gt C/y. The net carbon storage by the oceans will be some 0.6 Gt C/y greater than this CO2 flux due to carbon transported into the oceans by rivers. The corresponding estimate of air-to-biota CO2 flux is -2.5 +/- 0.9 Gt C/y implying a net storage of -1.3 Gt C/y after accounting for carbon lost from the biota via rivers or as CO. We find that within the range of approximately I Gt C/y our estimate of air-sea flux is very sensitive to the choice of data that are fitted. This confirms the appropriateness of our formal error estimates that are based on a priori statistics. These large uncertainties mean that our budget estimates must be regarded as preliminary and indicate the need for a refined statistical analysis of the observational data to assess their representativeness. A simple preliminary study of oxygen distributions is presented. The results indicate that, once the CO2 distribution is fitted, the spatial gradient of oxygen does not give significant additional discrimination between alternative carbon budgets and that the long-term trend of atmospheric oxygen will make the greatest contribution to resolving carbon budgets.
Author (revised)

N94-14103*# Umpqua Research Co., Myrtle Creek, OR. Aerospace Div.
DESTRUCTION OF PROBLEMATIC AIRBORNE CONTAMINANTS BY HYDROGEN REDUCTION USING A CATALYTICALLY ACTIVE, REGENERABLE SORBENT (CARS) Final Report
John O. Thompson and James R. Akse Jul. 1993 52 p
(Contract NAS2-13714)
(NASA-CR-194354; NAS 1.26:194354; URC-80436) Avail: CASI HC A04/MF A01

Thermally regenerable sorbent beds were demonstrated to be a highly efficient means for removal of toxic airborne trace organic contaminants aboard spacecraft. The utilization of the intrinsic weight savings available through this technology was not realized since many of the contaminants desorbed during thermal regeneration are poisons to the catalytic oxidizer or form highly toxic oxidation by-products in the Trace Contaminant Control System (TCCS). Included in this class of compounds are nitrogen, sulfur, silicon, and halogen containing organics. The catalytic reduction of these problematic contaminants using hydrogen at low temperatures (200-300 C)

offers an attractive route for their destruction since the by-products of such reactions, hydrocarbons and inorganic gases, are easily removed by existing technology. In addition, the catalytic oxidizer can be operated more efficiently due to the absence of potential poisons, and any posttreatment beds can be reduced in size. The incorporation of the catalyst within the sorbent bed further improves the system's efficiency. The demonstration of this technology provides the basis for an efficient regenerable TCCS for future NASA missions and can be used in more conventional settings to efficiently remove environmental pollutants.
Author (revised)

N94-14182# Department of Energy, Washington, DC. Environmental Sciences Div.
PROGRAM OPERATIONS PLAN
Apr. 1993 105 p
(DE93-012765; DOE/ER-0586T) Avail: CASI HC A06/MF A02

The Department of Energy's Atmospheric Chemistry Program (ACP) was initiated in 1991 to coordinate DOE's university and federal-laboratory atmospheric-chemistry research and to focus these efforts on national and international information requirements in the atmospheric-chemistry field. This Program Operations Plan describes the structure and vision of the effort designed to fulfill these needs, and is divided into two major components. The first of these is a Strategic Plan, which outlines the ACP's rationale, objectives, and vision, and describes its products that are anticipated over a future ten-year period. Although based on realistic appraisals of goals that are attainable given the financial, material, and intellectual resources of the ACP community, this Strategic Plan does not describe these resources themselves. The second component of the Program Operations Plan, the Implementation Plan, deals directly with these resource considerations. As such it focuses on practical implementation of Strategic-Plan elements at the individual research institutions, the anticipated scientific contributions of these groups, and their coordination within the ACP. In contrast to the Strategic Plan, this Implementation Plan extends only five years into the future. DOE

N94-14183# Sandia National Labs., Albuquerque, NM.
A LASER-BASED TECHNIQUE TO CONTINUOUSLY MONITOR METAL AEROSOL EMISSIONS
W. L. Flower, L. W. Peng, N. B. French, H. A. Johnsen, D. K. Ottesen, R. F. Renzi, and M. P. Bonin 1993 19 p Presented at the EPRI Workshop, Scottsdale, AZ, 19-22 May 1993
(Contract DE-AC04-76DR-00789)
(DE93-012836; SAND-93-8558C; CONF-9305183-1) Avail: CASI HC A03/MF A01

Sandia National Laboratories is developing an instrument to continuously monitor metal aerosol emissions. Applications for this monitor range from industrial process vents (e.g., exhaust stacks from electroplating baths) to waste treatment processes (incinerators), to boilers and industrial furnaces (coal-fired power plants). The monitoring technique is based on Laser Spark Spectroscopy ((LASS) also known as Laser-Induced Breakdown Spectroscopy--LIBS), in which a pulsed laser is used to rapidly heat a particle and produce a plasma (or laser 'spark'). The light emission from the spark is spectrally resolved and analyzed to identify the elemental constituents of the particle and quantify the abundance of the measured species. One feature of LASS is that it can measure atomic species embedded in either solid particles or fine liquid droplets, which account for a large percentage of metal emissions from applications of interest. Presented here are a description of the technique and initial results from laboratory simulations to determine sensitivity and to establish calibration procedures. Our project is currently focused on measuring chromium emissions from electroplating baths. This work forms the basis for future applications to incineration and fossil power plants since chromium is one of the more toxic metals under regulation by the Clean Air Act. DOE

N94-14459# Oak Ridge K-25 Site, TN.
LONG-RANGE GLOBAL WARMING IMPACT OF GASEOUS DIFFUSION PLANT OPERATION
L. D. Trowbridge Sep. 1992 40 p
(Contract DE-AC05-84OT-21400)
(DE93-011686; K/ETO-112) Avail: CASI HC A03/MF A01

The DOE gaseous diffusion plant complex makes extensive use of CFC-114 as a primary coolant. As this material is on the Montreal Protocol list of materials scheduled for production curtailment, a substitute must be found. In addition to physical cooling properties, the gaseous diffusion application imposes the unique requirement of chemical inertness to fluorinating agents. This has narrowed the selection of a near-term substitute to two fully fluorinated material, FC-318 and FC-3110, which are likely to be strong, long-lived greenhouse gases. In this document, calculations are presented showing, for a number of plausible scenarios of diffusion plant operation and coolant replacement strategy, the future course of coolant use, greenhouse gas emissions (including coolant and power-related indirect CO2 emissions), and the consequent global temperature impacts of these scenarios. DOE

N94-14477# California Univ., Berkeley. Lawrence Berkeley Lab.
APPLICATIONS OF THE ADVANCED LIGHT SOURCE TO PROBLEMS IN THE EARTH, SOIL, AND ENVIRONMENTAL SCIENCES
Oct. 1992 130 p Workshop held in San Francisco, CA, 11 Dec. 1991
(Contract DE-AC03-76SF-00098)
(DE93-015258; LBL-31852; CONF-911288) Avail: CASI HC A07/MF A02

The following topics are discussed: Advanced Light Source (ALS) status and research opportunities; advanced light source applications to geological materials; applications in the soil and environmental sciences; x-ray microprobe analysis; potential applications of the ALS in soil and environmental sciences; and x-ray spectroscopy using soft x-rays: applications to earth materials. DOE

N94-14508 Environmental Protection Agency, Washington, DC.
TOXIC SUBSTANCES CONTROL ACT (TSCA) CHEMICAL SUBSTANCES INVENTORY: REVISED INVENTORY SYNONYM AND PREFERRED NAME FILE, JAN. 1993 DOCUMENTATION
Jan. 1993 35 p Limited Reproducibility: More than 20% of this document may be affected by microfiche quality
(PB93-155166) Avail: CASI HC A03

The computer-readable TSCA Chemical Substance Inventory is issued periodically to provide chemical substance information for those substances on the non-confidential substance identity portion of the TSCA Master Inventory File. For a complete understanding of the data contained on these tapes, it is necessary to consult the introductory material of the printed 1985 Edition and the 1990 Supplement to 1985 Edition. These tapes contain no TSCA Confidential Business Information. They have been prepared by Chemical Abstracts Service, a Division of the American Chemical Society, under contract to the U.S. Environmental Protection Agency. The tapes consist of two files: Inventory Preferred Name File and Inventory Synonym Name File. The first file contains the CAS Registry Number, preferred CA Index Name, molecular formula, and other appropriate information for each non-confidential inventory chemical substance. The entries are in ascending CAS Registry Number order. The second file is a file of synonymous chemical names for the same substances listed in the Preferred Name File. Its entries are ordered alphabetically by name with each name accompanied by the same information for the substances as appears in the Preferred Name File. Author

N94-14516# Texas A&M Univ., College Station. Energy Systems Lab.
FOURTEENTH NATIONAL INDUSTRIAL ENERGY TECHNOLOGY CONFERENCE: PROCEEDINGS
1992 251 p Conference held in Houston, TX, 22-23 Apr. 1992
(DE93-016698; CONF-9204250) Avail: CASI HC A12/MF A03

Many short articles on various aspects of energy production, use, and conservation in industry are presented. The impacts of energy efficient equipment, recycling, pollution regulations, and energy auditing are discussed. The topics covered include: new generation sources and transmission issues, superconductivity applications, integrated resource planning, electrotechnology research, equipment and process improvement, environmental improvement, electric utility management, and recent European technology and conservation opportunities. Individual papers are indexed separately. DOE

N94-14523# Pacific Northwest Lab., Richland, WA.
SUMMARY OF CONCLUSIONS AND RECOMMENDATIONS FROM A VISIBILITY SCIENCE WORKSHOP
N. S. Laulainen Apr. 1993 49 p

(Contract DE-AC06-76RL-01830)
(DE93-012770; PNL-8606) Avail: CASI HC A03/MF A01

A workshop was held in Boulder, Colorado, on September 19-20, 1991, at the National Center for Atmospheric Research to assist the U.S. Department of Energy, Office of Fossil Energy, in developing a national assessment of visibility impairment. Participants reviewed the following: the current technical basis of the relationships between anthropogenic emissions of SO2, NO(x), and volatile organic compounds and visibility impairment; reviewed the major scientific issues and uncertainties related to visibility; impairing aerosols; and recommended technical approaches for performing such an assessment. DOE

N94-14723# Cologne Univ. (Germany). Inst. fuer Geophysik und Meteorologie.
IMPORTANCE OF SPRAYS FOR LONG RANGE TRANSPORT OF HARMFUL SUBSTANCES IN THE TROPOSPHERE [BEDEUTUNG DER AEROSOLE FUER DEN FERNTRANSPORT VON SCHADSTOFFEN IN DER TROPOSPHAERE]
Andreas Koetz 1991 156 p In GERMAN
(Mitt-81; ETN-93-94383) Avail: CASI HC A08/MF A02

Effects of aerosol phase in sulfate-nitrate-ammonium system on long range transport and deposition of sulfur and nitrogen in the troposphere are examined. Aerosol MARS (Model for an Aerosol Reacting System), which is based on thermodynamic concepts and allows aerosol composition to be calculated from relative humidity, sulfate formation rate in the gaseous phase and ammoniac and nitric acid concentrations, is described. Data about nitrogen and sulfur oxide emissions in Europe are presented using spatial distribution curves. A unidimensional model, which involves chemical reactions, emissions, deposition and vertical diffusion, was used for description of daily transport and vertical distribution of aerosol species; interactions between gaseous phase and sprays were considered as relaxation to the concentrations given by the thermodynamic equilibrium between both phases. Numerical spreading simulations were carried out with the three dimensional Euler model CTM2 (Chemistry Transport Model), derived from regional acid deposition model, in order to depict chemical transformations, and dry and wet deposition of trace particles in the troposphere. ESA

N94-14859# Oak Ridge National Lab., TN.
PATTERN AND PROCESS IN LANDSCAPE ECOLOGY: EIGHTH ANNUAL US LANDSCAPE ECOLOGY SYMPOSIUM Abstracts Only
1993 110 p Symposium held in Oak Ridge, TN, 24-27 Mar. 1993
(Contract DE-AC05-84OR-21400)
(DE93-014032; ORNL/M-2725; CONF-9303180-Absts) Avail: CASI HC A06/MF A02

Abstracts are presented from a meeting on landscape ecology. Topics include: conservation; climatic change; forest management; aquatic, wetland, rural, and urban landscapes; land use; and biodiversity. DOE

N94-14217# National Inst. for Resources and Environment, Ibaraki (Japan).
IMG: INTERFEROMETRIC MONITOR FOR GREENHOUSE GASES
R. Imasu, T. Ogawa (Tokyo Univ., Japan.), H. Shimoda (Tokai Univ., Tokyo, Japan.), and H. Kobayashi (Central Research Inst. of Electric Power Industry, Tokyo, Japan.) *In* Science and Technology Agency, Asia-Pacific ISY Conference, Volume 2 31 Mar. 1993 p 55-58 (For primary document see N94-14209 02-43)
Avail: CASI HC A01/MF A04

N94-14230# Tokyo Univ. (Japan). Center for Climate System Research.
THE EFFECTS OF ANTHROPOGENIC AEROSOLS ON OPTICAL THICKNESS AND PARTICLE SIZE OF CLOUDS. PART 1: RETRIEVAL ALGORITHM
Zhao Fengsheng and Teruyuki Nakajima *In* Science and Technology Agency, Asia-Pacific ISY Conference, Volume 2 31 Mar. 1993 p 111-116 (For primary document see N94-14209 02-43)
Avail: CASI HC A02/MF A04

N94-14236# United Nations Educational, Scientific and Cultural Organization, Paris (France). Div. of Earth Sciences.
SATELLITE TECHNOLOGY FOR ENVIRONMENTAL MONITORING IN DEVELOPING COUNTRIES
Kumon Tokumaru and Felix Kogan (National Oceanic and Atmospheric Administration, Washington, DC.) *In* Science and Technology Agency, Asia-Pacific ISY Conference, Volume 2 31 Mar. 1993 p 141-144 (For primary document see N94-14209 02-43)
Avail: CASI HC A01/MF A04

N94-14246# Byelorussian Scientific and Technical Centre of Environment Remote Diagnostics, Minsk.
STUDY OF THE CONSEQUENCES OF THE CHERNOBYL ACCIDENT AND TECHNOGENIC ACTIVITY IN THE REPUBLIC BELARUS USING AEROSPACE METHODS
Alexander Kovalyov *In* Science and Technology Agency, Asia-Pacific ISY Conference, Volume 2 31 Mar. 1993 p 189-192 (For primary document see N94-14209 02-43)
Avail: CASI HC A01/MF A04

N94-14250# Freie Univ., Berlin (Germany). Inst. for Meteorology.
THE ROLE OF THE DYNAMICS FOR THE DEVIATION OF THE TOTAL OZONE FROM THE LONG-TERM MEAN AT THE EDGE OF THE POLAR VORTEX
Karin Petzoldt *In* Science and Technology Agency, Asia-Pacific ISY Conference, Volume 2 31 Mar. 1993 p 211-214 Sponsored by BMFT (For primary document see N94-14209 02-43)
Avail: CASI HC A01/MF A04

N94-14251# Natural Environmental Research Council, Swindon (England).
THE EUROPEAN ARCTIC OZONE EXPERIMENT: AN INVESTIGATION OF NORTHERN HEMISPHERE OZONE DEPLETION
Richard A. Cox *In* Science and Technology Agency, Asia-Pacific ISY Conference, Volume 2 31 Mar. 1993 p 215-219 (For primary document see N94-14209 02-43)
Avail: CASI HC A01/MF A04

N94-14253# Institute of Atmospheric Physics, Beijing (China).
NEW EVIDENCES SUPPORTED THE WEI HYPOTHESIS ABOUT THE FORMATION OF THE ANTARCTIC OZONE HOLE
Ding-Wen Wei *In* Science and Technology Agency, Asia-Pacific ISY Conference, Volume 2 31 Mar. 1993 p 224-228 (For primary document see N94-14209 02-43)
Avail: CASI HC A01/MF A04

46 GEOPHYSICS

Includes aeronomy; upper and lower atmosphere studies; ionospheric and magnetospheric physics; and geomagnetism.

For space radiation see *93 Space Radiation.*

N94-12788*# Georgia Univ., Griffin. Dept. of Agronomy.
MEASURING SURFACE FLUXES IN CAPE Final Report, 23 Apr. 1991 - 22 Apr. 1992
E. T. Kanemasu, T. D-Shah, and Dalin Nie 1992 7 p
(Grant NAG8-880)
(NASA-CR-193664; NAS 1.26:193664) Avail: CASI HC A02/MF A01

Two stations (site 1612 and site 2008) were operated by the University of Georgia group from 6 July 1991 to 18 August 1991. The following data were collected continuously: surface energy fluxes (i.e., net radiation, soil heat fluxes, sensible heat flux and latent heat flux), air temperature, vapor pressure, soil temperature (at 1 cm depth), and precipitation. Canopy reflectance and light interception data were taken three times at each site between 6 July and 18 August. Soil moisture content was measured twice at each site. Author (revised)

N94-12794# Federal Coordinating Council for Science, Engineering and Technology, Washington, DC. Subcommittee on Atmospheric Research.
NATIONAL ATMOSPHERIC SCIENCES PROGRAM, FISCAL YEARS 1987-1990
24 Aug. 1992 142 p
(NSF-92-16) Avail: CASI HC A06/MF A02

This report describes the atmospheric sciences research programs of the SAR member agencies for Fiscal Years 1987-1990 with accompanying

fiscal data for those years. In addition there are appendices that include information on national and international atmospheric research and environmental organizations. Budgetary information also is presented for the U.S. Global Change Research Program (FY 1989 and 1990), for the National Acid Precipitation Assessment Program and the National Climate Program (FY 1987 through 1990). It is the latest in an ongoing series of reports which satisfy the responsibility for reviews of Federal R&D programs in the Earth Sciences as required by the FCCSET/CEES.

Derived from text

N94-12906# Argonne National Lab., IL.
INTEGRATED, FLEXIBLE, AND RAPID GEOPHYSICAL SURVEYING
S. F. Miller, L. D. McGinnis, M. D. Thompson, and C. Tome 1993 17 p Presented at the SAGEEP 1993 Symposium on the Application of Geophysics to Environmental and Engineering Problems, San Diego, CA, 18-21 Apr. 1993
(Contract W-31-109-eng-38)
(DE93-009989; ANL/ES/CP-77790; CONF-9304109-1) Avail: CASI HC A03/MF A01

Aberdeen Proving Ground (APG) is currently managing a comprehensive Installation Restoration Program involving more than 360 solid-waste managing units contained within 13 study areas. The Edgewood area and two landfills in the Aberdeen area appear on the National Priority List under the Comprehensive Environmental Response, Compensation, and Liability Act. Therefore, APG has entered into an interagency agreement with the US Environmental Protection Agency to address the listed areas. The West Branch of the Canal Creek area, located within the Edgewood area, is one of the areas that requires a Source Definition Study because there is an ongoing release of volatile organic compounds into the creek. A report prepared in 1989 included a list of 29 potentially contaminated buildings in the Edgewood area. Sixteen of the buildings contain known contaminants, nine buildings contain unknown contaminants, and four of the buildings are potentially clean. The EAI report recommended that a sampling and monitoring program be established to verify contamination levels in and around each building. Thirteen of the potentially contaminated buildings are in the West Branch of the Canal Creek area and are potential sources of volatile organic compounds. Operations have ceased, and the buildings have been abandoned, but processing equipment, sumps, drains, ventilation systems, and underground storage tanks remain. These appurtenances may contain liquid, solid, or vapor contaminants of unknown nature. DOE

N94-12952# Los Alamos National Lab., NM.
ION ANISOTROPY DRIVEN WAVES IN THE EARTH'S MAGNETOSHEATH AND PLASMA DEPLETION LAYER
R. E. Denton, M. K. Hudson (Dartmouth Coll., Hanover, NH.), B. J. Anderson (Johns Hopkins Univ., Laurel, MD.), and S. A. Fuselier (Lockheed Aircraft Corp., Palo Alto, CA.) 1993 17 p Presented at the AGU Monograph/Solar System Plasma Physics Meeting on Resolution of Processes in Space and Time, Yosemite, CA, Feb. 1993
(Contract W-7405-eng-36)
(DE93-012751; LA-UR-93-1470; CONF-9302115-3) Avail: CASI HC A03/MF A01

Recent studies of low frequency waves (omega(sub r) less than omega(sub p), where omega(sub p) is the proton gyrofrequency) observed by AMPTE/CCE in the plasma depletion layer and magnetosheath proper are reviewed. These waves are shown to be well identified with ion cyclotron and mirror mode waves. By statistically analyzing the transitions between the magnetopause and time intervals with ion cyclotron and mirror mode waves, it is established that the regions in which ion cyclotron waves occur are between the magnetopause and the regions where the mirror mode is observed. This result is shown to follow from the fact that the wave spectral properties are ordered with respect to the proton parallel beta, (beta)(sub (parallel)p). The later result is predicted by linear Vlasov theory using a simple model for the magnetosheath and plasma depletion layer. Thus, the observed spectral type can be associated with relative distance from the magnetopause. The anisotropy-beta relation, A(sub p) triple bond (T(perpendicular)/T(sub parallel))(sub p) - 1 = 0.50(beta)(sub (parallel)p)(sup -0.48) results from the fact that the waves pitch angle scatter the particles so that the plasma is near marginal stability and is a fundamental constraint on the plasma. DOE

N94-13092*# Smithsonian Astrophysical Observatory, Cambridge, MA.
DETERMINATION OF SPECTROSCOPIC PROPERTIES OF ATMOSPHERIC MOLECULES FROM HIGH RESOLUTION VACUUM ULTRAVIOLET CROSS SECTION AND WAVELENGTH MEASUREMENTS Semiannual Status Report No. 17, 1 Nov. 1992 - 30 Apr. 1993
W. H. Parkinson, K. Yoshino, and D. E. Freeman Jul. 1993 13 p
(Grant NAG5-484)
(NASA-CR-194024; NAS 1.26:194024) Avail: CASI HC A03/MF A01

An account is given of progress during the six-month period 1 Nov. 1992 to 30 Apr. 1993 on work on (1) cross section measurements of the Schumann-Runge continuum; (2) the determination of the predissociation linewidths of the Schumann-Runge bands of O2; (3) the determination of the molecular constants of the ground state of O2; (4) cross section measurements of CO2 in wavelength region 120-170 nm; and (4) determination of dissociation energy of O2. The experimental investigations are effected at high resolution with a 6.65 m scanning spectrometer which is, by virtue of its small instrumental width (FWHM = 0.0013 nm), uniquely suitable for cross section measurements of molecular bands with discrete rotational structure. Below 175 nm and in the region of the S-R continuum, synchrotron radiation is suitable for cross section measurements. All of these spectroscopic measurements are needed for accurate calculations of the production of atomic oxygen and penetration of solar radiation into the Earth's atmosphere. Author (revised)

N94-13212*# Cornell Univ., Ithaca, NY. Civil and Environmental Engineering Dept.
ATMOSPHERIC SOUNDINGS DURING THE WASHITA 1992 CAMPAIGN Final Technical Report, 1 Jun. - 30 Sep. 1992
W. Brutsaert 30 Sep. 1992 10 p
(Grant NAG5-1989)
(NASA-CR-194383; NAS 1.26:194383) Avail: CASI HC A02/MF A01

During the period June 9 through June 18, 1992, an intensive radiosounding program was conducted to measure atmospheric profiles of the wind velocity, the temperature and the specific humidity. The launch site was located near site MS000 in the northeastern part of the catchment of the Little Washita River; this location was selected in order to ensure that the measured profiles would reflect the catchment's surface features for the prevailing southwesterly winds during this time of the year. The launch times of the rawinsondes are shown. Derived from text

N94-13293*# Washington Univ., Seattle. College of Arts and Sciences.
ELECTRODYNAMICS OF THE MIDDLE ATMOSPHERE: SUPERPRESSURE BALLOON PROGRAM Final Report, 15 Apr. 1986 - 30 Jun. 1990; Abstract Only
Robert H. Holzworth 28 Aug. 1990 1 p
(Grants NAG5-635; NAGw-724; NSF ATM-80-17071; NSF ATM-82-12283; NSF ATM-84-11326; NSF ATM-86-15628)
(NASA-CR-193671; NAS 1.26:193671) Avail: CASI HC A01/MF A01

This project called Electrodynamics of the Middle Atmosphere (EMA): Superpressure Balloon Program was begun by the PI at the Aerospace Corporation in Los Angeles under joint NSF and NASA funding originally combined in one grant ATM80-17071 and has continued at the University of Washington under grants ATM8212283, ATM84-11326 and ATM86-15628 and NASA grants NAGW-724 and NAGS-635. In the EMA experiment a comprehensive set of electrical parameters was measured during eight long-duration balloon flights in the Southern Hemisphere stratosphere. These flights resulted in the largest vector electric field data set ever collected from the stratosphere which has been a treasure-trove of new phenomena. Since the stratosphere has never been electrodynamically sampled in this systematic manner before, it is perhaps not surprising that several new discoveries have been made and reported. Another way to measure the success of this first EMA project is to note that all together the total data rate was about 1 bit/sec/payload amounting to 12 MBytes (1/3 of 1 standard 1600 BPI magnetic tape) which nevertheless has resulted in 14 papers and 2 masters theses (so far! . Ten of these papers and one masters thesis specifically acknowledge the support by NASA grant NAGS-635 are discussed herein. Author

N94-13334*# American Geophysical Union, Washington, DC.
THE 1990 WESTERN PACIFIC GEOPHYSICS MEETING
1990 57 p Meeting was held in Kanazawa, Japan, 15-21 Aug. 1990

(Grant NAGw-2821)
(NASA-CR-193456; NAS 1.26:193456) Avail: CASI HC A04/MF A01

The 1990 Western Pacific Geophysics Meeting was held in Kanazawa, Japan from 15-21 Aug. 1990. This was the first meeting of a new series of meetings for the American Geophysical Union, and it proved to be very successful in terms of the scientific program and attendance, which included over 1,000 participants. The intent of this meeting was an effort on the part of the American Geophysical Union (AGU) and several Japanese geophysical societies to gather individual Earth and space scientists at a major scientific meeting to focus on geophysical problems being studied in the western Pacific rim. The meeting was organized along the lines of a typical AGU annual meeting with some invited talks, many contributed talks, poster sessions, and with emphasis on presentations and informal discussions. The program committee consisted of scientists from both the U.S. and Japan. This meeting provided ample opportunities for U.S. and Japanese scientists to get to know each other and their works on a one-to-one basis. It was also a valuable opportunity for students studying geophysics to get together and interact with each other and with scientists from both the U.S. and Japan. There were 939 abstracts submitted to the conference and a total of 102 sessions designed as a result of the abstracts received. The topics of interest are as follows: space geodetic and observatory measurements for earthquake and tectonic studies; gravity, sea level, and vertical motion; variations in earth rotation and earth dynamics; sedimentary magnetism; global processes and precipitation; subsurface contaminant transport; U.S. Western Pacific Rim initiatives in hydrology; shelf and coastal circulation; tectonics, magmatism, and hydrothermal processes; earthquake prediction and hazard assessment; seismic wave propagation in realistic media; and dynamics and structure of plate boundaries and of the Earth's deep interior. Author (revised)

N94-13335*# American Geophysical Union, Washington, DC.
THE AMERICAN GEOPHYSICAL UNION CHAPMAN CONFERENCE ON TECTONICS AND TOPOGRAPHY
1992 42 p Conference was held in Snowbird, UT, 31 Aug. - 4 Sep. 1992
(Grant NAGw-3089)
(NASA-CR-193454; NAS 1.26:193454) Avail: CASI HC A03/MF A01

The Chapman Conference on Tectonics and Topography was held 31 Aug. - 4 Sep. 1992. The conference was designed to bring together disparate groups of earth scientists who increasingly found themselves working on similar problems but in relative isolation. Thus, process geomorphologists found themselves face-to-face with numerical modelers and field geomorphologists, hydrologists encountered geologists, and tectonophysicists found people with related data. The keynote speakers represented a wide variety of disciplines, all of which were relevant to the interdisciplinary theme of the conference. One of the most surprising issues that surfaced was the relative dearth of data that exists about erosion--process and rates. This was exacerbated by a reminder that erosion is critical to the evaluation of surface uplift. Author (revised)

N94-13418*# Indiana Univ., Bloomington. Dept. of Biology.
GRAVITY AS A PROBE FOR UNDERSTANDING PATTERN SPECIFICATION Final Technical Report
George M. Malacinski and Anton W. Neff 28 Aug. 1993 9 p
(Grant NAGw-1548)
(NASA-CR-194142; NAS 1.26:194142) Avail: CASI HC A02/MF A01

Amphibian eggs from Xenopus laevis were employed as a model system. Xenopus embryos were demonstrated to be sensitive to novel force fields. Under clinostat-simulated weightlessness the location of the third cleavage furrow was shifted towards the equator; the dorsal lip was shifted closer to the vegetal pole; and head and eye dimensions of hatching tadpoles were enlarged. Effects of centrifuge-simulated hypergravity were the opposite of those of simulated weightlessness. Those morphological alterations had their own force-sensitive period, and a substantial spawning-to-spawning variation in sensitivity was observed. Despite those dramatic differences in embryogenesis, tadpoles at the feeding stage were largely indistinguishable from controls. Derived from text

N94-13465*# Washington Univ., Seattle. Dept. of Atmospheric Sciences.
THEORETICAL SUPPORT FOR THE AIRBORNE ANTARCTIC OZONE EXPERIMENT Final Report
Dennis L. Hartmann 3 Mar. 199
(Grant NAGw-1160)
(NASA-CR-193669; NAS 1.26:193669) Avail: CASI HC A01/MF A01

This investigation was to provide theoretical support during and after the deployment of NASA research aircraft to Punta Arenas, Chile during August and September of 1987 to conduct the Airborne Antarctic Ozone Experiment. The experiment was very successful in demonstrating the role of anthropogenic chlorine in producing the ozone hole over Antarctica during September and October of 1987. The PI worked primarily on using tracer data from the ER-2 aircraft to show that transport could not have caused the ozone hole in 1987, and that transport of chemical species into the polar vortex was very weak during the period of the experiment. The presence of gravity waves was also very apparent in the ER-2 data, and papers were published on this analysis and on the use of meteorological analyses to position the aircraft within the vortex. Author

N94-13620* National Aeronautics and Space Administration. Marshall Space Flight Center, Huntsville, AL.
CRRES TO BLAZE NEW TRAILS IN ORBIT (Videotape)
Jul. 1990 Videotape: 2 min. 5 sec. playing time, in color, with sound
(NASA-TM-109314; NONP-VT-93-185329) Avail: CASI VHS A01/BETA A22

The purpose of the Combined Release Radiation Effects Satellite in re-mapping and planning protection for future spacecraft is described. Author (revised)

N94-13622 Yale Univ., New Haven, CT.
MINIMAL MODELING OF THE BIMODALITY OF EXTRATROPICAL ATMOSPHERIC PLANETARY WAVES Ph.D. Thesis
Lionel Pandolfo 1992 294 p
Avail: Univ. Microfilms Order No. DA9308997

Recent analyses of atmospheric data have indicated that the amplitude of atmospheric waves of planetary scale can switch from a mode of large amplitudes to a mode of small ones and vice versa. This behavior is present in both, the Northern and Southern Hemispheres. These observations are described and situated in the context of low frequency, intraseasonal variability. Most theories of bimodality rely on the presence of an extratropical source of long Rossby waves and on their interaction with the forcing in order to achieve a resonance in the response of the planetary flow. The incompatibility of these theories with the observations characterizing global weather regimes is demonstrated. Then, a hierarchy of numerical, quasi-geostrophic models are developed in order to determine the simplest model containing the minimal physics sufficient for generating bimodal statistics for the planetary waves. The physical properties which allow the production of bimodal dynamics relate to the stability characteristics of the models' stationary solutions and to the tonal wavenumber(s) at which the lower boundary is felt. The latter is not a major catalyst for the appearance of dynamical instabilities in spectral models retaining a large number of components in the truncation, contrary to the results from low-order ones. Instabilities and bimodality appear in our model when it is run with no lower-boundary forcing. Asymmetries in the latter actually supply a phase-locking mechanism favoring the establishment of standing oscillations. The validity of models with channel geometry was questioned on the ground that they would allow for resonant behavior by preventing latitudinal wave propagation. The problem of the dispersion of perturbation energy across parallels of latitude from a source embedded in a fluctuating zonal-mean flow, using a linearized, non-divergent barotropic vorticity equation and a basic zonal-mean flow constructed from atmospheric data were studied. It was found that the spatial fluctuations of the basic tonal flow can offer a localizing mechanism that acts to confine wave propagation to a certain latitude band around the source of perturbation energy. The critical parameters characterizing the wave as propagating or confined consist of the amplitude and meridional scale of the fluctuations. Dissert. Abstr.

N94-13647 California Univ., Los Angeles.
NUMERICAL SIMULATION AND PARAMETERIZATION OF OROGRAPHIC GRAVITY WAVES Ph.D. Thesis
Young-Joon Kim 1992 283 p
Avail: Univ. Microfilms Order No. DA9310877

The problem of parameterizing gravity waves generated by subgrid-scale orography has recently been recognized important for large-scale models of the atmosphere. It was pointed out, for example, that excessively strong

westerlies may appear in the mid-latitude Northern Hemisphere winter if subgrid-scale orographic gravity-wave drag is neglected in high-resolution simulations. To date, parameterization schemes for orographic gravity waves were evaluated only on merits of overall improvement of simulated large-scale fields. A direct way of assessing parameterization schemes by using a numerical mesoscale gravity-wave model is followed: regarding a subdomain of the mesoscale model as a horizontal grid interval of a large-scale model, two vertical drag profiles - one estimated from a parameterization scheme applied to the subdomain-averaged variables and the other calculated directly from the variables at individual grid points of the mesoscale model - are compared. As a preparatory step, theoretical and numerical studies of gravity waves over mesoscale orography and the underlying ideas behind the parameterization of orographic gravity waves are reviewed. Then a two-dimensional numerical anelastic nonhydrostatic gravity wave model developed is described and results simulated by the model are presented. Through extensive comparisons with the numerically simulated results, it was found that the treatment of low-level wave-breaking and the choice of the parameters representing orography in existing parameterization schemes should be improved: We find that not only the standard deviation of orography, which is the only information regarding orography in existing schemes, but also higher moments of orography, such as the asymmetry and convexity of orography, should be considered. In an attempt to correct these problems, a revised scheme that uses the additional orographic statistics devised was proposed. First, the scheme for isolated orography cases was tested and encouraging results were found. Then complexities caused by the irregularity of orography were investigated and some important considerations on implementing the scheme are presented. Dissert. Abstr.

N94-13707*# Colorado Univ., Boulder.
MODELING OF THE PARTITIONING OF REACTIVE ODD NITROGEN IN THE LOWER STRATOSPHERE USING AIRCRAFT MEASUREMENTS OF NOy, NO, AND OTHER TRACE SPECIES Final Report, 1 May 1991 - 30 Sep. 1992
Stephan Randolph Kawa 1992 4 p
(Grant NAGw-2586)
(NASA-CR-194305; NAS 1.26:194305) Avail: CASI HC A01/MF A01

The objective of this research was to gain a more thorough understanding of the atmospheric processes which control the partitioning of species within the reactive nitrogen (NO(y)) reservoir in the lower stratosphere. This understanding is crucial to predicting ozone loss in the stratosphere. NO(y) is defined as NO + NO2 + HNO3 + N2O5 + ClONO2 + HO2NO2 + NO3 + particulate nitrate. The research focuses on deriving the partitioning among these species using the combined set of measurements from the NASA ER-2 aircraft during recent missions designed to study stratospheric ozone depletion. Author (revised)

N94-13709*# Alabama Univ., Huntsville.
DEVELOP RESEARCH PLAN FOR USE OF ATLAS DATA Final Report
Michael Newchurch 7 Aug. 1992 3 p
(Contract NAS8-36955)
(NASA-CR-194338; NAS 1.26:194338; UAH-5-32734; Rept-136) Avail: CASI HC A01/MF A01

This contract study is devoted to performing atmospheric photochemical modeling research in conjunction with the ATLAS missions. The purpose of the work was to provide scientific understanding of the stratospheric chemical measurements performed by the suite of ATLAS instruments. Photochemical model studies of the stratosphere were performed. SAGE and Dobson Umkehr ozone measurements were studied. Derived from text

N94-13793*# Aerospace Corp., El Segundo, CA. Engineering and Technology Group.
STORMTIME TRANSPORT OF RING CURRENT AND RADIATION BELT IONS
Margaret W. Chen, Michael Schulz, L. R. Lyons, and David J. Gorney 15 Apr. 1993 19 p See also A93-30815
(Grant NAGw-2126)
(NASA-CR-194416; NAS 1.26:194416; ATR-92(7190)-2) Avail: CASI HC A03/MF A01

This is an investigation of stormtime particle transport that leads to formation of the ring current. Our method is to trace the guiding-center motion of representative ions (having selected first adiabatic invariants mu) in response to model substorm-associated impulses in the convection electric field. We compare our simulation results qualitatively with existing analytically tractable idealizations of particle transport (direct convective access and radial diffusion) in order to assess the limits of validity of these approximations. For mu approximately less than 10 MeV/G (E approximately less than 10 keV at L equivalent to 3) the ion drift period on the final (ring-current) drift shell of interest (L equivalent to 3) exceeds the duration of the main phase of our model storm, and we find that the transport of ions to this drift shell is appropriately idealized as direct convective access, typically from open drift paths. Ion transport to a final closed drift path from an open (plasma-sheet) drift trajectory is possible for those portions of that drift path that lie outside the mean stormtime separatrix between closed and open drift trajectories, For mu approximately 10-25 MeV/G (110 keV approximately less than E approximately less than 280 keV at L equivalent to 3) the drift period at L equivalent to 3 is comparable to the postulated 3-hr duration of the storm, and the mode of transport is transitional between direct convective access and transport that resembles radial diffusion. (This particle population is transitional between the ring current and radiation belt). For mu approximately greater than 25 MeV/G (radiation-belt ions having E approximately greater than 280 keV at L equivalent to 3) the ion drift period is considerably shorter than the main phase of a typical storm, and ions gain access to the ring-current region essentially via radial diffusion. By computing the mean and mean-square cumulative changes in 1/L among (in this case) 12 representative ions equally spaced in drift time around the steady-state drift shell of interest (L equivalent to 3), we have estimated (from both our forward and our time-reversed simulations) the time-integrated radial-diffusion coefficients D(sup sim)(sub LL) for particles having selected values of mu approximately greater than 15 MeV/G. The results agree surprisingly well with the predictions (D(sup ql)(sub LL)) of quasilinear radial diffusion theory, despite the rather brief duration (approximately 3 hrs) of our model storm and despite the extreme variability (with frequency) of the spectral-density function that characterizes the applied electric field during our model storm. As expected, the values of D(sup sim)(sub LL) deduced (respectively) from our forward and time-reversed simulations agree even better with each other and with D(sup sim)(sub LL) when the impulse amplitudes which characterize the individual substorms of our model storm are systematically reduced. Author (revised)

N94-13816*# Smithsonian Astrophysical Observatory, Cambridge, MA.
MEASUREMENT OF HO2 AND OTHER TRACE GASES IN THE STRATOSPHERE USING A HIGH RESOLUTION FAR-INFRARED SPECTROMETER AT 28 km Semiannual Report No. 32, 1 Jan. - 30 Jun. 1993
Wesley A. Traub, Kelly V. Chance, David G. Johnson, Kenneth W. Jucks, and Steven C. Wofsy Aug. 1993 26 p
(Grant NsG-5175)
(NASA-CR-194175; NAS 1.26:194175) Avail: CASI HC A03/MF A01

This report covers the time period 1 January 1993 to 30 June 1993. During this reporting period we had our third Upper Atmosphere Research Satellite (UARS) correlative balloon flight and submitted the results from this flight to the Central Data Handling Facility (CDHF). We made a number of improvements in our data processing software in preparation for a new analysis of our old balloon data sets. Finally, we continue to analyze the data obtained during the second Airborne Arctic Stratospheric Expedition (AASE 2). Derived from text

N94-13825*# Texas Univ. at Dallas, Richardson. Center for Space Sciences.
ATOMIC HYDROGEN AND NITROGEN DISTRIBUTIONS FROM ATMOSPHERE EXPLORER MEASUREMENTS Final Technical Report
Edward L. Breig 13 Mar. 1992 7 p
(Grant NAGw-1571)
(NASA-CR-194336; NAS 1.26:194336) Avail: CASI HC A02/MF A01

We were selective as to our approach to research activities, and devoted primary attention to two investigations concerning the global behavior of atomic hydrogen in the Earth's upper atmosphere. We derive the thermospheric concentration of H by applying the condition of charge-exchange equilibrium between hydrogen and oxygen atoms and ions to in-situ measurements of F-region composition and temperature

from the series of Atmosphere Explorer (AE) aeronomy satellites. Progress and accomplishments on these chosen research projects are summarized. Author (revised)

N94-13826*# Johns Hopkins Univ., Laurel, MD. Applied Physics Lab.
ENERGETIC NEUTRAL ATOMS: IMAGING THE MAGNETOSPHERIC RING CURRENT Final Technical Report, 1 Jun. 1985 - 31 Oct. 1989
Edmond C. Roelof 1990 5 p
(Grants NAGw-773; NSF ATM-85-07034)
(NASA-CR-194339; NAS 1.26:194339) Avail: CASI HC A01/MF A01

Magnetospheric imaging is a new discipline whose goal is to make pictures of the energetic particle populations trapped in the magnetic field of Earth (or any other planet). This project demonstrated the technical feasibility and scientific validity of magnetospheric imaging using energetic neutral atoms (ENA) with the publication and quantitative analysis of the first ENA images ever obtained from space. ENA's are produced when singly-charged energetic (approximately 100 keV) trapped ions make an atomic collision with the neutral hydrogen atoms which boil of the top of the Earth's atmosphere. These hydrogen atoms suffuse the entire trapping volume of the magnetosphere. The energetic ion steals the electron from the atmospheric hydrogen, so the energetic ion is transformed into an energetic neutral atom with a velocity of several thousands of kilometers/second. Moreover, the new-born ENA preserves the velocity that the trapped ion had at the time of the collision. Consequently, any population of energetic ions emits ENA's. Derived from text

N94-13830# Defence Research Establishment Pacific, Victoria (British Columbia).
AEROMAGNETIC WORK IN THE LINCOLN SEA: 1991 SURVEY
J. Bradley Nelson Jul. 1991 16 p
(DSIS-93-00308; DREP-LN-91-06; CTN-93-60750) Avail: CASI HC A03

Aeromagnetic survey work in 1991 included completion of the Lincoln Sea Survey, begun in 1989, and the beginning of the Axel Heiberg Survey scheduled for completion in 1993. Total field, horizontal gradient, and some vertical gradient measurements were obtained. The 1991 total field measurements in the Lincoln Sea have been merged into the 1989 and 1990 data set. A levelled, gridded, total field map and depth to magnetic source analysis for the entire Lincoln Sea Survey area and a levelled, gridded, total field map of the 1991 portion of the Axel Heiberg Survey are presented. Analysis of the 1991 survey data indicates that the short wavelength, low amplitude anomalies just offshore from northern Greenland may be continuations of the faults or volcanics visible onshore. In addition, the magnetic anomalies at the mouth of the Robeson Channel are not consistent with the proposed Wegener Fault running northward into the center of the Lincoln Sea, but the anomaly pattern may be evidence for a motion of 40 km of Greenland relative to Ellesmere Island. Finally, the high amplitude, short wavelength anomalies just offshore from Axel Heiberg Island are continuations of onshore dike structures. Author (CISTI)

N94-13912# Pacific Northwest Lab., Richland, WA.
BOUNDARY LAYER STRUCTURE OVER AREAS OF HETEROGENEOUS HEAT FLUXES
J. C. Doran, F. J. Barnes (Los Alamos National Lab., NM.), R. L. Coulter (Argonne National Lab., IL.), and T. L. Crawford (National Oceanic and Atmospheric Administration, Oak Ridge, TN.) Jan. 1993 7 p Presented at the 4th American Meteorological Society Symposium on Global Change Studies, Anaheim, CA, 14-19 Jan. 1993
(Contracts DE-AC06-76RL-01830; W-31-109-eng-38; W-7405-eng-36)
(DE93-007887; PNL-SA-21377; CONF-930142-5) Avail: CASI HC A02/MF A01

In general circulation models (GCM's), some properties of a grid element are necessarily considered homogeneous. That is, for each grid volume there is associated a particular combination of boundary layer depth, vertical profiles of wind and temperature, surface fluxes of sensible and latent heat, etc. In reality, all of these quantities may exhibit significant spatial variations in the grid area, and the larger the area the greater the likely variations. In balancing the benefits of higher resolution against increased computational time and expense, it is useful to consider what the consequences of such subgrid-scale variability may be. Moreover, in interpreting the results of a simulation, one must be able to define an appropriate average value over a grid. There are two aspects of this latter problem: (1) in observations, how does one take a set of discrete or volume-averaged measurements and relate these to properties of the entire domain; and (2) in computations, how can subgrid-scale features be accounted for in the model parameterizations? To address these and related issues, two field campaigns were carried out near Boardman, Oregon, in June 1991 and 1992. These campaigns were designed to measure the surface fluxes of latent and sensible heat over adjacent areas with strongly contrasting surface types and to measure the response of the boundary layer to those fluxes. This paper discusses some initial findings from those campaigns. DOE

N94-13949# Norwegian Defence Research Establishment, Kjeller.
A ROCKET-BORNE LIDAR FOR STUDIES OF THE MIDDLE ATMOSPHERE
Torkild Eriksen 19 Oct. 1992 105 p
(FFI/RAPPORT-92/7034; ETN-93-93977) Avail: CASI HC A06/MF A02

The design of an engineering model for a rocketborne instrument for density measurements in the middle atmosphere is described. Such measurements are essential for the knowledge of the energy budget and dynamics in the atmosphere. Rocketborne measurements are a line of research which may improve the accuracy of the density resolution. Resolution calculations are executed for three available transmitters. Different receiver systems and detectors are discussed. Digital and analog signal processing techniques are considered. Analog signal processing with precision components is preferred due to a high signal rate. A complete description of the electronics is included. ESA

N94-13954*# Alabama Univ., Huntsville.
STUDIES ON EQUATORIAL SHOCK FORMATION DURING PLASMASPHERIC REFILLING Annual Report, from 1 Aug. 1992
Nagendra Singh 1993 54 p
(Grant NAGw-2128)
(NASA-CR-194392; NAS 1.26:194392) Avail: CASI HC A04/MF A01

During the grant period starting August 1, 1992, our major effort has been on examining the presence of equatorially trapped hot plasma on plasmaspheric refilling. We performed one-dimensional PIC simulations of cold plasmas expanding into a hot plasma, consisting of hot anisotropic ions and warm isotropic electrons, trapped in a region of minimum magnetic field. Simulations showed that the electric potential barrier built up by the anisotropy of the hot ion population facilitates in the formation of electrostatic shocks when the cold ion beams begin to come into contact with the hot plasma. The shock formation occurs even when the cold ion beams are highly supersonic with respect to the ion-acoustic speed. This finding is interesting because equatorial shock formation during the early stage of plasmaspheric refilling has been debated over about two decades. In the past ion-ion instability has been invoked as the main mechanism for the coupling between the cold ion beams approaching the equator from the conjugate ionspheres. This coupling occurs when the beams are sufficiently slow; the beam velocity being less than three times the ion-acoustic speed. In the presence of hot plasma, the beams slow down by the potential barrier. The slowing down and the reflection process lead to the formation of the electrostatic shock even for highly supersonic ion beams. The mixing of hot and cold plasma was also studied. Derived from text

N94-13956*# New Mexico Univ., Albuquerque. Biology Dept.
WIND EROSION IN SEMIARID LANDSCAPES: PREDICTIVE MODELS AND REMOTE SENSING METHODS FOR THE INFLUENCE OF VEGETATION Semiannual Status Report, 1 Jan. 1992 - 30 Jun. 1993
H. Brad Musick 30 Jun. 1993 10 p
(Grant NAG5-1833)
(NASA-CR-194029; NAS 1.26:194029) Avail: CASI HC A02/MF A01

The objectives of this research are: to develop and test predictive relations for the quantitative influence of vegetation canopy structure on wind erosion of semiarid rangeland soils, and to develop remote sensing methods for measuring the canopy structural parameters that determine sheltering against wind erosion. The influence of canopy structure on wind erosion will be investigated by means of wind-tunnel and field experiments using structural variables identified by the wind-tunnel and field experiments using model roughness elements to simulate plant canopies. The canopy structural variables identified by the wind-tunnel and field experiments as important in determining vegetative sheltering against wind erosion will then be measured at a number of naturally vegetated field sites and

compared with estimates of these variables derived from analysis of remotely sensed data. Author (revised)

N94-13960*# National Aeronautics and Space Administration. Goddard Space Flight Center, Greenbelt, MD.

SIMULTANEOUS SOLUTION FOR CORE MAGNETIC FIELD AND FLUID FLOW BENEATH AN ELECTRICALLY CONDUCTING MANTLE

Coerte V. Voorhies and Masahiro Nishihama (Hughes STX, Inc., Lanham, MD.) Sep. 1993 15 p Sponsored by NASA. Washington

(NASA-TM-4536; Rept-93E02367; NAS 1.15:4536) Avail: CASI HC A03/MF A01

The effects of laterally homogeneous mantle electrical conductivity were included in steady, frozen-flux core surface flow estimation along with refinements in method and weighting. The refined method allows simultaneous solution for both the initial radial geomagnetic field component at the core-mantle boundary (CMB) and the sub-adjacent fluid motion; it also features Gauss' method for solving the non-linear inverse problem associated with steady motional induction. The tradeoff between spatial complexity of the derived flows and misfit to the weighted Definitive Geomagnetic Reference Field models (DGRF's) is studied for various mantle conductivity profiles. For simple flow and a fixed initial geomagnetic condition, a fairly high deep-mantle conductivity performs better than either insulating or weakly conducting profiles; however, a thin, very high conductivity layer at the base of the mantle performs almost as well. Simultaneous solution for both initial geomagnetic field and flow reduces the misfit per degree of freedom even more than does changing the mantle conductivity profile. Moreover, when both core field and flow are estimated, the performance of the solutions and the derived flows become insensitive to the conductivity profile. Author

N94-13967*# Alabama Univ., Huntsville. College of Science.

THE ROLE OF IONOSPHERIC PLASMA IN THE MAGNETOSPHERE Final Report, Aug. 1990 - 1993

Gordon R. Wilson Sep. 1993 9 p

(Grant NAG8-822)

(NASA-CR-194404; NAS 1.26:194404) Avail: CASI HC A02/MF A01

During the course of this project we have made a great deal of progress developing and using a new plasma modeling technique which we now refer to as the Generalized Semikinetic (GSK) model. It has been used to study the development of plasma flows in the plasmasphere, the polar cap and auroral zones, and the transition region. Below we describe some of the major accomplishments of this grant. Derived from text

N94-13969*# California Inst. of Tech., Pasadena. Dept. of Geological and Planetary Sciences.

CHEMISTRY AND TRANSPORT IN A MULTI-DIMENSIONAL MODEL Annual Performance Report

Yuk L. Yung 1993 5 p

(Grant NAGw-413)

(NASA-CR-194425; NAS 1.26:194425) Avail: CASI HC A01/MF A01

The focus of our research program is the achievement of a quantitative understanding of the spatial distribution and temporal variation of chemical species in the terrestrial middle atmosphere, with emphasis on ozone. Although not directed at assessments of anthropogenic impacts, our activities contribute to a refinement of model descriptions of chemical and dynamical processes that are needed for assessment tasks. A unique feature of our research effort is a close interaction with the chemical kinetics group at JPL and the field measurement groups at JPL. The principal tools used in our investigations are I-D and 2-D photochemical models. The advective component of the meridional transport in these models is approximated by the diabatic circulation, which is derived diagnostically from the net radiative heating rates. We are developing accurate radiative transfer algorithms to find the net heating rates and the diabatic circulation for use in the 2-D model. Derived from text

N94-14049*# Colorado Univ., Boulder. Dept. of Aerospace Engineering Sciences.

IONOSPHERIC CALIBRATION FOR SINGLE FREQUENCY ALTIMETER MEASUREMENTS

William S. Schreiner and George H. Born 31 Aug. 1993 24 p

(Grant NAG1-1491)

(NASA-CR-194282; NAS 1.26:194282) Avail: CASI HC A03/MF A01

This report investigates the potential of using Global Positioning System (GPS) data and a model of the ionosphere to supply a measure of the sub-satellite Total Electron Current (TEC) of the required accuracy (10 TECU rms) for the purpose of calibrating single frequency radar altimeter measurements. Since climatological (monthly mean) models are known to be in error by as much as 50 percent, this work focused on the Parameterized Real-Time Ionospheric Specification Model (PRISM) which has the capability to improve model accuracy by ingesting (adjusting to) in situ ionospheric measurements. A set of globally distributed TEC measurements were generated using GPS data and were used as input to improve the accuracy of the PRISM model. The adjusted PRISM TEC values were compared to TOPEX dual frequency TEC measurements (which are considered truth) for a number of TOPEX sub-satellite tracks. The adjusted PRISM values generally compared to the TOPEX measurements within the 10 TECU accuracy requirements when the sub-satellite track passed within 300 to 400 km of the GPS TEC data or when the track passed through a night time ionosphere. However, when the sub-satellite points were greater than 300 to 400 km away from the GPS TEC data or when a local noon ionosphere was sampled, the adjusted PRISM values generally differed by greater than 10 TECU rms with data excursions from the TOPEX TEC measurements of as much as 40 TECU (an 8 cm path delay error at K band). Therefore, it can be concluded from this analysis that an unrealistically large number of GPS stations would be needed to predict sub-satellite TEC at the 10 TECU level in the day time ionosphere using a model such as PRISM. However, a technique currently being studied at the Jet Propulsion Laboratory (JPL) may provide a means of supplying adequate TEC data to meet the 10 TECU ionospheric correction accuracy when using a realistic number of ionospheric stations. This method involves using global GPS TEC data to estimate a global grid of vertical ionospheric TEC as a function of time (i.e. every one half hour) in a sun-fixed longitude frame. Working in a sun-fixed longitude frame, one is not limited by the spatial decorrelation distance of the ionosphere, but instead is limited more by the temporal correlations of the ionosphere in the sun-fixed frame which are a smaller effect. It is the opinion of the authors that using the global sun-fixed TEC grid data, in particular, ingesting it into PRISM, offers the best possibility of meeting the 10 TECU ionospheric correction accuracy requirement, and should be the subject of further study. Author (revised)

N94-14132# Deutsche Forschungsanstalt fuer Luft- und Raumfahrt, Oberpfaffenhofen (Germany). Abt. Meteorologische Flugmesssysteme.

FLUXES OF HEAT AND WATER VAPOUR IN A CONVECTIVE MIXED LAYER DURING EFEDA

Berenice I. Michels May 1992 81 p

(DLR-FB-92-21; ETN-93-93738) Avail: CASI HC A05/MF A01

A case study of the transport of sensible and latent heat in a convective boundary layer over complex terrain is presented. The method to analyze turbulence data from Falcon flights during the EFEDA (ECHIVAL Field Experiment for Desertification Threatened Areas) pilot study is described. For two flights of 23 Jun. 1991, a case study is made concerning the vertical flux profiles of heat and water vapor. Both flights include two different legs. The total fluxes are shown, together with a thermodynamic decomposition into different types of motions. The structural development of the atmospheric boundary layer is discussed. The results show different surface characteristics (evaporative fraction) for the two legs, resulting in an atmospheric boundary layer, which is horizontally not uniform but shows significantly different vertical flux profiles throughout the mixed layer. ESA

N94-14192# Office National d'Etudes et de Recherches Aerospatiales, Paris (France).

OPTICAL PROPAGATION THROUGH ATMOSPHERIC TURBULENCE. MODEL ANALYSIS OF ANISOPLANATISM AND APPLICATION TO ADAPTIVE OPTICS Ph.D. Thesis - Paris-Sud Univ. [PROPAGATION OPTIQUE A TRAVERS LA TURBULENCE ATMOSPHERIQUE. ETUDE MODALE DE L'ANISOPLANETISME ET APPLICATION A L'OPTIQUE ADAPTATIVE]

Francois Chassat Nov. 1992 204 p In FRENCH

(ONERA-P-1992-4; ETN-93-93967) Avail: CASI HC A10/MF A03

The correction capability of adaptive optics techniques is discussed. The correction capability of these techniques is limited by: no amplitude correction, difference between the sensing, the correcting wavelengths, and anisoplanatism effect. A theoretical analysis of this phenomenon is performed, considering the modal expansion of the wavefronts on the

Zernike polynomials. The spatial correlation of the modal expansion coefficients is derived. The results can be used: to characterize the performance of an adaptive optics system against anisoplanatism; to optimize this performance by tuning up the number of corrected modes; to limit the loss of correction quality due to anisoplanatism by feedback into the correction process. The possibility of working back from the wavefront measurements on a binary star to the profile of the refractive index fluctuations constant is explained. The experiments carried out to investigate the anisoplanatism effects and to validate the theory are presented. ESA

N94-14294# EG and G Energy Measurements, Inc., Las Vegas, NV. Remote Sensing Lab.

SURVEY OF SUBSURFACE GEOPHYSICAL EXPLORATION TECHNOLOGIES ADAPTABLE TO AN AIRBORNE PLATFORM

K. A. Taylor Dec. 1992 75 p

(Contract DE-AC08-88NV-10617)

(DE93-015080; EGG-10617-1216) Avail: CASI HC A04/MF A01

This report has been prepared by the US Department of Energy (DOE) as part of a Research Development Demonstration Testing and Evaluation (RDDT&E) project by EG&G Energy Measurement's (EG&G/EM) Remote Sensing Laboratory. It examines geophysical detection techniques which may be used in Environmental Restoration/Waste Management (ER/WM) surveys to locate buried waste, waste containers, potential waste migratory paths, and aquifer depths. Because of the Remote Sensing Laboratory's unique survey capabilities, only those technologies which have been adapted or are capable of being adapted to an airborne platform were studied. This survey describes several of the available subsurface survey technologies and discusses the basic capabilities of each: the target detectability, required geologic conditions, and associated survey methods. Because the airborne capabilities of these survey techniques have not been fully developed, the chapters deal mostly with the ground-based capabilities of each of the technologies, with reference made to the airborne capabilities where applicable. The information about each survey technique came from various contractors whose companies employ these specific technologies. EG&G/EM cannot guarantee or verify the accuracy of the contractor information; however, the data given is an indication of the technologies that are available. DOE

N94-14306*# Texas Univ., Austin. Center for Space Research.

THE DETERMINATION OF CRUSTAL MOTIONS USING LASER RANGING TO LAGEOS-2 AND LAGEOS-1 Annual Report, 1 Oct. 1992 - Jun. 1993

Byron D. Tapley and B. E. Schutz 1993 4 p

(Grant NAGw-1959)

(NASA-CR-193787; NAS 1.26:193787) Avail: CASI HC A01/MF A01

During the period October 1992 through June 1993, Center for Space Research efforts continued on four areas: (1) production of a solution for terrestrial reference frame including site positions, velocities, and Earth orientation and rotation spanning the entire Lageos-1 mission, (2) production of a solution for terrestrial reference frame including site positions and Earth orientation spanning the Lageos-2 mission, independently from Lageos-1, (3) evaluation of numerical characteristics of the integration of the Lageos-2 orbit, (4) evaluation of contributions of Lagecs-1 and Lageos-2 to temporal variations in the geopotential and 18.6 year tidal response of the Earth, and (5) attendence and participation in Lageos-2 Investigator Working Group Meetings and Committees. Author (revised)

N94-14328# Los Alamos National Lab., NM.

TERRESTRIAL MAGNETOSPHERIC IMAGING: NUMERICAL MODELING OF LOW ENERGY NEUTRAL ATOMS

K. R. Moore, H. O. Funsten, D. J. McComas, E. E. Scime, and M. F. Thomsen 1993 13 p Presented at the Annual Meeting of the Society of Photo-Optical Instrumentation Engineers, San Diego, 11-16 Jul. 1993

(Contract W-7405-eng-36)

(DE93-014561; LA-UR-93-1798; CONF-930722-3) Avail: CASI HC A03/MF A01

Imaging of the terrestrial magnetosphere can be performed by detection of low energy neutral atoms (LENA's) that are produced by charge exchange between magnetospheric plasma ions and cold neutral atoms of the Earth's geocorona. As a result of recent instrumentation advances it is now feasible to make energy-resolved measurements of LENA's from less than 1 keV to greater than 30 keV. To model expected LENA fluxes at a spacecraft, we initially used a simplistic, spherically symmetric magnetospheric plasma model. We now present improved calculations of both hydrogen and oxygen line-of-sight LENA fluxes expected on orbit for various plasma regimes as predicted by the Rice University Magnetospheric Specification Model. We also estimate expected image count rates based on realistic instrument geometric factors, energy passbands, and image accumulation intervals. The results indicate that presently proposed LENA instruments are capable of imaging of storm time ring current and potentially even quiet time ring current fluxes and that phenomena such as ion injections from the tail and subsequent drifts toward the dayside magnetopause may also be deduced. DOE

N94-14338# Indiana Univ., Bloomington.

ORGANIC GEOCHEMICAL AND TECTONIC EVOLUTION OF THE MIDCONTINENT RIFT SYSTEM

J. M. Hayes, L. M. Pratt, and A. H. Knoll (Harvard Univ., Cambridge, MA.) 1992 5 p

(Contract DE-FG02-88ER-13978)

(DE93-015093; DOE/ER-13978/4) Avail: CASI HC A01/MF A01

The older assemblages stand in contrast with the ca. 1000 Ma old Hunting Formation, Arctic Canada, which contains what may be the oldest evidence for modern algae - red algal fossils that compare closely with members of the extant family Bangiophyceae (Butterfield et al., 1990). Taken together the Nonesuch, Shaler, Hunting, and other assemblages support the hypothesis of a major episode of eukaryotic diversification ca. 1000 Ma ago. Prior to this time, eukaryotic primary producers must have been physiologically primitive (and now extinct) algae whose abundance in ecosystems is poorly constrained by analogies with the present oceans. Cyanobacteria were major primary producers in a wide range of marine environments. After 1000 Ma, diversifying red green and chromophyte algae contributed significantly to primary production in all save microbial mat communities in restricted environments. It bears mention that such mat communities remained significant potential sources of buried organic matter until the end of the Proterozoic, necessitating exploration strategies that differ from those commonly employed for younger rocks (Knoll, in press). As in Phanerozoic basins, petroleum exploration in Proterozoic rocks requires tools for stratigraphic correlation. In Neoproterozoic (less than 1000 Ma) rocks, biostratigraphy is possible, and it is aided significantly by C and Sr isotopic chemostratigraphy. New data from the Shaler Group contribute to the construction of C and Sr isotopic curves for Neoproterozoic time, making possible much improved chronostratigraphy for this time interval. DOE

N94-14424# Argonne National Lab., IL.

EVOLUTION OF THE LOWER PLANETARY BOUNDARY LAYER OVER STRONGLY CONTRASTING SURFACES

R. L. Coulter, W. Gao, T. J. Martin, J. D. Shannon, J. C. Doran (Pacific Northwest Lab., Richland, WA.), J. M. Hubbe (Pacific Northwest Lab., Richland, WA.), and W. M. Shaw (Pacific Northwest Lab., Richland, WA.) 1992 5 p Presented at the 72nd American Meteorological Society Conference, Atlanta, GA, 5-10 Jan. 1992

(Contract W-31-109-eng-38)

(DE93-010667; ANL/ER/CP-73469; CONF-920134-7) Avail: CASI HC A01/MF A01

In a multilaboratory field study held near Boardman, Oregon, in June 1991, various properties of the surface and lower atmospheric boundary layer over heavily irrigated cropland and adjacent desert steppe were investigated in the initial campaign of the Atmospheric Radiation Measurement (ARM) program. The locale was selected because its disparate characteristics over various spatial scales stress the ability of general circulation models (GCM's) to describe lower boundary conditions, particularly across the discontinuity between desert (in which turbulent flux of heat must be primarily as sensible heat) and large irrigated tracts (in which turbulent flux of latent heat should be the larger term). This campaign of ARM seeks to increase knowledge in three critical areas: (1) determination of the relationships between surface heat fluxes measured over multiple scales and the controlling surface parameters within each scale, (2) integration of local and nearly local heat flux estimates to produce estimates appropriate for GCM grid cells of 100-200 km horizontal dimension, and (3) characterization of the growth and development of the atmospheric boundary layer near transitions between surfaces with strongly contrasting moisture availabilities. DOE

N94-14425# National Oceanic and Atmospheric Administration, Oak Ridge, TN.
ATMOSPHERIC TURBULENCE AND DIFFUSION RESEARCH
R. P. Hosker, Jr. 31 Mar. 1993 66 p
(DE93-011842; ATDL-93011842) Avail: CASI HC A04/MF A01

The Atmospheric Turbulence and Diffusion Division (well known in the atmospheric dispersion community as the Atmospheric Turbulence and Diffusion Laboratory (ATDL)) is one of several field facilities of NOAA's Air Resources Laboratory, headquartered in Silver Spring, Maryland. The laboratory conducts research on matters of atmospheric diffusion and turbulent exchange, concerning air quality. ATDD focuses attention on the physics of the lower atmosphere, with special emphasis on the processes contributing to atmospheric transport, dispersion, deposition, and air-surface exchange, and on the development of predictive capabilities using the results of this research. Research is directed toward issues of national and global importance related to the missions of DOE, to DOE's Oak Ridge Field Office, and to NOAA. The program is divided into four major projects: plume transport and diffusion in the planetary boundary layer, complex topography, canopy micrometeorology, and air-surface exchange. DOE

N94-14518# Los Alamos National Lab., NM.
ATMOSPHERIC ACOUSTIC MODELING
E. M. D. Symbalisty, T. J. Fitzgerald, A. R. Jacobson, and R. W. Whitaker Jun. 1993 43 p
(Contract W-7405-eng-36)
(DE93-016727; LA-12566-MS) Avail: CASI HC A03/MF A01

We study the propagation of acoustic pulses in the atmosphere from the ground to the ionosphere, and to the time where part of the wave is headed back down to the ground. The study is accomplished via two computer codes, FLOTUBE and AADCAT. We include the effects of viscous dissipation and heat conduction and investigate the influence of the initial strength of the acoustic pulse. Wave flow through caustic regions is illustrated. DOE

47 METEOROLOGY AND CLIMATOLOGY

Includes weather forecasting and modification.

N94-12837# National Board of Waters and the Environment, Helsinki (Finland).
SNOW COVER MODELS IN OPERATIONAL WATERSHED FORECASTING
B. Vehvilaeinen 1992 112 p
(DE93-778332; VYH-PUB-11) Avail: CASI HC A06/MF A02

This study deals with water quality and acidification of 12 small lakes in the proposed national park area of Repovesi in 1990 - 1991. Water samples were taken also from two big lakes, Lake Repovesi and Lake Tihvetjaervi. Diatoms and metals were analyzed from a sediment profile of a small clearwater lake. The national acidification research project (HAPRO) included none of the lakes in the Repovesi area. The small lakes were mainly clearwater lakes with the exception of one humic pond. They were oligotrophic. The buffer capacity against acidification was very low. Two of the lakes were permanently acidic. Sulphate was the dominating anion except in the humic pond. Acid snowmelt waters increased markedly the nitrate nitrogen contents under the ice cover. Acidification models showed that alkalinity values have decreased much in the small lakes. Comparison between the old (from the 1960's) and new water quality results showed also the development of acidification e.g., in water color and in chemical oxygen demand. However, acidification was not evident in the paleolimnological investigations of one of the lakes. The diatoms reflected above all the clarity of water. The dominate species were Cyclotella kuetzingiana var. radiosa and C. kuetzingiana. The forestry measures in the nearby catchment area of the lake were poorly reflected in the diatom flora. Acidification in the Repovesi area is not as advanced as in the headwaters south of Salpausselkae or e.g., in the Nuuksio area in northern Espoo. The water quality of Lake Repovesi is classified as excellent. Lake Tihvetjaervi is mesotrophic. Risks to water protection consist of air pollution and of possible forestry measures. DOE

N94-12839*# Florida State Univ., Tallahassee. Dept. of Meteorology.
THE APPLICATION OF VAS SATELLITE IMAGERY TO THUNDERSTORM FORECASTING AT CAPE CANAVERAL Final Report, 1 Aug. 1988 - 29 Apr. 1993
Henry E. Fuelberg 12 Aug. 1993 4 p
(Grant NAG10-0047)
(NASA-CR-193563; NAS 1.26:193563; FSU-1338-592-26) Avail: CASI HC A01/MF A01

The Final Report on the application of VAS satellite imagery to thunderstorm forecasting at Cape Canaveral is presented. The objective of this research was to investigate whether satellite-derived imagery and derived products could be used advantageously in forecasting thunderstorms in the Cape Canaveral area. Specifically, data from the VISSR Atmospheric Sounder that is housed on the current series of GOES geostationary meteorological satellites was used. These satellite data were used extensively in the middle latitudes, but their utility over central Florida where the climate is more tropical had not been examined. Derived from text

N94-12903# Pacific Northwest Lab., Richland, WA.
A PARAMETERIZATION OF CLOUD DROPLET NUCLEATION
S. J. Ghan, C. Chuang, and J. E. Penner (Lawrence Livermore National Lab., CA.) Jan. 1993 7 p Presented at the 4th American Meteorological Society Symposium on Global Change Studies, Anaheim, CA, 14-19 Jan. 1993
(Contract DE-AC06-76RL-01830)
(DE93-007998; PNL-SA-20914; CONF-930142-4) Avail: CASI HC A02/MF A01

Droplet nucleation is a fundamental cloud process. The number of aerosols activated to form cloud droplets influences not only the number of aerosols scavenged by clouds but also the size of the cloud droplets. Cloud droplet size influences the cloud albedo and the conversion of cloud water to precipitation. Global aerosol models are presently being developed with the intention of coupling with global atmospheric circulation models to evaluate the influence of aerosols and aerosol-cloud interactions on climate. If these and other coupled models are to address issues of aerosol-cloud interactions, the droplet nucleation process must be adequately represented. Here we introduce a droplet nucleation parametrization that offers certain advantages over the popular Twomey parameterization. DOE

N94-12918# World Meteorological Organization, Geneva (Switzerland). World Climate Applications and Services Programme.
BIBLIOGRAPHY OF URBAN CLIMATE IN TROPICAL/SUBTROPICAL AREAS, 1981-1991
Ernesto Jauregui (Universidad Nacional Autonoma de Mexico, Mexico City.) May 1993 94 p
(WCASP-25; WMO/TD-552) Avail: CASI HC A05; print copy available at WMO, Geneva, Switzerland

Among the specific objectives of the first phase of the TRUCE project is the compilation of an inventory of available knowledge and on-going research related to urban climates in tropical areas. In conformity with this plan, the present writer has prepared an overview of development and bibliography on urban climate in tropical/subtropical areas for the period 1981-1991. The bibliography includes related areas of research such as urban air pollution, urban planning and energy consumption. The main source of information for this bibliography has been the scientific journal 'Meteorological and Geoastrophysical Abstracts' and other periodicals easily accessible in most university or institute libraries. Derived from text

N94-12957*# Alabama Univ., Huntsville. Earth System Science Lab.
DEVELOPMENT OF A GLOBAL BACKSCATTER MODEL FOR NASA'S LASER ATMOSPHERIC WIND SOUNDER Final Report, 31 Jan. 1989 - 30 Sep. 1992
David Bowdle, Laurie Collins, Douglas Mach, Richard McNider, and Aaron Song 1992 30 p
(Contract NAS8-37585)
(NASA-CR-192581; NAS 1.26:192581) Avail: CASI HC A03/MF A01

During the Contract Period April 1, 1989, to September 30, 1992, the Earth Systems Science Laboratory (ESSL) in the Research Institute at the University of Alabama in Huntsville (UAH) conducted a program of basic research on atmospheric backscatter characteristics, leading to the development of a global backscatter model. The ESSL research effort was

carried out in conjunction with the Earth System Observing Branch (ES43) at the National Aeronautics and Space Administration (NASA) Marshall Space Flight Center, as part of NASA Contract NAS8-37585 under the Atmospheric Dynamics Program at NASA Headquarters. This research provided important inputs to NASA's GLObal Backscatter Experiment (GLOBE) program, especially in the understanding of global aerosol life cycles, and to NASA's Doppler Lidar research program, especially the development program for their prospective space-based Laser Atmospheric Wind Sounder (LAWS). Derived from text

N94-12978# Phillips Lab., Hanscom AFB, MA.
DMSP F11 SSM/T-2 CALIBRATION AND VALIDATION Final Report, Jan. - Nov. 1992
V. Falcone, M. K. Griffin, R. G. Isaacs, J. D. Pickle, and J. F. Morrissey 29 Oct. 1992 447 p
(AF Proj. 6670)
(AD-A265817; PL-TR-92-2293; ERP-1111) Avail: CASI HC A19/MF A04

Calibration and validation of the Defense Meteorological Satellite Program (DMSP) Special Sensor Microwave Water Vapor Sounder (SSM/T-2) is investigated. The objective of the effort is to obtain simultaneous independent measurements of microwave radiance, water vapor mass, specific humidity, and relative humidity to quantitatively measure the performance of the instrument (calibration) and to validate the ability of the SSM/T-2 to measure the water vapor parameters, i.e. the environmental data records (EDRs) of Air Force Global Weather Central (AFGWC). Analysis of satellite and aircraft data for calibration using both underflights and radiative transfer calculation show that the SSM/T-2 is performing within or exceeds the original contract specifications (1K). The SSM/T-2 retrieved vertical moisture profiles (EDRs) are performing within the contract specification of +/- 30 RH when compared with collocated radiosonde data except over certain ocean atmospheres. DTIC

N94-12992# Air Force Inst. of Tech., Wright-Patterson AFB, OH.
ON THE VERTICAL STRUCTURE OF SEASONAL, INTERANNUAL AND INTRASEASONAL FLOWS M.S. Thesis
Steven R. Gilbert Dec. 1992 200 p
(AD-A265346; AFIT/CI/CIA-92-30D) Avail: CASI HC A09/MF A03

The vertical structure of the height and wind fields associated with the seasonal, interannual, and intraseasonal cycles is documented by making use of global ECMWF operational analyses for seven pressure levels (1000-100 mb) and spanning a 10 year period (1980-89). The role of tropical convection is examined for each of these time scales. The seasonal cycle is described through the structure of the geopotential height field standing waves, the vertical structure of the first seven wavenumbers of the rotational and divergent winds, and latitude/time cross-sections for the vertical structure of the planetary waves. The change in the vertical structure from the internal mode combinations found in the tropics to a dominant external mode of the extratropics occurs rapidly and within 10 deg of the convective source regions. Extensive use is made of a primitive equation (PE) model, as a diagnostic tool, to explore the extent to which tropical heating might influence the extratropical vertical structure. The PE response indicates the possibility that 25-40% of the Northern Hemisphere and 30-55% of the Southern Hemisphere kinematic vertical structure could be the result of tropical heating. Two significant El Nino Southern Oscillation (ENSO) events occur during this 10 year period and their vertical structures are examined. The cold phase is found to be dominated by higher internal modes than the warm phase. This may be linked to different air-sea interactive processes during cold and warm ENSO phases. DTIC

N94-13080# Nevada Univ., Reno. Desert Research Inst.
LINKAGE OF ANTHROPOGENIC AEROSOL TO CLOUDS AND CLIMATE
J. G. Hudson 14 Dec. 1992 24 p
(Contract DE-FG08-90ER-61012)
(DE93-016434; DOE/ER-61012/T3) Avail: CASI HC A03/MF A01

During the first year of this project, equipment was built to obtain direct droplet measurement data from a mobile platform in fog (or mountain impacted stratum) and to characterize CCN according to particle volatility (thermal processing). Since the start date, 15 July 1990, was during the California stratus season, and it was necessary to complete the construction of equipment and allow time before a field project, it was not possible to begin field work until the summer of 1991. This report discusses surface measurements made in 1991 and 1992 as well as the SEAHUNT (Shiptrail Evolution Above High Updraft Naval Targets) Project and the ASTEX (Atlantic Stratocumulus Transition Experiment) Project. DOE

N94-13119# Wisconsin Univ., Madison.
AN EXPERIMENTAL REGIONAL SCALE CLIMATE SIMULATION LABORATORY
1993 4 p
(Contract DE-FG02-92ER-61474)
(DE93-015935; DOE/ER-61474/1) Avail: CASI HC A01/MF A01

The major focus of this CHAMMP science team project is the development and in-model testing of new numerical methods and dynamical algorithms which are particularly well suited to massively parallel computers. The project includes efforts relevant to both global ocean circulation models and atmospheric General Circulation Models (GCM's) During the first year of the project we have been focusing on two basic areas. The first of these is the implementation and testing of a global non-linear dynamics code using the Local Spectral (LS) formalism. During the first year of the CHAMMP project we have been focusing on developing an efficient parallel implementation of a spherical LS code on a massively parallel computer. Our initial implementation platform has been the Thinking Machines CM5 system. We have completed an initial implementation of the LS system on the CM5 using a semi-spectral partitioning where the convolution sums in the LS kernel are computed using direct convolutions in the meridional direction and FFT based fast convolutions are performed using the Winnograd method in the zonal direction. A second element of the first year effort has been the evaluation of alternate dynamical systems for use in global ocean circulation models. In this area, we have concentrated our efforts on parabolic non-hydrostatic systems using artificial compressibility. DOE

N94-13175# Instituto de Pesquisas Espaciais, Sao Jose dos Campos (Brazil).
CYCLOGENESIS AND CYCLONE OVER SOUTH AMERICA Ph.D. Thesis [CICLOGENESES E CICLONES SOBRE A AMERICA DO SUL]
Manoel Alonso Gan Apr. 1992 212 p In PORTUGESE
(INPE-5400-TDI/479) Avail: CASI HC A10/MF A03

The propose of this study is to establish the most frequent place and season for cyclogenesis and to describe the mechanisms that cause cyclogenesis in South America region. A 10 year (1979-1988) climatological study of surface cyclogenesis is done. The results show that the higher frequency of cyclogenesis occurs during the winter and the lower frequency occurs during the summer time. The interannual variation was also examined. The winter of 1983, 1986, and 1987 'El Nino' years presented higher frequency of cyclogenesis while the winter of 1981 (positive Southern Oscillation Index) presented a minimum. Winters of maximum (minimum) frequency of cyclogenesis are associated with above (bellow) normal precipitation over Southern Brazil. The results of a linear quasi-geostrophic multilevel model, with latent heat release, show that the seasonal and interannual variations of the frequency of cyclogenesis are associated with baroclinics mechanisms. The two case studies (summer and winter) show that baroclinic and orographic mechanisms are responsible for cyclogenesis. The winter case shows that baroclinic mechanisms are responsible for cyclogenesis. The effect of topographic wave is noted in the cyclone's initial path. The summer case shows that cyclogenesis is caused by effects of orography and the cyclone intensification by baroclinic effects. A correlation analysis of both unfiltered and high-pass filtered geopotential height data showed the occurrence of a wavelike pattern moving to east and tilting to west with the height. The orographic effects appear when the wave gets close to the Andes Cordillera. The wavelike pattern that appears in the high-pass filtered data suggests a spatial structure and a displacement similar to the most unstable normal modes of quasi-geostrophic model with mountain range placed in north-south direction. Author

N94-13188 Tel-Aviv Univ. (Israel). Dept. of Interdisciplinary Studies.
LIGHTNING SIMULATION AND DETERMINATION OF EXPECTED STRIKING POINTS M.S. Thesis
Inna Nissenbaum Dec. 1991 73 p In HEBREW
(ITN-93-85202) Copyright Avail: Issuing Activity (Tel-Aviv Univ., Exact Sciences Library, Ramat Aviv 69978, Israel)

A dynamic model was developed for the propagation of a lightning

leader stroke, and a general algorithm was developed, which does not depend on boundary conditions. The numerical method was selected to match the calculation speed and memory capacity of an AT personal computer. In contrast to other models, which check field strength values at discrete points, the model described here facilitates calculations throughout the region of interest, and includes the nonlinear effects of local discharges. C language and BGI graphics are used and the software provides both color-graphic and numerical display of the results, comprising electric field strength and potential values. The model was used to calculate expected strike points. The results were not verified experimentally, but comparisons with published theoretical and field results indicated satisfactory agreement. ISA

N94-13404# Lawrence Livermore National Lab., CA.
PRELIMINARY METEOROLOGICAL RESULTS FOR 1992 WEST COAST SCOTLAND EXPERIMENT
H. F. Robey Jan. 1993 17 p
(Contract W-7405-eng-48)
(DE93-014677; UCRL-ID-112984) Avail: CASI HC A03/MF A01

This memo documents preliminary meteorological results from the 1992 West Coast Scotland Experiment, a joint US/UK radar ocean imaging experiment. Measurements of wind speed and direction are reported for both phases of the experiment covering the periods from 7-13 June and from 19-25 June. The measurements were obtained using a Campbell Scientific CR10 Datalogger and R. M. Young model 03001-5 anemometer and wind vane. The anemometer has a resolution of 0.1 m/s and the wind vane 1 deg, but the motion of the ship platform reduces the precision of the direction measurements to +/- 10 deg. Data were downloaded to an IBM PC-AT for final storage and analysis. The anemometer was mounted at a height of 10 meters above the mean water surface on top of a mast located at the bow of the Royal Marine Auxiliary Service (RMAS) tug, Cairn. The Cairn was moored at the center of the experiment site at 57 deg 7.13755 min N, 5 deg 44.88521 min W in the Sound of Sleat, nominally 200 meters from the ship track. Wind velocity and direction were recorded at a sample rate of 0.2 Hz, and the averaged value was output every 10 minutes from approximately 2 hours before the start of the first run to 2 hours after the end of the last run. Data are plotted in the following pages in 2 formats for a quick visual summary of the daily wind conditions. The top plot gives wind velocity (m/s) and direction (deg true) vs time given in minutes relative to the start of the first run which is designated as T. The lower plot gives a polar plot of the same data with velocity on the radial axis and direction on the azimuthal axis. The final two plots give a summary of the wind speed vs direction for phase 1 (7-13 June) and phase 2 (19-25 June). DOE

N94-13429# Instituto de Pesquisas Espaciais, Sao Jose dos Campos (Brazil).
SPATIAL VARIABILITY OF THROUGHFALL CHEMISTRY IN A TROPICAL RAINFOREST (CENTRAL AMAZONIA, BRAZIL)
Maria Cristina Forti and Colin Neal (Institute of Hydrology, Wallingford, England.) 1992 20 p Repr. from The Science of the Total Environment (Amsterdam, Netherlands, Elsevier Science Publishers B.V.), v. 120, 1992 p 245-259
(INPE-5431-PRE/1765) Avail: CASI HC A03/MF A01

A statistical analysis is made on throughfall data for a location in a 'terra firme' rain forest in central Amazonia. The results show a large variability in water and chemical fluxes. For all the ions there is a variance in the mean value due to the positions of sample collectors. Despite the large variability, throughfall volume is correlated with rainfall. This is not the case for any of the chemicals studied. The use of a transect design with collectors at variable positions is shown to be sound. It is concluded that to obtain flux estimates to within 10 percent of the mean at 90 percent confidence level, about 300 collections are required for the wet period and 200 collections are required for the dry period. It is proposed that in future studies, a minimum of 20 roving gages over as wide an area as practical be employed to achieve reliable estimates. Sampling programs should run for a period of at least one year. Author (revised)

N94-13516 Alberta Univ., Edmonton. Dept. of Geography.
REMOTE IDENTIFICATION OF RAIN AND HAIL WITH A POLARIZATION DIVERSITY RADAR Ph.D. Thesis
Kais J. L. Al-Jumily 1989 203 p
(ISBN-0-315-55623-4; CTN-93-60733) Copyright Avail: Micromedia Ltd., Technical Information Centre, 165 Hotel de Ville, Place du Portage, Phase 2, Hull, Quebec J8X 3X2, Canada HC/MF

Measurements made with a 2.88 GHz circular polarization diversity radar are compared with ground based observations of precipitation to improve the use of polarization methods for distinguishing hail from rain. Case studies involve light and heavy rain and rain/hail mixtures selected to represent the spectrum of precipitation rate, location, type, and duration. Propagation effects due to precipitation between the radar and target and the way in which they can be recognized and removed from radar measurements are incorporated into the evaluation. These improve data interpretation and thereby better determine the polarization characteristics of precipitation particles. Relations developed between the reflectivity factor and polarization parameters show that certain combinations of reflectivity and polarization measurements can be used to discriminate between rain and hail regions in storms and that neither reflectivity nor polarization measurements can be considered separately. A new technique, based on a combination of reflectivity and differential reflectivity derived from circular polarization measurements after propagation effects are removed, is developed for remote identification of rain and hail with radar. The method is tested on ground based observations. Results show that predicted hail regions correlate well with the surface hail pattern. Author (CISTI)

N94-13587# Institut Royal Meteorologique de Belgique, Brussels.
STORM PREDICTION THROUGH BAROMETRIC FIELD ANALYSIS [CONTRIBUTION A LA PREVISION DES ORAGES PAR L'ANALYSE DU CHAMP DE TENDANCE BAROMETRIQUE]
Martine Vertez 1992 62 p In FRENCH
(Publ-Ser-A-129; ETN-93-94379) Avail: CASI HC A04/MF A01

A study, whose aim was to bring more certitude to the prediction of when storms would break out and the extent of their violence, is reported. The theory of storms, what they are, and the different types that occur are considered. Theories of convection are discussed and meteorological observations of wind, pressure, rain, temperature, and humidity are considered. The use of satellite images in storm prediction is discussed. A case study which analyzes the information available at the time of the outbreak of the storm in the Brussels (Belgium) region on 2 Jul. 1991 is presented. The following are considered in this analysis: atmospheric situation, synoptic observations, radar maps, barometric maps, variations in temperature and humiduty, wind, and rain. ESA

N94-13589# Cologne Univ. (Germany). Inst. fuer Geophysik und Meteorologie.
DESCRIPTION OF THE EURAD CHEMISTRY-TRANSPORT MODEL. VERSION 2 (CTM2)
Heinz Hass 1991 106 p
(Rept-83; ETN-93-94384) Avail: CASI HC A06/MF A02

A limited area mesoscale Chemistry Transport Model (CTM), a comprehensive Eulerian air quality model, is described. This model simulates various chemical and physical processes that are thought to be important for understanding of the tropospheric trace gas distributions. Modeling the deposition of these gases is another important aspect in the CTM system. A description of the entire CTM2 modeling system in a more technical sense is given. The physical and chemical concepts of each submodule are described. Preprocessing information is given about how to run the model. Technical information like flow charts, array structures etc. are given in the appendix. ESA

N94-13614# Instituto de Pesquisas Espaciais, Sao Jose dos Campos (Brazil).
ESTIMATIONS OF TEMPERATURE AND HUMIDITY OF THE CANOPY IN AMAZON FOREST USING MICROWAVE DATA FROM SMMR SENSOR OF NIMBUS-7 SATELLITE M.S. Thesis [ESTIMATIVAS DA TEMPERATURA E UMIDADE DO DOSSEL NA FLORESTA AMAZONICA, UTILIZANDO DADOS DE MICROONDAS DO SENSOR SMMR DO SATELITE NIMBUS-7]
Jorge Luis Silva Brito Sep. 1992 108 p In PORTUGESE Original contains color illustrations
(INPE-5444-TDI/490) Avail: CASI HC A06/MF A02

The forest canopy humidity and temperature of the region of Manaus (3 deg S, 60 deg W) have been estimated for the 1985 wet (April-May) and dry (July-August) seasons at 12:00 and 00:00 local standard time,

from spaceborne microwave radiometer, along with microwave emission models. The satellite data consist of SMMR (Scanning Multichannel Microwave Radiometer) Nimbus-7 corrected brightness temperatures for the 6.6, 10.7, 18.0 and 37.0 GHz frequencies. To model the signal emitted by the forest canopy, two different numerical models were used: a discrete model, which calculates the scattering and absorbing coefficients of each bioelement of the canopy (stems, branches and leaves), and a continuous model, which uses a statistical description of the canopy dielectric properties canopy. Micrometeorological data obtained from the GTE/ABLE-2A (GLOBAL Tropospheric Experiment/Amazon Boundary Layer Experiment 2A), and ARME (Anglo-Brazilian Amazon Region Micrometeorological Experiment) at the Duck Reserve (2 deg 57 min S, 59 deg 57 min W) have been used. A sensitivity study of the models has also been conducted to evaluate the influence of the moisture, temperature gradient and vegetal biomass on the brightness temperatures simulated by the models. The sensitivity test has indicated that it is necessary to use both the 37.0 GHz and low frequencies to carry out the inversion of the structure parameters, moisture and temperature. The moisture values obtained through the inversion of the continuous model have been consistent with the ones obtained by other authors in field experiments in the Amazon region. A moisture index has been defined (normalized difference of the optimized moisture at 37.0 and 6.6 GHz frequencies), and has shown to be a good index of the vegetation stomatal resistance. Author

N94-13643# Meteorological Society of Japan, Tokyo.
STUDY ON TRMM DATA UTILIZATION FOR METEOROLOGY [TRMM DETA NO KISHOU BUNYA ENO RIYOU NI KANSURU CHOUSA KENTOU]
National Space Development Agency 31 Mar. 1993 72 p In JAPANESE
(NASDA-CNT-930007; JTN-93-80461) Avail: CASI HC A04/MF A01

TRMM (Tropical Rainfall Measuring Mission), which will be launched around 1996 jointly by Japan and the U.S., intends to observe three dimensional distributions of precipitation in the tropical and subtropical regions between 37 deg N and 37 deg S from space by using precipitation radar and other instruments. Data obtained by TRMM is expected to play an important role in research and operational fields related to precipitation. Especially, it is anticipated that TRMM data will be very useful for understanding the many varieties of meteorological phenomena, in which precipitation is a key factor. This report summarizes the expected research plans using TRMM data inside and outside Japan, based on the results of several scientific meetings. It became clear that about 100 scientists want to use TRMM data for their research works and that their research subjects are distributed very widely, such as precipitation climatology, precipitation systems in the tropics and subtropics, validation of the atmospheric general circulation models, improvement of numerical weather forecast model, flood forecast, and so on. Also, it can be noticed that about 50 members of the science team are actively performing the TRMM research programs in the U.S. and that other nations are also quite interested in TRMM.
Author (NASDA)

N94-13672# Instituto de Pesquisas Espaciais, Sao Jose dos Campos (Brazil).
CLIMATIC CHANGE DUE TO LAND SURFACE ALTERATIONS
Sergio H. Franchito and V. Brahmananda Rao 1992 38 p
(INPE-5495-PRE/1786) Avail: CASI HC A03/MF A01

A primitive equations global zonally averaged climate model is developed. The model includes biofeedback mechanisms. For the Northern Hemisphere the parameterization of biofeedback mechanisms is similar to that used by Gutman et al. For the Southern Hemisphere new parameterizations are derived. The model simulates reasonably well the mean annual zonally averaged climate and geobotanic zones. Deforestation, desertification, and irrigation experiments are performed. In the case of deforestation and desertification there is a reduction in the surface net radiation, evaporation, and precipitation and an increase in the surface temperature. In the case of irrigation experiment opposite changes occurred. In all the cases considered the changes in evapotranspiration overcome the effect of surface albedo modification. In all the experiments changes are smaller in the Southern Hemisphere. Author (revised)

N94-13675*# Pennsylvania State Univ., University Park. Dept. of Meteorology.
WEATHER FORECASTING SUPPORT FOR AASE-2 Final Report, 1 Oct. 1991 - 30 Mar. 1992
Gregory S. Forbes 22 Apr. 1992 5 p
(Grant NAGw-2792)
(NASA-CR-194342; NAS 1.26:194342) Avail: CASI HC A01/MF A01

The AFEAS Contract and NASA Grant were awarded to Penn State in order to obtain real-time weather forecasting support for the NASA AASE-II Project, which was conducted between October 1991 and March 1992. Because of the special weather sensitivities of the NASA ER-2 aircraft, AASE-II planners felt that public weather forecasts issued by the National Weather Service would not be adequate for mission planning purposes. A likely consequence of resorting to that medium would have been that scientists would have had to be at work by 4 AM day after day in the hope that the aircraft could fly, only to be frustrated by a great number of 'scrubbed' missions. Thus, the Pennsylvania State University was contracted to provide real-time weather support to the AASE-II mission.
Derived from text

N94-13686# World Meteorological Organization, Geneva (Switzerland).
MANUAL ON THE GLOBAL DATA-PROCESSING SYSTEM. VOLUME 1: (ANNEX 4 TO THE WMO REGULATIONS) GLOBAL ASPECTS (1992 EDITION)
1992 104 p
(WMO-485-Vol-1; ISBN-9-26-312485-X; ETN-93-94373) Copyright Avail: CASI MF A02; print copy available at WMO, Geneva, Switzerland

The manual on the Global Data Processing System (GDPS), which was designed to facilitate cooperation in data processing between members, to specify obligations of members in the implementation of the World Weather Watch (WWW) GDPS, and to ensure adequate uniformity and standardization in the practices and procedures employed in achieving the aforementioned, is presented. The manual consists of volumes 1 and 2, which deal with global and regional aspects respectively. Volume 1 of the manual covers: organization and functions of the GDPS; data processing for real time uses; and data processing for nonreal time uses which contain regulatory material for the global aspects of the WWW GDPS. The regulatory material stems from recommendations of the Commission for Basic Systems (CBS) as well as from decisions taken by Congress and the Executive Council. This volume, on global aspects, forms part of the Technical Regulations and is referred to as Annex 4 to the Technical Regulations. ESA

N94-13723*# Colorado Univ., Boulder. Cooperative Inst. for Research in the Environmental Sciences.
COHERENT DOPPLER LIDAR SIGNAL COVARIANCE INCLUDING WIND SHEAR AND WIND TURBULENCE
R. G. Frehlich 1 Sep. 1993 13 p Sponsored in part by NSF
(Grant NAG8-253)
(NASA-CR-194492; NAS 1.26:194492) Avail: CASI HC A03/MF A01

The performance of coherent Doppler lidar is determined by the statistics of the coherent Doppler signal. The derivation and calculation of the covariance of the Doppler lidar signal is presented for random atmospheric wind fields with wind shear. The random component is described by a Kolmogorov turbulence spectrum. The signal parameters are clarified for a general coherent Doppler lidar system. There are two distinct physical regimes: one where the transmitted pulse determines the signal statistics and the other where the wind field dominates the signal statistics. The Doppler shift of the signal is identified in terms of the wind field and system parameters. Author (revised)

N94-13914# Lawrence Livermore National Lab., CA.
AMIP: DIAGNOSTIC SUBPROJECT ON THE VARIABILITY IN THE TROPICS: SYNOPTIC TO INTRASEASONAL TIME SCALES
K. R. Sperber, J. M. Slingo, A. Matthews (European Centre for Medium-Range Weather Forecasts, Reading, England.), and T. N. Palmer Dec. 1992 6 p Presented at the 17th Annual Climate Diagnostics Conference, Norman, OK, 19-23 Oct. 1992
(Contract W-7405-eng-48)
(DE93-009287; UCRL-JC-112366; CONF-9210334-1) Avail: CASI HC A02/MF A01

The aim of this subproject is to evaluate the ability of GCM's to simulate the transient component of tropical convection and to increase

our understanding of the possible processes that govern the development, propagation, and dissipation of synoptic disturbances and the intraseasonal oscillation. A pilot study of the tropical variability in a high resolution version of the ECMWF model has already shown that a GCM may have considerable skill in simulating the observed distribution and periodicities of tropical disturbances. Verification of the model results will involve satellite data and NWP analyses. In particular, a similar study of the observed intraseasonal oscillation using EC analyses, being carried out as part of the Joint Diagnostics Project at Reading University, will form an important part of the verification of this subproject. In this paper we present a preliminary evaluation of the intraseasonal oscillation as simulated by the ECMWF model. This simulation, with a horizontal resolution of T42 (approximately 2.8 deg), was performed at Lawrence Livermore National Laboratory on behalf of the European Center for Medium-Range Weather Forecasts. DOE

N94-13926 Royal Netherlands Meteorological Inst., De Bilt.
NATIONAL USE OF THE GROUPS 7wwW1W2 AND 960ww FOR GROUND STATIONS [NATIONAAL GEBRUIK VAN DE GROEPEN 7WWW1W2 EN 960 WW VOOR LANDSTATIONS]
H. vanDrongelen (Koninklijke Inst. voor de Marine, The Hague, Netherlands.), A. Kamphuis (Koninklijke Luchtmacht, The Hague, Netherlands.), and P. Y. deVries Jan. 1992 44 p In DUTCH
(KNMI-Publ-181; ISBN-90-369-2016-7; ETN-93-93929) Copyright Avail: Royal Netherlands Meteorological Institute, P.O. Box 201, 3730 AE De Bilt, Wilhelminalaan 10, Netherlands

An operational manual for observers and meteorologists is presented. It is also an extra source of information for instructors and for users of codes. The present national and international rules are given, together with some clarifications and a few examples. Tables for the cancellation of announced phenomena using ww and w1w2 figures are given. ESA

N94-13985 Royal Netherlands Meteorological Inst., De Bilt. Afd. Centrale Weerdienst.
THE NOCTURNAL WIND MAXIMUM: AN INTERACTIVE FORECAST METHOD [HET NACHTELIJK WINDMAXIMUM: EEN INTERACTIEVE VERWACHTINGSMETHODE]
N. Maat and H. Bakker 1992 30 p In DUTCH
(KNMI-TR-142; ISBN-90-369-2014-0; ETN-93-93920) Copyright Avail: Royal Netherlands Meteorological Institute, P.O. Box 201, 3730 AE De Bilt, Wilhelminalaan 10, Netherlands

An interactive forecast method was developed for the nocturnal wind maximum at the upper side of the boundary layer at low altitude (low level jet). The theoretical basis for the forecast method is given. The numerical model is described. The testing of the model is illustrated through examples. It is shown that the stability of the boundary layer during the period of forecasting is essential. The computer program is presented. ESA

N94-13991 Royal Netherlands Meteorological Inst., De Bilt. Afd. Dynamische Meteorologie.
PRECIPITATION VERIFICATION LAM [NEERSLAGVERIFICATIE LAM]
W. C. deRooy and C. A. Engeldal 1992 27 p In DUTCH
(KNMI-TR-143; ISBN-90-369-2015-9; ETN-93-93921) Copyright Avail: Royal Netherlands Meteorological Institute, P.O. Box 201, 3730 AE De Bilt, Wilhelminalaan 10, Netherlands

The numerical weather forecasting model LAM, also called FMLAM (Fine Mesh Limited Area Model), was used for a short term precipitation forecast. A general description of the LAM is given. The comparison between the LAM forecasts and observations is described. The LAM can produce precipitation forecasts up to 30 hours in advance. The quality of the prognoses decreases only a little with the length of the period of forecasting. ESA

N94-13992 Royal Netherlands Meteorological Inst., De Bilt.
ADAPTATION OF HUMIDITY-CLOUD COVER RELATIONS IN THE LAM [AANPASSING VOCHT-BEDEKKINGSGRAADRELATIES IN HET LAM]
Wim C. deRooy 1992 25 p In DUTCH
(KNMI-TR-144; ISBN-90-369-2018-3; ETN-93-93922) Copyright Avail: Royal Netherlands Meteorological Institute, P.O. Box 201, 3730 AE De Bilt, Wilhelminalaan 10, Netherlands

A method to adapt the Ricketts relations between relative humidity and cloud cover to the Limited Area Model (LAM) is described. This adaptation was necessary because on days with low cloud cove, the minimum temperature analyzed and predicted by the LAM was too high. Using the Ricketts data and a theoretical limit, simple linear relations can be determined between relative humidity and cloud cover, taking into account the thickness of the cloud layer. ESA

N94-13993 Royal Netherlands Meteorological Inst., De Bilt.
A VERIFICATION OF THE EUROGUIDANCE: A GUIDANCE FORECAST FOR TRANSPORTATION AND TOURISM [EEN VERIFICATIE VAN DE EUROGIDS: DE GIDSVERWACHTING VOOR VERVOER EN TOERISME]
H. G. Theihzen 1992 67 p In DUTCH
(KNMI-TR-145; ISBN-90-369-2019-1; ETN-93-93923) Copyright Avail: Royal Netherlands Meteorological Institute, P.O. Box 201, 3730 AE De Bilt, Wilhelminalaan 10, Netherlands

Euroguidance, a guidance forecast for minimum and maximum temperatures and precipitation probability was verified for the period from 16 Oct. 1987 to 15 Oct. 1989. The verification shows that the forecasts are in general usable, but there are exceptions. An extension of the programming package using update techniques is in preparation. A reselection of the weather stations can be recommended (nine stations gave no satisfactory results during the verification period). ESA

N94-14057# Los Alamos National Lab., NM.
REGIONAL CLIMATOLOGY SENSITIVITY STUDIES
J. E. Bossert, C. Y. J. Kao, J. L. Winterkamp, J. O. Roads, and Shyh-C. Chen Feb. 1993 11 p Presented at the 3rd ARM Science Team Meeting, Norman, OK, 1-5 Mar. 1993
(Contract W-7405-eng-36)
(DE93-010712; LA-UR-93-857; CONF-9303122-1) Avail: CASI HC A03/MF A01

Recent interest in understanding climate and climate change at regional-scales has led to the application of mesoscale models for regional climatology studies. These models can provide an understanding of climate processes in a physically consistent way at much higher resolution than presently offered by GCM's. In recent work, we have tried to address questions in the RAMS mesoscale model to establish confidence in our modeling procedure. A more rigorous comparison of our modeling results with various data sets is reported. In the present paper, we use two simple numerical experiments to examine the impact of grid configuration on the predicted precipitation field from the RAMS model. We intend to demonstrate that the choice of the lateral boundaries and grid configurations can significantly impact the predicted fields of interest. DOE

N94-14071# World Meteorological Organization, Geneva (Switzerland).
MANUAL ON THE GLOBAL DATA-PROCESSING SYSTEM. VOLUME 2: REGIONAL ASPECTS (1992 EDITION)
1992 45 p
(WMO-485-Vol-2; ISBN-9-26-312485-X; ETN-93-94374) Copyright Avail: CASI MF A01: print copy available from World Meteorological Organization, Case Postale No. 5, CH-1211 Geneva 20, Switzerland

The manual on the Global Data Processing System (GDPS), which was designed to facilitate cooperation in data processing between members, to specify obligations of members in the implementation of the World Weather Watch (WWW) GDPS, and to ensure adequate uniformity and standardization in the practices and procedures employed in achieving the aforementioned, is presented. The manual consists of volumes 1 and 2, which deal with global and regional aspects respectively. Volume 2 contains the regional and national aspects of the WWW GDPS based on the practices and procedures adopted by the regional associations and by members concerned as well as relevant decisions of Congress, the Executive Council and the Commission for Basic Systems. This volume is divided into sections corresponding to the six regions of the World Meteorological Organization, namely: Africa, Asia, South America, North and Central America, south west Pacific, Europe. Each of these regions is divided into three parts: real time data processing (regional and national aspects); nonreal time processing (regional and national aspects); and monitoring of the GDPS (regional and national aspects). Data processing activities and meteorological services in the Antarctic are also covered. ESA

N94-14074*# National Aeronautics and Space Administration. Goddard Space Flight Center, Greenbelt, MD.
CIRCULATION AND RAINFALL CLIMATOLOGY OF A 10-YEAR (1979 - 1988) INTEGRATION WITH THE GODDARD LABORATORY FOR ATMOSPHERES GENERAL CIRCULATION MODEL
J.-H. Kim (Applied Research Corp., Landover, MD.) and Y. C. Sud Sep. 1993 228 p
(RTOP 913-00-00)
(NASA-TM-104591; Rept-93B00105; NAS 1.15:104591) Avail: CASI HC A11/MF A03

A 10-year (1979-1988) integration of Goddard Laboratory for Atmospheres (GLA) general circulation model (GCM) under Atmospheric Model Intercomparison Project (AMIP) is analyzed and compared with observation. The first momentum fields of circulation variables and also hydrological variables including precipitation, evaporation, and soil moisture are presented. Our goals are (1) to produce a benchmark documentation of the GLA GCM for future model improvements; (2) to examine systematic errors between the simulated and the observed circulation, precipitation, and hydrologic cycle; (3) to examine the interannual variability of the simulated atmosphere and compare it with observation; and (4) to examine the ability of the model to capture the major climate anomalies in response to events such as El Nino and La Nina. The 10-year mean seasonal and annual simulated circulation is quite reasonable compared to the analyzed circulation, except the polar regions and area of high orography. Precipitation over tropics are quite well simulated, and the signal of El Nino/La Nina episodes can be easily identified. The time series of evaporation and soil moisture in the 12 biomes of the biosphere also show reasonable patterns compared to the estimated evaporation and soil moisture.
Author (revised)

N94-14118# World Meteorological Organization, Geneva (Switzerland). World Climate Data and Monitoring Programme.
CCL WORKING GROUP ON CLIMATE DATA AND ITS RAPPORTEURS Final Report
Nov. 1992 86 p Presented at the Eleventh Session of the Commission for Climatology, Havana, Cuba, 15-26 Feb. 1993
(WCDMP-21; WMO-TD-523) Avail: CASI HC A05/MF A01; print copy available at WMO, Geneva, Switzerland

This collection of the Working Group's individual reports documents the progress being made in climate data management. The presented information includes pilot projects for improving data quality and product distribution for climate system monitoring; systematic monitoring of the global climate system; reference climatological stations (RCS); global and regional baseline data sets for climate change studies; climate data management in developing countries; CLICOM (climate computing); INFOCLIMA - a valuable approach to climate data sources; and climate related issues connected with the conversion of conventional meteorological stations to automatic ones.
CASI

N94-14189# Deutsche Forschungsanstalt fuer Luft- und Raumfahrt, Cologne (Germany). Hauptabt. Systemanalyse Raumfahrt.
WATER-VAPOUR, TOTAL WATER AND RAINRATE FROM PASSIVE MICROWAVE SATELLITE DATA OVER OCEAN Ph.D. Thesis - Hamburg Univ. [WASSERDAMPF, GESAMTWASSER UND NIEDERSCHLAGSRATE AUS DATEN PASSIVER MIKROWELLENRADIOMETER UEBER DEM OZEAN]
Peter Bauer Dec. 1992 135 p In GERMAN Original contains color illustrations
(DLR-FB-92-37; ETN-93-93964) Avail: CASI HC A07/MF A02

A radiative transfer model is developed for the simulation of millimeter wavelength radiances emerging from cloudy and precipitating atmospheres over oceans and different land surfaces. The model fully accounts for multiple scattering as well as for polarization effects caused by hydrometeors and the surface. A sensitivity analysis for the estimation of the influence of different surface types on the emitted radiation is carried out. For land surfaces only the variation of the vertical component of the emitted radiation with the surface conditions is small enough to be used for the retrieval of atmospheric parameters. A global set of 340 atmospheric radiosondes is used in order to simulate the dual polarized radiometer signals as measured in all spectra channels of the Special Sensor Microwave Imager (SSM/I). An error analysis of the effect of spatial inhomogeneity on the retrievals shows no systematic impact of fractional cloud and rain coverage within a pixel, except for water vapor, because of droplet absorption becoming effective also at frequencies of water vapor absorption. The retrieval algorithms are applied to SSM/I passive microwave soundings of Aug. 1987 for global maps of water vapor, precipitation and total water content. A preliminary comparison with surface climatologies, satellite measured rainrate from infrared soundings and an experiment with a general circulation model shows that the values are reliable within the range of sampling errors.
ESA

N94-14426# Lawrence Livermore National Lab., CA.
SEA SURFACE TEMPERATURE FORCING AND PHASE LOCKING OF NORDESTE PRECIPITATION
K. R. Sperber and S. Hameed (State Univ. of New York, Stony Brook.) Jul. 1992 4 p Presented at the 7th Brazilian Meteorological Congress: Climate Change and the Environment, San Paulo, Brazil, 28 Sep. - 2 Oct. 1992
(Contracts W-7405-eng-48; DE-FG02-85ER-60314)
(DE93-011873; UCRL-JC-109819; CONF-9209331-1) Avail: CASI HC A01/MF A01

Interannual variations of precipitation in several regions around the globe are known to be influenced by sea surface temperatures. We describe a procedure that elicits the same frequencies of variations in the sea surface temperatures as in precipitation. The modes of variations in the two fields are phase locked, allowing us to identify regions in the oceans that vary in unison with changes in precipitation on different time scales. The method is illustrated by application to northeast Brazil, the Nordeste, where flood and drought occur frequently.
DOE

N94-14546# Freie Univ., Berlin (Germany). Inst. fuer Meteorologie.
METEOROLOGICAL DATA, NEW SERIES A MONOGRAPHS. VOLUME 6, NO. 4: MODELIZATION OF HEAT FLUXES AT EARTH GROUND WITH CONSIDERATION OF VEGETATION Ph.D. Thesis [METEOROLOGISCHE ABHANDLUNGEN NEUE FOLGE SERIE A MONOGRAPHIEN. BAND 6, HEFT 4: MODELLIERUNG DER WAERMEFLUESSE AM ERDBODEN MIT BERUECKSICHTIGUNG VON VEGETATION]
Klaus Bluemel Jun. 1992 291 p In GERMAN
(Contract BMFT-07-KF-114-6)
(ETN-93-94169) Copyright Avail: CASI HC A13/MF A03

A 1-dimensional SVAT-model (Soil Vegetation Atmosphere Transfer Model) is presented. It is composed of three coupled submodels: a multilayer soil model, a vegetation model, and a multilayer model of the planetary boundary layer. The complete model can also be run without the planetary boundary model if wind, humidity, and temperature are prescribed at the upper boundary of the vegetation model. An additional driving force is the absorbed solar and atmospheric longwave radiation. The output are among other things the turbulent sensible and latent heat fluxes, the leaf temperature, profiles of soil temperature and soil water content and, if coupled with the boundary model, profiles of potential temperature, specific humidity and wind. The vegetation model is based upon the BATS (Biosphere Atmosphere and Transfer Scheme) model, in which many improvements and extensions were implemented. As for the soil, the equations of water and heavy transfer are solved. The model equations of the planetary boundary layer consist of Ekman equations and the balance equations for enthalpy and water vapor. To verify the model, the output is compared with data sampled in the field. The case of dense vegetation and relatively humid soil for three sunny days is treated. Altogether very good agreement is found.
ESA

N94-14707# Freie Univ., Berlin (Germany). Inst. fuer Meteorologie.
METEOROLOGICAL DATA, NEW SERIES A MONOGRAPHS. VOLUME 6, NO. 3: ESTIMATION OF INFLUENCE OF HIGH CLOUDS IN THE RADIATION FIELD AND THE CLIMAT BY ANALYSIS OF NOAA AVHRR DATA Ph.D. Thesis [METEOROLOGISCHE ABHANDLUNGEN NEUE FOLGE SERIE A MONOGRAPHIEN. BAND 6, HEFT 3: DIE BESTIMMUNG DES EINFLUSSES VON HOHEN WOLKEN AUF DAS STRAHLUNGSFELD UND AUF DAS KLIMA DURCH ANALYSE VON NOAA AVHRR-DATEN]
Franz Herbert Berger 1992 123 p In GERMAN
(Contracts BMFT-513-8320-KF-10110; BMFT-07-KFT-38/3)
(ETN-93-94170) Copyright Avail: CASI HC A06/MF A02

The influence of clouds on the radiation field and on climate is

investigated over the North Sea by analyzing NOAA AVHRR (Advanced Very High Resolution Radiometer) data. The main interest is on high clouds due to their ambivalent behavior in the radiation field. The first step was an accurate detailed cloud classification based on the infrared likelihood method. A further step is the determination of optical properties of high clouds. The derived information was applied to calculate the cloud-climate efficiency at the top of atmosphere and at the surface. The analysis of the data set shows that the monthly mean cloud forcing of Oct. 1990 is larger than in Oct. 1989 due to a larger amount of high clouds and less low level clouds in the North Sea. A first approach of a comparison of the increasing cloud forcing (heating of the Earth atmosphere system) and an analysis of the relative topography 300/850 hPa shows that the increase of the cloud forcing is well correlated with an increase of the temperature in this layer. The deviation from the long term mean of the pressure or temperature shows the same behavior. ESA

N94-14709# Max-Planck-Inst. fuer Meteorologie, Hamburg (Germany).
SIMULATION OF THE PRESENT-DAY CLIMATE WITH THE ECHAM MODEL: IMPACT OF MODEL PHYSICS AND RESOLUTION
Erich Roeckner, Klaus Arpe, Lennart Bengtsson, Sabine Brinkop (Deutsche Forschungsanstalt fuer Luft- und Raumfahrt, Oberpfaffenhofen, Germany.), Lydia Duemenil, Monika Esch, Edilbert Kirk (Hamburg Univ., Germany.), Frank Lunkeit (Hamburg Univ., Germany.), Michael Ponater (Deutsche Forschungsanstalt fuer Luft- und Raumfahrt, Oberpfaffenhofen, Germany.), and Burkhardt Rockel (GKSS-Forschungszentrum Geesthacht, Germany.) et al Oct. 1992 167 p
(Grant BMFT-07-KFT-05/6)
(Rept-93; ETN-93-94191) Avail: CASI HC A08/MF A02

A detailed description of the third generation atmospheric general circulation model ECHAM is presented. The climatology of ECHAM3, as simulated at low and high resolution (T21 and T42, respectively), is compared with ECMWF (European Center for Medium range Weather Forecasts) analyses (1981 to 1990) and also with the climatology of two earlier low resolution versions ECHAM1 and ECHAM2. At low resolution, the impact of the improved model physics is evident primarily in the simulated time-mean state which is more successfully reproduced by the more recent model versions, particularly by ECHAM3. The impact of increased horizontal resolution can be identified not only by a generally improved time-mean circulation, particularly in the southern hemisphere, but most significantly by the increased level of high frequency variability. In the low frequency range, however, the impact of increased horizontal resolution is modest, and all models fail to reproduce the observed level of low frequency intraseasonal variability. ESA

N94-14223*# National Aeronautics and Space Administration. Langley Research Center, Hampton, VA.
CLOUDS AND THE EARTH'S RADIANT ENERGY SYSTEM (CERES) ON THE TROPICAL RAINFALL MEASURING MISSION (TRMM)
Stephen L. Carman (TRW Space Technology Labs., Redondo Beach, CA.) and Leonard P. Kopia *In* Science and Technology Agency, Asia-Pacific ISY Conference, Volume 2 31 Mar. 1993 p 80-83 (For primary document see N94-14209 02-43)
Avail: CASI HC A01/MF A04

N94-14225# Tokyo Univ. (Japan). Center for Climate System Research.
ESTIMATE OF SAMPLING ERRORS OF TRMM RAINFALL OBSERVATION BY USING RADAR-AMeDAS COMPOSITE DATA
Akimasa Sumi, Riko Oki, and aikan Oki *In* Science and Technology Agency, Asia-Pacific ISY Conference, Volume 2 31 Mar. 1993 p 88-91 (For primary document see N94-14209 02-43)
Avail: CASI HC A01/MF A04

N94-14226# Ministry of Posts and Telecommunications, Tokyo (Japan). Communications Research Lab.
MULTIPARAMETER AIRBORNE RAIN RADAR DEVELOPMENT FOR TRMM VALIDATION AND TRMM-FOLLOW-ON STUDY
Hiroshi Kumagai, Kenichi Okamoto, Kenji Nakamura (Ministry of Posts and Telecommunications, Ibaraki, Japan.), Hiroshi Hanado (Ministry of Posts and Telecommunications, Ibaraki, Japan.), and Hiroaki Horie (Ministry of Posts and Telecommunications, Ibaraki, Japan.) *In* Science and Technology Agency, Asia-Pacific ISY Conference, Volume 2 31 Mar. 1993 p 92-95 (For primary document see N94-14209 02-43)
Avail: CASI HC A01/MF A04

N94-14231# National Oceanic and Atmospheric Administration, Washington, DC. National Environmental Satellite, Data, and Information Service.
CLIMATE PRODUCTS FROM NOAA OPERATIONAL SATELLITES
P. Krishna Rao and A. Gruber *In* Science and Technology Agency, Asia-Pacific ISY Conference, Volume 2 31 Mar. 1993 p 117-120 (For primary document see N94-14209 02-43)
Avail: CASI HC A01/MF A04

N94-14232# Institute of Disaster and Earth Sciences, Ibaraki (Japan).
SEASONAL CHANGE OF THE LAND-SURFACE TEMPERATURE OVER ASIAN CONTINENT DERIVED FROM GAC DATA ON NOAA-11 AVHRR
Kazurou Nakane *In* Science and Technology Agency, Asia-Pacific ISY Conference, Volume 2 31 Mar. 1993 p 122-125 (For primary document see N94-14209 02-43)
Avail: CASI HC A01/MF A04

N94-14233# National Oceanic and Atmospheric Administration, Washington, DC. Satellite Research Lab.
EARTH RADIATION BUDGET, CLOUD, AND AEROSOL PARAMETERS DERIVED FROM AVHRR AND TOVS MEASUREMENTS
Herbert Jacobowitz and Larry L. Stowe *In* Science and Technology Agency, Asia-Pacific ISY Conference, Volume 2 31 Mar. 1993 p 126-129 (For primary document see N94-14209 02-43)
Avail: CASI HC A01/MF A04

N94-14243# Chiba Univ. (Japan). Remote Sensing and Image Research Center.
EFFECTS OF TYPHOON ON TOMS DATA
Nobuo Takeuchi, Fumihiko Hiruma, and Kiyoshi Tsuchiya (Teikyo Univ., Utsunomiya, Japan.) *In* Science and Technology Agency, Asia-Pacific ISY Conference, Volume 2 31 Mar. 1993 p 177-180 (For primary document see N94-14209 02-43)
Avail: CASI HC A01/MF A04

N94-14269# Saga Univ. (Japan). Dept. of Information Science.
A METHOD FOR ESTIMATION OF PARTIAL CLOUD COVER WITHIN A PIXEL AND ITS EFFECT
Kouhei Arai *In* Science and Technology Agency, Asia-Pacific ISY Conference, Volume 2 31 Mar. 1993 p 307-310 (For primary document see N94-14209 02-43)
Avail: CASI HC A01/MF A04

N94-14663*# Johns Hopkins Univ., Laurel, MD. Applied Physics Lab.
RAIN RATE DURATION STATISTICS DERIVED FROM THE MID-ATLANTIC COAST RAIN GAUGE NETWORK
Julius Goldhirsh *In* JPL, Proceedings of the Seventeenth NASA Propagation Experimenters Meeting (NAPEX 17) and the Advanced Communications Technology Satellite (ACTS) Propagation Studies Miniworkshop 1 Aug. 1993 p 93-103 (For primary document see N94-14654 02-32)
(Contract N00039-91-C-0001)
Avail: CASI HC A03/MF A03

N94-14664*# Oklahoma Univ., Norman.
RAIN-RATE DATA BASE DEVELOPMENT AND RAIN-RATE CLIMATE ANALYSIS
Robert K. Crane *In* JPL, Proceedings of the Seventeenth NASA Propagation Experimenters Meeting (NAPEX 17) and the Advanced Communications Technology Satellite (ACTS) Propagation Studies Miniworkshop 1 Aug. 1993 p 105-128 (For primary document see N94-14654 02-32)
Avail: CASI HC A03/MF A03

48 OCEANOGRAPHY

Includes biological, dynamic, and physical oceanography; and marine resources.

For related information see also *43 Earth Resources and Remote Sensing.*

N94-12876# Lawrence Livermore National Lab., CA.
OCEAN ACOUSTIC PROCESSING: A MODEL-BASED APPROACH
J. V. Candy and E. J. Sullivan (Naval Underwater Systems Center, Newport, RI.) Jul. 1992 8 p Presented at the Oceans 1992, Newport, RI, 26-29 Oct. 1992 Revised
(Contract W-7405-eng-48)
(DE93-011902; UCRL-JC-107852-Rev-1; CONF-921066-3-Rev-1) Avail: CASI HC A02/MF A01

A model-based approach is proposed to solve the ocean acoustic signal processing problem that is based on a state-space representation of the normal-mode propagation model. This model is generalized to the stochastic case where an approximate Gauss-Markov model evolves which allows the inclusion of stochastic phenomena such as noise and modeling errors in a consistent manner. Based on this framework, investigations are made of model-based solutions to the signal enhancement and related parameter estimation problems. DOE

N94-12990# Naval Research Lab., Bay Saint Louis, MS. Oceanography Div.
CIRCULATION MODEL EXPERIMENTS OF THE GULF STREAM USING SATELLITE-DERIVED FIELDS Final Report
Daniel N. Fox, Michael R. Carnes, and Jimmy L. Mitchell Apr. 1993 48 p Limited Reproducibility: More than 20% of this document may be affected by microfiche quality
(AD-A266067; NRL/FR/7323-92-9412; NOARL-55) Avail: CASI HC A03

The ability to perform skillful forecasts of the space and time evolution of mesoscale ocean phenomena can significantly improve acoustic surveillance capabilities, search and rescue operators, the performance of weapon systems, and other aspects of naval operations. The Ocean Dynamics and Prediction Branch, Ocean Monitoring and Prediction Section of the Naval Research Laboratory (NRL), Stennis Space Center, MS, is developing an ocean nowcast/forecast capability to permit dynamical interpolation of the limited number of in situ and satellite observations available using a hierarchy of coupled hydrodynamic and thermodynamic models. A series of numerical experiments to predict the evolution of the Gulf Stream were performed. These experiments led to the first system to show significant skill in this area. The forecast system uses the NRL Northwest Atlantic regional primitive equation model and assimilation schemes. The schemes employ both a feature model and statistical correlations derived from the regional climatology of in situ data and long time-base numerical simulations. DTIC

N94-13500# Rome Univ. (Italy). Dipt. di Fisica.
PRELIMINARY RESULTS ON THE HYDROLOGICAL MEASUREMENTS IN THE AEGEAN SEA OFF CRETE: CRUISE, GEORGIA, 1989
Giuseppina Mattietti and Volfango Rupolo 1989 39 p
(Preprint-736; ETN-93-94372) Avail: CASI HC A03/MF A01

Data collected during the short oceanographical cruise 'Georgia 89' during which measurements of pure density and salinity were carried out are presented. These data were collected by means of a Kiel Multisonde ME 1500 bathysonde. The data were processed with an Olivetti m280 computer. Samples of deep marine water were also collected with a Rosette multisampler in order to measure the oxygen content at various depths. Together with the data, the following figures are presented: general map of the working zone with hydrological stations; bathymetric map of the working zone; diagrams of the hydrological stations; maps of potential temperature, salinity and density at various depths; isopycnals of the hydrological sections; vertical profiles of the oxygen values; maps of oxygen values at various depth; satellite thermal information of the sea surface. ESA

N94-13581# Environmental Research Inst. of Michigan, Ann Arbor.
RADAR IMAGING OF SUB-MESOSCALE OCEAN PHENOMENA Final Report, Feb. 1990 - Jan. 1993
Dave R. Lyzenga Mar. 1993 75 p
(Contract N00014-90-C-0071)
(AD-A266339; ERIM-225300-8-F) Avail: CASI HC A04/MF A01

A model for the short surface wave spectrum is presented, which includes the effects of wind forcing, surfactant damping, wave-current interactions, and wave breaking. A new analytical solution of the wave action equation was developed in order to account for wave-current interactions. The wave breaking model is based on a threshold criterion involving the vertical acceleration. The breaking fraction is then calculated as a function of the slope variance, and the backscatter is calculated from the Kirchhoff model by assuming a Gaussian correlation function within the breaking regions. Model predictions are compared with synthetic aperture radar observation made during the ONR/NRL High Resolution field experiment. DTIC

N94-13653# Japan Weather Association, Tokyo.
BUOY EXPERIMENTS TO OBTAIN THE SEA-TRUTH DATA FOR OCTS/NSCAT, PART 1 [OCTS/NSCAT NO TAME NO BUI NI YORU TURUSU DETA SHUTOKU JIKKEN]
National Space Development Agency 31 Mar. 1993 18 p In JAPANESE
(NASDA-CNT-930005-Pt-1; JTN-93-80459) Avail: CASI HC A03/MF A01

To verify the sensor data from OCTS (Ocean Color and Temperature Scanner) and NSCAT (NASA Scatterometer) onboard the ADEOS (Advanced Earth Observing Satellite), it is necessary to develop the ocean observation buoy system for sea truth data acquisition. This report describes the results for sea truth data acquisition experiment using the remodeled version of the existing ocean observation buoy. Outlines of the system configuration, installation process of the optical observation system, modification process of the buoy, and the existing climate and ocean phenomenon measurement system, and mooring device production process are described. Observed data such as optical data, ocean wave data, buoy movement, and their relations are studied. Author (NASDA)

N94-13728# Instituto de Pesquisas Espaciais, Sao Jose dos Campos (Brazil).
MAXIMUM ENTROPY SPECTRAL ANALYSIS OF THE GEOLOGICAL TIME SERIES OF THE OXYGEN ISOTOPE RECORD FROM DEEP-SEA CORES
Rajaram Purushotam Kane and Nalin Babulal Trivedi 1993 30 p Submitted for publication
(INPE-5465-PRE/1773) Avail: CASI HC A03/MF A01

A Maximum Entropy Spectral Analysis of the geological time series of the oxygen isotope 18 for the last 782,000 years showed 98,000 years as the most prominent periodicity, followed by 40,000 years of less than half the amplitude and still smaller peaks at 24,000, 67,000, 84,000, 107,000 and 786,000 years. Among the astronomical parameters, only eccentricity showed a similar periodicity viz. 96,000 years. Obliquity had a prominent periodicity at 41,000 years which was reflected in the oxygen isotope series also. Corresponding to the bimodal precession peaks (23,000 and 19,000 years), the oxygen isotope series showed a peak at 24,000 years and smaller peaks at 22,000 and 19,000 years. Our results compare well with those obtained by Thomson (1990) with a more sophisticated method. Author

N94-14090*# National Aeronautics and Space Administration. Goddard Space Flight Center, Greenbelt, MD.
VOLUME 14: THE FIRST SeaWiFS INTERCALIBRATION ROUND-ROBIN EXPERIMENT, SIRREX-1, JULY 1992
James L. Mueller (San Diego State Univ., CA.), Stanford B. Hooker, ed., and Elaine R. Firestone, ed. (General Sciences Corp., Laurel, MD.) Sep. 1993 62 p Its SeaWiFS Technical Report Series
(NASA-TM-104566; Rept-93B00117-Vol-14; NAS 1.15:104566) Avail: CASI HC A04/MF A01

The results of the first Sea-viewing Wide Field-of-view Sensor (SeaWiFS) Intercalibration Round-Robin Experiment (SIRREX-1), which was held at the Center for Hydro-Optics and Remote Sensing (CHORS) at San Diego State University (SDSU) on 27-31 July 1992 are presetend. Oceanographic radiometers to be used in the SeaWiFS Calibration and Validation Program will be calibrated by individuals from the National Aeronautics and Space Administration's (NASA's) Goddard Space Flight Center (GSFC), CHORS,

and seven other laboratories. The purpose of the SIRREX experiments is to assure the radiometric standards used in all of these laboratories are referenced to the same scales of spectral irradiance and radiance, which will be maintained by GSFC and periodically recalibrated by the National Institute of Standards and Technology (NIST). The spectral irradiance scale of GSFC's FEL lamp number F269 (recalibrated by NIST in October 1992) was transferred to lamps belonging to the 9 participating laboratories; I set of lamp transfer measurements (involving 4 of the lamps) was precise to within less than 1 percent and meets SeaWiFS goals, but a second set (involving another 14 lamps) did not. The spectral radiance scale of the GSFC 40-inch integrating sphere source was transferred to integrating sphere radiance sources belonging to four of the other laboratories. Reflectance plaques, used for irradiance-to-radiance transfer by five of the laboratories, were compared, but spectral bidirectional reflectance distribution functions (BRDF's) were not determined quantitatively. Also reported are results of similar comparisons (in October 1992) between the GSFC scales of spectral irradiance and radiance and those used by the Hughes/Santa Barbara Research Center (SBRC) to calibrate and characterize the SeaWiFS instrument. This first set of intercalibration round-robin experiments was a valuable learning experience for all participants, and led to several important procedural changes, which will be implemented in the second SIRREX, to be held at CHORS in June 1993. Author (revised)

N94-14205 New Brunswick Univ., Fredericton. Dept. of Surveying Engineering.
ON THE SPACE-TIME OCEAN CURRENT VARIABILITY AND ITS EFFECTS ON THE LENGTH-OF-DAY Ph.D. Thesis
Nikolaos Theodoros Christou Jul. 1990 355 p
(ISBN-0-315-59510-8; CTN-93-60856) Copyright Avail: Micromedia Ltd., Technical Information Centre, 165 Hotel de Ville, Place du Portage, Phase 2, Hull, Quebec J8X 3X2, Canada HC/MF

The time dependent perturbations of length of day (LOD), on time scales of about two years or less, associated with the space-time fluctuations of the global ocean circulation, are quantified. Estimates of the space-time variations of ocean currents were derived from both in-situ oceanographic data and two years of satellite altimetry observations from the GEOSAT Exact Repeat Mission. A new technique for extracting ocean current variability from satellite altimetry was developed, based on the gradient operator. The technique offers advantages over previous techniques on the recovery of oceanic variability in that it is conceptually simple and computationally efficient. Through analysis of ocean current variability, it is established that the oceanic excitation of LOD is at least at the level of 0.1 ms. Variations in the oceanic excitation of Delta-LOD have been identified and quantified at periods of 1 year and 0.5 years. At the annual period, the results indicate that the oceanic excitation appears large enough to account for the existing discrepancy between the observed (non-tidal) LOD and the atmospheric contribution. No significant oceanic excitation of Delta-LOD is found at the semiannual period. The results also indicate that there exist statistically significant higher frequency variations at about 121-, 107-, and 89-day periods. Author (CISTI)

N94-14775# Coastal Engineering Research Center, Vicksburg, MS.
COASTAL SCOUR PROBLEMS AND METHODS FOR PREDICTION OF MAXIMUM SCOUR Final Report
Jimmy E. Fowler May 1993 73 p
(AD-A266658; CERC-TR-93-8) Avail: CASI HC A04/MF A01

The most common coastal scour-related problems are to scour at rubble-mound structures and vertical seawalls and at the base of piles and horizontal pipelines. Existing scour prediction methods for these problems vary from rules of thumb to empirically derived equations to theoretically derived relationships. Recent studies at the U.S. Army Engineer Waterways Experiment Station's Coastal Engineering Research Center indicate that sufficient design guidance exists for vertical walls, pipelines, and vertical piles; however, additional research is still needed for rubble-mound structures. DTIC

N94-14261# Tsukuba Space Center, Ibaragi (Japan).
OUTLINE OF ISY SEA SURFACE TEMPERATURE DATA SETS
Korehiro Maeda and Hironori Maejima (National Space Development Agency, Ohashi, Japan.) *In* Science and Technology Agency, Asia-Pacific ISY Conference, Volume 2 31 Mar. 1993 p 269-273 (For primary document see N94-14209 02-43)
Avail: CASI HC A01/MF A04

N94-14262# Remote Sensing Technology Center, Tokyo (Japan).
INTEGRATION OF SST DATA SETS USING MOS-1 SATELLITE DATA: FOR VALIDATION AND MONITORING
Shouji Takeuchi, Yasunori Nakayama, and Tsuyoshi Tomita *In* Science and Technology Agency, Asia-Pacific ISY Conference, Volume 2 31 Mar. 1993 p 274-277 Sponsored by NASDA (For primary document see N94-14209 02-43)
Avail: CASI HC A01/MF A04

N94-14263# Commonwealth Scientific and Industrial Research Organization, Mordialoc (Australia). Atmospheric Research Div.
GEOPHYSICAL VALIDATION OF ATSR SEA SURFACE TEMPERATURES
I. J. Barton, D. T. Llewellyn-Jones (Rutherford Appleton Lab., Chilton, England.), A. J. Prata, and R. P. Cechet *In* Science and Technology Agency, Asia-Pacific ISY Conference, Volume 2 31 Mar. 1993 p 278-281 (For primary document see N94-14209 02-43)
Avail: CASI HC A01/MF A04

N94-14264# Iwate Univ., Morioka (Japan). Dept. of Computer and Information Science.
ACCURACY VALIDATION TEST OF ESTIMATED SEA SURFACE TEMPERATURE BY SATELLITE DATA
Sumio Tanba, Takashi Souma, Isao Yoshida, Takashi Watanabe, and Ryuuzou Yokoyama *In* Science and Technology Agency, Asia-Pacific ISY Conference, Volume 2 31 Mar. 1993 p 282-285 (For primary document see N94-14209 02-43)
Avail: CASI HC A01/MF A04

N94-14265# Iwate Univ., Morioka (Japan). Dept. of Computer Science.
SEA SURFACE EFFECT ON THE SEA SURFACE TEMPERATURE ESTIMATION BY SATELLITE DATA
Ryuuzou Yokoyama, Sumio Tanba, and Takashi Souma *In* Science and Technology Agency, Asia-Pacific ISY Conference, Volume 2 31 Mar. 1993 p 286-289 (For primary document see N94-14209 02-43)
Avail: CASI HC A01/MF A04

N94-14266# Maritime Safety Agency, Tokyo (Japan). Hydrographic Dept.
ON THE SEA TRUTH DATA OF THE KUROSHIO MEANDER AND COLD EDDY MOVEMENT
Masataka Hishida and Yutaka Michida *In* Science and Technology Agency, Asia-Pacific ISY Conference, Volume 2 31 Mar. 1993 p 290-298 (For primary document see N94-14209 02-43)
Avail: CASI HC A02/MF A04

N94-14267# Tohoku Regional Fisheries Research Lab., Miyagi (Japan).
TRACKING OF CHANGE OF A WARM-CORE RING STRUCTURE
Denzou Inagake and Akira Tomosada *In* Science and Technology Agency, Asia-Pacific ISY Conference, Volume 2 31 Mar. 1993 p 299-302 (For primary document see N94-14209 02-43)
Avail: CASI HC A01/MF A04

N94-14268# National Space Development Agency, Ohashi (Japan). Earth Observation Center.
OUTLINE OF ISY KUROSHIO OBSERVATION EXPERIMENT
Hironori Maejima, Hiroaki Ochiai (Toba Merchant Marine Coll., Japan.), and Hideo Tameishi (Japan Fisheries Information Service Center, Tokyo.) *In* Science and Technology Agency, Asia-Pacific ISY Conference, Volume 2 31 Mar. 1993 p 303-306 Prepared in cooperation with Tokyo Univ., Japan; Nakanihon Air Service Co. Ltd., Aichi, Japan; and Remote Sensing Technology Center, Tokyo, Japan (For primary document see N94-14209 02-43)
Avail: CASI HC A01/MF A04

N94-14270# Japan Fisheries Information Service Center, Tokyo.
WARM STREAMERS EXTENDED FROM WARM CORE RINGS (WCR'S) AND THEIR ROLE ON FISH MIGRATION AND FISHING GROUND FORMATION

Hideo Tameishi and Takeshige Sugimoto (Tokyo Univ., Japan.) *In* Science and Technology Agency, Asia-Pacific ISY Conference, Volume 2 31 Mar. 1993 p 311-316 (For primary document see N94-14209 02-43)
Avail: CASI HC A02/MF A04

N94-14271# Meteorological Research Inst., Tsukuba (Japan).
ATMOSPHERIC CORRECTION FOR SEA SURFACE TEMPERATURE BY APPLICATION OF MICROWAVE DUAL-CHANNEL TECHNIQUE TO VTIR DATA
Youzou Takayama *In* Science and Technology Agency, Asia-Pacific ISY Conference, Volume 2 31 Mar. 1993 p 317-320 (For primary document see N94-14209 02-43)
Avail: CASI HC A01/MF A04

51 LIFE SCIENCES (GENERAL)

N94-12793*# Jet Propulsion Lab., California Inst. of Tech., Pasadena.
CATALYSIS AND BIOCATALYSIS PROGRAM Final Report, May 1980 - 31 Dec. 1991
J. D. Ingham 1 May 1993 68 p
(Contract DE-AI01-86CE-90239)
(NASA-CR-194105; JPL-Publ-93-04; NAS 1.26:194105) Avail: CASI HC A04/MF A01

This final report presents a summary of research activities and accomplishments for the Catalysis and Biocatalysis Program, which was renamed the Biological and Chemical Technologies Research (BCTR) Program, currently of the Advanced Industrial Concepts Division (AICD), Office of Industrial Technologies of the Department of Energy (DOE). The Program was formerly under the Division of Energy Conversion and Utilization Technologies (ECUT) until the DOE reorganization in April, 1990. The goals of the BCTR Program are consistent with the initial ECUT goals, but represent an increased effort toward advances in chemical and biological technology transfer. In addition, the transition reflects a need for the BCTR Program to assume a greater R&D role in chemical catalysis as well as a need to position itself for a more encompassing involvement in a broader range of biological and chemical technology research. The mission of the AICD is to create a balanced Program of high risk, long-term, directed interdisciplinary research and development that will improve energy efficiency and enhance fuel flexibility in the industrial sector. Under AICD, the DOE Catalysis and Biocatalysis Program sponsors research and development in furthering industrial biotechnology applications and promotes the integrated participation of universities, industrial companies, and government research laboratories. Author (revised)

N94-12795*# Texas Univ., San Antonio.
MONOCLONAL ANTIBODIES DIRECTED AGAINST SURFACE MOLECULES OF MULTICELL SPHEROIDS Semiannual Status Report, 1 Jan. - 30 Jun. 1993
Andrew O. Martinez 1993 10 p
(Grant NAG2-819)
(NASA-CR-193560; NAS 1.26:193560) Avail: CASI HC A02/MF A01

The objective of this project is to generate a library of monoclonal antibodies (MAb's) to surface molecules involved in the cell-cell interactions of mammalian cells grown as multicell spheroids (MCS). MCS are highly organized 3-dimensional multicellular structures which exhibit many characteristics in vivo tissues not found in conventional monolayer or suspension culture. They also provide a functional assay for surface adhesion molecules. In brief, MCS combine the relevance of organized tissues with the accuracy of in vitro methodology. Further, one can manipulate these MCS experimentally to discern important information about their biology. Author (revised)

N94-12835# Pennsylvania State Univ., University Park. Dept. of Biology.
ROLE OF Ca(++)/CALMODULIN IN THE REGULATION OF MICROTUBULES IN HIGHER PLANTS
R. Cyr 1992 7 p
(Contract DE-FG02-91ER-20050)
(DE93-015885; DOE/ER-20050/T1) Avail: CASI HC A02/MF A01

The cytoskeleton including its microtubule (Mt) component participates in processes that directly affect growth and development in higher plants. Normal cytoskeletal function requires the precise and orderly arrangement of Mts into several cell cycle and developmentally specific arrays. The cortical array somehow directs the deposition of cellulose. Little molecular information is available regarding the formation of these arrays or the cellular signals to which they respond. Experimental data described here suggests that plant cells use calcium, in the form of a Ca(sup ++)/calmodulin complex, to affect the dynamics of Mts within the cortical array. Owing to the importance of Ca(sup ++) as a regulatory ion in higher plants we are probing for a putative Ca(sup ++)/Mt transduction pathway which may serve to integrate Mt activities within the growing and developing plant cell. We are using a lysed cell model in conjunction with immunocytochemical and biochemical methodologies to dissect how Ca(sup ++)/calmodulin interacts with Mts to affect their function. DOE

N94-13210*# Scripps Institution of Oceanography, La Jolla, CA.
EVOLUTION OF CATALYTIC RNA IN THE LABORATORY Final Technical Report, 1 Apr. 1989 - 31 Mar. 1992
Gerald F. Joyce 31 Mar. 1992 7 p
(Grant NAGw-1671)
(NASA-CR-194124; NAS 1.26:194124) Avail: CASI HC A02/MF A01

We are interested in the biochemistry of existing RNA enzymes and in the development of RNA enzymes with novel catalytic function. The focal point of our research program has been the design and operation of a laboratory system for the controlled evolution of catalytic RNA. This system serves as working model of RNA-based life and can be used to explore the catalytic potential of RNA. Evolution requires the integration of three chemical processes: amplification, mutation, and selection. Amplification results in additional copies of the genetic material. Mutation operates at the level of genotype to introduce variability, this variability in turn being expressed as a range of phenotypes. Selection operates at the level of phenotype to reduce variability by excluding those individuals that do not conform to the prevailing fitness criteria. These three processes must be linked so that only the selected individuals are amplified, subject to mutational error, to produce a progeny distribution of mutant individuals. We devised techniques for the amplification, mutation, and selection of catalytic RNA, all of which can be performed rapidly in vitro within a single reaction vessel. We integrated these techniques in such a way that they can be performed iteratively and routinely. This allowed us to conduct evolution experiments in response to artificially-imposed selection constraints. Our objective was to develop novel RNA enzymes by altering the selection constraints in a controlled manner. In this way we were able to expand the catalytic repertoire of RNA. Our long-range objective is to develop an RNA enzyme with RNA replicase activity. If such an enzyme had the ability to produce additional copies of itself, then RNA evolution would operate autonomously and the origin of life will have been realized in the laboratory. Derived from text

N94-13447*# National Aeronautics and Space Administration. Ames Research Center, Moffett Field, CA.
CLINICAL PHYSIOLOGY OF BED REST
John E. Greenleaf Apr. 1993 27 p
(RTOP 199-18-12-07)
(NASA-TM-104010; A-93058; NAS 1.15:104010) Avail: CASI HC A03/MF A01

Maintenance of optimal health in humans requires the proper balance between exercise, rest, and sleep as well as time in the upright position. About one-third of a lifetime is spent sleeping; and it is no coincidence that sleeping is performed in the horizontal position, the position in which gravitational influence on the body is minimal. Although enforced bed rest is necessary for the treatment of some ailments, in some cases it has probably been used unwisely. In addition to the lower hydrostatic pressure with the normally dependent regions of the cardiovascular system, body fuid compartments during bed rest in the horizontal body position, and virtual elimination of compression on the long bones of the skeletal system during bed rest (hypogravia), there is often reduction in energy metabolism due to the relative confinement (hypodynamia) and alteration of ambulatory circadian variations in metabolism, body temperature, and many hormonal systems. If patients are also moved to unfamiliar surroundings, they probably experience some feelings of anxiety and some sociopsychological problems. Adaptive physiological responses during bed rest are normal for that environment. They are attempts by the body to reduce unnecessary energy

expenditure, to optimize its function, and to enhance its survival potential. Many of the deconditioning responses begin within the first day or two of bed rest; these early responses have prompted physicians to insist upon early resumption of the upright posture and ambulation of bedridden patients. Author

N94-13473*# East Carolina Univ., Greenville, NC. School of Medicine.
PHYSIOLOGICAL ANATOMICAL RODENT EXPERIMENT (PARE) .04 FEASIBILITY TEST 1
Hubert W. Burden 22 Sep. 1993 73 p
(Contract NCC2-810)
(NASA-CR-194423; NAS 1.26:194423) Avail: CASI HC A04/MF A01

The objective of this feasibility study was to investigate the environmental/treatment stresses in the proposed PARE.04 experiments in a ground based study to determine if these stresses were of sufficient magnitude to compromise the planned shuttle experiments. Eighty pregnant Sprague-Dawley rats were received on day 2 (day I equals day of vaginal plug) of gestation (G2) and on G7 60 were laparotomized to determine the condition of pregnancy and allow assignment to test groups. The five test groups (N equals 10 each group) were as follows: Group 1, nominal flight; Group 2, laparotomy control; Group 3, hysterectomy control; Group 4, vivarium control; Group 5, caesarean delivery. On G17, groups 1, 2, and 5 were subjected to unilateral hysterectomy to obtain fetuses for evaluation. There was no difference in fetal crown-rump length, fetal weight, or placental weight in any of the test groups subjected to unilateral hysterectomy at G17. Animals were allowed to go to term and animals in each group delivered between the morning of G22 and the afternoon of G23. Rats assigned to Group 5 began delivering vaginally prior to the designated time for caesarean section, thus only 2 animals in this group were delivered by caesarean section. After delivery, a blood sample was taken from the dam, and they were euthanized and the thymus and adrenal glands weighed. Pups from experimental dams were tattooed for identification, the anogenital distance of male pups was photographed for later measurement, and all pups placed with foster dams and litter sizes were standardized to 10. On day 7, all pups were euthanized, and pup adrenal glands and thymus weighed. Laparotomy at G7 with or without unilateral hysterectomy at G17, had no effect on pregnancy maintenance or vaginal delivery. There was no difference in maternal adrenal or thymus weights or plasma levels of catecholamines, estradiol, progesterone, or corticosterone. Likewise, there was no difference in the anogenital distance (index of fetal stress) of neonatal male pups, between any of the experimental groups. From days 0-7, weight gain from dams in all experimental groups was similar. Lastly, there was no difference in weights of thymus and adrenal glands in pups euthanized at day 7. Collectively, these data indicate that treatment stresses inherent in the proposed PARE.04 experimental design should not compromise the planned shuttle experiments.

Author (revised)

N94-13562*# National Aeronautics and Space Administration. Ames Research Center, Moffett Field, CA.
THE EVOLUTION OF ENERGY-TRANSDUCING SYSTEMS: STUDIES WITH ARCHAEBACTERIA Semiannual Progress Report, Mar. - Aug. 1993
Helga Stan-Lotter Aug. 1993 5 p
(Contract NCC2-578)
(NASA-CR-194130; NAS 1.26:194130) Avail: CASI HC A01/MF A01

N-ethylmaleimide (NEM) inhibits the ATPase of H. saccharovorum in a nucleotide protectable manner. The bulk of 14C-NEM is incorporated into subunit 1. Inhibition kinetics indicated a single binding site. To determine the sequence around this site, cyanogen bromide peptides of NEM-labeled ATPase enzyme were prepared and separated on Tris-Tricine gels. Autoradiography indicated that the NEM binding site is probably located in a fragment of Mr 10-12 K. This result will be confirmed by N-terminal sequencing of the peptide. Since the cysteinyl residue, to which NEM is bound, may be located at the C-terminal end, purification and proteolytic treatment of the 10 K peptide will be required. One inhibitor of V-type ATPases, fluoresceinisothiocyanate (FITC) inhibited also the ATPase of H. saccharovorum. Preliminary results indicated protection against inhibition by nucleotides. Localization of the binding sited to the major subunits is in progress. An extraction procedure for the membrane sector of the ATPase complex of H. saccharovorum yielded a preparation which was enriched in a peptide of Mr 5 500. Experiments to test the immunological crossreaction with subunit c from the Escherichia coli F-type ATPase and the labeling with 14C-DCCD are currently carried out. Polyclonal antiserum to the smaller of the major subunits of the ATPase from H. saccharovorum (subunit II) reacts in Western blots strongly with the alpha and beta subunits of the F1 ATPase of E. coli, suggesting highly conserved regions on both types of ATPases. To elucidate further the regions of homology, cyanogen bromide peptides of the beta subunits were prepared for sequence analysis.

Derived from text

N94-13698# Gordon Research Conferences, Inc., Kingston, RI.
GORDON RESEARCH CONFERENCE ON CHRONOBIOLOGY, 1991 Final Report, 1 Aug. 1991 - 31 Jul. 1992
J. W. Hastings 31 Jul. 1992 9 p Conference held in Irsee, Germany, 29 Sep. - 4 Oct. 1991
(Grant AF-AFOSR-0280-91)
(AD-A266354; AFOSR-93-0447TR) Avail: CASI HC A02/MF A01

The 1991 Gordon Conference on Chronobiology was held at the Swabian Conference Center in Irsee, Germany, from 29 Sep. - 4 Oct. 1991. The possibility of holding the conference in Europe was known at the previous (1989) meeting, and conferees voted to do so if the opportunity materialized. Probably more than most, the field of chronobiology embraces many subdisciplines, ranging from molecular biology and genetics to physiology and ecology. It is also diverse in terms of biological material, including all Kingdoms and spanning the phylogenetic spectrum. It is relevant to many specific missions, such as medicine and pharmacology, agriculture, and insect control, as well as marine biology and oceanography. The program thus reflects the wish and the willingness of workers in this area to consider a diversity of functions and a diversity of systems, ranging from nitrogen fixation in bacteria, photosynthesis and luminescence in marine dinoflagellates and CAB gene expression in wheat, to conidiation in Neurospora, eclosion in Drosophila, and activity in rodents and man.

DTIC

N94-13823 Alberta Univ., Edmonton. Dept. of Zoology.
IMPROVING PHYSICAL PERFORMANCE BY CHEMICAL STIMULATION Final Report
Lawrence C. H. Wang 22 May 1992 34 p
(DSIS-92-03763; CTN-93-60770) Avail: CASI HC A03

The effectiveness of ginseng saponin (GS) as an ergogenic agent was evaluated and the mechanisms through which GS elicits its beneficial effect on exercise performance were elucidated. Short term (2-4 days) pretreatment with GS significantly prolonged the aerobic endurance of mature young and old rats exercising at 70 percent maximum oxygen volume. Results indicated that either a proto-panaxadiol triterpenoid or a proto-panaxatriol triterpenoid purified from GS were essential for eliciting the beneficial ergogenic effects of GS. Compared to saline treated control rats, GS significantly increased the plasma free fatty acid level of the animals at rest and during exercise. During exercise, the plasma glucose level of the control group declined progressively, whereas in the GS-treated animals it maintained a stable level. Both the liver and skeletal muscle glycogen levels of the GS-treated rats were slightly higher than those of the control animals after exhaustive exercise. These results indicate that GS enhances exercise endurance by altering fuel homeostasis during prolonged exercise, presumably by increasing free fatty acid utilization in preference of glucose for cellular energy production. Author (CISTI)

N94-13865*# Georgia State Univ., Atlanta. Language Research Center.
SELECTION OF BEHAVIORAL TASKS AND DEVELOPMENT OF SOFTWARE FOR EVALUATION OF RHESUS MONKEY BEHAVIOR DURING SPACEFLIGHT Semiannual Status Report, Mar. - Aug. 1993
Duane M. Rumbaugh and David A. Washburn Aug. 1993 7 p
(Grant NAG2-438)
(NASA-CR-194176; NAS 1.26:194176) Avail: CASI HC A02/MF A01

The results of several experiments were disseminated professionally during this semiannual period. These peer-reviewed papers that were accepted for publication represent the growth of our research areas, as follow-up experiments to previously published work in cognition and enrichment have been completed and are being published. The presentations not only reflect the latest interesting results that we have obtained, but also serve as a testament to the intense interest that is being expressed for our test system and findings. Derived from text

N94-14028*# Krug Life Sciences, Inc., Houston, TX.
METABOLIC RATE MEASUREMENTS COMPARING SUPINE WITH UPRIGHT UPPER-BODY EXERCISES
Suzanne M. Fortney, Michael C. Greenisen, Karin C. Loftin, Donya Beene, Sondra Freeman-Perez, and Linda Hnatt Sep. 1993 22 p
(Contract NAS9-18492)
(NASA-CR-4549; S-736; NAS 1.26:4549) Avail: CASI HC A03/MF A01

The ground-based study that tested the hypothesis that metabolic rates during supine and upright upper-body exercises are similar (mean value of 200 kcal/h) is presented. Six subjects each performed supine or upright exercise at three exercise stations, a hand-cycle ergometer, a rope-pull device, and a torque wrench. After a baseline measurement of the metabolic rate at rest, the metabolic rate was measured twice at each exercise station. The mean metabolic rates (kcal/h) during supine (n = 6) and upright control (n = 4) exercise stations were not significantly different except for the rope-pull station, 153.5 +/- 16.6 (supine) as compared to 247.0 +/- 21.7 (upright), p is less than 0.05. This difference may be due in part to an increased mechanical efficiency of supine exercises (15.0 +/- 0.7 percent) as compared to that of upright exercises (11.0 +/- 1.08 percent), p is less than 0.05. The net energy input was significantly smaller for the supine rope-pull exercise (64 +/- 18) as compared to upright (176 +/- 20). The relationship between best-rest exercises, metabolic rates, and the incidence of decompression sickness (DCS) should be examined to determine the true risk of DCS in spaceflight extravehicular activities.
Author (revised)

N94-14032*# National Aeronautics and Space Administration. Lyndon B. Johnson Space Center, Houston, TX.
VARIABILITY OF PREDICTION OF MAXIMAL OXYGEN CONCUMPTION ON THE CYCLE ERGOMETER USING STANDARD EQUATIONS
Michael C. Greenisen, Suzanne M. Fortney, Stuart M. C. Lee (Krug Life Sciences, Inc., Houston, TX.), Alan D. Moore (Krug Life Sciences, Inc., Houston, TX.), and Linda H. Barrows (Krug Life Sciences, Inc., Houston, TX.) Sep. 1993 11 p
(NASA-TP-3412; S-737; NAS 1.60:3412) Avail: CASI HC A03/MF A01

Several investigations within the Exercise Countermeasures Project at the NASA Johnson Space Center focused on the assessment of maximum oxygen consumption (VO2(sub max)) within the Astronaut Corps pre- and postspace flight. Investigations during the Apollo era suggested that there was a significant decrease in postflight VO2(sub max) when compared to preflight values, and current studies have documented that this trend continues in the Space Shuttle era. It is generally accepted and was confirmed in our laboratory that VO2(sub max) can be predicted from submaximal measures taken during graded exercise tests on the cycle ergometer with respect to populations. However, previous work had not examined the effect of day-to-day variations in the physiologic responses that might alter these predictions for individuals. Stability of individual submaximal data over serial tests is important so that predicted changes in VO2(sub max) are reflective of actual VO2(sub max) changes. Therefore, the purpose of this investigation was to determine which of the accepted equations to predict VO2(sub max) would be less affected by normal daily physiologic changes.
Author (revised)

N94-14097*# Alabama A & M Univ., Normal.
CHARACTERIZATION OF SPIRULINA BIOMASS FOR CELSS DIET POTENTIAL
Mahasin G. Tadros Aug. 1993 41 p
(Contract NCC2-501)
(NASA-CR-194123; NAS 1.26:194123) Avail: CASI HC A03/MF A01

Cyanobacteria, Spirulina maxima as a biogenerative photosynthetic and an edible alga for the space craft crew in a CELSS, was evaluated in an effort to increase the growth rate, biomass, yield, and chemical analysis in continuous cultures. The cell characteristics were determined for cultures maintained at steady state with respect to the substrate concentration. The productivity increased in experiments exposed to low light (30 uE m(exp -2)s(exp -1). Oxygen evolved and protein production were higher in cultures exposed to low light intensity. There was a relationship between nitrate concentration and the yield of the culture. Increasing the concentration of nitrate in the growth medium up to 20 mM was enough to produce a culture having the same chemical composition as that of complete medium. High light was inhibiting the yield of the culture. Increasing the concentration of phosphate beyond 1 mM did not improve the yield of the culture. Increasing the concentration of sodium chloride in the growth medium did not affect the growth of the alga up to 0.1 M but beyond that the culture started to be stressed. The response to stress appeared in high production of total carbohydrate on the expense of protein production. The oxygen production was also higher in cultures stressed with sodium chloride.
Author

N94-14128# National Defence Research Establishment, Umea (Sweden).
THE SURFACE-LOCATED YopN PROTEIN IS INVOLVED IN CALCIUM SIGNAL TRANSDUCTION IN YERSINIA PSEUDOTUBERCULOSIS
A. Forsberg, A.-M. Viitanen (Turku Univ., Finland.), M. Skurnik (Turku Univ., Finland.), and H. Wolf-Watz (Umea Univ., Sweden.) 1991 10 p Repr. from Molecular Microbiology, v. 5, no. 4, 1991 p 977-986 Sponsored by Sigrid Juselius Foundation; Emil Aaltonen Foundation; and Farmos Research and Science Foundation
(Grants SMRC-07490-040; BU-4426-30; STuF-90-00577)
(FOA-B-40416-4.4; ETN-93-93761) Avail: CASI HC A02/MF A01

The low calcium response is strongly conserved among the pathogenic Yersinia species and is observed when the pathogen is grown at 37 C in Ca(2+) depleted medium. This response is characterized by a general metabolic downshift and by a specific induction of virulence plasmid encoded Yop (Yersinia outer membrane protein) genes. Regulation of the Yop expression is exerted at a transcriptional level by a temperature regulated activator and by Ca(2+) regulated negative elements. The YopN gene was shown to encode a protein (formerly also designated Yop4b) which is surface located when Yersinia is grown at 37 C. YopN was found to be part of an operon that is induced during the low calcium response. Insertional inactivation of the YopN gene resulted in derepressed transcription of Yop genes. A hybrid plasmid containing the YopN gene under the control of the tac promoter fully restored the wild type phenotype of the YopN mutant. Thus, the surface located YopN somehow senses the calcium concentration and transmits a signal to shut off Yop transcription when the calcium concentration is high.
ESA

N94-14129# National Defence Research Establishment, Umea (Sweden). Cell and Microbiology Dept.
ANALYSIS OF THE V ANTIGEN lcrGVH-yopBD OPERON OF YERSINIA PSEUDOTUBERCULOSIS: EVIDENCE FOR A REGULATORY ROLE OF LcrH AND LcrV
Thomas Bergman (Umea Univ., Sweden.), Sebastian Haakansson (Umea Univ., Sweden.), Aake Forsberg, Lena Norlander, Anna Macellaro, Assar Baeckman (Umea Univ., Sweden.), Ingrid Boelin, and Hans Wolf-Watz (Umea Univ., Sweden.) 1991 10 p Repr. from Journal of Bacteriology, v. 173, no. 5, Mar. 1991 p 1607-1616
(Grants SMRC-07490-040; BU-4426-30; STuF-90-00577)
(FOA-B-40417-4.4; ETN-93-93762) Copyright Avail: CASI HC A02/MF A01

It is shown that the V antigen containing operon of Yersinia pseudotuberculosis is a polycistronic operon having the gene order lcrGVH-YopBD. Deoxyribonucleic Acid (DNA) sequencing analysis of lcrGVH revealed a high homology to the corresponding genes of Yersinia pestis. LcrG was conserved and LcrH showed only one amino acid different, while LcrV showed only 96.6% identity. The amino acid substitutions of LcrV occurred in the central domain of the protein, while the two ends of the protein were conserved. Northern (ribonucleic Acid (RNA)) blotting experiments showed that the operon is regulated at the transcriptional level by the extracellular stimuli temperature and calcium. One 4.6 Kb transcriptional product of the operon was identified. The mRNA is rapidly processed at its 5' end, resulting in different mRNA species of variable stability. By genetic analysis, the lcrV and lcrH gene products were found to be regulatory proteins having important roles in the Ca(2+) controlled regulation of Yop (Yersinia outer membrane protein) expression. The activity of LcrH is modulated by a gene product of the operon that inhibits the negative action of LcrH on Yop transcription in the absence of Ca(2+).
ESA

N94-14494*# Alabama Univ., Huntsville.
CELLULAR RESPONSES TO LOW-GRAVITY: PILOT STUDIES ON SUBORBITAL ROCKETS AND ORBITING SPACECRAFT Final Report, 1 Oct. 1991 - 30 Sep. 1993
Marian L. Lewis 30 Sep. 1993 40 p

(Grant NAGw-2739)
(NASA-CR-194402; NAS 1.26:194402) Avail: CASI HC A03/MF A01

The allocated funding supported, in part, experiments conducted on two Consort sounding rockets and five Shuttle flights. The primary parameters investigated were signal transduction in response to various mediators, cellular differentiation and metabolism in microgravity, and effect of microgravity on cytoskeletal morphology. Achievements include: demonstration of effect of spaceflight on the actin cytoskeleton in mouse osteoblasts and frog cells; confirmation that the T cell receptor-mediated signal transduction pathway in T lymphocytes is not affected by low-gravity compared to non-TCR-mediated stimulation (Con-A) which classically does not promote proliferative response; indication that microgravity may allow separation of proliferative signaling and secretory function in lymphocytes; demonstration that T lymphocytes and bone cells utilized less glucose indicating a shift in metabolism and confirming Spacelab results with WI-38 cells which used significantly less glucose, during spaceflight; confirmation that activation of human splenic B cells with a number of different mediators is not affected during spaceflight; demonstration of increased prostaglandin synthesis during reduced bone cell growth suggesting an effect of microgravity on prostaglandin-induced mitogenesis. The funding contributed significantly to the database described above and resulted in submission of six collaborative abstracts in 1993 (five to the ASGSB Annual Meeting and one to the ASCB Annual Meeting). Two abstracts were presented at the 1992 ASGSB Annual Meeting in Tucson. In addition, several peer reviewed papers are being generated and data will be included as background in preparation of future proposals, which hopefully will allow us to continue this type of extremely productive collaborative research.

Author (revised)

N94-14509# Yale Univ., New Haven, CT.
THE FIRST STEPS OF CHLOROPHYLL SYNTHESIS: RNA INVOLVEMENT AND REGULATION
D. Soell 1992 5 p
(Contract DE-FG02-87ER-13734)
(DE93-014398; DOE/ER-13734/4) Avail: CASI HC A01/MF A01

Glu-tRNA(sup Glu) is synthesized from glutamate and tRNA(sup Glu) by glutamyl-tRNA synthetase (GluRS). Recent work has demonstrated that Glu-tRNA(sup Glu) has dual functions and is a precursor for protein and 5-aminolevulinate (ALA) synthesis. Current data does not provide compelling evidence for the notion that GluRS is regulated by chlorophyll precursors or in concert with the other enzymes of ALA synthesis. We have redefined the C5-pathway as a two-step route to ALA starting with Glu-tRNA(sup Glu). Only two enzymes, Glu-tRNA reductase (GluTR) and GSA-2,1-amino-mutase (GSA-AM), are specifically involved in ALA synthesis. We have purified these enzymatic activities from Chlamydomonas and demonstrated that the two purified proteins in the presence of their cofactors NADPH and pyridoxal phosphate are sufficient for the in vitro Glu-tRNA (yields) ALA conversion. We have cloned the genes encoding GluTR. The sequences of the GluTR proteins deduced from these genes share highly conserved regions with those of bacterial origin. We have also cloned and analyzed the gene encoding GSA-AM from Arabidopsis. As in Salmonella typhimurium, there are indications of the existence of an additional pathway for ALA formation in E. coli. To shed light on the recognition of the single tRNA(sup Glu) by the chloroplast enzymes GluTR, GluRS, we characterized a chlorophyll-deficient mutant of Euglena having tRNA(sup Glu) with a point mutation in the T(Psi)C-loop. The altered tRNA supports protein but not ALA synthesis. DOE

N94-14596# Washington Univ., Seattle. Dept. of Applied Mathematics.
CHAOS AND MICROBIAL SYSTEMS
M. Kot Oct. 1992 5 p
(Contract DE-FG06-90ER-61034)
(DE93-016814; DOE/ER-61034/2) Avail: CASI HC A01/MF A01

The field of nonlinear dynamics has generated a variety of new techniques for identifying order in seemingly chaotic systems. These techniques have led to new insights for several ecological and epidemiological systems, most notably childhood disease epidemics. To better test the efficacy and relevance of these new techniques to population biology research with two components namely a mathematical analysis of some simple microbial models with chaotic dynamics; and experimental (chemostat) population studies to evaluate the accuracy of these models. I have completed a thorough analysis of the forced double-Monod model and of the phase-locking route to chaos that it exhibits. I have also analyzed a simpler pulsed system with mass action kinetics and a period-doubling route to chaos. This research also motivated detailed analyses of discrete-time predator-prey and dispersal models, and a fast new method for computing fractal dimension. My colleagues and I have assembled a complete laboratory system to determine the appropriateness of the forced double-Monod model. We have tested assays for concentration and density and have performed a variety of diagnostic tests on this system. We have measured growth parameters for bacteria and for protozoa in chemostat. DOE

N94-14802 Northwestern Univ., Evanston, IL.
STRUCTURES AND SHEAR RESPONSE OF LIPID MONOLAYERS
P. Dutta and J. B. Ketterson Feb. 1993 19 p Limited Reproducibility: More than 20% of this document may be affected by microfiche quality
(Contract DE-FG02-84ER-45125)
(DE93-015076; DOE/ER-45125/10) Avail: CASI HC A03

This report discusses our work during the last 3 years using x-ray diffraction and shear measurements to study lipid monolayers (membranes). The report is divided into: (1) structure--phase diagram of saturated fatty acid Langmuir monolayers, effect of head group interactions, and studies of transferred monolayers (LB films); and (2) mechanical properties--fiber optic capillary wave probe and centrosymmetric trough, mechanical behavior of heneicosanoic acid monolayer phases. DOE

N94-14852# Norwegian Defence Research Establishment, Kjeller. Div. for Environmental Toxicology,
A CHARACTERIZATION OF CARBOXYLESTERASES IN RAT AND GUINEA PIG: THEIR HETEROGENEITY AND ROLE IN DETOXICATION OF ORGANOPHOSPHORUS COMPOUNDS Ph.D. Thesis - Oslo Univ.
Rolf Gaustad Sep. 1993 51 p
(NDRE-Publ-93-1001) Avail: CASI HC A04/MF A01

The present study deals with the molecular properties of carboxylesterases (CarbEs) and the ability of the various isoenzymes to detoxify organophosphorus compounds. CarbE isoenzymes have been separated from lungs, livers, plasma and small intestines of rats and guinea pigs mainly by chromatofocusing. One of the isoenzymes in rat lung, pI 5.8, has been purified to near homogeneity. This isoenzyme has a molecular mass of approx 180 kDa with subunits of 60 kDa, and by Edman degradation the first 19 amino acid residues were determined. Monoclonal antibodies (MAbs) were prepared against the purified isoenzyme and used in enzyme-linked immunosorbent assays (ELISA) to distinguish between the CarbE isoenzymes in the different tissues. The molecular and immunological results showed a strong relationship between lung CarbE, pI 5.8, and the rat liver CarbE, pI 6.0. The MAbs were strongly bound to the high pI forms of the CarbE isoenzymes in plasma and small intestine from rats and guinea pigs, but not to the low pI forms. This indicates that at least two immunochemically distinct categories of isoenzymes are present in both plasma and intestine. Furthermore, the properties of the differenct CarbE isoenzymes with regard to inhibition by selected organophosphorus compounds were studied in vitro and in vivo. With some exemption the inhibition constants showed small differences between isoenzymes. Subcutaneous and intraperitonal administration of paraoxon and diisopropyl phospho fluoridate (DFP) rapidly inhibited the CarbE activity in guinea pig plasma, much higher doses were necessary to obtain a marked inhibition in lung and liver, and about 25 percent of CarbE activity in lung was resistant to inhibition. Gel filtration of lung homogenate after treatment with organophosphorus compuonds showed that CarbE activity in one of the molecular mass fractions was weakly inhibited. This might be due to different subcellular localization of the isoenzymes and thereby reduced accessibility to some of the lung CarbE isoenzyes. The experiments showed that the efficacy for detoxication is a function of the relative affinities of the organophosphorus compounds for CarbEs and acetyl cholinesterase (AChE). For compounds like paraoxon and DFP, with lower affinities for AChE than for CarbEs, also the lung and liver CarbEs contribute to the detoxication process. The distributions of CarbEs in separated rat liver cells were investigated by polyacrylamide gel electrophoresis (PAGE). All of the liver CarbE isoenzymes could be detected in the parenchymal cells, whereas in both Kupffer cells and endothelial cells only those with pI 6.4/6.2, also termed mono acylglyceral lipase, could be detected.

Author (revised)

N94-14862# European Space Agency. European Space Research and Technology Center, ESTEC, Noordwijk (Netherlands).
ETHOLOGY IN SPACE, A UNIQUE OPPORTUNITY FOR BEHAVIOURAL SCIENCE
R. E. Stark and S. R. Heerd, ed. Mar. 1993 99 p
(ESA-STM-246; ISBN-92-9092-208-7; ETN-93-94410) Copyright Avail: CASI HC A05/MF A02

The current status of experiments performed under space flight conditions using animals as subjects is reviewed and summarized. Some potential experimental approaches to study the behavioral responses and acclimatization of animals to the space environment are proposed. Future areas of required behavioral research are presented, and some of the peculiarities associated with the development of a life science experiment and its equipment specifically for behavioral studies in space are shown. The following are also advertized: the availability of the space environment to the European behavioral science community, to encourage behavioral scientists to think in terms of experimentation under microgravity conditions and to stimulate them in generating new ideas and proposals for flight experiments. ESA

N94-14899# San Diego State Univ., CA. Center for Hydro-Optics and Remote Sensing.
NONLINEAR RELATIONSHIPS BETWEEN PARTICULATE ABSORPTION AND CHLOROPHYLL: DETRITUS OR PIGMENT PACKAGING? Final Report
Joan S. Cleveland 15 Jun. 1993 21 p
(Contract N00014-92-J-1012)
(AD-A266806; TM-008-93) Avail: CASI HC A03/MF A01

Relationships for predicting phytoplanktonic absorption at 676 and 436 nm from chlorophyll alpha concentration have been developed for distinct geographic regions defined by latitude. The forms of the predictive equations are controlled by underlying biological mechanisms and lend insight into these mechanisms. Development of these region-specific models allows prediction of phytoplanktonic absorption from more easily measured parameters such as chlorophyll alpha concentration or in situ fluorescence and increases accuracy in modelling optical properties or primary production rate using specific absorption coefficients. Temperate and tropical regions exhibited nearly identical relationships at low chlorophyll so these regions were combined and treated as one. DTIC

N94-13760*# Osaka Univ. (Japan). Medical School.
SEPARATION OF BIOGENIC MATERIALS BY ELECTROPHORESIS UNDER ZERO GRAVITY (L-3)
Masao Kuroda *In* NASA. Marshall Space Flight Center, Spacelab J Experiment Descriptions Aug. 1993 p 155-160 (For primary document see N94-13732 02-29)
Avail: CASI HC A02/MF A03

N94-13763*# Tokyo Medical and Dental Univ. (Japan).
STUDIES ON THE EFFECTS OF MICROGRAVITY ON THE ULTRASTRUCTURE AND FUNCTIONS OF CULTURED MAMMALIAN CELLS (L-6)
Atsushige Sato *In* NASA. Marshall Space Flight Center, Spacelab J Experiment Descriptions Aug. 1993 p 171-172 (For primary document see N94-13732 02-29)
Avail: CASI HC A01/MF A03

N94-13764*# State Univ. of New York, Stony Brook.
GRAVITY, CHROMOSOMES, AND ORGANIZED DEVELOPMENT IN ASEPTICALLY CULTURED PLANT CELLS
Abraham D. Krikorian *In* NASA. Marshall Space Flight Center, Spacelab J Experiment Descriptions Aug. 1993 p 173-176 (For primary document see N94-13732 02-29)
Avail: CASI HC A01/MF A03

N94-13766*# Kyoto Univ. (Japan). Radiation Biology Center.
GENETIC EFFECTS OF HZE AND COSMIC RADIATION (L-9)
Mituo Ikenaga *In* NASA. Marshall Space Flight Center, Spacelab J Experiment Descriptions Aug. 1993 p 181-184 (For primary document see N94-13732 02-29)
Avail: CASI HC A01/MF A03

N94-13769*# Shizuoka Univ. (Japan).
A CIRCADIAN RHYTHM OF CONIDIATION IN NEUROSPORA CRASSA (L-12)
Yashuhiro Miyoshi *In* NASA. Marshall Space Flight Center, Spacelab J Experiment Descriptions Aug. 1993 p 197-200 (For primary document see N94-13732 02-29)
Avail: CASI HC A01/MF A03

N94-13770*# National Aeronautics and Space Administration. Ames Research Center, Moffett Field, CA.
AMPHIBIAN FERTILIZATION AND DEVELOPMENT IN MICROGRAVITY
Kenneth A. Souza *In* NASA. Marshall Space Flight Center, Spacelab J Experiment Descriptions Aug. 1993 p 201-207 (For primary document see N94-13732 02-29)
Avail: CASI HC A02/MF A03

52 AEROSPACE MEDICINE

Includes physiological factors; biological effects of radiation; and effects of weightlessness on man and animals.

N94-12832*# National Aeronautics and Space Administration. Lyndon B. Johnson Space Center, Houston, TX.
MEDICAL EVALUATIONS ON THE KC-135 1991 FLIGHT REPORT SUMMARY
Charles W. Lloyd Aug. 1993 240 p
(NASA-TM-104755; S-692; NAS 1.15:104755) Avail: CASI HC A11/MF A03

The medical investigations completed on the KC-135 during FY 1991 in support of the development of the Health Maintenance Facility and Medical Operations are presented. The experiments consisted of medical and engineering evaluations of medical hardware and procedures and were conducted by medical and engineering personnel. The hardware evaluated included prototypes of a crew medical restraint system and advanced life support pack, a shuttle orbiter medical system, an airway medical accessory kit, a supplementary extended duration orbiter medical kit, and a surgical overhead canopy. The evaluations will be used to design flight hardware and identify hardware-specific training requirements. The following procedures were evaluated: transport of an ill or injured crewmember at man-tended capability, surgical technique in microgravity, transfer of liquids in microgravity, advanced cardiac life support using man-tended capability Health Maintenance Facility hardware, medical transport using a model of the assured crew return vehicle, and evaluation of delivery mechanisms for aerosolized medications in microgravity. The results of these evaluation flights allow for a better understanding of the types of procedures that can be performed in a microgravity environment. Author (revised)

N94-12960*# Florida Agricultural and Mechanical Univ., Tallahassee. Coll. of Pharmacy.
CALCITONIN CONTROL OF CALCIUM METABOLISM DURING WEIGHTLESSNESS Final Report
Karam F. A. Soliman 1993 6 p
(Grant NAG2-411)
(NASA-CR-193622; NAS 1.26:193622) Avail: CASI HC A02/MF A01

The main objective of this proposal is to elucidate calcitonin role in calcium homeostasis during weightlessness. In this investigation our objectives are to study: the effect of weightlessness on thyroid and serum calcitonin, the effect of weightlessness on the circadian variation of calcitonin in serum and the thyroid gland, the role of light as zeitgeber for calcitonin circadian rhythm, the circadian pattern of thyroid sensitivity to release calcitonin in response to calcium load, and the role of serotonin and norepinephrine in the control of calcitonin release. The main objective of this research/proposal is to establish the role of calcitonin in calcium metabolism during weightlessness condition. Understanding the mechanism of these abnormalities will help in developing therapeutic means to counter calcium imbalance in spaceflights. Derived from text

N94-12972*# National Aeronautics and Space Administration. Ames Research Center, Moffett Field, CA.
GENDER DIFFERENCES IN ENDOCRINE RESPONSES TO POSTURE AND 7 DAYS OF 6 DEG HEAD DOWN BED REST

J. Vernikos, M. F. Dallman (California Univ., San Francisco.), L. C. Keil, D. OHara, and V. A. Convertino (National Aeronautics and Space Administration. John F. Kennedy Space Center, Cocoa Beach, FL.) Feb. 1993 20 p
(RTOP 199-18-12-09)
(NASA-TM-103991; A-93016; NAS 1.15:103991) Avail: CASI HC A03/MF A01

Endocrine regulation of fluids and electrolytes during seven days of 6 deg head down bed rest (HDBR) was compared in male (n = 8) and, for the first time, female (n = 8) volunteers. The subjects' responses to quiet standing for 2 hr before and after HDBR were also tested. In both sexes, diuresis and natriuresis were evident during the first 2-3 days of HDBR, resulting in a marked increase in the urinary Na/K ratio and significant Na retention on reambulation. After the first day of HDBR, plasma renin activity (PRA) was increased relative to aldosterone, plasma volume was decreased, and the renal response to aldosterone appeared to be appropriate. Circulating levels of arginine vasopressin (AVP), cortisol, and ACTH were unchanged during HDBR. Plasma testosterone decreased slightly on day 2 of HDBR in males. The ratio of AM ACTH to cortisol was lower in females than in males because ACTH was lower in females. Urinary cortisol increased and remained elevated throughout the HDBR in males only. There were no gender differences in the responses to 7 day HDBR, except those in the pituitary-adrenal system; those differences appeared unrelated to the postural change. The provocative cardiovascular test of quiet standing before and after bed rest revealed both sex differences and effects of HDBR. There were significant sex differences in cardiovascular responses to standing, before and after HDBR. Females had greater PRA and aldosterone responses to standing before bedrest and larger aldosterone responses to standing after HDBR than males. Cardiovascular responses to standing before and after bedrest differed markedly: arterial pressure and heart rates increased with standing before HDBR, by contrast, arterial pressure decreased, with greater increases in heart rates after HDBR. In both sexes, all hormonal responses to standing were greater after HDBR. The results show clearly that similar responses to standing as well as to HDBR occur in both sexes, but that females exhibit greater PRA and aldosterone responses than males. Author (revised)

N94-13038# Chicago Univ., IL. Dept. of Medicine.
PHASE-SHIFTING EFFECT OF LIGHT AND EXERCISE ON THE HUMAN CIRCADIAN CLOCK Annual Report, 1 Mar. 1991 - 28 Feb. 1993
Eve V. Cauter 18 May 1993 19 p
(Grant AF-AFOSR-0222-90)
(AD-A265732; AFOSR-93-0378TR) Avail: CASI HC A03/MF A01

The aim of the present study was to determine the magnitude and direction of immediate phaseshifts of human rhythms following a single exposure to a 3-hour pulse of bright light or physical activity. The pulse of light or activity was presented under constant routine conditions and measurement of the resultant phase-shifts were performed under the same constant routine conditions on the first day following pulse presentation. Four overt rhythms that are strongly dependent on circadian timing, i.e., the rhythms of plasma cortisol, plasma TSH, plasma melatonin, and body temperature, were monitored. Based on the analysis of the TSH profiles, our findings indicate that exposure to light around the time of the minimum of body temperature results in phase-advances averaging less than one hour in magnitude. Exposure to light approximately 3 hours before the time of the minimum of body temperature results in 1-2 hour phase delays. Preliminary analyses of the melatonin profiles confirm these observations. Our findings regarding the effects of exercise are still inconclusive. DTIC

N94-13061# Wyoming Univ., Laramie.
CELLULAR MECHANISM OF TURNOVER OF THE STRESS INDUCED PROTEIN HSP 70 Annual Report, 15 Apr. 1992 - 14 Apr. 1993
Nancy Petersen 17 May 1993 8 p
(Contract F49620-92-J-0234)
(AD-A265723; AFOSR-93-0383TR) Avail: CASI HC A02/MF A01

Synthesis of the heat shock protein, hsp7O, appears to be essential for recovery from heat and chemical stress. Both because of the role of this protein in cellular recovery from stress and because of the possibility of using levels of hsp7O synthesis or accumulation as a measurement of cellular response in stress, it is important to study the stability of hsp7O. We have shown that Drosophila hsp7O decays in vitro by an autoproteolytic mechanism. Autoproteolytic decay could be part of the feedback mechanism regulating the levels of hsp7O accumulation if it occurs in vivo. To determine whether autoproteolytic decay is occurring in vivo, we propose to identify the in vivo breakdown products of hsp7O and to compare their N-terminal sequences to those of the in vitro breakdown products. Precisely the same cutting site would indicate that the same protease may be responsible for the decay in both cases. We will also determine the site of the protease activity in hsp7O for the in vitro decay. DTIC

N94-13193# Oklahoma Univ., Norman. Dept. of Psychology.
READINESS TO PERFORM TESTING: A CRITICAL ANALYSIS OF THE CONCEPT AND CURRENT PRACTICES Final Report
Kirby Gilliland and Robert E. Schlegel Aug. 1993 77 p
(Contract DTFA02-92-P-23499)
(DOT/FAA/AM-93/13) Avail: CASI HC A05/MF A01

Readiness to Perform (RTP) testing has become an increasingly popular alternative to biochemical screening as a method for assessing risk factors (i.e., drug, alcohol, fatigue, etc.) in the workplace. The focus of RTP testing is on the assessment of worker performance capability prior to job engagement. Thus, RTP testing is a method of assessing the state of preparedness of workers for performing their jobs. Unfortunately, RTP testing is being distributed and applied in the workplace despite a lack of knowledge regarding its conceptual basis and use. A project that investigated the conceptual and methodological foundations of RTP testing is summarized. Based on their expertise and background in task battery research, development, and validation, the authors explored the principles and empirical research on which the concept and methods of RTP testing appear to be based. This evaluation included literature reviews, methodological assessments, and an analysis of popular RTP measures. First, a brief review of some of the background for RTP testing is provided and the difficult task of defining RTP is attempted. Specific issues and problems in conceptualizing and implementing RTP testing are addressed. Among the numerous issues addressed are the more important comprehensive factors of determining the appropriate criteria for RTP prediction and establishing the validity of RTP through various forms of empirical research. In addition, a number of the problems associated with implementing RTP testing are presented. Some examples of these problems are: testing methodology, comparative standards, time limits in testing, general versus restricted populations, and the hidden costs of RTP testing. Finally, two supporting literature reviews of areas that form the rational foundation for RTP testing are included. One review provides a summary of some of the major computerized performance assessment batteries from which many of the current RTP measures were derived. The other review surveys research literature on the influence of selected risk factors on human performance. Author (revised)

N94-13714*# National Aeronautics and Space Administration. Langley Research Center, Hampton, VA.
CELLULAR TRACK MODEL FOR STUDY OF HEAVY ION BEAMS
Judy L. Shinn, Robert Katz (Nebraska Univ., Lincoln.), Francis A. Cucinotta, John W. Wilson, and Duc M. Ngo (Old Dominion Univ., Norfolk, VA.) Washington Aug. 1993 15 p
(RTOP 199-45-16-11)
(NASA-TP-3351; L-17231; NAS 1.60:3351) Avail: CASI HC A03/MF A01

Track theory is combined with a realistic model of a heavy ion beam to study the effects of nuclear fragmentation on cell survival and biological effectiveness. The effects of secondary reaction products are studied as a function of depth in a water column. Good agreement is found with experimental results for the survival of human T-I cells exposed to monoenergetic carbon, neon, and argon beams under aerobic and hypoxia conditions. The present calculation, which includes the effect of target fragmentation, is a significant improvement over an earlier calculation because of the use of a vastly improved beam model with no change in the track theory or cellular response parameters. Author

N94-13782*# California Univ., San Francisco.
PSYCHOPHYSIOLOGICAL INVESTIGATIONS OF THE BIOMEDICAL PROBLEMS OF MANNED SPACEFLIGHT Final Technical Report, 1 Jan. 1990 - 28 Feb. 1993
15 May 1993 4 p
(Contract NCC2-115; RTOP 199-70-12-14)
(NASA-CR-194107; NAS 1.26:194107) Avail: CASI HC A01/MF A01

The Final Report on psychophysiological investigations of the biomedical

problems of manned spaceflight is presented. In the first project, statistical analyses of human autonomic data were performed. The objectives were the following: to establish a relational data base containing human psychophysiological data obtained from Shuttle flight experiments and ground-based research over a 20 year period; to enable multi-user access and retrieval of these data for subsequent analyses and for possible inclusion in the proposed Life Sciences Data Archive; and to enable/conduct statistical analyses across several experiments on large subject populations which can thereby provide definitive answers to questions on human autonomic and behavioral responses and adaptation to environmental stressors on Earth and in space. The second project studied motion sickness. The objectives were: to test/develop hardware and procedures to be incorporated into preflight training of crewmembers of Spacelab-J; and to examine spin-off applications of AFT. The third project studied orthostatic intolerance. The objective was to test the feasibility of applying autogenic-feedback training as a potential treatment for postflight orthostatic intolerance.

Derived from text

N94-13824*# California Univ., San Diego. Dept. of Medicine.
RENAL FUNCTION ALTERATIONS DURING SKELETAL MUSCLE DISUSE IN SIMULATED MICROGRAVITY Final Technical Report, 1 Jan. - 31 Oct. 1992
Bryan J. Tucker 31 Oct. 1992 5 p
(Contract NCC2-556)
(NASA-CR-194258; NAS 1.26:194258) Avail: CASI HC A01/MF A01

This project was to examine the alterations in renal functions during skeletal muscle disuse in simulated microgravity. Although this area could cover a wide range of investigative efforts, the limited funding resulted in the selection of two projects. These projects would result in data contributing to an area of research deemed high priority by NASA and would address issues of the alterations in renal response to vasoactive stimuli during conditions of skeletal muscle disuse as well as investigate the contribution of skeletal muscle disuse, conditions normally found in long term human exposure to microgravity, to the balance of fluid and macromolecules within the vasculature versus the interstitium. These two projects selected are as follows: investigate the role of angiotensin 2 on renal function during periods of simulated microgravity and skeletal muscle disuse to determine if the renal response is altered to changes in circulating concentrations of angiotensin 2 compared to appropriate controls; and determine if the shift of fluid balance from vasculature to the interstitium, the two components of extracelilular fluid volume, that occur during prolonged exposure to microgravity and skeletal muscle disuse is a result, in part, to alterations in the fluid and macromolecular balance in the peripheral capillary beds, of which the skeletal muscle contains the majority of recruitment capillaries. A recruitment capillary bed would be most sensitive to alterations in Starling forces and fluid and macromolecular permeability. Author (revised)

N94-13847# Alberta Univ., Edmonton. Dept. of Mechanical Engineering.
TRANSCRIPT OF WORKSHOP ON MACHINERY HEALTH MONITORING
A. Craggs, ed., R. J. Rogers, ed. (New Brunswick Univ., Fredericton.), and T. N. Moore, ed. (Queens Univ., Kingston, Ontario.) Mar. 1992 75 p
Workshop held in Calgary, Alberta, 27 Sep. 1988 Sponsored by National Research Council of Canada, Ottawa, Ontario
(IME-MET-TR-005; NRC-33557; CTN-93-60783) Avail: CASI HC A04/MF A01

At a workshop on machinery health monitoring, 15 speakers presented short, prepared talks on topics including vibration monitoring, plant machinery diagnostics, use of test equipment and interpretation of results, economic benefits of monitoring, expert systems, bearings, research programs, sensors, vibration frequency spectral analysis, vibration reduction, liner cavitation damage in engines, predictive and preventive maintenance, standards, and training. After the prepared talks, a free-ranging discussion explored the points introduced in the formal presentations and also addressed additional areas of concern. A transcript of the prepared talks and discussion session is presented. CISTI

N94-14043# Deutsche Forschungsanstalt fuer Luft- und Raumfahrt, Cologne (Germany). Inst. fuer Flugmedizin.
CIRCADIAN RHYTHMS DURING SIMULATION OF THE D2-SPACEFLIGHT Ph.D. Thesis - Tech. Hochschule Aachen [ZIRKADIANE RHYTHMIK BEI DER SIMULATION DES D-2-WELTRAUMFLUGES]
Henning Allmers Sep. 1992 148 p In GERMAN
(DLR-FB-92-27; ETN-93-93958) Avail: CASI HC A07/MF A02

Eight subjects were isolated from the outside world for 26 days, during which two time zone shifts were performed and seven days of six degree down tilt were achieved simulating weightlessness. The results show that the method to achieve time zone change by gradually shortening the day for one hour over a period of seven days is a valid procedure to accomplish a seven hour time zone shift in a easterly direction for some body functions such as heat rate and sodium excretion. Other parameters such as temperature and hydroxylmelatoninsulfate excretion only adapted during weightlessness simulation. The results show that the method did not achieve ideal adaptation of all circadian rhythms in the evaluated parameters at the simulated spaceflight launch date. ESA

N94-14141 Defence and Civil Inst. of Environmental Medicine, Downsview (Ontario).
DCIEM: THE FIRST FIFTY YEARS, 1939-1989
1989 112 p
(CTN-93-60767) Avail: CASI HC A06

Canada's Department of National Defence established the Associate Committee on Aviation Medical Research in 1939 and laboratory studies in pressure physiology began in Toronto. In 1940, research efforts were expanded with the formation of the No. 1 Clinical Investigation Unit, where a low-temperature low-pressure chamber was constructed to support research on human capabilities under cold and high-altitude conditions. The Unit was also the site of the first human centrifuge in the allied countries, which was used to develop the world's first anti-G flying suit to go into service. After the war, research in aviation medicine continued at the universities and at the Unit, now renamed the Royal Canadian Air Force Institute of Aviation Medicine. In 1968, this institute was again renamed to become the Canadian Forces Institute of Environmental Medicine (CFIEM). In 1971, CFIEM was merged with Defense Research Establishment Toronto to form the Defense and Civil Institute of Environmental Medicine (DCIEM). The history of DCIEM and its forerunners is presented in pictorial form, showing highlights of research activities and research facilities.

Author (CISTI)

N94-14412* National Aeronautics and Space Administration, Washington, DC.
AEROSPACE MEDICINE AND BIOLOGY: A CONTINUING BIBLIOGRAPHY WITH INDEXES (SUPPLEMENT 379)
Sep. 1993 106 p
(NASA-SP-7011(379); NAS 1.21:7011(379)) Avail: CASI HC A06

This bibliography lists 305 reports, articles, and other documents introduced into the NASA Scientific and Technical Information System during Sep. 1993. Subject coverage includes: aerospace medicine and physiology, life support systems and man/system technology, protective clothing, exobiology and extraterrestrial life, planetary biology, and flight crew behavior and performance. Author

N94-14860# European Space Agency, Paris (France).
PHYSICAL COUNTERMEASURES FOR LONG-TERM MANNED SPACE FLIGHTS
A. Gueell, G. Tallarida, H. Wegmann, and C. Barron, ed. Feb. 1993 93 p
(ESA-SP-1160; ISBN-92-9092-077-7; ETN-93-94409) Copyright Avail: CASI HC A05/MF A01

The physiological data that provide the most accurate description of the medical problems encountered during long term space flight, and data indicating a need for countermeasures to ameliorate the safety of astronauts, are ascertained. Ground studies that will best serve as a basis for future flight protocols are discussed. Physical countermeasures used during past safe flights are listed and new approaches are proposed. The need for long term bed rest studies necessary to gain more fundamental knowledge about the adaptive processes that occur during weightlessness, and to validate the ability of various proposed countermeasures to counteract these mechanisms is indicated. ESA

N94-14879# Naval Medical Research Inst., Bethesda, MD.
THYROID ALTERATIONS IN PORCINE AFTER PROLONGED EXPOSURE TO COLD OR HEAT

Bruce A. Young, Sarah J. Cosgrove, and Robert J. Christopherson 1992 28 p
(DA Proj. MM3-3-C-30)
(AD-A266840; NMRI-92-130) Avail: CASI HC A03/MF A01

Studies by the Naval Medical Research Institute on humans after prolonged Antarctic residence have shown possible intracellular thyroid hormone alternations. These studies demonstrated a rise in serum clearance of orally administered triiodothyronine (T3), T3 production, and T3 total volume distribution in naval personnel after a 42 week residence in Antarctica compared to a control period in California. The increased serum clearance and total pool of T3 indicated a possible intracellular response which could not be further investigated using human subjects. An animal model permitted prolonged confinement of subjects in temperature controlled chambers and the use of radioisotopes to label T3. DTIC

N94-13757*# National Space Development Agency, Tokyo (Japan).
HEALTH MONITORING OF JAPANESE PAYLOAD SPECIALIST: AUTONOMIC NERVOUS AND CARDIOVASCULAR RESPONSES UNDER REDUCED GRAVITY CONDITION (L-0)
Chiharu Sekiguchi *In* NASA. Marshall Space Flight Center, Spacelab J Experiment Descriptions Aug. 1993 p 139-144 (For primary document see N94-13732 02-29)
Avail: CASI HC A02/MF A03

N94-13758*# Nagoya Univ. (Japan).
ENDOCRINE AND METABOLIC CHANGES IN PAYLOAD SPECIALIST (L-1)
Nobuo Matsui *In* NASA. Marshall Space Flight Center, Spacelab J Experiment Descriptions Aug. 1993 p 145-149 (For primary document see N94-13732 02-29)
Avail: CASI HC A01/MF A03

N94-13759*# Nagoya Univ. (Japan). Research Inst. of Environmental Medicine.
NEUROPHYSIOLOGICAL STUDY ON VISUO-VESTIBULAR CONTROL OF POSTURE AND MOVEMENT IN FISH DURING ADAPTATION TO WEIGHTLESSNESS
Shigeo Mori *In* NASA. Marshall Space Flight Center, Spacelab J Experiment Descriptions Aug. 1993 p 151-153 (For primary document see N94-13732 02-29)
Avail: CASI HC A01/MF A03

N94-13761*# Nagoya Univ. (Japan).
COMPARATIVE MEASUREMENT OF VISUAL STABILITY IN EARTH AND COSMIC SPACE (L-4)
Kazugo Koga *In* NASA. Marshall Space Flight Center, Spacelab J Experiment Descriptions Aug. 1993 p 161-163 (For primary document see N94-13732 02-29)
Avail: CASI HC A01/MF A03

N94-13765*# Showa Univ., Tokyo (Japan).
EFFECT OF LOW GRAVITY ON CALCIUM METABOLISM AND BONE FORMATION (L-7)
Tatsuo Suda *In* NASA. Marshall Space Flight Center, Spacelab J Experiment Descriptions Aug. 1993 p 177-178 (For primary document see N94-13732 02-29)
Avail: CASI HC A01/MF A03

N94-13768*# National Space Development Agency, Tokyo (Japan).
STUDY ON THE BIOLOGICAL EFFECT OF COSMIC RADIATION AND THE DEVELOPMENT OF RADIATION PROTECTION TECHNOLOGY (L-11)
Shunji Nagaoka *In* NASA. Marshall Space Flight Center, Spacelab J Experiment Descriptions Aug. 1993 p 189-196 (For primary document see N94-13732 02-29)
Avail: CASI HC A02/MF A03

N94-13771*# Baylor Coll. of Medicine, Houston, TX. Dept. of Medicine.
MAGNETIC RESONANCE IMAGING AFTER EXPOSURE TO MICROGRAVITY
Adrian LeBlanc *In* NASA. Marshall Space Flight Center, Spacelab J Experiment Descriptions Aug. 1993 p 209-211 (For primary document see N94-13732 02-29)
Avail: CASI HC A01/MF A03

N94-13772*# National Aeronautics and Space Administration. Lyndon B. Johnson Space Center, Houston, TX.
COUNTERMEASURE FOR REDUCING POST-FLIGHT ORTHOSTATIC INTOLERANCE: LOWER BODY NEGATIVE PRESSURE (LBNP) EXPERIMENT E140
John B. Charles *In* NASA. Marshall Space Flight Center, Spacelab J Experiment Descriptions Aug. 1993 p 213-222 (For primary document see N94-13732 02-29)
Avail: CASI HC A02/MF A03

N94-13773*# Saint Louis Univ., MO. School of Medicine.
BONE CULTURE RESEARCH
Nicola C. Partridge *In* NASA. Marshall Space Flight Center, Spacelab J Experiment Descriptions Aug. 1993 p 223-226 (For primary document see N94-13732 02-29)
Avail: CASI HC A01/MF A03

N94-13774*# National Aeronautics and Space Administration. Lyndon B. Johnson Space Center, Houston, TX.
AUTOGENIC FEEDBACK TRAINING EXPERIMENT: A PREVENTATIVE METHOD FOR SPACE MOTION SICKNESS
Patricia S. Cowings *In* NASA. Marshall Space Flight Center, Spacelab J Experiment Descriptions Aug. 1993 p 227-248 (For primary document see N94-13732 02-29)
Avail: CASI HC A03/MF A03

53 BEHAVIORAL SCIENCES

Includes psychological factors; individual and group behavior; crew training and evaluation; and psychiatric research.

N94-12929 Air Force Inst. of Tech., Wright-Patterson AFB, OH.
THE EFFECTS OF EVALUATION AND PRODUCTION BLOCKING ON THE PERFORMANCE OF BRAINSTORMING GROUPS M.S. Thesis
Kevin D. Osten Aug. 1992 72 p Limited Reproducibility: Document partially illegible
(AD-A265495; AFIT/CI/CIA-92-134) Avail: Issuing Activity (Defense Technical Information Center (DTIC))

Evaluation apprehension and production blocking have been identified as possible factors leading to the reduced performance of brainstorming groups. In some experiments, high evaluation led to reduced group performance, while in other experiments performance was unaffected. The present experiment examined the effects of outside evaluation and production blocking of group performance. The resulting 2 x 2 design used responses from 171 introductory psychology students, run in same-gender groups of three. Contrary to the evaluation apprehension hypothesis, evaluation level had no significant adverse effect on group performance. In support of the production blocking hypothesis, low production blocking groups generated significantly more ideas than high production blocking groups. Satisfaction with the group experience and satisfaction with individuals and group performance were also examined. Explanations for the results are discussed as well as limitations and suggestions for future research. DTIC

N94-12975# Naval Aerospace Medical Research Lab., Pensacola, FL.
WORK/REST SCHEDULES AND PERFORMANCE OF S-3 AVIATORS DURING FLEET EXERCISE
David F. Neri and Scott A. Shappell Mar. 1993 18 p
(AD-A265807; NAMRL-1382) Avail: CASI HC A03/MF A01

We examined the effect that a fleet exercise has on the work/rest patterns, fatigue, and cognitive performance of S-3 aviators. For 10 days during Fleet Exercise 1992, twenty-one S-3 aviators from Carrier Air Wing Seventeen (CVW-17) aboard USS Saratoga (CV-60) completed detailed daily-activity logs while performing their usual tasks. Subjective measures of fatigue, quality of rest, and sleep need were also collected. A subset of eight aviators completed a brief battery of computer tasks as soon before flying as possible and again after flight debrief. Results indicated that,

although the fleet exercise appeared to be below average in difficulty, there were statistically significant performance changes from pre- to postflight on a fatigue-sensitive reaction time task. Average sleep onset was delayed over the course of the fleet exercise, peaking at past 0300 by day 8. A continuation of this pattern could lead to circadian desynchrony and serious sleep problems. Responses to questions on fatigue, sleep need, and readiness to fly a strike mission were consistent with circadian factors. Further research in this area is needed to determine the magnitude and extent of this problem. We recommend that additional data be collected on a variety of fleet exercises with particular effort made to include S-3 squadrons affected by the reductions in manning and increased tasking. The additional data will provide an objective means of fully evaluating the impact of these operational changes on the S-3 community. DTIC

N94-12982# Naval Aerospace Medical Research Lab., Pensacola, FL.
WORK/REST SCHEDULES AND PERFORMANCE OF F/A-18 AVIATORS DURING FLEET EXERCISE 1992
S. A. Shappell and D. F. Neri Apr. 1993 29 p
(AD-A265826; NAMRL-1383) Avail: CASI HC A03/MF A01

As a continuation of our previous work during Operation Desert Shield/Storm, we examined the effect a fleet exercise has on the work/rest patterns, fatigue, and cognitive performance of F/A-18 aviators. For 10 days during Fleet Exercise 1992, 25 pilots from VFA-81 and VFA-83 completed daily work/rest logs while performing their usual tasks. Subjective measure of fatigue, quality of rest, and sleep need were also collected. A subset of these F/A-18 pilots completed a brief battery of cognitive tasks as soon before flying as possible and again after the flight debrief. As a group, the pilots were adequately rested with little or no problem sleeping, and they operated on a typical work/rest schedule for deployed F/A-18 aviators. However, in some instances during which late night missions were flown, sleep onset was delayed, coupled with shorter sleep periods and additional sleep problems. Several work/rest and flight related parameters were related to subjective measures of aircrew combat readiness, including the following: (1) flight quartile, (2) number and order of flights per day, (3) flight duration, (4) flight hours during the 72 h before a mission, (5) total work during the 24 h before a mission, (6) total sleep during the 12 h before a mission, and (7) total hours continuously awake before a mission. All seven variables significantly contributed to a multiple regression model derived using subjective strike delay, accounting for 51 percent of the variance. Moreover, statistically significant changes were observed from pre- to postflight on a fatigue-sensitive reaction time task. DTIC

N94-13582# Aerospace Medical Research Labs., Brooks AFB, TX.
THE IDENTIFICATION OF ABILITY REQUIREMENTS AND SELECTION INSTRUMENTS FOR FIGHTER PILOT TRAINING Interim Report, Jan. - Aug. 1992
Thomas R. Carretta, Michael N. Rodgers, and Ivar Hansen Jun. 1993 48 p
(AD-A266340; AL/HR-TP-1993-0016) Avail: CASI HC A03/MF A01

Forty-three experienced fighter pilots from Canada, Norway, and the United States served as subject matter experts (SME's) in an effort to determine the relative importance of 27 personnel characteristics for fighter pilot performance. Inter-rater reliability estimates indicated an acceptable level of agreement for SME's within each country and between pairs of countries regarding the relative importance of the 27 characteristics. Because there was sufficient agreement among SME's from the three countries, the average ranking of the 27 characteristics was calculated. Based on these results, aviation psychologists from Canada, Denmark, the Netherlands, Norway, the United Kingdom, and the United States reviewed selection instruments currently in use in NATO member countries, to identify the most promising selection instruments for inclusion in a computer-based fighter pilot test battery. Their recommendations are summarized in the paper. DTIC

N94-13961*# National Aeronautics and Space Administration. Lyndon B. Johnson Space Center, Houston, TX.
AN EVALUATION OF NOISE AND ITS EFFECTS ON SHUTTLE CREWMEMBERS DURING STS-50/USML-1
Anton Koros (Lockheed Engineering and Sciences Co., Houston, TX.), Charles Wheelwright (Lockheed Engineering and Sciences Co., Houston, TX.), and Susan Adam Sep. 1993 51 p
(NASA-TM-104775; S-729; NAS 1.15:104775) Avail: CASI HC A04/MF A01

High noise levels can lead to physiological, psychological, and performance effects in man, ranging from irritability, annoyance, and sleep interference to interference with verbal communication and fatigue, and to temporary or permanent threshold shift at more extreme levels. The current study evaluated the acoustic environment of the STS50/USML-1 mission. The major objectives were to gain subjective assessments of the STS-50 noise levels, document impacts of noise upon crewmember performance, collect inflight sound level measurements, compare noise levels across missions, evaluate the current Shuttle acoustic criterion, and to make recommendations regarding noise specifications for SSF and other long-duration manned space missions. Sound measurements indicated that background noise levels were 60, 64, and 61 A-weighted decibels, respectively, on the Orbiter middeck, flight deck, and Space lab. All levels were rated acceptable, with the Spacelab environment rated the most favorably. Sleep stations afforded attenuation from airborne noise sources, although all crewmembers reported being awakened by crew activity on the middeck. Models of distance for acceptable speech communications were generated, identifying situations of compromised verbal communications to be avoided. Author

N94-14797# Carnegie-Mellon Univ., Pittsburgh, PA. Robotics Inst.
DEPTHS FROM FOCUSING AND DEFOCUSING
Nicola Muscettola Mar. 1993 29 p
(Contract F33615-90-C-1465; ARPA Order 7597)
(AD-A266644; CMU-RI-TR-93-07) Avail: CASI HC A03/MF A01

This paper studies the problem of obtaining depth information from focusing and defocusing, which have long been noticed as important sources of depth information for human and machine vision. In depth from focusing, we try to eliminate the local maxima problem which is the main source of inaccuracy in focusing; in depth from defocusing, a new computational model is proposed to achieve higher accuracy. The major contributions of this paper are as follows: (1) in depth from focusing, instead of the popular Fibonacci search which is often trapped in local maxima, we propose the combination of Fibonacci search and curve fitting, which leads to an unprecedentedly accurate result; (2) a new model of the blurring effect is presented which takes the geometric blurring as well as the imaging blurring into consideration and the calibration of the blurring model; and (3) in spectrogram-based depth from defocusing, an iterative estimation method is proposed to decrease or eliminate the window effect. This paper reports focus ranging with less than 1/1000 error and the defocus ranging with about 1/200 error. With this precision, depth from focus ranging is becoming competitive with stereo vision for reconstructing 3D depth information. DTIC

N94-14846# Federal Aviation Administration, Oklahoma City, OK. Civil Aeromedical Inst.
VALIDITY OF FAA-APPROVED COLOR VISION TESTS FOR CLASS 2 AND CLASS 3 AEROMEDICAL SCREENING Final Report
Henry W. Mertens and Nelda J. Milburn Sep. 1993 13 p
(DOT/FAA/AM-93/17) Avail: CASI HC A03/MF A01

All clinical color vision tests currently used in the medical examination of pilots were studied regarding validity for prediction of performance on practical tests of ability to discriminate the aviation signal colors, red, green, and white given under both day and night conditions. Those same practical tests are given to pilots with color vision deficiency who apply for a waiver of the Class 2 or Class 3 color vision standards. Subjects with varying type and degree of color vision deficiency (n=122) and subjects with normal color vision (n=120) were classified with the anomaloscope and given both practical and clinical tests. The clinical color vision tests included the American Optical Company plates (1965 and 1940 Editions), AOCHRR plates (2nd Edition), Ishihara plates (14-, 16-, 24-, and 38-plate tests), Dvorine plates, Richmond plates, Farnsworth Lantern, School of Aviation Medicine Color Threshold Tester, Titmus Tester, Titmus II Tester, OPTEC 2000 Tester, and Keystone Orthoscope/Telebinocular test. The criterion tests required naming the colors of actual signals produced by the Aviation Signal Light, with the same test procedures and viewing distances used in actual practical tests. The Farnsworth Lantern and several plate tests were the best clinical tests for predicting ability to identify the colors of aviation signals. Individuals with color vision deficiency identified

signal colors better at night than during the day. Recommendations for improving the disposition criteria of some clinical tests, and for discontinuing several obsolete tests are discussed. Author (revised)

N94-14854# Federal Aviation Administration, Oklahoma City, OK. Civil Aeromedical Inst.
VALIDATION OF AN INEXPENSIVE ILLUMINANT FOR AEROMEDICAL COLOR VISION SCREENING Final Report
Nelda J. Milburn and Henry W. Mertens Sep. 1993 9 p
(DOT/FAA/AM-93/16) Avail: CASI HC A02/MF A01

An inexpensive illuminant for color vision screening suggested by the NRC-NAS Committee on Vision was evaluated as a substitute for the Macbeth Easel Lamp. The Macbeth Easel Lamp is the recommended illuminant for pseudoisochromatic plate tests used in aeromedical color vision screening, but is no longer in production. Subjects included both normal trichromats (p=145) and persons with varying degrees and types of color vision deficiencies (p=152) as diagnosed with the Nagel Type I anomaloscope. Subjects were given the Dvorine Pseudo-Isochromatic Plate Test illuminated by each of the two light sources. One Verilux True Color Light tube (F15T8VLX) was installed in an adjustable fluorescent desk lamp and positioned at a height of 24 in above the center of the Dvorine test book to give a 270 lux illumination to match the illumination produced by the Macbeth light source. The two presentations of the Dvorine were separated by several other color vision tests. Each subject was given a different random order of plates 2-15 for each light source. Pass/Fail performance with the Dvorine test was virtually the same with the two light sources when criterion for failure was three or more errors. The Verilux True Color Light obtained a Kappa value of .97, and very low false positive (.021) and false negative (.006) rates when compared to the Macbeth Easel Lamp. Performance and possible applications of the Verilux True Color Light in aeromedical color vision screening are discussed.
Author (revised)

N94-13314*# National Aeronautics and Space Administration. Ames Research Center, Moffett Field, CA.
VISUAL INFORMATION FOR JUDGING TEMPORAL RANGE
Mary K. Kaiser and Lyn Mowafy (Dayton Univ. Research Inst., Higley, AZ.) *In its* Piloting Vertical Flight Aircraft: A Conference on Flying Qualities and Human Factors Jul. 1993 p 309-313 (For primary document see N94-13294 02-08)
Avail: CASI HC A01/MF A04

N94-13442# University of Electro-Communications, Tokyo (Japan).
HEIDEGGER'S THINKING
Ichiro Akanuma *In its* Bulletin of the University of Electro-Communications, Volume 6, No. 1, Serial No. 11 Jun. 1993 p 97-10 In JAPANESE (For primary document see N94-13432 02-61)
Avail: CASI HC A02/MF A02

54 MAN/SYSTEM TECHNOLOGY AND LIFE SUPPORT

Includes human engineering; biotechnology; and space suits and protective clothing.

For related information see also *16 Space Transportation.*

N94-12935 Systems Research Labs., Inc., Dayton, OH.
EVALUATION OF THE RETROGRADE INFLATION ANTI-G SUIT (RIAGS) Final Report, Oct. 1989 - 1992
Lloyd D. Tripp, Jr., Kathy McCloskey, Daniel Repperger, Stephen E. Popper, and Smith L. Johnston 18 Dec. 1992 16 p Limited Reproducibility: More than 20% of this document may be affected by microfiche quality
(Contract F33615-89-C-0574)
(AD-A265884; AL-TR-1992-0176) Avail: CASI HC A03

The Retrograde Inflation Anti-G Suit (RIAGS) was originally designed and fabricated in the early 1940's by Mr. David Clark and Dr. Earl Wood as The Progressive Arterial Occlusion Anti-g Suit. Testing of this suit on the Mayo Clinic centrifuge revealed that the suit provided more g protection than the fighter pilot of the era needed (+2.9 gz relaxed). This technology was revisited in 1987 by the Armstrong Laboratory and culminated in the development of a new version of the technology using modern methods and materials. The new suit consisted of a retrograde inflating anti-g suit which inflated cephaladward, arterial occlusive cuffs for the arms, and capstan sleeves. These suit combinations were compared to the standard Air Force issue CSU-13B/P anti-g suit. Endurance testing of the current suit involved exposing subjects to a continuous +4.5 to +7 gz Simulated Aerial Combat Maneuver. Results showed the RIAGS with capstan sleeves provided the maximum amount of protection to the subject in terms of endurance (p less than 0.013), followed by RIAGS alone (p less than 0.058), Standard CSU-13B/P and RIAGS with occlusion cuffs (p=0.28). In addition to the protection issue, RIAGS with sleeves also proved to be the most comfortable of all the g suit combinations evaluated. DTIC

N94-13132*# Vexcel Corp., Boulder, CO.
EOS WORKSTATION Final Report, 2 Jun. 1989 - 3 Jan. 1992
Franz Leberl, Milan Karspeck, Michel Millot, Kelly Maurice, and Matt Jackson 7 Apr. 1992 365 p
(Contract NAS7-1070; SBIR-07.07-0094)
(NASA-CR-191326; NAS 1.26:191326) Avail: CASI HC A16/MF A03

This final report summarizes the work done from mid-1989 until January 1992 to develop a prototype set of tools for the analysis of EOS-type images. Such images are characterized by great multiplicity and quantity. A single 'snapshot' of EOS-type imagery may contain several hundred component images so that on a particular pixel, one finds multiple gray values. A prototype EOS-sensor, AVIRIS, has 224 gray values at each pixel. The work focused on the ability to utilize very large images and continuously roam through those images, zoom and be able to hold more than one black and white or color image, for example for stereo viewing or for image comparisons. A second focus was the utilization of so-called 'image cubes', where multiple images need to be co-registered and then jointly analyzed, viewed, and manipulated. The target computer platform that was selected was a high-performance graphics superworkstation, Stardent 3000. This particular platform offered many particular graphics tools such as the Application Visualization System (AVS) or Dore, but it missed availability of commercial third-party software for relational data bases, image processing, etc. The project was able to cope with these limitations and a phase-3 activity is currently being negotiated to port the software and enhance it for use with a novel graphics superworkstation to be introduced into the market in the Spring of 1993. Author (revised)

N94-13229 Tel-Aviv Univ. (Israel). Dept. of Interdisciplinary Studies.
BODY/CUSHION CONTACT STRESS ANALYSIS DURING SITTING M.S. Thesis
Silviu Comisioneru Sep. 1991 154 p
(ITN-93-85204) Copyright Avail: Issuing Activity (Tel-Aviv Univ., Exact Sciences Library, Ramat Aviv 69978, Israel)

Suitably designed cushions could minimize body stresses experienced during sitting for long periods and the consequent discomfort and pain. A series of two-dimensional numerical models of the pelvis-cushion system and the stresses developed in the body as a result of sitting on various types of cushion were analysed by means of the ANSYS finite-element program. Experimental measurements were made by means of the Contact Pressure Display (CPD) and the Piezoresistive Sensor Array (PSA). It was shown that the use of composite cushions, comprising layers of various thicknesses, made of materials of various mechanical properties, could provide a quasi-uniform stress distribution, with consequently reduced stresses on the skeleton and soft tissues. It was demonstrated that the achievement of such a quasi-uniform stress distribution is a fundamental condition for comfort. Cushion design guidelines were developed based on the need to use softer materials in high-stress regions and stiffer materials in low-stress regions, with a lower layer sufficiently stiff to prevent contact between the ischial tuberosities and the rigid base. Other applications of composite cushion design are in protecting the human body against vibration and impact stresses and in protecting paraplegic and geriatric patients against pressure ulcer development, caused by prolonged sitting without change of posture. For such patients, the cushion design and optimization must be done on an individual basis. ISA

N94-13388# National Aerospace Lab., Tokyo (Japan). Space Technology Research Group.
EVALUATION FOR MEMBRANE COMPONENTS OF WATER RECYCLING SYSTEM [MIZU SAISEI JUNKAN SHISUTEMU YOUSO NO TOKUSEI HYOUKA]
Toshiharu Tanemura, Kouji Ootsubo, Mitsuo Oguchi, Akira Ashida (Hitachi Ltd., Tokyo, Japan.), Nobuo Hamano (Hitachi Ltd., Tokyo, Japan.), and Kenji Mitani (Hitachi Ltd., Tokyo, Japan.) Apr. 1992 33 p In JAPANESE
(NAL-TM-646; JTN-93-80481) Avail: CASI HC A03/MF A01

The water recycling system is a key subsystem of the integrated material recycling system which must be developed to obtain long-term, manned space activity. This paper presents the results of system study for designing water recycling system in which three kinds of membrane filters are introduced to purify waste water discharged from men, animals, and plants. In addition, the long duration processing tests utilizing artificial urine waste water were conducted to evaluate the appropriateness of adopting these membrane filters. Author (NASDA)

N94-13399*# National Aeronautics and Space Administration. Lyndon B. Johnson Space Center, Houston, TX.
ANALYSIS OF DIFFERENCES BETWEEN SEATING POSITIONS IN SIMULATORS AND ORBITERS
Philip T. Mongan Sep. 1993 13 p
(NASA-TM-104776; S-730; NAS 1.15:104776) Avail: CASI HC A03/MF A01

Crew comments indicate that Space Shuttle simulator seats place crewmembers in a position different from that of the actual Orbiter seats. The crew feel that they launch in a different position, and with a different reach and visibility, from that in which they had trained. This study examined three factors in differences between training and flight positions. Key dimensions, which were considered important to spatial orientation, were compared in the Orbiters and simulators. These were dimensions such as seat back to glare shield and seat pan to overhead. The differences between flight and training crew equipment, and how these differences may contribute to the problem were discussed with engineers and technicians responsible for the equipment. Eye position measurements were taken on subjects to assess any differences that could be attributed to different ingress methods in the Orbiters and the simulators. This report presents the data, analysis, and recommendations. Author (revised)

N94-13472# Japan Manned Space Systems Corp., Tokyo.
SURVEY AND STUDY ON ENVIRONMENTAL CONTROL AND LIFE SUPPORT (ECLS) TECHNOLOGIES, PART 2 [KANKYOU SEIGYO/SEIMEI IJI GIJUTSU NO CHOUSA KENTOU]
Tokyo, Japan 31 Mar. 1993 35 p In JAPANESE
(NASDA-CNT-930012-Pt-2; JTN-93-80466-Pt-2) Avail: CASI HC A03/MF A01

The survey and study on ECLS (Environmental Control and Life Support) technologies aiming at an ECLS to which the advanced technology at the present time is incorporated focusing on the air renewal technologies (such as removal of carbon dioxide, reduction of carbon dioxide, oxygen production, and toxic gas removal) and water recycle technologies (such as distillation and filtration) taking into the consideration a manned engineering test satellite (assuming the launch around 2000) is presented. The reference model establishment, recycling type ECLSS (Environmental Control and Life Support System) total system study, survey and study on subsystem technologies, planning of research and development projects, and visiting survey of ECLSS oriented facilities in and out of the country, and survey of the ECLSS related references is presented. An integrated research project for manned platform recycling type life support equipment is shown. Author (NASDA)

N94-13601* National Aeronautics and Space Administration. Lyndon B. Johnson Space Center, Houston, TX.
STS-30 MAGELLAN IUS/EVA TRAINING IN WETF (Videotape)
Apr. 1989 Videotape: 11 min. playing time, in color, with sound
(NASA-TM-109300; NONP-VT-93-185315) Avail: CASI VHS A01/BETA A22

Astronauts Thagard and Lee suit up and enter the WETF to practice working the Magellan mockup in a zero-g environment. Author

N94-13611* National Aeronautics and Space Administration, Washington, DC.
NEW PROSTHETIC DEVICES (Videotape)
May 1991 Videotape: 3 min. 36 sec. playing time, in color, with sound
(NASA-TM-109304; NONP-VT-93-185322) Avail: CASI VHS A01/BETA A22

Using robotic techniques, NASA researchers have developed end-effectors designed to meet individual needs of hand and below the elbow amputees that are more efficient than the traditional hook. Author

N94-13615* National Aeronautics and Space Administration, Washington, DC.
RECYCLING IN SPACE (Videotape)
May 1991 Videotape: 3 min. 11 sec. playing time, in color, with sound
(NASA-TM-109307; NONP-VT-93-185325) Avail: CASI VHS A01/BETA A22

NASA's effort to provide a completely enclosed life support system that offers food and recycled air, water, and waste for long-duration space travel or settlements is explained. Author (revised)

N94-13674*# Foster-Miller Associates, Inc., Waltham, MA.
DEVELOPMENT OF A NONAZEOTROPIC HEAT PUMP FOR CREW HYGIENE WATER HEATING Final Report, Jun. 1989 - Aug. 1991
David H. Walker and Glenn I. Deming Oct. 1991 98 p
(Contract NAS8-38407; SBIR-09.04-3200)
(NASA-CR-194189; NAS 1.26:194189; FM-9017-482) Avail: CASI HC A05/MF A02

A Phase 2 SBIR Program funded by the NASA Marshall Space Flight Center to develop a Nonazeotropic Heat Pump is described. The heat pump system which was designed, fabricated, and tested in the Foster-Miller laboratory, is capable of providing crew hygiene water heating for future manned missions. The heat pump utilizes a nonazeotropic refrigerant mixture which, in this application, provides a significant Coefficient of Performance improvement over a single-constituent working fluid. In order to take full advantage of the refrigerant mixture, compact tube-in-tube heat exchangers were designed. A high efficiency scroll compressor with a proprietary lubrication system was developed to meet the requirements of operation in zero-gravity. The prototype heat pump system consumes less than 200W of power compared to the alternative of electric cartridge heaters which would require 2 to 5 kW. Author (revised)

N94-13712*# Bionetics Corp., Cocoa Beach, FL.
BIOMASS PRODUCTION CHAMBER AIR ANALYSIS OF WHEAT STUDY (BWT931)
J. H. Batten, B. V. Peterson, E. Berdis, and E. M. Wheeler Aug. 1993 62 p
(Contract NAS10-11624)
(NASA-CR-194092; NAS 1.26:194092) Avail: CASI HC A04/MF A01

NASA's Controlled Ecological Life Support System (CELSS) biomass production chamber at John F. Kennedy Space Center provides a test bed for bioregenerative studies using plants to provide food, oxygen, carbon dioxide removal, and potable water to humans during long term space travel. Growing plants in enclosed environments has brought about concerns regarding the level of volatile organic compounds (VOC's) emitted from plants and the construction materials that make up the plant growth chambers. In such closed systems, the potential exists for some VOC's to reach toxic levels and lead to poor plant growth, plant death, or health problems for human inhabitants. This study characterized the air in an enclosed environment in which wheat cv. Yocora Rojo was grown. Ninty-four whole air samples were analyzed by gas chromatography/mass spectrometry throughout the eighty-four day planting. VOC emissions from plants and materials were characterized and quantified. Author (revised)

N94-13901# European Space Agency. European Space Research and Technology Center, ESTEC, Noordwijk (Netherlands). Thermal Control and Life Support Div.
LIFE SUPPORT AND HABITABILITY MANUAL, VOLUME 1
R. A. Binot Aug. 1991 563 p
(ESA-PSS-03-406-Issue-1-Vol-1; ETN-93-94406) Copyright Avail: CASI HC A24/MF A04

This manual is designed to serve the needs of researchers and engineers working in the field of manned space programs and covers various aspects

of life support and habitability. System needs are addressed and technologies associated with each of these systems are detailed by sets of data sheets that were designed to follow a standard format. The manual will be developed progressively and will be updated by issuing revised chapters and individual data sheets. It is offered to companies and research centers so that they may propose technical inputs to be used in the preparation of such updates. These inputs will be strictly technical, clear, complete, and will avoid any information of a commercial nature. In volume 1, requirements for life support, driving missions, and atmosphere revitalization are covered. ESA

N94-13902# European Space Agency. European Space Research and Technology Center, ESTEC, Noordwijk (Netherlands). Thermal Control and Life Support Div.

LIFE SUPPORT AND HABITABILITY MANUAL, VOLUME 2

R. A. Binot Aug. 1991 557 p

(ESA-PSS-03-406-Issue-1-Vol-2; ETN-93-94407) Copyright Avail: CASI HC A24/MF A04

This manual is designed to serve the needs of researchers and engineers working in the field of manned space programs and covers various aspects of life support and habitability. System needs are addressed and technologies associated with each of these systems are detailed by sets of data sheets that were designed to follow a standard format. The manual will be developed progressively and will be updated by issuing revised chapters and individual data sheets. It is offered to companies and research centers so that they may propose technical inputs to be used in the preparation of such updates. These inputs will be strictly technical, clear, complete, and will avoid any information of a commercial nature. In volume 2, atmosphere supply and control, and temperature and humidity control are covered. Information on equivalent weight and the determination of weight penalties, and on qualitative assessment methods, is given. ESA

N94-13972# Civil Aeromedical Inst., Oklahoma City, OK.

AN ASSESSMENT OF THE POTENTIAL FOR NECK INJURY DUE TO PADDING OF AIRCRAFT INTERIOR WALLS FOR HEAD IMPACT PROTECTION Final Report

R. Armenia-Cope, J. H. Marcus, R. V. Gowdy, and R. L. DeWeese Aug. 1993 13 p

(DOT/FAA/AM-93/14) Avail: CASI HC A03/MF A01

This report describes a short test program to assess the potential for neck injury induced by placing padding on the interior walls of an aircraft cabin to reduce the possibility of a head injury during a crash. Such padding is a possible mechanism of achieving the heightened impact protection requirements adopted by the Federal Aviation Administration in 1988. The report reviews the literature on impact induced neck injury, and reports neck injury criteria developed and reported by others. The type of test device to use with the neck injury criteria is also discussed. Using the reported neck injury criteria, and a Hybrid 3 test dummy with neck instrumentation, the testing program found that neck injury, with one exception, was not likely in either the tested pad or unpadded case. The one exception was neck extension injuries for which both the unpadded and padded tests exceeded the injury criteria. The tested pad, in comparison to the unpadded case, substantially decreased the neck extension moment, implying a reduction in neck injury risk. Author (revised)

N94-13979*# National Aeronautics and Space Administration. John F. Kennedy Space Center, Cocoa Beach, FL.

VALIDATED ENVIRONMENTAL AND PHYSIOLOGICAL DATA FROM THE CELSS BREADBOARD PROJECTS BIOMASS PRODUCTION CHAMBER. BWT931 (WHEAT CV. YECORA ROJO)

G. W. Stutte (Bionetics Corp., Cocoa Beach, FL.), C. L. Mackowiak (Bionetics Corp., Cocoa Beach, FL.), G. A. Markwell (Bionetics Corp., Cocoa Beach, FL.), R. M. Wheeler, and J. C. Sager Aug. 1993 9 p Revised

(Contract NAS10-11624)

(NASA-TM-109272; NAS 1.15:109272) Avail: CASI HC A02/MF A01

This KSC database is being made available to the scientific research community to facilitate the development of crop development models, to test monitoring and control strategies, and to identify environmental limitations in crop production systems. The KSC validated dataset consists of 17 parameters necessary to maintain bioregenerative life support functions: water purification, CO2 removal, O2 production, and biomass production. The data are available on disk as either a DATABASE SUBSET (one week of 5-minute data) or DATABASE SUMMARY (daily averages of parameters). Online access to the VALIDATED DATABASE will be made available to institutions with specific programmatic requirements. Availability and access to the KSC validated database are subject to approval and limitations implicit in KSC computer security policies. Author (revised)

N94-14023# Galaxy Scientific Corp., Pleasantville, NJ.

HUMAN FACTORS IN AVIATION MAINTENANCE: PHASE 3, VOLUME 1 Final Interim Report, Feb. - Dec. 1992

Aug. 1993 161 p

(Contract DTFA01-92-Y-01005)

(DOT/FAA/AM-93/15) Avail: CASI HC A08/MF A02

The third phase of research on Human Factors in Aviation Maintenance continued to look at the human's role in the aviation maintenance system via investigations, demonstrations, and evaluations of the research program outputs. An evaluation of a computer-based training simulation for troubleshooting an airliner environmental control system and an evaluation of the aircraft maintenance visual environment are described. A job aid for Aviation Safety Inspectors is also reported on, along with an evaluation of pen computers considered for the job aid. Also described is research on the following: ergonomic factors related to posture and fatigue; identification of characteristics of personnel best suited for inspection-oriented jobs; redesign of work control cards; and visual inspection and training alternatives in aviation maintenance. Author (revised)

N94-14335# Oak Ridge National Lab., TN.

EYE-GAZE AND INTENT: APPLICATION IN 3D INTERFACE CONTROL

J. C. Schryver and J. H. Goldberg (Pennsylvania State Univ., University Park.) 1993 7 p Presented at the 5th International Conference on Human-computer Interaction, Orlando, FL, 8-13 Aug. 1993

(Contract DE-AC05-84OR-21400)

(DE93-015210; CONF-9308124-1) Avail: CASI HC A02/MF A01

Computer interface control is typically accomplished with an input 'device' such as a keyboard, mouse, trackball, etc. An input device translates a users input actions, such as mouse clicks and key presses, into appropriate computer commands. To control the interface, the user must first convert intent into the syntax of the input device. A more natural means of computer control is possible when the computer can directly infer user intent, without need of intervening input devices. We describe an application of eye-gaze-contingent control of an interactive three-dimensional (3D) user interface. A salient feature of the user interface is natural input, with a heightened impression of controlling the computer directly by the mind. With this interface, input of rotation and translation are intuitive, whereas other abstract features, such as zoom, are more problematic to match with user intent. This paper describes successes with implementation to date and ongoing efforts to develop a more sophisticated intent inferencing methodology. DOE

N94-14451# Westinghouse Idaho Nuclear Co., Inc., Idaho Falls.

SHEAN (SIMPLIFIED HUMAN ERROR ANALYSIS CODE) AND AUTOMATED THERP

J. R. Wilson 1993 9 p Presented at the GOCO Database Meeting, Augusta, GA, 2-3 Feb. 1993

(Contract DE-AC07-84ID-12435)

(DE93-014904; WINCO-11908; CONF-9302122-1) Avail: CASI HC A02/MF A01

One of the most widely used human error analysis tools is THERP (Technique for Human Error Rate Prediction). Unfortunately, this tool has disadvantages. The Nuclear Regulatory Commission, realizing these drawbacks, commissioned Dr. Swain, the author of THERP, to create a simpler, more consistent tool for deriving human error rates. That effort produced the Accident Sequence Evaluation Program Human Reliability Analysis Procedure (ASEP), which is more conservative than THERP, but a valuable screening tool. ASEP involves answering simple questions about the scenario in question, and then looking up the appropriate human error rate in the indicated table (THERP also uses look-up tables, but four times as many). The advantages of ASEP are that human factors expertise is not required, and the training to use the method is minimal. Although not originally envisioned by Dr. Swain, the ASEP approach actually begs to be computerized. That WINCO did, calling the code SHEAN, for Simplified Human Error ANalysis. The code was done in TURBO Basic for IBM or IBM-compatible MS-DOS, for fast execution. WINCO is now in the process

of comparing this code against THERP for various scenarios. A discussion of SHEAN is reported. DOE

N94-14790* National Aeronautics and Space Administration. Lyndon B. Johnson Space Center, Houston, TX.
STS-35 EVA PAYLOAD TRAINING IN WETF (Videotape)
Apr. 1990 Videotape: 11 min. playing time, in color, with sound
(NASA-TM-109492; NONP-VT-93-190289) Avail: CASI VHS A01/BETA A22

Footage showing astronauts Lounge and Hoffman donning EVA suits while astronaut Durrance watches is presented. The footage also shows Lounge and Hoffman working on an ASTRO-1 mockup in the WETF. Author (revised)

N94-13315*# National Aeronautics and Space Administration. Ames Research Center, Moffett Field, CA.
VISUAL CUEING CONSIDERATIONS IN NAP-OF-THE-EARTH HELICOPTER FLIGHT HEAD-SLAVED HELMET-MOUNTED DISPLAYS
Arthur J. Grunwald and Silvia Kohn (Technion - Israel Inst. of Engineering, Haifa.) *In its* Piloting Vertical Flight Aircraft: A Conference on Flying Qualities and Human Factors Jul. 1993 p 315-327 (For primary document see N94-13294 02-08)
Avail: CASI HC A03/MF A04

N94-13319*# Helikopter Service A/S, Oslo (Norway).
HUMAN FACTOR IMPLICATIONS OF THE EUROCOPTER AS332L-1 SUPER PUMA COCKPIT
R. Randall Padfield *In* NASA. Ames Research Center, Piloting Vertical Flight Aircraft: A Conference on Flying Qualities and Human Factors Jul. 1993 p 377-392 Presented at the 15th European Rotorcraft Forum, Amsterdam, The Netherlands, 12-15 Sep. 1989 Previously announced in AIAA as A91-45400 (For primary document see N94-13294 02-08)
Avail: CASI HC A03/MF A04

N94-13767*# National Aerospace Lab., Tokyo (Japan).
MANUAL CONTROL IN SPACE RESEARCH ON PERCEPTUAL-MOTOR FUNCTIONS UNDER ZERO GRAVITY CONDITIONS (L-10)
Akira Tada *In* NASA. Marshall Space Flight Center, Spacelab J Experiment Descriptions Aug. 1993 p 185-187 (For primary document see N94-13732 02-29)
Avail: CASI HC A01/MF A03

N94-13775*# National Aeronautics and Space Administration. Lyndon B. Johnson Space Center, Houston, TX.
IN-FLIGHT DEMONSTRATION OF THE SPACE STATION FREEDOM HEALTH MAINTENANCE FACILITY FLUID THERAPY SYSTEM (E300/E05)
Charles W. Lloyd *In* NASA. Marshall Space Flight Center, Spacelab J Experiment Descriptions Aug. 1993 p 249-257 (For primary document see N94-13732 02-29)
Avail: CASI HC A02/MF A03

N94-14648*# National Aeronautics and Space Administration. Lyndon B. Johnson Space Center, Houston, TX.
COMPUTATIONAL CONTROL WORKSTATION: USERS' PERSPECTIVES
Carlos M. Roithmayr, Timothy M. Straube (Colorado Univ., Boulder.), and Jeffrey S. Tave (Lockheed Engineering and Sciences Co., Houston, TX.) *In* JPL, Proceedings of the Fifth NASA/NSF/DOD Workshop on Aerospace Computational Control 15 Feb. 1993 p 491-505 (For primary document see N94-14618 02-39)
Avail: CASI HC A03/MF A04

55 SPACE BIOLOGY

Includes exobiology; planetary biology; and extraterrestrial life.

N94-13086*# Georgia Inst. of Tech., Atlanta. School of Electrical Engineering.
SEARCH FOR EXTRATERRESTRIAL INTELLIGENCE/HIGH RESOLUTION MICROWAVE SURVEY TEAM MEMBER Semiannual Status Report No. 5, 1 Mar. - 31 Aug. 1993
Paul G. Steffes 1993 61 p
(Grant NAG2-700)
(NASA-CR-194177; NAS 1.26:194177) Avail: CASI HC A04/MF A01

This semiannual status report describes activities conducted by the Principal Investigator during the first half of this third year of the NASA High Resolution Microwave Survey (HRMS) Investigator Working Group (IWG). As a (HRMS) Team Member with primary interest in the Sky Survey activity, this investigator attended IWG meetings at NASA/Ames and U.C.-Santa Cruz in Apr. and Aug. 1992, and has traveled independently to NRAO/Kitt Peak, Arizona (April 1993) and Woodbury, Georgia (July 1993). During the July 1993 visit to the Georgia Tech Research Corporation/Woodbury Research Facility, an experiment was conducted to study the effects of interference from C-band (3.7 - 4.2 GHz) geostationary spacecraft on the Sky Survey operation in that band. At the first IWG meeting in April of this year, results of a SETI observation conducted at the 203 GHz positronium hyperfine resonance using the NRAO facility at Kitt Peak, AZ, were presented, as well as updates on the development of the spaceborne RFI data bases developed for the project. At the second meeting, results of the study of interference from C-band geostationary spacecraft were presented. Likewise, a presentation was made at the accompanying 1993 Bioastronomy Symposium describing the SETI observation at the positronium hyperfine resonance. Author (revised)

59 MATHEMATICAL AND COMPUTER SCIENCES (GENERAL)

N94-12838*# National Aeronautics and Space Administration. Ames Research Center, Moffett Field, CA.
ADVANCING AUTOMATION AND ROBOTICS TECHNOLOGY FOR THE SPACE STATION FREEDOM AND FOR THE U.S. ECONOMY Progress Report No.16, 17 Sep. 1992 - 16 Mar. 1993
May 1993 58 p
(RTOP 476-14-01)
(NASA-TM-104024; A-93084; NAS 1.15:104024) Avail: CASI HC A04/MF A01

In April 1985, as required by Public Law 98-371, the NASA Advanced Technology Advisory Committee (ATAC) reported to Congress the results of its studies on advanced automation and robotics technology for use on Space Station Freedom. This material was documented in the initial report (NASA Technical Memorandum 87566). A further requirement of the law was that ATAC follow NASA's progress in this area and report to Congress semiannually. This report is the sixteenth in a series of progress updates and covers the period between 15 Sep. 1992 - 16 Mar. 1993. The report describes the progress made by Levels 1, 2, and 3 of the Space Station Freedom in developing and applying advanced automation and robotics technology. Emphasis was placed upon the Space Station Freedom Program responses to specific recommendations made in ATAC Progress Report 15; and includes a status review of Space Station Freedom Launch Processing facilities at Kennedy Space Center. Assessments are presented for these and other areas as they apply to the advancement of automation and robotics technology for Space Station Freedom. Author (revised)

N94-12886*# National Aeronautics and Space Administration. Langley Research Center, Hampton, VA.
APPROACHES TO HIGH ASPECT RATIO TRIANGULATIONS
M.-A. Posenau Aug. 1993 21 p Presented at the 5th Canadian Conference on Computational Geometry, Waterloo, Ontario, 5-9 Aug. 1993
(RTOP 505-90-53-02)
(NASA-TM-107684; NAS 1.15:107684) Avail: CASI HC A03/MF A01

In aerospace computational fluid dynamics calculations, high aspect ratio, or stretched, triangulations are necessary to adequately resolve the features of a viscous flow around bodies. In this paper, we explore alternatives to the Delaunay triangulation which can be used to generate high aspect ratio triangulations of point sets. The method is based on a variation of the lifting map concept which derives Delaunay triangulations from convex hull calculations. Author (revised)

N94-12973*# National Aeronautics and Space Administration. Ames Research Center, Moffett Field, CA.
PARALLEL IMPLEMENTATION OF AN ALGORITHM FOR DELAUNAY TRIANGULATION
Marshal L. Merriam Jul. 1992 14 p
(RTOP 505-59-53)
(NASA-TM-103951; A-92144; NAS 1.15:103951) Avail: CASI HC A03/MF A01

The theory and practice of implementing Tanemura's algorithm for 3D Delaunay triangulation on Intel's Gamma prototype, a 128 processor MIMD computer, is described. Efficient implementation of Tanemura's algorithm on a conventional, vector processing supercomputer is problematic. It does not vectorize to any significant degree and requires indirect addressing. Efficient implementation on a parallel architecture is possible, however. Speeds in excess of 20 times a single processor Cray Y-MP are realized on 128 processors of the Intel Gamma prototype. Author (revised)

N94-13069# Massachusetts Univ., Amherst.
COMPUTATION AND GRAPHICS IN MATHEMATICAL RESEARCH
D. A. Hoffman and J. Spruck Jun. 1993 14 p
(Contract DE-FG02-86ER-25015)
(DE93-016512; DOE/ER-25015/T1) Avail: CASI HC A03/MF A01

Current research is described for the following topics: grain boundaries and dislocations in compound polymers, boundary value problems for hypersurfaces constant Gaussian curvature, and discrete computational geometry. DOE

N94-13200*# National Aeronautics and Space Administration. Ames Research Center, Moffett Field, CA.
THE NAS PARALLEL BENCHMARKS
David Bailey, ed., John Barton, ed., Thomas Lasinski, ed., and Horst Simon, ed. (Computer Sciences Corp., El Segundo, CA.) Jul. 1993 68 p
(RTOP 536-01-11)
(NASA-TM-103863; A-91148; NAS 1.15:103863) Avail: CASI HC A04/MF A01

A new set of benchmarks was developed for the performance evaluation of highly parallel supercomputers. These benchmarks consist of a set of kernels, the 'Parallel Kernels,' and a simulated application benchmark. Together they mimic the computation and data movement characteristics of large scale computational fluid dynamics (CFD) applications. The principal distinguishing feature of these benchmarks is their 'pencil and paper' specification - all details of these benchmarks are specified only algorithmically. In this way many of the difficulties associated with conventional benchmarking approaches on highly parallel systems are avoided. Author (revised)

60 COMPUTER OPERATIONS AND HARDWARE

Includes hardware for computer graphics, firmware, and data processing.

For components see *33 Electronics and Electrical Engineering.*

N94-13286# Los Alamos National Lab., NM.
ADVANCED COMPUTERS AND SIMULATION
R. D. Ryne 1993 5 p Presented at the International Particle Accelerator Conference, Washington, DC, 17-20 May 1993
(Contract W-7405-eng-36)
(DE93-014354; LA-UR-93-1961; CONF-930511-78) Avail: CASI HC A01/MF A01

Accelerator physicists today have access to computers that are far more powerful than those available just 10 years ago. In the early 1980's, desktop workstations performed less than one million floating point operations per second (Mflops), and the realized performance of vector supercomputers was at best a few hundred Mflops. Today vector processing is available on the desktop providing researchers with performance approaching 100 Mflops at a price that is measured in thousands of dollars. Furthermore, advances in Massively Parallel Processors (MPP) have made performance of over 10 gigaflops a reality, and at mid-decade, MPP's are expected to be capable of teraflops performance. Along with advances in MPP hardware, researchers have also made significant progress in developing algorithms and software for MPP's. These changes have had, and will continue to have, a significant impact on the work of computational accelerator physicists. Now, instead of running particle simulations with just a few thousand particles, we can perform desktop simulations with tens of thousands of simulation particles, and calculations with well over 1 million particles are being performed on MPP's. In the area of computational electromagnetics, simulations that used to be performed only on vector supercomputers now run in several hours on desktop workstations, and researchers are hoping to perform simulations with over one billion mesh points on future MPP's. In this paper we will discuss the latest advances and what can be expected in the near future in hardware, software, and applications codes for the advanced simulation of particle accelerators. DOE

N94-13363*# California Univ., Berkeley. Computer Science Div.
DISKLESS SUPERCOMPUTERS: SCALABLE, RELIABLE I/O FOR THE TERA-OP TECHNOLOGY BASE Final Report
Randy H. Katz, John K. Ousterhout, and David A. Patterson 1993 11 p
(Grant NAG2-591)
(NASA-CR-194089; NAS 1.26:194089) Avail: CASI HC A03/MF A01

Computing is seeing an unprecedented improvement in performance; over the last five years there has been an order-of-magnitude improvement in the speeds of workstation CPU's. At least another order of magnitude seems likely in the next five years, to machines with 500 MIPS or more. The goal of the ARPA Teraop program is to realize even larger, more powerful machines, executing as many as a trillion operations per second. Unfortunately, we have seen no comparable breakthroughs in I/O performance; the speeds of I/O devices and the hardware and software architectures for managing them have not changed substantially in many years. We have completed a program of research to demonstrate hardware and software I/O architectures capable of supporting the kinds of internetworked 'visualization' workstations and supercomputers that will appear in the mid 1990s. The project had three overall goals: high performance, high reliability, and scalable, multipurpose system.
Author (revised)

N94-13525# Center for Mathematics and Computer Science, Amsterdam (Netherlands). Computer Science/Algorithmics and Architecture Dept.
HASHING AND REHASHING IN EMULATED SHARED MEMORY
Joerg Keller (Center for Mathematics and Computer Science, Amsterdam, Netherlands.) Oct. 1992 18 p
(Contracts SFB-124-D4; NF-62-376)
(CWI-CS-R9240; ETN-93-94166) Copyright Avail: CASI HC A02/MF A02

The PRAM (Parallel Random Access Machine) model is widely used to formulate parallel algorithms because of its shared memory and its synchronous behavior. The model, however, bears little resemblance to real parallel machines. This has led to various approaches to emulating PRAM's on processor networks. A survey of the principles behind these emulations is presented, and it is shown why hashing is an important part of them. The commonly used types of hash functions and their theoretical properties are discussed and related to their behavior in simulations. Both synthetic and application based traces are used as input data for these simulations. The simulation results suggest the use of linear functions with randomly chosen coefficients. These functions also have the advantage of short evaluation time and bijectivity. But no matter which type of hash function is chosen, it may be necessary to choose a new hash function on the fly. An algorithm to rehash linear functions in optimal time without using shade memory or mass storage systems during rehashing is presented. ESA

N94-13546# National Research Council of Canada, Ottawa (Ontario). Inst. for Information Technology.
COLLECTION AND ANALYSIS OF DIALOGUE PROTOCOLS FOR THE QUESTION-ANSWERING FACILITY OF THE ENTITY-RELATIONSHIP MODELING ADVISOR
A. Parent Oct. 1990 61 p
(ERB-1032; NRC-31827; CTN-93-60825) Copyright Avail: CASI HC A04/MF A01

An experimental procedure was set up to simulate the conditions under which an intelligent computer facility could help a user create a conceptual data model. This was accomplished by having a human advisor give assistance within constraints similar to those of the computerized

facility. The semantics of the conceptual model were made available to the human expert so that heuristic rules associated with the area of application could be collected. The task consisted of designing a conceptual data model for an unsatisfactory condition report management system for use in equipment maintenance. The user had to develop a valid conceptual model of this system, in the entity relationship formalism, using the Silverrun-ERM automated modeling tool. To analyze the protocols, an adapted version of dialogue game theory was applied. Five question types were identified. The results show that the most important need of the user involves a validation question seeking the evaluation of a hypothetical or current state of the user's conceptual design. This activity will offer a basis for the functional specification of a computer facility capable of constructing an educational response to questions dealing with conceptual data design. CISTI

N94-13547# National Research Council of Canada, Ottawa (Ontario). Inst. for Information Technology.

MASS MARKET COMPUTERS FOR SOFTWARE DEVELOPMENT

W. M. Gentleman and M. Wein Nov. 1991 15 p Presented at the 1991 ACM Symposium of Personal and Small Computers, Toronto, Ontario, 12-14 Jun. 1991

(ERB-1035; NRC-33162; CTN-93-60826) Copyright Avail: CASI HC A03/MF A01

The mass market or appliance computer has become a plausible alternative to workstations for software development. While it is easy to use for software development, a different style of development emerges. By being truly personal, the mass market computer provides a focus for all the professional activities of a developer such as program development, documentation, and preparation of presentations. The primary form of software used on such computers is commercially available software; this has profound implications on how the software is used and the make-or-buy tradeoff takes on an entirely new meaning. The advantages of mass market computers are described. An environment consisting of a network of mass market computers is presented as an example of how these computers have influenced the development of a novel source management scheme. Author (CISTI)

N94-13609* National Aeronautics and Space Administration. Ames Research Center, Moffett Field, CA.

CRAY Y-MP (Videotape)

Nov. 1988 Videotape: 12 min. playing time, in color, with sound

(NASA-TM-109303; NONP-VT-93-185321) Avail: CASI VHS A01/BETA A22

This video shows the installation of the Cray Y-MP, a computer four times faster than any other computer at Ames. Computer room scenes, aeronautical and space applications, and other non-aerospace applications are also included. Author (revised)

N94-13788*# Hughes STX, Inc., Lanham, MD.

SPACE AND EARTH SCIENCES, COMPUTER SYSTEMS, AND SCIENTIFIC DATA ANALYSIS SUPPORT, VOLUME 1 Final Progress Report, 1 Jun. - 30 Sep. 1993

Ronald H. Estes, ed. 6 Oct. 1993 688 p

(Contract NAS5-30440)

(NASA-CR-194535; NAS 1.26:194535) Avail: CASI HC A99/MF A06

This Final Progress Report covers the specific technical activities of Hughes STX Corporation for the last contract triannual period of 1 June through 30 Sep. 1993, in support of assigned task activities at Goddard Space Flight Center (GSFC). It also provides a brief summary of work throughout the contract period of performance on each active task. Technical activity is presented in Volume 1, while financial and level-of-effort data is presented in Volume 2. Technical support was provided to all Division and Laboratories of Goddard's Space Sciences and Earth Sciences Directorates. Types of support include: scientific programming, systems programming, computer management, mission planning, scientific investigation, data analysis, data processing, data base creation and maintenance, instrumentation development, and management services. Mission and instruments supported include: ROSAT, Astro-D, BBXRT, XTE, AXAF, GRO, COBE, WIND, UIT, SMM, STIS, HEIDI, DE, URAP, CRRES, Voyagers, ISEE, San Marco, LAGEOS, TOPEX/Poseidon, Pioneer-Venus, Galileo, Cassini, Nimbus-7/TOMS, Meteor-3/TOMS, FIFE, BOREAS, TRMM, AVHRR, and Landsat. Accomplishments include: development of computing programs for mission science and data analysis, supercomputer applications support, computer network support, computational upgrades for data archival and analysis centers, end-to-end management for mission data flow, scientific modeling and results in the fields of space and Earth physics, planning and design of GSFC VO DAAC and VO IMS, fabrication, assembly, and testing of mission instrumentation, and design of mission operations center. Author (revised)

N94-13943*# Jet Propulsion Lab., California Inst. of Tech., Pasadena.

TEST REPORT FOR SINGLE EVENT EFFECTS OF THE 80386DX MICROPROCESSOR

R. Kevin Watson, Harvey R. Schwartz, and Donald K. Nichols 15 Feb. 1993 26 p

(Contract NAS7-918)

(NASA-CR-194509; JPL-Publ-93-12; NAS 1.26:194509) Avail: CASI HC A03/MF A01

The Jet Propulsion Laboratory Section 514 Single Event Effects (SEE) Testing and Analysis Group has performed a series of SEE tests of certain strategic registers of Intel's 80386DX CHMOS 4 microprocessor. Following a summary of the test techniques and hardware used to gather the data, we present the SEE heavy ion and proton test results. We also describe the registers tested, along with a system impact analysis should these registers experience a single event upset. Author (revised)

N94-14136*# Old Dominion Univ., Norfolk, VA. Dept. of Electrical and Computer Engineering.

A PERFORMANCE PREDICTION MODEL FOR A FAULT-TOLERANT COMPUTER DURING RECOVERY AND RESTORATION Ph.D. Thesis Report, 1 Jan. - 31 Dec. 1992

John W. Stoughton and Rodrigo A. Obando Sep. 1993 186 p

(Contract NCC1-136)

(NASA-CR-194490; NAS 1.26:194490) Avail: CASI HC A09/MF A02

The modeling and design of a fault-tolerant multiprocessor system is addressed. In particular, the behavior of the system during recovery and restoration after a fault has occurred is investigated. Given that a multicomputer system is designed using the Algorithm to Architecture to Mapping Model (ATAMM), and that a fault (death of a computing resource) occurs during its normal steady-state operation, a model is presented as a viable research tool for predicting the performance bounds of the system during its recovery and restoration phases. Furthermore, the bounds of the performance behavior of the system during this transient mode can be assessed. These bounds include: time to recover from the fault (t(sub rec)), time to restore the system (t(sub rec)) and whether there is a permanent delay in the system's Time Between Input and Output (TBIO) after the system has reached a steady state. An implementation of an ATAMM based computer was developed with the Generic VHSIC Spaceborne Computer (GVSC) as the target system. A simulation of the GVSC was also written based on the code used in ATAMM Multicomputer Operating System (AMOS). The simulation is in turn used to validate the new model in the usefulness and accuracy in tracking the propagation of the delay through the system and predicting the behavior in the transient state of recovery and restoration. The model is validated as an accurate method to predict the transient behavior of an ATAMM based multicomputer during recovery and restoration. Author (revised)

N94-14626*# DYNACS Engineering Co., Inc., Houston, TX.

COMPUTATIONAL CONTROLS WORKSTATION: ALGORITHMS AND HARDWARE

R. Venugopal and M. Kumar *In* JPL, Proceedings of the Fifth NASA/NSF/DOD Workshop on Aerospace Computational Control 15 Feb. 1993 p 117-123 (For primary document see N94-14618 02-39) Avail: CASI HC A02/MF A04

61 COMPUTER PROGRAMMING AND SOFTWARE

Includes computer programs, routines, alogorithms, and specific applications, e.g., CAD/CAM.

N94-12808*# Alabama Univ., Tuscaloosa. Dept. of Engineering Science and Mechanics.

ADAPTIVELY RESIZING POPULATIONS: ALGORITHM, ANALYSIS, AND FIRST RESULTS

Robert E. Smith and Ellen Smuda 13 Sep. 1993 57 p

(Grant NAG9-625)

(NASA-CR-194277; NAS 1.26:194277) Avail: CASI HC A04/MF A01

Deciding on an appropriate population size for a given Genetic Algorithm (GA) application can often be critical to the algorithm's success. Too small, and the GA can fall victim to sampling error, affecting the efficacy of its search. Too large, and the GA wastes computational resources. Although advice exists for sizing GA populations, much of this advice involves theoretical aspects that are not accessible to the novice user. An algorithm for adaptively resizing GA populations is suggested. This algorithm is based on recent theoretical developments that relate population size to schema fitness variance. The suggested algorithm is developed theoretically, and simulated with expected value equations. The algorithm is then tested on a problem where population sizing can mislead the GA. The work presented suggests that the population sizing algorithm may be a viable way to eliminate the population sizing decision from the application of GA's. Author (revised)

N94-12840# Lawrence Livermore National Lab., CA.

PACT USER'S GUIDE

S. A. Brown and D. Braddy Jan. 1993 26 p

(Contract W-7405-eng-48)

(DE93-013093; UCRL-MA-112087) Avail: CASI HC A03/MF A01

In a computing landscape which has many different hardware architectures and supporting software systems ranging from compilers to operating systems, there is an obvious and strong need for a philosophy of software development that lends itself to the design and construction of portable code systems. The current efforts to standardize software bear witness to this need. PACT is an effort to implement a software development environment which is itself portable and promotes the design and construction of portable applications. PACT does not include such important tools as editors and compilers. Well built tools of that kind are readily available across virtually all computer platforms. The areas that PACT addresses are at a higher level involving issues such as data portability, portable inter-process communication, and graphics. In its current conception, PACT is a set of 10 tools. Nine of these are implemented as libraries, and two of them provide both libraries and executable applications. PACT is entirely coded in C but was designed with a view toward support of other languages, notably FORTRAN. DOE

N94-12864# Lawrence Livermore National Lab., CA.

FORTRAN GRAPHICS ROUTINES FOR THE MACINTOSH

B. W. Shore Jun. 1992 15 p

(Contract W-7405-eng-48)

(DE93-013092; UCRL-MA-111145) Avail: CASI HC A03/MF A01

The Language Systems MPW FORTRAN is a popular FORTRAN compiler for the Macintosh. Unfortunately, it does not have any built-in calls to graphics routines (such as are available with Graflib on the NLTSS), so there is no simple way to make x-y plots from calls within FORTRAN. Instead, a file of data must be created and a commercial plotting routine (such as IGOR or KALEIDAGRAPH) or a spreadsheet with graphics (such as WINGZ) must be applied to post-process the data. The Macintosh does have available many built-in calls (to the Macintosh Toolbox) that allow drawing shapes and lines with quickdraw, but these are not designed for plotting functions and are difficult to learn to use. This work outlines some FORTRAN routines that can be called from LS FORTRAN to make the necessary calls to the Macintosh Toolbox to create simple two-dimensional plots or contour plots. The source code DEMOGRAF.F shows how these routines may be used. DEMOGRAF.F simply demonstrates some FORTRAN subroutines that can be called with language systems MPW FORTRAN on the Macintosh to plot arrays of numbers. The subroutines essentially mimic the functionality that has been available at LTSS and NLTSS and UNICOS at LLNL. The graphics primitives are kept in four separate files, each containing several subroutines. The subroutines are compiled and stored in a library file, LIBgraf.o. Makefile is used to link this library to the source code. A discussion is included on requirements for interactive plotting of functions. DOE

N94-12883# Lawrence Livermore National Lab., CA.

SMOOTH TRANSITIONS BETWEEN BUMP RENDERING ALGORITHMS

B. G. Becker and N. L. Max Jan. 1993 37 p Presented at the Siggraph 1993 Conference, Anaheim, CA, 2-6 Aug. 1993

(Contract W-7405-eng-48)

(DE93-012504; UCRL-JC-112601; CONF-930881-2) Avail: CASI HC A03/MF A01

A method is described for switching smoothly between rendering algorithms as required by the amount of visible surface detail. The result will be more realism with less computation for displaying objects whose surface detail can be described by one or more bump maps. The three rendering algorithms considered are bidirectional reflection distribution function (BRDF), bump-mapping, and displacement-mapping. The bump-mapping has been modified to make it consistent with the other two. For a given viewpoint, one of these algorithms will show a better trade-off between quality, computation time, and aliasing than the other two. Thus, it needs to be determined for any given viewpoint which regions of the object(s) will be rendered with each algorithm. The decision as to which algorithm is appropriate is a function of distance, viewing angle, and the frequency of bumps in the bump map. DOE

N94-12933 University of Southern California, Marina del Rey. Information Sciences Inst.

COMMON LISP FRAMEWORK Final Report, 1 Sep. 1987 - 31 May 1992

David S. Wile 8 Feb. 1993 21 p Limited Reproducibility: More than 20% of this document may be affected by microfiche quality

(Contract MDA903-87-C-0641; DARPA Order 6096)

(AD-A265878) Avail: Issuing Activity (Defense Technical Information Center (DTIC))

The principal goal of the COMMON LISP Framework project was to support Strategic Computing (SC) contractors with a comprehensive, state-of-the-art programming framework for the development and evolution of COMMON LISP programs. The CLF has affected the technical community by shaping both the structure of modern programming environments and the development paradigm they support. This structure rests upon an active objectbase which maintains integrity, integrated tools and provides persistence. CLF's integrity management is unique in providing declarative integrity condition statements--which can be reasoned about and analyzed--while still permitting efficient algorithmic maintenance of these conditions. Its declarative persistence mechanism, based on conceptual aggregations of objects, is also unique. Tools are integrated with the objectbase rather than each other. They gather their inputs from, and place their results back in, the objectbase and are invoked (demonically) by relative activity in the objectbase. DTIC

N94-12956# Sandia National Labs., Albuquerque, NM.

A GENERAL CONTACT DETECTION ALGORITHM FOR FINITE ELEMENT ANALYSIS

M. W. Heinstein, S. W. Attaway, J. W. Swegle, and F. J. Mello 1992 9 p Presented at the First International Conference in Contact Mechanics, Southampton, England, 13-15 Jul. 1993

(Contract DE-AC04-76DP-00789)

(DE93-012846; SAND-92-2059C; CONF-930782-1) Avail: CASI HC A02/MF A01

A contact detection algorithm has been developed to address difficulties associated with the numerical simulation of contact in nonlinear finite element structural analysis codes. Mechanics problems which have self-contacting surfaces, tearing and eroding surfaces, and multibody impact are solved using the new algorithm. The proposed algorithm is portable between dynamic and quasi-static codes and can efficiently model contact between a variety of finite element types including shells, bricks, beams and particles. The algorithm is composed of the following: (1) a location strategy that uses a global search to decide which slave nodes are in proximity to a

master surface; and (2) an accurate detailed contact check that uses the projected motions of both master surface and slave node. The capability of the new algorithm is illustrated with several example problems. DOE

N94-12974# Naval Command, Control and Ocean Surveillance Center, San Diego, CA.
ADVANCED DISPLAY OBJECT SELECTION METHODS FOR ENHANCING USER-COMPUTER PRODUCTIVITY
G. A. Osga Mar. 1993 6 p
(AD-A265806) Avail: CASI HC A02/MF A01

The User-Interface Technology Branch at NCCOSC RDT&E Division has been conducting a series of studies to address the suitability of commercial off-the-shelf (COTS) graphical user-interface (GUI) methods for efficiency and performance in critical naval combat systems. This paper presents an advanced selection algorithm and method developed to increase user performance when masking selections on tactical displays. The method has also been applied with considerable success to a variety of cursor and pointing tasks. Typical GUI's allow user selection by the following methods: (1) moving a cursor with a pointing device such as a mouse, trackball, joystick, touchscreen; and (2) placing the cursor on the object. Examples of GUI objects are the buttons, icons, folders, scroll bars, etc. used in many personal computer and workstation applications. This paper presents an improved method of selection and the theoretical basis for the significant performance gains achieved with various input devices tested. The method is applicable to all GUI styles and display sizes, and is particularly useful for selections on small screens such as notebook computers. Considering the amount of work-hours spent pointing and clicking across all styles of available graphic user-interfaces, the cost/benefit in applying this method to graphic user-interfaces is substantial, with the potential for increasing productivity across thousands of users and applications. DTIC

N94-12991# Arizona Univ., Tucson.
TREE RECONSTRUCTION FROM PARTIAL ORDERS
S. K. Kannan and T. J. Warnow (Sandia National Labs., Albuquerque, NM.) 1993 11 p Presented at the Workshop on Algorithms and Data Structures; International Congress on Automata and Language Processing, Montreal, Canada; Lund, Sweden, 11-13 Aug. 1993; Jul. 1993
(Contract DE-AC04-76DP-00789)
(DE93-009841; SAND-93-0689C; CONF-930884-1; CONF-930770-1) Avail: CASI HC A03/MF A01

The problem of constructing trees given a matrix of interleaf distances is motivated by applications in computational evolutionary biology and linguistics. The general problem is to find an edge-weighted tree which most closely approximates the distance matrix. Although the construction problem is easy when the tree exactly fits the distance matrix, optimization problems under all popular criteria are either known or conjectured to be NP-complete. In this paper we consider the related problem where we are given a partial order on the pairwise distances, and wish to construct (if possible) an edge-weighted tree realizing the partial order. In particular we are interested in partial orders which arise from experiments on triples of species, which determine either a linear ordering of the three pairwise distances (called Total Order Model or TOM experiments) or only the pair(s) of minimum distance apart (called Partial Order Model or POM experiments). The POM and TOM experimental model is inspired by the model proposed by Kannan, Lawler, and Warnow for constructing trees from experiments which determine the rooted topology for any triple of species. We examine issues of construction of trees and consistency of TOM and POM experiments, where the trees may either be weighted or unweighted. Using these experiments to construct unweighted trees without nodes of degree two is motivated by a similar problem studied by Winkler, called the Discrete Metric Realization problem, which he showed to be strongly NP-hard. We have the following results: Determining consistency of a set of TOM or POM experiments is NP-complete whether the tree is weighted or constrained to be unweighted and without degree two nodes. We can construct unweighted trees without degree two nodes from TOM experiments in optimal O(n(sup 3)) time and from POM experiments in O(n(sup 4)) time. DOE

N94-12999# Sandia National Labs., Albuquerque, NM.
DATA FUSION FOR ADAPTIVE CONTROL IN MANUFACTURING: IMPACT ON ENGINEERING INFORMATION MODELS
O. H. Bray 1992 11 p Presented at the 1993 ASME International Computers in Engineering Conference and Exposition, San Diego, CA, 8-12 Aug. 1993
(Contract DE-AC04-76DP-00789)
(DE93-011555; SAND-92-2405C; CONF-930862-2) Avail: CASI HC A03/MF A01

This paper addresses the impact of data fusion on engineering and manufacturing information systems. Data fusion is the integration and analysis of data from multiple sensors to develop a more accurate understanding of a situation and determine how to respond to it. Sensor fusion, a related term, has a somewhat different, more implementation oriented focus. The difference between these two concepts is addressed specifically in Section 1. Although data fusion can be applied in many situations, this paper focuses on its application to manufacturing and how it changes some of the more traditional, less adaptive information models that support the design and manufacturing functions. DOE

N94-13014# Allied-Signal Aerospace Co., Kansas City, MO.
KNOWLEDGE BASE TECHNOLOGY FOR CT-DIMS: REPORT 1
E. E. Kelley May 1993 40 p
(Contract DE-AC04-76DP-00613)
(DE93-013118; KCP-613-4984) Avail: CASI HC A03/MF A01

This report discusses progress on the Cutting Tool-Database and Information Management System (CT-DIMS) project being conducted by the University of Illinois Urbana-Champaign (UIUC) under contract to the Department of Energy. This project was initiated in October 1991 by UIUC. The Knowledge-Based Engineering Systems Research Laboratory (KBESRL) at UIUC is developing knowledge base technology and prototype software for the presentation and manipulation of the cutting tool databases at Allied-Signal Inc., Kansas City Division (KCD). The graphical tool selection capability being developed for CT-DIMS in the Intelligent Design Environment for Engineering Automation (IDEEA) will provide a concurrent environment for simultaneous access to tool databases, tool standard libraries, and cutting tool knowledge. DOE

N94-13023*# Purdue Univ., West Lafayette, IN. School of Electrical Engineering.
FEATURE EXTRACTION AND CLASSIFICATION ALGORITHMS FOR HIGH DIMENSIONAL DATA
Chulhee Lee and David Landgrebe Jan. 1993 226 p
(Grant NAGw-925)
(NASA-CR-194298; NAS 1.26:194298; TR-EE-93-1) Avail: CASI HC A11/MF A03

Feature extraction and classification algorithms for high dimensional data are investigated. Developments with regard to sensors for Earth observation are moving in the direction of providing much higher dimensional multispectral imagery than is now possible. In analyzing such high dimensional data, processing time becomes an important factor. With large increases in dimensionality and the number of classes, processing time will increase significantly. To address this problem, a multistage classification scheme is proposed which reduces the processing time substantially by eliminating unlikely classes from further consideration at each stage. Several truncation criteria are developed and the relationship between thresholds and the error caused by the truncation is investigated. Next an approach to feature extraction for classification is proposed based directly on the decision boundaries. It is shown that all the features needed for classification can be extracted from decision boundaries. A characteristic of the proposed method arises by noting that only a portion of the decision boundary is effective in discriminating between classes, and the concept of the effective decision boundary is introduced. The proposed feature extraction algorithm has several desirable properties: it predicts the minimum number of features necessary to achieve the same classification accuracy as in the original space for a given pattern recognition problem; and it finds the necessary feature vectors. The proposed algorithm does not deteriorate under the circumstances of equal means or equal covariances as some previous algorithms do. In addition, the decision boundary feature extraction algorithm can be used both for parametric and non-parametric classifiers. Finally, some problems encountered in analyzing high dimensional data are studied and possible solutions are proposed. First, the increased importance of the second order statistics in analyzing high dimensional data is recognized. By investigating the characteristics of high dimensional data, the reason why the second order statistics must be taken into account in high

dimensional data is suggested. Recognizing the importance of the second order statistics, there is a need to represent the second order statistics. A method to visualize statistics using a color code is proposed. By representing statistics using color coding, one can easily extract and compare the first and the second statistics. Author (revised)

N94-13024# Northwestern Univ., Evanston, IL.
OPTIMIZATION AND EIGENVALUE COMPUTATION WITH APPLICATION TO METEOROLOGY AND OCEANOGRAPHY
J. Nocedal May 1993 3 p
(Contract DE-FG02-87ER-25047)
(DE93-015310; DOE/ER-25047/5) Avail: CASI HC A01/MF A01

Our computational experience has shown that dynamic scaling techniques can have a dramatic effect in the efficiency of optimization algorithms, especially when the number of variables is very large. Conjugate gradient and limited memory methods do not have adequate information on the Hessian matrix, and dynamic scaling of the variables can supply some of this missing information. We developed a full-rank scaling technique for variable metric methods that is globally and superlinearly convergent on general problems. We have also proposed a new technique for accelerating the optimization process in the solution of data assimilation problems. This is an area where optimization plays a crucial role, since the four dimensional assimilation approach consists of using a nonlinear optimization code to adjust the initial conditions of the model so that measurements distributed in space and time can be adequately predicted. Each iteration of the optimization method requires a full simulation of the model a process that typically takes 1 hour on the CRAY 90. We have found that by computing a few extreme eigenvalues of the Hessian matrix, and by incorporating this information in a limited memory code, the number of simulations can be reduced by at least 50%. This is highly significant and represents a substantial contribution to the area of variational assimilation of data. We have also developed an extension of the limited memory BFGS method that is capable of handling simple bounds on the variables, providing more freedom to the modeler. This work was made possible by the development of compact matrix representations of limited memory matrices, which keep the computational cost of the iteration to a minimum. Indeed, we have shown that the operations with limited memory BFGS matrices are optimal in terms of arithmetic operations, since they can be rewritten as the reverse automatic differentiation of an auxiliary function. DOE

N94-13049# Carnegie-Mellon Univ., Pittsburgh, PA. Software Engineering Inst.
LECTURE NOTES ON SOFTWARE PROCESS IMPROVEMENT Final Report
Laurie H. Werth Feb. 1993 60 p
(Contract F19628-90-C-0003)
(AD-A265200; CMU/SEI-93-EM-8) Avail: CASI HC A04/MF A01

Software process improvement is not usually covered in standard software engineering textbooks. However, because it is a topic of great interest to the software industry, both faculty and students should be familiar with it. The goal of this package is to provide the basis for an introductory 30 to 60 minute lecture on the software process and its improvement. The material in the main body of the document is intended primarily for instructors. In conjunction with the student-oriented document described below, it provides technical information from which an instructor can prepare a lecture. Two appendices provide additional information for instructors. Appendix A is a brief description of the use of the software process material in a university software engineering class at the University of Texas at Austin. This classroom example might be used as an illustration for students to relate the process concepts to their own software development work. Appendix B presents the Software Engineering Institute's (SEI) process maturity questionnaire from which instructors and students can gain some insight into how a software process is assessed. DTIC

N94-13065*# College of William and Mary, Williamsburg, VA. Dept. of Computer Sciences.
A PATH-ORIENTED MATRIX-BASED KNOWLEDGE REPRESENTATION SYSTEM
Stefan Feyock and Stamos T. Karamouzis Washington NASA Sep. 1993 26 p
(Contract NCC1-159; RTOP 505-64-13-22)
(NASA-CR-4539; NAS 1.26:4539) Avail: CASI HC A03/MF A01

Experience has shown that designing a good representation is often the key to turning hard problems into simple ones. Most AI (Artificial Intelligence) search/representation techniques are oriented toward an infinite domain of objects and arbitrary relations among them. In reality much of what needs to be represented in AI can be expressed using a finite domain and unary or binary predicates. Well-known vector- and matrix-based representations can efficiently represent finite domains and unary/binary predicates, and allow effective extraction of path information by generalized transitive closure/path matrix computations. In order to avoid space limitations a set of abstract sparse matrix data types was developed along with a set of operations on them. This representation forms the basis of an intelligent information system for representing and manipulating relational data. Author

N94-13077# National Aeronautical Lab., Bangalore (India). Aerospace Electronics Div.
PC BASED A320 QUICK ACCESS RECORDER READOUT FACILITY
B. S. Adiga, S. J. Muralidhar, C. Ramesh, and Aravind (Indian Inst. of Tech., Madras.) Sep. 1991 21 p
(PD-AL-9109) Avail: CASI HC A03/MF A01

A Readout Facility was established at NAL for Indian Airlines for Decoding of A320 Quick Access Recorder Data which is presently in operation in India. This PC based system reads the data recorded on QAR, transfers the data to PC, converts the raw data into its appropriate engineering units and displays it on the screen. It also has the provision of graphical representation of various parameters with reference to altitude coarse. This system can be used to investigate any incident/day-to-day maintenance of A320 Aircraft. Author (revised)

N94-13113*# Georgia Inst. of Tech., Atlanta. Digital Signal Processing Lab.
IMAGE CODING USING ENTROPY-CONSTRAINED RESIDUAL VECTOR QUANTIZATION
Faouzi Kossentini, Mark J. T. Smith, and Christopher F. Barnes 15 Apr. 1993 31 p
(Grants NAG5-2187; NSF MIP-91-16113)
(NASA-CR-193728; NAS 1.26:193728) Avail: CASI HC A03/MF A01

The residual vector quantization (RVQ) structure is exploited to produce a variable length codeword RVQ. Necessary conditions for the optimality of this RVQ are presented, and a new entropy-constrained RVQ (ECRVQ) design algorithm is shown to be very effective in designing RVQ codebooks over a wide range of bit rates and vector sizes. The new EC-RVQ has several important advantages. It can outperform entropy-constrained VQ (ECVQ) in terms of peak signal-to-noise ratio (PSNR), memory, and computation requirements. It can also be used to design high rate codebooks and codebooks with relatively large vector sizes. Experimental results indicate that when the new EC-RVQ is applied to image coding, very high quality is achieved at relatively low bit rates. Author (revised)

N94-13120# Lawrence Livermore National Lab., CA.
ULTRA 2 USER'S MANUAL FOR ULTRA 2 REVISION 3.0
S. A. Brown, C. F. McMillan, D. Braddy, and P. Keller Jan. 1993 74 p Revised
(Contract W-7405-eng-48)
(DE93-015970; UCRL-MA-108967-Rev-1) Avail: CASI HC A04/MF A01

ULTRA 2 is a program for the presentation, manipulation, and analysis of 1D data sets (i.e., x, y pairs). Presentation refers to the capability to display and make hard copies of data plots. Manipulation refers to the capability to excerpt, shift, and scale data sets. Analysis refers to the capability to combine data sets in various ways to create new data sets. An example of this is the Fast Fourier Transform (FFT) capability in ULTRA 2. The principal object with which ULTRA 2 works is the curve. A curve is an object which consists of an array of x values, an array of y values, a number of points (the length of the x and y arrays), and an ASCII label. ULTRA 2 operates on curves. ULTRA II is a portable tool. It runs on machines from supercomputers to PC's. It runs under UNIX, DOS, and MAC OS. Its portability derives from the PACT libraries which provide the portable graphics and the SCHEME interpreter engine which are the main foundation of ULTRA 2. ULTRA 2 can read and write ASCII data files or PDB files with ULTRA curves in them. PDBLib is another PACT tool which

provides portable, self-describing, binary data files. PDBLib has specific functionality to write ULTRA curves. This provides an easy and convenient way for applications to produce ULTRA files. The advantage of PDB files over ASCII files is that PDB files are about 1/3 the size of a corresponding ASCII file and can be written or read about 10 times faster. Interested readers will find references to PACT documentation later in this manual.
DOE

N94-13130*# Coherent Research, Inc., Syracuse, NY.
A KNOWLEDGE-BASED EXPERT SYSTEM TO COORDINATE CAD/CAE WITH INTEGRATION AND TEST Final Technical Report
Charles D. Stormon 10 Jul. 1991 91 p
(Contract NAS7-1068; SBIR-06.06-0929)
(NASA-CR-191394; NAS 1.26:191394) Avail: CASI HC A05/MF A01

The objective of this project was to construct a prototype expert system to coordinate computer aided design and computer engineering (CAD/CAE) with integration and test. The prototype was intended to integrate existing CAD/CAE tools, provide the facility for integration with future CAD/CAE tools, and use a knowledge base to assist in simulation, testing, fault diagnosis, and design verification. In constructing this prototype, the approach was to build on experience gained from our Phase 1 effort, while maintaining a flow of new ideas from a close-knit collaboration with researchers at Syracuse University. The results from Phase 1 proved useful in terms of understanding some of the more difficult research issues, but major effort was required to create a prototype which provided the above functions. Much was learned in the process of creating this prototype, both in terms of what was feasible and what was useful. Ultimately, such a prototype was successfully constructed, and it is supplied along with this report. We believe that this prototype will allow NASA and CRi to address the issues of commercialization from a well-informed perspective.
Author (revised)

N94-13151# Los Alamos National Lab., NM.
ADAPTIVE TRANSFER FUNCTION NETWORKS
J. R. Goulding 1993 6 p Presented at the World Congress on Neural Networks, Portland, OR, 11-15 Jul. 1993
(Contract W-7405-eng-36)
(DE93-014344; LA-UR-93-1983; CONF-930741-3) Avail: CASI HC A02/MF A01

Real-time pattern classification and time-series forecasting applications continue to drive artificial neural network (ANN) technology. As ANNs increase in complexity, the throughput of digital computer simulations decreases. A novel ANN, the Adaptive Transfer Function Network (ATF-Net), directly addresses the issue of throughput. ATF-Nets are global mapping equations generated by the superposition of ensemblies of neurodes having arbitrary continuous functions receiving encoded input data. ATF-Nets may be implemented on parallel digital computers. An example is presented which illustrates a four-fold increase in computational throughput. DOE

N94-13185*# Institute for Computer Applications in Science and Engineering, Hampton, VA.
CALCULATING INTERSECTIONS OF SURFACES IN SCREEN SPACE Final Report
David C. Banks Washington Jul. 1993 15 p Submitted for publication
(Contract NAS1-19480; RTOP 505-90-52-01)
(NASA-CR-191498; NAS 1.26:191498; ICASE-93-41) Avail: CASI HC A03/MF A01

When surfaces intersect, one may desire to highlight the intersection curve in order to make the shape of the penetrating surfaces more visible. Highlighting the intersection is especially helpful when the surfaces become transparent, because transparency makes the intersections less evident. A technique for locating intersections in screen space using only the information locally available to a pixel is discussed. The technique is designed to exploit parallelism at the pixel level and was implemented on the Pixel-Planes 5 graphics supercomputer. Author (revised)

N94-13290# Stanford Univ., CA. Knowledge Systems Lab.
GENERIC SOFTWARE ARCHITECTURE BASED REDESIGN
Sanjay Bhansali 1992 6 p
Avail: CASI HC A02/MF A01

The design of software architecture is concerned with decomposing a software system into sub-systems or modules, defining the interface and the dependencies between the modules, allocating high-level tasks to agents, determining representation schemes for data, and other similar activities which enable the later implementation of the software to proceed in a modular and largely routine manner. Currently existing software methodologies and tools are generally adequate in constructing an initial design for a system that is well structured. However, they do not adequately capture the process or rationale underlying the design and hence later modifications to the system are difficult and error-prone. Since a major portion of a software's lifecycle is devoted to maintenance, significant payoffs could result if changes to a software artifact can be incorporated rapidly and reliably. Author (revised)

N94-13355*# Stanford Univ., CA. Dept. of Computer Science.
SOFTWARE SYNTHESIS USING GENERIC ARCHITECTURES
Sanjay Bhansali Aug. 1993 43 p
(Contract NCC2-749)
(NASA-CR-194201; NAS 1.26:194201; KSL-93-60) Avail: CASI HC A03/MF A01

A framework for synthesizing software systems based on abstracting software system designs and the design process is described. The result of such an abstraction process is a generic architecture and the process knowledge for customizing the architecture. The customization process knowledge is used to assist a designer in customizing the architecture as opposed to completely automating the design of systems. Our approach using an implemented example of a generic tracking architecture which was customized in two different domains is illustrated. How the designs produced using KASE compare to the original designs of the two systems, and current work and plans for extending KASE to other application areas are described. Author (revised)

N94-13356*# Stanford Univ., CA. Dept. of Computer Science.
ARCHITECTURE-DRIVEN REUSE OF CODE IN KASE
Sanjay Bhansali Apr. 1993 9 p
(Contract NCC2-7491)
(NASA-CR-194200; NAS 1.26:194200; KSL-93-35) Avail: CASI HC A02/MF A01

In order to support the synthesis of large, complex software systems, we need to focus on issues pertaining to the architectural design of a system in addition to algorithm and data structure design. An approach that is based on abstracting the architectural design of a set of problems in the form of a generic architecture, and providing tools that can be used to instantiate the generic architecture for specific problem instances is presented. Such an approach also facilitates reuse of code between different systems belonging to the same problem class. An application of our approach on a realistic problem is described; the results of the exercise are presented; and how our approach compares to other work in this area is discussed.
Author (revised)

N94-13357# Stanford Univ., CA. Knowledge Systems Lab.
THE KASE APPROACH TO DOMAIN-SPECIFIC SOFTWARE SYSTEMS
Sanjay Bhansali and H. Penny Nii 1992 5 p Previously announced as N93-17502
Avail: CASI HC A01/MF A01

Designing software systems, like all design activities, is a knowledge-intensive task. Several studies have found that the predominant cause of failures among system designers is lack of knowledge - knowledge about the application domain, knowledge about design schemes, and knowledge about design processes. The goal of domain specific software design systems is to explicitly represent knowledge relevant to a class of applications and use it to partially or completely automate various aspects of the design activity for designing systems within that domain. The hope is that this would reduce the intellectual burden on the human designers and lead to more efficient software development. A domain-specific system built on top of KASE, a knowledge-assisted software engineering environment being developed at the Stanford Knowledge Systems Laboratory is presented. The main ideas underlying the construction of domain specific systems within KASE are introduced; the application of the idea in the synthesis of a system for tracking aircrafts from radar signals is illustrated; and some of the issues in constructing domain-specific systems are discussed. Author (revised)

N94-13382# California Univ., Berkeley. Lawrence Berkeley Lab.
EGS (UNDERSCORE) WINDOWS 2: AN ENHANCED GRAPHICAL INTERFACE TO EGS
S. Chatterjee and R. J. Donahue Jan. 1993 14 p Presented at the International Conference on Monte Carlo Simulation in Nuclear and High Energy Physics, Tallahassee, FL, 22-26 Feb. 1993
(Contract DE-AC03-76SF-00098)
(DE93-010447; LBL-33429; CONF-9302113-1) Avail: CASI HC A03/MF A01

This report gives a general overview of the EGS-Windows2 program. The program is intended to be used to display individual particle histories of electrons, photons, and positrons generated by the EGS4 Code System. Much of this work is based on the earlier version of EGS-Windows2 from the Institute for National Measurement Standards at the National Research Council of Canada (NRCC). No attempt is made to modify their EGS subroutine WATCH, which is used to output the particle vectors to be read by EGS-Windows, or duplicate any of the documentation describing the subroutine. EGS-Windows2 reads data in the same format as produced by WATCH. Users of EGS-Windows2 are encouraged to obtain the original EGS-Windows report from the NRCC in addition to this report as complete documentation of EGS-Windows2. As in the original report, two levels of information are covered in this report: the user level, and the programmer level. The user level should be read by all users. It describes execution, operation, and capabilities. The programmer level should be read by those users who may want to modify the program or who would like a more detailed understanding. It describes briefly the routines and there function, as well as the major changes in the new release of the 3D graphics programming library Sun PHIGS 2.0. DOE

N94-13394# EG and G Energy Measurements, Inc., Idaho Falls.
CREATING A STRATEGIC PLAN FOR CONFIGURATION MANAGEMENT USING COMPUTER AIDED SOFTWARE ENGINEERING (CASE) TOOLS
P. R. Smith and R. Sarfaty 1993 26 p Presented at the 1993 DOE/Contractors and Facilities Data Acquisition and Control User's Group Meeting, Livermore, CA, 13-16 Apr. 1993
(Contract DE-AC07-76ID-01570)
(DE93-013663; EGG-M-93143; CONF-9304134-1) Avail: CASI HC A03/MF A01

This paper provides guidance in the definition, documentation, measurement, enhancement of processes, and validation of a strategic plan for configuration management (CM). The approach and methodology used in establishing a strategic plan is the same for any enterprise, including the Department of Energy (DOE), commercial nuclear plants, the Department of Defense (DOD), or large industrial complexes. The principles and techniques presented are used world wide by some of the largest corporations. The authors used industry knowledge and the areas of their current employment to illustrate and provide examples. Developing a strategic configuration and information management plan for DOE Idaho Field Office (DOE-ID) facilities is discussed in this paper. A good knowledge of CM principles is the key to successful strategic planning. This paper will describe and define CM elements and discuss how CM integrates the facility's physical configuration, design basis, and documentation. The strategic plan does not need the support of a computer aided software engineering (CASE) tool. However, the use of the CASE tool provides a methodology for consistency in approach, graphics, and database capability combined to form an encyclopedia and a method of presentation that is easily understood and aids the process of reengineering. CASE tools have much more capability than those stated above. Some examples are supporting a joint application development group (JAD) to prepare a software functional specification document and, if necessary, provide the capability to automatically generate software application code. This paper briefly discusses characteristics and capabilities of two CASE tools that use different methodologies to generate similar deliverables. DOE

N94-13426# Instituto de Pesquisas Espaciais, Sao Jose dos Campos (Brazil).
A MEASUREMENT AND EVALUATION PROCESS MODEL APPLIED TO SOFTWARE ENGINEERING ENVIRONMENTS [UM MODELO PARA O PROCESSO DE MEDICAO E AVALIACAO APLICADO EM AMBIENTES DE ENGENHARIA DE SOFTWARE]
Nilson SantAnna Apr. 1991 37 p In PORTUGESE
(INPE-5345-PUD/048) Avail: CASI HC A03/MF A01

In order to determine the software development processes, it is necessary to have available information about the processes models and the present technology. A possible way to do this is developing studies directed to project environments. These studies can be conducted based on measurement and evaluation mechanisms to capture useful information in order to improve the processes and products quality, increase the productivity and reduce the costs, among other goals. Concepts regarding software engineering area, as well as a model to measurement and evaluation mechanisms in such way that useful information about the processes models and the present technologies (methodologies and tools) can be collected in an organized form. Author

N94-13432# University of Electro-Communications, Tokyo (Japan).
BULLETIN OF THE UNIVERSITY OF ELECTRO-COMMUNICATIONS, VOLUME 6, NO. 1, SERIAL NO. 11
Jun. 1993 129 p In ENGLISH and JAPANESE
Avail: CASI HC A07/MF A02

The following topics are addressed: fabrication of AlGaAs/GaAs-light-emitting devices by selective metalorganic chemical vapor deposition using dialkylmetalchloride; student's works and power supplies in electronic circuit laboratory; on the construction and decoding of hyperelliptic codes; computational Russian morphological generation on Prolog: noun, pronoun, and adjective; designing and generating a GUI module using GUI; codes from an N-dimensional torus simplicially or cellularly decomposed; study of computer system as a musical instrument; analysis of fundamental frequency pattern in speech; reconsideration of the autonomous view of language; and Heidegger's thinking. For individual titles, see N94-13433 through N94-13442.

N94-13433# University of Electro-Communications, Tokyo (Japan).
FABRICATION OF AlGaAs/GaAs-LIGHT-EMITTING DEVICES BY SELECTIVE MOCVD USING DIALKYLMETALCHLORIDE **c33**
Koichi Yamaguchi, Shigeki Kishida, and Kotaro Okamoto *In its* Bulletin of the University of Electro-Communications, Volume 6, No. 1, Serial No. 11 Jun. 1993 p 1-8 In JAPANESE (For primary document see N94-13432 02-61)
Avail: CASI HC A02/MF A02

AlGaAs/GaAs-light-emitting devices were fabricated by selective metalorganic chemical vapor deposition (MOCVD) using dialkylmetalchloride. Polycrystal deposition was effectively suppressed on SiO2-mask surfaces even under atmospheric-pressure conditions. Ridged layers grown on side surfaces provided lateral current confinement and reduced edge leakage. As the results, stable light emission from the selective epitaxial layers was observed by current injection. It was found that it is a useful growth technique for application to integrated optical devices. Author (revised)

N94-13434# University of Electro-Communications, Tokyo (Japan).
STUDENT'S WORKS AND POWER SUPPLIES IN ELECTRONIC CIRCUIT LABORATORY **c33**
Kiyoomi Tanaka, Takashi Warashina, and Yoshihiko Hayakawa *In its* Bulletin of the University of Electro-Communications, Volume 6, No. 1, Serial No. 11 Jun. 1993 p 9-19 In JAPANESE (For primary document see N94-13432 02-61)
Avail: CASI HC A03/MF A02

We have been taking charge of the basic laboratory experiment in Department of Electronics Engineering of UEC and have been performing the maintenance and development of laboratory equipment. We have been taking up the various problems and have been improving the system of laboratory experiments. We are thinking basically as follows. As we provided the environment where students can conduct an experiment freely, they may study methods and skills of engineering according to the plan which he makes by himself. To realize this laboratory system, we have produced the careful selection of subjects, and the increase and improvement of laboratory equipment. We have completed the laboratory system where each student can obtain equipment for the experiment of electronic circuits. Now, we are opening the laboratory of the problem solving method. The faculty provides problems about the subjects, among which a student can choose some and solves them by conducting his experiment without a time limit. This paper describes how the laboratory of electronic circuit has been constructed, changed, and maintained. Author (revised)

N94-13435# University of Electro-Communications, Tokyo (Japan). Dept. of Computer Science and Information Mathematics.
ON THE CONSTRUCTION AND DECODING OF HYPERELLIPTIC CODES
Masazumi Kurihara *In its* Bulletin of the University of Electro-Communications, Volume 6, No. 1, Serial No. 11 Jun. 1993 p 21-28 (For primary document see N94-13432 02-61)
Avail: CASI HC A02/MF A02

Methods of construction and decoding of algebraic geometric codes from hyperelliptic curves are presented. The decoding is able to correct up to ((d*-1)/2) errors and the complexity is O(n(sup 2)), where d* is the designed distance of the code and n is the code length. We decompose t errors into some double errors, where t is less than or equal to ((d*-1)/2). We can treat their errors as ordinary double errors and in parallel.
Author (revised)

N94-13436# University of Electro-Communications, Tokyo (Japan).
COMPUTATIONAL RUSSIAN MORPHOLOGICAL GENERATION ON PROLOG: NOUN, PRONOUN, AND ADJECTIVE
Tetsuya Okamoto, Kayoko Yamamoto, and Yasuo Urai *In its* Bulletin of the University of Electro-Communications, Volume 6, No. 1, Serial No. 11 Jun. 1993 p 29-38 In JAPANESE (For primary document see N94-13432 02-61)
Avail: CASI HC A02/MF A02

An experimental Russian morphological generator on Prolog was outlined. The generator produces all Russian inflected forms, including allomorphs, with their accents. Word dictionary and morphological rewriting rules were defined based on Zaliznyak's theory as well as on school grammars. This word-form generating system was tested on 10,000 words (lexemes) from Karamzin's works. The noun, adjective and pronoun component of the system was described.
Author (revised)

N94-13437# University of Electro-Communications, Tokyo (Japan).
DESIGNING AND GENERATING A GUI MODULE USING GUI
Keita Oosima and Mituo Kobayasi *In its* Bulletin of the University of Electro-Communications, Volume 6, No. 1, Serial No. 11 Jun. 1993 p 39-47 In JAPANESE (For primary document see N94-13432 02-61)
Avail: CASI HC A02/MF A02

Programming of GUI (Graphical User Interface) of an application program is not so easy, that a typical GUI is constructed from ready-made GUI modules. However, a ready-made GUI module often does not fit an application. The authors propose a method of making a GUI module by means of GUI. Based on the method a software tool for designing and generating a GUI module is implemented on the X Window System. Experiments show that the system is useful to get an expected GUI module with ease.
Author

N94-13438# University of Electro-Communications, Tokyo (Japan).
CODES FROM AN N-DIMENSIONAL TORUS SIMPLICIALLY OR CELLULARLY DECOMPOSED
Yoshinori Shimizu and Hirobumi Mizuno *In its* Bulletin of the University of Electro-Communications, Volume 6, No. 1, Serial No. 11 Jun. 1993 p 49-57 In JAPANESE (For primary document see N94-13432 02-61)
Avail: CASI HC A02/MF A02

S. Thomeier showed that linear codes can be constructed on a chain complex. He constructed the codes on an acyclic chain complex. We construct the codes on a non-acyclic chain complex of n-dimensional torus simplicially or cellularly decomposed, and give lengths, dimensions, minimum distances, and generator matrices of the codes.
Author (revised)

N94-13439# University of Electro-Communications, Tokyo (Japan).
STUDY OF COMPUTER SYSTEM AS A MUSICAL INSTRUMENT
Daisuke Sugitani and Yoshimitu Takasawa *In its* Bulletin of the University of Electro-Communications, Volume 6, No. 1, Serial No. 11 Jun. 1993 p 59-68 In JAPANESE (For primary document see N94-13432 02-61)
Avail: CASI HC A02/MF A02

A Computer Music System has become very popular to the people in Japan. But they mostly use it only as something like a recording machine. In music, live performance is the most exciting and important. Why don't people make use of the system in live music ? The main reason is that the system can't respond to our instruction in real time. A new computer music player which follows a human sense through a mouse (input device) is presented. As a result of experiments, our system could play music with human musicians and we found new meanings of the MIDI (Musical Instruments Digital Interface) data.
Author (revised)

N94-13440# University of Electro-Communications, Tokyo (Japan).
ANALYSIS OF FUNDAMENTAL FREQUENCY PATTERN IN SPEECH **c32**
Takeshi Okudera and Yoshimitsu Takasawa *In its* Bulletin of the University of Electro-Communications, Volume 6, No. 1, Serial No. 11 Jun. 1993 p 69-78 In JAPANESE (For primary document see N94-13432 02-61)
Avail: CASI HC A02/MF A02

The fundamental frequency pattern is varied in speech. For example, when we speak angrily, the fundamental frequency is high, and the intonation comes to be deep. Is there a rule about the pattern and speech? The way to analyze the fundamental frequency pattern at an accent part with 2 intervals is suggested. Each interval is the ratio of 2 values of fundamental frequency per Japanese pattern with only 2 parameters. Then, in the experiment, we found out a rule when the pattern was varied in speech.
Author (revised)

N94-13441# University of Electro-Communications, Tokyo (Japan).
RECONSIDERATION OF THE AUTONOMOUS VIEW OF LANGUAGE **c32**
Eijiro Tsuboi *In its* Bulletin of the University of Electro-Communications, Volume 6, No. 1, Serial No. 11 Jun. 1993 p 79-96 In JAPANESE (For primary document see N94-13432 02-61)
Avail: CASI HC A03/MF A02

This paper aims to provide a critical examination of the autonomous view of language espoused in current generative grammar that attributes modular status to the faculty of language which is itself taken to comprise autonomous modular components. Several pieces of supposed evidence for the autonomous thesis are discussed, along with some other related topics, and shown to be critically flawed. It is suggested in conclusion that the status of language as a product of the processes of natural selection and syntacticization should be given more recognition in order to obtain a more realistic and integrating framework for natural language.
Author

N94-13442# University of Electro-Communications, Tokyo (Japan).
HEIDEGGER'S THINKING **c53**
Ichiro Akanuma *In its* Bulletin of the University of Electro-Communications, Volume 6, No. 1, Serial No. 11 Jun. 1993 p 97-10 In JAPANESE (For primary document see N94-13432 02-61)
Avail: CASI HC A02/MF A02

In Heidegger's 'Was heist Denken? (= What is called thinking?)', we meet with a shocking statement 'Die Wissenschaft denkt nicht (= Science does not think.)'. Considering what he truly means by these words, I would like to pursue his way of thinking and his ultimate aim in philosophy. In his lecture 'Gelassenheit (releasement)' given at his home town, Heidegger emphasizes the importance of 'Besinnung (meditative thinking)' in contrast with the overwhelming thinking of today, that is, 'das rechnende Denken (calculative thinking)'. This 'meditative thinking' is what Heidegger has in mind when he says 'science does not think.' I want to reflect upon the way of our life in the age of science and technology through listening to his speech carefully.
Author (revised)

N94-13443*# Stanford Univ., CA. Dept. of Computer Science.
SOFTWARE DESIGN BY REUSING ARCHITECTURES
Sanjay Bhansali and H. Penny Nii Jul. 1992 11 p Revised
(Contract NCC2-7491)
(NASA-CR-194151; NAS 1.26:194151; KSL-92-38) Avail: CASI HC A03/MF A01

Abstraction fosters reuse by providing a class of artifacts that can be instantiated or customized to produce a set of artifacts meeting different specific requirements. It is proposed that significant leverage can be obtained by abstracting software system designs and the design process. The result of such an abstraction is a generic architecture and a set of knowledge-based, customization tools that can be used to instantiate the generic architecture. An approach for designing software systems based on the above idea are described. The approach is illustrated through an implemented example, and the advantages and limitations of the approach are discussed.
Author (revised)

N94-13453# National Aerospace Lab., Tokyo (Japan). Computational Sciences Div.

ANALYSIS AND EFFECTS OF THE NUMBER OF NESTS OF DO LOOPS DURING VECTOR SUPERCOMPUTING [BEKUTORU KEISANKI NIOKERU TAJUU DO RUPU NO KOUSO KU SHORI KOUKA TO SONO KAISEKII]

Masahiro Yoshida Apr. 1992 29 p In JAPANESE
(NAL-TR-1146; JTN-93-80499) Avail: CASI HC A03/MF A01

This paper investigates the efficiency of a programming technique which reduces the number of nests of DO loops to obtain longer vector lengths and higher vectorization ratios in vector supercomputers. The technique is applied to a three dimensional Navier-Stokes code, LANS-3D, and run on a Fujitsu VP-400. Scalar and vector processing times of the original and modified DO loops are compared and analyzed. In addition, a criterion is proposed to determine the technique's effective applicability from using quantitative characteristics of the DO loops. Author (NASDA)

N94-13480# Allied-Signal Aerospace Co., Kansas City, MO.

RAPID INTELLIGENT INSPECTION PROCESS DEFINITION FOR DIMENSIONAL MEASUREMENT IN ADVANCED MANUFACTURING

C. W. Brown Mar. 1993 8 p Presented at the Advanced Technology Program Proposal Meeting, Arlington, TX, 19 Mar. 1993
(Contract DE-AC04-76DP-00613)
(DE93-011271; KCP-613-5172; CONF-9303165-1) Avail: CASI HC A02/MF A01

The Rapid Intelligent Inspection Process Definition (RIIPD) project is an industry-led effort to advance computer integrated manufacturing (CIM) systems for the creation and modification of inspection process definitions. The RIIPD project will define, design, develop, and demonstrate an automated tool (i.e., software) to generate inspection process plans and coordinate measuring machine (CMM) inspection programs, as well as produce support information for the dimensional measurement of piece parts. The goal of this project is to make the inspection and part verification function, specifically CMM measurements, a more effective production support tool by reducing inspection process definition flowtime, creating consistent and standard inspections, increasing confidence of measurement results, and capturing inspection expertise. This objective is accomplished through importing STEP geometry definitions, applying solid modeling, incorporating explicit tolerance representations, establishing dimensional inspection, techniques, embedding artificial intelligence techniques, and adhering to the Dimensional Measuring Interface Standard (DMIS) national standard. DOE

N94-13524# Center for Mathematics and Computer Science, Amsterdam (Netherlands). Computer Science/Software Technology Dept.

ON THE OCCUR-CHECK FREE PROLOG PROGRAMS

Krzysztof R. Apt (Amsterdam Univ., Netherlands.) and Alessandro Pellegrini (Padua Univ., Italy.) Oct. 1992 39 p
(CWI-CS-R9238; ETN-93-94164) Copyright Avail: CASI HC A03/MF A01

In most PROLOG implementations for the efficiency reasons, the so called check is omitted from the unification algorithm. Natural syntactic conditions which allow the occur-check to be safely omitted are presented. The established results apply to most well known PROLOG programs, including those that use difference-lists, and seem to explain why this omission does not lead in practice to any complications. When applying these results to general programs, their usefulness for proving absence of floundering is shown. A program transformation is proposed which transforms every program into a program for which only the calls to the built-in unification predicate need to be resolved by a unification algorithm with the occur-check. ESA

N94-13539 Tel-Aviv Univ. (Israel). Dept. of Solid Mechanics, Materials and Structures.

ROBOT PROGRAMMING, NATURAL COMPUTATION AND CONCEPTUAL GRAPHS M.S. Thesis

Alex Kapitanovsky May 1990 173 p
(ITN-93-85193) Copyright Avail: Issuing Activity (Tel-Aviv Univ., Exact Sciences Library, Ramat Aviv 69978, Israel)

A method is developed for robot program synthesis. Currently, the programming of a robot task is one of the major hurdles of robot application. The automation of robot program synthesis will ease industrial application of robots. In order to develop a support system for robot programming, it is proposed to consider the natural information processing by humans during synthesis and interpretation of robotic programs and then to construct an approximate conceptual model of the dynamically changing real world which is involved. Such a model must be suitable (i.e., representable and executable) for efficient computer processing. This approach enables the proposed system to provide a means for automated (knowledge guided) conversion of a user's request, expressed in a natural language, to the appropriate conceptual model of the required task. This model incorporates the information necessary for understanding, planning, and sensory-guided performance of the required robotic task. In Part A, the overall framework of the system is defined, together with the first phase of an assembly program synthesis: request specification, planning of the valid assembly sequences and determination of the required sources. Part B concerns the final phase of a robot program synthesis and its interpretation in changing conditions. A case study is presented, to illustrate this approach on the large family of multi-axisymmetric components. Author (ISA)

N94-13576# Lawrence Livermore National Lab., CA.

PROGRAMMING THE MULTIMODAL INTERFACE

E. P. Glinert and M. M. Blattner 10 Sep. 1992 8 p Presented at the INTERCHI 1993 Interact and Computation Human Interaction, Amsterdam, Netherlands, 24-29 Apr. 1993
(Contract W-7405-eng-48)
(DE93-013084; UCRL-JC-112195; CONF-9304147-1) Avail: CASI HC A02/MF A01

Fundamental problems will confront those who wish to take full advantage of the power of tomorrow's multimodal environments. We argue that our recently introduced concept of meta-widget, when embedded within a high level, networked user interface server, can support the effective implementation of complex multimedia applications. We develop algorithms which enable a multimodal system to select the 'best' combination of representations for the various 'information packets' in a display at any moment. If no acceptable - combination of available representations can be found, strategies are provided for creating a new and useful, if not beautiful, representation to resolve the impasse. A running example is provided to motivate and clarify the discussion. DOE

N94-13578# Sandia National Labs., Albuquerque, NM.

TEST/ANALYSIS CORRELATION AND MODEL UPDATING OF THE STARS 1 AND 2 MISSILE SYSTEMS

C. W. Fulcher, E. L. Marek, and R. L. Mayes 1992 12 p Presented at the 1st Dynamic Testing Agency/National Agency for Finite Element Methods and Standards International Conference, Milton Keynes, England, 7-9- Jul. 1993
(Contract DE-AC04-76DP-00789)
(DE93-013774; SAND-92-1891C; CONF-930786-1) Avail: CASI HC A03/MF A01

The testing, modeling, and test/analysis correlation of the STARS I & II missile systems is reviewed. The STARS project is described. The system identification methodology is discussed. A series of modal tests designed to characterize the various structural components is summarized. The development and updating of detailed finite element models, in a test/analysis correlation process, is presented. DOE

N94-13586*# Research Inst. for Advanced Computer Science, Moffett Field, CA.

FORMALLY BIORTHOGONAL POLYNOMIALS AND A LOOK-AHEAD LEVINSON ALGORITHM FOR GENERAL TOEPLITZ SYSTEMS

Roland W. Freund (Bell Telephone Labs., Inc., Murray Hill, NJ.) and Hongyuan Zha (Pennsylvania State Univ., University Park.) Sep. 1992 41 p Revised Submitted for publication
(Contracts NCC2-387; DAAL03-90-G-0105)
(NASA-CR-194297; NAS 1.26:194297; RIACS-TR-91-27) Avail: CASI HC A03/MF A01

Systems of linear equations with Toeplitz coefficient matrices arise in many important applications. The classical Levinson algorithm computes solutions of Toeplitz systems with only O(n(sub 2)) arithmetic operations, as compared to O(n(sub 3)) operations that are needed for solving general linear systems. However, the Levinson algorithm in its original form requires that all leading principal submatrices are nonsingular. An extension of the Levinson algorithm to general Toeplitz systems is presented. The algorithm

uses look-ahead to skip over exactly singular, as well as ill-conditioned leading submatrices, and, at the same time, it still fully exploits the Toeplitz structure. In our derivation of this algorithm, we make use of the intimate connection of Toeplitz matrices with formally biorthogonal polynomials.
Author (revised)

N94-13636* National Aeronautics and Space Administration. Lyndon B. Johnson Space Center, Houston, TX.
SIX DEGREE OF FREEDOM (Videotape)
Nov. 1990 Videotape: 7 min. 41 sec. playing time, in color, with sound
(NASA-TM-109295; NONP-VT-93-185310) Avail: CASI VHS A01/BETA A22

This animated clip shows operations of the Six Degree of Freedom (DOF) computer during a simulated mission. The clip is intercut with live video of a shuttle crew 'docking' with Space Station Freedom.
Author (revised)

N94-13688 National Physical Lab., Teddington (England). Materials Metrology Div.
SPECIMEN FILES IN VAMAS STANDARD DATA TRANSFER FORMAT (EXAMPLE 1.TXT TO EXAMPLE 4.TXT)
M. P. Seah and W. A. Dench Mar. 1993 20 p
(NPL-DMM(A)-90; ETN-93-94462) Copyright Avail: National Physical Laboratory, Teddington, Middlesex TW11 0W, United Kingdom HC

So that data may be transferred from institute to institute or from computer to computer, the VAMAS standard data transfer format was established. The VAMAS Format may be used for both exporting and importing data. To assist those writing the imported data software, four examples of files in the Format, which may then be read and manipulated by such software, are provided. If the files are correctly read, many of the basic functions of the reading program will have been tested. Four files are provided on IBM PC readable diskettes in the VAMAS Format, representative of different aspects of the use of the Format. The textual labels and the values of parameters in these examples have no particular significance and do not indicate the approval or support of any particular manufacturer or that any particular instrument can produce the data or conditions recorded in the files. All four examples are purely synthetic. The annotation of these files is given in the annex. ESA

N94-13700# Tulane Univ., New Orleans, LA.
THE 8TH WORKSHOP ON THE MATHEMATICAL FOUNDATIONS OF PROGRAMMING SEMANTICS Progress Report, 1 Apr. 1992 - 31 Mar. 1993
Michael W. Mislove 31 Mar. 1993 4 p Workshop held in Oxford, England, 6-10 Apr. 1992
(Contract N00014-92-J-1480)
(AD-A266436) Avail: CASI HC A01/MF A01

This grant provided support for the Eighth Workshop on the Mathematical Foundations of Programming Semantics, held at the University of Oxford from 6-10 April 1992. The Workshop attracted 101 participants from 13 countries including the United States. Twenty-nine of the participants were graduate students. There were six invited hour talks, and 38 contributed 30-minute talks. These talks ranged from talks on abstract mathematical topics such as topology and category theory, to work on the mathematical foundations underlying semantics issues, to applications of such theories to the semantics of various high-level programming languages. There were two Special Sessions at the Workshop. The first was organized by J.M. Woodcock (Oxford) on Formal Methods and featured a talk by Cliff Jones (Manchester). The second special session was on Linear Logic. It was organized by Samson Abramsky (Imperial College) and featured an address by J.-Y. Girard (Paris), as well as talks by Jean-Marc Andreoli (Muenchen) and Philip Scott (Edinburgh and Ottawa). DTIC

N94-13702# North Carolina Univ., Charlotte. Dept. of Mathematics.
MATHEMATICAL ALGORITHMS FOR MULTIDIMENSIONAL INVERSE SCATTERING PROBLEMS IN INHOMOGENEOUS MEDIUM
Michael V. Klibanov 1992 133 p
(Contract N00014-92-J-1008)
(AD-A266440) Avail: CASI HC A07/MF A02

Multidimensional inverse scattering problems (ISP) in inhomogeneous media have important and extensive applications in many areas of interest to the Navy. Among them are ocean acoustics, electromagnetic properties of sea ice, oceanic biology, and non-invasive testing of some materials, including semiconductors. From mathematical point of view the numerical methods must be based on robust and efficient mathematical algorithms. The development of such algorithms with rapid convergence rates is a challenging task in the theory of multidimensional ISP. In fact, ISP's represent an alternative to the conventional X-ray tomography. The major difficulty of the ISP's is that waves propagate in different (unknown) directions rather than just along straight lines, as it is in the case with X-ray tomography. Thus another term for ISP's is diffusion tomography. We have been working on theoretical studies and computational testing of numerical methods for Inverse Scattering Problems (ISP). Our main efforts have been concentrated on 3-Dimensional ISP. A more minor effort was devoted to 1-D phaseless ISP, that is ISP without phase information. DTIC

N94-13721*# Institute for Computer Applications in Science and Engineering, Hampton, VA.
A DATA DISTRIBUTED PARALLEL ALGORITHM FOR RAY-TRACED VOLUME RENDERING Final Report
Kwan-Liu Ma, James S. Painter (Utah Univ., Salt Lake City.), Charles D. Hansen (Los Alamos National Lab., NM.), and Michael F. Krogh (Los Alamos National Lab., NM.) Washington Aug. 1993 32 p Submitted for publication Sponsored in part by NSF
(Contract NAS1-19480; RTOP 505-90-52-01)
(NASA-CR-191520; NAS 1.26:191520; ICASE-93-59) Avail: CASI HC A03/MF A01

This paper presents a divide-and-conquer ray-traced volume rendering algorithm and a parallel image compositing method, along with their implementation and performance on the Connection Machine CM-5, and networked workstations. This algorithm distributes both the data and the computations to individual processing units to achieve fast, high-quality rendering of high-resolution data. The volume data, once distributed, is left intact. The processing nodes perform local ray tracing of their subvolume concurrently. No communication between processing units is needed during this locally ray-tracing process. A subimage is generated by each processing unit and the final image is obtained by compositing subimages in the proper order, which can be determined a priori. Test results on both the CM-5 and a group of networked workstations demonstrate the practicality of our rendering algorithm and compositing method. Derived from text

N94-13779# Carnegie-Mellon Univ., Pittsburgh, PA. School of Computer Science.
FAIL-SAFE PVM: A PORTABLE PACKAGE FOR DISTRIBUTED PROGRAMMING WITH TRANSPARENT RECOVERY
Juan Leon, Allan L. Fisher, and Peter Steenkiste Feb. 1993 25 p
(Contract MDA972-90-C-0035; ARPA Order 7330)
(AD-A266594; CMU-CS-93-124) Avail: CASI HC A03/MF A01

Through fail-safe PVM we seek to explore fault tolerance for distributed computation from a practical perspective. The fail-safety features are considered to be add-ons to an existing model from distributed computing, VIZ PVM in the prototype. We desire the following from the add-ons, with respect to the base model: (1) Application independence. Fail-safety is provided for arbitrary model programs; (2) Application transparency. Failures are invisible to applications that do not bypass the model; (3) Compatibility. The interfaces presented by the model and the modified model are compatible; (4) External to operating system. The implementation requires only the standard OS interface. This makes it portable, which in turn facilitates heterogeneity and the constitution of systems containing many machines from different administrative domains; (5) Minimal overhead. Minimize overhead during regular execution; and (6) Practicality. The whole system is considered. In particular, the existence of distributed stable storage is not assumed. DTIC

N94-13784*# Jet Propulsion Lab., California Inst. of Tech., Pasadena.
EVENT-DRIVEN SIMULATION IN SELMON: AN OVERVIEW OF EDSE
Nicolas F. Rouquette, Steve A. Chien, and Leonard Charest, Jr. Aug. 1992 19 p
(Contract NAS7-918)
(NASA-CR-194505; JPL-Publ-92-23; NAS 1.26:194505) Avail: CASI HC A03/MF A01

EDSE (event-driven simulation engine), a model-based event-driven simulator implemented for SELMON, a tool for sensor selection and anomaly detection in real-time monitoring is described. The simulator is used in

conjunction with a causal model to predict future behavior of the model from observed data. The behavior of the causal model is interpreted as equivalent to the behavior of the physical system being modeled. An overview of the functionality of the simulator and the model-based event-driven simulation paradigm on which it is based is provided. Included are high-level descriptions of the following key properties: event consumption and event creation, iterative simulation, synchronization and filtering of monitoring data from the physical system. Finally, how EDSE stands with respect to the relevant open issues of discrete-event and model-based simulation is discussed. Author (revised)

N94-13805 Politecnico di Milano (Italy). Dipt. di Elettronica e Informazione.

PROGRAMMING LANGUAGES MADE IN ITALY [I LINGUAGGI DI PROGRAMMAZIONE MADE IN ITALY]

Stefano CrespiReghizzi Jan. 1993 25 p In ITALIAN

(Rept-93-002; ETN-93-94511) Avail: Politecnico di Milano, Piazza Leonardo da Vinci 32, 20133 Milan, Italy HC

A survey of the programming languages and compilers designed in Italy in the early days and especially in the last five years is presented. These include the languages DRAGOON (Distributed Reusable Ada Generation from an Object Oriented Notation); MML/MME (Multi-Microprocessor Environment); ALGRES; Galileo (language for processing of databases based on the semantic concept model and having the structure of a functional language); PROTOB (language and object oriented graphic/icon environment for the design of real time systems, especially in industry); TRIO (real-time implicit O); and two other programming environments, KeyOne (an interactive environment for the design, programming, and documentation of C, C++, Ada, FORTRAN, etc.) and TIP (interactive programming environment in Modula-2 addressing, in particular, introductory courses in informatics). ESA

N94-13807 Politecnico di Milano (Italy). Dipt. di Elettronica e Informazione.

PARAMETER IDENTIFICATION OF A MODEL OF THE PROCESS OF SOFTWARE DEVELOPMENT [IDENTIFICAZIONE DEI PARAMETRI DI UN MODELLO DEL PROCESSO DI SVILUPPO DEL SOFTWARE]

Fabrizio Lorito 1993 16 p In ITALIAN

(Rept-93-008; ETN-93-94515) Avail: Politecnico di Milano, Piazza Leonardo da Vinci 32, 20133 Milan, Italy HC

A description of a dynamical integrated model for the analysis of the software design development process is presented. The possibility of using automatic parameter techniques from real-time data is analyzed. Various possible techniques (random or recursive schemes, with or without gradient use) are analyzed and discussed in relation to their applicability. ESA

N94-13822 Politecnico di Milano (Italy). Dipt. di Elettronica e Informazione.

HYPERTEXT COMPILING TOOLS (HCT): DEVELOPING MODEL BASED APPLICATIONS WITH STANDARD HYPERTEXT SYSTEMS

Andrea Caloini (Nippon Electric Co. Ltd., Kawasaki, Japan.) 1992 28 p

(Rept-92-049; ETN-93-94504) Avail: Politecnico di Milano, Piazza Leonardo da Vinci 32, 20133 Milan, Italy HC

The realization of applications requiring an intensive, organized, authoring effort, such as online documentation, electronic books, or kiosks, that need to be developed accordingly to classical software engineering requirements (maintainability, scalability, documentation, portability, integration, reuse of existing material, versioning, updatability, etc.) is addressed. HCT (Hypertext Compiling Tools), a set of tools to translate hypertext-hypermedia applications designed using a high level model (HDM, Hypermedia Design Model) into applications implemented by a commercial hypertext system (ToolBook), is presented. Although each single tool is specific to either HDM or ToolBook, the approach is presented in a more general way. Results obtained in application development are summarized. ESA

N94-13828*# Texas Univ., Brownsville. Dept. of Mathematics.

EXPLOITING STRUCTURE: INTRODUCTION AND MOTIVATION

Semiannual Status Report, 1 Mar. - 31 Aug. 1993

Zhong Ling Xu 3 Sep. 1993 10 p

(Grant NAG5-2210)

(NASA-CR-194199; NAS 1.26:194199) Avail: CASI HC A02/MF A01

Research activities performed during the period of 29 June 1993 through 31 Aug. 1993 are summarized. The Robust Stability of Systems where transfer function or characteristic polynomial are multilinear affine functions of parameters of interest in two directions, Algorithmic and Theoretical, was developed. In the algorithmic direction, a new approach that reduces the computational burden of checking the robust stability of the system with multilinear uncertainty is found. This technique is called 'Stability by linear process.' In fact, the 'Stability by linear process' described gives an algorithm. In analysis, we obtained a robustness criterion for the family of polynomials with coefficients of multilinear affine function in the coefficient space and obtained the result for the robust stability of diamond families of polynomials with complex coefficients also. We obtained the limited results for SPR design and we provide a framework for solving ACS. Finally, copies of the outline of our results are provided in the appendix. Also, there is an administration issue in the appendix. Author (revised)

N94-13858 Applied Silicon, Inc., Ottawa (Ontario).

VMEC30 PROGRAMMING LIBRARY: REFERENCE MANUAL

Hugh A. Parliament Apr. 1992 52 p

(DSIS-93-00350; CTN-93-60756) Avail: CASI HC A04

The library routines available to programmers developing software for the VMEC30 board in the Adaptive Signal Processing Testbed are described. The various routines are grouped into the following categories: general digital signal processing (DSP) functions, including Fourier transform calculations, power spectrum estimation, and filter calculations; routines available for performing DSP functions on the VMEC30 board or any other TMS320C30 based processing board; VMEC30 executive functions such as memory allocation, initialization, device driver interfaces, interrupt handling, interprocessor communications, and format conversion; and VMEC30 host/interface functions including downloading code, starting programs, resetting the VMEC30, and performing data table and command processing functions. Author (CISTI)

N94-13932*# Research Inst. for Advanced Computer Science, Moffett Field, CA.

USRA/RIACS Final Report, 1 Jul. - 31 Dec. 1992

Joseph Oliger 1992 27 p

(Contract NCC2-387)

(NASA-CR-194334; NAS 1.26:194334) Avail: CASI HC A03/MF A01

The Research Institute for Advanced Computer Science (RIACS) was established by the Universities Space Research Association (USRA) at the NASA Ames Research Center (ARC) on 6 June 1983. RIACS is privately operated by USRA, a consortium of universities with research programs in the aerospace sciences, under a cooperative agreement with NASA. The primary mission of RIACS is to provide research and expertise in computer science and scientific computing to support the scientific missions of NASA ARC. The research carried out at RIACS must change its emphasis from year to year in response to NASA ARC's changing needs and technological opportunities. A flexible scientific staff is provided through a university faculty visitor program, a post doctoral program, and a student visitor program. Not only does this provide appropriate expertise but it also introduces scientists outside of NASA to NASA problems. A small group of core RIACS staff provides continuity and interacts with an ARC technical monitor and scientific advisory group to determine the RIACS mission. RIACS activities are reviewed and monitored by a USRA advisory council and ARC technical monitor. Research at RIACS is currently being done in the following areas: Parallel Computing; Advanced Methods for Scientific Computing; Learning Systems; High Performance Networks and Technology; Graphics, Visualization, and Virtual Environments. Author (revised)

N94-13944 Applied Silicon, Inc., Ottawa (Ontario).

VMEC30 SOFTWARE DEVELOPMENT: TUTORIAL MANUAL

Hugh A. Parliament Sep. 1992 138 p

(DSIS-93-00351; CTN-93-60757) Avail: CASI HC A07

The VMEC30 board is a VME bus based processing board based on the TMS320C30 Digital Signal Processor. A self-contained and self-paced course is presented for learning how to develop software for the VMEC30 board. The tutorial starts with an overview of the VMEC30 hardware, including a memory map of the board and some important registers. The areas of memory that are usable for programs are outlined. The host utilities available for communicating with the VMEC30 monitor are reviewed,

with some information on the monitor commands as well as an example of downloading and running code. The Texas Instruments development tools are then described, detailing the compile/link procedure for software and the use of the simulator. An overview of the VMEC30 library routines available for use is presented, followed by a section on simple programming examples. Helpful hints and programming tips for developing software on the board are included. Author (CISTI)

N94-13990 Applied Silicon, Inc., Ottawa (Ontario).
DEMONSTRATION AND ACCEPTANCE TEST PLAN FOR REAL-TIME EXCISION SOFTWARE ON THE ADAPTIVE SIGNAL PROCESSING TESTBED
Hugh A. Parliament 20 Mar. 1992 9 p
(Contract DREO-W7714-0-9504)
(DSIS-93-00275; CTN-93-60813) Avail: CASI HC A02

The functions to be demonstrated for the acceptance test for the real-time excision software component on the Adaptive Signal Processing Testbed are described. A script outlines the steps to be performed in the demonstration and describes the expected results. A check list is included which indicates which sections were performed successfully and accepted. The operations to be demonstrated are the continuous acquisition mode with power spectrum estimation, the real-time excision software, and the off-line despreading and bit error rate determination software for post-run analysis of the excision system. Author (CISTI)

N94-13995# Laboratoire d'Automatique et d'Analyse des Systemes, Toulouse (France).
TRANSFORMATION AND COMPOSITION OF REFUSAL GRAPHS: TESTABILITY ANALYSIS Ph.D. Thesis - Toulouse Univ.
[TRANSFORMATION ET COMPOSITION DE GRAPHES DE REFUS: ANALYSE DE LA TESTABILITE]
Khalil Drira 1992 170 p In FRENCH
(LAAS-92435; ETN-93-94237) Avail: CASI HC A08/MF A02

Formal Description Techniques (FDT) were developed to assist in the design of complex computing systems. These techniques lead to rigorous validation approaches. The design and validation of distributed computing systems, in particular, that of communicating systems, are presented. Validation concerns the process of checking whether a system implementation conforms to the system's specification. In the framework of a design without within FDT, a homogeneous validation approach, which unified two approaches up to now distinguished, is proposed: verification and conformance testing. The use of a single conformance definition merges the advantages of both approaches: verification's discriminating power resulting from the internal knowledge of the system and conformance testing's generality which can be applied to any implementation. Validation is enhanced by a design assessment based on testability analysis. This consists of investigating testability for each component of a system whose global behavior specification results from the interconnection of several components. The proposed approach considers in the same way either standard testability criteria, or testability analysis of systems that are partially or totally controllable and observable. ESA

N94-14004# Center for Mathematics and Computer Science, Amsterdam (Netherlands). Operations Research, Statistics, and System Theory Dept.
THREE, FOUR, FIVE, SIX OR THE COMPLEXITY OF SCHEDULING WITH COMMUNICATION DELAYS
J. A. Hoogeveen (Princeton Univ., NJ.), J. Lenstra (Technische Univ., Eindhoven, Netherlands.), and B. Veltman Oct. 1992 11 p
(CWI-BS-R9229; ETN-93-94160) Copyright Avail: CASI HC A03/MF A01

A set of unit-time jobs has to be processed on identical parallel machines subject to precedence constraints and unit-time communication delays; does there exist a schedule of length at most L? The problem has two variants, depending on whether the number of machines is restrictively small or not. For the first variant, the question can be answered in polynomial time for $L = 3$ and is NP complete for $L = 4$. The second variant is solvable in polynomial for $L = 5$ and NP complete for $L = 6$. As a consequence, neither of these problems has a polynomial approximation scheme, unless $P = NP$. ESA

N94-14006# Messerschmitt-Boelkow-Blohm G.m.b.H., Munich (Germany). Military Aircraft Div.
MATHEMATICAL OPTIMIZATION: A TOOL FOR AIRCRAFT DESIGN
J. Krammer and O. Sensburg 24 Jul. 1992 14 p Presented at DGLR-Jahrestagung 1992, Bremen, Germany, 29 Sep. - 2 Oct. 1992
(MBB-LME-251-S-PUB-0492; ETN-93-94198) Copyright Avail: CASI HC A03/MF A01

Formal mathematical optimization methods developed for the structural design of aircraft are introduced. Together with reliable analysis programs like finite element methods they provide powerful tools for the structural design. They are efficient in at least two ways: producing designs that meet all specified requirements at minimum weight in one step; relieving the engineer from a time consuming search for modifications that give better results, they allow more creative design modifications. The practical architecture of multidisciplinary design optimization software is discussed. In the case of structural design this is based on three concepts: a structural model, an optimzation algorithm and an optimization model. A powerful optimization code called MBB-LAGRANGE which uses mathematical programming methods to fulfill different constraints simultaneously was developed. Some examples depicting the successful application of the MBB-LAGRANGE code are presented. Results of other optimization codes are also shown. ESA

N94-14014 Applied Silicon, Inc., Ottawa (Ontario).
ASPT SOFTWARE SOURCE CODE: SUN DRIVER PACKAGE
Hugh A. Parliament 17 Aug. 1992 65 p
(Contract DREO-W7714-0-9504)
(DSIS-93-00262; CTN-93-60811) Avail: CASI HC A04

The source code for the Sun driver package which is a component of the Adaptive Signal Processing Testbed is presented. The package consists of device drivers and configuration files, and includes files for generating a Unix kernel that supports access to the VMEC30 board as a Unix character device. CISTI

N94-14016 Applied Silicon, Inc., Ottawa (Ontario).
ASPT SOFTWARE SOURCE CODE: DEVELOPMENT SYSTEM PACKAGE, VME-C30 COMPONENT
Hugh A. Parliament 17 Aug. 1992 151 p
(Contract DREO-W7714-0-9504)
(DSIS-93-00276; CTN-93-60814) Avail: CASI HC A08

The source code for the development system package (VMEC30 component) which is part of the Adaptive Signal Processing Testbed is presented. The source code covers the on-board monitor program for the VMEC30 board. The monitor software consists of control files for building the monitor as well as a mixture of C and assembly language routines for the TMS320C30 digital signal processor. Author (CISTI)

N94-14017 Martec Ltd., Halifax (Nova Scotia).
CMAPP USER'S MANUAL, PART 2
J. C. Wallace and M. W. Chernuka Sep. 1990 42 p
(Contract DREA-W7707-0-0918/01-OSC)
(DSIS-93-00858-Pt-2; DREA-CR-90-442-Pt-2; CTN-93-60838) Avail: CASI HC A03

CMAPP (Composite Material Properties Prediction) is a menu-driven composite material analysis computer program capable of generating effective material properties for particulate, continuous fiber, and platelet composites. Constituent material properties can also be generated from composite properties. A collection of eight micromechanical material models has been incorporated into the CMAPP model library. A hierarchical arrangement of menus is used to guide the user through the process of defining various material parameters, entering all necessary material data, and storing or displaying the results. CMAPP will not only perform a single analysis, but will also perform analyses for a range of volume fractions. The latter option gives the user the ability to investigate the effect that a volume fraction change has on any desired material property. Continued development of CMAPP is expected. It will eventually be a comprehensive composite material property program that will deal with macro-mechanical as well as micro-mechanical properties and will calculate a wide range of material properties. Author (CISTI)

N94-14019# Sandia National Labs., Albuquerque, NM.
VFGEN: A PARALLEL VOLUME FRACTION GENERATOR FOR HYDROCODES
A. L. Ames, A. C. Robinson, and T. L. Edwards 1993 10 p Presented at the Object-Oriented Numerics Conference, Sunriver, OR, 25-27 Apr. 1993
(Contract DE-AC04-76DP-00789)
(DE93-011673; SAND-93-0044C; CONF-9304114-3) Avail: CASI HC A02/MF A01

Mesh generation for hypervelocity impact calculations involves computing the portion of the volume of each cell in a grid filled by a solid object. We have developed a volume fraction generator that supports three-dimensional regular Cartesian grids. It executes on both serial and massively parallel computers, and uses a commercial solid modeler (ACIS) to accurately compute the volume fractions. The volume fraction generator, VFGEN, was developed using an object-oriented paradigm facilitated by the ACIS C++ solid modeler toolkit. Although the underlying problem is embarrassingly parallel, a number of geometric optimizations have been developed to improve speed on serial architectures. The relationship of these optimizations to performance of the algorithm on parallel machines is described. DOE

N94-14039# Norwegian Defence Research Establishment, Kjeller.
DETERMINATION OF POSITION AND ORIENTATION OF RIGID BODIES FROM IMAGE SEGMENTS [BESTEMMELSE AV STIVE LEGEMERS POSISJON OG ORIENTERING UT FRA SEGMENTERTE BILDER]
Mads Egil Henriksveen 11 May 1992 115 p In NORWEGIAN
(FFI-92-4005; ETN-93-94451) Avail: CASI HC A06/MF A02

Scene analysis is connected to image processing and pattern recognition, and can be defined as the determination of a scene description from image data. Examples are determination of types of objects and their position and orientation in the scene. A method for determining the position and orientation (pose) of rigid bodies based on image segments is described. The method takes two inputs: a segment representing the silhouette of the imaged object, whose pose is to be determined; and a geometric model of the object. An estimate of object pose is found by minimizing a deviation measure for the segment and a silhouette of the object described by the geometric model. Results from testing the method on synthetic and real image segments are presented. ESA

N94-14051 Applied Silicon, Inc., Ottawa (Ontario).
VMEC30 SUN SOFTWARE DEVELOPMENT UTILITIES: USER'S MANUAL
Hugh A. Parliament Mar. 1992 30 p
(DSIS-93-00348; CTN-93-60754) Avail: CASI HC A03

The VMEC30 software development utilities consist of the VMEC30 monitor program, the TMS320C30 C compiler/assembler/linker, the Sun workstation based downloading programs, and the common object file format (COFF) utility programs. These utilities provide the necessary functionality for working with the VMEC30 board in the Sun environment. The utilities allow for compilation and linking of code, downloading the code to the board, running the code on the board, and obtaining information about the COFF files generated. The various software development utilities are described in separate sections and examples are presented of interactive sessions with the development tools. Author (CISTI)

N94-14052 Applied Silicon, Inc., Ottawa (Ontario).
VMEC30 SUN DEVICE DRIVERS: USER'S MANUAL
Hugh A. Parliament Mar. 1992 17 p
(DSIS-93-00349; CTN-93-60755) Avail: CASI HC A03

The VMEC30 board is a TMS320C30 processor board that interfaces to the VMEbus. The board may be installed in the VMEbus of a Sun workstation. In order to access and interface programs to the board, two SUNOS (UNIX) device drivers are provided for each board, the host port driver and the DMA port driver. The use of these drivers for input-output and for VMEC30 board control operations is described along with instructions on how to install them into the SUNOS kernel. Examples of accessing the boards are provided as a reference for the user. Author (CISTI)

N94-14088 Odyssey Research Associates, Inc., Ottawa (Ontario).
EVES: AN OVERVIEW
Dan Craigen, Sentot Kromodimoeljo, Irwin Meisels, Bill Pase, and Mark Saaltink 1 Mar. 1991 23 p
(Contract DSS-W2207-8-AF78)
(DSIS-93-00238; ORA-CP-91-5402-43; CTN-93-60804) Avail: CASI HC A03/MF A01

A new formal methods tool called EVES is described, consisting mainly of a set theoretic-based language called Verdi and an automated deduction system called NEVER. The primary purpose of the EVES project was to develop a software verification system, integrating state of the art techniques from automated deduction, mathematics, language design, and formal methods, so that the system is both sound and useful. An overview of the various aspects of EVES is presented and illustrated by two small examples. The success of the development of EVES has been demonstrated, in part, by the ability to specify, implement, and prove a substantial application: the PICO language interpreter. CISTI

N94-14139*# College of William and Mary, Williamsburg, VA. Dept. of Computer Science.
A DESIGN METHODOLOGY FOR PORTABLE SOFTWARE ON PARALLEL COMPUTERS Final Research Report
David M. Nicol, Keith W. Miller, and Dan A. Chrisman 9 Aug. 1993 59 p
(Grant NAG1-995)
(NASA-CR-194181; NAS 1.26:194181) Avail: CASI HC A04/MF A01

This final report for research that was supported by grant number NAG-1-995 documents our progress in addressing two difficulties in parallel programming. The first difficulty is developing software that will execute quickly on a parallel computer. The second difficulty is transporting software between dissimilar parallel computers. In general, we expect that more hardware-specific information will be included in software designs for parallel computers than in designs for sequential computers. This inclusion is an instance of portability being sacrificed for high performance. New parallel computers are being introduced frequently. Trying to keep one's software on the current high performance hardware, a software developer almost continually faces yet another expensive software transportation. The problem of the proposed research is to create a design methodology that helps designers to more precisely control both portability and hardware-specific programming details. The proposed research emphasizes programming for scientific applications. We completed our study of the parallelizability of a subsystem of the NASA Earth Radiation Budget Experiment (ERBE) data processing system. This work is summarized in section two. A more detailed description is provided in Appendix A ('Programming Practices to Support Eventual Parallelism'). Mr. Chrisman, a graduate student, wrote and successfully defended a Ph.D. dissertation proposal which describes our research associated with the issues of software portability and high performance. The list of research tasks are specified in the proposal. The proposal 'A Design Methodology for Portable Software on Parallel Computers' is summarized in section three and is provided in its entirety in Appendix B. We are currently studying a proposed subsystem of the NASA Clouds and the Earth's Radiant Energy System (CERES) data processing system. This software is the proof-of-concept for the Ph.D. dissertation. We have implemented and measured the performance of a portion of this subsystem on the Intel iPSC/2 parallel computer. These results are provided in section four. Our future work is summarized in section five, our acknowledgements are stated in section six, and references for published papers associated with NAG-1-995 are provided in section seven. Derived from text

N94-14176# Los Alamos National Lab., NM.
DISTRIBUTED PROCESSOR MONTE CARLO: MCNP RESULTS ON A 16-NODE IBM CLUSTER
G. W. McKinney 1993 8 p Presented at the Advanced Monte Carlo Computer Programs for Radiation Transport, Saclay, France, 27-29 Apr. 1993
(Contract W-7405-eng-36)
(DE93-012639; LA-UR-93-1338; CONF-9304131-1) Avail: CASI HC A02/MF A01

The advent of high-performance computer systems has brought to maturity programming concepts like vectorization, multiprocessing, and multitasking. Although there are many schools of thought as to the most significant factor in obtaining order-of-magnitude increases in performance, such speedup can only be achieved by integrating the computer system, and application code. Vectorization leads to faster manipulation of arrays by overlapping instruction CPU cycles. Discrete ordinates codes, which

require the solving of large matrices, have proved to be major benefactors of vectorization. Monte Carlo transport, on the other hand, typically contains numerous logic statements and requires extensive redevelopment to benefit from vectorization. Multiprocessing and multitasking provide additional CPU cycles via multiple processors. Such systems are generally designed with either common memory access or distributed memory access. In both cases, theoretical speedup, as a function of the number of processors (P) and the fraction of task time that multiprocesses (f), can be formulated using Amdahl's Law S(f, P) = 1/(1 (minus) f + f /P). However, for most applications this theoretical limit cannot be achieved, due to additional terms not included in Amdahl's Law. Monte Carlo transport is a natural candidate for multiprocessing, since the particle tracks are generally independent, and the precision of the result increases as the square root of the number of particles tracked. DOE

N94-14190# European Space Agency, Paris (France). ESA Board for Software Standardization and Control.
GUIDE TO THE SOFTWARE ARCHITECTURAL DESIGN PHASE
Jan. 1992 76 p
(ESA-PSS-05-04-Issue-1; ETN-93-93965) Copyright Avail: CASI HC A05/MF A01

The software engineering standards to be applied for all deliverable software implemented for the European Space Agency are described. The first phase of the software development, the output of this phase and the second phase, concerning the architecture design, are summarized. The architectural design phase defines the software in terms of the major software components and interfaces, and covers all the software requirements. The document is a guide on how to produce the architectural design. Methods, tools, and how to write the architectural design definition, starting from a template, are provided. The life cycle management activities and all relevant mandatory practices are included. ESA

N94-14191# European Space Agency, Paris (France).
GUIDE TO THE SOFTWARE DETAILED DESIGN AND PRODUCTION PHASE
May 1992 100 p
(ESA-PSS-05-05-Issue-1; ETN-93-93966) Copyright Avail: CASI HC A05/MF A02

The software engineering standards to be applied for all deliverable software implemented for the European Space Agency are described. The second phase of the software development concerning the architecture design, the output of this phase and the third phase, concerning production and design are summarized. The design phase can be called the implementation phase because developers code, document and test the software after detailing the design specified in the architectural design document. The document is a guide on how to produce the design document and the software user manual. Methods, tools and how to write the design document, starting from templates are provided. The life cycle management activities all relevant mandatory practives are included. ESA

N94-14197 Applied Silicon, Inc., Ottawa (Ontario).
ASPT SOFTWARE SOURCE CODE: HOST DEVELOPMENT SYSTEM PACKAGE
Hugh A. Parliament 17 Aug. 1992 120 p
(Contract DREO-W7714-0-9504)
(DSIS-93-00277; CTN-93-60815) Avail: CASI HC A06

The source code is presented for the development system package, host component, which is part of the Adaptive Signal Processing Testbed. The package consists of files grouped into three distinct modules: the VC30 downloader module, the remote terminal module, and the common object file format utilities. Author (CISTI)

N94-14200# National Research Council of Canada, Ottawa (Ontario). Inst. for Information Technology.
DISCRETE EVENT SIMULATION USING OBJECT-ORIENTED PROGRAMMING: APPLICATION TO MANUFACTURING
H. Atabakhsh and A. W. Chan May 1992 39 p
(ERB-1037; NRC-33188; CTN-93-60821) Copyright Avail: CASI HC A03/MF A01

Discrete event simulation following the traditional approach of event scheduling has been implemented using the object oriented paradigm. Concepts and terminology in object oriented programming are reviewed and implications of using this paradigm for discrete event simulation are discussed. To illustrate the concepts, an example in the field of discrete parts manufacturing has been implemented in Smalltalk-80. The approach used is, however, generic and can be implemented in other object oriented programming environments and applied to other domains in discrete event simulation. A brief comparison is also made between this approach and the implementation of discrete event simulation based on the multiprocessing approach proposed by Goldberg and Robson (1989). Author (CISTI)

N94-14207 Operational Research and Analysis Establishment, Ottawa (Ontario). Directorate of Land Operational Research.
GROUND ATTACK PROFILE SELECTOR PROGRAM, VERSION 3.0
Tom Whiteford Jan. 1993 93 p
(DSIS-93-00702; ORAE-DLOR-RN-92-4; CTN-93-60840) Avail: CASI HC A05

The Ground Attack Profile Selector version 3.0 is an interactive program written in C language which allows the user to construct a three dimensional flight profile of an aircraft. Perspective views of 100-m resolution digital terrain data from the Carmonette database were produced on a Silicon Graphics workstation to increase the realism of the flight profile. This new version expands on the overall graphics presentation of the terrain and translates the program to the lower level C programming code. The theory and the algorithms developed in the previous versions of the program are documented, and the new graphics routines are explained. A listing of the main program and subroutines is included. Author (CISTI)

N94-14289# Lawrence Livermore National Lab., CA.
PC VIRUSES: HOW DO THEY DO THAT?
K. Pichnarczyk Jul. 1992 10 p Presented at the Workshop on Computer Security Incident Handling, Denver, CO, Aug. 1992
(Contract W-7405-eng-48)
(DE93-012581; UCRL-JC-111212; CONF-9208108-2) Avail: CASI HC A02/MF A01

The topic of PC Viruses has been an issue for a number of years now. They've been reported in major newspapers, tabloids, television, and radio. People from all fields get viruses: government, private sector businesses, home computers, schools, and computer software suppliers. A definition is proposed to introduce the virus phenomenon. Virus authors come from a variety of communities. Motives and ideologies of authors are discussed, and examples of viruses are offered. Also mentioned is the growing number of viruses developed, isolated, and never distributed to the public at large, but kept within the antivirus research community. Virus examples are offered as well. Viruses are distributed not only through bulletin boards and shareware, but also from areas previously assumed to be safe, including the threat of receiving a virus through a standard in-house function, such as an in-house hardware maintenance shop. Three categories of viruses are presented: File Infecter viruses, Boot Sector Infecters, and the new category of Directory Entry Infecter virus. Also discussed are crossover viruses, that is, viruses which utilize a variety of techniques to ensure survival. An explanation of what is occurring within every stage of various viruses is given. Replication strategies common to all three types are noted, mainly the two different replication strategies of memory resident infecters and active selection infecters. A detailed definition, description, and application of a stealth virus is presented. Detection strategies are discussed as each topic in this section is completed; a high level schemata of the operation of various virus detection programs ispresented. Since most eradication today is done using virus detection/eradication software, this paper attempts to reveal the techniques used by these packages. Included in the paper is the topic of manual eradication. DOE

N94-14295# Sandia National Labs., Albuquerque, NM.
CENTER OF TRACE ALGORITHMS FOR EXTRACTING DIGITIZED WAVEFORMS FROM TWO-DIMENSIONAL IMAGES
J. W. Lee May 1993 27 p
(Contract DE-AC04-76DP-00789)
(DE93-015082; SAND-93-1011) Avail: CASI HC A03/MF A01

A class of recording instruments records high-frequency signals as a two-dimensional image rather than converting the analog signal directly to digital output. This report explores the task of reducing the two-dimensional trace to a uniformly sampled waveform that best represents the signal characteristics. Many recorders provide algorithms for locating the center

of trace. The author discusses these algorithms and alternative algorithms, comparing their effectiveness. DOE

N94-14368*# Research Inst. for Computing and Information Systems, Houston, TX.

INTEGRATING INTERFACE SLICING INTO SOFTWARE ENGINEERING PROCESSES

Jon Beck (West Virginia Univ., Morgantown.) 15 Aug. 1993 10 p
(Contract NCC9-16)
(NASA-CR-192761; NAS 1.26:192761) Avail: CASI HC A02/MF A01

Interface slicing is a tool which was developed to facilitate software engineering. As previously presented, it was described in terms of its techniques and mechanisms. The integration of interface slicing into specific software engineering activities is considered by discussing a number of potential applications of interface slicing. The applications discussed specifically address the problems, issues, or concerns raised in a previous project. Because a complete interface slicer is still under development, these applications must be phrased in future tenses. Nonetheless, the interface slicing techniques which were presented can be implemented using current compiler and static analysis technology. Whether implemented as a standalone tool or as a module in an integrated development or reverse engineering environment, they require analysis no more complex than that required for current system development environments. By contrast, conventional slicing is a methodology which, while showing much promise and intuitive appeal, has yet to be fully implemented in a production language environment despite 12 years of development. Author (revised)

N94-14399# Sandia National Labs., Albuquerque, NM.

AN EFFICIENT PARALLEL ALGORITHM FOR MATRIX-VECTOR MULTIPLICATION

B. Hendrickson, R. Leland, and S. Plimpton Mar. 1993 21 p
(Contract DE-AC04-76DP-00789)
(DE93-015125; SAND-92-2765) Avail: CASI HC A03/MF A01

The multiplication of a vector by a matrix is the kernel computation of many algorithms in scientific computation. A fast parallel algorithm for this calculation is therefore necessary if one is to make full use of the new generation of parallel supercomputers. This paper presents a high performance, parallel matrix-vector multiplication algorithm that is particularly well suited to hypercube multiprocessors. For an n x n matrix on p processors, the communication cost of this algorithm is O(n/(radical)p + log(p)), independent of the matrix sparsity pattern. The performance of the algorithm is demonstrated by employing it as the kernel in the well-known NAS conjugate gradient benchmark, where a run time of 6.09 seconds was observed. This is the best published performance on this benchmark achieved to date using a massively parallel supercomputer. DOE

N94-14435# Lawrence Livermore National Lab., CA.

COMPUTATIONAL MECHANICS AND SUPERCOMPUTING AT LLNL

G. L. Goudreau Oct. 1992 9 p Presented at the Winter Annual Meeting of the American Society of Mechanical Engineers, Anaheim, CA, 8-13 Nov. 1992
(Contract W-7405-eng-48)
(DE93-016453; UCRL-JC-112000; CONF-921110-52) Avail: CASI HC A02/MF A01

This report discusses: evolution of Methods Development Group (MDG) codes on CRAY computers; MDG collaborators program; transition to distributed computing; and new mechanics and new supercomputers. DOE

N94-14470# Westinghouse Savannah River Co., Aiken, SC.

REVIEWS OF COMPUTING TECHNOLOGY: OBJECT-ORIENTED TECHNOLOGY

D. C. Skeen 1 Mar. 1993 56 p
(Contract DE-AC09-89SR-18035)
(DE93-014740; WSRC-IM-90-83-9) Avail: CASI HC A04/MF A01

A useful metaphor in introducing object-oriented concepts is the idea of a computer hardware manufacturer assembling products from an existing stock of electronic parts. In this analogy, think of the parts as pieces of computer software and of the finished products as computer applications. Like its counterpart, the object is capable of performing its specific function in a wide variety of different applications. The advantages to assembling hardware using a set of prebuilt parts are obvious. The design process is greatly simplified in this scenario, since the designer needs only to carry the design down to the chip level, rather than to the transistor level. As a result, the designer is free to develop a more reliable and feature rich product. Also, since the component parts are reused in several different products, the parts can be made more robust and subjected to more rigorous testing than would be economically feasible for a part used in only one piece of equipment. Additionally, maintenance on the resulting systems is simplified because of the part-level consistency from one type of equipment to another. The remainder of this document introduces the techniques used to develop objects, the benefits of the technology, outstanding issues that remain with the technology, industry direction for the technology, and the impact that object-oriented technology is likely to have on the organization. While going through this material, the reader will find it useful to remember the parts analogy and to keep in mind that the overall purpose of object-oriented technology is to create software parts and to construct applications using those parts. DOE

N94-14472*# Research Inst. for Computing and Information Systems, Houston, TX.

ON-LINE UPGRADE OF PROGRAM MODULES USING AdaPT Technical Report, 1 May 1990 - 31 Mar. 1993

Raymond S. Waldrop (Texas A&M Univ., College Station.), Richard A. Volz (Texas A&M Univ., College Station.), Gary W. Smith (Texas A&M Univ., College Station.), Stephen J. Goldsack (Imperial Coll. of Science and Technology, London, England.), and A. A. Holzbach-Valero (Imperial Coll. of Science and Technology, London, England.) 17 Jun. 1993 34 p
(Contract NCC9-16; RICIS Proj. SE-35)
(NASA-CR-194331; NAS 1.26:194331) Avail: CASI HC A03/MF A01

One purpose of our research is the investigation of the effectiveness and expressiveness of AdaPT, a set of language extensions to Ada 83, for distributed systems. As a part of that effort, we are now investigating the subject of replacing, e.g. upgrading, software modules while the software system remains in operation. The AdaPT language extensions provide a good basis for this investigation for several reasons: they include the concept of specific, self-contained program modules which can be manipulated; support for program configuration is included in the language; and although the discussion will be in terms of the AdaPT language, the AdaPT to Ada 83 conversion methodology being developed as another part of this project will provide a basis for the application of our findings to Ada 83 and Ada 9X systems. The purpose of this investigation is to explore the basic mechanisms of the replacement process. With this purpose in mind, we will avoid including issues whose presence would obscure these basic mechanisms by introducing additional, unrelated concerns. Thus, while replacement in the presence of real-time deadlines, heterogeneous systems, and unreliable networks is certainly a topic of interest, we will first gain an understanding of the basic processes in the absence of such concerns. The extension of the replacement process to more complex situations can be made later. A previous report established an overview of the module replacement problem, a taxonomy of the various aspects of the replacement process, and a solution to one case in the replacement taxonomy. This report provides solutions to additional cases in the replacement process taxonomy: replacement of partitions with state and replacement of nodes. The solutions presented here establish the basic principles for module replacement. Extension of these solutions to other more complicated cases in the replacement taxonomy is direct, though requiring substantial work beyond the available funding. Derived from text

N94-14496 Institute for Aerospace Research, Ottawa (Ontario). Structures and Materials Lab.

A DESCRIPTION OF THE COMPUTER PROGRAM CALDK38 WHICH CONTROLS INSTRUMENTATION SET-UP AND DATA ACQUISITION DURING DEADWEIGHT CALIBRATION USING AN HBM DK 38 S6 DIGITAL MEASURING UNIT

C. W. MacKenzie Jul. 1993 147 p
(LTR-ST-1935; CTN-93-60862) Avail: Micromedia Ltd., Technical Information Centre, 165 Hotel de Ville, Place du Portage, Phase 2, Hull, Quebec J8X 3X2, Canada HC/MF

The calibration of force transducers, using deadweight machines to apply the force and electronic manually-read readout instruments to measure the transducer output, has been a tedious, time consuming task because of the more than 90 readings required for a typical calibration. High precision, computer controllable digital measuring systems can aid considerably in

this task. A description is presented of such a system (the DK 38 S6 by Hottinger Baldwin Messtechnik) and the computer code CALD38.BAS that was developed for it. CALD38.BAS is the main control and data acquisition program for performing a 3 run, 30 reading calibration. The measuring unit, computer hardware, and program modules are described with sufficient detail to allow a user to run the program and make minor programming modifications if required; however, a detailed calibration procedure or operations/reference manual is not provided. CISTI

N94-14505 Tel-Aviv Univ. (Israel). Dept. of Computer Science.
IMPLEMENTATION AND EXPERIMENTATION WITH A MOTION PLANNING SYSTEM M.S. Thesis
Amir Livne Jun. 1991 100 p
(ITN-93-85213) Copyright Avail: Issuing Activity (Tel-Aviv Univ., Exact Sciences Library, Ramat Aviv 69978, Israel)

In the present work, a system was implemented and used experimentally for solving the general motion planning problem with two degrees of freedom. The algorithm on which the work is based can solve any motion planning problem with two degrees of freedom; it is both asymptotically efficient, with a slightly super-linear running time, and relatively simple. Experiments with the system have shown that in some, non-trivial cases, the actual running time is favorable. The theoretical background of the work is described, with details of the implementation and experimental results. Chapter 1 is an introduction to the thesis. Chapter 2 outlines the theoretical background of the motion planning problem with two degrees of freedom and the general solution. Chapter 3 describes the implementation of the system. The goals of the implementation, mainly that the system work for real-life inputs and that the system will be easy to expand, are discussed. The input, ouput and logic of the system are also described. Chapter 4 describes experimentation with the system. A few instances of the motion planning problem with two degrees of freedom that the system is able to solve are discussed and performance-related data are given. Chapter 5 is a manual for a would-be user who may wish to expand or modify the system. The architecture, interfaces, and data-structures of the system are explained. A number of possible expansions of the system are described. Finally, in Chapter 6, various outputs of the system are given.
Author (ISA)

N94-14515# Oak Ridge National Lab., TN.
ORGBUG: A WINDOWS-BASED COMBINATORIAL GEOMETRY DEBUGGER
T. J. Burns Jun. 1993 21 p
(Contract DE-AC05-84OR-21400)
(DE93-016640; ORNL/TM-12020) Avail: CASI HC A03/MF A01

ORGBUG is the second half of a two part graphical display and debugging system for combinatorial geometry. The first part of the system consists of a 'view' generator, CGVIEW. ORGBUG itself is a Microsoft Windows-based application designed to run on a 386 personal computer and to display the 'view' produced by CGVIEW as an aid to debugging. ORGBUG also includes specific tools to facilitate the identification of geometric features which are inconsistent or in error. DOE

N94-14521# Lawrence Livermore National Lab., CA.
AN OVERVIEW OF PARALLEL SCIENTIFIC VISUALIZATION
S. Whitman Apr. 1993 12 p Presented at the 1st Bilkent Computer Graphics Conference: Advanced Techniques in Animation, Rendering, and Visualization, Ankara, Turkey, 12-14 Jul. 1993
(Contract W-7405-eng-48)
(DE93-017105; UCRL-JC-113690; CONF-9307104-1) Avail: CASI HC A03/MF A01

In this document, the usage of high performance computers (SIMD, MIMD, and vector) for scientific visualization is discussed. Various institutions and companies are investigating how to best utilize supercomputers and massively parallel processors for visualizing scientific data. Approaches which have been taken include the use of visualization servers, parallelizing existing commercial scientific visualization packages, and custom solutions utilizing various high performance computers. A synopsis of some recent approaches is included, and a brief analysis as to the applicability of the various efforts is offered. DOE

N94-14528# Sandia National Labs., Albuquerque, NM.
ENTERPRISE INTEGRATION: A TOOL'S PERSPECTIVE
J. Polito, A. Jones (National Inst. of Standards and Technology, Gaithersburg, MD.), and H. Grant (National Science Foundation, Washington, DC.) 1993 19 p Presented at the NATO Advanced Research Workshop on Integration: Information and Collaboration Models, Il Ciocca, Italy, 6-11 Jun. 1993
(Contract DE-AC04-76DP-00789)
(DE93-015651; SAND-93-1386C; CONF-9306195-1) Avail: CASI HC A03/MF A01

The advent of sophisticated automation equipment and computer hardware and software is changing the way manufacturing is performed. To compete in the global marketplace, manufacturing companies must integrate these new technologies into their factories. In addition, they must integrate the planning, control, and data management methodologies needed to make effective use of these technologies. This paper provides an overview of recent approaches to achieving this enterprise integration. It then describes, using simulation as a particular example, a new tool's perspective of enterprise integration. DOE

N94-14556 Tel-Aviv Univ. (Israel).
PARADIGMS FOR VERY FAST PARALLEL ALGORITHMS Ph.D. Thesis
Omer Berkman 1 Aug. 1989 116 p
(ITN-93-85212) Copyright Avail: Issuing Activity (Tel-Aviv Univ., Exact Sciences Library, Ramat Aviv 69978, Israel)

Unusually fast parallel algorithms are presented for several problems. All use abstract parallel computation models which are members of the parallel random access machine (PRAM) family. All the algorithms have a linear time-processor product and are, therefore, optimal. Merging and prefix-minima problems run in triply-logarithmic time. It is shown that, by using the fast algorithms for merging, two sorted arrays of numbers in the domain (1...s) can be merged in O(log log log s) time using an optimal number of processors and O(ns(exp epsilon)) space. An algorithm is given for the prefix-minima problem, which runs in O(log log log s) time, using an optimal number of processors and O(ns(exp epsilon)) space on a Priority CRCW PRAM. These new algorithms for merging and prefix-minima suggest that the current lower bounds for minimum and merging are not satisfactory and that future research should try to consider the domain of the input. Problems which run in log-star time include the level-ancestor and the prefix-minima problems. A class of algorithms was developed which run in Inverse-Ackerman time, O(alpha(n)) time, in which alpha(n) is the inverse of the extremely slow-growing Ackerman's function. These algorithms are enabled to run by means of the recursive star-tree parallel data structure. Star-tree applications include the Lowest-Common Ancestor, the Parentheses Matching and the Inverse-Ackerman Time Reducibilities problems. On the CRCW-bit PRAM, a non-standard PRAM version, the above three problems which require Inverse-Ackerman running time can be solved in constant time using n processors or in other words are fully-parallelizable. ISA

N94-14571# Pacific Northwest Lab., Richland, WA.
THEORY, MODELING, AND SIMULATION
May 1993 103 p
(Contract DE-AC06-76RL-01830)
(DE93-015607; PNL-8642) Avail: CASI HC A06/MF A02

This report briefly discusses research on the following topics: development of electronic structure methods; modeling molecular processes in clusters; modeling molecular processes in solution; modeling molecular processes in separations chemistry; modeling interfacial molecular processes; modeling molecular processes in the atmosphere; methods for periodic calculations on solids; chemistry and physics of minerals; graphical user interfaces for computational chemistry codes; visualization and analysis of molecular simulations; integrated computational chemistry environment; and benchmark computations. DOE

N94-14581# Superconducting Super Collider Lab., Dallas, TX.
INTEGRATING PAW, A GRAPHICAL ANALYSIS INTERFACE TO SYBASE
A. Fry and I. Chow Apr. 1993 10 p Presented at the 5th Annual International Industrial Symposium on the Super Collider and Exhibition, San Francisco, CA, 6-8 May 1993
(Contract DE-AC35-89ER-40486)
(DE93-014172; SSCL-Preprint-218; CONF-930537-35) Avail: CASI HC A02/MF A01

The program PAW (Physics Analysis Workstation) enjoys tremendous

popularity within the high energy physics community. It is implemented on a large number of platforms and is available to the high energy physics community free of charge from the CERN computing division. PAW combines extensive graphical display capability (HPLOT/HIGZ), with histogramming (HBOOK4), file and data handling (ZEBRA), vector arithmetic manipulation (SIGMA), user defined functions (COMIS), powerful function minimization (MINUIT), and a command interpreter (KUIP). To facilitate the possibility of using relational databases in physics analysis, we have added an SQL interface to PAW. This interface allows users to create PAW N-tuples from Sybase tables and vice versa. We discuss the implementations below. DOE

N94-14696# Oak Ridge National Lab., TN.
SWITCHOVER SOFTWARE RELIABILITY ESTIMATE FOR PADUCAH FREEZER/SUBLIMER COMPUTER SYSTEMS
D. M. Flanagan and J. N. Davis Apr. 1993 74 p
(Contract DE-AC05-84OR-21400)
(DE93-013844; ORNL/TM-12234) Avail: CASI HC A04/MF A01

The K-25 Engineering Division purchased a series of redundant computer systems and developed software for the purpose of providing continuous process monitoring and control for the Freezer/Sublimer equipment in the gaseous diffusion process at the Paducah Gaseous Diffusion Plant. The application software is loaded on two central processing units (CPU) so that in the event of the failure of the primary unit, the processing can switch to the backup unit and continue processing without error. It is the purpose of this document to demonstrate the reliability of this system with respect to its ability to switch properly between redundant CPUs. The total reliability estimation problem--which considers the computer hardware, the operating system software, and the application software--has been reduced to one that considers only the application software directly involved in the switchover process. Estimates are provided for software reliability and the testing coverage. Software and hardware reliability models and reliability growth models are considered in addition to Bayesian approaches. DOE

N94-14712# Laboratoire d'Automatique et d'Analyse des Systemes, Toulouse (France). Groupe Decentralisation, Hierarchisation, et Parallelisme en Optimisation et Commande.
ON THE SOLUTION OF A CLASS OF GRAPH PROBLEMS BY PARALLEL ALGORITHMS Ph.D. Thesis - Toulouse Univ. [CONTRIBUTION A LA RESOLUTION DE PROBLEMES D'OPTIMISATION DANS LES GRAPHES PAR DES ALGORITHMES PARALLELES]
Thierry Gayraud 1992 150 p In FRENCH
(LAAS-92514; ETN-93-94362) Avail: CASI HC A07/MF A02

Basic concepts on models of parallel computation and parallel computers are examined. The two parallel computers used for experiments are described: Sequent Balance machine (10 processors shared memory MIMD computer) and T-Node machine (32 processor distributed memory MIMD commuter). The parallel algorithms proposed to solve three graph problems are considered. The first problem is all-pairs shortest path problem. Two parallel algorithms are designed. The first one based on Floyd-Warshall sequential algorithm uses data partitioning. The second one based on Dijkstra algorithm uses a Fibonacci heap data structure in order to reduce algorithm complexity. Implementations on the two kinds of parallel computers are described. The second problem is the minimum spanning tree problelm. Two parallel algorithms are designed. They use a graph decomposition technique with overlapping and it is proved that the global solution is included into the unions of local solutions. One is based on Krustkal algorithm, the other on Prim algorithm and Fibonacci heap and their experimental results are discussed. The third problem is the Steiner minimum tree problem which is a NP-Complete problem. Only heuristics can be used to solve large instances. A new class of sequential and parallel heuristics based on shortest path techniques is proposed. The complexity of these heuristics was reduced by using Fibonacci heaps and the speed up of the parallel heuristics is almost linear. ESA

N94-14714# Laboratoire d'Automatique et d'Analyse des Systemes, Toulouse (France).
VERIFICATION OF CRITICAL SOFTWARE BY STATISTICAL TESTING Ph.D. Thesis - Toulouse Univ. [VERIFICATION DE LOGICIELS CRITIQUES PAR LE TEST STATISTIQUE]
Helene Waeselynck 1993 181 p In FRENCH
(LAAS-93006; ETN-93-94364) Avail: CASI HC A09/MF A02

The use of statistical testing as a verification technique for critical software, that is, software having ultra high dependability requirements, is considered. Statistical testing involves exercising a program with random inputs, the test profile and the number of generated inputs being determined according to criteria based on software structure or software functionalities: the probabilistic generation allows the imperfect connection of current criteria with respect to the faults they aim at tracking down to be compensated, making them quite insufficient for critical software. The potentialities of this approach are justified by studying the theoretical reasons for a test to be unsuccessful: its feasibility and efficiency are confirmed by experiments involving a software from the nuclear field. As regards unit testing, the proposed approach combines structural statistical testing with a separate deterministic test of extremal values. As regards testing complex software components, random input data are designed from behavioral models extracted from the specification. Classical models are first investigated (finite state machines and decision tables); then the approach is refined by considering more sophisticated models, namely Statecharts. ESA

N94-14813# Grenoble-1 Univ. (France). Inst. d'Informatique et Mathematiques Appliquees.
ROBUST NON CONVEX OPTIMIZATION ALGORITHMS: CODES AND NUMERICAL SIMULATION OF LARGE SCALE Ph.D. Thesis [ALGORITHMES ROBUSTES EN OPTIMISATION NON CONVEXE. CODES ET SIMULATIONS NUMERIQUES EN GRANDE DIMENSION]
Abderrazek Chine 1991 177 p In FRENCH
(ETN-93-94354) Avail: CASI HC A09/MF A02

Some non-convex optimization algorithms, the implementation of codes devoted to industrial application, and numerical simulations of concrete problems of large scale were studied. Quadratic problems (convex or not convex) with linear or quadratic constraints as well as constrained or unconstrained trust region methods to minimize a smooth function were studied. The non-convex optimization (classification, duality, stability and subgradient algorithms) were addressed. Numerical simulations of large scale concrete problems are presented and discussed. ESA

N94-14844 Argonne National Lab., IL.
TOWARD A VERIFIABLE APPROACH TO THE DESIGN OF CONCURRENT COMPUTATIONS
G. H. Chisholm 1993 13 p Presented at the 1993 International Simulators Conference on High Performance Computing, Arlington, VA, 29 Mar. - 1 Apr. 1993 Limited Reproducibility: More than 20% of this document may be affected by microfiche quality
(Contract W-31-109-eng-38)
(DE93-012908; ANL/MCS/CP-79562; CONF-930372-11) Avail: CASI HC A03

Distributed programs are dependent on explicit message passing between disjoint components of the computation. This paper is concerned with investigating an approach for proving correctness of distributed programs under an assumed data-exchange capability. Stated informally, the data exchange assumption is that every message is passed correctly, i.e., neither lost nor corrupted. One approach for constructing a proof under this assumption would be to embed an abstract model of the data communications mechanism into the program specification. The Message Passing Interface (MPI) standard provides a basis for such a model. In support of our investigations, we have developed a high-level specification using the ASLAN specification language. Our specification is based on a generalized communications model from which the MPI model may be derived. We describe the specification of this model and an approach to the specification of distributed programs with explicit message passing based on a verifiable data exchange model. DOE

N94-14864 Lawrence Livermore National Lab., CA.
GENERALIZED SMOOTH MODELS
J. Glosup 23 Jul. 1992 17 p Presented at the Joint Statistical Meetings of the American Statistical Association, the Biometric Society and the Institute of Mathematical Statistics, Boston, MA, 9-13 Aug. 1992 Limited Reproducibility: More than 20% of this document may be affected by microfiche quality
(Contract W-7405-eng-48)
(DE93-013045; UCRL-JC-111224; CONF-920893-7) Avail: CASI HC A03

The class of gene linear models is extended to develop a class of nonparametric regression models known as generalized smooth models. The technique of local scoring is used to estimate a generalized smooth model and the estimation procedure based on locally weighted regression is shown to produce local likelihood estimates. The asymptotically correct distribution of the deviance difference is derived and its use in comparing the fits of generalized linear models and generalized smooth models is illustrated. The relationship between generalized smooth models and generalized additive models is also discussed. DOE

N94-14866# Texas Univ., Austin. Fusion Research Center.
SPLINES, CONTOURS AND SVD SUBROUTINES
Emilia R. Solano and Holger St.John (General Atomic Co., San Diego, CA.) Jun. 1993 48 p
(Contracts DE-FG05-88ER-53266; DE-AC03-89ER-51114)
(DE93-016088; DOE/ER-53266/44; FRCR-435) Avail: CASI HC A03/MF A01

Portability of FORTRAN code is a major concern these days, since hardware and commercial software change faster than the codes themselves. Hence, using public domain, portable, mathematical subroutines is imperative. Here we present a collection of subroutines we have used in the past, and found to be particularly useful. They are: 2-dimensional splines, contour tracing of flux surface (based on 2-D spline), and singular Value Matrix Decomposition (for Chi-square minimization). DOE

N94-14871# Oak Ridge Y-12 Plant, TN.
CAD DATA EXCHANGE WITH MARTIN MARIETTA ENERGY SYSTEMS, INC., OAK RIDGE, TN
K. L. Smith Jun. 1993 33 p
(Contract DE-AC05-84OS-21400)
(DE93-017233; Y/EN-4612/R1) Avail: CASI HC A03/MF A01

This document has been developed to provide guidance in the interchange of electronic CAD data with Martin Marietta Energy Systems, Inc., Oak Ridge, Tennessee. It is not meant to be as comprehensive as the existing standards and specifications, but to provide a minimum set of practices that will enhance the success of the CAD data exchange. It is now a Department of Energy (DOE) Oak Ridge Field Office requirement that Architect-Engineering (A-E) firms prepare all new drawings using a Computer Aided Design (CAD) system that is compatible with the facility manager's (FM) CAD system. For Oak Ridge facilities, the CAD system used for facility design by the FM, Martin Marietta Energy Systems, Inc., is Intergraph. The format for interchange of CAD data for Oak Ridge facilities will be the Intergraph MicroStation format. DOE

N94-14162# Calspan Corp., Arnold AFS, TN.
COMPUTATIONAL TECHNIQUES AND CAPABILITIES
James R. Maus (Arnold Engineering Development Center, Arnold AFS, TN.) *In* VKI, Methodology of Hypersonic Testing 1993 18 p
Prepared in cooperation with Arnold Engineering Development Center, Arnold AFS, TN (For primary document see N94-14153 02-02)
Copyright Avail: CASI HC A03/MF A03

N94-14224# Ministry of Posts and Telecommunications, Tokyo (Japan). Communications Research Lab.
TRMM PRECIPITATION RADAR ALGORITHM
Kenichi Okamoto *In* Science and Technology Agency, Asia-Pacific ISY Conference, Volume 2 31 Mar. 1993 p 84-87 (For primary document see N94-14209 02-43)
Avail: CASI HC A01/MF A04

N94-14234# National Oceanic and Atmospheric Administration, Washington, DC. Satellite Research Lab.
THE DEVELOPMENT AND IMPLEMENTATION OF AN INTERACTIVE RETRIEVAL/ANALYSIS/FORECAST ALGORITHM
Henry E. Fleming, Mitchell D. Goldberg, Wayman E. Baker, John C. Derber, and Bert B. Katz (General Sciences Corp., Washington, DC.) *In* Science and Technology Agency, Asia-Pacific ISY Conference, Volume 2 31 Mar. 1993 p 130-133 (For primary document see N94-14209 02-43)
Avail: CASI HC A01/MF A04

N94-14611# National Aeronautical Lab., Bangalore (India). Computational and Theoretical Fluid Dynamics Div.
DEVELOPMENT OF PC-BASED AERONAUTICAL SOFTWARE (AEROWARE)
Premalatha Ramamoorthy and P. Ramamoorthy *In its* Proceedings of the Fluid Dynamics Symposium in Honour of Professor R. Narasimha on his 60th Birthday Jul. 1993 p 153-158 (For primary document see N94-14598 02-34)
Avail: CASI HC A02/MF A03

N94-14625*# Victoria Univ. (British Columbia). Dept. of Mechanical Engineering.
MODELLING ROBOTIC SYSTEMS WITH DADS
L. W. Churchill and I. Sharf *In* JPL, Proceedings of the Fifth NASA/NSF/DOD Workshop on Aerospace Computational Control 15 Feb. 1993 p 105-116 (For primary document see N94-14618 02-39)
Avail: CASI HC A03/MF A04

N94-14627*# Jet Propulsion Lab., California Inst. of Tech., Pasadena.
CAESY: A SOFTWARE TOOL FOR COMPUTER-AIDED ENGINEERING
Matt Wette *In its* Proceedings of the Fifth NASA/NSF/DOD Workshop on Aerospace Computational Control 15 Feb. 1993 p 125-130 (For primary document see N94-14618 02-39)
Avail: CASI HC A02/MF A04

N94-14628*# National Aeronautics and Space Administration. Goddard Space Flight Center, Greenbelt, MD.
ASTEC AND MODEL: CONTROLS SOFTWARE DEVELOPMENT AT GODDARD SPACE FLIGHT CENTER
John P. Downing, Frank H. Bauer, and Jeffrey L. Surber (Fairchild Space Co., Germantown, MD.) *In* JPL, Proceedings of the Fifth NASA/NSF/DOD Workshop on Aerospace Computational Control 15 Feb. 1993 p 131-141 (For primary document see N94-14618 02-39)
Avail: CASI HC A03/MF A04

N94-14629*# Boeing Defense and Space Group, Seattle, WA.
ANIMATION OF MULTI-FLEXIBLE BODY SYSTEMS AND ITS USE IN CONTROL SYSTEM DESIGN
Carl Juengst and Ron Stahlberg (Iowa Univ., Iowa City.) *In* JPL, Proceedings of the Fifth NASA/NSF/DOD Workshop on Aerospace Computational Control 15 Feb. 1993 p 143-151 (For primary document see N94-14618 02-39)
Avail: CASI HC A02/MF A04

N94-14630*# Air Force Academy, CO.
THE USE OF LINKED LISTS IN THE SIMULATION OF CONTROLLER-STRUCTURE INTERACTION
Ralph Quan *In* JPL, Proceedings of the Fifth NASA/NSF/DOD Workshop on Aerospace Computational Control 15 Feb. 1993 p 153-166 See also A93-44533 (For primary document see N94-14618 02-39)
Avail: CASI HC A03/MF A04

N94-14631*# Jet Propulsion Lab., California Inst. of Tech., Pasadena.
SPATIAL OPERATOR ALGEBRA FOR FLEXIBLE MULTIBODY DYNAMICS
A. Jain and G. Rodriguez *In its* Proceedings of the Fifth NASA/NSF/DOD Workshop on Aerospace Computational Control 15 Feb. 1993 p 167-183 (For primary document see N94-14618 02-39)
Avail: CASI HC A03/MF A04

N94-14636*# Jet Propulsion Lab., California Inst. of Tech., Pasadena.
PARALLEL O(LOG n) ALGORITHMS FOR OPEN- AND CLOSED-CHAIN RIGID MULTIBODY SYSTEMS BASED ON A NEW MASS MATRIX FACTORIZATION TECHNIQUE
Amir Fijany *In its* Proceedings of the Fifth NASA/NSF/DOD Workshop on Aerospace Computational Control 15 Feb. 1993 p 243-266 (For primary document see N94-14618 02-39)
Avail: CASI HC A03/MF A04

N94-14638*# Jet Propulsion Lab., California Inst. of Tech., Pasadena.
REAL-TIME DYNAMICS SIMULATION OF THE CASSINI SPACECRAFT USING DARTS. PART 1: FUNCTIONAL CAPABILITIES AND THE SPATIAL ALGEBRA ALGORITHM
A. Jain and G. K. Man *In its* Proceedings of the Fifth NASA/NSF/DOD Workshop on Aerospace Computational Control 15 Feb. 1993 p 297-306 (For primary document see N94-14618 02-39)
Avail: CASI HC A02/MF A04

N94-14639*# Jet Propulsion Lab., California Inst. of Tech., Pasadena.
REAL-TIME DYNAMIC SIMULATION OF THE CASSINI SPACECRAFT USING DARTS. PART 2: PARALLEL/VECTORIZED REAL-TIME IMPLEMENTATION
A. Fijany, J. A. Roberts, A. Jain, and G. K. Man *In its* Proceedings of the Fifth NASA/NSF/DOD Workshop on Aerospace Computational Control 15 Feb. 1993 p 307-326 (For primary document see N94-14618 02-39)
Avail: CASI HC A03/MF A04

N94-14641*# Jet Propulsion Lab., California Inst. of Tech., Pasadena.
SIMULATION OF LINEAR MECHANICAL SYSTEMS
S. W. Sirlin *In its* Proceedings of the Fifth NASA/NSF/DOD Workshop on Aerospace Computational Control 15 Feb. 1993 p 365-377 (For primary document see N94-14618 02-39)
Avail: CASI HC A03/MF A04

N94-14645*# Purdue Univ., West Lafayette, IN. Space Systems Control Lab.
AN APPLICATION OF THE IMC SOFTWARE TO CONTROLLER DESIGN FOR THE JPL LSCL EXPERIMENT FACILITY
Guoming Zhu and Robert E. Skelton *In* JPL, Proceedings of the Fifth NASA/NSF/DOD Workshop on Aerospace Computational Control 15 Feb. 1993 p 427-462 (For primary document see N94-14618 02-39)
Avail: CASI HC A03/MF A04

N94-14652*# National Aeronautics and Space Administration. Marshall Space Flight Center, Huntsville, AL.
A PROGRAM FOR THE INVESTIGATION OF THE MULTIBODY MODELING, VERIFICATION, AND CONTROL LABORATORY
Patrick A. Tobbe (Logicon Control Dynamics Co., Huntsville, AL.), Paul M. Christian (DYNACS Engineering Co., Inc., Huntsville, AL.), John M. Rakoczy, and Marlon L. Bulter *In* JPL, Proceedings of the Fifth NASA/NSF/DOD Workshop on Aerospace Computational Control 15 Feb. 1993 p 553-567 (For primary document see N94-14618 02-39)
Avail: CASI HC A03/MF A04

62 COMPUTER SYSTEMS

Includes computer networks and special application computer systems.

N94-12878# Sandia National Labs., Albuquerque, NM.
BEYOND CORE: MAKING PARALLEL COMPUTER I/O PRACTICAL
D. Womble, D. Greenberg, S. Wheat, and R. Riesen (New Mexico Univ., Albuquerque.) 1993 8 p Presented at the Parallel I/O and Databases Symposium, Hanover, NH, 21-30 Jun. 1993
(Contract DE-AC04-76DP-00789)
(DE93-012347; SAND-93-0956C; CONF-9306157-1) Avail: CASI HC A02/MF A01

The solution of Grand Challenge Problems will require computations which are too large to fit in the memories of even the largest machines. Inevitably, new designs of I/O systems will be necessary to support them. Through our implementations of an out-of-core LU factorization, we have learned several important lessons about what I/O systems should be like. In particular we believe that the I/O system must provide the programmer with the ability to explicitly manage storage. One method of doing so is to have a partitioned secondary storage in which each processor owns a logical disk. Along with operating system enhancements which allow overheads such as buffer copying to be avoided, this sort of I/O system meets the needs of high performance computing. DOE

N94-12917# Los Alamos National Lab., NM.
A NETWORK EVALUATION AND ANALYSIS TOOL
L. A. Stoltz, R. Whiteson, P. K. Fasel, R. Temple, and J. S. Dreicer 1993 5 p Presented at the 1993 Ninth International Conference on Systems Engineering, Las Vegas, NV, 14-16 Jul. 1993
(Contract W-7405-eng-36)
(DE93-012647; LA-UR-93-1287; CONF-930773-2) Avail: CASI HC A01/MF A01

The rapid emergence of large heterogeneous networks, distributed systems, and massively parallel computers has resulted in economies of scale, enhanced productivity, efficient communication, resource sharing, and increased reliability, which are computationally beneficial. In addition to these benefits, networking presents technical challenges and problems with respect to maintaining and ensuring the security, design, compatibility, integrity, functionality, and management of these systems. In this paper we describe a computer security tool, Network Evaluation and Analysis Tool (NEAT), that we have developed to address these concerns. DOE

N94-12930 BBN Systems and Technologies Corp., Cambridge, MA.
MULTICLUSTER Final Technical Report, Sep. 1990 - Feb. 1992
Edward F. Walker, Christopher E. Barber, James C. Berets, Susan K. Pawlowski, and Jonathan Cole Mar. 1993 33 p Limited Reproducibility: More than 20% of this document may be affected by microfiche quality
(Contract F30602-89-D-0050)
(AD-A265869; Rept-7725; RL-TR-93-9) Avail: CASI HC A03

The implementation of multicluster operation in the Cronus distributed computing environment is presented. A cluster is a collection of hosts on one or more networks. Clusters are formed to organize and control the relationship between organizations for reasons of security and administration. The mechanisms to support intercluster object addressing are presented; these mechanisms form the basis for multicluster operation. Object-oriented distributed computing environments strive to present a uniform environment for building distributed applications by providing host and network transparent access to resources. Previously, the Cronus distributed environment operated in an environment of different types of hosts executing across several local area networks connected by gateways. Cronus achieved a uniform environment by treating the set of hosts as a single system in terms of authentication and in binding object identifiers to their locations. To extend Cronus to large environments, it is necessary to decompose the environment into collections of hosts. Decomposition is crucial to system scalability. It speeds up the location of objects and reduces the number of global name spaces DTIC

N94-12938*# College of William and Mary, Newport News, VA.
PARALLELIZING TIMED PETRI NET SIMULATIONS Final Report
David M. Nicol 31 Aug. 1993 91 p
(Grant NAG1-1060)
(NASA-CR-194278; NAS 1.26:194278) Avail: CASI HC A05/MF A01

The possibility of using parallel processing to accelerate the simulation of Timed Petri Nets (TPN's) was studied. It was recognized that complex system development tools often transform system descriptions into TPN's or TPN-like models, which are then simulated to obtain information about system behavior. Viewed this way, it was important that the parallelization of TPN's be as automatic as possible, to admit the possibility of the parallelization being embedded in the system design tool. Later years of the grant were devoted to examining the problem of joint performance and reliability analysis, to explore whether both types of analysis could be accomplished within a single framework. In this final report, the results of our studies are summarized. We believe that the problem of parallelizing TPN's automatically for MIMD architectures has been almost completely solved for a large and important class of problems. Our initial investigations into joint performance/reliability analysis are two-fold; it was shown that Monte Carlo simulation, with importance sampling, offers promise of joint analysis in the context of a single tool, and methods for the parallel simulation of general Continuous Time Markov Chains, a model framework within which joint performance/reliability models can be cast, were developed. However, very much more work is needed to determine the scope and generality of these approaches. The results obtained in our two studies, future directions for this type of work, and a list of publications are included. Author (revised)

N94-13043# Sandia National Labs., Albuquerque, NM.
UNICOS(TRADE NAME) SECURITY TESTING
W. H. Vandevender 1993 9 p Presented at the 15th Computer Security Group Training Conference: Mission Possible - Connected and Protected, Albuquerque, NM, 3-6 May 1993
(Contract DE-AC04-76DP-00789)
(DE93-011680; SAND-93-0742C; CONF-9305151-2) Avail: CASI HC A02/MF A01 (US Sales Only)

Developing security plans and supporting security tests is a very important part of the Department of Energy accreditation process. This paper will discuss the general testing methodology that was used to achieve DOE accreditation of the Secure UNICOS environment at Sandia National Laboratories (NM). In addition, some specific security testing procedures, tests and problem areas will be described. DOE

N94-13052# Carnegie-Mellon Univ., Pittsburgh, PA. School of Computer Science.
MOBILE HOST INTERNETWORKING USING IP LOOSE SOURCE ROUTING
David B. Johnson Feb. 1993 23 p
(Contract MDA972-90-C-0035; ARPA Order 7330)
(AD-A265713; CMU-CS-93-128) Avail: CASI HC A03/MF A01

Internetworking protocols such as IP currently do not allow 'mobile hosts' to interoperate easily or conveniently with other hosts on the network. A host's IP address encodes the network number to which the host is connected, which prevents IP datagrams from reaching the host when it moves to a new location and connects to the Internet within a different network. A new protocol for allowing mobile hosts to transparently interoperate in the Internet using IP is presented. The protocol is designed to make use of existing facilities of the IP protocol architecture where possible, in order to minimize any changes necessary to existing protocol software. The protocol takes advantage of the standard IP loose source routing option for routing datagrams correctly to mobile hosts, while allowing the hosts to retain their normal 'home' IP address even when connected to a foreign network. The protocol is simple and scales well to large numbers of mobile hosts. It requires fewer changes to existing software and adds less overhead to the network than previous IP mobile host internetworking protocols. DTIC

N94-13177*# Proteon, Inc., Westborough, MA.
HIGH SPEED PACKET SWITCHING Final Report
Oct. 1991 43 p
(Contracts NAS5-30629; F30602-89-C-0014; SBIR-07.04-2800)
(NASA-CR-191334; NAS 1.26:191334) Avail: CASI HC A03/MF A01

This document constitutes the final report prepared by Proteon, Inc. of Westborough, Massachusetts under contract NAS 5-30629 entitled High-Speed Packet Switching (SBIR 87-1, Phase 2) prepared for NASA-Greenbelt, Maryland. The primary goal of this research project is to use the results of the SBIR Phase 1 effort to develop a sound, expandable hardware and software router architecture capable of forwarding 25,000 packets per second through the router and passing 300 megabits per second on the router's internal busses. The work being delivered under this contract received its funding from three different sources: the SNIPE/RIG contract (Contract Number F30602-89-C-0014, CDRL Sequence Number A002), the SBIR contract, and Proteon. The SNIPE/RIG and SBIR contracts had many overlapping requirements, which allowed the research done under SNIPE/RIG to be applied to SBIR. Proteon funded all of the work to develop new router interfaces other than FDDI, in addition to funding the productization of the router itself. The router being delivered under SBIR will be a fully product-quality machine. The work done during this contract produced many significant findings and results, summarized here and explained in detail in later sections of this report. The SNIPE/RIG contract was completed. That contract had many overlapping requirements with the SBIR contract, and resulted in the successful demonstration and delivery of a high speed router. The development that took place during the SNIPE/RIG contract produced findings that included the choice of processor and an understanding of the issues surrounding inter processor communications in a multiprocessor environment. Many significant speed enhancements to the router software were made during that time. Under the SBIR contract (and with help from Proteon-funded work), it was found that a single processor router achieved a throughput significantly higher than originally anticipated. For this reason, a single processor router was developed and the final delivery under this contract will include a single processor CNX-500 router. The router and its interface boards (2 FDDIs and 2 dual-ethernets) are all product-quality components. Derived from text

N94-13204*# MCAT Inst., San Jose, CA.
IMPLEMENTATION OF ADI: SCHEMES ON MIMD PARALLEL COMPUTERS
Rob F. VanderWijngaart Jul. 1993 23 p Proposed for presentation at the Supercomputing 1993 Conference, Portland, OR, 15-19 Nov. 1993 Original contains color illustrations
(Contract NCC2-752)
(NASA-CR-193720; NAS 1.26:193720; MCAT-93-13) Avail: CASI HC A03/MF A01; 1 functional color page

In order to simulate the effects of the impingement of hot exhaust jets of High Performance Aircraft on landing surfaces a multi-disciplinary computation coupling flow dynamics to heat conduction in the runway needs to be carried out. Such simulations, which are essentially unsteady, require very large computational power in order to be completed within a reasonable time frame of the order of an hour. Such power can be furnished by the latest generation of massively parallel computers. These remove the bottleneck of ever more congested data paths to one or a few highly specialized central processing units (CPU's) by having many off-the-shelf CPU's work independently on their own data, and exchange information only when needed. During the past year the first phase of this project was completed, in which the optimal strategy for mapping an ADI-algorithm for the three dimensional unsteady heat equation to a MIMD parallel computer was identified. This was done by implementing and comparing three different domain decomposition techniques that define the tasks for the CPU's in the parallel machine. These implementations were done for a Cartesian grid and Dirichlet boundary conditions. The most promising technique was then used to implement the heat equation solver on a general curvilinear grid with a suite of nontrivial boundary conditions. Finally, this technique was also used to implement the Scalar Penta-diagonal (SP) benchmark, which was taken from the NAS Parallel Benchmarks report. All implementations were done in the programming language C on the Intel iPSC/860 computer. Derived from text

N94-13450*# National Aeronautics and Space Administration. Langley Research Center, Hampton, VA.
A HARDWARE IMPLEMENTATION OF A PROVABLY CORRECT DESIGN OF A FAULT-TOLERANT CLOCK SYNCHRONIZATION CIRCUIT
Wilfredo Torres-Pomales Jul. 1993 14 p
(RTOP 505-64-10-10)
(NASA-TM-109001; NAS 1.15:109001) Avail: CASI HC A03/MF A01

A fault-tolerant clock synchronization system was designed to a proven correct formal specification. Formal methods were used in the development of this specification. A description of the system and an analysis of the tests performed are presented. Plots of typical experimental results are included. Author (revised)

N94-13470# Oak Ridge National Lab., TN.
THE KSR1: EXPERIMENTATION AND MODELING OF POSTSTORE
E. Rosti (Milan Univ., Italy.), E. Smirni, T. D. Wagner, A. W. Apon, and L. W. Dowdy Feb. 1993 34 p
(Contract DE-AC05-84OR-21400)
(DE93-012539; ORNL/TM-12287) Avail: CASI HC A03/MF A01

Kendall Square Research introduced the KSR1 system in 1991. The architecture is based on a ring of rings of 64-bit microprocessors. It is a distributed, shared memory system and is scalable. The memory structure is unique and is the key to understanding the system. Different levels of caching eliminate physical memory addressing and leads to the ALLCACHE(trademark) scheme. Since requested data may be found in any of several caches, the initial access time is variable. Once pulled into the local (sub)cache, subsequent access times are fixed and minimal. Thus, the KSR1 is a Cache-Only Memory Architecture (COMA) system. This paper describes experimentation and an analytic model of the KSR1. The focus is on the poststore programmer option. With the poststore option, the programmer can elect to broadcast the updated value of a variable to all processors that might have a copy. This may save time for threads on other processors, but it delays the broadcasting thread and

places additional traffic on the ring. The specific issue addressed is to determine under what conditions poststore is beneficial. The analytic model and the experimental observations are in good agreement. They indicate that the decision to use poststore depends both on the application and the current system load. DOE

N94-13921*# Research Inst. for Advanced Computer Science, Moffett Field, CA.

EFFICIENT, MASSIVELY PARALLEL EIGENVALUE COMPUTATION

Yan Huo (Princeton Univ., NJ.) and Robert Schreiber Jan. 1993 17 p Submitted for publication

(Contract NAS2-13721; NSF CDA-91-21709)

(NASA-CR-194289; NAS 1.26:194289; RIACS-TR-93-02) Avail: CASI HC A03/MF A01

In numerical simulations of disordered electronic systems, one of the most common approaches is to diagonalize random Hamiltonian matrices and to study the eigenvalues and eigenfunctions of a single electron in the presence of a random potential. An effort to implement a matrix diagonalization routine for real symmetric dense matrices on massively parallel SIMD computers, the Maspar MP-1 and MP-2 systems, is described. Results of numerical tests and timings are also presented.

Author (revised)

N94-13924# Center for Mathematics and Computer Science, Amsterdam (Netherlands). Computer Science Dept./Algorithmics and Architecture Dept.

FAST PARALLEL STRING PREFIX-MATCHING

Dany Breslauer Oct. 1992 11 p Sponsored in part by European Research Consortium for Informatics and Mathematics

(AD-A267758; CWI-CS-R9239; ETN-93-94165) Copyright Avail: CASI HC A03/MF A01

An O(log log m) time n log m/log log m processor CRCW-PRAM (Parallel Random Access Machine) algorithm for the string prefix-matching problem over a general alphabet is presented. The algorithm can also be used to compute the KMP (Kruth Morris Pratt) failure function in O(log log m) time on m log m/log log m processors. These results improve on the running time of the best previous algorithm for both problems, which was O(log m), while preserving the same number of operations. ESA

N94-14011# Sandia National Labs., Albuquerque, NM.

KERBEROS: A UNIX-TCP/IP NETWORK AUTHENTICATION SYSTEM

W. H. Rahe and G. D. Machin 1993 11 p Presented at the 15th Computer Security Group, Mission Possible, Connected and Protected Training Conference, Albuquerque, NM, 3-6 May 1993

(Contract DE-AC04-76DP-00789)

(DE93-011677; SAND-93-0908C; CONF-9305151-5) Avail: CASI HC A03/MF A01 (US Sales Only)

Vulnerabilities inherent in network transmissions reduce the security protections provided by multiple remote authentication processes. The 'trusted systems' concept also provides potential for inadvertent or deliberate abuse of computing resources. Additionally, since the owner of a workstation potentially has complete control of a particular workstation, including the ability to edit all files and add customer accounts through the use of privileged accounts, additional security concerns exist including file integrity, file privacy, and customer masquerade. In a networked computing environment, both the customer/client and the server identities become more difficult to assure. The possibility of disclosure and non-assurance of information integrity transmitted on the network media are markedly increased In recognition of these difficulties, Digital Equipment Corporation (DEC) and International Business Machines (IBM) provided funding for the creation of Project Athena at (MIT) whose charter was to address distributed computing including security. Kerberos is an application developed by this project to provide centralized 'third-party' authentication in a distributed network. Network access control may be provided by Kerberos for each of the computing resources within either a local or remote network. Kerberos contains a database of principals and encryption keys in a Key Distribution Center (KDC). The KDC contains the keys (passwords) or all customers and must reside on a tightly controlled, limited access system. The KDC provides non-corruptible authentication credentials which are used in conjunction with the local authorization file and local services to perform the authentication and authorization functions for local and remote customer requests. DOE

N94-14177# Los Alamos National Lab., NM.

QUANTUM MONTE CARLO BY MESSAGE PASSING

J. Bonca and J. E. Gubernatis 1993 13 p Presented at the Mardi Gras Conference on Concurrent Computing in the Physical Sciences, Baton Rouge, LA, 18-20 Feb. 1993

(Contract W-7405-eng-36)

(DE93-012645; LA-UR-93-1296; CONF-9302112-2) Avail: CASI HC A03/MF A01

We summarize results of quantum Monte Carlo simulations of the degenerate single-impurity Anderson model using the impurity algorithm of Hirsch and Fye. Using methods of Bayesian statistical inference, coupled with the principle of maximum entropy, we extracted the single-particle spectral density from the imaginary-time Green's function. The variations of resulting spectral densities with model parameters agree qualitatively with the spectral densities predicted by NCA calculations. All the simulations were performed on a cluster of 16 IBM R6000/560 workstations under the control of the message-passing software PVM. We described the trivial parallelization of our quantum Monte Carlo code both for the cluster and the CM-5 computer. Other issues for effective parallelization of the impurity algorithm are also discussed. DOE

N94-14187# Helsinki Univ. of Technology (Finland). Inst. of Mathematics.

THEORY FOR ITERATIVE SOLUTION OF LARGE DYNAMICAL SYSTEMS USING PARALLEL COMPUTATION Ph.D. Thesis

Ulla Miekkala Nov. 1991 22 p Sponsored by Academy of Finland, and Helsinki Univ. of Technology, Espoo

(TKK-MAT-A304; TKK-DISS-793; ISBN-951-22-0846-6; ETN-93-93483) Avail: CASI HC A03/MF A01

Convergence studies of Picard-Lindeloef type iteration methods are summarized. Picard-Lindeloef type iteration is also known as waveform relaxation or dynamic iteration methods. The dynamic iteration method is defined for the linear autonomous model problem. An overview of convergence results is given. The essential contents of four separate papers that also make up this thesis are presented, that is, the convergence study on infinite time interval for time continuous iteration of a linear initial value problem consisting of Ordinary Differential Equations (ODE's) or differential-algebraic equations, a similar study for discretized ODE's, and consideration of multirate discretization. Work done on different aspects of dynamic iteration methods is collected. ESA

N94-14315# Lawrence Livermore National Lab., CA.

UNIFORM USER AND GROUP IDs ON A LARGE NETWORK

K. Crispin Oct. 1992 7 p Presented at the CRAY User Group Meeting, Washington, DC, 9-13 Oct. 1992

(Contract W-7405-eng-48)

(DE93-013047; UCRL-JC-111883; CONF-9210353-1) Avail: CASI HC A02/MF A01

Over the past few years the Livermore Computer Center has converted from a 'home grown system' facility to a more or less standard UNIX environment. As a result we have several hundred UNIX systems on our network ranging from the UNICOS Crays to Sun workstations. For the usual reasons we want to maintain a single UID space across all these systems. This paper describes some of the problems and issues we have encountered in pursuit of this goal. DOE

N94-14475# IBM Federal Systems Div., Houston, TX.

THE NATIONAL STORAGE LABORATORY: A COLLABORATIVE RESEARCH PROJECT

R. A. Coyne, H. Hulen, and R. Watson (Lawrence Livermore National Lab., CA.) 17 Feb. 1993 5 p Presented at the 10th Conference on Computing in High Energy Physics, Annecy, France, 21-25 Sep. 1992

(Contract W-7405-eng-48)

(DE93-015099; UCRL-JC-111816-Rev-1; CONF-920966-25-Rev-1) Avail: CASI HC A01/MF A01

Large scientific, engineering, and commercial applications are straining storage and networking facilities, a condition compounded by new supercomputers, massively parallel processors, and workstations. An application driven, industry-led, collaborative, storage testbed project centered at Lawrence Livermore National Laboratory (LLNL), called the National Storage Laboratory, was organized to investigate, demonstrate, and commercialize technology to remove performance bottlenecks and to

provide new needed storage system functionality. The experience of the project will also contribute to the work of the IEEE Storage System Standards Working Group. DOE

N94-14476# Stanford Univ., CA. Linear Accelerator Center.
OVERVIEW OF THE SCALABLE COHERENT INTERFACE, IEEE STD 1596 (SCI)
D. B. Gustavson, D. V. James (Apple Computer, Inc., Cupertino, CA.), and H. A. Wiggers (Hewlett-Packard Co., Palo Alto, CA.) Oct. 1992 3 p Presented at the IEEE Nuclear Science Symposium and Medical Imaging Conference, Orlando, FL, 26-31 Oct. 1992
(Contract DE-AC03-76SF-00515)
(DE93-015247; SLAC-PUB-5967; CONF-921005-34) Avail: CASI HC A01/MF A01

The Scalable Coherent Interface standard defines a new generation of interconnection that spans the full range from supercomputer memory 'bus' to campus-wide network. SCI provides bus-like services and a shared-memory software model while using an underlying, packet protocol on many independent communication links. Initially these links are 1 GByte/s (wires) and 1 GBit/s (fiber), but the protocol scales well to future faster or lower-cost technologies. The interconnect may use switches, meshes, and rings. The SCI distributed-shared-memory model is simple and versatile, enabling for the first time a smooth integration of highly parallel multiprocessors, workstations, personal computers, I/O, networking, and data acquisition. DOE

N94-14716# Laboratoire d'Automatique et d'Analyse des Systemes, Toulouse (France). Equipe Outils et Logiciels pour la Communication.
EXECUTION METHODS, AND PARALLEL VIRTUAL MACHINES FOR DISTRIBUTED IMPLEMENTATION OF THE LCS PARALLEL PROGRAMMING LANGUAGE Ph.D. Thesis - Toulouse Univ. [METHODES D'EXECUTION ET MACHINES VIRTUELLES PARALLELES POUR L'IMPLANTATION DISTRIBUEE DU LANGAGE DE PROGRAMMATION PARALLELE LCS]
Thierry LeSergent 1993 161 p In FRENCH
(LAAS-93032; ETN-93-94365) Avail: CASI HC A08/MF A02

The implementation of a high level parallel programming language on parallel physical machines with shared or distributed memory is considered. The language support of the study, LCS, combines the high level concepts of the functional language Standard ML, and the CCS communicating processes paradigm. The operational semantics of LCS is defined by an abstract machine. The LCS compiler produces code for a virtual machine that implements this abstract machine. The parallel virtual machine is designed as a small number of elementary virtual sequential machines which share all the objects built in a heap. The main contributions concern the management of the shared memory and the management of the processes. The management of the shared heap uses a garbage collector executed on parallel on elementary machines, incrementally with computations on each of them. An original mechanism of scan credit, and distributed algorithms for allocations, lead to a total cooperation between machines. On target machines with distributed memory, the heap is built by the distributed shared virtual memory technique, efficiently integrated with the garbage collector by the use in both cases of access protections on memory pages. The number of the LCS processes can be very high and may quickly vary. The management of processes is distributed between the elementary machines. A load balancing algorithm, based on dynamic bounds, was designed. Its properties are proved, and the results confirmed by simulation. The implementation shows the qualities of the parallel garbage collector designed. ESA

N94-14614# National Aeronautical Lab., Bangalore (India). Computational and Theoretical Fluid Dynamics Div.
DEVELOPMENT OF PARALLEL PROCESSING AT NAL: A RETROSPECT
U. N. Sinha, V. R. Sarasamma, S. Rajalakshmy, C. R. Sreenivasan, and G. S. Dwarakanath *In its* Proceedings of the Fluid Dynamics Symposium in Honour of Professor R. Narasimha on his 60th Birthday Jul. 1993 p 181-190 (For primary document see N94-14598 02-34)
Avail: CASI HC A02/MF A03

N94-14637*# Ohio State Univ., Columbus. Dept. of Electrical Engineering.
PARALLEL METHODS FOR DYNAMIC SIMULATION OF MULTIPLE MANIPULATOR SYSTEMS
Scott McMillan, P. Sadayappan, and David E. Orin *In* JPL, Proceedings of the Fifth NASA/NSF/DOD Workshop on Aerospace Computational Control 15 Feb. 1993 p 267-281 (For primary document see N94-14618 02-39)
Avail: CASI HC A03/MF A04

63 CYBERNETICS

Includes feedback and control theory, artificial intelligence, robotics and expert systems.

For related information see also *54 Man/System Technology and Life Support.*

N94-12859# Los Alamos National Lab., NM.
COMPLETING FAULT MODELS FOR ABDUCTIVE DIAGNOSIS
E. Knill, P. T. Cox (Nova Scotia Technical Coll., Halifax.), and T. Pietrzykowski (Nova Scotia Technical Coll., Halifax.) Nov. 1992 21 p Presented at the 13th International Joint Conference on Artificial Intelligence, Chambery, Savoie, France, 29 Aug. - 3 Sep. 1993
(Contract W-7405-eng-36)
(DE93-003832; LA-UR-92-3770; CONF-930848-1) Avail: CASI HC A03/MF A01

In logic-based diagnosis, the consistency-based method is used to determine the possible sets of faulty devices. If the fault models of the devices are incomplete or nondeterministic, then this method does not necessarily yield abductive explanations of system behavior. Such explanations give additional information about faulty behavior and can be used for prediction. Unfortunately, system descriptions for the consistency-based method are often not suitable for abductive diagnosis. Methods for completing the fault models for abductive diagnosis have been suggested informally by Poole and by Cox et al. Here we formalize these methods by introducing a standard form for system descriptions. The properties of these methods are determined in relation to consistency-based diagnosis and compared to other ideas for integrating consistency-based and abductive diagnosis. DOE

N94-12889*# National Aeronautics and Space Administration. Ames Research Center, Moffett Field, CA.
EFFICIENT DYNAMIC OPTIMIZATION OF LOGIC PROGRAMS
Phil Laird Jun. 1992 7 p Submitted for publication
(NASA-TM-109251; FIA-92-20; NAS 1.15:109251) Avail: CASI HC A02/MF A01

A summary is given of the dynamic optimization approach to speed up learning for logic programs. The problem is to restructure a recursive program into an equivalent program whose expected performance is optimal for an unknown but fixed population of problem instances. We define the term 'optimal' relative to the source of input instances and sketch an algorithm that can come within a logarithmic factor of optimal with high probability. Finally, we show that finding high-utility unfolding operations (such as EBG) can be reduced to clause reordering. Author (revised)

N94-12890*# National Aeronautics and Space Administration. Ames Research Center, Moffett Field, CA.
ARTIFICIAL INTELLIGENCE SUPPORT FOR SCIENTIFIC MODEL-BUILDING
Richard M. Keller Aug. 1992 6 p Submitted for publication
(NASA-TM-109252; FIA-92-29; NAS 1.15:109252) Avail: CASI HC A02/MF A01

Scientific model-building can be a time-intensive and painstaking process, often involving the development of large and complex computer programs. Despite the effort involved, scientific models cannot easily be distributed and shared with other scientists. In general, implemented scientific models are complex, idiosyncratic, and difficult for anyone but the original scientific development team to understand. We believe that artificial intelligence techniques can facilitate both the model-building and model-sharing process. In this paper, we overview our effort to build a scientific modeling software tool that aids the scientist in developing and using models. This tool

includes an interactive intelligent graphical interface, a high-level domain specific modeling language, a library of physics equations and experimental datasets, and a suite of data display facilities. Author (revised)

N94-12969# Naval Command, Control and Ocean Surveillance Center, San Diego, CA. RDT and E Div.

AN ANALOG CLUSTERING NETWORK FROM A BIOLOGICAL MODEL

P. A. Shoemaker, C. G. Hutchens, and S. B. Patil Apr. 1993 4 p

(AD-A265637) Avail: CASI HC A01/MF A01

One reason for the recent resurgence of interest in neural network-like computational models has been the prospect of compact and fast implementations of these networks in integrated circuit form. While analog implementations offer considerable advantages with regard to speed and density, their precision and noise immunity are important concerns. Some researchers have built analogues of biological structures for early sensory processing, and they have emphasized that tolerance of noisy and imprecise components is a natural emergent feature of these networks. However, the ways in which higher or cognitive functions might be learned and computed with such components for the most part remains unknown. In addition, learning itself remains problematic in analog circuitry. Means proposed for long-term, modifiable analog weight storage (e.g., floating-gate MOS devices) are sensitive, difficult to control, and of limited precision. We have chosen to implement a model of olfactory processing which we believe to be an instructive paradigm for computation in a learning system with low-precision weights and weight changes. The model has been shown capable of performing a hierarchical clustering of vectors on its input space. This capability is of potential interest for a range of applications, from automatic target recognition (ATR) to surveillance and detection. The network requires only coarse-valued weights (three to five bits resolution) and its operation relies on the statistical properties of large assemblages of sparsely interconnected neurons, rather than high precision processing. DTIC

N94-13131*# Odetics, Inc., Anaheim, CA.

CONTROL ALGORITHM IMPLEMENTATION FOR A REDUNDANT DEGREE OF FREEDOM MANIPULATOR Final Report, 13 Jul. 1989 - 13 Oct. 1991

Steve Cohan 13 Oct. 1991 90 p

(Contract NAS7-1062; SBIR-05.01-0300A)

(NASA-CR-191339; NAS 1.26:191339) Avail: CASI HC A05/MF A01

This project's purpose is to develop and implement control algorithms for a kinematically redundant robotic manipulator. The manipulator is being developed concurrently by Odetics Inc., under internal research and development funding. This SBIR contract supports algorithm conception, development, and simulation, as well as software implementation and integration with the manipulator hardware. The Odetics Dexterous Manipulator is a lightweight, high strength, modular manipulator being developed for space and commercial applications. It has seven fully active degrees of freedom, is electrically powered, and is fully operational in 1 G. The manipulator consists of five self-contained modules. These modules join via simple quick-disconnect couplings and self-mating connectors which allow rapid assembly/disassembly for reconfiguration, transport, or servicing. Each joint incorporates a unique drive train design which provides zero backlash operation, is insensitive to wear, and is single fault tolerant to motor or servo amplifier failure. The sensing system is also designed to be single fault tolerant. Although the initial prototype is not space qualified, the design is well-suited to meeting space qualification requirements. The control algorithm design approach is to develop a hierarchical system with well defined access and interfaces at each level. The high level endpoint/configuration control algorithm transforms manipulator endpoint position/orientation commands to joint angle commands, providing task space motion. At the same time, the kinematic redundancy is resolved by controlling the configuration (pose) of the manipulator, using several different optimizing criteria. The center level of the hierarchy servos the joints to their commanded trajectories using both linear feedback and model-based nonlinear control techniques. The lowest control level uses sensed joint torque to close torque servo loops, with the goal of improving the manipulator dynamic behavior. The control algorithms are subjected to a dynamic simulation before implementation. Author (revised)

N94-13184*# Institute for Computer Applications in Science and Engineering, Hampton, VA.

PARAMETRIC BINARY DISSECTION Final Report

Shahid H. Bokhari (University of Engineering and Technology, Lahore, Pakistan.), Thomas W. Crockett (National Aeronautics and Space Administration. Langley Research Center, Hampton, VA.), and David M. Nicol (College of William and Mary, Williamsburg, VA.) Washington Jul. 1993 38 p Submitted for publication

(Contracts NAS1-19480; NAS1-18605; NSF CCR-92-01195; RTOP 505-90-52-01)

(NASA-CR-191496; NAS 1.26:191496; ICASE-93-39) Avail: CASI HC A03/MF A01

Binary dissection is widely used to partition non-uniform domains over parallel computers. This algorithm does not consider the perimeter, surface area, or aspect ratio of the regions being generated and can yield decompositions that have poor communication to computation ratio. Parametric Binary Dissection (PBD) is a new algorithm in which each cut is chosen to minimize load + lambda x(shape). In a 2 (or 3) dimensional problem, load is the amount of computation to be performed in a subregion and shape could refer to the perimeter (respectively surface) of that subregion. Shape is a measure of communication overhead and the parameter permits us to trade off load imbalance against communication overhead. When A is zero, the algorithm reduces to plain binary dissection. This algorithm can be used to partition graphs embedded in 2 or 3-d. Load is the number of nodes in a subregion, shape the number of edges that leave that subregion, and lambda the ratio of time to communicate over an edge to the time to compute at a node. An algorithm is presented that finds the depth d parametric dissection of an embedded graph with n vertices and e edges in O(max(n log n, de)) time, which is an improvement over the O(dn log n) time of plain binary dissection. Parallel versions of this algorithm are also presented; the best of these requires O(n/p) log(sup 3)p) time on a p processor hypercube, assuming graphs of bounded degree. How PBD is applied to 3-d unstructured meshes and yields partitions that are better than those obtained by plain dissection is described. Its application to the color image quantization problem is also discussed, in which samples in a high-resolution color space are mapped onto a lower resolution space in a way that minimizes the color error. Author (revised)

N94-13253*# Akron Univ., OH. Dept. of Mechanical Engineering.

ADAPTIVE CONTROL OF INTERFACE BY TEMPERATURE AND INTERFACE PROFILE FEEDBACK IN TRANSPARENT MULTI-ZONE CRYSTAL GROWTH FURNACE Final Technical Report, 25 Sep. 1989 - 31 May 1991

Celal Batur 1991 32 p

(Contract NCC3-150)

(NASA-CR-194140; NAS 1.26:194140) Avail: CASI HC A03/MF A01

The objective of this research is to control the dynamics of multizone programmable crystal growth furnaces. Due to the inevitable heat exchange among different heating zones and the transient nature of the process, the dynamics of multizone furnaces is time varying, distributed, and therefore complex in nature. Electrical power to heating zones and the translational speed of the ampoule are employed as inputs to control the dynamics. Structural properties of the crystal is the ultimate aim of this adaptive control system. These properties can be monitored in different ways. Following an order of complexity, these may include: (1) on line measurement of the material optical properties such as the refractive index of crystal; (2) on line x-ray imaging of the interface topology; (3) on line optical quantification of the interface profile such as the determination of concavity or convexity of the interface shape; and (4) on line temperature measurement at points closest to the material such as measurements of the ampoule's outside and inside surface temperatures. The research performed makes use of the temperature and optical measurements, specified in (3) and (4) as the outputs of furnace dynamics. However, if the instrumentation is available, the proposed control methodology can be extended to the measurements listed in (1) and (2). Author (revised)

N94-13329 Tel-Aviv Univ. (Israel). Dept. of Electronics, Communications, Control and Computer Systems.

SELF TUNING AND ADAPTIVE CONTROL: EVALUATIONS AND IMPROVEMENTS OF ALGORITHMS M.S. Thesis

Tzvika Friedman Oct. 1990 253 p

(ITN-93-85192) Copyright Avail: Issuing Activity (Tel-Aviv. Univ., Exact Sciences Library, Ramat Aviv 69978, Israel)

Astrom and Hagglund's self-tuning regulator (STR) theory, based on the relay feedback identification method, is examined and an extended theory is developed. The self-tuning procedure was successfully implemented on several industrial systems. Several methods for on-line identification for an adaptive control were tested, using a true electromechanical system in a closed loop. This eliminated nonlinear phenomena and ensured controllability of the system and a safe response in all identification phases. Furthermore, closed-loop identification complies with the identification and estimation forms for an adaptive control. A different approach was used for adaptive control, owing to the necessity for compromise between identification quality and system performance. The approach used combines a priori knowledge of the physical structure of the system and working conditions. The main feature of this approach is that there is on-line decision and incomplete identification or on-line updating of controller parameters at every sampling. The physical structure and phenomena of an electromechanical system are examined and identification methods which detect the working conditions in the system are presented. ISA

N94-13515 Windsor Univ. (Ontario). Dept. of Electrical Engineering.
CLOSE RANGE 3-D POSITION SENSING USING STEREO VISION AND POINT-OF-CORRESPONDANCE THROUGH MATHEMATICAL MORPHOLOGY Ph.D. Thesis
Mohamed T. Boraie 1989 154 p
(ISBN-0-315-61012-3; CTN-93-60720) Copyright Avail: Micromedia Ltd., Technical Information Centre, 165 Hotel de Ville, Place du Portage, Phase 2, Hull, Quebec J8X 3X2, Canada HC/MF

A procedure is introduced for calibrating two charge coupled device cameras for the purpose of close range position sensing. The procedure results in an over-determined set of linear algebraic equations that can be utilized in determining the coordinate position of some identifiable feature in the scene relative to any set of orthogonal axes. The proposed approach relaxes the geometrical constraint required by most of the available procedures. The performance is then evaluated and both accuracy and repeatability are examined. For the purpose of determining the feature position in a multi-feature image, the point of correspondence (POC) problem is discussed, and a procedure for the POC problem in stereoscopic vision is introduced. The procedure utilizes mathematical morphology as an image processing tool in finding edge-strength images and in determining the location of the POC. Finally, lens distortion parameters are introduced to the calibration process, and the effect of each parameter is illustrated.
Author (CISTI)

N94-13517# National Research Council of Canada, Ottawa (Ontario). Associate Committee on Artificial Intelligence.
ARTIFICIAL INTELLIGENCE IN CANADA: A DESCRIPTION BY THE MEMBERS OF THE ACAI
Jan. 1991 216 p
(NRC-31789; CTN-93-60828) Copyright Avail: CASI HC A10/MF A03

A composite description is provided of artificial intelligence research, development, and application as it exists in Canada today. The description is based on knowledge and information readily available to members of the Associate Committee on Artificial Intelligence of the National Research Council of Canada. Research and development activities, objectives, facilities, and other matters are reviewed in three main sections: consortia and other collaborative organizations; universities, government departments and agencies; and business and industry. In the aerospace field, of special interest are the activities of the Canadian Space Agency related to the Space Station Mobile Servicing System and its Strategic Technologies for Enhanced Automation and Robotics Program; Transport Canada's work on artificial intelligence in its Aviation Group; and CAE Electronics Ltd.'s FLITE program on aerodynamic simulation. Results of a Canadian artificial intelligence capability survey conducted in December 1989 are appended.
CISTI

N94-13529# National Aerospace Lab., Amsterdam (Netherlands). Informatics Div.
REASONING WITH UNCERTAIN AND INCOMPLETE INFORMATION IN AEROSPACE APPLICATIONS
J. C. Donker 25 Sep. 1991 21 p Presented at the AGARD symposium on Machine Intelligence for Aerospace Electronic Systems, Lisbon, Portugal, 16 May 1991
(NLR-TP-91366-U; ETN-93-94338) Avail: CASI HC A03/MF A01

The applicability of the Dempster-Shafer theory to reason with information that is uncertain or incomplete was investigated. Parts of the initiation and identification problems in multiradar tracking were modeled. It is shown that the Dempster-Shafer theory promises improvements over the Bayesian approach, but also that the latter currently is a more advanced theory than the former. Notions used in reasoning with incomplete or uncertain information are presented together with an overview of existing methods.
ESA

N94-13568 Tel-Aviv Univ. (Israel). Dept. of Interdisciplinary Studies.
ROBOT-TASK COMPLIANCE: THE ENERGY CRITERION M.S. Thesis
Eli Profeta Jan. 1991 133 p In HEBREW
(ITN-93-85196) Copyright Avail: Issuing Activity (Tel-Aviv Univ., Exact Sciences Library, Ramat Aviv 69978, Israel)

To help to define the criteria for selection of a robot for a task, robots are classified according to intelligence, manipulator type and drive system. The various tasks performed by robots are described and the special characteristics required of a robot to perform each task are noted. Limitations on the extensive use of robots are then described. In defining the criteria and composing the algorithms used in selection of a robot for a given task, special consideration is given to workspace requirements, degrees of freedom and manipulator design, from the point of view of their influence of the suitability of a robot to perform the task. The energy criterion was developed to enable all the above-mentioned considerations to be combined; it can be used to choose a robot for a task and to optimize the operation of the robot. This enables the inherently most efficient robot to be chosen for a task and for it then to be operated and controlled in the most energy efficient way. This criterion directly conflicts with time-optimal control of robot joints, and also with other optimization rules such as torque control, path optimization, trajectory or workspace optimization. Its benefit lies in lowering the stresses on moving parts and, hence, the wear on components; a further economic benefit is the reduced operational cost which arises from the low energy consumption of energy-efficient robots. Stages in developing the criterion are: Calculation of the task energy; comparison of that energy with the mechanical motion energy of the various types of robots, and then, after choosing the type of robot, programming its links to move in an energy efficient way by its electrical motors. ISA

N94-13603*# Research Inst. for Advanced Computer Science, Moffett Field, CA.
A REVIEW AND ANALYSIS OF NEURAL NETWORKS FOR CLASSIFICATION OF REMOTELY SENSED MULTISPECTRAL IMAGERY
Justin D. Paola and Robert A. Schowengerdt Jun. 1993 49 p
(Contract NAS2-13721; NAG5-2198)
(NASA-CR-194291; NAS 1.26:194291; RIACS-TR-93-05) Avail: CASI HC A03/MF A01

A literature survey and analysis of the use of neural networks for the classification of remotely sensed multispectral imagery is presented. As part of a brief mathematical review, the backpropagation algorithm, which is the most common method of training multi-layer networks, is discussed with an emphasis on its application to pattern recognition. The analysis is divided into five aspects of neural network classification: (1) input data preprocessing, structure, and encoding; (2) output encoding and extraction of classes; (3) network architecture, (4) training algorithms; and (5) comparisons to conventional classifiers. The advantages of the neural network method over traditional classifiers are its non-parametric nature, arbitrary decision boundary capabilities, easy adaptation to different types of data and input structures, fuzzy output values that can enhance classification, and good generalization for use with multiple images. The disadvantages of the method are slow training time, inconsistent results due to random initial weights, and the requirement of obscure initialization values (e.g., learning rate and hidden layer size). Possible techniques for ameliorating these problems are discussed. It is concluded that, although the neural network method has several unique capabilities, it will become a useful tool in remote sensing only if it is made faster, more predictable, and easier to use.
Author (revised)

N94-13704# Air Force Inst. of Tech., Wright-Patterson AFB, OH. School of Engineering.
ANNS: AN X WINDOW BASED VERSION OF THE AFIT NEURAL NETWORK SIMULATOR M.S. Thesis
Ching-Seh Wu Jun. 1993 172 p
(AD-A266540; AFIT/GCE/ENG/93J-01) Avail: CASI HC A08/MF A02

This thesis presents an X Window based neural network simulation environment developed at Air Force Institute of Technology (AFIT) using the techniques of modern software engineering. This artificial neural network simulator is a tool running on Sun SPARCstations and supporting two user modes: end-users and client-programmers. End-users interact with neural network paradigms developed by client-programmers for the purpose of studying and analyzing the execution of a particular Neural Network (NN) paradigm or class of NN algorithms. Client programmers maintain the system and use this environment for the development of new NN paradigms or algorithms for end-users. The development follows a hybrid software engineering paradigm which combines the best characteristics of the classic life cycle, prototype, and iterative methodologies through requirements, design, implementation, and testing. An object-oriented approach is used for the design including preliminary and detailed design. The system is implemented with the C programming language on Sun workstation and uses the XView window-based environment. It provides users with a variety of control and input options: simulation speed control, multiple and simultaneous NN algorithm simulations, and simulation environment control. DTIC

N94-13820# National Research Council of Canada, Ottawa (Ontario).
ARTIFICIAL INTELLIGENCE IN CANADA: A DESCRIPTION BY THE MEMBERS OF THE ACAI [INTELLIGENCE ARTIFICIELLE AU CANADA: MEMOIRE PREPARE PAR LES MEMBRES DU CAIA]
Jan. 1991 226 p In FRENCH
(CNR-31790; CTN-93-60827) Copyright Avail: CASI HC A11/MF A03

A composite description is provided of artificial intelligence research, development, and application as it exists in Canada today. The description is based on knowledge and information readily available to members of the Associate Committee on Artificial Intelligence of the National Research Council of Canada. Research and development activities, objectives, facilities, and other matters are reviewed in three main sections: consortia and other collaborative organizations; universities, government departments and agencies; and business and industry. In the aerospace field, of special interest are the activities of the Canadian Space Agency related to the Space Station Mobile Servicing System and its Strategic Technologies for Enhanced Automation and Robotics Program; Transport Canada's work on artificial intelligence in its Aviation Group; and CAE Electronics Ltd.'s FLITE program on aerodynamic simulation. Results of a Canadian artificial intelligence capability survey conducted in December 1989 are appended. CISTI

N94-13842 Ottawa Univ. (Ontario).
DEVELOPMENT OF A TACTILE AND VISION INTEGRATED SYSTEM, AND OBJECT IDENTIFICATION TECHNIQUES FOR SPDM APPLICATIONS
Emil Petriu, Niculae Trif, Yann Venne, and Michael Greenspan Mar. 1991 35 p
(Contract DSS-9F009-0-4015)
(DSIS-93-00153; CSA-DSM-CR-91-027; CTN-93-60801) Avail: CASI HC A03

The development and application of an experimental robotic tactile sensing system is described. The system is used for the active (exploratory) tactile perception of three dimensional object geometric profiles. The hardware developments consist of a 16-by-16 tactile probe and an instrumented passive compliant wrist. The software contributions consist of an interactive graphic display package and a library of basic image processing functions implemented as C-language programs. A two-dimensional correlation technique was developed to recover at the sub-pixel level the pose position errors occurring during the sequential tactile exploration of the large planar object surfaces. Author (CISTI)

N94-13844 Ottawa Univ. (Ontario).
DEVELOPMENT OF A COMPUTER VISION SYSTEM TO SUPPLEMENT THE ACTIVE TACTILE SENSING CAPABILITY IN A STRUCTURED ENVIRONMENT
Emil Petriu, Taco Bieseman, Niculae Trif, and Trevor James 1991 45 p
(DSIS-93-00072; CTN-93-60774) Avail: CASI HC A03

An orignal and nontraditional approach to the three dimensional object visual recognition problem is discussed. The proposed technique is based on a permanent encoding of all visible object surfaces with binary symbols corresponding to the terms of a large-size pseudo-random binary array. The applicability of the proposed method is restricted to applications such as space stations, nuclear plants, and hazardous but controllable environments which allow for object encoding and a-priori mapping of all encoded object surfaces in a geometric database. However, in these few recommended applications, the two-dimensional pseudo-random encoding provides a robust and computationally efficient means for visual object recognition. It would also allow for an easy integration with the tactile sensor system in a model-based multi-sensor data fusion system. Experiments were conducted on five encoded objects to validate the viability of the proposed method for object recognition in the space station environment. The results demonstrate the practicability of two-dimensional pseudo-random coding for visual recognition of three dimensional objects. Author (CISTI)

N94-13860# National Research Council of Canada, Ottawa (Ontario). Machinery and Engine Technology.
A DISTRIBUTED, VISUAL OBJECT SYSTEM USING AGGREGATION OBJECTS WITH A LOCAL NAMESPACE
David M. Morton Oct. 1992 38 p
(IME-MET-TR-007; NRCC-35853; CTN-93-60834) Avail: CASI HC A03/MF A01

A design for a distributed object system is described. Active objects are used to group other objects. Objects in the group may share specialized behavior and may reference each other by name. The distributed system is implemented in Audition, an object oriented language that extends the theatrical paradigm of performers and stages introduced in Rehearsal World. In Audition, Stages aggregate other objects and manage local namespaces; in Distributed Audition they are also active objects. Stages can themselves be named and can be members of a group of objects defined on another stage. Stages can be moved to any workstation on a network, thus, providing a global partitioned namespace. Stages maintain multiple threads and a queue of incoming messages. A potential intelligent simulation application is an air traffic control system. Author (CISTI)

N94-13999# Center for Mathematics and Computer Science, Amsterdam (Netherlands). Operations Research, Statistics, and System Theory Dept.
ON SOME RESULTS BY FUHRMANN ON HANKEL OPERATORS
Andrea Gombani (Consiglio Nazionale delle Ricerche, Padua, Italy.) Oct. 1992 9 p Sponsored in part by CNR, and NATO
(CWI-BS-R9224; ETN-93-94155) Copyright Avail: CASI HC A02/MF A01

Some generalizations and some simpler derivations of results by Fuhrmann are presented. In spite of the fact that Hankel operators have become, after the seminal paper of Adamjan, Arov and Krein, a central tool in systems theory and in interpolation theory, some of its features have been studied in detail only recently. Among the relevant results are the connection between restricted shift realizations and between the singular values of the original operator and those of its Nehari extension. A simple derivation of these results and some generalizations are presented. ESA

N94-14000# Center for Mathematics and Computer Science, Amsterdam (Netherlands). Operations Research, Statistics, and System Theory Dept.
ON RELATIONS BETWEEN SCHMIDT PAIRS ARISING IN ROBUST CONTROL
Andrea Gombani (Consiglio Nazionale delle Ricerche, Padua, Italy.) Oct. 1992 16 p Sponsored in part by CNR, and NATO
(CWI-BS-R9225; ETN-93-94156) Copyright Avail: CASI HC A03/MF A01

Some generalizations and some simpler derivations of results which appeared in Fuhrmann and Fuhrmann and Ober are presented. The main result is that the singular values and Schmidt vectors of the Hankel operator with symbol a normalized coprime factorization of a plant can be given an explicit representation in terms of the plant, of its optimally robust controller and of the Schmidt pairs of another scalar Hankel operator. ESA

N94-14001# Center for Mathematics and Computer Science, Amsterdam (Netherlands). Operations Research, Statistics, and System Theory Dept.
ON THE SCHMIDT PAIRS OF MULTIVARIABLE HANKEL OPERATORS AND ROBUST CONTROL
Andrea Gombani (Consiglio Nazionale delle Ricerche, Padua, Italy.) Oct. 1992 17 p Sponsored in part by CNR, and NATO
(CWI-BS-R9226; ETN-93-94157) Copyright Avail: CASI HC A03/MF A01

The multivariable version of a result which appeared in Fuhrmann and Ober is considered. It is shown that the singular values and the Schmidt vectors of the Hankel operator with symbol a normalized coprime factorization of a plant can be given an explicit representative in terms of the plant, of its superoptimally robust controller and of the Schmidt pairs of another Hankel operator. The derivation is obtained using techniques of superoptimal Nehari extension developed by Young. ESA

N94-14018# Center for Mathematics and Computer Science, Amsterdam (Netherlands). Operations Research, Statistics, and System Theory Dept.
TUNING OF GAUSSIAN STOCHASTIC CONTROL SYSTEMS
J. H. VanSchuppen Oct. 1992 32 p Submitted for publication
(CWI-BS-R9223; ETN-93-94154) Copyright Avail: CASI HC A03/MF A01

A study aimed at exploring the question of which adaptive controllers for Gaussian stochastic control systems achieve tuning in closed loop is presented. A closed loop consisting of a control system and an adaptive controller is called 'tuning' for a specified control objective if the real system and the ideal system defined below achieve the same value for the control objective. The 'real system' is the system consisting of the unknown control system in closed loop with the adaptive controller in which the parameters of the adaptive controller have been determined by identification under feedback or in closed loop. The 'ideal system' is the system consisting of the unknown control system in closed loop with a controller in which the controller has been synthesized with knowledge of the unknown control system and such that the closed loop system satisfies the control objective. For which adaptive controllers does tuning hold? This question is considered for both a Gaussian stochastic control system with full observations and with partial observations. The approach to the problem is based on stochastic realization theory for Gaussian systems. The question is answered positively for the control objectives of minimum variance control and pole placement. Necessary conditions for tuning are discussed. ESA

N94-14084# Instituto de Pesquisas Espaciais, Sao Jose dos Campos (Brazil).
SELF-TUNING CONTROL TECHNIQUES FOR MULTIVARIABLE SYSTEMS M.S. Thesis [TECNICAS DE CONTROLE AUTO-SINTONIZADO PARA SISTEMAS MULTIVARIAVEIS]
Suely Silva Feb. 1992 105 p In PORTUGESE
(INPE-5449-TDI/495) Avail: CASI HC A06/MF A02

This work presents the development of a control algorithm of the self-tuning type for the control of multivariable systems when the number of outputs is greater than the number of inputs. For its application, the system dynamics is supposed unknown and represented by a difference equation, accordingly to which the future observations are obtained from the past values observations and inputs. As a worked out example, the attitude control of a low altitude satellite with triaxial stabilization is given. The observations are provided by measurements supposedly acquired through solar and horizon sensors and gyrometers. An optimal algorithm uses them to estimate the parameters that define the attitude of the satellite. The inputs are the three control torques that are respectively applied on the three axes by means of gas jets and according to the attitude simulator used for the tests. Finally, the results of the tests that evaluate the feasibility of the proposed procedure are presented. Author

N94-14117# Los Alamos National Lab., NM.
KNOWLEDGE BASED SYSTEMS: FROM PROCESS CONTROL TO POLICY ANALYSIS
J. G. Marinuzzi 1993 6 p Presented at the Ideas in Science and Electronics Meeting, Albuquerque, NM, 11 May 1993
(Contract W-7405-eng-36)
(DE93-014582; LA-UR-93-1717; CONF-9305187-2) Avail: CASI HC A02/MF A01

Los Alamos has been pursuing the use of Knowledge Based Systems for many years. These systems are currently being used to support projects that range across many production and operations areas. By investing time and money in people and equipment, Los Alamos has developed one of the strongest knowledge based systems capabilities within the DOE. Staff of Los Alamos' Mechanical and Electronic Engineering Division are using these knowledge systems to increase capability, productivity, and competitiveness in areas of manufacturing quality control, robotics, process control, plant design, and management decision support. This paper describes some of these projects and associated technical program approaches, accomplishments, benefits, and future goals. DOE

N94-14201# National Research Council of Canada, Ottawa (Ontario). Inst. for Information Technology.
THE BIRIS SERVER: INTEGRATION OF A THREE-DIMENSIONAL RANGE SENSOR INTO A HARMONY-BASED REALTIME ARCHITECTURE
D. A. Green and F. Blais Apr. 1992 19 p
(ERB-1036; NRC-33183; CTN-93-60822) Copyright Avail: CASI HC A03/MF A01

The BIRIS three dimensional laser range sensor has been interfaced to a multiprocessor system running under the Harmony realtime operating system. The method and rationale used in the interfacing are described, with emphasis on a description of a server that presents to the application programmer a clear abstraction of the BIRIS system so that control of the device and access to its data are uncomplicated. The system described is a component of a mobile robot system developed by the Autonomous Systems Laboratory at the National Research Council of Canada. BIRIS is initially being implemented on the mobile robot using a single laser projector and two video fields per acquisition (azimuth scanning only). The BIRIS system configured for this application offers short range sensing limited to about 3.5 m. BIRIS will be used primarily as a source of realtime range data for local navigation purposes. Description of the BIRIS server includes the system hardware configuration, interface mechanics, Harmony task structure in the software configuration, high level software interface, and initialization of the server. CISTI

N94-14361# Center for Mathematics and Computer Science, Amsterdam (Netherlands). Operations Research, Statistics, and System Theory Dept.
STOCHASTIC BOUNDS FOR A POLLING SYSTEM
O. J. Boxma (Tilburg Univ., Netherlands.) and M. Kelbert Nov. 1992 15 p Submitted for publication Sponsored in part by the Commission of the European Communities
(CWI-BS-R9230; ETN-93-94161) Copyright Avail: CASI HC A03/MF A01

Two queueing systems are considered: a symmetric polling system with gated service at all N queues and with switchover times, and a single server single queue model with one arrival stream of ordinary customers and N additional permanently present customers. It is assumed that the combined arrival process at the queues of the polling system coincides with the arrival process of the ordinary customers in the single queue model, and that the service time and switchover time distributions of the polling mode coincide with the service time distributions of the ordinary and permanent customers, respectively, in the single queue model. A complete equivalence between both models is accomplished by the following queue insertion of arriving customers. In the single queue model, an arriving ordinary customer occupies with probability p(sub i) a position at the end of the queue section behind the i-th permanent customer, i = 1,...,N. In the cyclic polling model, an arriving customer with probability p(sub i) joins the end of the i-th queue to be visited by the server, measured from its present position. For the single queue model it is proved that, if two queue insertion distributions (p(sub i), i = 1, ..., N) and (q(sub i), i = 1,...,N) are stochastically ordered, then also the workload and queue length distribution in the corresponding two single queue versions are stochastically ordered. This immediately leads to equivalent stochastic orderings in polling models. The single queue model with Poisson arrivals and p(sub 1) = 1 is studied in detail. ESA

N94-14444*# Georgia Inst. of Tech., Atlanta. School of Aerospace Engineering.
DEVELOPMENT OF AN hp-VERSION FINITE ELEMENT METHOD FOR COMPUTATIONAL OPTIMAL CONTROL Semiannual Progress Report, 22 Feb. - 21 Aug. 1993
Dewey H. Hodges and Michael S. Warner 21 Aug. 1993 14 p
(Grant NAG1-1435)
(NASA-CR-194149; NAS 1.26:194149) Avail: CASI HC A03/MF A01

The purpose of this research effort is to develop a means to use, and to ultimately implement, hp-version finite elements in the numerical solution of optimal control problems. The hybrid MACSYMA/FORTRAN code GENCODE was developed which utilized h-version finite elements to successfully approximate solutions to a wide class of optimal control problems. In that code the means for improvement of the solution was the refinement of the time-discretization mesh. With the extension to hp-version finite elements, the degrees of freedom include both nodal values and extra interior values associated with the unknown states, co-states, and controls, the number of which depends on the order of the shape functions in each element. Author (revised)

N94-14568# Oak Ridge National Lab., TN.
DECENTRALIZED CONTROL OF UNCERTAIN SYSTEMS VIA SENSITIVITY MODELS
D. A. Schoenwald and U. Oezguener 1993 5 p Presented at the 12th IFAC World Congress, Sydney, Australia, 19-23 Jul. 1993
(Contract DE-AC05-84OR-21400)
(DE93-012963; CONF-930781-1) Avail: CASI HC A01/MF A01

In this paper, we present a decentralized strategy for optimal control of interconnected systems exhibiting parametric uncertainty. First, we demonstrate that sensitivity models for linear interconnected systems can be generated at each subsystem using only locally available information. Second, we present an optimal control law that incorporates sensitivity functions in the feedback path. The control scheme is completely decentralized and is proposed as a means of making the closed loop system less sensitive to parameter deviations. Finally, we give an example of an interconnected system and show how this control strategy is implemented. DOE

N94-14718# Rome Univ. (Italy). Dipt. di Fisica.
RETRIEVAL PROPERTIES OF NEURAL NETWORKS WITH INFINITELY MANY MARKED PATTERNS
Stam Nicolis (Istituto Nazionale di Fisica Nucleare, Rome, Italy.) 5 Mar. 1990 12 p Sponsored by EEC
(Preprint-729; ETN-93-94367) Avail: CASI HC A03/MF A01

An extension of the Hopfield model, where a certain number of 'privileged' (or 'marked') patterns enters the Hebb rule with weight 1, while the remaining enter with weight gamma less than 1, was studied. Both sets are infinite. Assuming replica symmetry, the zero temperature capacity minus gamma and overlap minus gamma diagrams are calculated and compared with numerical simulations, when both sets hold the same number of patterns. The transitions from the retrieval to the spin glass phase are found to be first order. ESA

N94-14737# Los Alamos National Lab., NM.
IDENTIFICATION OF CONTINUOUS-TIME DYNAMICAL SYSTEMS: NEURAL NETWORK BASED ALGORITHMS AND PARALLEL IMPLEMENTATION
R. M. Farber, A. S. Lapedes, R. Rico-Martinez (Princeton Univ., NJ.), and I. G. Kevrekidis (Princeton Univ., NJ.) 1993 5 p Presented at the 6th Society for Industrial and Applied Mathematics (SIAM) Conference on Parallel Processing for Scientific Computing, Norfolk, VA, 21-24 Mar. 1993
(Contract W-7405-eng-36)
(DE93-014427; LA-UR-93-1565; CONF-930331-11) Avail: CASI HC A01/MF A01

Time-delay mappings constructed using neural networks have proven successful performing nonlinear system identification; however, because of their discrete nature, their use in bifurcation analysis of continuous-tune systems is limited. This shortcoming can be avoided by embedding the neural networks in a training algorithm that mimics a numerical integrator. Both explicit and implicit integrators can be used. The former case is based on repeated evaluations of the network in a feedforward implementation; the latter relies on a recurrent network implementation. Here the algorithms and their implementation on parallel machines (SIMD and MIMD architectures) are discussed. DOE

N94-14777# SRI International Corp., Menlo Park, CA.
PASSIVE RECOVERY OF SCENE GEOMETRY FOR AN UNMANNED GROUND VEHICLE Annual Report, Nov. 1991 - Nov. 1992
Robert C. Bolles May 1993 34 p
(Contract DACA76-92-C-0003; DARPA Order 8323)
(AD-A266670; TEC-0033) Avail: CASI HC A03/MF A01

The primary goal of this project is to develop a passive technology for recovering scene geometry in order to support an Unmanned Ground Vehicle (UGV) operating in a general outdoor environment. We focus on our evaluation of current stereo techniques. We report the results of the first phase of this evaluation and discuss plans for the second phase. In addition, we briefly describe our progress in the following areas: development of new object tracking techniques; application of a new scene modeling technique (developed on a parallel contract at SRI) to UGV tasks; and development of two auxiliary techniques to support our research--a technique for generating synthetic stereo pairs and a technique for multiplexing imagery from a pair of moving cameras onto a single videotape. DTIC

N94-14785# BDM International, Inc., Arlington, VA.
SMART MATERIALS/STRUCTURES TECHNICAL ANALYSIS Final Report, 26 Nov. 1990 - 30 Nov. 1992
Phillip A. Parrish, Carlos J. Coe, and Norman M. Wereley 3 Jun. 1993 52 p
(Contract DAAL03-91-C-0002)
(AD-A266771; BDM-VAS-0784-93-TR; ARO-28608.1-MS) Avail: CASI HC A04/MF A01

'Smart' materials and structures have the capability to respond to their environment to a significant degree, by virtue of intrinsic properties and/or built-in sensor/actuator systems. The words 'smart' or 'intelligent' as applied to materials/structures are used in an idealistic and imprecise way to indicate an analogy with the integrated sensor/actuator/control systems evolved by living beings. The programmatic objectives of this proposal suggest the following definition of Smart materials/structures (SMS): Smart materials/structures (SMS) are structural systems based upon materials with the ability to 'sense' their own response to environmental and operational stimuli and able to modify that response in such as way as to maintain or optimize structural performance, utilizing embedded sensors and actuators interfaced with closed-loop adaptive control systems based on system stimulus-response models. In this effort, BDM Federal, Inc., a subsidiary of BDM International, Inc. conducted a technical analysis of Smart Materials and Structures in order to assist DARPA in planning a future initiative in this area. DTIC

N94-14882# Naval Command, Control and Ocean Surveillance Center, San Diego, CA. RDT and E Div.
DETERMINING NEURAL NETWORK CONNECTIVITY USING EVOLUTIONARY PROGRAMMING
John R. McDonnell and Don Waagen Mar. 1993 6 p
(AD-A266853) Avail: CASI HC A02/MF A01

This work investigates the application of evolutionary programming, a stochastic search technique, for determining connectivity in feedforward neural networks. The method is capable of simultaneously evolving both the connection scheme and the network weights. The number of synapses are incorporated into an objective function so that network parameter optimization is done with respect to a connectivity cost as well as mean pattern error. Experimental results are shown using feedforward networks for simple binary mapping problems. DTIC

N94-14634*# Toronto Univ. (Ontario). Inst. for Aerospace Studies.
A NEURAL-NETWORK APPROACH TO ROBOTIC CONTROL
D. P. W. Graham and G. M. T. DEleuterio *In* JPL, Proceedings of the Fifth NASA/NSF/DOD Workshop on Aerospace Computational Control 15 Feb. 1993 p 221-236 Sponsored by Natural Science and Engineering Research Council; Inst. for Robotics and Intelligent Systems; Inst. for Space and Terrestrial Science (For primary document see N94-14618 02-39)
Avail: CASI HC A03/MF A04

N94-14643*# California Univ., Los Angeles. Dept. of Chemical Engineering.
ON I(1): OPTIMAL DECENTRALIZED PERFORMANCE
Dennis Sourlas and Vasilios Manousiouthakis *In* JPL, Proceedings of the Fifth NASA/NSF/DOD Workshop on Aerospace Computational Control 15 Feb. 1993 p 395-411 (For primary document see N94-14618 02-39)
Avail: CASI HC A03/MF A04

N94-14651*# Computer Motion, Inc., Goleta, CA.
DESIGN AND CONTROL OF A MACRO-MICRO ROBOT FOR PRECISE FORCE APPLICATIONS
Yulun Wang, Amante Mangaser, Keith Laby, Steve Jordan, and Jeff Wilson *In* JPL, Proceedings of the Fifth NASA/NSF/DOD Workshop on Aerospace Computational Control 15 Feb. 1993 p 535-552 Sponsored in part by NSF (For primary document see N94-14618 02-39)
Avail: CASI HC A03/MF A04

64 NUMERICAL ANALYSIS

Includes iteration, difference equations, and numerical approximation.

N94-12895# International Centre for Theoretical Physics, Trieste (Italy).
SCALAR CURVATURE AND SPHERICAL-TYPE RIEMANNIAN MANIFOLDS
J. P. Ezin Oct. 1992 10 p
(DE93-622852; IC-92/317) Avail: CASI HC A02/MF A01 (US Sales Only)

In this paper after reporting on Tanno and Weber conditions linked with closed conformal vector fields for a Riemannian compact manifold to be isometric with Euclidean sphere, we prove that if a metric conformal to the induced one on a hypersurface of a (n + 1)-dimensional manifold with nonpositive constant sectional curvature has constant scalar curvature equal to 2n - 3, then the ambient space is Euclidean space. DOE

N94-13025# Utah State Univ., Logan. Dept. of Mathematics.
NEWTON ITERATIVE METHODS FOR LARGE SCALE NONLINEAR SYSTEMS
H. F. Walker and K. Turner 1993 5 p
(Contract DE-FG02-92ER-25136)
(DE93-015357; DOE/ER-25136/1) Avail: CASI HC A01/MF A01

The objective of this project is to develop robust, efficient Newton iterative methods for general large scale problems well suited for discretizations of partial differential equations, integral equations, and other continuous problems. A concomitant objective is to develop improved iterative linear algebra methods. We first outline research on Newton iterative methods and then review work on iterative linear algebra methods. DOE

N94-13202*# National Aeronautics and Space Administration. Langley Research Center, Hampton, VA.
A ROBUST MULTILEVEL SIMULTANEOUS EIGENVALUE SOLVER Final Report
Sorin Costiner (Weizmann Inst. of Science, Rehovoth, Israel.) and Shlomo Taasan Washington Jun. 1993 21 p
(Contracts NAS1-19480; NAS1-18605; RTOP 505-90-52-01)
(NASA-CR-191491; ICASE-93-35; NAS 1.26:191491) Avail: CASI HC A03/MF A01

Multilevel (ML) algorithms for eigenvalue problems are often faced with several types of difficulties such as: the mixing of approximated eigenvectors by the solution process, the approximation of incomplete clusters of eigenvectors, the poor representation of solution on coarse levels, and the existence of close or equal eigenvalues. Algorithms that do not treat appropriately these difficulties usually fail, or their performance degrades when facing them. These issues motivated the development of a robust adaptive ML algorithm which treats these difficulties, for the calculation of a few eigenvectors and their corresponding eigenvalues. The main techniques used in the new algorithm include: the adaptive completion and separation of the relevant clusters on different levels, the simultaneous treatment of solutions within each cluster, and the robustness tests which monitor the algorithm's efficiency and convergence. The eigenvectors' separation efficiency is based on a new ML projection technique generalizing the Rayleigh Ritz projection, combined with a technique, the backrotations. These separation techniques, when combined with an FMG formulation, in many cases lead to algorithms of O(qN) complexity, for q eigenvectors of size N on the finest level. Previously developed ML algorithms are less focused on the mentioned difficulties. Moreover, algorithms which employ fine level separation techniques are of O(q(sub 2)N) complexity and usually do not overcome all these difficulties. Computational examples are presented where Schrodinger type eigenvalue problems in 2-D and 3-D, having equal and closely clustered eigenvalues, are solved with the efficiency of the Poisson multigrid solver. A second order approximation is obtained in O(qN) work, where the total computational work is equivalent to only a few fine level relaxations per eigenvector. Author (revised)

N94-13223# Gosudarstvennyi Komitet po Ispolzovaniyu Atomnoi Energii, Moscow (USSR).
HYDRODYNAMIC ASYMPTOTICS OF GREEN FUNCTIONS IN MAGNETICS WITH SPONTANEOUSLY BROKEN SYMMETRY
M. Yu. Kovalevskij and A. L. Shishkin 1991 12 p In RUSSIAN
(DE93-621349; KFTI-91-10) Avail: CASI HC A03/MF A01 (US Sales Only)

Dynamic equations of magnetics with full spontaneous symmetry breaking in relation to spin rotations in presence of an external field are formulated on the basis of the Hamilton approach. Low-frequent asymptotic Green functions G(sub ab)(k-vector, omega) with arbitrary a,b dynamic values are found and spin wave spectra are obtained. DOE

N94-13284 Carnegie-Mellon Univ., Pittsburgh, PA. Dept. of Computer Science.
SOLVING INTEGER PROGRAMS FROM DEPENDENCE AND SYNCHRONIZATION PROBLEMS
Jaspal Subhlok Mar. 1993 21 p Limited Reproducibility: More than 20% of this document may be affected by microfiche quality
(Contract MDA972-90-C-0035; ARPA Order 7330)
(AD-A265702; CMU-CS-93-130) Avail: CASI HC A03

We present a method to determine whether a set of equations has a non-negative integer solution. The method is designed for the particular occurence of this problem in the context of compiler analysis of parallel programs. The system of equations is first transformed to Smith normal form to determine if any integer solutions exist. In case of multiple integer solutions, a parameterized solution space representing all non-negative solutions is obtained. Fourier-Motzkin elimination is employed to determine if the real solution space is empty. If the solution space is not empty, either the existence of an integer solution is readily verified, or a simplified convex region is obtained such that the original system of equations has a solution if and only if this convex region contains an integer point. The main result of the paper is a set of new heuristic search procedures that are used to identify an integer solution in a convex region, or to prove that no integer solution exists. These are based on the geometrical properties of convex regions that are not empty but do not contain integer points. This method is an exact and efficient way of solving integer programming problems arising in dependence and synchronization analysis of parallel programs. DTIC

N94-13289*# Institute for Computer Applications in Science and Engineering, Hampton, VA.
A HYBRID PADE-GALERKIN TECHNIQUE FOR DIFFERENTIAL EQUATIONS Final Report
James F. Geer and Carl M. Andersen (College of William and Mary, Williamsburg, VA.) Washington Jul. 1993 25 p Submitted for publication
(Contract NAS1-19480; RTOP 505-90-52-01)
(NASA-CR-191494; NAS 1.26:191494; ICASE-93-38) Avail: CASI HC A03/MF A01

A three-step hybrid analysis technique, which successively uses the regular perturbation expansion method, the Pade expansion method, and then a Galerkin approximation, is presented and applied to some model boundary value problems. In the first step of the method, the regular perturbation method is used to construct an approximation to the solution in the form of a finite power series in a small parameter epsilon associated with the problem. In the second step of the method, the series approximation obtained in step one is used to construct a Pade approximation in the

form of a rational function in the parameter epsilon. In the third step, the various powers of epsilon which appear in the Pade approximation are replaced by new (unknown) parameters (delta(sub j)). These new parameters are determined by requiring that the residual formed by substituting the new approximation into the governing differential equation is orthogonal to each of the perturbation coordinate functions used in step one. The technique is applied to model problems involving ordinary or partial differential equations. In general, the technique appears to provide good approximations to the solution even when the perturbation and Pade approximations fail to do so. The method is discussed and topics for future investigations are indicated. Author (revised)

N94-13354*# Institute for Computer Applications in Science and Engineering, Hampton, VA.

ACTIVE CONTROL OF ACOUSTIC PRESSURE FIELDS USING SMART MATERIAL TECHNOLOGIES Final Report

H. T. Banks (North Carolina State Univ., Raleigh.) and R. C. Smith (National Aeronautics and Space Administration. Langley Research Center, Hampton, VA.) Washington Jun. 1993 31 p Presented at the Workshop on Flow Control, Minneapolis, MN, 16-20 Nov. 1992 Submitted for publication

(Contracts NAS1-18605; NAS1-19480; AF-AFOSR-0091-90; RTOP 505-90-52-01)

(NASA-CR-191480; NAS 1.26:191480; ICASE-93-31) Avail: CASI HC A03/MF A01

An overview describing the use of piezoceramic patches in reducing noise in a structural acoustics setting is presented. The passive and active contributions due to patches which are bonded to an Euler-Bernoulli beam or thin shell are briefly discussed and the results are incorporated into a 2-D structural acoustics model. In this model, an exterior noise source causes structural vibrations which in turn lead to interior noise as a result of nonlinear fluid/structure coupling mechanism. Interior sound pressure levels are reduced via patches bonded to the flexible boundary (a beam in this case) which generate pure bending moments when an out-of-phase voltage is applied. Well-posedness results for the infinite dimensional system are discussed and a Galerkin scheme for approximating the system dynamics is outlined. Control is implemented by using linear quadratic regulator (LQR) optimal control theory to calculate gains for the linearized system and then feeding these gains back into the nonlinear system of interest. The effectiveness of this strategy for this problem is illustrated in an example. Author (revised)

N94-13391# Argonne National Lab., IL. Mathematics and Computer Science Div.

SIMPLIFICATION-DRIVEN AUTOMATED PARTIAL EVALUATION

J. M. Boyle 21 Nov. 1992 13 p Presented at the ACM SIGPLAN Symposium on Partial Evaluation and Semantics Based Program Manipulation, Gothenburg, Sweden, 14-16 Jun. 1993

(Contract W-31-109-eng-38)

(DE93-012890; ANL/MCS/CP-78726; CONF-9306162-1) Avail: CASI HC A03/MF A01

I describe an automated approach to partial evaluation based on simplification and implemented by program transformations. The approach emphasizes program algebra and relies on canonical forms and distributive laws to expose instances to which simplifications can be applied. I discuss some of the considerations that led to the design of this approach. This design discussion should be useful both in understanding the structure of the partial evaluation transformations and as an example of how to approach the design of automated program transformations in general. This approach to partial evaluation has been applied to a number of practical examples of moderate complexity, including the following: the running example used in this paper, proving an identity for lists, and eliminating a virtual data structure from a specification of practical interest. The chief practical barrier to its wider application is the growth of the intermediate program text during partial evaluation. Despite this limitation, this approach has the virtues of being implemented, automated, and able to partially evaluate specifications containing implicit data, including some specifications of practical interest. DOE

N94-13421*# Texas Univ., Brownsville.

ROBUST STABILITY OF DIAMOND FAMILIES OF POLYNOMIALS WITH COMPLEX COEFFICIENTS

Zhong Ling Xu 1993 16 p

(Grant NAG5-2210)

(NASA-CR-194132; NAS 1.26:194132) Avail: CASI HC A03/MF A01

Like the interval model of Kharitonov, the diamond model proves to be an alternative powerful device for taking into account the variation of parameters in prescribed ranges. The robust stability of some kinds of diamond polynomial families with complex coefficients are discussed. By exploiting the geometric characterizations of their value sets, we show that, for the family of polynomials with complex coefficients and both their real and imaginary parts lying in a diamond, the stability of eight specially selected extreme point polynomials is necessary as well as sufficient for the stability of the whole family. For the so-called simplex family of polynomials, four extreme point and four exposed edge polynomials of this family need to be checked for the stability of the entire family. The relations between the stability of various diamonds are also discussed. Author

N94-13496# Center for Mathematics and Computer Science, Amsterdam (Netherlands). Computer Science/Software Technology Dept.

THE SILENT STEP IN TIME

A. S. Klusener Jun. 1992 76 p

(CWI-CS-R9221; ETN-93-94163) Copyright Avail: CASI HC A05/MF A01

In untimed process algebras such as CCS and ACP (Algebra of Communicating Sequential Process), the silent step enables abstraction from internal actions. Several formalizations of abstraction have been introduced, such as observational congruence, delay bisimulation, and branching bisimulation. However, in real time process algebras such as ACP(rho), the silent step has not yet been solved. A formalization of these semantics regarding the silent step in real time process algebra is presented. The characterizing laws, which correspond closely to the untimed laws, are studied. An investigation as to which of the semantics is appropriate in the context of ACP(rho) is performed. Restriction is made to process terms without recursion and completeness, and decidability for branching bisimulation equivalence is obtained. ESA

N94-13499# Rome Univ. (Italy). Dipt. di Fisica.

INTEGRABLE SYSTEM DESCRIBING SURFACES OF NON-CONSTANT CURVATURE

D. Levi (Istituto Nazionale di Fisica Nucleare, Rome, Italy.) and A. Sym (Warsaw Univ., Poland.) 10 Apr. 1990 4 p

(Preprint-734; ETN-93-94371) Avail: CASI HC A01/MF A01

The soliton technique is applied to a system of partial differential equations describing the geometry of a special class of hyperbolic surfaces, that is surfaces in E cubed of negative curvature. The Darboux matrix is presented and a purely algebraic way to generate exact solutions to this system is described. ESA

N94-13526# Center for Mathematics and Computer Science, Amsterdam (Netherlands). Computer Science/Software Technology Dept.

ON THE FOUNDATIONS OF FINAL SEMANTICS: NON-STANDARD SETS, METRIC SPACES, PARTIAL ORDERS

Jan. J. M. M. Rutten and Daniele Turi Nov. 1992 56 p Submitted for publication Sponsored in part by Stichting voor Fundamenteel Onderzoek der Materie

(CWI-CS-R9241; ETN-93-94167) Copyright Avail: CASI HC A04/MF A01

Canonical solutions of domain equations are shown to be 'final coalgebras', not only in a category of nonstandard sets (as already known), but also in categories of metric spaces and partial orders. Coalgebras are simple categorical structures generalizing the notion of post-fixed point. They are also used here for giving a new comprehensive presentation of the (still) nonstandard theory of 'non-well-founded sets' (as non standard sets are usually called). This paper is meant to provide a basis to a more general project aiming at a full exploitation of the finality of the domains in the semantics of programming languages. Such a 'final semantics' enjoys uniformity and generality. For instance, semantic observational equivalences like bisimulation can be derived as instances of a single 'coalgebraic' definition (introduced elsewhere), which is parametric of the functor appearing in the domain equation. Some properties of this general form of equivalence are also studied. ESA

N94-13536# International Centre for Theoretical Physics, Trieste (Italy).
ON THE SYMMETRY ALGEBRA OF THE DISCRETE STATES IN d LESS THAN 2 CLOSED STRING THEORY
S. Panda (Groningen Rijksuniv., Netherlands.) and S. Roy Jan. 1993 13 p
(DE93-622903; IC-93/13; UG-1/93) Avail: CASI HC A03/MF A01 (US Sales Only)

The symmetry charges associated with the Lian-Zuckerman states for d less than 2 closed string theory are constructed. Unlike in the open string case, it is shown here that the symmetry charges commute among themselves and act trivially on all the physical states. DOE

N94-13545# Electrotechnical Lab., Tsukuba (Japan).
ROBUST FILTERS FOR IMAGE SMOOTHING
T. Kurita and P. Boulanger (National Research Council of Canada, Ottawa, Ontario.) Dec. 1990 35 p
(ERB-1033; NRC-31798; CTN-93-60824) Copyright Avail: CASI HC A03/MF A01

The properties of some rank filters such as median, least median squared, and trimmed median squared, are discussed in the context of robust statistics. The efficient computation of these filters is discussed and their stability to the outlier is compared with the standard median filter. Using the robust estimator as an outliers detector, a new type of filter can be designed which performs smoothing on the remaining pixels after removing the outliers. The Gaussian reweighted median (GRM) filter uses Gaussian weights inhibited at the outlier positions to smooth images. This filter inherits the properties of both median and Gaussian filters. Experimental results are presented showing comparisons between corrupted digital images and the same images processed by the various filters. It is demonstrated experimentally that the GRM filter is the best filter overall since it operates like a median filter on impulse noises and reduces the Gaussian noise. Comparison of the GRM filter and the Gaussian filter shows that the GRM filter can preserve sharp edges while small details of the image are smoothed. Subroutines for finding location estimates are appended.
Author (CISTI)

N94-13717*# National Aeronautics and Space Administration. Langley Research Center, Hampton, VA.
PRECONDITIONING AND THE LIMIT TO THE INCOMPRESSIBLE FLOW EQUATIONS
E. Turkel, A. Fiterman, and B. vanLeer Washington Jul. 1993 23 p Submitted for publication
(Contracts NAS1-18605; NAS1-19480; RTOP 505-90-52-01)
(NASA-CR-191500; ICASE-93-42; NAS 1.26:191500) Avail: CASI HC A03/MF A01

The use of preconditioning methods to accelerate the convergence to a steady state for both the incompressible and compressible fluid dynamic equations are considered. The relation between them for both the continuous problem and the finite difference approximation is also considered. The analysis relies on the inviscid equations. The preconditioning consists of a matrix multiplying the time derivatives. Hence, the steady state of the preconditioned system is the same as the steady state of the original system. For finite difference methods the preconditioning can change and improve the steady state solutions. An application to flow around an airfoil is presented. Author

N94-13722*# Institute for Computer Applications in Science and Engineering, Hampton, VA.
CANONICAL FORMS OF MULTIDIMENSIONAL STEADY INVISCID FLOWS Final Report
Shlomo Taasan Washington Jun. 1993 15 p Submitted for publication
(Contracts NAS1-19480; NAS1-18605; RTOP 505-90-52-01)
(NASA-CR-191488; NAS 1.26:191488; ICASE-93-34) Avail: CASI HC A03/MF A01

Canonical forms and canonical variables for inviscid flow problems are derived. In these forms the components of the system governed by different types of operators (elliptic and hyperbolic) are separated. Both the incompressible and compressible cases are analyzed, and their similarities and differences are discussed. The canonical forms obtained are block upper triangular operator form in which the elliptic and non-elliptic parts reside in different blocks. The full nonlinear equations are treated without using any linearization process. This form enables a better analysis of the equations as well as better numerical treatment. These forms are the analog of the decomposition of the one dimensional Euler equations into characteristic directions and Riemann invariants. Author (revised)

N94-13725*# Institute for Computer Applications in Science and Engineering, Hampton, VA.
THE CHEBYSHEV-LEGENDRE METHOD: IMPLEMENTING LEGENDRE METHODS ON CHEBYSHEV POINTS Final Report
Wai Sun Don (Brown Univ., Providence, RI.) and David Gottlieb (Brown Univ., Providence, RI.) Washington Jul. 1993 23 p Submitted for publication
(Contracts NAS1-19480; AF-AFOSR-0090-93; N00014-91-J-4016; NSF DMS-92-11820; RTOP 505-90-52-01)
(NASA-CR-191497; NAS 1.26:191497; ICASE-93-40) Avail: CASI HC A03/MF A01

We present a new collocation method for the numerical solution of partial differential equations. This method uses the Chebyshev collocation points, but because of the way the boundary conditions are implemented, it has all the advantages of the Legendre methods. In particular, L2 estimates can be obtained easily for hyperbolic and parabolic problems.
Author (revised)

N94-13731# Weidlinger Associates, New York, NY.
NON-UNIQUENESS IN DYNAMIC RATE-INDEPENDENT NON-ASSOCIATED PLASTICITY Technical Report, 15 Jun. 1989 - 31 Mar. 1992
Ivan S. Sandler and Thomas A. Pucik (Logicon R and D Associates, Los Angeles, CA.) 1 Jun. 1993 37 p
(Contract DNA001-89-C-0052)
(AD-A266342; WA-9204; DNA-TR-92-108) Avail: CASI HC A03/MF A01

Ground shock calculations often use rate-independent plasticity models with non-associated flow. By means of a 'constructive' mathematical proof, it is demonstrated here that this approach leads to multiple (and therefore spurious) solutions for dynamic initial/boundary value problems; in other words, uniqueness is lost. Although a simple class of multiple solutions is presented, the results are shown to be generally valid, implying that normality of flow is a necessary (as well as a sufficient) condition for uniqueness in dynamic applications of rate-independent plasticity. This finding implies an inherent lack of robustness in numerical analyses utilizing models based on non-associated flow. Because the use of such models is widespread in ground shock (and structural) calculations, the fact that uniqueness breaks down is significant; it casts serious doubt on any (and every) calculation based on these constitutive representations. It is strongly recommended that all ground shock calculators promptly abandon their reliance on such models. To describe the situation most bluntly, these models do not provide a rational basis for the computations needed for prediction, design and/or analysis applications. In all cases for which an associated flow rule is deemed inadequate to fit observed material behavior, an approach other than rate-independent plasticity must be sought in order to represent such behavior in a reliable, self-consistent and rational manner. DTIC

N94-13792*# Institute for Computer Applications in Science and Engineering, Hampton, VA.
HIGH ORDER HYBRID NUMERICAL SIMULATIONS OF TWO DIMENSIONAL DETONATION WAVES Final Report
Wei Cai (North Carolina Univ., Charlotte.) Washington Jul. 1993 42 p
(Contract NAS1-19480; RTOP 505-90-52-01; NSF ASC-91-13895)
(NASA-CR-191506; ICASE-93-47; NAS 1.26:191506) Avail: CASI HC A03/MF A01

In order to study multi-dimensional unstable detonation waves, a high order numerical scheme suitable for calculating the detailed transverse wave structures of multidimensional detonation waves was developed. The numerical algorithm uses a multi-domain approach so different numerical techniques can be applied for different components of detonation waves. The detonation waves are assumed to undergo an irreversible, unimolecular reaction A yields B. Several cases of unstable two dimensional detonation waves are simulated and detailed transverse wave interactions are documented. The numerical results show the importance of resolving the detonation front without excessive numerical viscosity in order to obtain the correct cellular patterns. Author (revised)

N94-13809 Politecnico di Milano (Italy). Dipt. di Elettronica e Informazione.
SIMULATED ANNEALING FOR THE PROBLEM OF MULTIRESOURCE LOCATION ON GRAPH [DOPPIO ANNEALING PER PROBLEMI DI LOCALIZZAZIONE MULTI-RISORSE SU GRAFO]
Giovanni Righini May 1993 14 p In ITALIAN Sponsored in part by Ministry of University and Scientific Research and Technology, Italy
(Rept-93-033; ETN-93-94579) Avail: Politecnico di Milano, Piazza Leonardo da Vinci 32, 20133 Milan, Italy HC

A simulated annealing methodology for the problem of multiresource absolute location on a graph is presented. The methodology can be applied to different functions/objectives; the classical problem of the P-median and the lesser known P-baricenter problem are referenced. Some experimental tests are summarized to show the validity of the illustrated technique. ESA

N94-13922*# Research Inst. for Advanced Computer Science, Moffett Field, CA.
ON THE SUPERCONVERGENCE OF GALERKIN METHODS FOR HYPERBOLIC IBVP
David Gottlieb (Brown Univ., Providence, RI.), Bertil Gustafsson (Uppsala Univ., Sweden.), Pelle Olsson, and Bo Strand (Uppsala Univ., Sweden.) Aug. 1993 22 p
(Contracts NAS2-13721; AF-AFOSR-0090-93; N00014-91-J-4016; NSF DMS-92-11820; NUTEK-89-02539P)
(NASA-CR-194293; NAS 1.26:194293; RIACS-TR-93-07) Avail: CASI HC A03/MF A01

Finite element Galerkin methods for periodic first order hyperbolic equations exhibit superconvergence on uniform grids at the nodes, i.e., there is an error estimate 0(h(sup 2r)) instead of the expected approximation order 0(h(sup r)). It will be shown that no matter how the approximating subspace S(sup h) is chosen, the superconvergence property is lost if there are characteristics leaving the domain. The implications of this result when constructing compact implicit difference schemes is also discussed. Author (revised)

N94-13971# Norwegian Defence Research Establishment, Kjeller.
OPEN BOUNDARY CONDITIONS FOR INCOMPLETELY PARABOLIC SYSTEMS
Ivar Lie 23 Sep. 1992 47 p
(FFI/RAPPORT-92/7029; ETN-93-93975) Avail: CASI HC A03/MF A01

A theory for the construction of open boundary conditions for incompletely parabolic perturbations of hyperbolic systems is presented, and the use of this theory on equations for nonlinear acoustic propagation in seawater is demonstrated. Comparisons with the correction method for hyperbolic systems are discussed. The boundary conditions derived contain first derivatives in space. Implementation of the open boundary conditions are discussed in the context of the Chebyshev spectral collocation method. Numerical experiments are presented to show that the boundary conditions work well in practice. ESA

N94-14002# Center for Mathematics and Computer Science, Amsterdam (Netherlands). Operations Research, Statistics, and System Theory Dept.
ON THE GEOMETRY OF EXTERNAL SPECTRAL FACTORS AND THE RICCATI INEQUALITY
Andrea Gombani (Consiglio Nazionale delle Ricerche, Padua, Italy.) Oct. 1992 15 p Sponsored in part by CNR, and NATO
(CWI-BS-R9227; ETN-93-94158) Copyright Avail: CASI HC A03/MF A01

The geometric structure of the spectral factors of a given spectral density is studied. It is shown that these factors can be associated to a set of invariant subspaces, and the manifold structure of this set is exhibited, providing also an explicit parametrization for it. Some connection with the set of solutions to the Riccati inequality is also made. ESA

N94-14003# Center for Mathematics and Computer Science, Amsterdam (Netherlands). Operations Research, Statistics, and System Theory Dept.
ON THE DIFFERENTIAL STRUCTURE OF MATRIX-VALUED RATIONAL INNER FUNCTIONS
D. Alpay (Ben Gurion Univ. of the Negev, Beersheva, Israel.), L. Baratchart (Institut National de Recherche d'Informatique et d'Automatique, Valbonne, France.), and Andrea Gombani (Consiglio Nazionale delle Ricerche, Padua, Italy.) Oct. 1992 43 p Submitted for publication Sponsored in part by NATO
(CWI-BS-R9228; ETN-93-94159) Copyright Avail: CASI HC A03/MF A01

The set I(sup p)(sub n) of p by p complex matrix valued rational inner functions of fixed McMillan degree is considered. This set is shown to have a smooth manifold structure, and two atlases for it are exhibited; one is based on realization theory and exhibits I(sub p)(sub n) as the product of the manifold of equivalence classes of observable pairs and the unitary group U(p); the second studies I(sub p)(sub n) as transfer functions and rests on Schur parameters. Similar results are obtained for the real valued functions. ESA

N94-14150# Technische Univ., Delft (Netherlands). Faculty of Technical Mathematics and Informatics.
ON A DIFFERENCE EQUATION FOR GENERALIZATIONS OF CHARLIER POLYNOMIALS
Herman Bavinck and Roelof Koekoek 1992 13 p
(Rept-92-101; ETN-93-94290) Copyright Avail: CASI HC A03/MF A01

A set of polynomials which are orthogonal with respect to the classical discrete weight function of the Charlier polynomials at which an extra point mass at $x = 0$ is added is obtained. A difference operator of infinite order for which these new discrete orthogonal polynomials are eigenfunctions is constructed. ESA

N94-14307*# Research Inst. for Advanced Computer Science, Moffett Field, CA.
ON THE SUPERCONVERGENCE OF GALERKIN METHODS FOR HYPERBOLIC IBPV
David Gottlieb (Brown Univ., Providence, RI.), Bertil Gustafsson (Uppsala Univ., Sweden.), Pelle Olsson, and Bo Strand (Uppsala Univ., Sweden.) Aug. 1993 22 p
(Contracts NAS2-13721; AD-AFOSR-0090-93; N00014-91-J-4016; NSF DMS-92-11820; NUTEK-89-02539P)
(NASA-CR-194488; NAS 1.26:194488) Avail: CASI HC A03/MF A01

Finite element Galerkin methods for periodic first order hyperbolic equations exhibit superconvergence on uniform grids at the nodes, i.e., there is an error estimate O(h(sup 2r)) instead of the expected approximation order O(h(sup r)). It will be shown that no matter how the approximating subspace S(sup h) is chosen, the superconvergence property is lost if there are characteristics leaving the domain. The implications of this result when constructing compact implicit difference schemes is also discussed. Author (revised)

N94-14407*# National Aeronautics and Space Administration. Lewis Research Center, Cleveland, OH.
LEAST-SQUARES FINITE ELEMENT SOLUTIONS FOR THREE-DIMENSIONAL BACKWARD-FACING STEP FLOW
Bo-Nan Jiang, Lin-Jun Hou, and Tsung-Liang Lin (Livermore Software Technology Corp., CA.) Aug. 1993 23 p Presented at the Fifth International Symposium on Computational Fluid Dynamics, Sendai, Japan, 31 Aug. - 3 Sep. 1993
(Contract NCC3-233; RTOP 505-90-5K)
(NASA-TM-106353; ICOMP-93-31; E-8136; NAS 1.15:106353) Avail: CASI HC A03/MF A01

Comprehensive numerical solutions of the steady state incompressible viscous flow over a three-dimensional backward-facing step up to Re equals 800 are presented. The results are obtained by the least-squares finite element method (LSFEM) which is based on the velocity-pressure-vorticity formulation. The computed model is of the same size as that of Armaly's experiment. Three-dimensional phenomena are observed even at low Reynolds number. The calculated values of the primary reattachment length are in good agreement with experimental results. Author (revised)

N94-14429*# Brown Univ., Providence, RI.
MULTI-DIMENSIONAL HIGH ORDER ESSENTIALLY NON-OSCILLATORY FINITE DIFFERENCE METHODS IN GENERALIZED COORDINATES Semiannual Progress Report, 1 Jan. - 30 Jun. 1992
Chi-Wang Shu 30 Jun. 1992 6 p
(Grant NAG1-1145)
(NASA-CR-194031; NAS 1.26:194031) Avail: CASI HC A02/MF A01

The nonlinear stability of compact schemes for shock calculations is

investigated. In recent years compact schemes were used in various numerical simulations including direct numerical simulation of turbulence. However to apply them to problems containing shocks, one has to resolve the problem of spurious numerical oscillation and nonlinear instability. A framework to apply nonlinear limiting to a local mean is introduced. The resulting scheme can be proven total variation (1D) or maximum norm (multi D) stable and produces nice numerical results in the test cases. The result is summarized in the preprint entitled 'Nonlinearly Stable Compact Schemes for Shock Calculations', which was submitted to SIAM Journal on Numerical Analysis. Research was continued on issues related to two and three dimensional essentially non-oscillatory (ENO) schemes. The main research topics include: parallel implementation of ENO schemes on Connection Machines; boundary conditions; shock interaction with hydrogen bubbles, a preparation for the full combustion simulation; and direct numerical simulation of compressible sheared turbulence. Author (revised)

N94-14506 Tel-Aviv Univ. (Israel). School of Mathematical Sciences.
EXTREMAL POLYGON CONTAINMENT PROBLEMS AND OTHER ISSUES IN PARAMETRIC SEARCHING M.S. Thesis
Sivan Toledo Apr. 1991 73 p
(ITN-93-85214) Copyright Avail: Issuing Activity (Tel-Aviv Univ., Exact Sciences Library, Ramat Aviv 69978, Israel)

A parametric search seeks a value for a parameter, in a problem whose solution depends on that parameter and on a known input. The value sought for the parameter is that which leads to a desired property of the solution. Several polygon containment problems are solved, in which a location is sought for the largest copy of a convex polygonal object, P, in an environment, Q, comprising polygonal obstacles. P must not intersect the polygons, following permitted translation, rotation and scaling. Solution of the general problem also involves solution of the fixed-size problem, which comprises determination of whether a fixed-size copy of P can be placed in Q. An algorithm is used which finds a superset of placements, not all of which are valid. The solution runs in time, O(k(exp 2)nlambda(sub 4)(kn)log(exp 3)(kn)log log(kn)), in which k and n are the complexities of P and Q, respectively, and lambda(sub q)(r) is the maximum length of an (r,q)-Davenport-Schinzel sequence, which is almost linear in r for any fixed q. Some restricted variants of the general case are solved. In one, Q is the interior of a convex polygon and P is not allowed to rotate; it is solved in a time which is linear in the sum of the complexities of P and Q. In a second variant, disjoint copies of two convex polygons, P(sub 1) and P(sub 2), which may not rotate, are placed inside a convex polygon, Q; the complexities are k(sub 1), k(sub 2) and n, respectively. This variant is solved in time, O(n + k(sub 1) + k(sub 2))log(exp 2)(n + k(sub 1) + k(sub 2)). ISA

N94-14589# Lawrence Livermore National Lab., CA.
LARGE SPATIAL, TEMPORAL, AND ALGORITHMIC ADAPTIVITY FOR IMPLICIT NONLINEAR FINITE ELEMENT ANALYSIS
B. E. Engelmann and R. G. Whirley 30 Jul. 1992 20 p Presented at the Winter Annual Meeting of the American Society of Mechanical Engineers (ASME), Anaheim, CA, 8-13 Nov. 1992
(Contract W-7405-eng-48)
(DE93-016438; UCRL-JC-107859; CONF-921110-51) Avail: CASI HC A03/MF A01

The development of effective solution strategies to solve the global nonlinear equations which arise in implicit finite element analysis has been the subject of much research in recent years. Robust algorithms are needed to handle the complex nonlinearities that arise in many implicit finite element applications such as metalforming process simulation. The authors experience indicates that robustness can best be achieved through adaptive solution strategies. In the course of their research, this adaptivity and flexibility has been refined into a production tool through the development of a solution control language called ISLAND. This paper discusses aspects of adaptive solution strategies including iterative procedures to solve the global equations and remeshing techniques to extend the domain of Lagrangian methods. Examples using the newly developed ISLAND language are presented to illustrate the advantages of embedding temporal, algorithmic, and spatial adaptivity in a modern implicit nonlinear finite element analysis code. DOE

N94-14731*# National Aeronautics and Space Administration. Lewis Research Center, Cleveland, OH.
ANALYSIS, APPROXIMATION, AND COMPUTATION OF A COUPLED SOLID/FLUID TEMPERATURE CONTROL PROBLEM
Max D. Gunzburger and Hyung C. Lee (Virginia Polytechnic Inst., Blacksburg.) Sep. 1993 35 p
(Contracts NCC3-233; N00014-91-J-1493; AF-AFOSR-0179-90; AF-AFOSR-0061-93)
(NASA-TM-106351; ICOMP-93-30; E-8132; NAS 1.15:106351) Avail: CASI HC A03/MF A01

An optimization problem is formulated motivated by the desire to remove temperature peaks, i.e., 'hot spots', along the bounding surfaces of containers of fluid flows. The heat equation of the solid container is coupled to the energy equations for the fluid. Heat sources can be located in the solid body, the fluid, or both. Control is effected by adjustments to the temperature of the fluid at the inflow boundary. Both mathematical analyses and computational experiments are given. Author (revised)

N94-14789# Texas A&M Univ., College Station. Dept. of Mathematics.
MATHEMATIC METHODS AND ALGORITHMS FOR REAL-TIME APPLICATIONS Final Report, 15 Apr. 1990 - 14 Apr. 1993
Charles K. Chui 1 Jun. 1993 10 p
(Contract DAAL03-90-G-0091)
(AD-A266776; ARO-27524.34-MA-SDI) Avail: CASI HC A02/MF A01

A general framework of scaling functions and wavelets is developed. From this framework, explicit formulas of interpolatory spline-wavelets, compactly supported spline-wavelets, their duals, wavelets on a bounded interval, and trigonometric wavelets are derived. On the other hand, by using the scale of 3 instead of 2, we are able to construct compactly supported orthonormal symmetric scaling functions and their corresponding pair of symmetric and antisymmetric wavelets. To avoid aliasing and other undesirable effects in wavelet decompositions, we introduce a continuous multiresolution analysis that generates the dyadic wavelets of Mallat and Zhong. Another approach is to consider frames. In this regard, we derive Littlewood-Paley inequalities and identities for frames. As an important application, we prove two oversampling theorems: one for generating frames from frames, and another to insure that tight frames remain tight. For further decomposition of the higher octave bands, wavelet packets are studied and a stability result is obtained. In a different project, we use ridge functions to construct neural networks with one hidden layer and prove that all such networks only give global approximations. Our study of systems reduction is again based on the AAK approach. We obtained rates of convergence of the rational symbol functions. DTIC

N94-14807# Technische Univ., Berlin (Germany). Fachbereich fuer Elektrotechnik.
UTILIZATION OF BOUNDARY ELEMENT METHOD FOR EXTRACTION OF FREQUENCY DEPENDENT CONDUCTIVITY PARAMETERS OF LOSSY INTRA-CHIP TRANSMISSION LINES Ph.D. Thesis [ANWENDUNG DER METHODE DER RANDELEMENTE ZUR EXTRAHIERUNG FREQUENZABHAENGIGER LEITUNGSPARAMETER VON VERLUSTBEHAFTETEN INTRA-CHIP-VERBINDUNGSLEITUNGEN]
Waldemar Wlodarczyk 1992 169 p In GERMAN
(ETN-93-94385) Avail: CASI HC A08/MF A02

The electric behavior of intra-chip transmission structures with any cross section is determined by means of an analysis of a field theory supported structure and a signal analysis in time area. Linear boundary elements were used for extraction of parameters like R, L, and C for some examples such as monoconductor, two conductor system, and multiconductor transmission lines with a dielectric interface. Conductor losses were examined by means of two dimensional simulations taking into account current penetration in conductors in terms of wideband skin and proximity effects. Current penetration problem was formulated with electrodynamic potentials. The influence of conductor profile deformation due to galvanic reinforcement or corrosion in alternative current impedance and capacity was discussed. Resulting transmission properties were included in a signal analysis for examining the behavior of pulses used as data support in digital systems. Pulse response is found to be strongly dependent on conductor cross section shape. ESA

N94-14840# Texas Univ., Arlington. Dept. of Mathematics.
FUNCTIONAL DIFFERENTIAL EQUATIONS WITH PIECEWISE CONTINUOUS ARGUMENT Final Report, 1 Sep. 1989 - 31 Dec. 1992
Gangaram S. Ladde and Joseph Wiener 15 Apr. 1993 35 p
(Contract DAAL03-89-G-0107)
(AD-A266660; ARO-26739.16-MA-SAH) Avail: CASI HC A03/MF A01

By developing certain auxiliary results, a modified version of the stochastic averaging principle is formulated to investigate stochastic dynamic systems consisting of fast and slow phenomena. Using the properties of optimal feedback control laws, the robust control problem of distributed parameter systems is analyzed. In addition, the stability analysis of a large-scale distributed parameter system is also investigated. Applications are given to illustrate the results. DTIC

N94-14886 Joint Inst. for Nuclear Research, Dubna (USSR). Lab. of Computing Techniques and Automation.
ON A CONVERGENCE OF ITERATIVE NEWTON'S SCHEME
T. Zhanlav and I. V. Puzynin 1991 8 p Limited Reproducibility: More than 20% of this document may be affected by microfiche quality
(DE93-626604; JINR-R-5-91-559) Avail: Issuing Activity (Department of Energy (DOE)) (US Sales Only)

The continuous analog of Newton's method is studied. The algorithm for calculating the iterative parameter is given and the convergence of iterative Newton's scheme for solving the nonlinear functional equation in Banach space is established. DOE

N94-14890 Joint Inst. for Nuclear Research, Dubna (USSR). Lab. of Theoretical Physics.
SPHERICAL ANHARMONIC OSCILLATOR IN SELF-SIMILAR APPROXIMATION
E. P. Yukalova and V. I. Yukalov 1992 16 p Limited Reproducibility: More than 20% of this document may be affected by microfiche quality
(DE93-626622; JINR-E-5-92-75) Avail: Issuing Activity (Department of Energy (DOE)) (US Sales Only)

The method of self-similar approximation is applied here for calculating the eigenvalues of the three-dimensional spherical anharmonic oscillator. The advantage of this method is in its simplicity and high accuracy. The comparison with other known analytical methods proves that this method is more simple and accurate. DOE

N94-14900# Carnegie-Mellon Univ., Pittsburgh, PA. School of Computer Science.
GENERATING KNIGHT'S TOURS WITHOUT BACKTRACKING FROM ERRORS
Jefferey A. Shufelt 21 May 1993 27 p
(Contract DAAH04-93-G-0092)
(AD-A266807; CMU-CS-93-161) Avail: CASI HC A03/MF A01

We describe research on the problem of generating multiple closed tours of an mxn chessboard by a knight, subject to the constraint that the search scheme used to solve the problem is non-backtracking; i.e., that the search engine never visits a node in the search tree that will ultimately lead to a dead end. We describe our experiences and results in the context of KTC, a search program developed to undertake this task. We describe the implementation of KTC, the search constraints we discovered, and KTC's performance to date, illustrating that a limited amount of domain knowledge can lead to near-perfect search on this class of Hamiltonian circuit construction problems. We close by suggesting promising directions for achieving a perfect search on this problem and the implications of such an achievement. DTIC

65 STATISTICS AND PROBABILITY

Includes data sampling and smoothing; Monte Carlo method; and stochastic processes.

N94-12896# International Centre for Theoretical Physics, Trieste (Italy).
STOCHASTIC DYNAMICS: CROSSOVER FROM 1/f(SUP 3) TO FLICKER NOISE
E. Canessa and V. L. Nguyen Jan. 1993 25 p
(DE93-622862; IC-93/8) Avail: CASI HC A03/MF A01 (US Sales Only)

Finite time processes within the limits of the Newton equation and zero inertia motion (i.e., road to chaos) are studied by numerically solving the ordinary, stochastic Langevin equation in 1D for a free particle with inertial moving in a medium with viscosity (gamma). In these simulations, the scaling behavior of particle trajectories chi(t) and velocities v(t) with time are derived and the inclusion of non-zero particle masses is shown to define the asymptotic time limit tau(sub c) at which - independently of gamma - the system evolves into the well-known statistically stationary state characterized by /chi(sup 2)(t)/ is proportional to t and flicker noise. The time tau(sub c) is further analyzed from the correlation length given by the 2-point autocorrelation function of the particle velocity at each value of gamma. It is found that the noise power spectrum of v(t) is characterized by flicker noise for frequencies f less than or = f(sub c) approx. 1/tau(sub c), whereas for f greater than f(sub c), the noise power spectra behave as 1/f(sup upsilon), where upsilon varies between the limits of Newton's equation (i.e., upsilon = 3) and road to chaos (i.e., upsilon = 1). Furthermore, at times tau less than tau(sub c) and 0 less than gamma less than infinity, an ad-hoc exponent for the scaling of the variance of particle velocities with time is shown to characterize a subset of multifractal dimensions d(sub f)(gamma) while the single particle trajectories are shown to display a rather different subset of exponents on increasing gamma. Generic features of this transition are nicely given by Poincare maps in the velocity space. DOE

N94-12919# Los Alamos National Lab., NM.
A NEW METHOD TO ASSESS MONTE CARLO CONVERGENCE
R. A. Forster, T. E. Booth, and S. P. Pederson 1993 12 p Presented at the Advanced Monte Carlo Computer Programs for Radiation Transport, Saclay, France, 27-29 Apr. 1993
(Contract W-7405-eng-36)
(DE93-012667; LA-UR-93-1446; CONF-9304131-3) Avail: CASI HC A03/MF A01

The central limit theorem can be applied to a Monte Carlo solution if the following two requirements are satisfied: (1) the random variable has a finite mean and a finite variance; and (2) the number N of independent observations grows large. When these are satisfied, a confidence interval based on the normal distribution with a specified coverage probability can be formed. The first requirement is generally satisfied by the knowledge of the type of Monte Carlo tally being used. The Monte Carlo practitioner has only a limited number of marginally quantifiable methods that use sampled values to assess the fulfillment of the second requirement; e.g., statistical error reduction proportional to 1/the square root of N with error magnitude guidelines. No consideration is given to what has not yet been sampled. A new method is presented here to assess the convergence of Monte Carlo solutions by analyzing the shape of the empirical probability density function (PDF) of history scores, f(x), where the random variable x is the score from one particle history and the integral evaluated from -infinity to infinity of f(x)dx = 1. Since f(x) is seldom known explicitly, Monte Carlo particle random walks sample f(x) implicitly. Unless there is a largest possible history score, the empirical f(x) must eventually decrease more steeply than 1/x(exp 3) for the second moment (the integral evaluated from -infinity to infinity of x(exp 2)f(x)dx) to exist. DOE

N94-13540 McGill Univ., Montreal (Quebec). Dept. of Electrical Engineering.
BAYESIAN ESTIMATION OF MOTION FIELDS FROM IMAGE SEQUENCES Ph.D. Thesis
Janusz Konrad Jun. 1989 257 p
(ISBN-0-315-57212-4; CTN-93-60724) Copyright Avail: Micromedia Ltd., Technical Information Centre, 165 Hotel de Ville, Place du Portage, Phase 2, Hull, Quebec J8X 3X2, Canada HC/MF

The ill-posed problem of estimating two dimensional motion in time varying images is addressed. The approach proposed uses the theory of stochastic processes at the formulation and solution stages. Independent Gaussian random variables are used to model the relationship between motion fields and images, and vector and binary Markov random fields are used to model motion and motion discontinuity fields, respectively. These models, combined using the Bayes rule, result in a Gibbsian a posteriori probability distribution from which the maximum a posteriori (MAP) and the minimum expected cost (MEC) estimation criteria are derived. Optimization of these criteria is performed using stochastic relaxation. The MAP estimation is extended to handle large displacements via a hierarchical approach. Deterministic approximations to some of the stochastic algorithms proposed

are derived and compared with their stochastic counterparts. The color information is incorporated into the estimation process. Numerous experimental results are presented. Two of the methods proposed are applied to motion compensated interpolation and shown to reduce certain types of errors. Author (CISTI)

N94-13585# Stanford Univ., CA. Dept. of Statistics.
MAXIMUM LIKELIHOOD ESTIMATION FOR CONSTRAINED OR MISSING DATA MODELS Technical Report
Alan E. Gelfand and Bradley P. Carlin 5 May 1993 20 p
(Contract N00025-92-J-1264)
(AD-A266563; TR-468) Avail: CASI HC A03/MF A01

In statistical models involving constrained or missing data, likelihoods constraining integrals emerge. In the case of both constrained and missing data, the result is a ratio of integrals, which for multivariate data may defy exact or approximate analytic expression. Seeking maximum likelihood estimates in such a setting, we propose Monte Carlo approximants for these integrals, and subsequently maximize the resulting approximate likelihood. Iteration of this strategy expedites the maximization, while the Gibbs sampler is useful for the required Monte Carlo generation. As a result, we handle a class of models broader than the customary EM setting without using an EM-type algorithm. Implementation of the methodology is illustrated in two numerical examples. DTIC

N94-13677# Center for Mathematics and Computer Science, Amsterdam (Netherlands). Operations Research, Statistics, and System Theory Dept.
STOCHASTIC REALIZATION OF FINITE-VALUED PROCESSES AND PRIMES IN THE POSITIVE MATRICES
G. Picci and J. H. VanSchuppen Oct. 1992 10 p Repr. from Recent Advances in Mathematical Theory of Systems, Control, Networks, and Signal Processing 2: Proceedings of the International Symposium MTNS-1991, (Tokyo, Japan, Mita Press), 1992 p 227-232 Presented at the International Symposium MTNS-1991, Tokyo, Japan, 1991
(CWI-BS-R9222; ETN-93-94153) Copyright Avail: CASI HC A02/MF A01

A study aimed at showing that the stochastic realization problem of finite valued processes reduces to the problem of factorization of positive matrices is presented. The stochastic realization problem of finite valued processes asks for the classification of all minimal finite stochastic systems such that the output process of such a system equals a given process in distribution. This problem is motivated by the use of stochastic models in signal processing, communication, and control. The problem of characterizing the minimal number of states in this problem leads to a factorization problem for positive matrices and hence to the study of positive linear algebra. The results are a characterization of primes in the positive matrices and examples of such primes. ESA

N94-13848# National Defence Headquarters, Ottawa (Ontario). Directorate of Mathematics and Statistics.
STATISTICAL ANALYSIS OF THE m RANKINGS PROBLEM: KENDALL'S PROTOTYPE AND THE GROUPING ESTIMATE METHOD BASED ON NORMAL SCORES
Tuan A. Vu Aug. 1992 44 p
(DSIS-93-00139; DMS-RN-4-92; CTN-93-60785) Avail: CASI HC A03/MF A01

The statistical analysis of the theory of ranks has been developed extensively over the past fifty years. This subject considers the relationship between the rankings that a group of m judges assigns to a set of n objects. Kendall's contributions to the m rankings problem are considered. These include the formulae of the correlation coefficient between two rankings, the coefficient of Concordance W among judges, and significance tests of W as well as the best estimate based on the order of the sums of natural number ranks for each object. Based on the concept of normal scores and order statistics, a new procedure to find the best estimate is developed in which groups of objects which should be ranked the same are formed, based on the test of consecutive order statistics of normal score ranks' sums for each object after sorting in ascending order. Computer program listings for performing various ranking calculations are appended. Author (CISTI)

N94-14005# Center for Mathematics and Computer Science, Amsterdam (Netherlands). Operations Research, Statistics, and System Theory Dept.
STOCHASTIC SCHEDULING GAMES WITH MARKOV DECISION ARRIVAL PROCESSES
Eitan Altman (Institut National de Recherche d'Informatique et d'Automatique, Valbonne, France.) and Ger Koole (Center for Mathematics and Computer Science, Amsterdam, Netherlands.) Nov. 1992 14 p Sponsored by the Commission of the European Communities
(CWI-BS-R9231; ETN-93-94162) Copyright Avail: CASI HC A03/MF A01

The dependent arrival processes MDAP (Markov Decision Arrival Processes) were introduced by Hordijk and Koole to model special arrival processes into controlled queueing networks. These were applied to solve control problems with several controllers having a common objective, where the output from one controlled network is fed into a second one. In case that objectives of the controllers are different, one may choose a min-max (worst case) approach where typically a controller tries to obtain the best performance under the worst possible (unknown) strategies of the other controllers. In this study MDAP is used to model such situations or situations of control in an unknown environment. This approach is applied to several scheduling problems, including scheduling of customers and scheduling of servers. Different information patterns including delayed information are considered. For all these models several structural results of the optimal policies are obtained. ESA

N94-14178# Los Alamos National Lab., NM.
HYBRID S(SUB N)/MONTE CARLO RESEARCH AND RESULTS
R. S. Baker 1993 13 p Presented at the Advanced Monte Carlo Computer Programs for Radiation Transport, Saclay, France, 27-29 Apr. 1993
(Contract W-7405-eng-36)
(DE93-012677; LA-UR-93-1392; CONF-9304131-2) Avail: CASI HC A03/MF A01

The neutral particle transport equation is solved by a hybrid method that iteratively couples regions where deterministic (S(sub N)) and stochastic (Monte Carlo) methods are applied. The Monte Carlo and S(sub N) regions are fully coupled in the sense that no assumption is made about geometrical separation or decoupling. The hybrid Monte Carlo/S(sub N) method provides a new means of solving problems involving both optically thick and optically thin regions that neither Monte Carlo nor S(sub N) is well suited for by themselves. The hybrid method has been successfully applied to realistic shielding problems. The vectorized Monte Carlo algorithm in the hybrid method has been ported to the massively parallel architecture of the Connection Machine. Comparisons of performance on a vector machine (Cray Y-MP) and the Connection Machine (CM-2) show that significant speedups are obtainable for vectorized Monte Carlo algorithms on massively parallel machines, even when realistic problems requiring variance reduction are considered. However, the architecture of the Connection Machine does place some limitations on the regime in which the Monte Carlo algorithm may be expected to perform well. DOE

N94-14314# Lawrence Livermore National Lab., CA.
DECONVOLUTION FOR POSITIVE SIGNALS
D. M. Goodman Oct. 1992 10 p Presented at the Symposium on Fundamentals of Discrete Time Systems, Chicago, IL, 26-27 Jun. 1992
(Contract W-7405-eng-48)
(DE93-013044; UCRL-JC-111956; CONF-9206371-1) Avail: CASI HC A02/MF A01

We consider estimating an unknown positive signal from an observed signal that has been corrupted by known linear dynamics and additive noise. In many experiments the goal is to estimate energy or power as a function of time; consequently, the positive deconvolution problem occurs frequently in a wide variety of scientific disciplines. We present two new methods. One is based on Mallows' C(sub L) statistic, and the other is based on conjugate gradients. We describe several other methods. This paper considers 'small sample' problems. This fact and the imposition of positivity constraints makes analytic comparisons of the methods impossible. Therefore, we include preliminary Monte-Carlo comparisons. DOE

N94-14320# Brookhaven National Lab., Upton, NY.
SELF ORGANIZED CRITICALITY
M. Creutz Mar. 1993 9 p Presented at the Madi Gras Conference on

Concurrent Computing in the Physical Sciences, Baton Rouge, LA, 18-20 Feb. 1993
(Contract DE-AC02-76CH-00016)
(DE93-013182; BNL-48759; CONF-9302112-1) Avail: CASI HC A02/MF A01

Self organized criticality refers to the tendency of highly dissipative systems to drive themselves to a critical state. This has been proposed to explain why observed physics often displays a wide disparity of length and time scales. The phenomenon can be studied in simple cellular automaton models. DOE

N94-14334# Oak Ridge National Lab., TN.
DEVELOPMENT AND APPLICATION OF THE AUTOMATED MONTE CARLO BIASING PROCEDURE IN SAS4
J. S. Tang and B. L. Broadhead 1993 21 p Presented at the Advanced Monte Carlo Computer Programs for Radiation Transport Conference, Saclay, France, 27-29 Apr. 1993
(Contract DE-AC05-84OR-21400)
(DE93-015205; CONF-9304131-7) Avail: CASI HC A03/MF A01

An automated approach for biasing Monte Carlo shielding calculations is described. In particular, adjoint fluxes from a one-dimensional discrete-ordinates calculation are used to generate biasing parameters for a three-dimensional Monte Carlo calculation. The automated procedure consisting of cross-section processing, adjoint flux determination, biasing parameter generation, and the initiation of a MORSE-SGC/S Monte Carlo calculation has been implemented in the SAS4 module of the SCALE computer code system. The automated procedure has been used extensively in the investigation of both computational and experimental benchmarks for the NEACRP working group on shielding assessment of transportation packages. The results of these studies indicate that with the automated biasing procedure, Monte Carlo shielding calculations of spent fuel casks can be easily performed with minimum effort and that accurate results can be obtained at reasonable computing cost. The systematic biasing approach described in this paper can also be applied to other similar shielding problems. DOE

N94-14441# Los Alamos National Lab., NM.
THE EFFECTS OF INTERNAL FLUCTUATIONS ON A CLASS OF NONEQUILIBRIUM STATISTICAL FIELD THEORIES
M. M. Millonas 1993 5 p Presented at the 12th International Conference on Noise in Physical Systems and 1/f Fluctuations, Saint Louis, MO, 16-20 Aug. 1993
(Contract W-7405-eng-36)
(DE93-016620; LA-UR-93-2132; CONF-930866-3) Avail: CASI HC A01/MF A01

A class of models with applications to swarm behavior as well as many other types of spatially extended complex biological and physical systems is studied. Internal fluctuations can play an active role in the organization of the phase structure of such systems. In particular, for the class of models studied here the effect of internal fluctuations due to finite size is a renormalized decrease in the temperature near the point of spontaneous symmetry breaking. DOE

N94-14502 Tel-Aviv Univ. (Israel). Statistics Dept.
OPTIMAL MAINTENANCE POLICIES OF A MARKOVIAN SYSTEM M.S. Thesis
Nir Douer Jun. 1991 69 p In HEBREW
(ITN-93-85216) Copyright Avail: Issuing Activity (Tel-Aviv Univ., Exact Sciences Library, Ramat Aviv 69978, Israel)

We consider a Markovian system, deteriorating in time, which can be either replaced or partially repaired after each inspection. After a repair or replacement, the system may also be found in a worse state (as a consequence of the maintenance activity). Under reasonable assumptions on the costs of operating, replacing or repairing the system, we show that there exists a generalized control limit rule such that there is a state i* below which no repair or replacement actions are taken and a state, j such that for j greater than or equal to i*, a maintenance action must be performed. We show the above for both discrete and continuous state space, and prove optimality of the generalized control limit rule policy for both the criteria: (1) total expected discounted cost; and (2) long run average cost. Author (ISA)

N94-14545# Groningen Rijksuniv. (Netherlands). Dept. of Mathematics and Computing Science.
DISTRIBUTIONAL INFERENCES FOR A LOCATION PARAMETER Thesis [VERDELINGSPRAKEN VOOR EEN LOCATIEPARAMETER]
H. J. Guichelarr Oct. 1992 30 p In DUTCH
(W-9219; ETN-93-94102) Avail: CASI HC A03/MF A01

Distribution inferences were made about a stochastic unknown in the form of a probability Q. An inference is evaluated by means of the risks for a loss function L(y, Q). Sometimes the real value of y can be found, allowing a real evaluation of the inferences. Distributional inferences were also made for location parameter problems. The choice of the optimal equivariance procedure to make distributional inferences is discussed. ESA

N94-14703# Technische Univ., Berlin (Germany). Fachbereich Informatik.
ROBUST ESTIMATORS AND TESTS IN ONE-SAMPLE LOCATION PROBLEM WITH PARTICULAR CONSIDERATION ON MODIFIED MAXIMUM LIKELIHOOD PROCESS Ph.D. Thesis [ROBUSTE SCHAETZER UND TESTS IM EINSTICHPROBEN-LAGEPROBLEM UNTER BESONDERER BERUECKSICHTIGUNG DES MODIFIZIERTEN MAXIMUM-LIKELIHOOD-VERFAHRENS]
Ung-Hee Lee 1992 195 p In GERMAN
(ETN-93-94391) Avail: CASI HC A09/MF A03

M, L, and R estimators are examined with the maxmin criterion for short and long tailed distributions and finite populations using Monte Carlo simulations. For L estimator, selector statistics were used for classification of distribution type data and trimming and winsorization medians were defined; the swindle method was introduced in a simulation in order to obtain precise results of the variance of location estimators. Several examples of possible influence functions for M estimators were given and a numerical estimation was performed using Newton method. Some alternative location tests instead of classical student tests were considered in which test robustness was examined under deviations of normal distributions for finite populations. For assessment of study reliability, assumptions of distribution symmetry and data dependence such as serial or constant correlation and autoregression were examined. ESA

N94-14788# Princeton Univ., NJ. Dept. of Statistics.
EXPLORATORY DATA ANALYSIS: PAST, PRESENT AND FUTURE
John W. Tukey Apr. 1993 68 p
(Contract DAAL03-91-G-0138)
(AD-A266775; ARO-26997.10-MA) Avail: CASI HC A04/MF A01

The following topics are discussed: the 1971-1977 early formulation of Exploratory Data Analysis, in terms of results of some of its techniques and considerations which underlay, at various depths, the choices realized in the books; the 1991-1995 development of Exploratory Analysis of Variance, described in its simplest (two-way table) form and barely sketched in general; discussion of the changes in apparent philosophy caused by the need to communicate more complicated things, notches, hints, the likely impact on a revised edition of Exploratory Data Analysis 1977; and dreams and targets for what might happen in 1996-2005, with emphasis on Exploratory Regression and the combined use of multiple description. DTIC

66 SYSTEMS ANALYSIS

Includes mathematical modeling; network analysis; and operations research.

N94-13549# Operational Research and Analysis Establishment, Ottawa (Ontario). Directorate of Logistics Analysis.
SPARE PARTS ANALYSIS OF THE MK.32B-751 AAR POD
Michael K. Ormrod Jan. 1993 15 p
(DSIS-93-00737; ORAE-PR-614; CTN-93-60839) Avail: CASI HC A03/MF A01

To provide air refuelling support, maintain airlift capability, and contribute to the modernization of the air reserves, Canada's Department of National Defence purchased five C130H tankers and outfitted them with Mk32B-751 air-to-air refuelling (AAR) pods. A study was undertaken to determine if the

quantity of spares initially procured for the AAR pods is adequate to maintain a 75 percent operational availability. The initial spares were analyzed using the ROSAM program which predicted the operational availability of the pod to be 98 percent. In addition, a sensitivity analysis of the estimated mean time before failure (MTBF), operating hours, and contractor repair time was also performed. By halving the MBTF of the parts or doubling the operating hours of the pod, availability fell to 90 percent. By doubling the time required for the contractor to repair any part, availability dropped to 92 percent. In all cases, the operational availability of the pod was well above the 75 percent target. CISTI

N94-13987# Technische Univ., Delft (Netherlands). Faculty of Aerospace Engineering.
GATE ASSIGNMENT USING LINEAR PROGRAMMING M.S. Thesis
C. G. vanRhee Jul. 1992 254 p
(LR-698; ETN-93-94010) Avail: CASI HC A12/MF A03

A method for optimizing the aircraft to gate assignment with the use of linear programming is presented. The Automatic Optimal Resource and Tarmac Allocation (AORTA) program is able to handle many real life assignment criteria. The purpose of the development of a program using linear programming was to investigate whether this method could be effectively used to provide a practical solution to the problem. This means that all kinds of practical constraints must be incorporated and all kinds of assignment rules must be taken into account. The effectiveness of the program is tested with data from Schiphol Airport. The results show that the AORTA program can be used to solve assignment problems. ESA

67 THEORETICAL MATHEMATICS

Includes topology and number theory.

N94-12843# Melbourne Univ., Parkville (Australia). School of Physics.
GAUGING THE OCTONION ALGEBRA
A. K. Waldron and G. C. Joshi 1992 19 p
(DE93-622864; UM-P-92/60) Avail: CASI HC A03/MF A01 (US Sales Only)

By considering representation theory for non-associative algebras the fundamental adjoint representations of the octonion algebra is constructed. It is then shown how these representations by associative matrices allow a consistent octonionic gauge theory to be realized. It was found that non-associativity implies the existence of new terms in the transformation laws of fields and the kinetic term of an octonionic Lagrangian. DOE

N94-12955# Oak Ridge National Lab., TN.
RARE ATTRIBUTES IN FINITE UNIVERSE: HYPOTHESES TESTING SPECIFICATION AND EXACT RANDOMIZED UPPER CONFIDENCE BOUNDS
T. Wright Mar. 1993 33 p
(Contract DE-AC05-84OR-21400)
(DE93-012783; ORNL/TM-12269) Avail: CASI HC A03/MF A01

When attributes are rare and few, or none are observed, in the selected sample from a finite universe, sampling statisticians are increasingly being challenged to use whatever methods are available to declare with high probability or confidence that the universe is near or completely attribute-free. This is especially true when the attribute is undesirable. Approximations such as those based on normal theory are frequently inadequate with rare attributes. For simple random sampling without replacement, an appropriate probability distribution for statistical inference is the hypergeometric distribution. But even with the hypergeometric distribution, the investigator is limited from making claims of attribute-free with high confidence unless the sample size is quite large using nonrandomized techniques. In the hypergeometric setting with rare attributes, exact randomized tests of hypothesis are investigated to determine the effect on power of how one specifies the null hypothesis. In particular, specifying the null hypothesis as zero attributes does not always yield maximum possible power. We also consider the hypothesis specification question under complex sampling designs including stratified random sampling and two-stage cluster sampling (one case involves random selection at first stage and another case involves probability proportional to size without replacement selection at first stage). Also under simple random sampling, this article defines and presents a simple algorithm for the construction of exact 'randomized' upper confidence bounds which permit one to possibly report tighter bounds than those exact bounds obtained using 'nonrandomized' methods. DOE

70 PHYSICS (GENERAL)

For precision time and time interval (PTTI) see *35 Instrumentation and Photography;* for geophysics, astrophysics or solar physics see *46 Geophysics, 90 Astrophysics,* or *92 Solar Physics.*

N94-12877# International Centre for Theoretical Physics, Trieste (Italy).
DETERMINATION OF CRITICAL DENSITY OF CHARGE
F. Vila Nov. 1992 10 p
(DE93-622897; IC-92/370) Avail: CASI HC A02/MF A01 (US Sales Only)

In this work is given a full theoretical treatment of the problem of how to determine the critical density of charge on nonconductive rectangular charged surfaces placed near a small spherical conductive and earthed surface. DOE

N94-13235# Polish Academy of Sciences, Warsaw. Inst. Podstawowych Problemow Techniki
STABILITY OF SUBHARMONICS AND ESCAPE PHENOMENA IN THE TWIN-WELL POTENTIAL DUFFING SYSTEM
J. Janicki and W. Szemplinska-Stupnicka Jun. 1993 67 p
Avail: CASI HC A04/MF A01

Low order subharmonic resonances in the twin-well potential Duffing system are studied: 1:1, 1:2, 1:3 of one-well motion and 1:1, 1:3 of cross-well motion. Solutions for the resonances are found using a modification of the near-linear perturbation method. Then Hill's variational equation allows us to examine stability of the solutions. Due to the above methods major bifurcations of subharmonics can be located approximately in the parameter space: folds, period-doublings and symmetry-breakings. Results of numerical experiment are included for comparison. They show that the analysis of the local bifurcations can estimate phenomena of escape from potential well. Two types of chaotic attractor catastrophes are also found in the system: one is invertible with respect to parameter changes, the other is not and involves hysteresis. The former type seems to be related to the local bifurcations of regular orbits, the latter corresponds to the boundary crisis. Author

N94-13508 International Centre for Theoretical Physics, Trieste (Italy).
THE GENERAL GRAVITATIONAL POTENTIAL FIELD OF A HOMOGENEOUS CYLINDER ROTATING ABOUT ITS AXIS
D. D. Bakwa Jan. 1993 8 p Limited Reproducibility: More than 20% of this document may be affected by microfiche quality
(DE93-622853; IC-93/14) Avail: CASI HC A02 (US Sales Only)

In the paper 'On the Gravitation of Moving Bodies' a new law of gravitation called the law of general gravitation was proposed. In this paper the general gravitational field of a homogeneous cylinder rotating uniformly about its axis is derived. DOE

N94-13627 Pennsylvania State Univ., New Kensington.
EVALUATION FOR RHEOLOGICAL CONSTITUTIVE RELATIONS, USING THE INDENTATION TECHNIQUE Ph.D. Thesis
Lei Fang 1992 185 p
Avail: Univ. Microfilms Order No. DA9311630

A simple experimental method of determining the rheological constitutive relations is proposed. The method relies upon an analysis of the frictionless contact of a rigid spherical indenter and the rheological materials. The proposal addresses problems in two fields: rheological constitutive models and contact mechanics. It attempts to evaluate the rheological constitutive relations using an indentation technique. A systematic, optimization-based material parameter/function indentation model is proposed. The identification algorithm is based on a modified Marquardt-Levenberg method. A new integral constitutive equation for viscoelastic materials is derived. The derivation is carried out so that a damage function is included in the model in a relatively convenient form. Inclusion of damage effects makes this constitutive equation considerably more general than the widely accepted K-BKZ integral model. The single-step and double-step stress relaxation indentation experiments on asphalt materials were performed. The K-BKZ,

Wagner, and nonlinear Volterra models were evaluated. It is demonstrated that the new integral constitutive model shows a very good agreement with the experimental data. The idea of damage function is introduced not only to have a better fit of data, but the damage (or irreversibility) is observed experimentally. Also, the creep indentation tests on composites were presented. A multiaxial theory of creep deformation for particle-strengthened metal matrix composites (Zhu-Weng Theory) was evaluated. The goal of the proposed research is to develop the indentation technique for use in basic mechanical studies. From the indentation test, material response is measured. The data are used in conjunction with the material parameter identification model to optimally back calculate the constitutive relations. Comparing the experimental data between the indentation test and other experiment method demonstrates the viability of the proposed approach. Dissert. Abstr.

N94-13897*# APD Cryogenics, Inc., Allentown, PA.
THREE-STAGE LINEAR, SPLIT-STIRLING CRYOCOOLER FOR 1 TO 2K MAGNETIC COLD STAGE
R. C. Longsworth Aug. 1993 101 p Original contains color illustrations
(Contract NAS2-13180)
(NASA-CR-4538; A-93105; NAS 1.26:4538) Avail: CASI HC A06/MF A02; 3 functional color pages

A long-life, linear, high efficiency 8K split Stirling cycle cryocooler was designed, built, and tested. The refrigerator is designed for cooling a 50 mW, 1.5K magnetic cold stage. Dual opposed piston compressors are driven by moving-coil linear motors. The three stage expander, although not completed, is also driven by a linear motor and is designed to produce 1 SW at 60K, 4W at 16K, and 1.2W at 8K. The cold regenerator employs a parallel gap construction for high efficiency. The key technology areas addressed include warm and cold flexible suspension bearings and a new cold regenerator geometry for high efficiency at 8K. Author (revised)

N94-14027*# National Aeronautics and Space Administration. Ames Research Center, Moffett Field, CA.
THERMAL CONDUCTANCE OF PRESSED METALLIC CONTACTS AUGMENTED WITH INDIUM FOIL OR APIEZON-N (TM) GREASE AT LIQUID HELIUM TEMPERATURES
Louis J. Salerno, Peter Kittel, and Alan L. Spivak (Trans-Bay Electronics, Richmond, CA.) Jul. 1993 11 p
(RTOP 582-09-11)
(NASA-TM-108779; A-93035; NAS 1.15:108779) Avail: CASI HC A03/MF A01

The thermal conductance of pressed contacts which have been augmented with Indium foil or Apiezon-N (tm) grease was measured over the temperature range of 1.6 to 6.0 K, with applied forces from 22 N to 670 N. The sample pairs were fabricated from OFHC copper, 6061-T6 aluminum, free-machining brass, and 304 stainless steel. Although the thermal conductance was found to increase with increasing applied contact force, the force dependence was less than in earlier work. The addition of Indium foil or Apiezon-NT grease between the contact surfaces resulted in an improvement over uncoated surfaces ranging from a factor of approximately 3 for stainless steel to an order of magnitude for copper contacts. Author (revised)

N94-14431# Joint Publications Research Service, Arlington, VA.
JPRS REPORT: SCIENCE AND TECHNOLOGY. CENTRAL EURASIA: ENGINEERING AND EQUIPMENT
17 Aug. 1993 26 p Transl. into ENGLISH from various Russian articles
(JPRS-UEQ-93-006) Avail: CASI HC A03/MF A01

Translated articles cover the following topics: on possibility of utilizing high-T(sub c) superconductivity phenomena in gyros; analytical investigation of dynamics equations of low-flying satellite by computer algebra methods; plane resonant motions of viscoelastic body in elliptical orbit; vibration damping of system containing unbalanced rotor; azimut' spectropolarimeter for remote sensing of natural objects; fiber optic loop-type interferometer-based logic gates; investigation of fuel combustion completeness in combustion chambers with film vaporizers; study of plane stratified flow around object; numerical investigation of flows in mixed spatial boundary layers of prolate spheroid in flow with angles of incidence; and turbulent boundary layer evolution under successive effect of shock wave and expansion fan. Author

N94-14584# California Univ., Berkeley. Lawrence Berkeley Lab.
THEORY OF THE NEGATIVE MAGNETORESISTANCE IN MAGNETIC METALLIC MULTILAYERS
R. Q. Hood and L. M. Falicov Apr. 1993 12 p Presented at the Spring Meeting of the MRS, San Francisco, CA, 12-16 Apr. 1993
(Contract DE-AC03-76SF-00098)
(DE93-013912; LBL-33948; CONF-930405-10) Avail: CASI HC A03/MF A01

The Boltzman equation is solved for a system consisting of alternating ferromagnetic normal metallic layers. The in-plane conductance of the film is calculated for two configurations: successive ferromagnetic layers aligned parallel and antiparallel to each other. Results explain the giant negative magnetoresistance encountered in these systems when an initial antiparallel arrangement is changed into a parallel configuration by application of an external magnetic field. The calculation depends on the following: geometric parameters (the thicknesses of the layers); intrinsic metal parameters (number of conduction electrons, magnetization and effective masses in the layers); bulk sample properties (conductivity relaxation times); and interface scattering properties (diffuse scattering versus potential scattering at the interfaces). It is found that a large negative magnetoresistance requires, in general, considerable asymmetry in the interface scattering for the two spin orietations. All qualitative features of the experiments are reproduced. Quantitative agreement can be achieved with sensible values of the parameters. The effect can be conceptually explained based on considerations of phase-space availability for an electron of a given spin orientation as it travels through the multilayer sample in the various configurations and traverses the interfaces. DOE

N94-14733*# National Aeronautics and Space Administration. Langley Research Center, Hampton, VA.
VIBRATIONAL RELAXATION IN HYPERSONIC FLOW FIELDS
Willard E. Meador, Gilda A. Miner, and John H. Heinbockel (Old Dominion Univ., Norfolk, VA.) Sep. 1993 23 p
(RTOP 506-40-62-01)
(NASA-TP-3367; L-17238; NAS 1.60:3367) Avail: CASI HC A03/MF A01

Mathematical formulations of vibrational relaxation are derived from first principles for application to fluid dynamic computations of hypersonic flow fields. Relaxation within and immediately behind shock waves is shown to be substantially faster than that described in current numerical codes. The result should be a significant reduction in nonequilibrium radiation overshoot in shock layers and in radiative heating of hypersonic vehicles; these results are precisely the trends needed to bring theoretical predictions more in line with flight data. Errors in existing formulations are identified and qualitative comparisons are made. Author

71 ACOUSTICS

Includes sound generation, transmission and attenuation.
For noise pollution see *45 Environmental Pollution.*

N94-13692# European Space Agency, Paris (France).
THE PROBLEM OF THE SONIC BOOM FOR FUTURE HIGH-SPEED TRANSPORT AIRCRAFT
Andre Auriol (Office National d'Etudes et de Recherches Aerospatiales, Paris, France.), Claude Lecomte (Office National d'Etudes et de Recherches Aerospatiales, Paris, France.), and Christian Thery (Office National d'Etudes et de Recherches Aerospatiales, Paris, France.) Apr. 1993 70 p Transl. into ENGLISH of Le probleme du bang sonique pour de futurs avions de transport a haute vitesse (Paris, France, ONERA) 1990 p 1-52 Original language document announced as N93-30020
(ESA-TT-1286; ONERA-NT-1990-3; ETN-93-94584) Avail: CASI HC A04/MF A01

The sonic boom origin and propagation in the atmosphere are reviewed. The main effects on structures and living creatures are described. The only appreciable nuisance resulting from the boom is due to the startle reaction. No acceptability threshold was defined up until now. However, the startle reactions appear to become rare for boom intensities less than 50 pascals or for booms having a low intensity forward shock front followed by progressive compression. The following studies are recommended to be

carried out: on the startle reactions so as to define tolerable booms of unconventional shapes; and on the aerodynamics of the shapes of aircraft liable to generate such booms. ESA

N94-13831 Calian Communications, Kanata (Ontario).
ACOUSTO-OPTICAL POST-PROCESSOR TIME-INTEGRATING CORRELATOR UPDATES Final Report
B. Baker 28 Mar. 1991 17 p
(DSIS-93-00314; DREO-17; CTN-93-60751) Avail: CASI HC A03

The updates to the acousto-optical signal processing development facility/time integrating correlator (TIC) system developed by Calian Communications Systems are described. One of the main functions of the post-processor in the TIC system is to control the acquisition of data by the photodetector array. The following three functions have been added to the post-processor of the TIC system: a detection statistics package; two methods of no phase shift pedestal removal; and a statistical analysis package. In addition, a corrected method of processing the correlation function is used when pedestal removal is inhibited. The changes to the supervisor task and the correlation display task are detailed. Sample screens are included for illustration. Author (CISTI)

N94-13885 National Physical Lab., Teddington (England). Radiation Science and Acoustics Div.
AN EXPERIMENTAL ASSESSMENT OF THE USE OF GROUND-LEVEL MICROPHONES TO MEASURE THE FLY-OVER NOISE OF JET-ENGINED AIRCRAFT
R. C. Payne Jan. 1993 38 p Sponsored by Dept. of Transport, London, United Kingdom
(NPL-RSA(EXT)-0039; ETN-93-94466) Copyright Avail: National Physical Laboratory, Teddington, Middlesex TW11 0LW, United Kingdom HC

During aircraft flight trials to measure the noise levels of six different military jet aircraft types in low altitude high speed operations, noise measurements were performed using microphones at ground level and at a height of 1.2 m. The program provided reliable data on the difference between sound pressure levels from the two microphone arrangements, for sound incident over a range of angles, from 0 deg (aircraft overhead) to approximately 80 deg. Substantial differences from ground level to 1.2 m were observed in measurements of maximum perceived noise level, effective perceived noise level and maximum A-weighted sound pressure level. For sound waves incident to the ground at angles less than approximately 60 deg from vertical, these differences were found to be independent of angle of incidence for all the six aircraft and all flight procedures. Within this range of sound incidence angles the ground plane arrangement produced data that closely approximated pressure doubled values. The conventional 1.2 m high microphone gave rise to noise levels approximately 4 dB lower. For sound incident at angles greater than 60 deg from vertical, the difference between noise levels measured using the two microphone configurations was found to depend on angle of incidence, reducing to zero at approximately 75 deg. When noise measurements are made using the ground plane arrangement, the effects of meteorological conditions must be considered in relation to sound incident at angles greater than approximately 60 deg. ESA

N94-14034# Technical Research Centre of Finland, Espoo. Heating and Ventilation Lab.
STUDY ON THE POSSIBILITIES TO APPLY SPECTRUMINDEX
Juhani Parmanen and Pauli Sysioe Aug. 1992 41 p Sponsored by NORDTEST
(VTT-PUBS-109; ISBN-9-51-384277-4; ETN-93-94483) Copyright Avail: CASI HC A03/MF A01

Possibilities to apply spectrumindex in building acoustics are studied. Spectrumindex refers to the difference of two sound pressure levels caused by the same sound field and measured using two separate frequency weightings. The purpose of the study is to develop a simple method in which one can apply the spectrumindex to evaluate the traffic noise reduction indices existing already in a NORDTEST method. The spectrumindex principle was applied to a test material of 20 different windows. Two alternatives were used as basic sound reduction indices. The equation including the best realizable sound insulation curves was chosen as the most feasible estimation method. It is shown that reliable estimation results can be obtained. The deviation is at the most 1 dB from the correct value calculated in accordance with the NORDTE[illegible] The study is completed by using a material consisting of 11 exterior doors and one single pane window. ESA

N94-14130 Southampton Univ. (England). Inst. of Sound and Vibration research.
UNDERWATER HEARING: A REVIEW
M. Al-Masri, A. Martin, and J. Nedwell May 1993 54 p Limited Reproducibility: More than 20% of this document may be affected by microfiche quality
(ISVR-TR-212) Copyright Avail: Issuing Activity

In view of the prevalence of hearing loss among commercial divers and the absence of widely accepted noise exposure limits for occupational underwater use, a review of studies of underwater hearing thresholds and hearing mechanisms was undertaken with the ultimate aim of developing noise exposure limits. Previous studies of underwater hearing thresholds appear to show that the ear underwater is less sensitive than compared with air. However, a surprisingly wide range of values for underwater hearing thresholds was reported, for example 35-90 dB SPL(re 20 MuPa) at 0.25 kHz and 30-80 dB at 1 kHz. No representative single threshold curve can be extracted with any validity. Possible reasons for such a wide scatter of results include high underwater ambient noise levels which may have masked the subjects underwater hearing thresholds, ill defined stimuli and underwater sound fields, and variable and informal audiometric methodology. Previous authors have proposed three somewhat interlinked theories to explain how sound is transmitted from water to the cochlea. These involve: the 'auricular' conduction pathway, the bone conduction pathway, and the dual conduction pathway. Up to this day, no one pathway has been shown to predominate, and all of them have been poorly evaluated. It is also possible that the presence of air bubbles in the ear canal and increased water depth may have significant effects on underwater hearing thresholds. These effects may be dependent on the underwater hearing mechanism. Again, the studies reviewed give conflicting results and no valid conclusion can be drawn. It is apparent that further experimental studies are required to establish underwater hearing thresholds and to provide an understanding of the mechanisms of hearing underwater. These should be based upon suitable facilities and methodologies for testing hearing thresholds underwater following modern and scientific audio metric practice. Author (revised)

N94-14360# JASCO Research Ltd., Sidney (British Columbia).
FLATDAN BEAMFORMER ENHANCEMENTS AND TESTING
Roberto Racca, Ian Schumacher, and P. Kraeutner Jul. 1992 46 p
(Contract DREP-W7708-1-0980-01-XSA)
(DSIS-93-00287; DREP-CR-92-47; CTN-93-60798) Avail: CASI HC A03

FLATDAN is a program that implements a Farfield Line Array Time Domain beamformer for processing large amounts of acoustic data. Upsampling is used to increase the time delay resolution beyond that of the input sampling frequency. However, decimation after the beamforming operation ensures that the output data rate per beam is the same as the input data rate per sensor. The beamformer can accommodate up to 256 input sensor channels and can provide output for up to 256 beams. The beamformer expects input data for all sensors to be in a single file written using the Defence Research Establishment Pacific Ocean Acoustics .DAT format. Beam output data is written in the same format. An information manual for FLATDAN users is presented, describing the beamformer design, program operation, and program structure. Modifications to the file input/output routines since the original introduction of FLATDAN are noted. A performance analysis of the beamformer code was conducted using a VAX performance and coverage analyzer utility. Results are given, showing how much total execution time is spent at given locations in the program. Sample plots from test runs using simulated input data are included. CISTI

N94-14481*# National Aeronautics and Space Administration. Langley Research Center, Hampton, VA.
ACTIVE CONTROL OF FAN-GENERATED PLANE WAVE NOISE
Carl H. Gerhold, William E. Nuckolls (Analytical Services and Materials, Inc., Hampton, VA.), Odillyn L. SantaMaria, and Scott D. Martinson Aug. 1993 28 p Sponsored by NASA. Washington
(RTOP 535-03-11-02)
(NASA-TM-109008; NAS 1.15:109008) Avail: CASI HC A03/MF A01

Subsonic propulsion systems for future aircraft may incorporate ultra-high

bypass ratio ducted fan engines whose dominant noise source is the fan with blade passage frequency less than 1000 Hz. This low frequency combines with the requirement of a short nacelle to diminish the effectiveness of passive duct liners. Active noise control is seen as a viable method to augment the conventional passive treatments. An experiment to control ducted fan noise using a time domain active adaptive system is reported. The control sound source consists of loudspeakers arrayed around the fan duct. The error sensor location is in the fan duct. The purpose of this experiment is to demonstrate that the in-duct error sensor reduces the mode spillover in the far field, thereby increasing the efficiency of the control system. In this first series of tests, the fan is configured so that predominantly zero order circumferential waves are generated. The control system is found to reduce the blade passage frequency tone significantly in the acoustic far field when the mode orders of the noise source and of the control source are the same. The noise reduction is not as great when the mode orders are not the same even though the noise source modes are evanescent, but the control system converges stably and global noise reduction is demonstrated in the far field. Further experimentation is planned in which the performance of the system will be evaluated when higher order radial and spinning modes are generated. Author (revised)

N94-14867# Los Alamos National Lab., NM.
STUDY OF CHEMICAL REACTIONS UNDER THE INFLUENCE OF ULTRASOUND
Kien-Yin Lee 1993 5 p Presented at the Ultrasonics International 1993, Vienna, Austria, 6-8 Jul. 1993
(Contract W-7405-eng-36)
(DE93-016458; LA-UR-93-2331; CONF-930799-1) Avail: CASI HC A01/MF A01

At Los Alamos, the author is interested in sonochemistry because there is potential for accelerating reactions involving the synthesis of certain nitro compounds and for reducing the possibility of decomposition under milder reaction conditions. The author has initiated the study of the nitration of 2,4-dihydro-3H-1,2,4-triazol-3-one with concentrated nitric acid under sonication. The preparation of 4,5-tetrazine, and oxidation of 3,6-diamino-1,2,4,5-tetrazine were also studied. Sonication reaction conditions and results of these reactions under ultrasound are discussed in detail. DOE

72 ATOMIC AND MOLECULAR PHYSICS

Includes atomic structure, electron properties, and molecular spectra.

N94-12845# Melbourne Univ., Parkville (Australia). School of Physics.
ELECTRIC CHARGE QUANTIZATION
R. Foot (Southampton Univ., England.), H. Lew (Purdue Univ., West Lafayette, IN.), and R. R. Volkas Jun. 1992 17 p
(DE93-622901; UM-P-92/52; OZ-92/19; SHEP-91/92) Avail: CASI HC A03/MF A01 (US Sales Only)

Experimentally it has been known for a long time that the electric charges of the observed particles appear to be quantized. An approach to understanding electric charge quantization that can be used for gauge theories with explicit U(1) factors - such as the standard model and its variants - is pedagogically reviewed and discussed in this article. This approach used the allowed invariances of the Lagrangian and their associated anomaly cancellation equations. It is demonstrated that charge may be de-quantized in the three-generation standard model with massless neutrinos, because differences in family-lepton-numbers are anomaly-free. The relevant experimental limits are also reviewed. This approach to charge quantization suggests that the minimal standard model should be extended so that family-lepton-number differences are explicitly broken. Some candidate extensions such as the minimal standard model augmented by Majorana right-handed neutrinos are also briefly discussed. DOE

N94-12847# Melbourne Univ., Parkville (Australia). School of Physics.
TOP QUARK POLARIZATION AND T-ODD SPIN CORRELATIONS AS TOOLS FOR TESTING (NON) STANDARD MODEL PREDICTIONS
W. Bernreuther (Ecole Polytechnique, Palaiseau, France.), J. P. Ma, and T. Schroeder (Heidelberg Univ., Germany.) 1992 17 p
(DE93-622956; UM-P-92/63; OZ-92/27; HD-THEP-92-30) Avail: CASI HC A03/MF A01 (US Sales Only)

In this paper a number of T-odd spin-momentum correlations are defined for t and t-bar quarks and directly measurable correlations involving the momenta of the charged leptons and/or b jets from t and t-bar decay are identified. It concentrates on observables which can be classified as being even under a CP symmetry transformation in the case of e(sup +)e(sup -) yields tt-bar X or pp-bar yields tt-bar X (unpolarized or transversely polarized beams). These correlations project onto absorptive parts of the scattering matrix which are induced by CP-conserving interactions. In order to estimate the effects of the Standard Model interactions the Quantum Chromodynamics and Higgs boson contributions were calculated to a number of these observables. Several of them are considered to be useful tools for a detailed study of the tt-bar system at future hadron colliders. DOE

N94-12848# Melbourne Univ., Parkville (Australia). School of Physics.
MEDIUM ENERGY HADRON-NUCLEUS SCATTERING IN THE 1/N EXPANSION FORMALISM
S. Kuyucak (Australian National Univ., Canberra.) and I. Morrison 1992 31 p
(DE93-622957; UM-P-92/66) Avail: CASI HC A03/MF A01 (US Sales Only)

The algebraic-eikonal approach to the medium energy hadron-nucleus scattering is generalized to arbitrary interactions and boson types using the 1/N expansion technique for the interacting boson model. The results are used in a comparative study of proton scattering from deformed nuclei in the sd and sdg boson models. The two models give almost identical results for a pure quadrupole interaction but widely differ when a hexadecapole interaction is included. DOE

N94-12858 Melbourne Univ., Parkville (Australia). School of Physics.
ELECTROMAGNETIC DEFLECTION OF SPINNING PARTICLES
J. P. Costella and B. H. J. McKellar 1992 13 p Limited Reproducibility: More than 20% of this document may be affected by microfiche quality
(DE93-622866; UM-P-92/93) Avail: CASI HC A03 (US Sales Only)

It is shown that it is possible to obtain self-consistent and physically acceptable relativistic classical equations of motion for a point-like spin-half particle possessing an electric charge and magnetic dipole moment, directly from a manifestly covariant Lagrangian, if the classical degrees of freedom are appropriately chosen. The equations obtained encompass the well-tested Lorentz force and Thomas-Bargmann-Michel-Telegdi spin equations, as well as providing a definite specification of the classical magnetic dipole force, whose exact form has been the subject of recent debate. Radiation reaction - the force and torque on an accelerated particle due to its self-interaction - is neglected at this stage. DOE

N94-12860# Fribourg Univ. (Switzerland).
DETECTION OF HOT MUONIC HYDROGEN ATOMS EMITTED IN VACUUM USING X-RAYS
R. Jacot-Guillarmod, J. M. Bailey (Liverpool Univ., England.), G. A. Beer (Victoria Univ., British Columbia.), P. E. Knowles (Victoria Univ., British Columbia.), G. R. Mason (Victoria Univ., British Columbia.), A. Olin (Victoria Univ., British Columbia.), J. L. Beveridge (Tri-Univ. Meson Facility, Vancouver, British Columbia.), G. M. Marshall (Tri-Univ. Meson Facility, Vancouver, British Columbia.), J. H. Brewer (British Columbia Univ., Vancouver.), and B. M. Forster (British Columbia Univ., Vancouver.) 1992 6 p Presented at the Ascona Workshop on Muonic Atomic and Molecules, Ascona, Switzerland, 5-9 Apr. 1992
(Contract DE-FG02-87ER-40333)
(DE93-010253; DOE/ER-40333/137; CONF-9204241-1) Avail: CASI HC A02/MF A01

Negative muons are stopped in solid layers of hydrogen and neon. Muonic hydrogen atoms can drift to the neon layer where the muon is immediately transferred. It was found that the time structure of the muonic neon X-rays follows the exponential law where the rate is the same as the disappearance rate of (mu)(-)p atoms. The pp(mu)-formation rate and the muon transfer rate to deuterium are deduced. DOE

N94-12879# International Centre for Theoretical Physics, Trieste (Italy).
SOLITONS AND 1/f NOISE IN MOLECULAR CHAINS

H. Rosu and E. Canessa Jan. 1993 15 p
(DE93-622898; IC-93/22) Avail: CASI HC A03/MF A01 (US Sales Only)

Davydov's model of solitons in (alpha)-helix protein chains is shown to display features of self-organized criticality (SOC), i.e., power law behavior of correlations in space and 1/f noise, as a consequence of considering random peptide group displacements from their (periodic) equilibrium positions along a chain. This may shed light on a basic mechanism leading to obtain flicker noise in (alpha)-helix protein chains and to predict a SOC regime in biomolecular structures from first principles. We believe our treat of 1/f noise to be of some relevance to recent findings due to Voss on DNA (Phys. Rev. Lett. 68, 3805 (1992)). DOE

N94-12882# International Centre for Theoretical Physics, Trieste (Italy).
CHARGED SCALAR PARTICLES AND (TAU) LEPTONIC DECAY
Zhijian Tao Feb. 1993 11 p
(DE93-622969; IC-93/31) Avail: CASI HC A03/MF A01 (US Sales Only)

Charged scalar particles introduced in some extensions of the standard model can induce (tau) leptonic at tree level. We find that with some charged SU(2)-singlet scalar particles, like ones introduced in Zee-type model, (tau) leptonic decay width is always smaller than what is predicted by the standard model, therefore they may offer a natural solution to (tau) decay puzzle. To be more specific, we examine some Zee-type models in detail to see if at the same time they are acceptable in particle physics, cosmology and astrophysics. It is shown that (tau) decay data do put some constraints on these models. DOE

N94-12894# Purdue Univ., West Lafayette, IN. Dept. of Chemistry.
MOLECULAR SOLVENT-DYNAMICAL EFFECTS ON ACTIVATED ELECTRON-TRANSFER KINETICS: HOW IMPORTANT IS SOLVENT FRICTION? Technical Report
Michael J. Weaver Apr. 1993 26 p
(Contract N00014-91-J-1409)
(AD-A265886; TR-142) Avail: CASI HC A03/MF A01

The likely extent of retardation exerted by solvent friction upon the rates of activated electron-transfer (ET) processes is explored and evaluated with reference to some extent solvent-dependent data for metallocene ET self exchanges. Barrier-crossing frequencies extracted from the experimental kinetic and barrier data for suitably adiabatic reactions are compared with solvent inertial frequencies (i.e. the zero-friction limit) as estimated from currently available analytic expressions. The additional extent of rate retardation seen in going from low-friction to ostensibly strongly overdamped solvents as deduced in this manner is seen to be substantially muted in comparison with the predictions of conventional Debye-continuum approaches, although follows a solvent functionality that is nevertheless roughly in accord with the latter. The likely importance of more rapid dynamics associated with short-range (molecular) solvation is addressed in the light of these findings. DTIC

N94-12940# Toledo Univ., OH. Dept. of Physics and Astronomy.
MEASUREMENTS OF SCATTERING PROCESSES IN NEGATIVE ION-ATOM COLLISIONS
T. J. Kvale 1993 13 p
(Contract DE-FG05-88ER-13971)
(DE93-013863; DOE/ER-13971/20) Avail: CASI HC A03/MF A01

This research project is designed to provide measurements of various scattering processes which occur in H(-) collisions with atomic (specifically, noble gas and atomic hydrogen) targets at intermediate energies. These processes include elastic scattering, single- and double-electron detachment, and target excitation/ionization. For the elastic and target inelastic processes where H(-) is scattered intact, the experimental technique of Ion Energy-Loss Spectroscopy (IELS) will be employed to identify the final target state(s). In most of the above processes, cross sections are unknown both experimentally and theoretically. The measurements in progress will provide either experimentally determined cross sections or set upper limits to those cross sections. In either case, these measurements will be stringent tests of our understanding in energetic negative ion-atom collisions. In addition secondary negative particle emission yields for H(sup 0) on Cu in the 3 to 50 keV range are shown. DOE

N94-12949# Los Alamos National Lab., NM.
NO-LOST THEOREM FOR PARITY VIOLATING NUCLEON-NUCLEON SCATTERING EXPERIMENTS
T. Goldman 1993 8 p Presented at the Future Directions in Particle and Nuclear Physics at Multi-GeV Hadron Beam Facilities, Upton, NY, 4-6 Mar. 1993
(Contract W-7405-eng-36)
(DE93-012737; LA-UR-93-1532; CONF-930389-10) Avail: CASI HC A02/MF A01

A purely left-chiral model of the weak interactions is used to show that the total parity-violating asymmetry in quark-quark scattering must grow with increasing energy. In the absence of other new physics, non-observation of a large asymmetry can therefore be used to infer an upper bound on the mass scale for new right-chiral weak vector bosons. Applying this idea to actual nucleon-nucleon scattering requires more involved calculations, as the dominant contribution appears to come from a component of diquark-quark scattering related to, but not identical to, wavefunction-mixing. Earlier criticism of this model by Simonius and Unger is refuted, and a new calculation is proposed as an additional check on the result. Finally, we argue that the so-called 'spin crisis' does not affect our conclusions. DOE

N94-12950# Los Alamos National Lab., NM.
LOW ENERGY NEUTRAL ATOM IMAGING TECHNIQUES
Herbert O. Funsten, David J. McComas, and Earl E. Scime 1993 13 p Presented at the Annual Meeting of the Society of Photo-Optical Instrumentation Engineers, San Diego, CA, 11-16 Jul. 1993
(Contract W-7405-eng-36)
(DE93-012744; LA-UR-93-1509; CONF-930722-1) Avail: CASI HC A03/MF A01

The potential scientific return from low energy neutral atom (LENA) imaging of the magnetosphere is extraordinary. The technical challenges of LENA detection include the following: (1) removal of LENA's from the tremendous ambient UV without losing information of their incident trajectories, (2) quantification of their trajectories, and (3) obtaining high sensitivity measurements. Two techniques that have been proposed for this purpose are based on fundamentally different atomic interaction mechanisms between LENA's and a solid: LENA transmission through an ultrathin foil and LENA reflection from a solid surface. Both of these methods provide LENA ionization (for subsequent removal from the UV by electrostatic deflection) and secondary electron emission (for start pulse generation for time-of-flight and/or coincidence). We present a comparative study of the transmission and reflection techniques based on differences in atomic interactions with solids and surfaces. We show that transmission methods yield an order of magnitude greater secondary electron emission than reflection methods. Transmission methods are shown to be sufficient for LENA energies of approximately 1 keV to greater than 30 keV. Reflection methods using low work function surfaces could be employed for LENA ionization for energies less than several keV. DOE

N94-12954# Fermi National Accelerator Lab., Batavia, IL.
A SEARCH FOR SCALAR LEPTOQUARKS IN D0
K. W. Merritt Nov. 1992 5 p Presented at the Meeting of the Division of Particles and Fields of the American Physical Society, Batavia, IL, 10-14 Nov. 1992
(Contract DE-AC02-76CH-03000)
(DE93-012780; FNAL/C-93/045/E; CONF-921122-52) Avail: CASI HC A01/MF A01

A search has been made using the data from the first run of the D0 detector at the Fermilab Tevatron for pair production of scalar leptoquarks, each decaying into electron plus quark (visible in the detector as electron plus jet). From a data sample representing 841 nb(exp -1), a limit of 74 GeV at 95% confidence level can be set on the mass of the first generation scalar leptoquark, for a particular calculation of the production cross section and a 100% branching fraction into electron plus quark. DOE

N94-12997# Washington Univ., Seattle. Dept. of Physics.
ASPECTS OF SYMMETRY VIOLATION
E. M. Henley 1992 11 p Presented at the 10th International Symposium on High-Energy Spin Physics, Nagoya, Japan, 9-14 Nov. 1992
(Contract DE-FG06-88ER-40427)

(DE93-011003; DOE/ER-40427/36-N92; CONF-921131-12) Avail: CASI HC A03/MF A01

Violations of symmetries have been used to determine, or test, theoretical dynamics or to study structure. Recent experiments on parity non-conservation and time reversal symmetry, experiments that depend on spin properties, are used to illustrate both applications. DOE

N94-13018 California Univ., Berkeley. Lawrence Berkeley Lab.
RADIATIVE CORRECTIONS IN THE STRONGLY INTERACTING LIMIT OF THE STANDARD ELECTROWEAK MODEL
M. K. Gaillard 19 Apr. 1993 16 p Presented at the International Symposium on 30 Years of Neutral Currents, Los Angeles, CA, 3-5 Feb. 1993 Limited Reproducibility: More than 20% of this document may be affected by poor print
(Contract DE-AC03-76SF-00098)
(DE93-013906; LBL-33976; UCB-PTH-93/14; NSF-ITP-93-42; CONF-930293-3) Avail: Issuing Activity (Department of Energy (DOE))

Radiative corrections to the parameters of the standard electroweak model are considered in case that there is no light Higgs particle. DOE

N94-13051# Minnesota Univ., Minneapolis. Dept. of Chemistry.
EXPERIMENTAL AND THEORETICAL STUDY OF INHOMOGENEOUS ELECTRON TRANSFER IN BETAINE: COMPARISONS OF MEASURED AND PREDICTED SPECTRAL DYNAMICS
Alan E. Johnson, Nancy E. Levinger, Wlodzimierz Jarzeba, Ralph E. Schlief, and Dahv A. Kliner 15 May 1993 63 p
(Contract N00014-89-J-1746)
(AD-A265703; TR-3) Avail: CASI HC A04/MF A01

New tunable pump and probe data are reported for the S(sub 1)-S(sub 0) reverse electron transfer in betaine in solution. The observed dynamics are a dramatic function of probe wavelength due to energy deposition into solute and solvent molecular degrees of freedom from the electron transfer. These data indicate that in nonpolar solvents, this energy is primarily deposited into intramolecular modes, but some is specifically deposited into polar collective motions of the solvent, i.e. the solvent coordinate. Modern theories of electron transfer that include diffusive motion along the solvent coordinate as a driving mechanism for electron transfer predict this specific energy deposition into the solvent coordinate. A model by Walker et al. is extended to predict the spectral dynamics due to solvent coordinate heating caused by the electron transfer and compare to experimental results. It is shown that the diffusive electron transfer mechanism creates a displaced distribution along the solvent coordinate that is characterized by an absorption spectrum that is red-shifted from the equilibrium ground-state distribution, in agreement with experimental observations. The model is not in quantitative agreement with experiment, however, because it neglects the contributions of vibrational heating of the intramolecular modes to the spectral dynamics. This type of vibrational heating is evident in the observed dynamics in nonpolar solvents. DTIC

N94-13071# Pittsburgh Univ., PA.
NEW INFRARED PHOTON ABSORPTION PROCESSES
J. E. Bayfield May 1993 12 p
(Contract DE-FG02-88ER-13960)
(DE93-017017; DOE/ER-13960/5) Avail: CASI HC A03/MF A01

The fast ionization of atoms by very short laser pulses, and its possible suppression at extreme pulse intensities, is an active new field of investigation at present. Described is an investigation of whether past techniques for infrared laser multiphoton ionization of excited hydrogen atoms and of one-dimensional microwave ionization of highly excited hydrogen atoms can be combined and extended to address the new issues. Although technically difficult and requiring further improvement of the apparatus, intense-field infrared laser experiments on excited hydrogen atoms are possible and can directly test theoretical and numerical results. DOE

N94-13097# Brookhaven National Lab., Upton, NY.
HIJET WITH AGS PHYSICS AND N(SUP *)'S
R. S. Longacre 11 Feb. 1993 9 p Presented at the HIPAGS Meeting, Cambridge, MA, 14-17 Jan. 1993
(Contracts DE-AC02-76CH-00016; DE-FG05-87ER-40309; DE-FG02-91ER-40645; DE-FG02-88ER-40413)
(DE93-014022; BNL-48648; CONF-930173-7) Avail: CASI HC A02/MF A01

We investigate the effects of secondary interactions in nucleus-nucleus and proton-nucleus collisions using a modified HIJET Monte Carlo generator. The effects of N(sup *) production is explored and it is found that the numbers of kaons can almost be explained by their inclusion. However the transverse momentum spectrum of the kaons is not explained, since their production in HIJET is a soft secondary scattering process and not a hot thermal process like the data. DOE

N94-13098# Brookhaven National Lab., Upton, NY.
NEUTRAL STRANGE PARTICLE PRODUCTION AT THE AGS
A. C. Saulys 11 Feb. 1993 8 p Presented at the HIPAGS Meeting, Cambridge, MA, 14-17 Jan. 1993
(Contracts DE-AC02-76CH-00016; DE-FG02-91ER-40645; DE-FG02-88ER-40413; DE-FG05-87ER-40309)
(DE93-014044; BNL-48649; CONF-930173-9) Avail: CASI HC A02/MF A01

We present the results of Lambda and K(sub s)(sup o) production from Si and Pb targets with 14.6 x Lambda Gev/c Si beams. The measured rapidity distributions and the transverse mass exponential slopes are presented and compared with models. DOE

N94-13101# Brookhaven National Lab., Upton, NY.
POLARIZATION AND COLOR TRANSPARENCY
G. Bunce 1993 4 p Presented at the Future Directions in Particle and Nuclear Physics At Multi-GeV Hadron Beam Facilities, Upton, NY, 4-6 Mar. 1993
(Contract DE-AC02-76CH-00016)
(DE93-014319; BNL-48832; CONF-930389-12) Avail: CASI HC A01/MF A01

Color transparency offers an interesting experimental test of our understanding of hadronic polarization effects which have been seen at high energy. Large polarization effects have been seen for exclusive high momentum transfer reactions which are incompatible with lowest order pQCD. It is proposed to filter these reactions by scattering inside a nucleus. We expect that only color transparent hadrons would survive, and that these should be products of 'hard' scattering. If the polarization arises from a non-perturbative 'soft' effect, the nucleus should filter these reaction products away. We should see no polarization remaining after the reaction is filtered by a large nucleus. DOE

N94-13149# Brookhaven National Lab., Upton, NY.
MEASUREMENT OF THE SPIN OF A PARTICLE USING UNDULATOR RADIATION
A. Luccio 1993 4 p Presented at the International Particle Accelerator Conference, Washington, DC, 17-20 May 1993
(Contract DE-AC02-76CH-00016)
(DE93-014334; BNL-48237; CONF-930511-75) Avail: CASI HC A01/MF A01

The use of many-period wigglers to rotate the spin of particles in accelerators has been proposed. An added advantage of this scheme is that a spectrum of synchrotron radiation will be produced that contains a contribution due to the spin, so that the device can be effectively used as spin polarimeter, with advantages compared to Compton backscattering methods. Results are presented for two high energy proton storage rings: RHIC and the SSC. DOE

N94-13173# Los Alamos National Lab., NM.
RECENT STUDY OF BEAM STABILITY IN THE PSR
T. S. F. Wang, R. Cooper, D. Fitzgerald, S. Frankle, T. Hardek, R. Hutson, R. Macek, C. Ohmori, M. Plum, and H. Thiessen et al 1993 4 p Presented at the International Particle Accelerator Conference, Washington, DC, 17-20 May 1993
(Contract W-7405-eng-36)
(DE93-014473; LA-UR-93-1874; CONF-930511-112) Avail: CASI HC A01/MF A01

A fast transverse instability with beam loss has been observed in the 800 MeV Los Alamos Pro Ring (PSR) when the injected beam intensity reaches 2 - 4(10)(exp 13) protons per pulse. Previous observations indicate that the instability is most likely driven by electrons trapped within the proton beam. Theoretical study shown that beam leakage into the inter-bunch gap leads to electron trapping. Recent experiments were carried out by using the newly implemented 'pinger' and by varying the machine transition

gamma to explore further the 'e-p' instability and the nature of the instability. This paper summarizes some of these recent experimental results and theoretical studies. DOE

N94-13205# Los Alamos National Lab., NM.
PRESENT STATUS OF SAGE
T. J. Bowles 1993 11 p Presented at the 13th Moriond Workshop on Perspectives in Neutrinos, Villars-sur-Ollon, Switzerland, 30 Jan. - 6 Feb. 1993
(Contract W-7405-eng-36)
(DE93-014350; LA-UR-93-1970; CONF-930187-5) Avail: CASI HC A03/MF A01

A radiochemical Ga-71-Ge-71 experiment to determine the primary flux of neutrinos from the Sun began measurements of the solar neutrino flux at the Baksan Neutrino Observatory in 1990. The number of Ge-71 atoms extracted from 30 tons of gallium in 1990 and from 57 tons of gallium in 1991 was measured in twelve runs during the period of Jan. 1990 to Dec. 1991. The combined 1990 and 1991 data sets give a value of 58 +17/-24 (stat) +/-14 (syst) SNU. This is to be compared with 132 SNU predicted by the Standard Solar Model. DOE

N94-13219# Brookhaven National Lab., Upton, NY.
NUCLEAR FUSION OF PROTONS WITH IONS OF BORON
A. G. Ruggiero 1993 4 p Presented at the International Particle Accelerator Conference, Washington, DC, 17-20 May 1993
(Contract DE-AC02-76CH-00016)
(DE93-014284; BNL-48374; CONF-930511-124) Avail: CASI HC A01/MF A01

This paper describes a method of extracting energy from the fusion events occurring between the collision of a beam of protons with a beam of ions of Boron-11. The two beams are circulating in separated and intersecting storage rings where they collide head-on in a common long-straight section. Requirements on the luminosity of the low-energy collider are shown. Limitations due to space-charge and intrabeam scattering are described. Very fast electron cooling is needed to compensate these effects. DOE

N94-13225# International Centre for Theoretical Physics, Trieste (Italy).
MOLECULAR DYNAMICS SIMULATION OF ELECTRONICALLY EXCITED POLYATOMIC MOLECULES
V. D. Vachev, B. A. Grishanin (International Laser Centre, Moscow, Russia.), and V. N. Zadkov (International Laser Centre, Moscow, Russia.) Jan. 1993 14 p
(DE93-623045; LAMP-93/1) Avail: CASI HC A03/MF A01 (US Sales Only)

A computer simulation method is proposed for MD study of the photoinduced intramolecular dynamics in polyatomic molecules electronically excited by ultrashort laser pulses. An efficient, partially analytical procedure for calculation of the absorption (emission) spectra is developed and used for determination of molecular potentials in accordance with the experimental supersonic jets spectra. DOE

N94-13241# Brookhaven National Lab., Upton, NY.
A SEARCH FOR STRONG-FIELD DIRECT TWO ELECTRON IONIZATION USING COINCIDENCE SPECTROSCOPY
P. Agostini, E. Mevel, P. Breger (Commissariat a l'Energie Atomique, Gif-sur-Yvette, France.), B. Walker, B. Yang, and L. F. DiMauro 1993 5 p Presented at the 5th Short Wavelength: Physics with Intense Laser Pulses, San Diego, CA, 29-31 Mar. 1993
(Contract DE-AC02-76CH-00016)
(DE93-013435; BNL-48940; CONF-9303119-2) Avail: CASI HC A01/MF A01

We report on our program in detecting two-electron ionization using electron-electron and electron-ion coincidence measurements. The coincidence techniques have been applied to the multiphoton ionization (MPI) of xenon atoms with 0.527 micron excitation. The results show that direct two electron ionization is not occurring which is in variance with an earlier report. We also present a polarization study on the MPI of helium at 0.62 micron and discuss these results in context of existing models. DOE

N94-13251# Lawrence Livermore National Lab., CA.
CHARGED-PARTICLE EVALUATION METHODOLOGY AT LAWRENCE LIVERMORE NATIONAL LABORATORY
D. A. Resler and R. M. White Oct. 1992 10 p Presented at the Symposium on Nuclear Data Evaluation Methodology, Upton, NY, 12-16 Oct. 1992
(Contract W-7405-eng-48)
(DE93-013429; UCRL-JC-112154; CONF-921046-18) Avail: CASI HC A02/MF A01

We recently completed charged-particle evaluations for reactions of hydrogen and helium that are important in fusion applications. In this paper we emphasize the methods developed which are unique to the evaluation of low-energy charged-particle data. In addition, we discuss general methods we developed to eliminate some of the tedious aspects of data evaluation such as the extraction of numerical values from graphs when tabulated experimental data are unavailable. We also discuss software tools developed for visualization of experimental data and to construct curves using a computer mouse or a variety of least-squares techniques ranging from simple polynomial and cubic-spline fits to R-matrix analyses. DOE

N94-13283 Indiana Univ., Bloomington.
HIGH RESOLUTION ELECTRON ENERGY LOSS STUDIES OF SURFACE VIBRATIONS
L. L. Kesmodel May 1993 8 p Limited Reproducibility: More than 20% of this document may be affected by microfiche quality
(Contract DE-FG02-84ER-45147)
(DE93-014441; DOE/ER-45147/8) Avail: CASI HC A02

New experimental investigations of surface vibrational properties of materials with high-resolution electron energy loss spectroscopy (EELS) are reported. This document summarizes progress over the three year project period on surface phonon measurements on copper (001); silver (111); ultrathin magnetic films; aluminum on silicon (111); and copper-oxide based superconductors. DOE

N94-13348# Montreal Univ. (Quebec). Dept. of Physics.
DOUBLE SEMI-LEPTONIC CHARM DECAY IN HELIOS-I 450 GeV/c p-Be DATA
A. Pierre and P. A. Pomianowski 1992 3 p Presented at the Meeting of the Division of Particles and Fields of the American Physical Society, Batavia, IL, 10-14 Nov. 1992
(Contract DE-FG02-91ER-40646)
(DE93-013493; CONF-921122-54-App-1) Avail: CASI HC A01/MF A01

Data taken in 1989 by HELIOS-I (NA34) at the CERN SPS (450 GeV/c proton beam on Be target) have been examined for e(+/-)(mu)(-/+) or mu(+-)(mu)(-+) pairs with the associated missing energy. Such pairs arise from semi-leptonic decay of both members of a c(bar-c) pair. The e(mu) and mu(mu) samples are consistent with expectations from charm decay, allowing a quantitative limit to be placed on other physics. DOE

N94-13349# Oak Ridge National Lab., TN.
BETA/GAMMA TEST PROBLEMS FOR ITS
G. T. Mei 1993 5 p Presented at the DOE Radiation Protection Conference, Las Vegas, NV, 13-15 Apr. 1993
(Contract DE-AC05-84OR-21400)
(DE93-013522; CONF-9304128-8) Avail: CASI HC A01/MF A01

The Integrated Tiger Series of Coupled Electron/Photon Monte Carlo Transport Codes (ITS 3.0, PC Version) was used at Oak Ridge National Laboratory (ORNL) to compare with and extend the experimental findings of the beta/gamma response of selected health physics instruments. In order to assure that ITS gives correct results, several beta/gamma problems have been tested. ITS was used to simulate these problems numerically, and results for each were compared to the problem's experimental or analytical results. ITS successfully predicted the experimental or analytical results of all tested problems within the statistical uncertainty inherent in the Monte Carlo method. DOE

N94-13350# Fermi National Accelerator Lab., Batavia, IL.
LOW ENERGY RESPONSE OF THE DO CALORIMETER AND JET ENERGY MEASUREMENT
P. C. Bhat Nov. 1992 5 p Presented at the Meeting of the Division of Particles and Fields of the American Physical Society, Batavia, IL, 10-14 Nov. 1992

(Contract DE-AC02-76CH-03000)
(DE93-013569; FNAL/C-93/049-E; CONF-921122-57) Avail: CASI HC A01/MF A01

Previous studies of the DO calorimeter with electron and hadron beams above 10 GeV/c have shown excellent linearity of response and AN e/pi ratio close to one. Here we report on our measurements of the response of the DO central calorimeter modules down to 2 GeV/c. The measured low energy response for electrons and pions are convoluted with jet fragmentation from the PYTHIA Monte Carlo code to obtain the corrections for jet energy. DOE

N94-13362 Gosudarstvennyi Komitet po Ispolzovaniyu Atomnoi Energii, Serpukhov (USSR).
FURTHER STUDY OF THE X(1910) MESON
D. Alde et al 1991 7 p Submitted for publication Limited Reproducibility: More than 20% of this document may be affected by microfiche quality
(DE93-621443; IFVE-OEF-91-40) Avail: CASI HC A02 (US Sales Only)

New data on eta' eta system produced in pi(sup -) p charge-exchange reaction at 38 GeV/c momentum are presented. The data confirm the existence of the narrow eta' eta resonance X(1910). The hypothesis of X(1910) quantum numbers to be J(sup PC)=1(sup -+), forbidden for qq-bar meson, is discussed to explain both extremely low limits obtained for X(1910) decays through pi(sup 0) pi(sup 0), eta eta and K(sub S)(sup 0) K(sub S)(sup 0) channels and flat t-dependence of X(1910) production cross section. DOE

N94-13409# Sandia National Labs., Albuquerque, NM.
VARIANCE REDUCTION UNIQUE TO COUPLED ELECTRON/PHOTON MONTE CARLO TRANSPORT
J. A. Halbleib, R. P. Kensek, and G. D. Valdez 1993 9 p Presented at the Advanced Monte Carlo Computer Programs for Radiation Transport, Saclay, France, 27-29 Apr. 1993
(Contract DE-AC04-76DP-00789)
(DE93-014999; SAND-93-0482C; CONF-9304131-5) Avail: CASI HC A02/MF A01

The disparity between the mean free paths of electrons and photons leads to unique variance-reduction procedures for coupled transport at intermediate energies. It is electrons that ultimately deposit charge and energy; yet electron transport is much more expensive than photon transport. The objective, then, is to control the variance of the energy, angular, and spatially dependent populations of the two species within the generation and transport of the cascade in such a way that all contributions to electron flux in the vicinity of the detector are represented to a degree commensurate with their importance. However, in beta/gamma transport, biasing techniques are often unique to one or the other of the species. DOE

N94-13412# Virginia Polytechnic Inst. and State Univ., Blacksburg. Dept. of Physics.
STUDY OF ELECTROWEAK INTERACTIONS
A. Abashian 1993 13 p
(Contract DE-AS05-80ER-10713)
(DE93-015067; DOE/ER-10713/T4) Avail: CASI HC A03/MF A01

This report is the final technical report for research conducted during the period 1 Feb. 1992 to 31 Jan. 1993. It covers three primary activities: the AMY experiment on the study of final states produced in e(+)e(-) collisions at the square root of s is approximately equal to 60 GeV, the MEGA/RHO experiment on the study of decay modes of the muon, and the R&D program on the development of resistive plate chambers for use at B factory electron colliders and possible SSC experiments. DOE

N94-13414# Rice Univ., Houston, TX.
QUASI-ELASTIC NEUTRON SCATTERING STUDIES OF PROTEIN DYNAMICS
H. E. Rorschach 25 May 1993 6 p
(Contract DE-FG05-88ER-60721)
(DE93-015074; DOE/ER-60721/6) Avail: CASI HC A02/MF A01

Results that shed new light on the study of protein dynamics were obtained by quasi-elastic neutron scattering. The triple axis instrument H-9 supplied by the cold source was used to perform a detailed study of the quasi-elastic spectrum and the Debye-Waller factor for trypsin in powder form, in solution, and in crystals. A preliminary study of myoglobin crystals was also done. A new way to view the results of quasi-elastic scattering experiments is sketched, and the data on trypsin are presented and analyzed according to this new picture. DOE

N94-13484# Argonne National Lab., IL.
ULTRAFAST PHOTOINDUCED ELECTRON TRANSFER REACTIONS IN SUPRAMOLECULAR ARRAYS: STUDIES OF ELECTRONIC COUPLING AND SOLVATION
M. R. Wasielewski, G. P. Wiederrecht, and W. A. Svec 1993 5 p Presented at the 17th Solar Photochemistry Research Conference, Brainerd, MN, 6-10 Jun. 1993
(Contract W-31-109-eng-38)
(DE93-012910; ANL/CHM/CP-79459; CONF-9306113-1) Avail: CASI HC A01/MF A01

Research in our laboratory focuses on developing supramolecular arrays that produce long-lived charge separation by limiting the electronic coupling between the separated charges, and on the role of solvation in determining the rates and energetics of photoinitiated electron transfer reactions. Arrays have been developed that closely mimic the electronic coupling that was observed only for long-lived radical pairs produced in photosynthetic glassy solids. A series of 36 fixed-distance donor-acceptor molecules using porphyrin donors, triptycene spacers, and 9 different acceptors has been prepared; these are used to probe the dependence of photoinduced charge separation rates on free energy of reaction as a function of solvent both in liquid and solid solution. Data were obtained on rates of charge separation in dioxane, MTHF, butyronitrile, toluene, chlorobenzene, and benzonitrile. DOE

N94-13485# Pacific Northwest Lab., Richland, WA.
ELECTRON EMISSION RESULTING FROM FAST ION IMPACT ON THIN METAL FOILS: IMPLICATIONS OF THESE DATA FOR DEVELOPMENT OF TRACK STRUCTURE MODELS
R. D. DuBois and C. G. Drexler Apr. 1993 31 p Presented at the DOE Monte Carlo Workshop, Irving, CA, 28-29 Apr. 1993
(Contract DE-AC06-76RL-01830)
(DE93-013506; PNL-SA-22200; CONF-9304148-1) Avail: CASI HC A03/MF A01

Experimental information useful in improving and testing theoretical models of energy deposition and redistribution in particle-condensed phase media is discussed. An overview of information available from previous, and ongoing, studies of the electron emission from thin foils is presented and the need for doubly differential electron energy and angular distribution data stressed. Existing data are used to demonstrate that precisely known, and controllable, surface and bulk conditions of the condensed-phase media are required for experimental studies of this type. Work in progress and improvements planned for future studies at the Pacific Northwest Laboratory are outlined. DOE

N94-13492# Los Alamos National Lab., NM.
ADVANCES IN LOW ENERGY NEUTRAL ATOM IMAGING TECHNIQUES
E. E. Scime, H. O. Funsten, D. J. McComas, K. R. Moore, and M. Gruntman 1993 11 p Presented at the Annual Meeting of the Society of Photo-Optical Instrumentation Engineers, San Diego, CA, 11-16 Jul. 1993
(Contract W-7405-eng-36)
(DE93-012745; LA-UR-93-1508; CONF-930722-2) Avail: CASI HC A03/MF A01

Recently proposed low energy neutral atom (LENA) imaging techniques use a collisional process to convert the low energy neutrals into ions before detection. At low energies, collisional processes limit the angular resolution and conversion efficiencies of these devices. However, if the intense ultraviolet light background can be suppressed, direct LENA detection is possible. We present results from a series of experiments designed to develop a novel filtering structure based on free-standing transmission gratings. If the grating period is sufficiently small, free standing transmission gratings can be employed to substantially polarize ultraviolet (UV) light in the wavelength range 300 to 1500 A. If a second grating is placed behind the first grating, with its axis of polarization oriented at a right angle to the first's, a substantial attenuation of UV radiation is achievable. The neutrals will pass through the remaining open area of two gratings and be detected without UV background complications. We have obtained nominal 2000 A period (1000 A bars with 1000 A slits) free standing, gold transmission

gratings and measured their UV and atomic transmission characteristics. The geometric factor of a LENA imager based on this technology is comparable to that of other proposed LENA imagers. In addition, this type of imager does not distort the neutral trajectories, allowing for high angular resolution. DOE

N94-13494# Fermi National Accelerator Lab., Batavia, IL.
INCLUSIVE SINGLE MUONS AT DO
K. A. Bazizi (California Univ., Riverside.) Nov. 1992 5 p Presented at the Meeting of the Division of Particles and Fields of the American Physical Society, Batavia, IL, 10-14 Nov. 1992
(Contract DE-AC02-76CH-03000)
(DE93-012779; FNAL/C-93/048/E; CONF-921122-53) Avail: CASI HC A01/MF A01

We report preliminary results on b-quark production in p(bar-p) collisions at (the square root of s) = 1.8 TeV from the current Run 1a of the Tevatron collider. Using an inclusive muon data sample which corresponds to an integrated luminosity of 50-70 nb(exp -1) and by further requiring the muon to be accompanied by a jet, we obtain an almost background free sample of muons consistent with b(bar-b) (yields) (mu)X decay. A preliminary p(sub T)(exp mu) spectrum and some characteristics of this decay, compared to the Monte Carlo expectations, are presented. DOE

N94-13506 Gosudarstvennyi Komitet po Ispolzovaniyu Atomnoi Energii, Serpukhov (USSR).
EFFECTS OF ADDITIONAL ISOSCALAR VECTOR BOSONS IN e(SUP +)e)(SUP -)(YIELDS)ff-BAR PROCESSES AT THE TRISTAN AND LEP ENERGIES
A. A. Pankov, S. S. Gershtejn, A. A. Likhoded, and O. P. Yushchenko 1991 15 p Submitted for publication Limited Reproducibility: More than 20% of this document may be affected by microfiche quality
(DE93-621451; IHEP-OTF-91-137) Avail: CASI HC A03 (US Sales Only)

The phenomenological manifestation of the additional Y(Y(sub L)) boson arising in the models with the composite structure of electroweak interactions is studied for the process e(sup +)e(sup -) yields ff-bar at the TRISTAN and LEP energies. It is shown that the presence of the additional isoscalar boson, yields a measurable effect in the cross-section of e(sup +)e(sup -) yields mu(sup +)mu(sup -) (hadrons) processes at LEP. This effect in the muon and hadron cross-sections at the energies M(sub Z) +/- Gamma(sub Z)/2 can be approx. 1.5-2% for small values of the gamma-Y mixing parameter. DOE

N94-13856*# Louisiana State Univ., Baton Rouge. Dept. of Physics and Astronomy.
A PROGRAM OF CORRELATED OBSERVATIONS USING THE EGRET INSTRUMENT ON GRO AND THE IMB NEUTRINO DETECTOR Final Technical Report
Robert C. Svoboda 1992 9 p
(Grant NAG5-1520)
(NASA-CR-194367; NAS 1.26:194367) Avail: CASI HC A02/MF A01

A reliable, real-time supernova monitoring system was devised using the IMB neutrino detector to serve as an 'early-warning' system for EGRET and other instruments on GRO. New methods and software were developed to allow the IMB monitoring computer in Cleveland to: recognize that a trigger burst had occurred; make a judgement on whether the burst was spurrious or an actual supernova; prepare brief summary files and 'quick-look' data so that a final disposition could be made by a trained scientist; and contact the 'watch' scientist via personal beeper in Baton Rouge. This system ran from Dec. 1990 to Apr. 1991, when the neutrino detector failed for unrelated reasons. In addition to the supernova system, high-energy neutrino data was prepared and formatted for comparison with EGRET gamma-ray data. Author (revised)

N94-13883 National Physical Lab., Teddington (England). Radiation Science and Acoustics Div.
MEASUREMENT OF THE Fe-56(n,p)Mn-56, Al-27(n,p)Mg-27 AND Al-27(n,ALPHA)Na-24 CROSS SECTIONS AT 16.0, 17.0 AND 18.3 MeV
P. Kolkowski, T. B. Ryves, and A. C. Hooley Dec. 1992 33 p
(NPL-RSA(EXT)-38; ETN-93-94465) Copyright Avail: National Physical Laboratory, Teddington, Middlesex TW11 0LW, United Kingdom HC

The cross sections of the Fe-56(n,p)Mn-56, Al-27(n,p)Mg-27, and the Al-27(n,alpha)Na-24 reactions were determined using the activation technique at neutron energies of 16.0, 17.0, and 18.3 MeV. The neutron fluences were measured using a proton recoil telescope, employing neutron-proton scattering cross section data from the most accurate values available. Corrections were applied for the effect of low energy neutrons produced by the d+D and other reactions. These ranged from under 0.2% at 16 and 17 MeV to 30% at 18.3 MeV for the worst case: that of the Al-27(n,p)Mg-27 reaction. The results are in good agreement with those found in the literature. At 18 MeV the results are less consistent probably on account of the increased effect of the low energy neutron component. ESA

N94-13884# Fermi National Accelerator Lab., Batavia, IL.
QUARK AND GLUON JETS AT CDF
N. Wainer Nov. 1992 5 p Presented at the Meeting of the Division of Particles and Fields of the American Physical Society, Batavia, IL, 10-14 Nov. 1992
(Contract DE-AC02-76CH-03000)
(DE93-014919; FNAL/C-92/345-E; CONF-921122-66) Avail: CASI HC A01/MF A01

Jet shapes at the square root of s = 1.8 TeV have been measured by CDF at the Fermilab Tevatron Collider. The jet shape is mainly formed by parton emission before hadronization. The jet shapes may also be used to differ between quark and gluon jets. Two approaches are tried. Jet shape variables are input to a feed forward neural network trained on QCD Monte Carlos. We observe a variation of the quark content of jets as a function of jet transverse energy. The second approach consists of constructing a likelihood function, based on Monte Carlo predictions, with the Mellin moments of the momentum of charged tracks in jets. Differences are found between gluon-like jets in 2-jet events and quark-like jets in photon-jet events. DOE

N94-13890# Argonne National Lab., IL.
ARE THERE ATMOSPHERIC NEUTRINO OSCILLATIONS?
M. C. Goodman 1993 3 p Presented at the International Cosmic Ray Conference, Calgary, Alberta, 19-20 Jul. 1993
(Contract W-31-109-eng-38)
(DE93-015550; ANL-HEP-CP-93-33; CONF-930779-17) Avail: CASI HC A01/MF A01

The neutrino oscillation explanation (nu(sub mu) yields nu(sub tau)) of the atmospheric neutrino deficit is often discussed but is far from widely accepted. This paper discusses several experimental observations and indicates how a consistent picture pointing towards neutrino oscillations might develop. DOE

N94-13893# Lawrence Livermore National Lab., CA.
CHARGE-EXCHANGE REACTIONS AND WEAK INTERACTION RATES FOR TYPE 2 SUPERNOVAE
M. B. Aufderheide Dec. 1992 19 p Presented at the Workshop on Nuclear Physics in the Universe, Oak Ridge, TN, 24-26 Sep. 1992
(Contract W-7405-eng-48)
(DE93-015104; UCRL-JC-111448; CONF-9209239-6) Avail: CASI HC A03/MF A01

The role of weak interactions, such as electron capture and beta decay on fp shell nuclei, during pre-supernova evolution of massive stars is examined. The utility of charge-exchange experiments for calibrating these rates is discussed. Recent (n,p) measurements indicate that the presently used rates need to be recalculated because the location of the Gamow-Teller resonances which dominate the rates in the presupernova environment could not be accurately determined. How these measurements allow us to calibrate our shell model calculations, and thus these rates, is explained. The general character of beta decay rates in this environment is then examined. It is shown that the creation and destruction rates for electrons appear to balance just after core silicon burning. A one zone model is used to examine how the beta decays will affect the evolution of the electron number and entropy. The consequences for collapse models are briefly examined. DOE

N94-13895# Fermi National Accelerator Lab., Batavia, IL.
OBSERVATION OF THE COALESCING OF BEAM INTO AN ASYMMETRIC RF BUCKET BY STOCHASTIC COOLING
A. M. Halling and Xian-Ping Lu May 1993 4 p Presented at the International Particle Accelerator Conference, Washington, DC, 17-20 May

1993
(Contract DE-AC02-76CH-03000)
(DE93-015133; FNAL/C-93/126; CONF-930511-135) Avail: CASI HC A01/MF A01

Antiprotons in the debuncher ring at Fermilab have been observed to be bunched outside of the 'barrier bucket' when cooled to small (Delta)p/p by stochastic cooling. This bunching occurs in the same location as a very small, stable bucket in the RF waveform. The stochastic cooling appears to be causing antiprotons that were originally uniformly distributed to be captured in this stable bucket. DOE

N94-13896# Argonne National Lab., IL.
RESONANT X RAY RAMAN SCATTERING FROM ATOMS AND MOLECULES
P. L. Cowan 1992 34 p Presented at the International Conference on Anomalous Scattering (ICAS) Conference, Hamburg, Germany, 17-21 Aug. 1992
(Contract W-31-109-eng-38)
(DE93-015158; ANL/PHY/CP-79637; CONF-9208186-3) Avail: CASI HC A03/MF A01

Inelastic x-ray scattering and elastic x-ray scattering are fundamentally related processes. When the x-ray photon energy is near the ionization threshold for an inner shell, the inelastic channel is dominated by resonant x-ray Raman scattering. Studies of this emission not only illuminate the resonant scattering process in general, they also point to new opportunities for spectral studies of electronic structure using x-rays. Atoms in the form of a free gas provide an ideal target for testing the current theoretical understanding of resonant x-ray Raman scattering. In addition, x-ray scattering from molecular gases demonstrates the effect of bonding symmetry on the polarization and angular distribution of the scattered x-rays. Comparisons of experimental data with theory demonstrate both the successes and limitations of simple, single-electron interpretations of the scattering process. DOE

N94-13927# Georgia Univ., Athens. Dept. of Physics and Astronomy.
HIGH ENERGY HADRON-HADRON COLLISIONS
T. T. Chou 1992 16 p
(Contract DE-FG09-84ER-40160)
(DE93-015584; DOE/ER-40160/9) Avail: CASI HC A03/MF A01

Results of a study on high energy collisions with the geometrical model are summarized in three parts: (1) the elastic hadron-hadron collision, (2) the inelastic hadron-hadron collision, and (3) e(sup +)e(sup (minus)) annihilation. For elastic scattering, a modified form for the hadronic matter form factor of the proton was proposed which is still dipole in form but contains an energy-dependent range parameter. This new expression of the opacity function fits the elastic (bar p)p scattering very well from the ISR to S(bar p)pS energies. Extrapolation of this theory also yielded results in good agreement with the (bar p)p differential cross section measured at the Tevatron. For inelastic hadron-hadron collisions, we have made a systematic investigation of the single-particle momentum spectra in the entire S(bar p)pS energy region. Results are useful for the extrapolation of angular distribution to the higher SSC energies. In e(sup +)e(sup (minus)) annihilation, a detailed analysis of all available experimental multiplicity data from PETRA to LEP energies has been performed. The cluster size of emitted hadrons increases gradually with energy. Aside from high-energy collisions, the giant fullerene molecules were studied and precise algebraic eigenvalue expressions of the Hueckel problem for carbon-240 were obtained. DOE

N94-13936# Aerospace Corp., El Segundo, CA. Space and Environment Technology Center.
DYNAMICAL MODEL FOR THE DISTRIBUTION OF GEOMAGNETICALLY TRAPPED ANOMALOUS-COMPONENT IONS
J. B. Blake, M. Schulz, and M. C. McNab 1 Jun. 1993 8 p
(ATR-91(9558)-6) Avail: CASI HC A02/MF A01

Geomagnetically trapped ions having energies E approximately equal to 1-10 MeV/nucleon are presumed to originate from the anomalous component of the cosmic-ray spectrum. The mechanism is straightforward: singly-charged anomalous component ions which happen to reach low altitude near their geomagnetic cutoffs may be stripped by the residual atmosphere. The stripping can reduce an ion's rigidity sufficiently to ensure durable trapping. Because the atmospheric grammage required to strip an anomalous-component ion is orders of magnitude smaller than that required to stop the ion, the newly-trapped ion can have a lifetime of days to weeks. The above-described suggestion of Blake and Friesen elicited little interest for years because of the dearth of available measurements. However, analysis of data from the Space Shuttle experiment TRIS, studies of observations from a long series of Soviet experiments, and the formation of the U.S.-U.S.S.R. Joint Working Group on the Charge State of the Anomalous Component have lead to renewed interest in studies of the anomalous component and the geomagnetic trapping of its constituent ions. It also seems clear that, because high-Z, low-energy solar particles are only partially ionized, this same mechanism will result in the trapping of energetic solar particles. Blake made an estimate of spectral shape, lifetime, and L-value distribution of the trapped anomalous component by invoking the formalism used to analyze the injection of Cosmic Ray Albedo Neutrons into the Earth's magnetosphere. The predicted spectral shape, in particular, appears to be borne out by the observations. Further positive results from the studies of the Joint Working Group argue for more rigorous theoretical studies. The purpose of this brief report is to describe some preliminary results of this latter work. Author (revised)

N94-13952# State Univ. of New York, Stony Brook. Dept. of Physics.
THE THEORY OF RELATIVISTIC HEAVY ION COLLISIONS
Jul. 1993 38 p
(Contract DE-FG02-93ER-40768)
(DE93-015934; DOE/ER-40768/1) Avail: CASI HC A03/MF A01

This program began in January 1993. Its primary goals are studies of highly excited matter and its production in nuclear collisions at very high energies. After a general orientation on the project, abstracts describing the contents of completed papers and providing some details of current projects are given. Principal topics of interest are the following: the dynamics of nuclear collisions at very high energies (RHIC and LHC), the dynamics of nuclear collisions at AGS energies, high-temperature QCD and the physics of the quark-gluon plasma, and the production of strangelets and other rare objects. DOE

N94-13983# Cornell Univ., Ithaca, NY. Dept. of Physics.
PHOTOCHEMICAL DYNAMICS OF SURFACE ORIENTED MOLECULES
W. Ho 1993 5 p
(Contract DE-FG02-91ER-14205)
(DE93-016289; DOE/ER-14205/2) Avail: CASI HC A01/MF A01

Photodesorption and photoreaction was investigated using a mass spectrometer, on O2 alone and co-adsorbed with CO on Pt(111) at 80 K. Desorption of O2 continues for 1 ps, indicating multiple excitation of adsorbed O2 by photogenerated hot electrons. The branching ratio for O2 desorption to CO2 product formation increases as the O2 is photoexcited by femtosecond light pulses, in contrast to the larger CO2 photoyield for nanosecond laser excitation. DOE

N94-14140# Lawrence Livermore National Lab., CA.
INDIRECT PROCESSES IN ELECTRON IMPACT IONIZATION OF Kr(24+) AND Kr(25+)
M. H. Chen and K. J. Reed Sep. 1992 4 p Presented at the 6th International Conference on Physics of Highly Charged Ions, Manhattan, KS, 28 Sep. - 2 Oct. 1992
(Contract W-7405-eng-48)
(DE93-014129; UCRL-JC-111717; CONF-920948-13) Avail: CASI HC A01/MF A01

Electron-impact ionization cross sections have been calculated for magnesium-like Kr(24+) and sodium-like Kr(25+). Electron-impact ionization is an important atomic process in hot dense plasmas. It can affect the ionization balance, electron temperature, electron density, and level population in the plasma. In the past decade, theoretical and experimental studies have revealed that indirect processes can make significant contributions to the cross sections for electron impact ionization of positive ions. The most important indirect process is excitation of an inner-shell electron followed by Auger emission. Higher-order processes such as resonant excitation followed by sequential double Auger emission can also contribute significantly. The contributions of excitation-autoionization and resonant excitation double autoionization (REDA) were included, in addition to the cross sections for direct ionization of a 3s electron. The calculations were carried out using the relativistic distorted wave methods and the multiconfiguration Dirac-Fock model. For Kr(25+), the total cross section

is about 5 times the direct ionization cross section. For the Kr(24+), the indirect contribution is about 2.5 times the direct ionization cross section. The REDA process produces many strong resonances and contributes about 20% to the average ionization cross section. DOE

N94-14144# Brookhaven National Lab., Upton, NY.
RESONANCES IN THE SIGMA NN SYSTEM
B. F. Gibson (Los Alamos National Lab., NM.) and I. R. Afnan 1993 7 p Presented at the Future Directions in Particle and Nuclear Physics at Multi-GeV Hadron Beam Facilities, Upton, NY, 4-6 Mar. 1993
(Contract W-7405-eng-36)
(DE93-014353; LA-UR-93-1965; CONF-930389-14) Avail: CASI HC A02/MF A01

We first review certain unique aspects of few-body Lambda-hypernuclei and then explore the physics of Sigma-hypernuclei that would produce structure near the Sigma threshold in few-body elastic scattering and reactions. In particular, we discuss a predicted enhancement in the lambda(d) cross section near the Sigma NN threshold in terms of poles in the Tau = 0 Y N N amplitude. A brief discussion of anticipated poles in the Tau = 1 amplitudes is also given. DOE

N94-14181# Los Alamos National Lab., NM.
THE (MU)(+) YIELDS E(+)GAMMA
M. D. Cooper 1993 5 p Presented at the International Workshop on Low Energy Muon Science (LEMS 1993), Santa Fe, NM, 4-8 Apr. 1993
(Contract W-7405-eng-36)
(DE93-012750; LA-UR-93-1471; CONF-9304145-1) Avail: CASI HC A01/MF A01

The MEGA experiment at LAMPF is the only current search for mu(+) yields e(+)(gamma) underway. The limit on this rare muon-decay process tests the standard model of electroweak interactions. This report covers the status of the analysis of data taken in 1992 and the prospects for future improvements. DOE

N94-14363# Brookhaven National Lab., Upton, NY.
THE E2 N(YIELDS)(DELTA) TRANSITION FROM POLARIZED COMPTON SCATTERING
A. M. Sandorfi, G. Blanpied (South Carolina Univ., Columbia.), M. C. Blecher (Virginia Polytechnic Inst. and State Univ., Blacksburg.), A. Caracappa, and C. Dijalali (South Carolina Univ., Columbia.) 1993 2 p Presented at the 13th International Conference on Particles and Nuclei, Peruigia, Italy, 27 Jun. - 3 Jul. 1993
(Contract DE-AC02-76CH-00016)
(DE93-012522; BNL-48717; CONF-930637-1) Avail: CASI HC A01/MF A01

The tensor interaction between the quarks in a proton is predicted to produce a D-wave component in its wave function, which breaks spherical symmetry and results in a static deformation for the proton's first excited state, the Delta resonance at approximately 320 MeV. The Delta is photo-excited mainly by M1 radiation. However, if its wavefunction contains a D-wave component, then the N approaches Delta transition can also be excited by E2 photons. The magnitude and sign of the E2/M1 mixing ration in the N approaches Delta transition are quite sensitive to the internal structure of the proton and have been of great interest in recent years. The extraction of a small E2 amplitude is complicated by the presence of non resonant background contributions. In elastic (Compton) scattering of polarized photons most background contributions cancel in the polarization asymmetry. This has not been previously exploited, since such measurements are technically demanding. Extraction of the E2 component is presently underway. Derived from text

N94-14366# Los Alamos National Lab., NM.
RARE MUON PROCESSES
M. D. Cooper 1993 4 p Presented at the Future Directions in Particle and Nuclear Physics At Multi-GeV Hadron Beam Facilities Conference, Upton, NY, 4-6 Mar. 1993
(Contract W-7405-eng-36)
(DE93-012646; LA-UR-93-1292; CONF-930389-4) Avail: CASI HC A01/MF A01

The status of rare muon processes as tests of the standard model is reviewed with the emphasis on results that are expected from experiments in the near future. DOE

N94-14419# Kentucky Univ., Lexington.
COHERENT EXCITATION OF AUTOIONIZING RESONANCES BY ELECTRON IMPACT
N. L. S. Martin Jun. 1993 4 p
(Contract DE-FG05-91ER-14214)
(DE93-018169; DOE/ER-14214/2) Avail: CASI HC A01/MF A01

Experimental investigations have been carried out into interference effects caused by coherent population, by electron impact, of cadmium autoionizing levels and continua of differing total angular momentum and parity. The work provides information on both the excitation mechanism by charged particle impact and the spectroscopy of autoionizing levels. DOE

N94-14420# Florida State Univ., Tallahassee. Dept. of Chemistry.
SELECTIVE EXCITATION, RELAXATION, AND ENERGY CHANNELING IN MOLECULAR SYSTEMS
W. C. Rhodes Aug. 1993 32 p
(Contract DE-FG05-86ER-60473)
(DE93-018819; DOE/ER-60473/7) Avail: CASI HC A03/MF A01

Research involves theoretical studies of response, relaxation, and correlated motion in time-dependent behavior of large molecular systems ranging from polyatomic molecules to protein molecules in their natural environment. The underlying theme is subsystem modulation dynamics. Another main idea is that quantum mechanical correlations between components of a system develop with time, playing a major role in determining the balance between coherent and dissipative forces. Central theme is interplay of coherence and dissipation in determining the nature of dynamic structuring and energy flow in molecular transformation mechanisms. Subsystem equations of motion are being developed to show how nonlinear, dissipative dynamics of a particular subsystem arise from correlated interactions with the rest of the system (substituent groups, solvent, lattice modes, etc.); one consequence is resonance structures and networks. Quantum dynamics and thermodynamics are being applied to understand control and energy transfer mechanisms in biological functions of protein molecules; these mechanisms are both global and local. Besides the above theory, the research deals with phenomenological aspects of molecular systems. DOE

N94-14466# Los Alamos National Lab., NM.
ANGULAR CORRELATIONS IN NEUTRON BETA DECAY
T. J. Bowles 1993 22 p Presented at the Colloquium in Honor of Walter Mampe, Grenoble (France), 29 Jan. 1993
(Contract W-7405-eng-36)
(DE93-014349; LA-UR-93-1971; CONF-9301111-1) Avail: CASI HC A03/MF A01

A new generation experiment searching for time reversal violation in polarized neutron beta decay is discussed, including theoretical description of polarized beta decay; measurement of angular correlations; theoretical implications; and future possibilities. DOE

N94-14468# Los Alamos National Lab., NM.
DYNAMICS OF PION-NUCLEUS SYSTEMS
M. B. Johnson 1993 7 p Presented at the Future Directions in Particle and Nuclear Physics at Multi-GeV Hadron Beam Facilities, Upton, NY, 4-6 Mar. 1993
(Contract W-7405-eng-36)
(DE93-014449; LA-UR-93-1692; CONF-930389-13) Avail: CASI HC A02/MF A01

The prospects for using high-energy pions to examine modifications of baryon resonances in nuclei, nuclear structure, exchange currents, short-range correlations, and to characterize pion propagation are discussed. DOE

N94-14471# Washington Univ., Seattle.
MEASURING STRANGENESS IN THE NUCLEON
E. M. Henley 1992 20 p Presented at the 35th Congresso Nacional de Fisica, Puebla, Mexico, Nov. 1992
(Contract DE-FG06-88ER-40427)
(DE93-014861; DOE/ER-40427/02-N93; CONF-9211243-1) Avail: CASI HC A03/MF A01

Evidence for strangeness matrix-elements in the proton are reviewed, and other measurements for specific strangeness matrix elements are presented. DOE

N94-14514# Los Alamos National Lab., NM.
MEASURING PARITY VIOLATION USING THE NEUTRON CAPTURE REACTION
C. M. Frankle, J. D. Bowman, S. J. Seestrom, N. R. Roberson (Duke Univ., Durham, NC.), and E. I. Sharapov (Joint Inst. for Nuclear Research, Dubna, USSR.) 1993 7 p *Presented at the International Workshop/Time Reversal Invariance and Parity Violation in Neutron Physics, Dubna, Russia, 4-7 May 1993*
(Contracts W-7405-eng-36; DE-FG05-88ER-40441; DE-FG05-91ER-40619) (DE93-016629; LA-UR-93-2066; CONF-9305235-1) Avail: CASI HC A02/MF A01

Measuring parity violation using the total capture reaction has certain advantages over neutron transmission experiments. Very much less material is required for targets, a necessity when dealing with separated isotopes. The capture reaction is also quite sensitive to very weak resonances. These advantages indicated the need to construct a near 4(pi) gamma ray detector for use at LANSCE. A design for such a detector has been completed. Issues influencing the design and the final design parameters are discussed in detail. DOE

N94-14524# Fermi National Accelerator Lab., Batavia, IL.
TOP QUARK SEARCH: RESULTS AND PROSPECTS AT FERMILAB
T. Rodrigo 1992 28 p
(Contract DE-AC02-76CH-03000)
(DE93-013016; DOE/FTR-93013016) Avail: CASI HC A03/MF A01 (US Sales Only)

A summary of the present experimental search for the top quark at the p(bar p) collider experiment CDF is reviewed. The prospects for finding top at the TEVA-TRON collider, in the near future, are discussed. DOE

N94-14526# Lawrence Livermore National Lab., CA.
MULTIPLE SCHROEDINGER CATS FROM MULTILEVEL ATOMS
P. L. Knight (Imperial Coll. of Science and Technology, London, England.) and B. W. Shore Oct. 1992 15 p
(Contract W-7405-eng-48)
(DE93-013412; UCRL-JC-112165) Avail: CASI HC A03/MF A01

We show that the generalization of the two-level Jaynes-Cummings model to a multiple-level atom leads to a generalization of the two-mode field to a multiple-mode field. The field modes correspond to macroscopic states of the field, attainable with large mean photon numbers. DOE

N94-14527# Washington Univ., Seattle. Dept. of Physics.
THE OFF SHELL (RHO)-(OMEGA) MIXING IN THE QCD SUM RULES
Testuo Hatsuda, Ernest M. Henley, Thomas Meissner, and Gastao Krein (Instituto de Fisica Teorica, Sao Paulo, Brazil.) 1993 39 p
(Contracts DE-FG06-88ER-40427; DE-FG06-90ER-40561)
(DE93-014845; DOE/ER/40427-09-N93; DOE/ER/40561-103) Avail: CASI HC A03/MF A01

The q(sup 2) dependence of the (rho) - (omega) mixing amplitude is analyzed with the use of the QCD sum rules and the dispersion relation. In going off shell the mixing decreases, changes sign at q(sup 2) approximately = 0.4 m(sub rho)(sup 2) greater than 0, and is negative in the space-like region. Implications of this result to the isospin breaking part of the nuclear force are discussed. DOE

N94-14549*# Hampton Univ., VA. Dept. of Physics.
[SCATTERING CALCULATIONS AND CONFINING INTERACTIONS] Final Report, 1984-1992
Warren W. Buck and Khin M. Maung 1993 70 p
(Grant NAG1-477)
(NASA-CR-194242; NAS 1.26:194242) Avail: CASI HC A04/MF A01

Most of the research work performed under this grant were concerned with strong interaction processes ranging from kaon-nucleon interaction to proton-nucleus scattering calculations. Research performed under this grant can be categorized into three groups: (1) parametrization of fundamental interactions, (2) development of formal theory, and (3) calculations based upon the first two. Parametrizations of certain fundamental interactions, such as kaon-nucleon interaction, for example, were necessary because kaon-nucleon scattering amplitude was needed to perform kaon-nucleus scattering calculations. It was possible to calculate kaon-nucleon amplitudes from the first principle, but it was unnecessary for the purpose of the project. Similar work was also done for example for anti-protons and anti-nuclei. Formal developments to some extent were also pursued so that consistent calculations can be done. For individual titles, see N94-14550 through N94-14552.

N94-14550*# National Aeronautics and Space Administration. Langley Research Center, Hampton, VA.
RELATIVISTIC PROTON-NUCLEUS SCATTERING AND ONE-BOSON-EXCHANGE MODELS
Khin Maung Maung (Hampton Univ., VA.), Franz Gross (College of William and Mary, Williamsburg, VA.), J. A. Tjon (Utrecht State Univ., Netherlands.), L. W. Townsend, and S. J. Wallace (Maryland Univ., College Park.) *In* Hampton Univ., Scattering Calculations and Confining Interactions 1993 11 p Repr. from Physical Review C (American Physical Society), v. 43, no. 3, Mar. 1991 p 1378-1388 Sponsored in part by DOE (For primary document see N94-14549 02-72)
Avail: CASI HC A03/MF A01

Relativistic p-(Ca-40) elastic scattering observables are calculated using four sets of relativistic NN amplitudes obtained from different one-boson-exchange (OBE) models. The first two sets are based upon a relativistic equation in which one particle is on mass shell and the other two sets are obtained from a quasipotential reduction of the Bethe-Salpeter equation. Results at 200, 300, and 500 MeV are presented for these amplitudes. Differences between the predictions of these models provide a study of the uncertainty in constructing Dirac optical potentials from OBE-based NN amplitudes. Author

N94-14551*# National Aeronautics and Space Administration. Langley Research Center, Hampton, VA.
THEORETICAL ANTIDEUTERON-NUCLEUS ABSORPTIVE CROSS SECTIONS
W. W. Buck (Hampton Univ., VA.), J. W. Norbury (Old Dominion Univ., Norfolk, VA.), L. W. Townsend, and J. W. Wilson *In* Hampton Univ., Scattering Calculations and Confining Interactions 1993 5 p Repr. from Physical Review C (American Physical Society), v. 33, no. 1, Jan. 1986 p 234-238 (For primary document see N94-14549 02-72)
(Contract NCC1-42)
Avail: CASI HC A01/MF A01

Antideuteron-nucleus absorptive cross sections for intermediate to high energies are calculated using an ion-ion optical model. Good agreement with experiment (within 15 percent) is obtained in this same model for (bar p)-nucleus cross sections at laboratory energies up to 15 GeV. We describe a technique for estimating antinucleus-nucleus cross sections from NN data and suggest that further cosmic ray studies to search for antideuterons and other antinuclei be undertaken. Author

N94-14552*# Hampton Univ., VA. Dept. of Physics.
ISOSPIN FLIP AS A RELATIVISTIC EFFECT: NN INTERACTIONS
W. W. Buck *In its* Scattering Calculations and Confining Interactions 1993 10 p Prepared in cooperation with Continuous Electron Beam Accelerator Facility, Newport New, VA. (For primary document see N94-14549 02-72)
(Grant NSF RII-87-04038)
(CEBAF-PR-89-023; HUPhy-89-1) Avail: CASI HC A02/MF A01

Results are presented of an analytic relativistic calculation of a OBE nucleon-nucleon (NN) interaction employing the Gross equation. The calculation consists of a non-relativistic reduction that keeps the negative energy states. The result is compared to purely non-relativistic OBEP results and the relativistic effects are separated out. One finds that the resulting relativistic effects are expressable as a power series in (tau(sub 1))(tau(sub 2)) that agrees, qualitatively, with NN scattering. Upon G-parity transforming this NN potential, one obtains, qualitatively, a short range NN spectroscopy in which the S-states are the lowest states. Author

N94-14569# Lawrence Livermore National Lab., CA.
SOME TOOLS OF THE TRADE WE'VE DEVELOPED FOR OUR CROSS-SECTION CALCULATIONS
D. G. Gardner and M. A. Gardner Nov. 1992 8 p Presented at the Symposium on Nuclear Data Evaluation Methodology, Upton, NY, 12-16 Oct. 1992
(Contract W-7405-eng-48)
(DE93-013835; UCRL-JC-110651; CONF-921046-19) Avail: CASI HC A02/MF A01

A number (seven) of compute codes have been modified or developed, both main-frame and PC. Three of the codes are discussed in some detail. They are as follows: a controller-driven, double-precision version of the coupled-channel code ECIS; the latest version of STAPRE, a precompound plus Hauser-Feshbach nuclear reaction code; and NUSTART, a PC code that analyzes large sets of discrete nuclear levels and the multipole transitions among them. All main-frame codes are now being converted to the UNICOS operating system. DOE

N94-14580# Brookhaven National Lab., Upton, NY.
EARLY BARYON AND MESON SPECTROSCOPY CULMINATING IN THE DISCOVERY OF THE OMEGA MINUS SU(3) AND QUARKS
N. P. Samios 1993 24 p Presented at the 3rd International Symposium on the History of Particle Physics: The Rise of the Standard Model, Stanford, CA, 24-27 Jun. 1993
(Contract DE-AC02-76CH-00016)
(DE93-014321; BNL-48871; CONF-9306168-1) Avail: CASI HC A03/MF A01

This report discusses the early experimental and theoretical research that resulted in the discovery of the omega minus particles, quarks, and other subatomic particles. DOE

N94-14588# Superconducting Super Collider Lab., Dallas, TX.
PROTON-PROTON SCATTERING CONTRIBUTION TO EMITTANCE GROWTH
T. Garavaglia May 1993 5 p Presented at the International Particle Accelerator Conference, Washington, DC, 17-20 May 1993 Submitted for publication
(Contract DE-AC35-89ER-40486)
(DE93-016090; SSCL-Preprint-409; CONF-930511-186) Avail: CASI HC A01/MF A01

Proton-proton scattering contributes to the emittance growth of the SSC. A formulation is given and used to estimate the mean scattering angle, which is used to determine the contribution to SSC emittance growth resulting from elastic pp scattering. The method is based upon Lorentz invariants, and it permits the determination of the cross section for scattering in the center of mass (c.m.) system, as well as scattering from a fixed target (f.t.). Also an example is given for the case of electromagnetic pp scattering, which results from single virtual photon exchange. DOE

N94-14691# Illinois Univ., Urbana. Fusion Studies Lab.
DIRECT DETERMINATION OF ALPHA PARTICLE TRANSPORT COEFFICIENTS
J. Guo and G. H. Miley 1992 10 p Presented at the Meeting of the Division of Plasma Physics of the American Physical Society, Seattle, WA, 16-20 Nov. 1992
(Contract DE-FG02-90ER-54092)
(DE93-013488; CONF-921103-12-App-A) Avail: CASI HC A02/MF A01

Many studies have been reported on the simulation of impurity transport phenomena in the Tokamak fusion plasma using the MIST code (1,2,3). The MIST code is to solve the multi-ionization state impurity transport equations by assuming that the transport fluxes of different ionization states are known. In most simulations, the transport fluxes of impurities are usually expressed in terms of diffusion coefficient and convective velocities. By considering the 'inverse' problem (vs.MIST), the basic idea of this research is to solve the one dimensional (ONE-D, with cylindrical geometry) impurity transport equations to determine the transport coefficients from the experimental impurity density evolution data. We have developed a computer code which is labelled as 'DASH' to solve this problem. The alpha particle transport coefficients can be obtained and inter-corrected by using the MIST and this DASH code. This code also provides a way to check the simulation results of MIST code. DOE

N94-14721# Rome Univ. (Italy). Dipt. di Fisica.
COMPARING THE Z(SUP 0) MASS AND INCLUSIVE WIDTHS TO THE STANDARD ELECTROWEAK THEORY
Arianna Borrelli (Istituto Nazionale di Fisica Nucleare, Rome, Italy.), Luciana Maiana (Istituto Nazionale di Fisica Nucleare, Rome, Italy.), and Renata Sisto (Istituto Nazionale di Fisica Nucleare, Rome, Italy.) 4 Apr. 1990 11 p Sponsored in part by Ministry of University and Scientific and Technological Research, Italy
(Preprint-731; ETN-93-94369) Avail: CASI HC A03/MF A01

The Z(sup 0) mass and inclusive widths measured by Large Electron-Positron (LEP) storage ring experiments are compared with the predictions of the standard electroweak theory. A strategy analogous to the one adopted by Ellis and Fogli is followed and the value of sine squared theta(sub w) as function of m(sub t) derived from each partial width is compared with that obtained from the Z(sup 0) mass. It is pointed out that the comparison is quite insensitive to m(sub t), but rather it can give a precise test of the theory itself. ESA

N94-14778# New Mexico State Univ., Las Cruces.
CHARGE STORAGE AND SWITCHING PHENOMENA WITH MOLECULAR ASSEMBLIES OF METAL COMPLEXES Final Report, Jan. 1990 - Apr. 1993
M. K. DeArmond 31 May 1993 14 p
(Contract DAAL03-90-G-0036)
(AD-A266673; ARO-26744.1-CH-SAH) Avail: CASI HC A03/MF A01

The central theme of the four research areas has been and is intramolecular and intermolecular charge separation in materials (metal complexes and oligomeric thiophene) directed towards the preparation of molecular assemblies useful in molecular electronics. The multi-electron redox materials study has been completed and the generality of the charge localization scheme proposed by us for (Ru(L3))(2+) materials has beenestablished for n = 1 through 5 electrons. The one and two electron reduction are best adapted as intramolecular switching molecules. The liquid-liquid media has been established as an appropriate media for intermolecular charge separation using an external electric field to control the charge switching. The use of sol-gel media in the liquid-liquid experimental arrangement allows durable and portable charge separation assemblies. The oligomer-polymer materials provide a concentrated and durable molecular species capable of intermolecular and intramolecular charge separation at interfaces (liquid-liquid) and in Langmuir-Blodgett assemblies. The pendant Ru(2) complexes and the orthogonal thiophene oligomers both possess the perpendicular arrangement of pi electron systems that can lead to charge storage and molecular switching. The mixed metal complex/fatty acid Langmuir-Blodgett films provide the organized molecular assembly system with the best potential for molecular electronics. Our development of a technique for producing durable and portable LB films with a great range of metal complex types implies that this approach may be preferable to the fluid solution L-L-sol-gel approach. DTIC

N94-14804# Los Alamos National Lab., NM.
THE LAHET CODE SYSTEM: INTRODUCTION, DEVELOPMENT, AND BENCHMARKING
R. E. Prael 1993 19 p Presented at the Simulating Accelerator Radiation Environments Workshop, Santa Fe, NM, 11-15 Jan. 1993
(Contract W-7405-eng-36)
(DE93-012657; LA-UR-93-1216; CONF-930168-6) Avail: CASI HC A03/MF A01

An introduction to the LAHET code system is presented, showing the function of each code and their interrelation. A summary is made of the principal physics models used in LAHET. Some recent results in benchmarking are shown for small-angle neutron emission from Li-7 for 800 MeV protons incident, neutron emission from Be-9 at several incident proton energies, and actinide and subactinide fission ratios. DOE

N94-14857# California Univ., Berkeley. Lawrence Berkeley Lab.
TESTS OF NON-LOCAL INTERFERENCES IN KAON PHYSICS AT ASYMMETRIC PHI-FACTORIES
P. H. Eberhard 16 Apr. 1993 34 p Presented at the UCLA Workshop on Asymmetric Phi Factories, Los Angeles, CA, 28 Oct. 1992
(Contract DE-AC03-76SF-00098)
(DE93-013905; LBL-33937; CONF-9210336-2) Avail: CASI HC A03/MF A01

Tests of non-local interference effects in the two-kaon system are proposed. The first kind of tests consists of measuring the amount of destructive interference between K(sub S) yields K(sub L) regeneration processes of two distant kaons. The second kind deals with constructive interference. These tests could be performed at an asymmetric phi-factory. Estimates are given of the number of events predicted by orthodox quantum mechanics and kaon regeneration theory in various suitable experimental conditions. The impact on local theories if the predictions of quantum mechanics hold is discussed. DOE

N94-14872# Brookhaven National Lab., Upton, NY.
CONSTRUCTION OF THE COURANT-SNYDER INVARIANTS FOR THE NON-LINEAR EQUATIONS OF MOTION UNDER PRESENCE OF THE LINEAR COUPLING
V. Garczynski 10 Jun. 1993 11 p
(Contract DE-AC02-76CH-00016)
(DE93-017565; BNL-49183; AGS/AD-93-9) Avail: CASI HC A03/MF A01

A single particle subjected to an arbitrary static magnetic field, which includes skew-quadrupole and solenoidal fields, is considered. The Courant-Snyder invariants are constructed, and the long-term stability of the beam in a storage ring is formulated in terms of the normal modes. The generalized Courant-Snyder invariants become Lyapunov functions when the new generalized B-functions admit non-zero lower and finite upper bounds. DOE

N94-14875 Academy of Sciences of the Ukraine, Kiev. Inst. Teoreticheskoj Fiziki.
ON THE STATISTICAL THEORY OF THE EVEN-EVEN NUCLEONS LEVELS' DENSITY
V. N. Malnev and V. K. Tartakovskij 1992 12 p Limited Reproducibility: More than 20% of this document may be affected by microfiche quality
(DE93-623990; ITF-92-9) Avail: CASI HC A03 (US Sales Only)

The thermodynamical functions and levels' density of the heavy even-even nucleons above the critical temperature of the superfluidity transition as well as below it are discussed on the basis of the general results of quantum statistics and thermodynamics applied to some nuclear models. DOE

N94-14881 Academy of Sciences of the Ukraine, Kiev. Fiziko-Tekhnicheskij Inst.
THE SPACE-TIME AND ENERGY PARAMETERS OF DEUTERIUM BRAKING BY THE CENTRAL COLLISION WITH ATOMS
V. F. Zelenskij and V. I. Nikiforov 1992 5 p Limited Reproducibility: More than 20% of this document may be affected by microfiche quality
(DE93-624144; KFTI-92-49) Avail: CASI HC A01 (US Sales Only)

Parameters of deuteron braking by frontal collisions with immobile boron, palladium, and gadolinium atoms were calculated using the programs and databases of the problem-oriented PERST system base version. Energy range of deuteron was 50-4000 eV, their slowing down was considered up to 0.01 eV kinetic energies. DOE

N94-14891 Joint Inst. for Nuclear Research, Dubna (USSR). Lab. of Theoretical Physics.
A HYDROGEN ATOM IN THE CURVED SPACE: ORTHOGONALITY OF RADIAL WAVE FUNCTIONS WITH RESPECT TO THE CRITICAL MOMENTUM
L. G. Mardoyan and A. N. Sisakyan 1992 6 p Limited Reproducibility: More than 20% of this document may be affected by microfiche quality
(DE93-626623; JINR-R-2-92-47) Avail: CASI HC A02 (US Sales Only)

The condition of orthogonality in the orbital momentum of radial wave functions of a hydrogen atom in the curved space of constant positive curvature. This condition of orthogonality is proved to be consequence of accidental degeneration of the energy spectrum. DOE

N94-14898# Fermi National Accelerator Lab., Batavia, IL.
E789 AND P865: HIGH-RATE FIXED-TARGET STUDIES OF CHARM AND BEAUTY
D. M. Kaplan Jun. 1993 6 p Presented at the HQ 1993: Heavy Quarks at Fixed Target, Frascati, Italy, 31 May - 2 Jun. 1993
(Contract DE-AC02-76CH-03000)
(DE93-017223; FNAL/C-93/162; CONF-9305240-1) Avail: CASI HC A02/MF A01

Experiment 789 at Fermilab used the high-rate E605/E772 spectrometer to study low-multiplicity charm and beauty decays. Preliminary results on charm and beauty production are presented based on analysis of approximately 100% of the charm data and approximately 50% of the beauty data. A new experiment is proposed to improve charm and beauty sensitivity by several orders of magnitude. DOE

N94-14905*# Alabama Univ., Huntsville. Center for Applied Optics.
ATOMIC RESEARCH Final Report
James B. Hadaway, Robert Connatser, Bobby Cothren, and R. B. Johnson 26 Jul. 1993 36 p
(Contract NAS8-38609)
(NASA-CR-193843; NAS 1.26:193843) Avail: CASI HC A03/MF A01

Work performed by the University of Alabama in Huntsville's (UAH) Center for Applied Optics (CAO) entitled Atomic Research is documented. Atomic oxygen (AO) effects on materials have long been a critical concern in designing spacecraft to withstand exposure to the Low Earth Orbit (LEO) environment. The objective of this research effort was to provide technical expertise in the design of instrumentation and experimental techniques for analyzing materials exposed to atomic oxygen in accelerated testing at NASA/MSFC. Such testing was required to answer fundamental questions concerning Space Station Freedom (SSF) candidate materials and materials exposed to atomic oxygen aboard the Long-Duration Exposure Facility (LDEF). The primary UAH task was to provide technical design, review, and analysis to MSFC in the development of a state-of-the-art 5eV atomic oxygen beam facility required to simulate the RAM-induced low earth orbit (LEO) AO environment. This development was to be accomplished primarily at NASA/MSFC. In support of this task, contamination effects and ultraviolet (UV) simulation testing was also to be carried out using NASA/MSFC facilities. Any materials analysis of LDEF samples was to be accomplished at UAH. Author (revised)

73 NUCLEAR AND HIGH-ENERGY PHYSICS

Includes elementary and nuclear particles; and reactor theory. For space radiation see *93 Space Radiation.*

N94-12817# Oak Ridge National Lab., TN.
MEASUREMENTS OF TRANSVERSE ENERGY AND FORWARD ENERGY IN HIGH-ENERGY NUCLEAR COLLISIONS
S. P. Sorensen (Tennessee Univ., Knoxville.) 1993 12 p Presented at the 2nd International Conference on Physics and Astrophysics of Quark-Gluon Plasma, Calcutta, India, 19-23 Jan. 1993
(Contract DE-AC05-84OR-21400)
(DE93-012755; CONF-9301109-1) Avail: CASI HC A03/MF A01

The experimental data on forward energy and transverse energy production in high energy nuclear collisions at the AGS and SPS accelerators are reviewed. DOE

N94-13103# Los Alamos National Lab., NM.
MEASUREMENT OF H ZERO EXCITED STATES PRODUCED BY FOIL STRIPPING OF 800-MeV H(-) IONS
J. B. Donahue, D. A. Clark, S. Cohen, D. Fitzgerald, S. C. Frankle, R. L. Huston, R. Macek, E. MacKerrow, O. vanDyck, and C. Wilkinson et al 1993 4 p Presented at the International Particle Accelerator Conference, Washington, DC, 17-20 May 1993
(Contract W-7405-eng-36)
(DE93-014391; LA-UR-93-2038; CONF-930511-45) Avail: CASI HC A01/MF A01

Foil stripping of H(-) directly to H(+) is being considered for proton injection in the next generation of high-current proton storage rings. This technique can result in significant losses because excited states of HO, which are also produced in the foil, are field stripped in the downstream bending magnets. Without due care in the injection system design, many of the resulting protons will be outside the acceptance of the storage ring and will be quickly lost. We measured the production of such H(sup 0) excited states at the LAMPF High Resolution Atomic Beam Facility. An 800-MeV H(-) beam was passed through carbon foils of thicknesses 70, 100, 200, and 300 (mu)g/cm(sup 2), and the excited states were analyzed by a special magnet downstream of the foil. The magnet had a linear field gradient so that the trajectories of the outgoing protons could be used to reconstruct the field values at which the various H(sup 0) stripped. We found that about 1% of the H(sup 0) emerge in excited states which can be stripped to protons by ring-bending magnets. DOE

N94-13208# Lawrence Livermore National Lab., CA.
EBIT TRAPPING PROGRAM
S. R. Elliott, B. Beck, P. Beiersdorfer, D. DeWitt, D. K. Knapp, R. E. Marrs, D. Schneider, D. Church, and L. Schweikhard 10 Mar. 1993 17 p Presented at the Workshop on Traps for Antimatter and Radioactive Nuclei,

Vancouver, Canada, 25-27 Feb. 1993
(Contract W-7405-eng-48)
(DE93-014422; UCRL-JC-113710; CONF-930274-2) Avail: CASI HC A03/MF A01

Since its inception in 1986, the Electron Beam Ion Trap (EBIT) at LLNL has been used to produce and study highly charged ions up to U-82(+). It has focused on the determination of electron-ion collision cross sections dielectronic recombination, electron-impact excitation, resonance excitation, and ionization as well as precise atomic structure models. The recent advance of SuperEBIT has extended the available ionization stages to bare U-92(+). An extraction system allows us to perform experiments outside EBIT. This includes experiments in an external Penning trap under construction. Furthermore, current x-ray spectroscopic techniques will be supplemented by the future addition of a Fourier-Transform Ion Cyclotron Resonance (FT-ICR) mass spectrometry system. EBIT is geared to study not only a large variety of atomic physics but also nuclear physics phenomena, such as the bound state beta decay of fully stripped (sup 163)Dy-66(+). DOE

N94-13209# Los Alamos National Lab., NM.
BEAM HALO FORMATION FROM SPACE-CHARGE DOMINATED BEAMS IN UNIFORM FOCUSING CHANNELS
J. S. OConnell (Booz-Allen and Hamilton, Inc., Washington, DC.), T. P. Wangler, R. S. Mills, and K. R. Crandall (AccSys Technology, Inc., Pleasanton, CA.) 1993 4 p Presented at the International Particle Accelerator Conference, Washington, DC, 17-20 May 1993
(Contract W-7405-eng-36)
(DE93-014458; LA-UR-93-1919; CONF-930511-49) Avail: CASI HC A01/MF A01

In space-charge dominated beams, the nonlinear space-charge forces produce a filamentation pattern, which results in a 2-component beam consisting of an inner core and an outer halo. The halo is very prominent in mismatched beams, and the potential for accelerator activation is of concern for a next generation of cw, high-power proton linacs that could be applied for intense neutron generators to process nuclear materials. We present new results about beam halo and the evolution of space-charge dominated beams from multiparticle simulation of initial laminar beams in a uniform linear focusing channel, and from a model consisting of single particle interactions with a uniform-density beam core. We study the energy gain from particle interactions with the space-charge field of the core, and we identify the resonant characteristic of this interaction as the basic cause of the separation of the beam into the two components. We identify three different particle-trajectory types, and we suggest that one of these types may lead to continuous halo growth, even after the halo is removed by collimators. DOE

N94-13220# Brookhaven National Lab., Upton, NY.
A NEW FORMULATION OF LONGITUDINAL COHERENT INSTABILITIES
S. Y. Zhang and W. T. Weng 1993 4 p Presented at the International Particle Accelerator Conference, Washington, DC, 17-20 May 1993
(Contract DE-AC02-76CH-00016)
(DE93-014288; BNL-48233; CONF-930511-127) Avail: CASI HC A01/MF A01

The quadrature response of longitudinal impedance is shown to be the effective impedance for the beam instability. The results of the application of this formulation are compared with that obtained using the Robinson-Pedersen approach and the Sacherer integral equation. The formulation is further generalized to the rigid bunch motion using the signal analysis method, where a form factor shows up naturally. Finally, the formulation is applied to solve the coupled bunch instabilities. Examples of the AGS Booster and the AGS coupled bunch instabilities are used to illustrate the applications of the formulation. DOE

N94-13327# Los Alamos National Lab., NM.
DESIGN FOR LOW BEAM LOSS IN ACCELERATORS FOR INTENSE NEUTRON SOURCE APPLICATIONS
R. A. Jameson 1993 6 p Presented at the International Particle Accelerator Conference, Washington, DC, 17-20 May 1993
(Contract W-7405-eng-36)
(DE93-014557; LA-UR-93-1816; CONF-930511-82) Avail: CASI HC A02/MF A01

Control of beam loss in intense ion linacs involves keeping beam spill below parts in 10(sup -5) - 10(sup -8)/m by preventing total beam size from extending to the limiting apertures. Starting from good rms design practices, new analysis of the machine architecture is described in terms of the effects of the machine tune with space-charge, free-energy constraint, and halo-producing mechanisms. It is shown that halos are produced by the time- (or position-) varying nature of common linac aspects (such as misalignment, mismatching, acceleration, and construction techniques) through collective core/single-particle interaction dynamics plus resonances. DOE

N94-13328# Los Alamos National Lab., NM.
BEAM HALO IN HIGH-INTENSITY BEAMS
T. P. Wangler 1993 11 p Presented at the Computational Accelerator Physics Conference (CAP93), Pleasanton, CA, 22-26 Feb. 1993
(Contract W-7405-eng-36)
(DE93-014565; LA-UR-93-1686; CONF-930269-14) Avail: CASI HC A03/MF A01

In space-charge dominated beams the nonlinear space-charge forces produce a filamentation pattern, which in projection to the 2-D phase spaces results in a 2-component beam consisting of an inner core and a diffuse outer halo. The beam-halo is of concern for a next generation of CW, high-power proton linacs that could be applied to intense neutron generators for nuclear materials processing. The author describes what has been learned about beam halo and the evolution of space-charge dominated beams using numerical simulations of initial laminar beams in uniform linear focusing channels. Initial results are presented from a study of beam entropy for an intense space-charge dominated beam. DOE

N94-13419*# Iowa Univ., Iowa City. Dept. of Physics and Astronomy.
THE MULTI-ION, MULTI-EVENT TEST OF ION CYCLOTRON RESONANCE HEATING Semiannual Status Report, 8 May - 30 Aug. 1993
Ann M. Persoon 30 Aug. 1993 3 p
(Grant NAGw-3576)
(NASA-CR-194134; NAS 1.26:194134) Avail: CASI HC A01/MF A01

The multi-ion, multi-event study of ion cyclotron resonance heating was funded to study ion energization through ion cyclotron resonance with low frequency broadband electromagnetic turbulence. The initial work on the ion cyclotron resonance heating (ICRH) of oxygen ions was presented in Crew et al. Crew and his co-authors developed a two-parameter representation of selected oxygen conic distributions and modeled the conic formation in terms of resonance heating. The first year seeks to extend the work of Crew and his co-authors by testing the applicability of the ICRH mechanism to helium ion conic distributions, using data obtained from the Energetic Ion Composition Spectrometer and the Plasma Wave Instrument on Dynamics Explorer 1. Author (revised)

N94-13727# Lawrence Livermore National Lab., CA.
LONGITUDINAL BEAM DYNAMICS FOR HEAVY ION FUSION
D. A. Callahan, A. B. Langdon, A. Friedman, and I. Haber (Naval Research Lab., Washington, DC.) 13 May 1993 3 p Presented at the International Particle Accelerator Conference, Washington, DC, 17-20 May 1993
(Contracts W-7405-eng-48; DE-AI05-83ER-40112; DE-AI05-92ER-54177)
(DE93-013850; UCRL-JC-112341; CONF-930511-69) Avail: CASI HC A01/MF A01

The longitudinal wall impedance instability is of great interest for a heavy ion fusion (HIF) driver because complete stabilization of this mode via momentum spread is impractical due to requirements of focusing the beam onto the inertial confinement fusion target. This instability is being studied with the WARPrz particle-in-cell code. The impedance of the induction linac modules is modeled as a wall impedance corresponding to a continuum of resistors and capacitors in parallel. We discuss simulations of this instability including reflections of perturbations off the beam end, the effects of finite temperature, and simulations of errors in intermittently-applied axial confining fields. We also present very long simulations in which we look for beam equilibria. DOE

N94-14460# Lawrence Livermore National Lab., CA.
ABSOLUTE DETECTION EFFICIENCY OF A MICRO-CHANNEL PLATE DETECTOR TO X RAYS IN THE 1-100 KeV ENERGY RANGE
G. A. Burginyon, B. A. Jacoby, J. K. Wobser, R. D. Ernst, D. S. Ancheta, and K. G. Tirsell 3 Sep. 1992 9 p Presented at the 37th Annual

Society of Photo-Optical Instrumentation Engineers (SPIE) International Symposium on Optical and Optoelectronic Applied Science and Engineering, San Diego, CA, 19-24 Jul. 1992
(Contract W-7405-eng-48)
(DE93-012592; UCRL-JC-108982; CONF-920792-58) Avail: CASI HC A02/MF A01

There is little information in the literature on the performance of working microchannel plate (MCP) detectors at high x-ray energies. We have measured the absolute efficiency of a microchannel-plate-intensified, subnanosecond, one dimensional unaging x-ray detector developed at LLNL in the 1 to 100 keV range and at 1.25 MeV. The detector consists of a gold photocathode deposited on the front surface of the MCP (optimized for Ni K(sub (alpha)) x-rays) to convert x-rays to electrons, an MCP to amplify the electrons, and a fast In:CdS phosphor that converts the electron's kinetic energy to light. The phosphor is coated on fiber-optic faceplate to transmit the light out of the vacuum system. Electrostatic focusing electrodes compress the electron current out of the MCP in one dimension while preserving spatial resolution in the other. The calibration geometry, dictated by a recent experiment, required grazing incidence x-rays (15.6(degree)) onto the MCP detector in order to maximize deliverable current. The experiment also used a second detector made up of 0.071 in. thick BC422 plastic scintillator material from the Bicron corporation. We compare the absolute efficiencies of these two detectors in units of optical W/sq cm into 4(pi) per x-ray, W/sq cm incident. At 7.47 keV and 900 volts MCP bias, the MCP detector delivers approximately 1400 times more light than the scintillator detector. DOE

N94-14843 Academy of Sciences of the Ukraine, Kiev. Inst. Yadernykh Issledovanij.
MULTIPLICITY SPECTROMETRY ON NEUTRON FILTERED BEAMS [SPEKTROMETRIYA MNOZHESTVENNOSTI NA FIL'TROVANNYKH PUCHKAKH NEJTRONOV]
Y. G. Shchepkin, T. A. Senchenko, and E. A. Pavlenko et al 1991 27 p In RUSSIAN Prepared in cooperation with Gosudarstvennyi Komitet po Ispolzovaniyu Atomnoi Energii, Moscow, Russia Limited Reproducibility: More than 20% of this document may be affected by microfiche quality
(DE93-617529; KIYal-91-36) Avail: CASI HC A03 (US Sales Only)

Multiplicity spectrometer using sodium iodine crystals for research neutron reactions on neutron reactions on neutron filtered beams of the reactor is described. Spectrometer parameters and the influence of experimental indeterminacies on parameter stability are presented. DOE

N94-14893# Lawrence Livermore National Lab., CA.
CHARACTERISTICS OF A HIGH ENERGY MUON(+)MUON(-) COLLIDER BASED ON ELECTRO-PRODUCTION OF MUONS
W. A. Barletta and A. M. Sessler (California Univ., Berkeley. Lawrence Berkeley Lab.) Feb. 1993 9 p Presented at the Mini Workshop on Muon(+)Muon(-) Colliders: Particle Physics and Design, Napa Valley, CA, 9-11 Dec. 1992
(Contracts W-7405-eng-48; DE-AC03-76SF-00098)
(DE93-017154; UCRL-JC-113093; CONF-921284-1) Avail: CASI HC A02/MF A01

This paper presents an analysis of the possibility of designing a high energy muon(+)muon(-) collider based on electro-production of muons. An analytic expression for the pair production cross-section yields an expression for the electron-to-muon conversion efficiency. This quantity is connected to the luminosity definition via the beam power on the production target. Sets of consistent parameters are then derived as a function of electron beam and collider characteristics. DOE

N94-14897# Indiana Univ., Bloomington. Cyclotron Facility.
THE EVOLUTION OF TENSOR POLARIZATION
H. Huang, S. Y. Lee, and L. Ratner (Brookhaven National Lab., Upton, NY.) 1993 3 p Presented at the International Particle Accelerator Conference, Washington, DC, 17-20 May 1993
(Contract DE-FG02-92ER-40747)
(DE93-017209; DOE/ER-40747/5; CONF-930511-236) Avail: CASI HC A01/MF A01

By using the equation of motion for the vector polarization, the spin transfer matrix for spin tensor polarization is derived. The evolution equation for the tensor polarization is studied in the presence of an isolate spin resonance and in the presence of a spin rotor or snake. DOE

74 OPTICS

Includes light phenomena; and optical devices.
For lasers see *36 Lasers and Masers.*

N94-12797*# Stanford Univ., CA. STAR Lab.
COLOR IMAGE PROCESSING FOR FLAT PANEL VISUAL DISPLAY MODELING Technical Report, 1 Nov. 1992 - 30 Apr. 1993
Allen M. Peterson and Ramin Samadani 1993 13 p
(Contract NCC2-777)
(NASA-CR-193660; NAS 1.26:193660) Avail: CASI HC A03/MF A01

Cathode ray tubes (CRT's), liquid crystal displays (LCD's) and many other flat panel displays use spatially separated color pixel components to produce color images. The new manufacturing techniques for flat panel displays support a wider range of possible pixel shapes and geometric layouts than those possible with CRT manufacturing technology. We describe an algorithm comprised of several image processing steps that allows the user to specify arbitrary color component shapes and to specify the geometrical description for the layout of these components. The algorithm is based in part on the theory of periodic plane tilings. This theory is quite general and it allows for the unified treatment of the display pixel shapes and layouts that may arise in practice. This algorithm may be used by display designers to simulate various display designs in order to study tradeoffs for the visibility of sampling and display reconstruction artifacts. Author (revised)

N94-12863 Naval Command, Control and Ocean Surveillance Center, San Diego, CA. Research, Development, Test and Evaluation Div.
LASER-INDUCED FLUORESCENCE OVER OPTICAL FIBERS FOR REAL TIME IN SITU MEASUREMENT OF PETROLEUM HYDROCARBONS IN SEAWATER
S. H. Lieberman, S. M. Inman, and G. A. Theriault Apr. 1993 8 p Limited Reproducibility: More than 20% of this document may be affected by microfiche quality
(AD-A265106) Avail: CASI HC A02

A fiber optic-based fluorometer system is described that uses a pulsed laser to induce fluorescence and a time-gated linear photodiode array coupled to a spectrograph for rapid measurement of fluorescence emission spectra and fluorescence decay times. Data is presented from studies conducted in San Diego Bay where the system has been used for real-time in situ measurements of temporal and spatial variability of petroleum hydrocarbons in seawater. Results show that the optical fiber fluorometer system is capable of direct quantification of low level (parts-per-billion diesel fuel marine equivalent) concentrations of petroleum hydrocarbons. Analysis times for measurement of complete fluorescence emission spectra are fast (tens of milliseconds) and compare with the temporal response characteristics for temperature and conductivity sensors that are used for measuring standard physical hydrographic parameters. Results obtained with the fiber optic fluorometer system during a mapping study in San Diego Bay show good correlation with GC-MS analysis of total polycyclic aromatic hydrocarbons (PAHs) measured on discrete samples collected during the study. DTIC

N94-12865# Lawrence Livermore National Lab., CA.
THE OPTICAL CONSTANTS AND SPECTRAL SPECULAR REFLECTIVITY OF HIGHLY ORIENTED PYROLYTIC GRAPHITE (HOPG)
M. A. Havstad, M. A. Schildbach, and W. McLean, II Oct. 1992 3 p Presented at the National Conference and Exposition on Heat Transfer, Atlanta, GA, 8-11 Aug. 1993
(Contract W-7405-eng-48)
(DE93-011894; UCRL-JC-111969; CONF-930830-11) Avail: CASI HC A01/MF A01

The measurements were made using two independent optical systems, and good agreement was obtained. The spectral directional-hemispherical reflectivity at normal incidence varies from 0.41 at 0.55 micron to 0.74 at 8.45 microns. Components of complex index of refraction increase smoothly with wavelength, the index increasing from 3.10 at 0.55 micron to 7.84 at 8.45 microns. Extinction coefficient varies from 2.01 to 6.66 over the same range. An attempt was made to fit the complex index to a model with both free and bound carriers. DOE

N94-12979# Army Research Lab., Aberdeen Proving Ground, MD.
INFRARED TRANSMISSION AND PATH RADIANCE THROUGH DUST AND FOG Final Report
James Williams Apr. 1993 31 p
(AD-A265825; ARL-MR-35) Avail: CASI HC A03/MF A01

The obscurant effects of dust and fog can significantly degrade the performance of infrared (IR) sensors engaged in target acquisition. To quantify these effects, computer runs were conducted using the EOSAEL model FCLOUD for the 3-5 and 8-12 micrometers wavebands. FCLOUD was used to calculate beam transmission and path radiance through homogeneous ellipsoidal dust and fog clouds. Both advective and radiative fogs were considered. The EOSAEL models XSCALE and LOWTRAN 7 were also run to calculate transmission over the same wavebands for fog. These results compare favorably with FCLOUD. This study suggests that the performance of IR sensors in the wavebands investigated will be severely degraded in the presence of heavy or moderate fog. Under the dust conditions studied, IR transmission is considerably better than for fog. There is an expected transmission loss, however, with the inclusion of multiple scattering effects and a progressively greater loss as the cloud path length increases. DTIC

N94-13015# Chicago Univ., IL.
FUNDAMENTALS AND TECHNIQUES OF NONIMAGING OPTICS
R. Winston Apr. 1993 53 p
(Contract DE-FG02-87ER-13726)
(DE93-013145; DOE/ER-13726/6) Avail: CASI HC A04/MF A01

For many tasks in illumination and collection, the acceptance angle is required to vary along the reflector. If the acceptance angle function is known, then the reflector profile can be calculated as a function of it. The total flux seen by an observer from a source and its brightness (radiance) is proportional to the sum of the view factor of the source and its reflection. This allows one to calculate the acceptance angle function necessary to produce a certain flux distribution and thereby construct the reflector profile. We demonstrate the method for several examples including finite size sources with reflectors directly joining the source. DOE

N94-13353*# Virginia Polytechnic Inst. and State Univ., Blacksburg. Fiber and Electro-Optics Research Center.
OPTICAL FIBER SENSORS FOR MATERIALS AND STRUCTURES CHARACTERIZATION Final Report
D. K. Lindner and R. O. Claus Sep. 1991 7 p
(Grant NAG1-1176)
(NASA-CR-194090; NAS 1.26:194090) Avail: CASI HC A02/MF A01

The final technical report on Optical Fiber Sensors for Materials and Structures Characterization, covering the period August 1990 through August 1991 is presented. Research programs in the following technical areas are described; sapphire optical fiber sensors; vibration analysis using two-mode elliptical core fibers and sensors; extrinsic Fabry-Perot interferometer development; and coatings for fluorescent-based sensor. Research progress in each of these areas was substantial, as evidenced by the technical publications which are included as appendices. CASI

N94-13482# Lawrence Livermore National Lab., CA.
MEASUREMENTS OF OPTICAL PROPERTIES OF WAVESHIFTING OPTICAL FIBER FOR LIQUID SCINTILLATOR HADRON CALORIMETRY
C. Cochran, M. Lowry, C. Wuest, P. Armatis, G. Graham, and E. Ables Sep. 1992 14 p Presented at the Society of Photo-Optical Instrumentation Engineers International Symposium on Optical Applied Science and Engineering, San Diego, CA, 19-24 Jul. 1992
(Contract W-7405-eng-48)
(DE93-012606; UCRL-JC-109421; CONF-920792-52) Avail: CASI HC A03/MF A01

Measurements have been made on optical properties of Bicron BCF-91 waveshifting optical fiber. This fiber is proposed as a means of converting UV and blue light emitted from a liquid scintillator when exposed to ionizing radiation. The conversion is accomplished by coiling the fiber in a reservoir filled with liquid scintillator and coated internally with reflective paint. The UV and blue light is absorbed by the waveshifting dyes in the fiber and reemitted light is channeled into the core of the fiber and output to photodetectors. It has been proposed to outfit the hadron calorimeter subsystem of the GEM detector to be built at the Superconducting Super Collider with 800,000 separate liquid scintillator/waveshifting fiber cells. The measurements described in this work deal with the optical performance of the fiber: spectral emission, response as a function of input wavelength, response as a function of irradiated length, propagation length, and output numerical aperture. The theoretical response of an ideal calorimeter cell is studied based on the results of the measurements presented. DOE

N94-13490 McMaster Univ., Hamilton (Ontario).
THREE DIMENSIONAL TRACKING OF FOUR POINT PLANAR PATTERNS USING CORNERS Ph.D. Thesis
Michael J. Frendo 1989 170 p
(ISBN-0-315-52149-X; CTN-93-60725) Copyright Avail: Issuing Activity (Micromedia Ltd., Technical Information Centre, 165 Hotel de Ville, Place du Portage, Phase 2, Hull, Quebec J8X 3X2, Canada HC)

Tracking of planar shapes using a single camera view is investigated. Two dimensional silhouette projections of planar shapes randomly oriented and positioned in the camera field of view are processed to determine their position and rotational orientation with respect to the camera. This information can then be provided to robots or automated guided vehicles for automated assembly, docking, shape identification, and retrieval. Silhouettes are initially encoded in the system as a linked list of vertex points representing changes in the direction of the contour. This contour is employed to get an initial estimate of the shape's position. Corner feature points of the shape are then more accurately located using a fast corner location algorithm. A photogrammetric solution is then applied to the projection points of the corners to determine the three dimensional position of the shape. The photogrammetric technique employed does not require a least squares fit as does the traditional photogrammetric approach. This new approach is contrasted with the traditional method in terms of accuracy and computational complexity. Author (CISTI)

N94-13664 Department of the Navy, Washington, DC.
A FOURIER TRANSFORM MICROSCOPE FOR X RAY AND/OR GAMMA RAY IMAGING Patent Application
Kent S. Wood, inventor (to Navy) 15 Mar. 1993 34 p Limited Reproducibility: More than 20% of this document may be affected by microfiche quality
(AD-D015742; US-Patent-Appl-SN-031410; Navy-Case-73566) Avail: CASI HC A03

A Fourier transform microscope for use in imaging a source of x-ray and/or gamma-ray radiation includes first and second grids arranged in proximity to the source. The first grid includes an arrangement of first subgrids elements with a first predetermined number n of approximately parallel, equally-spaced linear first radiation-transparent regions which are arranged in alternation with the first ribs. The second grid includes an arrangement of second subgrids elements which are larger than the first subgrids elements, and which have a common field of view with corresponding first subgrid elements. Each second subgrid element has a second predetermined number n + m of approximately parallel, equally-spaced linear second ribs which are opaque to the radiation of interest, and second radiation-transparent regions which alternate with the second ribs. Each first subgrid element and its corresponding second subgrid element is termed a 'subgrid system'. Each subgrid system can be used to derive an amplitude and phase of an associated Fourier component. A position-sensitive detector detects a Moire or fringe pattern from wach subgrids system and generates a signal indicative of the radiation intensity distribution image of the source in spatial frequency domain which can be converted into a radiation intensity distribution image of the source in spatial domain using a Fourier transform. DTIC

N94-13682*# Massachusetts Univ., Amherst.
HIGH SPEED ALL-OPTICAL NETWORKS Final Report, 1 May 1989 - 1 Feb. 1993
Imrich Chlamtac 1 Feb. 1993 5 p
(Grant NAG2-578)
(NASA-CR-194384; NAS 1.26:194384; UM-522746) Avail: CASI HC A01/MF A01

An inherent problem of conventional point-to-point WAN architectures is that they cannot translate optical transmission bandwidth into comparable user available throughput due to the limiting electronic processing speed of the switching nodes. This report presents the first solution to WDM based WAN networks that overcomes this limitation. The proposed Lightnet architecture takes into account the idiosyncrasies of WDM

switching/transmission leading to an efficient and pragmatic solution. The Lightnet architecture trades the ample WDM bandwidth for a reduction in the number of processing stages and a simplification of each switching stage, leading to drastically increased effective network throughputs.

Derived from text

N94-13719*# Daedalus Enterprises, Inc., Ann Arbor, MI.
MODIS-N AIRBORNE SIMULATOR Final Report, 1 Feb. - 1 May 1992
Steven D. Cech 22 May 1992 36 p
(Contract NAS5-31334)
(NASA-CR-194364; NAS 1.26:194364) Avail: CASI HC A03/MF A01

All required work associated with the above referenced contract has been successfully completed at this time. The Modis-N Airborne Simulator has been developed from existing AB184 Wildfire spectrometer parts as well as new detector arrays, optical components, and associated mechanical and electrical hardware. The various instrument components have been integrated into an operational system which has undergone extensive laboratory calibration and testing. The instrument has been delivered to NASA Ames where it will be installed on the NASA ER-2. The following paragraphs detail the specific tasks performed during the contract effort, the results obtained during the integration and testing of the instrument, and the conclusions which can be drawn from this effort.

Derived from text

N94-13845 Toronto Univ. (Ontario). Acousto-Optic Research Lab.
IMPLEMENTATION OF MANUFACTURING TECHNIQUES FOR PLANAR, SINGLE MODE WAVEGUIDES ON LITHIUM NIOBATE Final Report, 1 Jul. 1990 - 31 Mar. 1991
Velimir M. Ristic and Wujun Zhou Mar. 1991 55 p
(DSIS-93-00101; CTN-93-60776) Avail: CASI HC A04

An extensive study was conducted to examine the possibilities of eliminating or controlling optical damage in lithium niobate based optical waveguides. Impurities and thermal treatments are seen as key factors in optical damage (or photorefractive effect). Planar, single mode waveguides such as Mg:Ti:LiNbO3, Mg:Ti:Mg:LiNbO3, Ti:Mg:LiNbO3, and Zn:LiNbO3 were fabricated using vacuum deposition and thermal diffusion techniques with the highest purity materials available. The impurity levels in the materials were analyzed using secondary ion mass spectrometry and mass spectroscopy. The waveguide properties and optical damage were measured in the TM(0) and TE(0) modes using the Mach-Zehnder inteferometer. The study demonstrates the present day limitations in what can be achieved in improving the optical damage resistance in LiNbO3 based waveguides.

CISTI

N94-13868 Canadian Marconi Co. Ltd., Montreal (Quebec). Avionics Div.
INTEGRATED OPTICS TECHNOLOGY TRANSFER Final Report
Wen Y. Jiang 19 Apr. 1991 18 p
(Contract DSS-W7714-8-5713-01-ST)
(DSIS-93-00179; CMC-0867-1016; CTN-93-60806) Avail: CASI HC A03

The integrated optic spectrum analyzer (IOSA) performs a spectrum analysis of radio frequency (RF) signals in real time, with potential applications in electronic warfare receivers. The distinguising characteristics of the IOSA include small size, low weight, high rigidity, low cost, and low RF power requirements compared to bulk acoustic-optic devices. The IOSA consists of an optical waveguide, two integrated optic lenses, a surface acoustic wave (SAW) transducer, a laser diode, and a photodetector array. System design, waveguide design, and SAW transducer design are described, along with the processes used for fabrication of the lens, waveguide, and SAW transducer. The IOSA system was then tested and results are presented. The dynamic range of the system was over 30 dB. The acousto-optic diffraction efficiency of the SAW transducer was better than 50 percent/1 W RF. The 5-dB bandwidth of acousto-optic diffraction was around 350 MHz. The RF frequency resolution was 6.4 MHz. The test results showed that most specifications surpassed the design targets.

CISTI

N94-14317# Lawrence Livermore National Lab., CA.
GAMMA-INSENSITIVE OPTICAL FOCAL PLANE ARRAY
H. Kruger Oct. 1992 69 p
(Contract W-7405-eng-48)
(DE93-013100; UCRL-ID-112223) Avail: CASI HC A04/MF A01

Two types of optical focal plane array concepts are proposed which use semitransparent photocathodes and gas avalanche multiplication to count an optical photon or a gamma as submicrosecond pulses with a charge that can be adjusted to be as large as 106 electrons. Avalanche diameters are sufficiently small to allow use of pixel sizes of tens of microns. Currently available photocathode materials permit operation at ultraviolet/visible wavelengths with approximately 10-20% quantum efficiency and in the near-infrared with approximately 0.1-0.3% quantum efficiency. The dark current of these photocathodes is sufficiently low so that they can be operated at room temperature. The weight of these gas avalanche focal plane designs is small and negligible compared to that required for data processing. The first concept, using a quartz cathode plate, is a relatively simple mechanical design. It detects a gamma mainly through the Cerenkov photons radiated in the quartz by the high-energy end of the gamma-produced Compton electron spectrum. It can operate in a high gamma flux; however, it has little capability to discriminate between optical photon and gamma counts. The second concept uses scintillating fiberoptic cathode and anode plates to detect all the gamma-produced electrons. It is a more complicated design; however, it is inherently capable of discriminating between optical photon and gamma events on the basis of pulse height and pixel count pattern. It can operate in a gamma flux of 10(exp 10) to 10(exp 11) gammas/sq cm/sec if built with scintillating glass fibers. Use of plastic scintillation fibers increases the tolerable gamma flux to approximately 10(exp 12)-10(exp 13) gammas/sq cm/sec, but makes the mechanical design of the gas avalanche focal plane array more difficult. Prototype gas avalanche focal plane arrays need to be built and tested to verify feasibility of this optical sensor concept. DOE

N94-14367# Los Alamos National Lab., NM.
POLARIZATION EFFECTS IN OPTICAL FIBER CURRENT SENSORS BASED ON SAGNAC INTERFEROMETERS WITH 3 BY 3 COUPLERS
K. B. Rochford (National Inst. of Standards and Technology, Boulder, CO.), G. W. Day (National Inst. of Standards and Technology, Boulder, CO.), and P. R. Forman 1993 5 p Presented at the 9th Optical Fiber Sensors Conference, Firenze, Italy, 4-6 May 1993
(Contract W-7405-eng-36)
(DE93-012665; LA-UR-93-1449; CONF-930588-2) Avail: CASI HC A01/MF A01

Response functions of an ideal Sagnac optical fiber current sensor based on a 3 x 3 coupler fundamentally depend on the polarization state of light catering coupler, even for a zero birefringence system. The desired response functions, cosinusoids separated by 120(degrees) phase shifts, are obtained only for circularly polarized light. The response functions for linearly polarized and depolarized inputs are cosinusoids separated by 180(degrees), and yield only zero-slope small-signal responses. Also, two outputs are degenerate, so that the response is similar to that observed in 2 x 2 systems. Thus, 3 x 3 couplers offer no advantage over 2 x 2 systems for linear polarized light. This result increases system complexity in that polarization control optics are required to supply the proper polarization, even for an ideal, zero-birefringence system. DOE

N94-14438# Lawrence Livermore National Lab., CA.
BRILLOUIN SCATTERING FROM FLUCTUATIONS PRODUCED BY STIMULATED RAMAN SCATTERING
T. Kolber (Alberta Univ., Edmonton.), W. Rozmus (Alberta Univ., Edmonton.), V. T. Tikhonchuk (Academy of Sciences, USSR, Moscow.), H. A. Baldis, and K. Estabrook 1 Mar. 1993 9 p Presented at the OE/LASE 1993 International Society for Optical Engineering Conference, Los Angeles, CA, 16-23 Jan. 1993
(Contract W-7405-eng-48)
(DE93-016531; UCRL-JC-112700; CONF-930159-44) Avail: CASI HC A02/MF A01

We discuss the mechanism responsible for the enhancement of Brillouin backscattered light in the context of recent experimental observations. The scattering takes place from the fluctuations produced during the nonlinear evolution of stimulated Raman scattering. The frequency spectra of Brillouin light shows blue and red shifted components consistent with experimental observations. DOE

N94-14473*# Hughes Danbury Optical Systems, Inc., CT.
IMPACT OF SHORTER WAVELENGTHS ON OPTICAL QUALITY FOR LAWS Final Report
Alan B. Wissinger, Robert J. Noll, James G. Tsacoyeanes, and Jeanette

R. Tausanovitch Sep. 1993 35 p
(NASA Order H-20752-D)
(NASA-CR-193433; NAS 1.26:193433; PR-D15-0018) Copyright Avail: CASI HC A03/MF A01

This study explores parametrically as a function of wavelength the degrading effects of several common optical aberrations (defocus, astigmatism, wavefronttilts, etc.), using the heterodyne mixing efficiency factor as the merit function. A 60 cm diameter aperture beam expander with an expansion ratio of 15:1 and a primary mirror focal ratio of f/2 was designed for the study. An HDOS copyrighted analysis program determined the value of merit function for various optical misalignments. With sensitivities provided by the analysis, preliminary error budget and tolerance allocations were made for potential optical wavefront errors and boresight errors during laser shot transit time. These were compared with the baseline 1.5 m CO2 laws and the optical fabrication state of the art (SOA) as characterized by the Hubble Space Telescope. Reducing wavelength and changing optical design resulted in optical quality tolerances within the SOA both at 2 and 1 micrometer. However, advanced sensing and control devices would be necessary to be tightened by a factory of 1.8 for a 2 micrometer system and by 3.6 for a 1 micrometer system relative to the baseline CO2 LAWS. Available SOA components could be used for operation at 2 micrometers but operation at 1 micrometer does not appear feasible. Author

N94-14529# Brookhaven National Lab., Upton, NY.
RADIATION EFFECTS ON OPTOELECTRONIC ANALOG LINK FOR PARTICLE DETECTORS
T. Tsang May 1993 3 p Presented at the 2nd European Conference on Radiations and Their Effects on Devices and Systems, Saint Malo, France, 13-16 Sep. 1993
(Contract DE-AC02-76CH-00016)
(DE93-015794; BNL-49074; CONF-930953-1) Avail: CASI HC A01/MF A01

The successful operation of an optoelectronic analog link for transfer of particle detector signals in high radiation area requires a detailed radiation damage study. We present at this conference the study of Ti:LiNbO3 optical modulators with gamma-rays and neutrons. DOE

N94-14548*# Dynamic System Technologies, Inc., Huntsville, AL.
SMALL SCALE ADAPTIVE OPTICS EXPERIMENT SYSTEMS ENGINEERING Final Report
William H. Boykin 30 Sep. 1993 41 p
(Contract NAS8-39216)
(NASA-CR-194419; NAS 1.26:194419; HSV-93-0003) Avail: CASI HC A03/MF A01

Assessment of the current technology relating to the laser power beaming system which in full scale is called the Beam Transmission Optical System (BTOS). Evaluation of system integration efforts are being conducted by the various government agencies and industry. Concepts are being developed for prototypes of adaptive optics for a BTOS. Author

N94-14702# Pacific Northwest Lab., Richland, WA.
QUANTITATIVE LUMINESCENCE IMAGING SYSTEM
C. R. Batishko, K. A. Stahl, and B. A. Fecht 1992 48 p Presented at the Workshop on 3-dimensional Graphics Modeling of RFR Distribution in Humans, Brooks AFB, TX, 8-9 Dec. 1992
(Contract DE-AC06-76RL-01830)
(DE93-015691; PNL-SA-21677; CONF-921281-1) Avail: CASI HC A03/MF A01

The goal of the Measurement of Chemiluminescence project is to develop and deliver a suite of imaging radiometric instruments for measuring spatial distributions of chemiluminescence. Envisioned deliverables include instruments working at the microscopic, macroscopic, and life-sized scales. Both laboratory and field portable instruments are envisioned. The project also includes development of phantoms as enclosures for the diazoluminomelanin (DALM) chemiluminescent chemistry. A suite of either phantoms in a variety of typical poses, or phantoms that could be adjusted to a variety of poses, is envisioned. These are to include small mammals (rats), mid-sized mammals (monkeys), and human body parts. A complete human phantom that can be posed is a long-term goal of the development. Taken together, the chemistry and instrumentation provide a means for imaging rf dosimetry based on chemiluminescence induced by the heat resulting from rf energy absorption. The first delivered instrument, the Quantitative Luminescence Imaging System (QLIS), resulted in a patent, and an R&D Magazine 1991 R&D 100 award, recognizing it as one of the 100 most significant technological developments of 1991. The current status of the project is that three systems have been delivered, several related studies have been conducted, two preliminary human hand phantoms have been delivered, system upgrades have been implemented, and calibrations have been maintained. Current development includes sensitivity improvements to the microscope-based system; extension of the large-scale (potentially life-sized targets) system to field portable applications; extension of the 2-D large-scale system to 3-D measurement; imminent delivery of a more refined human hand phantom and a rat phantom; rf, thermal and imaging subsystem integration; and continued calibration and upgrade support. DOE

N94-14704# Technische Univ., Berlin (Germany). Fachbereich Elektrotechnik.
MANUFACTURING AND EXAMINATION OF INTEGRATED OPTICAL WAVEGUIDE COMPONENTS IN SILICON Ph.D. Thesis [HERSTELLUNG UND UNTERSUCHUNG INTEGRIERT OPTISCHER WELLENLEITERKOMPONENTEN IN SILIZIUM]
Joachim Schmidtchen 1992 127 p In GERMAN
(ETN-93-94393) Avail: CASI HC A07/MF A02

Waveguides are manufactured with a method developed for titanium diffused lithium niobate waveguides. Germanium was used for increasing refractivity and an alloy of germanium and silicon was employed as doping material in order to avoid problems in the beginning of the diffusion process. Waveguide losses inferior to 0.5 dB/cm were obtained by optimization of layer thickness and strip breath. Monomode rib waveguides were manufactured by isotropic and anisotropic etching of a silicon on insulator. SIMOX (Separation by Isolated Oxygen) process was used for production of a silica layer of 0.2 micrometers. The near field intensity profile of a rib waveguide was recorded and compared with a simulated equivalent waveguide. It is concluded that silicon can be used in optical communication technology for realization of integrated optoelectronic devices. ESA

N94-14856# Technische Univ., Berlin (Germany). Fachbereich Physik.
TWO DIMENSIONAL MEASUREMENT AND EVALUATION OF POINT IMAGES AT MICROSCOPE OBJECTIVES Ph.D. Thesis [ZWEIDIMENSIONALE MESSUNG UND AUSWERTUNG VON PUNKTBILDERN AN MIKROOBJEKTIVEN]
Roman Castaneda-Sepulveda 1993 153 p In GERMAN
(ETN-93-94397) Avail: CASI HC A08/MF A02

A process for two dimensional measurement and evaluation of point images is developed, which allows the reproduction quality of a given test object to be obtained on the basis of quantitative assessment of symmetry and energy distribution of the point image. The process was realized by considering the production of a test object with the Airy muster method, the measurement of axial and nonaxial point images with subpixel scanning, and the evaluation of point image by using the moment method. A digital image processing system was used as a receiver because of the simple positioning of charge coupled device cameras and the high velocity for recording two dimensional pictures. Corrections were made with difference image and low pass filtration methods in order to guarantee accuracy of measurements. Moments were calculated until the fourth order for estimation of symmetry parameters of point images, such as mean quadratic radius, eccentricities, energy and coma factors, which are shown to be invariant with coordinate transformations and are proved to be good estimators in the sense of Hertel definition of objective quality criteria. ESA

N94-14903*# Alabama Univ., Huntsville. Center for Applied Optics.
INVESTIGATION OF ZERODUR MATERIAL PROCESSING Final Report
R. Barry Johnson Jul. 1993 5 p
(Contract NAS8-38609)
(NASA-CR-193842; NAS 1.26:193842) Avail: CASI HC A01/MF A01

The Final Report of the Center for Applied Optics (CAO), of The University of Alabama (UAH) study entitled 'Investigation of Zerodur Material Processing' is presented. The objectives of the effort were to prepare glass samples by cutting, grinding, etching, and polishing block Zerodur to desired specifications using equipment located in the optical shop located in the Optical System Branch at NASA/MSFC; characterize samples for subsurface damage and surface roughness; utilize Zerodur samples for coating investigations; and perform investigations into enhanced optical

fabrication and metrology techniques. The results of this investigation will be used to support the Advanced X Ray Astrophysics Facility (AXAF) program as well as other NASA/MSFC research programs. The results of the technical effort are presented and discussed. Author (revised)

75 PLASMA PHYSICS

Includes magnetohydrodynamics and plasma fusion.

For ionospheric plasmas see *46 Geophysics*. For space plasmas see *90 Astrophysics*.

N94-12814# Los Alamos National Lab., NM.
TWO-DIMENSIONAL SIMULATIONS OF FOIL IMPLOSION EXPERIMENTS ON THE LOS ALAMOS CAPACITOR BANK
D. L. Peterson, R. L. Bowers, J. H. Brownell, A. E. Greene, H. Lee, and W. Matuska 1993 9 p Presented at the 3rd International Conference on Dense z-Pinches, London, England, 19-23 Apr. 1993
(Contract W-7405-eng-36)
(DE93-012676; LA-UR-93-1393; CONF-9304126-7) Avail: CASI HC A02/MF A01

A number of z-pinch experiments have been conducted at Los Alamos on the Pegasus capacitor bank in which 2-cm high, 5-cm radius, thin foil loads were imploded with currents in excess of 3 MA. Two-dimensional radiation magnetohydrodynamic (RMHD) simulations of these implosions have been performed to model the implosion dynamics and subsequent generation of an x-ray pulse. Comparison of the simulation instability development with visible light framing camera photographs show good agreement and illustrate the instability evolution from short to long wavelengths and a final disruption of the imploding plasma shell. The calculations also show good agreement with experimental timing and measured current and voltage waveforms, and also reproduce features characteristic of the x-ray output. These include a broad pulsewidth, and the presence of multiple peaks and small time scale structures, features which cannot be reproduced by one-dimensional models. X-ray spectra obtained from the calculated pinch also reproduce qualitative features in the measured spectra. DOE

N94-12846# Lawrence Livermore National Lab., CA.
A 3D GYROKINETIC PARTICLE-IN-CELL SIMULATION OF FUSION PLASMA MICROTURBULENCE ON PARALLEL COMPUTERS
T. J. Williams Dec. 1992 6 p Presented at the 1993 International Simulators Conference on High Performance Computing, Arlington, VA, 29 Mar. - 1 Apr. 1993
(Contract W-7405-eng-48)
(DE93-012503; UCRL-JC-111840; CONF-930372-10) Avail: CASI HC A02/MF A01

One of the grand challenge problems now supported by HPCC is the Numerical Tokamak Project. A goal of this project is the study of low-frequency micro-instabilities in tokamak plasmas, which are believed to cause energy loss via turbulent thermal transport across the magnetic field lines. An important tool in this study is gyrokinetic particle-in-cell (PIC) simulation. Gyrokinetic, as opposed to fully-kinetic, methods are particularly well suited to the task because they are optimized to study the frequency and wavelength domain of the microinstabilities. Furthermore, many researchers now employ low-noise delta(f) methods to greatly reduce statistical noise by modelling only the perturbation of the gyrokinetic distribution function from a fixed background, not the entire distribution function. In spite of the increased efficiency of these improved algorithms over conventional PIC algorithms, gyrokinetic PIC simulations of tokamak micro-turbulence are still highly demanding of computer power--even fully-vectorized codes on vector supercomputers. For this reason, we have worked for several years to redevelop these codes on massively parallel computers. We have developed 3D gyrokinetic PIC simulation codes for SIMD and MIMD parallel processors, using control-parallel, data-parallel, and domain-decomposition message-passing (DDMP) programming paradigms. This poster summarizes our earlier work on codes for the Connection Machine and BBN TC2000 and our development of a generic DDMP code for distributed-memory parallel machines. We discuss the memory-access issues which are of key importance in writing parallel PIC codes, with special emphasis on issues peculiar to gyrokinetic PIC. We outline the domain decompositions in our new DDMP code and discuss the interplay of different domain decompositions suited for the particle-pushing and field-solution components of the PIC algorithm. DOE

N94-12849# Los Alamos National Lab., NM.
ADVANCED MAGNETIC FLUX COMPRESSION GENERATOR DEVELOPMENT ISSUES: A COMPARISON OF COAXIAL AND DISK GENERATORS
M. G. Sheppard and B. L. Freeman Apr. 1993 33 p
(Contract W-7405-eng-36)
(DE93-014025; LA-12482-MS) Avail: CASI HC A03/MF A01

Three magnetic flux compression generator (FCG) geometries are reviewed and compared for their suitability as high-current, high-power drivers for z-pinch implosion programs at Los Alamos. They are the inside-out coaxial FCG, the disk FCG, and the outside-in coaxial FCG. A wide range of issues is discussed for each type FCG including current-carrying capability, current densities, robustness, explosive mass and shape, initiation schemes, efficiency, operating times, complexity, and expense associated with development and fabrication. Equations are derived and used in simple scaling studies. The results of these studies are supported by MHD calculations and references to relevant experiments both here and in Russia. The inside-out coaxial FCG is shown to be suitable, both for the very high current applications and for anticipated future Trailmaster concepts. Based upon this analysis and results reported in the Russian literature, the inside-out coaxial FCG is more suitable than the disk FCG for the high-current applications considered, and the two are roughly equivalent when applied to lower-current Trailmaster concepts. The outside-in coaxial FCG is unsuitable for either application because of its limited current-carrying capability and the large investment required for initial development. DOE

N94-12853# Gosudarstvennyi Komitet po Ispolzovaniyu Atomnoi Energii, Moscow (USSR).
EXCITATION OF COUPLED WAVES IN PLASMA PERIODIC STRUCTURES BY RELATIVISTIC ELECTRON BEAM AND ACCELERATION OF CHARGED PARTICLES
V. A. Balakirev and A. V. Borodkin 1991 24 p In RUSSIAN
(DE93-621657; KFTI-91-9) Avail: CASI HC A03/MF A01 (US Sales Only)

A process of electromagnetic excitation in plasma periodic structures by relativistic electron beam and a possibility of parametric excitation of plasma semi-space slow surface wave are investigated. Parametric coupling of external radiation and surface wave is realized by a periodic unhomogenity of plasma density which can be created by ion-sound wave excitation. A two-beam scheme of acceleration in coupled slowing down structures is proposed. DOE

N94-12854# Gosudarstvennyi Komitet po Ispolzovaniyu Atomnoi Energii, Moscow (USSR).
INVESTIGATION OF DYNAMICS OF PLASMA FLUXES GENERATED BY THE QUASI-STATIONARY PLASMA ACCELERATOR P-50
A. Yu. Voloshko, I. E. Garkusha, D. G. Solyakov, V. I. Tereshin, and V. V. Chebotarev 1991 16 p In RUSSIAN
(DE93-621665; KFTI-91-15) Avail: CASI HC A03/MF A01 (US Sales Only)

The results of experimental research on electric and magnetic field distribution in plasma fluxes generated by the P-50 accelerator in different work regimes are represented. Current vortices and regions with increased potential in plasma fluxes behind the accelerator cut are discovered. On the base of E and H-field experimental distribution, values of electron and ion local velocities and density in plasma flux were numerically calculated in the frame of MHD approximation. This research shows the advantages of pilot cathode compared with usual one and the necessity of anode gas supply in accelerating channel. DOE

N94-12862# STI Optronics, Bellevue, WA.
THEORY OF FIELD-REVERSED CONFIGURATIONS
L. C. Steinhauer 29 Jan. 1993 24 p
(Contract DE-AC06-80ER-53098)
(DE93-015611; DOE/ER-53098/T9) Avail: CASI HC A03/MF A01

This report summarizes results from the theoretical program on field reversed configurations (FRC) at STI Optronics. The program, which has spanned the last 13 years, has included analytical as well as computational

components. It has led to published papers on every major topic of FRC theory. The report is outlined to summarize results from each of these topic areas: formation, equilibrium, stability, and confinement. Also briefly described are Steinhauer's activities as Compact Toroid Theory Listening Post. Appendix A is a brief listing of the major advances achieved in this program. Attached at the back of this report is a collection of technical papers in archival journals that resulted from work in this program. The discussion within each subsection is given chronologically in order to give a historical sense of the evolution of understanding of FRC physics. DOE

N94-12901# Instituto de Pesquisas Espaciais, Sao Jose dos Campos (Brazil).

PLASMA DIFFUSION THROUGH MULTIDIPOLE MAGNETIC FIELDS

Jose Leonardo Ferreira 1993 24 p Submitted for publication

(INPE-5460-PRE/1768) Avail: CASI HC A03/MF A01

The diffusion of a cold plasma through multidipole fields of a magnetic picket fence is presented. The ion diffusion and trapping is determined by electric potentials inside the multidipole fields. The electron diffusion is regulated by an anomalous transport process driven by an ion acoustic instability inside the magnetic sheath. Particles drifting with velocities above the ion acoustic speed generates high amplitude turbulent waves responsible for all anomalous diffusion process. Author (revised)

N94-12944# Japan Atomic Energy Research Inst., Tokyo. Dept. of Fusion Engineering research.

TEST APPARATUS FOR ITER BLANKET COOLING WATER DISTRIBUTION DESIGN

Hiroshi Yoshida (Japan Atomic Energy Research Inst., Naka.), Mikio Enoeda (Japan Atomic Energy Research Inst., Naka.), Shingo Hirata (Kawasaki Heavy Industries Ltd., Tokyo, Japan.), and Hideki Ito (Kawasaki Heavy Industries Ltd., Tokyo, Japan.) May 1992 55 p

(DE93-753157; JAERI-M-92-070) Avail: CASI HC A04/MF A01

Current Japanese breeding blanket concept being developed for the ITER driver blanket is comprised of three breeding layers, nine multiplier layers and five water cooling panels. In order to meet design requirements of tritium release efficiency and material temperature restrictions, configuration of these layers should be designed to achieve optimum temperature profiles in the radial direction of the blanket. Such temperature conditions are attained by appropriate water flow rate distribution in each cooling panel. Furthermore, the cooling panel must be designed to accommodate variation of D-T burning plasma density during ITER operation. An engineering test apparatus composed of three parallel cooling panel models was developed. It was designed to examine performance of orifice type passive distributions for cooling header design. The apparatus can be operated under ITER blanket design conditions: temperature range: 60 - 100 C; water pressure: 1.5 MPa; flow rate: 0.5-5 m/s; pressure drop: up to 50 kPa; heat flux of heater: 20-2000 kW/m(sup 2). Author

N94-12953# General Atomics Technologies Corp., San Diego, CA.

DIMENSIONALLY SIMILAR DISCHARGES WITH CENTRAL RF HEATING ON THE D3-D TOKAMAK

C. C. Petty, T. C. Luce, and R. I. Pinsker Apr. 1993 4 p Presented at the 10th Topical Conference on Radio Frequency Power in Plasmas, Boston, MA, 1-3 Apr. 1993

(Contract DE-AC03-89ER-51114)

(DE93-012776; GA-A-21257; CONF-9304112-11) Avail: CASI HC A01/MF A01

The scaling of L-mode heat transport with normalized gyroradius is investigated on the D3-D tokamak using central RF heating. A toroidal field scan of dimensionally similar discharges with central ECH and/or fast wave heating show gyro-Bohm-like scaling both globally and locally. The main difference between these results and those using NBI heating on D3-D is that with RF heating the deposition profile is not very sensitive to the plasma density. Therefore central heating can be utilized for both the low-B and high-B discharges, whereas for NBI the power deposition is decidedly off-axis for the high-B discharge. DOE

N94-12984# City Univ. of New York, Staten Island.

GROWTH CURVE ANALYSIS FOR PLASMA PROFILES USING SMOOTHING SPLINES

K. Imre May 1993 14 p

(Contract DE-FG02-91ER-54131)

(DE93-015741; DOE/ER-54131/2) Avail: CASI HC A03/MF A01

We are developing a profile analysis code for the statistical estimation of the parametric dependencies of the temperature and density profiles in tokamaks. Our code uses advanced statistical techniques to determine the optimal fit, i.e. the fit which minimized the predictive error. For a forty TFTR Ohmic profile dataset, our preliminary results indicate that the profile shape depends almost exclusively on q(sub a') but that the shape dependencies are not Gaussian. We are now comparing various shape models on the TFTR data. In the first six months, we have completed the core modules of the code, including a B-spline package for variable knot locations, a data-based method to determine the optimal smoothing parameters, self-consistent estimation of the bias errors, and adaptive fitting near the plasma edge. Visualization graphics already include three dimensional surface plots, and discharge by discharge plots of the predicted curves with error bars together with the actual measurements values, and plots of the basis functions with errors. DOE

N94-12995# Lawrence Livermore National Lab., CA.

HIGHLY CHARGED IONS IN HOT, DENSE PLASMAS

A. L. Osterheld, R. S. Walling, B. K. F. Young, W. H. Goldstein, G. Shimkaveg, B. J. MacGowan, L. DaSilva, C. Keane, B. Hammel, and R. London et al Sep. 1992 12 p Presented at the 6th International Conference on Physics of Highly Charged Ions, Manhattan, KS, 28 Sep. - 2 Oct. 1992

(Contract W-7405-eng-48)

(DE93-013348; UCRL-JC-111868; CONF-920948-12) Avail: CASI HC A03/MF A01

Highly-charged ions play a critical role in hot, dense plasmas. They affect the energy balance and hydrodynamic evolution of transient plasmas. The radiation emitted by highly charged ions may be used in several practical applications, such as inertial confinement fusion, short wavelength lasers, and x-ray sources for lithography and microscopy applications. This radiation may also be used to diagnose the conditions in plasmas. In recent years, models have been developed to describe the atomic kinetics of complex ionization states of highly charged ions in plasmas. However, reliable atomic calculations and careful experiments which test both the fundamental atomic physics and the assumptions of the plasma emission models are required. DOE

N94-13017# Lawrence Livermore National Lab., CA.

INERTIAL CONFINEMENT FUSION

L. Powers, ed., R. Condouris, ed., M. Kotowski, ed., and P. W. Murphy, ed. 1992 62 p

(Contract W-7405-eng-48)

(DE93-013303; UCRL-LR-105821-92-4) Avail: CASI HC A04/MF A01

This issue of the ICF Quarterly contains seven articles that describe recent progress in Lawrence Livermore National Laboratory's ICF program. The Department of Energy recently initiated an effort to design a 1-2 MJ glass laser, the proposed National Ignition Facility (NIF). These articles span various aspects of a program which is aimed at moving forward toward such a facility by continuing to use the Nova laser to gain understanding of NIF-relevant target physics, by developing concepts for an NIF laser driver and by envisioning a variety of applications for larger ICF facilities. This report discusses research on the following topics: Stimulated Rotational Raman Scattering in Nitrogen; A Maxwell Equation Solver in LASNEX for the Simulation of Moderately Intense Ultrashort Pulse Experiments; Measurements of Radial Heat-Wave Propagation in Laser-Produced Plasmas; Laser-Seeded Modulation Growth on Directly Driven Foils; Stimulated Raman Scattering in Large-Aperture, High-Fluence Frequency-Conversion Crystals; Fission Product Hazard Reduction Using Inertial Fusion Energy; and the Use of Inertial Confinement Fusion for Nuclear Weapons Effects Simulations. DOE

N94-13033# Oak Ridge National Lab., TN.

ION CYCLOTRON HEATING EXPERIMENTS AND PLANS FOR THE ADVANCED TOROIDAL FACILITY (ATF)

D. A. Rasmussen, D. B. Batchelor, R. J. Goulding, D. J. Hoffman, E. F. Jaeger, J. A. Rome, and C. E. Thomas 1993 4 p Presented at the 10th Topical Conference on Radio Frequency Power in Plasmas, Boston, MA, 1-3 Apr. 1993

(Contract DE-AC05-84OR-21400)

(DE93-012965; CONF-9304112-10) Avail: CASI HC A01/MF A01

In the Advanced Toroidal Facility (ATF) Ion Cyclotron Resonant Frequency (ICRF) experiments to date, a single-strap tunable antenna with carbon limiters has been used at power densities up to 13.6 MW/m(sup 2) (900 kW). Hydrogen minority heating experiments at 14.4 MHz were performed in deuterium plasmas formed initially with both second-harmonic electron cyclotron heating (ECH) and helium neutral beam injection (NBI). No ICRF heating was observed in the low-density ECH target plasmas. Two distinct NBI plus ICRF operating modes are described. The moderate heating of these discharges is probably limited by impurities sputtered from the vessel walls and/or poorly confined orbits for the heated particles. A two-strap, phased antenna, designed to reduce impurities and capable of both minority and direct electron heating is described. A second antenna design for optimizing the coupling to well confined ion orbits, additional ICRF heating schemes, and methods for reducing the RF edge interactions in a stellarator geometry are also being considered. DOE

N94-13039# Illinois Univ., Urbana. Dept. of Mechanical and Industrial Engineer ing.

TWO TEMPERATURE MODELING AND EXPERIMENTAL MEASUREMENTS OF LASER SUSTAINED HYDROGEN PLASMAS Annual Report, 16 Jun. 1992 - 1 May 1993

Herman Krier and Ayhan E. Mertogul 1 May 1993 245 p

(Contract F49620-92-J-0448)

(AD-A265750; UILU-ENG-93-4015; AFOSR-93-0386TR) Avail: CASI HC A11/MF A03

Experiments have been performed which measured the global absorption and thermal efficiency of laser sustained hydrogen plasmas for the first time. Results include global absorption as high as 90% and thermal efficiency as high as 80%. These results validate laser propulsion as a feasible orbital transfer technology. A kinetic nonequilibrium model of laser sustained hydrogen plasmas has been formulated and solved. This model is the first of its kind and includes a discretized beam raytrace with a variable index of refraction based upon plasma electron number density. Model results have compared favorably with experimental results and the model has been used to provide predictions of LSP performance well outside the realm of experiments. Multiple model solutions have been obtained which are dependent upon initial conditions. No significant kinetic nonequilibrium was observed in LSP core regions for incident powers up to 700 kW. Beam refraction by the LSP has been observed to have a major effect on LSP performance. The methodology formulated in this document has direct applicability to two temperature modeling of arcjet plasmas, work which is currently underway at UIUC. DTIC

N94-13046# Oak Ridge National Lab., TN.

EQUILIBRIUM RECONSTRUCTION OF THE q-PROFILE IN TOKAMAKS FROM MOTIONAL STARK EFFECT DATA

S. P. Hirshman, D. K. Lee, F. M. Levinton, S. H. Batha (Fusion Physics and Technologies, Torrance, CA.), M. Okabayashi, and R. M. Wieland (Princeton Univ., NJ.) 1993 8 p Presented at the 20th European Conference on Contrrolled Fusion and Plasma Physics, Lisbon, Portugal, 26-30 Jul. 1993

(Contract DE-AC05-84OR-21400)

(DE93-015815; CONF-930720-12) Avail: CASI HC A02/MF A01

The motional Stark effect (MSE) diagnostic has been implemented on the Tokamak Fusion Test Reactor (TFIR) and the Princeton Beta Experiment (PBX-M) to obtain q-profile measurements in the presence of a finite-beta plasma. A multichannel MSE parameter system has obtained data for several plasma conditions including L-mode, Supershot, current ramps, and high beta(sub p). Accurate measurement of the q-profile is essential for analysis of the equilibrium, stability, and transport properties of a tokamak. Many externally observed phenomena, such as sawteeth and the beta collapse, can be analyzed principally in terms of the q and q' (i.e., shear) profiles. Thus, the MSE measurement supplements the standard diagnostic suite of external magnetic probes to provide a new set of internal profile data which was previously unavailable. Using the MSE data, together with magnetic probe data, it is possible to obtain a self-consistent equilibrium reconstruction of the q-profile. Before describing the reconstruction technique, a brief review of the MSE diagnostic will be presented in this paper. DOE

N94-13047# Naval Research Lab., Washington, DC.

INERTIAL CONFINEMENT FUSION PROGRAM

1992 8 p

(Contract DE-AI03-79DP-40092)

(DE93-013372; DOE/DP-40092/9) Avail: CASI HC A02/MF A01

The Nike laser system is progressing well. All of the amplifiers through the first E-beam pumped amplifier have been installed. The pulse-power reliability problems with the 20 cm e-beam amplifier have been solved, and this amplifier now operates in a highly-reproducible fashion at five minute intervals, at full power. A computerized control system and a computerized data acquisition system for monitoring the laser have been installed and successfully operated. A prototype computer-controlled automatic laser alignment system has been successfully tested. The assembly and testing of the large 60 cm amplifier pulsed power is progressing well. The optical system for the main NIKE beamlines is complete through the power discharge amplifiers. Sufficient optics have now arrived to test the full energy capability of the laser through the 20 cm amplifier using six 20 nsec angularly-multiplexed beams. DOE

N94-13081*# TRW Systems and Energy, Redondo Beach, CA. Applied Technology Div.

ICE/ISEE PLASMA WAVE DATA ANALYSIS Final Report, Jan. 1990 - Dec. 1991

E. W. Greenstadt Mar. 1992 8 p

(Contract NAS5-33046)

(NASA-CR-194375; NAS 1.26:194375) Avail: CASI HC A02/MF A01

The interval reported on, from Jan. 1990 to Dec. 1991, has been one of continued processing and archiving of ICE plasma wave (pw) data and transition from analysis of ISEE 3 and ICE cometary data to ICE data taken along its cruise trajectory, where coronal mass ejections are the focus of attention. We have continued to examine with great interest the last year of ISEE 3's precomet phase, when it spent considerable time far downwind from Earth, recording conditions upstream, downstream, and across the very weak, distant flank bow shock. Among other motivations was the apparent similarity of some shock and post shock structures to the signatures of the bow wave surrounding comet Giacobini-Zinner, whose ICE-phase data was revisited. While pursuing detailed, second-order scientific inquiries still pending from the late ISEE 3 recordings, we have also sought to position ourselves for study of CME's by instituting a data processing format new to the ISEE 3/ICE pw detector. Processed detector output has always been summarized and archived in 24-hour segments, with all pw channels individually plotted and stacked one above the next down in frequency, with each channel calibrated separately to keep all data patterns equally visible in the plots, regardless of gross differences in energy content at the various frequencies. Since CME's, with their preceding and following solar wind plasmas, can take more than one day to pass by the spacecraft, a more condensed synoptic view of the pw data is required to identify, let alone assess, CME characteristics than has been afforded by the traditional routines. This requirement is addressed in a major new processing initiative in the past two years. Besides our own ongoing and fresh investigations, we have cooperated, within our resources, with studies conducted extramurally by distant colleagues irrespective of the phase of the ISEE 3/ICE mission under scrutiny. The remainder of this report summarizes our processing activities, our investigations, both internal and cooperative, our scientific results, and our publication activity. Author (revised)

N94-13084*# Southwest Research Inst., San Antonio, TX. Dept. of Space Science.

INVESTIGATION OF PLASMA INSTABILITIES IN THE POLAR CUSP Semiannual Progress Report, 1 Mar. - 31 Aug. 1993

H. K. Wong 31 Aug. 1993 3 p

(Grant NAGw-1620; SwRI Proj. 15-2779)

(NASA-CR-194283; NAS 1.26:194283) Avail: CASI HC A01/MF A01

During the last six months, our efforts concentrated on studying the excitation of electromagnetic waves in the whistler frequency range by an anisotropic electron beam. A paper entitled 'Electron Cyclotron Wave Generation by Relativistic Electrons' was submitted to Journal of Geophysical Research and was accepted for publication. This paper is in collaboration with Dr. M. L. Goldstein at Goddard Space Flight Center. It was shown that an anisotropic electron beam (or gyrating electron beam) is capable of generating electron cyclotron waves with frequency from above to below the electron plasma frequency in a low density plasma. This instability may account for the observed Z mode and the electromagnetic component of auroral hiss in the Earth's polar region. The abstract of this paper is

enclosed. For a high density plasma in which the electron plasma frequency is considerably higher than the electron cyclotron frequency, a new left-hand electromagnetic wave at whistler frequencies, which is also driven unstable by an anisotropic electron beam, was found. The basic notion of this new instability is the significant change of the dispersion equation due to the contribution of the beam component, which can shift the usual right hand whistler waves into left hand waves. Author (revised)

N94-13100# Los Alamos National Lab., NM.
A PC-PCL-BASED CONTROL SYSTEM FOR THE HIGH-VOLTAGE PULSED-POWER OPERATION OF THE INTENSE DIAGNOSTIC NEUTRAL BEAM (IDNB) EXPERIMENT
R. Gribble Jun. 1993 15 p
(Contract W-7405-eng-36)
(DE93-014144; LA-12483-MS) Avail: CASI HC A03/MF A01

A stand-alone, semiautomated control system for the high-voltage pulsed-power energy sources on the Intense Diagnostic Neutral Beam Experiment at Los Alamos National Laboratory using personal computer (PC) and programmable logic controller (PLC) technology has been developed and implemented. The control system, consisting of a PC with the graphic operator interface, the network connecting the PC to the PLC, the PLC, the PLC I/O modules, fiber-optic interfaces and software, is described. DOE

N94-13144# Oak Ridge National Lab., TN.
EFFECT ON ANTENNA STRUCTURE OF HIGH POWER RF DURING PLASMA OPERATION
G. R. Haste, C. E. Thomas, A. Fadnek, M. D. Carter, B. Beaumont, A. Becoulet, H. Kuus, and B. Saoutic 1993 4 p Presented at the 10th Topical Conference on Radio Frequency Power in Plasmas, Boston, MA, 1-3 Apr. 1993
(Contract DE-AC05-84OR-21400)
(DE93-013278; CONF-9304112-12) Avail: CASI HC A01/MF A01

High-power, long-pulse operation on the Tore Supra tokamak results in considerable stress on the plasma-facing components. The ICH antennas must deliver high-power RF (up to 4 MW per antenna) in this environment. The antenna structure is therefore subjected to the power flux resulting from the interaction between RF and the edge plasma. The structure's response during operation is described, as is the condition of the antenna after prolonged use. DOE

N94-13207# Lawrence Livermore National Lab., CA.
KINETIC SIMULATIONS OF ULTRA-INTENSE LASER PLASMA INTERACTIONS AND A NOVEL METHOD OF GENERATING ODD HARMONICS
S. C. Wilks, W. L. Kruer, and W. B. Mori (California Univ., Los Angeles.) 11 Feb. 1993 9 p Presented at the OE/LASE 1993 International Society for Optical Engineering (SPIE) Conference, Los Angeles, CA, 16-23 Jan. 1993
(Contract W-7405-eng-48)
(DE93-014418; UCRL-JC-113163; CONF-930159-34) Avail: CASI HC A02/MF A01

We report on computer simulation results for a new laser plasma interaction regime. Our report concentrates on the collisionless, kinetic nature of the plasma motion. It is found that even for normal incidence, the absorption of the laser light by the plasma electrons near critical can be as high as 60%, and that, the temperature of the hot electrons produced can be predicted simply by knowing the associated ponderomotive potential of the incident laser. We also describe a new odd harmonic generation mechanism due to the interaction of the laser with the plasma electrons near critical. DOE

N94-13217# Lawrence Livermore National Lab., CA.
MAGNETIC FUSION COMPUTING: A PERSONAL RETROSPECTIVE VIEW
J. Killeen Aug. 1992 14 p Presented at the Joint Varenna-Lausanne International Workshop on Theory of Fusion Plasmas, Varenna, Italy, 24-28 Aug. 1992 Prepared in cooperation with California Univ., Davis
(Contract W-7405-eng-48)
(DE93-014147; UCRL-JC-111405; CONF-920813-3) Avail: CASI HC A03/MF A01

The association of computing with magnetic fusion research has a history of more than 30 years. Then, as now, the mathematical complexity of describing plasma phenomena has made the computer an indispensable tool in extending the theory. Our first area of application addressed fluid MHD models to represent ideal and resistive plasmas as well as equilibria. A second equally important area of research was in the solution of kinetic plasma models. Both Vlasov and Fokker-Planck models have been solved in the codes we developed, the latter allowing us to make realistic estimates of the transport of heat and particles in reacting fusion plasmas. The critical importance of computing to plasma physics research led us to the development of the dedicated computing facilities at NERSC (National Energy Research Supercomputer Center, Livermore). Aspects of these theoretical and institutional developments will be presented in a historical retrospective view. DOE

N94-13240 Academy of Sciences of the Ukraine, Kharkov.
ELECTRODYNAMICS OF HELICAL PLASMA STRUCTURES
A. K. Berezin, V. A. Buts, I. K. Kovalchuk, V. I. Kurilko, I. N. Onishchenko, A. P. Tolstoluzhskij, and Ya. B. Fajnberg 1991 35 p In RUSSIAN Limited Reproducibility: More than 20% of this document may be affected by microfiche quality
(DE93-620981; KFTI-91-52) Avail: Issuing Activity (Department of Energy (DOE)) (US Sales Only)

Electrodynamic properties of a hybrid slowing down structure consisting of co-axial beam and plasma were investigated theoretically. Dispersion relations for axial-symmetric waves in this system were found in hydrodynamic approximation. It was shown that in presence of a plasma column the phase velocity increases compared with that in case of a spiral in vacuum. Analytical expressions for increments of excited fields for beams of small and large density were obtained. At a sufficiently large beam density not only dispersion of the system changes, but the mechanism of vibration excitation changes too. Namely, with the beam density increase, splitting of its dispersion curve leads to disappearance of Cherenkov instability and appearance of anomal Doppler effect instability. Field topography for spiral-plasma system was investigated analytically and experimentally. DOE

N94-13393# Lawrence Livermore National Lab., CA.
PARAMETRIC INSTABILITIES IN LARGE NONUNIFORM LASER PLASMAS
H. A. Baldis, D. S. Montgomery, J. D. Moody, K. G. Estabrook, R. L. Berger, W. L. Kruer, C. Labaune, and S. H. Batha Sep. 1992 8 p Presented at the ICPP 1992 International Conference on Plasma Physics, Innsbruck, Austria, 29 Jun. - 3 Jul. 1992
(Contract W-7405-eng-48)
(DE93-013184; UCRL-JC-111546; CONF-920610-16) Avail: CASI HC A02/MF A01

The study of parametric instabilities in laser plasmas is of vital importance for inertial confinement fusion (ICF). The long scale-length plasma encountered in the corona of an ICF target provides ideal conditions for the growth of instabilities such as stimulated Brillouin scattering (SBS), stimulated Raman scattering (SRS), and filamentation. These instabilities can have detrimental effects in ICF, and their characterization and understanding is of importance. Scattering instabilities are driven through a feedback loop by which the beating between the electromagnetic EM fields of the laser and the scattered light matches the frequency of a local longitudinal mode of the plasma. Any process which interferes with the coherence of this mechanism can substantially alter the behavior of the instability. Of particular interest is the study of laser beam smoothing techniques on parametric instabilities. These techniques are used to improve irradiation uniformity which can suppress hydrodynamic instabilities. Laser beam smoothing techniques have the potential to control the scattering level from parametric instabilities since they provide not only a smoother laser intensity distribution, but also reduced coherence. Beam smoothing techniques that affect the growth of parametric instabilities include spatial smoothing and temporal smoothing by laser bandwidth. Spatial smoothing modifies the phase fronts and temporal distribution of intensities in the focal volume. The transverse intensity spectrum is shifted towards a higher spatial wavenumber and can significantly limit the growth of filamentation. Temporal smoothing reduces the coherence time and consequently limits the growth time. Laser bandwidth is required for most smoothing techniques and can have an independent effect on the instabilities as well. DOE

N94-13507 Academy of Sciences of the Ukraine, Kharkov.
INTERFEROMETRIC INVESTIGATION METHODS OF PLASMA SPATIAL CHARACTERISTICS ON STELLARATORS AND TOKAMAKS IN SUBMILLIMETER REGION
V. L. Berezhnyj, V. I. Kononenko, V. A. Epishin, and A. N. Topkov 1992 36 p In RUSSIAN Limited Reproducibility: More than 20% of this document may be affected by microfiche quality
(DE93-621606; INIS-mf-13479) Avail: CASI HC A03 (US Sales Only)

The review of interferometric methods of plasma investigation in the wave submillimeter range is given. The diagnostic schemes in stellarators and tokamaks designed for experienced thermonuclear reactors and also the perspective ones, which are still out of practice, are shown. The methods of these diagnostics, their physical principles, the main possibilities and restrictions at changes of electron density, magnetic fields (currents) and their spatial distributions are described. DOE

N94-13513# Los Alamos National Lab., NM.
INSTABILITY HEATING OF THE HDZP
R. H. Lovberg (California Univ., San Diego, La Jolla.), R. A. Riley, and J. S. Shlachter 1993 10 p Presented at the Third International Conference on Dense Z-Pinches, London, England, 19-23 Apr. 1993
(Contract W-7405-eng-36)
(DE93-012641; LA-UR-93-1318; CONF-9304126-5) Avail: CASI HC A02/MF A01

We present a model of dense Z-Pinch heating. For pinches of sufficiently small diameter and high current, direct ion heating by m = 0 instabilities becomes the principal channel for power input. This process is particularly important in the present generation of dense micro-pinches (e.g., HDZP-2) where instability growth times are much smaller than current risetimes, and a typical pinch diameter is several orders smaller than that of the chamber. Under these conditions, m = 0 formation is not disruptive; the large E(sub z) field reconnects the instability cusps externally, after which the ingested magnetic flux decays into turbulent kinetic energy of the plasma. The continuous process is analogous to boiling of a heated fluid. A simple analysis shows that an equivalent resistance R(sub t) = (l/4(the square root of (Nm(sub i))(mu(sub 0)/pi)(exp 3/2)I/r appears in the driving circuit, where I is the pinch current, N is the line density, l is the pinch length, m(sub i) is the ion mass, and r is the pinch radius. A corresponding heating term has been added to the ion energy equation in a 0-D, self-similar simulation, which had been written previously to estimate fusion yields and radial expansion of D(sub 2) fiber pinches. The simulation results agree well with the experimental results from HDZP-2, where the assumption of only joule heating produced gross disagreement. Turbulent ion heating should be the dominant process in any simple pinch carrying meg-ampere current that has a submillimeter radius. DOE

N94-13518# Saskatchewan Univ., Saskatoon. Plasma Physics Lab.
[ACTIVITIES OF THE UNIVERSITY OF SASKATCHEWAN, PLASMA PHYSICS LABORATORY] Progress Report, 1991-1992
G. D. Conway, A. Hirose, K. K. Jain, K. Mark, D. McColl, O. Mitarai (Kumamoto Inst. of Tech., Japan.), J. Ratzdaff, L. Schott, H. M. Skarsgard, and C. Xiao et al 1992 33 p Sponsored by Natural Sciences and Engineering Research Council; Office of the National Fusion Program; and Canadian Fusion Fuels Technology Project
(CTN-93-60831) Copyright Avail: CASI HC A03/MF A01

Detailed summaries of research projects conducted at the University of Saskatchewan's Plasma Physics Laboratory during 1991-92 are presented in the fields of tokamak experiments and reactor studies, basic plasma physics, and theories of instabilities and anomalous transport in tokamaks. The tokamak projects include discharge conditions and plasma diagnostics in the STOR-M tokamak, plasma modes and oscillations, edge density and magnetic fluctuations, diamagnetic measurements, and alternating current tokamak operation. Basic plasma physics projects include studies of radio frequency ion heating, parametric excitation of nonlinear asymmetric sheath oscillations, and dispersion function for a half-Maxwellian velocity distribution. Progress is also reported on developing the compact toroid fueller, intended for accelerating a compact toroid plasmoid to a velocity sufficient for central penetration into the Tokamak de Varennes, and on the compact torus injector project. The injector will be installed on the STOR-M tokamak to study compact torus injection into tokamak discharges. Abstracts of publications during 1991/92 are also included. CISTI

N94-13563# Saskatchewan Univ., Saskatoon. Plasma Physics Lab.
THE RESONANCE BROADENING THEORY REVISITED
A. Hirose and O. Ishihara (Texas Technological Univ., Lubbock.) Jan. 1993 12 p Presented at the Interdisciplinary Workshop on Statistical Description of Transport in Plasma, Astro- and Nuclear Physics, Les Houches, France, Feb. 1993
(PPL-134; CTN-93-60788) Avail: CASI HC A03/MF A01

It is shown that the velocity variance in one dimensional electrostatic turbulence is not pure Brownian but subdiffusive and increasing with time, with a corresponding diffusivity decreasing with time. The fractional Brownian motion associated with the diffusion process is attributed to non-Markovian statistics of particle trajectories. The anomalous spatial diffusivity across a sheared magnetic field caused by low frequency electric and/or magnetic fields is analogous to the velocity diffusivity and has the same scaling with the turbulence level and time. The theory has been tested favorably by numerical test particle simulations. Author (CISTI)

N94-13564# Saskatchewan Univ., Saskatoon. Plasma Physics Lab.
NONLINEAR EVOLUTION OF TEARING MODES IN INHOMOGENEOUS PLASMAS
A. I. Smolyakov Oct. 1992 48 p
(PPL-133; CTN-93-60789) Avail: CASI HC A03/MF A01

The effects of plasma gradients on the nonlinear dynamics of magnetic islands are considered. It is shown that the diamagnetic effects can substantially change island dynamics from the standard Rutherford's regime. In particular, the effects of plasma inhomogeneities can lead to the nonlinear excitation of magnetic islands with finite threshold in a situation when the linear drift-tearing modes are stable. Nonlinear differential equations are derived for the time evolution of magnetic island width and rotational frequency. Using these equations, it is found that the magnetic islands are stable in a wide range of plasma parameters. The general Grad-Shafranov type equation is also considered for neighboring equilibrium in a finite pressure plasma. Analysis of pressure effect on the saturation of m = 2 tearing modes in a tokamak gives an unexpected result in the non-monotonic behavior of the magnetic island width with a pressure rise. An equation is also derived for the nonlinear evolution of a m = 1 magnetic island. This saturated state is shown to be stable, and the combining effect of plasma pressure and toroidal magnetic field reduces the width of saturated islands. It is noted that the considered theory of nonlinear evolution of tearing modes could be used to understand the basic phenomena of plasma turbulence and anomalous transport. CISTI

N94-13577# Oak Ridge National Lab., TN.
FOLDED WAVEGUIDE DESIGNS FOR TOKAMAKS
D. J. Hoffman, T. S. Bigelow, C. H. Fogelman, J. J. Yugo, J. B. O. Caughman, W. L. Gardner, M. D. Carter, P. H. Probert, and E. Barbato 1993 5 p Presented at the 10th Topical Conference on Radio Frequency Power in Plasmas, Boston, MA, 1-3 Apr. 1993
(Contract DE-AC05-84OR-21400)
(DE93-013274; CONF-9304112-13) Avail: CASI HC A01/MF A01

The folded waveguide (FWG) has been tested to the megawatt level in RFTF and shows great promise for tokamak use. It has three primary advantages: low electric field (anywhere) per unit power coupled to the plasma, strong structural capabilities, and better spectral content than loops. A tokamak test is now needed. Potential candidates include C-Mod at 80 MHz and FTU at 433 MHz. The waveguide test on the first machine will be directed at conventional ion cyclotron heating, while the test on the latter will be directed at direct electron heating. In addition, a variation of the folded waveguide is proposed to be tested on Phaedrus-T. In this paper, we discuss the advantages of the waveguide, the design layout, some of the potential physics programs, and how these programs may have an impact on its potential use in ITER. DOE

N94-13678 Massachusetts Univ., Lowell.
INVESTIGATION OF AN ALTERNATING CURRENT PLASMA AS AN ELEMENT SELECTIVE ATOMIC EMISSION DETECTOR FOR HIGH-RESOLUTION CAPILLARY GAS CHROMATOGRAPHY AND AS A SOURCE FOR ATOMIC ABSORPTION AND ATOMIC EMISSION SPECTROMETRY Ph.D. Thesis
Jackson M. Ombaba 1992 223 p
Avail: Univ. Microfilms Order No. DA9305335

This thesis deals with the construction and evaluation of an alternating

current plasma (ACP) as an element-selective detector for high resolution capillary gas chromatography (GC) and as an excitation source for atomic absorption spectrometry (AAS) and atomic emission spectrometry (AES). The plasma, constrained in a quartz discharge tube at atmospheric pressure, is generated between two copper electrodes and utilizes helium as the plasma supporting gas. The alternating current plasma power source consists of a step-up transformer with a secondary output voltage of 14,000 V at a current of 23 mA. The device exhibits a stable signal because the plasma is self-seeding and reignites itself every half cycle. A tesla coil is not required to commence generation of the plasma if the ac voltage applied is greater than the breakdown voltage of the plasma-supporting gas. The chromatographic applications studied included the following: (1) the separation and selective detection of the organotin species, tributyltin chloride (TBT) and tetrabutyltin (TEBT), in environmental matrices including mussels (Mvutilus edullus) and sediment from Boston Harbor, industrial waste water and industrial sludge, and (2) the detection of methylcyclopentadienyl manganesetricarbonyl (MMT) and similar compounds used as gasoline additives. An ultrasonic nebulizer (common room humidifier) was utilized as a sample introduction device for aqueous solutions when the ACP was employed as an atomization source for atomic absorption spectrometry and as an excitation source for atomic emission spectrometry. Plasma diagnostic parameters studied include spatial electron number density across the discharge tube, electronic, excitation and ionization temperatures. Interference studies both in absorption and emission modes were also considered. Figures of merits of selected elements both in absorption and emission modes are reported. The evaluation of a computer-aided optimization program, Drylab GC, using spearmint oil and Environmental Protection Agency (EPA) standard mixture as probes is also discussed. The program supplied by LC Resources (Lafayette, CA) is used for separation optimization and prediction of gas chromatographic parameters. Column dead-time and average plate number were used as input data in conjunction with the retention times and peak areas of solutes at two different temperature programming rates. Once input data are entered into an IBM or IBM compatible personal computer, the program produces a 'relative resolution map' (RRM) which guides the analyst in selecting the most favorable temperature programming rate for the separation. Dissert. Abstr.

N94-13680 Princeton Univ., NJ.
STUDIES OF NON-INDUCTIVE CURRENT DRIVE IN THE CDX-U TOKAMAK Ph.D. Thesis
Yong-Seok Hwang 1993 127 p
Avail: Univ. Microfilms Order No. DA9311198

Two types of novel, non-inductive current drive concepts for starting-up and maintaining tokamak discharges, dc-helicity injection and internally-generated pressure-driven currents, have been developed on the CDX-U tokamak. To study the equilibrium and transport of these plasmas, a full set of magnetic diagnostics was installed. By applying a finite element method and a least squares error fitting technique, internal plasma current distributions are reconstructed from the measurements. Also, electron density distributions were obtained from 2 mm interferometer measurements by a similar least squares error technique utilizing magnetic flux configurations obtained by the magnetic analysis. Neoclassical pressure-driven currents in ECH plasmas are modeled with the reconstructed magnetic structure, using the electron density distribution and the electron temperature profile measured by a Langmuir probe. In a trapped particle geometry, precessional currents contribute significantly to the net toroidal plasma current. As closed flux surfaces are formed, particle detrapping generates bootstrap current as a major contributor while decreasing the precessional current. These neoclassical currents always predict a hollow profile, while the local and global magnetic measurements indicate a centrally-peaked profile. Indeed, we find that the non-hollow current density profile, with non-classical transport using Boozer's term in Ohm's law, gives better agreement to the internal magnetic structure measured by movable magnetic probes than does the hollow profile. This confirms the existence of a non-classical current transport. This non-classical current transport should be applicable to other forms of non-inductive current drive situations, including the helicity injected case. In the dc-helicity injection scheme, the need to increase injection current and maintain plasma equilibrium restricts possible arrangements. Several injection configurations were investigated, with the best found to be outside injection with a single divert or configuration, where the cathode is placed at the low field side of the x-point. In this geometry, plasma current as high as IO kA and edge safety factor q(sub a) similar to 5-10 were achieved. The formation of closed flux surfaces is shown by a two-dimensional magnetic reconstruction based on measurements. Experimental data and helicity balance show a good power efficiency and current drive efficiency independent of density. Both pressure-driven and dc-helicity injected tokamaks show the importance of plasma equilibrium in obtaining high plasma current. Noting that initial current generation requires smaller vertical fields in both techniques, programmed vertical field operation has proven to be very important in achieving high plasma current. These non-inductive current drive techniques show great potential as efficient current drive methods (due to their relatively density-independent efficiency) for future steady-state and/or long-pulse fusion reactors. Dissert. Abstr.

N94-13835# Saskatchewan Univ., Saskatoon. Plasma Physics Lab.
EXPERIMENTS ON THE CURRENT RAMPDOWN PHASE IN THE STOR-M TOKAMAK FOR AC OPERATION
O. Mitarai, G. Conway, A. Hirose, H. M. Skarsgard, C. Xiao, L. Zhang, and W. Zhang Oct. 1992 22 p
(PPL-132; CTN-93-60790) Avail: CASI HC A03/MF A01

The current rampdown phase followed by nondisruptive current termination is studied for future alternating current (AC) operations in the STOR-M tokamak. The plasma current is smoothly reduced to zero without disruptions with the rampdown rate of around minus 1.5 kA/ms. The plasma density in the current rampdown phase is controlled by gas puffing. The plasma current-density trace in the Hugill diagram follows a straight line, accompanied by slow inward shift in the major radius direction just before the current termination. At the current termination, a residual plasma density of (0.58 to 2.9)times 10 to the eighteenth per cubic meter is observed, with a corresponding Murakami parameter of ((0.41 to 2.1)times 10 to the eighteenth)/m2/T. After the current termination, the low density plasma remains for 5 to 20 ms, which would allow AC operation in the STOR-M tokamak if the radiation barrier does not affect the subsequent current evolution. Author (CISTI)

N94-13836# Saskatchewan Univ., Saskatoon. Plasma Physics Lab.
SMALL SCALE MAGNETIC ISLANDS IN COLLISIONLESS PLASMAS
A. I. Smolyakov and A. Hirose Sep. 1992 9 p
(PPL-131; CTN-93-60791) Avail: CASI HC A02/MF A01

Several investigations have indicated that skin-size electromagnetic turbulence is a plausible candidate responsible for anomalous transport in tokamaks. Results are presented from a study of nonlinearly saturated magnetic islands (spontaneous breaking of magnetic symmetry) having a characteristic dimension in the range of the skin depth, taking into account the longitudinal inertia of electrons. The existence of these islands is discussed in terms of a hydrodynamic nonlinear dispersion relation for a nonuniform plasma in a sheared magnetic field. A nonlinear equation to describe the steady-state magnetic island having a characteristic width of the order of skin depth is derived and solved. The anomalous electron thermal diffusivity based on the skin-size magnetic turbulence contains the electron temperature gradient (eta) in the form of 1/2 + 1/eta.
Author (CISTI)

N94-13849# Saskatchewan Univ., Saskatoon. Plasma Physics Lab.
PLASMA AUTO-BIASING DURING OHMIC H-MODE IN THE STOR-M TOKAMAK
W. Zhang, C. Xiao, and A. Hirose Mar. 1993 29 p Sponsored by Natural Sciences and Engineering Research Council and Atomic Energy of Canada Ltd.
(PPL-136; CTN-93-60786) Avail: CASI HC A03/MF A01

Application of a short current pulse on a nominal Ohmic discharge in the STOR-M tokamak triggers the Ohmic H-mode characterized by reduced H sub alpha radiation, increased electron density, and reduced edge density/magnetic fluctuations. Measurements of plasma floating potential at the plasma edge and in the scrape-off layer indicate that the Ohmic H-mode is accompanied by negative plasma autobiasing which leads to a steeper radial electric field profile at the edge. Since the duration of the current pulse is shorter than the resistive skin time of about 1 ms, preferential edge heating is expected, which is believed to be responsible for changes in the edge discharge condition favorable for inducing the Ohmic H-mode. The electron density profile becomes steeper at the edge during the H-mode, and clear formation of a density pedestal has been seen. The evolution of the density profile suggests the presence of particle pinch. It is found that

the electrostatic modes are dominant in the scrape-off layer while electromagnetic modes dominate in the main plasma. A similar H-mode is induced by external negative electrode biasing. Author (CISTI)

N94-13850# Saskatchewan Univ., Saskatoon. Plasma Physics Lab.
ON ENERGY TRANSPORT EQUATIONS FOR TURBULENT MAGNETIZED PLASMA
A. I. Smolyakov (Wisconsin Univ., Madison.) and A. Hirose Mar. 1993 21 p Sponsored in part by Natural Sciences and Engineering Research Council
(Contract DE-FG02-86ER-53218)
(PPL-135; CTN-93-60787) Avail: CASI HC A03/MF A01

By imposing drift ordering on the standard Braginskii magnetohydrodynamic equations, anomalous transport equations for a plasma in the presence of electromagnetic fluctuations are derived. The structure of convective energy fluxes and source terms in the energy balance equation is investigated in some detail. For low frequency electrostatic turbulence, the energy flux has a unique numerical factor 3/2 in its convective part. However, for magnetic turbulence, the convective energy flux, which is proportional to the particle flux induced by magnetic fluctuations, has a numerical factor 5/2. The physical meaning of the source terms in the energy balance equation is clarified. Author (CISTI)

N94-13851# Saskatchewan Univ., Saskatoon. Plasma Physics Lab.
SEMI-LOCAL KINETIC ANALYSIS OF THE TOROIDAL ION TEMPERATURE GRADIENT MODE
A. Hirose Jul. 1992 10 p
(PPL-130; CTN-93-60792) Avail: CASI HC A02/MF A01

In analyzing linear stability of plasma modes, the local approximation continues to be a useful method for making at least qualitative estimates of growth rates. The accuracy of this approximation improves if the norms of all differential operators are close to the exact values. A semi-local kinetic analysis is presented of the growth rate of the toroidal ion temperature gradient mode in tokamaks, with differential norms based on a simple eigenfunction. The semi-local kinetic dispersion relation is shown to yield growth rates in quantitative as well as qualitative agreement with the rigorous integral equation formulation. CISTI

N94-13852# Saskatchewan Univ., Saskatoon. Dept. of Physics.
ANOMALOUS TRANSPORT DUE TO THE ION ACOUSTIC INSTABILITY IN TOKAMAKS
A. Hirose, A. Smolyakov, and O. Ishihara (Texas Technological Univ., Lubbock.) Jul. 1992 16 p
(PPL-129; CTN-93-60793) Avail: CASI HC A03/MF A01

A hydrodynamic ion acoustic instability in isothermal tokamaks is analytically predicted and confirmed by a semi-local kinetic dispersion relation. The ion magnetic drift efficiently mitigates the ion Landau damping, and the marginally stable ion acoustic mode is strongly destabilized by trapped electron magnetic drift resonance. The quasilinear electron thermal diffusivity estimated for the instability is proportional to the 3/2 power of the electron temperature, divided by the product of the poloidal and toroidal magnetic fields. Author (CISTI)

N94-13853# Saskatchewan Univ., Saskatoon. Plasma Physics Lab.
COLLISIONAL EFFECTS OF TRAPPED ELECTRONS ON THE ANOMALOUS PARTICLE AND THERMAL PINCHES
A. Hirose May 1992 12 p
(PPL-128; CTN-93-60794) Avail: CASI HC A03/MF A01

A small collisionality parameter is shown to be sufficient to deactivate the anomalous pinch effects of particles and/or heat caused by drift-type, low frequency electrostatic modes of turbulence in tokamaks. As the parameter is increased from zero, deactivation of anomalous pinches occurs before instabilities are quenched. Therefore, a collisionless assumption remains qualitatively valid for instabilities themselves, although transport coefficients are sensitively dependent on the collisionality parameter. Author (CISTI)

N94-13854*# California Univ., San Diego, La Jolla.
NUMERICAL STUDIES OF COLLISIONLESS CURRENT LAYERS Final Technical Report
Kevin B. Quest 19 Jan. 1993 2 p Submitted for publication
(Grant NAGw-1712)
(NASA-CR-194337; NAS 1.26:194337) Avail: CASI HC A01/MF A01

The purpose of this proposal was to investigate collisionless current layers using a variety of analytic and numerical tools. The first year of the contract was dedicated to analytical studies, to the porting and adaption of codes being used in this study, and to the numerical simulation of collisionless current layers. The second year entailed the development of multi-dimensional hybrid algorithms as well as the re-examination of the problem of integro-differential equations that occur in the linear stage of plasma instabilities. Derived from text

N94-13877# Saskatchewan Univ., Saskatoon. Plasma Physics Lab.
ON MHD MODE EQUATIONS IN TOROIDAL PLASMAS
A. Hirose Jun. 1993 15 p
(PPL-139; CTN-93-60747) Avail: CASI HC A03/MF A01

It is shown that the electron density perturbation proposed by Hirose (1985) maintains the parallel electric field associated with ideal toroidal magnetohydrodynamic modes to order b, the finite ion Larmor radius parameter, while the electron density perturbation conventionally employed makes the parallel electric field much larger, on the order of the square root of b. The magnetohydrodynamic ballooning mode equation is unaffected by the degree of plasma compressibility and is given by the form known in the compressible limit. The stability boundary of the ballooning mode becomes dependent on the inverse aspect ratio, which has a stabilizing influence. Author (CISTI)

N94-13900# General Atomic Co., San Diego, CA.
DEPENDENCE OF BETA(TAU) ON PLASMA SHAPE IN D3-D
E. A. Lazarus (Oak Ridge National Lab., TN.) May 1993 4 p Presented at the 20th European Conference on Controlled Fusion and Plasma Physics, Lisbon, Portugal, 26-30 Jul. 1993
(Contracts DE-AC03-89ER-51114; DE-AC05-84OR-21400)
(DE93-015473; GA-A-21306; CONF-930720-6) Avail: CASI HC A01/MF A01

In this paper we discuss the observed variation in plasma performance with plasma shape; in particular, we shall compare single and double null diverted plasmas. The product (beta)(center dot)(tau) has been used as a figure-of-merit for comparing different toroidal magnetic configurations. Here we shall use it as the figure-of-merit for comparing differing configurations within the D3-D tokamak. DOE

N94-13908# Sandia National Labs., Albuquerque, NM.
PLASMA-ETCHING SCIENCE MEETS TECHNOLOGY IN THE MDL
K. E. Greenberg, P. A. Miller, R. Patteson, and B. K. Smith Mar. 1993 99 p
(Contract DE-AC04-76DP-00789)
(DE93-012086; SAND-93-0187) Avail: CASI HC A05/MF A02

Results from fundamental investigations of low-temperature plasma systems were used to improve chamber-to-chamber reproducibility and reliability in commercial plasma-etching equipment. The fundamental studies were performed with a GEC RF Reference Cell, a laboratory research system designed to facilitate experimental and theoretical studies of plasma systems. Results and diagnostics from the Reference Cell studies were then applied to analysis and rectification of chamber-to-chamber variability on a commercial, multichamber, plasma reactor. Pertinent results were transferred to industry. DOE

N94-13913# Argonne National Lab., IL.
HEAT AND SEED RECOVERY TECHNOLOGY PROJECT
W. M. Swift, M. Petrick, and K. Natesan 1993 14 p Presented at the MHD Contractor's Review Meeting, Pittsburgh, PA, 2-4 Feb. 1993
(Contract W-31-109-eng-38)
(DE93-009203; ANL/CMT/CP-78930; CONF-930270-1) Avail: CASI HC A03/MF A01

The objective of this work is to address technical issues related to both the MHD topping and bottoming cycles and to their integration. Design information will be obtained through modeling and experimentation. This information, together with the insults of long duration testing at DOE's Coal Fired Flow Facility (CFFF) and Component Development and Integration Facility (CDIF), can be used to reliably design the first-generation MHD retrofit plant. Work during the reporting period focused on the following tasks: (1) computer modeling of the integrated topping-cycle power train

(combustor/nozzle/channel/diffuser); (2) evaluation of materials for the bottoming steam cycle; (3) systems analysis of an MHD/CO2 cycle; and (4) the completion of a topical report on the reactivation of the ANL superconducting magnet system. Accomplishments in these areas are described briefly. DOE

N94-14024# Instituto de Pesquisas Espaciais, Sao Jose dos Campos (Brazil).

STABILITY AND CONFINEMENT PROPERTIES OF SMALL-ASPECT-RATIO TOKAMAK

Ricardo M. O. Galvao and Marisa Roberto (Universidade Estadual de Paulista, Guaratingueta, Brazil.) Nov. 1992 9 p

(INPE-5463-PRE/1771) Avail: CASI HC A02/MF A01

The stability of compact magnetic confinement configurations with axial symmetry is investigated with respect to ballooning modes using equilibrium profiles characteristic of high-beta discharges produced in large tokamaks. It is shown that average beta values (Beta factor is approximately 0.l0) are readily obtained for configurations with a substantial paramagnetic effect. The stability to trapped particle modes in the collisionless regime can also be achieved by reversal of single particle drifts caused by toroidal effects. Author (revised)

N94-14206# Saskatchewan Univ., Saskatoon. Plasma Physics Lab.

ANOMALOUS TRANSPORT DUE TO SMALL SCALE ELECTROMAGNETIC AND LARGE SCALE ELECTROSTATIC MODES IN TOKAMAKS

A. Hirose and A. I. Smolyakov (Wisconsin Univ., Madison.) Jul. 1993 16 p Presented at the Transport, Chaos, and Plasma Physics Workshop, Marseille, France, 5-9 Jul. 1993 Sponsored in part by Natural Sciences and Engineering Research Council

(Contract DE-FG02-86ER-53218)

(PPL-140; CTN-93-60858) Avail: CASI HC A03/MF A01

Stability of skin-size electromagnetic drift mode and long wavelength electrostatic ion acoustic transit mode in a low beta collisionless tokamak discharge was investigated in terms of a semi-local kinetic formulation in which kinetic resonances and nonlocal ballooning nature are implemented. Both modes are driven unstable through electron kinetic resonances under realistic discharge conditions. The ion acoustic mode persists even when ion temperature approximates electron temperature, as ion Landau damping is effectively suppressed by the ion magnetic drift provided the mode propagates in the electron diamagnetic drift. The anomalous electron thermal diffusivities estimated from the instabilities appear to explain some features of transport anomalies, including the radial profile of electron thermal diffusivity, particle pinch, isotope effect, and Bohm (rather than gyro-Bohm) scaling of the diffusivities. Author (CISTI)

N94-14293# General Atomic Co., San Diego, CA.

DIRECT ELECTRON HEATING AND CURRENT DRIVE WITH FAST WAVES IN D3-D

R. I. Pinsker, C. C. Petty, R. W. Callis, W. P. Cary, S. C. Chiu, R. L. Freeman, J. S. deGrassie, R. W. Harvey, T. C. Luce, and M. J. Mayberry et al Sep. 1992 9 p Presented at the 14th International Conference on Plasma Physics and Controlled Nuclear Fusion Research, Wurzburg, Germany, 30 Sep. - 7 Oct. 1992

(Contracts DE-AC03-89ER-51114; DE-AC05-84OR-21400; W-7405-eng-48)

(DE93-013028; GA-A-21046; CONF-9209290-9; IAEA-CN-56/E-2-4) Avail: CASI HC A02/MF A01

Experiments on the D3-D tokamak have been performed to evaluate noninductive current drive with direct electron absorption of the fast Alfven wave (FW) in the ion cyclotron range of frequencies. These experiments have employed a 2 MW 60 NM transmitter connected to a four-element toroidally phased array of loop antennas located at the outside midplane of the D3-D vacuum vessel. Efficient direct electron heating was obtained with (0, (pi), 0, (pi)) antenna phasing; H-mode confinement was obtained with direct electron absorption of the fast wave as the sole source of auxiliary heating. Current drive experiments were performed with (0, (pi)/2, (pi), 3(pi)/2) antenna phasing at fast wave power levels up to 1.2 MW. Preheating with 60 GHz ECH was used to increase the single-pass absorption of the fast wave with a directive spectrum. When the fast wave is launched in the direction that aids the inductively driven current (co-current drive), up to 40% of the 0.4 MA plasma current is sustained noninductively. Counter-current drive strongly affects the sawtoothing behavior and results in highly peaked electron temperature profiles (T(sub e)(0) approximately less than 6 keV) but much smaller driven currents. DOE

N94-14312# Lawrence Livermore National Lab., CA.

MEASURING OPACITY OF SHOCK GENERATED ARGON PLASMAS

D. Erskine, B. Rozsnyai, and M. Ross Sep. 1992 6 p Presented at the International Conference on the Physics of Strongly Coupled Plasmas, Rochester, NY, 17-21 Aug. 1992

(Contract W-7405-eng-48)

(DE93-013038; UCRL-JC-111903; CONF-9208135-5) Avail: CASI HC A02/MF A01

Plasmas are generated by passage of a strong planar shock wave through gas. Initial experiments in argon have produced plasmas with 2 eV temperature, 0.004 gm/cu cm density, and coupling parameter Gamma approximately 0.3 - 0.7. Plasmas having Gamma greater than 1 are attainable with greater initial gas pressure. The opacity of the plasma is measured versus wavelength by recording the risetime of emitted light. Initial measurements are in visible light. Preliminary results are compared with calculations using the HOPE code. DOE

N94-14342# Lawrence Livermore National Lab., CA.

IMPLICIT MULTI-FLUID SIMULATION OF INTERPENETRATING PLASMAS

P. W. Rambo and J. Denavit 3 Nov. 1992 13 p Presented at the 1992 Nuclear Explosives Code Developers Conference, Sunnyvale, CA, 2-6 Nov. 1992

(Contract W-7405-eng-48)

(DE93-013351; UCRL-JC-112302; CONF-9211128-8) Avail: CASI HC A03/MF A01

A one dimensional simulation code for interpenetrating multi-component plasmas is presented. Separate fluid equations for multiple species and the Poisson equation for the electric field are solved implicitly to allow stable accurate solutions over a wide range of the time scale parameters omega(sub p)(Delta)t and nu(sub c)(Delta)t (omega(sup p) is the plasma frequency, nu(sub c) a typical collision frequency, and (Delta)t the time step). In regions where omega(sub p)(Delta)t much less than 1 and nu(sub c)(Delta)t much less than 1, electron dynamics and space-charge effects are resolved, while in regions where omega(sub p)(Delta)t much greater than 1 and/or nu(sub c)(Delta)t much greater than 1, the ambipolar and/or diffusion models are recovered. In regions of low collisionality, particles may be created and deleted which are followed using particle and cell techniques combined with scatter and drag due to collisions with the fluids. Applications of this code to interpenetrating laser generated plasmas are presented. DOE

N94-14347# General Atomic Co., San Diego, CA.

VARIATION OF DIVERTOR PLASMA PARAMETERS WITH DIVERTOR DEPTH FOR H-MODE DISCHARGES IN D3-D

D. N. Hill (Lawrence Livermore National Lab., CA.), S. L. Allen (Lawrence Livermore National Lab., CA.), R. A. Jong (Lawrence Livermore National Lab., CA.), C. Lasnier (Lawrence Livermore National Lab., CA.), G. D. Porter (Lawrence Livermore National Lab., CA.), R. Wood (Lawrence Livermore National Lab., CA.), T. W. Petrie, N. H. Brooks, T. E. Evans, and A. W. Leonard et al May 1993 4 p Presented at the 20th European Conference on Controlled Fusion and Plasma Physics, Lisbon, Portugal, 26-30 Jul. 1993

(Contracts DE-AC03-89ER-51114; W-7405-eng-48; DE-AC04-76DP-00789; DE-FG03-89ER-51121)

(DE93-015475; GA-A-21311; CONF-930720-8) Avail: CASI HC A01/MF A01

We report here the results of experiments aimed at quantifying the advantages of increasing the X-point to target-plate distance in a diverter tokamak operating with H-mode confinement. Larger distances should lower the peak electron temperature at the target plates, thereby reducing sputtering and lowering the impurity concentration in the core plasma. When gas puffing is used to reduce the diverter heat flux, extra field-line length may increase the volume available for radiation and increase gas isolation between the core and diverter regions. DOE

N94-14349# Sandia National Labs., Albuquerque, NM.

PHYSICS OF GAS BREAKDOWN FOR ION BEAM TRANSPORT IN GAS

C. L. Olson, J. W. Poukey, D. D. Hinshelwood, D. V. Rose (JAYCOR, Vienna, VA.), R. F. Hubbard, M. Lampe, J. M. Neri, P. F. Ottinger, S. P. Slinker, and S. J. Stephanakis 1993 10 p Presented at the International Symposium on Heavy Ion Fusion, Frascati, Italy, 25-28 May 1993
(Contract DE-AC04-76DP-00789)
(DE93-015646; SAND-93-1289C; CONF-9305136-2) Avail: CASI HC A02/MF A01

Detailed analysis, experiments, and computer simulations are producing a new understanding of gas breakdown during intense ion beam transport in neutral gas. Charge neutralization of beam micro-clumps is shown to limit the net clump potentials to a non-zero value (pi)(sub min), which can lead to divergence growth and axial energy spreading. At pressures approximately greater than 1 Torr, plasma shielding should substantially reduce this effect. Current neutralization has been studied in experiments on the GAMBLE 2 accelerator. The importance of fast electrons (knockons and runaways) has been established in IPROP simulations, which are in agreement with the experiments. For light ion fusion parameters with pressures approximately greater than 1 Torr, very small net current fractions (much less than 1%) appear feasible, permitting ballistic transport in gas. Self-pinched requires higher net current fractions (greater than or equal to 2%) and preliminary IPROP code results indicate that this appears achievable for small-radius intense beams in lower pressure gases (approximately less than 1 Torr). Several self-pinched transport concepts look promising. The importance of these results for both light ion fusion and heavy ion fusion is discussed. DOE

N94-14519# General Atomic Co., San Diego, CA.
D3-D RESEARCH OPERATIONS
D. Baker, ed. May 1993 220 p
(Contract DE-AC03-89ER-51114)
(DE93-016729; GA-A-21186) Avail: CASI HC A10/MF A03

This report discusses research on the following topics: D3-D program overview; divertor and boundary research program; advanced tokamak studies; tokamak physics; operations; program development; support services; contribution to ITER physics R&D; and collaborative efforts. DOE

N94-14532# Los Alamos National Lab., NM.
REVIEW OF THE PROCYON EXPLOSIVE PULSED POWER SYSTEM
J. H. Goforth, H. Oona, and A. E. Greene et al 1993 39 p Presented at the 9th IEEE Pulsed Power Conference, Albuquerque, NM, 21-23 Jun. 1993
(Contract W-7405-eng-36)
(DE93-016562; LA-UR-93-2255; CONF-930616-10) Avail: CASI HC A03/MF A01

#he Procyon explosive pulsed power system is designed for powering plasma z-pinch experiments. It begins with a helical explosive-driven magnetic flux compression generator (MCG) for amplifying seed current from a capacitor bank into a storage inductor. One conductor element of the storage inductor is an explosively formed fuse (EFF) opening switch tailored to divert current to a plasma flow switch (PFS) in less than 3 microseconds. The PFS, in turn, delivers current to a z-pinch load. Experiments to date have concentrated on the explosive pulsed power components and PFS. This paper focuses on the results of a recent full energy MCG/EFF/PFS test. DOE

N94-14564# Lawrence Livermore National Lab., CA.
KINETIC SIMULATIONS OF ULTRA-INTENSE LASER PLASMA INTERACTIONS
W. L. Kruer and S. C. Wilks Jun. 1992 5 p Presented at the International Conference on Plasma Physics (ICPP) - Joint Conference of the 9th Kiev International Conference on Plasma Theory and the 9th International Congress on Waves and Stabilities in Plasma (ICWI), Innsbruck, Austria, 29 Jun.
(Contract W-7405-eng-48)
(DE93-014419; UCRL-JC-110953; CONF-9206359-1) Avail: CASI HC A01/MF A01

Kinetic simulations are used to investigate the interaction of an ultra-intense, small spot-size laser beam with a preformed plasma. The beam is sufficiently intense to drive the electrons relativistically and to impart a pressure in excess of hundreds of Mbars to the plasma. Key features of the interaction include generation of electrons and inward-directed ions with energies in the Mev range and strong hole boring which enhances the absorption. The simulations also show self-generated magnetic fields of order 10(exp 8) Gauss, a Rayleigh-Taylor like instability of the light-plasma interface, as well as self-focusing of the laser beam and strong Raman backscatter. DOE

N94-14567# Los Alamos National Lab., NM.
THE STATUS OF COLD FUSION
E. Storms 1993 6 p Presented at the 28th Intersociety Energy Conversion Engineering Conference, Atlanta, GA, 8-13 Aug. 1993
(Contract W-7405-eng-36)
(DE93-012731; LA-UR-93-1564; CONF-930804-1) Avail: CASI HC A02/MF A01

This report attempts to update the status of the phenomenon of cold fusion. The new field is continuing to grow as a variety of nuclear reactions are discovered to occur in a variety of chemical environments at modest temperatures. However, it must be cautioned that most scientists consider cold fusion as something akin to UFO's, ESP, and numerology. DOE

N94-14570# General Atomics Technologies Corp., San Diego, CA.
ACTIVE DENSITY CONTROL IN DIII-D H-MODE PLASMAS
M. A. Mahdavi, M. J. Schaffer, P. M. Anderson, C. B. Baxi, N. H. Brooks, K. H. Burrell, G. L. Campbell, J. S. deGrassie, T. E. Evans, and J. R. Ferron et al May 1993 4 p Presented at the 20th European Conference on Controlled Fusion and Plasma Physics, Lisbon, Portugal, 26-30 Jul. 1993
(Contracts DE-AC03-89ER-51114; W-7405-eng-48; DE-AC04-76DP-00789; DE-AC05-84OR-21400; DE-FG03-89ER-51121)
(DE93-015477; GA-A-21304; CONF-930720-9) Avail: CASI HC A01/MF A01

In this paper we present the first results of divertor cryopumping experiments in the absence of biasing on DIII-D H-mode plasmas. DOE

N94-14579# Massachusetts Inst. of Tech., Cambridge. Dept. of Physics and Plasma Fusion Center.
MEASUREMENTS OF EDGE FLUCTUATIONS BY PHASE CONTRAST IMAGING ON DIII-D
S. Coda, M. Porkolab, K. H. Burrell (General Atomic Co., San Diego, CA.), and T. N. Carlstrom (General Atomic Co., San Diego, CA.) May 1993 5 p Presented at the 20th European Conference on Controlled Fusion and Plasma Physics, Lisbon, Portugal, 26-30 Jul. 1993
(Contracts DE-AC03-89ER-51114; DE-FG02-91ER-54109)
(DE93-014018; GA-A-21316; CONF-930720-5) Avail: CASI HC A01/MF A01

A novel imaging diagnostic for the investigation of edge plasma density fluctuations was recently installed on the D3-D tokamak. The diagnostic, which is based on the Zernike phase contrast method, was developed in response to the need for spatially resolved, long wavelength fluctuation measurements. Unique features of this system include: Large bandwidth (100 MHz), high sensitivity ((tilde n)(sub e) is approximately equal to 10(exp 9) cm(exp -3)), and absolute calibration capability. Initial results are presented on the fluctuation suppression at the L- to H-mode transition and on the bursts of turbulent activity which occur during ELM's. DOE

N94-14583# General Atomic Co., San Diego, CA.
THE ROLE OF ELECTRIC FIELD SHEAR STABILIZATION OF TURBULENCE IN THE H-MODE TO VH-MODE TRANSITION IN D3-D
K. H. Burrell, T. H. Osborne, R. J. Groebner, and C. L. Rettig (California Univ., Los Angeles.) May 1993 4 p Presented at the 20th European Conference on Controlled Fusion and Plasma Physics, Lisbon, Portugal, 26-30 Jul. 1993
(Contract DE-AC03-89ER-51114)
(DE93-015474; GA-A-21308; CONF-930720-7) Avail: CASI HC A01/MF A01

VH-mode plasmas exhibit energy confinement times up to 2.4 times the DIII-D/JET H-mode scaling relation and up to 3.9 times the value given by ITER89-P L-mode scaling. If this confinement improvement can be exploited in reactor plasmas, smaller prototype reactors with significantly lower unit cost can be produced. Accordingly, understanding and optimizing the confinement improvement is of significant interest. One of the possible explanations for this bulk confinement improvement is stabilization of turbulence by shear in the radial electric field, similar to the present

explanation for the confinement improvement at the extreme plasma edge at the L to H transition. Preliminary measurements have shown that the region of the plasma where the electric field gradient is steepest broadens when the plasma goes from H-mode to V-mode. More recent measurements have confirmed this broadening and have shown that the change in the electric field gradient occurs prior to the change in the thermal transport. In addition, transport analysis shows that the electric field shear increases in the same region between magnetic flux coordinate rho = 0.6 and 0.9 where the local thermal transport decreases. Furthermore, far infrared (FIR) scattering measurements have detected density fluctuations in the region around rho = 0.8 which could be responsible for enhanced transport and which disappear at the time that the electric field shear increases. These fluctuations appear as bursts of density fluctuations in the 0.5 to 1.5 MHz range. The time between bursts increases as the electric field shear increases. Once these bursts disappear, the major change in confinement takes place in most discharges. When isolated bursts occur, the heat and angular momentum pulse connected with the burst are detectable on the plasma profile diagnostics. Derived from text

N94-14590# Lawrence Livermore National Lab., CA.
IMPEDANCE-POWER EFFECTS ON PLASMA POLYMER SURFACE FINISH USING A HELICAL RESONATOR DISCHARGE
R. Brusasco, S. W. Ferguson, and R. Stever Dec. 1992 8 p Presented at the 205th American Chemical Society National Meeting, Denver, CO, 28 Mar. - 2 Apr. 1993
(Contract W-7405-eng-48)
(DE93-016454; UCRL-JC-112361; CONF-930304-30) Avail: CASI HC A02/MF A01

Plasma polymerized organic coatings are used in the fabrication of targets for experiments in the Inertial Confinement Fusion (ICF) program at Lawrence Livermore National Laboratory. The authors are performing experiments to understand the process conditions leading to the preparation of smooth (approx. 100 Angstroms) plasma polymer surfaces while maintaining the highest deposition rate possible. It had been reported by Howling et al., that the formation of particulate matter in the deposition of silicon by the plasma reaction of silane affected the plasma impedance. This suggested that experiments designed to examine the correlation of surface texture with plasma impedance would be of interest. Furthermore, it is possible that an impedance change may cause a change in the power coupling efficiency from the transmitter to the plasma. Preliminary work in the authors laboratory indicated that the reactor temperature influenced the surface texture. The focus of this paper is to carefully examine the effects of reactor temperature on the surface texture of the plasma polymer, ensuring constant reactor conditions especially with respect to RF power. DOE

N94-14770 Oak Ridge National Lab., TN.
DESIGN OF THE ION CYCLOTRON SYSTEM FOR TPX
D. Swain, S. Shipley, J. Yugo, R. Goulding, D. Batchelor, D. Stallings, and E. Fredd (Princeton Univ., NJ.) 1993 4 p Presented at the 10th Topical Conference on Radio Frequency Power in Plasmas, Boston, MA, 1-3 Apr. 1993 Limited Reproducibility: More than 20% of this document may be affected by microfiche quality
(Contract DE-AC05-84OR-21400)
(DE93-012961; CONF-9304112-9) Avail: CASI HC A01

The TPX experiment will operate for very long pulse times (greater than or equal to 1000 s) and will require current drive of several different types to explore the advanced physics operating modes as one of its main missions. Fast wave current drive (FWCD) using ion cyclotron waves in the 40-80 MHz range will be used as one of the main current-drive mechanisms. For initial operation, 8 MW of RF will be supplied, along with 8 MW of neutral beams and 1.5 MW of lower hybrid power. The ion cyclotron (IC) system is a major part of the TPX heating and current drive system. The IC system must: supply 8 MW of power through two main horizontal ports; be upgradable to provide up to 12 MW of RF power through two ports; operate, for 1000-s pulses every 75 min; drive current using FWCD with high reliability; be bakeable to 350(degree)C for cleaning; and incorporate shielding to attenuate the neutron and gamma flux from DD operation so that hands-on maintenance can be performed exterior to the vacuum vessel. The system will consist of four modified FMIT power units that will be upgraded to deliver 2 MW each to the plasma. Two antennas, each with six current straps, will be located in adjacent ports. A sophisticated matching system is needed to provide experimental flexibility and reliability. DOE

N94-14865# Lawrence Livermore National Lab., CA.
THE 8 TO 11 keV X RAY SOURCES FOR IMAGING AND ABSORPTION EXPERIMENTS
J. D. Molitoris, D. W. Phillion, A. L. Osterheld, R. E. Stewart, and S. D. Rothman (Atomic Weapons Research Establishment, Aldermaston, England.) 30 Nov. 1992 17 p Presented at the 9th Topical Conference on High-Temperature Plasma Diagnostics, Santa Fe, NM, 15-19 Mar. 1992
(Contract W-7405-eng-48)
(DE93-015973; UCRL-JC-112307; CONF-920362-48) Avail: CASI HC A03/MF A01

We have measured the 8 to 11 keV emission spectra from plasmas produced by impinging 0.53 micron 100 and 200 ps FWHM Gaussian laser pulses on targets of different materials. The experimental spectra from W and Zn are identified by comparison with local thermodynamic equilibrium plasma emission calculations. DOE

N94-14874 Columbia Univ., New York, NY.
ANOMALOUS ION TRANSPORT AND FEEDBACK CONTROL
1993 25 p Limited Reproducibility: More than 20% of this document may be affected by microfiche quality
(Contract DE-FG02-87ER-53257)
(DE93-018324; DOE/ER-53257/6) Avail: CASI HC A03

The slab branch of the ITG mode was produced by a DC ion acceleration heating scheme and definitively identified in CLM under the previous DOE grant. A transit-time RF heating scheme was used to produce a more Maxwellian ion population to produce and identify a more predictable slab ITG mode. These experiments are partly based on some theoretical work on the substantial effects of anisotropy in eta(sub i) on the slab mode. The progress under the present DOE grant is described. DOE

N94-14894# Lawrence Livermore National Lab., CA.
TIME RESOLVED MEASUREMENT OF ELECTRON TEMPERATURES OF EXPLODING FOIL X RAY LASER PLASMAS
B. K. F. Young, A. L. Osterheld, G. M. Shimkaveg, R. L. Shepherd, R. S. Walling, W. H. Goldstein, and R. E. Stewart 14 Apr. 1993 15 p Presented at the Radiative Properties of Hot Dense Matter Conference, Santa Barbara, CA, 2-6 Nov. 1992
(Contract W-7405-eng-48)
(DE93-017161; UCRL-JC-111844; CONF-9211211-2) Avail: CASI HC A03/MF A01

The authors present results of recent experiments to measure the plasma conditions present in a neon-like x-ray laser plasma. They measure the time-resolved K-shell emission spectra of low Z tracer material doped into a yttrium exploding foil target. They determine the plasma conditions by analyzing the K-shell emission spectra assuming a quasi-steady state approximation. Two-dimensional LASNEX hydrodynamics simulations are in reasonable agreement with these time-resolved electron temperatures. DOE

76 SOLID-STATE PHYSICS

Includes superconductivity.

For related information, see also *33 Electronics and Electrical Engineering* and *36 Lasers and Masers.*

N94-12796*# Alabama Univ., Huntsville. Center for Microgravity and Materials Research.
BREADBOARD ACTIVITIES FOR ADVANCED PROTEIN CRYSTAL GROWTH Semiannual Report No. 2, 3 Feb. - 3 Aug. 1993
Franz Rosenberger and Michael Banish 1993 2 p
(Grant NAG8-931)
(NASA-CR-193559; NAS 1.26:193559) Avail: CASI HC A01/MF A01

The proposed work entails the design, assembly, testing, and delivery of a turn-key system for the semi-automated determination of protein solubilities as a function of temperature. The system will utilize optical scintillation as a means of detecting and monitoring nucleation and crystallite growth during temperature lowering (or raising, with retrograde solubility

systems). The deliverables of this contract are: (1) turn-key scintillation system for the semi-automatic determination of protein solubilities as a function of temperature, (2) instructions and software package for the operation of the scintillation system, and (3) one semi-annual and one final report including the test results obtained for ovostatin with the above scintillation system. Author (revised)

N94-12813# Sandia National Labs., Albuquerque, NM.
CRYSTALLOGRAPHIC PHASE IDENTIFICATION IN THE SCANNING ELECTRON MICROSCOPE: BACKSCATTERED ELECTRON KIKUCHI PATTERNS
J. R. Michael and R. P. Goehner 1993 3 p Presented at the Annual Meeting of the Electron Microscopy Society of America, Cincinnati, OH, 1-6 Aug. 1993
(Contract DE-AC04-76DP-00789)
(DE93-011574; SAND-93-0813C; CONF-930822-2) Avail: CASI HC A01/MF A01

Use of charge coupled device-based detector for acquisition of high-quality backscattered electron Kikuchi patterns (BEKP) allows on-line crystallographic phase identification in the SEM. Phase identification through combined BEKP and energy dispersive x-ray spectrometry is demonstrated using Ru oxide thin films on Si, which were identified as tetragonal RuO(sub 2). DOE

N94-12818# Oak Ridge National Lab., TN.
FLUX-PINNING RELATED DEFECT STRUCTURES IN MELT-PROCESSED YBa2Cu3O(7-x)
Z. L. Wang, R. Kontra, A. Goyal, D. M. Kroeger, and L. F. Allard 1993 3 p Presented at the Annual Meeting of the Electron Microscopy Society of America, Cincinnati, OH, 1-6 Aug. 1993
(Contract DE-AC05-84OR-21400)
(DE93-012759; CONF-930822-5) Avail: CASI HC A01/MF A01

High resolution transmission electron microscopy (HRTEM) was used to observe defects in Y123. Stacking faults lying parallel to the (001) basal plane are observed near the Y211/Y123 (Y2BaCu5O/YBa2Cu3O(7-delta)) interfaces in Y123. These stacking faults are produced by either excess single Cu-O layers or double Cu-O and Y-O layers. Y enrichment and Ba depletion were observed near the Y211/Y123 interface; this is consistent with dissolution of trapped Y211. Such diffusion effects and stress due to lattice mismatch at Y211/Y123 interfaces may be the mechanisms for generating stacking faults around the Y211 particles in the Y123 matrix. A new type of defect with displacement vector 1/6(032) or 1/6(302) was also observed. DOE

N94-12828 Academy of Sciences (USSR), Leningrad.
ON THE NEUTRON EDM SEARCH IN THE LAUE DIFFRACTION BY THE CRYSTAL WITHOUT A CENTRE OF SYMMETRY
V. V. Fedorov, V. V. Voronin, and E. G. Lapin 1991 30 p Limited Reproducibility: More than 20% of this document may be affected by microfiche quality
(DE93-622971; LIYaF-1644) Avail: CASI HC A03 (US Sales Only)

A new method of neutron electric dipole moment (EDM) searching is proposed. It is based on the spin dependence of the pendelous phase of a neutron diffracted by the noncentrosymmetric crystal. A two-crystal set up is proposed and analyzed to get the big enough luminosity. With the strong interplanar electric field of the crystal and the sufficiently long time of the neutron passage through the crystals for the Bragg angles close to (pi)/2 it makes possible to exceed the sensitivity achieved with the ultra cold neutron method. DOE

N94-12873*# Alabama Univ., Huntsville. Materials Processing Lab.
REDUCE FLUID EXPERIMENT SYSTEM FLIGHT DATA FROM IML-1 Final Report
Gary L. Workman, Andrea Passeur, and Sabrina Harper 28 Aug. 1993 39 p
(Contract NAS8-38609)
(NASA-CR-193835; NAS 1.26:193835) Avail: CASI HC A03/MF A01

Processing and data reduction of holographic images from Spacelab presents some interesting challenges in determining the effects of microgravity on crystal growth processes. Evaluation of several processing techniques, including the Computerized Holographic Image Processing System and the Software Development Package (SDP151) will provide fundamental information for holographic and schlieren analysis of the space flight data. Author (revised)

N94-12893# Australian Nuclear Science and Technology Organization, Lucas Heights.
LIQUID PHASE EPITAXY OF GALLIUM ARSENIDE: A REVIEW
D. Alexiev, M. Edmondson, K. S. A. Butcher (MacQuarie Univ., North Ryde, Australia.), and T. Tansley (MacQuarie Univ., North Ryde, Australia.) Jul. 1992 20 p
(DE93-622212; ANSTO-E-702) Avail: CASI HC A03/MF A01 (US Sales Only)

Liquid phase epitaxy of gallium arsenide has been investigated intensively from the late 1960's to the present and has now a special place in the manufacture of wide band, compound semiconductor radiation detectors. Although this particular process appears to have gained prominence in the last three decades, the authors point out that its origins reach back to 1836 when Frankenheim made his first observations. A brief review is presented from a semiconductor applications point of view on how this subject developed. DOE

N94-12934*# Fairchild Technical Support Center, Huntsville, AL.
ADVANCED PROTEIN CRYSTAL GROWTH PROGRAMMATIC SENSITIVITY STUDY Final Report
Jul. 1992 130 p
(Contract NAS8-39352)
(NASA-CR-193827; NAS 1.26:193827) Avail: CASI HC A07/MF A02

The purpose of this study is to define the costs of various APCG (Advanced Protein Crystal Growth) program options and to determine the parameters which, if changed, impact the costs and goals of the programs and to what extent. This was accomplished by developing and evaluating several alternate programmatic scenarios for the microgravity Advanced Protein Crystal Growth program transitioning from the present shuttle activity to the man tended Space Station to the permanently manned Space Station. These scenarios include selected variations in such sensitivity parameters as development and operational costs, schedules, technology issues, and crystal growth methods. This final report provides information that will aid in planning the Advanced Protein Crystal Growth Program. Author (revised)

N94-13003# North Carolina State Univ., Raleigh. Dept. of Materials Science and Engineering.
THE STUDY OF STRUCTURE-PROCESSING-PROPERTY RELATIONS IN COPPER OXIDE BASED HIGH (Tc) SUPERCONDUCTORS
A. I. Kingon Jun. 1993 6 p
(Contract DE-FG05-88ER-45359)
(DE93-015066; DOE/ER-45359/2) Avail: CASI HC A02/MF A01

The objective of this project is the investigation of critical current limiting processes in bulk superconductors. Since the grain boundaries play a key role here, we focus on the electrical characterization of single grain boundaries. Electrical contact to thin polished sections is established with thermosonic wire bonding. Laser cutting is used to isolate a single grain boundary. Results on YBa2Cu3O(x) showed that two different types of grain boundaries are present. Most grain boundaries showed current voltage characteristics typical for flux pinning effect and little or no change in low magnetic fields. However, the Josephson effect could also be found in some grain boundaries exhibiting a remarkable decrease of I(sub c) in low magnetic fields. Both types could be found in the same sample. Additionally we are working on Bi2Sr2CaCu2O(x) thick films grown on silver foil or MgO substrates. The films showed metallic behavior and T(sub c) = 80K. Preliminary results showed that the grain boundaries are of the flux pinning type. DOE

N94-13005# Purdue Univ., West Lafayette, IN. School of Materials Engineering.
STUDY OF MULTICOMPONENT DIFFUSION AND TRANSPORT PHENOMENA
1993 21 p
(Contract DE-FG02-84ER-45133)
(DE93-015095; DOE/ER-45133/5) Avail: CASI HC A03/MF A01

The major activities in this period concern the following topics: the percolation threshold in electronic conduction in (beta)-alumina type solid

electrolytes, mixed alkali effects in ion conducting binary glasses, chemical diffusion problems, semiconductors, and relaxation process in diffusion. The last topic constitutes the bulk of the recent progress. DOE

N94-13009# Oak Ridge National Lab., TN.
DETERMINATION OF CHANNELING PERSPECTIVES FOR COMPLEX CRYSTAL STRUCTURES
W. R. Allen Mar. 1993 27 p
(Contract DE-AC05-84OR-21400)
(DE93-012872; ORNL/TM-12170) Avail: CASI HC A03/MF A01

Specification of the atomic arrangement for axes and planes of high symmetry is essential for crystal alignment using Rutherford backscattering and for studies of the lattice location of impurities in single crystals. By rotation of an inscribed orthogonal coordinate system, a visual image for a given perspective of a crystal structure can be specified. Knowledge of the atomic arrangement permits qualitative channeling perspectives to be visualized and calculation of continuum potentials for channeling. Channeling angular-yield profiles can then be analytically modeled and, subsequently, shadowing by host atoms of positions within the unit cell predicted. Software to calculate transformed atom positions for a channeling perspective in a single crystal are described and illustrated for the spinel crystal structure. DOE

N94-13010# Lawrence Livermore National Lab., CA.
GRAIN-BOUNDARY ELECTRONIC STATES BY MULTIPLE-SCATTERING THEORY
E. C. Sowa and A. Gonis Aug. 1992 6 p Presented at the 2nd International Conference and Exhibition on Computer Applications to Materials and Molecular Science and Engineering, Yokohama, Japan, 22-25 Sep. 1992
(Contract W-7405-eng-48)
(DE93-013198; UCRL-JC-109651; CONF-920927-4) Avail: CASI HC A02/MF A01

In order to calculate the electronic structure of grain boundaries, it is necessary to treat properly the lack of translational symmetry in directions perpendicular to the interface between two half solids. This treatment can be provided on the basis of multiple-scattering theory. We have developed a formalism which allows the exact treatment of the Schroedinger equation for systems with reduced translational symmetry, yielding solutions which in the converged limit satisfy the proper boundary conditions imposed by the geometry of the system. We report the first application of this real-space multiple-scattering theory to the calculation of the local density of states (DOS) at metallic grain boundaries. We exhibit and compare local DOS's at selected sites for both unrelaxed and relaxed (Sigma)5 (100) 36.9 degrees twist and (Sigma)5 (310) tilt grain boundaries in Cu, where the atomic coordinates of the relaxed configurations were obtained with the Embedded Atom Method. We discuss briefly the mainfeatures of our method, and give our plans for future work. DOE

N94-13012# Oak Ridge National Lab., TN.
LATTICE SITE OF HELIUM IMPLANTED IN Si AND DIAMOND
W. R. Allen 1992 10 p Presented at the 16th Material Research Society International Symposium on the Scientific Basis for Nuclear Waste Management Fall Meeting, Boston, MA, 30 Nov. - 5 Dec. 1992
(Contract DE-AC05-84OR-21400)
(DE93-015365; CONF-921101-130) Avail: CASI HC A02/MF A01

Single crystals of silicon and diamond were implanted at 300K with 70 keV He-3. Ion channeling analyses were executed by application of Rutherford backscattering spectrometry and nuclear reaction analysis. Helium exhibits a non-random lattice site in the channeling angular distributions for silicon and diamond. A major fraction of the implanted He-3 was qualitatively identified to be near to the tetrahedral interstice in both materials. However, greater occupation of tetrahedral interstices was noted in Si. DOE

N94-13020# Stanford Linear Accelerator Center, CA.
PROCEEDINGS OF THE WORKSHOP ON APPLICATIONS OF SYNCHROTRON RADIATION TO TRACE IMPURITY ANALYSIS FOR ADVANCED SILICON PROCESSING
S. Laderman (Hewlett-Packard Co., Palo Alto, CA.) and P. Pianetta Mar. 1993 159 p Workshop held in Stanford, CA, 21 Oct. 1992
(Contract DE-AC03-76SF-00515)
(DE93-013389; SLAC-415; SLAC/SSRL-0009; CONF-9210277) Avail: CASI HC A08/MF A02

Wafer surface trace impurity analysis is essential for development of competitive Si circuit technologies. Today's grazing incidence x-ray fluorescence techniques with rotating anodes fall short of requirements for the future. Hewlett Packard/Toshiba experiments indicate that with second generation synchrotron sources such as SSRL, the techniques can be extended sufficiently to meet important needs of the leading edge Si circuit industry through nearly all of the 1990's. This workshop was held to identify people interested in use of synchrotron radiation-based methods and to document needs and concerns for further development. Viewgraphs are included for the following presentations: microcontamination needs in silicon technology, analytical methods for wafer surface contamination, trace impurity analysis of liquid drops using synchrotron radiation, TRXRF using synchrotron sources, potential role of synchrotron radiation TRXRF in Si process R&D, potential development of synchrotron radiation facilities, and identification of goals, needs, and concerns. DOE

N94-13037# Michigan Univ., Ann Arbor. Dept. of Electrical Engineering and Computer Science.
NONLINEAR LASER SPECTROSCOPY STUDIES OF SEMICONDUCTOR HETEROSTRUCTURES Final Report, 15 Dec. 1989 - 14 Jan. 1993
Duncan Steel 14 Jan. 1993 81 p
(Grant AF-AFOSR-0100-90)
(AD-A265728; AFOSR-93-0397TR) Avail: CASI HC A05/MF A01

Research progress in quantum optoelectronics has dominated much of the recent literature in semiconductors because of the new physical phenomena which can be observed and because of the potential for new smaller and higher speed devices of importance to communications, computing, and other high information density applications. Much of the work has focused on 3-5 compounds because it is believed these materials may provide improved performance over silicon. In addition since they are a direct band gap semiconductor, there are also potential optical applications. Under this AFOSR grant, our laboratory has been involved in the general area of the study of the optical physics of semiconductors. These studies have provided new insight into the nature of optical properties as well as material properties. The work has emphasized the application of coherent nonlinear laser spectroscopy methods in the study of bulk GaAs and GaAs/AlGaAs quantum wells. This work is based on frequency and time domain four-wave mixing techniques, many of which were developed by our group under earlier AFOSR support. These experiments are enabling us to measure many properties of these systems, as well as showing that in heterostructures, the effects of disorder must be included in order to provide a complete understanding. DTIC

N94-13102# Brookhaven National Lab., Upton, NY.
CANTED MAGNETIC MOMENTS AT THE Gd(0001) SURFACE
Dong-Gi Li (Syracuse Univ., NY.), Jian-Di Zhang (Syracuse Univ., NY.), P. A. Dowben (Syracuse Univ., NY.), K. Garrison, P. D. Johnson, H. Tang (California Univ., Irvine.), T. G. Walker (California Univ., Irvine.), and H. Hopster (California Univ., Irvine.) 1993 6 p Presented at the Spring Meeting of the Materials Research Society, San Francisco, CA, 12-16 Apr. 1993
(Contract DE-AC02-76CH-00016)
(DE93-014327; BNL-48954; CONF-930405-14) Avail: CASI HC A02/MF A01

With spin polarized electron spectroscopies, the authors have investigated ordered Gd(0001) films deposited on W(110). The photoemission features of the gadolinium 5d surface state, the 4f levels, and the background exhibit considerable spin polarization along the same direction in the plane of the film, indicative of ferromagnetic coupling between the surface and the bulk. The 4f spin polarized photoemission data provides strong evidence that the surface 4f polarization differs from the bulk 4f polarization for Gd(0001). The temperature dependent measurements with spin polarized secondary electron spectroscopy conclusively establishes that the surface of clean Gd(0001) possesses a perpendicular polarization component which persists to an enhanced surface Curie temperature. Small amounts of contamination at the surface result in the disappearance of the perpendicular component and, therefore, a more perfect ferromagnetic coupling between the surface and the bulk. DOE

N94-13136# Lawrence Livermore National Lab., CA.
ATOMIC STRUCTURE OF THE 310 TWIN IN NIOBIUM: THEORETICAL PREDICTIONS AND COMPARISON WITH EXPERIMENTAL OBSERVATION
G. H. Campbell, W. E. King, S. M. Foiles, and M. Ruehle Nov. 1992 8 p Presented at the 16th Material Research Society International Symposium on the Scientific Basis for Nuclear Waste Management Fall Meeting, Boston, MA, 30 Nov. - 5 Dec. 1992
(Contract W-7405-eng-48)
(DE93-013421; UCRL-JC-112067; CONF-921101-120) Avail: CASI HC A02/MF A01

High-resolution transmission electron microscopy (HREM) has been used to characterize the atomic structure of the symmetric 36.9(degrees) tilt grain boundary with zone (001) tilt axes forming a twin about (310) in Nb. The projected structure was imaged along two different directions in the plane of the boundary and was compared to model structures through high-resolution image simulation. The atomic structure of this (Sigma)-5 boundary was predicted with atomistic simulations using interatomic potentials derived from the Embedded Atom Method (EAM), Finnis-Sinclair (FS), and the Model Generalized Pseudopotential Theory (MGPT). The EAM and FS predicted structures with translations of the adjacent crystals which break mirror symmetry. The MGPT predicted one stable structure with mirror symmetry. The atomic structure of the (310) twin in Nb was found by HREM to be mirror symmetric. These findings indicate that the angular dependent interactions modeled in the MGPT are important for determining the grain boundary structures of bcc transition metals. DOE

N94-13150# Brookhaven National Lab., Upton, NY.
CRYSTALLOGRAPHIC AND METALLURGICAL CHARACTERIZATION OF RADIATION DETECTOR GRADE CADMIUM TELLURIDE MATERIALS
C. J. Johnson, E. E. Eissler, S. E. Cameron, Y. Kong, S. Fan, S. Jovanovic, and K. G. Lynn 1993 30 p Presented at the Spring Meeting of the Materials Research Society, San Francisco, CA, 12-16 Apr. 1993
(Contract DE-AC02-76CH-00016)
(DE93-014335; BNL-48960; CONF-930405-11) Avail: CASI HC A03/MF A01

Radiation detector grade CdTe crystals are characterized by several crystallographic and metallurgical techniques including infrared microscopy, dislocation etch pitting, and x-ray diffraction. Results are presented for a set of 50 detectors fabricated from an ingot produced by the High Pressure Bridgman method. Data on the temperature dependence of leakage current and pulse height analysis are presented, along with measurements of room temperature charge transport properties. Attempts to relate crystal structure to detector performance are discussed. DOE

N94-13152# Princeton Univ., NJ.
TRANSPORT PROPERTIES OF DISORDERED POROUS MEDIA FROM THE MICROSTRUCTURE
1993 9 p
(Contract DE-FG02-92ER-14275)
(DE93-016065; DOE/ER-14275/1) Avail: CASI HC A02/MF A01

Progress was made in 4 general areas: quantitative characterization of microstructure via n-point distribution functions; determination of bounds on effective properties that depend on these n-point functions (conductivity, NMR, permeability); derivation of cross- property relations; and development of efficient first-passage time algorithms (Brownian-motion simulations) to compute effective diffusion properties. DOE

N94-13213# Atomic Energy Commission, Damascus (Syria).
ANNEALING STUDY OF MAIN ELECTRON IRRADIATION-INDUCED DEFECTS (H4 AND H5) IN P-InP USING DLTS TECHNIQUE
B. Massarani, F. Awad, and M. Kaaka Dec. 1992 35 p In ARABIC
(DE93-623204; AECS-PH/FRSR-62) Avail: CASI HC A03/MF A01 (US Sales Only)

Thermal annealing of the two hole traps H(sub 4) and H(sub 5) in room-temperature electron-irradiated In P Schottky diodes was investigated. Electron-irradiation energy ranging between 0.15 and 1.5 MeV with doses ranging between 5 x 10(sup 14) and 10(sup 16) e/cm(sup 2). DLTS technique with double-phase detector was used in this study. Contrary to what is generally admitted, we found that H(sub 5) anneals out at about 150 C(sup o) with an activation energy of 1 eV. We have shown that H(sub 4) is a complex defect having two components that we could resolve. While the first one, having lower emission cross section and higher capture cross section with (Delta)E = 0.37 eV anneals out at about 110 C(sup o). The other component, with (Delta)E = 0.50 eV is thermally stable even above 170 C(sup o). DOE

N94-13226# Flinders Univ., Adelaide (Australia). Electronic Structure of Materials Center.
CALCULATION OF ELECTRON-LITHIUM SCATTERING USING THE COUPLED-CHANNEL OPTICAL METHOD
I. Bray, D. V. Fursa, and I. E. McCarthy Aug. 1992 24 p
(DE93-623049; ESM-48) Avail: CASI HC A03/MF A01 (US Sales Only)

This paper presents calculations of spin asymmetries for the elastic and 2(sup 2)P channels, differential and integrated cross sections for the elastic through to 4(sup 2)F channels, and total cross sections of electrons scattering on lithium at a range of energies from 1 to 200 eV. Very good agreement is found with available measurements at all energies, which for the spin asymmetries may only be achieved by the inclusion of coupling of the low-lying target states to the target continuum. DOE

N94-13228# International Centre for Theoretical Physics, Trieste (Italy).
COMMENT OF PARAMETER EXCITATION OF ALFVEN AND HELIICON WAVES IN A MAGNETOACTIVE COMPENSATED SEMICONDUCTOR BY MICROWAVE RADIATION
V. Skarka and C. Y. Chen Feb. 1993 4 p
(DE93-623203; IC-93/36) Avail: CASI HC A01/MF A01 (US Sales Only)

The solution of the linearized kinetic equation used by Mamun et al (Phys. Rev. B, 1991, 44, 8685) is incorrect since it is derived using an unjustified approximation which conflicts with the ordering given in the paper itself. This solution, in contrast with the standard gyrokinetic one, exhibits no features essential for a magnetized plasma. Therefore, it cannot be employed as a basis for the construction of the nonlinear response as well as for obtaining the linear dispersion relation. DOE

N94-13291*# MCAT Inst., San Jose, CA.
COLORIMETRIC QUALIFICATION OF SHEAR SENSITIVE LIQUID CRYSTAL COATINGS
Joseph J. Muratore, Jr. Aug. 1993 26 p Original contains color illustrations
(Contract NCC2-704)
(NASA-CR-194126; NAS 1.26:194126; MCAT-93-17) Avail: CASI HC A03/MF A01; 6 functional color pages

The work that has been done to date on the Shear Sensitive Liquid Crystal Project demonstrated that cholesteric liquid crystal coatings respond to both the direction and magnitude of a shearing force. The response of the coating is to selectively scatter incident white light into a spectrum of colors. Discernible color changes at a fixed angle of observation and illumination are the result of an applied shear stress. The intention was to be able to convert these observable color patterns from a flow visualization technique into a quantitative tool. One of the earlier intentions was to be able to use liquid crystals in dynamic flow fields. This was assumed possible because liquid crystals had made it possible to visualize transients in surface shear forces. Although the transients were visualized by color changes to an order one micro second, the time response of a coating to align to a shearing force is dependent on the magnitude of the change between its initial and final states. Unfortunately, the response is not instantaneous. It is for this reason any future attempt at quantifying the magnitude and directions of a shearing force are limited to surface shear stress vector fields in three dimensional steady state flows. This limitation does not significantly detract from the utility of liquid crystal coatings. The measurement of skin friction in the study of transition on wings, prediction of drag forces, performance assessment, and the investigation of boundary layer behavior is of great importance in aerodynamics. There exist numerous examples of techniques for the measurement of surface shear stress. Most techniques require arduous calibrations and necessitate extensive preparation of the receiving surfaces. However, the main draw back of instruments such as Preston tubes, hot films, buried wire gages, and floating element balances is that they only provide a point measurement. The advantages of capturing global shear data would be appreciable when compared with conventional point measurement sensors. It has yet to be

determined if a repeatable correlation exists between the measured color of a liquid crystal coating and the magnitude/directional components of a shear vector imposed onto it. Author (revised)

N94-13359 Harvard Univ., Cambridge, MA. Div. of Applied Sciences.
MEASUREMENTS ON TWO-DIMENSIONAL ARRAYS OF MESOSCOPIC JOSEPHSON JUNCTIONS Technical Report
Thomas S. Tighe Feb. 1993 190 p Limited Reproducibility: More than 20% of this document may be affected by microfiche quality
(Contracts N00014-89-J-1023; N00014-89-J-1565)
(AD-A265129; TR-35) Avail: CASI HC A09

Measurements on two-dimensional arrays of Josephson junctions with junction sizes down to 60 nm by 60 nm are reported. Due to their small size, these junctions belong to the class of mesoscopic systems: they show behavior which reveals the underlying quantum mechanical properties. Two energies characterize the junctions, the Josephson energy E(sub j) and the charging energy E(sub c). Arrays in which E(sub j) much greater than E(sub c) are superconducting around zero bias and at zero temperature, while arrays in which E(sub c) much greater than E(sub j), called charging arrays, are instead insulating. This is the basis of the superconductor-to-insulator (S-I) transition. Author (DTIC)

N94-13373# Georgia Inst. of Tech., Atlanta. School of Physics.
METASTABLE ENHANCEMENT OF C(+) AND O(+) CAPTURE REACTIONS
E. W. Thomas 31 Jul. 1992 7 p
(Contract DE-FG05-87ER-13745)
(DE93-015075; DOE/ER-13745/3) Avail: CASI HC A02/MF A01

The project is devoted to the study of charge transfer neutralization of carbon and oxygen ions in H and H2 gases at energies from 10 to 500 eV. A major motivation was to provide cross section data to support analysis of edge plasmas in Tokamak Fusion devices. The first objective was to measure cross sections for metastable, excited, singly charged ions separately from the cross sections for ground state ions. Previously published values are confusing because the beams used included unknown fractions of metastables, and these metastables have cross sections that are greatly different from the ground states. The program was fully accomplished, and metastable cross sections were found to be over an order of magnitude greater than ones for the ground state. The existing discrepancies in the literature were resolved. Considerable effort was devoted to the design and operation of ion source configurations where the metastable content of the ion beam was known. Subsequently, study progressed to the neutralization of multiply charged C and 0 ions in the same targets. First there has been a need to develop ion sources which can produce useful beams of multiply charged species. This has now been accomplished. The intent is to use these sources for the measurement of cross sections with an attempt to differentiate between the behavior of ground and metastably excited species. DOE

N94-13405# Lawrence Livermore National Lab., CA.
BARIUM FLUORIDE RESEARCH AND DEVELOPMENT AT LAWRENCE LIVERMORE NATIONAL LABORATORY
C. R. Wuest, B. A. Fuchs, and W. Kway 24 Jul. 1992 127 p
(Contract W-7405-eng-48)
(DE93-014682; UCRL-ID-113834) Avail: CASI HC A07/MF A02

Lawrence Livermore National Laboratory (LLNL) has been asked to provide R&D on new methods of barium fluoride (BaF2) crystal surface preparation, as well as optical coating methods to improve the efficiency of transport of scintillation light through the crystal to the photodetector. The goal of the R&D is to identify a method (or methods) for preparing the surface to eliminate the amorphous layer that has been found to be a product of the surface preparation techniques used when the crystals are manufactured in China and provide a crystalline surface free from oxygen and other contamination, with suitable flatness for optical coating. Ultraviolet reflective coatings have been identified that are suitable for the wavelengths of the scintillation light (220 nm peak). The coating consists of a layer of aluminum with a magnesium fluoride over-layer. This coating can be applied in a uniform layer or in a graded layer, with reflectance varying as a function of position. It is ultimately desired that the UV coating be applied with graded reflectance to linearize the response of the crystal along its length. DOE

N94-13444*# Universities Space Research Association, Huntsville, AL.
CRYSTAL GROWTH OF ZnSe AND RELATED TERNARY COMPOUND SEMICONDUCTORS BY PHYSICAL VAPOR TRANSPORT Final Report
Ching-Hua Su 23 Aug. 1993 41 p
(Contract NAS8-39718)
(NASA-CR-193834; NAS 1.26:193834) Avail: CASI HC A03/MF A01

The materials to be investigated are ZnSe and related ternary semiconducting alloys (e.g., ZnS(x)Se(1-x), ZnTe(x)Se(1-x), and Zn(1-x)Cd(x)Se). These materials are useful for opto-electronic applications such as high efficient light emitting diodes and low power threshold and high temperature lasers in the blue-green region of the visible spectrum. The recent demonstration of its optical bistable properties also makes ZnSe a possible candidate material for digital optical computers. The investigation consists of an extensive ground-based study followed by flight experimentation, and involves both experimental and theoretical work. The objectives of the ground-based work are to establish the characteristics of the crystals grown on Earth as a basis for subsequent comparative evaluations of the crystals grown in a low gravity environment and to obtain the experimental data and perform the analyses required to define the optimum parameters for the flight experiments. During the six months of the Preliminary Definition Phase, the research efforts were concentrated on the binary compound ZnSe - the purification of starting materials of Se by zone refining, the synthesis of ZnSe starting materials, the heat treatments of the starting materials, the vapor transport rate measurements, the vapor partial pressure measurements of ZnSe, the crystal growth of ZnSe by physical vapor transport, and various characterization on the grown ZnSe crystals. Author (revised)

N94-13510 International Centre for Theoretical Physics, Trieste (Italy).
EMPIRICAL TIGHT-BINDING PARAMETERS FOR SOLID C(SUB 60)
N. Tit and V. Kumar Jan. 1993 18 p Limited Reproducibility: More than 20% of this document may be affected by microfiche quality
(DE93-623061; IC-93/6) Avail: CASI HC A03 (US Sales Only)

We present a tight-binding model for the electronic structure of C(sub 60) using four (1s and 3p) orbitals per carbon atom. The model has been developed by fitting the tight-binding parameters to the ab-initio pseudopotential calculation of Troullier and Martins (Phys. Rev. B46, 1754 (1992)) in the face-centered cubic (Fm3-bar) phase. Following this, calculations of the energy bands and the density of electronic states have been carried out as a function of the lattice constant. Good agreement has been obtained with the observed lattice-constant dependence of T(sub c) using McMillan's formula. Furthermore, calculations of the electronic structure are presented in the simple cubic (Pa3-bar) phase. DOE

N94-13580# Rochester Univ., NY. Dept. of Electrical Engineering.
THEORETICAL SIS MIXER RESEARCH Final Technical Report, 1 Jun. 1990 - 30 Nov. 1992
Marc J. Feldman Jun. 1993 10 p
(Grant AF-AFOSR-0316-90)
(AD-A266323; AFOSR-93-0437TR) Avail: CASI HC A02/MF A01

Theoretical research has been conducted to elucidate the basic physics behind the properties of superconductor-insulator-superconductor (SIS) tunnel junction receiving devices. The properties of SIS mixers using nonideal junctions and finite LO power, were determined by analytic expansion of the equations of the quantum theory of mixing, and also by computer simulations of SIS receivers over the entire range of experimental parameters. The result is a new coherent and intuitive picture of SIS mixer behavior. Many of the outstanding mysteries and questions about SIS receivers are resolved, and this contributes greatly to the design and interpretation of SIS mixer experiments. Other calculations show how to achieve sub-quantum noise temperatures in the phase sensitive SIS mixer, an important step towards realization of ultra-low-noise detectors. A simplified model casts doubt on the superlative experimental results reported for the RF-series dc-parallel biased array SIS mixer. DTIC

N94-13590# Technische Univ., Berlin (Germany). Fachbereich Physik.
A CONTINUUM THEORY FOR LIQUID CRYSTALS DESCRIBING DIFFERENT DEGREES OF ORIENTATIONAL ORDER Ph.D. Thesis
Stefan Blenk 1992 126 p
(ETN-93-94392) Avail: CASI HC A07/MF A02

Starting out with the mesoscopic concept, the phenomenological orientational balance equations for liquid crystals in alignment tensor

formulation are rederived. The dissipation inequality is exploited by Coleman-Noll's method to get restrictions for the constitutive equations of nematics. The macroscopic concept yields beside the alignment tensor other macroscopic variable and constitutive equations being in connection with the alignment tensor balance. The latter is as well derived as the macroscopic spin balance. Equilibrium properties of the constitutive equations resulting from the dissipation inequality are investigated, and the stress tensor in equilibrium is determined. Also the Landau conditions for equilibrium in liquid crystals are derived and extended to inhomogeneous alignment. The free energy and the couple stress tensor are calculated and in the case of total alignment compared to Ericksen-Leslie's results. It turned out that using the mesoscopic concept, more information and more essential restrictions to constitutive equations are obtained than without it. Therefore the mesoscopic approach does not only give a better understanding of liquid crystal theories but does also give an efficient tool for investigating their constitutive equations. ESA

N94-13694# California Univ., Berkeley. Lawrence Berkeley Lab.
CHANGES IN ELECTRICAL DEVICE CHARACTERISTICS DURING THE FORMATION OF DISLOCATIONS IN SITU IN THE TEM
F. M. Ross, R. Hull, D. Bahnck, J. C. Bean, L. J. Peticolas, C. A. King, and R. R. Kola Mar. 1993 4 p Presented at the 8th Conference on Microscopy of Semiconducting Materials, Oxford, England, 5-8 Apr. 1993
(Contract DE-AC03-76SF-00098)
(DE93-013910; LBL-33886; CONF-9304150-1) Avail: CASI HC A01/MF A01

By adding electrical connections to a specimen heating holder for a transmission electron microscope, we have measured the characteristics of electronic devices such as diodes while they remain under observation in the microscope. We have made electron-transparent specimens from metastable GeSi/Si p-n junction diodes and introduced dislocations by heating in situ. The combination of electrical measurement and real-time observation of dislocation formation allows us to examine the electrical properties of dislocations in individual devices and the influence of defects on device performance. DOE

N94-13875*# Maryland Univ., College Park. Lab. for Global Remote Sensing Studies.
ADVANCED SOLID-STATE ARRAY SPECTRORADIOMETER DATA COLLECTION DURING HAPEX-2 SAHEL Progress Report
Charles L. Walthall, Rangshai N. Halthore (Hughes STX, Inc., Greenbelt, MD.), Carol Russell (Universities Space Research Association, Greenbelt, MD.), Phillip W. Dabney (National Aeronautics and Space Administration. Goddard Space Flight Center, Greenbelt, MD.), James R. Irons (National Aeronautics and Space Administration. Goddard Space Flight Center, Greenbelt, MD.), Bill Kovalick (Hughes STX, Inc., Greenbelt, MD.), David Graham (Hughes STX, Inc., Greenbelt, MD.), and Mike Bur (Hughes STX, Inc., Greenbelt, MD.) May 1993 23 p
(Grant NAGw-3139)
(NASA-CR-194144; NAS 1.26:194144) Avail: CASI HC A03/MF A01

Data collection using the Advanced Solid-state Array Spectroradiometer (ASAS) during the Hydrologic Atmospheric Pilot Experiment in the Sahel (HAPEX-II Sahel) field campaign in the Republic of Niger, West Central Africa from 22 Aug. to 19 Sep. 1992 is documented. Details on the ASAS system such as the hardware, data collection methods, information on system calibration, and data processing procedures are included. The ASAS configuration deployed for HAPEX-II Sahel contains several new components, including a new sensor array and pointing system. Because of this, new calibration procedures are being developed at the same time that the first ASAS images from HAPEX-II Sahel are being processed. These new calibration procedures will be documented in a future publication. Author (revised)

N94-13881# Lawrence Livermore National Lab., CA.
OPTICAL AND PHYSICAL PROPERTIES OF THE LiSrAlF6:Cr LASER CRYSTAL
L. K. Smith, S. A. Payne, J. B. Tassano, L. D. DeLoach, W. L. Kway, and W. F. Krupke 18 May 1993 5 p Presented at the 8th Optical Society of America (OSA) Meeting on Advanced Solid-State Lasers, New Orleans, LA, 1-3 Feb. 1993
(Contract W-7405-eng-48)
(DE93-014657; UCRL-JC-111851; CONF-9302116-2) Avail: CASI HC A01/MF A01

We have measured several of the physical and optical parameters of LiSrAlF6:Cr or Cr:LiSAF laser material. The parameters in question are the ones that are important to its laser performance including the thermomechanical properties, water durabilities, and Auger upconversion constants. A thermomechanical figure-of-merit has been determined from measurements of the fracture toughness, expansion coefficient, thermal conductivity, Young's modulus, and heat capacity. Tests of water durability suggest that a neutral pH of 7 is optimum to minimize water dissolution. The Auger effect was found to be a significant factor at higher Cr concentration, where excited-state migration leads to an increase in the upconversion rate. DOE

N94-13930# Oak Ridge National Lab., TN.
HIGH-RESOLUTION Z-CONTRAST IMAGING AND HOLE CONCENTRATION MAPPING OF YBCO THIN FILMS
S. J. Pennycook, N. D. Browning, S. Zhu, R. Feenstra, D. P. Norton, D. H. Lowndes, and M. F. Chisholm May 1993 5 p Presented at the International Workshop on Superconductivity, Hokkaido, Japan, 28 Jun. - 1 Jul. 1993
(Contract DE-AC05-84OR-21400)
(DE93-015803; CONF-930682-2) Avail: CASI HC A01/MF A01

Atomic-resolution Z-contrast electron microscopy provides a directly interpretable image showing the location of high-Z atomic columns without the need for any structural models. Usually, the type of column may be identified from its intensity, and the structure and morphology of interfaces, ultrathin films, and superlattices are directly revealed. This has generated many insights into growth and relaxation phenomena. Since the Z-contrast image uses only electrons scattered through large angles, electron energy loss spectroscopy may be performed simultaneously using the transmitted beam, providing information on the local hole concentration from the fine structure of the oxygen-K absorption edge. The resolution achieved is below the coherence length, allowing a microscopic interpretation of transport properties. DOE

N94-13938*# National Aeronautics and Space Administration. Marshall Space Flight Center, Huntsville, AL.
OPTIMIZATION OF THE PROCESSING PARAMETERS OF HIGH TEMPERATURE SUPERCONDUCTING GLASS-CERAMICS: CENTER DIRECTOR'S DISCRETIONARY FUND FINAL REPORT
E. C. Ethridge and W. F. Kaukler (Alabama Univ., Huntsville.) Sep. 1993 24 p
(NASA-TM-108421; NAS 1.15:108421) Avail: CASI HC A03/MF A01

A number of promising glass forming compositions of high Tc superconducting Ba-Sr-Ca-Cu-O (BSCCO) materials were evaluated for their glass-ceramic crystallization ability. The BSCCO ceramics belonging to the class of superconductors in the Ba-Sr-Ca-Cu-O system were the focus of this study. By first forming the superconducting material as a glass, subsequent devitrification into the crystalline (glass-ceramic) superconductor can be performed by thermal processing of the glass preform body. Glass formability and phase formation were determined by a variety of methods in another related study. This study focused on the nucleation and crystallization of the materials. Thermal analysis during rapid cooling aids in the evaluation of nucleation and crystallization behavior. Melt viscosity is used to predict glass formation ability. Author (revised)

N94-13973# Fermi National Accelerator Lab., Batavia, IL.
CESIUM IODIDE (CsI) CRYSTAL MANUFACTURE
S. R. Childress and R. E. Ray, Jr. 28 Aug. 1992 6 p
(Contract DE-AC02-76CH-03000)
(DE93-012146; DOE/FTR-93012146) Avail: CASI HC A02/MF A01 (US Sales Only)

The CsI calorimeter, which is to be assembled by the KTeV collaboration, is 2.0 meters by 2.0 meters square and consists of pure Cesium Iodide crystals. The crystals are 500 mm or 27 radiation lengths long and come in two transverse sizes: 25 mm square and 50 mm square. The crystals may be single units or they may be made from pairs of glued crystals. The mechanical tolerances and light output characteristics required of the crystals by KTeV are fairly stringent and are just at the edge of the state-of-the-art. We have visited the three companies who are bidding on

the KTeV CsI order in order to evaluate their abilities to produce crystals sufficient for our purposes as well as to evaluate their production capabilities. DOE

N94-13980# Michigan Technological Univ., Houghton.
BOUNDARY STABILITY UNDER NONEQUILIBRIUM CONDITIONS
1993 11 p
(Contract DE-FG02-87ER-45315)
(DE93-016259; DOE/ER-45315/17) Avail: CASI HC A03/MF A01

The purpose of this work is to study microscopic, nanometer-scale behavior of interfaces under nonequilibrium conditions prevailing during service or materials processing. The need is to study grain boundary and surface/thin film instabilities under applied stress and chemical diffusion. This document is divided into: grain boundaries (stability, dislocations under applied stress, structural stability of grain boundaries during DIGM and under applied stress) and surfaces/thin films (hillock growth on microcrystalline and single crystal surfaces, plate edge instabilities, coherently strained islands). DOE

N94-13981# State Univ. of New York, Alfred. Coll. of Ceramics.
COMBUSTION SYNTHESIS AND ENGINEERING OF NANOPARTICLES FOR ELECTRONIC, STRUCTURAL, AND SUPERCONDUCTOR APPLICATIONS
G. C. Stangle, V. R. W. Amarakoon, and W. A. Schulze 28 May 1993 21 p
(Contract DE-FG02-93ER-12128)
(DE93-016286; DOE/ER-12128/1) Avail: CASI HC A03/MF A01

Fully dense, nanocrystalline ceramic articles were prepared by the new nanofabrication process. The process consists of two steps: synthesis of ceramic nanoparticles and fabrication of dense, nanocrystalline ceramic parts. The synthesis step produced 10-nanometer-diameter crystallites, and is capable of being scaled up to kilogram/hour production rates. The fabrication step produced dense parts at significantly reduced sintering temperatures and times -- representing a factor of 10-100 reduction in process energy requirements. The process was demonstrated by producing ultrafine-grained yttria-stabilized ZrO2, an important material with a variety of energy-related applications (solid electrolytes, oxygen sensors, electrode materials, thermal barrier coatings, etc.). Results from this period clearly illustrate the capabilities of this energy-efficient and directly commercializable process for producing dense, nanocrystalline, multicomponent oxide ceramics. DOE

N94-14010# Norwegian Defence Research Establishment, Kjeller. Electronics Div.
ELECTRICAL AND OPTICAL PROPERTIES OF MULTIPLE QUANTUM WELL STRUCTURES AND THEIR APPLICATIONS TO INFRARED DETECTORS Ph.D. Thesis - Tech. Univ. Munich
Petter Helgsen 23 Oct. 1992 77 p
(FFI-92/7012; ETN-93-93972) Avail: CASI HC A05/MF A01

The subband nature of semiconductor Multiple Quantum Wells (MQW's) using photoconductance spectroscopy, optical absorption, and tunneling experiments combined with model calculations, is reported. The aim was to study and fabricate intersubband infrared detectors. Interband protoconductivity experiments on InGaAsP/InP MQW's led to a better understanding of the photoconductivity processes and to a very precise determination of the band offsets in this material system. The sequential tunneling is one of the major noise sources for well doped GaAs/AlGaAs MQW intersubband infrared detectors. The observed 1-5 characteristics of a MQW structure are described by taking the nonresonant tunneling properly into account. The design, fabrication, modeling, and characterization are described for both a bound-to-bound state and a bound-to-continuum state GaAs/AlGaAs intersubband detector. The intersubband absorption process is, in addition, examined separately with emphasis on the dependence of the integrated absorption and the linewidth on quantum well design parameters. The performances of GaAs/AlGaAs intersubband detectors and HgCdTe detectors are reviewed. Intersubband detectors are shown to be very promising with detection levels approaching those of state of the art HgCdTe detectors. ESA

N94-14079# Sandia National Labs., Albuquerque, NM.
FREE-EXCITON RECOMBINATION IN GaAs
D. J. Wolford, G. D. Gilliland, T. F. Kuech, J. A. Bradley (IBM Research Lab., Yorktown Heights, NY.), and H. P. Hjalmarson 1992 5 p Presented at the International Conference on the Physics of Semiconductors, Beijing, China, 10-14 Aug. 1993
(Contract DE-AC04-76DP-00789)
(DE93-009843; SAND-92-0824C; CONF-930880-3) Avail: CASI HC A01/MF A01

We have studied the kinetics of free-exciton recombination in 'ideal' GaAs structures. Our studies include detailed photoluminescence kinetics measurements versus laser excitation power, temperature, sample structure, and surface treatment. The primary goal in these studies is to understand the mechanism precipitating free-exciton recombination and the role, if any, that polaritons play. Additionally, we have assessed the effects free-carriers and a variety of different sample structures and surface treatments have on these kinetics. DOE

N94-14083# Sandia National Labs., Albuquerque, NM.
INTRINSIC AND INTERFACIAL RECOMBINATION IN OMVPE- AND MBE-PREPARED GaAs/Al(x)Ga(1-x)As HETEROSTRUCTURES
G. D. Gilliland, D. J. Wolford, T. F. Kuech, J. A. Bradley (IBM Research Lab., Yorktown Heights, NY.), J. Klem, and H. P. Hjalmarson 1993 4 p Presented at the International Conference on the Physics of Semiconductors, Beijing, China, 10-14 Aug. 1993
(Contract DE-AC04-76DP-00789)
(DE93-009844; SAND-93-0609C; CONF-930880-1) Avail: CASI HC A01/MF A01

We have studied intrinsic free-carrier recombination in a variety of GaAs structures, including: OMVPE- and MBE-prepared GaAs/Al(x)Ga(1-x)As double heterostructures, Na2S passivated GaAs structures and bare GaAs structures. We find OMVPE prepared structures are superior to all of these other structures with 300 K lifetimes of approximately 2.5 micro-s and negligible nonradiative interface and bulk recombination, and thus are truly surface-free (S less than 40 cm/s). Moreover, we observe systematic trends in optical properties versus growth conditions. Lastly, we find that the presence of free-exciton recombination in the low-temperature photoluminescence spectra is a necessary but not sufficient condition for optimal optical properties (i.e. long minority-carrier lifetimes). DOE

N94-14085# Midwest Research Inst., Golden, CO. National Renewable Energy Lab.
STRUCTURAL AND ELECTRONIC STUDIES OF a-SiGe:H ALLOYS
W. Paul Apr. 1993 64 p Prepared in cooperation with Harvard Univ., Cambridge, MA
(Contract DE-AC02-83CH-10093)
(DE93-010021; NREL/TP-411-5457) Avail: CASI HC A04/MF A01

This report describes work to produce alloys of a-Si(1-x)Ge(x):H of improved photoelectronic quality by plasma-enhanced chemical vapor deposition (PECVD). The goal was to discover optimum preparation conditions for the end-component, a-Ge:H, to establish whether modification of the usual practice of starting from a-Si:H preparation conditions was advisable. Such modification, found to be necessary, gave films of a-Ge:H with efficiency-mobility-lifetime products ((eta)(mu)(tau)) 10(exp 2) to 10(exp 3) higher than were earlier available, in homogeneous environmentally stable material. Both a-Ge:H and a-Si(1-x)Ge(x):H of large x were studied in detail. Alloy material was shown to have (eta)(mu)(tau) 10(exp 2) larger than found earlier. However, just as the (eta)(mu)(tau) of a-Si:H decreases when Ge is added, so also the (eta)(mu)(tau) of these alloys with Si addition. By contrast, the ambipolar diffusion lengths, L(sub o) which are governed by the hole mobility, vary by only a factor of two over the whole alloy series. Using the experimental finding of a small valence band offset between a-Si:H and a-Ge:H compositional fluctuations on a 10-mm scale are suggested to explain the behavior of (eta)(mu)(tau) and L(sub o). The implications for eventual improvement of the alloys are profound, but require direct experimental tests of the postulated compositional fluctuations. DOE

N94-14108# Sandia National Labs., Albuquerque, NM.
ANOMALOUS LOW-TEMPERATURE FREE-EXCITON TRANSPORT IN GaAs STRUCTURES
D. J. Wolford, G. D. Gilliland, T. F. Kuech, J. A. Bradley (IBM Research Lab., Yorktown Heights, NY.), and H. P. Hjalmarson 1992 4 p Presented at the International Conference on the Physics of Semiconductors, Beijing, China, 10-14 Aug. 1993

(Contract DE-AC04-76DP-00789)
(DE93-009845; SAND-92-0825C; CONF-930880-2) Avail: CASI HC A01/MF A01

Using an optical analogue to the classical Haynes-Schockley experiment, we have studied low-temperature free-exciton transport in several 'ideal' GaAs structures. We find the observed diffusion constants to be laser excitation power dependent below 50 K and independent of laser power at higher temperatures. We observe peak 2 K diffusivities of greater than 1000 sq cm/Vs. Possible mechanisms are discussed. DOE

N94-14122# Los Alamos National Lab., NM.
MEASUREMENT OF PENETRATION DEPTH LAMBDA(T) IN YBa2Cu3O(7-DELTA) THIN FILM
J. Y. Lee (Ohio State Univ., Columbus.), T. R. Lemberger (Ohio State Univ., Columbus.), S. Foltyn, and X. D. Wu 1993 3 p Presented at the Conference of the International Union of Pure and Applied Physics on Low Temperature Physics (LT 20), Eugene, OR, 1-11 Aug. 1993
(Contract W-7405-eng-36)
(DE93-014587; LA-UR-93-1705; CONF-930801-2) Avail: CASI HC A01/MF A01

We present the magnetic penetration depth lambda(T) in two laser ablated YBa2Cu3O(7-delta) thin films, determined by the two-coil method. The slope of 1/lambda(exp 2)(T) near T(sub c), the only exactly measurable quantity, extrapolates to 930 A at T = 0, which compares well with 830 A in the high quality single crystal recently reported and which exhibited a linear T dependence at low T. For T less than 30K, we find lambda(T)/lambda(0)-1 = a(T/T(sub c))(exp 2) where a = 0.5. DOE

N94-14125# Lawrence Livermore National Lab., CA.
LASER AND SPECTROSCOPIC PROPERTIES OF Yb-DOPED APATITE CRYSTALS
L. D. DeLoach, S. A. Payne, W. F. Krupke, L. K. Smith, W. L. Kway, J. B. Tassano, and B. H. T. Chai (University of Central Florida, Orlando.) 18 May 1993 4 p Presented at the 8th Optical Society of America (OSA) Meeting on Advanced Solid-State Lasers, New Orleans, LA, 1-3 Feb. 1993
(Contract W-7405-eng-48)
(DE93-014656; UCRL-JC-113407; CONF-9302116-1) Avail: CASI HC A01/MF A01

Favorable spectroscopic and laser properties were measured in several Yb-doped apatite crystals: Ca5(PO4)(sub 3)F, Sr5(PO4)(sub 3)F, and Ca(5-x)Sr(x)(PO4)(sub 3)F where (x = 1-3). The properties included absorption and emission spectra, and laser pumping (slope efficiency). DOE

N94-14185# Argonne National Lab., IL. Materials Science Div.
ON THE HARDENING AND SOFTENING OF NANOCRYSTALLINE MATERIALS
G. E. Fougere, J. R. Weertman, and R. W. Siegel Apr. 1993 7 p Presented at the Conference on Nanostructured Materials, Cancun, Mexico, 21-25 Sep. 1992
(Contracts W-31-109-eng-38; DE-FG02-86ER-45229)
(DE93-012901; ANL/MSD/CP-79532; CONF-920947-5) Avail: CASI HC A02/MF A01

Nanocrystalline Pd and Cu samples have been thermally treated to determine whether the relation between hardness and grain size depend on the method used to vary the grain sizes. Previous reports indicate that hardening with decreasing grain size resulted from data obtained using individual samples, while softening with decreasing grain size resulted from data from a given sample that had been thermally treated. Hardening and softening regimes were evident for the nanocrystalline Cu, and the hardness improvements over the original as-consolidated state were maintained throughout the thermal treatments. This review examines our hardness results for Cu and Pd and those for other nanocrystalline materials. DOE

N94-14193# Office National d'Etudes et de Recherches Aerospatiales, Paris (France).
PHYSICAL AND STRUCTURAL PROPERTIES OF A SPUTTERED ZIRCONIA-YTTRIA LAYER USED AS A THERMAL RESISTANCE Ph.D. Thesis - Paris 6 Univ. [PROPRIETES PHYSIQUES ET STRUCTURALES D'UNE RESISTANCE THERMIQUE EN ZIRCONE YTTRIEE OBTENUE PAR PULVERISATION CATHODIQUE]
Magali Clery Oct. 1992 208 p In FRENCH Original contains color illustrations
(ONERA-NT-1992-10; ETN-93-93969) Avail: CASI HC A10/MF A03

A ZrO2-7 wt % Y2O3 thin sputtered film is studied. The film is developed for use as the thermal resistance in a thermal fluxmeter. Microstructural characteristics are studied as a function of deposition parameters. The substrate temperature and bias during deposition are shown to have an influence on morphology, microstructure, crystalline structure and lattice parameters, texture, stresses and microstresses. The objectives are to obtain zirconia-yttria layers with smallest possible thermal conductivity, high electrical resistivity, and good mechanical properties when subjected to thermal aging. ESA

N94-14198# National Research Council of Canada, Ottawa (Ontario). Inst. for Microstructural Sciences.
[ACTIVITIES OF INSTITUTE FOR MICROSTRUCTURAL SCIENCES] Annual Report, 1991-1992
1992 92 p
(NRC-32815; CTN-93-60816) Copyright Avail: CASI HC A05/MF A01

The Institute for Microstructural Sciences (IMS) supports the mission of the National Research Council of Canada by providing leadership, in collaboration with industry, in the development of a strategic base for information technology. IMS achieves its objectives through such means as the performance of research and development, the development of vital expertise and knowledge, and making sophisticated infrastructure accessible in collaborative research projects. IMS's organization is based around ten functional groups in five program areas (advanced semiconductor devices, optoelectronics, acoustics, electronic and photonic materials, and solid state physics) subdivided into 25 major projects. Reports of activities in these programs are presented, including overall objectives, lists of specific projects, research facilities and capabilities, and lists of publications. Highlights of 1991/92 projects include development of a prototype ridge waveguide microwave spectrometer with 8 GHz resolution, successful construction of novel wavelength division demultiplexers, design and fabrication of a novel field effect transistor, and production of strained layer InGaAs/GaAs lasers having application in photonic integrated circuits. CISTI

N94-14199# National Research Council of Canada, Ottawa (Ontario). Inst. for Microstructural Sciences.
[ACTIVITIES OF INSTITUTE FOR MICROSTRUCTURAL SCIENCES] Annual Report, 1991-1992 [INSTITUT DE SCIENCES DES MICROSTRUCTURES: RAPPORT ANNUEL 1991/1992]
1992 97 p In FRENCH
(CNR-32815; CTN-93-60817) Copyright Avail: CASI HC A05/MF A02

The Institute for Microstructural Sciences (IMS) supports the mission of the National Research Council of Canada by providing leadership, in collaboration with industry, in the development of a strategic base for information technology. IMS achieves its objectives through such means as the performance of research and development, the development of vital expertise and knowledge, and making sophisticated infrastructure accessible in collaborative research projects. IMS's organization is based around ten functional groups in five program areas (advanced semiconductor devices, optoelectronics, acoustics, electronic and photonic materials, and solid state physics) subdivided into 25 major projects. Reports of activities in these programs are presented, including overall objectives, lists of specific projects, research facilities and capabilities, and lists of publications. Highlights of 1991/92 projects include development of a prototype ridge waveguide microwave spectrometer with 8 GHz resolution, successful construction of novel wavelength division demultiplexers, design and fabrication of a novel field effect transistor, and production of strained layer InGaAs/GaAs lasers having application in photonic integrated circuits. CISTI

N94-14203 Department of National Defence, Ottawa (Ontario). Directorate Research and Development Air.
A QUARTZ CRYSTAL MICROBALANCE STUDY OF LITHIUM INSERTION AND REMOVAL INTO EVAPORATED FILMS MO(Y) (M = Mo, Fe, AND V)
E. Andrukaitis and R. S. McMillan (National Research Council of Canada, Ottawa, Ontario.) 1991 11 p
(DSIS-93-00649; CTN-93-60841) Avail: CASI HC A03

The reversible Li insertion in WO3 containing MoO3, V2O5, and Fe2O3 evaporated films was examined using the electrochemical quartz crystal microbalance (EQCM) technique. Amorphous films in their highest oxidation state were thermally evaporated and vacuum deposited onto 5 MHz quartz crystals. The frequency (mass) change for Li intercalation followed the 1 e- transfer reaction given by: xLi+ + xe- + MO(y) = Li(x)MO(y), where M = Mo, Fe, V, and/or W. Initial insertion and removal cycles have a low utilization of the electrode surface, with the reversibility of the Li intercalation dependant on stoichiometry. The Li was found to accumulate in the film by the EQCM technique during the electrochemical reduction and oxidation of these films. Surface changes such as film dissolution and electrolyte decomposition were detected by the EQCM technique during constant current cycling. Author (CISTI)

N94-14296# Minnesota Univ., Minneapolis. Dept. of Chemical Engineering and Materials Science.

THEORY OF THE ELECTRONIC AND STRUCTURAL PROPERTIES OF SOLID STATE OXIDES

J. R. Chelikowsky 1993 34 p

(Contract DE-FG02-89ER-45391)

(DE93-016051; DOE/ER-45391/4) Avail: CASI HC A03/MF A01

Emphasis has been on the electronic materials: silica, titania, and ruthenia. Fundamental interest centered on nature of microstructure of these solids in the amorphous state, or mixed oxide state. New theoretical techniques have been implemented to examine such issues, based on ab initio pseudopotential methods and interatomic potentials. Some areas examined under this project are: (1) Nature of the amorphization transformation of quartz under pressure. Specific focus is on the microscopic nature of the amorphous material and the driving forces for amorphization. (2) Equation of states of crystalline silica polymorphs. (3) Elastic anomalies in silica. In particular, the existence of a 'negative' Poisson ratio in high temperature, low density forms of crystalline silica. (4) Optical and structural properties of titania and mixed oxides such as Ru(sub x)Ti(sub 1-x)O(sub 2). DOE

N94-14304# Argonne National Lab., IL. Materials Science Div.

PRISM-FILM COUPLING IN ANISOTROPIC PLANAR WAVEGUIDES OF EPITAXIAL (101) RUTILE THIN FILMS

C. M. Foster, S. K. Chan, H. L. M. Chang, R. P. Chiarello, and D. J. Lam Apr. 1993 7 p Presented at the Spring Meeting of the Materials Research Society, San Francisco, CA, 12-16 Apr. 1993

(Contract W-31-109-eng-38)

(DE93-012912; ANL/MSD/CP-78008; CONF-930405-4) Avail: CASI HC A02/MF A01

We report optical waveguiding in single-crystal, epitaxial (101) oriented rutile (TiO2) thin films grown on (1120) sapphire (alpha-Al2O3) substrates using the MOCVD technique. The propagation-constants for asymmetric planar waveguides composed of an anisotropic dielectric media applicable to these films are derived. Modifications to the prism-film coupling theory for this anisotropic case are also discussed. By application of this model to (101) oriented rutile thin films, we directly obtain values of the ordinary and extraordinary refractive indexes, n(sub o) and n(sub e), of the rutile thin films as well as film thicknesses. We obtain typical values of the refractive indexes (n(sub o) = 2.5701 +/- 0.0005; n(sub e)=2.934 +/- 0.001) near to those for bulk rutile single crystals indicating the exceptional quality of these films. DOE

N94-14313# Lawrence Livermore National Lab., CA.

MONTE CARLO SIMULATION OF THE OCP FREEZING TRANSITION

H. E. DeWitt, W. L. Slattery (Los Alamos National Lab., NM.), and Juxing Yang (Harvard Medical School, Boston, MA.) Sep. 1992 10 p Presented at the International Conference on the Physics of Strongly Coupled Plasmas, Rochester, NY, 17-21 Aug. 1992

(Contract W-7405-eng-48)

(DE93-013039; UCRL-JC-111904; CONF-9208135-6) Avail: CASI HC A02/MF A01

The One Component Plasma (OCP) in three dimensions is a system of classical point charges moving in a fixed uniform neutralizing background. In nature the OCP is a rough approximation of the conditions in a white dwarf star in which one has fully ionized nuclei such as carbon, oxygen, and smaller amounts of heavier elements up to iron all moving in a nearly uniform background provided by relativistically degenerate electrons. The OCP is also a mathematical limiting model for a non-neutral plasma of ions in a Penning trap and cooled to strongly coupled conditions. Similarly, a collection of charge colloidal suspensions in water can exhibit the Coulomb freezing behavior of the OCP. A single dimensionless parameter, Gamma, is sufficient to describe the system. For very weak coupling, Gamma much less than 1, the thermodynamic properties of the OCP are given rigorously by the Debye-Huckel theory. This paper reports on Monte Carlo simulation of the freezing of the OCP from a random start for particle numbers ranging from 500 to 2000. In one case the authors obtained a perfect bcc lattice, but in most cases the final state would be an imperfect crystal or two different microcrystals, fcc and bcc, growing into each other. With a cluster analysis program the authors looked at the formation of nucleating clusters, and followed the actual freezing process. Roughly 80 particles are needed in a cluster before it starts to grow rapidly and freeze. DOE

N94-14329# Los Alamos National Lab., NM.

SHOCK COMPRESSION AND QUASIELASTIC RELEASE IN TANTALUM

J. N. Johnson, R. S. Hixson, D. L. Tonks, and G. T. Gray, III 1993 5 p Presented at the 14th International Conference on High Pressure Science and Technology and the 1993 Technical Meeting of the Topical Group on Shock Compression of Condensed Matter, Colorado Springs, CO, 28 Jun. - 3 Jul. 1993

(Contract W-7405-eng-36)

(DE93-014566; LA-UR-93-1785; CONF-9306167-3) Avail: CASI HC A01/MF A01

Previous studies of quasielastic release in shock-loaded FCC metals have shown a strong influence of the defect state on the leading edge, or first observable arrival, of release wave, due to large density of pinned dislocation segments behind the shock front, their relatively large pinning separation, and a very short response time as determined by drag coefficient in shock-compressed state. This effect is entirely equivalent to problems associated with elastic moduli determination using ultrasonic methods. This is particularly true for FCC metals, which have an especially low Peierls stress, or inherent lattice resistance, that has little influence in pinning dislocation segments and inhibiting anelastic deformation. BCC metals, on the other hand, have a large Peierls stress that essentially holds dislocation segments in place at low net applied shear stresses and thus allows fully elastic deformation to occur in the complete absence of anelastic behavior. Shock-compression and release experiments have been performed on tantalum (BCC), with the observation that the leading release disturbance is indeed elastic. This conclusion is established by examination of experimental VISAR records taken at the tantalum/sapphire (window) interface in a symmetric-impact experiment which subjects the sample to a peak longitudinal stress of approximately 7.3 GPa, in comparison with characteristic code calculations. DOE

N94-14332# Lawrence Livermore National Lab., CA.

AN X RAY DETECTOR USING SUPERCONDUCTING ALUMINUM TUNNEL JUNCTIONS

W. C. Barber, R. W. Bland, J. W. Carpenter, R. T. Johnson, K. E. Laws, J. Lockhart, J. S. Lee, R. M. Watson, S. E. Labov, and C. E. Cunningham et al 1992 13 p Presented at the 37th Annual Society of Photo-Optical Instrumentation Engineers (SPIE) International Symposium on Optical and Optoelectronic Applied Science and Engineering, San Diego, CA, 19-24 Jul. 1992

(Contracts W-7405-eng-48; DE-FG03-92ER-40711)

(DE93-015103; UCRL-JC-111941; CONF-920792-63) Avail: CASI HC A03/MF A01

We report on tests of a prototype detector for 6-keV X-rays using series arrays of tunnel junction. Tests with higher-energy particles indicate an energy resolution of 4 keV, at 0.3K and with a warm pre-amp. At lower temperatures and with cooled FET, the resolution should approach 100 eV. DOE

N94-14339# Los Alamos National Lab., NM.

EFFECT OF SPONTANEOUS DECAY OF SUPERCONDUCTOR QUASIPARTICLES IN THE TUNNELING DENSITY OF STATES

D. Coffey 1993 9 p Presented at the Conference on Spectroscopies in Novel Superconductors, Santa Fe, NM, 17-19 Mar. 1993

(Contract W-7405-eng-36)

(DE93-012681; LA-UR-93-1384; CONF-930367-3) Avail: CASI HC A02/MF A01

Superconductivity has been successfully described with either the Landau-Ginzburg theory of second order phase transitions or with strong-coupling versions of the original BCS theory for almost fifty years. Recent tunneling and photoemission data on the cuprate oxide superconductors may now provide evidence of corrections to the mean field approximation. It has been shown by Zasadzinski et al. that there is a dip at eV (approx equal) 3(Delta)(sub 0) in the SIS tunneling conductance, which is the derivative of the current across a superconductor-insulator-superconductor junction with respect to the applied voltage, for a set of cuprate superconductors whose (Tc)'s range from 5.5 to 100 K. Recently L. Coffey and I proposed an explanation of this feature in terms of the spontaneous decay of mean field quasiparticles. We showed that corrections to the mean field approximation for a superconductor lead to different frequency thresholds for spontaneous quasiparticle decay with different superconductor order parameter symmetries. These effects lead to features in the superconductor density of states and in the SIS tunneling conductance and provide experimental evidence of d-wave symmetry for the superconductor order parameter in the cuprates. I discuss model and also evidence of quasiparticle decay in ARPES data on Bi2Sr2CaCu2O8.
DOE

N94-14344# Sandia National Labs., Albuquerque, NM.
EFFECTS OF GROWTH CONDITIONS AND SUBSTRATE ORIENTATION ON THE PROPERTIES OF InSb
R. M. Biefeld and K. C. Baucom 1992 7 p Presented at the Spring Meeting of the Materials Research Society, San Francisco, CA, 12-16 Apr. 1993
(Contract DE-AC04-76DP-00789)
(DE93-013766; SAND-92-2508C; CONF-930405-7) Avail: CASI HC A02/MF A01

Two new organometallic Sb sources, tris(dimethylamino)antimony (TDMASb), and tertiarybutyldimethylantimony (TBDMSb) are being investigated. Growth of InSb using TDMASb, or TBDMSb and TMIn was investigated at 350 to 475 C using a range of 5/3 ratios, growth rates and pressures. Misoriented InSb substrates were also used for selected growth conditions. The growth rates of InSb using TMIn and either TDMASb or TBDMSb at temperatures less than or equal to 425 C were proportional to both the TMIn flow rate and the temperature. The surface morphology of InSb grown using either TDMASb or TBDMSb was very rough for growth temperatures less than or equal to 425 C. This may be due to the complex decomposition mechanisms involved and the presence of methyl groups on the surface. Smoother backgrounds were generally found when using off axis substrates. The details of the defects observed on the surfaces were dependent on the type of misorientation and can be related to the atomic structure of the surface steps. Both n- and p-type InSb were grown using TBDMSb or TDMASb and TMIn with mobilities up to 68,990 and 7773 cm(exp 2)/Vs, respectively, at 77 K. The mobility for InSb using either TDMASb or TBDMSb was optimized by going to lower temperatures, pressures and 5/3 ratios. The opposite was true for surface morphology which improved with higher temperature, pressure, and 5/3 ratio. The growth of high mobility InSb with smooth surfaces at T less than or equal to 425 C was not achieved with TDMASb or TBDMSb and TMIn under the conditions investigated in this work.
DOE

N94-14345# Sandia National Labs., Albuquerque, NM.
MICROSTRUCTURAL MECHANISMS THAT ENHANCE ELECTROMIGRATION RESISTANCE IN Al-Cu THIN FILMS
D. R. Frear and J. R. Michael 1993 9 p Presented at the Spring Meeting of the Materials Research Society, San Francisco, CA, 12-16 Apr. 1993
(Contract DE-AC04-76DP-00789)
(DE93-013770; SAND-93-1013C; CONF-930405-8) Avail: CASI HC A02/MF A01

Evolution of the microstructure of Al-2wt.%Cu thin films is examined with respect to how the presence of copper can influence electromigration behavior. After an anneal that simulates a thin film sintering step, the microstructure of the Al-Cu films consisted of 1 micron aluminum grains with theta-phase Al2Cu precipitates at grain boundaries and triple points. The grain size and precipitation distribution did not change with subsequent heat treatments. Upon cooling to room temperature the heat treatment of the films near the Al/Al+ theta solvus temperature results in depletion of copper at the aluminum grain boundaries. Heat treatments lower in the two phase region (200 to 300 C) result in enrichment of copper at the aluminum grain boundaries. Here, it is proposed that electromigration behavior of aluminum is improved by adding copper because the copper enrichment in the form of Al2Cu phase may hinder aluminum diffusion along the grain boundaries.
DOE

N94-14348# Oak Ridge National Lab., TN.
KINETICS OF PHOTODEPOSITION OF SUPERCONDUCTING FILMS
C. H. Chen, R. C. Phillips, and P. W. Morrison (Advanced Fuel Research, Inc., East Hartford, CT.) 1992 6 p Presented at the 16th Material Research Society International Symposium on the Scientific Basis for Nuclear Waste Management Fall Meeting, Boston, MA, 30 Nov. - 5 Dec. 1992
(Contract DE-AC05-84OR-21400)
(DE93-015511; CONF-921101-129) Avail: CASI HC A02/MF A01

It is critical to understand the kinetics of photodeposition of metal-oxide superconducting films. The monitoring of surface conditions of superconducting films on substrates was primarily obtained by FTIR. Desorbed ions and neutral atoms are the primary species producing the films during the laser ablation process, and mass spectroscopy is effective for determining the desorbed species. Although efforts have been made to learn the process, no complete models have been arrived at. In general, the production of superconducting films is primarily due to deposition of neutral atoms and metal oxide molecules.
DOE

N94-14354# Minnesota Univ., Minneapolis. Dept. of Chemical Engineering and Materials Science.
A MICROSTRUCTURAL APPROACH TO FATIGUE CRACK PROCESSES IN POLY CRYSTALLINE BCC MATERIALS
W. W. Gerberich 1992 11 p
(Contract DE-FG02-84ER-45141)
(DE93-016666; DOE/ER-45141/9) Avail: CASI HC A03/MF A01

The objective of this project was to study fatigue where a combination of low temperature and cyclic loading produced cyclic cleavage in bcc Fe-base systems. The dislocation dynamics and quasi-statics of crack growth were probed. This document reviews progress over the past 6 years: hydrogen embrittlement and cleavage, computations (stress near crack tip), dislocation emission from grain boundaries, fracture process zones, and understanding brittle fracture at the atomistic/dislocation scales and at the microscopic/macroscopic scale.
DOE

N94-14362# Oak Ridge National Lab., TN.
EFFECTS OF DEPOSITON RATE ON Bi2Sr2CaCu2O(8+x) AND Bi2Sr(1.6)La(0.4)CuO(6+x) EPITAXIAL THIN FILM GROWTH BY PULSED-LASER ABLATION
S. Zhu (Tennessee Univ., Knoxville.), D. H. Lowndes, B. C. Chakoumakos, D. K. Christen, J. D. Budai, X. Y. Zheng, and R. J. Warmack 1993 7 p Presented at the 2nd International Conference on Laser Ablation, Knoxville, TN, 19-22 Apr. 1993
(Contract DE-AC05-84OR-21400)
(DE93-015797; CONF-9304144-4) Avail: CASI HC A02/MF A01

Bi2Sr2CaCu2O(8+x) and Bi2Sr(1.6)La(0.4)CuO(6+x) epitaxial films have been grown on (001) MgO and SrTiO3 substrates at different deposition rates by pulsed-laser ablation (PLA). Surface morphology, crystallinity and superconducting critical temperature of the films depend sensitively on deposition rate even though ablation target composition and substrate temperature were kept almost constant. Scanning election microscopy showed that density of particles generated by PLA is reduced by decreasing the deposition rate. Results show that the highest quality films of the highly anisotropic Bi-based materials are deposited by PLA at a low deposition rate, which results in film growth in a near-equilibrium state.
DOE

N94-14365# Los Alamos National Lab., NM.
PLOUGHING ON GOLD USING A SCANNING TUNNELING MICROSCOPE
R. D. Day and P. E. Russell (North Carolina State Univ., Raleigh.) 1993 5 p Presented at the Principles of Cutting Mechanics Conference, Tuscon, AZ, 13-15 Apr. 1993
(Contract W-7405-eng-36)
(DE93-012632; LA-UR-93-1150; CONF-9304138-1) Avail: CASI HC A01/MF A01

The purpose of the experiments is to measure the nominal force on

the sample induced by the tip as a function of voltage and tunneling current and use the imaging capabilities of the Scanning Tunneling Microscope (STM) to determine if the sample material's surface can be deformed plastically in a controlled manner by the tip. In our investigations we use the tip as a ploughing tool which can be moved in a line to create a furrow, or can be scanned in a plane to displace a pocket of material. This document describes how we measure the tunneling force, presents some of the data acquired to date, and shows evidence of plastic deformation caused by the tip. DOE

N94-14409*# National Aeronautics and Space Administration. Langley Research Center, Hampton, VA.

ROOM TEMPERATURE DEGRADATION OF YBa2Cu3O(7-x) SUPERCONDUCTORS IN VARYING RELATIVE HUMIDITY ENVIRONMENTS

M. W. Hooker (Clemson Univ., SC.), S. A. Wise, I. A. Carlberg, R. M. Stephens, R. T. Simchick (Lockheed Engineering and Sciences Co., Hampton, VA.), and A. Farjami (Christopher Newport Coll., Newport News, VA.) Sep. 1993 14 p

(RTOP 142-20-14-02)

(NASA-TP-3368; L-17203; NAS 1.60:3368) Avail: CASI HC A03/MF A01

An aging study was performed to determine the stability of YBa2Cu3O(7-x) ceramics in humid environments at 20 C. In this study, fired ceramic specimens were exposed to humidity levels ranging from 30.5 to 100 percent for 2-, 4-, and 6-week time intervals. After storage under these conditions, the specimens were characterized by X-ray diffraction (XRD), scanning electron microscopy (SEM), and electrical resistance measurements. At every storage condition evaluated, the fired ceramics were found to interact with H2O present in the surrounding environment, resulting in the decomposition of the YBa2Cu3O(7-x) phase. XRD data showed that BaCO3, CuO, and Y2BaCuO5 were present after aging and that the peak intensities of these impurity phases increased both with increasing humidity level and with increasing time of exposure. Additionally, SEM analyses of the ceramic microstructures after aging revealed the development of needle-like crystallites along the surface of the test specimens after aging. Furthermore, the superconducting transition temperature T(sub c) was found to decrease both with increasing humidity level and with increasing time of exposure. All the specimens aged at 30.5, 66, and 81 percent relative humidity exhibited superconducting transitions above 80 K, although these values were reduced by the exposure to the test conditions. Conversely, the specimens stored in direct contact with water (100 percent relative humidity) exhibited no superconducting transitions. Author (revised)

N94-14413# Los Alamos National Lab., NM.

STRUCTURE AND STABILITY OF MICROVOIDS IN A-Si:H

R. Biswas (Iowa State Univ. of Science and Technology, Ames.) and I. Kwon 1993 7 p Presented at the Spring Meeting of the Materials Research Society, San Francisco, CA, 12-16 Apr. 1993 Submitted for publication

(Contract W-7405-eng-36)

(DE93-016625; LA-UR-93-2091; CONF-930405-27) Avail: CASI HC A02/MF A01

Microvoids appear to be universally present in a-Si:H as demonstrated by small angle X-ray scattering including the presence of microvoids in device quality glow discharge a-Si:H. We have studied the structural properties of these microvoids with molecular dynamics simulations. Using molecular dynamics simulations with classical potentials, we have created microvoids by removing Si and H atoms from a computer generated a-Si:H network. The internal surfaces of the microvoids were passivated with additional H atoms and the microvoids were fully relaxed. Microvoids over a limited range of sizes (5 - 90 missing atoms) were examined. We obtained a relaxed microvoid structure with no dangling bonds for a microvoid with 17 missing atoms, whereas other sizes examined produced less relaxed models with short H-H distances at the microvoid surface. The strains near the microvoid surface are described. The microvoid model was stable to local excitations on weak bonds in the vicinity of the microvoid. DOE

N94-14439# Lawrence Livermore National Lab., CA.

COMPUTATIONAL DIAGNOSTICS FOR DETECTING PHASE TRANSITIONS DURING NANOINDENTATION

S. M. Lee, C. G. Hoover, J. S. Kallman, A. J. DeGroot, and W. G. Hoover Dec. 1992 8 p Presented at the 16th Material Research Society International Symposium on the Scientific Basis for Nuclear Waste Management, Boston, MA, 30 Nov. - 5 Dec. 1992

(Contract W-7405-eng-48)

(DE93-016536; UCRL-JC-110982; CONF-921101-136) Avail: CASI HC A02/MF A01

We studied nanoindentation of silicon using nonequilibrium molecular dynamics simulations with up to a million particles. Both crystalline and amorphous silicon samples are considered. We use computational diffraction patterns as a diagnostic tool for detecting phase transitions resulting from structural changes. Simulations of crystalline samples show a transition to the amorphous phase in a region a few atomic layers thick surrounding the lateral faces of the indenter, as has been suggested by experimental results. Our simulation results provide estimates for the yield strength (nanohardness) of silicon for a range of temperatures. DOE

N94-14440# Lawrence Livermore National Lab., CA.

METASTABILITY OF YTTRIUM-OXIDES

A. F. Jankowski, M. P. Stratman, E. M. Sedillo, J. P. Hayes, and G. F. Gallegos Apr. 1993 19 p Presented at the International Conference on Metallurgical Coatings and Thin Films, San Diego, CA, 19-23 Apr. 1993

(Contract W-7405-eng-48)

(DE93-016548; UCRL-JC-112829; CONF-930419-3) Avail: CASI HC A03/MF A01

Metastable yttrium-oxide films are synthesized using reactive sputter deposition. The yttrium concentration of the as-deposited film is found to vary as a function of the sputter deposition rate. In addition to the synthesis of the cubic equilibrium phase Y2O3, oxide compounds can be formed with 40-80 at.% yttrium. The crystalline state of the as-deposited film is dependent on the substrate temperature. A metastable, orthorhombic yttrium-rich oxide is formed on room temperature substrates. Substrates of Ta10W are coated with several microns of yttrium-oxide. The stability of these yttrium-oxide coatings are investigated as subjected to an atmospheric pressure of oxygen at an elevated temperature of 1773 K. The coatings and substrates are examined for stability of crystalline structure, composition, cracking, adhesion, and corrosion. A yttrium-rich oxide coating is found to offer the best corrosion protection to the Ta10W substrate. DOE

N94-14478# Oak Ridge National Lab., TN.

EVOLVING SURFACE CUSPS DURING STRAINED-LAYER EPITAXY

D. E. Jesson, S. J. Pennycook, J. M. Baribeau (National Research Council of Canada, Ottawa, Ontario.), and D. C. Houghton (National Research Council of Canada, Ottawa, Ontario.) Apr. 1993 7 p Presented at the Spring Meeting of the MRS, San Francisco, CA, 12-16 Apr. 1993

(Contract DE-AC05-84OR-21400)

(DE93-015430; CONF-930405-25) Avail: CASI HC A02/MF A01

Z-contrast imaging and Ge marker layer experiments were combined to study the evolving surface morphology of Si(x)Ge(1-x) alloys grown by molecular beam epitaxy (MBE). Surface cusps are seen to arise as the intersection lines between coherent islands. The potential implications of stress concentrations associated with cusps are considered with a view to strain relaxation in the film via dislocation nucleation. DOE

N94-14517# Brookhaven National Lab., Upton, NY.

IS K3C60 A LINE PHASE?

Q. Zhu (Pennsylvania Univ., Philadelphia.), J. E. Fischer (Pennsylvania Univ., Philadelphia.), and D. E. Cox 1993 5 p Presented at the IWEP-NM 1993: International Workshop on Electronic Polymers, Alw Materials, Kirchberg, Austria, Apr. 1993

(Contracts DE-FG02-86ER-45254; DE-FG05-90ER-75596; DE-AC02-76CH-00016)

(DE93-016700; BNL-49087; CONF-9304171-1) Avail: CASI HC A01/MF A01 ,

We present x-ray diffraction evidence that K(x)C60 with x as low as 1.6 exhibits phase-pure fcc structures over some temperature range. These results have implications for the equilibrium binary phase diagram, and for the possibility of testing the hypothesis that fullerene superconductors are doped Mott-Hubbard insulators. DOE

N94-14554 Tel-Aviv Univ. (Israel). School of Physics and Astronomy.
THE LINDEMANN CRITERION OF MELTING FOR PURE AND MIXED IONIC CRYSTALS M.S. Thesis
David Berrebi Nov. 1991 83 p
(ITN-93-85210) Copyright Avail: Issuing Activity (Tel-Aviv Univ., Exact Sciences Library, Ramat Aviv 69978, Israel)

Generalization of the Lindemann criterion of melting for disordered mixed crystals provides the possibility of predicting the diagram of state for different mixtures. In the present work, this criterion was adapted for pure ionic crystals and was generalized for mixed ionic crystals also. Use of the optical phonon mode instead of the acoustic phonon mode gave the same kind of Lindemann formula as for metals. However, the difference between an ionic crystal and a simple atomic one is that the mass which characterizes the lattice is the reduced mass of the two ions rather than their sum, i.e., M(sub r) = M(sub A)M(sub C)/(M(sub A) + M(sub C)) instead of M(sub s) = M(sub A) + M(sub C) in which M(sub C) and M(sub A) are the masses of the cation and anion, respectively. A melting criterion, equivalent to the Lindemann criterion, was formulated for mixed binary ionic crystals. For many binary and some ternary systems, the calculations gave azeotropic phase boundary lines or surfaces which were confirmed by the experimental data. The criterion for solubility derived from these calculations also agreed well with experimental results. There was a good correlation between the present results and other calculations based on thermochemical considerations. The Debye temperature and Lindemann parameters were calculated for more complex binary solids, having diamond, zinc blend and chalcopyrite structures. ISA

N94-14557 Tel-Aviv Univ. (Israel). School of Physics and Astronomy.
SMALL POLARON CONDUCTION IN Y2Ti2O7 M.S. Thesis
Nissan Fishbaum May 1990 67 p In HEBREW
(ITN-93-85221) Copyright Avail: Issuing Activity (Tel-Aviv Univ., Exact Sciences Library, Ramat Aviv 69978, Israel)

A low and activated electron mobility over a wide temperature range, measured in reduced single-crystal Y2Ti2O7, reflects the small polaron transport mechanism. Electrical conductivity and thermoelectric power measurements were employed in order to derive the temperature dependence of the mobility. Both conductivity and electron concentration (deduced from the thermoelectric power) are activated. The large difference in the activation energies (which is much larger than kT) implies significant activation of the mobility, indicative of small polarons. The formation of small polarons in this material is attributed to strong electron-phonon interaction and to a large oxygen vacancy concentration, which had been introduced into the material via a reduction process in hydrogen of high temperature. Experimental support for a strong electron-phonon interaction is found in the strong temperature dependence of the optical band-gap and in the large coupling constant estimated from our transport data. We assume that this interaction is due mainly to acoustical phonons. The large oxygen vacancy concentration - deduced from our measurements and from ionic conductivity measurements by others - stabilizes the small polaron and thus increases the likelihood for its formation. Also related to this large oxygen vacancy concentration is the ability of Y2Ti2O7 to incorporate large amounts of chromium (in contrast to other titanates that become unstable). A structural model which accounts for small polaron conduction in this material is proposed. Author (ISA)

N94-14559 Tel-Aviv Univ. (Israel). School of Physics and Astronomy.
A SUM-RULE OF LUMINESCENCE SPECTRUM M.S. Thesis
Pinchas Dahan Sep. 1991 71 p
(ITN-93-85223) Copyright Avail: Issuing Activity (Tel-Aviv Univ., Exact Sciences Library, Ramat Aviv 69978, Israel)

This work will discuss the sum rule of the luminescence spectrum, h nu(sub 1) + h nu(sub 2) = E(sub g), observed for semiconductors doped with transition metal impurities. h nu(sub 1) and h nu(sub 2), respectively, denote the photon energy of the zero phonon line (ZPL) in the infrared band and in the blue band. The sum of these two photon energy lines gives the band gap energy, E(sub g). The origin of the ZPL photon energy in the infrared band h nu(sub 1) is known and well explained by the intra-center transition between the two levels which results from the splitting by the ligand field potential. The origin of the ZPL photon energy in the blue band is explained in this work. The ZPL photon energy in the blue band is due to a second order process, which involves transition interference between the radiative term, P and the nonadiabatic term, L. The intensity of this process is essentially enhanced owing to a peculiar resonance of a Fermi type between the photon, phonons and the impurity transition. The essential conditions allowing this ZPL to be measured are that there is strong displacement in the Jahn-Teller effect and that the energy levels of the impurity are deep levels. Author (ISA)

N94-14597# Pittsburgh Univ., PA. Dept. of Chemistry.
QUANTUM STATE RESOLVED DESORPTION OF CO FROM SOLID SURFACES
K. C. Janda 1992 14 p
(Contract DE-FG02-88ER-13933)
(DE93-016876; DOE/ER-13933/3) Avail: CASI HC A03/MF A01

The work consisted of two major efforts. First, we studied the recombinative desorption of hydrogen atoms from a Si(100) surface. The desorption kinetics turned out to scale with the first power of the hydrogen atom coverage on the surface instead of the second power. The interpretation of these results is rather controversial. The second series of studies focus on mixing of isotopic composition between CO molecules on a Ni(111) surface. The isotopic mixing reaction was found to proceed at modest surface temperatures, but not to go to completion even at high surface temperatures. DOE

N94-14695# Sandia National Labs., Albuquerque, NM.
SOLUTION CHEMISTRY OPTIMIZATION OF SOL-GEL PROCESSED PZT THIN FILMS
S. J. Lockwood, R. W. Scwartz, B. A. Tuttle, and E. V. Thomas 1992 7 p Presented at the 1993 Spring Meeting of the MRS, San Francisco, CA, 12-16 May 1993
(Contract DE-AC04-76DP-00789)
(DE93-013776; SAND-92-2490C; CONF-9305195-1) Avail: CASI HC A02/MF A01

We have optimized the ferroelectric properties and microstructural characteristics of sol-gel PZT thin films used in a CMOS-integrated, 256 bit ferroelectric non-volatile memory. The sol-gel process utilized in our work involved the reaction of Zr n-butoxide, Ti isopropoxide, and Pb (4) acetate in a methanol/acetic acid solvent system. A 10-factor screening experiment identified solution concentration, acetic acid addition, and water volume as the solution chemistry factors having the most significant effects on the remanent polarization, coercive field, ferroelectric loop quality, and microstructural quality. The optimal values for these factors were determined by running a 3-factor uniform shell design, modeling the responses, and testing the models at the predicted optimal conditions. The optimized solution chemistry generated 3-layer, 300-400 nm thick films on RuO2 coated silicon substrates with coercive fields of less than 25 kv/cm (a 40-50% improvement over the original solution chemistry), a remanent polarization of 25-30 micro-C/cm and a reduction in the pyrochlore phase content below observable levels. DOE

N94-14697# Laboratoire d'Automatique et d'Analyse des Systemes, Toulouse (France). Groupe Microstructures et Microsystemes Integres.
MOLECULAR SIMULATOR: A BASIC TOOL FOR SUBMICRON MOS PROCESSES DEVELOPMENT Ph.D. Thesis - Toulouse Univ. [SIMULATEUR MOLECULAIRE: UN OUTIL DE BASE POUR LE DEVELOPPEMENT DES PROCEDES MOS SUBMICRONIQUES]
Heriniaina Roger Razafindratsita 1992 133 p In FRENCH
(LAAS-92484; ETN-93-94359) Avail: CASI HC A07/MF A02

Scaling down under micron of MOS (Metal Oxide Semiconductor) silicon devices is accomplished by fabricating oxide layers whose thickness is not in excess of a few tens of Angstrom. At this thickness, an atomic scale model capable of accounting for the microstrip and localized information is needed. A simulator based on energy models involving two body and three body interactions was completed and the Metropolis test was carried out. Many validity tests performed bore out the simulator's ability to simulate silicon and silicon oxide crystals. To analyze the growth of the first oxide monolayers, the oxygen atoms were deposited on the surface of the silicon substrate and the structure was relaxed. By converting the oxygen rate into the growth time, this method could then be applied to the practical example of oxide growth at room temperature and under atmospheric pressure on a Si(001) surface. It was found that the formation of the first oxide layers resulted from a distortion-relaxation process occurring between the oxygen and the silicon ones. From the simulated results, a logarithmic-linear law was formulated, approximating to within the

experimental results of oxide growth in the thickness range less than ten Angstrom. In addition, the introduction of point defects in the substrate allowed the model to be refined. In particular two cases of defect mixture, namely 1.5% of interstitials (that is, 3 interstitials for 200 silicon atoms of the substrate) and 6% of vacancies; and 6% of interstitials and 6% of vacancies enable the deviation between the simulated and experimental results to be reduced by half. ESA

N94-14699# California Univ., Berkeley. Lawrence Berkeley Lab.
DIRECT SUBMILLIMETER ABSORPTIVITY MEASUREMENTS ON EPITAXIAL Ba(1-x)K(x)BiO3 FILMS AT 2K
D. Miller, P. L. Richards, E. J. Nicol (California Univ., Santa Barbara.), E. S. Hellman (Bell Telephone Labs., Inc., Murray Hill, NJ.), E. H. Hartford, Jr. (Bell Telephone Labs., Inc., Murray Hill, NJ.), C. E. Platt (Illinois Univ., Urbana-Champaign.), R. A. Schweinfurth (Illinois Univ., Urbana-Champaign.), D. J. VanHarlingen (Illinois Univ., Urbana-Champaign.), and J. Amano (Hewlett-Packard Labs., Palo Alto, CA.) Apr. 1993 4 p Presented at the Conference on Spectroscopies in Novel Superconductors, Santa Fe, NM, 17-19 Mar. 1993
(Contract DE-AC03-76SF-00098)
(DE93-013904; LBL-33971; CONF-930367-5) Avail: CASI HC A01/MF A01

We have used a bolometric technique to obtain accurate low temperature loss data for epitaxial thin films of Ba(0.6)K(0.4)BiO3 from 30 to 700 cm(exp -1). These films were grown on MgO and SrTiO3 substrates by MBE, off-axis sputtering, and laser deposition techniques. All films show a strong absorption onset near the BCS tunneling gap of 3.5k(sub B)T(sub c). We have analyzed these data using a Kramers-Kronig transformation and have corrected for finite film thickness effects. Results indicate that the absorption onset is consistent with a superconducting energy gap. Comparison is made with predictions based on strong coupling Eliashberg theory using (alpha)(exp 2)F(omega) spectra obtained from the literature. While we are able to fit the overall measured absorptivity, we are unable to fit the structure observed in our data. DOE

N94-14705# Technische Univ., Berlin (Germany). Fachbereich Physik.
DYNAMIC JAHN-TELLER EFFECT: CALCULATION OF FINE STRUCTURE SPECTRUM, ISOTOPE SHIFT AND ZEEMAN BEHAVIOR AT DEEP CENTER Ni2+ IN CdS Ph.D. Thesis [DYNAMISCHER JAHN-TELLER-EFFEKT: BERECHNUNG DES FEINSTRUKTURSPEKTRUMS, DER ISOTOPIEVERSCHIEBUNG UND DES ZEEMAN-VERHALTENS AM TIEFEN ZENTRUM NI2+ IN CDS]
Juergen Schoepp 1992 160 p In GERMAN
(ETN-93-94394) Avail: CASI HC A08/MF A02

The internal transition of the deep center Ni2+ in II to IV semiconductor cadmium sulfide is examined with reference to crystal field theory. An algorithm was developed for calculation, in a basis fitted to trigonal symmetry, of fine structure operator matrix which is made of the sum of operators from spin trajectory coupling, trigonal field and electron phonon coupling. The dependence of energy level on the mass was calculated in order to examine the isotropy effect at Ni2+ transition. The mass dependence of phonon energy was estimated in an atomic cluster by using a valence force model from Keating for elastic energy. The Zeeman behavior of Ni2+ transition was examined for magnetic fields; the Zeeman operator was added to the fine structure operator and the resulting matrix was diagonalized. It is noticed that calculations are quantitatively and qualitatively in agreement with experiments. ESA

N94-14720# Rome Univ. (Italy). Dipt. di Fisica.
RENORMALIZED BAND STRUCTURE OF CuO2 LAYERS IN SUPERCONDUCTING COMPOUNDS: A MEAN FIELD APPROACH
M. Grilli, C. Castellani, and C. DiCastro 30 Mar. 1990 16 p
(Preprint-730; ETN-93-94368) Avail: CASI HC A03/MF A01

The band structure of a CuO2 plane including two copper orbitals (d(sub(x squared - y squared))) and d(sub(3z squared - r squared)) and two oxygen orbitals (p(sub x), p (sub y)) in tight binding approximation was analyzed. A Hubbard interaction between copper d holes was considered using a slave boson technique, while oxygen and copper holes interact via a nearest neighbors coulombic repulsion treated in Hartree-Fock approximation. The resulting band structure opens the way to a comparison with the experiments (ARPES (Angle Resolved Photoemission), XAS (X-Ray Absorption), infrared reflectivity) and to some theoretical implications on the pairing mechanism of high critical temperature superconductors. ESA

N94-14739# Ohio Univ., Athens.
ELECTRONIC STATES IN SYSTEMS OF REDUCED DIMENSIONALITY
S. E. Ulloa 20 May 1993 9 p
(Contract DE-FG02-87ER-45334)
(DE93-014440; DOE/ER-45334/6) Avail: CASI HC A02/MF A01

The common theme of the research is the effects of electronic interactions on the properties of systems. Specifically, work was done in the following areas: magnetically modulated systems, Raman and EELS in superlattices, ballistic quantum interference effects, quantum dot arrays, and optical response of undoped fullerene crystals. DOE

N94-14773# Los Alamos National Lab., NM.
MUON SPIN RELAXATION STUDIES OF HEAVY FERMION SUPERCONDUCTORS
R. H. Heffner 1993 7 p Presented at the International Workshop on Low Energy Muon Science (LEMS 1993), Santa Fe, NM, 4-8 Apr. 1993
(Contract W-7405-eng-36)
(DE93-014576; LA-UR-93-1736; CONF-9304145-2) Avail: CASI HC A02/MF A01

This talk will focus recent developments in our understanding of heavy fermion (HF) superconductors and the role that positive muon spin relaxation ((mu)SR) studies have played in helping to elucidate their properties. As illustrations two systems will be discussed: (1) UPd(sub 2)Al(sub 3), one of the most recently discovered HF superconductors, which also displays coexisting magnetic order, and (2) UBe(sub 3) doped with small quantities of Th substituted for U, which displays an interplay between its superconducting and magnetic ground states, leading to multiple superconducting states. DOE

N94-14798 Harvard Univ., Cambridge, MA. Div. of Applied Sciences.
MEASUREMENTS OF CRYSTAL GROWTH KINETICS AT EXTREME DEVIATIONS FROM EQUILIBRIUM
M. J. Aziz May 1993 6 p Limited Reproducibility: More than 20% of this document may be affected by microfiche quality
(Contract DE-FG02-89ER-45401)
(DE93-014526; DOE/ER-45401/4) Avail: CASI HC A02

We have measured solute trapping of Sn in Al over a wide enough range of velocities to make a quantitative test of theory. The Continuous Growth Model of Aziz is the only one-parameter model that fits the data. We have also measured the diffusive speed - the growth rate at which interfacial partitioning is in mid-transition between equilibrium partitioning and complete solute trapping - for several solutes in Al. We have found an inverse correlation between the equilibrium partition coefficient and the diffusive speed. Taken together, these results give us unprecedented predictive capability in modeling rapid solidification processing. We have also theoretically examined short-range diffusion-limited growth, characteristic of incomplete solute trapping, and interface-limited growth, characteristic of complete solute trapping, in alloy solidification and have shown that the two regimes fall naturally out of a single unified theory of solidification. DOE

N94-14825 Tel-Aviv Univ. (Israel).
MAGNETIC INTERACTIONS AND DISORDER - PHASE TRANSITIONS IN DILUTE SPIN-GLASSES AND HIGH TEMPERATURE SUPERCONDUCTORS Ph.D. Thesis
Lior Klein Sep. 1991 263 p
(ITN-93-85217) Copyright Avail: Issuing Activity (Tel-Aviv Univ., Exact Sciences Library, Ramat Aviv 69978, Israel)

Fifteenth-order high-temperature series expansions were developed for studying the critical behavior of the Ising spin glass with nearest-neighbor exchange interactions, each of which randomly assumes the values +J or -J. Series for the Edwards-Anderson spin glass susceptibility and two of its derivatives with respect to the ordering field were evaluated for hypercubic lattices in general dimensions, d, which extend previous general dimension series by five terms. Some measurable universal amplitude ratios were estimated from the new series and were also calculated analytically by means of the renormalization group and epsilon-expansion techniques. The results provide a smooth interpolation between the mean field results above six dimensions and experiments and simulations in physical dimensions.

Calculated derivatives are related to measurements of derivatives of the magnetization with respect to a uniform magnetic field. The properties of the dilute spin glass were studied, both at zero temperature and at finite temperatures. In high-temperature superconductors, the effect of the antiferromagnetic background of the Cu spins in the CuO2 planes on the spectrum of the mobile quasiparticles was studied. Several possible quasiparticles were studied, which involve the spin of the hole and the spins of the two neighboring copper ions. Using tight binding methods, four energy bands for each quasiparticle were obtained and the favored charge carrier to be a spin-one-half quasiparticle was found. ISA

N94-14826 Tel-Aviv Univ. (Israel).
PHASES AND PHASE TRANSITIONS OF POLYMERIC LIQUID CRYSTALS: A HIGH RESOLUTION X RAY DIFFRACTION AND LIGHT SCATTERING STUDY Ph.D. Thesis
Ehud Nachaliel 25 Mar. 1991 130 p In HEBREW
(ITN-93-85218) Copyright Avail: Issuing Activity (Tel-Aviv Univ., Exact Sciences Library, Ramat Aviv 69978, Israel)

Liquid crystal polymers (LCP) were compared with monomeric liquid crystals (MLC) by means of high-resolution x-ray (HIREX) and light scattering (LIS). Both HIREX and LIS were used to study the nematic-smectic(sub a) phase transition of P4.1 polysiloxane; the following critical exponents were determined: nu(sub parallel) = 0.77 +/-0.05; nu(sub normal) = 0.57 +/-0.08; gamma = 1.3 +/-0.10. The bare correlation lengths were found to be: xi(sup 0)(sub parallel) = 3.27 +/-0.08; xi(sup 0)(sub normal)q(sub 0) = 1.09 +/-0.14 which are unusually large in comparison with MLC. LIS experiments confirmed these values and indicated 'cross over' of nu(sub parallel) from 0.77 to 0.53. These results are typical of a system near to a tricritical point. HIREX was used to study the nematic-smectic(sub c) phase transition in C6-polysiloxane; the results were a good fit to Chen and Lubensky's mean field theory but the correlation lengths saturated near the transition to the nematic phase. A study of the smectic(sub a) phase of PA6 polyacrylate, near the transition to the nematic phase, showed that, except very close to the transition, the first and second harmonics of the x-ray structure factor were found to be consistent with the harmonic theory of de Gennes and Caille. This is thought to indicate the importance of anharmonic corrections near the phase transition. Fits to the experimental data yielded the compressibility constant, B and the splay elastic constant, K(sub s). B was found to obey a power law: B varies as t(sup phi) in which phi = 0.82 +/-0.08. In good agreement with theoretical predictions using exponents from the literature, but in disagreement with previous experimental results on MLC's. The splay elastic constant K(sub s) has roughly the same magnitude as in MLC's but tends to decrease by approximately 50% upon approaching the transition from below. This temperature dependence might give further evidence for the importance of anharmonicity in the system. Finally, the smectic(sub c) phase of C6 polysiloxane was studied, using HIREX. The tilt angle was found to decrease continuously upon decreasing temperature. This behavior, opposite to that observed in MLC's is caused by the stiffening in the plymeric backbone and spacers. ISA

N94-14839# North Carolina State Univ., Raleigh. Dept. of Materials Science and Engineering.
CHARACTERIZATION OF DIAMOND FILM GROWTH IN A COMBUSTION FLAME Final Report, 12 Mar. 1990 - 31 May 1993
John T. Prater and Jeffrey T. Glass 7 Jun. 1993 25 p
(Contract DAAL03-89-D-0003)
(AD-A266659; ARO-27810.9-MS) Avail: CASI HC A03/MF A01

This research has investigated the growth of diamond films in the combustion flame of an oxyacetylene torch. As a result of this research we now have a good understanding of the parameters that affect the growth of high quality diamond films and a better understanding of the nucleation process. Research resulting in the growth of highly textured, high quality diamond films on Si(100) substrates is reported. DTIC

N94-14868# California Univ., Berkeley. Lawrence Berkeley Lab.
QUENCHING AND ANNEALING EFFECTS ON THE SPECIFIC HEAT OF YBa2Cu3O(7-DELTA)
J. P. Emerson, R. A. Fisher, D. A. Wright, N. E. Phillips, J. E. Gordon (Amherst Coll., MA.), and E. M. McCarron, III (Du Pont de Nemours, E. I. and Co., Wilmington, DE.) Apr. 1993 8 p Presented at the Conference of the International Union of Pure and Applied Physics on Low Temperature Physics (LT 20), Eugene, OR, 1-11 Aug. 1993
(Contract DE-AC03-76SF-00098)
(DE93-016483; LBL-34029; CONF-930801-7) Avail: CASI HC A02/MF A01

The effect of heat treatments and quenching with no change in oxygen content was studied for a polycrystalline sample of YBCO. Quenching the sample changes the specific heat and resistivity, showing that nonsuperconducting regions, some of which are not associated with Cu(2+) moments, can be created in YBCO by heat treatment alone. DOE

77 THERMODYNAMICS AND STATISTICAL PHYSICS

Includes quantum mechanics; theoretical physics; and Bose and Fermi statistics.

For related information see also *25 Inorganic and Physical Chemistry* and *34 Fluid Mechanics and Heat Transfer.*

N94-12844# Melbourne Univ., Parkville (Australia). School of Physics.
QUATERNIONS AND THE HEURISTIC ROLE OF MATHEMATICAL STRUCTURES IN PHYSICS
Ronald Anderson (Boston Coll., Chestnut Hill, MA.) and G. C. Joshi Jul. 1992 39 p
(DE93-622865; UM-P-92/61; OZ-92/20) Avail: CASI HC A03/MF A01 (US Sales Only)

One of the important ways development takes place in mathematics is via a process of generalization. On the basis of a recent characterization of the process the authors propose that generalizations of mathematical structures that are already part of successful physical theories serve as good guides for the development of new physical theories. The principle is a more formal presentation and extension of a position stated earlier this century by Dirac. Quaternions form an excellent example of such a generalization, and a number of the ways in which their use in physical theories illustrates this principle, are discussed. DOE

N94-12855 Gosudarstvennyi Komitet po Ispolzovaniyu Atomnoi Energii, Moscow (USSR).
TO THE THEORY OF TRIPLET PAIRING IN FERMI-LIQUID MODEL [K TEORIL TRIPLETNOGO SPARIVANIYA V MODELI FERMI-ZHIDKOSTI]
A. A. Isaev and S. V. Peletminskij 1991 17 p In RUSSIAN Limited Reproducibility: More than 20% of this document may be affected by microfiche quality
(DE93-621770; KFTI-91-11) Avail: CASI HC A03 (US Sales Only)

A Fermi-liquid approach based on generalization of self-consistent field method to superfluid systems with triplet pairing is developed. Theory of Fermi-liquid for normal and superfluid states is based on a general expression for energy as a functional of normal and abnormal quasi-particle distribution functions. Under condition of thermodynamic potential minimum for a system, equations of self-consistency in triplet case describing superfluid phases with different symmetry properties are obtained. A detailed analysis of these equations for unitary and non-unitary states of superfluid Fermi-liquid is made. DOE

N94-13206# Los Alamos National Lab., NM.
DISCUSSION OF STRESS TENSOR NONUNIQUENESS WITH APPLICATION TO NONUNIFORM, PARTICULATE SYSTEMS
J. B. Aidun 1993 5 p Presented at the 14th International Conference on High Pressure Science and Technology and the 1993 Technical Meeting of the Topical Group on Shock Compression of Condensed Matter, Colorado Springs, CO, 28 Jun. - 3 Jul. 1993
(Contract W-7405-eng-36)
(DE93-014352; LA-UR-93-1968; CONF-9306167-1) Avail: CASI HC A01/MF A01

The indeterminacy of the mechanical stress tensor has been noted in several developments of expressions for stress in a system of particles. It is generally agreed that physical quantities related to the stress tensor must be insensitive to this nonuniqueness, but there is no definitive prescription for insuring it. Kroener's tensor decomposition theorem is applied to the mechanical stress tensor sigma(sub ij) to show that its complete determination requires specification of its 'incompatibility,' epsilon(sub ijk)

epsilon(sub lmn) delta(sub j) delta(sub m) sigma(sub kn), in addition to its divergence, which is obtained from the momentum conservation relation. For a particulate system, stress tensor incompatibility is shown to vanish to recover the correct expression for macroscopically observable traction. This result removes concern about nonuniqueness without requiring equilibrium or arbitrarily-defined force lines. DOE

N94-13479# Texas Univ., Austin. Center for Particle Physics.
THE GEOMETRIC PHASE IN QUANTUM PHYSICS
A. Bohm Mar. 1993 64 p Presented at the North Atlantic Treaty Organization-ASI Meeting on Recent Problems in Mathematical Physics, Salamanca, Spain, Jun. 1992
(Contract DE-FG03-93ER-40757)
(DE93-011121; DOE/ER-40757/004; CONF-9206360-1) Avail: CASI HC A04/MF A01

After an explanatory introduction, a quantum system in a classical time-dependent environment is discussed; an example is a magnetic moment in a classical magnetic field. At first, the general abelian case is discussed in the adiabatic approximation. Then the geometric phase for nonadiabatic change of the environment (Anandan-Aharonov phase) is introduced, and after that, general cyclic (nonadiabatic) evolution is discussed. The mathematics of fiber bundles is introduced, and some of its results are used to describe the relation between the adiabatic Berry phase and the geometric phase for general cyclic evolution of a pure state. The discussion is restricted to the abelian, U(1) phase. DOE

N94-13554 Toronto Univ. (Ontario).
THERMODYNAMIC STATUS OF STATIC AND DYNAMIC CONTACT ANGLES Ph.D. Thesis
Chester John Budziak 1992 247 p
(ISBN-0-315-73844-8) Avail: Univ. Microfilms Order No. DANN73844

A controversy about the meaning of contact angles and their lack of reproducibility is spread throughout the past century's literature of physics, chemistry and engineering. The majority of contact angle data available today is attributed to Zisman from work performed in the late 1940's and 1950's. His data is still in wide use today. Since Zisman considerable progress has been made in measuring contact angles. New procedures have been developed for surface and liquid preparations, as well as techniques for contact angle measurements. Non-ideal surfaces have been modeled allowing for thermodynamic interpretation of phenomenological contact angles. Still there is a need to incorporate all of these developments into a suitable methodology for measuring contact angles that are thermodynamically significant. The capillary rise at a vertical plate technique is best suited to the study of phenomenological contact angles. The precision of the capillary rise technique exceeds that of other contact angle measuring techniques since it is based on the measurement of a length, not an angle. It is also suited to the study of dynamic advancing, receding and static contact angles. The capillary rise technique has been unwanted in this thesis using digital image analysis in conjunction with high precision motor driven translational stages. The overall precision of the capillary rise at a vertical plate, h, using the automated cathetometer is equal to +/- 0.00001 cm. The corresponding precision in the contact angle is +/- 0.003 degrees. Three high quality solid surfaces were produced for studying contact angle phenomena: a dip-coating process was developed or coating a fluorocarbon solution (FC-721 produced by 3M) onto mica sheets; Teflon FEP was heat pressed against mica at elevated temperatures and pressures and microscope glass slides were siliconized. These surfaces exhibited less than +/- 0.1 degree variation in the contact angle over a 14 mm length of the surface. Dynamic advancing contact angles, measured on the above surfaces were found to be reproducible, independent of the velocity of the three phase contact line (for velocities less than 0.5 mm/min) and equal to the static contact angle. Contact angles measured by the capillary rise at a vertical plate technique were compared with contact angles of sessile drops measured by the Axisymmetric Drop Shape Analysis (ADSA). Excellent agreement has been found between contact angles obtained from the shape of a sessile drop and those obtained from the capillary rise on a vertical plate. The experimental contact angles were used to test two competing theories of determining the surface tension of solids from contact angles--the Fowkes surface component theory and the Neumann equation of state approach. It was found that the latter approach can be used to calculate the surface tension of solids and that an equation for interfacial tensions involves only the solid and 778 liquid surface tension. Author

N94-14417# Harvard Univ., Cambridge, MA.
MATHEMATICS AND STRING THEORY
A. Jaffe and Shing-Tung Yau 1993 8 p
(Contract DE-FG02-88ER-25065)
(DE93-017903; DOE/ER-25065/4) Avail: CASI HC A02/MF A01

Work on this grant was centered on connections between non-commutative geometry and physics. The following topics were covered: cyclic cohomology, non-commutative manifolds, index theory, reflection positivity, space quantization, quantum groups, and number theory. DOE

N94-14453# Sandia National Labs., Albuquerque, NM.
SIDEWALL THERMOMETRY PERTURBATIONS TO NONLINEAR HEAT TRANSPORT NEAR THE (LAMBDA) TRANSITION IN He-4
R. Duncan, R. Akau, S. Gianoulakis, U. Israelsson (Jet Propulsion Lab., California Inst. of Tech., Pasadena.), and T. Chui (Jet Propulsion Lab., California Inst. of Tech., Pasadena.) 1993 2 p Presented at the Conference of the International Union of Pure and Applied Physics on Low Temperature Physics (LT 20), Eugene, OR, 1-11 Aug. 1993
(Contract DE-AC04-76DP-00789)
(DE93-014990; SAND-93-1324C; CONF-930801-3) Avail: CASI HC A01/MF A01

The effect of a sidewall thermometry probe on heat transport measurements in liquid He-4 very close to the superfluid transition is simulated numerically. The effective thermal position of the probe changes with closeness of approach to the superfluid transition. The radial heat flux induced by the sidewall probe is calculated for specific probe designs. DOE

N94-14593# Los Alamos National Lab., NM.
STATISTICAL MECHANICAL THEORY OF LIQUID ENTROPY
D. C. Wallace 1993 15 p Presented at the 1st Congress of the International Society for Theoretical Chemistry and Physics, Gerona, Spain, 28 Jun. - 3 Jul. 1993
(Contract W-7405-eng-36)
(DE93-016524; LA-UR-93-2390; CONF-930680-1) Avail: CASI HC A03/MF A01

The multiparticle correlation expansion for the entropy of a classical monatomic liquid is presented. This entropy expresses the physical picture in which there is no free particle motion, but rather, each atom moves within a cage formed by its neighbors. The liquid expansion, including only pair correlations, gives an excellent account of the experimental entropy of most liquid metals, of liquid argon, and the hard sphere liquid. The pair correlation entropy is well approximated by a universal function of temperature. Higher order correlation entropy, due to n-particle irreducible correlations for n greater than or = 3, is significant in only a few liquid metals, and its occurrence suggests the presence of n-body forces. When the liquid theory is applied to the study of melting, the author discovers the important classification of normal and anomalous melting, according to whether there is not or is a significant change in the electronic structure upon melting, and he discovers the universal disordering entropy for melting of a monatomic crystal. Interesting directions for future research are: extension to include orientational correlations of molecules, theoretical calculation of the entropy of water, application to the entropy of the amorphous state, and correlational entropy of compressed argon. The author clarifies the relation among different entropy expansions in the recent literature. DOE

N94-14680# Carnegie-Mellon Univ., Pittsburgh, PA. Dept. of Mathematics.
NONLINEAR ANALYSIS, SCIENTIFIC COMPUTATION, AND CONTINUUM MECHANICS APPLIED TO THE SCIENCE OF MATERIALS Final Report, 9 Mar. 1990 - 9 Mar. 1993
Morton E. Gurtin and William O. Williams 9 Mar. 1993 12 p
(Contract MIPR-ARO-148-91)
(AD-A266641; ARO-27557.1-MA) Avail: CASI HC A03/MF A01

This grant enabled the department to form the Research Group in Mathematical Materials Science in 1990, a group that formed the nucleus of the Center for Nonlinear Analysis, established in 1991, by the ARO. The Center has created a vigorous environment for collaboration among

mathematicians and allied scientists. Within the international mathematics community the Center has assumed a leadership role, especially for questions related to materials science. The major research effort has focused toward developing, analyzing, and unifying mathematical models that characterize material behavior at a phenomenological level. The main thrust is applied nonlinear analysis, nonlinear continuum physics, and scientific computation. The educational goals have been to train young scientists and to train and involve female and minority students in the sciences.
DTIC

N94-14738# Stevens Inst. of Tech., Hoboken, NJ. Dept. of Physics and Engineering Physics.
INVESTIGATIONS OF TRANSITIONS FROM ORDER TO CHAOS IN DYNAMICAL SYSTEMS
G. Schmidt Mar. 1993 4 p
(Contract DE-FG02-87ER-13740)
(DE93-014438; DOE/ER-13740/11) Avail: CASI HC A01/MF A01
Work was carried out in the following areas: The Arter flow and fast dynamo in connection with astrophysical magnetic fields, chaotic ion motion in the magnetosphere, nonlinear waves in two-dimensional plasmas, stochastic webs and transport phenomena, and chaotic mixing. DOE

N94-14740# Los Alamos National Lab., NM.
THE FRACTIONAL QUANTUM HALL EFFECT AND THE SPHERICAL SHELL MODEL
J. N. Ginocchio 1993 17 p Presented at the From Spectroscopy to Chaos Symposium, Rochester, NY, 17 Apr. 1993
(Contract W-7405-eng-36)
(DE93-014553; LA-UR-93-1824; CONF-9304152-1) Avail: CASI HC A03/MF A01
We review the fractional quantum Hall effect in a spherical geometry and propose an ansatz for the many electron wavefunctions which may explain the fractional quantum Hall effect. DOE

N94-14887 Joint Inst. for Nuclear Research, Dubna (USSR). Lab. of Theoretical Physics.
SOLITON EQUATIONS AND SELF-DUAL GAUGE FIELDS
T. A. Ivanova and A. D. Popov 1992 12 p Limited Reproducibility: More than 20% of this document may be affected by microfiche quality
(DE93-626620; JINR-E-2-92-149) Avail: Issuing Activity (Department of Energy (DOE)) (US Sales Only)
The Boussinesq, N-wave, one-dimensional gas dynamics, matrix Korteweg-de Vries, and generalized nonlinear Schroedinger equations are shown to be reductions of the self-duality equations for gauge fields.
DOE

N94-14896# State Univ. of New York, Albany. Dept. of Physics.
STUDIES IN QUANTUM FIELD THEORY
D. G. Caldi Mar. 1993 3 p
(Contract DE-FG02-92ER-40741)
(DE93-017201; DOE/ER-40741/1) Avail: CASI HC A01/MF A01
A brief summary is given of work on the following topics: new phase of QED and the GSI peaks; conformal field theories, quantum groups, and integrable systems; and Q-quantum mechanics. DOE

80 SOCIAL SCIENCES (GENERAL)

Includes educational matters.

N94-13216 South Carolina Univ., Columbia.
WORKSHOP FOR COORDINATING SOUTH CAROLINA'S PRE-COLLEGE SYSTEMIC INITIATIVES IN SCIENCE AND MATHEMATICS
1992 13 p Presented at the Mathematics and Sciences Education Summit, Fripp Island, SC, 28-30 Aug. 1992 Limited Reproducibility: More than 20% of this document may be affected by poor print
(Contract DE-FG05-92ER-75842)
(DE93-012263; DOE/ER-75842/1; CONF-9208223) Avail: Issuing Activity (Department of Energy (DOE))
On 19 Dec. 1991, South Carolina's Governor, established the Governor's Mathematics and Sciences Advisory Board (MSAB) to articulate a vision and develop a statewide plan for improving science and mathematics education in South Carolina. The MSAB recognized that systemic change must occur if the achievement levels of students in South Carolina are to improve in a dramatic way. The MSAB holds two fundamental beliefs about systemic change: (1) all of the elements of the science and mathematics education system must be working in harmony towards the same vision; and (2) each element of the system must be held against high standards and progress must be assessed regularly against these standards.
DOE

N94-13427# Instituto de Pesquisas Espaciais, Sao Jose dos Campos (Brazil).
TECHNOLOGY PARKS AND THE COOPERATION AMONG UNIVERSITIES AND FIRMS: THE CASES OF CAMPINAS, SAO JOSE DOS CAMPOS E SAO CARLOS [OS POLOS TECNOLOGICOS DE CAMPINAS, SAO JOSE DOS CAMPOS E SAO CARLOS E A VINCULACAO UNIVERSIDADE-SETOR PRODUTIVO]
Jose Adelino Medeiros, Ana Lucia Vitale Torkomian, and Sergio Alves Perilo May 1991 39 p In PORTUGESE Presented at the 15th Simposio Nacional de Pesquisa de Administracao em Ciencia e Tecnologia, Sao Paulo, Brazil, 22-24 Oct. 1990
(INPE-5251-TAE/04) Avail: CASI HC A03/MF A01
This work presents the concept of technology parks and discusses three cases that exemplify the development of these structures in Brazil. General information about the cities where these experiences took place is made available and the relative importance of each park is discussed. It reviews the creation and development of universities and research institutes in each case and analyzes the existing organizational structures that promote the approximation between industry and research centers. The factors and the ways that led to the specialization of each technology park, the kinds of financing and governmental support received by each one and the role of scientists and entrepreneurs are discussed. Finally, a comparative analysis among the three cases is presented and the mechanisms that allowed the emergence of new technology base firms are highlighted. Author

N94-13619* National Aeronautics and Space Administration. John C. Stennis Space Center, Bay Saint Louis, MS.
TAECANNAUTICS: SHARING THE DREAM (Videotape)
Apr. 1989 Videotape: 13 min. 30 sec. playing time, in color, with sound
(NASA-TM-109309; NONP-VT-93-185328) Avail: CASI VHS A01/BETA A22
A week-long teacher workshop is described. Highlights include underwater simulation training, model rocket building and launching, map reading, and survival training. Author (revised)

N94-13984*# Science Applications International Corp., Washington, DC.
GENERIC RESULTS OF THE SPACE PHYSICS COMMUNITY SURVEY Final Report
Chris Thompson, ed., Rikhi R. Sharma, and Nathaniel B. Cohen Aug. 1993 133 p
(Contract NASw-4394)
(NASA-CR-194538; NAS 1.26:194538) Avail: CASI HC A07/MF A02
This report summarizes the results of a survey of the members of the space physics research community conducted in 1990-1991 to ascertain demographic information on the respondents and information on their views on a number of facets of their space physics research. The survey was conducted by questionnaire and the information received was compiled in a database and analyzed statistically. The statistical results are presented for the respondent population as a whole and by four different respondent cross sections: individual disciplines of space physics, type of employers, age groups, and research techniques employed. Data from a brief corresponding survey of the graduate students of respondents are also included. Author (revised)

N94-14462# Beleidscommissie Remote Sensing, Delft (Netherlands).
EDUCATIONAL MODULE FOR THE HIGHER AGRICULTURAL EDUCATION. PART 2: EUTROPHICATION OBSERVED BY REMOTE SENSING: AN EDUCATIONAL APPROACH TO WATER QUALITY MONITORING [ONDERWIJSMODULE VOOR HET HOGER AGRARISCH ONDERWIJS. DEEL 2: EUTROPHICATION OBSERVED BY REMOTE SENSING. AN EDUCATIONAL APPROACH TO WATER QUALITY MONITORING]

M. deBakker (Agrarische Univ., Friesland, Netherlands.) and P. Tempel (Agrarische Univ., Friesland, Netherlands.) Oct. 1992 23 p
(BCRS-92-11B; ISBN-9-05-411063-5; ETN-93-94088) Avail: CASI HC A03/MF A01

The eutrophication of surface waters, in particular of lakes in the Netherlands, were studied using remote sensing imagery. LANDSAT Thematic Mapper satellite images were studied to gain insight in the spatial patterns of eutrophication processes in the Frisian lakes as indicated by water coloring. The educational aspects of this study were managed with the image processing module of IDRISI, an educational, grid based geographic analysis system software package of Eastman. ESA

N94-14809# Beleidscommissie Remote Sensing, Delft (Netherlands).
EDUCATIONAL MODULE FOR THE HIGHER AGRICULTURAL EDUCATION. PART 1: LAND USE CLASSIFICATION USING SATELLITE PICTURES [ONDERWIJSMODULE VOOR HET HOGER AGRARISCH ONDERWIJS. DEEL 1: BODEMGEBRUIKSCLASSIFICATIE AAN DE HAND VAN SATELLIETBEELDEN]
A. vanRuiten and C. J. Pennekamp Oct. 1992 92 p In DUTCH
(BCRS-92-11a; ISBN-9-05-411049-X; ETN-93-94087) Avail: CASI HC A05/MF A01

The educational module--land use classification using satellite pictures--for students at higher agricultural schools without remote sensing experience is presented. The electromagnetic spectrum, spectral bands, and colors are introduced. Digital image improvement using the stretching technique is treated. The use of several bands for the reproduction of digital images is discussed. The density slicing method for the quantitative classification of satellite pictures is introduced. Land use classification based on the method of 'supervised classification' is explained. ESA

81 ADMINISTRATION AND MANAGEMENT

Includes management planning and research.

N94-13059# Ohio State Univ., Columbus. Research Foundation.
RELEGATION FOR DECENTRALIZED CONTROL Final Report, 1 Mar. 1989 - 30 Sep. 1992
U. Ozguner Feb. 1993 145 p
(Contract F49620-89-C-0046)
(AD-A265720; AFOSR-93-0390TR) Avail: CASI HC A07/MF A02

In this report, we describe the total effort at Ohio State on the Project Relegation for Decentralized Control. The first part of this reflects on one of the primary research topics which was considered in the first year of research. The work performed in the first year concentrated on optimal relegation. In the second part of the report, we concentrate on circuit analogies for large flexible space structures. Many large-scale systems such as flexible spacecraft appendages are nonlinear in behavior. But their large scale makes centralized control difficult. Thus, we propose several methods for designing decentralized control laws that take system nonlinearities into account. Equally important is the task of modeling large-scale systems. This motivated research on applying well-known circuit theory techniques to the problem of modeling flexible structures. The third part of this report describes work performed on another primary research topic which was considered in the first year of research-the use of singular perturbations for multi-time scale analysis of two-link structures. This work was developed for use in embedding active materials into the links and relegating the control tasks. DTIC

N94-13060# General Accounting Office, Washington, DC. Information Management and Technology Div.
JOHNSON SPACE CENTER PROCUREMENT: CONTROLS OVER PAYMENTS TO CONTRACTORS SHOULD BE STRENGTHENED
23 Oct. 1992 11 p
(AD-A265722; GAO/IMTEC-93-2) Avail: CASI HC A03/MF A01

The objective of this work was to determine if the JSC had adequate internal controls over the management of information processing contracts, grants, and purchase orders. We selected three cost-plus-award-fee contracts with significant information processing requirements for our review because they are, according to NASA procurement representatives, among the most complex to manage, and have products that are usually unique and sometimes difficult to objectively measure and evaluate. At JSC we select and review the management controls over these three contracts, currently valued at more than $425 million. Although JSC has various systems of internal controls in place, those used for paying contractors make JSC vulnerable to potential waste, abuse, and mismanagement. Specifically, JSC contracting officers and technical representatives do not link the receipt of products and services actually received against the cost vouchers contractors submit for payment. While JSC relies on a series of internal control mechanisms for assurances that contractors deliver high quality goods and services, none of these mechanisms is a sufficient substitute for periodic linking of contractors cost vouchers with products actually received. As a result, opportunities exist for JSC to be billed and pay for goods and services that were never received. DTIC

N94-13400*# National Aeronautics and Space Administration. Lyndon B. Johnson Space Center, Houston, TX.
USER OBSERVATIONS ON INFORMATION SHARING (CORPORATE KNOWLEDGE AND LESSONS LEARNED)
Ronald A. Montague, Lawrence A. Gregg (Webb, Murray and Associates, Inc., Houston, TX.), Shirley A. Martin (Webb, Murray and Associates, Inc., Houston, TX.), Leroy H. Underwood (Webb, Murray and Associates, Inc., Houston, TX.), and John M. McGee (Webb, Murray and Associates, Inc., Houston, TX.) Sep. 1993 92 p
(NASA-TM-104781; S-741; NAS 1.15:104781) Avail: CASI HC A05/MF A01

The sharing of 'corporate knowledge' and lessons learned in the NASA aerospace community has been identified by Johnson Space Center survey participants as a desirable tool. The concept of the program is based on creating a user friendly information system that will allow engineers, scientists, and managers at all working levels to share their information and experiences with other users irrespective of location or organization. The survey addresses potential end uses for such a system and offers some guidance on the development of subsequent processes to ensure the integrity of the information shared. This system concept will promote sharing of information between NASA centers, between NASA and its contractors, between NASA and other government agencies, and perhaps between NASA and institutions of higher learning. Author (revised)

N94-13629* National Aeronautics and Space Administration. Goddard Space Flight Center, Greenbelt, MD.
NASA EXPERIENCES IN THE GODDARD MMS (Videotape)
Jan. 1989 Videotape: 33 min. 20 sec. playing time, in color, with sound
(NASA-TM-109290; NONP-VT-93-185305) Avail: CASI VHS A01/BETA A22

The GSFC connection in the multi-mission spacecraft management field is explored. Author (revised)

N94-13982# National Science Foundation, Washington, DC. Div. of Science Resources Studies.
SELECTED DATA ON ACADEMIC SCIENCE AND ENGINEERING R AND D EXPENDITURES: FISCAL YEAR 1991
1991 30 p *Its* Surveys of Science Resources Series
(NSF-92-329) Avail: CASI HC A03/MF A01

The data presented in this summary are being released in advance of a more comprehensive detailed statistical tables publication and are compiled from the National Science Foundation's Survey of Scientific and Engineering Expenditures at Universities and Colleges Fiscal Year (FY) 1991. They refer to science and engineering (S&E) expenditures for separately budgeted research and development (R&D). The phrase 'separately budgeted research and development expenditures' refers to all funds that are expended for activities specifically organized to produce research outcomes and that are commissioned by an agency external to the institution or that are separately budgeted by an organizational unit within the institution. Data presented in these tables are assembled from the most recently completed survey and represent the latest totals available as of August 1992. Since both current-year and prior-year data are subject to revision in subsequent years, references to prior-years' data should be restricted to the latest data release. Derived from text

N94-14449# Technische Univ., Eindhoven (Netherlands).
DECISION SUPPORT FOR MATERIAL PLANNERS Ph.D. Thesis [BESLISSINGSONDERSTEUNING VOOR MATERIAALPLANNERS]

Adrianus Albertus An denBoer 1992 128 p In DUTCH
(ISBN-9-03-860201-4; ETN-93-94056) Copyright Avail: CASI HC A07/MF A02

The information processing and decision making behavior of material planners was analyzed in order to improve their logistic performance and to make recommendations for the (re)design of decision support systems. Insight was gained into the information processing and decision making behavior by comparative studies in different factories. The problem of the material planner was described in terms of theoretical decision science and psychological concepts. Possible improvements are discussed from a point of view of information technology and ergonomics. The recommended design for decision support is only operational as a prototype. Future developments are pointed out and recommendations for improving the decision support in general and for the material planner in particular are given. ESA

N94-14499# National Science Foundation, Washington, DC.
SCIENTISTS, ENGINEERS, AND TECHNICIANS IN NONMANUFACTURING INDUSTRIES: 1990. DETAILED STATISTICAL TABLES
Joseph P. Gannon 1990 88 p *Its* Surveys of Science Resources Series
(NSF-92-334) Avail: CASI HC A05/MF A01; SOD HC

Estimates are presented on the total number of scientists, engineers, and technicians (SET's) who were employed in nonmanufacturing industries in 1990. The estimates were developed from the Labor Department's Occupational Employment Statistics (OES) Survey, a Federal/State program that produces national and State estimates of employment by industry for nonfarm wage and salary workers. The Bureau of Labor Statistics (BLS) has the primary responsibility for developing OES survey procedures and providing technical guidance and assistance with survey problems. State Employment Security Agencies implement the survey at State levels and prepare current and projected employment statistics for these labor markets. Some States also prepare sub-State estimates. The National Science Foundation (NSF) has enhanced the BLS effort since 1977 by financing the collection of full details on the types of scientific and technical jobs filled by industry. Analysis of this information provides insight into the dynamics of the labor market. Author (revised)

N94-14796# Carnegie-Mellon Univ., Pittsburgh, PA. Robotics Inst.
AN EXPERIMENTAL ANALYSIS OF BOTTLENECK-CENTERED OPPORTUNISTIC SCHEDULING
Nicola Muscettola Mar. 1993 18 p
(Contract F30602-91-F-0016)
(AD-A266643; CMU-RI-TR-93-06) Avail: CASI HC A03/MF A01

Bottleneck-centered, opportunistic scheduling is an effective problem solving paradigm based on a fundamental Analyze-Focus-Decide cycle. Opportunistic schedulers have shown better overall performance than other scheduling systems adopting different paradigms. However, in order to make more significant progress, we need to better understand how the different phases of the opportunistic cycle interact during problem solving. This paper reports an extensive analysis of a specific embodiment of the opportunistic scheduling paradigm, the Conflict Partition Scheduling procedure. By analyzing the role of each phase of CPS proposing variations and anticipating expected effects on the performance of the algorithm, we aim to develop a better understanding of the importance of the different phases and of their interactions. The hypotheses on the performance of CPS are then verified in an experimental analysis. The results of this study provide hard evidence that supports the fundamental assumptions made by opportunistic scheduling. DTIC

82 DOCUMENTATION AND INFORMATION SCIENCE

Includes information management; information storage and retrieval technology; technical writing; graphic arts; and micrography.

For computer documentation see *61 Computer Programming and Software.*

N94-12801# Loyola Coll., Baltimore, MD. Japanese Technology Evaluation Center.
JTEC PANEL REPORT ON KNOWLEDGE-BASED SYSTEMS IN JAPAN Final Report
Michael J. DeHaemer, Geoffrey M. Holdridge, ed., Amy L. Bernstein, ed., and Robert S. Engelmore, ed. May 1993 218 p Sponsored in part by ARPA
(Grant NSF ENG-91-11333)
(PB93-170124; ISBN-1-883712-00-9) Avail: CASI HC A10/MF A03

This is the final report of the Japanese Technology Evaluation Center (JTEC) Panel on Knowledge-Based Systems in Japan, sponsored by the National Science Foundation and the Advanced Research Projects Agency. It examines Japanese expert systems applications and advanced knowledge-based (KB) systems R&D, and compares progress and trends with similar developments in the United States. The report includes an executive summary, an introductory chapter, and chapters on: applications; tools and infrastructure; advanced research; national projects; integration with conventional data processing systems; and business perspectives. Site reports on the visits made to Japanese corporate, government and university facilities are included as appendices. The panel observed some contrasts between U.S. and Japanese KB research and applications: Japanese computer manufacturers play a dominant role in the technology and business of expert systems. These large companies have mastered this technology as a core competence, and tend to use systems engineers rather than knowledge engineers to build systems. Consequently, integration with conventional information technology is handled routinely and smoothly. Japanese companies have more experience in applications of KB systems technology to heavy industry, particularly in steel and construction. Products based on the use of fuzzy control logic have had a big impact in Japanese consumer products. Japanese companies are continuing their substantial investments in KB systems technology and business. Compared to the U.S., the quantity of Japanese university research is considerably smaller, but the quality of the best work is as high. Author (revised)

N94-12907# Sandia National Labs., Albuquerque, NM.
MAKING THE CONNECTION BETWEEN INFORMATION MODELING AND IMPLEMENTATION
M. J. Eaton 1993 8 p Presented at the INGRES World 1993 Conference, Santa Clara, CA, 9-13 May 1993
(Contract DE-AC04-76DP-00789)
(DE93-011588; SAND-93-0869C; CONF-9305161-2) Avail: CASI HC A02/MF A01

Over the past several years, the Information Technology Department at Sandia Laboratories has developed information systems based on a solid foundation of information modeling and data administration. The output of the information modeling efforts is a fifth normal form relational table structure and associated data constraints. Developers would then implement the system by creating end-user application software. Traditionally, the development process combined the code necessary for maintaining data constraints with the code to provide the user interface (i.e. forms, windows, etc.). This approach has an adverse effect on the maintainability of the software as the system (i.e. the information model) changes over time. This paper will discuss the application of a direct connection between the information model and the implementation of a database with associated code to maintain required data constraints. The automated generation of this code allows the developers to concentrate on the user interface code development. The technique involves generating database procedure code automatically from the information modeling process. The database procedure code will enforce the data constraints defined in the information model. This has resulted in a fully functional database with complete rules enforcement within days of a completed information model. This work used the Knowledge Management Extensions of the Ingres database

software. Changes to the architecture of both Application By Forms (ABF) and Ingres Windows4GL client applications required by this process will also be discussed. DOE

N94-12936# Environmental Protection Agency, Washington, DC. Office of Solid Waste and Emergency Response.
VENDOR INFORMATION SYSTEM FOR INNOVATIVE TREATMENT TECHNOLOGIES. USER MANUAL (VISITT VERSION 2.0). NUMBER 2
Apr. 1993 71 p See also PB92-221647
(PB93-196640; EPA/542/R-93/001) Avail: CASI HC A04/MF A01

The Technology Innovation Office (TIO) of the U.S. Environmental Protection Agency (EPA) Office of Solid Waste and Emergency Response (OSWER) has developed the Vendor Information System for Innovative Treatment Technologies (VISITT) to provide current information on innovative treatment technology for the remediation of contaminated sites. VISITT contains technology information submitted by developers, manufacturers, and suppliers of innovative treatment technology equipment and services. The database provides a means for innovative technology vendors to make their products and capabilities known to state, Federal, and private sector professionals. The VISITT update, Version 2.0, contains approximately 230 technologies from more than 140 vendors. In addition to the increase in technologies and vendors, Version 2.0 also contains updated information on Version 1.0 vendors and enhanced printing capabilities that allow easier comparison of technologies and vendors. NTIS

N94-12958# Assistant Secretary of Defense (Communications Command Control and Intelligence), Washington, DC.
DEFENSE INFORMATION INFRASTRUCTURE: RATIONALE FOR DEFENSE MANAGEMENT REPORT DECISION 918 Final Report
Cynthia Kendall and Bill Beyer 26 May 1993 30 p
(AD-A266014) Avail: CASI HC A03/MF A01

On 15 Sep. 1993, the Deputy Secretary of Defense approved DMRD 918, 'Defense Information Infrastructure'. The objective of this DMRD is to establish an information infrastructure which provides a seamless, transparent, and protected end-to-end information transfer capability for DOD users. The paper Defense information Infrastructure: Rational for Defense Management Report Decision 918, Sep. 1992 provides the underlying assumption, principles, and strategy which provided the basis for the concept of the approved DRMD. The overall Defense Information Infrastructure (DII) and its role in support of joint operations is described. It defines those sub-elements of the Infrastructure for which the Defense information Systems Agency would have management responsibility (as envisioned in the development of the original DMRD), including a description of how the DISA could operate and finance theses functions. It outlines a potential sequence of actions to implement the information infrastructure that better support our joint and combined forces. The paper may be useful to anyone who has an interest in the genesis of the DMRD, especially as a baseline document from which informed discussion of the DMRD may proceed. DTIC

N94-12983# Superconducting Super Collider Lab., Dallas, TX.
BUILDING THE REPOSITORIES TO SERVE
D. Lersch Apr. 1993 5 p Presented at the International Particle Accelerator Conference, Washington, DC, 17-20 May 1993
(Contract DE-AC35-89ER-40486)
(DE93-014100; SSCL-Preprint-288; CONF-930511-90) Avail: CASI HC A01/MF A01

The project to design and build the Superconducting Super Collider (SSC) Laboratory also includes the exciting opportunity to implement client/server information systems. Lab technologists were eager to take advantage of the cost savings inherent in the open systems and a distributed, client server environment and, at the same time, conscious of the need to provide secure repositories for sensitive data as well as a schedule sensitive acquisition strategy for mission critical software. During the first year of project activity, micro-based project management and business support systems were acquired and implemented to support a small study project of less than 400 people allocating contracts of less than $1 million. The transition to modern business systems capable of supporting more than 10,000 participants (world wide) who would be researching and developing the new technologies that would support the world's largest scientific instrument, a 42 Tevatron, superconducting, super collider became a mission critical event. This paper will present the SSC Laboratory's strategy to balance our commitment to open systems, structured query language (SQL) standards and our success with acquiring commercial off the shelf software (COTS) to support our immediate goals. Included will be an outline of the vital roles played by other labs (Livermore, CERN, Brookhaven, Fermi and others) and a discussion of future collaboration potentials to leverage the information activities of all Department of Energy (DOE) funded labs. DOE

N94-13030*# Wisconsin Univ., Madison. Dept. of Computer Sciences.
[DEVELOPMENT OF ISO CONNECTION-ORIENTED/CORRECTIONLESS GATEWAYS] Final Report
Lawrence H. Landweber 4 Apr. 1991 1 p
(Grant NAGw-1318)
(NASA-CR-193667; NAS 1.26:193667) Avail: CASI HC A01/MF A01

The project had two goals, establishment of a gateway between French and U.S. academic networks and studies of issues related to the development of ISO connection-oriented/connectionless (CO/CL) gateways. The first component involved installation of a 56K bps line between Princeton Univ. and INRIA in France. The end-points of these lines were connected by Vitalink link level bridges. The Princeton end was then connected to the NSFNET via the John Von Neumann Supercomputer Center. The French end was connected to Transpac, the French X.25 public data network and to the French IP research internet. U.S. users may communicate with users of the French internet by e-mail and may access computational and data resources in France by use of remote login and file transfer. The connection to Transpac enables U.S. users to access the SIMBAD astronomical database outside of Paris. Access to this database from the U.S. can be via TCP/IP or DECNET (via a DECNET to TCP/IP gateway) protocols utilizing a TCP/IP to X.25 gateway developed and operated by INRIA. The second component of the project involved experiments aimed at understanding the issues involved is ISO CO/CL gateways. An experimental gateway was developed at Wisconsin and a preliminary report was prepared. Because of the need to devote most resources to the first component of the project, work in this area did not go beyond development of a prototype gateway. Author (revised)

N94-13041# Naval Research Lab., Bay Saint Louis, MS. Detachment Center.
KNOWLEDGE-BASED OCEANOGRAPHIC IMAGE COMPRESSION Final Report
Ronald J. Holyer and Juanita R. Chase Mar. 1993 30 p
(AD-A265752; NRL/MR/7240-93-7026) Avail: CASI HC A03/MF A01

The Navy has a requirement for image compression on the order of 30:1 for transmission of satellite imagery to the Fleet. Many common image compression algorithms will not retain the desired image fidelity at this compression ratio. This study investigates the use of domain specific oceanographic knowledge in the compression process as one means of achieving the required performance. A transform-based compression algorithm, which draws upon a large, representative image archive for a statistical description of oceanographic knowledge, is proposed and demonstrated. Very high compression ratios seem to be achievable by this method (much greater than 30:1), but the exact evaluation of performance potential requires further study. Among the unique characteristics of this approach is the ability to fill in cloudy areas with estimated image features. While knowledge-based image compression shows much promise for very high compression ratios, it does have significant drawbacks. The most significant of these are the requirement for a large image archive and much computation in order to build the region specific, knowledge-based algorithm. For these reasons, the compression approach demonstrated here is not seen as the single solution to all of the Navy's satellite image compression problems. However, in many applications the proposed algorithm could be very beneficial. In concert with other more generic image compression algorithms, knowledge-based image compression should play an important role. DTIC

N94-13057*# National Aeronautics and Space Administration. Langley Research Center, Hampton, VA.
NASA/DOD AEROSPACE KNOWLEDGE DIFFUSION RESEARCH PROJECT. REPORT 18: A COMPARISON OF THE TECHNICAL COMMUNICATION PRACTICES OF AEROSPACE ENGINEERS AND SCIENTISTS IN INDIA AND THE UNITED STATES
Thomas E. Pinelli, Rebecca O. Barclay (Rensselaer Polytechnic Inst., Troy,

NY.), and John M. Kennedy (Indiana Univ., Bloomington.) Washington Sep. 1993 69 p
(RTOP 505-90-00)
(NASA-TM-109006; NAS 1.15:109006) Avail: CASI HC A04/MF A01

As part of Phase 4 of the NASA/DoD Aerospace Knowledge Diffusion Research Project, two studies were conducted that investigated the technical communications practices of India and U.S. aerospace engineers and scientists. Both studies have the same seven objectives: first, to solicit the opinions of aerospace engineers and scientists regarding the importance of technical communications to their profession; second, to determine the use and production of technical communications by aerospace engineers and scientists; third, to seek their views about the appropriate content of an undergraduate course in technical communications; fourth, to determine aerospace engineers' and scientists' use of libraries, technical information centers, and on-line data bases; fifth, to determine the use and importance of computer and information technology to them; sixth, to determine their use of electronic networks; and seventh, to determine their use of foreign and domestically produced technical reports. A self-administered questionnaire was distributed to aerospace engineers and scientists at the Indian Institute of Science and the NASA Langley Research Center. The completion rates for the India and U.S. surveys were 48 and 53 percent, respectively. Responses of the India and U.S. participants to selected questions are presented in this report. Author

N94-13062*# Pennsylvania State Univ., University Park.
[ARCHIVING OF HEAO-1 DATA PRODUCTS AND THE CREATION OF A GENERAL USER'S GUIDE TO THE ARCHIVE] Final Technical Report
John A. Nousek 26 Feb. 1993 15 p
(Grant NAG8-758)
(NASA-CR-193415; NAS 1.26:193415) Avail: CASI HC A03/MF A01

The activities at Penn State University are described. Initiated at Penn State in Jan. 1989, the goal of this program was to preserve the results of the HEAO-1 mission by transforming the obsolete and disorganized data products into modern and documented forms. The result of this effort was an archive of top level data products, totalling 70 Mbytes; a general User's Guide to the archive, which is attached; and a hardcopy archive containing standardized plots and output of fits made to all the pointing data taken by the HEAO-1 A-2 LED experiment. A more detailed description of these activities is found in the following sections. Accompanying this document is a copy of the User's Guide which may provide additional detail. Author (revised)

N94-13105*# National Aeronautics and Space Administration, Washington, DC.
ACCESS TO JAPANESE AEROSPACE-RELATED SCIENTIFIC AND TECHNICAL INFORMATION: THE NASA AEROSPACE DATABASE
Glenn P. Hoetker and Thomas F. Lahr Oct. 1993 12 p
(NASA-TM-109413; NAS 1.15:109413) Avail: CASI HC A03/MF A01

With Japan's growing R&D strength in aerospace-related fields, it is increasingly important for U.S. researchers to be aware of Japanese advances. However, several factors make it difficult to do so. After reviewing the diffusion of aerospace STI in Japan, four factors which make it difficult for U.S. researchers to gather this information are discussed: language, the human network, information scatter, and document acquisition. NASA activities to alleviate these difficulties are described, beginning with a general overview of the NASA STI Program. The effects of the new National Level Agreement between NASA and NASDA are discussed. Author

N94-13107*# National Aeronautics and Space Administration, Washington, DC.
PROGRAM/PROJECT MANAGEMENT RESOURCE LISTS
Oct. 1993 63 p
(NASA-TM-109268; NAS 1.15:109268) Avail: CASI HC A04/MF A01

The Program/Project Management Collection at NASA Headquarters Library is part of a larger initiative by the Training and Development Division, Code FT, NASA Headquarters. The collection is being developed to support the Program/Project Management Initiative which includes the training of NASA managers. These PPM Resource Lists have proven to be a useful method of informing NASA employees nationwide about the subject coverage of the library collection. All resources included on the lists are available at or through NASA Headquarters Library. NASA employees at other Centers may request listed books through interlibrary loan, and listed articles by contacting me by phone, mail, or e-mail. Author

N94-13116*# Innovation Associates, Inc., Ann Arbor, MI.
VIEW GENERATED DATABASE Final Report
James G. Downward 1992 225 p
(Contract NAS7-1066; SBIR-05.01-8500)
(NASA-CR-191397; NAS 1.26:191397) Avail: CASI HC A10/MF A03

This document represents the final report for the View Generated Database (VGD) project, NAS7-1066. It documents the work done on the project up to the point at which all project work was terminated due to lack of project funds. The VGD was to provide the capability to accurately represent any real-world object or scene as a computer model. Such models include both an accurate spatial/geometric representation of surfaces of the object or scene, as well as any surface detail present on the object. Applications of such models are numerous, including acquisition and maintenance of work models for tele-autonomous systems, generation of accurate 3-D geometric/photometric models for various 3-D vision systems, and graphical models for realistic rendering of 3-D scenes via computer graphics. Author (revised)

N94-13121# Lawrence Livermore National Lab., CA.
SCORE USER'S MANUAL
S. A. Brown and D. Braddy Jan. 1993 42 p Revised
(Contract W-7405-eng-48)
(DE93-015987; UCRL-MA-108976-Rev-1) Avail: CASI HC A03/MF A01

PACT is a set of tools to facilitate the development of portable scientific software and to visualize scientific data. As with most constructs, PACT has a foundation. In this case that foundation is SCORE. SCORE (System CORE) has two main functions. The first and perhaps most important is to smooth over the differences between different C implementations and define the parameters which drive most of the conditional compilations in the rest of PACT. Second, it contains several groups of functionality that are used extensively throughout PACT. Although C is highly standardized now, that has not always been the case. Roughly speaking C compilers fall into three categories: ANSI standard; derivative of the Portable C Compiler (Kernighan and Ritchie); and the rest. PACT has been successfully ported to many ANSI and PCC systems. It has never been successfully ported to a system in the last category. The reason is mainly that the 'standard' C library supplied with such implementations is so far from true ANSI or PCC standard that PACT would have to include its own version of the standard C library in order to work at all. SCORE's job is to include the requisite standard headers and ensure that certain key standard library functions exist and function correctly so that, to applications which include the SCORE header(s) and load with SCORE, all C implementations look the same. Once SCORE has been successfully compiled, only the areas of graphics, IPC, and binary data handling require special handling. DOE

N94-13126*# Advanced Communications Technology, Inc., Silver Spring, MD.
VIEWCACHE: AN INCREMENTAL POINTER-BASE ACCESS METHOD FOR DISTRIBUTED DATABASES. PART 1: THE UNIVERSAL INDEX SYSTEM DESIGN DOCUMENT. PART 2: THE UNIVERSAL INDEX SYSTEM LOW-LEVEL DESIGN DOCUMENT. PART 3: USER'S GUIDE. PART 4: REFERENCE MANUAL. PART 5: UIMS TEST SUITE Final Report, 2 May 1989 - 31 Oct. 1992
Steve Kelley, Nick Roussopoulos, and Timos Sellis 10 Oct. 1992 238 p
(Contract NAS5-30628; SBIR-07.06-3759)
(NASA-CR-191788; NAS 1.26:191788) Avail: CASI HC A11/MF A03

The goal of the Universal Index System (UIS), is to provide an easy-to-use and reliable interface to many different kinds of database systems. The impetus for this system was to simplify database index management for users, thus encouraging the use of indexes. As the idea grew into an actual system design, the concept of increasing database performance by facilitating the use of time-saving techniques at the user level became a theme for the project. This Final Report describes the Design, the Implementation of UIS, and its Language Interfaces. It also includes the User's Guide and the Reference Manual. Author (revised)

N94-13192*# Purdue Univ., West Lafayette, IN. School of Electrical Engineering.

DESIGN OF PARTIALLY SUPERVISED CLASSIFIERS FOR MULTISPECTRAL IMAGE DATA

Byeungwoo Jeon and David Landgrebe Mar. 1993 87 p
(Grant NAGw-925)
(NASA-CR-194299; NAS 1.26:194299; TR-EE-93-11) Avail: CASI HC A05/MF A01

A partially supervised classification problem is addressed, especially when the class definition and corresponding training samples are provided a priori only for just one particular class. In practical applications of pattern classification techniques, a frequently observed characteristic is the heavy, often nearly impossible requirements on representative prior statistical class characteristics of all classes in a given data set. Considering the effort in both time and man-power required to have a well-defined, exhaustive list of classes with a corresponding representative set of training samples, this 'partially' supervised capability would be very desirable, assuming adequate classifier performance can be obtained. Two different classification algorithms are developed to achieve simplicity in classifier design by reducing the requirement of prior statistical information without sacrificing significant classifying capability. The first one is based on optimal significance testing, where the optimal acceptance probability is estimated directly from the data set. In the second approach, the partially supervised classification is considered as a problem of unsupervised clustering with initially one known cluster or class. A weighted unsupervised clustering procedure is developed to automatically define other classes and estimate their class statistics. The operational simplicity thus realized should make these partially supervised classification schemes very viable tools in pattern classification. Author (revised)

N94-13352# EG and G Energy Measurements, Inc., Idaho Falls.

GLOSSARY OF SSDC TERMS AND ACRONYMS

R. L. Horman Dec. 1992 159 p Revised
(Contract DE-AC07-76ID-01570)
(DE93-013697; DOE-76-45/28-Rev-1; SSDC-28-Rev-1) Avail: CASI HC A08/MF A02

This combination glossary and list of acronyms and abbreviations was compiled to provide the user a ready reference to System Safety Development Center (SSDC) terms. The acronyms are from the publication INEL Acronyms published by the Technical Publications Group. This group updates these acronyms periodically; the version used in this report was dated Oct. 1992. DOE

N94-13401*# National Aeronautics and Space Administration, Washington, DC.

NASA AEROSPACE DATABASE SUBJECT SCOPE: AN OVERVIEW

Sep. 1993 28 p
(NASA-SP-7107; NAS 1.21:7107) Avail: CASI HC A03/MF A01

Outlined here is the subject scope of the NASA Aerospace Database, a publicly available subset of the NASA Scientific and Technical (STI) Database. Topics of interest to NASA are outlined and placed within the framework of the following broad aerospace subject categories: aeronautics, astronautics, chemistry and materials, engineering, geosciences, life sciences, mathematical and computer sciences, physics, social sciences, space sciences, and general. A brief discussion of the subject scope is given for each broad area, followed by a similar explanation of each of the narrower subject fields that follow. The subject category code is listed for each entry. Author (revised)

N94-13406# Lawrence Livermore National Lab., CA.

DATAA: DATA ACQUISITION MADE EASY

R. L. Hodgin Oct. 1992 21 p
(Contract W-7405-eng-48)
(DE93-014683; UCRL-ID-113844) Avail: CASI HC A03/MF A01

DATAA was written to fill the need for a versatile, general purpose data acquisition program for digital scopes and data recorders. Unfortunately, a 'GPIB' software standard was only recently developed for such instruments. For operating the older, pre-standard digital scopes, different software for each instrument is usually required. The concept for this program is that the operator controls the instrument settings. The computer controls the data acquisition. 'Let the operators do what they do best, let the computer do what it does best.' In a research environment, the diagnostic setup requirements are constantly changing. Reliable, reproducible data is essential. DATAA accomplishes this task. Data is automatically stored, with setup information being included with each data file. A plotting routine allows for easy examination of all data. For hardcopies, data files are printed at 300DPI to a Laser Jet printer. This report contains a brief description of each main command. Included are figures showing the main display screens and sample waveform charts. DOE

N94-13461*# Jet Propulsion Lab., California Inst. of Tech., Pasadena.

PUBLICATIONS OF THE JET PROPULSION LABORATORY: 1990 AND 1991

15 Jun. 1993 59 p
(NASA-CR-193287; NAS 1.26:193287; JPL-BIBL-39-32) Avail: CASI HC A04/MF A01

JPL Bibliography 39-32 describes and indexes by primary author the externally distributed technical reporting, released during calendar years 1990 and 1991, that resulted from scientific and engineering work performed or managed by the Jet Propulsion Laboratory (JPL). Three classes of publications are included: (1) JPL publications (90- and 91-series) in which the information is complete for a specific accomplishment; (2) articles from the quarterly Telecommunications and Data Acquisition (TDA) Progress Report (42-series); and (3) articles published in the open literature. Author (revised)

N94-13701# Air Force Inst. of Tech., Wright-Patterson AFB, OH.

MAGIC MIRROR ON THE WALL, WHO'S THE FASTEST DATABASE OF THEM ALL? A SURVEY OF DATABASE BENCHMARKS

Timothy J. Halloran and Mark A. Roth 21 Jun. 1993 14 p
(AD-A266437; AFIT/EN-TR-93-5) Avail: CASI HC A03/MF A01

Benchmarks are important tools for measuring the performance of database management systems (DBMS) and for understanding vendor claims of performance. This paper performs the following tasks: defines DBMS benchmarks, explores the role of the Transaction Processing Performance Council as the only benchmark standards organization, and surveys eight existing DBMS benchmarks for on-line transaction processing, relational, and object-oriented databases. DTIC

N94-13806 Politecnico di Milano (Italy). Dipt. di Elettronica e Informazione.

INTEGRATION BETWEEN GEOGRAPHIC INFORMATION SYSTEMS AND ENVIRONMENTAL SIMULATION MODELS [INTEGRAZIONE TRA SISTEMI INFORMATIVI GEOGRAFICI E MODELLI DI SIMULAZIONE AMBIENTALI]

G. Calori 1993 29 p In ITALIAN
(Rept-93-004; ETN-93-94512) Avail: Politecnico di Milano, Piazza Leonardo da Vinci 32, 20133 Milan, Italy HC

The characteristics of a territorial information system aimed at supporting environmental simulation are outlined. Focusing on a reference architecture, a possible categorization of the information necessary to describe the world with data used by environmental simulation models, to support the conceptual design of an information system integrated with the management of geometrical and temporal aspects, is considered. The analysis applies specifically to simulation models of atmospheric pollution. ESA

N94-13863 Politecnico di Milano (Italy). Dipt. di Elettronica e Informazione.

THE OOA TECHNIQUE IN INFORMATION SYSTEMS [LE TECNICHE DI OOA NEI SISTEMI INFORMATIVI]

P. Fraternali 1992 25 p In ITALIAN
(Rept-72-92; ETN-93-94507) Avail: Politecnico di Milano, Piazza Leonardo da Vinci 32, 20133 Milan, Italy HC

The reasons for OOA and D (Object Oriented Analysis and Design) are addressed. Characteristics of complex systems, Structured Analysis and Design (SA/SD) and its limitations, the principal inspirations of OOA and D, a possible definition of OOA and D, and the advantages of OOA and D, are discussed. Cognitive processes and information organization based on OOA and D are discussed. The OO lifecycle is outlined. A proposed methodology for OOA is described. ESA

N94-13879 National Physical Lab., Teddington (England). Information Technology and Computing Div.

SECURITY CLAUSES IN THE WRITING AND ANALYSIS OF STANDARDS

Bronia Szczygiel and Andrew Harry Feb. 1993 17 p Sponsored by Dept. of Trade and Industry, London, United Kingdon

(NPL-DITC-216-93; ETN-93-94463) Copyright Avail: National Physical Laboratory, Teddington, Middlesex TW11 0LW, United Kingdom HC

Limitations in the power of formal methodologies in expressing security aspects of software led to the suggestion of the need for security clauses, these being statements within standards addressing the security properties that an implementation of the standard must demonstrate. The value of security clauses is discussed, and their relationship to formal specifications of standards is examined. The possible structure of such clauses and how they might be integrated into current methodologies are discussed and examples for a mechanistic and a protocol based standard are given.

ESA

N94-13915# Oak Ridge National Lab., TN.

A DATA BASE FOR AGING OF STRUCTURAL MATERIALS

C. B. Oland, D. J. Naus, and S. Jerath (North Dakota Univ., Grand Forks.) 1993 6 p *Presented at the 12th Biennial Conference for the International Association for Structural Mechanics in Reactor Technology, Stuttgart, Germany, 16-20 Aug. 1993*

(Contract DE-AC05-84OR-21400)

(DE93-009714; CONF-930803-5) Avail: CASI HC A02/MF A01

USNRC initiated a Structural Aging (SAG) Program at ORNL. The objective of the program is to provide assistance in identifying potential structural safety issues and to establish acceptance criteria for use in nuclear power plant evaluations for continued service. One part focuses on the development of a Structural Materials Information Center where long-term and environment-dependent material properties are being collected and assembled into a data base. This data base is presented in two complementary formats. The Structural Materials Handbook is an expandable, hard-copy reference document that contains the complete data base for each material. The Structural Materials Electronic Data Base is accessible using an IBM-compatible personal computer. This paper presents an overview of the Structural Materials Information Center and briefly describes the features of the handbook and the electronic data base. In addition, a proposed method for using the data base to establish current property values for materials in existing concrete structures and to estimate the future performance of these materials is also presented. DOE

N94-14048# Virginia Polytechnic Inst. and State Univ., Blacksburg. Dept. of Industrial and Systems Engineering.

INFORMATION REQUIREMENTS OF SELF-MANAGING TEAMS

E. M. VanAken 1992 12 p Presented at the International Conference on Self-Managing Teams, Dallas, TX, Sep. - Oct. 1992

(Contract DE-FG02-91NP-00119)

(DE93-010319; CONF-9209334-1) Avail: CASI HC A03/MF A01

In response to the significant challenges organizations face today, many managers have put in place continuous improvement efforts to help the organization to enhance its competitive position. A key element of continuous improvement efforts is employee involvement, and one of the most complex, mature, and effective forms of employee involvement is self-managing teams. A self-managing team is a group of employees, usually eight to fifteen, which is responsible for planning, implementing, controlling, and improving work processes. There are many characteristics of self-managing teams which are discussed frequently in the literature and are common topics of seminars and workshops on SMT's, including the role of the first-line supervisor, the structure of teams, the training necessary, and the pay system for SMT's. However, one area which has not been as widely researched is the role of information--what types of information do self-managing teams need? This paper addresses this question. Results from a multiple case study research project focusing on the information requirements of SMT's are presented. Specifically, seven types of information SMT's need are identified, as well as general characteristics of the information system. By information system, I mean very broadly, the system (both formal and informal) which provides information of any kind to a self-managing team. The results of this research can be thought of as 'design features' for an information system to support SMT's. Practicing managers can use these design features in two ways: they can design them into beginning SMT efforts; or, for SMT's already established, managers can compare them to the existing information system and adjust accordingly. DOE

N94-14069# National Research Council of Canada, Ottawa (Ontario).

[ACTIVITIES OF INSTITUTE FOR INFORMATION TECHNOLOGY] Annual Report, 1991-1992 [INSTITUT DE TECHNOLOGIE DE L'INFORMATION: RAPPORT ANNUEL 1991/1992]

Sep. 1992 55 p In FRENCH Original contains color illustrations

(CNR-35024; CTN-93-60818) Copyright Avail: CASI HC A04/MF A01

The Institute for Information Technology is part of Canada's National Research Council and has five laboratories, four in the Montreal-Ottawa corridor and one in British Columbia. The Institute's research programs comprise four elements: software engineering, including integrated and real-time systems, large-scale systems, and commercial software products; knowledge based systems, including intelligent advisor systems, diagnostic systems, and automatic learning; sensor-based automation, including robotics, sensor systems, and photonic systems; and systems integration, including manufacturing and resource industry support systems and electromagnetic protection. Activities of the Institute for 1991/92 are reviewed, and lists of publications, patents, and presentations are included.

CISTI

N94-14072# Nijmegen Univ. (Netherlands). Dept. of Informatics.

PSM: A NEW GENERATION OF DATA MODELING [PSM: DATAMODELLEREN, IN HET KWADRAAT]

A. H. M. terHofstede, H. A. Proper, and T. P. vanderWeide Jun. 1992 12 p In DUTCH

(TR-92-13; ETN-93-93867) Avail: CASI HC A03/MF A01

The data modeling technique PSM (Predicator Set Model) is presented. PSM is a general data modeling technique and serves as a basis for all modeling techniques based on the so called object role approach. PSM is an exponent of a new generation of data modeling techniques which is suited for complex data structures. The present generation fails in the modeling of complex application domains; such as hypermedia applications, CAD/CAM (Computer Aided Design/Manufacturing) systems, and meta-modeling. ESA

N94-14196# National Research Council of Canada, Ottawa (Ontario). Machinery and Engine Technology.

AN EXPERT SYSTEM CLASS LIBRARY FOR AUDITION [BIBLIOTHEQUE DU TYPE SYSTEME EXPERT POUR AUDITION]

David M. Morton and Andrew M. Drinnan Dec. 1992 13 p

(IME-MET-TR-008; CTN-93-60860) Avail: CASI HC A03/MF A01

An expert system class library for the object-oriented Audition environment has been created. The expert system is a forward chaining rule-based inference engine. It owns a set of static facts that are supplied by the user and a set of dynamic facts that the system has inferred. Dynamic facts are inferred from existing facts using a set of user-specified rules. User specified actions may also be executed based on the results of these inferences. To minimize inferencing time, rules are grouped into rulesets. Groups of rulesets that define complete sets of knowledge are organized into knowledge bases. An expert system may have multiple knowledge bases. A rule editor is provided for creating, editing and debugging. An overview is presented for the system applied for air traffic control. CISTI

N94-14202# National Research Council of Canada, Ottawa (Ontario). Inst. for Information Technology.

AN EVALUATION OF ZIM AND ENTITY-RELATIONAL MODELS IN MANAGING DATABASES FOR DECISION SUPPORT SYSTEMS

D. B. Kotak and T. B. Wong Apr. 1991 31 p

(ERB-1034; NRC-31835; CTN-93-60823) Copyright Avail: CASI HC A03/MF A01

ZIM is a fourth generation database management system developed by Zanthe Information Management and designed using the newest theory in database design, the entity relationship set theory. ZIM was evaluated as a potential candidate for use as a tool in developing a computer based decision support system for solving capacity flow problems. An overview of ZIM is presented, including software installation and the application generation process. The evaluation was carried out by building, as a test case, a database to support the vessel berthing information for the British

Columbia Grain Shippers' Clearance Association. ZIM is shown to be an extremely powerful and flexible system for developing standalone databases, particularly for developing daily production applications. Its procedural language, coupled with its excellent screen definition system, provides full flexibility in setting up user-oriented menus and displays. However, this flexibility is achieved at the cost of having to learn a completely new language, and ZIM's poor external language interface and hidden data file structure do not lend themselves to integration with other software packages. CISTI

N94-14331# Lawrence Livermore National Lab., CA.
STORAGE SYSTEMS FOR NATIONAL INFORMATION ASSETS
R. A. Coyne (IBM Federal Systems Div., Houston, TX.), H. Hulen (IBM Federal Systems Div., Houston, TX.), and R. Watson 17 Feb. 1993 10 p Presented at the ACM/IEEE Supercomputing Conference, Minneapolis, MN, 14-21 Nov. 1992
(Contract W-7405-eng-48)
(DE93-015101; UCRL-JC-111558-Rev-1; CONF-921125-7) Avail: CASI HC A02/MF A01

An industry-led collaborative project, called the National Storage Laboratory, has been organized to investigate technology for storage system that will be the future repositories for our national information assets. Lawrence Livermore National Laboratory through its National Energy Research Supercomputer Center (NERSC) is the operational site and the provider of applications. It is anticipated that the integrated testbed system will represent a significant advance in the technology for distributed storage system capable of handling gigabyte class files at gigabit-per-second data rates. DOE

N94-14433# California Univ., Berkeley. Lawrence Berkeley Lab.
PUBLIC CENSUS DATA ON CD-ROM AT LAWRENCE BERKELEY LABORATORY
D. W. Merrill Oct. 1992 15 p
(Contract DE-AC03-76SF-00098)
(DE93-015273; LBL-32165-Rev-2) Avail: CASI HC A03/MF A01

The Comprehensive Epidemiologic Data Resource (CEDR) and Populations at Risk to Environmental Pollution (PAREP) projects, of the Information and Computing Sciences Division (ICSD) at Lawrence Berkeley Laboratory (LBL), are using public socio-economic and geographic data files which are available to CEDR and PAREP collaborators via LBL's computing network. At this time, 70 CD-ROM diskettes (approximately 36 gigabytes) are on line via the Unix file server cedrcd. lbl. gov. Most of the files are from the US Bureau of the Census, and most pertain to the 1990 Census of Population and Housing. All the CD-ROM diskettes contain documentation in the form of ASCII text files. Printed documentation for most files is available for inspection at University of California Data and Technical Assistance (UC DATA), or the UC Documents Library. Many of the CD-ROM diskettes distributed by the Census Bureau contain software for PC compatible computers, for easily accessing the data. Shared access to the data is maintained through a collaboration among the CEDR and PAREP projects at LBL, and UC DATA, and the UC Documents Library. Via the Sun Network File System (NFS), these data can be exported to Internet computers for direct access by the user's application program(s). DOE

N94-14458# Oak Ridge National Lab., TN.
OAK RIDGE ENVIRONMENTAL INFORMATION SYSTEM (ORIES) SITE WORKSTATION INFORMATION PACKET FOR OREIS 6.2
L. D. Voorhees, R. A. McCord, R. C. Durfee, M. L. Land, R. J. Olson, M. R. Palmer, J. K. Thomas, E. P. Tinnel, and B. C. Zygmunt Feb. 1993 128 p
(Contract DE-AC05-84OR-21400)
(DE93-010761; ES/ER/TM-57) Avail: CASI HC A07/MF A02

The OREIS site workstation information packet was developed to accompany the OREIS site workstations, which are being delivered to the Environmental Restoration programs at the five DOE-OR sites. The packet is written specifically for the Site ER program staff at each of the five sites who have been designated the OREIS contact by their ER program manager, and is not intended for general distribution. The packet provides an overview of the components of OREIS, points to more detailed information provided in the accompanying vendor and OREIS developed manuals, and includes information on training opportunities and user support. DOE

N94-14485*# National Aeronautics and Space Administration. Langley Research Center, Hampton, VA.
NASA/DOD AEROSPACE KNOWLEDGE DIFFUSION RESEARCH PROJECT. PAPER 34: USERS AND USES OF DOD TECHNICAL REPORTS: A REPORT FROM THE FIELD
Thomas E. Pinelli, Rebecca O. Barclay (Rensselaer Polytechnic Inst., Troy, NY.), and John M. Kennedy (Indiana Univ., Bloomington.) 1993 23 p Presented at the 1993 Military Librarians Workshop, Albuquerque, NM, 15-19 Nov. 1993; sponsored by Phillips Lab. and Special Libraries Association
(NASA-TM-109327; NAS 1.15:109327) Avail: CASI HC A03/MF A01

The NASA/DoD Aerospace Knowledge Diffusion Research Project attempts to understand the information environment in which U.S. aerospace engineers and scientists work, the information-seeking behavior of U.S. aerospace engineers and scientists, and the factors that influence the use of scientific and technical information (STI) (Pinelli, Barclay, and Kennedy, 1991). Such an understanding could (1) lead to the development of practical theory, (2) contribute to the design and development of aerospace information systems, and (3) have practical implications for transferring the results of federally funded aerospace research and development (R&D) to the U.S. aerospace community. This paper presents data from two information-seeking behavior studies involving U.S. aerospace engineers and scientists that were undertaken as Phase 1 activities of the NASA/DoD Aerospace Knowledge Diffusion Research Project. Responses from three groups of respondents - DoD, other government, and industry - are presented for two sets of selected questions. One set focuses on DoD technical reports: their use and importance, reasons for non-use, the factors affecting their use, the sources used to find out about them and the sources used to physically obtain them, and the quality of DoD technical reports. The second set focuses on information sources used in problem solving: the use of U.S. government technical reports in problem solving and the information sources used to find out about U.S. government technical reports. Derived from text

N94-14486*# National Aeronautics and Space Administration. Langley Research Center, Hampton, VA.
NASA/DOD AEROSPACE KNOWLEDGE DIFFUSION RESEARCH PROJECT. PAPER 36: TECHNICAL UNCERTAINTY AS A CORRELATE OF INFORMATION USE BY US INDUSTRY-AFFILIATED AEROSPACE ENGINEERS AND SCIENTISTS
Thomas E. Pinelli, Nanci A. Glassman (Continental Research, Norfolk, VA.), Linda O. Affelder (Continental Research, Norfolk, VA.), Laura M. Hecht (Indiana Univ., Bloomington.), John M. Kennedy (Indiana Univ., Bloomington.), and Rebecca O. Barclay (Rensselaer Polytechnic Inst., Troy, NY.) 1994 10 p Proposed for presentation at the 32nd Aerospace Sciences Meeting and Exhibit of the American Institute of Aeronautics and Astronautics, Reno, NV, 11 Jan. 1994
(NASA-TM-109328; NAS 1.15:109328; AIAA Paper 94-0839) Avail: CASI HC A02/MF A01

This paper reports the results of an exploratory study that investigated the influence of technical uncertainty on the use of information and information sources by U.S. industry-affiliated aerospace engineers and scientists in completing or solving a project, task, or problem. Data were collected through a self-administered questionnaire. Survey participants were U.S. aerospace engineers and scientists whose names appeared on the Society of Automotive Engineers (SAE) mailing list. The results support the findings of previous research and the following study assumptions. Information and information-source use differ for projects, problems, and tasks with high and low technical uncertainty. As technical uncertainty increases, information-source use changes from internal to external and from informal to formal sources. As technical uncertainty increases, so too does the use of federally funded aerospace research and development (R&D). The use of formal information sources to learn about federally funded aerospace R&D differs for projects, problems, and tasks with high and low technical uncertainty. Author

N94-14487*# National Aeronautics and Space Administration. Langley Research Center, Hampton, VA.
NASA/DOD AEROSPACE KNOWLEDGE DIFFUSION RESEARCH PROJECT. PAPER 39: THE ROLE OF COMPUTER NETWORKS IN AEROSPACE ENGINEERING
Ann P. Bishop (Illinois Univ., Urbana-Champaign.) and Thomas E. Pinelli

1994 16 p Proposed for presentation at the 32nd Aerospace Sciences Meeting and Exhibit of the American Institute of Aeronautics and Astronautics, Reno, NV, 11 Jan. 1994
(NASA-TM-109331; NAS 1.15:109331; AIAA Paper 94-0841) Avail: CASI HC A03/MF A01

This paper presents selected results from an empirical investigation into the use of computer networks in aerospace engineering. Such networks allow aerospace engineers to communicate with people and access remote resources through electronic mail, file transfer, and remote log-in. The study drew its subjects from private sector, government and academic organizations in the U.S. aerospace industry. Data presented here were gathered in a mail survey, conducted in Spring 1993, that was distributed to aerospace engineers performing a wide variety of jobs. Results from the mail survey provide a snapshot of the current use of computer networks in the aerospace industry, suggest factors associated with the use of networks, and identify perceived impacts of networks on aerospace engineering work and communication. Author

N94-14488*# National Aeronautics and Space Administration. Langley Research Center, Hampton, VA.
NASA/DOD AEROSPACE KNOWLEDGE DIFFUSION RESEARCH PROJECT. PAPER 37: THE IMPACT OF POLITICAL CONTROL ON TECHNICAL COMMUNICATIONS: A COMPARATIVE STUDY OF RUSSIAN AND US AEROSPACE ENGINEERS AND SCIENTISTS
Rebecca O. Barclay (Rensselaer Polytechnic Inst., Troy, NY.), Thomas E. Pinelli, Madelyn Flammia (University of Central Florida, Orlando.), and John M. Kennedy (Indiana Univ., Bloomington.) 1994 12 p Proposed for presentation at the 32nd Aerospace Sciences Meeting and Exhibit of the American Institute of Aeronautics and Astronautics, Reno, NV, 11 Jan. 1994
(NASA-TM-109329; NAS 1.15:109329; AIAA Paper 94-0838) Avail: CASI HC A03/MF A01

Until the recent dissolution of the Soviet Union, the Communist Party exerted a strict control of access to and dissemination of scientific and technical information (STI). This article presents models of the Soviet-style information society and the Western-style information society and discusses the effects of centralized governmental control of information on Russian technical communication practices. The effects of political control on technical communication are then used to interpret the results of a survey of Russian and U.S. aerospace engineers and scientists concerning the time devoted to technical communication, their collaborative writing practices and their attitudes toward collaboration, the kinds of technical documents they produce and use, and their use of computer technology, and their use of and the importance to them of libraries and technical information centers. The data are discussed in terms of tentative conclusions drawn from the literature. Finally, we conclude with four questions concerning government policy, collaboration, and the flow of STI between Russian and U.S. aerospace engineers and scientists. Author

N94-14489*# National Aeronautics and Space Administration. Langley Research Center, Hampton, VA.
NASA/DOD AEROSPACE KNOWLEDGE DIFFUSION RESEARCH PROJECT. PAPER 38: COMPUTER MEDIATED COMMUNICATION (CMC) AND THE COMMUNICATION OF TECHNICAL INFORMATION IN AEROSPACE
Daniel J. Murphy (State Univ. of New York, Utica.) and Thomas E. Pinelli 1994 13 p Proposed for presentation at the 32nd Aerospace Sciences Meeting and Exhibit of the American Institute of Aeronautics and Astronautics, Reno, NV, 11 Jan. 1994
(NASA-TM-109330; NAS 1.15:109330; AIAA Paper 94-0840) Avail: CASI HC A03/MF A01

This paper discusses the use of computers as a medium for communication (CMC) used by aerospace engineers and scientists to obtain and/or provide technical information related to research and development activities. The data were obtained from a questionnaire survey that yielded 1006 mail responses. In addition to communication media, the research also investigates degrees of task uncertainty, environmental complexity, and other relevant variables that can affect aerospace workers' information-seeking strategies. While findings indicate that many individuals report CMC is an important function in their communication patterns, the research indicates that CMC is used less often and deemed less valuable than other more conventional media, such as paper documents, group meetings, telephone and face-to-face conversations. Fewer than one third of the individuals in the survey account for nearly eighty percent of the reported CMC use, and another twenty percent indicate they do not use the medium at all, its availability notwithstanding. These preliminary findings suggest that CMC is not as pervasive a communication medium among aerospace workers as the researcher expect a priori. The reasons underlying the reported media use are not yet fully known, and this suggests that continuing research in this area may be valuable. Author

N94-14498# National Oceanic and Atmospheric Administration, Washington, DC.
SUMMARY OF THE NOAA/NESDIS WORKSHOP ON DEVELOPMENT OF A GLOBAL SATELLITE/IN SITU ENVIRONMENTAL DATABASE
K. P. Gallo, ed. and D. A. Hastings, ed. (National Geophysical Data Center, Boulder, CO.) Aug. 1993 21 p Workshop held in Camp Springs, MD, 9-11 Sep. 1992
(NOAA-TR-NESDIS-72) Avail: CASI HC A03/MF A01

A Workshop was convened 9-11 Sep. 1992, at the NOAA Science Center, Camp Springs, Maryland, to discuss the development of a Global Satellite/In Situ Environmental Database (original workshop title 'Comprehensive Satellite/In Situ Climate Data Product') that would address the requirements of the climate modeling and diagnostics communities. The objectives of the workshop included review of the current products of the National Environmental Satellite, Data, and Information Service (NESDIS) and development of recommendations and requirements for a combined satellite and surface (in situ) global climatology data set. A group of approximately 35 individuals that represented the operational satellite measurements, climate modeling, and climate diagnostic communities participated in the workshop. The candidate data sets for inclusion in the Environmental Database included operational satellite products and, potentially, in situ data. Operational products discussed included Satellite Derived Atmospheric Soundings, Snow Cover, Sea Ice, Vegetation Index, Sea Surface Temperature, Ozone, Aerosols, and Planetary Radiation Budget Data Sets. Author (revised)

N94-14555 Tel-Aviv Univ. (Israel). Applied Math Dept.
REMOVING NOISE FROM DISCONTINUOUS DATA M.S. Thesis
Daphna Mizrachi Nov. 1991 59 p
(ITN-93-85211) Copyright Avail: Issuing Activity (Tel-Aviv Univ., Exact Sciences Library, Ramat Aviv 69978, Israel)

Most information sampling processes add noise to the sampled signal, usually in the form of small oscillations from the function which describes the information. Standard filtering methods can remove the noise from discontinuous data, but at the cost of smearing the discontinuities. In the present work, two methods are presented for removing noise without blurring discontinuities. The first method is based on the least square approximation, which removes noise from the signal by replacing it with a smooth polynomial function which minimizes the sum of the squared residuals. To preserve discontinuities and avoid the creation of a Gibbs phenomenon near them, the method starts by detecting all discontinuity points. Then a fit is found for each noisy but smooth part of the signal, assuming there is no correlation between the elements of the noise. Thus, the fit minimizes the squared residuals and also produces uncorrelated residuals. The second approach uses the fact that any data-compression algorithm contains an element of noise reduction; white noise is among the non-significant information removed in the compression process. A multi-resolution type of noise compression algorithm is used, in which the information content of the signal is decomposed into a hierarchy of scales. Noise in the signal shows up in the very high scales as rapid oscillations, with no contribution to the information content, i.e., as uncorrelated deviations from a mean value. An essentially non-oscillatory (ENO) interpolation technique is presented, ISA

N94-14562 Defense Information Systems Agency, Arlington, VA.
DEFENSE INFORMATION TECHNOLOGY SERVICES ORGANIZATION FY 1994 BUDGET ESTIMATES. INFORMATION TECHNOLOGY SYSTEMS BUDGET
Apr. 1993 284 p Limited Reproducibility: More than 20% of this document may be affected by microfiche quality
(PB93-199016) Avail: CASI HC A13

The following contents are presented: General Narrative; Report on Information Technology Systems; Summary Report on Collections; Summary Report on Development and Modernization; Summary Report on Operations

and Other Costs; Report on Operations and Other Cost Function Activities; Major Information Technology Acquisition Plans, ADP Requirements/Indefinite-Quantity Contract; and Central Design Activities.
NTIS

N94-14803 Georgia Univ., Athens. Complex Carbohydrate Research Center.
CarbBank: A STRUCTURAL AND BIBLIOGRAPHIC DATABASE FOR COMPLEX CARBOHYDRATES
P. Albersheim Jun. 1992 8 p Limited Reproducibility: More than 20% of this document may be affected by microfiche quality
(Contract DE-FG09-88ER-13970)
(DE93-015582; DOE/ER-13970/4) Avail: Issuing Activity (Department of Energy (DOE))
The CarbBank project has several key facets: building a computer database that presents carbohydrate sequence information derived from the published literature, programming to create computer applications that use the information in the database, creating software for multiple computer platforms, and distributing software to end users. DOE

N94-14880 International Atomic Energy Agency, Vienna (Austria). Nuclear Data Section.
INGDB-90. THE INTERNATIONAL NEUTRON NUCLEAR DATA BASE FOR GEOPHYSICS APPLICATIONS
N. P. Kocherov and P. K. McLaughline, comp. Jul. 1991 11 p Limited Reproducibility: More than 20% of this document may be affected by microfiche quality
(DE93-624095; IAEA-NDS-127(Rev-0)) Avail: CASI HC A03 (US Sales Only)
This document describes the contents of the International Neutron Nuclear Data Base for applications in nuclear geophysics, such as borehole logging and mineral analysis. It contains neutron cross-section data from 19 elements and their isotopes of primary importance in geophysics, plus a data file with neutron spectra of three frequently used neutron sources. The INGDB-90 file is available, cost free, from the IAEA Nuclear Data Section on PC diskettes or on magnetic tape. DOE

N94-14249# Ludwig-Maximilians-Univ., Munich (Germany). Dept. for General and Applied Geology.
DEVELOPMENT OF A REMOTE SENSING GEOGRAPHIC INFORMATION SYSTEM FOR LAND COVER CHANGES AND ASSESSMENT OF RISK DUE TO NATURAL AND MAN MADE HAZARDS COVERING THE AREA OF THE INNER DELTA OF THE YELLOW RIVER
A. Hirscheider, J. Bodechtel, C. Yuan, m1459168, W. Zhang (Ministry of Geology and Mineral Resources, Beijing, China.), T. Zhang (Geology Science Inst., Henan, China.), T. Chen (Geology Science Inst., Henan, China.), and W. Mauser *In* Science and Technology Agency, Asia-Pacific ISY Conference, Volume 2 31 Mar. 1993 p 204-207 (For primary document see N94-14209 02-43)
Avail: CASI HC A01/MF A04

83 ECONOMICS AND COST ANALYSIS

Includes cost effectiveness studies.

No abstracts in this category.

84 LAW, POLITICAL SCIENCE AND SPACE POLICY

Includes NASA appropriation hearings; aviation law; space law and policy; international law; international cooperation; and patent policy.

N94-12800*# Hernandez Engineering, Inc., Houston, TX.
WHERE NO FLAG HAS GONE BEFORE: POLITICAL AND TECHNICAL ASPECTS OF PLACING A FLAG ON THE MOON
Anne M. Platoff Aug. 1993 16 p Presented at the 26th Meeting of the North American Vexillological Association, San Antonio, TX, 11 Oct. 1992
(Contract NAS9-18263)
(NASA-CR-188251; NAS 1.26:188251) Avail: CASI HC A03/MF A01
The flag on the Moon represents an important event in vexillological history. The political and technical aspects of placing a flag on the Moon, focusing on the first Moon landing, is examined. During their historic extravehicular activity, the Apollo 11 crew planted the flag of the United States on the lunar surface. This flag-raising was strictly a symbolic activity, as the United Nations Treaty on Outer Space precluded any territorial claim. Nevertheless, there were domestic and international debates over the appropriateness of the event. Congress amended the agency's appropriations bill to prevent the National Aeronautics and Space Administration (NASA) from placing flags of other nations, or those of international associations, on the Moon during missions funded solely by the United States. Like any activity in space exploration, the Apollo flag-raising also provided NASA engineers with an interesting technical challenge. They designed a flagpole with a horizontal bar allowing the flag to 'fly' without the benefit of wind to overcome the effects of the Moon's lack of an atmosphere. Other factors considered in the design were weight, heat resistance, and ease of assembly by astronauts whose space suits restricted their range of movement and ability to grasp items. As NASA plans a return to the Moon and an expedition to Mars, we will likely see flags continue to go 'where no flag has gone before'. Author (revised)

N94-14115 National Academy of Sciences - National Research Council, Washington, DC. Committee on Science, Engineering and the Federal Government.
SCIENCE, TECHNOLOGY, AND THE FEDERAL GOVERNMENT: NATIONAL GOALS FOR A NEW ERA
Steve Olson, ed. 1993 60 p
Copyright Avail: Issuing Activity
This Committee on Science, Engineering, and Public Policy of the National Academy of Sciences, National Academy of Engineering, and Institute of Medicine presents five chapters and an appendix dealing with the federal funding of research and development in the United States. Each chapter presents different perspectives such as: The Changing Context for science and Technology, Science and Technology in Modern Society, National goals for Science, The Federal Role in the Development and adoption of Technology, and Conclusions and Next Steps. Some principles to be followed in achieving the goal of national leadership include the need for quality, adequacy and stability of funding, and the synergy between research and education. CASI

N94-14283# Ministry of Communications, Anyang (Republic of Korea). Radio Wave Div.
THE CURRENT SITUATION, TRENDS, INTERNATIONAL COOPERATION OF SPACE COMMUNICATION TECHNOLOGICAL DEVELOPMENT IN THE REPUBLIC OF KOREA
Moo-Gon Pyun and Jai-Rim Yuk *In* Science and Technology Agency, Asia-Pacific ISY Conference, Volume 2 31 Mar. 1993 p 385-388 (For primary document see N94-14209 02-43)
Avail: CASI HC A01/MF A04

85 URBAN TECHNOLOGY AND TRANSPORTATION

Includes applications of space technology to urban problems; technology transfer; technology assessment; and surface and mass transportation.

For related information see also *03 Air Transportation and Safety, 16 Space Transportation,* and *44 Energy Production and Conversion.*

N94-12931*# Allied-Signal Aerospace Co., Phoenix, AZ. Auxiliary Power Div.

ADVANCED TURBINE TECHNOLOGY APPLICATIONS PROJECT (ATTAP) Annual Report No. 5, 1992

Mar. 1993 153 p

(Contract DEN3-335)

(NASA-CR-191088; NAS 1.26:191088; Rept-31-8071(05)) Avail: CASI HC A08/MF A02

This report is the fifth in a series of Annual Technical Summary Reports for the Advanced Turbine Technology Applications Project (ATTAP), sponsored by the U.S. Department of Energy (DOE). The report was prepared by Garrett Auxiliary Power Division (GAPD), a unit of Allied-Signal Aerospace Company, a unit of Allied Signal, Inc. The report includes information provided by Garrett Ceramic Components, and the Norton Advanced Ceramics Company, (formerly Norton/TRW Ceramics), subcontractors to GAPD on the ATTAP. This report covers plans and progress on ceramics development for commercial automotive applications over the period 1 Jan. through 31 Dec. 1992. Project effort conducted under this contract is part of the DOE Gas Turbine Highway Vehicle System program. This program is directed to provide the U.S. automotive industry the high-risk, long-range technology necessary to produce gas turbine engines for automobiles with reduced fuel consumption, reduced environmental impact, and a decreased reliance on scarce materials and resources. The program is oriented toward developing the high-risk technology of ceramic structural component design and fabrication, such that industry can carry this technology forward to production in the 1990's. The ATTAP test bed engine, carried over from the previous AGT101 project, is being used for verification testing of the durability of next generation ceramic components, and their suitability for service at Reference Powertrain Design conditions. This document reports the technical effort conducted by GAPD and the ATTAP subcontractors during the fifth year of the project. Topics covered include ceramic processing definition and refinement, design improvements to the ATTAP test bed engine and test rigs, and the methodology development of ceramic impact and fracture mechanisms. Appendices include reports by ATTAP subcontractors in the development of silicon nitride materials and processes. Author (revised)

N94-13104*# Research Triangle Inst., Research Triangle Park, NC. Technology Applications Team.

TECHNOLOGY APPLICATIONS TEAM: APPLICATIONS OF AEROSPACE TECHNOLOGY Quarterly Report, Apr. - Jun. 1993

1993 75 p

(Contract NASw-4367)

(NASA-CR-194362; NAS 1.26:194362; RTI/4321/Q3-93) Avail: CASI HC A04/MF A01

Highlights of the Research Triangle Institute (RTI) Applications Team activities over the past quarter are presented in Section 1.0. The Team's progress in fulfilling the requirements of the contract is summarized in Section 2.0. In addition to our market-driven approach to applications project development, RTI has placed increased effort on activities to commercialize technologies developed at NASA Centers. These Technology Commercialization efforts are summarized in Section 3.0. New problem statements prepared by the Team in the reporting period are presented in Section 4.0. The Team's transfer activities for ongoing projects with the NASA Centers are presented in Section 5.0. Section 6.0 summarizes the status of four add-on tasks. Travel for the reporting period is described in Section 7.0. The RTI Team staff and consultants and their project responsibilities are listed in Appendix A. The authors gratefully acknowledge the contributions of many individuals to the RTI Technology Applications Team program. The time and effort contributed by managers, engineers, and scientists throughout NASA were essential to program success. Most important to the program has been a productive working relationship with the NASA Field Center Technology Utilization (TU) Offices. The RTI Team continues to strive for improved effectiveness as a resource to these offices. Industry managers, technical staff, medical researchers, and clinicians have been cooperative and open in their participation. The RTI Team looks forward to continuing expansion of its interaction with U.S. industry to facilitate the transfer of aerospace technology to the private sector. Derived from text

88 SPACE SCIENCES (GENERAL)

N94-13182# Joint Publications Research Service, Arlington, VA.

JPRS REPORT: SCIENCE AND TECHNOLOGY. CENTRAL EURASIA: SPACE

28 Jun. 1993 48 p Transl. into ENGLISH from various Russian articles (JPRS-USP-93-003) Avail: CASI HC A03/MF A01

Translations of articles in the following areas of science and technology are presented: space sciences; space applications; and space policy and administration. CASI

89 ASTRONOMY

Includes radio, gamma-ray, and infrared astronomy, and astrometry.

N94-12915*# National Aeronautics and Space Administration. Goddard Space Flight Center, Greenbelt, MD.

THE EVIDENCE FOR CLUMPY ACCRETION IN THE HERBIG Ae STAR HR 5999

M. R. Perez, C. A. Grady (Applied Research Corp., Landover, MD.), and P. S. The (Amsterdam Univ., Netherlands.) 1993 10 p

(Contracts NAS5-32059; NAS5-31841)

(NASA-TM-108257; NAS 1.15:108257) Avail: CASI HC A02/MF A01

Analysis of IUE high- and low-dispersion spectra of the young Herbig Ae star HR 5999 (HD 144668) covering 1978-1992 revealed dramatic changes in the Mg II h and k (2795.5, 2802.7 A) emission profiles, changes in the column density and distribution in radial velocity of accreting gas, and flux in the Ly(alpha), O I, and C IV emission lines, which are correlated with the UV excess luminosity. Variability in the spectral type inferred from the UV spectral energy distribution, ranging from A5 IV-III in high state to A7 III in the low state, was also observed. The trend of earlier inferred spectral type with decreasing wavelength and with increasing UV continuum flux has previously been noted as a signature of accretion disks in lower mass pre-main sequence stars (PMS) and in systems undergoing FU Orionis-type outbursts. Our data represent the first detection of similar phenomena in an intermediate mass (M greater than or equal to 2 solar mass) PMS star. Recent IUE spectra show gas accreting toward the star with velocities as high as plus 300 km/s, much as is seen toward beta Pic, and suggest that we also view this system through the debris disk. The absence of UV lines with the rotational broadening expected given the optical data (A7 IV, V sini=180 plus or minus 20 km/s for this system) also suggests that most of the UV light originates in the disk, even in the low continuum state. The dramatic variability in the column density of accreting gas, is consistent with clumpy accretion, such as has been observed toward beta Pic, is a hallmark of accretion onto young stars, and is not restricted to the clearing phase, since detectable amounts of accretion are present for stars with 0.5 Myr less than t(sub age) less than 2.8 Myr. The implications for models of beta Pic and similar systems are briefly discussed. Author (revised)

N94-12970*# Southwest Research Inst., San Antonio, TX.

MHD SHOCKS IN CORONAL MASS EJECTIONS Final Report, 25 May 1990 - 25 Nov. 1991

R. S. Steinolfson 25 Nov. 1991 10 p

(Contract NAS5-30930; SwRI Proj. 15-3578)

(NASA-CR-193418; NAS 1.26:193418) Avail: CASI HC A02/MF A01

The primary objective of this research program is the study of the magnetohydrodynamic (MHD) shocks and nonlinear simple waves produced

as a result of the interaction of ejected lower coronal plasma with the ambient corona. The types of shocks and nonlinear simple waves produced for representative coronal conditions and disturbance velocities were determined. The wave system and the interactions between the ejecta and ambient corona were studied using both analytic theory and numerical solutions of the time-dependent, nonlinear MHD equations. Observations from the SMM coronagraph/polarimeter provided both guidance and motivation and are used extensively in evaluating the results. As a natural consequence of the comparisons with the data, the simulations assisted in better understanding the physical interactions in coronal mass ejections (CME's). Author (revised)

N94-13178*# Columbia Univ., New York, NY. Astrophysics Lab.
GRO: BLACK HOLE MODELS FOR GAMMA RAY BURSTS Annual Report, 15 Jul. 1992 - 14 Jul. 1993
Jacob Shaham Jul. 1993 4 p
(Grant NAG5-2017)
(NASA-CR-193244; NAS 1.26:193244; CAL-2120) Avail: CASI HC A01/MF A01

This grant deals with the production of gamma-ray bursts (GRB's) close to horizons of black holes (BH's), mainly via accretion of small chunks of matter onto extreme Kerr BH's. In the past year, we laid the ground work for actual calculations close to Kerr BH's. Because of technical reasons, actual work has only started very recently. Following the detailed list of research subprojects as per our original proposal, we have performed research in the following areas: spectrum calculation; burst dynamics; tidal capture and primordial cloud collapse; halo density profile; and capture of other objects. Derived from text

N94-13181*# Columbia Univ., New York, NY. Dept. of Astronomy and Physics.
ROSAT: X RAY SURVEY OF COMPACT GROUPS Final Technical Report, period ending 31 Mar. 1993
Jacqueline vanGorkom Jul. 1993 4 p
(Grant NAG5-1954)
(NASA-CR-193297; NAS 1.26:193297; CAL-2122) Avail: CASI HC A01/MF A01

This is the final technical report on grant NAG5-1954, which was awarded under the NASA ROSAT Guest Investigator Program to Columbia University. This grant was awarded for a number of projects on two rather different topics: (1) an x-ray survey of compact groups of galaxies; and (2) the fate of gas in merging galaxies. Progress made in these projects is presented. Derived from text

N94-13231 Tel-Aviv Univ. (Israel).
A PHOTOMETRIC STUDY OF MASSIVE X-RAY BINARIES Ph.D. Thesis
Haim Mendelson 1992 172 p
(ITN-93-85207) Copyright Avail: Issuing Activity (Tel-Aviv Univ., Exact Sciences Library, Ramat Aviv 69978, Israel)

Massive X-ray binaries comprise a neutron star or black hole and an early-type star; their X-radiation is generated by the accretion of matter from the early-type star onto its companion. The X-ray spectra of such systems is usually hard, with exponentially fitted kT values exceeding about 15 keV. In many cases, the X-ray emission is pulsed, owing to the funneling of accreted matter towards the magnetic poles of the neutron star, whose magnetic axis is not aligned with its rotation axis. The systems are divided into two groups according to the luminosity class of the massive star: supergiant X-ray binaries (SXRB), with a spectral type earlier than B2; and Be X-ray binaries. The optical radiation of the system is dominated by the early-type star. Seven systems which could be readily observed from the Wise Observatory were monitored photometrically in the U, B, V, R, and I bands and in the H(sub alpha) radiation. The aim was to seek correlations between the changes in the X-ray and in the optical radiation and to detect long-term changes in system luminosities and orbital periods. The main conclusion is that a permanent or transient accretion disk may exist in Be binaries; a permanent disk may be associated with a highly eccentric system in which Roche-lobe overflows recur around periastron, or in close systems in which the neutron star moves within the flattened envelope of the Be star; a transient disk may form in large systems during the active phases of the Be star, when a large amount of matter is ejected from it. ISA

N94-13245# Instituto de Pesquisas Espaciais, Sao Jose dos Campos (Brazil).
THE DEVELOPMENT OF THE TIMAX PROJECT: A HARD X RAY IMAGING TELESCOPE Thesis [O DESENVOLVIMENTO DO PROJETO TIMAX: UM TELESCOPIO IMAGEADOR DE RAIOS X DUROS]
Flavio DAmico Aug. 1992 100 p In PORTUGESE
(INPE-5474-TDI/505) Avail: CASI HC A05/MF A02

The development of the TIMAX project, the first imaging telescope for hard x-rays built in the Southern Hemisphere, is described. A new and elegant manner of providing an antimask of the initial mask without the addition of extra weight to the experiment is shown and the advantages of this method are emphasized. The TIMAX experiment has an angular resolution of approximately 1 deg .7 in a 10 deg x 10 deg (FWHM) field of view with a sensitivity of 7 x 10(exp -5) photons cm(sup -2)s(sup -l)keV(sup -l) in the 30-100 keV range, for an integration time of 10(exp 4) s at a residual atmosphere of 3.5 g(cm(sup -2)). With this sensitivity images of the brightest sources in the Southern Hemisphere are able to be produced. We are particularly interested in the Galactic Center Region. New hard x-ray images of this poorly studied region of the sky are the main contributions of the experiment for the evolution of high energy astrophysics. Author (revised)

N94-13287*# Colorado Univ., Boulder. Joint Inst. for Lab. Astrophysics.
RADIATIVE TRANSFER IN THE DYNAMIC ATMOSPHERES OF MIRA-TYPE VARIABLES Final Report, 1 Oct. 1989 - 31 Sep. 1991
Jeffrey L. Linsky and Donald G. Luttermoser 29 Aug. 1991 3 p
(Grant NAG5-1305)
(NASA-CR-193324; NAS 1.26:193324) Avail: CASI HC A01/MF A01

This NASA grant covers our ADP research program, which involved detailed radiative transfer calculations of hydrodynamic models of pulsating asymptotic giant branch stars. Synthetic spectra resulting from these calculations are compared with International Ultraviolet Explorer (IUE) observations of these stars to test the validity of the models. Author (revised)

N94-13370# British Columbia Univ., Vancouver. Dept. of Geophysics and Astronomy.
A PHOTOMETRIC AND MORPHOLOGICAL STUDY OF COMPACT GROUPS OF GALAXIES AND THEIR ENVIRONMENTS Ph.D. Thesis
Enrico Kindl Feb. 1990 181 p
(ISBN-0-315-59601-5; CTN-93-60847) Copyright Avail: Micromedia Ltd., Technical Information Centre, 165 Hotel de Ville, Place du Portage, Phase 2, Hull, Quebec J8X 3X2, Canada HC/MF

Astrometry, photometry, and morphological classifications were derived from camera images for all 463 galaxies in a sample of 100 compact groups in Hickson's 1982 catalog. Some minor revisions to the catalog are made. Morphological concordance occurs among galaxies within a group; more galaxies are the same type (spiral or nonspiral) than would be expected by chance. Galaxy morphological type correlates with group optical luminosity and, more strongly, with velocity dispersion, but not with galaxy space density. These results imply that the morphological types of galaxies in compact groups are strongly influenced by the environment, and that this influence occurs mostly at the time of galaxy formation. Fields surrounding 97 compact groups with known redshifts were examined, and coordinates, magnitudes, diameters, and Hubble types were derived for 3,389 galaxies in these fields. Results indicate that most groups are dense dynamical entities. Monte Carlo simulations show that 35 percent of galaxy quintets are predicted to contain a single discordant redshift due to the chance alignment of an unrelated field galaxy. This is in agreement with the observed number of four discordant quintets in 10, and these results are consistent with the cosmological interpretation of galaxy redshifts. CISTI

N94-13371 Calgary Univ. (Alberta). Dept. of Physics and Astronomy.
A SURVEY OF COMPACT PLANETARY NEBULAE AT RADIO WAVELENGTHS Ph.D. Thesis
Orla Boje Aaquist Aug. 1990 181 p
(ISBN-0-315-61950-3; CTN-93-60848) Copyright Avail: Micromedia Ltd., Technical Information Centre, 165 Hotel de Ville, Place du Portage, Phase 2, Hull, Quebec J8X 3X2, Canada HC/MF

A radio continuum survey of 174 objects previously classified as possible or true planetary nebulae (PN) is reported. Of these sources, 114 were detected with the very large array radio telescope, and intensity contour

plots, radio flux densities at 5 GHz, diameters, and accurate positions are given. The survey leads to identification of a large number of high surface brightness objects which are likely candidates for very young PN. Modelling of the 2-dimensional brightness distributions shows that most of the survey detections can be reasonably well reproduced by a thin, prolate, ellipsoidal shell seen in projection. Examinations of other distant independent characteristics reveals that all of the surface brightness quantities are strongly correlated to each other, while all other correlations are very low. Significant differences do exist between these objects and the general population in a number of distant independent parameters. In terms of these parameters, the characteristics of the survey detections seem to be typical of other high surface brightness PN. A subgroup of 20 of the brighter, poorly resolved objects was reobserved at 15 GHz. One of these objects, K3-35, has mixed characteristics of both compact H II regions and young PN. Author (CISTI)

N94-13448*# Hughes Danbury Optical Systems, Inc., CT.
LUTE TELESCOPE STRUCTURAL DESIGN Study Report
Gregory Ruthven May 1993 53 p Revised
(NASA Order H-19671-D)
(NASA-CR-192594; NAS 1.26:192594; PR-D15-0015) Avail: CASI HC A04/MF A01

The major objective of the Lunar Ultraviolet Transit Experiment (LUTE) Telescope Structural Design Study was to investigate the feasibility of designing an ultralightweight 1-m aperture system within optical performance requirements and mass budget constraints. This study uses the results from our previous studies on LUTE as a basis for further developing the LUTE structural architecture. After summarizing our results in Section 2, Section 3 begins with the overall logic we used to determine which telescope 'structural form' should be adopted for further analysis and weight estimates. Specific telescope component analysis showing calculated fundamental frequencies and how they compare with our derived requirements are included. 'First-order' component stress analyses to ensure telescope optical and structural component (i.e. mirrors & main bulkhead) weights are realistic are presented. Layouts of both the primary and tertiary mirrors showing dimensions that are consistent with both our weight and frequency calculations also form part of Section 3. Section 4 presents our calculated values for the predicted thermally induced primary-to-secondary mirror despace motion due to the large temperature range over which LUTE must operate. Two different telescope design approaches (one which utilizes fused quartz metering rods and one which assumes the entire telescope is fabricated from beryllium) are considered in this analysis. We bound the secondary mirror focus mechanism range (in despace) based on these two telescope configurations. In Section 5 we show our overall design of the UVTA (Ultraviolet Telescope Assembly) via an 'exploded view' of the sub-system. The 'exploded view' is annotated to help aid in the understanding of each sub-assembly. We also include a two view layout of the UVTA from which telescope and telescope component dimensions can be measured. We conclude our study with a set of recommendations not only with respect to the LUTE structural architecture but also on other topics related to the overall feasibility of the LUTE telescope sub-system. Author (revised)

N94-13452# National Aerospace Lab., Tokyo (Japan). Aeroengine Div.
SOME FLOW PROPERTIES OF TELESCOPE ENCLOSURES ESTIMATED FROM WATER CHANNEL TESTS: APPLICATION OF THE FLOW VISUALIZATION TECHNIQUES
Shigemi Shindou, Kimio Sakata, Hiroyasu Andou (Tokyo Astronomical Observatory, Japan.), L. Barr (Tokyo Astronomical Observatory, Japan.), and Akihiko Miyashita (Tokyo Astronomical Observatory, Japan.) Sep. 1992 18 p Original contains color illustrations
(NAL-TR-1178T; JTN-93-80497) Avail: CASI HC A03/MF A01

Studies on the seeing conditions inside telescope domes indicate that substantial air ventilation is necessary to prevent image degradation due to thermal nonuniformity of the air within the dome, especially for a dome as large as the Japan National Large Telescope (JNLT). In traditional telescope enclosures, in which a cylinder is topped by a hemispherical dome, the air flow quality is influenced by factors such as temperature fluctuations and the distribution of dust contamination which affect the seeing conditions. To determine the best telescope shape from a perspective of achieving desirable air ventilation conditions, the National Aerospace Laboratory (NAL) and National Astronomical Observatory (NAO) jointly studied dome shapes. Flow visualization techniques were applied to the tests using a circulating water channel developed by the NAL Aeroengine Division in order to evaluate flow properties inside and outside models of a telescope enclosure. The hydrogen bubble method and dye injection technique with image processing were primarily utilized. Three types of enclosure models (one to 500 scale) were designed: (1) a traditional shape having a circular cylinder base topped by a hemisphere (HS); (2) a straight-sided trapezoidal shape (New Technology Telescope, NTT); and (3) a flat-roof cylinder with sidewall (Modified Enclosure, ME); subsequently tested in the circulating water channel. Flushing of the enclosure was also closely observed via dye-injection. Author (NASDA)

N94-13462*# Pennsylvania State Univ., University Park. Dept. of Astronomy and Astrophysics.
SEARCH FOR X RAY EMITTING YOUNG STARS OUTSIDE OF MASSIVE MOLECULAR CLOUDS Final Technical Report, 1 Aug. 1989 - 31 Dec. 1991
Eric D. Feigelson 31 Dec. 1991 3 p
(Grant NAG5-1212)
(NASA-CR-193609; NAS 1.26:193609) Avail: CASI HC A01/MF A01

This project is intended to determine whether X-ray surveys of the sky can uncover previously unrecognized populations of pre-main sequence stars outside of large well-known star forming regions. X-ray observations of large regions such as the Taurus-Auriga complex, Orion molecular cloud, Ophiuchi and Chamaeleon clouds had revealed that low mass pre-main sequence emit X-rays 10(exp 2)-10(exp 4) above main sequence levels, and that X-ray surveys select a large population of 'weak' T Tauri stars that are not easily found in traditional optical and infrared surveys. The present project sought to find 'weak' T Tauri stars around smaller and more distant molecular clouds. X-ray surveys potentially could elucidate the star forming capabilities of small clouds, which are not well understood. Derived from text

N94-13591 Hawaii Univ., Honolulu.
A NEAR-INFRARED FAINT GALAXY SURVEY: EVOLUTION AND THE COSMOLOGICAL GEOMETRY FROM K BAND PHOTOMETRY Ph.D. Thesis
Jonathan Perry Gardner 1992 161 p
Avail: Univ. Microfilms Order No. DA9312191

The results of four K band surveys of the extra galactic sky are presented. Each survey was designed to balance depth with area of coverage, and a sufficient number of galaxies was studied at each magnitude from K = 12 to K = 22 to provide good statistics. Each survey area was also observed in the B and I bands. Methods for making long exposures in the near-infrared and optical are described. The K band number counts are compiled. The excess seen in the B band number counts is not seen in the K band number counts, and a change in slope is seen in the K counts at K = 17. The number count data are shown to be consistent with the measured B-K color, as the K band selected sample becomes rapidly bluer after turning over at K = 17. The I-K colors are presented and it is argued that there is a deficiency of galaxies with the colors of unevolved ellipticals at z = 1. The B-K colors are shown to move away from the no-evolution model beginning at K = 17. The position of the galaxies on the B-I vs I-K plot are consistent with these arguments. The surface brightness of the galaxies is analyzed and it is argued that variation in surface brightness causes no systematic bias in the number count data. Various aspects of the data are compared with models of primeval galaxies and galaxy evolution. The K band number counts are compared with a model of pure luminosity evolution, a cosmological constant model and a merging model. It is argued that the merging model is the best explanation for all of the data, although the model needs to be modified before it will provide a good fit to the number counts. Dissert. Abstr.

N94-13605* National Aeronautics and Space Administration, Washington, DC.
THE FOUR GREAT OBSERVATORIES (Videotape)
Dec. 1986 Videotape: 5 min. 40 sec. playing time, in color, with sound
(NASA-TM-109311; NONP-VT-93-185318) Avail: CASI VHS A01/BETA A22

This video presentation introduces the Hubble Space Telescope, Gamma Ray Observatory, Advanced X-ray Astrophysics Facility (AXAF), and the Shuttle Infrared Telescope Facility (SIRTF). Author

N94-13646 Texas Univ., Austin.
TIME SERIES PHOTOMETRY OF FAINT CATACLYSMIC VARIABLES WITH A CCD Ph.D. Thesis
Timothy Mark Cameron Abbott 1992 217 p
Avail: Univ. Microfilms Order No. DA9309110

I describe a new hardware and software environment for the practice of time-series stellar photometry with the CCD systems available at McDonald Observatory. This instrument runs suitable CCD's in frame transfer mode and permits windowing on the CCD image to maximize the duty cycle of the photometer. Light curves may be extracted and analyzed in real time at the telescope and image data are stored for later, more thorough analysis. I describe a star tracking algorithm, which is optimized for a timeseries of images of the same stellar field. I explore the extraction of stellar brightness measures from these images using circular software apertures and develop a complete description of the noise properties of this technique. I show that scintillation and pixelization noise have a significant effect on high quality observations. I demonstrate that optimal sampling and profile fitting techniques are unnecessarily complex or detrimental methods of obtaining stellar brightness measures under conditions commonly encountered in timeseries CCD photometry. I compare CCD's and photomultiplier tubes as detectors for timeseries photometry using light curves of a variety of stars obtained simultaneously with both detectors and under equivalent conditions. A CCD can produce useful data under conditions when a photomultiplier tube cannot, and a CCD will often produce more reliable results even under photometric conditions. I prevent studies of the cataclysmic variables (CV's) AL Com, CP Eri, V Per, and DO Leo made using the time series CCD photometer. AL Com is a very faint CV at high Galactic latitude and a bona fide Population II CV. Some of the properties of AL Com are similar to the dwarf nova WZ Sge and others are similar to the intermediate polar EX Hya, but overall AL Com is unlike any other well-studied cataclysmic variable. CP Eri is shown to be the fifth known interacting binary white dwarf. V Per was the first CV found to have an orbital period near the middle of the gap in the orbital period distribution of CV's. DO Leo is an eclipsing CV which can reasonably be included in a sample of Population II CV candidates.
Dissert. Abstr.

N94-13657 Hawaii Univ., Honolulu.
THE 1 TO 5 MICRON IMAGING OF DEEPLY EMBEDDED YOUNG STELLAR OBJECTS Ph.D. Thesis
Michael Elvin Ressler 1992 231 p
Avail: Univ. Microfilms Order No. DA9312215

Spectral energy distributions (SEDs) are one of the primary tools for analyzing the natures of young stellar objects. Theoretical models of SEDs have achieved some success over a wide frequency range; however, the models often underpredict the near-infrared (NW, 1-5 micrometers) fluxes observed with single-element photometers by more than an order of magnitude. This observed 'extra' flux is generally thought to be radiation which is scattered into the observer's beam from anisotropically distributed material surrounding the protostar. I explore a sample of well-known protostars with a seeing-matched InSb photodiode array camera; fourteen objects have been imaged in the J through M broadband filters, and many of these were imaged through a circular variable filter scanned through the 3.08 micrometer water ice band or through a linear polarizer with the K filter. These images are used to separate the scattered light from the line-of-sight radiation which together make up the published singlebeam SEDs. While resolved, an isotropic scattering accounts for the NIR excesses in some objects, the general scenario is somewhat more complex. For instance, scattering from circumstellar material is seldom significant at wavelengths greater than 3 micrometers and thus will not explain excesses in the 3-5 micrometer region. Some objects appear completely point-like, yet have significant NIR excesses, implying that either scattering is significant on very small scales or that other processes are involved. The implications of these findings concerning models of YSOs and their SEDs are discussed. In addition, we find that approximately 40 percent of these objects (and of a larger sample) appear to be multiple, in rough agreement with the apparent frequency for Main Sequence stars. Finally, five of the fourteen objects appear to have varied significantly in intensity over periods ranging from months to years. We suggest several possible mechanisms for variations on these time scales. Dissert. Abstr.

N94-13668 Texas Univ., Austin.
THE SPECTROSCOPIC EVOLUTION OF NOVAE IN THE BULGE OF M31 AND A SEARCH FOR THEIR POSSIBLE ORIGIN IN THE M31 GLOBULAR CLUSTER SYSTEM Ph.D. Thesis
Austin Bede Tomaney 1992 257 p
Avail: Univ. Microfilms Order No. DA9309300

Results are presented from a three year (1987 to 1989) spectroscopic and photometric survey of novae in M31's bulge, the first comprehensive study of novae outside the Galactic and Magellanic Cloud systems. Nine novae were detected and monitored and their spectra cover a range of outburst states from early decline to the early nebular phases. Broad agreement in spectral morphology and evolution is found with Galactic novae. Since Galactic novae are mainly disk objects, this indicates that novae outburst properties are not critically dependent on the metallicity of the progenitor population. However, in this sample, and in a sample of four M31 nova spectra taken in 1983, no fast, violent outbursts frequently associated with nova systems containing ONeMg white dwarfs were found, suggestive of a systematic difference between the observed proportion of such outbursts between Galactic and M31 bulge novae. Three novae in the sample were observed on succeeding nights during the transition phase of their evolution. Extraordinary variations in some nightly line strengths, particularly the N III lines, were discovered. It is argued that this variability reflects the deposition of drag energy by the secondary star during the common envelope phase of nova evolution and is indicative of a key phase in mass loss from nova systems. Observations include the spectroscopic coverage of an extremely slow nova from 1987 to l990, during the object's evolution in the nebula phase. This provided a unique opportunity to make the first detailed comparison of the evolution and properties of an extra galactic nova with those in our own Galaxy. The roughly solar abundances obtained are typical of similar slow Galactic novae. Further observations are also presented of a unique outburst in 1988 that was independently discovered and reported by Rich et al. These data confirm the inferences of other observers that the outburst differed markedly from that of a typical classical nova. Finally an extensive spectroscopic survey of the M31 globular cluster system was made in an effort to find evidence of a previously suggested enhanced nova rate in these objects. No outbursts were detected during an effective survey time of one year for the entire system. Dissert. Abstr.

N94-13679*# California Univ., Berkeley. Dept. of Astronomy.
ULTRAVIOLET OBSERVATIONS OF NGC 4395, THE LEAST LUMINOUS AND NEAREST KNOWN SEYFERT 1 NUCLEUS Final Technical Report, 15 Jul. 1989 - 14 Jul. 1990
Alexei V. Filippenko 1990 2 p
(Grant NAG5-1171)
(NASA-CR-194304; NAS 1.26:194304) Avail: CASI HC A01/MF A01

The purpose of the grant was to obtain and analyze International Ultraviolet Explorer (IUE) spectra of the spiral galaxy NGC 4395, which contains the nearest and least luminous known Seyfert nucleus. The ultraviolet (UV) spectra was to be used to test the intriguing hypothesis that the 'activity' could be explained by purely stellar phenomena, and to further explore the unprecedented properties of this nucleus. To test the feasibility of the project (the nucleus of NGC 4395 is very faint), one IUE shift was allocated, with the possibility of three additional shifts later on. Ultraviolet observations were attempted with IUE on 4 June 1989. Unfortunately, it was found that the only available guide star could no longer be detected sufficiently well with the FES, whose present sensitivity is lower than it was at the beginning of the IUE mission. Thus, it is no longer possible to observe NGC 4395 with IUE. Given these circumstances, as well as the faintness of the nucleus of NGC 4395, a Cycle 2 HST proposal for observations of this object was submitted. Author (revised)

N94-13681*# Virginia Univ., Charlottesville. Dept. of Astronomy.
SPECTRA OF LATE TYPE DWARF STARS OF KNOWN ABUNDANCE FOR STELLAR POPULATION MODELS Final Technical Report, 1 Feb. 1988 - 31 May 1990
R. W. OConnell 1990 2 p
(Grant NAG5-1035)
(NASA-CR-194301; NAS 1.26:194301) Avail: CASI HC A01/MF A01

The project consisted of two parts. The first was to obtain new low-dispersion, long-wavelength, high S/N IUE spectra of F-G-K dwarf stars with previously determined abundances, temperatures, and gravities. To

insure high quality, the spectra are either trailed, or multiple exposures are taken within the large aperture. Second, the spectra are assembled into a library which combines the new data with existing IUE Archive data to yield mean spectral energy distributions for each important type of star. My principal responsibility is the construction and maintenance of this UV spectral library. It covers the spectral range 1200-3200A and is maintained in two parts: a version including complete wavelength coverage at the full spectral resolution of the Low Resolution cameras; and a selected bandpass version, consisting of the mean flux in pre-selected 20A bands. These bands are centered on spectral features or continuum regions of special utility - e.g. the C IV lambda 1550 or Mg II lambda 2800 feature. In the middle-UV region, special emphasis is given to those features (including continuum 'breaks') which are most useful in the study of F-G-K star spectra in the integrated light of old stellar populations. Derived from text

N94-13894*# Sonoma State Univ., Rohnert Park, CA. Dept. of Physics and Astronomy.

HIGH TIME RESOLUTION STUDIES OF BINARY X RAY PULSARS Semiannual Technical Report, 1 Sep. 1992 - 1 Aug. 1993

Lynn R. Cominsky 1 Oct. 1992 1 p

(Grant NAG5-1260)

(NASA-CR-194395; NAS 1.26:194395) Avail: CASI HC A01/MF A01

This report covers the period September 1, 1992 through August 1, 1993 for NASA grant NAG 5-1260 through the Astrophysics Data Program (ADP), for the project 'High Time Resolution Studies of Binary X-ray Pulsars'. During the past 11 months, we have concentrated on scientific analysis of the data, and have had to reanalyze several data sets, due to a newly discovered error in the unpacking of the count rate data. This error has now been corrected, but may have caused us to miss some scientific results, so we have gone back and reanalyzed the affected data sets, as well as continuing our analysis of other objects. Derived from text

N94-13966*# Johns Hopkins Univ., Baltimore, MD. Dept. of Physics and Astronomy.

ROCKET AND LABORATORY STUDIES IN ASTRONOMY Status Report, 1 Sep. 1992 - 31 Aug. 1993

P. D. Feldman 30 Sep. 1993 6 p

(Grant NAG5-619)

(NASA-CR-194410; NAS 1.26:194410) Avail: CASI HC A02/MF A01

This report covers the period from September 1, 1992 to August 31, 1993. During the reporting period we launched the Faint Object Telescope to measure absolute fluxes of two hot dwarf stars in the spectral range below 1200 A. Although all systems worked normally, a higher than anticipated pressure in the detector led to ion-feedback that masked the useable data from the source. We have identified the source of the problem and are preparing for a reflight in the Fall of 1993. Our laboratory program for the evaluation of the ultraviolet performance of charge-coupled-detector (CCD) arrays continued with the aim of including a UV-sensitive CCD in a payload to be flown in 1994, and we have begun the assembly of this payload. Work has continued on the analysis of data from previous rocket experiments and from the UVX experiment which flew on STS-61C in January 1986. Derived from text

N94-14146*# Colorado Univ., Boulder.

X RAY OBSERVATIONS OF LATE-TYPE STARS USING THE ROSAT ALL-SKY SURVEY Final Report

Jeffrey L. Linsky and Thomas A. Fleming 2 Mar. 1992 4 p

(Grant NAGw-1480)

(NASA-CR-193716; NAS 1.26:193716) Avail: CASI HC A01/MF A01

The ROSAT mission made the first x ray survey of the entire sky using an imaging detector. Although ROSAT is a joint NASA/German project and involves direct American participation during its second phase of pointed observations, the all-sky survey remains the sole property of the German investigators. NASA grant represented the first use of ROSAT data analysis funds to support direct American participation in the ROSAT all-sky survey. The project involved a collaborative agreement between the Joint Institute for Laboratory Astrophysics (JILA) and the Max-Planck-Institut fur Extraterrestrische Physik (MPE) where JILA supplied MPE with a post-doctoral research associate with experience in the field of stellar (coronal) x ray emission to work within their ROSAT group. In return, members of the cool star research group at JILA were given the opportunity to collaborate on projects involving ROSAT all-sky survey data. Both sides have benefitted (and still benefit) from this arrangement since MPE suffers from a shortage of researchers who are interested in x ray emission from 'normal' stars and white dwarfs. MPE has also drawn upon experience in optical identification of x ray sources from the Einstein Extended Medium Sensitivity Survey in planning their own identification strategies for the ROSAT all-sky survey. The JILA cool stars group has benefitted since access to all-sky survey data has expanded the scope of their already extensive research programs involving multiwavelength observations of late-type stars. ROSAT was successfully launched on 1 June 1990 and conducted the bulk of the survey from 30 July 1990 to 25 January 1991. Data gaps in the survey have subsequently been made up. At the time of this writing (February 1992), the survey data have been processed once with the Standard Analysis Software System (SASS). A second processing will soon begin with improvements made to the SASS to correct errors and bugs found while carrying out scientific projects with data from the first processing. We outline the major research activities of Dr. Fleming over the past year (detailed accounts of his activities during the first two years of this grant can be found in the first-year and second-year status reports on this grant). Regarding the three specific projects which were proposed in the original proposal, two of them (White Dwarfs and Late M Dwarfs) are near completion. The results are described in two conference proceedings which are appended. Author (revised)

N94-14305*# Smithsonian Astrophysical Observatory, Cambridge, MA.

AXAF FITS STANDARD FOR RAY TRACE INTERCHANGE Interim Report

Paul F. Hsieh 15 Jul. 1993 20 p

(Contract NAS8-36123)

(NASA-CR-194025; NAS 1.26:194025; SAO-AXAF-DR-93-039) Avail: CASI HC A03/MF A01

A standard data format for the archival and transport of x-ray events generated by ray trace models is described. Upon review and acceptance by the Advanced X-ray Astrophysics Facility (AXAF) Software Systems Working Group (SSWG), this standard shall become the official AXAF data format for ray trace events. The Flexible Image Transport System (FITS) is well suited for the purposes of the standard and was selected to be the basis of the standard. FITS is both flexible and efficient and is also widely used within the astronomical community for storage and transfer of data. In addition, software to read and write FITS format files are widely available. In selecting quantities to be included within the ray trace standard, the AXAF Mission Support team, Science Instruments team, and the other contractor teams were surveyed. From the results of this survey, the following requirements were established: (1) for the scientific needs, each photon should have associated with it: position, direction, energy, and statistical weight; the standard must also accommodate path length (relative phase), and polarization. (2) a unique photon identifier is necessary for bookkeeping purposes; (3) a log of individuals, organizations, and software packages that have modified the data must be maintained in order to create an audit trail; (4) a mechanism for extensions to the basic kernel should be provided; and (5) the ray trace standard should integrate with future AXAF data product standards. Author (revised)

N94-14357*# Sonoma State Univ., Rohnert Park, CA. Dept. of Physics and Astronomy.

ROSAT OBSERVATIONS OF THE BINARY Be-STAR/RADIO PULSAR PSR1259-63 Semiannual Technical Report, 15 Jan. - 1 Aug. 1993

Lynn R. Cominsky 1 Aug. 1993 1 p

(Grant NAG5-1684)

(NASA-CR-194394; NAS 1.26:194394) Avail: CASI HC A01/MF A01

This report covers the period January 15, 1993 through ROSAT Guest Investigator Program, for the August 1, 1993 for NASA grant NAG5-1684 project 'ROSAT Observations of the Binary received the standard output for both the initial Be-star/Radio Pulsar PSR1259-63'. We have now 10,713 second observation of PSR1259-63 (which occurred during 8/30/92 - 9/4/92) and the subsequent 36,108 second observation (during 2/7 - 16/93). The source was detected at the rate of 0.02 counts per second, or about 200 total photons in the first observation, and at about 0.03 counts per second for a total of 1200 additional photons during the second observation. In addition, significant variability, both temporal and spectral has occurred during the second data set. No pulsations at the radio period were found, with upper limits of 5-10 percent. This is in marked

contrast to the lack of detection in observations made by Bailes et al., during AO2 on 2/28/92. Derived from text

N94-14358*# Harvard-Smithsonian Center for Astrophysics, Cambridge, MA.

PHOTOMETRY AND SPECTROSCOPY IN THE OPEN CLUSTER ALPHA PERSEI, 2

Charles F. Prosser 1993 31 p

(Grant NAGw-2698)

(NASA-CR-193397; NAS 1.26:193397) Avail: CASI HC A03/MF A01

Results from a combination of new spectroscopic and photometric observations in the lower main-sequence and pre-main sequence of the open cluster alpha Persei are presented. New echelle spectroscopy has provided radial and rotational velocity information for thirteen candidate members, three of which are nonmembers based on radial velocity, absence of a Li 6707A feature, and absence of H-alpha emission. A set of revised rotational velocity estimates for several slowly rotating candidates identified earlier is given, yielding rotational velocities as low as 7 km/s for two apparent cluster members. VRI photometry for several pre-main sequence members is given; the new (V,V-I(sub K)) photometry yields a more clearly defined pre-main sequence. A list of approximately 43 new faint candidate members based on the (V,V-I(sub K)) CCD photometry is presented in an effort to identify additional cluster members at very low masses. Low-dispersion spectra obtained for several of these candidates provide in some cases supporting evidence for cluster membership. The single brown dwarf candidate in this cluster is for the first time placed in a color-magnitude diagram with other cluster members, providing a better means for establishing its true status. Stars from among the list of new photometric candidates may provide the means for establishing a sequence of cluster members down to very faint magnitudes (V approximately 21) and consequently very low masses. New coordinate determinations for previous candidate members and finding charts for the new photometric candidates are provided in appendices. Derived from text

N94-14359*# Catholic Univ. of America, Washington, DC. Robotics and Control Lab.

A CAPACIFLECTOR-BASED ROBOTIC SYSTEM Semiannual Technical Report, 1 Feb. - 1 Aug. 1993

Charles C. Nguyen and Paulo F. Uribe Aug. 1993 35 p

(Grant NAG5-780)

(NASA-CR-193783; NAS 1.26:193783) Avail: CASI HC A03/MF A01

This report presents preliminary results obtained from a research grant entitled 'Capaciflector-based Control and Imaging,' with Grant Number NAG 5-780, for the period between February 1, 1993 and August 1, 1993. This report deals with the development of a robotic system which is used to evaluate the feasibility of servicing and repairing the Hubble Space Telescope (HST) using robots. In particular, the task of opening the HST's toolbox is considered in this report. First the main components of the robotic system will be introduced. Then each component will be described in detail from low-level to high-level. Finally tasks that have been accomplished during the reporting period for the development of the robotic system will be presented. Listings of source codes for the accomplished tasks are given at the end of the report. Derived from text

N94-14405*# New Mexico State Univ., Las Cruces. Dept. of Astronomy.

ROSAT OBSERVATIONS OF CLUSTERS WITH WIDE-ANGLE TAILED RADIO SOURCES Progress Report

Jack O. Burns 30 Apr. 1993 12 p

(Grants NAG5-1737; NAG5-1819)

(NASA-CR-193784; NAS 1.26:193784) Avail: CASI HC A03/MF A01

The goal of these ROSAT PSPC pointed observations was to understand the nature of X-ray emission associated clusters that contain luminous wide-angle tailed (WAT) radio sources identified with the centrally dominant cluster galaxies. These 500 kpc diameter radio sources are strongly affected by confinement and interaction with the intracluster medium. So, a complete picture of the origin and evolution of these radio sources is not possible without detailed X-ray observations which sample the distribution and temperature of the surrounding hot gas. Two WAT clusters have been observed with the ROSAT PSPC to date. The first is Abell 2634 which contains the WAT 3C 465 and was approved for observations in AO-1. Unfortunately, these observations were broken into two widely separated pieces in time. The first data set containing about 9000 sec of integration arrived in mid-March, 1992. The second data set containing about 10,500 sec arrived just recently in early April (after a first tape was destroyed in the mail). The second cluster is 1919+479 which was approved for observations in AO-2. These ROSAT data arrived in October 1992. Derived from text

N94-14406*# Arizona State Univ., Tempe.

THE SOFT X RAY TRANSIENT CEN X-4 IN QUIESCENCE Final Report, 15 Aug. 1991 - 14 Feb. 1993

Paul C. Schmidtke 14 Feb. 1993 2 p

(Grant NAG5-1744)

(NASA-CR-194033; NAS 1.26:194033) Avail: CASI HC A01/MF A01

The initial goal of this project was to examine the quiescent X-ray light curve of the recurrent X-ray/optical nova Cen X-4 throughout its 15.1-hr orbital period. Using these observations the pre-outburst conditions of the binary would be investigated and the relationship between soft X-ray transients and persistent low-mass X-ray binaries would be established. ROSAT-PSPC observations were scheduled for 1991 August 9-13. Unfortunately, failure of the satellite's attitude control system near the end of the all-sky survey severely curtailed science operations for much of 1991, and the requested observations of Cen X-4 were never taken. Since the stated goal could not be accomplished, the time and resources of this project were used in support of two other ROSAT programs for which I am co-investigator: 'Identification of LMC X-ray Sources Using ROSAT-HRI Images' and 'X-ray Light Curve for an Eclipsing Black-Hole Binary'. The results of these investigations are described. Derived from text

N94-14493*# Lehigh Univ., Bethlehem, PA. Dept. of Mathematics.

ANALYSIS OF THE IUE SPECTRA OF THE STRONGLY INTERACTING BINARY BETA LYRAE Final Report

George E. McCluskey, Jr. 25 Aug. 1993 54 p

(Grant NsG-5386)

(NASA-CR-194118; NAS 1.26:194118) Avail: CASI HC A04/MF A01

The six-band ultraviolet light curves of beta Lyrae obtained with the Orbiting Astronomical Observatory A-2 in 1970 exhibited a very unusual behavior. The secondary minimum deepened at shorter wavelength, indicating that one was not observing light variations caused primarily by the eclipses of two stars having a roughly Planckian energy distribution. It was then suggested that the light variations were caused by a viewing angle effect of an optically-thick, ellipsoidal circumbinary gas cloud. Since 1978 beta Lyrae has been observed with the International Ultraviolet Explorer (IUE) satellite. We have constructed ultraviolet light curves from the IUE archival data for comparison with the OAO-A2 results. We find that they are in substantial agreement with each other. The Voyager ultraviolet spectrometer was also used to observe this binary during a period covered by IUE observations. The Voyager results agree with those of the two other satellite observatories at wavelengths longer than about 1350 A. However, in the wavelength region shorter than the Lyman-alpha line at 1216 A, the light curves at 1085 A and 965 A show virtually no light variation except an apparent flaring near phase 0.7, which is also in evidence at longer wavelengths. We suggest that the optically-thick circumbinary gas cloud, which envelops the two stars completely, assumes a roughly spherical shape when observed at these shorter wavelengths. Author

N94-14811# Belgian Royal Observatory, Brussels.

ROYAL BELGIUM OBSERVATORY CALENDAR: 156TH YEAR Annual Report [ANNUAIRE DE L'OBSERVATOIRE DE BELGIQUE: 156EME ANNEE]

1993 228 p In FRENCH and FLEMISH

(ETN-93-94221) Avail: CASI HC A11/MF A03

A multitude of astronomical dates and information for the year 1993 are presented and include the following: important dates in the Israelite, Gregorian, Julian, and Muslim calendars; religions and civil holidays and saints' days; astronomical seasons; the situation, rising, setting etc. of the Sun; the dates and times of certain positions of the Moon; planetary orbits and visibility; and conditions of observations of comets and meteorites.

ESA

90 ASTROPHYSICS

Includes cosmology; celestial mechanics; space plasmas; and interstellar and interplanetary gases and dust.

For related information see also *75 Plasma Physics*.

N94-12815# Los Alamos National Lab., NM.
A NEW LIMIT ON THE RATE-DENSITY OF EVAPORATING BLACK HOLES
1993 5 p Presented at the International Cosmic Ray Conference, Calgary, Alberta, 19-20 Jul. 1993
(Contract W-7405-eng-36)
(DE93-012716; LA-UR-93-1609; CONF-930779-9) Avail: CASI HC A01/MF A01

Data taken with the CYGNUS detector between 1989 and 1993 have been used to search for 1 second bursts of ultra-high energy (UHE) gamma rays from any point in the northern sky. There is no evidence for such bursts. Therefore the theory-dependent upper limit on the rate-density of evaporating black holes is 6.1 x 10(sup 5)pc(sup -3)yr(sup -1) at the 99% C.L. After renormalizing previous direct searches to the same theory, this limit is the most restrictive by more than 2 orders of magnitude. DOE

N94-12880# International Centre for Theoretical Physics, Trieste (Italy).
MOEBIUS INVERSE PROBLEM FOR DISTORTED BLACK HOLES
H. Rosu Jan. 1993 12 p
(DE93-622899; IC-93/27) Avail: CASI HC A03/MF A01 (US Sales Only)

Hawking 'thermal' radiation could be a means to detect black holes of micron sizes, which may be hovering through the universe. We consider these micro-black holes to be distorted by the presence of some distribution of matter representing a convolution factor for their Hawking radiation. One may hope to determine from their Hawking signals the temperature distribution of their material shells by the inverse black body problem. In 1990, Nan-xian Chen has used a so-called modified Moebius transform to solve the inverse black body problem. We discuss and apply this technique to Hawking radiation. Some comments on supersymmetric applications of Moebius function and transform are also added. DOE

N94-12971# Phillips Lab., Hanscom AFB, MA.
FORCE-FREE MAGNETIC FIELDS, CURL EIGENFUNCTIONS, AND THE SPHERE IN TRANSFORM SPACE, WITH APPLICATIONS TO FLUID DYNAMICS AND ELECTROMAGNETIC THEORY Interim Report
Malcolm A. MacLeod 8 Jan. 1993 34 p
(AD-A265805; AD-E201473; PL-TR-93-2009; ERP-1117; XC-PL/HANSCOM) Avail: CASI HC A03/MF A01

The mathematical foundation of a new description of force free magnetic fields (FFMF's) is given, using Moses' curl eigenfunctions, in preparation for an investigation of solar magnetic clouds and their interaction with the Earth's magnetosphere and perturbation of the radiation belts. Constant-alpha FFMF's are defined completely on the unit hemisphere in Fourier transform space. This reduces the three-dimensional physical space problem to a two-dimensional transform space problem. A scheme for classifying these fields by the dimensionality, symmetry, and complexity of their supporting sets in transform space is sketched. The fields corresponding to the simplest 0-, 1-, and 2-dimensional transform sphere sets are exhibited. Four applications illustrate the technique: (1) the constant-alpha FFMF vector potential is shown to be unimodal; (2) alpha is identified with a normalized magnetic helicity; (3) the helicity hierarchy for Trkalian fluids is shown to depend only on alpha and the mean kinetic energy; and (4) the Maxwell equations are reduced to an FFMF problem, providing a new point of view for electromagnetic theory. Speculative applications to turbulence and the laboratory modeling of astrophysical FFMF's are mentioned. Future directions for development are indicated, and extensive connections to related work are documented. DTIC

N94-12980# Fermi National Accelerator Lab., Batavia, IL.
REDSHIFT DISTORTIONS OF GALAXY CORRELATION FUNCTIONS
J. N. Fry and E. Gaztanaga 12 May 1993 30 p
(Contract DE-AC02-76CH-03000)
(DE93-014007; FNAL/Pub-93-097-A) Avail: CASI HC A03/MF A01

To examine how peculiar velocities can affect the 2-, 3-, and 4-point correlation functions, we evaluate volume-average correlations for configurations that emphasize and minimize distortions for four different volume-limited samples from each of the CfA, SSRS, and IRAS redshift catalogs. We present the results as the correlation length r(sub 0) and power index gamma of the 2-point correlation, bar-xi(sub 2) = (r(sub 0)/r) sup gamma), and as the hierarchical amplitudes of the 3- and 4-point functions, S(sub 3) = bar-xi(sub 3)/bar-xi(sub 2)(sup 2) and S(sub 4) = bar-xi/bar-xi)(sub 2)(sup 3). We find a characteristic distortion for bar-xi(sub 2): The slope gamma is flatter and the correlation length is larger in redshift space than in real space; that is, redshift distortions 'move' correlations from small to large scales. At the largest scales, extra power in the redshift distribution is compatible with Omega(sup 4/7)/b approx. 1; we find 0.53 plus/minus 0.15, 1.10 plus/minus 0.16 and 0.84 plus/minus 0.45 for the CfA, SSRS and IRAS catalogs. Higher order correlations bar-xi(sub 3) and bar-xi(sub 4) suffer similar redshift distortions, but in such a way that, within the accuracy of our analysis, the normalized amplitudes S(sub 3) and S(sub 4) are insensitive to this effect. The hierarchical amplitudes S(sub 3) and S(sub 4) are constant as a function of scale between 1-12 h(sup -1) Mpc and have similar values in all samples and catalogues, S(sub 3) approx. 2 and S(sub 4) approx. 6, despite the fact that bar-xi(sub 2), bar-xi(sub 3), and bar-xi(sub 4) differ from one sample to another by large factors. The agreement between the independent estimations of S(sub 3) and S(sub 4) is remarkable given the different criteria in the selection of galaxies and also the difference in the resulting range of densities, luminosities and locations between samples. DOE

N94-13011# Lawrence Livermore National Lab., CA.
ON INHOMOGENEOUS HALO COLLAPSE AND THE GLOBULAR CLUSTER METALLICITY GRADIENT
D. Hartmann, N. Miller, G. Mathews, and G. Malinie (Commissariat a l'Energie Atomique, Villeneuve-Saint-Georges, France.) Sep. 1992 7 p Presented at the Santa Cruz Workshop on the Galaxy-Globular Cluster Connection, Santa Cruz, CA, Jul. 1992
(Contract W-7405-eng-48)
(DE93-013090; UCRL-JC-111689; CONF-9207198-1) Avail: CASI HC A02/MF A01

Globular cluster systems hold vital information on the formation and early evolution of galaxies. In particular, any correlation between kinematics and composition might allow us to probe the most active periods of galactic chemo-dynamics (GCD). Using the detailed observations of the Galactic globular cluster system, we study GCD of the Galactic halo. Assuming that the sub-class of halo globulars traces the star formation history of the halo, we investigate the chemical evolution of a collapsing, centrally condensed proto-galaxy. The absence of a strong radial metallicity gradient is used to test inhomogeneous models. We find that violent relaxation and supernova heating wash out the metallicity gradient established during the collapse. Following cluster orbits during collapse, when the potential changes rapidly, and in a static potential thereafter, we find a very small present-day metallicity gradient, consistent with the observations. DOE

N94-13096# Fermi National Accelerator Lab., Batavia, IL.
INFLATION AFTER COBE: LECTURES ON INFLATIONARY COSMOLOGY
M. S. Turner (Chicago Univ., IL.) 1992 70 p Presented at the TASI Summer School; Cargese Summer School on Quantitative Particle Physics; Varenna Summer School on Galaxy Formation, Boulder, CO; Corsica, France; Varenna, Italy, 11-29 Jun. 1992; Jul. 1992; Jul. 1992
(Contract DE-AC02-76CH-03000)
(DE93-014008; FNAL/C-92/313-A; CONF-9206314-2; CONF-9207199-1; CONF-9207200-1) Avail: CASI HC A04/MF A01

In these lectures I review the standard hot big-bang cosmology, emphasizing its successes, its shortcomings, and its major challenge-a detailed understanding of the formation of structure in the Universe. I then discuss the motivations for and the fundamentals of inflationary cosmology, particularly emphasizing the quantum origin of metric (density and gravity-wave) perturbations. Inflation addresses the shortcomings of the standard cosmology and provides the 'initial data' for structure formation. I conclude by addressing the implications of inflation for structure formation, evaluating the various cold dark matter models in the light of the recent detection of temperature anisotropies in the cosmic background radiation by COBE. In the near term, the study of structure formation offers a powerful probe of inflation, as well as specific inflationary models. DOE

N94-13171*# Alabama Univ., Huntsville.
ROSAT GUEST INVESTIGATOR PROGRAM (AO-1). ON A SEARCH FOR CORONAL X RAY EMISSIONS FROM WHITE DWARFS Final Technical Report, period ending Jun. 1992
Z. E. Musielak Mar. 1992 2 p
(Grant NAG5-1651)
(NASA-CR-193654; NAS 1.26:193654) Avail: CASI HC A01/MF A01

We have suggested that cool magnetic white dwarfs may be sources of X-ray coronal emission and proposed several prominent candidates for this emission. One of these candidates (EG 250) was approved for the C-category observation by the National and International Committee and was observed by ROSAT on April 17, 1991. Unfortunately, the granted exposure time (1071 s) was much shorter than that which was required by theoretical predictions to observe coronal X-ray emission from this object. The tape containing the data was send to us in November 1991. Since then we have analyzed the data visiting the ROSAT Science Center at NASA Goddard Space Flight Center. The analysis of the data taken during this short observation show, as expected, no X-rays. It is our hope that EG 250 will be observed again during the AO-2 phase of pointed observations, as 10,000 s of observing time was granted to V. Trimble for the C-category observation of this star. We have a close contact with Dr. Trimble regarding this matter. Because our all targets (GD 90, KUV 2316-123 and GD 356) proposed for the observation during the AO-2 phase of pointed observations have been approved by the National and International Committee, we have installed the required software at NASA/MSFC to be able to carry out the data analysis in Huntsville. Two of our targets have already been observed (KUV 2316-123 was observed on Dec. 3, 1991 with 10,000 s of the exposure time, and GD 356 was observed on Jan 4, 1992 with 5,000 s of the exposure time). We just received the data and will begin the analysis soon. The results of our analysis will be reported to the scientific community by publishing papers in the Astrophysical Journal Letters. Our intention is to submit a paper when the analysis of the data taken during AO2 is completed. The data taken during the observation of EG 250 will be a part of this paper. Derived from text

N94-13174# Instituto de Pesquisas Espaciais, Sao Jose dos Campos (Brazil).
THE INTERPLANETARY ORIGINS AND THE MAIN-PHASE DEVELOPMENT OF MODERATE GEOMAGNETIC STORMS (1978 - 1979) Ph.D. Thesis [A ORIGEM INTERPLANETARIA E O DESENVOLVIMENTO DA FASE PRINCIPAL DAS TEMPESTADES GEOMAGNETICAS MODERADAS (1978 - 1979)]
Odim Mendes, Jr. Aug. 1992 296 p In PORTUGESE
(INPE-5445-TDI/491) Avail: CASI HC A13/MF A03

Geomagnetic storms are related to the ring current, which is driven by energy injection primarily during energetic solar wind-magnetosphere coupling due to reconnection at the magnetopause. This work identified the interplanetary origins of moderate geomagnetic storms (-100 nT less than or equal to Dst(MIN) less than -50 nT) and analyzed the coupling processes during the storm main phase. For this purpose the interplanetary magnetic field, solar-wind temperature, density and velocity data, obtained by the ISEE-3 satellite, were used together with the equatorial-Dst and auroral-AE geomagnetic indices, provided by the World Data Center, for the interval August/1978 - December/1979. 78 moderate storms were identified, in which 40 storm events (Dst beginning at approximately 0 nT) were selected. Related to these well defined events the following interplanetary origins were found: coronal mass ejections phenomena - CME (40 percent related to interplanetary shocks; 22.5 percent to single streams; 17.5 percent to streams interactions; 10 percent to non-compressive density enhancement) and non-CME phenomena (7.5 percent related to Alfven-like waves and 2.5 percent to no-identified feature). 47 percent of CME-phenomena occurred near the heliospheric current sheet. Regarding the main-phase development all energy coupling functions showed a similar behavior, that is, the south component of the interplanetary magnetic field (in the magnetospheric coordinate frame) controls basically this coupling. The best linear fits were given by Ey electric field-like and epsilon electric power-like functions. However the complexities in these coupling relations point to other simultaneous energy transfer processes such as non-proportional transference, viscous transference, and 'unloading' process.
Author (revised)

N94-13203*# Texas Univ., Austin. Inst. for Geophysics.
METEOROID ENVIRONMENT NEAR THE EARTH-MOON SYSTEM Final Technical Report, May 1987 - May 1991
Yosio Nakamura 10 Mar. 1992 8 p
(Grant NAGw-1064)
(NASA-CR-193670; NAS 1.26:193670) Avail: CASI HC A02/MF A01

We undertook a research program to investigate the properties of small objects crossing the orbit of the Earth-Moon system using a unique set of data obtained during the Apollo lunar landing missions with a network of seismic stations on the surface of the Moon. The primary objectives of the study were to find out the nature of these objects, whether they were of cometary or asteroidal origin based on their orbital distributions and seismic effects upon impacts, and then to infer the role these small objects play in the evolution of the solar system. In this final technical report, we briefly summarize the results of this study. Detailed results of the study have been published in a series of papers and a dissertation, which are listed in the PUBLICATIONS section. Abstracts of the published papers and the dissertation are attached as an appendix. Derived from text

N94-13230 Tel-Aviv Univ. (Israel). Faculty of Exact Sciences.
PLANNING OF A COMET SIMULATOR M.S. Thesis
Meir Reingewirtz Aug. 1991 70 p In HEBREW
(ITN-93-85206) Copyright Avail: Issuing Activity (Tel-Aviv Univ., Exact Sciences Library, Ramat Aviv 69978, Israel)

Cometary nuclei consist of mineral and organic dust, ice, and trapped gases. The low temperature at which comets were formed suggests that the ice was formed in the amorphous state. When a comet is heated as it approaches the sun, thermal processes in which the amorphous ice plays a dominant role affect the comet's behavior. Therefore, the gas-laden, amorphous ice appears to be worth extensive study. In previous studies, the microscopic properties of thin, isothermal layers of amorphous ice were investigated. The size of these samples was usually smaller than 1 gram, which is suitable for studying the processes of trapping and release of gases from the amorphous ice, but is too small for investigating properties such as thermal conductivity, specific heat, porosity, permeability to gases, and mechanical strength. In the KOSI experiments, thick samples were studied, but they were of crystalline, not amorphous ice. Therefore, the results cannot be directly applied to comets. Thus, it became necessary to build a device for producing large samples of amorphous ice. This work describes a simulator which can produce a sample of about 1 kg of gas-laden amorphous ice. The simulator, which is under construction at the University of Tel-Aviv, will enable properties of amorphous ice to be measured which cannot be measured with small samples. The apparatus will also be used for the study of crust building and for examining possible mechanisms for the sporadically observed outbursts in comets.
Author (ISA)

N94-13233*# Applied Research Corp., Landover, MD.
UV EXTINCTION PROPERTIES OF CARINA NEBULAR DUST Final Report, 9 Jan. 1991 - 8 Feb. 1993
Derck Massa 4 Feb. 1993 18 p
(Contract NAS5-31832)
(NASA-CR-193424; NAS 1.26:193424; R93-205) Avail: CASI HC A03/MF A01

I have performed an analysis of the UV extinction by dust along the line of sight to the young open cluster Tr 16. The observed curves are parameterized in order to extract quantitative information about the structure of the curves. Furthermore, by constructing differential extinction curves, obtained by differencing curves for stars which lie within a few arc seconds of each other on the sky, I was able to obtain a curve which is free of the effects of foreground extinction, and represents the extinction by the dust in the Tr 16 molecular cloud. I then show that this curve is nearly identical to one due to dust in the Orion molecular cloud. This result shows that dust in the Carina arm exhibits the same behavior as that in the local arm. Author

N94-13239*# Catholic Univ. of America, Washington, DC. Dept. of Physics.
PHYSICAL PROPERTIES OF GAS DISKS AROUND SHELL STARS WITH AND WITHOUT DUST Final Progress Report, 1 Jan. 1990 - 15 Apr. 1992

Carol A. Grady 1992 4 p
(Grant NAG5-1316)
(NASA-CR-193655; NAS 1.26:193655) Avail: CASI HC A01/MF A01

Analysis of archival IRAS and IUE data has resulted in: (1) identification of 8 new A star proto-planetary candidates; (2) detection of a mass outflow event around Beta Pic (subsequently confirmed by the 1991 July HST observation); and (3) confirmation of the suggestion by Waters et al. (1988) that 51 Oph is a protoplanetary system similar to beta Pic with the detection of high density, high velocity, collisionally ionized accreting gas in the line of sight toward this star. Derived from text

N94-13262# Los Alamos National Lab., NM.
EVOLUTION OF THE INTERPLANETARY MAGNETIC FIELD
D. J. McComas 1993 42 p Presented at the AGU Monograph/Solar System Plasma Physics Meeting on Resolution of Processes in Space and Time, Yosemite, CA, Feb. 1993
(Contract W-7405-eng-36)
(DE93-012631; LA-UR-93-1159; CONF-9302115-2) Avail: CASI HC A03/MF A01

Remote observations of magnetic field topologies in the solar corona and in situ observations of the solar wind and interplanetary magnetic field (IMF) in interplanetary space are used to examine the temporal evolution of the spatial distribution of open and closed field regions emanating from the Sun. The simple 'open' configuration of inward and outward pointing sectors in the IMF is periodically disrupted by magnetically distinct coronal mass ejections (CME's) which erupt from previously closed magnetic field regions in the corona into interplanetary space. At 1 AU, CME's contain counterstreaming halo electrons which indicate their distinct magnetic topologies. This topology is generally thought to be one of the following: plasmoids that are completely disconnected from the Sun; magnetic 'bottles,' still tied to the corona at both ends; or flux ropes which are only partially disconnected. Fully disconnected plasmoids would have no long term effect on the amount of open flux; however, both in situ observations of details of the halo electron distributions and remote coronagraph observations of radial fields following CME's indicate that CME's generally do retain at least partial attached to the Sun. Both the magnetic-bottle and flux rope geometries require some mitigating process to close off previously open fields in order to avoid a flux catastrophe. In addition, the average amount of magnetic flux observed in interplanetary space varies over the solar cycle, also indicating that there must be ways in which new flux is opened and previously open flux is closed off. The most likely scenario for closing off open magnetic fields is for reconnection to occur above helmet streamers, where oppositely directed field regions are juxtaposed in the corona. These events would serve to return closed field arches to the Sun and release open, U-shaped structures into the solar wind. DOE

N94-13332*# Texas Univ., Austin. Dept. of Astronomy.
ANALYSIS OF INTERSTELLAR CLOUD STRUCTURE BASED ON IRAS IMAGES Final Report, 15 Sep. 1989 - 14 Mar. 1992
John M. Scalo 1992 4 p
(Grant NAG5-1263)
(NASA-CR-194341; NAS 1.26:194341) Avail: CASI HC A01/MF A01

The goal of this project was to develop new tools for the analysis of the structure of densely sampled maps of interstellar star-forming regions. A particular emphasis was on the recognition and characterization of nested hierarchical structure and fractal irregularity, and their relation to the level of star formation activity. The panoramic IRAS images provided data with the required range in spatial scale, greater than a factor of 100, and in column density, greater than a factor of 50. In order to construct densely sampled column density maps of star-forming clouds, column density images of four nearby cloud complexes were constructed from IRAS data. The regions have various degrees of star formation activity, and most of them have probably not been affected much by the disruptive effects of young massive stars. The largest region, the Scorpius-Ophiuchus cloud complex, covers about 1000 square degrees (it was subdivided into a few smaller regions for analysis). Much of the work during the early part of the project focused on an 80 square degree region in the core of the Taurus complex, a well-studied region of low-mass star formation. Derived from text

N94-13361 International Centre for Theoretical Physics, Trieste (Italy).
DILATON QUANTUM COSMOLOGY IN TWO DIMENSIONS
F. D. Mazzitelli and J. G. Russo (Texas Univ., Austin.) Nov. 1992 22 p
Limited Reproducibility: More than 20% of this document may be affected by microfiche quality
(DE93-621377; IC-92/409; UTTG-28-92) Avail: CASI HC A03 (US Sales Only)

We consider a renormalizable two-dimensional model of dilaton gravity coupled to a set of conformal fields as a toy model for quantum cosmology. We discuss the cosmological solutions of the model and study the effect of including the back reaction due to quantum corrections. As a result, when the matter density is below some threshold new singularities form in a weak coupling region, which suggests that they will not be removed in full quantum theory. We also solve the Wheeler-DeWitt equation. Depending on the quantum state of the Universe, the singularities may appear in a quantum region where the wave function is not oscillatory, i.e., when there is not a well defined notion of classical spacetime. DOE

N94-13372 Laval Univ. (Quebec). Faculte des sciences et de genie.
ABUNDANCE MARKERS IN H II REGIONS OF LATE SPIRAL GALAXIES Ph.D. Thesis [LES INDICATEURS D'ABONDANCE DANS LES REGIONS HII DES GALAXIES SPIRALES TARDIVES]
Julien Belley Aug. 1990 406 p In FRENCH
(ISBN-0-315-62457-4; CTN-93-60849) Copyright Avail: Micromedia Ltd., Technical Information Centre, 165 Hotel de Ville, Place du Portage, Phase 2, Hull, Quebec J8X 3X2, Canada HC/MF

Large scale spectro photometric measurements were obtained for 130 and 160 H II regions from the spiral galaxies NGC628 (M74) and NGC6946 at the 1.6-m Mount Megantic Observatory telescope. The method of monochromatic imaging, carried out with the aid of narrow bandpass interference filters, has allowed integrating the flux in the spectral lines H-alpha, H-beta, O(III)(500.7 nm), and N(II)(658.4 nm). The O/H abundances and the abundance gradients were determined using the semi-empirical calibration of Edmunds and Pagel and O(III)/H-beta measurements in the H II regions observed. The high statistical reliability of the abundance gradients gives by extrapolation estimates of average abundance of 9.36 for NGC6946 and 9.20 for NGC628. The slopes of the two abundance gradients remain constant for all the radial domain covered in each galaxy. By comparing with the O/H abundance measurements of many other galaxies, it is shown that the gradient slopes, with a few exceptions, stay identical. The absence of correlation between the various gradients of the galaxies exists for all the physical parameters considered, in spite of the relatively wide domains of O/H abundance (8.4 and 9.4) and luminosity (9.5 to 10.5). CISTI

N94-13423*# Massachusetts Inst. of Tech., Cambridge.
THE PHYSICAL AND CHEMICAL EVOLUTION OF PROTOSTELLAR DISKS. THE GROWTH OF PROTOSTELLAR DISKS: PROGRESS TO DATE Final Report
Steven W. Stahler 25 Aug. 1993 3 p
(Grants NAGw-2322; NAGw-3107)
(NASA-CR-194111; NAS 1.26:194111) Avail: CASI HC A01/MF A01

This study constitutes one part of our multi-disciplinary approach to the evolution of planet-forming disks. The goal is to establish the disks' thermal and mechanical properties as they grow by the infall of their parent interstellar clouds. Thus far, significant advances toward establishing the evolving surface density of such disks was made. Author (revised)

N94-13446*# Smithsonian Astrophysical Observatory, Cambridge, MA.
THE ONSET OF GALACTIC WINDS IN EARLY-TYPE GALAXIES Final Report, 1 Aug. 1989 - 31 Jul. 1991 .
Christine Jones Jul. 1992 2 p
(Grant NAG5-1205)
(NASA-CR-193640; NAS 1.26:193640) Avail: CASI HC A01/MF A01

We completed the spectral analysis of 31 early-type galaxies to investigate whether their x-ray emission was predominantly due to thermal bremsstrahlung from a hot gaseous corona or emission from discrete, galactic sources such as x-ray binaries. If a corona dominates the x-ray emission, its spectra is expected to be relatively cool (0.5 - 1 keV) compared to the harder emission associated with x-ray binaries in our galaxy, the Magellanic Clouds and M31. While it is generally accepted that the x-ray emission in luminous E and S0 galaxies arises from hot coronae, the status of hot gas in lower luminosity (and hence lower mass) galaxies is less clear. Calculations show that, for a given supernova rate, a critical galaxy luminosity (mass) exists below which the gas cannot be gravitationally

confined and a galactic wind is predicted to be effective in expelling gas from the galaxy. Since significant mass (a dark halo) is required to hold a hot, gaseous corona around a galaxy, we expect that the faintest, smallest galaxies will not have a hot corona, but their x-ray emission will be dominated by galactic sources or by an active galactic nuclei. In the sample we tested which spanned the absolute magnitude range from -21.5 to -19.5, we found that except for two galaxies whose x-ray emission was dominated by an active nucleus, that the others were consistent with emission from hot gas. We also found that there is a correlation between gas temperature and galaxy magnitude (mass), such that the brighter, more luminous galaxies have hotter gas temperatures. Thus even at relatively faint magnitudes, the dominant emission from early-type galaxies appears to be hot gas. We also carried out an investigation of the x-ray surface brightness distribution of the x-ray emission for about 100 early type galaxies to determine whether the x-ray emission from galaxies are extended. Extended x-ray emission is expected if the emission is due to a hot gaseous corona. We determined the ratio of the source counts in two annuli (0-80 arc seconds and 80-160 arc seconds) for each galaxy and analyzed these ratios using a maximum likelihood estimator to determine the errors on the ratios. Even for weak sources, this ratio provides a sensitive test for source extent. We then compared these ratios to a sample of quasars (all unresolved sources) and have determined which galaxies are extended and which are consistent with point sources. A first paper including the Einstein x-ray fluxes for 147 early-type galaxies has been published in the Astrophysical Journal Supplement Series (with Roberts, Hogg, Bregman, Forman entitled 'Interstellar Matter in Early-Type Galaxies'). A second paper will describe the spectral and extent analysis carried out for this galaxy sample. These results also have been presented at scientific conferences and in colloquia. Derived from text

N94-13449# Instituto de Pesquisas Espaciais, Sao Jose dos Campos (Brazil).

SAMPLING OF GLOBULAR CLUSTERS AND THE DISTANCE TO THE GALACTIC CENTER M.S. Thesis [AMOSTRAGEM DE AGLOMERADOS GLOBULARES E A DISTANCIA AO CENTRO GALACTICO]

Camilo Tello Bohorquez Jul. 1992 111 p In PORTUGESE
(INPE-5446-TDI/492) Avail: CASI HC A06/MF A02

An up-to-date sample of 134 globular clusters with an error in magnitude of 0(sub m).40 was used to test a new model of estimation for the distance to the Galactic Center. The model is based upon a diagnosis of the selection effects in the local azimuthal distribution of clusters in order to redistribute them systematically around candidates to the center of symmetry of the system. The procedure tests subsamples of clusters of different spatial extent and uses the mean, the medium, and an average value weighted by binomial coefficients to estimate separately the displacement of the centroid in the altered systems. For each subsample the candidate with the smallest modulation of its mean joint displacement with the associated scatter is selected, and it is concluded from an analysis of weighted means that the most consistent result favors an estimate of R(sub o) = 6.90 +/- 0.33 kpc. Author (revised)

N94-13503# Belgian Royal Observatory, Brussels.

TIDAL INTERACTIONS IN THE EARTH MOON SYSTEM

P. Melchior 1992 41 p Presented at the Internation Union of Geodesy and Geophysics General Assembly Union Lecture, Vienna, Austria, Aug. 1991 Submitted for publication
(Communications-Ser-B-160; ETN-93-94377) Avail: CASI HC A03/MF A01

Three epochs in the development of man's knowledge of tidal interactions are discussed: the epoch of pioneers to the International Geophysical Year 'IGY1957'; a transition period from IGY1957 up to 1980 when there were not the powerful tools of today, but improved quartz clinometers, recording gravimeters, and the first 'electronic computer' (the glorious IBM650) existed; the present days with powerful computers, Very Long Base Interferometry (VLBI) superconducting gravimeters (1982), excellent models of the Earth's internal structure, and quite good models of the oceanic tides (1979). ESA

N94-13504# Belgian Royal Observatory, Brussels.

VARIATIONS COMMON TO THE INTERPLANETARY MAGNETIC FIELD, THE ZONAL ATMOSPHERIC CIRCULATION AND THE EARTH'S ROTATION

D. Djurovic (Belgrade Univ., Yugoslavia.) and P. Paquet 1991 16 p Repr. from Q.J.R. Meteorol. Soc., v. 117, 1991 p 571-586 See also A91-48941
(Communications-Ser-B-157; ETN-93-94378) Avail: CASI HC A03/MF A01

A study of the cyclic fluctuations in the Earth's rotation, the geomagnetic field, the global atmospheric circulation and solar activity which revealed the existence of 50 day and 120 day oscillations common to all is presented. The results, as well as the results obtained by radiometric measurements from the satellites Nimbus 7 and the Solar Maximum Mission, suggest that their origin lies in the physical processes in the Sun. The mechanism remains unexplained but from this work it follows that the role of the interplanetary magnetic field could very well be important. ESA

N94-13550 California Univ., Los Angeles.

POLARIZATION AND VARIABILITY OF ACTIVE GALAXIES AND QUASARS Ph.D. Thesis

Wayne Buell Webb 1992 261 p
Avail: Univ. Microfilms Order No. DA9310955

We measured UBVRI polarizations of 0.5-2.5 percent in more than a dozen 'normal' quasars and Seyfert 1 galaxies. In many cases the percentage of polarization increased with frequency. The position angle was wavelength-independent, suggesting the polarization in a given object originated in a single physical process. In nine of the quasars, the polarization was best understood as scattering off dust grains. The second most successful fit to the data was polarization proportional to the flux of the blue thermal component. The low level of polarization associated with the thermal ultraviolet component may be due to electron scattering in an accretion disk or torus. Using a Monte Carlo simulation, we calculated which accretion models are consistent with the observed low levels of polarization. We found that accretion flows shaped like flat disks and wedges produced too much polarization. Toroids and wedge-shaped disks (with half-angles of 30 degrees or more) produced lower levels of polarization, more consistent with the observations of normal quasars. We monitored 23 quasars and Seyfert 1 galaxies on short time scales: minutes, hours, days, weeks, and months. We found no evidence for intranight optical variations. However, we did find variability on a time scale of one to several days in II percent of the galaxies in both the blue and green, and in 26 percent of the AGNs observed in the red. We found optical variability common on a 60 day time scale, detectable in 60 percent of the AGNs in the blue filter and 40 percent in the red filter. Our sample suggests a weak anti-correlation of luminosity and FeII/H(sub beta) ratio with variability. Variability on the time scales of one day and 60 days are consistent with the dynamical and thermal time scales, respectively, of accretion flows about supermassive black holes. Author

N94-13551 California Univ., San Diego.

THE EXTENT AND CONTENT OF LOW-IONIZATION GAS IN GALAXIES Ph.D. Thesis

Donna Suzanne Womble 1992 321 p
Avail: Univ. Microfilms Order No. DA9312135

This dissertation reports combined observations of QSO absorption and H I emission from galaxies which comprise proximate pairs of background and foreground objects. The fortuitous juxtaposition of these QSO-galaxy 'pairs' provides unique opportunities to probe the extent and content of gas in foreground galaxies through evaluation of the incidence and strength of absorption lines in the spectra of the background QSOs. When combined with direct observations of the neutral hydrogen emission from galaxies, the high quality QSO absorption spectra help to quantify the relative distributions of hydrogen and metal-enriched gas in galaxies. We present optical, spectroscopic observations of a new sample of nine close QSO-galaxy pairs. Based on the results from previous studies, these objects were selected with strict limitations on the QSO-galaxy impact parameters. For a select subset of these galaxies, we present synthesis images of the H I emission distributions. These observations are combined with deep optical images and far-infrared fluxes of the galaxies to assess and interpret morphological and environmental conditions which may influence the absorption status. These observations are combined with the existing measurements for all pairs with similar impact parameters to form a 'complete' sample. Using the database from this sample of 22 close pairs, we provide a compilation of results for the individual sources and we draw a number of global conclusions. Naive assumptions regarding a direct

correspondence between the incidence and strength of Ca II absorption and the impact parameters are invalid for these data. There does not appear to be a sharp impact parameter limit beyond which Ca II absorption is never detected, nor is there a minimum separation below which absorption is always detected. Limits on the relative abundance of Ca II and H I indicate that the QSO-galaxy pair absorption systems have gas-phase abundances of calcium which are larger than in the majority of Galactic halo sightlines. We tentatively find that the absorbing galaxies may be more luminous in the optical and far-infrared than the non-absorbers. Combined with a qualitative assessment of the galaxy morphologies and environments, we find that these results are consistent with the absorbers being characteristically more active than the non-absorbed. Tidal interactions and active star-formation play important and perhaps crucial roles in the origin of the absorbing gas. We interpret these results in the context of calcium depletion, and we briefly compare the inferred properties with those seen in higher red shift QSO absorption systems. Author

N94-13648 Hawaii Univ., Honolulu.
MILLIMETER AND INFRARED STUDIES OF YOUNG STELLAR OBJECTS IN DARK CLOUD L1641 Ph.D. Thesis
Hua Chen 1992 237 p
Avail: Univ. Microfilms Order No. DA9312183

To understand the physical process of star formation, we address three questions: (1) what are the critical indicators of evolutionary states of young stellar objects?; (2) when and how are dense cores dissipated?; and (3) how are young stars distributed in a single molecular cloud? We selected 224 IRAS sources from the IRAS coadded images in dark cloud L1641. The IRAS data analysis suggested that the 122 sources inside L1641 are probably young stellar objects, while the sources outside L1641 are probably infrared cirrus. In (13)CO and HCO(+) millimeter observations, we found that most of the IRAS sources with CO outflows are associated with molecular dense cores, while most nonoutflow sources are not. This can be explained if dense cores are dissipated by the outflows before the driving sources become pre-main-sequence stars. Using near-IR array detectors, we imaged 59 IRAS sources in H and K', some of them also were imaged in narrow-band L and M. The most important result from the imaging is the detection of small groupings of 10-40 near-IR sources near 14 IRAS sources. These groupings, defined as stellar density enhancements (SDEs), are statistically significant compared to background stars. Most of the near-IR sources within the SDEs are low-mass pre-main-sequence stars physically associated with the IRAS sources. The SDEs probably result from pile-up of young stars due to continuous star formation within the dense cores, a phenomenon seen in the early stage of star formation. Our images showed that the young stars in L1641 can be characterized by a range of stellar densities, from a large cluster (the Trapezium Cluster) to the SDEs and to individual stars. The previously proposed cluster and isolated star formation modes are probably the high and low ends of the continuous distribution. With the near-IR imaging, we were able to identify the probable near-IR counterparts for 55 of the 59 IRAS sources. Forty-five of them are class I sources, and the other 10 sources are class II sources. Dissert. Abstr.

N94-13649 Toronto Univ. (Ontario).
COLD DARK MATTER HALOS Ph.D. Thesis
John Joseph Dubinski 1991 135 p
Avail: Univ. Microfilms Order No. DANN73881

The dark halos arising in the Cold Dark Matter (CDM) cosmology are simulated to investigate the relationship between the structure and kinematics of dark halos and galaxies. Realistic cosmological initial conditions and tidal field boundary conditions are used in N-body simulations of the collapse of density peaks to form dark halos. The core radii of dark halos are no greater than the softening radius, r(sub s) = 1.4 kpc. The density profiles can be fit with an analytical Hernquist (1990) profile with an effective power law which varies between -1 in the center to -4 at large radii. The rotation curves of dark halos resemble the flat rotation curves of spiral galaxies in the observed range, 1.5 approximately less than r approximately less than 30 kpc. The halos are strongly triaxial and very flat with (c/a) = 0.50 and (b/a) = 0.71. The distribution of ellipticities for dark halos reaches a maximum at epsilon = 0.5 in contrast to the distribution for elliptical galaxies which peaks at epsilon = 0.2 suggesting that ellipticals are much rounder than dark halos. Dark halos are generally flatter than their progenitor density peaks. The final shape and orientation of a dark halo are largely determined by tidal torquing and are sensitive to changes in the strength and orientation of a tidal field. Dark halos are pressure supported objects with negligible rotational support as indicated by the mean dimensionless spin, lamda = 0.042 +/- 0.024. The angular momentum vector tends to align with the true minor axis of dark halos. Elliptical galaxies have a similar behavior implied by the observation of the tendency for alignment of the rotation vector and the apparent minor axis. The origin of this behavior may be traced to the tendency for tidal torques to misalign with the major axis of a density peak. Tidal torques are found to isotropize the velocity ellipsoids of dark halos at large radii, contrary to the expectation of radially anisotropic velocity ellipsoids in cold collapse simulations. Overall, the properties of CDM halos are broadly consistent with the properties of dark halos derived from the observations of galaxies. Dissert. Abstr.

N94-13651 Texas Univ., Austin.
THE REIONIZATION OF THE INTERGALACTIC MEDIUM Ph.D. Thesis
Mark Laird Giroux 1992 384 p
Avail: Univ. Microfilms Order No. DA9309174

We have calculated in detail the thermal and ionization evolution of a uniform intergalactic medium (IGM) composed of H and He, undergoing 'reionization' in a post-recombination Friedmann universe, including the mean effect of gas clumps embedded in a smoothly distributed ambient gas. We have solved nonequilibrium rate equations for ionization and recombination, together with the equations of energy conservation, including the effects of cosmological expansion, radiative and Compton cooling, and the diffuse flux emitted by the gas, and radiative transfer. We have included the contribution to the continuum opacity of the universe due to the observed quasar absorption line clouds (QALC's). We have considered a variety of generic sources of photoionization, including quasars and primeval galaxies, as well as the possibility that hydrodynamical processes deposit thermal energy in the IGM. Our purpose is to elucidate the minimum requirements for reionizing the IGM by z approx. = 5 to the extent required by the Gunn-Peterson limit, by the energy release associated with cosmological structure formation. These minimum requirements are a significant constraint on theories of the origin of structure in the universe. We have calculated the time varying density of the IGM by coupling our detailed, numerical calculations of an evolving uniform IGM to the linearized equations for the growth of density fluctuations in both the gaseous and dark components in a Cold Dark Matter (CDM) universe, identifying the IGM density with the uncollapsed baryon fraction. The collapsed fraction is postulated to be a source of energy injection into the IGM by radiation or bulk hydrodynamical heating (e.g. via shocks) or both, at a rate which is marginally enough to satisfy the Gunn-Peterson constraint at z less than 5. We find that the IGM must have contained a substantial fraction of the total baryon density of the universe in a CDM model both during and after its reionization epoch. Self-consistent reionization of the IGM by the collapsed baryon fraction has a strong effect on the rate of collapse. Dissert. Abstr.

N94-13716*# Michigan Univ., Ann Arbor.
THE DISTANCE TO THE HIGH VELOCITY CLOUDS OF NEUTRAL HYDROGEN Final Report, 1 Oct. 1989 - 30 Sep. 1991
Joel N. Bregman 1992 14 p
(Grant NAG5-1268)
(NASA-CR-194343; NAS 1.26:194343; UM-026952) Avail: CASI HC A03/MF A01

The goal of this project was to determine the distance to high velocity gas clouds. These clouds are believed to lie in the halo of the galaxy, but this is a matter of controversy. The technique was used to look for the effect of absorption by these clouds against the light of stars at various distances along the line of sight to these clouds. This was done in the ultraviolet using the International Ultraviolet Explorer. Absorption at the velocity of the clouds was not found in any of the stars, which have kilcparsec distances. It was concluded that the vertical distance to these clouds is at least 1.5 kpc, putting them firmly in the halo of the galaxy. Author (revised)

N94-13781*# Columbia Univ., New York, NY.
THEORETICAL MOLECULAR STUDIES OF ASTROPHYSICAL INTEREST Final Technical Report, 1 Dec. 1974 - 30 Sep. 1991
George Flynn 30 Sep. 1991 13 p
(Grant NsG-7105)
(NASA-CR-193300; NAS 1.26:193300) Avail: CASI HC A03/MF A01

When work under this grant began in 1974 there was a great need for state-to-state collisional excitation rates for interstellar molecules observed by radio astronomers. These were required to interpret observed line intensities in terms of local temperatures and densities, but, owing to lack of experimental or theoretical values, estimates then being used for this purpose ranged over several orders of magnitude. A problem of particular interest was collisional excitation of formaldehyde; Townes and Cheung had suggested that the relative size of different state-to-state rates (propensity rules) was responsible for the anomalous absorption observed for this species. We believed that numerical molecular scattering techniques (in particular the close coupling or coupled channel method) could be used to obtain accurate results, and that these would be computationally feasible since only a few molecular rotational levels are populated at the low temperatures thought to prevail in the observed regions. Such calculations also require detailed knowledge of the intermolecular forces, but we thought that those could also be obtained with sufficient accuracy by theoretical (quantum chemical) techniques. Others, notably Roy Gordon at Harvard, had made progress in solving the molecular scattering equations, generally using semi-empirical intermolecular potentials. Work done under this grant generalized Gordon's scattering code, and introduced the use of theoretical interaction potentials obtained by solving the molecular Schroedinger equation. Earlier work had considered only the excitation of a diatomic molecule by collisions with an atom, and we extended the formalism to include excitation of more general molecular rotors (e.g., H2CO, NH2, and H2O) and also collisions of two rotors (e.g., H2-H2).

Author (revised)

N94-13864*# Virginia Polytechnic Inst. and State Univ., Blacksburg. Dept. of Physics.

SITES OF FINE-SCALE ELECTRON DENSITY TURBULENCE IN THE INTERSTELLAR MEDIUM Final Technical Report, 1 Oct. 1989 - 18 May 1992

John H. Simonetti 1992 8 p

(Grant NAG5-1275)

(NASA-CR-193708; NAS 1.26:193708) Avail: CASI HC A02/MF A01

Observations of radio-wave scattering effects probe interstellar electron-density turbulence. But with limited use of complementary data sets only broad conclusions have been obtained. The locations of this turbulence are unknown (phases, objects, etc.), as is the mechanism for its production, although it could play a role in various galactic processes. The IRAS data set was used to search for correlations between scattering and structures traced by infrared emitting dust. The existent HI (21-cm line emission), and 408-MHz radio-continuum all-sky surveys were used to search for correlations between scattering and structures traced by these emissions. Only lines of sight outside the galactic plane were considered (to better delimit the structures which might be causing scattering). No correlation is apparent between 21-cm line emission, or infrared continuum emission and interstellar scattering. However, a correlation exists between the scattering toward extragalactic radio sources and 408-MHz continuum emission.

Author (revised)

N94-14075# Technische Univ., Berlin (Germany). Fachbereich Physik.

DUST PRODUCTION IN THE ENVELOPES OF CARBON STARS: R CORONAE BOREALIS Ph.D. Thesis [STAUBBILDUNG IN DEN HUELLEN VON KOHLENSTOFFSTERNEN: R CORONAE BOREALIS]

Achim Goeres 1992 197 p In GERMAN

(ETN-93-94389) Avail: CASI HC A09/MF A03

A quantitative, analytic model of darkening events of R Coronae Borealis, based on phenomenological models of light decline by soot formation, with focus on causal relation between the pulsating atmosphere and episodic condensation processes, is presented. The most important properties of R Coronae Borealis, such as anisotropy of soot distribution, episodic occurrence of condensation processes and expansion motion of soot clouds, were recognized as a sequence of a chain of sensitive regulation mechanisms. It is ascertained, that small carbon clusters can absorb star thermal ultraviolet radiation and are so accelerated by radiation pressure, and that supersonic drift velocities are reached. The DRACON (Drift Regulated Anisotropic Condensation) model was used to establish that drift velocity is reduced by stellar pulsation in interaction between shock waves and validation field variations until effective condensation occurs. It is concluded that soot formation anisotropy is a consequence of the deterioration of spherical symmetry due to semiregular multiphase pulsations of R Coronae Borealis, and of the extreme sensitive conditions of condensation dependence on drift velocity.

ESA

N94-14116# Los Alamos National Lab., NM.

A CLASSICAL INSTABILITY FOR BLACK STRINGS AND p-BRANES

R. Gregory (Chicago Univ., IL.) and R. Laflamme 1993 5 p Presented at the Gravity and Relativistic Astrophysics, Waterloo, Ontario, 13-15 May 1993

(Contract W-7405-eng-36)

(DE93-014577; LA-UR-93-1732; CONF-9305199-1) Avail: CASI HC A01/MF A01

We investigate the evolution of small perturbations around black strings and branes which are low energy solutions of string theory. For simplicity, we focussed our attention on the zero charge case and showed that there are unstable modes for a range of time frequency and wavelength in the extra 10-D dimensions. These perturbations can be stabilized if the extra dimensions are compactified to a scale smaller than the minimum wavelength for which instability occurs and thus will not affect large astrophysical black holes in four dimensions. We comment on the implications of this result for the Cosmic Censorship Hypothesis.

DOE

N94-14330# State Univ. of New York, Stony Brook. Dept. of Physics.

RESEARCH IN THEORETICAL NUCLEAR PHYSICS

Jun. 1993 131 p

(Contract DE-FG02-88ER-40388)

(DE93-015096; DOE/ER-40388/102) Avail: CASI HC A07/MF A02

The introductory section describes the goals, main thrusts, and interrelationships between the various activities in the program and principal achievements of the Stony Brook Nuclear Theory Group during 1992-93. Details and specific accomplishments are related in abstract form. Current research is taking place in the following areas: strong interaction physics (the physics of hadrons, QCD and the nucleus, QCD at finite temperature and high density), relativistic heavy-ion physics, nuclear structure and nuclear many-body theory, and nuclear astrophysics.

DOE

N94-14341# Lawrence Livermore National Lab., CA.

WIND MASS AND ENERGY DEPOSITION

J. I. Castor , 21 Sep. 1992 13 p Presented at the 104th Annual Meeting of the Astronomical Society of the Pacific, Madison, WI, 20-25 Jun. 1992

(Contract W-7405-eng-48)

(DE93-013345; UCRL-JC-111860; CONF-9206370-1) Avail: CASI HC A03/MF A01

The subject of mass return to the interstellar medium by the winds of massive stars is reviewed from the viewpoint of calculations of stellar evolution with mass loss, combined with the birth rate function for stars of different masses (IMF). The uncertainties due to the IMF and in the assumed mass loss rates are discussed. The corresponding energy deposition rates from stellar winds are also estimated.

DOE

N94-14404*# Smithsonian Astrophysical Observatory, Cambridge, MA.

A LONG-TERM SPACE ASTROPHYSICS RESEARCH PROGRAM: THE EVOLUTION OF THE QUASAR CONTINUUM Semiannual Report No. 6, 1 Jan. - 30 Jun. 1993

M. Elvis Jul. 1993 74 p

(Grant NAGw-2201)

(NASA-CR-193714; NAS 1.26:193714) Avail: CASI HC A04/MF A01

The research program supported by this grant now has great momentum. Numerous papers are in progress, and a strong multi-wavelength observing program is rapidly accumulating data on samples of high redshift quasars across the spectrum. ROSAT spectra of quasars continue to yield surprises. Of four z = 3 quasars with X-ray spectra, three show strong absorption. This contrasts strongly with the situation for luminous AGN at low redshifts where fewer than 1 in 20 show X-ray absorption. A new site for this absorption is probably needed, either around the quasar (e.g. in a cluster cooling flow) or along the line of sight (e.g. in a Damped Lyman-alpha system). The unabsorbed quasar allows limits on the physical conditions in a damped Lyman-alpha cloud to be calculated, and will allow a X-ray Gunn-Peterson test to be applied that will limit the fraction of the closure mass in an intergalactic medium. The X-ray spectral indices of these z = 3 quasars show no change from those of similar objects at low z, suggesting

that 'short-lifetime' models apply. Eight other z = 3-4 quasars have been detected and their energy distributions from X-rays to Infrared (using new infrared spectrographs) have been compiled. These are now being compared with the low z continua from the 'Atlas of Quasar Energy Distributions' to search for evolutionary changes. The discovery of a likely warm absorber in 3C351 made recognition of another example simple. Also, modeling of the conditions in the absorber in 3C351 using the OVI absorption line from HST and the high ionization emission lines, suggests that the broad line region is indeed the origin of the warm absorber in this quasar, and by extension, others. Warm absorbers can now be used as a new diagnostic of this region. The X-ray spectrum of a 'Red Quasar', 3C212, has a cut-off spectrum, which could be fitted by an absorbed power-law, or more remarkably, by an unabsorbed black body. Using our quasi-simultaneous optical data and photoionization modeling we are able to rule out this latter possibility. The long-sought key to understanding red quasars has now been found. (Reddening was earlier ruled out because no 2175A absorption feature was seen. This is now seen to have been misleading.)

Derived from text

N94-14467# Lawrence Livermore National Lab., CA.

THE FIRST DATA FROM THE MACHO EXPERIMENT

D. P. Bennett, C. Akerlof (California Univ., Berkeley.), C. Alcock, R. Allsman, T. Axlerod, K. H. Cook, K. Freeman (Mount Stromlo and Siding Spring Observatory, Canberra, Australia.), K. Griest (California Univ., Berkeley.), S. Marshall (California Univ., Berkeley.), and H.-S. Park 17 Mar. 1993 7 p Presented at the Texas/PASCO 1992 International Conference, Berkeley, CA, 13-18 Dec. 1992

(Contract W-7405-eng-48)

(DE93-014423; UCRL-JC-113606; CONF-921266-2) Avail: CASI HC A02/MF A01

Massive Compact Halo Objects such as brown dwarfs, Jupiters, and black holes are prime candidates to comprise the dark halo of our galaxy. Paczynski noted that objects (dubbed MACHOS) with masses in the range 10(exp -6) solar mass less than M approximately less than 100 solar mass can be detected via gravitational microlensing of stars in the Magellanic Clouds with the caveat that only about one in 10(exp 6) stars will be lensed at any given time. Our group has recently begun a search for microlensing using a refurbished 1.27 meter telescope at the Mount Stromlo Observatory in Australia. Since the summer of 1992, we have been imaging up to 10(exp 7) stars a night in the Large Magellanic Cloud using our large format two-color 3.4 x 10(exp 7) pixel CCD camera. First results based on an analysis of approximately 10(exp 6) of these stars are reported. Although this is not enough data to make definitive statements about the nature of the dark matter, we are able to conclude that the rate of variable star background events is not larger than the expected MACHO signal.

DOE

N94-14482*# Colorado Univ., Boulder. Dept. of Computer Science.

VISUALIZATION TECHNIQUES TO AID IN THE ANALYSIS OF MULTI-SPECTRAL ASTROPHYSICAL DATA SETS Final Report

Edward W. Brugel, Gitta O. Domik (Paderborn Univ., Germany.), and Thomas R. Ayres Sep. 1993 105 p

(Grants NAGw-1902; NSF ASC-90-01115)

(NASA-CR-194489; NAS 1.26:194489) Avail: CASI HC A06/MF A02

The goal of this project was to support the scientific analysis of multi-spectral astrophysical data by means of scientific visualization. Scientific visualization offers its greatest value if it is not used as a method separate or alternative to other data analysis methods but rather in addition to these methods. Together with quantitative analysis of data, such as offered by statistical analysis, image or signal processing, visualization attempts to explore all information inherent in astrophysical data in the most effective way. Data visualization is one aspect of data analysis. Our taxonomy as developed in Section 2 includes identification and access to existing information, preprocessing and quantitative analysis of data, visual representation and the user interface as major components to the software environment of astrophysical data analysis. In pursuing our goal to provide methods and tools for scientific visualization of multi-spectral astrophysical data, we therefore looked at scientific data analysis as one whole process, adding visualization tools to an already existing environment and integrating the various components that define a scientific data analysis environment. As long as the software development process of each component is separate from all other components, users of data analysis software are constantly interrupted in their scientific work in order to convert from one data format to another, or to move from one storage medium to another, or to switch from one user interface to another. We also took an in-depth look at scientific visualization and its underlying concepts, current visualization systems, their contributions, and their shortcomings. The role of data visualization is to stimulate mental processes different from quantitative data analysis, such as the perception of spatial relationships or the discovery of patterns or anomalies while browsing through large data sets. Visualization often leads to an intuitive understanding of the meaning of data values and their relationships by sacrificing accuracy in interpreting the data values. In order to be accurate in the interpretation, data values need to be measured, computed on, and compared to theoretical or empirical models (quantitative analysis). If visualization software hampers quantitative analysis (which happens with some commercial visualization products), its use is greatly diminished for astrophysical data analysis. The software system STAR (Scientific Toolkit for Astrophysical Research) was developed as a prototype during the course of the project to better understand the pragmatic concerns raised in the project. STAR led to a better understanding on the importance of collaboration between astrophysicists and computer scientists.

Author (revised)

N94-14536# Los Alamos National Lab., NM.

MULTIPLICATIVE NOISE: APPLICATIONS IN COSMOLOGY AND FIELD THEORY

S. Habib 1993 21 p Presented at the 8th Annual Workshop in Nonlinear Astronomy, Gainesville, FL, 4-6 Feb. 1993

(Contract W-7405-eng-36)

(DE93-016624; LA-UR-93-2105; CONF-9302132-1) Avail: CASI HC A03/MF A01

Physical situations involving multiplicative noise arise generically in cosmology and field theory. In this paper, the focus is first on exact nonlinear Langevin equations, appropriate in a cosmological setting, for a system with one degree of freedom. The Langevin equations are derived using an appropriate time-dependent generalization of a model due to Zwanzig. These models are then extended to field theories and the generation of multiplicative noise in such a context is discussed. Important issues in both the cosmological and field theoretic cases are the fluctuation-dissipation relations and the relaxation time scale. Of some importance in cosmology is the fact that multiplicative noise can substantially reduce the relaxation time. In the field theoretic context, such a noise can lead to a significant enhancement in the nucleation rate of topological defects.

DOE

N94-14685*# Columbia Univ., New York, NY. Depts. of Astronomy and Physics.

WAS 49: MIRROR FOR A HIDDEN SEYFERT 1 GALAXY Final Technical Report, 15 Sep. 1992 - 14 Sep. 1993

Jules Halpern, E. Moran, L. Kay, and R. Antonucci Oct. 1993 12 p

(Grant NAG5-2092)

(NASA-CR-194537; NAS 1.26:194537; CAL-2139) Avail: CASI HC A03/MF A01

Was 49 is an interacting pair of Seyfert galaxies at z = 0.063, one of which contains a hidden Seyfert 1 nucleus as evidenced by the highly polarized broad wings on its Balmer lines. The disk of the main galaxy, Was 49a, appears to be globally photoionized by a powerful continuum source, undoubtedly the hidden Seyfert 1 companion, Was 49b. The intrinsic luminosity of Was 49b is at least 100 times larger than the observed (scattered) luminosity. A single SWP spectrum of the pair, which can be spatially resolved in the large aperture was obtained. A narrow Ly-alpha line was detected from Was 49b, the hidden Seyfert 1, at a flux level consistent with that of an unreddened Seyfert 2 galaxy. The lack of detection of a continuum is consistent with a power-law of v(sup -1) or steeper extrapolated from the optical, again consistent with the spectrum of other Seyfert 2 and hidden Seyfert 1 galaxies.

Author (revised)

N94-14688*# Columbia Univ., New York, NY. Depts. of Astronomy and Physics.

MULTIWAVELENGTH OBSERVATIONS OF UNIDENTIFIED HIGH ENERGY GAMMA RAY SOURCES Annual Status and Final Technical Report, 15 Aug. 1992 - 14 Oct. 1993

Jules P. Halpern Oct. 1993 29 p

(Grant NAG5-2051)
(NASA-CR-194536; NAS 1.26:194536; CAL-2140) Avail: CASI HC A03/MF A01

As was the case for COS B, the majority of high-energy (greater than 100 MeV) gamma-ray sources detected by the EGRET instrument on GRO are not immediately identifiable with cataloged objects at other wavelengths. These persistent gamma-ray sources are, next to the gamma-ray bursts, the least understood objects in the universe. Even a rudimentary understanding of their nature awaits identifications and follow-up work at other wavelengths to tell us what they are. The as yet unidentified sources are potentially the most interesting, since they may represent unrecognized new classes of astronomical objects, such as radio-quiet pulsars or new types of active galactic nuclei (AGN's). This two-year investigation is intended to support the analysis, correlation, and theoretical interpretation of data that we are obtaining at x ray, optical, and radio wavelengths in order to render the gamma-ray data interpretable. According to plan, in the first year concentration was on the identification and study of Geminga. The second year will be devoted to studies of similar unidentified gamma-ray sources which will become available in the first EGRET catalogs. The results obtained so far are presented in the two papers which are reproduced in the Appendix. In these papers, we discuss the pulse profiles of Geminga, the geometry and efficiency of the magnetospheric accelerator, the distance to Geminga, the implications for theories of polar cap heating, the effect of the magnetic field on the surface emission and environment of the neutron star, and possible interpretations of a radio-quiet Geminga. The implications of the other gamma-ray pulsars which were discovered to have high gamma-ray efficiency are also discussed, and the remaining unidentified COS B sources are attributed to a population of efficient gamma-ray sources, some of which may be radio quiet. Author (revised)

91 LUNAR AND PLANETARY EXPLORATION

Includes planetology; and manned and unmanned flights.

For spacecraft design or space stations see *18 Spacecraft Design, Testing and Performance.*

N94-12823*# Smithsonian Astrophysical Observatory, Cambridge, MA.
VENUS GRAVITY Final Report and Semiannual Status Report Nos. 1, 2 and 3, 1 Feb. 1991 - 31 Jan. 1993
Robert D. Reasenberg Jun. 1993 12 p See also A93-10559
(Grant NAGw-2361)
(NASA-CR-194077; NAS 1.26:194077) Avail: CASI HC A03/MF A01

The anomalous gravity field of Venus shows high correlation with surface features revealed by radar. We extract gravity models from the Doppler tracking data from the Pioneer Venus Orbiter (PVO) by means of a two-step process. In the first step, we solve the nonlinear spacecraft state estimation problem using a Kalman filter-smoother. The Kalman filter was evaluated through simulations. This evaluation and some unusual features of the filter are discussed. In the second step, we perform a geophysical inversion using a linear Bayesian estimator. To allow an unbiased comparison between gravity and topography, we use a simulation technique to smooth and distort the radar topographic data so as to yield maps having the same characteristics as our gravity maps. The maps presented cover 2/3 of the surface of Venus and display the strong topography-gravity correlation previously reported. The topography-gravity scatter plots show two distinct trends. Author (revised)

N94-13083*# National Aeronautics and Space Administration. Ames Research Center, Moffett Field, CA.
REDUCTION AND ANALYSIS OF SEASONS 15 AND 16 (1991 - 1992) PIONEER VENUS RADIO OCCULTATION DATA AND CORRELATIVE STUDIES WITH OBSERVATIONS OF THE NEAR-INFRARED EMISSION OF VENUS Semiannual Progress Report No. 1, 1 Apr. - 30 Sep. 1992
Jon M. Jenkins 1992 12 p
(Contract NCC2-753)
(NASA-CR-194128; NAS 1.26:194128) Avail: CASI HC A03/MF A01

Radio occultation experiments, and radio astronomical observations have suggested that significant variations (both spatial and temporal) in the abundances of sulfur-bearing gases are occurring below the Venus cloud layers. In addition, recent Near Infra-Red images of the nightside of Venus revealed large-scale features which sustain their shape over multiple rotations (the rotation periods of the features are 6.0 +/- 0.5 days). Presumably, the contrast variations in the NIR images are caused by variations in the abundance of large particles in the cloud deck. If these particles are composed of liquid sulfuric acid, one would expect a strong anticorrelation between regions with a high abundance of sulfuric acid vapor, and regions where there are large particles. One technique for monitoring the abundance and distribution of sulfuric acid vapor (H2SO4) at and below the main Venus cloud layer (altitudes below 50 km) is to measure the 13-cm wavelength opacity using Pioneer Venus Orbiter Radio Occultation Studies (PV-ORO). We are working to characterize variations in the abundance and distribution of subcloud H2SO4(g) in the Venus atmosphere by using a number of 13-cm radio occultation measurements conducted with the Pioneer Venus Orbiter near the inferior conjunction of 1991. When retrieved, the vertical profiles of the abundance of H2SO4(g) will be compared and correlated with NIR images of the night side of Venus made during the same period of time. Hopefully, the combination of these two different types of data will make it possible to constrain or identify the composition of the large particles causing the features observed in the NIR images. Considered on their own, however, the parameters retrieved from the radio occultation experiments are valuable science products. Author (revised)

N94-13088*# North Carolina State Univ., Raleigh.
MARS MISSION RESEARCH CENTER Annual Report No. 3, 1 Jul. 1990 - 30 Jun. 1991
Jul. 1991 75 p Prepared in cooperation with North Carolina Agricultural and Technical State Univ., Greensboro
(Grant NAGw-1331)
(NASA-CR-194034; NAS 1.26:194034) Avail: CASI HC A04/MF A01

The Mars Mission Research Center (M2RC) is one of nine University Space Engineering Research Centers established by NASA in June 1988. It is a cooperative effort between NCSU and A&T in Greensboro. The goal of the Center is to focus on research and educational technologies for planetary exploration with particular emphasis on Mars. The research combines Mission Analysis and Design, Hypersonic Aerodynamics and Propulsion, Structures and Controls, Composite Materials, and Fabrication Methods in a cross-disciplined program directed towards the development of space transportation systems for lunar and planetary travel. The activities of the students and faculty in the M2RC for the period 1 Jul. 1990 to 30 Jun. 1991 are described. Derived from text

N94-13183*# National Aeronautics and Space Administration. Ames Research Center, Moffett Field, CA.
PLANETARY PROTECTION IMPLEMENTATION ON FUTURE MARS LANDER MISSIONS
Robert Howell (Biotrack Corp., Mountain View, CA.) and Donald L. DeVincenzi Jun. 1993 30 p Workshop held in Palo Alto, CA, 13-15 Jul. 1992
(RTOP 199-59-12-05)
(NASA-CP-3216; A-93085; NAS 1.55:3216) Avail: CASI HC A03/MF A01

A workshop was convened to discuss the subject of planetary protection implementation for Mars lander missions. It was sponsored and organized by the Exobiology Implementation Team of the U.S./Russian Joint Working Group on Space Biomedical and Life Support Systems. The objective of the workshop was to discuss planetary protection issues for the Russian Mars '94 mission, which is currently under development, as well as for additional future Mars lander missions including the planned Mars '96 and U.S. MESUR Pathfinder and Network missions. A series of invited presentations was made to ensure that workshop participants had access to information relevant to the planned discussions. The topics summarized in this report include exobiology science objectives for Mars exploration, current international policy on planetary protection, planetary protection requirements developed for earlier missions, mission plans and designs for future U.S. and Russian Mars landers, biological contamination of spacecraft components, and techniques for spacecraft bioload reduction. In addition, the recent recommendations of the U.S. Space Studies Board (SSB) on this subject were also summarized. Much of the discussion focused on the recommendations of the SSB. The SSB proposed relaxing the planetary protection requirements for those Mars lander missions that do not contain life detection experiments, but maintaining Viking-like requirements for those missions that do contain life detection experiments. The SSB

recommendations were found to be acceptable as a guide for future missions, although many questions and concerns about interpretation were raised and are summarized. Significant among the concerns was the need for more quantitative guidelines to prevent misinterpretation by project offices and better access to and use of the Viking data base of bioassays to specify microbial burden targets. Among the questions raised were how will the SSB recommendations be integrated with existing Committee on Space Research (COSPAR) policy and how will they apply to and affect Mars '94, Mars '96, MESUR Pathfinder, and MESUR Network missions? One additional topic briefly considered at the workshop was the identification of some issues related to planetary protection considerations for Mars sample return missions. These issues will form the basis for a follow-on joint U.S./Russian workshop on that subject. Author (revised)

N94-13199*# National Air and Space Museum, Washington, DC. Center for Earth and Planetary Studies.

THE NATURE AND ORIGIN OF PERIODICALLY SPACED TECTONIC FEATURES ON MARS Final Report

Thomas R. Watters 29 Oct. 1991 4 p

(Grant NAGw-1106)

(NASA-CR-193821; NAS 1.26:193821) Avail: CASI HC A01/MF A01

The final report on the nature and origin of periodically spaced tectonic features on Mars is presented. The focus of this investigation was to characterize and model the periodically spaced wrinkle ridges observed in ridged plains material on Mars. The investigation centered on the wrinkle ridges in ridged plains material on the Tharsis Plateau. Wrinkle ridges are interpreted to be structural in origin, resulting from buckling followed by reverse or thrust faulting of the ridged plains material. The study extended beyond Tharsis to other ridged plains units, particularly those in Hesperia Planum. As a corollary, an analysis of the spacing of the anticlinal ridges of the Yakima Fold Belt of the Columbia Plateau in the NW United States was undertaken. Author (revised)

N94-13561*# Arizona State Univ., Tempe. Geology Dept.

REGIONAL TECTONIC ANALYSIS OF VENUS AS PART OF THE PIONEER VENUS GUEST INVESTIGATOR PROJECT Final Report

David R. Williams 9 Sep. 1991 4 p

(Grant NAG2-690)

(NASA-CR-194079; NAS 1.26:194079) Avail: CASI HC A01/MF A01

Over the past year, much of the tectonic analysis of Venus we have done has centered on global properties of the planet, in order to understand fundamental aspects of the dynamics of the mantle and lithosphere of Venus. We have developed convection models of the Earth and Venus. These models assume whole mantle internally-heated convection. The viscosity is temperature, volatile-content, and stress dependent. An initial temperature and volatile content is assumed, and the thermal evolution is tracked for 4.6 billion years. During this time, heating occurs by decay of radiogenic elements in the mantle, and degassing and regassing of volatiles takes place at the surface. For a model assuming plate tectonics as the primary heat loss mechanism, representing the Earth through most of it's history and perhaps Venus' earlier history, degassing of the mantle was found to occur rapidly (approximately 200 My) over a large range of parameters. Even for parameters chosen to represent extreme cases of an initially cool planet, low radiogenic heating, and large initial volatile complement, the mantle water content was degassed to an equilibrium value in about 2 By. These values may be applicable to the early Venus, if a large, Moon-forming impact on Earth resulted in efficient heating and loss of water, leaving Venus with a comparably greater volatile budget and less vigorous early convection. It may therefore be impossible to retain large amounts of water in the interior of Venus until the planet cools down enough for the 'cold-trap' effect to take place. This effect traps crust forming melts within the mantle due to a cusp in the solidus, causing these melts to refreeze at depth into a dense eclogite phase, which will inhibit ascent of this material to the surface. This effect, however, requires a hydrous mantle, so early loss of water might prevent it from taking place. Since without plate tectonics there is no mechanism for regassing volatiles into the mantle, as occurs on Earth at subduction zones, this means the interior of Venus would at present be almost completely dry. We have also calculated argon degassing, and mantle flow velocities. viscosities, and cooling rates in these models, and these values can provide constraints on present day mantle dynamics. Derived from text

N94-13613* National Aeronautics and Space Administration, Washington, DC.

EXPLORING MARS (Videotape)

Mar. 1987 Videotape: 5 min. 40 sec. playing time, in color, with sound

(NASA-TM-109306; NONP-VT-93-185324) Avail: CASI VHS A01/BETA A22

This presentation shows what researchers are designing (solar balloon and rover) to better explore Mars geography before sending a manned mission. Author (revised)

N94-13626* National Aeronautics and Space Administration. Lewis Research Center, Cleveland, OH.

NASA IMAGES 11 (Videotape)

Apr. 1988 Videotape: 27 min. 6 sec. playing time, in color, with sound

(NASA-TM-109287; NONP-VT-93-185303) Avail: CASI VHS A01/BETA A22

A look at unmanned spacecraft to explore planets is presented. The topics covered include Pioneer 10 and 11, Pioneer-Venus, Voyager, IUE, and HEAO. Author (revised)

N94-13655# Institute for Future Technology, Tokyo (Japan).

THE STUDIES ON LUNAR AND PLANETARY EXPLORATION AND UTILIZATION: THE STUDY ON LUNAR RESOURCES UTILIZATION [TSUKI WAKUSEI NO KAIHATSU RIYOU NO KENKYUU: TSUIKISHIGEN NO KAIHATSU RIYOU NO KENKYUU]

National Space Development Agency 31 Mar. 1993 24 p In JAPANESE

(NASDA-CNT-930014; JTN-93-80468) Avail: CASI HC A03/MF A01

The results of the gathering of various knowledge about the lunar resources (including the outline of lunar resource development and utilization, lunar topography and lunar surface environments, and physical properties and chemical compositions of the lunar surface soil) are described. The outline of processes for lunar resource utilization (including pre-processing of regolith (sorting and concentration)), separation of components (reduction, extraction and refinement), and case studies on lunar surface resource utilization systems (including scenarios of lunar base and lunar surface activities, and strategy for lunar resource utilization) is given. Major lunar dark mantle deposits, correlation between intensity of the ferromagnetic resonance for FeO amount and other maturity indices, drawing the Apollo 12 double drive-tube core, scanning electron micrograph of a composite volcanic glass droplet from Apollo 17 core, and lunar resource utilization processes, etc. are shown. Author (NASDA)

N94-13855*# Northeast Louisiana State Coll., Monroe. Dept. of Geosciences.

MARTIAN SEDIMENTARY DEPOSITS Final Technical Report

Rene DeHon 25 Mar. 1992 6 p

(Grant NsG-7534)

(NASA-CR-193266; NAS 1.26:193266) Avail: CASI HC A02/MF A01

The objectives are characterization of flow through outflow channels, sedimentation associated with Martian outflow systems, and documentation of Martian lakes. Over the period of the grant much, but not all, of the study centered on the Maja Valles outflow. Maja served as an example in which the effects of multiple channel routing and ponding could be studied. Maja Valles also served as the test case for calculating flow through an outflow system. Applying the lessons learned in Maja Valles and comparisons and contrast required a scrutiny of other channels. Author (revised)

N94-14298*# Lunar and Planetary Inst., Houston, TX.

WORKSHOP ON THE SPACE ENVIRONMENT: THE EFFECTS ON THE OPTICAL PROPERTIES OF AIRLESS BODIES

B. Hapke, ed. (Pittsburgh Univ., PA.), B. Clark, ed., G. Benedix, ed., D. Domingue, ed., and M. Cintala, ed. (National Aeronautics and Space Administration. Lyndon B. Johnson Space Center, Houston, TX.) 1993 18 p Workshop held in Houston, TX, 9-10 Nov. 1992

(Contract NASw-4574)

(NASA-CR-194417; NAS 1.26:194417; LPI/TR-93-01) Avail: CASI HC A03/MF A01

Reflectance spectrophotometry and polarimetry are major tools in remote sensing studies of surfaces of solar system bodies. The interpretations of such measurements are often based on laboratory studies of meteoritic, lunar, and terrestrial materials. However, the optical properties of regoliths

are known to be affected by the space environment. Thus, some of the major questions addressed in the workshop include identity of the soil component responsible for alteration of the optical properties, the process that produced this component, and how reliably the effects of these processes could be extrapolated to other bodies of the solar system. For individual titles, see N94-14299 through N94-14303.

N94-14299*# National Aeronautics and Space Administration. Lyndon B. Johnson Space Center, Houston, TX.

IMPACT MELTING AND VAPORIZATION IN PLANETARY REGOLITHS

Mark J. Cintala *In* Lunar and Planetary Inst., Workshop on the Space Environment: The Effects on the Optical Properties of Airless Bodies 1993 p 5-7 (For primary document see N94-14298 02-91)

Avail: CASI HC A01/MF A01

The thermal phenomena attending high-velocity impact have profound effects on virtually every aspect of the physical, chemical, and optical evolution of planetary regoliths. Not only do impacts pulverize, redistribute, and mix the various components of a regolith, but they also fuse and vaporize them - changing crystalline material to glass, releasing trapped or implanted gases, and spreading vaporized products across the planet's surface, among many other things. Those wishing to understand the details of regolith evolution must incorporate the effects of impact into their approach to the problem. Derived from a more extensive contribution, a short summary of the thermal processes accompanying impact into planetary regoliths, with the immediate acknowledgment that it is neither exhaustive in its consideration of the existing literature nor exact in any of its treatments, is presented. The reader desiring more information is directed to the relevant papers cited at the end; should they fail to provide satisfaction, he or she is then heartily encouraged to attack the problem immediately.

Author (revised)

N94-14300*# Rensselaer Polytechnic Inst., Troy, NY. Dept. of Earth and Environmental Sciences.

EXTRAPOLATION OF SPACE WEATHERING PROCESSES TO OTHER SMALL SOLAR SYSTEM BODIES

M. J. Gaffey *In* Lunar and Planetary Inst., Workshop on the Space Environment: The Effects on the Optical Properties of Airless Bodies 1993 p 7-8 (For primary document see N94-14298 02-91)

Avail: CASI HC A01/MF A01

A diverse range of processes were invoked as the dominant factor or as important contributory factors in the modification of the optical surface and regolith of the moon. These include impact vitrification by large and small projectiles, solar wind implantation and the reduction of oxidized iron during energetic events, sputtering and crystal lattice damage by energetic cosmic rays, shock metamorphism of minerals, mixing of diverse lithologies by impacts, and contamination by external materials. These processes are also potentially important on the rocky surfaces of other small solar system bodies. For icy bodies, several additional processes are also possible, including formation of complex organic compounds from methane and ammonia-bearing ices by ultraviolet irradiation and the condensation of vapor species to form frost layers in the polar or cooler regions of objects at appropriate heliocentric distances. The lunar case, even when completely understood, will not extend in a simple linear fashion to other small rocky objects, nor will the optical surfaces of those objects all be affected to the same degree by each process. The major factors that will control the relative efficacy of a possible mechanism include the efficiency of ejecta retention and the degree to which the regolith materials experience multiple events (primarily a function of body size, escape velocity, and impactor velocities); the mean duration of typical regolith particle exposure at the optical surface and within reach of the micrometeorite, cosmic ray, solar wind, or UV fluxes (a function of the rate and scale of regolith mixing, production, and removal processes); the incident flux of solar (low energy) cosmic rays, solar wind, or UV radiation (inverse square of heliocentric distance) or of galactic (high energy) cosmic rays (slowly increasing flux with heliocentric distance); and the compositional and mineralogical nature of the surface being affected. In general, those processes that depend upon either the retention of impact ejecta or on the presence of multigenerational regoliths should be substantially less effective on smaller bodies with lower escape velocities. However, there are important exceptions to this generalization. For example, a process that involves the hypervelocity impact of small particles into a fine-grained regolith may be able to effectively retain highly shocked or melted material due to the nature of shock wave propagation in such a heterogeneous material.

Author (revised)

N94-14301*# Pittsburgh Univ., PA.

LABORATORY SIMULATIONS OF LUNAR DARKENING PROCESSES

B. Hapke *In* Lunar and Planetary Inst., Workshop on the Space Environment: The Effects on the Optical Properties of Airless Bodies 1993 p 8-9 (For primary document see N94-14298 02-91)

Avail: CASI HC A01/MF A01

It was clear long before the Apollo missions that a darkening process occurs on the moon. However, its nature remains controversial and elusive. Current evidence implies that the darkening is associated with, and is probably caused by, submicroscopic metallic iron in the regolith. Questions discussed at the workshop include: (1) under what conditions will impact vitrification produce a dark glass; (2) what is the role of the submicroscopic metallic Fe (SMFe) in the lunar darkening process; (3) how is the SMFe produced; (4) is there a significant component of the regolith that has been deposited from a vapor, if so, what form is it in, and how can it be recognized, what are its effects on the chemistry of the regolith; (5) how do the processes of impact vitrification, vaporization, sputtering, and SMFe production vary as a function of distance from the sun and location in planetary magnetospheres; and (6) what other processes might affect optical properties. Ices have lower melting and boiling temperatures and sputtering yields several orders of magnitude larger than silicates. Hence, analogous processes will occur to an even greater extent on satellites of the outer planets, and these questions are relevant to those bodies as well.

Author (revised)

N94-14302*# National Aeronautics and Space Administration. Lyndon B. Johnson Space Center, Houston, TX.

DEPOSITION OF IMPACT-GENERATED VAPORS IN THE LUNAR REGOLITH

Lindsay P. Keller and David S. McKay *In* Lunar and Planetary Inst., Workshop on the Space Environment: The Effects on the Optical Properties of Airless Bodies 1993 p 9-10 (For primary document see N94-14298 02-91)

Avail: CASI HC A01/MF A01

The composition and structure of the finest grain sizes in lunar soils are strongly influenced by impact-associated processes such as comminution, melting, and vaporization. These factors in turn exert a strong influence on the optical properties of the materials. The literature regarding the fractionations that accompany the evaporation of silicate materials during impacts is reviewed, the evidence for vapor deposits in the lunar samples is considered, our own efforts to characterize vapor deposits in lunar soils using electron microscopy is described, and the implications of vapor deposits on the optical properties of the lunar fines are discussed.

Author (revised)

N94-14303*# Tennessee Univ., Knoxville. Dept. of Geological Sciences.

THE STATE OF Fe IN THE LUNAR REGOLITH AND ITS RELATIONSHIP TO THE SPECTRAL REFLECTANCE PROPERTIES OF THE MOON

Lawrence A. Taylor *In* Lunar and Planetary Inst., Workshop on the Space Environment: The Effects on the Optical Propertis of Airless Bodies 1993 p 10-11 (For primary document see N94-14298 02-91)

Avail: CASI HC A01/MF A01

Space weathering may have altered the surfaces of airless bodies such as asteroids and the moon, and effectively shock-darkened their surfaces, resulting in much lower reflectance and shallower absorption bands compared to those of simple, comminuted, and powdered rocks produced in the laboratory. Studies of lunar samples from the Apollo missions have led to the suggestion that these reflection properties are inherent to the fine-grained regolith which has recorded a wide variety of shock-metamorphic effects. In particular, the lunar soil (i.e., that part of the regolith with grain sizes below 1 mm) contains native Fe in quantities above those present in the rocks from which the soil was formed. The origin and nature of the native Fe in the soil is addressed, and speculations concerning its effects upon the soil's optical properties are presented. Portions of this discussion draw heavily from earlier papers by our research group. Author (revised)

92 SOLAR PHYSICS

Includes solar activity, solar flares, solar radiation and sunspots. For related information see *93 Space Radiation.*

N94-13146*# Teledyne Brown Engineering, Huntsville, AL.
ULTRAVIOLET SPECTROMETER AND POLARIMETER (UVSP) CATALOG OF OBSERVATIONS. VOLUME 3: EXPERIMENTS 63058-99771 (FEBRUARY 1988 - NOVEMBER 1989)
William Henze, Jr. Washington Jul. 1993 889 p
(Contract NAS8-35921)
(NASA-CR-4529; NAS 1.26:4529; M-724-Vol-3) Avail: CASI HC A99/MF A10

A catalog of a observations (experiments) obtained by the Ultraviolet Spectrometer and Polarimeter (UVSP) on the Solar Maximum Mission (SMM) from Nov. 1980 to Nov. 1989 is provided. The information for each entry includes the time of each observation, the observed position of the Sun, the spacecraft roll angle, the slit used, and instrument parameters such as raster size, pixel spacing, wavelength, polarimeter usage, gate time, etc. The document is split into three volumes: Volume 1 contains experiments 1-30719 (Feb. 1980 - Apr. 1985); Volume 2 contains experiments 30720-63057 (Apr. 1985 - Feb. 1988); and Volume 3 contains experiments 63058-99771 (Feb. 1988 - Nov. 1989). Author (revised)

N94-13234*# Joint Inst. for Lab. Astrophysics, Boulder, CO.
BASIC RESEARCH IN SOLAR PHYSICS Final Technical Report
Jeffrey L. Linsky 28 Apr. 1991 6 p
(Grant NGL-06-003-057)
(NASA-CR-193632; NAS 1.26:193632) Avail: CASI HC A02/MF A01

This grant, dating back more than 20 years has supported a variety of investigations of the chromospheres and coronae of the Sun and related cool stars by the Principal Investigator, his postdocs and graduate students, and colleagues at other institutions. This work involved studies of radiative transfer and spectral line formation theory, and the application of these techniques to the analysis of spectra obtained from space and ground-based observatories in the optical, ultraviolet, x-ray and radio portions of the spectrum. Space observations have included the analysis of spectra from OSO-7, Skylab, SMM, and the HRTS rocket experiments. Recent work has concentrated on the interaction of magnetic fields, plasma and radiation in the outer atmospheres of the Sun and other magnetically active stars with different fundamental parameters. Our study of phenomena common to the Sun and stars, the 'solar-stellar connection', can elucidate the fundamental physics, because spatially-resolved observations of the Sun provide us with the 'groundtruth,' while interpretation of stellar data permit us to isolate those parameters critical to stellar activity. Recently, we have studied the differences in physical properties between solar regions of high magnetic flux density and the surrounding plasma. High-resolution CN and CO spectroheliograms have been used to model the thermal inhomogeneities driven by unstable CO cooling, and we have analyzed spatially resolved UV spectra from HRTS to model the thermal structure and energy balance of small-scale structures. The study of nonlinear relations between atmospheric radiative losses and the photospheric magnetic flux density has been continued. We have also proposed a new model for the decay of plages by random walk diffusion of magnetic flux. Our analysis of phenomena common to the Sun and stars included the application of available spectroscopic diagnostics, establishing evidence that the atmospheres of the least active stars are heated at a 'basal' rate that is also found in the centers of solar supergranules, and using the Doppler-imaging technique to measure the position, size, and brightness of stellar active regions. We are computing multi-component models for solar and stellar atmospheres, and models for coronal loops and for the transition-region down flows. The study of solar and stellar flares permits us to assess the role of turbulent energy transport, to pinpoint the mechanism behind Type I radio bursts, to determine whether plasma radiation or cyclotron maser is responsible for microwave flares on M dwarfs, and to extend our knowledge of the basic physics pertinent to cyclotron-maser processes operating on the Sun. Derived from text

N94-13502# Belgian Royal Observatory, Brussels.
THE INFRARED SOLAR SPECTRUM
N. Grevesse (Liege Univ., Belgium.) and A. J. Sauval 1991 20 p
Repr. from The Infrared Spectral Region of Stars, Proceedings of the Montpellier Colloquium, Oct. 1990 (Cambridge, England, University Press), 1991 p 215-233 Proceedings of the Montpellier Colloquium held in Cambridge, England, 1991
(Communications-Ser-B-159; ETN-93-94376) Avail: CASI HC A03/MF A01

The spectrum of the quiet Sun at wavelengths larger than about 1 micrometer (or wavenumbers shorter than 10,000/cm) are described. The main characteristics of studying the solar spectrum in the infrared region are summarized. The new high resolution low noise solar spectra obtained by the Atmospheric Trace Molecule Spectroscopy (ATMOS) Fourier transform spectrometer experiment on board the Space Shuttle are considered. Atomic and molecular spectroscopy/line identification are discussed. Solar observations in the infrared are summarized. Recent analyses have led to a better understanding of the heterogeneous structure of the solar outer layers: thermal bifurcation between the cool photosphere and the hot flux tube chromosphere, convective motions in the photosphere, oscillations in the photosphere and chromosphere, magnetic fields and shapes of the flux tubes, etc. ESA

N94-13671*# California Univ., San Diego, La Jolla. Center for Astrophysics and Space Sciences.
DETERMINING THE SOLAR-FLARE PHOTOSPHERIC SCALE HEIGHT FROM SMM GAMMA-RAY MEASUREMENTS Final Technical Report, 1 Mar. 1990 - 28 Feb. 1991
Richard E. Lingenfelter 28 Feb. 1991 2 p
(Grant NAG5-1324)
(NASA-CR-194084; NAS 1.26:194084) Avail: CASI HC A01/MF A01

A connected series of Monte Carlo programs was developed to make systematic calculations of the energy, temporal and angular dependences of the gamma-ray line and neutron emission resulting from such accelerated ion interactions. Comparing the results of these calculations with the Solar Maximum Mission/Gamma Ray Spectrometer (SMM/GRS) measurements of gamma-ray line and neutron fluxes, the total number and energy spectrum of the flare-accelerated ions trapped on magnetic loops at the Sun were determined and the angular distribution, pitch angle scattering, and mirroring of the ions on loop fields were constrained. Comparing the calculations with measurements of the time dependence of the neutron capture line emission, a determination of the He-3/H ratio in the photosphere was also made. The diagnostic capabilities of the SMM/GRS measurements were extended by developing a new technique to directly determine the effective photospheric scale height in solar flares from the neutron capture gamma-ray line measurements, and critically test current atmospheric models in the flare region. Author (revised)

N94-13958*# California Inst. of Tech., Pasadena. Solar Astronomy.
HARD X RAY/MICROWAVE SPECTROSCOPY OF SOLAR FLARES Final Report, 1 Mar. 1990 - 29 Feb. 1992
Dale E. Gary May 1992 4 p
(Grant NAG5-1323)
(NASA-CR-194399; NAS 1.26:194399) Avail: CASI HC A01/MF A01

The joint study of hard x ray and microwave observations of solar flares is extremely important because the two complementary ways of viewing the accelerated electrons yield information that cannot be obtained using hard x rays or microwaves alone. The microwaves can provide spatial information lacking in the hard x rays, and the x ray data can give information on the energy distribution of electrons that remove ambiguities in the radio data. A prerequisite for combining the two data-sets, however, is to first understand which range of microwave frequencies correlate best with the hard x rays. This SMM Guest Investigator grant enabled us to combine multi-frequency OVRO data with calibrated hard x ray data to shed light on the relationship between the two emissions. In particular, the questions of which microwave frequencies correspond to which hard x ray energies, and what is the corresponding energy of the electrons that produce both types of emission are investigated. Author (revised)

N94-13963*# National Aeronautics and Space Administration. Goddard Space Flight Center, Greenbelt, MD.
NIMBUS-7 EARTH RADIATION BUDGET CALIBRATION HISTORY. PART 1: THE SOLAR CHANNELS
H. Lee Kyle, Douglas V. Hoyt (Research and Data Systems, Inc., Greenbelt, MD.), John R. Hickey (Eppley Lab., Inc., Newport, RI.), Robert H. Maschhoff (Gulton Industries, Inc., Albuquerque, NM.), and Brenda J. Vallette (Research

and Data Systems, Inc., Greenbelt, MD.) Sep. 1993 74 p
(Contract NAS5-31331; RTOP 665-10-70)
(NASA-RP-1316; Rept-93B00110; NAS 1.61:1316) Avail: CASI HC A04/MF A01

The Earth Radiation Budget (ERB) experiment on the Nimbus-7 satellite measured the total solar irradiance plus broadband spectral components on a nearly daily basis from 16 Nov. 1978, until 16 June 1992. Months of additional observations were taken in late 1992 and in 1993. The emphasis is on the electrically self calibrating cavity radiometer, channel 10c, which recorded accurate total solar irradiance measurements over the whole period. The spectral channels did not have inflight calibration adjustment capabilities. These channels can, with some additional corrections, be used for short-term studies (one or two solar rotations - 27 to 60 days), but not for long-term trend analysis. For channel 10c, changing radiometer pointing, the zero offsets, the stability of the gain, the temperature sensitivity, and the influences of other platform instruments are all examined and their effects on the measurements considered. Only the question of relative accuracy (not absolute) is examined. The final channel 10c product is also compared with solar measurements made by independent experiments on other satellites. The Nimbus experiment showed that the mean solar energy was about 0.1 percent (1.4 W/sqm) higher in the excited Sun years of 1979 and 1991 than in the quiet Sun years of 1985 and 1986. The error analysis indicated that the measured long-term trends may be as accurate as +/- 0.005 percent. The worse-case error estimate is +/- 0.03 percent. Author (revised)

N94-14479*# California Inst. of Tech., Pasadena. Div. of Geological and Planetary Sciences.
INTERACTIONS AMONG CONVECTION, MAGNETIC FIELDS AND p-MODE OSCILLATIONS IN THE SUN Annual Performance Report, 1 Jan. - 31 Dec. 1993
Peter Goldreich 31 Dec. 1993 4 p
(Grant NAGw-3018)
(NASA-CR-194477; NAS 1.26:194477) Avail: CASI HC A01/MF A01

Two papers on different aspects of the excitation and damping of solar oscillations were accepted for publication in the Astrophysical Journal. The first paper evaluates the rate at which turbulent convection feeds energy into individual p-modes. It is shown that stochastic excitation by turbulent convection provides a satisfactory fit to the product of the mode energies and linewidths. A somewhat surprising conclusion is that entropy fluctuations are about an order of magnitude more significant than are fluctuations of the Reynolds stress in exciting p-modes. However, entropy fluctuations cannot excite f-modes. This may account for the relatively low energies of the f-modes compared to those of the p-modes. The second paper explores the role of scattering of acoustic modes by turbulent velocity fluctuations. Scattering of a mode is concentrated near the top of its acoustic cavity. Because the turbulence has low Mach number, scattering couples modes having similar frequencies. Its net effects are to increase the linewidths of all modes and to transfer energy from p-modes to f-modes. Scattering is likely to be the dominant source for the linewidths of p-modes. In particular, it may account for the unexpectedly large linewidths measured for low frequency modes. Copies of preprints of the two papers referred to above are attached. The remainder of the report is devoted to a description of unpublished results. Author

N94-14492*# California Univ., Berkeley. Space Sciences Lab.
MEASUREMENTS OF THE SPATIAL STRUCTURE AND DIRECTIVITY OF 100 KeV PHOTON SOURCES IN SOLAR FLARES USING PVO AND ISEE-3 SPACECRAFT Final Report, 1 Apr. 1986 - 31 Mar. 1990
Kinsey A. Anderson 20 Feb. 1991 3 p
(Grant NAG2-393)
(NASA-CR-194080; NAS 1.26:194080) Avail: CASI HC A01/MF A01

The objective of this grant was to measure the spatial structure and directivity of the hard X-ray and low energy gamma-ray (100 keV-2 MeV) continuum sources in solar flares using stereoscopic observations made with spectrometers aboard the Pioneer Venus Orbiter (PVO) and Third International Sun Earth Explorer (ISEE-3) spacecraft. Since the hard X-ray emission is produced by energetic electrons through the bremsstrahlung process, the observed directivity can be directly related to the 'beaming' of electrons accelerated during the flare as they propagate from the acceleration region in the corona to the chromosphere/transition region. Some models (e.g., the thick-target model) predict that most of the impulsive hard X-ray/low energy gamma-ray source is located in the chromosphere, the effective height of the X-ray source above the photosphere increasing with the decrease in the photon energy. This can be verified by determining the height-dependence of the photon source through stereoscopic observations of those flares which are partially occulted from the view of one of the two spacecraft. Thus predictions about beaming of electrons as well as their spatial distributions could be tested through the analysis proposed under this grant. Derived from text

N94-14560 National Geophysical Data Center, Boulder, CO.
SOLAR-GEOPHYSICAL DATA NUMBER 584, APRIL 1993. PART 1: (PROMPT REPORTS). DATA FOR MARCH, FEBRUARY 1993, AND LATE DATA
Helen E. Coffey, ed. Apr. 1993 145 p See also PB93-198331 and PB93-188894 Limited Reproducibility: More than 20% of this document may be affected by microfiche quality
(PB93-198323; SGD-584-Pt-1) Avail: CASI HC A07

Data are provided for the following months: (1) March 1993--solar-terrestrial environment, IUWDS alert periods (advance and worldwide), solar activity indices, solar flares, solar radio emission, Stanford mean solar magnetic field; and (2) February 1993--solar active regions, sudden ionospheric disturbances, solar radio spectral observations, cosmic ray measurements by neutron monitor, and geomagnetic indices. NTIS

N94-14561 National Geophysical Data Center, Boulder, CO.
SOLAR-GEOPHYSICAL DATA NUMBER 584, APRIL 1993. PART 2: (COMPREHENSIVE REPORTS). DATA FOR OCTOBER 1992 AND MISCELLANEOUS
Helen E. Coffey, ed. Apr. 1993 65 p See also PB93-198323 and PB93-188902 Limited Reproducibility: More than 20% of this document may be affected by microfiche quality
(PB93-198331; SGD-584-Pt-2) Avail: CASI HC A04

Data are provided for October 1992: solar flares; solar radio bursts at fixed frequencies; solar x-ray radiation from GOES satellite graphs; mass ejections from the sun; and active prominences and filaments. NTIS

N94-14577*# Washington Univ., Seattle.
COMPARATIVE STUDY OF X RAY AND MICROWAVE EMISSIONS DURING SOLAR FLARES Final Report, 1 Jan. 1992 - 30 Jun. 1993
Robert M. Winglee 1993 3 p
(Grant NAGw-2819)
(NASA-CR-194532; NAS 1.26:194532) Avail: CASI HC A01/MF A01

The work supported by the grant consisted of two projects. The first project involved making detailed case studies of two flares using SMM data in conjunction with ground based observations. The first flare occurred at 1454 UT on June 20, 1989 and involved the eruption of a prominence near the limb. In the study we used data from many wavelength regimes including the radio, H-alpha, hard X-rays, and soft X-rays. We used a full gyrosynchrotron code to model the apparent presence of a 1.4 GHz source early in the flare that was in the form of a large coronal loop. The model results lead us to conclude that the initial acceleration occurs in small, dense loops which also produced the flare's hard X-ray emission. We also found evidence that a source at 1.4 GHz later in the event was due to second harmonic plasma emission. This source was adjacent to a leg of the prominence and comes from a dense column of material in the magnetic structure supporting the prominence. Finally, we investigated a source of microwaves and soft X-rays, occurring approximately 10 min after the hard X-ray peak, and calculate a lower limit for the density of the source. The second flare that was studied occurred at 2156 UT on June 20, 1989 and was observed with the VLA and the Owens Valley Radio Observatory (OVRO) Frequency Agile Array. We have developed a gyrosynchrotron model of the sources at flare peak using a new gyrosynchrotron approximation which is valid at very low harmonics of the gyrofrequency. We found that the accelerated particle densities of the sources decreased much more with radius from the source center than had been supposed in previous work, while the magnetic field varied less. We also used the available data to analyze a highly polarized source which appeared late in the flare. The second project involved compiling a statistical base for the relative timing of the hard X-ray peak, the turbulent and blue-shift velocities inferred from soft X-ray line emissions observed by SMM and the microwave peak as determined from ground-based observations. This timing was then used to aid the testing of newly developed global models for flares that

incorporate the global magnetic topology as well as the electron dynamics that are responsible for the hard X-rays and microwaves.

Derived from text

93 SPACE RADIATION

Includes cosmic radiation; and inner and outer earth's radiation belts.

For biological effects of radiation see *52 Aerospace Medicine.* For theory see *73 Nuclear and High-Energy Physics.*

N94-12816# Los Alamos National Lab., NM.
SEARCH FOR ULTRA-HIGH ENERGY EMISSION FROM GEMINGA AND FIVE UNIDENTIFIED EGRET SOURCES
1993 5 p Presented at the International Cosmic Ray Conference, Calgary, Alberta, 19-20 Jul. 1993
(Contract W-7405-eng-36)
(DE93-012717; LA-UR-93-1608; CONF-930779-6) Avail: CASI HC A01/MF A01

Data from the CYGNUS extensive air shower array were searched for continuous ultra-high energy (UHE) gamma radiation from five unidentified EGRET sources and from the Geminga pulsar. No evidence for continuous emission from any of these objects was found. Data in the Geminga source bin were also searched for pulsed emission using the recent EGRET ephemeris (237 ms period). No evidence of a periodic signal was found. The 90% confidence level upper limit on the continuous gamma-ray flux above 80 TeV for Geminga is 7.9 x 10(sup -14) cm(sup -2) s(sup -1).

DOE

N94-12826*# Washington Univ., Seattle. Dept. of Physics.
COSMIC PHYSICS DATA ANALYSIS PROGRAM Final Technical Report, 1 Mar. 1992 - 28 Feb. 1993
R. Jeffrey Wilkes 23 Sep. 1993 18 p
(Grant NAGw-3026)
(NASA-CR-194357; NAS 1.26:194357) Avail: CASI HC A03/MF A01

A data analysis program was carried out to investigate the intensity, propagation, and origin of primary Cosmic Ray Galactic electrons. Scanning was carried out on two new balloon flight experiments as well as the border area of previous experiments. The identification and evaluation of the energies of the primary electrons were carried out. A new analysis of these data were incorporated into an overall evaluation of the roll of electrons in the problem of the origin of cosmic rays. Recent measurements indicate that the earth may be within the expanding Geminga supernova shock wave which is expected to have a major effect upon the propagation and the energy spectrum of galactic electrons. Calculations with the Geminga model indicate that the cut-off energy may be very close to the observed highest energy electrons in our analysis. Author (revised)

N94-12875*# National Aeronautics and Space Administration. Langley Research Center, Hampton, VA.
EFFECTS OF RADIOBIOLOGICAL UNCERTAINTY ON VEHICLE AND HABITAT SHIELD DESIGN FOR MISSIONS TO THE MOON AND MARS
John W. Wilson, John E. Nealy, Walter Schimmerling, Francis A. Cucinotta, and James S. Wood Washington Aug. 1993 20 p
(RTOP 199-04-16-11)
(NASA-TP-3312; L-17188; NAS 1.60:3312) Avail: CASI HC A03/MF A01

Some consequences of uncertainties in radiobiological risk due to galactic cosmic ray (GCR) exposure are analyzed for their effect on engineering designs for the first lunar outpost and a mission to explore Mars. This report presents the plausible effect of biological uncertainties, the design changes necessary to reduce the uncertainties to acceptable levels for a safe mission, and an evaluation of the mission redesign cost. Estimates of the amount of shield mass required to compensate for radiobiological uncertainty are given for a simplified vehicle and habitat. The additional amount of shield mass required to provide a safety factor for uncertainty compensation is calculated from the expected response to GCR exposure. The amount of shield mass greatly increases in the estimated range of biological uncertainty, thus, escalating the estimated cost of the mission. The estimates are used as a quantitative example for the cost-effectiveness of research in radiation biophysics and radiation physics. Author (revised)

N94-12922# Los Alamos National Lab., NM.
SEARCH FOR UHE POINT-SOURCE EMISSION OVER VARIOUS TIME SCALES
1993 4 p Presented at the International Cosmic-Ray Conference, Calgary, Ontario, 19-20 Jul. 1993
(Contract W-7405-eng-36)
(DE93-012718; LA-UR-93-1607; CONF-930779-3) Avail: CASI HC A01/MF A01

A method has been developed to search for pulsed and/or unpulsed ultra high energy (UHE) emission from point sources over a range of time scales. This method has been applied to data accumulated with the CYGNUS extensive air-shower array for events associated with the directions of Cyg X-3, Her X-1, the Crab nebula, and a collection of 48 secondary source candidates. An examination of time scales ranging from minutes to years has yielded results consistent with background fluctuations. DOE

N94-12923# Los Alamos National Lab., NM.
SEARCH FOR EMISSION OF ULTRA HIGH ENERGY RADIATION FROM ACTIVE GALACTIC NUCLEI
1993 5 p Presented at the International Cosmic-Ray Conference, Calgary, Ontario, 19-20 Jul. 1993
(Contract W-7405-eng-36)
(DE93-012719; LA-UR-93-1606; CONF-930779-7) Avail: CASI HC A01/MF A01

A search for emission of ultra-high energy gamma radiation from 13 active galactic nuclei that were detected by EGRET, using the CYGNUS extensive air-shower array, is described. The data set has been searched for continuous emission, emission on the time scale of one week, and for emission on the time scale of one day. No evidence for emission from any of the AGN on any of the time scales examined was found. The 90% C.L. upper limit to the continuous flux from Mrk 421 above 50 TeV is 7.5(10)(exp -14) /sq cm-s. DOE

N94-12924# Los Alamos National Lab., NM.
SEARCH FOR UHE EMISSION FROM CYGNUS X-3
M. J. Stark 1993 4 p Presented at the International Cosmic-Ray Conference, Calgary, Ontario, 19-20 Jul. 1993
(Contract W-7405-eng-36)
(DE93-012720; LA-UR-93-1605; CONF-930779-5) Avail: CASI HC A01/MF A01

Data from the CYGNUS experiment has been searched for evidence of ultra high energy (UHE) emission from Cygnus X-3. An upper limit to continuous flux from the source is given. In addition, we find no evidence for episodic emission from Cygnus X-3 on any time scale from 3.3 minutes to 4 years. The results of searches for periodic emission from Cygnus X-3 will be presented at the conference. DOE

N94-12946# Los Alamos National Lab., NM.
ANGULAR RESOLUTION STUDIES OF THE CYGNUS ARRAY USING THE SHADOWS OF THE SUN AND MOON
A. L. Shoup 1993 5 p Presented at the International Cosmic-Ray Conference, Calgary, Ontario, 19-20 Jul. 1993
(Contract W-7405-eng-36)
(DE93-012723; LA-UR-93-1602; CONF-930779-2) Avail: CASI HC A01/MF A01

Using the cosmic ray shadows of the sun and moon, we have estimated the angular resolution of the CYGNUS extensive air shower array. With the event sample now available we estimate the angular resolution of the array to be 0.70(sub -0.06)(exp +0.07) degrees. The resolution depends on the total number of detected shower particles. A new parameterization of the measured shower-front timing structure and the use of counters with small pulse areas lead to a approximately 25% improvement in the resolution. The systematic pointing error of the array is less than 0.4 deg.

DOE

N94-12947# Los Alamos National Lab., NM.
SEARCH FOR CONTINUOUS AND SINGLE DAY EMISSION FROM ULTRA-HIGH-ENERGY SOURCES
Mei-Li Chen 1993 5 p Presented at the International Cosmic-Ray Conference, Calgary, Ontario, 19-20 Jul. 1993
(Contract W-7405-eng-36)

(DE93-012724; LA-UR-93-1601; CONF-930779-11) Avail: CASI HC A01/MF A01

Data from the CYGNUS experiment has been used to search the northern sky for point sources of continuous ultra-high-energy gamma radiation and to examine 51 candidate sources on a daily basis to search for episodic emission. In this paper, we make use of our most recent data to update our previously published results from these searches. The data sample is approximately twice as large as the published data set for continuous emission, and contains an additional year for the daily search. The latest results, up to the time of the conference, will be presented at the meeting. DOE

N94-12964# Los Alamos National Lab., NM.
SEARCH FOR ULTRA-HIGH-ENERGY RADIATION FROM GAMMA-RAY BURSTS
R. W. Schnee 1993 5 p Presented at the International Cosmic-Ray Conference, Calgary, Ontario, 19-20 Jul. 1993
(Contract W-7405-eng-36)
(DE93-012721; LA-UR-93-1604; CONF-930779-10) Avail: CASI HC A01/MF A01

Using data from the CYGNUS extensive air shower array, we have searched for evidence of the emission of ultra-high-energy radiation coincident with gamma-ray bursts observed by the BATSE instrument on the Compton Gamma-Ray Observatory. No statistically significant excess was found for any point in the sky within 4(sigma) of BATSE's best location coordinates for any of the 56 bursts examined. Furthermore, no events were seen in the 2.2 deg radius circular bin surrounding gamma-ray burst GRB 920720, whose location was determined accurately by the Compton/Ulysses/PVO Interplanetary Network of satellites. Flux upper limits depend greatly on the actual zenith angle of the burst. Typical fluence upper limits above 100 TeV are approximately 10(exp -6) erg/sq cm. The fluence upper limits for GRB 920720 is 2(10)(exp -6) erg/sq cm. DOE

N94-13087*# Hampden-Sydney Coll., VA. Dept. of Physics and Astronomy.
ANALYSIS OF DATA FROM THE ENERGETIC GAMMA-RAY EXPERIMENT ON THE GAMMA RAY OBSERVATORY Semiannual Status Report No. 4, 15 Feb. - 15 Aug. 1993
Donald A. Kniffen 15 Aug. 1993 9 p
(Grant NAG5-1742)
(NASA-CR-194178; NAS 1.26:194178) Avail: CASI HC A02/MF A01

The work under the Grant has involved continued participation with the Compton Gamma Ray Observatory Energetic Gamma-Ray Experiment Telescope (EGRET) Team in the analysis of data obtained during instrument operations and the preparation of scientific papers and proposals for future observations. The EGRET team was also successful on many proposals for the Phase 3 portion of the mission, including long high galactic latitude studies of the diffuse extragalactic radiation. These studies will be used in a effort to establish whether this radiation is truly diffuse or the sum of radiation from unresolved discrete sources such as radio-loud quasars. The effort involved working remotely by internet connection on the Goddard Space Flight Center Computers where the EGRET data are archived. Students have monitored instrument performance and analyzed data remotely and will continue to do so. The PI has completed the detailed analysis of five viewing periods to search for point sources and this work has been used in developing the first EGRET catalog of sources, soon to be released. Author (revised)

N94-13211*# California Inst. of Tech., Pasadena. Space Radiation Lab.
RESEARCH IN COSMIC AND GAMMA RAY ASTROPHYSICS: COSMIC PHYSICS PORTION Status Report, 1 Oct. 1992 - 30 Sep. 1993
Edward C. Stone, Richard A. Mewaldt, and Stephen Schindler 27 Aug. 1993 20 p
(Grant NAGw-1919)
(NASA-CR-194127; NAS 1.26:194127) Avail: CASI HC A03/MF A01

Research in particle astrophysics at the Space Radiation Laboratory (SRL) of the California Institute of Technology is supported under NASA Grant NAGW-1919. A three-year proposal for continuation of support was submitted a year ago and put into effect 1 October 1992. This report is the combined progress report and continuation application called for under the Federal Demonstration Project. Gamma-ray Astrophysics at SRL is separately supported under NAGW-1919 and will be separately summarized and proposed. This report will document progress and plans for our particle spectroscopy activities and for related data analysis, calibration, and community service activities. A bibliography and a budget will be attached as appendices. The Caltech SRL research program includes a heavy emphasis on elemental and isotopic spectroscopy of energetic particles in the cosmic radiation; in solar, interplanetary, and anomalous 'cosmic' radiation; and in planetary magnetospheres as discussed.

Derived from text

N94-13232 Tel-Aviv Univ. (Israel).
THE CONTINUUM EMISSION OF ACTIVE GALACTIC NUCLEI Ph.D. Thesis
Ari Laor Apr. 1990 150 p
(ITN-93-85208) Copyright Avail: Issuing Activity (Tel-Aviv Univ., Exact Sciences Library, Ramat Aviv 69978, Israel)

The structure and spectrum of massive, geometrically thin, bare accretion discs surrounding a massive black hole were calculated and the results were compared with observations of active galactic nuclei (AGN). The calculations apply to an alpha-disc and full relativistic corrections were applied. The radiative transfer equations were solved by the Eddington approximation for an atmosphere with a vertical temperature gradient. All disks considered were found to be radiation-pressure dominated throughout the self-gravity-dominated region. Owing to the vertical temperature gradient, the surface temperature was found to be close to the effective temperature, even where there were significant electron scattering effects, contrary to previous findings. Relativistic effects were found to modify the spectrum considerably at large viewing angles; the angular dependence may have important implications for the modeling of AGN emission lines. Theoretical calculations are presented for the continuum polarization. Classical calculations predict high polarization for thin accretion disk continua at large inclination angles, contrary to observations of most AGN. The polarization of such disks was calculated using an improved radiative transfer method, including a full general relativistic treatment of the radiation propagation and its effects on polarization. The overall polarization was found to be much less than previously suggested. ISA

N94-13263*# National Aeronautics and Space Administration. Langley Research Center, Hampton, VA.
SEMIEMPIRICAL FRAGMENTATION MODELS ON GALACTIC COSMIC RAY TRANSPORT CALCULATIONS WITH HYDROGEN TARGET
Judy L. Shinn, John W. Wilson, and Francis F. Badavi (Christopher Newport Coll., Newport News, VA.) Aug. 1993 18 p
(RTOP 199-45-16-11)
(NASA-TP-3350; L-17227; NAS 1.60:3350) Avail: CASI HC A03/MF A01

Nuclear fragmentation cross sections of Silberberg and Tsao that are more accurate for a hydrogen target were implemented in the data base to replace those of Rudstam for a galactic cosmic ray transport code (HZETRN). Sample calculations were made for the transported galactic cosmic ray flux through a liquid hydrogen shield at solar minimum condition to determine the effect of such a change. The transported flux based on the Silberberg-Tsao semiempirical formalism contains fewer high-LET (linear energy transfer) components but more low-LET components than the results based on Rudstam's formalism: and this disparity deepens as the shield thickness increases. A comparison of the results obtained from using both energy-dependent and energy-independent cross sections of Silberberg and Tsao indicates that the energy-independent assumption results in an underestimation of high-LET flux above 100 keV/micron by approximately 40 percent for a 15-g/cm(sup 2) thickness of liquid hydrogen. Similar results were obtained in a previous study when both energy-dependent and energy-independent cross sections of Rudstam were considered. Nonetheless, the present study found that an energy-independent calculation would be best accomplished by using Rudstam's cross sections as done in the past for various engineering applications. Author (revised)

N94-13288*# Delaware Univ., Newark. Bartol Research Inst.
X RAY EMISSION FROM DYNAMICAL SHOCK MODELS IN HOT-STAR WINDS Final Report, 1 Nov. 1988 - 31 Oct. 1991
Stanley P. Owocki 31 Oct. 1991 6 p
(Grant NAGw-1487)
(NASA-CR-194093; NAS 1.26:194093) Avail: CASI HC A02/MF A01

The principal aim of this project was to determine whether x ray

emission from instability-generated shocks in dynamical models of highly unstable hot-star winds could explain the x ray flux spectrum observed from such hot stars by Einstein and other x ray satellites. Our initial efforts focused on extending the earlier isothermal simulations of wind instabilities to include an explicit treatment of the energy balance between shock heating and simplified radiative cooling. It was found, however, that direct resolution of cooling regions behind shocks is often impractical, and thus additional, indirect methods for determining this shock x ray emission were also developed. The results indicate that the reverse shocks that dominate simple 1-D instability models typically have too little material undergoing a strong shock to produce the observed x ray emission. Other models with more strongly driven variability from the wind base sometimes show high-speed collisions between relatively dense clumps, and in these instances the computed x ray flux spectrum matches the observed spectrum quite well. This suggests that collisions between relatively large scale wind streams of different speeds may be more suited to producing the observed x rays than the reverse shocks arising from small-scale instabilities.

Author (revised)

N94-13476*# Radiophysics, Inc., Boulder, CO.

NEPTUNE HIGH-LATITUDE EMISSION: DEPENDENCE OF ANGLE ON FREQUENCY Final Report, 4 Jun. 1992 - 9 Jul. 1993

Constance Sawyer 9 Jul. 1993 11 p

(Contract NASw-4700)

(NASA-CR-193280; NAS 1.26:193280) Avail: CASI HC A03/MF A01

Smooth broadband radio emission reached a maximum and then cut off as Voyager approached the north magnetic pole of Neptune. The time of each event depends on frequency, yielding information on radio source location, and emission angle. In a preliminary analysis L-shell and magnetic longitude define radio-source locations in a dipole field. The emission angle at each frequency is identified with the angle between the magnetic-field direction at the source and the line of sight to Voyager 2 at the time of emission maximum. At each value of L in the range 6 less than L less than 9, there is one source longitude for which emission angle varies smoothly from greater or equal to 90 deg at 40 kHz to as low as 20 deg at 462 kHz. A more complex magnetic-field model can give a qualitatively different result. Author

N94-13483# Argonne National Lab., IL.

A POSITRON ANNIHILATION RADIATION TELESCOPE USING LAUE DIFFRACTION IN A CRYSTAL LENS

R. K. Smither and P. vonBallmoos Mar. 1993 20 p Presented at the International Gamma-Ray Astrophysics Laboratory Integral Workshop, Les Diablerets, Switzerland, 2-5 Feb. 1993

(Contract W-31-109-eng-38)

(DE93-012905; ANL/XFD/CP-79506; CONF-9302114-1) Avail: CASI HC A03/MF A01

We present a new type of gamma-ray telescope featuring a Laue diffraction lens, a detector module with a 3-by-3 germanium array, and a balloon gondola stabilized to 5 arc sec pointing accuracy. The instrument's lens is designed to collect 511 keV photons on its 150 sq cm effective area and focus them onto a small detector having only (approx) 14 cu cm of equivalent volume for background noise. As a result, this telescope overcomes the mass-sensitivity impasse of present detectors in which the collection areas are identical to the detection area. The sensitivity of our instrument is anticipated to be 3 (times) 10(exp -5) ph cm(exp -2) S(exp -1) at 511 keV with an angular resolution of 15 arc sec and an energy resolution of 2 keV. These features will allow the resolve of a possible energetically narrow 511 keV positron annihilation line both energy-wise and spatially within a Galactic Center 'microquasar' as 1EI740.7-2942 or GRS1758-258. In addition to the galactic 'microquasars', other prime objectives include Cyg X-1, X-ray binaries, pulsars, and AGNS. DOE

N94-13654 State Univ. of New York, Stony Brook.

THE ORIGIN OF THE FAR-INFRARED EMISSION FROM GALACTIC MOLECULAR CLOUDS Ph.D. Thesis

Thomas Joseph Mooney 1992 187 p

Avail: Univ. Microfilms Order No. DA9310049

In order to study the star formation process, the total far-IR luminosity, CO luminosity, and virial mass were measured for 78 first Galactic quadrant molecular clouds using the Massachusetts-Stony Brook CO Survey and the IRAS Galactic plane images. Fifty-one of the clouds are distinct IR sources (IR-strong) associated with H II regions. The remaining 27 clouds have low-IR surface brightnesses (IR-quiet), most of which contain weak radio continuum sources that are not cataloged H II regions. Estimates of the far-IR flux due to external heating of the clouds enabled a determination of the radial distribution of the Galactic interstellar radiation field, which has an approximate exponential scale length of 1.5-2.0 kpc, and a separation of the external and internal contributions to the clouds total far-IR luminosity. The total and internal far-IR luminosities of both IR-types are nearly proportional to the CO luminosity. IR-strong clouds are dominantly heated internally by embedded high-mass, ionizing stars of spectral types earlier than approximately B2, and IR-quiet clouds are mostly heated externally with internal intermediate-mass stars of spectral types later than approximately B3. An average equivalent to 1/3 of the total far-IR luminosity of IR-strong clouds, but nearly 3/4 of that of IR-quiet clouds, is due to external heating. The ratio of the far-IR luminosity to cloud mass -- a measure of the high-mass star formation activity of the clouds -- ranges over several orders of magnitude with a moderate maximum of approximately 20 (solar luminosity/solar mass), and is independent of cloud mass for both IR-types. High-mass star formation occurring in IR-strong clouds is equally efficient or inefficient across a wide range of cloud mass. The independence of high-mass star formation activity on cloud mass, and the long gas depletion times (approximately greater than 10(exp 9) years) expected from the modest average activity of 2-3 (solar luminosity/solar mass), exclude efficient self-induced, or cloud-cloud collision initiated star formation mechanisms. The evolutionary state of molecular clouds can be inferred from their IR/CO morphologies, far-IR properties, and observed internal populations. Driven primarily by high-mass star formation, molecular clouds evolve from recently formed massive cold clouds, through a cloud-destructive high-mass star formation phase, to post-OB star formation cloud remnants. IR-quiet clouds are most likely a mixture of old and young molecular clouds, with IR-strong clouds as the transition between these two IR-quiet phases. Dissert. Abstr.

N94-13695# California Univ., Berkeley. Lawrence Berkeley Lab.

THE BETA(+) DECAY AND COSMIC-RAY HALF-LIFE OF Mn-54

M. T. F. daCruz, E. B. Norman, Y. D. Chan, A. Garcia, R. M. Larimer, K. T. Lesko, R. G. Stokstad, and F. E. Wietfeldt 29 Mar. 1993 4 p Presented at the International Cosmic-Ray Conference, Calgary, Ontario, 19-20 Jul. 1993

(Contracts DE-AC03-76SF-00098; DE-FG05-87ER-40314)

(DE93-013913; LBL-33903; CONF-930779-13) Avail: CASI HC A01/MF A01

We performed a search for the beta(+) branch of Mn-54 decay. As a cosmic ray, Mn-54, deprived of its atomic electrons, can decay only via beta(+) and beta(-) decay, with a half-life of the order of 10(exp 6) yr. This turns Mn-54 into a suitable cosmic chronometer for the study of cosmic-ray confinement times. We searched for coincident back-to-back 511-keV gamma-rays using two germanium detectors inside a NaI(Tl) annulus. An upper limit of 2 x 10(exp -8) was found for the beta(+) decay branch, corresponding to a lower limit of 13.7 for the log ft value. DOE

N94-13708*# National Aeronautics and Space Administration. Goddard Space Flight Center, Greenbelt, MD.

ADP STUDY OF GAMMA-RAY BURSTS Final Report

Don Q. Lamb (Chicago Univ., IL.), John C. L. Wang (Canadian Inst. for Theoretical Astrophysics, Toronto, Ontario.), Geoffry J. Heuter (California Univ., San Diego.), Carlo Graziani (Chicago Univ., IL.), Tom Loredo (Chicago Univ., IL.), and Peter Freeman (Chicago Univ., IL.) 1991 2 p

(Grant NAG5-1177)

(NASA-CR-194311; NAS 1.26:194311) Avail: CASI HC A01/MF A01

This grant supported study of cyclotron scattering lines in the spectra of gamma-ray bursts through analysis of Ginga and HEAO-1 archival data, and modeling of the results in terms of radiation transfer calculations of cyclotron scattering in a strong magnetic field. A Monte Carlo radiation transfer code with which we are able to calculate the expected properties of cyclotron scattering lines in the spectra of gamma-ray bursts was developed. The extensive software necessary in order to carry out fits of these model spectra to gamma-ray burst spectral data, including folding of the model spectra through the detector response functions was also developed. Fits to Ginga satellite data on burst GB880205 were completed and fits to Ginga satellite data on burst GB870303 are being carried out. These fits have allowed us to test our software, as well as to garner new

scientific results. This work has demonstrated that cyclotron resonant scattering successfully accounts for the locations, strengths, and widths of the observed line features in GB870303 and GB880205. The success of the model provides compelling evidence that these gamma-ray bursts come from strongly magnetic neutron stars and are galactic in origin, resolving longstanding controversies about the nature and distance of the burst sources. These results were reported in two papers which are in press in the proceedings of the Taos Workshop on Gamma-Ray Bursts, and in a paper submitted for publication. Derived from text

N94-13965*# New Hampshire Univ., Durham. Space Science Center.
COSMIC AND SOLAR GAMMA RAY AND NEUTRON EXPERIMENTS Final Report, 1 Nov. 1991 - 31 Oct. 1992
Philip P. Dunphy and Edward L. Chupp 1992 5 p
(Grant NAGw-2734)
(NASA-CR-193359; NAS 1.26:193359) Avail: CASI HC A01/MF A01

This report summarizes the results of the research supported by NASA grant NAGW-2734 and lists the papers and publications produced through the grant. The basic goal of the work was to complete analysis of data from exposure of a large NaI scintillation detector to fast neutrons and to disseminate the results of the analysis. A secondary goal was to compare the measured detector response to neutrons with Monte Carlo calculations of the response. In Section 2.0, we discuss the goals of the research. In Section 3.0, we summarize the results of the research. In Section 4.0, we list the papers and publications produced under the grant. Preprints or reprints of the publications are attached as appendices. Derived from text

N94-14461# Los Alamos National Lab., NM.
RESULTS FROM A WATER-CERENKOV ARRAY
C. L. Dion (Maryland Univ., College Park.) 1993 5 p Presented at the International Cosmic-Ray Conference, Calgary, Alberta, 19-20 Jul. 1993
(Contract W-7405-eng-36)
(DE93-012715; LA-UR-93-1610; CONF-930779-4) Avail: CASI HC A01/MF A01

Five surface water-Cerenkov detectors (pools), running in coincidence with the CYGNUS extensive air shower array, are described. Preliminary results on the timing response and the estimated angular resolution of the pools are presented. Based on comparisons between the pools and the scintillator array, the angular resolution of the pools is estimated to be approximately 0.5 degrees which is consistent with Monte Carlo predictions. Pool trigger rates and photoelectron lateral distributions are also presented. DOE

N94-14553 Tel-Aviv Univ. (Israel).
EMISSION LINE VARIABILITY IN ACTIVE GALACTIC NUCLEI Ph.D. Thesis
Dan Maoz Apr. 1990 134 p
(ITN-93-85209) Copyright Avail: Issuing Activity (Tel-Aviv Univ., Exact Sciences Library, Ramat Aviv 69978, Israel)

This work investigates the size, structure and kinematics of the Broad Line Region (BLR) of Active Galactic Nuclei (AGN), as reflected through emission line variability. It includes an analysis of previous variability studies and new observational results, which are presented and analyzed. A numerical method is developed to evaluate the significance of the cross-correlation technique, as applied to the measurement of AGN emission line region sizes. It shows that such results and their significance are strongly dependent upon geometrical assumptions. When applied to published data for Akn 120 and NGC 4151, the method shows that estimates for the size of BLR do not significantly contradict the predictions of photoionization models, and that measurements with a much higher sampling frequency and lower measurement error are needed for this. An intensive monitoring project was carried out for 7 months at the Wise Observatory, in which a sample of 11 Seyfert 1 galaxies and three quasars was observed spectroscopically on an almost nightly basis. A novel calibration technique, in which each object was observed simultaneously with a field star, resulted in very accurate measurements. In terms of both the sampling rate and the measurement errors, this project constitutes a factor of 3-5 improvement over the best previous efforts. An accurate measurement of the size of the BLR in three objects which underwent large enough variations (Mrk 279, NGC 5548 and NGC 4151) confirms for the first time the small sizes suggested by the earlier studies. Author (ISA)

N94-14889 Joint Inst. for Nuclear Research, Dubna (USSR). Lab. of Theoretical Physics.
RADIATION PERTURBATION THEORY IN GRAVITY AND QUANTUM UNIVERSE AS A HYDROGEN ATOM
V. N. Pervushin 1992 7 p Limited Reproducibility: More than 20% of this document may be affected by microfiche quality
(DE93-626621; JINR-E-2-92-322) Avail: Issuing Activity (Department of Energy (DOE)) (US Sales Only)

In quantum theory of gravity of the (n+1)-dimensional space-time, the Faddeev-Popov functional integral is constructed for radiation perturbation theory. In this version, the Universe expansion looks as the collective superfluid motion of quantum space, and the vacuum energy density plays the role of the hidden mass. DOE

99 GENERAL

N94-13019# Lawrence Livermore National Lab., CA.
ENERGY AND TECHNOLOGY REVIEW, MARCH 1993
J. A. Sefcik, ed. and W. J. Quirk, ed. 1993 39 p
(Contract W-7405-eng-48)
(DE93-013941; UCRL-52000-93-3) Avail: CASI HC A03/MF A01

The Lawrence Livermore National Laboratory was established in 1952 to research on nuclear weapons and magnetic fusion energy. Since then, we have added other major programs, including fusion and laser isotope separation, biomedical and environmental science, strategic defense, and applied energy technology. These programs, in turn, require research in basic scientific disciplines, including chemistry and materials science, computer science and technology, engineering, and physics. This review is published monthly to report on unclassified work in all of our programs. This issue describes three endeavors. We have developed a multiple-frame, laser-illuminated, electro-optic camera system that produces sequential photographs of fast phenomena, such as the formation of shaped-charge jets, with unprecedented high resolution. Another project concerns a new rocket propulsion system for small spacecraft. This liquid rocket propulsion system won a 1992 R&D 100 award and features miniature pumps that can turn on and off and can change speed within a millisecond to meet a wide range of thrust requirements. The last project reported on pertains to computational integrated photonics: using numerical simulation to optimize photonic devices. DOE

N94-13376* National Aeronautics and Space Administration. Goddard Space Flight Center, Greenbelt, MD.
THE INTERNATIONAL COLLOQUIUM ON ATOMIC SPECTRA AND OSCILLATOR STRENGTHS FOR ASTROPHYSICAL AND LABORATORY PLASMAS Special Publication
J. Sugar (National Inst. of Standards and Technology, Gaithersburg, MD.) and D. Leckrone Apr. 1993 201 p Colloquium held in Gaithersburg, MD, 14-17 Sep. 1992 Limited Reproducibility: More than 20% of this document may be affected by microfiche quality
(NASA-TM-109255; NAS 1.15:109255; PB93-198422; NIST/SP-850)
Avail: CASI HC A10

This was the fourth in a series of colloquia begun at the University of Lund, Sweden in 1983 and subsequently held in Toledo, Ohio and Amsterdam, The Netherlands. The purpose of these meetings is to provide an international forum for communication between major users of atomic spectroscopic data and the providers of these data. These data include atomic wavelengths, line shapes, energy levels, lifetimes, and oscillator strengths. Speakers were selected from a wide variety of disciplines including astrophysics, laboratory plasma research, spectrochemistry, and theoretical and experimental atomic physics. NTIS

N94-13505# Hawker Siddeley Canada Ltd., Toronto (Ontario).
[ACTIVITIES OF HAWKER SIDDELEY CANADA INC.] Annual Report, 1992
1993 42 p Original contains color illustrations
(CTN-93-60865) Avail: CASI HC A03/MF A01

Hawker Siddeley Canada Inc. is a diversified industrial company with five divisions and seven subsidiaries in Canada, the United States, the United Kingdom, and Australia. These divisions and subsidiaries include

Orenda (Mississauga, Ontario), which repairs jet engine and industrial gas turbine components, provides engineering and laboratory testing services for the aerospace and other industries, and manufactures jet engine and gas turbine components; Windsor Aerospace (Windsor, Ontario), which manufactures precision gears and other components for the aerospace and other industries; and Middleton Aerospace Corp. (Middleton, MA), which manufactures engine components for the aerospace industry. Other divisions produce steel castings, lease and repair railcars, manufacture sawmill and mining equipment, and provide other products and services for mining and civil engineering. This report for the year ending December 31, 1992 highlights activities and presents financial statements. Total sales were $370 million, operating profit $43.4 million, and net earnings $15.4 million.

CISTI

N94-13519# Institute for Aerospace Research, Ottawa (Ontario). Flight Research Lab.

[ACTIVITIES OF INSTITUTE FOR AEROSPACE RESEARCH, FLIGHT RESEARCH LABORATORY] Annual Progress Report, 1992

B. Leach, ed. 1992 175 p

(CTN-93-60832) Avail: CASI HC A08/MF A02

A summary is presented of progress in the research projects of the Flight Research Laboratory during 1992 and a brief indication of future plans for continuing and new projects. Projects are described in the areas of flight mechanics, airborne science, and facility development, and major facilities at the Laboratory are also described. Subjects of specific projects include flight tests, simulator model development, microgravity experiments, flight dynamics and handling qualities, flight safety and operational problems, guidance and navigation systems, pilot-vehicle interface technologies, speech recognition, atmospheric geoscience, resource geoscience, and defense.

CISTI

N94-13548# Institute for Aerospace Research, Ottawa (Ontario). Structures and Materials Lab.

FINITE ELEMENT CALCULATION OF STRESS-INTENSITY FACTORS FOR THUMB-NAIL CRACKS IN DEN SPECIMENS

W. Beres and A. K. Koul Apr. 1993 50 p Sponsored by Dept. of National Defence

(LTR-ST-1929; CTN-93-60833) Avail: CASI HC A03/MF A01

The accepted techniques for stress intensity factor (SIF) extraction from three-dimensional finite element method (FEM) calculations are reviewed. Results are then summarized for thumbnail cracks emanating from a semicircular notch of double edge notch (DEN) specimens. Two different specimen geometries corresponding to AGARD and Institute of Aerospace Research dimensions were analyzed. In the AGARD specimen, the ratio of the notch radius to the specimen width (R/W) is 1/16 while in the other the R/W is 1/8. Three-dimensional models were run on NISA 2/DISPLAY 3 and ABAQUS FEM software packages to calculate SIFs. Results obtained for standard AGARD specimens are compared with the predictions of Newman's 1990 model and found to be very close. Graphs showing the absolute values of SIF for small thumbnail cracks emanating from semicircular notches of Institute DEN specimens and the dependence of SIFs on crack dimensions are also presented. The numerical results indicate that in the crack depth range of 0.3-0.4 mm, a semicircular crack will tend to grow into a semi-elliptical crack. An increase in R/W increases the SIF for a given crack depth and a/c ratio in the DEN specimens, where a is half of the surface crack length and c is the crack depth.

Author (CISTI)

N94-13612* National Aeronautics and Space Administration, Washington, DC.

HIGHLIGHTS, 1981 (Videotape)

Dec. 1981 Videotape: 14 min. 30 sec. playing time, in color, with sound

(NASA-TM-109305; NONP-VT-93-185323) Avail: CASI VHS A01/BETA A22

This video presentation covers Shuttle flights 1 and 2, Spacelab, mobile workstation, Voyager 2 Saturn, Infrared Astronomy Satellite, Hubble Space Telescope, Kuiper Airborne Observatory, High Altitude Earth Survey, Landsat, aerodynamic research, electric cars, wind energy, XV-15, Quiet Shorthaul Research Aircraft, X-14 BVTOL, 40 x 80 Wind Tunnel, and turboprop research.

Author (revised)

N94-13633* National Aeronautics and Space Administration. Hugh L. Dryden Flight Research Facility, Edwards, CA.

FLIGHT OPERATIONS HIGHLIGHTS, TAPES 1 AND 2 (Videotape)

Apr. 1990 Videotape: 1 hr. 40 min. playing time, in color, with sound

(NASA-TM-109293; NONP-VT-93-185308) Avail: CASI VHS A01/BETA A22

Historical film footage of the X-series aircraft (including Yeager's X-1 flight), lifting bodies, and early Apollo landing tests is presented.

Author (revised)

N94-13923*# National Aeronautics and Space Administration. Wallops Flight Facility, Wallops Island, VA.

BIRDS OF WALLOPS ISLAND, VIRGINIA, 1970 - 1992

Charles R. Vaughn Jul. 1993 46 p

(NASA-TM-104589; Rept-93B00111; NAS 1.15:104589) Avail: CASI HC A03/MF A01

This Technical Memorandum provides extensive data on birdlife at Wallops Island, a mid-Atlantic barrier island, and home to NASA Wallops Flight Facility's launch range. Variation in the distribution and abundance of many species is considerable in this region, which is centered along the north-south axis of the Delmarva Peninsula. Data (date of occurrence and general abundance) and analysis of the Island's diverse habitat structure are provided. A total of 244 species of birds are recorded; a summary of the records are given in the Species Accounts and the Appendix.

Author (revised)

N94-13962*# National Aeronautics and Space Administration. Langley Research Center, Hampton, VA.

RESEARCH AND TECHNOLOGHY HIGHLIGHTS, 1992

Mar. 1993 251 p Original contains color illustrations

(NASA-TM-4452; L-17200; NAS 1.15:4452) Avail: CASI HC A12/MF A03; 34 functional color pages

The mission of the NASA Langley Research Center is to increase the knowledge and capability of the United States in a full range of aeronautics disciplines and in selected space disciplines. This mission will be accomplished by performing innovative research relevant to national needs and Agency goals, transferring technology to users in a timely manner, and providing development support to other United States Government agencies, industry, and other NASA centers. Highlights of the major accomplishments and applications that have been made by Langley researchers and by our university and industry colleagues during the past year are presented. The highlights illustrate both the broad range of research and technology (R&T) activities supported by NASA Langley Research Center and the contributions of this work toward maintaining United States leadership in aeronautics and space research. Some of the Center's most important research and testing facilities are also described.

Author (revised)

N94-14060# Defence Research Establishment, Ottawa (Ontario). Protective Sciences Div.

A HISTORY OF THE DEFENCE RESEARCH ESTABLISHMENT, OTTAWA

Jim Norman, ed. and Rita M. Crow, ed. Mar. 1992 175 p

(CTN-93-60737) Avail: CASI HC A08/MF A02

The Defence Research Establishment Ottawa (DREO) has its roots in Canada's chemical and biological defense programs of the 1930's and 1940's. The earliest activity relating to DREO originated from the Department of National Defence's Master General of Ordnance, when it was decided to establish a gas mask respirator assembly plant in the late 1930's. In 1941, the plant and a technical laboratory working on chemical warfare were amalgamated into the Chemical Warfare Laboratories (CWL), DREO's direct forerunner. In 1947, the Defence Research Board was formed to handle defense-related scientific research, and the CWL became a research establishment of the Board. The Board changed the establishment's name to DREO in 1967 when it gave all its establishments geographically related names. DREO is currently organized into four divisions: Protective Sciences, Electronics, Electronic Warfare, and Radar. Details are presented on research conducted in these divisions and their forerunners in the following areas: nuclear, chemical, and biological defense; earth satellites; the SEASAT project; airborne and surface radar; energy conversion; and earth sciences.

CISTI

N94-14137# European Space Agency, Paris (France).
EUROPEAN SPACE FOR EXCLUSIVELY PEACEFUL PURPOSES
Norman Longdon, ed. 1992 24 p Original contains color illustrations
(ESA-BR-86; ISBN-9-29-092123-4; ETN-93-93946) Copyright Avail: CASI HC A03/MF A01

The European Space Agency (ESA) activities and programs are summarized. Information concerning major establishments, political management, budget, and planned investments is provided. Results from ESA scientific running programs and news from projects under development are presented. They include: Horizon 200 project, X-ray Multi-Mirror, Far Infrared Submillimeter Telescope, Infrared Space Observatory, Huygens Probe, Meteosat satellite, European Remote Sensing satellites, microgravity, and manned space flights. The role of ESA in the field of telecommunication is overviewed. The success of Ariane and the future market for ESA launchers are considered. ESA partnerships and international cooperation to develop human intervention in space are discussed. ESA

N94-14401# California Univ., Berkeley. Lawrence Berkeley Lab.
LAWRENCE BERKELEY LABORATORY CHEMICAL SCIENCES DIVISION Annual Report, 1991
Sep. 1992 83 p
(Contract DE-AC03-76SF-00098)
(DE93-015260; LBL-32387) Avail: CASI HC A05/MF A01

Summaries are given of research in the following fields: photochemistry of materials in stratosphere, energy transfer and structural studies of molecules on surfaces, laser sources and techniques, crossed molecular beams, molecular interactions, theory of atomic and molecular collision processes, selective photochemistry, photodissociation of free radicals, physical chemistry with emphasis on thermodynamic properties, chemical physics at high photon energies, high-energy atomic physics, atomic physics, high-energy oxidizers and delocalized-electron solids, catalytic hydrogenation of CO, transition metal-catalyzed conversion of CO, NO, H2, and organic molecules to fuels and petrochemicals, formation of oxyacids of sulfur from SO2, potentially catalytic and conducting organometallics, actinide chemistry, and molecular thermodynamics for phase equilibria in mixtures. Under exploratory R and D funds, the following are discussed: technical evaluation of beamlines and experimental stations for chemical dynamics applications at the ALS synchrotron, and molecular beam threshold time-of-flight spectroscopy of rare gas atoms. Research on normal and superconducting properties of high-(Tc) systems is reported under work for others. DOE

N94-14455# Midwest Research Inst., Golden, CO. National Renewable Energy Lab.
[ACTIVITIES OF THE BASIC SCIENCES BRANCH] Annual Report, 1 Oct. 1990 - 30 Sep. 1991
Apr. 1993 51 p
(Contract DE-AC02-83CH-10093)
(DE93-010012; NREL/TP-451-4961) Avail: CASI HC A04/MF A01

This report summarizes the progress of the Basic Sciences Branch of the National Renewable Energy Laboratory (NREL) from October 1, 1990, through September 30, 1991. Seven technical sections of the report cover these main areas of NREL's in-house research: Semiconductor Crystal Growth, Amorphous Silicon Research, Polycrystalline Thin Films, 3-5 High-Efficiency Photovoltaic Cells, Solid-State Theory, Solid-State Spectroscopy, and Superconductivity. Each section explains the purpose and major accomplishments of the work in the context of the US Department of Energy's National Photovoltaic Research Program plans. DOE

N94-14587# California Univ., Berkeley. Lawrence Berkeley Lab.
CURRENT TITLES
Apr. 1993 61 p
(Contract DE-AC03-76SF-00098)
(DE93-015859; LBL-PUB-719) Avail: CASI HC A04/MF A01

Approximately 116 abstracts are presented of work done with the electron microscope. NCEM is a DOE-designated national user facility and is available at no charge to qualified researchers (assess is controlled by a steering committee). DOE

N94-14791*# National Aeronautics and Space Administration. Goddard Space Flight Center, Greenbelt, MD.
THE 1991 RESEARCH AND TECHNOLOGY REPORT, GODDARD SPACE FLIGHT CENTER
Gerald Soffen, ed., Howard Ottenstein, ed., Harry Montgomery, ed., Walter Truszkowski, ed., Kenneth Frost, ed., Walter Sullivan, ed., and Charles Boyle, ed. 1991 238 p Original contains color illustrations
(NASA-TM-108738; NAS 1.15:108738) Avail: CASI HC A11/MF A03; 31 functional color pages

The 1991 Research and Technology Report for Goddard Space Flight Center is presented. Research covered areas such as (1) earth sciences including upper atmosphere, lower atmosphere, oceans, hydrology, and global studies; (2) space sciences including solar studies, planetary studies, Astro-1, gamma ray investigations, and astrophysics; (3) flight projects; (4) engineering including robotics, mechanical engineering, electronics, imaging and optics, thermal and cryogenic studies, and balloons; and (5) ground systems, networks, and communications including data and networks, TDRSS, mission planning and scheduling, and software development and test. CASI

N94-14276*# National Aeronautics and Space Administration, Washington, DC.
MY EXPERIENCES IN MANNED SPACE FLIGHT
Michel Weeks *In* Science and Technology Agency, Asia-Pacific ISY Conference, Volume 2 31 Mar. 1993 p 348-355 (For primary document see N94-14209 02-43)
Avail: CASI HC A02/MF A04

SUBJECT INDEX

Typical Subject Index Listing

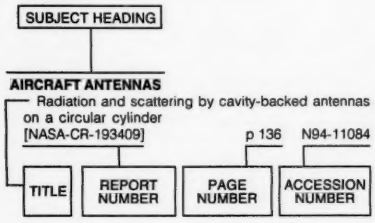

The subject heading is a key to the subject content of the document. Titles, report numbers, and accession numbers of pertinent documents are provided under each subject heading. When the title is insufficiently descriptive of the document content, a title extension is added, separated from the title by three hyphens. The report number helps to indicate the type of document cited (e.g., NASA report, NASA translation, NASA contractor report). The accession number is the number by which the document abstracts are arranged in this journal and by which the document is sold or requested. The page number helps you locate the citation in the abstract section. The titles, with title extensions if present, are arranged under each subject heading in ascending accession number order. The subject headings have been selected from the latest revision of the *NASA Thesaurus*.

A

A STARS
Physical properties of gas disks around shell stars with and without dust
[NASA-CR-193655] p 835 N94-13239

ABILITIES
Readiness to perform testing: A critical analysis of the concept and current practices
[DOT/FAA/AM-93/13] p 732 N94-13193

ABORTED MISSIONS
STS-55 pad abort: Engine 2011 oxidizer preburner augmented spark igniter check valve leak
[NASA-CR-193830] p 533 N94-12806

ABSORPTION CROSS SECTIONS
Determination of spectroscopic properties of atmospheric molecules from high resolution vacuum ultraviolet cross section and wavelength measurements
[NASA-CR-194024] p 712 N94-13092
Theoretical antideuteron-nucleus absorptive cross sections p 786 N94-14551
Signal and reference wavelengths for the elimination of SO2 cross sensitivity in remote measurements of tropospheric ozone with lidar
[GKSS/92/E/24] p 617 N94-14819

ABSORPTION SPECTRA
Determination of spectroscopic properties of atmospheric molecules from high resolution vacuum ultraviolet cross section and wavelength measurements
[NASA-CR-194024] p 712 N94-13092
Molecular dynamics simulation of electronically excited polyatomic molecules
[DE93-623045] p 781 N94-13225
Recent developments in multiple-scattering calculations of XAFS and XANES
[DE93-010999] p 563 N94-13477
Many-body corrections in XAFS
[DE93-011002] p 563 N94-13478
The extent and content of low-ionization gas in galaxies p 837 N94-13551
Optical properties of CO2 ice and CO2 snow in the ultraviolet, visible, and infrared
[NASA-CR-194110] p 686 N94-14081
Direct submillimeter absorptivity measurements on epitaxial Ba(1-x)K(x)BiO3 films at 2K
[DE93-013904] p 815 N94-14699
The mobile lidar system ARGOS for spatial resolution remote measuring of gaseous air pollutants
[GKSS/92/E/26] p 617 N94-14820

ABSORPTION SPECTROSCOPY
Infrared absorption spectroscopy and chemical kinetics of free radicals
[DE93-015078] p 562 N94-13004
Many-body corrections in XAFS
[DE93-011002] p 563 N94-13478
Investigation of an alternating current plasma as an element selective atomic emission detector for high-resolution capillary gas chromatography and as a source for atomic absorption and atomic emission spectrometry p 798 N94-13678
Ultra-soft x ray absorption spectroscopy: A bulk and surface probe of materials
[DE93-014325] p 566 N94-14582

ABSORPTIVITY
Optimization of transparent and reflecting electrodes for amorphous silicon solar cells
[DE93-010009] p 704 N94-14110
Direct submillimeter absorptivity measurements on epitaxial Ba(1-x)K(x)BiO3 films at 2K
[DE93-013904] p 815 N94-14699
Nonlinear relationships between particulate absorption and chlorophyll: Detritus or pigment packaging?
[AD-A266806] p 731 N94-14899

ABSTRACTS
ARTI Refrigerant Database
[DE93-014774] p 595 N94-13021
Fifteenth Combustion Research Conference
[DE93-015758] p 562 N94-13045
Large space structures and systems in the space station era: A bibliography with indexes (supplement 05)
[NASA-SP-7085(05)] p 543 N94-14411

ACCELERATED LIFE TESTS
Lifetime prediction of materials exposed to the natural space environment
[NASA-CR-193833] p 561 N94-12830
Dry film lubricant evaluation
[DE93-013114] p 578 N94-13118
Formal functional test designs with a test representation language p 609 N94-14383

ACCELERATION (PHYSICS)
Microgravity acceleration measurement environment characterization p 590 N94-13755

ACCELEROMETERS
Isolation of a piezoresistive accelerometer used in high acceleration tests
[DE93-013764] p 649 N94-13395
Microgravity acceleration measurement environment characterization p 590 N94-13755

ACCESS CONTROL
Kerberos: A UNIX-TCP/IP network authentication system
[DE93-011677] p 760 N94-14011

ACCESS TIME
The KSR1: Experimentation and modeling of poststore
[DE93-012539] p 759 N94-13470

ACCIDENTS
A model for fuel fire duration and application to the B-1B bomber
[DE93-013000] p 512 N94-14292

ACCRETION DISKS
The evidence for clumpy accretion in the Herbig Ae star HR 5999
[NASA-TM-108257] p 828 N94-12915
A photometric study of massive x-ray binaries
[ITN-93-85207] p 829 N94-13231
The continuum emission of active galactic nuclei
[ITN-93-85208] p 847 N94-13232
Physical properties of gas disks around shell stars with and without dust
[NASA-CR-193655] p 835 N94-13239
The physical and chemical evolution of protostellar disks. The growth of protostellar disks: Progress to date
[NASA-CR-194111] p 836 N94-13423

ACCUMULATORS
Technology assessments of advanced energy storage systems for electric and hybrid vehicles
[DE93-014395] p 701 N94-12913

ACCURACY
Methods for evaluating the predictive accuracy of structural dynamic models
[NASA-CR-191337] p 671 N94-13124
Calculation of the required sensor accuracy to obtain a specified state estimation accuracy
[NAL-TR-1173] p 649 N94-13343

ACIDITY
Snow cover models in operational watershed forecasting
[DE93-778332] p 718 N94-12837
Experimental and kinetic modeling of acid/base and redox reactions over oxide catalysts
[DE93-016203] p 563 N94-13375

ACOUSTIC EMISSION
Piston engine intake and exhaust system design
[ISVR-TR-222] p 663 N94-13874
Study of deferred acoustic emission in carbon epoxy composites
[ISAL-91-0078] p 560 N94-14815

ACOUSTIC FREQUENCIES
Portable acoustic wave sensor systems for real-time monitoring of volatile organic compounds
[DE93-013753] p 582 N94-14511

ACOUSTIC LEVITATION
Drop dynamics in space and interference with acoustic field (M-15) p 588 N94-13747
Preparation of optical materials used in non-visible region (M-17) p 589 N94-13749

ACOUSTIC MEASUREMENT
Study on the possibilities to apply spectrumindex
[VTT-PUBS-109] p 777 N94-14034
Activities report of the National Electrotechnical Institute Galileo Ferraris
[ETN-93-94224] p 627 N94-14812

ACOUSTIC PROPAGATION
Open boundary conditions for incompletely parabolic systems
[FFI/RAPPORT-92/7029] p 770 N94-13971

ACOUSTIC SCATTERING
Interactions among convection, magnetic fields and p-mode oscillations in the sun
[NASA-CR-194477] p 845 N94-14479

ACOUSTIC VELOCITY
Numerical simulation of velocity-coupled combustion response of solid rocket propellants p 585 N94-14490
Rapid distortion analysis and direct simulation of compressible homogeneous turbulence at finite Mach number p 645 N94-14757

ACOUSTICS
Ocean acoustic processing: A model-based approach
[DE93-011902] p 725 N94-12876
An 8-node axisymmetric acoustic finite element for non-axisymmetric fluid-structure interaction analysis
[FFA-TN-1993-03] p 673 N94-13689
Atmospheric acoustic modeling
[DE93-016727] p 718 N94-14518

ACOUSTO-OPTICS
Acousto-optical post-processor time-integrating correlator updates
[DSIS-93-00314] p 777 N94-13831
Integrated optics technology transfer
[DSIS-93-00179] p 792 N94-13868

ACRYLIC RESINS
Pore-size-distribution of cationic polyacrylamide hydrogels
[DE93-015218] p 581 N94-14400
Phases and phase transitions of polymeric liquid crystals: A high resolution x ray diffraction and light scattering study
[ITN-93-85218] p 816 N94-14826

ACTIVATED CARBON
Low pressure storage of natural gas on activated carbon
[DE93-014053] p 660 N94-12851
ACTIVATION ENERGY
A study of the role of homogeneous process in heterogeneous high explosives
[DE93-012733] p 585 N94-14180
ACTIVE CONTROL
Feasibility study of an orbiting laboratory for testing CSI technology
[NASA-CR-191524] p 540 N94-13016
Thermal Expert System (TEXSYS): Systems autonomy demonstration project, volume 1. Overview
[NASA-TM-102877] p 538 N94-13201
In-flight simulation of high agility through active control: Taming complexity by design p 523 N94-13306
Active control of acoustic pressure fields using smart material technologies
[NASA-CR-191480] p 768 N94-13354
Robust synthesis of discrete-time multivariable control systems with induced delays p 662 N94-13642
Thermal Expert System (TEXSYS): Systems autonomy demonstration project, volume 2. Results
[NASA-TM-102877] p 538 N94-13989
Active control of fan-generated plane wave noise
[NASA-TM-109008] p 777 N94-14481
Active density control in DIII-D H-mode plasmas
[DE93-015477] p 802 N94-14570
Animation of multi-flexible body systems and its use in control system design p 678 N94-14629
The use of linked lists in the simulation of controller-structure interaction p 679 N94-14630
ACTIVE GALACTIC NUCLEI
Search for emission of ultra high energy radiation from active galactic nuclei
[DE93-012719] p 846 N94-12923
The continuum emission of active galactic nuclei
[ITN-93-85208] p 847 N94-13232
Emission line variability in active galactic nuclei
[ITN-93-85209] p 849 N94-14553
ACTIVITY (BIOLOGY)
The role of human activity and land use change in atmospheric chemistry and air quality
[DE93-011871] p 709 N94-14022
ACTS
Proceedings of the Seventeenth NASA Propagation Experimenters Meeting (NAPEX 17) and the Advanced Communications Technology Satellite (ACTS) Propagation Studies Miniworkshop
[NASA-CR-194096] p 612 N94-14654
Opening remarks: Current and future activities p 612 N94-14655
Radiometric observations of atmospheric attenuation at 20.6 and 31.65 GHz: The Wave Propagation Laboratory data base p 613 N94-14660
Advanced Communications Technology Satellite (ACTS) program: ACTS project update p 615 N94-14673
The ACTS propagation terminal delivery and support p 615 N94-14674
Data collection with the ACTS propagation terminal p 615 N94-14675
Preprocessing data collected with the ACTS propagation terminal p 616 N94-14676
ACTS data center p 616 N94-14677
ACTS propagation experiment discussion: Ka-band propagation measurements using the ACTS propagation terminal and the CSU-CHILL and Space Communications Technology Center Florida propagation program p 616 N94-14678
ACTUATORS
Advanced electric motor technology flux mapping
[NASA-CR-193824] p 621 N94-13186
Actuator and aerodynamic modeling for high-angle-of-attack aeroservoelasticity
[NASA-TM-4493] p 520 N94-13255
Electrical Actuation Technology Bridging
[NASA-CP-3213] p 551 N94-13417
Design and performance of an automated video-based laser beam alignment system
[DE93-012571] p 656 N94-13481
Experimental and analytical analysis of the response of a smart beam to rate feedback
[AD-A266544] p 557 N94-13706
Design and application of electromechanical actuators for deep space missions
[NASA-CR-194145] p 663 N94-14134
Strategic avionics technology definition studies. Subtask 3-1A: Electrical Actuation (ELA) systems
[NASA-CR-194393] p 536 N94-14323
Superconductivity devices: Commercial use of space
[NASA-CR-194163] p 625 N94-14324
Cammatic: An approach to improve DSS 13 antenna gravity-loading performance p 608 N94-14374
Inverse dynamics: Simultaneous trajectory tracking and vibration reduction with distributed actuators p 678 N94-14624
PACE: A test bed for the dynamics and control of flexible multibody systems p 527 N94-14650
Smart materials/structures technical analysis
[AD-A266771] p 766 N94-14785
The further development and refinement of an expert-systems approach to the creative design of mechanisms and mechanical systems
[AD-A266812] p 665 N94-14901
ADA (PROGRAMMING LANGUAGE)
On-line upgrade of program modules using AdaPT
[NASA-CR-194331] p 754 N94-14472
ADAPTIVE CONTROL
Data fusion for adaptive control in manufacturing: Impact on engineering information models
[DE93-011555] p 743 N94-12999
Adaptive control of interface by temperature and interface profile feedback in transparent multi-zone crystal growth furnace
[NASA-CR-194140] p 762 N94-13253
Self tuning and adaptive control: Evaluations and improvements of algorithms
[ITN-93-85192] p 762 N94-13329
Tuning of Gaussian stochastic control systems
[CWI-BS-R9223] p 765 N94-14018
Eye-gaze and intent: Application in 3D interface control
[DE93-015210] p 738 N94-14335
Statistical results from the Virginia Tech propagation experiment using the Olympus 12, 20, and 30 GHz satellite beacons p 613 N94-14658
Early detection of insulation failure in electric motors
[PB93-198208] p 626 N94-14686
Smart materials/structures technical analysis
[AD-A266771] p 766 N94-14785
ADAPTIVE FILTERS
Spatially-varying IIR filter banks for image coding
[NASA-CR-193727] p 619 N94-12897
A combined analogue and digital pulse compression system using large time bandwidth product signals for use in synthetic aperture radar
[ISBN-0-315-54373-6] p 600 N94-13489
Adaptive Signal Processing Testbed
[DSIS-93-00258] p 604 N94-13869
Adaptive Signal Processing Testbed: Software design specification
[DSIS-93-00259] p 604 N94-13870
Adaptive Signal Processing Testbed signal excision software: User's manual
[DSIS-93-00260] p 606 N94-14037
ADAPTIVE OPTICS
Optical propagation through atmospheric turbulence. Model analysis of anisoplanatism and application to adaptive optics
[ONERA-P-1992-4] p 716 N94-14192
Experimental instrumentation system for the Phased Array Mirror Extendible Large Aperture (PAMELA) test program
[NASA-CR-194421] p 705 N94-14430
Small scale adaptive optics experiment systems engineering
[NASA-CR-194419] p 793 N94-14548
Wavefront sensing, control, and pointing p 546 N94-14833
Laser power beaming system analyses
[NASA-CR-193840] p 660 N94-14904
ADDITIVES
Surface analysis of bearings
[AD-A266800] p 661 N94-13122
Processing and testing of high toughness silicon nitride ceramics
[NASA-CR-191190] p 582 N94-14543
ADENOSINE TRIPHOSPHATE
The evolution of energy-transducing systems: Studies with archaebacteria
[NASA-CR-194130] p 728 N94-13562
ADHESION
Ohmic heating of composite candidate graphite-fiber/coating combinations
[NASA-TM-4491] p 554 N94-12871
Correlations of the growth, structure, and stress with the adhesion of diamond films on tungsten
[DE93-012855] p 576 N94-12912
Study of novel conductive paints for solar cell electromagnetic fields
[DE93-015088] p 581 N94-14337
ADHESION TESTS
System integration and demonstration of adhesive bonded high temperature aluminum alloys for aerospace structure, phase 2
[NASA-CR-191459] p 575 N94-12792
ADHESIVE BONDING
System integration and demonstration of adhesive bonded high temperature aluminum alloys for aerospace structure, phase 2
[NASA-CR-191459] p 575 N94-12792
Miniature mechanism assembly
[DE93-015595] p 624 N94-13928
ADIABATIC CONDITIONS
Adiabatic and non adiabatic effects in Free Electron Laser (FEL) non linear interactions
[ITN-93-85224] p 659 N94-14547
ADIABATIC EQUATIONS
The geometric phase in quantum physics
[DE93-011121] p 817 N94-13479
ADIPRENE (TRADEMARK)
Compatibility testing of vacuum seal materials
[DE93-014366] p 663 N94-14113
ADJOINTS
Gauging the octonion algebra
[DE93-622864] p 775 N94-12843
Differential Sensitivity Theory applied to the MESA code for high pressure interactions
[DE93-016460] p 676 N94-14591
ADSORBENTS
Low pressure storage of natural gas on activated carbon
[DE93-014053] p 660 N94-12851
Linear and nonlinear spectroscopic probing of solute interactions with chemically modified silica surface
[DE93-014648] p 562 N94-13001
ADSORPTION
Computer simulations for the adsorption of polymers onto surfaces
[DE93-016667] p 577 N94-13070
Experimental and kinetic modeling of acid/base and redox reactions over oxide catalysts
[DE93-016203] p 563 N94-13375
Photochemical dynamics of surface oriented molecules
[DE93-016289] p 784 N94-13983
ADVANCED SOLID ROCKET MOTOR (STS)
Results of wind tunnel tests of an ASRM configured 0.03 scale Space Shuttle integrated vehicle model (47-OTS) in the AEDC 16-foot transonic wind tunnel, volume 2
[NASA-CR-185697] p 534 N94-12965
Results of wind tunnel tests of an ASRM configured 0.03 scale Space Shuttle integrated vehicle model (47-OTS) in the AEDC 16-foot Transonic wind tunnel (IA613A), volume 1
[NASA-CR-185696] p 534 N94-13191
ADVANCED VERY HIGH RESOLUTION RADIOMETER
Degradation of the visible and near-infrared channels of the advanced very high resolution radiometer on the NOAA-9 spacecraft: Assessment and recommendations for corrections
[NOAA-TR-NESDIS-70] p 544 N94-13029
An algorithm for the remote sensing of fog using satellite-data and additional information
[DLR-FB-92-23] p 688 N94-14135
The effects of anthropogenic aerosols on optical thickness and particle size of clouds. Part 1: Retrieval algorithm p 691 N94-14230
Accuracy validation test of estimated sea surface temperature by satellite data p 696 N94-14264
AERIAL PHOTOGRAPHY
Computer vision and sensor fusion for detecting buried objects
[DE93-012605] p 700 N94-14566
Obtaining digital regional planning information from aerial pictures
[REPT-228] p 700 N94-14810
AERIAL RECONNAISSANCE
Application of transient airborne electromagnetic and ground resistivity methods to geological mapping in tropical terrains
[ISBN-0-315-57172-1] p 685 N94-13542
Computer vision and sensor fusion for detecting buried objects
[DE93-012605] p 700 N94-14566
AEROACOUSTICS
Results of wind tunnel tests of an ASRM configured 0.03 scale Space Shuttle integrated vehicle model (47-OTS) in the AEDC 16-foot transonic wind tunnel, volume 2
[NASA-CR-185697] p 534 N94-12965
Results of wind tunnel tests of an ASRM configured 0.03 scale Space Shuttle integrated vehicle model (47-OTS) in the AEDC 16-foot Transonic wind tunnel (IA613A), volume 1
[NASA-CR-185696] p 534 N94-13191
On the use of the method of matched asymptotic expansions in propeller aerodynamics and acoustics
[NLR-TP-91307-U] p 503 N94-13528

Mixing noise reduction for rectangular supersonic jets by nozzle shaping and induced screech mixing
[NASA-TM-106364] p 508 N94-14208

AEROASSIST
The MRIS feasibility study
[NASA-TM-107763] p 597 N94-12804
Guidance law development for aeroassisted transfer vehicles using matched asymptotic expansions
[NASA-CR-194523] p 508 N94-14538

AERODYNAMIC CHARACTERISTICS
A method of predicting quasi-steady aerodynamics for flutter analysis of high speed vehicles using steady CFD calculations
[NASA-TM-109009] p 514 N94-12850
Identifying the NAL spaceplane aerodynamic model using dynamic wind tunnel tests
[NAL-TR-1171] p 500 N94-12951
Aerodynamics of a sphere and an oblate spheroid for Mach numbers from 0.6 to 10.5 including some effects of test conditions
[NASA-TM-109016] p 500 N94-13172
SRISTI: The NAL method for the design and analysis of Natural Laminar Flow (NLF) airfoils p 516 N94-14615
VSAERO analysis of a Piper Cub aircraft p 516 N94-14616
Panel codes for aerodynamic analysis at NAL p 510 N94-14617

AERODYNAMIC COEFFICIENTS
Estimation of aircraft aerodynamic derivatives with the Total Least Squares Method
[NAL-TR-1150] p 502 N94-13392
Development of an automated film-reading system for ballistic ranges
[NASA-CR-194398] p 650 N94-13815
Techniques for estimating Space Station aerodynamic characteristics
[NASA-CR-193394] p 541 N94-13955
Numerical simulation of a powered-lift landing, tracking flow features using overset grids, and simulation of high lift devices on a fighter-lift-and-control wing
[NASA-CR-194260] p 527 N94-14322

AERODYNAMIC CONFIGURATIONS
Extrapolation of ground test data to flight p 507 N94-14170

AERODYNAMIC FORCES
A method of predicting quasi-steady aerodynamics for flutter analysis of high speed vehicles using steady CFD calculations
[NASA-TM-109009] p 514 N94-12850
Investigation of an aeroelastic oscillator: Analysis of one-degree-of-freedom galloping with combined translational and torsional effects
[LR-707] p 527 N94-13906
Techniques for estimating Space Station aerodynamic characteristics
[NASA-CR-193394] p 541 N94-13955

AERODYNAMIC HEATING
Improved aeroprediction code. Part 1: Summary of new methods and comparison with experiment
[AD-A266015] p 500 N94-12989
Test and evaluation methods p 506 N94-14163
Shock/boundary-layer/shock interactions p 507 N94-14172

AERODYNAMIC INTERFERENCE
A wall interference assessment/correction system
[NASA-CR-194174] p 500 N94-13076
Flow-field interference produced by an asymmetrical support strut
[IAR-AN-75] p 504 N94-14031
Wall interference studies: Revisited p 640 N94-14604

AERODYNAMIC LOADS
Results of experimental investigations to determine external tank protuberance loads using a 0.03-scale model of the Space Shuttle launch configuration (model 47-OTS) in the NASA/ARC unitary plan wind tunnel, volume 1
[NASA-CR-167690] p 534 N94-12810
Results of wind tunnel tests of an ASRM configured 0.03 scale Space Shuttle integrated vehicle model (47-OTS) in the AEDC 16-foot transonic wind tunnel, volume 2
[NASA-CR-185697] p 534 N94-12965
Results of wind tunnel tests of an ASRM configured 0.03 scale Space Shuttle integrated vehicle model (47-OTS) in the AEDC 16-foot Transonic wind tunnel (IA613A), volume 1
[NASA-CR-185696] p 534 N94-13191
Results of experimental investigations to determine external tank protuberance loads using a 0.03-scale model of the Space Shuttle launch configuration (Model 47-OTS) in the NASA/ARC unitary plan wind tunnel, volume 2
[NASA-CR-167691] p 536 N94-14047
Inflow characteristics associated with high-blade-loading events in a wind farm
[DE93-010042] p 704 N94-14423

AERODYNAMIC NOISE
Mixing noise reduction for rectangular supersonic jets by nozzle shaping and induced screech mixing
[NASA-TM-106364] p 508 N94-14208

AERODYNAMIC STABILITY
Actuator and aerodynamic modeling for high-angle-of-attack aeroservoelasticity
[NASA-TM-4493] p 520 N94-13255
Development of a high-speed mechanical drive system for oscillating an annular blade row in the bending mode
[NAL-TR-1170] p 502 N94-13342
Experimental studies of vortex flaps and vortex plates. Part 2: 1.15m span 60 deg delta wing
[NAL-TR-1180T-PT-2] p 502 N94-13454
Hypersonic aerodynamic characteristics of SSTO-type aerospace planes. Part 1: The NAL 0-th configuration
[NAL-TR-1186] p 514 N94-13459
Qualitative investigation of a generic fighter model in radio controlled gliding flight
[LM-AA-003] p 516 N94-13898
Turbulent diffusion in homogeneous shear flow with stable density stratification
[DLR-FB-92-26] p 639 N94-14443
A new treatment of periodic systems with applications to helicopter rotor blade dynamics
[AD-A266770] p 510 N94-14784

AERODYNAMIC STALLING
Numerical simulation of dynamic stall of NACA0012 airfoil oscillating near static stall angle using the Navier-Stokes equations
[DE93-767970] p 505 N94-14061

AERODYNAMICS
Proceedings of the Fluid Dynamics Symposium in honour of Professor R. Narasimha on his 60th birthday
[NAL-SP-9315] p 639 N94-14598

AEROELASTICITY
Investigation of an aeroelastic oscillator: Analysis of one-degree-of-freedom galloping with combined translational and torsional effects
[LR-707] p 527 N94-13906

AEROMAGNETISM
Aeromagnetic work in the Lincoln Sea: 1991 survey
[DSIS-93-00308] p 715 N94-13830

AERONAUTICAL ENGINEERING
Center of excellence in rotary wing technology
[AD-A266655] p 510 N94-14799

AEROSERVOELASTICITY
Actuator and aerodynamic modeling for high-angle-of-attack aeroservoelasticity
[NASA-TM-4493] p 520 N94-13255

AEROSOLS
A parameterization of cloud droplet nucleation
[DE93-007998] p 718 N94-12903
Development of a global backscatter model for NASA's laser atmospheric wind sounder
[NASA-CR-192581] p 718 N94-12957
Linkage of anthropogenic aerosol to clouds and climate
[DE93-016434] p 719 N94-13080
Novel Co:MgF2 lidar for aerosol profiler
[NASA-CR-191525] p 654 N94-13091
Binary homogeneous nucleation: Temperature and relative humidity fluctuations and non-linearity
[DE93-007884] p 709 N94-13911
A laser-based technique to continuously monitor metal aerosol emissions
[DE93-012836] p 710 N94-14183
Bridging the gap between the Rayleigh and Thomson limits for various convex bodies
[DSIS-93-00613] p 607 N94-14204
The effects of anthropogenic aerosols on optical thickness and particle size of clouds. Part 1: Retrieval algorithm p 691 N94-14230
Earth radiation budget, cloud, and aerosol parameters derived from AVHRR and TOVS measurements p 691 N94-14233
Summary of conclusions and recommendations from a visibility science workshop
[DE93-012770] p 710 N94-14523
Importance of sprays for long range transport of harmful substances in the troposphere
[MITT-81] p 711 N94-14723

AEROSPACE ENGINEERING
Approaches to high aspect ratio triangulations
[NASA-TM-107684] p 739 N94-12886
NASA/DOD Aerospace Knowledge Diffusion Research Project. Report 18: A comparison of the technical communication practices of aerospace engineers and scientists in India and the United States
[NASA-TM-109006] p 821 N94-13057
A survey and analysis of experimental hydrogen sensors
[NASA-TM-106300] p 648 N94-13135
JPRS report: Science and technology. Central Eurasia: Space
[JPRS-USP-93-003] p 828 N94-13182
Highlights, 1981
[NASA-TM-109305] p 850 N94-13612
Artificial intelligence in Canada: A description by the members of the ACAI
[CNR-31790] p 764 N94-13820
Research and technologhy highlights, 1992
[NASA-TM-4452] p 850 N94-13962
NASA/DOD Aerospace Knowledge Diffusion Research Project. Paper 34: Users and uses of DOD technical reports: A report from the field
[NASA-TM-109327] p 825 N94-14485
NASA/DOD Aerospace Knowledge Diffusion Research Project. Paper 36: Technical uncertainty as a correlate of information use by US industry-affiliated aerospace engineers and scientists
[NASA-TM-109328] p 825 N94-14486
NASA/DOD Aerospace Knowledge Diffusion Research Project. Paper 39: The role of computer networks in aerospace engineering
[NASA-TM-109331] p 825 N94-14487
NASA/DOD Aerospace Knowledge Diffusion Research Project. Paper 37: The impact of political control on technical communications: A comparative study of Russian and US aerospace engineers and scientists
[NASA-TM-109329] p 826 N94-14488
NASA/DOD Aerospace Knowledge Diffusion Research Project. Paper 38: Computer Mediated Communication (CMC) and the communication of technical information in aerospace
[NASA-TM-109330] p 826 N94-14489
The 1991 research and technology report, Goddard Space Flight Center
[NASA-TM-108738] p 851 N94-14791

AEROSPACE ENVIRONMENTS
Lifetime prediction of materials exposed to the natural space environment
[NASA-CR-193833] p 561 N94-12830
Thermal distortion measurement of TETRUS type thermal test model of large deployable antenna for mobile communications satellite p 529 N94-13270
Research on radiation resistance properties of structural materials for space use p 529 N94-13271
Development of modular cable mesh deployable antenna p 530 N94-13274
Study on superconducting basic technology for space application, part 1
[NASDA-CNT-930015-PT-1] p 622 N94-13425
Gravity, chromosomes, and organized development in aseptically cultured plant cells p 592 N94-13764
Interactions between spacecraft and their environments
[NASA-TM-106115] p 541 N94-13917
Test report for single event effects of the 80386DX microprocessor
[NASA-CR-194509] p 741 N94-13943
Workshop on the Space Environment: The Effects on the Optical Properties of Airless Bodies
[NASA-CR-194417] p 842 N94-14298
Ethology in space, a unique opportunity for behavioural science
[ESA-STM-246] p 731 N94-14862

AEROSPACE INDUSTRY
Technology Applications Team: Applications of aerospace technology
[NASA-CR-194362] p 828 N94-13104
Ninth Annual NASA/Contractors Conference on Quality and Productivity. World Class Excellence: The Journey Continues. Keynote presentations
[NASA-CR-194513] p 665 N94-13148
The power of cross-functional teams in driving total quality p 666 N94-13159
User observations on information sharing (corporate knowledge and lessons learned)
[NASA-TM-104781] p 819 N94-13400
Activities of Hawker Siddeley Canada Inc.
[CTN-93-60865] p 849 N94-13505
Artificial intelligence in Canada: A description by the members of the ACAI
[NRC-31789] p 763 N94-13517
Activities of Bombardier, Inc.
[ISBN-2-921393-11-5] p 499 N94-13520
JPRS report: Science and technology. Central Eurasia: Engineering and equipment
[JPRS-UEQ-93-006] p 776 N94-14431

AEROSPACE MEDICINE
Medical evaluations on the KC-135 1991 flight report summary
[NASA-TM-104755] p 731 N94-12832
Health monitoring of Japanese payload specialist: Autonomic nervous and cardiovascular responses under reduced gravity condition (L-0) p 591 N94-13757
Neurophysiological study on visuo-vestibular control of posture and movement in fish during adaptation to weightlessness p 591 N94-13759
Comparative measurement of visual stability in Earth and cosmic space (L-4) p 592 N94-13761

Autogenic feedback training experiment: A preventative method for space motion sickness p 595 N94-13774
In-flight demonstration of the Space Station Freedom Health Maintenance Facility fluid therapy system (E300/E05) p 595 N94-13775
DCIEM: The first fifty years, 1939-1989 [CTN-93-60767] p 733 N94-14141
Aerospace medicine and biology: A continuing bibliography with indexes (supplement 379) [NASA-SP-7011(379)] p 733 N94-14412

AEROSPACE PLANES
A method of predicting quasi-steady aerodynamics for flutter analysis of high speed vehicles using steady CFD calculations [NASA-TM-109009] p 514 N94-12850
Numerical simulation of hypersonic flow for the design of the H-2 orbiting plane (HOPE), part 3 [NAL-TR-1168-PT-3] p 499 N94-12948
Identifying the NAL spaceplane aerodynamic model using dynamic wind tunnel tests [NAL-TR-1171] p 500 N94-12951
Perspective on the National Aero-Space Plane Program instrumentation development [NASA-TM-4505] p 516 N94-13256
Flight evaluations of approach/landing navigation sensor systems: Summary of 1990 flight experiments [NAL-TR-1175] p 513 N94-13344
Hypersonic aerodynamic characteristics of SSTO-type aerospace planes. Part 1: The NAL 0-th configuration [NAL-TR-1186] p 514 N94-13459
HOPE real time flight operations analyses for return to earth phase, part B [NASDA-CNT-930011] p 535 N94-13599
HOPE conceptual design in FY 1991 [NASDA-CNT-930017] p 535 N94-13600
HOPE real time flight operations analyses for return to earth phase, part A [NASDA-CNT-930010-PT-A] p 535 N94-13645
Conceptual design on H-2 Orbiting Plane (HOPE) [NASDA-CNT-930018] p 535 N94-13656
The concept study of the space transportation system HOPE in FY 1991 [NASDA-CNT-930016] p 536 N94-14100
Trajectory optimization for the national aerospace plane [NASA-CR-194146] p 516 N94-14104
Research and development of space transportation systems in ISAS p 537 N94-14277
Contributions of winged re-entry vehicle to space activities p 537 N94-14278
Mission scenario of HOPE p 537 N94-14279
The status of the HOPE concept study p 537 N94-14280
Spaceplane program at NAL: System concept and related technology issues p 537 N94-14281

AEROSPACE SAFETY
STS-29 post-insertion/deorbit prep and crew bailout [NASA-TM-109299] p 535 N94-13641

AEROSPACE SCIENCES
JPRS report: Science and technology. Central Eurasia: Space [JPRS-USP-93-003] p 828 N94-13182
NASA aerospace database subject scope: An overview [NASA-SP-7107] p 823 N94-13401
Activities of Institute for Aerospace Research, Flight Research Laboratory [CTN-93-60832] p 850 N94-13519
Research and technologhy highlights, 1992 [NASA-TM-4452] p 850 N94-13962
Generic results of the space physics community survey [NASA-CR-194538] p 818 N94-13984
China's devotion to space science and applications p 532 N94-14273
The 1991 research and technology report, Goddard Space Flight Center [NASA-TM-108738] p 851 N94-14791

AEROSPACE SYSTEMS
Spacecraft COst REduction Team (SCORE): TQM/CI on a massive scale p 667 N94-13160
Thermal Expert System (TEXSYS): Systems autonomy demonstration project, volume 1. Overview [NASA-TM-102877] p 538 N94-13201
Electrical Actuation Technology Bridging [NASA-CP-3213] p 551 N94-13417
Mongoose ASIC microcontroller programming guide [NASA-RP-1319] p 623 N94-13871
An ultra-compact processor module based on the R3000 [DE93-012549] p 625 N94-14427
A program for the investigation of the Multibody Modeling, Verification, and Control Laboratory p 682 N94-14652

AEROSPACE TECHNOLOGY TRANSFER
Technology Applications Team: Applications of aerospace technology [NASA-CR-194362] p 828 N94-13104
Access to Japanese aerospace-related scientific and technical information: The NASA Aerospace Database [NASA-TM-109413] p 822 N94-13105

AEROSPACE VEHICLES
Multidisciplinary design techniques applied to conceptual aerospace vehicle design [NASA-CR-194409] p 515 N94-13618
Terrestrial environment (climatic) criteria guidelines for use in aerospace vehicle development, 1993 revision [NASA-TM-4511] p 533 N94-14824

AEROTHERMODYNAMICS
Methodology of Hypersonic Testing [VKI-LS-1993-03] p 505 N94-14153
Aerodynamic and aerothermal facilities 2. Part 1: Short-duration, high-enthalpy facilities p 506 N94-14159
Aerodynamic and aerothermal facilities 2: Continuous flow high enthalpy facilities p 506 N94-14160
Test and evaluation methods p 506 N94-14163
Materials/structures testing p 506 N94-14164
Hypersonic flight testing. Part 2: Aerothermal flight testing p 507 N94-14169

AGGREGATES
Small-angle scattering, contrast variation and the study of complex composite materials: A study of the structure of carbon black [DE93-012707] p 559 N94-14690

AGING (MATERIALS)
Lifetime prediction of materials exposed to the natural space environment [NASA-CR-193833] p 561 N94-12830
A data base for aging of structural materials [DE93-009714] p 824 N94-13915

AGRICULTURE
Integration of remote sensing and mathematical modelling in disaster mitigation p 692 N94-14239
Land evaluation for agricultural productivity in North-East Thailand using LANDSAT TM data and geographic information p 693 N94-14242
Educational module for the Higher Agricultural Education. Part 2: Eutrophication observed by remote sensing: An educational approach to water quality monitoring [BCRS-92-11B] p 818 N94-14462
Educational module for the higher agricultural education. Part 1: Land use classification using satellite pictures [BCRS-92-11A] p 819 N94-14809

AIR BREATHING ENGINES
Analysis of gas turbine engines using water and oxygen injection to achieve high Mach numbers and high thrust [NASA-TM-106270] p 518 N94-13143
An experimental investigation of mixing enhancement in a simulated scramjet combustor by use of swirling jets [NASA-TM-109246] p 518 N94-13190
Aeropropulsion facilities p 506 N94-14161

AIR CONDITIONING
ARTI Refrigerant Database [DE93-014774] p 595 N94-13021

AIR COOLING
Some flow properties of telescope enclosures estimated from water channel tests: Application of the flow visualization techniques [NAL-TR-1178T] p 830 N94-13452

AIR DEFENSE
HELSCAM V2.0: Development and application guide [DSIS-93-00137] p 515 N94-13867

AIR FLOW
Project AIRSTREAM: Trace gas [DE93-008849] p 706 N94-12904

AIR LAND INTERACTIONS
Effects of surface thermal forcing on stratified flow past an isolated obstacle p 633 N94-13553
Integration of space and in-situ observations to study atmosphere, ocean and land processes [NASA-CR-194495] p 683 N94-14500

AIR LAW
The international regulation of air transport: Changing regimes and price effects [ISBN-0-315-55958-6] p 511 N94-13543

AIR NAVIGATION
Flight evaluations of approach/landing navigation sensor systems: Summary of 1990 flight experiments [NAL-TR-1175] p 513 N94-13344
Determination of Loran-C/GPS human factors issues [PB93-199693] p 514 N94-14563

AIR POLLUTION
Bibliography of urban climate in tropical/subtropical areas, 1981-1991 [WCASP-25] p 718 N94-12918
The North Atlantic Regional Experiment (NARE) [DE93-010126] p 706 N94-13054
Diagnostic studies of the HxOy-NxOy-O3 photochemical system using data from NASA GTE field expeditions [NASA-CR-193672] p 706 N94-13170
AQUIS: A PC-based source information manager [DE93-012893] p 707 N94-13383
An examination of utility emissions contributions to elevated ozone concentrations in the Chicago area [DE93-012852] p 708 N94-13495
Destruction of problematic airborne contaminants by hydrogen reduction using a Catalytically Active, Regenerable Sorbent (CARS) [NASA-CR-194354] p 709 N94-14103
Program operations plan [DE93-012765] p 710 N94-14182
IMG: Interferometric monitor for greenhouse gases p 689 N94-14217
Long-range global warming impact of gaseous diffusion plant operation [DE93-011686] p 710 N94-14459
Summary of conclusions and recommendations from a visibility science workshop [DE93-012770] p 710 N94-14523
The mobile lidar system ARGOS for spatial resolution remote measuring of gaseous air pollutants [GKSS/92/E/26] p 617 N94-14820

AIR PURIFICATION
Survey and study on Environmental Control and Life Support (ECLS) technologies, part 2 [NASDA-CNT-930012-PT-2] p 737 N94-13472

AIR QUALITY
Molten carbonate fuel cell product development test environmental assessment/protection plan [DE93-000288] p 702 N94-13380
AQUIS: A PC-based source information manager [DE93-012893] p 707 N94-13383
An examination of utility emissions contributions to elevated ozone concentrations in the Chicago area [DE93-012852] p 708 N94-13495
Description of the EURAD chemistry-transport model. Version 2 (CTM2) [REPT-83] p 720 N94-13589
The role of human activity and land use change in atmospheric chemistry and air quality [DE93-011871] p 709 N94-14022
Status and future opportunities for conversion of synthesis gas to liquid energy fuels [DE93-010025] p 584 N94-14089
Atmospheric turbulence and diffusion research [DE93-011842] p 718 N94-14425
Summary of conclusions and recommendations from a visibility science workshop [DE93-012770] p 710 N94-14523

AIR SAMPLING
Project AIRSTREAM: Trace gas [DE93-008849] p 706 N94-12904
The footprint area influencing a high-volume air sampler [DE93-013947] p 706 N94-13095
Biomass production chamber air analysis of wheat study (BWT931) [NASA-CR-194092] p 737 N94-13712

AIR SEA ICE INTERACTIONS
Integration of space and in-situ observations to study atmosphere, ocean and land processes [NASA-CR-194495] p 683 N94-14500

AIR TO AIR REFUELING
Spare parts analysis of the MK.32B-751 AAR pod [DSIS-93-00737] p 774 N94-13549

AIR TRAFFIC CONTROL
Activities report of the Federal Administration for Flight Safety (Germany) [ETN-93-94208] p 511 N94-14008
The influence of ATC message length and timing on pilot communication [NASA-CR-177621] p 512 N94-14744

AIR TRANSPORTATION
The international regulation of air transport: Changing regimes and price effects [ISBN-0-315-55958-6] p 511 N94-13543

AIR WATER INTERACTIONS
Ocean uptake of carbon dioxide [DE93-012967] p 707 N94-13384
Binary homogeneous nucleation: Temperature and relative humidity fluctuations and non-linearity [DE93-007884] p 709 N94-13911
Synthesis inversion of atmospheric CO2 using the GISS tracer transport model [CSIRO-TP-29] p 709 N94-14095
Sea surface temperature forcing and phase locking of Nordeste precipitation [DE93-011873] p 723 N94-14426

AIRBORNE EQUIPMENT
EOS workstation [NASA-CR-191326] p 736 N94-13132

Development of an on-board aircraft optical fiber data bus system
[NAL-TR-1163] p 514 N94-13338
Performance evaluation tests of the GPS/DGPS navigation system installed in the NAL Dornier 228: Preliminary ground test results
[NAL-TM-649] p 513 N94-13346
Operational test of the airborne data acquisition system: SADA, the Bara Bonita experiment
[INPE-5451-NTC/305] p 685 N94-13610
NASA airborne satellite instrumentation calibrator (NASIC) technical reference
[NASA-RP-1315] p 545 N94-13713
Modis-N airborne simulator
[NASA-CR-194364] p 792 N94-13719

AIRBORNE SURVEILLANCE RADAR
Multiparameter airborne rain radar development for TRMM validation and TRMM-follow-on study
p 690 N94-14226

AIRBORNE/SPACEBORNE COMPUTERS
Functional categories for future flight deck designs
[NASA-TM-109005] p 517 N94-13710
Phase aligner for the Electronically Scanned Thinned Array Radiometer (ESTAR) instrument
[NASA-TM-4518] p 623 N94-13878
Test report for single event effects of the 80386DX microprocessor
[NASA-CR-194509] p 741 N94-13943

AIRCRAFT ACCIDENT INVESTIGATION
PC based A320 quick access recorder readout facility
[PD-AL-9109] p 744 N94-13077

AIRCRAFT ACCIDENTS
An assessment of the potential for neck injury due to padding of aircraft interior walls for head impact protection
[DOT/FAA/AM-93/14] p 738 N94-13972

AIRCRAFT COMMUNICATION
The influence of ATC message length and timing on pilot communication
[NASA-CR-177621] p 512 N94-14744

AIRCRAFT COMPARTMENTS
An assessment of the potential for neck injury due to padding of aircraft interior walls for head impact protection
[DOT/FAA/AM-93/14] p 738 N94-13972
Widebody cabin water spray optimization tests
[DOT/FAA/CT-TN93/29] p 511 N94-14186

AIRCRAFT CONFIGURATIONS
Hypersonic aerodynamic characteristics of SSTO-type aerospace planes. Part 1: The NAL 0-th configuration
[NAL-TR-1186] p 514 N94-13459
Analysis of the Harrier forebody/inlet design using computational techniques
[NASA-CR-193616] p 503 N94-13463

AIRCRAFT CONSTRUCTION MATERIALS
Electrophoretic and electrolytic deposition of ceramic particles on porous substrates
[AD-A265141] p 575 N94-12812
Role of microstructure on fatigue durability of aluminum aircraft alloys
[AD-A266350] p 571 N94-13697
Testing and analysis of curved frame specimens made from a Long Discontinuous Fiber (LDF) material
[NASA-TM-109014] p 557 N94-13711

AIRCRAFT CONTROL
Piloting Vertical Flight Aircraft: A Conference on Flying Qualities and Human Factors
[NASA-CP-3220] p 521 N94-13294
Design criteria for integrated flight/propulsion control systems for STOVL fighter aircraft p 521 N94-13297
Handling qualities effects of display latency p 517 N94-13316
Primary display latency criteria based on flying qualities and performance data p 525 N94-13318
Piloting considerations for terminal area operations of civil tiltwing and tiltrotor aircraft p 525 N94-13320
Evaluation of two cockpit display concepts for civil tiltrotor instrument operations on steep approaches p 517 N94-13323
Control system design of a cable-mounted model used for dynamic wind tunnel testing
[NAL-TR-1161] p 528 N94-13337
Development of a high-speed mechanical drive system for oscillating an annular blade row in the bending mode
[NAL-TR-1170] p 502 N94-13342
Rolling moment control in the NAL 10 cm x 10 cm magnetic suspension and balance system
[NAL-TR-1164] p 526 N94-13347
Flight path control for the approach and landing of the quiet STOL experimental aircraft ASKA
[NAL-TR-1183] p 513 N94-13457
Knowledge-based processing for aircraft flight control
[NASA-CR-194074] p 526 N94-13469
Optimal lateral escape maneuvers for microburst encounters during final approach
[LR-691] p 511 N94-13534
Simulator study of uncoupled control functions. Use of manual pointing modes when aiming at ground targets and oncoming airborne target
[FFA-TN-1992-18] p 528 N94-13588

AIRCRAFT DESIGN
Design criteria for integrated flight/propulsion control systems for STOVL fighter aircraft p 521 N94-13297
Analysis of the Harrier forebody/inlet design using computational techniques
[NASA-CR-193616] p 503 N94-13463
A future view of computational science in aircraft
[NASA-TM-109284] p 504 N94-13621
Development and application of a comprehensive, design-sensitive weight prediction method for wing structures of transport category aircraft
[LR-693] p 515 N94-13687
Mathematical optimization: A tool for aircraft design
[MBB-LME-251-S-PUB-0492] p 751 N94-14006
Development of PC-based Aeronautical Software (AEROWARE) p 641 N94-14611
SRISTI: The NAL method for the design and analysis of Natural Laminar Flow (NLF) airfoils p 516 N94-14615
Panel codes for aerodynamic analysis at NAL p 510 N94-14617

AIRCRAFT ENGINES
Aircraft engine type certification handbook: Advisory circular
[AC-33-2B] p 518 N94-13252
Futurepath 2
[NASA-TM-109285] p 518 N94-13623
Synthetic lubricants and high-performance functional fluids: Phosphazenes
[ARL-TR-45] p 580 N94-14126

AIRCRAFT EQUIPMENT
Modis-N airborne simulator
[NASA-CR-194364] p 792 N94-13719

AIRCRAFT FUEL SYSTEMS
Techniques for improving the performance of a simplified electronic fuel controller with incremental actuation for small gas turbine engines
[ISBN-0-315-56062-2] p 661 N94-13521

AIRCRAFT GUIDANCE
Knowledge-based processing for aircraft flight control
[NASA-CR-194074] p 526 N94-13469
Evaluation of infrared sensors for autonomous landing guidance
[AD-A266450] p 513 N94-13703

AIRCRAFT HAZARDS
Smart skin technology development for measuring ice accretion, stall, and high AOA aircraft performance. Part 1: Capacitive ice detector development
[NASA-CR-194252] p 511 N94-13424

AIRCRAFT INDUSTRY
Activities of Bombardier, Inc.
[ISBN-2-921393-11-5] p 499 N94-13520

AIRCRAFT INSTRUMENTS
Position error determination for the speedometer and altimeter of the NAL QSTOL experimental aircraft ASKA
[NAL-TR-1144] p 517 N94-13451
Photogrammetric methods for trajectory measurements
[NLR-TP-91166-U] p 650 N94-13527

AIRCRAFT LANDING
Implementation of ADI: Schemes on MIMD parallel computers
[NASA-CR-193720] p 759 N94-13204
Visual cueing aids for rotorcraft landings p 524 N94-13313
Flight path control for the approach and landing of the quiet STOL experimental aircraft ASKA
[NAL-TR-1183] p 513 N94-13457
Evaluation of infrared sensors for autonomous landing guidance
[AD-A266450] p 513 N94-13703

AIRCRAFT MAINTENANCE
Flight service evaluation of composite components on the Bell helicopter model 206L
[NASA-CR-191499] p 555 N94-13267
The development of inspection and repair methods for the C-17 aft cargo door
[LR-704] p 499 N94-13904
MSD in fuselage lap joints: Requirements for inspection intervals for typical fuselage lap joint panels with Multiple Site Damage
[LR-697] p 675 N94-13986
Human factors in aviation maintenance: Phase 3, volume 1
[DOT/FAA/AM-93/15] p 738 N94-14023

AIRCRAFT MANEUVERS
A piloted simulation investigation of the normal load factor and longitudinal thrust required for air-to-air acquisition and tracking p 522 N94-13301
The development and potential of inverse simulation for the quantitative assessment of helicopter handling qualities p 523 N94-13311

AIRCRAFT MODELS
Identifying the NAL spaceplane aerodynamic model using dynamic wind tunnel tests
[NAL-TR-1171] p 500 N94-12951
Control system design of a cable-mounted model used for dynamic wind tunnel testing
[NAL-TR-1161] p 528 N94-13337
Rolling moment control in the NAL 10 cm x 10 cm magnetic suspension and balance system
[NAL-TR-1164] p 526 N94-13347
Experimental studies of vortex flaps and vortex plates. Part 2: 1.15m span 60 deg delta wing
[NAL-TR-1180T-PT-2] p 502 N94-13454
Analysis of the Harrier forebody/inlet design using computational techniques
[NASA-CR-193616] p 503 N94-13463
Qualitative investigation of a generic fighter model in radio controlled gliding flight
[LM-AA-003] p 516 N94-13898

AIRCRAFT PARTS
Computational methods for reliable fatigue and damage tolerance dimensioning of aircraft structures
[FFA-TN-1993-05] p 515 N94-13690

AIRCRAFT PERFORMANCE
Piloting Vertical Flight Aircraft: A Conference on Flying Qualities and Human Factors
[NASA-CP-3220] p 521 N94-13294
Handling qualities effects of display latency p 517 N94-13316
Primary display latency criteria based on flying qualities and performance data p 525 N94-13318
Piloting considerations for terminal area operations of civil tiltwing and tiltrotor aircraft p 525 N94-13320
Performance seeking control: Program overview and future directions
[NASA-TM-4531] p 519 N94-14855

AIRCRAFT PILOTS
Work/rest schedules and performance of S-3 aviators during fleet exercise
[AD-A265807] p 734 N94-12975
Work/rest schedules and performance of F/A-18 aviators during Fleet Exercise 1992
[AD-A265826] p 735 N94-12982
The identification of ability requirements and selection instruments for fighter pilot training
[AD-A266340] p 735 N94-13582
Determination of Loran-C/GPS human factors issues
[PB93-199693] p 514 N94-14563
The influence of ATC message length and timing on pilot communication
[NASA-CR-177621] p 512 N94-14744

AIRCRAFT RELIABILITY
MSD in fuselage lap joints: Requirements for inspection intervals for typical fuselage lap joint panels with Multiple Site Damage
[LR-697] p 675 N94-13986

AIRCRAFT SAFETY
In-flight simulation of high agility through active control: Taming complexity by design p 523 N94-13306
Activities report of the Federal Administration for Flight Safety (Germany)
[ETN-93-94208] p 511 N94-14008
Widebody cabin water spray optimization tests
[DOT/FAA/CT-TN93/29] p 511 N94-14186

AIRCRAFT SPECIFICATIONS
ADS-33C related handling qualities research performed using the NRC Bell 205 airborne simulator p 521 N94-13295
MIL-H-8501B: Application to shipboard terminal operations p 521 N94-13296
Some lessons learned in three years with ADS-33C --- rotorcraft handling qualities specification p 521 N94-13299

AIRCRAFT STABILITY
MIL-H-8501B: Application to shipboard terminal operations p 521 N94-13296

AIRCRAFT STRUCTURES
Role of microstructure on fatigue durability of aluminum aircraft alloys
[AD-A265627] p 568 N94-12993
Role of microstructure on fatigue durability of aluminum aircraft alloys
[AD-A266350] p 571 N94-13697
Review of Canadian aeronautical fatigue work, 1991-1993
[LTR-ST-1932] p 674 N94-13861

AIRFOIL OSCILLATIONS
Development of a high-speed mechanical drive system for oscillating an annular blade row in the bending mode
[NAL-TR-1170] p 502 N94-13342
A survey of crack path stability criteria and their application to crack flapping phenomena in stiffened structures
[LR-681] p 675 N94-13929

Numerical simulation of dynamic stall of NACA0012 airfoil oscillating near static stall angle using the Navier-Stokes equations
[DE93-767970] p 505 N94-14061

AIRFOIL PROFILES
Fundamental study of shock wave/turbulent boundary layer interactions with passive control in transonic flows
[ESA-TT-1278] p 630 N94-13117

AIRFOILS
Clebsch variable model for unsteady, transonic flow; application to 2D airfoils
[NLR-TP-91387-U] p 503 N94-13530
Development of PC-based Aeronautical Software (AEROWARE) p 641 N94-14611

AIRFRAME MATERIALS
An experimental investigation into the damage resistance and compression-after-impact strength of T800H/3900-2
[LTR-ST-1909] p 675 N94-13945

AIRFRAMES
Actuator and aerodynamic modeling for high-angle-of-attack aeroservoelasticity
[NASA-TM-4493] p 520 N94-13255
Smart skin technology development for measuring ice accretion, stall, and high AOA aircraft performance. Part 1: Capacitive ice detector development
[NASA-CR-194252] p 511 N94-13424

AIRGLOW
Vacuum ultraviolet instrumentation for solar irradiance and thermospheric airglow
[NASA-CR-194525] p 652 N94-14684

AIRLINE OPERATIONS
The international regulation of air transport: Changing regimes and price effects
[ISBN-0-315-55958-6] p 511 N94-13543
Gate assignment using linear programming
[LR-698] p 775 N94-13987

AIRPORTS
Airport terminals: Optimum configurations and gate position requirement
[ISBN-0-315-61722-5] p 528 N94-13544
Evaluation of infrared sensors for autonomous landing guidance
[AD-A266450] p 513 N94-13703
Gate assignment using linear programming
[LR-698] p 775 N94-13987

AIRSPEED
Recent flight-test results of optical airdata techniques
[NASA-TM-4504] p 517 N94-13791

ALBEDO
A parameterization of cloud droplet nucleation
[DE93-007998] p 718 N94-12903

ALGAE
Biodiesel/aquatic species project report, FY 1992
[DE93-010024] p 709 N94-14087
Organic Geochemical and tectonic evolution of the Midcontinent Rift system
[DE93-015093] p 717 N94-14338

ALGEBRA
Gauging the octonion algebra
[DE93-622864] p 775 N94-12843
Simplification-driven automated partial evaluation
[DE93-012890] p 768 N94-13391
The silent step in time
[CWI-CS-R9221] p 768 N94-13496
On the foundations of final semantics: Non-standard sets, metric spaces, partial orders
[CWI-CS-R9241] p 768 N94-13526
On the symmetry algebra of the discrete states in d less than 2 closed string theory
[DE93-622903] p 769 N94-13536
Application of symbolic and algebraic manipulation software in solving applied mechanics problems
[NASA-CR-4544] p 596 N94-13798
Applications of computer algebra to distributed parameter systems p 677 N94-14623
Spatial operator algebra for flexible multibody dynamics p 679 N94-14631

ALGORITHMS
Adaptively resizing populations: Algorithm, analysis, and first results
[NASA-CR-194277] p 742 N94-12808
Smooth transitions between bump rendering algorithms
[DE93-012504] p 742 N94-12883
A general contact detection algorithm for finite element analysis
[DE93-012846] p 742 N94-12956
Optimization and eigenvalue computation with application to meteorology and oceanography
[DE93-015310] p 744 N94-13024
Knowledge-based oceanographic image compression
[AD-A265752] p 821 N94-13041
Control algorithm implementation for a redundant degree of freedom manipulator
[NASA-CR-191339] p 762 N94-13131
Estimation of aircraft aerodynamic derivatives with the Total Least Squares Method
[NAL-TR-1150] p 502 N94-13392
Analysis of the Harrier forebody/inlet design using computational techniques
[NASA-CR-193616] p 503 N94-13463
Three dimensional tracking of four point planar patterns using corners
[ISBN-0-315-52149-X] p 791 N94-13490
On the occur-check free PROLOG programs
[CWI-CS-R9238] p 748 N94-13524
Hashing and rehashing in emulated shared memory
[CWI-CS-R9240] p 740 N94-13525
Maximum likelihood estimation for constrained or missing data models
[AD-A266563] p 773 N94-13585
Study on TRMM data utilization for meteorology
[NASDA-CNT-930007] p 721 N94-13643
Mathematical algorithms for multidimensional inverse scattering problems in inhomogeneous medium
[AD-A266440] p 749 N94-13702
ANNS: An X Window based version of the AFIT neural network simulator
[AD-A266540] p 764 N94-13704
A data distributed parallel algorithm for ray-traced volume rendering
[NASA-CR-191520] p 749 N94-13721
Simulated annealing for the problem of multiresource location on graph
[REPT-93-033] p 770 N94-13809
Adaptive Signal Processing Testbed
[DSIS-93-00258] p 604 N94-13869
Fast parallel string prefix-matching
[AD-A267758] p 760 N94-13924
Adaptive Signal Processing Testbed signal excision software: User's manual
[DSIS-93-00260] p 606 N94-14037
An algorithm for the remote sensing of fog using satellite-data and additional information
[DLR-FB-92-23] p 688 N94-14135
Quantum Monte Carlo by message passing
[DE93-012645] p 760 N94-14177
An exact processing algorithm for wide beam spaceborne SAR data p 689 N94-14213
TRMM precipitation radar algorithm p 690 N94-14224
The effects of anthropogenic aerosols on optical thickness and particle size of clouds. Part 1: Retrieval algorithm p 691 N94-14230
The development and implementation of an interactive retrieval/analysis/forecast algorithm p 692 N94-14234
Integration of remote sensing and mathematical modelling in disaster mitigation p 692 N94-14239
Center of trace algorithms for extracting digitized waveforms from two-dimensional images
[DE93-015082] p 753 N94-14295
Domain connectivity among systems of overset grids
[NASA-CR-193390] p 508 N94-14326
Implementation and experimentation with a motion planning system
[ITN-93-85213] p 755 N94-14505
Guidance law development for aeroassisted transfer vehicles using matched asymptotic expansions
[NASA-CR-194523] p 508 N94-14538
Advanced ballistic range technology
[NASA-CR-194530] p 533 N94-14540
Large spatial, temporal, and algorithmic adaptivity for implicit nonlinear finite element analysis
[DE93-016438] p 771 N94-14589
A vertex-based finite-volume algorithm for the Navier-Stokes equations p 639 N94-14599
Computational Controls Workstation: Algorithms and hardware p 678 N94-14626
Caesy: A software tool for computer-aided engineering p 678 N94-14627
The use of linked lists in the simulation of controller-structure interaction p 679 N94-14630
Non-recursive augmented Lagrangian algorithms for the forward and inverse dynamics of constrained flexible multibodies p 679 N94-14633
Parallel O(log n) algorithms for open- and closed-chain rigid multibody systems based on a new mass matrix factorization technique p 679 N94-14636
Parallel methods for dynamic simulation of multiple manipulator systems p 680 N94-14637
On l(1): Optimal decentralized performance p 681 N94-14643
Control system design for flexible structures using data models p 527 N94-14646
Analysis, approximation, and computation of a coupled solid/fluid temperature control problem
[NASA-TM-106351] p 771 N94-14731
Mathematic methods and algorithms for real-time applications
[AD-A266776] p 771 N94-14789
An experimental analysis of bottleneck-centered opportunistic scheduling
[AD-A266643] p 820 N94-14796
Robust non convex optimization algorithms: Codes and numerical simulation of large scale
[ETN-93-94354] p 756 N94-14813

ALIGNMENT
Determination of channeling perspectives for complex crystal structures
[DE93-012872] p 805 N94-13009
Design and performance of an automated video-based laser beam alignment system
[DE93-012571] p 656 N94-13481
A continuum theory for liquid crystals describing different degrees of orientational order
[ETN-93-94392] p 807 N94-13590

ALKALI HALIDES
Ionic conductivity of alkali halides and their mixtures near liquid-solid phase transition
[ITN-93-85222] p 566 N94-14558

ALKALIES
Study of multicomponent diffusion and transport phenomena
[DE93-015095] p 804 N94-13005
Thermal history effects on electrical relaxation and conductivity for potassium silicate glass with low alkali concentrations
[NASA-TM-106324] p 583 N94-14845

ALKALINE EARTH METALS
Canonical correlation of waste glass compositions and durability, including pH
[DE93-012754] p 578 N94-13493
Fine-powder Al2O3 and SiO2 for preparation of multielement standards for rare-earth elements analysis
[DE93-625118] p 567 N94-14884

ALKANES
Theoretical treatment of the bulk and surface properties of fluids containing long, flexible molecules
[DE93-015560] p 575 N94-12861
Comparative ignition of hexane and octane isomers in a shock tube
[DE93-016535] p 566 N94-14869

ALKENES
Office of Naval Research/DARPA publications: Composite materials with improved properties in compression
[AD-A265509] p 560 N94-14794

ALLOYING
Preparation and characterization of rapidly solidified Al-Li alloys
[ISBN-0-315-58948-5] p 569 N94-13367
Study on solidification of immisible alloys (M-10) p 588 N94-13742

ALLOYS
Containerless processing of undercooled melts
[NASA-CR-194350] p 572 N94-14123

ALPHA PARTICLES
Direct determination of alpha particle transport coefficients
[DE93-013488] p 787 N94-14691

ALTERNATING CURRENT
Investigation of an alternating current plasma as an element selective atomic emission detector for high-resolution capillary gas chromatography and as a source for atomic absorption and atomic emission spectrometry p 798 N94-13678

ALTERNATING DIRECTION IMPLICIT METHODS
Implementation of ADI: Schemes on MIMD parallel computers
[NASA-CR-193720] p 759 N94-13204

ALTIMETERS
Position error determination for the speedometer and altimeter of the NAL QSTOL experimental aircraft ASKA
[NAL-TR-1144] p 517 N94-13451

ALUMINIDES
Insoluble coatings for Stirling engine heat pipe condenser surfaces
[NASA-CR-191188] p 554 N94-14771

ALUMINUM
Inhibiting corrosion in Gr/Al and Gr/Mg metal matrix composites using nonequilibrium alloying techniques
[AD-A266547] p 556 N94-13583
Development of test techniques to simulate high-frequency mechanical shock on weapon components
[KCP-613-4998] p 675 N94-13907
Measurements of crystal growth kinetics at extreme deviations from equilibrium
[DE93-014526] p 815 N94-14798

ALUMINUM ALLOYS
Effect of pressure on order and stability in alloys: The case of Al-Ge
[DE93-013842] p 567 N94-12899
A benchmark bending test of a thick specimen, Part 1: Experiments
[ARL-RR-6-PT-1] p 670 N94-12927

A benchmark bending test of a thick specimen. Part 2: Surface displacement measurements
[ARL-RR-6-PT-2] p 670 N94-12928
Role of microstructure on fatigue durability of aluminum aircraft alloys
[AD-A265627] p 568 N94-12993
Effect of microstructure on passive film formation and breakdown on Al alloys
[AD-A265339] p 569 N94-13050
The corrosion behavior of 8001 Al under heat-transfer conditions in an aqueous loop system
[DE93-013450] p 569 N94-13242
Preparation and characterization of rapidly solidified Al-Li alloys
[ISBN-0-315-58948-5] p 569 N94-13367
Modern aluminium sheet alloys for aerospace applications
[NLR-TP-92057-U] p 570 N94-13497
The ASCOR test: A simple automated method for stress corrosion testing of aluminium alloys
[NLR-TP-91438-U] p 570 N94-13532
UK interlaboratory tensile tests on Al alloy/SiC particulate metal matrix composites
[NPL-DMM(A)-77] p 570 N94-13666
Fatigue crack initiation and propagation in aluminum alloys 8090 and 2124 in hydrogenous atmospheres
p 570 N94-13670
Role of microstructure on fatigue durability of aluminum aircraft alloys
[AD-A266350] p 571 N94-13697
The microstructural response of near gamma-TiAl+W to heat treatment
[DSIS-93-00237] p 571 N94-13840
The influence of a microgravity environment on the dendritic morphology during directional solidification of hypoeutectic Al-Si alloys
[NASA-CR-194139] p 571 N94-13891
Fatigue design curves for 6061-T6 aluminum
[DE93-011849] p 571 N94-14021
Microstructural mechanisms that enhance electromigration resistance in Al-Cu thin films
[DE93-013770] p 812 N94-14345
The growth of short fatigue cracks in an aluminium alloy
[RAE-TR-92063] p 574 N94-14828
Multicrystalline silicon solar cells: Gettering optimization and characterization
[DE93-015001] p 705 N94-14861

ALUMINUM ARSENIDES
Anomalous low-temperature free-exciton transport in GaAs structures
[DE93-009845] p 809 N94-14108

ALUMINUM COMPOUNDS
Muon spin relaxation studies of heavy fermion superconductors
[DE93-014576] p 815 N94-14773

ALUMINUM GALLIUM ARSENIDES
Numerical simulation and analysis of electrical and optical properties of Al(x)Ga(1-x)As / GaAs
[ETN-93-94387] p 703 N94-13997

ALUMINUM OXIDES
Processing and mechanical properties of silicon carbide platelet reinforced alumina composites
p 556 N94-13557
Microwave hybrid heating of alumina filaments
[DE93-012642] p 581 N94-14327
Microwave sintering of large alumina bodies
[DE93-012752] p 581 N94-14340
Fine-powder Al2O3 and SiO2 for preparation of multielement standards for rare-earth elements analysis
[DE93-625118] p 567 N94-14884

ALUMINUM-LITHIUM ALLOYS
The feasibility of producing aluminum-lithium structures for cryogenic tankage applications by laser beam welding
[NASA-CR-191527] p 595 N94-14026
Microstructural origins and modeling of intergranular crack initiation in an Al-Li-Cu-Mg-(Zr) alloy
[ISAL-91-0012] p 574 N94-14814
Effect of thermal processing practices on the properties of superplastic Al-Li alloys
[NASA-CR-4548] p 574 N94-14850

AMAZON REGION (SOUTH AMERICA)
Modeling of biosphere-atmosphere interaction for forest and pastureland in the Amazon
[INPE-5454-TDI/496] p 707 N94-13330
Estimations of temperature and humidity of the canopy in Amazon Forest using microwave data from SMMR sensor of Nimbus-7 satellite
[INPE-5444-TDI/490] p 720 N94-13614

AMBIENT TEMPERATURE
A verification of the Euroguidance: A guidance forecast for transportation and tourism
[KNMI-TR-145] p 722 N94-13993

AMBIPOLAR DIFFUSION
Structural and electronic studies of a-SiGe:H alloys
[DE93-010021] p 809 N94-14085

AMINES
Experimental and kinetic modeling of acid/base and redox reactions over oxide catalysts
[DE93-016203] p 563 N94-13375

AMINO ACIDS
Characterization of 1:1 random copolymers obtained from 6-, 7-, 11-, and 12-carbon amino acids
[AD-A265827] p 577 N94-12985

AMMETERS
A high-precision direct current measuring device over a kiloampere range
[DE93-626409] p 627 N94-14885

AMORPHOUS MATERIALS
Amorphous sol-gel insulating films
[DE93-012859] p 576 N94-12866
Procedures for analysis of debris relative to Space Shuttle systems
[NASA-TM-109190] p 534 N94-12900
Planning of a comet simulator
[ITN-93-85206] p 835 N94-13230
Barium fluoride research and development at Lawrence Livermore National Laboratory
[DE93-014682] p 807 N94-13405
The 1.00 MeV proton radiation resistance studies of amorphous silicon-based alloy solar cells
p 703 N94-13639
Fabrication of Si-As-Te ternary amorphous semiconductor in the microgravity environment (M-13)
p 588 N94-13745
Structural and electronic studies of a-SiGe:H alloys
[DE93-010021] p 809 N94-14085
Activities of the Basic Sciences Branch
[DE93-010012] p 851 N94-14455

AMORPHOUS SEMICONDUCTORS
Fabrication of Si-As-Te ternary amorphous semiconductor in the microgravity environment (M-13)
p 588 N94-13745

AMORPHOUS SILICON
Photovoltaic Subcontract Program
[DE93-000092] p 700 N94-12868
The 1.00 MeV proton radiation resistance studies of amorphous silicon-based alloy solar cells
p 703 N94-13639
Continuous roll-to-roll a-Si photovoltaic manufacturing technology
[DE93-010006] p 704 N94-14109
Optimization of transparent and reflecting electrodes for amorphous silicon solar cells
[DE93-010009] p 704 N94-14110
Theory of the electronic and structural properties of solid state oxides
[DE93-016051] p 811 N94-14296
Structure and stability of microvoids in A-Si:H
[DE93-016625] p 813 N94-14413
Computational diagnostics for detecting phase transitions during nanoindentation
[DE93-016536] p 813 N94-14439

AMPLIFICATION
Evolution of catalytic RNA in the laboratory
[NASA-CR-194124] p 727 N94-13210
Independent adjustment of the higher order frequency dependent phase in chirped pulse amplification systems
[DE93-017106] p 625 N94-14522

AMPLIFIERS
Numerical simulations of Nd:YAG laser amplifiers
[FFI/RAPPORT-92/7028] p 657 N94-13970

AMPLITUDE MODULATION
Envelope and instantaneous frequency estimation of narrowband modulated signals
[DREO-TN-92-3] p 605 N94-14033

AMPOULES
Adaptive control of interface by temperature and interface profile feedback in transparent multi-zone crystal growth furnace
[NASA-CR-194140] p 762 N94-13253

ANALOG CIRCUITS
An analog clustering network from a biological model
[AD-A265637] p 762 N94-12969

ANALOG TO DIGITAL CONVERTERS
HYMOSS signal processing for pushbroom spectral imaging
[NASA-CR-191341] p 620 N94-13125
Center of trace algorithms for extracting digitized waveforms from two-dimensional images
[DE93-015082] p 753 N94-14295

ANALYSIS OF VARIANCE
Exploratory data analysis: Past, present and future
[AD-A266775] p 774 N94-14788

ANALYTICAL CHEMISTRY
Quality assurance for environmental chemistry, 1991, volume 1
[DE93-011791] p 709 N94-14020

ANDROMEDA GALAXY
The spectroscopic evolution of novae in the bulge of M31 and a search for their possible origin in the M31 globular cluster system p 831 N94-13668

ANELASTICITY
Shock compression and quasielastic release in tantalum
[DE93-014566] p 811 N94-14329

ANGLE OF ATTACK
Improved aeroprediction code. Part 1: Summary of new methods and comparison with experiment
[AD-A266015] p 500 N94-12989
Results of wind tunnel tests of an ASRM configured 0.03 scale Space Shuttle integrated vehicle model (47-OTS) in the AEDC 16-foot Transonic wind tunnel (IA613A), volume 1
[NASA-CR-185696] p 534 N94-13191

ANGLES (GEOMETRY)
Thermodynamic status of static and dynamic contact angles
[ISBN-0-315-73844-8] p 817 N94-13554

ANGULAR CORRELATION
Angular correlations in neutron beta decay
[DE93-014349] p 785 N94-14486

ANGULAR DISTRIBUTION
Resonant x ray Raman scattering from atoms and molecules
[DE93-015158] p 784 N94-13896

ANGULAR MOMENTUM
Coherent excitation of autoionizing resonances by electron impact
[DE93-018169] p 785 N94-14419
Predicting the vibrations of a spinning inflated membrane
[DE93-010690] p 676 N94-14456
The fractional quantum Hall effect and the spherical shell model
[DE93-014553] p 818 N94-14740
On transport of energy, momentum, orbital angular momentum and self-angular momentum of electromagnetic wave in dispersal media
[DE93-624179] p 617 N94-14883

ANGULAR RESOLUTION
Angular resolution studies of the CYGNUS array using the shadows of the Sun and Moon
[DE93-012723] p 846 N94-12946
Advances in low energy neutral atom imaging techniques
[DE93-012745] p 782 N94-13492
Results from a water-Cerenkov array
[DE93-012715] p 849 N94-14461

ANIMALS
Ethology in space, a unique opportunity for behavioural science
[ESA-STM-246] p 731 N94-14862

ANISOTROPIC MEDIA
Prism-film coupling in anisotropic planar waveguides of epitaxial (101) rutile thin films
[DE93-012912] p 811 N94-14304
On transport of energy, momentum, orbital angular momentum and self-angular momentum of electromagnetic wave in dispersal media
[DE93-624179] p 617 N94-14883

ANISOTROPIC PLATES
Nonlinear vibrations of thick composite plates: Higher-order shear deformation plate theory
p 556 N94-13558
Shear buckling of fiber metal laminates: Comparison between orthotropic and anisotropic plate models using finite element method
[LTR-ST-1934] p 671 N94-13565

ANISOTROPY
Ion anisotropy driven waves in the Earth's magnetosheath and plasma depletion layer
[DE93-012751] p 712 N94-12952
Field emitter array RF amplifier development project. Phase 1: Cathode technology development
[AD-A266346] p 622 N94-13776
Some aspects of sheet forming simulation using explicit finite element techniques
[DE93-012479] p 663 N94-13975
Prism-film coupling in anisotropic planar waveguides of epitaxial (101) rutile thin films
[DE93-012912] p 811 N94-14304
Anomalous ion transport and feedback control
[DE93-018324] p 803 N94-14874

ANNEALING
Annealing study of main electron irradiation-induced defects (H4 and H5) in P-InP using DLTS technique
[DE93-623204] p 806 N94-13213
Surfaces and interfaces of ceramics and metals
[DE93-014959] p 578 N94-13408
Microstructural mechanisms that enhance electromigration resistance in Al-Cu thin films
[DE93-013770] p 812 N94-14345

Influence of heat treatment on microstructure of Ti-35wt Al prepared by elemental powder metallurgy
[GKSS/92/E/27] p 574 N94-14821
Quenching and annealing effects on the specific heat of YBa2Cu3O(7-delta)
[DE93-016483] p 816 N94-14868
Yield properties of tungsten and tungsten heavy alloys
[AD-A266833] p 575 N94-14878

ANNIHILATION REACTIONS
High energy hadron-hadron collisions
[DE93-015584] p 784 N94-13927

ANNUAL VARIATIONS
On the vertical structure of seasonal, interannual and intraseasonal flows
[AD-A265346] p 719 N94-12992
Cyclogenesis and cyclone over South America
[INPE-5400-TDI/479] p 719 N94-13175
Circulation and rainfall climatology of a 10-year (1979 - 1988) integration with the Goddard Laboratory for atmospheres general circulation model
[NASA-TM-104591] p 723 N94-14074
Seasonal change of the land-surface temperature over Asian Continent derived from GAC data on NOAA-11 AVHRR p 691 N94-14232
Sea surface temperature forcing and phase locking of Nordeste precipitation
[DE93-011873] p 723 N94-14426
Solar radiation on Mars: Stationary photovoltaic array
[NASA-TM-106321] p 626 N94-14730

ANNULAR FLOW
Studies of momentum and energy transfer across wavy gas-liquid interfaces
[AD-A266432] p 635 N94-13699

ANNULAR PLATES
Development of a high-speed mechanical drive system for oscillating an annular blade row in the bending mode
[NAL-TR-1170] p 502 N94-13342
Nonlinear vibrations of thick composite plates: Higher-order shear deformation plate theory p 556 N94-13558

ANODES
Field emitter array RF amplifier development project. Phase 1: Cathode technology development
[AD-A266346] p 622 N94-13776

ANTARCTIC REGIONS
Theoretical support for the Airborne Antarctic Ozone Experiment
[NASA-CR-193669] p 713 N94-13465

ANTENNA ARRAYS
A hybrid finite element-boundary integral for the analysis of cavity-backed antennas of arbitrary shape
[NASA-CR-193719] p 599 N94-13236
Using a focal-plane array to estimate antenna pointing errors
[NASA-CR-194502] p 602 N94-13810
Phase aligner for the Electronically Scanned Thinned Array Radiometer (ESTAR) instrument
[NASA-TM-4518] p 623 N94-13878
A cryogenic seven-element HEMT front end for DSS 13 p 608 N94-14375
Layout and cabling considerations for a large communications antenna array p 611 N94-14395

ANTENNA COMPONENTS
Layout and cabling considerations for a large communications antenna array p 611 N94-14395
An initial study of using the 34-m antenna for lunar mission support p 611 N94-14396

ANTENNA DESIGN
The 24 GHz measurements of 2.2 lambda conical horn antennas illuminating a conducting sheet
[NASA-TM-109002] p 598 N94-12811
Ion cyclotron heating experiments and plans for the Advanced Toroidal Facility (ATF)
[DE93-012965] p 795 N94-13033
Effect on antenna structure of high power RF during plasma operation
[DE93-013278] p 797 N94-13144
A hybrid finite element-boundary integral for the analysis of cavity-backed antennas of arbitrary shape
[NASA-CR-193719] p 599 N94-13236
The Second Workshop on Deployment and Assembly Experiment of Large Space Structure on Orbit
[NASDA-CON-930003] p 529 N94-13268
Structural design of hexa-link truss deployable antenna p 529 N94-13269
Thermal distortion measurement of TETRUS type thermal test model of large deployable antenna for mobile communications satellite p 529 N94-13270
Development of modular cable mesh deployable antenna p 530 N94-13274
Trial manufacture model and in-space verification method of deployable antenna p 530 N94-13278
Electrical characterization of the JET A(sub 2) antenna: Comparison of model with measurements Wade, T.
[DE93-012964] p 607 N94-14291
Cammatic: An approach to improve DSS 13 antenna gravity-loading performance p 608 N94-14374
Layout and cabling considerations for a large communications antenna array p 611 N94-14395
An initial study of using the 34-m antenna for lunar mission support p 611 N94-14396
Feasibility study of a synthesis procedure for array feeds to improve radiation performance of large distorted reflector antennas
[NASA-CR-194491] p 612 N94-14501
Design of the ion cyclotron system for TPX
[DE93-012961] p 803 N94-14770

ANTENNA FEEDS
Feasibility study of a synthesis procedure for array feeds to improve radiation performance of large distorted reflector antennas
[NASA-CR-194491] p 612 N94-14501

ANTENNA RADIATION PATTERNS
A hybrid finite element-boundary integral for the analysis of cavity-backed antennas of arbitrary shape
[NASA-CR-193719] p 599 N94-13236
Antenna pattern control using impedance surfaces
[NASA-CR-194517] p 602 N94-13799
Analysis of microstrip patch antennas with nonzero surface resistance
[NASA-TP-3362] p 604 N94-13916
Radio metric errors due to mismatch and offset between a DSN antenna beam and the beam of a troposphere calibration instrument p 607 N94-14370

ANTENNAS
Design of the ion cyclotron system for TPX
[DE93-012961] p 803 N94-14770

ANTIBODIES
Monoclonal antibodies directed against surface molecules of multicell spheroids
[NASA-CR-193560] p 727 N94-12795

ANTIGENS
Analysis of the V antigen lcrGVH-yopBD operon of Yersinia pseudotuberculosis: Evidence for a regulatory role of LcrH and LcrV
[FOA-B-40417-4.4] p 729 N94-14129

ANTINUCLEONS
Isospin flip as a relativistic effect: NN interactions
[CEBAF-PR-89-023] p 786 N94-14552

ANTIPROTONS
Observation of the coalescing of beam into an asymmetric RF bucket by stochastic cooling
[DE93-015133] p 783 N94-13895

ANTIREFLECTION COATINGS
Project proposal for partial computational physics support for Survivability of Coatings program
[DE93-013788] p 576 N94-12939
Absorption and damage thresholds of low defect density hafnia deposited with activated oxygen
[DE93-013853] p 655 N94-13243
Laser-damage susceptibility of nodular defects in dielectric mirror coatings: AFM measurements and electric-field modeling
[DE93-014655] p 580 N94-14124
Materials and structures p 546 N94-14835
Multicrystalline silicon solar cells: Gettering optimization and characterization
[DE93-015001] p 705 N94-14861

APERTURES
Locally non-uniform finite-difference time domain with application to stealth, crosstalk, and narrow apertures
[DE93-013958] p 601 N94-13696
Fabrication p 546 N94-14834

APPLICATION SPECIFIC INTEGRATED CIRCUITS
HYMOSS signal processing for pushbroom spectral imaging
[NASA-CR-191341] p 620 N94-13125
Mongoose ASIC microcontroller programming guide
[NASA-RP-1319] p 623 N94-13871

APPLICATIONS PROGRAMS (COMPUTERS)
Making the connection between information modeling and implementation
[DE93-011588] p 820 N94-12907
GRO: Black hole models for gamma ray bursts
[NASA-CR-193244] p 829 N94-13178
Selection of behavioral tasks and development of software for evaluation of rhesus monkey behavior during spaceflight
[NASA-CR-194176] p 728 N94-13865
HELSCAM V2.0: Development and application guide
[DSIS-93-00137] p 515 N94-13867
Demonstration and acceptance test plan for real-time excision software on the Adaptive Signal Processing Testbed
[DSIS-93-00275] p 751 N94-13990
Adaptive Signal Processing Testbed application software: User's manual
[DSIS-93-00261] p 606 N94-14038
Development of software for composite materials analysis, phase 1, part 1
[DSIS-93-00857-PT-1-PHASE-1] p 558 N94-14105
Ground Attack Profile Selector Program, version 3.0
[DSIS-93-00702] p 753 N94-14207
A description of the computer program CALDK38 which controls instrumentation set-up and data acquisition during deadweight calibration using an HBM DK 38 S6 digital measuring unit
[LTR-ST-1935] p 754 N94-14496
Advanced ballistic range technology
[NASA-CR-194530] p 533 N94-14540
Development of PC-based Aeronautical Software (AEROWARE) p 641 N94-14611
Development of parallel processing at NAL: A retrospect p 641 N94-14614
SRISTI: The NAL method for the design and analysis of Natural Laminar Flow (NLF) airfoils p 516 N94-14615
Modelling robotic systems with DADS p 678 N94-14625
Animation of multi-flexible body systems and its use in control system design p 678 N94-14629
Switchover software reliability estimate for Paducah freezer/sublimer computer systems
[DE93-013844] p 756 N94-14696
Splines, contours and SVD subroutines
[DE93-016088] p 757 N94-14866

APPROACH AND LANDING TESTS (STS)
Flight evaluations of approach/landing navigation sensor systems: Summary of 1990 flight experiments
[NAL-TR-1175] p 513 N94-13344

APPROACH CONTROL
Compatibility of information and mode of control: The case for natural control systems p 523 N94-13307
Visual cueing aids for rotorcraft landings p 524 N94-13313
Evaluation of two cockpit display concepts for civil tiltrotor instrument operations on steep approaches p 517 N94-13323
Flight path control for the approach and landing of the quiet STOL experimental aircraft ASKA
[NAL-TR-1183] p 513 N94-13457
Optimal lateral escape maneuvers for microburst encounters during final approach
[LR-691] p 511 N94-13534
Helicopter precision approach capability using the Global Positioning System
[NASA-CR-194037] p 513 N94-13957

APPROXIMATION
Spherical anharmonic oscillator in self-similar approximation
[DE93-626622] p 772 N94-14890

AQUEOUS SOLUTIONS
The importance of hard core repulsion in models of activity coefficients in aqueous electrolyte solutions: Illustration in the case of hydration theory
[DE93-012476] p 561 N94-12881
Reverse micelle synthesis of nanoscale metal containing catalysts
[DE93-012869] p 572 N94-14184

AQUIFERS
BOAST 2 for the IBM 3090 and RISC 6000
[DE93-000138] p 638 N94-14351

ARC HEATING
Arc-heating tests of thermal protection system materials for the H-2 rocket fairing
[NAL-TR-1181] p 551 N94-13455
Aerodynamic and aerothermal facilities 2: Continuous flow high enthalpy facilities p 506 N94-14160

ARC JET ENGINES
Recent testing of 30 kW hydrogen arcjet thrusters
[NASA-TM-106214] p 551 N94-13430

ARC MELTING
A conduction model for the vacuum arc remelting process
[NPL-DMM(A)-98] p 639 N94-14464

ARC WELDING
Welding technologies as applied to nuclear manufacturing
[DE93-010924] p 664 N94-14565

ARCHAEBACTERIA
The evolution of energy-transducing systems: Studies with archaebacteria
[NASA-CR-194130] p 728 N94-13562

ARCHITECTURE
Airport terminals: Optimum configurations and gate position requirement
[ISBN-0-315-61722-5] p 528 N94-13544
Simulating the daylight performance of fenestration systems and spaces of arbitrary complexity: The IDC method
[DE93-015177] p 704 N94-14333

ARCHITECTURE (COMPUTERS)
PACT user's guide
[DE93-013093] p 742 N94-12840
Mobile host internetworking using IP loose source routing
[AD-A265713] p 759 N94-13052

High speed packet switching
[NASA-CR-191334] p 759 N94-13177
Architecture-driven reuse of code in KASE
[NASA-CR-194200] p 745 N94-13356
The KSR1: Experimentation and modeling of poststore
[DE93-012539] p 759 N94-13470
High speed all-optical networks
[NASA-CR-194384] p 791 N94-13682
Guide to the software architectural design phase
[ESA-PSS-05-04-ISSUE-1] p 753 N94-14190
The BIRIS server: Integration of a three-dimensional range sensor into a harmony-based realtime architecture
[ERB-1036] p 765 N94-14201
NASA Space Engineering Research Center for VLSI systems design
[NASA-CR-194035] p 625 N94-14325
Implementation and experimentation with a motion planning system
[ITN-93-85213] p 755 N94-14505
Determining neural network connectivity using evolutionary programming
[AD-A266853] p 766 N94-14882

ARCTIC REGIONS
Arctic ozone expedition
[NASA-TM-109301] p 708 N94-13602
Airborne Arctic stratospheric expedition: Ozone
[NASA-TM-109312] p 515 N94-13606
Weather forecasting support for AASE-2
[NASA-CR-194342] p 721 N94-13675
Aeromagnetic work in the Lincoln Sea: 1991 survey
[DSIS-93-00308] p 715 N94-13830
Organic Geochemical and tectonic evolution of the Midcontinent Rift system
[DE93-015093] p 717 N94-14338
Nonlinear relationships between particulate absorption and chlorophyll: Detritus or pigment packaging?
[AD-A266806] p 731 N94-14899

ARGON
Statistical mechanical theory of liquid entropy
[DE93-016524] p 817 N94-14593

ARGON PLASMA
Measuring opacity of shock generated argon plasmas
[DE93-013038] p 801 N94-14312

ARID LANDS
Wind erosion in semiarid landscapes: Predictive models and remote sensing methods for the influence of vegetation
[NASA-CR-194029] p 715 N94-13956

ARMOR
The 3-D massively parallel impact simulations using PCTH
[DE93-011593] p 670 N94-12908
Collisions and separations in 2D hydrodynamical code
[ITN-93-85225] p 639 N94-14503

ARPA COMPUTER NETWORK
Diskless supercomputers: Scalable, reliable I/O for the Tera-Op technology base
[NASA-CR-194089] p 740 N94-13363

ARSENIC
A review of the global emissions, transport, and effects of heavy metals in the environment
[DE93-013507] p 706 N94-12937

ARTIFICIAL INTELLIGENCE
Advancing automation and robotics technology for the Space Station Freedom and for the U.S. economy
[NASA-TM-104024] p 739 N94-12838
Completing fault models for abductive diagnosis
[DE93-003832] p 761 N94-12859
Artificial intelligence support for scientific model-building
[NASA-TM-109252] p 761 N94-12890
VISART: Artificial vision for industrial use. A comprehensive system
[INPE-5379-TDI/474] p 665 N94-12941
An analog clustering network from a biological model
[AD-A265637] p 762 N94-12969
A path-oriented matrix-based knowledge representation system
[NASA-CR-4539] p 744 N94-13065
Knowledge-based processing for aircraft flight control
[NASA-CR-194074] p 526 N94-13469
Artificial intelligence in Canada: A description by the members of the ACAI
[NRC-31789] p 763 N94-13517
Reasoning with uncertain and incomplete information in aerospace applications
[NLR-TP-91366-U] p 763 N94-13529
An expert system for integrated structural analysis and design optimization for aerospace structures
[NASA-CR-194225] p 673 N94-13673
Artificial intelligence in Canada: A description by the members of the ACAI
[CNR-31790] p 764 N94-13820
SCAILET: An intelligent assistant for satellite ground terminal operations
[NASA-TM-105879] p 538 N94-13918
Intelligent environment for interpretation tasks of remotely sensed images
[INPE-5466-PRE/1774] p 687 N94-14082
Knowledge based systems: From process control to policy analysis
[DE93-014582] p 765 N94-14117
Self organized criticality
[DE93-013182] p 773 N94-14320

ARTIFICIAL SATELLITES
The remarkable achievement of China satellite application p 692 N94-14235

ASCENT TRAJECTORIES
Trajectory optimization for the national aerospace plane
[NASA-CR-194146] p 516 N94-14104

ASPECT RATIO
Stability and confinement properties of small-aspect-ratio tokamak
[INPE-5463-PRE/1771] p 801 N94-14024

ASSEMBLING
Miniature mechanism assembly
[DE93-015595] p 624 N94-13928

ASSEMBLY LANGUAGE
Robot programming, natural computation and conceptual graphs
[ITN-93-85193] p 748 N94-13539

ASSOCIATIVE PROCESSING (COMPUTERS)
Retrieval properties of neural networks with infinitely many marked patterns
[PREPRINT-729] p 766 N94-14718

ASTEROIDS
Meteoroid environment near the Earth-Moon system
[NASA-CR-193670] p 835 N94-13203

ASTRO MISSIONS (STS)
STS-35 EVA payload training in WETF
[NASA-TM-109492] p 739 N94-14790

ASTRONAUT TRAINING
STS-35 EVA payload training in WETF
[NASA-TM-109492] p 739 N94-14790

ASTRONOMICAL CATALOGS
Ultraviolet Spectrometer and Polarimeter (UVSP) catalog of observations. Volume 3: Experiments 63058-99771 (February 1988 - November 1989)
[NASA-CR-4529] p 844 N94-13146
Royal Belgium observatory calendar: 156th year
[ETN-93-94221] p 833 N94-14811

ASTRONOMICAL INTERFEROMETRY
Planetary system detection by POINTS
[NASA-CR-194361] p 545 N94-13067

ASTRONOMICAL MODELS
GRO: Black hole models for gamma ray bursts
[NASA-CR-193244] p 829 N94-13178

ASTRONOMICAL OBSERVATORIES
The four great observatories
[NASA-TM-109311] p 830 N94-13605
Executive summary p 545 N94-14831

ASTRONOMICAL PHOTOMETRY
A photometric study of massive x-ray binaries
[ITN-93-85207] p 829 N94-13231
A photometric and morphological study of compact groups of galaxies and their environments
[ISBN-0-315-59601-5] p 829 N94-13370
A near-infrared faint galaxy survey: Evolution and the cosmological geometry from K band photometry p 830 N94-13591
Photometry and spectroscopy in the open cluster Alpha Persei, 2
[NASA-CR-193397] p 833 N94-14358

ASTRONOMICAL SATELLITES
ALFIS: Astronomical Low Frequency Interferometry Satellites. A feasibility study
[LR-699] p 542 N94-13988

ASTRONOMICAL SPECTROSCOPY
ROSAT guest investigator program (AO-1). On a search for coronal x ray emissions from white dwarfs
[NASA-CR-193654] p 835 N94-13171
UV extinction properties of carina nebular dust
[NASA-CR-193424] p 835 N94-13233
Basic research in solar physics
[NASA-CR-193632] p 844 N94-13234
Rocket and laboratory studies in astronomy
[NASA-CR-194410] p 832 N94-13966
Photometry and spectroscopy in the open cluster Alpha Persei, 2
[NASA-CR-193397] p 833 N94-14358
Emission line variability in active galactic nuclei
[ITN-93-85209] p 849 N94-14553

ASTROPHYSICS
Force-free magnetic fields, curl eigenfunctions, and the sphere in transform space, with applications to fluid dynamics and electromagnetic theory
[AD-A265805] p 834 N94-12971
Research in cosmic and gamma ray astrophysics: Cosmic physics portion
[NASA-CR-194127] p 847 N94-13211
The development of the TIMAX project: A hard x ray imaging telescope
[INPE-5474-TDI/505] p 829 N94-13245
The International Colloquium on Atomic Spectra and Oscillator Strengths for Astrophysical and Laboratory Plasmas
[NASA-TM-109255] p 849 N94-13376
Generic results of the space physics community survey
[NASA-CR-194538] p 818 N94-13984
Visualization techniques to aid in the analysis of multi-spectral astrophysical data sets
[NASA-CR-194489] p 840 N94-14482
Workshop Proceedings: Optical Systems Technology for Space Astrophysics in the 21st Century, volume 3
[NASA-CR-194102] p 545 N94-14830
The next century astrophysics program p 546 N94-14832
Wavefront sensing, control, and pointing p 546 N94-14833
Fabrication p 546 N94-14834
Optical systems integrated modeling p 547 N94-14837
Advanced optical instruments technology p 547 N94-14838

ASYMMETRY
Observation of the coalescing of beam into an asymmetric RF bucket by stochastic cooling
[DE93-015133] p 783 N94-13895

ASYMPTOTIC GIANT BRANCH STARS
Radiative transfer in the dynamic atmospheres of Mira-type variables
[NASA-CR-193324] p 829 N94-13287

ASYMPTOTIC METHODS
Hydrodynamic asymptotics of Green functions in magnetics with spontaneously broken symmetry
[DE93-621349] p 767 N94-13223

ASYMPTOTIC SERIES
On the use of the method of matched asymptotic expansions in propeller aerodynamics and acoustics
[NLR-TP-91307-U] p 503 N94-13528
Guidance law development for aeroassisted transfer vehicles using matched asymptotic expansions
[NASA-CR-194523] p 508 N94-14538
A small-scale turbulence model p 643 N94-14746

ATLANTIC OCEAN
Preliminary meteorological results for 1992 West Coast Scotland Experiment
[DE93-014677] p 720 N94-13404

ATMOSPHERIC ATTENUATION
Spectroscopic method and data reduction algorithm for laser long-path absorption measurements using RIS p 689 N94-14218
A method for estimation of partial cloud cover within a pixel and its effect p 697 N94-14269
Atmospheric correction for sea surface temperature by application of microwave dual-channel technique to VTIR data p 697 N94-14271
Hardware design for the Autonomous Visibility Monitoring (AVM) observatory p 533 N94-14394
Radiometric observations of atmospheric attenuation at 20.6 and 31.65 GHz: The Wave Propagation Laboratory data base p 613 N94-14660
Rain-rate data base development and rain-rate climate analysis p 614 N94-14664

ATMOSPHERIC BOUNDARY LAYER
Binary homogeneous nucleation: Temperature and relative humidity fluctuations and non-linearity
[DE93-007884] p 709 N94-13911
Fluxes of heat and water vapour in a convective mixed layer during EFEDA
[DLR-FB-92-21] p 716 N94-14132
Evolution of the lower planetary boundary layer over strongly contrasting surfaces
[DE93-010667] p 717 N94-14424
Meteorological data, new series A monographs. Volume 6, no. 4: Modelization of heat fluxes at Earth ground with consideration of vegetation
[ETN-93-94169] p 723 N94-14546

ATMOSPHERIC CHEMISTRY
Gathering and exchange information on atmospheric chemistry and polluted atmospheres
[DE93-009940] p 705 N94-12869
Determination of spectroscopic properties of atmospheric molecules from high resolution vacuum ultraviolet cross section and wavelength measurements
[NASA-CR-194024] p 712 N94-13092
Description of the EURAD chemistry-transport model. Version 2 (CTM2)
[REPT-83] p 720 N94-13589
Modeling of the partitioning of reactive odd nitrogen in the lower stratosphere using aircraft measurements of NOy, NO, and other trace species
[NASA-CR-194305] p 714 N94-13707
Develop research plan for use of atlas data
[NASA-CR-194338] p 714 N94-13709

Submillimeter, millimeter, and microwave spectral line catalogue, revision 3
[NASA-CR-194501] p 602 N94-13813
Atomic hydrogen and nitrogen distributions from atmosphere explorer measurements
[NASA-CR-194336] p 714 N94-13825
Chemistry and transport in a multi-dimensional model
[NASA-CR-194425] p 716 N94-13969
The role of human activity and land use change in atmospheric chemistry and air quality
[DE93-011871] p 709 N94-14022
Synthesis inversion of atmospheric CO2 using the GISS tracer transport model
[CSIRO-TP-29] p 709 N94-14095
Program operations plan
[DE93-012765] p 710 N94-14182
Importance of sprays for long range transport of harmful substances in the troposphere
[MITT-81] p 711 N94-14723
Terrestrial environment (climatic) criteria guidelines for use in aerospace vehicle development, 1993 revision
[NASA-TM-4511] p 533 N94-14824

ATMOSPHERIC CIRCULATION
Development of a global backscatter model for NASA's laser atmospheric wind sounder
[NASA-CR-192581] p 718 N94-12957
On the vertical structure of seasonal, interannual and intraseasonal flows
[AD-A265346] p 719 N94-12992
An experimental regional scale climate simulation laboratory
[DE93-015935] p 719 N94-13119
Atmospheric soundings during the Washita 1992 campaign
[NASA-CR-194383] p 712 N94-13212
Modeling of biosphere-atmosphere interaction for forest and pastureland in the Amazon
[INPE-5454-TDI/496] p 707 N94-13330
Preliminary meteorological results for 1992 West Coast Scotland Experiment
[DE93-014677] p 720 N94-13404
Variations common to the interplanetary magnetic field, the zonal atmospheric circulation and the Earth's rotation
[COMMUNICATIONS-SER-B-157] p 837 N94-13504
Effects of surface thermal forcing on stratified flow past an isolated obstacle p 633 N94-13553
Numerical simulation and parameterization of orographic gravity waves p 713 N94-13647
Coherent Doppler lidar signal covariance including wind shear and wind turbulence
[NASA-CR-194492] p 721 N94-13723
Boundary layer structure over areas of heterogeneous heat fluxes
[DE93-007887] p 715 N94-13912
AMIP: Diagnostic subproject on the variability in the tropics: Synoptic to intraseasonal time scales
[DE93-009287] p 721 N94-13914
Atmospheric turbulence and diffusion research
[DE93-011842] p 718 N94-14425
Meteorological data, new series A monographs. Volume 6, no. 4: Modelization of heat fluxes at Earth ground with consideration of vegetation
[ETN-93-94169] p 723 N94-14546
Simulation of the present-day climate with the ECHAM model: Impact of model physics and resolution
[REPT-93] p 724 N94-14709

ATMOSPHERIC COMPOSITION
Project AIRSTREAM: Trace gas
[DE93-008849] p 706 N94-12904
Diagnostic studies of the HxOy-NxOy-O3 photochemical system using data from NASA GTE field expeditions
[NASA-CR-193672] p 706 N94-13170
Modeling of the partitioning of reactive odd nitrogen in the lower stratosphere using aircraft measurements of NOy, NO, and other trace species
[NASA-CR-194305] p 714 N94-13707
Measurement of HO2 and other trace gases in the stratosphere using a high resolution far-infrared spectrometer at 28 km
[NASA-CR-194175] p 714 N94-13816
Atomic hydrogen and nitrogen distributions from atmosphere explorer measurements
[NASA-CR-194336] p 714 N94-13825
Chemistry and transport in a multi-dimensional model
[NASA-CR-194425] p 716 N94-13969
Synthesis inversion of atmospheric CO2 using the GISS tracer transport model
[CSIRO-TP-29] p 709 N94-14095
The role of the dynamics for the deviation of the total ozone from the long-term mean at the edge of the polar vortex p 694 N94-14250

ATMOSPHERIC CORRECTION
Ionospheric calibration for single frequency altimeter measurements
[NASA-CR-194282] p 716 N94-14049
A method for estimation of partial cloud cover within a pixel and its effect p 697 N94-14269
Atmospheric correction for sea surface temperature by application of microwave dual-channel technique to VTIR data p 697 N94-14271

ATMOSPHERIC DENSITY
Novel Co:MgF2 lidar for aerosol profiler
[NASA-CR-191525] p 654 N94-13091
A rocket-borne lidar for studies of the middle atmosphere
[FFI/RAPPORT-92/7034] p 715 N94-13949

ATMOSPHERIC DIFFUSION
Atmospheric turbulence and diffusion research
[DE93-011842] p 718 N94-14425

ATMOSPHERIC EFFECTS
An examination of utility emissions contributions to elevated ozone concentrations in the Chicago area
[DE93-012852] p 708 N94-13495
Image processing and analysis of airborne POLDER data p 689 N94-14219
Solar radiation on Mars: Stationary photovoltaic array
[NASA-TM-106321] p 626 N94-14730

ATMOSPHERIC ELECTRICITY
The interplanetary origins and the main-phase development of moderate geomagnetic storms (1978 - 1979)
[INPE-5445-TDI/491] p 835 N94-13174

ATMOSPHERIC GENERAL CIRCULATION MODELS
An experimental regional scale climate simulation laboratory
[DE93-015935] p 719 N94-13119
Minimal modeling of the bimodality of extratropical atmospheric planetary waves p 713 N94-13622
Boundary layer structure over areas of heterogeneous heat fluxes
[DE93-007887] p 715 N94-13912
AMIP: Diagnostic subproject on the variability in the tropics: Synoptic to intraseasonal time scales
[DE93-009287] p 721 N94-13914
Regional climatology sensitivity studies
[DE93-010712] p 722 N94-14057
Circulation and rainfall climatology of a 10-year (1979 - 1988) integration with the Goddard Laboratory for atmospheres general circulation model
[NASA-TM-104591] p 723 N94-14074
Evolution of the lower planetary boundary layer over strongly contrasting surfaces
[DE93-010667] p 717 N94-14424
Simulation of the present-day climate with the ECHAM model: Impact of model physics and resolution
[REPT-93] p 724 N94-14709

ATMOSPHERIC HEATING
The role of clouds and oceans in global greenhouse warming
[DE93-016206] p 706 N94-13079

ATMOSPHERIC MODELS
Soil erosion rates caused by wind and saltating sand stresses in a wind tunnel
[DE93-009154] p 706 N94-12905
Diagnostic studies of the HxOy-NxOy-O3 photochemical system using data from NASA GTE field expeditions
[NASA-CR-193672] p 706 N94-13170
Cyclogenesis and cyclone over South America
[INPE-5400-TDI/479] p 719 N94-13175
Modeling of biosphere-atmosphere interaction for forest and pastureland in the Amazon
[INPE-5454-TDI/496] p 707 N94-13330
Description of the EURAD chemistry-transport model. Version 2 (CTM2)
[REPT-83] p 720 N94-13589
Climatic change due to land surface alterations
[INPE-5495-PRE/1786] p 721 N94-13672
Develop research plan for use of atlas data
[NASA-CR-194338] p 714 N94-13709
The role of human activity and land use change in atmospheric chemistry and air quality
[DE93-011871] p 709 N94-14022
Ionospheric calibration for single frequency altimeter measurements
[NASA-CR-194282] p 716 N94-14049
New evidences supported the Wei hypothesis about the formation of the Antarctic ozone hole p 694 N94-14253
Atmospheric acoustic modeling
[DE93-016727] p 718 N94-14518
Meteorological data, new series A monographs. Volume 6, no. 4: Modelization of heat fluxes at Earth ground with consideration of vegetation
[ETN-93-94169] p 723 N94-14546
Rain-rate data base development and rain-rate climate analysis p 614 N94-14664
Terrestrial environment (climatic) criteria guidelines for use in aerospace vehicle development, 1993 revision
[NASA-TM-4511] p 533 N94-14824

ATMOSPHERIC MOISTURE
Adaptation of humidity-cloud cover relations in the LAM
[KNMI-TR-144] p 722 N94-13992
Water-vapour, total water and rainrate from passive microwave satellite data over ocean
[DLR-FB-92-37] p 723 N94-14189
Remote sensing of low level cloud optical characteristics p 691 N94-14229
The effects of anthropogenic aerosols on optical thickness and particle size of clouds. Part 1: Retrieval algorithm p 691 N94-14230
The development and implementation of an interactive retrieval/analysis/forecast algorithm p 692 N94-14234
Atmospheric correction for sea surface temperature by application of microwave dual-channel technique to VTIR data p 697 N94-14271

ATMOSPHERIC PHYSICS
Activities of Institute for Aerospace Research, Flight Research Laboratory
[CTN-93-60832] p 850 N94-13519
Description of the EURAD chemistry-transport model. Version 2 (CTM2)
[REPT-83] p 720 N94-13589
Generic results of the space physics community survey
[NASA-CR-194538] p 818 N94-13984

ATMOSPHERIC PRESSURE
On the vertical structure of seasonal, interannual and intraseasonal flows
[AD-A265346] p 719 N94-12992

ATMOSPHERIC RADIATION
Are there atmospheric neutrino oscillations?
[DE93-015550] p 783 N94-13890
Evolution of the lower planetary boundary layer over strongly contrasting surfaces
[DE93-010667] p 717 N94-14424

ATMOSPHERIC SCATTERING
Development of a global backscatter model for NASA's laser atmospheric wind sounder
[NASA-CR-192581] p 718 N94-12957

ATMOSPHERIC SOUNDING
The application of VAS satellite imagery to thunderstorm forecasting at Cape Canaveral
[NASA-CR-193563] p 718 N94-12839
DMSP F11 SSM/T-2 calibration and validation
[AD-A265817] p 719 N94-12978
Novel Co:MgF2 lidar for aerosol profiler
[NASA-CR-191525] p 654 N94-13091
Atmospheric soundings during the Washita 1992 campaign
[NASA-CR-194383] p 712 N94-13212
Electrodynamics of the middle atmosphere: Superpressure balloon program
[NASA-CR-193671] p 712 N94-13293
Measurement of HO2 and other trace gases in the stratosphere using a high resolution far-infrared spectrometer at 28 km
[NASA-CR-194175] p 714 N94-13816
A rocket-borne lidar for studies of the middle atmosphere
[FFI/RAPPORT-92/7034] p 715 N94-13949
Asia-Pacific ISY Conference, volume 2
[NASDA-CM-199-VOL-2] p 688 N94-14209
Remote sensing of low level cloud optical characteristics p 691 N94-14229
The effects of anthropogenic aerosols on optical thickness and particle size of clouds. Part 1: Retrieval algorithm p 691 N94-14230
Climate products from NOAA operational satellites p 691 N94-14231
Earth radiation budget, cloud, and aerosol parameters derived from AVHRR and TOVS measurements p 691 N94-14233
The role of the dynamics for the deviation of the total ozone from the long-term mean at the edge of the polar vortex p 694 N94-14250
The European Arctic ozone experiment: An investigation of Northern Hemisphere ozone depletion p 694 N94-14251
Space-based activities: SAM 2 and SAGE 2 p 694 N94-14252
New evidences supported the Wei hypothesis about the formation of the Antarctic ozone hole p 694 N94-14253

ATMOSPHERIC TEMPERATURE
The role of clouds and oceans in global greenhouse warming
[DE93-016206] p 706 N94-13079
Atmospheric soundings during the Washita 1992 campaign
[NASA-CR-194383] p 712 N94-13212

Estimations of temperature and humidity of the canopy in Amazon Forest using microwave data from SMMR sensor of Nimbus-7 satellite
| INPE-5444-TDI/490 | p 720 N94-13614
Binary homogeneous nucleation: Temperature and relative humidity fluctuations and non-linearity
| DE93-007884 | p 709 N94-13911
Boundary layer structure over areas of heterogeneous heat fluxes
| DE93-007887 | p 715 N94-13912
Seasonal change of the land-surface temperature over Asian Continent derived from GAC data on NOAA-11 AVHRR p 691 N94-14232
The development and implementation of an interactive retrieval/analysis/forecast algorithm p 692 N94-14234

ATMOSPHERIC TURBULENCE
Coherent Doppler lidar signal covariance including wind shear and wind turbulence
| NASA-CR-194492 | p 721 N94-13723
Fluxes of heat and water vapour in a convective mixed layer during EFEDA
| DLR-FB-92-21 | p 716 N94-14132
Optical propagation through atmospheric turbulence. Model analysis of anisoplanatism and application to adaptive optics
| ONERA-P-1992-4 | p 716 N94-14192
Atmospheric turbulence and diffusion research
| DE93-011842 | p 718 N94-14425
Interactions among convection, magnetic fields and p-mode oscillations in the sun
| NASA-CR-194477 | p 845 N94-14479
Results from a study of scintillation behavior at 12, 20, and 30 GHz using the results from the Virginia Tech Olympus receivers p 613 N94-14659

ATMOSPHERICS
Integration of space and in-situ observations to study atmosphere, ocean and land processes
| NASA-CR-194495 | p 683 N94-14500

ATOMIC BEAMS
Novel oxygen atom source for material degradation studies
| NASA-CR-191323 | p 562 N94-13115

ATOMIC COLLISIONS
Calculation of electron-lithium scattering using the coupled-channel optical method
| DE93-623049 | p 806 N94-13226
Energetic neutral atoms: Imaging the magnetospheric ring current
| NASA-CR-194339 | p 715 N94-13826
Lawrence Berkeley Laboratory Chemical Sciences Division
| DE93-015260 | p 851 N94-14401

ATOMIC ENERGY LEVELS
To the theory of triplet pairing in Fermi-liquid model
| DE93-621770 | p 816 N94-12855

ATOMIC EXCITATIONS
Measurements of scattering processes in negative ion-atom collisions
| DE93-013863 | p 779 N94-12940
Measurement of H zero excited states produced by foil stripping of 800-MeV H(-) ions
| DE93-014391 | p 788 N94-13103
EBIT Trapping Program
| DE93-014422 | p 788 N94-13208
Free-exciton recombination in GaAs
| DE93-009843 | p 809 N94-14079
Anomalous low-temperature free-exciton transport in GaAs structures
| DE93-009845 | p 809 N94-14108
Coherent excitation of autoionizing resonances by electron impact
| DE93-018169 | p 785 N94-14419
Selective excitation, relaxation, and energy channeling in molecular systems
| DE93-018819 | p 785 N94-14420
High-order harmonic generation with short-pulse lasers
| DE93-016532 | p 659 N94-14594

ATOMIC INTERACTIONS
Low energy neutral atom imaging techniques
| DE93-012744 | p 779 N94-12950

ATOMIC PHYSICS
Highly charged ions in hot, dense plasmas
| DE93-013348 | p 795 N94-12995
Indirect processes in electron impact ionization of Kr(24+) and Kr(25+)
| DE93-014129 | p 784 N94-14140
Atomic research
| NASA-CR-193843 | p 788 N94-14905

ATOMIC SPECTRA
The International Colloquium on Atomic Spectra and Oscillator Strengths for Astrophysical and Laboratory Plasmas
| NASA-TM-109255 | p 849 N94-13376
Investigation of an alternating current plasma as an element selective atomic emission detector for high-resolution capillary gas chromatography and as a source for atomic absorption and atomic emission spectrometry p 798 N94-13678

ATOMIC STRUCTURE
Structure stability and spectroscopy of metal clusters
| DE93-016142 | p 567 N94-12836
Determination of channeling perspectives for complex crystal structures
| DE93-012872 | p 805 N94-13009
Grain-boundary electronic states by multiple-scattering theory
| DE93-013198 | p 805 N94-13010
Automated crack identification for cement paste
| AD-A265753 | p 665 N94-13042
Atomic structure of the 310 twin in niobium: Theoretical predictions and comparison with experimental observation
| DE93-013421 | p 806 N94-13136
Electronic structure and phase stability properties in ternary substitutional alloys
| DE93-013848 | p 569 N94-13137
EBIT Trapping Program
| DE93-014422 | p 788 N94-13208
First-principles studies of phase stability and the structural and dynamical properties of hydrogen-metal systems
| DE93-016129 | p 570 N94-13374
Empirical tight-binding parameters for solid C(sub 60)
| DE93-623061 | p 807 N94-13510
Resonant x ray Raman scattering from atoms and molecules
| DE93-015158 | p 784 N94-13896
Spin polarized photoemission studies of interfacial and thin film magnetism
| DE93-014326 | p 580 N94-14142
Theory of the electronic and structural properties of solid state oxides
| DE93-016051 | p 811 N94-14296
Effects of growth conditions and substrate orientation on the properties of InSb
| DE93-013766 | p 812 N94-14344
Theory, modeling, and simulation
| DE93-015607 | p 755 N94-14571
Renormalized band structure of CuO2 layers in superconducting compounds: A mean field approach
| PREPRINT-730 | p 815 N94-14720

ATOMIZERS
A computer model for liquid jet atomization in rocket thrust chambers
| NASA-CR-194194 | p 627 N94-12803
Gas atomized Er3Ni powder for cryocooler applications
| DE93-011564 | p 568 N94-13000
Simulation of preburner sprays, volume 1
| NASA-CR-193844 | p 647 N94-14906

ATTENUATION COEFFICIENTS
The optical constants and spectral specular reflectivity of Highly Oriented Pyrolytic Graphite (HOPG)
| DE93-011894 | p 790 N94-12865
Quantitative mapping of pore fraction variations in silicon nitride using an ultrasonic contact scan technique
| NASA-TP-3377 | p 665 N94-13056

ATTITUDE (INCLINATION)
Attitude determination of stratospheric balloons using Kalman filters
| INPE-5498-TDI/513 | p 649 N94-13366
The effect of crystal tilt on high resolution micrographs of small metal particles
| DE93-013915 | p 574 N94-14795

ATTITUDE CONTROL
A superconducting large-angle magnetic suspension
| NASA-CR-189735 | p 596 N94-13141
Investigation of the effects of bandwidth and time delay on helicopter roll-axis handling qualities p 522 N94-13300
Handling qualities effects of display latency p 517 N94-13316
Dynamic Forms. Part 1: Functions
| NASA-TP-3397 | p 596 N94-13790
Self-tuning control techniques for multivariable systems
| INPE-5449-TDI/495 | p 765 N94-14084
Wavefront sensing, control, and pointing p 546 N94-14833

ATTITUDE STABILITY
Attitude determination of stratospheric balloons using Kalman filters
| INPE-5498-TDI/513 | p 649 N94-13366

AUDIO FREQUENCIES
Analysis of fundamental frequency pattern in speech p 618 N94-13440

AUDIO SIGNALS
Digital sound: The selection of critical programme material and preparation of recordings for CCIR tests on low bit-rate codecs
| BBC-RD-1993/1 | p 598 N94-12925
Digital sound: Subjective tests on commentary-quality codecs
| BBC-RD-1993/2 | p 598 N94-12926

AUGER SPECTROSCOPY
Analysis of samples of reflector materials which are multicoated and metal samples with oxide coatings which have been exposed the space environment in LDEF testing
| NASA-CR-193647 | p 575 N94-12789
Surface science instrumentation for the study of important catalytic and electrochemical interfaces
| DE93-015068 | p 563 N94-13413

AURORAL ZONES
The role of ionospheric plasma in the magnetosphere
| NASA-CR-194404 | p 716 N94-13967

AUSTENITIC STAINLESS STEELS
Materials compatibility of hydride storage materials with austenitic stainless steels
| DE93-013688 | p 703 N94-13691

AUTOIONIZATION
Indirect processes in electron impact ionization of Kr(24+) and Kr(25+)
| DE93-014129 | p 784 N94-14140

AUTOMATA THEORY
Self organized criticality
| DE93-013182 | p 773 N94-14320

AUTOMATIC CONTROL
Cognitive engineering in aerospace application: Pilot interaction with cockpit automation
| NASA-CR-177617 | p 510 N94-13247
Robot programming, natural computation and conceptual graphs
| ITN-93-85193 | p 748 N94-13539
Communications and control for electric power systems
| NASA-CR-194503 | p 622 N94-13811
Development of an automated film-reading system for ballistic ranges
| NASA-CR-194398 | p 650 N94-13815
Activities of Institute for Information Technology
| CNR-35024 | p 824 N94-14069
A high-precision direct current measuring device over a kiloampere range
| DE93-626409 | p 627 N94-14885

AUTOMATIC FLIGHT CONTROL
Design and pilot evaluation of the RAH-66 Comanche Core AFCS p 525 N94-13321

AUTOMATIC PILOTS
Knowledge-based processing for aircraft flight control
| NASA-CR-194074 | p 526 N94-13469

AUTOMATIC TEST EQUIPMENT
Design automation tools for testable VLSI circuits
| ISBN-0-315-61461-7 | p 621 N94-13333

AUTOMOBILE FUELS
Biofuels for transportation: The road from research to the marketplace
| DE93-000091 | p 585 N94-14454

AUTOMOBILES
Dynamics and design of nonholonomic robotic mechanical systems
| ISBN-0-315-72009-3 | p 662 N94-13597

AUTONOMOUS NAVIGATION
Evaluation of infrared sensors for autonomous landing guidance
| AD-A266450 | p 513 N94-13703

AUTONOMY
Reconsideration of the autonomous view of language p 618 N94-13441
Thermal Expert System (TEXSYS): Systems autonomy demonstration project, volume 2. Results
| NASA-TM-102877 | p 538 N94-13989

AUTORADIOGRAPHY
The evolution of energy-transducing systems: Studies with archaebacteria
| NASA-CR-194130 | p 728 N94-13562

AUTOREGRESSIVE PROCESSES
Signal design for data communication through rapidly varying linear channels
| ITN-93-85195 | p 601 N94-13567

AUXILIARY PROPULSION
Electric propulsion system technology
| NASA-CR-194099 | p 549 N94-13068

AVALANCHE DIODES
Design and optimization of high voltage lateral DMOS devices using RESURF technology
| LAAS-92511 | p 626 N94-14711

AVALANCHES
High counting rate resistive-plate chamber
| DE93-014928 | p 651 N94-14452

AVIATION METEOROLOGY
Flight crew interface aspects of forward-looking airborne windshear detection systems
[NASA-CR-191437] p 516 N94-12829
AVIATION PSYCHOLOGY
Work/rest schedules and performance of F/A-18 aviators during Fleet Exercise 1992
[AD-A265826] p 735 N94-12982
AVIONICS
Future developments of the NLR research flight simulator
[NLR-TP-92143-U] p 528 N94-13498
High flux heat exchanger
[AD-A266341] p 636 N94-13730
AWARDS
Measuring quality progress p 666 N94-13154
AXES OF ROTATION
Cold dark matter halos p 838 N94-13649
AXIAL FLOW TURBINES
Numerical simulation of steady three-dimensional flows in axial turbomachinery bladerows p 634 N94-13630
AXISYMMETRIC BODIES
An 8-node axisymmetric acoustic finite element for non-axisymmetric fluid-structure interaction analysis
[FFA-TN-1993-03] p 673 N94-13689
AXISYMMETRIC FLOW
A small-scale turbulence model p 643 N94-14746

B

BACKSCATTERING
Crystallographic phase identification in the scanning electron microscope: Backscattered electron Kikuchi patterns
[DE93-011574] p 804 N94-12813
Development of a global backscatter model for NASA's laser atmospheric wind sounder
[NASA-CR-192581] p 718 N94-12957
Determination of channeling perspectives for complex crystal structures
[DE93-012872] p 805 N94-13009
Automated crack identification for cement paste
[AD-A265753] p 665 N94-13042
Measurement of the spin of a particle using undulator radiation
[DE93-014334] p 780 N94-13149
Radar imaging of sub-mesoscale ocean phenomena
[AD-A266339] p 725 N94-13581
Brillouin scattering from fluctuations produced by stimulated Raman scattering
[DE93-016531] p 792 N94-14438
BACKWARD FACING STEPS
Development of a recursion RNG-based turbulence model
[NASA-CR-191511] p 636 N94-13718
Least-squares finite element solutions for three-dimensional backward-facing step flow
[NASA-TM-106353] p 770 N94-14407
BACTERIA
Dynamics of adaptive structures: Design through simulations
[NASA-CR-193724] p 540 N94-13112
Gordon Research Conference on Chronobiology, 1991
[AD-A266354] p 728 N94-13698
Characterization of Spirulina biomass for CELSS diet potential
[NASA-CR-194123] p 729 N94-14097
The surface-located YopN protein is involved in calcium signal transduction in Yersinia pseudotuberculosis
[FOA-B-40416-4.4] p 729 N94-14128
Analysis of the V antigen lcrGVH-yopBD operon of Yersinia pseudotuberculosis: Evidence for a regulatory role of LcrH and LcrV
[FOA-B-40417-4.4] p 729 N94-14129
Organic Geochemical and tectonic evolution of the Midcontinent Rift system
[DE93-015093] p 717 N94-14338
The first steps of chlorophyll synthesis: RNA involvement and regulation
[DE93-014398] p 730 N94-14509
Chaos and microbial systems
[DE93-016814] p 730 N94-14596
BACTERIOLOGY
Analysis of the V antigen lcrGVH-yopBD operon of Yersinia pseudotuberculosis: Evidence for a regulatory role of LcrH and LcrV
[FOA-B-40417-4.4] p 729 N94-14129
BAILOUT
STS-29 post-insertion/deorbit prep and crew bailout
[NASA-TM-109299] p 535 N94-13641
BAKING
Study of novel conductive paints for solar cell electromagnetic fields
[DE93-015088] p 581 N94-14337
BALANCE
Rolling moment control in the NAL 10 cm x 10 cm magnetic suspension and balance system
[NAL-TR-1164] p 526 N94-13347
BALL BEARINGS
Dry film lubricant evaluation
[DE93-013114] p 578 N94-13118
Surface analysis of bearings
[AD-A266800] p 661 N94-13122
BALLISTIC RANGES
Development of an automated film-reading system for ballistic ranges
[NASA-CR-194398] p 650 N94-13815
Advanced ballistic range technology
[NASA-CR-194396] p 532 N94-14068
Aerodynamic and aerothermal facilities 2. Part 1: Short-duration, high-enthalpy facilities p 506 N94-14159
Advanced ballistic range technology
[NASA-CR-194530] p 533 N94-14540
BALLISTICS
Electronic states in systems of reduced dimensionality
[DE93-014440] p 815 N94-14739
BALLOON FLIGHT
Measurement of HO2 and other trace gases in the stratosphere using a high resolution far-infrared spectrometer at 28 km
[NASA-CR-194175] p 714 N94-13816
BALLOON SOUNDING
Electrodynamics of the middle atmosphere: Superpressure balloon program
[NASA-CR-193671] p 712 N94-13293
Measurement of HO2 and other trace gases in the stratosphere using a high resolution far-infrared spectrometer at 28 km
[NASA-CR-194175] p 714 N94-13816
BALLOONING MODES
On MHD mode equations in toroidal plasmas
[PPL-139] p 800 N94-13877
Stability and confinement properties of small-aspect-ratio tokamak
[INPE-5463-PRE/1771] p 801 N94-14024
BALMER SERIES
Was 49: Mirror for a hidden Seyfert 1 galaxy
[NASA-CR-194537] p 840 N94-14685
BANACH SPACE
Contributions to numerical solution of Navier-Stokes equations in two and three dimensional flows
[ETN-93-94395] p 647 N94-14816
On a convergence of iterative Newton's scheme
[DE93-626604] p 772 N94-14886
BAND STRUCTURE OF SOLIDS
Structural and electronic studies of a-SiGe:H alloys
[DE93-010021] p 809 N94-14085
A sum-rule of luminescence spectrum
[ITN-93-85223] p 814 N94-14559
Renormalized band structure of CuO2 layers in superconducting compounds: A mean field approach
[PREPRINT-730] p 815 N94-14720
BANDPASS FILTERS
Insertion loss and noise-temperature contribution of high-temperature superconducting bandpass filters centered at 2.3 and 8.45 GHz p 608 N94-14376
BANDWIDTH
Investigation of the effects of bandwidth and time delay on helicopter roll-axis handling qualities p 522 N94-13300
Measurements of edge fluctuations by phase contrast imaging on DIII-D
[DE93-014018] p 802 N94-14579
H2S data reduction
[NASA-CR-193389] p 617 N94-14743
BANGLADESH
Application of satellite remote sensing technology in disaster mitigation: A case study of Bangladesh p 692 N94-14238
BARIUM FLUORIDES
Barium fluoride research and development at Lawrence Livermore National Laboratory
[DE93-014682] p 807 N94-13405
BARIUM OXIDES
Room temperature degradation of YBa2Cu3O(7-x) superconductors in varying relative humidity environments
[NASA-TP-3368] p 813 N94-14409
BARRELS (CONTAINERS)
Development and application of the automated Monte Carlo biasing procedure in SAS4
[DE93-015205] p 774 N94-14334
BARRIER LAYERS
Soil erosion rates caused by wind and saltating sand stresses in a wind tunnel
[DE93-009154] p 706 N94-12905
Studies on equatorial shock formation during plasmaspheric refilling
[NASA-CR-194392] p 715 N94-13954
BARYON RESONANCE
Dynamics of pion-nucleus systems
[DE93-014449] p 785 N94-14468
BARYONS
Early baryon and meson spectroscopy culminating in the discovery of the Omega minus SU(3) and quarks
[DE93-014321] p 787 N94-14580
BASE FLOW
A computational study of the base region flow field for the M865 projectile
[ARL-TR-109] p 504 N94-13795
BAYES THEOREM
Bayesian estimation of motion fields from image sequences
[ISBN-0-315-57212-4] p 772 N94-13540
Synthesis inversion of atmospheric CO2 using the GISS tracer transport model
[CSIRO-TP-29] p 709 N94-14095
Quantum Monte Carlo by message passing
[DE93-012645] p 760 N94-14177
BCS THEORY
Effect of spontaneous decay of superconductor quasiparticles in the tunneling density of states
[DE93-012681] p 811 N94-14339
BEAM CURRENTS
Low-current traveling wave tube for use in the microwave power module
[NASA-TP-3344] p 620 N94-13110
BEAM INJECTION
Wake-field and space charge effects on high brightness beams calculations and measured results for the laser driven photoelectrons at BNL-ATF
[DE93-015787] p 659 N94-14572
BEAM NEUTRALIZATION
Physics of gas breakdown for ion beam transport in gas
[DE93-015646] p 801 N94-14349
BEAM WAVEGUIDES
Predicted performance of a dc beam driven FEM oscillator designed for fusion applications at 200-250 GHz
[DE93-013414] p 655 N94-13145
HRMS sky survey wideband feed system design for DSS 24 beam waveguide antenna p 611 N94-14397
BEAMS (RADIATION)
A new formulation of longitudinal coherent instabilities
[DE93-014288] p 789 N94-13220
Laser beam control and diagnostic systems for the copper-pumped dye laser system at Lawrence Livermore National Laboratory
[DE93-016529] p 658 N94-14437
BEAMS (SUPPORTS)
Helical truss beam development for large space structure p 530 N94-13276
Some frequency and damping measurements of laminated beryllium beams
[DE93-015909] p 676 N94-14530
BEARINGS
Canadian Target Assembly (CTA) to Airborne Support Equipment (ASE) vibration test report
[IME-AMT-TR-001] p 663 N94-14195
BED REST
Gender differences in endocrine responses to posture and 7 days of 6 deg head down bed rest
[NASA-TM-103991] p 731 N94-12972
Clinical physiology of bed rest
[NASA-TM-104010] p 727 N94-13447
Countermeasure for reducing post-flight orthostatic intolerance: Lower Body Negative Pressure (LBNP) experiment E140 p 594 N94-13772
BEDS (PROCESS ENGINEERING)
Materials compatibility of hydride storage materials with austenitic stainless steels
[DE93-013688] p 703 N94-13691
BEHAVIOR
Selection of behavioral tasks and development of software for evaluation of rhesus monkey behavior during spaceflight
[NASA-CR-194176] p 728 N94-13865
Ethology in space, a unique opportunity for behavioural science
[ESA-STM-246] p 731 N94-14862
BELGIUM
Potential evapotranspiration in Belgium: Spatial and temporal variability
[PUBL-SER-A-130] p 686 N94-13994
BELL AIRCRAFT
Flight service evaluation of composite components on the Bell helicopter model 206L
[NASA-CR-191499] p 555 N94-13267
ADS-33C related handling qualities research performed using the NRC Bell 205 airborne simulator p 521 N94-13295

BEND TESTS
A benchmark bending test of a thick specimen, Part 1: Experiments
[ARL-RR-6-PT-1] p 670 N94-12927
A benchmark bending test of a thick specimen. Part 2: Surface displacement measurements
[ARL-RR-6-PT-2] p 670 N94-12928
Measuring methods for CFRP laminates' bending and torsion rigidities characteristics p 529 N94-13272
Testing and analysis of curved frame specimens made from a Long Discontinuous Fiber (LDF) material
[NASA-TM-109014] p 557 N94-13711
BENDING FATIGUE
Thermal gradient-induced deflection of a thick-walled cylinder with bending residual stresses
[AD-A266347] p 673 N94-13777
BENDING THEORY
Elastic-plastic mixed-iterative finite element analysis: Implementation and performance assessment
[NASA-TM-106164] p 675 N94-13919
BERYLLIUM
Double semi-leptonic charm decay in HELIOS-I 450 GeV/c p-Be data
[DE93-013493] p 781 N94-13348
Some frequency and damping measurements of laminated beryllium beams
[DE93-015909] p 676 N94-14530
BERYLLIUM COMPOUNDS
Muon spin relaxation studies of heavy fermion superconductors
[DE93-014576] p 815 N94-14773
BETA FACTOR
Stability and confinement properties of small-aspect-ratio tokamak
[INPE-5463-PRE/1771] p 801 N94-14024
BETA PARTICLES
Beta/gamma test problems for ITS
[DE93-013522] p 781 N94-13349
The beta(+) decay and cosmic-ray half-life of Mn-54
[DE93-013913] p 848 N94-13695
Charge-exchange reactions and weak interaction rates for Type 2 supernovae
[DE93-015104] p 783 N94-13893
Angular correlations in neutron beta decay
[DE93-014349] p 785 N94-14466
BETAINES
Experimental and theoretical study of inhomogeneous electron transfer in betaine: Comparisons of measured and predicted spectral dynamics
[AD-A265703] p 780 N94-13051
BETHE-SALPETER EQUATION
Relativistic proton-nucleus scattering and one-boson-exchange models p 786 N94-14550
BIAS
Performance evaluation of the honeywell GG1308 miniature ring laser gyroscope
[AD-A266694] p 653 N94-14782
BIBLIOGRAPHIES
Bibliography of urban climate in tropical/subtropical areas, 1981-1991
[WCASP-25] p 718 N94-12918
ARTI Refrigerant Database
[DE93-014774] p 595 N94-13021
Publications of the Jet Propulsion Laboratory: 1990 and 1991
[NASA-CR-193287] p 823 N94-13461
Flammability of clothing, volume 2
[DSIS-93-00036-VOL-2] p 564 N94-13819
Large space structures and systems in the space station era: A bibliography with indexes (supplement 05)
[NASA-SP-7085(05)] p 543 N94-14411
CarbBank: A structural and bibliographic database for complex carbohydrates
[DE93-015582] p 827 N94-14803
BIDIRECTIONAL REFLECTANCE
Smooth transitions between bump rendering algorithms
[DE93-012504] p 742 N94-12883
Spectral reflectance of soils from Sao Paulo State
[INPE-5424-PRP/172] p 684 N94-13377
Operational test of the airborne data acquisition system: SADA, the Bara Bonita experiment
[INPE-5451-NTC/305] p 685 N94-13610
BIG BANG COSMOLOGY
Inflation after COBE: Lectures on inflationary cosmology
[DE93-014008] p 834 N94-13096
BIMETALS
Anchoring strategies for bimetallic species in zeolites
[DE93-015622] p 567 N94-12834
Theory of the negative magnetoresistance in magnetic metallic multilayers
[DE93-013912] p 776 N94-14584
BINARY ALLOYS
Electronic structure and phase stability properties in ternary substitutional alloys
[DE93-013848] p 569 N94-13137
BINARY DATA
SCORE user's manual
[DE93-015987] p 822 N94-13121
Parametric binary dissection
[NASA-CR-191496] p 762 N94-13184
Obstacle detection by recognizing binary expansion patterns
[NASA-CR-194415] p 514 N94-14495
How to read a phase equilibrium diagram for high-temperature ceramics material as main object
[DE93-512333] p 582 N94-14513
Is K3C60 a line phase?
[DE93-016700] p 813 N94-14517
Determining neural network connectivity using evolutionary programming
[AD-A266853] p 766 N94-14882
BINARY STARS
High time resolution studies of binary x ray pulsars
[NASA-CR-194395] p 832 N94-13894
BINARY SYSTEMS (MATERIALS)
Study of multicomponent diffusion and transport phenomena
[DE93-015095] p 804 N94-13005
Crystal growth of ZnSe and related ternary compound semiconductors by physical vapor transport
[NASA-CR-193834] p 807 N94-13444
Diffusion in liquid state and solidification of binary system (M-7) p 587 N94-13739
Is K3C60 a line phase?
[DE93-016700] p 813 N94-14517
The Lindemann criterion of melting for pure and mixed ionic crystals
[ITN-93-85210] p 814 N94-14554
BINOMIALS
Computational problems with the binomial failure rate model and incomplete common cause failure reliability data
[DE93-014346] p 669 N94-14143
BIOCHEMISTRY
Role of Ca(++)/calmodulin in the regulation of microtubules in higher plants
[DE93-015885] p 727 N94-12835
BIOCONVERSION
Characterization of Spirulina biomass for CELSS diet potential
[NASA-CR-194123] p 729 N94-14097
Biofuels for transportation: The road from research to the marketplace
[DE93-000091] p 585 N94-14454
BIODYNAMICS
Flow limitation and flutter in membrane walled collapsible tubes: A model for expiratory wheezing
[ISBN-0-315-73875-8] p 635 N94-13662
BIOFEEDBACK
Autogenic feedback training experiment: A preventative method for space motion sickness p 595 N94-13774
Psychophysiological investigations of the biomedical problems of manned spaceflight
[NASA-CR-194107] p 732 N94-13782
BIOGEOCHEMISTRY
Organic Geochemical and tectonic evolution of the Midcontinent Rift system
[DE93-015093] p 717 N94-14338
BIOLOGICAL EFFECTS
Cellular track model for study of heavy ion beams
[NASA-TP-3351] p 732 N94-13714
Study on the biological effect of cosmic radiation and the development of radiation protection technology (L-11) p 593 N94-13768
Amphibian fertilization and development in microgravity p 594 N94-13770
Aerospace medicine and biology: A continuing bibliography with indexes (supplement 379)
[NASA-SP-7011(379)] p 733 N94-14412
Pattern and Process in Landscape Ecology: Eighth Annual US Landscape Ecology Symposium
[DE93-014032] p 711 N94-14859
BIOLOGICAL EVOLUTION
Evolution of catalytic RNA in the laboratory
[NASA-CR-194124] p 727 N94-13210
BIOLOGICAL MODELS (MATHEMATICS)
Flow limitation and flutter in membrane walled collapsible tubes: A model for expiratory wheezing
[ISBN-0-315-73875-8] p 635 N94-13662
BIOMASS
Biomass production chamber air analysis of wheat study (BWT931)
[NASA-CR-194092] p 737 N94-13712
Validated environmental and physiological data from the CELSS Breadboard Projects Biomass Production Chamber. BWT931 (Wheat cv. Yecora Rojo)
[NASA-TM-109272] p 738 N94-13979
Biodiesel/aquatic species project report, FY 1992
[DE93-010024] p 709 N94-14087
Status and future opportunities for conversion of synthesis gas to liquid energy fuels
[DE93-010025] p 584 N94-14089
Biofuels for transportation: The road from research to the marketplace
[DE93-000091] p 585 N94-14454
BIOMASS ENERGY PRODUCTION
The 1992 JSEE/JWEA Joint Conference
[DE93-793955] p 700 N94-12822
Characterization of Spirulina biomass for CELSS diet potential
[NASA-CR-194123] p 729 N94-14097
BIOMEDICAL DATA
Circadian rhythms during simulation of the D2-spaceflight
[DLR-FB-92-27] p 733 N94-14043
BIOPHYSICS
Effects of radiobiological uncertainty on vehicle and habitat shield design for missions to the moon and Mars
[NASA-TP-3312] p 646 N94-12875
BIOSPHERE
Modeling of biosphere-atmosphere interaction for forest and pastureland in the Amazon
[INPE-5454-TDI/496] p 707 N94-13330
Meteorological data, new series A monographs. Volume 6, no. 4: Modelization of heat fluxes at Earth ground with consideration of vegetation
[ETN-93-94169] p 723 N94-14546
BIOSYNTHESIS
Evolution of catalytic RNA in the laboratory
[NASA-CR-194124] p 727 N94-13210
The first steps of chlorophyll synthesis: RNA involvement and regulation
[DE93-014398] p 730 N94-14509
Biomimetic methane oxidation
[DE93-013196] p 705 N94-14510
BIOTECHNOLOGY
Catalysis and biocatalysis program
[NASA-CR-194105] p 727 N94-12793
Monoclonal antibodies directed against surface molecules of multicell spheroids
[NASA-CR-193560] p 727 N94-12795
Biomimetic methane oxidation
[DE93-013196] p 705 N94-14510
BIPOLAR TRANSISTORS
Electrical noise in microwave field effect and bipolar transistors
[LAAS-93042] p 616 N94-14717
BIRDS
Birds of Wallops Island, Virginia, 1970 - 1992
[NASA-TM-104589] p 850 N94-13923
BIREFRINGENCE
Poling of thin polymer films in electro optic applications
[AD-A266562] p 579 N94-13584
BISPHENOLS
Unexpectedly rapid hydrosilation polymerization of the diallyl derivative of bisphenol A and 2,6-diallylphenol
[AD-A265832] p 577 N94-12986
BLACK BODY RADIATION
Coupled thermal response of objects and participating media in fires and large combustion systems
[DE93-012848] p 561 N94-12819
Moebius inverse problem for distorted black holes
[DE93-622899] p 834 N94-12880
A calibration procedure for radiation budget radiometers and its influence on interpretation of measured values
[MITT-82] p 651 N94-14149
BLACK HOLES (ASTRONOMY)
A new limit on the rate-density of evaporating black holes
[DE93-012716] p 834 N94-12815
Moebius inverse problem for distorted black holes
[DE93-622899] p 834 N94-12880
GRO: Black hole models for gamma ray bursts
[NASA-CR-193244] p 829 N94-13178
The continuum emission of active galactic nuclei
[ITN-93-85208] p 847 N94-13232
The soft x ray transient Cen X-4 in quiescence
[NASA-CR-194033] p 833 N94-14406
The first data from the MACHO experiment
[DE93-014423] p 840 N94-14467
BLADE TIPS
Numerical simulation of steady three-dimensional flows in axial turbomachinery bladerows p 634 N94-13630
BLADES
On curve veering and flutter of rotating blades
[NASA-TM-106282] p 670 N94-12872
BLASIUS FLOW
The transient behavior of a boundary layer exposed to uniform suction
[ITN-93-85205] p 630 N94-13197

BLINDS
Simulating the daylight performance of fenestration systems and spaces of arbitrary complexity: The IDC method
[DE93-015177] p 704 N94-14333
BLOCKING
The effects of evaluation and production blocking on the performance of brainstorming groups
[AD-A265495] p 734 N94-12929
BLOOD PLASMA
Phase-shifting effect of light and exercise on the human circadian clock
[AD-A265732] p 732 N94-13038
BLOWING
Experimental investigation of the effects of blowing ratio parameter on heat transfer to a film-cooled flat plate
[AD-A266599] p 636 N94-13780
An experimental study on the effect of die geometry on swell and sag in the parison extrusion stage
[IMI-93RT-42400-1476-G] p 597 N94-14070
BLUE GREEN ALGAE
Characterization of Spirulina biomass for CELSS diet potential
[NASA-CR-194123] p 729 N94-14097
BLUNT BODIES
Aerodynamics of a sphere and an oblate spheroid for Mach numbers from 0.6 to 10.5 including some effects of test conditions
[NASA-TM-109016] p 500 N94-13172
BLURRING
Depths from focusing and defocusing
[AD-A266644] p 735 N94-14797
BODIES OF REVOLUTION
Computer code for scattering from impedance bodies of revolution. Part 3: Surface impedance with s and phi variation. Analytical and numerical results
[NASA-CR-193396] p 599 N94-13264
BODY CENTERED CUBIC LATTICES
Monte Carlo simulation of the OCP freezing transition
[DE93-013039] p 811 N94-14313
Shock compression and quasielastic release in tantalum
[DE93-014566] p 811 N94-14329
A microstructural approach to fatigue crack processes in poly crystalline BCC materials
[DE93-016666] p 812 N94-14354
Statics and kinetics of phase transformations in bcc Fe-Cr
[DE93-013839] p 574 N94-14793
BODY KINEMATICS
Proceedings of the Fifth NASA/NSF/DOD Workshop on Aerospace Computational Control
[NASA-CR-194515] p 677 N94-14618
Geometric stiffening in multibody dynamics formulations p 677 N94-14619
Stress stiffening and approximate equations in flexible multibody dynamics p 677 N94-14620
A component modes projection and assembly model reduction methodology for articulated, multi-flexible body structures p 677 N94-14622
Nonrecursive formulations of multibody dynamics and concurrent multiprocessing p 679 N94-14632
Parallel O(log n) algorithms for open- and closed-chain rigid multibody systems based on a new mass matrix factorization technique p 679 N94-14636
Parallel methods for dynamic simulation of multiple manipulator systems p 680 N94-14637
Space Station Common Berthing Mechanism, a multi-body simulation application p 544 N94-14640
Computational Control Workstation: Users' perspectives p 681 N94-14648
BODY TEMPERATURE
Phase-shifting effect of light and exercise on the human circadian clock
[AD-A265732] p 732 N94-13038
BODY-WING AND TAIL CONFIGURATIONS
VSAERO analysis of a Piper Cub aircraft p 516 N94-14616
BODY-WING CONFIGURATIONS
Improved aeroprediction code. Part 1: Summary of new methods and comparison with experiment
[AD-A266015] p 500 N94-12989
A robust quasi-simultaneous interaction method for a full potential flow with a boundary layer with application to wing/body configurations
[NLR-TP-91397-U] p 503 N94-13531
BOILERS
Fatigue design curves for 6061-T6 aluminum
[DE93-011849] p 571 N94-14021
BOLOMETERS
Direct submillimeter absorptivity measurements on epitaxial Ba(1-x)K(x)BiO3 films at 2K
[DE93-013904] p 815 N94-14699
BOLTZMANN TRANSPORT EQUATION
Theory of the negative magnetoresistance in magnetic metallic multilayers
[DE93-013912] p 776 N94-14584
BOMBER AIRCRAFT
A model for fuel fire duration and application to the B-1B bomber
[DE93-013000] p 512 N94-14292
BONDING
Office of Naval Research/DARPA publications: Composite materials with improved properties in compression
[AD-A265509] p 560 N94-14794
BONE DEMINERALIZATION
Calcitonin control of calcium metabolism during weightlessness
[NASA-CR-193622] p 731 N94-12960
Effect of low gravity on calcium metabolism and bone formation (L-7) p 593 N94-13765
Bone culture research p 595 N94-13773
BONE MARROW
Magnetic resonance imaging after exposure to microgravity p 594 N94-13771
BONES
Bone culture research p 595 N94-13773
BOOSTER ROCKET ENGINES
The conceptual study on future space transportation systems. Part A: Conceptual study of flyback booster
[NASDA-CNT-930013] p 536 N94-14099
BOREHOLES
INGDB-90. The International Neutron Nuclear Data Base for geophysics applications
[DE93-624095] p 827 N94-14880
BORESIGHT ERROR
Electromagnetic wave test p 508 N94-14173
BORON
Deposition of crystalline boron thick layers from gas phase
[DE93-620499] p 576 N94-12867
BORON ISOTOPES
Nuclear fusion of protons with ions of boron
[DE93-014284] p 781 N94-13219
BOROSILICATE GLASS
Canonical correlation of waste glass compositions and durability, including pH
[DE93-012754] p 578 N94-13493
Relationship between borosilicate glass composition, structure, and durability test response (SRS)
[DE93-013578] p 581 N94-14343
Modeling surface area to volume effects on borosilicate glass dissolution
[DE93-011891] p 581 N94-14432
BOSONS
Medium energy hadron-nucleus scattering in the 1/N expansion formalism
[DE93-622957] p 778 N94-12848
Radiative corrections in the strongly interacting limit of the standard electroweak model
[DE93-013906] p 780 N94-13018
Effects of additional isoscalar vector bosons in e(sup +)e)(sup -)(yields)ff-bar processes at the TRISTAN and LEP energies
[DE93-621451] p 783 N94-13506
Relativistic proton-nucleus scattering and one-boson-exchange models p 786 N94-14550
Characteristics of a high energy muon(+)muon(-) collider based on electro-production of muons
[DE93-017154] p 790 N94-14893
BOUNDARIES
Spatial and temporal variability of precipitation and chemistry: Case studies from the frontal boundary study
[DE93-007883] p 708 N94-13910
How to read a phase equilibrium diagram for high-temperature ceramics material as main object
[DE93-512333] p 582 N94-14513
BOUNDARY CONDITIONS
On the motion through a viscous fluid of a spherical particle touching a plane wall: Slip boundary conditions
[DE93-012540] p 628 N94-12961
Open boundary conditions for incompletely parabolic systems
[FFI/RAPPORT-92/7029] p 770 N94-13971
Boundary stability under nonequilibrium conditions
[DE93-016259] p 809 N94-13980
Domain connectivity among systems of overset grids
[NASA-CR-193390] p 508 N94-14326
Multigrid solution of internal flows using unstructured solution adaptive meshes
[NASA-CR-194233] p 638 N94-14356
Evolution of the lower planetary boundary layer over strongly contrasting surfaces
[DE93-010667] p 717 N94-14424
Multi-dimensional high order essentially non-oscillatory finite difference methods in generalized coordinates
[NASA-CR-194031] p 770 N94-14429
Wall interference studies: Revisited p 640 N94-14604
BOUNDARY ELEMENT METHOD
Micromechanical modeling of laminated composites with interfaces and woven composites using the boundary element method
[NASA-TM-106280] p 670 N94-13053
Boundary formulations for nonlinear design sensitivity analysis p 672 N94-13669
Torsion problem of elastostatics: An application of boundary element method and relation with conformal mapping
[DSIS-92-03794] p 674 N94-13833
Utilization of boundary element method for extraction of frequency dependent conductivity parameters of lossy intra-chip transmission lines
[ETN-93-94385] p 771 N94-14807
BOUNDARY INTEGRAL METHOD
A hybrid finite element-boundary integral for the analysis of cavity-backed antennas of arbitrary shape
[NASA-CR-193719] p 599 N94-13236
Boundary formulations for nonlinear design sensitivity analysis p 672 N94-13669
Scattering by a groove in an impedance plane
[NASA-CR-193362] p 602 N94-13720
BOUNDARY LAYER COMBUSTION
Homogeneous-hetergeneous combustion: Thermal and chemical coupling
[DE93-016050] p 565 N94-14403
Numerical simulation of velocity-coupled combustion response of solid rocket propellants p 585 N94-14490
BOUNDARY LAYER CONTROL
Transition prediction and control in subsonic flow over a hump
[NASA-CR-4543] p 629 N94-13066
Boundary-layer transition p 507 N94-14171
BOUNDARY LAYER EQUATIONS
Transition prediction and control in subsonic flow over a hump
[NASA-CR-4543] p 629 N94-13066
Research on chemical vapor deposition processes for advanced ceramic coatings
[NASA-CR-193613] p 577 N94-13089
A robust quasi-simultaneous interaction method for a full potential flow with a boundary layer with application to wing/body configurations
[NLR-TP-91397-U] p 503 N94-13531
BOUNDARY LAYER FLOW
Integration of viscous effects into inviscid computational methods
[NASA-CR-193677] p 629 N94-13007
Large-eddy simulation of laminar-turbulent breakdown at high speeds with dynamic subgrid-scale modeling
[NASA-CR-4533] p 629 N94-13064
Numerical study of the effects of icing on viscous flow over wings
[NASA-CR-193306] p 500 N94-13180
Numerical simulations of unsteady flows in turbomachines p 633 N94-13569
On the secondary instability of the most dangerous Goertler vortex
[NASA-CR-191504] p 636 N94-13785
Shock/boundary-layer/shock interactions p 507 N94-14172
Stability of spatially developing boundary layers p 640 N94-14605
BOUNDARY LAYER SEPARATION
Fundamental study of shock wave/turbulent boundary layer interactions with passive control in transonic flows
[ESA-TT-1278] p 630 N94-13117
Interaction of two glancing, crossing shock waves with a turbulent boundary-layer at various Mach numbers
[NASA-TM-103740] p 509 N94-14780
BOUNDARY LAYER STABILITY
Transition prediction and control in subsonic flow over a hump
[NASA-CR-4543] p 629 N94-13066
Three-Dimensional Boundary-Layer program (BL3D) for swept subsonic or supersonic wings with application to laminar flow control
[NASA-CR-4531] p 629 N94-13073
The effect of crossflow on Taylor vortices: A model problem
[NASA-CR-191487] p 630 N94-13128
High speed transition prediction
[NASA-CR-194125] p 502 N94-13422
Stability of spatially developing boundary layers p 640 N94-14605
BOUNDARY LAYER TRANSITION
Large-eddy simulation of laminar-turbulent breakdown at high speeds with dynamic subgrid-scale modeling
[NASA-CR-4533] p 629 N94-13064
Transition prediction and control in subsonic flow over a hump
[NASA-CR-4543] p 629 N94-13066

The effect of crossflow on Taylor vortices: A model problem
[NASA-CR-191487] p 630 N94-13128
High speed transition prediction
[NASA-CR-194125] p 502 N94-13422
High freestream turbulence effects on the transport of heat and momentum p 633 N94-13559
Boundary-layer transition p 507 N94-14171
Stability of spatially developing boundary layers p 640 N94-14605

BOUNDARY LAYERS
Experimental investigation of the effects of blowing ratio parameter on heat transfer to a film-cooled flat plate
[AD-A266599] p 636 N94-13780
Boundary layer structure over areas of heterogeneous heat fluxes
[DE93-007887] p 715 N94-13912

BOUNDARY VALUE PROBLEMS
Computation and graphics in mathematical research
[DE93-016512] p 740 N94-13069
A hybrid Pade-Galerkin technique for differential equations
[NASA-CR-191494] p 767 N94-13289
Evolution of disturbances in stagnation point flow
[NASA-CR-191516] p 636 N94-13724
On the orthotropicity assumption and discontinuity conditions of conical shells
[LR-703] p 673 N94-13787
Theory for iterative solution of large dynamical systems using parallel computation
[TKK-MAT-A304] p 760 N94-14187
Nonrecursive formulations of multibody dynamics and concurrent multiprocessing p 679 N94-14632

BRAIDED COMPOSITES
Graphite fiber textile preform/copper matrix composites
[NASA-CR-193797] p 558 N94-14050

BRAIN
Current distribution tomography for determination of internal current density distributions
[DE93-015463] p 604 N94-13899

BRAKING
Technology assessments of advanced energy storage systems for electric and hybrid vehicles
[DE93-014395] p 701 N94-12913

BRAYTON CYCLE
A modular gas-cooled cermet reactor system for planetary base power
[DE93-013672] p 550 N94-13351

BRAZIL
Sea surface temperature forcing and phase locking of Nordeste precipitation
[DE93-011873] p 723 N94-14426

BREADBOARD MODELS
Breadboard activities for advanced protein crystal growth
[NASA-CR-193559] p 803 N94-12796
Solid state laser systems for space application
[NASA-CR-194133] p 656 N94-13420
Trellis coding with Continuous Phase Modulation (CPM) for satellite-based land-mobile communications
[NASA-CR-191325] p 604 N94-13909
Validated environmental and physiological data from the CELSS Breadboard Projects Biomass Production Chamber. BWT931 (Wheat cv. Yecora Rojo)
[NASA-TM-109272] p 738 N94-13979
Plasma contactor technology for Space Station Freedom
[NASA-TM-106291] p 553 N94-14725

BREMSSTRAHLUNG
The space-time and energy parameters of deuterium braking by the central collision with atoms
[DE93-624144] p 788 N94-14881

BRIDGMAN METHOD
Crystallographic and metallurgical characterization of radiation detector grade cadmium telluride materials
[DE93-014335] p 806 N94-13150

BRIGHTNESS
Fundamentals and techniques of nonimaging optics
[DE93-013145] p 791 N94-13015

BRIGHTNESS TEMPERATURE
Estimations of temperature and humidity of the canopy in Amazon Forest using microwave data from SMMR sensor of Nimbus-7 satellite
[INPE-5444-TDI/490] p 720 N94-13614
Radiometric observations of atmospheric attenuation at 20.6 and 31.65 GHz: The Wave Propagation Laboratory data base p 613 N94-14660

BRILLOUIN EFFECT
Brillouin scattering from fluctuations produced by stimulated Raman scattering
[DE93-016531] p 792 N94-14438

BRITTLE MATERIALS
Micromechanical damage theories for brittle solids with interacting microcracks
[AD-A266348] p 673 N94-13778

BRITTLENESS
Wear-mechanism modelling
[DE93-012311] p 579 N94-13974
Machining and grinding: High rate deformation in practice
[DE93-010718] p 664 N94-14457

BROADBAND
Ionospheric effects on a wide-bandwidth, polarimetric, space-based, synthetic-aperture radar
[DE93-015084] p 612 N94-14512

BROADCASTING
Digital sound: The selection of critical programme material and preparation of recordings for CCIR tests on low bit-rate codecs
[BBC-RD-1993/1] p 598 N94-12925
Digital sound: Subjective tests on commentary-quality codecs
[BBC-RD-1993/2] p 598 N94-12926
Technological development for broadcasting satellites in NHK Laboratories p 618 N94-14288
Coverage aspects of a single frequency network designed for digital audio broadcasting
[BBC-RD-1993/3] p 616 N94-14742

BROKEN SYMMETRY
Hydrodynamic asymptotics of Green functions in magnetics with spontaneously broken symmetry
[DE93-621349] p 767 N94-13223
On a nonminimal gauge interaction of a scalar field in D=2+1 Chern-Simons-Maxwell theory
[DE93-621380] p 621 N94-13224
The effects of internal fluctuations on a class of nonequilibrium statistical field theories
[DE93-016620] p 774 N94-14441
Measuring parity violation using the neutron capture reaction
[DE93-016629] p 786 N94-14514
The off shell (rho)-(omega) mixing in the QCD sum rules
[DE93-014845] p 786 N94-14527

BROWN DWARF STARS
The first data from the MACHO experiment
[DE93-014423] p 840 N94-14467

BROWNIAN MOVEMENTS
Transport properties of disordered porous media from the microstructure
[DE93-016065] p 806 N94-13152
The resonance broadening theory revisited
[PPL-134] p 798 N94-13563

BRUSH SEALS
Rotordynamic and leakage characteristics of a 4-stage brush seal
[AD-A266012] p 660 N94-12988

BSCCO SUPERCONDUCTORS
Optimization of the processing parameters of high temperature superconducting glass-ceramics: Center Director's discretionary fund final report
[NASA-TM-108421] p 808 N94-13938
Superconductivity devices: Commercial use of space
[NASA-CR-194163] p 625 N94-14324
Effect of spontaneous decay of superconductor quasiparticles in the tunneling density of states
[DE93-012681] p 811 N94-14339

BUBBLE CHAMBERS
EGS (underscore) windows 2: An enhanced graphical interface to EGS
[DE93-010447] p 746 N94-13382

BUBBLES
Study of bubble behavior in weightlessness (effects of thermal gradient and acoustic stationary wave) (M-16) p 589 N94-13748

BUCKLING
A probabilistic method for the buckling assessment of stiffened composite shells
[NASA-TM-106286] p 671 N94-13379
Shear buckling of fiber metal laminates: Comparison between orthotropic and anisotropic plate models using finite element method
[LTR-ST-1934] p 671 N94-13565
On the orthotropicity assumption and discontinuity conditions of conical shells
[LR-703] p 673 N94-13787
Compressive buckling of curved, anisotropic panels stiffened in two directions. Part 1: Derivation of the governing equations
[LR-694] p 675 N94-13931
Structural change of graphite during electron irradiation
[DE93-015961] p 582 N94-14531
The effect of initial imperfections on shell stability: An updated review
[LR-695] p 682 N94-14692
Buckling analysis of laminated thin shells in a hot environment
[NASA-TM-106302] p 683 N94-14776

BUDGETING
Selected data on academic science and engineering R and D expenditures: Fiscal Year 1991
[NSF-92-329] p 819 N94-13982

BUFFETING
Measurements of wing and fin buffeting on the standard dynamics model
[IAR-AN-76] p 526 N94-13859

BUILDINGS
Study on the possibilities to apply spectrumindex
[VTT-PUBS-109] p 777 N94-14034
Transition of building energy consumption using multi-input, single-output dynamic model
[VTT-PUBS-116] p 597 N94-14055
Simulating the daylight performance of fenestration systems and spaces of arbitrary complexity: The IDC method
[DE93-015177] p 704 N94-14333

BUMPERS
Comparison of analytic Whipple bumper shield ballistic limits with CTH simulations
[DE93-015126] p 539 N94-13006
Simulation of orbital debris impacts on bumper shields
[DE93-013773] p 540 N94-13398
BALLIST: A computer program to empirically predict the bumper thickness required to prevent perforation of the Space Station by orbital debris
[NASA-CR-193825] p 543 N94-14120

BUNCHING
Observation of the coalescing of beam into an asymmetric RF bucket by stochastic cooling
[DE93-015133] p 783 N94-13895

BUOYS
Buoy experiments to obtain the sea-truth data for OCTS/NSCAT, part 1
[NASDA-CNT-930005-PT-1] p 725 N94-13653

BURNING RATE
Closed-chamber analysis of M5 propellant lot RAD-64597
[AD-A266321] p 585 N94-14145

BURNS (INJURIES)
Review of test methods for material flammability
[DSIS-93-00480] p 564 N94-13942

C

C (PROGRAMMING LANGUAGE)
SCORE user's manual
[DE93-015987] p 822 N94-13121

C BAND
Search for extraterrestrial intelligence/high resolution microwave survey team member
[NASA-CR-194177] p 739 N94-13086

CABLES (ROPES)
Identifying the NAL spaceplane aerodynamic model using dynamic wind tunnel tests
[NAL-TR-1171] p 500 N94-12951
Control system design of a cable-mounted model used for dynamic wind tunnel testing
[NAL-TR-1161] p 528 N94-13337

CADASTRAL MAPPING
Integration of remotely sensed data and cadastral ownership boundaries for land inventory purposes
[BCRS-92-16] p 687 N94-14127

CADMIUM
A review of the global emissions, transport, and effects of heavy metals in the environment
[DE93-013507] p 706 N94-12937

CADMIUM SULFIDES
Dynamic Jahn-Teller effect: Calculation of fine structure spectrum, isotope shift and Zeeman behavior at deep center Ni2+ in CdS
[ETN-93-94394] p 815 N94-14705

CADMIUM TELLURIDES
Crystallographic and metallurgical characterization of radiation detector grade cadmium telluride materials
[DE93-014335] p 806 N94-13150

CALCIUM
Role of Ca(++)/calmodulin in the regulation of microtubules in higher plants
[DE93-015885] p 727 N94-12835
Calcitonin control of calcium metabolism during weightlessness
[NASA-CR-193622] p 731 N94-12960
The surface-located YopN protein is involved in calcium signal transduction in Yersinia pseudotuberculosis
[FOA-B-40416-4.4] p 729 N94-14128

CALCIUM METABOLISM
Calcitonin control of calcium metabolism during weightlessness
[NASA-CR-193622] p 731 N94-12960
Effect of low gravity on calcium metabolism and bone formation (L-7) p 593 N94-13765

CALCIUM PHOSPHATES
Laser and spectroscopic properties of Yb-doped apatite crystals
[DE93-014656] p 810 N94-14125
CALENDARS
Royal Belgium observatory calendar: 156th year
[ETN-93-94221] p 833 N94-14811
CALIBRATING
DMSP F11 SSM/T-2 calibration and validation
[AD-A265817] p 719 N94-12978
Degradation of the visible and near-infrared channels of the advanced very high resolution radiometer on the NOAA-9 spacecraft: Assessment and recommendations for corrections
[NOAA-TR-NESDIS-70] p 544 N94-13029
Phobos/Harp post launch support
[NASA-CR-193676] p 540 N94-13109
Preparations for and first results of the calibration and interpretation of ERS-1 SAR imagery over land
[BCRS-92-13] p 684 N94-13123
HYMOSS signal processing for pushbroom spectral imaging
[NASA-CR-191341] p 620 N94-13125
Proceedings of the 11th Space Surveillance Workshop, volume 1
[AD-A265120] p 531 N94-13358
Isolation of a piezoresistive accelerometer used in high acceleration tests
[DE93-013764] p 649 N94-13395
NASA airborne satellite instrumentation calibrator (NASIC) technical reference
[NASA-RP-1315] p 545 N94-13713
Tomographic methods in flow diagnostics
[NASA-TM-106330] p 650 N94-13876
Camera calibration in a hazardous environment performed in situ with automated analysis and verification
[DE93-010274] p 651 N94-14046
Volume 14: The first SeaWiFS intercalibration round-robin experiment, SIRREX-1, July 1992
[NASA-TM-104566] p 725 N94-14090
Earth Observation Center Annual Report on Research and Development, Fiscal Year 1992
[EOC-92-01-0007] p 687 N94-14091
Calibration and in-house validation results of JERS-1 data p 687 N94-14092
A calibration procedure for radiation budget radiometers and its influence on interpretation of measured values
[MITT-82] p 651 N94-14149
Results from ERS-1 and JERS-1 SAR calibration experiments and data analysis p 688 N94-14210
Methods for calibration/validation of AVNIR p 689 N94-14216
Radio metric errors due to mismatch and offset between a DSN antenna beam and the beam of a troposphere calibration instrument p 607 N94-14370
Calibration of the receiver channel for the GOPEX precursor experiments p 610 N94-14387
A description of the computer program CALDK38 which controls instrumentation set-up and data acquisition during deadweight calibration using an HBM DK 38 S6 digital measuring unit
[LTR-ST-1935] p 754 N94-14496
Calibration of a magnetic induction system for measurement of hypervelocities
[DE93-013949] p 652 N94-14578
The 3D pneumatic and 2D dynamic probes: Their development and subsequent use in a transonic fan
[RAE-TM-AERO/PROP-22] p 653 N94-14827
CALMODULIN
Role of Ca(++)/calmodulin in the regulation of microtubules in higher plants
[DE93-015885] p 727 N94-12835
CALORIMETERS
Low energy response of the DO calorimeter and jet energy measurement
[DE93-013569] p 781 N94-13350
Measurements of optical properties of waveshifting optical fiber for liquid scintillator hadron calorimetry
[DE93-012606] p 791 N94-13482
Cesium iodide (CsI) crystal manufacture
[DE93-012146] p 808 N94-13973
Optical fibre Fabry-Perot interferometers for calorimetric heat transfer gauges
[RAE-TM-AERO/PROP-20] p 653 N94-14701
CAMERAS
Photogrammetric methods for trajectory measurements
[NLR-TP-91166-U] p 650 N94-13527
Suppression of bright objects using a spatial light modulator when imaging with CCD- and image intensified cameras
[FFI-93/7008] p 650 N94-13665
A widget based operations simulator for a planetary camera: A model for the high resolution stereo camera on Mars 94
[DLR-FB-92-30] p 651 N94-14044
Camera calibration in a hazardous environment performed in situ with automated analysis and verification
[DE93-010274] p 651 N94-14046
A fast frame rate 512 x 512 CCD digital camera system
[DE93-013048] p 653 N94-14792
Image motion photography
[DE93-013962] p 653 N94-14858
CANADA
A history of the Defence Research Establishment, Ottawa
[CTN-93-60737] p 850 N94-14060
Organic Geochemical and tectonic evolution of the Midcontinent Rift system
[DE93-015093] p 717 N94-14338
CANONICAL FORMS
Simplification-driven automated partial evaluation
[DE93-012890] p 768 N94-13391
Canonical forms of multidimensional steady inviscid flows
[NASA-CR-191488] p 769 N94-13722
CANOPIES (VEGETATION)
Analytical framework for modeling scale-related variabilities in remote sensing p 685 N94-13592
Estimations of temperature and humidity of the canopy in Amazon Forest using microwave data from SMMR sensor of Nimbus-7 satellite
[INPE-5444-TDI/490] p 720 N94-13614
Wind erosion in semiarid landscapes: Predictive models and remote sensing methods for the influence of vegetation
[NASA-CR-194029] p 715 N94-13956
CANTILEVER BEAMS
Experimental and analytical analysis of the response of a smart beam to rate feedback
[AD-A266544] p 557 N94-13706
CAPACITANCE
Development of UHF spark-switched L-C Oscillators
[DE93-015019] p 623 N94-13892
A capaciflector-based robotic system
[NASA-CR-193783] p 833 N94-14359
NASA metrology and calibration, 1993
[NASA-TM-109280] p 597 N94-14410
Moisture meter evaluation
[DE93-016581] p 652 N94-14534
CAPACITORS
Two-dimensional simulations of foil implosion experiments on the Los Alamos capacitor bank
[DE93-012676] p 794 N94-12814
Schemes for the use of conducting polymers as active materials in electrochemical supercapacitors
[DE93-012713] p 580 N94-14179
CAPILLARY FLOW
Capillary surfaces in a wedge: Differing contact angles
[DE93-013903] p 631 N94-13244
Thermodynamic status of static and dynamic contact angles
[ISBN-0-315-73844-8] p 817 N94-13554
CAPILLARY WAVES
Drop dynamics in space and interference with acoustic field (M-15) p 588 N94-13747
Structures and shear response of lipid monolayers
[DE93-015076] p 730 N94-14802
CAPTURE EFFECT
Measuring parity violation using the neutron capture reaction
[DE93-016629] p 786 N94-14514
CARBIDES
Conversion of light hydrocarbon gases to metal carbides for production of liquid fuels and chemicals
[DE93-014962] p 583 N94-13002
CARBOHYDRATE METABOLISM
Improving physical performance by chemical stimulation
[DSIS-92-03763] p 728 N94-13823
CARBOHYDRATES
CarbBank: A structural and bibliographic database for complex carbohydrates
[DE93-015582] p 827 N94-14803
CARBON
Forest management for fixing and sequestering carbon
[DE93-013520] p 707 N94-13486
Small-angle scattering, contrast variation and the study of complex composite materials: A study of the structure of carbon black
[DE93-012707] p 559 N94-14690
Office of Naval Research/DARPA publications: Composite materials with improved properties in compression
[AD-A265509] p 560 N94-14794
CARBON CYCLE
Ocean uptake of carbon dioxide
[DE93-012967] p 707 N94-13384
Forest management for fixing and sequestering carbon
[DE93-013520] p 707 N94-13486
CARBON DIOXIDE
Propulsion simulator for magnetically-suspended wind tunnel models
[NASA-CR-189560] p 527 N94-13127
Ocean uptake of carbon dioxide
[DE93-012967] p 707 N94-13384
Electrocatalysis issues in polymer electrolyte fuel cells
[DE93-014450] p 702 N94-13402
Photochemical dynamics of surface oriented molecules
[DE93-016289] p 784 N94-13983
Optical properties of CO2 ice and CO2 snow in the ultraviolet, visible, and infrared
[NASA-CR-194110] p 686 N94-14081
IMG: Interferometric monitor for greenhouse gases p 689 N94-14217
Sequestering carbon dioxide in industrial polymers: Building materials for the 21st century
[DE93-016087] p 580 N94-14297
Promotion of geothermal energy development in 1991
[DE93-799061] p 705 N94-14679
CARBON DIOXIDE CONCENTRATION
Ocean uptake of carbon dioxide
[DE93-012967] p 707 N94-13384
Synthesis inversion of atmospheric CO2 using the GISS tracer transport model
[CSIRO-TP-29] p 709 N94-14095
CARBON DIOXIDE LASERS
Laser CO2 beam transmission through hollow metallic waveguide coated by a thin internal dielectric layer
[ITN-93-85201] p 656 N94-13571
Study of speckle reduction when using a CO2 waveguide laser close to its threshold state
[DSIS-93-00250] p 657 N94-14067
JPRS report: Science and technology. Central Eurasia: Materials science
[JPRS-UMS-93-005] p 559 N94-14575
CARBON FIBER REINFORCED PLASTICS
Measuring methods for CFRP laminates' bending and torsion rigidities characteristics p 529 N94-13272
Development of time-dependent orthotropic constitutive law of a thermoplastic composite material p 556 N94-13595
Testing and analysis of curved frame specimens made from a Long Discontinuous Fiber (LDF) material
[NASA-TM-109014] p 557 N94-13711
Polymer infiltration studies
[NASA-CR-194521] p 582 N94-14539
JPRS report: Science and technology. Central Eurasia: Materials science
[JPRS-UMS-93-004] p 559 N94-14574
CARBON FIBERS
Ohmic heating of composite candidate graphite-fiber/coating combinations
[NASA-TM-4491] p 554 N94-12871
Modified carbon for improved corrosion resistance
[AD-D015741] p 556 N94-13663
Fabrication of very-low-density, high-stiffness carbon fiber/aluminum hybridized composite with ultra-low density and high stiffness (M-11) p 588 N94-13743
JPRS report: Science and technology. Central Eurasia: Materials science
[JPRS-UMS-93-006] p 558 N94-14573
CARBON MONOXIDE
Conversion of light hydrocarbon gases to metal carbides for production of liquid fuels and chemicals
[DE93-014962] p 583 N94-13002
Electrocatalysis issues in polymer electrolyte fuel cells
[DE93-014450] p 702 N94-13402
An examination of utility emissions contributions to elevated ozone concentrations in the Chicago area
[DE93-012852] p 708 N94-13495
The origin of the far-infrared emission from galactic molecular clouds p 848 N94-13654
Quantum state resolved desorption of CO from solid surfaces
[DE93-016876] p 814 N94-14597
CARBON STARS
Dust production in the envelopes of carbon stars: R Coronae Borealis
[ETN-93-94389] p 839 N94-14075
CARBON STEELS
A study of hydrogen effects on fracture behavior of radioactive waste storage tanks
[DE93-018171] p 574 N94-14873
CARBON-CARBON COMPOSITES
Electrophoretic and electrolytic deposition of ceramic particles on porous substrates
[AD-A265141] p 575 N94-12812

CARBONATES
Carbonate fuel cell endurance: Hardware corrosion and electrolyte management status
[DE93-013800] p 701 N94-13093
Molten carbonate fuel cell product development test environmental assessment/protection plan
[DE93-000288] p 702 N94-13380
Performance effects of coal-derived contaminants on the carbonate fuel cell
[DE93-013801] p 703 N94-13693
CARBONYL COMPOUNDS
Characterization of 1:1 random copolymers obtained from 6-, 7-, 11-, and 12-carbon amino acids
[AD-A265827] p 577 N94-12985
CARBOXYLIC ACIDS
A characterization of carboxylesterases in rat and guinea pig: Their heterogeneity and role in detoxication of organophosphorus compounds
[NDRE-PUBL-93-1001] p 730 N94-14852
CARDIOVASCULAR SYSTEM
Countermeasure for reducing post-flight orthostatic intolerance: Lower Body Negative Pressure (LBNP) experiment E140 p 594 N94-13772
CARRIER DENSITY (SOLID STATE)
Numerical simulation and analysis of electrical and optical properties of Al(x)Ga(1-x)As / GaAs
[ETN-93-94387] p 703 N94-13997
CARRIER MOBILITY
Effects of growth conditions and substrate orientation on the properties of InSb
[DE93-013766] p 812 N94-14344
CARRIER TRANSPORT (SOLID STATE)
Numerical simulation and analysis of electrical and optical properties of Al(x)Ga(1-x)As / GaAs
[ETN-93-94387] p 703 N94-13997
CASCADE FLOW
On the local nature of the energy cascade
p 643 N94-14748
CASCADE WIND TUNNELS
An experimental investigation of the redistribution of gas stream total temperature in a high turning angle transonic planar cascade
[ISBN-0-315-60791-2] p 502 N94-13369
CASE HISTORIES
Storm prediction through barometric field analysis
[PUBL-SER-A-129] p 720 N94-13587
CASSINI MISSION
Real-time dynamics simulation of the Cassini spacecraft using DARTS. Part 1: Functional capabilities and the spatial algebra algorithm p 680 N94-14638
Real-time dynamic simulation of the Cassini spacecraft using DARTS. Part 2: Parallel/vectorized real-time implementation p 680 N94-14639
CASTING
Characterization of 1:1 random copolymers obtained from 6-, 7-, 11-, and 12-carbon amino acids
[AD-A265827] p 577 N94-12985
Casting of superconducting composite materials (M-4)
p 586 N94-13736
CATACLYSMIC VARIABLES
Time series photometry of faint cataclysmic variables with a CCD p 831 N94-13646
CATALOGS (PUBLICATIONS)
Submillimeter, millimeter, and microwave spectral line catalogue, revision 3
[NASA-CR-194501] p 602 N94-13813
CATALYSIS
Catalysis and biocatalysis program
[NASA-CR-194105] p 727 N94-12793
Photocatalysis for the treatment of waste water: Applications involving the removal of metals
[DE93-011669] p 561 N94-12841
Electrocatalysis issues in polymer electrolyte fuel cells
[DE93-014450] p 702 N94-13402
Hydrogen peroxide safety issues
[DE93-013895] p 565 N94-14346
Catalytic arene hydrogenation using early transition metal hydride compounds
[DE93-015500] p 573 N94-14402
Biomimetic methane oxidation
[DE93-013196] p 705 N94-14510
Reactor studies of metal ions associated with chromatographic silica
[AD-A266675] p 573 N94-14779
CATALYSTS
Anchoring strategies for bimetallic species in zeolites
[DE93-015622] p 567 N94-12834
Unexpectedly rapid hydrosilation polymerization of the diallyl derivative of bisphenol A and 2,6-diallylphenol
[AD-A265832] p 577 N94-12986
Experimental and kinetic modeling of acid/base and redox reactions over oxide catalysts
[DE93-016203] p 563 N94-13375
Status and future opportunities for conversion of synthesis gas to liquid energy fuels
[DE93-010025] p 584 N94-14089
Reverse micelle synthesis of nanoscale metal containing catalysts
[DE93-012869] p 572 N94-14184
Hydrogen peroxide safety issues
[DE93-013895] p 565 N94-14346
Catalytic arene hydrogenation using early transition metal hydride compounds
[DE93-015500] p 573 N94-14402
Homogeneous-hetergeneous combustion: Thermal and chemical coupling
[DE93-016050] p 565 N94-14403
CATALYTIC ACTIVITY
Catalysis and biocatalysis program
[NASA-CR-194105] p 727 N94-12793
A survey and analysis of experimental hydrogen sensors
[NASA-TM-106300] p 648 N94-13135
Evolution of catalytic RNA in the laboratory
[NASA-CR-194124] p 727 N94-13210
Destruction of problematic airborne contaminants by hydrogen reduction using a Catalytically Active, Regenerable Sorbent (CARS)
[NASA-CR-194354] p 709 N94-14103
Reverse micelle synthesis of nanoscale metal containing catalysts
[DE93-012869] p 572 N94-14184
Lawrence Berkeley Laboratory Chemical Sciences Division
[DE93-015260] p 851 N94-14401
Biomimetic methane oxidation
[DE93-013196] p 705 N94-14510
CATASTROPHE THEORY
On curve veering and flutter of rotating blades
[NASA-TM-106282] p 670 N94-12872
CATENARIES
A photovoltaic catenary-tent array for the Martian surface
[NASA-TM-106306] p 621 N94-13194
CATHODES
Field emitter array RF amplifier development project. Phase 1: Cathode technology development
[AD-A266346] p 622 N94-13776
CATHODIC COATINGS
Physical and structural properties of a sputtered zirconia-yttria layer used as a thermal resistance
[ONERA-NT-1992-10] p 810 N94-14193
CATIONS
Infrared spectroscopy of organic free radicals related to combustion processes
[DE93-017086] p 562 N94-13222
CAUCHY PROBLEM
Full Riemann solution of the one- and two-dimensional Euler equations
[DLR-FB-92-34] p 638 N94-14188
A new Lagrangian method for three-dimensional steady supersonic flows
[NASA-TM-106068] p 510 N94-14847
CAVITIES
Long-pulse operation of a gyrotron with beam/RF separation
[DE93-015007] p 649 N94-13410
CD-ROM
Public census data on CD-ROM at Lawrence Berkeley Laboratory
[DE93-015273] p 825 N94-14433
CELL DIVISION
Gravity as a probe for understanding pattern specification
[NASA-CR-194142] p 713 N94-13418
Cellular responses to low-gravity: Pilot studies on suborbital rockets and orbiting spacecraft
[NASA-CR-194402] p 729 N94-14494
CELLS (BIOLOGY)
Monoclonal antibodies directed against surface molecules of multicell spheroids
[NASA-CR-193560] p 727 N94-12795
Studies on the effects of microgravity on the ultrastructure and functions of cultured mammalian cells (L-6) p 592 N94-13763
Gravity, chromosomes, and organized development in aseptically cultured plant cells p 592 N94-13764
CELLULOSE NITRATE
Closed-chamber analysis of M5 propellant lot RAD-64597
[AD-A266321] p 585 N94-14145
CEMENTS
Automated crack identification for cement paste
[AD-A265753] p 665 N94-13042
CENSUS
Public census data on CD-ROM at Lawrence Berkeley Laboratory
[DE93-015273] p 825 N94-14433
CENTRAL PROCESSING UNITS
Implementation of ADI: Schemes on MIMD parallel computers
[NASA-CR-193720] p 759 N94-13204
Some tools of the trade we've developed for our cross-section calculations
[DE93-013835] p 786 N94-14569
Switchover software reliability estimate for Paducah freezer/sublimer computer systems
[DE93-013844] p 756 N94-14696
CEPSTRAL ANALYSIS
Speaker independent recognition of isolated words using vector quantization and neural networks
[ETN-93-94390] p 616 N94-14724
CERAMIC BONDING
Problems and opportunities in microwave joining of ceramics
[DE93-014998] p 579 N94-13888
CERAMIC COATINGS
Electrophoretic and electrolytic deposition of ceramic particles on porous substrates
[AD-A265141] p 575 N94-12812
Research on chemical vapor deposition processes for advanced ceramic coatings
[NASA-CR-193613] p 577 N94-13089
JPRS report: Science and technology. Central Eurasia: Materials science
[JPRS-UMS-93-004] p 559 N94-14574
CERAMIC MATRIX COMPOSITES
Ceramic matrix composites by microwave assisted CVI
[DE93-012640] p 576 N94-12916
Development of nondestructive evaluation methods and prediction of effects of flaws on the fracture behavior of structural ceramics
[DE93-012942] p 577 N94-13032
Measurement of residual strain in composites by means of time-of-flight neutron diffraction
[DE93-012939] p 555 N94-13248
Thermal shock resistance of ceramic matrix composites
[NASA-CR-189136] p 557 N94-13920
CERAMICS
Ceramic matrix composites by microwave assisted CVI
[DE93-012640] p 576 N94-12916
Advanced Turbine Technology Applications Project (ATTAP)
[NASA-CR-191088] p 828 N94-12931
Modeling the impact behavior of AD85 ceramic under multi-axial loading
[AD-A265877] p 576 N94-12932
MMIC packaging technology development
[NASA-CR-194183] p 621 N94-13336
Surfaces and interfaces of ceramics and metals
[DE93-014959] p 578 N94-13408
Problems and opportunities in microwave joining of ceramics
[DE93-014998] p 579 N94-13888
Applications of surface science to solid lubricants
[SMC-TR-93-24] p 579 N94-13903
Optimization of the processing parameters of high temperature superconducting glass-ceramics: Center Director's discretionary fund final report
[NASA-TM-108421] p 808 N94-13938
Wear-mechanism modelling
[DE93-012311] p 579 N94-13974
Combustion synthesis and engineering of nanoparticles for electronic, structural, and superconductor applications
[DE93-016286] p 809 N94-13981
Superconductivity devices: Commercial use of space
[NASA-CR-194163] p 625 N94-14324
Microwave hybrid heating of alumina filaments
[DE93-012642] p 581 N94-14327
Nonlinear wave predictions in ceramics
[DE93-016516] p 582 N94-14436
How to read a phase equilibrium diagram for high-temperature ceramics material as main object
[DE93-512333] p 582 N94-14513
Processing and testing of high toughness silicon nitride ceramics
[NASA-CR-191190] p 582 N94-14543
CEREBELLUM
A neural-network approach to robotic control
p 679 N94-14634
CERENKOV COUNTERS
Research in cosmic and gamma ray astrophysics: Cosmic physics portion
[NASA-CR-194127] p 847 N94-13211
Gamma-insensitive optical focal plane array
[DE93-013100] p 792 N94-14317
Results from a water-Cerenkov array
[DE93-012715] p 849 N94-14461
CERENKOV RADIATION
Research in cosmic and gamma ray astrophysics: Cosmic physics portion
[NASA-CR-194127] p 847 N94-13211
CERMETS
A modular gas-cooled cermet reactor system for planetary base power
[DE93-013672] p 550 N94-13351

Preparation of particle-dispersion alloys (M-6)
p 587 N94-13738
Fabrication of very-low-density, high-stiffness carbon fiber/aluminum hybridized composite with ultra-low density and high stiffness (M-11) p 588 N94-13743

CERTIFICATION
Aircraft engine type certification handbook: Advisory circular
|AC-33-2B| p 518 N94-13252

CESIUM IODIDES
Cesium iodide (CsI) crystal manufacture
|DE93-012146| p 808 N94-13973

CHAINS
The design of chain links and slings
|NPL-DMM(A)-94| p 662 N94-13808

CHANGE DETECTION
Asia-Pacific ISY Conference, volume 2
|NASDA-CM-199-VOL-2| p 688 N94-14209
Climate products from NOAA operational satellites
p 691 N94-14231
Detecting land cover changes in Chiang-Mai area in Thailand p 693 N94-14241
Development of a remote sensing geographic information system for land cover changes and assessment of risk due to natural and man made hazards covering the area of the inner delta of the Yellow River
p 694 N94-14249
The Swedish ISY contribution p 695 N94-14256
Vegetation mapping of Indo-China Peninsula using MOS-1 MESSR and NOAA AVHRR p 695 N94-14257
Estimation of vegetation damage due to ash fall in Mt. Pinatubo area using MOS-1 data p 695 N94-14259

CHANNEL FLOW
Search for subgrid scale parameterization by projection pursuit regression p 643 N94-14749
Isotropy of small scale turbulence
p 644 N94-14752
Estimation of the vortex length scale and intensity from two-dimensional samples p 645 N94-14756
A transport equation for eddy viscosity
p 646 N94-14762

CHANNEL NOISE
The E2 N(yields)(Delta) transition from polarized Compton scattering
|DE93-012522| p 785 N94-14363

CHANNELS (DATA TRANSMISSION)
Application of new electro-optic technology to Space Station Freedom data management system
|NASA-CR-177622| p 538 N94-13257
Development of an on-board aircraft optical fiber data bus system
|NAL-TR-1163| p 514 N94-13338
Signal design for data communication through rapidly varying linear channels
|ITN-93-85195| p 601 N94-13567
Characterisation of the LMS propagation channel at L- and S-bands: Narrowband experimental data and channel modelling p 615 N94-14669

CHAOS
Modulational stability of periodic solutions of the Kuramoto-Sivaskinsky equation
|NASA-CR-191502| p 628 N94-12888
Chaos and microbial systems
|DE93-016814| p 730 N94-14596
Investigations of transitions from order to chaos in dynamical systems
|DE93-014438| p 818 N94-14738

CHARACTERIZATION
Battery testing at Argonne National Laboratory
|DE93-011761| p 624 N94-14012

CHARGE CARRIERS
Intrinsic and interfacial recombination in OMVPE- and MBE-prepared GaAs/Al(x)Ga(1-x)As heterostructures
|DE93-009844| p 809 N94-14083
Anomalous low-temperature free-exciton transport in GaAs structures
|DE93-009845| p 809 N94-14108
Magnetic interactions and disorder - phase transitions in dilute spin-glasses and high temperature superconductors
|ITN-93-85217| p 815 N94-14825

CHARGE COUPLED DEVICES
Crystallographic phase identification in the scanning electron microscope: Backscattered electron Kikuchi patterns
|DE93-011574| p 804 N94-12813
Time series photometry of faint cataclysmic variables with a CCD p 831 N94-13646
Suppression of bright objects using a spatial light modulator when imaging with CCD- and image intensified cameras
|FFI-93/7008| p 650 N94-13665
Rocket and laboratory studies in astronomy
|NASA-CR-194410| p 832 N94-13966
A widget based operations simulator for a planetary camera: A model for the high resolution stereo camera on Mars 94
|DLR-FB-92-30| p 651 N94-14044
A fast frame rate 512 x 512 CCD digital camera system
|DE93-013048| p 653 N94-14792

CHARGE EXCHANGE
Terrestrial magnetospheric imaging: Numerical modeling of low energy neutral atoms
|DE93-014561| p 717 N94-14328

CHARGE TRANSFER
Further study of the X(1910) meson
|DE93-621443| p 782 N94-13362
Metastable enhancement of C(+) and O(+) capture reactions
|DE93-015075| p 807 N94-13373
Charge-exchange reactions and weak interaction rates for Type 2 supernovae
|DE93-015104| p 783 N94-13893

CHARGE TRANSFER DEVICES
An acoustic charge transport imager for high definition television applications
|NASA-CR-194518| p 650 N94-14029

CHARGED PARTICLES
Excitation of coupled waves in plasma periodic structures by relativistic electron beam and acceleration of charged particles
|DE93-621657| p 794 N94-12853
Electromagnetic deflection of spinning particles
|DE93-622866| p 778 N94-12858
Charged scalar particles and (tau) leptonic decay
|DE93-622969| p 779 N94-12882
Stripping efficiencies for 277 MeV/amu gold beam on copper foils
|DE93-014306| p 569 N94-13221
Charged-particle evaluation methodology at Lawrence Livermore National Laboratory
|DE93-013429| p 781 N94-13251
Variance reduction unique to coupled electron/photon Monte Carlo transport
|DE93-014999| p 782 N94-13409
ROSAT observations of the binary Be-star/radio pulsar PSR1259-63
|NASA-CR-194394| p 832 N94-14357
Investigations of transitions from order to chaos in dynamical systems
|DE93-014438| p 818 N94-14738
Anomalous ion transport and feedback control
|DE93-018324| p 803 N94-14874

CHARM (PARTICLE PHYSICS)
Double semi-leptonic charm decay in HELIOS-I 450 GeV/c p-Be data
|DE93-013493| p 781 N94-13348
E789 and P865: High-rate fixed-target studies of charm and beauty
|DE93-017223| p 788 N94-14898

CHEBYSHEV APPROXIMATION
The Chebyshev-Legendre method: Implementing Legendre methods on Chebyshev points
|NASA-CR-191497| p 769 N94-13725
A new treatment of periodic systems with applications to helicopter rotor blade dynamics
|AD-A266770| p 510 N94-14784

CHELATES
Synthesis of organic ligands for f-element separations
|DE93-012915| p 554 N94-14290

CHELATION
Determination of trace elements in triglycine sulfate solutions
|NASA-CR-193481| p 562 N94-13048

CHEMICAL ANALYSIS
Gas atomized Er3Ni powder for cryocooler applications
|DE93-011564| p 568 N94-13000
Spectral reflectance of soils from Sao Paulo State
|INPE-5424-PRP/172| p 684 N94-13377
Surface science instrumentation for the study of important catalytic and electrochemical interfaces
|DE93-015068| p 563 N94-13413
Investigation of an alternating current plasma as an element selective atomic emission detector for high-resolution capillary gas chromatography and as a source for atomic absorption and atomic emission spectrometry p 798 N94-13678
Quality assurance for environmental chemistry, 1991, volume 1
|DE93-011791| p 709 N94-14020
Ultra-soft x ray absorption spectroscopy: A bulk and surface probe of materials
|DE93-014325| p 566 N94-14582
Procurement and execution of PCB analyses: Customer-analyst interactions
|DE93-009964| p 566 N94-14694

CHEMICAL BONDS
Infrared absorption spectroscopy and chemical kinetics of free radicals
|DE93-015078| p 562 N94-13004
Office of Naval Research/DARPA publications: Composite materials with improved properties in compression
|AD-A265509| p 560 N94-14794

CHEMICAL COMPOSITION
ARTI Refrigerant Database
|DE93-014774| p 595 N94-13021
Research in cosmic and gamma ray astrophysics: Cosmic physics portion
|NASA-CR-194127| p 847 N94-13211
Formation of deoxidization products in iron ingot by the addition of Al, Si, and/or Mn (M-5) p 587 N94-13737
Spatial and temporal variability of precipitation and chemistry: Case studies from the frontal boundary study
|DE93-007883| p 708 N94-13910
Synthetic lubricants and high-performance functional fluids: Phosphazenes
|ARL-TR-45| p 580 N94-14126
Relationship between borosilicate glass composition, structure, and durability test response (SRS)
|DE93-013578| p 581 N94-14343

CHEMICAL COMPOUNDS
Toxic Substances Control Act (TSCA) chemical substances inventory: Revised inventory synonym and preferred name file, Jan. 1993 documentation
|PB93-155166| p 710 N94-14508

CHEMICAL ENERGY
Lawrence Berkeley Laboratory Chemical Sciences Division
|DE93-015260| p 851 N94-14401

CHEMICAL EQUILIBRIUM
Computer program for thermal and transport properties of parahydrogen from 20 to 10,000 K
|NASA-TP-3378| p 552 N94-14102

CHEMICAL EVOLUTION
The physical and chemical evolution of protostellar disks. The growth of protostellar disks: Progress to date
|NASA-CR-194111| p 836 N94-13423

CHEMICAL EXPLOSIONS
Modeling ignition chemistry
|DE93-012340| p 561 N94-12910
Equation of state for detonation products
|DE93-012671| p 583 N94-12921
A study of the role of homogeneous process in heterogeneous high explosives
|DE93-012733| p 585 N94-14180
Atmospheric acoustic modeling
|DE93-016727| p 718 N94-14518
The 4th International Symposium on Analysis and Detection of Explosives
|DE93-620280| p 585 N94-14829

CHEMICAL PROPERTIES
Toxic Substances Control Act (TSCA) chemical substances inventory: Revised inventory synonym and preferred name file, Jan. 1993 documentation
|PB93-155166| p 710 N94-14508

CHEMICAL PROPULSION
Low thrust space propulsion
|NASA-TM-109286| p 552 N94-13625
Closed-chamber analysis of M5 propellant lot RAD-64597
|AD-A266321| p 585 N94-14145

CHEMICAL REACTIONS
Unexpectedly rapid hydrosilation polymerization of the diallyl derivative of bisphenol A and 2,6-diallylphenol
|AD-A265832| p 577 N94-12986
Conversion of light hydrocarbon gases to metal carbides for production of liquid fuels and chemicals
|DE93-014962| p 583 N94-13002
Fifteenth Combustion Research Conference
|DE93-015758| p 562 N94-13045
Research on chemical vapor deposition processes for advanced ceramic coatings
|NASA-CR-193613| p 577 N94-13089
Reduction of Pu(6) with hydrogen peroxide: Effects of plutonium, peroxide, and iron concentrations and of reaction time
|DE93-013598| p 564 N94-13487
Destruction of waste energetic materials using base hydrolysis
|DE93-012738| p 584 N94-13491
High order hybrid numerical simulations of two dimensional detonation waves
|NASA-CR-191506| p 769 N94-13792
Binary homogeneous nucleation: Temperature and relative humidity fluctuations and non-linearity
|DE93-007884| p 709 N94-13911
Interactions between spacecraft and their environments
|NASA-TM-106115| p 541 N94-13917
Hydrogen peroxide safety issues
|DE93-013895| p 565 N94-14346

Modeling surface area to volume effects on borosilicate glass dissolution
| DE93-011891 | p 581 N94-14432
Microchannel cooled heatsinks for high average power laser diode arrays
| DE93-016533 | p 658 N94-14442
Computation of nonequilibrium flows using PNS equations p 641 N94-14610
Numerical study of shock-induced combustion in methane-air mixtures
| NASA-TM-106354 | p 642 N94-14722
Numerical simulations of turbulent premixed H2/O2/N2 flames with complex chemistry p 567 N94-14765
Effect of finite-rate chemistry and unequal Schmidt numbers on turbulent non-premixed flames modeled with single-step chemistry p 567 N94-14766
Structure of turbulent non-premixed flames modeled with two-step chemistry p 567 N94-14767
Stochastic modeling of turbulent reacting flows p 647 N94-14768
Study of chemical reactions under the influence of ultrasound
| DE93-016458 | p 778 N94-14867

CHEMICAL REACTORS
Conversion of light hydrocarbon gases to metal carbides for production of liquid fuels and chemicals
| DE93-014962 | p 583 N94-13002
Reactor studies of metal ions associated with chromatographic silica
| AD-A266675 | p 573 N94-14779

CHEMICAL VAPOR INFILTRATION
Ceramic matrix composites by microwave assisted CVI
| DE93-012640 | p 576 N94-12916

CHEMICAL WARFARE
A history of the Defence Research Establishment, Ottawa
| CTN-93-60737 | p 850 N94-14060

CHEMILUMINESCENCE
Quantitative luminescence imaging system
| DE93-015691 | p 793 N94-14702

CHINA
China's devotion to space science and applications p 532 N94-14273

CHINESE SPACE PROGRAM
The remarkable achievement of China satellite application p 692 N94-14235
China's devotion to space science and applications p 532 N94-14273

CHIPS (ELECTRONICS)
Chip-level testability requirements guidelines
| AD-A262583 | p 619 N94-12967
High flux heat exchanger
| AD-A266341 | p 636 N94-13730
Alternate cleaning methods for LCCAs
| KCP-613-5045 | p 624 N94-13937
NASA Space Engineering Research Center for VLSI systems design
| NASA-CR-194035 | p 625 N94-14325
Utilization of boundary element method for extraction of frequency dependent conductivity parameters of lossy intra-chip transmission lines
| ETN-93-94385 | p 771 N94-14807

CHIRAL DYNAMICS
No-lost theorem for parity violating nucleon-nucleon scattering experiments
| DE93-012737 | p 779 N94-12949

CHIRP
Independent adjustment of the higher order frequency dependent phase in chirped pulse amplification systems
| DE93-017106 | p 625 N94-14522

CHIRP SIGNALS
Independent adjustment of the higher order frequency dependent phase in chirped pulse amplification systems
| DE93-017106 | p 625 N94-14522

CHLORINE
Theoretical support for the Airborne Antarctic Ozone Experiment
| NASA-CR-193669 | p 713 N94-13465

CHLOROFLUOROCARBONS
IMG: Interferometric monitor for greenhouse gases p 689 N94-14217
Long-range global warming impact of gaseous diffusion plant operation
| DE93-011686 | p 710 N94-14459

CHLOROPHYLLS
The first steps of chlorophyll synthesis: RNA involvement and regulation
| DE93-014398 | p 730 N94-14509
Nonlinear relationships between particulate absorption and chlorophyll: Detritus or pigment packaging?
| AD-A266806 | p 731 N94-14899

CHROMATOGRAPHY
Office of Naval Research/DARPA publications: Composite materials with improved properties in compression
| AD-A265509 | p 560 N94-14794

CHROMIUM
Radiation hardening and radiation-induced chromium depletion effects on intergranular stress corrosion cracking of austenitic stainless steels
| DE93-011602 | p 572 N94-14058
Tetravalent chromium (Cr(4+)) as laser-active ion for tunable solid-state lasers
| NASA-CR-194527 | p 659 N94-14576

CHROMIUM ALLOYS
Statics and kinetics of phase transformations in bcc Fe-Cr
| DE93-013839 | p 574 N94-14793

CHROMOSOMES
Gravity, chromosomes, and organized development in aseptically cultured plant cells p 592 N94-13764

CHROMOSPHERE
Basic research in solar physics
| NASA-CR-193632 | p 844 N94-13234

CIRCADIAN RHYTHMS
Calcitonin control of calcium metabolism during weightlessness
| NASA-CR-193622 | p 731 N94-12960
Work/rest schedules and performance of S-3 aviators during fleet exercise
| AD-A265807 | p 734 N94-12975
Work/rest schedules and performance of F/A-18 aviators during Fleet Exercise 1992
| AD-A265826 | p 735 N94-12982
Phase-shifting effect of light and exercise on the human circadian clock
| AD-A265732 | p 732 N94-13038
A circadian rhythm of conidiation in Neurospora crassa (L-12) p 593 N94-13769
Circadian rhythms during simulation of the D2-spaceflight
| DLR-FB-92-27 | p 733 N94-14043

CIRCUIT BOARDS
Solderability of surface mount devices
| AD-A265751 | p 620 N94-13040

CIRCUITS
Student's works and power supplies in electronic circuit laboratory p 627 N94-13434
Electronic schematics for the Donner 600 Crystal Tomograph
| DE93-015277 | p 625 N94-14336
A high voltage dielectrically isolated smart power technology based on silicon direct bonding
| LAAS-92492 | p 626 N94-14698
A high-precision direct current measuring device over a kiloampere range
| DE93-626409 | p 627 N94-14885

CIRCULAR CYLINDERS
The three-dimensional flow past a rapidly rotating circular cylinder
| NASA-CR-191512 | p 630 N94-13075

CIRCULAR POLARIZATION
The x ray dichroism experiments using circular polarization
| DE93-013195 | p 568 N94-13036
Polarization effects in optical fiber current sensors based on Sagnac interferometers with 3 by 3 couplers
| DE93-012665 | p 792 N94-14367

CIRCULAR WAVEGUIDES
Laser CO2 beam transmission through hollow metallic waveguide coated by a thin internal dielectric layer
| ITN-93-85201 | p 656 N94-13571

CIRCULATION CONTROL AIRFOILS
An experimental study of a turbulent boundary layer in the trailing edge region of a curculation-control airfoil
| NASA-CR-194522 | p 508 N94-14541

CIRCULATION DISTRIBUTION
An experimental investigation of shock wave/vortex interaction p 634 N94-13574

CITIES
Bibliography of urban climate in tropical/subtropical areas, 1981-1991
| WCASP-25 | p 718 N94-12918

CIVIL AVIATION
Piloting considerations for terminal area operations of civil tiltwing and tiltrotor aircraft p 525 N94-13320
The international regulation of air transport: Changing regimes and price effects
| ISBN-0-315-55958-6 | p 511 N94-13543

CLASSICAL MECHANICS
Stochastic dynamics: Crossover from 1/f(sup 3) to flicker noise
| DE93-622862 | p 772 N94-12896
Application of symbolic and algebraic manipulation software in solving applied mechanics problems
| NASA-CR-4544 | p 596 N94-13798

CLASSIFICATIONS
Satellite imagery and exogenous data integration by neural network in automation land-cover classification
| INPE-5480-PRE/1778 | p 686 N94-13729
Communications and control for electric power systems: Power flow classification for static security assessment
| NASA-CR-194512 | p 624 N94-13948
Integration of remotely sensed data and cadastral ownership boundaries for land inventory purposes
| BCRS-92-16 | p 687 N94-14127
Detecting land cover changes in Chiang-Mai area in Thailand p 693 N94-14241
Effects of typhoon on TOMS data p 693 N94-14243
Remote sensing for monitoring tropical moist forests in the Indo-Chinese region p 695 N94-14258
Mangrove afforestation monitoring using remote sensing p 695 N94-14260
Supervised classification of remotely sensed images
| DLR-FB-92-07 | p 700 N94-14428
Educational module for the higher agricultural education. Part 1: Land use classification using satellite pictures
| BCRS-92-11A | p 819 N94-14809

CLASSIFIERS
Feature discovery on segmented objects in SAR imagery using self-organizing neural networks
| DE93-010685 | p 686 N94-14056
Obstacle detection by recognizing binary expansion patterns
| NASA-CR-194415 | p 514 N94-14495
Computer vision and sensor fusion for detecting buried objects
| DE93-012605 | p 700 N94-14566

CLEANERS
Alternate cleaning methods for LCCAs
| KCP-613-5045 | p 624 N94-13937
Performance of gas turbine compressor cleaners
| NLR-TP-91291-U | p 519 N94-14450

CLEANING
Alternate cleaning methods for LCCAs
| KCP-613-5045 | p 624 N94-13937

CLEANLINESS
Determination of the surface cleanliness of metals by FT-IR spectroscopy
| DE93-013252 | p 565 N94-14525

CLEAVAGE
A microstructural approach to fatigue crack processes in poly crystalline BCC materials
| DE93-016666 | p 812 N94-14354
JPRS report: Science and technology. Central Eurasia: Materials science
| JPRS-UMS-93-005 | p 559 N94-14575

CLEBSCH-GORDAN COEFFICIENTS
Clebsch variable model for unsteady, transonic flow; application to 2D airfoils
| NLR-TP-91387-U | p 503 N94-13530

CLIMATE
Bibliography of urban climate in tropical/subtropical areas, 1981-1991
| WCASP-25 | p 718 N94-12918
Linkage of anthropogenic aerosol to clouds and climate
| DE93-016434 | p 719 N94-13080
An experimental regional scale climate simulation laboratory
| DE93-015935 | p 719 N94-13119
AMIP: Diagnostic subproject on the variability in the tropics: Synoptic to intraseasonal time scales
| DE93-009287 | p 721 N94-13914
The role of human activity and land use change in atmospheric chemistry and air quality
| DE93-011871 | p 709 N94-14022
CCl working group on climate data and its rapporteurs
| WCDMP-21 | p 723 N94-14118
Climate products from NOAA operational satellites p 691 N94-14231
Global assessment of human activities p 695 N94-14255
Rain-rate data base development and rain-rate climate analysis p 614 N94-14664

CLIMATE CHANGE
The role of clouds and oceans in global greenhouse warming
| DE93-016206 | p 706 N94-13079
Forest management for fixing and sequestering carbon
| DE93-013520 | p 707 N94-13486
Climatic change due to land surface alterations
| INPE-5495-PRE/1786 | p 721 N94-13672
The role of human activity and land use change in atmospheric chemistry and air quality
| DE93-011871 | p 709 N94-14022
Regional climatology sensitivity studies
| DE93-010712 | p 722 N94-14057
Climate products from NOAA operational satellites p 691 N94-14231
Global assessment of human activities p 695 N94-14255

Integration of space and in-situ observations to study atmosphere, ocean and land processes
|NASA-CR-194495| p 683 N94-14500
Pattern and Process in Landscape Ecology: Eighth Annual US Landscape Ecology Symposium
|DE93-014032| p 711 N94-14859

CLIMATOLOGY
Soil erosion rates caused by wind and saltating sand stresses in a wind tunnel
|DE93-009154| p 706 N94-12905
Bibliography of urban climate in tropical/subtropical areas, 1981-1991
|WCASP-25| p 718 N94-12918
The role of clouds and oceans in global greenhouse warming
|DE93-016206| p 706 N94-13079
Forest management for fixing and sequestering carbon
|DE93-013520| p 707 N94-13486
Estimations of temperature and humidity of the canopy in Amazon Forest using microwave data from SMMR sensor of Nimbus-7 satellite
|INPE-5444-TDI/490| p 720 N94-13614
Regional climatology sensitivity studies
|DE93-010712| p 722 N94-14057
Activities report of the Netherlands Remote Sensing Board
|ETN-93-93880| p 686 N94-14073
Circulation and rainfall climatology of a 10-year (1979 - 1988) integration with the Goddard Laboratory for atmospheres general circulation model
|NASA-TM-104591| p 723 N94-14074
CCI working group on climate data and its rapporteurs
|WCDMP-21| p 723 N94-14118
Meteorological data, new series A monographs. Volume 6, no. 3: Estimation of influence of high clouds in the radiation field and the climat by analysis of NOAA AVHRR data
|ETN-93-94170| p 723 N94-14707
Simulation of the present-day climate with the ECHAM model: Impact of model physics and resolution
|REPT-93| p 724 N94-14709

CLOCKS
A hardware implementation of a provably correct design of a fault-tolerant clock synchronization circuit
|NASA-TM-109001| p 759 N94-13450

CLOSED ECOLOGICAL SYSTEMS
Evaluation for membrane components of water recycling system
|NAL-TM-646| p 737 N94-13388
Survey and study on Environmental Control and Life Support (ECLS) technologies, part 2
|NASDA-CNT-930012-PT-2| p 737 N94-13472
Recycling in space
|NASA-TM-109307| p 737 N94-13615
Biomass production chamber air analysis of wheat study (BWT931)
|NASA-CR-194092| p 737 N94-13712
Validated environmental and physiological data from the CELSS Breadboard Projects Biomass Production Chamber. BWT931 (Wheat cv. Yecora Rojo)
|NASA-TM-109272| p 738 N94-13979

CLOTHING
Flammability of clothing, volume 2
|DSIS-93-00036-VOL-2| p 564 N94-13819

CLOUD COVER
The role of clouds and oceans in global greenhouse warming
|DE93-016206| p 706 N94-13079
Adaptation of humidity-cloud cover relations in the LAM
|KNMI-TR-144| p 722 N94-13992
A method for estimation of partial cloud cover within a pixel and its effect p 697 N94-14269

CLOUD PHYSICS
Gathering and exchange information on atmospheric chemistry and polluted atmospheres
|DE93-009940| p 705 N94-12869
A parameterization of cloud droplet nucleation
|DE93-007998| p 718 N94-12903
Remote sensing of low level cloud optical characteristics p 691 N94-14229

CLOUDS (METEOROLOGY)
Diagnostic studies of the HxOy-NxOy-O3 photochemical system using data from NASA GTE field expeditions
|NASA-CR-193672| p 706 N94-13170
An algorithm for the remote sensing of fog using satellite-data and additional information
|DLR-FB-92-23| p 688 N94-14135
The effects of anthropogenic aerosols on optical thickness and particle size of clouds. Part 1: Retrieval algorithm p 691 N94-14230
Earth radiation budget, cloud, and aerosol parameters derived from AVHRR and TOVS measurements p 691 N94-14233
A method for estimation of partial cloud cover within a pixel and its effect p 697 N94-14269
Meteorological data, new series A monographs. Volume 6, no. 3: Estimation of influence of high clouds in the radiation field and the climat by analysis of NOAA AVHRR data
|ETN-93-94170| p 723 N94-14707

CLUSTER ANALYSIS
Design of partially supervised classifiers for multispectral image data
|NASA-CR-194299| p 823 N94-13192

CLUSTERS
Structure stability and spectroscopy of metal clusters
|DE93-016142| p 567 N94-12836
Synthesis and properties of novel cluster phases
|DE93-017056| p 577 N94-13072
Thermochemistry of transition metal clusters
|DE93-016201| p 571 N94-13977

CLUTTER
Constant False Alarm Rate (CFAR) detection in Weibull clutter
|ITN-93-85190| p 600 N94-13537

COAL
Reverse micelle synthesis of nanoscale metal containing catalysts
|DE93-012869| p 572 N94-14184

COAL DERIVED GASES
Performance effects of coal-derived contaminants on the carbonate fuel cell
|DE93-013801| p 703 N94-13693
Status and future opportunities for conversion of synthesis gas to liquid energy fuels
|DE93-010025| p 584 N94-14089

COAL DERIVED LIQUIDS
Surfactant studies for bench-scale operation
|NASA-CR-194097| p 701 N94-13187

COAL GASIFICATION
Performance effects of coal-derived contaminants on the carbonate fuel cell
|DE93-013801| p 703 N94-13693

COAL LIQUEFACTION
Surfactant studies for bench-scale operation
|NASA-CR-194097| p 701 N94-13187
Surfactant studies for bench-scale operation
|NASA-CR-194511| p 564 N94-13947

COAL UTILIZATION
Surfactant studies for bench-scale operation
|NASA-CR-194097| p 701 N94-13187

COALESCING
Observation of the coalescing of beam into an asymmetric RF bucket by stochastic cooling
|DE93-015133| p 783 N94-13895

COASTS
Preliminary meteorological results for 1992 West Coast Scotland Experiment
|DE93-014677| p 720 N94-13404
Coastal scour problems and methods for prediction of maximum scour
|AD-A266658| p 726 N94-14775

COATING
Electrophoretic and electrolytic deposition of ceramic particles on porous substrates
|AD-A265141| p 575 N94-12812
Amorphous sol-gel insulating films
|DE93-012859| p 576 N94-12866
Polymer infiltration studies
|NASA-CR-194521| p 582 N94-14539
Impedance-power effects on plasma polymer surface finish using a helical resonator discharge
|DE93-016454| p 803 N94-14590

COATINGS
Computer code for scattering from impedance bodies of revolution. Part 3: Surface impedance with s and phi variation. Analytical and numerical results
|NASA-CR-193396| p 599 N94-13264
Reflective coatings for solar applications
|DE93-010026| p 702 N94-13381
Barium fluoride research and development at Lawrence Livermore National Laboratory
|DE93-014682| p 807 N94-13405
Impedance-power effects on plasma polymer surface finish using a helical resonator discharge
|DE93-016454| p 803 N94-14590
Solution chemistry optimization of sol-gel processed PZT thin films
|DE93-013776| p 814 N94-14695

COAXIAL CABLES
Microwave interconnection
|DE93-016580| p 625 N94-14533

COAXIAL NOZZLES
Simulation of preburner sprays, volume 1
|NASA-CR-193844| p 647 N94-14906

COBALT
Novel Co:MgF2 lidar for aerosol profiler
|NASA-CR-191525| p 654 N94-13091

COCHLEA
Underwater hearing: A review
|ISVR-TR-212| p 777 N94-14130

COCKPITS
Human factor implications of the Eurocopter AS332L-1 Super Puma cockpit p 525 N94-13319
Evaluation of two cockpit display concepts for civil tiltrotor instrument operations on steep approaches p 517 N94-13323

CODE DIVISION MULTIPLE ACCESS
User needs for propagation data p 613 N94-14657

CODERS
Digital sound: Subjective tests on commentary-quality codecs
|BBC-RD-1993/2| p 598 N94-12926
Exploiting the cannibalistic traits of Reed-Solomon codes p 609 N94-14378

CODES
Codes from an N-dimensional torus simplicially or cellularly decomposed p 747 N94-13438

CODING
PACT user's guide
|DE93-013093| p 742 N94-12840
Codes from an N-dimensional torus simplicially or cellularly decomposed p 747 N94-13438
Coding performance of the Probe-Orbiter-Earth communication link p 608 N94-14377
Estimating the size of Huffman code preambles p 609 N94-14379
Transform coding for space applications
|NASA-TM-106362| p 612 N94-14542

COEFFICIENTS
The importance of hard core repulsion in models of activity coefficients in aqueous electrolyte solutions: Illustration in the case of hydration theory
|DE93-012476| p 561 N94-12881

COGNITION
Heidegger's thinking p 736 N94-13442

COGNITIVE PSYCHOLOGY
Selection of behavioral tasks and development of software for evaluation of rhesus monkey behavior during spaceflight
|NASA-CR-194176| p 728 N94-13865

COLD FLOW TESTS
Design and evaluation of single and dual flow thrust vector nozzles with post exit vanes
|NASA-CR-193393| p 638 N94-14086
Numerical simulation of velocity-coupled combustion response of solid rocket propellants p 585 N94-14490

COLD GAS
Evaluation of dual flow thrust vector nozzles with exhaust stream impingement
|NASA-CR-193392| p 630 N94-13078

COLD NEUTRONS
Quasi-elastic neutron scattering studies of protein dynamics
|DE93-015074| p 782 N94-13414

COLD PLASMAS
Plasma diffusion through multidipole magnetic fields
|INPE-5460-PRE/1768| p 795 N94-12901
Implicit multi-fluid simulation of interpenetrating plasmas
|DE93-013351| p 801 N94-14342

COLLAPSE
The numerical simulation of the collapse process of axially compressed cylindrical shells with measured imperfections
|LR-705| p 674 N94-13905
The motion of a conical shaped liner driven by explosive load
|ITN-93-85215| p 585 N94-14507

COLLISION PARAMETERS
Collisional effects of trapped electrons on the anomalous particle and thermal pinches
|PPL-128| p 800 N94-13853
Measurement of the Fe-56(n,p)Mn-56, Al-27(n,p)Mg-27 and Al-27(n,alpha)Na-24 cross sections at 16.0, 17.0 and 18.3 MeV
|NPL-RSA(EXT)-38| p 783 N94-13883

COLLISIONLESS PLASMAS
Small scale magnetic islands in collisionless plasmas
|PPL-131| p 799 N94-13836
Numerical Studies of Collisionless Current Layers
|NASA-CR-194337| p 800 N94-13854

COLLISIONS
Collisions and separations in 2D hydrodynamical code
|ITN-93-85225| p 639 N94-14503
The space-time and energy parameters of deuterium braking by the central collision with atoms
|DE93-624144| p 788 N94-14881

COLLOCATION
The Chebyshev-Legendre method: Implementing Legendre methods on Chebyshev points
|NASA-CR-191497| p 769 N94-13725

COLOR
Color image processing for flat panel visual display modeling
[NASA-CR-193660] p 790 N94-12797
Validation of an inexpensive illuminant for aeromedical color vision screening
[DOT/FAA/AM-93/16] p 736 N94-14854
COLOR VISION
Validity of FAA-approved color vision tests for class 2 and class 3 aeromedical screening
[DOT/FAA/AM-93/17] p 735 N94-14846
Validation of an inexpensive illuminant for aeromedical color vision screening
[DOT/FAA/AM-93/16] p 736 N94-14854
COLORIMETRY
Colorimetric qualification of shear sensitive liquid crystal coatings
[NASA-CR-194126] p 806 N94-13291
Spectral reflectance of soils from Sao Paulo State
[INPE-5424-PRP/172] p 684 N94-13377
COMBINATORIAL ANALYSIS
ORGBUG: A Windows-based combinatorial geometry debugger
[DE93-016640] p 755 N94-14515
COMBUSTIBLE FLOW
Chemical reactions in scramjet engines: Reduced kinetic models for ignition, combustion and nozzle flow
[NAL-TR-1184] p 563 N94-13458
A technique for direct measurement of skin friction in supersonic combustion flow p 503 N94-13555
Numerical simulation of velocity-coupled combustion response of solid rocket propellants p 585 N94-14490
Analysis of reacting flowfields in low-thrust rocket engines and plumes p 552 N94-14491
Studying Turbulence Using Numerical Simulation Databases. 4: Proceedings of the 1992 Summer Program
[NASA-CR-194556] p 643 N94-14745
COMBUSTION
Infrared spectroscopy of organic free radicals related to combustion processes
[DE93-017086] p 562 N94-13222
Combustion synthesis and engineering of nanoparticles for electronic, structural, and superconductor applications
[DE93-016286] p 809 N94-13981
Characterization of diamond film growth in a combustion flame
[AD-A266659] p 816 N94-14839
COMBUSTION CHAMBERS
Combustor technology for future small gas turbine aircraft
[NASA-TM-106312] p 517 N94-13142
An experimental investigation of mixing enhancement in a simulated scramjet combustor by use of swirling jets
[NASA-TM-109246] p 518 N94-13190
Turbulent particle dispersion in confined swirling flows
[DLR-FB-92-32] p 637 N94-14045
Propulsion integration p 508 N94-14174
COMBUSTION CHEMISTRY
Modeling ignition chemistry
[DE93-012340] p 561 N94-12910
Fifteenth Combustion Research Conference
[DE93-015758] p 562 N94-13045
COMBUSTION EFFICIENCY
Effects of hydrogen addition on combustion performance of a LOX/kerosene rocket
[NAL-TR-1177] p 548 N94-12945
COMBUSTION PHYSICS
Coupled thermal response of objects and participating media in fires and large combustion systems
[DE93-012848] p 561 N94-12819
Modeling ignition chemistry
[DE93-012340] p 561 N94-12910
Fifteenth Combustion Research Conference
[DE93-015758] p 562 N94-13045
Infrared spectroscopy of organic free radicals related to combustion processes
[DE93-017086] p 562 N94-13222
A model for fuel fire duration and application to the B-1B bomber
[DE93-013000] p 512 N94-14292
Comparative ignition of hexane and octane isomers in a shock tube
[DE93-016535] p 566 N94-14869
COMBUSTION PRODUCTS
Equation of state for detonation products
[DE93-012671] p 583 N94-12921
Flamespreading in granular solid propellant: Design of an experiment
[AD-A266009] p 583 N94-12987
Ocean uptake of carbon dioxide
[DE93-012967] p 707 N94-13384
Estimation of the concentration versus the time profile of zinc chloride particles in smoke clouds generated by the Raufoss A/S instantaneous smoke RA-90 and DM-45 HC smoke generator
[FFI-93/6001] p 708 N94-13821
The role of human activity and land use change in atmospheric chemistry and air quality
[DE93-011871] p 709 N94-14022
Biodiesel/aquatic species project report, FY 1992
[DE93-010024] p 709 N94-14087
A laser-based technique to continuously monitor metal aerosol emissions
[DE93-012836] p 710 N94-14183
Three-dimensional modeling of diesel engine intake flow, combustion and emissions-2
[NASA-CR-191189] p 519 N94-14448
Summary of conclusions and recommendations from a visibility science workshop
[DE93-012770] p 710 N94-14523
COMBUSTION SYNTHESIS
Combustion synthesis and engineering of nanoparticles for electronic, structural, and superconductor applications
[DE93-016286] p 809 N94-13981
COMBUSTION WIND TUNNELS
Aerodynamic and aerothermal facilities 2: Continuous flow high enthalpy facilities p 506 N94-14160
COMET NUCLEI
Planning of a comet simulator
[ITN-93-85206] p 835 N94-13230
COMETS
Meteoroid environment near the Earth-Moon system
[NASA-CR-193670] p 835 N94-13203
Planning of a comet simulator
[ITN-93-85206] p 835 N94-13230
COMFORT
Body/cushion contact stress analysis during sitting
[ITN-93-85204] p 736 N94-13229
COMMITTEE ON SPACE RESEARCH
Planetary protection implementation on future Mars lander missions
[NASA-CP-3216] p 841 N94-13183
COMMUNICATING
The silent step in time
[CWI-CS-R9221] p 768 N94-13496
COMMUNICATION
Bulletin of the University of Electro-Communications, volume 6, no. 1, serial no. 11 p 746 N94-13432
NASA/DOD Aerospace Knowledge Diffusion Research Project. Paper 37: The impact of political control on technical communications: A comparative study of Russian and US aerospace engineers and scientists
[NASA-TM-109329] p 826 N94-14488
COMMUNICATION NETWORKS
Multicluster
[AD-A265869] p 758 N94-12930
On the end-to-end communication problem in unreliable networks
[ITN-93-85188] p 598 N94-13195
High speed all-optical networks
[NASA-CR-194384] p 791 N94-13682
Communications and control for electric power systems
[NASA-CR-194503] p 622 N94-13811
The developments of satellite communications of China p 618 N94-14282
The current situation, trends, international cooperation of space communication technological development in the Republic of Korea p 699 N94-14283
Joint experiments using ETS-5 p 618 N94-14284
NTT's activities in satellite communications technology development p 618 N94-14286
Future outlook on international satellite communications in Asia Pacific region p 618 N94-14287
Coding performance of the Probe-Orbiter-Earth communication link p 608 N94-14377
Overview of the Scalable Coherent Interface, IEEE STD 1596 (SCI)
[DE93-015247] p 761 N94-14476
NASA/DOD Aerospace Knowledge Diffusion Research Project. Paper 39: The role of computer networks in aerospace engineering
[NASA-TM-109331] p 825 N94-14487
NASA/DOD Aerospace Knowledge Diffusion Research Project. Paper 38: Computer Mediated Communication (CMC) and the communication of technical information in aerospace
[NASA-TM-109330] p 826 N94-14489
COMMUNICATION SATELLITES
Technical support for digital systems technology development. Task order 1: ISP contention analysis and control
[NASA-CR-190758] p 537 N94-12809
Fine time uplink synchronization for frequency-hopped spread spectrum satellite communication system
[ISBN-0-315-54370-1] p 600 N94-13488
Characteristics of the amateur radio means of the Arsene satellite
[CNES-NT-131] p 605 N94-13950
Multiple-symbol differential detection of DPSK with frequency offset
[DREO-TN-92-5] p 606 N94-14063
COMMUNICATION THEORY
Toward a verifiable approach to the design of concurrent computations
[DE93-012908] p 756 N94-14844
COMPACT GALAXIES
ROSAT: X ray survey of compact groups
[NASA-CR-193297] p 829 N94-13181
COMPATIBILITY
Materials compatibility of hydride storage materials with austenitic stainless steels
[DE93-013688] p 703 N94-13691
Study of the intermateability of Cannon and Souriau subminiature connectors
[CNES-NT-132] p 624 N94-13951
Compatibility testing of vacuum seal materials
[DE93-014366] p 663 N94-14113
Compatibility of refrigerants and lubricants with motor materials
[DE93-014768] p 583 N94-14801
COMPENSATORS
Electrical characterization of the JET A(sub 2) antenna: Comparison of model with measurements Wade, T.
[DE93-012964] p 607 N94-14291
COMPILERS
PACT user's guide
[DE93-013093] p 742 N94-12840
SCORE user's manual
[DE93-015987] p 822 N94-13121
Solving integer programs from dependence and synchronization problems
[AD-A265702] p 767 N94-13284
Programming languages made in Italy
[REPT-93-002] p 750 N94-13805
Hypertext Compiling Tools (HCT): Developing model based applications with standard hypertext systems
[REPT-92-049] p 750 N94-13822
COMPLEX COMPOUNDS
Charge storage and switching phenomena with molecular assemblies of metal complexes
[AD-A266673] p 787 N94-14778
CarbBank: A structural and bibliographic database for complex carbohydrates
[DE93-015582] p 827 N94-14803
COMPLEX SYSTEMS
Computational problems with the binomial failure rate model and incomplete common cause failure reliability data
[DE93-014346] p 669 N94-14143
The effects of internal fluctuations on a class of nonequilibrium statistical field theories
[DE93-016620] p 774 N94-14441
COMPLEXITY
Three, four, five, six or the complexity of scheduling with communication delays
[CWI-BS-R9229] p 751 N94-14004
COMPONENT RELIABILITY
Early detection of insulation failure in electric motors
[PB93-198208] p 626 N94-14686
COMPOSITE FUNCTIONS
Dynamic Forms. Part 1: Functions
[NASA-TP-3397] p 596 N94-13790
COMPOSITE MATERIALS
Flight service evaluation of composite components on the Bell helicopter model 206L
[NASA-CR-191499] p 555 N94-13267
Thermodiffusion in heterogeneous elastic solids and homogenization
[REPT-14/1993] p 578 N94-13468
Testing and analysis of curved frame specimens made from a Long Discontinuous Fiber (LDF) material
[NASA-TM-109014] p 557 N94-13711
Casting of superconducting composite materials (M-4) p 586 N94-13736
On the orthotropicity assumption and discontinuity conditions of conical shells
[LR-703] p 673 N94-13787
Review of Canadian aeronautical fatigue work, 1991-1993
[LTR-ST-1932] p 674 N94-13861
CMAPP user's manual, part 2
[DSIS-93-00858-PT-2] p 751 N94-14017
Development of software for composite materials analysis, phase 1, part 1
[DSIS-93-00857-PT-1-PHASE-1] p 558 N94-14105
Dynamic mechanical deformation of a SiC(sub p)/Al-Li (8090) composite
[DE93-014586] p 558 N94-14121
The structure and mechanical properties of Ru-Cu and Ru-Ti nanolayer composites
[DE93-014453] p 558 N94-14469

Small-angle scattering, contrast variation and the study of complex composite materials: A study of the structure of carbon black
[DE93-012707] p 559 N94-14690
A study of fiber volume fraction effects in notched unidirectional SCS-6/Ti-15V-3Cr-3Al-3Sn composite
[NASA-CR-191165] p 559 N94-14769
Materials and structures p 546 N94-14835

COMPOSITE STRUCTURES
Resin transfer molding of textile composites
[NASA-CR-191505] p 554 N94-12833
A probabilistic method for the buckling assessment of stiffened composite shells
[NASA-TM-106286] p 671 N94-13379
Finite element analysis of composite plates by use of modified complementary energy principle
p 672 N94-13596
Structural investigation of a damaged GRP/foam sandwich composite using x ray computed tomography
p 669 N94-13857
Hierarchical nonlinear behavior of hot composite structures
[NASA-TM-106229] p 676 N94-14041
Probabilistic micromechanics for high-temperature composites
[NASA-CR-191150] p 676 N94-14408
Buckling analysis of laminated thin shells in a hot environment
[NASA-TM-106302] p 683 N94-14776
Smart materials/structures technical analysis
[AD-A266771] p 766 N94-14785
Materials and structures p 546 N94-14835

COMPRESSED GAS
Low pressure storage of natural gas on activated carbon
[DE93-014053] p 660 N94-12851
Gas atomized Er3Ni powder for cryocooler applications
[DE93-011564] p 568 N94-13000
Aerodynamic and aerothermal facilities 2. Part 1: Short-duration, high-enthalpy facilities
p 506 N94-14159

COMPRESSIBILITY
Sub-grid scale modeling for large eddy simulations in analysis of shock-turbulence interactions
[DE93-013425] p 631 N94-13250
Response of a supersonic boundary layer to a compression corner p 645 N94-14759

COMPRESSIBILITY EFFECTS
Rapid distortion analysis and direct simulation of compressible homogeneous turbulence at finite Mach number p 645 N94-14757

COMPRESSIBLE BOUNDARY LAYER
Large-eddy simulation of laminar-turbulent breakdown at high speeds with dynamic subgrid-scale modeling
[NASA-CR-4533] p 629 N94-13064

COMPRESSIBLE FLOW
Three-Dimensional Boundary-Layer program (BL3D) for swept subsonic or supersonic wings with application to laminar flow control
[NASA-CR-4531] p 629 N94-13073
A time-accurate numerical method for chemically reacting flows at all Mach numbers p 500 N94-13198
A solution algorithm for the prediction of compressible laminar and turbulent shear flows p 634 N94-13635
Preconditioning and the limit to the incompressible flow equations
[NASA-CR-191500] p 769 N94-13717
Canonical forms of multidimensional steady inviscid flows
[NASA-CR-191488] p 769 N94-13722
CNSFV code development, virtual zone Navier-Stokes computations of oscillating control surfaces and computational support of the laminar flow supersonic wind tunnel
[NASA-CR-194259] p 504 N94-14030
Numerical simulation of velocity-coupled combustion response of solid rocket propellants
p 585 N94-14490
An implicit finite volume nodal point scheme for the solution of two-dimensional compressible Navier-Stokes equations p 640 N94-14603
Navier-Stokes simulation of transonic vortex flow over a delta wing p 640 N94-14606
A finite volume method for computation of viscous flow in complex configurations p 640 N94-14607
Development of an explicit multiblock/multigrid flow solver for viscous flows in complex geometries
[NASA-TM-106356] p 642 N94-14728
Studying Turbulence Using Numerical Simulation Databases. 4: Proceedings of the 1992 Summer Program
[NASA-CR-194556] p 643 N94-14745
Investigation of the dilatational dissipation in compressible homogeneous shear flow
p 645 N94-14758
Vortex-induced disturbance field in a compressible shear layer p 645 N94-14760
Toward a quasi-linear closure for compressible turbulence
[DE93-017185] p 647 N94-14895

COMPRESSION LOADS
Inelastic deformation mechanisms in SCS-6/Ti 15-3 MMC lamina under compression
[NASA-CR-191170] p 555 N94-13378
Buckling analysis of laminated thin shells in a hot environment
[NASA-TM-106302] p 683 N94-14776

COMPRESSION TESTS
The numerical simulation of the collapse process of axially compressed cylindrical shells with measured imperfections
[LR-705] p 674 N94-13905

COMPRESSIVE STRENGTH
An experimental investigation into the damage resistance and compression-after-impact strength of T800H/3900-2
[LTR-ST-1909] p 675 N94-13945
Effect of size, shape, and end condition of test specimen on compressive strength of high-strength concrete
[DE93-500412] p 682 N94-14653

COMPRESSOR BLADES
Performance of gas turbine compressor cleaners
[NLR-TP-91291-U] p 519 N94-14450

COMPRESSORS
Double inlet pulse tube cryocooler theory
[AD-A266832] p 597 N94-14877

COMPTON EFFECT
Gamma-insensitive optical focal plane array
[DE93-013100] p 792 N94-14317
The E2 N(yields)(Delta) transition from polarized Compton scattering
[DE93-012522] p 785 N94-14363

COMPUTATION
Smooth transitions between bump rendering algorithms
[DE93-012504] p 742 N94-12883
Computation and graphics in mathematical research
[DE93-016512] p 740 N94-13069

COMPUTATIONAL CHEMISTRY
Modeling and simulation of transport and combustion phenomena in a supersonic mixing layer
[ONERA-NT-1992-11] p 565 N94-14194
Theory, modeling, and simulation
[DE93-015607] p 755 N94-14571

COMPUTATIONAL FLUID DYNAMICS
A computer model for liquid jet atomization in rocket thrust chambers
[NASA-CR-194194] p 627 N94-12803
A method of predicting quasi-steady aerodynamics for flutter analysis of high speed vehicles using steady CFD calculations
[NASA-TM-109009] p 514 N94-12850
Approaches to high aspect ratio triangulations
[NASA-TM-107684] p 739 N94-12886
Integration of viscous effects into inviscid computational methods
[NASA-CR-193677] p 629 N94-13007
Large-eddy simulation of laminar-turbulent breakdown at high speeds with dynamic subgrid-scale modeling
[NASA-CR-4533] p 629 N94-13064
Three-Dimensional Boundary-Layer program (BL3D) for swept subsonic or supersonic wings with application to laminar flow control
[NASA-CR-4531] p 629 N94-13073
Surrogates for numerical simulations; optimization of eddy-promoter heat exchangers
[NASA-CR-191510] p 629 N94-13074
Averaging techniques for steady and unsteady calculations of a transonic fan stage
[NASA-TM-106231] p 499 N94-13108
Interacting scales and energy transfer in isotropic turbulence
[NASA-CR-191477] p 630 N94-13133
A time-accurate numerical method for chemically reacting flows at all Mach numbers p 500 N94-13198
The NAS parallel benchmarks
[NASA-TM-103863] p 740 N94-13200
Analysis of the Harrier forebody/inlet design using computational techniques
[NASA-CR-193616] p 503 N94-13463
Fully developed turbulent flow in rectangular interrupted-plate ducts
[ISBN-0-315-63594-0] p 632 N94-13474
A robust quasi-simultaneous interaction method for a full potential flow with a boundary layer with application to wing/body configurations
[NLR-TP-91397-U] p 503 N94-13531
A high-resolution Lax-Friedrichs scheme for hyperbolic conservation laws with source terms: Application to shallow water equations
[DM-62] p 632 N94-13535
Thermodynamic status of static and dynamic contact angles
[ISBN-0-315-73844-8] p 817 N94-13554
Numerical simulations of unsteady flows in turbomachines p 633 N94-13569
Topics on spatially high-order accurate methods and pre-conditioning for the Navier-Stokes equations with finite-rate chemistry p 633 N94-13572
Passage-averaged approximation of turbomachinery flows using vorticity-potential method
[ISBN-0-315-72716-0] p 634 N94-13598
Calculation of hypersonic shock structure using flux-split algorithms
[NASA-CR-194296] p 504 N94-13607
A future view of computational science in aircraft
[NASA-TM-109284] p 504 N94-13621
Numerical simulation of steady three-dimensional flows in axial turbomachinery bladerows p 634 N94-13630
A control volume finite element method for three-dimensional, incompressible, viscous fluid flow
[ISBN-0-315-72019-0] p 635 N94-13683
Numerical studies of spray combustion in liquid-fueled engines p 564 N94-13685
A computational study of the base region flow field for the M865 projectile
[ARL-TR-109] p 504 N94-13795
Images constructed from computed flow fields
[NASA-CR-194397] p 650 N94-13814
Numerical investigations in three-dimensional internal flows
[NASA-CR-194143] p 637 N94-13827
Tomographic methods in flow diagnostics
[NASA-TM-106330] p 650 N94-13876
CNSFV code development, virtual zone Navier-Stokes computations of oscillating control surfaces and computational support of the laminar flow supersonic wind tunnel
[NASA-CR-194259] p 504 N94-14030
The spectral viscosity method applied to simulation of waves in a stratified atmosphere
[FFI-92/7047] p 637 N94-14040
Computational techniques and capabilities
p 506 N94-14162
Extrapolation of ground test data to flight
p 507 N94-14170
Numerical simulation of a powered-lift landing, tracking flow features using overset grids, and simulation of high lift devices on a fighter-lift-and-control wing
[NASA-CR-194260] p 527 N94-14322
Domain connectivity among systems of overset grids
[NASA-CR-193390] p 508 N94-14326
Least-squares finite element solutions for three-dimensional backward-facing step flow
[NASA-TM-106353] p 770 N94-14407
An adaptive projection method for the incompressible Euler equations
[DE93-016428] p 639 N94-14434
Advanced ballistic range technology
[NASA-CR-194530] p 533 N94-14540
Proceedings of the Fluid Dynamics Symposium in honour of Professor R. Narasimha on his 60th birthday
[NAL-SP-9315] p 639 N94-14598
A vertex-based finite-volume algorithm for the Navier-Stokes equations p 639 N94-14599
Development of full-potential codes in the decade 1983-1993 p 639 N94-14600
The structure of laminar flow in a three-dimensional driven cavity p 640 N94-14601
A vortex method for viscous unsteady flows
p 640 N94-14602
An implicit finite volume nodal point scheme for the solution of two-dimensional compressible Navier-Stokes equations p 640 N94-14603
Wall interference studies: Revisited
p 640 N94-14604
Stability of spatially developing boundary layers
p 640 N94-14605
Navier-Stokes simulation of transonic vortex flow over a delta wing p 640 N94-14606
A finite volume method for computation of viscous flow in complex configurations p 640 N94-14607
A grid generation package for high aspect ratio wings
p 510 N94-14608
The phenomenon of vortex breakdown
p 510 N94-14609
Computation of nonequilibrium flows using PNS equations p 641 N94-14610
Hypersonic viscous flow computations
p 510 N94-14612
Development of a general purpose multigrid accelerated Navier-Stokes solver p 641 N94-14613
Development of parallel processing at NAL: A retrospect p 641 N94-14614
Panel codes for aerodynamic analysis at NAL
p 510 N94-14617

Numerical study of shock-induced combustion in methane-air mixtures
| NASA-TM-106354 | p 642 N94-14722
Development of an explicit multiblock/multigrid flow solver for viscous flows in complex geometries
| NASA-TM-106356 | p 642 N94-14728
Vibrational relaxation in hypersonic flow fields
| NASA-TP-3367 | p 776 N94-14733
Low altitude plume impingement handbook
| NASA-CR-194193 | p 643 N94-14741
LES versus DNS: A comparative study
p 644 N94-14753
Behavior of streamwise rib vortices in a three-dimensional mixing layer p 644 N94-14754
Estimation of the vortex length scale and intensity from two-dimensional samples p 645 N94-14756
DNS and modeling of the interaction between turbulent premixed flames and walls p 646 N94-14763
The evolution equation for the flame surface density in turbulent premixed combustion p 567 N94-14764
Numerical simulations of turbulent premixed H2/O2/N2 flames with complex chemistry p 567 N94-14765
Effect of finite-rate chemistry and unequal Schmidt numbers on turbulent non-premixed flames modeled with single-step chemistry p 567 N94-14766
Structure of turbulent non-premixed flames modeled with two-step chemistry p 567 N94-14767
Stochastic modeling of turbulent reacting flows
p 647 N94-14768
Contributions to numerical solution of Navier-Stokes equations in two and three dimensional flows
| ETN-93-94395 | p 647 N94-14816
A new Lagrangian method for three-dimensional steady supersonic flows
| NASA-TM-106068 | p 510 N94-14847
The development of a scalable parallel 3-D CFD algorithm for turbomachinery
| NASA-CR-193604 | p 664 N94-14848
Analytical description of the breakup of liquid jets in air
| NASA-CR-191503 | p 647 N94-14849

COMPUTATIONAL GEOMETRY
Approaches to high aspect ratio triangulations
| NASA-TM-107684 | p 739 N94-12886

COMPUTATIONAL GRIDS
Numerical simulation of a powered-lift landing, tracking flow features using overset grids, and simulation of high lift devices on a fighter-lift-and-control wing
| NASA-CR-194260 | p 527 N94-14322
Domain connectivity among systems of overset grids
| NASA-CR-193390 | p 508 N94-14326
Multigrid solution of internal flows using unstructured solution adaptive meshes
| NASA-CR-194233 | p 638 N94-14356
An adaptive projection method for the incompressible Euler equations
| DE93-016428 | p 639 N94-14434
Collisions and separations in 2D hydrodynamical code
| ITN-93-85225 | p 639 N94-14503
A grid generation package for high aspect ratio wings
p 510 N94-14608
Development of an explicit multiblock/multigrid flow solver for viscous flows in complex geometries
| NASA-TM-106356 | p 642 N94-14728

COMPUTER AIDED DESIGN
Method of characteristics design of a supersonic wind tunnel nozzle with square cross-section, supplement 3
| NASA-CR-194359 | p 527 N94-12824
A knowledge-based expert system to coordinate CAD/CAE with integration and test
| NASA-CR-191394 | p 745 N94-13130
Parachute system design, analysis, and simulation tool
| DE93-013755 | p 501 N94-13260
Software synthesis using generic architectures
| NASA-CR-194201 | p 745 N94-13355
The KASE approach to domain-specific software systems p 745 N94-13357
Creating a strategic plan for configuration management using computer aided software engineering (CASE) tools
| DE93-013663 | p 746 N94-13394
Designing and generating a GUI module using GUI
p 747 N94-13437
Software design by reusing architectures
| NASA-CR-194151 | p 747 N94-13443
Programming the multimodal interface
| DE93-013084 | p 748 N94-13576
Test/analysis correlation and model updating of the STARS 1 and 2 missile systems
| DE93-013774 | p 748 N94-13578
Mathematical optimization: A tool for aircraft design
| MBB-LME-251-S-PUB-0492 | p 751 N94-14006
Computer program for analysis of high speed, single row, angular contact, spherical roller bearing, SASHBEAN. Volume 1: User's guide
| NASA-CR-191183 | p 663 N94-14445
Computer program for analysis of high speed, single row, angular contact, spherical roller bearing, SASHBEAN. Volume 2: Mathematical formulation and analysis
| NASA-CR-191182 | p 664 N94-14446
Enterprise integration: A tool's perspective
| DE93-015651 | p 755 N94-14528
Development of PC-based Aeronautical Software (AEROWARE) p 641 N94-14611
SRISTI: The NAL method for the design and analysis of Natural Laminar Flow (NLF) airfoils
p 516 N94-14615
Proceedings of the Fifth NASA/NSF/DOD Workshop on Aerospace Computational Control
| NASA-CR-194515 | p 677 N94-14618
A component modes projection and assembly model reduction methodology for articulated, multi-flexible body structures p 677 N94-14622
Caesy: A software tool for computer-aided engineering
p 678 N94-14627
Control system design for flexible structures using data models p 527 N94-14646
Analysis of new composite architectures
| NASA-CR-194524 | p 559 N94-14715
Derated ion thruster development status
| NASA-TM-106292 | p 553 N94-14726
Optical systems integrated modeling
p 547 N94-14837
CAD data exchange with Martin Marietta Energy Systems, Inc., Oak Ridge, TN
| DE93-017233 | p 757 N94-14871
The further development and refinement of an expert-systems approach to the creative design of mechanisms and mechanical systems
| AD-A266812 | p 665 N94-14901

COMPUTER AIDED MANUFACTURING
Data fusion for adaptive control in manufacturing: Impact on engineering information models
| DE93-011555 | p 743 N94-12999
Rapid intelligent inspection process definition for dimensional measurement in advanced manufacturing
| DE93-011271 | p 748 N94-13480
Discrete event simulation using object-oriented programming: Application to manufacturing
| ERB-1037 | p 753 N94-14200
Enterprise integration: A tool's perspective
| DE93-015651 | p 755 N94-14528

COMPUTER AIDED TOMOGRAPHY
Tomographic methods in flow diagnostics
| NASA-TM-106330 | p 650 N94-13876

COMPUTER ANIMATION
Animation of multi-flexible body systems and its use in control system design p 678 N94-14629
Computational Control Workstation: Users' perspectives p 681 N94-14648

COMPUTER COMPATIBLE TAPES
Toxic Substances Control Act (TSCA) chemical substances inventory: Revised inventory synonym and preferred name file, Jan. 1993 documentation
| PB93-155166 | p 710 N94-14508

COMPUTER GRAPHICS
FORTRAN graphics routines for the Macintosh
| DE93-013092 | p 742 N94-12864
Smooth transitions between bump rendering algorithms
| DE93-012504 | p 742 N94-12883
VISART: Artificial vision for industrial use. A comprehensive system
| INPE-5379-TDI/474 | p 665 N94-12941
Computation and graphics in mathematical research
| DE93-016512 | p 740 N94-13069
View generated database
| NASA-CR-191397 | p 822 N94-13116
ULTRA 2 user's manual for ULTRA 2 revision 3.0
| DE93-015970 | p 744 N94-13120
Parametric binary dissection
| NASA-CR-191496 | p 762 N94-13184
Calculating intersections of surfaces in screen space
| NASA-CR-191498 | p 745 N94-13185
EGS (underscore) windows 2: An enhanced graphical interface to EGS
| DE93-010447 | p 746 N94-13382
Programming the multimodal interface
| DE93-013084 | p 748 N94-13576
Rotor stator CGI
| NASA-TM-109313 | p 518 N94-13608
A perspective on AVS in an engineering sciences environment
| DE93-015011 | p 596 N94-13889
USRA/RIACS
| NASA-CR-194334 | p 750 N94-13932
Ground Attack Profile Selector Program, version 3.0
| DSIS-93-00702 | p 753 N94-14207
An overview of parallel scientific visualization
| DE93-017105 | p 755 N94-14521

COMPUTER INFORMATION SECURITY
Multicluster
| AD-A265869 | p 758 N94-12930
UNICOS(trade name) security testing
| DE93-011680 | p 759 N94-13043
Security clauses in the writing and analysis of standards
| NPL-DITC-216-93 | p 824 N94-13879
Validated environmental and physiological data from the CELSS Breadboard Projects Biomass Production Chamber. BWT931 (Wheat cv. Yecora Rojo)
| NASA-TM-109272 | p 738 N94-13979
Kerberos: A UNIX-TCP/IP network authentication system
| DE93-011677 | p 760 N94-14011
Uniform user and group IDs on a large network
| DE93-013047 | p 760 N94-14315

COMPUTER NETWORKS
A network evaluation and analysis tool
| DE93-012647 | p 758 N94-12917
Multicluster
| AD-A265869 | p 758 N94-12930
Building the repositories to serve --- Superconducting Super Collider information system
| DE93-014100 | p 821 N94-12983
Development of ISO connection-oriented/correctionless gateways
| NASA-CR-193667 | p 821 N94-13030
UNICOS(trade name) security testing
| DE93-011680 | p 759 N94-13043
Mobile host internetworking using IP loose source routing
| AD-A265713 | p 759 N94-13052
Adaptive Transfer Function Networks
| DE93-014344 | p 745 N94-13151
High speed packet switching
| NASA-CR-191334 | p 759 N94-13177
High speed all-optical networks
| NASA-CR-194384 | p 791 N94-13682
A data distributed parallel algorithm for ray-traced volume rendering
| NASA-CR-191520 | p 749 N94-13721
Space and Earth sciences, computer systems, and scientific data analysis support, volume 1
| NASA-CR-194535 | p 741 N94-13788
USRA/RIACS
| NASA-CR-194334 | p 750 N94-13932
Kerberos: A UNIX-TCP/IP network authentication system
| DE93-011677 | p 760 N94-14011
Uniform user and group IDs on a large network
| DE93-013047 | p 760 N94-14315
Storage systems for national information assets
| DE93-015101 | p 825 N94-14331
Public census data on CD-ROM at Lawrence Berkeley Laboratory
| DE93-015273 | p 825 N94-14433
The National Storage Laboratory: A collaborative research project
| DE93-015099 | p 760 N94-14475
Overview of the Scalable Coherent Interface, IEEE STD 1596 (SCI)
| DE93-015247 | p 761 N94-14476
NASA/DOD Aerospace Knowledge Diffusion Research Project. Paper 39: The role of computer networks in aerospace engineering
| NASA-TM-109331 | p 825 N94-14487
NASA/DOD Aerospace Knowledge Diffusion Research Project. Paper 38: Computer Mediated Communication (CMC) and the communication of technical information in aerospace
| NASA-TM-109330 | p 826 N94-14489
An overview of parallel scientific visualization
| DE93-017105 | p 755 N94-14521

COMPUTER PROGRAMMING
PACT user's guide
| DE93-013093 | p 742 N94-12840
Beyond core: Making parallel computer I/O practical
| DE93-012347 | p 758 N94-12878
Artificial intelligence support for scientific model-building
| NASA-TM-109252 | p 761 N94-12890
Lecture notes on software process improvement
| AD-A265200 | p 744 N94-13049
Development of a portable multispectral thermal infrared camera
| NASA-CR-191340 | p 648 N94-13176
Solving integer programs from dependence and synchronization problems
| AD-A265702 | p 767 N94-13284
Generic software architecture based redesign
p 745 N94-13290
Programming the multimodal interface
| DE93-013084 | p 748 N94-13576

ANNS: An X Window based version of the AFIT neural network simulator
[AD-A266540] p 764 N94-13704
Adaptive Signal Processing Testbed: Software design specification
[DSIS-93-00259] p 604 N94-13870
Mongoose ASIC microcontroller programming guide
[NASA-RP-1319] p 623 N94-13871
VMEC30 software development: Tutorial manual
[DSIS-93-00351] p 750 N94-13944
Adaptive Signal Processing Testbed application software: User's manual
[DSIS-93-00261] p 606 N94-14038
Computational mechanics and supercomputing at LLNL
[DE93-016453] p 754 N94-14435
On-line upgrade of program modules using AdaPT
[NASA-CR-194331] p 754 N94-14472
ASTEC and MODEL: Controls software development at Goddard Space Flight Center p 678 N94-14628
Determining neural network connectivity using evolutionary programming
[AD-A266853] p 766 N94-14882

COMPUTER PROGRAMS
PACT user's guide
[DE93-013093] p 742 N94-12840
Reduce fluid experiment system flight data from IML-1
[NASA-CR-193835] p 804 N94-12873
Artificial intelligence support for scientific model-building
[NASA-TM-109252] p 761 N94-12890
Project proposal for partial computational physics support for Survivability of Coatings program
[DE93-013788] p 576 N94-12939
A path-oriented matrix-based knowledge representation system
[NASA-CR-4539] p 744 N94-13065
View generated database
[NASA-CR-191397] p 822 N94-13116
SCORE user's manual
[DE93-015987] p 822 N94-13121
Methods for evaluating the predictive accuracy of structural dynamic models
[NASA-CR-191337] p 671 N94-13124
Development of a portable multispectral thermal infrared camera
[NASA-CR-191340] p 648 N94-13176
High speed packet switching
[NASA-CR-191334] p 759 N94-13177
A hybrid finite element-boundary integral for the analysis of cavity-backed antennas of arbitrary shape
[NASA-CR-193719] p 599 N94-13236
Computer code for scattering from impedance bodies of revolution. Part 3: Surface impedance with s and phi variation. Analytical and numerical results
[NASA-CR-193396] p 599 N94-13264
Advanced computers and simulation
[DE93-014354] p 740 N94-13286
AQUIS: A PC-based source information manager
[DE93-012893] p 707 N94-13383
Finite element analysis of composite plates by use of modified complementary energy principle
p 672 N94-13596
Thermal Expert System (TEXSYS): Systems autonomy demonstration project, volume 2. Results
[NASA-TM-102877] p 538 N94-13989
CMAPP user's manual, part 2
[DSIS-93-00858-PT-2] p 751 N94-14017
Advanced ballistic range technology
[NASA-CR-194396] p 532 N94-14068
Intelligent environment for interpretation tasks of remotely sensed images
[INPE-5466-PRE/1774] p 687 N94-14082
EVES: An overview
[DSIS-93-00238] p 752 N94-14088
Computer program for thermal and transport properties of parahydrogen from 20 to 10,000 K
[NASA-TP-3378] p 552 N94-14102
Extrapolation of ground test data to flight
p 507 N94-14170
PC viruses: How do they do that?
[DE93-012581] p 753 N94-14289
BAKEOUT: A computer program for predicting diffusive outgassing from stainless steel
[DE93-012613] p 573 N94-14364
Nonlinear wave predictions in ceramics
[DE93-016516] p 582 N94-14436
Oak Ridge Environmental Information System (ORIES) site workstation information packet for OREIS 6.2
[DE93-010761] p 825 N94-14458
Atmospheric acoustic modeling
[DE93-016727] p 718 N94-14518
Enterprise integration: A tool's perspective
[DE93-015651] p 755 N94-14528
Some tools of the trade we've developed for our cross-section calculations
[DE93-013835] p 786 N94-14569
Theory, modeling, and simulation
[DE93-015607] p 755 N94-14571
VSAERO analysis of a Piper Cub aircraft
p 516 N94-14616
Panel codes for aerodynamic analysis at NAL
p 510 N94-14617
Switchover software reliability estimate for Paducah freezer/sublimer computer systems
[DE93-013844] p 756 N94-14696
A computer program to calculate growth rates for cracks at notches in regions of residual stress
[RAE-TM-MAT/STR-1207] p 683 N94-14818
Splines, contours and SVD subroutines
[DE93-016088] p 757 N94-14866

COMPUTER STORAGE DEVICES
The KSR1: Experimentation and modeling of poststore
[DE93-012539] p 759 N94-13470
Storage systems for national information assets
[DE93-015101] p 825 N94-14331
The National Storage Laboratory: A collaborative research project
[DE93-015099] p 760 N94-14475

COMPUTER SYSTEMS DESIGN
Fail-safe PVM: A portable package for distributed programming with transparent recovery
[AD-A266594] p 749 N94-13779
Transformation and composition of refusal graphs: Testability analysis
[LAAS-92435] p 751 N94-13995
Guide to the software architectural design phase
[ESA-PSS-05-04-ISSUE-1] p 753 N94-14190
Guide to the software detailed design and production phase
[ESA-PSS-05-05-ISSUE-1] p 753 N94-14191

COMPUTER SYSTEMS PERFORMANCE
UNICOS(trade name) security testing
[DE93-011680] p 759 N94-13043
Diskless supercomputers: Scalable, reliable I/O for the Tera-Op technology base
[NASA-CR-194089] p 740 N94-13363
Transformation and composition of refusal graphs: Testability analysis
[LAAS-92435] p 751 N94-13995
A design methodology for portable software on parallel computers
[NASA-CR-194181] p 752 N94-14139
Switchover software reliability estimate for Paducah freezer/sublimer computer systems
[DE93-013844] p 756 N94-14696

COMPUTER SYSTEMS PROGRAMS
Software synthesis using generic architectures
[NASA-CR-194201] p 745 N94-13355
ASPT software source code: SUN driver package
[DSIS-93-00262] p 751 N94-14014
ASPT software source code: Development system package, VME-C30 component
[DSIS-93-00276] p 751 N94-14016
A design methodology for portable software on parallel computers
[NASA-CR-194181] p 752 N94-14139
ASPT software source code: Host development system package
[DSIS-93-00277] p 753 N94-14197

COMPUTER SYSTEMS SIMULATION
Transformation and composition of refusal graphs: Testability analysis
[LAAS-92435] p 751 N94-13995

COMPUTER TECHNIQUES
A PC-PCL-based control system for the high-voltage pulsed-power operation of the Intense Diagnostic Neutral Beam (IDNB) Experiment
[DE93-014144] p 797 N94-13100
Study of computer system as a musical instrument
p 747 N94-13439
The identification of ability requirements and selection instruments for fighter pilot training
[AD-A266340] p 735 N94-13582
Thermal Expert System (TEXSYS): Systems autonomy demonstration project, volume 2. Results
[NASA-TM-102877] p 538 N94-13989

COMPUTER VISION
VISART: Artificial vision for industrial use. A comprehensive system
[INPE-5379-TDI/474] p 665 N94-12941
View generated database
[NASA-CR-191397] p 822 N94-13116
Non-scanned LADAR imaging and applications
[DE93-013772] p 655 N94-13261
Three dimensional tracking of four point planar patterns using corners
[ISBN-0-315-52149-X] p 791 N94-13490
Close range 3-D position sensing using stereo vision and point-of-correspondance through mathematical morphology
[ISBN-0-315-61012-3] p 763 N94-13515
Bayesian estimation of motion fields from image sequences
[ISBN-0-315-57212-4] p 772 N94-13540
Development of a tactile and vision integrated system, and object identification techniques for SPDM applications
[DSIS-93-00153] p 764 N94-13842
Development of a computer vision system to supplement the active tactile sensing capability in a structured environment
[DSIS-93-00072] p 764 N94-13844
Computer vision and sensor fusion for detecting buried objects
[DE93-012605] p 700 N94-14566
Passive recovery of scene geometry for an unmanned ground vehicle
[AD-A266670] p 766 N94-14777
Depths from focusing and defocusing
[AD-A266644] p 735 N94-14797

COMPUTERIZED SIMULATION
A computer model for liquid jet atomization in rocket thrust chambers
[NASA-CR-194194] p 627 N94-12803
A 3D gyrokinetic particle-in-cell simulation of fusion plasma microturbulence on parallel computers
[DE93-012503] p 794 N94-12846
MHD shocks in coronal mass ejections
[NASA-CR-193418] p 828 N94-12970
Comparison of analytic Whipple bumper shield ballistic limits with CTH simulations
[DE93-015126] p 539 N94-13006
Electric propulsion system technology
[NASA-CR-194100] p 549 N94-13055
Computer simulations for the adsorption of polymers onto surfaces
[DE93-016667] p 577 N94-13070
Surrogates for numerical simulations; optimization of eddy-promoter heat exchangers
[NASA-CR-191510] p 629 N94-13074
A wall interference assessment/correction system
[NASA-CR-194174] p 500 N94-13076
View generated database
[NASA-CR-191397] p 822 N94-13116
Control algorithm implementation for a redundant degree of freedom manipulator
[NASA-CR-191339] p 762 N94-13131
Adaptive Transfer Function Networks
[DE93-014344] p 745 N94-13151
Implementation of ADI: Schemes on MIMD parallel computers
[NASA-CR-193720] p 759 N94-13204
Kinetic simulations of ultra-intense laser plasma interactions and a novel method of generating odd harmonics
[DE93-014418] p 797 N94-13207
Magnetic fusion computing: A personal retrospective view
[DE93-014147] p 797 N94-13217
Molecular dynamics simulation of electronically excited polyatomic molecules
[DE93-623045] p 781 N94-13225
Application of new electro-optic technology to Space Station Freedom data management system
[NASA-CR-177622] p 538 N94-13257
Parachute system design, analysis, and simulation tool
[DE93-013755] p 501 N94-13260
Advanced computers and simulation
[DE93-014354] p 740 N94-13286
A model for rotorcraft flying qualities studies
p 523 N94-13308
Attitude determination of stratospheric balloons using Kalman filters
[INPE-5498-TDI/513] p 649 N94-13366
Future developments of the NLR research flight simulator
[NLR-TP-92143-U] p 528 N94-13498
Hashing and rehashing in emulated shared memory
[CWI-CS-R9240] p 740 N94-13525
On the foundations of final semantics: Non-standard sets, metric spaces, partial orders
[CWI-CS-R9241] p 768 N94-13526
Rotor stator CGI
[NASA-TM-109313] p 518 N94-13608
Numerical simulation of steady three-dimensional flows in axial turbomachinery bladerows p 634 N94-13630
Six degree of freedom
[NASA-TM-109295] p 749 N94-13636
Numerical simulation and parameterization of orographic gravity waves p 713 N94-13647
ANNS: An X Window based version of the AFIT neural network simulator
[AD-A266540] p 764 N94-13704

Numerical Studies of Collisionless Current Layers
[NASA-CR-194337] p 800 N94-13854
A perspective on AVS in an engineering sciences environment
[DE93-015011] p 596 N94-13889
Numerical simulations of Nd:YAG laser amplifiers
[FFI/RAPPORT-92/7028] p 657 N94-13970
Human factors in aviation maintenance: Phase 3, volume 1
[DOT/FAA/AM-93/15] p 738 N94-14023
Hierarchical nonlinear behavior of hot composite structures
[NASA-TM-106229] p 676 N94-14041
Computer program for thermal and transport properties of parahydrogen from 20 to 10,000 K
[NASA-TP-3378] p 552 N94-14102
Computational techniques and capabilities
p 506 N94-14162
Discrete event simulation using object-oriented programming: Application to manufacturing
[ERB-1037] p 753 N94-14200
Implicit multi-fluid simulation of interpenetrating plasmas
[DE93-013351] p 801 N94-14342
Cammatic: An approach to improve DSS 13 antenna gravity-loading performance p 608 N94-14374
Multi-dimensional high order essentially non-oscillatory finite difference methods in generalized coordinates
[NASA-CR-194031] p 770 N94-14429
Turbulent diffusion in homogeneous shear flow with stable density stratification
[DLR-FB-92-26] p 639 N94-14443
Sidewall thermometry perturbations to nonlinear heat transport near the (lambda) transition in He-4
[DE93-014990] p 817 N94-14453
Enterprise integration: A tool's perspective
[DE93-015651] p 755 N94-14528
Theory, modeling, and simulation
[DE93-015607] p 755 N94-14571
Development of PC-based Aeronautical Software (AEROWARE) p 641 N94-14611
VSAERO analysis of a Piper Cub aircraft
p 516 N94-14616
The use of linked lists in the simulation of controller-structure interaction p 679 N94-14630
Computational strategies in the dynamic simulation of constrained flexible MBS p 679 N94-14635
Parallel methods for dynamic simulation of multiple manipulator systems p 680 N94-14637
Real-time dynamics simulation of the Cassini spacecraft using DARTS. Part 1: Functional capabilities and the spatial algebra algorithm p 680 N94-14638
Real-time dynamic simulation of the Cassini spacecraft using DARTS. Part 2: Parallel/vectorized real-time implementation p 680 N94-14639
Simulation of linear mechanical systems
p 680 N94-14641
Simulation of hypersonic, reacting flow around reentry bodies: Comparisons of numerical and experimental results
[MBB-LME-211-S-PUB-507] p 509 N94-14710
Studying Turbulence Using Numerical Simulation Databases. 4: Proceedings of the 1992 Summer Program
[NASA-CR-194556] p 643 N94-14745
On the local nature of the energy cascade
p 643 N94-14748
Search for subgrid scale parameterization by projection pursuit regression p 643 N94-14749
Robust non convex optimization algorithms: Codes and numerical simulation of large scale
[ETN-93-94354] p 756 N94-14813

CONCATENATED CODES
Enhanced decoding for the Galileo S-band mission
p 609 N94-14380

CONCENTRATION (COMPOSITION)
Two color holographic interferometry for microgravity application
[NASA-CR-194424] p 651 N94-14447

CONCENTRATORS
High-flux testing of heat pipes for point-focus solar collector systems
[DE93-011581] p 628 N94-12884

CONCRETE STRUCTURES
A data base for aging of structural materials
[DE93-009714] p 824 N94-13915

CONCRETES
Effect of size, shape, and end condition of test specimen on compressive strength of high-strength concrete
[DE93-500412] p 682 N94-14653

CONCURRENT PROCESSING
Toward a verifiable approach to the design of concurrent computations
[DE93-012908] p 756 N94-14844

CONDENSATION
Planning of a comet simulator
[ITN-93-85206] p 835 N94-13230

CONDENSING
Dust production in the envelopes of carbon stars: R Coronae Borealis
[ETN-93-94389] p 839 N94-14075

CONDUCTING POLYMERS
Schemes for the use of conducting polymers as active materials in electrochemical supercapacitors
[DE93-012713] p 580 N94-14179

CONDUCTION ELECTRONS
Theory of the negative magnetoresistance in magnetic metallic multilayers
[DE93-013912] p 776 N94-14584

CONDUCTIVE HEAT TRANSFER
Coupled thermal response of objects and participating media in fires and large combustion systems
[DE93-012848] p 561 N94-12819
Project proposal for partial computational physics support for Survivability of Coatings program
[DE93-013788] p 576 N94-12939
Implementation of ADI: Schemes on MIMD parallel computers
[NASA-CR-193720] p 759 N94-13204
Meteorological data, new series A monographs. Volume 6, no. 4: Modelization of heat fluxes at Earth ground with consideration of vegetation
[ETN-93-94169] p 723 N94-14546
Thermal design of hybrid circuits: Tools and methodology
[LAAS-92515] p 626 N94-14713

CONDUCTIVITY
Modeling ignition chemistry
[DE93-012340] p 561 N94-12910

CONDUCTORS
Study of novel conductive paints for solar cell electromagnetic fields
[DE93-015088] p 581 N94-14337
Microwave interconnection
[DE93-016580] p 625 N94-14533
The electric field of a current-carrying conductor
[DE93-626637] p 617 N94-14892

CONFERENCES
The 1992 JSEE/JWEA Joint Conference
[DE93-793955] p 700 N94-12822
High-temperature corrosion and protection of materials
[DE93-011072] p 568 N94-12998
Proceedings of the Workshop on Applications of Synchrotron Radiation to Trace Impurity Analysis for Advanced Silicon Processing
[DE93-013389] p 805 N94-13020
Fifteenth Combustion Research Conference
[DE93-015758] p 562 N94-13045
Ninth Annual NASA/Contractors Conference on Quality and Productivity. World Class Excellence: The Journey Continues. Keynote presentations
[NASA-CR-194513] p 665 N94-13148
Ninth Annual NASA/Contractors Conference on Quality and Productivity. World Class Excellence: The Journey Continues. Conference presentations
[NASA-CR-194514] p 665 N94-13153
Piloting Vertical Flight Aircraft: A Conference on Flying Qualities and Human Factors
[NASA-CP-3220] p 521 N94-13294
The 1990 Western Pacific Geophysics meeting
[NASA-CR-193456] p 712 N94-13334
The American Geophysical Union Chapman Conference on Tectonics and Topography
[NASA-CR-193454] p 713 N94-13335
Proceedings of the 11th Space Surveillance Workshop, volume 1
[AD-A265120] p 531 N94-13358
Electrical Actuation Technology Bridging
[NASA-CP-3213] p 551 N94-13417
STS-32 post-flight press conference
[NASA-TM-109294] p 541 N94-13634
Gordon Research Conference on Chronobiology, 1991
[AD-A266354] p 728 N94-13698
The 8th Workshop on the Mathematical Foundations of Programming Semantics
[AD-A266436] p 749 N94-13700
Asia-Pacific ISY conference, volume 1
[NASDA-CM-199-1] p 532 N94-14098
CCI working group on climate data and its rapporteurs
[WCDMP-21] p 723 N94-14118
Methodology of Hypersonic Testing
[VKI-LS-1993-03] p 505 N94-14153
Asia-Pacific ISY Conference, volume 2
[NASDA-CM-199-VOL-2] p 688 N94-14209
The Eighth Annual NASA/Contractors Conference and 1991 National Symposium on Quality and Productivity: Extending the boundaries of total quality management
[NASA-TM-109276] p 669 N94-14321
Fourteenth National Industrial Energy Technology Conference: Proceedings
[DE93-016698] p 710 N94-14516
Proceedings of the Fluid Dynamics Symposium in honour of Professor R. Narasimha on his 60th birthday
[NAL-SP-9315] p 639 N94-14598
Proceedings of the Fifth NASA/NSF/DOD Workshop on Aerospace Computational Control
[NASA-CR-194515] p 677 N94-14618
STS-35 post-flight press conference
[NASA-TM-109490] p 537 N94-14736
Studying Turbulence Using Numerical Simulation Databases. 4: Proceedings of the 1992 Summer Program
[NASA-CR-194556] p 643 N94-14745
The 4th International Symposium on Analysis and Detection of Explosives
[DE93-620280] p 585 N94-14829
Pattern and Process in Landscape Ecology: Eighth Annual US Landscape Ecology Symposium
[DE93-014032] p 711 N94-14859

CONFIGURATION MANAGEMENT
Creating a strategic plan for configuration management using computer aided software engineering (CASE) tools
[DE93-013663] p 746 N94-13394

CONFINEMENT
Active density control in DIII-D H-mode plasmas
[DE93-015477] p 802 N94-14570
The role of electric field shear stabilization of turbulence in the H-mode to VH-mode transition in D3-D
[DE93-015474] p 802 N94-14583

CONFORMAL MAPPING
Scalar curvature and spherical-type Riemannian manifolds
[DE93-622852] p 767 N94-12895
Torsion problem of elastostatics: An application of boundary element method and relation with conformal mapping
[DSIS-92-03794] p 674 N94-13833

CONICAL BODIES
Predicting the vibrations of a spinning inflated membrane
[DE93-010690] p 676 N94-14456

CONJUGATE GRADIENT METHOD
Optimization and eigenvalue computation with application to meteorology and oceanography
[DE93-015310] p 744 N94-13024
Deconvolution for positive signals
[DE93-013044] p 773 N94-14314
Analysis, approximation, and computation of a coupled solid/fluid temperature control problem
[NASA-TM-106351] p 771 N94-14731

CONNECTION MACHINE
A 3D gyrokinetic particle-in-cell simulation of fusion plasma microturbulence on parallel computers
[DE93-012503] p 794 N94-12846
A data distributed parallel algorithm for ray-traced volume rendering
[NASA-CR-191520] p 749 N94-13721

CONSERVATION
Fourteenth National Industrial Energy Technology Conference: Proceedings
[DE93-016698] p 710 N94-14516

CONSERVATION EQUATIONS
A control volume finite element method for three-dimensional, incompressible, viscous fluid flow
[ISBN-0-315-72019-0] p 635 N94-13683
Review of mathematical and physical basis of two-phase flow modeling
[KFK-4759] p 642 N94-14708

CONSERVATION LAWS
A high-resolution Lax-Friedrichs scheme for hyperbolic conservation laws with source terms: Application to shallow water equations
[DM-62] p 632 N94-13535
A control volume finite element method for three-dimensional, incompressible, viscous fluid flow
[ISBN-0-315-72019-0] p 635 N94-13683
Full Riemann solution of the one- and two-dimensional Euler equations
[DLR-FB-92-34] p 638 N94-14188
On transport of energy, momentum, orbital angular momentum and self-angular momentum of electromagnetic wave in dispersal media
[DE93-624179] p 617 N94-14883

CONSTITUTIVE EQUATIONS
A continuum theory for liquid crystals describing different degrees of orientational order
[ETN-93-94392] p 807 N94-13590
Development of time-dependent orthotropic constitutive law of a thermoplastic composite material
p 556 N94-13595
Evaluation for rheological constitutive relations, using the indentation technique p 775 N94-13627

Probabilistic micromechanics for high-temperature composites
| NASA-CR-191150 | p 676 N94-14408
Microstructural influences on the mechanical properties of solder
| DE93-015044 | p 573 N94-14474
CONSTRAINTS
Kinematics and constraints associated with swashplate blade pitch control
| NASA-TM-102265 | p 520 N94-12820
Generating knight's tours without backtracking from errors
| AD-A266807 | p 772 N94-14900
CONSTRUCTION
Application of synchrotron radiation in chemical dynamics
| DE93-015040 | p 563 N94-13411
On the construction and decoding of hyperelliptic codes p 747 N94-13435
Construction of the Courant-Snyder invariants for the non-linear equations of motion under presence of the linear coupling
| DE93-017565 | p 788 N94-14872
CONSTRUCTION MATERIALS
Sequestering carbon dioxide in industrial polymers: Building materials for the 21st century
| DE93-016087 | p 580 N94-14297
Compatibility of refrigerants and lubricants with motor materials
| DE93-014768 | p 583 N94-14801
CONTACT LOADS
A vacuum four-ball tribometer to evaluate liquid lubricants for space applications
| NASA-TM-106264 | p 575 N94-12842
Some aspects of sheet forming simulation using explicit finite element techniques
| DE93-012479 | p 663 N94-13975
Computer program for analysis of high speed, single row, angular contact, spherical roller bearing, SASHBEAN. Volume 2: Mathematical formulation and analysis
| NASA-CR-191182 | p 664 N94-14446
CONTACTORS
Plasma contactor technology for Space Station Freedom
| NASA-TM-106291 | p 553 N94-14725
CONTAINERLESS MELTS
Stabilized electromagnetic levitator
| NASA-CR-194261 | p 586 N94-12805
Drop dynamics in space and interference with acoustic field (M-15) p 588 N94-13747
Preparation of optical materials used in non-visible region (M-17) p 589 N94-13749
Protein crystal growth p 591 N94-13756
Containerless processing of undercooled melts
| NASA-CR-194350 | p 572 N94-14123
CONTAMINANTS
AQUIS: A PC-based source information manager
| DE93-012893 | p 707 N94-13383
CONTAMINATION
Integrated, flexible, and rapid geophysical surveying
| DE93-009989 | p 712 N94-12906
Vendor information system for innovative treatment technologies. User manual (VISITT version 2.0). Number 2
| PB93-196640 | p 821 N94-12936
Proceedings of the Workshop on Applications of Synchrotron Radiation to Trace Impurity Analysis for Advanced Silicon Processing
| DE93-013389 | p 805 N94-13020
Stability of reference masses 1: Evidence for posiible variations in the mass of reference kilograms arising from mercury contamination
| NPL-DMM(A)-86 | p 708 N94-13667
A review of robust detection
| DSIS-93-00400 | p 603 N94-13829
Optical degradation issues for XUV projection lithography systems
| DE93-012658 | p 626 N94-14805
CONTINENTAL SHELVES
Overview: Gas hydrate geology and geography
| DE93-014043 | p 688 N94-14151
CONTINUITY EQUATION
Contributions to numerical solution of Navier-Stokes equations in two and three dimensional flows
| ETN-93-94395 | p 647 N94-14816
CONTINUOUS RADIATION
Predicted performance of a dc beam driven FEM oscillator designed for fusion applications at 200-250 GHz
| DE93-013414 | p 655 N94-13145
Beam halo formation from space-charge dominated beams in uniform focusing channels
| DE93-014458 | p 789 N94-13209
Long-pulse operation of a gyrotron with beam/RF separation
| DE93-015007 | p 649 N94-13410
Microchannel cooled heatsinks for high average power laser diode arrays
| DE93-016533 | p 658 N94-14442
Tetravalent chromium (Cr(4+)) as laser-active ion for tunable solid-state lasers
| NASA-CR-194527 | p 659 N94-14576
CONTINUOUS SPECTRA
The continuum emission of active galactic nuclei
| ITN-93-85208 | p 847 N94-13232
CONTINUUM MECHANICS
Microstructural influences on the mechanical properties of solder
| DE93-015044 | p 573 N94-14474
Differential Sensitivity Theory applied to the MESA code for high pressure interactions
| DE93-016460 | p 676 N94-14591
Computational strategies in the dynamic simulation of constrained flexible MBS p 679 N94-14635
Nonlinear analysis, scientific computation, and continuum mechanics applied to the science of materials
| AD-A266641 | p 817 N94-14680
Review of mathematical and physical basis of two-phase flow modeling
| KFK-4759 | p 642 N94-14708
CONTOURS
Splines, contours and SVD subroutines
| DE93-016088 | p 757 N94-14866
CONTRACT MANAGEMENT
Johnson Space Center procurement: Controls over payments to contractors should be strengthened
| AD-A265722 | p 819 N94-13060
Shared visions: Partnership of Rockwell International and NASA Cost Effectiveness Enhancements (CEE) for the space shuttle system integration program p 668 N94-13166
CONTRACTORS
Photovoltaics: Contract lists, fiscal year 1992
| DE93-000093 | p 701 N94-12902
Johnson Space Center procurement: Controls over payments to contractors should be strengthened
| AD-A265722 | p 819 N94-13060
Ninth Annual NASA/Contractors Conference on Quality and Productivity. World Class Excellence: The Journey Continues. Keynote presentations
| NASA-CR-194513 | p 665 N94-13148
Ninth Annual NASA/Contractors Conference on Quality and Productivity. World Class Excellence: The Journey Continues. Conference presentations
| NASA-CR-194514 | p 665 N94-13153
Kennedy Space Center's NASA/Contractor Team-Centered Total Quality Management Seminar: Results, methods, and lessons learned p 667 N94-13162
NASA Johnson Space Center: Total quality partnership p 668 N94-13165
NASA/contractor partnership on the second TDRSS ground terminal program: Breaking barriers p 668 N94-13168
The Eighth Annual NASA/Contractors Conference and 1991 National Symposium on Quality and Productivity: Extending the boundaries of total quality management
| NASA-TM-109276 | p 669 N94-14321
CONTROL BOARDS
Human factor implications of the Eurocopter AS332L-1 Super Puma cockpit p 525 N94-13319
CONTROL EQUIPMENT
Electrical Actuation Technology Bridging
| NASA-CP-3213 | p 551 N94-13417
Techniques for improving the performance of a simplified electronic fuel controller with incremental actuation for small gas turbine engines
| ISBN-0-315-56062-2 | p 661 N94-13521
Mongoose ASIC microcontroller programming guide
| NASA-RP-1319 | p 623 N94-13871
Laser beam control and diagnostic systems for the copper-pumped dye laser system at Lawrence Livermore National Laboratory
| DE93-016529 | p 658 N94-14437
Switchover software reliability estimate for Paducah freezer/sublimer computer systems
| DE93-013844 | p 756 N94-14696
CONTROL MOMENT GYROSCOPES
A superconducting large-angle magnetic suspension
| NASA-CR-189735 | p 596 N94-13141
CONTROL SIMULATION
Propulsion simulator for magnetically-suspended wind tunnel models
| NASA-CR-189560 | p 527 N94-13127
Simulator study of uncoupled control functions. Use of manual pointing modes when aiming at ground targets and oncoming airborne target
| FFA-TN-1992-18 | p 528 N94-13588
Real-time dynamics simulation of the Cassini spacecraft using DARTS. Part 1: Functional capabilities and the spatial algebra algorithm p 680 N94-14638
Real-time dynamic simulation of the Cassini spacecraft using DARTS. Part 2: Parallel/vectorized real-time implementation p 680 N94-14639
Control structural interaction testbed: A model for multiple flexible body verification p 544 N94-14649
CONTROL STABILITY
Development of a high-speed mechanical drive system for oscillating an annular blade row in the bending mode
| NAL-TR-1170 | p 502 N94-13342
Generalized impedance control of a redundant manipulator p 661 N94-13575
Robust synthesis of discrete-time multivariable control systems with induced delays p 662 N94-13642
Optimization-based controller design for rotorcraft p 527 N94-14642
CONTROL STICKS
The application of active side arm controllers in helicopters p 522 N94-13302
A four-axis hand controller for helicopter flight control p 522 N94-13305
CONTROL SURFACES
Actuator and aerodynamic modeling for high-angle-of-attack aeroservoelasticity
| NASA-TM-4493 | p 520 N94-13255
CNSFV code development, virtual zone Navier-Stokes computations of oscillating control surfaces and computational support of the laminar flow supersonic wind tunnel
| NASA-CR-194259 | p 504 N94-14030
CONTROL SYSTEMS DESIGN
Roller-gear drives for robotic manipulators design, fabrication and test
| NASA-CR-194248 | p 660 N94-12802
Feasibility study of an orbiting laboratory for testing CSI technology
| NASA-CR-191524 | p 540 N94-13016
Inertial confinement fusion program
| DE93-013372 | p 796 N94-13047
Force reflecting hand controller for manipulator teleoperation
| NASA-CR-191345 | p 661 N94-13129
A superconducting large-angle magnetic suspension
| NASA-CR-189735 | p 596 N94-13141
Design criteria for integrated flight/propulsion control systems for STOVL fighter aircraft p 521 N94-13297
Rotorcraft flying qualities improvement using advanced control p 522 N94-13303
Compatibility of information and mode of control: The case for natural control systems p 523 N94-13307
Control system design of a cable-mounted model used for dynamic wind tunnel testing
| NAL-TR-1161 | p 528 N94-13337
Transmission zeros of spacecraft attitude control system
| NAL-TR-1166 | p 540 N94-13339
Electrical Actuation Technology Bridging
| NASA-CP-3213 | p 551 N94-13417
A hardware implementation of a provably correct design of a fault-tolerant clock synchronization circuit
| NASA-TM-109001 | p 759 N94-13450
Dynamic Forms. Part 1: Functions
| NASA-TP-3397 | p 596 N94-13790
Piston engine intake and exhaust system design
| ISVR-TR-222 | p 663 N94-13874
Tuning of Gaussian stochastic control systems
| CWI-BS-R9223 | p 765 N94-14018
Self-tuning control techniques for multivariable systems
| INPE-5449-TDI/495 | p 765 N94-14084
Propulsion integration p 508 N94-14174
Strategic avionics technology definition studies. Subtask 3-1A: Electrical Actuation (ELA) systems
| NASA-CR-194393 | p 536 N94-14323
Large space structures and systems in the space station era: A bibliography with indexes (supplement 05)
| NASA-SP-7085(05) | p 543 N94-14411
Proceedings of the Fifth NASA/NSF/DOD Workshop on Aerospace Computational Control
| NASA-CR-194515 | p 677 N94-14618
A component modes projection and assembly model reduction methodology for articulated, multi-flexible body structures p 677 N94-14622
Caesy: A software tool for computer-aided engineering p 678 N94-14627
ASTEC and MODEL: Controls software development at Goddard Space Flight Center p 678 N94-14628
Animation of multi-flexible body systems and its use in control system design p 678 N94-14629
Real-time dynamic simulation of the Cassini spacecraft using DARTS. Part 2: Parallel/vectorized real-time implementation p 680 N94-14639
Optimization-based controller design for rotorcraft p 527 N94-14642
Control system design for flexible structures using data models p 527 N94-14646

PACE: A test bed for the dynamics and control of flexible multibody systems p 527 N94-14650
A program for the investigation of the Multibody Modeling, Verification, and Control Laboratory p 682 N94-14652
A new treatment of periodic systems with applications to helicopter rotor blade dynamics
| AD-A266770 | p 510 N94-14784

CONTROL THEORY
Relegation for decentralized control
| AD-A265720 | p 819 N94-13059
Active control of acoustic pressure fields using smart material technologies
| NASA-CR-191480 | p 768 N94-13354
Generalized impedance control of a redundant manipulator p 661 N94-13575
Stochastic realization of finite-valued processes and primes in the positive matrices
| CWI-BS-R9222 | p 773 N94-13677
Decentralized control of uncertain systems via sensitivity models
| DE93-012963 | p 766 N94-14568
Simulation of linear mechanical systems p 680 N94-14641
On l(1): Optimal decentralized performance p 681 N94-14643
PACE: A test bed for the dynamics and control of flexible multibody systems p 527 N94-14650

CONTROL VALVES
Electrical Actuation Technology Bridging
| NASA-CP-3213 | p 551 N94-13417

CONTROLLABILITY
Rotorcraft flying qualities improvement using advanced control p 522 N94-13303
In-flight simulation of high agility through active control: Taming complexity by design p 523 N94-13306
Improvements in hover display dynamics for a combat helicopter p 523 N94-13310
The development and potential of inverse simulation for the quantitative assessment of helicopter handling qualities p 523 N94-13311
Handling qualities effects of display latency p 517 N94-13316
Effects of simulator motion and visual characteristics on rotorcraft handling qualities evaluations p 524 N94-13317
Design and pilot evaluation of the RAH-66 Comanche Core AFCS p 525 N94-13321
Design and pilot evaluation of the RAH-66 Comanche selectable control modes p 525 N94-13322
Evaluation of two cockpit display concepts for civil tiltrotor instrument operations on steep approaches p 517 N94-13323
Flight testing and frequency domain analysis for rotorcraft handling qualities characteristics p 526 N94-13324
Low-speed wind tunnel tests on a joined-wing aircraft model with various upper-fin
| NAL-TR-1169 | p 501 N94-13341

CONTROLLED FUSION
Magnetic fusion computing: A personal retrospective view
| DE93-014147 | p 797 N94-13217
Nonlinear evolution of tearing modes in inhomogeneous plasmas
| PPL-133 | p 798 N94-13564
The status of cold fusion
| DE93-012731 | p 802 N94-14567

CONTROLLERS
Kinematics and constraints associated with swashplate blade pitch control
| NASA-TM-102265 | p 520 N94-12820
A PC-PCL-based control system for the high-voltage pulsed-power operation of the Intense Diagnostic Neutral Beam (iDNB) Experiment
| DE93-014144 | p 797 N94-13100
Force reflecting hand controller for manipulator teleoperation
| NASA-CR-191345 | p 661 N94-13129
The application of active side arm controllers in helicopters p 522 N94-13302
A four-axis hand controller for helicopter flight control p 522 N94-13305
Design and performance of an automated video-based laser beam alignment system
| DE93-012571 | p 656 N94-13481
Strategic avionics technology definition studies. Subtask 3-1A: Electrical Actuation (ELA) systems
| NASA-CR-194393 | p 536 N94-14323
The use of linked lists in the simulation of controller-structure interaction p 679 N94-14630
A neural-network approach to robotic control p 679 N94-14634
Optimization-based controller design for rotorcraft p 527 N94-14642
On l(1): Optimal decentralized performance p 681 N94-14643
An application of the IMC software to controller design for the JPL LSCL Experiment Facility p 681 N94-14645
Control system design for flexible structures using data models p 527 N94-14646
Design and control of a macro-micro robot for precise force applications p 682 N94-14651

CONVECTION
AMIP: Diagnostic subproject on the variability in the tropics: Synoptic to intraseasonal time scales
| DE93-009287 | p 721 N94-13914

CONVECTIVE FLOW
Fluxes of heat and water vapour in a convective mixed layer during EFEDA
| DLR-FB-92-21 | p 716 N94-14132
An adaptive projection method for the incompressible Euler equations
| DE93-016428 | p 639 N94-14434
Interactions among convection, magnetic fields and p-mode oscillations in the sun
| NASA-CR-194477 | p 845 N94-14479

CONVECTIVE HEAT TRANSFER
Experimental measurement of local heat transfer coefficients over discrete roughened plates using infrared thermography p 635 N94-13652
Fluxes of heat and water vapour in a convective mixed layer during EFEDA
| DLR-FB-92-21 | p 716 N94-14132

CONVERGENCE
A new method to assess Monte Carlo convergence
| DE93-012667 | p 772 N94-12919
Optimization and eigenvalue computation with application to meteorology and oceanography
| DE93-015310 | p 744 N94-13024
Topics on spatially high-order accurate methods and pre-conditioning for the Navier-Stokes equations with finite-rate chemistry p 633 N94-13572
Mathematical algorithms for multidimensional inverse scattering problems in inhomogeneous medium
| AD-A266440 | p 749 N94-13702
Preconditioning and the limit to the incompressible flow equations
| NASA-CR-191500 | p 769 N94-13717
On the superconvergence of Galerkin methods for hyperbolic IBVP
| NASA-CR-194293 | p 770 N94-13922
On the superconvergence of Galerkin methods for hyperbolic IBPV
| NASA-CR-194488 | p 770 N94-14307
On a convergence of iterative Newton's scheme
| DE93-626604 | p 772 N94-14886

CONVERGENT NOZZLES
Mixing noise reduction for rectangular supersonic jets by nozzle shaping and induced screech mixing
| NASA-TM-106364 | p 508 N94-14208

CONVERGENT-DIVERGENT NOZZLES
An experimental investigation of shock wave/vortex interaction p 634 N94-13574
Mixing noise reduction for rectangular supersonic jets by nozzle shaping and induced screech mixing
| NASA-TM-106364 | p 508 N94-14208

CONVEXITY
Approaches to high aspect ratio triangulations
| NASA-TM-107684 | p 739 N94-12886

CONVOLUTION INTEGRALS
Deconvolution for positive signals
| DE93-013044 | p 773 N94-14314

COOL STARS
Basic research in solar physics
| NASA-CR-193632 | p 844 N94-13234

COOLANTS
Long-range global warming impact of gaseous diffusion plant operation
| DE93-011686 | p 710 N94-14459

COOLERS
Double inlet pulse tube cryocooler theory
| AD-A266832 | p 597 N94-14677

COOLING
Observation of the coalescing of beam into an asymmetric RF bucket by stochastic cooling
| DE93-015133 | p 783 N94-13895
Containerless processing of undercooled melts
| NASA-CR-194350 | p 572 N94-14123

COOLING FLOWS (ASTROPHYSICS)
Studies of gas in cooling flow clusters
| NASA-CR-193597 | p 628 N94-12959

COOLING SYSTEMS
High flux heat exchanger
| AD-A266341 | p 636 N94-13730

COORDINATION
Program operations plan
| DE93-012765 | p 710 N94-14182

COPOLYMERS
Characterization of 1:1 random copolymers obtained from 6-, 7-, 11-, and 12-carbon amino acids
| AD-A265827 | p 577 N94-12985
Computer simulations for the adsorption of polymers onto surfaces
| DE93-016667 | p 577 N94-13070
Phase transition in polymer blends and structure of ionomers and copolymers
| DE93-016256 | p 579 N94-13978
Surface characterization of LDEF materials
| NASA-CR-194519 | p 543 N94-14683
Office of Naval Research/DARPA publications: Composite materials with improved properties in compression
| AD-A265509 | p 560 N94-14794

COPPER
Ohmic heating of composite candidate graphite-fiber/coating combinations
| NASA-TM-4491 | p 554 N94-12871
The x ray dichroism experiments using circular polarization
| DE93-013195 | p 568 N94-13036
On the hardening and softening of nanocrystalline materials
| DE93-012901 | p 810 N94-14185
Laser beam control and diagnostic systems for the copper-pumped dye laser system at Lawrence Livermore National Laboratory
| DE93-016529 | p 658 N94-14437
The structure and mechanical properties of Ru-Cu and Ru-Ti nanolayer composites
| DE93-014453 | p 558 N94-14469
Electrochemical planarization for microelectronic circuits
| DE93-017214 | p 627 N94-14870

COPPER ALLOYS
Microstructural mechanisms that enhance electromigration resistance in Al-Cu thin films
| DE93-013770 | p 812 N94-14345

COPPER OXIDES
The study of structure-processing-property relations in copper oxide based high (Tc) superconductors
| DE93-015066 | p 804 N94-13003

COPPER SELENIDES
Activities of the Basic Sciences Branch
| DE93-010012 | p 851 N94-14455

CORE FLOW
Simultaneous solution for core magnetic field and fluid flow beneath an electrically conducting mantle
| NASA-TM-4536 | p 716 N94-13960
Tracking of change of a warm-core ring structure p 696 N94-14267

CORE SAMPLING
Maximum entropy spectral analysis of the geological time series of the oxygen isotope record from deep-sea cores
| INPE-5465-PRE/1773 | p 725 N94-13728

CORONAL LOOPS
Comparative study of x ray and microwave emissions during solar flares
| NASA-CR-194532 | p 845 N94-14577

CORONAS
Parametric instabilities in large nonuniform laser plasmas
| DE93-013184 | p 797 N94-13393

CORRELATION
Correlations of the growth, structure, and stress with the adhesion of diamond films on tungsten
| DE93-012855 | p 576 N94-12912

CORRELATION COEFFICIENTS
Statistical analysis of the m rankings problem: Kendall's prototype and the grouping estimate method based on normal scores
| DSIS-93-00139 | p 773 N94-13848

CORRELATION DETECTION
Acousto-optical post-processor time-integrating correlator updates
| DSIS-93-00314 | p 777 N94-13831

CORROSION
Carbonate fuel cell endurance: Hardware corrosion and electrolyte management status
| DE93-013800 | p 701 N94-13093
The corrosion behavior of 8001 Al under heat-transfer conditions in an aqueous loop system
| DE93-013450 | p 569 N94-13242
A study of hydrogen effects on fracture behavior of radioactive waste storage tanks
| DE93-018171 | p 574 N94-14873

CORROSION PREVENTION
High-temperature corrosion and protection of materials
| DE93-011072 | p 568 N94-12998
Inhibiting corrosion in Gr/Al and Gr/Mg metal matrix composites using nonequilibrium alloying techniques
| AD-A266547 | p 556 N94-13583

Metastability of yttrium-oxides
[DE93-016548] p 813 N94-14440
Insoluble coatings for Stirling engine heat pipe condenser surfaces
[NASA-CR-191188] p 554 N94-14771
CORROSION RESISTANCE
High-temperature corrosion and protection of materials
[DE93-011072] p 568 N94-12998
Carbonate fuel cell endurance: Hardware corrosion and electrolyte management status
[DE93-013800] p 701 N94-13093
About the influence of inert gas ion implantation on metal corrosion stability
[DE93-620574] p 569 N94-13360
Modified carbon for improved corrosion resistance
[AD-D015741] p 556 N94-13663
The effect of TiN coatings on the rolling contact fatique behavior of M50 bearing steel
[ARL-TR-40] p 662 N94-13794
JPRS report: Science and technology. Central Eurasia: Materials science
[JPRS-UMS-93-005] p 559 N94-14575
CORROSION TESTS
Carbonate fuel cell endurance: Hardware corrosion and electrolyte management status
[DE93-013800] p 701 N94-13093
The corrosion behavior of 8001 Al under heat-transfer conditions in an aqueous loop system
[DE93-013450] p 569 N94-13242
Fatigue crack initiation and propagation in aluminum alloys 8090 and 2124 in hydrogenous atmospheres
p 570 N94-13670
COSMIC BACKGROUND EXPLORER SATELLITE
Inflation after COBE: Lectures on inflationary cosmology
[DE93-014008] p 834 N94-13096
COSMIC DUST
UV extinction properties of carina nebular dust
[NASA-CR-193424] p 835 N94-13233
Physical properties of gas disks around shell stars with and without dust
[NASA-CR-193655] p 835 N94-13239
Dust production in the envelopes of carbon stars: R Coronae Borealis
[ETN-93-94389] p 839 N94-14075
COSMIC GASES
ROSAT: X ray survey of compact groups
[NASA-CR-193297] p 829 N94-13181
The extent and content of low-ionization gas in galaxies p 837 N94-13551
COSMIC PLASMA
Research in cosmic and gamma ray astrophysics: Cosmic physics portion
[NASA-CR-194127] p 847 N94-13211
Physical properties of gas disks around shell stars with and without dust
[NASA-CR-193655] p 835 N94-13239
COSMIC RAY ALBEDO
Dynamical model for the distribution of geomagnetically trapped anomalous-component ions
[ATR-91(9558)-6] p 784 N94-13936
COSMIC RAY SHOWERS
Search for UHE point-source emission over various time scales
[DE93-012718] p 846 N94-12922
Search for emission of ultra high energy radiation from active galactic nuclei
[DE93-012719] p 846 N94-12923
Angular resolution studies of the CYGNUS array using the shadows of the Sun and Moon
[DE93-012723] p 846 N94-12946
Search for ultra-high-energy radiation from gamma-ray bursts
[DE93-012721] p 847 N94-12964
Results from a water-Cerenkov array
[DE93-012715] p 849 N94-14461
COSMIC RAYS
Search for UHE point-source emission over various time scales
[DE93-012718] p 846 N94-12922
Search for UHE emission from Cygnus X-3
[DE93-012720] p 846 N94-12924
Search for continuous and single day emission from ultra-high-energy sources
[DE93-012724] p 846 N94-12947
Research in cosmic and gamma ray astrophysics: Cosmic physics portion
[NASA-CR-194127] p 847 N94-13211
The beta(+) decay and cosmic-ray half-life of Mn-54
[DE93-013913] p 848 N94-13695
Cosmic and solar gamma ray and neutron experiments
[NASA-CR-193359] p 849 N94-13965
Results from a water-Cerenkov array
[DE93-012715] p 849 N94-14461
COSMOCHEMISTRY
On inhomogeneous halo collapse and the globular cluster metallicity gradient
[DE93-013090] p 834 N94-13011
COSMOLOGY
Inflation after COBE: Lectures on inflationary cosmology
[DE93-014008] p 834 N94-13096
GRO: Black hole models for gamma ray bursts
[NASA-CR-193244] p 829 N94-13178
Dilaton quantum cosmology in two dimensions
[DE93-621377] p 836 N94-13361
The reionization of the intergalactic medium
p 838 N94-13651
A classical instability for black strings and p-branes
[DE93-014577] p 839 N94-14116
Mathematics and string theory
[DE93-017903] p 817 N94-14417
Multiplicative noise: Applications in cosmology and field theory
[DE93-016624] p 840 N94-14536
Radiation perturbation theory in gravity and quantum universe as a hydrogen atom
[DE93-626621] p 849 N94-14889
COST ANALYSIS
Effects of radiobiological uncertainty on vehicle and habitat shield design for missions to the moon and Mars
[NASA-TP-3312] p 846 N94-12875
Advanced protein crystal growth programmatic sensitivity study
[NASA-CR-193827] p 804 N94-12934
Compendium of executive summaries from the maglev system concept definition
[PB93-154938/GAR] p 661 N94-13285
Field of solar collectors: Effect of shadowing on the optimal field design
[ITN-93-85197] p 702 N94-13570
Selected data on academic science and engineering R and D expenditures: Fiscal Year 1991
[NSF-92-329] p 819 N94-13982
Optimal maintenance policies of a Markovian system
[ITN-93-85216] p 774 N94-14502
COST EFFECTIVENESS
Shared visions: Partnership of Rockwell International and NASA Cost Effectiveness Enhancements (CEE) for the space shuttle system integration program
p 668 N94-13166
COST ESTIMATES
Effects of radiobiological uncertainty on vehicle and habitat shield design for missions to the moon and Mars
[NASA-TP-3312] p 846 N94-12875
COST REDUCTION
Johnson Space Center procurement: Controls over payments to contractors should be strengthened
[AD-A265722] p 819 N94-13060
Spacecraft COst REduction Team (SCORE): TQM/CI on a massive scale p 667 N94-13160
Shared visions: Partnership of Rockwell International and NASA Cost Effectiveness Enhancements (CEE) for the space shuttle system integration program
p 668 N94-13166
Continuous roll-to-roll a-Si photovoltaic manufacturing technology
[DE93-010006] p 704 N94-14109
Flexibility and costs in the design process: A decision support model
[ISBN-9-06-814522-3] p 597 N94-14808
COUETTE FLOW
Stability of oscillatory two phase Couette flow
[NASA-CR-191501] p 636 N94-13817
COUNTERFLOW
A coherent flame model of premixed turbulent combustion in a counterflow geometry
[CUED/A-THERMO/TR.60] p 562 N94-13085
COUNTERMEASURES
Physical countermeasures for long-term manned space flights
[ESA-SP-1160] p 733 N94-14860
COUPLERS
Flex-gear electrical power transmission
[NASA-CR-194422] p 661 N94-13445
Polarization effects in optical fiber current sensors based on Sagnac interferometers with 3 by 3 couplers
[DE93-012665] p 792 N94-14367
COUPLING
Coupled thermal response of objects and participating media in fires and large combustion systems
[DE93-012848] p 561 N94-12819
COVALENT BONDS
Poling of thin polymer films in electro optic applications
[AD-A266562] p 579 N94-13584
COVARIANCE
Coherent Doppler lidar signal covariance including wind shear and wind turbulence
[NASA-CR-194492] p 721 N94-13723
Decentralized control of uncertain systems via sensitivity models
[DE93-012963] p 766 N94-14568
CRACK GEOMETRY
A survey of crack path stability criteria and their application to crack flapping phenomena in stiffened structures
[LR-681] p 675 N94-13929
CRACK INITIATION
Fatigue crack initiation and propagation in aluminum alloys 8090 and 2124 in hydrogenous atmospheres
p 570 N94-13670
Contribution to comparison of methods for determining welding procedures for the avoidance of hydrogen cracking
[VTT-PUBS-107] p 674 N94-13887
Fatigue predictions and scatter
[LR-696] p 675 N94-13933
A study of fiber volume fraction effects in notched unidirectional SCS-6/Ti-15V-3Cr-3Al-3Sn composite
[NASA-CR-191165] p 559 N94-14769
Microstructural origins and modeling of intergranular crack initiation in an Al-Li-Cu-Mg-(Zr) alloy
[ISAL-91-0012] p 574 N94-14814
CRACK PROPAGATION
Automated crack identification for cement paste
[AD-A265753] p 665 N94-13042
Modern aluminium sheet alloys for aerospace applications
[NLR-TP-92057-U] p 570 N94-13497
Combustion-induced crack/debond propagation in solid propellants p 584 N94-13560
Investigation of criteria for ductile fracture under fully-plastic conditions p 672 N94-13593
Fatigue crack initiation and propagation in aluminum alloys 8090 and 2124 in hydrogenous atmospheres
p 570 N94-13670
Some computational tools for the analysis of through cracks in stiffened fuselage shells
[LR-701] p 673 N94-13726
Micromechanical damage theories for brittle solids with interacting microcracks
[AD-A266348] p 673 N94-13778
A survey of crack path stability criteria and their application to crack flapping phenomena in stiffened structures
[LR-681] p 675 N94-13929
Fatigue predictions and scatter
[LR-696] p 675 N94-13933
MSD in fuselage lap joints: Requirements for inspection intervals for typical fuselage lap joint panels with Multiple Site Damage
[LR-697] p 675 N94-13986
A microstructural approach to fatigue crack processes in poly crystalline BCC materials
[DE93-016666] p 812 N94-14354
A study of fiber volume fraction effects in notched unidirectional SCS-6/Ti-15V-3Cr-3Al-3Sn composite
[NASA-CR-191165] p 559 N94-14769
A computer program to calculate growth rates for cracks at notches in regions of residual stress
[RAE-TM-MAT/STR-1207] p 683 N94-14818
The growth of short fatigue cracks in an aluminium alloy
[RAE-TR-92063] p 574 N94-14828
CRACK TIPS
A survey of crack path stability criteria and their application to crack flapping phenomena in stiffened structures
[LR-681] p 675 N94-13929
A microstructural approach to fatigue crack processes in poly crystalline BCC materials
[DE93-016666] p 812 N94-14354
CRACKING (FRACTURING)
The ASCOR test: A simple automated method for stress corrosion testing of aluminium alloys
[NLR-TP-91438-U] p 570 N94-13532
CRACKS
Role of microstructure on fatigue durability of aluminum aircraft alloys
[AD-A265627] p 568 N94-12993
Fracture behavior of vanadium/vanadium silicide in-situ composites
[DE93-013422] p 556 N94-13389
Theoretical studies of breakdown in random media
[DE93-018107] p 558 N94-14418
CRASHES
An assessment of the potential for neck injury due to padding of aircraft interior walls for head impact protection
[DOT/FAA/AM-93/14] p 738 N94-13972
CRASHWORTHINESS
Design and application of a quasistatic crush test fixture for investigating scale effects in energy absorbing composite plates
[NASA-CR-4526] p 670 N94-13063

CRAY COMPUTERS
Cray Y-MP
| NASA-TM-109303 | p 741 N94-13609
Computational mechanics and supercomputing at LLNL
| DE93-016453 | p 754 N94-14435
CREEP PROPERTIES
Development of time-dependent orthotropic constitutive law of a thermoplastic composite material
p 556 N94-13595
Computational strategies in the dynamic simulation of constrained flexible MBS p 679 N94-14635
CREEP TESTS
Development of time-dependent orthotropic constitutive law of a thermoplastic composite material
p 556 N94-13595
Evaluation for rheological constitutive relations, using the indentation technique p 775 N94-13627
CREW PROCEDURES (INFLIGHT)
Flight crew interface aspects of forward-looking airborne windshear detection systems
| NASA-CR-191437 | p 516 N94-12829
CRITICAL EXPERIMENTS
MCNP benchmark analyses of critical experiments for the Space Nuclear Thermal Propulsion program
| DE93-014046 | p 548 N94-12981
CRITICAL LOADING
Investigation of criteria for ductile fracture under fully-plastic conditions p 672 N94-13593
CRITICAL TEMPERATURE
Effects of depositon rate on Bi2Sr2CaCu2O(8+x) and Bi2Sr(1.6)La(0.4)CuO(6+x) epitaxial thin film growth by pulsed-laser ablation
| DE93-015797 | p 812 N94-14362
On the statistical theory of the even-even nucleons levels' density
| DE93-623990 | p 788 N94-14875
CROP GROWTH
Validated environmental and physiological data from the CELSS Breadboard Projects Biomass Production Chamber. BWT931 (Wheat cv. Yecora Rojo)
| NASA-TM-109272 | p 738 N94-13979
CROPS
Preparations for and first results of the calibration and interpretation of ERS-1 SAR imagery over land
| BCRS-92-13 | p 684 N94-13123
CROSS FLOW
The effect of crossflow on Taylor vortices: A model problem
| NASA-CR-191487 | p 630 N94-13128
CROSSTALK
Locally non-uniform finite-difference time domain with application to stealth, crosstalk, and narrow apertures
| DE93-013958 | p 601 N94-13696
CRRES (SATELLITE)
CRRES to blaze new trails in orbit
| NASA-TM-109314 | p 713 N94-13620
CRUDE OIL
Biodiesel/aquatic species project report, FY 1992
| DE93-010024 | p 709 N94-14087
BOAST 2 for the IBM 3090 and RISC 6000
| DE93-000138 | p 638 N94-14351
CRYOGENIC COOLING
Three-stage linear, split-Stirling cryocooler for 1 to 2K magnetic cold stage
| NASA-CR-4538 | p 776 N94-13897
A recuperative superfluid Stirling refrigerator
| DE93-016521 | p 597 N94-14592
CRYOGENIC EQUIPMENT
Residual contact restraints in cryogenics
| ETN-93-94375 | p 671 N94-13501
Sloshing dynamics on rotating helium dewar tank
| NASA-CR-194403 | p 637 N94-13959
Double inlet pulse tube cryocooler theory
| AD-A266832 | p 597 N94-14877
CRYOGENIC FLUID STORAGE
The feasibility of producing aluminum-lithium structures for cryogenic tankage applications by laser beam welding
| NASA-CR-191527 | p 595 N94-14026
CRYOGENIC FLUIDS
Cryogenic fluid film bearing tester development study
| NASA-CR-192586 | p 660 N94-12791
CFM technologies for space transportation: Multipurpose hydrogen testbed system definition and tank procurement
| NASA-CR-194355 | p 539 N94-12827
CRYOGENIC ROCKET PROPELLANTS
CFM technologies for space transportation: Multipurpose hydrogen testbed system definition and tank procurement
| NASA-CR-194355 | p 539 N94-12827
Effects of hydrogen addition on combustion performance of a LOX/kerosene rocket
| NAL-TR-1177 | p 548 N94-12945
CRYOGENIC TEMPERATURE
Thermal conductance of pressed metallic contacts augmented with Indium foil or Apiezon-N (tm) grease at liquid helium temperatures
| NASA-TM-108779 | p 776 N94-14027
CRYOGENICS
Thermal conductance of pressed metallic contacts augmented with Indium foil or Apiezon-N (tm) grease at liquid helium temperatures
| NASA-TM-108779 | p 776 N94-14027
A cryogenic seven-element HEMT front end for DSS 13 p 608 N94-14375
CRYOSTATS
Gas atomized Er3Ni powder for cryocooler applications
| DE93-011564 | p 568 N94-13000
CRYSTAL DEFECTS
Flux-pinning related defect structures in melt-processed YBa2Cu3O(7-x)
| DE93-012759 | p 804 N94-12818
Deposition of crystalline boron thick layers from gas phase
| DE93-620499 | p 576 N94-12867
Atomic structure of the 310 twin in niobium: Theoretical predictions and comparison with experimental observation
| DE93-013421 | p 806 N94-13136
Annealing study of main electron irradiation-induced defects (H4 and H5) in P-InP using DLTS technique
| DE93-623204 | p 806 N94-13213
Growth experiment of narrow band-gap semiconductor PbSnTe single crystals in space (M-1)
p 586 N94-13733
Effects of growth conditions and substrate orientation on the properties of InSb
| DE93-013766 | p 812 N94-14344
CRYSTAL FIELD THEORY
Protein crystal growth p 591 N94-13756
CRYSTAL GROWTH
Reduce fluid experiment system flight data from IML-1
| NASA-CR-193835 | p 804 N94-12873
Correlations of the growth, structure, and stress with the adhesion of diamond films on tungsten
| DE93-012855 | p 576 N94-12912
Adaptive control of interface by temperature and interface profile feedback in transparent multi-zone crystal growth furnace
| NASA-CR-194140 | p 762 N94-13253
Low temperature metal-organic chemical vapor deposition growth processes for high efficiency solar cells
| DE92-010562 | p 702 N94-13386
Fabrication of AlGaAs/GaAs-light-emitting devices by selective MOCVD using dialkylmetalchloride
p 627 N94-13433
Crystal growth of ZnSe and related ternary compound semiconductors by physical vapor transport
| NASA-CR-193834 | p 807 N94-13444
Growth experiment of narrow band-gap semiconductor PbSnTe single crystals in space (M-1)
p 586 N94-13733
Growth of PbSnTe single crystal by traveling-zone method in low gravity (M-2) p 586 N94-13734
Growth of semiconductor compound single crystal InSb by floating zone method (M-3) p 586 N94-13735
Growth of Si spherical crystals and the surface oxidation (M-9) p 587 N94-13741
Solidification of eutectic system alloys in space (M-19)
p 589 N94-13751
Growth of samarskite crystal under microgravity conditions (M-20) p 590 N94-13752
Growth experiment of organic metal crystal in low gravity (M-21) p 590 N94-13753
Crystal growth of compound semiconductors in a low-gravity environment (InGaAs crystals) (M-22)
p 590 N94-13754
Cesium iodide (CsI) crystal manufacture
| DE93-012146 | p 808 N94-13973
Effects of depositon rate on Bi2Sr2CaCu2O(8+x) and Bi2Sr(1.6)La(0.4)CuO(6+x) epitaxial thin film growth by pulsed-laser ablation
| DE93-015797 | p 812 N94-14362
Two color holographic interferometry for microgravity application
| NASA-CR-194424 | p 651 N94-14447
Activities of the Basic Sciences Branch
| DE93-010012 | p 851 N94-14455
Molecular simulator: A basic tool for submicron MOS processes development
| LAAS-92484 | p 814 N94-14697
Measurements of crystal growth kinetics at extreme deviations from equilibrium
| DE93-014526 | p 815 N94-14798
CRYSTAL LATTICES
Deposition of crystalline boron thick layers from gas phase
| DE93-620499 | p 576 N94-12867
Structural change of graphite during electron irradiation
| DE93-015961 | p 582 N94-14531
The Lindemann criterion of melting for pure and mixed ionic crystals
| ITN-93-85210 | p 814 N94-14554
Ionic conductivity of alkali halides and their mixtures near liquid-solid phase transition
| ITN-93-85222 | p 566 N94-14558
Magnetic interactions and disorder - phase transitions in dilute spin-glasses and high temperature superconductors
| ITN-93-85217 | p 815 N94-14825
Phases and phase transitions of polymeric liquid crystals: A high resolution x ray diffraction and light scattering study
| ITN-93-85218 | p 816 N94-14826
CRYSTAL STRUCTURE
Recovery of materials impacted at high velocity
| DE93-014150 | p 576 N94-12885
Correlations of the growth, structure, and stress with the adhesion of diamond films on tungsten
| DE93-012855 | p 576 N94-12912
Determination of channeling perspectives for complex crystal structures
| DE93-012872 | p 805 N94-13009
Atomic structure of the 310 twin in niobium: Theoretical predictions and comparison with experimental observation
| DE93-013421 | p 806 N94-13136
Crystallographic and metallurgical characterization of radiation detector grade cadmium telluride materials
| DE93-014335 | p 806 N94-13150
A continuum theory for liquid crystals describing different degrees of orientational order
| ETN-93-94392 | p 807 N94-13590
Theory of the electronic and structural properties of solid state oxides
| DE93-016051 | p 811 N94-14296
Metastability of yttrium-oxides
| DE93-016548 | p 813 N94-14440
The Lindemann criterion of melting for pure and mixed ionic crystals
| ITN-93-85210 | p 814 N94-14554
Ion assisted sputter deposition of Mo-Si multilayers
| DE93-013830 | p 583 N94-14693
CRYSTAL SURFACES
Adaptive control of interface by temperature and interface profile feedback in transparent multi-zone crystal growth furnace
| NASA-CR-194140 | p 762 N94-13253
Barium fluoride research and development at Lawrence Livermore National Laboratory
| DE93-014682 | p 807 N94-13405
Boundary stability under nonequilibrium conditions
| DE93-016259 | p 809 N94-13980
CRYSTALLINITY
Photovoltaic Subcontract Program
| DE93-000092 | p 700 N94-12868
On the hardening and softening of nanocrystalline materials
| DE93-012901 | p 810 N94-14185
A microstructural approach to fatigue crack processes in poly crystalline BCC materials
| DE93-016666 | p 812 N94-14354
CRYSTALLITES
Procedures for analysis of debris relative to Space Shuttle systems
| NASA-TM-109190 | p 534 N94-12900
Characterization of 1:1 random copolymers obtained from 6-, 7-, 11-, and 12-carbon amino acids
| AD-A265827 | p 577 N94-12985
Reverse micelle synthesis of nanoscale metal containing catalysts
| DE93-012869 | p 572 N94-14184
CRYSTALLIZATION
Optimization of the processing parameters of high temperature superconducting glass-ceramics: Center Director's discretionary fund final report
| NASA-TM-108421 | p 808 N94-13938
Theory of the electronic and structural properties of solid state oxides
| DE93-016051 | p 811 N94-14296
Ionic conductivity of alkali halides and their mixtures near liquid-solid phase transition
| ITN-93-85222 | p 566 N94-14558
CRYSTALLOGRAPHY
Crystallographic phase identification in the scanning electron microscope: Backscattered electron Kikuchi patterns
| DE93-011574 | p 804 N94-12813

Crystallographic and metallurgical characterization of radiation detector grade cadmium telluride materials
| DE93-014335 | p 806 N94-13150
The effect of crystal tilt on high resolution micrographs of small metal particles
| DE93-013915 | p 574 N94-14795

CRYSTALS
Crystallographic and metallurgical characterization of radiation detector grade cadmium telluride materials
| DE93-014335 | p 806 N94-13150
Barium fluoride research and development at Lawrence Livermore National Laboratory
| DE93-014682 | p 807 N94-13405
Quasi-elastic neutron scattering studies of protein dynamics
| DE93-015074 | p 782 N94-13414
A positron annihilation radiation telescope using Laue diffraction in a crystal lens
| DE93-012905 | p 848 N94-13483
Optical and physical properties of the LiSrAlF6:Cr laser crystal
| DE93-014657 | p 808 N94-13881
Cesium iodide (CsI) crystal manufacture
| DE93-012146 | p 808 N94-13973
Optical properties of CO2 ice and CO2 snow in the ultraviolet, visible, and infrared
| NASA-CR-194110 | p 686 N94-14081
Electronic schematics for the Donner 600 Crystal Tomograph
| DE93-015277 | p 625 N94-14336
The effect of crystal tilt on high resolution micrographs of small metal particles
| DE93-013915 | p 574 N94-14795
Multiplicity spectrometry on neutron filtered beams
| DE93-617529 | p 790 N94-14843

CUES
Visual cueing aids for rotorcraft landings p 524 N94-13313
Visual information for judging temporal range p 524 N94-13314
Visual cueing considerations in Nap-of-the-Earth helicopter flight head-slaved helmet-mounted displays p 524 N94-13315
Primary display latency criteria based on flying qualities and performance data p 525 N94-13318

CULTURE (SOCIAL SCIENCES)
Here's the beef: A case study in organizational transformation p 667 N94-13163
Building a quality culture in the Office of Space Flight: Approach, lessons learned and implications for the future p 667 N94-13164

CULTURE TECHNIQUES
Studies on the effects of microgravity on the ultrastructure and functions of cultured mammalian cells (L-6) p 592 N94-13763
Gravity, chromosomes, and organized development in aseptically cultured plant cells p 592 N94-13764
Bone culture research p 595 N94-13773

CUMULUS CLOUDS
Remote sensing of low level cloud optical characteristics p 691 N94-14229

CURRENT DENSITY
Advanced magnetic flux compression generator development issues: A comparison of coaxial and disk generators
| DE93-014025 | p 794 N94-12849
Metal oxide varistor feasibility study
| DE93-012921 | p 620 N94-13031
Electrocatalysis issues in polymer electrolyte fuel cells
| DE93-014450 | p 702 N94-13402
Current distribution tomography for determination of internal current density distributions
| DE93-015463 | p 604 N94-13899
Ploughing on gold using a Scanning Tunneling Microscope
| DE93-012632 | p 812 N94-14365

CURRENT DISTRIBUTION
Studies of non-inductive current drive in the CDX-U tokamak p 799 N94-13680
Current distribution tomography for determination of internal current density distributions
| DE93-015463 | p 604 N94-13899

CURRENT REGULATORS
Multi-output flyback converter with ultrafast current protection
| CNES-NT-133 | p 625 N94-14138

CURTAINS
Polymer infiltration studies
| NASA-CR-194521 | p 582 N94-14539

CURVATURE
Scalar curvature and spherical-type Riemannian manifolds
| DE93-622852 | p 767 N94-12895
Exploratory study of in-plane streamline curvature effects on a turbulent boundary layer at a Mach number of 3
| NASA-CR-193673 | p 501 N94-13292
Integrable system describing surfaces of non-constant curvature
| PREPRINT-734 | p 768 N94-13499
A hydrogen atom in the curved space: Orthogonality of radial wave functions with respect to the critical momentum
| DE93-626623 | p 788 N94-14891

CURVE FITTING
Removing noise from discontinuous data
| ITN-93-85211 | p 826 N94-14555

CURVED PANELS
Testing and analysis of curved frame specimens made from a Long Discontinuous Fiber (LDF) material
| NASA-TM-109014 | p 557 N94-13711

CUSHIONS
Body/cushion contact stress analysis during sitting
| ITN-93-85204 | p 736 N94-13229
An assessment of the potential for neck injury due to padding of aircraft interior walls for head impact protection
| DOT/FAA/AM-93/14 | p 738 N94-13972

CUTTING
Recent results from material processing studies on new generation lasers
| DE93-013841 | p 653 N94-12898
Knowledge base technology for CT-DIMS: Report 1
| DE93-013118 | p 743 N94-13014

CYANATES
The evolution of energy-transducing systems: Studies with archaebacteria
| NASA-CR-194130 | p 728 N94-13562

CYCLIC LOADS
A microstructural approach to fatigue crack processes in poly crystalline BCC materials
| DE93-016666 | p 812 N94-14354

CYCLOGENESIS
Cyclogenesis and cyclone over South America
| INPE-5400-TDI/479 | p 719 N94-13175

CYCLOHEXANE
Small-angle scattering, contrast variation and the study of complex composite materials: A study of the structure of carbon black
| DE93-012707 | p 559 N94-14690

CYCLONES
Cyclogenesis and cyclone over South America
| INPE-5400-TDI/479 | p 719 N94-13175

CYCLOTRON FREQUENCY
Direct electron heating and current drive with fast waves in D3-D
| DE93-013028 | p 801 N94-14293

CYCLOTRON RESONANCE
The multi-ion, multi-event test of ion cyclotron resonance heating
| NASA-CR-194134 | p 789 N94-13419
The de Haas-van Alphen studies and Fermi surface properties of organic superconductors (ET)2X
| DE93-015157 | p 623 N94-13925

CYCLOTRON RESONANCE DEVICES
Microwave generation for magnetic fusion energy applications
| DE93-013864 | p 654 N94-13058
Long-pulse operation of a gyrotron with beam/RF separation
| DE93-015007 | p 649 N94-13410

CYCLOTRONS
The de Haas-van Alphen studies and Fermi surface properties of organic superconductors (ET)2X
| DE93-015157 | p 623 N94-13925

CYGNUS CONSTELLATION
Search for UHE emission from Cygnus X-3
| DE93-012720 | p 846 N94-12924
Angular resolution studies of the CYGNUS array using the shadows of the Sun and Moon
| DE93-012723 | p 846 N94-12946

CYLINDRICAL BODIES
Capillary surfaces in a wedge: Differing contact angles
| DE93-013903 | p 631 N94-13244
Thermal gradient-induced deflection of a thick-walled cylinder with bending residual stresses
| AD-A266347 | p 673 N94-13777
Current distribution tomography for determination of internal current density distributions
| DE93-015463 | p 604 N94-13899
The accuracy of approximating radiative heat transfer using a temperature dependent thermal conductivity
| DE93-013105 | p 638 N94-14318
Dynamic soil pressures on rigid cylindrical vaults
| DE93-013930 | p 676 N94-14585

CYLINDRICAL SHELLS
A probabilistic method for the buckling assessment of stiffened composite shells
| NASA-TM-106286 | p 671 N94-13379
The numerical simulation of the collapse process of axially compressed cylindrical shells with measured imperfections
| LR-705 | p 674 N94-13905

D

DAMAGE
Micromechanical damage theories for brittle solids with interacting microcracks
| AD-A266348 | p 673 N94-13778
Theoretical studies of breakdown in random media
| DE93-018107 | p 558 N94-14418
Study of deferred acoustic emission in carbon epoxy composites
| ISAL-91-0078 | p 560 N94-14815

DAMAGE ASSESSMENT
An advanced test technique to quantify thermomechanical fatigue damage accumulation in composite materials
| NASA-CR-191147 | p 555 N94-13139
Micromechanical damage theories for brittle solids with interacting microcracks
| AD-A266348 | p 673 N94-13778
Integration of remote sensing and mathematical modelling in disaster mitigation p 692 N94-14239
Satellite remote sensing for disaster mitigation p 693 N94-14244
A concept for the world environment and disaster observation system p 693 N94-14245
Estimation of vegetation damage due to ash fall in Mt. Pinatubo area using MOS-1 data p 695 N94-14259
Secondary impact hazard assessment
| NASA-CR-188261 | p 543 N94-14483
Optimal maintenance policies of a Markovian system
| ITN-93-85216 | p 774 N94-14502

DARK MATTER
Cold dark matter halos p 838 N94-13649
The reionization of the intergalactic medium p 838 N94-13651
The first data from the MACHO experiment
| DE93-014423 | p 840 N94-14467

DARKENING
Laboratory simulations of lunar darkening processes p 843 N94-14301

DARKNESS
A circadian rhythm of conidiation in Neurospora crassa (L-12) p 593 N94-13769

DATA ACQUISITION
DATAA: Data acquisition made easy
| DE93-014683 | p 823 N94-13406
Arctic ozone expedition
| NASA-TM-109301 | p 708 N94-13602
Operational test of the airborne data acquisition system: SADA, the Bara Bonita experiment
| INPE-5451-NTC/305 | p 685 N94-13610
Buoy experiments to obtain the sea-truth data for OCTS/NSCAT, part 1
| NASDA-CNT-930005-PT-1 | p 725 N94-13653
Adaptive Signal Processing Testbed
| DSIS-93-00258 | p 604 N94-13869
Advanced solid-state array spectroradiometer data collection during HAPEX-2 Sahel
| NASA-CR-194144 | p 808 N94-13875
An experimental assessment of the use of ground-level microphones to measure the fly-over noise of jet-engined aircraft
| NPL-RSA(EXT)-0039 | p 777 N94-13885
Adaptive Signal Processing Testbed application software: User's manual
| DSIS-93-00261 | p 606 N94-14038
Earth Observation Center Annual Report on Research and Development, Fiscal Year 1992
| EOC-92-01-0007 | p 687 N94-14091
CCI working group on climate data and its rapporteurs
| WCDMP-21 | p 723 N94-14118
Geologic application of JERS-1 SAR data p 688 N94-14211
Outline of ISY sea surface temperature data sets p 696 N94-14261
The Telecommunications and Data Acquisition Report
| NASA-CR-194388 | p 607 N94-14369
Overview of the Scalable Coherent Interface, IEEE STD 1596 (SCI)
| DE93-015247 | p 761 N94-14476
A description of the computer program CALDK38 which controls instrumentation set-up and data acquisition during deadweight calibration using an HBM DK 38 S6 digital measuring unit
| LTR-ST-1935 | p 754 N94-14496
Data collection with the ACTS propagation terminal p 615 N94-14675
A fast frame rate 512 x 512 CCD digital camera system
| DE93-013048 | p 653 N94-14792

DATA BASE MANAGEMENT SYSTEMS
Making the connection between information modeling and implementation
| DE93-011588 | p 820 N94-12907
Knowledge base technology for CT-DIMS: Report 1
| DE93-013118 | p 743 N94-13014
AQUIS: A PC-based source information manager
| DE93-012893 | p 707 N94-13383
Magic mirror on the wall, who's the fastest database of them all? A survey of database benchmarks
| AD-A266437 | p 823 N94-13701
An evaluation of ZIM and entity-relational models in managing databases for decision support systems
| ERB-1034 | p 824 N94-14202
Oak Ridge Environmental Information System (ORIES) site workstation information packet for OREIS 6.2
| DE93-010761 | p 825 N94-14458
Earth science and application
| NASA-CR-184381 | p 683 N94-14484
Enterprise integration: A tool's perspective
| DE93-015651 | p 755 N94-14528
Integrating PAW, a graphical analysis interface to Sybase
| DE93-014172 | p 755 N94-14581

DATA BASES
Making the connection between information modeling and implementation
| DE93-011588 | p 820 N94-12907
Vendor information system for innovative treatment technologies. User manual (VISITT version 2.0). Number 2
| PB93-196640 | p 821 N94-12936
Knowledge base technology for CT-DIMS: Report 1
| DE93-013118 | p 743 N94-13014
ARTI Refrigerant Database
| DE93-014774 | p 595 N94-13021
Development of ISO connection-oriented/correctionless gateways
| NASA-CR-193667 | p 821 N94-13030
Archiving of HEAO-1 data products and the creation of a general user's guide to the archive
| NASA-CR-193415 | p 822 N94-13062
View generated database
| NASA-CR-191397 | p 822 N94-13116
Methods for evaluating the predictive accuracy of structural dynamic models
| NASA-CR-191337 | p 671 N94-13124
VIEWCACHE: An incremental pointer-base access method for distributed databases. Part 1: The universal index system design document. Part 2: The universal index system low-level design document. Part 3: User's guide. Part 4: Reference manual. Part 5: UIMS test suite
| NASA-CR-191788 | p 822 N94-13126
EOS workstation
| NASA-CR-191326 | p 736 N94-13132
Parachute system design, analysis, and simulation tool
| DE93-013755 | p 501 N94-13260
Creating a strategic plan for configuration management using computer aided software engineering (CASE) tools
| DE93-013663 | p 746 N94-13394
NASA aerospace database subject scope: An overview
| NASA-SP-7107 | p 823 N94-13401
Magic mirror on the wall, who's the fastest database of them all? A survey of database benchmarks
| AD-A266437 | p 823 N94-13701
Space and Earth sciences, computer systems, and scientific data analysis support, volume 1
| NASA-CR-194535 | p 741 N94-13788
The DREO Elint Browser Utility (DEBU) reference manual
| DSIS-92-03900 | p 603 N94-13837
A data base for aging of structural materials
| DE93-009714 | p 824 N94-13915
Validated environmental and physiological data from the CELSS Breadboard Projects Biomass Production Chamber. BWT931 (Wheat cv. Yecora Rojo)
| NASA-TM-109272 | p 738 N94-13979
Generic results of the space physics community survey
| NASA-CR-194538 | p 818 N94-13984
Summary of the NOAA/NESDIS Workshop on Development of a Global Satellite/In Situ Environmental Database
| NOAA-TR-NESDIS-72 | p 826 N94-14498
A database for propagation models
p 614 N94-14665
ACTS data center p 616 N94-14677
Studying Turbulence Using Numerical Simulation Databases. 4: Proceedings of the 1992 Summer Program
| NASA-CR-194556 | p 643 N94-14745
CarbBank: A structural and bibliographic database for complex carbohydrates
| DE93-015582 | p 827 N94-14803
INGDB-90. The International Neutron Nuclear Data Base for geophysics applications
| DE93-624095 | p 827 N94-14880
The space-time and energy parameters of deuterium braking by the central collision with atoms
| DE93-624144 | p 788 N94-14881

DATA COMPRESSION
Knowledge-based oceanographic image compression
| AD-A265752 | p 821 N94-13041
Image coding using entropy-constrained residual vector quantization
| NASA-CR-193728 | p 744 N94-13113
Estimating the size of Huffman code preambles
p 609 N94-14379
Transform coding for space applications
| NASA-TM-106362 | p 612 N94-14542

DATA CONVERSION ROUTINES
FORTRAN graphics routines for the Macintosh
| DE93-013092 | p 742 N94-12864

DATA FLOW ANALYSIS
Signal design for data communication through rapidly varying linear channels
| ITN-93-85195 | p 601 N94-13567
Simulator for heterogeneous dataflow architectures
| NASA-CR-191545 | p 622 N94-13797
Adaptive Signal Processing Testbed: Software design specification
| DSIS-93-00259 | p 604 N94-13870

DATA INTEGRATION
Data fusion for adaptive control in manufacturing: Impact on engineering information models
| DE93-011555 | p 743 N94-12999
Satellite imagery and exogenous data integration by neural network in automation land-cover classification
| INPE-5480-PRE/1778 | p 686 N94-13729
Nonlinear aspects of data integration for land-cover classification in a neural network environment
| INPE-5479-PRE/1778 | p 686 N94-13789
Advanced Communications ESM System (ACES) testbed: Integration study
| DSIS-93-00345 | p 604 N94-13939
Computer vision and sensor fusion for detecting buried objects
| DE93-012605 | p 700 N94-14566

DATA LINKS
Development of ISO connection-oriented/correctionless gateways
| NASA-CR-193667 | p 821 N94-13030
Characteristics of the amateur radio means of the Arsene satellite
| CNES-NT-131 | p 605 N94-13950
Asynchronous transfer mode link performance over ground networks p 610 N94-14385
Overview of the Scalable Coherent Interface, IEEE STD 1596 (SCI)
| DE93-015247 | p 761 N94-14476

DATA MANAGEMENT
Application of new electro-optic technology to Space Station Freedom data management system
| NASA-CR-177622 | p 538 N94-13257
CCI working group on climate data and its rapporteurs
| WCDMP-21 | p 723 N94-14118
Satellite technology for environmental monitoring in developing countries p 692 N94-14236
A concept for the world environment and disaster observation system p 693 N94-14245
Development of a remote sensing geographic information system for land cover changes and assessment of risk due to natural and man made hazards covering the area of the inner delta of the Yellow River p 694 N94-14249

DATA PROCESSING
JTEC Panel report on knowledge-based systems in Japan
| PB93-170124 | p 820 N94-12801
ICE/ISEE plasma wave data analysis
| NASA-CR-194375 | p 796 N94-13081
SCORE user's manual
| DE93-015987 | p 822 N94-13121
J2000.0 modelling of GEOAIM in the analysis of VLBI data from the NASA crustal dynamics project
| ISBN-0-315-59463-2 | p 684 N94-13368
Magic mirror on the wall, who's the fastest database of them all? A survey of database benchmarks
| AD-A266437 | p 823 N94-13701
Space and Earth sciences, computer systems, and scientific data analysis support, volume 1
| NASA-CR-194535 | p 741 N94-13788
Measurement of HO2 and other trace gases in the stratosphere using a high resolution far-infrared spectrometer at 28 km
| NASA-CR-194175 | p 714 N94-13816
Theory of post-block 2 VLBI observable extraction
| NASA-CR-194543 | p 686 N94-13872
PSM: A new generation of data modeling
| TR-92-13 | p 824 N94-14072
Overview of the ILAS operational data processing system p 690 N94-14220
Visualization techniques to aid in the analysis of multi-spectral astrophysical data sets
| NASA-CR-194489 | p 840 N94-14482
Preprocessing data collected with the ACTS propagation terminal p 616 N94-14676
ACTS data center p 616 N94-14677

DATA PROCESSING EQUIPMENT
Manual on the global data-processing system. Volume 1: (Annex 4 to the WMO regulations) global aspects (1992 edition)
| WMO-485-VOL-1 | p 721 N94-13686
Manual on the global data-processing system. Volume 2: Regional aspects (1992 edition)
| WMO-485-VOL-2 | p 722 N94-14071
The BIRIS server: Integration of a three-dimensional range sensor into a harmony-based realtime architecture
| ERB-1036 | p 765 N94-14201

DATA RECORDERS
PC based A320 quick access recorder readout facility
| PD-AL-9109 | p 744 N94-13077
DATAA: Data acquisition made easy
| DE93-014683 | p 823 N94-13406
Center of trace algorithms for extracting digitized waveforms from two-dimensional images
| DE93-015082 | p 753 N94-14295

DATA REDUCTION
Reduce fluid experiment system flight data from IML-1
| NASA-CR-193835 | p 804 N94-12873
Study on TRMM data utilization for meteorology
| NASDA-CNT-930007 | p 721 N94-13643
Theory of post-block 2 VLBI observable extraction
| NASA-CR-194543 | p 686 N94-13872
Earth Observation Center Annual Report on Research and Development, Fiscal Year 1992
| EOC-92-01-0007 | p 687 N94-14091
Calibration and in-house validation results of JERS-1 data p 687 N94-14092
Earth observation experiment data analysis
p 687 N94-14093
Results from ERS-1 and JERS-1 SAR calibration experiments and data analysis p 688 N94-14210
Geologic application of JERS-1 SAR data
p 688 N94-14211
An exact processing algorithm for wide beam spaceborne SAR data p 689 N94-14213
Image processing and analysis of airborne POLDER data p 689 N94-14219
Overview of the ILAS operational data processing system p 690 N94-14220
TRMM precipitation radar algorithm
p 690 N94-14224
Estimate of sampling errors of TRMM rainfall observation by using radar-AMeDAS composite data
p 690 N94-14225
Integration of SST data sets using MOS-1 satellite data: For validation and monitoring p 696 N94-14262
Visualization techniques to aid in the analysis of multi-spectral astrophysical data sets
| NASA-CR-194489 | p 840 N94-14482
H2S data reduction
| NASA-CR-193389 | p 617 N94-14743
Exploratory data analysis: Past, present and future
| AD-A266775 | p 774 N94-14788
Image motion photography
| DE93-013962 | p 653 N94-14858

DATA RETRIEVAL
A path-oriented matrix-based knowledge representation system
| NASA-CR-4539 | p 744 N94-13065
The DREO Elint Browser Utility (DEBU) reference manual
| DSIS-92-03900 | p 603 N94-13837

DATA SAMPLING
Estimate of sampling errors of TRMM rainfall observation by using radar-AMeDAS composite data
p 690 N94-14225

DATA STORAGE
Archiving of HEAO-1 data products and the creation of a general user's guide to the archive
| NASA-CR-193415 | p 822 N94-13062
Satellite technology for environmental monitoring in developing countries p 692 N94-14236
The National Storage Laboratory: A collaborative research project
| DE93-015099 | p 760 N94-14475
Earth science and application
| NASA-CR-184381 | p 683 N94-14484
Data collection with the ACTS propagation terminal
p 615 N94-14675

DATA STRUCTURES
PSM: A new generation of data modeling
| TR-92-13 | p 824 N94-14072
AXAF FITS standard for ray trace interchange
| NASA-CR-194025 | p 832 N94-14305

Earth science and application
| NASA-CR-184361 | p 683 N94-14484
Implementation and experimentation with a motion planning system
| ITN-93-85213 | p 755 N94-14505
The use of linked lists in the simulation of controller-structure interaction p 679 N94-14630

DATA SYSTEMS
PC based A320 quick access recorder readout facility
| PD-AL-9109 | p 744 N94-13077
Manual on the global data-processing system. Volume 1: (Annex 4 to the WMO regulations) global aspects (1992 edition)
| WMO-485-VOL-1 | p 721 N94-13686
Mongoose ASIC microcontroller programming guide
| NASA-RP-1319 | p 623 N94-13871
Manual on the global data-processing system. Volume 2: Regional aspects (1992 edition)
| WMO-485-VOL-2 | p 722 N94-14071
Payload/GSE/data system interface: Users guide for the VPF (Vertical Processing Facility)
| NASA-CR-194385 | p 532 N94-14148
Asia-Pacific ISY Conference, volume 2
| NASDA-CM-199-VOL-2 | p 688 N94-14209
Sensor operation of Advanced Earth Observing Satellite (ADEOS) p 689 N94-14215
Overview of the ILAS operational data processing system p 690 N94-14220
TRMM precipitation radar algorithm p 690 N94-14224
Development of a remote sensing geographic information system for land cover changes and assessment of risk due to natural and man made hazards covering the area of the inner delta of the Yellow River p 694 N94-14249
Control system design for flexible structures using data models p 527 N94-14646

DATA TRANSFER (COMPUTERS)
Specimen files in VAMAS standard data transfer format (EXAMPLE 1.TXT to EXAMPLE 4.TXT)
| NPL-DMM(A)-90 | p 749 N94-13688

DATA TRANSMISSION
On the end-to-end communication problem in unreliable networks
| ITN-93-85188 | p 598 N94-13195
Application of new electro-optic technology to Space Station Freedom data management system
| NASA-CR-177622 | p 538 N94-13257
Transmission zeros of spacecraft attitude control system
| NAL-TR-1166 | p 540 N94-13339
Signal design for data communication through rapidly varying linear channels
| ITN-93-85195 | p 601 N94-13567
The developments of satellite communications of China p 618 N94-14282
The current situation, trends, international cooperation of space communication technological development in the Republic of Korea p 699 N94-14283
Joint experiments using ETS-5 p 618 N94-14284
Space communications technology research in CRL p 618 N94-14285
NTT's activities in satellite communications technology development p 618 N94-14286
Future outlook on international satellite communications in Asia Pacific region p 618 N94-14287
Technological development for broadcasting satellites in NHK Laboratories p 618 N94-14288
Large space structures and systems in the space station era: A bibliography with indexes (supplement 05)
| NASA-SP-7085(05) | p 543 N94-14411
Transform coding for space applications
| NASA-TM-106362 | p 612 N94-14542
CAD data exchange with Martin Marietta Energy Systems, Inc., Oak Ridge, TN
| DE93-017233 | p 757 N94-14871

DAYTIME
Simulating the daylight performance of fenestration systems and spaces of arbitrary complexity: The IDC method
| DE93-015177 | p 704 N94-14333

DEBONDING (MATERIALS)
Combustion-induced crack/debond propagation in solid propellants p 584 N94-13560
Enhanced NDE systems
| NASA-CR-192603 | p 669 N94-14101

DEBYE-HUCKEL THEORY
Monte Carlo simulation of the OCP freezing transition
| DE93-013039 | p 811 N94-14313

DECAY
Charged scalar particles and (tau) leptonic decay
| DE93-622969 | p 779 N94-12882

DECISION MAKING
Reasoning with uncertain and incomplete information in aerospace applications
| NLR-TP-91366-U | p 763 N94-13529
Decision support for material planners
| ISBN-9-03-860201-4 | p 819 N94-14449
Flexibility and costs in the design process: A decision support model
| ISBN-9-06-814522-3 | p 597 N94-14808

DECISION THEORY
Tree reconstruction from partial orders
| DE93-009841 | p 743 N94-12991
Generating knight's tours without backtracking from errors
| AD-A266807 | p 772 N94-14900

DECODERS
Digital sound: Subjective tests on commentary-quality codecs
| BBC-RD-1993/2 | p 598 N94-12926

DECODING
On the construction and decoding of hyperelliptic codes p 747 N94-13435
Enhanced decoding for the Galileo S-band mission p 609 N94-14380

DECOMPOSITION
Discussion of stress tensor nonuniqueness with application to nonuniform, particulate systems
| DE93-014352 | p 816 N94-13206
On the construction and decoding of hyperelliptic codes p 747 N94-13435
Room temperature degradation of YBa2Cu3O(7-x) superconductors in varying relative humidity environments
| NASA-TP-3368 | p 813 N94-14409
How to read a phase equilibrium diagram for high-temperature ceramics material as main object
| DE93-512333 | p 582 N94-14513
Mathematic methods and algorithms for real-time applications
| AD-A266776 | p 771 N94-14789

DECOMPRESSION SICKNESS
Metabolic rate measurements comparing supine with upright upper-body exercises
| NASA-CR-4549 | p 729 N94-14028

DECONDITIONING
Health monitoring of Japanese payload specialist: Autonomic nervous and cardiovascular responses under reduced gravity condition (L-0) p 591 N94-13757

DECONTAMINATION
Camera calibration in a hazardous environment performed in situ with automated analysis and verification
| DE93-010274 | p 651 N94-14046

DECOUPLING
Hybrid S(sub N)/Monte Carlo research and results
| DE93-012677 | p 773 N94-14178

DEEP SPACE
Design and application of electromechanical actuators for deep space missions
| NASA-CR-194145 | p 663 N94-14134
Preliminary design and implementation of the baseline digital baseband architecture for advanced deep space transponders p 611 N94-14393
Optimizing interplanetary trajectories with deep space maneuvers
| NASA-CR-4546 | p 532 N94-14851

DEEP SPACE NETWORK
Environmental projects. Volume 15: Environmental assessment: Proposed 1-megawatt radar transmitter at the Mars site
| NASA-CR-194098 | p 598 N94-13090
Sequential ranging: How it works
| NASA-CR-194508 | p 532 N94-13796
The Telecommunications and Data Acquisition Report
| NASA-CR-194388 | p 607 N94-14369
Radio metric errors due to mismatch and offset between a DSN antenna beam and the beam of a troposphere calibration instrument p 607 N94-14370
A cryogenic seven-element HEMT front end for DSS 13 p 608 N94-14375
Insertion loss and noise-temperature contribution of high-temperature superconducting bandpass filters centered at 2.3 and 8.45 GHz p 608 N94-14376
Stability measurements of the radio science system at the 34-m high-efficiency antennas p 609 N94-14381
Performance results of a digital test signal generator p 609 N94-14382
PC4CAST: A tool for DSN load forecasting and capacity planning p 610 N94-14384
Asynchronous transfer mode link performance over ground networks p 610 N94-14385
An overview of the Galileo Optical Experiment (GOPEX) p 610 N94-14386
Galileo Optical Experiment (GOPEX) optical train: Design and validation at the Table Mountain Facility p 610 N94-14390
Preliminary design and implementation of the baseline digital baseband architecture for advanced deep space transponders p 611 N94-14393
Layout and cabling considerations for a large communications antenna array p 611 N94-14395
The flight performance of the Galileo orbiter USO p 611 N94-14398

DEFECTS
1/f noise and oxide traps in MOSFETs
| DE93-007581 | p 619 N94-12942
Development of nondestructive evaluation methods and prediction of effects of flaws on the fracture behavior of structural ceramics
| DE93-012942 | p 577 N94-13032
Changes in electrical device characteristics during the formation of dislocations in situ in the TEM
| DE93-013910 | p 808 N94-13694
Laser-damage susceptibility of nodular defects in dielectric mirror coatings: AFM measurements and electric-field modeling
| DE93-014655 | p 580 N94-14124
Shock compression and quasielastic release in tantalum
| DE93-014566 | p 811 N94-14329
The effect of initial imperfections on shell stability: An updated review
| LR-695 | p 682 N94-14692

DEFENSE PROGRAM
Defense information infrastructure: Rationale for defense management report decision 918
| AD-A266014 | p 821 N94-12958
STS-28 crew presentation clip
| NASA-TM-109298 | p 531 N94-13640
A history of the Defence Research Establishment, Ottawa
| CTN-93-60737 | p 850 N94-14060
An ultra-compact processor module based on the R3000
| DE93-012549 | p 625 N94-14427

DEFLECTION
Electromagnetic deflection of spinning particles
| DE93-622866 | p 778 N94-12858
Thermal gradient-induced deflection of a thick-walled cylinder with bending residual stresses
| AD-A266347 | p 673 N94-13777
Computer program for analysis of high speed, single row, angular contact, spherical roller bearing, SASHBEAN. Volume 1: User's guide
| NASA-CR-191183 | p 663 N94-14445
Computer program for analysis of high speed, single row, angular contact, spherical roller bearing, SASHBEAN. Volume 2: Mathematical formulation and analysis
| NASA-CR-191182 | p 664 N94-14446

DEFOCUSING
Depths from focusing and defocusing
| AD-A266644 | p 735 N94-14797

DEFORESTATION
Modeling of biosphere-atmosphere interaction for forest and pastureland in the Amazon
| INPE-5454-TDI/496 | p 707 N94-13330
Climatic change due to land surface alterations
| INPE-5495-PRE/1786 | p 721 N94-13672

DEFORMATION
Micromechanical strength effects in shock compression of solids
| DE93-014425 | p 670 N94-12887
The 3-D massively parallel impact simulations using PCTH
| DE93-011593 | p 670 N94-12908
Using a focal-plane array to estimate antenna pointing errors
| NASA-CR-194502 | p 602 N94-13810
Dynamic mechanical deformation of a SiC(sub p)/Al-Li (8090) composite
| DE93-014586 | p 558 N94-14121
Machining and grinding: High rate deformation in practice
| DE93-010718 | p 664 N94-14457
Yield properties of tungsten and tungsten heavy alloys
| AD-A266833 | p 575 N94-14878

DEGASSING
Regional tectonic analysis of Venus as part of the Pioneer Venus guest investigator project
| NASA-CR-194079 | p 842 N94-13561
BAKEOUT: A computer program for predicting diffusive outgassing from stainless steel
| DE93-012613 | p 573 N94-14364

DEGRADATION
Degradation of the visible and near-infrared channels of the advanced very high resolution radiometer on the NOAA-9 spacecraft: Assessment and recommendations for corrections
| NOAA-TR-NESDIS-70 | p 544 N94-13029
Room temperature degradation of YBa2Cu3O(7-x) superconductors in varying relative humidity environments
| NASA-TP-3368 | p 813 N94-14409
Ion assisted sputter deposition of Mo-Si multilayers
| DE93-013830 | p 583 N94-14693

Optical degradation issues for XUV projection lithography systems
[DE93-012658] p 626 N94-14805

DEGREES OF FREEDOM
Control algorithm implementation for a redundant degree of freedom manipulator
[NASA-CR-191339] p 762 N94-13131
Generalized impedance control of a redundant manipulator p 661 N94-13575
Six degree of freedom
[NASA-TM-109295] p 749 N94-13636
Self organized criticality
[DE93-013182] p 773 N94-14320
Implementation and experimentation with a motion planning system
[ITN-93-85213] p 755 N94-14505

DELAY
Three, four, five, six or the complexity of scheduling with communication delays
[CWI-BS-R9229] p 751 N94-14004
Radio metric errors due to mismatch and offset between a DSN antenna beam and the beam of a troposphere calibration instrument p 607 N94-14370

DELAY LINES
Processing, fabrication and demonstration of HTS integrated microwave circuits
[AD-A265789] p 619 N94-12892

DELTA FUNCTION
Toward a quasi-linear closure for compressible turbulence
[DE93-017185] p 647 N94-14895

DELTA WINGS
Estimation of critical values and vibration characteristics on supersonic delta wings. Part 2: Locally-stationary time series analysis of nonstationary random responses
[NAL-TR-1179] p 502 N94-13345
Experimental studies of vortex flaps and vortex plates. Part 2: 1.15m span 60 deg delta wing
[NAL-TR-1180T-PT-2] p 502 N94-13454
Experimental studies of vortex flaps and vortex plates. Part 1: 0.53 m span 60 deg delta wing
[DE93-767969] p 505 N94-14059
Numerical simulation of a powered-lift landing, tracking flow features using overset grids, and simulation of high lift devices on a fighter-lift-and-control wing
[NASA-CR-194260] p 527 N94-14322
Navier-Stokes simulation of transonic vortex flow over a delta wing p 640 N94-14606

DEMODULATION
Multiple-symbol differential detection of DPSK with frequency offset
[DREO-TN-92-5] p 606 N94-14063
I/Q demodulation of radar signals with calibration and filtering
[DREO-RN-1119] p 606 N94-14064

DEMODULATORS
Digital quadrature demodulation for radar ESM applications
[DREO-TN-92-10] p 603 N94-13838
Multiple-symbol differential detection of DPSK with frequency offset
[DREO-TN-92-5] p 606 N94-14063
I/Q demodulation of radar signals with calibration and filtering
[DREO-RN-1119] p 606 N94-14064

DEMOGRAPHY
Generic results of the space physics community survey
[NASA-CR-194538] p 818 N94-13984

DENDRITIC CRYSTALS
The influence of a microgravity environment on the dendritic morphology during directional solidification of hypoeutectic Al-Si alloys
[NASA-CR-194139] p 571 N94-13891

DENSE PLASMAS
The 24 GHz measurements of 2.2 lambda conical horn antennas illuminating a conducting sheet
[NASA-TM-109002] p 598 N94-12811
Highly charged ions in hot, dense plasmas
[DE93-013348] p 795 N94-12995
Indirect processes in electron impact ionization of Kr(24+) and Kr(25+)
[DE93-014129] p 784 N94-14140
Implicit multi-fluid simulation of interpenetrating plasmas
[DE93-013351] p 801 N94-14342

DENSITY (MASS/VOLUME)
Preliminary results on the hydrological measurements in the Aegean Sea off Crete: Cruise, Georgia, 1989
[PREPRINT-736] p 725 N94-13500

DENSITY DISTRIBUTION
Analysis of interstellar cloud structure based on IRAS images
[NASA-CR-194341] p 836 N94-13332
Cold dark matter halos p 838 N94-13649
The use of polarised neutron reflection for unique density profile determination in thin films
[PB93-187136] p 579 N94-13783
Current distribution tomography for determination of internal current density distributions
[DE93-015463] p 604 N94-13899

DENSITY MEASUREMENT
Novel Co:MgF2 lidar for aerosol profiler
[NASA-CR-191525] p 654 N94-13091
A rocket-borne lidar for studies of the middle atmosphere
[FFI/RAPPORT-92/7034] p 715 N94-13949

DEOXIDIZING
Formation of deoxidization products in iron ingot by the addition of Al, Si, and/or Mn (M-5) p 587 N94-13737

DEOXYRIBONUCLEIC ACID
Analysis of the V antigen lcrGVH-yopBD operon of Yersinia pseudotuberculosis: Evidence for a regulatory role of LcrH and LcrV
[FOA-B-40417-4.4] p 729 N94-14129

DEPOSITION
Role of Ca(++)/calmodulin in the regulation of microtubules in higher plants
[DE93-015885] p 727 N94-12835
Amorphous sol-gel insulating films
[DE93-012859] p 576 N94-12866
Impedance-power effects on plasma polymer surface finish using a helical resonator discharge
[DE93-016454] p 803 N94-14590
Ion assisted sputter deposition of Mo-Si multilayers
[DE93-013830] p 583 N94-14693

DEPTH
Measurement of penetration depth lambda(T) in YBa2Cu3O(7-delta) thin film
[DE93-014587] p 810 N94-14122
Depths from focusing and defocusing
[AD-A266644] p 735 N94-14797

DEPTH MEASUREMENT
Depths from focusing and defocusing
[AD-A266644] p 735 N94-14797

DESCENT TRAJECTORIES
Visual cueing aids for rotorcraft landings p 524 N94-13313
Optimal lateral escape maneuvers for microburst encounters during final approach
[LR-691] p 511 N94-13534

DESERTIFICATION
Climatic change due to land surface alterations
[INPE-5495-PRE/1786] p 721 N94-13672

DESERTS
Evolution of the lower planetary boundary layer over strongly contrasting surfaces
[DE93-010667] p 717 N94-14424

DESIGN ANALYSIS
A knowledge-based expert system to coordinate CAD/CAE with integration and test
[NASA-CR-191394] p 745 N94-13130
Parachute system design, analysis, and simulation tool
[DE93-013755] p 501 N94-13260
Multidisciplinary design techniques applied to conceptual aerospace vehicle design
[NASA-CR-194409] p 515 N94-13618
Galileo Optical Experiment (GOPEX) optical train: Design and validation at the Table Mountain Facility p 610 N94-14390
Impact of shorter wavelengths on optical quality for laws
[NASA-CR-193433] p 792 N94-14473
The further development and refinement of an expert-systems approach to the creative design of mechanisms and mechanical systems
[AD-A266812] p 665 N94-14901

DESORPTION
Photochemical dynamics of surface oriented molecules
[DE93-016289] p 784 N94-13983
Construction and test of a facility for photon-stimulated field description using excimer laser and time of flight
[ETN-93-94386] p 657 N94-13996
Quantum state resolved desorption of CO from solid surfaces
[DE93-016876] p 814 N94-14597

DESTRUCTIVE TESTS
Review of test methods for material flammability
[DSIS-93-00480] p 564 N94-13942

DETECTION
A general contact detection algorithm for finite element analysis
[DE93-012846] p 742 N94-12956
Early detection of insulation failure in electric motors
[PB93-198208] p 626 N94-14686
The 4th International Symposium on Analysis and Detection of Explosives
[DE93-620280] p 585 N94-14829

DETERIORATION
Optimal maintenance policies of a Markovian system
[ITN-93-85216] p 774 N94-14502

DETONATION
Equation of state for detonation products
[DE93-012671] p 583 N94-12921
Hydrogen peroxide safety issues
[DE93-013895] p 565 N94-14346

DETONATION WAVES
High order hybrid numerical simulations of two dimensional detonation waves
[NASA-CR-191506] p 769 N94-13792
Numerical study of shock-induced combustion in methane-air mixtures
[NASA-TM-106354] p 642 N94-14722

DEUTERIUM
Charged-particle evaluation methodology at Lawrence Livermore National Laboratory
[DE93-013429] p 781 N94-13251
The space-time and energy parameters of deuterium braking by the central collision with atoms
[DE93-624144] p 788 N94-14881

DEUTERONS
The space-time and energy parameters of deuterium braking by the central collision with atoms
[DE93-624144] p 788 N94-14881
The evolution of tensor polarization
[DE93-017209] p 790 N94-14897

DIAGNOSIS
Completing fault models for abductive diagnosis
[DE93-003832] p 761 N94-12859

DIALLYL COMPOUNDS
Unexpectedly rapid hydrosilation polymerization of the diallyl derivative of bisphenol A and 2,6-diallylphenol
[AD-A265832] p 577 N94-12986

DIAMOND FILMS
Correlations of the growth, structure, and stress with the adhesion of diamond films on tungsten
[DE93-012855] p 576 N94-12912
Scanning tunneling microscopy studies of diamond films and optoelectronic materials
[NASA-CR-194363] p 578 N94-13246
Characterization of diamond film growth in a combustion flame
[AD-A266659] p 816 N94-14839

DIAMONDS
Lattice site of helium implanted in Si and diamond
[DE93-015365] p 805 N94-13012
Simulation studies for surfaces and materials strength
[NASA-CR-193305] p 671 N94-13179
Scanning tunneling microscopy studies of diamond films and optoelectronic materials
[NASA-CR-194363] p 578 N94-13246
Machining aspects of nickel-phosphorus coatings
[DE93-013037] p 580 N94-14311

DIATOMIC GASES
Calculation of hypersonic shock structure using flux-split algorithms
[NASA-CR-194296] p 504 N94-13607

DICHROISM
The x ray dichroism experiments using circular polarization
[DE93-013195] p 568 N94-13036

DICTIONARIES
Glossary of SSDC terms and acronyms
[DE93-013697] p 823 N94-13352

DIELECTRIC PROPERTIES
Amorphous sol-gel insulating films
[DE93-012859] p 576 N94-12866
Moisture meter evaluation
[DE93-016581] p 652 N94-14534
Shielded open-circuited sample holders for dielectric and magnetic measurements of liquids and powders
[PB93-198851] p 652 N94-14687
A high voltage dielectrically isolated smart power technology based on silicon direct bonding
[LAAS-92492] p 626 N94-14698

DIELECTRICS
Laser CO2 beam transmission through hollow metallic waveguide coated by a thin internal dielectric layer
[ITN-93-85201] p 656 N94-13571
Theoretical investigation of scattering by homogeneous or coated dielectric spheres illuminated with a steady state or pulsed laser beam p 657 N94-13624
Laser-damage susceptibility of nodular defects in dielectric mirror coatings: AFM measurements and electric-field modeling
[DE93-014655] p 580 N94-14124
Prism-film coupling in anisotropic planar waveguides of epitaxial (101) rutile thin films
[DE93-012912] p 811 N94-14304
Theoretical studies of breakdown in random media
[DE93-018107] p 558 N94-14418
Moisture meter evaluation
[DE93-016581] p 652 N94-14534

Shielded open-circuited sample holders for dielectric and magnetic measurements of liquids and powders
| PB93-198851 | p 652 N94-14687
Materials and structures p 546 N94-14835
Electrochemical planarization for microelectronic circuits
| DE93-017214 | p 627 N94-14870

DIES
An experimental study on the effect of die geometry on swell and sag in the parison extrusion stage
| IMI-93RT-42400-1476-G | p 597 N94-14070

DIESEL ENGINES
Futurepath 2
| NASA-TM-109285 | p 518 N94-13623
Biodiesel/aquatic species project report, FY 1992
| DE93-010024 | p 709 N94-14087
Three-dimensional modeling of diesel engine intake flow, combustion and emissions-2
| NASA-CR-191189 | p 519 N94-14448

DIESEL FUELS
Biodiesel/aquatic species project report, FY 1992
| DE93-010024 | p 709 N94-14087
Biofuels for transportation: The road from research to the marketplace
| DE93-000091 | p 585 N94-14454

DIFFERENCE EQUATIONS
Preconditioning and the limit to the incompressible flow equations
| NASA-CR-191500 | p 769 N94-13717
Self-tuning control techniques for multivariable systems
| INPE-5449-TDI/495 | p 765 N94-14084
On a difference equation for generalizations of Charlier polynomials
| REPT-92-101 | p 770 N94-14150

DIFFERENTIAL EQUATIONS
A hybrid Pade-Galerkin technique for differential equations
| NASA-CR-191494 | p 767 N94-13289
Theory for iterative solution of large dynamical systems using parallel computation
| TKK-MAT-A304 | p 760 N94-14187
An adaptive projection method for the incompressible Euler equations
| DE93-016428 | p 639 N94-14434
ASTEC and MODEL: Controls software development at Goddard Space Flight Center p 678 N94-14628
Functional differential equations with piecewise continuous argument
| AD-A266660 | p 772 N94-14840

DIFFERENTIAL GEOMETRY
On the differential structure of matrix-valued rational inner functions
| CWI-BS-R9228 | p 770 N94-14003

DIFFRACTION
On the neutron EDM search in the Laue diffraction by the crystal without a centre of symmetry
| DE93-622971 | p 804 N94-12828
A positron annihilation radiation telescope using Laue diffraction in a crystal lens
| DE93-012905 | p 848 N94-13483
Fabrication p 546 N94-14834

DIFFRACTION PATTERNS
A Fourier transform microscope for x ray and/or gamma ray imaging
| AD-D015742 | p 791 N94-13664
Advanced ballistic range technology
| NASA-CR-194530 | p 533 N94-14540

DIFFRACTOMETERS
Measurement of strain in individual phases of composites before, during, and after mechanical loading
| DE93-014585 | p 558 N94-14119

DIFFUSE RADIATION
Analysis of data from the energetic gamma-ray experiment on the gamma ray observatory
| NASA-CR-194178 | p 847 N94-13087
NREL solar radiation resource assessment project: Status and outlook
| DE93-010034 | p 704 N94-14422

DIFFUSION
Study of multicomponent diffusion and transport phenomena
| DE93-015095 | p 804 N94-13005
Transport properties of disordered porous media from the microstructure
| DE93-016065 | p 806 N94-13152
Mathematical algorithms for multidimensional inverse scattering problems in inhomogeneous medium
| AD-A266440 | p 749 N94-13702
Gas-evaporation in low-gravity field (cogelation mechanism of metal vapors) (M-14) p 588 N94-13746
Growth experiment of organic metal crystal in low gravity (M-21) p 590 N94-13753
Crystal growth of compound semiconductors in a low-gravity environment (InGaAs crystals) (M-22) p 590 N94-13754
Boundary stability under nonequilibrium conditions
| DE93-016259 | p 809 N94-13980

DIFFUSION COEFFICIENT
Stormtime transport of ring current and radiation belt ions
| NASA-CR-194416 | p 714 N94-13793
Contribution to comparison of methods for determining welding procedures for the avoidance of hydrogen cracking
| VTT-PUBS-107 | p 674 N94-13887
Direct determination of alpha particle transport coefficients
| DE93-013488 | p 787 N94-14691
Manufacturing and examination of integrated optical waveguide components in silicon
| ETN-93-94393 | p 793 N94-14704

DIFFUSION FLAMES
Structure of turbulent non-premixed flames modeled with two-step chemistry p 567 N94-14767

DIFFUSION THEORY
Stochastic dynamics: Crossover from 1/f(sup 3) to flicker noise
| DE93-622862 | p 772 N94-12896

DIFFUSIVITY
Temperature dependence of diffusivities, preliminary definition phase
| NASA-CR-192613 | p 648 N94-13326
The resonance broadening theory revisited
| PPL-134 | p 798 N94-13563

DIGITAL COMPUTERS
Adaptive Transfer Function Networks
| DE93-014344 | p 745 N94-13151

DIGITAL DATA
Digital sound: The selection of critical programme material and preparation of recordings for CCIR tests on low bit-rate codecs
| BBC-RD-1993/1 | p 598 N94-12925
Digital sound: Subjective tests on commentary-quality codecs
| BBC-RD-1993/2 | p 598 N94-12926
Evaluation of beta-spline interpolation in digital terrain models
| INPE-5475-TDI/506 | p 684 N94-13364
DATAA: Data acquisition made easy
| DE93-014683 | p 823 N94-13406
Study of computer system as a musical instrument p 747 N94-13439
Net radiation mapping of mountainous terrain using Landsat-5 thematic mapper imagery and digital terrain data
| ISBN-0-315-57755-X | p 685 N94-13475
Development of an automated film-reading system for ballistic ranges
| NASA-CR-194398 | p 650 N94-13815
Advanced Communications ESM System (ACES) testbed: Integration study
| DSIS-93-00345 | p 604 N94-13939
EWTEST signal excision testbed: System evaluation
| DSIS-93-00346 | p 607 N94-14065
Obtaining digital regional planning information from aerial pictures
| REPT-228 | p 700 N94-14810

DIGITAL FILTERS
Spatially-varying IIR filter banks for image coding
| NASA-CR-193727 | p 619 N94-12897
Recursive time-varying filter banks for subband image coding
| NASA-CR-193726 | p 598 N94-12920
A combined analogue and digital pulse compression system using large time bandwidth product signals for use in synthetic aperture radar
| ISBN-0-315-54373-6 | p 600 N94-13489
Robust filters for image smoothing
| ERB-1033 | p 769 N94-13545

DIGITAL RADAR SYSTEMS
A combined analogue and digital pulse compression system using large time bandwidth product signals for use in synthetic aperture radar
| ISBN-0-315-54373-6 | p 600 N94-13489

DIGITAL SIMULATION
Numerical simulation of hypersonic flow for the design of the H-2 orbiting plane (HOPE), part 3
| NAL-TR-1168-PT-3 | p 499 N94-12948
Transmission zeros of spacecraft attitude control system
| NAL-TR-1166 | p 540 N94-13339
The nocturnal wind maximum: An interactive forecast method
| KNMI-TR-142 | p 722 N94-13985
Precipitation verification LAM
| KNMI-TR-143 | p 722 N94-13991
Turbulent particle dispersion in confined swirling flows
| DLR-FB-92-32 | p 637 N94-14045
Numerical simulation of dynamic stall of NACA0012 airfoil oscillating near static stall angle using the Navier-Stokes equations
| DE93-767970 | p 505 N94-14061
Turbulent diffusion in homogeneous shear flow with stable density stratification
| DLR-FB-92-26 | p 639 N94-14443

DIGITAL SYSTEMS
Destination-directed, packet-switched architecture for a geostationary communications satellite network
| NASA-TP-3379 | p 538 N94-13111
Techniques for improving the performance of a simplified electronic fuel controller with incremental actuation for small gas turbine engines
| ISBN-0-315-56062-2 | p 661 N94-13521
Digital quadrature demodulation for radar ESM applications
| DREO-TN-92-10 | p 603 N94-13838
Preliminary design and implementation of the baseline digital baseband architecture for advanced deep space transponders p 611 N94-14393
Coverage aspects of a single frequency network designed for digital audio broadcasting
| BBC-RD-1993/3 | p 616 N94-14742
A fast frame rate 512 x 512 CCD digital camera system
| DE93-013048 | p 653 N94-14792

DIGITAL TECHNIQUES
Intelligent environment for interpretation tasks of remotely sensed images
| INPE-5466-PRE/1774 | p 687 N94-14082

DIGITAL TELEVISION
Optimization of a subband coding for high definition television with motion controlled three dimensional frequency band decomposition
| ETN-93-94396 | p 617 N94-14817

DIMENSIONAL ANALYSIS
Integration of space and in-situ observations to study atmosphere, ocean and land processes
| NASA-CR-194495 | p 683 N94-14500

DIMENSIONAL MEASUREMENT
Rapid intelligent inspection process definition for dimensional measurement in advanced manufacturing
| DE93-011271 | p 748 N94-13480
The use of polarised neutron reflection for unique density profile determination in thin films
| PB93-187136 | p 579 N94-13783

DIMETHYL COMPOUNDS
Office of Naval Research/DARPA publications: Composite materials with improved properties in compression
| AD-A265509 | p 560 N94-14794

DIODES
Numerical simulation and analysis of electrical and optical properties of Al(x)Ga(1-x)As / GaAs
| ETN-93-94387 | p 703 N94-13997

DIPOLE MOMENTS
On the neutron EDM search in the Laue diffraction by the crystal without a centre of symmetry
| DE93-622971 | p 804 N94-12828

DIPOLES
Plasma diffusion through multidipole magnetic fields
| INPE-5460-PRE/1768 | p 795 N94-12901

DIRAC EQUATION
Relativistic proton-nucleus scattering and one-boson-exchange models p 786 N94-14550

DIRECT BROADCAST SATELLITES
The current situation, trends, international cooperation of space communication technological development in the Republic of Korea p 699 N94-14283

DIRECT CURRENT
Studies of non-inductive current drive in the CDX-U tokamak p 799 N94-13680
Direct electron heating and current drive with fast waves in D3-D
| DE93-013028 | p 801 N94-14293
A high-precision direct current measuring device over a kiloampere range
| DE93-626409 | p 627 N94-14885

DIRECTION FINDING
Portable multipath measurement system
| DSIS-93-00177 | p 603 N94-13843

DIRECTIONAL SOLIDIFICATION (CRYSTALS)
The influence of a microgravity environment on the dendritic morphology during directional solidification of hypoeutectic Al-Si alloys
| NASA-CR-194139 | p 571 N94-13891
Immiscible phase incorporation during directional solidification of hypermonotectics
| NASA-CR-194412 | p 565 N94-14480

DIRECTIVITY
Measurements of the spatial structure and directivity of 100 KeV photon sources in solar flares using PVO and ISEE-3 spacecraft
| NASA-CR-194080 | p 845 N94-14492

DIRICHLET PROBLEM
Modulational stability of periodic solutions of the Kuramoto-Sivaskinsky equation
| NASA-CR-191502 | p 628 N94-12888
DISASTERS
Application of satellite remote sensing technology in disaster mitigation: A case study of Bangladesh
p 692 N94-14238
Integration of remote sensing and mathematical modelling in disaster mitigation p 692 N94-14239
Satellite remote sensing for disaster mitigation
p 693 N94-14244
A concept for the world environment and disaster observation system p 693 N94-14245
A tentative plan on China and Asian-Pacific satellite system for disaster reduction p 693 N94-14247
DISCONTINUITY
Removing noise from discontinuous data
| ITN-93-85211 | p 826 N94-14555
DISLOCATIONS (MATERIALS)
Boundary stability under nonequilibrium conditions
| DE93-016259 | p 809 N94-13980
DISPERSING
A model for fuel fire duration and application to the B-1B bomber
| DE93-013000 | p 512 N94-14292
DISPLACEMENT
Sampling of globular clusters and the distance to the galactic center
| INPE-5446-TDI/492 | p 837 N94-13449
DISPLACEMENT MEASUREMENT
A benchmark bending test of a thick specimen, Part 1: Experiments
| ARL-RR-6-PT-1 | p 670 N94-12927
A benchmark bending test of a thick specimen. Part 2: Surface displacement measurements
| ARL-RR-6-PT-2 | p 670 N94-12928
DISPLAY DEVICES
Color image processing for flat panel visual display modeling
| NASA-CR-193660 | p 790 N94-12797
Advanced display object selection methods for enhancing user-computer productivity
| AD-A265806 | p 743 N94-12974
PC based A320 quick access recorder readout facility
| PD-AL-9109 | p 744 N94-13077
A perspective on the FAA approval process: Integrating rotorcraft displays, controls and workload
p 521 N94-13298
Improvements in hover display dynamics for a combat helicopter p 523 N94-13310
Handling qualities effects of display latency
p 517 N94-13316
Primary display latency criteria based on flying qualities and performance data p 525 N94-13318
Human factor implications of the Eurocopter AS332L-1 Super Puma cockpit p 525 N94-13319
Evaluation of two cockpit display concepts for civil tiltrotor instrument operations on steep approaches
p 517 N94-13323
Programming the multimodal interface
| DE93-013084 | p 748 N94-13576
Eye-gaze and intent: Application in 3D interface control
| DE93-015210 | p 738 N94-14335
An overview of parallel scientific visualization
| DE93-017105 | p 755 N94-14521
DISSOLVING
Synthesis and properties of novel cluster phases
| DE93-017056 | p 577 N94-13072
Modeling surface area to volume effects on borosilicate glass dissolution
| DE93-011891 | p 581 N94-14432
DISTORTION
Electromagnetic wave test p 508 N94-14173
DISTRIBUTED PARAMETER SYSTEMS
Applications of computer algebra to distributed parameter systems p 677 N94-14623
DISTRIBUTED PROCESSING
A network evaluation and analysis tool
| DE93-012647 | p 758 N94-12917
Multicluster
| AD-A265869 | p 758 N94-12930
VIEWCACHE: An incremental pointer-base access method for distributed databases. Part 1: The universal index system design document. Part 2: The universal index system low-level design document. Part 3: User's guide. Part 4: Reference manual. Part 5: UIMS test suite
| NASA-CR-191788 | p 822 N94-13126
The KSR1: Experimentation and modeling of poststore
| DE93-012539 | p 759 N94-13470
Fail-safe PVM: A portable package for distributed programming with transparent recovery
| AD-A266594 | p 749 N94-13779
A distributed, visual object system using aggregation objects with a local namespace
| IME-MET-TR-007 | p 764 N94-13860
Distributed processor Monte Carlo: MCNP results on a 16-node IBM cluster
| DE93-012639 | p 752 N94-14176
Storage systems for national information assets
| DE93-015101 | p 825 N94-14331
Computational mechanics and supercomputing at LLNL
| DE93-016453 | p 754 N94-14435
Toward a verifiable approach to the design of concurrent computations
| DE93-012908 | p 756 N94-14844
DISTRIBUTION FUNCTIONS
Smooth transitions between bump rendering algorithms
| DE93-012504 | p 742 N94-12883
Fatigue predictions and scatter
| LR-696 | p 675 N94-13933
DISULFIDES
Dry film lubricant evaluation
| DE93-013114 | p 578 N94-13118
DIVERGENCE
Discussion of stress tensor nonuniqueness with application to nonuniform, particulate systems
| DE93-014352 | p 816 N94-13206
DIVERTERS
Dependence of beta(tau) on plasma shape in D3-D
| DE93-015473 | p 800 N94-13900
Electrical characterization of the JET A(sub 2) antenna: Comparison of model with measurements Wade, T.
| DE93-012964 | p 607 N94-14291
Variation of divertor plasma parameters with divertor depth for H-mode discharges in D3-D
| DE93-015475 | p 801 N94-14347
D3-D research operations
| DE93-016729 | p 802 N94-14519
DMSP SATELLITES
DMSP F11 SSM/T-2 calibration and validation
| AD-A265817 | p 719 N94-12978
DOCUMENTATION
Goddard Space Flight Center robotics demo
| NASA-TM-109302 | p 662 N94-13604
PSM: A new generation of data modeling
| TR-92-13 | p 824 N94-14072
DOCUMENTS
Glossary of SSDC terms and acronyms
| DE93-013697 | p 823 N94-13352
DOMAINS
Domain connectivity among systems of overset grids
| NASA-CR-193390 | p 508 N94-14326
DOMES (STRUCTURAL FORMS)
Some flow properties of telescope enclosures estimated from water channel tests: Application of the flow visualization techniques
| NAL-TR-1178T | p 830 N94-13452
DOMESTIC SATELLITE COMMUNICATIONS SYSTEMS
The developments of satellite communications of China p 618 N94-14282
The current situation, trends, international cooperation of space communication technological development in the Republic of Korea p 699 N94-14283
DOORS
The development of inspection and repair methods for the C-17 aft cargo door
| LR-704 | p 499 N94-13904
DOPED CRYSTALS
Poling of thin polymer films in electro optic applications
| AD-A266562 | p 579 N94-13584
Optimization of transparent and reflecting electrodes for amorphous silicon solar cells
| DE93-010009 | p 704 N94-14110
Laser and spectroscopic properties of Yb-doped apatite crystals
| DE93-014656 | p 810 N94-14125
Schemes for the use of conducting polymers as active materials in electrochemical supercapacitors
| DE93-012713 | p 580 N94-14179
Structure and stability of microvoids in A-Si:H
| DE93-016625 | p 813 N94-14413
Is K3C60 a line phase?
| DE93-016700 | p 813 N94-14517
Time resolved measurement of electron temperatures of exploding foil x ray laser plasmas
| DE93-017161 | p 803 N94-14894
DOPPLER EFFECT
Trellis coding with Continuous Phase Modulation (CPM) for satellite-based land-mobile communications
| NASA-CR-191325 | p 604 N94-13909
DOPPLER RADAR
Venus gravity
| NASA-CR-194077 | p 841 N94-12823
Development of a global backscatter model for NASA's laser atmospheric wind sounder
| NASA-CR-192581 | p 718 N94-12957
Coherent Doppler lidar signal covariance including wind shear and wind turbulence
| NASA-CR-194492 | p 721 N94-13723
DORNIER AIRCRAFT
Flight evaluations of approach/landing navigation sensor systems: Summary of 1990 flight experiments
| NAL-TR-1175 | p 513 N94-13344
Performance evaluation tests of the GPS/DGPS navigation system installed in the NAL Dornier 228: Preliminary ground test results
| NAL-TM-649 | p 513 N94-13346
DOSIMETERS
Study on the biological effect of cosmic radiation and the development of radiation protection technology (L-11) p 593 N94-13768
Investigations of low-temperature neutron embrittlement of ferritic steels
| DE93-015460 | p 573 N94-14700
DOUBLE SIDEBAND TRANSMISSION
The MRIS feasibility study
| NASA-TM-107763 | p 597 N94-12804
DOWNLINKING
Sequential ranging: How it works
| NASA-CR-194508 | p 532 N94-13796
Simulation of downlink synchronization for a frequency-hopped satellite communication system
| DSIS-93-00477 | p 605 N94-13941
Stability measurements of the radio science system at the 34-m high-efficiency antennas p 609 N94-14381
Transform coding for space applications
| NASA-TM-106362 | p 612 N94-14542
DRAG MEASUREMENT
Aerodynamics of a sphere and an oblate spheroid for Mach numbers from 0.6 to 10.5 including some effects of test conditions
| NASA-TM-109016 | p 500 N94-13172
DRAG REDUCTION
Direct simulation of polymer drag reduction in free shear flows and vortex dipoles p 644 N94-14755
DRAINAGE
BOAST 2 for the IBM 3090 and RISC 6000
| DE93-000138 | p 638 N94-14351
DRILLING
Recent results from material processing studies on new generation lasers
| DE93-013841 | p 653 N94-12898
Promotion of geothermal energy development in 1991
| DE93-799057 | p 701 N94-13214
Overview: Gas hydrate geology and geography
| DE93-014043 | p 688 N94-14151
DROP SIZE
A parameterization of cloud droplet nucleation
| DE93-007998 | p 718 N94-12903
Experimental determination of droplets local mean diameter of a sprag from impinging jets
| INPE-5469-TDI/500 | p 631 N94-13365
DROPS (LIQUIDS)
A parameterization of cloud droplet nucleation
| DE93-007998 | p 718 N94-12903
Linkage of anthropogenic aerosol to clouds and climate
| DE93-016434 | p 719 N94-13080
Experimental determination of droplets local mean diameter of a sprag from impinging jets
| INPE-5469-TDI/500 | p 631 N94-13365
Numerical studies of spray combustion in liquid-fueled engines p 564 N94-13685
Drop dynamics in space and interference with acoustic field (M-15) p 588 N94-13747
Liquid metal drop ejection
| NASA-CR-193718 | p 572 N94-14133
Droplet-turbulence interactions in sprays exposed to supercritical environmental conditions
| NASA-CR-194408 | p 638 N94-14308
DROSOPHILA
Genetic effects of HZE and cosmic radiation (L-9)
p 593 N94-13766
DROUGHT
Sea surface temperature forcing and phase locking of Nordeste precipitation
| DE93-011873 | p 723 N94-14426
DRY HEAT
Hot Dry Rock energy
| DE93-014452 | p 702 N94-13403
DRYING
Characterization of 1:1 random copolymers obtained from 6-, 7-, 11-, and 12-carbon amino acids
| AD-A265827 | p 577 N94-12985
DUAL THRUST NOZZLES
Evaluation of dual flow thrust vector nozzles with exhaust stream impingement
| NASA-CR-193392 | p 630 N94-13078

Design and evaluation of single and dual flow thrust vector nozzles with post exit vanes
[NASA-CR-193393] p 638 N94-14086
DUCTED FAN ENGINES
Active control of fan-generated plane wave noise
[NASA-TM-109008] p 777 N94-14481
DUCTED FLOW
Fully developed turbulent flow in rectangular interrupted-plate ducts
[ISBN-0-315-63594-0] p 632 N94-13474
DUCTED ROCKET ENGINES
Hypersonic propulsion characterization p 505 N94-14156
DUCTILITY
Fracture behavior of vanadium/vanadium silicide in-situ composites
[DE93-013422] p 556 N94-13389
Investigation of criteria for ductile fracture under fully-plastic conditions p 672 N94-13593
Machining and grinding: High rate deformation in practice
[DE93-010718] p 664 N94-14457
DUCTS
Fully developed turbulent flow in rectangular interrupted-plate ducts
[ISBN-0-315-63594-0] p 632 N94-13474
DUFFING DIFFERENTIAL EQUATION
Stability of subharmonics and escape phenomena in the twin-well potential duffing system p 775 N94-13235
DUMMIES
An assessment of the potential for neck injury due to padding of aircraft interior walls for head impact protection
[DOT/FAA/AM-93/14] p 738 N94-13972
DURABILITY
Role of microstructure on fatigue durability of aluminum aircraft alloys
[AD-A265627] p 568 N94-12993
Reflective coatings for solar applications
[DE93-010026] p 702 N94-13381
Canonical correlation of waste glass compositions and durability, including pH
[DE93-012754] p 578 N94-13493
Role of microstructure on fatigue durability of aluminum aircraft alloys
[AD-A266350] p 571 N94-13697
Optical and physical properties of the LiSrAlF6:Cr laser crystal
[DE93-014657] p 808 N94-13881
Relationship between borosilicate glass composition, structure, and durability test response (SRS)
[DE93-013578] p 581 N94-14343
JPRS report: Science and technology. Central Eurasia: Materials science
[JPRS-UMS-93-004] p 559 N94-14574
DUST
Infrared transmission and path radiance through dust and fog
[AD-A265825] p 791 N94-12979
DWARF STARS
Spectra of late type dwarf stars of known abundance for stellar population models
[NASA-CR-194301] p 831 N94-13681
Rocket and laboratory studies in astronomy
[NASA-CR-194410] p 832 N94-13966
DYE LASERS
Recent results from material processing studies on new generation lasers
[DE93-013841] p 653 N94-12898
Design and performance of an automated video-based laser beam alignment system
[DE93-012571] p 656 N94-13481
Single event effects and laser simulation studies
[NASA-CR-194506] p 657 N94-13812
Laser beam control and diagnostic systems for the copper-pumped dye laser system at Lawrence Livermore National Laboratory
[DE93-016529] p 658 N94-14437
DYNAMIC CHARACTERISTICS
System identification for Space Station Freedom using observer/Kalman filter Markov parameters
[NASA-CR-191521] p 539 N94-12976
Investigation of an aeroelastic oscillator: Analysis of one-degree-of-freedom galloping with combined translational and torsional effects
[LR-707] p 527 N94-13906
Computational diagnostics for detecting phase transitions during nanoindentation
[DE93-016536] p 813 N94-14439
DYNAMIC CONTROL
A component modes projection and assembly model reduction methodology for articulated, multi-flexible body structures p 677 N94-14622
Computational Controls Workstation: Algorithms and hardware p 678 N94-14626
Control system design for flexible structures using data models p 527 N94-14646
PACE: A test bed for the dynamics and control of flexible multibody systems p 527 N94-14650
DYNAMIC LOADS
Experimental and analytical analysis of the response of a smart beam to rate feedback
[AD-A266544] p 557 N94-13706
Computer program for analysis of high speed, single row, angular contact, spherical roller bearing, SASHBEAN. Volume 1: User's guide
[NASA-CR-191183] p 663 N94-14445
DYNAMIC MODELS
Methods for evaluating the predictive accuracy of structural dynamic models
[NASA-CR-191337] p 671 N94-13124
X ray emission from dynamical shock models in hot-star winds
[NASA-CR-194093] p 847 N94-13288
A model for rotorcraft flying qualities studies p 523 N94-13308
An analytic modeling and system identification study of rotor/fuselage dynamics at hover p 524 N94-13312
Attitude determination of stratospheric balloons using Kalman filters
[INPE-5498-TDI/513] p 649 N94-13366
Dynamics and design of nonholonomic robotic mechanical systems
[ISBN-0-315-72009-3] p 662 N94-13597
Transition of building energy consumption using multi-input, single-output dynamic model
[VTT-PUBS-116] p 597 N94-14055
Stress stiffening and approximate equations in flexible multibody dynamics p 677 N94-14620
DYNAMIC PRESSURE
Dynamic soil pressures on rigid cylindrical vaults
[DE93-013930] p 676 N94-14585
DYNAMIC PROGRAMMING
Parameter identification of a model of the process of software development
[REPT-93-008] p 750 N94-13807
Speaker independent recognition of isolated words using vector quantization and neural networks
[ETN-93-94390] p 616 N94-14724
DYNAMIC RESPONSE
Structural design/margin assessment
[NASA-TP-3410] p 669 N94-12831
Molecular solvent-dynamical effects on activated electron-transfer kinetics: How important is solvent friction?
[AD-A265886] p 779 N94-12894
Movement of deployable truss p 531 N94-13280
Development of test techniques to simulate high-frequency mechanical shock on weapon components
[KCP-613-4998] p 675 N94-13907
Some aspects of sheet forming simulation using explicit finite element techniques
[DE93-012479] p 663 N94-13975
Spatial operator algebra for flexible multibody dynamics p 679 N94-14631
Non-recursive augmented Lagrangian algorithms for the forward and inverse dynamics of constrained flexible multibodies p 679 N94-14633
Computational strategies in the dynamic simulation of constrained flexible MBS p 679 N94-14635
Simulation of linear mechanical systems p 680 N94-14641
DYNAMIC STABILITY
Movement of deployable truss p 531 N94-13280
Study of a one-dimensional deployable structure employing telescopic members p 531 N94-13282
DYNAMIC STRUCTURAL ANALYSIS
A method of predicting quasi-steady aerodynamics for flutter analysis of high speed vehicles using steady CFD calculations
[NASA-TM-109009] p 514 N94-12850
Dynamics of adaptive structures: Design through simulations
[NASA-CR-193724] p 540 N94-13112
Methods for evaluating the predictive accuracy of structural dynamic models
[NASA-CR-191337] p 671 N94-13124
Actuator and aerodynamic modeling for high-angle-of-attack aeroservoelasticity
[NASA-TM-4493] p 520 N94-13255
Optical fiber sensors for materials and structures characterization
[NASA-CR-194090] p 791 N94-13353
Variational approach to probabilistic finite elements
[NASA-CR-187179] p 674 N94-13873
Some frequency and damping measurements of laminated beryllium beams
[DE93-015909] p 676 N94-14530
Proceedings of the Fifth NASA/NSF/DOD Workshop on Aerospace Computational Control
[NASA-CR-194515] p 677 N94-14618
Stress stiffening and approximate equations in flexible multibody dynamics p 677 N94-14620
Some experiences with Krylov vectors and Lanczos vectors p 677 N94-14621
Spatial operator algebra for flexible multibody dynamics p 679 N94-14631
Non-recursive augmented Lagrangian algorithms for the forward and inverse dynamics of constrained flexible multibodies p 679 N94-14633
Computational strategies in the dynamic simulation of constrained flexible MBS p 679 N94-14635
Parallel O(log n) algorithms for open- and closed-chain rigid multibody systems based on a new mass matrix factorization technique p 679 N94-14636
Parallel methods for dynamic simulation of multiple manipulator systems p 680 N94-14637
Space Station Common Berthing Mechanism, a multi-body simulation application p 544 N94-14640
Simulation of linear mechanical systems p 680 N94-14641
Computational issues in optimal tuning and placement of passive dampers p 681 N94-14647
Computational Control Workstation: Users' perspectives p 681 N94-14648
DYNAMIC TESTS
Identifying the NAL spaceplane aerodynamic model using dynamic wind tunnel tests
[NAL-TR-1171] p 500 N94-12951
Movement of deployable truss p 531 N94-13280
Study of a one-dimensional deployable structure employing telescopic members p 531 N94-13282
Smart skin technology development for measuring ice accretion, stall, and high AOA aircraft performance. Part 1: Capacitive ice detector development
[NASA-CR-194252] p 511 N94-13424
Machinery dynamics activities in Canadian industries
[IME-MET-TR-006] p 663 N94-14147
A program for the investigation of the Multibody Modeling, Verification, and Control Laboratory p 682 N94-14652
DYNAMICAL SYSTEMS
Theory for iterative solution of large dynamical systems using parallel computation
[TKK-MAT-A304] p 760 N94-14187
Identification of continuous-time dynamical systems: Neural network based algorithms and parallel implementation
[DE93-014427] p 766 N94-14737
Investigations of transitions from order to chaos in dynamical systems
[DE93-014438] p 818 N94-14738

E

EARLY STARS
A photometric study of massive x-ray binaries
[ITN-93-85207] p 829 N94-13231
EARLY WARNING SYSTEMS
A program of correlated observations using the EGRET instrument on GRO and the IMB neutrino detector
[NASA-CR-194367] p 783 N94-13856
EARTH ATMOSPHERE
National atmospheric sciences program, fiscal years 1987-1990
[NSF-92-16] p 711 N94-12794
Determination of spectroscopic properties of atmospheric molecules from high resolution vacuum ultraviolet cross section and wavelength measurements
[NASA-CR-194024] p 712 N94-13092
Modeling of biosphere-atmosphere interaction for forest and pastureland in the Amazon
[INPE-5454-TDI/496] p 707 N94-13330
Boundary layer structure over areas of heterogeneous heat fluxes
[DE93-007887] p 715 N94-13912
Terrestrial environment (climatic) criteria guidelines for use in aerospace vehicle development, 1993 revision
[NASA-TM-4511] p 533 N94-14824
EARTH CORE
Simultaneous solution for core magnetic field and fluid flow beneath an electrically conducting mantle
[NASA-TM-4536] p 716 N94-13960
EARTH CRUST
J2000.0 modelling of GEOAIM in the analysis of VLBI data from the NASA crustal dynamics project
[ISBN-0-315-59463-2] p 684 N94-13368
The determination of crustal motions using laser ranging to Lageos-2 and Lageos-1
[NASA-CR-193787] p 717 N94-14306

EARTH ENVIRONMENT
National atmospheric sciences program, fiscal years 1987-1990
| NSF-92-16 | p 711 N94-12794
A concept for the world environment and disaster observation system p 693 N94-14245
EARTH IONOSPHERE
The role of ionospheric plasma in the magnetosphere
| NASA-CR-194404 | p 716 N94-13967
Ionospheric calibration for single frequency altimeter measurements
| NASA-CR-194282 | p 716 N94-14049
Ionospheric effects on a wide-bandwidth, polarimetric, space-based, synthetic-aperture radar
| DE93-015084 | p 612 N94-14512
EARTH MAGNETOSPHERE
Force-free magnetic fields, curl eigenfunctions, and the sphere in transform space, with applications to fluid dynamics and electromagnetic theory
| AD-A265805 | p 834 N94-12971
TROPIX: A solar electric propulsion flight experiment
| NASA-TM-106297 | p 534 N94-13028
Advances in low energy neutral atom imaging techniques
| DE93-012745 | p 782 N94-13492
Stormtime transport of ring current and radiation belt ions
| NASA-CR-194416 | p 714 N94-13793
Energetic neutral atoms: Imaging the magnetospheric ring current
| NASA-CR-194339 | p 715 N94-13826
The role of ionospheric plasma in the magnetosphere
| NASA-CR-194404 | p 716 N94-13967
Investigations of transitions from order to chaos in dynamical systems
| DE93-014438 | p 818 N94-14738
EARTH MANTLE
Simultaneous solution for core magnetic field and fluid flow beneath an electrically conducting mantle
| NASA-TM-4536 | p 716 N94-13960
EARTH MOVEMENTS
Dynamic soil pressures on rigid cylindrical vaults
| DE93-013930 | p 676 N94-14585
EARTH OBSERVATIONS (FROM SPACE)
Estimations of temperature and humidity of the canopy in Amazon Forest using microwave data from SMMR sensor of Nimbus-7 satellite
| INPE-5444-TDI/490 | p 720 N94-13614
Minutes of the Sixth CEOS Plenary Meeting
| NASA-TM-108252 | p 542 N94-14112
Some potentials of the Indonesian region for Earth observation p 692 N94-14237
Earth observation from low-inclination orbit as a necessary complement to polar missions p 694 N94-14248
ERS-1 system
| ESA-SP-1146 | p 699 N94-14353
EARTH OBSERVING SYSTEM (EOS)
EOS workstation
| NASA-CR-191326 | p 736 N94-13132
Phase aligner for the Electronically Scanned Thinned Array Radiometer (ESTAR) instrument
| NASA-TM-4518 | p 623 N94-13878
Minutes of the Sixth CEOS Plenary Meeting
| NASA-TM-108252 | p 542 N94-14112
EARTH ORBITAL ENVIRONMENTS
Analysis of samples of reflector materials which are multicoated and metal samples with oxide coatings which have been exposed the space environment in LDEF testing
| NASA-CR-193647 | p 575 N94-12789
Meteoroid environment near the Earth-Moon system
| NASA-CR-193670 | p 835 N94-13203
Surface characterization of LDEF materials
| NASA-CR-194519 | p 543 N94-14683
Atomic research
| NASA-CR-193843 | p 788 N94-14905
EARTH ORIENTATION
The determination of crustal motions using laser ranging to Lageos-2 and Lageos-1
| NASA-CR-193787 | p 717 N94-14306
Use of global positioning system measurements to determine geocentric coordinates and variations in Earth orientation p 514 N94-14372
EARTH RADIATION BUDGET
Nimbus-7 Earth radiation budget calibration history. Part 1: The solar channels
| NASA-RP-1316 | p 844 N94-13963
Space measurements for determining the Earth's energy and water cycles p 690 N94-14227
Earth radiation budget, cloud, and aerosol parameters derived from AVHRR and TOVS measurements p 691 N94-14233
EARTH RADIATION BUDGET EXPERIMENT
Nimbus-7 Earth radiation budget calibration history. Part 1: The solar channels
| NASA-RP-1316 | p 844 N94-13963
EARTH RESOURCES
Minutes of the Sixth CEOS Plenary Meeting
| NASA-TM-108252 | p 542 N94-14112
Pattern and Process in Landscape Ecology: Eighth Annual US Landscape Ecology Symposium
| DE93-014032 | p 711 N94-14859
EARTH ROTATION
The 1990 Western Pacific Geophysics meeting
| NASA-CR-193456 | p 712 N94-13334
Variations common to the interplanetary magnetic field, the zonal atmospheric circulation and the Earth's rotation
| COMMUNICATIONS-SER-B-157 | p 837 N94-13504
On the space-time ocean current variability and its effects on the length-of-day
| ISBN-0-315-59510-8 | p 726 N94-14205
The determination of crustal motions using laser ranging to Lageos-2 and Lageos-1
| NASA-CR-193787 | p 717 N94-14306
EARTH SCIENCES
National atmospheric sciences program, fiscal years 1987-1990
| NSF-92-16 | p 711 N94-12794
A history of the Defence Research Establishment, Ottawa
| CTN-93-60737 | p 850 N94-14060
Applications of the Advanced Light Source to problems in the earth, soil, and environmental sciences
| DE93-015258 | p 710 N94-14477
The 1991 research and technology report, Goddard Space Flight Center
| NASA-TM-108738 | p 851 N94-14791
EARTH SURFACE
Climatic change due to land surface alterations
| INPE-5495-PRE/1786 | p 721 N94-13672
Advanced solid-state array spectroradiometer data collection during HAPEX-2 Sahel
| NASA-CR-194144 | p 808 N94-13875
EARTH TERMINALS
SCAILET: An intelligent assistant for satellite ground terminal operations
| NASA-TM-105879 | p 538 N94-13918
The ACTS propagation terminal delivery and support p 615 N94-14674
ACTS propagation experiment discussion: Ka-band propagation measurements using the ACTS propagation terminal and the CSU-CHILL and Space Communications Technology Center Florida propagation program p 616 N94-14678
EARTH TIDES
Tidal interactions in the Earth Moon system
| COMMUNICATIONS-SER-B-160 | p 837 N94-13503
EARTH-MOON SYSTEM
Meteoroid environment near the Earth-Moon system
| NASA-CR-193670 | p 835 N94-13203
Tidal interactions in the Earth Moon system
| COMMUNICATIONS-SER-B-160 | p 837 N94-13503
EARTHQUAKES
The 1990 Western Pacific Geophysics meeting
| NASA-CR-193456 | p 712 N94-13334
Dynamic soil pressures on rigid cylindrical vaults
| DE93-013930 | p 676 N94-14585
EBERT SPECTROMETERS
NASA airborne satellite instrumentation calibrator (NASIC) technical reference
| NASA-RP-1315 | p 545 N94-13713
ECHELLE GRATINGS
Photometry and spectroscopy in the open cluster Alpha Persei, 2
| NASA-CR-193397 | p 833 N94-14358
ECLIPSING BINARY STARS
The soft x ray transient Cen X-4 in quiescence
| NASA-CR-194033 | p 833 N94-14406
Analysis of the IUE spectra of the strongly interacting binary beta Lyrae
| NASA-CR-194118 | p 833 N94-14493
ECOLOGY
Molten carbonate fuel cell product development test environmental assessment/protection plan
| DE93-000288 | p 702 N94-13380
Gordon Research Conference on Chronobiology, 1991
| AD-A266354 | p 728 N94-13698
Minutes of the Sixth CEOS Plenary Meeting
| NASA-TM-108252 | p 542 N94-14112
Pattern and Process in Landscape Ecology: Eighth Annual US Landscape Ecology Symposium
| DE93-014032 | p 711 N94-14859
ECONOMIC ANALYSIS
Hot Dry Rock energy
| DE93-014452 | p 702 N94-13403
Field of solar collectors: Effect of shadowing on the optimal field design
| ITN-93-85197 | p 702 N94-13570
Status and future opportunities for conversion of synthesis gas to liquid energy fuels
| DE93-010025 | p 584 N94-14089
ECONOMIC DEVELOPMENT
Fourteenth National Industrial Energy Technology Conference: Proceedings
| DE93-016698 | p 710 N94-14516
ECONOMIC FACTORS
Sequestering carbon dioxide in industrial polymers: Building materials for the 21st century
| DE93-016087 | p 580 N94-14297
ECOSYSTEMS
Organic Geochemical and tectonic evolution of the Midcontinent Rift system
| DE93-015093 | p 717 N94-14338
Pattern and Process in Landscape Ecology: Eighth Annual US Landscape Ecology Symposium
| DE93-014032 | p 711 N94-14859
EDDY VISCOSITY
Two-dimensional Navier-Stokes heat transfer analysis for rough turbine blades
| NASA-TM-106008 | p 629 N94-13027
A multiple-scale turbulence model for incompressible flow
| NASA-TM-106113 | p 631 N94-13385
An implicit finite volume nodal point scheme for the solution of two-dimensional compressible Navier-Stokes equations p 640 N94-14603
Search for subgrid scale parameterization by projection pursuit regression p 643 N94-14749
LES versus DNS: A comparative study p 644 N94-14753
A transport equation for eddy viscosity p 646 N94-14762
EDGE DETECTION
Feature extraction and classification algorithms for high dimensional data
| NASA-CR-194298 | p 743 N94-13023
EDUCATION
Lecture notes on software process improvement
| AD-A265200 | p 744 N94-13049
Workshop for coordinating South Carolina's pre-college systemic initiatives in science and mathematics
| DE93-012263 | p 818 N94-13216
Selected data on academic science and engineering R and D expenditures: Fiscal Year 1991
| NSF-92-329 | p 819 N94-13982
Oak Ridge Environmental Information System (ORIES) site workstation information packet for OREIS 6.2
| DE93-010761 | p 825 N94-14458
Educational module for the Higher Agricultural Education. Part 2: Eutrophication observed by remote sensing: An educational approach to water quality monitoring
| BCRS-92-11B | p 818 N94-14462
Nonlinear analysis, scientific computation, and continuum mechanics applied to the science of materials
| AD-A266641 | p 817 N94-14680
Center of excellence in rotary wing technology
| AD-A266655 | p 510 N94-14799
Educational module for the higher agricultural education. Part 1: Land use classification using satellite pictures
| BCRS-92-11A | p 819 N94-14809
EFFECTIVE PERCEIVED NOISE LEVELS
Noise levels from a model turbofan engine with simulated noise control measures applied
| NASA-TM-106318 | p 518 N94-14036
EFFICIENCY
Robot-task compliance: The energy criterion
| ITN-93-85196 | p 763 N94-13568
EFFUSIVES
Estimation of vegetation damage due to ash fall in Mt. Pinatubo area using MOS-1 data p 695 N94-14259
EGGS
Amphibian fertilization and development in microgravity p 594 N94-13770
EIGENVALUES
On curve veering and flutter of rotating blades
| NASA-TM-106282 | p 670 N94-12872
Optimization and eigenvalue computation with application to meteorology and oceanography
| DE93-015310 | p 744 N94-13024
A robust multilevel simultaneous eigenvalue solver
| NASA-CR-191491 | p 767 N94-13202
Some experiences with Krylov vectors and Lanczos vectors p 677 N94-14621
On I(1): Optimal decentralized performance p 681 N94-14643
Spherical anharmonic oscillator in self-similar approximation
| DE93-626622 | p 772 N94-14890

EIGENVECTORS
Force-free magnetic fields, curl eigenfunctions, and the sphere in transform space, with applications to fluid dynamics and electromagnetic theory
|AD-A265805| p 834 N94-12971
A robust multilevel simultaneous eigenvalue solver
|NASA-CR-191491| p 767 N94-13202
EJECTION
Liquid metal drop ejection
|NASA-CR-193718| p 572 N94-14133
ELASTIC DEFORMATION
Stress stiffening and approximate equations in flexible multibody dynamics p 677 N94-14620
ELASTIC MEDIA
Thermodiffusion in heterogeneous elastic solids and homogenization
|REPT-14/1993| p 578 N94-13468
ELASTIC PROPERTIES
Modeling the impact behavior of AD85 ceramic under multi-axial loading
|AD-A265877| p 576 N94-12932
A process for evaluation of mechanical behavior of surface films
|W-1/92| p 579 N94-14007
ELASTIC SCATTERING
Measurements of scattering processes in negative ion-atom collisions
|DE93-013863| p 779 N94-12940
Calculation of electron-lithium scattering using the coupled-channel optical method
|DE93-623049| p 806 N94-13226
High energy hadron-hadron collisions
|DE93-015584| p 784 N94-13927
Resonances in the Sigma NN system
|DE93-014353| p 785 N94-14144
The E2 N(yields)(Delta) transition from polarized Compton scattering
|DE93-012522| p 785 N94-14363
Scattering calculations and confining interactions
|NASA-CR-194242| p 786 N94-14549
Relativistic proton-nucleus scattering and one-boson-exchange models p 786 N94-14550
Proton-proton scattering contribution to emittance growth
|DE93-016090| p 787 N94-14588
ELASTIC WAVES
Micromechanical strength effects in shock compression of solids
|DE93-014425| p 670 N94-12887
ELASTOMERS
Compatibility testing of vacuum seal materials
|DE93-014366| p 663 N94-14113
Small-angle scattering, contrast variation and the study of complex composite materials: A study of the structure of carbon black
|DE93-012707| p 559 N94-14690
ELASTOPLASTICITY
Variational approach to probabilistic finite elements
|NASA-CR-187179| p 674 N94-13873
Elastic-plastic mixed-iterative finite element analysis: Implementation and performance assessment
|NASA-TM-106164| p 675 N94-13919
A process for evaluation of mechanical behavior of surface films
|W-1/92| p 579 N94-14007
ELASTOSTATICS
Torsion problem of elastostatics: An application of boundary element method and relation with conformal mapping
|DSIS-92-03794| p 674 N94-13833
ELECTRIC BATTERIES
Battery testing at Argonne National Laboratory
|DE93-011761| p 624 N94-14012
ELECTRIC CHARGE
Electric charge quantization
|DE93-622901| p 778 N94-12845
Determination of critical density of charge
|DE93-622897| p 775 N94-12877
A method for determination of the superficial charge density
|DE93-622896| p 619 N94-12891
Stripping efficiencies for 277 MeV/amu gold beam on copper foils
|DE93-014306| p 569 N94-13221
Schemes for the use of conducting polymers as active materials in electrochemical supercapacitors
|DE93-012713| p 580 N94-14179
The electric field of a current-carrying conductor
|DE93-626637| p 617 N94-14892
ELECTRIC CONDUCTORS
Mutual inductance between partially wound tori and a bifilar conductor
|ETN-93-94388| p 624 N94-13998
Utilization of boundary element method for extraction of frequency dependent conductivity parameters of lossy intra-chip transmission lines
|ETN-93-94385| p 771 N94-14807
ELECTRIC CONNECTORS
Rigid-flexible printed wiring boards
|DE93-013938| p 620 N94-13094
Flex-gear electrical power transmission
|NASA-CR-194422| p 661 N94-13445
Changes in electrical device characteristics during the formation of dislocations in situ in the TEM
|DE93-013910| p 808 N94-13694
Study of the intermateability of Cannon and Souriau subminiature connectors
|CNES-NT-132| p 624 N94-13951
Microwave interconnection
|DE93-016580| p 625 N94-14533
ELECTRIC CONTACTS
Flex-gear electrical power transmission
|NASA-CR-194422| p 661 N94-13445
Miniature mechanism assembly
|DE93-015595| p 624 N94-13928
Study of novel conductive paints for solar cell electromagnetic fields
|DE93-015088| p 581 N94-14337
ELECTRIC CURRENT
Advanced magnetic flux compression generator development issues: A comparison of coaxial and disk generators
|DE93-014025| p 794 N94-12849
Electron beam probe measurements of electric fields in rf discharges p 601 N94-13661
Polarization effects in optical fiber current sensors based on Sagnac interferometers with 3 by 3 couplers
|DE93-012665| p 792 N94-14367
The electric field of a current-carrying conductor
|DE93-626637| p 617 N94-14892
ELECTRIC DIPOLES
On the neutron EDM search in the Laue diffraction by the crystal without a centre of symmetry
|DE93-622971| p 804 N94-12828
ELECTRIC DISCHARGES
Determination of critical density of charge
|DE93-622897| p 775 N94-12877
Lightning simulation and determination of expected striking points
|ITN-93-85202| p 719 N94-13188
Electron beam probe measurements of electric fields in rf discharges p 601 N94-13661
ELECTRIC FIELD STRENGTH
Lightning simulation and determination of expected striking points
|ITN-93-85202| p 719 N94-13188
Induced voltages at air gaps due to electromagnetic field caused by direct and indirect lightning strokes
|ITN-93-85203| p 599 N94-13237
ELECTRIC FIELDS
Investigation of dynamics of plasma fluxes generated by the quasi-stationary plasma accelerator P-50
|DE93-621665| p 794 N94-12854
Electrodynamics of the middle atmosphere: Superpressure balloon program
|NASA-CR-193671| p 712 N94-13293
Folded waveguide designs for tokamaks
|DE93-013274| p 798 N94-13577
Electron beam probe measurements of electric fields in rf discharges p 601 N94-13661
Field emitter array RF amplifier development project. Phase 1: Cathode technology development
|AD-A266346| p 622 N94-13776
Analysis of microstrip patch antennas with nonzero surface resistance
|NASA-TP-3362| p 604 N94-13916
Implicit multi-fluid simulation of interpenetrating plasmas
|DE93-013351| p 801 N94-14342
Absolute detection efficiency of a micro-channel plate detector to x rays in the 1-100 KeV energy range
|DE93-012592| p 789 N94-14460
The role of electric field shear stabilization of turbulence in the H-mode to VH-mode transition in D3-D
|DE93-015474| p 802 N94-14583
The electric field of a current-carrying conductor
|DE93-626637| p 617 N94-14892
ELECTRIC HYBRID VEHICLES
Technology assessments of advanced energy storage systems for electric and hybrid vehicles
|DE93-014395| p 701 N94-12913
ELECTRIC MOTOR VEHICLES
Battery testing at Argonne National Laboratory
|DE93-011761| p 624 N94-14012
ELECTRIC MOTORS
Advanced electric motor technology flux mapping
|NASA-CR-193824| p 621 N94-13186
Compatibility of refrigerants and lubricants with motor materials
|DE93-014768| p 583 N94-14801
ELECTRIC POTENTIAL
The study of structure-processing-property relations in copper oxide based high (Tc) superconductors
|DE93-015066| p 804 N94-13003
Lightning simulation and determination of expected striking points
|ITN-93-85202| p 719 N94-13188
Induced voltages at air gaps due to electromagnetic field caused by direct and indirect lightning strokes
|ITN-93-85203| p 599 N94-13237
Electron beam probe measurements of electric fields in rf discharges p 601 N94-13661
Separation of biogenic materials by electrophoresis under zero gravity (L-3) p 592 N94-13760
Development of UHF spark-switched L-C Oscillators
|DE93-015019| p 623 N94-13892
Ploughing on gold using a Scanning Tunneling Microscope
|DE93-012632| p 812 N94-14365
NASA metrology and calibration, 1993
|NASA-TM-109280| p 597 N94-14410
Kinetic simulations of ultra-intense laser plasma interactions
|DE93-014419| p 802 N94-14564
Plasma contactor technology for Space Station Freedom
|NASA-TM-106291| p 553 N94-14725
The electric field of a current-carrying conductor
|DE93-626637| p 617 N94-14892
ELECTRIC POWER SUPPLIES
Student's works and power supplies in electronic circuit laboratory p 627 N94-13434
Communications and control for electric power systems
|NASA-CR-194503| p 622 N94-13811
Communications and control for electric power systems: Power flow classification for static security assessment
|NASA-CR-194512| p 624 N94-13948
ELECTRIC PROPULSION
Recent testing of 30 kW hydrogen arcjet thrusters
|NASA-TM-106214| p 551 N94-13430
Low thrust space propulsion
|NASA-TM-109286| p 552 N94-13625
Battery testing at Argonne National Laboratory
|DE93-011761| p 624 N94-14012
ELECTRIC ROCKET ENGINES
Low power pulsed MPD thruster system analysis and applications
|NASA-CR-191187| p 550 N94-13415
ELECTRIC SWITCHES
Miniature mechanism assembly
|DE93-015595| p 624 N94-13928
Design and optimization of high voltage lateral DMOS devices using RESURF technology
|LAAS-92511| p 626 N94-14711
ELECTRIC WIRE
Microwave interconnection
|DE93-016580| p 625 N94-14533
ELECTRICAL ENGINEERING
Bulletin of the University of Electro-Communications, volume 6, no. 1, serial no. 11 p 746 N94-13432
ELECTRICAL FAULTS
Early detection of insulation failure in electric motors
|PB93-198208| p 626 N94-14686
A high voltage dielectrically isolated smart power technology based on silicon direct bonding
|LAAS-92492| p 626 N94-14698
ELECTRICAL IMPEDANCE
Utilization of boundary element method for extraction of frequency dependent conductivity parameters of lossy intra-chip transmission lines
|ETN-93-94385| p 771 N94-14807
ELECTRICAL INSULATION
Amorphous sol-gel insulating films
|DE93-012859| p 576 N94-12866
Early detection of insulation failure in electric motors
|PB93-198208| p 626 N94-14686
ELECTRICAL MEASUREMENT
A method for determination of the superficial charge density
|DE93-622896| p 619 N94-12891
Electrodynamics of the middle atmosphere: Superpressure balloon program
|NASA-CR-193671| p 712 N94-13293
Electron beam probe measurements of electric fields in rf discharges p 601 N94-13661
Changes in electrical device characteristics during the formation of dislocations in situ in the TEM
|DE93-013910| p 808 N94-13694
A high-precision direct current measuring device over a kiloampere range
|DE93-626409| p 627 N94-14885

ELECTRICAL PROPERTIES
Changes in electrical device characteristics during the formation of dislocations in situ in the TEM
| DE93-013910 | p 808 N94-13694
The Large Area Pulsed Solar Simulator (LAPSS)
| NASA-CR-194507 | p 703 N94-13940
Structural and electronic studies of a-SiGe:H alloys
| DE93-010021 | p 809 N94-14085
Optimization of transparent and reflecting electrodes for amorphous silicon solar cells
| DE93-010009 | p 704 N94-14110
Schemes for the use of conducting polymers as active materials in electrochemical supercapacitors
| DE93-012713 | p 580 N94-14179
Effects of growth conditions and substrate orientation on the properties of InSb
| DE93-013766 | p 812 N94-14344

ELECTRICAL RESISTANCE
Room temperature degradation of YBa2Cu3O(7-x) superconductors in varying relative humidity environments
| NASA-TP-3368 | p 813 N94-14409
Design and optimization of high voltage lateral DMOS devices using RESURF technology
| LAAS-92511 | p 626 N94-14711

ELECTRICAL RESISTIVITY
Non-linear effects in vortex viscous flow in superconductors-role of finite heat removal velocity
| DE93-621785 | p 618 N94-12856
Application of transient airborne electromagnetic and ground resistivity methods to geological mapping in tropical terrains
| ISBN-0-315-57172-1 | p 685 N94-13542
Study of novel conductive paints for solar cell electromagnetic fields
| DE93-015088 | p 581 N94-14337
High counting rate resistive-plate chamber
| DE93-014928 | p 651 N94-14452
Thermal history effects on electrical relaxation and conductivity for potassium silicate glass with low alkali concentrations
| NASA-TM-106324 | p 583 N94-14845

ELECTRICITY
Flex-gear electrical power transmission
| NASA-CR-194422 | p 661 N94-13445

ELECTRO-OPTICS
Energy and technology review, March 1993
| DE93-013941 | p 849 N94-13019
Nonlinear laser spectroscopy studies of semiconductor heterostructures
| AD-A265728 | p 805 N94-13037
Application of new electro-optic technology to Space Station Freedom data management system
| NASA-CR-177622 | p 538 N94-13257
Radiation effects on optoelectronic analog link for particle detectors
| DE93-015794 | p 793 N94-14529

ELECTROCATALYSTS
Electrocatalysis issues in polymer electrolyte fuel cells
| DE93-014450 | p 702 N94-13402

ELECTROCHEMICAL CELLS
Surface science instrumentation for the study of important catalytic and electrochemical interfaces
| DE93-015068 | p 563 N94-13413
Electrochemical noise in lithium primary cells
| DSIS-93-00236 | p 623 N94-13846

ELECTROCHEMICAL CORROSION
Inhibiting corrosion in Gr/Al and Gr/Mg metal matrix composites using nonequilibrium alloying techniques
| AD-A266547 | p 556 N94-13583

ELECTROCHEMICAL MACHINING
Electrochemical planarization for microelectronic circuits
| DE93-017214 | p 627 N94-14870

ELECTRODE MATERIALS
Carbonate fuel cell endurance: Hardware corrosion and electrolyte management status
| DE93-013800 | p 701 N94-13093
Combustion synthesis and engineering of nanoparticles for electronic, structural, and superconductor applications
| DE93-016286 | p 809 N94-13981

ELECTRODEPOSITION
Electrophoretic and electrolytic deposition of ceramic particles on porous substrates
| AD-A265141 | p 575 N94-12812

ELECTRODES
Separation of biogenic materials by electrophoresis under zero gravity (L-3) p 592 N94-13760
Optimization of transparent and reflecting electrodes for amorphous silicon solar cells
| DE93-010009 | p 704 N94-14110
High counting rate resistive-plate chamber
| DE93-014928 | p 651 N94-14452

ELECTRODYNAMICS
Electrodynamics of helical plasma structures
| DE93-620981 | p 797 N94-13240
Electrodynamics of the middle atmosphere: Superpressure balloon program
| NASA-CR-193671 | p 712 N94-13293

ELECTROKINETICS
Electrophoretic and electrolytic deposition of ceramic particles on porous substrates
| AD-A265141 | p 575 N94-12812

ELECTROLYSIS
Primary and secondary electrical space power based on advanced PEM systems
| DE93-012643 | p 553 N94-14689

ELECTROLYTES
The importance of hard core repulsion in models of activity coefficients in aqueous electrolyte solutions: Illustration in the case of hydration theory
| DE93-012476 | p 561 N94-12881
Schemes for the use of conducting polymers as active materials in electrochemical supercapacitors
| DE93-012713 | p 580 N94-14179

ELECTROLYTIC CELLS
Electrocatalysis issues in polymer electrolyte fuel cells
| DE93-014450 | p 702 N94-13402
Status of SOFC development in USA
| DE93-015568 | p 704 N94-14355

ELECTROMAGNETIC ABSORPTION
Gathering and exchange information on atmospheric chemistry and polluted atmospheres
| DE93-009940 | p 705 N94-12869
Kinetic simulations of ultra-intense laser plasma interactions and a novel method of generating odd harmonics
| DE93-014418 | p 797 N94-13207
Absorption and damage thresholds of low defect density hafnia deposited with activated oxygen
| DE93-013853 | p 655 N94-13243
Quantitative luminescence imaging system
| DE93-015691 | p 793 N94-14702

ELECTROMAGNETIC COUPLING
Ultrafast photoinduced electron transfer reactions in supramolecular arrays: Studies of electronic coupling and solvation
| DE93-012910 | p 782 N94-13484

ELECTROMAGNETIC ENVIRONMENT EXPERIMENT
Stabilized electromagnetic levitator
| NASA-CR-194261 | p 586 N94-12805

ELECTROMAGNETIC FIELDS
Parametric instabilities in large nonuniform laser plasmas
| DE93-013184 | p 797 N94-13393
Laser-damage susceptibility of nodular defects in dielectric mirror coatings: AFM measurements and electric-field modeling
| DE93-014655 | p 580 N94-14124
Study of novel conductive paints for solar cell electromagnetic fields
| DE93-015088 | p 581 N94-14337
Multiple Schroedinger cats from multilevel atoms
| DE93-013412 | p 786 N94-14526
On transport of energy, momentum, orbital angular momentum and self-angular momentum of electromagnetic wave in dispersal media
| DE93-624179 | p 617 N94-14883

ELECTROMAGNETIC INTERACTIONS
Electromagnetic deflection of spinning particles
| DE93-622866 | p 778 N94-12858
Study of electroweak interactions
| DE93-015067 | p 782 N94-13412
The (mu)(+) yields e(+)gamma
| DE93-012750 | p 785 N94-14181
Wake-field and space charge effects on high brightness beams calculations and measured results for the laser driven photoelectrons at BNL-ATF
| DE93-015787 | p 659 N94-14572

ELECTROMAGNETIC INTERFERENCE
Induced voltages at air gaps due to electromagnetic field caused by direct and indirect lightning strokes
| ITN-93-85203 | p 599 N94-13237
Kalman filter based architectures for interference excision
| DSIS-93-00034 | p 603 N94-13818
A comparison of recursive least squares and Kalman filtering excisors for swept tone interference
| DSIS-93-00362 | p 606 N94-14054

ELECTROMAGNETIC MEASUREMENT
High temperature electromagnetic characterization of thermal protection system tile materials
| NASA-CR-189687 | p 578 N94-13431
Application of transient airborne electromagnetic and ground resistivity methods to geological mapping in tropical terrains
| ISBN-0-315-57172-1 | p 685 N94-13542
Measurement electronics of industrial microwave resonator sensors
| TKK-S-RAD-S194 | p 625 N94-14096
Survey of subsurface geophysical exploration technologies adaptable to an airborne platform
| DE93-015080 | p 717 N94-14294

ELECTROMAGNETIC NOISE
1/f noise and oxide traps in MOSFETs
| DE93-007581 | p 619 N94-12942
Flex-gear electrical power transmission
| NASA-CR-194422 | p 661 N94-13445
Electrochemical noise in lithium primary cells
| DSIS-93-00236 | p 623 N94-13846
Electrical noise in microwave field effect and bipolar transistors
| LAAS-93042 | p 616 N94-14717

ELECTROMAGNETIC PROPULSION
Electromagnetic propulsion for spacecraft
| NASA-CR-191186 | p 551 N94-13416

ELECTROMAGNETIC RADIATION
Investigation of plasma instabilities in the Polar cusp
| NASA-CR-194283 | p 796 N94-13084
A hybrid finite element-boundary integral for the analysis of cavity-backed antennas of arbitrary shape
| NASA-CR-193719 | p 599 N94-13236
The propagation characteristics and instability properties of low-frequency electromagnetic waves in the Io plasma torus p 601 N94-13650
Electromagnetic wave test p 508 N94-14173
Ionospheric effects on a wide-bandwidth, polarimetric, space-based, synthetic-aperture radar
| DE93-015084 | p 612 N94-14512
Quantitative luminescence imaging system
| DE93-015691 | p 793 N94-14702

ELECTROMAGNETIC SCATTERING
Computer code for scattering from impedance bodies of revolution. Part 3: Surface impedance with s and phi variation. Analytical and numerical results
| NASA-CR-193396 | p 599 N94-13264
Theoretical investigation of scattering by homogeneous or coated dielectric spheres illuminated with a steady state or pulsed laser beam p 657 N94-13624
Portable multipath measurement system
| DSIS-93-00177 | p 603 N94-13843
Shielded open-circuited sample holders for dielectric and magnetic measurements of liquids and powders
| PB93-198851 | p 652 N94-14687

ELECTROMAGNETIC WAVE TRANSMISSION
Theoretical investigation of scattering by homogeneous or coated dielectric spheres illuminated with a steady state or pulsed laser beam p 657 N94-13624

ELECTROMECHANICAL DEVICES
Self tuning and adaptive control: Evaluations and improvements of algorithms
| ITN-93-85192 | p 762 N94-13329
Design and application of electromechanical actuators for deep space missions
| NASA-CR-194145 | p 663 N94-14134
Superconductivity devices: Commercial use of space
| NASA-CR-194163 | p 625 N94-14324

ELECTROMECHANICS
Activities report of the National Electrotechnical Institute Galileo Ferraris
| ETN-93-94224 | p 627 N94-14812

ELECTROMIGRATION
Microstructural mechanisms that enhance electromigration resistance in Al-Cu thin films
| DE93-013770 | p 812 N94-14345

ELECTRON BEAM WELDING
Welding technologies as applied to nuclear manufacturing
| DE93-010924 | p 664 N94-14565

ELECTRON BEAMS
Inertial confinement fusion program
| DE93-013372 | p 796 N94-13047
Microwave generation for magnetic fusion energy applications
| DE93-013864 | p 654 N94-13058
Investigation of plasma instabilities in the Polar cusp
| NASA-CR-194283 | p 796 N94-13084
EBIT Trapping Program
| DE93-014422 | p 788 N94-13208
Research on radiation resistance properties of structural materials for space use p 529 N94-13271
Low energy response of the DO calorimeter and jet energy measurement
| DE93-013569 | p 781 N94-13350
Long-pulse operation of a gyrotron with beam/RF separation
| DE93-015007 | p 649 N94-13410
Electron beam probe measurements of electric fields in rf discharges p 601 N94-13661
Structural change of graphite during electron irradiation
| DE93-015961 | p 582 N94-14531

Adiabatic and non adiabatic effects in Free Electron Laser (FEL) non linear interactions
| ITN-93-85224 | p 659 N94-14547
Characteristics of a high energy muon(+)muon(-) collider based on electro-production of muons
| DE93-017154 | p 790 N94-14893

ELECTRON BUNCHING
Wake-field and space charge effects on high brightness beams calculations and measured results for the laser driven photoelectrons at BNL-ATF
| DE93-015787 | p 659 N94-14572

ELECTRON CAPTURE
Metastable enhancement of C(+) and O(+) capture reactions
| DE93-015075 | p 807 N94-13373
Charge-exchange reactions and weak interaction rates for Type 2 supernovae
| DE93-015104 | p 783 N94-13893

ELECTRON CYCLOTRON HEATING
Dimensionally similar discharges with central RF heating on the D3-D tokamak
| DE93-012776 | p 795 N94-12953
Ion cyclotron heating experiments and plans for the Advanced Toroidal Facility (ATF)
| DE93-012965 | p 795 N94-13033
Long-pulse operation of a gyrotron with beam/RF separation
| DE93-015007 | p 649 N94-13410
Studies of non-inductive current drive in the CDX-U tokamak p 799 N94-13680
Direct electron heating and current drive with fast waves in D3-D
| DE93-013028 | p 801 N94-14293
Active density control in DIII-D H-mode plasmas
| DE93-015477 | p 802 N94-14570

ELECTRON DENSITY (CONCENTRATION)
The MRIS feasibility study
| NASA-TM-107763 | p 597 N94-12804
Sites of fine-scale electron density turbulence in the interstellar medium
| NASA-CR-193708 | p 839 N94-13864
On MHD mode equations in toroidal plasmas
| PPL-139 | p 800 N94-13877
The fractional quantum Hall effect and the spherical shell model
| DE93-014553 | p 818 N94-14740

ELECTRON DENSITY PROFILES
Active density control in DIII-D H-mode plasmas
| DE93-015477 | p 802 N94-14570

ELECTRON EMISSION
Electron emission resulting from fast ion impact on thin metal foils: Implications of these data for development of track structure models
| DE93-013506 | p 782 N94-13485
Indirect processes in electron impact ionization of Kr(24+) and Kr(25+)
| DE93-014129 | p 784 N94-14140

ELECTRON ENERGY
Cosmic physics data analysis program
| NASA-CR-194357 | p 846 N94-12826
Phobos/Harp post launch support
| NASA-CR-193676 | p 540 N94-13109
Kinetic simulations of ultra-intense laser plasma interactions and a novel method of generating odd harmonics
| DE93-014418 | p 797 N94-13207
A search for strong-field direct two electron ionization using coincidence spectroscopy
| DE93-013435 | p 781 N94-13241
High resolution electron energy loss studies of surface vibrations
| DE93-014441 | p 781 N94-13283
Electron emission resulting from fast ion impact on thin metal foils: Implications of these data for development of track structure models
| DE93-013506 | p 782 N94-13485
Folded waveguide designs for tokamaks
| DE93-013274 | p 798 N94-13577
Small scale magnetic islands in collisionless plasmas
| PPL-131 | p 799 N94-13836
Dependence of beta(tau) on plasma shape in D3-D
| DE93-015473 | p 800 N94-13900
Direct electron heating and current drive with fast waves in D3-D
| DE93-013028 | p 801 N94-14293
Absolute detection efficiency of a micro-channel plate detector to x rays in the 1-100 KeV energy range
| DE93-012592 | p 789 N94-14460
Structural change of graphite during electron irradiation
| DE93-015961 | p 582 N94-14531
Adiabatic and non adiabatic effects in Free Electron Laser (FEL) non linear interactions
| ITN-93-85224 | p 659 N94-14547
Time resolved measurement of electron temperatures of exploding foil x ray laser plasmas
| DE93-017161 | p 803 N94-14894

ELECTRON IMPACT
EBIT Trapping Program
| DE93-014422 | p 788 N94-13208
Indirect processes in electron impact ionization of Kr(24+) and Kr(25+)
| DE93-014129 | p 784 N94-14140
Coherent excitation of autoionizing resonances by electron impact
| DE93-018169 | p 785 N94-14419

ELECTRON IRRADIATION
Annealing study of main electron irradiation-induced defects (H4 and H5) in P-InP using DLTS technique
| DE93-623204 | p 806 N94-13213
Structural change of graphite during electron irradiation
| DE93-015961 | p 582 N94-14531

ELECTRON MICROSCOPES
Current titles --- National Center for Electron Microscopy
| DE93-015859 | p 851 N94-14587
Laser lithography by photon scanning tunneling microscopy
| DE93-015962 | p 660 N94-14863

ELECTRON MICROSCOPY
Procedures for analysis of debris relative to Space Shuttle systems
| NASA-TM-109190 | p 534 N94-12900
High spatial resolution x ray microanalysis: Comparison of experiment and incoherent scattering calculations
| DE93-011685 | p 648 N94-13044
Current titles --- National Center for Electron Microscopy
| DE93-015859 | p 851 N94-14587

ELECTRON MOBILITY
Anomalous low-temperature free-exciton transport in GaAs structures
| DE93-009845 | p 809 N94-14108
Small polaron conduction in Y2Ti2O7
| ITN-93-85221 | p 814 N94-14557

ELECTRON PHONON INTERACTIONS
Small polaron conduction in Y2Ti2O7
| ITN-93-85221 | p 814 N94-14557
Dynamic Jahn-Teller effect: Calculation of fine structure spectrum, isotope shift and Zeeman behavior at deep center Ni2+ in CdS
| ETN-93-94394 | p 815 N94-14705

ELECTRON PROBES
Electron beam probe measurements of electric fields in rf discharges p 601 N94-13661

ELECTRON SCATTERING
Calculation of electron-lithium scattering using the coupled-channel optical method
| DE93-623049 | p 806 N94-13226
High-resolution Z-contrast imaging and hole concentration mapping of YBCO thin films
| DE93-015803 | p 808 N94-13930
The E2 N(yields)(Delta) transition from polarized Compton scattering
| DE93-012522 | p 785 N94-14363

ELECTRON SPECTROSCOPY
High-resolution Z-contrast imaging and hole concentration mapping of YBCO thin films
| DE93-015803 | p 808 N94-13930

ELECTRON STATES
Grain-boundary electronic states by multiple-scattering theory
| DE93-013198 | p 805 N94-13010
Infrared spectroscopy of organic free radicals related to combustion processes
| DE93-017086 | p 562 N94-13222
Empirical tight-binding parameters for solid C(sub 60)
| DE93-623061 | p 807 N94-13510
Electronic states in systems of reduced dimensionality
| DE93-014440 | p 815 N94-14739

ELECTRON TRANSFER
Molecular solvent-dynamical effects on activated electron-transfer kinetics: How important is solvent friction?
| AD-A265886 | p 779 N94-12894
Project proposal for partial computational physics support for Survivability of Coatings program
| DE93-013788 | p 576 N94-12939
Experimental and theoretical study of inhomogeneous electron transfer in betaine: Comparisons of measured and predicted spectral dynamics
| AD-A265703 | p 780 N94-13051
Variance reduction unique to coupled electron/photon Monte Carlo transport
| DE93-014999 | p 782 N94-13409
Ultrafast photoinduced electron transfer reactions in supramolecular arrays: Studies of electronic coupling and solvation
| DE93-012910 | p 782 N94-13484
Schemes for the use of conducting polymers as active materials in electrochemical supercapacitors
| DE93-012713 | p 580 N94-14179

ELECTRON TRANSITIONS
A sum-rule of luminescence spectrum
| ITN-93-85223 | p 814 N94-14559
Dynamic Jahn-Teller effect: Calculation of fine structure spectrum, isotope shift and Zeeman behavior at deep center Ni2+ in CdS
| ETN-93-94394 | p 815 N94-14705

ELECTRON TUBES
Field emitter array RF amplifier development project. Phase 1: Cathode technology development
| AD-A266346 | p 622 N94-13776

ELECTRON TUNNELING
Electrical and optical properties of multiple quantum well structures and their applications to infrared detectors
| FFI-92/7012 | p 809 N94-14010
Ploughing on gold using a Scanning Tunneling Microscope
| DE93-012632 | p 812 N94-14365
Laser lithography by photon scanning tunneling microscopy
| DE93-015962 | p 660 N94-14863

ELECTRON-ION RECOMBINATION
EBIT Trapping Program
| DE93-014422 | p 788 N94-13208

ELECTRON-POSITRON PAIRS
Top quark search: Results and prospects at Fermilab
| DE93-013016 | p 786 N94-14524

ELECTRONIC CONTROL
Electrical Actuation Technology Bridging
| NASA-CP-3213 | p 551 N94-13417
Techniques for improving the performance of a simplified electronic fuel controller with incremental actuation for small gas turbine engines
| ISBN-0-315-56062-2 | p 661 N94-13521
Performance seeking control: Program overview and future directions
| NASA-TM-4531 | p 519 N94-14855

ELECTRONIC EQUIPMENT
Center of trace algorithms for extracting digitized waveforms from two-dimensional images
| DE93-015082 | p 753 N94-14295

ELECTRONIC EQUIPMENT TESTS
Chip-level testability requirements guidelines
| AD-A262583 | p 619 N94-12967
Design automation tools for testable VLSI circuits
| ISBN-0-315-61461-7 | p 621 N94-13333

ELECTRONIC MAIL
NASA/DOD Aerospace Knowledge Diffusion Research Project. Paper 38: Computer Mediated Communication (CMC) and the communication of technical information in aerospace
| NASA-TM-109330 | p 826 N94-14489

ELECTRONIC MODULES
An ultra-compact processor module based on the R3000
| DE93-012549 | p 625 N94-14427

ELECTRONIC PACKAGING
Solderability of surface mount devices
| AD-A265751 | p 620 N94-13040
MMIC packaging technology development
| NASA-CR-194183 | p 621 N94-13336
An ultra-compact processor module based on the R3000
| DE93-012549 | p 625 N94-14427

ELECTRONIC WARFARE
Advanced Communications ESM System (ACES) testbed: Integration study
| DSIS-93-00345 | p 604 N94-13939
Simulation of downlink synchronization for a frequency-hopped satellite communication system
| DSIS-93-00477 | p 605 N94-13941
A history of the Defence Research Establishment, Ottawa
| CTN-93-60737 | p 850 N94-14060

ELECTRONS
Low energy response of the DO calorimeter and jet energy measurement
| DE93-013569 | p 781 N94-13350
EGS (underscore) windows 2: An enhanced graphical interface to EGS
| DE93-010447 | p 746 N94-13382
Variance reduction unique to coupled electron/photon Monte Carlo transport
| DE93-014999 | p 782 N94-13409
Monte Carlo simulation of the OCP freezing transition
| DE93-013039 | p 811 N94-14313
Physics of gas breakdown for ion beam transport in gas
| DE93-015646 | p 801 N94-14349
Coherent excitation of autoionizing resonances by electron impact
| DE93-018169 | p 785 N94-14419

Structural change of graphite during electron irradiation
[DE93-015961] p 582 N94-14531

ELECTROPHORESIS
Electrophoretic and electrolytic deposition of ceramic particles on porous substrates
[AD-A265141] p 575 N94-12812
Separation of biogenic materials by electrophoresis under zero gravity (L-3) p 592 N94-13760
Microstructural mechanisms that enhance electromigration resistance in Al-Cu thin films
[DE93-013770] p 812 N94-14345

ELECTROPLATING
Design and testing of planar magnetic micromotors fabricated by deep x ray lithography and electroplating
[DE93-012856] p 618 N94-12821
A laser-based technique to continuously monitor metal aerosol emissions
[DE93-012836] p 710 N94-14183
Electrochemical planarization for microelectronic circuits
[DE93-017214] p 627 N94-14870

ELECTRORHEOLOGICAL FLUIDS
Synthetic lubricants and high-performance functional fluids: Phosphazenes
[ARL-TR-45] p 580 N94-14126

ELECTROSTATICS
Determination of critical density of charge
[DE93-622897] p 775 N94-12877
Studies on equatorial shock formation during plasmaspheric refilling
[NASA-CR-194392] p 715 N94-13954

ELECTROSTRICTION
Superconductivity devices: Commercial use of space
[NASA-CR-194163] p 625 N94-14324

ELEMENTARY EXCITATIONS
Effect of spontaneous decay of superconductor quasiparticles in the tunneling density of states
[DE93-012681] p 811 N94-14339

ELEMENTARY PARTICLE INTERACTIONS
Top quark search: Results and prospects at Fermilab
[DE93-013016] p 786 N94-14524
Scattering calculations and confining interactions
[NASA-CR-194242] p 786 N94-14549

ELEMENTARY PARTICLES
E789 and P865: High-rate fixed-target studies of charm and beauty
[DE93-017223] p 788 N94-14898

ELEVATION ANGLE
Characterisation of the LMS propagation channel at L- and S-bands: Narrowband experimental data and channel modelling p 615 N94-14669
Results of multiband (L, S, Ku band) propagation measurements and model for high elevation angle land mobile satellite channel p 615 N94-14670

ELLIPSOMETRY
Effect of microstructure on passive film formation and breakdown on Al alloys
[AD-A265339] p 569 N94-13050

ELLIPTICITY
Cold dark matter halos p 838 N94-13649

ELUTION
Direct probing of chromatography columns by laser-induced fluorescence
[DE93-015208] p 654 N94-13022
Reactor studies of metal ions associated with chromatographic silica
[AD-A266675] p 573 N94-14779

EMBEDDING
Experimental and analytical analysis of the response of a smart beam to rate feedback
[AD-A266544] p 557 N94-13706

EMBRITTLEMENT
Investigations of low-temperature neutron embrittlement of ferritic steels
[DE93-015460] p 573 N94-14700

EMBRYOLOGY
Gravity as a probe for understanding pattern specification
[NASA-CR-194142] p 713 N94-13418

EMISSION
Three dimensional time-dependent hydrodynamic and propagation modeling of x ray laser emission
[DE93-012575] p 654 N94-12962

EMISSION SPECTRA
Laser-induced fluorescence over optical fibers for real time in situ measurement of petroleum hydrocarbons in seawater
[AD-A265106] p 790 N94-12863
The evidence for clumpy accretion in the Herbig Ae star HR 5999
[NASA-TM-108257] p 828 N94-12915
Search for UHE emission from Cygnus X-3
[DE93-012720] p 846 N94-12924
Studies of gas in cooling flow clusters
[NASA-CR-193597] p 628 N94-12959
Molecular dynamics simulation of electronically excited polyatomic molecules
[DE93-623045] p 781 N94-13225
The continuum emission of active galactic nuclei
[ITN-93-85208] p 847 N94-13232
Analysis of interstellar cloud structure based on IRAS images
[NASA-CR-194341] p 836 N94-13332
The onset of galactic winds in early-type galaxies
[NASA-CR-193640] p 836 N94-13446
The infrared solar spectrum
[COMMUNICATIONS-SER-B-159] p 844 N94-13502
The extent and content of low-ionization gas in galaxies p 837 N94-13551
Investigation of an alternating current plasma as an element selective atomic emission detector for high-resolution capillary gas chromatography and as a source for atomic absorption and atomic emission spectrometry p 798 N94-13678
Laser and spectroscopic properties of Yb-doped apatite crystals
[DE93-014656] p 810 N94-14125
Emission line variability in active galactic nuclei
[ITN-93-85209] p 849 N94-14553
Comparative study of x ray and microwave emissions during solar flares
[NASA-CR-194532] p 845 N94-14577
Was 49: Mirror for a hidden Seyfert 1 galaxy
[NASA-CR-194537] p 840 N94-14685
The 8 to 11 keV x ray sources for imaging and absorption experiments
[DE93-015973] p 803 N94-14865
Time resolved measurement of electron temperatures of exploding foil x ray laser plasmas
[DE93-017161] p 803 N94-14894

EMITTANCE
The optical constants and spectral specular reflectivity of Highly Oriented Pyrolytic Graphite (HOPG)
[DE93-011894] p 790 N94-12865
Measuring opacity of shock generated argon plasmas
[DE93-013038] p 801 N94-14312
Proton-proton scattering contribution to emittance growth
[DE93-016090] p 787 N94-14588

EMITTERS
Field emitter array RF amplifier development project. Phase 1: Cathode technology development
[AD-A266346] p 622 N94-13776
Emitter Wrap-Through solar cell
[DE93-014996] p 703 N94-13886

ENCLOSURES
Some flow properties of telescope enclosures estimated from water channel tests: Application of the flow visualization techniques
[NAL-TR-1178T] p 830 N94-13452

END EFFECTORS
Force reflecting hand controller for manipulator teleoperation
[NASA-CR-191345] p 661 N94-13129
New prosthetic devices
[NASA-TM-109304] p 737 N94-13611
The further development and refinement of an expert-systems approach to the creative design of mechanisms and mechanical systems
[AD-A266812] p 665 N94-14901

END-TO-END DATA SYSTEMS
On the end-to-end communication problem in unreliable networks
[ITN-93-85188] p 598 N94-13195

ENDANGERED SPECIES
Birds of Wallops Island, Virginia, 1970 - 1992
[NASA-TM-104589] p 850 N94-13923

ENDOCRINE SYSTEMS
Gender differences in endocrine responses to posture and 7 days of 6 deg head down bed rest
[NASA-TM-103991] p 731 N94-12972

ENDOCRINOLOGY
Gender differences in endocrine responses to posture and 7 days of 6 deg head down bed rest
[NASA-TM-103991] p 731 N94-12972
Endocrine and metabolic changes in payload specialist (L-1) p 591 N94-13758

ENERGETIC PARTICLES
Energetic neutral atoms: Imaging the magnetospheric ring current
[NASA-CR-194339] p 715 N94-13826

ENERGY ABSORPTION
Design and application of a quasistatic crush test fixture for investigating scale effects in energy absorbing composite plates
[NASA-CR-4526] p 670 N94-13063
The 8 to 11 keV x ray sources for imaging and absorption experiments
[DE93-015973] p 803 N94-14865

ENERGY BANDS
Empirical tight-binding parameters for solid C(sub 60)
[DE93-623061] p 807 N94-13510
Liquid and gas evanescent wave spectroscopy via tunable lasers and silver halide fibers
[ITN-93-85226] p 565 N94-14465
Magnetic interactions and disorder - phase transitions in dilute spin-glasses and high temperature superconductors
[ITN-93-85217] p 815 N94-14825

ENERGY BUDGETS
Highly charged ions in hot, dense plasmas
[DE93-013348] p 795 N94-12995

ENERGY CONSERVATION
Simulating the daylight performance of fenestration systems and spaces of arbitrary complexity: The IDC method
[DE93-015177] p 704 N94-14333
Fourteenth National Industrial Energy Technology Conference: Proceedings
[DE93-016698] p 710 N94-14516

ENERGY CONSUMPTION
Bibliography of urban climate in tropical/subtropical areas, 1981-1991
[WCASP-25] p 718 N94-12918
Transition of building energy consumption using multi-input, single-output dynamic model
[VTT-PUBS-116] p 597 N94-14055

ENERGY CONVERSION
Catalysis and biocatalysis program
[NASA-CR-194105] p 727 N94-12793
Solar dynamic power system development for Space Station Freedom
[NASA-RP-1310] p 548 N94-12807
A history of the Defence Research Establishment, Ottawa
[CTN-93-60737] p 850 N94-14060

ENERGY CONVERSION EFFICIENCY
Low temperature metal-organic chemical vapor deposition growth processes for high efficiency solar cells
[DE92-010562] p 702 N94-13386
Emitter Wrap-Through solar cell
[DE93-014996] p 703 N94-13886
Colorado State University program for developing, testing, evaluating, and optimizing solar heating and cooling systems
[DE93-016018] p 705 N94-14504

ENERGY DISSIPATION
A 3D gyrokinetic particle-in-cell simulation of fusion plasma microturbulence on parallel computers
[DE93-012503] p 794 N94-12846
Numerical simulations and experiments on physics of high Mach number shockwave: Turbulent flow interactions
[DE93-013424] p 631 N94-13249
Surfaces and interfaces of ceramics and metals
[DE93-014959] p 578 N94-13408
Investigation of criteria for ductile fracture under fully-plastic conditions p 672 N94-13593
Predicting the vibrations of a spinning inflated membrane
[DE93-010690] p 676 N94-14456
Structural change of graphite during electron irradiation
[DE93-015961] p 582 N94-14531
A study of the fine scale motions of incompressible time-developing mixing layers p 644 N94-14751

ENERGY DISTRIBUTION
Spectra of late type dwarf stars of known abundance for stellar population models
[NASA-CR-194301] p 831 N94-13681

ENERGY GAPS (SOLID STATE)
Structural and electronic studies of a-SiGe:H alloys
[DE93-010021] p 809 N94-14085

ENERGY LEVELS
The International Colloquium on Atomic Spectra and Oscillator Strengths for Astrophysical and Laboratory Plasmas
[NASA-TM-109255] p 849 N94-13376
A study of the role of homogeneous process in heterogeneous high explosives
[DE93-012733] p 585 N94-14180
Multiple Schroedinger cats from multilevel atoms
[DE93-013412] p 786 N94-14526
Isospin flip as a relativistic effect: NN interactions
[CEBAF-PR-89-023] p 786 N94-14552
Dynamic Jahn-Teller effect: Calculation of fine structure spectrum, isotope shift and Zeeman behavior at deep center Ni2+ in CdS
[ETN-93-94394] p 815 N94-14705
On the statistical theory of the even-even nucleons levels' density
[DE93-623990] p 788 N94-14875

ENERGY METHODS
Some computational tools for the analysis of through cracks in stiffened fuselage shells
| LR-701 | p 673 N94-13726
Compressive buckling of curved, anisotropic panels stiffened in two directions. Part 1: Derivation of the governing equations
| LR-694 | p 675 N94-13931
ENERGY POLICY
Program operations plan
| DE93-012765 | p 710 N94-14182
Fourteenth National Industrial Energy Technology Conference: Proceedings
| DE93-016698 | p 710 N94-14516
ENERGY REQUIREMENTS
Strategic avionics technology definition studies. Subtask 3-1A: Electrical Actuation (ELA) systems
| NASA-CR-194393 | p 536 N94-14323
ENERGY SPECTRA
Research in cosmic and gamma ray astrophysics: Cosmic physics portion
| NASA-CR-194127 | p 847 N94-13211
A multiple-scale turbulence model for incompressible flow
| NASA-TM-106113 | p 631 N94-13385
Rare muon processes
| DE93-012646 | p 785 N94-14366
ENERGY STORAGE
NASA handbook for nickel-hydrogen batteries
| NASA-RP-1314 | p 550 N94-13265
ENERGY TECHNOLOGY
Photovoltaic Subcontract Program
| DE93-000092 | p 700 N94-12868
Energy and technology review, March 1993
| DE93-013941 | p 849 N94-13019
Study on superconducting basic technology for space application, part 1
| NASDA-CNT-930015-PT-1 | p 622 N94-13425
Status of SOFC development in USA
| DE93-015568 | p 704 N94-14355
NREL solar radiation resource assessment project: Status and outlook
| DE93-010034 | p 704 N94-14422
Colorado State University program for developing, testing, evaluating, and optimizing solar heating and cooling systems
| DE93-016018 | p 705 N94-14504
Fourteenth National Industrial Energy Technology Conference: Proceedings
| DE93-016698 | p 710 N94-14516
ENERGY TRANSFER
Experimental and theoretical study of inhomogeneous electron transfer in betaine: Comparisons of measured and predicted spectral dynamics
| AD-A265703 | p 780 N94-13051
Interacting scales and energy transfer in isotropic turbulence
| NASA-CR-191477 | p 630 N94-13133
The interplanetary origins and the main-phase development of moderate geomagnetic storms (1978 - 1979)
| INPE-5445-TDI/491 | p 835 N94-13174
Sub-grid scale modeling for large eddy simulations in analysis of shock-turbulence interactions
| DE93-013425 | p 631 N94-13250
Variance reduction unique to coupled electron/photon Monte Carlo transport
| DE93-014999 | p 782 N94-13409
Electron emission resulting from fast ion impact on thin metal foils: Implications of these data for development of track structure models
| DE93-013506 | p 782 N94-13485
Studies of momentum and energy transfer across wavy gas-liquid interfaces
| AD-A266432 | p 635 N94-13699
On energy transport equations for turbulent magnetized plasma
| PPL-135 | p 800 N94-13850
A study of the role of homogeneous process in heterogeneous high explosives
| DE93-012733 | p 585 N94-14180
Wind mass and energy deposition
| DE93-013345 | p 839 N94-14341
Lawrence Berkeley Laboratory Chemical Sciences Division
| DE93-015260 | p 851 N94-14401
Selective excitation, relaxation, and energy channeling in molecular systems
| DE93-018819 | p 785 N94-14420
Adiabatic and non adiabatic effects in Free Electron Laser (FEL) non linear interactions
| ITN-93-85224 | p 659 N94-14547
The role of electric field shear stabilization of turbulence in the H-mode to VH-mode transition in D3-D
| DE93-015474 | p 802 N94-14583
Search for subgrid scale parameterization by projection pursuit regression p 643 N94-14749
Triad interactions in the dissipation range p 644 N94-14750
On transport of energy, momentum, orbital angular momentum and self-angular momentum of electromagnetic wave in dispersal media
| DE93-624179 | p 617 N94-14883
ENGINE AIRFRAME INTEGRATION
Propulsion integration p 508 N94-14174
ENGINE DESIGN
Advanced Turbine Technology Applications Project (ATTAP)
| NASA-CR-191088 | p 828 N94-12931
Electric propulsion system technology
| NASA-CR-194099 | p 549 N94-13068
Combustor technology for future small gas turbine aircraft
| NASA-TM-106312 | p 517 N94-13142
Low thrust space propulsion
| NASA-TM-109286 | p 552 N94-13625
Gas core nuclear thermal rocket engine research and development in the former USSR
| DE93-012165 | p 552 N94-14013
Noise levels from a model turbofan engine with simulated noise control measures applied
| NASA-TM-106318 | p 518 N94-14036
Aeropropulsion facilities p 506 N94-14161
Derated ion thruster development status
| NASA-TM-106292 | p 553 N94-14726
A hot dynamic seal rig for measuring hypersonic engine seal durability and flow performance
| NASA-TM-106294 | p 664 N94-14727
ENGINE FAILURE
Identification and interpretation of patterns in rocket engine data
| NASA-CR-194534 | p 552 N94-14309
ENGINE INLETS
Analysis of the Harrier forebody/inlet design using computational techniques
| NASA-CR-193616 | p 503 N94-13463
Piston engine intake and exhaust system design
| ISVR-TR-222 | p 663 N94-13874
Three-dimensional modeling of diesel engine intake flow, combustion and emissions-2
| NASA-CR-191189 | p 519 N94-14448
ENGINE MONITORING INSTRUMENTS
Strain sensing technology for high temperature applications
| NASA-TM-4498 | p 648 N94-12874
ENGINE NOISE
Mixing noise reduction for rectangular supersonic jets by nozzle shaping and induced screech mixing
| NASA-TM-106364 | p 508 N94-14208
Active control of fan-generated plane wave noise
| NASA-TM-109008 | p 777 N94-14481
ENGINE PARTS
NDE of titanium alloy MMC rings for gas turbine engines
| NASA-TM-106188 | p 555 N94-13138
Compatibility of refrigerants and lubricants with motor materials
| DE93-014768 | p 583 N94-14801
ENGINE TESTS
Advanced Turbine Technology Applications Project (ATTAP)
| NASA-CR-191088 | p 828 N94-12931
Electric propulsion system technology
| NASA-CR-194099 | p 549 N94-13068
Aircraft engine type certification handbook: Advisory circular
| AC-33-2B | p 518 N94-13252
ENGINEERING
Selected data on academic science and engineering R and D expenditures: Fiscal Year 1991
| NSF-92-329 | p 819 N94-13982
Science, technology, and the federal government: National goals for a new era p 627 N94-14115
ENGINEERING DRAWINGS
CAD data exchange with Martin Marietta Energy Systems, Inc., Oak Ridge, TN
| DE93-017233 | p 757 N94-14871
ENGINEERS
NASA/DOD Aerospace Knowledge Diffusion Research Project. Report 18: A comparison of the technical communication practices of aerospace engineers and scientists in India and the United States
| NASA-TM-109006 | p 821 N94-13057
Generic results of the space physics community survey
| NASA-CR-194538 | p 818 N94-13984
NASA/DOD Aerospace Knowledge Diffusion Research Project. Paper 34: Users and uses of DOD technical reports: A report from the field
| NASA-TM-109327 | p 825 N94-14485
NASA/DOD Aerospace Knowledge Diffusion Research Project. Paper 36: Technical uncertainty as a correlate of information use by US industry-affiliated aerospace engineers and scientists
| NASA-TM-109328 | p 825 N94-14486
NASA/DOD Aerospace Knowledge Diffusion Research Project. Paper 39: The role of computer networks in aerospace engineering
| NASA-TM-109331 | p 825 N94-14487
NASA/DOD Aerospace Knowledge Diffusion Research Project. Paper 37: The impact of political control on technical communications: A comparative study of Russian and US aerospace engineers and scientists
| NASA-TM-109329 | p 826 N94-14488
NASA/DOD Aerospace Knowledge Diffusion Research Project. Paper 38: Computer Mediated Communication (CMC) and the communication of technical information in aerospace
| NASA-TM-109330 | p 826 N94-14489
Scientists, engineers, and technicians in nonmanufacturing industries: 1990. Detailed statistical tables
| NSF-92-334 | p 820 N94-14499
ENTROPY
Beam halo in high-intensity beams
| DE93-014565 | p 789 N94-13328
A multiphase model for shock-induced flow in low density foam
| DE93-013767 | p 632 N94-13397
Statistical mechanical theory of liquid entropy
| DE93-016524 | p 817 N94-14593
ENVIRONMENT EFFECTS
Laser-induced fluorescence over optical fibers for real time in situ measurement of petroleum hydrocarbons in seawater
| AD-A265106 | p 790 N94-12863
A review of the global emissions, transport, and effects of heavy metals in the environment
| DE93-013507 | p 706 N94-12937
Environmental projects. Volume 15: Environmental assessment: Proposed 1-megawatt radar transmitter at the Mars site
| NASA-CR-194098 | p 598 N94-13090
Promotion of geothermal energy development in 1991
| DE93-799057 | p 701 N94-13214
Promotion of geothermal energy development in 1991
| DE93-799058 | p 701 N94-13215
Pollution prevention through total quality
| DE93-013814 | p 707 N94-13390
Birds of Wallops Island, Virginia, 1970 - 1992
| NASA-TM-104589 | p 850 N94-13923
IMG: Interferometric monitor for greenhouse gases p 689 N94-14217
Long-range global warming impact of gaseous diffusion plant operation
| DE93-011686 | p 710 N94-14459
Summary of conclusions and recommendations from a visibility science workshop
| DE93-012770 | p 710 N94-14523
Promotion of geothermal energy development in 1991
| DE93-799061 | p 705 N94-14679
ENVIRONMENT MANAGEMENT
Environmental awareness
| DE93-014192 | p 707 N94-13218
Survey of subsurface geophysical exploration technologies adaptable to an airborne platform
| DE93-015080 | p 717 N94-14294
Fourteenth National Industrial Energy Technology Conference: Proceedings
| DE93-016698 | p 710 N94-14516
ENVIRONMENT MODELS
Modeling of biosphere-atmosphere interaction for forest and pastureland in the Amazon
| INPE-5454-TDI/496 | p 707 N94-13330
Integration between geographic information systems and environmental simulation models
| REPT-93-004 | p 823 N94-13806
Summary of the NOAA/NESDIS Workshop on Development of a Global Satellite/In Situ Environmental Database
| NOAA-TR-NESDIS-72 | p 826 N94-14498
ENVIRONMENT POLLUTION
Snow cover models in operational watershed forecasting
| DE93-778332 | p 718 N94-12837
Spatial and temporal variability of precipitation and chemistry: Case studies from the frontal boundary study
| DE93-007883 | p 708 N94-13910
Status and future opportunities for conversion of synthesis gas to liquid energy fuels
| DE93-010025 | p 584 N94-14089
Study of the consequences of the Chernobyl accident and technogenic activity in the Republic Belarus using aerospace methods p 693 N94-14246

ENVIRONMENT PROTECTION
Vendor information system for innovative treatment technologies. User manual (VISITT version 2.0). Number 2
| PB93-196640 | p 821 N94-12936
Planetary protection implementation on future Mars lander missions
| NASA-CP-3216 | p 841 N94-13183
Environmental awareness
| DE93-014192 | p 707 N94-13218
Multisensor remote sensing data and GIS techniques for monitoring preservation areas: A case study
| INPE-5317-PRE/1714 | p 688 N94-14131
Long-range global warming impact of gaseous diffusion plant operation
| DE93-011686 | p 710 N94-14459
Toxic Substances Control Act (TSCA) chemical substances inventory: Revised inventory synonym and preferred name file, Jan. 1993 documentation
| PB93-155166 | p 710 N94-14508

ENVIRONMENT SIMULATION
Planning of a comet simulator
| ITN-93-85206 | p 835 N94-13230
Taecannautics: Sharing the dream
| NASA-TM-109309 | p 818 N94-13619

ENVIRONMENTAL CHEMISTRY
Spatial variability of throughfall chemistry in a tropical rainforest (Central Amazonia, Brazil)
| INPE-5431-PRE/1765 | p 720 N94-13429
Quality assurance for environmental chemistry, 1991, volume 1
| DE93-011791 | p 709 N94-14020

ENVIRONMENTAL ENGINEERING
Recycling in space
| NASA-TM-109307 | p 737 N94-13615

ENVIRONMENTAL MONITORING
Preparations for and first results of the calibration and interpretation of ERS-1 SAR imagery over land
| BCRS-92-13 | p 684 N94-13123
Molten carbonate fuel cell product development test environmental assessment/protection plan
| DE93-000288 | p 702 N94-13380
Environmental radioactivity intercomparison 1992
| NPL-RSA(EXT)-37 | p 708 N94-13880
Minutes of the Sixth CEOS Plenary Meeting
| NASA-TM-108252 | p 542 N94-14112
CCI working group on climate data and its rapporteurs
| WCDMP-21 | p 723 N94-14118
Asia-Pacific ISY Conference, volume 2
| NASDA-CM-199-VOL-2 | p 688 N94-14209
IMG: Interferometric monitor for greenhouse gases p 689 N94-14217
TRMM system overview and status in the United States p 690 N94-14221
TRMM Project in Japan: Overview and status p 690 N94-14222
Clouds and the Earth's Radiant Energy System (CERES) on the Tropical Rainfall Measuring Mission (TRMM) p 690 N94-14223
Climate products from NOAA operational satellites p 691 N94-14231
Satellite technology for environmental monitoring in developing countries p 692 N94-14236
Application of satellite remote sensing technology in disaster mitigation: A case study of Bangladesh p 692 N94-14238
Integration of remote sensing and mathematical modelling in disaster mitigation p 692 N94-14239
Soil erosion mapping using remote sensing and GIS techniques p 692 N94-14240
Detecting land cover changes in Chiang-Mai area in Thailand p 693 N94-14241
Land evaluation for agricultural productivity in North-East Thailand using LANDSAT TM data and geographic information p 693 N94-14242
Satellite remote sensing for disaster mitigation p 693 N94-14244
A concept for the world environment and disaster observation system p 693 N94-14245
Study of the consequences of the Chernobyl accident and technogenic activity in the Republic Belarus using aerospace methods p 693 N94-14246
A tentative plan on China and Asian-Pacific satellite system for disaster reduction p 693 N94-14247
Earth observation from low-inclination orbit as a necessary complement to polar missions p 694 N94-14248
Development of a remote sensing geographic information system for land cover changes and assessment of risk due to natural and man made hazards covering the area of the inner delta of the Yellow River p 694 N94-14249
Some thoughts on the space programs in the Asia Pacific regions p 697 N94-14272
Summary of the NOAA/NESDIS Workshop on Development of a Global Satellite/In Situ Environmental Database
| NOAA-TR-NESDIS-72 | p 826 N94-14498
The National Remote Sensing Program (NRSP-2 1991 - 2000): The 1992 annual plan of the Netherlands Remote Sensing Board
| BCRS-92-22 | p 700 N94-14544
Terrestrial environment (climatic) criteria guidelines for use in aerospace vehicle development, 1993 revision
| NASA-TM-4511 | p 533 N94-14824

ENVIRONMENTAL QUALITY
Performance of gas turbine compressor cleaners
| NLR-TP-91291-U | p 519 N94-14450

ENVIRONMENTAL RESEARCH SATELLITES
Summary of the NOAA/NESDIS Workshop on Development of a Global Satellite/In Situ Environmental Database
| NOAA-TR-NESDIS-72 | p 826 N94-14498

ENVIRONMENTAL SURVEYS
Promotion of geothermal energy development in 1991
| DE93-799057 | p 701 N94-13214
Rover imaging system for the Mars rover/sample return mission
| NASA-CR-193413 | p 649 N94-13464
Activities report of the Netherlands Remote Sensing Board
| ETN-93-93880 | p 686 N94-14073

ENVIRONMENTAL TESTS
Analysis of samples of reflector materials which are multicoated and metal samples with oxide coatings which have been exposed the space environment in LDEF testing
| NASA-CR-193647 | p 575 N94-12789
Study on improvement of flammability, odor and offgassing tests for materials
| NASDA-CNT-930009 | p 563 N94-13471
Test report for single event effects of the 80386DX microprocessor
| NASA-CR-194509 | p 741 N94-13943
Development of an advanced spacecraft tandem mass spectrometer
| NASA-CR-194195 | p 545 N94-13953
Materials/structures testing p 506 N94-14164

ENZYME ACTIVITY
The evolution of energy-transducing systems: Studies with archaebacteria
| NASA-CR-194130 | p 728 N94-13562
The first steps of chlorophyll synthesis: RNA involvement and regulation
| DE93-014398 | p 730 N94-14509

ENZYMES
Evolution of catalytic RNA in the laboratory
| NASA-CR-194124 | p 727 N94-13210
Crystal growth of enzymes in low gravity (L-5) p 592 N94-13762
Biomimetic methane oxidation
| DE93-013196 | p 705 N94-14510
A characterization of carboxylesterases in rat and guinea pig: Their heterogeneity and role in detoxication of organophosphorus compounds
| NDRE-PUBL-93-1001 | p 730 N94-14852

EPITAXY
Scanning tunneling microscopy studies of diamond films and optoelectronic materials
| NASA-CR-194363 | p 578 N94-13246
Prism-film coupling in anisotropic planar waveguides of epitaxial (101) rutile thin films
| DE93-012912 | p 811 N94-14304
Formation of textured YBCO films by laser ablation
| DE93-013131 | p 581 N94-14319
Manufacturing and examination of integrated optical waveguide components in silicon
| ETN-93-94393 | p 793 N94-14704

EPOXY MATRIX COMPOSITES
Study of deferred acoustic emission in carbon epoxy composites
| ISAL-91-0078 | p 560 N94-14815

EPOXY RESINS
Automated crack identification for cement paste
| AD-A265753 | p 665 N94-13042
Miniature mechanism assembly
| DE93-015595 | p 624 N94-13928

EQUATIONS OF MOTION
Electromagnetic deflection of spinning particles
| DE93-622866 | p 778 N94-12858
Nonlinear vibrations of thick composite plates: Higher-order shear deformation plate theory p 556 N94-13558
PACE: A test bed for the dynamics and control of flexible multibody systems p 527 N94-14650
Construction of the Courant-Snyder invariants for the non-linear equations of motion under presence of the linear coupling
| DE93-017565 | p 788 N94-14872
The evolution of tensor polarization
| DE93-017209 | p 790 N94-14897

EQUATIONS OF STATE
Theoretical treatment of the bulk and surface properties of fluids containing long, flexible molecules
| DE93-015560 | p 575 N94-12861
Equation of state for detonation products
| DE93-012671 | p 583 N94-12921
Multiphase equation of state for iron
| DE93-013956 | p 568 N94-12977
Direct determination of alpha particle transport coefficients
| DE93-013488 | p 787 N94-14691

EQUILIBRIUM FLOW
Least-squares finite element solutions for three-dimensional backward-facing step flow
| NASA-TM-106353 | p 770 N94-14407
The structure of intense vorticity in homogeneous isotropic turbulence p 643 N94-14747

EQUIPMENT
Activities of Hawker Siddeley Canada Inc.
| CTN-93-60865 | p 849 N94-13505

EQUIPMENT SPECIFICATIONS
The study on large space structure assembly technology: The study on deployable truss structure, part 2 and 3
| NASDA-TMR-930003-PT-2-3 | p 541 N94-13659
High performance multi-mode radar altimeter for future spaceborne application p 548 N94-14214

ERROR ANALYSIS
Completing fault models for abductive diagnosis
| DE93-003832 | p 761 N94-12859
Methods for evaluating the predictive accuracy of structural dynamic models
| NASA-CR-191337 | p 671 N94-13124
Lower bounds on time of arrival estimation of pulse compression waveforms
| ITN-93-85189 | p 599 N94-13196
Error analysis of real time and post processed or bit determination of GFO using GPS tracking
| NASA-CR-193646 | p 512 N94-13238
A priori error estimates for an hp-version of the discontinuous Galerkin method for hyperbolic conservation laws
| NASA-TM-108993 | p 632 N94-13467
GPS satellite sky distribution: Impact on the propagation of some important errors in precise relative positioning
| ISBN-0-315-51838-3 | p 513 N94-13541
Bounds on time delay estimation given unknown signal spectral parameters
| ITN-93-85194 | p 601 N94-13566
Topics on spatially high-order accurate methods and pre-conditioning for the Navier-Stokes equations with finite-rate chemistry p 633 N94-13572
Orbit determination error analysis based on the requirements of ADEOS mission
| NASDA-CNT-930008 | p 532 N94-13644
Theory of post-block 2 VLBI observable extraction
| NASA-CR-194543 | p 686 N94-13872
Test report for single event effects of the 80386DX microprocessor
| NASA-CR-194509 | p 741 N94-13943
Estimate of sampling errors of TRMM rainfall observation by using radar-AMeDAS composite data p 690 N94-14225
SHEAN (Simplified Human Error Analysis code) and automated THERP
| DE93-014904 | p 738 N94-14451

ERROR CORRECTING CODES
Investigation for improving Global Positioning System (GPS) orbits using a discrete sequential estimator and stochastic models of selected physical processes
| NASA-CR-194167 | p 512 N94-13082

ERROR CORRECTING DEVICES
Telescope pointing for GOPEX p 610 N94-14389

ERRORS
On the construction and decoding of hyperelliptic codes p 747 N94-13435
Design and performance of an automated video-based laser beam alignment system
| DE93-012571 | p 656 N94-13481
HOPE real time flight operations analyses for return to earth phase, part B
| NASDA-CNT-930011 | p 535 N94-13599
HOPE real time flight operations analyses for return to earth phase, part A
| NASDA-CNT-930010-PT-A | p 535 N94-13645
Estimate of sampling errors of TRMM rainfall observation by using radar-AMeDAS composite data p 690 N94-14225
Radio metric errors due to mismatch and offset between a DSN antenna beam and the beam of a troposphere calibration instrument p 607 N94-14370
Small scale adaptive optics experiment systems engineering
| NASA-CR-194419 | p 793 N94-14548

H2S data reduction
[NASA-CR-193389] p 617 N94-14743
Generating knight's tours without backtracking from errors
[AD-A266807] p 772 N94-14900

ERS-1 (ESA SATELLITE)
Preparations for and first results of the calibration and interpretation of ERS-1 SAR imagery over land
[BCRS-92-13] p 684 N94-13123
ERS-1 system
[ESA-SP-1146] p 699 N94-14353

ESA SPACECRAFT
Space transportation systems within ESA programmes: Current status and perspectives p 537 N94-14275

ESSENTIALLY NON-OSCILLATORY SCHEMES
A comparison of two formulations for high-order accurate essentially non-oscillatory schemes
[NASA-CR-191476] p 499 N94-12852
A high-resolution Lax-Friedrichs scheme for hyperbolic conservation laws with source terms: Application to shallow water equations
[DM-62] p 632 N94-13535
Topics on spatially high-order accurate methods and pre-conditioning for the Navier-Stokes equations with finite-rate chemistry p 633 N94-13572
Multi-dimensional high order essentially non-oscillatory finite difference methods in generalized coordinates
[NASA-CR-194031] p 770 N94-14429
Removing noise from discontinuous data
[ITN-93-85211] p 826 N94-14555

ESTIMATES
Scientists, engineers, and technicians in nonmanufacturing industries: 1990. Detailed statistical tables
[NSF-92-334] p 820 N94-14499

ESTIMATING
Investigation for improving Global Positioning System (GPS) orbits using a discrete sequential estimator and stochastic models of selected physical processes
[NASA-CR-194167] p 512 N94-13082
Estimation of aircraft aerodynamic derivatives with the Total Least Squares Method
[NAL-TR-1150] p 502 N94-13392
Kalman filter input estimation
[NAL-TR-1182] p 649 N94-13456
Bounds on time delay estimation given unknown signal spectral parameters
[ITN-93-85194] p 601 N94-13566

ETA-MESONS
Further study of the X(1910) meson
[DE93-621443] p 782 N94-13362

ETCHING
Crystallographic and metallurgical characterization of radiation detector grade cadmium telluride materials
[DE93-014335] p 806 N94-13150
Field emitter array RF amplifier development project. Phase 1: Cathode technology development
[AD-A266346] p 622 N94-13776
Microchannel cooled heatsinks for high average power laser diode arrays
[DE93-016533] p 658 N94-14442

ETHYL ALCOHOL
Biofuels for transportation: The road from research to the marketplace
[DE93-000091] p 585 N94-14454

EUKARYOTES
Organic Geochemical and tectonic evolution of the Midcontinent Rift system
[DE93-015093] p 717 N94-14338

EULER EQUATIONS OF MOTION
Clebsch variable model for unsteady, transonic flow; application to 2D airfoils
[NLR-TP-91387-U] p 503 N94-13530
Canonical forms of multidimensional steady inviscid flows
[NASA-CR-191488] p 769 N94-13722
Full Riemann solution of the one- and two-dimensional Euler equations
[DLR-FB-92-34] p 638 N94-14188
Nonlinear wave predictions in ceramics
[DE93-016516] p 582 N94-14436
Collisions and separations in 2D hydrodynamical code
[ITN-93-85225] p 639 N94-14503
Analytical description of the breakup of liquid jets in air
[NASA-CR-191503] p 647 N94-14849

EUROPEAN COMMUNICATIONS SATELLITE
ECS: Eighth year in orbit
[ESA-BR-82] p 543 N94-14352

EUROPEAN SPACE AGENCY
European space for exclusively peaceful purposes
[ESA-BR-86] p 851 N94-14137

EUROPEAN SPACE PROGRAMS
European space for exclusively peaceful purposes
[ESA-BR-86] p 851 N94-14137
Space transportation systems within ESA programmes: Current status and perspectives p 537 N94-14275

EUTECTIC ALLOYS
Solidification of eutectic system alloys in space (M-19) p 589 N94-13751
Influence of heat treatment on microstructure of Ti-35wt Al prepared by elemental powder metallurgy
[GKSS/92/E/27] p 574 N94-14821

EUTROPHICATION
Educational module for the Higher Agricultural Education. Part 2: Eutrophication observed by remote sensing: An educational approach to water quality monitoring
[BCRS-92-11B] p 818 N94-14462

EVALUATION
A knowledge-based expert system to coordinate CAD/CAE with integration and test
[NASA-CR-191394] p 745 N94-13130
A measurement and evaluation process model applied to software engineering environments
[INPE-5345-PUD/048] p 746 N94-13428

EVAPORATION
Promotion of geothermal energy development in 1991
[DE93-799058] p 701 N94-13215
Numerical studies of spray combustion in liquid-fueled engines p 564 N94-13685

EVAPOTRANSPIRATION
Potential evapotranspiration in Belgium: Spatial and temporal variability
[PUBL-SER-A-130] p 686 N94-13994

EVEN-EVEN NUCLEI
On the statistical theory of the even-even nucleons levels' density
[DE93-623990] p 788 N94-14875

EXCIMER LASERS
Kinetic studies following state-selective laser excitation
[DE93-012970] p 654 N94-13013
Excimer laser surface processing of titanium
[DE93-012633] p 570 N94-13512

EXCITATION
Excitation of coupled waves in plasma periodic structures by relativistic electron beam and acceleration of charged particles
[DE93-621657] p 794 N94-12853
Comment of parameter excitation of Alfven and Heliicon waves in a magnetoactive compensated semiconductor by microwave radiation
[DE93-623203] p 806 N94-13228

EXCITONS
Free-exciton recombination in GaAs
[DE93-009843] p 809 N94-14079
Intrinsic and interfacial recombination in OMVPE- and MBE-prepared GaAs/Al(x)Ga(1-x)As heterostructures
[DE93-009844] p 809 N94-14083
Anomalous low-temperature free-exciton transport in GaAs structures
[DE93-009845] p 809 N94-14108

EXERCISE PHYSIOLOGY
Metabolic rate measurements comparing supine with upright upper-body exercises
[NASA-CR-4549] p 729 N94-14028
Variability of prediction of maximal oxygen concumption on the cycle ergometer using standard equations
[NASA-TP-3412] p 729 N94-14032

EXHAUST EMISSION
AQUIS: A PC-based source information manager
[DE93-012893] p 707 N94-13383
Piston engine intake and exhaust system design
[ISVR-TR-222] p 663 N94-13874
Long-range global warming impact of gaseous diffusion plant operation
[DE93-011686] p 710 N94-14459

EXHAUST GASES
Propulsion simulator for magnetically-suspended wind tunnel models
[NASA-CR-189560] p 527 N94-13127
Combustor technology for future small gas turbine aircraft
[NASA-TM-106312] p 517 N94-13142
AQUIS: A PC-based source information manager
[DE93-012893] p 707 N94-13383
Long-range global warming impact of gaseous diffusion plant operation
[DE93-011686] p 710 N94-14459
Portable acoustic wave sensor systems for real-time monitoring of volatile organic compounds
[DE93-013753] p 582 N94-14511
Terrestrial environment (climatic) criteria guidelines for use in aerospace vehicle development, 1993 revision
[NASA-TM-4511] p 533 N94-14824

EXHAUST NOZZLES
Electrophoretic and electrolytic deposition of ceramic particles on porous substrates
[AD-A265141] p 575 N94-12812

EXHAUST SYSTEMS
Piston engine intake and exhaust system design
[ISVR-TR-222] p 663 N94-13874

EXHAUST VELOCITY
Investigation of the feasibility of optical diagnostic measurements at the exit of the SSME
[NASA-CR-193832] p 553 N94-14682

EXOBIOLOGY
Planetary protection implementation on future Mars lander missions
[NASA-CP-3216] p 841 N94-13183
Studies on the effects of microgravity on the ultrastructure and functions of cultured mammalian cells (L-6) p 592 N94-13763
Aerospace medicine and biology: A continuing bibliography with indexes (supplement 379)
[NASA-SP-7011(379)] p 733 N94-14412

EXOTHERMIC REACTIONS
Chemical reactions in scramjet engines: Reduced kinetic models for ignition, combustion and nozzle flow
[NAL-TR-1184] p 563 N94-13458

EXPANDABLE STRUCTURES
The Second Workshop on Deployment and Assembly Experiment of Large Space Structure on Orbit
[NASDA-CON-930003] p 529 N94-13268
Structural design of hexa-link truss deployable antenna p 529 N94-13269
Thermal distortion measurement of TETRUS type thermal test model of large deployable antenna for mobile communications satellite p 529 N94-13270
Development of modular cable mesh deployable antenna p 530 N94-13274
Helical truss beam development for large space structure p 530 N94-13276
Trial manufacture model and in-space verification method of deployable antenna p 530 N94-13278
A concept on on-orbit experiments of deployable structures utilizing JEM/HOPE p 531 N94-13279
Movement of deployable truss p 531 N94-13280
Development and application of one dimensional deployable truss p 531 N94-13281
The study on large space structure assembly technology: The study on deployable truss structure, part 1
[NASDA-TMR-930002] p 541 N94-13658
The study on large space structure assembly technology: The study on deployable truss structure, part 2 and 3
[NASDA-TMR-930003-PT-2-3] p 541 N94-13659

EXPEDITIONS
Airborne Arctic stratospheric expedition: Ozone
[NASA-TM-109312] p 515 N94-13606

EXPERIMENT DESIGN
A benchmark bending test of a thick specimen, Part 1: Experiments
[ARL-RR-6-PT-1] p 670 N94-12927
Heavy section steel irradiation experiment
[DE93-015517] p 573 N94-14537

EXPERIMENTATION
Development of experimental demonstration processes for laminar-turbulent flow states at wing profiles in free flight
[ILR-MITT-280(1993)] p 510 N94-14800

EXPERT SYSTEMS
JTEC Panel report on knowledge-based systems in Japan
[PB93-170124] p 820 N94-12801
Advancing automation and robotics technology for the Space Station Freedom and for the U.S. economy
[NASA-TM-104024] p 739 N94-12838
Knowledge base technology for CT-DIMS: Report 1
[DE93-013118] p 743 N94-13014
A knowledge-based expert system to coordinate CAD/CAE with integration and test
[NASA-CR-191394] p 745 N94-13130
Thermal Expert System (TEXSYS): Systems autonomy demonstration project, volume 1. Overview
[NASA-TM-102877] p 538 N94-13201
Collection and analysis of dialogue protocols for the question-answering facility of the entity-relationship modeling advisor
[ERB-1032] p 740 N94-13546
An expert system for integrated structural analysis and design optimization for aerospace structures
[NASA-CR-194225] p 673 N94-13673
SCAILET: An intelligent assistant for satellite ground terminal operations
[NASA-TM-105879] p 538 N94-13918
Gate assignment using linear programming
[LR-698] p 775 N94-13987
Thermal Expert System (TEXSYS): Systems autonomy demonstration project, volume 2. Results
[NASA-TM-102877] p 538 N94-13989
An expert system class library for Audition
[IME-MET-TR-008] p 824 N94-14196
Identification and interpretation of patterns in rocket engine data
[NASA-CR-194534] p 552 N94-14309

An integrated knowledge system for the Space Shuttle hazardous gas detection system
| NASA-CR-194533 | p 536 N94-14310
The further development and refinement of an expert-systems approach to the creative design of mechanisms and mechanical systems
| AD-A266812 | p 665 N94-14901

EXPIRATION
Flow limitation and flutter in membrane walled collapsible tubes: A model for expiratory wheezing
| ISBN-0-315-73875-8 | p 635 N94-13662

EXPLOSIONS
The motion of a conical shaped liner driven by explosive load
| ITN-93-85215 | p 585 N94-14507

EXPLOSIVES
Synthesis and characterization of 1,4-dinitroglycoluril (DINGU)
| DE93-014111 | p 584 N94-13099
Destruction of waste energetic materials using base hydrolysis
| DE93-012738 | p 584 N94-13491
A study of the role of homogeneous process in heterogeneous high explosives
| DE93-012733 | p 585 N94-14180
Nonlinear wave predictions in ceramics
| DE93-016516 | p 582 N94-14436
The 4th International Symposium on Analysis and Detection of Explosives
| DE93-620280 | p 585 N94-14829

EXPOSURE
Phase-shifting effect of light and exercise on the human circadian clock
| AD-A265732 | p 732 N94-13038

EXTENSOMETERS
Strain sensing technology for high temperature applications
| NASA-TM-4498 | p 648 N94-12874

EXTERNAL TANKS
Results of experimental investigations to determine external tank protuberance loads using a 0.03-scale model of the Space Shuttle launch configuration (model 47-OTS) in the NASA/ARC unitary plan wind tunnel, volume 1
| NASA-CR-167690 | p 534 N94-12810
Results of wind tunnel tests of an ASRM configured 0.03 scale Space Shuttle integrated vehicle model (47-OTS) in the AEDC 16-foot transonic wind tunnel, volume 2
| NASA-CR-185697 | p 534 N94-12965
Results of experimental investigations to determine external tank protuberance loads using a 0.03-scale model of the Space Shuttle launch configuration (Model 47-OTS) in the NASA/ARC unitary plan wind tunnel, volume 2
| NASA-CR-167691 | p 536 N94-14047

EXTINCTION
Homogeneous-hetergeneous combustion: Thermal and chemical coupling
| DE93-016050 | p 565 N94-14403

EXTRAGALACTIC RADIO SOURCES
Sites of fine-scale electron density turbulence in the interstellar medium
| NASA-CR-193708 | p 839 N94-13864

EXTRAPOLATION
Extrapolation of ground test data to flight
p 507 N94-14170

EXTRATERRESTRIAL INTELLIGENCE
Search for extraterrestrial intelligence/high resolution microwave survey team member
| NASA-CR-194177 | p 739 N94-13086

EXTRATERRESTRIAL RADIATION
Research in cosmic and gamma ray astrophysics: Cosmic physics portion
| NASA-CR-194127 | p 847 N94-13211
Genetic effects of HZE and cosmic radiation (L-9)
p 593 N94-13766
Single Event Upset (SEU) testing of semiconductor components at the McMaster Accelerator Laboratory
| DSIS-93-00071 | p 623 N94-13834

EXTRATERRESTRIAL RESOURCES
The studies on lunar and planetary exploration and utilization: The study on lunar resources utilization
| NASDA-CNT-930014 | p 842 N94-13655

EXTRAVEHICULAR ACTIVITY
STS-30 Magellan IUS/EVA training in WETF
| NASA-TM-109300 | p 737 N94-13601
Metabolic rate measurements comparing supine with upright upper-body exercises
| NASA-CR-4549 | p 729 N94-14028
Large space structures and systems in the space station era: A bibliography with indexes (supplement 05)
| NASA-SP-7085(05) | p 543 N94-14411
STS-35 EVA payload training in WETF
| NASA-TM-109492 | p 739 N94-14790

EXTREME ULTRAVIOLET RADIATION
Vacuum ultraviolet instrumentation for solar irradiance and thermospheric airglow
| NASA-CR-194525 | p 652 N94-14684
Optical degradation issues for XUV projection lithography systems
| DE93-012658 | p 626 N94-14805

EXTREMELY HIGH FREQUENCIES
A near-infrared faint galaxy survey: Evolution and the cosmological geometry from K band photometry
p 830 N94-13591

EXTRUDING
An experimental study on the effect of die geometry on swell and sag in the parison extrusion stage
| IMI-93RT-42400-1476-G | p 597 N94-14070

EYE MOVEMENTS
Manual control in space research on perceptual-motor functions under zero gravity conditions (L-10)
p 593 N94-13767
Eye-gaze and intent: Application in 3D interface control
| DE93-015210 | p 738 N94-14335

EYE PROTECTION
Novel Co:MgF2 lidar for aerosol profiler
| NASA-CR-191525 | p 654 N94-13091

F

F-15 AIRCRAFT
Preliminary flight results of a fly-by-throttle emergency flight control system on an F-15 airplane
| NASA-TM-4503 | p 520 N94-13254

FABRICATION
Roller-gear drives for robotic manipulators design, fabrication and test
| NASA-CR-194248 | p 660 N94-12802
Design and testing of planar magnetic micromotors fabricated by deep x ray lithography and electroplating
| DE93-012856 | p 618 N94-12821
Processing, fabrication and demonstration of HTS integrated microwave circuits
| AD-A265789 | p 619 N94-12892
Rigid-flexible printed wiring boards
| DE93-013938 | p 620 N94-13094
Fabrication of AlGaAs/GaAs-light-emitting devices by selective MOCVD using dialkylmetalchloride
p 627 N94-13433
Fabrication of very-low-density, high-stiffness carbon fiber/aluminum hybridized composite with ultra-low density and high stiffness (M-11) p 588 N94-13743
Fabrication of Si-As-Te ternary amorphous semiconductor in the microgravity environment (M-13)
p 588 N94-13745
Combustion synthesis and engineering of nanoparticles for electronic, structural, and superconductor applications
| DE93-016286 | p 809 N94-13981
Measurement of strain in individual phases of composites before, during, and after mechanical loading
| DE93-014585 | p 558 N94-14119
Machining aspects of nickel-phosphorus coatings
| DE93-013037 | p 580 N94-14311
Fabrication p 546 N94-14834
Investigation of Zerodur material processing
| NASA-CR-193842 | p 793 N94-14903

FABRICS
Review of test methods for material flammability
| DSIS-93-00480 | p 564 N94-13942

FABRY-PEROT INTERFEROMETERS
Optical fiber sensors for materials and structures characterization
| NASA-CR-194090 | p 791 N94-13353
Optical fibre Fabry-Perot interferometers for calorimetric heat transfer gauges
| RAE-TM-AERO/PROP-20 | p 653 N94-14701

FACE CENTERED CUBIC LATTICES
Determination of channeling perspectives for complex crystal structures
| DE93-012872 | p 805 N94-13009
Monte Carlo simulation of the OCP freezing transition
| DE93-013039 | p 811 N94-14313
Is K3C60 a line phase?
| DE93-016700 | p 813 N94-14517

FACTORIAL DESIGN
Effect of size, shape, and end condition of test specimen on compressive strength of high-strength concrete
| DE93-500412 | p 682 N94-14653

FACTORIZATION
Beyond core: Making parallel computer I/O practical
| DE93-012347 | p 758 N94-12878
On relations between Schmidt pairs arising in robust control
| CWI-BS-R9225 | p 764 N94-14000

FAIL-SAFE SYSTEMS
Fail-safe PVM: A portable package for distributed programming with transparent recovery
| AD-A266594 | p 749 N94-13779

FAILURE
Theoretical studies of breakdown in random media
| DE93-018107 | p 558 N94-14418

FAILURE ANALYSIS
STS-55 pad abort: Engine 2011 oxidizer preburner augmented spark igniter check valve leak
| NASA-CR-193830 | p 533 N94-12806
Surface analysis of bearings
| AD-A266800 | p 661 N94-13122
MSD in fuselage lap joints: Requirements for inspection intervals for typical fuselage lap joint panels with Multiple Site Damage
| LR-697 | p 675 N94-13986
An improved approach for flight readiness certification: Methodology for failure risk assessment and application examples, volume 1
| NASA-CR-194498 | p 542 N94-14076
An improved approach for flight readiness certification: Methodology for failure risk assessment and application examples. Volume 2: Software documentation
| NASA-CR-194499 | p 542 N94-14077
An improved approach for flight readiness certification: Methodology for failure risk assessment and application examples. Volume 3: Structure and listing of programs
| NASA-CR-194500 | p 542 N94-14078
Machining and grinding: High rate deformation in practice
| DE93-010718 | p 664 N94-14457
An improved approach for flight readiness certification: Probabilistic models for flaw propagation and turbine blade failure. Volume 1: Methodology and applications
| NASA-CR-194496 | p 519 N94-14841
An improved approach for flight readiness certification: Probabilistic models for flaw propagation and turbine blade failure. Volume 2: Software documentation
| NASA-CR-194497 | p 519 N94-14842

FAILURE MODES
Inelastic deformation mechanisms in SCS-6/Ti 15-3 MMC lamina under compression
| NASA-CR-191170 | p 555 N94-13378
Role of microstructure on fatigue durability of aluminum aircraft alloys
| AD-A266350 | p 571 N94-13697
Failure modes of reduced-order orbit determination filters and their remedies p 532 N94-14373
An improved approach for flight readiness certification: Probabilistic models for flaw propagation and turbine blade failure. Volume 1: Methodology and applications
| NASA-CR-194496 | p 519 N94-14841
An improved approach for flight readiness certification: Probabilistic models for flaw propagation and turbine blade failure. Volume 2: Software documentation
| NASA-CR-194497 | p 519 N94-14842

FAINT OBJECTS
A near-infrared faint galaxy survey: Evolution and the cosmological geometry from K band photometry
p 830 N94-13591
Rocket and laboratory studies in astronomy
| NASA-CR-194410 | p 832 N94-13966

FAIRINGS
Arc-heating tests of thermal protection system materials for the H-2 rocket fairing
| NAL-TR-1181 | p 551 N94-13455

FALKNER-SKAN EQUATION
Stability of spatially developing boundary layers
p 640 N94-14605

FALSE ALARMS
Constant False Alarm Rate (CFAR) detection in Weibull clutter
| ITN-93-85190 | p 600 N94-13537
Stochastic performance modeling and evaluation of obstacle detectability with imaging range sensors
| NASA-CR-194510 | p 605 N94-13946

FAR FIELDS
New vortex dynamics methods for rotor free wake analysis
| AD-A266656 | p 509 N94-14774

FAR INFRARED RADIATION
Analysis of interstellar cloud structure based on IRAS images
| NASA-CR-194341 | p 836 N94-13332
The origin of the far-infrared emission from galactic molecular clouds p 848 N94-13654

FAR ULTRAVIOLET RADIATION
Vacuum ultraviolet instrumentation for solar irradiance and thermospheric airglow
| NASA-CR-194525 | p 652 N94-14684

FARM CROPS
Validated environmental and physiological data from the CELSS Breadboard Projects Biomass Production Chamber. BWT931 (Wheat cv. Yecora Rojo)
| NASA-TM-109272 | p 738 N94-13979

FARMLANDS
Evolution of the lower planetary boundary layer over strongly contrasting surfaces
| DE93-010667 | p 717 N94-14424
FAST FOURIER TRANSFORMATIONS
An experimental regional scale climate simulation laboratory
| DE93-015935 | p 719 N94-13119
ULTRA 2 user's manual for ULTRA 2 revision 3.0
| DE93-015970 | p 744 N94-13120
FAST NEUTRONS
Cosmic and solar gamma ray and neutron experiments
| NASA-CR-193359 | p 849 N94-13965
Radiation hardening and radiation-induced chromium depletion effects on intergranular stress corrosion cracking of austenitic stainless steels
| DE93-011602 | p 572 N94-14058
AlGaAs diode laser blue shift resulting from fast neutron irradiation
| AD-A266642 | p 659 N94-14681
FATIGUE (MATERIALS)
Fatigue crack initiation and propagation in aluminum alloys 8090 and 2124 in hydrogenous atmospheres
p 570 N94-13670
Computational methods for reliable fatigue and damage tolerance dimensioning of aircraft structures
| FFA-TN-1993-05 | p 515 N94-13690
Fatigue and residual strength characteristics of fiber metal laminates subjected to incidental damage
| LR-708 | p 674 N94-13803
Review of Canadian aeronautical fatigue work, 1991-1993
| LTR-ST-1932 | p 674 N94-13861
A microstructural approach to fatigue crack processes in poly crystalline BCC materials
| DE93-016666 | p 812 N94-14354
Inflow characteristics associated with high-blade-loading events in a wind farm
| DE93-010042 | p 704 N94-14423
A study of fiber volume fraction effects in notched unidirectional SCS-6/Ti-15V-3Cr-3Al-3Sn composite
| NASA-CR-191165 | p 559 N94-14769
Thermomechanical and isothermal fatigue behavior of a (90)sub 8 titanium matrix composite
| NASA-CR-191196 | p 560 N94-14822
FATIGUE LIFE
Fatigue predictions and scatter
| LR-696 | p 675 N94-13933
Computer program for analysis of high speed, single row, angular contact, spherical roller bearing, SASHBEAN. Volume 1: User's guide
| NASA-CR-191183 | p 663 N94-14445
Computer program for analysis of high speed, single row, angular contact, spherical roller bearing, SASHBEAN. Volume 2: Mathematical formulation and analysis
| NASA-CR-191182 | p 664 N94-14446
Thermomechanical and isothermal fatigue behavior of a (90)sub 8 titanium matrix composite
| NASA-CR-191196 | p 560 N94-14822
FATIGUE TESTS
An advanced test technique to quantify thermomechanical fatigue damage accumulation in composite materials
| NASA-CR-191147 | p 555 N94-13139
Fatigue crack initiation and propagation in aluminum alloys 8090 and 2124 in hydrogenous atmospheres
p 570 N94-13670
Role of microstructure on fatigue durability of aluminum aircraft alloys
| AD-A266350 | p 571 N94-13697
The effect of TiN coatings on the rolling contact fatigue behavior of M50 bearing steel
| ARL-TR-40 | p 662 N94-13794
Thermomechanical and isothermal fatigue behavior of a (90)sub 8 titanium matrix composite
| NASA-CR-191196 | p 560 N94-14822
The growth of short fatigue cracks in an aluminium alloy
| RAE-TR-92063 | p 574 N94-14828
FATTY ACIDS
Direct probing of chromatography columns by laser-induced fluorescence
| DE93-015208 | p 654 N94-13022
Structures and shear response of lipid monolayers
| DE93-015076 | p 730 N94-14802
FAULT DETECTION
Thermal Expert System (TEXSYS): Systems automony demonstration project, volume 1. Overview
| NASA-TM-102877 | p 538 N94-13201
Identification and interpretation of patterns in rocket engine data
| NASA-CR-194534 | p 552 N94-14309
An integrated knowledge system for the Space Shuttle hazardous gas detection system
| NASA-CR-194533 | p 536 N94-14310
FAULT TOLERANCE
A hardware implementation of a provably correct design of a fault-tolerant clock synchronization circuit
| NASA-TM-109001 | p 759 N94-13450
Fail-safe PVM: A portable package for distributed programming with transparent recovery
| AD-A266594 | p 749 N94-13779
A performance prediction model for a fault-tolerant computer during recovery and restoration
| NASA-CR-194490 | p 741 N94-14136
FAULT TREES
Completing fault models for abductive diagnosis
| DE93-003832 | p 761 N94-12859
FEASIBILITY ANALYSIS
The MRIS feasibility study
| NASA-TM-107763 | p 597 N94-12804
Feasibility study of an orbiting laboratory for testing CSI technology
| NASA-CR-191524 | p 540 N94-13016
Hot Dry Rock energy
| DE93-014452 | p 702 N94-13403
Physiological Anatomical Rodent Experiment (PARE) .04 Feasibility Test 1
| NASA-CR-194423 | p 728 N94-13473
Feasibility study of a synthesis procedure for array feeds to improve radiation performance of large distorted reflector antennas
| NASA-CR-194491 | p 612 N94-14501
FEDERAL BUDGETS
National atmospheric sciences program, fiscal years 1987-1990
| NSF-92-16 | p 711 N94-12794
Defense Information Technology Services organization FY 1994 budget estimates. Information Technology Systems budget
| PB93-199016 | p 826 N94-14562
FEEDBACK
Cellular mechanism of turnover of the stress induced protein HSP 70
| AD-A265723 | p 732 N94-13061
Characteristics of semiconductor lasers with optical feedback
| ISBN-0-315-55435-5 | p 656 N94-13522
Experimental and analytical analysis of the response of a smart beam to rate feedback
| AD-A266544 | p 557 N94-13706
FEEDBACK CONTROL
Self tuning and adaptive control: Evaluations and improvements of algorithms
| ITN-93-85192 | p 762 N94-13329
Design and performance of an automated video-based laser beam alignment system
| DE93-012571 | p 656 N94-13481
Experimental and analytical analysis of the response of a smart beam to rate feedback
| AD-A266544 | p 557 N94-13706
Dynamic Forms. Part 1: Functions
| NASA-TP-3397 | p 596 N94-13790
Decentralized control of uncertain systems via sensitivity models
| DE93-012963 | p 766 N94-14568
On l(1): Optimal decentralized performance
p 681 N94-14643
Smart materials/structures technical analysis
| AD-A266771 | p 766 N94-14785
Functional differential equations with piecewise continuous argument
| AD-A266660 | p 772 N94-14840
Anomalous ion transport and feedback control
| DE93-018324 | p 803 N94-14874
FEEDFORWARD CONTROL
Dynamics and design of nonholonomic robotic mechanical systems
| ISBN-0-315-72009-3 | p 662 N94-13597
Identification of continuous-time dynamical systems: Neural network based algorithms and parallel implementation
| DE93-014427 | p 766 N94-14737
Determining neural network connectivity using evolutionary programming
| AD-A266853 | p 766 N94-14882
FERMI LIQUIDS
To the theory of triplet pairing in Fermi-liquid model
| DE93-621770 | p 816 N94-12855
FERMI SURFACES
The de Haas-van Alphen studies and Fermi surface properties of organic superconductors (ET)2X
| DE93-015157 | p 623 N94-13925
FERMIONS
Muon spin relaxation studies of heavy fermion superconductors
| DE93-014576 | p 815 N94-14773
FERRIC IONS
Reactor studies of metal ions associated with chromatographic silica
| AD-A266675 | p 573 N94-14779
FERRITIC STAINLESS STEELS
Investigations of low-temperature neutron embrittlement of ferritic steels
| DE93-015460 | p 573 N94-14700
FERROELECTRICITY
Solution chemistry optimization of sol-gel processed PZT thin films
| DE93-013776 | p 814 N94-14695
FERROMAGNETIC MATERIALS
Spin polarized photoemission studies of interfacial and thin film magnetism
| DE93-014326 | p 580 N94-14142
Theory of the negative magnetoresistance in magnetic metallic multilayers
| DE93-013912 | p 776 N94-14584
FERROMAGNETISM
Canted magnetic moments at the Gd(0001) surface
| DE93-014327 | p 805 N94-13102
FERTILIZATION
Amphibian fertilization and development in microgravity p 594 N94-13770
FERTILIZERS
Environmental awareness
| DE93-014192 | p 707 N94-13218
FIBER COMPOSITES
Ohmic heating of composite candidate graphite-fiber/coating combinations
| NASA-TM-4491 | p 554 N94-12871
Development of nondestructive evaluation methods and prediction of effects of flaws on the fracture behavior of structural ceramics
| DE93-012942 | p 577 N94-13032
Inelastic deformation mechanisms in SCS-6/Ti 15-3 MMC lamina under compression
| NASA-CR-191170 | p 555 N94-13378
Inhibiting corrosion in Gr/Al and Gr/Mg metal matrix composites using nonequilibrium alloying techniques
| AD-A266547 | p 556 N94-13583
A stochastic model for behavior analysis of fiber-reinforced quasi-brittle materials
p 672 N94-13594
Modified carbon for improved corrosion resistance
| AD-D015741 | p 556 N94-13663
Fatigue and residual strength characteristics of fiber metal laminates subjected to incidental damage
| LR-708 | p 674 N94-13803
Characterization of composite materials for aerospace structures
| ESA-TT-1260 | p 557 N94-13804
Probabilistic micromechanics for high-temperature composites
| NASA-CR-191150 | p 676 N94-14408
Immiscible phase incorporation during directional solidification of hypermonotectics
| NASA-CR-194412 | p 565 N94-14480
Thermoelastic response of metal matrix composites with large-diameter fibers subjected to thermal gradients
| NASA-TM-106344 | p 560 N94-14823
FIBER OPTICS
Laser-induced fluorescence over optical fibers for real time in situ measurement of petroleum hydrocarbons in seawater
| AD-A265106 | p 790 N94-12863
Application of new electro-optic technology to Space Station Freedom data management system
| NASA-CR-177622 | p 538 N94-13257
Proceedings of the 11th Space Surveillance Workshop, volume 1
| AD-A265120 | p 531 N94-13358
Polarization effects in optical fiber current sensors based on Sagnac interferometers with 3 by 3 couplers
| DE93-012665 | p 792 N94-14367
Absolute detection efficiency of a micro-channel plate detector to x rays in the 1-100 KeV energy range
| DE93-012592 | p 789 N94-14460
Advanced optical instruments technology
p 547 N94-14838
FIBER ORIENTATION
Development of nondestructive evaluation methods and prediction of effects of flaws on the fracture behavior of structural ceramics
| DE93-012942 | p 577 N94-13032
FIBER STRENGTH
Development of nondestructive evaluation methods and prediction of effects of flaws on the fracture behavior of structural ceramics
| DE93-012942 | p 577 N94-13032
FIBER VOLUME FRACTION
A study of fiber volume fraction effects in notched unidirectional SCS-6/Ti-15V-3Cr-3Al-3Sn composite
| NASA-CR-191165 | p 559 N94-14769
FIELD EFFECT TRANSISTORS
1/f noise and oxide traps in MOSFETs
| DE93-007581 | p 619 N94-12942

An x ray detector using superconducting aluminum tunnel junctions
| DE93-015103 | p 811 N94-14332
Electrical noise in microwave field effect and bipolar transistors
| LAAS-93042 | p 616 N94-14717

FIELD OF VIEW
Visual cueing considerations in Nap-of-the-Earth helicopter flight head-slaved helmet-mounted displays
p 524 N94-13315

FIELD THEORY (PHYSICS)
Force-free magnetic fields, curl eigenfunctions, and the sphere in transform space, with applications to fluid dynamics and electromagnetic theory
| AD-A265805 | p 834 N94-12971
The effects of internal fluctuations on a class of nonequilibrium statistical field theories
| DE93-016620 | p 774 N94-14441
Multiple Schroedinger cats from multilevel atoms
| DE93-013412 | p 786 N94-14526
Multiplicative noise: Applications in cosmology and field theory
| DE93-016624 | p 840 N94-14536
Renormalized band structure of CuO2 layers in superconducting compounds: A mean field approach
| PREPRINT-730 | p 815 N94-14720
Soliton equations and self-dual gauge fields
| DE93-626620 | p 818 N94-14887
Studies in quantum field theory
| DE93-017201 | p 818 N94-14896

FIGHTER AIRCRAFT
Design criteria for integrated flight/propulsion control systems for STOVL fighter aircraft p 521 N94-13297
The identification of ability requirements and selection instruments for fighter pilot training
| AD-A266340 | p 735 N94-13582
High flux heat exchanger
| AD-A266341 | p 636 N94-13730
Qualitative investigation of a generic fighter model in radio controlled gliding flight
| LM-AA-003 | p 516 N94-13898

FIGURE OF MERIT
Robot-task compliance: The energy criterion
| ITN-93-85196 | p 763 N94-13568

FILE MAINTENANCE (COMPUTERS)
Generic software architecture based redesign
p 745 N94-13290

FILM COOLING
Experimental investigation of the effects of blowing ratio parameter on heat transfer to a film-cooled flat plate
| AD-A266599 | p 636 N94-13780

FILM THICKNESS
Effect of microstructure on passive film formation and breakdown on Al alloys
| AD-A265339 | p 569 N94-13050
The use of polarised neutron reflection for unique density profile determination in thin films
| PB93-187136 | p 579 N94-13783
Direct submillimeter absorptivity measurements on epitaxial Ba(1-x)K(x)BiO3 films at 2K
| DE93-013904 | p 815 N94-14699

FILMS
A process for evaluation of mechanical behavior of surface films
| W-1/92 | p 579 N94-14007

FINANCIAL MANAGEMENT
Selected data on academic science and engineering R and D expenditures: Fiscal Year 1991
| NSF-92-329 | p 819 N94-13982

FINE STRUCTURE
Recent developments in multiple-scattering calculations of XAFS and XANES
| DE93-010999 | p 563 N94-13477
Many-body corrections in XAFS
| DE93-011002 | p 563 N94-13478

FINITE DIFFERENCE THEORY
A comparison of two formulations for high-order accurate essentially non-oscillatory schemes
| NASA-CR-191476 | p 499 N94-12852
Locally non-uniform finite-difference time domain with application to stealth, crosstalk, and narrow apertures
| DE93-013958 | p 601 N94-13696
Modelling of the temperature distribution in a copper roll for the design of a system of cooled rolls adapted to vertical strip casting
| IMI-93RT-21200-1436-G | p 557 N94-13866
Multi-dimensional high order essentially non-oscillatory finite difference methods in generalized coordinates
| NASA-CR-194031 | p 770 N94-14429
An adaptive projection method for the incompressible Euler equations
| DE93-016428 | p 639 N94-14434
Nonlinear wave predictions in ceramics
| DE93-016516 | p 582 N94-14436
Computation of nonequilibrium flows using PNS equations p 641 N94-14610
A new Lagrangian method for three-dimensional steady supersonic flows
| NASA-TM-106068 | p 510 N94-14847

FINITE ELEMENT METHOD
Thermosolutal convection and macrosegregation in dendritic alloys
| NASA-CR-194039 | p 567 N94-12825
Modeling the impact behavior of AD85 ceramic under multi-axial loading
| AD-A265877 | p 576 N94-12932
A general contact detection algorithm for finite element analysis
| DE93-012846 | p 742 N94-12956
Advanced electric motor technology flux mapping
| NASA-CR-193824 | p 621 N94-13186
Body/cushion contact stress analysis during sitting
| ITN-93-85204 | p 736 N94-13229
A hybrid finite element-boundary integral for the analysis of cavity-backed antennas of arbitrary shape
| NASA-CR-193719 | p 599 N94-13236
A priori error estimates for an hp-version of the discontinuous Galerkin method for hyperbolic conservation laws
| NASA-TM-108993 | p 632 N94-13467
Fully developed turbulent flow in rectangular interrupted-plate ducts
| ISBN-0-315-63594-0 | p 632 N94-13474
Finite element calculation of stress-intensity factors for thumb-nail cracks in DEN specimens
| LTR-ST-1929 | p 850 N94-13548
Nonlinear vibrations of thick composite plates: Higher-order shear deformation plate theory
p 556 N94-13558
Shear buckling of fiber metal laminates: Comparison between orthotropic and anisotropic plate models using finite element method
| LTR-ST-1934 | p 671 N94-13565
Finite element analysis of composite plates by use of modified complementary energy principle
p 672 N94-13596
An expert system for integrated structural analysis and design optimization for aerospace structures
| NASA-CR-194225 | p 673 N94-13673
A control volume finite element method for three-dimensional, incompressible, viscous fluid flow
| ISBN-0-315-72019-0 | p 635 N94-13683
An 8-node axisymmetric acoustic finite element for non-axisymmetric fluid-structure interaction analysis
| FFA-TN-1993-03 | p 673 N94-13689
Computational methods for reliable fatigue and damage tolerance dimensioning of aircraft structures
| FFA-TN-1993-05 | p 515 N94-13690
Testing and analysis of curved frame specimens made from a Long Discontinuous Fiber (LDF) material
| NASA-TM-109014 | p 557 N94-13711
Application of symbolic and algebraic manipulation software in solving applied mechanics problems
| NASA-CR-4544 | p 596 N94-13798
Variational approach to probabilistic finite elements
| NASA-CR-187179 | p 674 N94-13873
Elastic-plastic mixed-iterative finite element analysis: Implementation and performance assessment
| NASA-TM-106164 | p 675 N94-13919
On the superconvergence of Galerkin methods for hyperbolic IBVP
| NASA-CR-194293 | p 770 N94-13922
Some aspects of sheet forming simulation using explicit finite element techniques
| DE93-012479 | p 663 N94-13975
A process for evaluation of mechanical behavior of surface films
| W-1/92 | p 579 N94-14007
Finite element calculation of stress-intensity factors for thru-thickness cracks in DEN specimens
| LTR-ST-1905 | p 675 N94-14035
On the superconvergence of Galerkin methods for hyperbolic IBPV
| NASA-CR-194488 | p 770 N94-14307
Least-squares finite element solutions for three-dimensional backward-facing step flow
| NASA-TM-106353 | p 770 N94-14407
Probabilistic micromechanics for high-temperature composites
| NASA-CR-191150 | p 676 N94-14408
Development of an hp-version finite element method for computational optimal control
| NASA-CR-194149 | p 766 N94-14444
Welding technologies as applied to nuclear manufacturing
| DE93-010924 | p 664 N94-14565
Large spatial, temporal, and algorithmic adaptivity for implicit nonlinear finite element analysis
| DE93-016438 | p 771 N94-14589
Analysis of new composite architectures
| NASA-CR-194524 | p 559 N94-14715
Elastic-plastic finite element analyses of an unidirectional, 9 vol percent tungsten fiber reinforced copper matrix composite
| NASA-TM-106304 | p 559 N94-14719
Analysis, approximation, and computation of a coupled solid/fluid temperature control problem
| NASA-TM-106351 | p 771 N94-14731
Buckling analysis of laminated thin shells in a hot environment
| NASA-TM-106302 | p 683 N94-14776
Nonlinear wave forces on large ocean structures
| AD-A266820 | p 683 N94-14902

FINITE VOLUME METHOD
A comparison of two formulations for high-order accurate essentially non-oscillatory schemes
| NASA-CR-191476 | p 499 N94-12852
A solution algorithm for the prediction of compressible laminar and turbulent shear flows p 634 N94-13635
CNSFV code development, virtual zone Navier-Stokes computations of oscillating control surfaces and computational support of the laminar flow supersonic wind tunnel
| NASA-CR-194259 | p 504 N94-14030
Analysis of reacting flowfields in low-thrust rocket engines and plumes p 552 N94-14491
A vertex-based finite-volume algorithm for the Navier-Stokes equations p 639 N94-14599
An implicit finite volume nodal point scheme for the solution of two-dimensional compressible Navier-Stokes equations p 640 N94-14603
Navier-Stokes simulation of transonic vortex flow over a delta wing p 640 N94-14606
A finite volume method for computation of viscous flow in complex configurations p 640 N94-14607

FINNED BODIES
Low-speed wind tunnel tests on a joined-wing aircraft model with various upper-fin
| NAL-TR-1169 | p 501 N94-13341

FINS
Measurements of wing and fin buffeting on the standard dynamics model
| IAR-AN-76 | p 526 N94-13859

FIR FILTERS
Exact reconstruction analysis/synthesis filter banks with time-varying filters
| NASA-CR-193725 | p 600 N94-13466
Digital quadrature demodulation for radar ESM applications
| DREO-TN-92-10 | p 603 N94-13838

FIRES
Coupled thermal response of objects and participating media in fires and large combustion systems
| DE93-012848 | p 561 N94-12819
A model for fuel fire duration and application to the B-1B bomber
| DE93-013000 | p 512 N94-14292

FISHES
Neurophysiological study on visuo-vestibular control of posture and movement in fish during adaptation to weightlessness p 591 N94-13759
Warm streamers extended from Warm Core Rings (WCR's) and their role on fish migration and fishing ground formation p 697 N94-14270

FISHING
Warm streamers extended from Warm Core Rings (WCR's) and their role on fish migration and fishing ground formation p 697 N94-14270

FIXED WINGS
Measurements of wing and fin buffeting on the standard dynamics model
| IAR-AN-76 | p 526 N94-13859

FIXTURES
Design and application of a quasistatic crush test fixture for investigating scale effects in energy absorbing composite plates
| NASA-CR-4526 | p 670 N94-13063

FLAME PROPAGATION
Flamespreading in granular solid propellant: Design of an experiment
| AD-A266009 | p 583 N94-12987
A coherent flame model of premixed turbulent combustion in a counterflow geometry
| CUED/A-THERMO/TR.60 | p 562 N94-13085
Effect of finite-rate chemistry and unequal Schmidt numbers on turbulent non-premixed flames modeled with single-step chemistry p 567 N94-14766

FLAME RETARDANTS
Flammability of clothing, volume 2
| DSIS-93-00036-VOL-2 | p 564 N94-13819
Review of test methods for material flammability
| DSIS-93-00480 | p 564 N94-13942
Synthetic lubricants and high-performance functional fluids: Phosphazenes
| ARL-TR-45 | p 580 N94-14126

FLAMES
Characterization of diamond film growth in a combustion flame
| AD-A266659 | p 816 N94-14839
FLAMMABILITY
Study on improvement of flammability, odor and offgassing tests for materials
| NASDA-CNT-930009 | p 563 N94-13471
Flammability of clothing, volume 2
| DSIS-93-00036-VOL-2 | p 564 N94-13819
Review of test methods for material flammability
| DSIS-93-00480 | p 564 N94-13942
FLAPPING
A survey of crack path stability criteria and their application to crack flapping phenomena in stiffened structures
| LR-681 | p 675 N94-13929
FLARE STARS
A photometric study of massive x-ray binaries
| ITN-93-85207 | p 829 N94-13231
FLAT PLATES
An analytical investigation of transient effects on rewetting of heated thin flat plates
| NASA-TM-106120 | p 628 N94-12968
Design and application of a quasistatic crush test fixture for investigating scale effects in energy absorbing composite plates
| NASA-CR-4526 | p 670 N94-13063
Experimental investigation of the effects of blowing ratio parameter on heat transfer to a film-cooled flat plate
| AD-A266599 | p 636 N94-13780
FLAT SURFACES
Determination of the surface cleanliness of metals by FT-IR spectroscopy
| DE93-013252 | p 565 N94-14525
FLEXIBILITY
Rigid-flexible printed wiring boards
| DE93-013938 | p 620 N94-13094
FLEXIBLE BODIES
Nonlinear damping model for flexible structures
| NASA-CR-193711 | p 539 N94-12790
Relegation for decentralized control
| AD-A265720 | p 819 N94-13059
Flex-gear electrical power transmission
| NASA-CR-194422 | p 661 N94-13445
Geometric stiffening in multibody dynamics formulations p 677 N94-14619
Stress stiffening and approximate equations in flexible multibody dynamics p 677 N94-14620
Some experiences with Krylov vectors and Lanczos vectors p 677 N94-14621
Computational Controls Workstation: Algorithms and hardware p 678 N94-14626
Animation of multi-flexible body systems and its use in control system design p 678 N94-14629
Spatial operator algebra for flexible multibody dynamics p 679 N94-14631
Nonrecursive formulations of multibody dynamics and concurrent multiprocessing p 679 N94-14632
Non-recursive augmented Lagrangian algorithms for the forward and inverse dynamics of constrained flexible multibodies p 679 N94-14633
Computational strategies in the dynamic simulation of constrained flexible MBS p 679 N94-14635
Real-time dynamics simulation of the Cassini spacecraft using DARTS. Part 1: Functional capabilities and the spatial algebra algorithm p 680 N94-14638
Control system design for flexible structures using data models p 527 N94-14646
PACE: A test bed for the dynamics and control of flexible multibody systems p 527 N94-14650
A program for the investigation of the Multibody Modeling, Verification, and Control Laboratory p 682 N94-14652
FLEXIBLE SPACECRAFT
Relegation for decentralized control
| AD-A265720 | p 819 N94-13059
Dynamics of adaptive structures: Design through simulations
| NASA-CR-193724 | p 540 N94-13112
Proceedings of the Fifth NASA/NSF/DOD Workshop on Aerospace Computational Control
| NASA-CR-194515 | p 677 N94-14618
Spatial operator algebra for flexible multibody dynamics p 679 N94-14631
An application of the IMC software to controller design for the JPL LSCL Experiment Facility p 681 N94-14645
Control structural interaction testbed: A model for multiple flexible body verification p 544 N94-14649
FLIGHT CHARACTERISTICS
Piloting Vertical Flight Aircraft: A Conference on Flying Qualities and Human Factors
| NASA-CP-3220 | p 521 N94-13294
ADS-33C related handling qualities research performed using the NRC Bell 205 airborne simulator p 521 N94-13295
MIL-H-8501B: Application to shipboard terminal operations p 521 N94-13296
Design criteria for integrated flight/propulsion control systems for STOVL fighter aircraft p 521 N94-13297
A perspective on the FAA approval process: Integrating rotorcraft displays, controls and workload p 521 N94-13298
Some lessons learned in three years with ADS-33C --- rotorcraft handling qualities specification p 521 N94-13299
A piloted simulation investigation of the normal load factor and longitudinal thrust required for air-to-air acquisition and tracking p 522 N94-13301
The application of active side arm controllers in helicopters p 522 N94-13302
Rotorcraft flying qualities improvement using advanced control p 522 N94-13303
The impact of flying qualities on helicopter operational agility p 522 N94-13304
In-flight simulation of high agility through active control: Taming complexity by design p 523 N94-13306
A model for rotorcraft flying qualities studies p 523 N94-13308
Interpreted Cooper-Harper for broader use p 523 N94-13309
Improvements in hover display dynamics for a combat helicopter p 523 N94-13310
Handling qualities effects of display latency p 517 N94-13316
Effects of simulator motion and visual characteristics on rotorcraft handling qualities evaluations p 524 N94-13317
Primary display latency criteria based on flying qualities and performance data p 525 N94-13318
Piloting considerations for terminal area operations of civil tiltwing and tiltrotor aircraft p 525 N94-13320
Design and pilot evaluation of the RAH-66 Comanche Core AFCS p 525 N94-13321
Design and pilot evaluation of the RAH-66 Comanche selectable control modes p 525 N94-13322
Flight testing and frequency domain analysis for rotorcraft handling qualities characteristics p 526 N94-13324
Qualitative investigation of a generic fighter model in radio controlled gliding flight
| LM-AA-003 | p 516 N94-13898
The flight performance of the Galileo orbiter USO p 611 N94-14398
FLIGHT CLOTHING
Evaluation of the Retrograde Inflation Anti-G Suit (RIAGS)
| AD-A265884 | p 736 N94-12935
FLIGHT CONTROL
Preliminary flight results of a fly-by-throttle emergency flight control system on an F-15 airplane
| NASA-TM-4503 | p 520 N94-13254
Actuator and aerodynamic modeling for high-angle-of-attack aeroservoelasticity
| NASA-TM-4493 | p 520 N94-13255
Piloting Vertical Flight Aircraft: A Conference on Flying Qualities and Human Factors
| NASA-CP-3220 | p 521 N94-13294
Design criteria for integrated flight/propulsion control systems for STOVL fighter aircraft p 521 N94-13297
Investigation of the effects of bandwidth and time delay on helicopter roll-axis handling qualities p 522 N94-13300
The application of active side arm controllers in helicopters p 522 N94-13302
Rotorcraft flying qualities improvement using advanced control p 522 N94-13303
A four-axis hand controller for helicopter flight control p 522 N94-13305
In-flight simulation of high agility through active control: Taming complexity by design p 523 N94-13306
Compatibility of information and mode of control: The case for natural control systems p 523 N94-13307
Visual information for judging temporal range p 524 N94-13314
Piloting considerations for terminal area operations of civil tiltwing and tiltrotor aircraft p 525 N94-13320
Preliminary design features of the RASCAL: A NASA /Army rotorcraft in-flight simulator p 526 N94-13325
Flight path control for the approach and landing of the quiet STOL experimental aircraft ASKA
| NAL-TR-1183 | p 513 N94-13457
Dynamic Forms. Part 1: Functions
| NASA-TP-3397 | p 596 N94-13790
Mongoose ASIC microcontroller programming guide
| NASA-RP-1319 | p 623 N94-13871
The development and flight test of a deployable precision landing system for spacecraft recovery
| NASA-TM-4525 | p 537 N94-14853
FLIGHT CREWS
Work/rest schedules and performance of S-3 aviators during fleet exercise
| AD-A265807 | p 734 N94-12975
FLIGHT ENVELOPES
The impact of flying qualities on helicopter operational agility p 522 N94-13304
FLIGHT INSTRUMENTS
Rover imaging system for the Mars rover/sample return mission
| NASA-CR-193413 | p 649 N94-13464
FLIGHT MANAGEMENT SYSTEMS
Flight crew interface aspects of forward-looking airborne windshear detection systems
| NASA-CR-191437 | p 516 N94-12829
Cognitive engineering in aerospace application: Pilot interaction with cockpit automation
| NASA-CR-177617 | p 510 N94-13247
FLIGHT MECHANICS
Activities of Institute for Aerospace Research, Flight Research Laboratory
| CTN-93-60832 | p 850 N94-13519
FLIGHT OPERATIONS
Flight operations highlights, tapes 1 and 2
| NASA-TM-109293 | p 850 N94-13633
FLIGHT PATHS
Flight path control for the approach and landing of the quiet STOL experimental aircraft ASKA
| NAL-TR-1183 | p 513 N94-13457
Ground Attack Profile Selector Program, version 3.0
| DSIS-93-00702 | p 753 N94-14207
FLIGHT RECORDERS
PC based A320 quick access recorder readout facility
| PD-AL-9109 | p 744 N94-13077
FLIGHT SAFETY
In-flight simulation of high agility through active control: Taming complexity by design p 523 N94-13306
Preliminary nuclear safety assessment of the NEPST (Topaz 2) space reactor program
| DE93-012853 | p 551 N94-13514
Activities report of the Federal Administration for Flight Safety (Germany)
| ETN-93-94208 | p 511 N94-14008
FLIGHT SIMULATION
Vertical motion simulator familiarization guide
| NASA-TM-103923 | p 527 N94-13008
A piloted simulation investigation of the normal load factor and longitudinal thrust required for air-to-air acquisition and tracking p 522 N94-13301
The application of active side arm controllers in helicopters p 522 N94-13302
In-flight simulation of high agility through active control: Taming complexity by design p 523 N94-13306
Interpreted Cooper-Harper for broader use p 523 N94-13309
Improvements in hover display dynamics for a combat helicopter p 523 N94-13310
The development and potential of inverse simulation for the quantitative assessment of helicopter handling qualities p 523 N94-13311
Visual cueing aids for rotorcraft landings p 524 N94-13313
Visual information for judging temporal range p 524 N94-13314
Visual cueing considerations in Nap-of-the-Earth helicopter flight head-slaved helmet-mounted displays p 524 N94-13315
Handling qualities effects of display latency p 517 N94-13316
Effects of simulator motion and visual characteristics on rotorcraft handling qualities evaluations p 524 N94-13317
Primary display latency criteria based on flying qualities and performance data p 525 N94-13318
Design and pilot evaluation of the RAH-66 Comanche Core AFCS p 525 N94-13321
Design and pilot evaluation of the RAH-66 Comanche selectable control modes p 525 N94-13322
Evaluation of two cockpit display concepts for civil tiltrotor instrument operations on steep approaches p 517 N94-13323
Control system design of a cable-mounted model used for dynamic wind tunnel testing
| NAL-TR-1161 | p 528 N94-13337
HELSCAM V2.0: Development and application guide
| DSIS-93-00137 | p 515 N94-13867
Laboratory simulation of spacecraft charging in the plasma wake region
| FFI-93-7007 | p 542 N94-14107
Ground Attack Profile Selector Program, version 3.0
| DSIS-93-00702 | p 753 N94-14207
FLIGHT SIMULATORS
ADS-33C related handling qualities research performed using the NRC Bell 205 airborne simulator p 521 N94-13295

Effects of simulator motion and visual characteristics on rotorcraft handling qualities evaluations
p 524 N94-13317
Preliminary design features of the RASCAL: A NASA /Army rotorcraft in-flight simulator p 526 N94-13325
Future developments of the NLR research flight simulator
[NLR-TP-92143-U] p 528 N94-13498
Simulator study of uncoupled control functions. Use of manual pointing modes when aiming at ground targets and oncoming airborne target
[FFA-TN-1992-18] p 528 N94-13588
Modis-N airborne simulator
[NASA-CR-194364] p 792 N94-13719

FLIGHT STABILITY TESTS
Flight evaluations of approach/landing navigation sensor systems: Summary of 1990 flight experiments
[NAL-TR-1175] p 513 N94-13344
Flight path control for the approach and landing of the quiet STOL experimental aircraft ASKA
[NAL-TR-1183] p 513 N94-13457

FLIGHT TEST INSTRUMENTS
Photogrammetric methods for trajectory measurements
[NLR-TP-91166-U] p 650 N94-13527

FLIGHT TESTS
TROPIX: A solar electric propulsion flight experiment
[NASA-TM-106297] p 534 N94-13028
Preliminary flight results of a fly-by-throttle emergency flight control system on an F-15 airplane
[NASA-TM-4503] p 520 N94-13254
Flight service evaluation of composite components on the Bell helicopter model 206L
[NASA-CR-191499] p 555 N94-13267
ADS-33C related handling qualities research performed using the NRC Bell 205 airborne simulator
p 521 N94-13295
In-flight simulation of high agility through active control: Taming complexity by design p 523 N94-13306
Flight testing and frequency domain analysis for rotorcraft handling qualities characteristics
p 526 N94-13324
Preliminary design features of the RASCAL: A NASA /Army rotorcraft in-flight simulator p 526 N94-13325
Flight evaluations of approach/landing navigation sensor systems: Summary of 1990 flight experiments
[NAL-TR-1175] p 513 N94-13344
Estimation of aircraft aerodynamic derivatives with the Total Least Squares Method
[NAL-TR-1150] p 502 N94-13392
Electromagnetic propulsion for spacecraft
[NASA-CR-191186] p 551 N94-13416
Modis-N airborne simulator
[NASA-CR-194364] p 792 N94-13719
Recent flight-test results of optical airdata techniques
[NASA-TM-4504] p 517 N94-13791
Flight validation of a pulsed smoke flow visualization system
[NASA-CR-186026] p 516 N94-14106
Methodology of Hypersonic Testing
[VKI-LS-1993-03] p 505 N94-14153
Aeropropulsion test and evaluation methods
p 506 N94-14165
Hypersonic flight test. Part 1: Propulsion flight testing
p 507 N94-14168
Hypersonic flight testing. Part 2: Aerothermal flight testing p 507 N94-14169
Extrapolation of ground test data to flight
p 507 N94-14170
The development and flight test of a deployable precision landing system for spacecraft recovery
[NASA-TM-4525] p 537 N94-14853
Performance seeking control: Program overview and future directions
[NASA-TM-4531] p 519 N94-14855

FLIGHT TRAINING
Work/rest schedules and performance of S-3 aviators during fleet exercise
[AD-A265807] p 734 N94-12975

FLOAT ZONES
Growth of semiconductor compound single crystal InSb by floating zone method (M-3) p 586 N94-13735
Growth of samarskite crystal under microgravity conditions (M-20) p 590 N94-13752

FLOODS
Sea surface temperature forcing and phase locking of Nordeste precipitation
[DE93-011873] p 723 N94-14426

FLOQUET THEOREM
Stability of oscillatory two phase Couette flow
[NASA-CR-191501] p 636 N94-13817

FLOW CHAMBERS
Flamespreading in granular solid propellant: Design of an experiment
[AD-A266009] p 583 N94-12987

FLOW CHARACTERISTICS
Numerical simulations and experiments on physics of high Mach number shockwave: Turbulent flow interactions
[DE93-013424] p 631 N94-13249
Flow limitation and flutter in membrane walled collapsible tubes: A model for expiratory wheezing
[ISBN-0-315-73875-8] p 635 N94-13662
Design and evaluation of single and dual flow thrust vector nozzles with post exit vanes
[NASA-CR-193393] p 638 N94-14086
Characterization of flow fields in hypersonic ground test facilities p 505 N94-14157
Search for subgrid scale parameterization by projection pursuit regression p 643 N94-14749

FLOW DISTRIBUTION
Turbulence modeling of free shear layers for high-performance aircraft
[NASA-CR-193659] p 520 N94-12799
Large-eddy simulation of laminar-turbulent breakdown at high speeds with dynamic subgrid-scale modeling
[NASA-CR-4533] p 629 N94-13064
A wall interference assessment/correction system
[NASA-CR-194174] p 500 N94-13076
Averaging techniques for steady and unsteady calculations of a transonic fan stage
[NASA-TM-106231] p 499 N94-13108
Interacting scales and energy transfer in isotropic turbulence
[NASA-CR-191477] p 630 N94-13133
Colorimetric qualification of shear sensitive liquid crystal coatings
[NASA-CR-194126] p 806 N94-13291
Some flow properties of telescope enclosures estimated from water channel tests: Application of the flow visualization techniques
[NAL-TR-1178T] p 830 N94-13452
A three-dimensional supersonic turbulent boundary layer generated by an isentropic compression
p 503 N94-13556
Calculation of hypersonic shock structure using flux-split algorithms
[NASA-CR-194296] p 504 N94-13607
Rotor stator CGI
[NASA-TM-109313] p 518 N94-13608
Recent flight-test results of optical airdata techniques
[NASA-TM-4504] p 517 N94-13791
A computational study of the base region flow field for the M865 projectile
[ARL-TR-109] p 504 N94-13795
Images constructed from computed flow fields
[NASA-CR-194397] p 650 N94-13814
Numerical investigations in three-dimensional internal flows
[NASA-CR-194143] p 637 N94-13827
Results of experimental investigations to determine external tank protuberance loads using a 0.03-scale model of the Space Shuttle launch configuration (Model 47-OTS) in the NASA/ARC unitary plan wind tunnel, volume 2
[NASA-CR-167691] p 536 N94-14047
Design and evaluation of single and dual flow thrust vector nozzles with post exit vanes
[NASA-CR-193393] p 638 N94-14086
Characterization of flow fields in hypersonic ground test facilities p 505 N94-14157
Hypersonic flow field measurements: Intrusive
p 507 N94-14166
Hypersonic flow-field measurements: Nonintrusive
p 507 N94-14167
Numerical simulation of velocity-coupled combustion response of solid rocket propellants
p 585 N94-14490
Analysis of reacting flowfields in low-thrust rocket engines and plumes p 552 N94-14491
Advanced ballistic range technology
[NASA-CR-194530] p 533 N94-14540
The structure of laminar flow in a three-dimensional driven cavity p 640 N94-14601
Vibrational relaxation in hypersonic flow fields
[NASA-TP-3367] p 776 N94-14733
Low altitude plume impingement handbook
[NASA-CR-194193] p 643 N94-14741
The structure of intense vorticity in homogeneous isotropic turbulence p 643 N94-14747
Effect of finite-rate chemistry and unequal Schmidt numbers on turbulent non-premixed flames modeled with single-step chemistry p 567 N94-14766
The 3D pneumatic and 2D dynamic probes: Their development and subsequent use in a transonic fan
[RAE-TM-AERO/PROP-22] p 653 N94-14827
The development of a scalable parallel 3-D CFD algorithm for turbomachinery
[NASA-CR-193604] p 664 N94-14848

FLOW EQUATIONS
Thermal gravitational modelling and scaling of two-phase heat transport systems: Similarity considerations and useful equations predictions versus experimental results
[NLR-TP-91477-U] p 632 N94-13533
Preconditioning and the limit to the incompressible flow equations
[NASA-CR-191500] p 769 N94-13717
The method of Laplace Transform MultiQuadrics (LTMQ) for the solution of the groundwater flow equation
[DE93-010408] p 637 N94-14053
Proceedings of the Fluid Dynamics Symposium in honour of Professor R. Narasimha on his 60th birthday
[NAL-SP-9315] p 639 N94-14598
Development of full-potential codes in the decade 1983-1993 p 639 N94-14600
Review of mathematical and physical basis of two-phase flow modeling
[KFK-4759] p 642 N94-14708

FLOW MEASUREMENT
Three-dimensional structure of straight and curved plane wakes
[NASA-CR-194420] p 501 N94-13266
Hypersonic flow field measurements: Intrusive
p 507 N94-14166
Hypersonic flow-field measurements: Nonintrusive
p 507 N94-14167
NASA metrology and calibration, 1993
[NASA-TM-109280] p 597 N94-14410
An experimental study of a turbulent boundary layer in the trailing edge region of a curculation-control airfoil
[NASA-CR-194522] p 508 N94-14541
Investigation of the feasibility of optical diagnostic measurements at the exit of the SSME
[NASA-CR-193832] p 553 N94-14682
Intra-blade quantitative transonic flow measurements at the DRA Pyestock Isentropic Light Piston Facility using PIV (Particle Image Velocimetry)
[RAE-TM-AERO/PROP-21] p 509 N94-14706

FLOW STABILITY
High speed transition prediction
[NASA-CR-194125] p 502 N94-13422
Studies of turbulent shear flows and their control
[NASA-CR-194114] p 635 N94-13676
Evolution of disturbances in stagnation point flow
[NASA-CR-191516] p 636 N94-13724
Stability of oscillatory two phase Couette flow
[NASA-CR-191501] p 636 N94-13817
The phenomenon of vortex breakdown
p 510 N94-14609
Linear instability of curved free shear layers
[NASA-TM-106290] p 642 N94-14729
The structure of intense vorticity in homogeneous isotropic turbulence p 643 N94-14747

FLOW VELOCITY
On the theory of the decaying developed turbulence with spontaneous parity violation
[DE93-623190] p 632 N94-13511
Widebody cabin water spray optimization tests
[DOT/FAA/CT-TN93/29] p 511 N94-14186
Effects of growth conditions and substrate orientation on the properties of InSb
[DE93-013766] p 812 N94-14344
Upgrading of raw natural gas using high-performance polymer membranes
[DE93-014041] p 566 N94-14586

FLOW VISUALIZATION
Colorimetric qualification of shear sensitive liquid crystal coatings
[NASA-CR-194126] p 806 N94-13291
Exploratory study of in-plane streamline curvature effects on a turbulent boundary layer at a Mach number of 3
[NASA-CR-193673] p 501 N94-13292
Low-speed wind tunnel tests on a joined-wing aircraft model with various upper-fin
[NAL-TR-1169] p 501 N94-13341
Some flow properties of telescope enclosures estimated from water channel tests: Application of the flow visualization techniques
[NAL-TR-1178T] p 830 N94-13452
Hypersonic aerodynamic characteristics of SSTO-type aerospace planes. Part 1: The NAL 0-th configuration
[NAL-TR-1186] p 514 N94-13459
A three-dimensional supersonic turbulent boundary layer generated by an isentropic compression
p 503 N94-13556
Marangoni effect induced convection in material processing under microgravity (M-18)
p 589 N94-13750
Images constructed from computed flow fields
[NASA-CR-194397] p 650 N94-13814
Flow-field interference produced by an asymmetrical support strut
[IAR-AN-75] p 504 N94-14031

Experimental studies of vortex flaps and vortex plates. Part 1: 0.53 m span 60 deg delta wing
| DE93-767969 | p 505 N94-14059
Advanced ballistic range technology
| NASA-CR-194396 | p 532 N94-14068
Design and evaluation of single and dual flow thrust vector nozzles with post exit vanes
| NASA-CR-193393 | p 638 N94-14086
Flight validation of a pulsed smoke flow visualization system
| NASA-CR-186026 | p 516 N94-14106
Hypersonic flow field measurements: Intrusive p 507 N94-14166
An overview of parallel scientific visualization
| DE93-017105 | p 755 N94-14521
Intra-blade quantitative transonic flow measurements at the DRA Pyestock Isentropic Light Piston Facility using PIV (Particle Image Velocimetry)
| RAE-TM-AERO/PROP-21 | p 509 N94-14706
Interaction of two glancing, crossing shock waves with a turbulent boundary-layer at various Mach numbers
| NASA-TM-103740 | p 509 N94-14780

FLUENCE
Search for ultra-high-energy radiation from gamma-ray bursts
| DE93-012721 | p 847 N94-12964
Novel oxygen atom source for material degradation studies
| NASA-CR-191323 | p 562 N94-13115
Measurement of the Fe-56(n,p)Mn-56, Al-27(n,p)Mg-27 and Al-27(n,alpha)Na-24 cross sections at 16.0, 17.0 and 18.3 MeV
| NPL-RSA(EXT)-38 | p 783 N94-13883
UV and IR laser ablation for inductively coupled plasma mass spectrometry
| DE93-017124 | p 658 N94-14415

FLUID BOUNDARIES
Analysis, approximation, and computation of a coupled solid/fluid temperature control problem
| NASA-TM-106351 | p 771 N94-14731

FLUID DYNAMICS
Studies of turbulent shear flows and their control
| NASA-CR-194114 | p 635 N94-13676
Research and technoloqhy highlights, 1992
| NASA-TM-4452 | p 850 N94-13962
Flight validation of a pulsed smoke flow visualization system
| NASA-CR-186026 | p 516 N94-14106
Hypersonic overview p 505 N94-14154
A study of thin liquid sheet flows
| NASA-TM-106323 | p 642 N94-14732

FLUID FILMS
Cryogenic fluid film bearing tester development study
| NASA-CR-192586 | p 660 N94-12791
A study of thin liquid sheet flows
| NASA-TM-106323 | p 642 N94-14732

FLUID FILTERS
Evaluation for membrane components of water recycling system
| NAL-TM-646 | p 737 N94-13388

FLUID FLOW
The method of Laplace Transform MultiQuadrics (LTMQ) for the solution of the groundwater flow equation
| DE93-010408 | p 637 N94-14053

FLUID JETS
The motion of a conical shaped liner driven by explosive load
| ITN-93-85215 | p 585 N94-14507
Analytical description of the breakup of liquid jets in air
| NASA-CR-191503 | p 647 N94-14849

FLUID MANAGEMENT
CFM technologies for space transportation: Multipurpose hydrogen testbed system definition and tank procurement
| NASA-CR-194355 | p 539 N94-12827

FLUID MECHANICS
Modulational stability of periodic solutions of the Kuramoto-Sivaskinsky equation
| NASA-CR-191502 | p 628 N94-12888
The method of Laplace Transform MultiQuadrics (LTMQ) for the solution of the groundwater flow equation
| DE93-010408 | p 637 N94-14053
JPRS report: Science and technology. Central Eurasia: Engineering and equipment
| JPRS-UEQ-93-006 | p 776 N94-14431

FLUID-SOLID INTERACTIONS
Thermodynamic status of static and dynamic contact angles
| ISBN-0-315-73844-8 | p 817 N94-13554
An 8-node axisymmetric acoustic finite element for non-axisymmetric fluid-structure interaction analysis
| FFA-TN-1993-03 | p 673 N94-13689
Analysis, approximation, and computation of a coupled solid/fluid temperature control problem
| NASA-TM-106351 | p 771 N94-14731

FLUORESCENCE
Ultra-soft x ray absorption spectroscopy: A bulk and surface probe of materials
| DE93-014325 | p 566 N94-14582

FLUORINE ORGANIC COMPOUNDS
Schemes for the use of conducting polymers as active materials in electrochemical supercapacitors
| DE93-012713 | p 580 N94-14179

FLUOROPOLYMERS
Highly fluorinated polymers
| NASA-CR-194147 | p 579 N94-13964

FLUTTER
On curve veering and flutter of rotating blades
| NASA-TM-106282 | p 670 N94-12872
Flow limitation and flutter in membrane walled collapsible tubes: A model for expiratory wheezing
| ISBN-0-315-73875-8 | p 635 N94-13662

FLUTTER ANALYSIS
A method of predicting quasi-steady aerodynamics for flutter analysis of high speed vehicles using steady CFD calculations
| NASA-TM-109009 | p 514 N94-12850
On curve veering and flutter of rotating blades
| NASA-TM-106282 | p 670 N94-12872
Estimation of critical values and vibration characteristics on supersonic delta wings. Part 2: Locally-stationary time series analysis of nonstationary random responses
| NAL-TR-1179 | p 502 N94-13345

FLUX (RATE)
Phobos/Harp post launch support
| NASA-CR-193676 | p 540 N94-13109

FLUX DENSITY
Advanced electric motor technology flux mapping
| NASA-CR-193824 | p 621 N94-13186
Meteoroid environment near the Earth-Moon system
| NASA-CR-193670 | p 835 N94-13203
Schemes for the use of conducting polymers as active materials in electrochemical supercapacitors
| DE93-012713 | p 580 N94-14179
Radiation perturbation theory in gravity and quantum universe as a hydrogen atom
| DE93-626621 | p 849 N94-14889

FLUX PINNING
Flux-pinning related defect structures in melt-processed YBa2Cu3O(7-x)
| DE93-012759 | p 804 N94-12818
The study of structure-processing-property relations in copper oxide based high (Tc) superconductors
| DE93-015066 | p 804 N94-13003

FLUX VECTOR SPLITTING
Calculation of hypersonic shock structure using flux-split algorithms
| NASA-CR-194296 | p 504 N94-13607
A comparison of computational and experimental data for a subscale high speed propulsive nozzle at low mach numbers
| AD-A266543 | p 504 N94-13705

FLY BY WIRE CONTROL
Preliminary flight results of a fly-by-throttle emergency flight control system on an F-15 airplane
| NASA-TM-4503 | p 520 N94-13254

FLYWHEELS
Technology assessments of advanced energy storage systems for electric and hybrid vehicles
| DE93-014395 | p 701 N94-12913

FOAMS
A multiphase model for shock-induced flow in low density foam
| DE93-013767 | p 632 N94-13397

FOCAL PLANE DEVICES
Using a focal-plane array to estimate antenna pointing errors
| NASA-CR-194502 | p 602 N94-13810
Gamma-insensitive optical focal plane array
| DE93-013100 | p 792 N94-14317

FOG
Infrared transmission and path radiance through dust and fog
| AD-A265825 | p 791 N94-12979
An algorithm for the remote sensing of fog using satellite-data and additional information
| DLR-FB-92-23 | p 688 N94-14135

FOKKER-PLANCK EQUATION
Nonlinear damping model for flexible structures
| NASA-CR-193711 | p 539 N94-12790

FOLDING STRUCTURES
Folded waveguide designs for tokamaks
| DE93-013274 | p 798 N94-13577

FORCE DISTRIBUTION
Techniques for estimating Space Station aerodynamic characteristics
| NASA-CR-193394 | p 541 N94-13955

FORCE-FREE MAGNETIC FIELDS
Force-free magnetic fields, curl eigenfunctions, and the sphere in transform space, with applications to fluid dynamics and electromagnetic theory
| AD-A265805 | p 834 N94-12971

FORECASTING
Snow cover models in operational watershed forecasting
| DE93-778332 | p 718 N94-12837
Circulation model experiments of the Gulf Stream using satellite-derived fields
| AD-A266067 | p 725 N94-12990
Application of satellite remote sensing technology in disaster mitigation: A case study of Bangladesh p 692 N94-14238

FOREST FIRE DETECTION
Multisensor remote sensing data and GIS techniques for monitoring preservation areas: A case study
| INPE-5317-PRE/1714 | p 688 N94-14131

FOREST MANAGEMENT
Dendrometric variables estimation in homogeneous forests using LANDSAT TM data
| INPE-5455-TDI/497 | p 684 N94-13331
Forest management for fixing and sequestering carbon
| DE93-013520 | p 707 N94-13486
Multi-source national forest inventory of Finland p 694 N94-14254
Global assessment of human activities p 695 N94-14255
The Swedish ISY contribution p 695 N94-14256
Vegetation mapping of Indo-China Peninsula using MOS-1 MESSR and NOAA AVHRR p 695 N94-14257
Remote sensing for monitoring tropical moist forests in the Indo-Chinese region p 695 N94-14258
Mangrove afforestation monitoring using remote sensing p 695 N94-14260
Pattern and Process in Landscape Ecology: Eighth Annual US Landscape Ecology Symposium
| DE93-014032 | p 711 N94-14859

FORESTS
Dendrometric variables estimation in homogeneous forests using LANDSAT TM data
| INPE-5455-TDI/497 | p 684 N94-13331
Forest management for fixing and sequestering carbon
| DE93-013520 | p 707 N94-13486
Moisture meter evaluation
| DE93-016581 | p 652 N94-14534

FORMALDEHYDE
Theoretical molecular studies of astrophysical interest
| NASA-CR-193300 | p 838 N94-13781

FORMALISM
Dynamic Forms. Part 1: Functions
| NASA-TP-3397 | p 596 N94-13790
Wake-field and space charge effects on high brightness beams calculations and measured results for the laser driven photoelectrons at BNL-ATF
| DE93-015787 | p 659 N94-14572

FORMAT
Specimen files in VAMAS standard data transfer format (EXAMPLE 1.TXT to EXAMPLE 4.TXT)
| NPL-DMM(A)-90 | p 749 N94-13688

FORMING TECHNIQUES
Processing and mechanical properties of silicon carbide platelet reinforced alumina composites p 556 N94-13557
Polymer infiltration studies
| NASA-CR-194521 | p 582 N94-14539

FORTRAN
FORTRAN graphics routines for the Macintosh
| DE93-013092 | p 742 N94-12864
ASTEC and MODEL: Controls software development at Goddard Space Flight Center p 678 N94-14628
Splines, contours and SVD subroutines
| DE93-016088 | p 757 N94-14866

FORWARD SCATTERING
Meteor forward scatter studies
| DSIS-93-00382 | p 602 N94-13801
A study of meteor scatter communications
| DSIS-93-00151 | p 603 N94-13841

FOSSIL FUELS
Ocean uptake of carbon dioxide
| DE93-012967 | p 707 N94-13384
The role of human activity and land use change in atmospheric chemistry and air quality
| DE93-011871 | p 709 N94-14022
Summary of conclusions and recommendations from a visibility science workshop
| DE93-012770 | p 710 N94-14523

FOSSILS
Organic Geochemical and tectonic evolution of the Midcontinent Rift system
| DE93-015093 | p 717 N94-14338

FOUR-WAVE MIXING
Nonlinear laser spectroscopy studies of semiconductor heterostructures
[AD-A265728] p 805 N94-13037
FOURIER TRANSFORMATION
Force-free magnetic fields, curl eigenfunctions, and the sphere in transform space, with applications to fluid dynamics and electromagnetic theory
[AD-A265805] p 834 N94-12971
Solid state laser systems for space application
[NASA-CR-194133] p 656 N94-13420
A Fourier transform microscope for x ray and/or gamma ray imaging
[AD-D015742] p 791 N94-13664
Imaging Fourier transform spectrometer
[DE93-017193] p 651 N94-14416
Liquid and gas evanescent wave spectroscopy via tunable lasers and silver halide fibers
[ITN-93-85226] p 585 N94-14465
Determination of the surface cleanliness of metals by FT-IR spectroscopy
[DE93-013252] p 565 N94-14525
Image reconstruction for x ray holographic microscopy
[DE93-013094] p 653 N94-14772
FRACTALS
Analysis of interstellar cloud structure based on IRAS images
[NASA-CR-194341] p 836 N94-13332
Self organized criticality
[DE93-013182] p 773 N94-14320
FRACTIONATION
Deposition of impact-generated vapors in the lunar regolith p 843 N94-14302
UV and IR laser ablation for inductively coupled plasma mass spectrometry
[DE93-017124] p 658 N94-14415
The first steps of chlorophyll synthesis: RNA involvement and regulation
[DE93-014398] p 730 N94-14509
FRACTOGRAPHY
Fracture behavior of vanadium/vanadium silicide in-situ composites
[DE93-013422] p 556 N94-13389
Role of microstructure on fatigue durability of aluminum aircraft alloys
[AD-A266350] p 571 N94-13697
FRACTURE MECHANICS
Role of microstructure on fatigue durability of aluminum aircraft alloys
[AD-A265627] p 568 N94-12993
Development of nondestructive evaluation methods and prediction of effects of flaws on the fracture behavior of structural ceramics
[DE93-012942] p 577 N94-13032
Fracture behavior of vanadium/vanadium silicide in-situ composites
[DE93-013422] p 556 N94-13389
Processing and mechanical properties of silicon carbide platelet reinforced alumina composites
p 556 N94-13557
Investigation of criteria for ductile fracture under fully-plastic conditions p 672 N94-13593
Computational methods for reliable fatigue and damage tolerance dimensioning of aircraft structures
[FFA-TN-1993-05] p 515 N94-13690
Review of Canadian aeronautical fatigue work, 1991-1993
[LTR-ST-1932] p 674 N94-13861
Thermal shock resistance of ceramic matrix composites
[NASA-CR-189136] p 557 N94-13920
An investigation of the role of second phase particles in the design of ultra high strength steels of improved toughness
[AD-A266774] p 573 N94-14786
A study of hydrogen effects on fracture behavior of radioactive waste storage tanks
[DE93-018171] p 574 N94-14873
FRACTURE STRENGTH
Fracture behavior of vanadium/vanadium silicide in-situ composites
[DE93-013422] p 556 N94-13389
Modern aluminium sheet alloys for aerospace applications
[NLR-TP-92057-U] p 570 N94-13497
Processing and testing of high toughness silicon nitride ceramics
[NASA-CR-191190] p 582 N94-14543
A study of fiber volume fraction effects in notched unidirectional SCS-6/Ti-15V-3Cr-3Al-3Sn composite
[NASA-CR-191165] p 559 N94-14769
An investigation of the role of second phase particles in the design of ultra high strength steels of improved toughness
[AD-A266774] p 573 N94-14786
FRACTURING
Nonlinear wave predictions in ceramics
[DE93-016516] p 582 N94-14436
FRAGMENTATION
Semiempirical fragmentation models on galactic cosmic ray transport calculations with hydrogen target
[NASA-TP-3350] p 847 N94-13263
FREE BOUNDARIES
Heat flows and harmonic maps with a free boundary
[DE93-622856] p 632 N94-13509
FREE CONVECTION
Contributions to numerical solution of Navier-Stokes equations in two and three dimensional flows
[ETN-93-94395] p 647 N94-14816
FREE ELECTRON LASERS
Microwave generation for magnetic fusion energy applications
[DE93-013864] p 654 N94-13058
Predicted performance of a dc beam driven FEM oscillator designed for fusion applications at 200-250 GHz
[DE93-013414] p 655 N94-13145
Multi-bunch beam-break-up studies for a SWFEL/TBA
[DE93-016973] p 658 N94-14414
The standing wave FEL/TBA: Realistic cavity geometry and energy extraction
[DE93-016972] p 659 N94-14520
Adiabatic and non adiabatic effects in Free Electron Laser (FEL) non linear interactions
[ITN-93-85224] p 659 N94-14547
FREE FLIGHT
Development of experimental demonstration processes for laminar-turbulent flow states at wing profiles in free flight
[ILR-MITT-280(1993)] p 510 N94-14800
FREE FLOW
High freestream turbulence effects on the transport of heat and momentum p 633 N94-13559
Recent flight-test results of optical airdata techniques
[NASA-TM-4504] p 517 N94-13791
FREE MOLECULAR FLOW
Techniques for estimating Space Station aerodynamic characteristics
[NASA-CR-193394] p 541 N94-13955
FREE RADICALS
Infrared absorption spectroscopy and chemical kinetics of free radicals
[DE93-015078] p 562 N94-13004
Infrared spectroscopy of organic free radicals related to combustion processes
[DE93-017086] p 562 N94-13222
FREEZING
Monte Carlo simulation of the OCP freezing transition
[DE93-013039] p 811 N94-14313
Ionic conductivity of alkali halides and their mixtures near liquid-solid phase transition
[ITN-93-85222] p 566 N94-14558
FRENCH SPACE PROGRAM
Characteristics of the amateur radio means of the Arsene satellite
[CNES-NT-131] p 605 N94-13950
FREQUENCIES
Rotordynamic and leakage characteristics of a 4-stage brush seal
[AD-A266012] p 660 N94-12988
FREQUENCY ASSIGNMENT
New challenges in propagation research in the US
p 612 N94-14656
FREQUENCY DISCRIMINATORS
Envelope and instantaneous frequency estimation of narrowband modulated signals
[DREO-TN-92-3] p 605 N94-14033
FREQUENCY DISTRIBUTION
Testing various time-frequency distribution techniques
[DREO-TN-92-17] p 606 N94-14062
FREQUENCY DIVISION MULTIPLE ACCESS
Technical support for digital systems technology development. Task order 1: ISP contention analysis and control
[NASA-CR-190758] p 537 N94-12809
User needs for propagation data p 613 N94-14657
FREQUENCY DIVISION MULTIPLEXING
Coverage aspects of a single frequency network designed for digital audio broadcasting
[BBC-RD-1993/3] p 616 N94-14742
FREQUENCY HOPPING
Fine time uplink synchronization for frequency-hopped spread spectrum satellite communication system
[ISBN-0-315-54370-1] p 600 N94-13488
Simulation of downlink synchronization for a frequency-hopped satellite communication system
[DSIS-93-00477] p 605 N94-13941
FREQUENCY MEASUREMENT
Some frequency and damping measurements of laminated beryllium beams
[DE93-015909] p 676 N94-14530
Activities report of the National Electrotechnical Institute Galileo Ferraris
[ETN-93-94224] p 627 N94-14812
FREQUENCY MODULATION
Envelope and instantaneous frequency estimation of narrowband modulated signals
[DREO-TN-92-3] p 605 N94-14033
Coverage aspects of a single frequency network designed for digital audio broadcasting
[BBC-RD-1993/3] p 616 N94-14742
FREQUENCY RANGES
Electrical characterization of the JET A(sub 2) antenna: Comparison of model with measurements Wade, T.
[DE93-012964] p 607 N94-14291
FREQUENCY RESPONSE
A rational interpolation method to compute frequency response p 681 N94-14644
FREQUENCY SCANNING
Optimization of a subband coding for high definition television with motion controlled three dimensional frequency band decomposition
[ETN-93-94396] p 617 N94-14817
FREQUENCY SHIFT
Trellis coding with Continuous Phase Modulation (CPM) for satellite-based land-mobile communications
[NASA-CR-191325] p 604 N94-13909
Multiple-symbol differential detection of DPSK with frequency offset
[DREO-TN-92-5] p 606 N94-14063
FREQUENCY STABILITY
Stability measurements of the radio science system at the 34-m high-efficiency antennas p 609 N94-14381
The flight performance of the Galileo orbiter USO
p 611 N94-14398
FRESNEL REFLECTORS
Horizontal-cavity surface-emitting lasers, superluminescent LEDs, and amplifiers, and parabolic gain unstable resonator semiconductor lasers
p 656 N94-13573
FRETTING
Autofrettage: Stress distribution under load and retained stresses after depressurization. A modified plane-strain case
[AD-A266320] p 671 N94-13579
FRICTION
Molecular solvent-dynamical effects on activated electron-transfer kinetics: How important is solvent friction?
[AD-A265886] p 779 N94-12894
FRICTION MEASUREMENT
A technique for direct measurement of skin friction in supersonic combustion flow p 503 N94-13555
FROGS
Amphibian fertilization and development in microgravity p 594 N94-13770
FROUDE NUMBER
Effects of surface thermal forcing on stratified flow past an isolated obstacle p 633 N94-13553
FUEL CELL POWER PLANTS
Molten carbonate fuel cell product development test environmental assessment/protection plan
[DE93-000288] p 702 N94-13380
FUEL CELLS
Carbonate fuel cell endurance: Hardware corrosion and electrolyte management status
[DE93-013800] p 701 N94-13093
Molten carbonate fuel cell product development test environmental assessment/protection plan
[DE93-000288] p 702 N94-13380
Electrocatalysis issues in polymer electrolyte fuel cells
[DE93-014450] p 702 N94-13402
Performance effects of coal-derived contaminants on the carbonate fuel cell
[DE93-013801] p 703 N94-13693
Status of SOFC development in USA
[DE93-015568] p 704 N94-14355
FUEL COMBUSTION
Combustor technology for future small gas turbine aircraft
[NASA-TM-106312] p 517 N94-13142
Numerical studies of spray combustion in liquid-fueled engines p 564 N94-13685
Three-dimensional modeling of diesel engine intake flow, combustion and emissions-2
[NASA-CR-191189] p 519 N94-14448
Comparative ignition of hexane and octane isomers in a shock tube
[DE93-016535] p 566 N94-14869
FUEL CONSUMPTION
Trajectory optimization for the national aerospace plane
[NASA-CR-194146] p 516 N94-14104

FUEL CONTROL
Techniques for improving the performance of a simplified electronic fuel controller with incremental actuation for small gas turbine engines
[ISBN-0-315-56062-2] p 661 N94-13521

FUEL CORROSION
Review of nuclear thermal propulsion carbide reactor fuel corrosion and exhibit
[DE93-016605] p 585 N94-14535

FUEL INJECTION
A computer model for liquid jet atomization in rocket thrust chambers
[NASA-CR-194194] p 627 N94-12803
Effects of hydrogen addition on combustion performance of a LOX/kerosene rocket
[NAL-TR-1177] p 548 N94-12945
Combustor technology for future small gas turbine aircraft
[NASA-TM-106312] p 517 N94-13142

FUEL PRODUCTION
Biofuels for transportation: The road from research to the marketplace
[DE93-000091] p 585 N94-14454

FUEL SPRAYS
A computer model for liquid jet atomization in rocket thrust chambers
[NASA-CR-194194] p 627 N94-12803
Numerical studies of spray combustion in liquid-fueled engines p 564 N94-13685

FUEL SYSTEMS
A model for fuel fire duration and application to the B-1B bomber
[DE93-013000] p 512 N94-14292

FUEL TESTS
Space reactor fuel element testing in upgraded TREAT
[DE93-012524] p 554 N94-14806

FULL SCALE TESTS
Technical Evaluation Motor No. 10 (TEM-10)
[NASA-CR-193846] p 554 N94-14907

FULLERENES
Empirical tight-binding parameters for solid C(sub 60)
[DE93-623061] p 807 N94-13510
Is K3C60 a line phase?
[DE93-016700] p 813 N94-14517
Electronic states in systems of reduced dimensionality
[DE93-014440] p 815 N94-14739

FUNCTIONAL DESIGN SPECIFICATIONS
Creating a strategic plan for configuration management using computer aided software engineering (CASE) tools
[DE93-013663] p 746 N94-13394
Functional categories for future flight deck designs
[NASA-TM-109005] p 517 N94-13710
Formal functional test designs with a test representation language p 609 N94-14383

FUNCTIONS (MATHEMATICS)
On the foundations of final semantics: Non-standard sets, metric spaces, partial orders
[CWI-CS-R9241] p 768 N94-13526
On the differential structure of matrix-valued rational inner functions
[CWI-BS-R9228] p 770 N94-14003

FURNACES
Adaptive control of interface by temperature and interface profile feedback in transparent multi-zone crystal growth furnace
[NASA-CR-194140] p 762 N94-13253

FUSELAGES
Some computational tools for the analysis of through cracks in stiffened fuselage shells
[LR-701] p 673 N94-13726
Compressive buckling of curved, anisotropic panels stiffened in two directions. Part 1: Derivation of the governing equations
[LR-694] p 675 N94-13931
MSD in fuselage lap joints: Requirements for inspection intervals for typical fuselage lap joint panels with Multiple Site Damage
[LR-697] p 675 N94-13986

FUSION (MELTING)
The Lindemann criterion of melting for pure and mixed ionic crystals
[ITN-93-85210] p 814 N94-14554

FUSION REACTORS
Growth curve analysis for plasma profiles using smoothing splines
[DE93-015741] p 795 N94-12984
Equilibrium reconstruction of the q-profile in tokamaks from motional Stark effect data
[DE93-015815] p 796 N94-13046
Physics of gas breakdown for ion beam transport in gas
[DE93-015646] p 801 N94-14349

FUSION WEAPONS
Inertial Confinement Fusion
[DE93-013303] p 795 N94-13017

FUZZY SETS
Supervised classification of remotely sensed images
[DLR-FB-92-07] p 700 N94-14428

FUZZY SYSTEMS
JTEC Panel report on knowledge-based systems in Japan
[PB93-170124] p 820 N94-12801

G

GADOLINIUM
Canted magnetic moments at the Gd(0001) surface
[DE93-014327] p 805 N94-13102

GALACTIC BULGE
The spectroscopic evolution of novae in the bulge of M31 and a search for their possible origin in the M31 globular cluster system p 831 N94-13668

GALACTIC CLUSTERS
Studies of gas in cooling flow clusters
[NASA-CR-193597] p 628 N94-12959
Redshift distortions of galaxy correlation functions
[DE93-014007] p 834 N94-12980
ROSAT: X ray survey of compact groups
[NASA-CR-193297] p 829 N94-13181
UV extinction properties of carina nebular dust
[NASA-CR-193424] p 835 N94-13233
A photometric and morphological study of compact groups of galaxies and their environments
[ISBN-0-315-59601-5] p 829 N94-13370
Sampling of globular clusters and the distance to the galactic center
[INPE-5446-TDI/492] p 837 N94-13449
ROSAT observations of clusters with wide-angle tailed radio sources
[NASA-CR-193784] p 833 N94-14405

GALACTIC COSMIC RAYS
Cosmic physics data analysis program
[NASA-CR-194357] p 846 N94-12826
Effects of radiobiological uncertainty on vehicle and habitat shield design for missions to the moon and Mars
[NASA-TP-3312] p 846 N94-12875
Semiempirical fragmentation models on galactic cosmic ray transport calculations with hydrogen target
[NASA-TP-3350] p 847 N94-13263

GALACTIC EVOLUTION
On inhomogeneous halo collapse and the globular cluster metallicity gradient
[DE93-013090] p 834 N94-13011
A near-infrared faint galaxy survey: Evolution and the cosmological geometry from K band photometry p 830 N94-13591
The reionization of the intergalactic medium p 838 N94-13651

GALACTIC HALOS
The onset of galactic winds in early-type galaxies
[NASA-CR-193640] p 836 N94-13446
Cold dark matter halos p 838 N94-13649
The first data from the MACHO experiment
[DE93-014423] p 840 N94-14467

GALACTIC MASS
The onset of galactic winds in early-type galaxies
[NASA-CR-193640] p 836 N94-13446

GALACTIC NUCLEI
Was 49: Mirror for a hidden Seyfert 1 galaxy
[NASA-CR-194537] p 840 N94-14685

GALACTIC RADIATION
Analysis of data from the energetic gamma-ray experiment on the gamma ray observatory
[NASA-CR-194178] p 847 N94-13087
The onset of galactic winds in early-type galaxies
[NASA-CR-193640] p 836 N94-13446
The extent and content of low-ionization gas in galaxies p 837 N94-13551

GALACTIC STRUCTURE
Analysis of interstellar cloud structure based on IRAS images
[NASA-CR-194341] p 836 N94-13332
The distance to the high velocity clouds of neutral hydrogen
[NASA-CR-194343] p 838 N94-13716
Emission line variability in active galactic nuclei
[ITN-93-85209] p 849 N94-14553

GALAXIES
Redshift distortions of galaxy correlation functions
[DE93-014007] p 834 N94-12980
The onset of galactic winds in early-type galaxies
[NASA-CR-193640] p 836 N94-13446
The extent and content of low-ionization gas in galaxies p 837 N94-13551
A near-infrared faint galaxy survey: Evolution and the cosmological geometry from K band photometry p 830 N94-13591

GALERKIN METHOD
A hybrid Pade-Galerkin technique for differential equations
[NASA-CR-191494] p 767 N94-13289
A priori error estimates for an hp-version of the discontinuous Galerkin method for hyperbolic conservation laws
[NASA-TM-108993] p 632 N94-13467
On the superconvergence of Galerkin methods for hyperbolic IBVP
[NASA-CR-194293] p 770 N94-13922
On the superconvergence of Galerkin methods for hyperbolic IBPV
[NASA-CR-194488] p 770 N94-14307

GALILEO PROJECT
Enhanced decoding for the Galileo S-band mission p 609 N94-14380

GALILEO SPACECRAFT
Coding performance of the Probe-Orbiter-Earth communication link p 608 N94-14377
An overview of the Galileo Optical Experiment (GOPEX) p 610 N94-14386
Telescope pointing for GOPEX p 610 N94-14389
Galileo Optical Experiment (GOPEX) optical train: Design and validation at the Table Mountain Facility p 610 N94-14390
GOPEX laser transmission and monitoring systems p 611 N94-14391
GOPEX at the Starfire Optical Range p 611 N94-14392
The flight performance of the Galileo orbiter USO p 611 N94-14398

GALLIUM ARSENIDES
Liquid phase epitaxy of gallium arsenide: A review
[DE93-622212] p 804 N94-12893
Numerical simulation and analysis of electrical and optical properties of Al(x)Ga(1-x)As / GaAs
[ETN-93-94387] p 703 N94-13997
Free-exciton recombination in GaAs
[DE93-009843] p 809 N94-14079
Intrinsic and interfacial recombination in OMVPE- and MBE-prepared GaAs/Al(x)Ga(1-x)As heterostructures
[DE93-009844] p 809 N94-14083
Anomalous low-temperature free-exciton transport in GaAs structures
[DE93-009845] p 809 N94-14108
Activities of the Basic Sciences Branch
[DE93-010012] p 851 N94-14455

GALLIUM ISOTOPES
Present status of SAGE
[DE93-014350] p 781 N94-13205

GAME THEORY
Stochastic scheduling games with Markov decision arrival processes
[CWI-BS-R9231] p 773 N94-14005
Generating knight's tours without backtracking from errors
[AD-A266807] p 772 N94-14900

GAMMA RAY ASTRONOMY
Search for ultra-high energy emission from Geminga and five unidentified EGRET sources
[DE93-012717] p 846 N94-12816
Search for emission of ultra high energy radiation from active galactic nuclei
[DE93-012719] p 846 N94-12923
Search for UHE emission from Cygnus X-3
[DE93-012720] p 846 N94-12924
Search for continuous and single day emission from ultra-high-energy sources
[DE93-012724] p 846 N94-12947
Research in cosmic and gamma ray astrophysics: Cosmic physics portion
[NASA-CR-194127] p 847 N94-13211
Multiwavelength observations of unidentified high energy gamma ray sources
[NASA-CR-194536] p 840 N94-14688

GAMMA RAY BURSTS
A new limit on the rate-density of evaporating black holes
[DE93-012716] p 834 N94-12815
Search for emission of ultra high energy radiation from active galactic nuclei
[DE93-012719] p 846 N94-12923
Search for ultra-high-energy radiation from gamma-ray bursts
[DE93-012721] p 847 N94-12964
GRO: Black hole models for gamma ray bursts
[NASA-CR-193244] p 829 N94-13178
ADP study of gamma-ray bursts
[NASA-CR-194311] p 848 N94-13708

GAMMA RAY OBSERVATORY
Analysis of data from the energetic gamma-ray experiment on the gamma ray observatory
[NASA-CR-194178] p 847 N94-13087
The four great observatories
[NASA-TM-109311] p 830 N94-13605

GAMMA RAY SPECTRA
ADP study of gamma-ray bursts
[NASA-CR-194311] p 848 N94-13708
GAMMA RAY SPECTROMETERS
Determining the solar-flare photospheric scale height from SMM gamma-ray measurements
[NASA-CR-194084] p 844 N94-13671
GAMMA RAY TELESCOPES
Search for emission of ultra high energy radiation from active galactic nuclei
[DE93-012719] p 846 N94-12923
Analysis of data from the energetic gamma-ray experiment on the gamma ray observatory
[NASA-CR-194178] p 847 N94-13087
A positron annihilation radiation telescope using Laue diffraction in a crystal lens
[DE93-012905] p 848 N94-13483
GAMMA RAYS
Search for ultra-high energy emission from Geminga and five unidentified EGRET sources
[DE93-012717] p 846 N94-12816
Search for continuous and single day emission from ultra-high-energy sources
[DE93-012724] p 846 N94-12947
Search for ultra-high-energy radiation from gamma-ray bursts
[DE93-012721] p 847 N94-12964
Metal-semiconductor, composite radiation detectors
[DE93-013313] p 619 N94-12994
Beta/gamma test problems for ITS
[DE93-013522] p 781 N94-13349
A positron annihilation radiation telescope using Laue diffraction in a crystal lens
[DE93-012905] p 848 N94-13483
Cosmic and solar gamma ray and neutron experiments
[NASA-CR-193359] p 849 N94-13965
Gamma-insensitive optical focal plane array
[DE93-013100] p 792 N94-14317
Measurements of the spatial structure and directivity of 100 KeV photon sources in solar flares using PVO and ISEE-3 spacecraft
[NASA-CR-194080] p 845 N94-14492
Measuring parity violation using the neutron capture reaction
[DE93-016629] p 786 N94-14514
Radiation effects on optoelectronic analog link for particle detectors
[DE93-015794] p 793 N94-14529
Multiwavelength observations of unidentified high energy gamma ray sources
[NASA-CR-194536] p 840 N94-14688
GARBAGE
STS-35 crew trash compactor briefing
[NASA-TM-109487] p 533 N94-14735
GAS ANALYSIS
An integrated knowledge system for the Space Shuttle hazardous gas detection system
[NASA-CR-194533] p 536 N94-14310
Portable acoustic wave sensor systems for real-time monitoring of volatile organic compounds
[DE93-013753] p 582 N94-14511
GAS ATOMIZATION
Gas atomized Er3Ni powder for cryocooler applications
[DE93-011564] p 568 N94-13000
GAS CHROMATOGRAPHY
Investigation of an alternating current plasma as an element selective atomic emission detector for high-resolution capillary gas chromatography and as a source for atomic absorption and atomic emission spectrometry p 798 N94-13678
Procurement and execution of PCB analyses: Customer-analyst interactions
[DE93-009964] p 566 N94-14694
GAS COMPOSITION
An examination of utility emissions contributions to elevated ozone concentrations in the Chicago area
[DE93-012852] p 708 N94-13495
GAS DETECTORS
A survey and analysis of experimental hydrogen sensors
[NASA-TM-106300] p 648 N94-13135
An integrated knowledge system for the Space Shuttle hazardous gas detection system
[NASA-CR-194533] p 536 N94-14310
GAS DISSOCIATION
Physics of gas breakdown for ion beam transport in gas
[DE93-015646] p 801 N94-14349
GAS DYNAMICS
ROSAT: X ray survey of compact groups
[NASA-CR-193297] p 829 N94-13181
An experimental investigation of shock wave/vortex interaction p 634 N94-13574
Hypersonic flow phenomenology p 505 N94-14155
Full Riemann solution of the one- and two-dimensional Euler equations
[DLR-FB-92-34] p 638 N94-14188
JPRS report: Science and technology. Central Eurasia: Engineering and equipment
[JPRS-UEQ-93-006] p 776 N94-14431
Soliton equations and self-dual gauge fields
[DE93-626620] p 818 N94-14887
GAS EVOLUTION
Hydrogen peroxide safety issues
[DE93-013895] p 565 N94-14346
GAS EXCHANGE
Ocean uptake of carbon dioxide
[DE93-012967] p 707 N94-13384
GAS FLOW
Studies of momentum and energy transfer across wavy gas-liquid interfaces
[AD-A266432] p 635 N94-13699
Hypersonic propulsion characterization p 505 N94-14156
GAS GUNS
High velocity gas gun
[NASA-TM-109296] p 541 N94-13637
Development of test techniques to simulate high-frequency mechanical shock on weapon components
[KCP-613-4998] p 675 N94-13907
GAS HEATING
Upgrading of raw natural gas using high-performance polymer membranes
[DE93-014041] p 566 N94-14586
GAS INJECTION
Analysis of gas turbine engines using water and oxygen injection to achieve high Mach numbers and high thrust
[NASA-TM-106270] p 518 N94-13143
BOAST 2 for the IBM 3090 and RISC 6000
[DE93-000138] p 638 N94-14351
GAS IONIZATION
New infrared photon absorption processes
[DE93-017017] p 780 N94-13071
A search for strong-field direct two electron ionization using coincidence spectroscopy
[DE93-013435] p 781 N94-13241
GAS LASERS
Kinetic studies following state-selective laser excitation
[DE93-012970] p 654 N94-13013
GAS MIXTURES
Numerical study of shock-induced combustion in methane-air mixtures
[NASA-TM-106354] p 642 N94-14722
H2S data reduction
[NASA-CR-193389] p 617 N94-14743
GAS PRESSURE
Measuring opacity of shock generated argon plasmas
[DE93-013038] p 801 N94-14312
GAS RECOVERY
BOAST 2 for the IBM 3090 and RISC 6000
[DE93-000138] p 638 N94-14351
GAS SPECTROSCOPY
Liquid and gas evanescent wave spectroscopy via tunable lasers and silver halide fibers
[ITN-93-85226] p 565 N94-14465
GAS STREAMS
Evaluation of dual flow thrust vector nozzles with exhaust stream impingement
[NASA-CR-193392] p 630 N94-13078
Upgrading of raw natural gas using high-performance polymer membranes
[DE93-014041] p 566 N94-14586
GAS TEMPERATURE
Coupled thermal response of objects and participating media in fires and large combustion systems
[DE93-012848] p 561 N94-12819
Investigation of the feasibility of optical diagnostic measurements at the exit of the SSME
[NASA-CR-193832] p 553 N94-14682
GAS TRANSPORT
Modeling ignition chemistry
[DE93-012340] p 561 N94-12910
BAKEOUT: A computer program for predicting diffusive outgassing from stainless steel
[DE93-012613] p 573 N94-14364
GAS TURBINE ENGINES
Advanced Turbine Technology Applications Project (ATTAP)
[NASA-CR-191088] p 828 N94-12931
NDE of titanium alloy MMC rings for gas turbine engines
[NASA-TM-106188] p 555 N94-13138
Combustor technology for future small gas turbine aircraft
[NASA-TM-106312] p 517 N94-13142
Techniques for improving the performance of a simplified electronic fuel controller with incremental actuation for small gas turbine engines
[ISBN-0-315-56062-2] p 661 N94-13521
Review of Canadian aeronautical fatigue work, 1991-1993
[LTR-ST-1932] p 674 N94-13861
GAS TURBINES
Performance of gas turbine compressor cleaners
[NLR-TP-91291-U] p 519 N94-14450
GASEOUS DIFFUSION
Long-range global warming impact of gaseous diffusion plant operation
[DE93-011686] p 710 N94-14459
Switchover software reliability estimate for Paducah freezer/sublimer computer systems
[DE93-013844] p 756 N94-14696
GASEOUS FUELS
Low pressure storage of natural gas on activated carbon
[DE93-014053] p 660 N94-12851
GASEOUS ROCKET PROPELLANTS
Analysis of reacting flowfields in low-thrust rocket engines and plumes p 552 N94-14491
GATES (CIRCUITS)
Phase aligner for the Electronically Scanned Thinned Array Radiometer (ESTAR) instrument
[NASA-TM-4518] p 623 N94-13878
GATES (OPENINGS)
Airport terminals: Optimum configurations and gate position requirement
[ISBN-0-315-61722-5] p 528 N94-13544
GAUGE INVARIANCE
Aspects of symmetry violation
[DE93-011003] p 779 N94-12997
On a nonminimal gauge interaction of a scalar field in D=2+1 Chern-Simons-Maxwell theory
[DE93-621380] p 621 N94-13224
Soliton equations and self-dual gauge fields
[DE93-626620] p 818 N94-14887
GAUGE THEORY
Gauging the octonion algebra
[DE93-622864] p 775 N94-12843
Electric charge quantization
[DE93-622901] p 778 N94-12845
On a nonminimal gauge interaction of a scalar field in D=2+1 Chern-Simons-Maxwell theory
[DE93-621380] p 621 N94-13224
Soliton equations and self-dual gauge fields
[DE93-626620] p 818 N94-14887
GAUSS EQUATION
The electric field of a current-carrying conductor
[DE93-626637] p 617 N94-14892
GEARS
Roller-gear drives for robotic manipulators design, fabrication and test
[NASA-CR-194248] p 660 N94-12802
GELS
Pore-size-distribution of cationic polyacrylamide hydrogels
[DE93-015218] p 581 N94-14400
GENE EXPRESSION
The surface-located YopN protein is involved in calcium signal transduction in Yersinia pseudotuberculosis
[FOA-B-40416-4.4] p 729 N94-14128
Analysis of the V antigen lcrGVH-yopBD operon of Yersinia pseudotuberculosis: Evidence for a regulatory role of LcrH and LcrV
[FOA-B-40417-4.4] p 729 N94-14129
GENERAL AVIATION AIRCRAFT
Determination of Loran-C/GPS human factors issues
[PB93-199693] p 514 N94-14563
GENETIC ALGORITHMS
An analytic modeling and system identification study of rotor/fuselage dynamics at hover p 524 N94-13312
GENETIC CODE
Analysis of the V antigen lcrGVH-yopBD operon of Yersinia pseudotuberculosis: Evidence for a regulatory role of LcrH and LcrV
[FOA-B-40417-4.4] p 729 N94-14129
GENETIC ENGINEERING
The first steps of chlorophyll synthesis: RNA involvement and regulation
[DE93-014398] p 730 N94-14509
GENETICS
Adaptively resizing populations: Algorithm, analysis, and first results
[NASA-CR-194277] p 742 N94-12808
Evolution of catalytic RNA in the laboratory
[NASA-CR-194124] p 727 N94-13210
Gordon Research Conference on Chronobiology, 1991
[AD-A266354] p 728 N94-13698
Genetic effects of HZE and cosmic radiation (L-9) p 593 N94-13766

Analysis of the V antigen lcrGVH-yopBD operon of Yersinia pseudotuberculosis: Evidence for a regulatory role of LcrH and LcrV
[FOA-B-40417-4.4] p 729 N94-14129

GEOBOTANY
A knowledge-based model for the integration of remote sensing into a mineral exploration program
[ISBN-0-315-58982-5] p 685 N94-13523

GEOCENTRIC COORDINATES
Improved treatment of global positioning system force parameters in precise orbit determination applications
p 514 N94-14371
Use of global positioning system measurements to determine geocentric coordinates and variations in Earth orientation p 514 N94-14372

GEOCHRONOLOGY
Maximum entropy spectral analysis of the geological time series of the oxygen isotope record from deep-sea cores
[INPE-5465-PRE/1773] p 725 N94-13728

GEOCORONAL EMISSIONS
Terrestrial magnetospheric imaging: Numerical modeling of low energy neutral atoms
[DE93-014561] p 717 N94-14328

GEODETIC SURVEYS
The 1990 Western Pacific Geophysics meeting
[NASA-CR-193456] p 712 N94-13334

GEODYNAMICS
J2000.0 modelling of GEOAIM in the analysis of VLB1 data from the NASA crustal dynamics project
[ISBN-0-315-59463-2] p 684 N94-13368
The determination of crustal motions using laser ranging to Lageos-2 and Lageos-1
[NASA-CR-193787] p 717 N94-14306

GEOGRAPHIC INFORMATION SYSTEMS
Integration between geographic information systems and environmental simulation models
[REPT-93-004] p 823 N94-13806
Multisensor remote sensing data and GIS techniques for monitoring preservation areas: A case study
[INPE-5317-PRE/1714] p 688 N94-14131

GEOGRAPHY
Overview: Gas hydrate geology and geography
[DE93-014043] p 688 N94-14151

GEOLOGICAL FAULTS
Organic Geochemical and tectonic evolution of the Midcontinent Rift system
[DE93-015093] p 717 N94-14338

GEOLOGICAL SURVEYS
Integrated, flexible, and rapid geophysical surveying
[DE93-009989] p 712 N94-12906
Promotion of geothermal energy development in 1991
[DE93-799057] p 701 N94-13214
Activities of Institute for Aerospace Research, Flight Research Laboratory
[CTN-93-60832] p 850 N94-13519
Application of transient airborne electromagnetic and ground resistivity methods to geological mapping in tropical terrains
[ISBN-0-315-57172-1] p 685 N94-13542
Geologic application of JERS-1 SAR data
p 688 N94-14211
Survey of subsurface geophysical exploration technologies adaptable to an airborne platform
[DE93-015080] p 717 N94-14294
Promotion of geothermal energy development in 1991
[DE93-799061] p 705 N94-14679

GEOLOGY
Overview: Gas hydrate geology and geography
[DE93-014043] p 688 N94-14151
Applications of the Advanced Light Source to problems in the earth, soil, and environmental sciences
[DE93-015258] p 710 N94-14477

GEOMAGNETISM
The interplanetary origins and the main-phase development of moderate geomagnetic storms (1978 - 1979)
[INPE-5445-TDI/491] p 835 N94-13174
Variations common to the interplanetary magnetic field, the zonal atmospheric circulation and the Earth's rotation
[COMMUNICATIONS-SER-B-157] p 837 N94-13504
Energetic neutral atoms: Imaging the magnetospheric ring current
[NASA-CR-194339] p 715 N94-13826
Aeromagnetic work in the Lincoln Sea: 1991 survey
[DSIS-93-00308] p 715 N94-13830
Dynamical model for the distribution of geomagnetically trapped anomalous-component ions
[ATR-91(9558)-6] p 784 N94-13936
Simultaneous solution for core magnetic field and fluid flow beneath an electrically conducting mantle
[NASA-TM-4536] p 716 N94-13960
Solar-geophysical data number 584, April 1993. Part 1: (Prompt reports). Data for March, February 1993, and late data
[PB93-198323] p 845 N94-14560

GEOMETRIC RECTIFICATION (IMAGERY)
Supervised classification of remotely sensed images
[DLR-FB-92-07] p 700 N94-14428

GEOMETRICAL OPTICS
Three dimensional time-dependent hydrodynamic and propagation modeling of x ray laser emission
[DE93-012575] p 654 N94-12962
Optimization study of x ray laser coherence in Ni-like Ta
[DE93-016419] p 660 N94-14888

GEOMETRICAL THEORY OF DIFFRACTION
The 24 GHz measurements of 2.2 lambda conical horn antennas illuminating a conducting sheet
[NASA-TM-109002] p 598 N94-12811

GEOMETRY
The geometric phase in quantum physics
[DE93-011121] p 817 N94-13479
Integrable system describing surfaces of non-constant curvature
[PREPRINT-734] p 768 N94-13499
Extremal polygon containment problems and other issues in parametric searching
[ITN-93-85214] p 771 N94-14506

GEOMORPHOLOGY
The American Geophysical Union Chapman Conference on Tectonics and Topography
[NASA-CR-193454] p 713 N94-13335

GEOPHYSICS
Integrated, flexible, and rapid geophysical surveying
[DE93-009989] p 712 N94-12906
The 1990 Western Pacific Geophysics meeting
[NASA-CR-193456] p 712 N94-13334
The American Geophysical Union Chapman Conference on Tectonics and Topography
[NASA-CR-193454] p 713 N94-13335
Solar-geophysical data number 584, April 1993. Part 1: (Prompt reports). Data for March, February 1993, and late data
[PB93-198323] p 845 N94-14560
Solar-geophysical data number 584, April 1993. Part 2: (Comprehensive reports). Data for October 1992 and miscellaneous
[PB93-198331] p 845 N94-14561
INGDB-90. The International Neutron Nuclear Data Base for geophysics applications
[DE93-624095] p 827 N94-14880

GEOPOTENTIAL HEIGHT
Cyclogenesis and cyclone over South America
[INPE-5400-TDI/479] p 719 N94-13175

GEOSAT SATELLITES
Error analysis of real time and post processed or bit determination of GFO using GPS tracking
[NASA-CR-193646] p 512 N94-13238

GEOTHERMAL ENERGY CONVERSION
Hot Dry Rock energy
[DE93-014452] p 702 N94-13403

GEOTHERMAL ENERGY EXTRACTION
Hot Dry Rock energy
[DE93-014452] p 702 N94-13403

GEOTHERMAL RESOURCES
Promotion of geothermal energy development in 1991
[DE93-799057] p 701 N94-13214
Promotion of geothermal energy development in 1991
[DE93-799058] p 701 N94-13215
Hot Dry Rock energy
[DE93-014452] p 702 N94-13403

GEOTHERMAL TECHNOLOGY
Hot Dry Rock energy
[DE93-014452] p 702 N94-13403

GERMANIUM
Manufacturing and examination of integrated optical waveguide components in silicon
[ETN-93-94393] p 793 N94-14704

GERMANIUM ALLOYS
Effect of pressure on order and stability in alloys: The case of Al-Ge
[DE93-013842] p 567 N94-12899
Structural and electronic studies of a-SiGe:H alloys
[DE93-010021] p 809 N94-14085
Evolving surface cusps during strained-layer epitaxy
[DE93-015430] p 813 N94-14478

GERMANIUM ISOTOPES
Present status of SAGE
[DE93-014350] p 781 N94-13205

GETTERS
Multicrystalline silicon solar cells: Gettering optimization and characterization
[DE93-015001] p 705 N94-14861

GIACOBINI-ZINNER COMET
ICE/ISEE plasma wave data analysis
[NASA-CR-194375] p 796 N94-13081

GLASS
Procedures for analysis of debris relative to Space Shuttle systems
[NASA-TM-109190] p 534 N94-12900
Poling of thin polymer films in electro optic applications
[AD-A266562] p 579 N94-13584
High temperature behavior of glass (M-8)
p 587 N94-13740
Fabrication of Si-As-Te ternary amorphous semiconductor in the microgravity environment (M-13)
p 588 N94-13745
Preparation of optical materials used in non-visible region (M-17) p 589 N94-13749
Optimization of the processing parameters of high temperature superconducting glass-ceramics: Center Director's discretionary fund final report
[NASA-TM-108421] p 808 N94-13938
Theoretical studies of breakdown in random media
[DE93-018107] p 558 N94-14418
High counting rate resistive-plate chamber
[DE93-014928] p 651 N94-14452
Investigation of Zerodur material processing
[NASA-CR-193842] p 793 N94-14903

GLASS FIBER REINFORCED PLASTICS
Structural investigation of a damaged GRP/foam sandwich composite using x ray computed tomography
p 669 N94-13857

GLASS FIBERS
Gamma-insensitive optical focal plane array
[DE93-013100] p 792 N94-14317

GLASS LASERS
Inertial Confinement Fusion
[DE93-013303] p 795 N94-13017

GLASS TRANSITION TEMPERATURE
Ionic conductivity of alkali halides and their mixtures near liquid-solid phase transition
[ITN-93-85222] p 566 N94-14558
Office of Naval Research/DARPA publications: Composite materials with improved properties in compression
[AD-A265509] p 560 N94-14794

GLIDE PATHS
Visual cueing aids for rotorcraft landings
p 524 N94-13313
Evaluation of two cockpit display concepts for civil tiltrotor instrument operations on steep approaches
p 517 N94-13323

GLIDING
Qualitative investigation of a generic fighter model in radio controlled gliding flight
[LM-AA-003] p 516 N94-13898

GLOBAL POSITIONING SYSTEM
Investigation for improving Global Positioning System (GPS) orbits using a discrete sequential estimator and stochastic models of selected physical processes
[NASA-CR-194167] p 512 N94-13082
Error analysis of real time and post processed or bit determination of GFO using GPS tracking
[NASA-CR-193646] p 512 N94-13238
Performance evaluation tests of the GPS/DGPS navigation system installed in the NAL Dornier 228: Preliminary ground test results
[NAL-TM-649] p 513 N94-13346
GPS satellite sky distribution: Impact on the propagation of some important errors in precise relative positioning
[ISBN-0-315-51838-3] p 513 N94-13541
Helicopter precision approach capability using the Global Positioning System
[NASA-CR-194037] p 513 N94-13957
Ionospheric calibration for single frequency altimeter measurements
[NASA-CR-194282] p 716 N94-14049
Improved treatment of global positioning system force parameters in precise orbit determination applications
p 514 N94-14371
Use of global positioning system measurements to determine geocentric coordinates and variations in Earth orientation p 514 N94-14372
Determination of Loran-C/GPS human factors issues
[PB93-199693] p 514 N94-14563
The development and flight test of a deployable precision landing system for spacecraft recovery
[NASA-TM-4525] p 537 N94-14853

GLOBAL WARMING
The role of clouds and oceans in global greenhouse warming
[DE93-016206] p 706 N94-13079
Sequestering carbon dioxide in industrial polymers: Building materials for the 21st century
[DE93-016087] p 580 N94-14297
Long-range global warming impact of gaseous diffusion plant operation
[DE93-011686] p 710 N94-14459

GLOBULAR CLUSTERS
On inhomogeneous halo collapse and the globular cluster metallicity gradient
[DE93-013090] p 834 N94-13011
Sampling of globular clusters and the distance to the galactic center
[INPE-5446-TDI/492] p 837 N94-13449
The spectroscopic evolution of novae in the bulge of M31 and a search for their possible origin in the M31 globular cluster system p 831 N94-13668
GLOW DISCHARGES
Structural and electronic studies of a-SiGe:H alloys
[DE93-010021] p 809 N94-14085
GLUCOSIDES
Improving physical performance by chemical stimulation
[DSIS-92-03763] p 728 N94-13823
GLUONS
No-lost theorem for parity violating nucleon-nucleon scattering experiments
[DE93-012737] p 779 N94-12949
Quark and gluon jets at CDF
[DE93-014919] p 783 N94-13884
GLUTAMATES
The first steps of chlorophyll synthesis: RNA involvement and regulation
[DE93-014398] p 730 N94-14509
GLYCINE
Determination of trace elements in triglycine sulfate solutions
[NASA-CR-193481] p 562 N94-13048
GOERTLER INSTABILITY
The effect of crossflow on Taylor vortices: A model problem
[NASA-CR-191487] p 630 N94-13128
On the secondary instability of the most dangerous Goertler vortex
[NASA-CR-191504] p 636 N94-13785
Linear instability of curved free shear layers
[NASA-TM-106290] p 642 N94-14729
GOES 7
Solar-geophysical data number 584, April 1993. Part 2: (Comprehensive reports). Data for October 1992 and miscellaneous
[PB93-198331] p 845 N94-14561
GOLD
Incomplete melting of the Au(100) surface
[DE93-623192] p 569 N94-13227
Ploughing on gold using a Scanning Tunneling Microscope
[DE93-012632] p 812 N94-14365
GOLD ISOTOPES
Stripping efficiencies for 277 MeV/amu gold beam on copper foils
[DE93-014306] p 569 N94-13221
GOVERNMENT/INDUSTRY RELATIONS
Shared visions: Partnership of Rockwell International and NASA Cost Effectiveness Enhancements (CEE) for the space shuttle system integration program p 668 N94-13166
Government/contractor partnerships for continuous improvement. A Goddard Space Flight Center example p 669 N94-13169
George M. Low Trophy: NASA's quality and excellence award. 1992 recipients: Honeywell Clearwater, IBM Houston
[NASA-TM-109265] p 669 N94-13396
User observations on information sharing (corporate knowledge and lessons learned)
[NASA-TM-104781] p 819 N94-13400
Technology parks and the cooperation among universities and firms: The cases of Campinas, Sao Jose dos Campos e Sao Carlos
[INPE-5251-TAE/04] p 818 N94-13427
GRAIN BOUNDARIES
The study of structure-processing-property relations in copper oxide based high (Tc) superconductors
[DE93-015066] p 804 N94-13003
Grain-boundary electronic states by multiple-scattering theory
[DE93-013198] p 805 N94-13010
Interfacial precipitation, segregation and deformation in alloy 600: Implications on primary-side IGSCC
[DE93-013161] p 568 N94-13035
Computation and graphics in mathematical research
[DE93-016512] p 740 N94-13069
Atomic structure of the 310 twin in niobium: Theoretical predictions and comparison with experimental observation
[DE93-013421] p 806 N94-13136
Microstructural evolution of NARloy-Z at elevated temperatures
[NASA-TM-108419] p 571 N94-13715
Boundary stability under nonequilibrium conditions
[DE93-016259] p 809 N94-13980
GRAIN SIZE
On the hardening and softening of nanocrystalline materials
[DE93-012901] p 810 N94-14185
GRAMMARS
Reconsideration of the autonomous view of language p 618 N94-13441
GRAPH THEORY
Transformation and composition of refusal graphs: Testability analysis
[LAAS-92435] p 751 N94-13995
On the solution of a class of graph problems by parallel algorithms
[LAAS-92514] p 756 N94-14712
GRAPHICAL USER INTERFACE
Artificial intelligence support for scientific model-building
[NASA-TM-109252] p 761 N94-12890
Advanced display object selection methods for enhancing user-computer productivity
[AD-A265806] p 743 N94-12974
Designing and generating a GUI module using GUI p 747 N94-13437
Mass market computers for software development
[ERB-1035] p 741 N94-13547
Programming the multimodal interface
[DE93-013084] p 748 N94-13576
Integrating PAW, a graphical analysis interface to Sybase
[DE93-014172] p 755 N94-14581
GRAPHITE
Ohmic heating of composite candidate graphite-fiber/coating combinations
[NASA-TM-4491] p 554 N94-12871
Scanning tunneling microscopy studies of diamond films and optoelectronic materials
[NASA-CR-194363] p 578 N94-13246
Inhibiting corrosion in Gr/Al and Gr/Mg metal matrix composites using nonequilibrium alloying techniques
[AD-A266547] p 556 N94-13583
Development of time-dependent orthotropic constitutive law of a thermoplastic composite material p 556 N94-13595
Structural change of graphite during electron irradiation
[DE93-015961] p 582 N94-14531
GRAPHITE-EPOXY COMPOSITES
Design and application of a quasistatic crush test fixture for investigating scale effects in energy absorbing composite plates
[NASA-CR-4526] p 670 N94-13063
Experimental and analytical analysis of the response of a smart beam to rate feedback
[AD-A266544] p 557 N94-13706
An experimental investigation into the damage resistance and compression-after-impact strength of T800H/3900-2
[LTR-ST-1909] p 675 N94-13945
GRAPHS (CHARTS)
Simulated annealing for the problem of multiresource location on graph
[REPT-93-033] p 770 N94-13809
GRASSLANDS
Modeling of biosphere-atmosphere interaction for forest and pastureland in the Amazon
[INPE-5454-TDI/496] p 707 N94-13330
GRATINGS (SPECTRA)
Advances in low energy neutral atom imaging techniques
[DE93-012745] p 782 N94-13492
Advanced optical instruments technology p 547 N94-14838
GRAVELS
Stochastic performance modeling and evaluation of obstacle detectability with imaging range sensors
[NASA-CR-194510] p 605 N94-13946
GRAVIMETRY
Survey of subsurface geophysical exploration technologies adaptable to an airborne platform
[DE93-015080] p 717 N94-14294
GRAVITATION
The 1990 Western Pacific Geophysics meeting
[NASA-CR-193456] p 712 N94-13334
Dilaton quantum cosmology in two dimensions
[DE93-621377] p 836 N94-13361
On the symmetry algebra of the discrete states in d less than 2 closed string theory
[DE93-622903] p 769 N94-13536
Radiation perturbation theory in gravity and quantum universe as a hydrogen atom
[DE93-626621] p 849 N94-14889
GRAVITATION THEORY
The general gravitational potential field of a homogeneous cylinder rotating about its axis
[DE93-622853] p 775 N94-13508
Radiation perturbation theory in gravity and quantum universe as a hydrogen atom
[DE93-626621] p 849 N94-14889
GRAVITATIONAL COLLAPSE
On inhomogeneous halo collapse and the globular cluster metallicity gradient
[DE93-013090] p 834 N94-13011
GRAVITATIONAL EFFECTS
Evaluation of the Retrograde Inflation Anti-G Suit (RIAGS)
[AD-A265884] p 736 N94-12935
Calcitonin control of calcium metabolism during weightlessness
[NASA-CR-193622] p 731 N94-12960
Gravity as a probe for understanding pattern specification
[NASA-CR-194142] p 713 N94-13418
Spacelab J experiment descriptions
[NASA-TM-4517] p 586 N94-13732
The influence of a microgravity environment on the dendritic morphology during directional solidification of hypoeutectic Al-Si alloys
[NASA-CR-194139] p 571 N94-13891
GRAVITATIONAL FIELDS
The general gravitational potential field of a homogeneous cylinder rotating about its axis
[DE93-622853] p 775 N94-13508
GRAVITATIONAL PHYSIOLOGY
Calcitonin control of calcium metabolism during weightlessness
[NASA-CR-193622] p 731 N94-12960
Gravity as a probe for understanding pattern specification
[NASA-CR-194142] p 713 N94-13418
Endocrine and metabolic changes in payload specialist (L-1) p 591 N94-13758
GRAVITY ANOMALIES
Venus gravity
[NASA-CR-194077] p 841 N94-12823
GRAVITY WAVES
Theoretical support for the Airborne Antarctic Ozone Experiment
[NASA-CR-193669] p 713 N94-13465
Numerical simulation and parameterization of orographic gravity waves p 713 N94-13647
The spectral viscosity method applied to simulation of waves in a stratified atmosphere
[FFI-92/7047] p 637 N94-14040
GRAY GAS
Coupled thermal response of objects and participating media in fires and large combustion systems
[DE93-012848] p 561 N94-12819
GRAZING
Determination of the surface cleanliness of metals by FT-IR spectroscopy
[DE93-013252] p 565 N94-14525
GRAZING INCIDENCE
Proceedings of the Workshop on Applications of Synchrotron Radiation to Trace Impurity Analysis for Advanced Silicon Processing
[DE93-013389] p 805 N94-13020
GREEN'S FUNCTIONS
Hydrodynamic asymptotics of Green functions in magnetics with spontaneously broken symmetry
[DE93-621349] p 767 N94-13223
Radiation perturbation theory in gravity and quantum universe as a hydrogen atom
[DE93-626621] p 849 N94-14889
GREENHOUSE EFFECT
The role of clouds and oceans in global greenhouse warming
[DE93-016206] p 706 N94-13079
Forest management for fixing and sequestering carbon
[DE93-013520] p 707 N94-13486
IMG: Interferometric monitor for greenhouse gases p 689 N94-14217
Long-range global warming impact of gaseous diffusion plant operation
[DE93-011686] p 710 N94-14459
GRENADES
Estimation of the concentration versus the time profile of zinc chloride particles in smoke clouds generated by the Raufoss A/S instantaneous smoke RA-90 and DM-45 HC smoke generator
[FFI-93/6001] p 708 N94-13821
GRID GENERATION (MATHEMATICS)
Parallel implementation of an algorithm for Delaunay triangulation
[NASA-TM-103951] p 740 N94-12973
Numerical simulation of steady three-dimensional flows in axial turbomachinery bladerows p 634 N94-13630
Locally non-uniform finite-difference time domain with application to stealth, crosstalk, and narrow apertures
[DE93-013958] p 601 N94-13696

Numerical investigations in three-dimensional internal flows
[NASA-CR-194143] p 637 N94-13827
A perspective on AVS in an engineering sciences environment
[DE93-015011] p 596 N94-13889
Some aspects of sheet forming simulation using explicit finite element techniques
[DE93-012479] p 663 N94-13975
VFGEN: A parallel volume fraction generator for hydrocodes
[DE93-011673] p 752 N94-14019
Computational techniques and capabilities
p 506 N94-14162
Domain connectivity among systems of overset grids
[NASA-CR-193390] p 508 N94-14326
Multigrid solution of internal flows using unstructured solution adaptive meshes
[NASA-CR-194233] p 638 N94-14356
An adaptive projection method for the incompressible Euler equations
[DE93-016428] p 639 N94-14434
Predicting the vibrations of a spinning inflated membrane
[DE93-010690] p 676 N94-14456
A grid generation package for high aspect ratio wings
p 510 N94-14608

GROOVES
Scattering by a groove in an impedance plane
[NASA-CR-193362] p 602 N94-13720

GROUND EFFECT (AERODYNAMICS)
Numerical simulation of a powered-lift landing, tracking flow features using overset grids, and simulation of high lift devices on a fighter-lift-and-control wing
[NASA-CR-194260] p 527 N94-14322

GROUND OPERATIONAL SUPPORT SYSTEM
Sensor operation of Advanced Earth Observing Satellite (ADEOS) p 689 N94-14215

GROUND STATE
Metastable enhancement of C(+) and O(+) capture reactions
[DE93-015075] p 807 N94-13373

GROUND STATIONS
National use of the groups 7wwW1W2 and 960ww for ground stations
[KNMI-PUBL-181] p 722 N94-13926
Sensor operation of Advanced Earth Observing Satellite (ADEOS) p 689 N94-14215

GROUND SUPPORT EQUIPMENT
An experimental assessment of the use of ground-level microphones to measure the fly-over noise of jet-engined aircraft
[NPL-RSA(EXT)-0039] p 777 N94-13885
Payload/GSE/data system interface: Users guide for the VPF (Vertical Processing Facility)
[NASA-CR-194385] p 532 N94-14148

GROUND SUPPORT SYSTEMS
Control system design of a cable-mounted model used for dynamic wind tunnel testing
[NAL-TR-1161] p 528 N94-13337
Space and Earth sciences, computer systems, and scientific data analysis support, volume 1
[NASA-CR-194535] p 741 N94-13788
Sensor operation of Advanced Earth Observing Satellite (ADEOS) p 689 N94-14215
Asynchronous transfer mode link performance over ground networks p 610 N94-14385

GROUND TESTS
Performance evaluation tests of the GPS/DGPS navigation system installed in the NAL Dornier 228: Preliminary ground test results
[NAL-TM-649] p 513 N94-13346
Methodology of Hypersonic Testing
[VKI-LS-1993-03] p 505 N94-14153
Computational techniques and capabilities
p 506 N94-14162
Test and evaluation methods p 506 N94-14163
Materials/structures testing p 506 N94-14164
Aeropropulsion test and evaluation methods
p 506 N94-14165
Extrapolation of ground test data to flight
p 507 N94-14170
Control structural interaction testbed: A model for multiple flexible body verification p 544 N94-14649
A program for the investigation of the Multibody Modeling, Verification, and Control Laboratory
p 682 N94-14652

GROUND TRUTH
Evaluation of infrared sensors for autonomous landing guidance
[AD-A266450] p 513 N94-13703
Integration of remotely sensed data and cadastral ownership boundaries for land inventory purposes
[BCRS-92-16] p 687 N94-14127

GROUND WATER
Integrated, flexible, and rapid geophysical surveying
[DE93-009989] p 712 N94-12906
The method of Laplace Transform MultiQuadrics (LTMQ) for the solution of the groundwater flow equation
[DE93-010408] p 637 N94-14053
Promotion of geothermal energy development in 1991
[DE93-799061] p 705 N94-14679

GROUND-AIR-GROUND COMMUNICATION
The influence of ATC message length and timing on pilot communication
[NASA-CR-177621] p 512 N94-14744

GROUP DYNAMICS
The effects of evaluation and production blocking on the performance of brainstorming groups
[AD-A265495] p 734 N94-12929

GROUP THEORY
Mathematics and string theory
[DE93-017903] p 817 N94-14417

GUIDE VANES
Numerical simulations of unsteady flows in turbomachines p 633 N94-13569

GULF STREAM
Circulation model experiments of the Gulf Stream using satellite-derived fields
[AD-A266067] p 725 N94-12990

GUN PROPELLANTS
Flamespreading in granular solid propellant: Design of an experiment
[AD-A266009] p 583 N94-12987

GYROFREQUENCY
Ion anisotropy driven waves in the Earth's magnetosheath and plasma depletion layer
[DE93-012751] p 712 N94-12952
Comparative study of x ray and microwave emissions during solar flares
[NASA-CR-194532] p 845 N94-14577

GYROSCOPES
Performance evaluation of the honeywell GG1308 miniature ring laser gyroscope
[AD-A266694] p 653 N94-14782

GYROTROPISM
On transport of energy, momentum, orbital angular momentum and self-angular momentum of electromagnetic wave in dispersal media
[DE93-624179] p 617 N94-14883

H

H I REGIONS
The extent and content of low-ionization gas in galaxies p 837 N94-13551

H II REGIONS
Abundance markers in H II regions of late spiral galaxies
[ISBN-0-315-62457-4] p 836 N94-13372

H-60 HELICOPTER
Optimization-based controller design for rotorcraft
p 527 N94-14642

HABITABILITY
Life support and habitability manual, volume 1
[ESA-PSS-03-406-ISSUE-1-VOL] p 737 N94-13901
Life support and habitability manual, volume 2
[ESA-PSS-03-406-ISSUE-1-VOL] p 738 N94-13902

HABITATS
Birds of Wallops Island, Virginia, 1970 - 1992
[NASA-TM-104589] p 850 N94-13923
Pattern and Process in Landscape Ecology: Eighth Annual US Landscape Ecology Symposium
[DE93-014032] p 711 N94-14859

HADRONS
Top quark polarization and T-odd spin correlations as tools for testing (non) Standard Model predictions
[DE93-622956] p 778 N94-12847
Medium energy hadron-nucleus scattering in the 1/N expansion formalism
[DE93-622957] p 778 N94-12848
Polarization and color transparency
[DE93-014319] p 780 N94-13101
Low energy response of the DO calorimeter and jet energy measurement
[DE93-013569] p 781 N94-13350
Measurements of optical properties of waveshifting optical fiber for liquid scintillator hadron calorimetry
[DE93-012606] p 791 N94-13482
High energy hadron-hadron collisions
[DE93-015584] p 784 N94-13927
Research in theoretical nuclear physics
[DE93-015096] p 839 N94-14330
Top quark search: Results and prospects at Fermilab
[DE93-013016] p 786 N94-14524
Comparing the Z(sup 0) mass and inclusive widths to the standard electroweak theory
[PREPRINT-731] p 787 N94-14721

HAFNIUM OXIDES
Absorption and damage thresholds of low defect density hafnia deposited with activated oxygen
[DE93-013853] p 655 N94-13243

HAIL
Remote identification of rain and hail with a polarization diversity radar
[ISBN-0-315-55623-4] p 720 N94-13516

HALF LIFE
The beta(+) decay and cosmic-ray half-life of Mn-54
[DE93-013913] p 848 N94-13695

HALL EFFECT
Effects of growth conditions and substrate orientation on the properties of InSb
[DE93-013766] p 812 N94-14344
The fractional quantum Hall effect and the spherical shell model
[DE93-014553] p 818 N94-14740

HALOS
On inhomogeneous halo collapse and the globular cluster metallicity gradient
[DE93-013090] p 834 N94-13011
Beam halo formation from space-charge dominated beams in uniform focusing channels
[DE93-014458] p 789 N94-13209
Evolution of the interplanetary magnetic field
[DE93-012631] p 836 N94-13262
Design for low beam loss in accelerators for intense neutron source applications
[DE93-014557] p 789 N94-13327
Beam halo in high-intensity beams
[DE93-014565] p 789 N94-13328

HAMILTON-JACOBI EQUATION
Guidance law development for aeroassisted transfer vehicles using matched asymptotic expansions
[NASA-CR-194523] p 508 N94-14538

HAMILTONIAN FUNCTIONS
Hydrodynamic asymptotics of Green functions in magnetics with spontaneously broken symmetry
[DE93-621349] p 767 N94-13223
Nonlinear vibrations of thick composite plates: Higher-order shear deformation plate theory
p 556 N94-13558
Quantum Monte Carlo by message passing
[DE93-012645] p 760 N94-14177
Multiplicative noise: Applications in cosmology and field theory
[DE93-016624] p 840 N94-14536
Construction of the Courant-Snyder invariants for the non-linear equations of motion under presence of the linear coupling
[DE93-017565] p 788 N94-14872
Spherical anharmonic oscillator in self-similar approximation
[DE93-626622] p 772 N94-14890

HANDBOOKS
Aircraft engine type certification handbook: Advisory circular
[AC-33-2B] p 518 N94-13252
NASA handbook for nickel-hydrogen batteries
[NASA-RP-1314] p 550 N94-13265

HANDLING EQUIPMENT
An experimental study of tether reel system: A laboratory model
[NAL-TR-1176T] p 539 N94-12943

HANKEL FUNCTIONS
On some results by Fuhrmann on Hankel operators
[CWI-BS-R9224] p 764 N94-13999
On relations between Schmidt pairs arising in robust control
[CWI-BS-R9225] p 764 N94-14000
On the Schmidt pairs of multivariable Hankel operators and robust control
[CWI-BS-R9226] p 765 N94-14001

HARDNESS
A process for evaluation of mechanical behavior of surface films
[W-1/92] p 579 N94-14007
On the hardening and softening of nanocrystalline materials
[DE93-012901] p 810 N94-14185

HARDNESS TESTS
The structure and mechanical properties of Ru-Cu and Ru-Ti nanolayer composites
[DE93-014453] p 558 N94-14469

HARDWARE
Hardware design for the Autonomous Visibility Monitoring (AVM) observatory p 533 N94-14394

HARMONIC FUNCTIONS
An 8-node axisymmetric acoustic finite element for non-axisymmetric fluid-structure interaction analysis
[FFA-TN-1993-03] p 673 N94-13689

HARMONIC GENERATIONS
Kinetic simulations of ultra-intense laser plasma interactions and a novel method of generating odd harmonics
[DE93-014418] p 797 N94-13207
High-order harmonic generation with short-pulse lasers
[DE93-016532] p 659 N94-14594
HARMONIC OSCILLATORS
Stability of subharmonics and escape phenomena in the twin-well potential duffing system p 775 N94-13235
Spherical anharmonic oscillator in self-similar approximation
[DE93-626622] p 772 N94-14890
HARRIER AIRCRAFT
Analysis of the Harrier forebody/inlet design using computational techniques
[NASA-CR-193616] p 503 N94-13463
HAZARDS
Integrated, flexible, and rapid geophysical surveying
[DE93-009989] p 712 N94-12906
Environmental awareness
[DE93-014192] p 707 N94-13218
HEAD DOWN TILT
Circadian rhythms during simulation of the D2-spaceflight
[DLR-FB-92-27] p 733 N94-14043
HEALTH PHYSICS
Beta/gamma test problems for ITS
[DE93-013522] p 781 N94-13349
HEAO
NASA images 11
[NASA-TM-109287] p 842 N94-13626
HEARING
Underwater hearing: A review
[ISVR-TR-212] p 777 N94-14130
HEAT ENGINES
Insoluble coatings for Stirling engine heat pipe condenser surfaces
[NASA-CR-191188] p 554 N94-14771
HEAT EXCHANGERS
Surrogates for numerical simulations; optimization of eddy-promoter heat exchangers
[NASA-CR-191510] p 629 N94-13074
High flux heat exchanger
[AD-A266341] p 636 N94-13730
Colorado State University program for developing, testing, evaluating, and optimizing solar heating and cooling systems
[DE93-016018] p 705 N94-14504
HEAT FLUX
Measuring surface fluxes in CAPE
[NASA-CR-193664] p 711 N94-12788
Test apparatus for ITER blanket cooling water distribution design
[DE93-753157] p 795 N94-12944
A technique for direct measurement of skin friction in supersonic combustion flow p 503 N94-13555
Experimental measurement of local heat transfer coefficients over discrete roughened plates using infrared thermography p 635 N94-13652
Boundary layer structure over areas of heterogeneous heat fluxes
[DE93-007887] p 715 N94-13912
Fluxes of heat and water vapour in a convective mixed layer during EFEDA
[DLR-FB-92-21] p 716 N94-14132
Sidewall thermometry perturbations to nonlinear heat transport near the (lambda) transition in He-4
[DE93-014990] p 817 N94-14453
Optical fibre Fabry-Perot interferometers for calorimetric heat transfer gauges
[RAE-TM-AERO/PROP-20] p 653 N94-14701
HEAT MEASUREMENT
Measuring surface fluxes in CAPE
[NASA-CR-193664] p 711 N94-12788
Measurements of optical properties of waveshifting optical fiber for liquid scintillator hadron calorimetry
[DE93-012606] p 791 N94-13482
The status of cold fusion
[DE93-012731] p 802 N94-14567
HEAT PIPES
High-flux testing of heat pipes for point-focus solar collector systems
[DE93-011581] p 628 N94-12884
An analytical investigation of transient effects on rewetting of heated thin flat plates
[NASA-TM-106120] p 628 N94-12968
Insoluble coatings for Stirling engine heat pipe condenser surfaces
[NASA-CR-191188] p 554 N94-14771
HEAT PUMPS
Development of a nonazeotropic heat pump for crew hygiene water heating
[NASA-CR-194189] p 737 N94-13674
HEAT RESISTANT ALLOYS
System integration and demonstration of adhesive bonded high temperature aluminum alloys for aerospace structure, phase 2
[NASA-CR-191459] p 575 N94-12792
High-temperature corrosion and protection of materials
[DE93-011072] p 568 N94-12998
HEAT SINKS
Microchannel cooled heatsinks for high average power laser diode arrays
[DE93-016533] p 658 N94-14442
HEAT STORAGE
Colorado State University program for developing, testing, evaluating, and optimizing solar heating and cooling systems
[DE93-016018] p 705 N94-14504
HEAT TOLERANCE
Cellular mechanism of turnover of the stress induced protein HSP 70
[AD-A265723] p 732 N94-13061
HEAT TRANSFER
Study of possible mechanisms of instability due to heat transfer
[INPE-5448-TDI/494] p 628 N94-12966
Magnetic fusion computing: A personal retrospective view
[DE93-014147] p 797 N94-13217
The corrosion behavior of 8001 Al under heat-transfer conditions in an aqueous loop system
[DE93-013450] p 569 N94-13242
A multiphase model for shock-induced flow in low density foam
[DE93-013767] p 632 N94-13397
Heat flows and harmonic maps with a free boundary
[DE93-622856] p 632 N94-13509
Thermal gravitational modelling and scaling of two-phase heat transport systems: Similarity considerations and useful equations predictions versus experimental results
[NLR-TP-91477-U] p 632 N94-13533
Experimental investigation of the effects of blowing ratio parameter on heat transfer to a film-cooled flat plate
[AD-A266599] p 636 N94-13780
Sidewall thermometry perturbations to nonlinear heat transport near the (lambda) transition in He-4
[DE93-014990] p 817 N94-14453
A conduction model for the vacuum arc remelting process
[NPL-DMM(A)-98] p 639 N94-14464
Colorado State University program for developing, testing, evaluating, and optimizing solar heating and cooling systems
[DE93-016018] p 705 N94-14504
HEAT TRANSFER COEFFICIENTS
Experimental measurement of local heat transfer coefficients over discrete roughened plates using infrared thermography p 635 N94-13652
High frame rate thermal imager for hypersonic wind tunnel applications
[ONERA-NT-1992-12] p 650 N94-14009
A conduction model for the vacuum arc remelting process
[NPL-DMM(A)-98] p 639 N94-14464
HEAT TRANSMISSION
Recent results from material processing studies on new generation lasers
[DE93-013841] p 653 N94-12898
HEAT TREATMENT
Microstructural evolution of NARloy-Z at elevated temperatures
[NASA-TM-108419] p 571 N94-13715
The microstructural response of near gamma-TiAl+W to heat treatment
[DSIS-93-00237] p 571 N94-13840
Microstructural mechanisms that enhance electromigration resistance in Al-Cu thin films
[DE93-013770] p 812 N94-14345
Effect of thermal processing practices on the properties of superplastic Al-Li alloys
[NASA-CR-4548] p 574 N94-14850
Quenching and annealing effects on the specific heat of YBa2Cu3O(7-delta)
[DE93-016483] p 816 N94-14868
HEATING
The multi-ion, multi-event test of ion cyclotron resonance heating
[NASA-CR-194134] p 789 N94-13419
Problems and opportunities in microwave joining of ceramics
[DE93-014998] p 579 N94-13888
Microwave hybrid heating of alumina filaments
[DE93-012642] p 581 N94-14327
HEATING EQUIPMENT
Development of a nonazeotropic heat pump for crew hygiene water heating
[NASA-CR-194189] p 737 N94-13674
HEAVY IONS
Evolution of high-repetition-rate induction accelerators through advancements in switching
[DE93-012599] p 654 N94-12963
Neutral strange particle production at the AGS
[DE93-014044] p 780 N94-13098
Cellular track model for study of heavy ion beams
[NASA-TP-3351] p 732 N94-13714
Longitudinal beam dynamics for heavy ion fusion
[DE93-013850] p 789 N94-13727
Single event effects and laser simulation studies
[NASA-CR-194506] p 657 N94-13812
The theory of relativistic heavy ion collisions
[DE93-015934] p 784 N94-13952
Physics of gas breakdown for ion beam transport in gas
[DE93-015646] p 801 N94-14349
HEAVY NUCLEI
On the statistical theory of the even-even nucleons levels' density
[DE93-623990] p 788 N94-14875
HELICAL FLOW
Studies of non-inductive current drive in the CDX-U tokamak p 799 N94-13680
HELICOPTER CONTROL
Kinematics and constraints associated with swashplate blade pitch control
[NASA-TM-102265] p 520 N94-12820
Piloting Vertical Flight Aircraft: A Conference on Flying Qualities and Human Factors
[NASA-CP-3220] p 521 N94-13294
ADS-33C related handling qualities research performed using the NRC Bell 205 airborne simulator p 521 N94-13295
MIL-H-8501B: Application to shipboard terminal operations p 521 N94-13296
A perspective on the FAA approval process: Integrating rotorcraft displays, controls and workload p 521 N94-13298
Some lessons learned in three years with ADS-33C --- rotorcraft handling qualities specification p 521 N94-13299
Investigation of the effects of bandwidth and time delay on helicopter roll-axis handling qualities p 522 N94-13300
A piloted simulation investigation of the normal load factor and longitudinal thrust required for air-to-air acquisition and tracking p 522 N94-13301
The application of active side arm controllers in helicopters p 522 N94-13302
Rotorcraft flying qualities improvement using advanced control p 522 N94-13303
The impact of flying qualities on helicopter operational agility p 522 N94-13304
A four-axis hand controller for helicopter flight control p 522 N94-13305
In-flight simulation of high agility through active control: Taming complexity by design p 523 N94-13306
Compatibility of information and mode of control: The case for natural control systems p 523 N94-13307
A model for rotorcraft flying qualities studies p 523 N94-13308
Interpreted Cooper-Harper for broader use p 523 N94-13309
Improvements in hover display dynamics for a combat helicopter p 523 N94-13310
The development and potential of inverse simulation for the quantitative assessment of helicopter handling qualities p 523 N94-13311
An analytic modeling and system identification study of rotor/fuselage dynamics at hover p 524 N94-13312
Visual cueing aids for rotorcraft landings p 524 N94-13313
Visual information for judging temporal range p 524 N94-13314
Visual cueing considerations in Nap-of-the-Earth helicopter flight head-slaved helmet-mounted displays p 524 N94-13315
Effects of simulator motion and visual characteristics on rotorcraft handling qualities evaluations p 524 N94-13317
Human factor implications of the Eurocopter AS332L-1 Super Puma cockpit p 525 N94-13319
Design and pilot evaluation of the RAH-66 Comanche selectable control modes p 525 N94-13322
Flight testing and frequency domain analysis for rotorcraft handling qualities characteristics p 526 N94-13324
Preliminary design features of the RASCAL: A NASA /Army rotorcraft in-flight simulator p 526 N94-13325

HELICOPTER DESIGN
The impact of flying qualities on helicopter operational agility p 522 N94-13304
Design and pilot evaluation of the RAH-66 Comanche Core AFCS p 525 N94-13321
Preliminary design features of the RASCAL: A NASA /Army rotorcraft in-flight simulator p 526 N94-13325

HELICOPTER PERFORMANCE
Piloting Vertical Flight Aircraft: A Conference on Flying Qualities and Human Factors
[NASA-CP-3220] p 521 N94-13294
ADS-33C related handling qualities research performed using the NRC Bell 205 airborne simulator p 521 N94-13295
MIL-H-8501B: Application to shipboard terminal operations p 521 N94-13296
A perspective on the FAA approval process: Integrating rotorcraft displays, controls and workload p 521 N94-13298
Some lessons learned in three years with ADS-33C --- rotorcraft handling qualities specification p 521 N94-13299
Investigation of the effects of bandwidth and time delay on helicopter roll-axis handling qualities p 522 N94-13300
A piloted simulation investigation of the normal load factor and longitudinal thrust required for air-to-air acquisition and tracking p 522 N94-13301
The application of active side arm controllers in helicopters p 522 N94-13302
Rotorcraft flying qualities improvement using advanced control p 522 N94-13303
The impact of flying qualities on helicopter operational agility p 522 N94-13304
In-flight simulation of high agility through active control: Taming complexity by design p 523 N94-13306
A model for rotorcraft flying qualities studies p 523 N94-13308
Interpreted Cooper-Harper for broader use p 523 N94-13309
Improvements in hover display dynamics for a combat helicopter p 523 N94-13310
The development and potential of inverse simulation for the quantitative assessment of helicopter handling qualities p 523 N94-13311
Effects of simulator motion and visual characteristics on rotorcraft handling qualities evaluations p 524 N94-13317
Design and pilot evaluation of the RAH-66 Comanche selectable control modes p 525 N94-13322
Flight testing and frequency domain analysis for rotorcraft handling qualities characteristics p 526 N94-13324
An analysis of helicopter attrition using a low level combat simulation
[DSIS-93-00282] p 515 N94-13839

HELICOPTER WAKES
New vortex dynamics methods for rotor free wake analysis
[AD-A266656] p 509 N94-14774
Free-wake computation of helicopter rotor flowfield for general flight regimes
[AD-A266692] p 509 N94-14781

HELICOPTERS
Flight service evaluation of composite components on the Bell helicopter model 206L
[NASA-CR-191499] p 555 N94-13267
Human factor implications of the Eurocopter AS332L-1 Super Puma cockpit p 525 N94-13319
Helicopter precision approach capability using the Global Positioning System
[NASA-CR-194037] p 513 N94-13957
New vortex dynamics methods for rotor free wake analysis
[AD-A266656] p 509 N94-14774
A new treatment of periodic systems with applications to helicopter rotor blade dynamics
[AD-A266770] p 510 N94-14784
Center of excellence in rotary wing technology
[AD-A266655] p 510 N94-14799

HELIUM
Lattice site of helium implanted in Si and diamond
[DE93-015365] p 805 N94-13012

HELIUM IONS
The multi-ion, multi-event test of ion cyclotron resonance heating
[NASA-CR-194134] p 789 N94-13419
High-order harmonic generation with short-pulse lasers
[DE93-016532] p 659 N94-14594

HELIUM ISOTOPES
Charged-particle evaluation methodology at Lawrence Livermore National Laboratory
[DE93-013429] p 781 N94-13251
Sidewall thermometry perturbations to nonlinear heat transport near the (lambda) transition in He-4
[DE93-014990] p 817 N94-14453

HELIUM PLASMA
Investigation of an alternating current plasma as an element selective atomic emission detector for high-resolution capillary gas chromatography and as a source for atomic absorption and atomic emission spectrometry p 798 N94-13678

HELIUM-NEON LASERS
Laser lithography by photon scanning tunneling microscopy
[DE93-015962] p 660 N94-14863

HELMET MOUNTED DISPLAYS
Improvements in hover display dynamics for a combat helicopter p 523 N94-13310
Visual cueing considerations in Nap-of-the-Earth helicopter flight head-slaved helmet-mounted displays p 524 N94-13315

HEMODYNAMIC RESPONSES
Health monitoring of Japanese payload specialist: Autonomic nervous and cardiovascular responses under reduced gravity condition (L-0) p 591 N94-13757

HERMETIC SEALS
MMIC packaging technology development
[NASA-CR-194183] p 621 N94-13336

HERTZSPRUNG-RUSSELL DIAGRAM
X ray observations of late-type stars using the ROSAT all-sky survey
[NASA-CR-193716] p 832 N94-14146

HESSIAN MATRICES
Optimization and eigenvalue computation with application to meteorology and oceanography
[DE93-015310] p 744 N94-13024

HETEROGENEITY
Thermodiffusion in heterogeneous elastic solids and homogenization
[REPT-14/1993] p 578 N94-13468
Boundary layer structure over areas of heterogeneous heat fluxes
[DE93-007887] p 715 N94-13912
A study of the role of homogeneous process in heterogeneous high explosives
[DE93-012733] p 585 N94-14180
Small-angle scattering, contrast variation and the study of complex composite materials: A study of the structure of carbon black
[DE93-012707] p 559 N94-14690
A characterization of carboxylesterases in rat and guinea pig: Their heterogeneity and role in detoxication of organophosphorus compounds
[NDRE-PUBL-93-1001] p 730 N94-14852

HETEROJUNCTIONS
Intrinsic and interfacial recombination in OMVPE- and MBE-prepared GaAs/Al(x)Ga(1-x)As heterostructures
[DE93-009844] p 809 N94-14083

HEURISTIC METHODS
Quaternions and the heuristic role of mathematical structures in physics
[DE93-622865] p 816 N94-12844
Solving integer programs from dependence and synchronization problems
[AD-A265702] p 767 N94-13284
Extremal polygon containment problems and other issues in parametric searching
[ITN-93-85214] p 771 N94-14506

HIERARCHIES
Analysis of interstellar cloud structure based on IRAS images
[NASA-CR-194341] p 836 N94-13332

HIGH ACCELERATION
Isolation of a piezoresistive accelerometer used in high acceleration tests
[DE93-013764] p 649 N94-13395

HIGH ASPECT RATIO
Approaches to high aspect ratio triangulations
[NASA-TM-107684] p 739 N94-12886

HIGH CURRENT
Advanced magnetic flux compression generator development issues: A comparison of coaxial and disk generators
[DE93-014025] p 794 N94-12849
Instability heating of the HDZP
[DE93-012641] p 798 N94-13513
Multi-bunch beam-break-up studies for a SWFEL/TBA
[DE93-016973] p 658 N94-14414

HIGH DEFINITION TELEVISION
An acoustic charge transport imager for high definition television applications
[NASA-CR-194518] p 650 N94-14029
Optimization of a subband coding for high definition television with motion controlled three dimensional frequency band decomposition
[ETN-93-94396] p 617 N94-14817

HIGH ELECTRON MOBILITY TRANSISTORS
A cryogenic seven-element HEMT front end for DSS 13 p 608 N94-14375

HIGH ENERGY INTERACTIONS
Measurements of transverse energy and forward energy in high-energy nuclear collisions
[DE93-012755] p 788 N94-12817
Quark and gluon jets at CDF
[DE93-014919] p 783 N94-13884
High energy hadron-hadron collisions
[DE93-015584] p 784 N94-13927
The theory of relativistic heavy ion collisions
[DE93-015934] p 784 N94-13952
Workshop on Formation of Supermolecular Structures in Composite Fluid: Phase Rule and Dynamics
[DE93-782887] p 581 N94-14421
Wake-field and space charge effects on high brightness beams calculations and measured results for the laser driven photoelectrons at BNL-ATF
[DE93-015787] p 659 N94-14572
Integrating PAW, a graphical analysis interface to Sybase
[DE93-014172] p 755 N94-14581
The next century astrophysics program p 546 N94-14832
Characteristics of a high energy muon(+)muon(-) collider based on electro-production of muons
[DE93-017154] p 790 N94-14893

HIGH FREQUENCIES
Measurement electronics of industrial microwave resonator sensors
[TKK-S-RAD-S194] p 625 N94-14096

HIGH GRAVITY ENVIRONMENTS
Gravity as a probe for understanding pattern specification
[NASA-CR-194142] p 713 N94-13418

HIGH POWER LASERS
Microchannel cooled heatsinks for high average power laser diode arrays
[DE93-016533] p 658 N94-14442

HIGH PRESSURE
Differential Sensitivity Theory applied to the MESA code for high pressure interactions
[DE93-016460] p 676 N94-14591

HIGH RESOLUTION
High resolution electron energy loss studies of surface vibrations
[DE93-014441] p 781 N94-13283
High time resolution studies of binary x ray pulsars
[NASA-CR-194395] p 832 N94-13894
High-resolution Z-contrast imaging and hole concentration mapping of YBCO thin films
[DE93-015803] p 808 N94-13930
A widget based operations simulator for a planetary camera: A model for the high resolution stereo camera on Mars 94
[DLR-FB-92-30] p 651 N94-14044
The effect of crystal tilt on high resolution micrographs of small metal particles
[DE93-013915] p 574 N94-14795

HIGH REYNOLDS NUMBER
Three-dimensional structure of straight and curved plane wakes
[NASA-CR-194420] p 501 N94-13266

HIGH SPEED CAMERAS
Energy and technology review, March 1993
[DE93-013941] p 849 N94-13019
High frame rate thermal imager for hypersonic wind tunnel applications
[ONERA-NT-1992-12] p 650 N94-14009

HIGH SPEED PHOTOGRAPHY
Energy and technology review, March 1993
[DE93-013941] p 849 N94-13019

HIGH STRENGTH STEELS
An investigation of the role of second phase particles in the design of ultra high strength steels of improved toughness
[AD-A266774] p 573 N94-14786

HIGH TEMPERATURE
High-temperature corrosion and protection of materials
[DE93-011072] p 568 N94-12998
High temperature electromagnetic characterization of thermal protection system tile materials
[NASA-CR-189687] p 578 N94-13431
High temperature behavior of glass (M-8) p 587 N94-13740
Statics and kinetics of phase transformations in bcc Fe-Cr
[DE93-013839] p 574 N94-14793

HIGH TEMPERATURE ENVIRONMENTS
Thermosolutal convection and macrosegregation in dendritic alloys
[NASA-CR-194039] p 567 N94-12825

Strain sensing technology for high temperature applications
[NASA-TM-4498] p 648 N94-12874
Interfacial precipitation, segregation and deformation in alloy 600: implications on primary-side IGSCC
[DE93-013161] p 568 N94-13035
A technique for direct measurement of skin friction in supersonic combustion flow p 503 N94-13555
Buckling analysis of laminated thin shells in a hot environment
[NASA-TM-106302] p 683 N94-14776

HIGH TEMPERATURE GAS COOLED REACTORS
A modular gas-cooled cermet reactor system for planetary base power
[DE93-013672] p 550 N94-13351

HIGH TEMPERATURE GASES
The onset of galactic winds in early-type galaxies
[NASA-CR-193640] p 836 N94-13446
Hypersonic flow phenomenology p 505 N94-14155
ROSAT observations of clusters with wide-angle tailed radio sources
[NASA-CR-193784] p 833 N94-14405

HIGH TEMPERATURE LUBRICANTS
A vacuum four-ball tribometer to evaluate liquid lubricants for space applications
[NASA-TM-106264] p 575 N94-12842
Synthetic lubricants and high-performance functional fluids: Phosphazenes
[ARL-TR-45] p 580 N94-14126

HIGH TEMPERATURE PLASMAS
Highly charged ions in hot, dense plasmas
[DE93-013348] p 795 N94-12995
Studies on equatorial shock formation during plasmaspheric refilling
[NASA-CR-194392] p 715 N94-13954
Indirect processes in electron impact ionization of Kr(24+) and Kr(25+)
[DE93-014129] p 784 N94-14140

HIGH TEMPERATURE SUPERCONDUCTORS
Processing, fabrication and demonstration of HTS integrated microwave circuits
[AD-A265789] p 619 N94-12892
Analysis and characterizations of planar transmission structures and components for superconducting and monolithic integrated circuits
[NASA-CR-193675] p 619 N94-13026
Effect of spontaneous decay of superconductor quasiparticles in the tunneling density of states
[DE93-012681] p 811 N94-14339
Kinetics of photodeposition of superconducting films
[DE93-015511] p 812 N94-14348
Insertion loss and noise-temperature contribution of high-temperature superconducting bandpass filters centered at 2.3 and 8.45 GHz p 608 N94-14376
Direct submillimeter absorptivity measurements on epitaxial Ba(1-x)K(x)BiO3 films at 2K
[DE93-013904] p 815 N94-14699
Renormalized band structure of CuO2 layers in superconducting compounds: A mean field approach
[PREPRINT-730] p 815 N94-14720

HIGH TEMPERATURE TESTS
Thermal distortion measurement of TETRUS type thermal test model of large deployable antenna for mobile communications satellite p 529 N94-13270
Aerodynamic and aerothermal facilities 2: Continuous flow high enthalpy facilities p 506 N94-14160
A hot dynamic seal rig for measuring hypersonic engine seal durability and flow performance
[NASA-TM-106294] p 664 N94-14727

HIGH VOLTAGES
Development of UHF spark-switched L-C Oscillators
[DE93-015019] p 623 N94-13892
A high voltage dielectrically isolated smart power technology based on silicon direct bonding
[LAAS-92492] p 626 N94-14698
Design and optimization of high voltage lateral DMOS devices using RESURF technology
[LAAS-92511] p 626 N94-14711

HISTORIES
Magnetic fusion computing: A personal retrospective view
[DE93-014147] p 797 N94-13217
Tidal interactions in the Earth Moon system
[COMMUNICATIONS-SER-B-160] p 837 N94-13503
Flight operations highlights, tapes 1 and 2
[NASA-TM-109293] p 850 N94-13633
A history of the Defence Research Establishment, Ottawa
[CTN-93-60737] p 850 N94-14060
My experiences in manned space flight p 698 N94-14276
Early baryon and meson spectroscopy culminating in the discovery of the Omega minus SU(3) and quarks
[DE93-014321] p 787 N94-14580

HOLDERS
Shielded open-circuited sample holders for dielectric and magnetic measurements of liquids and powders
[PB93-198851] p 652 N94-14687

HOLE DISTRIBUTION (MECHANICS)
Quantitative mapping of pore fraction variations in silicon nitride using an ultrasonic contact scan technique
[NASA-TP-3377] p 665 N94-13056

HOLE MOBILITY
Structural and electronic studies of a-SiGe:H alloys
[DE93-010021] p 809 N94-14085

HOLES (ELECTRON DEFICIENCIES)
High-resolution Z-contrast imaging and hole concentration mapping of YBCO thin films
[DE93-015803] p 808 N94-13930
Renormalized band structure of CuO2 layers in superconducting compounds: A mean field approach
[PREPRINT-730] p 815 N94-14720
Magnetic interactions and disorder - phase transitions in dilute spin-glasses and high temperature superconductors
[ITN-93-85217] p 815 N94-14825

HOLES (MECHANICS)
A classical instability for black strings and p-branes
[DE93-014577] p 839 N94-14116

HOLLOW CATHODES
Plasma contactor technology for Space Station Freedom
[NASA-TM-106291] p 553 N94-14725

HOLOGRAPHIC INTERFEROMETRY
Two color holographic interferometry for microgravity application
[NASA-CR-194424] p 651 N94-14447

HOLOGRAPHY
Reduce fluid experiment system flight data from IML-1
[NASA-CR-193835] p 804 N94-12873
Measuring methods for CFRP laminates' bending and torsion rigidities characteristics p 529 N94-13272
Image reconstruction for x ray holographic microscopy
[DE93-013094] p 653 N94-14772
Optimization study of x ray laser coherence in Ni-like Ta
[DE93-016419] p 660 N94-14888

HOMEOSTASIS
Calcitonin control of calcium metabolism during weightlessness
[NASA-CR-193622] p 731 N94-12960

HOMOGENEOUS TURBULENCE
A multiple-scale turbulence model for incompressible flow
[NASA-TM-106113] p 631 N94-13385
Turbulent diffusion in homogeneous shear flow with stable density stratification
[DLR-FB-92-26] p 639 N94-14443
The structure of intense vorticity in homogeneous isotropic turbulence p 643 N94-14747
Rapid distortion analysis and direct simulation of compressible homogeneous turbulence at finite Mach number p 645 N94-14757

HOMOGENIZING
Thermodiffusion in heterogeneous elastic solids and homogenization
[REPT-14/1993] p 578 N94-13468

HOMOLOGY
On the symmetry algebra of the discrete states in d less than 2 closed string theory
[DE93-622903] p 769 N94-13536

HONEYCOMB STRUCTURES
Theoretical studies of breakdown in random media
[DE93-018107] p 558 N94-14418

HORIZON SCANNERS
Low cost attitude control system reaction wheel development
[NASA-CR-191332] p 540 N94-13140

HORIZONTAL FLIGHT
Free-wake computation of helicopter rotor flowfield for general flight regimes
[AD-A266692] p 509 N94-14781

HORMONE METABOLISMS
Calcitonin control of calcium metabolism during weightlessness
[NASA-CR-193622] p 731 N94-12960
Gender differences in endocrine responses to posture and 7 days of 6 deg head down bed rest
[NASA-TM-103991] p 731 N94-12972

HORMONES
Calcitonin control of calcium metabolism during weightlessness
[NASA-CR-193622] p 731 N94-12960
Endocrine and metabolic changes in payload specialist (L-1) p 591 N94-13758
Bone culture research p 595 N94-13773
Thyroid alterations in porcine after prolonged exposure to cold or heat
[AD-A266840] p 733 N94-14879

HORN ANTENNAS
The 24 GHz measurements of 2.2 lambda conical horn antennas illuminating a conducting sheet
[NASA-TM-109002] p 598 N94-12811
Antenna pattern control using impedance surfaces
[NASA-CR-194517] p 602 N94-13799
Using a focal-plane array to estimate antenna pointing errors
[NASA-CR-194502] p 602 N94-13810

HORNS
HRMS sky survey wideband feed system design for DSS 24 beam waveguide antenna p 611 N94-14397

HOT ATOMS
Detection of hot muonic hydrogen atoms emitted in vacuum using x-rays
[DE93-010253] p 778 N94-12860

HOT ELECTRONS
Kinetic simulations of ultra-intense laser plasma interactions and a novel method of generating odd harmonics
[DE93-014418] p 797 N94-13207
Photochemical dynamics of surface oriented molecules
[DE93-016289] p 784 N94-13983

HOT ISOSTATIC PRESSING
Influence of heat treatment on microstructure of Ti-35wt Al prepared by elemental powder metallurgy
[GKSS/92/E/27] p 574 N94-14821

HOT PRESSING
Gas atomized Er3Ni powder for cryocooler applications
[DE93-011564] p 568 N94-13000

HOT STARS
X ray emission from dynamical shock models in hot-star winds
[NASA-CR-194093] p 847 N94-13288
Rocket and laboratory studies in astronomy
[NASA-CR-194410] p 832 N94-13966

HOTSHOT WIND TUNNELS
Aerodynamic and aerothermal facilities 2. Part 1: Short-duration, high-enthalpy facilities p 506 N94-14159

HOVERING
Improvements in hover display dynamics for a combat helicopter p 523 N94-13310
An analytic modeling and system identification study of rotor/fuselage dynamics at hover p 524 N94-13312
Visual cueing aids for rotorcraft landings p 524 N94-13313
Optimization-based controller design for rotorcraft p 527 N94-14642
Free-wake computation of helicopter rotor flowfield for general flight regimes
[AD-A266692] p 509 N94-14781

HUBBLE SPACE TELESCOPE
The four great observatories
[NASA-TM-109311] p 830 N94-13605
A capacifiector-based robotic system
[NASA-CR-193783] p 833 N94-14359

HULLS (STRUCTURES)
Approaches to high aspect ratio triangulations
[NASA-TM-107684] p 739 N94-12886
Structural investigation of a damaged GRP/foam sandwich composite using x ray computed tomography p 669 N94-13857

HUMAN BEHAVIOR
Psychophysiological investigations of the biomedical problems of manned spaceflight
[NASA-CR-194107] p 732 N94-13782

HUMAN BODY
Body/cushion contact stress analysis during sitting
[ITN-93-85204] p 736 N94-13229

HUMAN FACTORS ENGINEERING
Evaluation of the Retrograde Inflation Anti-G Suit (RIAGS)
[AD-A265884] p 736 N94-12935
Piloting Vertical Flight Aircraft: A Conference on Flying Qualities and Human Factors
[NASA-CP-3220] p 521 N94-13294
The application of active side arm controllers in helicopters p 522 N94-13302
A four-axis hand controller for helicopter flight control p 522 N94-13305
Human factor implications of the Eurocopter AS332L-1 Super Puma cockpit p 525 N94-13319
Analysis of differences between seating positions in simulators and orbiters
[NASA-TM-104776] p 737 N94-13399
Human factors in aviation maintenance: Phase 3, volume 1
[DOT/FAA/AM-93/15] p 738 N94-14023
SHEAN (Simplified Human Error Analysis code) and automated THERP
[DE93-014904] p 738 N94-14451
Determination of Loran-C/GPS human factors issues
[PB93-199693] p 514 N94-14563

HUMAN PERFORMANCE
Readiness to perform testing: A critical analysis of the concept and current practices
[DOT/FAA/AM-93/13] p 732 N94-13193
Functional categories for future flight deck designs
[NASA-TM-109005] p 517 N94-13710
An evaluation of noise and its effects on shuttle crewmembers during STS-50/USML-1
[NASA-TM-104775] p 735 N94-13961
Human factors in aviation maintenance: Phase 3, volume 1
[DOT/FAA/AM-93/15] p 738 N94-14023
SHEAN (Simplified Human Error Analysis code) and automated THERP
[DE93-014904] p 738 N94-14451

HUMAN TOLERANCES
Evaluation of the Retrograde Inflation Anti-G Suit (RIAGS)
[AD-A265884] p 736 N94-12935
Psychophysiological investigations of the biomedical problems of manned spaceflight
[NASA-CR-194107] p 732 N94-13782
An assessment of the potential for neck injury due to padding of aircraft interior walls for head impact protection
[DOT/FAA/AM-93/14] p 738 N94-13972

HUMIDITY
Atmospheric soundings during the Washita 1992 campaign
[NASA-CR-194383] p 712 N94-13212
Estimations of temperature and humidity of the canopy in Amazon Forest using microwave data from SMMR sensor of Nimbus-7 satellite
[INPE-5444-TDI/490] p 720 N94-13614
Binary homogeneous nucleation: Temperature and relative humidity fluctuations and non-linearity
[DE93-007884] p 709 N94-13911
Room temperature degradation of YBa2Cu3O(7-x) superconductors in varying relative humidity environments
[NASA-TP-3368] p 813 N94-14409

HUMIDITY MEASUREMENT
NASA metrology and calibration, 1993
[NASA-TM-109280] p 597 N94-14410

HYBRID CIRCUITS
Thermal design of hybrid circuits: Tools and methodology
[LAAS-92515] p 626 N94-14713

HYBRID COMPOSITES
Design and application of a quasistatic crush test fixture for investigating scale effects in energy absorbing composite plates
[NASA-CR-4526] p 670 N94-13063

HYBRID PROPULSION
Battery testing at Argonne National Laboratory
[DE93-011761] p 624 N94-14012

HYDRATES
Overview: Gas hydrate geology and geography
[DE93-014043] p 688 N94-14151

HYDRATION
The importance of hard core repulsion in models of activity coefficients in aqueous electrolyte solutions: Illustration in the case of hydration theory
[DE93-012476] p 561 N94-12881

HYDRAULIC FLUIDS
Synthetic lubricants and high-performance functional fluids: Phosphazenes
[ARL-TR-45] p 580 N94-14126

HYDRIDES
First-principles studies of phase stability and the structural and dynamical properties of hydrogen-metal systems
[DE93-016129] p 570 N94-13374

HYDROBALLISTICS
Collisions and separations in 2D hydrodynamical code
[ITN-93-85225] p 639 N94-14503

HYDROCARBONS
Laser-induced fluorescence over optical fibers for real time in situ measurement of petroleum hydrocarbons in seawater
[AD-A265106] p 790 N94-12863
Direct probing of chromatography columns by laser-induced fluorescence
[DE93-015208] p 654 N94-13022
Overview: Gas hydrate geology and geography
[DE93-014043] p 688 N94-14151

HYDRODYNAMIC EQUATIONS
On MHD mode equations in toroidal plasmas
[PPL-139] p 800 N94-13877
Collisions and separations in 2D hydrodynamical code
[ITN-93-85225] p 639 N94-14503

HYDRODYNAMICS
The 3-D massively parallel impact simulations using PCTH
[DE93-011593] p 670 N94-12908
Three dimensional time-dependent hydrodynamic and propagation modeling of x ray laser emission
[DE93-012575] p 654 N94-12962
Highly charged ions in hot, dense plasmas
[DE93-013348] p 795 N94-12995
Comparison of analytic Whipple bumper shield ballistic limits with CTH simulations
[DE93-015126] p 539 N94-13006
Inertial confinement fusion program
[DE93-013372] p 796 N94-13047
Hydrodynamic asymptotics of Green functions in magnetics with spontaneously broken symmetry
[DE93-621349] p 767 N94-13223
Gas core nuclear thermal rocket engine research and development in the former USSR
[DE93-012165] p 552 N94-14013
A study of the role of homogeneous process in heterogeneous high explosives
[DE93-012733] p 585 N94-14180
Nonlinear wave predictions in ceramics
[DE93-016516] p 582 N94-14436
Collisions and separations in 2D hydrodynamical code
[ITN-93-85225] p 639 N94-14503
Nonlinear wave forces on large ocean structures
[AD-A266820] p 683 N94-14902

HYDROGEN
Effects of hydrogen addition on combustion performance of a LOX/kerosene rocket
[NAL-TR-1177] p 548 N94-12945
Measurement of H zero excited states produced by foil stripping of 800-MeV H(-) ions
[DE93-014391] p 788 N94-13103
A survey and analysis of experimental hydrogen sensors
[NASA-TM-106300] p 648 N94-13135
Destruction of problematic airborne contaminants by hydrogen reduction using a Catalytically Active, Regenerable Sorbent (CARS)
[NASA-CR-194354] p 709 N94-14103
BAKEOUT: A computer program for predicting diffusive outgassing from stainless steel
[DE93-012613] p 573 N94-14364
A hydrogen atom in the curved space: Orthogonality of radial wave functions with respect to the critical momentum
[DE93-626623] p 788 N94-14891

HYDROGEN ATOMS
Detection of hot muonic hydrogen atoms emitted in vacuum using x-rays
[DE93-010253] p 778 N94-12860
Measurements of scattering processes in negative ion-atom collisions
[DE93-013863] p 779 N94-12940
Atomic hydrogen and nitrogen distributions from atmosphere explorer measurements
[NASA-CR-194336] p 714 N94-13825
Energetic neutral atoms: Imaging the magnetospheric ring current
[NASA-CR-194339] p 715 N94-13826
Quantum state resolved desorption of CO from solid surfaces
[DE93-016876] p 814 N94-14597
Radiation perturbation theory in gravity and quantum universe as a hydrogen atom
[DE93-626621] p 849 N94-14889
A hydrogen atom in the curved space: Orthogonality of radial wave functions with respect to the critical momentum
[DE93-626623] p 788 N94-14891

HYDROGEN CLOUDS
The distance to the high velocity clouds of neutral hydrogen
[NASA-CR-194343] p 838 N94-13716

HYDROGEN EMBRITTLEMENT
A microstructural approach to fatigue crack processes in poly crystalline BCC materials
[DE93-016666] p 812 N94-14354
A study of hydrogen effects on fracture behavior of radioactive waste storage tanks
[DE93-018171] p 574 N94-14873

HYDROGEN FUELS
Computer program for thermal and transport properties of parahydrogen from 20 to 10,000 K
[NASA-TP-3378] p 552 N94-14102

HYDROGEN IONS
Measurements of scattering processes in negative ion-atom collisions
[DE93-013863] p 779 N94-12940
Measurement of H zero excited states produced by foil stripping of 800-MeV H(-) ions
[DE93-014391] p 788 N94-13103

HYDROGEN OXYGEN ENGINES
Tensile properties of LE-7 engine material with welded joint
[NAL-TR-1188] p 570 N94-13460
Analysis of reacting flowfields in low-thrust rocket engines and plumes p 552 N94-14491

HYDROGEN PEROXIDE
Reduction of Pu(6) with hydrogen peroxide: Effects of plutonium, peroxide, and iron concentrations and of reaction time
[DE93-013598] p 564 N94-13487
Hydrogen peroxide safety issues
[DE93-013895] p 565 N94-14346

HYDROGEN PLASMA
Two temperature modeling and experimental measurements of laser sustained hydrogen plasmas
[AD-A265750] p 796 N94-13039

HYDROGEN SULFIDE
Promotion of geothermal energy development in 1991
[DE93-799061] p 705 N94-14679

HYDROGENATION
Catalytic arene hydrogenation using early transition metal hydride compounds
[DE93-015500] p 573 N94-14402

HYDROLOGICAL CYCLE
Circulation and rainfall climatology of a 10-year (1979 - 1988) integration with the Goddard Laboratory for atmospheres general circulation model
[NASA-TM-104591] p 723 N94-14074
Space measurements for determining the Earth's energy and water cycles p 690 N94-14227
Integration of space and in-situ observations to study atmosphere, ocean and land processes
[NASA-CR-194495] p 683 N94-14500

HYDROLOGY
Promotion of geothermal energy development in 1991
[DE93-799057] p 701 N94-13214
Promotion of geothermal energy development in 1991
[DE93-799058] p 701 N94-13215
The 1990 Western Pacific Geophysics meeting
[NASA-CR-193456] p 712 N94-13334
The American Geophysical Union Chapman Conference on Tectonics and Topography
[NASA-CR-193454] p 713 N94-13335

HYDROLYSIS
Destruction of waste energetic materials using base hydrolysis
[DE93-012738] p 584 N94-13491

HYDROSTATICS
Technology assessments of advanced energy storage systems for electric and hybrid vehicles
[DE93-014395] p 701 N94-12913

HYGIENE
Development of a nonazeotropic heat pump for crew hygiene water heating
[NASA-CR-194189] p 737 N94-13674

HYPERBOLIC DIFFERENTIAL EQUATIONS
A high-resolution Lax-Friedrichs scheme for hyperbolic conservation laws with source terms: Application to shallow water equations
[DM-62] p 632 N94-13535
On the superconvergence of Galerkin methods for hyperbolic IBVP
[NASA-CR-194293] p 770 N94-13922
On the superconvergence of Galerkin methods for hyperbolic IBPV
[NASA-CR-194488] p 770 N94-14307

HYPERBOLIC FUNCTIONS
A priori error estimates for an hp-version of the discontinuous Galerkin method for hyperbolic conservation laws
[NASA-TM-108993] p 632 N94-13467

HYPERCUBE MULTIPROCESSORS
An efficient parallel algorithm for matrix-vector multiplication
[DE93-015125] p 754 N94-14399

HYPERGEOMETRIC FUNCTIONS
Rare attributes in finite universe: Hypotheses testing specification and exact randomized upper confidence bounds
[DE93-012783] p 775 N94-12955

HYPERNUCLEI
Resonances in the Sigma NN system
[DE93-014353] p 785 N94-14144

HYPERSONIC BOUNDARY LAYER
Hypersonic flow phenomenology p 505 N94-14155
Hypersonic propulsion characterization p 505 N94-14156

HYPERSONIC COMBUSTION
Numerical study of shock-induced combustion in methane-air mixtures
[NASA-TM-106354] p 642 N94-14722

HYPERSONIC FLIGHT
Methodology of Hypersonic Testing
[VKI-LS-1993-03] p 505 N94-14153
Hypersonic overview p 505 N94-14154
Aerodynamic and aerothermal facilities 1: Hypersonic wind tunnels p 506 N94-14158
Hypersonic flight test. Part 1: Propulsion flight testing p 507 N94-14168

Hypersonic flight testing. Part 2: Aerothermal flight testing p 507 N94-14169
Shock/boundary-layer/shock interactions p 507 N94-14172

HYPERSONIC FLOW
Numerical simulation of hypersonic flow for the design of the H-2 orbiting plane (HOPE), part 3 [NAL-TR-1168-PT-3] p 499 N94-12948
Hypersonic aerodynamic characteristics of SSTO-type aerospace planes. Part 1: The NAL 0-th configuration [NAL-TR-1186] p 514 N94-13459
Methodology of Hypersonic Testing [VKI-LS-1993-03] p 505 N94-14153
Hypersonic overview p 505 N94-14154
Hypersonic flow phenomenology p 505 N94-14155
Aerodynamic and aerothermal facilities 1: Hypersonic wind tunnels p 506 N94-14158
Computational techniques and capabilities p 506 N94-14162
Hypersonic flow field measurements: Intrusive p 507 N94-14166
Hypersonic flow-field measurements: Nonintrusive p 507 N94-14167
Shock/boundary-layer/shock interactions p 507 N94-14172
Computation of nonequilibrium flows using PNS equations p 641 N94-14610
Hypersonic viscous flow computations p 510 N94-14612
Simulation of hypersonic, reacting flow around reentry bodies: Comparisons of numerical and experimental results [MBB-LME-211-S-PUB-507] p 509 N94-14710
Numerical study of shock-induced combustion in methane-air mixtures [NASA-TM-106354] p 642 N94-14722
A hot dynamic seal rig for measuring hypersonic engine seal durability and flow performance [NASA-TM-106294] p 664 N94-14727
Vibrational relaxation in hypersonic flow fields [NASA-TP-3367] p 776 N94-14733

HYPERSONIC HEAT TRANSFER
Test and evaluation methods p 506 N94-14163

HYPERSONIC NOZZLES
A comparison of computational and experimental data for a subscale high speed propulsive nozzle at low mach numbers [AD-A266543] p 504 N94-13705

HYPERSONIC SHOCK
Numerical simulations and experiments on physics of high Mach number shockwave: Turbulent flow interactions [DE93-013424] p 631 N94-13249
Sub-grid scale modeling for large eddy simulations in analysis of shock-turbulence interactions [DE93-013425] p 631 N94-13250
Calculation of hypersonic shock structure using flux-split algorithms [NASA-CR-194296] p 504 N94-13607

HYPERSONIC SPEED
Electromagnetic wave test p 508 N94-14173

HYPERSONIC TEST APPARATUS
Methodology of Hypersonic Testing [VKI-LS-1993-03] p 505 N94-14153
Characterization of flow fields in hypersonic ground test facilities p 505 N94-14157
Aerodynamic and aerothermal facilities 1: Hypersonic wind tunnels p 506 N94-14158
Aerodynamic and aerothermal facilities 2. Part 1: Short-duration, high-enthalpy facilities p 506 N94-14159
Aerodynamic and aerothermal facilities 2: Continuous flow high enthalpy facilities p 506 N94-14160
Aeropropulsion facilities p 506 N94-14161

HYPERSONIC VEHICLES
Strain sensing technology for high temperature applications [NASA-TM-4498] p 648 N94-12874
Hypersonic propulsion characterization p 505 N94-14156
Materials/structures testing p 506 N94-14164
Aeropropulsion test and evaluation methods p 506 N94-14165
Boundary-layer transition p 507 N94-14171
Propulsion integration p 508 N94-14174
Vibrational relaxation in hypersonic flow fields [NASA-TP-3367] p 776 N94-14733

HYPERSONIC WIND TUNNELS
Numerical simulation of hypersonic flow for the design of the H-2 orbiting plane (HOPE), part 3 [NAL-TR-1168-PT-3] p 499 N94-12948
High frame rate thermal imager for hypersonic wind tunnel applications [ONERA-NT-1992-12] p 650 N94-14009
Methodology of Hypersonic Testing [VKI-LS-1993-03] p 505 N94-14153
Characterization of flow fields in hypersonic ground test facilities p 505 N94-14157
Aerodynamic and aerothermal facilities 1: Hypersonic wind tunnels p 506 N94-14158
Test and evaluation methods p 506 N94-14163

HYPERSONICS
Hypersonic aerodynamic characteristics of SSTO-type aerospace planes. Part 1: The NAL 0-th configuration [NAL-TR-1186] p 514 N94-13459
A comparison of computational and experimental data for a subscale high speed propulsive nozzle at low mach numbers [AD-A266543] p 504 N94-13705
Hypersonic overview p 505 N94-14154
Hypersonic viscous flow computations p 510 N94-14612

HYPERVELOCITY GUNS
High velocity gas gun [NASA-TM-109296] p 541 N94-13637

HYPERVELOCITY IMPACT
Recovery of materials impacted at high velocity [DE93-014150] p 576 N94-12885
The 3-D massively parallel impact simulations using PCTH [DE93-011593] p 670 N94-12908
VFGEN: A parallel volume fraction generator for hydrocodes [DE93-011673] p 752 N94-14019

HYPERVELOCITY LAUNCHERS
Experimental technique to simulate orbital-debris impact on space shields at impact velocities over 10 km/s [DE93-011619] p 539 N94-12909

HYPERVELOCITY PROJECTILES
Experimental technique to simulate orbital-debris impact on space shields at impact velocities over 10 km/s [DE93-011619] p 539 N94-12909
Comparison of analytic Whipple bumper shield ballistic limits with CTH simulations [DE93-015126] p 539 N94-13006
Simulation of orbital debris impacts on bumper shields [DE93-013773] p 540 N94-13398
Calibration of a magnetic induction system for measurement of hypervelocities [DE93-013949] p 652 N94-14578

HYPODYNAMIA
Clinical physiology of bed rest [NASA-TM-104010] p 727 N94-13447

I

ICE
Planning of a comet simulator [ITN-93-85206] p 835 N94-13230
Optical properties of CO2 ice and CO2 snow in the ultraviolet, visible, and infrared [NASA-CR-194110] p 686 N94-14081

ICE FORMATION
Numerical study of the effects of icing on viscous flow over wings [NASA-CR-193306] p 500 N94-13180
Smart skin technology development for measuring ice accretion, stall, and high AOA aircraft performance. Part 1: Capacitive ice detector development [NASA-CR-194252] p 511 N94-13424

ICE MAPPING
Outline of ISY sea surface temperature data sets p 696 N94-14261

IDEAL GAS
A comparison of computational and experimental data for a subscale high speed propulsive nozzle at low mach numbers [AD-A266543] p 504 N94-13705

IGNITERS
STS-55 pad abort: Engine 2011 oxidizer preburner augmented spark igniter check valve leak [NASA-CR-193830] p 533 N94-12806

IGNITION
Modeling ignition chemistry [DE93-012340] p 561 N94-12910
Flamespreading in granular solid propellant: Design of an experiment [AD-A266009] p 583 N94-12987
Inertial Confinement Fusion [DE93-013303] p 795 N94-13017
Chemical reactions in scramjet engines: Reduced kinetic models for ignition, combustion and nozzle flow [NAL-TR-1184] p 563 N94-13458
Homogeneous-hetergeneous combustion: Thermal and chemical coupling [DE93-016050] p 565 N94-14403
Three-dimensional modeling of diesel engine intake flow, combustion and emissions-2 [NASA-CR-191189] p 519 N94-14448
Comparative ignition of hexane and octane isomers in a shock tube [DE93-016535] p 566 N94-14869

ILLUMINANCE
Fundamentals and techniques of nonimaging optics [DE93-013145] p 791 N94-13015
Simulating the daylight performance of fenestration systems and spaces of arbitrary complexity: The IDC method [DE93-015177] p 704 N94-14333

ILLUMINATING
Phase-shifting effect of light and exercise on the human circadian clock [AD-A265732] p 732 N94-13038
Validation of an inexpensive illuminant for aeromedical color vision screening [DOT/FAA/AM-93/16] p 736 N94-14854

IMAGE ANALYSIS
View generated database [NASA-CR-191397] p 822 N94-13116
EOS workstation [NASA-CR-191326] p 736 N94-13132
Bayesian estimation of motion fields from image sequences [ISBN-0-315-57212-4] p 772 N94-13540
Evaluation of the Shuttle remote manipulator [NASA-CR-194351] p 662 N94-13800
Determination of position and orientation of rigid bodies from image segments [FFI-92-4005] p 752 N94-14039
Intelligent environment for interpretation tasks of remotely sensed images [INPE-5466-PRE/1774] p 687 N94-14082
Asia-Pacific ISY Conference, volume 2 [NASDA-CM-199-VOL-2] p 688 N94-14209
Image processing and analysis of airborne POLDER data p 689 N94-14219
Data analysis for GOPEX image frames p 610 N94-14388
Obstacle detection by recognizing binary expansion patterns [NASA-CR-194415] p 514 N94-14495

IMAGE CLASSIFICATION
Feature extraction and classification algorithms for high dimensional data [NASA-CR-194298] p 743 N94-13023
Design of partially supervised classifiers for multispectral image data [NASA-CR-194299] p 823 N94-13192
A review and analysis of neural networks for classification of remotely sensed multispectral imagery [NASA-CR-194291] p 763 N94-13603
Nonlinear aspects of data integration for land-cover classification in a neural network environment [INPE-5479-PRE/1778] p 686 N94-13789

IMAGE CORRELATORS
Acousto-optical post-processor time-integrating correlator updates [DSIS-93-00314] p 777 N94-13831

IMAGE ENHANCEMENT
Advanced ballistic range technology [NASA-CR-194530] p 533 N94-14540

IMAGE FILTERS
Robust filters for image smoothing [ERB-1033] p 769 N94-13545

IMAGE FURNACES
High temperature behavior of glass (M-8) p 587 N94-13740

IMAGE INTENSIFIERS
Suppression of bright objects using a spatial light modulator when imaging with CCD- and image intensified cameras [FFI-93/7008] p 650 N94-13665

IMAGE MOTION COMPENSATION
Image motion photography [DE93-013962] p 653 N94-14858

IMAGE PROCESSING
Color image processing for flat panel visual display modeling [NASA-CR-193660] p 790 N94-12797
Reduce fluid experiment system flight data from IML-1 [NASA-CR-193835] p 804 N94-12873
Spatially-varying IIR filter banks for image coding [NASA-CR-193727] p 619 N94-12897
Recursive time-varying filter banks for subband image coding [NASA-CR-193726] p 598 N94-12920
Feature extraction and classification algorithms for high dimensional data [NASA-CR-194298] p 743 N94-13023
Knowledge-based oceanographic image compression [AD-A265752] p 821 N94-13041
Preparations for and first results of the calibration and interpretation of ERS-1 SAR imagery over land [BCRS-92-13] p 684 N94-13123

EOS workstation
[NASA-CR-191326] p 736 N94-13132
Development of a portable multispectral thermal infrared camera
[NASA-CR-191340] p 648 N94-13176
Exact reconstruction analysis/synthesis filter banks with time-varying filters
[NASA-CR-193725] p 600 N94-13466
Design and performance of an automated video-based laser beam alignment system
[DE93-012571] p 656 N94-13481
Three dimensional tracking of four point planar patterns using corners
[ISBN-0-315-52149-X] p 791 N94-13490
Close range 3-D position sensing using stereo vision and point-of-correspondance through mathematical morphology
[ISBN-0-315-61012-3] p 763 N94-13515
Robust filters for image smoothing
[ERB-1033] p 769 N94-13545
A data distributed parallel algorithm for ray-traced volume rendering
[NASA-CR-191520] p 749 N94-13721
Feature discovery on segmented objects in SAR imagery using self-organizing neural networks
[DE93-010685] p 686 N94-14056
Intelligent environment for interpretation tasks of remotely sensed images
[INPE-5466-PRE/1774] p 687 N94-14082
Asia-Pacific ISY Conference, volume 2
[NASDA-CM-199-VOL-2] p 688 N94-14209
Results from ERS-1 and JERS-1 SAR calibration experiments and data analysis p 688 N94-14210
Geologic application of JERS-1 SAR data p 688 N94-14211
An exact processing algorithm for wide beam spaceborne SAR data p 689 N94-14213
Image processing and analysis of airborne POLDER data p 689 N94-14219
Integration of SST data sets using MOS-1 satellite data: For validation and monitoring p 696 N94-14262
Center of trace algorithms for extracting digitized waveforms from two-dimensional images
[DE93-015082] p 753 N94-14295
Data analysis for GOPEX image frames p 610 N94-14388
Laser beam control and diagnostic systems for the copper-pumped dye laser system at Lawrence Livermore National Laboratory
[DE93-016529] p 658 N94-14437
Obstacle detection by recognizing binary expansion patterns
[NASA-CR-194415] p 514 N94-14495
Image reconstruction for x ray holographic microscopy
[DE93-013094] p 653 N94-14772
A fast frame rate 512 x 512 CCD digital camera system
[DE93-013048] p 653 N94-14792
Two dimensional measurement and evaluation of point images at microscope objectives
[ETN-93-94397] p 793 N94-14856
Image motion photography
[DE93-013962] p 653 N94-14858

IMAGE RECONSTRUCTION
Image reconstruction for x ray holographic microscopy
[DE93-013094] p 653 N94-14772
Optimization of a subband coding for high definition television with motion controlled three dimensional frequency band decomposition
[ETN-93-94396] p 617 N94-14817

IMAGE RESOLUTION
Confocal profilometer with nanometric vertical resolution
[DE93-622698] p 653 N94-12857
Image coding using entropy-constrained residual vector quantization
[NASA-CR-193728] p 744 N94-13113
Parametric binary dissection
[NASA-CR-191496] p 762 N94-13184
Mathematic methods and algorithms for real-time applications
[AD-A266776] p 771 N94-14789
Two dimensional measurement and evaluation of point images at microscope objectives
[ETN-93-94397] p 793 N94-14856

IMAGERY
A review and analysis of neural networks for classification of remotely sensed multispectral imagery
[NASA-CR-194291] p 763 N94-13603

IMAGES
Advanced ballistic range technology
[NASA-CR-194530] p 533 N94-14540

IMAGING RADAR
Proceedings of the 11th Space Surveillance Workshop, volume 1
[AD-A265120] p 531 N94-13358

IMAGING SPECTROMETERS
Spectral analysis for automated exploration and sample acquisition
[NASA-CR-194095] p 545 N94-13189
Imaging Fourier transform spectrometer
[DE93-017193] p 651 N94-14416

IMAGING TECHNIQUES
Low energy neutral atom imaging techniques
[DE93-012744] p 779 N94-12950
Automated crack identification for cement paste
[AD-A265753] p 665 N94-13042
HYMOSS signal processing for pushbroom spectral imaging
[NASA-CR-191341] p 620 N94-13125
The development of the TIMAX project: A hard x ray imaging telescope
[INPE-5474-TDI/505] p 829 N94-13245
Imaging microscopy with x ray lasers at Lawrence Livermore National Laboratory
[DE93-013419] p 655 N94-13258
Non-scanned LADAR imaging and applications
[DE93-013772] p 655 N94-13261
Advances in low energy neutral atom imaging techniques
[DE93-012745] p 782 N94-13492
Operational test of the airborne data acquisition system: SADA, the Bara Bonita experiment
[INPE-5451-NTC/305] p 685 N94-13610
The 1 to 5 micron imaging of deeply embedded young stellar objects p 831 N94-13657
Magnetic resonance imaging after exposure to microgravity p 594 N94-13771
Energetic neutral atoms: Imaging the magnetospheric ring current
[NASA-CR-194339] p 715 N94-13826
Development of a computer vision system to supplement the active tactile sensing capability in a structured environment
[DSIS-93-00072] p 764 N94-13844
Current distribution tomography for determination of internal current density distributions
[DE93-015463] p 604 N94-13899
High-resolution Z-contrast imaging and hole concentration mapping of YBCO thin films
[DE93-015803] p 808 N94-13930
Stochastic performance modeling and evaluation of obstacle detectability with imaging range sensors
[NASA-CR-194510] p 605 N94-13946
An acoustic charge transport imager for high definition television applications
[NASA-CR-194518] p 650 N94-14029
Study of speckle reduction when using a CO2 waveguide laser close to its threshold state
[DSIS-93-00250] p 657 N94-14067
Droplet-turbulence interactions in sprays exposed to supercritical environmental conditions
[NASA-CR-194408] p 638 N94-14308
Terrestrial magnetospheric imaging: Numerical modeling of low energy neutral atoms
[DE93-014561] p 717 N94-14328
Data analysis for GOPEX image frames p 610 N94-14388
Supervised classification of remotely sensed images
[DLR-FB-92-07] p 700 N94-14428
The first data from the MACHO experiment
[DE93-014423] p 840 N94-14467
Measurements of edge fluctuations by phase contrast imaging on DIII-D
[DE93-014018] p 802 N94-14579
Quantitative luminescence imaging system
[DE93-015691] p 793 N94-14702
Intra-blade quantitative transonic flow measurements at the DRA Pyestock Isentropic Light Piston Facility using PIV (Particle Image Velocimetry)
[RAE-TM-AERO/PROP-21] p 509 N94-14706
Depths from focusing and defocusing
[AD-A266644] p 735 N94-14797
The 8 to 11 keV x ray sources for imaging and absorption experiments
[DE93-015973] p 803 N94-14865
Optimization study of x ray laser coherence in Ni-like Ta
[DE93-016419] p 660 N94-14888

IMMUNE SYSTEMS
Cellular track model for study of heavy ion beams
[NASA-TP-3351] p 732 N94-13714
Cellular responses to low-gravity: Pilot studies on suborbital rockets and orbiting spacecraft
[NASA-CR-194402] p 729 N94-14494

IMPACT DAMAGE
Modeling the impact behavior of AD85 ceramic under multi-axial loading
[AD-A265877] p 576 N94-12932
Comparison of analytic Whipple bumper shield ballistic limits with CTH simulations
[DE93-015126] p 539 N94-13006
Simulation of orbital debris impacts on bumper shields
[DE93-013773] p 540 N94-13398
Secondary impact hazard assessment
[NASA-CR-188261] p 543 N94-14483

IMPACT LOADS
Modeling the impact behavior of AD85 ceramic under multi-axial loading
[AD-A265877] p 576 N94-12932

IMPACT MELTS
Impact melting and vaporization in planetary regoliths p 843 N94-14299

IMPACT PREDICTION
Differential Sensitivity Theory applied to the MESA code for high pressure interactions
[DE93-016460] p 676 N94-14591

IMPACT RESISTANCE
An assessment of the potential for neck injury due to padding of aircraft interior walls for head impact protection
[DOT/FAA/AM-93/14] p 738 N94-13972

IMPACT STRENGTH
An experimental investigation into the damage resistance and compression-after-impact strength of T800H/3900-2
[LTR-ST-1909] p 675 N94-13945

IMPACT TESTS
Recovery of materials impacted at high velocity
[DE93-014150] p 576 N94-12885
The 3-D massively parallel impact simulations using PCTH
[DE93-011593] p 670 N94-12908
Experimental technique to simulate orbital-debris impact on space shields at impact velocities over 10 km/s
[DE93-011619] p 539 N94-12909
A general contact detection algorithm for finite element analysis
[DE93-012846] p 742 N94-12956
Isolation of a piezoresistive accelerometer used in high acceleration tests
[DE93-013764] p 649 N94-13395
Evaluation for rheological constitutive relations, using the indentation technique p 775 N94-13627
Fatigue and residual strength characteristics of fiber metal laminates subjected to incidental damage
[LR-708] p 674 N94-13803
An assessment of the potential for neck injury due to padding of aircraft interior walls for head impact protection
[DOT/FAA/AM-93/14] p 738 N94-13972
Materials/structures testing p 506 N94-14164
Secondary impact hazard assessment
[NASA-CR-188261] p 543 N94-14483

IMPEDANCE
Effect of microstructure on passive film formation and breakdown on Al alloys
[AD-A265339] p 569 N94-13050
A new formulation of longitudinal coherent instabilities
[DE93-014288] p 789 N94-13220
Generalized impedance control of a redundant manipulator p 661 N94-13575
Scattering by a groove in an impedance plane
[NASA-CR-193362] p 602 N94-13720
Longitudinal beam dynamics for heavy ion fusion
[DE93-013850] p 789 N94-13727
Design and control of a macro-micro robot for precise force applications p 682 N94-14651

IMPELLERS
Numerical simulations of unsteady flows in turbomachines p 633 N94-13569

IMPINGEMENT
A multiphase model for shock-induced flow in low density foam
[DE93-013767] p 632 N94-13397
The 8 to 11 keV x ray sources for imaging and absorption experiments
[DE93-015973] p 803 N94-14865

IMPLOSIONS
Two-dimensional simulations of foil implosion experiments on the Los Alamos capacitor bank
[DE93-012676] p 794 N94-12814
Advanced magnetic flux compression generator development issues: A comparison of coaxial and disk generators
[DE93-014025] p 794 N94-12849
Shock-free acceleration of laser driven targets
[DE93-008050] p 655 N94-13387
Review of the Procyon explosive pulsed power system
[DE93-016562] p 802 N94-14532
Toward a quasi-linear closure for compressible turbulence
[DE93-017185] p 647 N94-14895

IMPURITIES
Proceedings of the Workshop on Applications of Synchrotron Radiation to Trace Impurity Analysis for Advanced Silicon Processing
[DE93-013389] p 805 N94-13020

Performance effects of coal-derived contaminants on the carbonate fuel cell
[DE93-013801] p 703 N94-13693
Room temperature degradation of YBa2Cu3O(7-x) superconductors in varying relative humidity environments
[NASA-TP-3368] p 813 N94-14409
Direct determination of alpha particle transport coefficients
[DE93-013488] p 787 N94-14691
Investigations of low-temperature neutron embrittlement of ferritic steels
[DE93-015460] p 573 N94-14700

IN SITU MEASUREMENT
Laser-induced fluorescence over optical fibers for real time in situ measurement of petroleum hydrocarbons in seawater
[AD-A265106] p 790 N94-12863
Portable acoustic wave sensor systems for real-time monitoring of volatile organic compounds
[DE93-013753] p 582 N94-14511

INCLUSIONS
An investigation of the role of second phase particles in the design of ultra high strength steels of improved toughness
[AD-A266774] p 573 N94-14786

INCOHERENT SCATTERING
High spatial resolution x ray microanalysis: Comparison of experiment and incoherent scattering calculations
[DE93-011685] p 648 N94-13044

INCOMPRESSIBLE FLOW
A multiple-scale turbulence model for incompressible flow
[NASA-TM-106113] p 631 N94-13385
On the theory of the decaying developed turbulence with spontaneous parity violation
[DE93-623190] p 632 N94-13511
Studies of turbulent shear flows and their control
[NASA-CR-194114] p 635 N94-13676
A control volume finite element method for three-dimensional, incompressible, viscous fluid flow
[ISBN-0-315-72019-0] p 635 N94-13683
Preconditioning and the limit to the incompressible flow equations
[NASA-CR-191500] p 769 N94-13717
Canonical forms of multidimensional steady inviscid flows
[NASA-CR-191488] p 769 N94-13722
Evolution of disturbances in stagnation point flow
[NASA-CR-191516] p 636 N94-13724
Least-squares finite element solutions for three-dimensional backward-facing step flow
[NASA-TM-106353] p 770 N94-14407
An adaptive projection method for the incompressible Euler equations
[DE93-016428] p 639 N94-14434
A finite volume method for computation of viscous flow in complex configurations p 640 N94-14607
Analysis, approximation, and computation of a coupled solid/fluid temperature control problem
[NASA-TM-106351] p 771 N94-14731
Investigations of transitions from order to chaos in dynamical systems
[DE93-014438] p 818 N94-14738
A study of the fine scale motions of incompressible time-developing mixing layers p 644 N94-14751

INCOMPRESSIBLE FLUIDS
Study of possible mechanisms of instability due to heat transfer
[INPE-5448-TDI/494] p 628 N94-12966
Studies of turbulent shear flows and their control
[NASA-CR-194114] p 635 N94-13676

INCONEL (TRADEMARK)
Interfacial precipitation, segregation and deformation in alloy 600: Implications on primary-side IGSCC
[DE93-013161] p 568 N94-13035
Tensile properties of LE-7 engine material with welded joint
[NAL-TR-1188] p 570 N94-13460

INDENTATION
A process for evaluation of mechanical behavior of surface films
[W-1/92] p 579 N94-14007
Computational diagnostics for detecting phase transitions during nanoindentation
[DE93-016536] p 813 N94-14439

INDEPENDENT VARIABLES
Extremal polygon containment problems and other issues in parametric searching
[ITN-93-85214] p 771 N94-14506

INDEXES (DOCUMENTATION)
VIEWCACHE: An incremental pointer-base access method for distributed databases. Part 1: The universal index system design document. Part 2: The universal index system low-level design document. Part 3: User's guide. Part 4: Reference manual. Part 5: UIMS test suite
[NASA-CR-191788] p 822 N94-13126
Publications of the Jet Propulsion Laboratory: 1990 and 1991
[NASA-CR-193287] p 823 N94-13461
Toxic Substances Control Act (TSCA) chemical substances inventory: Revised inventory synonym and preferred name file, Jan. 1993 documentation
[PB93-155166] p 710 N94-14508

INDIA
NASA/DOD Aerospace Knowledge Diffusion Research Project. Report 18: A comparison of the technical communication practices of aerospace engineers and scientists in India and the United States
[NASA-TM-109006] p 821 N94-13057

INDIUM
Thermal conductance of pressed metallic contacts augmented with Indium foil or Apiezon-N (tm) grease at liquid helium temperatures
[NASA-TM-108779] p 776 N94-14027

INDIUM ANTIMONIDES
Effects of growth conditions and substrate orientation on the properties of InSb
[DE93-013766] p 812 N94-14344

INDIUM PHOSPHIDES
Annealing study of main electron irradiation-induced defects (H4 and H5) in P-InP using DLTS technique
[DE93-623204] p 806 N94-13213
Activities of the Basic Sciences Branch
[DE93-010012] p 851 N94-14455

INDONESIAN SPACE PROGRAM
Some potentials of the Indonesian region for Earth observation p 692 N94-14237

INDUCTANCE
Development of UHF spark-switched L-C Oscillators
[DE93-015019] p 623 N94-13892
Mutual inductance between partially wound tori and a bifilar conductor
[ETN-93-94388] p 624 N94-13998
Multi-output flyback converter with ultrafast current protection
[CNES-NT-133] p 625 N94-14138

INDUCTION MOTORS
Design and application of electromechanical actuators for deep space missions
[NASA-CR-194145] p 663 N94-14134
Early detection of insulation failure in electric motors
[PB93-198208] p 626 N94-14686

INDUSTRIAL ENERGY
Fourteenth National Industrial Energy Technology Conference: Proceedings
[DE93-016698] p 710 N94-14516

INDUSTRIAL MANAGEMENT
Ninth Annual NASA/Contractors Conference on Quality and Productivity. World Class Excellence: The Journey Continues. Keynote presentations
[NASA-CR-194513] p 665 N94-13148
The power of cross-functional teams in driving total quality p 666 N94-13159
Pollution prevention through total quality
[DE93-013814] p 707 N94-13390

INDUSTRIAL PLANTS
A laser-based technique to continuously monitor metal aerosol emissions
[DE93-012836] p 710 N94-14183
Enterprise integration: A tool's perspective
[DE93-015651] p 755 N94-14528

INDUSTRIAL WASTES
Photocatalysis for the treatment of waste water: Applications involving the removal of metals
[DE93-011669] p 561 N94-12841
A review of the global emissions, transport, and effects of heavy metals in the environment
[DE93-013507] p 706 N94-12937
Pollution prevention through total quality
[DE93-013814] p 707 N94-13390

INDUSTRIES
Photovoltaics: Program overview, fiscal year 1992
[DE93-000055] p 701 N94-12914
A review of the global emissions, transport, and effects of heavy metals in the environment
[DE93-013507] p 706 N94-12937
ARTI Refrigerant Database
[DE93-014774] p 595 N94-13021
Pollution prevention through total quality
[DE93-013814] p 707 N94-13390
Scientists, engineers, and technicians in nonmanufacturing industries: 1990. Detailed statistical tables
[NSF-92-334] p 820 N94-14499
Promotion of geothermal energy development in 1991
[DE93-799061] p 705 N94-14679

INELASTIC COLLISIONS
Many-body corrections in XAFS
[DE93-011002] p 563 N94-13478
High energy hadron-hadron collisions
[DE93-015584] p 784 N94-13927

INELASTIC SCATTERING
Many-body corrections in XAFS
[DE93-011002] p 563 N94-13478
Resonant x ray Raman scattering from atoms and molecules
[DE93-015158] p 784 N94-13896

INEQUALITIES
On the geometry of external spectral factors and the Riccati inequality
[CWI-BS-R9227] p 770 N94-14002

INERTIAL CONFINEMENT FUSION
Highly charged ions in hot, dense plasmas
[DE93-013348] p 795 N94-12995
Inertial Confinement Fusion
[DE93-013303] p 795 N94-13017
Inertial confinement fusion program
[DE93-013372] p 796 N94-13047
Parametric instabilities in large nonuniform laser plasmas
[DE93-013184] p 797 N94-13393
Longitudinal beam dynamics for heavy ion fusion
[DE93-013850] p 789 N94-13727
Toward a quasi-linear closure for compressible turbulence
[DE93-017185] p 647 N94-14895

INERTIAL NAVIGATION
Helicopter precision approach capability using the Global Positioning System
[NASA-CR-194037] p 513 N94-13957
Some frequency and damping measurements of laminated beryllium beams
[DE93-015909] p 676 N94-14530
Performance evaluation of the honeywell GG1308 miniature ring laser gyroscope
[AD-A266694] p 653 N94-14782

INERTIAL UPPER STAGE
STS-30 Magellan IUS/EVA training in WETF
[NASA-TM-109300] p 737 N94-13601

INFERENCE
Distributional inferences for a location parameter
[W-9219] p 774 N94-14545

INFILTRATION
Polymer infiltration studies
[NASA-CR-194521] p 582 N94-14539

INFLATABLE STRUCTURES
Research on inflatable structure for space use p 530 N94-13275
Materials and structures p 546 N94-14835

INFORMATION
Information requirements of self-managing teams
[DE93-010319] p 824 N94-14048

INFORMATION DISSEMINATION
NASA/DOD Aerospace Knowledge Diffusion Research Project. Report 18: A comparison of the technical communication practices of aerospace engineers and scientists in India and the United States
[NASA-TM-109006] p 821 N94-13057
Access to Japanese aerospace-related scientific and technical information: The NASA Aerospace Database
[NASA-TM-109413] p 822 N94-13105
Public census data on CD-ROM at Lawrence Berkeley Laboratory
[DE93-015273] p 825 N94-14433
NASA/DOD Aerospace Knowledge Diffusion Research Project. Paper 34: Users and uses of DOD technical reports: A report from the field
[NASA-TM-109327] p 825 N94-14485
NASA/DOD Aerospace Knowledge Diffusion Research Project. Paper 36: Technical uncertainty as a correlate of information use by US industry-affiliated aerospace engineers and scientists
[NASA-TM-109328] p 825 N94-14486
NASA/DOD Aerospace Knowledge Diffusion Research Project. Paper 39: The role of computer networks in aerospace engineering
[NASA-TM-109331] p 825 N94-14487
NASA/DOD Aerospace Knowledge Diffusion Research Project. Paper 37: The impact of political control on technical communications: A comparative study of Russian and US aerospace engineers and scientists
[NASA-TM-109329] p 826 N94-14488
NASA/DOD Aerospace Knowledge Diffusion Research Project. Paper 38: Computer Mediated Communication (CMC) and the communication of technical information in aerospace
[NASA-TM-109330] p 826 N94-14489

INFORMATION FLOW
Application of new electro-optic technology to Space Station Freedom data management system
[NASA-CR-177622] p 538 N94-13257
ACTS data center p 616 N94-14677
INFORMATION MANAGEMENT
Making the connection between information modeling and implementation
[DE93-011588] p 820 N94-12907
Defense information infrastructure: Rationale for defense management report decision 918
[AD-A266014] p 821 N94-12958
Knowledge base technology for CT-DIMS: Report 1
[DE93-013118] p 743 N94-13014
Creating a strategic plan for configuration management using computer aided software engineering (CASE) tools
[DE93-013663] p 746 N94-13394
Quality assurance for environmental chemistry, 1991, volume 1
[DE93-011791] p 709 N94-14020
INFORMATION RETRIEVAL
NASA aerospace database subject scope: An overview
[NASA-SP-7107] p 823 N94-13401
INFORMATION SYSTEMS
Vendor information system for innovative treatment technologies. User manual (VISITT version 2.0). Number 2
[PB93-196640] p 821 N94-12936
Defense information infrastructure: Rationale for defense management report decision 918
[AD-A266014] p 821 N94-12958
Building the repositories to serve --- Superconducting Super Collider information system
[DE93-014100] p 821 N94-12983
Data fusion for adaptive control in manufacturing: Impact on engineering information models
[DE93-011555] p 743 N94-12999
ARTI Refrigerant Database
[DE93-014774] p 595 N94-13021
Johnson Space Center procurement: Controls over payments to contractors should be strengthened
[AD-A265722] p 819 N94-13060
A path-oriented matrix-based knowledge representation system
[NASA-CR-4539] p 744 N94-13065
Measuring quality progress p 666 N94-13154
User observations on information sharing (corporate knowledge and lessons learned)
[NASA-TM-104781] p 819 N94-13400
NASA aerospace database subject scope: An overview
[NASA-SP-7107] p 823 N94-13401
The OOA technique in information systems
[REPT-72-92] p 823 N94-13863
Information requirements of self-managing teams
[DE93-010319] p 824 N94-14048
Activities of Institute for Information Technology
[CNR-35024] p 824 N94-14069
PSM: A new generation of data modeling
[TR-92-13] p 824 N94-14072
CCI working group on climate data and its rapporteurs
[WCDMP-21] p 723 N94-14118
Public census data on CD-ROM at Lawrence Berkeley Laboratory
[DE93-015273] p 825 N94-14433
Oak Ridge Environmental Information System (ORIES) site workstation information packet for OREIS 6.2
[DE93-010761] p 825 N94-14458
Toxic Substances Control Act (TSCA) chemical substances inventory: Revised inventory synonym and preferred name file, Jan. 1993 documentation
[PB93-155166] p 710 N94-14508
Defense Information Technology Services organization FY 1994 budget estimates. Information Technology Systems budget
[PB93-199016] p 826 N94-14562
CarbBank: A structural and bibliographic database for complex carbohydrates
[DE93-015582] p 827 N94-14803
INFORMATION THEORY
Reasoning with uncertain and incomplete information in aerospace applications
[NLR-TP-91366-U] p 763 N94-13529
INFORMATION TRANSFER
Vendor information system for innovative treatment technologies. User manual (VISITT version 2.0). Number 2
[PB93-196640] p 821 N94-12936
NASA/DOD Aerospace Knowledge Diffusion Research Project. Report 18: A comparison of the technical communication practices of aerospace engineers and scientists in India and the United States
[NASA-TM-109006] p 821 N94-13057
User observations on information sharing (corporate knowledge and lessons learned)
[NASA-TM-104781] p 819 N94-13400
NASA/DOD Aerospace Knowledge Diffusion Research Project. Paper 34: Users and uses of DOD technical reports: A report from the field
[NASA-TM-109327] p 825 N94-14485
NASA/DOD Aerospace Knowledge Diffusion Research Project. Paper 36: Technical uncertainty as a correlate of information use by US industry-affiliated aerospace engineers and scientists
[NASA-TM-109328] p 825 N94-14486
NASA/DOD Aerospace Knowledge Diffusion Research Project. Paper 39: The role of computer networks in aerospace engineering
[NASA-TM-109331] p 825 N94-14487
NASA/DOD Aerospace Knowledge Diffusion Research Project. Paper 37: The impact of political control on technical communications: A comparative study of Russian and US aerospace engineers and scientists
[NASA-TM-109329] p 826 N94-14488
NASA/DOD Aerospace Knowledge Diffusion Research Project. Paper 38: Computer Mediated Communication (CMC) and the communication of technical information in aerospace
[NASA-TM-109330] p 826 N94-14489
INFRARED ABSORPTION
Infrared absorption spectroscopy and chemical kinetics of free radicals
[DE93-015078] p 562 N94-13004
New infrared photon absorption processes
[DE93-017017] p 780 N94-13071
Electrical and optical properties of multiple quantum well structures and their applications to infrared detectors
[FFI-92/7012] p 809 N94-14010
INFRARED ASTRONOMY
Physical properties of gas disks around shell stars with and without dust
[NASA-CR-193655] p 835 N94-13239
Analysis of interstellar cloud structure based on IRAS images
[NASA-CR-194341] p 836 N94-13332
A near-infrared faint galaxy survey: Evolution and the cosmological geometry from K band photometry p 830 N94-13591
Millimeter and infrared studies of young stellar objects in dark cloud L1641 p 838 N94-13648
The origin of the far-infrared emission from galactic molecular clouds p 848 N94-13654
The 1 to 5 micron imaging of deeply embedded young stellar objects p 831 N94-13657
The next century astrophysics program p 546 N94-14832
INFRARED DETECTORS
Proceedings of the 11th Space Surveillance Workshop, volume 1
[AD-A265120] p 531 N94-13358
Evaluation of infrared sensors for autonomous landing guidance
[AD-A266450] p 513 N94-13703
High frame rate thermal imager for hypersonic wind tunnel applications
[ONERA-NT-1992-12] p 650 N94-14009
Electrical and optical properties of multiple quantum well structures and their applications to infrared detectors
[FFI-92/7012] p 809 N94-14010
INFRARED IMAGERY
Reduction and analysis of seasons 15 and 16 (1991 - 1992) Pioneer Venus radio occultation data and correlative studies with observations of the near-infrared emission of Venus
[NASA-CR-194128] p 841 N94-13083
Development of a portable multispectral thermal infrared camera
[NASA-CR-191340] p 648 N94-13176
Millimeter and infrared studies of young stellar objects in dark cloud L1641 p 838 N94-13648
Experimental measurement of local heat transfer coefficients over discrete roughened plates using infrared thermography p 635 N94-13652
The 1 to 5 micron imaging of deeply embedded young stellar objects p 831 N94-13657
Study of speckle reduction when using a CO2 waveguide laser close to its threshold state
[DSIS-93-00250] p 657 N94-14067
INFRARED INSPECTION
Measuring methods for CFRP laminates' bending and torsion rigidities characteristics p 529 N94-13272
INFRARED INSTRUMENTS
Development of a portable multispectral thermal infrared camera
[NASA-CR-191340] p 648 N94-13176
Imaging Fourier transform spectrometer
[DE93-017193] p 651 N94-14416
INFRARED LASERS
Kinetic studies following state-selective laser excitation
[DE93-012970] p 654 N94-13013
New infrared photon absorption processes
[DE93-017017] p 780 N94-13071
UV and IR laser ablation for inductively coupled plasma mass spectrometry
[DE93-017124] p 658 N94-14415
INFRARED PHOTOMETRY
A near-infrared faint galaxy survey: Evolution and the cosmological geometry from K band photometry p 830 N94-13591
INFRARED RADIATION
Infrared transmission and path radiance through dust and fog
[AD-A265825] p 791 N94-12979
A fast frame rate 512 x 512 CCD digital camera system
[DE93-013048] p 653 N94-14792
INFRARED RADIOMETERS
Methods for calibration/validation of AVNIR p 689 N94-14216
Future TRMM follow-on mission p 691 N94-14228
INFRARED REFLECTION
Liquid and gas evanescent wave spectroscopy via tunable lasers and silver halide fibers
[ITN-93-85226] p 565 N94-14465
INFRARED SOURCES (ASTRONOMY)
A near-infrared faint galaxy survey: Evolution and the cosmological geometry from K band photometry p 830 N94-13591
Millimeter and infrared studies of young stellar objects in dark cloud L1641 p 838 N94-13648
The origin of the far-infrared emission from galactic molecular clouds p 848 N94-13654
INFRARED SPECTRA
The infrared solar spectrum
[COMMUNICATIONS-SER-B-159] p 844 N94-13502
Optical properties of CO2 ice and CO2 snow in the ultraviolet, visible, and infrared
[NASA-CR-194110] p 686 N94-14081
Spectroscopic method and data reduction algorithm for laser long-path absorption measurements using RIS p 689 N94-14218
Kinetics of photodeposition of superconducting films
[DE93-015511] p 812 N94-14348
Imaging Fourier transform spectrometer
[DE93-017193] p 651 N94-14416
A sum-rule of luminescence spectrum
[ITN-93-85223] p 814 N94-14559
INFRARED SPECTROMETERS
EOS workstation
[NASA-CR-191326] p 736 N94-13132
Measurement of HO2 and other trace gases in the stratosphere using a high resolution far-infrared spectrometer at 28 km
[NASA-CR-194175] p 714 N94-13816
Overview of the ILAS operational data processing system p 690 N94-14220
Determination of the surface cleanliness of metals by FT-IR spectroscopy
[DE93-013252] p 565 N94-14525
INFRARED SPECTROSCOPY
Infrared spectroscopy of organic free radicals related to combustion processes
[DE93-017086] p 562 N94-13222
Measurement of HO2 and other trace gases in the stratosphere using a high resolution far-infrared spectrometer at 28 km
[NASA-CR-194175] p 714 N94-13816
Spectroscopic method and data reduction algorithm for laser long-path absorption measurements using RIS p 689 N94-14218
Liquid and gas evanescent wave spectroscopy via tunable lasers and silver halide fibers
[ITN-93-85226] p 565 N94-14465
Determination of the surface cleanliness of metals by FT-IR spectroscopy
[DE93-013252] p 565 N94-14525
Office of Naval Research/DARPA publications: Composite materials with improved properties in compression
[AD-A265509] p 560 N94-14794
INGOTS
Crystallographic and metallurgical characterization of radiation detector grade cadmium telluride materials
[DE93-014335] p 806 N94-13150
Formation of deoxidization products in iron ingot by the addition of Al, Si, and/or Mn (M-5) p 587 N94-13737
INJECTION MOLDING
Effect of stabilization on the recycling of polyolefins in blow moulding
[IMI-93RT-42400-1477-G] p 596 N94-13684

An experimental study on the effect of die geometry on swell and sag in the parison extrusion stage
[IMI-93RT-42400-1476-G] p 597 N94-14070

INJURIES
An assessment of the potential for neck injury due to padding of aircraft interior walls for head impact protection
[DOT/FAA/AM-93/14] p 738 N94-13972

INLET AIRFRAME CONFIGURATIONS
Analysis of the Harrier forebody/inlet design using computational techniques
[NASA-CR-193616] p 503 N94-13463
Propulsion integration p 508 N94-14174

INLET PRESSURE
Rotordynamic and leakage characteristics of a 4-stage brush seal
[AD-A266012] p 660 N94-12988

INORGANIC COMPOUNDS
Amorphous sol-gel insulating films
[DE93-012859] p 576 N94-12866

INPUT
Kalman filter input estimation
[NAL-TR-1182] p 649 N94-13456
Implementation and experimentation with a motion planning system
[ITN-93-85213] p 755 N94-14505

INPUT/OUTPUT ROUTINES
Beyond core: Making parallel computer I/O practical
[DE93-012347] p 758 N94-12878
VMEC30 SUN device drivers: User's manual
[DSIS-93-00349] p 752 N94-14052

INSERTION LOSS
MMIC packaging technology development
[NASA-CR-194183] p 621 N94-13336
Insertion loss and noise-temperature contribution of high-temperature superconducting bandpass filters centered at 2.3 and 8.45 GHz p 608 N94-14376

INSOLATION
Field of solar collectors: Effect of shadowing on the optimal field design
[ITN-93-85197] p 702 N94-13570

INSPECTION
VISART: Artificial vision for industrial use. A comprehensive system
[INPE-5379-TDI/474] p 665 N94-12941
Rapid intelligent inspection process definition for dimensional measurement in advanced manufacturing
[DE93-011271] p 748 N94-13480
The development of inspection and repair methods for the C-17 aft cargo door
[LR-704] p 499 N94-13904

INSTALLING
ORGBUG: A Windows-based combinatorial geometry debugger
[DE93-016640] p 755 N94-14515

INSTRUCTION SETS (COMPUTERS)
Test report for single event effects of the 80386DX microprocessor
[NASA-CR-194509] p 741 N94-13943

INSTRUCTORS
Lecture notes on software process improvement
[AD-A265200] p 744 N94-13049
Taecannautics: Sharing the dream
[NASA-TM-109309] p 818 N94-13619

INSTRUMENT APPROACH
Evaluation of two cockpit display concepts for civil tiltrotor instrument operations on steep approaches p 517 N94-13323

INSTRUMENT COMPENSATION
Earth Observation Center Annual Report on Research and Development, Fiscal Year 1992
[EOC-92-01-0007] p 687 N94-14091
Calibration and in-house validation results of JERS-1 data p 687 N94-14092
Results from ERS-1 and JERS-1 SAR calibration experiments and data analysis p 688 N94-14210
Methods for calibration/validation of AVNIR p 689 N94-14216

INSTRUMENT ERRORS
Estimation of aircraft aerodynamic derivatives with the Total Least Squares Method
[NAL-TR-1150] p 502 N94-13392
Position error determination for the speedometer and altimeter of the NAL QSTOL experimental aircraft ASKA
[NAL-TR-1144] p 517 N94-13451

INSTRUMENT FLIGHT RULES
A perspective on the FAA approval process: Integrating rotorcraft displays, controls and workload p 521 N94-13298

INTAKE SYSTEMS
Piston engine intake and exhaust system design
[ISVR-TR-222] p 663 N94-13874

INTEGERS
Solving integer programs from dependence and synchronization problems
[AD-A265702] p 767 N94-13284

INTEGRAL EQUATIONS
Newton iterative methods for large scale nonlinear systems
[DE93-015357] p 767 N94-13025
Computer code for scattering from impedance bodies of revolution. Part 3: Surface impedance with s and phi variation. Analytical and numerical results
[NASA-CR-193396] p 599 N94-13264
Evaluation for rheological constitutive relations, using the indentation technique p 775 N94-13627

INTEGRALS
Maximum likelihood estimation for constrained or missing data models
[AD-A266563] p 773 N94-13585

INTEGRATED CIRCUITS
Processing, fabrication and demonstration of HTS integrated microwave circuits
[AD-A265789] p 619 N94-12892
An analog clustering network from a biological model
[AD-A265637] p 762 N94-12969
Analysis and characterizations of planar transmission structures and components for superconducting and monolithic integrated circuits
[NASA-CR-193675] p 619 N94-13026
MMIC packaging technology development
[NASA-CR-194183] p 621 N94-13336
Plasma-etching science meets technology in the MDL
[DE93-012086] p 800 N94-13908
Optical degradation issues for XUV projection lithography systems
[DE93-012658] p 626 N94-14805
Electrochemical planarization for microelectronic circuits
[DE93-017214] p 627 N94-14870

INTEGRATED OPTICS
Energy and technology review, March 1993
[DE93-013941] p 849 N94-13019
Integrated optics technology transfer
[DSIS-93-00179] p 792 N94-13868

INTERACTING GALAXIES
Was 49: Mirror for a hidden Seyfert 1 galaxy
[NASA-CR-194537] p 840 N94-14685

INTERACTIONS
Tidal interactions in the Earth Moon system
[COMMUNICATIONS-SER-B-160] p 837 N94-13503

INTERATOMIC FORCES
Atomic structure of the 310 twin in niobium: Theoretical predictions and comparison with experimental observation
[DE93-013421] p 806 N94-13136
Ploughing on gold using a Scanning Tunneling Microscope
[DE93-012632] p 812 N94-14365

INTERCALATION
A quartz crystal microbalance study of lithium insertion and removal into evaporated films MO(y) (M = Mo, Fe, and V)
[DSIS-93-00649] p 810 N94-14203

INTERFACIAL TENSION
Pinching solutions of slender cylindrical jets
[NASA-CR-191482] p 630 N94-13114
Thermodynamic status of static and dynamic contact angles
[ISBN-0-315-73844-8] p 817 N94-13554
Drop dynamics in space and interference with acoustic field (M-15) p 588 N94-13747
Study of bubble behavior in weightlessness (effects of thermal gradient and acoustic stationary wave) (M-16) p 589 N94-13748
Marangoni effect induced convection in material processing under microgravity (M-18) p 589 N94-13750
A study of thin liquid sheet flows
[NASA-TM-106323] p 642 N94-14732

INTERFEROMETERS
Polarization effects in optical fiber current sensors based on Sagnac interferometers with 3 by 3 couplers
[DE93-012665] p 792 N94-14367

INTERFEROMETRY
Confocal profilometer with nanometric vertical resolution
[DE93-622698] p 653 N94-12857
Solid state laser systems for space application
[NASA-CR-194133] p 656 N94-13420
Interferometric investigation methods of plasma spatial characteristics on stellarators and tokamaks in submillimeter region
[DE93-621606] p 798 N94-13507
Images constructed from computed flow fields
[NASA-CR-194397] p 650 N94-13814
Tomographic methods in flow diagnostics
[NASA-TM-106330] p 650 N94-13876
Advanced ballistic range technology
[NASA-CR-194396] p 532 N94-14068
Advanced ballistic range technology
[NASA-CR-194530] p 533 N94-14540

INTERGALACTIC MEDIA
The reionization of the intergalactic medium p 838 N94-13651

INTERGRANULAR CORROSION
Interfacial precipitation, segregation and deformation in alloy 600: Implications on primary-side IGSCC
[DE93-013161] p 568 N94-13035
Radiation hardening and radiation-induced chromium depletion effects on intergranular stress corrosion cracking of austenitic stainless steels
[DE93-011602] p 572 N94-14058

INTERMEDIATE FREQUENCIES
Performance results of a digital test signal generator p 609 N94-14382

INTERMETALLICS
Fracture behavior of vanadium/vanadium silicide in-situ composites
[DE93-013422] p 556 N94-13389

INTERMOLECULAR FORCES
Marangoni effect induced convection in material processing under microgravity (M-18) p 589 N94-13750

INTERNAL COMBUSTION ENGINES
A computer model for liquid jet atomization in rocket thrust chambers
[NASA-CR-194194] p 627 N94-12803

INTERNAL ENERGY
Equation of state for detonation products
[DE93-012671] p 583 N94-12921

INTERNAL PRESSURE
Autofrettage: Stress distribution under load and retained stresses after depressurization. A modified plane-strain case
[AD-A266320] p 671 N94-13579

INTERNATIONAL COOPERATION
Where no flag has gone before: Political and technical aspects of placing a flag on the Moon
[NASA-CR-188251] p 827 N94-12800
The North Atlantic Regional Experiment (NARE)
[DE93-010126] p 706 N94-13054
The design of chain links and slings
[NPL-DMM(A)-94] p 662 N94-13808
Asia-Pacific ISY conference, volume 1
[NASDA-CM-199-1] p 532 N94-14098
Minutes of the Sixth CEOS Plenary Meeting
[NASA-TM-108252] p 542 N94-14112
European space for exclusively peaceful purposes
[ESA-BR-86] p 851 N94-14137

INTERNATIONAL LAW
Planetary protection implementation on future Mars lander missions
[NASA-CP-3216] p 841 N94-13183
The international regulation of air transport: Changing regimes and price effects
[ISBN-0-315-55958-6] p 511 N94-13543
Long-range global warming impact of gaseous diffusion plant operation
[DE93-011686] p 710 N94-14459

INTERNATIONAL RELATIONS
Where no flag has gone before: Political and technical aspects of placing a flag on the Moon
[NASA-CR-188251] p 827 N94-12800

INTERNATIONAL SPACE YEAR
Asia-Pacific ISY conference, volume 1
[NASDA-CM-199-1] p 532 N94-14098
Asia-Pacific ISY Conference, volume 2
[NASDA-CM-199-VOL-2] p 688 N94-14209
Image processing and analysis of airborne POLDER data p 689 N94-14219
Future TRMM follow-on mission p 691 N94-14228
Outline of ISY sea surface temperature data sets p 696 N94-14261
Outline of ISY Kuroshio observation experiment p 697 N94-14268
Joint experiments using ETS-5 p 618 N94-14284

INTERORBITAL TRAJECTORIES
Guidance law development for aeroassisted transfer vehicles using matched asymptotic expansions
[NASA-CR-194523] p 508 N94-14538

INTERPLANETARY MAGNETIC FIELDS
Ion anisotropy driven waves in the Earth's magnetosheath and plasma depletion layer
[DE93-012751] p 712 N94-12952
The interplanetary origins and the main-phase development of moderate geomagnetic storms (1978 - 1979)
[INPE-5445-TDI/491] p 835 N94-13174
Evolution of the interplanetary magnetic field
[DE93-012631] p 836 N94-13262
Variations common to the interplanetary magnetic field, the zonal atmospheric circulation and the Earth's rotation
[COMMUNICATIONS-SER-B-157] p 837 N94-13504

INTERPLANETARY SPACECRAFT
Electric propulsion system technology
[NASA-CR-194100] p 549 N94-13055

INTERPLANETARY TRAJECTORIES
Optimizing interplanetary trajectories with deep space maneuvers
[NASA-CR-4546] p 532 N94-14851
INTERPOLATION
Evaluation of beta-spline interpolation in digital terrain models
[INPE-5475-TDI/506] p 684 N94-13364
A rational interpolation method to compute frequency response p 681 N94-14644
INTERPROCESSOR COMMUNICATION
Three, four, five, six or the complexity of scheduling with communication delays
[CWI-BS-R9229] p 751 N94-14004
Adaptive Signal Processing Testbed: VME-based DSP board market survey
[DSIS-93-00274] p 605 N94-14015
EWTEST signal excision testbed: System evaluation
[DSIS-93-00346] p 607 N94-14065
On the solution of a class of graph problems by parallel algorithms
[LAAS-92514] p 756 N94-14712
Toward a verifiable approach to the design of concurrent computations
[DE93-012908] p 756 N94-14844
INTERSECTIONS
Calculating intersections of surfaces in screen space
[NASA-CR-191498] p 745 N94-13185
INTERSTELLAR EXTINCTION
UV extinction properties of carina nebular dust
[NASA-CR-193424] p 835 N94-13233
INTERSTELLAR GAS
Physical properties of gas disks around shell stars with and without dust
[NASA-CR-193655] p 835 N94-13239
The reionization of the intergalactic medium p 838 N94-13651
Analysis of the IUE spectra of the strongly interacting binary beta Lyrae
[NASA-CR-194118] p 833 N94-14493
INTERSTELLAR MATTER
The distance to the high velocity clouds of neutral hydrogen
[NASA-CR-194343] p 838 N94-13716
Sites of fine-scale electron density turbulence in the interstellar medium
[NASA-CR-193708] p 839 N94-13864
INTERSTELLAR SPACE
The beta(+) decay and cosmic-ray half-life of Mn-54
[DE93-013913] p 848 N94-13695
INTERSTITIALS
Lattice site of helium implanted in Si and diamond
[DE93-015365] p 805 N94-13012
INTERVERTEBRAL DISKS
Magnetic resonance imaging after exposure to microgravity p 594 N94-13771
INTRAVENOUS PROCEDURES
In-flight demonstration of the Space Station Freedom Health Maintenance Facility fluid therapy system (E300/E05) p 595 N94-13775
INTRUSION
Hypersonic flow field measurements: Intrusive p 507 N94-14166
INVARIANCE
The electric field of a current-carrying conductor
[DE93-626637] p 617 N94-14892
INVENTORIES
Toxic Substances Control Act (TSCA) chemical substances inventory: Revised inventory synonym and preferred name file, Jan. 1993 documentation
[PB93-155166] p 710 N94-14508
INVERSE KINEMATICS
Generalized impedance control of a redundant manipulator p 661 N94-13575
Inverse dynamics: Simultaneous trajectory tracking and vibration reduction with distributed actuators p 678 N94-14624
Non-recursive augmented Lagrangian algorithms for the forward and inverse dynamics of constrained flexible multibodies p 679 N94-14633
Design and control of a macro-micro robot for precise force applications p 682 N94-14651
INVERSE SCATTERING
Mathematical algorithms for multidimensional inverse scattering problems in inhomogeneous medium
[AD-A266440] p 749 N94-13702
INVERSIONS
Synthesis inversion of atmospheric CO2 using the GISS tracer transport model
[CSIRO-TP-29] p 709 N94-14095
INVISCID FLOW
Integration of viscous effects into inviscid computational methods
[NASA-CR-193677] p 629 N94-13007
Three-Dimensional Boundary-Layer program (BL3D) for swept subsonic or supersonic wings with application to laminar flow control
[NASA-CR-4531] p 629 N94-13073
Pinching solutions of slender cylindrical jets
[NASA-CR-191482] p 630 N94-13114
Numerical simulations of unsteady flows in turbomachines p 633 N94-13569
Canonical forms of multidimensional steady inviscid flows
[NASA-CR-191488] p 769 N94-13722
Evolution of disturbances in stagnation point flow
[NASA-CR-191516] p 636 N94-13724
On the secondary instability of the most dangerous Goertler vortex
[NASA-CR-191504] p 636 N94-13785
The spectral viscosity method applied to simulation of waves in a stratified atmosphere
[FFI-92/7047] p 637 N94-14040
Hypersonic flow phenomenology p 505 N94-14155
Extrapolation of ground test data to flight p 507 N94-14170
An adaptive projection method for the incompressible Euler equations
[DE93-016428] p 639 N94-14434
Linear instability of curved free shear layers
[NASA-TM-106290] p 642 N94-14729
Analytical description of the breakup of liquid jets in air
[NASA-CR-191503] p 647 N94-14849
IO
The propagation characteristics and instability properties of low-frequency electromagnetic waves in the Io plasma torus p 601 N94-13650
IODINE
Multiplicity spectrometry on neutron filtered beams
[DE93-617529] p 790 N94-14843
ION ACOUSTIC WAVES
Anomalous transport due to the ion acoustic instability in tokamaks
[PPL-129] p 800 N94-13852
ION BEAMS
EBIT Trapping Program
[DE93-014422] p 788 N94-13208
Nuclear fusion of protons with ions of boron
[DE93-014284] p 781 N94-13219
Design for low beam loss in accelerators for intense neutron source applications
[DE93-014557] p 789 N94-13327
Metastable enhancement of C(+) and O(+) capture reactions
[DE93-015075] p 807 N94-13373
Cellular track model for study of heavy ion beams
[NASA-TP-3351] p 732 N94-13714
Longitudinal beam dynamics for heavy ion fusion
[DE93-013850] p 789 N94-13727
Physics of gas breakdown for ion beam transport in gas
[DE93-015646] p 801 N94-14349
The evolution of tensor polarization
[DE93-017209] p 790 N94-14897
ION CURRENTS
Ionic conductivity of alkali halides and their mixtures near liquid-solid phase transition
[ITN-93-85222] p 566 N94-14558
ION CYCLOTRON RADIATION
Ion anisotropy driven waves in the Earth's magnetosheath and plasma depletion layer
[DE93-012751] p 712 N94-12952
Ion cyclotron heating experiments and plans for the Advanced Toroidal Facility (ATF)
[DE93-012965] p 795 N94-13033
Effect on antenna structure of high power RF during plasma operation
[DE93-013278] p 797 N94-13144
The multi-ion, multi-event test of ion cyclotron resonance heating
[NASA-CR-194134] p 789 N94-13419
Folded waveguide designs for tokamaks
[DE93-013274] p 798 N94-13577
The propagation characteristics and instability properties of low-frequency electromagnetic waves in the Io plasma torus p 601 N94-13650
Direct electron heating and current drive with fast waves in D3-D
[DE93-013028] p 801 N94-14293
Design of the ion cyclotron system for TPX
[DE93-012961] p 803 N94-14770
ION ENGINES
Electric propulsion system technology
[NASA-CR-194100] p 549 N94-13055
Electric propulsion system technology
[NASA-CR-194099] p 549 N94-13068
Derated ion thruster development status
[NASA-TM-106292] p 553 N94-14726
ION EXCHANGING
Canonical correlation of waste glass compositions and durability, including pH
[DE93-012754] p 578 N94-13493
Modeling surface area to volume effects on borosilicate glass dissolution
[DE93-011891] p 581 N94-14432
ION IMPACT
Electron emission resulting from fast ion impact on thin metal foils: Implications of these data for development of track structure models
[DE93-013506] p 782 N94-13485
ION IMPLANTATION
Lattice site of helium implanted in Si and diamond
[DE93-015365] p 805 N94-13012
About the influence of inert gas ion implantation on metal corrosion stability
[DE93-620574] p 569 N94-13360
ION IRRADIATION
Ion assisted sputter deposition of Mo-Si multilayers
[DE93-013830] p 583 N94-14693
ION MOTION
Investigations of transitions from order to chaos in dynamical systems
[DE93-014438] p 818 N94-14738
ION PLATING
Ion assisted sputter deposition of Mo-Si multilayers
[DE93-013830] p 583 N94-14693
ION PROPULSION
Electric propulsion system technology
[NASA-CR-194100] p 549 N94-13055
Electric propulsion system technology
[NASA-CR-194099] p 549 N94-13068
Plasma contactor technology for Space Station Freedom
[NASA-TM-106291] p 553 N94-14725
Derated ion thruster development status
[NASA-TM-106292] p 553 N94-14726
ION SOURCES
Novel oxygen atom source for material degradation studies
[NASA-CR-191323] p 562 N94-13115
ION TEMPERATURE
Semi-local kinetic analysis of the toroidal ion temperature gradient mode
[PPL-130] p 800 N94-13851
The role of electric field shear stabilization of turbulence in the H-mode to VH-mode transition in D3-D
[DE93-015474] p 802 N94-14583
IONIC COLLISIONS
Measurements of transverse energy and forward energy in high-energy nuclear collisions
[DE93-012755] p 788 N94-12817
Measurements of scattering processes in negative ion-atom collisions
[DE93-013863] p 779 N94-12940
Neutral strange particle production at the AGS
[DE93-014044] p 780 N94-13098
Energetic neutral atoms: Imaging the magnetospheric ring current
[NASA-CR-194339] p 715 N94-13826
The theory of relativistic heavy ion collisions
[DE93-015934] p 784 N94-13952
IONIC CRYSTALS
The Lindemann criterion of melting for pure and mixed ionic crystals
[ITN-93-85210] p 814 N94-14554
IONIC MOBILITY
Ionic conductivity of alkali halides and their mixtures near liquid-solid phase transition
[ITN-93-85222] p 566 N94-14558
IONIZATION
Low energy neutral atom imaging techniques
[DE93-012744] p 779 N94-12950
New infrared photon absorption processes
[DE93-017017] p 780 N94-13071
Infrared spectroscopy of organic free radicals related to combustion processes
[DE93-017086] p 562 N94-13222
A search for strong-field direct two electron ionization using coincidence spectroscopy
[DE93-013435] p 781 N94-13241
IONIZATION CROSS SECTIONS
Indirect processes in electron impact ionization of Kr(24+) and Kr(25+)
[DE93-014129] p 784 N94-14140
IONIZING RADIATION
Measurements of optical properties of waveshifting optical fiber for liquid scintillator hadron calorimetry
[DE93-012606] p 791 N94-13482
JPRS report: Science and technology. Central Eurasia: Materials science
[JPRS-UMS-93-004] p 559 N94-14574

IONOSPHERIC ELECTRON DENSITY
Ionospheric calibration for single frequency altimeter measurements
[NASA-CR-194282] p 716 N94-14049
IONOSPHERIC PROPAGATION
Ionospheric effects on a wide-bandwidth, polarimetric, space-based, synthetic-aperture radar
[DE93-015084] p 612 N94-14512
IONS
Highly charged ions in hot, dense plasmas
[DE93-013348] p 795 N94-12995
Spatial variability of throughfall chemistry in a tropical rainforest (Central Amazonia, Brazil)
[INPE-5431-PRE/1765] p 720 N94-13429
Advances in low energy neutral atom imaging techniques
[DE93-012745] p 782 N94-13492
Synthesis of organic ligands for f-element separations
[DE93-012915] p 554 N94-14290
High-order harmonic generation with short-pulse lasers
[DE93-016532] p 659 N94-14594
IRIDIUM
Stability of reference masses 1: Evidence for posible variations in the mass of reference kilograms arising from mercury contamination
[NPL-DMM(A)-86] p 708 N94-13667
IRON
Multiphase equation of state for iron
[DE93-013956] p 568 N94-12977
The x ray dichroism experiments using circular polarization
[DE93-013195] p 568 N94-13036
Formation of deoxidization products in iron ingot by the addition of Al, Si, and/or Mn (M-5) p 587 N94-13737
Laboratory simulations of lunar darkening processes p 843 N94-14301
The state of Fe in the lunar regolith and its relationship to the spectral reflectance properties of the moon p 843 N94-14303
IRON ALLOYS
Propulsion simulator for magnetically-suspended wind tunnel models
[NASA-CR-189560] p 527 N94-13127
Statics and kinetics of phase transformations in bcc Fe-Cr
[DE93-013839] p 574 N94-14793
IRON OXIDES
A quartz crystal microbalance study of lithium insertion and removal into evaporated films MO(y) (M = Mo, Fe, and V)
[DSIS-93-00649] p 810 N94-14203
IRRADIANCE
Nimbus-7 Earth radiation budget calibration history. Part 1: The solar channels
[NASA-RP-1316] p 844 N94-13963
Volume 14: The first SeaWiFS intercalibration round-robin experiment, SIRREX-1, July 1992
[NASA-TM-104566] p 725 N94-14090
IRRADIATION
Novel oxygen atom source for material degradation studies
[NASA-CR-191323] p 562 N94-13115
Molecular dynamics simulation of electronically excited polyatomic molecules
[DE93-623045] p 781 N94-13225
Heavy section steel irradiation experiment
[DE93-015517] p 573 N94-14537
IRREGULARITIES
Estimation of critical values and vibration characteristics on supersonic delta wings. Part 2: Locally-stationary time series analysis of nonstationary random responses
[NAL-TR-1179] p 502 N94-13345
IRRIGATION
Climatic change due to land surface alterations
[INPE-5495-PRE/1786] p 721 N94-13672
Evolution of the lower planetary boundary layer over strongly contrasting surfaces
[DE93-010667] p 717 N94-14424
ISENTROPE
Equation of state for detonation products
[DE93-012671] p 583 N94-12921
ISENTROPIC PROCESSES
A three-dimensional supersonic turbulent boundary layer generated by an isentropic compression p 503 N94-13556
Intra-blade quantitative transonic flow measurements at the DRA Pyestock Isentropic Light Piston Facility using PIV (Particle Image Velocimetry)
[RAE-TM-AERO/PROP-21] p 509 N94-14706
ISING MODEL
Statics and kinetics of phase transformations in bcc Fe-Cr
[DE93-013839] p 574 N94-14793
ISOLATION
Isolation of a piezoresistive accelerometer used in high acceleration tests
[DE93-013764] p 649 N94-13395
Catalytic arene hydrogenation using early transition metal hydride compounds
[DE93-015500] p 573 N94-14402
A high voltage dielectrically isolated smart power technology based on silicon direct bonding
[LAAS-92492] p 626 N94-14698
ISOMERS
Comparative ignition of hexane and octane isomers in a shock tube
[DE93-016535] p 566 N94-14869
ISOPROPYL ALCOHOL
Alternate cleaning methods for LCCAs
[KCP-613-5045] p 624 N94-13937
ISOTHERMAL FLOW
BOAST 2 for the IBM 3090 and RISC 6000
[DE93-000138] p 638 N94-14351
ISOTOPE SEPARATION
Laser beam control and diagnostic systems for the copper-pumped dye laser system at Lawrence Livermore National Laboratory
[DE93-016529] p 658 N94-14437
ISOTOPIC SPIN
Isospin flip as a relativistic effect: NN interactions
[CEBAF-PR-89-023] p 786 N94-14552
ISOTROPIC TURBULENCE
Interacting scales and energy transfer in isotropic turbulence
[NASA-CR-191477] p 630 N94-13133
On the theory of the decaying developed turbulence with spontaneous parity violation
[DE93-623190] p 632 N94-13511
The structure of intense vorticity in homogeneous isotropic turbulence p 643 N94-14747
On the local nature of the energy cascade p 643 N94-14748
Search for subgrid scale parameterization by projection pursuit regression p 643 N94-14749
Isotropy of small scale turbulence p 644 N94-14752
LES versus DNS: A comparative study p 644 N94-14753
Evolution of the shock front and turbulence structures in the shock/turbulence interaction p 645 N94-14761
Stochastic modeling of turbulent reacting flows p 647 N94-14768
ISOTROPY
Isotropy of small scale turbulence p 644 N94-14752
ITERATIVE SOLUTION
Newton iterative methods for large scale nonlinear systems
[DE93-015357] p 767 N94-13025
Calculation of the required sensor accuracy to obtain a specified state estimation accuracy
[NAL-TR-1173] p 649 N94-13343
Elastic-plastic mixed-iterative finite element analysis: Implementation and performance assessment
[NASA-TM-106164] p 675 N94-13919
Hybrid S(sub N)/Monte Carlo research and results
[DE93-012677] p 773 N94-14178
Theory for iterative solution of large dynamical systems using parallel computation
[TKK-MAT-A304] p 760 N94-14187
Computational mechanics and supercomputing at LLNL
[DE93-016453] p 754 N94-14435
Large spatial, temporal, and algorithmic adaptivity for implicit nonlinear finite element analysis
[DE93-016438] p 771 N94-14589
On a convergence of iterative Newton's scheme
[DE93-626604] p 772 N94-14886
IUE
NASA images 11
[NASA-TM-109287] p 842 N94-13626

J

J INTEGRAL
Investigation of criteria for ductile fracture under fully-plastic conditions p 672 N94-13593
JAHN-TELLER EFFECT
Dynamic Jahn-Teller effect: Calculation of fine structure spectrum, isotope shift and Zeeman behavior at deep center Ni2+ in CdS
[ETN-93-94394] p 815 N94-14705
JAPAN
The 1990 Western Pacific Geophysics meeting
[NASA-CR-193456] p 712 N94-13334
JAPANESE SPACE PROGRAM
Access to Japanese aerospace-related scientific and technical information: The NASA Aerospace Database
[NASA-TM-109413] p 822 N94-13105
Space transportation systems and space activities in the 21st century p 537 N94-14274
JAPANESE SPACECRAFT
A concept on on-orbit experiments of deployable structures utilizing JEM/HOPE p 531 N94-13279
Arc-heating tests of thermal protection system materials for the H-2 rocket fairing
[NAL-TR-1181] p 551 N94-13455
Tensile properties of LE-7 engine material with welded joint
[NAL-TR-1188] p 570 N94-13460
Study on improvement of flammability, odor and offgassing tests for materials
[NASDA-CNT-930009] p 563 N94-13471
HOPE real time flight operations analyses for return to earth phase, part B
[NASDA-CNT-930011] p 535 N94-13599
HOPE conceptual design in FY 1991
[NASDA-CNT-930017] p 535 N94-13600
Orbit determination error analysis based on the requirements of ADEOS mission
[NASDA-CNT-930008] p 532 N94-13644
HOPE real time flight operations analyses for return to earth phase, part A
[NASDA-CNT-930010-PT-A] p 535 N94-13645
Conceptual design on H-2 Orbiting Plane (HOPE)
[NASDA-CNT-930018] p 535 N94-13656
Earth Observation Center Annual Report on Research and Development, Fiscal Year 1992
[EOC-92-01-0007] p 687 N94-14091
Calibration and in-house validation results of JERS-1 data p 687 N94-14092
Earth observation experiment data analysis p 687 N94-14093
ADEOS project p 687 N94-14094
The conceptual study on future space transportation systems. Part A: Conceptual study of flyback booster
[NASDA-CNT-930013] p 536 N94-14099
The concept study of the space transportation system HOPE in FY 1991
[NASDA-CNT-930016] p 536 N94-14100
Asia-Pacific ISY Conference, volume 2
[NASDA-CM-199-VOL-2] p 688 N94-14209
Results from ERS-1 and JERS-1 SAR calibration experiments and data analysis p 688 N94-14210
Geologic application of JERS-1 SAR data p 688 N94-14211
Research and development of space transportation systems in ISAS p 537 N94-14277
Contributions of winged re-entry vehicle to space activities p 537 N94-14278
Mission scenario of HOPE p 537 N94-14279
The status of the HOPE concept study p 537 N94-14280
Spaceplane program at NAL: System concept and related technology issues p 537 N94-14281
JET AIRCRAFT NOISE
An experimental assessment of the use of ground-level microphones to measure the fly-over noise of jet-engined aircraft
[NPL-RSA(EXT)-0039] p 777 N94-13885
Mixing noise reduction for rectangular supersonic jets by nozzle shaping and induced screech mixing
[NASA-TM-106364] p 508 N94-14208
JET ENGINES
Rotor stator CGI
[NASA-TM-109313] p 518 N94-13608
JET EXHAUST
Implementation of ADI: Schemes on MIMD parallel computers
[NASA-CR-193720] p 759 N94-13204
JET FLOW
Pinching solutions of slender cylindrical jets
[NASA-CR-191482] p 630 N94-13114
Analytical description of the breakup of liquid jets in air
[NASA-CR-191503] p 647 N94-14849
JET IMPINGEMENT
Implementation of ADI: Schemes on MIMD parallel computers
[NASA-CR-193720] p 759 N94-13204
Experimental determination of droplets local mean diameter of a sprag from impinging jets
[INPE-5469-TDI/500] p 631 N94-13365
Low altitude plume impingement handbook
[NASA-CR-194193] p 643 N94-14741
JET LAG
Circadian rhythms during simulation of the D2-spaceflight
[DLR-FB-92-27] p 733 N94-14043

JET MIXING FLOW
An experimental investigation of mixing enhancement in a simulated scramjet combustor by use of swirling jets
[NASA-TM-109246] p 518 N94-13190
Mixing noise reduction for rectangular supersonic jets by nozzle shaping and induced screech mixing
[NASA-TM-106364] p 508 N94-14208
JET PROPULSION
A technique for direct measurement of skin friction in supersonic combustion flow p 503 N94-13555
JOINED WINGS
Low-speed wind tunnel tests on four types of joined-wing aircraft models
[NAL-TR-1167] p 501 N94-13340
Low-speed wind tunnel tests on a joined-wing aircraft model with various upper-fin
[NAL-TR-1169] p 501 N94-13341
JOINTS (JUNCTIONS)
Flex-gear electrical power transmission
[NASA-CR-194422] p 661 N94-13445
Problems and opportunities in microwave joining of ceramics
[DE93-014998] p 579 N94-13888
Canadian Target Assembly (CTA) to Airborne Support Equipment (ASE) vibration test report
[IME-AMT-TR-001] p 663 N94-14195
JOSEPHSON JUNCTIONS
Measurements on two-dimensional arrays of mesoscopic Josephson junctions
[AD-A265129] p 807 N94-13359
Theoretical SIS mixer research
[AD-A266323] p 807 N94-13580
An x ray detector using superconducting aluminum tunnel junctions
[DE93-015103] p 811 N94-14332
JUNCTION DIODES
Changes in electrical device characteristics during the formation of dislocations in situ in the TEM
[DE93-013910] p 808 N94-13694
AlGaAs diode laser blue shift resulting from fast neutron irradiation
[AD-A266642] p 659 N94-14681

K

K-EPSILON TURBULENCE MODEL
Turbulence modeling of free shear layers for high-performance aircraft
[NASA-CR-193659] p 520 N94-12799
A solution algorithm for the prediction of compressible laminar and turbulent shear flows p 634 N94-13635
Numerical simulation of velocity-coupled combustion response of solid rocket propellants p 585 N94-14490
Response of a supersonic boundary layer to a compression corner p 645 N94-14759
KALMAN FILTERS
Calculation of the required sensor accuracy to obtain a specified state estimation accuracy
[NAL-TR-1173] p 649 N94-13343
Attitude determination of stratospheric balloons using Kalman filters
[INPE-5498-TDI/513] p 649 N94-13366
Kalman filter input estimation
[NAL-TR-1182] p 649 N94-13456
Kalman filter based architectures for interference excision
[DSIS-93-00034] p 603 N94-13818
A comparison of recursive least squares and Kalman filtering excisors for swept tone interference
[DSIS-93-00362] p 606 N94-14054
KAONS
HIJET with AGS physics and N(sup *)'s
[DE93-014022] p 780 N94-13097
Tests of non-local interferences in kaon physics at asymmetric phi-factories
[DE93-013905] p 787 N94-14857
KAPTON (TRADEMARK)
Surface characterization of LDEF materials
[NASA-CR-194519] p 543 N94-14683
KELVIN-HELMHOLTZ INSTABILITY
Pinching solutions of slender cylindrical jets
[NASA-CR-191482] p 630 N94-13114
Linear instability of curved free shear layers
[NASA-TM-106290] p 642 N94-14729
KEROSENE
Effects of hydrogen addition on combustion performance of a LOX/kerosene rocket
[NAL-TR-1177] p 548 N94-12945
KINEMATICS
Kinematics and constraints associated with swashplate blade pitch control
[NASA-TM-102265] p 520 N94-12820
Dynamics and design of nonholonomic robotic mechanical systems
[ISBN-0-315-72009-3] p 662 N94-13597
KINETIC ENERGY
The space-time and energy parameters of deuterium braking by the central collision with atoms
[DE93-624144] p 788 N94-14881
KINETICS
Statics and kinetics of phase transformations in bcc Fe-Cr
[DE93-013839] p 574 N94-14793
Measurements of crystal growth kinetics at extreme deviations from equilibrium
[DE93-014526] p 815 N94-14798
KNOWLEDGE BASED SYSTEMS
JTEC Panel report on knowledge-based systems in Japan
[PB93-170124] p 820 N94-12801
Knowledge-based oceanographic image compression
[AD-A265752] p 821 N94-13041
A path-oriented matrix-based knowledge representation system
[NASA-CR-4539] p 744 N94-13065
Software synthesis using generic architectures
[NASA-CR-194201] p 745 N94-13355
Architecture-driven reuse of code in KASE
[NASA-CR-194200] p 745 N94-13356
The KASE approach to domain-specific software systems p 745 N94-13357
Software design by reusing architectures
[NASA-CR-194151] p 747 N94-13443
Knowledge-based processing for aircraft flight control
[NASA-CR-194074] p 526 N94-13469
A knowledge-based model for the integration of remote sensing into a mineral exploration program
[ISBN-0-315-58982-5] p 685 N94-13523
Activities of Institute for Information Technology
[CNR-35024] p 824 N94-14069
Knowledge based systems: From process control to policy analysis
[DE93-014582] p 765 N94-14117
An integrated knowledge system for the Space Shuttle hazardous gas detection system
[NASA-CR-194533] p 536 N94-14310
KNOWLEDGE BASES (ARTIFICIAL INTELLIGENCE)
A path-oriented matrix-based knowledge representation system
[NASA-CR-4539] p 744 N94-13065
Thermal Expert System (TEXSYS): Systems autonomy demonstration project, volume 2. Results
[NASA-TM-102877] p 538 N94-13989
An expert system class library for Audition
[IME-MET-TR-008] p 824 N94-14196
KNOWLEDGE REPRESENTATION
A path-oriented matrix-based knowledge representation system
[NASA-CR-4539] p 744 N94-13065
An expert system for integrated structural analysis and design optimization for aerospace structures
[NASA-CR-194225] p 673 N94-13673
KOLMOGOROV THEORY
Interacting scales and energy transfer in isotropic turbulence
[NASA-CR-191477] p 630 N94-13133
On the theory of the decaying developed turbulence with spontaneous parity violation
[DE93-623190] p 632 N94-13511
Coherent Doppler lidar signal covariance including wind shear and wind turbulence
[NASA-CR-194492] p 721 N94-13723
The structure of intense vorticity in homogeneous isotropic turbulence p 643 N94-14747
Triad interactions in the dissipation range p 644 N94-14750
KONDO EFFECT
Quantum Monte Carlo by message passing
[DE93-012645] p 760 N94-14177
KRAMERS-KRONIG FORMULA
Direct submillimeter absorptivity measurements on epitaxial Ba(1-x)K(x)BiO3 films at 2K
[DE93-013904] p 815 N94-14699
KRYPTON
Kinetic studies following state-selective laser excitation
[DE93-012970] p 654 N94-13013
KRYPTON FLUORIDE LASERS
Inertial confinement fusion program
[DE93-013372] p 796 N94-13047

L

LABORATORIES
Photovoltaics: Contract lists, fiscal year 1992
[DE93-000093] p 701 N94-12902
Preliminary design features of the RASCAL: A NASA /Army rotorcraft in-flight simulator p 526 N94-13325
Publications of the Jet Propulsion Laboratory: 1990 and 1991
[NASA-CR-193287] p 823 N94-13461
Activities of the University of Saskatchewan, Plasma Physics Laboratory
[CTN-93-60831] p 798 N94-13518
A perspective on AVS in an engineering sciences environment
[DE93-015011] p 596 N94-13889
Quality assurance for environmental chemistry, 1991, volume 1
[DE93-011791] p 709 N94-14020
A laser-based technique to continuously monitor metal aerosol emissions
[DE93-012836] p 710 N94-14183
Uniform user and group IDs on a large network
[DE93-013047] p 760 N94-14315
LABORATORY EQUIPMENT
Student's works and power supplies in electronic circuit laboratory p 627 N94-13434
Plasma-etching science meets technology in the MDL
[DE93-012086] p 800 N94-13908
Laser beam control and diagnostic systems for the copper-pumped dye laser system at Lawrence Livermore National Laboratory
[DE93-016529] p 658 N94-14437
LAGRANGE COORDINATES
A new Lagrangian method for three-dimensional steady supersonic flows
[NASA-TM-106068] p 510 N94-14847
LAGRANGIAN FUNCTION
Electric charge quantization
[DE93-622901] p 778 N94-12845
Electromagnetic deflection of spinning particles
[DE93-622866] p 778 N94-12858
Non-recursive augmented Lagrangian algorithms for the forward and inverse dynamics of constrained flexible multibodies p 679 N94-14633
On the local nature of the energy cascade p 643 N94-14748
LAKES
Snow cover models in operational watershed forecasting
[DE93-778332] p 718 N94-12837
Educational module for the Higher Agricultural Education. Part 2: Eutrophication observed by remote sensing: An educational approach to water quality monitoring
[BCRS-92-11B] p 818 N94-14462
LAMINAR BOUNDARY LAYER
Three-Dimensional Boundary-Layer program (BL3D) for swept subsonic or supersonic wings with application to laminar flow control
[NASA-CR-4531] p 629 N94-13073
LAMINAR FLOW
Transition prediction and control in subsonic flow over a hump
[NASA-CR-4543] p 629 N94-13066
The transient behavior of a boundary layer exposed to uniform suction
[ITN-93-85205] p 630 N94-13197
A solution algorithm for the prediction of compressible laminar and turbulent shear flows p 634 N94-13635
A comparison of computational and experimental data for a subscale high speed propulsive nozzle at low mach numbers
[AD-A266543] p 504 N94-13705
CNSFV code development, virtual zone Navier-Stokes computations of oscillating control surfaces and computational support of the laminar flow supersonic wind tunnel
[NASA-CR-194259] p 504 N94-14030
The structure of laminar flow in a three-dimensional driven cavity p 640 N94-14601
An implicit finite volume nodal point scheme for the solution of two-dimensional compressible Navier-Stokes equations p 640 N94-14603
Navier-Stokes simulation of transonic vortex flow over a delta wing p 640 N94-14606
Computation of nonequilibrium flows using PNS equations p 641 N94-14610
DNS and modeling of the interaction between turbulent premixed flames and walls p 646 N94-14763
Development of experimental demonstration processes for laminar-turbulent flow states at wing profiles in free flight
[ILR-MITT-280(1993)] p 510 N94-14800
LAMINAR FLOW AIRFOILS
SRISTI: The NAL method for the design and analysis of Natural Laminar Flow (NLF) airfoils p 516 N94-14615

LAMINATES
Micromechanical modeling of laminated composites with interfaces and woven composites using the boundary element method
[NASA-TM-106280] p 670 N94-13053
Measuring methods for CFRP laminates' bending and torsion rigidities characteristics p 529 N94-13272
Inelastic deformation mechanisms in SCS-6/Ti 15-3 MMC lamina under compression
[NASA-CR-191170] p 555 N94-13378
Shear buckling of fiber metal laminates: Comparison between orthotropic and anisotropic plate models using finite element method
[LTR-ST-1934] p 671 N94-13565
Finite element analysis of composite plates by use of modified complementary energy principle
p 672 N94-13596
Fatigue and residual strength characteristics of fiber metal laminates subjected to incidental damage
[LR-708] p 674 N94-13803
Optimal synthesis of hot composite laminates with interphase layers
[NASA-TM-106326] p 557 N94-14042
Probabilistic micromechanics for high-temperature composites
[NASA-CR-191150] p 676 N94-14408
Polymer infiltration studies
[NASA-CR-194521] p 582 N94-14539
Buckling analysis of laminated thin shells in a hot environment
[NASA-TM-106302] p 683 N94-14776

LAND
Seasonal change of the land-surface temperature over Asian Continent derived from GAC data on NOAA-11 AVHRR p 691 N94-14232

LAND MANAGEMENT
Forest management for fixing and sequestering carbon
[DE93-013520] p 707 N94-13486
Application of satellite remote sensing technology in disaster mitigation: A case study of Bangladesh
p 692 N94-14238
Integration of remote sensing and mathematical modelling in disaster mitigation p 692 N94-14239
Soil erosion mapping using remote sensing and GIS techniques p 692 N94-14240
Detecting land cover changes in Chiang-Mai area in Thailand p 693 N94-14241
Land evaluation for agricultural productivity in North-East Thailand using LANDSAT TM data and geographic information p 693 N94-14242
Satellite remote sensing for disaster mitigation
p 693 N94-14244
A concept for the world environment and disaster observation system p 693 N94-14245
A tentative plan on China and Asian-Pacific satellite system for disaster reduction p 693 N94-14247
Development of a remote sensing geographic information system for land cover changes and assessment of risk due to natural and man made hazards covering the area of the inner delta of the Yellow River
p 694 N94-14249
Multi-source national forest inventory of Finland
p 694 N94-14254
Global assessment of human activities
p 695 N94-14255
The Swedish ISY contribution p 695 N94-14256
Vegetation mapping of Indo-China Peninsula using MOS-1 MESSR and NOAA AVHRR p 695 N94-14257
Remote sensing for monitoring tropical moist forests in the Indo-Chinese region p 695 N94-14258
Estimation of vegetation damage due to ash fall in Mt. Pinatubo area using MOS-1 data p 695 N94-14259
Mangrove afforestation monitoring using remote sensing p 695 N94-14260

LAND MOBILE SATELLITE SERVICE
Contribution towards a draft revision of recommendations 681: Propagation data required for the design of Earth-space land mobile telecommunications systems p 614 N94-14666
Characterisation of the LMS propagation channel at L- and S-bands: Narrowband experimental data and channel modelling p 615 N94-14669
Results of multiband (L, S, Ku band) propagation measurements and model for high elevation angle land mobile satellite channel p 615 N94-14670

LAND USE
Forest management for fixing and sequestering carbon
[DE93-013520] p 707 N94-13486
The role of human activity and land use change in atmospheric chemistry and air quality
[DE93-011871] p 709 N94-14022
Activities report of the Netherlands Remote Sensing Board
[ETN-93-93880] p 686 N94-14073
Integration of remotely sensed data and cadastral ownership boundaries for land inventory purposes
[BCRS-92-16] p 687 N94-14127
Pattern and Process in Landscape Ecology: Eighth Annual US Landscape Ecology Symposium
[DE93-014032] p 711 N94-14859

LANDAU-GINZBURG EQUATIONS
Effect of spontaneous decay of superconductor quasiparticles in the tunneling density of states
[DE93-012681] p 811 N94-14339

LANDFILLS
Integrated, flexible, and rapid geophysical surveying
[DE93-009989] p 712 N94-12906

LANDFORMS
The nature and origin of periodically spaced tectonic features on Mars
[NASA-CR-193821] p 842 N94-13199

LANDING AIDS
Evaluation of infrared sensors for autonomous landing guidance
[AD-A266450] p 513 N94-13703

LANDING SIMULATION
Visual cueing aids for rotorcraft landings
p 524 N94-13313
Numerical simulation of a powered-lift landing, tracking flow features using overset grids, and simulation of high lift devices on a fighter-lift-and-control wing
[NASA-CR-194260] p 527 N94-14322

LANDSAT 5
Net radiation mapping of mountainous terrain using Landsat-5 thematic mapper imagery and digital terrain data
[ISBN-0-315-57755-X] p 685 N94-13475

LANGEVIN FORMULA
Stochastic dynamics: Crossover from 1/f(sup 3) to flicker noise
[DE93-622862] p 772 N94-12896
Multiplicative noise: Applications in cosmology and field theory
[DE93-016624] p 840 N94-14536

LANGUAGE PROGRAMMING
Programming languages made in Italy
[REPT-93-002] p 750 N94-13805
EVES: An overview
[DSIS-93-00238] p 752 N94-14088

LANGUAGES
Reconsideration of the autonomous view of language
p 618 N94-13441

LAPLACE EQUATION
Torsion problem of elastostatics: An application of boundary element method and relation with conformal mapping
[DSIS-92-03794] p 674 N94-13833
Mutual inductance between partially wound tori and a bifilar conductor
[ETN-93-94388] p 624 N94-13998

LAPLACE TRANSFORMATION
The method of Laplace Transform MultiQuadrics (LTMQ) for the solution of the groundwater flow equation
[DE93-010408] p 637 N94-14053

LARGE SCALE INTEGRATION
Electrochemical planarization for microelectronic circuits
[DE93-017214] p 627 N94-14870

LARGE SPACE STRUCTURES
Relegation for decentralized control
[AD-A265720] p 819 N94-13059
Methods for evaluating the predictive accuracy of structural dynamic models
[NASA-CR-191337] p 671 N94-13124
The Second Workshop on Deployment and Assembly Experiment of Large Space Structure on Orbit
[NASDA-CON-930003] p 529 N94-13268
Structural design of hexa-link truss deployable antenna p 529 N94-13269
Thermal distortion measurement of TETRUS type thermal test model of large deployable antenna for mobile communications satellite p 529 N94-13270
Development of modular cable mesh deployable antenna p 530 N94-13274
Research on inflatable structure for space use
p 530 N94-13275
Helical truss beam development for large space structure p 530 N94-13276
Application of intelligently adaptable structure and robot to large space structure p 530 N94-13277
A concept on on-orbit experiments of deployable structures utilizing JEM/HOPE p 531 N94-13279
Movement of deployable truss p 531 N94-13280
Development and application of one dimensional deployable truss p 531 N94-13281
Study of a one-dimensional deployable structure employing telescopic members p 531 N94-13282
The study on large space structure assembly technology: The study on deployable truss structure, part 1
[NASDA-TMR-930002] p 541 N94-13658
The study on large space structure assembly technology: The study on deployable truss structure, part 2 and 3
[NASDA-TMR-930003-PT-2-3] p 541 N94-13659
Large space structures and systems in the space station era: A bibliography with indexes (supplement 05)
[NASA-SP-7085(05)] p 543 N94-14411
Proceedings of the Fifth NASA/NSF/DOD Workshop on Aerospace Computational Control
[NASA-CR-194515] p 677 N94-14618
The use of linked lists in the simulation of controller-structure interaction p 679 N94-14630
An application of the IMC software to controller design for the JPL LSCL Experiment Facility
p 681 N94-14645
Computational issues in optimal tuning and placement of passive dampers p 681 N94-14647
Control structural interaction testbed: A model for multiple flexible body verification p 544 N94-14649
A program for the investigation of the Multibody Modeling, Verification, and Control Laboratory
p 682 N94-14652

LASER ABLATION
Shock-free acceleration of laser driven targets
[DE93-008050] p 655 N94-13387
Measurement of penetration depth lambda(T) in YBa2Cu3O(7-delta) thin film
[DE93-014587] p 810 N94-14122
Formation of textured YBCO films by laser ablation
[DE93-013131] p 581 N94-14319
Kinetics of photodeposition of superconducting films
[DE93-015511] p 812 N94-14348
Effects of depositon rate on Bi2Sr2CaCu2O(8+x) and Bi2Sr(1.6)La(0.4)CuO(6+x) epitaxial thin film growth by pulsed-laser ablation
[DE93-015797] p 812 N94-14362
UV and IR laser ablation for inductively coupled plasma mass spectrometry
[DE93-017124] p 658 N94-14415

LASER APPLICATIONS
Kinetic studies following state-selective laser excitation
[DE93-012970] p 654 N94-13013
Non-scanned LADAR imaging and applications
[DE93-013772] p 655 N94-13261
Single event effects and laser simulation studies
[NASA-CR-194506] p 657 N94-13812
Miniature mechanism assembly
[DE93-015595] p 624 N94-13928
Photochemical dynamics of surface oriented molecules
[DE93-016289] p 784 N94-13983
The Livermore x ray laser program
[DE93-014118] p 658 N94-14152
Laser beam control and diagnostic systems for the copper-pumped dye laser system at Lawrence Livermore National Laboratory
[DE93-016529] p 658 N94-14437
Impact of shorter wavelengths on optical quality for laws
[NASA-CR-193433] p 792 N94-14473
JPRS report: Science and technology. Central Eurasia: Materials science
[JPRS-UMS-93-006] p 558 N94-14573
JPRS report: Science and technology. Central Eurasia: Materials science
[JPRS-UMS-93-005] p 559 N94-14575
Intra-blade quantitative transonic flow measurements at the DRA Pyestock Isentropic Light Piston Facility using PIV (Particle Image Velocimetry)
[RAE-TM-AERO/PROP-21] p 509 N94-14706
Laser lithography by photon scanning tunneling microscopy
[DE93-015962] p 660 N94-14863
Optimization study of x ray laser coherence in Ni-like Ta
[DE93-016419] p 660 N94-14888

LASER BEAMS
Non-scanned LADAR imaging and applications
[DE93-013772] p 655 N94-13261
Design and performance of an automated video-based laser beam alignment system
[DE93-012571] p 656 N94-13481
Theoretical investigation of scattering by homogeneous or coated dielectric spheres illuminated with a steady state or pulsed laser beam p 657 N94-13624
The interaction of intense femtosecond laser pulses with solid targets
[DE93-014415] p 658 N94-14114
Telescope pointing for GOPEX p 610 N94-14389
GOPEX at the Starfire Optical Range
p 611 N94-14392
Laser beam control and diagnostic systems for the copper-pumped dye laser system at Lawrence Livermore National Laboratory
[DE93-016529] p 658 N94-14437

Impact of shorter wavelengths on optical quality for laws
[NASA-CR-193433] p 792 N94-14473
Small scale adaptive optics experiment systems engineering
[NASA-CR-194419] p 793 N94-14548
Kinetic simulations of ultra-intense laser plasma interactions
[DE93-014419] p 802 N94-14564

LASER CAVITIES
Characteristics of semiconductor lasers with optical feedback
[ISBN-0-315-55435-5] p 656 N94-13522
Horizontal-cavity surface-emitting lasers, superluminescent LEDs, and amplifiers, and parabolic gain unstable resonator semiconductor lasers
p 656 N94-13573
The standing wave FEL/TBA: Realistic cavity geometry and energy extraction
[DE93-016972] p 659 N94-14520

LASER DAMAGE
Absorption and damage thresholds of low defect density hafnia deposited with activated oxygen
[DE93-013853] p 655 N94-13243
Laser-damage susceptibility of nodular defects in dielectric mirror coatings: AFM measurements and electric-field modeling
[DE93-014655] p 580 N94-14124

LASER DOPPLER VELOCIMETERS
An experimental study of a turbulent boundary layer in the trailing edge region of a curculation-control airfoil
[NASA-CR-194522] p 508 N94-14541

LASER DRILLING
Recent results from material processing studies on new generation lasers
[DE93-013841] p 653 N94-12898
Emitter Wrap-Through solar cell
[DE93-014996] p 703 N94-13886

LASER FUSION
Shock-free acceleration of laser driven targets
[DE93-008050] p 655 N94-13387

LASER GYROSCOPES
Performance evaluation of the honeywell GG1308 miniature ring laser gyroscope
[AD-A266694] p 653 N94-14782

LASER HEATING
High temperature electromagnetic characterization of thermal protection system tile materials
[NASA-CR-189687] p 578 N94-13431
Excimer laser surface processing of titanium
[DE93-012633] p 570 N94-13512

LASER INDUCED FLUORESCENCE
Laser-induced fluorescence over optical fibers for real time in situ measurement of petroleum hydrocarbons in seawater
[AD-A265106] p 790 N94-12863
Gathering and exchange information on atmospheric chemistry and polluted atmospheres
[DE93-009940] p 705 N94-12869
Direct probing of chromatography columns by laser-induced fluorescence
[DE93-015208] p 654 N94-13022

LASER MATERIALS
Optical and physical properties of the LiSrAlF6:Cr laser crystal
[DE93-014657] p 808 N94-13881
Laser and spectroscopic properties of Yb-doped apatite crystals
[DE93-014656] p 810 N94-14125
Independent adjustment of the higher order frequency dependent phase in chirped pulse amplification systems
[DE93-017106] p 625 N94-14522

LASER MICROSCOPY
The x ray lasers as sources for x ray microscopy
[DE93-013420] p 655 N94-13259

LASER MODE LOCKING
Tetravalent chromium (Cr(4+)) as laser-active ion for tunable solid-state lasers
[NASA-CR-194527] p 659 N94-14576

LASER MODES
Characteristics of semiconductor lasers with optical feedback
[ISBN-0-315-55435-5] p 656 N94-13522
Impact of shorter wavelengths on optical quality for laws
[NASA-CR-193433] p 792 N94-14473

LASER OUTPUTS
Three dimensional time-dependent hydrodynamic and propagation modeling of x ray laser emission
[DE93-012575] p 654 N94-12962
Novel Co:MgF2 lidar for aerosol profiler
[NASA-CR-191525] p 654 N94-13091
Parametric instabilities in large nonuniform laser plasmas
[DE93-013184] p 797 N94-13393
Optical and physical properties of the LiSrAlF6:Cr laser crystal
[DE93-014657] p 808 N94-13881
GOPEX laser transmission and monitoring systems
p 611 N94-14391
Laser beam control and diagnostic systems for the copper-pumped dye laser system at Lawrence Livermore National Laboratory
[DE93-016529] p 658 N94-14437
Impact of shorter wavelengths on optical quality for laws
[NASA-CR-193433] p 792 N94-14473
The standing wave FEL/TBA: Realistic cavity geometry and energy extraction
[DE93-016972] p 659 N94-14520
Experimental measurements of selenium x-ray laser spectral line profiles
[DE93-016543] p 659 N94-14595
Optimization study of x ray laser coherence in Ni-like Ta
[DE93-016419] p 660 N94-14888

LASER PLASMA INTERACTIONS
Three dimensional time-dependent hydrodynamic and propagation modeling of x ray laser emission
[DE93-012575] p 654 N94-12962
Kinetic simulations of ultra-intense laser plasma interactions and a novel method of generating odd harmonics
[DE93-014418] p 797 N94-13207
Parametric instabilities in large nonuniform laser plasmas
[DE93-013184] p 797 N94-13393
Oscillator-amplifier experiments in neon-like yttrium
[DE93-012577] p 657 N94-13976
UV and IR laser ablation for inductively coupled plasma mass spectrometry
[DE93-017124] p 658 N94-14415
Kinetic simulations of ultra-intense laser plasma interactions
[DE93-014419] p 802 N94-14564

LASER PLASMAS
Two temperature modeling and experimental measurements of laser sustained hydrogen plasmas
[AD-A265750] p 796 N94-13039
Parametric instabilities in large nonuniform laser plasmas
[DE93-013184] p 797 N94-13393
Implicit multi-fluid simulation of interpenetrating plasmas
[DE93-013351] p 801 N94-14342
Brillouin scattering from fluctuations produced by stimulated Raman scattering
[DE93-016531] p 792 N94-14438
Optical degradation issues for XUV projection lithography systems
[DE93-012658] p 626 N94-14805
Time resolved measurement of electron temperatures of exploding foil x ray laser plasmas
[DE93-017161] p 803 N94-14894

LASER POWER BEAMING
Small scale adaptive optics experiment systems engineering
[NASA-CR-194419] p 793 N94-14548
Laser power beaming system analyses
[NASA-CR-193840] p 660 N94-14904

LASER PROPULSION
Two temperature modeling and experimental measurements of laser sustained hydrogen plasmas
[AD-A265750] p 796 N94-13039

LASER PUMPING
Inertial Confinement Fusion
[DE93-013303] p 795 N94-13017
Numerical simulations of Nd:YAG laser amplifiers
[FFI/RAPPORT-92/7028] p 657 N94-13970
Laser and spectroscopic properties of Yb-doped apatite crystals
[DE93-014656] p 810 N94-14125
Laser beam control and diagnostic systems for the copper-pumped dye laser system at Lawrence Livermore National Laboratory
[DE93-016529] p 658 N94-14437

LASER RANGE FINDERS
Non-scanned LADAR imaging and applications
[DE93-013772] p 655 N94-13261
The BIRIS server: Integration of a three-dimensional range sensor into a harmony-based realtime architecture
[ERB-1036] p 765 N94-14201
The determination of crustal motions using laser ranging to Lageos-2 and Lageos-1
[NASA-CR-193787] p 717 N94-14306

LASER SPECTROSCOPY
Linear and nonlinear spectroscopic probing of solute interactions with chemically modified silica surface
[DE93-014648] p 562 N94-13001
Direct probing of chromatography columns by laser-induced fluorescence
[DE93-015208] p 654 N94-13022
Nonlinear laser spectroscopy studies of semiconductor heterostructures
[AD-A265728] p 805 N94-13037
A laser-based technique to continuously monitor metal aerosol emissions
[DE93-012836] p 710 N94-14183
Lawrence Berkeley Laboratory Chemical Sciences Division
[DE93-015260] p 851 N94-14401
Liquid and gas evanescent wave spectroscopy via tunable lasers and silver halide fibers
[ITN-93-85226] p 565 N94-14465

LASER STABILITY
Horizontal-cavity surface-emitting lasers, superluminescent LEDs, and amplifiers, and parabolic gain unstable resonator semiconductor lasers
p 656 N94-13573

LASER TARGET INTERACTIONS
The optical constants and spectral specular reflectivity of Highly Oriented Pyrolytic Graphite (HOPG)
[DE93-011894] p 790 N94-12865
Shock-free acceleration of laser driven targets
[DE93-008050] p 655 N94-13387
The interaction of intense femtosecond laser pulses with solid targets
[DE93-014415] p 658 N94-14114

LASER TARGETS
Inertial Confinement Fusion
[DE93-013303] p 795 N94-13017
Shock-free acceleration of laser driven targets
[DE93-008050] p 655 N94-13387
Parametric instabilities in large nonuniform laser plasmas
[DE93-013184] p 797 N94-13393
The interaction of intense femtosecond laser pulses with solid targets
[DE93-014415] p 658 N94-14114
UV and IR laser ablation for inductively coupled plasma mass spectrometry
[DE93-017124] p 658 N94-14415
Impedance-power effects on plasma polymer surface finish using a helical resonator discharge
[DE93-016454] p 803 N94-14590
Optical degradation issues for XUV projection lithography systems
[DE93-012658] p 626 N94-14805
The 8 to 11 keV x ray sources for imaging and absorption experiments
[DE93-015973] p 803 N94-14865

LASER WELDING
The feasibility of producing aluminum-lithium structures for cryogenic tankage applications by laser beam welding
[NASA-CR-191527] p 595 N94-14026
Welding technologies as applied to nuclear manufacturing
[DE93-010924] p 664 N94-14565

LASING
Oscillator-amplifier experiments in neon-like yttrium
[DE93-012577] p 657 N94-13976
Microchannel cooled heatsinks for high average power laser diode arrays
[DE93-016533] p 658 N94-14442
AlGaAs diode laser blue shift resulting from fast neutron irradiation
[AD-A266642] p 659 N94-14681

LATE STARS
X ray observations of late-type stars using the ROSAT all-sky survey
[NASA-CR-193716] p 832 N94-14146

LATENT HEAT
Measuring surface fluxes in CAPE
[NASA-CR-193664] p 711 N94-12788
Boundary layer structure over areas of heterogeneous heat fluxes
[DE93-007887] p 715 N94-13912

LATERAL CONTROL
Investigation of the effects of bandwidth and time delay on helicopter roll-axis handling qualities
p 522 N94-13300
Rolling moment control in the NAL 10 cm x 10 cm magnetic suspension and balance system
[NAL-TR-1164] p 526 N94-13347

LATITUDE
Solar radiation on Mars: Stationary photovoltaic array
[NASA-TM-106321] p 626 N94-14730

LAUE METHOD
On the neutron EDM search in the Laue diffraction by the crystal without a centre of symmetry
[DE93-622971] p 804 N94-12828
A positron annihilation radiation telescope using Laue diffraction in a crystal lens
[DE93-012905] p 848 N94-13483

LAUNCH VEHICLES
Results of wind tunnel tests of an ASRM configured 0.03 scale Space Shuttle integrated vehicle model (47-OTS) in the AEDC 16-foot transonic wind tunnel, volume 2
[NASA-CR-185697] p 534 N94-12965
Electrical Actuation Technology Bridging
[NASA-CP-3213] p 551 N94-13417
Arc-heating tests of thermal protection system materials for the H-2 rocket fairing
[NAL-TR-1181] p 551 N94-13455
Tensile properties of LE-7 engine material with welded joint
[NAL-TR-1188] p 570 N94-13460
HOPE real time flight operations analyses for return to earth phase, part B
[NASDA-CNT-930011] p 535 N94-13599
HOPE real time flight operations analyses for return to earth phase, part A
[NASDA-CNT-930010-PT-A] p 535 N94-13645
LAUNCHERS
HL-20 personnel launch system
[NASA-TM-109292] p 504 N94-13632
LEACHING
Canonical correlation of waste glass compositions and durability, including pH
[DE93-012754] p 578 N94-13493
Relationship between borosilicate glass composition, structure, and durability test response (SRS)
[DE93-013578] p 581 N94-14343
LEAD ALLOYS
Thermosolutal convection and macrosegregation in dendritic alloys
[NASA-CR-194039] p 567 N94-12825
LEAD TELLURIDES
Growth experiment of narrow band-gap semiconductor PbSnTe single crystals in space (M-1)
p 586 N94-13733
Growth of PbSnTe single crystal by traveling-zone method in low gravity (M-2) p 586 N94-13734
LEAD ZIRCONATE TITANATES
Superconductivity devices: Commercial use of space
[NASA-CR-194163] p 625 N94-14324
LEADING EDGES
Numerical study of the effects of icing on viscous flow over wings
[NASA-CR-193306] p 500 N94-13180
Low-speed wind tunnel tests on four types of joined-wing aircraft models
[NAL-TR-1167] p 501 N94-13340
Numerical simulation of dynamic stall of NACA0012 airfoil oscillating near static stall angle using the Navier-Stokes equations
[DE93-767970] p 505 N94-14061
LEAKAGE
STS-55 pad abort: Engine 2011 oxidizer preburner augmented spark igniter check valve leak
[NASA-CR-193830] p 533 N94-12806
Rotordynamic and leakage characteristics of a 4-stage brush seal
[AD-A266012] p 660 N94-12988
A survey and analysis of experimental hydrogen sensors
[NASA-TM-106300] p 648 N94-13135
LEARNING
Modelling robotic systems with DADS
p 678 N94-14625
LEAST SQUARES METHOD
Estimation of aircraft aerodynamic derivatives with the Total Least Squares Method
[NAL-TR-1150] p 502 N94-13392
A comparison of recursive least squares and Kalman filtering excisors for swept tone interference
[DSIS-93-00362] p 606 N94-14054
Least-squares finite element solutions for three-dimensional backward-facing step flow
[NASA-TM-106353] p 770 N94-14407
Removing noise from discontinuous data
[ITN-93-85211] p 826 N94-14555
LECTURES
Lecture notes on software process improvement
[AD-A265200] p 744 N94-13049
LEDGES
Simulation studies for surfaces and materials strength
[NASA-CR-193305] p 671 N94-13179
LEGENDRE FUNCTIONS
The Chebyshev-Legendre method: Implementing Legendre methods on Chebyshev points
[NASA-CR-191497] p 769 N94-13725
LEIDENFROST PHENOMENON
An analytical investigation of transient effects on rewetting of heated thin flat plates
[NASA-TM-106120] p 628 N94-12968
LENGTH
Solid state laser systems for space application
[NASA-CR-194133] p 656 N94-13420
LENS DESIGN
Integrated optics technology transfer
[DSIS-93-00179] p 792 N94-13868
LENSES
A positron annihilation radiation telescope using Laue diffraction in a crystal lens
[DE93-012905] p 848 N94-13483
LEPTONS
Top quark polarization and T-odd spin correlations as tools for testing (non) Standard Model predictions
[DE93-622956] p 778 N94-12847
Charged scalar particles and (tau) leptonic decay
[DE93-622969] p 779 N94-12882
A search for scalar leptoquarks in D0
[DE93-012780] p 779 N94-12954
Top quark search: Results and prospects at Fermilab
[DE93-013016] p 786 N94-14524
Comparing the Z(sup 0) mass and inclusive widths to the standard electroweak theory
[PREPRINT-731] p 787 N94-14721
LEVITATION MELTING
Stabilized electromagnetic levitator
[NASA-CR-194261] p 586 N94-12805
LIAPUNOV FUNCTIONS
Construction of the Courant-Snyder invariants for the non-linear equations of motion under presence of the linear coupling
[DE93-017565] p 788 N94-14872
LIBRARIES
Satellite technology for environmental monitoring in developing countries p 692 N94-14236
Public census data on CD-ROM at Lawrence Berkeley Laboratory
[DE93-015273] p 825 N94-14433
LIE GROUPS
Gauging the octonion algebra
[DE93-622864] p 775 N94-12843
Soliton equations and self-dual gauge fields
[DE93-626620] p 818 N94-14887
LIFE (DURABILITY)
A hot dynamic seal rig for measuring hypersonic engine seal durability and flow performance
[NASA-TM-106294] p 664 N94-14727
LIFE CYCLE COSTS
Chip-level testability requirements guidelines
[AD-A262583] p 619 N94-12967
Optimal maintenance policies of a Markovian system
[ITN-93-85216] p 774 N94-14502
LIFE SCIENCES
Aerospace medicine and biology: A continuing bibliography with indexes (supplement 379)
[NASA-SP-7011(379)] p 733 N94-14412
Cellular responses to low-gravity: Pilot studies on suborbital rockets and orbiting spacecraft
[NASA-CR-194402] p 729 N94-14494
LIFE SUPPORT SYSTEMS
Medical evaluations on the KC-135 1991 flight report summary
[NASA-TM-104755] p 731 N94-12832
Life support and habitability manual, volume 1
[ESA-PSS-03-406-ISSUE-1-VOL] p 737 N94-13901
Life support and habitability manual, volume 2
[ESA-PSS-03-406-ISSUE-1-VOL] p 738 N94-13902
Aerospace medicine and biology: A continuing bibliography with indexes (supplement 379)
[NASA-SP-7011(379)] p 733 N94-14412
LIFT
Experimental studies of vortex flaps and vortex plates. Part 1: 0.53 m span 60 deg delta wing
[DE93-767969] p 505 N94-14059
Numerical simulation of dynamic stall of NACA0012 airfoil oscillating near static stall angle using the Navier-Stokes equations
[DE93-767970] p 505 N94-14061
Numerical simulation of a powered-lift landing, tracking flow features using overset grids, and simulation of high lift devices on a fighter-lift-and-control wing
[NASA-CR-194260] p 527 N94-14322
LIFTING BODIES
HL-20 personnel launch system
[NASA-TM-109292] p 504 N94-13632
LIFTING REENTRY VEHICLES
HL-20 personnel launch system
[NASA-TM-109292] p 504 N94-13632
LIGANDS
Synthesis and properties of novel cluster phases
[DE93-017056] p 577 N94-13072
Thermochemistry of transition metal clusters
[DE93-016201] p 571 N94-13977
Synthesis of organic ligands for f-element separations
[DE93-012915] p 554 N94-14290
LIGHT (VISIBLE RADIATION)
The Large Area Pulsed Solar Simulator (LAPSS)
[NASA-CR-194507] p 703 N94-13940
Photovoltaic advanced research and development project: Solar radiation research
[DE92-016430] p 704 N94-14350
LIGHT AMPLIFIERS
Horizontal-cavity surface-emitting lasers, superluminescent LEDs, and amplifiers, and parabolic gain unstable resonator semiconductor lasers
p 656 N94-13573
LIGHT CURVE
The soft x ray transient Cen X-4 in quiescence
[NASA-CR-194033] p 833 N94-14406
Analysis of the IUE spectra of the strongly interacting binary beta Lyrae
[NASA-CR-194118] p 833 N94-14493
LIGHT EMISSION
Studies of gas in cooling flow clusters
[NASA-CR-193597] p 628 N94-12959
Fabrication of AlGaAs/GaAs-light-emitting devices by selective MOCVD using dialkylmetalchloride
p 627 N94-13433
LIGHT EMITTING DIODES
Horizontal-cavity surface-emitting lasers, superluminescent LEDs, and amplifiers, and parabolic gain unstable resonator semiconductor lasers
p 656 N94-13573
LIGHT GAS GUNS
Experimental technique to simulate orbital-debris impact on space shields at impact velocities over 10 km/s
[DE93-011619] p 539 N94-12909
Calibration of a magnetic induction system for measurement of hypervelocities
[DE93-013949] p 652 N94-14578
LIGHT IONS
Physics of gas breakdown for ion beam transport in gas
[DE93-015646] p 801 N94-14349
LIGHT SCATTERING
Experimental determination of droplets local mean diameter of a sprag from impinging jets
[INPE-5469-TDI/500] p 631 N94-13365
Image processing and analysis of airborne POLDER data p 689 N94-14219
Brillouin scattering from fluctuations produced by stimulated Raman scattering
[DE93-016531] p 792 N94-14438
Image reconstruction for x ray holographic microscopy
[DE93-013094] p 653 N94-14772
LIGHT SOURCES
Fundamentals and techniques of nonimaging optics
[DE93-013145] p 791 N94-13015
Applications of the Advanced Light Source to problems in the earth, soil, and environmental sciences
[DE93-015258] p 710 N94-14477
Validation of an inexpensive illuminant for aeromedical color vision screening
[DOT/FAA/AM-93/16] p 736 N94-14854
LIGHT TRANSMISSION
Gathering and exchange information on atmospheric chemistry and polluted atmospheres
[DE93-009940] p 705 N94-12869
Optical propagation through atmospheric turbulence. Model analysis of anisoplanatism and application to adaptive optics
[ONERA-P-1992-4] p 716 N94-14192
LIGHT TRANSPORT AIRCRAFT
SRISTI: The NAL method for the design and analysis of Natural Laminar Flow (NLF) airfoils
p 516 N94-14615
LIGHT WATER
Nuclear thermal propulsion engine based on particle bed reactor using light water steam as a propellant
[DE93-014336] p 552 N94-14111
LIGHT WATER REACTORS
Radiation hardening and radiation-induced chromium depletion effects on intergranular stress corrosion cracking of austenitic stainless steels
[DE93-011602] p 572 N94-14058
LIGHTNING
Lightning simulation and determination of expected striking points
[ITN-93-85202] p 719 N94-13188
LINE SHAPE
Experimental measurements of selenium x-ray laser spectral line profiles
[DE93-016543] p 659 N94-14595
LINE SPECTRA
Studies of gas in cooling flow clusters
[NASA-CR-193597] p 628 N94-12959
Basic research in solar physics
[NASA-CR-193632] p 844 N94-13234
The infrared solar spectrum
[COMMUNICATIONS-SER-B-159] p 844 N94-13502
Submillimeter, millimeter, and microwave spectral line catalogue, revision 3
[NASA-CR-194501] p 602 N94-13813

Emission line variability in active galactic nuclei
[ITN-93-85209] p 849 N94-14553

LINEAR ACCELERATORS
Evolution of high-repetition-rate induction accelerators through advancements in switching
[DE93-012599] p 654 N94-12963
Beam halo formation from space-charge dominated beams in uniform focusing channels
[DE93-014458] p 789 N94-13209
Design for low beam loss in accelerators for intense neutron source applications
[DE93-014557] p 789 N94-13327
Beam halo in high-intensity beams
[DE93-014565] p 789 N94-13328
Longitudinal beam dynamics for heavy ion fusion
[DE93-013850] p 789 N94-13727
The standing wave FEL/TBA: Realistic cavity geometry and energy extraction
[DE93-016972] p 659 N94-14520

LINEAR ENERGY TRANSFER (LET)
Single event effects and laser simulation studies
[NASA-CR-194506] p 657 N94-13812
Single Event Upset (SEU) testing of semiconductor components at the McMaster Accelerator Laboratory
[DSIS-93-00071] p 623 N94-13834

LINEAR EQUATIONS
Formally biorthogonal polynomials and a look-ahead Levinson algorithm for general Toeplitz systems
[NASA-CR-194297] p 748 N94-13586

LINEAR PROGRAMMING
Gate assignment using linear programming
[LR-698] p 775 N94-13987

LINEAR QUADRATIC REGULATOR
Active control of acoustic pressure fields using smart material technologies
[NASA-CR-191480] p 768 N94-13354
Robust synthesis of discrete-time multivariable control systems with induced delays p 662 N94-13642

LINEAR SYSTEMS
Calculation of the required sensor accuracy to obtain a specified state estimation accuracy
[NAL-TR-1173] p 649 N94-13343
Decentralized control of uncertain systems via sensitivity models
[DE93-012963] p 766 N94-14568
Simulation of linear mechanical systems p 680 N94-14641
Optimization-based controller design for rotorcraft p 527 N94-14642
A rational interpolation method to compute frequency response p 681 N94-14644
A new treatment of periodic systems with applications to helicopter rotor blade dynamics
[AD-A266770] p 510 N94-14784

LINKAGES
The design of chain links and slings
[NPL-DMM(A)-94] p 662 N94-13808

LIPIDS
Biodiesel/aquatic species project report, FY 1992
[DE93-010024] p 709 N94-14087
Structures and shear response of lipid monolayers
[DE93-015076] p 730 N94-14802

LIQUEFACTION
Reverse micelle synthesis of nanoscale metal containing catalysts
[DE93-012869] p 572 N94-14184
Ionic conductivity of alkali halides and their mixtures near liquid-solid phase transition
[ITN-93-85222] p 566 N94-14558

LIQUEFIED GASES
Statistical mechanical theory of liquid entropy
[DE93-016524] p 817 N94-14593

LIQUID ALLOYS
Solidification of eutectic system alloys in space (M-19) p 589 N94-13751

LIQUID ATOMIZATION
A computer model for liquid jet atomization in rocket thrust chambers
[NASA-CR-194194] p 627 N94-12803

LIQUID BEARINGS
Cryogenic fluid film bearing tester development study
[NASA-CR-192586] p 660 N94-12791

LIQUID CHROMATOGRAPHY
Linear and nonlinear spectroscopic probing of solute interactions with chemically modified silica surface
[DE93-014648] p 562 N94-13001
Direct probing of chromatography columns by laser-induced fluorescence
[DE93-015208] p 654 N94-13022
Reactor studies of metal ions associated with chromatographic silica
[AD-A266675] p 573 N94-14779

LIQUID COOLING
Test apparatus for ITER blanket cooling water distribution design
[DE93-753157] p 795 N94-12944

LIQUID CRYSTALS
Colorimetric qualification of shear sensitive liquid crystal coatings
[NASA-CR-194126] p 806 N94-13291
A continuum theory for liquid crystals describing different degrees of orientational order
[ETN-93-94392] p 807 N94-13590
Suppression of bright objects using a spatial light modulator when imaging with CCD- and image intensified cameras
[FFI-93/7008] p 650 N94-13665
Workshop on Formation of Supermolecular Structures in Composite Fluid: Phase Rule and Dynamics
[DE93-782887] p 581 N94-14421
Phases and phase transitions of polymeric liquid crystals: A high resolution x ray diffraction and light scattering study
[ITN-93-85218] p 816 N94-14826

LIQUID FLOW
Stability of oscillatory two phase Couette flow
[NASA-CR-191501] p 636 N94-13817
Microchannel cooled heatsinks for high average power laser diode arrays
[DE93-016533] p 658 N94-14442
A study of thin liquid sheet flows
[NASA-TM-106323] p 642 N94-14732

LIQUID FUELS
A computer model for liquid jet atomization in rocket thrust chambers
[NASA-CR-194194] p 627 N94-12803
Conversion of light hydrocarbon gases to metal carbides for production of liquid fuels and chemicals
[DE93-014962] p 583 N94-13002
Status and future opportunities for conversion of synthesis gas to liquid energy fuels
[DE93-010025] p 584 N94-14089

LIQUID HELIUM
Three-stage linear, split-Stirling cryocooler for 1 to 2K magnetic cold stage
[NASA-CR-4538] p 776 N94-13897

LIQUID HELIUM 2
Sloshing dynamics on rotating helium dewar tank
[NASA-CR-194403] p 637 N94-13959

LIQUID HYDROGEN
CFM technologies for space transportation: Multipurpose hydrogen testbed system definition and tank procurement
[NASA-CR-194355] p 539 N94-12827
Semiempirical fragmentation models on galactic cosmic ray transport calculations with hydrogen target
[NASA-TP-3350] p 847 N94-13263

LIQUID INJECTION
Analysis of gas turbine engines using water and oxygen injection to achieve high Mach numbers and high thrust
[NASA-TM-106270] p 518 N94-13143

LIQUID METALS
Diffusion in liquid state and solidification of binary system (M-7) p 587 N94-13739
Liquid metal drop ejection
[NASA-CR-193718] p 572 N94-14133
Statistical mechanical theory of liquid entropy
[DE93-016524] p 817 N94-14593

LIQUID OXYGEN
Effects of hydrogen addition on combustion performance of a LOX/kerosene rocket
[NAL-TR-1177] p 548 N94-12945

LIQUID PHASE EPITAXY
Liquid phase epitaxy of gallium arsenide: A review
[DE93-622212] p 804 N94-12893

LIQUID PHASE SINTERING
Study on the mechanism of liquid phase sintering (M-12) p 588 N94-13744

LIQUID PHASES
Multiphase equation of state for iron
[DE93-013956] p 568 N94-12977
Growth of samarskite crystal under microgravity conditions (M-20) p 590 N94-13752

LIQUID PROPELLANT ROCKET ENGINES
Energy and technology review, March 1993
[DE93-013941] p 849 N94-13019
Numerical studies of spray combustion in liquid-fueled engines p 564 N94-13685

LIQUID ROCKET PROPELLANTS
A computer model for liquid jet atomization in rocket thrust chambers
[NASA-CR-194194] p 627 N94-12803
Numerical studies of spray combustion in liquid-fueled engines p 564 N94-13685
Nuclear thermal propulsion engine based on particle bed reactor using light water steam as a propellant
[DE93-014336] p 552 N94-14111

LIQUID SLOSHING
Sloshing dynamics on rotating helium dewar tank
[NASA-CR-194403] p 637 N94-13959

LIQUID SURFACES
Capillary surfaces in a wedge: Differing contact angles
[DE93-013903] p 631 N94-13244

LIQUID-GAS MIXTURES
Studies of momentum and energy transfer across wavy gas-liquid interfaces
[AD-A266432] p 635 N94-13699

LIQUID-SOLID INTERFACES
An analytical investigation of transient effects on rewetting of heated thin flat plates
[NASA-TM-106120] p 628 N94-12968
Thermodynamic status of static and dynamic contact angles
[ISBN-0-315-73844-8] p 817 N94-13554
Immiscible phase incorporation during directional solidification of hypermonotectics
[NASA-CR-194412] p 565 N94-14480

LIQUID-VAPOR INTERFACES
Studies of momentum and energy transfer across wavy gas-liquid interfaces
[AD-A266432] p 635 N94-13699
Sloshing dynamics on rotating helium dewar tank
[NASA-CR-194403] p 637 N94-13959

LIQUIDS
Shielded open-circuited sample holders for dielectric and magnetic measurements of liquids and powders
[PB93-198851] p 652 N94-14687

LISP (PROGRAMMING LANGUAGE)
Common lisp framework
[AD-A265878] p 742 N94-12933

LITHIUM
Calculation of electron-lithium scattering using the coupled-channel optical method
[DE93-623049] p 806 N94-13226
A quartz crystal microbalance study of lithium insertion and removal into evaporated films MO(y) (M = Mo, Fe, and V)
[DSIS-93-00649] p 810 N94-14203

LITHIUM ALLOYS
Preparation and characterization of rapidly solidified Al-Li alloys
[ISBN-0-315-58948-5] p 569 N94-13367

LITHIUM HYDRIDES
Generation of neutronic thermal data in support of space nuclear propulsion
[DE93-013148] p 549 N94-13034

LITHIUM NIOBATES
Implementation of manufacturing techniques for planar, single mode waveguides on lithium niobate
[DSIS-93-00101] p 792 N94-13845
Liquid metal drop ejection
[NASA-CR-193718] p 572 N94-14133

LITHOGRAPHY
Design and testing of planar magnetic micromotors fabricated by deep x ray lithography and electroplating
[DE93-012856] p 618 N94-12821
Optical degradation issues for XUV projection lithography systems
[DE93-012658] p 626 N94-14805
Laser lithography by photon scanning tunneling microscopy
[DE93-015962] p 660 N94-14863

LITHOSPHERE
Regional tectonic analysis of Venus as part of the Pioneer Venus guest investigator project
[NASA-CR-194079] p 842 N94-13561

LIVER
A characterization of carboxylesterases in rat and guinea pig: Their heterogeneity and role in detoxication of organophosphorus compounds
[NDRE-PUBL-93-1001] p 730 N94-14852

LOAD TESTS
A benchmark bending test of a thick specimen. Part 2: Surface displacement measurements
[ARL-RR-6-PT-2] p 670 N94-12928

LOADS (FORCES)
Structural design/margin assessment
[NASA-TP-3410] p 669 N94-12831
A piloted simulation investigation of the normal load factor and longitudinal thrust required for air-to-air acquisition and tracking p 522 N94-13301
Autofrettage: Stress distribution under load and retained stresses after depressurization. A modified plane-strain case
[AD-A266320] p 671 N94-13579
An 8-node axisymmetric acoustic finite element for non-axisymmetric fluid-structure interaction analysis
[FFA-TN-1993-03] p 673 N94-13689
Nonlinear wave forces on large ocean structures
[AD-A266820] p 683 N94-14902

LOCAL THERMODYNAMIC EQUILIBRIUM
The 8 to 11 keV x ray sources for imaging and absorption experiments
[DE93-015973] p 803 N94-14865

LOGIC PROGRAMMING
Completing fault models for abductive diagnosis
[DE93-003832] p 761 N94-12859
Efficient dynamic optimization of logic programs
[NASA-TM-109251] p 761 N94-12889
LOGISTICS MANAGEMENT
Decision support for material planners
[ISBN-9-03-860201-4] p 819 N94-14449
LONG DURATION EXPOSURE FACILITY
Analysis of samples of reflector materials which are multicoated and metal samples with oxide coatings which have been exposed the space environment in LDEF testing
[NASA-CR-193647] p 575 N94-12789
STS-32 mission highlights resource tape
[NASA-TM-109291] p 531 N94-13631
Partial analysis of LDEF experiment A-0114
[NASA-CR-193826] p 564 N94-14025
Surface characterization of LDEF materials
[NASA-CR-194519] p 543 N94-14683
LONG DURATION SPACE FLIGHT
Recycling in space
[NASA-TM-109307] p 737 N94-13615
Magnetic resonance imaging after exposure to microgravity p 594 N94-13771
An evaluation of noise and its effects on shuttle crewmembers during STS-50/USML-1
[NASA-TM-104775] p 735 N94-13961
Physical countermeasures for long-term manned space flights
[ESA-SP-1160] p 733 N94-14860
LONG TERM EFFECTS
Surface characterization of LDEF materials
[NASA-CR-194519] p 543 N94-14683
LOOP ANTENNAS
Direct electron heating and current drive with fast waves in D3-D
[DE93-013028] p 801 N94-14293
LOOPS
Analysis and effects of the number of nests of DO loops during vector supercomputing
[NAL-TR-1146] p 748 N94-13453
LORAN C
Determination of Loran-C/GPS human factors issues
[PB93-199693] p 514 N94-14563
LOSSES
Recent study of beam stability in the PSR
[DE93-014473] p 780 N94-13173
LOSSY MEDIA
Utilization of boundary element method for extraction of frequency dependent conductivity parameters of lossy intra-chip transmission lines
[ETN-93-94385] p 771 N94-14807
LOW ALTITUDE
Low altitude plume impingement handbook
[NASA-CR-194193] p 643 N94-14741
LOW CARBON STEELS
Investigation of criteria for ductile fracture under fully-plastic conditions p 672 N94-13593
LOW CONCENTRATIONS
Reduction of Pu(6) with hydrogen peroxide: Effects of plutonium, peroxide, and iron concentrations and of reaction time
[DE93-013598] p 564 N94-13487
LOW CURRENTS
Low-current traveling wave tube for use in the microwave power module
[NASA-TP-3344] p 620 N94-13110
LOW DENSITY MATERIALS
Fabrication of very-low-density, high-stiffness carbon fiber/aluminum hybridized composite with ultra-low density and high stiffness (M-11) p 588 N94-13743
LOW FREQUENCIES
A 3D gyrokinetic particle-in-cell simulation of fusion plasma microturbulence on parallel computers
[DE93-012503] p 794 N94-12846
1/f noise and oxide traps in MOSFETs
[DE93-007581] p 619 N94-12942
The propagation characteristics and instability properties of low-frequency electromagnetic waves in the Io plasma torus p 601 N94-13650
LOW FREQUENCY BANDS
ALFIS: Astronomical Low Frequency Interferometry Satellites. A feasibility study
[LR-699] p 542 N94-13988
LOW NOISE
Flex-gear electrical power transmission
[NASA-CR-194422] p 661 N94-13445
Position error determination for the speedometer and altimeter of the NAL QSTOL experimental aircraft ASKA
[NAL-TR-1144] p 517 N94-13451
LOW PASS FILTERS
Spatially-varying IIR filter banks for image coding
[NASA-CR-193727] p 619 N94-12897
LOW PRESSURE
Low pressure storage of natural gas on activated carbon
[DE93-014053] p 660 N94-12851
NASA metrology and calibration, 1993
[NASA-TM-109280] p 597 N94-14410
LOW REYNOLDS NUMBER
Least-squares finite element solutions for three-dimensional backward-facing step flow
[NASA-TM-106353] p 770 N94-14407
LOW SPEED
Low-speed wind tunnel tests on four types of joined-wing aircraft models
[NAL-TR-1167] p 501 N94-13340
LOW SPEED WIND TUNNELS
A guide to the DRA 13 ft x 9 ft Low Speed Wind Tunnel Facility
[AD-A267739] p 528 N94-14876
LOW TEMPERATURE
Low temperature metal-organic chemical vapor deposition growth processes for high efficiency solar cells
[DE92-010562] p 702 N94-13386
A microstructural approach to fatigue crack processes in poly crystalline BCC materials
[DE93-016666] p 812 N94-14354
LOW THRUST
Analysis of reacting flowfields in low-thrust rocket engines and plumes p 552 N94-14491
LOW THRUST PROPULSION
Low thrust space propulsion
[NASA-TM-109286] p 552 N94-13625
LOWER ATMOSPHERE
Atmospheric turbulence and diffusion research
[DE93-011842] p 718 N94-14425
LOWER BODY NEGATIVE PRESSURE
Health monitoring of Japanese payload specialist: Autonomic nervous and cardiovascular responses under reduced gravity condition (L-0) p 591 N94-13757
Countermeasure for reducing post-flight orthostatic intolerance: Lower Body Negative Pressure (LBNP) experiment E140 p 594 N94-13772
LUBRICANT TESTS
A vacuum four-ball tribometer to evaluate liquid lubricants for space applications
[NASA-TM-106264] p 575 N94-12842
Dry film lubricant evaluation
[DE93-013114] p 578 N94-13118
Surface analysis of bearings
[AD-A266800] p 661 N94-13122
LUBRICANTS
Surface analysis of bearings
[AD-A266800] p 661 N94-13122
Miscibility of lubricants with refrigerants, phase 1
[DE93-014766-PHASE-1] p 596 N94-13407
Canadian Target Assembly (CTA) to Airborne Support Equipment (ASE) vibration test report
[IME-AMT-TR-001] p 663 N94-14195
Compatibility of refrigerants and lubricants with motor materials
[DE93-014768] p 583 N94-14801
LUBRICATING OILS
Synthetic lubricants and high-performance functional fluids: Phosphazenes
[ARL-TR-45] p 580 N94-14126
LUMINESCENCE
Gordon Research Conference on Chronobiology, 1991
[AD-A266354] p 728 N94-13698
A sum-rule of luminescence spectrum
[ITN-93-85223] p 814 N94-14559
LUMINOSITY
The evidence for clumpy accretion in the Herbig Ae star HR 5999
[NASA-TM-108257] p 828 N94-12915
A search for scalar leptoquarks in D0
[DE93-012780] p 779 N94-12954
Inclusive single muons at DO
[DE93-012779] p 783 N94-13494
The origin of the far-infrared emission from galactic molecular clouds p 848 N94-13654
LUMINOUS INTENSITY
Photocatalysis for the treatment of waste water: Applications involving the removal of metals
[DE93-011669] p 561 N94-12841
Characterization of Spirulina biomass for CELSS diet potential
[NASA-CR-194123] p 729 N94-14097
LUNAR BASES
Effects of radiobiological uncertainty on vehicle and habitat shield design for missions to the moon and Mars
[NASA-TP-3312] p 846 N94-12875
LUNAR COMPOSITION
Deposition of impact-generated vapors in the lunar regolith p 843 N94-14302
LUNAR ENVIRONMENT
Laboratory simulations of lunar darkening processes p 843 N94-14301
LUNAR EXPLORATION
The studies on lunar and planetary exploration and utilization: The study on lunar resources utilization
[NASDA-CNT-930014] p 842 N94-13655
LUNAR GEOLOGY
Laboratory simulations of lunar darkening processes p 843 N94-14301
Deposition of impact-generated vapors in the lunar regolith p 843 N94-14302
The state of Fe in the lunar regolith and its relationship to the spectral reflectance properties of the moon p 843 N94-14303
LUNAR LANDING
Where no flag has gone before: Political and technical aspects of placing a flag on the Moon
[NASA-CR-188251] p 827 N94-12800
LUNAR RESOURCES
The studies on lunar and planetary exploration and utilization: The study on lunar resources utilization
[NASDA-CNT-930014] p 842 N94-13655
LUNAR ROCKS
The state of Fe in the lunar regolith and its relationship to the spectral reflectance properties of the moon p 843 N94-14303
LUNAR ROVING VEHICLES
Asynchronous transfer mode link performance over ground networks p 610 N94-14385
LUNAR SEISMOGRAPHS
Meteoroid environment near the Earth-Moon system
[NASA-CR-193670] p 835 N94-13203
LUNAR SHADOW
Angular resolution studies of the CYGNUS array using the shadows of the Sun and Moon
[DE93-012723] p 846 N94-12946
LUNAR SOIL
Deposition of impact-generated vapors in the lunar regolith p 843 N94-14302
The state of Fe in the lunar regolith and its relationship to the spectral reflectance properties of the moon p 843 N94-14303
LUNAR SURFACE
The studies on lunar and planetary exploration and utilization: The study on lunar resources utilization
[NASDA-CNT-930014] p 842 N94-13655
Laboratory simulations of lunar darkening processes p 843 N94-14301
LUNGS
Flow limitation and flutter in membrane walled collapsible tubes: A model for expiratory wheezing
[ISBN-0-315-73875-8] p 635 N94-13662
A characterization of carboxylesterases in rat and guinea pig: Their heterogeneity and role in detoxication of organophosphorus compounds
[NDRE-PUBL-93-1001] p 730 N94-14852
LYMPHOCYTES
Cellular responses to low-gravity: Pilot studies on suborbital rockets and orbiting spacecraft
[NASA-CR-194402] p 729 N94-14494
LYRA CONSTELLATION
Analysis of the IUE spectra of the strongly interacting binary beta Lyrae
[NASA-CR-194118] p 833 N94-14493

M

MACH NUMBER
Improved aeroprediction code. Part 1: Summary of new methods and comparison with experiment
[AD-A266015] p 500 N94-12989
A time-accurate numerical method for chemically reacting flows at all Mach numbers p 500 N94-13198
Numerical simulations and experiments on physics of high Mach number shockwave: Turbulent flow interactions
[DE93-013424] p 631 N94-13249
Topics on spatially high-order accurate methods and pre-conditioning for the Navier-Stokes equations with finite-rate chemistry p 633 N94-13572
A solution algorithm for the prediction of compressible laminar and turbulent shear flows p 634 N94-13635
A comparison of computational and experimental data for a subscale high speed propulsive nozzle at low mach numbers
[AD-A266543] p 504 N94-13705
MACHINE LEARNING
Efficient dynamic optimization of logic programs
[NASA-TM-109251] p 761 N94-12889
An analog clustering network from a biological model
[AD-A265637] p 762 N94-12969
Obstacle detection by recognizing binary expansion patterns
[NASA-CR-194415] p 514 N94-14495

MACHINERY
Transcript of workshop on machinery health monitoring
[IME-MET-TR-005] p 733 N94-13847
Machinery dynamics activities in Canadian industries
[IME-MET-TR-006] p 663 N94-14147
MACHINING
Machining aspects of nickel-phosphorus coatings
[DE93-013037] p 580 N94-14311
Computational diagnostics for detecting phase transitions during nanoindentation
[DE93-016536] p 813 N94-14439
Machining and grinding: High rate deformation in practice
[DE93-010718] p 664 N94-14457
MAGELLAN PROJECT (NASA)
STS-30 Magellan IUS/EVA training in WETF
[NASA-TM-109300] p 737 N94-13601
MAGELLANIC CLOUDS
The first data from the MACHO experiment
[DE93-014423] p 840 N94-14467
MAGNESIUM
Inhibiting corrosion in Gr/Al and Gr/Mg metal matrix composites using nonequilibrium alloying techniques
[AD-A266547] p 556 N94-13583
MAGNESIUM FLUORIDES
Novel Co:MgF2 lidar for aerosol profiler
[NASA-CR-191525] p 654 N94-13091
MAGNETIC ANOMALIES
Aeromagnetic work in the Lincoln Sea: 1991 survey
[DSIS-93-00308] p 715 N94-13830
Dynamical model for the distribution of geomagnetically trapped anomalous-component ions
[ATR-91(9558)-6] p 784 N94-13936
MAGNETIC BEARINGS
Cryogenic fluid film bearing tester development study
[NASA-CR-192586] p 660 N94-12791
MAGNETIC CIRCUITS
Advanced electric motor technology flux mapping
[NASA-CR-193824] p 621 N94-13186
MAGNETIC DIPOLES
Neptune high-latitude emission: Dependence of angle on frequency
[NASA-CR-193280] p 848 N94-13476
MAGNETIC EFFECTS
Multiwavelength observations of unidentified high energy gamma ray sources
[NASA-CR-194536] p 840 N94-14688
MAGNETIC ENERGY STORAGE
Technology assessments of advanced energy storage systems for electric and hybrid vehicles
[DE93-014395] p 701 N94-12913
MAGNETIC FIELD CONFIGURATIONS
Theory of field-reversed configurations
[DE93-015611] p 794 N94-12862
Evolution of the interplanetary magnetic field
[DE93-012631] p 836 N94-13262
Studies of non-inductive current drive in the CDX-U tokamak p 799 N94-13680
Current distribution tomography for determination of internal current density distributions
[DE93-015463] p 604 N94-13899
Stability and confinement properties of small-aspect-ratio tokamak
[INPE-5463-PRE/1771] p 801 N94-14024
MAGNETIC FIELD RECONNECTION
The interplanetary origins and the main-phase development of moderate geomagnetic storms (1978 - 1979)
[INPE-5445-TDI/491] p 835 N94-13174
MAGNETIC FIELDS
A 3D gyrokinetic particle-in-cell simulation of fusion plasma microturbulence on parallel computers
[DE93-012503] p 794 N94-12846
Investigation of dynamics of plasma fluxes generated by the quasi-stationary plasma accelerator P-50
[DE93-621665] p 794 N94-12854
Plasma diffusion through multidipole magnetic fields
[INPE-5460-PRE/1768] p 795 N94-12901
Kinetic simulations of ultra-intense laser plasma interactions and a novel method of generating odd harmonics
[DE93-014418] p 797 N94-13207
Evolution of the interplanetary magnetic field
[DE93-012631] p 836 N94-13262
Neptune high-latitude emission: Dependence of angle on frequency
[NASA-CR-193280] p 848 N94-13476
The geometric phase in quantum physics
[DE93-011121] p 817 N94-13479
ADP study of gamma-ray bursts
[NASA-CR-194311] p 848 N94-13708
Casting of superconducting composite materials (M-4)
p 586 N94-13736
Energetic neutral atoms: Imaging the magnetospheric ring current
[NASA-CR-194339] p 715 N94-13826
Mutual inductance between partially wound tori and a bifilar conductor
[ETN-93-94388] p 624 N94-13998
Multi-bunch beam-break-up studies for a SWFEL/TBA
[DE93-016973] p 658 N94-14414
Interactions among convection, magnetic fields and p-mode oscillations in the sun
[NASA-CR-194477] p 845 N94-14479
Kinetic simulations of ultra-intense laser plasma interactions
[DE93-014419] p 802 N94-14564
Theory of the negative magnetoresistance in magnetic metallic multilayers
[DE93-013912] p 776 N94-14584
Investigations of transitions from order to chaos in dynamical systems
[DE93-014438] p 818 N94-14738
Construction of the Courant-Snyder invariants for the non-linear equations of motion under presence of the linear coupling
[DE93-017565] p 788 N94-14872
MAGNETIC FLUX
Advanced magnetic flux compression generator development issues: A comparison of coaxial and disk generators
[DE93-014025] p 794 N94-12849
The study of structure-processing-property relations in copper oxide based high (Tc) superconductors
[DE93-015066] p 804 N94-13003
Instability heating of the HDZP
[DE93-012641] p 798 N94-13513
Review of the Procyon explosive pulsed power system
[DE93-016562] p 802 N94-14532
MAGNETIC INDUCTION
Simultaneous solution for core magnetic field and fluid flow beneath an electrically conducting mantle
[NASA-TM-4536] p 716 N94-13960
Survey of subsurface geophysical exploration technologies adaptable to an airborne platform
[DE93-015080] p 717 N94-14294
Calibration of a magnetic induction system for measurement of hypervelocities
[DE93-013949] p 652 N94-14578
MAGNETIC LEVITATION VEHICLES
Compendium of executive summaries from the maglev system concept definition
[PB93-154938/GAR] p 661 N94-13285
MAGNETIC MEASUREMENT
Survey of subsurface geophysical exploration technologies adaptable to an airborne platform
[DE93-015080] p 717 N94-14294
Shielded open-circuited sample holders for dielectric and magnetic measurements of liquids and powders
[PB93-198851] p 652 N94-14687
A high-precision direct current measuring device over a kiloampere range
[DE93-626409] p 627 N94-14885
MAGNETIC MOMENTS
Canted magnetic moments at the Gd(0001) surface
[DE93-014327] p 805 N94-13102
The geometric phase in quantum physics
[DE93-011121] p 817 N94-13479
Quantum Monte Carlo by message passing
[DE93-012645] p 760 N94-14177
MAGNETIC PERMEABILITY
Quantum Monte Carlo by message passing
[DE93-012645] p 760 N94-14177
A high-precision direct current measuring device over a kiloampere range
[DE93-626409] p 627 N94-14885
MAGNETIC PROPERTIES
The 1990 Western Pacific Geophysics meeting
[NASA-CR-193456] p 712 N94-13334
Spin polarized photoemission studies of interfacial and thin film magnetism
[DE93-014326] p 580 N94-14142
Magnetic interactions and disorder - phase transitions in dilute spin-glasses and high temperature superconductors
[ITN-93-65217] p 815 N94-14825
MAGNETIC RESONANCE
Magnetic resonance imaging after exposure to microgravity p 594 N94-13771
MAGNETIC STARS
ROSAT guest investigator program (AO-1). On a search for coronal x ray emissions from white dwarfs
[NASA-CR-193654] p 835 N94-13171
MAGNETIC STORMS
The interplanetary origins and the main-phase development of moderate geomagnetic storms (1978 - 1979)
[INPE-5445-TDI/491] p 835 N94-13174
MAGNETIC SURVEYS
Application of transient airborne electromagnetic and ground resistivity methods to geological mapping in tropical terrains
[ISBN-0-315-57172-1] p 685 N94-13542
Aeromagnetic work in the Lincoln Sea: 1991 survey
[DSIS-93-00308] p 715 N94-13830
MAGNETIC SUSPENSION
Propulsion simulator for magnetically-suspended wind tunnel models
[NASA-CR-189560] p 527 N94-13127
A superconducting large-angle magnetic suspension
[NASA-CR-189735] p 596 N94-13141
Compendium of executive summaries from the maglev system concept definition
[PB93-154938/GAR] p 661 N94-13285
Rolling moment control in the NAL 10 cm x 10 cm magnetic suspension and balance system
[NAL-TR-1164] p 526 N94-13347
MAGNETIC SWITCHING
Evolution of high-repetition-rate induction accelerators through advancements in switching
[DE93-012599] p 654 N94-12963
MAGNETIZATION
Theory of the negative magnetoresistance in magnetic metallic multilayers
[DE93-013912] p 776 N94-14584
MAGNETOHYDRODYNAMIC FLOW
The role of ionospheric plasma in the magnetosphere
[NASA-CR-194404] p 716 N94-13967
Implicit multi-fluid simulation of interpenetrating plasmas
[DE93-013351] p 801 N94-14342
Review of the Procyon explosive pulsed power system
[DE93-016562] p 802 N94-14532
MAGNETOHYDRODYNAMIC GENERATORS
Advanced magnetic flux compression generator development issues: A comparison of coaxial and disk generators
[DE93-014025] p 794 N94-12849
Heat and seed recovery technology project
[DE93-009203] p 800 N94-13913
MAGNETOHYDRODYNAMIC STABILITY
Two-dimensional simulations of foil implosion experiments on the Los Alamos capacitor bank
[DE93-012676] p 794 N94-12814
Theory of field-reversed configurations
[DE93-015611] p 794 N94-12862
Plasma diffusion through multidipole magnetic fields
[INPE-5460-PRE/1768] p 795 N94-12901
Equilibrium reconstruction of the q-profile in tokamaks from motional Stark effect data
[DE93-015815] p 796 N94-13046
Investigation of plasma instabilities in the Polar cusp
[NASA-CR-194283] p 796 N94-13084
Recent study of beam stability in the PSR
[DE93-014473] p 780 N94-13173
Parametric instabilities in large nonuniform laser plasmas
[DE93-013184] p 797 N94-13393
Instability heating of the HDZP
[DE93-012641] p 798 N94-13513
Nonlinear evolution of tearing modes in inhomogeneous plasmas
[PPL-133] p 798 N94-13564
The propagation characteristics and instability properties of low-frequency electromagnetic waves in the Io plasma torus p 601 N94-13650
Longitudinal beam dynamics for heavy ion fusion
[DE93-013850] p 789 N94-13727
Small scale magnetic islands in collisionless plasmas
[PPL-131] p 799 N94-13836
Semi-local kinetic analysis of the toroidal ion temperature gradient mode
[PPL-130] p 800 N94-13851
Anomalous transport due to the ion acoustic instability in tokamaks
[PPL-129] p 800 N94-13852
Numerical Studies of Collisionless Current Layers
[NASA-CR-194337] p 800 N94-13854
On MHD mode equations in toroidal plasmas
[PPL-139] p 800 N94-13877
Stability and confinement properties of small-aspect-ratio tokamak
[INPE-5463-PRE/1771] p 801 N94-14024
Anomalous transport due to small scale electromagnetic and large scale electrostatic modes in tokamaks
[PPL-140] p 801 N94-14206
Implicit multi-fluid simulation of interpenetrating plasmas
[DE93-013351] p 801 N94-14342
The role of electric field shear stabilization of turbulence in the H-mode to VH-mode transition in D3-D
[DE93-015474] p 802 N94-14583
Anomalous ion transport and feedback control
[DE93-018324] p 803 N94-14874

MAGNETOHYDRODYNAMIC TURBULENCE
On energy transport equations for turbulent magnetized plasma
[PPL-135] p 800 N94-13850
MAGNETOHYDRODYNAMIC WAVES
Comment of parameter excitation of Alfven and Heliicon waves in a magnetoactive compensated semiconductor by microwave radiation
[DE93-623203] p 806 N94-13228
Investigations of transitions from order to chaos in dynamical systems
[DE93-014438] p 818 N94-14738
MAGNETOHYDRODYNAMICS
MHD shocks in coronal mass ejections
[NASA-CR-193418] p 828 N94-12970
Magnetic fusion computing: A personal retrospective view
[DE93-014147] p 797 N94-13217
Heat and seed recovery technology project
[DE93-009203] p 800 N94-13913
Investigations of transitions from order to chaos in dynamical systems
[DE93-014438] p 818 N94-14738
MAGNETOPAUSE
Ion anisotropy driven waves in the Earth's magnetosheath and plasma depletion layer
[DE93-012751] p 712 N94-12952
The interplanetary origins and the main-phase development of moderate geomagnetic storms (1978 - 1979)
[INPE-5445-TDI/491] p 835 N94-13174
Terrestrial magnetospheric imaging: Numerical modeling of low energy neutral atoms
[DE93-014561] p 717 N94-14328
MAGNETOPLASMADYNAMICS
Electric propulsion system technology
[NASA-CR-194099] p 549 N94-13068
Low power pulsed MPD thruster system analysis and applications
[NASA-CR-191187] p 550 N94-13415
MAGNETORESISTIVITY
Theory of the negative magnetoresistance in magnetic metallic multilayers
[DE93-013912] p 776 N94-14584
MAGNETOSHEATH
Ion anisotropy driven waves in the Earth's magnetosheath and plasma depletion layer
[DE93-012751] p 712 N94-12952
MAGNETRON SPUTTERING
Ion assisted sputter deposition of Mo-Si multilayers
[DE93-013830] p 583 N94-14693
MAGNETS
Calibration of a magnetic induction system for measurement of hypervelocities
[DE93-013949] p 652 N94-14578
MAGNONS
Hydrodynamic asymptotics of Green functions in magnetics with spontaneously broken symmetry
[DE93-621349] p 767 N94-13223
MAINTENANCE
Activities of Hawker Siddeley Canada Inc.
[CTN-93-60865] p 849 N94-13505
Transcript of workshop on machinery health monitoring
[IME-MET-TR-005] p 733 N94-13847
Optimal maintenance policies of a Markovian system
[ITN-93-85216] p 774 N94-14502
MAINTENANCE TRAINING
Human factors in aviation maintenance: Phase 3, volume 1
[DOT/FAA/AM-93/15] p 738 N94-14023
MAN ENVIRONMENT INTERACTIONS
Chemistry and transport in a multi-dimensional model
[NASA-CR-194425] p 716 N94-13969
Summary of conclusions and recommendations from a visibility science workshop
[DE93-012770] p 710 N94-14523
MAN MACHINE SYSTEMS
Flight crew interface aspects of forward-looking airborne windshear detection systems
[NASA-CR-191437] p 516 N94-12829
Cognitive engineering in aerospace application: Pilot interaction with cockpit automation
[NASA-CR-177617] p 510 N94-13247
Compatibility of information and mode of control: The case for natural control systems p 523 N94-13307
Future developments of the NLR research flight simulator
[NLR-TP-92143-U] p 528 N94-13498
Aerospace medicine and biology: A continuing bibliography with indexes (supplement 379)
[NASA-SP-7011(379)] p 733 N94-14412
MAN-COMPUTER INTERFACE
Common lisp framework
[AD-A265878] p 742 N94-12933
Advanced display object selection methods for enhancing user-computer productivity
[AD-A265806] p 743 N94-12974
Collection and analysis of dialogue protocols for the question-answering facility of the entity-relationship modeling advisor
[ERB-1032] p 740 N94-13546
Programming the multimodal interface
[DE93-013084] p 748 N94-13576
Functional categories for future flight deck designs
[NASA-TM-109005] p 517 N94-13710
SCAILET: An intelligent assistant for satellite ground terminal operations
[NASA-TM-105879] p 538 N94-13918
Intelligent environment for interpretation tasks of remotely sensed images
[INPE-5466-PRE/1774] p 687 N94-14082
Payload/GSE/data system interface: Users guide for the VPF (Vertical Processing Facility)
[NASA-CR-194385] p 532 N94-14148
Eye-gaze and intent: Application in 3D interface control
[DE93-015210] p 738 N94-14335
An overview of parallel scientific visualization
[DE93-017105] p 755 N94-14521
MANAGEMENT
Discovery management workshop
[NASA-TM-108244] p 531 N94-14080
MANAGEMENT INFORMATION SYSTEMS
Making the connection between information modeling and implementation
[DE93-011588] p 820 N94-12907
Building the repositories to serve --- Superconducting Super Collider information system
[DE93-014100] p 821 N94-12983
Knowledge base technology for CT-DIMS: Report 1
[DE93-013118] p 743 N94-13014
Program/project management resource lists
[NASA-TM-109268] p 822 N94-13107
MANAGEMENT METHODS
Ninth Annual NASA/Contractors Conference on Quality and Productivity. World Class Excellence: The Journey Continues. Conference presentations
[NASA-CR-194514] p 665 N94-13153
Measuring quality progress p 666 N94-13154
Defining the performance gap: Conducting a self-assessment p 666 N94-13155
What's the bottom line payback for TQM? p 666 N94-13156
Partnership with the customer p 666 N94-13157
Strategic planning as a focus for continuous improvement. A case study p 666 N94-13158
The power of cross-functional teams in driving total quality p 666 N94-13159
Kennedy Space Center's NASA/Contractor Team-Centered Total Quality Management Seminar: Results, methods, and lessons learned p 667 N94-13162
Here's the beef: A case study in organizational transformation p 667 N94-13163
NASA Johnson Space Center: Total quality partnership p 668 N94-13165
The Eighth Annual NASA/Contractors Conference and 1991 National Symposium on Quality and Productivity: Extending the boundaries of total quality management
[NASA-TM-109276] p 669 N94-14321
MANAGEMENT PLANNING
Strategic planning as a focus for continuous improvement. A case study p 666 N94-13158
Building a quality culture in the Office of Space Flight: Approach, lessons learned and implications for the future p 667 N94-13164
Creating a strategic plan for configuration management using computer aided software engineering (CASE) tools
[DE93-013663] p 746 N94-13394
Forest management for fixing and sequestering carbon
[DE93-013520] p 707 N94-13486
Space and Earth sciences, computer systems, and scientific data analysis support, volume 1
[NASA-CR-194535] p 741 N94-13788
Fourteenth National Industrial Energy Technology Conference: Proceedings
[DE93-016698] p 710 N94-14516
MANAGEMENT SYSTEMS
Measuring quality progress p 666 N94-13154
Teamwork for Oversight of Processes and Systems (TOPS). Implementation guide for TOPS version 2.0, 10 August 1992 p 668 N94-13167
Quality assurance for environmental chemistry, 1991, volume 1
[DE93-011791] p 709 N94-14020
MANEUVERABILITY
A piloted simulation investigation of the normal load factor and longitudinal thrust required for air-to-air acquisition and tracking p 522 N94-13301
In-flight simulation of high agility through active control: Taming complexity by design p 523 N94-13306
MANGANESE ISOTOPES
The beta(+) decay and cosmic-ray half-life of Mn-54
[DE93-013913] p 848 N94-13695
MANIPULATORS
Roller-gear drives for robotic manipulators design, fabrication and test
[NASA-CR-194248] p 660 N94-12802
Force reflecting hand controller for manipulator teleoperation
[NASA-CR-191345] p 661 N94-13129
Control algorithm implementation for a redundant degree of freedom manipulator
[NASA-CR-191339] p 762 N94-13131
Robot-task compliance: The energy criterion
[ITN-93-85196] p 763 N94-13568
Generalized impedance control of a redundant manipulator p 661 N94-13575
Decentralized control of uncertain systems via sensitivity models
[DE93-012963] p 766 N94-14568
Modelling robotic systems with DADS p 678 N94-14625
Parallel methods for dynamic simulation of multiple manipulator systems p 680 N94-14637
MANNED MARS MISSIONS
Design, qualification and operation of nuclear rockets for safe Mars missions
[DE93-010792] p 549 N94-12996
Mirror fusion propulsion system: A performance comparison with alternate propulsion systems for the manned Mars Mission
[NASA-TM-109248] p 550 N94-13147
Optimizing interplanetary trajectories with deep space maneuvers
[NASA-CR-4546] p 532 N94-14851
MANNED SPACE FLIGHT
Development of a nonazeotropic heat pump for crew hygiene water heating
[NASA-CR-194189] p 737 N94-13674
Life support and habitability manual, volume 1
[ESA-PSS-03-406-ISSUE-1-VOL] p 737 N94-13901
Life support and habitability manual, volume 2
[ESA-PSS-03-406-ISSUE-1-VOL] p 738 N94-13902
An evaluation of noise and its effects on shuttle crewmembers during STS-50/USML-1
[NASA-TM-104775] p 735 N94-13961
My experiences in manned space flight p 698 N94-14276
The problem of traveling in outer space: The rocket motor
[NASA-TT-10002] p 552 N94-14463
Physical countermeasures for long-term manned space flights
[ESA-SP-1160] p 733 N94-14860
MANNED SPACECRAFT
Development of an advanced spacecraft tandem mass spectrometer
[NASA-CR-194195] p 545 N94-13953
MANUAL CONTROL
Evaluation of two cockpit display concepts for civil tiltrotor instrument operations on steep approaches p 517 N94-13323
Simulator study of uncoupled control functions. Use of manual pointing modes when aiming at ground targets and oncoming airborne target
[FFA-TN-1992-18] p 528 N94-13588
Manual control in space research on perceptual-motor functions under zero gravity conditions (L-10) p 593 N94-13767
MANUALS
Environmental awareness
[DE93-014192] p 707 N94-13218
Manual on the global data-processing system. Volume 1: (Annex 4 to the WMO regulations) global aspects (1992 edition)
[WMO-485-VOL-1] p 721 N94-13686
Life support and habitability manual, volume 1
[ESA-PSS-03-406-ISSUE-1-VOL] p 737 N94-13901
Life support and habitability manual, volume 2
[ESA-PSS-03-406-ISSUE-1-VOL] p 738 N94-13902
National use of the groups 7wwW1W2 and 960ww for ground stations
[KNMI-PUBL-181] p 722 N94-13926
Manual on the global data-processing system. Volume 2: Regional aspects (1992 edition)
[WMO-485-VOL-2] p 722 N94-14071
Oak Ridge Environmental Information System (ORIES) site workstation information packet for OREIS 6.2
[DE93-010761] p 825 N94-14458
A guide to the DRA 13 ft x 9 ft Low Speed Wind Tunnel Facility
[AD-A267739] p 528 N94-14876

MANUFACTURING
Photovoltaics: Contract lists, fiscal year 1992
[DE93-000093] p 701 N94-12902
Role of microstructure on fatigue durability of aluminum aircraft alloys
[AD-A265627] p 568 N94-12993
Knowledge base technology for CT-DIMS: Report 1
[DE93-013118] p 743 N94-13014
Rigid-flexible printed wiring boards
[DE93-013938] p 620 N94-13094
Pollution prevention through total quality
[DE93-013814] p 707 N94-13390
Rapid intelligent inspection process definition for dimensional measurement in advanced manufacturing
[DE93-011271] p 748 N94-13480
Activities of Hawker Siddeley Canada Inc.
[CTN-93-60865] p 849 N94-13505
Cesium iodide (CsI) crystal manufacture
[DE93-012146] p 808 N94-13973
Continuous roll-to-roll a-Si photovoltaic manufacturing technology
[DE93-010006] p 704 N94-14109
Knowledge based systems: From process control to policy analysis
[DE93-014582] p 765 N94-14117
Welding technologies as applied to nuclear manufacturing
[DE93-010924] p 664 N94-14565
MANY BODY PROBLEM
Many-body corrections in XAFS
[DE93-011002] p 563 N94-13478
MAPPING
Quantitative mapping of pore fraction variations in silicon nitride using an ultrasonic contact scan technique
[NASA-TP-3377] p 665 N94-13056
Error analysis of real time and post processed or bit determination of GFO using GPS tracking
[NASA-CR-193646] p 512 N94-13238
MARANGONI CONVECTION
Marangoni effect induced convection in material processing under microgravity (M-18)
p 589 N94-13750
Contributions to numerical solution of Navier-Stokes equations in two and three dimensional flows
[ETN-93-94395] p 647 N94-14816
MARINE BIOLOGY
Remote sensing of aquatic system
[INPE-5271-PRP/159] p 684 N94-13426
Nonlinear relationships between particulate absorption and chlorophyll: Detritus or pigment packaging?
[AD-A266806] p 731 N94-14899
MARINE ENVIRONMENTS
Remote sensing of aquatic system
[INPE-5271-PRP/159] p 684 N94-13426
MARINE METEOROLOGY
Binary homogeneous nucleation: Temperature and relative humidity fluctuations and non-linearity
[DE93-007884] p 709 N94-13911
MARINE TECHNOLOGY
Coastal scour problems and methods for prediction of maximum scour
[AD-A266658] p 726 N94-14775
MARKET RESEARCH
Photovoltaics: Program overview, fiscal year 1992
[DE93-000055] p 701 N94-12914
MARKOV CHAINS
Optimal maintenance policies of a Markovian system
[ITN-93-85216] p 774 N94-14502
MARKOV PROCESSES
Stochastic scheduling games with Markov decision arrival processes
[CWI-BS-R9231] p 773 N94-14005
The effects of internal fluctuations on a class of nonequilibrium statistical field theories
[DE93-016620] p 774 N94-14441
Optimal maintenance policies of a Markovian system
[ITN-93-85216] p 774 N94-14502
MARS (PLANET)
MARS Mission research center
[NASA-CR-194034] p 841 N94-13088
Solar radiation on Mars: Stationary photovoltaic array
[NASA-TM-106321] p 626 N94-14730
MARS ATMOSPHERE
Optical properties of CO2 ice and CO2 snow in the ultraviolet, visible, and infrared
[NASA-CR-194110] p 686 N94-14081
MARS LANDING
Planetary protection implementation on future Mars lander missions
[NASA-CP-3216] p 841 N94-13183
MARS PHOTOGRAPHS
Rover imaging system for the Mars rover/sample return mission
[NASA-CR-193413] p 649 N94-13464
MARS PROBES
Exploring Mars
[NASA-TM-109306] p 842 N94-13613
MARS SURFACE
The nature and origin of periodically spaced tectonic features on Mars
[NASA-CR-193821] p 842 N94-13199
Martian sedimentary deposits
[NASA-CR-193266] p 842 N94-13855
A widget based operations simulator for a planetary camera: A model for the high resolution stereo camera on Mars 94
[DLR-FB-92-30] p 651 N94-14044
Optical properties of CO2 ice and CO2 snow in the ultraviolet, visible, and infrared
[NASA-CR-194110] p 686 N94-14081
MASS
Stability of reference masses 1: Evidence for posiible variations in the mass of reference kilograms arising from mercury contamination
[NPL-DMM(A)-86] p 708 N94-13667
MASS SPECTROMETERS
Development of an advanced spacecraft tandem mass spectrometer
[NASA-CR-194195] p 545 N94-13953
MASS SPECTROSCOPY
EBIT Trapping Program
[DE93-014422] p 788 N94-13208
Research in cosmic and gamma ray astrophysics: Cosmic physics portion
[NASA-CR-194127] p 847 N94-13211
Low temperature metal-organic chemical vapor deposition growth processes for high efficiency solar cells
[DE92-010562] p 702 N94-13386
Construction and test of a facility for photon-stimulated field description using excimer laser and time of flight
[ETN-93-94386] p 657 N94-13996
UV and IR laser ablation for inductively coupled plasma mass spectrometry
[DE93-017124] p 658 N94-14415
MASS TRANSFER
Research on chemical vapor deposition processes for advanced ceramic coatings
[NASA-CR-193613] p 577 N94-13089
The corrosion behavior of 8001 Al under heat-transfer conditions in an aqueous loop system
[DE93-013450] p 569 N94-13242
Destruction of waste energetic materials using base hydrolysis
[DE93-012738] p 584 N94-13491
Studies of momentum and energy transfer across wavy gas-liquid interfaces
[AD-A266432] p 635 N94-13699
Wind mass and energy deposition
[DE93-013345] p 839 N94-14341
MASSIVE STARS
A photometric study of massive x-ray binaries
[ITN-93-85207] p 829 N94-13231
Charge-exchange reactions and weak interaction rates for Type 2 supernovae
[DE93-015104] p 783 N94-13893
MASSIVELY PARALLEL PROCESSORS
The 3-D massively parallel impact simulations using PCTH
[DE93-011593] p 670 N94-12908
A network evaluation and analysis tool
[DE93-012647] p 758 N94-12917
An experimental regional scale climate simulation laboratory
[DE93-015935] p 719 N94-13119
Implementation of ADI: Schemes on MIMD parallel computers
[NASA-CR-193720] p 759 N94-13204
Advanced computers and simulation
[DE93-014354] p 740 N94-13286
A data distributed parallel algorithm for ray-traced volume rendering
[NASA-CR-191520] p 749 N94-13721
Efficient, massively parallel eigenvalue computation
[NASA-CR-194289] p 760 N94-13921
VFGEN: A parallel volume fraction generator for hydrocodes
[DE93-011673] p 752 N94-14019
Hybrid S(sub N)/Monte Carlo research and results
[DE93-012677] p 773 N94-14178
An efficient parallel algorithm for matrix-vector multiplication
[DE93-015125] p 754 N94-14399
An overview of parallel scientific visualization
[DE93-017105] p 755 N94-14521
MATCHING
Screening of solar cells
[NASA-TM-106298] p 620 N94-13134
MATERIALS HANDLING
Hydrogen peroxide safety issues
[DE93-013895] p 565 N94-14346
MATERIALS SCIENCE
Recovery of materials impacted at high velocity
[DE93-014150] p 576 N94-12885
Nonlinear analysis, scientific computation, and continuum mechanics applied to the science of materials
[AD-A266641] p 817 N94-14680
MATERIALS TESTS
Ohmic heating of composite candidate graphite-fiber/coating combinations
[NASA-TM-4491] p 554 N94-12871
Flight service evaluation of composite components on the Bell helicopter model 206L
[NASA-CR-191499] p 555 N94-13267
Effect of thermal processing practices on the properties of superplastic Al-Li alloys
[NASA-CR-4548] p 574 N94-14850
Atomic research
[NASA-CR-193843] p 788 N94-14905
MATHEMATICAL LOGIC
Rare attributes in finite universe: Hypotheses testing specification and exact randomized upper confidence bounds
[DE93-012783] p 775 N94-12955
MATHEMATICAL MODELS
A computer model for liquid jet atomization in rocket thrust chambers
[NASA-CR-194194] p 627 N94-12803
The 24 GHz measurements of 2.2 lambda conical horn antennas illuminating a conducting sheet
[NASA-TM-109002] p 598 N94-12811
Venus gravity
[NASA-CR-194077] p 841 N94-12823
Thermosolutal convection and macrosegregation in dendritic alloys
[NASA-CR-194039] p 567 N94-12825
Artificial intelligence support for scientific model-building
[NASA-TM-109252] p 761 N94-12890
An analytical investigation of transient effects on rewetting of heated thin flat plates
[NASA-TM-106120] p 628 N94-12968
Tree reconstruction from partial orders
[DE93-009841] p 743 N94-12991
Surrogates for numerical simulations; optimization of eddy-promoter heat exchangers
[NASA-CR-191510] p 629 N94-13074
The three-dimensional flow past a rapidly rotating circular cylinder
[NASA-CR-191512] p 630 N94-13075
A coherent flame model of premixed turbulent combustion in a counterflow geometry
[CUED/A-THERMO/TR.60] p 562 N94-13085
Dynamics of adaptive structures: Design through simulations
[NASA-CR-193724] p 540 N94-13112
Diagnostic studies of the HxOy-NxOy-O3 photochemical system using data from NASA GTE field expeditions
[NASA-CR-193672] p 706 N94-13170
Lightning simulation and determination of expected striking points
[ITN-93-85202] p 719 N94-13188
Radiative transfer in the dynamic atmospheres of Mira-type variables
[NASA-CR-193324] p 829 N94-13287
A model for rotorcraft flying qualities studies
p 523 N94-13308
The development and potential of inverse simulation for the quantitative assessment of helicopter handling qualities p 523 N94-13311
An analytic modeling and system identification study of rotor/fuselage dynamics at hover p 524 N94-13312
Calculation of the required sensor accuracy to obtain a specified state estimation accuracy
[NAL-TR-1173] p 649 N94-13343
Neptune high-latitude emission: Dependence of angle on frequency
[NASA-CR-193280] p 848 N94-13476
Electron emission resulting from fast ion impact on thin metal foils: Implications of these data for development of track structure models
[DE93-013506] p 782 N94-13485
Tidal interactions in the Earth Moon system
[COMMUNICATIONS-SER-B-160] p 837 N94-13503
A knowledge-based model for the integration of remote sensing into a mineral exploration program
[ISBN-0-315-58982-5] p 685 N94-13523
Analytical framework for modeling scale-related variabilities in remote sensing p 685 N94-13592
A stochastic model for behavior analysis of fiber-reinforced quasi-brittle materials
p 672 N94-13594

Passage-averaged approximation of turbomachinery flows using vorticity-potential method
[ISBN-0-315-72716-0] p 634 N94-13598
Minimal modeling of the bimodality of extratropical atmospheric planetary waves p 713 N94-13622
Evaluation for rheological constitutive relations, using the indentation technique p 775 N94-13627
Develop research plan for use of atlas data
[NASA-CR-194338] p 714 N94-13709
Theoretical molecular studies of astrophysical interest
[NASA-CR-193300] p 838 N94-13781
Event-driven simulation in SELMON: An overview of EDSE
[NASA-CR-194505] p 749 N94-13784
Antenna pattern control using impedance surfaces
[NASA-CR-194517] p 602 N94-13799
A review of robust detection
[DSIS-93-00400] p 603 N94-13829
Modelling of the temperature distribution in a copper roll for the design of a system of cooled rolls adapted to vertical strip casting
[IMI-93RT-21200-1436-G] p 557 N94-13866
Stochastic performance modeling and evaluation of obstacle detectability with imaging range sensors
[NASA-CR-194510] p 605 N94-13946
Wind erosion in semiarid landscapes: Predictive models and remote sensing methods for the influence of vegetation
[NASA-CR-194029] p 715 N94-13956
Sloshing dynamics on rotating helium dewar tank
[NASA-CR-194403] p 637 N94-13959
Simultaneous solution for core magnetic field and fluid flow beneath an electrically conducting mantle
[NASA-TM-4536] p 716 N94-13960
The role of ionospheric plasma in the magnetosphere
[NASA-CR-194404] p 716 N94-13967
Computer program for thermal and transport properties of parahydrogen from 20 to 10,000 K
[NASA-TP-3378] p 552 N94-14102
A performance prediction model for a fault-tolerant computer during recovery and restoration
[NASA-CR-194490] p 741 N94-14136
Computational techniques and capabilities
p 506 N94-14162
Integration of remote sensing and mathematical modelling in disaster mitigation p 692 N94-14239
Nonlinear wave predictions in ceramics
[DE93-016516] p 582 N94-14436
Three-dimensional modeling of diesel engine intake flow, combustion and emissions-2
[NASA-CR-191189] p 519 N94-14448
A conduction model for the vacuum arc remelting process
[NPL-DMM(A)-98] p 639 N94-14464
The motion of a conical shaped liner driven by explosive load
[ITN-93-85215] p 585 N94-14507
Atmospheric acoustic modeling
[DE93-016727] p 718 N94-14518
Scattering calculations and confining interactions
[NASA-CR-194242] p 786 N94-14549
Long duration measurements of fading on a low elevation angle, 11-GHz satellite path p 613 N94-14661
A database for propagation models
p 614 N94-14665
Contribution towards a draft revision of recommendations 681: Propagation data required for the design of Earth-space land mobile telecommunications systems p 614 N94-14666
Characterisation of the LMS propagation channel at L- and S-bands: Narrowband experimental data and channel modelling p 615 N94-14669
ACTS propagation experiment discussion: Ka-band propagation measurements using the ACTS propagation terminal and the CSU-CHILL and Space Communications Technology Center Florida propagation program
p 616 N94-14678
Nonlinear analysis, scientific computation, and continuum mechanics applied to the science of materials
[AD-A266641] p 817 N94-14680
A study of thin liquid sheet flows
[NASA-TM-106323] p 642 N94-14732
Robust non convex optimization algorithms: Codes and numerical simulation of large scale
[ETN-93-94354] p 756 N94-14813
Optical systems integrated modeling
p 547 N94-14837
Double inlet pulse tube cryocooler theory
[AD-A266832] p 597 N94-14877
Toward a quasi-linear closure for compressible turbulence
[DE93-017185] p 647 N94-14895

MATHEMATICAL PROGRAMMING

The 8th Workshop on the Mathematical Foundations of Programming Semantics
[AD-A266436] p 749 N94-13700
Mathematical optimization: A tool for aircraft design
[MBB-LME-251-S-PUB-0492] p 751 N94-14006

MATHEMATICS

Workshop for coordinating South Carolina's pre-college systemic initiatives in science and mathematics
[DE93-012263] p 818 N94-13216

MATRICES (MATHEMATICS)

Tree reconstruction from partial orders
[DE93-009841] p 743 N94-12991
A path-oriented matrix-based knowledge representation system
[NASA-CR-4539] p 744 N94-13065
Codes from an N-dimensional torus simplicially or cellularly decomposed p 747 N94-13438
Formally biorthogonal polynomials and a look-ahead Levinson algorithm for general Toeplitz systems
[NASA-CR-194297] p 748 N94-13586
Stochastic realization of finite-valued processes and primes in the positive matrices
[CWI-BS-R9222] p 773 N94-13677
Efficient, massively parallel eigenvalue computation
[NASA-CR-194289] p 760 N94-13921
On the differential structure of matrix-valued rational inner functions
[CWI-BS-R9228] p 770 N94-14003
An efficient parallel algorithm for matrix-vector multiplication
[DE93-015125] p 754 N94-14399
The use of linked lists in the simulation of controller-structure interaction p 679 N94-14630
Parallel O(log n) algorithms for open- and closed-chain rigid multibody systems based on a new mass matrix factorization technique p 679 N94-14636
Splines, contours and SVD subroutines
[DE93-016088] p 757 N94-14866

MATRIX MATERIALS

Ceramic matrix composites by microwave assisted CVI
[DE93-012640] p 576 N94-12916
Graphite fiber textile preform/copper matrix composites
[NASA-CR-193797] p 558 N94-14050

MATRIX METHODS

Development of time-dependent orthotropic constitutive law of a thermoplastic composite material
p 556 N94-13595

MAXIMUM ENTROPY METHOD

Maximum entropy spectral analysis of the geological time series of the oxygen isotope record from deep-sea cores
[INPE-5465-PRE/1773] p 725 N94-13728
Quantum Monte Carlo by message passing
[DE93-012645] p 760 N94-14177

MAXIMUM LIKELIHOOD ESTIMATES

Cancellation of multipath for monopulse radars
[ITN-93-85191] p 600 N94-13538
Maximum likelihood estimation for constrained or missing data models
[AD-A266563] p 773 N94-13585
Enhanced decoding for the Galileo S-band mission
p 609 N94-14380
Supervised classification of remotely sensed images
[DLR-FB-92-07] p 700 N94-14428
Robust estimators and tests in one-sample location problem with particular consideration on modified maximum likelihood process
[ETN-93-94391] p 774 N94-14703
Generalized smooth models
[DE93-013045] p 756 N94-14864

MEAN FREE PATH

Variance reduction unique to coupled electron/photon Monte Carlo transport
[DE93-014999] p 782 N94-13409

MEASURE AND INTEGRATION

An adaptive projection method for the incompressible Euler equations
[DE93-016428] p 639 N94-14434

MEASUREMENT

A measurement and evaluation process model applied to software engineering environments
[INPE-5345-PUD/048] p 746 N94-13428

MEASURING INSTRUMENTS

Phobos/Harp post launch support
[NASA-CR-193676] p 540 N94-13109
Perspective on the National Aero-Space Plane Program instrumentation development
[NASA-TM-4505] p 516 N94-13256
Calculation of the required sensor accuracy to obtain a specified state estimation accuracy
[NAL-TR-1173] p 649 N94-13343
DATAA: Data acquisition made easy
[DE93-014683] p 823 N94-13406
The 3D pneumatic and 2D dynamic probes: Their development and subsequent use in a transonic fan
[RAE-TM-AERO/PROP-22] p 653 N94-14827
A high-precision direct current measuring device over a kiloampere range
[DE93-626409] p 627 N94-14885

MECHANICAL DRIVES

Roller-gear drives for robotic manipulators design, fabrication and test
[NASA-CR-194248] p 660 N94-12802
Development of a high-speed mechanical drive system for oscillating an annular blade row in the bending mode
[NAL-TR-1170] p 502 N94-13342

MECHANICAL ENGINEERING

Machinery dynamics activities in Canadian industries
[IME-MET-TR-006] p 663 N94-14147

MECHANICAL IMPEDANCE

Computer code for scattering from impedance bodies of revolution. Part 3: Surface impedance with s and phi variation. Analytical and numerical results
[NASA-CR-193396] p 599 N94-13264

MECHANICAL PROPERTIES

Simulation studies for surfaces and materials strength
[NASA-CR-193305] p 671 N94-13179
Measurements on two-dimensional arrays of mesoscopic Josephson junctions
[AD-A265129] p 807 N94-13359
Measurement of strain in individual phases of composites before, during, and after mechanical loading
[DE93-014585] p 558 N94-14119
Dynamic mechanical deformation of a SiC(sub p)/Al-Li (8090) composite
[DE93-014586] p 558 N94-14121
Physical and structural properties of a sputtered zirconia-yttria layer used as a thermal resistance
[ONERA-NT-1992-10] p 810 N94-14193
Nonlinear wave predictions in ceramics
[DE93-016516] p 582 N94-14436
Machining and grinding: High rate deformation in practice
[DE93-010718] p 664 N94-14457
The structure and mechanical properties of Ru-Cu and Ru-Ti nanolayer composites
[DE93-014453] p 558 N94-14469
Microstructural influences on the mechanical properties of solder
[DE93-015044] p 573 N94-14474
Structures and shear response of lipid monolayers
[DE93-015076] p 730 N94-14802
Yield properties of tungsten and tungsten heavy alloys
[AD-A266833] p 575 N94-14878

MECHANICAL SHOCK

Development of test techniques to simulate high-frequency mechanical shock on weapon components
[KCP-613-4998] p 675 N94-13907

MEDIAN (STATISTICS)

Robust estimators and tests in one-sample location problem with particular consideration on modified maximum likelihood process
[ETN-93-94391] p 774 N94-14703

MEDICAL EQUIPMENT

Medical evaluations on the KC-135 1991 flight report summary
[NASA-TM-104755] p 731 N94-12832

MEDICAL SCIENCE

Clinical physiology of bed rest
[NASA-TM-104010] p 727 N94-13447
Thyroid alterations in porcine after prolonged exposure to cold or heat
[AD-A266840] p 733 N94-14879

MEDICAL SERVICES

In-flight demonstration of the Space Station Freedom Health Maintenance Facility fluid therapy system (E300/E05) p 595 N94-13775

MEDICINE

Science, technology, and the federal government: National goals for a new era p 827 N94-14115

MELT SPINNING

Preparation and characterization of rapidly solidified Al-Li alloys
[ISBN-0-315-58948-5] p 569 N94-13367

MELTING

Incomplete melting of the Au(100) surface
[DE93-623192] p 569 N94-13227
High temperature behavior of glass (M-8)
p 587 N94-13740
Microwave hybrid heating of alumina filaments
[DE93-012642] p 581 N94-14327
Statistical mechanical theory of liquid entropy
[DE93-016524] p 817 N94-14593

MELTS (CRYSTAL GROWTH)

Growth experiment of narrow band-gap semiconductor PbSnTe single crystals in space (M-1)
p 586 N94-13733
Growth of Si spherical crystals and the surface oxidation (M-9) p 587 N94-13741

Crystal growth of compound semiconductors in a low-gravity environment (InGaAs crystals) (M-22)
p 590 N94-13754
Containerless processing of undercooled melts
[NASA-CR-194350] p 572 N94-14123

MEMBRANE STRUCTURES
Evaluation for membrane components of water recycling system
[NAL-TM-646] p 737 N94-13388

MEMBRANES
Predicting the vibrations of a spinning inflated membrane
[DE93-010690] p 676 N94-14456
Upgrading of raw natural gas using high-performance polymer membranes
[DE93-014041] p 566 N94-14586
Primary and secondary electrical space power based on advanced PEM systems
[DE93-012643] p 553 N94-14689
Structures and shear response of lipid monolayers
[DE93-015076] p 730 N94-14802

MEMORY (COMPUTERS)
Beyond core: Making parallel computer I/O practical
[DE93-012347] p 758 N94-12878
The KSR1: Experimentation and modeling of poststore
[DE93-012539] p 759 N94-13470
Hashing and rehashing in emulated shared memory
[CWI-CS-R9240] p 740 N94-13525
The National Storage Laboratory: A collaborative research project
[DE93-015099] p 760 N94-14475
Execution methods, and parallel virtual machines for distributed implementation of the LCS parallel programming language
[LAAS-93032] p 761 N94-14716

MENTAL PERFORMANCE
Work/rest schedules and performance of S-3 aviators during fleet exercise
[AD-A265807] p 734 N94-12975
Work/rest schedules and performance of F/A-18 aviators during Fleet Exercise 1992
[AD-A265826] p 735 N94-12982
Selection of behavioral tasks and development of software for evaluation of rhesus monkey behavior during spaceflight
[NASA-CR-194176] p 728 N94-13865
The influence of ATC message length and timing on pilot communication
[NASA-CR-177621] p 512 N94-14744

MERCURY (METAL)
Stability of reference masses 1: Evidence for posiible variations in the mass of reference kilograms arising from mercury contamination
[NPL-DMM(A)-86] p 708 N94-13667

MERGING ROUTINES
Paradigms for very fast parallel algorithms
[ITN-93-85212] p 755 N94-14556

MESON RESONANCE
Further study of the X(1910) meson
[DE93-621443] p 782 N94-13362

MESON-NUCLEON INTERACTIONS
Dynamics of pion-nucleus systems
[DE93-014449] p 785 N94-14468

MESONS
Aspects of symmetry violation
[DE93-011003] p 779 N94-12997
Further study of the X(1910) meson
[DE93-621443] p 782 N94-13362
The off shell (rho)-(omega) mixing in the QCD sum rules
[DE93-014845] p 786 N94-14527
Early baryon and meson spectroscopy culminating in the discovery of the Omega minus SU(3) and quarks
[DE93-014321] p 787 N94-14580
Tests of non-local interferences in kaon physics at asymmetric phi-factories
[DE93-013905] p 787 N94-14857

MESOSCALE PHENOMENA
Circulation model experiments of the Gulf Stream using satellite-derived fields
[AD-A266067] p 725 N94-12990
Effects of surface thermal forcing on stratified flow past an isolated obstacle p 633 N94-13553
Numerical simulation and parameterization of orographic gravity waves p 713 N94-13647
Regional climatology sensitivity studies
[DE93-010712] p 722 N94-14057

MESSAGE PROCESSING
Fail-safe PVM: A portable package for distributed programming with transparent recovery
[AD-A266594] p 749 N94-13779
The influence of ATC message length and timing on pilot communication
[NASA-CR-177621] p 512 N94-14744

MESSAGES
The influence of ATC message length and timing on pilot communication
[NASA-CR-177621] p 512 N94-14744
Toward a verifiable approach to the design of concurrent computations
[DE93-012908] p 756 N94-14844

METABOLISM
Clinical physiology of bed rest
[NASA-TM-104010] p 727 N94-13447
Endocrine and metabolic changes in payload specialist (L-1) p 591 N94-13758
Metabolic rate measurements comparing supine with upright upper-body exercises
[NASA-CR-4549] p 729 N94-14028
Cellular responses to low-gravity: Pilot studies on suborbital rockets and orbiting spacecraft
[NASA-CR-194402] p 729 N94-14494

METAL COATINGS
Analysis of samples of reflector materials which are multicoated and metal samples with oxide coatings which have been exposed the space environment in LDEF testing
[NASA-CR-193647] p 575 N94-12789
Ohmic heating of composite candidate graphite-fiber/coating combinations
[NASA-TM-4491] p 554 N94-12871
Absorption and damage thresholds of low defect density hafnia deposited with activated oxygen
[DE93-013853] p 655 N94-13243
Laser CO2 beam transmission through hollow metallic waveguide coated by a thin internal dielectric layer
[ITN-93-85201] p 656 N94-13571
Metastability of yttrium-oxides
[DE93-016548] p 813 N94-14440
JPRS report: Science and technology. Central Eurasia: Materials science
[JPRS-UMS-93-006] p 558 N94-14573
JPRS report: Science and technology. Central Eurasia: Materials science
[JPRS-UMS-93-004] p 559 N94-14574
Materials and structures p 546 N94-14835

METAL CRYSTALS
Atomic structure of the 310 twin in niobium: Theoretical predictions and comparison with experimental observation
[DE93-013421] p 806 N94-13136
Growth experiment of organic metal crystal in low gravity (M-21) p 590 N94-13753

METAL FATIGUE
Role of microstructure on fatigue durability of aluminum aircraft alloys
[AD-A265627] p 568 N94-12993
Role of microstructure on fatigue durability of aluminum aircraft alloys
[AD-A266350] p 571 N94-13697
Fatigue design curves for 6061-T6 aluminum
[DE93-011849] p 571 N94-14021

METAL FIBERS
Elastic-plastic finite element analyses of an unidirectional, 9 vol percent tungsten fiber reinforced copper matrix composite
[NASA-TM-106304] p 559 N94-14719

METAL FILMS
The x ray dichroism experiments using circular polarization
[DE93-013195] p 568 N94-13036
Microstructural mechanisms that enhance electromigration resistance in Al-Cu thin films
[DE93-013770] p 812 N94-14345

METAL FOILS
Two-dimensional simulations of foil implosion experiments on the Los Alamos capacitor bank
[DE93-012676] p 794 N94-12814
Stripping efficiencies for 277 MeV/amu gold beam on copper foils
[DE93-014306] p 569 N94-13221
Electron emission resulting from fast ion impact on thin metal foils: Implications of these data for development of track structure models
[DE93-013506] p 782 N94-13485
Thermal conductance of pressed metallic contacts augmented with Indium foil or Apiezon-N (tm) grease at liquid helium temperatures
[NASA-TM-108779] p 776 N94-14027

METAL HYDRIDES
Materials compatibility of hydride storage materials with austenitic stainless steels
[DE93-013688] p 703 N94-13691
Catalytic arene hydrogenation using early transition metal hydride compounds
[DE93-015500] p 573 N94-14402

METAL IONS
Thermochemistry of transition metal clusters
[DE93-016201] p 571 N94-13977
Tetravalent chromium (Cr(4+)) as laser-active ion for tunable solid-state lasers
[NASA-CR-194527] p 659 N94-14576
Reactor studies of metal ions associated with chromatographic silica
[AD-A266675] p 573 N94-14779

METAL MATRIX COMPOSITES
Ohmic heating of composite candidate graphite-fiber/coating combinations
[NASA-TM-4491] p 554 N94-12871
NDE of titanium alloy MMC rings for gas turbine engines
[NASA-TM-106188] p 555 N94-13138
An advanced test technique to quantify thermomechanical fatigue damage accumulation in composite materials
[NASA-CR-191147] p 555 N94-13139
Inelastic deformation mechanisms in SCS-6/Ti 15-3 MMC lamina under compression
[NASA-CR-191170] p 555 N94-13378
Inhibiting corrosion in Gr/Al and Gr/Mg metal matrix composites using nonequilibrium alloying techniques
[AD-A266547] p 556 N94-13583
Evaluation for rheological constitutive relations, using the indentation technique p 775 N94-13627
Modified carbon for improved corrosion resistance
[AD-D015741] p 556 N94-13663
UK interlaboratory tensile tests on Al alloy/SiC particulate metal matrix composites
[NPL-DMM(A)-77] p 570 N94-13666
Preparation of particle-dispersion alloys (M-6)
p 587 N94-13738
Fabrication of very-low-density, high-stiffness carbon fiber/aluminum hybridized composite with ultra-low density and high stiffness (M-11) p 588 N94-13743
Fatigue and residual strength characteristics of fiber metal laminates subjected to incidental damage
[LR-708] p 674 N94-13803
Modelling of the temperature distribution in a copper roll for the design of a system of cooled rolls adapted to vertical strip casting
[IMI-93RT-21200-1436-G] p 557 N94-13866
Hierarchical nonlinear behavior of hot composite structures
[NASA-TM-106229] p 676 N94-14041
Optimal synthesis of hot composite laminates with interphase layers
[NASA-TM-106326] p 557 N94-14042
Elastic-plastic finite element analyses of an unidirectional, 9 vol percent tungsten fiber reinforced copper matrix composite
[NASA-TM-106304] p 559 N94-14719
Thermomechanical and isothermal fatigue behavior of a (90)sub 8 titanium matrix composite
[NASA-CR-191196] p 560 N94-14822
Thermoelastic response of metal matrix composites with large-diameter fibers subjected to thermal gradients
[NASA-TM-106344] p 560 N94-14823

METAL OXIDE SEMICONDUCTORS
1/f noise and oxide traps in MOSFETs
[DE93-007581] p 619 N94-12942
Molecular simulator: A basic tool for submicron MOS processes development
[LAAS-92484] p 814 N94-14697
Design and optimization of high voltage lateral DMOS devices using RESURF technology
[LAAS-92511] p 626 N94-14711

METAL OXIDES
Kinetics of photodeposition of superconducting films
[DE93-015511] p 812 N94-14348

METAL PARTICLES
The effect of crystal tilt on high resolution micrographs of small metal particles
[DE93-013915] p 574 N94-14795

METAL PLATES
Experimental technique to simulate orbital-debris impact on space shields at impact velocities over 10 km/s
[DE93-011619] p 539 N94-12909
Development of test techniques to simulate high-frequency mechanical shock on weapon components
[KCP-613-4998] p 675 N94-13907
High counting rate resistive-plate chamber
[DE93-014928] p 651 N94-14452
Heavy section steel irradiation experiment
[DE93-015517] p 573 N94-14537

METAL POWDER
Study on the mechanism of liquid phase sintering (M-12) p 588 N94-13744
Reverse micelle synthesis of nanoscale metal containing catalysts
[DE93-012869] p 572 N94-14184

METAL PROPELLANTS
Combustion-induced crack/debond propagation in solid propellants p 584 N94-13560

METAL SURFACES
Incomplete melting of the Au(100) surface
[DE93-623192] p 569 N94-13227
About the influence of inert gas ion implantation on metal corrosion stability
[DE93-620574] p 569 N94-13360
Surfaces and interfaces of ceramics and metals
[DE93-014959] p 578 N94-13408
Excimer laser surface processing of titanium
[DE93-012633] p 570 N94-13512
Materials compatibility of hydride storage materials with austenitic stainless steels
[DE93-013688] p 703 N94-13691
Determination of the surface cleanliness of metals by FT-IR spectroscopy
[DE93-013252] p 565 N94-14525
Quantum state resolved desorption of CO from solid surfaces
[DE93-016876] p 814 N94-14597
METAL VAPOR LASERS
Recent results from material processing studies on new generation lasers
[DE93-013841] p 653 N94-12898
Absorption and damage thresholds of low defect density hafnia deposited with activated oxygen
[DE93-013853] p 655 N94-13243
Laser beam control and diagnostic systems for the copper-pumped dye laser system at Lawrence Livermore National Laboratory
[DE93-016529] p 658 N94-14437
METAL VAPORS
Gas-evaporation in low-gravity field (cogelation mechanism of metal vapors) (M-14) p 588 N94-13746
METAL-GAS SYSTEMS
First-principles studies of phase stability and the structural and dynamical properties of hydrogen-metal systems
[DE93-016129] p 570 N94-13374
METAL-METAL BONDING
A high voltage dielectrically isolated smart power technology based on silicon direct bonding
[LAAS-92492] p 626 N94-14698
METALLICITY
On inhomogeneous halo collapse and the globular cluster metallicity gradient
[DE93-013090] p 834 N94-13011
METALLIZING
Electrochemical planarization for microelectronic circuits
[DE93-017214] p 627 N94-14870
METALLOGRAPHY
Estimation of strain in 1-kW primary containment vessels by microstructural examination
[DE93-013053] p 573 N94-14316
METALORGANIC CHEMICAL VAPOR DEPOSITION
Low temperature metal-organic chemical vapor deposition growth processes for high efficiency solar cells
[DE92-010562] p 702 N94-13386
Fabrication of AlGaAs/GaAs-light-emitting devices by selective MOCVD using dialkylmetalchloride p 627 N94-13433
METALS
Structure stability and spectroscopy of metal clusters
[DE93-016142] p 567 N94-12836
A benchmark bending test of a thick specimen. Part 2: Surface displacement measurements
[ARL-RR-6-PT-2] p 670 N94-12928
Metal-semiconductor, composite radiation detectors
[DE93-013313] p 619 N94-12994
Boundary stability under nonequilibrium conditions
[DE93-016259] p 809 N94-13980
Machining and grinding: High rate deformation in practice
[DE93-010718] p 664 N94-14457
The effect of crystal tilt on high resolution micrographs of small metal particles
[DE93-013915] p 574 N94-14795
METASTABLE STATE
Metastable enhancement of C(+) and O(+) capture reactions
[DE93-015075] p 807 N94-13373
Metastability of yttrium-oxides
[DE93-016548] p 813 N94-14440
METEOROID CONCENTRATION
Meteoroid environment near the Earth-Moon system
[NASA-CR-193670] p 835 N94-13203
METEOROID PROTECTION
Comparison of analytic Whipple bumper shield ballistic limits with CTH simulations
[DE93-015126] p 539 N94-13006
BALLIST: A computer program to empirically predict the bumper thickness required to prevent perforation of the Space Station by orbital debris
[NASA-CR-193825] p 543 N94-14120
METEOROID SHOWERS
Meteoroid environment near the Earth-Moon system
[NASA-CR-193670] p 835 N94-13203
METEOROIDS
Meteor forward scatter studies
[DSIS-93-00382] p 602 N94-13801
METEOROLOGICAL BALLOONS
Attitude determination of stratospheric balloons using Kalman filters
[INPE-5498-TDI/513] p 649 N94-13366
METEOROLOGICAL PARAMETERS
Bibliography of urban climate in tropical/subtropical areas, 1981-1991
[WCASP-25] p 718 N94-12918
The role of clouds and oceans in global greenhouse warming
[DE93-016206] p 706 N94-13079
Study on TRMM data utilization for meteorology
[NASDA-CNT-930007] p 721 N94-13643
National use of the groups 7wwW1W2 and 960ww for ground stations
[KNMI-PUBL-181] p 722 N94-13926
METEOROLOGICAL RADAR
Preliminary meteorological results for 1992 West Coast Scotland Experiment
[DE93-014677] p 720 N94-13404
Remote identification of rain and hail with a polarization diversity radar
[ISBN-0-315-55623-4] p 720 N94-13516
TRMM precipitation radar algorithm p 690 N94-14224
Estimate of sampling errors of TRMM rainfall observation by using radar-AMeDAS composite data p 690 N94-14225
Multiparameter airborne rain radar development for TRMM validation and TRMM-follow-on study p 690 N94-14226
Future TRMM follow-on mission p 691 N94-14228
METEOROLOGICAL SERVICES
Weather forecasting support for AASE-2
[NASA-CR-194342] p 721 N94-13675
METEOROLOGY
Optimization and eigenvalue computation with application to meteorology and oceanography
[DE93-015310] p 744 N94-13024
Preliminary meteorological results for 1992 West Coast Scotland Experiment
[DE93-014677] p 720 N94-13404
Evaluation of infrared sensors for autonomous landing guidance
[AD-A266450] p 513 N94-13703
Activities report of the Netherlands Remote Sensing Board
[ETN-93-93880] p 686 N94-14073
CCI working group on climate data and its rapporteurs
[WCDMP-21] p 723 N94-14118
METHANE
Conversion of light hydrocarbon gases to metal carbides for production of liquid fuels and chemicals
[DE93-014962] p 583 N94-13002
IMG: Interferometric monitor for greenhouse gases p 689 N94-14217
Biomimetic methane oxidation
[DE93-013196] p 705 N94-14510
METHOD OF CHARACTERISTICS
Method of characteristics design of a supersonic wind tunnel nozzle with square cross-section, supplement 3
[NASA-CR-194359] p 527 N94-12824
METHOD OF MOMENTS
Antenna pattern control using impedance surfaces
[NASA-CR-194517] p 602 N94-13799
METHYL ALCOHOL
Biofuels for transportation: The road from research to the marketplace
[DE93-000091] p 585 N94-14454
Biomimetic methane oxidation
[DE93-013196] p 705 N94-14510
METHYL COMPOUNDS
Experimental and kinetic modeling of acid/base and redox reactions over oxide catalysts
[DE93-016203] p 563 N94-13375
METRIC SPACE
On the foundations of final semantics: Non-standard sets, metric spaces, partial orders
[CWI-CS-R9241] p 768 N94-13526
METROLOGY
Activities report of the National Electrotechnical Institute Galileo Ferraris
[ETN-93-94224] p 627 N94-14812
Investigation of Zerodur material processing
[NASA-CR-193842] p 793 N94-14903
MICHELSON INTERFEROMETERS
IMG: Interferometric monitor for greenhouse gases p 689 N94-14217
MICROANALYSIS
Procedures for analysis of debris relative to Space Shuttle systems
[NASA-TM-109190] p 534 N94-12900
High spatial resolution x ray microanalysis: Comparison of experiment and incoherent scattering calculations
[DE93-011685] p 648 N94-13044
Microstructural evolution of NARloy-Z at elevated temperatures
[NASA-TM-108419] p 571 N94-13715
MICROBALANCES
A quartz crystal microbalance study of lithium insertion and removal into evaporated films MO(y) (M = Mo, Fe, and V)
[DSIS-93-00649] p 810 N94-14203
MICROBIOLOGY
Chaos and microbial systems
[DE93-016814] p 730 N94-14596
MICROBURSTS (METEOROLOGY)
Optimal lateral escape maneuvers for microburst encounters during final approach
[LR-691] p 511 N94-13534
MICROCHANNEL PLATES
Absolute detection efficiency of a micro-channel plate detector to x rays in the 1-100 KeV energy range
[DE93-012592] p 789 N94-14460
MICROCHANNELS
Microchannel cooled heatsinks for high average power laser diode arrays
[DE93-016533] p 658 N94-14442
MICROCRACKS
Modeling the impact behavior of AD85 ceramic under multi-axial loading
[AD-A265877] p 576 N94-12932
Automated crack identification for cement paste
[AD-A265753] p 665 N94-13042
A stochastic model for behavior analysis of fiber-reinforced quasi-brittle materials p 672 N94-13594
Micromechanical damage theories for brittle solids with interacting microcracks
[AD-A266348] p 673 N94-13778
MICROCRYSTALS
Boundary stability under nonequilibrium conditions
[DE93-016259] p 809 N94-13980
MICROELECTRONICS
Solderability of surface mount devices
[AD-A265751] p 620 N94-13040
Mongoose ASIC microcontroller programming guide
[NASA-RP-1319] p 623 N94-13871
An ultra-compact processor module based on the R3000
[DE93-012549] p 625 N94-14427
Microwave interconnection
[DE93-016580] p 625 N94-14533
Electrochemical planarization for microelectronic circuits
[DE93-017214] p 627 N94-14870
MICROGRAVITY
Monoclonal antibodies directed against surface molecules of multicell spheroids
[NASA-CR-193560] p 727 N94-12795
Medical evaluations on the KC-135 1991 flight report summary
[NASA-TM-104755] p 731 N94-12832
Reduce fluid experiment system flight data from IML-1
[NASA-CR-193835] p 804 N94-12873
Advanced protein crystal growth programmatic sensitivity study
[NASA-CR-193827] p 804 N94-12934
Calcitonin control of calcium metabolism during weightlessness
[NASA-CR-193622] p 731 N94-12960
Capillary surfaces in a wedge: Differing contact angles
[DE93-013903] p 631 N94-13244
Temperature dependence of diffusivities, preliminary definition phase
[NASA-CR-192613] p 648 N94-13326
Crystal growth of ZnSe and related ternary compound semiconductors by physical vapor transport
[NASA-CR-193834] p 807 N94-13444
Thermal gravitational modelling and scaling of two-phase heat transport systems: Similarity considerations and useful equations predictions versus experimental results
[NLR-TP-91477-U] p 632 N94-13533
STS-30 Magellan IUS/EVA training in WETF
[NASA-TM-109300] p 737 N94-13601
Spacelab J experiment descriptions
[NASA-TM-4517] p 586 N94-13732
Growth experiment of narrow band-gap semiconductor PbSnTe single crystals in space (M-1) p 586 N94-13733
Growth of PbSnTe single crystal by traveling-zone method in low gravity (M-2) p 586 N94-13734

Growth of semiconductor compound single crystal InSb by floating zone method (M-3) p 586 N94-13735
Casting of superconducting composite materials (M-4) p 586 N94-13736
Formation of deoxidization products in iron ingot by the addition of Al, Si, and/or Mn (M-5) p 587 N94-13737
Preparation of particle-dispersion alloys (M-6) p 587 N94-13738
Diffusion in liquid state and solidification of binary system (M-7) p 587 N94-13739
High temperature behavior of glass (M-8) p 587 N94-13740
Growth of Si spherical crystals and the surface oxidation (M-9) p 587 N94-13741
Study on solidification of immisible alloys (M-10) p 588 N94-13742
Fabrication of very-low-density, high-stiffness carbon fiber/aluminum hybridized composite with ultra-low density and high stiffness (M-11) p 588 N94-13743
Study on the mechanism of liquid phase sintering (M-12) p 588 N94-13744
Fabrication of Si-As-Te ternary amorphous semiconductor in the microgravity environment (M-13) p 588 N94-13745
Gas-evaporation in low-gravity field (cogelation mechanism of metal vapors) (M-14) p 588 N94-13746
Drop dynamics in space and interference with acoustic field (M-15) p 588 N94-13747
Study of bubble behavior in weightlessness (effects of thermal gradient and acoustic stationary wave) (M-16) p 589 N94-13748
Preparation of optical materials used in non-visible region (M-17) p 589 N94-13749
Marangoni effect induced convection in material processing under microgravity (M-18) p 589 N94-13750
Solidification of eutectic system alloys in space (M-19) p 589 N94-13751
Growth of samarskite crystal under microgravity conditions (M-20) p 590 N94-13752
Growth experiment of organic metal crystal in low gravity (M-21) p 590 N94-13753
Crystal growth of compound semiconductors in a low-gravity environment (InGaAs crystals) (M-22) p 590 N94-13754
Microgravity acceleration measurement environment characterization p 590 N94-13755
Protein crystal growth p 591 N94-13756
Health monitoring of Japanese payload specialist: Autonomic nervous and cardiovascular responses under reduced gravity condition (L-0) p 591 N94-13757
Neurophysiological study on visuo-vestibular control of posture and movement in fish during adaptation to weightlessness p 591 N94-13759
Separation of biogenic materials by electrophoresis under zero gravity (L-3) p 592 N94-13760
Comparative measurement of visual stability in Earth and cosmic space (L-4) p 592 N94-13761
Crystal growth of enzymes in low gravity (L-5) p 592 N94-13762
Studies on the effects of microgravity on the ultrastructure and functions of cultured mammalian cells (L-6) p 592 N94-13763
Gravity, chromosomes, and organized development in aseptically cultured plant cells p 592 N94-13764
Effect of low gravity on calcium metabolism and bone formation (L-7) p 593 N94-13765
Manual control in space research on perceptual-motor functions under zero gravity conditions (L-10) p 593 N94-13767
Study on the biological effect of cosmic radiation and the development of radiation protection technology (L-11) p 593 N94-13768
Amphibian fertilization and development in microgravity p 594 N94-13770
Magnetic resonance imaging after exposure to microgravity p 594 N94-13771
Countermeasure for reducing post-flight orthostatic intolerance: Lower Body Negative Pressure (LBNP) experiment E140 p 594 N94-13772
Bone culture research p 595 N94-13773
Autogenic feedback training experiment: A preventative method for space motion sickness p 595 N94-13774
In-flight demonstration of the Space Station Freedom Health Maintenance Facility fluid therapy system (E300/E05) p 595 N94-13775
Renal function alterations during skeletal muscle disuse in simulated microgravity [NASA-CR-194258] p 733 N94-13824
The influence of a microgravity environment on the dendritic morphology during directional solidification of hypoeutectic Al-Si alloys [NASA-CR-194139] p 571 N94-13891
Sloshing dynamics on rotating helium dewar tank [NASA-CR-194403] p 637 N94-13959
Cellular responses to low-gravity: Pilot studies on suborbital rockets and orbiting spacecraft [NASA-CR-194402] p 729 N94-14494

MICROGRAVITY APPLICATIONS
Stabilized electromagnetic levitator [NASA-CR-194261] p 586 N94-12805
Reduce fluid experiment system flight data from IML-1 [NASA-CR-193835] p 804 N94-12873

MICROHARDNESS
Fracture behavior of vanadium/vanadium silicide in-situ composites [DE93-013422] p 556 N94-13389

MICROMECHANICS
Micromechanical strength effects in shock compression of solids [DE93-014425] p 670 N94-12887
A stochastic model for behavior analysis of fiber-reinforced quasi-brittle materials p 672 N94-13594
Micromechanical damage theories for brittle solids with interacting microcracks [AD-A266348] p 673 N94-13778
Hierarchical nonlinear behavior of hot composite structures [NASA-TM-106229] p 676 N94-14041
Probabilistic micromechanics for high-temperature composites [NASA-CR-191150] p 676 N94-14408
Elastic-plastic finite element analyses of an unidirectional, 9 vol percent tungsten fiber reinforced copper matrix composite [NASA-TM-106304] p 559 N94-14719
Thermoelastic response of metal matrix composites with large-diameter fibers subjected to thermal gradients [NASA-TM-106344] p 560 N94-14823

MICROMETEOROIDS
Interactions between spacecraft and their environments [NASA-TM-106115] p 541 N94-13917
Secondary impact hazard assessment [NASA-CR-188261] p 543 N94-14483

MICROMETEOROLOGY
The footprint area influencing a high-volume air sampler [DE93-013947] p 706 N94-13095
Atmospheric turbulence and diffusion research [DE93-011842] p 718 N94-14425

MICROMOTORS
Design and testing of planar magnetic micromotors fabricated by deep x ray lithography and electroplating [DE93-012856] p 618 N94-12821

MICROORGANISMS
Biodiesel/aquatic species project report, FY 1992 [DE93-010024] p 709 N94-14087

MICROPOROSITY
Amorphous sol-gel insulating films [DE93-012859] p 576 N94-12866
Quantitative mapping of pore fraction variations in silicon nitride using an ultrasonic contact scan technique [NASA-TP-3377] p 665 N94-13056

MICROPROCESSORS
The KSR1: Experimentation and modeling of poststore [DE93-012539] p 759 N94-13470
Mongoose ASIC microcontroller programming guide [NASA-RP-1319] p 623 N94-13871
Test report for single event effects of the 80386DX microprocessor [NASA-CR-194509] p 741 N94-13943
Adaptive Signal Processing Testbed: VME-based DSP board market survey [DSIS-93-00274] p 605 N94-14015
An ultra-compact processor module based on the R3000 [DE93-012549] p 625 N94-14427

MICROSCOPES
A Fourier transform microscope for x ray and/or gamma ray imaging [AD-D015742] p 791 N94-13664

MICROSCOPY
Crystallographic and metallurgical characterization of radiation detector grade cadmium telluride materials [DE93-014335] p 806 N94-13150
Imaging micrcscopy with x ray lasers at Lawrence Livermore National Laboratory [DE93-013419] p 655 N94-13258
Laser-damage susceptibility of nodular defects in dielectric mirror coatings: AFM measurements and electric-field modeling [DE93-014655] p 580 N94-14124
Image reconstruction for x ray holographic microscopy [DE93-013094] p 653 N94-14772

MICROSTRIP ANTENNAS
Analysis of microstrip patch antennas with nonzero surface resistance [NASA-TP-3362] p 604 N94-13916

MICROSTRIP TRANSMISSION LINES
Analysis and characterizations of planar transmission structures and components for superconducting and monolithic integrated circuits [NASA-CR-193675] p 619 N94-13026

MICROSTRUCTURE
Amorphous sol-gel insulating films [DE93-012859] p 576 N94-12866
Deposition of crystalline boron thick layers from gas phase [DE93-620499] p 576 N94-12867
Recovery of materials impacted at high velocity [DE93-014150] p 576 N94-12885
Role of microstructure on fatigue durability of aluminum aircraft alloys [AD-A265627] p 568 N94-12993
Gas atomized Er3Ni powder for cryocooler applications [DE93-011564] p 568 N94-13000
Effect of microstructure on passive film formation and breakdown on Al alloys [AD-A265339] p 569 N94-13050
Transport properties of disordered porous media from the microstructure [DE93-016065] p 806 N94-13152
Fracture behavior of vanadium/vanadium silicide in-situ composites [DE93-013422] p 556 N94-13389
Tensile properties of LE-7 engine material with welded joint [NAL-TR-1188] p 570 N94-13460
Excimer laser surface processing of titanium [DE93-012633] p 570 N94-13512
Processing and mechanical properties of silicon carbide platelet reinforced alumina composites p 556 N94-13557
Role of microstructure on fatigue durability of aluminum aircraft alloys [AD-A266350] p 571 N94-13697
Microstructural evolution of NARloy-Z at elevated temperatures [NASA-TM-108419] p 571 N94-13715
The microstructural response of near gamma-TiAl+W to heat treatment [DSIS-93-00237] p 571 N94-13840
The influence of a microgravity environment on the dendritic morphology during directional solidification of hypoeutectic Al-Si alloys [NASA-CR-194139] p 571 N94-13891
High-resolution Z-contrast imaging and hole concentration mapping of YBCO thin films [DE93-015803] p 808 N94-13930
Radiation hardening and radiation-induced chromium depletion effects on intergranular stress corrosion cracking of austenitic stainless steels [DE93-011602] p 572 N94-14058
Physical and structural properties of a sputtered zirconia-yttria layer used as a thermal resistance [ONERA-NT-1992-10] p 810 N94-14193
Theory of the electronic and structural properties of solid state oxides [DE93-016051] p 811 N94-14296
Estimation of strain in 1-kW primary containment vessels by microstructural examination [DE93-013053] p 573 N94-14316
Microstructural mechanisms that enhance electromigration resistance in Al-Cu thin films [DE93-013770] p 812 N94-14345
A microstructural approach to fatigue crack processes in poly crystalline BCC materials [DE93-016666] p 812 N94-14354
Pore-size-distribution of cationic polyacrylamide hydrogels [DE93-015218] p 581 N94-14400
Room temperature degradation of YBa2Cu3O(7-x) superconductors in varying relative humidity environments [NASA-TP-3368] p 813 N94-14409
Theoretical studies of breakdown in random media [DE93-018107] p 558 N94-14418
Computational diagnostics for detecting phase transitions during nanoindentation [DE93-016536] p 813 N94-14439
Microstructural influences on the mechanical properties of solder [DE93-015044] p 573 N94-14474
Processing and testing of high toughness silicon nitride ceramics [NASA-CR-191190] p 582 N94-14543
Current titles --- National Center for Electron Microscopy [DE93-015859] p 851 N94-14587
Solution chemistry optimization of sol-gel processed PZT thin films [DE93-013776] p 814 N94-14695

Molecular simulator: A basic tool for submicron MOS processes development
[LAAS-92484] p 814 N94-14697
An investigation of the role of second phase particles in the design of ultra high strength steels of improved toughness
[AD-A266774] p 573 N94-14786
Office of Naval Research/DARPA publications: Composite materials with improved properties in compression
[AD-A265509] p 560 N94-14794
Microstructural origins and modeling of intergranular crack initiation in an Al-Li-Cu-Mg-(Zr) alloy
[ISAL-91-0012] p 574 N94-14814
Influence of heat treatment on microstructure of Ti-35wt Al prepared by elemental powder metallurgy
[GKSS/92/E/27] p 574 N94-14821
Phases and phase transitions of polymeric liquid crystals: A high resolution x ray diffraction and light scattering study
[ITN-93-85218] p 816 N94-14826

MICROWAVE ABSORPTION
H2S data reduction
[NASA-CR-193389] p 617 N94-14743

MICROWAVE AMPLIFIERS
Microwave generation for magnetic fusion energy applications
[DE93-013864] p 654 N94-13058

MICROWAVE ANTENNAS
Enhanced decoding for the Galileo S-band mission
p 609 N94-14380

MICROWAVE CIRCUITS
Processing, fabrication and demonstration of HTS integrated microwave circuits
[AD-A265789] p 619 N94-12892
A millimeter-wave tunneladder TWT
[NASA-CR-182183] p 620 N94-13106
MMIC packaging technology development
[NASA-CR-194183] p 621 N94-13336
Electrical noise in microwave field effect and bipolar transistors
[LAAS-93042] p 616 N94-14717

MICROWAVE EMISSION
Estimations of temperature and humidity of the canopy in Amazon Forest using microwave data from SMMR sensor of Nimbus-7 satellite
[INPE-5444-TDI/490] p 720 N94-13614
Comparative study of x ray and microwave emissions during solar flares
[NASA-CR-194532] p 845 N94-14577

MICROWAVE EQUIPMENT
Microwave interconnection
[DE93-016580] p 625 N94-14533

MICROWAVE FREQUENCIES
Hard x ray/microwave spectroscopy of solar flares
[NASA-CR-194399] p 844 N94-13958

MICROWAVE LANDING SYSTEMS
Flight evaluations of approach/landing navigation sensor systems: Summary of 1990 flight experiments
[NAL-TR-1175] p 513 N94-13344

MICROWAVE POWER BEAMING
Low-current traveling wave tube for use in the microwave power module
[NASA-TP-3344] p 620 N94-13110

MICROWAVE RADIOMETERS
Estimations of temperature and humidity of the canopy in Amazon Forest using microwave data from SMMR sensor of Nimbus-7 satellite
[INPE-5444-TDI/490] p 720 N94-13614
Phase aligner for the Electronically Scanned Thinned Array Radiometer (ESTAR) instrument
[NASA-TM-4518] p 623 N94-13878
Future TRMM follow-on mission p 691 N94-14228
Radiometric observations of atmospheric attenuation at 20.6 and 31.65 GHz: The Wave Propagation Laboratory data base p 613 N94-14660

MICROWAVE REFLECTOMETERS
The MRIS feasibility study
[NASA-TM-107763] p 597 N94-12804
Scattering of reflectometer signals from rippled surfaces
[PPL-138] p 602 N94-13802

MICROWAVE RESONANCE
Measurement electronics of industrial microwave resonator sensors
[TKK-S-RAD-S194] p 625 N94-14096

MICROWAVE SCATTERING
Scattering of reflectometer signals from rippled surfaces
[PPL-138] p 602 N94-13802

MICROWAVE SENSORS
Measurement electronics of industrial microwave resonator sensors
[TKK-S-RAD-S194] p 625 N94-14096
ERS-1 system
[ESA-SP-1146] p 699 N94-14353

MICROWAVE SOUNDING
DMSP F11 SSM/T-2 calibration and validation
[AD-A265817] p 719 N94-12978
Water-vapour, total water and rainrate from passive microwave satellite data over ocean
[DLR-FB-92-37] p 723 N94-14189

MICROWAVE SPECTRA
Submillimeter, millimeter, and microwave spectral line catalogue, revision 3
[NASA-CR-194501] p 602 N94-13813

MICROWAVES
Ceramic matrix composites by microwave assisted CVI
[DE93-012640] p 576 N94-12916
Search for extraterrestrial intelligence/high resolution microwave survey team member
[NASA-CR-194177] p 739 N94-13086
Comment of parameter excitation of Alfven and Heliicon waves in a magnetoactive compensated semiconductor by microwave radiation
[DE93-623203] p 806 N94-13228
Problems and opportunities in microwave joining of ceramics
[DE93-014998] p 579 N94-13888
Microwave hybrid heating of alumina filaments
[DE93-012642] p 581 N94-14327
Microwave sintering of large alumina bodies
[DE93-012752] p 581 N94-14340
Microwave interconnection
[DE93-016580] p 625 N94-14533

MIDDLE ATMOSPHERE
Electrodynamics of the middle atmosphere: Superpressure balloon program
[NASA-CR-193671] p 712 N94-13293
A rocket-borne lidar for studies of the middle atmosphere
[FFI/RAPPORT-92/7034] p 715 N94-13949
Chemistry and transport in a multi-dimensional model
[NASA-CR-194425] p 716 N94-13969

MIE SCATTERING
Bridging the gap between the Rayleigh and Thomson limits for various convex bodies
[DSIS-93-00613] p 607 N94-14204

MILITARY HELICOPTERS
ADS-33C related handling qualities research performed using the NRC Bell 205 airborne simulator
p 521 N94-13295
MIL-H-8501B: Application to shipboard terminal operations p 521 N94-13296
Some lessons learned in three years with ADS-33C --- rotorcraft handling qualities specification
p 521 N94-13299
Investigation of the effects of bandwidth and time delay on helicopter roll-axis handling qualities
p 522 N94-13300
Improvements in hover display dynamics for a combat helicopter p 523 N94-13310
Design and pilot evaluation of the RAH-66 Comanche Core AFCS p 525 N94-13321
Design and pilot evaluation of the RAH-66 Comanche selectable control modes p 525 N94-13322
An analysis of helicopter attrition using a low level combat simulation
[DSIS-93-00282] p 515 N94-13839
HELSCAM V2.0: Development and application guide
[DSIS-93-00137] p 515 N94-13867

MILITARY TECHNOLOGY
Solderability of surface mount devices
[AD-A265751] p 620 N94-13040
Knowledge-based oceanographic image compression
[AD-A265752] p 821 N94-13041

MILLIMETER WAVES
A millimeter-wave tunneladder TWT
[NASA-CR-182183] p 620 N94-13106
Long-pulse operation of a gyrotron with beam/RF separation
[DE93-015007] p 649 N94-13410
Millimeter and infrared studies of young stellar objects in dark cloud L1641 p 838 N94-13648
Submillimeter, millimeter, and microwave spectral line catalogue, revision 3
[NASA-CR-194501] p 602 N94-13813

MIMD (COMPUTERS)
Parallelizing Timed Petri Net simulations
[NASA-CR-194278] p 758 N94-12938
Parallel implementation of an algorithm for Delaunay triangulation
[NASA-TM-103951] p 740 N94-12973
Implementation of ADI: Schemes on MIMD parallel computers
[NASA-CR-193720] p 759 N94-13204
An overview of parallel scientific visualization
[DE93-017105] p 755 N94-14521
On the solution of a class of graph problems by parallel algorithms
[LAAS-92514] p 756 N94-14712
Identification of continuous-time dynamical systems: Neural network based algorithms and parallel implementation
[DE93-014427] p 766 N94-14737

MIMO (CONTROL SYSTEMS)
Transmission zeros of spacecraft attitude control system
[NAL-TR-1166] p 540 N94-13339
Control system design for flexible structures using data models p 527 N94-14646

MINERAL EXPLORATION
A knowledge-based model for the integration of remote sensing into a mineral exploration program
[ISBN-0-315-58982-5] p 685 N94-13523

MINERALOGY
Spectral analysis for automated exploration and sample acquisition
[NASA-CR-194095] p 545 N94-13189

MINIATURIZATION
Performance evaluation of the honeywell GG1308 miniature ring laser gyroscope
[AD-A266694] p 653 N94-14782

MINORITY CARRIERS
Intrinsic and interfacial recombination in OMVPE- and MBE-prepared GaAs/Al(x)Ga(1-x)As heterostructures
[DE93-009844] p 809 N94-14083
Multicrystalline silicon solar cells: Gettering optimization and characterization
[DE93-015001] p 705 N94-14861

MIRROR FUSION
Mirror fusion propulsion system: A performance comparison with alternate propulsion systems for the manned Mars Mission
[NASA-TM-109248] p 550 N94-13147

MIRRORS
Project proposal for partial computational physics support for Survivability of Coatings program
[DE93-013788] p 576 N94-12939
Reflective coatings for solar applications
[DE93-010026] p 702 N94-13381
Design and performance of an automated video-based laser beam alignment system
[DE93-012571] p 656 N94-13481
Laser-damage susceptibility of nodular defects in dielectric mirror coatings: AFM measurements and electric-field modeling
[DE93-014655] p 580 N94-14124
Determination of the surface cleanliness of metals by FT-IR spectroscopy
[DE93-013252] p 565 N94-14525
Fabrication p 546 N94-14834

MISSILE CONTROL
Test/analysis correlation and model updating of the STARS 1 and 2 missile systems
[DE93-013774] p 748 N94-13578

MISSILE DESIGN
Test/analysis correlation and model updating of the STARS 1 and 2 missile systems
[DE93-013774] p 748 N94-13578

MISSILE LAUNCHERS
Test/analysis correlation and model updating of the STARS 1 and 2 missile systems
[DE93-013774] p 748 N94-13578

MISSILE SYSTEMS
Test/analysis correlation and model updating of the STARS 1 and 2 missile systems
[DE93-013774] p 748 N94-13578

MISSILES
Test/analysis correlation and model updating of the STARS 1 and 2 missile systems
[DE93-013774] p 748 N94-13578
Electromagnetic wave test p 508 N94-14173

MISSION PLANNING
MARS Mission research center
[NASA-CR-194034] p 841 N94-13088
Present status of JEM utilization projects
p 530 N94-13273
Earth Observation Center Annual Report on Research and Development, Fiscal Year 1992
[EOC-92-01-0007] p 687 N94-14091
Earth observation experiment data analysis
p 687 N94-14093
ADEOS project p 687 N94-14094
Asia-Pacific ISY conference, volume 1
[NASDA-CM-199-1] p 532 N94-14098
European space for exclusively peaceful purposes
[ESA-BR-86] p 851 N94-14137
TRMM system overview and status in the United States p 690 N94-14221
TRMM Project in Japan: Overview and status
p 690 N94-14222
Future TRMM follow-on mission p 691 N94-14228
Space transportation systems within ESA programmes: Current status and perspectives p 537 N94-14275
Mission scenario of HOPE p 537 N94-14279

Primary and secondary electrical space power based on advanced PEM systems
[DE93-012643] p 553 N94-14689

MIXED CRYSTALS
The Lindemann criterion of melting for pure and mixed ionic crystals
[ITN-93-85210] p 814 N94-14554

MIXING CIRCUITS
Theoretical SIS mixer research
[AD-A266323] p 807 N94-13580

MIXING LAYERS (FLUIDS)
A multiple-scale turbulence model for incompressible flow
[NASA-TM-106113] p 631 N94-13385
Modeling and simulation of transport and combustion phenomena in a supersonic mixing layer
[ONERA-NT-1992-11] p 565 N94-14194
Linear instability of curved free shear layers
[NASA-TM-106290] p 642 N94-14729
A study of the fine scale motions of incompressible time-developing mixing layers p 644 N94-14751
Behavior of streamwise rib vortices in a three-dimensional mixing layer p 644 N94-14754
Direct simulation of polymer drag reduction in free shear flows and vortex dipoles p 644 N94-14755
Investigation of the dilatational dissipation in compressible homogeneous shear flow p 645 N94-14758

MOBILE COMMUNICATION SYSTEMS
Trellis coding with Continuous Phase Modulation (CPM) for satellite-based land-mobile communications
[NASA-CR-191325] p 604 N94-13909
Opening remarks: Current and future activities p 612 N94-14655
Propagation issues for emerging mobile and portable communications: A systems perspective p 614 N94-14667
Propagation considerations in the American Mobile Satellite system design p 614 N94-14668
Tree attenuation at 20 GHz: Foliage effects p 615 N94-14672

MODAL RESPONSE
System identification for Space Station Freedom using observer/Kalman filter Markov parameters
[NASA-CR-191521] p 539 N94-12976
A component modes projection and assembly model reduction methodology for articulated, multi-flexible body structures p 677 N94-14622

MODEL REFERENCE ADAPTIVE CONTROL
Control algorithm implementation for a redundant degree of freedom manipulator
[NASA-CR-191339] p 762 N94-13131

MODELS
An experimental study of tether reel system: A laboratory model
[NAL-TR-1176T] p 539 N94-12943

MODERATORS
Generation of neutronic thermal data in support of space nuclear propulsion
[DE93-013148] p 549 N94-13034

MODULATION
Modulational stability of periodic solutions of the Kuramoto-Sivaskinsky equation
[NASA-CR-191502] p 628 N94-12888

MODULATORS
Radiation effects on optoelectronic analog link for particle detectors
[DE93-015794] p 793 N94-14529

MODULES
On-line upgrade of program modules using AdaPT
[NASA-CR-194331] p 754 N94-14472

MODULUS OF ELASTICITY
An advanced test technique to quantify thermomechanical fatigue damage accumulation in composite materials
[NASA-CR-191147] p 555 N94-13139
Micromechanical damage theories for brittle solids with interacting microcracks
[AD-A266348] p 673 N94-13778
Optical and physical properties of the LiSrAlF6:Cr laser crystal
[DE93-014657] p 808 N94-13881
Shock compression and quasielastic release in tantalum
[DE93-014566] p 811 N94-14329

MOIRE FRINGES
A Fourier transform microscope for x ray and/or gamma ray imaging
[AD-D015742] p 791 N94-13664

MOISTURE
Moisture meter evaluation
[DE93-016581] p 652 N94-14534

MOISTURE CONTENT
Measuring surface fluxes in CAPE
[NASA-CR-193664] p 711 N94-12788
Moisture meter evaluation
[DE93-016581] p 652 N94-14534

MOISTURE METERS
Moisture meter evaluation
[DE93-016581] p 652 N94-14534

MOLECULAR BEAM EPITAXY
Intrinsic and interfacial recombination in OMVPE- and MBE-prepared GaAs/Al(x)Ga(1-x)As heterostructures
[DE93-009844] p 809 N94-14083
Evolving surface cusps during strained-layer epitaxy
[DE93-015430] p 813 N94-14478

MOLECULAR BEAMS
Lawrence Berkeley Laboratory Chemical Sciences Division
[DE93-015260] p 851 N94-14401

MOLECULAR BIOLOGY
Solitons and 1/f noise in molecular chains
[DE93-622898] p 778 N94-12879
Gordon Research Conference on Chronobiology, 1991
[AD-A266354] p 728 N94-13698

MOLECULAR CHAINS
Theoretical treatment of the bulk and surface properties of fluids containing long, flexible molecules
[DE93-015560] p 575 N94-12861
Solitons and 1/f noise in molecular chains
[DE93-622898] p 778 N94-12879
Computer simulations for the adsorption of polymers onto surfaces
[DE93-016667] p 577 N94-13070

MOLECULAR CLOUDS
UV extinction properties of carina nebular dust
[NASA-CR-193424] p 835 N94-13233
Analysis of interstellar cloud structure based on IRAS images
[NASA-CR-194341] p 836 N94-13332
Search for x ray emitting young stars outside of massive molecular clouds
[NASA-CR-193609] p 830 N94-13462
The origin of the far-infrared emission from galactic molecular clouds p 848 N94-13654
Analysis of the IUE spectra of the strongly interacting binary beta Lyrae
[NASA-CR-194118] p 833 N94-14493

MOLECULAR COLLISIONS
Theoretical molecular studies of astrophysical interest
[NASA-CR-193300] p 838 N94-13781
Lawrence Berkeley Laboratory Chemical Sciences Division
[DE93-015260] p 851 N94-14401

MOLECULAR ELECTRONICS
Charge storage and switching phenomena with molecular assemblies of metal complexes
[AD-A266673] p 787 N94-14778

MOLECULAR EXCITATION
Kinetic studies following state-selective laser excitation
[DE93-012970] p 654 N94-13013
Molecular dynamics simulation of electronically excited polyatomic molecules
[DE93-623045] p 781 N94-13225
Theoretical molecular studies of astrophysical interest
[NASA-CR-193300] p 838 N94-13781
Photochemical dynamics of surface oriented molecules
[DE93-016289] p 784 N94-13983
Structure and stability of microvoids in A-Si:H
[DE93-016625] p 813 N94-14413

MOLECULAR GASES
Resonant x ray Raman scattering from atoms and molecules
[DE93-015158] p 784 N94-13896
Charge storage and switching phenomena with molecular assemblies of metal complexes
[AD-A266673] p 787 N94-14778

MOLECULAR INTERACTIONS
Molecular solvent-dynamical effects on activated electron-transfer kinetics: How important is solvent friction?
[AD-A265886] p 779 N94-12894
Theory, modeling, and simulation
[DE93-015607] p 755 N94-14571

MOLECULAR ORBITALS
Charge storage and switching phenomena with molecular assemblies of metal complexes
[AD-A266673] p 787 N94-14778

MOLECULAR PHYSICS
Experimental and theoretical study of inhomogeneous electron transfer in betaine: Comparisons of measured and predicted spectral dynamics
[AD-A265703] p 780 N94-13051
Phase transition in polymer blends and structure of ionomers and copolymers
[DE93-016256] p 579 N94-13978
Computational diagnostics for detecting phase transitions during nanoindentation
[DE93-016536] p 813 N94-14439

MOLECULAR RELAXATION
Vibrational relaxation in hypersonic flow fields
[NASA-TP-3367] p 776 N94-14733

MOLECULAR SPECTROSCOPY
Kinetic studies following state-selective laser excitation
[DE93-012970] p 654 N94-13013
The infrared solar spectrum
[COMMUNICATIONS-SER-B-159] p 844 N94-13502

MOLECULAR STRUCTURE
Resonant x ray Raman scattering from atoms and molecules
[DE93-015158] p 784 N94-13896
Workshop on Formation of Supermolecular Structures in Composite Fluid: Phase Rule and Dynamics
[DE93-782887] p 581 N94-14421
Theory, modeling, and simulation
[DE93-015607] p 755 N94-14571
CarbBank: A structural and bibliographic database for complex carbohydrates
[DE93-015582] p 827 N94-14803

MOLECULAR THEORY
Theory, modeling, and simulation
[DE93-015607] p 755 N94-14571

MOLECULAR WEIGHT
Characterization of 1:1 random copolymers obtained from 6-, 7-, 11-, and 12-carbon amino acids
[AD-A265827] p 577 N94-12985

MOLECULES
Ultrafast photoinduced electron transfer reactions in supramolecular arrays: Studies of electronic coupling and solvation
[DE93-012910] p 782 N94-13484
Selective excitation, relaxation, and energy channeling in molecular systems
[DE93-018819] p 785 N94-14420

MOLTEN SALT ELECTROLYTES
Carbonate fuel cell endurance: Hardware corrosion and electrolyte management status
[DE93-013800] p 701 N94-13093

MOLYBDENUM
Optical degradation issues for XUV projection lithography systems
[DE93-012658] p 626 N94-14805

MOLYBDENUM DISULFIDES
Dry film lubricant evaluation
[DE93-013114] p 578 N94-13118
Applications of surface science to solid lubricants
[SMC-TR-93-24] p 579 N94-13903

MOLYBDENUM OXIDES
A quartz crystal microbalance study of lithium insertion and removal into evaporated films MO(y) (M = Mo, Fe, and V)
[DSIS-93-00649] p 810 N94-14203

MOMENT DISTRIBUTION
Techniques for estimating Space Station aerodynamic characteristics
[NASA-CR-193394] p 541 N94-13955

MOMENTUM
On transport of energy, momentum, orbital angular momentum and self-angular momentum of electromagnetic wave in dispersal media
[DE93-624179] p 617 N94-14883

MOMENTUM THEORY
Dynamics of adaptive structures: Design through simulations
[NASA-CR-193724] p 540 N94-13112
Pinching solutions of slender cylindrical jets
[NASA-CR-191482] p 630 N94-13114

MOMENTUM TRANSFER
High freestream turbulence effects on the transport of heat and momentum p 633 N94-13559
Studies of momentum and energy transfer across wavy gas-liquid interfaces
[AD-A266432] p 635 N94-13699
The role of electric field shear stabilization of turbulence in the H-mode to VH-mode transition in D3-D
[DE93-015474] p 802 N94-14583
On transport of energy, momentum, orbital angular momentum and self-angular momentum of electromagnetic wave in dispersal media
[DE93-624179] p 617 N94-14883

MONATOMIC GASES
Measurements of scattering processes in negative ion-atom collisions
[DE93-013863] p 779 N94-12940
Calculation of hypersonic shock structure using flux-split algorithms
[NASA-CR-194296] p 504 N94-13607

MONITORS
A high-precision direct current measuring device over a kiloampere range
[DE93-626409] p 627 N94-14885

MONKEYS
Selection of behavioral tasks and development of software for evaluation of rhesus monkey behavior during spaceflight
[NASA-CR-194176] p 728 N94-13865
MONOMERS
Unexpectedly rapid hydrosilation polymerization of the diallyl derivative of bisphenol A and 2,6-diallylphenol
[AD-A265832] p 577 N94-12986
Poling of thin polymer films in electro optic applications
[AD-A266562] p 579 N94-13584
Phases and phase transitions of polymeric liquid crystals: A high resolution x ray diffraction and light scattering study
[ITN-93-85218] p 816 N94-14826
MONOPULSE RADAR
Cancellation of multipath for monopulse radars
[ITN-93-85191] p 600 N94-13538
MONOTECTIC ALLOYS
Study on solidification of immisible alloys (M-10)
p 588 N94-13742
Immiscible phase incorporation during directional solidification of hypermonotectics
[NASA-CR-194412] p 565 N94-14480
MONTE CARLO METHOD
A new method to assess Monte Carlo convergence
[DE93-012667] p 772 N94-12919
Parallelizing Timed Petri Net simulations
[NASA-CR-194278] p 758 N94-12938
HIJET with AGS physics and N(sup *)'s
[DE93-014022] p 780 N94-13097
GRO: Black hole models for gamma ray bursts
[NASA-CR-193244] p 829 N94-13178
Beta/gamma test problems for ITS
[DE93-013522] p 781 N94-13349
Variance reduction unique to coupled electron/photon Monte Carlo transport
[DE93-014999] p 782 N94-13409
Maximum likelihood estimation for constrained or missing data models
[AD-A266563] p 773 N94-13585
Determining the solar-flare photospheric scale height from SMM gamma-ray measurements
[NASA-CR-194084] p 844 N94-13671
ADP study of gamma-ray bursts
[NASA-CR-194311] p 848 N94-13708
Distributed processor Monte Carlo: MCNP results on a 16-node IBM cluster
[DE93-012639] p 752 N94-14176
Quantum Monte Carlo by message passing
[DE93-012645] p 760 N94-14177
Hybrid S(sub N)/Monte Carlo research and results
[DE93-012677] p 773 N94-14178
Monte Carlo simulation of the OCP freezing transition
[DE93-013039] p 811 N94-14313
Deconvolution for positive signals
[DE93-013044] p 773 N94-14314
Development and application of the automated Monte Carlo biasing procedure in SAS4
[DE93-015205] p 774 N94-14334
Results from a water-Cerenkov array
[DE93-012715] p 849 N94-14461
Measuring parity violation using the neutron capture reaction
[DE93-016629] p 786 N94-14514
Robust estimators and tests in one-sample location problem with particular consideration on modified maximum likelihood process
[ETN-93-94391] p 774 N94-14703
Statics and kinetics of phase transformations in bcc Fe-Cr
[DE93-013839] p 574 N94-14793
The LAHET code system: Introduction, development, and benchmarking
[DE93-012657] p 787 N94-14804
MOON
Tidal interactions in the Earth Moon system
[COMMUNICATIONS-SER-B-160] p 837 N94-13503
The studies on lunar and planetary exploration and utilization: The study on lunar resources utilization
[NASDA-CNT-930014] p 842 N94-13655
Extrapolation of space weathering processes to other small solar system bodies p 843 N94-14300
MORPHOLOGY
Gravity as a probe for understanding pattern specification
[NASA-CR-194142] p 713 N94-13418
Formation of deoxidization products in iron ingot by the addition of Al, Si, and/or Mn (M-5) p 587 N94-13737
Ion assisted sputter deposition of Mo-Si multilayers
[DE93-013830] p 583 N94-14693
MOTION PERCEPTION
Bayesian estimation of motion fields from image sequences
[ISBN-0-315-57212-4] p 772 N94-13540
Comparative measurement of visual stability in Earth and cosmic space (L-4) p 592 N94-13761
MOTION SICKNESS
Health monitoring of Japanese payload specialist: Autonomic nervous and cardiovascular responses under reduced gravity condition (L-0) p 591 N94-13757
Neurophysiological study on visuo-vestibular control of posture and movement in fish during adaptation to weightlessness p 591 N94-13759
Comparative measurement of visual stability in Earth and cosmic space (L-4) p 592 N94-13761
Autogenic feedback training experiment: A preventative method for space motion sickness p 595 N94-13774
Psychophysiological investigations of the biomedical problems of manned spaceflight
[NASA-CR-194107] p 732 N94-13782
MOTION SIMULATION
Vertical motion simulator familiarization guide
[NASA-TM-103923] p 527 N94-13008
Computational Control Workstation: Users' perspectives p 681 N94-14648
MOTION SIMULATORS
Future developments of the NLR research flight simulator
[NLR-TP-92143-U] p 528 N94-13498
MOUNTAINS
Net radiation mapping of mountainous terrain using Landsat-5 thematic mapper imagery and digital terrain data
[ISBN-0-315-57755-X] p 685 N94-13475
MULTIGRID METHODS
Analysis of the Harrier forebody/inlet design using computational techniques
[NASA-CR-193616] p 503 N94-13463
Development of a general purpose multigrid accelerated Navier-Stokes solver p 641 N94-14613
Development of an explicit multiblock/multigrid flow solver for viscous flows in complex geometries
[NASA-TM-106356] p 642 N94-14728
MULTILAYER INSULATION
CFM technologies for space transportation: Multipurpose hydrogen testbed system definition and tank procurement
[NASA-CR-194355] p 539 N94-12827
MULTIMEDIA
Programming the multimodal interface
[DE93-013084] p 748 N94-13576
Hypertext Compiling Tools (HCT): Developing model based applications with standard hypertext systems
[REPT-92-049] p 750 N94-13822
MULTIMISSION MODULAR SPACECRAFT
NASA experiences in the Goddard MMS
[NASA-TM-109290] p 819 N94-13629
MULTIPATH TRANSMISSION
Cancellation of multipath for monopulse radars
[ITN-93-85191] p 600 N94-13538
MUSIC and maximum likelihood using a refined propagation model: Performance comparison for radar low-angle tracking
[DREO-RN-1122] p 603 N94-13832
Portable multipath measurement system
[DSIS-93-00177] p 603 N94-13843
Results of multiband (L, S, Ku band) propagation measurements and model for high elevation angle land mobile satellite channel p 615 N94-14670
Coverage aspects of a single frequency network designed for digital audio broadcasting
[BBC-RD-1993/3] p 616 N94-14742
MULTIPHASE FLOW
A multiphase model for shock-induced flow in low density foam
[DE93-013767] p 632 N94-13397
Implicit multi-fluid simulation of interpenetrating plasmas
[DE93-013351] p 801 N94-14342
MULTIPHOTON ABSORPTION
New infrared photon absorption processes
[DE93-017017] p 780 N94-13071
A search for strong-field direct two electron ionization using coincidence spectroscopy
[DE93-013435] p 781 N94-13241
MULTIPLE BEAM INTERVAL SCANNERS
An initial study of using the 34-m antenna for lunar mission support p 611 N94-14396
MULTIPLEXING
HYMOSS signal processing for pushbroom spectral imaging
[NASA-CR-191341] p 620 N94-13125
MULTIPLICATION
An efficient parallel algorithm for matrix-vector multiplication
[DE93-015125] p 754 N94-14399
MULTIPROCESSING (COMPUTERS)
High speed packet switching
[NASA-CR-191334] p 759 N94-13177
Simulator for heterogeneous dataflow architectures
[NASA-CR-191545] p 622 N94-13797
A performance prediction model for a fault-tolerant computer during recovery and restoration
[NASA-CR-194490] p 741 N94-14136
Distributed processor Monte Carlo: MCNP results on a 16-node IBM cluster
[DE93-012639] p 752 N94-14176
Nonrecursive formulations of multibody dynamics and concurrent multiprocessing p 679 N94-14632
On the solution of a class of graph problems by parallel algorithms
[LAAS-92514] p 756 N94-14712
MULTISENSOR APPLICATIONS
Non-scanned LADAR imaging and applications
[DE93-013772] p 655 N94-13261
Reasoning with uncertain and incomplete information in aerospace applications
[NLR-TP-91366-U] p 763 N94-13529
Computer vision and sensor fusion for detecting buried objects
[DE93-012605] p 700 N94-14566
MULTISPECTRAL BAND CAMERAS
Development of a portable multispectral thermal infrared camera
[NASA-CR-191340] p 648 N94-13176
MULTIVARIABLE CONTROL
Rotorcraft flying qualities improvement using advanced control p 522 N94-13303
Robust synthesis of discrete-time multivariable control systems with induced delays p 662 N94-13642
Self-tuning control techniques for multivariable systems
[INPE-5449-TDI/495] p 765 N94-14084
MUON SPIN ROTATION
Muon spin relaxation studies of heavy fermion superconductors
[DE93-014576] p 815 N94-14773
MUONS
Detection of hot muonic hydrogen atoms emitted in vacuum using x-rays
[DE93-010253] p 778 N94-12860
Double semi-leptonic charm decay in HELIOS-I 450 GeV/c p-Be data
[DE93-013493] p 781 N94-13348
Study of electroweak interactions
[DE93-015067] p 782 N94-13412
Inclusive single muons at DO
[DE93-012779] p 783 N94-13494
Effects of additional isoscalar vector bosons in e(sup +)e)(sup -)(yields)ff-bar processes at the TRISTAN and LEP energies
[DE93-621451] p 783 N94-13506
The (mu)(+) yields e(+)gamma
[DE93-012750] p 785 N94-14181
Rare muon processes
[DE93-012646] p 785 N94-14366
Characteristics of a high energy muon(+)muon(-) collider based on electro-production of muons
[DE93-017154] p 790 N94-14893
MUSCLES
Magnetic resonance imaging after exposure to microgravity p 594 N94-13771
MUSCULOSKELETAL SYSTEM
Body/cushion contact stress analysis during sitting
[ITN-93-85204] p 736 N94-13229
Effect of low gravity on calcium metabolism and bone formation (L-7) p 593 N94-13765
Renal function alterations during skeletal muscle disuse in simulated microgravity
[NASA-CR-194258] p 733 N94-13824
MUSIC
Study of computer system as a musical instrument
p 747 N94-13439
MUTATIONS
Evolution of catalytic RNA in the laboratory
[NASA-CR-194124] p 727 N94-13210
MYOGLOBIN
Quasi-elastic neutron scattering studies of protein dynamics
[DE93-015074] p 782 N94-13414

N

N-TYPE SEMICONDUCTORS
Effects of growth conditions and substrate orientation on the properties of InSb
[DE93-013766] p 812 N94-14344
NAP-OF-THE-EARTH NAVIGATION
Visual cueing considerations in Nap-of-the-Earth helicopter flight head-slaved helmet-mounted displays
p 524 N94-13315

NASA PROGRAMS
National atmospheric sciences program, fiscal years 1987-1990
[NSF-92-16] p 711 N94-12794
Technology Applications Team: Applications of aerospace technology
[NASA-CR-194362] p 828 N94-13104
Program/project management resource lists
[NASA-TM-109268] p 822 N94-13107
Ninth Annual NASA/Contractors Conference on Quality and Productivity. World Class Excellence: The Journey Continues. Keynote presentations
[NASA-CR-194513] p 665 N94-13148
Ninth Annual NASA/Contractors Conference on Quality and Productivity. World Class Excellence: The Journey Continues. Conference presentations
[NASA-CR-194514] p 665 N94-13153
Strategic planning as a focus for continuous improvement. A case study p 666 N94-13158
Building a quality culture in the Office of Space Flight: Approach, lessons learned and implications for the future p 667 N94-13164
NASA Johnson Space Center: Total quality partnership p 668 N94-13165
Shared visions: Partnership of Rockwell International and NASA Cost Effectiveness Enhancements (CEE) for the space shuttle system integration program p 668 N94-13166
NASA/contractor partnership on the second TDRSS ground terminal program: Breaking barriers p 668 N94-13168
Government/contractor partnerships for continuous improvement. A Goddard Space Flight Center example p 669 N94-13169
User observations on information sharing (corporate knowledge and lessons learned)
[NASA-TM-104781] p 819 N94-13400
NASA aerospace database subject scope: An overview
[NASA-SP-7107] p 823 N94-13401
Goddard Space Flight Center robotics demo
[NASA-TM-109302] p 662 N94-13604
Highlights, 1981
[NASA-TM-109305] p 850 N94-13612
NASA experiences in the Goddard MMS
[NASA-TM-109290] p 819 N94-13629
The Eighth Annual NASA/Contractors Conference and 1991 National Symposium on Quality and Productivity: Extending the boundaries of total quality management
[NASA-TM-109276] p 669 N94-14321
NASA Space Engineering Research Center for VLSI systems design
[NASA-CR-194035] p 625 N94-14325

NASA SPACE PROGRAMS
Access to Japanese aerospace-related scientific and technical information: The NASA Aerospace Database
[NASA-TM-109413] p 822 N94-13105
Highlights, 1981
[NASA-TM-109305] p 850 N94-13612
Research and technologhy highlights, 1992
[NASA-TM-4452] p 850 N94-13962

NATIONAL AEROSPACE PLANE PROGRAM
Perspective on the National Aero-Space Plane Program instrumentation development
[NASA-TM-4505] p 516 N94-13256
Trajectory optimization for the national aerospace plane
[NASA-CR-194146] p 516 N94-14104

NATIONAL AIRSPACE SYSTEM
Determination of Loran-C/GPS human factors issues
[PB93-199693] p 514 N94-14563

NATIONAL PARKS
Multisensor remote sensing data and GIS techniques for monitoring preservation areas: A case study
[INPE-5317-PRE/1714] p 688 N94-14131

NATURAL GAS
Low pressure storage of natural gas on activated carbon
[DE93-014053] p 660 N94-12851
Overview: Gas hydrate geology and geography
[DE93-014043] p 688 N94-14151
Upgrading of raw natural gas using high-performance polymer membranes
[DE93-014041] p 566 N94-14586

NAVIER-STOKES EQUATION
Turbulence modeling of free shear layers for high-performance aircraft
[NASA-CR-193659] p 520 N94-12799
Numerical simulation of hypersonic flow for the design of the H-2 orbiting plane (HOPE), part 3
[NAL-TR-1168-PT-3] p 499 N94-12948
Integration of viscous effects into inviscid computational methods
[NASA-CR-193677] p 629 N94-13007
Two-dimensional Navier-Stokes heat transfer analysis for rough turbine blades
[NASA-TM-106008] p 629 N94-13027
Averaging techniques for steady and unsteady calculations of a transonic fan stage
[NASA-TM-106231] p 499 N94-13108
Analysis of the Harrier forebody/inlet design using computational techniques
[NASA-CR-193616] p 503 N94-13463
Topics on spatially high-order accurate methods and pre-conditioning for the Navier-Stokes equations with finite-rate chemistry p 633 N94-13572
Passage-averaged approximation of turbomachinery flows using vorticity-potential method
[ISBN-0-315-72716-0] p 634 N94-13598
A computational study of the base region flow field for the M865 projectile
[ARL-TR-109] p 504 N94-13795
CNSFV code development, virtual zone Navier-Stokes computations of oscillating control surfaces and computational support of the laminar flow supersonic wind tunnel
[NASA-CR-194259] p 504 N94-14030
Multigrid solution of internal flows using unstructured solution adaptive meshes
[NASA-CR-194233] p 638 N94-14356
Analysis of reacting flowfields in low-thrust rocket engines and plumes p 552 N94-14491
A vertex-based finite-volume algorithm for the Navier-Stokes equations p 639 N94-14599
The structure of laminar flow in a three-dimensional driven cavity p 640 N94-14601
An implicit finite volume nodal point scheme for the solution of two-dimensional compressible Navier-Stokes equations p 640 N94-14603
Navier-Stokes simulation of transonic vortex flow over a delta wing p 640 N94-14606
Computation of nonequilibrium flows using PNS equations p 641 N94-14610
Hypersonic viscous flow computations p 510 N94-14612
Development of a general purpose multigrid accelerated Navier-Stokes solver p 641 N94-14613
Analysis, approximation, and computation of a coupled solid/fluid temperature control problem
[NASA-TM-106351] p 771 N94-14731
Low altitude plume impingement handbook
[NASA-CR-194193] p 643 N94-14741
DNS and modeling of the interaction between turbulent premixed flames and walls p 646 N94-14763
Contributions to numerical solution of Navier-Stokes equations in two and three dimensional flows
[ETN-93-94395] p 647 N94-14816
Analytical description of the breakup of liquid jets in air
[NASA-CR-191503] p 647 N94-14849
Toward a quasi-linear closure for compressible turbulence
[DE93-017185] p 647 N94-14895

NAVIGATION AIDS
Flight evaluations of approach/landing navigation sensor systems: Summary of 1990 flight experiments
[NAL-TR-1175] p 513 N94-13344
Some frequency and damping measurements of laminated beryllium beams
[DE93-015909] p 676 N94-14530

NAVIGATION INSTRUMENTS
Flight evaluations of approach/landing navigation sensor systems: Summary of 1990 flight experiments
[NAL-TR-1175] p 513 N94-13344
Performance evaluation tests of the GPS/DGPS navigation system installed in the NAL Dornier 228: Preliminary ground test results
[NAL-TM-649] p 513 N94-13346

NEAR INFRARED RADIATION
A near-infrared faint galaxy survey: Evolution and the cosmological geometry from K band photometry p 830 N94-13591
Millimeter and infrared studies of young stellar objects in dark cloud L1641 p 838 N94-13648
The 1 to 5 micron imaging of deeply embedded young stellar objects p 831 N94-13657

NECK (ANATOMY)
An assessment of the potential for neck injury due to padding of aircraft interior walls for head impact protection
[DOT/FAA/AM-93/14] p 738 N94-13972

NEGATIVE IONS
Measurements of scattering processes in negative ion-atom collisions
[DE93-013863] p 779 N94-12940

NEODYMIUM LASERS
Numerical simulations of Nd:YAG laser amplifiers
[FFI/RAPPORT-92/7028] p 657 N94-13970
The interaction of intense femtosecond laser pulses with solid targets
[DE93-014415] p 658 N94-14114

NEON
High-order harmonic generation with short-pulse lasers
[DE93-016532] p 659 N94-14594

NEPTUNE (PLANET)
Neptune high-latitude emission: Dependence of angle on frequency
[NASA-CR-193280] p 848 N94-13476

NERVOUS SYSTEM
An analog clustering network from a biological model
[AD-A265637] p 762 N94-12969

NETWORK ANALYSIS
A network evaluation and analysis tool
[DE93-012647] p 758 N94-12917
Proceedings of the 11th Space Surveillance Workshop, volume 1
[AD-A265120] p 531 N94-13358

NETWORK CONTROL
Communications and control for electric power systems
[NASA-CR-194503] p 622 N94-13811

NEURAL NETS
An analog clustering network from a biological model
[AD-A265637] p 762 N94-12969
Adaptive Transfer Function Networks
[DE93-014344] p 745 N94-13151
A review and analysis of neural networks for classification of remotely sensed multispectral imagery
[NASA-CR-194291] p 763 N94-13603
ANNS: An X Window based version of the AFIT neural network simulator
[AD-A266540] p 764 N94-13704
Satellite imagery and exogenous data integration by neural network in automation land-cover classification
[INPE-5480-PRE/1778] p 686 N94-13729
Nonlinear aspects of data integration for land-cover classification in a neural network environment
[INPE-5479-PRE/1778] p 686 N94-13789
Tomographic methods in flow diagnostics
[NASA-TM-106330] p 650 N94-13876
Communications and control for electric power systems: Power flow classification for static security assessment
[NASA-CR-194512] p 624 N94-13948
Feature discovery on segmented objects in SAR imagery using self-organizing neural networks
[DE93-010685] p 686 N94-14056
Identification and interpretation of patterns in rocket engine data
[NASA-CR-194534] p 552 N94-14309
Obstacle detection by recognizing binary expansion patterns
[NASA-CR-194415] p 514 N94-14495
Computer vision and sensor fusion for detecting buried objects
[DE93-012605] p 700 N94-14566
A neural-network approach to robotic control p 679 N94-14634
Retrieval properties of neural networks with infinitely many marked patterns
[PREPRINT-729] p 766 N94-14718
Speaker independent recognition of isolated words using vector quantization and neural networks
[ETN-93-94390] p 616 N94-14724
Identification of continuous-time dynamical systems: Neural network based algorithms and parallel implementation
[DE93-014427] p 766 N94-14737
Mathematic methods and algorithms for real-time applications
[AD-A266776] p 771 N94-14789
Determining neural network connectivity using evolutionary programming
[AD-A266853] p 766 N94-14882

NEURONS
An analog clustering network from a biological model
[AD-A265637] p 762 N94-12969

NEUROPHYSIOLOGY
Neurophysiological study on visuo-vestibular control of posture and movement in fish during adaptation to weightlessness p 591 N94-13759
Feature discovery on segmented objects in SAR imagery using self-organizing neural networks
[DE93-010685] p 686 N94-14056

NEUROSPORA
A circadian rhythm of conidiation in Neurospora crassa (L-12) p 593 N94-13769

NEUTRAL ATOMS
Low energy neutral atom imaging techniques
[DE93-012744] p 779 N94-12950
Advances in low energy neutral atom imaging techniques
[DE93-012745] p 782 N94-13492

Energetic neutral atoms: Imaging the magnetospheric ring current
[NASA-CR-194339] p 715 N94-13826
Terrestrial magnetospheric imaging: Numerical modeling of low energy neutral atoms
[DE93-014561] p 717 N94-14328
Kinetics of photodeposition of superconducting films
[DE93-015511] p 812 N94-14348

NEUTRAL BEAMS
A PC-PCL-based control system for the high-voltage pulsed-power operation of the Intense Diagnostic Neutral Beam (IDNB) Experiment
[DE93-014144] p 797 N94-13100

NEUTRAL CURRENTS
The electric field of a current-carrying conductor
[DE93-626637] p 617 N94-14892

NEUTRAL GASES
The distance to the high velocity clouds of neutral hydrogen
[NASA-CR-194343] p 838 N94-13716
Physics of gas breakdown for ion beam transport in gas
[DE93-015646] p 801 N94-14349

NEUTRAL PARTICLES
Neutral strange particle production at the AGS
[DE93-014044] p 780 N94-13098
Measurement of H zero excited states produced by foil stripping of 800-MeV H(-) ions
[DE93-014391] p 788 N94-13103
Advances in low energy neutral atom imaging techniques
[DE93-012745] p 782 N94-13492
Hybrid S(sub N)/Monte Carlo research and results
[DE93-012677] p 773 N94-14178
Terrestrial magnetospheric imaging: Numerical modeling of low energy neutral atoms
[DE93-014561] p 717 N94-14328

NEUTRINOS
Charged scalar particles and (tau) leptonic decay
[DE93-622969] p 779 N94-12882
A program of correlated observations using the EGRET instrument on GRO and the IMB neutrino detector
[NASA-CR-194367] p 783 N94-13856
Are there atmospheric neutrino oscillations?
[DE93-015550] p 783 N94-13890
Angular correlations in neutron beta decay
[DE93-014349] p 785 N94-14466

NEUTRON ABSORBERS
Generation of neutronic thermal data in support of space nuclear propulsion
[DE93-013148] p 549 N94-13034

NEUTRON ACTIVATION ANALYSIS
Fine-powder Al2O3 and SiO2 for preparation of multielement standards for rare-earth elements analysis
[DE93-625118] p 567 N94-14884

NEUTRON BEAMS
Measurement of the Fe-56(n,p)Mn-56, Al-27(n,p)Mg-27 and Al-27(n,alpha)Na-24 cross sections at 16.0, 17.0 and 18.3 MeV
[NPL-RSA(EXT)-38] p 783 N94-13883
Multiplicity spectrometry on neutron filtered beams
[DE93-617529] p 790 N94-14843

NEUTRON DECAY
Angular correlations in neutron beta decay
[DE93-014349] p 785 N94-14466

NEUTRON DIFFRACTION
Measurement of residual strain in composites by means of time-of-flight neutron diffraction
[DE93-012939] p 555 N94-13248
Quasi-elastic neutron scattering studies of protein dynamics
[DE93-015074] p 782 N94-13414
Measurement of strain in individual phases of composites before, during, and after mechanical loading
[DE93-014585] p 558 N94-14119
Workshop on Formation of Supermolecular Structures in Composite Fluid: Phase Rule and Dynamics
[DE93-782887] p 581 N94-14421

NEUTRON EMISSION
The LAHET code system: Introduction, development, and benchmarking
[DE93-012657] p 787 N94-14804

NEUTRON IRRADIATION
AlGaAs diode laser blue shift resulting from fast neutron irradiation
[AD-A266642] p 659 N94-14681
Investigations of low-temperature neutron embrittlement of ferritic steels
[DE93-015460] p 573 N94-14700

NEUTRON SCATTERING
Generation of neutronic thermal data in support of space nuclear propulsion
[DE93-013148] p 549 N94-13034
Quasi-elastic neutron scattering studies of protein dynamics
[DE93-015074] p 782 N94-13414
The use of polarised neutron reflection for unique density profile determination in thin films
[PB93-187136] p 579 N94-13783
Workshop on Formation of Supermolecular Structures in Composite Fluid: Phase Rule and Dynamics
[DE93-782887] p 581 N94-14421
Small-angle scattering, contrast variation and the study of complex composite materials: A study of the structure of carbon black
[DE93-012707] p 559 N94-14690

NEUTRON SOURCES
Design for low beam loss in accelerators for intense neutron source applications
[DE93-014557] p 789 N94-13327
Beam halo in high-intensity beams
[DE93-014565] p 789 N94-13328
INGDB-90. The International Neutron Nuclear Data Base for geophysics applications
[DE93-624095] p 827 N94-14880

NEUTRON SPECTROMETERS
Multiplicity spectrometry on neutron filtered beams
[DE93-617529] p 790 N94-14843

NEUTRON STARS
A photometric study of massive x-ray binaries
[ITN-93-85207] p 829 N94-13231

NEUTRONS
On the neutron EDM search in the Laue diffraction by the crystal without a centre of symmetry
[DE93-622971] p 804 N94-12828
Workshop on Formation of Supermolecular Structures in Composite Fluid: Phase Rule and Dynamics
[DE93-782887] p 581 N94-14421
Measuring parity violation using the neutron capture reaction
[DE93-016629] p 786 N94-14514
The status of cold fusion
[DE93-012731] p 802 N94-14567
Multiplicity spectrometry on neutron filtered beams
[DE93-617529] p 790 N94-14843
INGDB-90. The International Neutron Nuclear Data Base for geophysics applications
[DE93-624095] p 827 N94-14880

NEWTON METHODS
Newton iterative methods for large scale nonlinear systems
[DE93-015357] p 767 N94-13025
Calculation of the required sensor accuracy to obtain a specified state estimation accuracy
[NAL-TR-1173] p 649 N94-13343
On a convergence of iterative Newton's scheme
[DE93-626604] p 772 N94-14886

NEWTON-RAPHSON METHOD
Evaluation of the Shuttle remote manipulator
[NASA-CR-194351] p 662 N94-13800

NICKEL
Quantum state resolved desorption of CO from solid surfaces
[DE93-016876] p 814 N94-14597
Optimization study of x ray laser coherence in Ni-like Ta
[DE93-016419] p 660 N94-14888

NICKEL ALLOYS
JPRS report: Science and technology. Central Eurasia: Materials science
[JPRS-UMS-93-004] p 559 N94-14574

NICKEL COATINGS
JPRS report: Science and technology. Central Eurasia: Materials science
[JPRS-UMS-93-005] p 559 N94-14575
Insoluble coatings for Stirling engine heat pipe condenser surfaces
[NASA-CR-191188] p 554 N94-14771

NICKEL HYDROGEN BATTERIES
NASA handbook for nickel-hydrogen batteries
[NASA-RP-1314] p 550 N94-13265

NIOBIUM
Atomic structure of the 310 twin in niobium: Theoretical predictions and comparison with experimental observation
[DE93-013421] p 806 N94-13136

NITINOL ALLOYS
Experimental and analytical analysis of the response of a smart beam to rate feedback
[AD-A266544] p 557 N94-13706

NITRATES
Characterization of Spirulina biomass for CELSS diet potential
[NASA-CR-194123] p 729 N94-14097

NITRATION
Study of chemical reactions under the influence of ultrasound
[DE93-016458] p 778 N94-14867

NITRIC ACID
Reduction of Pu(6) with hydrogen peroxide: Effects of plutonium, peroxide, and iron concentrations and of reaction time
[DE93-013598] p 564 N94-13487
Study of chemical reactions under the influence of ultrasound
[DE93-016458] p 778 N94-14867

NITRO COMPOUNDS
Synthesis and characterization of 1,4-dinitroglycoluril (DINGU)
[DE93-014111] p 584 N94-13099
Study of chemical reactions under the influence of ultrasound
[DE93-016458] p 778 N94-14867

NITROGEN
Characterization of 1:1 random copolymers obtained from 6-, 7-, 11-, and 12-carbon amino acids
[AD-A265827] p 577 N94-12985
Modeling of the partitioning of reactive odd nitrogen in the lower stratosphere using aircraft measurements of NOy, NO, and other trace species
[NASA-CR-194305] p 714 N94-13707

NITROGEN COMPOUNDS
Importance of sprays for long range transport of harmful substances in the troposphere
[MITT-81] p 711 N94-14723

NITROGEN DIOXIDE
The mobile lidar system ARGOS for spatial resolution remote measuring of gaseous air pollutants
[GKSS/92/E/26] p 617 N94-14820

NITROGEN OXIDES
An examination of utility emissions contributions to elevated ozone concentrations in the Chicago area
[DE93-012852] p 708 N94-13495
IMG: Interferometric monitor for greenhouse gases
p 689 N94-14217
Summary of conclusions and recommendations from a visibility science workshop
[DE93-012770] p 710 N94-14523

NITROGENATION
Gordon Research Conference on Chronobiology, 1991
[AD-A266354] p 728 N94-13698

NITROGLYCERIN
Closed-chamber analysis of M5 propellant lot RAD-64597
[AD-A266321] p 585 N94-14145

NOAA SATELLITES
An algorithm for the remote sensing of fog using satellite-data and additional information
[DLR-FB-92-23] p 688 N94-14135

NOBLE METALS
Spin polarized photoemission studies of interfacial and thin film magnetism
[DE93-014326] p 580 N94-14142

NOISE INTENSITY
1/f noise and oxide traps in MOSFETs
[DE93-007581] p 619 N94-12942
An evaluation of noise and its effects on shuttle crewmembers during STS-50/USML-1
[NASA-TM-104775] p 735 N94-13961
Underwater hearing: A review
[ISVR-TR-212] p 777 N94-14130

NOISE MEASUREMENT
An experimental assessment of the use of ground-level microphones to measure the fly-over noise of jet-engined aircraft
[NPL-RSA(EXT)-0039] p 777 N94-13885
An evaluation of noise and its effects on shuttle crewmembers during STS-50/USML-1
[NASA-TM-104775] p 735 N94-13961

NOISE REDUCTION
An analog clustering network from a biological model
[AD-A265637] p 762 N94-12969
Active control of acoustic pressure fields using smart material technologies
[NASA-CR-191480] p 768 N94-13354
Piston engine intake and exhaust system design
[ISVR-TR-222] p 663 N94-13874
Study on the possibilities to apply spectrumindex
[VTT-PUBS-109] p 777 N94-14034
Noise levels from a model turbofan engine with simulated noise control measures applied
[NASA-TM-106318] p 518 N94-14036
Study of speckle reduction when using a CO2 waveguide laser close to its threshold state
[DSIS-93-00250] p 657 N94-14067
Mixing noise reduction for rectangular supersonic jets by nozzle shaping and induced screech mixing
[NASA-TM-106364] p 508 N94-14208
Active control of fan-generated plane wave noise
[NASA-TM-109008] p 777 N94-14481
Removing noise from discontinuous data
[ITN-93-85211] p 826 N94-14555

NOISE SPECTRA
1/f noise and oxide traps in MOSFETs
[DE93-007581] p 619 N94-12942
NOISE TEMPERATURE
Insertion loss and noise-temperature contribution of high-temperature superconducting bandpass filters centered at 2.3 and 8.45 GHz p 608 N94-14376
NOISE TOLERANCE
An evaluation of noise and its effects on shuttle crewmembers during STS-50/USML-1
[NASA-TM-104775] p 735 N94-13961
NONADIABATIC CONDITIONS
The geometric phase in quantum physics
[DE93-011121] p 817 N94-13479
Adiabatic and non adiabatic effects in Free Electron Laser (FEL) non linear interactions
[ITN-93-85224] p 659 N94-14547
NONDESTRUCTIVE TESTS
Development of nondestructive evaluation methods and prediction of effects of flaws on the fracture behavior of structural ceramics
[DE93-012942] p 577 N94-13032
Quantitative mapping of pore fraction variations in silicon nitride using an ultrasonic contact scan technique
[NASA-TP-3377] p 665 N94-13056
NDE of titanium alloy MMC rings for gas turbine engines
[NASA-TM-106188] p 555 N94-13138
Structural investigation of a damaged GRP/foam sandwich composite using x ray computed tomography p 669 N94-13857
The development of inspection and repair methods for the C-17 aft cargo door
[LR-704] p 499 N94-13904
High frame rate thermal imager for hypersonic wind tunnel applications
[ONERA-NT-1992-12] p 650 N94-14009
Enhanced NDE systems
[NASA-CR-192603] p 669 N94-14101
JPRS report: Science and technology. Central Eurasia: Materials science
[JPRS-UMS-93-006] p 558 N94-14573
Study of deferred acoustic emission in carbon epoxy composites
[ISAL-91-0078] p 560 N94-14815
NONEQUILIBRIUM CONDITIONS
Boundary stability under nonequilibrium conditions
[DE93-016259] p 809 N94-13980
Characterization of flow fields in hypersonic ground test facilities p 505 N94-14157
NONEQUILIBRIUM FLOW
Computation of nonequilibrium flows using PNS equations p 641 N94-14610
NONEQUILIBRIUM THERMODYNAMICS
Topics on spatially high-order accurate methods and pre-conditioning for the Navier-Stokes equations with finite-rate chemistry p 633 N94-13572
NONHOLONOMIC EQUATIONS
Dynamics and design of nonholonomic robotic mechanical systems
[ISBN-0-315-72009-3] p 662 N94-13597
NONINTRUSIVE MEASUREMENT
Hypersonic flow-field measurements: Nonintrusive p 507 N94-14167
NONLINEAR EQUATIONS
Open boundary conditions for incompletely parabolic systems
[FFI/RAPPORT-92/7029] p 770 N94-13971
Multiplicative noise: Applications in cosmology and field theory
[DE93-016624] p 840 N94-14536
Large spatial, temporal, and algorithmic adaptivity for implicit nonlinear finite element analysis
[DE93-016438] p 771 N94-14589
Construction of the Courant-Snyder invariants for the non-linear equations of motion under presence of the linear coupling
[DE93-017565] p 788 N94-14872
On a convergence of iterative Newton's scheme
[DE93-626604] p 772 N94-14886
NONLINEAR OPTICS
Nonlinear laser spectroscopy studies of semiconductor heterostructures
[AD-A265728] p 805 N94-13037
Beam halo formation from space-charge dominated beams in uniform focusing channels
[DE93-014458] p 789 N94-13209
Poling of thin polymer films in electro optic applications
[AD-A266562] p 579 N94-13584
NONLINEAR PROGRAMMING
Boundary formulations for nonlinear design sensitivity analysis p 672 N94-13669
NONLINEAR SYSTEMS
Modulational stability of periodic solutions of the Kuramoto-Sivaskinsky equation
[NASA-CR-191502] p 628 N94-12888
Newton iterative methods for large scale nonlinear systems
[DE93-015357] p 767 N94-13025
Relegation for decentralized control
[AD-A265720] p 819 N94-13059
Stability of subharmonics and escape phenomena in the twin-well potential duffing system p 775 N94-13235
Nonlinear vibrations of thick composite plates: Higher-order shear deformation plate theory p 556 N94-13558
Nonlinear aspects of data integration for land-cover classification in a neural network environment
[INPE-5479-PRE/1778] p 686 N94-13789
Multi-dimensional high order essentially non-oscillatory finite difference methods in generalized coordinates
[NASA-CR-194031] p 770 N94-14429
Nonlinear wave predictions in ceramics
[DE93-016516] p 582 N94-14436
Chaos and microbial systems
[DE93-016814] p 730 N94-14596
Identification of continuous-time dynamical systems: Neural network based algorithms and parallel implementation
[DE93-014427] p 766 N94-14737
A new treatment of periodic systems with applications to helicopter rotor blade dynamics
[AD-A266770] p 510 N94-14784
NONLINEARITY
A general contact detection algorithm for finite element analysis
[DE93-012846] p 742 N94-12956
Linear and nonlinear spectroscopic probing of solute interactions with chemically modified silica surface
[DE93-014648] p 562 N94-13001
Beam halo formation from space-charge dominated beams in uniform focusing channels
[DE93-014458] p 789 N94-13209
Brillouin scattering from fluctuations produced by stimulated Raman scattering
[DE93-016531] p 792 N94-14438
Kinetic simulations of ultra-intense laser plasma interactions
[DE93-014419] p 802 N94-14564
Stress stiffening and approximate equations in flexible multibody dynamics p 677 N94-14620
Nonrecursive formulations of multibody dynamics and concurrent multiprocessing p 679 N94-14632
Nonlinear analysis, scientific computation, and continuum mechanics applied to the science of materials
[AD-A266641] p 817 N94-14680
NONUNIFORM PLASMAS
Parametric instabilities in large nonuniform laser plasmas
[DE93-013184] p 797 N94-13393
NONUNIFORMITY
Locally non-uniform finite-difference time domain with application to stealth, crosstalk, and narrow apertures
[DE93-013958] p 601 N94-13696
Machining and grinding: High rate deformation in practice
[DE93-010718] p 664 N94-14457
NORMAL DENSITY FUNCTIONS
A new method to assess Monte Carlo convergence
[DE93-012667] p 772 N94-12919
NORMAL SHOCK WAVES
An experimental investigation of shock wave/vortex interaction p 634 N94-13574
NORTHERN SKY
Search for continuous and single day emission from ultra-high-energy sources
[DE93-012724] p 846 N94-12947
NOTCHES
A computer program to calculate growth rates for cracks at notches in regions of residual stress
[RAE-TM-MAT/STR-1207] p 683 N94-14818
NOVAE
The spectroscopic evolution of novae in the bulge of M31 and a search for their possible origin in the M31 globular cluster system p 831 N94-13668
NOZZLE DESIGN
Method of characteristics design of a supersonic wind tunnel nozzle with square cross-section, supplement 3
[NASA-CR-194359] p 527 N94-12824
Propulsion integration p 508 N94-14174
Qualification test of the Ross Double Planetary Mixer
[NASA-CR-192600] p 652 N94-14497
NOZZLE FLOW
An experimental investigation of the redistribution of gas stream total temperature in a high turning angle transonic planar cascade
[ISBN-0-315-60791-2] p 502 N94-13369
Chemical reactions in scramjet engines: Reduced kinetic models for ignition, combustion and nozzle flow
[NAL-TR-1184] p 563 N94-13458
Investigation of the feasibility of optical diagnostic measurements at the exit of the SSME
[NASA-CR-193832] p 553 N94-14682
NOZZLE GEOMETRY
Mixing noise reduction for rectangular supersonic jets by nozzle shaping and induced screech mixing
[NASA-TM-106364] p 508 N94-14208
NUCLEAR ASTROPHYSICS
Research in theoretical nuclear physics
[DE93-015096] p 839 N94-14330
NUCLEAR BINDING ENERGY
Simulation studies for surfaces and materials strength
[NASA-CR-193305] p 671 N94-13179
Thermochemistry of transition metal clusters
[DE93-016201] p 571 N94-13977
Spin polarized photoemission studies of interfacial and thin film magnetism
[DE93-014326] p 580 N94-14142
NUCLEAR ENERGY
JPRS report: Science and technology. Central Eurasia: Engineering and equipment
[JPRS-UEQ-93-006] p 776 N94-14431
NUCLEAR ENGINE FOR ROCKET VEHICLES
Nuclear propulsion systems engineering
[DE93-010791] p 548 N94-12870
NUCLEAR EXPLOSIONS
Atmospheric acoustic modeling
[DE93-016727] p 718 N94-14518
NUCLEAR FISSION
A modular gas-cooled cermet reactor system for planetary base power
[DE93-013672] p 550 N94-13351
The LAHET code system: Introduction, development, and benchmarking
[DE93-012657] p 787 N94-14804
NUCLEAR FUELS
Review of nuclear thermal propulsion carbide reactor fuel corrosion and exhibit
[DE93-016605] p 585 N94-14535
Space reactor fuel element testing in upgraded TREAT
[DE93-012524] p 554 N94-14806
NUCLEAR FUSION
Microwave generation for magnetic fusion energy applications
[DE93-013864] p 654 N94-13058
Nuclear fusion of protons with ions of boron
[DE93-014284] p 781 N94-13219
Long-pulse operation of a gyrotron with beam/RF separation
[DE93-015007] p 649 N94-13410
The status of cold fusion
[DE93-012731] p 802 N94-14567
NUCLEAR INTERACTIONS
Measurements of transverse energy and forward energy in high-energy nuclear collisions
[DE93-012755] p 788 N94-12817
HIJET with AGS physics and N(sup *)'s
[DE93-014022] p 780 N94-13097
Scattering calculations and confining interactions
[NASA-CR-194242] p 786 N94-14549
NUCLEAR MAGNETIC RESONANCE
Development of nondestructive evaluation methods and prediction of effects of flaws on the fracture behavior of structural ceramics
[DE93-012942] p 577 N94-13032
Transport properties of disordered porous media from the microstructure
[DE93-016065] p 806 N94-13152
Office of Naval Research/DARPA publications: Composite materials with improved properties in compression
[AD-A265509] p 560 N94-14794
NUCLEAR PHYSICS
Advanced computers and simulation
[DE93-014354] p 740 N94-13286
Research in theoretical nuclear physics
[DE93-015096] p 839 N94-14330
Some tools of the trade we've developed for our cross-section calculations
[DE93-013835] p 786 N94-14569
NUCLEAR POWER PLANTS
A data base for aging of structural materials
[DE93-009714] p 824 N94-13915
Computational problems with the binomial failure rate model and incomplete common cause failure reliability data
[DE93-014346] p 669 N94-14143
NUCLEAR PROPULSION
Nuclear propulsion systems engineering
[DE93-010791] p 548 N94-12870

MCNP benchmark analyses of critical experiments for the Space Nuclear Thermal Propulsion program
[DE93-014046] p 548 N94-12981
Design, qualification and operation of nuclear rockets for safe Mars missions
[DE93-010792] p 549 N94-12996
Generation of neutronic thermal data in support of space nuclear propulsion
[DE93-013148] p 549 N94-13034
Gas core nuclear thermal rocket engine research and development in the former USSR
[DE93-012165] p 552 N94-14013
Computer program for thermal and transport properties of parahydrogen from 20 to 10,000 K
[NASA-TP-3378] p 552 N94-14102
Nuclear thermal propulsion engine based on particle bed reactor using light water steam as a propellant
[DE93-014336] p 552 N94-14111
Review of nuclear thermal propulsion carbide reactor fuel corrosion and exhibit
[DE93-016605] p 585 N94-14535
Space reactor fuel element testing in upgraded TREAT
[DE93-012524] p 554 N94-14806

NUCLEAR REACTIONS
Semiempirical fragmentation models on galactic cosmic ray transport calculations with hydrogen target
[NASA-TP-3350] p 847 N94-13263
The theory of relativistic heavy ion collisions
[DE93-015934] p 784 N94-13952
Angular correlations in neutron beta decay
[DE93-014349] p 785 N94-14466
Measuring parity violation using the neutron capture reaction
[DE93-016629] p 786 N94-14514
Some tools of the trade we've developed for our cross-section calculations
[DE93-013835] p 786 N94-14569
Multiplicity spectrometry on neutron filtered beams
[DE93-617529] p 790 N94-14843
INGDB-90. The International Neutron Nuclear Data Base for geophysics applications
[DE93-624095] p 827 N94-14880

NUCLEAR REACTORS
The corrosion behavior of 8001 Al under heat-transfer conditions in an aqueous loop system
[DE93-013450] p 569 N94-13242
A modular gas-cooled cermet reactor system for planetary base power
[DE93-013672] p 550 N94-13351
Fatigue design curves for 6061-T6 aluminum
[DE93-011849] p 571 N94-14021
Estimation of strain in 1-kW primary containment vessels by microstructural examination
[DE93-013053] p 573 N94-14316
Welding technologies as applied to nuclear manufacturing
[DE93-010924] p 664 N94-14565

NUCLEAR ROCKET ENGINES
Gas core nuclear thermal rocket engine research and development in the former USSR
[DE93-012165] p 552 N94-14013
Space reactor fuel element testing in upgraded TREAT
[DE93-012524] p 554 N94-14806

NUCLEAR SCATTERING
Medium energy hadron-nucleus scattering in the 1/N expansion formalism
[DE93-622957] p 778 N94-12848

NUCLEAR STRUCTURE
Research in theoretical nuclear physics
[DE93-015096] p 839 N94-14330
Dynamics of pion-nucleus systems
[DE93-014449] p 785 N94-14468

NUCLEAR WEAPONS
Inertial Confinement Fusion
[DE93-013303] p 795 N94-13017
A model for fuel fire duration and application to the B-1B bomber
[DE93-013000] p 512 N94-14292

NUCLEATION
A parameterization of cloud droplet nucleation
[DE93-007998] p 718 N94-12903
Binary homogeneous nucleation: Temperature and relative humidity fluctuations and non-linearity
[DE93-007884] p 709 N94-13911
Optimization of the processing parameters of high temperature superconducting glass-ceramics: Center Director's discretionary fund final report
[NASA-TM-108421] p 808 N94-13938
Containerless processing of undercooled melts
[NASA-CR-194350] p 572 N94-14123
Multiplicative noise: Applications in cosmology and field theory
[DE93-016624] p 840 N94-14536
Characterization of diamond film growth in a combustion flame
[AD-A266659] p 816 N94-14839

NUCLEI (NUCLEAR PHYSICS)
Research in cosmic and gamma ray astrophysics: Cosmic physics portion
[NASA-CR-194127] p 847 N94-13211

NUCLEON-NUCLEON INTERACTIONS
HIJET with AGS physics and N(sup *)'s
[DE93-014022] p 780 N94-13097
Resonances in the Sigma NN system
[DE93-014353] p 785 N94-14144
The off shell (rho)-(omega) mixing in the QCD sum rules
[DE93-014845] p 786 N94-14527
Relativistic proton-nucleus scattering and one-boson-exchange models p 786 N94-14550
Theoretical antideuteron-nucleus absorptive cross sections p 786 N94-14551
Isospin flip as a relativistic effect: NN interactions
[CEBAF-PR-89-023] p 786 N94-14552
The LAHET code system: Introduction, development, and benchmarking
[DE93-012657] p 787 N94-14804

NUCLEON-NUCLEON SCATTERING
No-lost theorem for parity violating nucleon-nucleon scattering experiments
[DE93-012737] p 779 N94-12949
Theoretical antideuteron-nucleus absorptive cross sections p 786 N94-14551
Isospin flip as a relativistic effect: NN interactions
[CEBAF-PR-89-023] p 786 N94-14552

NUCLEONS
Measuring strangeness in the nucleon
[DE93-014861] p 785 N94-14471
Isospin flip as a relativistic effect: NN interactions
[CEBAF-PR-89-023] p 786 N94-14552
On the statistical theory of the even-even nucleons levels' density
[DE93-623990] p 788 N94-14875

NULL HYPOTHESIS
Rare attributes in finite universe: Hypotheses testing specification and exact randomized upper confidence bounds
[DE93-012783] p 775 N94-12955

NUMBER THEORY
Mathematics and string theory
[DE93-017903] p 817 N94-14417

NUMERICAL ANALYSIS
MHD shocks in coronal mass ejections
[NASA-CR-193418] p 828 N94-12970
Combustor technology for future small gas turbine aircraft
[NASA-TM-106312] p 517 N94-13142
Magnetic fusion computing: A personal retrospective view
[DE93-014147] p 797 N94-13217
A probabilistic method for the buckling assessment of stiffened composite shells
[NASA-TM-106286] p 671 N94-13379
Numerical simulation and parameterization of orographic gravity waves p 713 N94-13647
Mathematical algorithms for multidimensional inverse scattering problems in inhomogeneous medium
[AD-A266440] p 749 N94-13702
A comparison of computational and experimental data for a subscale high speed propulsive nozzle at low mach numbers
[AD-A266543] p 504 N94-13705
High order hybrid numerical simulations of two dimensional detonation waves
[NASA-CR-191506] p 769 N94-13792
The numerical simulation of the collapse process of axially compressed cylindrical shells with measured imperfections
[LR-705] p 674 N94-13905
Numerical simulations of Nd:YAG laser amplifiers
[FFI/RAPPORT-92/7028] p 657 N94-13970

NUMERICAL CONTROL
An experimental study of tether reel system: A laboratory model
[NAL-TR-1176T] p 539 N94-12943
Data fusion for adaptive control in manufacturing: Impact on engineering information models
[DE93-011555] p 743 N94-12999
Inertial confinement fusion program
[DE93-013372] p 796 N94-13047
A PC-PCL-based control system for the high-voltage pulsed-power operation of the Intense Diagnostic Neutral Beam (IDNB) Experiment
[DE93-014144] p 797 N94-13100
DATAA: Data acquisition made easy
[DE93-014683] p 823 N94-13406
Knowledge based systems: From process control to policy analysis
[DE93-014582] p 765 N94-14117
Eye-gaze and intent: Application in 3D interface control
[DE93-015210] p 738 N94-14335
Laser beam control and diagnostic systems for the copper-pumped dye laser system at Lawrence Livermore National Laboratory
[DE93-016529] p 658 N94-14437
A fast frame rate 512 x 512 CCD digital camera system
[DE93-013048] p 653 N94-14792
Performance seeking control: Program overview and future directions
[NASA-TM-4531] p 519 N94-14855

NUMERICAL FLOW VISUALIZATION
High speed transition prediction
[NASA-CR-194125] p 502 N94-13422
Rotor stator CGI
[NASA-TM-109313] p 518 N94-13608
Numerical simulation of steady three-dimensional flows in axial turbomachinery bladerows p 634 N94-13630
Analysis of reacting flowfields in low-thrust rocket engines and plumes p 552 N94-14491
Simulation of hypersonic, reacting flow around reentry bodies: Comparisons of numerical and experimental results
[MBB-LME-211-S-PUB-507] p 509 N94-14710

NUMERICAL STABILITY
Modulational stability of periodic solutions of the Kuramoto-Sivaskinsky equation
[NASA-CR-191502] p 628 N94-12888
Stability of subharmonics and escape phenomena in the twin-well potential duffing system p 775 N94-13235

NUMERICAL WEATHER FORECASTING
The nocturnal wind maximum: An interactive forecast method
[KNMI-TR-142] p 722 N94-13985
Precipitation verification LAM
[KNMI-TR-143] p 722 N94-13991
Adaptation of humidity-cloud cover relations in the LAM
[KNMI-TR-144] p 722 N94-13992
A verification of the Euroguidance: A guidance forecast for transportation and tourism
[KNMI-TR-145] p 722 N94-13993

NUTRITIONAL REQUIREMENTS
Characterization of Spirulina biomass for CELSS diet potential
[NASA-CR-194123] p 729 N94-14097

O

OBJECT PROGRAMS
A distributed, visual object system using aggregation objects with a local namespace
[IME-MET-TR-007] p 764 N94-13860
Reviews of computing technology: Object-oriented technology
[DE93-014740] p 754 N94-14470

OBJECT-ORIENTED PROGRAMMING
Object-oriented productivity metrics p 667 N94-13161
Programming languages made in Italy
[REPT-93-002] p 750 N94-13805
A distributed, visual object system using aggregation objects with a local namespace
[IME-MET-TR-007] p 764 N94-13860
The OOA technique in information systems
[REPT-72-92] p 823 N94-13863
Efficient, massively parallel eigenvalue computation
[NASA-CR-194289] p 760 N94-13921
Discrete event simulation using object-oriented programming: Application to manufacturing
[ERB-1037] p 753 N94-14200
Reviews of computing technology: Object-oriented technology
[DE93-014740] p 754 N94-14470

OBLIQUE SHOCK WAVES
An experimental investigation of shock wave/vortex interaction p 634 N94-13574

OBSERVATORIES
Search for ultra-high-energy radiation from gamma-ray bursts
[DE93-012721] p 847 N94-12964

OBSTACLE AVOIDANCE
Obstacle detection by recognizing binary expansion patterns
[NASA-CR-194415] p 514 N94-14495

OCEAN CURRENTS
Circulation model experiments of the Gulf Stream using satellite-derived fields
[AD-A266067] p 725 N94-12990
An experimental regional scale climate simulation laboratory
[DE93-015935] p 719 N94-13119

Ocean uptake of carbon dioxide
[DE93-012967] p 707 N94-13384
Tidal interactions in the Earth Moon system
[COMMUNICATIONS-SER-B-160] p 837 N94-13503
Radar imaging of sub-mesoscale ocean phenomena
[AD-A266339] p 725 N94-13581
On the space-time ocean current variability and its effects on the length-of-day
[ISBN-0-315-59510-8] p 726 N94-14205
On the sea truth data of the Kuroshio meander and cold eddy movement p 696 N94-14266
Tracking of change of a warm-core ring structure p 696 N94-14267
Outline of ISY Kuroshio observation experiment p 697 N94-14268
Warm streamers extended from Warm Core Rings (WCR's) and their role on fish migration and fishing ground formation p 697 N94-14270

OCEAN DATA ACQUISITIONS SYSTEMS
Buoy experiments to obtain the sea-truth data for OCTS/NSCAT, part 1
[NASDA-CNT-930005-PT-1] p 725 N94-13653
Phase aligner for the Electronically Scanned Thinned Array Radiometer (ESTAR) instrument
[NASA-TM-4518] p 623 N94-13878
ERS-1 system
[ESA-SP-1146] p 699 N94-14353

OCEAN DYNAMICS
Circulation model experiments of the Gulf Stream using satellite-derived fields
[AD-A266067] p 725 N94-12990
An experimental regional scale climate simulation laboratory
[DE93-015935] p 719 N94-13119
Integration of space and in-situ observations to study atmosphere, ocean and land processes
[NASA-CR-194495] p 683 N94-14500
Nonlinear wave forces on large ocean structures
[AD-A266820] p 683 N94-14902

OCEAN MODELS
Circulation model experiments of the Gulf Stream using satellite-derived fields
[AD-A266067] p 725 N94-12990
Radar imaging of sub-mesoscale ocean phenomena
[AD-A266339] p 725 N94-13581

OCEAN SURFACE
DMSP F11 SSM/T-2 calibration and validation
[AD-A265817] p 719 N94-12978
Error analysis of real time and post processed or bit determination of GFO using GPS tracking
[NASA-CR-193646] p 512 N94-13238
Radar imaging of sub-mesoscale ocean phenomena
[AD-A266339] p 725 N94-13581
Artificial oil pollution detection and wave observation in the sea adjacent to Japan by ERS-1 SAR p 688 N94-14212
Image processing and analysis of airborne POLDER data p 689 N94-14219
Outline of ISY sea surface temperature data sets p 696 N94-14261
Integration of SST data sets using MOS-1 satellite data: For validation and monitoring p 696 N94-14262
Geophysical validation of ATSR sea surface temperatures p 696 N94-14263
Accuracy validation test of estimated sea surface temperature by satellite data p 696 N94-14264
Sea surface effect on the sea surface temperature estimation by satellite data p 696 N94-14265
On the sea truth data of the Kuroshio meander and cold eddy movement p 696 N94-14266
Tracking of change of a warm-core ring structure p 696 N94-14267
Outline of ISY Kuroshio observation experiment p 697 N94-14268
Warm streamers extended from Warm Core Rings (WCR's) and their role on fish migration and fishing ground formation p 697 N94-14270

OCEANOGRAPHY
Ocean acoustic processing: A model-based approach
[DE93-011902] p 725 N94-12876
Optimization and eigenvalue computation with application to meteorology and oceanography
[DE93-015310] p 744 N94-13024
Knowledge-based oceanographic image compression
[AD-A265752] p 821 N94-13041
An experimental regional scale climate simulation laboratory
[DE93-015935] p 719 N94-13119
Activities report of the Netherlands Remote Sensing Board
[ETN-93-93880] p 686 N94-14073
Volume 14: The first SeaWiFS intercalibration round-robin experiment, SIRREX-1, July 1992
[NASA-TM-104566] p 725 N94-14090

OCEANS
The role of clouds and oceans in global greenhouse warming
[DE93-016206] p 706 N94-13079
Error analysis of real time and post processed or bit determination of GFO using GPS tracking
[NASA-CR-193646] p 512 N94-13238
Ocean uptake of carbon dioxide
[DE93-012967] p 707 N94-13384

OCTANE
Comparative ignition of hexane and octane isomers in a shock tube
[DE93-016535] p 566 N94-14869

ODORS
Study on improvement of flammability, odor and offgassing tests for materials
[NASDA-CNT-930009] p 563 N94-13471

OFFGASSING
Study on improvement of flammability, odor and offgassing tests for materials
[NASDA-CNT-930009] p 563 N94-13471

OFFSHORE PLATFORMS
Nonlinear wave forces on large ocean structures
[AD-A266820] p 683 N94-14902

OHMIC DISSIPATION
Ohmic heating of composite candidate graphite-fiber/coating combinations
[NASA-TM-4491] p 554 N94-12871

OIL POLLUTION
Artificial oil pollution detection and wave observation in the sea adjacent to Japan by ERS-1 SAR p 688 N94-14212

OIL RECOVERY
BOAST 2 for the IBM 3090 and RISC 6000
[DE93-000138] p 638 N94-14351

OIL SLICKS
Artificial oil pollution detection and wave observation in the sea adjacent to Japan by ERS-1 SAR p 688 N94-14212

OLIGOMERS
Unexpectedly rapid hydrosilation polymerization of the diallyl derivative of bisphenol A and 2,6-diallylphenol
[AD-A265832] p 577 N94-12986
Charge storage and switching phenomena with molecular assemblies of metal complexes
[AD-A266673] p 787 N94-14778

ON-LINE SYSTEMS
Transition of building energy consumption using multi-input, single-output dynamic model
[VTT-PUBS-116] p 597 N94-14055
On-line upgrade of program modules using AdaPT
[NASA-CR-194331] p 754 N94-14472
Portable acoustic wave sensor systems for real-time monitoring of volatile organic compounds
[DE93-013753] p 582 N94-14511

ONBOARD DATA PROCESSING
ALFIS: Astronomical Low Frequency Interferometry Satellites. A feasibility study
[LR-699] p 542 N94-13988

OPACITY
H2S data reduction
[NASA-CR-193389] p 617 N94-14743

OPEN CLUSTERS
UV extinction properties of carina nebular dust
[NASA-CR-193424] p 835 N94-13233
Photometry and spectroscopy in the open cluster Alpha Persei, 2
[NASA-CR-193397] p 833 N94-14358

OPERATING COSTS
Robot-task compliance: The energy criterion
[ITN-93-85196] p 763 N94-13568
Optimal maintenance policies of a Markovian system
[ITN-93-85216] p 774 N94-14502

OPERATIONS RESEARCH
Gate assignment using linear programming
[LR-698] p 775 N94-13987

OPERATORS (MATHEMATICS)
On some results by Fuhrmann on Hankel operators
[CWI-BS-R9224] p 764 N94-13999
On relations between Schmidt pairs arising in robust control
[CWI-BS-R9225] p 764 N94-14000
On the Schmidt pairs of multivariable Hankel operators and robust control
[CWI-BS-R9226] p 765 N94-14001

OPTICAL BISTABILITY
Characteristics of semiconductor lasers with optical feedback
[ISBN-0-315-55435-5] p 656 N94-13522

OPTICAL COMMUNICATION
Development of an on-board aircraft optical fiber data bus system
[NAL-TR-1163] p 514 N94-13338
An overview of the Galileo Optical Experiment (GOPEX) p 610 N94-14386
Galileo Optical Experiment (GOPEX) optical train: Design and validation at the Table Mountain Facility p 610 N94-14390
GOPEX laser transmission and monitoring systems p 611 N94-14391
GOPEX at the Starfire Optical Range p 611 N94-14392

OPTICAL CONTROL
Executive summary p 545 N94-14831
Wavefront sensing, control, and pointing p 546 N94-14833

OPTICAL DATA PROCESSING
Development of an on-board aircraft optical fiber data bus system
[NAL-TR-1163] p 514 N94-13338
High speed all-optical networks
[NASA-CR-194384] p 791 N94-13682

OPTICAL EQUIPMENT
Fabrication of AlGaAs/GaAs-light-emitting devices by selective MOCVD using dialkylmetalchloride p 627 N94-13433
Optical degradation issues for XUV projection lithography systems
[DE93-012658] p 626 N94-14805
Optical testing p 547 N94-14836
Optical systems integrated modeling p 547 N94-14837
Advanced optical instruments technology p 547 N94-14838

OPTICAL FIBERS
Development of an on-board aircraft optical fiber data bus system
[NAL-TR-1163] p 514 N94-13338
Optical fiber sensors for materials and structures characterization
[NASA-CR-194090] p 791 N94-13353
Measurements of optical properties of waveshifting optical fiber for liquid scintillator hadron calorimetry
[DE93-012606] p 791 N94-13482
Liquid and gas evanescent wave spectroscopy via tunabie lasers and silver halide fibers
[ITN-93-85226] p 565 N94-14465
Radiation effects on optoelectronic analog link for particle detectors
[DE93-015794] p 793 N94-14529
Optical fibre Fabry-Perot interferometers for calorimetric heat transfer gauges
[RAE-TM-AERO/PROP-20] p 653 N94-14701

OPTICAL FILTERS
Advanced optical instruments technology p 547 N94-14838

OPTICAL FLOW (IMAGE ANALYSIS)
Compatibility of information and mode of control: The case for natural control systems p 523 N94-13307

OPTICAL HETERODYNING
Impact of shorter wavelengths on optical quality for laws
[NASA-CR-193433] p 792 N94-14473

OPTICAL MATERIALS
Effect of microstructure on passive film formation and breakdown on Al alloys
[AD-A265339] p 569 N94-13050
Optical fiber sensors for materials and structures characterization
[NASA-CR-194090] p 791 N94-13353
Reflective coatings for solar applications
[DE93-010026] p 702 N94-13381
Barium fluoride research and development at Lawrence Livermore National Laboratory
[DE93-014682] p 807 N94-13405
Preparation of optical materials used in non-visible region (M-17) p 589 N94-13749
Workshop Proceedings: Optical Systems Technology for Space Astrophysics in the 21st Century, volume 3
[NASA-CR-194102] p 545 N94-14830
Executive summary p 545 N94-14831
Materials and structures p 546 N94-14835
Advanced optical instruments technology p 547 N94-14838
Investigation of Zerodur material processing
[NASA-CR-193842] p 793 N94-14903

OPTICAL MEASUREMENT
Adaptive control of interface by temperature and interface profile feedback in transparent multi-zone crystal growth furnace
[NASA-CR-194140] p 762 N94-13253
Tomographic methods in flow diagnostics
[NASA-TM-106330] p 650 N94-13876
Investigation of the feasibility of optical diagnostic measurements at the exit of the SSME
[NASA-CR-193832] p 553 N94-14682
Executive summary p 545 N94-14831

OPTICAL MEASURING INSTRUMENTS
Recent flight-test results of optical airdata techniques
[NASA-TM-4504] p 517 N94-13791

Tomographic methods in flow diagnostics
[NASA-TM-106330] p 650 N94-13876
Earth Observation Center Annual Report on Research and Development, Fiscal Year 1992
[EOC-92-01-0007] p 687 N94-14091
Calibration and in-house validation results of JERS-1 data p 687 N94-14092
Earth observation experiment data analysis p 687 N94-14093
ADEOS project p 687 N94-14094
Spectroscopic method and data reduction algorithm for laser long-path absorption measurements using RIS p 689 N94-14218
Image processing and analysis of airborne POLDER data p 689 N94-14219
Intra-blade quantitative transonic flow measurements at the DRA Pyestock Isentropic Light Piston Facility using PIV (Particle Image Velocimetry)
[RAE-TM-AERO/PROP-21] p 509 N94-14706
Workshop Proceedings: Optical Systems Technology for Space Astrophysics in the 21st Century, volume 3
[NASA-CR-194102] p 545 N94-14830
Executive summary p 545 N94-14831
Optical testing p 547 N94-14836

OPTICAL MICROSCOPES
Two dimensional measurement and evaluation of point images at microscope objectives
[ETN-93-94397] p 793 N94-14856

OPTICAL POLARIZATION
The continuum emission of active galactic nuclei
[ITN-93-85208] p 847 N94-13232

OPTICAL PROPERTIES
Measurements of optical properties of waveshifting optical fiber for liquid scintillator hadron calorimetry
[DE93-012606] p 791 N94-13482
Optical and physical properties of the LiSrAlF6:Cr laser crystal
[DE93-014657] p 808 N94-13881
Optimization of transparent and reflecting electrodes for amorphous silicon solar cells
[DE93-010009] p 704 N94-14110
Laser and spectroscopic properties of Yb-doped apatite crystals
[DE93-014656] p 810 N94-14125
Theory of the electronic and structural properties of solid state oxides
[DE93-016051] p 811 N94-14296
Workshop on the Space Environment: The Effects on the Optical Properties of Airless Bodies
[NASA-CR-194417] p 842 N94-14298
Impact of shorter wavelengths on optical quality for laws
[NASA-CR-193433] p 792 N94-14473
Relativistic proton-nucleus scattering and one-boson-exchange models p 786 N94-14550
Theoretical antideuteron-nucleus absorptive cross sections p 786 N94-14551

OPTICAL PUMPING
The Livermore x ray laser program
[DE93-014118] p 658 N94-14152

OPTICAL RADAR
Novel Co:MgF2 lidar for aerosol profiler
[NASA-CR-191525] p 654 N94-13091
Non-scanned LADAR imaging and applications
[DE93-013772] p 655 N94-13261
Coherent Doppler lidar signal covariance including wind shear and wind turbulence
[NASA-CR-194492] p 721 N94-13723
A rocket-borne lidar for studies of the middle atmosphere
[FFI/RAPPORT-92/7034] p 715 N94-13949
Signal and reference wavelengths for the elimination of SO2 cross sensitivity in remote measurements of tropospheric ozone with lidar
[GKSS/92/E/24] p 617 N94-14819
The mobile lidar system ARGOS for spatial resolution remote measuring of gaseous air pollutants
[GKSS/92/E/26] p 617 N94-14820

OPTICAL REFLECTION
Determination of the surface cleanliness of metals by FT-IR spectroscopy
[DE93-013252] p 565 N94-14525

OPTICAL RESONATORS
Horizontal-cavity surface-emitting lasers, superluminescent LEDs, and amplifiers, and parabolic gain unstable resonator semiconductor lasers p 656 N94-13573
Theoretical investigation of scattering by homogeneous or coated dielectric spheres illuminated with a steady state or pulsed laser beam p 657 N94-13624

OPTICAL THICKNESS
The effects of anthropogenic aerosols on optical thickness and particle size of clouds. Part 1: Retrieval algorithm p 691 N94-14230
Earth radiation budget, cloud, and aerosol parameters derived from AVHRR and TOVS measurements p 691 N94-14233
Solar radiation on Mars: Stationary photovoltaic array
[NASA-TM-106321] p 626 N94-14730

OPTICAL TRACKING
DMSP F11 SSM/T-2 calibration and validation
[AD-A265817] p 719 N94-12978
Three dimensional tracking of four point planar patterns using corners
[ISBN-0-315-52149-X] p 791 N94-13490
Electromagnetic wave test p 508 N94-14173

OPTICAL WAVEGUIDES
Implementation of manufacturing techniques for planar, single mode waveguides on lithium niobate
[DSIS-93-00101] p 792 N94-13845
Integrated optics technology transfer
[DSIS-93-00179] p 792 N94-13868
Liquid and gas evanescent wave spectroscopy via tunable lasers and silver halide fibers
[ITN-93-85226] p 565 N94-14465
Manufacturing and examination of integrated optical waveguide components in silicon
[ETN-93-94393] p 793 N94-14704

OPTIMAL CONTROL
Active control of acoustic pressure fields using smart material technologies
[NASA-CR-191480] p 768 N94-13354
Optimal lateral escape maneuvers for microburst encounters during final approach
[LR-691] p 511 N94-13534
On some results by Fuhrmann on Hankel operators
[CWI-BS-R9224] p 764 N94-13999
On relations between Schmidt pairs arising in robust control
[CWI-BS-R9225] p 764 N94-14000
On the Schmidt pairs of multivariable Hankel operators and robust control
[CWI-BS-R9226] p 765 N94-14001
Development of an hp-version finite element method for computational optimal control
[NASA-CR-194149] p 766 N94-14444
Decentralized control of uncertain systems via sensitivity models
[DE93-012963] p 766 N94-14568
Analysis, approximation, and computation of a coupled solid/fluid temperature control problem
[NASA-TM-106351] p 771 N94-14731
Functional differential equations with piecewise continuous argument
[AD-A266660] p 772 N94-14840
Performance seeking control: Program overview and future directions
[NASA-TM-4531] p 519 N94-14855

OPTIMIZATION
Efficient dynamic optimization of logic programs
[NASA-TM-109251] p 761 N94-12889
Tree reconstruction from partial orders
[DE93-009841] p 743 N94-12991
Surrogates for numerical simulations; optimization of eddy-promoter heat exchangers
[NASA-CR-191510] p 629 N94-13074
Multidisciplinary design techniques applied to conceptual aerospace vehicle design
[NASA-CR-194409] p 515 N94-13618
An expert system for integrated structural analysis and design optimization for aerospace structures
[NASA-CR-194225] p 673 N94-13673
Fast parallel string prefix-matching
[AD-A267758] p 760 N94-13924
Mathematical optimization: A tool for aircraft design
[MBB-LME-251-S-PUB-0492] p 751 N94-14006
VFGEN: A parallel volume fraction generator for hydrocodes
[DE93-011673] p 752 N94-14019
Optimal synthesis of hot composite laminates with interphase layers
[NASA-TM-106326] p 557 N94-14042
Development of an hp-version finite element method for computational optimal control
[NASA-CR-194149] p 766 N94-14444
Paradigms for very fast parallel algorithms
[ITN-93-85212] p 755 N94-14556
Computational issues in optimal tuning and placement of passive dampers p 681 N94-14647

OPTOELECTRONIC DEVICES
Activities of Institute for Microstructural Sciences
[NRC-32815] p 810 N94-14198
Activities of Institute for Microstructural Sciences
[CNR-32815] p 810 N94-14199
Radiation effects on optoelectronic analog link for particle detectors
[DE93-015794] p 793 N94-14529

ORBIT CALCULATION
Investigation for improving Global Positioning System (GPS) orbits using a discrete sequential estimator and stochastic models of selected physical processes
[NASA-CR-194167] p 512 N94-13082
Error analysis of real time and post processed or bit determination of GFO using GPS tracking
[NASA-CR-193646] p 512 N94-13238
Improved treatment of global positioning system force parameters in precise orbit determination applications p 514 N94-14371
Failure modes of reduced-order orbit determination filters and their remedies p 532 N94-14373

ORBIT TRANSFER VEHICLES
Low power pulsed MPD thruster system analysis and applications
[NASA-CR-191187] p 550 N94-13415
Guidance law development for aeroassisted transfer vehicles using matched asymptotic expansions
[NASA-CR-194523] p 508 N94-14538

ORBITAL ASSEMBLY
The Second Workshop on Deployment and Assembly Experiment of Large Space Structure on Orbit
[NASDA-CON-930003] p 529 N94-13268
Structural design of hexa-link truss deployable antenna p 529 N94-13269
Thermal distortion measurement of TETRUS type thermal test model of large deployable antenna for mobile communications satellite p 529 N94-13270
Development of modular cable mesh deployable antenna p 530 N94-13274
Research on inflatable structure for space use p 530 N94-13275
Helical truss beam development for large space structure p 530 N94-13276
Application of intelligently adaptable structure and robot to large space structure p 530 N94-13277
Trial manufacture model and in-space verification method of deployable antenna p 530 N94-13278
Development and application of one dimensional deployable truss p 531 N94-13281
The study on large space structure assembly technology: The study on deployable truss structure, part 1
[NASDA-TMR-930002] p 541 N94-13658
The study on large space structure assembly technology: The study on deployable truss structure, part 2 and 3
[NASDA-TMR-930003-PT-2-3] p 541 N94-13659
Large space structures and systems in the space station era: A bibliography with indexes (supplement 05)
[NASA-SP-7085(05)] p 543 N94-14411

ORBITAL MANEUVERS
Guidance law development for aeroassisted transfer vehicles using matched asymptotic expansions
[NASA-CR-194523] p 508 N94-14538

ORBITAL POSITION ESTIMATION
Orbit determination error analysis based on the requirements of ADEOS mission
[NASDA-CNT-930008] p 532 N94-13644

ORBITAL RENDEZVOUS
STS-32 mission highlights resource tape
[NASA-TM-109291] p 531 N94-13631

ORDER-DISORDER TRANSFORMATIONS
Effect of pressure on order and stability in alloys: The case of Al-Ge
[DE93-013842] p 567 N94-12899
Transport properties of disordered porous media from the microstructure
[DE93-016065] p 806 N94-13152

ORGANIC COMPOUNDS
Integrated, flexible, and rapid geophysical surveying
[DE93-009989] p 712 N94-12906
Biomass production chamber air analysis of wheat study (BWT931)
[NASA-CR-194092] p 737 N94-13712
Development of an advanced spacecraft tandem mass spectrometer
[NASA-CR-194195] p 545 N94-13953
Portable acoustic wave sensor systems for real-time monitoring of volatile organic compounds
[DE93-013753] p 582 N94-14511

ORGANIC PHOSPHORUS COMPOUNDS
A characterization of carboxylesterases in rat and guinea pig: Their heterogeneity and role in detoxication of organophosphorus compounds
[NDRE-PUBL-93-1001] p 730 N94-14852

ORGANIC SUPERCONDUCTORS
The de Haas-van Alphen studies and Fermi surface properties of organic superconductors (ET)2X
[DE93-015157] p 623 N94-13925

ORGANIZATIONS
Here's the beef: A case study in organizational transformation p 667 N94-13163

ORGANOMETALLIC COMPOUNDS
Anchoring strategies for bimetallic species in zeolites
[DE93-015622] p 567 N94-12834

Growth experiment of organic metal crystal in low gravity (M-21) p 590 N94-13753
Effects of growth conditions and substrate orientation on the properties of InSb
[DE93-013766] p 812 N94-14344

OROGRAPHY
Numerical simulation and parameterization of orographic gravity waves p 713 N94-13647

ORR-SOMMERFELD EQUATIONS
Stability of spatially developing boundary layers p 640 N94-14605

ORTHOGONALITY
On a difference equation for generalizations of Charlier polynomials
[REPT-92-101] p 770 N94-14150
A hydrogen atom in the curved space: Orthogonality of radial wave functions with respect to the critical momentum
[DE93-626623] p 788 N94-14891

ORTHONORMAL FUNCTIONS
Mathematic methods and algorithms for real-time applications
[AD-A266776] p 771 N94-14789

ORTHOTROPIC PLATES
Measuring methods for CFRP laminates' bending and torsion rigidities characteristics p 529 N94-13272

ORTHOTROPIC SHELLS
On the orthotropicity assumption and discontinuity conditions of conical shells
[LR-703] p 673 N94-13787

OSCILLATING FLOW
Study of possible mechanisms of instability due to heat transfer
[INPE-5448-TDI/494] p 628 N94-12966
Stability of oscillatory two phase Couette flow
[NASA-CR-191501] p 636 N94-13817

OSCILLATIONS
Are there atmospheric neutrino oscillations?
[DE93-015550] p 783 N94-13890
Predicting the vibrations of a spinning inflated membrane
[DE93-010690] p 676 N94-14456

OSCILLATOR STRENGTHS
The International Colloquium on Atomic Spectra and Oscillator Strengths for Astrophysical and Laboratory Plasmas
[NASA-TM-109255] p 849 N94-13376

OSCILLATORS
Predicted performance of a dc beam driven FEM oscillator designed for fusion applications at 200-250 GHz
[DE93-013414] p 655 N94-13145
Development of UHF spark-switched L-C Oscillators
[DE93-015019] p 623 N94-13892
Investigation of an aeroelastic oscillator: Analysis of one-degree-of-freedom galloping with combined translational and torsional effects
[LR-707] p 527 N94-13906

OUTGASSING
BAKEOUT: A computer program for predicting diffusive outgassing from stainless steel
[DE93-012613] p 573 N94-14364

OUTPUT
Implementation and experimentation with a motion planning system
[ITN-93-85213] p 755 N94-14505

OVERVOLTAGE
Induced voltages at air gaps due to electromagnetic field caused by direct and indirect lightning strokes
[ITN-93-85203] p 599 N94-13237

OXIDATION
Absorption and damage thresholds of low defect density hafnia deposited with activated oxygen
[DE93-013853] p 655 N94-13243
Reduction of Pu(6) with hydrogen peroxide: Effects of plutonium, peroxide, and iron concentrations and of reaction time
[DE93-013598] p 564 N94-13487
Growth of Si spherical crystals and the surface oxidation (M-9) p 587 N94-13741
Homogeneous-hetergeneous combustion: Thermal and chemical coupling
[DE93-016050] p 565 N94-14403
Biomimetic methane oxidation
[DE93-013196] p 705 N94-14510
Molecular simulator: A basic tool for submicron MOS processes development
[LAAS-92484] p 814 N94-14697
Study of chemical reactions under the influence of ultrasound
[DE93-016458] p 778 N94-14867

OXIDATION RESISTANCE
Electrophoretic and electrolytic deposition of ceramic particles on porous substrates
[AD-A265141] p 575 N94-12812

OXIDATION-REDUCTION REACTIONS
Photocatalysis for the treatment of waste water: Applications involving the removal of metals
[DE93-011669] p 561 N94-12841
Experimental and kinetic modeling of acid/base and redox reactions over oxide catalysts
[DE93-016203] p 563 N94-13375
Charge storage and switching phenomena with molecular assemblies of metal complexes
[AD-A266673] p 787 N94-14778

OXIDE FILMS
Analysis of samples of reflector materials which are multicoated and metal samples with oxide coatings which have been exposed the space environment in LDEF testing
[NASA-CR-193647] p 575 N94-12789
Metastability of yttrium-oxides
[DE93-016548] p 813 N94-14440

OXIDES
Experimental and kinetic modeling of acid/base and redox reactions over oxide catalysts
[DE93-016203] p 563 N94-13375
Synthesis of organic ligands for f-element separations
[DE93-012915] p 554 N94-14290

OXYGEN
Preliminary results on the hydrological measurements in the Aegean Sea off Crete: Cruise, Georgia, 1989
[PREPRINT-736] p 725 N94-13500

OXYGEN ATOMS
Novel oxygen atom source for material degradation studies
[NASA-CR-191323] p 562 N94-13115
Atomic hydrogen and nitrogen distributions from atmosphere explorer measurements
[NASA-CR-194336] p 714 N94-13825
Atomic research
[NASA-CR-193843] p 788 N94-14905

OXYGEN CONSUMPTION
Variability of prediction of maximal oxygen concumption on the cycle ergometer using standard equations
[NASA-TP-3412] p 729 N94-14032

OXYGEN ISOTOPES
Maximum entropy spectral analysis of the geological time series of the oxygen isotope record from deep-sea cores
[INPE-5465-PRE/1773] p 725 N94-13728

OXYGEN PRODUCTION
Characterization of Spirulina biomass for CELSS diet potential
[NASA-CR-194123] p 729 N94-14097

OZONE
An examination of utility emissions contributions to elevated ozone concentrations in the Chicago area
[DE93-012852] p 708 N94-13495
Arctic ozone expedition
[NASA-TM-109301] p 708 N94-13602
Develop research plan for use of atlas data
[NASA-CR-194338] p 714 N94-13709
Chemistry and transport in a multi-dimensional model
[NASA-CR-194425] p 716 N94-13969
Effects of typhoon on TOMS data p 693 N94-14243
The role of the dynamics for the deviation of the total ozone from the long-term mean at the edge of the polar vortex p 694 N94-14250
The European Arctic ozone experiment: An investigation of Northern Hemisphere ozone depletion p 694 N94-14251
Space-based activities: SAM 2 and SAGE 2 p 694 N94-14252
New evidences supported the Wei hypothesis about the formation of the Antarctic ozone hole p 694 N94-14253
Signal and reference wavelengths for the elimination of SO2 cross sensitivity in remote measurements of tropospheric ozone with lidar
[GKSS/92/E/24] p 617 N94-14819
The mobile lidar system ARGOS for spatial resolution remote measuring of gaseous air pollutants
[GKSS/92/E/26] p 617 N94-14820

OZONE DEPLETION
Theoretical support for the Airborne Antarctic Ozone Experiment
[NASA-CR-193669] p 713 N94-13465
Airborne Arctic stratospheric expedition: Ozone
[NASA-TM-109312] p 515 N94-13606
Modeling of the partitioning of reactive odd nitrogen in the lower stratosphere using aircraft measurements of NOy, NO, and other trace species
[NASA-CR-194305] p 714 N94-13707
The role of the dynamics for the deviation of the total ozone from the long-term mean at the edge of the polar vortex p 694 N94-14250
The European Arctic ozone experiment: An investigation of Northern Hemisphere ozone depletion p 694 N94-14251
Space-based activities: SAM 2 and SAGE 2 p 694 N94-14252
New evidences supported the Wei hypothesis about the formation of the Antarctic ozone hole p 694 N94-14253
Long-range global warming impact of gaseous diffusion plant operation
[DE93-011686] p 710 N94-14459

P

P-N JUNCTIONS
Changes in electrical device characteristics during the formation of dislocations in situ in the TEM
[DE93-013910] p 808 N94-13694

P-TYPE SEMICONDUCTORS
Effects of growth conditions and substrate orientation on the properties of InSb
[DE93-013766] p 812 N94-14344

PACIFIC OCEAN
Linkage of anthropogenic aerosol to clouds and climate
[DE93-016434] p 719 N94-13080

PACKET SWITCHING
Technical support for digital systems technology development. Task order 1: ISP contention analysis and control
[NASA-CR-190758] p 537 N94-12809
Destination-directed, packet-switched architecture for a geostationary communications satellite network
[NASA-TP-3379] p 538 N94-13111
High speed packet switching
[NASA-CR-191334] p 759 N94-13177

PACKET TRANSMISSION
Characteristics of the amateur radio means of the Arsene satellite
[CNES-NT-131] p 605 N94-13950

PACKETS (COMMUNICATION)
Technical support for digital systems technology development. Task order 1: ISP contention analysis and control
[NASA-CR-190758] p 537 N94-12809
Mathematic methods and algorithms for real-time applications
[AD-A266776] p 771 N94-14789

PADE APPROXIMATION
A hybrid Pade-Galerkin technique for differential equations
[NASA-CR-191494] p 767 N94-13289

PAINTS
Study of novel conductive paints for solar cell electromagnetic fields
[DE93-015088] p 581 N94-14337

PAIR PRODUCTION
Top quark polarization and T-odd spin correlations as tools for testing (non) Standard Model predictions
[DE93-622956] p 778 N94-12847
A search for scalar leptoquarks in D0
[DE93-012780] p 779 N94-12954
Characteristics of a high energy muon(+)muon(-) collider based on electro-production of muons
[DE93-017154] p 790 N94-14893

PALLADIUM ALLOYS
A survey and analysis of experimental hydrogen sensors
[NASA-TM-106300] p 648 N94-13135

PALLADIUM COMPOUNDS
Muon spin relaxation studies of heavy fermion superconductors
[DE93-014576] p 815 N94-14773

PANEL METHOD (FLUID DYNAMICS)
VSAERO analysis of a Piper Cub aircraft p 516 N94-14616
Panel codes for aerodynamic analysis at NAL p 510 N94-14617

PANELS
The feasibility of producing aluminum-lithium structures for cryogenic tankage applications by laser beam welding
[NASA-CR-191527] p 595 N94-14026

PANORAMIC CAMERAS
Rover imaging system for the Mars rover/sample return mission
[NASA-CR-193413] p 649 N94-13464

PARABOLIC ANTENNAS
Environmental projects. Volume 15: Environmental assessment: Proposed 1-megawatt radar transmitter at the Mars site
[NASA-CR-194098] p 598 N94-13090
Structural design of hexa-link truss deployable antenna p 529 N94-13269
Thermal distortion measurement of TETRUS type thermal test model of large deployable antenna for mobile communications satellite p 529 N94-13270

PARABOLIC DIFFERENTIAL EQUATIONS
Open boundary conditions for incompletely parabolic systems
[FFI/RAPPORT-92/7029] p 770 N94-13971
The method of Laplace Transform MultiQuadrics (LTMQ) for the solution of the groundwater flow equation
[DE93-010408] p 637 N94-14053
Computation of nonequilibrium flows using PNS equations p 641 N94-14610
PARABOLIC REFLECTORS
High-flux testing of heat pipes for point-focus solar collector systems
[DE93-011581] p 628 N94-12884
Environmental projects. Volume 15: Environmental assessment: Proposed 1-megawatt radar transmitter at the Mars site
[NASA-CR-194098] p 598 N94-13090
Development of UHF spark-switched L-C Oscillators
[DE93-015019] p 623 N94-13892
PARACHUTES
Parachute system design, analysis, and simulation tool
[DE93-013755] p 501 N94-13260
PARALLEL COMPUTERS
Turbulence modeling of free shear layers for high-performance aircraft
[NASA-CR-193659] p 520 N94-12799
Beyond core: Making parallel computer I/O practical
[DE93-012347] p 758 N94-12878
Surrogates for numerical simulations; optimization of eddy-promoter heat exchangers
[NASA-CR-191510] p 629 N94-13074
Adaptive Transfer Function Networks
[DE93-014344] p 745 N94-13151
Parametric binary dissection
[NASA-CR-191496] p 762 N94-13184
The NAS parallel benchmarks
[NASA-TM-103863] p 740 N94-13200
USRA/RIACS
[NASA-CR-194334] p 750 N94-13932
A design methodology for portable software on parallel computers
[NASA-CR-194181] p 752 N94-14139
Development of parallel processing at NAL: A retrospect p 641 N94-14614
PARALLEL PLATES
Stability of oscillatory two phase Couette flow
[NASA-CR-191501] p 636 N94-13817
High counting rate resistive-plate chamber
[DE93-014928] p 651 N94-14452
PARALLEL PROCESSING (COMPUTERS)
Beyond core: Making parallel computer I/O practical
[DE93-012347] p 758 N94-12878
The 3-D massively parallel impact simulations using PCTH
[DE93-011593] p 670 N94-12908
A network evaluation and analysis tool
[DE93-012647] p 758 N94-12917
Parallelizing Timed Petri Net simulations
[NASA-CR-194278] p 758 N94-12938
Parallel implementation of an algorithm for Delaunay triangulation
[NASA-TM-103951] p 740 N94-12973
An experimental regional scale climate simulation laboratory
[DE93-015935] p 719 N94-13119
Parametric binary dissection
[NASA-CR-191496] p 762 N94-13184
Implementation of ADI: Schemes on MIMD parallel computers
[NASA-CR-193720] p 759 N94-13204
Advanced computers and simulation
[DE93-014354] p 740 N94-13286
A data distributed parallel algorithm for ray-traced volume rendering
[NASA-CR-191520] p 749 N94-13721
Tomographic methods in flow diagnostics
[NASA-TM-106330] p 650 N94-13876
Efficient, massively parallel eigenvalue computation
[NASA-CR-194289] p 760 N94-13921
USRA/RIACS
[NASA-CR-194334] p 750 N94-13932
Three, four, five, six or the complexity of scheduling with communication delays
[CWI-BS-R9229] p 751 N94-14004
VFGEN: A parallel volume fraction generator for hydrocodes
[DE93-011673] p 752 N94-14019
Quantum Monte Carlo by message passing
[DE93-012645] p 760 N94-14177
Hybrid S(sub N)/Monte Carlo research and results
[DE93-012677] p 773 N94-14178
An efficient parallel algorithm for matrix-vector multiplication
[DE93-015125] p 754 N94-14399
An overview of parallel scientific visualization
[DE93-017105] p 755 N94-14521
Paradigms for very fast parallel algorithms
[ITN-93-85212] p 755 N94-14556
Development of parallel processing at NAL: A retrospect p 641 N94-14614
Parallel O(log n) algorithms for open- and closed-chain rigid multibody systems based on a new mass matrix factorization technique p 679 N94-14636
On the solution of a class of graph problems by parallel algorithms
[LAAS-92514] p 756 N94-14712
Identification of continuous-time dynamical systems: Neural network based algorithms and parallel implementation
[DE93-014427] p 766 N94-14737
The development of a scalable parallel 3-D CFD algorithm for turbomachinery
[NASA-CR-193604] p 664 N94-14848
PARALLEL PROGRAMMING
Calculating intersections of surfaces in screen space
[NASA-CR-191498] p 745 N94-13185
Hashing and rehashing in emulated shared memory
[CWI-CS-R9240] p 740 N94-13525
Fast parallel string prefix-matching
[AD-A267758] p 760 N94-13924
A design methodology for portable software on parallel computers
[NASA-CR-194181] p 752 N94-14139
Paradigms for very fast parallel algorithms
[ITN-93-85212] p 755 N94-14556
Execution methods, and parallel virtual machines for distributed implementation of the LCS parallel programming language
[LAAS-93032] p 761 N94-14716
PARAMETER IDENTIFICATION
Bounds on time delay estimation given unknown signal spectral parameters
[ITN-93-85194] p 601 N94-13566
Parameter identification of a model of the process of software development
[REPT-93-008] p 750 N94-13807
PARAMETERIZATION
A parameterization of cloud droplet nucleation
[DE93-007998] p 718 N94-12903
Extremal polygon containment problems and other issues in parametric searching
[ITN-93-85214] p 771 N94-14506
Scattering calculations and confining interactions
[NASA-CR-194242] p 786 N94-14549
On l(1): Optimal decentralized performance p 661 N94-14643
Search for subgrid scale parameterization by projection pursuit regression p 643 N94-14749
PARITY
No-lost theorem for parity violating nucleon-nucleon scattering experiments
[DE93-012737] p 779 N94-12949
On the theory of the decaying developed turbulence with spontaneous parity violation
[DE93-623190] p 632 N94-13511
Coherent excitation of autoionizing resonances by electron impact
[DE93-018169] p 785 N94-14419
Measuring parity violation using the neutron capture reaction
[DE93-016629] p 786 N94-14514
PARTIAL DIFFERENTIAL EQUATIONS
Newton iterative methods for large scale nonlinear systems
[DE93-015357] p 767 N94-13025
Simplification-driven automated partial evaluation
[DE93-012890] p 768 N94-13391
Integrable system describing surfaces of non-constant curvature
[PREPRINT-734] p 768 N94-13499
PARTIAL PRESSURE
Binary homogeneous nucleation: Temperature and relative humidity fluctuations and non-linearity
[DE93-007884] p 709 N94-13911
PARTICLE ACCELERATION
Wake-field and space charge effects on high brightness beams calculations and measured results for the laser driven photoelectrons at BNL-ATF
[DE93-015787] p 659 N94-14572
PARTICLE ACCELERATOR TARGETS
Charged-particle evaluation methodology at Lawrence Livermore National Laboratory
[DE93-013429] p 781 N94-13251
Application of synchrotron radiation in chemical dynamics
[DE93-015040] p 563 N94-13411
Longitudinal beam dynamics for heavy ion fusion
[DE93-013850] p 789 N94-13727
Characteristics of a high energy muon(+)muon(-) collider based on electro-production of muons
[DE93-017154] p 790 N94-14893
E789 and P865: High-rate fixed-target studies of charm and beauty
[DE93-017223] p 788 N94-14898
PARTICLE ACCELERATORS
Stripping efficiencies for 277 MeV/amu gold beam on copper foils
[DE93-014306] p 569 N94-13221
Study of electroweak interactions
[DE93-015067] p 782 N94-13412
Characteristics of a high energy muon(+)muon(-) collider based on electro-production of muons
[DE93-017154] p 790 N94-14893
PARTICLE BEAMS
Stripping efficiencies for 277 MeV/amu gold beam on copper foils
[DE93-014306] p 569 N94-13221
Intra-blade quantitative transonic flow measurements at the DRA Pyestock Isentropic Light Piston Facility using PIV (Particle Image Velocimetry)
[RAE-TM-AERO/PROP-21] p 509 N94-14706
PARTICLE COLLISIONS
Measurements of transverse energy and forward energy in high-energy nuclear collisions
[DE93-012755] p 788 N94-12817
Low energy neutral atom imaging techniques
[DE93-012744] p 779 N94-12950
Kinetic studies following state-selective laser excitation
[DE93-012970] p 654 N94-13013
EBIT Trapping Program
[DE93-014422] p 788 N94-13208
Nuclear fusion of protons with ions of boron
[DE93-014284] p 781 N94-13219
Metastable enhancement of C(+) and O(+) capture reactions
[DE93-015075] p 807 N94-13373
Study of electroweak interactions
[DE93-015067] p 782 N94-13412
Electron emission resulting from fast ion impact on thin metal foils: Implications of these data for development of track structure models
[DE93-013506] p 782 N94-13485
Inclusive single muons at DO
[DE93-012779] p 783 N94-13494
High energy hadron-hadron collisions
[DE93-015584] p 784 N94-13927
Top quark search: Results and prospects at Fermilab
[DE93-013016] p 786 N94-14524
Scattering calculations and confining interactions
[NASA-CR-194242] p 786 N94-14549
Theoretical antideuteron-nucleus absorptive cross sections p 786 N94-14551
PARTICLE DENSITY (CONCENTRATION)
Effects of depositon rate on Bi2Sr2CaCu2O(8+x) and Bi2Sr(1.6)La(0.4)CuO(6+x) epitaxial thin film growth by pulsed-laser ablation
[DE93-015797] p 812 N94-14362
PARTICLE DIFFUSION
Diffusion in liquid state and solidification of binary system (M-7) p 587 N94-13739
Turbulent particle dispersion in confined swirling flows
[DLR-FB-92-32] p 637 N94-14045
PARTICLE INTERACTIONS
Predicted performance of a dc beam driven FEM oscillator designed for fusion applications at 200-250 GHz
[DE93-013414] p 655 N94-13145
Beam halo formation from space-charge dominated beams in uniform focusing channels
[DE93-014458] p 789 N94-13209
Measuring strangeness in the nucleon
[DE93-014861] p 785 N94-14471
PARTICLE MASS
Comparing the Z(sup 0) mass and inclusive widths to the standard electroweak theory
[PREPRINT-731] p 787 N94-14721
PARTICLE MOTION
Stochastic dynamics: Crossover from 1/f(sup 3) to flicker noise
[DE93-622862] p 772 N94-12896
Kinetic simulations of ultra-intense laser plasma interactions and a novel method of generating odd harmonics
[DE93-014418] p 797 N94-13207
Numerical studies of spray combustion in liquid-fueled engines p 564 N94-13685
Stormtime transport of ring current and radiation belt ions
[NASA-CR-194416] p 714 N94-13793
PARTICLE PRODUCTION
Detection of hot muonic hydrogen atoms emitted in vacuum using x-rays
[DE93-010253] p 778 N94-12860
HIJET with AGS physics and N(sup *)'s
[DE93-014022] p 780 N94-13097

Neutral strange particle production at the AGS
[DE93-014044] p 780 N94-13098
Further study of the X(1910) meson
[DE93-621443] p 782 N94-13362
Study of electroweak interactions
[DE93-015067] p 782 N94-13412
Inclusive single muons at DO
[DE93-012779] p 783 N94-13494
Effects of additional isoscalar vector bosons in e(sup +)e)(sup -)(yields)ff-bar processes at the TRISTAN and LEP energies
[DE93-621451] p 783 N94-13506
Top quark search: Results and prospects at Fermilab
[DE93-013016] p 786 N94-14524
E789 and P865: High-rate fixed-target studies of charm and beauty
[DE93-017223] p 788 N94-14898

PARTICLE SPIN
Top quark polarization and T-odd spin correlations as tools for testing (non) Standard Model predictions
[DE93-622956] p 778 N94-12847
Electromagnetic deflection of spinning particles
[DE93-622866] p 778 N94-12858
Aspects of symmetry violation
[DE93-011003] p 779 N94-12997
Calculation of electron-lithium scattering using the coupled-channel optical method
[DE93-623049] p 806 N94-13226
Magnetic interactions and disorder - phase transitions in dilute spin-glasses and high temperature superconductors
[ITN-93-85217] p 815 N94-14825

PARTICLE THEORY
Electric charge quantization
[DE93-622901] p 778 N94-12845
Radiative corrections in the strongly interacting limit of the standard electroweak model
[DE93-013906] p 780 N94-13018
Comparing the Z(sup 0) mass and inclusive widths to the standard electroweak theory
[PREPRINT-731] p 787 N94-14721

PARTICLE TRACKS
EGS (underscore) windows 2: An enhanced graphical interface to EGS
[DE93-010447] p 746 N94-13382
Distributed processor Monte Carlo: MCNP results on a 16-node IBM cluster
[DE93-012639] p 752 N94-14176

PARTICLE TRAJECTORIES
Low energy neutral atom imaging techniques
[DE93-012744] p 779 N94-12950

PARTICLES
Bridging the gap between the Rayleigh and Thomson limits for various convex bodies
[DSIS-93-00613] p 607 N94-14204

PARTICULATES
Discussion of stress tensor nonuniqueness with application to nonuniform, particulate systems
[DE93-014352] p 816 N94-13206
Nonlinear relationships between particulate absorption and chlorophyll: Detritus or pigment packaging?
[AD-A266806] p 731 N94-14899

PARTITIONS (MATHEMATICS)
Parametric binary dissection
[NASA-CR-191496] p 762 N94-13184

PARTONS
Quark and gluon jets at CDF
[DE93-014919] p 783 N94-13884

PASSIVITY
Effect of microstructure on passive film formation and breakdown on Al alloys
[AD-A265339] p 569 N94-13050

PASTES
Automated crack identification for cement paste
[AD-A265753] p 665 N94-13042

PATTERN RECOGNITION
VISART: Artificial vision for industrial use. A comprehensive system
[INPE-5379-TDI/474] p 665 N94-12941
Feature extraction and classification algorithms for high dimensional data
[NASA-CR-194298] p 743 N94-13023
View generated database
[NASA-CR-191397] p 822 N94-13116
Design of partially supervised classifiers for multispectral image data
[NASA-CR-194299] p 823 N94-13192
Close range 3-D position sensing using stereo vision and point-of-correspondance through mathematical morphology
[ISBN-0-315-61012-3] p 763 N94-13515
A review and analysis of neural networks for classification of remotely sensed multispectral imagery
[NASA-CR-194291] p 763 N94-13603
Fast parallel string prefix-matching
[AD-A267758] p 760 N94-13924
Determination of position and orientation of rigid bodies from image segments
[FFI-92-4005] p 752 N94-14039
Feature discovery on segmented objects in SAR imagery using self-organizing neural networks
[DE93-010685] p 686 N94-14056
Identification and interpretation of patterns in rocket engine data
[NASA-CR-194534] p 552 N94-14309
Obstacle detection by recognizing binary expansion patterns
[NASA-CR-194415] p 514 N94-14495
Computer vision and sensor fusion for detecting buried objects
[DE93-012605] p 700 N94-14566
Retrieval properties of neural networks with infinitely many marked patterns
[PREPRINT-729] p 766 N94-14718
Speaker independent recognition of isolated words using vector quantization and neural networks
[ETN-93-94390] p 616 N94-14724

PAYLOADS
Temperature dependence of diffusivities, preliminary definition phase
[NASA-CR-192613] p 648 N94-13326
STS-53 Space Shuttle mission report
[NASA-CR-193101] p 535 N94-13934
Payload/GSE/data system interface: Users guide for the VPF (Vertical Processing Facility)
[NASA-CR-194385] p 532 N94-14148
ECS: Eighth year in orbit
[ESA-BR-82] p 543 N94-14352
STS-35 EVA payload training in WETF
[NASA-TM-109492] p 739 N94-14790

PEBBLE BED REACTORS
Nuclear thermal propulsion engine based on particle bed reactor using light water steam as a propellant
[DE93-014336] p 552 N94-14111

PEEK
Development of time-dependent orthotropic constitutive law of a thermoplastic composite material
p 556 N94-13595

PENETRATION
Measurement of penetration depth lambda(T) in YBa2Cu3O(7-delta) thin film
[DE93-014587] p 810 N94-14122
Collisions and separations in 2D hydrodynamical code
[ITN-93-85225] p 639 N94-14503
The motion of a conical shaped liner driven by explosive load
[ITN-93-85215] p 585 N94-14507

PEPTIDES
Solitons and 1/f noise in molecular chains
[DE93-622898] p 778 N94-12879
The evolution of energy-transducing systems: Studies with archaebacteria
[NASA-CR-194130] p 728 N94-13562

PERCOLATION
Study of multicomponent diffusion and transport phenomena
[DE93-015095] p 804 N94-13005

PERFORMANCE
Defining the performance gap: Conducting a self-assessment p 666 N94-13155

PERFORMANCE PREDICTION
The identification of ability requirements and selection instruments for fighter pilot training
[AD-A266340] p 735 N94-13582
Stochastic performance modeling and evaluation of obstacle detectability with imaging range sensors
[NASA-CR-194510] p 605 N94-13946
A performance prediction model for a fault-tolerant computer during recovery and restoration
[NASA-CR-194490] p 741 N94-14136
Aeropropulsion test and evaluation methods
p 506 N94-14165

PERFORMANCE TESTS
Digital sound: The selection of critical programme material and preparation of recordings for CCIR tests on low bit-rate codecs
[BBC-RD-1993/1] p 598 N94-12925
Digital sound: Subjective tests on commentary-quality codecs
[BBC-RD-1993/2] p 598 N94-12926
Evaluation for membrane components of water recycling system
[NAL-TM-646] p 737 N94-13388
Arc-heating tests of thermal protection system materials for the H-2 rocket fairing
[NAL-TR-1181] p 551 N94-13455
Selection of behavioral tasks and development of software for evaluation of rhesus monkey behavior during spaceflight
[NASA-CR-194176] p 728 N94-13865
The Large Area Pulsed Solar Simulator (LAPSS)
[NASA-CR-194507] p 703 N94-13940
Stochastic performance modeling and evaluation of obstacle detectability with imaging range sensors
[NASA-CR-194510] p 605 N94-13946
Battery testing at Argonne National Laboratory
[DE93-011761] p 624 N94-14012
Aerodynamic and aerothermal facilities 2: Continuous flow high enthalpy facilities p 506 N94-14160
Aeropropulsion test and evaluation methods
p 506 N94-14165
Qualification test of the Ross Double Planetary Mixer
[NASA-CR-192600] p 652 N94-14497
Control structural interaction testbed: A model for multiple flexible body verification p 544 N94-14649
Performance evaluation of the honeywell GG1308 miniature ring laser gyroscope
[AD-A266694] p 653 N94-14782

PERIODIC VARIATIONS
Variations common to the interplanetary magnetic field, the zonal atmospheric circulation and the Earth's rotation
[COMMUNICATIONS-SER-B-157] p 837 N94-13504
Maximum entropy spectral analysis of the geological time series of the oxygen isotope record from deep-sea cores
[INPE-5465-PRE/1773] p 725 N94-13728
AMIP: Diagnostic subproject on the variability in the tropics: Synoptic to intraseasonal time scales
[DE93-009287] p 721 N94-13914
On the space-time ocean current variability and its effects on the length-of-day
[ISBN-0-315-59510-8] p 726 N94-14205
ROSAT observations of the binary Be-star/radio pulsar PSR1259-63
[NASA-CR-194394] p 832 N94-14357
Structural change of graphite during electron irradiation
[DE93-015961] p 582 N94-14531

PERMEABILITY
Transport properties of disordered porous media from the microstructure
[DE93-016065] p 806 N94-13152
Locally non-uniform finite-difference time domain with application to stealth, crosstalk, and narrow apertures
[DE93-013958] p 601 N94-13696
Upgrading of raw natural gas using high-performance polymer membranes
[DE93-014041] p 566 N94-14586

PERMITTIVITY
Locally non-uniform finite-difference time domain with application to stealth, crosstalk, and narrow apertures
[DE93-013958] p 601 N94-13696

PEROXIDES
Measurement of HO2 and other trace gases in the stratosphere using a high resolution far-infrared spectrometer at 28 km
[NASA-CR-194175] p 714 N94-13816

PERSONAL COMPUTERS
A PC-PCL-based control system for the high-voltage pulsed-power operation of the Intense Diagnostic Neutral Beam (IDNB) Experiment
[DE93-014144] p 797 N94-13100
Mass market computers for software development
[ERB-1035] p 741 N94-13547
Development of an automated film-reading system for ballistic ranges
[NASA-CR-194398] p 650 N94-13815
PC viruses: How do they do that?
[DE93-012581] p 753 N94-14289
Some tools of the trade we've developed for our cross-section calculations
[DE93-013835] p 786 N94-14569
ASTEC and MODEL: Controls software development at Goddard Space Flight Center p 678 N94-14628

PERSONNEL
Building a quality culture in the Office of Space Flight: Approach, lessons learned and implications for the future p 667 N94-13164
Environmental awareness
[DE93-014192] p 707 N94-13218
Information requirements of self-managing teams
[DE93-010319] p 824 N94-14048

PERSONNEL DEVELOPMENT
Program/project management resource lists
[NASA-TM-109268] p 822 N94-13107

PERSONNEL MANAGEMENT
Information requirements of self-managing teams
[DE93-010319] p 824 N94-14048

PERSONNEL SELECTION
Readiness to perform testing: A critical analysis of the concept and current practices
[DOT/FAA/AM-93/13] p 732 N94-13193

PERTURBATION
A 3D gyrokinetic particle-in-cell simulation of fusion plasma microturbulence on parallel computers
[DE93-012503] p 794 N94-12846

A classical instability for black strings and p-branes
[DE93-014577] p 839 N94-14116
PERTURBATION THEORY
Stability of subharmonics and escape phenomena in the twin-well potential duffing system p 775 N94-13235
A hybrid Pade-Galerkin technique for differential equations
[NASA-CR-191494] p 767 N94-13289
A classical instability for black strings and p-branes
[DE93-014577] p 839 N94-14116
Radiation perturbation theory in gravity and quantum universe as a hydrogen atom
[DE93-626621] p 849 N94-14889
PETRI NETS
Parallelizing Timed Petri Net simulations
[NASA-CR-194278] p 758 N94-12938
Simulator for heterogeneous dataflow architectures
[NASA-CR-191545] p 622 N94-13797
PETROLEUM PRODUCTS
Laser-induced fluorescence over optical fibers for real time in situ measurement of petroleum hydrocarbons in seawater
[AD-A265106] p 790 N94-12863
PH
Promotion of geothermal energy development in 1991
[DE93-799058] p 701 N94-13215
Canonical correlation of waste glass compositions and durability, including pH
[DE93-012754] p 578 N94-13493
PHASE CONTRAST
Measurements of edge fluctuations by phase contrast imaging on DIII-D
[DE93-014018] p 802 N94-14579
PHASE CONTROL
Proceedings of the 11th Space Surveillance Workshop, volume 1
[AD-A265120] p 531 N94-13358
PHASE DIAGRAMS
Multiphase equation of state for iron
[DE93-013956] p 568 N94-12977
First-principles studies of phase stability and the structural and dynamical properties of hydrogen-metal systems
[DE93-016129] p 570 N94-13374
How to read a phase equilibrium diagram for high-temperature ceramics material as main object
[DE93-512333] p 582 N94-14513
Is K3C60 a line phase?
[DE93-016700] p 813 N94-14517
Statics and kinetics of phase transformations in bcc Fe-Cr
[DE93-013839] p 574 N94-14793
Influence of heat treatment on microstructure of Ti-35wt Al prepared by elemental powder metallurgy
[GKSS/92/E/27] p 574 N94-14821
PHASE ERROR
Ionospheric effects on a wide-bandwidth, polarimetric, space-based, synthetic-aperture radar
[DE93-015084] p 612 N94-14512
PHASE LOCKED SYSTEMS
Sea surface temperature forcing and phase locking of Nordeste precipitation
[DE93-011873] p 723 N94-14426
PHASE MODULATION
Trellis coding with Continuous Phase Modulation (CPM) for satellite-based land-mobile communications
[NASA-CR-191325] p 604 N94-13909
PHASE RULE
Workshop on Formation of Supermolecular Structures in Composite Fluid: Phase Rule and Dynamics
[DE93-782887] p 581 N94-14421
How to read a phase equilibrium diagram for high-temperature ceramics material as main object
[DE93-512333] p 582 N94-14513
PHASE SEPARATION (MATERIALS)
The Lindemann criterion of melting for pure and mixed ionic crystals
[ITN-93-85210] p 814 N94-14554
PHASE SHIFT
The MRIS feasibility study
[NASA-TM-107763] p 597 N94-12804
Non-scanned LADAR imaging and applications
[DE93-013772] p 655 N94-13261
Advanced ballistic range technology
[NASA-CR-194530] p 533 N94-14540
PHASE SHIFT KEYING
Envelope and instantaneous frequency estimation of narrowband modulated signals
[DREO-TN-92-3] p 605 N94-14033
Multiple-symbol differential detection of DPSK with frequency offset
[DREO-TN-92-5] p 606 N94-14063
PHASE STABILITY (MATERIALS)
Electronic structure and phase stability properties in ternary substitutional alloys
[DE93-013848] p 569 N94-13137
PHASE TRANSFORMATIONS
Recovery of materials impacted at high velocity
[DE93-014150] p 576 N94-12885
Effect of pressure on order and stability in alloys: The case of Al-Ge
[DE93-013842] p 567 N94-12899
First-principles studies of phase stability and the structural and dynamical properties of hydrogen-metal systems
[DE93-016129] p 570 N94-13374
The microstructural response of near gamma-TiAl+W to heat treatment
[DSIS-93-00237] p 571 N94-13840
Phase transition in polymer blends and structure of ionomers and copolymers
[DE93-016256] p 579 N94-13978
Monte Carlo simulation of the OCP freezing transition
[DE93-013039] p 811 N94-14313
Effect of spontaneous decay of superconductor quasiparticles in the tunneling density of states
[DE93-012681] p 811 N94-14339
Workshop on Formation of Supermolecular Structures in Composite Fluid: Phase Rule and Dynamics
[DE93-782887] p 581 N94-14421
Computational diagnostics for detecting phase transitions during nanoindentation
[DE93-016536] p 813 N94-14439
Immiscible phase incorporation during directional solidification of hypermonotectics
[NASA-CR-194412] p 565 N94-14480
Statics and kinetics of phase transformations in bcc Fe-Cr
[DE93-013839] p 574 N94-14793
Phases and phase transitions of polymeric liquid crystals: A high resolution x ray diffraction and light scattering study
[ITN-93-85218] p 816 N94-14826
PHASED ARRAYS
Electrical characterization of the JET A(sub 2) antenna: Comparison of model with measurements Wade, T.
[DE93-012964] p 607 N94-14291
Direct electron heating and current drive with fast waves in D3-D
[DE93-013028] p 801 N94-14293
Experimental instrumentation system for the Phased Array Mirror Extendible Large Aperture (PAMELA) test program
[NASA-CR-194421] p 705 N94-14430
PHENOLOGY
Analytical framework for modeling scale-related variabilities in remote sensing p 685 N94-13592
PHENOMENOLOGY
Nonlinear analysis, scientific computation, and continuum mechanics applied to the science of materials
[AD-A266641] p 817 N94-14680
PHILOSOPHY
Heidegger's thinking p 736 N94-13442
PHOSPHAZENE
Synthetic lubricants and high-performance functional fluids: Phosphazenes
[ARL-TR-45] p 580 N94-14126
PHOSPHORUS
Machining aspects of nickel-phosphorus coatings
[DE93-013037] p 580 N94-14311
Multicrystalline silicon solar cells: Gettering optimization and characterization
[DE93-015001] p 705 N94-14861
PHOTOCATHODES
Gamma-insensitive optical focal plane array
[DE93-013100] p 792 N94-14317
Absolute detection efficiency of a micro-channel plate detector to x rays in the 1-100 KeV energy range
[DE93-012592] p 789 N94-14460
PHOTOCHEMICAL REACTIONS
Infrared absorption spectroscopy and chemical kinetics of free radicals
[DE93-015078] p 562 N94-13004
Diagnostic studies of the HxOy-NxOy-O3 photochemical system using data from NASA GTE field expeditions
[NASA-CR-193672] p 706 N94-13170
Modeling of the partitioning of reactive odd nitrogen in the lower stratosphere using aircraft measurements of NOy, NO, and other trace species
[NASA-CR-194305] p 714 N94-13707
Chemistry and transport in a multi-dimensional model
[NASA-CR-194425] p 716 N94-13969
Photochemical dynamics of surface oriented molecules
[DE93-016289] p 784 N94-13983
Lawrence Berkeley Laboratory Chemical Sciences Division
[DE93-015260] p 851 N94-14401
PHOTOCONDUCTIVITY
Electrical and optical properties of multiple quantum well structures and their applications to infrared detectors
[FFI-92/7012] p 809 N94-14010
PHOTODIODES
An acoustic charge transport imager for high definition television applications
[NASA-CR-194518] p 650 N94-14029
Vacuum ultraviolet instrumentation for solar irradiance and thermospheric airglow
[NASA-CR-194525] p 652 N94-14684
PHOTODISSOCIATION
Application of synchrotron radiation in chemical dynamics
[DE93-015040] p 563 N94-13411
Thermochemistry of transition metal clusters
[DE93-016201] p 571 N94-13977
Lawrence Berkeley Laboratory Chemical Sciences Division
[DE93-015260] p 851 N94-14401
Investigation of the feasibility of optical diagnostic measurements at the exit of the SSME
[NASA-CR-193832] p 553 N94-14682
PHOTOELECTRIC EMISSION
Canted magnetic moments at the Gd(0001) surface
[DE93-014327] p 805 N94-13102
Spin polarized photoemission studies of interfacial and thin film magnetism
[DE93-014326] p 580 N94-14142
Effect of spontaneous decay of superconductor quasiparticles in the tunneling density of states
[DE93-012681] p 811 N94-14339
High-order harmonic generation with short-pulse lasers
[DE93-016532] p 659 N94-14594
PHOTOELECTROCHEMICAL DEVICES
Surface science instrumentation for the study of important catalytic and electrochemical interfaces
[DE93-015068] p 563 N94-13413
PHOTOELECTROCHEMISTRY
Surface science instrumentation for the study of important catalytic and electrochemical interfaces
[DE93-015068] p 563 N94-13413
PHOTOELECTRON SPECTROSCOPY
Analysis of samples of reflector materials which are multicoated and metal samples with oxide coatings which have been exposed the space environment in LDEF testing
[NASA-CR-193647] p 575 N94-12789
Surface science instrumentation for the study of important catalytic and electrochemical interfaces
[DE93-015068] p 563 N94-13413
Applications of surface science to solid lubricants
[SMC-TR-93-24] p 579 N94-13903
Vacuum ultraviolet instrumentation for solar irradiance and thermospheric airglow
[NASA-CR-194525] p 652 N94-14684
PHOTOELECTRONS
Research in cosmic and gamma ray astrophysics: Cosmic physics portion
[NASA-CR-194127] p 847 N94-13211
Surface science instrumentation for the study of important catalytic and electrochemical interfaces
[DE93-015068] p 563 N94-13413
Many-body corrections in XAFS
[DE93-011002] p 563 N94-13478
Results from a water-Cerenkov array
[DE93-012715] p 849 N94-14461
PHOTOEXCITATION
Ultrafast photoinduced electron transfer reactions in supramolecular arrays: Studies of electronic coupling and solvation
[DE93-012910] p 782 N94-13484
Photochemical dynamics of surface oriented molecules
[DE93-016289] p 784 N94-13983
The E2 N(yields)(Delta) transition from polarized Compton scattering
[DE93-012522] p 785 N94-14363
PHOTOGRAMMETRY
Photogrammetric methods for trajectory measurements
[NLR-TP-91166-U] p 650 N94-13527
Obtaining digital regional planning information from aerial pictures
[REPT-228] p 700 N94-14810
PHOTOGRAPHIC FILM
Development of an automated film-reading system for ballistic ranges
[NASA-CR-194398] p 650 N94-13815
PHOTOGRAPHY
Image motion photography
[DE93-013962] p 653 N94-14858
PHOTOINTERPRETATION
Preparations for and first results of the calibration and interpretation of ERS-1 SAR imagery over land
[BCRS-92-13] p 684 N94-13123
PHOTOIONIZATION
New infrared photon absorption processes
[DE93-017017] p 780 N94-13071

A search for strong-field direct two electron ionization using coincidence spectroscopy
[DE93-013435] p 781 N94-13241
The reionization of the intergalactic medium
p 838 N94-13651
Was 49: Mirror for a hidden Seyfert 1 galaxy
[NASA-CR-194537] p 840 N94-14685

PHOTOLITHOGRAPHY
Field emitter array RF amplifier development project. Phase 1: Cathode technology development
[AD-A266346] p 622 N94-13776

PHOTOLUMINESCENCE
Free-exciton recombination in GaAs
[DE93-009843] p 809 N94-14079

PHOTOLYSIS
Photocatalysis for the treatment of waste water: Applications involving the removal of metals
[DE93-011669] p 561 N94-12841
Application of synchrotron radiation in chemical dynamics
[DE93-015040] p 563 N94-13411
Thermochemistry of transition metal clusters
[DE93-016201] p 571 N94-13977

PHOTOMETERS
Barium fluoride research and development at Lawrence Livermore National Laboratory
[DE93-014682] p 807 N94-13405
Investigation of the feasibility of optical diagnostic measurements at the exit of the SSME
[NASA-CR-193832] p 553 N94-14682

PHOTOMETRY
Simulating the daylight performance of fenestration systems and spaces of arbitrary complexity: The IDC method
[DE93-015177] p 704 N94-14333
Activities report of the National Electrotechnical Institute Galileo Ferraris
[ETN-93-94224] p 627 N94-14812

PHOTOMICROGRAPHY
The effect of crystal tilt on high resolution micrographs of small metal particles
[DE93-013915] p 574 N94-14795

PHOTOMULTIPLIER TUBES
Calibration of the receiver channel for the GOPEX precursor experiments p 610 N94-14387
Absolute detection efficiency of a micro-channel plate detector to x rays in the 1-100 KeV energy range
[DE93-012592] p 789 N94-14460

PHOTON-ELECTRON INTERACTION
Variance reduction unique to coupled electron/photon Monte Carlo transport
[DE93-014999] p 782 N94-13409
Adiabatic and non adiabatic effects in Free Electron Laser (FEL) non linear interactions
[ITN-93-85224] p 659 N94-14547

PHOTONICS
Energy and technology review, March 1993
[DE93-013941] p 849 N94-13019

PHOTONS
Metal-semiconductor, composite radiation detectors
[DE93-013313] p 619 N94-12994
New infrared photon absorption processes
[DE93-017017] p 780 N94-13071
EGS (underscore) windows 2: An enhanced graphical interface to EGS
[DE93-010447] p 746 N94-13382
Variance reduction unique to coupled electron/photon Monte Carlo transport
[DE93-014999] p 782 N94-13409
A positron annihilation radiation telescope using Laue diffraction in a crystal lens
[DE93-012905] p 848 N94-13483
ROSAT observations of the binary Be-star/radio pulsar PSR1259-63
[NASA-CR-194394] p 832 N94-14357
The E2 N(yields)(Delta) transition from polarized Compton scattering
[DE93-012522] p 785 N94-14363
Measurements of the spatial structure and directivity of 100 KeV photon sources in solar flares using PVO and ISEE-3 spacecraft
[NASA-CR-194080] p 845 N94-14492
Multiple Schroedinger cats from multilevel atoms
[DE93-013412] p 786 N94-14526
Laser lithography by photon scanning tunneling microscopy
[DE93-015962] p 660 N94-14863

PHOTONUCLEAR REACTIONS
Some tools of the trade we've developed for our cross-section calculations
[DE93-013835] p 786 N94-14569

PHOTOSYNTHESIS
Ultrafast photoinduced electron transfer reactions in supramolecular arrays: Studies of electronic coupling and solvation
[DE93-012910] p 782 N94-13484
Gordon Research Conference on Chronobiology, 1991
[AD-A266354] p 728 N94-13698
Characterization of Spirulina biomass for CELSS diet potential
[NASA-CR-194123] p 729 N94-14097

PHOTOTHERMAL CONVERSION
High-flux testing of heat pipes for point-focus solar collector systems
[DE93-011581] p 628 N94-12884

PHOTOVOLTAIC CELLS
Photovoltaics: Contract lists, fiscal year 1992
[DE93-000093] p 701 N94-12902
Photovoltaics: Program overview, fiscal year 1992
[DE93-000055] p 701 N94-12914
A photovoltaic catenary-tent array for the Martian surface
[NASA-TM-106306] p 621 N94-13194
Activities of the Basic Sciences Branch
[DE93-010012] p 851 N94-14455

PHOTOVOLTAIC CONVERSION
The 1992 JSEE/JWEA Joint Conference
[DE93-793955] p 700 N94-12822
Photovoltaic Subcontract Program
[DE93-000092] p 700 N94-12868
Photovoltaics: Contract lists, fiscal year 1992
[DE93-000093] p 701 N94-12902
Photovoltaics: Program overview, fiscal year 1992
[DE93-000055] p 701 N94-12914
Low temperature metal-organic chemical vapor deposition growth processes for high efficiency solar cells
[DE92-010562] p 702 N94-13386
Photovoltaic advanced research and development project: Solar radiation research
[DE92-016430] p 704 N94-14350
Activities of the Basic Sciences Branch
[DE93-010012] p 851 N94-14455

PHYSICAL EXERCISE
Work/rest schedules and performance of F/A-18 aviators during Fleet Exercise 1992
[AD-A265826] p 735 N94-12982
Metabolic rate measurements comparing supine with upright upper-body exercises
[NASA-CR-4549] p 729 N94-14028
Variability of prediction of maximal oxygen concumption on the cycle ergometer using standard equations
[NASA-TP-3412] p 729 N94-14032

PHYSICAL FACTORS
Review of mathematical and physical basis of two-phase flow modeling
[KFK-4759] p 642 N94-14708

PHYSICAL FITNESS
Improving physical performance by chemical stimulation
[DSIS-92-03763] p 728 N94-13823

PHYSICAL PROPERTIES
Synthetic lubricants and high-performance functional fluids: Phosphazenes
[ARL-TR-45] p 580 N94-14126

PHYSICS
Event-driven simulation in SELMON: An overview of EDSE
[NASA-CR-194505] p 749 N94-13784
Generic results of the space physics community survey
[NASA-CR-194538] p 818 N94-13984

PHYSIOLOGICAL EFFECTS
Calcitonin control of calcium metabolism during weightlessness
[NASA-CR-193622] p 731 N94-12960
Physiological Anatomical Rodent Experiment (PARE).04 Feasibility Test 1
[NASA-CR-194423] p 728 N94-13473
The problem of the sonic boom for future high-speed transport aircraft
[ESA-TT-1286] p 776 N94-13692
An evaluation of noise and its effects on shuttle crewmembers during STS-50/USML-1
[NASA-TM-104775] p 735 N94-13961
Variability of prediction of maximal oxygen concumption on the cycle ergometer using standard equations
[NASA-TP-3412] p 729 N94-14032
Physical countermeasures for long-term manned space flights
[ESA-SP-1160] p 733 N94-14860
Thyroid alterations in porcine after prolonged exposure to cold or heat
[AD-A266840] p 733 N94-14879

PHYSIOLOGICAL RESPONSES
Gender differences in endocrine responses to posture and 7 days of 6 deg head down bed rest
[NASA-TM-103991] p 731 N94-12972
Gravity as a probe for understanding pattern specification
[NASA-CR-194142] p 713 N94-13418
Clinical physiology of bed rest
[NASA-TM-104010] p 727 N94-13447
Physiological Anatomical Rodent Experiment (PARE).04 Feasibility Test 1
[NASA-CR-194423] p 728 N94-13473
Endocrine and metabolic changes in payload specialist (L-1) p 591 N94-13758
Manual control in space research on perceptual-motor functions under zero gravity conditions (L-10)
p 593 N94-13767
Psychophysiological investigations of the biomedical problems of manned spaceflight
[NASA-CR-194107] p 732 N94-13782
Renal function alterations during skeletal muscle disuse in simulated microgravity
[NASA-CR-194258] p 733 N94-13824
Thyroid alterations in porcine after prolonged exposure to cold or heat
[AD-A266840] p 733 N94-14879

PHYSIOLOGICAL TESTS
Validation of an inexpensive illuminant for aeromedical color vision screening
[DOT/FAA/AM-93/16] p 736 N94-14854

PHYSIOLOGY
Validated environmental and physiological data from the CELSS Breadboard Projects Biomass Production Chamber, BWT931 (Wheat cv. Yecora Rojo)
[NASA-TM-109272] p 738 N94-13979

PHYTOPLANKTON
Nonlinear relationships between particulate absorption and chlorophyll: Detritus or pigment packaging?
[AD-A266806] p 731 N94-14899

PIEZOELECTRIC CERAMICS
Active control of acoustic pressure fields using smart material technologies
[NASA-CR-191480] p 768 N94-13354
Experimental and analytical analysis of the response of a smart beam to rate feedback
[AD-A266544] p 557 N94-13706

PIEZOELECTRICITY
An acoustic charge transport imager for high definition television applications
[NASA-CR-194518] p 650 N94-14029

PILOT PERFORMANCE
Cognitive engineering in aerospace application: Pilot interaction with cockpit automation
[NASA-CR-177617] p 510 N94-13247
Piloting Vertical Flight Aircraft: A Conference on Flying Qualities and Human Factors
[NASA-CP-3220] p 521 N94-13294
A perspective on the FAA approval process: Integrating rotorcraft displays, controls and workload
p 521 N94-13298
Improvements in hover display dynamics for a combat helicopter p 523 N94-13310
Visual information for judging temporal range
p 524 N94-13314
Visual cueing considerations in Nap-of-the-Earth helicopter flight head-slaved helmet-mounted displays
p 524 N94-13315
Primary display latency criteria based on flying qualities and performance data p 525 N94-13318
Human factor implications of the Eurocopter AS332L-1 Super Puma cockpit p 525 N94-13319
Piloting considerations for terminal area operations of civil tiltwing and tiltrotor aircraft p 525 N94-13320
The identification of ability requirements and selection instruments for fighter pilot training
[AD-A266340] p 735 N94-13582
The influence of ATC message length and timing on pilot communication
[NASA-CR-177621] p 512 N94-14744
Validity of FAA-approved color vision tests for class 2 and class 3 aeromedical screening
[DOT/FAA/AM-93/17] p 735 N94-14846

PILOT SELECTION
The identification of ability requirements and selection instruments for fighter pilot training
[AD-A266340] p 735 N94-13582

PILOT TRAINING
Cognitive engineering in aerospace application: Pilot interaction with cockpit automation
[NASA-CR-177617] p 510 N94-13247
The identification of ability requirements and selection instruments for fighter pilot training
[AD-A266340] p 735 N94-13582
Determination of Loran-C/GPS human factors issues
[PB93-199693] p 514 N94-14563

PIONEER PROJECT
NASA images 11
[NASA-TM-109287] p 842 N94-13626

PIONS
Low energy response of the DO calorimeter and jet energy measurement
[DE93-013569] p 781 N94-13350

Dynamics of pion-nucleus systems
[DE93-014449] p 785 N94-14468

PIPE FLOW
Potential flow in in-line and staggered tube banks
[IME-CRE-TR-006] p 637 N94-13862

PIPELINES
Upgrading of raw natural gas using high-performance polymer membranes
[DE93-014041] p 566 N94-14586

PIPER AIRCRAFT
VSAERO analysis of a Piper Cub aircraft
p 516 N94-14616

PIPES (TUBES)
Potential flow in in-line and staggered tube banks
[IME-CRE-TR-006] p 637 N94-13862

PISTON ENGINES
Piston engine intake and exhaust system design
[ISVR-TR-222] p 663 N94-13874

PISTONS
Double inlet pulse tube cryocooler theory
[AD-A266832] p 597 N94-14877

PITCHING MOMENTS
Numerical simulation of dynamic stall of NACA0012 airfoil oscillating near static stall angle using the Navier-Stokes equations
[DE93-767970] p 505 N94-14061

PITTING
Crystallographic and metallurgical characterization of radiation detector grade cadmium telluride materials
[DE93-014335] p 806 N94-13150

PIXELS
Color image processing for flat panel visual display modeling
[NASA-CR-193660] p 790 N94-12797
Two dimensional measurement and evaluation of point images at microscope objectives
[ETN-93-94397] p 793 N94-14856

PLANE STRAIN
Autofrettage: Stress distribution under load and retained stresses after depressurization. A modified plane-strain case
[AD-A266320] p 671 N94-13579

PLANE WAVES
Computer code for scattering from impedance bodies of revolution. Part 3: Surface impedance with s and phi variation. Analytical and numerical results
[NASA-CR-193396] p 599 N94-13264
Active control of fan-generated plane wave noise
[NASA-TM-109008] p 777 N94-14481

PLANETARY BASES
A modular gas-cooled cermet reactor system for planetary base power
[DE93-013672] p 550 N94-13351

PLANETARY BOUNDARY LAYER
Evolution of the lower planetary boundary layer over strongly contrasting surfaces
[DE93-010667] p 717 N94-14424
Atmospheric turbulence and diffusion research
[DE93-011842] p 718 N94-14425

PLANETARY EVOLUTION
Regional tectonic analysis of Venus as part of the Pioneer Venus guest investigator project
[NASA-CR-194079] p 842 N94-13561
Organic Geochemical and tectonic evolution of the Midcontinent Rift system
[DE93-015093] p 717 N94-14338

PLANETARY GEOLOGY
Spectral analysis for automated exploration and sample acquisition
[NASA-CR-194095] p 545 N94-13189
The nature and origin of periodically spaced tectonic features on Mars
[NASA-CR-193821] p 842 N94-13199
Exploring Mars
[NASA-TM-109306] p 842 N94-13613
Martian sedimentary deposits
[NASA-CR-193266] p 842 N94-13855
Workshop on the Space Environment: The Effects on the Optical Properties of Airless Bodies
[NASA-CR-194417] p 842 N94-14298
Impact melting and vaporization in planetary regoliths
p 843 N94-14299
Extrapolation of space weathering processes to other small solar system bodies p 843 N94-14300

PLANETARY GRAVITATION
Venus gravity
[NASA-CR-194077] p 841 N94-12823

PLANETARY MANTLES
Regional tectonic analysis of Venus as part of the Pioneer Venus guest investigator project
[NASA-CR-194079] p 842 N94-13561

PLANETARY NEBULAE
A survey of compact planetary nebulae at radio wavelengths
[ISBN-0-315-61950-3] p 829 N94-13371

PLANETARY SURFACES
Spectral analysis for automated exploration and sample acquisition
[NASA-CR-194095] p 545 N94-13189
Impact melting and vaporization in planetary regoliths
p 843 N94-14299
Extrapolation of space weathering processes to other small solar system bodies p 843 N94-14300

PLANETARY SYSTEMS
Planetary system detection by POINTS
[NASA-CR-194361] p 545 N94-13067

PLANETARY TEMPERATURE
Regional tectonic analysis of Venus as part of the Pioneer Venus guest investigator project
[NASA-CR-194079] p 842 N94-13561

PLANETARY WAVES
Minimal modeling of the bimodality of extratropical atmospheric planetary waves p 713 N94-13622

PLANT DESIGN
Field of solar collectors: Effect of shadowing on the optimal field design
[ITN-93-85197] p 702 N94-13570
Knowledge based systems: From process control to policy analysis
[DE93-014582] p 765 N94-14117

PLANTING
Forest management for fixing and sequestering carbon
[DE93-013520] p 707 N94-13486

PLANTS (BOTANY)
Role of Ca(++)/calmodulin in the regulation of microtubules in higher plants
[DE93-015885] p 727 N94-12835
Gravity, chromosomes, and organized development in aseptically cultured plant cells p 592 N94-13764
The first steps of chlorophyll synthesis: RNA involvement and regulation
[DE93-014398] p 730 N94-14509

PLASMA ACCELERATION
Investigation of dynamics of plasma fluxes generated by the quasi-stationary plasma accelerator P-50
[DE93-621665] p 794 N94-12854

PLASMA ACCELERATORS
Investigation of dynamics of plasma fluxes generated by the quasi-stationary plasma accelerator P-50
[DE93-621665] p 794 N94-12854

PLASMA COMPOSITION
Highly charged ions in hot, dense plasmas
[DE93-013348] p 795 N94-12995
Variation of divertor plasma parameters with divertor depth for H-mode discharges in D3-D
[DE93-015475] p 801 N94-14347
Direct determination of alpha particle transport coefficients
[DE93-013488] p 787 N94-14691

PLASMA COMPRESSION
On MHD mode equations in toroidal plasmas
[PPL-139] p 800 N94-13877

PLASMA CONTROL
Theory of field-reversed configurations
[DE93-015611] p 794 N94-12862
Growth curve analysis for plasma profiles using smoothing splines
[DE93-015741] p 795 N94-12984
Nonlinear evolution of tearing modes in inhomogeneous plasmas
[PPL-133] p 798 N94-13564
Studies of non-inductive current drive in the CDX-U tokamak p 799 N94-13680
Experiments on the current rampdown phase in the STOR-M tokamak for AC operation
[PPL-132] p 799 N94-13835
Dependence of beta(tau) on plasma shape in D3-D
[DE93-015473] p 800 N94-13900
Stability and confinement properties of small-aspect-ratio tokamak
[INPE-5463-PRE/1771] p 801 N94-14024
Variation of divertor plasma parameters with divertor depth for H-mode discharges in D3-D
[DE93-015475] p 801 N94-14347
D3-D research operations
[DE93-016729] p 802 N94-14519
Review of the Procyon explosive pulsed power system
[DE93-016562] p 802 N94-14532
Active density control in DIII-D H-mode plasmas
[DE93-015477] p 802 N94-14570
Measurements of edge fluctuations by phase contrast imaging on DIII-D
[DE93-014018] p 802 N94-14579
The role of electric field shear stabilization of turbulence in the H-mode to VH-mode transition in D3-D
[DE93-015474] p 802 N94-14583
Toward a quasi-linear closure for compressible turbulence
[DE93-017185] p 647 N94-14895

PLASMA CURRENTS
Studies of non-inductive current drive in the CDX-U tokamak p 799 N94-13680
Experiments on the current rampdown phase in the STOR-M tokamak for AC operation
[PPL-132] p 799 N94-13835
Numerical Studies of Collisionless Current Layers
[NASA-CR-194337] p 800 N94-13854
Active density control in DIII-D H-mode plasmas
[DE93-015477] p 802 N94-14570

PLASMA DENSITY
Excitation of coupled waves in plasma periodic structures by relativistic electron beam and acceleration of charged particles
[DE93-621657] p 794 N94-12853
Dimensionally similar discharges with central RF heating on the D3-D tokamak
[DE93-012776] p 795 N94-12953
Growth curve analysis for plasma profiles using smoothing splines
[DE93-015741] p 795 N94-12984
Active density control in DIII-D H-mode plasmas
[DE93-015477] p 802 N94-14570
Measurements of edge fluctuations by phase contrast imaging on DIII-D
[DE93-014018] p 802 N94-14579

PLASMA DIAGNOSTICS
Equilibrium reconstruction of the q-profile in tokamaks from motional Stark effect data
[DE93-015815] p 796 N94-13046
A PC-PCL-based control system for the high-voltage pulsed-power operation of the Intense Diagnostic Neutral Beam (IDNB) Experiment
[DE93-014144] p 797 N94-13100
Interferometric investigation methods of plasma spatial characteristics on stellarators and tokamaks in submillimeter region
[DE93-621606] p 798 N94-13507
Plasma-etching science meets technology in the MDL
[DE93-012086] p 800 N94-13908
Measuring opacity of shock generated argon plasmas
[DE93-013038] p 801 N94-14312
D3-D research operations
[DE93-016729] p 802 N94-14519
Measurements of edge fluctuations by phase contrast imaging on DIII-D
[DE93-014018] p 802 N94-14579
The 8 to 11 keV x ray sources for imaging and absorption experiments
[DE93-015973] p 803 N94-14865

PLASMA DIFFUSION
Plasma diffusion through multidipole magnetic fields
[INPE-5460-PRE/1768] p 795 N94-12901
The resonance broadening theory revisited
[PPL-134] p 798 N94-13563

PLASMA DRIFT
On energy transport equations for turbulent magnetized plasma
[PPL-135] p 800 N94-13850
Anomalous transport due to small scale electromagnetic and large scale electrostatic modes in tokamaks
[PPL-140] p 801 N94-14206

PLASMA DYNAMICS
Investigation of dynamics of plasma fluxes generated by the quasi-stationary plasma accelerator P-50
[DE93-621665] p 794 N94-12854
Electrodynamics of helical plasma structures
[DE93-620981] p 797 N94-13240
The resonance broadening theory revisited
[PPL-134] p 798 N94-13563
Nonlinear evolution of tearing modes in inhomogeneous plasmas
[PPL-133] p 798 N94-13564

PLASMA ENGINES
Electromagnetic propulsion for spacecraft
[NASA-CR-191186] p 551 N94-13416

PLASMA EQUILIBRIUM
Theory of field-reversed configurations
[DE93-015611] p 794 N94-12862
Stability and confinement properties of small-aspect-ratio tokamak
[INPE-5463-PRE/1771] p 801 N94-14024

PLASMA ETCHING
Plasma-etching science meets technology in the MDL
[DE93-012086] p 800 N94-13908

PLASMA FREQUENCIES
Investigation of plasma instabilities in the Polar cusp
[NASA-CR-194283] p 796 N94-13084
Implicit multi-fluid simulation of interpenetrating plasmas
[DE93-013351] p 801 N94-14342

PLASMA GUNS
Investigation of dynamics of plasma fluxes generated by the quasi-stationary plasma accelerator P-50
[DE93-621665] p 794 N94-12854

PLASMA HEATING
Dimensionally similar discharges with central RF heating on the D3-D tokamak
[DE93-012776] p 795 N94-12953
Evolution of high-repetition-rate induction accelerators through advancements in switching
[DE93-012599] p 654 N94-12963
Ion cyclotron heating experiments and plans for the Advanced Toroidal Facility (ATF)
[DE93-012965] p 795 N94-13033
Effect on antenna structure of high power RF during plasma operation
[DE93-013278] p 797 N94-13144
Predicted performance of a dc beam driven FEM oscillator designed for fusion applications at 200-250 GHz
[DE93-013414] p 655 N94-13145
Instability heating of the HDZP
[DE93-012641] p 798 N94-13513
Folded waveguide designs for tokamaks
[DE93-013274] p 798 N94-13577
Studies on equatorial shock formation during plasmaspheric refilling
[NASA-CR-194392] p 715 N94-13954
Electrical characterization of the JET A(sub 2) antenna: Comparison of model with measurements Wade, T.
[DE93-012964] p 607 N94-14291
D3-D research operations
[DE93-016729] p 802 N94-14519
Design of the ion cyclotron system for TPX
[DE93-012961] p 803 N94-14770

PLASMA INTERACTION EXPERIMENT
TROPIX: A solar electric propulsion flight experiment
[NASA-TM-106297] p 534 N94-13028
Laboratory simulation of spacecraft charging in the plasma wake region
[FFI-93-7007] p 542 N94-14107

PLASMA INTERACTIONS
Interactions between spacecraft and their environments
[NASA-TM-106115] p 541 N94-13917
Studies on equatorial shock formation during plasmaspheric refilling
[NASA-CR-194392] p 715 N94-13954
Ionospheric effects on a wide-bandwidth, polarimetric, space-based, synthetic-aperture radar
[DE93-015084] p 612 N94-14512

PLASMA LAYERS
Ion anisotropy driven waves in the Earth's magnetosheath and plasma depletion layer
[DE93-012751] p 712 N94-12952
Variation of divertor plasma parameters with divertor depth for H-mode discharges in D3-D
[DE93-015475] p 801 N94-14347
D3-D research operations
[DE93-016729] p 802 N94-14519

PLASMA PHYSICS
Magnetic fusion computing: A personal retrospective view
[DE93-014147] p 797 N94-13217
Metastable enhancement of C(+) and O(+) capture reactions
[DE93-015075] p 807 N94-13373
The International Colloquium on Atomic Spectra and Oscillator Strengths for Astrophysical and Laboratory Plasmas
[NASA-TM-109255] p 849 N94-13376
Activities of the University of Saskatchewan, Plasma Physics Laboratory
[CTN-93-60831] p 798 N94-13518
The resonance broadening theory revisited
[PPL-134] p 798 N94-13563
Numerical Studies of Collisionless Current Layers
[NASA-CR-194337] p 800 N94-13854
Implicit multi-fluid simulation of interpenetrating plasmas
[DE93-013351] p 801 N94-14342
Physics of gas breakdown for ion beam transport in gas
[DE93-015646] p 801 N94-14349
Review of the Procyon explosive pulsed power system
[DE93-016562] p 802 N94-14532

PLASMA PINCH
Collisional effects of trapped electrons on the anomalous particle and thermal pinches
[PPL-128] p 800 N94-13853

PLASMA POTENTIALS
Plasma auto-biasing during Ohmic H-mode in the STOR-M tokamak
[PPL-136] p 799 N94-13849
Studies on equatorial shock formation during plasmaspheric refilling
[NASA-CR-194392] p 715 N94-13954

PLASMA PRESSURE
Nonlinear evolution of tearing modes in inhomogeneous plasmas
[PPL-133] p 798 N94-13564

PLASMA PROPULSION
Low power pulsed MPD thruster system analysis and applications
[NASA-CR-191187] p 550 N94-13415
Electromagnetic propulsion for spacecraft
[NASA-CR-191186] p 551 N94-13416
Plasma contactor technology for Space Station Freedom
[NASA-TM-106291] p 553 N94-14725

PLASMA RADIATION
Highly charged ions in hot, dense plasmas
[DE93-013348] p 795 N94-12995
Comparative study of x ray and microwave emissions during solar flares
[NASA-CR-194532] p 845 N94-14577
The 8 to 11 keV x ray sources for imaging and absorption experiments
[DE93-015973] p 803 N94-14865

PLASMA SHEATHS
Plasma diffusion through multidipole magnetic fields
[INPE-5460-PRE/1768] p 795 N94-12901

PLASMA SPRAYING
Microstructural evolution of NARloy-Z at elevated temperatures
[NASA-TM-108419] p 571 N94-13715

PLASMA TEMPERATURE
Growth curve analysis for plasma profiles using smoothing splines
[DE93-015741] p 795 N94-12984
Two temperature modeling and experimental measurements of laser sustained hydrogen plasmas
[AD-A265750] p 796 N94-13039

PLASMA TURBULENCE
A 3D gyrokinetic particle-in-cell simulation of fusion plasma microturbulence on parallel computers
[DE93-012503] p 794 N94-12846
Plasma diffusion through multidipole magnetic fields
[INPE-5460-PRE/1768] p 795 N94-12901
Instability heating of the HDZP
[DE93-012641] p 798 N94-13513
The resonance broadening theory revisited
[PPL-134] p 798 N94-13563
Collisional effects of trapped electrons on the anomalous particle and thermal pinches
[PPL-128] p 800 N94-13853
The role of electric field shear stabilization of turbulence in the H-mode to VH-mode transition in D3-D
[DE93-015474] p 802 N94-14583

PLASMA WAVES
Excitation of coupled waves in plasma periodic structures by relativistic electron beam and acceleration of charged particles
[DE93-621657] p 794 N94-12853
Ion anisotropy driven waves in the Earth's magnetosheath and plasma depletion layer
[DE93-012751] p 712 N94-12952
ICE/ISEE plasma wave data analysis
[NASA-CR-194375] p 796 N94-13081
Investigations of transitions from order to chaos in dynamical systems
[DE93-014438] p 818 N94-14738

PLASMA-ELECTROMAGNETIC INTERACTION
Scattering of reflectometer signals from rippled surfaces
[PPL-138] p 602 N94-13802

PLASMA-PARTICLE INTERACTIONS
Excitation of coupled waves in plasma periodic structures by relativistic electron beam and acceleration of charged particles
[DE93-621657] p 794 N94-12853
Electrodynamics of helical plasma structures
[DE93-620981] p 797 N94-13240

PLASMAS (PHYSICS)
Two-dimensional simulations of foil implosion experiments on the Los Alamos capacitor bank
[DE93-012676] p 794 N94-12814
A 3D gyrokinetic particle-in-cell simulation of fusion plasma microturbulence on parallel computers
[DE93-012503] p 794 N94-12846
Inertial Confinement Fusion
[DE93-013303] p 795 N94-13017
Comment of parameter excitation of Alfven and Heliicon waves in a magnetoactive compensated semiconductor by microwave radiation
[DE93-623203] p 806 N94-13228
On energy transport equations for turbulent magnetized plasma
[PPL-135] p 800 N94-13850
Dependence of beta(tau) on plasma shape in D3-D
[DE93-015473] p 800 N94-13900
Oscillator-amplifier experiments in neon-like yttrium
[DE93-012577] p 657 N94-13976
The interaction of intense femtosecond laser pulses with solid targets
[DE93-014415] p 658 N94-14114
Monte Carlo simulation of the OCP freezing transition
[DE93-013039] p 811 N94-14313
Variation of divertor plasma parameters with divertor depth for H-mode discharges in D3-D
[DE93-015475] p 801 N94-14347
Direct determination of alpha particle transport coefficients
[DE93-013488] p 787 N94-14691
Anomalous ion transport and feedback control
[DE93-018324] p 803 N94-14874

PLASMASPHERE
Studies on equatorial shock formation during plasmaspheric refilling
[NASA-CR-194392] p 715 N94-13954
The role of ionospheric plasma in the magnetosphere
[NASA-CR-194404] p 716 N94-13967

PLASTIC DEFORMATION
A benchmark bending test of a thick specimen, Part 1: Experiments
[ARL-RR-6-PT-1] p 670 N94-12927
A benchmark bending test of a thick specimen. Part 2: Surface displacement measurements
[ARL-RR-6-PT-2] p 670 N94-12928
Inelastic deformation mechanisms in SCS-6/Ti 15-3 MMC lamina under compression
[NASA-CR-191170] p 555 N94-13378
A stochastic model for behavior analysis of fiber-reinforced quasi-brittle materials
p 672 N94-13594
Non-uniqueness in dynamic rate-independent non-associated plasticity
[AD-A266342] p 769 N94-13731
Thermal gradient-induced deflection of a thick-walled cylinder with bending residual stresses
[AD-A266347] p 673 N94-13777
Ploughing on gold using a Scanning Tunneling Microscope
[DE93-012632] p 812 N94-14365
Elastic-plastic finite element analyses of an unidirectional, 9 vol percent tungsten fiber reinforced copper matrix composite
[NASA-TM-106304] p 559 N94-14719

PLASTIC FLOW
An experimental study on the effect of die geometry on swell and sag in the parison extrusion stage
[IMI-93RT-42400-1476-G] p 597 N94-14070

PLASTIC PROPERTIES
A benchmark bending test of a thick specimen, Part 1: Experiments
[ARL-RR-6-PT-1] p 670 N94-12927
A benchmark bending test of a thick specimen. Part 2: Surface displacement measurements
[ARL-RR-6-PT-2] p 670 N94-12928
Modeling the impact behavior of AD85 ceramic under multi-axial loading
[AD-A265877] p 576 N94-12932
Investigation of criteria for ductile fracture under fully-plastic conditions p 672 N94-13593
Non-uniqueness in dynamic rate-independent non-associated plasticity
[AD-A266342] p 769 N94-13731
Elastic-plastic finite element analyses of an unidirectional, 9 vol percent tungsten fiber reinforced copper matrix composite
[NASA-TM-106304] p 559 N94-14719

PLATE THEORY
Nonlinear vibrations of thick composite plates: Higher-order shear deformation plate theory
p 556 N94-13558
Finite element analysis of composite plates by use of modified complementary energy principle
p 672 N94-13596

PLATES
Experimental measurement of local heat transfer coefficients over discrete roughened plates using infrared thermography p 635 N94-13652

PLATES (STRUCTURAL MEMBERS)
Finite element analysis of composite plates by use of modified complementary energy principle
p 672 N94-13596
Probabilistic micromechanics for high-temperature composites
[NASA-CR-191150] p 676 N94-14408

PLATES (TECTONICS)
Regional tectonic analysis of Venus as part of the Pioneer Venus guest investigator project
[NASA-CR-194079] p 842 N94-13561

PLATINUM
Electrocatalysis issues in polymer electrolyte fuel cells
[DE93-014450] p 702 N94-13402

Stability of reference masses 1: Evidence for posiible variations in the mass of reference kilograms arising from mercury contamination
[NPL-DMM(A)-86] p 708 N94-13667
Photochemical dynamics of surface oriented molecules
[DE93-016289] p 784 N94-13983

PLOTTERS
FORTRAN graphics routines for the Macintosh
[DE93-013092] p 742 N94-12864

PLOTTING
FORTRAN graphics routines for the Macintosh
[DE93-013092] p 742 N94-12864

PLUMES
UV and IR laser ablation for inductively coupled plasma mass spectrometry
[DE93-017124] p 658 N94-14415

PLUTONIUM
Reduction of Pu(6) with hydrogen peroxide: Effects of plutonium, peroxide, and iron concentrations and of reaction time
[DE93-013598] p 564 N94-13487
A model for fuel fire duration and application to the B-1B bomber
[DE93-013000] p 512 N94-14292

PLY ORIENTATION
Buckling analysis of laminated thin shells in a hot environment
[NASA-TM-106302] p 683 N94-14776

PNEUMATIC PROBES
The 3D pneumatic and 2D dynamic probes: Their development and subsequent use in a transonic fan
[RAE-TM-AERO/PROP-22] p 653 N94-14827

PODS (EXTERNAL STORES)
Spare parts analysis of the MK.32B-751 AAR pod
[DSIS-93-00737] p 774 N94-13549

POINT SOURCES
Search for UHE point-source emission over various time scales
[DE93-012718] p 846 N94-12922
Search for continuous and single day emission from ultra-high-energy sources
[DE93-012724] p 846 N94-12947

POINTING CONTROL SYSTEMS
Simulator study of uncoupled control functions. Use of manual pointing modes when aiming at ground targets and oncoming airborne target
[FFA-TN-1992-18] p 528 N94-13588
Telescope pointing for GOPEX p 610 N94-14389
Wavefront sensing, control, and pointing p 546 N94-14833

POISSON EQUATION
Numerical simulation and analysis of electrical and optical properties of Al(x)Ga(1-x)As / GaAs
[ETN-93-94387] p 703 N94-13997
Implicit multi-fluid simulation of interpenetrating plasmas
[DE93-013351] p 801 N94-14342

POISSON RATIO
Quantitative mapping of pore fraction variations in silicon nitride using an ultrasonic contact scan technique
[NASA-TP-3377] p 665 N94-13056
Theory of the electronic and structural properties of solid state oxides
[DE93-016051] p 811 N94-14296

POLAR CAPS
The role of ionospheric plasma in the magnetosphere
[NASA-CR-194404] p 716 N94-13967

POLAR METEOROLOGY
Arctic ozone expedition
[NASA-TM-109301] p 708 N94-13602

POLAR ORBITS
Earth observation from low-inclination orbit as a necessary complement to polar missions p 694 N94-14248

POLARIMETERS
Measurement of the spin of a particle using undulator radiation
[DE93-014334] p 780 N94-13149

POLARIMETRY
Ionospheric effects on a wide-bandwidth, polarimetric, space-based, synthetic-aperture radar
[DE93-015084] p 612 N94-14512

POLARITY
Direct probing of chromatography columns by laser-induced fluorescence
[DE93-015208] p 654 N94-13022

POLARIZATION
Polarization and color transparency
[DE93-014319] p 780 N94-13101
Polarization and variability of active galaxies and quasars p 837 N94-13550

POLARIZATION (CHARGE SEPARATION)
Ultrafast photoinduced electron transfer reactions in supramolecular arrays: Studies of electronic coupling and solvation
[DE93-012910] p 782 N94-13484
Charge storage and switching phenomena with molecular assemblies of metal complexes
[AD-A266673] p 787 N94-14778

POLARIZATION (SPIN ALIGNMENT)
Top quark polarization and T-odd spin correlations as tools for testing (non) Standard Model predictions
[DE93-622956] p 778 N94-12847
The evolution of tensor polarization
[DE93-017209] p 790 N94-14897

POLARIZATION (WAVES)
The E2 N(yields)(Delta) transition from polarized Compton scattering
[DE93-012522] p 785 N94-14363

POLARIZED ELECTROMAGNETIC RADIATION
Remote identification of rain and hail with a polarization diversity radar
[ISBN-0-315-55623-4] p 720 N94-13516

POLARIZED LIGHT
Polarization effects in optical fiber current sensors based on Sagnac interferometers with 3 by 3 couplers
[DE93-012665] p 792 N94-14367

POLARIZED RADIATION
The continuum emission of active galactic nuclei
[ITN-93-85208] p 847 N94-13232

POLARONS
Small polaron conduction in Y2Ti2O7
[ITN-93-85221] p 814 N94-14557

POLICIES
Planetary protection implementation on future Mars lander missions
[NASA-CP-3216] p 841 N94-13183
An examination of utility emissions contributions to elevated ozone concentrations in the Chicago area
[DE93-012852] p 708 N94-13495
Preliminary nuclear safety assessment of the NEPST (Topaz 2) space reactor program
[DE93-012853] p 551 N94-13514
Science, technology, and the federal government: National goals for a new era p 827 N94-14115

POLISHING
Field emitter array RF amplifier development project. Phase 1: Cathode technology development
[AD-A266346] p 622 N94-13776

POLITICS
Where no flag has gone before: Political and technical aspects of placing a flag on the Moon
[NASA-CR-188251] p 827 N94-12800
NASA/DOD Aerospace Knowledge Diffusion Research Project. Paper 37: The impact of political control on technical communications: A comparative study of Russian and US aerospace engineers and scientists
[NASA-TM-109329] p 826 N94-14488

POLLUTION CONTROL
A review of the global emissions, transport, and effects of heavy metals in the environment
[DE93-013507] p 706 N94-12937
AQUIS: A PC-based source information manager
[DE93-012893] p 707 N94-13383
Pollution prevention through total quality
[DE93-013814] p 707 N94-13390

POLLUTION MONITORING
Laser-induced fluorescence over optical fibers for real time in situ measurement of petroleum hydrocarbons in seawater
[AD-A265106] p 790 N94-12863
Gathering and exchange information on atmospheric chemistry and polluted atmospheres
[DE93-009940] p 705 N94-12869
The North Atlantic Regional Experiment (NARE)
[DE93-010126] p 706 N94-13054
AQUIS: A PC-based source information manager
[DE93-012893] p 707 N94-13383
Spatial and temporal variability of precipitation and chemistry: Case studies from the frontal boundary study
[DE93-007883] p 708 N94-13910
Study of the consequences of the Chernobyl accident and technogenic activity in the Republic Belarus using aerospace methods p 693 N94-14246

POLLUTION TRANSPORT
The North Atlantic Regional Experiment (NARE)
[DE93-010126] p 706 N94-13054
Diagnostic studies of the HxOy-NxOy-O3 photochemical system using data from NASA GTE field expeditions
[NASA-CR-193672] p 706 N94-13170
Importance of sprays for long range transport of harmful substances in the troposphere
[MITT-81] p 711 N94-14723

POLYAMIDE RESINS
Highly fluorinated polymers
[NASA-CR-194147] p 579 N94-13964
Pore-size-distribution of cationic polyacrylamide hydrogels
[DE93-015218] p 581 N94-14400

POLYATOMIC MOLECULES
Molecular dynamics simulation of electronically excited polyatomic molecules
[DE93-623045] p 781 N94-13225
Selective excitation, relaxation, and energy channeling in molecular systems
[DE93-018819] p 785 N94-14420

POLYCARBONATES
Sequestering carbon dioxide in industrial polymers: Building materials for the 21st century
[DE93-016087] p 580 N94-14297

POLYCHLORINATED BIPHENYLS
Procurement and execution of PCB analyses: Customer-analyst interactions
[DE93-009964] p 566 N94-14694

POLYCRYSTALS
Photovoltaic Subcontract Program
[DE93-000092] p 700 N94-12868
Activities of the Basic Sciences Branch
[DE93-010012] p 851 N94-14455
Quenching and annealing effects on the specific heat of YBa2Cu3O(7-delta)
[DE93-016483] p 816 N94-14868

POLYESTERS
Highly fluorinated polymers
[NASA-CR-194147] p 579 N94-13964

POLYETHER RESINS
Highly fluorinated polymers
[NASA-CR-194147] p 579 N94-13964

POLYETHYLENES
Effect of stabilization on the recycling of polyolefins in blow moulding
[IMI-93RT-42400-1477-G] p 596 N94-13684

POLYGONS
Extremal polygon containment problems and other issues in parametric searching
[ITN-93-85214] p 771 N94-14506

POLYIMIDE RESINS
Research on radiation resistance properties of structural materials for space use p 529 N94-13271

POLYIMIDES
Research on radiation resistance properties of structural materials for space use p 529 N94-13271

POLYMER BLENDS
Phase transition in polymer blends and structure of ionomers and copolymers
[DE93-016256] p 579 N94-13978

POLYMER CHEMISTRY
Effect of stabilization on the recycling of polyolefins in blow moulding
[IMI-93RT-42400-1477-G] p 596 N94-13684
Office of Naval Research/DARPA publications: Composite materials with improved properties in compression
[AD-A265509] p 560 N94-14794

POLYMER MATRIX COMPOSITES
The Second Workshop on Deployment and Assembly Experiment of Large Space Structure on Orbit
[NASDA-CON-930003] p 529 N94-13268
Research on radiation resistance properties of structural materials for space use p 529 N94-13271
Characterization of composite materials for aerospace structures
[ESA-TT-1260] p 557 N94-13804

POLYMER PHYSICS
Theoretical treatment of the bulk and surface properties of fluids containing long, flexible molecules
[DE93-015560] p 575 N94-12861

POLYMERIC FILMS
Amorphous sol-gel insulating films
[DE93-012859] p 576 N94-12866
Poling of thin polymer films in electro optic applications
[AD-A266562] p 579 N94-13584
The use of polarised neutron reflection for unique density profile determination in thin films
[PB93-187136] p 579 N94-13783
Impedance-power effects on plasma polymer surface finish using a helical resonator discharge
[DE93-016454] p 803 N94-14590

POLYMERIZATION
Unexpectedly rapid hydrosilation polymerization of the diallyl derivative of bisphenol A and 2,6-diallylphenol
[AD-A265832] p 577 N94-12986
Reverse micelle synthesis of nanoscale metal containing catalysts
[DE93-012869] p 572 N94-14184
Impedance-power effects on plasma polymer surface finish using a helical resonator discharge
[DE93-016454] p 803 N94-14590

POLYMERS
Electrocatalysis issues in polymer electrolyte fuel cells
[DE93-014450] p 702 N94-13402

Sequestering carbon dioxide in industrial polymers: Building materials for the 21st century
[DE93-016087] p 580 N94-14297
Direct simulation of polymer drag reduction in free shear flows and vortex dipoles p 644 N94-14755

POLYNOMIALS
Robust stability of diamond families of polynomials with complex coefficients
[NASA-CR-194132] p 768 N94-13421
Formally biorthogonal polynomials and a look-ahead Levinson algorithm for general Toeplitz systems
[NASA-CR-194297] p 748 N94-13586
The Chebyshev-Legendre method: Implementing Legendre methods on Chebyshev points
[NASA-CR-191497] p 769 N94-13725
Exploiting structure: Introduction and motivation
[NASA-CR-194199] p 750 N94-13828
On a difference equation for generalizations of Charlier polynomials
[REPT-92-101] p 770 N94-14150

POLYPROPYLENE
Effect of stabilization on the recycling of polyolefins in blow moulding
[IMI-93RT-42400-1477-G] p 596 N94-13684

POLYSACCHARIDES
CarbBank: A structural and bibliographic database for complex carbohydrates
[DE93-015582] p 827 N94-14803

POLYSILOXANES
Phases and phase transitions of polymeric liquid crystals: A high resolution x ray diffraction and light scattering study
[ITN-93-85218] p 816 N94-14826

POLYURETHANE RESINS
A multiphase model for shock-induced flow in low density foam
[DE93-013767] p 632 N94-13397

PONDEROMOTIVE FORCES
Adiabatic and non adiabatic effects in Free Electron Laser (FEL) non linear interactions
[ITN-93-85224] p 659 N94-14547

POPULATION THEORY
Chaos and microbial systems
[DE93-016814] p 730 N94-14596

POPULATIONS
Adaptively resizing populations: Algorithm, analysis, and first results
[NASA-CR-194277] p 742 N94-12808
Coherent excitation of autoionizing resonances by electron impact
[DE93-018169] p 785 N94-14419
Public census data on CD-ROM at Lawrence Berkeley Laboratory
[DE93-015273] p 825 N94-14433

POROSITY
Transport properties of disordered porous media from the microstructure
[DE93-016065] p 806 N94-13152
A multiphase model for shock-induced flow in low density foam
[DE93-013767] p 632 N94-13397
The method of Laplace Transform MultiQuadrics (LTMQ) for the solution of the groundwater flow equation
[DE93-010408] p 637 N94-14053
Pore-size-distribution of cationic polyacrylamide hydrogels
[DE93-015218] p 581 N94-14400

POROUS BOUNDARY LAYER CONTROL
The transient behavior of a boundary layer exposed to uniform suction
[ITN-93-85205] p 630 N94-13197

POROUS MATERIALS
Electrophoretic and electrolytic deposition of ceramic particles on porous substrates
[AD-A265141] p 575 N94-12812
Transport properties of disordered porous media from the microstructure
[DE93-016065] p 806 N94-13152
The method of Laplace Transform MultiQuadrics (LTMQ) for the solution of the groundwater flow equation
[DE93-010408] p 637 N94-14053
Theoretical studies of breakdown in random media
[DE93-018107] p 558 N94-14418

POROUS WALLS
Wall interference studies: Revisited
p 640 N94-14604

PORTABLE EQUIPMENT
Development of a portable multispectral thermal infrared camera
[NASA-CR-191340] p 648 N94-13176
Portable acoustic wave sensor systems for real-time monitoring of volatile organic compounds
[DE93-013753] p 582 N94-14511

POSITION (LOCATION)
Design and performance of an automated video-based laser beam alignment system
[DE93-012571] p 656 N94-13481
Simulated annealing for the problem of multiresource location on graph
[REPT-93-033] p 770 N94-13809
Computational issues in optimal tuning and placement of passive dampers p 681 N94-14647

POSITION ERRORS
Position error determination for the speedometer and altimeter of the NAL QSTOL experimental aircraft ASKA
[NAL-TR-1144] p 517 N94-13451
GPS satellite sky distribution: Impact on the propagation of some important errors in precise relative positioning
[ISBN-0-315-51838-3] p 513 N94-13541
Orbit determination error analysis based on the requirements of ADEOS mission
[NASDA-CNT-930008] p 532 N94-13644

POSITION SENSING
Performance evaluation tests of the GPS/DGPS navigation system installed in the NAL Dornier 228: Preliminary ground test results
[NAL-TM-649] p 513 N94-13346
Close range 3-D position sensing using stereo vision and point-of-correspondance through mathematical morphology
[ISBN-0-315-61012-3] p 763 N94-13515
Development of a tactile and vision integrated system, and object identification techniques for SPDM applications
[DSIS-93-00153] p 764 N94-13842

POSITIONING
GPS satellite sky distribution: Impact on the propagation of some important errors in precise relative positioning
[ISBN-0-315-51838-3] p 513 N94-13541

POSITIVE IONS
Role of Ca(++)/calmodulin in the regulation of microtubules in higher plants
[DE93-015885] p 727 N94-12835
Indirect processes in electron impact ionization of Kr(24+) and Kr(25+)
[DE93-014129] p 784 N94-14140

POSITRON ANNIHILATION
A positron annihilation radiation telescope using Laue diffraction in a crystal lens
[DE93-012905] p 848 N94-13483
Effects of additional isoscalar vector bosons in e(sup +)e)(sup -)(yields)ff-bar processes at the TRISTAN and LEP energies
[DE93-621451] p 783 N94-13506

POSITRONS
EGS (underscore) windows 2: An enhanced graphical interface to EGS
[DE93-010447] p 746 N94-13382
A positron annihilation radiation telescope using Laue diffraction in a crystal lens
[DE93-012905] p 848 N94-13483
Rare muon processes
[DE93-012646] p 785 N94-14366

POSTFLIGHT ANALYSIS
STS-53 Space Shuttle mission report
[NASA-CR-193101] p 535 N94-13934
STS-54 Space Shuttle mission report
[NASA-CR-194116] p 535 N94-13935

POSTMISSION ANALYSIS (SPACECRAFT)
STS-53 Space Shuttle mission report
[NASA-CR-193101] p 535 N94-13934
STS-54 Space Shuttle mission report
[NASA-CR-194116] p 535 N94-13935

POSTURE
Gender differences in endocrine responses to posture and 7 days of 6 deg head down bed rest
[NASA-TM-103991] p 731 N94-12972
Neurophysiological study on visuo-vestibular control of posture and movement in fish during adaptation to weightlessness p 591 N94-13759

POTASSIUM
Is K3C60 a line phase?
[DE93-016700] p 813 N94-14517

POTASSIUM SILICATES
Thermal history effects on electrical relaxation and conductivity for potassium silicate glass with low alkali concentrations
[NASA-TM-106324] p 583 N94-14845

POTENTIAL ENERGY
Incomplete melting of the Au(100) surface
[DE93-623192] p 569 N94-13227
Predicting the vibrations of a spinning inflated membrane
[DE93-010690] p 676 N94-14456

POTENTIAL FIELDS
The general gravitational potential field of a homogeneous cylinder rotating about its axis
[DE93-622853] p 775 N94-13508

POTENTIAL FLOW
A robust quasi-simultaneous interaction method for a full potential flow with a boundary layer with application to wing/body configurations
[NLR-TP-91397-U] p 503 N94-13531
Potential flow in in-line and staggered tube banks
[IME-CRE-TR-006] p 637 N94-13862

POWDER (PARTICLES)
Flamespreading in granular solid propellant: Design of an experiment
[AD-A266009] p 583 N94-12987
Gas atomized Er3Ni powder for cryocooler applications
[DE93-011564] p 568 N94-13000
Destruction of waste energetic materials using base hydrolysis
[DE93-012738] p 584 N94-13491
Measurement of strain in individual phases of composites before, during, and after mechanical loading
[DE93-014585] p 558 N94-14119
Reverse micelle synthesis of nanoscale metal containing catalysts
[DE93-012869] p 572 N94-14184
Polymer infiltration studies
[NASA-CR-194521] p 582 N94-14539
Shielded open-circuited sample holders for dielectric and magnetic measurements of liquids and powders
[PB93-198851] p 652 N94-14687
Fine-powder Al2O3 and SiO2 for preparation of multielement standards for rare-earth elements analysis
[DE93-625118] p 567 N94-14884

POWDER METALLURGY
Preparation of particle-dispersion alloys (M-6)
p 587 N94-13738
Study on the mechanism of liquid phase sintering (M-12) p 588 N94-13744
Gas-evaporation in low-gravity field (cogelation mechanism of metal vapors) (M-14) p 588 N94-13746

POWER AMPLIFIERS
Inertial confinement fusion program
[DE93-013372] p 796 N94-13047
Design and performance of the terawatt Cr:LiSrAlF6 laser system
[DE93-014678] p 657 N94-13882

POWER BEAMING
Two temperature modeling and experimental measurements of laser sustained hydrogen plasmas
[AD-A265750] p 796 N94-13039

POWER CONDITIONING
High flux heat exchanger
[AD-A266341] p 636 N94-13730

POWER CONVERTERS
Power converters for the 120 V bus supply control
[CNES-NT-134] p 622 N94-13552
Operation of high power converters in parallel
[NASA-CR-191096] p 622 N94-13786
Multi-output flyback converter with ultrafast current protection
[CNES-NT-133] p 625 N94-14138

POWER EFFICIENCY
Electromagnetic propulsion for spacecraft
[NASA-CR-191186] p 551 N94-13416

POWER SPECTRA
Maximum entropy spectral analysis of the geological time series of the oxygen isotope record from deep-sea cores
[INPE-5465-PRE/1773] p 725 N94-13728

POWER TRANSMISSION
Flex-gear electrical power transmission
[NASA-CR-194422] p 661 N94-13445
Communications and control for electric power systems: Power flow classification for static security assessment
[NASA-CR-194512] p 624 N94-13948

POWERED LIFT AIRCRAFT
Design criteria for integrated flight/propulsion control systems for STOVL fighter aircraft p 521 N94-13297
Numerical simulation of a powered-lift landing, tracking flow features using overset grids, and simulation of high lift devices on a fighter-lift-and-control wing
[NASA-CR-194260] p 527 N94-14322

PRASEODYMIUM
Synthesis of organic ligands for f-element separations
[DE93-012915] p 554 N94-14290

PRE-MAIN SEQUENCE STARS
The evidence for clumpy accretion in the Herbig Ae star HR 5999
[NASA-TM-108257] p 828 N94-12915
Search for x ray emitting young stars outside of massive molecular clouds
[NASA-CR-193609] p 830 N94-13462
Millimeter and infrared studies of young stellar objects in dark cloud L1641 p 838 N94-13648

PREBURNERS
STS-55 pad abort: Engine 2011 oxidizer preburner augmented spark igniter check valve leak
[NASA-CR-193830] p 533 N94-12806

Simulation of preburner sprays, volume 1
[NASA-CR-193844] p 647 N94-14906
PRECIPITATES
Effect of microstructure on passive film formation and breakdown on Al alloys
[AD-A265339] p 569 N94-13050
PRECIPITATION (CHEMISTRY)
Interfacial precipitation, segregation and deformation in alloy 600: Implications on primary-side IGSCC
[DE93-013161] p 568 N94-13035
PRECIPITATION (METEOROLOGY)
Measuring surface fluxes in CAPE
[NASA-CR-193664] p 711 N94-12788
Precipitation verification LAM
[KNMI-TR-143] p 722 N94-13991
A verification of the Euroguidance: A guidance forecast for transportation and tourism
[KNMI-TR-145] p 722 N94-13993
Circulation and rainfall climatology of a 10-year (1979 - 1988) integration with the Goddard Laboratory for atmospheres general circulation model
[NASA-TM-104591] p 723 N94-14074
PRECIPITATION HARDENING
Microstructural mechanisms that enhance electromigration resistance in Al-Cu thin films
[DE93-013770] p 812 N94-14345
PRECONDITIONING
Topics on spatially high-order accurate methods and pre-conditioning for the Navier-Stokes equations with finite-rate chemistry p 633 N94-13572
Preconditioning and the limit to the incompressible flow equations
[NASA-CR-191500] p 769 N94-13717
PREDICATE LOGIC
A path-oriented matrix-based knowledge representation system
[NASA-CR-4539] p 744 N94-13065
PREDICTION ANALYSIS TECHNIQUES
A method of predicting quasi-steady aerodynamics for flutter analysis of high speed vehicles using steady CFD calculations
[NASA-TM-109009] p 514 N94-12850
Improved aeroprediction code. Part 1: Summary of new methods and comparison with experiment
[AD-A266015] p 500 N94-12989
Transition prediction and control in subsonic flow over a hump
[NASA-CR-4543] p 629 N94-13066
Research on chemical vapor deposition processes for advanced ceramic coatings
[NASA-CR-193613] p 577 N94-13089
Methods for evaluating the predictive accuracy of structural dynamic models
[NASA-CR-191337] p 671 N94-13124
Simulation of orbital debris impacts on bumper shields
[DE93-013773] p 540 N94-13398
Piston engine intake and exhaust system design
[ISVR-TR-222] p 663 N94-13874
Transition of building energy consumption using multi-input, single-output dynamic model
[VTT-PUBS-116] p 597 N94-14055
Extrapolation of ground test data to flight p 507 N94-14170
Boundary-layer transition p 507 N94-14171
Electromagnetic wave test p 508 N94-14173
Nonlinear wave predictions in ceramics
[DE93-016516] p 582 N94-14436
Predicting the vibrations of a spinning inflated membrane
[DE93-010690] p 676 N94-14456
Long duration measurements of fading on a low elevation angle, 11-GHz satellite path p 613 N94-14661
Coastal scour problems and methods for prediction of maximum scour
[AD-A266658] p 726 N94-14775
Measurements of crystal growth kinetics at extreme deviations from equilibrium
[DE93-014526] p 815 N94-14798
A computer program to calculate growth rates for cracks at notches in regions of residual stress
[RAE-TM-MAT/STR-1207] p 683 N94-14818
PREDICTOR-CORRECTOR METHODS
Parallel methods for dynamic simulation of multiple manipulator systems p 680 N94-14637
PREFORMS
Optimization of the processing parameters of high temperature superconducting glass-ceramics: Center Director's discretionary fund final report
[NASA-TM-108421] p 808 N94-13938
Graphite fiber textile preform/copper matrix composites
[NASA-CR-193797] p 558 N94-14050
PREGNANCY
Physiological Anatomical Rodent Experiment (PARE) .04 Feasibility Test 1
[NASA-CR-194423] p 728 N94-13473
PREMIXED FLAMES
A coherent flame model of premixed turbulent combustion in a counterflow geometry
[CUED/A-THERMO/TR.60] p 562 N94-13085
DNS and modeling of the interaction between turbulent premixed flames and walls p 646 N94-14763
The evolution equation for the flame surface density in turbulent premixed combustion p 567 N94-14764
Numerical simulations of turbulent premixed H2/O2/N2 flames with complex chemistry p 567 N94-14765
PREPREGS
Polymer infiltration studies
[NASA-CR-194521] p 582 N94-14539
PREPROCESSING
Preprocessing data collected with the ACTS propagation terminal p 616 N94-14676
PRESSURE
Test and evaluation methods p 506 N94-14163
The motion of a conical shaped liner driven by explosive load
[ITN-93-85215] p 585 N94-14507
PRESSURE CHAMBERS
Combustion-induced crack/debond propagation in solid propellants p 584 N94-13560
PRESSURE DISTRIBUTION
Results of wind tunnel tests of an ASRM configured 0.03 scale Space Shuttle integrated vehicle model (47-OTS) in the AEDC 16-foot transonic wind tunnel, volume 2
[NASA-CR-185697] p 534 N94-12965
Exploratory study of in-plane streamline curvature effects on a turbulent boundary layer at a Mach number of 3
[NASA-CR-193673] p 501 N94-13292
Numerical simulations of unsteady flows in turbomachines p 633 N94-13569
Flow-field interference produced by an asymmetrical support strut
[IAR-AN-75] p 504 N94-14031
The motion of a conical shaped liner driven by explosive load
[ITN-93-85215] p 585 N94-14507
VSAERO analysis of a Piper Cub aircraft p 516 N94-14616
Vortex-induced disturbance field in a compressible shear layer p 645 N94-14760
PRESSURE EFFECTS
Effect of pressure on order and stability in alloys: The case of Al-Ge
[DE93-013842] p 567 N94-12899
A multiphase model for shock-induced flow in low density foam
[DE93-013767] p 632 N94-13397
PRESSURE GRADIENTS
Thermal gravitational modelling and scaling of two-phase heat transport systems: Similarity considerations and useful equations predictions versus experimental results
[NLR-TP-91477-U] p 632 N94-13533
A three-dimensional supersonic turbulent boundary layer generated by an isentropic compression p 503 N94-13556
Interaction of two glancing, crossing shock waves with a turbulent boundary-layer at various Mach numbers
[NASA-TM-103740] p 509 N94-14780
PRESSURE MEASUREMENT
Results of experimental investigations to determine external tank protuberance loads using a 0.03-scale model of the Space Shuttle launch configuration (model 47-OTS) in the NASA/ARC unitary plan wind tunnel, volume 1
[NASA-CR-167690] p 534 N94-12810
A wall interference assessment/correction system
[NASA-CR-194174] p 500 N94-13076
NASA metrology and calibration, 1993
[NASA-TM-109280] p 597 N94-14410
Interaction of two glancing, crossing shock waves with a turbulent boundary-layer at various Mach numbers
[NASA-TM-103740] p 509 N94-14780
PRESSURE RATIO
Rotordynamic and leakage characteristics of a 4-stage brush seal
[AD-A266012] p 660 N94-12988
A comparison of computational and experimental data for a subscale high speed propulsive nozzle at low mach numbers
[AD-A266543] p 504 N94-13705
PRESSURE REDUCTION
Autofrettage: Stress distribution under load and retained stresses after depressurization. A modified plane-strain case
[AD-A266320] p 671 N94-13579
PRESSURE SUITS
Evaluation of the Retrograde Inflation Anti-G Suit (RIAGS)
[AD-A265884] p 736 N94-12935
PRESSURE VESSELS
Autofrettage: Stress distribution under load and retained stresses after depressurization. A modified plane-strain case
[AD-A266320] p 671 N94-13579
Fatigue design curves for 6061-T6 aluminum
[DE93-011849] p 571 N94-14021
Estimation of strain in 1-kW primary containment vessels by microstructural examination
[DE93-013053] p 573 N94-14316
Heavy section steel irradiation experiment
[DE93-015517] p 573 N94-14537
PREVENTION
A tentative plan on China and Asian-Pacific satellite system for disaster reduction p 693 N94-14247
PRINTED CIRCUITS
Solderability of surface mount devices
[AD-A265751] p 620 N94-13040
Rigid-flexible printed wiring boards
[DE93-013938] p 620 N94-13094
PROBABILITY DENSITY FUNCTIONS
Numerical studies of spray combustion in liquid-fueled engines p 564 N94-13685
PROBABILITY DISTRIBUTION FUNCTIONS
Stochastic bounds for a polling system
[CWI-BS-R9230] p 765 N94-14361
Distributional inferences for a location parameter
[W-9219] p 774 N94-14545
PROBABILITY THEORY
Efficient dynamic optimization of logic programs
[NASA-TM-109251] p 761 N94-12889
Rare attributes in finite universe: Hypotheses testing specification and exact randomized upper confidence bounds
[DE93-012783] p 775 N94-12955
A probabilistic method for the buckling assessment of stiffened composite shells
[NASA-TM-106286] p 671 N94-13379
An improved approach for flight readiness certification: Methodology for failure risk assessment and application examples, volume 1
[NASA-CR-194498] p 542 N94-14076
An improved approach for flight readiness certification: Methodology for failure risk assessment and application examples. Volume 2: Software documentation
[NASA-CR-194499] p 542 N94-14077
An improved approach for flight readiness certification: Methodology for failure risk assessment and application examples. Volume 3: Structure and listing of programs
[NASA-CR-194500] p 542 N94-14078
Computational problems with the binomial failure rate model and incomplete common cause failure reliability data
[DE93-014346] p 669 N94-14143
A model for fuel fire duration and application to the B-1B bomber
[DE93-013000] p 512 N94-14292
Self organized criticality
[DE93-013182] p 773 N94-14320
Probabilistic micromechanics for high-temperature composites
[NASA-CR-191150] p 676 N94-14408
Distributional inferences for a location parameter
[W-9219] p 774 N94-14545
An improved approach for flight readiness certification: Probabilistic models for flaw propagation and turbine blade failure. Volume 1: Methodology and applications
[NASA-CR-194496] p 519 N94-14841
An improved approach for flight readiness certification: Probabilistic models for flaw propagation and turbine blade failure. Volume 2: Software documentation
[NASA-CR-194497] p 519 N94-14842
PROBLEM SOLVING
The effects of evaluation and production blocking on the performance of brainstorming groups
[AD-A265495] p 734 N94-12929
Application of symbolic and algebraic manipulation software in solving applied mechanics problems
[NASA-CR-4544] p 596 N94-13798
An experimental analysis of bottleneck-centered opportunistic scheduling
[AD-A266643] p 820 N94-14796
Generating knight's tours without backtracking from errors
[AD-A266807] p 772 N94-14900
PROCEDURES
Study on improvement of flammability, odor and offgassing tests for materials
[NASDA-CNT-930009] p 563 N94-13471
PROCESS CONTROL (INDUSTRY)
Pollution prevention through total quality
[DE93-013814] p 707 N94-13390
PROCUREMENT
Johnson Space Center procurement: Controls over payments to contractors should be strengthened
[AD-A265722] p 819 N94-13060

Procurement and execution of PCB analyses: Customer-analyst interactions
[DE93-009964] p 566 N94-14694

PRODUCT DEVELOPMENT
Rigid-flexible printed wiring boards
[DE93-013938] p 620 N94-13094
Molten carbonate fuel cell product development test environmental assessment/protection plan
[DE93-000288] p 702 N94-13380

PRODUCTION COSTS
Spacecraft COst REduction Team (SCORE): TQM/CI on a massive scale p 667 N94-13160
Status and future opportunities for conversion of synthesis gas to liquid energy fuels
[DE93-010025] p 584 N94-14089
Continuous roll-to-roll a-Si photovoltaic manufacturing technology
[DE93-010006] p 704 N94-14109

PRODUCTION ENGINEERING
Rigid-flexible printed wiring boards
[DE93-013938] p 620 N94-13094

PRODUCTION MANAGEMENT
Ninth Annual NASA/Contractors Conference on Quality and Productivity. World Class Excellence: The Journey Continues. Keynote presentations
[NASA-CR-194513] p 665 N94-13148
The power of cross-functional teams in driving total quality p 666 N94-13159

PRODUCTION PLANNING
Miniature mechanism assembly
[DE93-015595] p 624 N94-13928
Decision support for material planners
[ISBN-9-03-860201-4] p 819 N94-14449

PRODUCTIVITY
Ninth Annual NASA/Contractors Conference on Quality and Productivity. World Class Excellence: The Journey Continues. Keynote presentations
[NASA-CR-194513] p 665 N94-13148
Ninth Annual NASA/Contractors Conference on Quality and Productivity. World Class Excellence: The Journey Continues. Conference presentations
[NASA-CR-194514] p 665 N94-13153
Measuring quality progress p 666 N94-13154
Object-oriented productivity metrics p 667 N94-13161
Miniature mechanism assembly
[DE93-015595] p 624 N94-13928
Land evaluation for agricultural productivity in North-East Thailand using LANDSAT TM data and geographic information p 693 N94-14242

PROFILOMETERS
Confocal profilometer with nanometric vertical resolution
[DE93-622698] p 653 N94-12857

PROGRAM VERIFICATION (COMPUTERS)
Demonstration and acceptance test plan for real-time excision software on the Adaptive Signal Processing Testbed
[DSIS-93-00275] p 751 N94-13990
EVES: An overview
[DSIS-93-00238] p 752 N94-14088
ORGBUG: A Windows-based combinatorial geometry debugger
[DE93-016640] p 755 N94-14515
Verification of critical software by statistical testing
[LAAS-93006] p 756 N94-14714
Toward a verifiable approach to the design of concurrent computations
[DE93-012908] p 756 N94-14844

PROGRAMMING ENVIRONMENTS
Common lisp framework
[AD-A265878] p 742 N94-12933
The KASE approach to domain-specific software systems p 745 N94-13357
A measurement and evaluation process model applied to software engineering environments
[INPE-5345-PUD/048] p 746 N94-13428
Caesy: A software tool for computer-aided engineering p 678 N94-14627

PROGRAMMING LANGUAGES
Simplification-driven automated partial evaluation
[DE93-012890] p 768 N94-13391
The 8th Workshop on the Mathematical Foundations of Programming Semantics
[AD-A266436] p 749 N94-13700
Execution methods, and parallel virtual machines for distributed implementation of the LCS parallel programming language
[LAAS-93032] p 761 N94-14716

PROJECT MANAGEMENT
Program/project management resource lists
[NASA-TM-109268] p 822 N94-13107
Spacecraft COst REduction Team (SCORE): TQM/CI on a massive scale p 667 N94-13160
NASA/contractor partnership on the second TDRSS ground terminal program: Breaking barriers p 668 N94-13168
Creating a strategic plan for configuration management using computer aided software engineering (CASE) tools
[DE93-013663] p 746 N94-13394
Information requirements of self-managing teams
[DE93-010319] p 824 N94-14048
Program operations plan
[DE93-012765] p 710 N94-14182
NREL solar radiation resource assessment project: Status and outlook
[DE93-010034] p 704 N94-14422
Advanced Communications Technology Satellite (ACTS) program: ACTS project update p 615 N94-14673

PROJECT PLANNING
The North Atlantic Regional Experiment (NARE)
[DE93-010126] p 706 N94-13054
Present status of JEM utilization projects p 530 N94-13273
Heat and seed recovery technology project
[DE93-009203] p 800 N94-13913
Program operations plan
[DE93-012765] p 710 N94-14182
Space transportation systems within ESA programmes: Current status and perspectives p 537 N94-14275

PROJECT SETI
Search for extraterrestrial intelligence/high resolution microwave survey team member
[NASA-CR-194177] p 739 N94-13086

PROJECTILES
A computational study of the base region flow field for the M865 projectile
[ARL-TR-109] p 504 N94-13795
Development of test techniques to simulate high-frequency mechanical shock on weapon components
[KCP-613-4998] p 675 N94-13907
Collisions and separations in 2D hydrodynamical code
[ITN-93-85225] p 639 N94-14503

PROLOG (PROGRAMMING LANGUAGE)
Computational Russian morphological generation on Prolog: Noun, pronoun, and adjective p 747 N94-13436
On the occur-check free PROLOG programs
[CWI-CS-R9238] p 748 N94-13524

PROPAGATION MODES
Combustion-induced crack/debond propagation in solid propellants p 584 N94-13560

PROPARGYL GROUPS
Infrared absorption spectroscopy and chemical kinetics of free radicals
[DE93-015078] p 562 N94-13004

PROPELLANT COMBUSTION
A computer model for liquid jet atomization in rocket thrust chambers
[NASA-CR-194194] p 627 N94-12803
Chemical reactions in scramjet engines: Reduced kinetic models for ignition, combustion and nozzle flow
[NAL-TR-1184] p 563 N94-13458
Numerical studies of spray combustion in liquid-fueled engines p 564 N94-13685
Closed-chamber analysis of M5 propellant lot RAD-64597
[AD-A266321] p 585 N94-14145
Droplet-turbulence interactions in sprays exposed to supercritical environmental conditions
[NASA-CR-194408] p 638 N94-14308

PROPELLANTS
Destruction of waste energetic materials using base hydrolysis
[DE93-012738] p 584 N94-13491

PROPELLERS
On the use of the method of matched asymptotic expansions in propeller aerodynamics and acoustics
[NLR-TP-91307-U] p 503 N94-13528

PROPULSION SYSTEM CONFIGURATIONS
Nuclear propulsion systems engineering
[DE93-010791] p 548 N94-12870
Mirror fusion propulsion system: A performance comparison with alternate propulsion systems for the manned Mars Mission
[NASA-TM-109248] p 550 N94-13147
Recent testing of 30 kW hydrogen arcjet thrusters
[NASA-TM-106214] p 551 N94-13430
Gas core nuclear thermal rocket engine research and development in the former USSR
[DE93-012165] p 552 N94-14013
Hypersonic propulsion characterization p 505 N94-14156
Aeropropulsion facilities p 506 N94-14161
Propulsion integration p 508 N94-14174
Active control of fan-generated plane wave noise
[NASA-TM-109008] p 777 N94-14481

PROPULSION SYSTEM PERFORMANCE
Nuclear propulsion systems engineering
[DE93-010791] p 548 N94-12870
Effects of hydrogen addition on combustion performance of a LOX/kerosene rocket
[NAL-TR-1177] p 548 N94-12945
Propulsion simulator for magnetically-suspended wind tunnel models
[NASA-CR-189560] p 527 N94-13127
Mirror fusion propulsion system: A performance comparison with alternate propulsion systems for the manned Mars Mission
[NASA-TM-109248] p 550 N94-13147
Electromagnetic propulsion for spacecraft
[NASA-CR-191186] p 551 N94-13416
Piston engine intake and exhaust system design
[ISVR-TR-222] p 663 N94-13874
Gas core nuclear thermal rocket engine research and development in the former USSR
[DE93-012165] p 552 N94-14013
Closed-chamber analysis of M5 propellant lot RAD-64597
[AD-A266321] p 585 N94-14145
Hypersonic propulsion characterization p 505 N94-14156
Aeropropulsion test and evaluation methods p 506 N94-14165
Hypersonic flight test. Part 1: Propulsion flight testing p 507 N94-14168

PROPULSIVE EFFICIENCY
Propulsion integration p 508 N94-14174

PROPYLENE
Surface characterization of LDEF materials
[NASA-CR-194519] p 543 N94-14683

PROSTHETIC DEVICES
New prosthetic devices
[NASA-TM-109304] p 737 N94-13611

PROTEASE
Cellular mechanism of turnover of the stress induced protein HSP 70
[AD-A265723] p 732 N94-13061

PROTECTION
An assessment of the potential for neck injury due to padding of aircraft interior walls for head impact protection
[DOT/FAA/AM-93/14] p 738 N94-13972

PROTECTIVE CLOTHING
Flammability of clothing, volume 2
[DSIS-93-00036-VOL-2] p 564 N94-13819
Review of test methods for material flammability
[DSIS-93-00480] p 564 N94-13942
Aerospace medicine and biology: A continuing bibliography with indexes (supplement 379)
[NASA-SP-7011(379)] p 733 N94-14412

PROTECTIVE COATINGS
High-temperature corrosion and protection of materials
[DE93-011072] p 568 N94-12998
Dry film lubricant evaluation
[DE93-013114] p 578 N94-13118
The effect of TiN coatings on the rolling contact fatique behavior of M50 bearing steel
[ARL-TR-40] p 662 N94-13794
JPRS report: Science and technology. Central Eurasia: Materials science
[JPRS-UMS-93-006] p 558 N94-14573
JPRS report: Science and technology. Central Eurasia: Materials science
[JPRS-UMS-93-005] p 559 N94-14575

PROTEIN CRYSTAL GROWTH
Breadboard activities for advanced protein crystal growth
[NASA-CR-193559] p 803 N94-12796
Advanced protein crystal growth programmatic sensitivity study
[NASA-CR-193827] p 804 N94-12934
Protein crystal growth p 591 N94-13756
Crystal growth of enzymes in low gravity (L-5) p 592 N94-13762

PROTEIN SYNTHESIS
Cellular mechanism of turnover of the stress induced protein HSP 70
[AD-A265723] p 732 N94-13061
The first steps of chlorophyll synthesis: RNA involvement and regulation
[DE93-014398] p 730 N94-14509

PROTEINS
Solitons and 1/f noise in molecular chains
[DE93-622898] p 778 N94-12879
Cellular mechanism of turnover of the stress induced protein HSP 70
[AD-A265723] p 732 N94-13061
Protein crystal growth p 591 N94-13756
Characterization of Spirulina biomass for CELSS diet potential
[NASA-CR-194123] p 729 N94-14097

The surface-located YopN protein is involved in calcium signal transduction in Yersinia pseudotuberculosis
[FOA-B-40416-4.4] p 729 N94-14128
Selective excitation, relaxation, and energy channeling in molecular systems
[DE93-018819] p 785 N94-14420
The first steps of chlorophyll synthesis: RNA involvement and regulation
[DE93-014398] p 730 N94-14509
Biomimetic methane oxidation
[DE93-013196] p 705 N94-14510

PROTOCOL (COMPUTERS)
Mobile host internetworking using IP loose source routing
[AD-A265713] p 759 N94-13052
On the end-to-end communication problem in unreliable networks
[ITN-93-85188] p 598 N94-13195
Kerberos: A UNIX-TCP/IP network authentication system
[DE93-011677] p 760 N94-14011
Overview of the Scalable Coherent Interface, IEEE STD 1596 (SCI)
[DE93-015247] p 761 N94-14476

PROTON BEAMS
Measurement of H zero excited states produced by foil stripping of 800-MeV H(-) ions
[DE93-014391] p 788 N94-13103
Recent study of beam stability in the PSR
[DE93-014473] p 780 N94-13173
Nuclear fusion of protons with ions of boron
[DE93-014284] p 781 N94-13219
Beam halo in high-intensity beams
[DE93-014565] p 789 N94-13328
Double semi-leptonic charm decay in HELIOS-I 450 GeV/c p-Be data
[DE93-013493] p 791 N94-13348
Proton-proton scattering contribution to emittance growth
[DE93-016090] p 787 N94-14588

PROTON ENERGY
The LAHET code system: Introduction, development, and benchmarking
[DE93-012657] p 787 N94-14804

PROTON IRRADIATION
The 1.00 MeV proton radiation resistance studies of amorphous silicon-based alloy solar cells
p 703 N94-13639

PROTON SCATTERING
Medium energy hadron-nucleus scattering in the 1/N expansion formalism
[DE93-622957] p 778 N94-12848
Relativistic proton-nucleus scattering and one-boson-exchange models p 786 N94-14550
Proton-proton scattering contribution to emittance growth
[DE93-016090] p 787 N94-14588

PROTON-PROTON REACTIONS
Polarization and color transparency
[DE93-014319] p 780 N94-13101

PROTONS
Ion anisotropy driven waves in the Earth's magnetosheath and plasma depletion layer
[DE93-012751] p 712 N94-12952
Measurement of H zero excited states produced by foil stripping of 800-MeV H(-) ions
[DE93-014391] p 788 N94-13103
Measurement of the spin of a particle using undulator radiation
[DE93-014334] p 780 N94-13149
The E2 N(yields)(Delta) transition from polarized Compton scattering
[DE93-012522] p 785 N94-14363
Primary and secondary electrical space power based on advanced PEM systems
[DE93-012643] p 553 N94-14689
The LAHET code system: Introduction, development, and benchmarking
[DE93-012657] p 787 N94-14804

PROTOPLANETS
Physical properties of gas disks around shell stars with and without dust
[NASA-CR-193655] p 835 N94-13239

PROTOSTARS
The physical and chemical evolution of protostellar disks. The growth of protostellar disks: Progress to date
[NASA-CR-194111] p 836 N94-13423
Millimeter and infrared studies of young stellar objects in dark cloud L1641 p 838 N94-13648
The 1 to 5 micron imaging of deeply embedded young stellar objects p 831 N94-13657

PROTOZOA
Chaos and microbial systems
[DE93-016814] p 730 N94-14596

PROTUBERANCES
Results of experimental investigations to determine external tank protuberance loads using a 0.03-scale model of the Space Shuttle launch configuration (model 47-OTS) in the NASA/ARC unitary plan wind tunnel, volume 1
[NASA-CR-167690] p 534 N94-12810
Results of experimental investigations to determine external tank protuberance loads using a 0.03-scale model of the Space Shuttle launch configuration (Model 47-OTS) in the NASA/ARC unitary plan wind tunnel, volume 2
[NASA-CR-167691] p 536 N94-14047

PROVING
A knowledge-based expert system to coordinate CAD/CAE with integration and test
[NASA-CR-191394] p 745 N94-13130
Methods for calibration/validation of AVNIR
p 689 N94-14216

PSEUDOPOTENTIALS
First-principles studies of phase stability and the structural and dynamical properties of hydrogen-metal systems
[DE93-016129] p 570 N94-13374

PSYCHOLOGICAL EFFECTS
An evaluation of noise and its effects on shuttle crewmembers during STS-50/USML-1
[NASA-TM-104775] p 735 N94-13961

PSYCHOLOGICAL TESTS
Work/rest schedules and performance of S-3 aviators during fleet exercise
[AD-A265807] p 734 N94-12975
Work/rest schedules and performance of F/A-18 aviators during Fleet Exercise 1992
[AD-A265826] p 735 N94-12982

PSYCHOLOGY
The effects of evaluation and production blocking on the performance of brainstorming groups
[AD-A265495] p 734 N94-12929

PSYCHOPHYSIOLOGY
Psychophysiological investigations of the biomedical problems of manned spaceflight
[NASA-CR-194107] p 732 N94-13782

PULSARS
Search for ultra-high energy emission from Geminga and five unidentified EGRET sources
[DE93-012717] p 846 N94-12816
High time resolution studies of binary x ray pulsars
[NASA-CR-194395] p 832 N94-13894
ROSAT observations of the binary Be-star/radio pulsar PSR1259-63
[NASA-CR-194394] p 832 N94-14357
Multiwavelength observations of unidentified high energy gamma ray sources
[NASA-CR-194536] p 840 N94-14688

PULSE COMMUNICATION
DSP software development environments for the Adaptive Signal Processing Testbed
[DSIS-93-00347] p 607 N94-14066
Space communications technology research in CRL
p 618 N94-14285
NTT's activities in satellite communications technology development p 618 N94-14286
Future outlook on international satellite communications in Asia Pacific region p 618 N94-14287
Technological development for broadcasting satellites in NHK Laboratories p 618 N94-14288

PULSE COMPRESSION
Lower bounds on time of arrival estimation of pulse compression waveforms
[ITN-93-85189] p 599 N94-13196
A combined analogue and digital pulse compression system using large time bandwidth product signals for use in synthetic aperture radar
[ISBN-0-315-54373-6] p 600 N94-13489
Design and performance of the terawatt Cr:LiSrAlF6 laser system
[DE93-014678] p 657 N94-13882
Independent adjustment of the higher order frequency dependent phase in chirped pulse amplification systems
[DE93-017106] p 625 N94-14522

PULSE DURATION
Design and performance of the terawatt Cr:LiSrAlF6 laser system
[DE93-014678] p 657 N94-13882
Tetravalent chromium (Cr(4+)) as laser-active ion for tunable solid-state lasers
[NASA-CR-194527] p 659 N94-14576

PULSE GENERATORS
A PC-PCL-based control system for the high-voltage pulsed-power operation of the Intense Diagnostic Neutral Beam (IDNB) Experiment
[DE93-014144] p 797 N94-13100
Review of the Procyon explosive pulsed power system
[DE93-016562] p 802 N94-14532
A high-precision direct current measuring device over a kiloampere range
[DE93-626409] p 627 N94-14885

PULSE RATE
Evolution of high-repetition-rate induction accelerators through advancements in switching
[DE93-012599] p 654 N94-12963

PULSED JET ENGINES
Low power pulsed MPD thruster system analysis and applications
[NASA-CR-191187] p 550 N94-13415

PULSED LASERS
Inertial confinement fusion program
[DE93-013372] p 796 N94-13047
New infrared photon absorption processes
[DE93-017017] p 780 N94-13071
Imaging microscopy with x ray lasers at Lawrence Livermore National Laboratory
[DE93-013419] p 655 N94-13258
Shock-free acceleration of laser driven targets
[DE93-008050] p 655 N94-13387
Excimer laser surface processing of titanium
[DE93-012633] p 570 N94-13512
Theoretical investigation of scattering by homogeneous or coated dielectric spheres illuminated with a steady state or pulsed laser beam p 657 N94-13624
Single event effects and laser simulation studies
[NASA-CR-194506] p 657 N94-13812
The interaction of intense femtosecond laser pulses with solid targets
[DE93-014415] p 658 N94-14114
A laser-based technique to continuously monitor metal aerosol emissions
[DE93-012836] p 710 N94-14183
Effects of depositon rate on Bi2Sr2CaCu2O(8+x) and Bi2Sr(1.6)La(0.4)CuO(6+x) epitaxial thin film growth by pulsed-laser ablation
[DE93-015797] p 812 N94-14362
Data analysis for GOPEX image frames
p 610 N94-14388
Independent adjustment of the higher order frequency dependent phase in chirped pulse amplification systems
[DE93-017106] p 625 N94-14522
High-order harmonic generation with short-pulse lasers
[DE93-016532] p 659 N94-14594
The 8 to 11 keV x ray sources for imaging and absorption experiments
[DE93-015973] p 803 N94-14865

PULSED RADIATION
Two-dimensional simulations of foil implosion experiments on the Los Alamos capacitor bank
[DE93-012676] p 794 N94-12814
The Large Area Pulsed Solar Simulator (LAPSS)
[NASA-CR-194507] p 703 N94-13940

PURSUIT TRACKING
A piloted simulation investigation of the normal load factor and longitudinal thrust required for air-to-air acquisition and tracking p 522 N94-13301

PYROLYTIC GRAPHITE
The optical constants and spectral specular reflectivity of Highly Oriented Pyrolytic Graphite (HOPG)
[DE93-011894] p 790 N94-12865
Structural change of graphite during electron irradiation
[DE93-015961] p 582 N94-14531

PYROTECHNICS
Destruction of waste energetic materials using base hydrolysis
[DE93-012738] p 584 N94-13491

Q

Q FACTORS
H2S data reduction
[NASA-CR-193389] p 617 N94-14743

Q SWITCHED LASERS
Novel Co:MgF2 lidar for aerosol profiler
[NASA-CR-191525] p 654 N94-13091

QUADRATURES
A new formulation of longitudinal coherent instabilities
[DE93-014288] p 789 N94-13220
I/Q demodulation of radar signals with calibration and filtering
[DREO-RN-1119] p 606 N94-14064

QUALIFICATIONS
Design, qualification and operation of nuclear rockets for safe Mars missions
[DE93-010792] p 549 N94-12996

QUALITY
Digital sound: The selection of critical programme material and preparation of recordings for CCIR tests on low bit-rate codecs
[BBC-RD-1993/1] p 598 N94-12925
Digital sound: Subjective tests on commentary-quality codecs
[BBC-RD-1993/2] p 598 N94-12926

Ninth Annual NASA/Contractors Conference on Quality and Productivity. World Class Excellence: The Journey Continues. Keynote presentations
[NASA-CR-194513] p 665 N94-13148
QUALITY CONTROL
Project AIRSTREAM: Trace gas
[DE93-008849] p 706 N94-12904
Johnson Space Center procurement: Controls over payments to contractors should be strengthened
[AD-A265722] p 819 N94-13060
NASA Johnson Space Center: Total quality partnership p 668 N94-13165
Teamwork for Oversight of Processes and Systems (TOPS). Implementation guide for TOPS version 2.0, 10 August 1992 p 668 N94-13167
George M. Low Trophy: NASA's quality and excellence award. 1992 recipients: Honeywell Clearwater, IBM Houston
[NASA-TM-109265] p 669 N94-13396
The Large Area Pulsed Solar Simulator (LAPSS)
[NASA-CR-194507] p 703 N94-13940
Quality assurance for environmental chemistry, 1991, volume 1
[DE93-011791] p 709 N94-14020
An improved approach for flight readiness certification: Methodology for failure risk assessment and application examples, volume 1
[NASA-CR-194498] p 542 N94-14076
An improved approach for flight readiness certification: Methodology for failure risk assessment and application examples. Volume 2: Software documentation
[NASA-CR-194499] p 542 N94-14077
An improved approach for flight readiness certification: Methodology for failure risk assessment and application examples. Volume 3: Structure and listing of programs
[NASA-CR-194500] p 542 N94-14078
Knowledge based systems: From process control to policy analysis
[DE93-014582] p 765 N94-14117
Procurement and execution of PCB analyses: Customer-analyst interactions
[DE93-009964] p 566 N94-14694
An improved approach for flight readiness certification: Probabilistic models for flaw propagation and turbine blade failure. Volume 1: Methodology and applications
[NASA-CR-194496] p 519 N94-14841
An improved approach for flight readiness certification: Probabilistic models for flaw propagation and turbine blade failure. Volume 2: Software documentation
[NASA-CR-194497] p 519 N94-14842
QUANTITATIVE ANALYSIS
Procedures for analysis of debris relative to Space Shuttle systems
[NASA-TM-109190] p 534 N94-12900
QUANTUM CHROMODYNAMICS
Top quark polarization and T-odd spin correlations as tools for testing (non) Standard Model predictions
[DE93-622956] p 778 N94-12847
Polarization and color transparency
[DE93-014319] p 780 N94-13101
Quark and gluon jets at CDF
[DE93-014919] p 783 N94-13884
The theory of relativistic heavy ion collisions
[DE93-015934] p 784 N94-13952
Research in theoretical nuclear physics
[DE93-015096] p 839 N94-14330
Top quark search: Results and prospects at Fermilab
[DE93-013016] p 786 N94-14524
The off shell (rho)-(omega) mixing in the QCD sum rules
[DE93-014845] p 786 N94-14527
QUANTUM EFFICIENCY
The 1.00 MeV proton radiation resistance studies of amorphous silicon-based alloy solar cells p 703 N94-13639
Numerical simulation and analysis of electrical and optical properties of Al(x)Ga(1-x)As / GaAs
[ETN-93-94387] p 703 N94-13997
Gamma-insensitive optical focal plane array
[DE93-013100] p 792 N94-14317
QUANTUM ELECTRODYNAMICS
Studies in quantum field theory
[DE93-017201] p 818 N94-14896
QUANTUM MECHANICS
Quaternions and the heuristic role of mathematical structures in physics
[DE93-622865] p 816 N94-12844
Electromagnetic deflection of spinning particles
[DE93-622866] p 778 N94-12858
The geometric phase in quantum physics
[DE93-011121] p 817 N94-13479
Selective excitation, relaxation, and energy channeling in molecular systems
[DE93-018819] p 785 N94-14420
Multiple Schroedinger cats from multilevel atoms
[DE93-013412] p 786 N94-14526
The fractional quantum Hall effect and the spherical shell model
[DE93-014553] p 818 N94-14740
Tests of non-local interferences in kaon physics at asymmetric phi-factories
[DE93-013905] p 787 N94-14857
Studies in quantum field theory
[DE93-017201] p 818 N94-14896
QUANTUM STATISTICS
On the statistical theory of the even-even nucleons levels' density
[DE93-623990] p 788 N94-14875
QUANTUM THEORY
Gauging the octonion algebra
[DE93-622864] p 775 N94-12843
Measurements on two-dimensional arrays of mesoscopic Josephson junctions
[AD-A265129] p 807 N94-13359
Dilaton quantum cosmology in two dimensions
[DE93-621377] p 836 N94-13361
Mathematics and string theory
[DE93-017903] p 817 N94-14417
Electronic states in systems of reduced dimensionality
[DE93-014440] p 815 N94-14739
Radiation perturbation theory in gravity and quantum universe as a hydrogen atom
[DE93-626621] p 849 N94-14889
Studies in quantum field theory
[DE93-017201] p 818 N94-14896
QUANTUM WELLS
Nonlinear laser spectroscopy studies of semiconductor heterostructures
[AD-A265728] p 805 N94-13037
Surfaces and interfaces of ceramics and metals
[DE93-014959] p 578 N94-13408
Electrical and optical properties of multiple quantum well structures and their applications to infrared detectors
[FFI-92/7012] p 809 N94-14010
Spin polarized photoemission studies of interfacial and thin film magnetism
[DE93-014326] p 580 N94-14142
QUARK MODELS
Measuring strangeness in the nucleon
[DE93-014861] p 785 N94-14471
QUARKS
Measurements of transverse energy and forward energy in high-energy nuclear collisions
[DE93-012755] p 788 N94-12817
Top quark polarization and T-odd spin correlations as tools for testing (non) Standard Model predictions
[DE93-622956] p 778 N94-12847
No-lost theorem for parity violating nucleon-nucleon scattering experiments
[DE93-012737] p 779 N94-12949
A search for scalar leptoquarks in D0
[DE93-012780] p 779 N94-12954
Inclusive single muons at DO
[DE93-012779] p 783 N94-13494
Quark and gluon jets at CDF
[DE93-014919] p 783 N94-13884
Top quark search: Results and prospects at Fermilab
[DE93-013016] p 786 N94-14524
Early baryon and meson spectroscopy culminating in the discovery of the Omega minus SU(3) and quarks
[DE93-014321] p 787 N94-14580
QUARTZ
Recovery of materials impacted at high velocity
[DE93-014150] p 576 N94-12885
Theory of the electronic and structural properties of solid state oxides
[DE93-016051] p 811 N94-14296
QUASARS
Polarization and variability of active galaxies and quasars p 837 N94-13550
The extent and content of low-ionization gas in galaxies p 837 N94-13551
A long-term space astrophysics research program: The evolution of the quasar continuum
[NASA-CR-193714] p 839 N94-14404
QUASI-STEADY STATES
Time resolved measurement of electron temperatures of exploding foil x ray laser plasmas
[DE93-017161] p 803 N94-14894
QUATERNIONS
Quaternions and the heuristic role of mathematical structures in physics
[DE93-622865] p 816 N94-12844
QUENCHING
Quenching and annealing effects on the specific heat of YBa2Cu3O(7-delta)
[DE93-016483] p 816 N94-14868
QUEUEING THEORY
Stochastic scheduling games with Markov decision arrival processes
[CWI-BS-R9231] p 773 N94-14005
Stochastic bounds for a polling system
[CWI-BS-R9230] p 765 N94-14361

R

R CORONAE BOREALIS STARS
Dust production in the envelopes of carbon stars: R Coronae Borealis
[ETN-93-94389] p 839 N94-14075
RADAR
Multiparameter airborne rain radar development for TRMM validation and TRMM-follow-on study p 690 N94-14226
RADAR CROSS SECTIONS
Scattering by a groove in an impedance plane
[NASA-CR-193362] p 602 N94-13720
Analysis of microstrip patch antennas with nonzero surface resistance
[NASA-TP-3362] p 604 N94-13916
RADAR DETECTION
Digital quadrature demodulation for radar ESM applications
[DREO-TN-92-10] p 603 N94-13838
Survey of subsurface geophysical exploration technologies adaptable to an airborne platform
[DE93-015080] p 717 N94-14294
RADAR IMAGERY
Preparations for and first results of the calibration and interpretation of ERS-1 SAR imagery over land
[BCRS-92-13] p 684 N94-13123
EOS workstation
[NASA-CR-191326] p 736 N94-13132
Radar imaging of sub-mesoscale ocean phenomena
[AD-A266339] p 725 N94-13581
Feature discovery on segmented objects in SAR imagery using self-organizing neural networks
[DE93-010685] p 686 N94-14056
An exact processing algorithm for wide beam spaceborne SAR data p 689 N94-14213
RADAR MEASUREMENT
Remote identification of rain and hail with a polarization diversity radar
[ISBN-0-315-55623-4] p 720 N94-13516
RADAR SCATTERING
Scattering by a groove in an impedance plane
[NASA-CR-193362] p 602 N94-13720
RADAR SIGNATURES
I/Q demodulation of radar signals with calibration and filtering
[DREO-RN-1119] p 606 N94-14064
RADAR TRACKING
Venus gravity
[NASA-CR-194077] p 841 N94-12823
Reasoning with uncertain and incomplete information in aerospace applications
[NLR-TP-91366-U] p 763 N94-13529
MUSIC and maximum likelihood using a refined propagation model: Performance comparison for radar low-angle tracking
[DREO-RN-1122] p 603 N94-13832
RADAR TRANSMISSION
MUSIC and maximum likelihood using a refined propagation model: Performance comparison for radar low-angle tracking
[DREO-RN-1122] p 603 N94-13832
RADIAL VELOCITY
Photometry and spectroscopy in the open cluster Alpha Persei, 2
[NASA-CR-193397] p 833 N94-14358
RADIANCE
Recent results from material processing studies on new generation lasers
[DE93-013841] p 653 N94-12898
Infrared transmission and path radiance through dust and fog
[AD-A265825] p 791 N94-12979
Volume 14: The first SeaWiFS intercalibration round-robin experiment, SIRREX-1, July 1992
[NASA-TM-104566] p 725 N94-14090
RADIANT COOLING
X ray emission from dynamical shock models in hot-star winds
[NASA-CR-194093] p 847 N94-13288
Recent testing of 30 kW hydrogen arcjet thrusters
[NASA-TM-106214] p 551 N94-13430
RADIANT FLUX DENSITY
The 1 to 5 micron imaging of deeply embedded young stellar objects p 831 N94-13657
RADIANT HEATING
Measuring surface fluxes in CAPE
[NASA-CR-193664] p 711 N94-12788

RADIATION BELTS
Force-free magnetic fields, curl eigenfunctions, and the sphere in transform space, with applications to fluid dynamics and electromagnetic theory
[AD-A265805] p 834 N94-12971
Stormtime transport of ring current and radiation belt ions
[NASA-CR-194416] p 714 N94-13793
Dynamical model for the distribution of geomagnetically trapped anomalous-component ions
[ATR-91(9558)-6] p 784 N94-13936

RADIATION COUNTERS
Search for UHE point-source emission over various time scales
[DE93-012718] p 846 N94-12922
A program of correlated observations using the EGRET instrument on GRO and the IMB neutrino detector
[NASA-CR-194367] p 783 N94-13856
Radiation effects on optoelectronic analog link for particle detectors
[DE93-015794] p 793 N94-14529

RADIATION DAMAGE
About the influence of inert gas ion implantation on metal corrosion stability
[DE93-620574] p 569 N94-13360
Growth of samarskite crystal under microgravity conditions (M-20) p 590 N94-13752
Radiation effects on optoelectronic analog link for particle detectors
[DE93-015794] p 793 N94-14529

RADIATION DETECTORS
Crystallographic and metallurgical characterization of radiation detector grade cadmium telluride materials
[DE93-014335] p 806 N94-13150
Absolute detection efficiency of a micro-channel plate detector to x rays in the 1-100 KeV energy range
[DE93-012592] p 789 N94-14460
Results from a water-Cerenkov array
[DE93-012715] p 849 N94-14461
Measuring parity violation using the neutron capture reaction
[DE93-016629] p 786 N94-14514
Radiation effects on optoelectronic analog link for particle detectors
[DE93-015794] p 793 N94-14529

RADIATION DISTRIBUTION
Study of the consequences of the Chernobyl accident and technogenic activity in the Republic Belarus using aerospace methods p 693 N94-14246
Meteorological data, new series A monographs. Volume 6, no. 3: Estimation of influence of high clouds in the radiation field and the climat by analysis of NOAA AVHRR data
[ETN-93-94170] p 723 N94-14707

RADIATION DOSAGE
Temperature dependence of diffusivities, preliminary definition phase
[NASA-CR-192613] p 648 N94-13326
Genetic effects of HZE and cosmic radiation (L-9) p 593 N94-13766
Development and application of the automated Monte Carlo biasing procedure in SAS4
[DE93-015205] p 774 N94-14334

RADIATION EFFECTS
Project proposal for partial computational physics support for Survivability of Coatings program
[DE93-013788] p 576 N94-12939
Annealing study of main electron irradiation-induced defects (H4 and H5) in P-InP using DLTS technique
[DE93-623204] p 806 N94-13213
Comment of parameter excitation of Alfven and Heliicon waves in a magnetoactive compensated semiconductor by microwave radiation
[DE93-623203] p 806 N94-13228
About the influence of inert gas ion implantation on metal corrosion stability
[DE93-620574] p 569 N94-13360
Cellular track model for study of heavy ion beams
[NASA-TP-3351] p 732 N94-13714
Genetic effects of HZE and cosmic radiation (L-9) p 593 N94-13766
Study on the biological effect of cosmic radiation and the development of radiation protection technology (L-11) p 593 N94-13768
Interactions between spacecraft and their environments
[NASA-TM-106115] p 541 N94-13917
Radiation hardening and radiation-induced chromium depletion effects on intergranular stress corrosion cracking of austenitic stainless steels
[DE93-011602] p 572 N94-14058
Radiation effects on optoelectronic analog link for particle detectors
[DE93-015794] p 793 N94-14529
Structural change of graphite during electron irradiation
[DE93-015961] p 582 N94-14531
JPRS report: Science and technology. Central Eurasia: Materials science
[JPRS-UMS-93-004] p 559 N94-14574
AlGaAs diode laser blue shift resulting from fast neutron irradiation
[AD-A266642] p 659 N94-14681
Investigations of low-temperature neutron embrittlement of ferritic steels
[DE93-015460] p 573 N94-14700
Quantitative luminescence imaging system
[DE93-015691] p 793 N94-14702

RADIATION HARDENING
1/f noise and oxide traps in MOSFETs
[DE93-007581] p 619 N94-12942
Mongoose ASIC microcontroller programming guide
[NASA-RP-1319] p 623 N94-13871
Radiation hardening and radiation-induced chromium depletion effects on intergranular stress corrosion cracking of austenitic stainless steels
[DE93-011602] p 572 N94-14058

RADIATION MEASUREMENT
Measuring surface fluxes in CAPE
[NASA-CR-193664] p 711 N94-12788
Evolution of the lower planetary boundary layer over strongly contrasting surfaces
[DE93-010667] p 717 N94-14424

RADIATION MEASURING INSTRUMENTS
A Fourier transform microscope for x ray and/or gamma ray imaging
[AD-D015742] p 791 N94-13664

RADIATION PRESSURE
Improved treatment of global positioning system force parameters in precise orbit determination applications p 514 N94-14371

RADIATION PROTECTION
A photovoltaic catenary-tent array for the Martian surface
[NASA-TM-106306] p 621 N94-13194
Beta/gamma test problems for ITS
[DE93-013522] p 781 N94-13349
Preliminary nuclear safety assessment of the NEPST (Topaz 2) space reactor program
[DE93-012853] p 551 N94-13514
CRRES to blaze new trails in orbit
[NASA-TM-109314] p 713 N94-13620
Study on the biological effect of cosmic radiation and the development of radiation protection technology (L-11) p 593 N94-13768

RADIATION SHIELDING
Effects of radiobiological uncertainty on vehicle and habitat shield design for missions to the moon and Mars
[NASA-TP-3312] p 846 N94-12875
Semiempirical fragmentation models on galactic cosmic ray transport calculations with hydrogen target
[NASA-TP-3350] p 847 N94-13263
Development and application of the automated Monte Carlo biasing procedure in SAS4
[DE93-015205] p 774 N94-14334
Measuring parity violation using the neutron capture reaction
[DE93-016629] p 786 N94-14514

RADIATION SOURCES
Two-dimensional simulations of foil implosion experiments on the Los Alamos capacitor bank
[DE93-012676] p 794 N94-12814

RADIATION SPECTRA
Operational test of the airborne data acquisition system: SADA, the Bara Bonita experiment
[INPE-5451-NTC/305] p 685 N94-13610

RADIATION TOLERANCE
The Second Workshop on Deployment and Assembly Experiment of Large Space Structure on Orbit
[NASDA-CON-930003] p 529 N94-13268
Research on radiation resistance properties of structural materials for space use p 529 N94-13271
The 1.00 MeV proton radiation resistance studies of amorphous silicon-based alloy solar cells p 703 N94-13639

RADIATION TRANSPORT
A new method to assess Monte Carlo convergence
[DE93-012667] p 772 N94-12919
Three dimensional time-dependent hydrodynamic and propagation modeling of x ray laser emission
[DE93-012575] p 654 N94-12962
MCNP benchmark analyses of critical experiments for the Space Nuclear Thermal Propulsion program
[DE93-014046] p 548 N94-12981
Semiempirical fragmentation models on galactic cosmic ray transport calculations with hydrogen target
[NASA-TP-3350] p 847 N94-13263
Beta/gamma test problems for ITS
[DE93-013522] p 781 N94-13349
Distributed processor Monte Carlo: MCNP results on a 16-node IBM cluster
[DE93-012639] p 752 N94-14176
Development and application of the automated Monte Carlo biasing procedure in SAS4
[DE93-015205] p 774 N94-14334
The LAHET code system: Introduction, development, and benchmarking
[DE93-012657] p 787 N94-14804

RADIATIVE HEAT TRANSFER
Chemistry and transport in a multi-dimensional model
[NASA-CR-194425] p 716 N94-13969
The accuracy of approximating radiative heat transfer using a temperature dependent thermal conductivity
[DE93-013105] p 638 N94-14318

RADIATIVE TRANSFER
DMSP F11 SSM/T-2 calibration and validation
[AD-A265817] p 719 N94-12978
The continuum emission of active galactic nuclei
[ITN-93-85208] p 847 N94-13232
Basic research in solar physics
[NASA-CR-193632] p 844 N94-13234
Radiative transfer in the dynamic atmospheres of Mira-type variables
[NASA-CR-193324] p 829 N94-13287
ADP study of gamma-ray bursts
[NASA-CR-194311] p 848 N94-13708
Water-vapour, total water and rainrate from passive microwave satellite data over ocean
[DLR-FB-92-37] p 723 N94-14189

RADICALS
Application of synchrotron radiation in chemical dynamics
[DE93-015040] p 563 N94-13411

RADIO ALTIMETERS
Ionospheric calibration for single frequency altimeter measurements
[NASA-CR-194282] p 716 N94-14049
High performance multi-mode radar altimeter for future spaceborne application p 548 N94-14214

RADIO ASTRONOMY
Neptune high-latitude emission: Dependence of angle on frequency
[NASA-CR-193280] p 848 N94-13476
Theoretical molecular studies of astrophysical interest
[NASA-CR-193300] p 838 N94-13781
The next century astrophysics program p 548 N94-14832

RADIO ATTENUATION
Statistical results from the Virginia Tech propagation experiment using the Olympus 12, 20, and 30 GHz satellite beacons p 613 N94-14658
Long duration measurements of fading on a low elevation angle, 11-GHz satellite path p 613 N94-14661
Large-scale rainfall diversity for ACTS p 613 N94-14662
Rain-rate data base development and rain-rate climate analysis p 614 N94-14664
Propagation issues for emerging mobile and portable communications: A systems perspective p 614 N94-14667

RADIO COMMUNICATION
Measurement of wave propagation for VHF/UHF and a comparison between measured and predicted values
[FFI/RAPPORT-92/7024] p 605 N94-13968
The developments of satellite communications of China p 618 N94-14282
The current situation, trends, international cooperation of space communication technological development.in the Republic of Korea p 699 N94-14283
Space communications technology research in CRL p 618 N94-14285
Future outlook on international satellite communications in Asia Pacific region p 618 N94-14287
Technological development for broadcasting satellites in NHK Laboratories p 618 N94-14288
Proceedings of the Seventeenth NASA Propagation Experimenters Meeting (NAPEX 17) and the Advanced Communications Technology Satellite (ACTS) Propagation Studies Miniworkshop
[NASA-CR-194096] p 612 N94-14654
Opening remarks: Current and future activities p 612 N94-14655
New challenges in propagation research in the US p 612 N94-14656
Statistical results from the Virginia Tech propagation experiment using the Olympus 12, 20, and 30 GHz satellite beacons p 613 N94-14658
Long duration measurements of fading on a low elevation angle, 11-GHz satellite path p 613 N94-14661
A database for propagation models p 614 N94-14665
Contribution towards a draft revision of recommendations 681: Propagation data required for the design of Earth-space land mobile telecommunications systems p 614 N94-14666

Propagation considerations in the American Mobile Satellite system design p 614 N94-14668
Coverage aspects of a single frequency network designed for digital audio broadcasting [BBC-RD-1993/3] p 616 N94-14742

RADIO DIRECTION FINDERS
Portable multipath measurement system [DSIS-93-00177] p 603 N94-13843

RADIO ECHOES
A study of meteor scatter communications [DSIS-93-00151] p 603 N94-13841

RADIO EMISSION
Neptune high-latitude emission: Dependence of angle on frequency [NASA-CR-193280] p 848 N94-13476

RADIO EQUIPMENT
Development of UHF spark-switched L-C Oscillators [DE93-015019] p 623 N94-13892

RADIO FREQUENCIES
Dimensionally similar discharges with central RF heating on the D3-D tokamak [DE93-012776] p 795 N94-12953
Design for low beam loss in accelerators for intense neutron source applications [DE93-014557] p 789 N94-13327
Electron beam probe measurements of electric fields in rf discharges p 601 N94-13661
Field emitter array RF amplifier development project. Phase 1: Cathode technology development [AD-A266346] p 622 N94-13776
Plasma-etching science meets technology in the MDL [DE93-012086] p 800 N94-13908
Ionospheric calibration for single frequency altimeter measurements [NASA-CR-194282] p 716 N94-14049

RADIO FREQUENCY HEATING
Ion cyclotron heating experiments and plans for the Advanced Toroidal Facility (ATF) [DE93-012965] p 795 N94-13033
Effect on antenna structure of high power RF during plasma operation [DE93-013278] p 797 N94-13144
Electrical characterization of the JET A(sub 2) antenna: Comparison of model with measurements Wade, T. [DE93-012964] p 607 N94-14291
Microwave sintering of large alumina bodies [DE93-012752] p 581 N94-14340
Design of the ion cyclotron system for TPX [DE93-012961] p 803 N94-14770
Anomalous ion transport and feedback control [DE93-018324] p 803 N94-14874

RADIO GALAXIES
ROSAT observations of clusters with wide-angle tailed radio sources [NASA-CR-193784] p 833 N94-14405

RADIO METEORS
Meteor forward scatter studies [DSIS-93-00382] p 602 N94-13801
A study of meteor scatter communications [DSIS-93-00151] p 603 N94-13841

RADIO NAVIGATION
Environmental projects. Volume 15: Environmental assessment: Proposed 1-megawatt radar transmitter at the Mars site [NASA-CR-194098] p 598 N94-13090

RADIO OBSERVATION
Reduction and analysis of seasons 15 and 16 (1991 - 1992) Pioneer Venus radio occultation data and correlative studies with observations of the near-infrared emission of Venus [NASA-CR-194128] p 841 N94-13083

RADIO OCCULTATION
Reduction and analysis of seasons 15 and 16 (1991 - 1992) Pioneer Venus radio occultation data and correlative studies with observations of the near-infrared emission of Venus [NASA-CR-194128] p 841 N94-13083

RADIO RECEIVERS
Theoretical SIS mixer research [AD-A266323] p 807 N94-13580
Results from a study of scintillation behavior at 12, 20, and 30 GHz using the results from the Virginia Tech Olympus receivers p 613 N94-14659

RADIO SIGNALS
Coverage aspects of a single frequency network designed for digital audio broadcasting [BBC-RD-1993/3] p 616 N94-14742

RADIO SOURCES (ASTRONOMY)
A survey of compact planetary nebulae at radio wavelengths [ISBN-0-315-61950-3] p 829 N94-13371

RADIO TELEMETRY
Characteristics of the amateur radio means of the Arsene satellite [CNES-NT-131] p 605 N94-13950

RADIO TRANSMISSION
Measurement of wave propagation for VHF/UHF and a comparison between measured and predicted values [FFI/RAPPORT-92/7024] p 605 N94-13968

RADIO WAVES
Proceedings of the Seventeenth NASA Propagation Experimenters Meeting (NAPEX 17) and the Advanced Communications Technology Satellite (ACTS) Propagation Studies Miniworkshop [NASA-CR-194096] p 612 N94-14654
Opening remarks: Current and future activities p 612 N94-14655

RADIOACTIVE DECAY
Double semi-leptonic charm decay in HELIOS-I 450 GeV/c p-Be data [DE93-013493] p 781 N94-13348
The beta(+) decay and cosmic-ray half-life of Mn-54 [DE93-013913] p 848 N94-13695
Are there atmospheric neutrino oscillations? [DE93-015550] p 783 N94-13890
Charge-exchange reactions and weak interaction rates for Type 2 supernovae [DE93-015104] p 783 N94-13893
The (mu)(+) yields e(+)gamma [DE93-012750] p 785 N94-14181
Rare muon processes [DE93-012646] p 785 N94-14366
E789 and P865: High-rate fixed-target studies of charm and beauty [DE93-017223] p 788 N94-14898

RADIOACTIVE ISOTOPES
Project AIRSTREAM: Trace gas [DE93-008849] p 706 N94-12904
Research in cosmic and gamma ray astrophysics: Cosmic physics portion [NASA-CR-194127] p 847 N94-13211
Study of the consequences of the Chernobyl accident and technogenic activity in the Republic Belarus using aerospace methods p 693 N94-14246
The LAHET code system: Introduction, development, and benchmarking [DE93-012657] p 787 N94-14804

RADIOACTIVE MATERIALS
Research in cosmic and gamma ray astrophysics: Cosmic physics portion [NASA-CR-194127] p 847 N94-13211

RADIOACTIVE WASTES
Canonical correlation of waste glass compositions and durability, including pH [DE93-012754] p 578 N94-13493
Environmental radioactivity intercomparison 1992 [NPL-RSA(EXT)-37] p 708 N94-13880
Camera calibration in a hazardous environment performed in situ with automated analysis and verification [DE93-010274] p 651 N94-14046
Relationship between borosilicate glass composition, structure, and durability test response (SRS) [DE93-013578] p 581 N94-14343
Modeling surface area to volume effects on borosilicate glass dissolution [DE93-011891] p 581 N94-14432
Dynamic soil pressures on rigid cylindrical vaults [DE93-013930] p 676 N94-14585
A study of hydrogen effects on fracture behavior of radioactive waste storage tanks [DE93-018171] p 574 N94-14873

RADIOBIOLOGY
Effects of radiobiological uncertainty on vehicle and habitat shield design for missions to the moon and Mars [NASA-TP-3312] p 846 N94-12875

RADIOGRAPHY
Real time radiography of Titan 4 booster [DE93-012450] p 548 N94-12911

RADIOMETERS
Nimbus-7 Earth radiation budget calibration history. Part 1: The solar channels [NASA-RP-1316] p 844 N94-13963
Volume 14: The first SeaWiFS intercalibration round-robin experiment, SIRREX-1, July 1992 [NASA-TM-104566] p 725 N94-14090
Earth Observation Center Annual Report on Research and Development, Fiscal Year 1992 [EOC-92-01-0007] p 687 N94-14091
Earth observation experiment data analysis p 687 N94-14093
ADEOS project p 687 N94-14094
A calibration procedure for radiation budget radiometers and its influence on interpretation of measured values [MITT-82] p 651 N94-14149
Clouds and the Earth's Radiant Energy System (CERES) on the Tropical Rainfall Measuring Mission (TRMM) p 690 N94-14223

RADIOMETRIC CORRECTION
Analytical framework for modeling scale-related variabilities in remote sensing p 685 N94-13592
Radio metric errors due to mismatch and offset between a DSN antenna beam and the beam of a troposphere calibration instrument p 607 N94-14370

RADIOSONDES
DMSP F11 SSM/T-2 calibration and validation [AD-A265817] p 719 N94-12978

RAIL TRANSPORTATION
Activities of Bombardier, Inc. [ISBN-2-921393-11-5] p 499 N94-13520

RAIN
Remote identification of rain and hail with a polarization diversity radar [ISBN-0-315-55623-4] p 720 N94-13516
Spatial and temporal variability of precipitation and chemistry: Case studies from the frontal boundary study [DE93-007883] p 708 N94-13910
Water-vapour, total water and rainrate from passive microwave satellite data over ocean [DLR-FB-92-37] p 723 N94-14189
TRMM system overview and status in the United States p 690 N94-14221
TRMM Project in Japan: Overview and status p 690 N94-14222
TRMM precipitation radar algorithm p 690 N94-14224
Estimate of sampling errors of TRMM rainfall observation by using radar-AMeDAS composite data p 690 N94-14225
Multiparameter airborne rain radar development for TRMM validation and TRMM-follow-on study p 690 N94-14226
Future TRMM follow-on mission p 691 N94-14228
Large-scale rainfall diversity for ACTS p 613 N94-14662
Rain rate duration statistics derived from the Mid-Atlantic coast rain gauge network p 614 N94-14663
Rain-rate data base development and rain-rate climate analysis p 614 N94-14664

RAIN FORESTS
Modeling of biosphere-atmosphere interaction for forest and pastureland in the Amazon [INPE-5454-TDI/496] p 707 N94-13330
Spatial variability of throughfall chemistry in a tropical rainforest (Central Amazonia, Brazil) [INPE-5431-PRE/1765] p 720 N94-13429
Estimations of temperature and humidity of the canopy in Amazon Forest using microwave data from SMMR sensor of Nimbus-7 satellite [INPE-5444-TDI/490] p 720 N94-13614

RAIN GAGES
Rain rate duration statistics derived from the Mid-Atlantic coast rain gauge network p 614 N94-14663

RAMAN SPECTRA
Inertial Confinement Fusion [DE93-013303] p 795 N94-13017
Resonant x ray Raman scattering from atoms and molecules [DE93-015158] p 784 N94-13896
Brillouin scattering from fluctuations produced by stimulated Raman scattering [DE93-016531] p 792 N94-14438
Investigation of the feasibility of optical diagnostic measurements at the exit of the SSME [NASA-CR-193832] p 553 N94-14682

RAMAN SPECTROSCOPY
Scanning tunneling microscopy studies of diamond films and optoelectronic materials [NASA-CR-194363] p 578 N94-13246

RANDOM ACCESS MEMORY
Hashing and rehashing in emulated shared memory [CWI-CS-R9240] p 740 N94-13525
Single event effects and laser simulation studies [NASA-CR-194506] p 657 N94-13812
Paradigms for very fast parallel algorithms [ITN-93-85212] p 755 N94-14556

RANDOM PROCESSES
Investigation for improving Global Positioning System (GPS) orbits using a discrete sequential estimator and stochastic models of selected physical processes [NASA-CR-194167] p 512 N94-13082

RANDOM SAMPLING
Rare attributes in finite universe: Hypotheses testing specification and exact randomized upper confidence bounds [DE93-012783] p 775 N94-12955

RANDOM VARIABLES
A new method to assess Monte Carlo convergence [DE93-012667] p 772 N94-12919

RANDOM VIBRATION
Estimation of critical values and vibration characteristics on supersonic delta wings. Part 2: Locally-stationary time series analysis of nonstationary random responses [NAL-TR-1179] p 502 N94-13345

RANGE (EXTREMES)
Robust stability of diamond families of polynomials with complex coefficients
[NASA-CR-194132] p 768 N94-13421
RANGEFINDING
Sequential ranging: How it works
[NASA-CR-194508] p 532 N94-13796
RANK TESTS
Statistical analysis of the m rankings problem: Kendall's prototype and the grouping estimate method based on normal scores
[DSIS-93-00139] p 773 N94-13848
RANKING
Statistical analysis of the m rankings problem: Kendall's prototype and the grouping estimate method based on normal scores
[DSIS-93-00139] p 773 N94-13848
RAPID QUENCHING (METALLURGY)
Measurements of crystal growth kinetics at extreme deviations from equilibrium
[DE93-014526] p 815 N94-14798
RARE EARTH COMPOUNDS
Fine-powder Al2O3 and SiO2 for preparation of multielement standards for rare-earth elements analysis
[DE93-625118] p 567 N94-14884
RARE EARTH ELEMENTS
Fine-powder Al2O3 and SiO2 for preparation of multielement standards for rare-earth elements analysis
[DE93-625118] p 567 N94-14884
RARE GASES
Measurements of scattering processes in negative ion-atom collisions
[DE93-013863] p 779 N94-12940
About the influence of inert gas ion implantation on metal corrosion stability
[DE93-620574] p 569 N94-13360
RAREFIED GAS DYNAMICS
Techniques for estimating Space Station aerodynamic characteristics
[NASA-CR-193394] p 541 N94-13955
RASTER SCANNING
Confocal profilometer with nanometric vertical resolution
[DE93-622698] p 653 N94-12857
RATES (PER TIME)
Adaptive Signal Processing Testbed
[DSIS-93-00258] p 604 N94-13869
RATS
Physiological Anatomical Rodent Experiment (PARE).04 Feasibility Test 1
[NASA-CR-194423] p 728 N94-13473
Improving physical performance by chemical stimulation
[DSIS-92-03763] p 728 N94-13823
RAWINSONDES
Atmospheric soundings during the Washita 1992 campaign
[NASA-CR-194383] p 712 N94-13212
RAY TRACING
The propagation characteristics and instability properties of low-frequency electromagnetic waves in the Io plasma torus p 601 N94-13650
A data distributed parallel algorithm for ray-traced volume rendering
[NASA-CR-191520] p 749 N94-13721
AXAF FITS standard for ray trace interchange
[NASA-CR-194025] p 832 N94-14305
RAYLEIGH WAVES
On the secondary instability of the most dangerous Goertler vortex
[NASA-CR-191504] p 636 N94-13785
RAYLEIGH-RITZ METHOD
A robust multilevel simultaneous eigenvalue solver
[NASA-CR-191491] p 767 N94-13202
REACTING FLOW
A time-accurate numerical method for chemically reacting flows at all Mach numbers p 500 N94-13198
Topics on spatially high-order accurate methods and pre-conditioning for the Navier-Stokes equations with finite-rate chemistry p 633 N94-13572
Hypersonic overview p 505 N94-14154
Computation of nonequilibrium flows using PNS equations p 641 N94-14610
Simulation of hypersonic, reacting flow around reentry bodies: Comparisons of numerical and experimental results
[MBB-LME-211-S-PUB-507] p 509 N94-14710
Studying Turbulence Using Numerical Simulation Databases. 4: Proceedings of the 1992 Summer Program
[NASA-CR-194556] p 643 N94-14745
DNS and modeling of the interaction between turbulent premixed flames and walls p 646 N94-14763
The evolution equation for the flame surface density in turbulent premixed combustion p 567 N94-14764
Effect of finite-rate chemistry and unequal Schmidt numbers on turbulent non-premixed flames modeled with single-step chemistry p 567 N94-14766
Stochastic modeling of turbulent reacting flows p 647 N94-14768
REACTION KINETICS
Molecular solvent-dynamical effects on activated electron-transfer kinetics: How important is solvent friction?
[AD-A265886] p 779 N94-12894
Modeling ignition chemistry
[DE93-012340] p 561 N94-12910
Conversion of light hydrocarbon gases to metal carbides for production of liquid fuels and chemicals
[DE93-014962] p 583 N94-13002
Infrared absorption spectroscopy and chemical kinetics of free radicals
[DE93-015078] p 562 N94-13004
Fifteenth Combustion Research Conference
[DE93-015758] p 562 N94-13045
A coherent flame model of premixed turbulent combustion in a counterflow geometry
[CUED/A-THERMO/TR.60] p 562 N94-13085
Research on chemical vapor deposition processes for advanced ceramic coatings
[NASA-CR-193613] p 577 N94-13089
Absorption and damage thresholds of low defect density hafnia deposited with activated oxygen
[DE93-013853] p 655 N94-13243
Low temperature metal-organic chemical vapor deposition growth processes for high efficiency solar cells
[DE92-010562] p 702 N94-13386
Application of synchrotron radiation in chemical dynamics
[DE93-015040] p 563 N94-13411
Chemical reactions in scramjet engines: Reduced kinetic models for ignition, combustion and nozzle flow
[NAL-TR-1184] p 563 N94-13458
Reduction of Pu(6) with hydrogen peroxide: Effects of plutonium, peroxide, and iron concentrations and of reaction time
[DE93-013598] p 564 N94-13487
Chemistry and transport in a multi-dimensional model
[NASA-CR-194425] p 716 N94-13969
Hypersonic overview p 505 N94-14154
Hydrogen peroxide safety issues
[DE93-013895] p 565 N94-14346
Modeling surface area to volume effects on borosilicate glass dissolution
[DE93-011891] p 581 N94-14432
Numerical simulation of velocity-coupled combustion response of solid rocket propellants p 585 N94-14490
Numerical simulations of turbulent premixed H2/O2/N2 flames with complex chemistry p 567 N94-14765
Study of chemical reactions under the influence of ultrasound
[DE93-016458] p 778 N94-14867
Comparative ignition of hexane and octane isomers in a shock tube
[DE93-016535] p 566 N94-14869
REACTION TIME
Reduction of Pu(6) with hydrogen peroxide: Effects of plutonium, peroxide, and iron concentrations and of reaction time
[DE93-013598] p 564 N94-13487
REACTION WHEELS
Low cost attitude control system reaction wheel development
[NASA-CR-191332] p 540 N94-13140
REACTIVITY
Applications of surface science to solid lubricants
[SMC-TR-93-24] p 579 N94-13903
Metastability of yttrium-oxides
[DE93-016548] p 813 N94-14440
REACTOR CORES
Heavy section steel irradiation experiment
[DE93-015517] p 573 N94-14537
REACTOR MATERIALS
A data base for aging of structural materials
[DE93-009714] p 824 N94-13915
Estimation of strain in 1-kW primary containment vessels by microstructural examination
[DE93-013053] p 573 N94-14316
Investigations of low-temperature neutron embrittlement of ferritic steels
[DE93-015460] p 573 N94-14700
REACTOR SAFETY
Preliminary nuclear safety assessment of the NEPST (Topaz 2) space reactor program
[DE93-012853] p 551 N94-13514
A data base for aging of structural materials
[DE93-009714] p 824 N94-13915
SHEAN (Simplified Human Error Analysis code) and automated THERP
[DE93-014904] p 738 N94-14451
REACTOR TECHNOLOGY
Test apparatus for ITER blanket cooling water distribution design
[DE93-753157] p 795 N94-12944
READERS
Development of an automated film-reading system for ballistic ranges
[NASA-CR-194398] p 650 N94-13815
REAGENTS
Unexpectedly rapid hydrosilation polymerization of the diallyl derivative of bisphenol A and 2,6-diallylphenol
[AD-A265832] p 577 N94-12986
REAL TIME OPERATION
Laser-induced fluorescence over optical fibers for real time in situ measurement of petroleum hydrocarbons in seawater
[AD-A265106] p 790 N94-12863
Real time radiography of Titan 4 booster
[DE93-012450] p 548 N94-12911
Development of a portable multispectral thermal infrared camera
[NASA-CR-191340] p 648 N94-13176
Thermal Expert System (TEXSYS): Systems automony demonstration project, volume 1. Overview
[NASA-TM-102877] p 538 N94-13201
Error analysis of real time and post processed or bit determination of GFO using GPS tracking
[NASA-CR-193646] p 512 N94-13238
The silent step in time
[CWI-CS-R9221] p 768 N94-13496
Weather forecasting support for AASE-2
[NASA-CR-194342] p 721 N94-13675
Communications and control for electric power systems: Power flow classification for static security assessment
[NASA-CR-194512] p 624 N94-13948
Portable acoustic wave sensor systems for real-time monitoring of volatile organic compounds
[DE93-013753] p 582 N94-14511
Real-time dynamic simulation of the Cassini spacecraft using DARTS. Part 2: Parallel/vectorized real-time implementation p 680 N94-14639
Design and control of a macro-micro robot for precise force applications p 682 N94-14651
Identification of continuous-time dynamical systems: Neural network based algorithms and parallel implementation
[DE93-014427] p 766 N94-14737
Mathematic methods and algorithms for real-time applications
[AD-A266776] p 771 N94-14789
RECEIVERS
Adaptive Signal Processing Testbed
[DSIS-93-00258] p 604 N94-13869
Calibration of the receiver channel for the GOPEX precursor experiments p 610 N94-14387
RECONNAISSANCE AIRCRAFT
Design and pilot evaluation of the RAH-66 Comanche Core AFCS p 525 N94-13321
Design and pilot evaluation of the RAH-66 Comanche selectable control modes p 525 N94-13322
An analysis of helicopter attrition using a low level combat simulation
[DSIS-93-00282] p 515 N94-13839
RECORDS MANAGEMENT
Making the connection between information modeling and implementation
[DE93-011588] p 820 N94-12907
RECOVERABLE LAUNCH VEHICLES
HOPE conceptual design in FY 1991
[NASDA-CNT-930017] p 535 N94-13600
Conceptual design on H-2 Orbiting Plane (HOPE)
[NASDA-CNT-930018] p 535 N94-13656
The concept study of the space transportation system HOPE in FY 1991
[NASDA-CNT-930016] p 536 N94-14100
RECTANGLES
Fully developed turbulent flow in rectangular interrupted-plate ducts
[ISBN-0-315-63594-0] p 632 N94-13474
RECTANGULAR PLATES
Measuring methods for CFRP laminates' bending and torsion rigidities characteristics p 529 N94-13272
RECTIFICATION
Plasma-etching science meets technology in the MDL
[DE93-012086] p 800 N94-13908
RECURSIVE FUNCTIONS
Spatially-varying IIR filter banks for image coding
[NASA-CR-193727] p 619 N94-12897
Recursive time-varying filter banks for subband image coding
[NASA-CR-193726] p 598 N94-12920

RECYCLING
Evaluation for membrane components of water recycling system
[NAL-TM-646] p 737 N94-13388
Survey and study on Environmental Control and Life Support (ECLS) technologies, part 2
[NASDA-CNT-930012-PT-2] p 737 N94-13472
Recycling in space
[NASA-TM-109307] p 737 N94-13615
Effect of stabilization on the recycling of polyolefins in blow moulding
[IMI-93RT-42400-1477-G] p 596 N94-13684
Fourteenth National Industrial Energy Technology Conference: Proceedings
[DE93-016698] p 710 N94-14516

RED SHIFT
Redshift distortions of galaxy correlation functions
[DE93-014007] p 834 N94-12980
A photometric and morphological study of compact groups of galaxies and their environments
[ISBN-0-315-59601-5] p 829 N94-13370
The flight performance of the Galileo orbiter USO
p 611 N94-14398
A long-term space astrophysics research program: The evolution of the quasar continuum
[NASA-CR-193714] p 839 N94-14404
Brillouin scattering from fluctuations produced by stimulated Raman scattering
[DE93-016531] p 792 N94-14438

REDUCED ORDER FILTERS
Failure modes of reduced-order orbit determination filters and their remedies p 532 N94-14373
A component modes projection and assembly model reduction methodology for articulated, multi-flexible body structures p 677 N94-14622

REDUNDANCY
Exploiting the cannibalistic traits of Reed-Solomon codes p 609 N94-14378

REDUNDANT COMPONENTS
Generalized impedance control of a redundant manipulator p 661 N94-13575

REED-SOLOMON CODES
Exploiting the cannibalistic traits of Reed-Solomon codes p 609 N94-14378
Enhanced decoding for the Galileo S-band mission
p 609 N94-14380

REELS
An experimental study of tether reel system: A laboratory model
[NAL-TR-1176T] p 539 N94-12943

REENTRY VEHICLES
High temperature electromagnetic characterization of thermal protection system tile materials
[NASA-CR-189687] p 578 N94-13431
Simulation of hypersonic, reacting flow around reentry bodies: Comparisons of numerical and experimental results
[MBB-LME-211-S-PUB-507] p 509 N94-14710

REFERENCE STARS
Optical propagation through atmospheric turbulence. Model analysis of anisoplanatism and application to adaptive optics
[ONERA-P-1992-4] p 716 N94-14192

REFILLING
Studies on equatorial shock formation during plasmaspheric refilling
[NASA-CR-194392] p 715 N94-13954

REFLECTANCE
Reflective coatings for solar applications
[DE93-010026] p 702 N94-13381
Optimization of transparent and reflecting electrodes for amorphous silicon solar cells
[DE93-010009] p 704 N94-14110
Determination of the surface cleanliness of metals by FT-IR spectroscopy
[DE93-013252] p 565 N94-14525
Shielded open-circuited sample holders for dielectric and magnetic measurements of liquids and powders
[PB93-198851] p 652 N94-14687

REFLECTION
The 24 GHz measurements of 2.2 lambda conical horn antennas illuminating a conducting sheet
[NASA-TM-109002] p 598 N94-12811

REFLECTOR ANTENNAS
An initial study of using the 34-m antenna for lunar mission support p 611 N94-14396
Feasibility study of a synthesis procedure for array feeds to improve radiation performance of large distorted reflector antennas
[NASA-CR-194491] p 612 N94-14501

REFLECTORS
Analysis of samples of reflector materials which are multicoated and metal samples with oxide coatings which have been exposed the space environment in LDEF testing
[NASA-CR-193647] p 575 N94-12789
Fundamentals and techniques of nonimaging optics
[DE93-013145] p 791 N94-13015
Research on inflatable structure for space use
p 530 N94-13275
Reflective coatings for solar applications
[DE93-010026] p 702 N94-13381

REFRACTION
Optimization study of x ray laser coherence in Ni-like Ta
[DE93-016419] p 660 N94-14888

REFRACTIVITY
The optical constants and spectral specular reflectivity of Highly Oriented Pyrolytic Graphite (HOPG)
[DE93-011894] p 790 N94-12865
Optical properties of CO2 ice and CO2 snow in the ultraviolet, visible, and infrared
[NASA-CR-194110] p 686 N94-14081
Manufacturing and examination of integrated optical waveguide components in silicon
[ETN-93-94393] p 793 N94-14704

REFRACTORIES
How to read a phase equilibrium diagram for high-temperature ceramics material as main object
[DE93-512333] p 582 N94-14513

REFRACTORY COATINGS
Research on chemical vapor deposition processes for advanced ceramic coatings
[NASA-CR-193613] p 577 N94-13089

REFRACTORY MATERIALS
High-temperature corrosion and protection of materials
[DE93-011072] p 568 N94-12998
How to read a phase equilibrium diagram for high-temperature ceramics material as main object
[DE93-512333] p 582 N94-14513

REFRACTORY METAL ALLOYS
JPRS report: Science and technology. Central Eurasia: Materials science
[JPRS-UMS-93-006] p 558 N94-14573

REFRIGERANTS
ARTI Refrigerant Database
[DE93-014774] p 595 N94-13021
Miscibility of lubricants with refrigerants, phase 1
[DE93-014766-PHASE-1] p 596 N94-13407
Compatibility of refrigerants and lubricants with motor materials
[DE93-014768] p 583 N94-14801

REFRIGERATING
ARTI Refrigerant Database
[DE93-014774] p 595 N94-13021
Double inlet pulse tube cryocooler theory
[AD-A266832] p 597 N94-14877

REFRIGERATORS
Three-stage linear, split-Stirling cryocooler for 1 to 2K magnetic cold stage
[NASA-CR-4538] p 776 N94-13897
A recuperative superfluid Stirling refrigerator
[DE93-016521] p 597 N94-14592
Double inlet pulse tube cryocooler theory
[AD-A266832] p 597 N94-14877

REGENERATION (ENGINEERING)
Destruction of problematic airborne contaminants by hydrogen reduction using a Catalytically Active, Regenerable Sorbent (CARS)
[NASA-CR-194354] p 709 N94-14103

REGENERATION (PHYSIOLOGY)
Validated environmental and physiological data from the CELSS Breadboard Projects Biomass Production Chamber. BWT931 (Wheat cv. Yecora Rojo)
[NASA-TM-109272] p 738 N94-13979

REGENERATIVE COOLING
Recent testing of 30 kW hydrogen arcjet thrusters
[NASA-TM-106214] p 551 N94-13430

REGENERATIVE FUEL CELLS
Primary and secondary electrical space power based on advanced PEM systems
[DE93-012643] p 553 N94-14689

REGIONAL PLANNING
Obtaining digital regional planning information from aerial pictures
[REPT-228] p 700 N94-14810

REGOLITH
Workshop on the Space Environment: The Effects on the Optical Properties of Airless Bodies
[NASA-CR-194417] p 842 N94-14298
Impact melting and vaporization in planetary regoliths
p 843 N94-14299
Extrapolation of space weathering processes to other small solar system bodies p 843 N94-14300
Laboratory simulations of lunar darkening processes
p 843 N94-14301
Deposition of impact-generated vapors in the lunar regolith p 843 N94-14302
The state of Fe in the lunar regolith and its relationship to the spectral reflectance properties of the moon
p 843 N94-14303

REGRESSION ANALYSIS
Exploratory data analysis: Past, present and future
[AD-A266775] p 774 N94-14788
Generalized smooth models
[DE93-013045] p 756 N94-14864

REGULATIONS
Environmental awareness
[DE93-014192] p 707 N94-13218
Fourteenth National Industrial Energy Technology Conference: Proceedings
[DE93-016698] p 710 N94-14516

REINFORCING FIBERS
Characterization of composite materials for aerospace structures
[ESA-TT-1260] p 557 N94-13804
Thermal shock resistance of ceramic matrix composites
[NASA-CR-189136] p 557 N94-13920

RELATIVISTIC ELECTRON BEAMS
Excitation of coupled waves in plasma periodic structures by relativistic electron beam and acceleration of charged particles
[DE93-621657] p 794 N94-12853
Stripping efficiencies for 277 MeV/amu gold beam on copper foils
[DE93-014306] p 569 N94-13221

RELATIVISTIC PARTICLES
Investigation of plasma instabilities in the Polar cusp
[NASA-CR-194283] p 796 N94-13084
The theory of relativistic heavy ion collisions
[DE93-015934] p 784 N94-13952

RELATIVISTIC THEORY
The electric field of a current-carrying conductor
[DE93-626637] p 617 N94-14892

RELAXATION (MECHANICS)
Muon spin relaxation studies of heavy fermion superconductors
[DE93-014576] p 815 N94-14773
Thermal history effects on electrical relaxation and conductivity for potassium silicate glass with low alkali concentrations
[NASA-TM-106324] p 583 N94-14845

RELAXATION METHOD (MATHEMATICS)
Theory for iterative solution of large dynamical systems using parallel computation
[TKK-MAT-A304] p 760 N94-14187

RELIABILITY
Computational problems with the binomial failure rate model and incomplete common cause failure reliability data
[DE93-014346] p 669 N94-14143

RELIABILITY ANALYSIS
Chip-level testability requirements guidelines
[AD-A262583] p 619 N94-12967
Switchover software reliability estimate for Paducah freezer/sublimer computer systems
[DE93-013844] p 756 N94-14696
Verification of critical software by statistical testing
[LAAS-93006] p 756 N94-14714

RELIABILITY ENGINEERING
Defining the performance gap: Conducting a self-assessment p 666 N94-13155
On the end-to-end communication problem in unreliable networks
[ITN-93-85188] p 598 N94-13195
Study of the intermateability of Cannon and Souriau subminiature connectors
[CNES-NT-132] p 624 N94-13951
Computational problems with the binomial failure rate model and incomplete common cause failure reliability data
[DE93-014346] p 669 N94-14143
An improved approach for flight readiness certification: Probabilistic models for flaw propagation and turbine blade failure. Volume 1: Methodology and applications
[NASA-CR-194496] p 519 N94-14841
An improved approach for flight readiness certification: Probabilistic models for flaw propagation and turbine blade failure. Volume 2: Software documentation
[NASA-CR-194497] p 519 N94-14842

REMOTE CONTROL
Heavy section steel irradiation experiment
[DE93-015517] p 573 N94-14537

REMOTE MANIPULATOR SYSTEM
Application of intelligently adaptable structure and robot to large space structure p 530 N94-13277
Space Station Common Berthing Mechanism, a multi-body simulation application p 544 N94-14640

REMOTE SENSING
Knowledge-based oceanographic image compression
[AD-A265752] p 821 N94-13041
Linkage of anthropogenic aerosol to clouds and climate
[DE93-016434] p 719 N94-13080
Novel Co:MgF2 lidar for aerosol profiler
[NASA-CR-191525] p 654 N94-13091

Development of a portable multispectral thermal infrared camera
[NASA-CR-191340] p 648 N94-13176
Design of partially supervised classifiers for multispectral image data
[NASA-CR-194299] p 823 N94-13192
Dendrometric variables estimation in homogeneous forests using LANDSAT TM data
[INPE-5455-TDI/497] p 684 N94-13331
Spectral reflectance of soils from Sao Paulo State
[INPE-5424-PRP/172] p 684 N94-13377
Remote sensing of aquatic system
[INPE-5271-PRP/159] p 684 N94-13426
Net radiation mapping of mountainous terrain using Landsat-5 thematic mapper imagery and digital terrain data
[ISBN-0-315-57755-X] p 685 N94-13475
Remote identification of rain and hail with a polarization diversity radar
[ISBN-0-315-55623-4] p 720 N94-13516
A knowledge-based model for the integration of remote sensing into a mineral exploration program
[ISBN-0-315-58982-5] p 685 N94-13523
Analytical framework for modeling scale-related variabilities in remote sensing p 685 N94-13592
A review and analysis of neural networks for classification of remotely sensed multispectral imagery
[NASA-CR-194291] p 763 N94-13603
Operational test of the airborne data acquisition system: SADA, the Bara Bonita experiment
[INPE-5451-NTC/305] p 685 N94-13610
Estimations of temperature and humidity of the canopy in Amazon Forest using microwave data from SMMR sensor of Nimbus-7 satellite
[INPE-5444-TDI/490] p 720 N94-13614
Study on TRMM data utilization for meteorology
[NASDA-CNT-930007] p 721 N94-13643
Advanced solid-state array spectroradiometer data collection during HAPEX-2 Sahel
[NASA-CR-194144] p 808 N94-13875
Wind erosion in semiarid landscapes: Predictive models and remote sensing methods for the influence of vegetation
[NASA-CR-194029] p 715 N94-13956
Activities report of the Netherlands Remote Sensing Board
[ETN-93-93880] p 686 N94-14073
Intelligent environment for interpretation tasks of remotely sensed images
[INPE-5466-PRE/1774] p 687 N94-14082
Volume 14: The first SeaWiFS intercalibration round-robin experiment, SIRREX-1, July 1992
[NASA-TM-104566] p 725 N94-14090
Minutes of the Sixth CEOS Plenary Meeting
[NASA-TM-108252] p 542 N94-14112
Integration of remotely sensed data and cadastral ownership boundaries for land inventory purposes
[BCRS-92-16] p 687 N94-14127
Multisensor remote sensing data and GIS techniques for monitoring preservation areas: A case study
[INPE-5317-PRE/1714] p 688 N94-14131
An algorithm for the remote sensing of fog using satellite-data and additional information
[DLR-FB-92-23] p 688 N94-14135
Water-vapour, total water and rainrate from passive microwave satellite data over ocean
[DLR-FB-92-37] p 723 N94-14189
Asia-Pacific ISY Conference, volume 2
[NASDA-CM-199-VOL-2] p 688 N94-14209
Artificial oil pollution detection and wave observation in the sea adjacent to Japan by ERS-1 SAR p 688 N94-14212
High performance multi-mode radar altimeter for future spaceborne application p 548 N94-14214
IMG: Interferometric monitor for greenhouse gases p 689 N94-14217
Spectroscopic method and data reduction algorithm for laser long-path absorption measurements using RIS p 689 N94-14218
Image processing and analysis of airborne POLDER data p 689 N94-14219
Overview of the ILAS operational data processing system p 690 N94-14220
TRMM system overview and status in the United States p 690 N94-14221
TRMM Project in Japan: Overview and status p 690 N94-14222
Clouds and the Earth's Radiant Energy System (CERES) on the Tropical Rainfall Measuring Mission (TRMM) p 690 N94-14223
TRMM precipitation radar algorithm p 690 N94-14224
Estimate of sampling errors of TRMM rainfall observation by using radar-AMeDAS composite data p 690 N94-14225
Space measurements for determining the Earth's energy and water cycles p 690 N94-14227
Future TRMM follow-on mission p 691 N94-14228
Remote sensing of low level cloud optical characteristics p 691 N94-14229
The effects of anthropogenic aerosols on optical thickness and particle size of clouds. Part 1: Retrieval algorithm p 691 N94-14230
Climate products from NOAA operational satellites p 691 N94-14231
Seasonal change of the land-surface temperature over Asian Continent derived from GAC data on NOAA-11 AVHRR p 691 N94-14232
Earth radiation budget, cloud, and aerosol parameters derived from AVHRR and TOVS measurements p 691 N94-14233
Some potentials of the Indonesian region for Earth observation p 692 N94-14237
Application of satellite remote sensing technology in disaster mitigation: A case study of Bangladesh p 692 N94-14238
Integration of remote sensing and mathematical modelling in disaster mitigation p 692 N94-14239
Soil erosion mapping using remote sensing and GIS techniques p 692 N94-14240
Detecting land cover changes in Chiang-Mai area in Thailand p 693 N94-14241
Land evaluation for agricultural productivity in North-East Thailand using LANDSAT TM data and geographic information p 693 N94-14242
Effects of typhoon on TOMS data p 693 N94-14243
Satellite remote sensing for disaster mitigation p 693 N94-14244
A concept for the world environment and disaster observation system p 693 N94-14245
Study of the consequences of the Chernobyl accident and technogenic activity in the Republic Belarus using aerospace methods p 693 N94-14246
A tentative plan on China and Asian-Pacific satellite system for disaster reduction p 693 N94-14247
Earth observation from low-inclination orbit as a necessary complement to polar missions p 694 N94-14248
Development of a remote sensing geographic information system for land cover changes and assessment of risk due to natural and man made hazards covering the area of the inner delta of the Yellow River p 694 N94-14249
The role of the dynamics for the deviation of the total ozone from the long-term mean at the edge of the polar vortex p 694 N94-14250
The European Arctic ozone experiment: An investigation of Northern Hemisphere ozone depletion p 694 N94-14251
Space-based activities: SAM 2 and SAGE 2 p 694 N94-14252
New evidences supported the Wei hypothesis about the formation of the Antarctic ozone hole p 694 N94-14253
Multi-source national forest inventory of Finland p 694 N94-14254
Global assessment of human activities p 695 N94-14255
The Swedish ISY contribution p 695 N94-14256
Vegetation mapping of Indo-China Peninsula using MOS-1 MESSR and NOAA AVHRR p 695 N94-14257
Remote sensing for monitoring tropical moist forests in the Indo-Chinese region p 695 N94-14258
Estimation of vegetation damage due to ash fall in Mt. Pinatubo area using MOS-1 data p 695 N94-14259
Mangrove afforestation monitoring using remote sensing p 695 N94-14260
Outline of ISY sea surface temperature data sets p 696 N94-14261
Integration of SST data sets using MOS-1 satellite data: For validation and monitoring p 696 N94-14262
Geophysical validation of ATSR sea surface temperatures p 696 N94-14263
Accuracy validation test of estimated sea surface temperature by satellite data p 696 N94-14264
Sea surface effect on the sea surface temperature estimation by satellite data p 696 N94-14265
On the sea truth data of the Kuroshio meander and cold eddy movement p 696 N94-14266
Tracking of change of a warm-core ring structure p 696 N94-14267
Outline of ISY Kuroshio observation experiment p 697 N94-14268
A method for estimation of partial cloud cover within a pixel and its effect p 697 N94-14269
Warm streamers extended from Warm Core Rings (WCR's) and their role on fish migration and fishing ground formation p 697 N94-14270
Atmospheric correction for sea surface temperature by application of microwave dual-channel technique to VTIR data p 697 N94-14271
Some thoughts on the space programs in the Asia Pacific regions p 697 N94-14272
China's devotion to space science and applications p 532 N94-14273
Survey of subsurface geophysical exploration technologies adaptable to an airborne platform
[DE93-015080] p 717 N94-14294
Workshop on the Space Environment: The Effects on the Optical Properties of Airless Bodies
[NASA-CR-194417] p 842 N94-14298
ERS-1 system
[ESA-SP-1146] p 699 N94-14353
Supervised classification of remotely sensed images
[DLR-FB-92-07] p 700 N94-14428
Educational module for the Higher Agricultural Education. Part 2: Eutrophication observed by remote sensing: An educational approach to water quality monitoring
[BCRS-92-11B] p 818 N94-14462
Determination of the surface cleanliness of metals by FT-IR spectroscopy
[DE93-013252] p 565 N94-14525
The National Remote Sensing Program (NRSP-2 1991 - 2000): The 1992 annual plan of the Netherlands Remote Sensing Board
[BCRS-92-22] p 700 N94-14544
Computer vision and sensor fusion for detecting buried objects
[DE93-012605] p 700 N94-14566
Educational module for the higher agricultural education. Part 1: Land use classification using satellite pictures
[BCRS-92-11A] p 819 N94-14809
Obtaining digital regional planning information from aerial pictures
[REPT-228] p 700 N94-14810
Signal and reference wavelengths for the elimination of SO2 cross sensitivity in remote measurements of tropospheric ozone with lidar
[GKSS/92/E/24] p 617 N94-14819

REMOTE SENSORS

Buoy experiments to obtain the sea-truth data for OCTS/NSCAT, part 1
[NASDA-CNT-930005-PT-1] p 725 N94-13653
Microgravity acceleration measurement environment characterization p 590 N94-13755
Evaluation of the Shuttle remote manipulator
[NASA-CR-194351] p 662 N94-13800
Earth Observation Center Annual Report on Research and Development, Fiscal Year 1992
[EOC-92-01-0007] p 687 N94-14091
Calibration and in-house validation results of JERS-1 data p 687 N94-14092
Earth observation experiment data analysis p 687 N94-14093
ADEOS project p 687 N94-14094
Asia-Pacific ISY Conference, volume 2
[NASDA-CM-199-VOL-2] p 688 N94-14209
Results from ERS-1 and JERS-1 SAR calibration experiments and data analysis p 688 N94-14210
Geologic application of JERS-1 SAR data p 688 N94-14211
High performance multi-mode radar altimeter for future spaceborne application p 548 N94-14214
Sensor operation of Advanced Earth Observing Satellite (ADEOS) p 689 N94-14215
Methods for calibration/validation of AVNIR p 689 N94-14216
Overview of the ILAS operational data processing system p 690 N94-14220
Clouds and the Earth's Radiant Energy System (CERES) on the Tropical Rainfall Measuring Mission (TRMM) p 690 N94-14223
Multiparameter airborne rain radar development for TRMM validation and TRMM-follow-on study p 690 N94-14226
Hardware design for the Autonomous Visibility Monitoring (AVM) observatory p 533 N94-14394

RENAL FUNCTION

Renal function alterations during skeletal muscle disuse in simulated microgravity
[NASA-CR-194258] p 733 N94-13824

RENORMALIZATION GROUP METHODS

Development of a recursion RNG-based turbulence model
[NASA-CR-191511] p 636 N94-13718

REPLACING

On-line upgrade of program modules using AdaPT
[NASA-CR-194331] p 754 N94-14472

REPORTS

NASA/DOD Aerospace Knowledge Diffusion Research Project. Paper 34: Users and uses of DOD technical reports: A report from the field
[NASA-TM-109327] p 825 N94-14485

RESEARCH AIRCRAFT
Preliminary design features of the RASCAL: A NASA /Army rotorcraft in-flight simulator p 526 N94-13325
Performance evaluation tests of the GPS/DGPS navigation system installed in the NAL Dornier 228: Preliminary ground test results
[NAL-TM-649] p 513 N94-13346
Position error determination for the speedometer and altimeter of the NAL QSTOL experimental aircraft ASKA
[NAL-TR-1144] p 517 N94-13451
Theoretical support for the Airborne Antarctic Ozone Experiment
[NASA-CR-193669] p 713 N94-13465
Flight validation of a pulsed smoke flow visualization system
[NASA-CR-186026] p 516 N94-14106
RESEARCH AND DEVELOPMENT
National atmospheric sciences program, fiscal years 1987-1990
[NSF-92-16] p 711 N94-12794
Here's the beef: A case study in organizational transformation p 667 N94-13163
JPRS report: Science and technology. Central Eurasia: Space
[JPRS-USP-93-003] p 828 N94-13182
Publications of the Jet Propulsion Laboratory: 1990 and 1991
[NASA-CR-193287] p 823 N94-13461
Artificial intelligence in Canada: A description by the members of the ACAI
[NRC-31789] p 763 N94-13517
Highlights, 1981
[NASA-TM-109305] p 850 N94-13612
Artificial intelligence in Canada: A description by the members of the ACAI
[CNR-31790] p 764 N94-13820
Research and technologhy highlights, 1992
[NASA-TM-4452] p 850 N94-13962
Selected data on academic science and engineering R and D expenditures: Fiscal Year 1991
[NSF-92-329] p 819 N94-13982
Science, technology, and the federal government: National goals for a new era p 827 N94-14115
Activities of Institute for Microstructural Sciences
[NRC-32815] p 810 N94-14198
Activities of Institute for Microstructural Sciences
[CNR-32815] p 810 N94-14199
Storage systems for national information assets
[DE93-015101] p 825 N94-14331
NASA/DOD Aerospace Knowledge Diffusion Research Project. Paper 36: Technical uncertainty as a correlate of information use by US industry-affiliated aerospace engineers and scientists
[NASA-TM-109328] p 825 N94-14486
The 1991 research and technology report, Goddard Space Flight Center
[NASA-TM-108738] p 851 N94-14791
RESEARCH FACILITIES
Vertical motion simulator familiarization guide
[NASA-TM-103923] p 527 N94-13008
Technology parks and the cooperation among universities and firms: The cases of Campinas, Sao Jose dos Campos e Sao Carlos
[INPE-5251-TAE/04] p 818 N94-13427
Activities of Institute for Aerospace Research, Flight Research Laboratory
[CTN-93-60832] p 850 N94-13519
Cray Y-MP
[NASA-TM-109303] p 741 N94-13609
A future view of computational science in aircraft
[NASA-TM-109284] p 504 N94-13621
A history of the Defence Research Establishment, Ottawa
[CTN-93-60737] p 850 N94-14060
DCIEM: The first fifty years, 1939-1989
[CTN-93-60767] p 733 N94-14141
Uniform user and group IDs on a large network
[DE93-013047] p 760 N94-14315
Current titles --- National Center for Electron Microscopy
[DE93-015859] p 851 N94-14587
A guide to the DRA 13 ft x 9 ft Low Speed Wind Tunnel Facility
[AD-A267739] p 528 N94-14876
RESEARCH MANAGEMENT
Selected data on academic science and engineering R and D expenditures: Fiscal Year 1991
[NSF-92-329] p 819 N94-13982
The National Remote Sensing Program (NRSP-2 1991 - 2000): The 1992 annual plan of the Netherlands Remote Sensing Board
[BCRS-92-22] p 700 N94-14544
RESERVOIRS
BOAST 2 for the IBM 3090 and RISC 6000
[DE93-000138] p 638 N94-14351
RESIDUAL STRENGTH
Fatigue and residual strength characteristics of fiber metal laminates subjected to incidental damage
[LR-708] p 674 N94-13803
The development of inspection and repair methods for the C-17 aft cargo door
[LR-704] p 499 N94-13904
RESIDUAL STRESS
Measurement of residual strain in composites by means of time-of-flight neutron diffraction
[DE93-012939] p 555 N94-13248
Residual contact restraints in cryogenics
[ETN-93-94375] p 671 N94-13501
Thermal gradient-induced deflection of a thick-walled cylinder with bending residual stresses
[AD-A266347] p 673 N94-13777
Hierarchical nonlinear behavior of hot composite structures
[NASA-TM-106229] p 676 N94-14041
Optimal synthesis of hot composite laminates with interphase layers
[NASA-TM-106326] p 557 N94-14042
RESIDUES
Promotion of geothermal energy development in 1991
[DE93-799058] p 701 N94-13215
RESIN BONDING
Polymer infiltration studies
[NASA-CR-194521] p 582 N94-14539
RESIN TRANSFER MOLDING
Resin transfer molding of textile composites
[NASA-CR-191505] p 554 N94-12833
RESINS
Polymer infiltration studies
[NASA-CR-194521] p 582 N94-14539
RESISTANCE HEATING
Ohmic heating of composite candidate graphite-fiber/coating combinations
[NASA-TM-4491] p 554 N94-12871
Instability heating of the HDZP
[DE93-012641] p 798 N94-13513
RESONANCE
Stability of subharmonics and escape phenomena in the twin-well potential duffing system p 775 N94-13235
Resonances in the Sigma NN system
[DE93-014353] p 785 N94-14144
Measuring parity violation using the neutron capture reaction
[DE93-016629] p 786 N94-14514
RESONANCE SCATTERING
Resonant x ray Raman scattering from atoms and molecules
[DE93-015158] p 784 N94-13896
RESONANT FREQUENCIES
Predicting the vibrations of a spinning inflated membrane
[DE93-010690] p 676 N94-14456
Applications of computer algebra to distributed parameter systems p 677 N94-14623
RESONANT VIBRATION
Adiabatic and non adiabatic effects in Free Electron Laser (FEL) non linear interactions
[ITN-93-85224] p 659 N94-14547
RESONATORS
Measurement electronics of industrial microwave resonator sensors
[TKK-S-RAD-S194] p 625 N94-14096
H2S data reduction
[NASA-CR-193389] p 617 N94-14743
RESOURCE ALLOCATION
PC4CAST: A tool for DSN load forecasting and capacity planning p 610 N94-14384
RESOURCES MANAGEMENT
Hot Dry Rock energy
[DE93-014452] p 702 N94-13403
Quality assurance for environmental chemistry, 1991, volume 1
[DE93-011791] p 709 N94-14020
An evaluation of ZIM and entity-relational models in managing databases for decision support systems
[ERB-1034] p 824 N94-14202
Sequestering carbon dioxide in industrial polymers: Building materials for the 21st century
[DE93-016087] p 580 N94-14297
Fourteenth National Industrial Energy Technology Conference: Proceedings
[DE93-016698] p 710 N94-14516
Pattern and Process in Landscape Ecology: Eighth Annual US Landscape Ecology Symposium
[DE93-014032] p 711 N94-14859
RESPONSE TIME (COMPUTERS)
Analysis and effects of the number of nests of DO loops during vector supercomputing
[NAL-TR-1146] p 748 N94-13453
A design methodology for portable software on parallel computers
[NASA-CR-194181] p 752 N94-14139
RESTORATION
Integrated, flexible, and rapid geophysical surveying
[DE93-009989] p 712 N94-12906
RETURN TO EARTH SPACE FLIGHT
HOPE real time flight operations analyses for return to earth phase, part B
[NASDA-CNT-930011] p 535 N94-13599
HOPE real time flight operations analyses for return to earth phase, part A
[NASDA-CNT-930010-PT-A] p 535 N94-13645
REUSABLE HEAT SHIELDING
High temperature electromagnetic characterization of thermal protection system tile materials
[NASA-CR-189687] p 578 N94-13431
REUSABLE LAUNCH VEHICLES
HOPE conceptual design in FY 1991
[NASDA-CNT-930017] p 535 N94-13600
Conceptual design on H-2 Orbiting Plane (HOPE)
[NASDA-CNT-930018] p 535 N94-13656
The concept study of the space transportation system HOPE in FY 1991
[NASDA-CNT-930016] p 536 N94-14100
Research and development of space transportation systems in ISAS p 537 N94-14277
Contributions of winged re-entry vehicle to space activities p 537 N94-14278
REUSABLE ROCKET ENGINES
The conceptual study on future space transportation systems. Part A: Conceptual study of flyback booster
[NASDA-CNT-930013] p 536 N94-14099
REUSABLE SPACECRAFT
The concept study of the space transportation system HOPE in FY 1991
[NASDA-CNT-930016] p 536 N94-14100
REVERSE ENGINEERING
Integrating interface slicing into software engineering processes
[NASA-CR-192761] p 754 N94-14368
REVERSE FIELD PINCH
Theory of field-reversed configurations
[DE93-015611] p 794 N94-12862
REVERSE OSMOSIS
Evaluation for membrane components of water recycling system
[NAL-TM-646] p 737 N94-13388
REYNOLDS NUMBER
A solution algorithm for the prediction of compressible laminar and turbulent shear flows p 634 N94-13635
Boundary-layer transition p 507 N94-14171
The structure of laminar flow in a three-dimensional driven cavity p 640 N94-14601
The structure of intense vorticity in homogeneous isotropic turbulence p 643 N94-14747
REYNOLDS STRESS
Sub-grid scale modeling for large eddy simulations in analysis of shock-turbulence interactions
[DE93-013425] p 631 N94-13250
Development of a recursion RNG-based turbulence model
[NASA-CR-191511] p 636 N94-13718
Vortex-induced disturbance field in a compressible shear layer p 645 N94-14760
RHEOLOGY
Workshop on Formation of Supermolecular Structures in Composite Fluid: Phase Rule and Dynamics
[DE93-782887] p 581 N94-14421
RHYTHM (BIOLOGY)
Gordon Research Conference on Chronobiology, 1991
[AD-A266354] p 728 N94-13698
RIBBONS
Polymer infiltration studies
[NASA-CR-194521] p 582 N94-14539
RIBONUCLEIC ACIDS
Evolution of catalytic RNA in the laboratory
[NASA-CR-194124] p 727 N94-13210
Analysis of the V antigen lcrGVH-yopBD operon of Yersinia pseudotuberculosis: Evidence for a regulatory role of LcrH and LcrV
[FOA-B-40417-4.4] p 729 N94-14129
The first steps of chlorophyll synthesis: RNA involvement and regulation
[DE93-014398] p 730 N94-14509
RICCATI EQUATION
Kalman filter input estimation
[NAL-TR-1182] p 649 N94-13456
On the geometry of external spectral factors and the Riccati inequality
[CWI-BS-R9227] p 770 N94-14002
RIEMANN MANIFOLD
Scalar curvature and spherical-type Riemannian manifolds
[DE93-622852] p 767 N94-12895
Heat flows and harmonic maps with a free boundary
[DE93-622856] p 632 N94-13509

A hydrogen atom in the curved space: Orthogonality of radial wave functions with respect to the critical momentum
[DE93-626623] p 788 N94-14891

RIEMANN WAVES
Full Riemann solution of the one- and two-dimensional Euler equations
[DLR-FB-92-34] p 638 N94-14188

RIGID STRUCTURES
Determination of position and orientation of rigid bodies from image segments
[FFI-92-4005] p 752 N94-14039
Predicting the vibrations of a spinning inflated membrane
[DE93-010690] p 676 N94-14456
Animation of multi-flexible body systems and its use in control system design p 678 N94-14629
Nonrecursive formulations of multibody dynamics and concurrent multiprocessing p 679 N94-14632
Parallel O(log n) algorithms for open- and closed-chain rigid multibody systems based on a new mass matrix factorization technique p 679 N94-14636
Real-time dynamics simulation of the Cassini spacecraft using DARTS. Part 1: Functional capabilities and the spatial algebra algorithm p 680 N94-14638
Computational Control Workstation: Users' perspectives p 681 N94-14648

RING CURRENTS
The interplanetary origins and the main-phase development of moderate geomagnetic storms (1978 - 1979)
[INPE-5445-TDI/491] p 835 N94-13174
Stormtime transport of ring current and radiation belt ions
[NASA-CR-194416] p 714 N94-13793
Energetic neutral atoms: Imaging the magnetospheric ring current
[NASA-CR-194339] p 715 N94-13826
Terrestrial magnetospheric imaging: Numerical modeling of low energy neutral atoms
[DE93-014561] p 717 N94-14328

RING LASERS
Performance evaluation of the honeywell GG1308 miniature ring laser gyroscope
[AD-A266694] p 653 N94-14782

ROADS
Stochastic performance modeling and evaluation of obstacle detectability with imaging range sensors
[NASA-CR-194510] p 605 N94-13946

ROBOT ARMS
Roller-gear drives for robotic manipulators design, fabrication and test
[NASA-CR-194248] p 660 N94-12802
Control algorithm implementation for a redundant degree of freedom manipulator
[NASA-CR-191339] p 762 N94-13131
Modelling robotic systems with DADS
p 678 N94-14625

ROBOT CONTROL
Roller-gear drives for robotic manipulators design, fabrication and test
[NASA-CR-194248] p 660 N94-12802
Application of intelligently adaptable structure and robot to large space structure p 530 N94-13277
Robot programming, natural computation and conceptual graphs
[ITN-93-85193] p 748 N94-13539
Robot-task compliance: The energy criterion
[ITN-93-85196] p 763 N94-13568
Goddard Space Flight Center robotics demo
[NASA-TM-109302] p 662 N94-13604
A capaciflector-based robotic system
[NASA-CR-193783] p 833 N94-14359
Inverse dynamics: Simultaneous trajectory tracking and vibration reduction with distributed actuators
p 678 N94-14624
A neural-network approach to robotic control
p 679 N94-14634
Design and control of a macro-micro robot for precise force applications p 682 N94-14651

ROBOT DYNAMICS
Dynamics and design of nonholonomic robotic mechanical systems
[ISBN-0-315-72009-3] p 662 N94-13597
Inverse dynamics: Simultaneous trajectory tracking and vibration reduction with distributed actuators
p 678 N94-14624
Modelling robotic systems with DADS
p 678 N94-14625
A neural-network approach to robotic control
p 679 N94-14634
Parallel methods for dynamic simulation of multiple manipulator systems p 680 N94-14637
Design and control of a macro-micro robot for precise force applications p 682 N94-14651

ROBOT SENSORS
A capaciflector-based robotic system
[NASA-CR-193783] p 833 N94-14359

ROBOTICS
Roller-gear drives for robotic manipulators design, fabrication and test
[NASA-CR-194248] p 660 N94-12802
Advancing automation and robotics technology for the Space Station Freedom and for the U.S. economy
[NASA-TM-104024] p 739 N94-12838
Flex-gear electrical power transmission
[NASA-CR-194422] p 661 N94-13445
Robot programming, natural computation and conceptual graphs
[ITN-93-85193] p 748 N94-13539
Dynamics and design of nonholonomic robotic mechanical systems
[ISBN-0-315-72009-3] p 662 N94-13597
Goddard Space Flight Center robotics demo
[NASA-TM-109302] p 662 N94-13604
New prosthetic devices
[NASA-TM-109304] p 737 N94-13611
Development of a tactile and vision integrated system, and object identification techniques for SPDM applications
[DSIS-93-00153] p 764 N94-13842
Activities of Institute for Information Technology
[CNR-35024] p 824 N94-14069
Knowledge based systems: From process control to policy analysis
[DE93-014582] p 765 N94-14117
A capaciflector-based robotic system
[NASA-CR-193783] p 833 N94-14359
Large space structures and systems in the space station era: A bibliography with indexes (supplement 05)
[NASA-SP-7085(05)] p 543 N94-14411
Proceedings of the Fifth NASA/NSF/DOD Workshop on Aerospace Computational Control
[NASA-CR-194515] p 677 N94-14618
Modelling robotic systems with DADS
p 678 N94-14625
Spatial operator algebra for flexible multibody dynamics p 679 N94-14631
A neural-network approach to robotic control
p 679 N94-14634
Design and control of a macro-micro robot for precise force applications p 682 N94-14651
The further development and refinement of an expert-systems approach to the creative design of mechanisms and mechanical systems
[AD-A266812] p 665 N94-14901

ROBOTS
Application of intelligently adaptable structure and robot to large space structure p 530 N94-13277
Robot-task compliance: The energy criterion
[ITN-93-85196] p 763 N94-13568
The BIRIS server: Integration of a three-dimensional range sensor into a harmony-based realtime architecture
[ERB-1036] p 765 N94-14201
Design and control of a macro-micro robot for precise force applications p 682 N94-14651

ROBUSTNESS (MATHEMATICS)
A robust multilevel simultaneous eigenvalue solver
[NASA-CR-191491] p 767 N94-13202
Robust stability of diamond families of polynomials with complex coefficients
[NASA-CR-194132] p 768 N94-13421
Robust synthesis of discrete-time multivariable control systems with induced delays p 662 N94-13642
Exploiting structure: Introduction and motivation
[NASA-CR-194199] p 750 N94-13828
A review of robust detection
[DSIS-93-00400] p 603 N94-13829
Robust estimators and tests in one-sample location problem with particular consideration on modified maximum likelihood process
[ETN-93-94391] p 774 N94-14703

ROCKET ENGINE DESIGN
The conceptual study on future space transportation systems. Part A: Conceptual study of flyback booster
[NASDA-CNT-930013] p 536 N94-14099

ROCKET ENGINES
Low thrust space propulsion
[NASA-TM-109286] p 552 N94-13625
Nuclear thermal propulsion engine based on particle bed reactor using light water steam as a propellant
[DE93-014336] p 552 N94-14111
The problem of traveling in outer space: The rocket motor
[NASA-TT-10002] p 552 N94-14463

ROCKET EXHAUST
Analysis of reacting flowfields in low-thrust rocket engines and plumes p 552 N94-14491
Investigation of the feasibility of optical diagnostic measurements at the exit of the SSME
[NASA-CR-193832] p 553 N94-14682
Low altitude plume impingement handbook
[NASA-CR-194193] p 643 N94-14741

ROCKET NOSE CONES
Arc-heating tests of thermal protection system materials for the H-2 rocket fairing
[NAL-TR-1181] p 551 N94-13455

ROCKET NOZZLES
Qualification test of the Ross Double Planetary Mixer
[NASA-CR-192600] p 652 N94-14497

ROCKET OXIDIZERS
STS-55 pad abort: Engine 2011 oxidizer preburner augmented spark igniter check valve leak
[NASA-CR-193830] p 533 N94-12806
Effects of hydrogen addition on combustion performance of a LOX/kerosene rocket
[NAL-TR-1177] p 548 N94-12945

ROCKET-BORNE INSTRUMENTS
A rocket-borne lidar for studies of the middle atmosphere
[FFI/RAPPORT-92/7034] p 715 N94-13949

ROCKETS
The problem of traveling in outer space: The rocket motor
[NASA-TT-10002] p 552 N94-14463

ROCKS
Hot Dry Rock energy
[DE93-014452] p 702 N94-13403
BOAST 2 for the IBM 3090 and RISC 6000
[DE93-000138] p 638 N94-14351

ROLL
Investigation of the effects of bandwidth and time delay on helicopter roll-axis handling qualities
p 522 N94-13300

ROLLER BEARINGS
The effect of TiN coatings on the rolling contact fatique behavior of M50 bearing steel
[ARL-TR-40] p 662 N94-13794
Computer program for analysis of high speed, single row, angular contact, spherical roller bearing, SASHBEAN. Volume 1: User's guide
[NASA-CR-191183] p 663 N94-14445
Computer program for analysis of high speed, single row, angular contact, spherical roller bearing, SASHBEAN. Volume 2: Mathematical formulation and analysis
[NASA-CR-191182] p 664 N94-14446

ROLLERS
Roller-gear drives for robotic manipulators design, fabrication and test
[NASA-CR-194248] p 660 N94-12802
Modelling of the temperature distribution in a copper roll for the design of a system of cooled rolls adapted to vertical strip casting
[IMI-93RT-21200-1436-G] p 557 N94-13866

ROLLING CONTACT LOADS
The effect of TiN coatings on the rolling contact fatique behavior of M50 bearing steel
[ARL-TR-40] p 662 N94-13794

ROLLING MOMENTS
Rolling moment control in the NAL 10 cm x 10 cm magnetic suspension and balance system
[NAL-TR-1164] p 526 N94-13347

ROOM TEMPERATURE
Room temperature degradation of YBa2Cu3O(7-x) superconductors in varying relative humidity environments
[NASA-TP-3368] p 813 N94-14409

ROSAT MISSION
ROSAT: X ray survey of compact groups
[NASA-CR-193297] p 829 N94-13181
X ray observations of late-type stars using the ROSAT all-sky survey
[NASA-CR-193716] p 832 N94-14146

ROTARY WING AIRCRAFT
MIL-H-8501B: Application to shipboard terminal operations p 521 N94-13296
A perspective on the FAA approval process: Integrating rotorcraft displays, controls and workload
p 521 N94-13298
Some lessons learned in three years with ADS-33C --- rotorcraft handling qualities specification
p 521 N94-13299
A model for rotorcraft flying qualities studies
p 523 N94-13308
Visual cueing aids for rotorcraft landings
p 524 N94-13313
Effects of simulator motion and visual characteristics on rotorcraft handling qualities evaluations
p 524 N94-13317
Flight testing and frequency domain analysis for rotorcraft handling qualities characteristics
p 526 N94-13324
Preliminary design features of the RASCAL: A NASA /Army rotorcraft in-flight simulator p 526 N94-13325

ROTARY WINGS
Free-wake computation of helicopter rotor flowfield for general flight regimes
[AD-A266692] p 509 N94-14781
A new treatment of periodic systems with applications to helicopter rotor blade dynamics
[AD-A266770] p 510 N94-14784
Center of excellence in rotary wing technology
[AD-A266655] p 510 N94-14799
ROTATING BODIES
On curve veering and flutter of rotating blades
[NASA-TM-106282] p 670 N94-12872
Flex-gear electrical power transmission
[NASA-CR-194422] p 661 N94-13445
ROTATING CYLINDERS
The three-dimensional flow past a rapidly rotating circular cylinder
[NASA-CR-191512] p 630 N94-13075
The general gravitational potential field of a homogeneous cylinder rotating about its axis
[DE93-622853] p 775 N94-13508
ROTATING SPHERES
On the motion through a viscous fluid of a spherical particle touching a plane wall: Slip boundary conditions
[DE93-012540] p 628 N94-12961
ROTATION
On the motion through a viscous fluid of a spherical particle touching a plane wall: Slip boundary conditions
[DE93-012540] p 628 N94-12961
ROTOR AERODYNAMICS
On the use of the method of matched asymptotic expansions in propeller aerodynamics and acoustics
[NLR-TP-91307-U] p 503 N94-13528
New vortex dynamics methods for rotor free wake analysis
[AD-A266656] p 509 N94-14774
Free-wake computation of helicopter rotor flowfield for general flight regimes
[AD-A266692] p 509 N94-14781
ROTOR BLADES (TURBOMACHINERY)
Development of a high-speed mechanical drive system for oscillating an annular blade row in the bending mode
[NAL-TR-1170] p 502 N94-13342
ROTOR BODY INTERACTIONS
An analytic modeling and system identification study of rotor/fuselage dynamics at hover p 524 N94-13312
ROTOR DYNAMICS
Cryogenic fluid film bearing tester development study
[NASA-CR-192586] p 660 N94-12791
Rotordynamic and leakage characteristics of a 4-stage brush seal
[AD-A266012] p 660 N94-12988
An analytic modeling and system identification study of rotor/fuselage dynamics at hover p 524 N94-13312
A new treatment of periodic systems with applications to helicopter rotor blade dynamics
[AD-A266770] p 510 N94-14784
ROTORS
Rotor stator CGI
[NASA-TM-109313] p 518 N94-13608
ROVING VEHICLES
Exploring Mars
[NASA-TM-109306] p 842 N94-13613
ROWLAND CIRCLES
Vacuum ultraviolet instrumentation for solar irradiance and thermospheric airglow
[NASA-CR-194525] p 652 N94-14684
RULES
An expert system class library for Audition
[IME-MET-TR-008] p 824 N94-14196
Generating knight's tours without backtracking from errors
[AD-A266807] p 772 N94-14900
RUNGE-KUTTA METHOD
Analysis of reacting flowfields in low-thrust rocket engines and plumes p 552 N94-14491
A vertex-based finite-volume algorithm for the Navier-Stokes equations p 639 N94-14599
Navier-Stokes simulation of transonic vortex flow over a delta wing p 640 N94-14606
A new treatment of periodic systems with applications to helicopter rotor blade dynamics
[AD-A266770] p 510 N94-14784
RUNWAYS
Evaluation of infrared sensors for autonomous landing guidance
[AD-A266450] p 513 N94-13703
RUPTURING
Residual contact restraints in cryogenics
[ETN-93-94375] p 671 N94-13501
RURAL LAND USE
Educational module for the higher agricultural education. Part 1: Land use classification using satellite pictures
[BCRS-92-11A] p 819 N94-14809
Obtaining digital regional planning information from aerial pictures
[REPT-228] p 700 N94-14810
RUSSIAN FEDERATION
JPRS report: Science and technology. Central Eurasia: Space
[JPRS-USP-93-003] p 828 N94-13182
Computational Russian morphological generation on Prolog: Noun, pronoun, and adjective p 747 N94-13436
NASA/DOD Aerospace Knowledge Diffusion Research Project. Paper 37: The impact of political control on technical communications: A comparative study of Russian and US aerospace engineers and scientists
[NASA-TM-109329] p 826 N94-14488
RUTHENIUM
The structure and mechanical properties of Ru-Cu and Ru-Ti nanolayer composites
[DE93-014453] p 558 N94-14469
RUTILE
Prism-film coupling in anisotropic planar waveguides of epitaxial (101) rutile thin films
[DE93-012912] p 811 N94-14304

S

S MATRIX THEORY
Recent developments in multiple-scattering calculations of XAFS and XANES
[DE93-010999] p 563 N94-13477
S-3 AIRCRAFT
Work/rest schedules and performance of S-3 aviators during fleet exercise
[AD-A265807] p 734 N94-12975
SAFETY
Hydrogen peroxide safety issues
[DE93-013895] p 565 N94-14346
SAFETY FACTORS
Structural design/margin assessment
[NASA-TP-3410] p 669 N94-12831
Effects of radiobiological uncertainty on vehicle and habitat shield design for missions to the moon and Mars
[NASA-TP-3312] p 846 N94-12875
Design, qualification and operation of nuclear rockets for safe Mars missions
[DE93-010792] p 549 N94-12996
Early detection of insulation failure in electric motors
[PB93-198208] p 626 N94-14686
SAGE SATELLITE
Present status of SAGE
[DE93-014350] p 781 N94-13205
SAGNAC EFFECT
Polarization effects in optical fiber current sensors based on Sagnac interferometers with 3 by 3 couplers
[DE93-012665] p 792 N94-14367
SALINITY
Preliminary results on the hydrological measurements in the Aegean Sea off Crete: Cruise, Georgia, 1989
[PREPRINT-736] p 725 N94-13500
Phase aligner for the Electronically Scanned Thinned Array Radiometer (ESTAR) instrument
[NASA-TM-4518] p 623 N94-13878
SAMPLERS
Maximum likelihood estimation for constrained or missing data models
[AD-A266563] p 773 N94-13585
SAMPLING
Sampling of globular clusters and the distance to the galactic center
[INPE-5446-TDI/492] p 837 N94-13449
SANDS
Soil erosion rates caused by wind and saltating sand stresses in a wind tunnel
[DE93-009154] p 706 N94-12905
SANDWICH STRUCTURES
System integration and demonstration of adhesive bonded high temperature aluminum alloys for aerospace structure, phase 2
[NASA-CR-191459] p 575 N94-12792
Structural investigation of a damaged GRP/foam sandwich composite using x ray computed tomography p 669 N94-13857
SATELLITE ALTIMETRY
On the space-time ocean current variability and its effects on the length-of-day
[ISBN-0-315-59510-8] p 726 N94-14205
SATELLITE ANTENNAS
The Second Workshop on Deployment and Assembly Experiment of Large Space Structure on Orbit
[NASDA-CON-930003] p 529 N94-13268
Structural design of hexa-link truss deployable antenna p 529 N94-13269
Thermal distortion measurement of TETRUS type thermal test model of large deployable antenna for mobile communications satellite p 529 N94-13270
Development of modular cable mesh deployable antenna p 530 N94-13274
Trial manufacture model and in-space verification method of deployable antenna p 530 N94-13278
SATELLITE ATTITUDE CONTROL
Low cost attitude control system reaction wheel development
[NASA-CR-191332] p 540 N94-13140
Transmission zeros of spacecraft attitude control system
[NAL-TR-1166] p 540 N94-13339
SATELLITE COMMUNICATION
Destination-directed, packet-switched architecture for a geostationary communications satellite network
[NASA-TP-3379] p 538 N94-13111
Fine time uplink synchronization for frequency-hopped spread spectrum satellite communication system
[ISBN-0-315-54370-1] p 600 N94-13488
Trellis coding with Continuous Phase Modulation (CPM) for satellite-based land-mobile communications
[NASA-CR-191325] p 604 N94-13909
SCAILET: An intelligent assistant for satellite ground terminal operations
[NASA-TM-105879] p 538 N94-13918
Simulation of downlink synchronization for a frequency-hopped satellite communication system
[DSIS-93-00477] p 605 N94-13941
ALFIS: Astronomical Low Frequency Interferometry Satellites. A feasibility study
[LR-699] p 542 N94-13988
Multiple-symbol differential detection of DPSK with frequency offset
[DREO-TN-92-5] p 606 N94-14063
Asia-Pacific ISY Conference, volume 2
[NASDA-CM-199-VOL-2] p 688 N94-14209
The developments of satellite communications of China p 618 N94-14282
The current situation, trends, international cooperation of space communication technological development in the Republic of Korea p 699 N94-14283
Joint experiments using ETS-5 p 618 N94-14284
Space communications technology research in CRL p 618 N94-14285
NTT's activities in satellite communications technology development p 618 N94-14286
Future outlook on international satellite communications in Asia Pacific region p 618 N94-14287
Technological development for broadcasting satellites in NHK Laboratories p 618 N94-14288
New challenges in propagation research in the US p 612 N94-14656
User needs for propagation data p 613 N94-14657
Statistical results from the Virginia Tech propagation experiment using the Olympus 12, 20, and 30 GHz satellite beacons p 613 N94-14658
Results from a study of scintillation behavior at 12, 20, and 30 GHz using the results from the Virginia Tech Olympus receivers p 613 N94-14659
Large-scale rainfall diversity for ACTS p 613 N94-14662
Contribution towards a draft revision of recommendations 681: Propagation data required for the design of Earth-space land mobile telecommunications systems p 614 N94-14666
Propagation issues for emerging mobile and portable communications: A systems perspective p 614 N94-14667
Characterisation of the LMS propagation channel at L- and S-bands: Narrowband experimental data and channel modelling p 615 N94-14669
Results of multiband (L, S, Ku band) propagation measurements and model for high elevation angle land mobile satellite channel p 615 N94-14670
Effects of the equatorial ionosphere on L-band Earth-space transmissions p 615 N94-14671
Tree attenuation at 20 GHz: Foliage effects p 615 N94-14672
Preprocessing data collected with the ACTS propagation terminal p 616 N94-14676
ACTS data center p 616 N94-14677
NASA images 8
[NASA-TM-109416] p 544 N94-14783
The 1991 research and technology report, Goddard Space Flight Center
[NASA-TM-108738] p 851 N94-14791
SATELLITE CONFIGURATIONS
ALFIS: Astronomical Low Frequency Interferometry Satellites. A feasibility study
[LR-699] p 542 N94-13988
SATELLITE DESIGN
Earth Observation Center Annual Report on Research and Development, Fiscal Year 1992
[EOC-92-01-0007] p 687 N94-14091
ADEOS project p 687 N94-14094
Propagation considerations in the American Mobile Satellite system design p 614 N94-14668

SATELLITE IMAGERY
The application of VAS satellite imagery to thunderstorm forecasting at Cape Canaveral
[NASA-CR-193563] p 718 N94-12839
Knowledge-based oceanographic image compression
[AD-A265752] p 821 N94-13041
EOS workstation
[NASA-CR-191326] p 736 N94-13132
Dendrometric variables estimation in homogeneous forests using LANDSAT TM data
[INPE-5455-TDI/497] p 684 N94-13331
Net radiation mapping of mountainous terrain using Landsat-5 thematic mapper imagery and digital terrain data
[ISBN-0-315-57755-X] p 685 N94-13475
Satellite imagery and exogenous data integration by neural network in automation land-cover classification
[INPE-5480-PRE/1778] p 686 N94-13729
Nonlinear aspects of data integration for land-cover classification in a neural network environment
[INPE-5479-PRE/1778] p 686 N94-13789
Integration of remotely sensed data and cadastral ownership boundaries for land inventory purposes
[BCRS-92-16] p 687 N94-14127
Asia-Pacific ISY Conference, volume 2
[NASDA-CM-199-VOL-2] p 688 N94-14209
Artificial oil pollution detection and wave observation in the sea adjacent to Japan by ERS-1 SAR
p 688 N94-14212
Seasonal change of the land-surface temperature over Asian Continent derived from GAC data on NOAA-11 AVHRR p 691 N94-14232
Detecting land cover changes in Chiang-Mai area in Thailand p 693 N94-14241
Land evaluation for agricultural productivity in North-East Thailand using LANDSAT TM data and geographic information p 693 N94-14242
Effects of typhoon on TOMS data
p 693 N94-14243
Multi-source national forest inventory of Finland
p 694 N94-14254
Global assessment of human activities
p 695 N94-14255
Remote sensing for monitoring tropical moist forests in the Indo-Chinese region p 695 N94-14258
Estimation of vegetation damage due to ash fall in Mt. Pinatubo area using MOS-1 data p 695 N94-14259
Outline of ISY sea surface temperature data sets
p 696 N94-14261
Integration of SST data sets using MOS-1 satellite data: For validation and monitoring p 696 N94-14262
Geophysical validation of ATSR sea surface temperatures p 696 N94-14263
Accuracy validation test of estimated sea surface temperature by satellite data p 696 N94-14264
Tracking of change of a warm-core ring structure
p 696 N94-14267
A method for estimation of partial cloud cover within a pixel and its effect p 697 N94-14269
Warm streamers extended from Warm Core Rings (WCR's) and their role on fish migration and fishing ground formation p 697 N94-14270
Atmospheric correction for sea surface temperature by application of microwave dual-channel technique to VTIR data p 697 N94-14271
Meteorological data, new series A monographs. Volume 6, no. 3: Estimation of influence of high clouds in the radiation field and the climat by analysis of NOAA AVHRR data
[ETN-93-94170] p 723 N94-14707
NASA images 8
[NASA-TM-109416] p 544 N94-14783

SATELLITE INSTRUMENTS
NASA airborne satellite instrumentation calibrator (NASIC) technical reference
[NASA-RP-1315] p 545 N94-13713
ALFIS: Astronomical Low Frequency Interferometry Satellites. A feasibility study
[LR-699] p 542 N94-13988
ECS: Eighth year in orbit
[ESA-BR-82] p 543 N94-14352

SATELLITE NETWORKS
The 1991 research and technology report, Goddard Space Flight Center
[NASA-TM-108738] p 851 N94-14791

SATELLITE OBSERVATION
Circulation model experiments of the Gulf Stream using satellite-derived fields
[AD-A266067] p 725 N94-12990
Degradation of the visible and near-infrared channels of the advanced very high resolution radiometer on the NOAA-9 spacecraft: Assessment and recommendations for corrections
[NOAA-TR-NESDIS-70] p 544 N94-13029
Study on TRMM data utilization for meteorology
[NASDA-CNT-930007] p 721 N94-13643
Activities report of the Netherlands Remote Sensing Board
[ETN-93-93880] p 686 N94-14073
Calibration and in-house validation results of JERS-1 data p 687 N94-14092
Earth observation experiment data analysis
p 687 N94-14093
Asia-Pacific ISY conference, volume 1
[NASDA-CM-199-1] p 532 N94-14098
Asia-Pacific ISY Conference, volume 2
[NASDA-CM-199-VOL-2] p 688 N94-14209
Artificial oil pollution detection and wave observation in the sea adjacent to Japan by ERS-1 SAR
p 688 N94-14212
IMG: Interferometric monitor for greenhouse gases
p 689 N94-14217
Spectroscopic method and data reduction algorithm for laser long-path absorption measurements using RIS
p 689 N94-14218
TRMM system overview and status in the United States p 690 N94-14221
TRMM Project in Japan: Overview and status
p 690 N94-14222
Clouds and the Earth's Radiant Energy System (CERES) on the Tropical Rainfall Measuring Mission (TRMM)
p 690 N94-14223
TRMM precipitation radar algorithm
p 690 N94-14224
Estimate of sampling errors of TRMM rainfall observation by using radar-AMeDAS composite data
p 690 N94-14225
Space measurements for determining the Earth's energy and water cycles p 690 N94-14227
Future TRMM follow-on mission p 691 N94-14228
The effects of anthropogenic aerosols on optical thickness and particle size of clouds. Part 1: Retrieval algorithm p 691 N94-14230
Climate products from NOAA operational satellites
p 691 N94-14231
Seasonal change of the land-surface temperature over Asian Continent derived from GAC data on NOAA-11 AVHRR p 691 N94-14232
Earth radiation budget, cloud, and aerosol parameters derived from AVHRR and TOVS measurements
p 691 N94-14233
The development and implementation of an interactive retrieval/analysis/forecast algorithm
p 692 N94-14234
Satellite technology for environmental monitoring in developing countries p 692 N94-14236
Some potentials of the Indonesian region for Earth observation p 692 N94-14237
Application of satellite remote sensing technology in disaster mitigation: A case study of Bangladesh
p 692 N94-14238
Integration of remote sensing and mathematical modelling in disaster mitigation p 692 N94-14239
Soil erosion mapping using remote sensing and GIS techniques p 692 N94-14240
Detecting land cover changes in Chiang-Mai area in Thailand p 693 N94-14241
Land evaluation for agricultural productivity in North-East Thailand using LANDSAT TM data and geographic information p 693 N94-14242
Effects of typhoon on TOMS data
p 693 N94-14243
Satellite remote sensing for disaster mitigation
p 693 N94-14244
A concept for the world environment and disaster observation system p 693 N94-14245
Study of the consequences of the Chernobyl accident and technogenic activity in the Republic Belarus using aerospace methods p 693 N94-14246
A tentative plan on China and Asian-Pacific satellite system for disaster reduction p 693 N94-14247
Earth observation from low-inclination orbit as a necessary complement to polar missions
p 694 N94-14248
Development of a remote sensing geographic information system for land cover changes and assessment of risk due to natural and man made hazards covering the area of the inner delta of the Yellow River
p 694 N94-14249
The role of the dynamics for the deviation of the total ozone from the long-term mean at the edge of the polar vortex p 694 N94-14250
The European Arctic ozone experiment: An investigation of Northern Hemisphere ozone depletion
p 694 N94-14251
Space-based activities: SAM 2 and SAGE 2
p 694 N94-14252
New evidences supported the Wei hypothesis about the formation of the Antarctic ozone hole
p 694 N94-14253
Multi-source national forest inventory of Finland
p 694 N94-14254
Global assessment of human activities
p 695 N94-14255
The Swedish ISY contribution p 695 N94-14256
Vegetation mapping of Indo-China Peninsula using MOS-1 MESSR and NOAA AVHRR p 695 N94-14257
Remote sensing for monitoring tropical moist forests in the Indo-Chinese region p 695 N94-14258
Estimation of vegetation damage due to ash fall in Mt. Pinatubo area using MOS-1 data p 695 N94-14259
Mangrove afforestation monitoring using remote sensing p 695 N94-14260
Outline of ISY sea surface temperature data sets
p 696 N94-14261
Integration of SST data sets using MOS-1 satellite data: For validation and monitoring p 696 N94-14262
Geophysical validation of ATSR sea surface temperatures p 696 N94-14263
Accuracy validation test of estimated sea surface temperature by satellite data p 696 N94-14264
Tracking of change of a warm-core ring structure
p 696 N94-14267
Outline of ISY Kuroshio observation experiment
p 697 N94-14268
A method for estimation of partial cloud cover within a pixel and its effect p 697 N94-14269
Warm streamers extended from Warm Core Rings (WCR's) and their role on fish migration and fishing ground formation p 697 N94-14270
Atmospheric correction for sea surface temperature by application of microwave dual-channel technique to VTIR data p 697 N94-14271
Some thoughts on the space programs in the Asia Pacific regions p 697 N94-14272
Summary of the NOAA/NESDIS Workshop on Development of a Global Satellite/In Situ Environmental Database
[NOAA-TR-NESDIS-72] p 826 N94-14498
Educational module for the higher agricultural education. Part 1: Land use classification using satellite pictures
[BCRS-92-11A] p 819 N94-14809

SATELLITE ORBITS
Orbit determination error analysis based on the requirements of ADEOS mission
[NASDA-CNT-930008] p 532 N94-13644

SATELLITE ORIENTATION
Self-tuning control techniques for multivariable systems
[INPE-5449-TDI/495] p 765 N94-14084

SATELLITE POWER TRANSMISSION
Small scale adaptive optics experiment systems engineering
[NASA-CR-194419] p 793 N94-14548

SATELLITE SOUNDING
The application of VAS satellite imagery to thunderstorm forecasting at Cape Canaveral
[NASA-CR-193563] p 718 N94-12839

SATELLITE TRACKING
NASA images 8
[NASA-TM-109416] p 544 N94-14783

SATELLITE TRANSMISSION
The developments of satellite communications of China p 618 N94-14282
The current situation, trends, international cooperation of space communication technological development in the Republic of Korea p 699 N94-14283
Joint experiments using ETS-5 p 618 N94-14284
Space communications technology research in CRL
p 618 N94-14285
NTT's activities in satellite communications technology development p 618 N94-14286
Future outlook on international satellite communications in Asia Pacific region p 618 N94-14287
Technological development for broadcasting satellites in NHK Laboratories p 618 N94-14288
Effects of the equatorial ionosphere on L-band Earth-space transmissions p 615 N94-14671

SATELLITE-BORNE INSTRUMENTS
NASA airborne satellite instrumentation calibrator (NASIC) technical reference
[NASA-RP-1315] p 545 N94-13713
Methods for calibration/validation of AVNIR
p 689 N94-14216
IMG: Interferometric monitor for greenhouse gases
p 689 N94-14217
Spectroscopic method and data reduction algorithm for laser long-path absorption measurements using RIS
p 689 N94-14218
Overview of the ILAS operational data processing system p 690 N94-14220
Multiparameter airborne rain radar development for TRMM validation and TRMM-follow-on study
p 690 N94-14226
Wavefront sensing, control, and pointing
p 546 N94-14833

SATELLITE-BORNE PHOTOGRAPHY
Mangrove afforestation monitoring using remote sensing p 695 N94-14260
SATELLITE-BORNE RADAR
A calibration procedure for radiation budget radiometers and its influence on interpretation of measured values [MITT-82] p 651 N94-14149
An exact processing algorithm for wide beam spaceborne SAR data p 689 N94-14213
High performance multi-mode radar altimeter for future spaceborne application p 548 N94-14214
SCALARS
Scalar curvature and spherical-type Riemannian manifolds [DE93-622852] p 767 N94-12895
A search for scalar leptoquarks in D0 [DE93-012780] p 779 N94-12954
On a nonminimal gauge interaction of a scalar field in D=2+1 Chern-Simons-Maxwell theory [DE93-621380] p 621 N94-13224
SCALE (RATIO)
Analytical framework for modeling scale-related variabilities in remote sensing p 685 N94-13592
SCALE HEIGHT
Determining the solar-flare photospheric scale height from SMM gamma-ray measurements [NASA-CR-194084] p 844 N94-13671
SCALE MODELS
Results of experimental investigations to determine external tank protuberance loads using a 0.03-scale model of the Space Shuttle launch configuration (model 47-OTS) in the NASA/ARC unitary plan wind tunnel, volume 1 [NASA-CR-167690] p 534 N94-12810
Results of wind tunnel tests of an ASRM configured 0.03 scale Space Shuttle integrated vehicle model (47-OTS) in the AEDC 16-foot transonic wind tunnel, volume 2 [NASA-CR-185697] p 534 N94-12965
Results of wind tunnel tests of an ASRM configured 0.03 scale Space Shuttle integrated vehicle model (47-OTS) in the AEDC 16-foot Transonic wind tunnel (IA613A), volume 1 [NASA-CR-185696] p 534 N94-13191
Surfactant studies for bench-scale operation [NASA-CR-194511] p 564 N94-13947
Results of experimental investigations to determine external tank protuberance loads using a 0.03-scale model of the Space Shuttle launch configuration (Model 47-OTS) in the NASA/ARC unitary plan wind tunnel, volume 2 [NASA-CR-167691] p 536 N94-14047
Design and evaluation of single and dual flow thrust vector nozzles with post exit vanes [NASA-CR-193393] p 638 N94-14086
Simulating the daylight performance of fenestration systems and spaces of arbitrary complexity: The IDC method [DE93-015177] p 704 N94-14333
Effect of size, shape, and end condition of test specimen on compressive strength of high-strength concrete [DE93-500412] p 682 N94-14653
SCALING LAWS
Thermal gravitational modelling and scaling of two-phase heat transport systems: Similarity considerations and useful equations predictions versus experimental results [NLR-TP-91477-U] p 632 N94-13533
Anomalous ion transport and feedback control [DE93-018324] p 803 N94-14874
SCANNING ELECTRON MICROSCOPY
Crystallographic phase identification in the scanning electron microscope: Backscattered electron Kikuchi patterns [DE93-011574] p 804 N94-12813
Procedures for analysis of debris relative to Space Shuttle systems [NASA-TM-109190] p 534 N94-12900
High-resolution Z-contrast imaging and hole concentration mapping of YBCO thin films [DE93-015803] p 808 N94-13930
Room temperature degradation of YBa2Cu3O(7-x) superconductors in varying relative humidity environments [NASA-TP-3368] p 813 N94-14409
SCANNING TUNNELING MICROSCOPY
Scanning tunneling microscopy studies of diamond films and optoelectronic materials [NASA-CR-194363] p 578 N94-13246
Ploughing on gold using a Scanning Tunneling Microscope [DE93-012632] p 812 N94-14365
Laser lithography by photon scanning tunneling microscopy [DE93-015962] p 660 N94-14863
SCATTER PROPAGATION
Meteor forward scatter studies [DSIS-93-00382] p 602 N94-13801
A study of meteor scatter communications [DSIS-93-00151] p 603 N94-13841
SCATTERING
Grain-boundary electronic states by multiple-scattering theory [DE93-013198] p 805 N94-13010
ADP study of gamma-ray bursts [NASA-CR-194311] p 848 N94-13708
Theoretical molecular studies of astrophysical interest [NASA-CR-193300] p 838 N94-13781
Dynamics of pion-nucleus systems [DE93-014449] p 785 N94-14468
SCATTERING AMPLITUDE
The E2 N(yields)(Delta) transition from polarized Compton scattering [DE93-012522] p 785 N94-14363
Scattering calculations and confining interactions [NASA-CR-194242] p 786 N94-14549
Relativistic proton-nucleus scattering and one-boson-exchange models p 786 N94-14550
SCATTERING CROSS SECTIONS
Calculation of electron-lithium scattering using the coupled-channel optical method [DE93-623049] p 806 N94-13226
Recent developments in multiple-scattering calculations of XAFS and XANES [DE93-010999] p 563 N94-13477
Measurement of the Fe-56(n,p)Mn-56, Al-27(n,p)Mg-27 and Al-27(n,alpha)Na-24 cross sections at 16.0, 17.0 and 18.3 MeV [NPL-RSA(EXT)-38] p 783 N94-13883
SCATTEROMETERS
Earth Observation Center Annual Report on Research and Development, Fiscal Year 1992 [EOC-92-01-0007] p 687 N94-14091
ADEOS project p 687 N94-14094
SCENE ANALYSIS
Determination of position and orientation of rigid bodies from image segments [FFI-92-4005] p 752 N94-14039
Passive recovery of scene geometry for an unmanned ground vehicle [AD-A266670] p 766 N94-14777
SCHEDULES
Work/rest schedules and performance of S-3 aviators during fleet exercise [AD-A265807] p 734 N94-12975
Work/rest schedules and performance of F/A-18 aviators during Fleet Exercise 1992 [AD-A265826] p 735 N94-12982
SCHEDULING
Present status of JEM utilization projects p 530 N94-13273
Three, four, five, six or the complexity of scheduling with communication delays [CWI-BS-R9229] p 751 N94-14004
Stochastic scheduling games with Markov decision arrival processes [CWI-BS-R9231] p 773 N94-14005
An experimental analysis of bottleneck-centered opportunistic scheduling [AD-A266643] p 820 N94-14796
SCHLIEREN PHOTOGRAPHY
Fundamental study of shock wave/turbulent boundary layer interactions with passive control in transonic flows [ESA-TT-1278] p 630 N94-13117
Images constructed from computed flow fields [NASA-CR-194397] p 650 N94-13814
Advanced ballistic range technology [NASA-CR-194396] p 532 N94-14068
Advanced ballistic range technology [NASA-CR-194530] p 533 N94-14540
SCHMIDT TELESCOPES
Hardware design for the Autonomous Visibility Monitoring (AVM) observatory p 533 N94-14394
SCHOOLS
Workshop for coordinating South Carolina's pre-college systemic initiatives in science and mathematics [DE93-012263] p 818 N94-13216
SCHOTTKY DIODES
Annealing study of main electron irradiation-induced defects (H4 and H5) in P-InP using DLTS technique [DE93-623204] p 806 N94-13213
SCHROEDINGER EQUATION
Grain-boundary electronic states by multiple-scattering theory [DE93-013198] p 805 N94-13010
Multiple Schroedinger cats from multilevel atoms [DE93-013412] p 786 N94-14526
Soliton equations and self-dual gauge fields [DE93-626620] p 818 N94-14887
SCHUMANN-RUNGE BANDS
Determination of spectroscopic properties of atmospheric molecules from high resolution vacuum ultraviolet cross section and wavelength measurements [NASA-CR-194024] p 712 N94-13092
SCIENCE
Selected data on academic science and engineering R and D expenditures: Fiscal Year 1991 [NSF-92-329] p 819 N94-13982
Science, technology, and the federal government: National goals for a new era p 827 N94-14115
SCIENTIFIC VISUALIZATION
ULTRA 2 user's manual for ULTRA 2 revision 3.0 [DE93-015970] p 744 N94-13120
SCORE user's manual [DE93-015987] p 822 N94-13121
Charged-particle evaluation methodology at Lawrence Livermore National Laboratory [DE93-013429] p 781 N94-13251
A perspective on AVS in an engineering sciences environment [DE93-015011] p 596 N94-13889
Visualization techniques to aid in the analysis of multi-spectral astrophysical data sets [NASA-CR-194489] p 840 N94-14482
Earth science and application [NASA-CR-184381] p 683 N94-14484
An overview of parallel scientific visualization [DE93-017105] p 755 N94-14521
SCIENTISTS
NASA/DOD Aerospace Knowledge Diffusion Research Project. Report 18: A comparison of the technical communication practices of aerospace engineers and scientists in India and the United States [NASA-TM-109006] p 821 N94-13057
Generic results of the space physics community survey [NASA-CR-194538] p 818 N94-13984
NASA/DOD Aerospace Knowledge Diffusion Research Project. Paper 34: Users and uses of DOD technical reports: A report from the field [NASA-TM-109327] p 825 N94-14485
NASA/DOD Aerospace Knowledge Diffusion Research Project. Paper 36: Technical uncertainty as a correlate of information use by US industry-affiliated aerospace engineers and scientists [NASA-TM-109328] p 825 N94-14486
NASA/DOD Aerospace Knowledge Diffusion Research Project. Paper 39: The role of computer networks in aerospace engineering [NASA-TM-109331] p 825 N94-14487
NASA/DOD Aerospace Knowledge Diffusion Research Project. Paper 37: The impact of political control on technical communications: A comparative study of Russian and US aerospace engineers and scientists [NASA-TM-109329] p 826 N94-14488
NASA/DOD Aerospace Knowledge Diffusion Research Project. Paper 38: Computer Mediated Communication (CMC) and the communication of technical information in aerospace [NASA-TM-109330] p 826 N94-14489
Scientists, engineers, and technicians in nonmanufacturing industries: 1990. Detailed statistical tables [NSF-92-334] p 820 N94-14499
SCINTILLATING FIBERS
Gamma-insensitive optical focal plane array [DE93-013100] p 792 N94-14317
SCINTILLATION
Barium fluoride research and development at Lawrence Livermore National Laboratory [DE93-014682] p 807 N94-13405
Gamma-insensitive optical focal plane array [DE93-013100] p 792 N94-14317
Results from a study of scintillation behavior at 12, 20, and 30 GHz using the results from the Virginia Tech Olympus receivers p 613 N94-14659
Effects of the equatorial ionosphere on L-band Earth-space transmissions p 615 N94-14671
SCINTILLATION COUNTERS
Measurements of optical properties of waveshifting optical fiber for liquid scintillator hadron calorimetry [DE93-012606] p 791 N94-13482
Cosmic and solar gamma ray and neutron experiments [NASA-CR-193359] p 849 N94-13965
Absolute detection efficiency of a micro-channel plate detector to x rays in the 1-100 KeV energy range [DE93-012592] p 789 N94-14460
Results from a water-Cerenkov array [DE93-012715] p 849 N94-14461
SCORING
Generalized smooth models [DE93-013045] p 756 N94-14864
SCOUT LAUNCH VEHICLE
Scout: The unsung hero of space [NASA-TM-109289] p 540 N94-13628
SCOUT PROJECT
Scout: The unsung hero of space [NASA-TM-109289] p 540 N94-13628

SEA LEVEL
The 1990 Western Pacific Geophysics meeting
[NASA-CR-193456] p 712 N94-13334
SEA STATES
Buoy experiments to obtain the sea-truth data for OCTS/NSCAT, part 1
[NASDA-CNT-930005-PT-1] p 725 N94-13653
Sea surface effect on the sea surface temperature estimation by satellite data p 696 N94-14265
SEA SURFACE TEMPERATURE
Outline of ISY sea surface temperature data sets p 696 N94-14261
Integration of SST data sets using MOS-1 satellite data: For validation and monitoring p 696 N94-14262
Geophysical validation of ATSR sea surface temperatures p 696 N94-14263
Accuracy validation test of estimated sea surface temperature by satellite data p 696 N94-14264
Sea surface effect on the sea surface temperature estimation by satellite data p 696 N94-14265
On the sea truth data of the Kuroshio meander and cold eddy movement p 696 N94-14266
A method for estimation of partial cloud cover within a pixel and its effect p 697 N94-14269
Atmospheric correction for sea surface temperature by application of microwave dual-channel technique to VTIR data p 697 N94-14271
Sea surface temperature forcing and phase locking of Nordeste precipitation
[DE93-011873] p 723 N94-14426
SEA TRUTH
Buoy experiments to obtain the sea-truth data for OCTS/NSCAT, part 1
[NASDA-CNT-930005-PT-1] p 725 N94-13653
Sea surface effect on the sea surface temperature estimation by satellite data p 696 N94-14265
On the sea truth data of the Kuroshio meander and cold eddy movement p 696 N94-14266
SEA WATER
Laser-induced fluorescence over optical fibers for real time in situ measurement of petroleum hydrocarbons in seawater
[AD-A265106] p 790 N94-12863
Preliminary results on the hydrological measurements in the Aegean Sea off Crete: Cruise, Georgia, 1989
[PREPRINT-736] p 725 N94-13500
Open boundary conditions for incompletely parabolic systems
[FFI/RAPPORT-92/7029] p 770 N94-13971
SEALS (STOPPERS)
Compatibility testing of vacuum seal materials
[DE93-014366] p 663 N94-14113
A hot dynamic seal rig for measuring hypersonic engine seal durability and flow performance
[NASA-TM-106294] p 664 N94-14727
SEARCHING
Extremal polygon containment problems and other issues in parametric searching
[ITN-93-85214] p 771 N94-14506
SEASONS
Royal Belgium observatory calendar: 156th year
[ETN-93-94221] p 833 N94-14811
SEATS
Analysis of differences between seating positions in simulators and orbiters
[NASA-TM-104776] p 737 N94-13399
SECONDARY EMISSION
Measurements of scattering processes in negative ion-atom collisions
[DE93-013863] p 779 N94-12940
SECONDARY RADAR
Activities report of the Federal Administration for Flight Safety (Germany)
[ETN-93-94208] p 511 N94-14008
SEDIMENT TRANSPORT
Coastal scour problems and methods for prediction of maximum scour
[AD-A266658] p 726 N94-14775
SEDIMENTS
Martian sedimentary deposits
[NASA-CR-193266] p 842 N94-13855
Overview: Gas hydrate geology and geography
[DE93-014043] p 688 N94-14151
Coastal scour problems and methods for prediction of maximum scour
[AD-A266658] p 726 N94-14775
SEISMIC WAVES
The 1990 Western Pacific Geophysics meeting
[NASA-CR-193456] p 712 N94-13334
SELENIUM
Selenium x ray laser line profile measurements
[DE93-012580] p 658 N94-14175
Experimental measurements of selenium x-ray laser spectral line profiles
[DE93-016543] p 659 N94-14595
SELF CONSISTENT FIELDS
To the theory of triplet pairing in Fermi-liquid model
[DE93-621770] p 816 N94-12855
SELF FOCUSING
Kinetic simulations of ultra-intense laser plasma interactions
[DE93-014419] p 802 N94-14564
SELF LUBRICATING MATERIALS
Canadian Target Assembly (CTA) to Airborne Support Equipment (ASE) vibration test report
[IME-AMT-TR-001] p 663 N94-14195
SELF ORGANIZING SYSTEMS
Communications and control for electric power systems: Power flow classification for static security assessment
[NASA-CR-194512] p 624 N94-13948
Self organized criticality
[DE93-013182] p 773 N94-14320
SELF TESTS
Design automation tools for testable VLSI circuits
[ISBN-0-315-61461-7] p 621 N94-13333
SEMANTICS
The silent step in time
[CWI-CS-R9221] p 768 N94-13496
On the foundations of final semantics: Non-standard sets, metric spaces, partial orders
[CWI-CS-R9241] p 768 N94-13526
The 8th Workshop on the Mathematical Foundations of Programming Semantics
[AD-A266436] p 749 N94-13700
Programming languages made in Italy
[REPT-93-002] p 750 N94-13805
SEMICONDUCTOR DEVICES
Proceedings of the Workshop on Applications of Synchrotron Radiation to Trace Impurity Analysis for Advanced Silicon Processing
[DE93-013389] p 805 N94-13020
Surfaces and interfaces of ceramics and metals
[DE93-014959] p 578 N94-13408
Growth of Si spherical crystals and the surface oxidation (M-9) p 587 N94-13741
Single Event Upset (SEU) testing of semiconductor components at the McMaster Accelerator Laboratory
[DSIS-93-00071] p 623 N94-13834
Activities of Institute for Microstructural Sciences
[NRC-32815] p 810 N94-14198
Activities of Institute for Microstructural Sciences
[CNR-32815] p 810 N94-14199
NASA Space Engineering Research Center for VLSI systems design
[NASA-CR-194035] p 625 N94-14325
SEMICONDUCTOR LASERS
Gathering and exchange information on atmospheric chemistry and polluted atmospheres
[DE93-009940] p 705 N94-12869
Non-scanned LADAR imaging and applications
[DE93-013772] p 655 N94-13261
Characteristics of semiconductor lasers with optical feedback
[ISBN-0-315-55435-5] p 656 N94-13522
Horizontal-cavity surface-emitting lasers, superluminescent LEDs, and amplifiers, and parabolic gain unstable resonator semiconductor lasers p 656 N94-13573
Microchannel cooled heatsinks for high average power laser diode arrays
[DE93-016533] p 658 N94-14442
AlGaAs diode laser blue shift resulting from fast neutron irradiation
[AD-A266642] p 659 N94-14681
SEMICONDUCTORS (MATERIALS)
Liquid phase epitaxy of gallium arsenide: A review
[DE93-622212] p 804 N94-12893
Metal-semiconductor, composite radiation detectors
[DE93-013313] p 619 N94-12994
Nonlinear laser spectroscopy studies of semiconductor heterostructures
[AD-A265728] p 805 N94-13037
Crystallographic and metallurgical characterization of radiation detector grade cadmium telluride materials
[DE93-014335] p 806 N94-13150
Comment of parameter excitation of Alfven and Heliicon waves in a magnetoactive compensated semiconductor by microwave radiation
[DE93-623203] p 806 N94-13228
Surfaces and interfaces of ceramics and metals
[DE93-014959] p 578 N94-13408
Crystal growth of ZnSe and related ternary compound semiconductors by physical vapor transport
[NASA-CR-193834] p 807 N94-13444
Spacelab J experiment descriptions
[NASA-TM-4517] p 586 N94-13732
Growth experiment of narrow band-gap semiconductor PbSnTe single crystals in space (M-1) p 586 N94-13733
Growth of PbSnTe single crystal by traveling-zone method in low gravity (M-2) p 586 N94-13734
Growth of semiconductor compound single crystal InSb by floating zone method (M-3) p 586 N94-13735
Crystal growth of compound semiconductors in a low-gravity environment (InGaAs crystals) (M-22) p 590 N94-13754
Activities of the Basic Sciences Branch
[DE93-010012] p 851 N94-14455
A sum-rule of luminescence spectrum
[ITN-93-85223] p 814 N94-14559
Dynamic Jahn-Teller effect: Calculation of fine structure spectrum, isotope shift and Zeeman behavior at deep center Ni2+ in CdS
[ETN-93-94394] p 815 N94-14705
SENSITIVITY
Regional climatology sensitivity studies
[DE93-010712] p 722 N94-14057
Decentralized control of uncertain systems via sensitivity models
[DE93-012963] p 766 N94-14568
Differential Sensitivity Theory applied to the MESA code for high pressure interactions
[DE93-016460] p 676 N94-14591
SEPARATED FLOW
A solution algorithm for the prediction of compressible laminar and turbulent shear flows p 634 N94-13635
Numerical studies of spray combustion in liquid-fueled engines p 564 N94-13685
Development of a recursion RNG-based turbulence model
[NASA-CR-191511] p 636 N94-13718
Measurements of wing and fin buffeting on the standard dynamics model
[IAR-AN-76] p 526 N94-13859
Numerical simulation of dynamic stall of NACA0012 airfoil oscillating near static stall angle using the Navier-Stokes equations
[DE93-767970] p 505 N94-14061
SEQUENCING
Cellular mechanism of turnover of the stress induced protein HSP 70
[AD-A265723] p 732 N94-13061
SEQUENTIAL COMPUTERS
A design methodology for portable software on parallel computers
[NASA-CR-194181] p 752 N94-14139
SERIES EXPANSION
Medium energy hadron-nucleus scattering in the 1/N expansion formalism
[DE93-622957] p 778 N94-12848
Magnetic interactions and disorder - phase transitions in dilute spin-glasses and high temperature superconductors
[ITN-93-85217] p 815 N94-14825
SERVICE LIFE
Battery testing at Argonne National Laboratory
[DE93-011761] p 624 N94-14012
Inflow characteristics associated with high-blade-loading events in a wind farm
[DE93-010042] p 704 N94-14423
Derated ion thruster development status
[NASA-TM-106292] p 553 N94-14726
SET THEORY
On the foundations of final semantics: Non-standard sets, metric spaces, partial orders
[CWI-CS-R9241] p 768 N94-13526
SEX FACTOR
Gender differences in endocrine responses to posture and 7 days of 6 deg head down bed rest
[NASA-TM-103991] p 731 N94-12972
SEYFERT GALAXIES
Polarization and variability of active galaxies and quasars p 837 N94-13550
Ultraviolet observations of NGC 4395, the least luminous and nearest known Seyfert 1 nucleus
[NASA-CR-194304] p 831 N94-13679
Was 49: Mirror for a hidden Seyfert 1 galaxy
[NASA-CR-194537] p 840 N94-14685
SHADOWGRAPH PHOTOGRAPHY
Images constructed from computed flow fields
[NASA-CR-194397] p 650 N94-13814
Development of an automated film-reading system for ballistic ranges
[NASA-CR-194398] p 650 N94-13815
Advanced ballistic range technology
[NASA-CR-194396] p 532 N94-14068
Advanced ballistic range technology
[NASA-CR-194530] p 533 N94-14540
SHADOWS
Field of solar collectors: Effect of shadowing on the optimal field design
[ITN-93-85197] p 702 N94-13570
SHAFTS (MACHINE ELEMENTS)
Rotordynamic and leakage characteristics of a 4-stage brush seal
[AD-A266012] p 660 N94-12988

SHALES
Overview: Gas hydrate geology and geography
[DE93-014043] p 688 N94-14151
SHALLOW WATER
Nonlinear wave forces on large ocean structures
[AD-A266820] p 683 N94-14902
SHAPE FUNCTIONS
Boundary formulations for nonlinear design sensitivity analysis p 672 N94-13669
SHAPED CHARGES
The motion of a conical shaped liner driven by explosive load
[ITN-93-85215] p 585 N94-14507
SHAPES
Effect of size, shape, and end condition of test specimen on compressive strength of high-strength concrete
[DE93-500412] p 682 N94-14653
SHEAR FLOW
Studies of turbulent shear flows and their control
[NASA-CR-194114] p 635 N94-13676
Turbulent diffusion in homogeneous shear flow with stable density stratification
[DLR-FB-92-26] p 639 N94-14443
Search for subgrid scale parameterization by projection pursuit regression p 643 N94-14749
A study of the fine scale motions of incompressible time-developing mixing layers p 644 N94-14751
Direct simulation of polymer drag reduction in free shear flows and vortex dipoles p 644 N94-14755
Investigation of the dilatational dissipation in compressible homogeneous shear flow p 645 N94-14758
SHEAR LAYERS
Turbulence modeling of free shear layers for high-performance aircraft
[NASA-CR-193659] p 520 N94-12799
Linear instability of curved free shear layers
[NASA-TM-106290] p 642 N94-14729
A study of the fine scale motions of incompressible time-developing mixing layers p 644 N94-14751
Vortex-induced disturbance field in a compressible shear layer p 645 N94-14760
SHEAR PROPERTIES
Shear buckling of fiber metal laminates: Comparison between orthotropic and anisotropic plate models using finite element method
[LTR-ST-1934] p 671 N94-13565
Studies of momentum and energy transfer across wavy gas-liquid interfaces
[AD-A266432] p 635 N94-13699
An experimental study on the effect of die geometry on swell and sag in the parison extrusion stage
[IMI-93RT-42400-1476-G] p 597 N94-14070
Machining and grinding: High rate deformation in practice
[DE93-010718] p 664 N94-14457
Structures and shear response of lipid monolayers
[DE93-015076] p 730 N94-14802
SHEAR STRAIN
Nonlinear vibrations of thick composite plates: Higher-order shear deformation plate theory p 556 N94-13558
Computer program for analysis of high speed, single row, angular contact, spherical roller bearing, SASHBEAN. Volume 1: User's guide
[NASA-CR-191183] p 663 N94-14445
SHEAR STRENGTH
System integration and demonstration of adhesive bonded high temperature aluminum alloys for aerospace structure, phase 2
[NASA-CR-191459] p 575 N94-12792
SHEAR STRESS
Colorimetric qualification of shear sensitive liquid crystal coatings
[NASA-CR-194126] p 806 N94-13291
Finite element analysis of composite plates by use of modified complementary energy principle p 672 N94-13596
Non-uniqueness in dynamic rate-independent non-associated plasticity
[AD-A266342] p 769 N94-13731
Shock compression and quasielastic release in tantalum
[DE93-014566] p 811 N94-14329
Computer program for analysis of high speed, single row, angular contact, spherical roller bearing, SASHBEAN. Volume 2: Mathematical formulation and analysis
[NASA-CR-191182] p 664 N94-14446
Vortex-induced disturbance field in a compressible shear layer p 645 N94-14760
SHEARING
A stochastic model for behavior analysis of fiber-reinforced quasi-brittle materials p 672 N94-13594
SHELL STABILITY
A survey of crack path stability criteria and their application to crack flapping phenomena in stiffened structures
[LR-681] p 675 N94-13929
The effect of initial imperfections on shell stability: An updated review
[LR-695] p 682 N94-14692
SHELL STARS
Physical properties of gas disks around shell stars with and without dust
[NASA-CR-193655] p 835 N94-13239
SHELLS (STRUCTURAL FORMS)
Probabilistic micromechanics for high-temperature composites
[NASA-CR-191150] p 676 N94-14408
SHOCK FRONTS
Numerical simulations and experiments on physics of high Mach number shockwave: Turbulent flow interactions
[DE93-013424] p 631 N94-13249
Shock compression and quasielastic release in tantalum
[DE93-014566] p 811 N94-14329
Evolution of the shock front and turbulence structures in the shock/turbulence interaction p 645 N94-14761
SHOCK HEATING
X ray emission from dynamical shock models in hot-star winds
[NASA-CR-194093] p 847 N94-13288
SHOCK LOADS
Micromechanical strength effects in shock compression of solids
[DE93-014425] p 670 N94-12887
Shock compression and quasielastic release in tantalum
[DE93-014566] p 811 N94-14329
Nonlinear wave predictions in ceramics
[DE93-016516] p 582 N94-14436
SHOCK RESISTANCE
Thermal shock resistance of ceramic matrix composites
[NASA-CR-189136] p 557 N94-13920
SHOCK SPECTRA
Development of test techniques to simulate high-frequency mechanical shock on weapon components
[KCP-613-4998] p 675 N94-13907
SHOCK TESTS
Shock-free accele·ation of laser driven targets
[DE93-008050] p 655 N94-13387
Development of test techniques to simulate high-frequency mechanical shock on weapon components
[KCP-613-4998] p 675 N94-13907
Thermal shock resistance of ceramic matrix composites
[NASA-CR-189136] p 557 N94-13920
SHOCK TUBES
A multiphase model for shock-induced flow in low density foam
[DE93-013767] p 632 N94-13397
Experimental investigation of the effects of blowing ratio parameter on heat transfer to a film-cooled flat plate
[AD-A266599] p 636 N94-13780
Comparative ignition of hexane and octane isomers in a shock tube
[DE93-016535] p 566 N94-14869
SHOCK TUNNELS
Numerical simulation of hypersonic flow for the design of the H-2 orbiting plane (HOPE), part 3
[NAL-TR-1168-PT-3] p 499 N94-12948
Aerodynamic and aerothermal facilities 2. Part 1: Short-duration, high-enthalpy facilities p 506 N94-14159
SHOCK WAVE INTERACTION
Fundamental study of shock wave/turbulent boundary layer interactions with passive control in transonic flows
[ESA-TT-1278] p 630 N94-13117
Sub-grid scale modeling for large eddy simulations in analysis of shock-turbulence interactions
[DE93-013425] p 631 N94-13250
Shock/boundary-layer/shock interactions p 507 N94-14172
Multi-dimensional high order essentially non-oscillatory finite difference methods in generalized coordinates
[NASA-CR-194031] p 770 N94-14429
Evolution of the shock front and turbulence structures in the shock/turbulence interaction p 645 N94-14761
Interaction of two glancing, crossing shock waves with a turbulent boundary-layer at various Mach numbers
[NASA-TM-103740] p 509 N94-14780
SHOCK WAVE PROPAGATION
Modeling the impact behavior of AD85 ceramic under multi-axial loading
[AD-A265877] p 576 N94-12932
MHD shocks in coronal mass ejections
[NASA-CR-193418] p 828 N94-12970
Studies on equatorial shock formation during plasmaspheric refilling
[NASA-CR-194392] p 715 N94-13954
SHOCK WAVES
Recovery of materials impacted at high velocity
[DE93-014150] p 576 N94-12885
Micromechanical strength effects in shock compression of solids
[DE93-014425] p 670 N94-12887
The 3-D massively parallel impact simulations using PCTH
[DE93-011593] p 670 N94-12908
MHD shocks in coronal mass ejections
[NASA-CR-193418] p 828 N94-12970
Fundamental study of shock wave/turbulent boundary layer interactions with passive control in transonic flows
[ESA-TT-1278] p 630 N94-13117
Numerical simulations and experiments on physics of high Mach number shockwave: Turbulent flow interactions
[DE93-013424] p 631 N94-13249
Sub-grid scale modeling for large eddy simulations in analysis of shock-turbulence interactions
[DE93-013425] p 631 N94-13250
A multiphase model for shock-induced flow in low density foam
[DE93-013767] p 632 N94-13397
Measuring opacity of shock generated argon plasmas
[DE93-013038] p 801 N94-14312
Nonlinear wave predictions in ceramics
[DE93-016516] p 582 N94-14436
Atmospheric acoustic modeling
[DE93-016727] p 718 N94-14518
Comparative ignition of hexane and octane isomers in a shock tube
[DE93-016535] p 566 N94-14869
SHORT CRACKS
Finite element calculation of stress-intensity factors for thumb-nail cracks in DEN specimens
[LTR-ST-1929] p 850 N94-13548
Finite element calculation of stress-intensity factors for thru-thickness cracks in DEN specimens
[LTR-ST-1905] p 675 N94-14035
The growth of short fatigue cracks in an aluminium alloy
[RAE-TR-92063] p 574 N94-14828
SHORT TAKEOFF AIRCRAFT
Position error determination for the speedometer and altimeter of the NAL QSTOL experimental aircraft ASKA
[NAL-TR-1144] p 517 N94-13451
Flight path control for the approach and landing of the quiet STOL experimental aircraft ASKA
[NAL-TR-1183] p 513 N94-13457
SHROUDED PROPELLERS
Noise levels from a model turbofan engine with simulated noise control measures applied
[NASA-TM-106318] p 518 N94-14036
SHROUDS
Cammatic: An approach to improve DSS 13 antenna gravity-loading performance p 608 N94-14374
SHUTTLE MISSION SIMULATOR
Analysis of differences between seating positions in simulators and orbiters
[NASA-TM-104776] p 737 N94-13399
SIGNAL ANALYSIS
A new formulation of longitudinal coherent instabilities
[DE93-014288] p 789 N94-13220
The DREO Elint Browser Utility (DEBU) reference manual
[DSIS-92-03900] p 603 N94-13837
Advanced Communications ESM System (ACES) testbed: Integration study
[DSIS-93-00345] p 604 N94-13939
Envelope and instantaneous frequency estimation of narrowband modulated signals
[DREO-TN-92-3] p 605 N94-14033
Deconvolution for positive signals
[DE93-013044] p 773 N94-14314
Utilization of boundary element method for extraction of frequency dependent conductivity parameters of lossy intra-chip transmission lines
[ETN-93-94385] p 771 N94-14807
Optimization of a subband coding for high definition television with motion controlled three dimensional frequency band decomposition
[ETN-93-94396] p 617 N94-14817
SIGNAL ANALYZERS
Adaptive Signal Processing Testbed
[DSIS-93-00258] p 604 N94-13869
SIGNAL DETECTION
Signal design for data communication through rapidly varying linear channels
[ITN-93-85195] p 601 N94-13567

A review of robust detection
[DSIS-93-00400] p 603 N94-13829
Trellis coding with Continuous Phase Modulation (CPM) for satellite-based land-mobile communications
[NASA-CR-191325] p 604 N94-13909
Advanced Communications ESM System (ACES) testbed: Integration study
[DSIS-93-00345] p 604 N94-13939
Determining neural network connectivity using evolutionary programming
[AD-A266853] p 766 N94-14882

SIGNAL DETECTORS
Portable acoustic wave sensor systems for real-time monitoring of volatile organic compounds
[DE93-013753] p 582 N94-14511

SIGNAL ENCODING
Recursive time-varying filter banks for subband image coding
[NASA-CR-193726] p 598 N94-12920
Digital sound: The selection of critical programme material and preparation of recordings for CCIR tests on low bit-rate codecs
[BBC-RD-1993/1] p 598 N94-12925
Digital sound: Subjective tests on commentary-quality codecs
[BBC-RD-1993/2] p 598 N94-12926
Exact reconstruction analysis/synthesis filter banks with time-varying filters
[NASA-CR-193725] p 600 N94-13466
Speaker independent recognition of isolated words using vector quantization and neural networks
[ETN-93-94390] p 616 N94-14724
Optimization of a subband coding for high definition television with motion controlled three dimensional frequency band decomposition
[ETN-93-94396] p 617 N94-14817

SIGNAL FADING
Long duration measurements of fading on a low elevation angle, 11-GHz satellite path p 613 N94-14661
Large-scale rainfall diversity for ACTS p 613 N94-14662
Rain rate duration statistics derived from the Mid-Atlantic coast rain gauge network p 614 N94-14663
Contribution towards a draft revision of recommendations 681: Propagation data required for the design of Earth-space land mobile telecommunications systems p 614 N94-14666
Characterisation of the LMS propagation channel at L- and S-bands: Narrowband experimental data and channel modelling p 615 N94-14669
Results of multiband (L, S, Ku band) propagation measurements and model for high elevation angle land mobile satellite channel p 615 N94-14670
Tree attenuation at 20 GHz: Foliage effects p 615 N94-14672

SIGNAL GENERATORS
Performance results of a digital test signal generator p 609 N94-14382
The flight performance of the Galileo orbiter USO p 611 N94-14398

SIGNAL MEASUREMENT
Measurement of wave propagation for VHF/UHF and a comparison between measured and predicted values
[FFI/RAPPORT-92/7024] p 605 N94-13968

SIGNAL PROCESSING
Ocean acoustic processing: A model-based approach
[DE93-011902] p 725 N94-12876
Digital sound: The selection of critical programme material and preparation of recordings for CCIR tests on low bit-rate codecs
[BBC-RD-1993/1] p 598 N94-12925
Digital sound: Subjective tests on commentary-quality codecs
[BBC-RD-1993/2] p 598 N94-12926
An experimental study of tether reel system: A laboratory model
[NAL-TR-1176T] p 539 N94-12943
HYMOSS signal processing for pushbroom spectral imaging
[NASA-CR-191341] p 620 N94-13125
Exact reconstruction analysis/synthesis filter banks with time-varying filters
[NASA-CR-193725] p 600 N94-13466
Signal design for data communication through rapidly varying linear channels
[ITN-93-85195] p 601 N94-13567
Kalman filter based architectures for interference excision
[DSIS-93-00034] p 603 N94-13818
Acousto-optical post-processor time-integrating correlator updates
[DSIS-93-00314] p 777 N94-13831
Digital quadrature demodulation for radar ESM applications
[DREO-TN-92-10] p 603 N94-13838
VMEC30 programming library: Reference manual
[DSIS-93-00350] p 750 N94-13858
Adaptive Signal Processing Testbed
[DSIS-93-00258] p 604 N94-13869
Adaptive Signal Processing Testbed: Software design specification
[DSIS-93-00259] p 604 N94-13870
Advanced Communications ESM System (ACES) testbed: Integration study
[DSIS-93-00345] p 604 N94-13939
VMEC30 software development: Tutorial manual
[DSIS-93-00351] p 750 N94-13944
A rocket-borne lidar for studies of the middle atmosphere
[FFI/RAPPORT-92/7034] p 715 N94-13949
Demonstration and acceptance test plan for real-time excision software on the Adaptive Signal Processing Testbed
[DSIS-93-00275] p 751 N94-13990
ASPT software source code: SUN driver package
[DSIS-93-00262] p 751 N94-14014
Adaptive Signal Processing Testbed: VME-based DSP board market survey
[DSIS-93-00274] p 605 N94-14015
ASPT software source code: Development system package, VME-C30 component
[DSIS-93-00276] p 751 N94-14016
Adaptive Signal Processing Testbed signal excision software: User's manual
[DSIS-93-00260] p 606 N94-14037
Adaptive Signal Processing Testbed application software: User's manual
[DSIS-93-00261] p 606 N94-14038
VMEC30 SUN software development utilities: User's manual
[DSIS-93-00348] p 752 N94-14051
VMEC30 SUN device drivers: User's manual
[DSIS-93-00349] p 752 N94-14052
Testing various time-frequency distribution techniques
[DREO-TN-92-17] p 606 N94-14062
I/Q demodulation of radar signals with calibration and filtering
[DREO-RN-1119] p 606 N94-14064
EWTEST signal excision testbed: System evaluation
[DSIS-93-00346] p 607 N94-14065
DSP software development environments for the Adaptive Signal Processing Testbed
[DSIS-93-00347] p 607 N94-14066
ASPT software source code: Host development system package
[DSIS-93-00277] p 753 N94-14197
An exact processing algorithm for wide beam spaceborne SAR data p 689 N94-14213
Deconvolution for positive signals
[DE93-013044] p 773 N94-14314
FLATDAN beamformer enhancements and testing
[DSIS-93-00287] p 777 N94-14360
Stability measurements of the radio science system at the 34-m high-efficiency antennas p 609 N94-14381
Preliminary design and implementation of the baseline digital baseband architecture for advanced deep space transponders p 611 N94-14393
Determining neural network connectivity using evolutionary programming
[AD-A266853] p 766 N94-14882

SIGNAL RECEPTION
Calibration of the receiver channel for the GOPEX precursor experiments p 610 N94-14387

SIGNAL TO NOISE RATIOS
Lower bounds on time of arrival estimation of pulse compression waveforms
[ITN-93-85189] p 599 N94-13196
Performance results of a digital test signal generator p 609 N94-14382

SIGNAL TRANSMISSION
Ocean acoustic processing: A model-based approach
[DE93-011902] p 725 N94-12876
Digital sound: The selection of critical programme material and preparation of recordings for CCIR tests on low bit-rate codecs
[BBC-RD-1993/1] p 598 N94-12925
Trellis coding with Continuous Phase Modulation (CPM) for satellite-based land-mobile communications
[NASA-CR-191325] p 604 N94-13909
Calibration of the receiver channel for the GOPEX precursor experiments p 610 N94-14387
GOPEX laser transmission and monitoring systems p 611 N94-14391

SIGNATURES
Effects of typhoon on TOMS data p 693 N94-14243

SIGNS AND SYMPTOMS
Autogenic feedback training experiment: A preventative method for space motion sickness p 595 N94-13774

SILICA GLASS
Thermal history effects on electrical relaxation and conductivity for potassium silicate glass with low alkali concentrations
[NASA-TM-106324] p 583 N94-14845

SILICATES
Deposition of impact-generated vapors in the lunar regolith p 843 N94-14302

SILICIDES
Fracture behavior of vanadium/vanadium silicide in-situ composites
[DE93-013422] p 556 N94-13389

SILICON
Metal-semiconductor, composite radiation detectors
[DE93-013313] p 619 N94-12994
Lattice site of helium implanted in Si and diamond
[DE93-015365] p 805 N94-13012
Fracture behavior of vanadium/vanadium silicide in-situ composites
[DE93-013422] p 556 N94-13389
Computational diagnostics for detecting phase transitions during nanoindentation
[DE93-016536] p 813 N94-14439
Quantum state resolved desorption of CO from solid surfaces
[DE93-016876] p 814 N94-14597
A high voltage dielectrically isolated smart power technology based on silicon direct bonding
[LAAS-92492] p 626 N94-14698
Manufacturing and examination of integrated optical waveguide components in silicon
[ETN-93-94393] p 793 N94-14704
Multicrystalline silicon solar cells: Gettering optimization and characterization
[DE93-015001] p 705 N94-14861

SILICON ALLOYS
The 1.00 MeV proton radiation resistance studies of amorphous silicon-based alloy solar cells p 703 N94-13639
The influence of a microgravity environment on the dendritic morphology during directional solidification of hypoeutectic Al-Si alloys
[NASA-CR-194139] p 571 N94-13891
Evolving surface cusps during strained-layer epitaxy
[DE93-015430] p 813 N94-14478

SILICON CARBIDES
Micromechanical modeling of laminated composites with interfaces and woven composites using the boundary element method
[NASA-TM-106280] p 670 N94-13053
Processing and mechanical properties of silicon carbide platelet reinforced alumina composites p 556 N94-13557
Problems and opportunities in microwave joining of ceramics
[DE93-014998] p 579 N94-13888
Dynamic mechanical deformation of a SiC(sub p)/Al-Li (8090) composite
[DE93-014586] p 558 N94-14121

SILICON DIOXIDE
1/f noise and oxide traps in MOSFETs
[DE93-007581] p 619 N94-12942
Linear and nonlinear spectroscopic probing of solute interactions with chemically modified silica surface
[DE93-014648] p 562 N94-13001
Theory of the electronic and structural properties of solid state oxides
[DE93-016051] p 811 N94-14296
Molecular simulator: A basic tool for submicron MOS processes development
[LAAS-92484] p 814 N94-14697
Reactor studies of metal ions associated with chromatographic silica
[AD-A266675] p 573 N94-14779
Fine-powder Al2O3 and SiO2 for preparation of multielement standards for rare-earth elements analysis
[DE93-625118] p 567 N94-14884

SILICON FILMS
Ion assisted sputter deposition of Mo-Si multilayers
[DE93-013830] p 583 N94-14693

SILICON ISOTOPES
Office of Naval Research/DARPA publications: Composite materials with improved properties in compression
[AD-A265509] p 560 N94-14794

SILICON NITRIDES
Quantitative mapping of pore fraction variations in silicon nitride using an ultrasonic contact scan technique
[NASA-TP-3377] p 665 N94-13056
Processing and testing of high toughness silicon nitride ceramics
[NASA-CR-191190] p 582 N94-14543

SILICON OXIDES
Multicrystalline silicon solar cells: Gettering optimization and characterization
[DE93-015001] p 705 N94-14861

Electrochemical planarization for microelectronic circuits
[DE93-017214] p 627 N94-14870

SILICON RADIATION DETECTORS
Metal-semiconductor, composite radiation detectors
[DE93-013313] p 619 N94-12994
Proceedings of the Workshop on Applications of Synchrotron Radiation to Trace Impurity Analysis for Advanced Silicon Processing
[DE93-013389] p 805 N94-13020

SILICONES
Qualification test of the Ross Double Planetary Mixer
[NASA-CR-192600] p 652 N94-14497

SILOXANES
Unexpectedly rapid hydrosilation polymerization of the diallyl derivative of bisphenol A and 2,6-diallylphenol
[AD-A265832] p 577 N94-12986

SIMD (COMPUTERS)
Efficient, massively parallel eigenvalue computation
[NASA-CR-194289] p 760 N94-13921
An overview of parallel scientific visualization
[DE93-017105] p 755 N94-14521
Identification of continuous-time dynamical systems: Neural network based algorithms and parallel implementation
[DE93-014427] p 766 N94-14737

SIMPLIFICATION
Simplification-driven automated partial evaluation
[DE93-012890] p 768 N94-13391

SIMULATED ANNEALING
Simulated annealing for the problem of multiresource location on graph
[REPT-93-033] p 770 N94-13809

SIMULATION
Simulation studies for surfaces and materials strength
[NASA-CR-193305] p 671 N94-13179
Lightning simulation and determination of expected striking points
[ITN-93-85202] p 719 N94-13188
Event-driven simulation in SELMON: An overview of EDSE
[NASA-CR-194505] p 749 N94-13784
Development of test techniques to simulate high-frequency mechanical shock on weapon components
[KCP-613-4998] p 675 N94-13907
Laboratory simulations of lunar darkening processes p 843 N94-14301
Modeling surface area to volume effects on borosilicate glass dissolution
[DE93-011891] p 581 N94-14432
Computational diagnostics for detecting phase transitions during nanoindentation
[DE93-016536] p 813 N94-14439

SIMULATORS
Propulsion simulator for magnetically-suspended wind tunnel models
[NASA-CR-189560] p 527 N94-13127
Event-driven simulation in SELMON: An overview of EDSE
[NASA-CR-194505] p 749 N94-13784
Simulator for heterogeneous dataflow architectures
[NASA-CR-191545] p 622 N94-13797

SINGLE CRYSTALS
Determination of channeling perspectives for complex crystal structures
[DE93-012872] p 805 N94-13009
Lattice site of helium implanted in Si and diamond
[DE93-015365] p 805 N94-13012
Spacelab J experiment descriptions
[NASA-TM-4517] p 586 N94-13732
Growth experiment of narrow band-gap semiconductor PbSnTe single crystals in space (M-1) p 586 N94-13733
Growth of PbSnTe single crystal by traveling-zone method in low gravity (M-2) p 586 N94-13734
Growth of semiconductor compound single crystal InSb by floating zone method (M-3) p 586 N94-13735
Growth of Si spherical crystals and the surface oxidation (M-9) p 587 N94-13741
Growth of samarskite crystal under microgravity conditions (M-20) p 590 N94-13752
Growth experiment of organic metal crystal in low gravity (M-21) p 590 N94-13753
Crystal growth of enzymes in low gravity (L-5) p 592 N94-13762
Emitter Wrap-Through solar cell
[DE93-014996] p 703 N94-13886
Measurement of penetration depth lambda(T) in YBa2Cu3O(7-delta) thin film
[DE93-014587] p 810 N94-14122
Prism-film coupling in anisotropic planar waveguides of epitaxial (101) rutile thin films
[DE93-012912] p 811 N94-14304
Small polaron conduction in Y2Ti2O7
[ITN-93-85221] p 814 N94-14557

SINGLE EVENT UPSETS
Single event effects and laser simulation studies
[NASA-CR-194506] p 657 N94-13812
Single Event Upset (SEU) testing of semiconductor components at the McMaster Accelerator Laboratory
[DSIS-93-00071] p 623 N94-13834
Test report for single event effects of the 80386DX microprocessor
[NASA-CR-194509] p 741 N94-13943

SINGLE SIDEBAND TRANSMISSION
Envelope and instantaneous frequency estimation of narrowband modulated signals
[DREO-TN-92-3] p 605 N94-14033

SINGLE STAGE TO ORBIT VEHICLES
Hypersonic aerodynamic characteristics of SSTO-type aerospace planes. Part 1: The NAL 0-th configuration
[NAL-TR-1186] p 514 N94-13459
Multidisciplinary design techniques applied to conceptual aerospace vehicle design
[NASA-CR-194409] p 515 N94-13618
Spaceplane program at NAL: System concept and related technology issues p 537 N94-14281

SINTERING
Microwave hybrid heating of alumina filaments
[DE93-012642] p 581 N94-14327
Microwave sintering of large alumina bodies
[DE93-012752] p 581 N94-14340
How to read a phase equilibrium diagram for high-temperature ceramics material as main object
[DE93-512333] p 582 N94-14513
Processing and testing of high toughness silicon nitride ceramics
[NASA-CR-191190] p 582 N94-14543

SIS (SUPERCONDUCTORS)
Measurements on two-dimensional arrays of mesoscopic Josephson junctions
[AD-A265129] p 807 N94-13359
Theoretical SIS mixer research
[AD-A266323] p 807 N94-13580

SISO (CONTROL SYSTEMS)
Kalman filter input estimation
[NAL-TR-1182] p 649 N94-13456

SITTING POSITION
Clinical physiology of bed rest
[NASA-TM-104010] p 727 N94-13447

SIZE DETERMINATION
Adaptively resizing populations: Algorithm, analysis, and first results
[NASA-CR-194277] p 742 N94-12808
Emission line variability in active galactic nuclei
[ITN-93-85209] p 849 N94-14553

SIZE DISTRIBUTION
Experimental determination of droplets local mean diameter of a sprag from impinging jets
[INPE-5469-TDI/500] p 631 N94-13365
Pore-size-distribution of cationic polyacrylamide hydrogels
[DE93-015218] p 581 N94-14400

SKEWNESS
Evolution of the shock front and turbulence structures in the shock/turbulence interaction p 645 N94-14761

SKIN FRICTION
A technique for direct measurement of skin friction in supersonic combustion flow p 503 N94-13555
High freestream turbulence effects on the transport of heat and momentum p 633 N94-13559

SKIN TEMPERATURE (NON-BIOLOGICAL)
The development and implementation of an interactive retrieval/analysis/forecast algorithm p 692 N94-14234

SKY SURVEYS (ASTRONOMY)
Archiving of HEAO-1 data products and the creation of a general user's guide to the archive
[NASA-CR-193415] p 822 N94-13062
Search for extraterrestrial intelligence/high resolution microwave survey team member
[NASA-CR-194177] p 739 N94-13086
ROSAT guest investigator program (AO-1). On a search for coronal x ray emissions from white dwarfs
[NASA-CR-193654] p 835 N94-13171
A survey of compact planetary nebulae at radio wavelengths
[ISBN-0-315-61950-3] p 829 N94-13371
A near-infrared faint galaxy survey: Evolution and the cosmological geometry from K band photometry p 830 N94-13591
Sites of fine-scale electron density turbulence in the interstellar medium
[NASA-CR-193708] p 839 N94-13864
X ray observations of late-type stars using the ROSAT all-sky survey
[NASA-CR-193716] p 832 N94-14146
HRMS sky survey wideband feed system design for DSS 24 beam waveguide antenna p 611 N94-14397

SLEEP
Work/rest schedules and performance of S-3 aviators during fleet exercise
[AD-A265807] p 734 N94-12975
Work/rest schedules and performance of F/A-18 aviators during Fleet Exercise 1992
[AD-A265826] p 735 N94-12982

SLEEP DEPRIVATION
Work/rest schedules and performance of S-3 aviators during fleet exercise
[AD-A265807] p 734 N94-12975
Work/rest schedules and performance of F/A-18 aviators during Fleet Exercise 1992
[AD-A265826] p 735 N94-12982

SLENDER WINGS
A grid generation package for high aspect ratio wings p 510 N94-14608

SLICING
Integrating interface slicing into software engineering processes
[NASA-CR-192761] p 754 N94-14368

SLIDING
Wear-mechanism modelling
[DE93-012311] p 579 N94-13974

SLIDING FRICTION
JPRS report: Science and technology. Central Eurasia: Materials science
[JPRS-UMS-93-005] p 559 N94-14575

SLURRIES
Reverse micelle synthesis of nanoscale metal containing catalysts
[DE93-012869] p 572 N94-14184

SMART STRUCTURES
Feasibility study of an orbiting laboratory for testing CSI technology
[NASA-CR-191524] p 540 N94-13016
Smart skin technology development for measuring ice accretion, stall, and high AOA aircraft performance. Part 1: Capacitive ice detector development
[NASA-CR-194252] p 511 N94-13424
Smart materials/structures technical analysis
[AD-A266771] p 766 N94-14785

SMOKE
Estimation of the concentration versus the time profile of zinc chloride particles in smoke clouds generated by the Raufoss A/S instantaneous smoke RA-90 and DM-45 HC smoke generator
[FFI-93/6001] p 708 N94-13821
Flight validation of a pulsed smoke flow visualization system
[NASA-CR-186026] p 516 N94-14106

SMOOTHING
Shock-free acceleration of laser driven targets
[DE93-008050] p 655 N94-13387

SNOW
Optical properties of CO2 ice and CO2 snow in the ultraviolet, visible, and infrared
[NASA-CR-194110] p 686 N94-14081

SNOW COVER
Snow cover models in operational watershed forecasting
[DE93-778332] p 718 N94-12837

SODIUM
Multiplicity spectrometry on neutron filtered beams
[DE93-617529] p 790 N94-14843

SOFTENING
On the hardening and softening of nanocrystalline materials
[DE93-012901] p 810 N94-14185

SOFTWARE ENGINEERING
Generic software architecture based redesign p 745 N94-13290
Software synthesis using generic architectures
[NASA-CR-194201] p 745 N94-13355
Architecture-driven reuse of code in KASE
[NASA-CR-194200] p 745 N94-13356
The KASE approach to domain-specific software systems p 745 N94-13357
Creating a strategic plan for configuration management using computer aided software engineering (CASE) tools
[DE93-013663] p 746 N94-13394
A measurement and evaluation process model applied to software engineering environments
[INPE-5345-PUD/048] p 746 N94-13428
Software design by reusing architectures
[NASA-CR-194151] p 747 N94-13443
Mass market computers for software development
[ERB-1035] p 741 N94-13547
Space and Earth sciences, computer systems, and scientific data analysis support, volume 1
[NASA-CR-194535] p 741 N94-13788
Parameter identification of a model of the process of software development
[REPT-93-008] p 750 N94-13807

Hypertext Compiling Tools (HCT): Developing model based applications with standard hypertext systems
[REPT-92-049] p 750 N94-13822
Activities of Institute for Information Technology
[CNR-35024] p 824 N94-14069
Guide to the software architectural design phase
[ESA-PSS-05-04-ISSUE-1] p 753 N94-14190
Guide to the software detailed design and production phase
[ESA-PSS-05-05-ISSUE-1] p 753 N94-14191
PC viruses: How do they do that?
[DE93-012581] p 753 N94-14289
AXAF FITS standard for ray trace interchange
[NASA-CR-194025] p 832 N94-14305
Integrating interface slicing into software engineering processes
[NASA-CR-192761] p 754 N94-14368
Formal functional test designs with a test representation language p 609 N94-14383
PC4CAST: A tool for DSN load forecasting and capacity planning p 610 N94-14384
Visualization techniques to aid in the analysis of multi-spectral astrophysical data sets
[NASA-CR-194489] p 840 N94-14482
A database for propagation models p 614 N94-14665
Verification of critical software by statistical testing
[LAAS-93006] p 756 N94-14714
Determining neural network connectivity using evolutionary programming
[AD-A266853] p 766 N94-14882

SOFTWARE RELIABILITY
Diskless supercomputers: Scalable, reliable I/O for the Tera-Op technology base
[NASA-CR-194089] p 740 N94-13363
Switchover software reliability estimate for Paducah freezer/sublimer computer systems
[DE93-013844] p 756 N94-14696
Verification of critical software by statistical testing
[LAAS-93006] p 756 N94-14714

SOFTWARE REUSE
Software synthesis using generic architectures
[NASA-CR-194201] p 745 N94-13355
Architecture-driven reuse of code in KASE
[NASA-CR-194200] p 745 N94-13356
Software design by reusing architectures
[NASA-CR-194151] p 747 N94-13443
Integrating interface slicing into software engineering processes
[NASA-CR-192761] p 754 N94-14368

SOFTWARE TOOLS
Artificial intelligence support for scientific model-building
[NASA-TM-109252] p 761 N94-12890
Parachute system design, analysis, and simulation tool
[DE93-013755] p 501 N94-13260
Architecture-driven reuse of code in KASE
[NASA-CR-194200] p 745 N94-13356
The KASE approach to domain-specific software systems p 745 N94-13357
Creating a strategic plan for configuration management using computer aided software engineering (CASE) tools
[DE93-013663] p 746 N94-13394
Designing and generating a GUI module using GUI p 747 N94-13437
Software design by reusing architectures
[NASA-CR-194151] p 747 N94-13443
Rapid intelligent inspection process definition for dimensional measurement in advanced manufacturing
[DE93-011271] p 748 N94-13480
Some computational tools for the analysis of through cracks in stiffened fuselage shells
[LR-701] p 673 N94-13726
Hypertext Compiling Tools (HCT): Developing model based applications with standard hypertext systems
[REPT-92-049] p 750 N94-13822
VMEC30 programming library: Reference manual
[DSIS-93-00350] p 750 N94-13858
VMEC30 software development: Tutorial manual
[DSIS-93-00351] p 750 N94-13944
A widget based operations simulator for a planetary camera: A model for the high resolution stereo camera on Mars 94
[DLR-FB-92-30] p 651 N94-14044
VMEC30 SUN software development utilities: User's manual
[DSIS-93-00348] p 752 N94-14051
DSP software development environments for the Adaptive Signal Processing Testbed
[DSIS-93-00347] p 607 N94-14066
EVES: An overview
[DSIS-93-00238] p 752 N94-14088
Guide to the software architectural design phase
[ESA-PSS-05-04-ISSUE-1] p 753 N94-14190
Guide to the software detailed design and production phase
[ESA-PSS-05-05-ISSUE-1] p 753 N94-14191
PC4CAST: A tool for DSN load forecasting and capacity planning p 610 N94-14384
Computational Controls Workstation: Algorithms and hardware p 678 N94-14626
Caesy: A software tool for computer-aided engineering p 678 N94-14627
ASTEC and MODEL: Controls software development at Goddard Space Flight Center p 678 N94-14628
An application of the IMC software to controller design for the JPL LSCL Experiment Facility p 681 N94-14645

SOIL EROSION
Soil erosion rates caused by wind and saltating sand stresses in a wind tunnel
[DE93-009154] p 706 N94-12905
Soil erosion mapping using remote sensing and GIS techniques p 692 N94-14240

SOIL MAPPING
Spectral reflectance of soils from Sao Paulo State
[INPE-5424-PRP/172] p 684 N94-13377
Soil erosion mapping using remote sensing and GIS techniques p 692 N94-14240
Land evaluation for agricultural productivity in North-East Thailand using LANDSAT TM data and geographic information p 693 N94-14242

SOIL MECHANICS
Dynamic soil pressures on rigid cylindrical vaults
[DE93-013930] p 676 N94-14585

SOIL MOISTURE
Measuring surface fluxes in CAPE
[NASA-CR-193664] p 711 N94-12788
Phase aligner for the Electronically Scanned Thinned Array Radiometer (ESTAR) instrument
[NASA-TM-4518] p 623 N94-13878
Circulation and rainfall climatology of a 10-year (1979 - 1988) integration with the Goddard Laboratory for atmospheres general circulation model
[NASA-TM-104591] p 723 N94-14074

SOIL SCIENCE
Applications of the Advanced Light Source to problems in the earth, soil, and environmental sciences
[DE93-015258] p 710 N94-14477

SOILS
Measuring surface fluxes in CAPE
[NASA-CR-193664] p 711 N94-12788
Spectral reflectance of soils from Sao Paulo State
[INPE-5424-PRP/172] p 684 N94-13377
Land evaluation for agricultural productivity in North-East Thailand using LANDSAT TM data and geographic information p 693 N94-14242
Survey of subsurface geophysical exploration technologies adaptable to an airborne platform
[DE93-015080] p 717 N94-14294
Dynamic soil pressures on rigid cylindrical vaults
[DE93-013930] p 676 N94-14585
Coastal scour problems and methods for prediction of maximum scour
[AD-A266658] p 726 N94-14775

SOL-GEL PROCESSES
Amorphous sol-gel insulating films
[DE93-012859] p 576 N94-12866
Solution chemistry optimization of sol-gel processed PZT thin films
[DE93-013776] p 814 N94-14695
Charge storage and switching phenomena with molecular assemblies of metal complexes
[AD-A266673] p 787 N94-14778

SOLAR ACTIVITY
Variations common to the interplanetary magnetic field, the zonal atmospheric circulation and the Earth's rotation
[COMMUNICATIONS-SER-B-157] p 837 N94-13504

SOLAR ACTIVITY EFFECTS
Determining the solar-flare photospheric scale height from SMM gamma-ray measurements
[NASA-CR-194084] p 844 N94-13671

SOLAR ARRAYS
Screening of solar cells
[NASA-TM-106298] p 620 N94-13134
A photovoltaic catenary-tent array for the Martian surface
[NASA-TM-106306] p 621 N94-13194
Solar radiation on Mars: Stationary photovoltaic array
[NASA-TM-106321] p 626 N94-14730

SOLAR CELLS
The 1992 JSEE/JWEA Joint Conference
[DE93-793955] p 700 N94-12822
Photovoltaic Subcontract Program
[DE93-000092] p 700 N94-12868
Photovoltaics: Contract lists, fiscal year 1992
[DE93-000093] p 701 N94-12902
Photovoltaics: Program overview, fiscal year 1992
[DE93-000055] p 701 N94-12914
Screening of solar cells
[NASA-TM-106298] p 620 N94-13134
Low temperature metal-organic chemical vapor deposition growth processes for high efficiency solar cells
[DE92-010562] p 702 N94-13386
The 1.00 MeV proton radiation resistance studies of amorphous silicon-based alloy solar cells p 703 N94-13639
Emitter Wrap-Through solar cell
[DE93-014996] p 703 N94-13886
The Large Area Pulsed Solar Simulator (LAPSS)
[NASA-CR-194507] p 703 N94-13940
Numerical simulation and analysis of electrical and optical properties of Al(x)Ga(1-x)As / GaAs
[ETN-93-94387] p 703 N94-13997
Structural and electronic studies of a-SiGe:H alloys
[DE93-010021] p 809 N94-14085
Continuous roll-to-roll a-Si photovoltaic manufacturing technology
[DE93-010006] p 704 N94-14109
Optimization of transparent and reflecting electrodes for amorphous silicon solar cells
[DE93-010009] p 704 N94-14110
Study of novel conductive paints for solar cell electromagnetic fields
[DE93-015088] p 581 N94-14337
Photovoltaic advanced research and development project: Solar radiation research
[DE92-016430] p 704 N94-14350
Activities of the Basic Sciences Branch
[DE93-010012] p 851 N94-14455
Solar radiation on Mars: Stationary photovoltaic array
[NASA-TM-106321] p 626 N94-14730
Multicrystalline silicon solar cells: Gettering optimization and characterization
[DE93-015001] p 705 N94-14861

SOLAR COLLECTORS
The 1992 JSEE/JWEA Joint Conference
[DE93-793955] p 700 N94-12822
High-flux testing of heat pipes for point-focus solar collector systems
[DE93-011581] p 628 N94-12884
Reflective coatings for solar applications
[DE93-010026] p 702 N94-13381
Field of solar collectors: Effect of shadowing on the optimal field design
[ITN-93-85197] p 702 N94-13570
Colorado State University program for developing, testing, evaluating, and optimizing solar heating and cooling systems
[DE93-016018] p 705 N94-14504

SOLAR COOLING
Colorado State University program for developing, testing, evaluating, and optimizing solar heating and cooling systems
[DE93-016018] p 705 N94-14504

SOLAR CORONA
Basic research in solar physics
[NASA-CR-193632] p 844 N94-13234
Evolution of the interplanetary magnetic field
[DE93-012631] p 836 N94-13262
Measurements of the spatial structure and directivity of 100 KeV photon sources in solar flares using PVO and ISEE-3 spacecraft
[NASA-CR-194080] p 845 N94-14492

SOLAR DYNAMIC POWER SYSTEMS
Solar dynamic power system development for Space Station Freedom
[NASA-RP-1310] p 548 N94-12807

SOLAR ELECTRIC PROPULSION
TROPIX: A solar electric propulsion flight experiment
[NASA-TM-106297] p 534 N94-13028

SOLAR ELECTRONS
Measurements of the spatial structure and directivity of 100 KeV photon sources in solar flares using PVO and ISEE-3 spacecraft
[NASA-CR-194080] p 845 N94-14492

SOLAR ENERGY
Solar dynamic power system development for Space Station Freedom
[NASA-RP-1310] p 548 N94-12807
Photovoltaic Subcontract Program
[DE93-000092] p 700 N94-12868
Reflective coatings for solar applications
[DE93-010026] p 702 N94-13381
Nimbus-7 Earth radiation budget calibration history. Part 1: The solar channels
[NASA-RP-1316] p 844 N94-13963
Solar radiation on Mars: Stationary photovoltaic array
[NASA-TM-106321] p 626 N94-14730

SOLAR ENERGY CONVERSION
The 1992 JSEE/JWEA Joint Conference
[DE93-793955] p 700 N94-12822

Field of solar collectors: Effect of shadowing on the optimal field design
[ITN-93-85197] p 702 N94-13570
Colorado State University program for developing, testing, evaluating, and optimizing solar heating and cooling systems
[DE93-016018] p 705 N94-14504

SOLAR FLARES
Determining the solar-flare photospheric scale height from SMM gamma-ray measurements
[NASA-CR-194084] p 844 N94-13671
Hard x ray/microwave spectroscopy of solar flares
[NASA-CR-194399] p 844 N94-13958
Measurements of the spatial structure and directivity of 100 KeV photon sources in solar flares using PVO and ISEE-3 spacecraft
[NASA-CR-194080] p 845 N94-14492
Solar-geophysical data number 584, April 1993. Part 1: (Prompt reports). Data for March, February 1993, and late data
[PB93-198323] p 845 N94-14560
Comparative study of x ray and microwave emissions during solar flares
[NASA-CR-194532] p 845 N94-14577

SOLAR FLUX
Present status of SAGE
[DE93-014350] p 781 N94-13205

SOLAR GENERATORS
Field of solar collectors: Effect of shadowing on the optimal field design
[ITN-93-85197] p 702 N94-13570

SOLAR HEATING
Colorado State University program for developing, testing, evaluating, and optimizing solar heating and cooling systems
[DE93-016018] p 705 N94-14504

SOLAR INSTRUMENTS
Vacuum ultraviolet instrumentation for solar irradiance and thermospheric airglow
[NASA-CR-194525] p 652 N94-14684

SOLAR MAGNETIC FIELD
Basic research in solar physics
[NASA-CR-193632] p 844 N94-13234
Solar-geophysical data number 584, April 1993. Part 1: (Prompt reports). Data for March, February 1993, and late data
[PB93-198323] p 845 N94-14560
Comparative study of x ray and microwave emissions during solar flares
[NASA-CR-194532] p 845 N94-14577

SOLAR MAXIMUM MISSION
Ultraviolet Spectrometer and Polarimeter (UVSP) catalog of observations. Volume 3: Experiments 63058-99771 (February 1988 - November 1989)
[NASA-CR-4529] p 844 N94-13146
Determining the solar-flare photospheric scale height from SMM gamma-ray measurements
[NASA-CR-194084] p 844 N94-13671

SOLAR NEUTRINOS
Present status of SAGE
[DE93-014350] p 781 N94-13205

SOLAR NEUTRONS
Cosmic and solar gamma ray and neutron experiments
[NASA-CR-193359] p 849 N94-13965

SOLAR OSCILLATIONS
Interactions among convection, magnetic fields and p-mode oscillations in the sun
[NASA-CR-194477] p 845 N94-14479

SOLAR PHYSICS
Present status of SAGE
[DE93-014350] p 781 N94-13205
Basic research in solar physics
[NASA-CR-193632] p 844 N94-13234
Solar-geophysical data number 584, April 1993. Part 1: (Prompt reports). Data for March, February 1993, and late data
[PB93-198323] p 845 N94-14560
Solar-geophysical data number 584, April 1993. Part 2: (Comprehensive reports). Data for October 1992 and miscellaneous
[PB93-198331] p 845 N94-14561

SOLAR POWER SATELLITES
Large space structures and systems in the space station era: A bibliography with indexes (supplement 05)
[NASA-SP-7085(05)] p 543 N94-14411

SOLAR RADIATION
Photocatalysis for the treatment of waste water: Applications involving the removal of metals
[DE93-011669] p 561 N94-12841
Basic research in solar physics
[NASA-CR-193632] p 844 N94-13234
Net radiation mapping of mountainous terrain using Landsat-5 thematic mapper imagery and digital terrain data
[ISBN-0-315-57755-X] p 685 N94-13475
Nimbus-7 Earth radiation budget calibration history. Part 1: The solar channels
[NASA-RP-1316] p 844 N94-13963
Photovoltaic advanced research and development project: Solar radiation research
[DE92-016430] p 704 N94-14350
NREL solar radiation resource assessment project: Status and outlook
[DE93-010034] p 704 N94-14422
Vacuum ultraviolet instrumentation for solar irradiance and thermospheric airglow
[NASA-CR-194525] p 652 N94-14684

SOLAR RADIO BURSTS
Solar-geophysical data number 584, April 1993. Part 2: (Comprehensive reports). Data for October 1992 and miscellaneous
[PB93-198331] p 845 N94-14561

SOLAR RADIO EMISSION
Solar-geophysical data number 584, April 1993. Part 1: (Prompt reports). Data for March, February 1993, and late data
[PB93-198323] p 845 N94-14560

SOLAR REFLECTORS
Continuous roll-to-roll a-Si photovoltaic manufacturing technology
[DE93-010006] p 704 N94-14109

SOLAR SIMULATORS
The Large Area Pulsed Solar Simulator (LAPSS)
[NASA-CR-194507] p 703 N94-13940

SOLAR SPECTRA
The infrared solar spectrum
[COMMUNICATIONS-SER-B-159] p 844 N94-13502
Vacuum ultraviolet instrumentation for solar irradiance and thermospheric airglow
[NASA-CR-194525] p 652 N94-14684

SOLAR SYSTEM
Discovery management workshop
[NASA-TM-108244] p 531 N94-14080
The problem of traveling in outer space: The rocket motor
[NASA-TT-10002] p 552 N94-14463

SOLAR TERRESTRIAL INTERACTIONS
The interplanetary origins and the main-phase development of moderate geomagnetic storms (1978 - 1979)
[INPE-5445-TDI/491] p 835 N94-13174
Solar-geophysical data number 584, April 1993. Part 1: (Prompt reports). Data for March, February 1993, and late data
[PB93-198323] p 845 N94-14560

SOLAR WIND
ICE/ISEE plasma wave data analysis
[NASA-CR-194375] p 796 N94-13081
The interplanetary origins and the main-phase development of moderate geomagnetic storms (1978 - 1979)
[INPE-5445-TDI/491] p 835 N94-13174
Basic research in solar physics
[NASA-CR-193632] p 844 N94-13234
Evolution of the interplanetary magnetic field
[DE93-012631] p 836 N94-13262

SOLAR X-RAYS
Measurements of the spatial structure and directivity of 100 KeV photon sources in solar flares using PVO and ISEE-3 spacecraft
[NASA-CR-194080] p 845 N94-14492
Solar-geophysical data number 584, April 1993. Part 2: (Comprehensive reports). Data for October 1992 and miscellaneous
[PB93-198331] p 845 N94-14561

SOLDERED JOINTS
Microstructural influences on the mechanical properties of solder
[DE93-015044] p 573 N94-14474

SOLDERING
Solderability of surface mount devices
[AD-A265751] p 620 N94-13040

SOLID ELECTROLYTES
Study of multicomponent diffusion and transport phenomena
[DE93-015095] p 804 N94-13005
Electrocatalysis issues in polymer electrolyte fuel cells
[DE93-014450] p 702 N94-13402
Combustion synthesis and engineering of nanoparticles for electronic, structural, and superconductor applications
[DE93-016286] p 809 N94-13981
Status of SOFC development in USA
[DE93-015568] p 704 N94-14355

SOLID LUBRICANTS
Dry film lubricant evaluation
[DE93-013114] p 578 N94-13118
Applications of surface science to solid lubricants
[SMC-TR-93-24] p 579 N94-13903

SOLID MECHANICS
Thermal gradient-induced deflection of a thick-walled cylinder with bending residual stresses
[AD-A266347] p 673 N94-13777
Variational approach to probabilistic finite elements
[NASA-CR-187179] p 674 N94-13873
Elastic-plastic mixed-iterative finite element analysis: Implementation and performance assessment
[NASA-TM-106164] p 675 N94-13919
JPRS report: Science and technology. Central Eurasia: Engineering and equipment
[JPRS-UEQ-93-006] p 776 N94-14431

SOLID PHASES
Crystallographic phase identification in the scanning electron microscope: Backscattered electron Kikuchi patterns
[DE93-011574] p 804 N94-12813
Multiphase equation of state for iron
[DE93-013956] p 568 N94-12977
Automated crack identification for cement paste
[AD-A265753] p 665 N94-13042
Thermodiffusion in heterogeneous elastic solids and homogenization
[REPT-14/1993] p 578 N94-13468

SOLID PROPELLANT COMBUSTION
Combustion-induced crack/debond propagation in solid propellants p 584 N94-13560
Numerical simulation of velocity-coupled combustion response of solid rocket propellants p 585 N94-14490

SOLID PROPELLANT ROCKET ENGINES
Combustion-induced crack/debond propagation in solid propellants p 584 N94-13560
Test/analysis correlation and model updating of the STARS 1 and 2 missile systems
[DE93-013774] p 748 N94-13578
Numerical simulation of velocity-coupled combustion response of solid rocket propellants p 585 N94-14490
Qualification test of the Ross Double Planetary Mixer
[NASA-CR-192600] p 652 N94-14497
Technical Evaluation Motor No. 10 (TEM-10)
[NASA-CR-193846] p 554 N94-14907

SOLID PROPELLANTS
Flamespreading in granular solid propellant: Design of an experiment
[AD-A266009] p 583 N94-12987
Closed-chamber analysis of M5 propellant lot RAD-64597
[AD-A266321] p 585 N94-14145

SOLID ROCKET PROPELLANTS
Numerical simulation of velocity-coupled combustion response of solid rocket propellants p 585 N94-14490

SOLID SOLUTIONS
Effect of microstructure on passive film formation and breakdown on Al alloys
[AD-A265339] p 569 N94-13050
First-principles studies of phase stability and the structural and dynamical properties of hydrogen-metal systems
[DE93-016129] p 570 N94-13374
Ionic conductivity of alkali halides and their mixtures near liquid-solid phase transition
[ITN-93-85222] p 566 N94-14558
Statics and kinetics of phase transformations in bcc Fe-Cr
[DE93-013839] p 574 N94-14793

SOLID STATE
Characterization of 1:1 random copolymers obtained from 6-, 7-, 11-, and 12-carbon amino acids
[AD-A265827] p 577 N94-12985
Theory of the electronic and structural properties of solid state oxides
[DE93-016051] p 811 N94-14296

SOLID STATE DEVICES
Metal-semiconductor, composite radiation detectors
[DE93-013313] p 619 N94-12994

SOLID STATE LASERS
Novel Co:MgF2 lidar for aerosol profiler
[NASA-CR-191525] p 654 N94-13091
Solid state laser systems for space application
[NASA-CR-194133] p 656 N94-13420
Design and performance of the terawatt Cr:LiSrAlF6 laser system
[DE93-014678] p 657 N94-13882
Impact of shorter wavelengths on optical quality for laws
[NASA-CR-193433] p 792 N94-14473
Independent adjustment of the higher order frequency dependent phase in chirped pulse amplification systems
[DE93-017106] p 625 N94-14522

SOLID STATE PHYSICS
Activities of Institute for Microstructural Sciences
[NRC-32815] p 810 N94-14198

Activities of Institute for Microstructural Sciences
[CNR-32815] p 810 N94-14199

SOLID SURFACES
Low energy neutral atom imaging techniques
[DE93-012744] p 779 N94-12950
Thermodynamic status of static and dynamic contact angles
[ISBN-0-315-73844-8] p 817 N94-13554
Construction and test of a facility for photon-stimulated field description using excimer laser and time of flight
[ETN-93-94386] p 657 N94-13996
Quantum state resolved desorption of CO from solid surfaces
[DE93-016876] p 814 N94-14597

SOLID WASTES
Integrated, flexible, and rapid geophysical surveying
[DE93-009989] p 712 N94-12906
Vendor information system for innovative treatment technologies. User manual (VISITT version 2.0). Number 2
[PB93-196640] p 821 N94-12936
Environmental awareness
[DE93-014192] p 707 N94-13218

SOLID-SOLID INTERFACES
Surfaces and interfaces of ceramics and metals
[DE93-014959] p 578 N94-13408

SOLIDIFICATION
Thermosolutal convection and macrosegregation in dendritic alloys
[NASA-CR-194039] p 567 N94-12825
Formation of deoxidization products in iron ingot by the addition of Al, Si, and/or Mn (M-5) p 587 N94-13737
Diffusion in liquid state and solidification of binary system (M-7) p 587 N94-13739
Study on solidification of immisible alloys (M-10) p 588 N94-13742
Study on the mechanism of liquid phase sintering (M-12) p 588 N94-13744
Solidification of eutectic system alloys in space (M-19) p 589 N94-13751
Crystal growth of compound semiconductors in a low-gravity environment (InGaAs crystals) (M-22) p 590 N94-13754
Containerless processing of undercooled melts
[NASA-CR-194350] p 572 N94-14123
Measurements of crystal growth kinetics at extreme deviations from equilibrium
[DE93-014526] p 815 N94-14798

SOLIDS
Micromechanical strength effects in shock compression of solids
[DE93-014425] p 670 N94-12887

SOLITARY WAVES
Solitons and 1/f noise in molecular chains
[DE93-622898] p 778 N94-12879
Soliton equations and self-dual gauge fields
[DE93-626620] p 818 N94-14887

SOLUBILITY
Breadboard activities for advanced protein crystal growth
[NASA-CR-193559] p 803 N94-12796
Miscibility of lubricants with refrigerants, phase 1
[DE93-014766-PHASE-1] p 596 N94-13407
Destruction of waste energetic materials using base hydrolysis
[DE93-012738] p 584 N94-13491
Study on solidification of immisible alloys (M-10) p 588 N94-13742
The Lindemann criterion of melting for pure and mixed ionic crystals
[ITN-93-85210] p 814 N94-14554

SOLUTES
The importance of hard core repulsion in models of activity coefficients in aqueous electrolyte solutions: Illustration in the case of hydration theory
[DE93-012476] p 561 N94-12881
Linear and nonlinear spectroscopic probing of solute interactions with chemically modified silica surface
[DE93-014648] p 562 N94-13001
Direct probing of chromatography columns by laser-induced fluorescence
[DE93-015208] p 654 N94-13022
Pore-size-distribution of cationic polyacrylamide hydrogels
[DE93-015218] p 581 N94-14400
Reactor studies of metal ions associated with chromatographic silica
[AD-A266675] p 573 N94-14779
Measurements of crystal growth kinetics at extreme deviations from equilibrium
[DE93-014526] p 815 N94-14798

SOLUTIONS
Solution chemistry optimization of sol-gel processed PZT thin films
[DE93-013776] p 814 N94-14695

SOLVATION
Ultrafast photoinduced electron transfer reactions in supramolecular arrays: Studies of electronic coupling and solvation
[DE93-012910] p 782 N94-13484

SOLVENT EXTRACTION
Synthesis of organic ligands for f-element separations
[DE93-012915] p 554 N94-14290
Theory, modeling, and simulation
[DE93-015607] p 755 N94-14571

SOLVENTS
Molecular solvent-dynamical effects on activated electron-transfer kinetics: How important is solvent friction?
[AD-A265886] p 779 N94-12894
Experimental and theoretical study of inhomogeneous electron transfer in betaine: Comparisons of measured and predicted spectral dynamics
[AD-A265703] p 780 N94-13051
Computer simulations for the adsorption of polymers onto surfaces
[DE93-016667] p 577 N94-13070
Synthesis and properties of novel cluster phases
[DE93-017056] p 577 N94-13072
Destruction of waste energetic materials using base hydrolysis
[DE93-012738] p 584 N94-13491
Synthesis of organic ligands for f-element separations
[DE93-012915] p 554 N94-14290
Workshop on Formation of Supermolecular Structures in Composite Fluid: Phase Rule and Dynamics
[DE93-782887] p 581 N94-14421
Solution chemistry optimization of sol-gel processed PZT thin films
[DE93-013776] p 814 N94-14695

SONIC BOOMS
The problem of the sonic boom for future high-speed transport aircraft
[ESA-TT-1286] p 776 N94-13692

SOOT
Dust production in the envelopes of carbon stars: R Coronae Borealis
[ETN-93-94389] p 839 N94-14075

SORPTION
Ocean uptake of carbon dioxide
[DE93-012967] p 707 N94-13384
Portable acoustic wave sensor systems for real-time monitoring of volatile organic compounds
[DE93-013753] p 582 N94-14511

SOUND FIELDS
Underwater hearing: A review
[ISVR-TR-212] p 777 N94-14130

SOUND PRESSURE
Active control of acoustic pressure fields using smart material technologies
[NASA-CR-191480] p 768 N94-13354
Study on the possibilities to apply spectrumindex
[VTT-PUBS-109] p 777 N94-14034

SOUND PROPAGATION
The problem of the sonic boom for future high-speed transport aircraft
[ESA-TT-1286] p 776 N94-13692

SOUND WAVES
Ocean acoustic processing: A model-based approach
[DE93-011902] p 725 N94-12876
Study of bubbie behavior in weightlessness (effects of thermal gradient and acoustic stationary wave) (M-16) p 589 N94-13748
Liquid metal drop ejection
[NASA-CR-193718] p 572 N94-14133
Portable acoustic wave sensor systems for real-time monitoring of volatile organic compounds
[DE93-013753] p 582 N94-14511
Atmospheric acoustic modeling
[DE93-016727] p 718 N94-14518
Investigation of the dilatational dissipation in compressible homogeneous shear flow p 645 N94-14758

SOURCE PROGRAMS
ASPT software source code: SUN driver package
[DSIS-93-00262] p 751 N94-14014
ASPT software source code: Development system package, VME-C30 component
[DSIS-93-00276] p 751 N94-14016
ASPT software source code: Host development system package
[DSIS-93-00277] p 753 N94-14197

SOUTH AMERICA
Cyclogenesis and cyclone over South America
[INPE-5400-TDI/479] p 719 N94-13175

SOUTH CAROLINA
Workshop for coordinating South Carolina's pre-college systemic initiatives in science and mathematics
[DE93-012263] p 818 N94-13216

SPACE BASED RADAR
Ionospheric effects on a wide-bandwidth, polarimetric, space-based, synthetic-aperture radar
[DE93-015084] p 612 N94-14512

SPACE CHARGE
Beam halo formation from space-charge dominated beams in uniform focusing channels
[DE93-014458] p 789 N94-13209
Beam halo in high-intensity beams
[DE93-014565] p 789 N94-13328
Wake-field and space charge effects on high brightness beams calculations and measured results for the laser driven photoelectrons at BNL-ATF
[DE93-015787] p 659 N94-14572

SPACE COMMERCIALIZATION
Technology Applications Team: Applications of aerospace technology
[NASA-CR-194362] p 828 N94-13104
Large space structures and systems in the space station era: A bibliography with indexes (supplement 05)
[NASA-SP-7085(05)] p 543 N94-14411

SPACE COMMUNICATION
Environmental projects. Volume 15: Environmental assessment: Proposed 1-megawatt radar transmitter at the Mars site
[NASA-CR-194098] p 598 N94-13090
A millimeter-wave tunneladder TWT
[NASA-CR-182183] p 620 N94-13106
The Telecommunications and Data Acquisition Report
[NASA-CR-194388] p 607 N94-14369
Layout and cabling considerations for a large communications antenna array p 611 N94-14395
ACTS propagation experiment discussion: Ka-band propagation measurements using the ACTS propagation terminal and the CSU-CHILL and Space Communications Technology Center Florida propagation program p 616 N94-14678

SPACE COOLING (BUILDINGS)
Transition of building energy consumption using multi-input, single-output dynamic model
[VTT-PUBS-116] p 597 N94-14055

SPACE DEBRIS
Procedures for analysis of debris relative to Space Shuttle systems
[NASA-TM-109190] p 534 N94-12900
Experimental technique to simulate orbital-debris impact on space shields at impact velocities over 10 km/s
[DE93-011619] p 539 N94-12909
Comparison of analytic Whipple bumper shield ballistic limits with CTH simulations
[DE93-015126] p 539 N94-13006
Simulation of orbital debris impacts on bumper shields
[DE93-013773] p 540 N94-13398
High velocity gas gun
[NASA-TM-109296] p 541 N94-13637
Interactions between spacecraft and their environments
[NASA-TM-106115] p 541 N94-13917
BALLIST: A computer program to empirically predict the bumper thickness required to prevent perforation of the Space Station by orbital debris
[NASA-CR-193825] p 543 N94-14120
Secondary impact hazard assessment
[NASA-CR-188261] p 543 N94-14483

SPACE ENVIRONMENT SIMULATION
Novel oxygen atom source for material degradation studies
[NASA-CR-191323] p 562 N94-13115
Laboratory simulation of spacecraft charging in the plasma wake region
[FFI-93-7007] p 542 N94-14107
Atomic research
[NASA-CR-193843] p 788 N94-14905

SPACE ERECTABLE STRUCTURES
The Second Workshop on Deployment and Assembly Experiment of Large Space Structure on Orbit
[NASDA-CON-930003] p 529 N94-13268
Structural design of hexa-link truss deployable antenna p 529 N94-13269
Thermal distortion measurement of TETRUS type thermal test model of large deployable antenna for mobile communications satellite p 529 N94-13270
Development of modular cable mesh deployable antenna p 530 N94-13274
Research on inflatable structure for space use p 530 N94-13275
Helical truss beam development for large space structure p 530 N94-13276
Trial manufacture model and in-space verification method of deployable antenna p 530 N94-13278
A concept on on-orbit experiments of deployable structures utilizing JEM/HOPE p 531 N94-13279
Movement of deployable truss p 531 N94-13280
Development and application of one dimensional deployable truss p 531 N94-13281

Study of a one-dimensional deployable structure employing telescopic members p 531 N94-13282
The study on large space structure assembly technology: The study on deployable truss structure, part 1
[NASDA-TMR-930002] p 541 N94-13658
The study on large space structure assembly technology: The study on deployable truss structure, part 2 and 3
[NASDA-TMR-930003-PT-2-3] p 541 N94-13659

SPACE EXPLORATION
Where no flag has gone before: Political and technical aspects of placing a flag on the Moon
[NASA-CR-188251] p 827 N94-12800
Effects of radiobiological uncertainty on vehicle and habitat shield design for missions to the moon and Mars
[NASA-TP-3312] p 846 N94-12875
MARS Mission research center
[NASA-CR-194034] p 841 N94-13088
A modular gas-cooled cermet reactor system for planetary base power
[DE93-013672] p 550 N94-13351
NASA images 11
[NASA-TM-109287] p 842 N94-13626
Discovery management workshop
[NASA-TM-108244] p 531 N94-14080
Asia-Pacific ISY conference, volume 1
[NASDA-CM-199-1] p 532 N94-14098
Space transportation systems and space activities in the 21st century p 537 N94-14274

SPACE FLIGHT
Countermeasure for reducing post-flight orthostatic intolerance: Lower Body Negative Pressure (LBNP) experiment E140 p 594 N94-13772
Psychophysiological investigations of the biomedical problems of manned spaceflight
[NASA-CR-194107] p 732 N94-13782
An improved approach for flight readiness certification: Methodology for failure risk assessment and application examples, volume 1
[NASA-CR-194498] p 542 N94-14076
An improved approach for flight readiness certification: Methodology for failure risk assessment and application examples. Volume 2: Software documentation
[NASA-CR-194499] p 542 N94-14077
An improved approach for flight readiness certification: Methodology for failure risk assessment and application examples. Volume 3: Structure and listing of programs
[NASA-CR-194500] p 542 N94-14078
Laboratory simulation of spacecraft charging in the plasma wake region
[FFI-93-7007] p 542 N94-14107

SPACE FLIGHT STRESS
Selection of behavioral tasks and development of software for evaluation of rhesus monkey behavior during spaceflight
[NASA-CR-194176] p 728 N94-13865

SPACE HABITATS
Effects of radiobiological uncertainty on vehicle and habitat shield design for missions to the moon and Mars
[NASA-TP-3312] p 846 N94-12875
Life support and habitability manual, volume 1
[ESA-PSS-03-406-ISSUE-1-VOL] p 737 N94-13901
Life support and habitability manual, volume 2
[ESA-PSS-03-406-ISSUE-1-VOL] p 738 N94-13902

SPACE HEATING (BUILDINGS)
Transition of building energy consumption using multi-input, single-output dynamic model
[VTT-PUBS-116] p 597 N94-14055

SPACE INFRARED TELESCOPE FACILITY
The four great observatories
[NASA-TM-109311] p 830 N94-13605

SPACE LABORATORIES
Present status of JEM utilization projects p 530 N94-13273
Study on improvement of flammability, odor and offgassing tests for materials
[NASDA-CNT-930009] p 563 N94-13471

SPACE LAW
Where no flag has gone before: Political and technical aspects of placing a flag on the Moon
[NASA-CR-188251] p 827 N94-12800

SPACE MANUFACTURING
The studies on lunar and planetary exploration and utilization: The study on lunar resources utilization
[NASDA-CNT-930014] p 842 N94-13655
Asia-Pacific ISY conference, volume 1
[NASDA-CM-199-1] p 532 N94-14098
China's devotion to space science and applications p 532 N94-14273

SPACE MISSIONS
Present status of JEM utilization projects p 530 N94-13273
Gas core nuclear thermal rocket engine research and development in the former USSR
[DE93-012165] p 552 N94-14013
Asia-Pacific ISY conference, volume 1
[NASDA-CM-199-1] p 532 N94-14098
Design and application of electromechanical actuators for deep space missions
[NASA-CR-194145] p 663 N94-14134
China's devotion to space science and applications p 532 N94-14273
Space transportation systems and space activities in the 21st century p 537 N94-14274

SPACE NAVIGATION
Proceedings of the 11th Space Surveillance Workshop, volume 1
[AD-A265120] p 531 N94-13358
The development and flight test of a deployable precision landing system for spacecraft recovery
[NASA-TM-4525] p 537 N94-14853

SPACE OBSERVATIONS (FROM EARTH)
Optical propagation through atmospheric turbulence. Model analysis of anisoplanatism and application to adaptive optics
[ONERA-P-1992-4] p 716 N94-14192

SPACE PLASMAS
The International Colloquium on Atomic Spectra and Oscillator Strengths for Astrophysical and Laboratory Plasmas
[NASA-TM-109255] p 849 N94-13376
The propagation characteristics and instability properties of low-frequency electromagnetic waves in the Io plasma torus p 601 N94-13650
The role of ionospheric plasma in the magnetosphere
[NASA-CR-194404] p 716 N94-13967
Terrestrial magnetospheric imaging: Numerical modeling of low energy neutral atoms
[DE93-014561] p 717 N94-14328

SPACE POWER REACTORS
A modular gas-cooled cermet reactor system for planetary base power
[DE93-013672] p 550 N94-13351
Preliminary nuclear safety assessment of the NEPST (Topaz 2) space reactor program
[DE93-012853] p 551 N94-13514
Space reactor fuel element testing in upgraded TREAT
[DE93-012524] p 554 N94-14806

SPACE PROBES
Real-time dynamics simulation of the Cassini spacecraft using DARTS. Part 1: Functional capabilities and the spatial algebra algorithm p 680 N94-14638

SPACE PROCESSING
Reduce fluid experiment system flight data from IML-1
[NASA-CR-193835] p 804 N94-12873
Marangoni effect induced convection in material processing under microgravity (M-18) p 589 N94-13750
Solidification of eutectic system alloys in space (M-19) p 589 N94-13751
Growth of samarskite crystal under microgravity conditions (M-20) p 590 N94-13752
Growth experiment of organic metal crystal in low gravity (M-21) p 590 N94-13753
Containerless processing of undercooled melts
[NASA-CR-194350] p 572 N94-14123
Two color holographic interferometry for microgravity application
[NASA-CR-194424] p 651 N94-14447

SPACE PROGRAMS
Asia-Pacific ISY conference, volume 1
[NASDA-CM-199-1] p 532 N94-14098
My experiences in manned space flight p 698 N94-14276

SPACE SHUTTLE ASCENT STAGE
Results of wind tunnel tests of an ASRM configured 0.03 scale Space Shuttle integrated vehicle model (47-OTS) in the AEDC 16-foot transonic wind tunnel, volume 2
[NASA-CR-185697] p 534 N94-12965
Results of wind tunnel tests of an ASRM configured 0.03 scale Space Shuttle integrated vehicle model (47-OTS) in the AEDC 16-foot Transonic wind tunnel (IA613A), volume 1
[NASA-CR-185696] p 534 N94-13191

SPACE SHUTTLE MAIN ENGINE
STS-55 pad abort: Engine 2011 oxidizer preburner augmented spark igniter check valve leak
[NASA-CR-193830] p 533 N94-12806
SSME testing at Stennis Space Center
[NASA-TM-109310] p 552 N94-13617
Identification and interpretation of patterns in rocket engine data
[NASA-CR-194534] p 552 N94-14309
An integrated knowledge system for the Space Shuttle hazardous gas detection system
[NASA-CR-194533] p 536 N94-14310
Investigation of the feasibility of optical diagnostic measurements at the exit of the SSME
[NASA-CR-193832] p 553 N94-14682
Simulation of preburner sprays, volume 1
[NASA-CR-193844] p 647 N94-14906

SPACE SHUTTLE MISSION 61-A
STS-30 Magellan IUS/EVA training in WETF
[NASA-TM-109300] p 737 N94-13601
STS-29 post-insertion/deorbit prep and crew bailout
[NASA-TM-109299] p 535 N94-13641

SPACE SHUTTLE MISSIONS
STS-55 pad abort: Engine 2011 oxidizer preburner augmented spark igniter check valve leak
[NASA-CR-193830] p 533 N94-12806
STS-32 mission highlights resource tape
[NASA-TM-109291] p 531 N94-13631
Launch, entry, and landing resource clip
[NASA-TM-109297] p 535 N94-13638

SPACE SHUTTLE ORBITERS
Results of wind tunnel tests of an ASRM configured 0.03 scale Space Shuttle integrated vehicle model (47-OTS) in the AEDC 16-foot transonic wind tunnel, volume 2
[NASA-CR-185697] p 534 N94-12965
Results of wind tunnel tests of an ASRM configured 0.03 scale Space Shuttle integrated vehicle model (47-OTS) in the AEDC 16-foot Transonic wind tunnel (IA613A), volume 1
[NASA-CR-185696] p 534 N94-13191
Analysis of differences between seating positions in simulators and orbiters
[NASA-TM-104776] p 737 N94-13399
Six degree of freedom
[NASA-TM-109295] p 749 N94-13636
Microgravity acceleration measurement environment characterization p 590 N94-13755
Strategic avionics technology definition studies. Subtask 3-1A: Electrical Actuation (ELA) systems
[NASA-CR-194393] p 536 N94-14323

SPACE SHUTTLE PAYLOADS
STS-30 Magellan IUS/EVA training in WETF
[NASA-TM-109300] p 737 N94-13601
Mid-deck experiments, STS-26
[NASA-TM-109308] p 570 N94-13616

SPACE SHUTTLES
Results of experimental investigations to determine external tank protuberance loads using a 0.03-scale model of the Space Shuttle launch configuration (model 47-OTS) in the NASA/ARC unitary plan wind tunnel, volume 1
[NASA-CR-167690] p 534 N94-12810
Procedures for analysis of debris relative to Space Shuttle systems
[NASA-TM-109190] p 534 N94-12900
Results of wind tunnel tests of an ASRM configured 0.03 scale Space Shuttle integrated vehicle model (47-OTS) in the AEDC 16-foot Transonic wind tunnel (IA613A), volume 1
[NASA-CR-185696] p 534 N94-13191
Analysis of differences between seating positions in simulators and orbiters
[NASA-TM-104776] p 737 N94-13399
STS-53 Space Shuttle mission report
[NASA-CR-193101] p 535 N94-13934
STS-54 Space Shuttle mission report
[NASA-CR-194116] p 535 N94-13935
Results of experimental investigations to determine external tank protuberance loads using a 0.03-scale model of the Space Shuttle launch configuration (Model 47-OTS) in the NASA/ARC unitary plan wind tunnel, volume 2
[NASA-CR-167691] p 536 N94-14047
STS-33 launch and landing clip
[NASA-TM-109468] p 536 N94-14734

SPACE STATION FREEDOM
Solar dynamic power system development for Space Station Freedom
[NASA-RP-1310] p 548 N94-12807
Advancing automation and robotics technology for the Space Station Freedom and for the U.S. economy
[NASA-TM-104024] p 739 N94-12838
System identification for Space Station Freedom using observer/Kalman filter Markov parameters
[NASA-CR-191521] p 539 N94-12976
In-flight demonstration of the Space Station Freedom Health Maintenance Facility fluid therapy system (E300/E05) p 595 N94-13775
Space Station Common Berthing Mechanism, a multi-body simulation application p 544 N94-14640
Plasma contactor technology for Space Station Freedom
[NASA-TM-106291] p 553 N94-14725

SPACE STATION STRUCTURES
Secondary impact hazard assessment
[NASA-CR-188261] p 543 N94-14483

SPACE STATIONS
Transmission zeros of spacecraft attitude control system
[NAL-TR-1166] p 540 N94-13339
Asia-Pacific ISY conference, volume 1
[NASDA-CM-199-1] p 532 N94-14098

BALLIST: A computer program to empirically predict the bumper thickness required to prevent perforation of the Space Station by orbital debris
[NASA-CR-193825] p 543 N94-14120
Large space structures and systems in the space station era: A bibliography with indexes (supplement 05)
[NASA-SP-7085(05)] p 543 N94-14411
Computational Controls Workstation: Algorithms and hardware p 678 N94-14626

SPACE TECHNOLOGY EXPERIMENTS
Present status of JEM utilization projects p 530 N94-13273
Trial manufacture model and in-space verification method of deployable antenna p 530 N94-13278
Study on superconducting basic technology for space application, part 1
[NASDA-CNT-930015-PT-1] p 622 N94-13425

SPACE TRANSPORTATION
Space transportation systems within ESA programmes: Current status and perspectives p 537 N94-14275

SPACE TRANSPORTATION SYSTEM
STS-55 pad abort: Engine 2011 oxidizer preburner augmented spark igniter check valve leak
[NASA-CR-193830] p 533 N94-12806
STS-32 post-flight press conference
[NASA-TM-109294] p 541 N94-13634
Asia-Pacific ISY Conference, volume 2
[NASDA-CM-199-VOL-2] p 688 N94-14209
Space transportation systems and space activities in the 21st century p 537 N94-14274
Research and development of space transportation systems in ISAS p 537 N94-14277
Contributions of winged re-entry vehicle to space activities p 537 N94-14278
Mission scenario of HOPE p 537 N94-14279
The status of the HOPE concept study p 537 N94-14280
Spaceplane program at NAL: System concept and related technology issues p 537 N94-14281
STS-33 launch and landing clip
[NASA-TM-109468] p 536 N94-14734
STS-35 post-flight press conference
[NASA-TM-109490] p 537 N94-14736
STS-35 integrated sim in SMS and MOCR
[NASA-TM-109491] p 533 N94-14787

SPACE TRANSPORTATION SYSTEM FLIGHTS
STS-32 mission highlights resource tape
[NASA-TM-109291] p 531 N94-13631
STS-32 post-flight press conference
[NASA-TM-109294] p 541 N94-13634
STS-28 crew presentation clip
[NASA-TM-109298] p 531 N94-13640
STS-53 Space Shuttle mission report
[NASA-CR-193101] p 535 N94-13934
STS-54 Space Shuttle mission report
[NASA-CR-194116] p 535 N94-13935
STS-35 post-flight press conference
[NASA-TM-109490] p 537 N94-14736
STS-35 integrated sim in SMS and MOCR
[NASA-TM-109491] p 533 N94-14787

SPACE-TIME FUNCTIONS
Aspects of symmetry violation
[DE93-011003] p 779 N94-12997
The space-time and energy parameters of deuterium braking by the central collision with atoms
[DE93-624144] p 788 N94-14881

SPACEBORNE ASTRONOMY
Planetary system detection by POINTS
[NASA-CR-194361] p 545 N94-13067
Measurements of the spatial structure and directivity of 100 KeV photon sources in solar flares using PVO and ISEE-3 spacecraft
[NASA-CR-194080] p 845 N94-14492
Analysis of the IUE spectra of the strongly interacting binary beta Lyrae
[NASA-CR-194118] p 833 N94-14493

SPACEBORNE EXPERIMENTS
Reduce fluid experiment system flight data from IML-1
[NASA-CR-193835] p 804 N94-12873
Present status of JEM utilization projects p 530 N94-13273
Trial manufacture model and in-space verification method of deployable antenna p 530 N94-13278
A concept on on-orbit experiments of deployable structures utilizing JEM/HOPE p 531 N94-13279
Study on superconducting basic technology for space application, part 1
[NASDA-CNT-930015-PT-1] p 622 N94-13425
Mid-deck experiments, STS-26
[NASA-TM-109308] p 570 N94-13616
Preparation of particle-dispersion alloys (M-6) p 587 N94-13738
Study on solidification of immisible alloys (M-10) p 588 N94-13742
Microgravity acceleration measurement environment characterization p 590 N94-13755
Neurophysiological study on visuo-vestibular control of posture and movement in fish during adaptation to weightlessness p 591 N94-13759
Crystal growth of enzymes in low gravity (L-5) p 592 N94-13762
Studies on the effects of microgravity on the ultrastructure and functions of cultured mammalian cells (L-6) p 592 N94-13763
Effect of low gravity on calcium metabolism and bone formation (L-7) p 593 N94-13765
A circadian rhythm of conidiation in Neurospora crassa (L-12) p 593 N94-13769
Partial analysis of LDEF experiment A-0114
[NASA-CR-193826] p 564 N94-14025
Ethology in space, a unique opportunity for behavioural science
[ESA-STM-246] p 731 N94-14862

SPACEBORNE TELESCOPES
The four great observatories
[NASA-TM-109311] p 830 N94-13605
An overview of the Galileo Optical Experiment (GOPEX) p 610 N94-14386
Galileo Optical Experiment (GOPEX) optical train: Design and validation at the Table Mountain Facility p 610 N94-14390
Fabrication p 546 N94-14834
Laser power beaming system analyses
[NASA-CR-193840] p 660 N94-14904

SPACECRAFT ANTENNAS
Layout and cabling considerations for a large communications antenna array p 611 N94-14395

SPACECRAFT CHARGING
Interactions between spacecraft and their environments
[NASA-TM-106115] p 541 N94-13917
Laboratory simulation of spacecraft charging in the plasma wake region
[FFI-93-7007] p 542 N94-14107

SPACECRAFT COMMUNICATION
Sensor operation of Advanced Earth Observing Satellite (ADEOS) p 689 N94-14215
Transform coding for space applications
[NASA-TM-106362] p 612 N94-14542

SPACECRAFT COMPONENTS
The Second Workshop on Deployment and Assembly Experiment of Large Space Structure on Orbit
[NASDA-CON-930003] p 529 N94-13268
Research on inflatable structure for space use p 530 N94-13275
Helical truss beam development for large space structure p 530 N94-13276
Application of intelligently adaptable structure and robot to large space structure p 530 N94-13277
Trial manufacture model and in-space verification method of deployable antenna p 530 N94-13278
A concept on on-orbit experiments of deployable structures utilizing JEM/HOPE p 531 N94-13279
Movement of deployable truss p 531 N94-13280
Development and application of one dimensional deployable truss p 531 N94-13281
Study of a one-dimensional deployable structure employing telescopic members p 531 N94-13282
Study on improvement of flammability, odor and offgassing tests for materials
[NASDA-CNT-930009] p 563 N94-13471
The study on large space structure assembly technology: The study on deployable truss structure, part 1
[NASDA-TMR-930002] p 541 N94-13658
The study on large space structure assembly technology: The study on deployable truss structure, part 2 and 3
[NASDA-TMR-930003-PT-2-3] p 541 N94-13659
The study on test of docking mechanism system, part 1 and 2
[NASDA-TMR-930004-PT-1-2] p 541 N94-13660

SPACECRAFT CONSTRUCTION MATERIALS
The Second Workshop on Deployment and Assembly Experiment of Large Space Structure on Orbit
[NASDA-CON-930003] p 529 N94-13268
Research on radiation resistance properties of structural materials for space use p 529 N94-13271
Measuring methods for CFRP laminates' bending and torsion rigidities characteristics p 529 N94-13272
Arc-heating tests of thermal protection system materials for the H-2 rocket fairing
[NAL-TR-1181] p 551 N94-13455
Tensile properties of LE-7 engine material with welded joint
[NAL-TR-1188] p 570 N94-13460
The study on large space structure assembly technology: The study on deployable truss structure, part 1
[NASDA-TMR-930002] p 541 N94-13658
The study on large space structure assembly technology: The study on deployable truss structure, part 2 and 3
[NASDA-TMR-930003-PT-2-3] p 541 N94-13659
Materials/structures testing p 506 N94-14164

SPACECRAFT CONTAMINATION
Atomic research
[NASA-CR-193843] p 788 N94-14905

SPACECRAFT CONTROL
Low cost attitude control system reaction wheel development
[NASA-CR-191332] p 540 N94-13140
A superconducting large-angle magnetic suspension
[NASA-CR-189735] p 596 N94-13141
Application of intelligently adaptable structure and robot to large space structure p 530 N94-13277
Electrical Actuation Technology Bridging
[NASA-CP-3213] p 551 N94-13417
HOPE real time flight operations analyses for return to earth phase, part B
[NASDA-CNT-930011] p 535 N94-13599
HOPE real time flight operations analyses for return to earth phase, part A
[NASDA-CNT-930010-PT-A] p 535 N94-13645
Manual control in space research on perceptual-motor functions under zero gravity conditions (L-10) p 593 N94-13767
Mongoose ASIC microcontroller programming guide
[NASA-RP-1319] p 623 N94-13871
Strategic avionics technology definition studies. Subtask 3-1A: Electrical Actuation (ELA) systems
[NASA-CR-194393] p 536 N94-14323
Large space structures and systems in the space station era: A bibliography with indexes (supplement 05)
[NASA-SP-7085(05)] p 543 N94-14411
Real-time dynamics simulation of the Cassini spacecraft using DARTS. Part 1: Functional capabilities and the spatial algebra algorithm p 680 N94-14638
An application of the IMC software to controller design for the JPL LSCL Experiment Facility p 681 N94-14645
Control structural interaction testbed: A model for multiple flexible body verification p 544 N94-14649

SPACECRAFT DESIGN
Dynamics of adaptive structures: Design through simulations
[NASA-CR-193724] p 540 N94-13112
Spacecraft COst REduction Team (SCORE): TQM/CI on a massive scale p 667 N94-13160
Study of a one-dimensional deployable structure employing telescopic members p 531 N94-13282
HOPE conceptual design in FY 1991
[NASDA-CNT-930017] p 535 N94-13600
Exploring Mars
[NASA-TM-109306] p 842 N94-13613
Conceptual design on H-2 Orbiting Plane (HOPE)
[NASDA-CNT-930018] p 535 N94-13656
The study on large space structure assembly technology: The study on deployable truss structure, part 1
[NASDA-TMR-930002] p 541 N94-13658
The study on large space structure assembly technology: The study on deployable truss structure, part 2 and 3
[NASDA-TMR-930003-PT-2-3] p 541 N94-13659
The study on test of docking mechanism system, part 1 and 2
[NASDA-TMR-930004-PT-1-2] p 541 N94-13660
An improved approach for flight readiness certification: Methodology for failure risk assessment and application examples, volume 1
[NASA-CR-194498] p 542 N94-14076
An improved approach for flight readiness certification: Methodology for failure risk assessment and application examples. Volume 2: Software documentation
[NASA-CR-194499] p 542 N94-14077
An improved approach for flight readiness certification: Methodology for failure risk assessment and application examples. Volume 3: Structure and listing of programs
[NASA-CR-194500] p 542 N94-14078
The concept study of the space transportation system HOPE in FY 1991
[NASDA-CNT-930016] p 536 N94-14100
Research and development of space transportation systems in ISAS p 537 N94-14277
The status of the HOPE concept study p 537 N94-14280
Spaceplane program at NAL: System concept and related technology issues p 537 N94-14281
An improved approach for flight readiness certification: Probabilistic models for flaw propagation and turbine blade failure. Volume 1: Methodology and applications
[NASA-CR-194496] p 519 N94-14841
An improved approach for flight readiness certification: Probabilistic models for flaw propagation and turbine blade failure. Volume 2: Software documentation
[NASA-CR-194497] p 519 N94-14842
The development and flight test of a deployable precision landing system for spacecraft recovery
[NASA-TM-4525] p 537 N94-14853

SPACECRAFT DOCKING
Six degree of freedom
[NASA-TM-109295] p 749 N94-13636

The study on test of docking mechanism system, part 1 and 2
[NASDA-TMR-930004-PT-1-2] p 541 N94-13660
Space Station Common Berthing Mechanism, a multi-body simulation application p 544 N94-14640

SPACECRAFT ELECTRONIC EQUIPMENT
Study of the intermateability of Cannon and Souriau subminiature connectors
[CNES-NT-132] p 624 N94-13951

SPACECRAFT EQUIPMENT
An experimental study of tether reel system: A laboratory model
[NAL-TR-1176T] p 539 N94-12943
Structural design of hexa-link truss deployable antenna p 529 N94-13269
Thermal distortion measurement of TETRUS type thermal test model of large deployable antenna for mobile communications satellite p 529 N94-13270
Development of modular cable mesh deployable antenna p 530 N94-13274
Trial manufacture model and in-space verification method of deployable antenna p 530 N94-13278
Survey and study on Environmental Control and Life Support (ECLS) technologies, part 2
[NASDA-CNT-930012-PT-2] p 737 N94-13472
The study on test of docking mechanism system, part 1 and 2
[NASDA-TMR-930004-PT-1-2] p 541 N94-13660
Future TRMM follow-on mission p 691 N94-14228

SPACECRAFT GUIDANCE
HOPE real time flight operations analyses for return to earth phase, part B
[NASDA-CNT-930011] p 535 N94-13599
HOPE real time flight operations analyses for return to earth phase, part A
[NASDA-CNT-930010-PT-A] p 535 N94-13645
Guidance law development for aeroassisted transfer vehicles using matched asymptotic expansions
[NASA-CR-194523] p 508 N94-14538

SPACECRAFT INSTRUMENTS
Perspective on the National Aero-Space Plane Program instrumentation development
[NASA-TM-4505] p 516 N94-13256
Phase aligner for the Electronically Scanned Thinned Array Radiometer (ESTAR) instrument
[NASA-TM-4518] p 623 N94-13878
Development of an advanced spacecraft tandem mass spectrometer
[NASA-CR-194195] p 545 N94-13953
Future TRMM follow-on mission p 691 N94-14228

SPACECRAFT LANDING
Launch, entry, and landing resource clip
[NASA-TM-109297] p 535 N94-13638
STS-33 launch and landing clip
[NASA-TM-109468] p 536 N94-14734

SPACECRAFT LAUNCHING
Proceedings of the 11th Space Surveillance Workshop, volume 1
[AD-A265120] p 531 N94-13358
Preliminary nuclear safety assessment of the NEPST (Topaz 2) space reactor program
[DE93-012853] p 551 N94-13514
STS-32 mission highlights resource tape
[NASA-TM-109291] p 531 N94-13631
HL-20 personnel launch system
[NASA-TM-109292] p 504 N94-13632
Launch, entry, and landing resource clip
[NASA-TM-109297] p 535 N94-13638
STS-28 crew presentation clip
[NASA-TM-109298] p 531 N94-13640
STS-33 launch and landing clip
[NASA-TM-109468] p 536 N94-14734

SPACECRAFT MANEUVERS
Optimizing interplanetary trajectories with deep space maneuvers
[NASA-CR-4546] p 532 N94-14851

SPACECRAFT MODELS
Results of wind tunnel tests of an ASRM configured 0.03 scale Space Shuttle integrated vehicle model (47-OTS) in the AEDC 16-foot transonic wind tunnel, volume 2
[NASA-CR-185697] p 534 N94-12965
Results of wind tunnel tests of an ASRM configured 0.03 scale Space Shuttle integrated vehicle model (47-OTS) in the AEDC 16-foot Transonic wind tunnel (IA613A), volume 1
[NASA-CR-185696] p 534 N94-13191
HL-20 personnel launch system
[NASA-TM-109292] p 504 N94-13632
Failure modes of reduced-order orbit determination filters and their remedies p 532 N94-14373
Real-time dynamics simulation of the Cassini spacecraft using DARTS. Part 1: Functional capabilities and the spatial algebra algorithm p 680 N94-14638

SPACECRAFT MOTION
Sloshing dynamics on rotating helium dewar tank
[NASA-CR-194403] p 637 N94-13959

SPACECRAFT PERFORMANCE
ECS: Eighth year in orbit
[ESA-BR-82] p 543 N94-14352
The flight performance of the Galileo orbiter USO p 611 N94-14398

SPACECRAFT POWER SUPPLIES
An experimental study of tether reel system: A laboratory model
[NAL-TR-1176T] p 539 N94-12943
Spacecraft COst REduction Team (SCORE): TQM/CI on a massive scale p 667 N94-13160
A photovoltaic catenary-tent array for the Martian surface
[NASA-TM-106306] p 621 N94-13194
NASA handbook for nickel-hydrogen batteries
[NASA-RP-1314] p 550 N94-13265
Power converters for the 120 V bus supply control
[CNES-NT-134] p 622 N94-13552
Futurepath 2
[NASA-TM-109285] p 518 N94-13623
The Large Area Pulsed Solar Simulator (LAPSS)
[NASA-CR-194507] p 703 N94-13940
Large space structures and systems in the space station era: A bibliography with indexes (supplement 05)
[NASA-SP-7085(05)] p 543 N94-14411
Small scale adaptive optics experiment systems engineering
[NASA-CR-194419] p 793 N94-14548
Primary and secondary electrical space power based on advanced PEM systems
[DE93-012643] p 553 N94-14689

SPACECRAFT PROPULSION
Nuclear propulsion systems engineering
[DE93-010791] p 548 N94-12870
MCNP benchmark analyses of critical experiments for the Space Nuclear Thermal Propulsion program
[DE93-014046] p 548 N94-12981
Design, qualification and operation of nuclear rockets for safe Mars missions
[DE93-010792] p 549 N94-12996
Generation of neutronic thermal data in support of space nuclear propulsion
[DE93-013148] p 549 N94-13034
Two temperature modeling and experimental measurements of laser sustained hydrogen plasmas
[AD-A265750] p 796 N94-13039
Mirror fusion propulsion system: A performance comparison with alternate propulsion systems for the manned Mars Mission
[NASA-TM-109248] p 550 N94-13147
Electrical Actuation Technology Bridging
[NASA-CP-3213] p 551 N94-13417
Low thrust space propulsion
[NASA-TM-109286] p 552 N94-13625
The Large Area Pulsed Solar Simulator (LAPSS)
[NASA-CR-194507] p 703 N94-13940
Gas core nuclear thermal rocket engine research and development in the former USSR
[DE93-012165] p 552 N94-14013
Aeropropulsion facilities p 506 N94-14161
Large space structures and systems in the space station era: A bibliography with indexes (supplement 05)
[NASA-SP-7085(05)] p 543 N94-14411
Space reactor fuel element testing in upgraded TREAT
[DE93-012524] p 554 N94-14806

SPACECRAFT RADIATORS
An analytical investigation of transient effects on rewetting of heated thin flat plates
[NASA-TM-106120] p 628 N94-12968

SPACECRAFT RECOVERY
STS-32 mission highlights resource tape
[NASA-TM-109291] p 531 N94-13631
The development and flight test of a deployable precision landing system for spacecraft recovery
[NASA-TM-4525] p 537 N94-14853

SPACECRAFT REENTRY
HOPE real time flight operations analyses for return to earth phase, part B
[NASDA-CNT-930011] p 535 N94-13599
Launch, entry, and landing resource clip
[NASA-TM-109297] p 535 N94-13638
HOPE real time flight operations analyses for return to earth phase, part A
[NASDA-CNT-930010-PT-A] p 535 N94-13645

SPACECRAFT SHIELDING
Simulation of orbital debris impacts on bumper shields
[DE93-013773] p 540 N94-13398
High temperature electromagnetic characterization of thermal protection system tile materials
[NASA-CR-189687] p 578 N94-13431
CRRES to blaze new trails in orbit
[NASA-TM-109314] p 713 N94-13620

SPACECRAFT STRUCTURES
Experimental technique to simulate orbital-debris impact on space shields at impact velocities over 10 km/s
[DE93-011619] p 539 N94-12909
Methods for evaluating the predictive accuracy of structural dynamic models
[NASA-CR-191337] p 671 N94-13124
The Second Workshop on Deployment and Assembly Experiment of Large Space Structure on Orbit
[NASDA-CON-930003] p 529 N94-13268
Research on inflatable structure for space use p 530 N94-13275
Application of intelligently adaptable structure and robot to large space structure p 530 N94-13277
Movement of deployable truss p 531 N94-13280
Study of a one-dimensional deployable structure employing telescopic members p 531 N94-13282
The study on test of docking mechanism system, part 1 and 2
[NASDA-TMR-930004-PT-1-2] p 541 N94-13660
Characterization of composite materials for aerospace structures
[ESA-TT-1260] p 557 N94-13804
Control structural interaction testbed: A model for multiple flexible body verification p 544 N94-14649

SPACECRAFT TRACKING
Sequential ranging: How it works
[NASA-CR-194508] p 532 N94-13796
The Telecommunications and Data Acquisition Report
[NASA-CR-194388] p 607 N94-14369

SPACECREWS
STS-29 post-insertion/deorbit prep and crew bailout
[NASA-TM-109299] p 535 N94-13641
STS-35 crew trash compactor briefing
[NASA-TM-109487] p 533 N94-14735
STS-35 EVA payload training in WETF
[NASA-TM-109492] p 739 N94-14790

SPACELAB
Reduce fluid experiment system flight data from IML-1
[NASA-CR-193835] p 804 N94-12873
Spacelab J experiment descriptions
[NASA-TM-4517] p 586 N94-13732
Study on the biological effect of cosmic radiation and the development of radiation protection technology (L-11) p 593 N94-13768

SPARE PARTS
Spare parts analysis of the MK.32B-751 AAR pod
[DSIS-93-00737] p 774 N94-13549

SPARK GAPS
Evolution of high-repetition-rate induction accelerators through advancements in switching
[DE93-012599] p 654 N94-12963
Development of UHF spark-switched L-C Oscillators
[DE93-015019] p 623 N94-13892

SPATIAL DISTRIBUTION
Spatial and temporal variability of precipitation and chemistry: Case studies from the frontal boundary study
[DE93-007883] p 708 N94-13910
Chemistry and transport in a multi-dimensional model
[NASA-CR-194425] p 716 N94-13969
Potential evapotranspiration in Belgium: Spatial and temporal variability
[PUBL-SER-A-130] p 686 N94-13994
The role of the dynamics for the deviation of the total ozone from the long-term mean at the edge of the polar vortex p 694 N94-14250
The European Arctic ozone experiment: An investigation of Northern Hemisphere ozone depletion p 694 N94-14251
Space-based activities: SAM 2 and SAGE 2 p 694 N94-14252
New evidences supported the Wei hypothesis about the formation of the Antarctic ozone hole p 694 N94-14253
Measurements of the spatial structure and directivity of 100 KeV photon sources in solar flares using PVO and ISEE-3 spacecraft
[NASA-CR-194080] p 845 N94-14492
Quantitative luminescence imaging system
[DE93-015691] p 793 N94-14702

SPATIAL FILTERING
Estimation of the vortex length scale and intensity from two-dimensional samples p 645 N94-14756
Optimization of a subband coding for high definition television with motion controlled three dimensional frequency band decomposition
[ETN-93-94396] p 617 N94-14817

SPATIAL RESOLUTION
Confocal profilometer with nanometric vertical resolution
[DE93-622698] p 653 N94-12857
High spatial resolution x ray microanalysis: Comparison of experiment and incoherent scattering calculations
[DE93-011685] p 648 N94-13044

Optical propagation through atmospheric turbulence. Model analysis of anisoplanatism and application to adaptive optics
[ONERA-P-1992-4] p 716 N94-14192
Imaging Fourier transform spectrometer
[DE93-017193] p 651 N94-14416

SPECIFIC HEAT
Gas atomized Er3Ni powder for cryocooler applications
[DE93-011564] p 568 N94-13000
Optical and physical properties of the LiSrAlF6:Cr laser crystal
[DE93-014657] p 808 N94-13881

SPECIFIC IMPULSE
Electromagnetic propulsion for spacecraft
[NASA-CR-191186] p 551 N94-13416

SPECIFICATIONS
Design, qualification and operation of nuclear rockets for safe Mars missions
[DE93-010792] p 549 N94-12996
The design of chain links and slings
[NPL-DMM(A)-94] p 662 N94-13808
Security clauses in the writing and analysis of standards
[NPL-DITC-216-93] p 824 N94-13879

SPECKLE INTERFEROMETRY
Strain sensing technology for high temperature applications
[NASA-TM-4498] p 648 N94-12874

SPECKLE PATTERNS
Study of speckle reduction when using a CO2 waveguide laser close to its threshold state
[DSIS-93-00250] p 657 N94-14067

SPECTRA
Inclusive single muons at DO
[DE93-012779] p 783 N94-13494
A sum-rule of luminescence spectrum
[ITN-93-85223] p 814 N94-14559

SPECTRAL BANDS
New challenges in propagation research in the US p 612 N94-14656

SPECTRAL CORRELATION
Nonlinear damping model for flexible structures
[NASA-CR-193711] p 539 N94-12790

SPECTRAL EMISSION
Measurements of optical properties of waveshifting optical fiber for liquid scintillator hadron calorimetry
[DE93-012606] p 791 N94-13482
A calibration procedure for radiation budget radiometers and its influence on interpretation of measured values
[MITT-82] p 651 N94-14149

SPECTRAL ENERGY DISTRIBUTION
The 1 to 5 micron imaging of deeply embedded young stellar objects p 831 N94-13657
A long-term space astrophysics research program: The evolution of the quasar continuum
[NASA-CR-193714] p 839 N94-14404

SPECTRAL LINE WIDTH
Selenium x ray laser line profile measurements
[DE93-012580] p 658 N94-14175
Experimental measurements of selenium x-ray laser spectral line profiles
[DE93-016543] p 659 N94-14595

SPECTRAL METHODS
The Chebyshev-Legendre method: Implementing Legendre methods on Chebyshev points
[NASA-CR-191497] p 769 N94-13725
On the geometry of external spectral factors and the Riccati inequality
[CWI-BS-R9227] p 770 N94-14002
The spectral viscosity method applied to simulation of waves in a stratified atmosphere
[FFI-92/7047] p 637 N94-14040

SPECTRAL REFLECTANCE
The optical constants and spectral specular reflectivity of Highly Oriented Pyrolytic Graphite (HOPG)
[DE93-011894] p 790 N94-12865
Quantitative mapping of pore fraction variations in silicon nitride using an ultrasonic contact scan technique
[NASA-TP-3377] p 665 N94-13056
Spectral reflectance of soils from Sao Paulo State
[INPE-5424-PRP/172] p 684 N94-13377
Analytical framework for modeling scale-related variabilities in remote sensing p 685 N94-13592
Operational test of the airborne data acquisition system: SADA, the Bara Bonita experiment
[INPE-5451-NTC/305] p 685 N94-13610
The state of Fe in the lunar regolith and its relationship to the spectral reflectance properties of the moon p 843 N94-14303

SPECTRAL SENSITIVITY
Imaging Fourier transform spectrometer
[DE93-017193] p 651 N94-14416

SPECTROGRAPHS
Vacuum ultraviolet instrumentation for solar irradiance and thermospheric airglow
[NASA-CR-194525] p 652 N94-14684

SPECTROMETERS
Modis-N airborne simulator
[NASA-CR-194364] p 792 N94-13719
E789 and P865: High-rate fixed-target studies of charm and beauty
[DE93-017223] p 788 N94-14898

SPECTROPHOTOMETERS
Vacuum ultraviolet instrumentation for solar irradiance and thermospheric airglow
[NASA-CR-194525] p 652 N94-14684

SPECTRORADIOMETERS
Colorimetric qualification of shear sensitive liquid crystal coatings
[NASA-CR-194126] p 806 N94-13291
Spectral reflectance of soils from Sao Paulo State
[INPE-5424-PRP/172] p 684 N94-13377
Operational test of the airborne data acquisition system: SADA, the Bara Bonita experiment
[INPE-5451-NTC/305] p 685 N94-13610
Advanced solid-state array spectroradiometer data collection during HAPEX-2 Sahel
[NASA-CR-194144] p 808 N94-13875

SPECTROSCOPIC ANALYSIS
Procedures for analysis of debris relative to Space Shuttle systems
[NASA-TM-109190] p 534 N94-12900
The evidence for clumpy accretion in the Herbig Ae star HR 5999
[NASA-TM-108257] p 828 N94-12915
Determination of trace elements in triglycine sulfate solutions
[NASA-CR-193481] p 562 N94-13048
Quantitative mapping of pore fraction variations in silicon nitride using an ultrasonic contact scan technique
[NASA-TP-3377] p 665 N94-13056
Determination of spectroscopic properties of atmospheric molecules from high resolution vacuum ultraviolet cross section and wavelength measurements
[NASA-CR-194024] p 712 N94-13092
Scanning tunneling microscopy studies of diamond films and optoelectronic materials
[NASA-CR-194363] p 578 N94-13246
Colorimetric qualification of shear sensitive liquid crystal coatings
[NASA-CR-194126] p 806 N94-13291
The International Colloquium on Atomic Spectra and Oscillator Strengths for Astrophysical and Laboratory Plasmas
[NASA-TM-109255] p 849 N94-13376
Hard x ray/microwave spectroscopy of solar flares
[NASA-CR-194399] p 844 N94-13958
E789 and P865: High-rate fixed-target studies of charm and beauty
[DE93-017223] p 788 N94-14898

SPECTROSCOPY
Development of nondestructive evaluation methods and prediction of effects of flaws on the fracture behavior of structural ceramics
[DE93-012942] p 577 N94-13032
Fifteenth Combustion Research Conference
[DE93-015758] p 562 N94-13045
A search for strong-field direct two electron ionization using coincidence spectroscopy
[DE93-013435] p 781 N94-13241
Early baryon and meson spectroscopy culminating in the discovery of the Omega minus SU(3) and quarks
[DE93-014321] p 787 N94-14580
Multiplicity spectrometry on neutron filtered beams
[DE93-617529] p 790 N94-14843

SPECTRUM ANALYSIS
Spectral analysis for automated exploration and sample acquisition
[NASA-CR-194095] p 545 N94-13189
Basic research in solar physics
[NASA-CR-193632] p 844 N94-13234
Dendrometric variables estimation in homogeneous forests using LANDSAT TM data
[INPE-5455-TDI/497] p 684 N94-13331
The onset of galactic winds in early-type galaxies
[NASA-CR-193640] p 836 N94-13446
Bounds on time delay estimation given unknown signal spectral parameters
[ITN-93-85194] p 601 N94-13566
Spectra of late type dwarf stars of known abundance for stellar population models
[NASA-CR-194301] p 831 N94-13681
Maximum entropy spectral analysis of the geological time series of the oxygen isotope record from deep-sea cores
[INPE-5465-PRE/1773] p 725 N94-13728
Analysis of microstrip patch antennas with nonzero surface resistance
[NASA-TP-3362] p 604 N94-13916
Testing various time-frequency distribution techniques
[DREO-TN-92-17] p 606 N94-14062
An exact processing algorithm for wide beam spaceborne SAR data p 689 N94-14213
Spectroscopic method and data reduction algorithm for laser long-path absorption measurements using RIS p 689 N94-14218
Analysis of the IUE spectra of the strongly interacting binary beta Lyrae
[NASA-CR-194118] p 833 N94-14493
H2S data reduction
[NASA-CR-193389] p 617 N94-14743

SPEECH
Analysis of fundamental frequency pattern in speech p 618 N94-13440

SPEECH RECOGNITION
Speaker independent recognition of isolated words using vector quantization and neural networks
[ETN-93-94390] p 616 N94-14724

SPEED INDICATORS
Position error determination for the speedometer and altimeter of the NAL QSTOL experimental aircraft ASKA
[NAL-TR-1144] p 517 N94-13451

SPENT FUELS
Development and application of the automated Monte Carlo biasing procedure in SAS4
[DE93-015205] p 774 N94-14334

SPHERES
Force-free magnetic fields, curl eigenfunctions, and the sphere in transform space, with applications to fluid dynamics and electromagnetic theory
[AD-A265805] p 834 N94-12971
Theoretical investigation of scattering by homogeneous or coated dielectric spheres illuminated with a steady state or pulsed laser beam p 657 N94-13624

SPHERICAL HARMONICS
Project proposal for partial computational physics support for Survivability of Coatings program
[DE93-013788] p 576 N94-12939
Spherical anharmonic oscillator in self-similar approximation
[DE93-626622] p 772 N94-14890

SPHERICAL SHELLS
The fractional quantum Hall effect and the spherical shell model
[DE93-014553] p 818 N94-14740

SPIN DECOUPLING
The de Haas-van Alphen studies and Fermi surface properties of organic superconductors (ET)2X
[DE93-015157] p 623 N94-13925

SPIN GLASS
Retrieval properties of neural networks with infinitely many marked patterns
[PREPRINT-729] p 766 N94-14718
Magnetic interactions and disorder - phase transitions in dilute spin-glasses and high temperature superconductors
[ITN-93-85217] p 815 N94-14825

SPIN RESONANCE
The evolution of tensor polarization
[DE93-017209] p 790 N94-14897

SPIRAL ANTENNAS
A hybrid finite element-boundary integral for the analysis of cavity-backed antennas of arbitrary shape
[NASA-CR-193719] p 599 N94-13236

SPIRAL GALAXIES
Abundance markers in H II regions of late spiral galaxies
[ISBN-0-315-62457-4] p 836 N94-13372
Ultraviolet observations of NGC 4395, the least luminous and nearest known Seyfert 1 nucleus
[NASA-CR-194304] p 831 N94-13679

SPLINE FUNCTIONS
Growth curve analysis for plasma profiles using smoothing splines
[DE93-015741] p 795 N94-12984
Evaluation of beta-spline interpolation in digital terrain models
[INPE-5475-TDI/506] p 684 N94-13364

SPLINES
Splines, contours and SVD subroutines
[DE93-016088] p 757 N94-14866

SPRAY CHARACTERISTICS
Simulation of preburner sprays, volume 1
[NASA-CR-193844] p 647 N94-14906

SPRAY NOZZLES
Widebody cabin water spray optimization tests
[DOT/FAA/CT-TN93/29] p 511 N94-14186
Simulation of preburner sprays, volume 1
[NASA-CR-193844] p 647 N94-14906

SPRAYERS
A computer model for liquid jet atomization in rocket thrust chambers
[NASA-CR-194194] p 627 N94-12803
Widebody cabin water spray optimization tests
[DOT/FAA/CT-TN93/29] p 511 N94-14186
Simulation of preburner sprays, volume 1
[NASA-CR-193844] p 647 N94-14906
SPREAD SPECTRUM TRANSMISSION
Fine time uplink synchronization for frequency-hopped spread spectrum satellite communication system
[ISBN-0-315-54370-1] p 600 N94-13488
Kalman filter based architectures for interference excision
[DSIS-93-00034] p 603 N94-13818
Adaptive Signal Processing Testbed
[DSIS-93-00258] p 604 N94-13869
Adaptive Signal Processing Testbed: Software design specification
[DSIS-93-00259] p 604 N94-13870
Simulation of downlink synchronization for a frequency-hopped satellite communication system
[DSIS-93-00477] p 605 N94-13941
Adaptive Signal Processing Testbed signal excision software: User's manual
[DSIS-93-00260] p 606 N94-14037
A comparison of recursive least squares and Kalman filtering excisors for swept tone interference
[DSIS-93-00362] p 606 N94-14054
SPRINGS (ELASTIC)
Miniature mechanism assembly
[DE93-015595] p 624 N94-13928
SPRINGS (WATER)
Promotion of geothermal energy development in 1991
[DE93-799058] p 701 N94-13215
SPUTTERING
Metastability of yttrium-oxides
[DE93-016548] p 813 N94-14440
Multicrystalline silicon solar cells: Gettering optimization and characterization
[DE93-015001] p 705 N94-14861
STABILITY
Effect of pressure on order and stability in alloys: The case of Al-Ge
[DE93-013842] p 567 N94-12899
A new formulation of longitudinal coherent instabilities
[DE93-014288] p 789 N94-13220
Stability of reference masses 1: Evidence for posiible variations in the mass of reference kilograms arising from mercury contamination
[NPL-DMM(A)-86] p 708 N94-13667
Exploiting structure: Introduction and motivation
[NASA-CR-194199] p 750 N94-13828
STABILITY TESTS
Functional differential equations with piecewise continuous argument
[AD-A266660] p 772 N94-14840
STAGNATION POINT
Evolution of disturbances in stagnation point flow
[NASA-CR-191516] p 636 N94-13724
STAINLESS STEELS
BAKEOUT: A computer program for predicting diffusive outgassing from stainless steel
[DE93-012613] p 573 N94-14364
Welding technologies as applied to nuclear manufacturing
[DE93-010924] p 664 N94-14565
STANDARDS
VIEWCACHE: An incremental pointer-base access method for distributed databases. Part 1: The universal index system design document. Part 2: The universal index system low-level design document. Part 3: User's guide. Part 4: Reference manual. Part 5: UIMS test suite
[NASA-CR-191788] p 822 N94-13126
Specimen files in VAMAS standard data transfer format (EXAMPLE 1.TXT to EXAMPLE 4.TXT)
[NPL-DMM(A)-90] p 749 N94-13688
The design of chain links and slings
[NPL-DMM(A)-94] p 662 N94-13808
STANDING WAVES
Multi-bunch beam-break-up studies for a SWFEL/TBA
[DE93-016973] p 658 N94-14414
The standing wave FEL/TBA: Realistic cavity geometry and energy extraction
[DE93-016972] p 659 N94-14520
STAR FORMATION
Analysis of interstellar cloud structure based on IRAS images
[NASA-CR-194341] p 836 N94-13332
Search for x ray emitting young stars outside of massive molecular clouds
[NASA-CR-193609] p 830 N94-13462
Millimeter and infrared studies of young stellar objects in dark cloud L1641 p 838 N94-13648
The origin of the far-infrared emission from galactic molecular clouds p 848 N94-13654
STAR TRACKERS
Time series photometry of faint cataclysmic variables with a CCD p 831 N94-13646
STARK EFFECT
Equilibrium reconstruction of the q-profile in tokamaks from motional Stark effect data
[DE93-015815] p 796 N94-13046
STATE ESTIMATION
Calculation of the required sensor accuracy to obtain a specified state estimation accuracy
[NAL-TR-1173] p 649 N94-13343
Attitude determination of stratospheric balloons using Kalman filters
[INPE-5498-TDI/513] p 649 N94-13366
STATE VECTORS
A rational interpolation method to compute frequency response p 681 N94-14644
STATIC PRESSURE
A wall interference assessment/correction system
[NASA-CR-194174] p 500 N94-13076
Exploratory study of in-plane streamline curvature effects on a turbulent boundary layer at a Mach number of 3
[NASA-CR-193673] p 501 N94-13292
STATIC STABILITY
Test and evaluation methods p 506 N94-14163
STATIC TESTS
Technical Evaluation Motor No. 10 (TEM-10)
[NASA-CR-193846] p 554 N94-14907
STATICS
Statics and kinetics of phase transformations in bcc Fe-Cr
[DE93-013839] p 574 N94-14793
STATISTICAL ANALYSIS
Feature extraction and classification algorithms for high dimensional data
[NASA-CR-194298] p 743 N94-13023
Degradation of the visible and near-infrared channels of the advanced very high resolution radiometer on the NOAA-9 spacecraft: Assessment and recommendations for corrections
[NOAA-TR-NESDIS-70] p 544 N94-13029
Object-oriented productivity metrics p 667 N94-13161
Spatial variability of throughfall chemistry in a tropical rainforest (Central Amazonia, Brazil)
[INPE-5431-PRE/1765] p 720 N94-13429
Trellis coding with Continuous Phase Modulation (CPM) for satellite-based land-mobile communications
[NASA-CR-191325] p 604 N94-13909
Stochastic performance modeling and evaluation of obstacle detectability with imaging range sensors
[NASA-CR-194510] p 605 N94-13946
Generic results of the space physics community survey
[NASA-CR-194538] p 818 N94-13984
An improved approach for flight readiness certification: Methodology for failure risk assessment and application examples, volume 1
[NASA-CR-194498] p 542 N94-14076
An improved approach for flight readiness certification: Methodology for failure risk assessment and application examples. Volume 2: Software documentation
[NASA-CR-194499] p 542 N94-14077
An improved approach for flight readiness certification: Methodology for failure risk assessment and application examples. Volume 3: Structure and listing of programs
[NASA-CR-194500] p 542 N94-14078
A method for estimation of partial cloud cover within a pixel and its effect p 697 N94-14269
Atmospheric correction for sea surface temperature by application of microwave dual-channel technique to VTIR data p 697 N94-14271
Statistical results from the Virginia Tech propagation experiment using the Olympus 12, 20, and 30 GHz satellite beacons p 613 N94-14658
Results of multiband (L, S, Ku band) propagation measurements and model for high elevation angle land mobile satellite channel p 615 N94-14670
An improved approach for flight readiness certification: Probabilistic models for flaw propagation and turbine blade failure. Volume 1: Methodology and applications
[NASA-CR-194496] p 519 N94-14841
An improved approach for flight readiness certification: Probabilistic models for flaw propagation and turbine blade failure. Volume 2: Software documentation
[NASA-CR-194497] p 519 N94-14842
On the statistical theory of the even-even nucleons levels' density
[DE93-623990] p 788 N94-14875
STATISTICAL CORRELATION
Statistical analysis of the m rankings problem: Kendall's prototype and the grouping estimate method based on normal scores
[DSIS-93-00139] p 773 N94-13848
STATISTICAL DISTRIBUTIONS
An analog clustering network from a biological model
[AD-A265637] p 762 N94-12969
STATISTICAL MECHANICS
Discussion of stress tensor nonuniqueness with application to nonuniform, particulate systems
[DE93-014352] p 816 N94-13206
Statistical mechanical theory of liquid entropy
[DE93-016524] p 817 N94-14593
Retrieval properties of neural networks with infinitely many marked patterns
[PREPRINT-729] p 766 N94-14718
STATISTICAL TESTS
Robust estimators and tests in one-sample location problem with particular consideration on modified maximum likelihood process
[ETN-93-94391] p 774 N94-14703
STATISTICS
Selected data on academic science and engineering R and D expenditures: Fiscal Year 1991
[NSF-92-329] p 819 N94-13982
STATORS
Rotor stator CGI
[NASA-TM-109313] p 518 N94-13608
STEADY FLOW
Averaging techniques for steady and unsteady calculations of a transonic fan stage
[NASA-TM-106231] p 499 N94-13108
Canonical forms of multidimensional steady inviscid flows
[NASA-CR-191488] p 769 N94-13722
The structure of laminar flow in a three-dimensional driven cavity p 640 N94-14601
A new Lagrangian method for three-dimensional steady supersonic flows
[NASA-TM-106068] p 510 N94-14847
STEADY STATE
Preconditioning and the limit to the incompressible flow equations
[NASA-CR-191500] p 769 N94-13717
STEAM
Nuclear thermal propulsion engine based on particle bed reactor using light water steam as a propellant
[DE93-014336] p 552 N94-14111
STEELS
Applications of surface science to solid lubricants
[SMC-TR-93-24] p 579 N94-13903
Heavy section steel irradiation experiment
[DE93-015517] p 573 N94-14537
A study of hydrogen effects on fracture behavior of radioactive waste storage tanks
[DE93-018171] p 574 N94-14873
STELLAR ACTIVITY
Ultraviolet observations of NGC 4395, the least luminous and nearest known Seyfert 1 nucleus
[NASA-CR-194304] p 831 N94-13679
STELLAR COLOR
Polarization and variability of active galaxies and quasars p 837 N94-13550
STELLAR COMPOSITION
Abundance markers in H II regions of late spiral galaxies
[ISBN-0-315-62457-4] p 836 N94-13372
STELLAR CORES
Millimeter and infrared studies of young stellar objects in dark cloud L1641 p 838 N94-13648
STELLAR CORONAS
Studies of gas in cooling flow clusters
[NASA-CR-193597] p 628 N94-12959
ROSAT guest investigator program (AO-1). On a search for coronal x ray emissions from white dwarfs
[NASA-CR-193654] p 835 N94-13171
STELLAR EVOLUTION
Analysis of interstellar cloud structure based on IRAS images
[NASA-CR-194341] p 836 N94-13332
The physical and chemical evolution of protostellar disks. The growth of protostellar disks: Progress to date
[NASA-CR-194111] p 836 N94-13423
The spectroscopic evolution of novae in the bulge of M31 and a search for their possible origin in the M31 globular cluster system p 831 N94-13668
Charge-exchange reactions and weak interaction rates for Type 2 supernovae
[DE93-015104] p 783 N94-13893
Wind mass and energy deposition
[DE93-013345] p 839 N94-14341
ROSAT observations of clusters with wide-angle tailed radio sources
[NASA-CR-193784] p 833 N94-14405
STELLAR LUMINOSITY
Time series photometry of faint cataclysmic variables with a CCD p 831 N94-13646

STELLAR MAGNITUDE
Search for x ray emitting young stars outside of massive molecular clouds
[NASA-CR-193609] p 830 N94-13462
Photometry and spectroscopy in the open cluster Alpha Persei, 2
[NASA-CR-193397] p 833 N94-14358
STELLAR MASS EJECTION
MHD shocks in coronal mass ejections
[NASA-CR-193418] p 828 N94-12970
ICE/ISEE plasma wave data analysis
[NASA-CR-194375] p 796 N94-13081
The interplanetary origins and the main-phase development of moderate geomagnetic storms (1978 - 1979)
[INPE-5445-TDI/491] p 835 N94-13174
Evolution of the interplanetary magnetic field
[DE93-012631] p 836 N94-13262
Solar-geophysical data number 584, April 1993. Part 2: (Comprehensive reports). Data for October 1992 and miscellaneous
[PB93-198331] p 845 N94-14561
STELLAR MODELS
Analysis of interstellar cloud structure based on IRAS images
[NASA-CR-194341] p 836 N94-13332
Spectra of late type dwarf stars of known abundance for stellar population models
[NASA-CR-194301] p 831 N94-13681
STELLAR RADIATION
Search for ultra-high energy emission from Geminga and five unidentified EGRET sources
[DE93-012717] p 846 N94-12816
The soft x ray transient Cen X-4 in quiescence
[NASA-CR-194033] p 833 N94-14406
STELLAR ROTATION
Photometry and spectroscopy in the open cluster Alpha Persei, 2
[NASA-CR-193397] p 833 N94-14358
STELLAR SPECTRA
Physical properties of gas disks around shell stars with and without dust
[NASA-CR-193655] p 835 N94-13239
The spectroscopic evolution of novae in the bulge of M31 and a search for their possible origin in the M31 globular cluster system p 831 N94-13668
Spectra of late type dwarf stars of known abundance for stellar population models
[NASA-CR-194301] p 831 N94-13681
A long-term space astrophysics research program: The evolution of the quasar continuum
[NASA-CR-193714] p 839 N94-14404
Analysis of the IUE spectra of the strongly interacting binary beta Lyrae
[NASA-CR-194118] p 833 N94-14493
Solar-geophysical data number 584, April 1993. Part 1: (Prompt reports). Data for March, February 1993, and late data
[PB93-198323] p 845 N94-14560
STELLAR SPECTROPHOTOMETRY
Abundance markers in H II regions of late spiral galaxies
[ISBN-0-315-62457-4] p 836 N94-13372
Time series photometry of faint cataclysmic variables with a CCD p 831 N94-13646
The spectroscopic evolution of novae in the bulge of M31 and a search for their possible origin in the M31 globular cluster system p 831 N94-13668
STELLAR WINDS
The onset of galactic winds in early-type galaxies
[NASA-CR-193640] p 836 N94-13446
Wind mass and energy deposition
[DE93-013345] p 839 N94-14341
STELLARATORS
Ion cyclotron heating experiments and plans for the Advanced Toroidal Facility (ATF)
[DE93-012965] p 795 N94-13033
Interferometric investigation methods of plasma spatial characteristics on stellarators and tokamaks in submillimeter region
[DE93-621606] p 798 N94-13507
STEPPES
Evolution of the lower planetary boundary layer over strcngly contrasting surfaces
[DE93-010667] p 717 N94-14424
STEREOPHOTOGRAPHY
A widget based operations simulator for a planetary camera: A model for the high resolution stereo camera on Mars 94
[DLR-FB-92-30] p 651 N94-14044
STEREOSCOPIC VISION
Close range 3-D position sensing using stereo vision and point-of-correspondance through mathematical morphology
[ISBN-0-315-61012-3] p 763 N94-13515
Stochastic performance modeling and evaluation of obstacle detectability with imaging range sensors
[NASA-CR-194510] p 605 N94-13946
Depths from focusing and defocusing
[AD-A266644] p 735 N94-14797
STEREOSCOPY
EOS workstation
[NASA-CR-191326] p 736 N94-13132
Measurements of the spatial structure and directivity of 100 KeV photon sources in solar flares using PVO and ISEE-3 spacecraft
[NASA-CR-194080] p 845 N94-14492
STEROIDS
Phase-shifting effect of light and exercise on the human circadian clock
[AD-A265732] p 732 N94-13038
STIFFENING
Geometric stiffening in multibody dynamics formulations p 677 N94-14619
STIFFNESS
Measuring methods for CFRP laminates' bending and torsion rigidities characteristics p 529 N94-13272
Some frequency and damping measurements of laminated beryllium beams
[DE93-015909] p 676 N94-14530
STIRLING CYCLE
Three-stage linear, split-Stirling cryocooler for 1 to 2K magnetic cold stage
[NASA-CR-4538] p 776 N94-13897
A recuperative superfluid Stirling refrigerator
[DE93-016521] p 597 N94-14592
STIRLING ENGINES
Futurepath 2
[NASA-TM-109285] p 518 N94-13623
Insoluble coatings for Stirling engine heat pipe condenser surfaces
[NASA-CR-191188] p 554 N94-14771
STOCHASTIC PROCESSES
Ocean acoustic processing: A model-based approach
[DE93-011902] p 725 N94-12876
Stochastic dynamics: Crossover from 1/f(sup 3) to flicker noise
[DE93-622862] p 772 N94-12896
Investigation for improving Global Positioning System (GPS) orbits using a discrete sequential estimator and stochastic models of selected physical processes
[NASA-CR-194167] p 512 N94-13082
A stochastic model for behavior analysis of fiber-reinforced quasi-brittle materials
p 672 N94-13594
Robust synthesis of discrete-time multivariable control systems with induced delays p 662 N94-13642
Stochastic realization of finite-valued processes and primes in the positive matrices
[CWI-BS-R9222] p 773 N94-13677
Observation of the coalescing of beam into an asymmetric RF bucket by stochastic cooling
[DE93-015133] p 783 N94-13895
Stochastic performance modeling and evaluation of obstacle detectability with imaging range sensors
[NASA-CR-194510] p 605 N94-13946
On the geometry of external spectral factors and the Riccati inequality
[CWI-BS-R9227] p 770 N94-14002
Stochastic scheduling games with Markov decision arrival processes
[CWI-BS-R9231] p 773 N94-14005
Tuning of Gaussian stochastic control systems
[CWI-BS-R9223] p 765 N94-14018
Hybrid S(sub N)/Monte Carlo research and results
[DE93-012677] p 773 N94-14178
Stochastic bounds for a polling system
[CWI-BS-R9230] p 765 N94-14361
Inflow characteristics associated with high-blade-loading events in a wind farm
[DE93-010042] p 704 N94-14423
Investigations of transitions from order to chaos in dynamical systems
[DE93-014438] p 818 N94-14738
Stochastic modeling of turbulent reacting flows
p 647 N94-14768
Functional differential equations with piecewise continuous argument
[AD-A266660] p 772 N94-14840
Determining neural network connectivity using evolutionary programming
[AD-A266853] p 766 N94-14882
STOICHIOMETRY
Unexpectedly rapid hydrosilation polymerization of the diallyl derivative of bisphenol A and 2,6-diallylphenol
[AD-A265832] p 577 N94-12986
Gas atomized Er3Ni powder for cryocooler applications
[DE93-011564] p 568 N94-13000
STORAGE BATTERIES
Primary and secondary electrical space power based on advanced PEM systems
[DE93-012643] p 553 N94-14689
STORAGE RINGS (PARTICLE ACCELERATORS)
Recent study of beam stability in the PSR
[DE93-014473] p 780 N94-13173
Construction of the Courant-Snyder invariants for the non-linear equations of motion under presence of the linear coupling
[DE93-017565] p 788 N94-14872
STORAGE STABILITY
A study of hydrogen effects on fracture behavior of radioactive waste storage tanks
[DE93-018171] p 574 N94-14873
STORAGE TANKS
The feasibility of producing aluminum-lithium structures for cryogenic tankage applications by laser beam welding
[NASA-CR-191527] p 595 N94-14026
A study of hydrogen effects on fracture behavior of radioactive waste storage tanks
[DE93-018171] p 574 N94-14873
STORMS (METEOROLOGY)
Storm prediction through barometric field analysis
[PUBL-SER-A-129] p 720 N94-13587
STOVL AIRCRAFT
Design criteria for integrated flight/propulsion control systems for STOVL fighter aircraft p 521 N94-13297
STRAIN DISTRIBUTION
Estimation of strain in 1-kW primary containment vessels by microstructural examination
[DE93-013053] p 573 N94-14316
STRAIN ENERGY METHODS
Geometric stiffening in multibody dynamics formulations p 677 N94-14619
STRAIN GAGES
Strain sensing technology for high temperature applications
[NASA-TM-4498] p 648 N94-12874
The ASCOR test: A simple automated method for stress corrosion testing of aluminium alloys
[NLR-TP-91438-U] p 570 N94-13532
A technique for direct measurement of skin friction in supersonic combustion flow p 503 N94-13555
STRAIN MEASUREMENT
Strain sensing technology for high temperature applications
[NASA-TM-4498] p 648 N94-12874
Correlations of the growth, structure, and stress with the adhesion of diamond films on tungsten
[DE93-012855] p 576 N94-12912
Measurement of residual strain in composites by means of time-of-flight neutron diffraction
[DE93-012939] p 555 N94-13248
Measurement of strain in individual phases of composites before, during, and after mechanical loading
[DE93-014585] p 558 N94-14119
Cammatic: An approach to improve DSS 13 antenna gravity-loading performance p 608 N94-14374
STRAIN RATE
A stochastic model for behavior analysis of fiber-reinforced quasi-brittle materials
p 672 N94-13594
Non-uniqueness in dynamic rate-independent non-associated plasticity
[AD-A266342] p 769 N94-13731
Dynamic mechanical deformation of a SiC(sub p)/Al-Li (8090) composite
[DE93-014586] p 558 N94-14121
Machining and grinding: High rate deformation in practice
[DE93-010718] p 664 N94-14457
Search for subgrid scale parameterization by projection pursuit regression p 643 N94-14749
Yield properties of tungsten and tungsten heavy alloys
[AD-A266833] p 575 N94-14878
STRAKES
Measurements of wing and fin buffeting on the standard dynamics model
[IAR-AN-76] p 526 N94-13859
STRANGE ATTRACTORS
Stability of subharmonics and escape phenomena in the twin-well potential duffing system p 775 N94-13235
STRANGENESS
Neutral strange particle production at the AGS
[DE93-014044] p 780 N94-13098
Measuring strangeness in the nucleon
[DE93-014861] p 785 N94-14471
STRATA
Dynamic soil pressures on rigid cylindrical vaults
[DE93-013930] p 676 N94-14585
STRATIFICATION
Turbulent diffusion in homogeneous shear flow with stable density stratification
[DLR-FB-92-26] p 639 N94-14443

STRATIFIED FLOW
Effects of surface thermal forcing on stratified flow past an isolated obstacle p 633 N94-13553
STRATOCUMULUS CLOUDS
Linkage of anthropogenic aerosol to clouds and climate
[DE93-016434] p 719 N94-13080
Remote sensing of low level cloud optical characteristics p 691 N94-14229
STRATOSPHERE
Project AIRSTREAM: Trace gas
[DE93-008849] p 706 N94-12904
Airborne Arctic stratospheric expedition: Ozone
[NASA-TM-109312] p 515 N94-13606
Weather forecasting support for AASE-2
[NASA-CR-194342] p 721 N94-13675
Modeling of the partitioning of reactive odd nitrogen in the lower stratosphere using aircraft measurements of NOy, NO, and other trace species
[NASA-CR-194305] p 714 N94-13707
Measurement of HO2 and other trace gases in the stratosphere using a high resolution far-infrared spectrometer at 28 km
[NASA-CR-194175] p 714 N94-13816
Space-based activities: SAM 2 and SAGE 2 p 694 N94-14252
New evidences supported the Wei hypothesis about the formation of the Antarctic ozone hole p 694 N94-14253
STREAK CAMERAS
Image motion photography
[DE93-013962] p 653 N94-14858
STREAM FUNCTIONS (FLUIDS)
Contributions to numerical solution of Navier-Stokes equations in two and three dimensional flows
[ETN-93-94395] p 647 N94-14816
STREAMLINING
Exploratory study of in-plane streamline curvature effects on a turbulent boundary layer at a Mach number of 3
[NASA-CR-193673] p 501 N94-13292
STREAMS
Tracking of change of a warm-core ring structure p 696 N94-14267
Warm streamers extended from Warm Core Rings (WCR's) and their role on fish migration and fishing ground formation p 697 N94-14270
STRESS (PHYSIOLOGY)
Cellular mechanism of turnover of the stress induced protein HSP 70
[AD-A265723] p 732 N94-13061
Physiological Anatomical Rodent Experiment (PARE) .04 Feasibility Test 1
[NASA-CR-194423] p 728 N94-13473
Variability of prediction of maximal oxygen concumption on the cycle ergometer using standard equations
[NASA-TP-3412] p 729 N94-14032
STRESS ANALYSIS
Body/cushion contact stress analysis during sitting
[ITN-93-85204] p 736 N94-13229
LUTE telescope structural design
[NASA-CR-192594] p 830 N94-13448
Autofrettage: Stress distribution under load and retained stresses after depressurization. A modified plane-strain case
[AD-A266320] p 671 N94-13579
Finite element analysis of composite plates by use of modified complementary energy principle p 672 N94-13596
Computational methods for reliable fatigue and damage tolerance dimensioning of aircraft structures
[FFA-TN-1993-05] p 515 N94-13690
Some computational tools for the analysis of through cracks in stiffened fuselage shells
[LR-701] p 673 N94-13726
Thermal gradient-induced deflection of a thick-walled cylinder with bending residual stresses
[AD-A266347] p 673 N94-13777
Contribution to comparison of methods for determining welding procedures for the avoidance of hydrogen cracking
[VTT-PUBS-107] p 674 N94-13887
Compressive buckling of curved, anisotropic panels stiffened in two directions. Part 1: Derivation of the governing equations
[LR-694] p 675 N94-13931
Stress stiffening and approximate equations in flexible multibody dynamics p 677 N94-14620
The effect of initial imperfections on shell stability: An updated review
[LR-695] p 682 N94-14692
Analysis of new composite architectures
[NASA-CR-194524] p 559 N94-14715
STRESS CONCENTRATION
Evolving surface cusps during strained-layer epitaxy
[DE93-015430] p 813 N94-14478
STRESS CORROSION
The ASCOR test: A simple automated method for stress corrosion testing of aluminium alloys
[NLR-TP-91438-U] p 570 N94-13532
STRESS CORROSION CRACKING
Interfacial precipitation, segregation and deformation in alloy 600: Implications on primary-side IGSCC
[DE93-013161] p 568 N94-13035
Radiation hardening and radiation-induced chromium depletion effects on intergranular stress corrosion cracking of austenitic stainless steels
[DE93-011602] p 572 N94-14058
JPRS report: Science and technology. Central Eurasia: Materials science
[JPRS-UMS-93-005] p 559 N94-14575
STRESS DISTRIBUTION
Body/cushion contact stress analysis during sitting
[ITN-93-85204] p 736 N94-13229
Numerical simulations and experiments on physics of high Mach number shockwave: Turbulent flow interactions
[DE93-013424] p 631 N94-13249
Autofrettage: Stress distribution under load and retained stresses after depressurization. A modified plane-strain case
[AD-A266320] p 671 N94-13579
A process for evaluation of mechanical behavior of surface films
[W-1/92] p 579 N94-14007
Machining and grinding: High rate deformation in practice
[DE93-010718] p 664 N94-14457
STRESS FUNCTIONS
Elastic-plastic mixed-iterative finite element analysis: Implementation and performance assessment
[NASA-TM-106164] p 675 N94-13919
STRESS INTENSITY FACTORS
Finite element calculation of stress-intensity factors for thumb-nail cracks in DEN specimens
[LTR-ST-1929] p 850 N94-13548
Finite element calculation of stress-intensity factors for thru-thickness cracks in DEN specimens
[LTR-ST-1905] p 675 N94-14035
STRESS MEASUREMENT
Residual contact restraints in cryogenics
[ETN-93-94375] p 671 N94-13501
STRESS RELAXATION
Lifetime prediction of materials exposed to the natural space environment
[NASA-CR-193833] p 561 N94-12830
Evolving surface cusps during strained-layer epitaxy
[DE93-015430] p 813 N94-14478
STRESS TENSORS
Discussion of stress tensor nonuniqueness with application to nonuniform, particulate systems
[DE93-014352] p 816 N94-13206
STRESS-STRAIN RELATIONSHIPS
Autofrettage: Stress distribution under load and retained stresses after depressurization. A modified plane-strain case
[AD-A266320] p 671 N94-13579
Micromechanical damage theories for brittle solids with interacting microcracks
[AD-A266348] p 673 N94-13778
Measurement of strain in individual phases of composites before, during, and after mechanical loading
[DE93-014585] p 558 N94-14119
Elastic-plastic finite element analyses of an unidirectional, 9 vol percent tungsten fiber reinforced copper matrix composite
[NASA-TM-106304] p 559 N94-14719
STRETCHING
JPRS report: Science and technology. Central Eurasia: Materials science
[JPRS-UMS-93-005] p 559 N94-14575
Investigation of the dilatational dissipation in compressible homogeneous shear flow p 645 N94-14758
Response of a supersonic boundary layer to a compression corner p 645 N94-14759
Vortex-induced disturbance field in a compressible shear layer p 645 N94-14760
STRING THEORY
On the symmetry algebra of the discrete states in d less than 2 closed string theory
[DE93-622903] p 769 N94-13536
A classical instability for black strings and p-branes
[DE93-014577] p 839 N94-14116
Mathematics and string theory
[DE93-017903] p 817 N94-14417
STRINGS
A classical instability for black strings and p-branes
[DE93-014577] p 839 N94-14116
STRONG INTERACTIONS (FIELD THEORY)
Top quark polarization and T-odd spin correlations as tools for testing (non) Standard Model predictions
[DE93-622956] p 778 N94-12847
STRUCTURAL ANALYSIS
Structural design/margin assessment
[NASA-TP-3410] p 669 N94-12831
A general contact detection algorithm for finite element analysis
[DE93-012846] p 742 N94-12956
Relegation for decentralized control
[AD-A265720] p 819 N94-13059
Test/analysis correlation and model updating of the STARS 1 and 2 missile systems
[DE93-013774] p 748 N94-13578
Finite element analysis of composite plates by use of modified complementary energy principle p 672 N94-13596
Boundary formulations for nonlinear design sensitivity analysis p 672 N94-13669
Some computational tools for the analysis of through cracks in stiffened fuselage shells
[LR-701] p 673 N94-13726
The development of inspection and repair methods for the C-17 aft cargo door
[LR-704] p 499 N94-13904
Hierarchical nonlinear behavior of hot composite structures
[NASA-TM-106229] p 676 N94-14041
Materials/structures testing p 506 N94-14164
Control system design for flexible structures using data models p 527 N94-14646
STRUCTURAL DESIGN
Structural design/margin assessment
[NASA-TP-3410] p 669 N94-12831
Advanced Turbine Technology Applications Project (ATTAP)
[NASA-CR-191088] p 828 N94-12931
A photovoltaic catenary-tent array for the Martian surface
[NASA-TM-106306] p 621 N94-13194
The Second Workshop on Deployment and Assembly Experiment of Large Space Structure on Orbit
[NASDA-CON-930003] p 529 N94-13268
Structural design of hexa-link truss deployable antenna p 529 N94-13269
Thermal distortion measurement of TETRUS type thermal test model of large deployable antenna for mobile communications satellite p 529 N94-13270
Development of modular cable mesh deployable antenna p 530 N94-13274
Research on inflatable structure for space use p 530 N94-13275
Helical truss beam development for large space structure p 530 N94-13276
A concept on on-orbit experiments of deployable structures utilizing JEM/HOPE p 531 N94-13279
Movement of deployable truss p 531 N94-13280
Development and application of one dimensional deployable truss p 531 N94-13281
Study of a one-dimensional deployable structure employing telescopic members p 531 N94-13282
LUTE telescope structural design
[NASA-CR-192594] p 830 N94-13448
Poling of thin polymer films in electro optic applications
[AD-A266562] p 579 N94-13584
The study on large space structure assembly technology: The study on deployable truss structure, part 1
[NASDA-TMR-930002] p 541 N94-13658
The study on large space structure assembly technology: The study on deployable truss structure, part 2 and 3
[NASDA-TMR-930003-PT-2-3] p 541 N94-13659
The study on test of docking mechanism system, part 1 and 2
[NASDA-TMR-930004-PT-1-2] p 541 N94-13660
Mathematical optimization: A tool for aircraft design
[MBB-LME-251-S-PUB-0492] p 751 N94-14006
Large space structures and systems in the space station era: A bibliography with indexes (supplement 05)
[NASA-SP-7085(05)] p 543 N94-14411
Animation of multi-flexible body systems and its use in control system design p 678 N94-14629
Flexibility and costs in the design process: A decision support model
[ISBN-9-06-814522-3] p 597 N94-14808
STRUCTURAL DESIGN CRITERIA
Development and application of a comprehensive, design-sensitive weight prediction method for wing structures of transport category aircraft
[LR-693] p 515 N94-13687
The effect of initial imperfections on shell stability: An updated review
[LR-695] p 682 N94-14692

STRUCTURAL ENGINEERING
An improved approach for flight readiness certification: Methodology for failure risk assessment and application examples, volume 1
[NASA-CR-194498] p 542 N94-14076
An improved approach for flight readiness certification: Methodology for failure risk assessment and application examples. Volume 2: Software documentation
[NASA-CR-194499] p 542 N94-14077
An improved approach for flight readiness certification: Methodology for failure risk assessment and application examples. Volume 3: Structure and listing of programs
[NASA-CR-194500] p 542 N94-14078
STRUCTURAL FAILURE
Comparison of analytic Whipple bumper shield ballistic limits with CTH simulations
[DE93-015126] p 539 N94-13006
The numerical simulation of the collapse process of axially compressed cylindrical shells with measured imperfections
[LR-705] p 674 N94-13905
MSD in fuselage lap joints: Requirements for inspection intervals for typical fuselage lap joint panels with Multiple Site Damage
[LR-697] p 675 N94-13986
The effect of initial imperfections on shell stability: An updated review
[LR-695] p 682 N94-14692
An improved approach for flight readiness certification: Probabilistic models for flaw propagation and turbine blade failure. Volume 1: Methodology and applications
[NASA-CR-194496] p 519 N94-14841
An improved approach for flight readiness certification: Probabilistic models for flaw propagation and turbine blade failure. Volume 2: Software documentation
[NASA-CR-194497] p 519 N94-14842
STRUCTURAL PROPERTIES (GEOLOGY)
The nature and origin of periodically spaced tectonic features on Mars
[NASA-CR-193821] p 842 N94-13199
STRUCTURAL STABILITY
Measuring methods for CFRP laminates' bending and torsion rigidities characteristics p 529 N94-13272
Boundary stability under nonequilibrium conditions
[DE93-016259] p 809 N94-13980
STRUCTURAL STRAIN
JPRS report: Science and technology. Central Eurasia: Materials science
[JPRS-UMS-93-004] p 559 N94-14574
STRUCTURAL VIBRATION
On curve veering and flutter of rotating blades
[NASA-TM-106282] p 670 N94-12872
System identification for Space Station Freedom using observer/Kalman filter Markov parameters
[NASA-CR-191521] p 539 N94-12976
Active control of acoustic pressure fields using smart material technologies
[NASA-CR-191480] p 768 N94-13354
Nonlinear vibrations of thick composite plates: Higher-order shear deformation plate theory
p 556 N94-13558
Some frequency and damping measurements of laminated beryllium beams
[DE93-015909] p 676 N94-14530
STRUCTURED PROGRAMMING
Guide to the software architectural design phase
[ESA-PSS-05-04-ISSUE-1] p 753 N94-14190
Guide to the software detailed design and production phase
[ESA-PSS-05-05-ISSUE-1] p 753 N94-14191
STRUTS
Flow-field interference produced by an asymmetrical support strut
[IAR-AN-75] p 504 N94-14031
STUDENTS
Lecture notes on software process improvement
[AD-A265200] p 744 N94-13049
Workshop for coordinating South Carolina's pre-college systemic initiatives in science and mathematics
[DE93-012263] p 818 N94-13216
Characteristics of the amateur radio means of the Arsene satellite
[CNES-NT-131] p 605 N94-13950
Center of excellence in rotary wing technology
[AD-A266655] p 510 N94-14799
SUBHARMONIC GENERATORS
Stability of subharmonics and escape phenomena in the twin-well potential duffing system p 775 N94-13235
SUBMILLIMETER WAVES
Interferometric investigation methods of plasma spatial characteristics on stellarators and tokamaks in submillimeter region
[DE93-621606] p 798 N94-13507
Instability heating of the HDZP
[DE93-012641] p 798 N94-13513
Theoretical SIS mixer research
[AD-A266323] p 807 N94-13580
Submillimeter, millimeter, and microwave spectral line catalogue, revision 3
[NASA-CR-194501] p 602 N94-13813
Direct submillimeter absorptivity measurements on epitaxial Ba(1-x)K(x)BiO3 films at 2K
[DE93-013904] p 815 N94-14699
SUBROUTINES
FORTRAN graphics routines for the Macintosh
[DE93-013092] p 742 N94-12864
Splines, contours and SVD subroutines
[DE93-016088] p 757 N94-14866
SUBSONIC AIRCRAFT
Strain sensing technology for high temperature applications
[NASA-TM-4498] p 648 N94-12874
SUBSONIC FLOW
Study of possible mechanisms of instability due to heat transfer
[INPE-5448-TDI/494] p 628 N94-12966
Transition prediction and control in subsonic flow over a hump
[NASA-CR-4543] p 629 N94-13066
Development of a general purpose multigrid accelerated Navier-Stokes solver p 641 N94-14613
SUBSONIC SPEED
Performance seeking control: Program overview and future directions
[NASA-TM-4531] p 519 N94-14855
SUBSTRATES
Electrophoretic and electrolytic deposition of ceramic particles on porous substrates
[AD-A265141] p 575 N94-12812
Project proposal for partial computational physics support for Survivability of Coatings program
[DE93-013788] p 576 N94-12939
The study of structure-processing-property relations in copper oxide based high (Tc) superconductors
[DE93-015066] p 804 N94-13003
Effects of growth conditions and substrate orientation on the properties of InSb
[DE93-013766] p 812 N94-14344
Kinetics of photodeposition of superconducting films
[DE93-015511] p 812 N94-14348
Metastability of yttrium-oxides
[DE93-016548] p 813 N94-14440
Ion assisted sputter deposition of Mo-Si multilayers
[DE93-013830] p 583 N94-14693
Solution chemistry optimization of sol-gel processed PZT thin films
[DE93-013776] p 814 N94-14695
Characterization of diamond film growth in a combustion flame
[AD-A266659] p 816 N94-14839
SUCTION
The transient behavior of a boundary layer exposed to uniform suction
[ITN-93-85205] p 630 N94-13197
SUDDEN IONOSPHERIC DISTURBANCES
Solar-geophysical data number 584, April 1993. Part 1: (Prompt reports). Data for March, February 1993, and late data
[PB93-198323] p 845 N94-14560
SULFATES
Determination of trace elements in triglycine sulfate solutions
[NASA-CR-193481] p 562 N94-13048
SULFIDES
An investigation of the role of second phase particles in the design of ultra high strength steels of improved toughness
[AD-A266774] p 573 N94-14786
SULFUR COMPOUNDS
Performance effects of coal-derived contaminants on the carbonate fuel cell
[DE93-013801] p 703 N94-13693
Importance of sprays for long range transport of harmful substances in the troposphere
[MITT-81] p 711 N94-14723
SULFUR DIOXIDES
An examination of utility emissions contributions to elevated ozone concentrations in the Chicago area
[DE93-012852] p 708 N94-13495
Summary of conclusions and recommendations from a visibility science workshop
[DE93-012770] p 710 N94-14523
Promotion of geothermal energy development in 1991
[DE93-799061] p 705 N94-14679
Signal and reference wavelengths for the elimination of SO2 cross sensitivity in remote measurements of tropospheric ozone with lidar
[GKSS/92/E/24] p 617 N94-14819
The mobile lidar system ARGOS for spatial resolution remote measuring of gaseous air pollutants
[GKSS/92/E/26] p 617 N94-14820
SULFURIC ACID
Reduction and analysis of seasons 15 and 16 (1991 - 1992) Pioneer Venus radio occultation data and correlative studies with observations of the near-infrared emission of Venus
[NASA-CR-194128] p 841 N94-13083
SUM RULES
The off shell (rho)-(omega) mixing in the QCD sum rules
[DE93-014845] p 786 N94-14527
SUPERCOMPUTERS
The NAS parallel benchmarks
[NASA-TM-103863] p 740 N94-13200
Advanced computers and simulation
[DE93-014354] p 740 N94-13286
Diskless supercomputers: Scalable, reliable I/O for the Tera-Op technology base
[NASA-CR-194089] p 740 N94-13363
Analysis and effects of the number of nests of DO loops during vector supercomputing
[NAL-TR-1146] p 748 N94-13453
Computational mechanics and supercomputing at LLNL
[DE93-016453] p 754 N94-14435
An overview of parallel scientific visualization
[DE93-017105] p 755 N94-14521
SUPERCONDUCTING FILMS
Non-linear effects in vortex viscous flow in superconductors-role of finite heat removal velocity
[DE93-621785] p 618 N94-12856
High-resolution Z-contrast imaging and hole concentration mapping of YBCO thin films
[DE93-015803] p 808 N94-13930
Measurement of penetration depth lambda(T) in YBa2Cu3O(7-delta) thin film
[DE93-014587] p 810 N94-14122
Formation of textured YBCO films by laser ablation
[DE93-013131] p 581 N94-14319
Superconductivity devices: Commercial use of space
[NASA-CR-194163] p 625 N94-14324
Kinetics of photodeposition of superconducting films
[DE93-015511] p 812 N94-14348
Effects of depositon rate on Bi2Sr2CaCu2O(8+x) and Bi2Sr(1.6)La(0.4)CuO(6+x) epitaxial thin film growth by pulsed-laser ablation
[DE93-015797] p 812 N94-14362
SUPERCONDUCTING MAGNETS
Technology assessments of advanced energy storage systems for electric and hybrid vehicles
[DE93-014395] p 701 N94-12913
Heat and seed recovery technology project
[DE93-009203] p 800 N94-13913
SUPERCONDUCTING SUPER COLLIDER
Building the repositories to serve — Superconducting Super Collider information system
[DE93-014100] p 821 N94-12983
Integrating PAW, a graphical analysis interface to Sybase
[DE93-014172] p 755 N94-14581
Proton-proton scattering contribution to emittance growth
[DE93-016090] p 787 N94-14588
SUPERCONDUCTIVITY
To the theory of triplet pairing in Fermi-liquid model
[DE93-621770] p 816 N94-12855
A superconducting large-angle magnetic suspension
[NASA-CR-189735] p 596 N94-13141
Study on superconducting basic technology for space application, part 1
[NASDA-CNT-930015-PT-1] p 622 N94-13425
Theoretical SIS mixer research
[AD-A266323] p 807 N94-13580
Direct submillimeter absorptivity measurements on epitaxial Ba(1-x)K(x)BiO3 films at 2K
[DE93-013904] p 815 N94-14699
Muon spin relaxation studies of heavy fermion superconductors
[DE93-014576] p 815 N94-14773
SUPERCONDUCTORS
Study on superconducting basic technology for space application, part 1
[NASDA-CNT-930015-PT-1] p 622 N94-13425
Empirical tight-binding parameters for solid C(sub 60)
[DE93-623061] p 807 N94-13510
Casting of superconducting composite materials (M-4)
p 586 N94-13736
Combustion synthesis and engineering of nanoparticles for electronic, structural, and superconductor applications
[DE93-016286] p 809 N94-13981
Superconductivity devices: Commercial use of space
[NASA-CR-194163] p 625 N94-14324
Theoretical studies of breakdown in random media
[DE93-018107] p 558 N94-14418
Is K3C60 a line phase?
[DE93-016700] p 813 N94-14517

Muon spin relaxation studies of heavy fermion superconductors
[DE93-014576] p 815 N94-14773
SUPERCRITICAL FLOW
Droplet-turbulence interactions in sprays exposed to supercritical environmental conditions
[NASA-CR-194408] p 638 N94-14308
SUPERFLUIDITY
To the theory of triplet pairing in Fermi-liquid model
[DE93-621770] p 816 N94-12855
Sidewall thermometry perturbations to nonlinear heat transport near the (lambda) transition in He-4
[DE93-014990] p 817 N94-14453
On the statistical theory of the even-even nucleons levels' density
[DE93-623990] p 788 N94-14875
SUPERHIGH FREQUENCIES
Rain rate duration statistics derived from the Mid-Atlantic coast rain gauge network p 614 N94-14663
Tree attenuation at 20 GHz: Foliage effects p 615 N94-14672
SUPERLATTICES
Surfaces and interfaces of ceramics and metals
[DE93-014959] p 578 N94-13408
Electronic states in systems of reduced dimensionality
[DE93-014440] p 815 N94-14739
SUPERNOVAE
Cosmic physics data analysis program
[NASA-CR-194357] p 846 N94-12826
A program of correlated observations using the EGRET instrument on GRO and the IMB neutrino detector
[NASA-CR-194367] p 783 N94-13856
Charge-exchange reactions and weak interaction rates for Type 2 supernovae
[DE93-015104] p 783 N94-13893
SUPERPLASTICITY
Effect of thermal processing practices on the properties of superplastic Al-Li alloys
[NASA-CR-4548] p 574 N94-14850
SUPERPRESSURE BALLOONS
Electrodynamics of the middle atmosphere: Superpressure balloon program
[NASA-CR-193671] p 712 N94-13293
SUPERSONIC AIRCRAFT
Turbulence modeling of free shear layers for high-performance aircraft
[NASA-CR-193659] p 520 N94-12799
High flux heat exchanger
[AD-A266341] p 636 N94-13730
SUPERSONIC AIRFOILS
Estimation of critical values and vibration characteristics on supersonic delta wings. Part 2: Locally-stationary time series analysis of nonstationary random responses
[NAL-TR-1179] p 502 N94-13345
SUPERSONIC BOUNDARY LAYERS
Exploratory study of in-plane streamline curvature effects on a turbulent boundary layer at a Mach number of 3
[NASA-CR-193673] p 501 N94-13292
A three-dimensional supersonic turbulent boundary layer generated by an isentropic compression p 503 N94-13556
Investigation of the dilatational dissipation in compressible homogeneous shear flow p 645 N94-14758
Response of a supersonic boundary layer to a compression corner p 645 N94-14759
SUPERSONIC COMBUSTION
Chemical reactions in scramjet engines: Reduced kinetic models for ignition, combustion and nozzle flow
[NAL-TR-1184] p 563 N94-13458
A technique for direct measurement of skin friction in supersonic combustion flow p 503 N94-13555
Modeling and simulation of transport and combustion phenomena in a supersonic mixing layer
[ONERA-NT-1992-11] p 565 N94-14194
SUPERSONIC COMBUSTION RAMJET ENGINES
An experimental investigation of mixing enhancement in a simulated scramjet combustor by use of swirling jets
[NASA-TM-109246] p 518 N94-13190
Chemical reactions in scramjet engines: Reduced kinetic models for ignition, combustion and nozzle flow
[NAL-TR-1184] p 563 N94-13458
A technique for direct measurement of skin friction in supersonic combustion flow p 503 N94-13555
SUPERSONIC DRAG
Aerodynamics of a sphere and an oblate spheroid for Mach numbers from 0.6 to 10.5 including some effects of test conditions
[NASA-TM-109016] p 500 N94-13172
SUPERSONIC FLIGHT
The problem of the sonic boom for future high-speed transport aircraft
[ESA-TT-1286] p 776 N94-13692
Performance seeking control: Program overview and future directions
[NASA-TM-4531] p 519 N94-14855
SUPERSONIC FLOW
An experimental investigation of mixing enhancement in a simulated scramjet combustor by use of swirling jets
[NASA-TM-109246] p 518 N94-13190
High speed transition prediction
[NASA-CR-194125] p 502 N94-13422
An experimental investigation of shock wave/vortex interaction p 634 N94-13574
Development of a general purpose multigrid accelerated Navier-Stokes solver p 641 N94-14613
Response of a supersonic boundary layer to a compression corner p 645 N94-14759
A new Lagrangian method for three-dimensional steady supersonic flows
[NASA-TM-106068] p 510 N94-14847
SUPERSONIC FLUTTER
Development of a high-speed mechanical drive system for oscillating an annular blade row in the bending mode
[NAL-TR-1170] p 502 N94-13342
SUPERSONIC JET FLOW
Mixing noise reduction for rectangular supersonic jets by nozzle shaping and induced screech mixing
[NASA-TM-106364] p 508 N94-14208
SUPERSONIC NOZZLES
Chemical reactions in scramjet engines: Reduced kinetic models for ignition, combustion and nozzle flow
[NAL-TR-1184] p 563 N94-13458
Mixing noise reduction for rectangular supersonic jets by nozzle shaping and induced screech mixing
[NASA-TM-106364] p 508 N94-14208
SUPERSONIC SPEED
A comparison of computational and experimental data for a subscale high speed propulsive nozzle at low mach numbers
[AD-A266543] p 504 N94-13705
A computational study of the base region flow field for the M865 projectile
[ARL-TR-109] p 504 N94-13795
SUPERSONIC WIND TUNNELS
CNSFV code development, virtual zone Navier-Stokes computations of oscillating control surfaces and computational support of the laminar flow supersonic wind tunnel
[NASA-CR-194259] p 504 N94-14030
SUPPORT INTERFERENCE
Flow-field interference produced by an asymmetrical support strut
[IAR-AN-75] p 504 N94-14031
SUPPORT SYSTEMS
Building the repositories to serve --- Superconducting Super Collider information system
[DE93-014100] p 821 N94-12983
An evaluation of ZIM and entity-relational models in managing databases for decision support systems
[ERB-1034] p 824 N94-14202
SURFACE ACOUSTIC WAVE DEVICES
Integrated optics technology transfer
[DSIS-93-00179] p 792 N94-13868
Portable acoustic wave sensor systems for real-time monitoring of volatile organic compounds
[DE93-013753] p 582 N94-14511
SURFACE COOLING
Excimer laser surface processing of titanium
[DE93-012633] p 570 N94-13512
Modelling of the temperature distribution in a copper roll for the design of a system of cooled rolls adapted to vertical strip casting
[IMI-93RT-21200-1436-G] p 557 N94-13866
SURFACE DEFECTS
Absorption and damage thresholds of low defect density hafnia deposited with activated oxygen
[DE93-013853] p 655 N94-13243
SURFACE DISTORTION
A benchmark bending test of a thick specimen, Part 1: Experiments
[ARL-RR-6-PT-1] p 670 N94-12927
A benchmark bending test of a thick specimen. Part 2: Surface displacement measurements
[ARL-RR-6-PT-2] p 670 N94-12928
SURFACE EMITTING LASERS
Horizontal-cavity surface-emitting lasers, superluminescent LEDs, and amplifiers, and parabolic gain unstable resonator semiconductor lasers p 656 N94-13573
SURFACE ENERGY
Measuring surface fluxes in CAPE
[NASA-CR-193664] p 711 N94-12788
SURFACE FINISHING
Impedance-power effects on plasma polymer surface finish using a helical resonator discharge
[DE93-016454] p 803 N94-14590
Electrochemical planarization for microelectronic circuits
[DE93-017214] p 627 N94-14870
SURFACE GEOMETRY
Multigrid solution of internal flows using unstructured solution adaptive meshes
[NASA-CR-194233] p 638 N94-14356
SURFACE LAYERS
Incomplete melting of the Au(100) surface
[DE93-623192] p 569 N94-13227
About the influence of inert gas ion implantation on metal corrosion stability
[DE93-620574] p 569 N94-13360
SURFACE NAVIGATION
Passive recovery of scene geometry for an unmanned ground vehicle
[AD-A266670] p 766 N94-14777
SURFACE PROPERTIES
Theoretical treatment of the bulk and surface properties of fluids containing long, flexible molecules
[DE93-015560] p 575 N94-12861
Procedures for analysis of debris relative to Space Shuttle systems
[NASA-TM-109190] p 534 N94-12900
Computer simulations for the adsorption of polymers onto surfaces
[DE93-016667] p 577 N94-13070
Surface analysis of bearings
[AD-A266800] p 661 N94-13122
Computer code for scattering from impedance bodies of revolution. Part 3: Surface impedance with s and phi variation. Analytical and numerical results
[NASA-CR-193396] p 599 N94-13264
High resolution electron energy loss studies of surface vibrations
[DE93-014441] p 781 N94-13283
Barium fluoride research and development at Lawrence Livermore National Laboratory
[DE93-014682] p 807 N94-13405
Surfaces and interfaces of ceramics and metals
[DE93-014959] p 578 N94-13408
Surface science instrumentation for the study of important catalytic and electrochemical interfaces
[DE93-015068] p 563 N94-13413
Excimer laser surface processing of titanium
[DE93-012633] p 570 N94-13512
Applications of surface science to solid lubricants
[SMC-TR-93-24] p 579 N94-13903
Analysis of microstrip patch antennas with nonzero surface resistance
[NASA-TP-3362] p 604 N94-13916
The de Haas-van Alphen studies and Fermi surface properties of organic superconductors (ET)2X
[DE93-015157] p 623 N94-13925
Kinetics of photodeposition of superconducting films
[DE93-015511] p 812 N94-14348
Ploughing on gold using a Scanning Tunneling Microscope
[DE93-012632] p 812 N94-14365
Determination of the surface cleanliness of metals by FT-IR spectroscopy
[DE93-013252] p 565 N94-14525
Ultra-soft x ray absorption spectroscopy: A bulk and surface probe of materials
[DE93-014325] p 566 N94-14582
Surface characterization of LDEF materials
[NASA-CR-194519] p 543 N94-14683
SURFACE REACTIONS
Applications of surface science to solid lubricants
[SMC-TR-93-24] p 579 N94-13903
Machining and grinding: High rate deformation in practice
[DE93-010718] p 664 N94-14457
Quantum state resolved desorption of CO from solid surfaces
[DE93-016876] p 814 N94-14597
SURFACE ROUGHNESS
Transition prediction and control in subsonic flow over a hump
[NASA-CR-4543] p 629 N94-13066
Processing and mechanical properties of silicon carbide platelet reinforced alumina composites p 556 N94-13557
Experimental measurement of local heat transfer coefficients over discrete roughened plates using infrared thermography p 635 N94-13652
Impedance-power effects on plasma polymer surface finish using a helical resonator discharge
[DE93-016454] p 803 N94-14590
Investigation of Zerodur material processing
[NASA-CR-193842] p 793 N94-14903
SURFACE ROUGHNESS EFFECTS
Two-dimensional Navier-Stokes heat transfer analysis for rough turbine blades
[NASA-TM-106008] p 629 N94-13027

Transition prediction and control in subsonic flow over a hump
[NASA-CR-4543] p 629 N94-13066

SURFACE TEMPERATURE
Measuring surface fluxes in CAPE
[NASA-CR-193664] p 711 N94-12788
Coupled thermal response of objects and participating media in fires and large combustion systems
[DE93-012848] p 561 N94-12819
Effects of surface thermal forcing on stratified flow past an isolated obstacle p 633 N94-13553
Experimental investigation of the effects of blowing ratio parameter on heat transfer to a film-cooled flat plate
[AD-A266599] p 636 N94-13780
Wear-mechanism modelling
[DE93-012311] p 579 N94-13974
The accuracy of approximating radiative heat transfer using a temperature dependent thermal conductivity
[DE93-013105] p 638 N94-14318

SURFACE TREATMENT
Excimer laser surface processing of titanium
[DE93-012633] p 570 N94-13512
Free-exciton recombination in GaAs
[DE93-009843] p 809 N94-14079

SURFACE WATER
Educational module for the Higher Agricultural Education. Part 2: Eutrophication observed by remote sensing: An educational approach to water quality monitoring
[BCRS-92-11B] p 818 N94-14462

SURFACE WAVES
Excitation of coupled waves in plasma periodic structures by relativistic electron beam and acceleration of charged particles
[DE93-621657] p 794 N94-12853

SURFACES
Calculating intersections of surfaces in screen space
[NASA-CR-191498] p 745 N94-13185

SURFACTANTS
Computer simulations for the adsorption of polymers onto surfaces
[DE93-016667] p 577 N94-13070
Surfactant studies for bench-scale operation
[NASA-CR-194097] p 701 N94-13187
Surfactant studies for bench-scale operation
[NASA-CR-194511] p 564 N94-13947

SURVEYS
NASA/DOD Aerospace Knowledge Diffusion Research Project. Report 18: A comparison of the technical communication practices of aerospace engineers and scientists in India and the United States
[NASA-TM-109006] p 821 N94-13057
Defining the performance gap: Conducting a self-assessment p 666 N94-13155
User observations on information sharing (corporate knowledge and lessons learned)
[NASA-TM-104781] p 819 N94-13400
Magic mirror on the wall, who's the fastest database of them all? A survey of database benchmarks
[AD-A266437] p 823 N94-13701
A review of robust detection
[DSIS-93-00400] p 603 N94-13829
Selected data on academic science and engineering R and D expenditures: Fiscal Year 1991
[NSF-92-329] p 819 N94-13982
Generic results of the space physics community survey
[NASA-CR-194538] p 818 N94-13984

SWEDEN
The Swedish ISY contribution p 695 N94-14256

SWELLING
An experimental study on the effect of die geometry on swell and sag in the parison extrusion stage
[IMI-93RT-42400-1476-G] p 597 N94-14070

SWEPT WINGS
Three-Dimensional Boundary-Layer program (BL3D) for swept subsonic or supersonic wings with application to laminar flow control
[NASA-CR-4531] p 629 N94-13073

SWIRLING
An experimental investigation of mixing enhancement in a simulated scramjet combustor by use of swirling jets
[NASA-TM-109246] p 518 N94-13190

SWITCHES
Development of UHF spark-switched L-C Oscillators
[DE93-015019] p 623 N94-13892

SWITCHING
Charge storage and switching phenomena with molecular assemblies of metal complexes
[AD-A266673] p 787 N94-14778

SWITCHING CIRCUITS
Evolution of high-repetition-rate induction accelerators through advancements in switching
[DE93-012599] p 654 N94-12963

SYMBOLS
Application of symbolic and algebraic manipulation software in solving applied mechanics problems
[NASA-CR-4544] p 596 N94-13798

SYMMETRY
Aspects of symmetry violation
[DE93-011003] p 779 N94-12997
Determination of channeling perspectives for complex crystal structures
[DE93-012872] p 805 N94-13009
Resonant x ray Raman scattering from atoms and molecules
[DE93-015158] p 784 N94-13896

SYNAPSES
Determining neural network connectivity using evolutionary programming
[AD-A266853] p 766 N94-14882

SYNCHRONISM
Solving integer programs from dependence and synchronization problems
[AD-A265702] p 767 N94-13284
A hardware implementation of a provably correct design of a fault-tolerant clock synchronization circuit
[NASA-TM-109001] p 759 N94-13450
Fine time uplink synchronization for frequency-hopped spread spectrum satellite communication system
[ISBN-0-315-54370-1] p 600 N94-13488
Simulation of downlink synchronization for a frequency-hopped satellite communication system
[DSIS-93-00477] p 605 N94-13941

SYNCHRONOUS MOTORS
Design and application of electromechanical actuators for deep space missions
[NASA-CR-194145] p 663 N94-14134

SYNCHROTRON RADIATION
Proceedings of the Workshop on Applications of Synchrotron Radiation to Trace Impurity Analysis for Advanced Silicon Processing
[DE93-013389] p 805 N94-13020
Measurement of the spin of a particle using undulator radiation
[DE93-014334] p 780 N94-13149
Application of synchrotron radiation in chemical dynamics
[DE93-015040] p 563 N94-13411
Applications of surface science to solid lubricants
[SMC-TR-93-24] p 579 N94-13903
Comparative study of x ray and microwave emissions during solar flares
[NASA-CR-194532] p 845 N94-14577

SYNCHROTRONS
Proceedings of the Workshop on Applications of Synchrotron Radiation to Trace Impurity Analysis for Advanced Silicon Processing
[DE93-013389] p 805 N94-13020
A new formulation of longitudinal coherent instabilities
[DE93-014288] p 789 N94-13220
The evolution of tensor polarization
[DE93-017209] p 790 N94-14897

SYNCOM 4 SATELLITE
STS-32 mission highlights resource tape
[NASA-TM-109291] p 531 N94-13631

SYNOPTIC METEOROLOGY
Storm prediction through barometric field analysis
[PUBL-SER-A-129] p 720 N94-13587
AMIP: Diagnostic subproject on the variability in the tropics: Synoptic to intraseasonal time scales
[DE93-009287] p 721 N94-13914

SYNTHESIS (CHEMISTRY)
Correlations of the growth, structure, and stress with the adhesion of diamond films on tungsten
[DE93-012855] p 576 N94-12912
Synthesis inversion of atmospheric CO2 using the GISS tracer transport model
[CSIRO-TP-29] p 709 N94-14095
Catalytic arene hydrogenation using early transition metal hydride compounds
[DE93-015500] p 573 N94-14402

SYNTHETIC APERTURE RADAR
Preparations for and first results of the calibration and interpretation of ERS-1 SAR imagery over land
[BCRS-92-13] p 684 N94-13123
A combined analogue and digital pulse compression system using large time bandwidth product signals for use in synthetic aperture radar
[ISBN-0-315-54373-6] p 600 N94-13489
Phase aligner for the Electronically Scanned Thinned Array Radiometer (ESTAR) instrument
[NASA-TM-4518] p 623 N94-13878
Feature discovery on segmented objects in SAR imagery using self-organizing neural networks
[DE93-010685] p 686 N94-14056
Testing various time-frequency distribution techniques
[DREO-TN-92-17] p 606 N94-14062
Earth Observation Center Annual Report on Research and Development, Fiscal Year 1992
[EOC-92-01-0007] p 687 N94-14091
Calibration and in-house validation results of JERS-1 data p 687 N94-14092
Results from ERS-1 and JERS-1 SAR calibration experiments and data analysis p 688 N94-14210
Geologic application of JERS-1 SAR data p 688 N94-14211
Artificial oil pollution detection and wave observation in the sea adjacent to Japan by ERS-1 SAR p 688 N94-14212
An exact processing algorithm for wide beam spaceborne SAR data p 689 N94-14213
Survey of subsurface geophysical exploration technologies adaptable to an airborne platform
[DE93-015080] p 717 N94-14294
Ionospheric effects on a wide-bandwidth, polarimetric, space-based, synthetic-aperture radar
[DE93-015084] p 612 N94-14512
Microwave interconnection
[DE93-016580] p 625 N94-14533

SYNTHETIC FUELS
Status and future opportunities for conversion of synthesis gas to liquid energy fuels
[DE93-010025] p 584 N94-14089

SYSTEM FAILURES
STS-55 pad abort: Engine 2011 oxidizer preburner augmented spark igniter check valve leak
[NASA-CR-193830] p 533 N94-12806
Computational problems with the binomial failure rate model and incomplete common cause failure reliability data
[DE93-014346] p 669 N94-14143

SYSTEM IDENTIFICATION
System identification for Space Station Freedom using observer/Kalman filter Markov parameters
[NASA-CR-191521] p 539 N94-12976
Feasibility study of an orbiting laboratory for testing CSI technology
[NASA-CR-191524] p 540 N94-13016
An analytic modeling and system identification study of rotor/fuselage dynamics at hover p 524 N94-13312
Flight testing and frequency domain analysis for rotorcraft handling qualities characteristics p 526 N94-13324
Test/analysis correlation and model updating of the STARS 1 and 2 missile systems
[DE93-013774] p 748 N94-13578
Identification of continuous-time dynamical systems: Neural network based algorithms and parallel implementation
[DE93-014427] p 766 N94-14737

SYSTEMS ANALYSIS
Nuclear propulsion systems engineering
[DE93-010791] p 548 N94-12870
Analysis and effects of the number of nests of DO loops during vector supercomputing
[NAL-TR-1146] p 748 N94-13453
The OOA technique in information systems
[REPT-72-92] p 823 N94-13863
Heat and seed recovery technology project
[DE93-009203] p 800 N94-13913
Transformation and composition of refusal graphs: Testability analysis
[LAAS-92435] p 751 N94-13995
Optical systems integrated modeling p 547 N94-14837
Laser power beaming system analyses
[NASA-CR-193840] p 660 N94-14904

SYSTEMS ENGINEERING
Solar dynamic power system development for Space Station Freedom
[NASA-RP-1310] p 548 N94-12807
Nuclear propulsion systems engineering
[DE93-010791] p 548 N94-12870
Design, qualification and operation of nuclear rockets for safe Mars missions
[DE93-010792] p 549 N94-12996
Glossary of SSDC terms and acronyms
[DE93-013697] p 823 N94-13352
Electrical Actuation Technology Bridging
[NASA-CP-3213] p 551 N94-13417
Space and Earth sciences, computer systems, and scientific data analysis support, volume 1
[NASA-CR-194535] p 741 N94-13788
Hypersonic overview p 505 N94-14154
Integrating interface slicing into software engineering processes
[NASA-CR-192761] p 754 N94-14368
Formal functional test designs with a test representation language p 609 N94-14383
The further development and refinement of an expert-systems approach to the creative design of mechanisms and mechanical systems
[AD-A266812] p 665 N94-14901

SYSTEMS INTEGRATION
System integration and demonstration of adhesive bonded high temperature aluminum alloys for aerospace structure, phase 2
[NASA-CR-191459] p 575 N94-12792
Electric propulsion system technology
[NASA-CR-194100] p 549 N94-13055
Integration between geographic information systems and environmental simulation models
[REPT-93-004] p 823 N94-13806
Advanced Communications ESM System (ACES) testbed: Integration study
[DSIS-93-00345] p 604 N94-13939
Activities of Institute for Information Technology
[CNR-35024] p 824 N94-14069
Experimental instrumentation system for the Phased Array Mirror Extendible Large Aperture (PAMELA) test program
[NASA-CR-194421] p 705 N94-14430
Small scale adaptive optics experiment systems engineering
[NASA-CR-194419] p 793 N94-14548
Optical systems integrated modeling
p 547 N94-14837

SYSTEMS SIMULATION
Real-time dynamic simulation of the Cassini spacecraft using DARTS. Part 2: Parallel/vectorized real-time implementation p 680 N94-14639
Space Station Common Berthing Mechanism, a multi-body simulation application p 544 N94-14640

T

T TAURI STARS
Search for x ray emitting young stars outside of massive molecular clouds
[NASA-CR-193609] p 830 N94-13462

TABLES (DATA)
A benchmark bending test of a thick specimen. Part 2: Surface displacement measurements
[ARL-RR-6-PT-2] p 670 N94-12928
Royal Belgium observatory calendar: 156th year
[ETN-93-94221] p 833 N94-14811

TACTILE SENSORS (ROBOTICS)
Development of a tactile and vision integrated system, and object identification techniques for SPDM applications
[DSIS-93-00153] p 764 N94-13842
Development of a computer vision system to supplement the active tactile sensing capability in a structured environment
[DSIS-93-00072] p 764 N94-13844

TAIL ASSEMBLIES
Low-speed wind tunnel tests on four types of joined-wing aircraft models
[NAL-TR-1167] p 501 N94-13340

TANKER AIRCRAFT
Spare parts analysis of the MK.32B-751 AAR pod
[DSIS-93-00737] p 774 N94-13549

TANTALUM
Shock compression and quasielastic release in tantalum
[DE93-014566] p 811 N94-14329

TANTALUM ALLOYS
Metastability of yttrium-oxides
[DE93-016548] p 813 N94-14440

TARGET ACQUISITION
Infrared transmission and path radiance through dust and fog
[AD-A265825] p 791 N94-12979
A piloted simulation investigation of the normal load factor and longitudinal thrust required for air-to-air acquisition and tracking p 522 N94-13301

TASK PLANNING (ROBOTICS)
Robot programming, natural computation and conceptual graphs
[ITN-93-85193] p 748 N94-13539
Robot-task compliance: The energy criterion
[ITN-93-85196] p 763 N94-13568

TASKS
Work/rest schedules and performance of F/A-18 aviators during Fleet Exercise 1992
[AD-A265826] p 735 N94-12982

TEARING MODES (PLASMAS)
Nonlinear evolution of tearing modes in inhomogeneous plasmas
[PPL-133] p 798 N94-13564

TECHNOLOGIES
JPRS report: Science and technology. Central Eurasia: Space
[JPRS-USP-93-003] p 828 N94-13182
Heidegger's thinking p 736 N94-13442
Science, technology, and the federal government: National goals for a new era p 827 N94-14115

TECHNOLOGY ASSESSMENT
Where no flag has gone before: Political and technical aspects of placing a flag on the Moon
[NASA-CR-188251] p 827 N94-12800
Technology assessments of advanced energy storage systems for electric and hybrid vehicles
[DE93-014395] p 701 N94-12913
Compendium of executive summaries from the maglev system concept definition
[PB93-154938/GAR] p 661 N94-13285
Status and future opportunities for conversion of synthesis gas to liquid energy fuels
[DE93-010025] p 584 N94-14089
Optical systems integrated modeling
p 547 N94-14837
Advanced optical instruments technology
p 547 N94-14838

TECHNOLOGY TRANSFER
Catalysis and biocatalysis program
[NASA-CR-194105] p 727 N94-12793
Integrated optics technology transfer
[DSIS-93-00179] p 792 N94-13868
Center of excellence in rotary wing technology
[AD-A266655] p 510 N94-14799

TECHNOLOGY UTILIZATION
Technology Applications Team: Applications of aerospace technology
[NASA-CR-194362] p 828 N94-13104
Technology parks and the cooperation among universities and firms: The cases of Campinas, Sao Jose dos Campos e Sao Carlos
[INPE-5251-TAE/04] p 818 N94-13427
Sequestering carbon dioxide in industrial polymers: Building materials for the 21st century
[DE93-016087] p 580 N94-14297
NASA/DOD Aerospace Knowledge Diffusion Research Project. Paper 38: Computer Mediated Communication (CMC) and the communication of technical information in aerospace
[NASA-TM-109330] p 826 N94-14489
Transform coding for space applications
[NASA-TM-106362] p 612 N94-14542
Workshop Proceedings: Optical Systems Technology for Space Astrophysics in the 21st Century, volume 3
[NASA-CR-194102] p 545 N94-14830

TECTONICS
The nature and origin of periodically spaced tectonic features on Mars
[NASA-CR-193821] p 842 N94-13199
The 1990 Western Pacific Geophysics meeting
[NASA-CR-193456] p 712 N94-13334
The American Geophysical Union Chapman Conference on Tectonics and Topography
[NASA-CR-193454] p 713 N94-13335
Regional tectonic analysis of Venus as part of the Pioneer Venus guest investigator project
[NASA-CR-194079] p 842 N94-13561
Overview: Gas hydrate geology and geography
[DE93-014043] p 688 N94-14151
Organic Geochemical and tectonic evolution of the Midcontinent Rift system
[DE93-015093] p 717 N94-14338

TELECOMMUNICATION
Adaptive Signal Processing Testbed
[DSIS-93-00258] p 604 N94-13869

TELEOPERATORS
Force reflecting hand controller for manipulator teleoperation
[NASA-CR-191345] p 661 N94-13129

TELEROBOTICS
Force reflecting hand controller for manipulator teleoperation
[NASA-CR-191345] p 661 N94-13129

TELESCOPES
Some flow properties of telescope enclosures estimated from water channel tests: Application of the flow visualization techniques
[NAL-TR-1178T] p 830 N94-13452
Rocket and laboratory studies in astronomy
[NASA-CR-194410] p 832 N94-13966
Telescope pointing for GOPEX p 610 N94-14389
Experimental instrumentation system for the Phased Array Mirror Extendible Large Aperture (PAMELA) test program
[NASA-CR-194421] p 705 N94-14430
Small scale adaptive optics experiment systems engineering
[NASA-CR-194419] p 793 N94-14548

TEMPERATE REGIONS
Nonlinear relationships between particulate absorption and chlorophyll: Detritus or pigment packaging?
[AD-A266806] p 731 N94-14899

TEMPERATURE CONTROL
Thermal Expert System (TEXSYS): Systems automony demonstration project, volume 1. Overview
[NASA-TM-102877] p 538 N94-13201
Miscibility of lubricants with refrigerants, phase 1
[DE93-014766-PHASE-1] p 596 N94-13407
Thermal Expert System (TEXSYS): Systems autonomy demonstration project, volume 2. Results
[NASA-TM-102877] p 538 N94-13989
Propulsion integration p 508 N94-14174
Microchannel cooled heatsinks for high average power laser diode arrays
[DE93-016533] p 658 N94-14442
Thermal design of hybrid circuits: Tools and methodology
[LAAS-92515] p 626 N94-14713
Analysis, approximation, and computation of a coupled solid/fluid temperature control problem
[NASA-TM-106351] p 771 N94-14731

TEMPERATURE DEPENDENCE
Breadboard activities for advanced protein crystal growth
[NASA-CR-193559] p 803 N94-12796
Modeling ignition chemistry
[DE93-012340] p 561 N94-12910
Temperature dependence of diffusivities, preliminary definition phase
[NASA-CR-192613] p 648 N94-13326
High temperature electromagnetic characterization of thermal protection system tile materials
[NASA-CR-189687] p 578 N94-13431
High temperature behavior of glass (M-8)
p 587 N94-13740
A circadian rhythm of conidiation in Neurospora crassa (L-12) p 593 N94-13769
The accuracy of approximating radiative heat transfer using a temperature dependent thermal conductivity
[DE93-013105] p 638 N94-14318

TEMPERATURE DISTRIBUTION
Modelling of the temperature distribution in a copper roll for the design of a system of cooled rolls adapted to vertical strip casting
[IMI-93RT-21200-1436-G] p 557 N94-13866
ROSAT observations of clusters with wide-angle tailed radio sources
[NASA-CR-193784] p 833 N94-14405

TEMPERATURE EFFECTS
Non-linear effects in vortex viscous flow in superconductors-role of finite heat removal velocity
[DE93-621785] p 618 N94-12856
Quantitative mapping of pore fraction variations in silicon nitride using an ultrasonic contact scan technique
[NASA-TP-3377] p 665 N94-13056
Thermal gradient-induced deflection of a thick-walled cylinder with bending residual stresses
[AD-A266347] p 673 N94-13777
Materials/structures testing p 506 N94-14164
Multiwavelength observations of unidentified high energy gamma ray sources
[NASA-CR-194536] p 840 N94-14688
Phases and phase transitions of polymeric liquid crystals: A high resolution x ray diffraction and light scattering study
[ITN-93-85218] p 816 N94-14826
Thermal history effects on electrical relaxation and conductivity for potassium silicate glass with low alkali concentrations
[NASA-TM-106324] p 583 N94-14845
Quenching and annealing effects on the specific heat of YBa2Cu3O(7-delta)
[DE93-016483] p 816 N94-14868
Thyroid alterations in porcine after prolonged exposure to cold or heat
[AD-A266840] p 733 N94-14879

TEMPERATURE GRADIENTS
Ceramic matrix composites by microwave assisted CVI
[DE93-012640] p 576 N94-12916
Study of bubble behavior in weightlessness (effects of thermal gradient and acoustic stationary wave) (M-16)
p 589 N94-13748
Thermal gradient-induced deflection of a thick-walled cylinder with bending residual stresses
[AD-A266347] p 673 N94-13777
The accuracy of approximating radiative heat transfer using a temperature dependent thermal conductivity
[DE93-013105] p 638 N94-14318
Thermoelastic response of metal matrix composites with large-diameter fibers subjected to thermal gradients
[NASA-TM-106344] p 560 N94-14823
Anomalous ion transport and feedback control
[DE93-018324] p 803 N94-14874

TEMPERATURE MEASUREMENT
Ohmic heating of composite candidate graphite-fiber/coating combinations
[NASA-TM-4491] p 554 N94-12871
Two temperature modeling and experimental measurements of laser sustained hydrogen plasmas
[AD-A265750] p 796 N94-13039

The corrosion behavior of 8001 Al under heat-transfer conditions in an aqueous loop system
[DE93-013450] p 569 N94-13242
Adaptive control of interface by temperature and interface profile feedback in transparent multi-zone crystal growth furnace
[NASA-CR-194140] p 762 N94-13253
An experimental investigation of the redistribution of gas stream total temperature in a high turning angle transonic planar cascade
[ISBN-0-315-60791-2] p 502 N94-13369
Experimental measurement of local heat transfer coefficients over discrete roughened plates using infrared thermography p 635 N94-13652
Recent flight-test results of optical airdata techniques
[NASA-TM-4504] p 517 N94-13791
High frame rate thermal imager for hypersonic wind tunnel applications
[ONERA-NT-1992-12] p 650 N94-14009
NASA metrology and calibration, 1993
[NASA-TM-109280] p 597 N94-14410
Two color holographic interferometry for microgravity application
[NASA-CR-194424] p 651 N94-14447
Investigation of the feasibility of optical diagnostic measurements at the exit of the SSME
[NASA-CR-193832] p 553 N94-14682
Time resolved measurement of electron temperatures of exploding foil x ray laser plasmas
[DE93-017161] p 803 N94-14894

TEMPERATURE PROFILES
Study of possible mechanisms of instability due to heat transfer
[INPE-5448-TDI/494] p 628 N94-12966

TEMPORAL DISTRIBUTION
Spatial and temporal variability of precipitation and chemistry: Case studies from the frontal boundary study
[DE93-007883] p 708 N94-13910
Chemistry and transport in a multi-dimensional model
[NASA-CR-194425] p 716 N94-13969
Potential evapotranspiration in Belgium: Spatial and temporal variability
[PUBL-SER-A-130] p 686 N94-13994

TEMPORAL RESOLUTION
High time resolution studies of binary x ray pulsars
[NASA-CR-194395] p 832 N94-13894
Supervised classification of remotely sensed images
[DLR-FB-92-07] p 700 N94-14428

TENSILE PROPERTIES
Tensile properties of LE-7 engine material with welded joint
[NAL-TR-1188] p 570 N94-13460
UK interlaboratory tensile tests on Al alloy/SiC particulate metal matrix composites
[NPL-DMM(A)-77] p 570 N94-13666
Effect of thermal processing practices on the properties of superplastic Al-Li alloys
[NASA-CR-4548] p 574 N94-14850

TENSILE STRESS
Non-uniqueness in dynamic rate-independent non-associated plasticity
[AD-A266342] p 769 N94-13731

TENSILE TESTS
UK interlaboratory tensile tests on Al alloy/SiC particulate metal matrix composites
[NPL-DMM(A)-77] p 570 N94-13666
The feasibility of producing aluminum-lithium structures for cryogenic tankage applications by laser beam welding
[NASA-CR-191527] p 595 N94-14026
Elastic-plastic finite element analyses of an unidirectional, 9 vol percent tungsten fiber reinforced copper matrix composite
[NASA-TM-106304] p 559 N94-14719

TENSOR ANALYSIS
The evolution of tensor polarization
[DE93-017209] p 790 N94-14897

TENSORS
The evolution of tensor polarization
[DE93-017209] p 790 N94-14897

TERMINAL BALLISTICS
The motion of a conical shaped liner driven by explosive load
[ITN-93-85215] p 585 N94-14507

TERMINAL FACILITIES
Airport terminals: Optimum configurations and gate position requirement
[ISBN-0-315-61722-5] p 528 N94-13544

TERMINAL VELOCITY
On the motion through a viscous fluid of a spherical particle touching a plane wall: Slip boundary conditions
[DE93-012540] p 628 N94-12961

TERMINOLOGY
Glossary of SSDC terms and acronyms
[DE93-013697] p 823 N94-13352

TERMS
Glossary of SSDC terms and acronyms
[DE93-013697] p 823 N94-13352

TERNARY ALLOYS
Electronic structure and phase stability properties in ternary substitutional alloys
[DE93-013848] p 569 N94-13137
Crystal growth of ZnSe and related ternary compound semiconductors by physical vapor transport
[NASA-CR-193834] p 807 N94-13444

TERNARY SYSTEMS
Fabrication of Si-As-Te ternary amorphous semiconductor in the microgravity environment (M-13) p 588 N94-13745

TERRAIN
Evaluation of beta-spline interpolation in digital terrain models
[INPE-5475-TDI/506] p 684 N94-13364
Net radiation mapping of mountainous terrain using Landsat-5 thematic mapper imagery and digital terrain data
[ISBN-0-315-57755-X] p 685 N94-13475

TERRAIN ANALYSIS
Spectral reflectance of soils from Sao Paulo State
[INPE-5424-PRP/172] p 684 N94-13377
Satellite imagery and exogenous data integration by neural network in automation land-cover classification
[INPE-5480-PRE/1778] p 686 N94-13729
Nonlinear aspects of data integration for land-cover classification in a neural network environment
[INPE-5479-PRE/1778] p 686 N94-13789

TEST EQUIPMENT
CFM technologies for space transportation: Multipurpose hydrogen testbed system definition and tank procurement
[NASA-CR-194355] p 539 N94-12827
The Large Area Pulsed Solar Simulator (LAPSS)
[NASA-CR-194507] p 703 N94-13940

TEST FACILITIES
Molten carbonate fuel cell product development test environmental assessment/protection plan
[DE93-000288] p 702 N94-13380
Miscibility of lubricants with refrigerants, phase 1
[DE93-014766-PHASE-1] p 596 N94-13407
Development of test techniques to simulate high-frequency mechanical shock on weapon components
[KCP-613-4998] p 675 N94-13907
Heat and seed recovery technology project
[DE93-009203] p 800 N94-13913
Advanced Communications ESM System (ACES) testbed: Integration study
[DSIS-93-00345] p 604 N94-13939
EWTEST signal excision testbed: System evaluation
[DSIS-93-00346] p 607 N94-14065
A program for the investigation of the Multibody Modeling, Verification, and Control Laboratory p 682 N94-14652
A guide to the DRA 13 ft x 9 ft Low Speed Wind Tunnel Facility
[AD-A267739] p 528 N94-14876

TEST FIRING
SSME testing at Stennis Space Center
[NASA-TM-109310] p 552 N94-13617
A computational study of the base region flow field for the M865 projectile
[ARL-TR-109] p 504 N94-13795
Technical Evaluation Motor No. 10 (TEM-10)
[NASA-CR-193846] p 554 N94-14907

TEST STANDS
Advanced Turbine Technology Applications Project (ATTAP)
[NASA-CR-191088] p 828 N94-12931

TESTS
Goddard Space Flight Center robotics demo
[NASA-TM-109302] p 662 N94-13604
Optical testing p 547 N94-14836

TETHERED SATELLITES
An experimental study of tether reel system: A laboratory model
[NAL-TR-1176T] p 539 N94-12943

TETHERING
An experimental study of tether reel system: A laboratory model
[NAL-TR-1176T] p 539 N94-12943

TETHERLINES
An experimental study of tether reel system: A laboratory model
[NAL-TR-1176T] p 539 N94-12943

TETRAGONS
Low-speed wind tunnel tests on four types of joined-wing aircraft models
[NAL-TR-1167] p 501 N94-13340
Low-speed wind tunnel tests on a joined-wing aircraft model with various upper-fin
[NAL-TR-1169] p 501 N94-13341

TEXTILES
Resin transfer molding of textile composites
[NASA-CR-191505] p 554 N94-12833
Flammability of clothing, volume 2
[DSIS-93-00036-VOL-2] p 564 N94-13819
Graphite fiber textile preform/copper matrix composites
[NASA-CR-193797] p 558 N94-14050
Analysis of new composite architectures
[NASA-CR-194524] p 559 N94-14715

TEXTS
Hypertext Compiling Tools (HCT): Developing model based applications with standard hypertext systems
[REPT-92-049] p 750 N94-13822

THAILAND
Detecting land cover changes in Chiang-Mai area in Thailand p 693 N94-14241
Land evaluation for agricultural productivity in North-East Thailand using LANDSAT TM data and geographic information p 693 N94-14242

THEMATIC MAPPERS (LANDSAT)
Dendrometric variables estimation in homogeneous forests using LANDSAT TM data
[INPE-5455-TDI/497] p 684 N94-13331

THEMATIC MAPPING
Dendrometric variables estimation in homogeneous forests using LANDSAT TM data
[INPE-5455-TDI/497] p 684 N94-13331
Net radiation mapping of mountainous terrain using Landsat-5 thematic mapper imagery and digital terrain data
[ISBN-0-315-57755-X] p 685 N94-13475
Satellite imagery and exogenous data integration by neural network in automation land-cover classification
[INPE-5480-PRE/1778] p 686 N94-13729

THEOREM PROVING
EVES: An overview
[DSIS-93-00238] p 752 N94-14088

THEOREMS
No-lost theorem for parity violating nucleon-nucleon scattering experiments
[DE93-012737] p 779 N94-12949
Fast parallel string prefix-matching
[AD-A267758] p 760 N94-13924

THEORETICAL PHYSICS
Quaternions and the heuristic role of mathematical structures in physics
[DE93-622865] p 816 N94-12844
Research in theoretical nuclear physics
[DE93-015096] p 839 N94-14330

THERMAL ANALYSIS
Lifetime prediction of materials exposed to the natural space environment
[NASA-CR-193833] p 561 N94-12830
Ohmic heating of composite candidate graphite-fiber/coating combinations
[NASA-TM-4491] p 554 N94-12871
Boundary formulations for nonlinear design sensitivity analysis p 672 N94-13669
Optimization of the processing parameters of high temperature superconducting glass-ceramics: Center Director's discretionary fund final report
[NASA-TM-108421] p 808 N94-13938
Computer program for analysis of high speed, single row, angular contact, spherical roller bearing, SASHBEAN. Volume 1: User's guide
[NASA-CR-191183] p 663 N94-14445
Computer program for analysis of high speed, single row, angular contact, spherical roller bearing, SASHBEAN. Volume 2: Mathematical formulation and analysis
[NASA-CR-191182] p 664 N94-14446

THERMAL CONDUCTIVITY
Experimental investigation of the effects of blowing ratio parameter on heat transfer to a film-cooled flat plate
[AD-A266599] p 636 N94-13780
Optical and physical properties of the LiSrAlF6:Cr laser crystal
[DE93-014657] p 808 N94-13881
Thermal conductance of pressed metallic contacts augmented with Indium foil or Apiezon-N (tm) grease at liquid helium temperatures
[NASA-TM-108779] p 776 N94-14027
Physical and structural properties of a sputtered zirconia-yttria layer used as a thermal resistance
[ONERA-NT-1992-10] p 810 N94-14193
The accuracy of approximating radiative heat transfer using a temperature dependent thermal conductivity
[DE93-013105] p 638 N94-14318
Anomalous ion transport and feedback control
[DE93-018324] p 803 N94-14874

THERMAL CONTROL COATINGS
Combustion synthesis and engineering of nanoparticles for electronic, structural, and superconductor applications
[DE93-016286] p 809 N94-13981

THERMAL DECOMPOSITION
Low temperature metal-organic chemical vapor deposition growth processes for high efficiency solar cells
[DE92-010562] p 702 N94-13386
THERMAL DEGRADATION
Effect of stabilization on the recycling of polyolefins in blow moulding
[IMI-93RT-42400-1477-G] p 596 N94-13684
THERMAL DIFFUSION
Thermodiffusion in heterogeneous elastic solids and homogenization
[REPT-14/1993] p 578 N94-13468
Implementation of manufacturing techniques for planar, single mode waveguides on lithium niobate
[DSIS-93-00101] p 792 N94-13845
The role of electric field shear stabilization of turbulence in the H-mode to VH-mode transition in D3-D
[DE93-015474] p 802 N94-14583
THERMAL DIFFUSIVITY
Small scale magnetic islands in collisionless plasmas
[PPL-131] p 799 N94-13836
Collisional effects of trapped electrons on the anomalous particle and thermal pinches
[PPL-128] p 800 N94-13853
Anomalous transport due to small scale electromagnetic and large scale electrostatic modes in tokamaks
[PPL-140] p 801 N94-14206
Numerical simulations of turbulent premixed H2/O2/N2 flames with complex chemistry p 567 N94-14765
THERMAL ENERGY
Transition of building energy consumption using multi-input, single-output dynamic model
[VTT-PUBS-116] p 597 N94-14055
THERMAL ENVIRONMENTS
Low altitude plume impingement handbook
[NASA-CR-194193] p 643 N94-14741
THERMAL EXPANSION
An advanced test technique to quantify thermomechanical fatigue damage accumulation in composite materials
[NASA-CR-191147] p 555 N94-13139
JPRS report: Science and technology. Central Eurasia: Materials science
[JPRS-UMS-93-006] p 558 N94-14573
THERMAL INSTABILITY
Study of possible mechanisms of instability due to heat transfer
[INPE-5448-TDI/494] p 628 N94-12966
THERMAL INSULATION
Arc-heating tests of thermal protection system materials for the H-2 rocket fairing
[NAL-TR-1181] p 551 N94-13455
THERMAL MAPPING
High frame rate thermal imager for hypersonic wind tunnel applications
[ONERA-NT-1992-12] p 650 N94-14009
THERMAL NOISE
Using a focal-plane array to estimate antenna pointing errors
[NASA-CR-194502] p 602 N94-13810
THERMAL PROTECTION
High temperature electromagnetic characterization of thermal protection system tile materials
[NASA-CR-189687] p 578 N94-13431
Arc-heating tests of thermal protection system materials for the H-2 rocket fairing
[NAL-TR-1181] p 551 N94-13455
Flammability of clothing, volume 2
[DSIS-93-00036-VOL-2] p 564 N94-13819
Review of test methods for material flammability
[DSIS-93-00480] p 564 N94-13942
THERMAL REACTORS
Review of nuclear thermal propulsion carbide reactor fuel corrosion and exhibit
[DE93-016605] p 585 N94-14535
THERMAL RESISTANCE
Arc-heating tests of thermal protection system materials for the H-2 rocket fairing
[NAL-TR-11ь1] p 551 N94-13455
JPRS report: Science and technology. Central Eurasia: Materials science
[JPRS-UMS-93-004] p 559 N94-14574
THERMAL SHOCK
Cellular mechanism of turnover of the stress induced protein HSP 70
[AD-A265723] p 732 N94-13061
Thermal shock resistance of ceramic matrix composites
[NASA-CR-189136] p 557 N94-13920
THERMAL STABILITY
Structure stability and spectroscopy of metal clusters
[DE93-016142] p 567 N94-12836
Cellular mechanism of turnover of the stress induced protein HSP 70
[AD-A265723] p 732 N94-13061
Thermal design of hybrid circuits: Tools and methodology
[LAAS-92515] p 626 N94-14713
THERMAL STRESSES
Thermal gradient-induced deflection of a thick-walled cylinder with bending residual stresses
[AD-A266347] p 673 N94-13777
Thermal shock resistance of ceramic matrix composites
[NASA-CR-189136] p 557 N94-13920
Computational strategies in the dynamic simulation of constrained flexible MBS p 679 N94-14635
THERMOCHEMICAL PROPERTIES
Closed-chamber analysis of M5 propellant lot RAD-64597
[AD-A266321] p 585 N94-14145
THERMOCHEMISTRY
Conversion of light hydrocarbon gases to metal carbides for production of liquid fuels and chemicals
[DE93-014962] p 583 N94-13002
Performance effects of coal-derived contaminants on the carbonate fuel cell
[DE93-013801] p 703 N94-13693
Thermochemistry of transition metal clusters
[DE93-016201] p 571 N94-13977
THERMOCOUPLES
Widebody cabin water spray optimization tests
[DOT/FAA/CT-TN93/29] p 511 N94-14186
THERMODYNAMIC COUPLING
Homogeneous-hetergeneous combustion: Thermal and chemical coupling
[DE93-016050] p 565 N94-14403
THERMODYNAMIC CYCLES
Combustor technology for future small gas turbine aircraft
[NASA-TM-106312] p 517 N94-13142
THERMODYNAMIC EFFICIENCY
Two temperature modeling and experimental measurements of laser sustained hydrogen plasmas
[AD-A265750] p 796 N94-13039
THERMODYNAMIC PROPERTIES
Theoretical treatment of the bulk and surface properties of fluids containing long, flexible molecules
[DE93-015560] p 575 N94-12861
A time-accurate numerical method for chemically reacting flows at all Mach numbers p 500 N94-13198
Performance effects of coal-derived contaminants on the carbonate fuel cell
[DE93-013801] p 703 N94-13693
Thermochemistry of transition metal clusters
[DE93-016201] p 571 N94-13977
Lawrence Berkeley Laboratory Chemical Sciences Division
[DE93-015260] p 851 N94-14401
Review of nuclear thermal propulsion carbide reactor fuel corrosion and exhibit
[DE93-016605] p 585 N94-14535
Yield properties of tungsten and tungsten heavy alloys
[AD-A266833] p 575 N94-14878
THERMODYNAMICS
Implementation of ADI: Schemes on MIMD parallel computers
[NASA-CR-193720] p 759 N94-13204
Thermodynamic status of static and dynamic contact angles
[ISBN-0-315-73844-8] p 817 N94-13554
Optical and physical properties of the LiSrAlF6:Cr laser crystal
[DE93-014657] p 808 N94-13881
Selective excitation, relaxation, and energy channeling in molecular systems
[DE93-018819] p 785 N94-14420
Statistical mechanical theory of liquid entropy
[DE93-016524] p 817 N94-14593
Analysis, approximation, and computation of a coupled solid/fluid temperature control problem
[NASA-TM-106351] p 771 N94-14731
Thermomechanical and isothermal fatigue behavior of a (90)sub 8 titanium matrix composite
[NASA-CR-191196] p 560 N94-14822
On the statistical theory of the even-even nucleons levels' density
[DE93-623990] p 788 N94-14875
THERMOELASTICITY
Thermoelastic response of metal matrix composites with large-diameter fibers subjected to thermal gradients
[NASA-TM-106344] p 560 N94-14823
THERMOGRAPHY
Experimental measurement of local heat transfer coefficients over discrete roughened plates using infrared thermography p 635 N94-13652
High frame rate thermal imager for hypersonic wind tunnel applications
[ONERA-NT-1992-12] p 650 N94-14009
THERMONUCLEAR REACTIONS
Nuclear fusion of protons with ions of boron
[DE93-014284] p 781 N94-13219
Charged-particle evaluation methodology at Lawrence Livermore National Laboratory
[DE93-013429] p 781 N94-13251
The status of cold fusion
[DE93-012731] p 802 N94-14567
THERMOPHYSICAL PROPERTIES
Multiphase equation of state for iron
[DE93-013956] p 568 N94-12977
THERMOPLASTICITY
Development of time-dependent orthotropic constitutive law of a thermoplastic composite material
p 556 N94-13595
THERMOSPHERE
Atomic hydrogen and nitrogen distributions from atmosphere explorer measurements
[NASA-CR-194336] p 714 N94-13825
THICK FILMS
Deposition of crystalline boron thick layers from gas phase
[DE93-620499] p 576 N94-12867
Superconductivity devices: Commercial use of space
[NASA-CR-194163] p 625 N94-14324
Solution chemistry optimization of sol-gel processed PZT thin films
[DE93-013776] p 814 N94-14695
THICK PLATES
Nonlinear vibrations of thick composite plates: Higher-order shear deformation plate theory
p 556 N94-13558
Role of microstructure on fatigue durability of aluminum aircraft alloys
[AD-A266350] p 571 N94-13697
THICKNESS
The use of polarised neutron reflection for unique density profile determination in thin films
[PB93-187136] p 579 N94-13783
BALLIST: A computer program to empirically predict the bumper thickness required to prevent perforation of the Space Station by orbital debris
[NASA-CR-193825] p 543 N94-14120
THIN FILMS
Amorphous sol-gel insulating films
[DE93-012859] p 576 N94-12866
Photovoltaic Subcontract Program
[DE93-000092] p 700 N94-12868
Recovery of materials impacted at high velocity
[DE93-014150] p 576 N94-12885
Processing, fabrication and demonstration of HTS integrated microwave circuits
[AD-A265789] p 619 N94-12892
Canted magnetic moments at the Gd(0001) surface
[DE93-014327] p 805 N94-13102
Electrocatalysis issues in polymer electrolyte fuel cells
[DE93-014450] p 702 N94-13402
Poling of thin polymer films in electro optic applications
[AD-A266562] p 579 N94-13584
Studies of momentum and energy transfer across wavy gas-liquid interfaces
[AD-A266432] p 635 N94-13699
High-resolution Z-contrast imaging and hole concentration mapping of YBCO thin films
[DE93-015803] p 808 N94-13930
Boundary stability under nonequilibrium conditions
[DE93-016259] p 809 N94-13980
Measurement of penetration depth lambda(T) in YBa2Cu3O(7-delta) thin film
[DE93-014587] p 810 N94-14122
Spin polarized photoemission studies of interfacial and thin film magnetism
[DE93-014326] p 580 N94-14142
A quartz crystal microbalance study of lithium insertion and removal into evaporated films MO(y) (M = Mo, Fe, and V)
[DSIS-93-00649] p 810 N94-14203
Prism-film coupling in anisotropic planar waveguides of epitaxial (101) rutile thin films
[DE93-012912] p 811 N94-14304
Formation of textured YBCO films by laser ablation
[DE93-013131] p 581 N94-14319
Microstructural mechanisms that enhance electromigration resistance in Al-Cu thin films
[DE93-013770] p 812 N94-14345
Effects of depositon rate on Bi2Sr2CaCu2O(8+x) and Bi2Sr(1.6)La(0.4)CuO(6+x) epitaxial thin film growth by pulsed-laser ablation
[DE93-015797] p 812 N94-14362
Ion assisted sputter deposition of Mo-Si multilayers
[DE93-013830] p 583 N94-14693
Solution chemistry optimization of sol-gel processed PZT thin films
[DE93-013776] p 814 N94-14695

Molecular simulator: A basic tool for submicron MOS processes development
[LAAS-92484] p 814 N94-14697
Direct submillimeter absorptivity measurements on epitaxial Ba(1-x)K(x)BiO3 films at 2K
[DE93-013904] p 815 N94-14699
A study of thin liquid sheet flows
[NASA-TM-106323] p 642 N94-14732

THIN PLATES
Experimental technique to simulate orbital-debris impact on space shields at impact velocities over 10 km/s
[DE93-011619] p 539 N94-12909
Role of microstructure on fatigue durability of aluminum aircraft alloys
[AD-A266350] p 571 N94-13697

THIN WALLED SHELLS
Buckling analysis of laminated thin shells in a hot environment
[NASA-TM-106302] p 683 N94-14776

THIN WALLS
Study of possible mechanisms of instability due to heat transfer
[INPE-5448-TDI/494] p 628 N94-12966

THOMSON SCATTERING
Bridging the gap between the Rayleigh and Thomson limits for various convex bodies
[DSIS-93-00613] p 607 N94-14204

THORIUM COMPOUNDS
Muon spin relaxation studies of heavy fermion superconductors
[DE93-014576] p 815 N94-14773

THREE DIMENSIONAL BOUNDARY LAYER
Numerical study of the effects of icing on viscous flow over wings
[NASA-CR-193306] p 500 N94-13180
High speed transition prediction
[NASA-CR-194125] p 502 N94-13422
A three-dimensional supersonic turbulent boundary layer generated by an isentropic compression
p 503 N94-13556

THREE DIMENSIONAL FLOW
Three-Dimensional Boundary-Layer program (BL3D) for swept subsonic or supersonic wings with application to laminar flow control
[NASA-CR-4531] p 629 N94-13073
The three-dimensional flow past a rapidly rotating circular cylinder
[NASA-CR-191512] p 630 N94-13075
Three-dimensional structure of straight and curved plane wakes
[NASA-CR-194420] p 501 N94-13266
Numerical simulation of steady three-dimensional flows in axial turbomachinery bladerows p 634 N94-13630
A control volume finite element method for three-dimensional, incompressible, viscous fluid flow
[ISBN-0-315-72019-0] p 635 N94-13683
Evolution of disturbances in stagnation point flow
[NASA-CR-191516] p 636 N94-13724
Images constructed from computed flow fields
[NASA-CR-194397] p 650 N94-13814
Numerical investigations in three-dimensional internal flows
[NASA-CR-194143] p 637 N94-13827
Multigrid solution of internal flows using unstructured solution adaptive meshes
[NASA-CR-194233] p 638 N94-14356
Least-squares finite element solutions for three-dimensional backward-facing step flow
[NASA-TM-106353] p 770 N94-14407
An experimental study of a turbulent boundary layer in the trailing edge region of a curculation-control airfoil
[NASA-CR-194522] p 508 N94-14541
Navier-Stokes simulation of transonic vortex flow over a delta wing p 640 N94-14606
A finite volume method for computation of viscous flow in complex configurations p 640 N94-14607
Behavior of streamwise rib vortices in a three-dimensional mixing layer p 644 N94-14754
A new Lagrangian method for three-dimensional steady supersonic flows
[NASA-TM-106068] p 510 N94-14847
The development of a scalable parallel 3-D CFD algorithm for turbomachinery
[NASA-CR-193604] p 664 N94-14848

THREE DIMENSIONAL MODELS
The 3-D massively parallel impact simulations using PCTH
[DE93-011593] p 670 N94-12908
Numerical simulation of hypersonic flow for the design of the H-2 orbiting plane (HOPE), part 3
[NAL-TR-1168-PT-3] p 499 N94-12948
View generated database
[NASA-CR-191397] p 822 N94-13116
Imaging microscopy with x ray lasers at Lawrence Livermore National Laboratory
[DE93-013419] p 655 N94-13258
Micromechanical damage theories for brittle solids with interacting microcracks
[AD-A266348] p 673 N94-13778
Eye-gaze and intent: Application in 3D interface control
[DE93-015210] p 738 N94-14335
Three-dimensional modeling of diesel engine intake flow, combustion and emissions-2
[NASA-CR-191189] p 519 N94-14448
Liquid and gas evanescent wave spectroscopy via tunable lasers and silver halide fibers
[ITN-93-85226] p 565 N94-14465
Statics and kinetics of phase transformations in bcc Fe-Cr
[DE93-013839] p 574 N94-14793
Nonlinear wave forces on large ocean structures
[AD-A266820] p 683 N94-14902

THRESHOLD CURRENTS
AlGaAs diode laser blue shift resulting from fast neutron irradiation
[AD-A266642] p 659 N94-14681

THRESHOLDS (PERCEPTION)
Underwater hearing: A review
[ISVR-TR-212] p 777 N94-14130

THROTTLING
Electric propulsion system technology
[NASA-CR-194100] p 549 N94-13055

THRUST CONTROL
Preliminary flight results of a fly-by-throttle emergency flight control system on an F-15 airplane
[NASA-TM-4503] p 520 N94-13254
Design criteria for integrated flight/propulsion control systems for STOVL fighter aircraft p 521 N94-13297
A piloted simulation investigation of the normal load factor and longitudinal thrust required for air-to-air acquisition and tracking p 522 N94-13301
A four-axis hand controller for helicopter flight control p 522 N94-13305

THRUST VECTOR CONTROL
Evaluation of dual flow thrust vector nozzles with exhaust stream impingement
[NASA-CR-193392] p 630 N94-13078
Advanced electric motor technology flux mapping
[NASA-CR-193824] p 621 N94-13186
Electrical Actuation Technology Bridging
[NASA-CP-3213] p 551 N94-13417
Design and evaluation of single and dual flow thrust vector nozzles with post exit vanes
[NASA-CR-193393] p 638 N94-14086
Design and application of electromechanical actuators for deep space missions
[NASA-CR-194145] p 663 N94-14134

THUNDERSTORMS
The application of VAS satellite imagery to thunderstorm forecasting at Cape Canaveral
[NASA-CR-193563] p 718 N94-12839

THYROID GLAND
Calcitonin control of calcium metabolism during weightlessness
[NASA-CR-193622] p 731 N94-12960
Thyroid alterations in porcine after prolonged exposure to cold or heat
[AD-A266840] p 733 N94-14879

TIDAL WAVES
Artificial oil pollution detection and wave observation in the sea adjacent to Japan by ERS-1 SAR
p 688 N94-14212

TIDES
Cold dark matter halos p 838 N94-13649

TILES
High temperature electromagnetic characterization of thermal protection system tile materials
[NASA-CR-189687] p 578 N94-13431

TILT ROTOR AIRCRAFT
Piloting considerations for terminal area operations of civil tiltwing and tiltrotor aircraft p 525 N94-13320
Evaluation of two cockpit display concepts for civil tiltrotor instrument operations on steep approaches
p 517 N94-13323

TILT WING AIRCRAFT
Piloting considerations for terminal area operations of civil tiltwing and tiltrotor aircraft p 525 N94-13320

TIMBER IDENTIFICATION
Mangrove afforestation monitoring using remote sensing p 695 N94-14260

TIMBER INVENTORY
Dendrometric variables estimation in homogeneous forests using LANDSAT TM data
[INPE-5455-TDI/497] p 684 N94-13331

TIME DEPENDENCE
Three dimensional time-dependent hydrodynamic and propagation modeling of x ray laser emission
[DE93-012575] p 654 N94-12962
Development of time-dependent orthotropic constitutive law of a thermoplastic composite material
p 556 N94-13595
Deconvolution for positive signals
[DE93-013044] p 773 N94-14314
Selective excitation, relaxation, and energy channeling in molecular systems
[DE93-018819] p 785 N94-14420
An adaptive projection method for the incompressible Euler equations
[DE93-016428] p 639 N94-14434
A conduction model for the vacuum arc remelting process
[NPL-DMM(A)-98] p 639 N94-14464
Multiplicative noise: Applications in cosmology and field theory
[DE93-016624] p 840 N94-14536
Time resolved measurement of electron temperatures of exploding foil x ray laser plasmas
[DE93-017161] p 803 N94-14894

TIME DIVISION MULTIPLE ACCESS
Destination-directed, packet-switched architecture for a geostationary communications satellite network
[NASA-TP-3379] p 538 N94-13111
User needs for propagation data p 613 N94-14657

TIME DIVISION MULTIPLEXING
Technical support for digital systems technology development. Task order 1: ISP contention analysis and control
[NASA-CR-190758] p 537 N94-12809
Destination-directed, packet-switched architecture for a geostationary communications satellite network
[NASA-TP-3379] p 538 N94-13111

TIME LAG
Investigation of the effects of bandwidth and time delay on helicopter roll-axis handling qualities
p 522 N94-13300
Handling qualities effects of display latency
p 517 N94-13316
Primary display latency criteria based on flying qualities and performance data p 525 N94-13318
Bounds on time delay estimation given unknown signal spectral parameters
[ITN-93-85194] p 601 N94-13566

TIME MEASUREMENT
Activities report of the National Electrotechnical Institute Galileo Ferraris
[ETN-93-94224] p 627 N94-14812
Time resolved measurement of electron temperatures of exploding foil x ray laser plasmas
[DE93-017161] p 803 N94-14894

TIME OF FLIGHT SPECTROMETERS
Construction and test of a facility for photon-stimulated field description using excimer laser and time of flight
[ETN-93-94386] p 657 N94-13996

TIME SERIES ANALYSIS
Adaptive Transfer Function Networks
[DE93-014344] p 745 N94-13151
Estimation of critical values and vibration characteristics on supersonic delta wings. Part 2: Locally-stationary time series analysis of nonstationary random responses
[NAL-TR-1179] p 502 N94-13345
Time series photometry of faint cataclysmic variables with a CCD p 831 N94-13646
Maximum entropy spectral analysis of the geological time series of the oxygen isotope record from deep-sea cores
[INPE-5465-PRE/1773] p 725 N94-13728

TIN ALLOYS
Thermosolutal convection and macrosegregation in dendritic alloys
[NASA-CR-194039] p 567 N94-12825

TIN TELLURIDES
Growth of PbSnTe single crystal by traveling-zone method in low gravity (M-2) p 586 N94-13734

TISSUES (BIOLOGY)
Monoclonal antibodies directed against surface molecules of multicell spheroids
[NASA-CR-193560] p 727 N94-12795

TITAN 4 LAUNCH VEHICLE
Real time radiography of Titan 4 booster
[DE93-012450] p 548 N94-12911

TITANATES
Small polaron conduction in Y2Ti2O7
[ITN-93-85221] p 814 N94-14557

TITANIUM
An advanced test technique to quantify thermomechanical fatigue damage accumulation in composite materials
[NASA-CR-191147] p 555 N94-13139
The structure and mechanical properties of Ru-Cu and Ru-Ti nanolayer composites
[DE93-014453] p 558 N94-14469
Thermomechanical and isothermal fatigue behavior of a (90)sub 8 titanium matrix composite
[NASA-CR-191196] p 560 N94-14822

TITANIUM ALLOYS
Electronic structure and phase stability properties in ternary substitutional alloys
[DE93-013848] p 569 N94-13137
NDE of titanium alloy MMC rings for gas turbine engines
[NASA-TM-106188] p 555 N94-13138
Excimer laser surface processing of titanium
[DE93-012633] p 570 N94-13512
The microstructural response of near gamma-TiAl+W to heat treatment
[DSIS-93-00237] p 571 N94-13840
TITANIUM COMPOUNDS
Inelastic deformation mechanisms in SCS-6/Ti 15-3 MMC lamina under compression
[NASA-CR-191170] p 555 N94-13378
TITANIUM OXIDES
Photocatalysis for the treatment of waste water: Applications involving the removal of metals
[DE93-011669] p 561 N94-12841
TOKAMAK DEVICES
A 3D gyrokinetic particle-in-cell simulation of fusion plasma microturbulence on parallel computers
[DE93-012503] p 794 N94-12846
Test apparatus for ITER blanket cooling water distribution design
[DE93-753157] p 795 N94-12944
Dimensionally similar discharges with central RF heating on the D3-D tokamak
[DE93-012776] p 795 N94-12953
Growth curve analysis for plasma profiles using smoothing splines
[DE93-015741] p 795 N94-12984
Equilibrium reconstruction of the q-profile in tokamaks from motional Stark effect data
[DE93-015815] p 796 N94-13046
Effect on antenna structure of high power RF during plasma operation
[DE93-013278] p 797 N94-13144
Interferometric investigation methods of plasma spatial characteristics on stellarators and tokamaks in submillimeter region
[DE93-621606] p 798 N94-13507
Activities of the University of Saskatchewan, Plasma Physics Laboratory
[CTN-93-60831] p 798 N94-13518
Nonlinear evolution of tearing modes in inhomogeneous plasmas
[PPL-133] p 798 N94-13564
Folded waveguide designs for tokamaks
[DE93-013274] p 798 N94-13577
Studies of non-inductive current drive in the CDX-U tokamak p 799 N94-13680
Scattering of reflectometer signals from rippled surfaces
[PPL-138] p 602 N94-13802
Experiments on the current rampdown phase in the STOR-M tokamak for AC operation
[PPL-132] p 799 N94-13835
Plasma auto-biasing during Ohmic H-mode in the STOR-M tokamak
[PPL-136] p 799 N94-13849
Semi-local kinetic analysis of the toroidal ion temperature gradient mode
[PPL-130] p 800 N94-13851
Anomalous transport due to the ion acoustic instability in tokamaks
[PPL-129] p 800 N94-13852
Dependence of beta(tau) on plasma shape in D3-D
[DE93-015473] p 800 N94-13900
Stability and confinement properties of small-aspect-ratio tokamak
[INPE-5463-PRE/1771] p 801 N94-14024
Anomalous transport due to small scale electromagnetic and large scale electrostatic modes in tokamaks
[PPL-140] p 801 N94-14206
Electrical characterization of the JET A(sub 2) antenna: Comparison of model with measurements Wade, T.
[DE93-012964] p 607 N94-14291
Direct electron heating and current drive with fast waves in D3-D
[DE93-013028] p 801 N94-14293
Variation of divertor plasma parameters with divertor depth for H-mode discharges in D3-D
[DE93-015475] p 801 N94-14347
D3-D research operations
[DE93-016729] p 802 N94-14519
Measurements of edge fluctuations by phase contrast imaging on DIII-D
[DE93-014018] p 802 N94-14579
Design of the ion cyclotron system for TPX
[DE93-012961] p 803 N94-14770
Anomalous ion transport and feedback control
[DE93-018324] p 803 N94-14874
TOMOGRAPHY
Mathematical algorithms for multidimensional inverse scattering problems in inhomogeneous medium
[AD-A266440] p 749 N94-13702
Current distribution tomography for determination of internal current density distributions
[DE93-015463] p 604 N94-13899
Electronic schematics for the Donner 600 Crystal Tomograph
[DE93-015277] p 625 N94-14336
TOPOGRAPHY
Venus gravity
[NASA-CR-194077] p 841 N94-12823
Cyclogenesis and cyclone over South America
[INPE-5400-TDI/479] p 719 N94-13175
Error analysis of real time and post processed or bit determination of GFO using GPS tracking
[NASA-CR-193646] p 512 N94-13238
The American Geophysical Union Chapman Conference on Tectonics and Topography
[NASA-CR-193454] p 713 N94-13335
TOPOLOGY
Evolution of the interplanetary magnetic field
[DE93-012631] p 836 N94-13262
Heat flows and harmonic maps with a free boundary
[DE93-622856] p 632 N94-13509
Nonrecursive formulations of multibody dynamics and concurrent multiprocessing p 679 N94-14632
TOROIDAL PLASMAS
Dimensionally similar discharges with central RF heating on the D3-D tokamak
[DE93-012776] p 795 N94-12953
Nonlinear evolution of tearing modes in inhomogeneous plasmas
[PPL-133] p 798 N94-13564
The propagation characteristics and instability properties of low-frequency electromagnetic waves in the Io plasma torus p 601 N94-13650
Studies of non-inductive current drive in the CDX-U tokamak p 799 N94-13680
Plasma auto-biasing during Ohmic H-mode in the STOR-M tokamak
[PPL-136] p 799 N94-13849
On MHD mode equations in toroidal plasmas
[PPL-139] p 800 N94-13877
Dependence of beta(tau) on plasma shape in D3-D
[DE93-015473] p 800 N94-13900
D3-D research operations
[DE93-016729] p 802 N94-14519
TOROIDS
Mutual inductance between partially wound tori and a bifilar conductor
[ETN-93-94388] p 624 N94-13998
TORQUE
On the motion through a viscous fluid of a spherical particle touching a plane wall: Slip boundary conditions
[DE93-012540] p 628 N94-12961
Design and control of a macro-micro robot for precise force applications p 682 N94-14651
TORSION
Measuring methods for CFRP laminates' bending and torsion rigidities characteristics p 529 N94-13272
TOTAL OZONE MAPPING SPECTROMETER
Effects of typhoon on TOMS data p 693 N94-14243
TOTAL QUALITY MANAGEMENT
Lecture notes on software process improvement
[AD-A265200] p 744 N94-13049
Ninth Annual NASA/Contractors Conference on Quality and Productivity. World Class Excellence: The Journey Continues. Keynote presentations
[NASA-CR-194513] p 665 N94-13148
Ninth Annual NASA/Contractors Conference on Quality and Productivity. World Class Excellence: The Journey Continues. Conference presentations
[NASA-CR-194514] p 665 N94-13153
Measuring quality progress p 666 N94-13154
Defining the performance gap: Conducting a self-assessment p 666 N94-13155
What's the bottom line payback for TQM? p 666 N94-13156
Partnership with the customer p 666 N94-13157
Strategic planning as a focus for continuous improvement. A case study p 666 N94-13158
The power of cross-functional teams in driving total quality p 666 N94-13159
Spacecraft COst REduction Team (SCORE): TQM/CI on a massive scale p 667 N94-13160
Object-oriented productivity metrics p 667 N94-13161
Kennedy Space Center's NASA/Contractor Team-Centered Total Quality Management Seminar: Results, methods, and lessons learned p 667 N94-13162
Here's the beef: A case study in organizational transformation p 667 N94-13163
Building a quality culture in the Office of Space Flight: Approach, lessons learned and implications for the future p 667 N94-13164
NASA Johnson Space Center: Total quality partnership p 668 N94-13165
Teamwork for Oversight of Processes and Systems (TOPS). Implementation guide for TOPS version 2.0, 10 August 1992 p 668 N94-13167
NASA/contractor partnership on the second TDRSS ground terminal program: Breaking barriers p 668 N94-13168
Government/contractor partnerships for continuous improvement. A Goddard Space Flight Center example p 669 N94-13169
Pollution prevention through total quality
[DE93-013814] p 707 N94-13390
George M. Low Trophy: NASA's quality and excellence award. 1992 recipients: Honeywell Clearwater, IBM Houston
[NASA-TM-109265] p 669 N94-13396
The Eighth Annual NASA/Contractors Conference and 1991 National Symposium on Quality and Productivity: Extending the boundaries of total quality management
[NASA-TM-109276] p 669 N94-14321
TOUGHNESS
Processing and testing of high toughness silicon nitride ceramics
[NASA-CR-191190] p 582 N94-14543
An investigation of the role of second phase particles in the design of ultra high strength steels of improved toughness
[AD-A266774] p 573 N94-14786
TOWNSEND DISCHARGE
High counting rate resistive-plate chamber
[DE93-014928] p 651 N94-14452
TOXIC HAZARDS
Estimation of the concentration versus the time profile of zinc chloride particles in smoke clouds generated by the Raufoss A/S instantaneous smoke RA-90 and DM-45 HC smoke generator
[FFI-93/6001] p 708 N94-13821
Toxic Substances Control Act (TSCA) chemical substances inventory: Revised inventory synonym and preferred name file, Jan. 1993 documentation
[PB93-155166] p 710 N94-14508
TOXICITY
Biomass production chamber air analysis of wheat study (BWT931)
[NASA-CR-194092] p 737 N94-13712
Synthetic lubricants and high-performance functional fluids: Phosphazenes
[ARL-TR-45] p 580 N94-14126
Toxic Substances Control Act (TSCA) chemical substances inventory: Revised inventory synonym and preferred name file, Jan. 1993 documentation
[PB93-155166] p 710 N94-14508
TOXICITY AND SAFETY HAZARD
Toxic Substances Control Act (TSCA) chemical substances inventory: Revised inventory synonym and preferred name file, Jan. 1993 documentation
[PB93-155166] p 710 N94-14508
TRACE CONTAMINANTS
Project AIRSTREAM: Trace gas
[DE93-008849] p 706 N94-12904
Performance effects of coal-derived contaminants on the carbonate fuel cell
[DE93-013801] p 703 N94-13693
Destruction of problematic airborne contaminants by hydrogen reduction using a Catalytically Active, Regenerable Sorbent (CARS)
[NASA-CR-194354] p 709 N94-14103
Importance of sprays for long range transport of harmful substances in the troposphere
[MITT-81] p 711 N94-14723
TRACE ELEMENTS
Project AIRSTREAM: Trace gas
[DE93-008849] p 706 N94-12904
Determination of trace elements in triglycine sulfate solutions
[NASA-CR-193481] p 562 N94-13048
Modeling of the partitioning of reactive odd nitrogen in the lower stratosphere using aircraft measurements of NOy, NO, and other trace species
[NASA-CR-194305] p 714 N94-13707
Measurement of HO2 and other trace gases in the stratosphere using a high resolution far-infrared spectrometer at 28 km
[NASA-CR-194175] p 714 N94-13816
TRACKING RADAR
Cancellation of multipath for monopulse radars
[ITN-93-85191] p 600 N94-13538
TRACKING STATIONS
Use of global positioning system measurements to determine geocentric coordinates and variations in Earth orientation p 514 N94-14372

TRAILING EDGES
An experimental study of a turbulent boundary layer in the trailing edge region of a curculation-control airfoil
[NASA-CR-194522] p 508 N94-14541
TRAJECTORIES
Parachute system design, analysis, and simulation tool
[DE93-013755] p 501 N94-13260
Inverse dynamics: Simultaneous trajectory tracking and vibration reduction with distributed actuators
p 678 N94-14624
TRAJECTORY MEASUREMENT
Photogrammetric methods for trajectory measurements
[NLR-TP-91166-U] p 650 N94-13527
TRAJECTORY OPTIMIZATION
Trajectory optimization for the national aerospace plane
[NASA-CR-194146] p 516 N94-14104
Optimizing interplanetary trajectories with deep space maneuvers
[NASA-CR-4546] p 532 N94-14851
TRAJECTORY PLANNING
Implementation and experimentation with a motion planning system
[ITN-93-85213] p 755 N94-14505
TRANSCENDENTAL FUNCTIONS
Applications of computer algebra to distributed parameter systems p 677 N94-14623
TRANSDUCERS
Liquid metal drop ejection
[NASA-CR-193718] p 572 N94-14133
A description of the computer program CALDK38 which controls instrumentation set-up and data acquisition during deadweight calibration using an HBM DK 38 S6 digital measuring unit
[LTR-ST-1935] p 754 N94-14496
TRANSFER FUNCTIONS
Adaptive Transfer Function Networks
[DE93-014344] p 745 N94-13151
Exploiting structure: Introduction and motivation
[NASA-CR-194199] p 750 N94-13828
Water-vapour, total water and rainrate from passive microwave satellite data over ocean
[DLR-FB-92-37] p 723 N94-14189
Selective excitation, relaxation, and energy channeling in molecular systems
[DE93-018819] p 785 N94-14420
TRANSFER ORBITS
Two temperature modeling and experimental measurements of laser sustained hydrogen plasmas
[AD-A265750] p 796 N94-13039
TRANSFORMATIONS (MATHEMATICS)
Analytical framework for modeling scale-related variabilities in remote sensing p 685 N94-13592
Transform coding for space applications
[NASA-TM-106362] p 612 N94-14542
TRANSIENT OSCILLATIONS
The soft x ray transient Cen X-4 in quiescence
[NASA-CR-194033] p 833 N94-14406
TRANSIENT PRESSURES
NASA metrology and calibration, 1993
[NASA-TM-109280] p 597 N94-14410
TRANSIENT RESPONSE
The transient behavior of a boundary layer exposed to uniform suction
[ITN-93-85205] p 630 N94-13197
Some aspects of sheet forming simulation using explicit finite element techniques
[DE93-012479] p 663 N94-13975
TRANSISTOR AMPLIFIERS
A cryogenic seven-element HEMT front end for DSS 13 p 608 N94-14375
TRANSISTORS
Design and optimization of high voltage lateral DMOS devices using RESURF technology
[LAAS-92511] p 626 N94-14711
TRANSITION FLIGHT
Design criteria for integrated flight/propulsion control systems for STOVL fighter aircraft p 521 N94-13297
TRANSITION FLOW
Large-eddy simulation of laminar-turbulent breakdown at high speeds with dynamic subgrid-scale modeling
[NASA-CR-4533] p 629 N94-13064
Transition prediction and control in subsonic flow over a hump
[NASA-CR-4543] p 629 N94-13066
High speed transition prediction
[NASA-CR-194125] p 502 N94-13422
Effects of surface thermal forcing on stratified flow past an isolated obstacle p 633 N94-13553
TRANSITION METALS
Determination of trace elements in triglycine sulfate solutions
[NASA-CR-193481] p 562 N94-13048
Thermochemistry of transition metal clusters
[DE93-016201] p 571 N94-13977
Reactor studies of metal ions associated with chromatographic silica
[AD-A266675] p 573 N94-14779
TRANSITION POINTS
Transition prediction and control in subsonic flow over a hump
[NASA-CR-4543] p 629 N94-13066
TRANSITION TEMPERATURE
Room temperature degradation of YBa2Cu3O(7-x) superconductors in varying relative humidity environments
[NASA-TP-3368] p 813 N94-14409
Muon spin relaxation studies of heavy fermion superconductors
[DE93-014576] p 815 N94-14773
TRANSLATING
On the motion through a viscous fluid of a spherical particle touching a plane wall: Slip boundary conditions
[DE93-012540] p 628 N94-12961
TRANSLATIONAL MOTION
Implementation and experimentation with a motion planning system
[ITN-93-85213] p 755 N94-14505
TRANSMISSION
Laser CO2 beam transmission through hollow metallic waveguide coated by a thin internal dielectric layer
[ITN-93-85201] p 656 N94-13571
TRANSMISSION ELECTRON MICROSCOPY
Flux-pinning related defect structures in melt-processed YBa2Cu3O(7-x)
[DE93-012759] p 804 N94-12818
Changes in electrical device characteristics during the formation of dislocations in situ in the TEM
[DE93-013910] p 808 N94-13694
The effect of crystal tilt on high resolution micrographs of small metal particles
[DE93-013915] p 574 N94-14795
TRANSMISSION LINES
Locally non-uniform finite-difference time domain with application to stealth, crosstalk, and narrow apertures
[DE93-013958] p 601 N94-13696
The developments of satellite communications of China p 618 N94-14282
The current situation, trends, international cooperation of space communication technological development in the Republic of Korea p 699 N94-14283
Joint experiments using ETS-5 p 618 N94-14284
Space communications technology research in CRL
p 618 N94-14285
NTT's activities in satellite communications technology development p 618 N94-14286
Future outlook on international satellite communications in Asia Pacific region p 618 N94-14287
Utilization of boundary element method for extraction of frequency dependent conductivity parameters of lossy intra-chip transmission lines
[ETN-93-94385] p 771 N94-14807
TRANSMISSION LOSS
Infrared transmission and path radiance through dust and fog
[AD-A265825] p 791 N94-12979
Measurement of wave propagation for VHF/UHF and a comparison between measured and predicted values
[FFI/RAPPORT-92/7024] p 605 N94-13968
TRANSMISSIONS (MACHINE ELEMENTS)
Roller-gear drives for robotic manipulators design, fabrication and test
[NASA-CR-194248] p 660 N94-12802
TRANSMITTER RECEIVERS
Development of an on-board aircraft optical fiber data bus system
[NAL-TR-1163] p 514 N94-13338
TRANSMITTERS
Development of UHF spark-switched L-C Oscillators
[DE93-015019] p 623 N94-13892
TRANSONIC COMPRESSORS
The 3D pneumatic and 2D dynamic probes: Their development and subsequent use in a transonic fan
[RAE-TM-AERO/PROP-22] p 653 N94-14827
TRANSONIC FLIGHT
The problem of the sonic boom for future high-speed transport aircraft
[ESA-TT-1286] p 776 N94-13692
TRANSONIC FLOW
Fundamental study of shock wave/turbulent boundary layer interactions with passive control in transonic flows
[ESA-TT-1278] p 630 N94-13117
An experimental investigation of the redistribution of gas stream total temperature in a high turning angle transonic planar cascade
[ISBN-0-315-60791-2] p 502 N94-13369
Analysis of the Harrier forebody/inlet design using computational techniques
[NASA-CR-193616] p 503 N94-13463
Clebsch variable model for unsteady, transonic flow; application to 2D airfoils
[NLR-TP-91387-U] p 503 N94-13530
A robust quasi-simultaneous interaction method for a full potential flow with a boundary layer with application to wing/body configurations
[NLR-TP-91397-U] p 503 N94-13531
Development of full-potential codes in the decade 1983-1993 p 639 N94-14600
Navier-Stokes simulation of transonic vortex flow over a delta wing p 640 N94-14606
Development of a general purpose multigrid accelerated Navier-Stokes solver p 641 N94-14613
Intra-blade quantitative transonic flow measurements at the DRA Pyestock Isentropic Light Piston Facility using PIV (Particle Image Velocimetry)
[RAE-TM-AERO/PROP-21] p 509 N94-14706
TRANSONIC SPEED
Results of wind tunnel tests of an ASRM configured 0.03 scale Space Shuttle integrated vehicle model (47-OTS) in the AEDC 16-foot Transonic wind tunnel (IA613A), volume 1
[NASA-CR-185696] p 534 N94-13191
TRANSPARENCE
Optimization of transparent and reflecting electrodes for amorphous silicon solar cells
[DE93-010009] p 704 N94-14110
TRANSPONDERS
Preliminary design and implementation of the baseline digital baseband architecture for advanced deep space transponders p 611 N94-14393
TRANSPORT AIRCRAFT
Evaluation of two cockpit display concepts for civil tiltrotor instrument operations on steep approaches
p 517 N94-13323
TRANSPORT PROPERTIES
Modeling ignition chemistry
[DE93-012340] p 561 N94-12910
Equilibrium reconstruction of the q-profile in tokamaks from motional Stark effect data
[DE93-015815] p 796 N94-13046
Research on chemical vapor deposition processes for advanced ceramic coatings
[NASA-CR-193613] p 577 N94-13089
Transport properties of disordered porous media from the microstructure
[DE93-016065] p 806 N94-13152
A time-accurate numerical method for chemically reacting flows at all Mach numbers p 500 N94-13198
Measurements on two-dimensional arrays of mesoscopic Josephson junctions
[AD-A265129] p 807 N94-13359
On energy transport equations for turbulent magnetized plasma
[PPL-135] p 800 N94-13850
Direct determination of alpha particle transport coefficients
[DE93-013488] p 787 N94-14691
TRANSPORT THEORY
Study of multicomponent diffusion and transport phenomena
[DE93-015095] p 804 N94-13005
Variance reduction unique to coupled electron/photon Monte Carlo transport
[DE93-014999] p 782 N94-13409
Dynamical model for the distribution of geomagnetically trapped anomalous-component ions
[ATR-91(9558)-6] p 784 N94-13936
A transport equation for eddy viscosity
p 646 N94-14762
Toward a quasi-linear closure for compressible turbulence
[DE93-017185] p 647 N94-14895
TRANSPORTATION
Activities of Bombardier, Inc.
[ISBN-2-921393-11-5] p 499 N94-13520
A verification of the Euroguidance: A guidance forecast for transportation and tourism
[KNMI-TR-145] p 722 N94-13993
TRANSPORTATION ENERGY
Low pressure storage of natural gas on activated carbon
[DE93-014053] p 660 N94-12851
TRAPPED PARTICLES
Energetic neutral atoms: Imaging the magnetospheric ring current
[NASA-CR-194339] p 715 N94-13826
Collisional effects of trapped electrons on the anomalous particle and thermal pinches
[PPL-128] p 800 N94-13853
Studies on equatorial shock formation during plasmaspheric refilling
[NASA-CR-194392] p 715 N94-13954
TRAPPING
EBIT Trapping Program
[DE93-014422] p 788 N94-13208

TRAVELING WAVE TUBES
A millimeter-wave tunneladder TWT
[NASA-CR-182183] p 620 N94-13106
Low-current traveling wave tube for use in the microwave power module
[NASA-TP-3344] p 620 N94-13110
TREES (MATHEMATICS)
Tree reconstruction from partial orders
[DE93-009841] p 743 N94-12991
TRELLIS CODING
Trellis coding with Continuous Phase Modulation (CPM) for satellite-based land-mobile communications
[NASA-CR-191325] p 604 N94-13909
TRIANGULATION
Approaches to high aspect ratio triangulations
[NASA-TM-107684] p 739 N94-12886
Parallel implementation of an algorithm for Delaunay triangulation
[NASA-TM-103951] p 740 N94-12973
TRIBOLOGY
A vacuum four-ball tribometer to evaluate liquid lubricants for space applications
[NASA-TM-106264] p 575 N94-12842
Applications of surface science to solid lubricants
[SMC-TR-93-24] p 579 N94-13903
TRIGGER CIRCUITS
Results from a water-Cerenkov array
[DE93-012715] p 849 N94-14461
TRIGONOMETRIC FUNCTIONS
Mathematic methods and algorithms for real-time applications
[AD-A266776] p 771 N94-14789
TRITIUM
Charged-particle evaluation methodology at Lawrence Livermore National Laboratory
[DE93-013429] p 781 N94-13251
Materials compatibility of hydride storage materials with austenitic stainless steels
[DE93-013688] p 703 N94-13691
A study of hydrogen effects on fracture behavior of radioactive waste storage tanks
[DE93-018171] p 574 N94-14873
TROPICAL REGIONS
The application of VAS satellite imagery to thunderstorm forecasting at Cape Canaveral
[NASA-CR-193563] p 718 N94-12839
Bibliography of urban climate in tropical/subtropical areas, 1981-1991
[WCASP-25] p 718 N94-12918
Spectral reflectance of soils from Sao Paulo State
[INPE-5424-PRP/172] p 684 N94-13377
Spatial variability of throughfall chemistry in a tropical rainforest (Central Amazonia, Brazil)
[INPE-5431-PRE/1765] p 720 N94-13429
AMIP: Diagnostic subproject on the variability in the tropics: Synoptic to intraseasonal time scales
[DE93-009287] p 721 N94-13914
TRMM system overview and status in the United States p 690 N94-14221
TRMM Project in Japan: Overview and status p 690 N94-14222
Clouds and the Earth's Radiant Energy System (CERES) on the Tropical Rainfall Measuring Mission (TRMM) p 690 N94-14223
TRMM precipitation radar algorithm p 690 N94-14224
Estimate of sampling errors of TRMM rainfall observation by using radar-AMeDAS composite data p 690 N94-14225
Future TRMM follow-on mission p 691 N94-14228
Nonlinear relationships between particulate absorption and chlorophyll: Detritus or pigment packaging?
[AD-A266806] p 731 N94-14899
TROPOSPHERE
Project AIRSTREAM: Trace gas
[DE93-008849] p 706 N94-12904
Description of the EURAD chemistry-transport model. Version 2 (CTM2)
[REPT-83] p 720 N94-13589
AMIP: Diagnostic subproject on the variability in the tropics: Synoptic to intraseasonal time scales
[DE93-009287] p 721 N94-13914
Radio metric errors due to mismatch and offset between a DSN antenna beam and the beam of a troposphere calibration instrument p 607 N94-14370
Importance of sprays for long range transport of harmful substances in the troposphere
[MITT-81] p 711 N94-14723
Signal and reference wavelengths for the elimination of SO2 cross sensitivity in remote measurements of tropospheric ozone with lidar
[GKSS/92/E/24] p 617 N94-14819
TROPOSPHERIC SCATTERING
Results from a study of scintillation behavior at 12, 20, and 30 GHz using the results from the Virginia Tech Olympus receivers p 613 N94-14659
TRUSSES
Feasibility study of an orbiting laboratory for testing CSI technology
[NASA-CR-191524] p 540 N94-13016
The Second Workshop on Deployment and Assembly Experiment of Large Space Structure on Orbit
[NASDA-CON-930003] p 529 N94-13268
Helical truss beam development for large space structure p 530 N94-13276
Movement of deployable truss p 531 N94-13280
Development and application of one dimensional deployable truss p 531 N94-13281
Study of a one-dimensional deployable structure employing telescopic members p 531 N94-13282
TRYPSIN
Quasi-elastic neutron scattering studies of protein dynamics
[DE93-015074] p 782 N94-13414
TUBE HEAT EXCHANGERS
Study of possible mechanisms of instability due to heat transfer
[INPE-5448-TDI/494] p 628 N94-12966
TUMBLING MOTION
Predicting the vibrations of a spinning inflated membrane
[DE93-010690] p 676 N94-14456
TUNABLE LASERS
Gathering and exchange information on atmospheric chemistry and polluted atmospheres
[DE93-009940] p 705 N94-12869
Novel Co:MgF2 lidar for aerosol profiler
[NASA-CR-191525] p 654 N94-13091
Predicted performance of a dc beam driven FEM oscillator designed for fusion applications at 200-250 GHz
[DE93-013414] p 655 N94-13145
Tetravalent chromium (Cr(4+)) as laser-active ion for tunable solid-state lasers
[NASA-CR-194527] p 659 N94-14576
AlGaAs diode laser blue shift resulting from fast neutron irradiation
[AD-A266642] p 659 N94-14681
TUNGSTEN
Correlations of the growth, structure, and stress with the adhesion of diamond films on tungsten
[DE93-012855] p 576 N94-12912
TUNGSTEN ALLOYS
Metastability of yttrium-oxides
[DE93-016548] p 813 N94-14440
Yield properties of tungsten and tungsten heavy alloys
[AD-A266833] p 575 N94-14878
TUNGSTEN COMPOUNDS
Dry film lubricant evaluation
[DE93-013114] p 578 N94-13118
TUNGSTEN OXIDES
A quartz crystal microbalance study of lithium insertion and removal into evaporated films MO(y) (M = Mo, Fe, and V)
[DSIS-93-00649] p 810 N94-14203
TUNING
Self tuning and adaptive control: Evaluations and improvements of algorithms
[ITN-93-85192] p 762 N94-13329
Tuning of Gaussian stochastic control systems
[CWI-BS-R9223] p 765 N94-14018
Computational issues in optimal tuning and placement of passive dampers p 681 N94-14647
TUNNEL JUNCTIONS
Theoretical SIS mixer research
[AD-A266323] p 807 N94-13580
TURBINE BLADES
Two-dimensional Navier-Stokes heat transfer analysis for rough turbine blades
[NASA-TM-106008] p 629 N94-13027
Numerical simulations of unsteady flows in turbomachines p 633 N94-13569
Numerical simulation of steady three-dimensional flows in axial turbomachinery bladerows p 634 N94-13630
Multigrid solution of internal flows using unstructured solution adaptive meshes
[NASA-CR-194233] p 638 N94-14356
Inflow characteristics associated with high-blade-loading events in a wind farm
[DE93-010042] p 704 N94-14423
JPRS report: Science and technology. Central Eurasia: Materials science
[JPRS-UMS-93-006] p 558 N94-14573
TURBINE ENGINES
Turbulent particle dispersion in confined swirling flows
[DLR-FB-92-32] p 637 N94-14045
TURBINE WHEELS
JPRS report: Science and technology. Central Eurasia: Materials science
[JPRS-UMS-93-006] p 558 N94-14573
TURBOFAN ENGINES
Analysis of gas turbine engines using water and oxygen injection to achieve high Mach numbers and high thrust
[NASA-TM-106270] p 518 N94-13143
Noise levels from a model turbofan engine with simulated noise control measures applied
[NASA-TM-106318] p 518 N94-14036
TURBOJET ENGINES
Analysis of gas turbine engines using water and oxygen injection to achieve high Mach numbers and high thrust
[NASA-TM-106270] p 518 N94-13143
Development of a high-speed mechanical drive system for oscillating an annular blade row in the bending mode
[NAL-TR-1170] p 502 N94-13342
A hot dynamic seal rig for measuring hypersonic engine seal durability and flow performance
[NASA-TM-106294] p 664 N94-14727
TURBOMACHINERY
Averaging techniques for steady and unsteady calculations of a transonic fan stage
[NASA-TM-106231] p 499 N94-13108
Residual contact restraints in cryogenics
[ETN-93-94375] p 671 N94-13501
Numerical simulations of unsteady flows in turbomachines p 633 N94-13569
Passage-averaged approximation of turbomachinery flows using vorticity-potential method
[ISBN-0-315-72716-0] p 634 N94-13598
The development of a scalable parallel 3-D CFD algorithm for turbomachinery
[NASA-CR-193604] p 664 N94-14848
TURBOPROP ENGINES
Futurepath 2
[NASA-TM-109285] p 518 N94-13623
TURBORAMJET ENGINES
Hypersonic propulsion characterization p 505 N94-14156
TURBULENCE
Sites of fine-scale electron density turbulence in the interstellar medium
[NASA-CR-193708] p 839 N94-13864
An experimental study of a turbulent boundary layer in the trailing edge region of a curculation-control airfoil
[NASA-CR-194522] p 508 N94-14541
Studying Turbulence Using Numerical Simulation Databases. 4: Proceedings of the 1992 Summer Program
[NASA-CR-194556] p 643 N94-14745
A small-scale turbulence model p 643 N94-14746
Triad interactions in the dissipation range p 644 N94-14750
Isotropy of small scale turbulence p 644 N94-14752
Estimation of the vortex length scale and intensity from two-dimensional samples p 645 N94-14756
Toward a quasi-linear closure for compressible turbulence
[DE93-017185] p 647 N94-14895
TURBULENCE EFFECTS
High freestream turbulence effects on the transport of heat and momentum p 633 N94-13559
Numerical studies of spray combustion in liquid-fueled engines p 564 N94-13685
TURBULENCE MODELS
Force-free magnetic fields, curl eigenfunctions, and the sphere in transform space, with applications to fluid dynamics and electromagnetic theory
[AD-A265805] p 834 N94-12971
Two-dimensional Navier-Stokes heat transfer analysis for rough turbine blades
[NASA-TM-106008] p 629 N94-13027
Averaging techniques for steady and unsteady calculations of a transonic fan stage
[NASA-TM-106231] p 499 N94-13108
A multiple-scale turbulence model for incompressible flow
[NASA-TM-106113] p 631 N94-13385
Numerical simulation of steady three-dimensional flows in axial turbomachinery bladerows p 634 N94-13630
A control volume finite element method for three-dimensional, incompressible, viscous fluid flow
[ISBN-0-315-72019-0] p 635 N94-13683
Development of a recursion RNG-based turbulence model
[NASA-CR-191511] p 636 N94-13718
Analysis of reacting flowfields in low-thrust rocket engines and plumes p 552 N94-14491
Studying Turbulence Using Numerical Simulation Databases. 4: Proceedings of the 1992 Summer Program
[NASA-CR-194556] p 643 N94-14745
A small-scale turbulence model p 643 N94-14746
On the local nature of the energy cascade p 643 N94-14748
Search for subgrid scale parameterization by projection pursuit regression p 643 N94-14749

Triad interactions in the dissipation range
p 644 N94-14750
Rapid distortion analysis and direct simulation of compressible homogeneous turbulence at finite Mach number p 645 N94-14757
Investigation of the dilatational dissipation in compressible homogeneous shear flow
p 645 N94-14758
The evolution equation for the flame surface density in turbulent premixed combustion p 567 N94-14764
Numerical simulations of turbulent premixed H2/O2/N2 flames with complex chemistry p 567 N94-14765
Structure of turbulent non-premixed flames modeled with two-step chemistry p 567 N94-14767

TURBULENT BOUNDARY LAYER
The transient behavior of a boundary layer exposed to uniform suction
[ITN-93-85205] p 630 N94-13197
Three-dimensional structure of straight and curved plane wakes
[NASA-CR-194420] p 501 N94-13266
Exploratory study of in-plane streamline curvature effects on a turbulent boundary layer at a Mach number of 3
[NASA-CR-193673] p 501 N94-13292
A technique for direct measurement of skin friction in supersonic combustion flow p 503 N94-13555
A three-dimensional supersonic turbulent boundary layer generated by an isentropic compression
p 503 N94-13556
High freestream turbulence effects on the transport of heat and momentum p 633 N94-13559
An experimental study of a turbulent boundary layer in the trailing edge region of a curculation-control airfoil
[NASA-CR-194522] p 508 N94-14541
Direct simulation of polymer drag reduction in free shear flows and vortex dipoles p 644 N94-14755
Response of a supersonic boundary layer to a compression corner p 645 N94-14759
A transport equation for eddy viscosity
p 646 N94-14762
Interaction of two glancing, crossing shock waves with a turbulent boundary-layer at various Mach numbers
[NASA-TM-103740] p 509 N94-14780

TURBULENT COMBUSTION
A coherent flame model of premixed turbulent combustion in a counterflow geometry
[CUED/A-THERMO/TR.60] p 562 N94-13085
Analysis of reacting flowfields in low-thrust rocket engines and plumes p 552 N94-14491
Studying Turbulence Using Numerical Simulation Databases. 4: Proceedings of the 1992 Summer Program
[NASA-CR-194556] p 643 N94-14745
The evolution equation for the flame surface density in turbulent premixed combustion p 567 N94-14764
Numerical simulations of turbulent premixed H2/O2/N2 flames with complex chemistry p 567 N94-14765
Structure of turbulent non-premixed flames modeled with two-step chemistry p 567 N94-14767

TURBULENT DIFFUSION
Sub-grid scale modeling for large eddy simulations in analysis of shock-turbulence interactions
[DE93-013425] p 631 N94-13250
Turbulent diffusion in homogeneous shear flow with stable density stratification
[DLR-FB-92-26] p 639 N94-14443
Structure of turbulent non-premixed flames modeled with two-step chemistry p 567 N94-14767

TURBULENT FLOW
Transition prediction and control in subsonic flow over a hump
[NASA-CR-4543] p 629 N94-13066
Numerical simulations and experiments on physics of high Mach number shockwave: Turbulent flow interactions
[DE93-013424] p 631 N94-13249
Sub-grid scale modeling for large eddy simulations in analysis of shock-turbulence interactions
[DE93-013425] p 631 N94-13250
Fully developed turbulent flow in rectangular interrupted-plate ducts
[ISBN-0-315-63594-0] p 632 N94-13474
An experimental investigation of shock wave/vortex interaction p 634 N94-13574
Numerical simulation of steady three-dimensional flows in axial turbomachinery bladerows p 634 N94-13630
A solution algorithm for the prediction of compressible laminar and turbulent shear flows p 634 N94-13635
Studies of turbulent shear flows and their control
[NASA-CR-194114] p 635 N94-13676
Numerical studies of spray combustion in liquid-fueled engines p 564 N94-13685
Development of a recursion RNG-based turbulence model
[NASA-CR-191511] p 636 N94-13718
Experimental investigation of the effects of blowing ratio parameter on heat transfer to a film-cooled flat plate
[AD-A266599] p 636 N94-13780
Turbulent particle dispersion in confined swirling flows
[DLR-FB-92-32] p 637 N94-14045
Droplet-turbulence interactions in sprays exposed to supercritical environmental conditions
[NASA-CR-194408] p 638 N94-14308
Inflow characteristics associated with high-blade-loading events in a wind farm
[DE93-010042] p 704 N94-14423
Interactions among convection, magnetic fields and p-mode oscillations in the sun
[NASA-CR-194477] p 845 N94-14479
An implicit finite volume nodal point scheme for the solution of two-dimensional compressible Navier-Stokes equations p 640 N94-14603
Development of an explicit multiblock/multigrid flow solver for viscous flows in complex geometries
[NASA-TM-106356] p 642 N94-14728
Studying Turbulence Using Numerical Simulation Databases. 4: Proceedings of the 1992 Summer Program
[NASA-CR-194556] p 643 N94-14745
A small-scale turbulence model p 643 N94-14746
The structure of intense vorticity in homogeneous isotropic turbulence p 643 N94-14747
On the local nature of the energy cascade
p 643 N94-14748
Search for subgrid scale parameterization by projection pursuit regression p 643 N94-14749
Triad interactions in the dissipation range
p 644 N94-14750
A study of the fine scale motions of incompressible time-developing mixing layers p 644 N94-14751
Isotropy of small scale turbulence
p 644 N94-14752
LES versus DNS: A comparative study
p 644 N94-14753
Behavior of streamwise rib vortices in a three-dimensional mixing layer p 644 N94-14754
Direct simulation of polymer drag reduction in free shear flows and vortex dipoles p 644 N94-14755
Estimation of the vortex length scale and intensity from two-dimensional samples p 645 N94-14756
Investigation of the dilatational dissipation in compressible homogeneous shear flow
p 645 N94-14758
A transport equation for eddy viscosity
p 646 N94-14762
DNS and modeling of the interaction between turbulent premixed flames and walls p 646 N94-14763
The evolution equation for the flame surface density in turbulent premixed combustion p 567 N94-14764
Structure of turbulent non-premixed flames modeled with two-step chemistry p 567 N94-14767
Stochastic modeling of turbulent reacting flows
p 647 N94-14768
Development of experimental demonstration processes for laminar-turbulent flow states at wing profiles in free flight
[ILR-MITT-280(1993)] p 510 N94-14800
Toward a quasi-linear closure for compressible turbulence
[DE93-017185] p 647 N94-14895

TURBULENT HEAT TRANSFER
Two-dimensional Navier-Stokes heat transfer analysis for rough turbine blades
[NASA-TM-106008] p 629 N94-13027
High freestream turbulence effects on the transport of heat and momentum p 633 N94-13559

TURBULENT MIXING
Radar imaging of sub-mesoscale ocean phenomena
[AD-A266339] p 725 N94-13581
Modeling and simulation of transport and combustion phenomena in a supersonic mixing layer
[ONERA-NT-1992-11] p 565 N94-14194
Turbulent diffusion in homogeneous shear flow with stable density stratification
[DLR-FB-92-26] p 639 N94-14443
Analysis of reacting flowfields in low-thrust rocket engines and plumes p 552 N94-14491
Stochastic modeling of turbulent reacting flows
p 647 N94-14768

TVD SCHEMES
Numerical simulation of dynamic stall of NACA0012 airfoil oscillating near static stall angle using the Navier-Stokes equations
[DE93-767970] p 505 N94-14061
Hypersonic viscous flow computations
p 510 N94-14612

TWINNING
Deposition of crystalline boron thick layers from gas phase
[DE93-620499] p 576 N94-12867
Atomic structure of the 310 twin in niobium: Theoretical predictions and comparison with experimental observation
[DE93-013421] p 806 N94-13136

TWO DIMENSIONAL FLOW
Transition prediction and control in subsonic flow over a hump
[NASA-CR-4543] p 629 N94-13066
Clebsch variable model for unsteady, transonic flow; application to 2D airfoils
[NLR-TP-91387-U] p 503 N94-13530
Images constructed from computed flow fields
[NASA-CR-194397] p 650 N94-13814
Stability of spatially developing boundary layers
p 640 N94-14605
Development of a general purpose multigrid accelerated Navier-Stokes solver p 641 N94-14613
A small-scale turbulence model p 643 N94-14746

TWO DIMENSIONAL MODELS
Two-dimensional simulations of foil implosion experiments on the Los Alamos capacitor bank
[DE93-012676] p 794 N94-12814
Body/cushion contact stress analysis during sitting
[ITN-93-85204] p 736 N94-13229
Dilaton quantum cosmology in two dimensions
[DE93-621377] p 836 N94-13361
Chemistry and transport in a multi-dimensional model
[NASA-CR-194425] p 716 N94-13969
The motion of a conical shaped liner driven by explosive load
[ITN-93-85215] p 585 N94-14507
An implicit finite volume nodal point scheme for the solution of two-dimensional compressible Navier-Stokes equations p 640 N94-14603
Time resolved measurement of electron temperatures of exploding foil x ray laser plasmas
[DE93-017161] p 803 N94-14894

TWO PHASE FLOW
Thermal gravitational modelling and scaling of two-phase heat transport systems: Similarity considerations and useful equations predictions versus experimental results
[NLR-TP-91477-U] p 632 N94-13533
Studies of momentum and energy transfer across wavy gas-liquid interfaces
[AD-A266432] p 635 N94-13699
Stability of oscillatory two phase Couette flow
[NASA-CR-191501] p 636 N94-13817
Turbulent particle dispersion in confined swirling flows
[DLR-FB-92-32] p 637 N94-14045
Review of mathematical and physical basis of two-phase flow modeling
[KFK-4759] p 642 N94-14708

TYPHOONS
Effects of typhoon on TOMS data
p 693 N94-14243

U

U.S.S.R.
Gas core nuclear thermal rocket engine research and development in the former USSR
[DE93-012165] p 552 N94-14013

U.S.S.R. SPACE PROGRAM
JPRS report: Science and technology. Central Eurasia: Space
[JPRS-USP-93-003] p 828 N94-13182

U-2 AIRCRAFT
Weather forecasting support for AASE-2
[NASA-CR-194342] p 721 N94-13675
Modis-N airborne simulator
[NASA-CR-194364] p 792 N94-13719

UBV SPECTRA
Polarization and variability of active galaxies and quasars p 837 N94-13550

UH-60A HELICOPTER
Preliminary design features of the RASCAL: A NASA /Army rotorcraft in-flight simulator p 526 N94-13325

ULTRAHIGH FREQUENCIES
Development of UHF spark-switched L-C Oscillators
[DE93-015019] p 623 N94-13892
Effects of the equatorial ionosphere on L-band Earth-space transmissions p 615 N94-14671
Tree attenuation at 20 GHz: Foliage effects
p 615 N94-14672

ULTRAHIGH VACUUM
Scanning tunneling microscopy studies of diamond films and optoelectronic materials
[NASA-CR-194363] p 578 N94-13246

ULTRASHORT PULSED LASERS
Tetravalent chromium (Cr(4+)) as laser-active ion for tunable solid-state lasers
[NASA-CR-194527] p 659 N94-14576

ULTRASONIC FLAW DETECTION
Resin transfer molding of textile composites
[NASA-CR-191505] p 554 N94-12833
Quantitative mapping of pore fraction variations in silicon nitride using an ultrasonic contact scan technique
[NASA-TP-3377] p 665 N94-13056
Enhanced NDE systems
[NASA-CR-192603] p 669 N94-14101
ULTRASONIC RADIATION
Study of chemical reactions under the influence of ultrasound
[DE93-016458] p 778 N94-14867
ULTRASONIC SCANNERS
Quantitative mapping of pore fraction variations in silicon nitride using an ultrasonic contact scan technique
[NASA-TP-3377] p 665 N94-13056
ULTRASONICS
Study of chemical reactions under the influence of ultrasound
[DE93-016458] p 778 N94-14867
ULTRAVIOLET ABSORPTION
Gathering and exchange information on atmospheric chemistry and polluted atmospheres
[DE93-009940] p 705 N94-12869
ULTRAVIOLET ASTRONOMY
UV extinction properties of carina nebular dust
[NASA-CR-193424] p 835 N94-13233
Physical properties of gas disks around shell stars with and without dust
[NASA-CR-193655] p 835 N94-13239
Radiative transfer in the dynamic atmospheres of Mira-type variables
[NASA-CR-193324] p 829 N94-13287
Analysis of the IUE spectra of the strongly interacting binary beta Lyrae
[NASA-CR-194118] p 833 N94-14493
The next century astrophysics program
p 546 N94-14832
ULTRAVIOLET LASERS
UV and IR laser ablation for inductively coupled plasma mass spectrometry
[DE93-017124] p 658 N94-14415
ULTRAVIOLET RADIATION
UV extinction properties of carina nebular dust
[NASA-CR-193424] p 835 N94-13233
Advances in low energy neutral atom imaging techniques
[DE93-012745] p 782 N94-13492
ULTRAVIOLET SPECTRA
The evidence for clumpy accretion in the Herbig Ae star HR 5999
[NASA-TM-108257] p 828 N94-12915
UV extinction properties of carina nebular dust
[NASA-CR-193424] p 835 N94-13233
Ultraviolet observations of NGC 4395, the least luminous and nearest known Seyfert 1 nucleus
[NASA-CR-194304] p 831 N94-13679
Spectra of late type dwarf stars of known abundance for stellar population models
[NASA-CR-194301] p 831 N94-13681
The distance to the high velocity clouds of neutral hydrogen
[NASA-CR-194343] p 838 N94-13716
Optical properties of CO2 ice and CO2 snow in the ultraviolet, visible, and infrared
[NASA-CR-194110] p 686 N94-14081
Analysis of the IUE spectra of the strongly interacting binary beta Lyrae
[NASA-CR-194118] p 833 N94-14493
ULTRAVIOLET TELESCOPES
LUTE telescope structural design
[NASA-CR-192594] p 830 N94-13448
UNDERGROUND EXPLOSIONS
Atmospheric acoustic modeling
[DE93-016727] p 718 N94-14518
UNDERGROUND STRUCTURES
Promotion of geothermal energy development in 1991
[DE93-799058] p 701 N94-13215
UNDERWATER ACOUSTICS
Mathematical algorithms for multidimensional inverse scattering problems in inhomogeneous medium
[AD-A266440] p 749 N94-13702
Underwater hearing: A review
[ISVR-TR-212] p 777 N94-14130
FLATDAN beamformer enhancements and testing
[DSIS-93-00287] p 777 N94-14360
UNIFORM FLOW
The three-dimensional flow past a rapidly rotating circular cylinder
[NASA-CR-191512] p 630 N94-13075
UNIQUENESS
Non-uniqueness in dynamic rate-independent non-associated plasticity
[AD-A266342] p 769 N94-13731
UNITED STATES
NASA/DOD Aerospace Knowledge Diffusion Research Project. Report 18: A comparison of the technical communication practices of aerospace engineers and scientists in India and the United States
[NASA-TM-109006] p 821 N94-13057
Science, technology, and the federal government: National goals for a new era p 827 N94-14115
NASA/DOD Aerospace Knowledge Diffusion Research Project. Paper 37: The impact of political control on technical communications: A comparative study of Russian and US aerospace engineers and scientists
[NASA-TM-109329] p 826 N94-14488
UNIVERSE
Rare attributes in finite universe: Hypotheses testing specification and exact randomized upper confidence bounds
[DE93-012783] p 775 N94-12955
Redshift distortions of galaxy correlation functions
[DE93-014007] p 834 N94-12980
Inflation after COBE: Lectures on inflationary cosmology
[DE93-014008] p 834 N94-13096
Dilaton quantum cosmology in two dimensions
[DE93-621377] p 836 N94-13361
Radiation perturbation theory in gravity and quantum universe as a hydrogen atom
[DE93-626621] p 849 N94-14889
UNIVERSITIES
Technology parks and the cooperation among universities and firms: The cases of Campinas, Sao Jose dos Campos e Sao Carlos
[INPE-5251-TAE/04] p 818 N94-13427
Selected data on academic science and engineering R and D expenditures: Fiscal Year 1991
[NSF-92-329] p 819 N94-13982
UNIVERSITY PROGRAM
Weather forecasting support for AASE-2
[NASA-CR-194342] p 721 N94-13675
UNIX (OPERATING SYSTEM)
Kerberos: A UNIX-TCP/IP network authentication system
[DE93-011677] p 760 N94-14011
Uniform user and group IDs on a large network
[DE93-013047] p 760 N94-14315
UNMANNED SPACECRAFT
NASA images 11
[NASA-TM-109287] p 842 N94-13626
Contributions of winged re-entry vehicle to space activities p 537 N94-14278
Mission scenario of HOPE p 537 N94-14279
The status of the HOPE concept study
p 537 N94-14280
UNSTEADY AERODYNAMICS
A method of predicting quasi-steady aerodynamics for flutter analysis of high speed vehicles using steady CFD calculations
[NASA-TM-109009] p 514 N94-12850
Actuator and aerodynamic modeling for high-angle-of-attack aeroservoelasticity
[NASA-TM-4493] p 520 N94-13255
Numerical simulation of dynamic stall of NACA0012 airfoil oscillating near static stall angle using the Navier-Stokes equations
[DE93-767970] p 505 N94-14061
Domain connectivity among systems of overset grids
[NASA-CR-193390] p 508 N94-14326
UNSTEADY FLOW
Averaging techniques for steady and unsteady calculations of a transonic fan stage
[NASA-TM-106231] p 499 N94-13108
Clebsch variable model for unsteady, transonic flow; application to 2D airfoils
[NLR-TP-91387-U] p 503 N94-13530
Numerical simulations of unsteady flows in turbomachines p 633 N94-13569
A comparison of computational and experimental data for a subscale high speed propulsive nozzle at low mach numbers
[AD-A266543] p 504 N94-13705
Numerical simulation of a powered-lift landing, tracking flow features using overset grids, and simulation of high lift devices on a fighter-lift-and-control wing
[NASA-CR-194260] p 527 N94-14322
A vortex method for viscous unsteady flows
p 640 N94-14602
An implicit finite volume nodal point scheme for the solution of two-dimensional compressible Navier-Stokes equations p 640 N94-14603
UPLINKING
Sequential ranging: How it works
[NASA-CR-194508] p 532 N94-13796
Stability measurements of the radio science system at the 34-m high-efficiency antennas p 609 N94-14381
An overview of the Galileo Optical Experiment (GOPEX) p 610 N94-14386
Data analysis for GOPEX image frames
p 610 N94-14388
Galileo Optical Experiment (GOPEX) optical train: Design and validation at the Table Mountain Facility
p 610 N94-14390
GOPEX at the Starfire Optical Range
p 611 N94-14392
UPPER SURFACE BLOWING
Flight path control for the approach and landing of the quiet STOL experimental aircraft ASKA
[NAL-TR-1183] p 513 N94-13457
UPSTREAM
Evolution of the shock front and turbulence structures in the shock/turbulence interaction p 645 N94-14761
UPWIND SCHEMES (MATHEMATICS)
Hypersonic viscous flow computations
p 510 N94-14612
URANIUM COMPOUNDS
Muon spin relaxation studies of heavy fermion superconductors
[DE93-014576] p 815 N94-14773
URBAN RESEARCH
Bibliography of urban climate in tropical/subtropical areas, 1981-1991
[WCASP-25] p 718 N94-12918
USER MANUALS (COMPUTER PROGRAMS)
PACT user's guide
[DE93-013093] p 742 N94-12840
Vendor information system for innovative treatment technologies. User manual (VISITT version 2.0). Number 2
[PB93-196640] p 821 N94-12936
Archiving of HEAO-1 data products and the creation of a general user's guide to the archive
[NASA-CR-193415] p 822 N94-13062
ULTRA 2 user's manual for ULTRA 2 revision 3.0
[DE93-015970] p 744 N94-13120
SCORE user's manual
[DE93-015987] p 822 N94-13121
VIEWCACHE: An incremental pointer-base access method for distributed databases. Part 1: The universal index system design document. Part 2: The universal index system low-level design document. Part 3: User's guide. Part 4: Reference manual. Part 5: UIMS test suite
[NASA-CR-191788] p 822 N94-13126
The DREO Elint Browser Utility (DEBU) reference manual
[DSIS-92-03900] p 603 N94-13837
VMEC30 programming library: Reference manual
[DSIS-93-00350] p 750 N94-13858
HELSCAM V2.0: Development and application guide
[DSIS-93-00137] p 515 N94-13867
VMEC30 software development: Tutorial manual
[DSIS-93-00351] p 750 N94-13944
CMAPP user's manual, part 2
[DSIS-93-00858-PT-2] p 751 N94-14017
Adaptive Signal Processing Testbed signal excision software: User's manual
[DSIS-93-00260] p 606 N94-14037
Adaptive Signal Processing Testbed application software: User's manual
[DSIS-93-00261] p 606 N94-14038
VMEC30 SUN software development utilities: User's manual
[DSIS-93-00348] p 752 N94-14051
VMEC30 SUN device drivers: User's manual
[DSIS-93-00349] p 752 N94-14052
Payload/GSE/data system interface: Users guide for the VPF (Vertical Processing Facility)
[NASA-CR-194385] p 532 N94-14148
FLATDAN beamformer enhancements and testing
[DSIS-93-00287] p 777 N94-14360
USER REQUIREMENTS
Advanced display object selection methods for enhancing user-computer productivity
[AD-A265806] p 743 N94-12974
Information requirements of self-managing teams
[DE93-010319] p 824 N94-14048
UTILITIES
An examination of utility emissions contributions to elevated ozone concentrations in the Chicago area
[DE93-012852] p 708 N94-13495

V

V-22 AIRCRAFT
Handling qualities effects of display latency
p 517 N94-13316
VACUUM
Compatibility testing of vacuum seal materials
[DE93-014366] p 663 N94-14113
A study of thin liquid sheet flows
[NASA-TM-106323] p 642 N94-14732

VACUUM CHAMBERS
Scanning tunneling microscopy studies of diamond films and optoelectronic materials
[NASA-CR-194363] p 578 N94-13246
VACUUM DEPOSITION
Implementation of manufacturing techniques for planar, single mode waveguides on lithium niobate
[DSIS-93-00101] p 792 N94-13845
VACUUM MELTING
A conduction model for the vacuum arc remelting process
[NPL-DMM(A)-98] p 639 N94-14464
VACUUM SYSTEMS
Compatibility testing of vacuum seal materials
[DE93-014366] p 663 N94-14113
BAKEOUT: A computer program for predicting diffusive outgassing from stainless steel
[DE93-012613] p 573 N94-14364
VACUUM TESTS
A vacuum four-ball tribometer to evaluate liquid lubricants for space applications
[NASA-TM-106264] p 575 N94-12842
Ohmic heating of composite candidate graphite-fiber/coating combinations
[NASA-TM-4491] p 554 N94-12871
VALVES
STS-55 pad abort: Engine 2011 oxidizer preburner augmented spark igniter check valve leak
[NASA-CR-193830] p 533 N94-12806
VANADIUM
Fracture behavior of vanadium/vanadium silicide in-situ composites
[DE93-013422] p 556 N94-13389
VANADIUM ALLOYS
Electronic structure and phase stability properties in ternary substitutional alloys
[DE93-013848] p 569 N94-13137
Fracture behavior of vanadium/vanadium silicide in-situ composites
[DE93-013422] p 556 N94-13389
VANADIUM OXIDES
A quartz crystal microbalance study of lithium insertion and removal into evaporated films MO(y) (M = Mo, Fe, and V)
[DSIS-93-00649] p 810 N94-14203
VANES
Multigrid solution of internal flows using unstructured solution adaptive meshes
[NASA-CR-194233] p 638 N94-14356
VAPOR DEPOSITION
Deposition of crystalline boron thick layers from gas phase
[DE93-620499] p 576 N94-12867
Research on chemical vapor deposition processes for advanced ceramic coatings
[NASA-CR-193613] p 577 N94-13089
Scanning tunneling microscopy studies of diamond films and optoelectronic materials
[NASA-CR-194363] p 578 N94-13246
Effects of growth conditions and substrate orientation on the properties of InSb
[DE93-013766] p 812 N94-14344
Electrochemical planarization for microelectronic circuits
[DE93-017214] p 627 N94-14870
VAPOR PHASES
Multiphase equation of state for iron
[DE93-013956] p 568 N94-12977
Research on chemical vapor deposition processes for advanced ceramic coatings
[NASA-CR-193613] p 577 N94-13089
Hydrogen peroxide safety issues
[DE93-013895] p 565 N94-14346
VAPOR PRESSURE
Measuring surface fluxes in CAPE
[NASA-CR-193664] p 711 N94-12788
Binary homogeneous nucleation: Temperature and relative humidity fluctuations and non-linearity
[DE93-007884] p 709 N94-13911
VAPORIZING
Gas-evaporation in low-gravity field (cogelation mechanism of metal vapors) (M-14) p 588 N94-13746
Impact melting and vaporization in planetary regoliths p 843 N94-14299
VAPORS
Deposition of impact-generated vapors in the lunar regolith p 843 N94-14302
VARIABILITY
Spatial variability of throughfall chemistry in a tropical rainforest (Central Amazonia, Brazil)
[INPE-5431-PRE/1765] p 720 N94-13429
Polarization and variability of active galaxies and quasars p 837 N94-13550
Analytical framework for modeling scale-related variabilities in remote sensing p 685 N94-13592
Spatial and temporal variability of precipitation and chemistry: Case studies from the frontal boundary study
[DE93-007883] p 708 N94-13910
VARIABLE STARS
A photometric study of massive x-ray binaries
[ITN-93-85207] p 829 N94-13231
Analysis of the IUE spectra of the strongly interacting binary beta Lyrae
[NASA-CR-194118] p 833 N94-14493
VARIANCE (STATISTICS)
Robust estimators and tests in one-sample location problem with particular consideration on modified maximum likelihood process
[ETN-93-94391] p 774 N94-14703
VARIATIONAL PRINCIPLES
Variational approach to probabilistic finite elements
[NASA-CR-187179] p 674 N94-13873
VARISTORS
Metal oxide varistor feasibility study
[DE93-012921] p 620 N94-13031
VECTOR PROCESSING (COMPUTERS)
A path-oriented matrix-based knowledge representation system
[NASA-CR-4539] p 744 N94-13065
Advanced computers and simulation
[DE93-014354] p 740 N94-13286
Analysis and effects of the number of nests of DO loops during vector supercomputing
[NAL-TR-1146] p 748 N94-13453
Obstacle detection by recognizing binary expansion patterns
[NASA-CR-194415] p 514 N94-14495
An overview of parallel scientific visualization
[DE93-017105] p 755 N94-14521
VECTOR QUANTIZATION
Image coding using entropy-constrained residual vector quantization
[NASA-CR-193728] p 744 N94-13113
Speaker independent recognition of isolated words using vector quantization and neural networks
[ETN-93-94390] p 616 N94-14724
VECTOR SPACES
Numerical simulation of hypersonic flow for the design of the H-2 orbiting plane (HOPE), part 3
[NAL-TR-1168-PT-3] p 499 N94-12948
On the symmetry algebra of the discrete states in d less than 2 closed string theory
[DE93-622903] p 769 N94-13536
VECTORS (MATHEMATICS)
On relations between Schmidt pairs arising in robust control
[CWI-BS-R9225] p 764 N94-14000
On the Schmidt pairs of multivariable Hankel operators and robust control
[CWI-BS-R9226] p 765 N94-14001
An efficient parallel algorithm for matrix-vector multiplication
[DE93-015125] p 754 N94-14399
Some experiences with Krylov vectors and Lanczos vectors p 677 N94-14621
VEGETATION
Wind erosion in semiarid landscapes: Predictive models and remote sensing methods for the influence of vegetation
[NASA-CR-194029] p 715 N94-13956
Meteorological data, new series A monographs. Volume 6, no. 4: Modelization of heat fluxes at Earth ground with consideration of vegetation
[ETN-93-94169] p 723 N94-14546
VEGETATION GROWTH
Biomass production chamber air analysis of wheat study (BWT931)
[NASA-CR-194092] p 737 N94-13712
VEGETATIVE INDEX
Vegetation mapping of Indo-China Peninsula using MOS-1 MESSR and NOAA AVHRR p 695 N94-14257
Estimation of vegetation damage due to ash fall in Mt. Pinatubo area using MOS-1 data p 695 N94-14259
VELOCITY
The motion of a conical shaped liner driven by explosive load
[ITN-93-85215] p 585 N94-14507
VELOCITY DISTRIBUTION
On the theory of the decaying developed turbulence with spontaneous parity violation
[DE93-623190] p 632 N94-13511
Cold dark matter halos p 838 N94-13649
Least-squares finite element solutions for three-dimensional backward-facing step flow
[NASA-TM-106353] p 770 N94-14407
The motion of a conical shaped liner driven by explosive load
[ITN-93-85215] p 585 N94-14507
Vortex-induced disturbance field in a compressible shear layer p 645 N94-14760
VELOCITY MEASUREMENT
Quantitative mapping of pore fraction variations in silicon nitride using an ultrasonic contact scan technique
[NASA-TP-3377] p 665 N94-13056
A three-dimensional supersonic turbulent boundary layer generated by an isentropic compression p 503 N94-13556
High freestream turbulence effects on the transport of heat and momentum p 633 N94-13559
Droplet-turbulence interactions in sprays exposed to supercritical environmental conditions
[NASA-CR-194408] p 638 N94-14308
Calibration of a magnetic induction system for measurement of hypervelocities
[DE93-013949] p 652 N94-14578
Investigation of the feasibility of optical diagnostic measurements at the exit of the SSME
[NASA-CR-193832] p 553 N94-14682
Intra-blade quantitative transonic flow measurements at the DRA Pyestock Isentropic Light Piston Facility using PIV (Particle Image Velocimetry)
[RAE-TM-AERO/PROP-21] p 509 N94-14706
VENTILATION
Some flow properties of telescope enclosures estimated from water channel tests: Application of the flow visualization techniques
[NAL-TR-1178T] p 830 N94-13452
VENUS (PLANET)
Venus gravity
[NASA-CR-194077] p 841 N94-12823
Regional tectonic analysis of Venus as part of the Pioneer Venus guest investigator project
[NASA-CR-194079] p 842 N94-13561
VENUS ATMOSPHERE
Reduction and analysis of seasons 15 and 16 (1991 - 1992) Pioneer Venus radio occultation data and correlative studies with observations of the near-infrared emission of Venus
[NASA-CR-194128] p 841 N94-13083
VENUS CLOUDS
Reduction and analysis of seasons 15 and 16 (1991 - 1992) Pioneer Venus radio occultation data and correlative studies with observations of the near-infrared emission of Venus
[NASA-CR-194128] p 841 N94-13083
VENUS SURFACE
Regional tectonic analysis of Venus as part of the Pioneer Venus guest investigator project
[NASA-CR-194079] p 842 N94-13561
VERSATILITY
Flexibility and costs in the design process: A decision support model
[ISBN-9-06-814522-3] p 597 N94-14808
VERTICAL AIR CURRENTS
Linkage of anthropogenic aerosol to clouds and climate
[DE93-016434] p 719 N94-13080
Modeling of biosphere-atmosphere interaction for forest and pastureland in the Amazon
[INPE-5454-TDI/496] p 707 N94-13330
VERTICAL DISTRIBUTION
On the vertical structure of seasonal, interannual and intraseasonal flows
[AD-A265346] p 719 N94-12992
Fluxes of heat and water vapour in a convective mixed layer during EFEDA
[DLR-FB-92-21] p 716 N94-14132
Meteorological data, new series A monographs. Volume 6, no. 3: Estimation of influence of high clouds in the radiation field and the climat by analysis of NOAA AVHRR data
[ETN-93-94170] p 723 N94-14707
VERTICAL FLIGHT
Piloting Vertical Flight Aircraft: A Conference on Flying Qualities and Human Factors
[NASA-CP-3220] p 521 N94-13294
Design criteria for integrated flight/propulsion control systems for STOVL fighter aircraft p 521 N94-13297
VERTICAL LANDING
MIL-H-8501B: Application to shipboard terminal operations p 521 N94-13296
Evaluation of two cockpit display concepts for civil tiltrotor instrument operations on steep approaches p 517 N94-13323
VERTICAL MOTION SIMULATORS
Vertical motion simulator familiarization guide
[NASA-TM-103923] p 527 N94-13008
Effects of simulator motion and visual characteristics on rotorcraft handling qualities evaluations p 524 N94-13317
VERTICAL TAKEOFF AIRCRAFT
Piloting Vertical Flight Aircraft: A Conference on Flying Qualities and Human Factors
[NASA-CP-3220] p 521 N94-13294

VERY LARGE SCALE INTEGRATION
Design automation tools for testable VLSI circuits
[ISBN-0-315-61461-7] p 621 N94-13333
NASA Space Engineering Research Center for VLSI systems design
[NASA-CR-194035] p 625 N94-14325
VERY LONG BASE INTERFEROMETRY
J2000.0 modelling of GEOAIM in the analysis of VLBI data from the NASA crustal dynamics project
[ISBN-0-315-59463-2] p 684 N94-13368
Theory of post-block 2 VLBI observable extraction
[NASA-CR-194543] p 686 N94-13872
VIBRATION
High resolution electron energy loss studies of surface vibrations
[DE93-014441] p 781 N94-13283
Predicting the vibrations of a spinning inflated membrane
[DE93-010690] p 676 N94-14456
Applications of computer algebra to distributed parameter systems p 677 N94-14623
Free-wake computation of helicopter rotor flowfield for general flight regimes
[AD-A266692] p 509 N94-14781
VIBRATION DAMPING
Nonlinear damping model for flexible structures
[NASA-CR-193711] p 539 N94-12790
Kinematics and constraints associated with swashplate blade pitch control
[NASA-TM-102265] p 520 N94-12820
On curve veering and flutter of rotating blades
[NASA-TM-106282] p 670 N94-12872
Development and application of one dimensional deployable truss p 531 N94-13281
Some frequency and damping measurements of laminated beryllium beams
[DE93-015909] p 676 N94-14530
Inverse dynamics: Simultaneous trajectory tracking and vibration reduction with distributed actuators p 678 N94-14624
VIBRATION EFFECTS
Machinery dynamics activities in Canadian industries
[IME-MET-TR-006] p 663 N94-14147
VIBRATION ISOLATORS
Feasibility study of an orbiting laboratory for testing CSI technology
[NASA-CR-191524] p 540 N94-13016
VIBRATION MEASUREMENT
Transcript of workshop on machinery health monitoring
[IME-MET-TR-005] p 733 N94-13847
Machinery dynamics activities in Canadian industries
[IME-MET-TR-006] p 663 N94-14147
VIBRATION MODE
On curve veering and flutter of rotating blades
[NASA-TM-106282] p 670 N94-12872
A component modes projection and assembly model reduction methodology for articulated, multi-flexible body structures p 677 N94-14622
VIBRATION TESTS
Estimation of critical values and vibration characteristics on supersonic delta wings. Part 2: Locally-stationary time series analysis of nonstationary random responses
[NAL-TR-1179] p 502 N94-13345
Canadian Target Assembly (CTA) to Airborne Support Equipment (ASE) vibration test report
[IME-AMT-TR-001] p 663 N94-14195
VIBRATIONAL SPECTRA
Infrared spectroscopy of organic free radicals related to combustion processes
[DE93-017086] p 562 N94-13222
First-principles studies of phase stability and the structural and dynamical properties of hydrogen-metal systems
[DE93-016129] p 570 N94-13374
Dynamic Jahn-Teller effect: Calculation of fine structure spectrum, isotope shift and Zeeman behavior at deep center Ni2+ in CdS
[ETN-93-94394] p 815 N94-14705
VIRTUAL MEMORY SYSTEMS
Execution methods, and parallel virtual machines for distributed implementation of the LCS parallel programming language
[LAAS-93032] p 761 N94-14716
VIRTUAL REALITY
USRA/RIACS
[NASA-CR-194334] p 750 N94-13932
VIRUSES
PC viruses: How do they do that?
[DE93-012581] p 753 N94-14289
VISCOELASTICITY
Characterization of composite materials for aerospace structures
[ESA-TT-1260] p 557 N94-13804
Predicting the vibrations of a spinning inflated membrane
[DE93-010690] p 676 N94-14456
Dynamic soil pressures on rigid cylindrical vaults
[DE93-013930] p 676 N94-14585
VISCOSITY
Stability of oscillatory two phase Couette flow
[NASA-CR-191501] p 636 N94-13817
The spectral viscosity method applied to simulation of waves in a stratified atmosphere
[FFI-92/7047] p 637 N94-14040
VISCOUS DAMPING
Computational issues in optimal tuning and placement of passive dampers p 681 N94-14647
VISCOUS DRAG
Experimental studies of vortex flaps and vortex plates. Part 1: 0.53 m span 60 deg delta wing
[DE93-767969] p 505 N94-14059
VISCOUS FLOW
Non-linear effects in vortex viscous flow in superconductors-role of finite heat removal velocity
[DE93-621785] p 618 N94-12856
Approaches to high aspect ratio triangulations
[NASA-TM-107684] p 739 N94-12886
Integration of viscous effects into inviscid computational methods
[NASA-CR-193677] p 629 N94-13007
Numerical study of the effects of icing on viscous flow over wings
[NASA-CR-193306] p 500 N94-13180
A robust quasi-simultaneous interaction method for a full potential flow with a boundary layer with application to wing/body configurations
[NLR-TP-91397-U] p 503 N94-13531
Numerical simulations of unsteady flows in turbomachines p 633 N94-13569
Passage-averaged approximation of turbomachinery flows using vorticity-potential method
[ISBN-0-315-72716-0] p 634 N94-13598
A control volume finite element method for three-dimensional, incompressible, viscous fluid flow
[ISBN-0-315-72019-0] p 635 N94-13683
Hypersonic flow phenomenology p 505 N94-14155
Extrapolation of ground test data to flight p 507 N94-14170
Least-squares finite element solutions for three-dimensional backward-facing step flow
[NASA-TM-106353] p 770 N94-14407
A vortex method for viscous unsteady flows p 640 N94-14602
A finite volume method for computation of viscous flow in complex configurations p 640 N94-14607
Hypersonic viscous flow computations p 510 N94-14612
Development of an explicit multiblock/multigrid flow solver for viscous flows in complex geometries
[NASA-TM-106356] p 642 N94-14728
Analytical description of the breakup of liquid jets in air
[NASA-CR-191503] p 647 N94-14849
VISCOUS FLUIDS
On the motion through a viscous fluid of a spherical particle touching a plane wall: Slip boundary conditions
[DE93-012540] p 628 N94-12961
Stability of oscillatory two phase Couette flow
[NASA-CR-191501] p 636 N94-13817
VISIBILITY
Hardware design for the Autonomous Visibility Monitoring (AVM) observatory p 533 N94-14394
Summary of conclusions and recommendations from a visibility science workshop
[DE93-012770] p 710 N94-14523
VISIBLE SPECTRUM
Optical properties of CO2 ice and CO2 snow in the ultraviolet, visible, and infrared
[NASA-CR-194110] p 686 N94-14081
VISUAL AIDS
Visual cueing aids for rotorcraft landings p 524 N94-13313
VISUAL CONTROL
Compatibility of information and mode of control: The case for natural control systems p 523 N94-13307
Visual information for judging temporal range p 524 N94-13314
Visual cueing considerations in Nap-of-the-Earth helicopter flight head-slaved helmet-mounted displays p 524 N94-13315
Primary display latency criteria based on flying qualities and performance data p 525 N94-13318
VISUAL FIELDS
Visual cueing considerations in Nap-of-the-Earth helicopter flight head-slaved helmet-mounted displays p 524 N94-13315
Effects of simulator motion and visual characteristics on rotorcraft handling qualities evaluations p 524 N94-13317
VISUAL PERCEPTION
Comparative measurement of visual stability in Earth and cosmic space (L-4) p 592 N94-13761
Validity of FAA-approved color vision tests for class 2 and class 3 aeromedical screening
[DOT/FAA/AM-93/17] p 735 N94-14846
Validation of an inexpensive illuminant for aeromedical color vision screening
[DOT/FAA/AM-93/16] p 736 N94-14854
VISUAL STIMULI
Visual information for judging temporal range p 524 N94-13314
Primary display latency criteria based on flying qualities and performance data p 525 N94-13318
VISUAL TASKS
Validity of FAA-approved color vision tests for class 2 and class 3 aeromedical screening
[DOT/FAA/AM-93/17] p 735 N94-14846
VITERBI DECODERS
Coding performance of the Probe-Orbiter-Earth communication link p 608 N94-14377
VITRIFICATION
Relationship between borosilicate glass composition, structure, and durability test response (SRS)
[DE93-013578] p 581 N94-14343
VOICE COMMUNICATION
Analysis of fundamental frequency pattern in speech p 618 N94-13440
Propagation considerations in the American Mobile Satellite system design p 614 N94-14668
VOIDS
Structure and stability of microvoids in A-Si:H
[DE93-016625] p 813 N94-14413
VOLATILITY
Regional tectonic analysis of Venus as part of the Pioneer Venus guest investigator project
[NASA-CR-194079] p 842 N94-13561
VOLCANOES
Estimation of vegetation damage due to ash fall in Mt. Pinatubo area using MOS-1 data p 695 N94-14259
VOLT-AMPERE CHARACTERISTICS
Screening of solar cells
[NASA-TM-106298] p 620 N94-13134
The 1.00 MeV proton radiation resistance studies of amorphous silicon-based alloy solar cells p 703 N94-13639
VOLTAGE CONVERTERS (DC TO DC)
Power converters for the 120 V bus supply control
[CNES-NT-134] p 622 N94-13552
Operation of high power converters in parallel
[NASA-CR-191096] p 622 N94-13786
VOLTAGE REGULATORS
Operation of high power converters in parallel
[NASA-CR-191096] p 622 N94-13786
Multi-output flyback converter with ultrafast current protection
[CNES-NT-133] p 625 N94-14138
VORTEX AVOIDANCE
Optimal lateral escape maneuvers for microburst encounters during final approach
[LR-691] p 511 N94-13534
VORTEX BREAKDOWN
The effect of crossflow on Taylor vortices: A model problem
[NASA-CR-191487] p 630 N94-13128
The phenomenon of vortex breakdown p 510 N94-14609
Behavior of streamwise rib vortices in a three-dimensional mixing layer p 644 N94-14754
VORTEX FILAMENTS
New vortex dynamics methods for rotor free wake analysis
[AD-A266656] p 509 N94-14774
VORTEX FLAPS
Experimental studies of vortex flaps and vortex plates. Part 2: 1.15m span 60 deg delta wing
[NAL-TR-1180T-PT-2] p 502 N94-13454
Experimental studies of vortex flaps and vortex plates. Part 1: 0.53 m span 60 deg delta wing
[DE93-767969] p 505 N94-14059
VORTEX GENERATORS
Experimental studies of vortex flaps and vortex plates. Part 2: 1.15m span 60 deg delta wing
[NAL-TR-1180T-PT-2] p 502 N94-13454
VORTICES
Non-linear effects in vortex viscous flow in superconductors-role of finite heat removal velocity
[DE93-621785] p 618 N94-12856
Sub-grid scale modeling for large eddy simulations in analysis of shock-turbulence interactions
[DE93-013425] p 631 N94-13250
An experimental investigation of shock wave/vortex interaction p 634 N94-13574
On the secondary instability of the most dangerous Goertler vortex
[NASA-CR-191504] p 636 N94-13785

Flight validation of a pulsed smoke flow visualization system
[NASA-CR-186026] p 516 N94-14106
A vortex method for viscous unsteady flows
p 640 N94-14602
Navier-Stokes simulation of transonic vortex flow over a delta wing p 640 N94-14606
The phenomenon of vortex breakdown
p 510 N94-14609
Linear instability of curved free shear layers
[NASA-TM-106290] p 642 N94-14729
A small-scale turbulence model p 643 N94-14746
The structure of intense vorticity in homogeneous isotropic turbulence p 643 N94-14747
On the local nature of the energy cascade
p 643 N94-14748
Behavior of streamwise rib vortices in a three-dimensional mixing layer p 644 N94-14754
Direct simulation of polymer drag reduction in free shear flows and vortex dipoles p 644 N94-14755
Estimation of the vortex length scale and intensity from two-dimensional samples p 645 N94-14756
Vortex-induced disturbance field in a compressible shear layer p 645 N94-14760
Evolution of the shock front and turbulence structures in the shock/turbulence interaction p 645 N94-14761
New vortex dynamics methods for rotor free wake analysis
[AD-A266656] p 509 N94-14774
Free-wake computation of helicopter rotor flowfield for general flight regimes
[AD-A266692] p 509 N94-14781

VORTICITY
Passage-averaged approximation of turbomachinery flows using vorticity-potential method
[ISBN-0-315-72716-0] p 634 N94-13598
A vortex method for viscous unsteady flows
p 640 N94-14602
A small-scale turbulence model p 643 N94-14746
The structure of intense vorticity in homogeneous isotropic turbulence p 643 N94-14747
Search for subgrid scale parameterization by projection pursuit regression p 643 N94-14749
Isotropy of small scale turbulence
p 644 N94-14752
Vortex-induced disturbance field in a compressible shear layer p 645 N94-14760
Evolution of the shock front and turbulence structures in the shock/turbulence interaction p 645 N94-14761
Free-wake computation of helicopter rotor flowfield for general flight regimes
[AD-A266692] p 509 N94-14781

VORTICITY EQUATIONS
Free-wake computation of helicopter rotor flowfield for general flight regimes
[AD-A266692] p 509 N94-14781

VOYAGER PROJECT
NASA images 11
[NASA-TM-109287] p 842 N94-13626

W

WAFERS
Field emitter array RF amplifier development project. Phase 1: Cathode technology development
[AD-A266346] p 622 N94-13776

WAKES
Three-dimensional structure of straight and curved plane wakes
[NASA-CR-194420] p 501 N94-13266
Laboratory simulation of spacecraft charging in the plasma wake region
[FFI-93-7007] p 542 N94-14107
An experimental study of a turbulent boundary layer in the trailing edge region of a curculation-control airfoil
[NASA-CR-194522] p 508 N94-14541
Wake-field and space charge effects on high brightness beams calculations and measured results for the laser driven photoelectrons at BNL-ATF
[DE93-015787] p 659 N94-14572

WALL FLOW
A wall interference assessment/correction system
[NASA-CR-194174] p 500 N94-13076
An experimental study of a turbulent boundary layer in the trailing edge region of a curculation-control airfoil
[NASA-CR-194522] p 508 N94-14541
Analysis, approximation, and computation of a coupled solid/fluid temperature control problem
[NASA-TM-106351] p 771 N94-14731
A transport equation for eddy viscosity
p 646 N94-14762
DNS and modeling of the interaction between turbulent premixed flames and walls p 646 N94-14763

WALL PRESSURE
Autofrettage: Stress distribution under load and retained stresses after depressurization. A modified plane-strain case
[AD-A266320] p 671 N94-13579

WALLOPS ISLAND
Birds of Wallops Island, Virginia, 1970 - 1992
[NASA-TM-104589] p 850 N94-13923

WALLS
On the motion through a viscous fluid of a spherical particle touching a plane wall: Slip boundary conditions
[DE93-012540] p 628 N94-12961
An assessment of the potential for neck injury due to padding of aircraft interior walls for head impact protection
[DOT/FAA/AM-93/14] p 738 N94-13972

WARNING SYSTEMS
A tentative plan on China and Asian-Pacific satellite system for disaster reduction p 693 N94-14247

WARPAGE
Polymer infiltration studies
[NASA-CR-194521] p 582 N94-14539

WASTE DISPOSAL
Environmental awareness
[DE93-014192] p 707 N94-13218
A laser-based technique to continuously monitor metal aerosol emissions
[DE93-012836] p 710 N94-14183
Survey of subsurface geophysical exploration technologies adaptable to an airborne platform
[DE93-015080] p 717 N94-14294
STS-35 crew trash compactor briefing
[NASA-TM-109487] p 533 N94-14735
A study of hydrogen effects on fracture behavior of radioactive waste storage tanks
[DE93-018171] p 574 N94-14873

WASTE TREATMENT
Photocatalysis for the treatment of waste water: Applications involving the removal of metals
[DE93-011669] p 561 N94-12841
A laser-based technique to continuously monitor metal aerosol emissions
[DE93-012836] p 710 N94-14183
Survey of subsurface geophysical exploration technologies adaptable to an airborne platform
[DE93-015080] p 717 N94-14294
Relationship between borosilicate glass composition, structure, and durability test response (SRS)
[DE93-013578] p 581 N94-14343

WASTE WATER
Photocatalysis for the treatment of waste water: Applications involving the removal of metals
[DE93-011669] p 561 N94-12841

WATER
Alternate cleaning methods for LCCAs
[KCP-613-5045] p 624 N94-13937
Widebody cabin water spray optimization tests
[DOT/FAA/CT-TN93/29] p 511 N94-14186
Room temperature degradation of YBa2Cu3O(7-x) superconductors in varying relative humidity environments
[NASA-TP-3368] p 813 N94-14409
Modeling surface area to volume effects on borosilicate glass dissolution
[DE93-011891] p 581 N94-14432
Moisture meter evaluation
[DE93-016581] p 652 N94-14534

WATER COOLED REACTORS
Test apparatus for ITER blanket cooling water distribution design
[DE93-753157] p 795 N94-12944
Nuclear thermal propulsion engine based on particle bed reactor using light water steam as a propellant
[DE93-014336] p 552 N94-14111

WATER DEPRIVATION
Soil erosion rates caused by wind and saltating sand stresses in a wind tunnel
[DE93-009154] p 706 N94-12905

WATER EROSION
Coastal scour problems and methods for prediction of maximum scour
[AD-A266658] p 726 N94-14775

WATER HEATING
Development of a nonazeotropic heat pump for crew hygiene water heating
[NASA-CR-194189] p 737 N94-13674
Colorado State University program for developing, testing, evaluating, and optimizing solar heating and cooling systems
[DE93-016018] p 705 N94-14504
Promotion of geothermal energy development in 1991
[DE93-799061] p 705 N94-14679

WATER INJECTION
Analysis of gas turbine engines using water and oxygen injection to achieve high Mach numbers and high thrust
[NASA-TM-106270] p 518 N94-13143
BOAST 2 for the IBM 3090 and RISC 6000
[DE93-000138] p 638 N94-14351

WATER MODERATED REACTORS
MCNP benchmark analyses of critical experiments for the Space Nuclear Thermal Propulsion program
[DE93-014046] p 548 N94-12981

WATER POLLUTION
Laser-induced fluorescence over optical fibers for real time in situ measurement of petroleum hydrocarbons in seawater
[AD-A265106] p 790 N94-12863

WATER QUALITY
Snow cover models in operational watershed forecasting
[DE93-778332] p 718 N94-12837
Activities report of the Netherlands Remote Sensing Board
[ETN-93-93880] p 686 N94-14073
Educational module for the Higher Agricultural Education. Part 2: Eutrophication observed by remote sensing: An educational approach to water quality monitoring
[BCRS-92-11B] p 818 N94-14462

WATER RECLAMATION
Evaluation for membrane components of water recycling system
[NAL-TM-646] p 737 N94-13388

WATER TREATMENT
Photocatalysis for the treatment of waste water: Applications involving the removal of metals
[DE93-011669] p 561 N94-12841
Evaluation for membrane components of water recycling system
[NAL-TM-646] p 737 N94-13388
Survey and study on Environmental Control and Life Support (ECLS) technologies, part 2
[NASDA-CNT-930012-PT-2] p 737 N94-13472

WATER TUNNEL TESTS
Some flow properties of telescope enclosures estimated from water channel tests: Application of the flow visualization techniques
[NAL-TR-1178T] p 830 N94-13452

WATER VAPOR
A parameterization of cloud droplet nucleation
[DE93-007998] p 718 N94-12903
DMSP F11 SSM/T-2 calibration and validation
[AD-A265817] p 719 N94-12978
Binary homogeneous nucleation: Temperature and relative humidity fluctuations and non-linearity
[DE93-007884] p 709 N94-13911
Water-vapour, total water and rainrate from passive microwave satellite data over ocean
[DLR-FB-92-37] p 723 N94-14189
The development and implementation of an interactive retrieval/analysis/forecast algorithm
p 692 N94-14234
Atmospheric correction for sea surface temperature by application of microwave dual-channel technique to VTIR data p 697 N94-14271

WATER WAVES
Radar imaging of sub-mesoscale ocean phenomena
[AD-A266339] p 725 N94-13581
Nonlinear wave forces on large ocean structures
[AD-A266820] p 683 N94-14902

WATERSHEDS
Snow cover models in operational watershed forecasting
[DE93-778332] p 718 N94-12837
Pattern and Process in Landscape Ecology: Eighth Annual US Landscape Ecology Symposium
[DE93-014032] p 711 N94-14859

WAVE ATTENUATION
Portable acoustic wave sensor systems for real-time monitoring of volatile organic compounds
[DE93-013753] p 582 N94-14511

WAVE DISPERSION
Electrodynamics of helical plasma structures
[DE93-620981] p 797 N94-13240
Ionospheric effects on a wide-bandwidth, polarimetric, space-based, synthetic-aperture radar
[DE93-015084] p 612 N94-14512
The off shell (rho)-(omega) mixing in the QCD sum rules
[DE93-014845] p 786 N94-14527
On transport of energy, momentum, orbital angular momentum and self-angular momentum of electromagnetic wave in dispersal media
[DE93-624179] p 617 N94-14883

WAVE EQUATIONS
Radar imaging of sub-mesoscale ocean phenomena
[AD-A266339] p 725 N94-13581

WAVE FRONTS
Laser beam control and diagnostic systems for the copper-pumped dye laser system at Lawrence Livermore National Laboratory
[DE93-016529] p 658 N94-14437

Wavefront sensing, control, and pointing p 546 N94-14833

WAVE FUNCTIONS
Multiple Schroedinger cats from multilevel atoms [DE93-013412] p 786 N94-14526
The fractional quantum Hall effect and the spherical shell model [DE93-014553] p 818 N94-14740
Radiation perturbation theory in gravity and quantum universe as a hydrogen atom [DE93-626621] p 849 N94-14889
A hydrogen atom in the curved space: Orthogonality of radial wave functions with respect to the critical momentum [DE93-626623] p 788 N94-14891

WAVE GENERATION
Investigation of plasma instabilities in the Polar cusp [NASA-CR-194283] p 796 N94-13084

WAVE INTERACTION
MHD shocks in coronal mass ejections [NASA-CR-193418] p 828 N94-12970
A millimeter-wave tunneladder TWT [NASA-CR-182183] p 620 N94-13106
Radar imaging of sub-mesoscale ocean phenomena [AD-A266339] p 725 N94-13581

WAVE PACKETS
On transport of energy, momentum, orbital angular momentum and self-angular momentum of electromagnetic wave in dispersal media [DE93-624179] p 617 N94-14883

WAVE PROPAGATION
Ocean acoustic processing: A model-based approach [DE93-011902] p 725 N94-12876
The 3-D massively parallel impact simulations using PCTH [DE93-011593] p 670 N94-12908
Modeling the impact behavior of AD85 ceramic under multi-axial loading [AD-A265877] p 576 N94-12932
Numerical simulations and experiments on physics of high Mach number shockwave: Turbulent flow interactions [DE93-013424] p 631 N94-13249
The propagation characteristics and instability properties of low-frequency electromagnetic waves in the Io plasma torus p 601 N94-13650
Locally non-uniform finite-difference time domain with application to stealth, crosstalk, and narrow apertures [DE93-013958] p 601 N94-13696
Non-uniqueness in dynamic rate-independent non-associated plasticity [AD-A266342] p 769 N94-13731
High order hybrid numerical simulations of two dimensional detonation waves [NASA-CR-191506] p 769 N94-13792
Measurement of wave propagation for VHF/UHF and a comparison between measured and predicted values [FFI/RAPPORT-92/7024] p 605 N94-13968
Nonlinear wave predictions in ceramics [DE93-016516] p 582 N94-14436
Ionospheric effects on a wide-bandwidth, polarimetric, space-based, synthetic-aperture radar [DE93-015084] p 612 N94-14512
Atmospheric acoustic modeling [DE93-016727] p 718 N94-14518
Kinetic simulations of ultra-intense laser plasma interactions [DE93-014419] p 802 N94-14564
Proceedings of the Seventeenth NASA Propagation Experimenters Meeting (NAPEX 17) and the Advanced Communications Technology Satellite (ACTS) Propagation Studies Miniworkshop [NASA-CR-194096] p 612 N94-14654
Opening remarks: Current and future activities p 612 N94-14655
New challenges in propagation research in the US p 612 N94-14656
User needs for propagation data p 613 N94-14657
Statistical results from the Virginia Tech propagation experiment using the Olympus 12, 20, and 30 GHz satellite beacons p 613 N94-14658
Radiometric observations of atmospheric attenuation at 20.6 and 31.65 GHz: The Wave Propagation Laboratory data base p 613 N94-14660
Long duration measurements of fading on a low elevation angle, 11-GHz satellite path p 613 N94-14661
A database for propagation models p 614 N94-14665
Propagation issues for emerging mobile and portable communications: A systems perspective p 614 N94-14667
Propagation considerations in the American Mobile Satellite system design p 614 N94-14668
The ACTS propagation terminal delivery and support p 615 N94-14674
ACTS propagation experiment discussion: Ka-band propagation measurements using the ACTS propagation terminal and the CSU-CHILL and Space Communications Technology Center Florida propagation program p 616 N94-14678

WAVE SCATTERING
Sites of fine-scale electron density turbulence in the interstellar medium [NASA-CR-193708] p 839 N94-13864

WAVE-PARTICLE INTERACTIONS
Studies on equatorial shock formation during plasmaspheric refilling [NASA-CR-194392] p 715 N94-13954

WAVEFORMS
Lower bounds on time of arrival estimation of pulse compression waveforms [ITN-93-85189] p 599 N94-13196
DATAA: Data acquisition made easy [DE93-014683] p 823 N94-13406
Center of trace algorithms for extracting digitized waveforms from two-dimensional images [DE93-015082] p 753 N94-14295

WAVEGUIDE ANTENNAS
Folded waveguide designs for tokamaks [DE93-013274] p 798 N94-13577
HRMS sky survey wideband feed system design for DSS 24 beam waveguide antenna p 611 N94-14397

WAVEGUIDE LASERS
Study of speckle reduction when using a CO2 waveguide laser close to its threshold state [DSIS-93-00250] p 657 N94-14067

WAVEGUIDES
Analysis and characterizations of planar transmission structures and components for superconducting and monolithic integrated circuits [NASA-CR-193675] p 619 N94-13026
A millimeter-wave tunneladder TWT [NASA-CR-182183] p 620 N94-13106
Laser CO2 beam transmission through hollow metallic waveguide coated by a thin internal dielectric layer [ITN-93-85201] p 656 N94-13571
Folded waveguide designs for tokamaks [DE93-013274] p 798 N94-13577
Prism-film coupling in anisotropic planar waveguides of epitaxial (101) rutile thin films [DE93-012912] p 811 N94-14304

WAVELENGTH DIVISION MULTIPLEXING
Application of new electro-optic technology to Space Station Freedom data management system [NASA-CR-177622] p 538 N94-13257

WAVELENGTHS
Impact of shorter wavelengths on optical quality for laws [NASA-CR-193433] p 792 N94-14473

WAVELET ANALYSIS
Recursive time-varying filter banks for subband image coding [NASA-CR-193726] p 598 N94-12920

WAVERIDERS
Numerical investigations in three-dimensional internal flows [NASA-CR-194143] p 637 N94-13827

WEAK INTERACTIONS (FIELD THEORY)
Radiative corrections in the strongly interacting limit of the standard electroweak model [DE93-013906] p 780 N94-13018
Study of electroweak interactions [DE93-015067] p 782 N94-13412
Effects of additional isoscalar vector bosons in e(sup +)e)(sup -)(yields)ff-bar processes at the TRISTAN and LEP energies [DE93-621451] p 783 N94-13506
The (mu)(+) yields e(+)gamma [DE93-012750] p 785 N94-14181
Comparing the Z(sup 0) mass and inclusive widths to the standard electroweak theory [PREPRINT-731] p 787 N94-14721

WEAR
Wear-mechanism modelling [DE93-012311] p 579 N94-13974
Machining aspects of nickel-phosphorus coatings [DE93-013037] p 580 N94-14311

WEAR RESISTANCE
The effect of TiN coatings on the rolling contact fatique behavior of M50 bearing steel [ARL-TR-40] p 662 N94-13794

WEAR TESTS
Dry film lubricant evaluation [DE93-013114] p 578 N94-13118
Surface analysis of bearings [AD-A266800] p 661 N94-13122
Wear-mechanism modelling [DE93-012311] p 579 N94-13974
Canadian Target Assembly (CTA) to Airborne Support Equipment (ASE) vibration test report [IME-AMT-TR-001] p 663 N94-14195

WEATHER
Preliminary meteorological results for 1992 West Coast Scotland Experiment [DE93-014677] p 720 N94-13404
Weather forecasting support for AASE-2 [NASA-CR-194342] p 721 N94-13675

WEATHER FORECASTING
The application of VAS satellite imagery to thunderstorm forecasting at Cape Canaveral [NASA-CR-193563] p 718 N94-12839
Storm prediction through barometric field analysis [PUBL-SER-A-129] p 720 N94-13587
Weather forecasting support for AASE-2 [NASA-CR-194342] p 721 N94-13675

WEATHER STATIONS
CCl working group on climate data and its rapporteurs [WCDMP-21] p 723 N94-14118

WEATHERING
Extrapolation of space weathering processes to other small solar system bodies p 843 N94-14300

WEDGES
Capillary surfaces in a wedge: Differing contact angles [DE93-013903] p 631 N94-13244

WEIBULL DENSITY FUNCTIONS
Constant False Alarm Rate (CFAR) detection in Weibull clutter [ITN-93-85190] p 600 N94-13537

WEIGHT (MASS)
Development and application of a comprehensive, design-sensitive weight prediction method for wing structures of transport category aircraft [LR-693] p 515 N94-13687

WEIGHT ANALYSIS
Development and application of a comprehensive, design-sensitive weight prediction method for wing structures of transport category aircraft [LR-693] p 515 N94-13687

WEIGHTLESSNESS
Calcitonin control of calcium metabolism during weightlessness [NASA-CR-193622] p 731 N94-12960
Capillary surfaces in a wedge: Differing contact angles [DE93-013903] p 631 N94-13244
Spacelab J experiment descriptions [NASA-TM-4517] p 586 N94-13732
Drop dynamics in space and interference with acoustic field (M-15) p 588 N94-13747
Study of bubble behavior in weightlessness (effects of thermal gradient and acoustic stationary wave) (M-16) p 589 N94-13748
Endocrine and metabolic changes in payload specialist (L-1) p 591 N94-13758
Separation of biogenic materials by electrophoresis under zero gravity (L-3) p 592 N94-13760
Manual control in space research on perceptual-motor functions under zero gravity conditions (L-10) p 593 N94-13767
Bone culture research p 595 N94-13773

WEIGHTLESSNESS SIMULATION
Gravity as a probe for understanding pattern specification [NASA-CR-194142] p 713 N94-13418
STS-30 Magellan IUS/EVA training in WETF [NASA-TM-109300] p 737 N94-13601
Circadian rhythms during simulation of the D2-spaceflight [DLR-FB-92-27] p 733 N94-14043
STS-35 EVA payload training in WETF [NASA-TM-109492] p 739 N94-14790

WELD STRENGTH
Contribution to comparison of methods for determining welding procedures for the avoidance of hydrogen cracking [VTT-PUBS-107] p 674 N94-13887

WELD TESTS
Dry film lubricant evaluation [DE93-013114] p 578 N94-13118

WELDED JOINTS
Tensile properties of LE-7 engine material with welded joint [NAL-TR-1188] p 570 N94-13460
Fatigue design curves for 6061-T6 aluminum [DE93-011849] p 571 N94-14021
Estimation of strain in 1-kW primary containment vessels by microstructural examination [DE93-013053] p 573 N94-14316

WELDING
Recent results from material processing studies on new generation lasers [DE93-013841] p 653 N94-12898

WELLS
Promotion of geothermal energy development in 1991 [DE93-799057] p 701 N94-13214
Promotion of geothermal energy development in 1991 [DE93-799058] p 701 N94-13215

WETLANDS
Pattern and Process in Landscape Ecology: Eighth Annual US Landscape Ecology Symposium
[DE93-014032] p 711 N94-14859
WETTABILITY
Incomplete melting of the Au(100) surface
[DE93-623192] p 569 N94-13227
WETTING
An analytical investigation of transient effects on rewetting of heated thin flat plates
[NASA-TM-106120] p 628 N94-12968
WHEAT
Gordon Research Conference on Chronobiology, 1991
[AD-A266354] p 728 N94-13698
Biomass production chamber air analysis of wheat study (BWT931)
[NASA-CR-194092] p 737 N94-13712
Validated environmental and physiological data from the CELSS Breadboard Projects Biomass Production Chamber. BWT931 (Wheat cv. Yecora Rojo)
[NASA-TM-109272] p 738 N94-13979
WHISKERS (CRYSTALS)
Processing and testing of high toughness silicon nitride ceramics
[NASA-CR-191190] p 582 N94-14543
WHITE DWARF STARS
ROSAT guest investigator program (AO-1). On a search for coronal x ray emissions from white dwarfs
[NASA-CR-193654] p 835 N94-13171
Monte Carlo simulation of the OCP freezing transition
[DE93-013039] p 811 N94-14313
WIDE ANGLE LENSES
Rover imaging system for the Mars rover/sample return mission
[NASA-CR-193413] p 649 N94-13464
WIGGLER MAGNETS
Microwave generation for magnetic fusion energy applications
[DE93-013864] p 654 N94-13058
Predicted performance of a dc beam driven FEM oscillator designed for fusion applications at 200-250 GHz
[DE93-013414] p 655 N94-13145
Measurement of the spin of a particle using undulator radiation
[DE93-014334] p 780 N94-13149
Multi-bunch beam-break-up studies for a SWFEL/TBA
[DE93-016973] p 658 N94-14414
WIND (METEOROLOGY)
Atmospheric soundings during the Washita 1992 campaign
[NASA-CR-194383] p 712 N94-13212
Coherent Doppler lidar signal covariance including wind shear and wind turbulence
[NASA-CR-194492] p 721 N94-13723
Boundary layer structure over areas of heterogeneous heat fluxes
[DE93-007887] p 715 N94-13912
The nocturnal wind maximum: An interactive forecast method
[KNMI-TR-142] p 722 N94-13985
WIND DIRECTION
Preliminary meteorological results for 1992 West Coast Scotland Experiment
[DE93-014677] p 720 N94-13404
WIND EROSION
Soil erosion rates caused by wind and saltating sand stresses in a wind tunnel
[DE93-009154] p 706 N94-12905
Wind erosion in semiarid landscapes: Predictive models and remote sensing methods for the influence of vegetation
[NASA-CR-194029] p 715 N94-13956
WIND PROFILES
Development of a global backscatter model for NASA's laser atmospheric wind sounder
[NASA-CR-192581] p 718 N94-12957
On the vertical structure of seasonal, interannual and intraseasonal flows
[AD-A265346] p 719 N94-12992
WIND SHEAR
Flight crew interface aspects of forward-looking airborne windshear detection systems
[NASA-CR-191437] p 516 N94-12829
Coherent Doppler lidar signal covariance including wind shear and wind turbulence
[NASA-CR-194492] p 721 N94-13723
WIND TUNNEL APPARATUS
Identifying the NAL spaceplane aerodynamic model using dynamic wind tunnel tests
[NAL-TR-1171] p 500 N94-12951
Control system design of a cable-mounted model used for dynamic wind tunnel testing
[NAL-TR-1161] p 528 N94-13337
WIND TUNNEL MODELS
Results of experimental investigations to determine external tank protuberance loads using a 0.03-scale model of the Space Shuttle launch configuration (model 47-OTS) in the NASA/ARC unitary plan wind tunnel, volume 1
[NASA-CR-167690] p 534 N94-12810
Propulsion simulator for magnetically-suspended wind tunnel models
[NASA-CR-189560] p 527 N94-13127
Control system design of a cable-mounted model used for dynamic wind tunnel testing
[NAL-TR-1161] p 528 N94-13337
Aerodynamic and aerothermal facilities 1: Hypersonic wind tunnels p 506 N94-14158
WIND TUNNEL NOZZLES
Method of characteristics design of a supersonic wind tunnel nozzle with square cross-section, supplement 3
[NASA-CR-194359] p 527 N94-12824
WIND TUNNEL STABILITY TESTS
Estimation of critical values and vibration characteristics on supersonic delta wings. Part 2: Locally-stationary time series analysis of nonstationary random responses
[NAL-TR-1179] p 502 N94-13345
WIND TUNNEL TESTS
Soil erosion rates caused by wind and saltating sand stresses in a wind tunnel
[DE93-009154] p 706 N94-12905
Identifying the NAL spaceplane aerodynamic model using dynamic wind tunnel tests
[NAL-TR-1171] p 500 N94-12951
Propulsion simulator for magnetically-suspended wind tunnel models
[NASA-CR-189560] p 527 N94-13127
Aerodynamics of a sphere and an oblate spheroid for Mach numbers from 0.6 to 10.5 including some effects of test conditions
[NASA-TM-109016] p 500 N94-13172
Results of wind tunnel tests of an ASRM configured 0.03 scale Space Shuttle integrated vehicle model (47-OTS) in the AEDC 16-foot Transonic wind tunnel (IA613A), volume 1
[NASA-CR-185696] p 534 N94-13191
Exploratory study of in-plane streamline curvature effects on a turbulent boundary layer at a Mach number of 3
[NASA-CR-193673] p 501 N94-13292
Low-speed wind tunnel tests on four types of joined-wing aircraft models
[NAL-TR-1167] p 501 N94-13340
Low-speed wind tunnel tests on a joined-wing aircraft model with various upper-fin
[NAL-TR-1169] p 501 N94-13341
Rolling moment control in the NAL 10 cm x 10 cm magnetic suspension and balance system
[NAL-TR-1164] p 526 N94-13347
Experimental studies of vortex flaps and vortex plates. Part 2: 1.15m span 60 deg delta wing
[NAL-TR-1180T-PT-2] p 502 N94-13454
Hypersonic aerodynamic characteristics of SSTO-type aerospace planes. Part 1: The NAL 0-th configuration
[NAL-TR-1186] p 514 N94-13459
An experimental investigation of shock wave/vortex interaction p 634 N94-13574
Measurements of wing and fin buffeting on the standard dynamics model
[IAR-AN-76] p 526 N94-13859
Flow-field interference produced by an asymmetrical support strut
[IAR-AN-75] p 504 N94-14031
Noise levels from a model turbofan engine with simulated noise control measures applied
[NASA-TM-106318] p 518 N94-14036
Results of experimental investigations to determine external tank protuberance loads using a 0.03-scale model of the Space Shuttle launch configuration (Model 47-OTS) in the NASA/ARC unitary plan wind tunnel, volume 2
[NASA-CR-167691] p 536 N94-14047
Experimental studies of vortex flaps and vortex plates. Part 1: 0.53 m span 60 deg delta wing
[DE93-767969] p 505 N94-14059
Aerodynamic and aerothermal facilities 1: Hypersonic wind tunnels p 506 N94-14158
Computational techniques and capabilities p 506 N94-14162
An experimental study of a turbulent boundary layer in the trailing edge region of a curculation-control airfoil
[NASA-CR-194522] p 508 N94-14541
Optical fibre Fabry-Perot interferometers for calorimetric heat transfer gauges
[RAE-TM-AERO/PROP-20] p 653 N94-14701
WIND TUNNEL WALLS
A wall interference assessment/correction system
[NASA-CR-194174] p 500 N94-13076
Wall interference studies: Revisited p 640 N94-14604
WIND TUNNELS
Soil erosion rates caused by wind and saltating sand stresses in a wind tunnel
[DE93-009154] p 706 N94-12905
Propulsion simulator for magnetically-suspended wind tunnel models
[NASA-CR-189560] p 527 N94-13127
WIND TURBINES
The 1992 JSEE/JWEA Joint Conference
[DE93-793955] p 700 N94-12822
Inflow characteristics associated with high-blade-loading events in a wind farm
[DE93-010042] p 704 N94-14423
WIND VANES
Preliminary meteorological results for 1992 West Coast Scotland Experiment
[DE93-014677] p 720 N94-13404
WIND VELOCITY
Atmospheric soundings during the Washita 1992 campaign
[NASA-CR-194383] p 712 N94-13212
Preliminary meteorological results for 1992 West Coast Scotland Experiment
[DE93-014677] p 720 N94-13404
WINDOWS (APERTURES)
Simulating the daylight performance of fenestration systems and spaces of arbitrary complexity: The IDC method
[DE93-015177] p 704 N94-14333
WINDOWS (COMPUTER PROGRAMS)
EGS (underscore) windows 2: An enhanced graphical interface to EGS
[DE93-010447] p 746 N94-13382
ANNS: An X Window based version of the AFIT neural network simulator
[AD-A266540] p 764 N94-13704
ORGBUG: A Windows-based combinatorial geometry debugger
[DE93-016640] p 755 N94-14515
WINDPOWERED GENERATORS
Inflow characteristics associated with high-blade-loading events in a wind farm
[DE93-010042] p 704 N94-14423
WING FLAPS
Numerical simulation of a powered-lift landing, tracking flow features using overset grids, and simulation of high lift devices on a fighter-lift-and-control wing
[NASA-CR-194260] p 527 N94-14322
WING PROFILES
Development and application of a comprehensive, design-sensitive weight prediction method for wing structures of transport category aircraft
[LR-693] p 515 N94-13687
Development of experimental demonstration processes for laminar-turbulent flow states at wing profiles in free flight
[ILR-MITT-280(1993)] p 510 N94-14800
WING SPAN
Low-speed wind tunnel tests on four types of joined-wing aircraft models
[NAL-TR-1167] p 501 N94-13340
WINGS
A method of predicting quasi-steady aerodynamics for flutter analysis of high speed vehicles using steady CFD calculations
[NASA-TM-109009] p 514 N94-12850
Numerical study of the effects of icing on viscous flow over wings
[NASA-CR-193306] p 500 N94-13180
WIRE
Casting of superconducting composite materials (M-4) p 586 N94-13736
WIRING
Rigid-flexible printed wiring boards
[DE93-013938] p 620 N94-13094
Electronic schematics for the Donner 600 Crystal Tomograph
[DE93-015277] p 625 N94-14336
WOOD
Moisture meter evaluation
[DE93-016581] p 652 N94-14534
WORDS (LANGUAGE)
Computational Russian morphological generation on Prolog: Noun, pronoun, and adjective p 747 N94-13436
WORK FUNCTIONS
Low energy neutral atom imaging techniques
[DE93-012744] p 779 N94-12950
WORKLOADS (PSYCHOPHYSIOLOGY)
A perspective on the FAA approval process: Integrating rotorcraft displays, controls and workload p 521 N94-13298
Functional categories for future flight deck designs
[NASA-TM-109005] p 517 N94-13710

The influence of ATC message length and timing on pilot communication
[NASA-CR-177621] p 512 N94-14744
WORKSTATIONS
EOS workstation
[NASA-CR-191326] p 736 N94-13132
Advanced computers and simulation
[DE93-014354] p 740 N94-13286
A data distributed parallel algorithm for ray-traced volume rendering
[NASA-CR-191520] p 749 N94-13721
Kerberos: A UNIX-TCP/IP network authentication system
[DE93-011677] p 760 N94-14011
A widget based operations simulator for a planetary camera: A model for the high resolution stereo camera on Mars 94
[DLR-FB-92-30] p 651 N94-14044
Oak Ridge Environmental Information System (ORIES) site workstation information packet for OREIS 6.2
[DE93-010761] p 825 N94-14458
Integrating PAW, a graphical analysis interface to Sybase
[DE93-014172] p 755 N94-14581
Computational Controls Workstation: Algorithms and hardware p 678 N94-14626
Computational Control Workstation: Users' perspectives p 681 N94-14648
WORLD METEOROLOGICAL ORGANIZATION
Manual on the global data-processing system. Volume 1: (Annex 4 to the WMO regulations) global aspects (1992 edition)
[WMO-485-VOL-1] p 721 N94-13686
Manual on the global data-processing system. Volume 2: Regional aspects (1992 edition)
[WMO-485-VOL-2] p 722 N94-14071
WOVEN COMPOSITES
Micromechanical modeling of laminated composites with interfaces and woven composites using the boundary element method
[NASA-TM-106280] p 670 N94-13053
Analysis of new composite architectures
[NASA-CR-194524] p 559 N94-14715
WROUGHT ALLOYS
Microstructural evolution of NARloy-Z at elevated temperatures
[NASA-TM-108419] p 571 N94-13715

X

X RAY ABSORPTION
The x ray dichroism experiments using circular polarization
[DE93-013195] p 568 N94-13036
Recent developments in multiple-scattering calculations of XAFS and XANES
[DE93-010999] p 563 N94-13477
A long-term space astrophysics research program: The evolution of the quasar continuum
[NASA-CR-193714] p 839 N94-14404
Ultra-soft x ray absorption spectroscopy: A bulk and surface probe of materials
[DE93-014325] p 566 N94-14582
X RAY ANALYSIS
Real time radiography of Titan 4 booster
[DE93-012450] p 548 N94-12911
Project proposal for partial computational physics support for Survivability of Coatings program
[DE93-013788] p 576 N94-12939
High spatial resolution x ray microanalysis: Comparison of experiment and incoherent scattering calculations
[DE93-011685] p 648 N94-13044
X RAY ASTRONOMY
Search for UHE point-source emission over various time scales
[DE93-012718] p 846 N94-12922
ROSAT guest investigator program (AO-1). On a search for coronal x ray emissions from white dwarfs
[NASA-CR-193654] p 835 N94-13171
ROSAT: X ray survey of compact groups
[NASA-CR-193297] p 829 N94-13181
X ray emission from dynamical shock models in hot-star winds
[NASA-CR-194093] p 847 N94-13288
Search for x ray emitting young stars outside of massive molecular clouds
[NASA-CR-193609] p 830 N94-13462
ROSAT observations of the binary Be-star/radio pulsar PSR1259-63
[NASA-CR-194394] p 832 N94-14357
A long-term space astrophysics research program: The evolution of the quasar continuum
[NASA-CR-193714] p 839 N94-14404
ROSAT observations of clusters with wide-angle tailed radio sources
[NASA-CR-193784] p 833 N94-14405
The soft x ray transient Cen X-4 in quiescence
[NASA-CR-194033] p 833 N94-14406
X RAY ASTROPHYSICS FACILITY
The four great observatories
[NASA-TM-109311] p 830 N94-13605
AXAF FITS standard for ray trace interchange
[NASA-CR-194025] p 832 N94-14305
X RAY BINARIES
A photometric study of massive x-ray binaries
[ITN-93-85207] p 829 N94-13231
High time resolution studies of binary x ray pulsars
[NASA-CR-194395] p 832 N94-13894
ROSAT observations of the binary Be-star/radio pulsar PSR1259-63
[NASA-CR-194394] p 832 N94-14357
The soft x ray transient Cen X-4 in quiescence
[NASA-CR-194033] p 833 N94-14406
X RAY DETECTORS
Metal-semiconductor, composite radiation detectors
[DE93-013313] p 619 N94-12994
An x ray detector using superconducting aluminum tunnel junctions
[DE93-015103] p 811 N94-14332
Absolute detection efficiency of a micro-channel plate detector to x rays in the 1-100 KeV energy range
[DE93-012592] p 789 N94-14460
X RAY DIFFRACTION
Analysis of samples of reflector materials which are multicoated and metal samples with oxide coatings which have been exposed the space environment in LDEF testing
[NASA-CR-193647] p 575 N94-12789
Crystallographic and metallurgical characterization of radiation detector grade cadmium telluride materials
[DE93-014335] p 806 N94-13150
Room temperature degradation of YBa2Cu3O(7-x) superconductors in varying relative humidity environments
[NASA-TP-3368] p 813 N94-14409
Is K3C60 a line phase?
[DE93-016700] p 813 N94-14517
X RAY FLUORESCENCE
ROSAT observations of clusters with wide-angle tailed radio sources
[NASA-CR-193784] p 833 N94-14405
Measurements of the spatial structure and directivity of 100 KeV photon sources in solar flares using PVO and ISEE-3 spacecraft
[NASA-CR-194080] p 845 N94-14492
Comparative study of x ray and microwave emissions during solar flares
[NASA-CR-194532] p 845 N94-14577
X RAY IMAGERY
The development of the TiMAX project: A hard x ray imaging telescope
[INPE-5474-TDI/505] p 829 N94-13245
Adaptive control of interface by temperature and interface profile feedback in transparent multi-zone crystal growth furnace
[NASA-CR-194140] p 762 N94-13253
The x ray lasers as sources for x ray microscopy
[DE93-013420] p 655 N94-13259
X ray observations of late-type stars using the ROSAT all-sky survey
[NASA-CR-193716] p 832 N94-14146
Image reconstruction for x ray holographic microscopy
[DE93-013094] p 653 N94-14772
X RAY IRRADIATION
Design and testing of planar magnetic micromotors fabricated by deep x ray lithography and electroplating
[DE93-012856] p 618 N94-12821
X RAY LASERS
Three dimensional time-dependent hydrodynamic and propagation modeling of x ray laser emission
[DE93-012575] p 654 N94-12962
Imaging microscopy with x ray lasers at Lawrence Livermore National Laboratory
[DE93-013419] p 655 N94-13258
The x ray lasers as sources for x ray microscopy
[DE93-013420] p 655 N94-13259
Oscillator-amplifier experiments in neon-like yttrium
[DE93-012577] p 657 N94-13976
The Livermore x ray laser program
[DE93-014118] p 658 N94-14152
Selenium x ray laser line profile measurements
[DE93-012580] p 658 N94-14175
Experimental measurements of selenium x-ray laser spectral line profiles
[DE93-016543] p 659 N94-14595
Optimization study of x ray laser coherence in Ni-like Ta
[DE93-016419] p 660 N94-14888
Time resolved measurement of electron temperatures of exploding foil x ray laser plasmas
[DE93-017161] p 803 N94-14894
X RAY SCATTERING
Resonant x ray Raman scattering from atoms and molecules
[DE93-015158] p 784 N94-13896
Structure and stability of microvoids in A-Si:H
[DE93-016625] p 813 N94-14413
X RAY SOURCES
Search for UHE point-source emission over various time scales
[DE93-012718] p 846 N94-12922
Studies of gas in cooling flow clusters
[NASA-CR-193597] p 628 N94-12959
The x ray lasers as sources for x ray microscopy
[DE93-013420] p 655 N94-13259
The onset of galactic winds in early-type galaxies
[NASA-CR-193640] p 836 N94-13446
X ray observations of late-type stars using the ROSAT all-sky survey
[NASA-CR-193716] p 832 N94-14146
An x ray detector using superconducting aluminum tunnel junctions
[DE93-015103] p 811 N94-14332
The 8 to 11 keV x ray sources for imaging and absorption experiments
[DE93-015973] p 803 N94-14865
X RAY SPECTRA
Studies of gas in cooling flow clusters
[NASA-CR-193597] p 628 N94-12959
ROSAT guest investigator program (AO-1). On a search for coronal x ray emissions from white dwarfs
[NASA-CR-193654] p 835 N94-13171
Selenium x ray laser line profile measurements
[DE93-012580] p 658 N94-14175
A long-term space astrophysics research program: The evolution of the quasar continuum
[NASA-CR-193714] p 839 N94-14404
X RAY SPECTROSCOPY
Analysis of samples of reflector materials which are multicoated and metal samples with oxide coatings which have been exposed the space environment in LDEF testing
[NASA-CR-193647] p 575 N94-12789
Surface science instrumentation for the study of important catalytic and electrochemical interfaces
[DE93-015068] p 563 N94-13413
Recent developments in multiple-scattering calculations of XAFS and XANES
[DE93-010999] p 563 N94-13477
Many-body corrections in XAFS
[DE93-011002] p 563 N94-13478
Applications of surface science to solid lubricants
[SMC-TR-93-24] p 579 N94-13903
Hard x ray/microwave spectroscopy of solar flares
[NASA-CR-194399] p 844 N94-13958
Ultra-soft x ray absorption spectroscopy: A bulk and surface probe of materials
[DE93-014325] p 566 N94-14582
X RAY STARS
ROSAT guest investigator program (AO-1). On a search for coronal x ray emissions from white dwarfs
[NASA-CR-193654] p 835 N94-13171
Search for x ray emitting young stars outside of massive molecular clouds
[NASA-CR-193609] p 830 N94-13462
X RAY TELESCOPES
The development of the TIMAX project: A hard x ray imaging telescope
[INPE-5474-TDI/505] p 829 N94-13245
X RAYS
Two-dimensional simulations of foil implosion experiments on the Los Alamos capacitor bank
[DE93-012676] p 794 N94-12814
Detection of hot muonic hydrogen atoms emitted in vacuum using x-rays
[DE93-010253] p 778 N94-12860
Absolute detection efficiency of a micro-channel plate detector to x rays in the 1-100 KeV energy range
[DE93-012592] p 789 N94-14460
XENON
Kinetic studies following state-selective laser excitation
[DE93-012970] p 654 N94-13013

Y

YAG LASERS
Tetravalent chromium (Cr(4+)) as laser-active ion for tunable solid-state lasers
[NASA-CR-194527] p 659 N94-14576

YAW
The 3D pneumatic and 2D dynamic probes: Their development and subsequent use in a transonic fan
[RAE-TM-AERO/PROP-22] p 653 N94-14827
YBCO SUPERCONDUCTORS
Flux-pinning related defect structures in melt-processed YBa2Cu3O(7-x)
[DE93-012759] p 804 N94-12818
The study of structure-processing-property relations in copper oxide based high (Tc) superconductors
[DE93-015066] p 804 N94-13003
Measurement of residual strain in composites by means of time-of-flight neutron diffraction
[DE93-012939] p 555 N94-13248
Measurement of penetration depth lambda(T) in YBa2Cu3O(7-delta) thin film
[DE93-014587] p 810 N94-14122
Formation of textured YBCO films by laser ablation
[DE93-013131] p 581 N94-14319
Superconductivity devices: Commercial use of space
[NASA-CR-194163] p 625 N94-14324
Room temperature degradation of YBa2Cu3O(7-x) superconductors in varying relative humidity environments
[NASA-TP-3368] p 813 N94-14409
Quenching and annealing effects on the specific heat of YBa2Cu3O(7-delta)
[DE93-016483] p 816 N94-14868
YIELD POINT
Absorption and damage thresholds of low defect density hafnia deposited with activated oxygen
[DE93-013853] p 655 N94-13243
YIELD STRENGTH
Radiation hardening and radiation-induced chromium depletion effects on intergranular stress corrosion cracking of austenitic stainless steels
[DE93-011602] p 572 N94-14058
Yield properties of tungsten and tungsten heavy alloys
[AD-A266833] p 575 N94-14878
YTTERBIUM
Laser and spectroscopic properties of Yb-doped apatite crystals
[DE93-014656] p 810 N94-14125
YTTRIUM
First-principles studies of phase stability and the structural and dynamical properties of hydrogen-metal systems
[DE93-016129] p 570 N94-13374
Oscillator-amplifier experiments in neon-like yttrium
[DE93-012577] p 657 N94-13976
YTTRIUM COMPOUNDS
Small polaron conduction in Y2Ti2O7
[ITN-93-85221] p 814 N94-14557
YTTRIUM OXIDES
Combustion synthesis and engineering of nanoparticles for electronic, structural, and superconductor applications
[DE93-016286] p 809 N94-13981
Physical and structural properties of a sputtered zirconia-yttria layer used as a thermal resistance
[ONERA-NT-1992-10] p 810 N94-14193
Metastability of yttrium-oxides
[DE93-016548] p 813 N94-14440

Z

ZEEMAN EFFECT
Dynamic Jahn-Teller effect: Calculation of fine structure spectrum, isotope shift and Zeeman behavior at deep center Ni2+ in CdS
[ETN-93-94394] p 815 N94-14705
ZEOLITES
Anchoring strategies for bimetallic species in zeolites
[DE93-015622] p 567 N94-12834
Experimental and kinetic modeling of acid/base and redox reactions over oxide catalysts
[DE93-016203] p 563 N94-13375
ZETA PINCH
Two-dimensional simulations of foil implosion experiments on the Los Alamos capacitor bank
[DE93-012676] p 794 N94-12814
Advanced magnetic flux compression generator development issues: A comparison of coaxial and disk generators
[DE93-014025] p 794 N94-12849
Instability heating of the HDZP
[DE93-012641] p 798 N94-13513
Review of the Procyon explosive pulsed power system
[DE93-016562] p 802 N94-14532
ZINC ALLOYS
Crystal growth of ZnSe and related ternary compound semiconductors by physical vapor transport
[NASA-CR-193834] p 807 N94-13444
ZINC CHLORIDES
Estimation of the concentration versus the time profile of zinc chloride particles in smoke clouds generated by the Raufoss A/S instantaneous smoke RA-90 and DM-45 HC smoke generator
[FFI-93/6001] p 708 N94-13821
ZIRCONIUM OXIDES
Combustion synthesis and engineering of nanoparticles for electronic, structural, and superconductor applications
[DE93-016286] p 809 N94-13981
Physical and structural properties of a sputtered zirconia-yttria layer used as a thermal resistance
[ONERA-NT-1992-10] p 810 N94-14193
ZONE MELTING
Growth of semiconductor compound single crystal InSb by floating zone method (M-3) p 586 N94-13735

PERSONAL AUTHOR INDEX

Typical Personal Author Index Listing

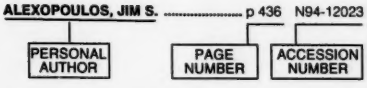

Listings in this index are arranged alphabetically by personal author. The page number helps you locate the citation in the abstract section. The accession number denotes the number by which the citation is identified.

A

AAQUIST, ORLA BOJE ..... p 829 N94-13371
ABASHIAN, A. ..... p 782 N94-13412
ABBATE, S. F. ..... p 609 N94-14381
ABBOTT, TERENCE S. ..... p 517 N94-13710
ABBOTT, TIMOTHY MARK CAMERON ..... p 831 N94-13646
ABDULAZIZ, SALMAN SAIB ..... p 703 N94-13639
ABEL, PHILLIP B. ..... p 554 N94-12871
ABERLE, BERND ..... p 651 N94-14044
ABLES, E. ..... p 791 N94-13482
ABOU-ZEID, MOHAMED N. ..... p 665 N94-13042
ABOUDI, JACOB ..... p 560 N94-14823
ABSI, ANTHONY E. ..... p 513 N94-13703
ABUMERI, GALIB H. ..... p 671 N94-13379
ACHAREKAR, M. A. ..... p 654 N94-13091
ADAM, SUSAN ..... p 735 N94-13961
ADAMS, B. E. ..... p 624 N94-13937
ADAMS, C. A. ..... p 514 N94-14563
ADAMS, R. J. ..... p 514 N94-14563
ADHEM, SAMAN M. I. ..... p 621 N94-13333
ADIGA, B. S. ..... p 744 N94-13077
ADKINS, D. R. ..... p 628 N94-12884
ADZHEMYAN, L. T. ..... p 632 N94-13511
AFFELDER, LINDA O. ..... p 825 N94-14486
AFJEH, ABDOLLAH A. ..... p 642 N94-14732
AFNAN, I. R. ..... p 785 N94-14144
AFOLABI, DARE ..... p 670 N94-12872
AFSHARI, PAYMAN ..... p 672 N94-13596
AGGARWAL, ARUN K. ..... p 663 N94-14445
..... p 664 N94-14446
AGOSTINI, P. ..... p 781 N94-13241
AGRONIN, MICHAEL ..... p 546 N94-14833
AIDUN, J. B. ..... p 816 N94-13206
AIKEN, EDWIN W. ..... p 526 N94-13325
AISAKA, TATSUYOSHI ..... p 529 N94-13270
AJAZ, H. ..... p 613 N94-14658
AJER, HALVOR ..... p 657 N94-13970
AKANUMA, ICHIRO ..... p 736 N94-13442
AKAU, R. ..... p 817 N94-14453
AKERLOF, C. ..... p 840 N94-14467
AKIYAMA, TSUYOSHI ..... p 693 N94-14242
AKSE, JAMES R. ..... p 709 N94-14103
AL-JAMILY, GHANIM ..... p 546 N94-14835
AL-JUMILY, KAIS J. L. ..... p 720 N94-13516
AL-MASRI, M. ..... p 777 N94-14130
ALAM, M. ..... p 576 N94-12912
ALBERSHEIM, P. ..... p 827 N94-14803
ALCOCK, C. ..... p 840 N94-14467
ALDE, D. ..... p 782 N94-13362
ALEXANDER, S. ..... p 540 N94-13112
ALEXIEV, D. ..... p 804 N94-12893
ALFANO, ROBERT R. ..... p 659 N94-14576
ALIAGA, DAVID ALFREDO ..... p 635 N94-13652
ALLARD, L. F. ..... p 804 N94-12818
ALLEN, S. L. ..... p 801 N94-14347
ALLEN, S. M. ..... p 569 N94-13137
ALLEN, W. R. ..... p 805 N94-13009
..... p 805 N94-13012
ALLISON, J. E. ..... p 558 N94-14119
ALLMERS, HENNING ..... p 733 N94-14043
ALLSMAN, R. ..... p 840 N94-14467
ALMEIDA, F. J. D. ..... p 623 N94-13834
ALMGREN, A. S. ..... p 639 N94-14434
ALPAY, D. ..... p 770 N94-14003
ALTMAN, EITAN ..... p 773 N94-14005
ALVELID, MAGNUS ..... p 673 N94-13689
AMANO, J. ..... p 815 N94-14699
AMARAKOON, V. R. W. ..... p 809 N94-13981
AMENDT, P. ..... p 660 N94-14888
AMES, A. L. ..... p 752 N94-14019
AMIROUCHE, F. M. L. ..... p 679 N94-14635
ANASTAS, GEORGE V., JR. ..... p 596 N94-13141
ANCHETA, D. S. ..... p 789 N94-14460
ANDERSEN, CARL M. ..... p 767 N94-13289
ANDERSEN, E. ..... p 655 N94-13258
ANDERSON, A. ..... p 506 N94-14158
ANDERSON, B. J. ..... p 712 N94-12952
ANDERSON, C. D. ..... p 586 N94-12805
ANDERSON, CHARLES D. ..... p 516 N94-12829
ANDERSON, D. F. ..... p 651 N94-14452
ANDERSON, I. E. ..... p 568 N94-13000
ANDERSON, JAMES S. ..... p 623 N94-13846
ANDERSON, KINSEY A. ..... p 845 N94-14492
ANDERSON, P. M. ..... p 802 N94-14570
ANDERSON, RONALD ..... p 816 N94-12844
ANDERSON, WILLIAM J. ..... p 660 N94-12802
ANDERSSON, BOERJE ..... p 515 N94-13690
ANDOU, HIROYASU ..... p 830 N94-13452
ANDOU, KAZUHIDE ..... p 530 N94-13274
ANDOU, YASUKATSU ..... p 502 N94-13345
ANDRE, ANTHONY D. ..... p 524 N94-13313
ANDREASSEN, OEYVIND ..... p 637 N94-14040
ANDREWS, HAL ..... p 523 N94-13309
ANDREWS, J. BARRY ..... p 565 N94-14480
ANDRIULLI, J. ..... p 676 N94-14530
ANDRUKAITIS, E. ..... p 810 N94-14203
ANGEL, PAUL W. ..... p 583 N94-14845
ANGEL, ROGER ..... p 546 N94-14834
ANTHES, JOHN P. ..... p 655 N94-13261
ANTONIA, R. A. ..... p 644 N94-14752
ANTONSEN, T. M., JR. ..... p 654 N94-13058
ANTONUCCI, R. ..... p 840 N94-14685
ANZAI, HIROYUKI ..... p 590 N94-13753
APON, A. W. ..... p 759 N94-13470
APPELBAUM, J. ..... p 620 N94-13134
..... p 621 N94-13194
..... p 626 N94-14730
APRIL, ERIC ..... p 603 N94-13829
APT, KRZYSZTOF R. ..... p 748 N94-13524
ARAI, KOUHEI ..... p 689 N94-14216
..... p 697 N94-14269
ARAVIND ..... p 744 N94-13077
ARBOCZ, J. ..... p 682 N94-14692
ARBOCZ, JOHANN ..... p 673 N94-13787
ARMATIS, P. ..... p 791 N94-13482
ARMENIA-COPE, R. ..... p 738 N94-13972
ARMENTROUT, P. B. ..... p 571 N94-13977
ARNOLD, JOE ..... p 546 N94-14835
ARNOLD, STEVEN M. ..... p 560 N94-14823
ARPE, KLAUS ..... p 724 N94-14709
ARROWOOD, J. L., JR. ..... p 600 N94-13466
ARTYUKH, V. G. ..... p 569 N94-13360
ASHBY, M. F. ..... p 579 N94-13974
ASHIDA, AKIRA ..... p 737 N94-13388
ASHLEY, C. S. ..... p 576 N94-12866
ASHTON, W. B. ..... p 706 N94-12937
ASIDA, SHIMON ..... p 639 N94-14503
ASKELAND, BJOERN ..... p 605 N94-13968
ASMAR, S. W. ..... p 611 N94-14398
ATABAKHSH, H. ..... p 753 N94-14200
ATKINS, H. L. ..... p 499 N94-12852
ATTAWAY, S. W. ..... p 742 N94-12956
AUFDERHEIDE, M. B. ..... p 783 N94-13893
AURAND, J. F. ..... p 623 N94-13892
AURIOL, ANDRE ..... p 776 N94-13692
AVERY, WILLIAM ..... p 554 N94-12833
AVITZUR, BOAZ ..... p 671 N94-13579
AWAD, F. ..... p 806 N94-13213
AXLEROD, T. ..... p 840 N94-14467
AYON, JUAN A. ..... p 545 N94-14830
..... p 545 N94-14831
AYRES, THOMAS R. ..... p 840 N94-14482
AZAIEZ, J. ..... p 644 N94-14755
AZIZ, M. J. ..... p 815 N94-14798
AZUMA, H. ..... p 589 N94-13748

B

BAAKLINI, GEORGE Y. ..... p 555 N94-13138
BACHAR, TOMER ..... p 630 N94-13197
BADAVI, FRANCIS F. ..... p 847 N94-13263
BAECKMAN, ASSAR ..... p 729 N94-14129
BAER, M. R. ..... p 561 N94-12910
..... p 632 N94-13397
BAHNCK, D. ..... p 808 N94-13694
BAILEY, DAVID ..... p 740 N94-13200
BAILEY, J. M. ..... p 778 N94-12860
BAILEY, M. C. ..... p 604 N94-13916
BAILEY, SCOTT M. ..... p 652 N94-14684
BAILLIE, STEWART W. ..... p 521 N94-13295
BAKER-JARVIS, J. ..... p 652 N94-14687
BAKER, B. ..... p 777 N94-13831
BAKER, D. ..... p 802 N94-14519
BAKER, R. S. ..... p 773 N94-14178
BAKER, WAYMAN E. ..... p 692 N94-14234
BAKKER, H. ..... p 722 N94-13985
BAKWA, D. D. ..... p 775 N94-13508
BALAKIREV, V. A. ..... p 794 N94-12853
BALANIS, CONSTANTINE A. ..... p 602 N94-13799
BALAZS, A. C. ..... p 577 N94-13070
BALDIS, H. A. ..... p 797 N94-13393
..... p 792 N94-14438
BALHORN, R. ..... p 655 N94-13258
BALL, R. M. ..... p 548 N94-12981
BANDARA, J. M. S. J. ..... p 528 N94-13544
BANGASSER, CARL ..... p 536 N94-14310
BANISH, MICHAEL ..... p 803 N94-12796
BANISH, R. MICHAEL ..... p 648 N94-13326
BANKS, DAVID C. ..... p 745 N94-13185
BANKS, H. T. ..... p 768 N94-13354
BARAM, YORAM ..... p 514 N94-14495
BARATCHART, L. ..... p 770 N94-14003
BARBATO, E. ..... p 798 N94-13577
BARBE, STEPHANE ..... p 650 N94-14009
BARBEE, T. W., JR. ..... p 655 N94-13258
BARBEE, TROY ..... p 546 N94-14835
BARBER, CHRISTOPHER E. ..... p 758 N94-12930
BARBER, W. C. ..... p 811 N94-14332
BARCLAY, REBECCA O. ..... p 821 N94-13057
..... p 825 N94-14485
..... p 825 N94-14486
..... p 826 N94-14488
BARIBEAU, J. M. ..... p 813 N94-14478
BARLETTA, W. A. ..... p 790 N94-14893
BARLOW, J. ..... p 527 N94-14642
BARNABA, ALPHONSE ..... p 625 N94-14138
BARNES, C. ..... p 657 N94-13812
BARNES, CHRISTOPHER F. ..... p 744 N94-13113
BARNES, F. J. ..... p 715 N94-13912
BARNIV, YAIR ..... p 514 N94-14495
BARONGO, JUSTUS OBIKO ..... p 685 N94-13542
BARR, L. ..... p 830 N94-13452
BARRON, C. ..... p 733 N94-14860
BARROS, MARIA SUELENA S. ..... p 686 N94-13729
..... p 686 N94-13789
BARROWS, LINDA H. ..... p 729 N94-14032
BARTON, I. J. ..... p 696 N94-14263
BARTON, J. S. ..... p 653 N94-14701
BARTON, JOHN ..... p 740 N94-13200
BARUCH, MENAHEM ..... p 673 N94-13787
BASORE, P. A. ..... p 703 N94-13886
BASSOM, ANDREW P. ..... p 630 N94-13128
BASSON, ANTON HERMAN ..... p 634 N94-13630
BASTON, D. W. ..... p 543 N94-14352
BATCHELOR, D. ..... p 803 N94-14770
BATCHELOR, D. B. ..... p 795 N94-13033
BATEMAN, V. I. ..... p 649 N94-13395
BATHA, S. H. ..... p 796 N94-13046
..... p 797 N94-13393
BATISHKO, C. R. ..... p 793 N94-14702
BATSON, P. J. ..... p 658 N94-14175
..... p 659 N94-14595

BATTEN, J. H.	p 737	N94-13712
BATTRICK, BRUCE	p 699	N94-14353
BATUR, CELAL	p 762	N94-13253
BAUCHAU, O.	p 510	N94-14799
BAUCOM, K. C.	p 812	N94-14344
BAUER, FRANK H.	p 678	N94-14628
BAUER, PETER	p 723	N94-14189
BAUER, ROBERT	p 615	N94-14673
BAUGH, HAROLD W.	p 532	N94-13796
BAUM, M.	p 567	N94-14765
BAUTISTA, J. J.	p 608	N94-14376
BAVINCK, HERMAN	p 770	N94-14150
BAXI, C. B.	p 802	N94-14570
BAYFIELD, J. E.	p 780	N94-13071
BAYO, EDUARDO	p 678	N94-14624
	p 679	N94-14633
BAZIZI, K. A.	p 783	N94-13494
BEACH, R.	p 658	N94-14442
BEALE, S. B.	p 637	N94-13862
BEAN, J. C.	p 808	N94-13694
BEAUMONT, B.	p 797	N94-13144
BEAVER, JOHN	p 616	N94-14678
BECK, B.	p 788	N94-13208
BECK, CORIN P.	p 525	N94-13318
BECK, JON	p 754	N94-14368
BECKER, B. G.	p 742	N94-12883
BECOULET, A.	p 797	N94-13144
BEDDHU, MURALI	p 634	N94-13635
BEDDOES, J.	p 571	N94-13840
BEENE, DONYA	p 729	N94-14028
BEENEN, RICHARD	p 542	N94-13988
BEER, G. A.	p 778	N94-12860
BEIER, BERNHARD	p 557	N94-13804
BEIERSDORFER, P.	p 788	N94-13208
BEIN, T.	p 567	N94-12834
BEJMUK, BOHDAN I.	p 668	N94-13166
BELL, C. P.	p 616	N94-14742
BELL, J. B.	p 639	N94-14434
BELLEY, JULIEN	p 836	N94-13372
BELONGIE, M.	p 609	N94-14380
BELOUS, V. A.	p 569	N94-13360
BELTRAN, L.	p 704	N94-14333
BELY, PIERRE	p 546	N94-14833
BELYTSCHKO, T.	p 674	N94-13873
BEN-IVRI, ISRAEL	p 599	N94-13196
BENEDIX, G.	p 842	N94-14298
BENGTSSON, LENNART	p 724	N94-14709
BENNET, B. A.	p 567	N94-14884
BENNETT, C. L.	p 651	N94-14416
BENNETT, D. P.	p 840	N94-14467
BENNETT, E. G.	p 570	N94-13666
BENNETT, R. G.	p 552	N94-14013
BENNETT, W. J.	p 658	N94-14442
BENZIGER, T. M.	p 584	N94-13491
BERAN, DIETER	p 694	N94-14248
BERDIS, E.	p 737	N94-13712
BERES, W.	p 850	N94-13548
	p 675	N94-14035
BERETS, JAMES C.	p 758	N94-12930
BEREZHNYJ, V. L.	p 798	N94-13507
BEREZIN, A. K.	p 797	N94-13240
BERGER, FRANZ HERBERT	p 723	N94-14707
BERGER, R. L.	p 797	N94-13393
BERGMAN, THOMAS	p 729	N94-14129
BERKENBOSCH, L. J.	p 596	N94-13407
BERKMAN, OMER	p 755	N94-14556
BERLA, DAVID	p 599	N94-13237
BERNARD, PIERRE	p 657	N94-14067
BERNHARDT, A. F.	p 627	N94-14870
BERNREUTHER, W.	p 778	N94-12847
BERNSTEIN, AMY L.	p 820	N94-12801
BERREBI, DAVID	p 814	N94-14554
BEST, R. W. B.	p 655	N94-13145
BESTERFIELD, G.	p 674	N94-13873
BEVERIDGE, J. L.	p 778	N94-12860
BEY, KIM S.	p 632	N94-13467
BEYER, BILL	p 821	N94-12958
BEYERS, M. E.	p 504	N94-14031
BEZLER, P.	p 554	N94-14806
BEZUGLYJ, A. I.	p 618	N94-12856
BHANSALI, SANJAY	p 745	N94-13290
	p 745	N94-13355
	p 745	N94-13356
	p 745	N94-13357
	p 747	N94-13443
BHAT, B. N.	p 571	N94-13715
BHAT, P. C.	p 781	N94-13350
BHATNAGAR, V.	p 607	N94-14291
BHUIYAN, A. K. M. FARIDUDDIN	p 695	N94-14260
BIALKE, WILLIAM	p 540	N94-13140
BICKFORD, D. F.	p 578	N94-13493
BICOS, ANDREW S.	p 540	N94-13016
BIEBERICH, MARY JO	p 580	N94-14126
BIEFELD, R. M.	p 812	N94-14344
BIESEMAN, TACO	p 764	N94-13844
BIGELOW, T. S.	p 798	N94-13577
BILALBEGOVIC, G.	p 569	N94-13227
BILBRO, JIM	p 546	N94-14834
BINDER, JANN OLUF	p 656	N94-13522
BINDIGANAVALE, SUNIL	p 602	N94-13720
BINOT, R. A.	p 737	N94-13901
	p 738	N94-13902
BISHOP, ANN P.	p 825	N94-14487
BISHOP, DENNIS	p 614	N94-14666
BISLING, PETER	p 617	N94-14819
	p 617	N94-14820
BISWAS, A.	p 610	N94-14387
BISWAS, R.	p 813	N94-14413
BLAIS, F.	p 765	N94-14201
BLAISDELL, G. A.	p 645	N94-14758
BLAKE, J. B.	p 784	N94-13936
BLAKE, KENNETH R.	p 638	N94-14356
BLAKE, R. D.	p 581	N94-14340
BLANCH, JAN H.	p 708	N94-13821
BLAND, R. W.	p 811	N94-14332
BLANKEN, CHRIS L.	p 521	N94-13299
	p 522	N94-13300
BLANKEN, CHRISTOPHER L.	p 521	N94-13294
BLANPIED, G.	p 785	N94-14363
BLATTNER, M. M.	p 748	N94-13576
BLECHER, M. C.	p 785	N94-14363
BLENK, STEFAN	p 807	N94-13590
BLEWITT, G.	p 514	N94-14371
BLISS, DONALD B.	p 509	N94-14774
BLISS, E. S.	p 656	N94-13481
	p 658	N94-14437
BLUEMCKE, ERICH WALTER	p 637	N94-14045
BLUEMEL, KLAUS	p 723	N94-14546
BOBINSKY, ERIC A.	p 538	N94-13111
BODECHTEL, J.	p 694	N94-14249
BOEDEKER, LAURENCE R.	p 553	N94-14682
BOELIN, INGRID	p 729	N94-14129
BOGDONOFF, SEYMOUR M.	p 501	N94-13292
BOGUE, RODNEY K.	p 516	N94-13256
	p 517	N94-13791
BOHM, A.	p 817	N94-13479
BOHORQUEZ, CAMILO TELLO	p 837	N94-13449
BOKHARI, SHAHID H.	p 762	N94-13184
BOLLES, ROBERT C.	p 766	N94-14777
BONCA, J.	p 760	N94-14177
BONIN, M. P.	p 710	N94-14183
BOOTH, T. E.	p 772	N94-12919
BORAIE, MOHAMED T.	p 763	N94-13515
BORKOWSKI, J. A.	p 550	N94-13351
BORN, GEORGE H.	p 716	N94-14049
BORODKIN, A. V.	p 794	N94-12853
BORRELLI, ARIANNA	p 787	N94-14721
BOSLOUGH, M. B.	p 539	N94-12909
BOSSE, ELOI	p 603	N94-13832
BOSSERT, J. E.	p 722	N94-14057
BOTTONI, M.	p 642	N94-14708
BOUANANE, MOHAMED EL AMINE	p 626	N94-14711
BOUDREAU, ALBERT H.	p 505	N94-14157
BOULANGER, P.	p 769	N94-13545
BOURCIER, W. L.	p 581	N94-14432
BOURGES-VERDU, CATHERINE	p 574	N94-14814
BOURGOYNE, A. T., JR.	p 638	N94-14351
BOURKE, M. A.M.	p 558	N94-14119
BOUTBOUL, THIERRY	p 656	N94-13571
BOWDLE, DAVID	p 718	N94-12957
BOWEN, J.	p 608	N94-14375
BOWERS, R. L.	p 794	N94-12814
BOWLER, DENNIS PATRICK	p 656	N94-13573
BOWLES, T. J.	p 781	N94-13205
	p 785	N94-14466
BOWMAN, J. D.	p 786	N94-14514
BOXMA, O. J.	p 765	N94-14361
BOYCE, R. R.	p 509	N94-14710
BOYD, ALFRED A.	p 668	N94-13165
BOYKIN, WILLIAM H.	p 793	N94-14548
BOYKIN, WILLIAM H., JR.	p 705	N94-14430
BOYLE, CHARLES	p 851	N94-14791
BOYLE, J. M.	p 768	N94-13391
BOYLE, R. J.	p 629	N94-13027
BRADDY, D.	p 742	N94-12840
	p 744	N94-13120
	p 822	N94-13121
BRADLEY, J. A.	p 809	N94-14079
	p 809	N94-14083
	p 809	N94-14108
BRADLEY, ROY	p 523	N94-13306
	p 523	N94-13311
BRAGA, CLAUDIA ZUCCARI FERNANDES	p 684	N94-13426
BRASE, J.	p 653	N94-14772
BRASWELL, DOROTHY O.	p 500	N94-13172
BRATMAN, V. L.	p 655	N94-13145
BRAY, I.	p 806	N94-13226
BRAY, K. N. C.	p 562	N94-13085
BRAY, O. H.	p 743	N94-12999
BRAY, RICHARD S.	p 517	N94-13323
BRAYMER, SUSAN A.	p 666	N94-13155
BREAULT, ROBERT	p 547	N94-14836
BREEZE, S. P.	p 652	N94-14578
BREGER, P.	p 781	N94-13241
BREGMAN, JOEL N.	p 838	N94-13716
BREIDENTHAL, J. C.	p 609	N94-14381
BREIG, EDWARD L.	p 714	N94-13825
BRENNAN, KEVIN F.	p 650	N94-14029
BRENNER, H.	p 628	N94-12961
BRENNER, MARTIN J.	p 520	N94-13255
BRESLAUER, DANY	p 760	N94-13924
BREWER, J. H.	p 778	N94-12860
BREWER, SI	p 547	N94-14837
BRINGI, V. N.	p 616	N94-14678
BRINKER, C. J.	p 576	N94-12866
BRINKOP, SABINE	p 724	N94-14709
BRISSON, J. G.	p 597	N94-14592
BRITO, JORGE LUIS SILVA	p 720	N94-13614
BRITT, JOHN E.	p 675	N94-13907
BROADHEAD, B. L.	p 774	N94-14334
BROCK, B. C.	p 612	N94-14512
BROCKENBROUGH, J. R.	p 568	N94-12993
BROGAN, F. A.	p 673	N94-13726
	p 674	N94-13905
BROOKES, DANIEL	p 603	N94-13832
BROOKES, N. B.	p 580	N94-14142
BROOKS, G. H.	p 709	N94-14020
BROOKS, N. H.	p 801	N94-14347
	p 802	N94-14570
BROPHY, JOHN R.	p 549	N94-13055
	p 549	N94-13068
BROUWER, H. H.	p 503	N94-13528
BROWN, C. W.	p 748	N94-13480
BROWN, F. A.	p 649	N94-13395
BROWN, JEFF	p 508	N94-14541
BROWN, L.	p 709	N94-14087
BROWN, NORMAN	p 546	N94-14834
BROWN, S. A.	p 742	N94-12840
	p 744	N94-13120
	p 822	N94-13121
BROWNELL, J. H.	p 794	N94-12814
BROWNING, N. D.	p 808	N94-13930
BRUEMMER, S. M.	p 568	N94-13035
	p 572	N94-14058
BRUGEL, EDWARD W.	p 840	N94-14482
BRUSASCO, R.	p 803	N94-14590
BRUTSAERT, W.	p 712	N94-13212
BRYAN, R. M.	p 578	N94-13118
BRYANSTON-CROSS, P. J.	p 509	N94-14706
BRYCE, J. D.	p 653	N94-14827
BRYFOGLE, MARK D.	p 661	N94-13129
BUCCI, R. J.	p 568	N94-12993
BUCK, W. W.	p 786	N94-14551
	p 786	N94-14552
BUCK, WARREN W.	p 786	N94-14549
BUCKINGHAM, A. C.	p 631	N94-13249
	p 631	N94-13250
BUCKNALL, D. G.	p 579	N94-13783
BUDAI, J. D.	p 812	N94-14362
BUDEN, D.	p 549	N94-12996
BUDINGER, T. F.	p 625	N94-14336
BUDZIAK, CHESTER JOHN	p 817	N94-13554
BUGG, CHARLES E.	p 591	N94-13756
BUHL, M. R.	p 700	N94-14566
BUKLEY, ANGELIA P.	p 527	N94-14646
BULBECK, C. J.	p 644	N94-14754
BULLARD, JERRY D.	p 667	N94-13160
BULTER, MARLON L.	p 682	N94-14652
BUNCE, G.	p 780	N94-13101
BUNTAIN, G. A.	p 584	N94-13491
BUONOMO, SERGIO	p 615	N94-14669
BUR, MIKE	p 808	N94-13875
BUR, REYNALD	p 630	N94-13117
BURCAT, A.	p 566	N94-14869
BURCHAM, FRANK W., JR.	p 520	N94-13254
BURDEN, HUBERT W.	p 728	N94-13473
BURGINYON, G. A.	p 789	N94-14460
BURKE, W. R.	p 543	N94-14352
BURNS, JACK O.	p 833	N94-14405
BURNS, T. J.	p 755	N94-14515
BURRELL, K. H.	p 802	N94-14570
	p 802	N94-14579
	p 802	N94-14583
BURROWS, CHRIS	p 547	N94-14837
BUSHKO, DARIUSZ A.	p 596	N94-13141
BUTCHER, K. S. A.	p 804	N94-12893
BUTLER, D. J.	p 653	N94-12857
BUTS, V. A.	p 797	N94-13240
BUTT, D. P.	p 585	N94-14535
BUTT, G.	p 615	N94-14670
BUTTON, P.	p 543	N94-14352
BUTTRAM, M. T.	p 623	N94-13892
BYRANT, M. G.	p 707	N94-13390

C

CAHOON, J. L. ..... p 625 N94-14336
CAI, H. J. ..... p 504 N94-14031
CAI, WEI ..... p 769 N94-13792
CAIN, J. M. ..... p 595 N94-13021
CALDI, D. G. ..... p 818 N94-14896
CALEDONIA, G. E. ..... p 562 N94-13115
CALFO, FREDERICK D. ..... p 642 N94-14732
CALISE, ANTHONY J. ..... p 508 N94-14538
CALLAHAN, D. A. ..... p 789 N94-13727
CALLIS, R. W. ..... p 801 N94-14293
CALOINI, ANDREA ..... p 750 N94-13822
CALORI, G. ..... p 823 N94-13806
CAMBON, C. ..... p 645 N94-14757
CAMERON, S. E. ..... p 806 N94-13150
CAMPARO, J. C. ..... p 659 N94-14681
CAMPBELL, G. H. ..... p 806 N94-13136
CAMPBELL, G. L. ..... p 802 N94-14570
CAMPBELL, WARREN ..... p 621 N94-13186
CANDY, J. V. ..... p 725 N94-12876
CANESSA, E. ..... p 778 N94-12879
p 772 N94-12896
CANNON, T. ..... p 704 N94-14350
CANTWELL, B. J. ..... p 644 N94-14751
CAPLAN, M. ..... p 655 N94-13145
CAPORASO, G. J. ..... p 654 N94-12963
CAPPETTA, A. N. ..... p 521 N94-13296
CARACAPPA, A. ..... p 785 N94-14363
CARBAUGH, DAVID C. ..... p 516 N94-12829
CARLBERG, I. A. ..... p 813 N94-14409
CARLIN, BRADLEY P. ..... p 773 N94-13585
CARLSON, K. D. ..... p 623 N94-13925
CARLSTROM, T. N. ..... p 802 N94-14579
CARMAN, STEPHEN L. ..... p 690 N94-14223
CARNES, MICHAEL R. ..... p 725 N94-12990
CARPENTER, J. W. ..... p 811 N94-14332
CARPENTER, SCOTT A. ..... p 550 N94-13147
CARPENTER, THOMAS W. ..... p 630 N94-13078
p 638 N94-14086
CARPER, D. M. ..... p 557 N94-13920
CARRETTA, THOMAS R. ..... p 735 N94-13582
CARSCALLEN, WILLIAM EDWARD
p 502 N94-13369
CARTER, M. D. ..... p 797 N94-13144
p 798 N94-13577
CARTER, M. R. ..... p 654 N94-12962
p 657 N94-13976
p 651 N94-14416
CARY, W. P. ..... p 801 N94-14293
CASPER, JAY ..... p 499 N94-12852
CASSIDY, PATRICK E. ..... p 579 N94-13964
CASTANEDA-SEPULVEDA, ROMAN
p 793 N94-14856
CASTELLANI, C. ..... p 815 N94-14720
CASTELLI, MICHAEL G. ..... p 555 N94-13139
p 560 N94-14822
CASTOR, J. I. ..... p 839 N94-14341
CATTAFESTA, LOUIS NICHOLAS, III
p 634 N94-13574
CAUGHMAN, J. B. O. ..... p 798 N94-13577
CAUTER, EVE V. ..... p 732 N94-13038
CECH, STEVEN D. ..... p 792 N94-13719
CECHET, R. P. ..... p 696 N94-14263
CEGIELSKI, ERIC ..... p 536 N94-14310
CERBONE, R. J. ..... p 548 N94-12981
CERNOSEK, R. W. ..... p 582 N94-14511
CHA, A. ..... p 611 N94-14396
CHADWELL, C. DAVID ..... p 512 N94-13082
CHAI, B. H. T. ..... p 810 N94-14125
CHAIT, A. ..... p 620 N94-13134
CHAKOUMAKOS, B. C. ..... p 812 N94-14362
CHAKRABARTTY, S. K. ..... p 639 N94-14598
p 639 N94-14599
p 510 N94-14608
CHALLIS, K. ..... p 669 N94-13857
CHAMEIDES, W. L. ..... p 706 N94-13170
CHAMIS, C. C. ..... p 676 N94-14041
CHAMIS, CHRISTOS C. ..... p 671 N94-13379
p 675 N94-13919
p 557 N94-14042
CHAN, A. ..... p 603 N94-13843
CHAN, A. W. ..... p 753 N94-14200
CHAN, S. K. ..... p 811 N94-14304
CHAN, Y. D. ..... p 848 N94-13695
CHANA, K. S. ..... p 653 N94-14701
p 509 N94-14706
CHANCE, KELLY V. ..... p 714 N94-13816
CHANDRASEKAR, V. ..... p 616 N94-14678
CHANG, H. L. M. ..... p 811 N94-14304
CHANG, LANG-MANN ..... p 583 N94-12987
CHANG, Y. ..... p 580 N94-14142
CHAREST, LEONARD, JR. ..... p 749 N94-13784
CHARLES, JOHN B. ..... p 594 N94-13772
CHASE, JUANITA R. ..... p 821 N94-13041
CHASNOV, J. ..... p 643 N94-14748
CHASNOV, J. R. ..... p 644 N94-14753
CHASSAT, FRANCOIS ..... p 716 N94-14192
CHATTERJEE, S. ..... p 746 N94-13382
CHAWLA, KALPANA ..... p 527 N94-14322
CHEBOTAREV, V. V. ..... p 794 N94-12854
CHELIKOWSKY, J. R. ..... p 811 N94-14296
CHEN, C. H. ..... p 812 N94-14348
CHEN, C. Y. ..... p 806 N94-13228
CHEN, CHAUR-FONG ..... p 685 N94-13592
CHEN, HUA ..... p 838 N94-13648
CHEN, J. H. ..... p 567 N94-14766
p 567 N94-14767
CHEN, M. H. ..... p 784 N94-14140
CHEN, MARGARET W. ..... p 714 N94-13793
CHEN, MEI-LI ..... p 846 N94-12947
CHEN, QISHENG ..... p 702 N94-13386
CHEN, SEN PAL ..... p 567 N94-14884
CHEN, SHYH-C. ..... p 722 N94-14057
CHEN, T. ..... p 694 N94-14249
CHENG, LI-JEN ..... p 547 N94-14838
CHENG, W. P. ..... p 645 N94-14756
CHERNUKA, M. W. ..... p 751 N94-14017
p 558 N94-14105
CHERRETT, M. A. ..... p 653 N94-14827
CHHABILDAS, L. C. ..... p 539 N94-12909
CHIARELLO, R. P. ..... p 811 N94-14304
CHIEN, STEVE A. ..... p 749 N94-13784
CHILDRESS, S. R. ..... p 808 N94-13973
CHILDS, D. W. ..... p 660 N94-12988
CHIMA, R. V. ..... p 499 N94-13108
CHINAEVA, V. P. ..... p 567 N94-14884
CHINE, ABDERRAZEK ..... p 756 N94-14813
CHISHOLM, G. H. ..... p 756 N94-14844
CHISHOLM, M. F. ..... p 808 N94-13930
CHIU, S. C. ..... p 801 N94-14293
CHLAMTAC, IMRICH ..... p 791 N94-13682
CHOI, SUNG R. ..... p 582 N94-14543
CHONG, M. S. ..... p 644 N94-14751
CHORY, M. A. ..... p 544 N94-14649
CHOU, M. Y. ..... p 570 N94-13374
CHOU, T. T. ..... p 784 N94-13927
CHOU, YEONG-SHYUNG ..... p 556 N94-13557
CHOW, CHUEN-YEN ..... p 503 N94-13463
CHOW, E. T. ..... p 610 N94-14385
CHOW, I. ..... p 755 N94-14581
CHOW, R. ..... p 655 N94-13243
CHREN, WILLIAM A., JR. ..... p 623 N94-13878
CHRISMAN, DAN A. ..... p 752 N94-14139
CHRISP, MICHAEL ..... p 547 N94-14838
CHRISTEN, D. K. ..... p 812 N94-14362
CHRISTENSON, T. R. ..... p 618 N94-12821
CHRISTIAN, PAUL M. ..... p 682 N94-14652
CHRISTOPHERSON, ROBERT J. .. p 733 N94-14879
CHRISTOU, NIKOLAOS THEODOROS
p 726 N94-14205
CHROSTOWSKI, JON D. ..... p 671 N94-13124
CHU, C. C. ..... p 681 N94-14647
CHU, T. S. ..... p 649 N94-13410
CHUANG, C. ..... p 718 N94-12903
CHUBB, DONALD L. ..... p 642 N94-14732
CHUECH, S. ..... p 627 N94-12803
CHUI, CHARLES K. ..... p 771 N94-14789
CHUI, T. ..... p 817 N94-14453
CHUNG, WILSON C. ..... p 619 N94-12897
p 598 N94-12920
CHUPP, EDWARD L. ..... p 849 N94-13965
CHURCH, D. ..... p 788 N94-13208
CHURCHILL, L. W. ..... p 678 N94-14625
CIARLO, D. ..... p 658 N94-14442
CINTALA, M. ..... p 842 N94-14298
CINTALA, MARK J. ..... p 843 N94-14299
CIVINSKAS, K. C. ..... p 629 N94-13027
CLAMPIN, MARK ..... p 546 N94-14833
CLARK, B. ..... p 842 N94-14298
CLARK, D. A. ..... p 788 N94-13103
CLARK, E. A. ..... p 703 N94-13691
CLARK, G. A. ..... p 700 N94-14566
CLAUS, R. O. ..... p 791 N94-13353
CLEMENT, SERGE ..... p 624 N94-13951
CLERY, MAGALI ..... p 810 N94-14193
CLEVELAND, JOAN S. ..... p 731 N94-14899
CLINARD, J. A. ..... p 569 N94-13242
COCHRAN, C. ..... p 791 N94-13482
CODA, S. ..... p 802 N94-14579
COE, CARLOS J. ..... p 766 N94-14785
COFFEY, D. ..... p 811 N94-14339
COFFEY, HELEN E. ..... p 845 N94-14560
p 845 N94-14561
COHAN, STEVE ..... p 762 N94-13131
COHEN, A. L. ..... p 544 N94-14649
COHEN, E. A. ..... p 602 N94-13813
COHEN, NATHANIEL B. ..... p 818 N94-13984
COHEN, S. ..... p 788 N94-13103
COLAVITA, MARK ..... p 546 N94-14833
COLE, JONATHAN ..... p 758 N94-12930
COLELLA, P. ..... p 639 N94-14434
COLEMAN, G. N. ..... p 645 N94-14757
COLINA ..... p 625 N94-14336
COLLINS, LAURIE ..... p 718 N94-12957
COLLINS, O. ..... p 609 N94-14378
COLOZZA, ANTHONY J. ..... p 621 N94-13194
COMANZO, H. A. ..... p 620 N94-13031
COMBS, R. ..... p 625 N94-14522
COMEDI, D. ..... p 623 N94-13834
COMINSKY, LYNN R. ..... p 832 N94-13894
p 832 N94-14357
COMISIONERU, SILVIU ..... p 736 N94-13229
CONCUS, P. ..... p 631 N94-13244
CONDER, A. ..... p 653 N94-14792
CONDOURIS, R. ..... p 795 N94-13017
CONN, J. J. ..... p 564 N94-13942
CONNATSER, ROBERT ..... p 788 N94-14905
CONNELL, JOHN L. ..... p 667 N94-13161
CONNER, K. J. ..... p 660 N94-12988
CONNER, W. V. ..... p 565 N94-14346
CONOVER, HELEN ..... p 683 N94-14484
CONTOLINI, R. J. ..... p 627 N94-14870
CONVERTINO, V. A. ..... p 731 N94-12972
CONWAY, G. ..... p 799 N94-13835
CONWAY, G. D. ..... p 798 N94-13518
p 602 N94-13802
COOK, K. H. ..... p 840 N94-14467
COOK, R. ..... p 683 N94-14818
p 574 N94-14828
COOPER, ALFRED R. ..... p 583 N94-14845
COOPER, M. D. ..... p 785 N94-14181
p 785 N94-14366
COOPER, P. M. ..... p 570 N94-13666
COOPER, R. ..... p 780 N94-13173
COSGROVE, SARAH J. ..... p 733 N94-14879
COSS, J. ..... p 657 N94-13812
COSTELLA, J. P. ..... p 778 N94-12858
COSTELLO, MARK F. ..... p 523 N94-13308
COSTERUS, B. ..... p 548 N94-12911
COSTINER, SORIN ..... p 767 N94-13202
COTHREN, BOBBY ..... p 788 N94-14905
COULTER, DAN ..... p 546 N94-14835
COULTER, R. L. ..... p 715 N94-13912
p 717 N94-14424
COVEY, STEVEN J. ..... p 559 N94-14769
COWAN, P. L. ..... p 784 N94-13896
COWARD, ADRIAN V. ..... p 636 N94-13817
COWIE, LENNOX L. ..... p 628 N94-12959
COWINGS, PATRICIA S. ..... p 595 N94-13774
COWLES, K. ..... p 533 N94-14394
COX, D. E. ..... p 813 N94-14517
COX, P. T. ..... p 761 N94-12859
COX, RICHARD A. ..... p 694 N94-14251
COYNE, R. A. ..... p 825 N94-14331
p 760 N94-14475
CRABTREE, G. W. ..... p 623 N94-13925
CRAGGS, A. ..... p 733 N94-13847
CRAIG, ROY R., JR. ..... p 677 N94-14621
CRAIGEN, DAN ..... p 752 N94-14088
CRAMER, P. ..... p 611 N94-14396
CRANDALL, K. R. ..... p 789 N94-13209
CRANE, ROBERT K. ..... p 614 N94-14664
CRAPO, J. A. ..... p 538 N94-13918
CRAWFORD, ROGER ..... p 505 N94-14156
p 506 N94-14160
p 508 N94-14174
CRAWFORD, T. L. ..... p 715 N94-13912
CRAXTON, R. S. ..... p 654 N94-12962
CREAGER, M. ..... p 542 N94-14076
p 542 N94-14077
p 542 N94-14078
p 519 N94-14841
p 519 N94-14842
CREIGHTON, J. R. ..... p 638 N94-14318
CRESPIREGHIZZI, STEFANO ..... p 750 N94-13805
CRETEGNY, J. F. ..... p 671 N94-13501
CREUTZ, M. ..... p 773 N94-14320
CRIMINALE, WILLIAM O. ..... p 636 N94-13724
CRISPIN, K. ..... p 760 N94-14315
CROCKETT, THOMAS W. ..... p 762 N94-13184
CROSS, A. E. ..... p 598 N94-12811
CROSS, AUBREY E. ..... p 597 N94-12804
CROW, RITA M. ..... p 850 N94-14060
CROWE, W. R. ..... p 623 N94-13892
CROWN, E. M. ..... p 564 N94-13819
CRUTCHIK, M. ..... p 621 N94-13194
CRUTCHIK, MARCOS ..... p 702 N94-13570
CUCINOTTA, FRANCIS A. ..... p 846 N94-12875
p 732 N94-13714
CUISIN, ANDRE ..... p 605 N94-13950
CUMMINGS, VIRGINIA J. ..... p 534 N94-12900
CUMPSON, P. J. ..... p 708 N94-13667
CUNNINGHAM, C. E. ..... p 811 N94-14332
CURL, R. F. ..... p 562 N94-13004
CURRIER, R. P. ..... p 576 N94-12916
CURTISS, H. C., JR. ..... p 524 N94-13312

CYR, R. ..... p 727 N94-12835

D

D-SHAH, T. ..... p 711 N94-12788
DABNEY, PHILLIP W. ..... p 808 N94-13875
DACRUZ, M. T. F. ..... p 848 N94-13695
DAHAN, PINCHAS ..... p 814 N94-14559
DAHMS, M. ..... p 574 N94-14821
DALE, J. D. ..... p 564 N94-13819
DALE, V. ..... p 707 N94-13486
DALLMAN, M. F. ..... p 731 N94-12972
DAMICO, FLAVIO ..... p 829 N94-13245
DAN, T. ..... p 587 N94-13739
DANA, M. T. ..... p 708 N94-13910
DANEK, GEORGE L. ..... p 527 N94-13008
DANLEY, T. J. ..... p 586 N94-12805
DANNEVIK, W. P. ..... p 647 N94-14895
DAPKUS, P. D. ..... p 702 N94-13386
DARAB, J. G. ..... p 572 N94-14184
DARLOW, M. ..... p 510 N94-14799
DARROW, C. ..... p 658 N94-14114
DARWIN, DAVID ..... p 665 N94-13042
DAS, ALOK ..... p 527 N94-14650
DASILVA, CRESPO M. ..... p 510 N94-14799
DASILVA, L. ..... p 795 N94-12995
p 658 N94-14175
DASILVA, L. B. ..... p 655 N94-13258
p 659 N94-14595
DAUM, P. ..... p 706 N94-13054
DAVARIAN, FARAMAZ ..... p 612 N94-14654
p 612 N94-14655
p 612 N94-14656
p 614 N94-14666
DAVEY, J. ..... p 580 N94-14179
DAVIE, N. T. ..... p 649 N94-13395
DAVIES, J. A. ..... p 623 N94-13834
DAVIES, P. O. A. L. ..... p 663 N94-13874
DAVIS, A. M. J. ..... p 628 N94-12961
DAVIS, J. N. ..... p 756 N94-14696
DAVIS, J. R. ..... p 669 N94-13857
DAVIS, W. C. ..... p 583 N94-12921
DAY, G. W. ..... p 792 N94-14367
DAY, R. D. ..... p 812 N94-14365
DAY, R. S. ..... p 564 N94-13487
DAYTON, JAMES A. ..... p 620 N94-13110
DEAN, GARVIN ..... p 621 N94-13186
DEARMOND, M. K. ..... p 787 N94-14778
DEBAKKER, M. ..... p 818 N94-14462
DEBOER, DAVID ..... p 617 N94-14743
DEBRITOALVES, SDNEI ..... p 665 N94-12941
DECKER, ARTHUR J. ..... p 650 N94-13876
DECKER, D. K. ..... p 622 N94-13786
DECKER, WILLIAM A. ..... p 525 N94-13320
p 517 N94-13323
DEFORD, J. F. ..... p 580 N94-14124
DEGRASSIE, J. S. ..... p 801 N94-14293
p 802 N94-14570
DEGROOT, A. J. ..... p 813 N94-14439
DEHAEMER, MICHAEL J. ..... p 820 N94-12801
DEHON, RENE ..... p 842 N94-13855
DEKOVEN, B. M. ..... p 566 N94-14582
DELAHAIS, MAURICE ..... p 537 N94-14275
DELCAMP, S. B. ..... p 659 N94-14681
DELEUTERIO, G. M. T. ..... p 679 N94-14634
DELGRANDE, N. K. ..... p 700 N94-14566
DELIL, A. A. M. ..... p 632 N94-13533
DELOACH, L. D. ..... p 808 N94-13881
p 810 N94-14125
DELOMBARD, RICHARD ..... p 590 N94-13755
DELUCA, W. H. ..... p 624 N94-14012
DEMAIO, JOE ..... p 522 N94-13305
DEMELENNE, B. ..... p 543 N94-14352
DEMING, GLENN I. ..... p 737 N94-13674
DEMONICAULT, J. M. ..... p 671 N94-13501
DEMORISSONVALERIANO, MARCIO
p 684 N94-13377
DENAVIT, J. ..... p 801 N94-14342
DENBOER, ADRIANUS ALBERTUS ANTOINE
p 819 N94-14449
DENCH, W. A. ..... p 749 N94-13688
DENIER, JAMES P. ..... p 630 N94-13075
p 636 N94-13785
DENISOV, G. G. ..... p 655 N94-13145
DENTON, R. E. ..... p 712 N94-12952
DEOLIVEIRA, CARLOS ALBERTO ..... p 687 N94-14082
DEOLIVEIRA, JOAO BERTOLDO ..... p 684 N94-13377
DEPIERO, F. W. ..... p 651 N94-14046
DEQUEIROZ, LUIZ CARLOS ..... p 631 N94-13365
DERBER, JOHN C. ..... p 692 N94-14234
DERBYSHIRE, K. R. ..... p 543 N94-14352
DERENZO, S. E. ..... p 625 N94-14336
DEROOY, W. C. ..... p 722 N94-13991
DEROOY, WIM C. ..... p 722 N94-13992
DEROUIN, C. R. ..... p 702 N94-13402
DESAI, S. S. ..... p 639 N94-14598
p 639 N94-14600
p 510 N94-14617
DESHPANDE, M. D. ..... p 640 N94-14601
DESIQUEIRAMARTINSFILHO, LUIZ
p 649 N94-13366
DESNOS, Y.-L. ..... p 688 N94-14210
DESTLER, W. W. ..... p 654 N94-13058
DETURRIS, DIANNE JOAN ..... p 503 N94-13555
DEVASIA, SANTOSH ..... p 678 N94-14624
DEVENY, MARC E. ..... p 550 N94-13147
DEVINCENZI, DONALD L. ..... p 841 N94-13183
DEVLIN, D. J. ..... p 576 N94-12916
DEVRIES, P. Y. ..... p 722 N94-13926
DEWEESE, R. L. ..... p 738 N94-13972
DEWITT, D. ..... p 788 N94-13208
DEWITT, H. E. ..... p 811 N94-14313
DEWULF, ROBERT ..... p 695 N94-14258
DEXTER, ROBERT JOSEPH ..... p 672 N94-13593
DHANALAKSHMI, K. ..... p 639 N94-14599
DIAZ, A. F. ..... p 583 N94-13002
DICASTRO, C. ..... p 815 N94-14720
DIDZIULIS, S. V. ..... p 661 N94-13122
DIDZIULIS, STEPHEN V. ..... p 579 N94-13903
DIECKMAN, S. L. ..... p 577 N94-13032
DIJALALI, C. ..... p 785 N94-14363
DIMAURO, L. F. ..... p 781 N94-13241
DINI, J. W. ..... p 580 N94-14311
DION, C. L. ..... p 849 N94-14461
DIRADDO, R. W. ..... p 596 N94-13684
p 597 N94-14070
DISALVO, F. ..... p 577 N94-13072
DITMIRE, T. ..... p 657 N94-13882
DIVSALAR, D. ..... p 608 N94-14377
DJUROVIC, D. ..... p 837 N94-13504
DOANE, DOUGLAS H. ..... p 526 N94-13325
DOANE, GEORGE B., III ..... p 621 N94-13186
DOBBINS, SEAN ..... p 630 N94-13078
p 638 N94-14086
DODGE, JAMES C. ..... p 690 N94-14227
DOERR, R. ..... p 583 N94-14801
DOLAN, K. ..... p 548 N94-12911
DOLGIN, BEN ..... p 546 N94-14835
DOLINAR, S. ..... p 608 N94-14377
p 609 N94-14380
DOMIK, GITTA O. ..... p 840 N94-14482
DOMINGUE, D. ..... p 842 N94-14298
DOMONKOS, MATTHEW ..... p 550 N94-13415
DON, WAI SUN ..... p 769 N94-13725
DONAHUE, J. B. ..... p 788 N94-13103
DONAHUE, R. J. ..... p 746 N94-13382
DONALDSON, GEORGE J. ..... p 623 N94-13846
DONKER, J. C. ..... p 763 N94-13529
DORAN, J. C. ..... p 715 N94-13912
p 717 N94-14424
DOREY, S. ..... p 683 N94-14818
DORNEY, DANIEL JOSEPH ..... p 633 N94-13569
DORSETT, KENNETH M. ..... p 516 N94-14106
DOUER, NIR ..... p 774 N94-14502
DOWBEN, P. A. ..... p 805 N94-13102
DOWDING, ROBERT J. ..... p 575 N94-14878
DOWDY, L. W. ..... p 759 N94-13470
DOWNER, JAMES R. ..... p 596 N94-13141
DOWNING, JOHN P. ..... p 678 N94-14628
DOWNWARD, JAMES G. ..... p 822 N94-13116
DRAGON, E. P. ..... p 653 N94-12898
DREICER, J. S. ..... p 758 N94-12917
DRESNER, MARTIN ELLIOT ..... p 511 N94-13543
DRESSENDORFER, PAUL V. ..... p 655 N94-13261
DREW, RUSSELL C. ..... p 545 N94-13953
DREXLER, C. G. ..... p 782 N94-13485
DRINNAN, ANDREW M. ..... p 824 N94-14196
DRIRA, KHALIL ..... p 751 N94-13995
DROEGE, M. W. ..... p 705 N94-14510
DRYFOOS, JAMES B. ..... p 525 N94-13322
DUBINSKI, JOHN JOSEPH ..... p 838 N94-13649
DUBOIS, R. D. ..... p 782 N94-13485
DUCK, PETER W. ..... p 630 N94-13075
DUEMENIL, LYDIA ..... p 724 N94-14709
DUGUAY, CLAUDE R. ..... p 685 N94-13475
DUKLER, A. E. ..... p 635 N94-13699
DUNAHAY, T. ..... p 709 N94-14087
DUNCAN, B. S. ..... p 631 N94-13385
DUNCAN, R. ..... p 817 N94-14453
DUNLOP, JAMES D. ..... p 550 N94-13265
DUNPHY, PHILIP P. ..... p 849 N94-13965
DURBIN, P. A. ..... p 646 N94-14762
DURFEE, R. C. ..... p 825 N94-14458
DURSCH, HARRY ..... p 554 N94-12833
DUSSINGER, PETER M. ..... p 554 N94-14771
DUTTA, P. ..... p 730 N94-14802
DUTTA, P. K. ..... p 640 N94-14602
DUTTA, VIMALA ..... p 640 N94-14603
DUXBURY, P. M. ..... p 558 N94-14418
DWARAKANATH, G. S. ..... p 641 N94-14614
p 516 N94-14615

E

EADS, JEANNETTE ..... p 667 N94-13162
EASTER, R. C. ..... p 709 N94-13911
EATON, M. J. ..... p 820 N94-12907
EBBELER, D. H. ..... p 542 N94-14076
p 542 N94-14077
p 542 N94-14078
p 519 N94-14841
p 519 N94-14842
EBERHARD, P. H. ..... p 787 N94-14857
EBERLEIN, SUSAN ..... p 545 N94-13189
EBERT, W. L. ..... p 581 N94-14432
EBIHARA, BEN ..... p 575 N94-12842
EBIHARA, BEN T. ..... p 620 N94-13110
EBISUI, TAKASHI ..... p 529 N94-13269
p 530 N94-13278
EDELSTEIN, ALAN S. ..... p 556 N94-13663
EDMONDSON, M. ..... p 804 N94-12893
EDWARDS, T. L. ..... p 752 N94-14019
EGGERS, D. M. ..... p 707 N94-13390
EGGLESTONE, G. T. ..... p 669 N94-13857
EGUCHI, AKIHIRO ..... p 537 N94-14280
EIRIK, ROE ..... p 542 N94-14107
EISSLER, E. E. ..... p 806 N94-13150
EJIRI, HIROSHI ..... p 502 N94-13345
EL-GENK, M. S. ..... p 585 N94-14535
EL-HADY, NABIL M. ..... p 629 N94-13064
ELDREDGE, D. ..... p 514 N94-14563
ELISABELAR, CHRISTIAN ..... p 622 N94-13552
ELLEMAN, T. S. ..... p 574 N94-14873
ELLER, NANCY ..... p 667 N94-13161
ELLINGSON, W. A. ..... p 577 N94-13032
ELLIOTT, S. R. ..... p 788 N94-13208
ELLIS, K. A. ..... p 602 N94-13801
ELVIS, M. ..... p 839 N94-14404
EMANUEL, M. ..... p 658 N94-14442
EMBURY, J. D. ..... p 558 N94-14469
EMERSON, J. P. ..... p 816 N94-14868
ENG, SVERRE ..... p 546 N94-14834
p 547 N94-14838
ENGELDAL, C. A. ..... p 722 N94-13991
ENGELMANN, B. E. ..... p 663 N94-13975
p 771 N94-14589
ENGELMORE, ROBERT S. ..... p 820 N94-12801
ENGLISH, R. E., JR. ..... p 656 N94-13481
ENOEDA, MIKIO ..... p 795 N94-12944
ENTING, I. G. ..... p 709 N94-14095
ENYA, S. ..... p 589 N94-13750
EPIPHANIO, JOSE CARLOS NEVES
p 684 N94-13377
EPISHIN, V. A. ..... p 798 N94-13507
EPPARD, W. M. ..... p 504 N94-13607
EPPS, HARLAN ..... p 547 N94-14837
ERBES, GERHARD ..... p 632 N94-13535
ERBLAND, PETER ..... p 516 N94-13256
ERICKSON, M. D. ..... p 566 N94-14694
ERIKSEN, TORKILD ..... p 715 N94-13949
ERNST, R. D. ..... p 789 N94-14460
ERSKINE, D. ..... p 801 N94-14312
ESCH, MONIKA ..... p 724 N94-14709
ESCHRICH, HEINZ ..... p 703 N94-13997
ESDAR, TORSTEN ..... p 694 N94-14248
ESHOW, MICHELLE M. ..... p 523 N94-13310
p 526 N94-13325
ESTABROOK, K. ..... p 792 N94-14438
ESTABROOK, K. G. ..... p 797 N94-13393
ESTES, RONALD H. ..... p 741 N94-13788
ETHRIDGE, E. C. ..... p 808 N94-13938
EVANGELISTA, ARLENE M. ..... p 695 N94-14259
EVANS, B. T. N. ..... p 607 N94-14204
EVANS, BARRY G. ..... p 615 N94-14670
EVANS, T. E. ..... p 801 N94-14347
p 802 N94-14570
EVERETT, LOUIS J. ..... p 662 N94-13800
EVERETT, RICHARD K. ..... p 556 N94-13663
EZERS, ROLANDS ERIKS ..... p 600 N94-13488
EZIN, J. P. ..... p 767 N94-12895

F

FADNEK, A. ..... p 797 N94-13144
FAJNBERG, YA. B. ..... p 797 N94-13240
FALABELLA, S. ..... p 655 N94-13243
FALCONE, ANTHONY ..... p 575 N94-12792
p 554 N94-12833
FALCONE, V. ..... p 719 N94-12978
FALICOV, L. M. ..... p 776 N94-14584
FAN, M. K. H. ..... p 527 N94-14642
FAN, S. ..... p 806 N94-13150
FANG, H. E. ..... p 670 N94-12908
FANG, LEI ..... p 775 N94-13627
FARBER, R. M. ..... p 766 N94-14737
FARJAMI, A. ..... p 813 N94-14409

FARMER, O. T. ..... p 658 N94-14415
FAROOQUE, M. ..... p 701 N94-13093
FARRELL, K. ..... p 573 N94-14700
FARRINGTON, MICHAEL D. ..... p 623 N94-13846
FASEL, P. K. ..... p 758 N94-12917
FAULKNER, A. ..... p 522 N94-13302
FECHT, B. A. ..... p 793 N94-14702
FEDOROV, V. V. ..... p 804 N94-12828
FEENSTRA, R. ..... p 808 N94-13930
FEIGELSON, ERIC D. ..... p 830 N94-13462
FEINSTEIN, J. ..... p 649 N94-13410
FEIT, M. D. ..... p 654 N94-12962
FELCH, K. ..... p 649 N94-13410
FELDE, D. K. ..... p 569 N94-13242
FELDMAN, MARC J. ..... p 807 N94-13580
FELDMAN, P. D. ..... p 832 N94-13966
FENG, X. ..... p 581 N94-14432
FENGSHENG, ZHAO ..... p 691 N94-14230
FENSKY, CONNIE ..... p 536 N94-14310
FERGUSON, DALE C. ..... p 541 N94-13917
FERGUSON, S. W. ..... p 803 N94-14590
FERNAU, M. E. ..... p 708 N94-13495
FERRARIS, J. P. ..... p 580 N94-14179
FERREIRA, JOSE LEONARDO ..... p 795 N94-12901
FERRELL, T. L. ..... p 660 N94-14863
FERRISS, D. H. ..... p 639 N94-14464
FERRON, J. R. ..... p 802 N94-14570
FEYOCK, STEFAN ..... p 744 N94-13065
FICHTER, BUCK ..... p 546 N94-14835
FIELDS, D. J. ..... p 651 N94-14416
FIJANY, A. ..... p 680 N94-14639
FIJANY, AMIR ..... p 679 N94-14636
FILATOVS, G. J. ..... p 558 N94-14050
FILIPPENKO, ALEXEI V. ..... p 831 N94-13679
FINN, R. ..... p 631 N94-13244
FINNEY, J. M. ..... p 670 N94-12927
p 670 N94-12928
FIRESTONE, ELAINE R. ..... p 725 N94-14090
FISCHER, D. A. ..... p 566 N94-14582
FISCHER, J. E. ..... p 813 N94-14517
FISHBAUM, NISSAN ..... p 814 N94-14557
FISHER, ALLAN L. ..... p 749 N94-13779
FISHER, R. A. ..... p 816 N94-14868
FITERMAN, A. ..... p 769 N94-13717
FITZGERALD, D. ..... p 788 N94-13103
p 780 N94-13173
FITZGERALD, T. J. ..... p 718 N94-14518
FLAMMIA, MADELYN ..... p 826 N94-14488
FLANAGAN, D. M. ..... p 756 N94-14696
FLEETWOOD, D. M. ..... p 619 N94-12942
FLEISCHAUER, PAUL D. ..... p 579 N94-13903
FLEMING, HENRY E. ..... p 692 N94-14234
FLEMING, THOMAS A. ..... p 832 N94-14146
FLOCK, WARREN L. ..... p 615 N94-14671
FLOWER, W. L. ..... p 710 N94-14183
FLYNN, EDWARD M. ..... p 636 N94-13730
FLYNN, FREDERICK J. ..... p 596 N94-13141
FLYNN, GEORGE ..... p 838 N94-13781
FOGELMAN, C. H. ..... p 798 N94-13577
FOGLER, DONALD L., JR. ..... p 525 N94-13321
FOGLER, R. J. ..... p 686 N94-14056
FOILES, S. M. ..... p 806 N94-13136
FOLLANSBEE, P. S. ..... p 664 N94-14457
FOLTYN, S. ..... p 810 N94-14122
FOOT, R. ..... p 778 N94-12845
FORBES, GREGORY S. ..... p 721 N94-13675
FORCE, DALE A. ..... p 620 N94-13110
FORD, BARBARA ..... p 603 N94-13837
FORMAGGIO, ANTONIO ROBERTO
p 684 N94-13377
FORMAN, G. A. ..... p 625 N94-14427
FORMAN, P. R. ..... p 792 N94-14367
FORSBERG, A. ..... p 729 N94-14128
FORSBERG, AAKE ..... p 729 N94-14129
FORSTER, B. M. ..... p 778 N94-12860
FORSTER, R. A. ..... p 772 N94-12919
FORTI, MARIA CRISTINA ..... p 720 N94-13429
FORTNEY, SUZANNE M. ..... p 729 N94-14028
p 729 N94-14032
FOSTER, C. M. ..... p 811 N94-14304
FOSTER, L. ..... p 570 N94-13512
FOSTER, N. ..... p 522 N94-13303
FOSTER, P. A. ..... p 663 N94-14113
FOUGERE, G. E. ..... p 810 N94-14185
FOURNIER, G. R. ..... p 607 N94-14204
FOWLER, JIMMY E. ..... p 726 N94-14775
FOX, DANIEL N. ..... p 725 N94-12990
FOX, E. C. ..... p 539 N94-12827
FOX, R. O. ..... p 647 N94-14768
FRANCEY, R. J. ..... p 709 N94-14095
FRANCHITO, SERGIO H. ..... p 721 N94-13672
FRANKLE, C. M. ..... p 786 N94-14514
FRANKLE, S. ..... p 780 N94-13173
FRANKLE, S. C. ..... p 788 N94-13103
FRANKLIN, JAMES A. ..... p 521 N94-13297
FRATERNALI, P. ..... p 823 N94-13863
FRAZIER, W. GARTH ..... p 527 N94-14646
FREAR, D. R. ..... p 812 N94-14345
FREDD, E. ..... p 803 N94-14770
FREDELL, ROBERT ..... p 674 N94-13803
FREEMAN-PEREZ, SONDRA ..... p 499 N94-13904
FREEMAN, B. L. ..... p 729 N94-14028
FREEMAN, D. E. ..... p 794 N94-12849
FREEMAN, K. ..... p 712 N94-13092
FREEMAN, PETER ..... p 840 N94-14467
FREEMAN, R. L. ..... p 848 N94-13708
FREHLICH, R. G. ..... p 801 N94-14293
FREITAS, B. L. ..... p 721 N94-13723
FRENCH, N. B. ..... p 658 N94-14442
FRENDO, MICHAEL J. ..... p 710 N94-14183
FREUDENSTEIN, FERDINAND ..... p 791 N94-13490
FREUND, ROLAND W. ..... p 665 N94-14901
FRICKE, ROBERT W., JR. ..... p 748 N94-13586
p 535 N94-13934
FRIEDMAN, A. ..... p 535 N94-13935
FRIEDMAN, J. R. ..... p 789 N94-13727
FRIEDMAN, TZVIKA ..... p 706 N94-12937
FRIEND, H. ..... p 762 N94-13329
FRONTASYEVA, M. V. ..... p 622 N94-13811
FROST, C. A. ..... p 567 N94-14884
FROST, KENNETH ..... p 623 N94-13892
FRUEHOLZ, R. P. ..... p 851 N94-14791
FRY, A. ..... p 659 N94-14681
FRY, J. N. ..... p 755 N94-14581
FRY, P. E. ..... p 834 N94-12980
FRYE, G. C. ..... p 625 N94-14533
FUCHS, B. A. ..... p 582 N94-14511
FUELBERG, HENRY E. ..... p 807 N94-13405
FUESS, D. ..... p 718 N94-12839
FUGATE, R. Q. ..... p 619 N94-12994
FUGONO, NOBUYOSHI ..... p 611 N94-14392
FUJIEDA, HIROTOSHI ..... p 691 N94-14228
p 501 N94-13340
FUJITA, TAKESHI ..... p 501 N94-13341
FUJITA, TOSHIMI ..... p 551 N94-13455
p 501 N94-13340
FUKAZAWA, AKIRA ..... p 501 N94-13341
FUKUSHIMA, YUKIO ..... p 587 N94-13737
FULCHER, C. W. ..... p 551 N94-13455
FULLER, GERALD G. ..... p 748 N94-13578
FULLERTON, C. GORDON ..... p 579 N94-13584
FULTON, J. L. ..... p 520 N94-13254
FUNES-GALLANZI, M. ..... p 572 N94-14184
FUNK, JOHN D., JR. ..... p 509 N94-14706
FUNSTEN, H. O. ..... p 525 N94-13318
p 782 N94-13492
FUNSTEN, HERBERT O. ..... p 717 N94-14328
FURMAN, EUGENE ..... p 779 N94-12950
FURSA, D. V. ..... p 625 N94-14324
FURUKAWA, KOUICHI ..... p 806 N94-13226
FUSELIER, S. A. ..... p 529 N94-13270
FUTTERMAN, J. A. H. ..... p 712 N94-12952
p 647 N94-14895

G

GAFF, DOUG ..... p 616 N94-14676
GAFFEY, M. J. ..... p 843 N94-14300
GAILEY, P. C. ..... p 604 N94-13899
GAILLARD, M. K. ..... p 780 N94-13018
GAL-OR, L. ..... p 575 N94-12812
GALKA, A. ..... p 578 N94-13468
GALLAGHER, DONALD W. ..... p 523 N94-13309
GALLEGOS, G. F. ..... p 813 N94-14440
GALLO, K. P. ..... p 826 N94-14498
GALLOP, L. D. ..... p 653 N94-14782
GALVAO, RICARDO M. O. ..... p 801 N94-14024
GAMA, FABIO FURLAN ..... p 685 N94-13610
GAN, MANOEL ALONSO ..... p 719 N94-13175
GANNON, JOSEPH P. ..... p 820 N94-14499
GAO, F. ..... p 647 N94-14768
GAO, W. ..... p 717 N94-14424
GARAVAGLIA, T. ..... p 787 N94-14588
GARBUTT, KEITH ..... p 527 N94-13127
GARCIA, A. ..... p 848 N94-13695
GARCIA, PHIL ..... p 655 N94-13261
GARCZYNSKI, V. ..... p 788 N94-14872
GARDNER, CHARLES K. ..... p 526 N94-13324
GARDNER, D. G. ..... p 786 N94-14569
GARDNER, JONATHAN PERRY ..... p 830 N94-13591
GARDNER, M. A. ..... p 786 N94-14569
GARDNER, W. L. ..... p 798 N94-13577
GARKUSHA, I. E. ..... p 794 N94-12854
GARNER, CHARLES E. ..... p 549 N94-13055
p 549 N94-13068
GARRISON, K. ..... p 805 N94-13102
p 580 N94-14142
GARRISON, WARREN M., JR. ..... p 573 N94-14786
GARY, DALE E. ..... p 844 N94-13958
GASPERAS, GEDIMINIS ..... p 502 N94-13422
GAUSTAD, ROLF ..... p 730 N94-14852
GAUTIER, M. A. ..... p 709 N94-14020
GAYRAUD, THIERRY ..... p 756 N94-14712
GAZTANAGA, E. ..... p 834 N94-12980
GEE, J. M. ..... p 703 N94-13886
GEER, JAMES F. ..... p 767 N94-13289
GEISER, U. ..... p 623 N94-13925
GELFAND, ALAN E. ..... p 773 N94-13585
GELLENS-MEULLENBERGHS, F. ..... p 686 N94-13994
GELLENS, D. ..... p 686 N94-13994
GENTLEMAN, W. M. ..... p 741 N94-13547
GEORGANTAS, ANTANIOS IOANNOU
p 661 N94-13521
GEORGE, PATRICIA ..... p 546 N94-14835
GERARDI, JOSEPH J. ..... p 511 N94-13424
GERBERICH, W. W. ..... p 812 N94-14354
GERHOLD, CARL H. ..... p 777 N94-14481
GERMOND, A. ..... p 624 N94-13948
GERSHTEJN, S. S. ..... p 783 N94-13506
GEYER, A. B. ..... p 625 N94-14336
GHAN, S. J. ..... p 718 N94-12903
GIANOULAKIS, S. ..... p 817 N94-14453
GIARDINO, MARCO J. ..... p 667 N94-13163
GIBSON, B. F. ..... p 785 N94-14144
GILBERT, D. W. ..... p 582 N94-14511
GILBERT, STEVEN R. ..... p 719 N94-12992
GILCHRIST, IAN ..... p 516 N94-14616
GILCHRIST, N. H. C. ..... p 598 N94-12925
p 598 N94-12926
GILLAND, JAMES H. ..... p 550 N94-13415
GILLIE, K. R. ..... p 624 N94-14012
GILLILAND, G. D. ..... p 809 N94-14079
p 809 N94-14083
p 809 N94-14108
GILLILAND, KIRBY ..... p 732 N94-13193
GILYARD, GLENN B. ..... p 519 N94-14855
GINOCCHIO, J. N. ..... p 818 N94-14740
GIRARD, M. M. ..... p 538 N94-13257
GIRIDHARAN, M. G. ..... p 627 N94-12803
GIROUX, MARK LAIRD ..... p 838 N94-13651
GLADNEY, E. S. ..... p 709 N94-14020
GLAND, J. L. ..... p 566 N94-14582
GLASS, B. J. ..... p 538 N94-13201
p 538 N94-13989
GLASS, G. P. ..... p 562 N94-13004
GLASS, JEFFREY T. ..... p 816 N94-14839
GLASS, M. W. ..... p 596 N94-13889
GLASSMAN, NANCI A. ..... p 825 N94-14486
GLAUER, JUERGEN ..... p 617 N94-14820
GLAVICH, THOMAS ..... p 547 N94-14838
GLINERT, E. P. ..... p 748 N94-13576
GLOSUP, J. ..... p 756 N94-14864
GLOVER, DANIEL ..... p 612 N94-14542
GOAD, CLYDE C. ..... p 512 N94-13082
GOAD, LARRY ..... p 547 N94-14838
GODBOLE, PUSHKAR E. ..... p 600 N94-13489
GODFREY, ANDREW GRADY ..... p 633 N94-13572
GOEHNER, R. P. ..... p 804 N94-12813
GOERES, ACHIM ..... p 839 N94-14075
GOERS, UTA-BARBARA ..... p 617 N94-14820
GOETTSCHE, A. ..... p 622 N94-13811
GOFORTH, J. H. ..... p 802 N94-14532
GOLD, PHILLIP J. ..... p 525 N94-13322
GOLDBERG, J. H. ..... p 738 N94-14335
GOLDBERG, MITCHELL D. ..... p 692 N94-14234
GOLDBERG, ROBERT K. ..... p 670 N94-13053
GOLDEY, C. L. ..... p 527 N94-13127
GOLDHIRSH, JULIUS ..... p 614 N94-14663
p 615 N94-14672
GOLDIE, JAMES H. ..... p 596 N94-13141
GOLDMAN, T. ..... p 779 N94-12949
GOLDREICH, PETER ..... p 845 N94-14479
GOLDSACK, STEPHEN J. ..... p 754 N94-14472
GOLDSTEIN, J. L. F. ..... p 573 N94-14474
GOLDSTEIN, W. H. ..... p 795 N94-12995
p 803 N94-14894
GOLDSTONE, J. A. ..... p 558 N94-14119
GOLSHAN, NASSER ..... p 614 N94-14667
GOMBANI, ANDREA ..... p 764 N94-13999
p 764 N94-14000
p 765 N94-14001
p 770 N94-14002
p 770 N94-14003
GOMESDAROCHA, INOCENCIO ..... p 628 N94-12966
GONDHALEKAR, VIJAY ..... p 596 N94-13141
GONG, JIAN ..... p 599 N94-13236
GONG, SHANGLONG ..... p 665 N94-13042
GONIS, A. ..... p 805 N94-13010
GOODFELLOW, KEITH D. ..... p 549 N94-13055
p 549 N94-13068
GOODMAN, D. M. ..... p 773 N94-14314
GOODMAN, M. C. ..... p 783 N94-13890
GOODYER, M. ..... p 527 N94-13127
GOOSSENS, ROLAND ..... p 695 N94-14258
GOPALAKRISHNA, M. RAO ..... p 550 N94-13265
GOPINATH, R. ..... p 640 N94-14604
GORDON-WINKLER, LYN ..... p 666 N94-13158

GORDON, J. E. p 816 N94-14868
GORDON, R. G. p 704 N94-14110
GORENSTEIN, PAUL p 546 N94-14835
GORLEY, T. A. E. p 662 N94-13808
GORNEY, DAVID J. p 714 N94-13793
GOTSIS, PASCAL K. p 683 N94-14776
GOTTESFELD, S. p 702 N94-13402
p 580 N94-14179
GOTTLIEB, DAVID p 769 N94-13725
p 770 N94-13922
p 770 N94-14307
GOUDER, T. p 568 N94-13036
GOUDREAU, G. L. p 754 N94-14435
GOUGH, R. W. p 707 N94-13390
GOULD, R. p 675 N94-13945
GOULDING, J. R. p 745 N94-13151
GOULDING, R. p 803 N94-14770
GOULDING, R. H. p 607 N94-14291
GOULDING, R. J. p 795 N94-13033
GOUVEIA, F. p 706 N94-13095
GOVINDARAJAN, RAMA p 640 N94-14605
GOWDY, R. V. p 738 N94-13972
GOYAL, A. p 804 N94-12818
GRACE, JOHN A. p 695 N94-14259
GRADY, C. A. p 828 N94-12915
GRADY, CAROL A. p 835 N94-13239
GRAHAM, D. P. W. p 679 N94-14634
GRAHAM, DAVID p 808 N94-13875
GRAHAM, G. p 791 N94-13482
GRAHAM, R. p 707 N94-13486
GRAMMER, HOLLY LITTLE p 543 N94-14683
GRANATSTEIN, V. L. p 654 N94-13058
GRANDJEAN, PIERRICK p 605 N94-13946
GRANEK, H. p 709 N94-14095
GRANT, G. A. p 564 N94-13942
GRANT, H. p 755 N94-14528
GRATZ, A. J. p 576 N94-12885
GRAVES, SARA J. p 683 N94-14484
GRAY, G. T., III p 811 N94-14329
GRAY, J. p 655 N94-13258
GRAZIANI, CARLO p 848 N94-13708
GREEN, D. A. p 765 N94-14201
GREEN, DAVID L. p 521 N94-13298
p 523 N94-13309
GREENBERG, D. p 758 N94-12878
GREENBERG, K. E. p 800 N94-13908
GREENE, A. E. p 794 N94-12814
p 802 N94-14532
GREENISEN, MICHAEL C. p 729 N94-14028
p 729 N94-14032
GREENLEAF, JOHN E. p 727 N94-13447
GREENSPAN, MICHAEL p 764 N94-13842
GREENSTADT, E. W. p 796 N94-13081
GREGG, LAWRENCE A. p 819 N94-13400
GREGORY, JOHN C. p 564 N94-14025
GREGORY, R. p 839 N94-14116
GREIVENKAMP, JOHN p 547 N94-14836
GREVESSE, N. p 844 N94-13502
GRIBBLE, R. p 797 N94-13100
GRIEST, K. p 840 N94-14467
GRIFFIN, M. K. p 719 N94-12978
GRILLI, M. p 815 N94-14720
GRISHANIN, B. A. p 781 N94-13225
GRITZO, L. A. p 561 N94-12819
GROEBNER, R. J. p 802 N94-14583
GROEDER, TORBJOERN p 650 N94-13665
GROEP, F. F. p 570 N94-13532
GROOT, J. S. p 684 N94-13123
GROSS, FRANZ p 786 N94-14550
GROSS, R. J. p 561 N94-12910
GROSSMAN, B. p 504 N94-13607
GRUBER, A. p 691 N94-14231
GRUBER, ROBERT P. p 620 N94-13110
GRUGEL, RICHARD N. p 571 N94-13891
GRUN, J. p 631 N94-13249
p 631 N94-13250
GRUNTMAN, M. p 782 N94-13492
GRUNWALD, ARTHUR J. p 524 N94-13315
GSCHNEIDNER, K. A., JR. p 568 N94-13000
GUBERNATIS, J. E. p 760 N94-14177
GUCKEL, H. p 618 N94-12821
GUEELL, A. p 733 N94-14860
GUICHELARR, H. J. p 774 N94-14545
GUNZBURGER, MAX D. p 771 N94-14731
GUO, J. p 787 N94-14691
GUPTIL, JAMES D. p 683 N94-14776
GURTIN, MORTON E. p 817 N94-14680
GUSAKOV, YU. V. p 627 N94-14885
GUSTAFSSON, BERTIL p 770 N94-13922
p 770 N94-14307
GUSTAVSON, D. B. p 761 N94-14476
GUTIERREZ-LUACES, B. O. p 609 N94-14382
GUZIEL, K. A. p 708 N94-13495
GWINN, K. W. p 501 N94-13260

H

HAAG, THOMAS W. p 551 N94-13430
p 553 N94-14726
HAAKANSSON, SEBASTIAN p 729 N94-14129
HABER, I. p 789 N94-13727
HABER, S. p 575 N94-12812
HABIB, S. p 840 N94-14536
HADAWAY, JAMES B. p 788 N94-14905
HAERTLING, GENE p 625 N94-14324
HAIDARA, F. p 613 N94-14659
HAILEY, C. E. p 501 N94-13260
HAJELA, P. p 510 N94-14799
HAJJAJI, MOHAMED p 569 N94-13367
HALBLEIB, J. A. p 782 N94-13409
HALES, STEPHEN J. p 574 N94-14850
HALICIOGLU, TIMUR p 671 N94-13179
HALL, DAVID G. p 518 N94-14036
HALLING, A. M. p 783 N94-13895
HALLORAN, TIMOTHY J. p 823 N94-13701
HALPERN, JULES p 840 N94-14685
HALPERN, JULES P. p 840 N94-14688
HALTHORE, RANGSHAI N. p 808 N94-13875
HAM, JOHNNIE A. p 526 N94-13324
HAMAKAWA, YOSHIHIRO p 588 N94-13745
HAMANO, NOBUO p 737 N94-13388
HAMEED, S. p 723 N94-14426
HAMLEY, JOHN A. p 553 N94-14725
HAMMEL, B. p 795 N94-12995
HAMMOND, E. p 704 N94-14422
HAMMOND, MONICA p 551 N94-13417
HANADO, HIROSHI p 690 N94-14226
HANN, RAIFORD E. p 583 N94-14845
HANSAKDI, EKKANIT p 693 N94-14242
HANSELKA, HOLGER p 557 N94-13804
HANSEN, CHARLES D. p 749 N94-13721
HANSEN, IVAR p 735 N94-13582
HAPKE, B. p 842 N94-14298
p 843 N94-14301
HARDEK, T. p 780 N94-13173
HARDIN, DANNY p 683 N94-14484
HARDY, GORDON H. p 525 N94-13320
HARGROVE, R. S. p 653 N94-12898
HARLAN, CHARLIE p 668 N94-13165
HARPER, SABRINA p 804 N94-12873
HARRY, ANDREW p 824 N94-13879
HARSTAD, E. N. p 676 N94-14591
HART, DANIEL C. p 524 N94-13317
HART, JAKE p 521 N94-13298
HARTFORD, E. H., JR. p 815 N94-14699
HARTMANN, D. p 834 N94-13011
HARTMANN, DENNIS L. p 713 N94-13465
HARVEY, JAMES p 546 N94-14833
HARVEY, R. W. p 801 N94-14293
HASHIMOTO, TOMOYUKI p 570 N94-13460
HASKEW, TIM A. p 663 N94-14134
HASS, HEINZ p 720 N94-13589
HASSELMAN, TIMOTHY K. p 671 N94-13124
HASTE, G. R. p 797 N94-13144
HASTINGS, D. A. p 826 N94-14498
HASTINGS, J. W. p 728 N94-13698
HATSUDA, TESTUO p 786 N94-14527
HAVSTAD, M. A. p 790 N94-12865
HAWKEY, TIMOTHY J. p 596 N94-13141
HAWKINS, LAWRENCE A. p 660 N94-12791
HAWORTH, D. C. p 646 N94-14763
p 567 N94-14765
HAYAKAWA, J. p 589 N94-13749
HAYAKAWA, YOSHIHIKO p 627 N94-13434
HAYASAKA, TADAHIRO p 691 N94-14229
HAYES, J. M. p 717 N94-14338
HAYES, J. P. p 813 N94-14440
HEARN, C. P. p 598 N94-12811
HEBERT, P. p 638 N94-14351
HECHT, LAURA M. p 825 N94-14486
HEDSTROM, J. C. p 553 N94-14689
HEERD, S. R. p 731 N94-14862
HEFFNER, R. H. p 815 N94-14773
HEFLIN, M. B. p 514 N94-14371
HEIL, GARRETT G. p 578 N94-13431
HEIMANN, P. p 563 N94-13411
HEINBOCKEL, JOHN H. p 776 N94-14733
HEINRICH, J. C. p 567 N94-12825
HEINSTEIN, M. W. p 742 N94-12956
HELGSEN, PETTER p 809 N94-14010
HELLMAN, E. S. p 815 N94-14699
HELMICK, LARRY S. p 575 N94-12842
HELMKEN, HENRY F. p 616 N94-14678
HELMS, RICHARD p 546 N94-14834
HENDRICKSON, B. p 754 N94-14399
HENKE, H. p 658 N94-14414
p 659 N94-14520
HENKNER, JENS p 651 N94-14044
HENLEY, E. M. p 779 N94-12997
p 785 N94-14471
HENLEY, ERNEST M. p 786 N94-14527
HENNEBERRY, HUGH M. p 518 N94-13143
HENNESSEY, MICHAEL PETER p 661 N94-13575
HENNING, RUDY p 616 N94-14678
HENNINGER, R. J. p 676 N94-14591
HENRIKSVEEN, MADS EGIL p 752 N94-14039
HENSHALL, G. A. p 556 N94-13389
HENZE, WILLIAM, JR. p 844 N94-13146
HERMAN, S. p 657 N94-13882
HERNANDEZ, J. p 651 N94-14416
HERNANDEZ, J. E. p 700 N94-14566
HERTEL, E. S., JR. p 539 N94-13006
p 540 N94-13398
HEUTER, GEOFFRY J. p 848 N94-13708
HEUZEY, M.-C. p 557 N94-13866
HICKEY, GREGORY S. p 701 N94-13187
p 564 N94-13947
HICKEY, JOHN R. p 844 N94-13963
HICKMAN, GAIL A. p 511 N94-13424
HICKMAN, J. MARK p 534 N94-13028
HIDAYAT, BAMBANG p 697 N94-14272
HILL, D. N. p 801 N94-14347
HILL, J. C. p 647 N94-14768
HILL, R. J. p 515 N94-13839
HILLARD, G. BARRY p 534 N94-13028
HILLIARD, ORVAL H. p 570 N94-13670
HILTON, M. R. p 661 N94-13122
HINDSON, WILLIAM S. p 525 N94-13320
p 526 N94-13325
HINGST, WARREN R. p 509 N94-14780
HINKLE, A. J. p 568 N94-12993
HINMAN, STEVE p 546 N94-14834
HINSHELWOOD, D. D. p 801 N94-14349
HIRABAYASHI, NORIAKI p 551 N94-13455
HIRATA, SHINGO p 795 N94-12944
HIROSE, A. p 798 N94-13518
p 798 N94-13563
p 799 N94-13835
p 799 N94-13836
p 799 N94-13849
p 800 N94-13850
p 800 N94-13851
p 800 N94-13852
p 800 N94-13853
p 800 N94-13877
p 801 N94-14206
HIRSCHEIDER, A. p 694 N94-14249
HIRSCHEL, E. H. p 509 N94-14710
HIRSHMAN, S. P. p 796 N94-13046
HIRUMA, FUMIHIKO p 693 N94-14243
HISHIDA, MASATAKA p 696 N94-14266
HIXSON, R. S. p 811 N94-14329
HJALMARSON, H. P. p 809 N94-14079
p 809 N94-14083
p 809 N94-14108
HJELM, R. P., JR. p 559 N94-14690
HNATICH, M. p 632 N94-13511
HNATT, LINDA p 729 N94-14028
HO, M. H. p 625 N94-14336
HO, W. p 784 N94-13983
HOBBS, M. L. p 561 N94-12910
HOCHBERG, ERIC p 547 N94-14836
HOCKNEY, RICHARD L. p 596 N94-13141
HODGES, DEWEY H. p 766 N94-14444
HODGIN, R. L. p 823 N94-13406
HODGKINSON, JOHN p 522 N94-13304
HODSON, H. P. p 653 N94-14827
HOELTZEL, DAVID p 665 N94-14901
HOETKER, GLENN P. p 822 N94-13105
HOFFERT, M. I. p 706 N94-13079
HOFFMAN, D. A. p 740 N94-13069
HOFFMAN, D. J. p 795 N94-13033
p 798 N94-13577
HOFFMAN, TERANCE J. p 557 N94-13706
HOH, ROGER H. p 521 N94-13299
HOLDER, NANETTE S. p 620 N94-13040
HOLDRIDGE, GEOFFREY M. p 820 N94-12801
HOLLOWAY, D. L. p 577 N94-13032
HOLYER, RONALD J. p 821 N94-13041
HOLZBACH-VALERO, A. A. p 754 N94-14472
HOLZMANN, IDO p 585 N94-14507
HOLZWORTH, ROBERT H. p 712 N94-13293
HOMCE, G. T. p 626 N94-14686
HOMSY, G. M. p 644 N94-14755
HONDA, YOSHIAKI p 695 N94-14255
p 695 N94-14257
HONG, STEVEN W. p 524 N94-13312
HOOD, R. Q. p 776 N94-14584
HOOGEVEEN, J. A. p 751 N94-14004
HOOIE, D. T. p 704 N94-14355
HOOKER, M. W. p 813 N94-14409
HOOKER, STANFORD B. p 725 N94-14090
HOOLEY, A. C. p 708 N94-13880
p 783 N94-13883
HOOVER, C. G. p 813 N94-14439
HOOVER, W. G. p 813 N94-14439

HOOVLER, G. S. p 548 N94-12981
HOPKINS, DALE A. p 670 N94-13053
HOPS, J. M. p 609 N94-14383
HOPSTER, H. p 805 N94-13102
HORIE, HIROAKI p 690 N94-14226
HORMAN, R. L. p 823 N94-13352
HORNSBY, JOHN KEITH p 685 N94-13523
HORSFALL, A. p 653 N94-12857
HORVATH, D. p 632 N94-13511
HOSKER, R. P., JR. p 718 N94-14425
HOSOMURA, T. p 693 N94-14241
HOU, LIN-JUN p 770 N94-14407
HOUGHTON, D. C. p 813 N94-14478
HOULIHAN, S. R. p 534 N94-12810
p 536 N94-14047
HOVMARK, GUNNAR p 528 N94-13588
HOWARD, J. B. p 583 N94-13002
HOWARD, STEPHEN L. p 583 N94-12987
HOWELL, L. H. p 639 N94-14434
HOWELL, ROBERT p 841 N94-13183
HOWITT, J. p 522 N94-13303
HOYT, DOUGLAS V. p 844 N94-13963
HOZUMI, KOUICHI p 514 N94-13459
HOZUMI, KOUKI p 514 N94-13338
HRYNEVYCH, M. p 653 N94-12857
HSI, CHI-SHIUNG p 625 N94-14324
HSIEH, PAUL F. p 832 N94-14305
HU, ESTHER M. p 628 N94-12959
HU, THOMAS S. Z. p 674 N94-13833
HUANG, ERICK T. p 683 N94-14902
HUANG, H. p 790 N94-14897
HUANG, P. J. p 662 N94-13794
HUBBARD, K. p 558 N94-14469
HUBBARD, K. M. p 570 N94-13512
HUBBARD, R. F. p 801 N94-14349
HUBBE, J. M. p 717 N94-14424
HUBER, C. C. p 707 N94-13383
HUDSON, J. G. p 719 N94-13080
HUDSON, M. K. p 712 N94-12952
HUESMAN, R. H. p 625 N94-14336
HUEY, H. p 649 N94-13410
HUFF, J. R. p 553 N94-14689
HUI, BERTRAM p 622 N94-13776
HULEN, H. p 825 N94-14331
p 760 N94-14475
HULL-ALLEN, GREG p 546 N94-14834
HULL, R. p 808 N94-13694
HULSTROM, R. p 704 N94-14350
HUNG, R. J. p 637 N94-13959
HUNT, GARY p 547 N94-14836
HUNT, WILLIAM D. p 650 N94-14029
HUNTER, GARY W. p 648 N94-13135
HUNTER, M. H. p 528 N94-14876
HUNTLEY, M. S. p 514 N94-14563
HUO, YAN p 760 N94-13921
HURST, M. T. p 573 N94-14537
HUSBANDS, C. R. p 538 N94-13257
HUSEONICA, WILLIAM F. p 667 N94-13163
HUSH, D. R. p 686 N94-14056
HUSTON, R. L. p 788 N94-13103
HUTCHENS, C. G. p 762 N94-12969
HUTSON, R. p 780 N94-13173
HWANG, YONG-SEOK p 799 N94-13680
HWOSCHINSKY, PETER p 521 N94-13298
HYDEN, AAKE p 528 N94-13588
HYMER, THOMAS C. p 500 N94-12989
HYUN, YONGHEE p 504 N94-13705

I

IANNO, N. J. p 581 N94-14337
IBRAHIM, E. p 627 N94-12803
IDELL, PAUL p 546 N94-14833
IIDA, TAKASHI p 618 N94-14285
IKEDA, HIRONOBU p 581 N94-14421
IKEDA, NOBUKAZU p 526 N94-13347
IKENAGA, MITUO p 593 N94-13766
ILLINGWORTH, GARTH p 547 N94-14837
IMASU, R. p 689 N94-14217
IMRE, K. p 795 N94-12984
INAGAKE, DENZOU p 696 N94-14267
INAGAKI, TOSHIHARU p 514 N94-13338
p 513 N94-13344
INGHAM, J. D. p 727 N94-12793
INGRAM, RICK E. p 604 N94-13939
p 605 N94-14015
p 607 N94-14065
INKOL, ROBERT p 603 N94-13838
INMAN, S. M. p 790 N94-12863
INOKUCHI, HAMAKI p 517 N94-13451
INOUYE, L. Y. p 622 N94-13786
IPATTI, A. p 682 N94-14653
IRIKADO, HIROSHI p 531 N94-13281
IRONS, JAMES R. p 808 N94-13875
IRWIN, R. DENNIS p 527 N94-14646
ISAACS, R. G. p 719 N94-12978
ISAEV, A. A. p 816 N94-12855
ISHIDA, KIYOMICHI p 502 N94-13345
ISHIHARA, O. p 798 N94-13563
p 800 N94-13852
ISHIKAWA, KAZUTOSHI p 514 N94-13338
p 513 N94-13344
p 513 N94-13346
ISLAM, M. JINNAHTUL p 695 N94-14260
ISMAILIDIS, T. p 704 N94-14422
ISOGAI, KOUJI p 505 N94-14061
ISRAELSSON, U. p 817 N94-14453
ITO, HIDEKI p 795 N94-12944
ITOH, TATSUO p 619 N94-13026
ITOU, YASUHIKO p 618 N94-14287
IVANCIC, WILLIAM D. p 538 N94-13111
IVANOVA, T. A. p 818 N94-14887
IWASAKI, AKIHITO p 501 N94-13340
p 501 N94-13341
IWASAKI, NOBUO p 689 N94-14215
IYER, VENKIT p 629 N94-13066
p 629 N94-13073
IZU, M. p 704 N94-14109

J

JACKSON, DARRYL J. p 668 N94-13167
JACKSON, K. J. p 561 N94-12881
JACKSON, MATT p 736 N94-13132
JACKSON, THOMAS L. p 636 N94-13724
JACOBOWITZ, HERBERT p 691 N94-14233
JACOBS, STEPHEN p 546 N94-14834
JACOBSEN, ROBERT A. p 526 N94-13325
JACOBSON, A. R. p 718 N94-14518
JACOBSON, MARK D. p 613 N94-14660
JACOBY, B. A. p 789 N94-14460
JACOT-GUILLARMOD, R. p 778 N94-12860
JAEGER, E. F. p 795 N94-13033
JAFFE, A. p 817 N94-14417
JAHSHAN, S. N. p 550 N94-13351
JAIN, A. p 679 N94-14631
p 680 N94-14638
p 680 N94-14639
JAIN, K. K. p 798 N94-13518
JAMES, D. V. p 761 N94-14476
JAMES, TREVOR p 764 N94-13844
JAMESON, R. A. p 789 N94-13327
JANDA, K. C. p 814 N94-14597
JANEZIC, M. D. p 652 N94-14687
JANICKI, J. p 775 N94-13235
JANKOWSKI, A. p 568 N94-13036
JANKOWSKI, A. F. p 581 N94-14319
p 813 N94-14440
JANSEN, C. J. p 528 N94-13498
JANSEN, RALPH p 575 N94-12842
JANSSEN, LUCAS L. F. p 687 N94-14127
JANTZEN, C. M. p 581 N94-14343
JARVIS, E. p 709 N94-14087
JARZEBA, WLODZIMIERZ p 780 N94-13051
JAUREGUI, ERNESTO p 718 N94-12918
JEGLEY, DAWN C. p 557 N94-13711
JENKINS, JON M. p 841 N94-13083
JEON, BYEUNGWOO p 823 N94-13192
JERATH, S. p 824 N94-13915
JERMAN, G. p 571 N94-13715
JEROME, S. M. p 708 N94-13880
JERVIS, T. R. p 570 N94-13512
p 558 N94-14469
p 813 N94-14478
JESSON, D. E. p 770 N94-14407
JIANG, BO-NAN p 792 N94-13868
JIANG, WEN Y. p 643 N94-14747
JIMENEZ, J. p 689 N94-14213
JIN, MICHAEL Y. p 521 N94-13296
JOHNS, J. B. p 525 N94-13318
JOHNS, JOHN B. p 710 N94-14183
JOHNSEN, H. A. p 701 N94-13093
JOHNSEN, R. p 780 N94-13051
JOHNSON, ALAN E. p 577 N94-12985
JOHNSON, C. G. p 806 N94-13150
JOHNSON, C. J. p 533 N94-14824
JOHNSON, D. L. p 759 N94-13052
JOHNSON, DAVID B. p 714 N94-13816
JOHNSON, DAVID G. p 670 N94-12887
JOHNSON, J. N. p 811 N94-14329
p 785 N94-14468
JOHNSON, M. B. p 805 N94-13102
JOHNSON, P. D. p 580 N94-14142
p 788 N94-14905
JOHNSON, R. B. p 793 N94-14903
JOHNSON, R. BARRY p 811 N94-14332
JOHNSON, R. T. p 524 N94-13313
JOHNSON, WALTER W. p 622 N94-13811
JOHNSTON, A. p 736 N94-12935
JOHNSTON, SMITH L. p 755 N94-14528
JONES, A. p 547 N94-14838
JONES, BILL p 836 N94-13446
JONES, CHRISTINE p 603 N94-13837
JONES, DAVID p 709 N94-14020
JONES, E. A. p 602 N94-13801
JONES, J. p 603 N94-13841
p 653 N94-14701
JONES, J. D. C. p 538 N94-13918
JONES, R. E. p 575 N94-12842
JONES, WILLIAM R., JR. p 801 N94-14347
JONG, R. A. p 682 N94-14651
JORDAN, STEVE p 702 N94-13381
JORGENSEN, G. p 649 N94-13410
JORY, H. p 775 N94-12843
JOSHI, G. C. p 812 N94-12844
p 527 N94-13127
JOSHI, P. B. p 806 N94-13150
JOVANOVIC, S. p 727 N94-13210
JOYCE, GERALD F. p 673 N94-13778
JU, JIANN-WEN p 714 N94-13816
JUCKS, KENNETH W. p 678 N94-14629
JUENGST, CARL p 675 N94-13907
JUMP, ROBERT D.

K

KAAKA, M. p 806 N94-13213
KAARAT, PHILIP p 547 N94-14838
KAISER, MARY K. p 524 N94-13314
KALLMAN, J. S. p 813 N94-14439
KALTENBACH, HANS-JAKOB p 639 N94-14443
KAMIO, AKIHIKO p 588 N94-13742
KAMPHUIS, A. p 722 N94-13926
KANAPOULIS, NICK p 619 N94-12967
KANE, R. J. p 700 N94-14566
KANE, RAJARAM PURUSHOTAM p 725 N94-13726
KANEMASU, E. T. p 711 N94-12788
KANNAN, S. K. p 743 N94-12991
KANSA, E. p 637 N94-14053
KANT, R. A. p 662 N94-13794
KANTAK, ANIL V. p 614 N94-14665
KAO, C. Y. J. p 722 N94-14057
KAPITANOVSKY, ALEX p 748 N94-13539
KAPLAN, D. M. p 788 N94-14898
KARAMOUZIS, STAMOS T. p 744 N94-13065
KARNOWSKY, M. p 618 N94-12821
KARPPI, RISTO A. p 674 N94-13887
KARSPECK, MILAN p 736 N94-13132
KARTZ, M. W. p 656 N94-13481
KASAI, YUMI p 687 N94-14092
KASCHMITTER, J. L. p 625 N94-14427
KATO, W. Y. p 554 N94-14806
KATOU, SUMIO p 530 N94-13275
p 531 N94-13282
KATZ, BERT B. p 692 N94-14234
KATZ, J. D. p 581 N94-14340
KATZ, JOSEPH p 629 N94-13007
KATZ, RANDY H. p 740 N94-13363
KATZ, ROBERT p 732 N94-13714
KAUFMANN, DAVID N. p 513 N94-13957
KAUKLER, W. F. p 808 N94-13938
KAUTZ, D. D. p 653 N94-12898
KAUTZ, HAROLD E. p 555 N94-13138
KAWA, STEPHAN RANDOLPH p 714 N94-13707
KAWAI, YASUSHI p 537 N94-14279
KAWALKO, STEPHEN F. p 599 N94-13264
KAWATA, Y. p 689 N94-14219
KAY, L. p 840 N94-14685
KAY, RICHARD B. p 656 N94-13420
KAYE, A. p 607 N94-14291
KAZMIERCZAK, MARCOS LEANDRO p 684 N94-13331
KEANE, C. p 795 N94-12995
KEARNEY, P. D. p 653 N94-12857
KEEMAN, DENNIS M. p 687 N94-14127
KEIL, L. C. p 731 N94-12972
KEIM, ROBERT p 546 N94-14834
KELBERT, M. p 765 N94-14361
KELLER, JAMES F. p 525 N94-13321
KELLER, JOERG p 740 N94-13525
KELLER, LINDSAY P. p 843 N94-14302
KELLER, P. p 744 N94-13120
KELLER, RICHARD M. p 761 N94-12890
KELLEY, E. E. p 743 N94-13014
KELLEY, N. D. p 704 N94-14423
KELLEY, STEVE p 822 N94-13126
KENDALL, CYNTHIA p 821 N94-12958
KENNEDY, JOHN M. p 821 N94-13057
p 825 N94-14485
p 825 N94-14486
p 826 N94-14488
KENNEY, CHARLES p 681 N94-14644
KENSEK, R. P. p 782 N94-13409
KERLEY, G. I. p 568 N94-12977
KERWIN, DAVID P. p 665 N94-13056
KESMODEL, L. L. p 781 N94-13283

KETCHAM, KIRK W. p 665 N94-13042
KETO, J. W. p 654 N94-13013
KETTERSON, J. B. p 730 N94-14802
KEVLAHAN, N. p 645 N94-14761
KEVREKIDIS, I. G. p 766 N94-14737
KEY, DAVID L. p 521 N94-13299
KEZIRIAN, M. T. p 628 N94-12961
KHALED, ELSAYED ESAM M. p 657 N94-13624
KHATKHATE, ATEEN A. p 511 N94-13424
KHREBTOV, V. L. p 576 N94-12867
KHURI-YAKUB, B. T. p 572 N94-14133
KIDA, S. p 644 N94-14750
KIDA, TAKASHI p 540 N94-13339
KIDD, S. R. p 653 N94-14701
KIEFEL, E. R. p 539 N94-12827
KIKUCHI, NOBORU p 596 N94-13798
KILLEEN, J. p 797 N94-13217
KIM, HAE SOO p 534 N94-12900
KIM, HEECHUL p 538 N94-13111
KIM, HYOUNG M. p 677 N94-14621
KIM, J. p 644 N94-14752
KIM, J. S. p 658 N94-14414
KIM, J.-H. p 723 N94-14074
KIM, JIN-SOO p 659 N94-14520
KIM, PAUL Y. p 663 N94-14147
KIM, Q. p 657 N94-13812
KIM, YONG-HOON p 548 N94-14214
KIM, YOUNG-JOON p 713 N94-13647
KINDL, ENRICO p 829 N94-13370
KING, C. A. p 808 N94-13694
KING, DAVID W. p 517 N94-13316
KING, W. E. p 806 N94-13136
KINGON, A. I. p 804 N94-13003
KINLAW, DENNIS C. p 667 N94-13162
KINTER, J. L., III p 683 N94-14500
KIRBIE, H. C. p 654 N94-12963
KIRCHHOF, WERNER p 694 N94-14248
KIRK, EDILBERT p 724 N94-14709
KIRKHAM, H. p 622 N94-13811
KISER, JAMES D. p 665 N94-13056
KISHI, SHINKICHI p 693 N94-14244
KISHIDA, SHIGEKI p 627 N94-13433
KITAMURA, TAKAYUKI p 530 N94-13276
KITTEL, PETER p 776 N94-14027
KITTIVER, CHARLES p 614 N94-14668
KLEIN, J. p 618 N94-12821
KLEIN, LIOR p 815 N94-14825
KLEM, D. E. p 658 N94-14114
KLEM, J. p 809 N94-14083
KLEPKO, ROBERT p 606 N94-14062
KLIBANOV, MICHAEL V. p 749 N94-13702
KLINER, DAHV A. p 780 N94-13051
KLOPFER, GOETZ H. p 504 N94-14030
KLOPPMANN, C. p 641 N94-14613
KLUSENER, A. S. p 768 N94-13496
KNAPP, D. K. p 788 N94-13208
KNIFFEN, DONALD A. p 847 N94-13087
KNIGHT, P. L. p 786 N94-14526
KNILL, E. p 761 N94-12859
KNOLL, A. H. p 717 N94-14338
KNORR, R. p 522 N94-13302
KNOWLES, P. E. p 778 N94-12860
KOBAYASHI, H. p 689 N94-14217
KOBAYASHI, HIROSHI p 502 N94-13342
KOBAYASHI, SHIGEO p 530 N94-13273
p 537 N94-14274
KOBAYASI, MITUO p 747 N94-13437
KOCH, J. A. p 655 N94-13258
p 658 N94-14175
p 659 N94-14595
KOCH, M. W. p 686 N94-14056
KOCHEROV, N. P. p 827 N94-14880
KOEHLER, SUNDOLF p 617 N94-14820
KOEHLINGER, M. W. p 552 N94-14013
KOEKOEK, ROELOF p 770 N94-14150
KOETZ, ANDREAS p 711 N94-14723
KOGA, KAZUGO p 592 N94-13761
KOGA, TATSUZOU p 529 N94-13272
KOGAN, FELIX p 692 N94-14236
KOGUMA, HIROYUKI p 687 N94-14093
KOHARA, S. p 588 N94-13744
KOHN, SILVIA p 524 N94-13315
KOIKE, J. p 582 N94-14531
KOIKE, M. p 563 N94-13411
KOIZUMI, SHINKICHI p 693 N94-14245
KOLA, R. R. p 808 N94-13694
KOLBER, T. p 792 N94-14438
KOLKMAN, H. J. p 519 N94-14450
KOLKOWSKI, P. p 783 N94-13883
KONG, Y. p 806 N94-13150
KONONENKO, V. I. p 798 N94-13507
KONRAD, JANUSZ p 772 N94-13540
KONRAD, WOLFGANG p 503 N94-13556
KONTRA, R. p 804 N94-12818
KOOKER, DOUGLAS E. p 583 N94-12987
KOOLE, GER p 773 N94-14005
KOPIA, LEONARD P. p 690 N94-14223
KOPPENAAL, D. W. p 658 N94-14415
KOROS, ANTON p 735 N94-13961
KORSCH, DIETRICH p 547 N94-14837
KORUKOV, N. A. p 627 N94-14885
KOSKI, N. L. p 709 N94-14020
KOSSENTINI, FAOUZI p 744 N94-13113
KOT, M. p 730 N94-14596
KOTAK, D. B. p 824 N94-14202
KOTOWSKI, M. p 795 N94-13017
KOUCHIYAMA, JIROU p 537 N94-14280
KOUL, A. K. p 850 N94-13548
p 675 N94-14035
KOVALCHUK, I. K. p 797 N94-13240
KOVALEVSKIJ, M. YU. p 767 N94-13223
KOVALICK, BILL p 808 N94-13875
KOVALYOV, ALEXANDER p 693 N94-14246
KOWAL, E. p 670 N94-12927
p 670 N94-12928
KOYAMA, TADAO p 514 N94-13459
KOZLOWSKI, M. R. p 655 N94-13243
p 580 N94-14124
KOZMINCHUK, BRIAN p 603 N94-13818
p 606 N94-14054
KRAEUTNER, P. p 777 N94-14360
KRAICHNAN, ROBERT H. p 644 N94-14750
KRAMMER, J. p 751 N94-14006
KRAUS, DONNA KAREN p 518 N94-13190
KRAUSE, J. L. p 659 N94-14594
KRECH, R. H. p 562 N94-13115
KREIN, GASTAO p 786 N94-14527
KREMER, M. p 581 N94-14400
KREMPL, E. p 510 N94-14799
KREN, LAWRENCE A. p 664 N94-14727
KRESS, R. L. p 651 N94-14046
KRIER, HERMAN p 796 N94-13039
KRIKORIAN, ABRAHAM D. p 592 N94-13764
KRISHER, T. P. p 611 N94-14398
KRISHNAKUMAR, S. p 671 N94-13565
KRISHNAN, A. p 627 N94-12803
KROEGER, D. M. p 804 N94-12818
KROGH, MICHAEL F. p 749 N94-13721
KROMODIMOELJO, SENTOT p 752 N94-14088
KRUER, W. L. p 797 N94-13207
p 797 N94-13393
p 802 N94-14564
KRUGER, H. p 792 N94-14317
KRUGER, J. p 569 N94-13050
KRUPKE, W. F. p 808 N94-13881
p 810 N94-14125
KUECH, T. F. p 809 N94-14079
p 809 N94-14083
p 809 N94-14108
KUJAK, S. p 583 N94-14801
KULAGA, J. E. p 624 N94-14012
KULANDER, K. C. p 659 N94-14594
KUMAGAI, HIROSHI p 690 N94-14226
KUMAKAWA, AKINAGA p 548 N94-12945
KUMAR, ANAND p 640 N94-14606
KUMAR, M. p 678 N94-14626
KUMAR, V. p 807 N94-13510
KUNG, A. H. p 563 N94-13411
KUNG, H. p 558 N94-14469
KUPPERMAN, D. S. p 555 N94-13248
KURDILA, ANDREW J. p 679 N94-14632
KURIHARA, MASAZUMI p 747 N94-13435
KURILKO, V. I. p 797 N94-13240
KURITA, T. p 769 N94-13545
KUROCHKIN, YU. A. p 617 N94-14883
KURODA, MASAO p 592 N94-13760
KURODA, TAKAJI p 693 N94-14245
KURZYDLO, ARTUR STANISLAW p 672 N94-13594
KUSAKA, T. p 689 N94-14219
KUUS, H. p 797 N94-13144
KUYUCAK, S. p 778 N94-12848
KVALE, T. J. p 779 N94-12940
KVAM, P. H. p 669 N94-14143
KWAK, MOON K. p 527 N94-14650
KWAN, S. p 651 N94-14452
KWAY, W. p 807 N94-13405
KWAY, W. L. p 808 N94-13881
p 810 N94-14125
KWON, I. p 813 N94-14413
KYLE, H. LEE p 844 N94-13963

L

LAAKSO, JOHN H. p 575 N94-12792
LABAUNE, C. p 797 N94-13393
LABOV, S. E. p 811 N94-14332
LABRANCHE, BRUNO p 657 N94-14067
LABY, KEITH p 682 N94-14651
LACHAPELL, M. p 548 N94-12911
LADDE, GANGARAM S. p 772 N94-14840
LADERMAN, S. p 805 N94-13020
LAFLAMME, R. p 839 N94-14116
LAHMANN, WILHELM p 617 N94-14820
LAHR, THOMAS F. p 822 N94-13105
LAI, L. p 603 N94-13843
LAIRD, PHIL p 761 N94-12889
LAM, D. J. p 811 N94-14304
LAMB, DON Q. p 848 N94-13708
LAMBERT, LARRY D. p 666 N94-13154
LAMBRINEAS, P. p 669 N94-13857
LAMONTAGNE, RENE p 605 N94-14033
LAMPE, M. p 801 N94-14349
LAND, M. L. p 825 N94-14458
LANDGREBE, DAVID p 743 N94-13023
p 823 N94-13192
LANDIS, G. A. p 626 N94-14730
LANDROE, STIG p 657 N94-13970
LANDWEBER, LAWRENCE H. p 821 N94-13030
LANE, S. p 658 N94-14114
LANGDON, A. B. p 789 N94-13727
LANGENBECK, SHARON L. p 546 N94-14835
LANGER, STANLEY H. p 573 N94-14779
LAOR, ARI p 847 N94-13232
LAPEAN, J. p 612 N94-14501
LAPEDES, A. S. p 766 N94-14737
LAPIN, E. G. p 804 N94-12828
LAPPOS, NICK p 522 N94-13304
LARIMER, R. M. p 848 N94-13695
LASINSKI, THOMAS p 740 N94-13200
LASKIN, ROBERT A. p 547 N94-14837
LASNIER, C. p 801 N94-14347
LASSEIGNE, D. GLENN p 636 N94-13724
LASTER, J. p 613 N94-14658
LATINSKIJ, S. M. p 621 N94-13224
LAUB, ALAN J. p 681 N94-14644
LAULAINEN, N. S. p 710 N94-14523
LAVOIE, J. ANDRE p 670 N94-13063
LAWS, K. E. p 811 N94-14332
LAWSON, A. C. p 558 N94-14119
LAXPATI, SHARAD R. p 599 N94-13264
LAZARUS, E. A. p 800 N94-13900
LE, CHOUNG p 614 N94-14665
LEACH, B. p 850 N94-13519
LEAODEMORAESNOVO, EVLYN MARCIA p 684 N94-13426
LEBERL, FRANZ p 736 N94-13132
LEBLANC, ADRIAN p 594 N94-13771
LECKRONE, D. p 849 N94-13376
LECOMTE, CLAUDE p 776 N94-13692
LEDESMA, RAGNAR p 679 N94-14633
LEDNICER, DAVID p 516 N94-14616
LEE, ALLAN Y. p 677 N94-14622
LEE, CHULHEE p 743 N94-13023
LEE, D. K. p 796 N94-13046
LEE, DAVID CHUNG LIANG p 688 N94-14131
LEE, H. p 794 N94-12814
LEE, HYUNG C. p 771 N94-14731
LEE, I. p 660 N94-14863
LEE, J. G. p 627 N94-12803
LEE, J. S. p 811 N94-14332
LEE, J. W. p 753 N94-14295
LEE, J. Y. p 810 N94-14122
LEE, JIM P. Y. p 606 N94-14064
LEE, KIEN-YIN p 778 N94-14867
LEE, P. R. p 611 N94-14397
LEE, R. W. p 659 N94-14595
LEE, S. p 645 N94-14761
LEE, S. M. p 813 N94-14439
LEE, S. Y. p 790 N94-14897
LEE, STUART M. C. p 729 N94-14032
LEE, T. p 660 N94-12851
LEE, UNG-HEE p 774 N94-14703
LEGGETT, P. J. p 543 N94-14352
LEIFER, R. p 706 N94-12904
LELAND, R. p 754 N94-14399
LELE, S. K. p 645 N94-14760
LEMBERGER, T. R. p 810 N94-14122
LEMOINE, P. p 534 N94-12965
p 534 N94-13191
LENSTRA, J. p 751 N94-14004
LENTJES, P. G. p 700 N94-14810
LEON, JUAN p 749 N94-13779
LEONARD, A. W. p 801 N94-14347
LERSCH, D. p 821 N94-12983
LESERGENT, THIERRY p 761 N94-14716
LESH, J. R. p 610 N94-14386
LESKO, K. T. p 848 N94-13695
LEVI, D. p 768 N94-13499
LEVINE, B. M. p 610 N94-14388
LEVINE, B. MARTIN p 547 N94-14837
LEVINGER, NANCY E. p 780 N94-13051
LEVINSON, L. M. p 620 N94-13031
LEVINTON, F. M. p 796 N94-13046
LEVUSH, B. p 654 N94-13058
LEVY, R. p 608 N94-14374
LEW, H. p 778 N94-12845
LEWIS, CHARLES M. p 577 N94-12986

LEWIS, MARIAN L. p 729 N94-14494
LEYLAND, JANE A. p 520 N94-12820
LI, CHEL ZU p 567 N94-14884
LI, DONG-GI p 805 N94-13102
LI, GUANG p 625 N94-14324
LI, JIAYU p 632 N94-13509
LI, K. p 621 N94-13336
LIA, CHIEN-CHAIN p 556 N94-13595
LICHTEN, S. M. p 514 N94-14371
p 514 N94-14372
LIE, IVAR p 770 N94-13971
p 637 N94-14040
LIEBERMAN, S. H. p 790 N94-12863
LIGOTKE, M. W. p 706 N94-12905
LIKHODED, A. A. p 783 N94-13506
LILLARD, R. S. p 569 N94-13050
LIN, H. P. p 613 N94-14662
LIN, TSUNG-LIANG p 770 N94-14407
LINDNER, D. K. p 791 N94-13353
LINEHAN, J. C. p 572 N94-14184
LINFIELD, R. P. p 607 N94-14370
LINGENFELTER, RICHARD E. p 844 N94-13671
LINSKY, JEFFREY L. p 844 N94-13234
p 829 N94-13287
p 832 N94-14146
LIOU, M. S. p 642 N94-14728
LIOU, MENG-SING p 510 N94-14847
LIOU, W. W. p 631 N94-13385
LIOU, WILLIAM W. p 642 N94-14729
LIPPARD, HENRY E. p 574 N94-14850
LITVA, J. p 603 N94-13843
LIU, J. p 568 N94-12993
LIU, JOSEPH T. C. p 635 N94-13676
LIU, KEFENG p 602 N94-13799
LIU, SHEN p 618 N94-14282
LIU, W. K. p 674 N94-13873
LIUBOVICH, S. p 575 N94-12812
LIVNE, AMIR p 755 N94-14505
LLEWELLYN-JONES, D. T. p 696 N94-14263
LLOYD, CHARLES W. p 731 N94-12832
p 595 N94-13775
LO, C. F. p 552 N94-14309
LO, CHING F. p 500 N94-13076
p 536 N94-14310
LO, T. p 603 N94-13843
LOBODA, GREGORY G. p 540 N94-13016
LOCKHART, J. p 811 N94-14332
LOCKWOOD, S. J. p 814 N94-14695
LOEHMAN, R. E. p 579 N94-13888
LOFTIN, KARIN C. p 729 N94-14028
LOGAN, M. N. p 576 N94-12866
LOGAN, R. T., JR. p 611 N94-14395
LOGAN, R. W. p 663 N94-13975
LOH, CHING-YUEN p 510 N94-14847
LOISELET, M. p 688 N94-14210
LONDON, R. p 795 N94-12995
LONDON, R. A. p 654 N94-12962
p 659 N94-14595
p 660 N94-14888
LONDON, R. R p 657 N94-13976
LONGACRE, R. S. p 780 N94-13097
LONGDON, NORMAN p 851 N94-14137
LONGSWORTH, R. C. p 776 N94-13897
LOOMIS, G. E. p 655 N94-13243
LOPEZ, J. M. p 644 N94-14754
LORD, J. D. p 570 N94-13666
LOREDO, TOM p 848 N94-13708
LORITO, FABRIZIO p 750 N94-13807
LOVBERG, R. H. p 798 N94-13513
LOWE, STEPHEN T. p 686 N94-13872
LOWNDES, D. H. p 808 N94-13930
p 812 N94-14362
LOWRY, M. p 791 N94-13482
LOYOLA, S. J. p 610 N94-14384
LU, HUNG-YU p 556 N94-13558
LU, PING p 516 N94-14104
LU, XIAN-PING p 783 N94-13895
LUCAS, S. E. M. p 708 N94-13880
LUCCIO, A. p 780 N94-13149
LUCE, T. C. p 795 N94-12953
p 801 N94-14293
LUDEWIG, H. p 548 N94-12981
p 549 N94-13034
p 552 N94-14111
p 554 N94-14806
LUDWIG, DAVID E. p 620 N94-13125
LUEDERS, KURT F. p 652 N94-14497
LUKE, EDWARD ALLEN p 664 N94-14848
LUM, BEN T. F. p 536 N94-14323
LUND, T. S. p 643 N94-14748
p 643 N94-14749
LUNDGREN, T. S. p 643 N94-14746
LUNDSTROM, J. M. p 623 N94-13892
LUNKEIT, FRANK p 724 N94-14709
LUTTERMOSER, DONALD G. p 829 N94-13287
LUXMOORE, R. p 707 N94-13486
LYKE, J. C. p 625 N94-14427
LYNN, K. G. p 806 N94-13150
LYONS, L. R. p 714 N94-13793
LYONS, VALERIE J. p 517 N94-13142
LYSHER, K. G. p 595 N94-14026
LYZENGA, DAVE R. p 725 N94-13581

M

MA, J. P. p 778 N94-12847
MA, KWAN-LIU p 749 N94-13721
MAAT, N. p 722 N94-13985
MACARY, VERONIQUE p 626 N94-14698
MACEK, R. p 788 N94-13103
p 780 N94-13173
MACELLARO, ANNA p 729 N94-14129
MACGOWAN, B. J. p 795 N94-12995
p 655 N94-13258
p 655 N94-13259
p 658 N94-14175
p 659 N94-14595
MACH, DOUGLAS p 718 N94-12957
MACHIN, G. D. p 760 N94-14011
MACKENZIE, C. W. p 754 N94-14496
MACKERROW, E. p 788 N94-13103
MACKOWIAK, C. L. p 738 N94-13979
MACKOWSKI, MICHAEL J. p 636 N94-13730
MACLEOD, MALCOLM A. p 834 N94-12971
MADSEN, W. W. p 548 N94-12870
p 549 N94-12996
MAEDA, KOREHIRO p 696 N94-14261
MAEJIMA, HIRONORI p 687 N94-14093
p 696 N94-14261
p 697 N94-14268
MAGNOLI, D. E. p 512 N94-14292
MAGNUSEN, P. E. p 568 N94-12993
MAHAJAN, VINI p 547 N94-14837
MAHALINGAM, S. p 567 N94-14766
p 567 N94-14767
MAHDAVI, M. A. p 802 N94-14570
MAHESH, K. p 645 N94-14761
MAHMOOD, NIK NASRUDDIN p 692 N94-14240
MAHMOOD, S. T. p 573 N94-14700
MAIANA, LUCIANA p 787 N94-14721
MAINE, TRINDEL A. p 520 N94-13254
MAISE, G. p 552 N94-14111
MAITA, MASATAKA p 537 N94-14281
MAJUMDAR, BHASKAR S. p 555 N94-13378
MAJUMDAR, S. p 555 N94-13248
p 639 N94-14598
MAJUMDAR, SEKHAR p 640 N94-14607
MALACINSKI, GEORGE M. p 713 N94-13418
MALEKPOUR, MAHYAR R. p 622 N94-13797
MALINIE, G. p 834 N94-13011
MALLA, R. P. p 514 N94-14372
MALM, J. O. p 574 N94-14795
MALNEV, V. N. p 788 N94-14875
MALONE, R. D. p 688 N94-14151
MALONSON, M. R. p 527 N94-13127
MAN, G. K. p 677 N94-14618
p 680 N94-14638
p 680 N94-14639
MANDELL, D. A. p 582 N94-14436
MANGASER, AMANTE p 682 N94-14651
MANI, A. p 674 N94-13873
MANNING, R. A. p 544 N94-14649
MANOUSIOUTHAKIS, VASILIOS p 681 N94-14643
MANSOUR, N. N. p 645 N94-14757
MANSUR, L. K. p 573 N94-14700
MAOZ, DAN p 849 N94-14553
MARCHELLO, JOSEPH M. p 582 N94-14539
MARCUS, J. H. p 738 N94-13972
MARDOYAN, L. G. p 788 N94-14891
MAREK, E. L. p 748 N94-13578
MARINA, M. p 609 N94-14382
MARINUZZI, J. G. p 765 N94-14117
MARION, B. p 704 N94-14422
MARK, K. p 798 N94-13518
MARKER, TIMOTHY R. p 511 N94-14186
MARKLEY, R. W. p 610 N94-14385
MARKWELL, G. A. p 738 N94-13979
MARLAND, G. p 707 N94-13486
MARLAND, S. p 707 N94-13486
MARROQUIN, J. p 534 N94-12965
p 534 N94-13191
MARRS, R. E. p 788 N94-13208
MARSH, S. F. p 564 N94-13487
MARSHALL, A. C. p 551 N94-13514
MARSHALL, G. M. p 778 N94-12860
MARSHALL, R. E. p 598 N94-12811
MARSHALL, S. p 840 N94-14467
MARTIN, A. p 777 N94-14130
MARTIN, N. L. S. p 785 N94-14419
MARTIN, SHIRLEY A. p 819 N94-13400
MARTIN, T. J. p 717 N94-14424
MARTINEZ, ANDREW O. p 727 N94-12795
MARTINEZ, E. A. p 564 N94-13487
MARTINSON, SCOTT D. p 777 N94-14481
MARTUKANITZ, R. P. p 595 N94-14026
MARU, H. p 701 N94-13093
MARUYAMA, BENJI p 556 N94-13663
MASAD, JAMAL A. p 629 N94-13066
MASCHHOFF, ROBERT H. p 844 N94-13963
MASON, G. R. p 778 N94-12860
MASON, PETE p 547 N94-14836
MASSA, DERCK p 835 N94-13233
MASSARANI, B. p 806 N94-13213
MASTERS, K. p 611 N94-14391
MASUI, KAZUYA p 502 N94-13392
p 517 N94-13451
MASUKO, HARUNOBU p 688 N94-14212
MASUKO, MASABUMI p 575 N94-12842
MATHEWS, G. p 834 N94-13011
MATHIAS, LON J. p 577 N94-12985
p 577 N94-12986
MATHUR, J. S. p 510 N94-14608
MATSUI, NOBUO p 591 N94-13758
MATSUSHIMA, KOUICHI p 513 N94-13344
MATSUZAKI, TAKASHI p 551 N94-13455
MATSUZAKI, YUUJI p 502 N94-13345
MATTHEWS, A. p 721 N94-13914
MATTHEWS, D. L. p 655 N94-13258
p 658 N94-14152
p 658 N94-14175
p 659 N94-14595
MATTHEWS, I. W. p 653 N94-14701
p 509 N94-14706
MATTHEWS, R. K. p 506 N94-14158
p 506 N94-14163
p 506 N94-14164
p 507 N94-14166
p 507 N94-14169
p 507 N94-14171
p 508 N94-14173
MATTHIES, LARRY p 605 N94-13946
MATTIETTI, GIUSEPPINA p 725 N94-13500
MATUSKA, W. p 794 N94-12814
MAUDLIN, P. J. p 676 N94-14591
MAUNG, KHIN M. p 786 N94-14549
MAUNG, KHIN MAUNG p 786 N94-14550
MAURICE, KELLY p 736 N94-13132
MAUS, JAMES R. p 505 N94-14155
p 506 N94-14159
p 506 N94-14162
p 507 N94-14170
MAUSER, W. p 694 N94-14249
MAX, N. L. p 742 N94-12883
MAXWELL, E. p 704 N94-14422
MAYANAGI, MITSUYOSHI p 514 N94-13338
MAYBERRY, M. J. p 801 N94-14293
MAYER, S. T. p 627 N94-14870
MAYES, R. L. p 748 N94-13578
MAZZITELLI, F. D. p 836 N94-13361
MCBRIDE, D. D. p 501 N94-13260
MCBRIEN, ROBERT KEVIN p 632 N94-13474
MCCARRON, E. M., III p 816 N94-14868
MCCARTHY, I. E. p 806 N94-13226
MCCARTNEY, L. N. p 570 N94-13666
MCCARTY, K. p 657 N94-13812
MCCLOSKEY, KATHY p 736 N94-12935
MCCLUNG, TIM M. p 666 N94-13159
MCCLUSKEY, GEORGE E., JR. p 833 N94-14493
MCCOLL, D. p 798 N94-13518
MCCOMAS, D. J. p 836 N94-13262
p 782 N94-13492
p 717 N94-14328
MCCOMAS, DAVID J. p 779 N94-12950
MCCONLEY, MARC W. p 642 N94-14732
MCCORD, R. A. p 825 N94-14458
MCDERMOTT, WILLIAM A. p 536 N94-14323
MCDONNELL, JOHN R. p 766 N94-14882
MCELIECE, R. J. p 609 N94-14379
MCFEE, M. T. p 569 N94-13242
MCGEE, JOHN M. p 819 N94-13400
MCGINNIS, L. D. p 712 N94-12906
MCGUFFIN, V. L. p 654 N94-13022
MCGUIRE, JAMES p 547 N94-14836
MCINTIRE, GERRY p 545 N94-13713
MCINTOSH, G. L. p 539 N94-12827
MCINVILLE, ROY M. p 500 N94-12989
MCKAY, DAVID S. p 843 N94-14302
MCKELLAR, B. H. J. p 778 N94-12858
MCKINNEY, G. W. p 752 N94-14176
MCLAUGHLIN, S. p 707 N94-13486
MCLAUGHLINE, P. K. p 827 N94-14880
MCLEAN, W., II p 790 N94-12865
MCMASTER, MATTHEW S. p 642 N94-14732
MCMASTER, TOM J. p 666 N94-13159
MCMILLAN, C. F. p 744 N94-13120
MCMILLAN, R. S. p 810 N94-14203
MCMILLAN, SCOTT p 680 N94-14637

MCNAB, M. C. p 784 N94-13936
MCNIDER, RICHARD p 718 N94-12957
MEADOR, WILLARD E. p 776 N94-14733
MEAKIN, ROBERT L. p 508 N94-14326
MEDEIROS, JOSE ADELINO p 818 N94-13427
MEDINA, ENRIQUE A. p 527 N94-14646
MEGURO, AKIRA p 530 N94-13274
MEHMED, ORAL p 670 N94-12872
MEHTA, RABINDRA D. p 501 N94-13266
MEI, G. T. p 781 N94-13349
MEI, YI p 601 N94-13650
MEI, Z. p 573 N94-14474
MEIER, H. p 543 N94-14352
MEINEL, ADEN p 547 N94-14836
MEISELS, IRWIN p 752 N94-14088
MEISENHEIMER, T. L. p 619 N94-12942
MEISSNER, THOMAS p 786 N94-14527
MELAMED, NAHUM p 508 N94-14538
MELCHIOR, P. p 837 N94-13503
MELLO, F. J. p 742 N94-12956
MELZ, C. p 522 N94-13302
MENDELSON, HAIM p 829 N94-13231
MENDES, ODIM, JR. p 835 N94-13174
MENEVEAU, C. p 643 N94-14748
p 643 N94-14749
MENON, RAMESH p 679 N94-14632
MERKLEY, D. R. p 586 N94-12805
MERRIAM, MARSHAL L. p 740 N94-12973
MERRICK, ROGER A. p 565 N94-14480
MERRILL, D. W. p 825 N94-14433
MERRITT, K. W. p 779 N94-12954
MERTEN, C. W. p 573 N94-14316
MERTENS, HENRY W. p 735 N94-14846
p 736 N94-14854
MERTOGUL, AYHAN E. p 796 N94-13039
MESSICA, AVI p 565 N94-14465
MESSNER, R. M. p 558 N94-14469
METZLER, R. A. p 652 N94-14534
MEVEL, E. p 781 N94-13241
MEWALDT, RICHARD A. p 847 N94-13211
MEYER, GEORGE p 596 N94-13790
MEYER, H. M., III p 565 N94-14525
MEYER, H. S. p 566 N94-14586
MICHAEL, J. R. p 804 N94-12813
p 648 N94-13044
p 812 N94-14345
MICHAELIS, WALFRIED p 617 N94-14820
MICHELS, BERENICE I. p 716 N94-14132
MICHIDA, YUTAKA p 696 N94-14266
MIDDLETON, R. M. p 662 N94-13794
MIEKKALA, ULLA p 760 N94-14187
MILBURN, NELDA J. p 735 N94-14846
p 736 N94-14854
MILEY, G. H. p 787 N94-14691
MILLER, D. p 815 N94-14699
MILLER, JEFFREY H. p 664 N94-14727
MILLER, KEITH W. p 752 N94-14139
MILLER, N. p 834 N94-13011
MILLER, P. A. p 800 N94-13908
MILLER, P. L. p 556 N94-13583
MILLER, R. W. p 531 N94-13358
MILLER, S. F. p 712 N94-12906
MILLER, TERESA Y. p 586 N94-13732
MILLONAS, M. M. p 774 N94-14441
MILLOT, MICHEL p 736 N94-13132
MILLS, G. p 584 N94-14089
MILLS, R. S. p 789 N94-13209
MILMAN, M. H. p 681 N94-14647
MINATO, ATSUSHI p 689 N94-14218
MINEGISHI, MASAKATSU p 502 N94-13345
MINER, GILDA A. p 776 N94-14733
MIRELS, HAROLD p 597 N94-14877
MIROW, P. p 510 N94-14800
MISLOVE, MICHAEL W. p 749 N94-13700
MITANI, KENJI p 737 N94-13388
MITANI, TOORU p 563 N94-13458
MITARAI, O. p 798 N94-13518
p 799 N94-13835
MITCHELL, DAVID G. p 524 N94-13317
MITCHELL, G. E. p 566 N94-14582
MITCHELL, JERREL R. p 527 N94-14646
MITCHELL, JIMMY L. p 725 N94-12990
MITCHELL, R. p 653 N94-14792
MITCHELL, T. E. p 558 N94-14469
MITSUGI, JIN p 530 N94-13274
MITTAL, MANOJ p 523 N94-13308
MIURA, HIROSHI p 531 N94-13280
MIURA, KOURYOU p 530 N94-13275
MIYASHITA, AKIHIKO p 830 N94-13452
MIYAZAWA, YOSHIKAZU p 513 N94-13344
MIYOSHI, YASHUHIRO p 593 N94-13769
MIZRACHI, DAPHNA p 826 N94-14555
MIZUNO, HIROBUMI p 747 N94-13438
MODESTINO, A. J. p 583 N94-13002
MOIN, PARVIZ p 643 N94-14749
MOLITORIS, J. D. p 803 N94-14865
MOLTON, P. M. p 580 N94-14297
MONGAN, PHILIP T. p 737 N94-13399
MONTAGUE, RONALD A. p 819 N94-13400
MONTGOMERY, D. S. p 797 N94-13393
MONTGOMERY, HARRY p 851 N94-14791
MOODENBAUGH, ARNIE R. p 566 N94-14582
MOODY, J. D. p 797 N94-13393
MOONEY, THOMAS JOSEPH p 848 N94-13654
MOORE, ALAN D. p 729 N94-14032
MOORE, FRANK G. p 500 N94-12989
MOORE, K. R. p 782 N94-13492
p 717 N94-14328
MOORE, N. R. p 542 N94-14076
p 542 N94-14077
p 542 N94-14078
p 519 N94-14841
p 519 N94-14842
MOORE, T. N. p 733 N94-13847
MORABITO, D. D. p 611 N94-14398
MORAN, E. p 840 N94-14685
MORGAN, J. MURRAY p 521 N94-13295
MORI, SHIGEO p 591 N94-13759
MORI, W. B. p 797 N94-13207
MORIDIS, G. J. p 637 N94-14053
MORIN, MICHEL p 657 N94-14067
MORINO, YOSHIKI p 529 N94-13271
p 531 N94-13279
p 531 N94-13280
p 531 N94-13281
p 531 N94-13282
MORISHITA, YOUJI p 618 N94-14288
MORITA, YUHEI p 592 N94-13762
MORIYAMA, TAKASHI p 687 N94-14092
p 687 N94-14093
p 687 N94-14094
MORRIS, J. W., JR. p 573 N94-14474
MORRIS, MIKE p 547 N94-14836
MORRISON, I. p 778 N94-12848
MORRISON, P. W. p 812 N94-14348
MORRISSEY, J. F. p 719 N94-12978
MORROW, DANIEL p 512 N94-14744
MORTON, DAVID M. p 764 N94-13860
p 824 N94-14196
MORTON, JOHN p 670 N94-13063
MOSER, R. D. p 647 N94-14768
MOSES, W. W. p 625 N94-14336
MOSHIER, W. C. p 556 N94-13583
MOSS, W. D. p 709 N94-14020
MOTLOCH, C. G. p 552 N94-14013
MOWAFY, LYN p 524 N94-13314
MOYA, M. M. p 686 N94-14056
MROWKA, S. p 655 N94-13258
p 658 N94-14175
p 659 N94-14595
MUDKAVI, VIDYADHAR Y. p 510 N94-14609
MUELLER, EUGENE A. p 616 N94-14678
MUELLER, JAMES L. p 725 N94-14090
MUELLER, JOHANNES p 651 N94-14149
MUELLER, R. L. p 703 N94-13940
MUELLERSCHOEN, R. J. p 514 N94-14371
MUGHABGHAB, S. p 549 N94-13034
MUGHABGHAB, S. F. p 548 N94-12981
MUKAI, S. p 690 N94-14220
MULLENHOFF, D. J. p 625 N94-14427
MUNDT, C. p 509 N94-14710
MURAGISHI, OSAMU p 530 N94-13275
p 531 N94-13282
MURAI, SHUNJI p 695 N94-14255
p 695 N94-14257
MURALIDHAR, S. J. p 744 N94-13077
MURAMATSU, YUJI p 587 N94-13738
MURATA, MASAAKI p 513 N94-13344
MURATORE, JOSEPH J., JR. p 806 N94-13291
MUROTSU, YOSHISADA p 530 N94-13277
MURPHY, BRIAN T. p 660 N94-12791
MURPHY, DANIEL J. p 826 N94-14489
MURPHY, P. W. p 795 N94-13017
MURRAY, JAMES E. p 537 N94-14853
MURTHY, P. L. N. p 676 N94-14041
MURTY, K. L. p 574 N94-14873
MUSCETTOLA, NICOLA p 820 N94-14796
p 735 N94-14797
MUSICK, H. BRAD p 715 N94-13956
MUSIELAK, Z. E. p 835 N94-13171
MYERS, D. p 704 N94-14422
MYERS, ROGER M. p 550 N94-13415
p 551 N94-13416
MYLVAGANAM, KANAGA SABAPATHY p 624 N94-13998

N

NACHALIEL, EHUD p 816 N94-14826
NADARAJAH, ARUNAN p 648 N94-13326
NAGAOKA, SHUNJI p 593 N94-13768
NAGARAJARAO, C. R. p 544 N94-13029
NAGAYASU, MASAHIKO p 528 N94-13337
p 649 N94-13343
p 649 N94-13456
NAGY, ANDREW p 540 N94-13109
NAKAI, MASAO p 687 N94-14092
p 688 N94-14212
NAKAJIMA, T. p 690 N94-14220
NAKAJIMA, TERUYUKI p 691 N94-14229
p 691 N94-14230
NAKAMURA, KENJI p 688 N94-14212
p 690 N94-14226
NAKAMURA, TOMIHISA p 551 N94-13455
NAKAMURA, YOSIO p 835 N94-13203
NAKANE, KAZUROU p 691 N94-14232
NAKANISHI, ISAO p 687 N94-14094
NAKATA, MUTSUMI p 618 N94-14284
NAKATANI, I. p 586 N94-13735
NAKAYA, YUKIHIRO p 687 N94-14093
NAKAYAMA, YASUNORI p 696 N94-14262
NARAYANA, C. L. p 510 N94-14617
NARIGON, M. L. p 544 N94-14649
NASTASI, M. p 570 N94-13512
p 558 N94-14469
NATESAN, K. p 800 N94-13913
NATORI, MICHIHIRO p 530 N94-13275
p 530 N94-13276
NAUS, D. J. p 824 N94-13915
NAVAGH, JOHN p 532 N94-14851
NAZAROV, V. M. p 567 N94-14884
NEAL, COLIN p 720 N94-13429
NEALY, JOHN E. p 846 N94-12875
NEDWELL, J. p 777 N94-14130
NEECE, R. T. p 598 N94-12811
NEECE, ROBERT T. p 597 N94-12804
NEELY, W. C. p 575 N94-12789
NEFF, ANTON W. p 713 N94-13418
NEFF, D. p 608 N94-14375
NEILSON, J. p 649 N94-13410
NEIN, MAX p 547 N94-14838
NELLIS, W. J. p 576 N94-12885
NELSON, AMY p 553 N94-14725
NELSON, B. p 613 N94-14658
NELSON, D. A. p 580 N94-14297
NELSON, J. BRADLEY p 715 N94-13830
NELSON, KARL p 554 N94-12833
NERI, D. F. p 735 N94-12982
NERI, DAVID F. p 734 N94-12975
NERI, J. M. p 801 N94-14349
NERY, CARLOS EDUARDO p 684 N94-13364
NEUFELD, DAVID C. p 537 N94-14853
NEUMAN, J. E. p 548 N94-12870
NEUMANN, W. E. p 543 N94-14352
NEVASMAA, PEKKA p 674 N94-13887
NEWAZ, GOLAM M. p 555 N94-13378
NEWCHURCH, MICHAEL p 714 N94-13709
NEWLIN, L. E. p 542 N94-14076
p 542 N94-14077
p 542 N94-14078
p 519 N94-14841
p 519 N94-14842
NEWMAN, L. p 705 N94-12869
NEWNAM, B. E. p 626 N94-14805
NEWTON, M. A. p 654 N94-12963
NG, C. Y. p 563 N94-13411
NGO, DUC M. p 732 N94-13714
NGUYEN, CHARLES C. p 833 N94-14359
NGUYEN, H. p 657 N94-13882
NGUYEN, T. M. p 611 N94-14393
NGUYEN, V. L. p 772 N94-12896
NICHOLS, DONALD K. p 741 N94-13943
NICOL, DAVID M. p 758 N94-12938
p 762 N94-13184
p 752 N94-14139
NICOL, E. J. p 815 N94-14699
NICOLETTE, V. F. p 561 N94-12819
NICOLIS, STAM p 766 N94-14718
NIE, DALIN p 711 N94-12788
NIEBUR, D. p 622 N94-13811
p 624 N94-13948
NIED, H. F. p 557 N94-13920
NIEDZWIECKI, RICHARD W. p 517 N94-13142
NIEUWENHUIZEN, M. P. p 542 N94-13988
NII, H. PENNY p 745 N94-13357
p 747 N94-13443
NIKIFOROV, V. I. p 788 N94-14881
NIP, WING S. p 623 N94-13846
NISHIHAMA, MASAHIRO p 716 N94-13960
NISHINAGA, TATAU p 587 N94-13741
NISSENBAUM, INNA p 719 N94-13188
NITSCHE, W. p 510 N94-14800
NIXON, A. E. p 564 N94-13487
NOCEDAL, J. p 744 N94-13024
NODA, JUNICHI p 502 N94-13345
NOLL, ROBERT J. p 792 N94-14473
NOORDUNG, HERMANN p 552 N94-14463

NORBURY, J. W. p 786 N94-14551
NORBY, R. p 707 N94-13486
NORDINE, P. C. p 586 N94-12805
NORLANDER, LENA p 729 N94-14129
NORMAN, E. B. p 848 N94-13695
NORMAN, JIM p 850 N94-14060
NORTON, D. P. p 808 N94-13930
NOUSEK, JOHN A. p 822 N94-13062
NOVO, EVLYN M. L. M. p 685 N94-13610
NUCKOLLS, WILLIAM E. p 777 N94-14481
NUGENT, K. A. p 653 N94-12857

O

OBANDO, RODRIGO A. p 741 N94-14136
OBERLE, WILLIAM F. p 585 N94-14145
OBERMAYER, M. p 522 N94-13302
OCHIAI, HIROAKI p 697 N94-14268
OCONNELL, J. S. p 789 N94-13209
OCONNELL, R. W. p 831 N94-13681
OCONNELL, T. p 550 N94-13147
ODEN, J. TINSLEY p 632 N94-13467
OEKSOY, D. p 578 N94-13493
OESTERLUND, H. p 695 N94-14256
OEZGUENER, U. p 766 N94-14568
OGAWA, T. p 689 N94-14217
OGIER, RICHARD G. p 537 N94-12809
OGUCHI, MITSUO p 737 N94-13388
OHARA, D. p 731 N94-12972
OHARA, G. P. p 673 N94-13777
OHLHAUSEN, J. A. p 576 N94-12912
OHLINGER, WAYNE L. p 553 N94-14725
OHMORI, C. p 780 N94-13173
OHNO, ATSUMI p 589 N94-13751
OHTA, TAKAO p 581 N94-14421
OINUMA, HIDESHI p 502 N94-13342
OKABAYASHI, M. p 796 N94-13046
OKADA, NORIAKI p 513 N94-13457
OKAMOTO, G. p 611 N94-14391
OKAMOTO, KENICHI p 688 N94-14212
p 690 N94-14224
p 690 N94-14226
OKAMOTO, KOTARO p 627 N94-13433
OKAMOTO, OSAMU p 539 N94-12943
OKAMOTO, TERUKI p 529 N94-13269
p 529 N94-13270
p 530 N94-13278
OKAMOTO, TETSUYA p 747 N94-13436
OKEEFE, M. A. p 574 N94-14795
OKI, RIKO p 690 N94-14225
OKI,TAIKAN p 690 N94-14225
OKUDERA, TAKESHI p 618 N94-13440
OKUNO, YOSHINORI p 513 N94-13344
OLAF, J. M. p 579 N94-14007
OLAND, C. B. p 824 N94-13915
OLDS, JOHN ROBERT p 515 N94-13618
OLESON, STEVEN R. p 534 N94-13028
OLIGER, JOSEPH p 750 N94-13932
OLIN, A. p 778 N94-12860
OLSEN, B. L. p 581 N94-14319
OLSON, C. L. p 801 N94-14349
OLSON, R. J. p 825 N94-14458
OLSON, STEVE p 827 N94-14115
OLSON, T. S. p 549 N94-12996
OLSSON, PELLE p 770 N94-13922
p 770 N94-14307
OMALLEY, B. T. p 709 N94-14020
OMBABA, JACKSON M. p 798 N94-13678
ONEILL, JOHN W. p 666 N94-13158
ONISHCHENKO, I. N. p 797 N94-13240
ONO, FUMIEI p 548 N94-12945
ONO, TAKATSUGU p 513 N94-13344
p 513 N94-13346
ONODA, JUNJIROU p 537 N94-14277
OOKAWA, YOSHIYUKI p 529 N94-13269
OONA, H. p 802 N94-14532
OOSIMA, KEITA p 747 N94-13437
OOTA, TOYOYUKI p 530 N94-13275
OOTSUBO, KOUJI p 737 N94-13388
ORELLANA, OSCAR p 630 N94-13114
ORIKASA, TERUAKI p 529 N94-13270
p 530 N94-13278
ORIN, DAVID E. p 680 N94-14637
ORKNEY, L. P. p 570 N94-13666
ORLANDI, P. p 644 N94-14755
ORME, JOHN S. p 519 N94-14855
ORMROD, MICHAEL K. p 774 N94-13549
ORVIS, W. J. p 619 N94-12994
OSBORNE, M. G. p 568 N94-13000
OSBORNE, T. H. p 802 N94-14583
OSGA, G. A. p 743 N94-12974
OSTEN, KEVIN D. p 734 N94-12929
OSTERHELD, A. L. p 654 N94-12962
p 795 N94-12995
p 803 N94-14865
p 803 N94-14894
OSTERWISCH, FREDERICK G. p 648 N94-13176
OTTENSTEIN, HOWARD p 851 N94-14791
OTTESEN, D. K. p 710 N94-14183
OTTINGER, P. F. p 801 N94-14349
OTTO, S. R. p 630 N94-13128
p 636 N94-13785
OUSTERHOUT, JOHN K. p 740 N94-13363
OVERBEY, GLENN p 536 N94-14310
OWEN, DEAN H. p 523 N94-13307
OWEN, W. M., JR. p 610 N94-14389
OWOCKI, STANLEY P. p 847 N94-13288
OXENHAM, A. J. p 598 N94-12926
OZGUNER, U. p 819 N94-13059

P

PADFIELD, GARETH D. p 522 N94-13304
p 523 N94-13306
PADFIELD, R. RANDALL p 525 N94-13319
PADILLA, CARLOS E. p 677 N94-14620
PAINE, R. T. p 554 N94-14290
PAINTER, JAMES S. p 749 N94-13721
PAINTER, JOHN H. p 526 N94-13469
PAKANEN, JOUKO p 597 N94-14055
PALLEWATTA, P. K. M. M. p 693 N94-14241
PALMATIER, T. H. p 609 N94-14379
PALMER, M. R. p 825 N94-14458
PALMER, RAYMOND W. p 620 N94-13110
PALMER, T. N. p 721 N94-13914
PANDA, S. p 769 N94-13536
PANDOLFO, LIONEL p 713 N94-13622
PANKOV, A. A. p 783 N94-13506
PAOLA, JUSTIN D. p 763 N94-13603
PAPADOPOULOS, MICHAEL p 539 N94-12976
PAPAGEORGIOU, DEMETRIOS T. p 628 N94-12888
p 630 N94-13114
p 636 N94-13817
p 647 N94-14849
PAPAMICHAEL, K. p 704 N94-14333
PAPAMOSCHOU, D. p 645 N94-14760
PAPANICOLAOU, GEORGE C. p 628 N94-12888
PAPPAS, D. P. p 568 N94-13036
PAQUET, P. p 837 N94-13504
PARENT, A. p 740 N94-13546
PARHAM, B. p 609 N94-14382
PARK, H.-S. p 840 N94-14467
PARK, K. C. p 540 N94-13112
PARKES, JAMES p 553 N94-14725
PARKINSON, W. H. p 712 N94-13092
PARKS, M. A. N. p 615 N94-14670
PARLIAMENT, HUGH A. p 750 N94-13858
p 604 N94-13869
p 604 N94-13870
p 604 N94-13939
p 750 N94-13944
p 751 N94-13990
p 751 N94-14014
p 751 N94-14016
p 606 N94-14037
p 606 N94-14038
p 752 N94-14051
p 752 N94-14052
p 607 N94-14066
p 753 N94-14197
PARMA, E. J. p 548 N94-12981
PARMANEN, JUHANI p 777 N94-14034
PARRISH, PHILLIP A. p 766 N94-14785
PARRY, S. p 567 N94-14884
PARSA, Z. p 659 N94-14572
PARTRIDGE, NICOLA C. p 595 N94-13773
PASE, BILL p 752 N94-14088
PASSEUR, ANDREA p 804 N94-12873
PATE, M. B. p 596 N94-13407
PATERA, ANTHONY p 629 N94-13074
PATERA, ANTHONY T. p 629 N94-13074
PATIL, S. B. p 762 N94-12969
PATOKIN, A. P. p 576 N94-12867
PATRABOY, TIMOTHY J. p 623 N94-13846
PATTERSON, DAVID A. p 740 N94-13363
PATTERSON, F. G. p 625 N94-14522
PATTERSON, MICHAEL J. p 553 N94-14725
p 553 N94-14726
PATTERSON, P. E. p 623 N94-13892
PATTESON, R. p 800 N94-13908
PAUL, W. p 809 N94-14085
PAUSDER, HEINZ-JUERGEN p 522 N94-13300
PAVLENKO, E. A. p 790 N94-14843
PAWEL, R. E. p 569 N94-13242
PAWLOWSKI, SUSAN K. p 758 N94-12930
PAYNE, R. C. p 777 N94-13885
PAYNE, S. A. p 808 N94-13881
p 810 N94-14125
PECORA, L. p 596 N94-13684
p 597 N94-14070
PEDERSON, S. P. p 772 N94-12919
PEDRAZA, D. F. p 582 N94-14531
PEEBLES, D. E. p 576 N94-12912
PELETMINSKIJ, S. V. p 816 N94-12855
PELLACIO, D. p 585 N94-14535
PELLEGRINI, ALESSANDRO p 748 N94-13524
PENFOLD, J. p 579 N94-13783
PENG, L. W. p 710 N94-14183
PENG, T. K. p 609 N94-14381
PENG, TSUNG-HUNG p 707 N94-13384
PENNA, P. J. p 516 N94-13898
p 504 N94-14031
PENNEKAMP, C. J. p 819 N94-14809
PENNER, J. E. p 718 N94-12903
p 709 N94-14022
PENNYCOOK, S. J. p 808 N94-13930
p 813 N94-14478
PEPPER, STEPHEN V. p 575 N94-12842
PERCIVAL, LARRY D. p 555 N94-13138
PEREPEZKO, J. H. p 572 N94-14123
PEREZ, JOSE M. p 578 N94-13246
PEREZ, M. R. p 828 N94-12915
PERILO, SERGIO ALVES p 818 N94-13427
PERITT, JONATHAN p 661 N94-13445
PERKINS, D. p 548 N94-12911
PERRY, A. E. p 644 N94-14751
PERRY, M. D. p 657 N94-13882
p 658 N94-14114
PERSOON, ANN M. p 789 N94-13419
PERVUSHIN, V. N. p 849 N94-14889
PESKOV, V. p 651 N94-14452
PETERS, L. K. p 709 N94-13911
PETERS, W. A. p 583 N94-13002
PETERSEN, NANCY p 732 N94-13061
PETERSON, ALLEN M. p 790 N94-12797
PETERSON, B. V. p 737 N94-13712
PETERSON, D. L. p 794 N94-12814
PETERSON, R. L. p 656 N94-13481
p 658 N94-14437
p 808 N94-13694
PETICOLAS, L. J. p 659 N94-14576
PETRICEVIC, V. p 800 N94-13913
PETRICK, M. p 801 N94-14347
PETRIE, T. W. p 538 N94-13918
PETRIK, E. J. p 764 N94-13842
PETRIU, EMIL p 764 N94-13844
PETTY, C. C. p 795 N94-12953
p 801 N94-14293
PETZOLDT, KARIN p 694 N94-14250
PHAM, T. T. p 609 N94-14381
PHILLION, D. W. p 803 N94-14865
PHILLIPS, N. E. p 816 N94-14868
PHILLIPS, R. C. p 812 N94-14348
PIANETTA, P. p 805 N94-13020
PICCI, G. p 773 N94-13677
PICHNARCZYK, K. p 753 N94-14289
PICKETT, H. M. p 602 N94-13813
PICKLE, J. D. p 719 N94-12978
PIERCE, JOE T. p 655 N94-13261
PIERRE, A. p 781 N94-13348
PIETRZYKOWSKI, T. p 761 N94-12859
PIGEAUD, A. p 703 N94-13693
PINDERA, MAREK-JERZY p 560 N94-14823
PINELLI, THOMAS E. p 821 N94-13057
p 825 N94-14485
p 825 N94-14486
p 825 N94-14487
p 826 N94-14488
p 826 N94-14489
PINSKER, R. I. p 795 N94-12953
p 801 N94-14293
PITTS, THOMAS p 546 N94-14833
PITZ, W. J. p 566 N94-14869
PIVIROTTO, THOMAS J. p 549 N94-13068
PIYAPONGSE, PONGPIT p 693 N94-14242
PLANA, ROBERT p 616 N94-14717
PLATOFF, ANNE M. p 827 N94-12800
PLATT, C. E. p 815 N94-14699
PLATT, J. A. p 628 N94-12968
PLIMPTON, S. p 754 N94-14399
PLUM, M. p 780 N94-13173
POINSOT, T. p 567 N94-14764
POINSOT, T. J. p 646 N94-14763
p 567 N94-14765
POIRIER, DAVID R. p 567 N94-12825
POLITO, J. p 755 N94-14528
POLK, JAMES E. p 549 N94-13068
POLLARA, F. p 608 N94-14377
POMIANOWSKI, P. A. p 781 N94-13348
PONATER, MICHAEL p 724 N94-14709
POND, CHARLES L. p 536 N94-14323
POOLE, LAMONT R. p 694 N94-14252
POON, C. p 675 N94-13945
POORMAN, R. p 571 N94-13715
POPOV, A. D. p 818 N94-14887
POPPER, STEPHEN E. p 736 N94-12935
PORKOLAB, M. p 802 N94-14579

PORTER, G. D. ..... p 801 N94-14347
POSENAU, M.-A. ..... p 739 N94-12886
POSNER, EDWARD C. ..... p 607 N94-14369
POST, W. M. ..... p 707 N94-13486
POSTLETHWAITE, I. ..... p 522 N94-13303
POTOTZKY, ANTHONY S. ..... p 514 N94-12850
POUKEY, J. W. ..... p 801 N94-14349
POVINELLI, L. A. ..... p 642 N94-14728
POWELL, G. L. ..... p 565 N94-14525
POWELL, J. R. ..... p 552 N94-14111
POWELL, WILLIAM C. ..... p 666 N94-13155
POWERS, L. ..... p 795 N94-13017
POYNTER, R. L. ..... p 602 N94-13813
PRABHU, D. K. ..... p 639 N94-14598
PRABHU, DINESH K. ..... p 641 N94-14610
PRAEL, R. E. ..... p 787 N94-14804
PRAIRIE, M. R. ..... p 561 N94-12841
PRAMANIK, M. A. H. ..... p 692 N94-14238
PRATA, A. J. ..... p 696 N94-14263
PRATER, J. L. ..... p 608 N94-14376
PRATER, JOHN T. ..... p 816 N94-14839
PRATT, L. M. ..... p 717 N94-14338
PRATT, TIMOTHY ..... p 613 N94-14658
p 613 N94-14659
PRAUSNITZ, J. M. ..... p 581 N94-14400
PRICE, D. F. ..... p 625 N94-14522
PRINS, MATTHIJS ..... p 597 N94-14808
PROBERT, P. H. ..... p 798 N94-13577
PROFETA, ELI ..... p 763 N94-13568
PROPER, H. A. ..... p 824 N94-14072
PROSSER, CHARLES F. ..... p 833 N94-14358
PRUZAN, DANIEL A. ..... p 511 N94-13424
PRZEKWAS, A. J. ..... p 627 N94-12803
PUCIK, THOMAS A. ..... p 769 N94-13731
PURI, I. K. ..... p 567 N94-14766
p 567 N94-14767
PUZYNIN, I. V. ..... p 772 N94-14886
PYE, L. D. ..... p 578 N94-13493
PYUN, MOO-GON ..... p 699 N94-14283

Q

QUAN, RALPH ..... p 679 N94-14630
QUEST, KEVIN B. ..... p 800 N94-13854
QUINTANA, JORGE A. ..... p 538 N94-13111
QUIRK, W. J. ..... p 849 N94-13019

R

RABINOWITZ, MARTIN J. ..... p 642 N94-14722
RABZAK, CHRISTOPHER ..... p 557 N94-14042
RACCA, ROBERTO ..... p 777 N94-14360
RAHE, W. H. ..... p 760 N94-14011
RAHMAN, MOHAMMAD REZAUR ..... p 692 N94-14239
RAINER, F. ..... p 655 N94-13243
RAJALAKSHMY, S. ..... p 641 N94-14614
RAJENDRAN, A. M. ..... p 576 N94-12932
RAKOCZY, JOHN M. ..... p 682 N94-14652
RAMACHANDRAN, KRISHNA ..... p 509 N94-14781
RAMAMOORTHY, P. ..... p 641 N94-14611
p 516 N94-14615
RAMAMOORTHY, PREMALATHA ..... p 641 N94-14611
RAMAN, GANESH ..... p 508 N94-14208
RAMBO, P. W. ..... p 801 N94-14342
RAMESH, C. ..... p 744 N94-13077
RAMESH, V. ..... p 510 N94-14617
RAMINS, PETER ..... p 620 N94-13110
RAMSEY, W. G. ..... p 578 N94-13493
p 581 N94-14343
RANGARAJAN, R. ..... p 639 N94-14600
p 510 N94-14617
RANKIN, C. C. ..... p 673 N94-13726
p 674 N94-13905
RAO, P. KRISHNA ..... p 691 N94-14231
RAO, V. BRAHMANANDA ..... p 721 N94-13672
RAPOPORT, R. D. ..... p 706 N94-12937
RASMUSSEN, D. A. ..... p 795 N94-13033
RATNER, L. ..... p 790 N94-14897
RATOWSKY, R. P. ..... p 654 N94-12962
RATZDAFF, J. ..... p 798 N94-13518
RAVID, RAFI ..... p 600 N94-13537
RAY, R. E., JR. ..... p 808 N94-13973
RAZAFINDRATSITA, HERINIAINA ROGER
p 814 N94-14697
REASENBERG, ROBERT D. ..... p 841 N94-12823
p 545 N94-13067
REDD, L. R. ..... p 549 N94-12996
REDDY, J. N. ..... p 676 N94-14408
REDFIELD, R. C. ..... p 662 N94-13800
REED, K. J. ..... p 784 N94-14140
REED, R. DALE ..... p 537 N94-14853
REHR, J. J. ..... p 563 N94-13477
p 563 N94-13478
REILLY, H. F. ..... p 611 N94-14397
REINGEWIRTZ, MEIR ..... p 835 N94-13230
REINHARD, L. ..... p 574 N94-14793
REINHART, R. C. ..... p 538 N94-13918
REISNER, JON ..... p 633 N94-13553
REITZ, R. D. ..... p 519 N94-14448
REITZE, D. H. ..... p 625 N94-14522
REKOVA, L. P. ..... p 569 N94-13360
REMAKLUS, WILL ..... p 615 N94-14675
RENNE, D. ..... p 704 N94-14422
RENZI, R. F. ..... p 710 N94-14183
REPPERGER, DANIEL ..... p 736 N94-12935
RESLER, D. A. ..... p 781 N94-13251
RESSLER, MICHAEL ELVIN ..... p 831 N94-13657
RETTIG, C. L. ..... p 802 N94-14583
REUSS, D. L. ..... p 645 N94-14756
REY, C. A. ..... p 586 N94-12805
RHOADES, C. E., JR. ..... p 576 N94-12939
RHODES, W. C. ..... p 785 N94-14420
RHUDY, R. W. ..... p 506 N94-14163
RIBEIRODAROCHA, HUMBERTO ..... p 707 N94-13330
RICE, EDWARD J. ..... p 508 N94-14208
RICHARDS, P. L. ..... p 815 N94-14699
RICHARDSON, J. ..... p 555 N94-13248
RICHHARIA, M. ..... p 615 N94-14670
RICO-MARTINEZ, R. ..... p 766 N94-14737
RIESEN, R. ..... p 758 N94-12878
RIGHINI, GIOVANNI ..... p 770 N94-13809
RIKS, E. ..... p 673 N94-13726
p 674 N94-13905
RILEY, D. J. ..... p 601 N94-13696
RILEY, R. A. ..... p 798 N94-13513
RIMMER, CHUCK ..... p 547 N94-14837
RINEHART, L. F. ..... p 623 N94-13892
RINOIE, KENICHI ..... p 502 N94-13454
p 505 N94-14059
RIORDAN, C. ..... p 704 N94-14350
p 704 N94-14422
RIPPIN, BOAZ ..... p 601 N94-13567
RISTIC, VELIMIR M. ..... p 792 N94-13845
ROADS, J. O. ..... p 722 N94-14057
ROBERSON, N. R. ..... p 786 N94-14514
ROBERTO, MARISA ..... p 801 N94-14024
ROBERTODOSSANTOS, JOAO ..... p 688 N94-14131
ROBERTS, C. SHANNON ..... p 667 N94-13164
ROBERTS, J. A. ..... p 680 N94-14639
ROBEY, H. F. ..... p 720 N94-13404
ROBINSON, A. C. ..... p 670 N94-12908
p 752 N94-14019
ROBINSON, WILLIAM ..... p 547 N94-14838
ROCHAT-RETOURNE, NATHALIE ..... p 560 N94-14815
ROCHFORD, K. B. ..... p 792 N94-14367
ROCKEL, BURKHARDT ..... p 724 N94-14709
ROCKWELL, S. T. ..... p 609 N94-14381
RODGERS, MICHAEL N. ..... p 735 N94-13582
RODIN, W. A. ..... p 663 N94-14113
RODRIGO, T. ..... p 786 N94-14524
RODRIGUES, VALTER ..... p 686 N94-13789
RODRIGUEZ, G. ..... p 679 N94-14631
RODVOLD, MICHELLE ..... p 512 N94-14744
ROEBUCK, B. ..... p 570 N94-13666
ROECKNER, ERICH ..... p 724 N94-14709
ROELOF, EDMOND C. ..... p 715 N94-13826
ROESSLER, P. ..... p 709 N94-14087
ROGALLO, R. S. ..... p 643 N94-14747
p 644 N94-14750
ROGERS, L. C. ..... p 676 N94-14530
ROGERS, M. M. ..... p 647 N94-14768
ROGERS, R. J. ..... p 733 N94-13847
ROGERS, ROBERT J. ..... p 663 N94-14147
ROITHMAYR, CARLOS M. ..... p 681 N94-14648
ROME, J. A. ..... p 795 N94-13033
ROMERO, FRANCISCO A. ..... p 665 N94-13042
ROMIG, A. D., JR. ..... p 648 N94-13044
ROOKE, D. P. ..... p 683 N94-14818
ROPER, J. R. ..... p 664 N94-14565
RORSCHACH, H. E. ..... p 782 N94-13414
ROSE, D. V. ..... p 801 N94-14349
ROSE, WILLIAM C. ..... p 637 N94-13827
ROSEN, ADI ..... p 598 N94-13195
ROSEN, R. S. ..... p 583 N94-14693
ROSENBERGER, FRANZ ..... p 803 N94-12796
p 648 N94-13326
ROSENQVIST, A. ..... p 695 N94-14256
ROSER, T. ..... p 569 N94-13221
ROSNER, DANIEL E. ..... p 577 N94-13089
ROSS, F. M. ..... p 808 N94-13694
ROSS, J. E. ..... p 663 N94-14195
ROSS, M. ..... p 801 N94-14312
ROSTI, E. ..... p 759 N94-13470
ROSU, H. ..... p 778 N94-12879
p 834 N94-12880
ROTH, DON J. ..... p 665 N94-13056
ROTH, MARK A. ..... p 823 N94-13701
ROTHMAN, S. D. ..... p 803 N94-14865
ROTHWELL, I. P. ..... p 573 N94-14402
ROTTMAN, GARY J. ..... p 652 N94-14684
ROUQUETTE, NICOLAS F. ..... p 749 N94-13784
ROUSSOPOULOS, NICK ..... p 822 N94-13126
ROY, S. ..... p 769 N94-13536
ROYALS, MARK ..... p 619 N94-12967
ROZMUS, W. ..... p 792 N94-14438
ROZSNYAI, B. ..... p 801 N94-14312
RUDGE, A. ..... p 580 N94-14179
RUEHLE, M. ..... p 806 N94-13136
RUGGIERO, A. G. ..... p 781 N94-13219
RULE, WILLIAM KEITH ..... p 543 N94-14120
RUMBAUGH, DUANE M. ..... p 728 N94-13865
RUNDLE, W. J. ..... p 656 N94-13481
RUPOLO, VOLFANGO ..... p 725 N94-13500
RUSSELL, CAROL ..... p 808 N94-13875
RUSSELL, P. E. ..... p 812 N94-14365
RUSSO, J. G. ..... p 836 N94-13361
RUTHVEN, GREGORY ..... p 830 N94-13448
RUTLAND, C. J. ..... p 519 N94-14448
RUTTEN, JAN. J. M. M. ..... p 768 N94-13526
RYAN, KENNETH F. ..... p 575 N94-14878
RYAN, P. M. ..... p 607 N94-14291
RYAN, R. S. ..... p 669 N94-12831
RYCKMAN, S. J., JR. ..... p 707 N94-13383
RYMES, M. ..... p 704 N94-14422
RYNE, R. D. ..... p 740 N94-13286
RYVES, T. B. ..... p 783 N94-13883

S

SAABAS, HELMUT JOHN ..... p 635 N94-13683
SAALTINK, MARK ..... p 752 N94-14088
SACCO, G. P. ..... p 527 N94-13127
SADAYAPPAN, P. ..... p 680 N94-14637
SAEGUSA, HIROSHI ..... p 531 N94-13279
SAFAAI-JAZI, A. ..... p 613 N94-14658
SAFFMAN, P. G. ..... p 643 N94-14747
SAGALOVICH, V. V. ..... p 576 N94-12867
SAGER, J. C. ..... p 738 N94-13979
SAGHAFI, JAHAN ..... p 516 N94-14616
SAHA, SUBIR KUMAR ..... p 662 N94-13597
SAHU, JUBARAJ ..... p 504 N94-13795
SAIGAL, A. ..... p 555 N94-13248
SAITO, THEODORE T. ..... p 546 N94-14835
SAITOU, GENYA ..... p 693 N94-14242
p 695 N94-14259
SAJFULIN, SH. Z. ..... p 627 N94-14885
SAKAKIBARA, SEIZOU ..... p 502 N94-13345
SAKAMAKI, MASAMORI ..... p 530 N94-13275
SAKAMOTO, HIROSHI ..... p 548 N94-12945
SAKAMOTO, MITSUMASA ..... p 570 N94-13460
SAKATA, KIMIO ..... p 830 N94-13452
SALERNO, LOUIS J. ..... p 776 N94-14027
SALMON, J. T. ..... p 658 N94-14437
SAMADANI, RAMIN ..... p 790 N94-12797
SAMEJIMA, SHUUICHI ..... p 618 N94-14286
SAMIOS, N. P. ..... p 787 N94-14580
SANCHEZ, J. A. ..... p 584 N94-13099
p 584 N94-13491
SANDERS, WILLIAM A. ..... p 582 N94-14543
SANDLER, DAVE ..... p 546 N94-14833
SANDLER, IVAN S. ..... p 769 N94-13731
SANDORFI, A. M. ..... p 785 N94-14363
SANFELIZ, JOSE G. ..... p 559 N94-14719
SANKAR, L. N. ..... p 500 N94-13180
SANTAMARIA, ODILLYN L. ..... p 777 N94-14481
SANTANNA, NILSON ..... p 746 N94-13428
SANTAVICCA, DOMENIC A. ..... p 638 N94-14308
SANTERRE, ROCK ..... p 513 N94-13541
SAOUTIC, B. ..... p 797 N94-13144
SAPER, RON ..... p 603 N94-13838
SARASAMMA, V. R. ..... p 641 N94-14614
SARAVANOS, DIMITRIS A. ..... p 557 N94-14042
SARFATY, R. ..... p 746 N94-13394
SARTER, NADINE R. ..... p 510 N94-13247
SARVER-VERHEY, TIMOTHY ..... p 553 N94-14725
SASA, SHUUICHI ..... p 528 N94-13337
p 649 N94-13343
p 649 N94-13456
SASAKI, MASAKI ..... p 548 N94-12945
SASANO, Y. ..... p 690 N94-14220
SASANO, YASUHIRO ..... p 689 N94-14218
SASUGA, TSUNEO ..... p 529 N94-13271
SATCHER, J. H. ..... p 705 N94-14510
SATO, ARTHUR HIDEYUKI ..... p 601 N94-13661
SATO, ATSUSHIGE ..... p 592 N94-13763
SATO, KAZUO ..... p 548 N94-12945
SAULYS, A. C. ..... p 780 N94-13098
SAUVAL, A. J. ..... p 844 N94-13502
SAWADA, HIDEO ..... p 526 N94-13347
SAWYER, CONSTANCE ..... p 848 N94-13476
SAXENA, S. K. ..... p 639 N94-14598
p 510 N94-14612
SCALO, JOHN M. ..... p 836 N94-13332
SCHAEDLICH, STEPHAN ..... p 688 N94-14135
SCHAFER, K. J. ..... p 659 N94-14594

SCHAFFER, M. J. ..... p 802 N94-14570
SCHAFFNER, MICHAEL S. ..... p 553 N94-14725
SCHAICH, P. C. ..... p 700 N94-14566
SCHAMEL, GUENTER ..... p 617 N94-14817
SCHARRER, JOSEPH K. ..... p 660 N94-12791
SCHEERES, D. J. ..... p 532 N94-14373
SCHERR, LARRY ..... p 547 N94-14836
SCHIJVE, J. ..... p 675 N94-13933
SCHILDBACH, M. A. ..... p 790 N94-12865
SCHIMMERLING, WALTER ..... p 846 N94-12875
SCHINDLER, STEPHEN ..... p 847 N94-13211
SCHLEGEL, ROBERT E. ..... p 732 N94-13193
SCHLEGELMILCH, R. F. ..... p 538 N94-13918
SCHLEITWEILER, P. M. ..... p 573 N94-14316
SCHLIEF, RALPH E. ..... p 780 N94-13051
SCHLOSBERG, W. H. ..... p 707 N94-13390
SCHMIDT, E. ..... p 548 N94-12981
p 549 N94-13034
SCHMIDT, G. ..... p 818 N94-14738
SCHMIDTCHEN, JOACHIM ..... p 793 N94-14704
SCHMIDTKE, PAUL C. ..... p 833 N94-14406
SCHNEE, R. W. ..... p 847 N94-12964
SCHNEIDER, D. ..... p 788 N94-13208
SCHNEIDER, STEVEN P. ..... p 527 N94-12824
SCHOENWALD, D. A. ..... p 766 N94-14568
SCHOEPP, JUERGEN ..... p 815 N94-14705
SCHOTT, L. ..... p 798 N94-13518
SCHOWENGERDT, ROBERT A. .... p 763 N94-13603
SCHRA, L. ..... p 570 N94-13497
p 570 N94-13532
SCHRADER, JAMES H. ..... p 597 N94-12804
SCHRECENGOST, T. R. ..... p 556 N94-13583
SCHREIBER, ROBERT ..... p 760 N94-13921
SCHREINER, WILLIAM S. ..... p 512 N94-13238
p 716 N94-14049
SCHROEDER, JEFFREY A. ..... p 523 N94-13310
SCHROEDER, T. ..... p 778 N94-12847
SCHRYVER, J. C. ..... p 738 N94-14335
SCHUBERT, W. K. ..... p 703 N94-13886
p 705 N94-14861
SCHULTE, H. ..... p 653 N94-14792
SCHULZ, M. ..... p 784 N94-13936
SCHULZ, MICHAEL ..... p 714 N94-13793
SCHULZE, NORMAN R. ..... p 550 N94-13147
SCHULZE, W. A. ..... p 809 N94-13981
SCHUMACHER, HELMUT ..... p 700 N94-14428
SCHUMACHER, IAN ..... p 777 N94-14360
SCHUMACHER, R. ..... p 649 N94-13410
SCHUTZ, B. E. ..... p 717 N94-14306
SCHWAMBORN, D. ..... p 641 N94-14613
SCHWARTZ, H. ..... p 657 N94-13812
SCHWARTZ, HARVEY R. ..... p 741 N94-13943
SCHWARZ, GOTTFRIED ..... p 651 N94-14044
SCHWEIKHARD, L. ..... p 788 N94-13208
SCHWEINFURTH, R. A. ..... p 815 N94-14699
SCIME, E. E. ..... p 782 N94-13492
p 717 N94-14328
SCIME, EARL E. ..... p 779 N94-12950
SCOFIELD, J. H. ..... p 619 N94-12942
SCOTT, ROBERT C. ..... p 514 N94-12850
SCWARTZ, R. W. ..... p 814 N94-14695
SEAH, M. P. ..... p 708 N94-13667
p 749 N94-13688
SEARLE, IAN ..... p 544 N94-14640
SEAS, A. ..... p 659 N94-14576
SEDILLO, E. M. ..... p 813 N94-14440
SEEGER, P. A. ..... p 559 N94-14690
SEESTROM, S. J. ..... p 786 N94-14514
SEFCIK, J. A. ..... p 849 N94-13019
SEGALMAN, D. J. ..... p 676 N94-14456
SEGAWA, Y. ..... p 586 N94-13734
SEGUCHI, TADAO ..... p 529 N94-13271
SEHMER, A. A. ..... p 653 N94-14858
SEKIGUCHI, CHIHARU ..... p 591 N94-13757
SEKINE, HIDEO ..... p 502 N94-13345
SEKINE, KOUJI ..... p 531 N94-13281
SELCOW, E. C. ..... p 548 N94-12981
SELLIS, TIMOS ..... p 822 N94-13126
SENCHENKO, T. A. ..... p 790 N94-14843
SENDA, KEI ..... p 530 N94-13277
SENGPIEL, W. ..... p 642 N94-14708
SENGUPTA, S. K. ..... p 700 N94-14566
SENSBURG, O. ..... p 751 N94-14006
SEPPALA, L. ..... p 625 N94-14522
SESSLER, A. M. ..... p 658 N94-14414
p 659 N94-14520
p 790 N94-14893
SEVASTON, GEORGE ..... p 546 N94-14833
SFORZA, MARIO ..... p 615 N94-14669
SHAHAM, JACOB ..... p 829 N94-13178
SHAHIDI, A. K. ..... p 538 N94-13918
SHAIK, K. S. ..... p 610 N94-14388
SHALKHAUSER, MARY JO ..... p 538 N94-13111
SHANG, HUAN-MIN ..... p 564 N94-13685
SHANKAR, P. N. ..... p 639 N94-14598
p 640 N94-14601
SHANNON, J. D. ..... p 717 N94-14424
SHANNON, ROBERT R. ..... p 547 N94-14837
SHAO, M. ..... p 610 N94-14390
SHAO, MIKE ..... p 547 N94-14838
SHAPPELL, S. A. ..... p 735 N94-12982
SHAPPELL, SCOTT A. ..... p 734 N94-12975
SHARAPOV, E. I. ..... p 786 N94-14514
SHARF, I. ..... p 678 N94-14625
SHARF, INNA ..... p 677 N94-14619
SHARKEY, JOHN ..... p 551 N94-13417
SHARMA, PRAMOD K. ..... p 701 N94-13187
p 564 N94-13947
SHARMA, RIKHI R. ..... p 818 N94-13984
SHARP, W. M. ..... p 659 N94-14520
SHARPE, J. B. ..... p 539 N94-12827
SHASHA, ELI ..... p 566 N94-14558
SHAW, B. A. ..... p 556 N94-13583
SHAW, W. M. ..... p 717 N94-14424
SHCHEPKIN, Y. G. ..... p 790 N94-14843
SHEAHAN, D. R. ..... p 539 N94-12827
SHEENA, ZVI ..... p 659 N94-14547
SHEN, B. ..... p 612 N94-14501
SHEN, HONG ..... p 662 N94-13642
SHEPHERD, R. L. ..... p 625 N94-14522
p 803 N94-14894
SHEPPARD, M. G. ..... p 794 N94-12849
SHERMAN, I. ..... p 626 N94-14730
SHERWOOD, R. J. ..... p 700 N94-14566
SHI, GEORGE Z. ..... p 536 N94-14310
SHI, NING ..... p 558 N94-14119
SHIAO, MICHAEL C. ..... p 671 N94-13379
SHIBATA, AKIRA ..... p 688 N94-14212
SHIBAYAMA, YUUZOU ..... p 531 N94-13281
SHIBUTA, SHIGETO ..... p 531 N94-13279
p 531 N94-13280
p 531 N94-13282
SHIH, T. H. ..... p 631 N94-13385
SHIMABUKURO, YOSIO EDEMIR . p 688 N94-14131
SHIMADA, MASANOBU ..... p 687 N94-14092
p 688 N94-14212
SHIMIZU, YOSHINORI ..... p 747 N94-13438
SHIMKAVEG, G. ..... p 795 N94-12995
SHIMKAVEG, G. M. ..... p 654 N94-12962
p 657 N94-13976
SHIMODA, H. ..... p 803 N94-14894
SHIMOMURA, TAKASHI ..... p 689 N94-14217
SHINDOU, SHIGEMI ..... p 528 N94-13337
SHINGUU, HIROKIMI ..... p 830 N94-13452
SHINN, J. ..... p 513 N94-13344
SHINN, JUDY L. ..... p 706 N94-13095
p 847 N94-13263
SHIPITALO, WILLIAM ..... p 732 N94-13714
SHIPLEY, S. ..... p 660 N94-12802
SHIRLEY, JOHN A. ..... p 803 N94-14770
SHISHKIN, A. L. ..... p 553 N94-14682
SHIVELY, DAVID G. ..... p 767 N94-13223
SHKLOVSKIJ, V. A. ..... p 604 N94-13916
SHLACHTER, J. S. ..... p 618 N94-12856
SHOEMAKER, H. D. ..... p 798 N94-13513
SHOEMAKER, P. A. ..... p 566 N94-14586
SHORE, B. W. ..... p 762 N94-12969
p 742 N94-12864
SHOUP, A. L. ..... p 786 N94-14526
SHTILMAN, L. ..... p 846 N94-12946
SHU, CHI-WANG ..... p 644 N94-14753
p 499 N94-12852
p 770 N94-14429
SHUFELT, JEFFEREY A. ..... p 772 N94-14900
SHUKLA, J. ..... p 683 N94-14500
SIEGEL, R. W. ..... p 810 N94-14185
SIGLER, CHARLES E., JR. ..... p 614 N94-14668
SILVA, SUELY ..... p 765 N94-14084
SIM, ALEX G. ..... p 537 N94-14853
SIMCHICK, R. T. ..... p 813 N94-14409
SIMMONS, RICKEY C. ..... p 517 N94-13323
SIMON, HORST ..... p 740 N94-13200
SIMONEN, E. P. ..... p 572 N94-14058
SIMONETTI, JOHN H. ..... p 839 N94-13864
SIMONS, WIM ..... p 542 N94-13988
SIMPSON, D. L. ..... p 674 N94-13861
SINGH, D. ..... p 577 N94-13032
SINGH, J. ..... p 571 N94-13715
SINGH, J. P. ..... p 577 N94-13032
p 641 N94-14613
SINGH, NAGENDRA ..... p 715 N94-13954
SINGHAL, S. N. ..... p 676 N94-14041
SINGHAL, SURENDRA N. ..... p 671 N94-13379
SINGLER, ROBERT E. ..... p 580 N94-14126
SINHA, SUBBASH C. ..... p 510 N94-14784
SINHA, U. N. ..... p 641 N94-14614
SIRLIN, S. W. ..... p 680 N94-14641
SIROCKY, PAUL J. ..... p 664 N94-14727
SISAKYAN, A. N. ..... p 788 N94-14891
SISTO, RENATA ..... p 787 N94-14721
SIVERS, E. A. ..... p 577 N94-13032
SIVIA, D. S. ..... p 579 N94-13783
SKARKA, V. ..... p 806 N94-13228
SKARSGARD, H. M. ..... p 798 N94-13518
p 799 N94-13835
SKEEN, D. C. ..... p 754 N94-14470
SKELTON, ROBERT E. ..... p 681 N94-14645
SKROBIS, K. J. ..... p 618 N94-12821
SKURNIK, M. ..... p 729 N94-14128
SLATTERY, W. L. ..... p 811 N94-14313
SLAVIN, A. ..... p 676 N94-14456
SLINGO, J. M. ..... p 721 N94-13914
SLINKER, S. P. ..... p 801 N94-14349
SLUITER, M. ..... p 567 N94-12899
p 569 N94-13137
SMAGA, J. A. ..... p 624 N94-14012
SMIRNI, E. ..... p 759 N94-13470
SMITH, A. E. ..... p 707 N94-13383
SMITH, B. K. ..... p 800 N94-13908
SMITH, BRIAN S. ..... p 623 N94-13871
SMITH, ERNEST K. ..... p 615 N94-14671
SMITH, G. ALLAN ..... p 596 N94-13790
SMITH, GARY W. ..... p 754 N94-14472
SMITH, K. L. ..... p 757 N94-14871
SMITH, L. K. ..... p 808 N94-13881
p 810 N94-14125
SMITH, M. J. T. ..... p 600 N94-13466
SMITH, M. R. ..... p 658 N94-14415
SMITH, MARK J. T. ..... p 619 N94-12897
p 598 N94-12920
p 744 N94-13113
SMITH, MONTY J. ..... p 527 N94-14650
SMITH, P. R. ..... p 746 N94-13394
SMITH, R. C. ..... p 768 N94-13354
SMITH, ROBERT E. ..... p 742 N94-12808
SMITH, SHELDON D. ..... p 643 N94-14741
SMITH, VIRGIL K., III ..... p 505 N94-14154
p 507 N94-14168
p 507 N94-14172
SMITH, WAYNE A. ..... p 638 N94-14356
SMITHER, R. K. ..... p 848 N94-13483
SMOLYAKOV, A. ..... p 800 N94-13852
SMOLYAKOV, A. I. ..... p 798 N94-13564
p 799 N94-13836
p 800 N94-13850
p 801 N94-14206
SMUDA, ELLEN ..... p 742 N94-12808
SMYRLIS, YIORGOS S. ..... p 628 N94-12888
SNIDER, J. B. ..... p 613 N94-14660
SNYDER, CHRISTOPHER A. ..... p 518 N94-13143
SOELL, D. ..... p 730 N94-14509
SOENARJO, J. H. ..... p 692 N94-14237
SOFFEN, GERALD ..... p 851 N94-14791
SOGA, NAOHIRO ..... p 587 N94-13740
SOLANO, EMILIA R. ..... p 757 N94-14866
SOLARZ, R. ..... p 658 N94-14442
SOLIMAN, KARAM F. A. ..... p 731 N94-12960
SOLOMON, STANLEY C. ..... p 652 N94-14684
SOLYAKOV, D. G. ..... p 794 N94-12854
SONDAK, DOUGLAS L. ..... p 520 N94-12799
SONDERGAARD, R. ..... p 644 N94-14751
SONG, AARON ..... p 718 N94-12957
SONG, SUN-DAL ..... p 657 N94-13996
SONI, NITIN J. ..... p 538 N94-13111
SORENSEN, S. P. ..... p 788 N94-12817
SORIA, J. ..... p 644 N94-14751
SOROKIN, D. P. ..... p 621 N94-13224
SOUKUP, R. J. ..... p 581 N94-14337
SOULAS, GEORGE C. ..... p 553 N94-14725
SOUMA, TAKASHI ..... p 696 N94-14264
p 696 N94-14265
SOURLAS, DENNIS ..... p 681 N94-14643
SOUTH, D. W. ..... p 708 N94-13495
SOUZA, KENNETH A. ..... p 594 N94-13770
SOWA, E. C. ..... p 805 N94-13010
SPEARMAN, M. LEROY ..... p 500 N94-13172
SPECTOR, V. A. ..... p 544 N94-14649
SPERBER, K. R. ..... p 721 N94-13914
p 723 N94-14426
SPINKS, DEBRA ..... p 643 N94-14745
SPIVAK, ALAN L. ..... p 776 N94-14027
SPONTARELLI, T. ..... p 584 N94-13491
SPRAGUE, S. ..... p 709 N94-14087
SPRUCK, J. ..... p 740 N94-13069
SREENIVASAN, C. R. ..... p 641 N94-14614
SRIDHARAN, R. ..... p 531 N94-13358
SRILATHA, K. R. ..... p 516 N94-14615
SRIVASTAVA, ASHOK ..... p 516 N94-14616
ST.JOHN, HOLGER ..... p 757 N94-14866
STAFFORD, R. B. ..... p 652 N94-14687
STAGGS, M. C. ..... p 580 N94-14124
STAHL, K. A. ..... p 793 N94-14702
STAHLBERG, RON ..... p 678 N94-14629
STAHLER, STEVEN W. ..... p 836 N94-13423
STALLINGS, D. ..... p 803 N94-14770
STAN-LOTTER, HELGA ..... p 728 N94-13562
STANGE, B. M. ..... p 561 N94-12841
STANGLE, G. C. ..... p 809 N94-13981

STANTON, P. H. p 611 N94-14397
STARK, J. W. p 623 N94-13834
STARK, M. J. p 846 N94-12924
STARK, R. E. p 731 N94-14862
STEARNS, D. G. p 583 N94-14693
STEEL, DUNCAN p 805 N94-13037
STEENKISTE, PETER p 749 N94-13779
STEFFEN, CARLOS ALBERTO p 685 N94-13610
STEFFES, PAUL G. p 739 N94-13086
STEHLE, ROY H. p 537 N94-12809
STEHLIK, M. p 632 N94-13511
STEINETZ, BRUCE M. p 664 N94-14727
STEINHAUER, L. C. p 794 N94-12862
STEINHOFF, JOHN p 509 N94-14781
STEINOLFSON, R. S. p 828 N94-12970
STEINTHORSSON, E. p 642 N94-14728
STENERSEN, KNUT p 657 N94-13970
STEPANEK, S. A. p 508 N94-14173
STEPANOV, K. N. p 617 N94-14883
STEPHANAKIS, S. J. p 801 N94-14349
STEPHENS, R. M. p 813 N94-14409
STERN, S. A. p 566 N94-14586
STERNE, P. A. p 568 N94-13036
STEVER, R. p 803 N94-14590
STEWART, LYNNE M. p 665 N94-13153
p 669 N94-14321
STEWART, R. E. p 657 N94-13976
p 803 N94-14865
p 803 N94-14894
STILL, WILLIAM T. p 669 N94-14321
STINECIPHER, M. M. p 584 N94-13099
STOCKS, G. M. p 567 N94-12899
STOFFEL, T. p 704 N94-14350
p 704 N94-14422
STOKSTAD, R. G. p 848 N94-13695
STOLLER, R. E. p 573 N94-14700
STOLLERY, JOHN L. p 502 N94-13454
STOLTZ, D. L. p 707 N94-13390
STOLTZ, L. A. p 758 N94-12917
STOLZ, C. J. p 655 N94-13243
STONE, EDWARD C. p 847 N94-13211
STONER, DAVID L. p 666 N94-13155
STORCH, JOEL A. p 677 N94-14623
STORMON, CHARLES D. p 745 N94-13130
STORMS, E. p 802 N94-14567
STOUGHTON, JOHN W. p 741 N94-14136
STOWE, LARRY L. p 691 N94-14233
STRAIN, D. p 608 N94-14374
STRAND, ALBERT A. p 668 N94-13167
STRAND, BO p 770 N94-13922
p 770 N94-14307
STRATMAN, M. P. p 813 N94-14440
STRAUBE, TIMOTHY M. p 681 N94-14648
STRAUSS, M. p 660 N94-14888
STRAZNICKY, P. V. p 675 N94-13945
STREINZ, C. C. p 569 N94-13050
STRELTSOV, V. N. p 617 N94-14892
STRETZ, L. A. p 584 N94-13099
STROH, K. R. p 553 N94-14689
STRUM, M. J. p 556 N94-13389
STUBBERUD, STEPHEN p 681 N94-14644
STUBENHOFER, R. L. p 624 N94-13928
STUTTE, G. W. p 738 N94-13979
STUTZMAN, W. L. p 612 N94-14501
STUTZMAN, WARREN L. p 613 N94-14658
p 615 N94-14674
SU, CHING-HUA p 807 N94-13444
SU, TZU-JENG p 677 N94-14621
SUBHLOK, JASPAL p 767 N94-13284
SUD, Y. C. p 723 N94-14074
SUDA, TATSUO p 593 N94-13765
SUENAGA, HISASHI p 526 N94-13347
SUENDERMANN, B. p 669 N94-13857
SUGAR, J. p 849 N94-13376
SUGIMOTO, NOBUO p 689 N94-14218
SUGIMOTO, TAKESHIGE p 697 N94-14270
SUGITANI, DAISUKE p 747 N94-13439
SULLIVAN, E. J. p 725 N94-12876
SULLIVAN, THOMAS M. p 613 N94-14657
SULLIVAN, WALTER p 851 N94-14791
SUMI, AKIMASA p 690 N94-14225
SUMMERS, CHRISTOPHER J. p 650 N94-14029
SUNDBERG, W. D. p 501 N94-13260
SURBER, JEFFREY L. p 678 N94-14628
SUTHARSHANA, S. p 542 N94-14076
p 542 N94-14077
p 542 N94-14078
p 519 N94-14841
p 519 N94-14842
SUTJAHJO, EDHI p 675 N94-13919
SUTTON, S. p 658 N94-14442
SUWITRA, KRISJANI p 614 N94-14665
SUZUKI, M. p 690 N94-14220
SUZUKI, SHINICHI p 687 N94-14094
SUZUKI, TAKAYUKI p 526 N94-13347
SUZUKI, TOMOO p 588 N94-13743
SVEC, W. A. p 782 N94-13484
SVOBODA, ROBERT C. p 783 N94-13856
SWAIN, D. p 803 N94-14770
SWANSON, PAUL N. p 546 N94-14832
SWEGLE, J. W. p 742 N94-12956
SWICKARD, SUZANNE M. p 665 N94-13056
SWIFT, G. W. p 597 N94-14592
SWIFT, W. M. p 800 N94-13913
SYDOW, E. V. p 620 N94-13094
SYED, ALI p 616 N94-14677
SYM, A. p 768 N94-13499
SYMBALISTY, E. M. D. p 718 N94-14518
SYSIOE, PAULI p 777 N94-14034
SZATMARY, STEVEN A. p 665 N94-13056
SZCZYGIEL, BRONIA p 824 N94-13879
SZEMPLINSKA-STUPNICKA, W. p 775 N94-13235

T

TAASAN, SHLOMO p 767 N94-13202
p 769 N94-13722
TABATA, MASAKI p 529 N94-13269
TADA, AKIRA p 593 N94-13767
TADROS, MAHASIN G. p 729 N94-14097
TADROS, SHAWKY H. p 562 N94-13048
TAGLER, RICHARD C. p 669 N94-13169
TAKAGI, MASATAKA p 695 N94-14257
TAKAHASHI, TARO p 707 N94-13384
TAKAMATSU, HIDEO p 690 N94-14222
TAKAMIZAWA, K. p 612 N94-14501
TAKASAWA, YOSHIMITSU p 618 N94-13440
TAKASAWA, YOSHIMITU p 747 N94-13439
TAKAYAMA, YOUZOU p 697 N94-14271
TAKEKAWA, S. p 590 N94-13752
TAKEUCHI, KENJI p 537 N94-14279
TAKEUCHI, NOBUO p 693 N94-14243
TAKEUCHI, SHOUJI p 696 N94-14262
TAKEUCHI, YOSHINARI p 530 N94-13276
TAKEYA, H. p 568 N94-13000
TAKIZAWA, M. p 689 N94-14219
TAKIZAWA, MINORU p 514 N94-13338
TAKIZAWA, NAOTO p 501 N94-13340
p 501 N94-13341
TALLANT, D. R. p 576 N94-12912
TALLARIDA, G. p 733 N94-14860
TAMEISHI, HIDEO p 697 N94-14268
p 697 N94-14270
TAMURA, HIROSHI p 548 N94-12945
TAN, XIN p 684 N94-13368
TANAKA, FUMIHIKO p 581 N94-14421
TANAKA, KIYOOMI p 627 N94-13434
TANBA, SUMIO p 696 N94-14264
p 696 N94-14265
TANEMURA, TOSHIHARU p 737 N94-13388
TANG, H. p 805 N94-13102
TANG, J. S. p 774 N94-14334
TANG, P. K. p 585 N94-14180
TANIAI, HITOSHI p 529 N94-13269
TANIZAWA, KAZUO p 529 N94-13269
TANSLEY, T. p 804 N94-12893
TAO, ZHIJIAN p 779 N94-12882
TAPLEY, BYRON D. p 717 N94-14306
TARTAKOVSKIJ, V. K. p 788 N94-14875
TASSANO, J. B. p 808 N94-13881
p 810 N94-14125
TATE, ATSUSHI p 502 N94-13345
TATSUMI, MASAMI p 590 N94-13754
TAUSANOVITCH, JEANETTE R. p 792 N94-14473
TAVE, JEFFREY S. p 681 N94-14648
TAYLOR, K. A. p 717 N94-14294
TAYLOR, LAWRENCE A. p 843 N94-14303
TAYLOR, R. T. p 705 N94-14510
TAYLOR, T. D. p 581 N94-14343
TELEGA, J. J. p 578 N94-13468
TEMPEL, P. p 818 N94-14462
TEMPLE, R. p 758 N94-12917
TEMPLETON, GEOFFREY B. p 665 N94-13148
p 665 N94-13153
p 669 N94-14321
TERESHIN, V. I. p 794 N94-12854
TERHOFSTEDE, A. H. M. p 824 N94-14072
TESMER, J. R. p 570 N94-13512
THANGAM, S. p 636 N94-13718
THART, W. G. T. p 570 N94-13497
THE, P. S. p 828 N94-12915
THEIHZEN, H. G. p 722 N94-13993
THEON, JOHN S. p 690 N94-14221
p 691 N94-14228
THERIAULT, G. A. p 790 N94-12863
THERY, CHRISTIAN p 776 N94-13692
THIESSEN, H. p 780 N94-13173
THOLE, KAREN ANN p 633 N94-13559
THOMAS, C. E. p 795 N94-13033
p 797 N94-13144
THOMAS, E. V. p 814 N94-14695
THOMAS, E. W. p 807 N94-13373
THOMAS, J. K. p 825 N94-14458
THOMAS, R. A. p 658 N94-14437
THOMAS, RICHARD E. p 541 N94-13955
THOMPSON, CHRIS p 818 N94-13984
THOMPSON, D. A. p 620 N94-13134
THOMPSON, G. R. p 656 N94-13481
THOMPSON, JOHN O. p 709 N94-14103
THOMPSON, M. D. p 712 N94-12906
THOMSEN, M. F. p 717 N94-14328
THOMSEN, OLAF p 617 N94-14819
THOMSON, DOUGLAS G. p 523 N94-13311
THOMSON, K. R. p 669 N94-13857
THORNE, LARRY F. p 675 N94-13907
TICEHURST, J. M. p 657 N94-13976
TIERNEY, PAUL G. p 668 N94-13168
TIGHE, THOMAS S. p 807 N94-13359
TIKARE, VEENA p 582 N94-14543
TIKHONCHUK, V. T. p 792 N94-14438
TILMANS, E. p 543 N94-14352
TINNEL, E. P. p 825 N94-14458
TIRKAS, PANAYIOTIS A. p 602 N94-13799
TIRSELL, K. G. p 789 N94-14460
TISCHLER, M. B. p 527 N94-14642
TISCHLER, MARK B. p 526 N94-13324
TIT, N. p 807 N94-13510
TITS, A. L. p 527 N94-14642
TJON, J. A. p 786 N94-14550
TOBBE, PATRICK A. p 682 N94-14652
TOBIN, J. G. p 568 N94-13036
TODOSOW, M. p 548 N94-12981
p 554 N94-14806
TOGANO, KAZUMASA p 586 N94-13736
TOKUMARU, KUMON p 692 N94-14236
TOLEDO, SIVAN p 771 N94-14506
TOLSON, ROBERT H. p 539 N94-12976
TOLSTOLUZHSKIJ, A. P. p 797 N94-13240
TOMANEY, AUSTIN BEDE p 831 N94-13668
TOME, C. p 712 N94-12906
TOMITA, TSUYOSHI p 696 N94-14262
TOMOSADA, AKIRA p 696 N94-14267
TOMPPO, ERKKI p 694 N94-14254
TONKS, D. L. p 811 N94-14329
TOPKOV, A. N. p 798 N94-13507
TORENBEEK, E. p 515 N94-13687
TORKOMIAN, ANA LUCIA VITALE p 818 N94-13427
TORRENCE, GEOFFREY W. p 613 N94-14661
TORRES-POMALES, WILFREDO p 759 N94-13450
TORTI, RICHARD P. p 596 N94-13141
TORTORELLI, P. F. p 568 N94-12998
TOSATTI, E. p 569 N94-13227
TOUNSI, PATRICK p 626 N94-14713
TOWNSEND, L. W. p 786 N94-14550
p 786 N94-14551
TRACHTA, GREGORY S. p 666 N94-13157
TRAIBER, A. J. S. p 569 N94-13137
TRAN, KHANH N. p 606 N94-14062
TRAUB, WESLEY A. p 714 N94-13816
TREBES, J. p 653 N94-14772
TREBES, J. E. p 655 N94-13258
TRIF, NICULAE p 764 N94-13842
p 764 N94-13844
TRIPP, LLOYD D., JR. p 736 N94-12935
TRIVEDI, NALIN BABULAL p 725 N94-13728
TROEIM, JAN p 542 N94-14107
TROLINGER, JAMES D. p 651 N94-14447
TROUVE, A. p 567 N94-14764
TROWBRIDGE, L. D. p 710 N94-14459
TRUDINGER, C. M. p 709 N94-14095
TRUSZKOWSKI, WALTER p 851 N94-14791
TSACOYEANES, JAMES G. p 792 N94-14473
TSAI, WEN-LANG p 596 N94-13798
TSANG, T. p 793 N94-14529
TSCHANZ, J. p 707 N94-13383
TSCHAPLINSKI, T. p 707 N94-13486
TSENG, I-SHIH p 585 N94-14490
TSING, N.-K. p 527 N94-14642
TSRUYA, SHALOM p 601 N94-13566
TSUBOI, EIJIRO p 618 N94-13441
TSUCHIYA, KIYOSHI p 693 N94-14243
TSUDA, SHOUICHI p 514 N94-13459
TSUHA, WALTER S. p 677 N94-14622
TUCKER, BRYAN J. p 733 N94-13824
TUCKER, GEORGE E. p 525 N94-13320
p 517 N94-13323
TUKEY, JOHN W. p 774 N94-14788
TUMMILLO, A. F. p 624 N94-14012
TURCHI, P. E. A. p 567 N94-12899
p 569 N94-13137
TURENNE, S. p 557 N94-13866
TURGEON, MARTIN p 606 N94-14063
TURI, DANIELE p 768 N94-13526
TURK, JOSEPH p 616 N94-14678
TURKEL, E. p 769 N94-13717
TURKO, B. T. p 625 N94-14336
TURNER, D. p 548 N94-12911

TURNER, K. p 767 N94-13025
TURNER, M. S. p 834 N94-13096
TURNER, ROSS M. p 603 N94-13832
TUSKAN, J. p 707 N94-13486
TUTTLE, B. A. p 814 N94-14695
TWARDY, HARALD p 557 N94-13804
TWEEDT, D. L. p 499 N94-13108
TYLER, J. p 638 N94-14351
TZASKOMA, PATRICIA p 556 N94-13663

U

UBER, D. C. p 625 N94-14336
UCHIDA, TADAO p 514 N94-13338
p 513 N94-13344
UDAGAWA, AKIRA p 529 N94-13271
UHLICH, D. M. p 656 N94-13481
ULLOA, S. E. p 815 N94-14739
ULMER, MELVILLE p 546 N94-14833
p 546 N94-14834
UNDERWOOD, J. H. p 658 N94-14175
p 659 N94-14595
UNDERWOOD, JOHN H. p 673 N94-13777
UNDERWOOD, LEROY H. p 819 N94-13400
UNRUH, W. P. p 581 N94-14327
URAI, YASUO p 747 N94-13436
URBANUS, W. H. p 655 N94-13145
URIBE, PAULO F. p 833 N94-14359
USILANER, BRIAN p 666 N94-13156
USLENGHI, PIERGIORGIO L. E. p 599 N94-13264

V

VACCAREZZA, STEPHEN E. p 638 N94-14086
VACCAREZZA, STEVEN p 630 N94-13078
VACHEV, V. D. p 781 N94-13225
VAHALA, GEORGE p 636 N94-13718
VAIDYA, R. U. p 558 N94-14121
VAINIKAINEN, PERTTI V. p 625 N94-14096
VALDEZ, G. D. p 782 N94-13409
VALENCIA, MARCO R. p 636 N94-13780
VALERIO, J. A. p 702 N94-13402
VALLETTE, BRENDA J. p 844 N94-13963
VANAKEN, E. M. p 824 N94-14048
VANBLEEK, B. J. p 700 N94-14810
VANDENBROEK, A. C. p 684 N94-13123
VANDERAAR, MARK p 538 N94-13111
VANDERBORGH, N. E. p 553 N94-14689
VANDERWEES, A. J. p 503 N94-13531
VANDERWEIDE, T. P. p 824 N94-14072
VANDERWIEL, M. J. p 655 N94-13145
VANDERWIJNGAART, ROB F. p 759 N94-13204
VANDEVENDER, W. H. p 759 N94-13043
VANDROMME, D. p 645 N94-14759
VANDRONGELEN, H. p 722 N94-13926
VANDYCK, O. p 788 N94-13103
VANGORKOM, JACQUELINE p 829 N94-13181
VANHAFTEN, D. H. p 548 N94-12870
VANHARLINGEN, D. J. p 815 N94-14699
VANLEER, B. p 769 N94-13717
VANMUIJDEN, J. p 503 N94-13531
VANOUDHEUSDEN, B. W. p 527 N94-13906
VANRHEE, C. G. p 775 N94-13987
VANRUITEN, A. p 819 N94-14809
VANSCHUPPEN, J. H. p 773 N94-13677
p 765 N94-14018
VASS, PAM p 699 N94-14353
VAUGHN, CHARLES R. p 850 N94-13923
VEHVILAEINEN, B. p 718 N94-12837
VELETSOS, A. S. p 676 N94-14585
VELTMAN, B. p 751 N94-14004
VENKATARAMAN, V. K. p 566 N94-14586
VENNE, YANN p 764 N94-13842
VENUGOPAL, R. p 678 N94-14626
VERBIST, BRUNO p 695 N94-14258
VERBRUGGEN, MARC p 674 N94-13803
VERHOEVEN, A. G. A. p 655 N94-13145
VERNIKOS, J. p 731 N94-12972
VERNON, S. P. p 583 N94-14693
VEROLME, J. L. p 675 N94-13931
VERTEZ, MARTINE p 720 N94-13587
VERVISCH, L. p 567 N94-14766
p 567 N94-14767
VIDDELEER, R. p 543 N94-14352
VIETINGHOFF, H. p 675 N94-13945
VIGUE, Y. p 514 N94-14371
VIITANEN, A.-M. p 729 N94-14128
VILA, F. p 775 N94-12877
p 619 N94-12891
VILNROTTER, V. A. p 602 N94-13810
VINNINS, M. F. p 653 N94-14782
VISSER, H. G. p 511 N94-13534
VISWANATHAN, S. p 510 N94-14617
VLOT, AD p 674 N94-13803
VOEVODIN, M. A. p 627 N94-14885
VOGEL, WOLFHARD J. p 613 N94-14661
p 613 N94-14662
p 615 N94-14672
p 616 N94-14677
VOGT, G. J. p 581 N94-14327
VOLAKIS, JOHN L. p 599 N94-13236
p 602 N94-13720
VOLKAS, R. R. p 778 N94-12845
VOLOSHKO, A. YU. p 794 N94-12854
VOLZ, RICHARD A. p 754 N94-14472
VONBALLMOOS, P. p 848 N94-13483
VONFLOTOW, ANDREAS H. p 677 N94-14620
VOORHEES, L. D. p 825 N94-14458
VOORHIES, COERTE V. p 716 N94-13960
VORONIN, V. V. p 804 N94-12828
VRANISH, JOHN p 661 N94-13445
VU, TUAN A. p 773 N94-13848
VUILLERMOZ, PATRICK p 565 N94-14194

W

WAAGEN, DON p 766 N94-14882
WADA, N. p 588 N94-13746
WADDILL, G. D. p 568 N94-13036
WADE, T. p 607 N94-14291
WAESELYNCK, HELENE p 756 N94-14714
WAGER, PAUL p 538 N94-13111
WAGNER, G. R. p 619 N94-12892
WAGNER, J. W. p 569 N94-13050
WAGNER, LYLE p 605 N94-13941
WAGNER, T. D. p 759 N94-13470
WAINER, N. p 783 N94-13884
WAITE, T. p 583 N94-14801
WAKEFIELD, M. E. p 539 N94-12827
WALBERG, GERALD D. p 515 N94-13618
WALDRON, A. K. p 775 N94-12843
WALDROP, RAYMOND S. p 754 N94-14472
WALEFFE, F. p 644 N94-14750
WALKER, B. p 781 N94-13241
WALKER, D. p 522 N94-13303
WALKER, DAVID H. p 737 N94-13674
WALKER, EDWARD F. p 758 N94-12930
WALKER, H. F. p 767 N94-13025
WALKER, T. G. p 805 N94-13102
WALLACE, D. C. p 817 N94-14593
WALLACE, J. C. p 751 N94-14017
p 558 N94-14105
WALLACE, S. J. p 786 N94-14550
WALLACE, W. p 571 N94-13840
WALLING, R. S. p 654 N94-12962
p 795 N94-12995
p 657 N94-13976
p 803 N94-14894
WALSH, COLIN p 635 N94-13662
WALTERS, J. L. p 538 N94-13918
WALTHALL, CHARLES L. p 808 N94-13875
WALTON, JAMES T. p 552 N94-14102
WAMPLER, W. A. p 559 N94-14690
WANDER, JOHN p 663 N94-14134
WANG, DA-HENG p 532 N94-14273
WANG, G.-X. p 574 N94-14821
WANG, H. H. p 623 N94-13925
WANG, H. T. G. p 599 N94-13236
WANG, HUA p 672 N94-13669
WANG, JOHN C. L. p 848 N94-13708
WANG, LAWRENCE C. H. p 728 N94-13823
WANG, T. S. F. p 780 N94-13173
WANG, YULUN p 682 N94-14651
WANG, Z. L. p 804 N94-12818
WANGLER, T. P. p 789 N94-13209
p 789 N94-13328
WANHILL, R. J. H. p 570 N94-13497
WARASHINA, TAKASHI p 627 N94-13434
WARD, DONALD T. p 516 N94-14106
WARD, JOHN L. p 545 N94-13713
WARMACK, R. J. p 812 N94-14362
p 660 N94-14863
WARNER, MICHAEL S. p 766 N94-14444
WARNOW, T. J. p 743 N94-12991
WARREN, STEPHEN p 686 N94-14081
WARREN, W. L. p 576 N94-12866
WASBERG, CARL ERIK p 637 N94-14040
WASHBURN, DAVID A. p 728 N94-13865
WASIELEWSKI, M. R. p 782 N94-13484
WATANABE, MITSUNORI p 502 N94-13345
WATANABE, SHIGEYA p 514 N94-13459
WATANABE, TAKASHI p 696 N94-14264
WATANABE, YOSHIAKI p 570 N94-13460
WATKINS, B. E. p 705 N94-14510
WATSON, R. p 825 N94-14331
p 760 N94-14475
WATSON, R. KEVIN p 741 N94-13943
WATSON, R. M. p 811 N94-14332
WATTERS, THOMAS R. p 842 N94-13199
WATTERSON, JAMES W. p 619 N94-12967
WAYE, D. E. p 501 N94-13260
WEAVER, MICHAEL J. p 779 N94-12894
WEBB, D. J. p 568 N94-13036
WEBB, WAYNE BUELL p 837 N94-13550
WEBER, WILLIAM P. p 560 N94-14794
WEBSTER, A. R. p 602 N94-13801
p 603 N94-13841
WEBSTER, C. E. p 624 N94-14012
WEBSTER, J. R. P. p 579 N94-13783
WEEKS, MICHEL p 698 N94-14276
WEERTMAN, J. R. p 810 N94-14185
WEGMANN, H. p 733 N94-14860
WEGNER, WOLFGANG p 638 N94-14188
WEGRZYN, J. p 660 N94-12851
WEI, DING-WEN p 694 N94-14253
WEIN, M. p 741 N94-13547
WEIS, M. P. p 573 N94-14364
WEISS, JONATHAN MITCHELL p 552 N94-14491
WEISSHAAR, J. C. p 562 N94-13222
WEITKAMP, CLAUS p 617 N94-14819
p 617 N94-14820
p 647 N94-14816
WELCHLIN, LUTZ p 520 N94-13254
WELLS, EDWARD A. p 662 N94-13794
WELLS, M. G. H. p 669 N94-13857
WELLS, P. p 556 N94-13583
WENDT, R. G. p 789 N94-13220
WENG, W. T. p 766 N94-14785
WERELEY, NORMAN M. p 612 N94-14501
WERNTZ, P. p 744 N94-13049
WERTH, LAURIE H. p 653 N94-12898
WERVE, M. E. p 566 N94-14869
WESTBROOK, C. K. p 503 N94-13530
WESTLAND, J. p 613 N94-14660
WESTWATER, E. R. p 677 N94-14618
WETTE, M. p 678 N94-14627
WETTE, MATT p 506 N94-14161
WETTLAUFER, BRIAN p 506 N94-14165
WEYGANDT, JAMES H. p 501 N94-13266
WHALLEY, MATTHEW S. p 521 N94-13294
p 522 N94-13301
WHEAT, S. p 758 N94-12878
WHEELER, E. M. p 737 N94-13712
WHEELER, R. M. p 738 N94-13979
WHEELWRIGHT, CHARLES p 735 N94-13961
WHIRLEY, R. G. p 663 N94-13975
p 771 N94-14589
WHITAKER, R. W. p 718 N94-14518
WHITCOMB, JOHN D. p 559 N94-14715
WHITE, M. G. p 563 N94-13411
WHITE, R. M. p 781 N94-13251
WHITE, W. E. p 625 N94-14522
WHITEFORD, TOM p 753 N94-14207
WHITEHEAD, B. A. p 552 N94-14309
WHITESON, R. p 758 N94-12917
WHITMAN, S. p 755 N94-14521
WHITTUM, D. H. p 658 N94-14414
WIEDERRECHT, G. P. p 782 N94-13484
WIELAND, R. M. p 796 N94-13046
WIENER, JOSEPH p 772 N94-14840
WIESMANN, H. p 660 N94-12851
WIETFELDT, F. E. p 848 N94-13695
WIGGERS, H. A. p 761 N94-14476
WIGHTMAN, J. P. p 543 N94-14683
WILCOX, J. Z. p 607 N94-14370
WILCOX, S. p 704 N94-14422
WILE, DAVID S. p 742 N94-12933
WILEMSKI, G. p 703 N94-13693
WILKES, R. JEFFREY p 846 N94-12826
WILKINSON, C. p 788 N94-13103
WILKS, S. C. p 797 N94-13207
p 802 N94-14564
WILLEKENS, A. J. L. p 650 N94-13527
WILLIAMS, DAVID R. p 842 N94-13561
WILLIAMS, GEORGE J., JR. p 553 N94-14726
WILLIAMS, J. M. p 623 N94-13925
WILLIAMS, JAMES p 791 N94-12979
WILLIAMS, KEVIN E. p 509 N94-14780
WILLIAMS, LARRY p 668 N94-13166
WILLIAMS, T. J. p 794 N94-12846
WILLIAMS, W. D. p 507 N94-14167
WILLIAMS, W. DAN p 648 N94-12874
WILLIAMS, W. F. p 616 N94-14742
WILLIAMS, WILLIAM O. p 817 N94-14680
WILSON, D. p 620 N94-13106
WILSON, GORDON R. p 716 N94-13967
WILSON, HENRY p 555 N94-13267
WILSON, J. R. p 738 N94-14451
WILSON, J. W. p 786 N94-14551
WILSON, JEFF p 682 N94-14651
WILSON, JOHN W. p 846 N94-12875
p 847 N94-13263
p 732 N94-13714
WILSON, K. E. p 610 N94-14386
WILSON, M. S. p 702 N94-13402

WINCHESTER, W. W. ..... p 702 N94-13403
WINGLEE, ROBERT M. ..... p 845 N94-14577
WINSTON, R. ..... p 791 N94-13015
WINTERKAMP, J. L. ..... p 722 N94-14057
WISE, S. A. ..... p 813 N94-14409
WISSINGER, ALAN B. ..... p 792 N94-14473
WIT, G. P. ..... p 675 N94-13986
WITHINGTON, JAMES P. ..... p 500 N94-13198
WLODARCZYK, WALDEMAR ..... p 771 N94-14807
WOBSER, J. K. ..... p 789 N94-14460
WODTKE, A. ..... p 563 N94-13411
WOFSY, STEVEN C. ..... p 714 N94-13816
WOJNAR, R. ..... p 578 N94-13468
WOLERY, T. J. ..... p 561 N94-12881
WOLF-WATZ, H. ..... p 729 N94-14128
WOLF-WATZ, HANS ..... p 729 N94-14129
WOLFORD, D. J. ..... p 809 N94-14079
p 809 N94-14083
p 809 N94-14108
WOMBLE, D. ..... p 758 N94-12878
WOMBLE, DONNA SUZANNE ..... p 837 N94-13551
WONG, H. K. ..... p 796 N94-13084
WONG, T. B. ..... p 824 N94-14202
WOO, A. C. ..... p 599 N94-13236
WOOD, JAMES S. ..... p 846 N94-12875
WOOD, KENT S. ..... p 791 N94-13664
WOOD, R. ..... p 801 N94-14347
WOODS, DAVID D. ..... p 510 N94-13247
WOODS, M. J. ..... p 708 N94-13880
WOODS, THOMAS N. ..... p 652 N94-14684
WOODWARD, R. L. ..... p 669 N94-13857
WOODWARD, RICHARD P. ..... p 518 N94-14036
WORKMAN, GARY L. ..... p 804 N94-12873
WOSNITZA, J. ..... p 623 N94-13925
WRAY, A. A. ..... p 643 N94-14747
WRIGHT, D. A. ..... p 816 N94-14868
WRIGHT, T. ..... p 775 N94-12955
WU, A. S. ..... p 562 N94-13085
WU, CHING-SEH ..... p 764 N94-13704
WU, K. ..... p 552 N94-14309
WU, MEI-RONG ..... p 692 N94-14235
WU, S.-C. ..... p 514 N94-14372
WU, SENG-RUNG ..... p 584 N94-13560
WU, X. D. ..... p 810 N94-14122
WUEST, C. ..... p 791 N94-13482
WUEST, C. R. ..... p 807 N94-13405
WYANT, JAMES ..... p 547 N94-14836
WYSS, M. L. ..... p 499 N94-13108

X

XIAO, C. ..... p 798 N94-13518
p 799 N94-13835
p 799 N94-13849
XIE, M. ..... p 679 N94-14635
XU, ZHONG LING ..... p 768 N94-13421
p 750 N94-13828

Y

YAHR, G. T. ..... p 571 N94-14021
YALOVOJ, I. N. ..... p 627 N94-14885
YAMADA, TOMOAKI ..... p 586 N94-13733
YAMADA, YASUHARU ..... p 693 N94-14242
YAMAGUCHI, A. ..... p 582 N94-14513
YAMAGUCHI, ISAO ..... p 540 N94-13339
YAMAGUCHI, KOICHI ..... p 627 N94-13433
YAMAGUCHI, YASUSHI ..... p 688 N94-14211
YAMAMOTO, KAYOKO ..... p 747 N94-13436
YAMAMOTO, YUKIMITSU ..... p 499 N94-12948
YAMANAKA, TATSUO ..... p 588 N94-13747
YAN, T.-Y. ..... p 610 N94-14388
YANAGIHARA, MASAAKI ..... p 500 N94-12951
p 528 N94-13337
p 537 N94-14278
YANAI, HIDEO ..... p 530 N94-13276
YANCEY, ROBERT N. ..... p 555 N94-13138
YANG, B. ..... p 781 N94-13241
YANG, H. Q. ..... p 627 N94-12803
YANG, JUXING ..... p 811 N94-14313
YANG, Z. ..... p 646 N94-14762
YATES, GIGI ..... p 545 N94-13189
YATES, LESLIE A. ..... p 650 N94-13814
p 650 N94-13815
p 532 N94-14068
p 533 N94-14540
YATSUYANAGI, NOBUYUKI ..... p 548 N94-12945
YAU, SHING-TUNG ..... p 817 N94-14417
YAZAWA, KENJI ..... p 517 N94-13451
YEE, J. H. ..... p 619 N94-12994
YEH, A. T. ..... p 566 N94-14582
YEH, H.-G. ..... p 611 N94-14393
YEHUDAR, YUVAL ..... p 600 N94-13538
YI, THOMAS Y. ..... p 550 N94-13265
YOKOTA, T. ..... p 690 N94-14220
YOKOYAMA, RYUUZOU ..... p 696 N94-14264
p 696 N94-14265
YONGHU, WENREN ..... p 509 N94-14781
YORKEY, T. ..... p 653 N94-14772
YOSHIDA, HIROSHI ..... p 795 N94-12944
YOSHIDA, ISAO ..... p 696 N94-14264
YOSHIDA, MASAHIRO ..... p 748 N94-13453
YOSHIMURA, SHOICHI ..... p 539 N94-12943
YOSHINO, K. ..... p 712 N94-13092
YOSHIZAWA, AKIRA ..... p 514 N94-13459
YOUNAN, A. H. ..... p 676 N94-14585
YOUNG, B. K. F. ..... p 795 N94-12995
p 803 N94-14894
YOUNG, BRUCE A. ..... p 733 N94-14879
YOUNG, P. J. ..... p 515 N94-13839
p 515 N94-13867
YU, J. ..... p 610 N94-14390
YU, S. S. ..... p 654 N94-12963
YUAN, C. ..... p 694 N94-14249
YUAN, S. ..... p 621 N94-13336
YUDATE, KOUZOU ..... p 529 N94-13271
YUGO, J. ..... p 803 N94-14770
YUGO, J. J. ..... p 798 N94-13577
YUH, C. ..... p 701 N94-13093
YUK, JAI-RIM ..... p 699 N94-14283
YUKALOV, V. I. ..... p 772 N94-14890
YUKALOVA, E. P. ..... p 772 N94-14890
YUNG, YUK L. ..... p 716 N94-13969
YUNGSTER, SHAYE ..... p 642 N94-14722
YUSHCHENKO, O. P. ..... p 783 N94-13506

Z

ZAAL, K. J. J. M. ..... p 675 N94-13929
ZADKOV, V. N. ..... p 781 N94-13225
ZALME, DESIREE ..... p 651 N94-14044
ZAN, S. J. ..... p 526 N94-13859
ZANG, WEIJIAN ..... p 539 N94-12790
ZATARSKI, M. M. ..... p 586 N94-12805
ZEE, RALPH ..... p 561 N94-12830
ZEIDERS, GLENN W., JR. ..... p 660 N94-14904
ZEILER, K. ..... p 709 N94-14087
ZELENSKIJ, V. F. ..... p 788 N94-14881
ZEMAN, O. ..... p 645 N94-14758
p 645 N94-14759
ZHA, HONGYUAN ..... p 748 N94-13586
ZHANG, GUO QI ..... p 673 N94-13787
ZHANG, GUO-FU ..... p 693 N94-14247
ZHANG, JIAN-DI ..... p 805 N94-13102
ZHANG, L. ..... p 799 N94-13835
ZHANG, S. Y. ..... p 789 N94-13220
ZHANG, T. ..... p 694 N94-14249
ZHANG, W. ..... p 799 N94-13835
p 799 N94-13849
p 694 N94-14249
ZHANG, XUDONG ..... p 634 N94-13598
ZHANLAV, T. ..... p 772 N94-14886
ZHAO, L. ..... p 571 N94-13840
ZHENG, SHANG-MIN ..... p 693 N94-14247
ZHENG, X. Y. ..... p 812 N94-14362
ZHOU, WUJUN ..... p 792 N94-13845
ZHOU, Y. ..... p 644 N94-14750
ZHOU, YE ..... p 630 N94-13133
p 636 N94-13718
ZHU, GUOMING ..... p 681 N94-14645
ZHU, MING ..... p 616 N94-14724
ZHU, Q. ..... p 813 N94-14517
ZHU, S. ..... p 808 N94-13930
p 812 N94-14362
ZOCCO, T. G. ..... p 570 N94-13512
ZOHAR, S. ..... p 602 N94-13810
ZOMBERG, BRIAN G. ..... p 623 N94-13878
ZOZ, S. C. ..... p 596 N94-13407
ZUREK, A. K. ..... p 558 N94-14121
ZYGMUNT, B. C. ..... p 825 N94-14458

Typical Corporate Source Index Listing

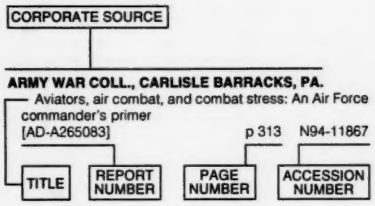

Listings in this index are arranged alphabetically by corporate source. The title of the document provides the user with a brief description of the subject matter. The report number helps to indicate the type of document cited (e.g., NASA report, translation, NASA contractor report). The accession number denotes the number by which the citation is identified. The page number helps you locate the citation in the abstract section. The titles are arranged under each corporate source in ascending accession number order.

A

ABACUS TECHNOLOGY CORP., CHEVY CHASE, MD.
Technology assessments of advanced energy storage systems for electric and hybrid vehicles
[DE93-014395] p 701 N94-12913

ACADEMIA SINICA, BEIJING (CHINA).
China's devotion to space science and applications p 532 N94-14273

ACADEMY OF SCIENCES OF THE UKRAINE, KHARKOV.
Non-linear effects in vortex viscous flow in superconductors-role of finite heat removal velocity
[DE93-621785] p 618 N94-12856
Deposition of crystalline boron thick layers from gas phase
[DE93-620499] p 576 N94-12867
Electrodynamics of helical plasma structures
[DE93-620981] p 797 N94-13240
About the influence of inert gas ion implantation on metal corrosion stability
[DE93-620574] p 569 N94-13360
Interferometric investigation methods of plasma spatial characteristics on stellarators and tokamaks in submillimeter region
[DE93-621606] p 798 N94-13507
On transport of energy, momentum, orbital angular momentum and self-angular momentum of electromagnetic wave in dispersal media
[DE93-624179] p 617 N94-14883

ACADEMY OF SCIENCES OF THE UKRAINE, KIEV.
Multiplicity spectrometry on neutron filtered beams
[DE93-617529] p 790 N94-14843
On the statistical theory of the even-even nucleons levels' density
[DE93-623990] p 788 N94-14875
The space-time and energy parameters of deuterium braking by the central collision with atoms
[DE93-624144] p 788 N94-14881

ACADEMY OF SCIENCES (USSR), LENINGRAD.
On the neutron EDM search in the Laue diffraction by the crystal without a centre of symmetry
[DE93-622971] p 804 N94-12828

ADVANCED AVIATION CONCEPTS, JUPITER, FL.
Determination of Loran-C/GPS human factors issues
[PB93-199693] p 514 N94-14563

ADVANCED COMMUNICATIONS TECHNOLOGY, INC., SILVER SPRING, MD.
VIEWCACHE: An incremental pointer-base access method for distributed databases. Part 1: The universal index system design document. Part 2: The universal index system low-level design document. Part 3: User's guide. Part 4: Reference manual. Part 5: UIMS test suite
[NASA-CR-191788] p 822 N94-13126

AERONAUTICAL RESEARCH INST. OF SWEDEN, STOCKHOLM.
Simulator study of uncoupled control functions. Use of manual pointing modes when aiming at ground targets and oncoming airborne target
[FFA-TN-1992-18] p 528 N94-13588
An 8-node axisymmetric acoustic finite element for non-axisymmetric fluid-structure interaction analysis
[FFA-TN-1993-03] p 673 N94-13689
Computational methods for reliable fatigue and damage tolerance dimensioning of aircraft structures
[FFA-TN-1993-05] p 515 N94-13690

AERONAUTICAL RESEARCH LABS., MELBOURNE (AUSTRALIA).
A benchmark bending test of a thick specimen, Part 1: Experiments
[ARL-RR-6-PT-1] p 670 N94-12927
A benchmark bending test of a thick specimen. Part 2: Surface displacement measurements
[ARL-RR-6-PT-2] p 670 N94-12928
Behavior of streamwise rib vortices in a three-dimensional mixing layer p 644 N94-14754

AEROSPACE CORP., EL SEGUNDO, CA.
Surface analysis of bearings
[AD-A266800] p 661 N94-13122
Stormtime transport of ring current and radiation belt ions
[NASA-CR-194416] p 714 N94-13793
Applications of surface science to solid lubricants
[SMC-TR-93-24] p 579 N94-13903
Dynamical model for the distribution of geomagnetically trapped anomalous-component ions
[ATR-91(9558)-6] p 784 N94-13936
AlGaAs diode laser blue shift resulting from fast neutron irradiation
[AD-A266642] p 659 N94-14681
Double inlet pulse tube cryocooler theory
[AD-A266832] p 597 N94-14877

AEROSPACE MEDICAL RESEARCH LABS., BROOKS AFB, TX.
The identification of ability requirements and selection instruments for fighter pilot training
[AD-A266340] p 735 N94-13582

AGENCY OF INDUSTRIAL SCIENCE AND TECHNOLOGY, TSUKUBA (JAPAN).
Growth experiment of organic metal crystal in low gravity (M-21) p 590 N94-13753

AIR-CONDITIONING AND REFRIGERATION TECHNOLOGY INST., INC., ARLINGTON, VA.
ARTI Refrigerant Database
[DE93-014774] p 595 N94-13021
Miscibility of lubricants with refrigerants, phase 1
[DE93-014766-PHASE-1] p 596 N94-13407
Compatibility of refrigerants and lubricants with motor materials
[DE93-014768] p 583 N94-14801

AIR FORCE ACADEMY, CO.
The use of linked lists in the simulation of controller-structure interaction p 679 N94-14630

AIR FORCE INST. OF TECH., WRIGHT-PATTERSON AFB, OH.
The effects of evaluation and production blocking on the performance of brainstorming groups
[AD-A265495] p 734 N94-12929
On the vertical structure of seasonal, interannual and intraseasonal flows
[AD-A265346] p 719 N94-12992
Magic mirror on the wall, who's the fastest database of them all? A survey of database benchmarks
[AD-A266437] p 823 N94-13701
ANNS: An X Window based version of the AFIT neural network simulator
[AD-A266540] p 764 N94-13704
A comparison of computational and experimental data for a subscale high speed propulsive nozzle at low mach numbers
[AD-A266543] p 504 N94-13705
Experimental and analytical analysis of the response of a smart beam to rate feedback
[AD-A266544] p 557 N94-13706
Experimental investigation of the effects of blowing ratio parameter on heat transfer to a film-cooled flat plate
[AD-A266599] p 636 N94-13780

AKRON UNIV., OH.
Adaptive control of interface by temperature and interface profile feedback in transparent multi-zone crystal growth furnace
[NASA-CR-194140] p 762 N94-13253

ALABAMA A & M UNIV., NORMAL.
Determination of trace elements in triglycine sulfate solutions
[NASA-CR-193481] p 562 N94-13048
Characterization of Spirulina biomass for CELSS diet potential
[NASA-CR-194123] p 729 N94-14097

ALABAMA UNIV., BIRMINGHAM.
Protein crystal growth p 591 N94-13756
Immiscible phase incorporation during directional solidification of hypermonotectics
[NASA-CR-194412] p 565 N94-14480

ALABAMA UNIV., HUNTSVILLE.
Breadboard activities for advanced protein crystal growth
[NASA-CR-193559] p 803 N94-12796
Reduce fluid experiment system flight data from IML-1
[NASA-CR-193835] p 804 N94-12873
Development of a global backscatter model for NASA's laser atmospheric wind sounder
[NASA-CR-192581] p 718 N94-12957
ROSAT guest investigator program (AO-1). On a search for coronal x ray emissions from white dwarfs
[NASA-CR-193654] p 835 N94-13171
Advanced electric motor technology flux mapping
[NASA-CR-193824] p 621 N94-13186
Temperature dependence of diffusivities, preliminary definition phase
[NASA-CR-192613] p 648 N94-13326
Numerical studies of spray combustion in liquid-fueled engines p 584 N94-13685
Develop research plan for use of atlas data
[NASA-CR-194338] p 714 N94-13709
Studies on equatorial shock formation during plasmaspheric refilling
[NASA-CR-194392] p 715 N94-13954
Sloshing dynamics on rotating helium dewar tank
[NASA-CR-194403] p 637 N94-13959
The role of ionospheric plasma in the magnetosphere
[NASA-CR-194404] p 716 N94-13967
Partial analysis of LDEF experiment A-0114
[NASA-CR-193826] p 564 N94-14025
BALLIST: A computer program to empirically predict the bumper thickness required to prevent perforation of the Space Station by orbital debris
[NASA-CR-193825] p 543 N94-14120
Earth science and application
[NASA-CR-184381] p 683 N94-14484
Cellular responses to low-gravity: Pilot studies on suborbital rockets and orbiting spacecraft
[NASA-CR-194402] p 729 N94-14494
Investigation of Zerodur material processing
[NASA-CR-193842] p 793 N94-14903
Atomic research
[NASA-CR-193843] p 788 N94-14905

ALABAMA UNIV., TUSCALOOSA.
Adaptively resizing populations: Algorithm, analysis, and first results
[NASA-CR-194277] p 742 N94-12806

Design and application of electromechanical actuators for deep space missions
[NASA-CR-194145] p 663 N94-14134

ALBERTA UNIV., EDMONTON.
Remote identification of rain and hail with a polarization diversity radar
[ISBN-0-315-55623-4] p 720 N94-13516
Characteristics of semiconductor lasers with optical feedback
[ISBN-0-315-55435-5] p 656 N94-13522
Flammability of clothing, volume 2
[DSIS-93-00036-VOL-2] p 564 N94-13819
improving physical performance by chemical stimulation
[DSIS-92-03763] p 728 N94-13823
Transcript of workshop on machinery health monitoring
[IME-MET-TR-005] p 733 N94-13847

ALLIED-SIGNAL AEROSPACE CANADA, TORONTO (ONTARIO).
The power of cross-functional teams in driving total quality p 666 N94-13159

ALLIED-SIGNAL AEROSPACE CO., KANSAS CITY, MO.
Knowledge base technology for CT-DIMS: Report 1
[DE93-013118] p 743 N94-13014
Rigid-flexible printed wiring boards
[DE93-013938] p 620 N94-13094
Dry film lubricant evaluation
[DE93-013114] p 578 N94-13118
Pollution prevention through total quality
[DE93-013814] p 707 N94-13390
Rapid intelligent inspection process definition for dimensional measurement in advanced manufacturing
[DE93-011271] p 748 N94-13480
Development of test techniques to simulate high-frequency mechanical shock on weapon components
[KCP-613-4998] p 675 N94-13907
Miniature mechanism assembly
[DE93-015595] p 624 N94-13928
Alternate cleaning methods for LCCAs
[KCP-613-5045] p 624 N94-13937
Microwave interconnection
[DE93-016580] p 625 N94-14533
Moisture meter evaluation
[DE93-016581] p 652 N94-14534

ALLIED-SIGNAL AEROSPACE CO., PHOENIX, AZ.
Advanced Turbine Technology Applications Project (ATTAP)
[NASA-CR-191088] p 828 N94-12931

ALUMINUM CO. OF AMERICA, ALCOA CENTER, PA.
Role of microstructure on fatigue durability of aluminum aircraft alloys
[AD-A265627] p 568 N94-12993
Role of microstructure on fatigue durability of aluminum aircraft alloys
[AD-A266350] p 571 N94-13697

AMERICAN GEOPHYSICAL UNION, WASHINGTON, DC.
The 1990 Western Pacific Geophysics meeting
[NASA-CR-193456] p 712 N94-13334
The American Geophysical Union Chapman Conference on Tectonics and Topography
[NASA-CR-193454] p 713 N94-13335

AMERICAN MOBILE SATELLITE CORP., WASHINGTON, DC.
Propagation considerations in the American Mobile Satellite system design p 614 N94-14668

AMERICAN PRODUCTIVITY AND AIR QUALITY CENTER, HOUSTON, TX.
Measuring quality progress p 666 N94-13154

AMERICAN UNIV., WASHINGTON, DC.
Solid state laser systems for space application
[NASA-CR-194133] p 656 N94-13420

AMES LAB., IA.
Gas atomized Er3Ni powder for cryocooler applications
[DE93-011564] p 568 N94-13000

ANALYTICAL SERVICES AND MATERIALS, INC., HAMPTON, VA.
Large-eddy simulation of laminar-turbulent breakdown at high speeds with dynamic subgrid-scale modeling
[NASA-CR-4533] p 629 N94-13064
Effect of thermal processing practices on the properties of superplastic Al-Li alloys
[NASA-CR-4548] p 574 N94-14850

APD CRYOGENICS, INC., ALLENTOWN, PA.
Three-stage linear, split-Stirling cryocooler for 1 to 2K magnetic cold stage
[NASA-CR-4538] p 776 N94-13897

APPLIED RESEARCH, INC., HUNTSVILLE, AL.
Enhanced NDE systems
[NASA-CR-192603] p 669 N94-14101

APPLIED RESEARCH CORP., LANDOVER, MD.
UV extinction properties of carina nebular dust
[NASA-CR-193424] p 835 N94-13233

APPLIED SILICON, INC., OTTAWA (ONTARIO).
VMEC30 programming library: Reference manual
[DSIS-93-00350] p 750 N94-13858
Adaptive Signal Processing Testbed
[DSIS-93-00258] p 604 N94-13869
Adaptive Signal Processing Testbed: Software design specification
[DSIS-93-00259] p 604 N94-13870
Advanced Communications ESM System (ACES) testbed: Integration study
[DSIS-93-00345] p 604 N94-13939
VMEC30 software development: Tutorial manual
[DSIS-93-00351] p 750 N94-13944
Demonstration and acceptance test plan for real-time excision software on the Adaptive Signal Processing Testbed
[DSIS-93-00275] p 751 N94-13990
ASPT software source code: SUN driver package
[DSIS-93-00262] p 751 N94-14014
Adaptive Signal Processing Testbed: VME-based DSP board market survey
[DSIS-93-00274] p 605 N94-14015
ASPT software source code: Development system package, VME-C30 component
[DSIS-93-00276] p 751 N94-14016
Adaptive Signal Processing Testbed signal excision software: User's manual
[DSIS-93-00260] p 606 N94-14037
Adaptive Signal Processing Testbed application software: User's manual
[DSIS-93-00261] p 606 N94-14038
VMEC30 SUN software development utilities: User's manual
[DSIS-93-00348] p 752 N94-14051
VMEC30 SUN device drivers: User's manual
[DSIS-93-00349] p 752 N94-14052
EWTEST signal excision testbed: System evaluation
[DSIS-93-00346] p 607 N94-14065
DSP software development environments for the Adaptive Signal Processing Testbed
[DSIS-93-00347] p 607 N94-14066
ASPT software source code: Host development system package
[DSIS-93-00277] p 753 N94-14197

ARGONNE NATIONAL LAB., IL.
Integrated, flexible, and rapid geophysical surveying
[DE93-009989] p 712 N94-12906
Development of nondestructive evaluation methods and prediction of effects of flaws on the fracture behavior of structural ceramics
[DE93-012942] p 577 N94-13032
Measurement of residual strain in composites by means of time-of-flight neutron diffraction
[DE93-012939] p 555 N94-13248
AQUIS: A PC-based source information manager
[DE93-012893] p 707 N94-13383
Simplification-driven automated partial evaluation
[DE93-012890] p 768 N94-13391
A positron annihilation radiation telescope using Laue diffraction in a crystal lens
[DE93-012905] p 848 N94-13483
Ultrafast photoinduced electron transfer reactions in supramolecular arrays: Studies of electronic coupling and solvation
[DE93-012910] p 782 N94-13484
An examination of utility emissions contributions to elevated ozone concentrations in the Chicago area
[DE93-012852] p 708 N94-13495
Are there atmospheric neutrino oscillations?
[DE93-015550] p 783 N94-13890
Resonant x ray Raman scattering from atoms and molecules
[DE93-015158] p 784 N94-13896
Heat and seed recovery technology project
[DE93-009203] p 800 N94-13913
The de Haas-van Alphen studies and Fermi surface properties of organic superconductors (ET)2X
[DE93-015157] p 623 N94-13925
Wear-mechanism modelling
[DE93-012311] p 579 N94-13974
Battery testing at Argonne National Laboratory
[DE93-011761] p 624 N94-14012
On the hardening and softening of nanocrystalline materials
[DE93-012901] p 810 N94-14185
Prism-film coupling in anisotropic planar waveguides of epitaxial (101) rutile thin films
[DE93-012912] p 811 N94-14304
Evolution of the lower planetary boundary layer over strongly contrasting surfaces
[DE93-010667] p 717 N94-14424
Procurement and execution of PCB analyses: Customer-analyst interactions
[DE93-009964] p 566 N94-14694
Toward a verifiable approach to the design of concurrent computations
[DE93-012908] p 756 N94-14844

ARIZONA STATE UNIV., TEMPE.
Surfaces and interfaces of ceramics and metals
[DE93-014959] p 578 N94-13408
Regional tectonic analysis of Venus as part of the Pioneer Venus guest investigator project
[NASA-CR-194079] p 842 N94-13561
Antenna pattern control using impedance surfaces
[NASA-CR-194517] p 602 N94-13799
The soft x ray transient Cen X-4 in quiescence
[NASA-CR-194033] p 833 N94-14406

ARIZONA UNIV., TUCSON.
Thermosolutal convection and macrosegregation in dendritic alloys
[NASA-CR-194039] p 567 N94-12825
Tree reconstruction from partial orders
[DE93-009841] p 743 N94-12991
Optical systems integrated modeling
p 547 N94-14837

ARMY ARMAMENT RESEARCH, DEVELOPMENT AND ENGINEERING CENTER, PICATINNY ARSENAL, NJ.
Solderability of surface mount devices
[AD-A265751] p 620 N94-13040

ARMY ARMAMENT RESEARCH, DEVELOPMENT AND ENGINEERING CENTER, WATERVLIET, NY.
Autofrettage: Stress distribution under load and retained stresses after depressurization. A modified plane-strain case
[AD-A266320] p 671 N94-13579
Thermal gradient-induced deflection of a thick-walled cylinder with bending residual stresses
[AD-A266347] p 673 N94-13777

ARMY AVIATION SYSTEMS COMMAND, MOFFETT FIELD, CA.
Some lessons learned in three years with ADS-33C
p 521 N94-13299
A piloted simulation investigation of the normal load factor and longitudinal thrust required for air-to-air acquisition and tracking p 522 N94-13301

ARMY AVIATION TECHNICAL TEST CENTER, FORT RUCKER, AL.
Flight testing and frequency domain analysis for rotorcraft handling qualities characteristics
p 526 N94-13324

ARMY RESEARCH LAB., ABERDEEN PROVING GROUND, MD.
Infrared transmission and path radiance through dust and fog
[AD-A265825] p 791 N94-12979
Flamespreading in granular solid propellant: Design of an experiment
[AD-A266009] p 583 N94-12987
A computational study of the base region flow field for the M865 projectile
[ARL-TR-109] p 504 N94-13795
Closed-chamber analysis of M5 propellant lot RAD-64597
[AD-A266321] p 585 N94-14145

ARMY RESEARCH LAB., CLEVELAND, OH.
Two-dimensional Navier-Stokes heat transfer analysis for rough turbine blades
[NASA-TM-106008] p 629 N94-13027

ARMY RESEARCH LAB., WATERTOWN, MA.
Modeling the impact behavior of AD85 ceramic under multi-axial loading
[AD-A265877] p 576 N94-12932
The effect of TiN coatings on the rolling contact fatique behavior of M50 bearing steel
[ARL-TR-40] p 662 N94-13794
Synthetic lubricants and high-performance functional fluids: Phosphazenes
[ARL-TR-45] p 580 N94-14126
Yield properties of tungsten and tungsten heavy alloys
[AD-A266833] p 575 N94-14878

ARNOLD ENGINEERING DEVELOPMENT CENTER, ARNOLD AFS, TN.
Hypersonic overview p 505 N94-14154
Hypersonic flow phenomenology p 505 N94-14155
Characterization of flow fields in hypersonic ground test facilities p 505 N94-14157
Aerodynamic and aerothermal facilities 1: Hypersonic wind tunnels p 506 N94-14158
Aerodynamic and aerothermal facilities 2. Part 1: Short-duration, high-enthalpy facilities
p 506 N94-14159
Aeropropulsion facilities p 506 N94-14161
Computational techniques and capabilities
p 506 N94-14162
Test and evaluation methods p 506 N94-14163
Materials/structures testing p 506 N94-14164
Aeropropulsion test and evaluation methods
p 506 N94-14165
Hypersonic flow field measurements: Intrusive
p 507 N94-14166

Hypersonic flow-field measurements: Nonintrusive
p 507 N94-14167
Hypersonic flight test. Part 1: Propulsion flight testing
p 507 N94-14168
Hypersonic flight testing. Part 2: Aerothermal flight testing
p 507 N94-14169
Extrapolation of ground test data to flight
p 507 N94-14170
Boundary-layer transition
p 507 N94-14171
Shock/boundary-layer/shock interactions
p 507 N94-14172
Electromagnetic wave test
p 508 N94-14173

ASIAN INST. OF TECH., BANGKOK (THAILAND).
Detecting land cover changes in Chiang-Mai area in Thailand
p 693 N94-14241

ASSISTANT SECRETARY OF DEFENSE (COMMUNICATIONS COMMAND CONTROL AND INTELLIGENCE), WASHINGTON, DC.
Defense information infrastructure: Rationale for defense management report decision 918
[AD-A266014] p 821 N94-12958

ATLANTIC RESEARCH CORP., LANDOVER, MD.
User needs for propagation data
p 613 N94-14657

ATOMIC ENERGY COMMISSION, DAMASCUS (SYRIA).
Annealing study of main electron irradiation-induced defects (H4 and H5) in P-InP using DLTS technique
[DE93-623204] p 806 N94-13213

AUBURN UNIV., AL.
Analysis of samples of reflector materials which are multicoated and metal samples with oxide coatings which have been exposed the space environment in LDEF testing
[NASA-CR-193647] p 575 N94-12789
Lifetime prediction of materials exposed to the natural space environment
[NASA-CR-193833] p 561 N94-12830
A new treatment of periodic systems with applications to helicopter rotor blade dynamics
[AD-A266770] p 510 N94-14784

AUSTRALIAN NUCLEAR SCIENCE AND TECHNOLOGY ORGANIZATION, LUCAS HEIGHTS.
Liquid phase epitaxy of gallium arsenide: A review
[DE93-622212] p 804 N94-12893

B

BANGLADESH SPACE RESEARCH AND REMOTE SENSING ORGANIZATION, DHAKA.
Mangrove afforestation monitoring using remote sensing
p 695 N94-14260

BANGLADESH UNIV. OF ENGINEERING AND TECHNOLOGY, DHAKA.
Integration of remote sensing and mathematical modelling in disaster mitigation
p 692 N94-14239

BATTELLE MEMORIAL INST., COLUMBUS, OH.
Inelastic deformation mechanisms in SCS-6/Ti 15-3 MMC lamina under compression
[NASA-CR-191170] p 555 N94-13378

BAYLOR COLL. OF MEDICINE, HOUSTON, TX.
Magnetic resonance imaging after exposure to microgravity
p 594 N94-13771

BBN SYSTEMS AND TECHNOLOGIES CORP., CAMBRIDGE, MA.
Multicluster
[AD-A265869] p 758 N94-12930

BDM INTERNATIONAL, INC., ARLINGTON, VA.
Smart materials/structures technical analysis
[AD-A266771] p 766 N94-14785

BECHTEL CORP., VERNON, CA.
Compendium of executive summaries from the maglev system concept definition
[PB93-154938/GAR] p 661 N94-13285

BELEIDSCOMMISSIE REMOTE SENSING, DELFT (NETHERLANDS).
Preparations for and first results of the calibration and interpretation of ERS-1 SAR imagery over land
[BCRS-92-13] p 684 N94-13123
Activities report of the Netherlands Remote Sensing Board
[ETN-93-93880] p 686 N94-14073
Integration of remotely sensed data and cadastral ownership boundaries for land inventory purposes
[BCRS-92-16] p 687 N94-14127
Educational module for the Higher Agricultural Education. Part 2: Eutrophication observed by remote sensing: An educational approach to water quality monitoring
[BCRS-92-11B] p 818 N94-14462
The National Remote Sensing Program (NRSP-2 1991 - 2000): The 1992 annual plan of the Netherlands Remote Sensing Board
[BCRS-92-22] p 700 N94-14544
Educational module for the higher agricultural education. Part 1: Land use classification using satellite pictures
[BCRS-92-11A] p 819 N94-14809

BELGIAN ROYAL OBSERVATORY, BRUSSELS.
The infrared solar spectrum
[COMMUNICATIONS-SER-B-159] p 844 N94-13502
Tidal interactions in the Earth Moon system
[COMMUNICATIONS-SER-B-160] p 837 N94-13503
Variations common to the interplanetary magnetic field, the zonal atmospheric circulation and the Earth's rotation
[COMMUNICATIONS-SER-B-157] p 837 N94-13504
Royal Belgium observatory calendar: 156th year
[ETN-93-94221] p 833 N94-14811

BELL HELICOPTER CO., FORT WORTH, TX.
Flight service evaluation of composite components on the Bell helicopter model 206L
[NASA-CR-191499] p 555 N94-13267

BIONETICS CORP., COCOA BEACH, FL.
Biomass production chamber air analysis of wheat study (BWT931)
[NASA-CR-194092] p 737 N94-13712

BOEING COMMERCIAL AIRPLANE CO., SEATTLE, WA.
Flight crew interface aspects of forward-looking airborne windshear detection systems
[NASA-CR-191437] p 516 N94-12829

BOEING DEFENSE AND SPACE GROUP, PHILADELPHIA, PA.
Handling qualities effects of display latency
p 517 N94-13316

BOEING DEFENSE AND SPACE GROUP, SEATTLE, WA.
System integration and demonstration of adhesive bonded high temperature aluminum alloys for aerospace structure, phase 2
[NASA-CR-191459] p 575 N94-12792
Resin transfer molding of textile composites
[NASA-CR-191505] p 554 N94-12833
Animation of multi-flexible body systems and its use in control system design
p 678 N94-14629
Space Station Common Berthing Mechanism, a multi-body simulation application
p 544 N94-14640

BOMBARDIER, INC., MONTREAL (QUEBEC).
Activities of Bombardier, Inc.
[ISBN-2-921393-11-5] p 499 N94-13520

BRITISH BROADCASTING CORP., KINGSWOOD (ENGLAND).
Digital sound: The selection of critical programme material and preparation of recordings for CCIR tests on low bit-rate codecs
[BBC-RD-1993/1] p 598 N94-12925
Digital sound: Subjective tests on commentary-quality codecs
[BBC-RD-1993/2] p 598 N94-12926
Coverage aspects of a single frequency network designed for digital audio broadcasting
[BBC-RD-1993/3] p 616 N94-14742

BRITISH COLUMBIA UNIV., VANCOUVER.
A photometric and morphological study of compact groups of galaxies and their environments
[ISBN-0-315-59601-5] p 829 N94-13370
The international regulation of air transport: Changing regimes and price effects
[ISBN-0-315-55958-6] p 511 N94-13543

BROOKHAVEN NATIONAL LAB., UPTON, NY.
Low pressure storage of natural gas on activated carbon
[DE93-014053] p 660 N94-12851
Gathering and exchange information on atmospheric chemistry and polluted atmospheres
[DE93-009940] p 705 N94-12869
MCNP benchmark analyses of critical experiments for the Space Nuclear Thermal Propulsion program
[DE93-014046] p 548 N94-12981
Generation of neutronic thermal data in support of space nuclear propulsion
[DE93-013148] p 549 N94-13034
Fifteenth Combustion Research Conference
[DE93-015758] p 562 N94-13045
The North Atlantic Regional Experiment (NARE)
[DE93-010126] p 706 N94-13054
HIJET with AGS physics and N(sup *)'s
[DE93-014022] p 780 N94-13097
Neutral strange particle production at the AGS
[DE93-014044] p 780 N94-13098
Polarization and color transparency
[DE93-014319] p 780 N94-13101
Canted magnetic moments at the Gd(0001) surface
[DE93-014327] p 805 N94-13102
Measurement of the spin of a particle using undulator radiation
[DE93-014334] p 780 N94-13149
Crystallographic and metallurgical characterization of radiation detector grade cadmium telluride materials
[DE93-014335] p 806 N94-13150
Nuclear fusion of protons with ions of boron
[DE93-014284] p 781 N94-13219
A new formulation of longitudinal coherent instabilities
[DE93-014288] p 789 N94-13220
Stripping efficiencies for 277 MeV/amu gold beam on copper foils
[DE93-014306] p 569 N94-13221
A search for strong-field direct two electron ionization using coincidence spectroscopy
[DE93-013435] p 781 N94-13241
Nuclear thermal propulsion engine based on particle bed reactor using light water steam as a propellant
[DE93-014336] p 552 N94-14111
Spin polarized photoemission studies of interfacial and thin film magnetism
[DE93-014326] p 580 N94-14142
Resonances in the Sigma NN system
[DE93-014353] p 785 N94-14144
Self organized criticality
[DE93-013182] p 773 N94-14320
The E2 N(yields)(Delta) transition from polarized Compton scattering
[DE93-012522] p 785 N94-14363
Is K3C60 a line phase?
[DE93-016700] p 813 N94-14517
Radiation effects on optoelectronic analog link for particle detectors
[DE93-015794] p 793 N94-14529
Wake-field and space charge effects on high brightness beams calculations and measured results for the laser driven photoelectrons at BNL-ATF
[DE93-015787] p 659 N94-14572
Early baryon and meson spectroscopy culminating in the discovery of the Omega minus SU(3) and quarks
[DE93-014321] p 787 N94-14580
Dynamic soil pressures on rigid cylindrical vaults
[DE93-013930] p 676 N94-14585
Space reactor fuel element testing in upgraded TREAT
[DE93-012524] p 554 N94-14806
Construction of the Courant-Snyder invariants for the non-linear equations of motion under presence of the linear coupling
[DE93-017565] p 788 N94-14872

BROWN UNIV., PROVIDENCE, RI.
Studies of turbulent shear flows and their control
[NASA-CR-194114] p 635 N94-13676
Multi-dimensional high order essentially non-oscillatory finite difference methods in generalized coordinates
[NASA-CR-194031] p 770 N94-14429

BUNDESANSTALT FUER FLUGSICHERUNG, FRANKFURT AM MAIN (GERMANY).
Activities report of the Federal Administration for Flight Safety (Germany)
[ETN-93-94208] p 511 N94-14008

BUREAU OF MINES, NORRIS, TN.
Early detection of insulation failure in electric motors
[PB93-198208] p 626 N94-14686

BYELORUSSIAN SCIENTIFIC AND TECHNICAL CENTRE OF ENVIRONMENT REMOTE DIAGNOSTICS, MINSK.
Study of the consequences of the Chernobyl accident and technogenic activity in the Republic Belarus using aerospace methods
p 693 N94-14246

C

CALGARY UNIV. (ALBERTA).
A survey of compact planetary nebulae at radio wavelengths
[ISBN-0-315-61950-3] p 829 N94-13371
Airport terminals: Optimum configurations and gate position requirement
[ISBN-0-315-61722-5] p 528 N94-13544

CALIAN COMMUNICATIONS, KANATA (ONTARIO).
Acousto-optical post-processor time-integrating correlator updates
[DSIS-93-00314] p 777 N94-13831

CALIFORNIA INST. OF TECH., PASADENA.
Research in cosmic and gamma ray astrophysics: Cosmic physics portion
[NASA-CR-194127] p 847 N94-13211
Surface science instrumentation for the study of important catalytic and electrochemical interfaces
[DE93-015068] p 563 N94-13413
Hard x ray/microwave spectroscopy of solar flares
[NASA-CR-194399] p 844 N94-13958
Chemistry and transport in a multi-dimensional model
[NASA-CR-194425] p 716 N94-13969
Interactions among convection, magnetic fields and p-mode oscillations in the sun
[NASA-CR-194477] p 845 N94-14479

CALIFORNIA POLYTECHNIC STATE UNIV., SAN LUIS OBISPO.
Evaluation of dual flow thrust vector nozzles with exhaust stream impingement
[NASA-CR-193392] p 630 N94-13078

Design and evaluation of single and dual flow thrust vector nozzles with post exit vanes
[NASA-CR-193393] p 638 N94-14086

CALIFORNIA UNIV., BERKELEY.
Diskless supercomputers: Scalable, reliable I/O for the Tera-Op technology base
[NASA-CR-194089] p 740 N94-13363
Electron beam probe measurements of electric fields in rf discharges p 601 N94-13661
Ultraviolet observations of NGC 4395, the least luminous and nearest known Seyfert 1 nucleus
[NASA-CR-194304] p 831 N94-13679
Measurements of the spatial structure and directivity of 100 KeV photon sources in solar flares using PVO and ISEE-3 spacecraft
[NASA-CR-194080] p 845 N94-14492

CALIFORNIA UNIV., BERKELEY. LAWRENCE BERKELEY LAB.
Radiative corrections in the strongly interacting limit of the standard electroweak model
[DE93-013906] p 780 N94-13018
Capillary surfaces in a wedge: Differing contact angles
[DE93-013903] p 631 N94-13244
EGS (underscore) windows 2: An enhanced graphical interface to EGS
[DE93-010447] p 746 N94-13382
Application of synchrotron radiation in chemical dynamics
[DE93-015040] p 563 N94-13411
Changes in electrical device characteristics during the formation of dislocations in situ in the TEM
[DE93-013910] p 808 N94-13694
The beta(+) decay and cosmic-ray half-life of Mn-54
[DE93-013913] p 848 N94-13695
The method of Laplace Transform MultiQuadrics (LTMQ) for the solution of the groundwater flow equation
[DE93-010408] p 637 N94-14053
Simulating the daylight performance of fenestration systems and spaces of arbitrary complexity: The IDC method
[DE93-015177] p 704 N94-14333
Electronic schematics for the Donner 600 Crystal Tomograph
[DE93-015277] p 625 N94-14336
Pore-size-distribution of cationic polyacrylamide hydrogels
[DE93-015218] p 581 N94-14400
Lawrence Berkeley Laboratory Chemical Sciences Division
[DE93-015260] p 851 N94-14401
Multi-bunch beam-break-up studies for a SWFEL/TBA
[DE93-016973] p 658 N94-14414
Public census data on CD-ROM at Lawrence Berkeley Laboratory
[DE93-015273] p 825 N94-14433
Microstructural influences on the mechanical properties of solder
[DE93-015044] p 573 N94-14474
Applications of the Advanced Light Source to problems in the earth, soil, and environmental sciences
[DE93-015258] p 710 N94-14477
The standing wave FEL/TBA: Realistic cavity geometry and energy extraction
[DE93-016972] p 659 N94-14520
Theory of the negative magnetoresistance in magnetic metallic multilayers
[DE93-013912] p 776 N94-14584
Current titles
[DE93-015859] p 851 N94-14587
Direct submillimeter absorptivity measurements on epitaxial Ba(1-x)K(x)BiO3 films at 2K
[DE93-013904] p 815 N94-14699
The effect of crystal tilt on high resolution micrographs of small metal particles
[DE93-013915] p 574 N94-14795
Tests of non-local interferences in kaon physics at asymmetric phi-factories
[DE93-013905] p 787 N94-14857
Quenching and annealing effects on the specific heat of YBa2Cu3O(7-delta)
[DE93-016483] p 816 N94-14868

CALIFORNIA UNIV., DAVIS.
Magnetic fusion computing: A personal retrospective view
[DE93-014147] p 797 N94-13217

CALIFORNIA UNIV., IRVINE.
Vortex-induced disturbance field in a compressible shear layer p 645 N94-14760

CALIFORNIA UNIV., LOS ANGELES.
Nonlinear damping model for flexible structures
[NASA-CR-193711] p 539 N94-12790
Analysis and characterizations of planar transmission structures and components for superconducting and monolithic integrated circuits
[NASA-CR-193675] p 619 N94-13026
Polarization and variability of active galaxies and quasars p 837 N94-13550
Horizontal-cavity surface-emitting lasers, superluminescent LEDs, and amplifiers, and parabolic gain unstable resonator semiconductor lasers
p 656 N94-13573
Numerical simulation and parameterization of orographic gravity waves p 713 N94-13647
The propagation characteristics and instability properties of low-frequency electromagnetic waves in the Io plasma torus p 601 N94-13650
On l(1): Optimal decentralized performance
p 681 N94-14643

CALIFORNIA UNIV., SAN DIEGO.
The extent and content of low-ionization gas in galaxies p 837 N94-13551
Renal function alterations during skeletal muscle disuse in simulated microgravity
[NASA-CR-194258] p 733 N94-13824

CALIFORNIA UNIV., SAN DIEGO, LA JOLLA.
Determining the solar-flare photospheric scale height from SMM gamma-ray measurements
[NASA-CR-194084] p 844 N94-13671
Numerical Studies of Collisionless Current Layers
[NASA-CR-194337] p 800 N94-13854

CALIFORNIA UNIV., SAN FRANCISCO.
Psychophysiological investigations of the biomedical problems of manned spaceflight
[NASA-CR-194107] p 732 N94-13782

CALIFORNIA UNIV., SANTA BARBARA.
Inverse dynamics: Simultaneous trajectory tracking and vibration reduction with distributed actuators
p 678 N94-14624
Non-recursive augmented Lagrangian algorithms for the forward and inverse dynamics of constrained flexible multibodies p 679 N94-14633
A rational interpolation method to compute frequency response p 681 N94-14644

CALM (JAMES M.), GREAT FALLS, VA.
ARTI Refrigerant Database
[DE93-014774] p 595 N94-13021

CALSPAN CORP., ARNOLD AFS, TN.
Hypersonic flow phenomenology p 505 N94-14155
Aerodynamic and aerothermal facilities 1: Hypersonic wind tunnels p 506 N94-14158
Aerodynamic and aerothermal facilities 2. Part 1: Short-duration, high-enthalpy facilities
p 506 N94-14159
Computational techniques and capabilities
p 506 N94-14162
Test and evaluation methods p 506 N94-14163
Materials/structures testing p 506 N94-14164
Hypersonic flow field measurements: Intrusive
p 507 N94-14166
Hypersonic flow-field measurements: Nonintrusive
p 507 N94-14167
Hypersonic flight testing. Part 2: Aerothermal flight testing p 507 N94-14169
Extrapolation of ground test data to flight
p 507 N94-14170
Boundary-layer transition p 507 N94-14171
Electromagnetic wave test p 508 N94-14173

CAMBRIDGE UNIV. (ENGLAND).
A coherent flame model of premixed turbulent combustion in a counterflow geometry
[CUED/A-THERMO/TR.60] p 562 N94-13085
Wear-mechanism modelling
[DE93-012311] p 579 N94-13974
Evolution of the shock front and turbulence structures in the shock/turbulence interaction p 645 N94-14761

CANADIAN MARCONI CO. LTD., MONTREAL (QUEBEC).
Integrated optics technology transfer
[DSIS-93-00179] p 792 N94-13868

CANTERBURY UNIV., CHRISTCHURCH (NEW ZEALAND).
Compatibility of information and mode of control: The case for natural control systems p 523 N94-13307

CARLETON UNIV., OTTAWA (ONTARIO).
Fine time uplink synchronization for frequency-hopped spread spectrum satellite communication system
[ISBN-0-315-54370-1] p 600 N94-13488
A combined analogue and digital pulse compression system using large time bandwidth product signals for use in synthetic aperture radar
[ISBN-0-315-54373-6] p 600 N94-13489
A knowledge-based model for the integration of remote sensing into a mineral exploration program
[ISBN-0-315-58982-5] p 685 N94-13523
The microstructural response of near gamma-TiAl+W to heat treatment
[DSIS-93-00237] p 571 N94-13840
An experimental investigation into the damage resistance and compression-after-impact strength of T800H/3900-2
[LTR-ST-1909] p 675 N94-13945

CARNEGIE-MELLON UNIV., PITTSBURGH, PA.
Lecture notes on software process improvement
[AD-A265200] p 744 N94-13049
Mobile host internetworking using IP loose source routing
[AD-A265713] p 759 N94-13052
Solving integer programs from dependence and synchronization problems
[AD-A265702] p 767 N94-13284
Fail-safe PVM: A portable package for distributed programming with transparent recovery
[AD-A266594] p 749 N94-13779
Nonlinear analysis, scientific computation, and continuum mechanics applied to the science of materials
[AD-A266641] p 817 N94-14680
An investigation of the role of second phase particles in the design of ultra high strength steels of improved toughness
[AD-A266774] p 573 N94-14786
An experimental analysis of bottleneck-centered opportunistic scheduling
[AD-A266643] p 820 N94-14796
Depths from focusing and defocusing
[AD-A266644] p 735 N94-14797
Generating knight's tours without backtracking from errors
[AD-A266807] p 772 N94-14900

CASE WESTERN RESERVE UNIV., CLEVELAND, OH.
Processing and testing of high toughness silicon nitride ceramics
[NASA-CR-191190] p 582 N94-14543

CATHOLIC UNIV. OF AMERICA, WASHINGTON, DC.
Physical properties of gas disks around shell stars with and without dust
[NASA-CR-193655] p 835 N94-13239
A capaciflector-based robotic system
[NASA-CR-193783] p 833 N94-14359

CENTER FOR MATHEMATICS AND COMPUTER SCIENCE, AMSTERDAM (NETHERLANDS).
The silent step in time
[CWI-CS-R9221] p 768 N94-13496
On the occur-check free PROLOG programs
[CWI-CS-R9238] p 748 N94-13524
Hashing and rehashing in emulated shared memory
[CWI-CS-R9240] p 740 N94-13525
On the foundations of final semantics: Non-standard sets, metric spaces, partial orders
[CWI-CS-R9241] p 768 N94-13526
Stochastic realization of finite-valued processes and primes in the positive matrices
[CWI-BS-R9222] p 773 N94-13677
Fast parallel string prefix-matching
[AD-A267758] p 760 N94-13924
On some results by Fuhrmann on Hankel operators
[CWI-BS-R9224] p 764 N94-13999
On relations between Schmidt pairs arising in robust control
[CWI-BS-R9225] p 764 N94-14000
On the Schmidt pairs of multivariable Hankel operators and robust control
[CWI-BS-R9226] p 765 N94-14001
On the geometry of external spectral factors and the Riccati inequality
[CWI-BS-R9227] p 770 N94-14002
On the differential structure of matrix-valued rational inner functions
[CWI-BS-R9228] p 770 N94-14003
Three, four, five, six or the complexity of scheduling with communication delays
[CWI-BS-R9229] p 751 N94-14004
Stochastic scheduling games with Markov decision arrival processes
[CWI-BS-R9231] p 773 N94-14005
Tuning of Gaussian stochastic control systems
[CWI-BS-R9223] p 765 N94-14018
Stochastic bounds for a polling system
[CWI-BS-R9230] p 765 N94-14361

CENTRE NATIONAL D'ETUDES SPATIALES, TOULOUSE (FRANCE).
Power converters for the 120 V bus supply control
[CNES-NT-134] p 622 N94-13552
Characteristics of the amateur radio means of the Arsene satellite
[CNES-NT-131] p 605 N94-13950
Study of the intermateability of Cannon and Souriau subminiature connectors
[CNES-NT-132] p 624 N94-13951
Multi-output flyback converter with ultrafast current protection
[CNES-NT-133] p 625 N94-14138

CHIBA INST. OF TECH., NARASHINO (JAPAN).
Solidification of eutectic system alloys in space (M-19)
p 589 N94-13751

CHIBA UNIV. (JAPAN).
Effects of typhoon on TOMS data
p 693 N94-14243

CHICAGO UNIV., IL.
Fundamentals and techniques of nonimaging optics
[DE93-013145] p 791 N94-13015
Phase-shifting effect of light and exercise on the human circadian clock
[AD-A265732] p 732 N94-13038
Computer code for scattering from impedance bodies of revolution. Part 3: Surface impedance with s and phi variation. Analytical and numerical results
[NASA-CR-193396] p 599 N94-13264

CHINA CENTRE FOR RESOURCES SATELLITE DATA AND APPLICATION, BEIJING.
The remarkable achievement of China satellite application p 692 N94-14235

CHINESE ACADEMY OF SPACE TECHNOLOGY, BEIJING.
A tentative plan on China and Asian-Pacific satellite system for disaster reduction p 693 N94-14247

CHRYSLER TECHNOLOGIES AIRBORNE SYSTEMS, INC., NEW ORLEANS, LA.
Results of experimental investigations to determine external tank protuberance loads using a 0.03-scale model of the Space Shuttle launch configuration (model 47-OTS) in the NASA/ARC unitary plan wind tunnel, volume 1
[NASA-CR-167690] p 534 N94-12810
Results of wind tunnel tests of an ASRM configured 0.03 scale Space Shuttle integrated vehicle model (47-OTS) in the AEDC 16-foot transonic wind tunnel, volume 2
[NASA-CR-185697] p 534 N94-12965
Results of wind tunnel tests of an ASRM configured 0.03 scale Space Shuttle integrated vehicle model (47-OTS) in the AEDC 16-foot Transonic wind tunnel (IA613A), volume 1
[NASA-CR-185696] p 534 N94-13191
Results of experimental investigations to determine external tank protuberance loads using a 0.03-scale model of the Space Shuttle launch configuration (Model 47-OTS) in the NASA/ARC unitary plan wind tunnel, volume 2
[NASA-CR-167691] p 536 N94-14047

CINCINNATI UNIV., OH.
A study of fiber volume fraction effects in notched unidirectional SCS-6/Ti-15V-3Cr-3Al-3Sn composite
[NASA-CR-191165] p 559 N94-14769

CITY COLL. OF THE CITY UNIV. OF NEW YORK, NY.
Tetravalent chromium (Cr(4+)) as laser-active ion for tunable solid-state lasers
[NASA-CR-194527] p 659 N94-14576

CITY UNIV. OF NEW YORK, STATEN ISLAND.
Growth curve analysis for plasma profiles using smoothing splines
[DE93-015741] p 795 N94-12984

CIVIL AEROMEDICAL INST., OKLAHOMA CITY, OK.
An assessment of the potential for neck injury due to padding of aircraft interior walls for head impact protection
[DOT/FAA/AM-93/14] p 738 N94-13972

CLARKSON UNIV., POTSDAM, NY.
Theoretical investigation of scattering by homogeneous or coated dielectric spheres illuminated with a steady state or pulsed laser beam p 657 N94-13624
Boundary formulations for nonlinear design sensitivity analysis p 672 N94-13669

CLEMSON UNIV., SC.
Superconductivity devices: Commercial use of space
[NASA-CR-194163] p 625 N94-14324

COASTAL ENGINEERING RESEARCH CENTER, VICKSBURG, MS.
Coastal scour problems and methods for prediction of maximum scour
[AD-A266658] p 726 N94-14775

COHERENT RESEARCH, INC., SYRACUSE, NY.
A knowledge-based expert system to coordinate CAD/CAE with integration and test
[NASA-CR-191394] p 745 N94-13130

COLLEGE OF WILLIAM AND MARY, NEWPORT NEWS, VA.
Parallelizing Timed Petri Net simulations
[NASA-CR-194278] p 758 N94-12938

COLLEGE OF WILLIAM AND MARY, WILLIAMSBURG, VA.
A path-oriented matrix-based knowledge representation system
[NASA-CR-4539] p 744 N94-13065
A design methodology for portable software on parallel computers
[NASA-CR-194181] p 752 N94-14139

COLOGNE UNIV. (GERMANY).
Description of the EURAD chemistry-transport model. Version 2 (CTM2)
[REPT-83] p 720 N94-13589
A calibration procedure for radiation budget radiometers and its influence on interpretation of measured values
[MITT-82] p 651 N94-14149
Importance of sprays for long range transport of harmful substances in the troposphere
[MITT-81] p 711 N94-14723

COLORADO STATE UNIV., FORT COLLINS.
Colorado State University program for developing, testing, evaluating, and optimizing solar heating and cooling systems
[DE93-016018] p 705 N94-14504
ACTS propagation experiment discussion: Ka-band propagation measurements using the ACTS propagation terminal and the CSU-CHILL and Space Communications Technology Center Florida propagation program p 616 N94-14678

COLORADO UNIV., BOULDER.
Dynamics of adaptive structures: Design through simulations
[NASA-CR-193724] p 540 N94-13112
Error analysis of real time and post processed or bit determination of GFO using GPS tracking
[NASA-CR-193646] p 512 N94-13238
Radiative transfer in the dynamic atmospheres of Mira-type variables
[NASA-CR-193324] p 829 N94-13287
Analysis of the Harrier forebody/inlet design using computational techniques
[NASA-CR-193616] p 503 N94-13463
Modeling of the partitioning of reactive odd nitrogen in the lower stratosphere using aircraft measurements of NOy, NO, and other trace species
[NASA-CR-194305] p 714 N94-13707
Coherent Doppler lidar signal covariance including wind shear and wind turbulence
[NASA-CR-194492] p 721 N94-13723
Ionospheric calibration for single frequency altimeter measurements
[NASA-CR-194282] p 716 N94-14049
X ray observations of late-type stars using the ROSAT all-sky survey
[NASA-CR-193716] p 832 N94-14146
Visualization techniques to aid in the analysis of multi-spectral astrophysical data sets
[NASA-CR-194489] p 840 N94-14482
Effects of the equatorial ionosphere on L-band Earth-space transmissions p 615 N94-14671

COLUMBIA UNIV., NEW YORK, NY.
GRO: Black hole models for gamma ray bursts
[NASA-CR-193244] p 829 N94-13178
ROSAT: X ray survey of compact groups
[NASA-CR-193297] p 829 N94-13181
Theoretical molecular studies of astrophysical interest
[NASA-CR-193300] p 838 N94-13781
Was 49: Mirror for a hidden Seyfert 1 galaxy
[NASA-CR-194537] p 840 N94-14685
Multiwavelength observations of unidentified high energy gamma ray sources
[NASA-CR-194536] p 840 N94-14688
Anomalous ion transport and feedback control
[DE93-018324] p 803 N94-14874
The further development and refinement of an expert-systems approach to the creative design of mechanisms and mechanical systems
[AD-A266812] p 665 N94-14901

COMMITTEE ON EARTH OBSERVATIONS SATELLITES, LONDON (ENGLAND).
Minutes of the Sixth CEOS Plenary Meeting
[NASA-TM-108252] p 542 N94-14112

COMMONWEALTH SCIENTIFIC AND INDUSTRIAL RESEARCH ORGANIZATION, HIGHETT (AUSTRALIA).
A study of the fine scale motions of incompressible time-developing mixing layers p 644 N94-14751

COMMONWEALTH SCIENTIFIC AND INDUSTRIAL RESEARCH ORGANIZATION, MORDIALOC (AUSTRALIA).
Geophysical validation of ATSR sea surface temperatures p 696 N94-14263

COMMONWEALTH SCIENTIFIC AND INDUSTRIAL RESEARCH ORGANIZATION, SYDNEY (AUSTRALIA).
Synthesis inversion of atmospheric CO2 using the GISS tracer transport model
[CSIRO-TP-29] p 709 N94-14095

COMPUTATIONAL FLUID DYNAMICS RESEARCH CORP., HUNTSVILLE, AL.
A computer model for liquid jet atomization in rocket thrust chambers
[NASA-CR-194194] p 627 N94-12803

COMPUTER MOTION, INC., GOLETA, CA.
Design and control of a macro-micro robot for precise force applications p 682 N94-14651

CONCORDIA UNIV., MONTREAL (QUEBEC).
Techniques for improving the performance of a simplified electronic fuel controller with incremental actuation for small gas turbine engines
[ISBN-0-315-56062-2] p 661 N94-13521

CONTINUOUS ELECTRON BEAM ACCELERATOR FACILITY, NEWPORT NEW, VA.
Isospin flip as a relativistic effect: NN interactions
[CEBAF-PR-89-023] p 786 N94-14552

CORNELL UNIV., ITHACA, NY.
Synthesis and properties of novel cluster phases
[DE93-017056] p 577 N94-13072
Atmospheric soundings during the Washita 1992 campaign
[NASA-CR-194383] p 712 N94-13212
Rover imaging system for the Mars rover/sample return mission
[NASA-CR-193413] p 649 N94-13464
Photochemical dynamics of surface oriented molecules
[DE93-016289] p 784 N94-13983

D

DAEDALUS ENTERPRISES, INC., ANN ARBOR, MI.
Development of a portable multispectral thermal infrared camera
[NASA-CR-191340] p 648 N94-13176
Modis-N airborne simulator
[NASA-CR-194364] p 792 N94-13719

DECISION SYSTEMS, INC., LOS ALTOS, CA.
The influence of ATC message length and timing on pilot communication
[NASA-CR-177621] p 512 N94-14744

DEFENCE AND CIVIL INST. OF ENVIRONMENTAL MEDICINE, DOWNSVIEW (ONTARIO).
DCIEM: The first fifty years, 1939-1989
[CTN-93-60767] p 733 N94-14141

DEFENCE RESEARCH AGENCY, BEDFORD (ENGLAND).
The impact of flying qualities on helicopter operational agility p 522 N94-13304
In-flight simulation of high agility through active control: Taming complexity by design p 523 N94-13306
A guide to the DRA 13 ft x 9 ft Low Speed Wind Tunnel Facility
[AD-A267739] p 528 N94-14876

DEFENCE RESEARCH ESTABLISHMENT ATLANTIC, DARTMOUTH (NOVA SCOTIA).
Torsion problem of elastostatics: An application of boundary element method and relation with conformal mapping
[DSIS-92-03794] p 674 N94-13833

DEFENCE RESEARCH ESTABLISHMENT, OTTAWA (ONTARIO).
Kalman filter based architectures for interference excision
[DSIS-93-00034] p 603 N94-13818
A review of robust detection
[DSIS-93-00400] p 603 N94-13829
MUSIC and maximum likelihood using a refined propagation model: Performance comparison for radar low-angle tracking
[DREO-RN-1122] p 603 N94-13832
The DREO Elint Browser Utility (DEBU) reference manual
[DSIS-92-03900] p 603 N94-13837
Digital quadrature demodulation for radar ESM applications
[DREO-TN-92-10] p 603 N94-13838
Simulation of downlink synchronization for a frequency-hopped satellite communication system
[DSIS-93-00477] p 605 N94-13941
Review of test methods for material flammability
[DSIS-93-00480] p 564 N94-13942
Envelope and instantaneous frequency estimation of narrowband modulated signals
[DREO-TN-92-3] p 605 N94-14033
A comparison of recursive least squares and Kalman filtering excisors for swept tone interference
[DSIS-93-00362] p 606 N94-14054
A history of the Defence Research Establishment, Ottawa
[CTN-93-60737] p 850 N94-14060
Testing various time-frequency distribution techniques
[DREO-TN-92-17] p 606 N94-14062
Multiple-symbol differential detection of DPSK with frequency offset
[DREO-TN-92-5] p 606 N94-14063
I/Q demodulation of radar signals with calibration and filtering
[DREO-RN-1119] p 606 N94-14064
Performance evaluation of the honeywell GG1308 miniature ring laser gyroscope
[AD-A266694] p 653 N94-14782

DEFENCE RESEARCH ESTABLISHMENT PACIFIC, VICTORIA (BRITISH COLUMBIA).
Aeromagnetic work in the Lincoln Sea: 1991 survey
[DSIS-93-00308] p 715 N94-13830

DEFENCE RESEARCH ESTABLISHMENT VALCARTIER (QUEBEC).
Bridging the gap between the Rayleigh and Thomson limits for various convex bodies
[DSIS-93-00613] p 607 N94-14204
DEFENSE INFORMATION SYSTEMS AGENCY, ARLINGTON, VA.
Defense Information Technology Services organization FY 1994 budget estimates. Information Technology Systems budget
[PB93-199016] p 826 N94-14562
DELAWARE UNIV., NEWARK.
Linear and nonlinear spectroscopic probing of solute interactions with chemically modified silica surface
[DE93-014648] p 562 N94-13001
X ray emission from dynamical shock models in hot-star winds
[NASA-CR-194093] p 847 N94-13288
Status and future opportunities for conversion of synthesis gas to liquid energy fuels
[DE93-010025] p 584 N94-14089
DEPARTMENT OF ENERGY, MORGANTOWN, WV.
Overview: Gas hydrate geology and geography
[DE93-014043] p 688 N94-14151
Status of SOFC development in USA
[DE93-015568] p 704 N94-14355
DEPARTMENT OF ENERGY, NEW YORK, NY.
Project AIRSTREAM: Trace gas
[DE93-008849] p 706 N94-12904
DEPARTMENT OF ENERGY, WASHINGTON, DC.
Program operations plan
[DE93-012765] p 710 N94-14182
DEPARTMENT OF NATIONAL DEFENCE, OTTAWA (ONTARIO).
A quartz crystal microbalance study of lithium insertion and removal into evaporated films MO(y) (M = Mo, Fe, and V)
[DSIS-93-00649] p 810 N94-14203
DEPARTMENT OF THE NAVY, WASHINGTON, DC.
Modified carbon for improved corrosion resistance
[AD-D015741] p 556 N94-13663
A Fourier transform microscope for x ray and/or gamma ray imaging
[AD-D015742] p 791 N94-13664
DEUTSCHE FORSCHUNGS- UND VERSUCHSANSTALT FUER LUFT- UND RAUMFAHRT, BRUNSWICK (GERMANY).
Investigation of the effects of bandwidth and time delay on helicopter roll-axis handling qualities
p 522 N94-13300
DEUTSCHE FORSCHUNGSANSTALT FUER LUFT- UND RAUMFAHRT, COLOGNE (GERMANY).
Circadian rhythms during simulation of the D2-spaceflight
[DLR-FB-92-27] p 733 N94-14043
Turbulent particle dispersion in confined swirling flows
[DLR-FB-92-32] p 637 N94-14045
Water-vapour, total water and rainrate from passive microwave satellite data over ocean
[DLR-FB-92-37] p 723 N94-14189
DEUTSCHE FORSCHUNGSANSTALT FUER LUFT- UND RAUMFAHRT, GOETTINGEN (GERMANY).
Full Riemann solution of the one- and two-dimensional Euler equations
[DLR-FB-92-34] p 638 N94-14188
DEUTSCHE FORSCHUNGSANSTALT FUER LUFT- UND RAUMFAHRT, OBERPFAFFENHOFEN (GERMANY).
A widget based operations simulator for a planetary camera: A model for the high resolution stereo camera on Mars 94
[DLR-FB-92-30] p 651 N94-14044
Fluxes of heat and water vapour in a convective mixed layer during EFEDA
[DLR-FB-92-21] p 716 N94-14132
An algorithm for the remote sensing of fog using satellite-data and additional information
[DLR-FB-92-23] p 688 N94-14135
Supervised classification of remotely sensed images
[DLR-FB-92-07] p 700 N94-14428
Turbulent diffusion in homogeneous shear flow with stable density stratification
[DLR-FB-92-26] p 639 N94-14443
DEUTSCHE VERSUCHSANSTALT FUER LUFT- UND RAUMFAHRT, OBERPFAFFENHOFEN (GERMANY).
Earth observation from low-inclination orbit as a necessary complement to polar missions
p 694 N94-14248
DRAPER (CHARLES STARK) LAB., INC., CAMBRIDGE, MA.
Applications of computer algebra to distributed parameter systems p 677 N94-14623
DUKE UNIV., DURHAM, NC.
New vortex dynamics methods for rotor free wake analysis
[AD-A266656] p 509 N94-14774
DYNACS ENGINEERING CO., INC., HOUSTON, TX.
Computational Controls Workstation: Algorithms and hardware p 678 N94-14626
DYNAMIC SYSTEM TECHNOLOGIES, INC., HUNTSVILLE, AL.
Small scale adaptive optics experiment systems engineering
[NASA-CR-194419] p 793 N94-14548
DYNAMIC SYSTEMS RESEARCH AND TRAINING CORP., HUNTSVILLE, AL.
Experimental instrumentation system for the Phased Array Mirror Extendible Large Aperture (PAMELA) test program
[NASA-CR-194421] p 705 N94-14430

E

EAGLE ENGINEERING, INC., HOUSTON, TX.
Secondary impact hazard assessment
[NASA-CR-188261] p 543 N94-14483
EAST CAROLINA UNIV., GREENVILLE, NC.
Physiological Anatomical Rodent Experiment (PARE) .04 Feasibility Test 1
[NASA-CR-194423] p 728 N94-13473
ECOLE CENTRALE DE LYON (FRANCE).
Numerical simulations of turbulent premixed H2/O2/N2 flames with complex chemistry p 567 N94-14765
ECOLE POLYTECHNIQUE, MONTREAL (QUEBEC).
Passage-averaged approximation of turbomachinery flows using vorticity-potential method
[ISBN-0-315-72716-0] p 634 N94-13598
Modelling of the temperature distribution in a copper roll for the design of a system of cooled rolls adapted to vertical strip casting
[IMI-93RT-21200-1436-G] p 557 N94-13866
EG AND G ENERGY MEASUREMENTS, INC., IDAHO FALLS.
Nuclear propulsion systems engineering
[DE93-010791] p 548 N94-12870
Design, qualification and operation of nuclear rockets for safe Mars missions
[DE93-010792] p 549 N94-12996
A modular gas-cooled cermet reactor system for planetary base power
[DE93-013672] p 550 N94-13351
Glossary of SSDC terms and acronyms
[DE93-013697] p 823 N94-13352
Creating a strategic plan for configuration management using computer aided software engineering (CASE) tools
[DE93-013663] p 746 N94-13394
Gas core nuclear thermal rocket engine research and development in the former USSR
[DE93-012165] p 552 N94-14013
EG AND G ENERGY MEASUREMENTS, INC., LAS VEGAS, NV.
Survey of subsurface geophysical exploration technologies adaptable to an airborne platform
[DE93-015080] p 717 N94-14294
EG AND G ROCKY FLATS, INC., GOLDEN, CO.
Hydrogen peroxide safety issues
[DE93-013895] p 565 N94-14346
Welding technologies as applied to nuclear manufacturing
[DE93-010924] p 664 N94-14565
ELECTROTECHNICAL LAB., TSUKUBA (JAPAN).
Robust filters for image smoothing
[ERB-1033] p 769 N94-13545
ELORET CORP., SUNNYVALE, CA.
Simulation studies for surfaces and materials strength
[NASA-CR-193305] p 671 N94-13179
Images constructed from computed flow fields
[NASA-CR-194397] p 650 N94-13814
Development of an automated film-reading system for ballistic ranges
[NASA-CR-194398] p 650 N94-13815
Advanced ballistic range technology
[NASA-CR-194396] p 532 N94-14068
Advanced ballistic range technology
[NASA-CR-194530] p 533 N94-14540
An experimental study of a turbulent boundary layer in the trailing edge region of a curculation-control airfoil
[NASA-CR-194522] p 508 N94-14541
ENERGY CONVERSION DEVICES, INC., TROY, MI.
Continuous roll-to-roll a-Si photovoltaic manufacturing technology
[DE93-010006] p 704 N94-14109
Optimization of transparent and reflecting electrodes for amorphous silicon solar cells
[DE93-010009] p 704 N94-14110
ENERGY RESEARCH CORP., DANBURY, CT.
Carbonate fuel cell endurance: Hardware corrosion and electrolyte management status
[DE93-013800] p 701 N94-13093
Performance effects of coal-derived contaminants on the carbonate fuel cell
[DE93-013801] p 703 N94-13693
ENGINEERING MECHANICS ASSOCIATION, INC., TORRANCE, CA.
Methods for evaluating the predictive accuracy of structural dynamic models
[NASA-CR-191337] p 671 N94-13124
ENVIRONMENTAL PROTECTION AGENCY, WASHINGTON, DC.
Vendor information system for innovative treatment technologies. User manual (VISITT version 2.0). Number 2
[PB93-196640] p 821 N94-12936
Toxic Substances Control Act (TSCA) chemical substances inventory: Revised inventory synonym and preferred name file, Jan. 1993 documentation
[PB93-155166] p 710 N94-14508
ENVIRONMENTAL RESEARCH INST. OF MICHIGAN, ANN ARBOR.
Radar imaging of sub-mesoscale ocean phenomena
[AD-A266339] p 725 N94-13581
EUROCOPTER DEUTSCHLAND G.M.B.H., MUNICH (GERMANY).
The application of active side arm controllers in helicopters p 522 N94-13302
EUROPEAN SPACE AGENCY, PARIS (FRANCE).
Fundamental study of shock wave/turbulent boundary layer interactions with passive control in transonic flows
[ESA-TT-1278] p 630 N94-13117
The problem of the sonic boom for future high-speed transport aircraft
[ESA-TT-1286] p 776 N94-13692
Characterization of composite materials for aerospace structures
[ESA-TT-1260] p 557 N94-13804
European space for exclusively peaceful purposes
[ESA-BR-86] p 851 N94-14137
Guide to the software architectural design phase
[ESA-PSS-05-04-ISSUE-1] p 753 N94-14190
Guide to the software detailed design and production phase
[ESA-PSS-05-05-ISSUE-1] p 753 N94-14191
Space transportation systems within ESA programmes: Current status and perspectives p 537 N94-14275
ECS: Eighth year in orbit
[ESA-BR-82] p 543 N94-14352
Physical countermeasures for long-term manned space flights
[ESA-SP-1160] p 733 N94-14860
EUROPEAN SPACE AGENCY. ESRIN, FRASCATI (ITALY).
ERS-1 system
[ESA-SP-1146] p 699 N94-14353
EUROPEAN SPACE AGENCY. EUROPEAN SPACE RESEARCH AND TECHNOLOGY CENTER, ESTEC, NOORDWIJK (NETHERLANDS).
Life support and habitability manual, volume 1
[ESA-PSS-03-406-ISSUE-1-VOL] p 737 N94-13901
Life support and habitability manual, volume 2
[ESA-PSS-03-406-ISSUE-1-VOL] p 738 N94-13902
Results from ERS-1 and JERS-1 SAR calibration experiments and data analysis p 688 N94-14210
Characterisation of the LMS propagation channel at L- and S-bands: Narrowband experimental data and channel modelling p 615 N94-14669
Ethology in space, a unique opportunity for behavioural science
[ESA-STM-246] p 731 N94-14862

F

FAIRCHILD TECHNICAL SUPPORT CENTER, HUNTSVILLE, AL.
Advanced protein crystal growth programmatic sensitivity study
[NASA-CR-193827] p 804 N94-12934
FEDERAL AVIATION ADMINISTRATION, ATLANTIC CITY, NJ.
Widebody cabin water spray optimization tests
[DOT/FAA/CT-TN93/29] p 511 N94-14186
FEDERAL AVIATION ADMINISTRATION, CAMBRIDGE, MA.
Determination of Loran-C/GPS human factors issues
[PB93-199693] p 514 N94-14563
FEDERAL AVIATION ADMINISTRATION, OKLAHOMA CITY, OK.
Validity of FAA-approved color vision tests for class 2 and class 3 aeromedical screening
[DOT/FAA/AM-93/17] p 735 N94-14846
Validation of an inexpensive illuminant for aeromedical color vision screening
[DOT/FAA/AM-93/16] p 736 N94-14854

FEDERAL AVIATION ADMINISTRATION, WASHINGTON, DC.
Aircraft engine type certification handbook: Advisory circular
[AC-33-2B] p 518 N94-13252
FEDERAL COORDINATING COUNCIL FOR SCIENCE, ENGINEERING AND TECHNOLOGY, WASHINGTON, DC.
National atmospheric sciences program, fiscal years 1987-1990
[NSF-92-16] p 711 N94-12794
FERMI NATIONAL ACCELERATOR LAB., BATAVIA, IL.
A search for scalar leptoquarks in D0
[DE93-012780] p 779 N94-12954
Redshift distortions of galaxy correlation functions
[DE93-014007] p 834 N94-12980
Inflation after COBE: Lectures on inflationary cosmology
[DE93-014008] p 834 N94-13096
Low energy response of the DO calorimeter and jet energy measurement
[DE93-013569] p 781 N94-13350
Inclusive single muons at DO
[DE93-012779] p 783 N94-13494
Quark and gluon jets at CDF
[DE93-014919] p 783 N94-13884
Observation of the coalescing of beam into an asymmetric RF bucket by stochastic cooling
[DE93-015133] p 783 N94-13895
Cesium iodide (CsI) crystal manufacture
[DE93-012146] p 808 N94-13973
High counting rate resistive-plate chamber
[DE93-014928] p 651 N94-14452
Top quark search: Results and prospects at Fermilab
[DE93-013016] p 786 N94-14524
E789 and P865: High-rate fixed-target studies of charm and beauty
[DE93-017223] p 788 N94-14898
FLINDERS UNIV., ADELAIDE (AUSTRALIA).
Calculation of electron-lithium scattering using the coupled-channel optical method
[DE93-623049] p 806 N94-13226
FLORIDA AGRICULTURAL AND MECHANICAL UNIV., TALLAHASSEE.
Calcitonin control of calcium metabolism during weightlessness
[NASA-CR-193622] p 731 N94-12960
FLORIDA STATE UNIV., TALLAHASSEE.
The application of VAS satellite imagery to thunderstorm forecasting at Cape Canaveral
[NASA-CR-193563] p 718 N94-12839
Selective excitation, relaxation, and energy channeling in molecular systems
[DE93-018819] p 785 N94-14420
FLOW ANALYSIS, INC., BROOKLYN, NY.
Free-wake computation of helicopter rotor flowfield for general flight regimes
[AD-A266692] p 509 N94-14781
FLUENT, INC., LEBANON, NH.
Multigrid solution of internal flows using unstructured solution adaptive meshes
[NASA-CR-194233] p 638 N94-14356
FOREST RESEARCH INST., HELSINKI (FINLAND).
Multi-source national forest inventory of Finland
p 694 N94-14254
FOSTER-MILLER ASSOCIATES, INC., WALTHAM, MA.
Development of a nonazeotropic heat pump for crew hygiene water heating
[NASA-CR-194189] p 737 N94-13674
FRAUNHOFER INST. FUER WERKSTOFFMECHANIK, FREIBURG (GERMANY).
A process for evaluation of mechanical behavior of surface films
[W-1/92] p 579 N94-14007
FREIE UNIV., BERLIN (GERMANY).
The role of the dynamics for the deviation of the total ozone from the long-term mean at the edge of the polar vortex p 694 N94-14250
Meteorological data, new series A monographs. Volume 6, no. 4: Modelization of heat fluxes at Earth ground with consideration of vegetation
[ETN-93-94169] p 723 N94-14546
Meteorological data, new series A monographs. Volume 6, no. 3: Estimation of influence of high clouds in the radiation field and the climat by analysis of NOAA AVHRR data
[ETN-93-94170] p 723 N94-14707
FRIBOURG UNIV. (SWITZERLAND).
Detection of hot muonic hydrogen atoms emitted in vacuum using x-rays
[DE93-010253] p 778 N94-12860
FUJI HEAVY INDUSTRIES LTD., TOKYO (JAPAN).
Movement of deployable truss p 531 N94-13280
Conceptual design on H-2 Orbiting Plane (HOPE)
[NASDA-CNT-930018] p 535 N94-13656
FUJI OIL CO. LTD., TSUKUBA (JAPAN).
Crystal growth of enzymes in low gravity (L-5)
p 592 N94-13762

G

GALAXY SCIENTIFIC CORP., PLEASANTVILLE, NJ.
Human factors in aviation maintenance: Phase 3, volume 1
[DOT/FAA/AM-93/15] p 738 N94-14023
GENERAL ACCOUNTING OFFICE, WASHINGTON, DC.
Johnson Space Center procurement: Controls over payments to contractors should be strengthened
[AD-A265722] p 819 N94-13060
GENERAL ATOMIC CO., SAN DIEGO, CA.
Dependence of beta(tau) on plasma shape in D3-D
[DE93-015473] p 800 N94-13900
Direct electron heating and current drive with fast waves in D3-D
[DE93-013028] p 801 N94-14293
Variation of divertor plasma parameters with divertor depth for H-mode discharges in D3-D
[DE93-015475] p 801 N94-14347
D3-D research operations
[DE93-016729] p 802 N94-14519
The role of electric field shear stabilization of turbulence in the H-mode to VH-mode transition in D3-D
[DE93-015474] p 802 N94-14583
GENERAL ATOMICS TECHNOLOGIES CORP., SAN DIEGO, CA.
Dimensionally similar discharges with central RF heating on the D3-D tokamak
[DE93-012776] p 795 N94-12953
Active density control in DIII-D H-mode plasmas
[DE93-015477] p 802 N94-14570
GENERAL ELECTRIC CO., CINCINNATI, OH.
Thermal shock resistance of ceramic matrix composites
[NASA-CR-189136] p 557 N94-13920
GENERAL MOTORS CORP., WARREN, MI.
Estimation of the vortex length scale and intensity from two-dimensional samples p 645 N94-14756
GEOLOGICAL SURVEY OF JAPAN, IBARAKI.
Geologic application of JERS-1 SAR data
p 688 N94-14211
GEORGE WASHINGTON UNIV., HAMPTON, VA.
System identification for Space Station Freedom using observer/Kalman filter Markov parameters
[NASA-CR-191521] p 539 N94-12976
Optimizing interplanetary trajectories with deep space maneuvers
[NASA-CR-4546] p 532 N94-14851
GEORGIA INST. OF TECH., ATLANTA.
Spatially-varying IIR filter banks for image coding
[NASA-CR-193727] p 619 N94-12897
Recursive time-varying filter banks for subband image coding
[NASA-CR-193726] p 598 N94-12920
Search for extraterrestrial intelligence/high resolution microwave survey team member
[NASA-CR-194177] p 739 N94-13086
Image coding using entropy-constrained residual vector quantization
[NASA-CR-193728] p 744 N94-13113
Diagnostic studies of the HxOy-NxOy-O3 photochemical system using data from NASA GTE field expeditions
[NASA-CR-193672] p 706 N94-13170
Numerical study of the effects of icing on viscous flow over wings
[NASA-CR-193306] p 500 N94-13180
A model for rotorcraft flying qualities studies
p 523 N94-13308
Metastable enhancement of C(+) and O(+) capture reactions
[DE93-015075] p 807 N94-13373
First-principles studies of phase stability and the structural and dynamical properties of hydrogen-metal systems
[DE93-016129] p 570 N94-13374
Exact reconstruction analysis/synthesis filter banks with time-varying filters
[NASA-CR-193725] p 600 N94-13466
Development of an hp-version finite element method for computational optimal control
[NASA-CR-194149] p 766 N94-14444
Guidance law development for aeroassisted transfer vehicles using matched asymptotic expansions
[NASA-CR-194523] p 508 N94-14538
H2S data reduction
[NASA-CR-193389] p 617 N94-14743
GEORGIA STATE UNIV., ATLANTA.
Selection of behavioral tasks and development of software for evaluation of rhesus monkey behavior during spaceflight
[NASA-CR-194176] p 728 N94-13865
GEORGIA TECH RESEARCH INST., ATLANTA.
An acoustic charge transport imager for high definition television applications
[NASA-CR-194518] p 650 N94-14029
GEORGIA UNIV., ATHENS.
High energy hadron-hadron collisions
[DE93-015584] p 784 N94-13927
CarbBank: A structural and bibliographic database for complex carbohydrates
[DE93-015582] p 827 N94-14803
GEORGIA UNIV., GRIFFIN.
Measuring surface fluxes in CAPE
[NASA-CR-193664] p 711 N94-12788
GHENT UNIV. (BELGIUM).
Remote sensing for monitoring tropical moist forests in the Indo-Chinese region p 695 N94-14258
GKSS-FORSCHUNGSZENTRUM GEESTHACHT (GERMANY).
Signal and reference wavelengths for the elimination of SO2 cross sensitivity in remote measurements of tropospheric ozone with lidar
[GKSS/92/E/24] p 617 N94-14819
The mobile lidar system ARGOS for spatial resolution remote measuring of gaseous air pollutants
[GKSS/92/E/26] p 617 N94-14820
Influence of heat treatment on microstructure of Ti-35wt Al prepared by elemental powder metallurgy
[GKSS/92/E/27] p 574 N94-14821
GLASGOW UNIV. (SCOTLAND).
The development and potential of inverse simulation for the quantitative assessment of helicopter handling qualities p 523 N94-13311
GORDON RESEARCH CONFERENCES, INC., KINGSTON, RI.
Gordon Research Conference on Chronobiology, 1991
[AD-A266354] p 728 N94-13698
GOSUDARSTVENNYI KOMITET PO ISPOLZOVANIYU ATOMNOI ENERGII, MOSCOW (USSR).
Excitation of coupled waves in plasma periodic structures by relativistic electron beam and acceleration of charged particles
[DE93-621657] p 794 N94-12853
Investigation of dynamics of plasma fluxes generated by the quasi-stationary plasma accelerator P-50
[DE93-621665] p 794 N94-12854
To the theory of triplet pairing in Fermi-liquid model
[DE93-621770] p 816 N94-12855
Hydrodynamic asymptotics of Green functions in magnetics with spontaneously broken symmetry
[DE93-621349] p 767 N94-13223
On a nonminimal gauge interaction of a scalar field in D=2+1 Chern-Simons-Maxwell theory
[DE93-621380] p 621 N94-13224
Multiplicity spectrometry on neutron filtered beams
[DE93-617529] p 790 N94-14843
GOSUDARSTVENNYI KOMITET PO ISPOLZOVANIYU ATOMNOI ENERGII, SERPUKHOV (USSR).
Further study of the X(1910) meson
[DE93-621443] p 782 N94-13362
Effects of additional isoscalar vector bosons in e(sup +)e)(sup -)(yields)ff-bar processes at the TRISTAN and LEP energies
[DE93-621451] p 783 N94-13506
GOVERNMENT INDUSTRIAL RESEARCH INST., OSAKA (JAPAN).
Preparation of optical materials used in non-visible region (M-17) p 589 N94-13749
GRENOBLE-1 UNIV. (FRANCE).
Robust non convex optimization algorithms: Codes and numerical simulation of large scale
[ETN-93-94354] p 756 N94-14813
GRONINGEN RIJKSUNIV. (NETHERLANDS).
Distributional inferences for a location parameter
[W-9219] p 774 N94-14545

H

HAMPDEN-SYDNEY COLL., VA.
Analysis of data from the energetic gamma-ray experiment on the gamma ray observatory
[NASA-CR-194178] p 847 N94-13087
HAMPTON UNIV., VA.
Scattering calculations and confining interactions
[NASA-CR-194242] p 786 N94-14549
Isospin flip as a relativistic effect: NN interactions
[CEBAF-PR-89-023] p 786 N94-14552
HARVARD-SMITHSONIAN CENTER FOR ASTROPHYSICS, CAMBRIDGE, MA.
Photometry and spectroscopy in the open cluster Alpha Persei, 2
[NASA-CR-193397] p 833 N94-14358
HARVARD UNIV., CAMBRIDGE, MA.
Measurements on two-dimensional arrays of mesoscopic Josephson junctions
[AD-A265129] p 807 N94-13359

Structural and electronic studies of a-SiGe:H alloys
[DE93-010021] p 809 N94-14085
Mathematics and string theory
[DE93-017903] p 817 N94-14417
Measurements of crystal growth kinetics at extreme deviations from equilibrium
[DE93-014526] p 815 N94-14798

HAWAII UNIV., HONOLULU.
Studies of gas in cooling flow clusters
[NASA-CR-193597] p 628 N94-12959
A near-infrared faint galaxy survey: Evolution and the cosmological geometry from K band photometry
p 830 N94-13591
Millimeter and infrared studies of young stellar objects in dark cloud L1641 p 838 N94-13648
The 1 to 5 micron imaging of deeply embedded young stellar objects p 831 N94-13657

HAWKER SIDDELEY CANADA LTD., TORONTO (ONTARIO).
Activities of Hawker Siddeley Canada Inc.
[CTN-93-60865] p 849 N94-13505

HELIKOPTER SERVICE A/S, OSLO (NORWAY).
Human factor implications of the Eurocopter AS332L-1 Super Puma cockpit p 525 N94-13319

HELSINKI UNIV. OF TECHNOLOGY, ESPOO (FINLAND).
Measurement electronics of industrial microwave resonator sensors
[TKK-S-RAD-S194] p 625 N94-14096

HELSINKI UNIV. OF TECHNOLOGY (FINLAND).
Theory for iterative solution of large dynamical systems using parallel computation
[TKK-MAT-A304] p 760 N94-14187

HERNANDEZ ENGINEERING, INC., HOUSTON, TX.
Where no flag has gone before: Political and technical aspects of placing a flag on the Moon
[NASA-CR-188251] p 827 N94-12800

HIGH TECHNOLOGY CORP., HAMPTON, VA.
Transition prediction and control in subsonic flow over a hump
[NASA-CR-4543] p 629 N94-13066

HOUSTON UNIV., TX.
Studies of momentum and energy transfer across wavy gas-liquid interfaces
[AD-A266432] p 635 N94-13699

HUGHES AIRCRAFT CO., TORRANCE, CA.
MMIC packaging technology development
[NASA-CR-194183] p 621 N94-13336

HUGHES DANBURY OPTICAL SYSTEMS, INC., CT.
LUTE telescope structural design
[NASA-CR-192594] p 830 N94-13448
Impact of shorter wavelengths on optical quality for laws
[NASA-CR-193433] p 792 N94-14473

HUGHES STX, INC., LANHAM, MD.
Space and Earth sciences, computer systems, and scientific data analysis support, volume 1
[NASA-CR-194535] p 741 N94-13788

I

IBM FEDERAL SYSTEMS DIV., HOUSTON, TX.
The National Storage Laboratory: A collaborative research project
[DE93-015099] p 760 N94-14475

IDAHO UNIV., MOSCOW.
Fatigue crack initiation and propagation in aluminum alloys 8090 and 2124 in hydrogenous atmospheres
p 570 N94-13670
NASA Space Engineering Research Center for VLSI systems design
[NASA-CR-194035] p 625 N94-14325

ILLINOIS INST. OF TECH., CHICAGO.
A stochastic model for behavior analysis of fiber-reinforced quasi-brittle materials
p 672 N94-13594

ILLINOIS UNIV., CHICAGO.
Finite element analysis of composite plates by use of modified complementary energy principle
p 672 N94-13596
Computational strategies in the dynamic simulation of constrained flexible MBS p 679 N94-14635

ILLINOIS UNIV., URBANA.
Two temperature modeling and experimental measurements of laser sustained hydrogen plasmas
[AD-A265750] p 796 N94-13039
Direct determination of alpha particle transport coefficients
[DE93-013488] p 787 N94-14691

IMATRAN VOIMA OY, HELSINKI (FINLAND).
Effect of size, shape, and end condition of test specimen on compressive strength of high-strength concrete
[DE93-500412] p 682 N94-14653

IMPERIAL COLL. OF SCIENCE AND TECHNOLOGY, LONDON (ENGLAND).
Simulation of preburner sprays, volume 1
[NASA-CR-193844] p 647 N94-14906

INDIANA UNIV., BLOOMINGTON.
High resolution electron energy loss studies of surface vibrations
[DE93-014441] p 781 N94-13283
Gravity as a probe for understanding pattern specification
[NASA-CR-194142] p 713 N94-13418
Organic Geochemical and tectonic evolution of the Midcontinent Rift system
[DE93-015093] p 717 N94-14338
The evolution of tensor polarization
[DE93-017209] p 790 N94-14897

INDONESIAN NATIONAL INST. OF AERONAUTICS AND SPACE, JAKARTA.
Some potentials of the Indonesian region for Earth observation p 692 N94-14237

INNOVATION ASSOCIATES, INC., ANN ARBOR, MI.
View generated database
[NASA-CR-191397] p 822 N94-13116

INNOVATIVE DYNAMICS, ITHACA, NY.
Smart skin technology development for measuring ice accretion, stall, and high AOA aircraft performance. Part 1: Capacitive ice detector development
[NASA-CR-194252] p 511 N94-13424

INSTITUT DE MECANIQUE DES FLUIDES DE TOULOUSE (FRANCE).
DNS and modeling of the interaction between turbulent premixed flames and walls p 646 N94-14763

INSTITUT NATIONAL DES SCIENCES APPLIQUEES, ROUTEN (FRANCE).
Response of a supersonic boundary layer to a compression corner p 645 N94-14759

INSTITUT NATIONAL DES SCIENCES APPLIQUEES DE LYON, VILLEURBANNE (FRANCE).
Microstructural origins and modeling of intergranular crack initiation in an Al-Li-Cu-Mg-(Zr) alloy
[ISAL-91-0012] p 574 N94-14814
Study of deferred acoustic emission in carbon epoxy composites
[ISAL-91-0078] p 560 N94-14815

INSTITUT ROYAL METEOROLOGIQUE DE BELGIQUE, BRUSSELS.
Storm prediction through barometric field analysis
[PUBL-SER-A-129] p 720 N94-13587
Potential evapotranspiration in Belgium: Spatial and temporal variability
[PUBL-SER-A-130] p 686 N94-13994

INSTITUTE FOR AEROSPACE RESEARCH, OTTAWA (ONTARIO).
Activities of Institute for Aerospace Research, Flight Research Laboratory
[CTN-93-60832] p 850 N94-13519
Finite element calculation of stress-intensity factors for thumb-nail cracks in DEN specimens
[LTR-ST-1929] p 850 N94-13548
Shear buckling of fiber metal laminates: Comparison between orthotropic and anisotropic plate models using finite element method
[LTR-ST-1934] p 671 N94-13565
Measurements of wing and fin buffeting on the standard dynamics model
[IAR-AN-76] p 526 N94-13859
Review of Canadian aeronautical fatigue work, 1991-1993
[LTR-ST-1932] p 674 N94-13861
Qualitative investigation of a generic fighter model in radio controlled gliding flight
[LM-AA-003] p 516 N94-13898
Flow-field interference produced by an asymmetrical support strut
[IAR-AN-75] p 504 N94-14031
Finite element calculation of stress-intensity factors for thru-thickness cracks in DEN specimens
[LTR-ST-1905] p 675 N94-14035
A description of the computer program CALDK38 which controls instrumentation set-up and data acquisition during deadweight calibration using an HBM DK 38 S6 digital measuring unit
[LTR-ST-1935] p 754 N94-14496

INSTITUTE FOR COMPUTER APPLICATIONS IN SCIENCE AND ENGINEERING, HAMPTON, VA.
A comparison of two formulations for high-order accurate essentially non-oscillatory schemes
[NASA-CR-191476] p 499 N94-12852
Modulational stability of periodic solutions of the Kuramoto-Sivaskinsky equation
[NASA-CR-191502] p 628 N94-12888
Surrogates for numerical simulations; optimization of eddy-promoter heat exchangers
[NASA-CR-191510] p 629 N94-13074
The three-dimensional flow past a rapidly rotating circular cylinder
[NASA-CR-191512] p 630 N94-13075
Pinching solutions of slender cylindrical jets
[NASA-CR-191482] p 630 N94-13114
The effect of crossflow on Taylor vortices: A model problem
[NASA-CR-191487] p 630 N94-13128
Interacting scales and energy transfer in isotropic turbulence
[NASA-CR-191477] p 630 N94-13133
Parametric binary dissection
[NASA-CR-191496] p 762 N94-13184
Calculating intersections of surfaces in screen space
[NASA-CR-191498] p 745 N94-13185
A hybrid Pade-Galerkin technique for differential equations
[NASA-CR-191494] p 767 N94-13289
Active control of acoustic pressure fields using smart material technologies
[NASA-CR-191480] p 768 N94-13354
A data distributed parallel algorithm for ray-traced volume rendering
[NASA-CR-191520] p 749 N94-13721
Canonical forms of multidimensional steady inviscid flows
[NASA-CR-191488] p 769 N94-13722
Evolution of disturbances in stagnation point flow
[NASA-CR-191516] p 636 N94-13724
The Chebyshev-Legendre method: Implementing Legendre methods on Chebyshev points
[NASA-CR-191497] p 769 N94-13725
On the secondary instability of the most dangerous Goertler vortex
[NASA-CR-191504] p 636 N94-13785
High order hybrid numerical simulations of two dimensional detonation waves
[NASA-CR-191506] p 769 N94-13792
Stability of oscillatory two phase Couette flow
[NASA-CR-191501] p 636 N94-13817
Analytical description of the breakup of liquid jets in air
[NASA-CR-191503] p 647 N94-14849

INSTITUTE FOR FUTURE TECHNOLOGY, TOKYO (JAPAN).
The studies on lunar and planetary exploration and utilization: The study on lunar resources utilization
[NASDA-CNT-930014] p 842 N94-13655

INSTITUTE OF ATMOSPHERIC PHYSICS, BEIJING (CHINA).
New evidences supported the Wei hypothesis about the formation of the Antarctic ozone hole
p 694 N94-14253

INSTITUTE OF DISASTER AND EARTH SCIENCES, IBARAKI (JAPAN).
Seasonal change of the land-surface temperature over Asian Continent derived from GAC data on NOAA-11 AVHRR p 691 N94-14232

INSTITUTE OF DISASTER AND EARTH SCIENCES, TSUKUBA (JAPAN).
Satellite remote sensing for disaster mitigation
p 693 N94-14244

INSTITUTE OF PHYSICAL AND CHEMICAL RESEARCH, SAITAMA (JAPAN).
Growth of PbSnTe single crystal by traveling-zone method in low gravity (M-2) p 586 N94-13734

INSTITUTO DE PESQUISAS ESPACIAIS, SAO JOSE DOS CAMPOS (BRAZIL).
Plasma diffusion through multidipole magnetic fields
[INPE-5460-PRE/1768] p 795 N94-12901
VISART: Artificial vision for industrial use. A comprehensive system
[INPE-5379-TDI/474] p 665 N94-12941
Study of possible mechanisms of instability due to heat transfer
[INPE-5448-TDI/494] p 628 N94-12966
The interplanetary origins and the main-phase development of moderate geomagnetic storms (1978 - 1979)
[INPE-5445-TDI/491] p 835 N94-13174
Cyclogenesis and cyclone over South America
[INPE-5400-TDI/479] p 719 N94-13175
The development of the TIMAX project: A hard x ray imaging telescope
[INPE-5474-TDI/505] p 829 N94-13245
Modeling of biosphere-atmosphere interaction for forest and pastureland in the Amazon
[INPE-5454-TDI/496] p 707 N94-13330
Dendrometric variables estimation in homogeneous forests using LANDSAT TM data
[INPE-5455-TDI/497] p 684 N94-13331
Evaluation of beta-spline interpolation in digital terrain models
[INPE-5475-TDI/506] p 684 N94-13364

Experimental determination of droplets local mean diameter of a sprag from impinging jets
[INPE-5469-TDI/500] p 631 N94-13365
Attitude determination of stratospheric balloons using Kalman filters
[INPE-5498-TDI/513] p 649 N94-13366
Spectral reflectance of soils from Sao Paulo State
[INPE-5424-PRP/172] p 684 N94-13377
Remote sensing of aquatic system
[INPE-5271-PRP/159] p 684 N94-13426
Technology parks and the cooperation among universities and firms: The cases of Campinas, Sao Jose dos Campos e Sao Carlos
[INPE-5251-TAE/04] p 818 N94-13427
A measurement and evaluation process model applied to software engineering environments
[INPE-5345-PUD/048] p 746 N94-13428
Spatial variability of throughfall chemistry in a tropical rainforest (Central Amazonia, Brazil)
[INPE-5431-PRE/1765] p 720 N94-13429
Sampling of globular clusters and the distance to the galactic center
[INPE-5446-TDI/492] p 837 N94-13449
Operational test of the airborne data acquisition system: SADA, the Bara Bonita experiment
[INPE-5451-NTC/305] p 685 N94-13610
Estimations of temperature and humidity of the canopy in Amazon Forest using microwave data from SMMR sensor of Nimbus-7 satellite
[INPE-5444-TDI/490] p 720 N94-13614
Climatic change due to land surface alterations
[INPE-5495-PRE/1786] p 721 N94-13672
Maximum entropy spectral analysis of the geological time series of the oxygen isotope record from deep-sea cores
[INPE-5465-PRE/1773] p 725 N94-13728
Satellite imagery and exogenous data integration by neural network in automation land-cover classification
[INPE-5480-PRE/1778] p 686 N94-13729
Nonlinear aspects of data integration for land-cover classification in a neural network environment
[INPE-5479-PRE/1778] p 686 N94-13789
Stability and confinement properties of small-aspect-ratio tokamak
[INPE-5463-PRE/1771] p 801 N94-14024
Intelligent environment for interpretation tasks of remotely sensed images
[INPE-5466-PRE/1774] p 687 N94-14082
Self-tuning control techniques for multivariable systems
[INPE-5449-TDI/495] p 765 N94-14084
Multisensor remote sensing data and GIS techniques for monitoring preservation areas: A case study
[INPE-5317-PRE/1714] p 688 N94-14131

INTERNATIONAL ATOMIC ENERGY AGENCY, VIENNA (AUSTRIA).
INGDB-90. The International Neutron Nuclear Data Base for geophysics applications
[DE93-624095] p 827 N94-14880

INTERNATIONAL CENTRE FOR THEORETICAL PHYSICS, TRIESTE (ITALY).
Determination of critical density of charge
[DE93-622897] p 775 N94-12877
Solitons and 1/f noise in molecular chains
[DE93-622898] p 778 N94-12879
Moebius inverse problem for distorted black holes
[DE93-622899] p 834 N94-12880
Charged scalar particles and (tau) leptonic decay
[DE93-622969] p 779 N94-12882
A method for determination of the superficial charge density
[DE93-622896] p 619 N94-12891
Scalar curvature and spherical-type Riemannian manifolds
[DE93-622852] p 767 N94-12895
Stochastic dynamics: Crossover from 1/f(sup 3) to flicker noise
[DE93-622862] p 772 N94-12896
Molecular dynamics simulation of electronically excited polyatomic molecules
[DE93-623045] p 781 N94-13225
Incomplete melting of the Au(100) surface
[DE93-623192] p 569 N94-13227
Comment of parameter excitation of Alfven and Heliicon waves in a magnetoactive compensated semiconductor by microwave radiation
[DE93-623203] p 806 N94-13228
Dilaton quantum cosmology in two dimensions
[DE93-621377] p 836 N94-13361
The general gravitational potential field of a homogeneous cylinder rotating about its axis
[DE93-622853] p 775 N94-13508
Heat flows and harmonic maps with a free boundary
[DE93-622856] p 632 N94-13509
Empirical tight-binding parameters for solid C(sub 60)
[DE93-623061] p 807 N94-13510
On the theory of the decaying developed turbulence with spontaneous parity violation
[DE93-623190] p 632 N94-13511
On the symmetry algebra of the discrete states in d less than 2 closed string theory
[DE93-622903] p 769 N94-13536

INTERNATIONAL SPACE YEAR ASSOCIATION, TOKYO (JAPAN).
Asia-Pacific ISY Conference, volume 2
[NASDA-CM-199-VOL-2] p 688 N94-14209

INTERSONICS, INC., NORTHBROOK, IL.
Stabilized electromagnetic levitator
[NASA-CR-194261] p 586 N94-12805

IOWA STATE UNIV. OF SCIENCE AND TECHNOLOGY, AMES.
Miscibility of lubricants with refrigerants, phase 1
[DE93-014766-PHASE-1] p 596 N94-13407
Effects of surface thermal forcing on stratified flow past an isolated obstacle p 633 N94-13553
Trajectory optimization for the national aerospace plane
[NASA-CR-194146] p 516 N94-14104

IOWA UNIV., IOWA CITY.
The multi-ion, multi-event test of ion cyclotron resonance heating
[NASA-CR-194134] p 789 N94-13419

IRVINE SENSORS CORP., COSTA MESA, CA.
HYMOSS signal processing for pushbroom spectral imaging
[NASA-CR-191341] p 620 N94-13125

ISHIKAWAJIMA-HARIMA HEAVY INDUSTRIES CO. LTD., TOKYO (JAPAN).
Marangoni effect induced convection in material processing under microgravity (M-18)
p 589 N94-13750

ISRAEL NATIONAL POLICE, JERUSALEM.
The 4th International Symposium on Analysis and Detection of Explosives
[DE93-620280] p 585 N94-14829

ISTITUTO ELETTROTECNICO NAZIONALE (GALILEO FERRARIS), TURIN (ITLAY).
Activities report of the National Electrotechnical Institute Galileo Ferraris
[ETN-93-94224] p 627 N94-14812

ITEK CORP., LEXINGTON, MA.
Wavefront sensing, control, and pointing
p 546 N94-14833

ITHACO, INC., ITHACA, NY.
Low cost attitude control system reaction wheel development
[NASA-CR-191332] p 540 N94-13140

IWATE UNIV., MORIOKA (JAPAN).
Accuracy validation test of estimated sea surface temperature by satellite data p 696 N94-14264
Sea surface effect on the sea surface temperature estimation by satellite data p 696 N94-14265

J

JAPAN ATOMIC ENERGY RESEARCH INST., TOKYO.
Test apparatus for ITER blanket cooling water distribution design
[DE93-753157] p 795 N94-12944

JAPAN BROADCASTING CORP., TOKYO.
Technological development for broadcasting satellites in NHK Laboratories p 618 N94-14288

JAPAN FISHERIES INFORMATION SERVICE CENTER, TOKYO.
Warm streamers extended from Warm Core Rings (WCR's) and their role on fish migration and fishing ground formation p 697 N94-14270

JAPAN MANNED SPACE SYSTEMS CORP., TOKYO.
Study on improvement of flammability, odor and offgassing tests for materials
[NASDA-CNT-930009] p 563 N94-13471
Survey and study on Environmental Control and Life Support (ECLS) technologies, part 2
[NASDA-CNT-930012-PT-2] p 737 N94-13472

JAPAN SOLAR ENERGY SOCIETY, TOKYO.
The 1992 JSEE/JWEA Joint Conference
[DE93-793955] p 700 N94-12822

JAPAN WEATHER ASSOCIATION, TOKYO.
Buoy experiments to obtain the sea-truth data for OCTS/NSCAT, part 1
[NASDA-CNT-930005-PT-1] p 725 N94-13653

JAPAN WIND ENERGY ASSOCIATION, TOKYO.
The 1992 JSEE/JWEA Joint Conference
[DE93-793955] p 700 N94-12822

JASCO RESEARCH LTD., SIDNEY (BRITISH COLUMBIA).
FLATDAN beamformer enhancements and testing
[DSIS-93-00287] p 777 N94-14360

JET PROPULSION LAB., CALIFORNIA INST. OF TECH., PASADENA.
Catalysis and biocatalysis program
[NASA-CR-194105] p 727 N94-12793
Electric propulsion system technology
[NASA-CR-194100] p 549 N94-13055
Electric propulsion system technology
[NASA-CR-194099] p 549 N94-13068
Environmental projects. Volume 15: Environmental assessment: Proposed 1-megawatt radar transmitter at the Mars site
[NASA-CR-194098] p 598 N94-13090
Ninth Annual NASA/Contractors Conference on Quality and Productivity. World Class Excellence: The Journey Continues. Keynote presentations
[NASA-CR-194513] p 665 N94-13148
Ninth Annual NASA/Contractors Conference on Quality and Productivity. World Class Excellence: The Journey Continues. Conference presentations
[NASA-CR-194514] p 665 N94-13153
Surfactant studies for bench-scale operation
[NASA-CR-194097] p 701 N94-13187
Spectral analysis for automated exploration and sample acquisition
[NASA-CR-194095] p 545 N94-13189
Publications of the Jet Propulsion Laboratory: 1990 and 1991
[NASA-CR-193287] p 823 N94-13461
Event-driven simulation in SELMON: An overview of EDSE
[NASA-CR-194505] p 749 N94-13784
Sequential ranging: How it works
[NASA-CR-194508] p 532 N94-13796
Using a focal-plane array to estimate antenna pointing errors
[NASA-CR-194502] p 602 N94-13810
Communications and control for electric power systems
[NASA-CR-194503] p 622 N94-13811
Single event effects and laser simulation studies
[NASA-CR-194506] p 657 N94-13812
Submillimeter, millimeter, and microwave spectral line catalogue, revision 3
[NASA-CR-194501] p 602 N94-13813
Theory of post-block 2 VLBI observable extraction
[NASA-CR-194543] p 686 N94-13872
The Large Area Pulsed Solar Simulator (LAPSS)
[NASA-CR-194507] p 703 N94-13940
Test report for single event effects of the 80386DX microprocessor
[NASA-CR-194509] p 741 N94-13943
Stochastic performance modeling and evaluation of obstacle detectability with imaging range sensors
[NASA-CR-194510] p 605 N94-13946
Surfactant studies for bench-scale operation
[NASA-CR-194511] p 564 N94-13947
Communications and control for electric power systems: Power flow classification for static security assessment
[NASA-CR-194512] p 624 N94-13948
An improved approach for flight readiness certification: Methodology for failure risk assessment and application examples, volume 1
[NASA-CR-194498] p 542 N94-14076
An improved approach for flight readiness certification: Methodology for failure risk assessment and application examples. Volume 2: Software documentation
[NASA-CR-194499] p 542 N94-14077
An improved approach for flight readiness certification: Methodology for failure risk assessment and application examples. Volume 3: Structure and listing of programs
[NASA-CR-194500] p 542 N94-14078
An exact processing algorithm for wide beam spaceborne SAR data p 689 N94-14213
The Telecommunications and Data Acquisition Report
[NASA-CR-194388] p 607 N94-14369
Radio metric errors due to mismatch and offset between a DSN antenna beam and the beam of a troposphere calibration instrument p 607 N94-14370
Improved treatment of global positioning system force parameters in precise orbit determination applications p 514 N94-14371
Use of global positioning system measurements to determine geocentric coordinates and variations in Earth orientation p 514 N94-14372
Failure modes of reduced-order orbit determination filters and their remedies p 532 N94-14373
Cammatic: An approach to improve DSS 13 antenna gravity-loading performance p 608 N94-14374
A cryogenic seven-element HEMT front end for DSS 13 p 608 N94-14375
Insertion loss and noise-temperature contribution of high-temperature superconducting bandpass filters centered at 2.3 and 8.45 GHz p 608 N94-14376
Coding performance of the Probe-Orbiter-Earth communication link p 608 N94-14377

Exploiting the cannibalistic traits of Reed-Solomon codes p 609 N94-14378
Estimating the size of Huffman code preambles p 609 N94-14379
Enhanced decoding for the Galileo S-band mission p 609 N94-14380
Stability measurements of the radio science system at the 34-m high-efficiency antennas p 609 N94-14381
Performance results of a digital test signal generator p 609 N94-14382
Formal functional test designs with a test representation language p 609 N94-14383
PC4CAST: A tool for DSN load forecasting and capacity planning p 610 N94-14384
Asynchronous transfer mode link performance over ground networks p 610 N94-14385
An overview of the Galileo Optical Experiment (GOPEX) p 610 N94-14386
Calibration of the receiver channel for the GOPEX precursor experiments p 610 N94-14387
Data analysis for GOPEX image frames p 610 N94-14388
Telescope pointing for GOPEX p 610 N94-14389
Galileo Optical Experiment (GOPEX) optical train: Design and validation at the Table Mountain Facility p 610 N94-14390
GOPEX laser transmission and monitoring systems p 611 N94-14391
Preliminary design and implementation of the baseline digital baseband architecture for advanced deep space transponders p 611 N94-14393
Hardware design for the Autonomous Visibility Monitoring (AVM) observatory p 533 N94-14394
Layout and cabling considerations for a large communications antenna array p 611 N94-14395
An initial study of using the 34-m antenna for lunar mission support p 611 N94-14396
HRMS sky survey wideband feed system design for DSS 24 beam waveguide antenna p 611 N94-14397
The flight performance of the Galileo orbiter USO p 611 N94-14398
Proceedings of the Fifth NASA/NSF/DOD Workshop on Aerospace Computational Control
[NASA-CR-194515] p 677 N94-14618
A component modes projection and assembly model reduction methodology for articulated, multi-flexible body structures p 677 N94-14622
Caesy: A software tool for computer-aided engineering p 678 N94-14627
Spatial operator algebra for flexible multibody dynamics p 679 N94-14631
Parallel O(log n) algorithms for open- and closed-chain rigid multibody systems based on a new mass matrix factorization technique p 679 N94-14636
Real-time dynamics simulation of the Cassini spacecraft using DARTS. Part 1: Functional capabilities and the spatial algebra algorithm p 680 N94-14638
Real-time dynamic simulation of the Cassini spacecraft using DARTS. Part 2: Parallel/vectorized real-time implementation p 680 N94-14639
Simulation of linear mechanical systems p 680 N94-14641
Computational issues in optimal tuning and placement of passive dampers p 681 N94-14647
Proceedings of the Seventeenth NASA Propagation Experimenters Meeting (NAPEX 17) and the Advanced Communications Technology Satellite (ACTS) Propagation Studies Miniworkshop
[NASA-CR-194096] p 612 N94-14654
Opening remarks: Current and future activities p 612 N94-14655
New challenges in propagation research in the US p 612 N94-14656
A database for propagation models p 614 N94-14665
Contribution towards a draft revision of recommendations 681: Propagation data required for the design of Earth-space land mobile telecommunications systems p 614 N94-14666
Propagation issues for emerging mobile and portable communications: A systems perspective p 614 N94-14667
Workshop Proceedings: Optical Systems Technology for Space Astrophysics in the 21st Century, volume 3
[NASA-CR-194102] p 545 N94-14830
Executive summary p 545 N94-14831
The next century astrophysics program p 546 N94-14832
An improved approach for flight readiness certification: Probabilistic models for flaw propagation and turbine blade failure. Volume 1: Methodology and applications
[NASA-CR-194496] p 519 N94-14841
An improved approach for flight readiness certification: Probabilistic models for flaw propagation and turbine blade failure. Volume 2: Software documentation
[NASA-CR-194497] p 519 N94-14842

JOHNS HOPKINS UNIV., BALTIMORE, MD.
Effect of microstructure on passive film formation and breakdown on Al alloys
[AD-A265339] p 569 N94-13050
Rocket and laboratory studies in astronomy
[NASA-CR-194410] p 832 N94-13966
Exploiting the cannibalistic traits of Reed-Solomon codes p 609 N94-14378
On the local nature of the energy cascade p 643 N94-14748
Search for subgrid scale parameterization by projection pursuit regression p 643 N94-14749

JOHNS HOPKINS UNIV., LAUREL, MD.
Energetic neutral atoms: Imaging the magnetospheric ring current
[NASA-CR-194339] p 715 N94-13826
Rain rate duration statistics derived from the Mid-Atlantic coast rain gauge network p 614 N94-14663

JOINT INST. FOR LAB. ASTROPHYSICS, BOULDER, CO.
Basic research in solar physics
[NASA-CR-193632] p 844 N94-13234

JOINT INST. FOR NUCLEAR RESEARCH, DUBNA (USSR).
Fine-powder Al2O3 and SiO2 for preparation of multielement standards for rare-earth elements analysis
[DE93-625118] p 567 N94-14884
A high-precision direct current measuring device over a kiloampere range
[DE93-626409] p 627 N94-14885
On a convergence of iterative Newton's scheme
[DE93-626604] p 772 N94-14886
Soliton equations and self-dual gauge fields
[DE93-626620] p 818 N94-14887
Radiation perturbation theory in gravity and quantum universe as a hydrogen atom
[DE93-626621] p 849 N94-14889
Spherical anharmonic oscillator in self-similar approximation
[DE93-626622] p 772 N94-14890
A hydrogen atom in the curved space: Orthogonality of radial wave functions with respect to the critical momentum
[DE93-626623] p 788 N94-14891
The electric field of a current-carrying conductor
[DE93-626637] p 617 N94-14892

JOINT PUBLICATIONS RESEARCH SERVICE, ARLINGTON, VA.
JPRS report: Science and technology. Central Eurasia: Space
[JPRS-USP-93-003] p 828 N94-13182
JPRS report: Science and technology. Central Eurasia: Engineering and equipment
[JPRS-UEQ-93-006] p 776 N94-14431
JPRS report: Science and technology. Central Eurasia: Materials science
[JPRS-UMS-93-006] p 558 N94-14573
JPRS report: Science and technology. Central Eurasia: Materials science
[JPRS-UMS-93-004] p 559 N94-14574
JPRS report: Science and technology. Central Eurasia: Materials science
[JPRS-UMS-93-005] p 559 N94-14575

K

KANAZAWA INST. OF TECH. (JAPAN).
Image processing and analysis of airborne POLDER data p 689 N94-14219

KANSAS STATE UNIV., MANHATTAN.
Nonlinear vibrations of thick composite plates: Higher-order shear deformation plate theory p 556 N94-13558

KANSAS UNIV., LAWRENCE.
Automated crack identification for cement paste
[AD-A265753] p 665 N94-13042

KAWASAKI HEAVY INDUSTRIES LTD., KAGAMIHARA (JAPAN).
Study of a one-dimensional deployable structure employing telescopic members p 531 N94-13282

KAWASAKI HEAVY INDUSTRIES LTD., KOBE (JAPAN).
Research on inflatable structure for space use p 530 N94-13275
HOPE real time flight operations analyses for return to earth phase, part B
[NASDA-CNT-930011] p 535 N94-13599
HOPE conceptual design in FY 1991
[NASDA-CNT-930017] p 535 N94-13600

KENTUCKY UNIV., LEXINGTON.
Coherent excitation of autoionizing resonances by electron impact
[DE93-018169] p 785 N94-14419

KERNFORSCHUNGSZENTRUM G.M.B.H., KARLSRUHE (GERMANY).
Review of mathematical and physical basis of two-phase flow modeling
[KFK-4759] p 642 N94-14708

KINLAW ASSOCIATES, NORFOLK, VA.
Kennedy Space Center's NASA/Contractor Team-Centered Total Quality Management Seminar: Results, methods, and lessons learned p 667 N94-13162

KOKUSAI DENSHIN DENWA CO. LTD., SAITAMA (JAPAN).
Future outlook on international satellite communications in Asia Pacific region p 618 N94-14287

KOREA AEROSPACE RESEARCH INST., TAEJON (REPUBLIC OF KOREA).
High performance multi-mode radar altimeter for future spaceborne application p 548 N94-14214

KRUG LIFE SCIENCES, INC., HOUSTON, TX.
Metabolic rate measurements comparing supine with upright upper-body exercises
[NASA-CR-4549] p 729 N94-14028

KYOTO UNIV. (JAPAN).
High temperature behavior of glass (M-8) p 587 N94-13740
Genetic effects of HZE and cosmic radiation (L-9) p 593 N94-13766

L

LABORATOIRE D'AUTOMATIQUE ET D'ANALYSE DES SYSTEMES, TOULOUSE (FRANCE).
Transformation and composition of refusal graphs: Testability analysis
[LAAS-92435] p 751 N94-13995
Molecular simulator: A basic tool for submicron MOS processes development
[LAAS-92484] p 814 N94-14697
A high voltage dielectrically isolated smart power technology based on silicon direct bonding
[LAAS-92492] p 626 N94-14698
Design and optimization of high voltage lateral DMOS devices using RESURF technology
[LAAS-92511] p 626 N94-14711
On the solution of a class of graph problems by parallel algorithms
[LAAS-92514] p 756 N94-14712
Thermal design of hybrid circuits: Tools and methodology
[LAAS-92515] p 626 N94-14713
Verification of critical software by statistical testing
[LAAS-93006] p 756 N94-14714
Execution methods, and parallel virtual machines for distributed implementation of the LCS parallel programming language
[LAAS-93032] p 761 N94-14716
Electrical noise in microwave field effect and bipolar transistors
[LAAS-93042] p 616 N94-14717

LAVAL UNIV. (QUEBEC).
Abundance markers in H II regions of late spiral galaxies
[ISBN-0-315-62457-4] p 836 N94-13372

LAWRENCE LIVERMORE NATIONAL LAB., CA.
PACT user's guide
[DE93-013093] p 742 N94-12840
A 3D gyrokinetic particle-in-cell simulation of fusion plasma microturbulence on parallel computers
[DE93-012503] p 794 N94-12846
FORTRAN graphics routines for the Macintosh
[DE93-013092] p 742 N94-12864
The optical constants and spectral specular reflectivity of Highly Oriented Pyrolytic Graphite (HOPG)
[DE93-011894] p 790 N94-12865
Ocean acoustic processing: A model-based approach
[DE93-011902] p 725 N94-12876
The importance of hard core repulsion in models of activity coefficients in aqueous electrolyte solutions: Illustration in the case of hydration theory
[DE93-012476] p 561 N94-12881
Smooth transitions between bump rendering algorithms
[DE93-012504] p 742 N94-12883
Recovery of materials impacted at high velocity
[DE93-014150] p 576 N94-12885
Recent results from material processing studies on new generation lasers
[DE93-013841] p 653 N94-12898
Effect of pressure on order and stability in alloys: The case of Al-Ge
[DE93-013842] p 567 N94-12899
Real time radiography of Titan 4 booster
[DE93-012450] p 548 N94-12911

Project proposal for partial computational physics support for Survivability of Coatings program
[DE93-013788] p 576 N94-12939
Three dimensional time-dependent hydrodynamic and propagation modeling of x ray laser emission
[DE93-012575] p 654 N94-12962
Evolution of high-repetition-rate induction accelerators through advancements in switching
[DE93-012599] p 654 N94-12963
Metal-semiconductor, composite radiation detectors
[DE93-013313] p 619 N94-12994
Highly charged ions in hot, dense plasmas
[DE93-013348] p 795 N94-12995
Grain-boundary electronic states by multiple-scattering theory
[DE93-013198] p 805 N94-13010
On inhomogeneous halo collapse and the globular cluster metallicity gradient
[DE93-013090] p 834 N94-13011
Inertial Confinement Fusion
[DE93-013303] p 795 N94-13017
Energy and technology review, March 1993
[DE93-013941] p 849 N94-13019
The x ray dichroism experiments using circular polarization
[DE93-013195] p 568 N94-13036
The footprint area influencing a high-volume air sampler
[DE93-013947] p 706 N94-13095
ULTRA 2 user's manual for ULTRA 2 revision 3.0
[DE93-015970] p 744 N94-13120
SCORE user's manual
[DE93-015987] p 822 N94-13121
Atomic structure of the 310 twin in niobium: Theoretical predictions and comparison with experimental observation
[DE93-013421] p 806 N94-13136
Electronic structure and phase stability properties in ternary substitutional alloys
[DE93-013848] p 569 N94-13137
Predicted performance of a dc beam driven FEM oscillator designed for fusion applications at 200-250 GHz
[DE93-013414] p 655 N94-13145
Kinetic simulations of ultra-intense laser plasma interactions and a novel method of generating odd harmonics
[DE93-014418] p 797 N94-13207
EBIT Trapping Program
[DE93-014422] p 788 N94-13208
Magnetic fusion computing: A personal retrospective view
[DE93-014147] p 797 N94-13217
Absorption and damage thresholds of low defect density hafnia deposited with activated oxygen
[DE93-013853] p 655 N94-13243
Numerical simulations and experiments on physics of high Mach number shockwave: Turbulent flow interactions
[DE93-013424] p 631 N94-13249
Sub-grid scale modeling for large eddy simulations in analysis of shock-turbulence interactions
[DE93-013425] p 631 N94-13250
Charged-particle evaluation methodology at Lawrence Livermore National Laboratory
[DE93-013429] p 781 N94-13251
Imaging microscopy with x ray lasers at Lawrence Livermore National Laboratory
[DE93-013419] p 655 N94-13258
The x ray lasers as sources for x ray microscopy
[DE93-013420] p 655 N94-13259
Fracture behavior of vanadium/vanadium silicide in-situ composites
[DE93-013422] p 556 N94-13389
Parametric instabilities in large nonuniform laser plasmas
[DE93-013184] p 797 N94-13393
Preliminary meteorological results for 1992 West Coast Scotland Experiment
[DE93-014677] p 720 N94-13404
Barium fluoride research and development at Lawrence Livermore National Laboratory
[DE93-014682] p 807 N94-13405
DATAA: Data acquisition made easy
[DE93-014683] p 823 N94-13406
Long-pulse operation of a gyrotron with beam/RF separation
[DE93-015007] p 649 N94-13410
Design and performance of an automated video-based laser beam alignment system
[DE93-012571] p 656 N94-13481
Measurements of optical properties of waveshifting optical fiber for liquid scintillator hadron calorimetry
[DE93-012606] p 791 N94-13482
Programming the multimodal interface
[DE93-013084] p 748 N94-13576
Longitudinal beam dynamics for heavy ion fusion
[DE93-013850] p 789 N94-13727
Optical and physical properties of the LiSrAlF6:Cr laser crystal
[DE93-014657] p 808 N94-13881
Design and performance of the terawatt Cr:LiSrAlF6 laser system
[DE93-014678] p 657 N94-13882
Charge-exchange reactions and weak interaction rates for Type 2 supernovae
[DE93-015104] p 783 N94-13893
AMIP: Diagnostic subproject on the variability in the tropics: Synoptic to intraseasonal time scales
[DE93-009287] p 721 N94-13914
Some aspects of sheet forming simulation using explicit finite element techniques
[DE93-012479] p 663 N94-13975
Oscillator-amplifier experiments in neon-like yttrium
[DE93-012577] p 657 N94-13976
The role of human activity and land use change in atmospheric chemistry and air quality
[DE93-011871] p 709 N94-14022
The interaction of intense femtosecond laser pulses with solid targets
[DE93-014415] p 658 N94-14114
Laser-damage susceptibility of nodular defects in dielectric mirror coatings: AFM measurements and electric-field modeling
[DE93-014655] p 580 N94-14124
Laser and spectroscopic properties of Yb-doped apatite crystals
[DE93-014656] p 810 N94-14125
Indirect processes in electron impact ionization of Kr(24+) and Kr(25+)
[DE93-014129] p 784 N94-14140
The Livermore x ray laser program
[DE93-014118] p 658 N94-14152
Selenium x ray laser line profile measurements
[DE93-012580] p 658 N94-14175
PC viruses: How do they do that?
[DE93-012581] p 753 N94-14289
A model for fuel fire duration and application to the B-1B bomber
[DE93-013000] p 512 N94-14292
Machining aspects of nickel-phosphorus coatings
[DE93-013037] p 580 N94-14311
Measuring opacity of shock generated argon plasmas
[DE93-013038] p 801 N94-14312
Monte Carlo simulation of the OCP freezing transition
[DE93-013039] p 811 N94-14313
Deconvolution for positive signals
[DE93-013044] p 773 N94-14314
Uniform user and group IDs on a large network
[DE93-013047] p 760 N94-14315
Gamma-insensitive optical focal plane array
[DE93-013100] p 792 N94-14317
The accuracy of approximating radiative heat transfer using a temperature dependent thermal conductivity
[DE93-013105] p 638 N94-14318
Formation of textured YBCO films by laser ablation
[DE93-013131] p 581 N94-14319
Storage systems for national information assets
[DE93-015101] p 825 N94-14331
An x ray detector using superconducting aluminum tunnel junctions
[DE93-015103] p 811 N94-14332
Wind mass and energy deposition
[DE93-013345] p 839 N94-14341
Implicit multi-fluid simulation of interpenetrating plasmas
[DE93-013351] p 801 N94-14342
Imaging Fourier transform spectrometer
[DE93-017193] p 651 N94-14416
Sea surface temperature forcing and phase locking of Nordeste precipitation
[DE93-011873] p 723 N94-14426
An ultra-compact processor module based on the R3000
[DE93-012549] p 625 N94-14427
Modeling surface area to volume effects on borosilicate glass dissolution
[DE93-011891] p 581 N94-14432
An adaptive projection method for the incompressible Euler equations
[DE93-016428] p 639 N94-14434
Computational mechanics and supercomputing at LLNL
[DE93-016453] p 754 N94-14435
Laser beam control and diagnostic systems for the copper-pumped dye laser system at Lawrence Livermore National Laboratory
[DE93-016529] p 658 N94-14437
Brillouin scattering from fluctuations produced by stimulated Raman scattering
[DE93-016531] p 792 N94-14438
Computational diagnostics for detecting phase transitions during nanoindentation
[DE93-016536] p 813 N94-14439
Metastability of yttrium-oxides
[DE93-016548] p 813 N94-14440
Microchannel cooled heatsinks for high average power laser diode arrays
[DE93-016533] p 658 N94-14442
Absolute detection efficiency of a micro-channel plate detector to x rays in the 1-100 KeV energy range
[DE93-012592] p 789 N94-14460
The first data from the MACHO experiment
[DE93-014423] p 840 N94-14467
Biomimetic methane oxidation
[DE93-013196] p 705 N94-14510
An overview of parallel scientific visualization
[DE93-017105] p 755 N94-14521
Independent adjustment of the higher order frequency dependent phase in chirped pulse amplification systems
[DE93-017106] p 625 N94-14522
Multiple Schroedinger cats from multilevel atoms
[DE93-013412] p 786 N94-14526
Kinetic simulations of ultra-intense laser plasma interactions
[DE93-014419] p 802 N94-14564
Computer vision and sensor fusion for detecting buried objects
[DE93-012605] p 700 N94-14566
Some tools of the trade we've developed for our cross-section calculations
[DE93-013835] p 786 N94-14569
Large spatial, temporal, and algorithmic adaptivity for implicit nonlinear finite element analysis
[DE93-016438] p 771 N94-14589
Impedance-power effects on plasma polymer surface finish using a helical resonator discharge
[DE93-016454] p 803 N94-14590
High-order harmonic generation with short-pulse lasers
[DE93-016532] p 659 N94-14594
Experimental measurements of selenium x-ray laser spectral line profiles
[DE93-016543] p 659 N94-14595
Ion assisted sputter deposition of Mo-Si multilayers
[DE93-013830] p 583 N94-14693
Image reconstruction for x ray holographic microscopy
[DE93-013094] p 653 N94-14772
A fast frame rate 512 x 512 CCD digital camera system
[DE93-013048] p 653 N94-14792
Statics and kinetics of phase transformations in bcc Fe-Cr
[DE93-013839] p 574 N94-14793
Generalized smooth models
[DE93-013045] p 756 N94-14864
The 8 to 11 keV x ray sources for imaging and absorption experiments
[DE93-015973] p 803 N94-14865
Electrochemical planarization for microelectronic circuits
[DE93-017214] p 627 N94-14870
Optimization study of x ray laser coherence in Ni-like Ta
[DE93-016419] p 660 N94-14888
Characteristics of a high energy muon(+)muon(-) collider based on electro-production of muons
[DE93-017154] p 790 N94-14893
Time resolved measurement of electron temperatures of exploding foil x ray laser plasmas
[DE93-017161] p 803 N94-14894
Toward a quasi-linear closure for compressible turbulence
[DE93-017185] p 647 N94-14895

LEHIGH UNIV., BETHLEHEM, PA.
Analysis of the IUE spectra of the strongly interacting binary beta Lyrae
[NASA-CR-194118] p 833 N94-14493

LEICESTER UNIV. (ENGLAND).
Rotorcraft flying qualities improvement using advanced control p 522 N94-13303

LOCKHEED ENGINEERING AND SCIENCES CO., HAMPTON, VA.
Simulator for heterogeneous dataflow architectures
[NASA-CR-191545] p 622 N94-13797

LOCKHEED ENGINEERING AND SCIENCES CO., HOUSTON, TX.
STS-53 Space Shuttle mission report
[NASA-CR-193101] p 535 N94-13934
STS-54 Space Shuttle mission report
[NASA-CR-194116] p 535 N94-13935

LOS ALAMOS NATIONAL LAB., NM.
Two-dimensional simulations of foil implosion experiments on the Los Alamos capacitor bank
[DE93-012676] p 794 N94-12814

A new limit on the rate-density of evaporating black holes
[DE93-012716] p 834 N94-12815
Search for ultra-high energy emission from Geminga and five unidentified EGRET sources
[DE93-012717] p 846 N94-12816
Advanced magnetic flux compression generator development issues: A comparison of coaxial and disk generators
[DE93-014025] p 794 N94-12849
Completing fault models for abductive diagnosis
[DE93-003832] p 761 N94-12859
Micromechanical strength effects in shock compression of solids
[DE93-014425] p 670 N94-12887
Ceramic matrix composites by microwave assisted CVI
[DE93-012640] p 576 N94-12916
A network evaluation and analysis tool
[DE93-012647] p 758 N94-12917
A new method to assess Monte Carlo convergence
[DE93-012667] p 772 N94-12919
Equation of state for detonation products
[DE93-012671] p 583 N94-12921
Search for UHE point-source emission over various time scales
[DE93-012718] p 846 N94-12922
Search for emission of ultra high energy radiation from active galactic nuclei
[DE93-012719] p 846 N94-12923
Search for UHE emission from Cygnus X-3
[DE93-012720] p 846 N94-12924
Angular resolution studies of the CYGNUS array using the shadows of the Sun and Moon
[DE93-012723] p 846 N94-12946
Search for continuous and single day emission from ultra-high-energy sources
[DE93-012724] p 846 N94-12947
No-lost theorem for parity violating nucleon-nucleon scattering experiments
[DE93-012737] p 779 N94-12949
Low energy neutral atom imaging techniques
[DE93-012744] p 779 N94-12950
Ion anisotropy driven waves in the Earth's magnetosheath and plasma depletion layer
[DE93-012751] p 712 N94-12952
Search for ultra-high-energy radiation from gamma-ray bursts
[DE93-012721] p 847 N94-12964
Metal oxide varistor feasibility study
[DE93-012921] p 620 N94-13031
Synthesis and characterization of 1,4-dinitroglycoluril (DINGU)
[DE93-014111] p 584 N94-13099
A PC-PCL-based control system for the high-voltage pulsed-power operation of the Intense Diagnostic Neutral Beam (IDNB) Experiment
[DE93-014144] p 797 N94-13100
Measurement of H zero excited states produced by foil stripping of 800-MeV H(-) ions
[DE93-014391] p 788 N94-13103
Adaptive Transfer Function Networks
[DE93-014344] p 745 N94-13151
Recent study of beam stability in the PSR
[DE93-014473] p 780 N94-13173
Present status of SAGE
[DE93-014350] p 781 N94-13205
Discussion of stress tensor nonuniqueness with application to nonuniform, particulate systems
[DE93-014352] p 816 N94-13206
Beam halo formation from space-charge dominated beams in uniform focusing channels
[DE93-014458] p 789 N94-13209
Evolution of the interplanetary magnetic field
[DE93-012631] p 836 N94-13262
Advanced computers and simulation
[DE93-014354] p 740 N94-13286
Design for low beam loss in accelerators for intense neutron source applications
[DE93-014557] p 789 N94-13327
Beam halo in high-intensity beams
[DE93-014565] p 789 N94-13328
Electrocatalysis issues in polymer electrolyte fuel cells
[DE93-014450] p 702 N94-13402
Hot Dry Rock energy
[DE93-014452] p 702 N94-13403
Reduction of Pu(6) with hydrogen peroxide: Effects of plutonium, peroxide, and iron concentrations and of reaction time
[DE93-013598] p 564 N94-13487
Destruction of waste energetic materials using base hydrolysis
[DE93-012738] p 584 N94-13491
Advances in low energy neutral atom imaging techniques
[DE93-012745] p 782 N94-13492
Excimer laser surface processing of titanium
[DE93-012633] p 570 N94-13512
Instability heating of the HDZP
[DE93-012641] p 798 N94-13513
Quality assurance for environmental chemistry, 1991, volume 1
[DE93-011791] p 709 N94-14020
Regional climatology sensitivity studies
[DE93-010712] p 722 N94-14057
A classical instability for black strings and p-branes
[DE93-014577] p 839 N94-14116
Knowledge based systems: From process control to policy analysis
[DE93-014582] p 765 N94-14117
Measurement of strain in individual phases of composites before, during, and after mechanical loading
[DE93-014585] p 558 N94-14119
Dynamic mechanical deformation of a SiC(sub p)/Al-Li (8090) composite
[DE93-014586] p 558 N94-14121
Measurement of penetration depth lambda(T) in YBa2Cu3O(7-delta) thin film
[DE93-014587] p 810 N94-14122
Computational problems with the binomial failure rate model and incomplete common cause failure reliability data
[DE93-014346] p 669 N94-14143
Distributed processor Monte Carlo: MCNP results on a 16-node IBM cluster
[DE93-012639] p 752 N94-14176
Quantum Monte Carlo by message passing
[DE93-012645] p 760 N94-14177
Hybrid S(sub N)/Monte Carlo research and results
[DE93-012677] p 773 N94-14178
Schemes for the use of conducting polymers as active materials in electrochemical supercapacitors
[DE93-012713] p 580 N94-14179
A study of the role of homogeneous process in heterogeneous high explosives
[DE93-012733] p 585 N94-14180
The (mu)(+) yields e(+)gamma
[DE93-012750] p 785 N94-14181
Synthesis of organic ligands for f-element separations
[DE93-012915] p 554 N94-14290
Microwave hybrid heating of alumina filaments
[DE93-012642] p 581 N94-14327
Terrestrial magnetospheric imaging: Numerical modeling of low energy neutral atoms
[DE93-014561] p 717 N94-14328
Shock compression and quasielastic release in tantalum
[DE93-014566] p 811 N94-14329
Effect of spontaneous decay of superconductor quasiparticles in the tunneling density of states
[DE93-012681] p 811 N94-14339
Microwave sintering of large alumina bodies
[DE93-012752] p 581 N94-14340
Ploughing on gold using a Scanning Tunneling Microscope
[DE93-012632] p 812 N94-14365
Rare muon processes
[DE93-012646] p 785 N94-14366
Polarization effects in optical fiber current sensors based on Sagnac interferometers with 3 by 3 couplers
[DE93-012665] p 792 N94-14367
Structure and stability of microvoids in A-Si:H
[DE93-016625] p 813 N94-14413
Nonlinear wave predictions in ceramics
[DE93-016516] p 582 N94-14436
The effects of internal fluctuations on a class of nonequilibrium statistical field theories
[DE93-016620] p 774 N94-14441
Machining and grinding: High rate deformation in practice
[DE93-010718] p 664 N94-14457
Results from a water-Cerenkov array
[DE93-012715] p 849 N94-14461
Angular correlations in neutron beta decay
[DE93-014349] p 785 N94-14466
Dynamics of pion-nucleus systems
[DE93-014449] p 785 N94-14468
The structure and mechanical properties of Ru-Cu and Ru-Ti nanolayer composites
[DE93-014453] p 558 N94-14469
Measuring parity violation using the neutron capture reaction
[DE93-016629] p 786 N94-14514
Atmospheric acoustic modeling
[DE93-016727] p 718 N94-14518
Review of the Procyon explosive pulsed power system
[DE93-016562] p 802 N94-14532
Review of nuclear thermal propulsion carbide reactor fuel corrosion and exhibit
[DE93-016605] p 585 N94-14535
Multiplicative noise: Applications in cosmology and field theory
[DE93-016624] p 840 N94-14536
The status of cold fusion
[DE93-012731] p 802 N94-14567
Differential Sensitivity Theory applied to the MESA code for high pressure interactions
[DE93-016460] p 676 N94-14591
A recuperative superfluid Stirling refrigerator
[DE93-016521] p 597 N94-14592
Statistical mechanical theory of liquid entropy
[DE93-016524] p 817 N94-14593
Primary and secondary electrical space power based on advanced PEM systems
[DE93-012643] p 553 N94-14689
Small-angle scattering, contrast variation and the study of complex composite materials: A study of the structure of carbon black
[DE93-012707] p 559 N94-14690
Identification of continuous-time dynamical systems: Neural network based algorithms and parallel implementation
[DE93-014427] p 766 N94-14737
The fractional quantum Hall effect and the spherical shell model
[DE93-014553] p 818 N94-14740
Muon spin relaxation studies of heavy fermion superconductors
[DE93-014576] p 815 N94-14773
The LAHET code system: Introduction, development, and benchmarking
[DE93-012657] p 787 N94-14804
Optical degradation issues for XUV projection lithography systems
[DE93-012658] p 626 N94-14805
Study of chemical reactions under the influence of ultrasound
[DE93-016458] p 778 N94-14867
Comparative ignition of hexane and octane isomers in a shock tube
[DE93-016535] p 566 N94-14869

LOUISIANA STATE UNIV., BATON ROUGE.
A program of correlated observations using the EGRET instrument on GRO and the IMB neutrino detector
[NASA-CR-194367] p 783 N94-13856
BOAST 2 for the IBM 3090 and RISC 6000
[DE93-000138] p 638 N94-14351

LOYOLA COLL., BALTIMORE, MD.
JTEC Panel report on knowledge-based systems in Japan
[PB93-170124] p 820 N94-12801

LUDWIG-MAXIMILIANS-UNIV., MUNICH (GERMANY).
Development of a remote sensing geographic information system for land cover changes and assessment of risk due to natural and man made hazards covering the area of the inner delta of the Yellow River
p 694 N94-14249

LUNAR AND PLANETARY INST., HOUSTON, TX.
Workshop on the Space Environment: The Effects on the Optical Properties of Airless Bodies
[NASA-CR-194417] p 842 N94-14298

M

M-C POWER CORP., BURR RIDGE, IL.
Molten carbonate fuel cell product development test environmental assessment/protection plan
[DE93-000288] p 702 N94-13380

MALAYAN CENTRE FOR REMOTE SENSING, KUALA-LAMPUR.
Soil erosion mapping using remote sensing and GIS techniques p 692 N94-14240

MARITIME SAFETY AGENCY, TOKYO (JAPAN).
On the sea truth data of the Kuroshio meander and cold eddy movement p 696 N94-14266

MARTEC LTD., HALIFAX (NOVA SCOTIA).
CMAPP user's manual, part 2
[DSIS-93-00858-PT-2] p 751 N94-14017
Development of software for composite materials analysis, phase 1, part 1
[DSIS-93-00857-PT-1-PHASE-1] p 558 N94-14105

MARTIN MARIETTA CORP., DENVER, CO.
CFM technologies for space transportation: Multipurpose hydrogen testbed system definition and tank procurement
[NASA-CR-194355] p 539 N94-12827

MARYLAND UNIV., COLLEGE PARK.
Microwave generation for magnetic fusion energy applications
[DE93-013864] p 654 N94-13058
Flex-gear electrical power transmission
[NASA-CR-194422] p 661 N94-13445
Advanced solid-state array spectroradiometer data collection during HAPEX-2 Sahel
[NASA-CR-194144] p 808 N94-13875

Integration of space and in-situ observations to study atmosphere, ocean and land processes
[NASA-CR-194495] p 683 N94-14500

MASON AND HANGER-SILAS MASON CO., INC., AMARILLO, TX.
Compatibility testing of vacuum seal materials
[DE93-014366] p 663 N94-14113

MASSACHUSETTS INST. OF TECH., CAMBRIDGE.
On the motion through a viscous fluid of a spherical particle touching a plane wall: Slip boundary conditions
[DE93-012540] p 628 N94-12961
The physical and chemical evolution of protostellar disks. The growth of protostellar disks: Progress to date
[NASA-CR-194111] p 636 N94-13423
Measurements of edge fluctuations by phase contrast imaging on DIII-D
[DE93-014018] p 802 N94-14579

MASSACHUSETTS INST. OF TECH., LEXINGTON.
Proceedings of the 11th Space Surveillance Workshop, volume 1
[AD-A265120] p 531 N94-13358

MASSACHUSETTS UNIV., AMHERST.
Computation and graphics in mathematical research
[DE93-016512] p 740 N94-13069
High speed all-optical networks
[NASA-CR-194384] p 791 N94-13682

MASSACHUSETTS UNIV., LOWELL.
Investigation of an alternating current plasma as an element selective atomic emission detector for high-resolution capillary gas chromatography and as a source for atomic absorption and atomic emission spectrometry p 798 N94-13678

MATERIALS RESEARCH LABS., ASCOT VALE (AUSTRALIA).
Structural investigation of a damaged GRP/foam sandwich composite using x ray computed tomography p 669 N94-13857

MAX-PLANCK-INST. FUER METEOROLOGIE, HAMBURG (GERMANY).
Simulation of the present-day climate with the ECHAM model: Impact of model physics and resolution
[REPT-93] p 724 N94-14709

MCAT INST., SAN JOSE, CA.
Turbulence modeling of free shear layers for high-performance aircraft
[NASA-CR-193659] p 520 N94-12799
Implementation of ADI: Schemes on MIMD parallel computers
[NASA-CR-193720] p 759 N94-13204
Colorimetric qualification of shear sensitive liquid crystal coatings
[NASA-CR-194126] p 806 N94-13291
High speed transition prediction
[NASA-CR-194125] p 502 N94-13422
CNSFV code development, virtual zone Navier-Stokes computations of oscillating control surfaces and computational support of the laminar flow supersonic wind tunnel
[NASA-CR-194259] p 504 N94-14030
Numerical simulation of a powered-lift landing, tracking flow features using overset grids, and simulation of high lift devices on a fighter-lift-and-control wing
[NASA-CR-194260] p 527 N94-14322

MCDONNELL-DOUGLAS CORP., HUNTINGTON BEACH, CA.
Feasibility study of an orbiting laboratory for testing CSI technology
[NASA-CR-191524] p 540 N94-13016
Mirror fusion propulsion system: A performance comparison with alternate propulsion systems for the manned Mars Mission
[NASA-TM-109248] p 550 N94-13147

MCDONNELL-DOUGLAS CORP., SAINT LOUIS, MO.
High temperature electromagnetic characterization of thermal protection system tile materials
[NASA-CR-189687] p 578 N94-13431

MCDONNELL-DOUGLAS HELICOPTER CO., MESA, AZ.
A four-axis hand controller for helicopter flight control p 522 N94-13305

MCDONNELL-DOUGLAS MISSILE SYSTEMS CO., SAINT LOUIS, MO.
High flux heat exchanger
[AD-A266341] p 636 N94-13730

MCDONNELL-DOUGLAS SPACE SYSTEMS CO., COCOA BEACH, FL.
Payload/GSE/data system interface: Users guide for the VPF (Vertical Processing Facility)
[NASA-CR-194385] p 532 N94-14148

MCGILL MFG. CO., VALPARAISO, IN.
Computer program for analysis of high speed, single row, angular contact, spherical roller bearing, SASHBEAN. Volume 1: User's guide
[NASA-CR-191183] p 663 N94-14445
Computer program for analysis of high speed, single row, angular contact, spherical roller bearing, SASHBEAN. Volume 2: Mathematical formulation and analysis
[NASA-CR-191182] p 664 N94-14446

MCGILL UNIV., MONTREAL (QUEBEC).
Fully developed turbulent flow in rectangular interrupted-plate ducts
[ISBN-0-315-63594-0] p 632 N94-13474
Bayesian estimation of motion fields from image sequences
[ISBN-0-315-57212-4] p 772 N94-13540
Application of transient airborne electromagnetic and ground resistivity methods to geological mapping in tropical terrains
[ISBN-0-315-57172-1] p 685 N94-13542
Dynamics and design of nonholonomic robotic mechanical systems
[ISBN-0-315-72009-3] p 662 N94-13597
A control volume finite element method for three-dimensional, incompressible, viscous fluid flow
[ISBN-0-315-72019-0] p 635 N94-13683

MCMASTER UNIV., HAMILTON (ONTARIO).
Three dimensional tracking of four point planar patterns using corners
[ISBN-0-315-52149-X] p 791 N94-13490
Single Event Upset (SEU) testing of semiconductor components at the McMaster Accelerator Laboratory
[DSIS-93-00071] p 623 N94-13834
Portable multipath measurement system
[DSIS-93-00177] p 603 N94-13843

MELBOURNE UNIV., PARKVILLE (AUSTRALIA).
Gauging the octonion algebra
[DE93-622864] p 775 N94-12843
Quaternions and the heuristic role of mathematical structures in physics
[DE93-622865] p 816 N94-12844
Electric charge quantization
[DE93-622901] p 778 N94-12845
Top quark polarization and T-odd spin correlations as tools for testing (non) Standard Model predictions
[DE93-622956] p 778 N94-12847
Medium energy hadron-nucleus scattering in the 1/N expansion formalism
[DE93-622957] p 778 N94-12848
Confocal profilometer with nanometric vertical resolution
[DE93-622698] p 653 N94-12857
Electromagnetic deflection of spinning particles
[DE93-622866] p 778 N94-12858

MERIDIAN CORP., ALEXANDRIA, VA.
Force reflecting hand controller for manipulator teleoperation
[NASA-CR-191345] p 661 N94-13129

MESSERSCHMITT-BOELKOW-BLOHM G.M.B.H., MUNICH (GERMANY).
Mathematical optimization: A tool for aircraft design
[MBB-LME-251-S-PUB-0492] p 751 N94-14006
Simulation of hypersonic, reacting flow around reentry bodies: Comparisons of numerical and experimental results
[MBB-LME-211-S-PUB-507] p 509 N94-14710

METEOROLOGICAL RESEARCH INST., TSUKUBA (JAPAN).
Atmospheric correction for sea surface temperature by application of microwave dual-channel technique to VTIR data p 697 N94-14271

METEOROLOGICAL SOCIETY OF JAPAN, TOKYO.
Study on TRMM data utilization for meteorology
[NASDA-CNT-930007] p 721 N94-13643

METROLASER, IRVINE, CA.
Two color holographic interferometry for microgravity application
[NASA-CR-194424] p 651 N94-14447

MICHIGAN STATE UNIV., EAST LANSING.
Direct probing of chromatography columns by laser-induced fluorescence
[DE93-015208] p 654 N94-13022
Theoretical studies of breakdown in random media
[DE93-018107] p 558 N94-14418

MICHIGAN TECHNOLOGICAL UNIV., HOUGHTON.
Boundary stability under nonequilibrium conditions
[DE93-016259] p 809 N94-13980

MICHIGAN UNIV., ANN ARBOR.
Nonlinear laser spectroscopy studies of semiconductor heterostructures
[AD-A265728] p 805 N94-13037
Phobos/Harp post launch support
[NASA-CR-193676] p 540 N94-13109
A hybrid finite element-boundary integral for the analysis of cavity-backed antennas of arbitrary shape
[NASA-CR-193719] p 599 N94-13236
The distance to the high velocity clouds of neutral hydrogen
[NASA-CR-194343] p 838 N94-13716
Scattering by a groove in an impedance plane
[NASA-CR-193362] p 602 N94-13720
Application of symbolic and algebraic manipulation software in solving applied mechanics problems
[NASA-CR-4544] p 596 N94-13798

MICROELECTRONICS CENTER OF NORTH CAROLINA, RESEARCH TRIANGLE PARK.
Field emitter array RF amplifier development project. Phase 1: Cathode technology development
[AD-A266346] p 622 N94-13776

MIDWEST RESEARCH INST., GOLDEN, CO.
Photovoltaic Subcontract Program
[DE93-000092] p 700 N94-12868
Photovoltaics: Contract lists, fiscal year 1992
[DE93-000093] p 701 N94-12902
Photovoltaics: Program overview, fiscal year 1992
[DE93-000055] p 701 N94-12914
Reflective coatings for solar applications
[DE93-010026] p 702 N94-13381
Low temperature metal-organic chemical vapor deposition growth processes for high efficiency solar cells
[DE92-010562] p 702 N94-13386
Structural and electronic studies of a-SiGe:H alloys
[DE93-010021] p 809 N94-14085
Biodiesel/aquatic species project report, FY 1992
[DE93-010024] p 709 N94-14087
Status and future opportunities for conversion of synthesis gas to liquid energy fuels
[DE93-010025] p 584 N94-14089
Continuous roll-to-roll a-Si photovoltaic manufacturing technology
[DE93-010006] p 704 N94-14109
Optimization of transparent and reflecting electrodes for amorphous silicon solar cells
[DE93-010009] p 704 N94-14110
Photovoltaic advanced research and development project: Solar radiation research
[DE92-016430] p 704 N94-14350
NREL solar radiation resource assessment project: Status and outlook
[DE93-010034] p 704 N94-14422
Inflow characteristics associated with high-blade-loading events in a wind farm
[DE93-010042] p 704 N94-14423
Biofuels for transportation: The road from research to the marketplace
[DE93-000091] p 585 N94-14454
Activities of the Basic Sciences Branch
[DE93-010012] p 851 N94-14455

MINISTRY OF COMMUNICATIONS, ANYANG (REPUBLIC OF KOREA).
The current situation, trends, international cooperation of space communication technological development in the Republic of Korea p 699 N94-14283

MINISTRY OF EDUCATION, KANAGAWA (JAPAN).
Helical truss beam development for large space structure p 530 N94-13276

MINISTRY OF POSTS AND TELECOMMUNICATIONS, BEIJING (CHINA).
The developments of satellite communications of China p 618 N94-14282

MINISTRY OF POSTS AND TELECOMMUNICATIONS, TOKYO (JAPAN).
Artificial oil pollution detection and wave observation in the sea adjacent to Japan by ERS-1 SAR p 688 N94-14212
TRMM precipitation radar algorithm p 690 N94-14224
Multiparameter airborne rain radar development for TRMM validation and TRMM-follow-on study p 690 N94-14226
Joint experiments using ETS-5 p 618 N94-14284
Space communications technology research in CRL p 618 N94-14285

MINNESOTA UNIV., MINNEAPOLIS.
Experimental and theoretical study of inhomogeneous electron transfer in betaine: Comparisons of measured and predicted spectral dynamics
[AD-A265703] p 780 N94-13051
Generalized impedance control of a redundant manipulator p 661 N94-13575
Theory of the electronic and structural properties of solid state oxides
[DE93-016051] p 811 N94-14296
A microstructural approach to fatigue crack processes in poly crystalline BCC materials
[DE93-016666] p 812 N94-14354
Homogeneous-hetergeneous combustion: Thermal and chemical coupling
[DE93-016050] p 565 N94-14403
A small-scale turbulence model p 643 N94-14746

MISSISSIPPI STATE UNIV., MISSISSIPPI STATE.
The development of a scalable parallel 3-D CFD algorithm for turbomachinery
[NASA-CR-193604] p 664 N94-14848

MISSISSIPPI STATE UNIV., STATE COLLEGE.
A solution algorithm for the prediction of compressible laminar and turbulent shear flows p 634 N94-13635
MITRE CORP., BEDFORD, MA.
Application of new electro-optic technology to Space Station Freedom data management system
[NASA-CR-177622] p 538 N94-13257
MITSUBISHI ELECTRIC CORP., TOKYO (JAPAN).
Structural design of hexa-link truss deployable antenna p 529 N94-13269
Thermal distortion measurement of TETRUS type thermal test model of large deployable antenna for mobile communications satellite p 529 N94-13270
Trial manufacture model and in-space verification method of deployable antenna p 530 N94-13278
MITSUBISHI HEAVY INDUSTRIES LTD., TOKYO (JAPAN).
HOPE real time flight operations analyses for return to earth phase, part A
[NASDA-CNT-930010-PT-A] p 535 N94-13645
The conceptual study on future space transportation systems. Part A: Conceptual study of flyback booster
[NASDA-CNT-930013] p 536 N94-14099
The concept study of the space transportation system HOPE in FY 1991
[NASDA-CNT-930016] p 536 N94-14100
MITSUBISHI RESEARCH INST., INC., TOKYO (JAPAN).
Mission scenario of HOPE p 537 N94-14279
MITSUBISHI SPACE SOFTWARE CORP. (JAPAN).
Orbit determination error analysis based on the requirements of ADEOS mission
[NASDA-CNT-930008] p 532 N94-13644
MONTREAL UNIV. (QUEBEC).
Double semi-leptonic charm decay in HELIOS-I 450 GeV/c p-Be data
[DE93-013493] p 781 N94-13348
Preparation and characterization of rapidly solidified Al-Li alloys
[ISBN-0-315-58948-5] p 569 N94-13367
MOUND LAB., MIAMISBURG, OH.
Estimation of strain in 1-kW primary containment vessels by microstructural examination
[DE93-013053] p 573 N94-14316

N

NAGOYA UNIV. (JAPAN).
Gas-evaporation in low-gravity field (cogelation mechanism of metal vapors) (M-14) p 588 N94-13746
Endocrine and metabolic changes in payload specialist (L-1) p 591 N94-13758
Neurophysiological study on visuo-vestibular control of posture and movement in fish during adaptation to weightlessness p 591 N94-13759
Comparative measurement of visual stability in Earth and cosmic space (L-4) p 592 N94-13761
How to read a phase equilibrium diagram for high-temperature ceramics material as main object
[DE93-512333] p 582 N94-14513
NAKANIHON AIR SERVICE CO. LTD., AICHI (JAPAN).
Outline of ISY Kuroshio observation experiment p 697 N94-14268
NASTEC, INC., CLEVELAND, OH.
Roller-gear drives for robotic manipulators design, fabrication and test
[NASA-CR-194248] p 660 N94-12802
NATIONAL ACADEMY OF SCIENCES - NATIONAL RESEARCH COUNCIL, WASHINGTON, DC.
Science, technology, and the federal government: National goals for a new era p 827 N94-14115
NATIONAL AERONAUTICAL LAB., BANGALORE (INDIA).
PC based A320 quick access recorder readout facility
[PD-AL-9109] p 744 N94-13077
Proceedings of the Fluid Dynamics Symposium in honour of Professor R. Narasimha on his 60th birthday
[NAL-SP-9315] p 639 N94-14598
A vertex-based finite-volume algorithm for the Navier-Stokes equations p 639 N94-14599
Development of full-potential codes in the decade 1983-1993 p 639 N94-14600
The structure of laminar flow in a three-dimensional driven cavity p 640 N94-14601
A vortex method for viscous unsteady flows p 640 N94-14602
An implicit finite volume nodal point scheme for the solution of two-dimensional compressible Navier-Stokes equations p 640 N94-14603
Wall interference studies: Revisited p 640 N94-14604
Stability of spatially developing boundary layers p 640 N94-14605
Navier-Stokes simulation of transonic vortex flow over a delta wing p 640 N94-14606
A finite volume method for computation of viscous flow in complex configurations p 640 N94-14607
A grid generation package for high aspect ratio wings p 510 N94-14608
The phenomenon of vortex breakdown p 510 N94-14609
Computation of nonequilibrium flows using PNS equations p 641 N94-14610
Development of PC-based Aeronautical Software (AEROWARE) p 641 N94-14611
Hypersonic viscous flow computations p 510 N94-14612
Development of a general purpose multigrid accelerated Navier-Stokes solver p 641 N94-14613
Development of parallel processing at NAL: A retrospect p 641 N94-14614
SRISTI: The NAL method for the design and analysis of Natural Laminar Flow (NLF) airfoils p 516 N94-14615
VSAERO analysis of a Piper Cub aircraft p 516 N94-14616
Panel codes for aerodynamic analysis at NAL p 510 N94-14617
NATIONAL AERONAUTICS AND SPACE ADMINISTRATION, WASHINGTON, DC.
Access to Japanese aerospace-related scientific and technical information: The NASA Aerospace Database
[NASA-TM-109413] p 822 N94-13105
Program/project management resource lists
[NASA-TM-109268] p 822 N94-13107
Building a quality culture in the Office of Space Flight: Approach, lessons learned and implications for the future p 667 N94-13164
George M. Low Trophy: NASA's quality and excellence award. 1992 recipients: Honeywell Clearwater, IBM Houston
[NASA-TM-109265] p 669 N94-13396
NASA aerospace database subject scope: An overview
[NASA-SP-7107] p 823 N94-13401
The four great observatories
[NASA-TM-109311] p 830 N94-13605
New prosthetic devices
[NASA-TM-109304] p 737 N94-13611
Highlights, 1981
[NASA-TM-109305] p 850 N94-13612
Exploring Mars
[NASA-TM-109306] p 842 N94-13613
Recycling in space
[NASA-TM-109307] p 737 N94-13615
Discovery management workshop
[NASA-TM-108244] p 531 N94-14080
TRMM system overview and status in the United States p 690 N94-14221
Space measurements for determining the Earth's energy and water cycles p 690 N94-14227
Future TRMM follow-on mission p 691 N94-14228
My experiences in manned space flight p 698 N94-14276
NASA metrology and calibration, 1993
[NASA-TM-109280] p 597 N94-14410
Large space structures and systems in the space station era: A bibliography with indexes (supplement 05)
[NASA-SP-7085(05)] p 543 N94-14411
Aerospace medicine and biology: A continuing bibliography with indexes (supplement 379)
[NASA-SP-7011(379)] p 733 N94-14412
The problem of traveling in outer space: The rocket motor
[NASA-TT-10002] p 552 N94-14463
NATIONAL AERONAUTICS AND SPACE ADMINISTRATION. AMES RESEARCH CENTER, MOFFETT FIELD, CA.
Kinematics and constraints associated with swashplate blade pitch control
[NASA-TM-102265] p 520 N94-12820
Advancing automation and robotics technology for the Space Station Freedom and for the U.S. economy
[NASA-TM-104024] p 739 N94-12838
Efficient dynamic optimization of logic programs
[NASA-TM-109251] p 761 N94-12889
Artificial intelligence support for scientific model-building
[NASA-TM-109252] p 761 N94-12890
Gender differences in endocrine responses to posture and 7 days of 6 deg head down bed rest
[NASA-TM-103991] p 731 N94-12972
Parallel implementation of an algorithm for Delaunay triangulation
[NASA-TM-103951] p 740 N94-12973
Vertical motion simulator familiarization guide
[NASA-TM-103923] p 527 N94-13008
Reduction and analysis of seasons 15 and 16 (1991 - 1992) Pioneer Venus radio occultation data and correlative studies with observations of the near-infrared emission of Venus
[NASA-CR-194128] p 841 N94-13083
Planetary protection implementation on future Mars lander missions
[NASA-CP-3216] p 841 N94-13183
The NAS parallel benchmarks
[NASA-TM-103863] p 740 N94-13200
Thermal Expert System (TEXSYS): Systems automony demonstration project, volume 1. Overview
[NASA-TM-102877] p 538 N94-13201
Piloting Vertical Flight Aircraft: A Conference on Flying Qualities and Human Factors
[NASA-CP-3220] p 521 N94-13294
Design criteria for integrated flight/propulsion control systems for STOVL fighter aircraft p 521 N94-13297
Improvements in hover display dynamics for a combat helicopter p 523 N94-13310
Visual cueing aids for rotorcraft landings p 524 N94-13313
Visual information for judging temporal range p 524 N94-13314
Visual cueing considerations in Nap-of-the-Earth helicopter flight head-slaved helmet-mounted displays p 524 N94-13315
Piloting considerations for terminal area operations of civil tiltwing and tiltrotor aircraft p 525 N94-13320
Evaluation of two cockpit display concepts for civil tiltrotor instrument operations on steep approaches p 517 N94-13323
Preliminary design features of the RASCAL: A NASA /Army rotorcraft in-flight simulator p 526 N94-13325
Clinical physiology of bed rest
[NASA-TM-104010] p 727 N94-13447
The evolution of energy-transducing systems: Studies with archaebacteria
[NASA-CR-194130] p 728 N94-13562
Airborne Arctic stratospheric expedition: Ozone
[NASA-TM-109312] p 515 N94-13606
Rotor stator CGI
[NASA-TM-109313] p 518 N94-13608
Cray Y-MP
[NASA-TM-109303] p 741 N94-13609
Amphibian fertilization and development in microgravity p 594 N94-13770
Dynamic Forms. Part 1: Functions
[NASA-TP-3397] p 596 N94-13790
Helicopter precision approach capability using the Global Positioning System
[NASA-CR-194037] p 513 N94-13957
Thermal Expert System (TEXSYS): Systems autonomy demonstration project, volume 2. Results
[NASA-TM-102877] p 538 N94-13989
Thermal conductance of pressed metallic contacts augmented with Indium foil or Apiezon-N (tm) grease at liquid helium temperatures
[NASA-TM-108779] p 776 N94-14027
Optimization-based controller design for rotorcraft p 527 N94-14642
The structure of intense vorticity in homogeneous isotropic turbulence p 643 N94-14747
Triad interactions in the dissipation range p 644 N94-14750
Isotropy of small scale turbulence p 644 N94-14752
Rapid distortion analysis and direct simulation of compressible homogeneous turbulence at finite Mach number p 645 N94-14757
Stochastic modeling of turbulent reacting flows p 647 N94-14768
NATIONAL AERONAUTICS AND SPACE ADMINISTRATION. GODDARD SPACE FLIGHT CENTER, GREENBELT, MD.
The evidence for clumpy accretion in the Herbig Ae star HR 5999
[NASA-TM-108257] p 828 N94-12915
NASA/contractor partnership on the second TDRSS ground terminal program: Breaking barriers p 668 N94-13168
Government/contractor partnerships for continuous improvement. A Goddard Space Flight Center example p 669 N94-13169
NASA handbook for nickel-hydrogen batteries
[NASA-RP-1314] p 550 N94-13265
The International Colloquium on Atomic Spectra and Oscillator Strengths for Astrophysical and Laboratory Plasmas
[NASA-TM-109255] p 849 N94-13376
Arctic ozone expedition
[NASA-TM-109301] p 708 N94-13602
Goddard Space Flight Center robotics demo
[NASA-TM-109302] p 662 N94-13604
NASA experiences in the Goddard MMS
[NASA-TM-109290] p 819 N94-13629

ADP study of gamma-ray bursts
[NASA-CR-194311] p 848 N94-13708
Mongoose ASIC microcontroller programming guide
[NASA-RP-1319] p 623 N94-13871
Phase aligner for the Electronically Scanned Thinned Array Radiometer (ESTAR) instrument
[NASA-TM-4518] p 623 N94-13878
Simultaneous solution for core magnetic field and fluid flow beneath an electrically conducting mantle
[NASA-TM-4536] p 716 N94-13960
Nimbus-7 Earth radiation budget calibration history. Part 1: The solar channels
[NASA-RP-1316] p 844 N94-13963
Circulation and rainfall climatology of a 10-year (1979 - 1988) integration with the Goddard Laboratory for atmospheres general circulation model
[NASA-TM-104591] p 723 N94-14074
Volume 14: The first SeaWiFS intercalibration round-robin experiment, SIRREX-1, July 1992
[NASA-TM-104566] p 725 N94-14090
ASTEC and MODEL: Controls software development at Goddard Space Flight Center p 678 N94-14628
The 1991 research and technology report, Goddard Space Flight Center
[NASA-TM-108738] p 851 N94-14791

NATIONAL AERONAUTICS AND SPACE ADMINISTRATION. HUGH L. DRYDEN FLIGHT RESEARCH CENTER, EDWARDS, CA.

Recent flight-test results of optical airdata techniques
[NASA-TM-4504] p 517 N94-13791

NATIONAL AERONAUTICS AND SPACE ADMINISTRATION. HUGH L. DRYDEN FLIGHT RESEARCH FACILITY, EDWARDS, CA.

Preliminary flight results of a fly-by-throttle emergency flight control system on an F-15 airplane
[NASA-TM-4503] p 520 N94-13254
Actuator and aerodynamic modeling for high-angle-of-attack aeroservoelasticity
[NASA-TM-4493] p 520 N94-13255
Perspective on the National Aero-Space Plane Program instrumentation development
[NASA-TM-4505] p 516 N94-13256
Flight operations highlights, tapes 1 and 2
[NASA-TM-109293] p 850 N94-13633
The development and flight test of a deployable precision landing system for spacecraft recovery
[NASA-TM-4525] p 537 N94-14853
Performance seeking control: Program overview and future directions
[NASA-TM-4531] p 519 N94-14855

NATIONAL AERONAUTICS AND SPACE ADMINISTRATION. JOHN C. STENNIS SPACE CENTER, BAY SAINT LOUIS, MS.

Here's the beef: A case study in organizational transformation p 667 N94-13163
SSME testing at Stennis Space Center
[NASA-TM-109310] p 552 N94-13617
Taecannautics: Sharing the dream
[NASA-TM-109309] p 818 N94-13619

NATIONAL AERONAUTICS AND SPACE ADMINISTRATION. JOHN F. KENNEDY SPACE CENTER, COCOA BEACH, FL.

Procedures for analysis of debris relative to Space Shuttle systems
[NASA-TM-109190] p 534 N94-12900
Validated environmental and physiological data from the CELSS Breadboard Projects Biomass Production Chamber. BWT931 (Wheat cv. Yecora Rojo)
[NASA-TM-109272] p 738 N94-13979

NATIONAL AERONAUTICS AND SPACE ADMINISTRATION. LYNDON B. JOHNSON SPACE CENTER, HOUSTON, TX.

Medical evaluations on the KC-135 1991 flight report summary
[NASA-TM-104755] p 731 N94-12832
Defining the performance gap: Conducting a self-assessment p 666 N94-13155
Strategic planning as a focus for continuous improvement. A case study p 666 N94-13158
NASA Johnson Space Center: Total quality partnership p 668 N94-13165
Shared visions: Partnership of Rockwell International and NASA Cost Effectiveness Enhancements (CEE) for the space shuttle system integration program p 668 N94-13166
Analysis of differences between seating positions in simulators and orbiters
[NASA-TM-104776] p 737 N94-13399
User observations on information sharing (corporate knowledge and lessons learned)
[NASA-TM-104781] p 819 N94-13400
STS-30 Magellan IUS/EVA training in WETF
[NASA-TM-109300] p 737 N94-13601
STS-32 mission highlights resource tape
[NASA-TM-109291] p 531 N94-13631
STS-32 post-flight press conference
[NASA-TM-109294] p 541 N94-13634
Six degree of freedom
[NASA-TM-109295] p 749 N94-13636
High velocity gas gun
[NASA-TM-109296] p 541 N94-13637
Launch, entry, and landing resource clip
[NASA-TM-109297] p 535 N94-13638
STS-28 crew presentation clip
[NASA-TM-109298] p 531 N94-13640
STS-29 post-insertion/deorbit prep and crew bailout
[NASA-TM-109299] p 535 N94-13641
Countermeasure for reducing post-flight orthostatic intolerance: Lower Body Negative Pressure (LBNP) experiment E140 p 594 N94-13772
Autogenic feedback training experiment: A preventative method for space motion sickness p 595 N94-13774
In-flight demonstration of the Space Station Freedom Health Maintenance Facility fluid therapy system (E300/E05) p 595 N94-13775
An evaluation of noise and its effects on shuttle crewmembers during STS-50/USML-1
[NASA-TM-104775] p 735 N94-13961
Variability of prediction of maximal oxygen concumption on the cycle ergometer using standard equations
[NASA-TP-3412] p 729 N94-14032
Impact melting and vaporization in planetary regoliths p 843 N94-14299
Deposition of impact-generated vapors in the lunar regolith p 843 N94-14302
The Eighth Annual NASA/Contractors Conference and 1991 National Symposium on Quality and Productivity: Extending the boundaries of total quality management
[NASA-TM-109276] p 669 N94-14321
Computational Control Workstation: Users' perspectives p 681 N94-14648
STS-33 launch and landing clip
[NASA-TM-109468] p 536 N94-14734
STS-35 crew trash compactor briefing
[NASA-TM-109487] p 533 N94-14735
STS-35 post-flight press conference
[NASA-TM-109490] p 537 N94-14736
STS-35 integrated sim in SMS and MOCR
[NASA-TM-109491] p 533 N94-14787
STS-35 EVA payload training in WETF
[NASA-TM-109492] p 739 N94-14790

NATIONAL AERONAUTICS AND SPACE ADMINISTRATION. LANGLEY RESEARCH CENTER, HAMPTON, VA.

The MRIS feasibility study
[NASA-TM-107763] p 597 N94-12804
The 24 GHz measurements of 2.2 lambda conical horn antennas illuminating a conducting sheet
[NASA-TM-109002] p 598 N94-12811
A method of predicting quasi-steady aerodynamics for flutter analysis of high speed vehicles using steady CFD calculations
[NASA-TM-109009] p 514 N94-12850
Effects of radiobiological uncertainty on vehicle and habitat shield design for missions to the moon and Mars
[NASA-TP-3312] p 846 N94-12875
Approaches to high aspect ratio triangulations
[NASA-TM-107684] p 739 N94-12886
NASA/DOD Aerospace Knowledge Diffusion Research Project. Report 18: A comparison of the technical communication practices of aerospace engineers and scientists in India and the United States
[NASA-TM-109006] p 821 N94-13057
Aerodynamics of a sphere and an oblate spheroid for Mach numbers from 0.6 to 10.5 including some effects of test conditions
[NASA-TM-109016] p 500 N94-13172
An experimental investigation of mixing enhancement in a simulated scramjet combustor by use of swirling jets
[NASA-TM-109246] p 518 N94-13190
A robust multilevel simultaneous eigenvalue solver
[NASA-CR-191491] p 767 N94-13202
Semiempirical fragmentation models on galactic cosmic ray transport calculations with hydrogen target
[NASA-TP-3350] p 847 N94-13263
A hardware implementation of a provably correct design of a fault-tolerant clock synchronization circuit
[NASA-TM-109001] p 759 N94-13450
A priori error estimates for an hp-version of the discontinuous Galerkin method for hyperbolic conservation laws
[NASA-TM-108993] p 632 N94-13467
Scout: The unsung hero of space
[NASA-TM-109289] p 540 N94-13628
HL-20 personnel launch system
[NASA-TM-109292] p 504 N94-13632
Functional categories for future flight deck designs
[NASA-TM-109005] p 517 N94-13710
Testing and analysis of curved frame specimens made from a Long Discontinuous Fiber (LDF) material
[NASA-TM-109014] p 557 N94-13711
Cellular track model for study of heavy ion beams
[NASA-TP-3351] p 732 N94-13714
Preconditioning and the limit to the incompressible flow equations
[NASA-CR-191500] p 769 N94-13717
Development of a recursion RNG-based turbulence model
[NASA-CR-191511] p 636 N94-13718
Analysis of microstrip patch antennas with nonzero surface resistance
[NASA-TP-3362] p 604 N94-13916
Research and technologhy highlights, 1992
[NASA-TM-4452] p 850 N94-13962
Clouds and the Earth's Radiant Energy System (CERES) on the Tropical Rainfall Measuring Mission (TRMM) p 690 N94-14223
Space-based activities: SAM 2 and SAGE 2 p 694 N94-14252
Room temperature degradation of YBa2Cu3O(7-x) superconductors in varying relative humidity environments
[NASA-TP-3368] p 813 N94-14409
Active control of fan-generated plane wave noise
[NASA-TM-109008] p 777 N94-14481
NASA/DOD Aerospace Knowledge Diffusion Research Project. Paper 34: Users and uses of DOD technical reports: A report from the field
[NASA-TM-109327] p 825 N94-14485
NASA/DOD Aerospace Knowledge Diffusion Research Project. Paper 36: Technical uncertainty as a correlate of information use by US industry-affiliated aerospace engineers and scientists
[NASA-TM-109328] p 825 N94-14486
NASA/DOD Aerospace Knowledge Diffusion Research Project. Paper 39: The role of computer networks in aerospace engineering
[NASA-TM-109331] p 825 N94-14487
NASA/DOD Aerospace Knowledge Diffusion Research Project. Paper 37: The impact of political control on technical communications: A comparative study of Russian and US aerospace engineers and scientists
[NASA-TM-109329] p 826 N94-14488
NASA/DOD Aerospace Knowledge Diffusion Research Project. Paper 38: Computer Mediated Communication (CMC) and the communication of technical information in aerospace
[NASA-TM-109330] p 826 N94-14489
Relativistic proton-nucleus scattering and one-boson-exchange models p 786 N94-14550
Theoretical antideuteron-nucleus absorptive cross sections p 786 N94-14551
Some experiences with Krylov vectors and Lanczos vectors p 677 N94-14621
Vibrational relaxation in hypersonic flow fields
[NASA-TP-3367] p 776 N94-14733
Materials and structures p 546 N94-14835

NATIONAL AERONAUTICS AND SPACE ADMINISTRATION. LEWIS RESEARCH CENTER, CLEVELAND, OH.

Solar dynamic power system development for Space Station Freedom
[NASA-RP-1310] p 548 N94-12807
A vacuum four-ball tribometer to evaluate liquid lubricants for space applications
[NASA-TM-106264] p 575 N94-12842
Ohmic heating of composite candidate graphite-fiber/coating combinations
[NASA-TM-4491] p 554 N94-12871
On curve veering and flutter of rotating blades
[NASA-TM-106282] p 670 N94-12872
Strain sensing technology for high temperature applications
[NASA-TM-4498] p 648 N94-12874
An analytical investigation of transient effects on rewetting of heated thin flat plates
[NASA-TM-106120] p 628 N94-12968
Two-dimensional Navier-Stokes heat transfer analysis for rough turbine blades
[NASA-TM-106008] p 629 N94-13027
TROPIX: A solar electric propulsion flight experiment
[NASA-TM-106297] p 534 N94-13028
Micromechanical modeling of laminated composites with interfaces and woven composites using the boundary element method
[NASA-TM-106280] p 670 N94-13053
Quantitative mapping of pore fraction variations in silicon nitride using an ultrasonic contact scan technique
[NASA-TP-3377] p 665 N94-13056
Averaging techniques for steady and unsteady calculations of a transonic fan stage
[NASA-TM-106231] p 499 N94-13108
Low-current traveling wave tube for use in the microwave power module
[NASA-TP-3344] p 620 N94-13110

Destination-directed, packet-switched architecture for a geostationary communications satellite network
[NASA-TP-3379] p 538 N94-13111
Screening of solar cells
[NASA-TM-106298] p 620 N94-13134
A survey and analysis of experimental hydrogen sensors
[NASA-TM-106300] p 648 N94-13135
NDE of titanium alloy MMC rings for gas turbine engines
[NASA-TM-106188] p 555 N94-13138
Combustor technology for future small gas turbine aircraft
[NASA-TM-106312] p 517 N94-13142
Analysis of gas turbine engines using water and oxygen injection to achieve high Mach numbers and high thrust
[NASA-TM-106270] p 518 N94-13143
A photovoltaic catenary-tent array for the Martian surface
[NASA-TM-106306] p 621 N94-13194
A probabilistic method for the buckling assessment of stiffened composite shells
[NASA-TM-106286] p 671 N94-13379
A multiple-scale turbulence model for incompressible flow
[NASA-TM-106113] p 631 N94-13385
Recent testing of 30 kW hydrogen arcjet thrusters
[NASA-TM-106214] p 551 N94-13430
A future view of computational science in aircraft
[NASA-TM-109284] p 504 N94-13621
Futurepath 2
[NASA-TM-109285] p 518 N94-13623
Low thrust space propulsion
[NASA-TM-109286] p 552 N94-13625
NASA images 11
[NASA-TM-109287] p 842 N94-13626
Microgravity acceleration measurement environment characterization p 590 N94-13755
Tomographic methods in flow diagnostics
[NASA-TM-106330] p 650 N94-13876
Interactions between spacecraft and their environments
[NASA-TM-106115] p 541 N94-13917
SCAILET: An intelligent assistant for satellite ground terminal operations
[NASA-TM-105879] p 538 N94-13918
Elastic-plastic mixed-iterative finite element analysis: Implementation and performance assessment
[NASA-TM-106164] p 675 N94-13919
Noise levels from a model turbofan engine with simulated noise control measures applied
[NASA-TM-106318] p 518 N94-14036
Hierarchical nonlinear behavior of hot composite structures
[NASA-TM-106229] p 676 N94-14041
Optimal synthesis of hot composite laminates with interphase layers
[NASA-TM-106326] p 557 N94-14042
Computer program for thermal and transport properties of parahydrogen from 20 to 10,000 K
[NASA-TP-3378] p 552 N94-14102
Mixing noise reduction for rectangular supersonic jets by nozzle shaping and induced screech mixing
[NASA-TM-106364] p 508 N94-14208
Least-squares finite element solutions for three-dimensional backward-facing step flow
[NASA-TM-106353] p 770 N94-14407
Transform coding for space applications
[NASA-TM-106362] p 612 N94-14542
Advanced Communications Technology Satellite (ACTS) program: ACTS project update p 615 N94-14673
Elastic-plastic finite element analyses of an unidirectional, 9 vol percent tungsten fiber reinforced copper matrix composite
[NASA-TM-106304] p 559 N94-14719
Numerical study of shock-induced combustion in methane-air mixtures
[NASA-TM-106354] p 642 N94-14722
Plasma contactor technology for Space Station Freedom
[NASA-TM-106291] p 553 N94-14725
Derated ion thruster development status
[NASA-TM-106292] p 553 N94-14726
A hot dynamic seal rig for measuring hypersonic engine seal durability and flow performance
[NASA-TM-106294] p 664 N94-14727
Development of an explicit multiblock/multigrid flow solver for viscous flows in complex geometries
[NASA-TM-106356] p 642 N94-14728
Linear instability of curved free shear layers
[NASA-TM-106290] p 642 N94-14729
Solar radiation on Mars: Stationary photovoltaic array
[NASA-TM-106321] p 626 N94-14730
Analysis, approximation, and computation of a coupled solid/fluid temperature control problem
[NASA-TM-106351] p 771 N94-14731
A study of thin liquid sheet flows
[NASA-TM-106323] p 642 N94-14732
A transport equation for eddy viscosity p 646 N94-14762
Buckling analysis of laminated thin shells in a hot environment
[NASA-TM-106302] p 683 N94-14776
Interaction of two glancing, crossing shock waves with a turbulent boundary-layer at various Mach numbers
[NASA-TM-103740] p 509 N94-14780
NASA images 8
[NASA-TM-109416] p 544 N94-14783
Thermoelastic response of metal matrix composites with large-diameter fibers subjected to thermal gradients
[NASA-TM-106344] p 560 N94-14823
Thermal history effects on electrical relaxation and conductivity for potassium silicate glass with low alkali concentrations
[NASA-TM-106324] p 583 N94-14845
A new Lagrangian method for three-dimensional steady supersonic flows
[NASA-TM-106068] p 510 N94-14847

NATIONAL AERONAUTICS AND SPACE ADMINISTRATION. MARSHALL SPACE FLIGHT CENTER, HUNTSVILLE, AL.

Structural design/margin assessment
[NASA-TP-3410] p 669 N94-12831
Electrical Actuation Technology Bridging
[NASA-CP-3213] p 551 N94-13417
Mid-deck experiments, STS-26
[NASA-TM-109308] p 570 N94-13616
CRRES to blaze new trails in orbit
[NASA-TM-109314] p 713 N94-13620
Microstructural evolution of NARloy-Z at elevated temperatures
[NASA-TM-108419] p 571 N94-13715
Spacelab J experiment descriptions
[NASA-TM-4517] p 586 N94-13732
Optimization of the processing parameters of high temperature superconducting glass-ceramics: Center Director's discretionary fund final report
[NASA-TM-108421] p 808 N94-13938
Control system design for flexible structures using data models p 527 N94-14646
A program for the investigation of the Multibody Modeling, Verification, and Control Laboratory p 682 N94-14652
Terrestrial environment (climatic) criteria guidelines for use in aerospace vehicle development, 1993 revision
[NASA-TM-4511] p 533 N94-14824
Fabrication p 546 N94-14834
Optical testing p 547 N94-14836
Advanced optical instruments technology p 547 N94-14838

NATIONAL AERONAUTICS AND SPACE ADMINISTRATION. WALLOPS FLIGHT FACILITY, WALLOPS ISLAND, VA.

NASA airborne satellite instrumentation calibrator (NASIC) technical reference
[NASA-RP-1315] p 545 N94-13713
Birds of Wallops Island, Virginia, 1970 - 1992
[NASA-TM-104589] p 850 N94-13923

NATIONAL AEROSPACE LAB., AMSTERDAM (NETHERLANDS).

Modern aluminium sheet alloys for aerospace applications
[NLR-TP-92057-U] p 570 N94-13497
Future developments of the NLR research flight simulator
[NLR-TP-92143-U] p 528 N94-13498
Photogrammetric methods for trajectory measurements
[NLR-TP-91166-U] p 650 N94-13527
On the use of the method of matched asymptotic expansions in propeller aerodynamics and acoustics
[NLR-TP-91307-U] p 503 N94-13528
Reasoning with uncertain and incomplete information in aerospace applications
[NLR-TP-91366-U] p 763 N94-13529
Clebsch variable model for unsteady, transonic flow; application to 2D airfoils
[NLR-TP-91387-U] p 503 N94-13530
A robust quasi-simultaneous interaction method for a full potential flow with a boundary layer with application to wing/body configurations
[NLR-TP-91397-U] p 503 N94-13531
The ASCOR test: A simple automated method for stress corrosion testing of aluminium alloys
[NLR-TP-91438-U] p 570 N94-13532
Thermal gravitational modelling and scaling of two-phase heat transport systems: Similarity considerations and useful equations predictions versus experimental results
[NLR-TP-91477-U] p 632 N94-13533
Performance of gas turbine compressor cleaners
[NLR-TP-91291-U] p 519 N94-14450

NATIONAL AEROSPACE LAB., KAKUDA (JAPAN).

Effects of hydrogen addition on combustion performance of a LOX/kerosene rocket
[NAL-TR-1177] p 548 N94-12945
Chemical reactions in scramjet engines: Reduced kinetic models for ignition, combustion and nozzle flow
[NAL-TR-1184] p 563 N94-13458
Tensile properties of LE-7 engine material with welded joint
[NAL-TR-1188] p 570 N94-13460

NATIONAL AEROSPACE LAB., TOKYO (JAPAN).

An experimental study of tether reel system: A laboratory model
[NAL-TR-1176T] p 539 N94-12943
Numerical simulation of hypersonic flow for the design of the H-2 orbiting plane (HOPE), part 3
[NAL-TR-1168-PT-3] p 499 N94-12948
Identifying the NAL spaceplane aerodynamic model using dynamic wind tunnel tests
[NAL-TR-1171] p 500 N94-12951
Control system design of a cable-mounted model used for dynamic wind tunnel testing
[NAL-TR-1161] p 528 N94-13337
Development of an on-board aircraft optical fiber data bus system
[NAL-TR-1163] p 514 N94-13338
Transmission zeros of spacecraft attitude control system
[NAL-TR-1166] p 540 N94-13339
Low-speed wind tunnel tests on four types of joined-wing aircraft models
[NAL-TR-1167] p 501 N94-13340
Low-speed wind tunnel tests on a joined-wing aircraft model with various upper-fin
[NAL-TR-1169] p 501 N94-13341
Development of a high-speed mechanical drive system for oscillating an annular blade row in the bending mode
[NAL-TR-1170] p 502 N94-13342
Calculation of the required sensor accuracy to obtain a specified state estimation accuracy
[NAL-TR-1173] p 649 N94-13343
Flight evaluations of approach/landing navigation sensor systems: Summary of 1990 flight experiments
[NAL-TR-1175] p 513 N94-13344
Estimation of critical values and vibration characteristics on supersonic delta wings. Part 2: Locally-stationary time series analysis of nonstationary random responses
[NAL-TR-1179] p 502 N94-13345
Performance evaluation tests of the GPS/DGPS navigation system installed in the NAL Dornier 228: Preliminary ground test results
[NAL-TM-649] p 513 N94-13346
Rolling moment control in the NAL 10 cm x 10 cm magnetic suspension and balance system
[NAL-TR-1164] p 526 N94-13347
Evaluation for membrane components of water recycling system
[NAL-TM-646] p 737 N94-13388
Estimation of aircraft aerodynamic derivatives with the Total Least Squares Method
[NAL-TR-1150] p 502 N94-13392
Position error determination for the speedometer and altimeter of the NAL QSTOL experimental aircraft ASKA
[NAL-TR-1144] p 517 N94-13451
Some flow properties of telescope enclosures estimated from water channel tests: Application of the flow visualization techniques
[NAL-TR-1178T] p 830 N94-13452
Analysis and effects of the number of nests of DO loops during vector supercomputing
[NAL-TR-1146] p 748 N94-13453
Experimental studies of vortex flaps and vortex plates. Part 2: 1.15m span 60 deg delta wing
[NAL-TR-1180T-PT-2] p 502 N94-13454
Arc-heating tests of thermal protection system materials for the H-2 rocket fairing
[NAL-TR-1181] p 551 N94-13455
Kalman filter input estimation
[NAL-TR-1182] p 649 N94-13456
Flight path control for the approach and landing of the quiet STOL experimental aircraft ASKA
[NAL-TR-1183] p 513 N94-13457
Hypersonic aerodynamic characteristics of SSTO-type aerospace planes. Part 1: The NAL 0-th configuration
[NAL-TR-1186] p 514 N94-13459
Drop dynamics in space and interference with acoustic field (M-15) p 588 N94-13747
Study of bubble behavior in weightlessness (effects of thermal gradient and acoustic stationary wave) (M-16) p 589 N94-13748
Manual control in space research on perceptual-motor functions under zero gravity conditions (L-10) p 593 N94-13767
Experimental studies of vortex flaps and vortex plates. Part 1: 0.53 m span 60 deg delta wing
[DE93-767969] p 505 N94-14059

Numerical simulation of dynamic stall of NACA0012 airfoil oscillating near static stall angle using the Navier-Stokes equations
[DE93-767970] p 505 N94-14061
Spaceplane program at NAL: System concept and related technology issues p 537 N94-14281

NATIONAL AIR AND SPACE MUSEUM, WASHINGTON, DC.
The nature and origin of periodically spaced tectonic features on Mars
[NASA-CR-193821] p 842 N94-13199

NATIONAL BOARD OF WATERS AND THE ENVIRONMENT, HELSINKI (FINLAND).
Snow cover models in operational watershed forecasting
[DE93-778332] p 718 N94-12837

NATIONAL CENTER FOR ATMOSPHERIC RESEARCH, BOULDER, CO.
Vacuum ultraviolet instrumentation for solar irradiance and thermospheric airglow
[NASA-CR-194525] p 652 N94-14684

NATIONAL DEFENCE HEADQUARTERS, OTTAWA (ONTARIO).
Electrochemical noise in lithium primary cells
[DSIS-93-00236] p 623 N94-13846
Statistical analysis of the m rankings problem: Kendall's prototype and the grouping estimate method based on normal scores
[DSIS-93-00139] p 773 N94-13848

NATIONAL DEFENCE RESEARCH ESTABLISHMENT, UMEA (SWEDEN).
The surface-located YopN protein is involved in calcium signal transduction in Yersinia pseudotuberculosis
[FOA-B-40416-4.4] p 729 N94-14128
Analysis of the V antigen lcrGVH-yopBD operon of Yersinia pseudotuberculosis: Evidence for a regulatory role of LcrH and LcrV
[FOA-B-40417-4.4] p 729 N94-14129

NATIONAL FERTILIZER DEVELOPMENT CENTER, MUSCLE SHOALS, AL.
Environmental awareness
[DE93-014192] p 707 N94-13218

NATIONAL GEOPHYSICAL DATA CENTER, BOULDER, CO.
Solar-geophysical data number 584, April 1993. Part 1: (Prompt reports). Data for March, February 1993, and late data
[PB93-198323] p 845 N94-14560
Solar-geophysical data number 584, April 1993. Part 2: (Comprehensive reports). Data for October 1992 and miscellaneous
[PB93-198331] p 845 N94-14561

NATIONAL INST. FOR ENVIRONMENTAL STUDIES, TSUKUBA (JAPAN).
Spectroscopic method and data reduction algorithm for laser long-path absorption measurements using RIS p 689 N94-14218
Overview of the ILAS operational data processing system p 690 N94-14220

NATIONAL INST. FOR RESEARCH IN INORGANIC MATERIALS, TOKYO (JAPAN).
Growth of samarskite crystal under microgravity conditions (M-20) p 590 N94-13752

NATIONAL INST. FOR RESOURCES AND ENVIRONMENT, IBARAKI (JAPAN).
IMG: Interferometric monitor for greenhouse gases p 689 N94-14217

NATIONAL INST. OF AGRO-ENVIRONMENTAL SCIENCE, IBARAKI (JAPAN).
Land evaluation for agricultural productivity in North-East Thailand using LANDSAT TM data and geographic information p 693 N94-14242
Estimation of vegetation damage due to ash fall in Mt. Pinatubo area using MOS-1 data p 695 N94-14259

NATIONAL INST. OF STANDARDS AND TECHNOLOGY, BOULDER, CO.
Shielded open-circuited sample holders for dielectric and magnetic measurements of liquids and powders
[PB93-198851] p 652 N94-14687

NATIONAL INST. OF STANDARDS AND TECHNOLOGY, GAITHERSBURG, MD.
Ultra-soft x ray absorption spectroscopy: A bulk and surface probe of materials
[DE93-014325] p 566 N94-14582

NATIONAL LAB. FOR HIGH ENERGY PHYSICS, IBARAKI (JAPAN).
Workshop on Formation of Supermolecular Structures in Composite Fluid: Phase Rule and Dynamics
[DE93-782887] p 581 N94-14421

NATIONAL OCEANIC AND ATMOSPHERIC ADMINISTRATION, BOULDER, CO.
Radiometric observations of atmospheric attenuation at 20.6 and 31.65 GHz: The Wave Propagation Laboratory data base p 613 N94-14660

NATIONAL OCEANIC AND ATMOSPHERIC ADMINISTRATION, OAK RIDGE, TN.
Atmospheric turbulence and diffusion research
[DE93-011842] p 718 N94-14425

NATIONAL OCEANIC AND ATMOSPHERIC ADMINISTRATION, WASHINGTON, DC.
Degradation of the visible and near-infrared channels of the advanced very high resolution radiometer on the NOAA-9 spacecraft: Assessment and recommendations for corrections
[NOAA-TR-NESDIS-70] p 544 N94-13029
Climate products from NOAA operational satellites p 691 N94-14231
Earth radiation budget, cloud, and aerosol parameters derived from AVHRR and TOVS measurements p 691 N94-14233
The development and implementation of an interactive retrieval/analysis/forecast algorithm p 692 N94-14234
Summary of the NOAA/NESDIS Workshop on Development of a Global Satellite/In Situ Environmental Database
[NOAA-TR-NESDIS-72] p 826 N94-14498

NATIONAL OPTICS INST., STE-FOY (QUEBEC).
Study of speckle reduction when using a CO2 waveguide laser close to its threshold state
[DSIS-93-00250] p 657 N94-14067

NATIONAL PHYSICAL LAB., TEDDINGTON (ENGLAND).
UK interlaboratory tensile tests on Al alloy/SiC particulate metal matrix composites
[NPL-DMM(A)-77] p 570 N94-13666
Stability of reference masses 1: Evidence for posiible variations in the mass of reference kilograms arising from mercury contamination
[NPL-DMM(A)-86] p 708 N94-13667
Specimen files in VAMAS standard data transfer format (EXAMPLE 1.TXT to EXAMPLE 4.TXT)
[NPL-DMM(A)-90] p 749 N94-13688
The design of chain links and slings
[NPL-DMM(A)-94] p 662 N94-13808
Security clauses in the writing and analysis of standards
[NPL-DITC-216-93] p 824 N94-13879
Environmental radioactivity intercomparison 1992
[NPL-RSA(EXT)-37] p 708 N94-13880
Measurement of the Fe-56(n,p)Mn-56, Al-27(n,p)Mg-27 and Al-27(n,alpha)Na-24 cross sections at 16.0, 17.0 and 18.3 MeV
[NPL-RSA(EXT)-38] p 783 N94-13883
An experimental assessment of the use of ground-level microphones to measure the fly-over noise of jet-engined aircraft
[NPL-RSA(EXT)-0039] p 777 N94-13885
A conduction model for the vacuum arc remelting process
[NPL-DMM(A)-98] p 639 N94-14464

NATIONAL RESEARCH COUNCIL OF CANADA, OTTAWA (ONTARIO).
ADS-33C related handling qualities research performed using the NRC Bell 205 airborne simulator p 521 N94-13295
Artificial intelligence in Canada: A description by the members of the ACAI
[NRC-31789] p 763 N94-13517
Collection and analysis of dialogue protocols for the question-answering facility of the entity-relationship modeling advisor
[ERB-1032] p 740 N94-13546
Mass market computers for software development
[ERB-1035] p 741 N94-13547
Effect of stabilization on the recycling of polyolefins in blow moulding
[IMI-93RT-42400-1477-G] p 596 N94-13684
Artificial intelligence in Canada: A description by the members of the ACAI
[CNR-31790] p 764 N94-13820
A distributed, visual object system using aggregation objects with a local namespace
[IME-MET-TR-007] p 764 N94-13860
Potential flow in in-line and staggered tube banks
[IME-CRE-TR-006] p 637 N94-13862
Activities of Institute for Information Technology
[CNR-35024] p 824 N94-14069
An experimental study on the effect of die geometry on swell and sag in the parison extrusion stage
[IMI-93RT-42400-1476-G] p 597 N94-14070
Canadian Target Assembly (CTA) to Airborne Support Equipment (ASE) vibration test report
[IME-AMT-TR-001] p 663 N94-14195
An expert system class library for Audition
[IME-MET-TR-008] p 824 N94-14196
Activities of Institute for Microstructural Sciences
[NRC-32815] p 810 N94-14198
Activities of Institute for Microstructural Sciences
[CNR-32815] p 810 N94-14199
Discrete event simulation using object-oriented programming: Application to manufacturing
[ERB-1037] p 753 N94-14200
The BIRIS server: Integration of a three-dimensional range sensor into a harmony-based realtime architecture
[ERB-1036] p 765 N94-14201
An evaluation of ZIM and entity-relational models in managing databases for decision support systems
[ERB-1034] p 824 N94-14202

NATIONAL RESEARCH INST. FOR METALS, TOKYO (JAPAN).
Growth of semiconductor compound single crystal InSb by floating zone method (M-3) p 586 N94-13735
Formation of deoxidization products in iron ingot by the addition of Al, Si, and/or Mn (M-5) p 587 N94-13737
Preparation of particle-dispersion alloys (M-6) p 587 N94-13738
Diffusion in liquid state and solidification of binary system (M-7) p 587 N94-13739

NATIONAL RESEARCH INST. FOR METALS, TSUKUBA (JAPAN).
Casting of superconducting composite materials (M-4) p 586 N94-13736

NATIONAL SCIENCE FOUNDATION, WASHINGTON, DC.
Selected data on academic science and engineering R and D expenditures: Fiscal Year 1991
[NSF-92-329] p 819 N94-13982
Scientists, engineers, and technicians in nonmanufacturing industries: 1990. Detailed statistical tables
[NSF-92-334] p 820 N94-14499

NATIONAL SPACE DEVELOPMENT AGENCY, IBARAKI (JAPAN).
The Second Workshop on Deployment and Assembly Experiment of Large Space Structure on Orbit
[NASDA-CON-930003] p 529 N94-13268
The study on large space structure assembly technology: The study on deployable truss structure, part 1
[NASDA-TMR-930002] p 541 N94-13658
The study on large space structure assembly technology: The study on deployable truss structure, part 2 and 3
[NASDA-TMR-930003-PT-2-3] p 541 N94-13659
The study on test of docking mechanism system, part 1 and 2
[NASDA-TMR-930004-PT-1-2] p 541 N94-13660

NATIONAL SPACE DEVELOPMENT AGENCY, OHASHI (JAPAN).
Outline of ISY Kuroshio observation experiment p 697 N94-14268

NATIONAL SPACE DEVELOPMENT AGENCY, SAITAMA (JAPAN).
Earth Observation Center Annual Report on Research and Development, Fiscal Year 1992
[EOC-92-01-0007] p 687 N94-14091
Calibration and in-house validation results of JERS-1 data p 687 N94-14092
Earth observation experiment data analysis p 687 N94-14093
ADEOS project p 687 N94-14094

NATIONAL SPACE DEVELOPMENT AGENCY, TOKYO (JAPAN).
Numerical simulation of hypersonic flow for the design of the H-2 orbiting plane (HOPE), part 3
[NAL-TR-1168-PT-3] p 499 N94-12948
Research on radiation resistance properties of structural materials for space use p 529 N94-13271
A concept on on-orbit experiments of deployable structures utilizing JEM/HOPE p 531 N94-13279
Flight evaluations of approach/landing navigation sensor systems: Summary of 1990 flight experiments
[NAL-TR-1175] p 513 N94-13344
Health monitoring of Japanese payload specialist: Autonomic nervous and cardiovascular responses under reduced gravity condition (L-0) p 591 N94-13757
Study on the biological effect of cosmic radiation and the development of radiation protection technology (L-11) p 593 N94-13768
Asia-Pacific ISY Conference, volume 2
[NASDA-CM-199-VOL-2] p 688 N94-14209
Sensor operation of Advanced Earth Observing Satellite (ADEOS) p 689 N94-14215
TRMM Project in Japan: Overview and status p 690 N94-14222

NATURAL ENVIRONMENTAL RESEARCH COUNCIL, SWINDON (ENGLAND).
The European Arctic ozone experiment: An investigation of Northern Hemisphere ozone depletion p 694 N94-14251

NAVAL AEROSPACE MEDICAL RESEARCH LAB., PENSACOLA, FL.
Work/rest schedules and performance of S-3 aviators during fleet exercise
[AD-A265807] p 734 N94-12975

Work/rest schedules and performance of F/A-18 aviators during Fleet Exercise 1992
[AD-A265826] p 735 N94-12982

NAVAL AIR WARFARE CENTER, WARMINSTER, PA.
MIL-H-8501B: Application to shipboard terminal operations p 521 N94-13296
Primary display latency criteria based on flying qualities and performance data p 525 N94-13318

NAVAL CIVIL ENGINEERING LAB., PORT HUENEME, CA.
Nonlinear wave forces on large ocean structures
[AD-A266820] p 683 N94-14902

NAVAL COMMAND, CONTROL AND OCEAN SURVEILLANCE CENTER, SAN DIEGO, CA.
Laser-induced fluorescence over optical fibers for real time in situ measurement of petroleum hydrocarbons in seawater
[AD-A265106] p 790 N94-12863
An analog clustering network from a biological model
[AD-A265637] p 762 N94-12969
Advanced display object selection methods for enhancing user-computer productivity
[AD-A265806] p 743 N94-12974
Determining neural network connectivity using evolutionary programming
[AD-A266853] p 766 N94-14882

NAVAL MEDICAL RESEARCH INST., BETHESDA, MD.
Thyroid alterations in porcine after prolonged exposure to cold or heat
[AD-A266840] p 733 N94-14879

NAVAL RESEARCH LAB., BAY SAINT LOUIS, MS.
Circulation model experiments of the Gulf Stream using satellite-derived fields
[AD-A266067] p 725 N94-12990
Knowledge-based oceanographic image compression
[AD-A265752] p 821 N94-13041

NAVAL RESEARCH LAB., WASHINGTON, DC.
Inertial confinement fusion program
[DE93-013372] p 796 N94-13047
Shock-free acceleration of laser driven targets
[DE93-008050] p 655 N94-13387

NAVAL SURFACE WARFARE CENTER, DAHLGREN, VA.
Improved aeroprediction code. Part 1: Summary of new methods and comparison with experiment
[AD-A266015] p 500 N94-12989

NEBRASKA UNIV., LINCOLN.
Study of novel conductive paints for solar cell electromagnetic fields
[DE93-015088] p 581 N94-14337

NEVADA UNIV., RENO.
Linkage of anthropogenic aerosol to clouds and climate
[DE93-016434] p 719 N94-13080
Numerical investigations in three-dimensional internal flows
[NASA-CR-194143] p 637 N94-13827

NEW BRUNSWICK UNIV., FREDERICTON.
J2000.0 modelling of GEOAIM in the analysis of VLB1 data from the NASA crustal dynamics project
[ISBN-0-315-59463-2] p 684 N94-13368
GPS satellite sky distribution: Impact on the propagation of some important errors in precise relative positioning
[ISBN-0-315-51838-3] p 513 N94-13541
Machinery dynamics activities in Canadian industries
[IME-MET-TR-006] p 663 N94-14147
On the space-time ocean current variability and its effects on the length-of-day
[ISBN-0-315-59510-8] p 726 N94-14205

NEW ENERGY AND INDUSTRIAL TECHNOLOGY DEVELOPMENT ORGANIZATION, TOKYO (JAPAN).
Promotion of geothermal energy development in 1991
[DE93-799057] p 701 N94-13214
Promotion of geothermal energy development in 1991
[DE93-799058] p 701 N94-13215
Promotion of geothermal energy development in 1991
[DE93-799061] p 705 N94-14679

NEW HAMPSHIRE UNIV., DURHAM.
Cosmic and solar gamma ray and neutron experiments
[NASA-CR-193359] p 849 N94-13965

NEW MEXICO STATE UNIV., LAS CRUCES.
ROSAT observations of clusters with wide-angle tailed radio sources
[NASA-CR-193784] p 833 N94-14405
Charge storage and switching phenomena with molecular assemblies of metal complexes
[AD-A266673] p 787 N94-14778

NEW MEXICO UNIV., ALBUQUERQUE.
Wind erosion in semiarid landscapes: Predictive models and remote sensing methods for the influence of vegetation
[NASA-CR-194029] p 715 N94-13956

NEW YORK UNIV., NEW YORK.
The role of clouds and oceans in global greenhouse warming
[DE93-016206] p 706 N94-13079

NIJMEGEN UNIV. (NETHERLANDS).
PSM: A new generation of data modeling
[TR-92-13] p 824 N94-14072

NIPPON ELECTRIC CO. LTD., TOKYO (JAPAN).
Development and application of one dimensional deployable truss p 531 N94-13281
Flight evaluations of approach/landing navigation sensor systems: Summary of 1990 flight experiments
[NAL-TR-1175] p 513 N94-13344

NIPPON ELECTRIC CO. LTD., YOKOHAMA (JAPAN).
A concept for the world environment and disaster observation system p 693 N94-14245

NIPPON TELEGRAPH AND TELEPHONE PUBLIC CORP., TOKYO (JAPAN).
Growth experiment of narrow band-gap semiconductor PbSnTe single crystals in space (M-1)
p 586 N94-13733

NIPPON TELEGRAPH AND TELEPHONE PUBLIC CORP., YOKOSUKA (JAPAN).
Development of modular cable mesh deployable antenna p 530 N94-13274
NTT's activities in satellite communications technology development p 618 N94-14286

NORTH CAROLINA AGRICULTURAL AND TECHNICAL STATE UNIV., GREENSBORO.
MARS Mission research center
[NASA-CR-194034] p 841 N94-13088
Graphite fiber textile preform/copper matrix composites
[NASA-CR-193797] p 558 N94-14050

NORTH CAROLINA STATE UNIV., RALEIGH.
Theoretical treatment of the bulk and surface properties of fluids containing long, flexible molecules
[DE93-015560] p 575 N94-12861
The study of structure-processing-property relations in copper oxide based high (Tc) superconductors
[DE93-015066] p 804 N94-13003
Infrared absorption spectroscopy and chemical kinetics of free radicals
[DE93-015078] p 562 N94-13004
MARS Mission research center
[NASA-CR-194034] p 841 N94-13088
Multidisciplinary design techniques applied to conceptual aerospace vehicle design
[NASA-CR-194409] p 515 N94-13618
Characterization of diamond film growth in a combustion flame
[AD-A266659] p 816 N94-14839
A study of hydrogen effects on fracture behavior of radioactive waste storage tanks
[DE93-018171] p 574 N94-14873

NORTH CAROLINA UNIV., CHARLOTTE.
Mathematical algorithms for multidimensional inverse scattering problems in inhomogeneous medium
[AD-A266440] p 749 N94-13702

NORTHEAST LOUISIANA STATE COLL., MONROE.
Martian sedimentary deposits
[NASA-CR-193266] p 842 N94-13855

NORTHWESTERN UNIV., EVANSTON, IL.
Optimization and eigenvalue computation with application to meteorology and oceanography
[DE93-015310] p 744 N94-13024
Variational approach to probabilistic finite elements
[NASA-CR-187179] p 674 N94-13873
Structures and shear response of lipid monolayers
[DE93-015076] p 730 N94-14802

NORWEGIAN DEFENCE RESEARCH ESTABLISHMENT, KJELLER.
Suppression of bright objects using a spatial light modulator when imaging with CCD- and image intensified cameras
[FFI-93/7008] p 650 N94-13665
Estimation of the concentration versus the time profile of zinc chloride particles in smoke clouds generated by the Raufoss A/S instantaneous smoke RA-90 and DM-45 HC smoke generator
[FFI-93/6001] p 708 N94-13821
A rocket-borne lidar for studies of the middle atmosphere
[FFI/RAPPORT-92/7034] p 715 N94-13949
Measurement of wave propagation for VHF/UHF and a comparison between measured and predicted values
[FFI/RAPPORT-92/7024] p 605 N94-13968
Numerical simulations of Nd:YAG laser amplifiers
[FFI/RAPPORT-92/7028] p 657 N94-13970
Open boundary conditions for incompletely parabolic systems
[FFI/RAPPORT-92/7029] p 770 N94-13971
Electrical and optical properties of multiple quantum well structures and their applications to infrared detectors
[FFI-92/7012] p 809 N94-14010
Determination of position and orientation of rigid bodies from image segments
[FFI-92-4005] p 752 N94-14039
The spectral viscosity method applied to simulation of waves in a stratified atmosphere
[FFI-92/7047] p 637 N94-14040
Laboratory simulation of spacecraft charging in the plasma wake region
[FFI-93-7007] p 542 N94-14107
A characterization of carboxylesterases in rat and guinea pig: Their heterogeneity and role in detoxication of organophosphorus compounds
[NDRE-PUBL-93-1001] p 730 N94-14852

O

OAK RIDGE K-25 SITE, TN.
Long-range global warming impact of gaseous diffusion plant operation
[DE93-011686] p 710 N94-14459

OAK RIDGE NATIONAL LAB., TN.
Measurements of transverse energy and forward energy in high-energy nuclear collisions
[DE93-012755] p 788 N94-12817
Flux-pinning related defect structures in melt-processed YBa2Cu3O(7-x)
[DE93-012759] p 804 N94-12818
Rare attributes in finite universe: Hypotheses testing specification and exact randomized upper confidence bounds
[DE93-012783] p 775 N94-12955
High-temperature corrosion and protection of materials
[DE93-011072] p 568 N94-12998
Conversion of light hydrocarbon gases to metal carbides for production of liquid fuels and chemicals
[DE93-014962] p 583 N94-13002
Determination of channeling perspectives for complex crystal structures
[DE93-012872] p 805 N94-13009
Lattice site of helium implanted in Si and diamond
[DE93-015365] p 805 N94-13012
Ion cyclotron heating experiments and plans for the Advanced Toroidal Facility (ATF)
[DE93-012965] p 795 N94-13033
Equilibrium reconstruction of the q-profile in tokamaks from motional Stark effect data
[DE93-015815] p 796 N94-13046
Effect on antenna structure of high power RF during plasma operation
[DE93-013278] p 797 N94-13144
The corrosion behavior of 8001 Al under heat-transfer conditions in an aqueous loop system
[DE93-013450] p 569 N94-13242
Beta/gamma test problems for ITS
[DE93-013522] p 781 N94-13349
Ocean uptake of carbon dioxide
[DE93-012967] p 707 N94-13384
The KSR1: Experimentation and modeling of poststore
[DE93-012539] p 759 N94-13470
Forest management for fixing and sequestering carbon
[DE93-013520] p 707 N94-13486
Folded waveguide designs for tokamaks
[DE93-013274] p 798 N94-13577
Current distribution tomography for determination of internal current density distributions
[DE93-015463] p 604 N94-13899
A data base for aging of structural materials
[DE93-009714] p 824 N94-13915
High-resolution Z-contrast imaging and hole concentration mapping of YBCO thin films
[DE93-015803] p 808 N94-13930
Fatigue design curves for 6061-T6 aluminum
[DE93-011849] p 571 N94-14021
Camera calibration in a hazardous environment performed in situ with automated analysis and verification
[DE93-010274] p 651 N94-14046
Electrical characterization of the JET A(sub 2) antenna: Comparison of model with measurements Wade, T.
[DE93-012964] p 607 N94-14291
Development and application of the automated Monte Carlo biasing procedure in SAS4
[DE93-015205] p 774 N94-14334
Eye-gaze and intent: Application in 3D interface control
[DE93-015210] p 738 N94-14335
Kinetics of photodeposition of superconducting films
[DE93-015511] p 812 N94-14348
Effects of depositon rate on Bi2Sr2CaCu2O(8+x) and Bi2Sr(1.6)La(0.4)CuO(6+x) epitaxial thin film growth by pulsed-laser ablation
[DE93-015797] p 812 N94-14362

Oak Ridge Environmental Information System (ORIES) site workstation information packet for OREIS 6.2
[DE93-010761] p 825 N94-14458
Evolving surface cusps during strained-layer epitaxy
[DE93-015430] p 813 N94-14478
ORGBUG: A Windows-based combinatorial geometry debugger
[DE93-016640] p 755 N94-14515
Some frequency and damping measurements of laminated beryllium beams
[DE93-015909] p 676 N94-14530
Structural change of graphite during electron irradiation
[DE93-015961] p 582 N94-14531
Heavy section steel irradiation experiment
[DE93-015517] p 573 N94-14537
Decentralized control of uncertain systems via sensitivity models
[DE93-012963] p 766 N94-14568
Switchover software reliability estimate for Paducah freezer/sublimer computer systems
[DE93-013844] p 756 N94-14696
Investigations of low-temperature neutron embrittlement of ferritic steels
[DE93-015460] p 573 N94-14700
Design of the ion cyclotron system for TPX
[DE93-012961] p 803 N94-14770
Pattern and Process in Landscape Ecology: Eighth Annual US Landscape Ecology Symposium
[DE93-014032] p 711 N94-14859
Laser lithography by photon scanning tunneling microscopy
[DE93-015962] p 660 N94-14863

OAK RIDGE Y-12 PLANT, TN.
Determination of the surface cleanliness of metals by FT-IR spectroscopy
[DE93-013252] p 565 N94-14525
CAD data exchange with Martin Marietta Energy Systems, Inc., Oak Ridge, TN
[DE93-017233] p 757 N94-14871

OBSERVATORIUM BOSSCHA, BANDUNG (INDONESIA).
Some thoughts on the space programs in the Asia Pacific regions p 697 N94-14272

ODETICS, INC., ANAHEIM, CA.
Control algorithm implementation for a redundant degree of freedom manipulator
[NASA-CR-191339] p 762 N94-13131

ODYSSEY RESEARCH ASSOCIATES, INC., OTTAWA (ONTARIO).
EVES: An overview
[DSIS-93-00238] p 752 N94-14088

OFFICE NATIONAL D'ETUDES ET DE RECHERCHES AEROSPATIALES, PARIS (FRANCE).
High frame rate thermal imager for hypersonic wind tunnel applications
[ONERA-NT-1992-12] p 650 N94-14009
Optical propagation through atmospheric turbulence. Model analysis of anisoplanatism and application to adaptive optics
[ONERA-P-1992-4] p 716 N94-14192
Physical and structural properties of a sputtered zirconia-yttria layer used as a thermal resistance
[ONERA-NT-1992-10] p 810 N94-14193
Modeling and simulation of transport and combustion phenomena in a supersonic mixing layer
[ONERA-NT-1992-11] p 565 N94-14194

OHIO STATE UNIV., COLUMBUS.
Relegation for decentralized control
[AD-A265720] p 819 N94-13059
Investigation for improving Global Positioning System (GPS) orbits using a discrete sequential estimator and stochastic models of selected physical processes
[NASA-CR-194167] p 512 N94-13082
Cognitive engineering in aerospace application: Pilot interaction with cockpit automation
[NASA-CR-177617] p 510 N94-13247
Parallel methods for dynamic simulation of multiple manipulator systems p 680 N94-14637

OHIO UNIV., ATHENS.
Electronic states in systems of reduced dimensionality
[DE93-014440] p 815 N94-14739

OKLAHOMA UNIV., NORMAN.
Readiness to perform testing: A critical analysis of the concept and current practices
[DOT/FAA/AM-93/13] p 732 N94-13193
Rain-rate data base development and rain-rate climate analysis p 614 N94-14664

OLD DOMINION UNIV., NORFOLK, VA.
A performance prediction model for a fault-tolerant computer during recovery and restoration
[NASA-CR-194490] p 741 N94-14136
Polymer infiltration studies
[NASA-CR-194521] p 582 N94-14539

OPERATIONAL RESEARCH AND ANALYSIS ESTABLISHMENT, OTTAWA (ONTARIO).
Spare parts analysis of the MK 32B-751 AAR pod
[DSIS-93-00737] p 774 N94-13549
An analysis of helicopter attrition using a low level combat simulation
[DSIS-93-00282] p 515 N94-13839
HELSCAM V2.0: Development and application guide
[DSIS-93-00137] p 515 N94-13867
Ground Attack Profile Selector Program, version 3.0
[DSIS-93-00702] p 753 N94-14207

OREGON STATE UNIV., CORVALLIS.
Analytical framework for modeling scale-related variabilities in remote sensing p 685 N94-13592

OSAKA PREFECTURE UNIV., SAKAI (JAPAN).
Application of intelligently adaptable structure and robot to large space structure p 530 N94-13277

OSAKA UNIV. (JAPAN).
Separation of biogenic materials by electrophoresis under zero gravity (L-3) p 592 N94-13760

OSAKA UNIV., TOYONAKA (JAPAN).
Fabrication of Si-As-Te ternary amorphous semiconductor in the microgravity environment (M-13) p 588 N94-13745

OTTAWA UNIV. (ONTARIO).
Development of a tactile and vision integrated system, and object identification techniques for SPDM applications
[DSIS-93-00153] p 764 N94-13842
Development of a computer vision system to supplement the active tactile sensing capability in a structured environment
[DSIS-93-00072] p 764 N94-13844

OVERSET METHODS, INC., VACAVILLE, CA.
Domain connectivity among systems of overset grids
[NASA-CR-193390] p 508 N94-14326

P

PACIFIC NORTHWEST LAB., RICHLAND, WA.
A parameterization of cloud droplet nucleation
[DE93-007998] p 718 N94-12903
Soil erosion rates caused by wind and saltating sand stresses in a wind tunnel
[DE93-009154] p 706 N94-12905
A review of the global emissions, transport, and effects of heavy metals in the environment
[DE93-013507] p 706 N94-12937
Interfacial precipitation, segregation and deformation in alloy 600: Implications on primary-side IGSCC
[DE93-013161] p 568 N94-13035
Electron emission resulting from fast ion impact on thin metal foils: Implications of these data for development of track structure models
[DE93-013506] p 782 N94-13485
Spatial and temporal variability of precipitation and chemistry: Case studies from the frontal boundary study
[DE93-007883] p 708 N94-13910
Binary homogeneous nucleation: Temperature and relative humidity fluctuations and non-linearity
[DE93-007884] p 709 N94-13911
Boundary layer structure over areas of heterogeneous heat fluxes
[DE93-007887] p 715 N94-13912
Radiation hardening and radiation-induced chromium depletion effects on intergranular stress corrosion cracking of austenitic stainless steels
[DE93-011602] p 572 N94-14058
Reverse micelle synthesis of nanoscale metal containing catalysts
[DE93-012869] p 572 N94-14184
Sequestering carbon dioxide in industrial polymers: Building materials for the 21st century
[DE93-016087] p 580 N94-14297
UV and IR laser ablation for inductively coupled plasma mass spectrometry
[DE93-017124] p 658 N94-14415
Summary of conclusions and recommendations from a visibility science workshop
[DE93-012770] p 710 N94-14523
Theory, modeling, and simulation
[DE93-015607] p 755 N94-14571
Quantitative luminescence imaging system
[DE93-015691] p 793 N94-14702

PARAMAX SYSTEMS CORP., HOUSTON, TX.
Partnership with the customer p 666 N94-13157

PENNSYLVANIA STATE UNIV., NEW KENSINGTON.
Evaluation for rheological constitutive relations, using the indentation technique p 775 N94-13627

PENNSYLVANIA STATE UNIV., STATE COLLEGE.
The feasibility of producing aluminum-lithium structures for cryogenic tankage applications by laser beam welding
[NASA-CR-191527] p 595 N94-14026

PENNSYLVANIA STATE UNIV., UNIVERSITY PARK.
Role of Ca(++)/calmodulin in the regulation of microtub[illegible] plants
[DE93-015885] p 727 N94-12835
Archiving of HEAO-1 data products and the creation of a general user's guide to the archive
[NASA-CR-193415] p 822 N94-13062
A time-accurate numerical method for chemically reacting flows at all Mach numbers p 500 N94-13198
Search for x ray emitting young stars outside of massive molecular clouds
[NASA-CR-193609] p 830 N94-13462
Processing and mechanical properties of silicon carbide platelet reinforced alumina composites p 556 N94-13557
Combustion-induced crack/debond propagation in solid propellants p 584 N94-13560
Numerical simulations of unsteady flows in turbomachines p 633 N94-13569
An experimental investigation of shock wave/vortex interaction p 634 N94-13574
Numerical simulation of steady three-dimensional flows in axial turbomachinery bladerows p 634 N94-13630
Robust synthesis of discrete-time multivariable control systems with induced delays p 662 N94-13642
Weather forecasting support for AASE-2
[NASA-CR-194342] p 721 N94-13675
Droplet-turbulence interactions in sprays exposed to supercritical environmental conditions
[NASA-CR-194408] p 638 N94-14308
Numerical simulation of velocity-coupled combustion response of solid rocket propellants p 585 N94-14490
Analysis of reacting flowfields in low-thrust rocket engines and plumes p 552 N94-14491

PENNSYLVANIA TRANSPORTATION INST., UNIVERSITY PARK.
Inhibiting corrosion in Gr/Al and Gr/Mg metal matrix composites using nonequilibrium alloying techniques
[AD-A266547] p 556 N94-13583

PHILLIPS LAB., EDWARDS AFB, CA.
PACE: A test bed for the dynamics and control of flexible multibody systems p 527 N94-14650

PHILLIPS LAB., HANSCOM AFB, MA.
Force-free magnetic fields, curl eigenfunctions, and the sphere in transform space, with applications to fluid dynamics and electromagnetic theory
[AD-A265805] p 834 N94-12971
DMSP F11 SSM/T-2 calibration and validation
[AD-A265817] p 719 N94-12978

PHILLIPS LAB., KIRTLAND AFB, NM.
GOPEX at the Starfire Optical Range p 611 N94-14392

PHOTON RESEARCH ASSOCIATES, INC., CAMBRIDGE, MA.
Stress stiffening and approximate equations in flexible multibody dynamics p 677 N94-14620

PHYSICAL SCIENCES, INC., ANDOVER, MA.
Novel oxygen atom source for material degradation studies
[NASA-CR-191323] p 562 N94-13115
Propulsion simulator for magnetically-suspended wind tunnel models
[NASA-CR-189560] p 527 N94-13127

PITTSBURGH UNIV., PA.
Computer simulations for the adsorption of polymers onto surfaces
[DE93-016667] p 577 N94-13070
New infrared photon absorption processes
[DE93-017017] p 780 N94-13071
Laboratory simulations of lunar darkening processes p 843 N94-14301
Quantum state resolved desorption of CO from solid surfaces
[DE93-016876] p 814 N94-14597

POLISH ACADEMY OF SCIENCES, WARSAW.
Stability of subharmonics and escape phenomena in the twin-well potential duffing system p 775 N94-13235
Thermodiffusion in heterogeneous elastic solids and homogenization
[REPT-14/1993] p 578 N94-13468

POLITECNICO DI MILANO (ITALY).
Programming languages made in Italy
[REPT-93-002] p 750 N94-13805
Integration between geographic information systems and environmental simulation models
[REPT-93-004] p 823 N94-13806
Parameter identification of a model of the process of software development
[REPT-93-008] p 750 N94-13807
Simulated annealing for the problem of multiresource location on graph
[REPT-93-033] p 770 N94-13809
Hypertext Compiling Tools (HCT): Developing model based applications with standard hypertext systems
[REPT-92-049] p 750 N94-13822

The OOA technique in information systems
[REPT-72-92] p 823 N94-13863

PRINCETON UNIV., NJ.
Transport properties of disordered porous media from the microstructure
[DE93-016065] p 806 N94-13152
Exploratory study of in-plane streamline curvature effects on a turbulent boundary layer at a Mach number of 3
[NASA-CR-193673] p 501 N94-13292
A three-dimensional supersonic turbulent boundary layer generated by an isentropic compression
p 503 N94-13556
Studies of non-inductive current drive in the CDX-U tokamak p 799 N94-13680
Micromechanical damage theories for brittle solids with interacting microcracks
[AD-A266348] p 673 N94-13778
Exploratory data analysis: Past, present and future
[AD-A266775] p 774 N94-14788

PROTEON, INC., WESTBOROUGH, MA.
High speed packet switching
[NASA-CR-191334] p 759 N94-13177

PURDUE UNIV., WEST LAFAYETTE, IN.
Method of characteristics design of a supersonic wind tunnel nozzle with square cross-section, supplement 3
[NASA-CR-194359] p 527 N94-12824
Anchoring strategies for bimetallic species in zeolites
[DE93-015622] p 567 N94-12834
Molecular solvent-dynamical effects on activated electron-transfer kinetics: How important is solvent friction?
[AD-A265886] p 779 N94-12894
Study of multicomponent diffusion and transport phenomena
[DE93-015095] p 804 N94-13005
Feature extraction and classification algorithms for high dimensional data
[NASA-CR-194298] p 743 N94-13023
Design of partially supervised classifiers for multispectral image data
[NASA-CR-194299] p 823 N94-13192
Catalytic arene hydrogenation using early transition metal hydride compounds
[DE93-015500] p 573 N94-14402
An application of the IMC software to controller design for the JPL LSCL Experiment Facility
p 681 N94-14645
Investigation of the dilatational dissipation in compressible homogeneous shear flow
p 645 N94-14758

Q

QUEENS UNIV., KINGSTON (ONTARIO).
Design automation tools for testable VLSI circuits
[ISBN-0-315-61461-7] p 621 N94-13333
An experimental investigation of the redistribution of gas stream total temperature in a high turning angle transonic planar cascade
[ISBN-0-315-60791-2] p 502 N94-13369

R

RADIOPHYSICS, INC., BOULDER, CO.
Neptune high-latitude emission: Dependence of angle on frequency
[NASA-CR-193280] p 848 N94-13476

REMOTE SENSING APPLICATIONS CENTRE, JAKARTA (INDONESIA).
Some thoughts on the space programs in the Asia Pacific regions p 697 N94-14272

REMOTE SENSING TECHNOLOGY CENTER, TOKYO (JAPAN).
Integration of SST data sets using MOS-1 satellite data: For validation and monitoring p 696 N94-14262
Outline of ISY Kuroshio observation experiment
p 697 N94-14268

REMTECH, INC., HUNTSVILLE, AL.
Low altitude plume impingement handbook
[NASA-CR-194193] p 643 N94-14741

RENSSELAER POLYTECHNIC INST., TROY, NY.
Extrapolation of space weathering processes to other small solar system bodies p 843 N94-14300
Center of excellence in rotary wing technology
[AD-A266655] p 510 N94-14799

RESEARCH INST. FOR ADVANCED COMPUTER SCIENCE, MOFFETT FIELD, CA.
Formally biorthogonal polynomials and a look-ahead Levinson algorithm for general Toeplitz systems
[NASA-CR-194297] p 748 N94-13586
A review and analysis of neural networks for classification of remotely sensed multispectral imagery
[NASA-CR-194291] p 763 N94-13603
Efficient, massively parallel eigenvalue computation
[NASA-CR-194289] p 760 N94-13921
On the superconvergence of Galerkin methods for hyperbolic IBVP
[NASA-CR-194293] p 770 N94-13922
USRA/RIACS
[NASA-CR-194334] p 750 N94-13932
On the superconvergence of Galerkin methods for hyperbolic IBPV
[NASA-CR-194488] p 770 N94-14307

RESEARCH INST. FOR COMPUTING AND INFORMATION SYSTEMS, HOUSTON, TX.
Integrating interface slicing into software engineering processes
[NASA-CR-192761] p 754 N94-14368
On-line upgrade of program modules using AdaPT
[NASA-CR-194331] p 754 N94-14472

RESEARCH TRIANGLE INST., RESEARCH TRIANGLE PARK, NC.
Chip-level testability requirements guidelines
[AD-A262583] p 619 N94-12967
Technology Applications Team: Applications of aerospace technology
[NASA-CR-194362] p 828 N94-13104

RICE UNIV., HOUSTON, TX.
Quasi-elastic neutron scattering studies of protein dynamics
[DE93-015074] p 782 N94-13414

ROCHESTER UNIV., NY.
Theoretical SIS mixer research
[AD-A266323] p 807 N94-13580

ROCKWELL INTERNATIONAL CORP., CANOGA PARK, CA.
STS-55 pad abort: Engine 2011 oxidizer preburner augmented spark igniter check valve leak
[NASA-CR-193830] p 533 N94-12806

ROCKWELL INTERNATIONAL CORP., DOWNEY, CA.
Strategic avionics technology definition studies. Subtask 3-1A: Electrical Actuation (ELA) systems
[NASA-CR-194393] p 536 N94-14323

ROME UNIV. (ITALY).
Integrable system describing surfaces of non-constant curvature
[PREPRINT-734] p 768 N94-13499
Preliminary results on the hydrological measurements in the Aegean Sea off Crete: Cruise, Georgia, 1989
[PREPRINT-736] p 725 N94-13500
Retrieval properties of neural networks with infinitely many marked patterns
[PREPRINT-729] p 766 N94-14718
Renormalized band structure of CuO2 layers in superconducting compounds: A mean field approach
[PREPRINT-730] p 815 N94-14720
Comparing the Z(sup 0) mass and inclusive widths to the standard electroweak theory
[PREPRINT-731] p 787 N94-14721
Direct simulation of polymer drag reduction in free shear flows and vortex dipoles p 644 N94-14755

ROTORDYNAMICS-SEAL RESEARCH, INC., SIMI VALLEY, CA.
Cryogenic fluid film bearing tester development study
[NASA-CR-192586] p 660 N94-12791

ROYAL AEROSPACE ESTABLISHMENT, FARNBOROUGH (ENGLAND).
Optical fibre Fabry-Perot interferometers for calorimetric heat transfer gauges
[RAE-TM-AERO/PROP-20] p 653 N94-14701
Intra-blade quantitative transonic flow measurements at the DRA Pyestock Isentropic Light Piston Facility using PIV (Particle Image Velocimetry)
[RAE-TM-AERO/PROP-21] p 509 N94-14706
A computer program to calculate growth rates for cracks at notches in regions of residual stress
[RAE-TM-MAT/STR-1207] p 683 N94-14818
The 3D pneumatic and 2D dynamic probes: Their development and subsequent use in a transonic fan
[RAE-TM-AERO/PROP-22] p 653 N94-14827
The growth of short fatigue cracks in an aluminium alloy
[RAE-TR-92063] p 574 N94-14828

ROYAL NETHERLANDS METEOROLOGICAL INST., DE BILT.
National use of the groups 7wwW1W2 and 960ww for ground stations
[KNMI-PUBL-181] p 722 N94-13926
The nocturnal wind maximum: An interactive forecast method
[KNMI-TR-142] p 722 N94-13985
Precipitation verification LAM
[KNMI-TR-143] p 722 N94-13991
Adaptation of humidity-cloud cover relations in the LAM
[KNMI-TR-144] p 722 N94-13992
A verification of the Euroguidance: A guidance forecast for transportation and tourism
[KNMI-TR-145] p 722 N94-13993

RUTHERFORD APPLETON LAB., CHILTON (ENGLAND).
The use of polarised neutron reflection for unique density profile determination in thin films
[PB93-187136] p 579 N94-13783

S

SAGA UNIV. (JAPAN).
Methods for calibration/validation of AVNIR
p 689 N94-14216
A method for estimation of partial cloud cover within a pixel and its effect p 697 N94-14269

SAINT LOUIS UNIV., MO.
Bone culture research p 595 N94-13773

SAN DIEGO STATE UNIV., CA.
Integration of viscous effects into inviscid computational methods
[NASA-CR-193677] p 629 N94-13007
Nonlinear relationships between particulate absorption and chlorophyll: Detritus or pigment packaging?
[AD-A266806] p 731 N94-14899

SAN JOSE STATE UNIV., CA.
Obstacle detection by recognizing binary expansion patterns
[NASA-CR-194415] p 514 N94-14495

SANDIA NATIONAL LABS., ALBUQUERQUE, NM.
Crystallographic phase identification in the scanning electron microscope: Backscattered electron Kikuchi patterns
[DE93-011574] p 804 N94-12813
Coupled thermal response of objects and participating media in fires and large combustion systems
[DE93-012848] p 561 N94-12819
Design and testing of planar magnetic micromotors fabricated by deep x ray lithography and electroplating
[DE93-012856] p 618 N94-12821
Photocatalysis for the treatment of waste water: Applications involving the removal of metals
[DE93-011669] p 561 N94-12841
Amorphous sol-gel insulating films
[DE93-012859] p 576 N94-12866
Beyond core: Making parallel computer I/O practical
[DE93-012347] p 758 N94-12878
High-flux testing of heat pipes for point-focus solar collector systems
[DE93-011581] p 628 N94-12884
Making the connection between information modeling and implementation
[DE93-011588] p 820 N94-12907
The 3-D massively parallel impact simulations using PCTH
[DE93-011593] p 670 N94-12908
Experimental technique to simulate orbital-debris impact on space shields at impact velocities over 10 km/s
[DE93-011619] p 539 N94-12909
Modeling ignition chemistry
[DE93-012340] p 561 N94-12910
Correlations of the growth, structure, and stress with the adhesion of diamond films on tungsten
[DE93-012855] p 576 N94-12912
1/f noise and oxide traps in MOSFETs
[DE93-007581] p 619 N94-12942
A general contact detection algorithm for finite element analysis
[DE93-012846] p 742 N94-12956
Multiphase equation of state for iron
[DE93-013956] p 568 N94-12977
Data fusion for adaptive control in manufacturing: Impact on engineering information models
[DE93-011555] p 743 N94-12999
Comparison of analytic Whipple bumper shield ballistic limits with CTH simulations
[DE93-015126] p 539 N94-13006
UNICOS(trade name) security testing
[DE93-011680] p 759 N94-13043
High spatial resolution x ray microanalysis: Comparison of experiment and incoherent scattering calculations
[DE93-011685] p 648 N94-13044
Parachute system design, analysis, and simulation tool
[DE93-013755] p 501 N94-13260
Non-scanned LADAR imaging and applications
[DE93-013772] p 655 N94-13261
Isolation of a piezoresistive accelerometer used in high acceleration tests
[DE93-013764] p 649 N94-13395
A multiphase model for shock-induced flow in low density foam
[DE93-013767] p 632 N94-13397
Simulation of orbital debris impacts on bumper shields
[DE93-013773] p 540 N94-13398
Variance reduction unique to coupled electron/photon Monte Carlo transport
[DE93-014999] p 782 N94-13409

Preliminary nuclear safety assessment of the NEPST (Topaz 2) space reactor program
[DE93-012853] p 551 N94-13514
Test/analysis correlation and model updating of the STARS 1 and 2 missile systems
[DE93-013774] p 748 N94-13578
Locally non-uniform finite-difference time domain with application to stealth, crosstalk, and narrow apertures
[DE93-013958] p 601 N94-13696
Emitter Wrap-Through solar cell
[DE93-014996] p 703 N94-13886
Problems and opportunities in microwave joining of ceramics
[DE93-014998] p 579 N94-13888
A perspective on AVS in an engineering sciences environment
[DE93-015011] p 596 N94-13889
Development of UHF spark-switched L-C Oscillators
[DE93-015019] p 623 N94-13892
Plasma-etching science meets technology in the MDL
[DE93-012086] p 800 N94-13908
Kerberos: A UNIX-TCP/IP network authentication system
[DE93-011677] p 760 N94-14011
VFGEN: A parallel volume fraction generator for hydrocodes
[DE93-011673] p 752 N94-14019
Feature discovery on segmented objects in SAR imagery using self-organizing neural networks
[DE93-010685] p 686 N94-14056
Free-exciton recombination in GaAs
[DE93-009843] p 809 N94-14079
Intrinsic and interfacial recombination in OMVPE- and MBE-prepared GaAs/Al(x)Ga(1-x)As heterostructures
[DE93-009844] p 809 N94-14083
Anomalous low-temperature free-exciton transport in GaAs structures
[DE93-009845] p 809 N94-14108
A laser-based technique to continuously monitor metal aerosol emissions
[DE93-012836] p 710 N94-14183
Center of trace algorithms for extracting digitized waveforms from two-dimensional images
[DE93-015082] p 753 N94-14295
Effects of growth conditions and substrate orientation on the properties of InSb
[DE93-013766] p 812 N94-14344
Microstructural mechanisms that enhance electromigration resistance in Al-Cu thin films
[DE93-013770] p 812 N94-14345
Physics of gas breakdown for ion beam transport in gas
[DE93-015646] p 801 N94-14349
An efficient parallel algorithm for matrix-vector multiplication
[DE93-015125] p 754 N94-14399
Sidewall thermometry perturbations to nonlinear heat transport near the (lambda) transition in He-4
[DE93-014990] p 817 N94-14453
Predicting the vibrations of a spinning inflated membrane
[DE93-010690] p 676 N94-14456
Portable acoustic wave sensor systems for real-time monitoring of volatile organic compounds
[DE93-013753] p 582 N94-14511
Ionospheric effects on a wide-bandwidth, polarimetric, space-based, synthetic-aperture radar
[DE93-015084] p 612 N94-14512
Enterprise integration: A tool's perspective
[DE93-015651] p 755 N94-14528
Calibration of a magnetic induction system for measurement of hypervelocities
[DE93-013949] p 652 N94-14578
Solution chemistry optimization of sol-gel processed PZT thin films
[DE93-013776] p 814 N94-14695
Effect of finite-rate chemistry and unequal Schmidt numbers on turbulent non-premixed flames modeled with single-step chemistry p 567 N94-14766
Structure of turbulent non-premixed flames modeled with two-step chemistry p 567 N94-14767
Image motion photography
[DE93-013962] p 653 N94-14858
Multicrystalline silicon solar cells: Gettering optimization and characterization
[DE93-015001] p 705 N94-14861

SASKATCHEWAN UNIV., SASKATOON.
Activities of the University of Saskatchewan, Plasma Physics Laboratory
[CTN-93-60831] p 798 N94-13518
The resonance broadening theory revisited
[PPL-134] p 798 N94-13563
Nonlinear evolution of tearing modes in inhomogeneous plasmas
[PPL-133] p 798 N94-13564
Scattering of reflectometer signals from rippled surfaces
[PPL-138] p 602 N94-13802
Experiments on the current rampdown phase in the STOR-M tokamak for AC operation
[PPL-132] p 799 N94-13835
Small scale magnetic islands in collisionless plasmas
[PPL-131] p 799 N94-13836
Plasma auto-biasing during Ohmic H-mode in the STOR-M tokamak
[PPL-136] p 799 N94-13849
On energy transport equations for turbulent magnetized plasma
[PPL-135] p 800 N94-13850
Semi-local kinetic analysis of the toroidal ion temperature gradient mode
[PPL-130] p 800 N94-13851
Anomalous transport due to the ion acoustic instability in tokamaks
[PPL-129] p 800 N94-13852
Collisional effects of trapped electrons on the anomalous particle and thermal pinches
[PPL-128] p 800 N94-13853
On MHD mode equations in toroidal plasmas
[PPL-139] p 800 N94-13877
Anomalous transport due to small scale electromagnetic and large scale electrostatic modes in tokamaks
[PPL-140] p 801 N94-14206

SATCON TECHNOLOGY CORP., CAMBRIDGE, MA.
A superconducting large-angle magnetic suspension
[NASA-CR-189735] p 596 N94-13141

SCHWARTZ ELECTRO-OPTICS, INC., ORLANDO, FL.
Novel Co:MgF2 lidar for aerosol profiler
[NASA-CR-191525] p 654 N94-13091

SCIENCE AND TECHNOLOGY AGENCY, TOKYO (JAPAN).
Asia-Pacific ISY conference, volume 1
[NASDA-CM-199-1] p 532 N94-14098
Asia-Pacific ISY Conference, volume 2
[NASDA-CM-199-VOL-2] p 688 N94-14209
Contributions of winged re-entry vehicle to space activities p 537 N94-14278

SCIENCE APPLICATIONS INTERNATIONAL CORP., WASHINGTON, DC.
Generic results of the space physics community survey
[NASA-CR-194538] p 818 N94-13984

SCIENCE UNIV. OF TOKYO (JAPAN).
Space transportation systems and space activities in the 21st century p 537 N94-14274

SCIENTIFIC RESEARCH ASSOCIATES, INC., GLASTONBURY, CT.
Simulation of preburner sprays, volume 1
[NASA-CR-193844] p 647 N94-14906

SCITRAN, INC., SANTA BARBARA, CA.
The problem of traveling in outer space: The rocket motor
[NASA-TT-10002] p 552 N94-14463

SCRIPPS INSTITUTION OF OCEANOGRAPHY, LA JOLLA, CA.
Evolution of catalytic RNA in the laboratory
[NASA-CR-194124] p 727 N94-13210

SECA, INC., HUNTSVILLE, AL.
Low altitude plume impingement handbook
[NASA-CR-194193] p 643 N94-14741

SHIZUOKA UNIV. (JAPAN).
A circadian rhythm of conidiation in Neurospora crassa (L-12) p 593 N94-13769

SHOWA UNIV., TOKYO (JAPAN).
Effect of low gravity on calcium metabolism and bone formation (L-7) p 593 N94-13765

SIKORSKY AIRCRAFT, STRATFORD, CT.
Design and pilot evaluation of the RAH-66 Comanche Core AFCS p 525 N94-13321
Design and pilot evaluation of the RAH-66 Comanche selectable control modes p 525 N94-13322
Computer program for analysis of high speed, single row, angular contact, spherical roller bearing, SASHBEAN. Volume 1: User's guide
[NASA-CR-191183] p 663 N94-14445
Computer program for analysis of high speed, single row, angular contact, spherical roller bearing, SASHBEAN. Volume 2: Mathematical formulation and analysis
[NASA-CR-191182] p 664 N94-14446

SIRIUS GROUP, PEABODY, MA.
Laser power beaming system analyses
[NASA-CR-193840] p 660 N94-14904

SIROTA AND ALPER ASSOCIATES, INC., BETHESDA, MD.
What's the bottom line payback for TQM?
p 666 N94-13156

SMITHSONIAN ASTROPHYSICAL OBSERVATORY, CAMBRIDGE, MA.
Venus gravity
[NASA-CR-194077] p 841 N94-12823
Planetary system detection by POINTS
[NASA-CR-194361] p 545 N94-13067
Determination of spectroscopic properties of atmospheric molecules from high resolution vacuum ultraviolet cross section and wavelength measurements
[NASA-CR-194024] p 712 N94-13092
The onset of galactic winds in early-type galaxies
[NASA-CR-193640] p 836 N94-13446
Measurement of HO2 and other trace gases in the stratosphere using a high resolution far-infrared spectrometer at 28 km
[NASA-CR-194175] p 714 N94-13816
AXAF FITS standard for ray trace interchange
[NASA-CR-194025] p 832 N94-14305
A long-term space astrophysics research program: The evolution of the quasar continuum
[NASA-CR-193714] p 839 N94-14404

SOCIETE EUROPEENNE DE PROPULSION, VERNON (FRANCE).
Residual contact restraints in cryogenics
[ETN-93-94375] p 671 N94-13501

SOCIETY OF NON-TRADITIONAL TECHNOLOGY, TOKYO (JAPAN).
Study on superconducting basic technology for space application, part 1
[NASDA-CNT-930015-PT-1] p 622 N94-13425

SONOMA STATE UNIV., ROHNERT PARK, CA.
High time resolution studies of binary x ray pulsars
[NASA-CR-194395] p 832 N94-13894
ROSAT observations of the binary Be-star/radio pulsar PSR1259-63
[NASA-CR-194394] p 832 N94-14357

SOUTH CAROLINA UNIV., COLUMBIA.
Workshop for coordinating South Carolina's pre-college systemic initiatives in science and mathematics
[DE93-012263] p 818 N94-13216

SOUTHAMPTON UNIV. (ENGLAND).
Piston engine intake and exhaust system design
[ISVR-TR-222] p 663 N94-13874
Underwater hearing: A review
[ISVR-TR-212] p 777 N94-14130

SOUTHWEST RESEARCH INST., SAN ANTONIO, TX.
MHD shocks in coronal mass ejections
[NASA-CR-193418] p 828 N94-12970
Investigation of plasma instabilities in the Polar cusp
[NASA-CR-194283] p 796 N94-13084

SOUTHWEST TEXAS STATE UNIV., SAN MARCOS.
Highly fluorinated polymers
[NASA-CR-194147] p 579 N94-13964

SRI INTERNATIONAL CORP., MENLO PARK, CA.
Technical support for digital systems technology development. Task order 1: ISP contention analysis and control
[NASA-CR-190758] p 537 N94-12809
Passive recovery of scene geometry for an unmanned ground vehicle
[AD-A266670] p 766 N94-14777

STANFORD LINEAR ACCELERATOR CENTER, CA.
Proceedings of the Workshop on Applications of Synchrotron Radiation to Trace Impurity Analysis for Advanced Silicon Processing
[DE93-013389] p 805 N94-13020

STANFORD UNIV., CA.
Color image processing for flat panel visual display modeling
[NASA-CR-193660] p 790 N94-12797
Three-dimensional structure of straight and curved plane wakes
[NASA-CR-194420] p 501 N94-13266
Generic software architecture based redesign
p 745 N94-13290
Software synthesis using generic architectures
[NASA-CR-194201] p 745 N94-13355
Architecture-driven reuse of code in KASE
[NASA-CR-194200] p 745 N94-13356
The KASE approach to domain-specific software systems p 745 N94-13357
Software design by reusing architectures
[NASA-CR-194151] p 747 N94-13443
Poling of thin polymer films in electro optic applications
[AD-A266562] p 579 N94-13584
Maximum likelihood estimation for constrained or missing data models
[AD-A266563] p 773 N94-13585
Liquid metal drop ejection
[NASA-CR-193718] p 572 N94-14133
Overview of the Scalable Coherent Interface, IEEE STD 1596 (SCI)
[DE93-015247] p 761 N94-14476
Studying Turbulence Using Numerical Simulation Databases. 4: Proceedings of the 1992 Summer Program
[NASA-CR-194556] p 643 N94-14745
The evolution equation for the flame surface density in turbulent premixed combustion p 567 N94-14764

STARMARK CORP., ARLINGTON, VA.
A perspective on the FAA approval process: Integrating rotorcraft displays, controls and workload p 521 N94-13298
Interpreted Cooper-Harper for broader use p 523 N94-13309
STATE UNIV. OF NEW YORK, ALBANY.
Studies in quantum field theory [DE93-017201] p 818 N94-14896
STATE UNIV. OF NEW YORK, ALFRED.
Combustion synthesis and engineering of nanoparticles for electronic, structural, and superconductor applications [DE93-016286] p 809 N94-13981
STATE UNIV. OF NEW YORK, STONY BROOK.
The origin of the far-infrared emission from galactic molecular clouds p 848 N94-13654
Gravity, chromosomes, and organized development in aseptically cultured plant cells p 592 N94-13764
The theory of relativistic heavy ion collisions [DE93-015934] p 784 N94-13952
Phase transition in polymer blends and structure of ionomers and copolymers [DE93-016256] p 579 N94-13978
Research in theoretical nuclear physics [DE93-015096] p 839 N94-14330
STERLING SOFTWARE, INC., PALO ALTO, CA.
Object-oriented productivity metrics p 667 N94-13161
STEVENS INST. OF TECH., HOBOKEN, NJ.
Investigations of transitions from order to chaos in dynamical systems [DE93-014438] p 818 N94-14738
STI OPTRONICS, BELLEVUE, WA.
Theory of field-reversed configurations [DE93-015611] p 794 N94-12862
STOCKHOLM UNIV. (SWEDEN).
A high-resolution Lax-Friedrichs scheme for hyperbolic conservation laws with source terms: Application to shallow water equations [DM-62] p 632 N94-13535
STRUCTURAL ANALYSIS TECHNOLOGY, INC., SANTA CLARA, CA.
An expert system for integrated structural analysis and design optimization for aerospace structures [NASA-CR-194225] p 673 N94-13673
SUMITOMO ELECTRIC INDUSTRIES LTD., OSAKA (JAPAN).
Crystal growth of compound semiconductors in a low-gravity environment (InGaAs crystals) (M-22) p 590 N94-13754
SUPERCONDUCTING SUPER COLLIDER LAB., DALLAS, TX.
Building the repositories to serve [DE93-014100] p 821 N94-12983
Integrating PAW, a graphical analysis interface to Sybase [DE93-014172] p 755 N94-14581
Proton-proton scattering contribution to emittance growth [DE93-016090] p 787 N94-14588
SURREY UNIV., GUILDFORD (ENGLAND).
Results of multiband (L, S, Ku band) propagation measurements and model for high elevation angle land mobile satellite channel p 615 N94-14670
SVERDRUP TECHNOLOGY, INC., ARNOLD AFS, TN.
Hypersonic overview p 505 N94-14154
Aeropropulsion facilities p 506 N94-14161
Aeropropulsion test and evaluation methods p 506 N94-14165
Hypersonic flight test. Part 1: Propulsion flight testing p 507 N94-14168
Shock/boundary-layer/shock interactions p 507 N94-14172
SVERDRUP TECHNOLOGY, INC., BROOK PARK, OH.
An advanced test technique to quantify thermomechanical fatigue damage accumulation in composite materials [NASA-CR-191147] p 555 N94-13139
Low power pulsed MPD thruster system analysis and applications [NASA-CR-191187] p 550 N94-13415
Electromagnetic propulsion for spacecraft [NASA-CR-191186] p 551 N94-13416
Thermomechanical and isothermal fatigue behavior of a (90)sub 8 titanium matrix composite [NASA-CR-191196] p 560 N94-14822
SWEDISH SPACE CORP., SOLNA.
The Swedish ISY contribution p 695 N94-14256
SYRACUSE UNIV., NY.
Upgrading of raw natural gas using high-performance polymer membranes [DE93-014041] p 566 N94-14586
SYSTEMS RESEARCH LABS., INC., DAYTON, OH.
Evaluation of the Retrograde Inflation Anti-G Suit (RIAGS) [AD-A265884] p 736 N94-12935
SYSTEMS TECHNOLOGY, INC., HAWTHORNE, CA.
Effects of simulator motion and visual characteristics on rotorcraft handling qualities evaluations p 524 N94-13317

T

TECHNICAL RESEARCH CENTRE OF FINLAND, ESPOO.
Contribution to comparison of methods for determining welding procedures for the avoidance of hydrogen cracking [VTT-PUBS-107] p 674 N94-13887
Study on the possibilities to apply spectrumindex [VTT-PUBS-109] p 777 N94-14034
Transition of building energy consumption using multi-input, single-output dynamic model [VTT-PUBS-116] p 597 N94-14055
TECHNION RESEARCH AND DEVELOPMENT FOUNDATION LTD., HAIFA (ISRAEL).
Electrophoretic and electrolytic deposition of ceramic particles on porous substrates [AD-A265141] p 575 N94-12812
TECHNISCHE UNIV., BERLIN (GERMANY).
A continuum theory for liquid crystals describing different degrees of orientational order [ETN-93-94392] p 807 N94-13590
Construction and test of a facility for photon-stimulated field description using excimer laser and time of flight [ETN-93-94386] p 657 N94-13996
Numerical simulation and analysis of electrical and optical properties of Al(x)Ga(1-x)As / GaAs [ETN-93-94387] p 703 N94-13997
Mutual inductance between partially wound tori and a bifilar conductor [ETN-93-94388] p 624 N94-13998
Dust production in the envelopes of carbon stars: R Coronae Borealis [ETN-93-94389] p 839 N94-14075
Robust estimators and tests in one-sample location problem with particular consideration on modified maximum likelihood process [ETN-93-94391] p 774 N94-14703
Manufacturing and examination of integrated optical waveguide components in silicon [ETN-93-94393] p 793 N94-14704
Dynamic Jahn-Teller effect: Calculation of fine structure spectrum, isotope shift and Zeeman behavior at deep center Ni2+ in CdS [ETN-93-94394] p 815 N94-14705
Speaker independent recognition of isolated words using vector quantization and neural networks [ETN-93-94390] p 616 N94-14724
Development of experimental demonstration processes for laminar-turbulent flow states at wing profiles in free flight [ILR-MITT-280(1993)] p 510 N94-14800
Utilization of boundary element method for extraction of frequency dependent conductivity parameters of lossy intra-chip transmission lines [ETN-93-94385] p 771 N94-14807
Contributions to numerical solution of Navier-Stokes equations in two and three dimensional flows [ETN-93-94395] p 647 N94-14816
Optimization of a subband coding for high definition television with motion controlled three dimensional frequency band decomposition [ETN-93-94396] p 617 N94-14817
Two dimensional measurement and evaluation of point images at microscope objectives [ETN-93-94397] p 793 N94-14856
TECHNISCHE UNIV., DELFT (NETHERLANDS).
Optimal lateral escape maneuvers for microburst encounters during final approach [LR-691] p 511 N94-13534
Development and application of a comprehensive, design-sensitive weight prediction method for wing structures of transport category aircraft [LR-693] p 515 N94-13687
Some computational tools for the analysis of through cracks in stiffened fuselage shells [LR-701] p 673 N94-13726
On the orthotropicity assumption and discontinuity conditions of conical shells [LR-703] p 673 N94-13787
Fatigue and residual strength characteristics of fiber metal laminates subjected to incidental damage [LR-708] p 674 N94-13803
The development of inspection and repair methods for the C-17 aft cargo door [LR-704] p 499 N94-13904
The numerical simulation of the collapse process of axially compressed cylindrical shells with measured imperfections [LR-705] p 674 N94-13905
Investigation of an aeroelastic oscillator: Analysis of one-degree-of-freedom galloping with combined translational and torsional effects [LR-707] p 527 N94-13906
A survey of crack path stability criteria and their application to crack flapping phenomena in stiffened structures [LR-681] p 675 N94-13929
Compressive buckling of curved, anisotropic panels stiffened in two directions. Part 1: Derivation of the governing equations [LR-694] p 675 N94-13931
Fatigue predictions and scatter [LR-696] p 675 N94-13933
MSD in fuselage lap joints: Requirements for inspection intervals for typical fuselage lap joint panels with Multiple Site Damage [LR-697] p 675 N94-13986
Gate assignment using linear programming [LR-698] p 775 N94-13987
ALFIS: Astronomical Low Frequency Interferometry Satellites. A feasibility study [LR-699] p 542 N94-13988
On a difference equation for generalizations of Charlier polynomials [REPT-92-101] p 770 N94-14150
The effect of initial imperfections on shell stability: An updated review [LR-695] p 682 N94-14692
TECHNISCHE UNIV., EINDHOVEN (NETHERLANDS).
Decision support for material planners [ISBN-9-03-860201-4] p 819 N94-14449
Flexibility and costs in the design process: A decision support model [ISBN-9-06-814522-3] p 597 N94-14808
TECHNOLOGY GROUP, LOS ANGELES, CA.
Trellis coding with Continuous Phase Modulation (CPM) for satellite-based land-mobile communications [NASA-CR-191325] p 604 N94-13909
TEL-AVIV UNIV. (ISRAEL).
Lightning simulation and determination of expected striking points [ITN-93-85202] p 719 N94-13188
On the end-to-end communication problem in unreliable networks [ITN-93-85188] p 598 N94-13195
Lower bounds on time of arrival estimation of pulse compression waveforms [ITN-93-85189] p 599 N94-13196
The transient behavior of a boundary layer exposed to uniform suction [ITN-93-85205] p 630 N94-13197
Body/cushion contact stress analysis during sitting [ITN-93-85204] p 736 N94-13229
Planning of a comet simulator [ITN-93-85206] p 835 N94-13230
A photometric study of massive x-ray binaries [ITN-93-85207] p 829 N94-13231
The continuum emission of active galactic nuclei [ITN-93-85208] p 847 N94-13232
Induced voltages at air gaps due to electromagnetic field caused by direct and indirect lightning strokes [ITN-93-85203] p 599 N94-13237
Self tuning and adaptive control: Evaluations and improvements of algorithms [ITN-93-85192] p 762 N94-13329
Constant False Alarm Rate (CFAR) detection in Weibull clutter [ITN-93-85190] p 600 N94-13537
Cancellation of multipath for monopulse radars [ITN-93-85191] p 600 N94-13538
Robot programming, natural computation and conceptual graphs [ITN-93-85193] p 748 N94-13539
Bounds on time delay estimation given unknown signal spectral parameters [ITN-93-85194] p 601 N94-13566
Signal design for data communication through rapidly varying linear channels [ITN-93-85195] p 601 N94-13567
Robot-task compliance: The energy criterion [ITN-93-85196] p 763 N94-13568
Field of solar collectors: Effect of shadowing on the optimal field design [ITN-93-85197] p 702 N94-13570
Laser CO2 beam transmission through hollow metallic waveguide coated by a thin internal dielectric layer [ITN-93-85201] p 656 N94-13571
Liquid and gas evanescent wave spectroscopy via tunable lasers and silver halide fibers [ITN-93-85226] p 565 N94-14465

Optimal maintenance policies of a Markovian system
[ITN-93-85216] p 774 N94-14502
Collisions and separations in 2D hydrodynamical code
[ITN-93-85225] p 639 N94-14503
Implementation and experimentation with a motion planning system
[ITN-93-85213] p 755 N94-14505
Extremal polygon containment problems and other issues in parametric searching
[ITN-93-85214] p 771 N94-14506
The motion of a conical shaped liner driven by explosive load
[ITN-93-85215] p 585 N94-14507
Adiabatic and non adiabatic effects in Free Electron Laser (FEL) non linear interactions
[ITN-93-85224] p 659 N94-14547
Emission line variability in active galactic nuclei
[ITN-93-85209] p 849 N94-14553
The Lindemann criterion of melting for pure and mixed ionic crystals
[ITN-93-85210] p 814 N94-14554
Removing noise from discontinuous data
[ITN-93-85211] p 826 N94-14555
Paradigms for very fast parallel algorithms
[ITN-93-85212] p 755 N94-14556
Small polaron conduction in Y2Ti2O7
[ITN-93-85221] p 814 N94-14557
Ionic conductivity of alkali halides and their mixtures near liquid-solid phase transition
[ITN-93-85222] p 566 N94-14558
A sum-rule of luminescence spectrum
[ITN-93-85223] p 814 N94-14559
LES versus DNS: A comparative study
p 644 N94-14753
Magnetic interactions and disorder - phase transitions in dilute spin-glasses and high temperature superconductors
[ITN-93-85217] p 815 N94-14825
Phases and phase transitions of polymeric liquid crystals: A high resolution x ray diffraction and light scattering study
[ITN-93-85218] p 816 N94-14826

TELEDYNE BROWN ENGINEERING, HUNTSVILLE, AL.
Ultraviolet Spectrometer and Polarimeter (UVSP) catalog of observations. Volume 3: Experiments 63058-99771 (February 1988 - November 1989)
[NASA-CR-4529] p 844 N94-13146

TENNESSEE UNIV., KNOXVILLE.
The state of Fe in the lunar regolith and its relationship to the spectral reflectance properties of the moon
p 843 N94-14303

TENNESSEE UNIV. SPACE INST., TULLAHOMA.
A wall interference assessment/correction system
[NASA-CR-194174] p 500 N94-13076
Hypersonic propulsion characterization
p 505 N94-14156
Aerodynamic and aerothermal facilities 2: Continuous flow high enthalpy facilities p 506 N94-14160
Propulsion integration p 508 N94-14174
Identification and interpretation of patterns in rocket engine data
[NASA-CR-194534] p 552 N94-14309
An integrated knowledge system for the Space Shuttle hazardous gas detection system
[NASA-CR-194533] p 536 N94-14310

TEXAS A&M UNIV., COLLEGE STATION.
Rotordynamic and leakage characteristics of a 4-stage brush seal
[AD-A266012] p 660 N94-12988
Knowledge-based processing for aircraft flight control
[NASA-CR-194074] p 526 N94-13469
Evaluation of the Shuttle remote manipulator
[NASA-CR-194351] p 662 N94-13800
Techniques for estimating Space Station aerodynamic characteristics
[NASA-CR-193394] p 541 N94-13955
Flight validation of a pulsed smoke flow visualization system
[NASA-CR-186026] p 516 N94-14106
Fourteenth National Industrial Energy Technology Conference: Proceedings
[DE93-016698] p 710 N94-14516
Nonrecursive formulations of multibody dynamics and concurrent multiprocessing p 679 N94-14632
Analysis of new composite architectures
[NASA-CR-194524] p 559 N94-14715
Mathematic methods and algorithms for real-time applications
[AD-A266776] p 771 N94-14789

TEXAS UNIV., ARLINGTON.
Functional differential equations with piecewise continuous argument
[AD-A266660] p 772 N94-14840

TEXAS UNIV., AUSTIN.
Kinetic studies following state-selective laser excitation
[DE93-012970] p 654 N94-13013
Meteoroid environment near the Earth-Moon system
[NASA-CR-193670] p 835 N94-13203
Analysis of interstellar cloud structure based on IRAS images
[NASA-CR-194341] p 836 N94-13332
The geometric phase in quantum physics
[DE93-011121] p 817 N94-13479
High freestream turbulence effects on the transport of heat and momentum p 633 N94-13559
Investigation of criteria for ductile fracture under fully-plastic conditions p 672 N94-13593
Time series photometry of faint cataclysmic variables with a CCD p 831 N94-13646
The reionization of the intergalactic medium
p 838 N94-13651
Experimental measurement of local heat transfer coefficients over discrete roughened plates using infrared thermography p 635 N94-13652
The spectroscopic evolution of novae in the bulge of M31 and a search for their possible origin in the M31 globular cluster system p 831 N94-13668
The determination of crustal motions using laser ranging to Lageos-2 and Lageos-1
[NASA-CR-193787] p 717 N94-14306
Long duration measurements of fading on a low elevation angle, 11-GHz satellite path p 613 N94-14661
Large-scale rainfall diversity for ACTS
p 613 N94-14662
Tree attenuation at 20 GHz: Foliage effects
p 615 N94-14672
ACTS data center p 616 N94-14677
Splines, contours and SVD subroutines
[DE93-016088] p 757 N94-14866

TEXAS UNIV., BROWNSVILLE.
Robust stability of diamond families of polynomials with complex coefficients
[NASA-CR-194132] p 768 N94-13421
Exploiting structure: Introduction and motivation
[NASA-CR-194199] p 750 N94-13828

TEXAS UNIV., SAN ANTONIO.
Monoclonal antibodies directed against surface molecules of multicell spheroids
[NASA-CR-193560] p 727 N94-12795

TEXAS UNIV. AT DALLAS, RICHARDSON.
Atomic hydrogen and nitrogen distributions from atmosphere explorer measurements
[NASA-CR-194336] p 714 N94-13825

THERMACORE, INC., LANCASTER, PA.
Insoluble coatings for Stirling engine heat pipe condenser surfaces
[NASA-CR-191188] p 554 N94-14771

THIOKOL CORP., BRIGHAM CITY, UT.
Qualification test of the Ross Double Planetary Mixer
[NASA-CR-192600] p 652 N94-14497
Technical Evaluation Motor No. 10 (TEM-10)
[NASA-CR-193846] p 554 N94-14907

TOHOKU REGIONAL FISHERIES RESEARCH LAB., MIYAGI (JAPAN).
Tracking of change of a warm-core ring structure
p 696 N94-14267

TOKYO INST. OF TECH. (JAPAN).
Study on solidification of immisible alloys (M-10)
p 588 N94-13742
Fabrication of very-low-density, high-stiffness carbon fiber/aluminum hybridized composite with ultra-low density and high stiffness (M-11) p 588 N94-13743

TOKYO MEDICAL AND DENTAL UNIV. (JAPAN).
Studies on the effects of microgravity on the ultrastructure and functions of cultured mammalian cells (L-6) p 592 N94-13763

TOKYO SCIENCE UNIV. (JAPAN).
Present status of JEM utilization projects
p 530 N94-13273

TOKYO UNIV. (JAPAN).
Growth of Si spherical crystals and the surface oxidation (M-9) p 587 N94-13741
Study on the mechanism of liquid phase sintering (M-12) p 588 N94-13744
Estimate of sampling errors of TRMM rainfall observation by using radar-AMeDAS composite data
p 690 N94-14225
Remote sensing of low level cloud optical characteristics p 691 N94-14229
The effects of anthropogenic aerosols on optical thickness and particle size of clouds. Part 1: Retrieval algorithm p 691 N94-14230
Application of satellite remote sensing technology in disaster mitigation: A case study of Bangladesh
p 692 N94-14238
Global assessment of human activities
p 695 N94-14255
Vegetation mapping of Indo-China Peninsula using MOS-1 MESSR and NOAA AVHRR p 695 N94-14257
Outline of ISY Kuroshio observation experiment
p 697 N94-14268

TOKYO UNIV., SAGAMIHARA (JAPAN).
Asia-Pacific ISY Conference, volume 2
[NASDA-CM-199-VOL-2] p 688 N94-14209
Research and development of space transportation systems in ISAS p 537 N94-14277

TOLEDO UNIV., OH.
Measurements of scattering processes in negative ion-atom collisions
[DE93-013863] p 779 N94-12940

TORONTO UNIV. (ONTARIO).
Thermodynamic status of static and dynamic contact angles
[ISBN-0-315-73844-8] p 817 N94-13554
Cold dark matter halos p 838 N94-13649
Flow limitation and flutter in membrane walled collapsible tubes: A model for expiratory wheezing
[ISBN-0-315-73875-8] p 635 N94-13662
Implementation of manufacturing techniques for planar, single mode waveguides on lithium niobate
[DSIS-93-00101] p 792 N94-13845
A neural-network approach to robotic control
p 679 N94-14634

TOSHIBA CORP., TOKYO (JAPAN).
Flight evaluations of approach/landing navigation sensor systems: Summary of 1990 flight experiments
[NAL-TR-1175] p 513 N94-13344

TRANE CO., LACROSSE, WI.
Compatibility of refrigerants and lubricants with motor materials
[DE93-014768] p 583 N94-14801

TRW, INC., REDONDO BEACH, CA.
Control structural interaction testbed: A model for multiple flexible body verification p 544 N94-14649

TRW ELECTRONIC SYSTEMS GROUP, REDONDO BEACH, CA.
Teamwork for Oversight of Processes and Systems (TOPS). Implementation guide for TOPS version 2.0, 10 August 1992 p 668 N94-13167

TRW SPACE TECHNOLOGY LABS., REDONDO BEACH, CA.
Spacecraft COst REduction Team (SCORE): TQM/CI on a massive scale p 667 N94-13160

TRW SYSTEMS AND ENERGY, REDONDO BEACH, CA.
ICE/ISEE plasma wave data analysis
[NASA-CR-194375] p 796 N94-13081

TRW SYSTEMS GROUP, REDONDO BEACH, CA.
Operation of high power converters in parallel
[NASA-CR-191096] p 622 N94-13786

TSUKUBA SPACE CENTER, IBARAGI (JAPAN).
Outline of ISY sea surface temperature data sets
p 696 N94-14261
The status of the HOPE concept study
p 537 N94-14280

TSUKUBA UNIV., IBARAKI (JAPAN).
Measuring methods for CFRP laminates' bending and torsion rigidities characteristics p 529 N94-13272

TULANE UNIV., NEW ORLEANS, LA.
The 8th Workshop on the Mathematical Foundations of Programming Semantics
[AD-A266436] p 749 N94-13700

U

UMPQUA RESEARCH CO., MYRTLE CREEK, OR.
Destruction of problematic airborne contaminants by hydrogen reduction using a Catalytically Active, Regenerable Sorbent (CARS)
[NASA-CR-194354] p 709 N94-14103

UNITED NATIONS EDUCATIONAL, SCIENTIFIC AND CULTURAL ORGANIZATION, PARIS (FRANCE).
Satellite technology for environmental monitoring in developing countries p 692 N94-14236

UNITED TECHNOLOGIES RESEARCH CENTER, EAST HARTFORD, CT.
An analytic modeling and system identification study of rotor/fuselage dynamics at hover p 524 N94-13312
Investigation of the feasibility of optical diagnostic measurements at the exit of the SSME
[NASA-CR-193832] p 553 N94-14682

UNIVERSITIES SPACE RESEARCH ASSOCIATION, HUNTSVILLE, AL.
Crystal growth of ZnSe and related ternary compound semiconductors by physical vapor transport
[NASA-CR-193834] p 807 N94-13444

UNIVERSITY OF ELECTRO-COMMUNICATIONS, TOKYO (JAPAN).
Bulletin of the University of Electro-Communications, volume 6, no. 1, serial no. 11 p 746 N94-13432
Fabrication of AlGaAs/GaAs-light-emitting devices by selective MOCVD using dialkylmetalchloride
p 627 N94-13433

Student's works and power supplies in electronic circuit laboratory p 627 N94-13434
On the construction and decoding of hyperelliptic codes p 747 N94-13435
Computational Russian morphological generation cn Prolog: Noun, pronoun, and adjective p 747 N94-13436
Designing and generating a GUI module using GUI p 747 N94-13437
Codes from an N-dimensional torus simplicially or cellularly decomposed p 747 N94-13438
Study of computer system as a musical instrument p 747 N94-13439
Analysis of fundamental frequency pattern in speech p 618 N94-13440
Reconsideration of the autonomous view of language p 618 N94-13441
Heidegger's thinking p 736 N94-13442

UNIVERSITY OF NORTH TEXAS, DENTON.
Scanning tunneling microscopy studies of diamond films and optoelectronic materials
[NASA-CR-194363] p 578 N94-13246

UNIVERSITY OF SOUTHERN CALIFORNIA, LOS ANGELES.
Office of Naval Research/DARPA publications: Composite materials with improved properties in compression
[AD-A265509] p 560 N94-14794

UNIVERSITY OF SOUTHERN CALIFORNIA, MARINA DEL REY.
Common lisp framework
[AD-A265878] p 742 N94-12933

UNIVERSITY OF SOUTHERN ILLINOIS, CARBONDALE.
Development of time-dependent orthotropic constitutive law of a thermoplastic composite material p 556 N94-13595

UNIVERSITY OF SOUTHERN MISSISSIPPI, HATTIESBURG.
Characterization of 1:1 random copolymers obtained from 6-, 7-, 11-, and 12-carbon amino acids
[AD-A265827] p 577 N94-12985
Unexpectedly rapid hydrosilation polymerization of the diallyl derivative of bisphenol A and 2,6-diallylphenol
[AD-A265832] p 577 N94-12986

UNIVERSITY OF WESTERN ONTARIO, LONDON.
Meteor forward scatter studies
[DSIS-93-00382] p 602 N94-13801
A study of meteor scatter communications
[DSIS-93-00151] p 603 N94-13841

UTAH STATE UNIV., LOGAN.
Newton iterative methods for large scale nonlinear systems
[DE93-015357] p 767 N94-13025

UTAH UNIV., SALT LAKE CITY.
Thermochemistry of transition metal clusters
[DE93-016201] p 571 N94-13977

V

VANDERBILT UNIV., NASHVILLE, TN.
The influence of a microgravity environment on the dendritic morphology during directional solidification of hypoeutectic Al-Si alloys
[NASA-CR-194139] p 571 N94-13891

VARIAN ASSOCIATES, PALO ALTO, CA.
A millimeter-wave tunneladder TWT
[NASA-CR-182183] p 620 N94-13106
Long-pulse operation of a gyrotron with beam/RF separation
[DE93-015007] p 649 N94-13410

VEXCEL CORP., BOULDER, CO.
EOS workstation
[NASA-CR-191326] p 736 N94-13132

VICTORIA UNIV. (BRITISH COLUMBIA).
Geometric stiffening in multibody dynamics formulations p 677 N94-14619
Modelling robotic systems with DADS p 678 N94-14625

VIGYAN RESEARCH ASSOCIATES, INC., HAMPTON, VA.
Three-Dimensional Boundary-Layer program (BL3D) for swept subsonic or supersonic wings with application to laminar flow control
[NASA-CR-4531] p 629 N94-13073

VIKING INSTRUMENTS CORP., RESTON, VA.
Development of an advanced spacecraft tandem mass spectrometer
[NASA-CR-194195] p 545 N94-13953

VIRGINIA COMMONWEALTH UNIV., RICHMOND.
Structure stability and spectroscopy of metal clusters
[DE93-016142] p 567 N94-12836

VIRGINIA POLYTECHNIC INST., BLACKSBURG.
Probabilistic micromechanics for high-temperature composites
[NASA-CR-191150] p 676 N94-14408

VIRGINIA POLYTECHNIC INST. AND STATE UNIV., BLACKSBURG.
Design and application of a quasistatic crush test fixture for investigating scale effects in energy absorbing composite plates
[NASA-CR-4526] p 670 N94-13063
Optical fiber sensors for materials and structures characterization
[NASA-CR-194090] p 791 N94-13353
Study of electroweak interactions
[DE93-015067] p 782 N94-13412
A technique for direct measurement of skin friction in supersonic combustion flow p 503 N94-13555
Topics on spatially high-order accurate methods and pre-conditioning for the Navier-Stokes equations with finite-rate chemistry p 633 N94-13572
Calculation of hypersonic shock structure using flux-split algorithms
[NASA-CR-194296] p 504 N94-13607
Sites of fine-scale electron density turbulence in the interstellar medium
[NASA-CR-193708] p 839 N94-13864
Information requirements of self-managing teams
[DE93-010319] p 824 N94-14048
Feasibility study of a synthesis procedure for array feeds to improve radiation performance of large distorted reflector antennas
[NASA-CR-194491] p 612 N94-14501
Statistical results from the Virginia Tech propagation experiment using the Olympus 12, 20, and 30 GHz satellite beacons p 613 N94-14658
Results from a study of scintillation behavior at 12, 20, and 30 GHz using the results from the Virginia Tech Olympus receivers p 613 N94-14659
The ACTS propagation terminal delivery and support p 615 N94-14674
Data collection with the ACTS propagation terminal p 615 N94-14675
Preprocessing data collected with the ACTS propagation terminal p 616 N94-14676
Surface characterization of LDEF materials
[NASA-CR-194519] p 543 N94-14683

VIRGINIA UNIV., CHARLOTTESVILLE.
Spectra of late type dwarf stars of known abundance for stellar population models
[NASA-CR-194301] p 831 N94-13681

VON KARMAN INST. FOR FLUID DYNAMICS, RHODE-SAINT-GENESE (BELGIUM).
Methodology of Hypersonic Testing
[VKI-LS-1993-03] p 505 N94-14153

W

WASHINGTON UNIV., SEATTLE.
Cosmic physics data analysis program
[NASA-CR-194357] p 846 N94-12826
Aspects of symmetry violation
[DE93-011003] p 779 N94-12997
Electrodynamics of the middle atmosphere: Superpressure balloon program
[NASA-CR-193671] p 712 N94-13293
Theoretical support for the Airborne Antarctic Ozone Experiment
[NASA-CR-193669] p 713 N94-13465
Recent developments in multiple-scattering calculations of XAFS and XANES
[DE93-010999] p 563 N94-13477
Many-body corrections in XAFS
[DE93-011002] p 563 N94-13478
Optical properties of CO2 ice and CO2 snow in the ultraviolet, visible, and infrared
[NASA-CR-194110] p 686 N94-14081
Measuring strangeness in the nucleon
[DE93-014861] p 785 N94-14471
The off shell (rho)-(omega) mixing in the QCD sum rules
[DE93-014845] p 786 N94-14527
Comparative study of x ray and microwave emissions during solar flares
[NASA-CR-194532] p 845 N94-14577
Chaos and microbial systems
[DE93-016814] p 730 N94-14596

WATERLOO UNIV. (ONTARIO).
Net radiation mapping of mountainous terrain using Landsat-5 thematic mapper imagery and digital terrain data
[ISBN-0-315-57755-X] p 685 N94-13475

WAYNE STATE UNIV., DETROIT, MI.
The 1.00 MeV proton radiation resistance studies of amorphous silicon-based alloy solar cells p 703 N94-13639

WEIDLINGER ASSOCIATES, NEW YORK, NY.
Non-uniqueness in dynamic rate-independent non-associated plasticity
[AD-A266342] p 769 N94-13731

WEIZMANN INST. OF SCIENCE, REHOVOTH (ISRAEL).
The 4th International Symposium on Analysis and Detection of Explosives
[DE93-620280] p 585 N94-14829

WESTINGHOUSE ELECTRIC CORP., PITTSBURGH, PA.
Processing, fabrication and demonstration of HTS integrated microwave circuits
[AD-A265789] p 619 N94-12892

WESTINGHOUSE HANFORD CO., RICHLAND, WA.
BAKEOUT: A computer program for predicting diffusive outgassing from stainless steel
[DE93-012613] p 573 N94-14364

WESTINGHOUSE IDAHO NUCLEAR CO., INC., IDAHO FALLS.
SHEAN (Simplified Human Error Analysis code) and automated THERP
[DE93-014904] p 738 N94-14451

WESTINGHOUSE SAVANNAH RIVER CO., AIKEN, SC.
Canonical correlation of waste glass compositions and durability, including pH
[DE93-012754] p 578 N94-13493
Materials compatibility of hydride storage materials with austenitic stainless steels
[DE93-013688] p 703 N94-13691
Relationship between borosilicate glass composition, structure, and durability test response (SRS)
[DE93-013578] p 581 N94-14343
Reviews of computing technology: Object-oriented technology
[DE93-014740] p 754 N94-14470

WINAND STARING CENTRE, WAGENINGEN (NETHERLANDS).
Obtaining digital regional planning information from aerial pictures
[REPT-228] p 700 N94-14810

WINDSOR UNIV. (ONTARIO).
Close range 3-D position sensing using stereo vision and point-of-correspondance through mathematical morphology
[ISBN-0-315-61012-3] p 763 N94-13515

WISCONSIN UNIV., MADISON.
Development of ISO connection-oriented/correctionless gateways
[NASA-CR-193667] p 821 N94-13030
An experimental regional scale climate simulation laboratory
[DE93-015935] p 719 N94-13119
Infrared spectroscopy of organic free radicals related to combustion processes
[DE93-017086] p 562 N94-13222
Experimental and kinetic modeling of acid/base and redox reactions over oxide catalysts
[DE93-016203] p 563 N94-13375
Containerless processing of undercooled melts
[NASA-CR-194350] p 572 N94-14123
Three-dimensional modeling of diesel engine intake flow, combustion and emissions-2
[NASA-CR-191189] p 519 N94-14448
Reactor studies of metal ions associated with chromatographic silica
[AD-A266675] p 573 N94-14779

WORLD METEOROLOGICAL ORGANIZATION, GENEVA (SWITZERLAND).
Bibliography of urban climate in tropical/subtropical areas, 1981-1991
[WCASP-25] p 718 N94-12918
Manual on the global data-processing system. Volume 1: (Annex 4 to the WMO regulations) global aspects (1992 edition)
[WMO-485-VOL-1] p 721 N94-13686
Manual on the global data-processing system. Volume 2: Regional aspects (1992 edition)
[WMO-485-VOL-2] p 722 N94-14071
CCl working group on climate data and its rapporteurs
[WCDMP-21] p 723 N94-14118

WRIGHT LAB., WRIGHT-PATTERSON AFB, OH.
Evaluation of infrared sensors for autonomous landing guidance
[AD-A266450] p 513 N94-13703

WYOMING UNIV., LARAMIE.
Cellular mechanism of turnover of the stress induced protein HSP 70
[AD-A265723] p 732 N94-13061

Y

YALE UNIV., NEW HAVEN, CT.
Research on chemical vapor deposition processes for advanced ceramic coatings
[NASA-CR-193613] p 577 N94-13089
Minimal modeling of the bimodality of extratropical atmospheric planetary waves p 713 N94-13622
The first steps of chlorophyli synthesis: RNA involvement and regulation
[DE93-014398] p 730 N94-14509

Typical Contract Number Index Listing

AF PROJ. 2306 ..... p 92 N94-11866

CONTRACT NUMBER | PAGE NUMBER | ACCESSION NUMBER

Listings in this index are arranged alphanumerically by contract number. Under each contract number the accession numbers denoting documents that have been produced as a result of research done under that contract are arranged in ascending order. The page number helps to locate the citation in the abstract section. The accession number denotes the number by which the citation is identified.

AD-AFOSR-0090-93 ..... p 770 N94-14307
AF PROJ. 6670 ..... p 719 N94-12978
AF-AFOSR-0061-93 ..... p 771 N94-14731
AF-AFOSR-0090-93 ..... p 769 N94-13725
p 770 N94-13922
AF-AFOSR-0091-90 ..... p 768 N94-13354
AF-AFOSR-0100-90 ..... p 805 N94-13037
AF-AFOSR-0179-90 ..... p 771 N94-14731
AF-AFOSR-0180-91 ..... p 636 N94-13724
AF-AFOSR-0222-90 ..... p 732 N94-13038
AF-AFOSR-0240-91 ..... p 681 N94-14644
AF-AFOSR-0280-91 ..... p 728 N94-13698
AF-AFOSR-0296-89 ..... p 665 N94-13042
AF-AFOSR-0316-90 ..... p 807 N94-13580
AF-AFOSR-0336-90 ..... p 673 N94-13778
AF-AFOSR-0474-89 ..... p 575 N94-12812
ARPA ORDER 7330 ..... p 759 N94-13052
p 767 N94-13284
p 749 N94-13779
ARPA ORDER 7597 ..... p 735 N94-14797
BCRS PROJ. 3.1/TO-01 ..... p 687 N94-14127
BMFT-01-QS-88168 ..... p 651 N94-14149
BMFT-07-KF-114-6 ..... p 723 N94-14546
BMFT-07-KFT-05/6 ..... p 724 N94-14709
BMFT-07-KFT-38/3 ..... p 723 N94-14707
BMFT-412-7491-K-0275-5 ..... p 617 N94-14817
BMFT-513-8320-KF-10110 ..... p 723 N94-14707
BU-4426-30 ..... p 729 N94-14128
p 729 N94-14129
DA PROJ. MM3-3-C-30 ..... p 733 N94-14879
DA PROJ. R00-0-NO ..... p 683 N94-14902
DA PROJ. 1L1-62211-A-47-A ..... p 663 N94-14445
p 664 N94-14446
DAAH04-93-G-0092 ..... p 772 N94-14900
DAAL03-88-C-0004 ..... p 510 N94-14799
DAAL03-88-K-0062 ..... p 509 N94-14774
DAAL03-89-C-0027 ..... p 509 N94-14781
DAAL03-89-D-0003 ..... p 816 N94-14839
DAAL03-89-G-0107 ..... p 772 N94-14840
DAAL03-89-K-0172 ..... p 510 N94-14784
DAAL03-89-K-0175 ..... p 573 N94-14786
DAAL03-90-G-0036 ..... p 787 N94-14778
DAAL03-90-G-0081 ..... p 579 N94-13584
DAAL03-90-G-0091 ..... p 771 N94-14789
DAAL03-90-G-0105 ..... p 748 N94-13586
DAAL03-90-G-0123 ..... p 573 N94-14779
DAAL03-90-G-0130 ..... p 665 N94-14901
DAAL03-91-C-0002 ..... p 766 N94-14785
DAAL03-91-G-0138 ..... p 774 N94-14788
DACA76-92-C-0003 ..... p 766 N94-14777
DARPA ORDER 6096 ..... p 742 N94-12933
DARPA ORDER 8323 ..... p 766 N94-14777
DE-AC01-91CE-50337 ..... p 701 N94-12913
DE-AC02-76CH-00016 ..... p 660 N94-12851
p 705 N94-12869
p 548 N94-12981
p 549 N94-13034
p 562 N94-13045
p 706 N94-13054
p 780 N94-13097
p 780 N94-13098
p 780 N94-13101
p 805 N94-13102
p 780 N94-13149
p 806 N94-13150
p 781 N94-13219
p 789 N94-13220
p 569 N94-13221
p 781 N94-13241
p 552 N94-14111
p 580 N94-14142
p 773 N94-14320
p 785 N94-14363
p 813 N94-14517
p 793 N94-14529
p 659 N94-14572
p 787 N94-14580
p 566 N94-14582
p 676 N94-14585
p 554 N94-14806
p 788 N94-14872
DE-AC02-76CH-03000 ..... p 779 N94-12954
p 834 N94-12980
p 834 N94-13096
p 781 N94-13350
p 783 N94-13494
p 783 N94-13884
p 783 N94-13895
p 808 N94-13973
p 651 N94-14452
p 786 N94-14524
p 788 N94-14898
DE-AC02-83CH-10093 ..... p 700 N94-12868
p 701 N94-12902
p 701 N94-12914
p 702 N94-13381
p 702 N94-13386
p 809 N94-14085
p 709 N94-14087
p 584 N94-14089
p 704 N94-14109
p 704 N94-14110
p 704 N94-14350
p 704 N94-14422
p 704 N94-14423
p 585 N94-14454
p 851 N94-14455
DE-AC03-76SF-00098 ..... p 780 N94-13018
p 631 N94-13244
p 746 N94-13382
p 563 N94-13411
p 808 N94-13694
p 848 N94-13695
p 637 N94-14053
p 658 N94-14175
p 704 N94-14333
p 625 N94-14336
p 581 N94-14400
p 851 N94-14401
p 658 N94-14414
p 825 N94-14433
p 573 N94-14474
p 710 N94-14477
p 659 N94-14520
p 776 N94-14584
p 851 N94-14587
p 659 N94-14595
p 815 N94-14699
p 574 N94-14795
p 787 N94-14857
p 816 N94-14868
p 790 N94-14893
DE-AC03-76SF-00515 ..... p 805 N94-13020
p 761 N94-14476
DE-AC03-89ER-51114 ..... p 795 N94-12953
p 800 N94-13900
p 801 N94-14293
p 801 N94-14347
p 802 N94-14519
p 802 N94-14570
p 802 N94-14579
p 802 N94-14583
p 757 N94-14866
DE-AC04-76DP-00613 ..... p 743 N94-13014
p 620 N94-13094
p 578 N94-13118
p 707 N94-13390
p 748 N94-13480
p 675 N94-13907
p 624 N94-13928
p 624 N94-13937
p 625 N94-14533
p 652 N94-14534
DE-AC04-76DP-00789 ..... p 804 N94-12813
p 561 N94-12819
p 618 N94-12821
p 561 N94-12841
p 576 N94-12866
p 758 N94-12878
p 628 N94-12884
p 820 N94-12907
p 670 N94-12908
p 539 N94-12909
p 561 N94-12910
p 576 N94-12912
p 619 N94-12942
p 742 N94-12956
p 568 N94-12977
p 743 N94-12991
p 743 N94-12999
p 539 N94-13006
p 759 N94-13043
p 648 N94-13044
p 501 N94-13260
p 655 N94-13261
p 649 N94-13395
p 632 N94-13397
p 540 N94-13398
p 782 N94-13409
p 551 N94-13514
p 748 N94-13578
p 601 N94-13696
p 703 N94-13886
p 579 N94-13888
p 596 N94-13889
p 623 N94-13892
p 800 N94-13908
p 760 N94-14011
p 752 N94-14019
p 686 N94-14056
p 809 N94-14079
p 809 N94-14083
p 809 N94-14108
p 753 N94-14295
p 812 N94-14344
p 812 N94-14345
p 801 N94-14347
p 801 N94-14349
p 754 N94-14399
p 817 N94-14453
p 676 N94-14456
p 582 N94-14511
p 612 N94-14512
p 755 N94-14528
p 802 N94-14570
p 652 N94-14578
p 814 N94-14695
p 653 N94-14858
p 705 N94-14861
DE-AC04-76DR-00789 ..... p 710 N94-14183
DE-AC04-88DP-43495 ..... p 573 N94-14316
DE-AC04-91AL-65030 ..... p 663 N94-14113
DE-AC05-84OR-21400 ..... p 788 N94-12817
p 804 N94-12818
p 567 N94-12899
p 775 N94-12955
p 568 N94-12998
p 805 N94-13009
p 805 N94-13012
p 795 N94-13033
p 796 N94-13046
p 797 N94-13144
p 569 N94-13242
p 781 N94-13349
p 707 N94-13384
p 759 N94-13470
p 707 N94-13486

	p 798	N94-13577	
	p 604	N94-13899	
	p 800	N94-13900	
	p 824	N94-13915	
	p 808	N94-13930	
	p 571	N94-14021	
	p 651	N94-14046	
	p 607	N94-14291	
	p 801	N94-14293	
	p 774	N94-14334	
	p 738	N94-14335	
	p 812	N94-14348	
	p 812	N94-14362	
	p 825	N94-14458	
	p 813	N94-14478	
	p 755	N94-14515	
	p 676	N94-14530	
	p 582	N94-14531	
	p 573	N94-14537	
	p 766	N94-14568	
	p 802	N94-14570	
	p 756	N94-14696	
	p 573	N94-14700	
	p 803	N94-14770	
	p 711	N94-14859	
	p 660	N94-14863	
DE-AC05-84OS-21400	p 565	N94-14525	
	p 757	N94-14871	
DE-AC05-84OT-21400	p 710	N94-14459	
DE-AC06-76RL-01830	p 718	N94-12903	
	p 706	N94-12905	
	p 706	N94-12937	
	p 568	N94-13035	
	p 782	N94-13485	
	p 708	N94-13910	
	p 709	N94-13911	
	p 715	N94-13912	
	p 572	N94-14058	
	p 572	N94-14184	
	p 580	N94-14297	
	p 658	N94-14415	
	p 710	N94-14523	
	p 755	N94-14571	
	p 793	N94-14702	
DE-AC06-80ER-53098	p 794	N94-12862	
DE-AC06-87RL-10930	p 573	N94-14364	
DE-AC07-76ID-01570	p 548	N94-12870	
	p 549	N94-12996	
	p 550	N94-13351	
	p 823	N94-13352	
	p 746	N94-13394	
	p 552	N94-14013	
DE-AC07-84ID-12435	p 738	N94-14451	
DE-AC08-88NV-10617	p 717	N94-14294	
DE-AC09-89SR-18035	p 578	N94-13493	
	p 703	N94-13691	
	p 581	N94-14343	
	p 754	N94-14470	
DE-AC21-90MC-27168	p 701	N94-13093	
	p 703	N94-13693	
DE-AC22-92PC-92111	p 583	N94-13002	
DE-AC34-90DP-62349	p 565	N94-14346	
	p 664	N94-14565	
DE-AC35-89ER-40486	p 821	N94-12983	
	p 755	N94-14581	
	p 787	N94-14588	
DE-AI01-86CE-90239	p 727	N94-12793	
DE-AI01-91CE-50306	p 519	N94-14448	
DE-AI03-79DP-40092	p 796	N94-13047	
	p 655	N94-13387	
DE-AI05-83ER-40112	p 789	N94-13727	
DE-AI05-92ER-54177	p 789	N94-13727	
DE-AI21-92PC-92150	p 701	N94-13187	
DE-AS05-80ER-10713	p 782	N94-13412	
DE-FC21-92MC-28065	p 702	N94-13380	
DE-FG01-92CE-15974	p 581	N94-14337	
DE-FG02-84ER-13183	p 563	N94-13375	
DE-FG02-84ER-45125	p 730	N94-14802	
DE-FG02-84ER-45133	p 804	N94-13005	
DE-FG02-84ER-45141	p 812	N94-14354	
DE-FG02-84ER-45147	p 781	N94-13283	
DE-FG02-85ER-60314	p 723	N94-14426	
DE-FG02-86ER-25015	p 740	N94-13069	
DE-FG02-86ER-45228	p 578	N94-13408	
DE-FG02-86ER-45229	p 810	N94-14185	
DE-FG02-86ER-45237	p 579	N94-13978	
DE-FG02-86ER-45254	p 813	N94-14517	
DE-FG02-86ER-53218	p 800	N94-13850	
	p 801	N94-14206	
DE-FG02-86SF-16306	p 705	N94-14504	
DE-FG02-87ER-13726	p 791	N94-13015	
DE-FG02-87ER-13734	p 730	N94-14509	
DE-FG02-87ER-13740	p 818	N94-14738	
DE-FG02-87ER-25047	p 744	N94-13024	
DE-FG02-87ER-40333	p 778	N94-12860	
DE-FG02-87ER-45298	p 577	N94-13072	
DE-FG02-87ER-45315	p 809	N94-13980	
DE-FG02-87ER-45334	p 815	N94-14739	
DE-FG02-87ER-53257	p 803	N94-14874	
DE-FG02-88ER-13878	p 565	N94-14403	
DE-FG02-88ER-13896	p 628	N94-12961	
DE-FG02-88ER-13933	p 814	N94-14597	
DE-FG02-88ER-13960	p 780	N94-13071	
DE-FG02-88ER-13978	p 717	N94-14338	
DE-FG02-88ER-25065	p 817	N94-14417	
DE-FG02-88ER-40388	p 839	N94-14330	
DE-FG02-88ER-40413	p 780	N94-13097	
	p 780	N94-13098	
DE-FG02-89ER-14056	p 654	N94-13022	
DE-FG02-89ER-45391	p 811	N94-14296	
DE-FG02-89ER-45401	p 815	N94-14798	
DE-FG02-90ER-45418	p 558	N94-14418	
DE-FG02-90ER-45438	p 577	N94-13070	
DE-FG02-90ER-54092	p 787	N94-14691	
DE-FG02-90ER-61014	p 706	N94-13079	
DE-FG02-91CE-23810	p 595	N94-13021	
	p 596	N94-13407	
DE-FG02-91ER-14187	p 583	N94-14801	
DE-FG02-91ER-14193	p 562	N94-13001	
DE-FG02-91ER-14205	p 571	N94-13977	
DE-FG02-91ER-20050	p 784	N94-13983	
DE-FG02-91ER-40645	p 727	N94-12835	
	p 780	N94-13097	
DE-FG02-91ER-40646	p 780	N94-13098	
DE-FG02-91ER-54109	p 781	N94-13348	
DE-FG02-91ER-54131	p 802	N94-14579	
DE-FG02-91NP-00119	p 795	N94-12984	
DE-FG02-92ER-14275	p 824	N94-14048	
DE-FG02-92ER-14280	p 806	N94-13152	
DE-FG02-92ER-14281	p 573	N94-14402	
DE-FG02-92ER-14306	p 567	N94-12834	
DE-FG02-92ER-25136	p 562	N94-13222	
DE-FG02-92ER-40741	p 767	N94-13025	
DE-FG02-92ER-40747	p 818	N94-14896	
DE-FG02-92ER-61474	p 790	N94-14897	
DE-FG02-93ER-12128	p 719	N94-13119	
DE-FG02-93ER-40768	p 809	N94-13981	
DE-FG03-89ER-51121	p 784	N94-13952	
	p 801	N94-14347	
DE-FG03-92ER-25140	p 802	N94-14570	
DE-FG03-92ER-40711	p 639	N94-14434	
DE-FG03-93ER-14348	p 811	N94-14332	
DE-FG03-93ER-40757	p 654	N94-13013	
DE-FG05-84ER-13191	p 817	N94-13479	
DE-FG05-85ER-13439	p 654	N94-13013	
DE-FG05-86ER-60473	p 562	N94-13004	
DE-FG05-87ER-13745	p 785	N94-14420	
DE-FG05-87ER-40309	p 807	N94-13373	
	p 780	N94-13097	
DE-FG05-87ER-40314	p 780	N94-13098	
DE-FG05-87ER-45316	p 848	N94-13695	
DE-FG05-87ER-52147	p 567	N94-12836	
DE-FG05-88ER-13971	p 654	N94-13058	
DE-FG05-88ER-40441	p 779	N94-12940	
DE-FG05-88ER-45359	p 786	N94-14514	
DE-FG05-88ER-53266	p 804	N94-13003	
DE-FG05-88ER-60721	p 757	N94-14866	
DE-FG05-90ER-45431	p 782	N94-13414	
DE-FG05-90ER-75582	p 570	N94-13374	
DE-FG05-90ER-75596	p 563	N94-13413	
DE-FG05-91ER-14181	p 813	N94-14517	
DE-FG05-91ER-14214	p 575	N94-12861	
DE-FG05-91ER-40619	p 785	N94-14419	
DE-FG05-92ER-75784	p 786	N94-14514	
DE-FG05-92ER-75842	p 574	N94-14873	
DE-FG06-88ER-40427	p 818	N94-13216	
	p 779	N94-12997	
DE-FG06-90ER-40561	p 785	N94-14471	
DE-FG06-90ER-45415	p 786	N94-14527	
	p 786	N94-14527	
DE-FG06-90ER-61034	p 563	N94-13477	
DE-FG07-89ID-12842	p 563	N94-13478	
DE-FG08-90ER-61012	p 730	N94-14596	
DE-FG09-84ER-40160	p 638	N94-14351	
DE-FG09-88ER-13970	p 719	N94-13080	
DEN3-335	p 784	N94-13927	
DFG-SO-104/9-1	p 827	N94-14803	
DFG-SO-104/9-2	p 828	N94-12931	
DNA001-89-C-0052	p 579	N94-14007	
DREA-W7707-0-0918/01-OSC	p 579	N94-14007	
	p 769	N94-13731	
DREO-W7714-0-9504	p 751	N94-14017	
	p 558	N94-14105	
	p 604	N94-13869	
	p 604	N94-13870	
	p 751	N94-13990	
	p 751	N94-14014	
	p 605	N94-14015	
	p 751	N94-14016	
	p 606	N94-14037	
	p 606	N94-14038	
	p 753	N94-14197	
DREP-W7708-1-0980-01-XSA	p 777	N94-14360	
DSS-W2207-8-AF78	p 752	N94-14088	
DSS-W7702-1-R289-01-XSG	p 657	N94-14067	
DSS-W7714-0-9383-01-SS	p 603	N94-13843	
DSS-W7714-8-5713-01-ST	p 792	N94-13868	
DSS-36001-9-3601-01-SS	p 603	N94-13841	
DSS-9F009-0-4015	p 764	N94-13842	
DTFA01-92-Y-01005	p 738	N94-14023	
DTFA02-92-P-23499	p 732	N94-13193	
ESTEC-7989/88/NL/PB(SC)	p 542	N94-14107	
ESTEC-9307/91/NL/PP(SC)	p 673	N94-13689	
FMV-FLYG-82450-87-348-24-001	p 528	N94-13588	
FMV-FLYG-82450-88-341-73-0	p 528	N94-13588	
FNDCT-246/91	p 630	N94-13114	
F04701-88-C-0089	p 661	N94-13122	
	p 579	N94-13903	
	p 659	N94-14681	
F19628-90-C-0002	p 531	N94-13358	
F19628-90-C-0003	p 744	N94-13049	
F30602-89-C-0014	p 759	N94-13177	
F30602-89-D-0050	p 758	N94-12930	
F30602-90-D-0097	p 619	N94-12967	
F30602-91-F-0016	p 820	N94-14796	
F33615-88-C-2908	p 660	N94-12988	
F33615-89-C-0574	p 736	N94-12935	
F33615-90-C-1465	p 735	N94-14797	
F33615-90-C-2054	p 636	N94-13730	
F33615-92-C-5915	p 568	N94-12993	
F49620-89-C-0046	p 819	N94-13059	
F49620-91-C-0095	p 678	N94-14624	
	p 679	N94-14633	
F49620-92-J-0023	p 628	N94-12888	
F49620-92-J-0234	p 732	N94-13061	
F49620-92-J-0448	p 796	N94-13039	
JPL-956520	p 615	N94-14672	
MDA903-87-C-0641	p 742	N94-12933	
MDA972-90-C-0035	p 759	N94-13052	
	p 767	N94-13284	
	p 749	N94-13779	
MDA972-91-C-0028	p 622	N94-13776	
MIPR-ARO-148-91	p 817	N94-14680	
NAGW-1064	p 835	N94-13203	
NAGW-1106	p 842	N94-13199	
NAGW-1160	p 713	N94-13465	
NAGW-1166	p 683	N94-14500	
NAGW-1318	p 821	N94-13030	
NAGW-1331	p 841	N94-13088	
NAGW-1355	p 545	N94-13067	
NAGW-1406	p 625	N94-14325	
NAGW-1480	p 832	N94-14146	
NAGW-1487	p 847	N94-13288	
NAGW-1548	p 713	N94-13418	
NAGW-1571	p 714	N94-13825	
NAGW-1620	p 796	N94-13084	
NAGW-1671	p 727	N94-13210	
NAGW-1712	p 800	N94-13854	
NAGW-1734	p 686	N94-14081	
NAGW-1902	p 840	N94-14482	
NAGW-1919	p 847	N94-13211	
NAGW-1959	p 717	N94-14306	
NAGW-2022	p 621	N94-13194	
	p 626	N94-14730	
NAGW-2126	p 714	N94-13793	
NAGW-2128	p 715	N94-13954	
NAGW-2201	p 839	N94-14404	
NAGW-2317	p 682	N94-14692	
NAGW-2322	p 836	N94-13423	
NAGW-2361	p 841	N94-12823	
NAGW-2540	p 571	N94-13891	
NAGW-2586	p 714	N94-13707	
NAGW-2698	p 833	N94-14358	
NAGW-2734	p 849	N94-13965	
NAGW-2739	p 729	N94-14494	
NAGW-2753	p 650	N94-14029	
NAGW-2792	p 721	N94-13675	
NAGW-2819	p 845	N94-14577	
NAGW-2821	p 712	N94-13334	
NAGW-3018	p 845	N94-14479	
NAGW-3026	p 846	N94-12826	
NAGW-3089	p 713	N94-13335	
NAGW-3107	p 836	N94-13423	
NAGW-3139	p 808	N94-13875	
NAGW-3576	p 789	N94-13419	
NAGW-413	p 716	N94-13969	
NAGW-533	p 617	N94-14743	
NAGW-631	p 540	N94-13109	
NAGW-724	p 712	N94-13293	
NAGW-773	p 715	N94-13826	
NAGW-925	p 743	N94-13023	
	p 823	N94-13192	
NAG1-1060	p 758	N94-12938	
NAG1-1066	p 526	N94-13469	
NAG1-1067	p 582	N94-14539	
NAG1-1133	p 527	N94-12824	
NAG1-1139	p 508	N94-14538	
NAG1-1145	p 499	N94-12852	

p 770 N94-14429
NAG1-1176 p 791 N94-13353
NAG1-1183 p 602 N94-13799
NAG1-1186 p 543 N94-14683
NAG1-1255 p 516 N94-14104
NAG1-1301 p 625 N94-14324
NAG1-1313 p 575 N94-12789
NAG1-1346 p 659 N94-14576
NAG1-1416 p 539 N94-12976
NAG1-1435 p 766 N94-14444
NAG1-1468 p 578 N94-13246
NAG1-1478 p 602 N94-13720
NAG1-1491 p 716 N94-14049
NAG1-343 p 670 N94-13063
NAG1-477 p 786 N94-14549
NAG1-631 p 579 N94-13964
NAG1-776 p 504 N94-13607
NAG1-786 p 706 N94-13170
NAG1-859 p 612 N94-14501
NAG1-961 p 501 N94-13292
NAG1-995 p 752 N94-14139
NAG10-0047 p 718 N94-12839
NAG2-393 p 845 N94-14492
NAG2-411 p 731 N94-12960
NAG2-438 p 728 N94-13865
NAG2-544 p 599 N94-13264
NAG2-578 p 791 N94-13682
NAG2-591 p 740 N94-13363
NAG2-690 p 842 N94-13561
NAG2-700 p 739 N94-13086
NAG2-733 p 500 N94-13076
NAG2-778 p 630 N94-13078
NAG2-819 p 727 N94-12795
NAG3-1016 p 635 N94-13676
NAG3-1060 p 567 N94-12825
NAG3-1073 p 664 N94-14848
NAG3-1087 p 519 N94-14448
NAG3-1253 p 572 N94-14133
NAG3-1270 p 559 N94-14715
NAG3-1432 p 558 N94-14050
NAG3-535 p 674 N94-13873
NAG3-768 p 500 N94-13180
NAG3-884 p 577 N94-13089
NAG3-933 p 676 N94-14408
NAG5-1035 p 831 N94-13681
NAG5-1171 p 831 N94-13679
NAG5-1177 p 848 N94-13708
NAG5-1205 p 836 N94-13446
NAG5-1212 p 830 N94-13462
NAG5-1257 p 628 N94-12959
NAG5-1260 p 832 N94-13894
NAG5-1263 p 836 N94-13332
NAG5-1268 p 838 N94-13716
NAG5-1275 p 839 N94-13864
NAG5-1305 p 829 N94-13287
NAG5-1316 p 835 N94-13239
NAG5-1319 p 656 N94-13420
NAG5-1323 p 844 N94-13958
NAG5-1324 p 844 N94-13671
NAG5-1520 p 783 N94-13856
NAG5-1651 p 835 N94-13171
NAG5-1684 p 832 N94-14357
NAG5-1737 p 833 N94-14405
NAG5-1742 p 847 N94-13087
NAG5-1744 p 833 N94-14406
NAG5-1819 p 833 N94-14405
NAG5-1833 p 715 N94-13956
NAG5-1954 p 829 N94-13181
NAG5-1989 p 712 N94-13212
NAG5-2004 p 661 N94-13445
NAG5-2017 p 829 N94-13178
NAG5-2041 p 512 N94-13082
NAG5-2051 p 840 N94-14688
NAG5-2092 p 840 N94-14685
NAG5-2187 p 619 N94-12897
p 598 N94-12920
p 744 N94-13113
p 600 N94-13466
NAG5-2198 p 763 N94-13603
NAG5-2210 p 768 N94-13421
p 750 N94-13828
NAG5-484 p 712 N94-13092
NAG5-619 p 832 N94-13966
NAG5-635 p 712 N94-13293
NAG5-676 p 652 N94-14684
NAG5-780 p 833 N94-14359
NAG8-129 p 637 N94-13959
NAG8-160 p 638 N94-14308
NAG8-166 p 552 N94-14309
NAG8-204 p 562 N94-13048
NAG8-240 p 663 N94-14134
NAG8-253 p 721 N94-13723
NAG8-758 p 822 N94-13062
NAG8-768 p 565 N94-14480
NAG8-771 p 572 N94-14123
NAG8-822 p 716 N94-13967
NAG8-835 p 536 N94-14310
NAG8-880 p 711 N94-12788
NAG8-931 p 803 N94-12796
NAG9-357 p 677 N94-14621
NAG9-386 p 541 N94-13955
NAG9-450 p 662 N94-13800
NAG9-574 p 540 N94-13112
NAG9-625 p 742 N94-12808
NAL PROJ. CF-0-900 p 639 N94-14598
NAL PROJ. CF-1-121 p 510 N94-14612
NASA ORDER H-19671-D p 830 N94-13448
NASA ORDER H-19675-D p 660 N94-12791
NASA ORDER H-20752-D p 792 N94-14473
NASA ORDER H-20780-D p 660 N94-14904
NASA ORDER L-4409-D p 595 N94-14026
NASA ORDER T-256M p 543 N94-14483
NASA ORDER 1504 p 643 N94-14741
NASA ORDER 1575 p 643 N94-14741
NASA ORDER 1633 p 643 N94-14741
NASA ORDER 1688 p 643 N94-14741
NASA ORDER 1808 p 643 N94-14741
NASW-4358 p 538 N94-13257
NASW-4367 p 828 N94-13104
NASW-4394 p 818 N94-13984
NASW-4574 p 842 N94-14298
NASW-4693 p 552 N94-14463
NASW-4700 p 848 N94-13476
NAS1-15279 p 555 N94-13267
NAS1-18027 p 516 N94-12829
NAS1-18560 p 575 N94-12792
NAS1-18605 p 628 N94-12888
p 630 N94-13114
p 762 N94-13184
p 767 N94-13202
p 768 N94-13354
p 769 N94-13717
p 769 N94-13722
NAS1-18763 p 540 N94-13016
p 578 N94-13431
NAS1-18845 p 527 N94-13127
NAS1-18853 p 596 N94-13141
NAS1-19000 p 622 N94-13797
NAS1-19247 p 554 N94-12833
NAS1-19299 p 629 N94-13066
NAS1-19300 p 654 N94-13091
NAS1-19320 p 629 N94-13064
NAS1-19399 p 574 N94-14850
NAS1-19480 p 499 N94-12852
p 628 N94-12888
p 629 N94-13074
p 630 N94-13075
p 630 N94-13114
p 630 N94-13128
p 630 N94-13133
p 762 N94-13184
p 745 N94-13185
p 767 N94-13202
p 767 N94-13289
p 768 N94-13354
p 769 N94-13717
p 636 N94-13718
p 749 N94-13721
p 769 N94-13722
p 636 N94-13724
p 769 N94-13725
p 636 N94-13785
p 769 N94-13792
p 636 N94-13817
p 647 N94-14849
NAS1-19672 p 499 N94-12852
p 629 N94-13066
p 629 N94-13073
NAS10-11400 p 532 N94-14148
NAS10-11624 p 737 N94-13712
p 738 N94-13979
NAS2-13180 p 776 N94-13897
NAS2-13210 p 512 N94-14744
NAS2-13714 p 709 N94-14103
NAS2-13721 p 763 N94-13603
p 760 N94-13921
p 770 N94-13922
p 770 N94-14307
NAS3-133 p 582 N94-14543
NAS3-23347 p 620 N94-13106
NAS3-25093 p 622 N94-13786
NAS3-25266 p 555 N94-13139
p 621 N94-13194
p 550 N94-13415
p 551 N94-13416
p 508 N94-14208
p 626 N94-14730
p 560 N94-14822
NAS3-25423 p 663 N94-14445
p 664 N94-14446
NAS3-25640 p 557 N94-13920
NAS3-25642 p 673 N94-13673
NAS3-25785 p 638 N94-14356
NAS3-25803 p 660 N94-12802
NAS3-25864 p 621 N94-13336
NAS3-25934 p 537 N94-12809
NAS3-25966 p 511 N94-13424
NAS3-26325 p 554 N94-14771
NAS3-26494 p 555 N94-13378
NAS5-30307 p 540 N94-13140
NAS5-30440 p 741 N94-13788
NAS5-30628 p 822 N94-13126
NAS5-30629 p 759 N94-13177
NAS5-30930 p 828 N94-12970
NAS5-31331 p 844 N94-13963
NAS5-31334 p 792 N94-13719
NAS5-31832 p 835 N94-13233
NAS5-31841 p 828 N94-12915
NAS5-32059 p 828 N94-12915
NAS5-33046 p 796 N94-13081
NAS7-1003 p 604 N94-13909
NAS7-1062 p 762 N94-13131
NAS7-1063 p 648 N94-13176
NAS7-1064 p 671 N94-13124
NAS7-1065 p 620 N94-13125
NAS7-1066 p 822 N94-13116
NAS7-1068 p 745 N94-13130
NAS7-1069 p 661 N94-13129
NAS7-1070 p 736 N94-13132
NAS7-918 p 598 N94-13090
p 749 N94-13784
p 532 N94-13796
p 602 N94-13810
p 622 N94-13811
p 657 N94-13812
p 602 N94-13813
p 703 N94-13940
p 741 N94-13943
p 605 N94-13946
p 564 N94-13947
p 624 N94-13948
p 542 N94-14076
p 612 N94-14654
p 519 N94-14841
p 519 N94-14842
NAS7-963 p 562 N94-13115
NAS8-35921 p 844 N94-13146
NAS8-36123 p 832 N94-14305
NAS8-36645 p 564 N94-14025
NAS8-36861 p 553 N94-14682
NAS8-36955 p 714 N94-13709
p 683 N94-14484
NAS8-37585 p 718 N94-12957
NAS8-38100 p 652 N94-14497
p 554 N94-14907
NAS8-38407 p 737 N94-13674
NAS8-38422 p 545 N94-13953
NAS8-38423 p 643 N94-14741
NAS8-38425 p 627 N94-12803
NAS8-38555 p 543 N94-14120
NAS8-38609 p 804 N94-12873
p 621 N94-13186
p 793 N94-14903
p 788 N94-14905
NAS8-38872 p 647 N94-14906
NAS8-38958 p 586 N94-12805
NAS8-39131 p 561 N94-12830
NAS8-39201 p 539 N94-12827
NAS8-39216 p 793 N94-14548
NAS8-39218 p 705 N94-14430
NAS8-39352 p 804 N94-12934
NAS8-39394 p 669 N94-14101
NAS8-39402 p 651 N94-14447
NAS8-39716 p 648 N94-13326
NAS8-39718 p 807 N94-13444
NAS8-40000 p 533 N94-12806
NAS9-17840 p 534 N94-12810
p 534 N94-12965
p 534 N94-13191
p 536 N94-14047
NAS9-18263 p 827 N94-12800
NAS9-18492 p 729 N94-14028
NAS9-18880 p 536 N94-14323
NATO-CRG-920097 p 628 N94-12888
NCA2-136 p 596 N94-13798
NCA2-653 p 599 N94-13236
NCC1-104 p 532 N94-14851
NCC1-136 p 741 N94-14136
NCC1-159 p 744 N94-13065
NCC1-168 p 515 N94-13618
NCC1-42 p 786 N94-14551
NCC2-115 p 732 N94-13782
NCC2-297 p 671 N94-13179
NCC2-387 p 748 N94-13586
p 750 N94-13932
NCC2-458 p 629 N94-13007
NCC2-460 p 643 N94-14745
NCC2-501 p 729 N94-14097

NCC2-507 ..... p 637 N94-13827
NCC2-545 ..... p 508 N94-14541
NCC2-556 ..... p 733 N94-13824
NCC2-55 ..... p 501 N94-13266
NCC2-563 ..... p 527 N94-14322
NCC2-578 ..... p 728 N94-13562
NCC2-583 ..... p 650 N94-13814
p 650 N94-13815
p 532 N94-14068
p 533 N94-14540
NCC2-592 ..... p 510 N94-13247
NCC2-616 ..... p 504 N94-14030
NCC2-663 ..... p 520 N94-12799
NCC2-703 ..... p 514 N94-14495
NCC2-704 ..... p 806 N94-13291
p 502 N94-13422
NCC2-714 ..... p 503 N94-13463
NCC2-742 ..... p 516 N94-14106
NCC2-748 ..... p 638 N94-14086
NCC2-7491 ..... p 745 N94-13356
p 747 N94-13443
NCC2-749 ..... p 745 N94-13355
NCC2-752 ..... p 759 N94-13204
NCC2-753 ..... p 841 N94-13083
NCC2-775 ..... p 513 N94-13957
NCC2-777 ..... p 790 N94-12797
NCC2-783 ..... p 508 N94-14326
NCC2-810 ..... p 728 N94-13473
NCC3-104 ..... p 620 N94-13134
NCC3-150 ..... p 762 N94-13253
NCC3-192 ..... p 619 N94-13026
NCC3-233 ..... p 670 N94-12872
p 770 N94-14407
p 642 N94-14722
p 642 N94-14728
p 642 N94-14729
p 771 N94-14731
NCC9-16 ..... p 754 N94-14368
p 754 N94-14472
NF-62-376 ..... p 740 N94-13525
NGL-06-003-057 ..... p 844 N94-13234
NGT-40016 ..... p 559 N94-14769
NGT-50623 ..... p 512 N94-13238
NIVR-01802N ..... p 503 N94-13531
NIVR-01904N ..... p 503 N94-13530
NSF ASC-90-01115 ..... p 840 N94-14482
NSF ASC-91-13895 ..... p 769 N94-13792
NSF ATM-80-17071 ..... p 712 N94-13293
NSF ATM-82-12283 ..... p 712 N94-13293
NSF ATM-84-11326 ..... p 712 N94-13293
NSF ATM-85-07034 ..... p 715 N94-13826
NSF ATM-86-15628 ..... p 712 N94-13293
NSF CCR-92-01195 ..... p 762 N94-13184
NSF CDA-91-21709 ..... p 760 N94-13921
NSF CTS-91-13048 ..... p 643 N94-14748
p 643 N94-14749
NSF CTS-91-58124 ..... p 647 N94-14768
NSF DMS-90-03227 ..... p 628 N94-12888
NSF DMS-92-11820 ..... p 769 N94-13725
p 770 N94-13922
p 770 N94-14307
NSF ECS-93-0000N ..... p 599 N94-13264
NSF ENG-91-11333 ..... p 820 N94-12801
NSF MIP-91-16113 ..... p 619 N94-12897
p 598 N94-12920
p 744 N94-13113
p 600 N94-13466
NSF RII-87-04038 ..... p 786 N94-14552
NSG-4015 ..... p 539 N94-12790
NSG-5175 ..... p 714 N94-13816
NSG-5386 ..... p 833 N94-14493
NSG-7105 ..... p 838 N94-13781
NSG-7534 ..... p 842 N94-13855
NUTEK-89-02539P ..... p 770 N94-13922
p 770 N94-14307
N00014-89-J-1023 ..... p 807 N94-13359
N00014-89-J-1180 ..... p 569 N94-13050
N00014-89-J-1225 ..... p 577 N94-12985
p 577 N94-12986
N00014-89-J-1229 ..... p 702 N94-13386
N00014-89-J-1565 ..... p 807 N94-13359
N00014-89-J-1610 ..... p 629 N94-13074
N00014-89-J-1746 ..... p 780 N94-13051
N00014-89-J-1961 ..... p 560 N94-14794
N00014-90-C-0071 ..... p 725 N94-13581
N00014-90-J-1090 ..... p 635 N94-13699
N00014-90-J-4124 ..... p 629 N94-13074
N00014-91-C-0112 ..... p 619 N94-12892
N00014-91-C-0128 ..... p 571 N94-13697
N00014-91-J-1196 ..... p 556 N94-13583
N00014-91-J-1409 ..... p 779 N94-12894
N00014-91-J-1493 ..... p 771 N94-14731
N00014-91-J-1889 ..... p 629 N94-13074
N00014-91-J-4016 ..... p 769 N94-13725
p 770 N94-13922
p 770 N94-14307
N00014-92-J-1008 ..... p 749 N94-13702
N00014-92-J-1012 ..... p 731 N94-14899
N00014-92-J-1109 ..... p 643 N94-14748
p 643 N94-14749
N00014-92-J-1480 ..... p 749 N94-13700
N00025-92-J-1264 ..... p 773 N94-13585
N00039-91-C-0001 ..... p 614 N94-14663
p 615 N94-14672
RF PROJ. 760126/72687 ..... p 512 N94-13082
RICIS PROJ. SE-35 ..... p 754 N94-14472
RTOP 142-20-14-02 ..... p 813 N94-14409
RTOP 144-10-10 ..... p 612 N94-14542
RTOP 199-04-16-11 ..... p 846 N94-12875
RTOP 199-18-12-07 ..... p 727 N94-13447
RTOP 199-18-12-09 ..... p 731 N94-12972
RTOP 199-45-16-11 ..... p 847 N94-13263
p 732 N94-13714
RTOP 199-59-12-05 ..... p 841 N94-13183
RTOP 199-70-12-14 ..... p 732 N94-13782
RTOP 310-10-60-93-01 ..... p 607 N94-14370
RTOP 310-10-61-84-02 ..... p 514 N94-14371
p 514 N94-14372
RTOP 310-10-63-50-00 ..... p 532 N94-14373
RTOP 310-20-65-86-04 ..... p 608 N94-14374
RTOP 310-20-66-91-02 ..... p 608 N94-14375
RTOP 310-20-66-92-01 ..... p 608 N94-14376
RTOP 310-30-71-83-02 ..... p 609 N94-14378
p 609 N94-14379
RTOP 310-30-71-83-04 ..... p 608 N94-14377
RTOP 314-30-61-02-07 ..... p 609 N94-14380
RTOP 314-30-69-40-06 ..... p 611 N94-14397
RTOP 314-40-31-30-26 ..... p 611 N94-14398
RTOP 314-40-41-11-06 ..... p 609 N94-14381
p 609 N94-14382
RTOP 314-40-41-21-03 ..... p 609 N94-14383
RTOP 315-90-22-70-19 ..... p 610 N94-14384
RTOP 315-91-10-13-08 ..... p 611 N94-14393
RTOP 315-91-60-10-03 ..... p 610 N94-14386
p 610 N94-14387
p 610 N94-14388
p 610 N94-14389
p 610 N94-14390
p 611 N94-14391
p 611 N94-14392
RTOP 315-91-60-10-06 ..... p 533 N94-14394
RTOP 315-91-60-10-07 ..... p 611 N94-14395
RTOP 316-30-19-41-04 ..... p 610 N94-14385
RTOP 316-30-19-41-05 ..... p 611 N94-14396
RTOP 324-01-00 ..... p 554 N94-14771
RTOP 324-02-01 ..... p 596 N94-13141
RTOP 474-42-10 ..... p 622 N94-13786
RTOP 474-46-10 ..... p 553 N94-14725
RTOP 474-52-10 ..... p 548 N94-12807
RTOP 476-14-01 ..... p 739 N94-12838
RTOP 505-33-13 ..... p 575 N94-12842
RTOP 505-43-31 ..... p 632 N94-13467
RTOP 505-59-50-01 ..... p 629 N94-13064
RTOP 505-59-52 ..... p 521 N94-13294
RTOP 505-59-53 ..... p 740 N94-12973
RTOP 505-59-54-01 ..... p 527 N94-13127
RTOP 505-61-51 ..... p 520 N94-12820
RTOP 505-62-27 ..... p 642 N94-14728
RTOP 505-62-31 ..... p 509 N94-14780
RTOP 505-62-40 ..... p 631 N94-13385
RTOP 505-62-50 ..... p 648 N94-12874
p 650 N94-13876
RTOP 505-62-52 ..... p 629 N94-13027
p 510 N94-14847
RTOP 505-62-70 ..... p 583 N94-14845
RTOP 505-63-20-01 ..... p 575 N94-12792
RTOP 505-63-36 ..... p 663 N94-14445
p 664 N94-14446
RTOP 505-63-5A ..... p 582 N94-14543
RTOP 505-63-5B ..... p 674 N94-13873
p 676 N94-14041
RTOP 505-63-50-03 ..... p 595 N94-14026
p 574 N94-14850
RTOP 505-63-50-08 ..... p 557 N94-13711
RTOP 505-63-50-09 ..... p 670 N94-13063
RTOP 505-63-50-15 ..... p 514 N94-12850
RTOP 505-63-53 ..... p 675 N94-13919
RTOP 505-64-10-10 ..... p 759 N94-13450
RTOP 505-64-12-01 ..... p 516 N94-12829
RTOP 505-64-12-04 ..... p 597 N94-12804
p 598 N94-12811
RTOP 505-64-13-22 ..... p 744 N94-13065
RTOP 505-64-20-54 ..... p 604 N94-13916
RTOP 505-64-29 ..... p 527 N94-13008
RTOP 505-64-52 ..... p 596 N94-13790
RTOP 505-64-53-02 ..... p 517 N94-13710
RTOP 505-68-50 ..... p 517 N94-13791
p 537 N94-14853
RTOP 505-69-20-01 ..... p 500 N94-13172
RTOP 505-70-00 ..... p 518 N94-13143
RTOP 505-90-00 ..... p 821 N94-13057
RTOP 505-90-5K ..... p 670 N94-12872
RTOP 505-90-52-01 ..... p 770 N94-14407
p 642 N94-14722
p 642 N94-14729
p 499 N94-12852
p 628 N94-12888
p 629 N94-13074
p 630 N94-13075
p 630 N94-13114
p 630 N94-13128
p 630 N94-13133
p 762 N94-13184
p 745 N94-13185
p 767 N94-13202
p 767 N94-13289
p 768 N94-13354
p 769 N94-13717
p 636 N94-13718
p 749 N94-13721
p 769 N94-13722
p 636 N94-13724
p 769 N94-13725
p 636 N94-13785
p 769 N94-13792
p 636 N94-13817
p 647 N94-14849
RTOP 505-90-53-02 ..... p 739 N94-12886
RTOP 506-40-62-01 ..... p 776 N94-14733
RTOP 506-41-11 ..... p 620 N94-13134
p 621 N94-13194
p 626 N94-14730
p 642 N94-14732
RTOP 506-41-52 ..... p 541 N94-13917
RTOP 506-42-31 ..... p 550 N94-13415
p 551 N94-13416
p 551 N94-13430
p 553 N94-14726
RTOP 506-43-11 ..... p 554 N94-12871
p 665 N94-13056
RTOP 506-49-11-01 ..... p 532 N94-14851
RTOP 506-61-42 ..... p 620 N94-13106
RTOP 506-72-00 ..... p 620 N94-13110
RTOP 506-72-1D ..... p 538 N94-13918
RTOP 506-72-21 ..... p 538 N94-13111
RTOP 510-01-50 ..... p 670 N94-13053
p 555 N94-13138
p 555 N94-13139
p 555 N94-13378
p 557 N94-13920
p 557 N94-14042
p 676 N94-14408
p 559 N94-14719
p 559 N94-14769
p 560 N94-14822
p 560 N94-14823
RTOP 510-02-12-10 ..... p 554 N94-12833
RTOP 510-02-12 ..... p 671 N94-13379
RTOP 533-02-34 ..... p 520 N94-13254
RTOP 533-02-35 ..... p 520 N94-13255
p 516 N94-14106
RTOP 533-02-39 ..... p 519 N94-14855
RTOP 535-03-10 ..... p 518 N94-14036
RTOP 535-03-11-02 ..... p 777 N94-14481
RTOP 535-05-10 ..... p 499 N94-13108
p 517 N94-13142
RTOP 536-01-11 ..... p 740 N94-13200
RTOP 536-06-37-03 ..... p 555 N94-13267
RTOP 537-02-22 ..... p 508 N94-14208
RTOP 537-03-23-03 ..... p 629 N94-13066
p 629 N94-13073
RTOP 537-04-20 ..... p 683 N94-14776
RTOP 549-03-11 ..... p 538 N94-13201
p 538 N94-13989
RTOP 553-02-01 ..... p 519 N94-14841
p 519 N94-14842
RTOP 582-09-11 ..... p 776 N94-14027
RTOP 585-03-11-08 ..... p 540 N94-13016
RTOP 586-03-11-31 ..... p 622 N94-13797
RTOP 590-14-31-01 ..... p 539 N94-12976
RTOP 590-21-11 ..... p 648 N94-13135
RTOP 592-01-11-12 ..... p 578 N94-13431
RTOP 593-71-11 ..... p 552 N94-14102
RTOP 665-10-70 ..... p 844 N94-13963
RTOP 674-24-05 ..... p 628 N94-12968
RTOP 690-60-21 ..... p 537 N94-12809
RTOP 730-00-00 ..... p 550 N94-13265
RTOP 763-21-41 ..... p 516 N94-13256
RTOP 763-22-41 ..... p 664 N94-14727
RTOP 778-34-2A ..... p 519 N94-14448
RTOP 889-54-62-01-00 ..... p 611 N94-14398
RTOP 913-00-00 ..... p 723 N94-14074
RTOP 920-20-08 ..... p 534 N94-13028
SBIR-01.01-3800 ..... p 638 N94-14356
SBIR-02.02-9030 ..... p 527 N94-13127
SBIR-02.08-8581A ..... p 643 N94-14741
SBIR-03.01-0533 ..... p 511 N94-13424
SBIR-04.04-1319 ..... p 673 N94-13673

SBIR-04.10-2551 ..... p 671 N94-13124
SBIR-04.14-9030 ..... p 562 N94-13115
SBIR-05.01-0300A ..... p 762 N94-13131
SBIR-05.01-3600 ..... p 661 N94-13129
SBIR-05.01-8500 ..... p 822 N94-13116
SBIR-05.03-1391A ..... p 660 N94-12802
SBIR-06.06-0929 ..... p 745 N94-13130
SBIR-07.04-2800 ..... p 759 N94-13177
SBIR-07.06-3759 ..... p 822 N94-13126
SBIR-07.07-0094 ..... p 736 N94-13132
SBIR-08.01-8211 ..... p 620 N94-13125
SBIR-08.06-5649 ..... p 648 N94-13176
SBIR-08.10-2214A ..... p 545 N94-13953
SBIR-09.01-0540A ..... p 596 N94-13141
SBIR-09.04-3200 ..... p 737 N94-13674
SBIR-09.20-7640 ..... p 540 N94-13140
SBIR-11.04-6576C ..... p 627 N94-12803
SBIR-14.05-6455 ..... p 604 N94-13909
SFB-124-D4 ..... p 740 N94-13525
SMRC-07490-040 ..... p 729 N94-14128
p 729 N94-14129
STUF-90-00577 ..... p 729 N94-14128
p 729 N94-14129
SWRI PROJ. 15-2779 ..... p 796 N94-13084
SWRI PROJ. 15-3578 ..... p 828 N94-12970
W-31-109-ENG-38 ..... p 712 N94-12906
p 577 N94-13032
p 555 N94-13248
p 707 N94-13383
p 768 N94-13391
p 848 N94-13483
p 782 N94-13484
p 708 N94-13495
p 783 N94-13890
p 784 N94-13896
p 715 N94-13912
p 800 N94-13913
p 623 N94-13925
p 579 N94-13974
p 624 N94-14012
p 810 N94-14185
p 811 N94-14304
p 717 N94-14424
p 581 N94-14432
p 566 N94-14694
p 756 N94-14844
W-7405-ENG-36 ..... p 794 N94-12814
p 834 N94-12815
p 846 N94-12816
p 794 N94-12849
p 761 N94-12859
p 670 N94-12887
p 576 N94-12916
p 758 N94-12917
p 772 N94-12919
p 583 N94-12921
p 846 N94-12922
p 846 N94-12923
p 846 N94-12924
p 846 N94-12946
p 846 N94-12947
p 779 N94-12949
p 779 N94-12950
p 712 N94-12952
p 847 N94-12964
p 620 N94-13031
p 584 N94-13099
p 797 N94-13100
p 788 N94-13103
p 745 N94-13151
p 780 N94-13173
p 781 N94-13205
p 816 N94-13206
p 789 N94-13209
p 836 N94-13262
p 740 N94-13286
p 789 N94-13327
p 789 N94-13328
p 702 N94-13402
p 702 N94-13403
p 564 N94-13487
p 782 N94-13492
p 570 N94-13512
p 798 N94-13513
p 715 N94-13912
p 709 N94-14020
p 722 N94-14057
p 839 N94-14116
p 765 N94-14117
p 558 N94-14119
p 558 N94-14121
p 810 N94-14122
p 669 N94-14143
p 785 N94-14144
p 752 N94-14176
p 760 N94-14177
p 773 N94-14178
p 580 N94-14179
p 585 N94-14180
p 785 N94-14181
p 554 N94-14290
p 581 N94-14327
p 717 N94-14328
p 811 N94-14329
p 811 N94-14339
p 581 N94-14340
p 812 N94-14365
p 785 N94-14366
p 792 N94-14367
p 813 N94-14413
p 582 N94-14436
p 774 N94-14441
p 664 N94-14457
p 849 N94-14461
p 785 N94-14466
p 785 N94-14468
p 558 N94-14469
p 786 N94-14514
p 718 N94-14518
p 802 N94-14532
p 585 N94-14535
p 840 N94-14536
p 802 N94-14567
p 676 N94-14591
p 597 N94-14592
p 817 N94-14593
p 553 N94-14689
p 559 N94-14690
p 766 N94-14737
p 818 N94-14740
p 815 N94-14773
p 787 N94-14804
p 626 N94-14805
p 778 N94-14867
W-7405-ENG-48 ..... p 742 N94-12840
p 794 N94-12846
p 742 N94-12864
p 790 N94-12865
p 725 N94-12876
p 561 N94-12881
p 742 N94-12883
p 576 N94-12885
p 653 N94-12898
p 567 N94-12899
p 548 N94-12911
p 576 N94-12939
p 654 N94-12962
p 654 N94-12963
p 619 N94-12994
p 795 N94-12995
p 805 N94-13010
p 834 N94-13011
p 795 N94-13017
p 849 N94-13019
p 568 N94-13036
p 706 N94-13095
p 744 N94-13120
p 822 N94-13121
p 806 N94-13136
p 569 N94-13137
p 655 N94-13145
p 797 N94-13207
p 788 N94-13208
p 797 N94-13217
p 655 N94-13243
p 631 N94-13249
p 631 N94-13250
p 781 N94-13251
p 655 N94-13258
p 655 N94-13259
p 556 N94-13389
p 797 N94-13393
p 720 N94-13404
p 807 N94-13405
p 823 N94-13406
p 649 N94-13410
p 656 N94-13481
p 791 N94-13482
p 584 N94-13491
p 748 N94-13576
p 789 N94-13727
p 808 N94-13881
p 657 N94-13882
p 783 N94-13893
p 721 N94-13914
p 663 N94-13975
p 657 N94-13976
p 709 N94-14022
p 658 N94-14114
p 580 N94-14124
p 810 N94-14125
p 784 N94-14140
p 658 N94-14152
p 658 N94-14175
p 753 N94-14289
p 512 N94-14292
p 801 N94-14293
p 580 N94-14311
p 801 N94-14312
p 811 N94-14313
p 773 N94-14314
p 760 N94-14315
p 792 N94-14317
p 638 N94-14318
p 581 N94-14319
p 825 N94-14331
p 811 N94-14332
p 839 N94-14341
p 801 N94-14342
p 801 N94-14347
p 651 N94-14416
p 723 N94-14426
p 625 N94-14427
p 581 N94-14432
p 639 N94-14434
p 754 N94-14435
p 658 N94-14437
p 792 N94-14438
p 813 N94-14439
p 813 N94-14440
p 658 N94-14442
p 789 N94-14460
p 840 N94-14467
p 760 N94-14475
p 705 N94-14510
p 755 N94-14521
p 625 N94-14522
p 786 N94-14526
p 802 N94-14564
p 700 N94-14566
p 786 N94-14569
p 802 N94-14570
p 771 N94-14589
p 803 N94-14590
p 659 N94-14594
p 659 N94-14595
p 583 N94-14693
p 653 N94-14772
p 653 N94-14792
p 574 N94-14793
p 756 N94-14864
p 803 N94-14865
p 566 N94-14869
p 627 N94-14870
p 660 N94-14888
p 790 N94-14893
p 803 N94-14894
p 647 N94-14895
W-7405-ENG-82 ..... p 568 N94-13000

REPORT NUMBER INDEX

Typical Report Number Index Listing

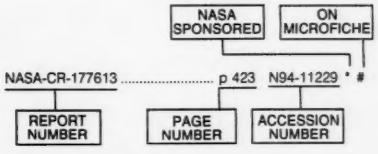

Listings in this index are arranged alphanumerically by report number. The accession number denotes the number by which the citation is identified. The page number helps to locate the citation in the abstract section. An asterisk (*) indicates that the item is a NASA report. A pound sign (#) indicates that the item is available on microfiche.

A-90033 p 520 N94-12820 * #
A-90319-VOL-1 p 538 N94-13201 * #
A-90319-VOL-2 p 538 N94-13989 * #
A-91148 p 740 N94-13200 * #
A-92031 p 527 N94-13008 * #
A-92144 p 740 N94-12973 * #
A-93016 p 731 N94-12972 * #
A-93035 p 776 N94-14027 * #
A-93058 p 727 N94-13447 * #
A-93074 p 521 N94-13294 * #
A-93078 p 596 N94-13790 * #
A-93084 p 739 N94-12838 * #
A-93085 p 841 N94-13183 * #
A-93105 p 776 N94-13897 * #
A-93108 p 510 N94-13247 * #
A-93112 p 596 N94-13798 * #
A-93115 p 512 N94-14744 * #
A-93117 p 538 N94-13257 * #

AC-33-2B p 518 N94-13252 #

AD-A259606 p 605 N94-13941
AD-A259650 p 603 N94-13818
AD-A259913 p 606 N94-14054
AD-A260153 p 606 N94-14064 #
AD-A260166 p 603 N94-13838 #
AD-A262583 p 619 N94-12967 #
AD-A265106 p 790 N94-12863
AD-A265120 p 531 N94-13358
AD-A265129 p 807 N94-13359
AD-A265141 p 575 N94-12812
AD-A265200 p 744 N94-13049 #
AD-A265339 p 569 N94-13050 #
AD-A265346 p 719 N94-12992 #
AD-A265495 p 734 N94-12929
AD-A265509 p 560 N94-14794 #
AD-A265627 p 568 N94-12993 #
AD-A265637 p 762 N94-12969 #
AD-A265702 p 767 N94-13284
AD-A265703 p 780 N94-13051 #
AD-A265713 p 759 N94-13052 #
AD-A265720 p 819 N94-13059 #
AD-A265722 p 819 N94-13060 #
AD-A265723 p 732 N94-13061 #
AD-A265728 p 805 N94-13037 #
AD-A265732 p 732 N94-13038 #
AD-A265750 p 796 N94-13039 #
AD-A265751 p 620 N94-13040 #
AD-A265752 p 821 N94-13041 #
AD-A265753 p 665 N94-13042 #
AD-A265789 p 619 N94-12892 #
AD-A265805 p 834 N94-12971 #
AD-A265806 p 743 N94-12974 #
AD-A265807 p 734 N94-12975 #
AD-A265817 p 719 N94-12978 #
AD-A265825 p 791 N94-12979 #
AD-A265826 p 735 N94-12982 #
AD-A265827 p 577 N94-12985 #
AD-A265832 p 577 N94-12986 #
AD-A265869 p 758 N94-12930
AD-A265877 p 576 N94-12932
AD-A265878 p 742 N94-12933
AD-A265884 p 736 N94-12935
AD-A265886 p 779 N94-12894 #
AD-A266009 p 583 N94-12987 #
AD-A266012 p 660 N94-12988 #
AD-A266014 p 821 N94-12958 #
AD-A266015 p 500 N94-12989 #
AD-A266067 p 725 N94-12990 #
AD-A266320 p 671 N94-13579 #
AD-A266321 p 585 N94-14145 #
AD-A266323 p 807 N94-13580 #
AD-A266339 p 725 N94-13581 #
AD-A266340 p 735 N94-13582 #
AD-A266341 p 636 N94-13730 #
AD-A266342 p 769 N94-13731 #
AD-A266346 p 622 N94-13776 #
AD-A266347 p 673 N94-13777 #
AD-A266348 p 673 N94-13778 #
AD-A266350 p 571 N94-13697 #
AD-A266354 p 728 N94-13698 #
AD-A266432 p 635 N94-13699 #
AD-A266436 p 749 N94-13700 #
AD-A266437 p 823 N94-13701 #
AD-A266440 p 749 N94-13702 #
AD-A266450 p 513 N94-13703 #
AD-A266540 p 764 N94-13704 #
AD-A266543 p 504 N94-13705 #
AD-A266544 p 557 N94-13706 #
AD-A266547 p 556 N94-13583 #
AD-A266562 p 579 N94-13584 #
AD-A266563 p 773 N94-13585 #
AD-A266594 p 749 N94-13779 #
AD-A266599 p 636 N94-13780 #
AD-A266641 p 817 N94-14680 #
AD-A266642 p 659 N94-14681 #
AD-A266643 p 820 N94-14796 #
AD-A266644 p 735 N94-14797 #
AD-A266655 p 510 N94-14799 #
AD-A266656 p 509 N94-14774 #
AD-A266658 p 726 N94-14775 #
AD-A266659 p 816 N94-14839 #
AD-A266660 p 772 N94-14840 #
AD-A266670 p 766 N94-14777 #
AD-A266673 p 787 N94-14778 #
AD-A266675 p 573 N94-14779 #
AD-A266692 p 509 N94-14781 #
AD-A266694 p 653 N94-14782 #
AD-A266770 p 510 N94-14784 #
AD-A266771 p 766 N94-14785 #
AD-A266774 p 573 N94-14786 #
AD-A266775 p 774 N94-14788 #
AD-A266776 p 771 N94-14789 #
AD-A266800 p 661 N94-13122 #
AD-A266806 p 731 N94-14899 #
AD-A266807 p 772 N94-14900 #
AD-A266812 p 665 N94-14901 #
AD-A266820 p 683 N94-14902 #
AD-A266832 p 597 N94-14877 #
AD-A266833 p 575 N94-14878 #
AD-A266840 p 733 N94-14879 #
AD-A266853 p 766 N94-14882 #
AD-A267563 p 579 N94-13903 #
AD-A267739 p 528 N94-14876
AD-A267758 p 760 N94-13924 #

AD-D015741 p 556 N94-13663
AD-D015742 p 791 N94-13664

AD-E201473 p 834 N94-12971 #

AECS-PH/FRSR-62 p 806 N94-13213 #

AFIT/CI/CIA-92-134 p 734 N94-12929
AFIT/CI/CIA-92-30D p 719 N94-12992 #

AFIT/EN-TR-93-5 p 823 N94-13701 #

AFIT/GA/ENY/93J-01 p 557 N94-13706 #

AFIT/GAE/ENY/93J-01 p 636 N94-13780 #
AFIT/GAE/ENY/93J-02 p 504 N94-13705 #

AFIT/GCE/ENG/93J-01 p 764 N94-13704 #

AFOSR-93-0344TR p 575 N94-12812
AFOSR-93-0378TR p 732 N94-13038 #
AFOSR-93-0383TR p 732 N94-13061 #
AFOSR-93-0385TR p 665 N94-13042 #
AFOSR-93-0386TR p 796 N94-13039 #
AFOSR-93-0390TR p 819 N94-13059 #
AFOSR-93-0397TR p 805 N94-13037 #
AFOSR-93-0434TR p 673 N94-13778 #
AFOSR-93-0437TR p 807 N94-13580 #
AFOSR-93-0447TR p 728 N94-13698 #

AGS/AD-93-9 p 788 N94-14872 #

AIAA PAPER 91-2129 p 629 N94-13027 * #
AIAA PAPER 93-03252 p 642 N94-14729 * #
AIAA PAPER 93-0705 p 541 N94-13917 * #
AIAA PAPER 93-1086 p 551 N94-13416 * #
AIAA PAPER 93-1346 p 664 N94-14727 * #
AIAA PAPER 93-1419 p 520 N94-13255 * #
AIAA PAPER 93-1820 p 520 N94-13254 * #
AIAA PAPER 93-1902 p 551 N94-13430 * #
AIAA PAPER 93-1917 p 642 N94-14722 * #
AIAA PAPER 93-2094 p 550 N94-13147 * #
AIAA PAPER 93-2225 p 553 N94-14726 * #
AIAA PAPER 93-2228 p 553 N94-14725 * #
AIAA PAPER 93-2380 p 642 N94-14728 * #
AIAA PAPER 93-2391 p 550 N94-13415 * #
AIAA PAPER 93-3065 p 499 N94-13108 * #
AIAA PAPER 93-3765 p 519 N94-14855 * #
AIAA PAPER 93-4322 p 508 N94-14208 * #
AIAA PAPER 93-4401 p 518 N94-14036 * #
AIAA PAPER 93-4670 p 612 N94-14542 * #
AIAA PAPER 94-0838 p 826 N94-14488 * #
AIAA PAPER 94-0839 p 825 N94-14486 * #
AIAA PAPER 94-0840 p 826 N94-14489 * #
AIAA PAPER 94-0841 p 825 N94-14487 * #

AIAA PAPER-93-1208 p 501 N94-13260 #

AL-TR-1992-0176 p 736 N94-12935

AL/HR-TP-1993-0016 p 735 N94-13582 #

ANE-110 p 518 N94-13252 #

ANL-HEP-CP-93-33 p 783 N94-13890 #

ANL/CHM/CP-79459 p 782 N94-13484 #

ANL/CMT/CP-78930 p 800 N94-13913 #
ANL/CMT/CP-79338 p 624 N94-14012 #

ANL/EAIS/CP-78850 p 707 N94-13383 #
ANL/EAIS/CP-78927 p 708 N94-13495 #

ANL/ER/CP-73469 p 717 N94-14424 #
ANL/ER/CP-77861 p 566 N94-14694 #

ANL/ES/CP-77790 p 712 N94-12906 #

ANL/MCS/CP-78726 p 768 N94-13391 #
ANL/MCS/CP-79562 p 756 N94-14844

ANL/MCT/CP-78715 p 555 N94-13248 #
ANL/MCT/CP-79029 p 577 N94-13032 #

ANL/MSD/CP-78008 p 811 N94-14304 #
ANL/MSD/CP-79532 p 810 N94-14185 #
ANL/MSD/CP-79640 p 623 N94-13925 #

ANL/OTM/CR-3 p 579 N94-13974 #

ANL/PHY/CP-79637 p 784 N94-13896 #

ANL/XFD/CP-79506 p 848 N94-13483 #

ANSTO-E-702 ..... p 804 N94-12893 #

AR-008-363 ..... p 670 N94-12927
AR-008-364 ..... p 670 N94-12928

ARCCB-TR-93015 ..... p 671 N94-13579 #
ARCCB-TR-93017 ..... p 673 N94-13777 #

ARFSD-TR-93001 ..... p 620 N94-13040 #

ARL-CR-81-VOL-2 ..... p 664 N94-14446 * #
ARL-CR-82-VOL-1 ..... p 663 N94-14445 * #

ARL-MR-14 ..... p 629 N94-13027 * #
ARL-MR-35 ..... p 791 N94-12979 #
ARL-MR-83 ..... p 585 N94-14145 #

ARL-RR-6-PT-1 ..... p 670 N94-12927
ARL-RR-6-PT-2 ..... p 670 N94-12928

ARL-TR-109 ..... p 504 N94-13795 #
ARL-TR-137 ..... p 576 N94-12932
ARL-TR-143 ..... p 575 N94-14878 #
ARL-TR-40 ..... p 662 N94-13794 #
ARL-TR-45 ..... p 580 N94-14126 #

ARO-25462.13-EG-RW ..... p 510 N94-14799 #
ARO-25623.4-EG-S ..... p 509 N94-14781 #
ARO-25747.1-EG ..... p 509 N94-14774 #
ARO-26061.15-EG ..... p 510 N94-14784 #
ARO-26739.16-MA-SAH ..... p 772 N94-14840 #
ARO-26744.1-CH-SAH ..... p 787 N94-14778 #
ARO-26883.2-MS ..... p 579 N94-13584 #
ARO-26995.3-EG ..... p 665 N94-14901 #
ARO-26997.10-MA ..... p 774 N94-14788 #
ARO-27407.1-MS ..... p 573 N94-14786 #
ARO-27524.34-MA-SDI ..... p 771 N94-14789 #
ARO-27557.1-MA ..... p 817 N94-14680 #
ARO-27600.9-CH ..... p 573 N94-14779 #
ARO-27810.9-MS ..... p 816 N94-14839 #
ARO-28608.1-MS ..... p 766 N94-14785 #

ATDL-93011842 ..... p 718 N94-14425 #

ATR-91(9558)-6 ..... p 784 N94-13936 #
ATR-92(7190)-2 ..... p 714 N94-13793 * #
ATR-93(8399)-2 ..... p 597 N94-14877 #

BBC-RD-1993/1 ..... p 598 N94-12925
BBC-RD-1993/2 ..... p 598 N94-12926
BBC-RD-1993/3 ..... p 616 N94-14742

BCRS-92-11A ..... p 819 N94-14809 #
BCRS-92-11B ..... p 818 N94-14462 #
BCRS-92-13 ..... p 684 N94-13123 #
BCRS-92-16 ..... p 687 N94-14127 #
BCRS-92-22 ..... p 700 N94-14544 #

BDM-VAS-0784-93-TR ..... p 766 N94-14785 #

BER-550-248 ..... p 543 N94-14120 * #
BER-597-163 ..... p 663 N94-14134 * #

BNL-48218 ..... p 569 N94-13221 #
BNL-48233 ..... p 789 N94-13220 #
BNL-48237 ..... p 780 N94-13149 #
BNL-48374 ..... p 781 N94-13219 #
BNL-48540 ..... p 549 N94-13034 #
BNL-48648 ..... p 780 N94-13097 #
BNL-48649 ..... p 780 N94-13098 #
BNL-48667 ..... p 552 N94-14111 #
BNL-48685 ..... p 660 N94-12851 #
BNL-48698 ..... p 548 N94-12981 #
BNL-48700 ..... p 554 N94-14806 #
BNL-48717 ..... p 785 N94-14363 #
BNL-48759 ..... p 773 N94-14320 #
BNL-48832 ..... p 780 N94-13101 #
BNL-48871 ..... p 787 N94-14580 #
BNL-48887 ..... p 566 N94-14582 #
BNL-48923 ..... p 562 N94-13045 #
BNL-48940 ..... p 781 N94-13241 #
BNL-48953 ..... p 580 N94-14142 #
BNL-48954 ..... p 805 N94-13102 #
BNL-48958 ..... p 659 N94-14572 #
BNL-48960 ..... p 806 N94-13150 #
BNL-49074 ..... p 793 N94-14529 #
BNL-49087 ..... p 813 N94-14517 #
BNL-49183 ..... p 788 N94-14872 #
BNL-52372 ..... p 676 N94-14585 #
BNL-70246 ..... p 705 N94-12869 #
BNL-70309 ..... p 706 N94-13054 #

BR315742 ..... p 574 N94-14828 #
BR315905 ..... p 653 N94-14827 #
BR316329 ..... p 509 N94-14706 #
BR316512 ..... p 683 N94-14818 #
BR316596 ..... p 653 N94-14701 #

BU-RI-9450 ..... p 626 N94-14686

CAL-2120 ..... p 829 N94-13178 * #
CAL-2122 ..... p 829 N94-13181 * #
CAL-2139 ..... p 840 N94-14685 * #
CAL-2140 ..... p 840 N94-14688 * #

CAP-95-ATF-93C ..... p 659 N94-14572 #

CEBAF-PR-89-023 ..... p 786 N94-14552 * #

CECOM-TR-93-E-2 ..... p 604 N94-13916 * #

CERC-TR-93-8 ..... p 726 N94-14775 #

CFDRC-4041/1 ..... p 627 N94-12803 * #

CJ5-07 ..... p 674 N94-13861 #

CMC-0867-1016 ..... p 792 N94-13868

CMOTT-93-11 ..... p 642 N94-14729 * #
CMOTT-93-3 ..... p 631 N94-13385 * #

CMU-CS-93-124 ..... p 749 N94-13779 #
CMU-CS-93-128 ..... p 759 N94-13052 #
CMU-CS-93-130 ..... p 767 N94-13284
CMU-CS-93-161 ..... p 772 N94-14900 #

CMU-RI-TR-93-06 ..... p 820 N94-14796 #
CMU-RI-TR-93-07 ..... p 735 N94-14797 #

CMU/SEI-93-EM-8 ..... p 744 N94-13049 #

CNES-NT-131 ..... p 605 N94-13950 #
CNES-NT-132 ..... p 624 N94-13951 #
CNES-NT-133 ..... p 625 N94-14138 #
CNES-NT-134 ..... p 622 N94-13552 #

CNR-31790 ..... p 764 N94-13820 #
CNR-32815 ..... p 810 N94-14199 #
CNR-35024 ..... p 824 N94-14069 #
CNR-35325 ..... p 557 N94-13866 #

COMMUNICATIONS-SER-B-157 . p 837 N94-13504 #
COMMUNICATIONS-SER-B-159 . p 844 N94-13502 #
COMMUNICATIONS-SER-B-160 . p 837 N94-13503 #

CONF-9107235-1 ..... p 709 N94-14022 #
CONF-9109349-2 ..... p 659 N94-14572 #
CONF-911288 ..... p 710 N94-14477 #
CONF-920134-7 ..... p 717 N94-14424 #
CONF-920362-48 ..... p 803 N94-14865 #
CONF-9204120-9-REV-1 ..... p 583 N94-14693 #
CONF-9204241-1 ..... p 778 N94-12860 #
CONF-9204250 ..... p 710 N94-14516 #
CONF-920523-10 ..... p 658 N94-14175 #
CONF-920523-12 ..... p 654 N94-12962 #
CONF-920523-13 ..... p 657 N94-13976 #
CONF-920523-14 ..... p 658 N94-14152 #
CONF-920523-16 ..... p 660 N94-14888 #
CONF-920610-16 ..... p 797 N94-13393 #
CONF-9206202-7 ..... p 574 N94-14793
CONF-9206314-2 ..... p 834 N94-13096 #
CONF-9206359-1 ..... p 802 N94-14564 #
CONF-9206360-1 ..... p 817 N94-13479 #
CONF-9206370-1 ..... p 839 N94-14341 #
CONF-9206371-1 ..... p 773 N94-14314 #
CONF-9207190 ..... p 581 N94-14421
CONF-9207198-1 ..... p 834 N94-13011 #
CONF-9207199-1 ..... p 834 N94-13096 #
CONF-9207200-1 ..... p 834 N94-13096 #
CONF-9207205-1 ..... p 566 N94-14869 #
CONF-920761-17 ..... p 561 N94-12881 #
CONF-920792-52 ..... p 791 N94-13482 #
CONF-920792-56 ..... p 653 N94-14772
CONF-920792-57 ..... p 656 N94-13481 #
CONF-920792-58 ..... p 789 N94-14460 #
CONF-920792-59 ..... p 655 N94-13258 #
CONF-920792-60 ..... p 655 N94-13259 #
CONF-920792-63 ..... p 811 N94-14332 #
CONF-920803-17 ..... p 548 N94-12870 #
CONF-9208108-2 ..... p 753 N94-14289 #
CONF-9208109-88 ..... p 654 N94-12963 #
CONF-920813-3 ..... p 797 N94-13217 #
CONF-9208132-13 ..... p 623 N94-13925 #
CONF-9208135-5 ..... p 801 N94-14312 #
CONF-9208135-6 ..... p 811 N94-14313 #
CONF-9208142-22 ..... p 655 N94-13145 #
CONF-9208160-7 ..... p 563 N94-13477 #
CONF-9208186-3 ..... p 784 N94-13896 #
CONF-9208221-2 ..... p 563 N94-13478 #
CONF-9208223 ..... p 818 N94-13216
CONF-9208225-1 ..... p 568 N94-13036 #

CONF-920893-7 ..... p 756 N94-14864
CONF-9209239-6 ..... p 783 N94-13893 #
CONF-920927-4 ..... p 805 N94-13010 #
CONF-9209290-9 ..... p 801 N94-14293 #
CONF-9209325 ..... p 585 N94-14829
CONF-9209331-1 ..... p 723 N94-14426 #
CONF-9209334-1 ..... p 824 N94-14048 #
CONF-9209344-1 ..... p 628 N94-12961 #
CONF-9209360-1 ..... p 573 N94-14474 #
CONF-920947-5 ..... p 810 N94-14185 #
CONF-920948-12 ..... p 795 N94-12995 #
CONF-920948-13 ..... p 784 N94-14140 #
CONF-920966-25-REV-1 ..... p 760 N94-14475 #
CONF-921005-34 ..... p 761 N94-14476 #
CONF-921007-32 ..... p 573 N94-14700 #
CONF-9210231-4 ..... p 700 N94-14566 #
CONF-9210277 ..... p 805 N94-13020 #
CONF-9210334-1 ..... p 721 N94-13914 #
CONF-9210336-2 ..... p 787 N94-14857 #
CONF-9210353-1 ..... p 760 N94-14315 #
CONF-9210356-1 ..... p 655 N94-13243 #
CONF-921046-18 ..... p 781 N94-13251 #
CONF-921046-19 ..... p 786 N94-14569 #
CONF-921047-3 ..... p 626 N94-14805 #
CONF-921066-3-REV-1 ..... p 725 N94-12876 #
CONF-921101-111 ..... p 581 N94-14432 #
CONF-921101-114 ..... p 576 N94-12866 #
CONF-921101-115 ..... p 567 N94-12899 #
CONF-921101-118 ..... p 581 N94-14319 #
CONF-921101-119 ..... p 556 N94-13389 #
CONF-921101-120 ..... p 806 N94-13136 #
CONF-921101-122 ..... p 569 N94-13137 #
CONF-921101-129 ..... p 812 N94-14348 #
CONF-921101-130 ..... p 805 N94-13012 #
CONF-921101-134 ..... p 582 N94-14531 #
CONF-921101-136 ..... p 813 N94-14439 #
CONF-921103-12-APP-A ..... p 787 N94-14691 #
CONF-921110-49 ..... p 663 N94-13975 #
CONF-921110-51 ..... p 771 N94-14589 #
CONF-921110-52 ..... p 754 N94-14435 #
CONF-9211106-2 ..... p 625 N94-14427 #
CONF-9211117-7 ..... p 580 N94-14311 #
CONF-9211128-8 ..... p 801 N94-14342 #
CONF-9211211-2 ..... p 803 N94-14894 #
CONF-921122-52 ..... p 779 N94-12954 #
CONF-921122-53 ..... p 783 N94-13494 #
CONF-921122-54-APP-1 ..... p 781 N94-13348 #
CONF-921122-57 ..... p 781 N94-13350 #
CONF-921122-66 ..... p 783 N94-13884 #
CONF-9211240-1 ..... p 660 N94-12851 #
CONF-9211243-1 ..... p 785 N94-14471 #
CONF-921125-7 ..... p 825 N94-14331 #
CONF-921130-2 ..... p 568 N94-13000 #
CONF-921131-12 ..... p 779 N94-12997 #
CONF-921152-14 ..... p 705 N94-14510 #
CONF-921162-16 ..... p 576 N94-12885 #
CONF-921256-5 ..... p 659 N94-14595 #
CONF-921266-2 ..... p 840 N94-14467 #
CONF-921276 ..... p 700 N94-12822 #
CONF-921281-1 ..... p 793 N94-14702 #
CONF-921284-1 ..... p 790 N94-14893 #
CONF-930103-31 ..... p 549 N94-12996 #
CONF-930103-33 ..... p 550 N94-13351 #
CONF-930103-36 ..... p 554 N94-14806 #
CONF-930103-37 ..... p 549 N94-13034 #
CONF-930103-38 ..... p 548 N94-12981 #
CONF-930103-40 ..... p 552 N94-14111 #
CONF-9301109-1 ..... p 788 N94-12817 #
CONF-9301111-1 ..... p 785 N94-14466 #
CONF-930133-10 ..... p 708 N94-13910 #
CONF-930133-9 ..... p 709 N94-13911 #
CONF-930142-4 ..... p 718 N94-12903 #
CONF-930142-5 ..... p 715 N94-13912 #
CONF-930159-34 ..... p 797 N94-13207 #
CONF-930159-41 ..... p 658 N94-14437 #
CONF-930159-42 ..... p 658 N94-14442 #
CONF-930159-43 ..... p 659 N94-14594 #
CONF-930159-44 ..... p 792 N94-14438 #
CONF-930163-2 ..... p 653 N94-14792
CONF-930168-6 ..... p 787 N94-14804 #
CONF-930173-7 ..... p 780 N94-13097 #
CONF-930173-9 ..... p 780 N94-13098 #
CONF-930187-5 ..... p 781 N94-13205 #
CONF-9302103-2 ..... p 570 N94-13512 #
CONF-9302107-SUMM ..... p 563 N94-13411 #
CONF-9302112-1 ..... p 773 N94-14320 #
CONF-9302112-2 ..... p 760 N94-14177 #
CONF-9302113-1 ..... p 746 N94-13382 #
CONF-9302114-1 ..... p 848 N94-13483 #
CONF-9302115-2 ..... p 836 N94-13262 #
CONF-9302115-3 ..... p 712 N94-12952 #
CONF-9302116-1 ..... p 810 N94-14125 #
CONF-9302116-2 ..... p 808 N94-13881 #
CONF-9302122-1 ..... p 738 N94-14451 #
CONF-9302129-1 ..... p 676 N94-14530 #
CONF-9302132-1 ..... p 840 N94-14536 #

CONF-930269-14 ..... p 789 N94-13328 #
CONF-930270-1 ..... p 800 N94-13913 #
CONF-930274-2 ..... p 788 N94-13208 #
CONF-930285-1 ..... p 707 N94-13486 #
CONF-930293-3 ..... p 780 N94-13018
CONF-930304-19 ..... p 572 N94-14184 #
CONF-930304-30 ..... p 803 N94-14590 #
CONF-9303119-2 ..... p 781 N94-13241 #
CONF-9303119-3 ..... p 658 N94-14114 #
CONF-9303119-4 ..... p 625 N94-14522 #
CONF-9303122-1 ..... p 722 N94-14057 #
CONF-9303123-1 ..... p 566 N94-14694 #
CONF-9303126-3 ..... p 631 N94-13249 #
CONF-9303126-6 ..... p 647 N94-14895 #
CONF-9303137-1 ..... p 624 N94-14012 #
CONF-9303165-1 ..... p 748 N94-13480 #
CONF-930318-9 ..... p 572 N94-14058 #
CONF-9303180-ABSTS ..... p 711 N94-14859 #
CONF-9303182-1 ..... p 604 N94-13899 #
CONF-9303188-1 ..... p 573 N94-14537 #
CONF-9303198-1 ..... p 627 N94-14870 #
CONF-930331-11 ..... p 766 N94-14737 #
CONF-930367-3 ..... p 811 N94-14339 #
CONF-930367-5 ..... p 815 N94-14699 #
CONF-930372-10 ..... p 794 N94-12846 #
CONF-930372-11 ..... p 756 N94-14844
CONF-930389-10 ..... p 779 N94-12949 #
CONF-930389-12 ..... p 780 N94-13101 #
CONF-930389-13 ..... p 785 N94-14468 #
CONF-930389-14 ..... p 785 N94-14144 #
CONF-930389-4 ..... p 785 N94-14366 #
CONF-930403-39 ..... p 651 N94-14046 #
CONF-930405-10 ..... p 776 N94-14584 #
CONF-930405-11 ..... p 806 N94-13150 #
CONF-930405-12 ..... p 566 N94-14582 #
CONF-930405-13 ..... p 580 N94-14142 #
CONF-930405-14 ..... p 805 N94-13102 #
CONF-930405-15 ..... p 558 N94-14469 #
CONF-930405-25 ..... p 813 N94-14478 #
CONF-930405-27 ..... p 813 N94-14413 #
CONF-930405-4 ..... p 811 N94-14304 #
CONF-930405-7 ..... p 812 N94-14344 #
CONF-930405-8 ..... p 812 N94-14345 #
CONF-9304103-6 ..... p 565 N94-14525 #
CONF-9304106-1 ..... p 664 N94-14457 #
CONF-9304109-1 ..... p 712 N94-12906 #
CONF-9304112-10 ..... p 795 N94-13033 #
CONF-9304112-11 ..... p 795 N94-12953 #
CONF-9304112-12 ..... p 797 N94-13144 #
CONF-9304112-13 ..... p 798 N94-13577 #
CONF-9304112-8 ..... p 607 N94-14291 #
CONF-9304112-9 ..... p 803 N94-14770
CONF-9304114-3 ..... p 752 N94-14019 #
CONF-9304126-5 ..... p 798 N94-13513 #
CONF-9304126-7 ..... p 794 N94-12814 #
CONF-9304128-8 ..... p 781 N94-13349 #
CONF-9304131-1 ..... p 752 N94-14176 #
CONF-9304131-2 ..... p 773 N94-14178 #
CONF-9304131-3 ..... p 772 N94-12919 #
CONF-9304131-5 ..... p 782 N94-13409 #
CONF-9304131-7 ..... p 774 N94-14334 #
CONF-9304134-1 ..... p 746 N94-13394 #
CONF-9304135-1 ..... p 539 N94-12909 #
CONF-9304135-2 ..... p 540 N94-13398 #
CONF-9304138-1 ..... p 812 N94-14365 #
CONF-9304142-1 ..... p 553 N94-14689 #
CONF-9304144-1 ..... p 580 N94-14124 #
CONF-9304144-4 ..... p 812 N94-14362 #
CONF-9304144-8 ..... p 660 N94-14863 #
CONF-9304144-9 ..... p 658 N94-14415 #
CONF-9304145-1 ..... p 785 N94-14181 #
CONF-9304145-2 ..... p 815 N94-14773 #
CONF-9304146-1 ..... p 568 N94-13035 #
CONF-9304147-1 ..... p 748 N94-13576 #
CONF-9304148-1 ..... p 782 N94-13485 #
CONF-9304149-1 ..... p 702 N94-13381 #
CONF-9304150-1 ..... p 808 N94-13694 #
CONF-9304152-1 ..... p 818 N94-14740 #
CONF-9304154-1 ..... p 669 N94-14143 #
CONF-9304171-1 ..... p 813 N94-14517 #
CONF-930419-1 ..... p 576 N94-12912 #
CONF-930419-3 ..... p 813 N94-14440 #
CONF-930438-14 ..... p 576 N94-12916 #
CONF-930438-19 ..... p 581 N94-14343 #
CONF-930438-23 ..... p 579 N94-13888 #
CONF-930438-6 ..... p 581 N94-14340 #
CONF-930438-8 ..... p 578 N94-13493 #
CONF-930438-9 ..... p 581 N94-14327 #
CONF-930445-14 ..... p 655 N94-13261 #
CONF-930445-18 ..... p 651 N94-14416 #
CONF-930445-1 ..... p 686 N94-14056 #
CONF-930483-7 ..... p 707 N94-13390 #
CONF-9305101-1 ..... p 703 N94-13693 #
CONF-9305101-3 ..... p 704 N94-14355 #
CONF-930511-112 ..... p 780 N94-13173 #
CONF-930511-124 ..... p 781 N94-13219 #
CONF-930511-127 ..... p 789 N94-13220 #
CONF-930511-129 ..... p 569 N94-13221 #
CONF-930511-135 ..... p 783 N94-13895 #
CONF-930511-186 ..... p 787 N94-14588 #
CONF-930511-223 ..... p 659 N94-14520 #
CONF-930511-234 ..... p 658 N94-14414 #
CONF-930511-236 ..... p 790 N94-14897 #
CONF-930511-45 ..... p 788 N94-13103 #
CONF-930511-49 ..... p 789 N94-13209 #
CONF-930511-69 ..... p 789 N94-13727 #
CONF-930511-75 ..... p 780 N94-13149 #
CONF-930511-78 ..... p 740 N94-13286 #
CONF-930511-82 ..... p 789 N94-13327 #
CONF-930511-90 ..... p 821 N94-12983 #
CONF-9305135-3 ..... p 577 N94-13032 #
CONF-9305136-2 ..... p 801 N94-14349 #
CONF-9305151-2 ..... p 759 N94-13043 #
CONF-9305151-5 ..... p 760 N94-14011 #
CONF-9305161-2 ..... p 820 N94-12907 #
CONF-9305166-2 ..... p 566 N94-14586 #
CONF-9305168-3 ..... p 596 N94-13889 #
CONF-9305177-5 ..... p 558 N94-14119 #
CONF-9305179-1 ..... p 551 N94-13514 #
CONF-9305183-1 ..... p 710 N94-14183 #
CONF-9305185-1 ..... p 559 N94-14690 #
CONF-9305186-1 ..... p 618 N94-12821 #
CONF-9305187-2 ..... p 765 N94-14117 #
CONF-9305188-1 ..... p 555 N94-13248 #
CONF-9305189-3 ..... p 561 N94-12910 #
CONF-9305195-1 ..... p 814 N94-14695 #
CONF-9305197-1 ..... p 631 N94-13244 #
CONF-9305199-1 ..... p 839 N94-14116 #
CONF-9305235-1 ..... p 786 N94-14514 #
CONF-9305240-1 ..... p 788 N94-14898 #
CONF-9305243-1 ..... p 704 N94-14423 #
CONF-930537-35 ..... p 755 N94-14581 #
CONF-930540-3 ..... p 703 N94-13886 #
CONF-930540-7 ..... p 705 N94-14861 #
CONF-930557-1 ..... p 582 N94-14511 #
CONF-930571-13 ..... p 701 N94-13093 #
CONF-930571-14 ..... p 580 N94-14179 #
CONF-930572-3 ..... p 584 N94-13491 #
CONF-930580-3 ..... p 501 N94-13260 #
CONF-930588-2 ..... p 792 N94-14367 #
CONF-9306113-1 ..... p 782 N94-13484 #
CONF-9306153-1 ..... p 637 N94-14053 #
CONF-9306157-1 ..... p 758 N94-12878 #
CONF-930616-10 ..... p 802 N94-14532 #
CONF-930616-2 ..... p 623 N94-13892 #
CONF-9306162-1 ..... p 768 N94-13391 #
CONF-9306164-1 ..... p 574 N94-14795
CONF-9306167-1 ..... p 816 N94-13206 #
CONF-9306167-2 ..... p 558 N94-14121 #
CONF-9306167-3 ..... p 811 N94-14329 #
CONF-9306167-4 ..... p 670 N94-12887 #
CONF-9306167-5 ..... p 676 N94-14591 #
CONF-9306168-1 ..... p 787 N94-14580 #
CONF-9306170-1 ..... p 649 N94-13395 #
CONF-9306172 ..... p 562 N94-13045 #
CONF-9306195-1 ..... p 755 N94-14528 #
CONF-930633-1 ..... p 585 N94-14535 #
CONF-930637-1 ..... p 785 N94-14363 #
CONF-930647-2 ..... p 708 N94-13495 #
CONF-930647-3 ..... p 707 N94-13383 #
CONF-930658-1 ..... p 653 N94-12898 #
CONF-930680-1 ..... p 817 N94-14593 #
CONF-930682-2 ..... p 808 N94-13930 #
CONF-930687-2 ..... p 688 N94-14151 #
CONF-930702-14 ..... p 571 N94-14021 #
CONF-930702-24 ..... p 573 N94-14364 #
CONF-930703-2 ..... p 597 N94-14592 #
CONF-9307104-1 ..... p 755 N94-14521 #
CONF-930713-10 ..... p 585 N94-14180 #
CONF-930713-8 ..... p 583 N94-12921 #
CONF-930714-2 ..... p 639 N94-14434 #
CONF-930720-12 ..... p 796 N94-13046 #
CONF-930720-5 ..... p 802 N94-14579 #
CONF-930720-6 ..... p 800 N94-13900 #
CONF-930720-7 ..... p 802 N94-14583 #
CONF-930720-8 ..... p 801 N94-14347 #
CONF-930720-9 ..... p 802 N94-14570 #
CONF-930722-1 ..... p 779 N94-12950 #
CONF-930722-2 ..... p 782 N94-13492 #
CONF-930722-3 ..... p 717 N94-14328 #
CONF-930741-3 ..... p 745 N94-13151 #
CONF-930765-2 ..... p 670 N94-12908 #
CONF-930770-1 ..... p 743 N94-12991 #
CONF-930773-2 ..... p 758 N94-12917 #
CONF-930779-10 ..... p 847 N94-12964 #
CONF-930779-11 ..... p 846 N94-12947 #
CONF-930779-13 ..... p 848 N94-13695 #
CONF-930779-17 ..... p 783 N94-13890 #
CONF-930779-2 ..... p 846 N94-12946 #
CONF-930779-3 ..... p 846 N94-12922 #
CONF-930779-4 ..... p 849 N94-14461 #
CONF-930779-5 ..... p 846 N94-12924 #
CONF-930779-6 ..... p 846 N94-12816 #
CONF-930779-7 ..... p 846 N94-12923 #
CONF-930779-9 ..... p 834 N94-12815 #
CONF-930781-1 ..... p 766 N94-14568 #
CONF-930782-1 ..... p 742 N94-12956 #
CONF-930785-1 ..... p 631 N94-13250 #
CONF-930786-1 ..... p 748 N94-13578 #
CONF-930788-1 ..... p 632 N94-13397 #
CONF-930799-1 ..... p 778 N94-14867 #
CONF-930801-2 ..... p 810 N94-14122 #
CONF-930801-3 ..... p 817 N94-14453 #
CONF-930801-7 ..... p 816 N94-14868 #
CONF-930803-5 ..... p 824 N94-13915 #
CONF-930804-1 ..... p 802 N94-14567 #
CONF-930804-2 ..... p 702 N94-13402 #
CONF-9308111-1 ..... p 704 N94-14333 #
CONF-9308124-1 ..... p 738 N94-14335 #
CONF-9308130-1 ..... p 582 N94-14436 #
CONF-930822-1 ..... p 648 N94-13044 #
CONF-930822-2 ..... p 804 N94-12813 #
CONF-930822-5 ..... p 804 N94-12818 #
CONF-930830-11 ..... p 790 N94-12865 #
CONF-930830-13 ..... p 628 N94-12884 #
CONF-930830-14 ..... p 561 N94-12841 #
CONF-930830-16 ..... p 561 N94-12819 #
CONF-930830-17 ..... p 707 N94-13384 #
CONF-930848-1 ..... p 761 N94-12859 #
CONF-930862-2 ..... p 743 N94-12999 #
CONF-930866-1 ..... p 619 N94-12942 #
CONF-930866-3 ..... p 774 N94-14441 #
CONF-930880-1 ..... p 809 N94-14083 #
CONF-930880-2 ..... p 809 N94-14108 #
CONF-930880-3 ..... p 809 N94-14079 #
CONF-930881-2 ..... p 742 N94-12883 #
CONF-930884-1 ..... p 743 N94-12991 #
CONF-9309116-2 ..... p 676 N94-14456 #
CONF-930953-1 ..... p 793 N94-14529 #

CRL-233 ..... p 603 N94-13843

CSA-DSM-CR-91-027 ..... p 764 N94-13842

CSIRO-TP-29 ..... p 709 N94-14095

CTN-93-60718 ..... p 621 N94-13333
CTN-93-60719 ..... p 661 N94-13521
CTN-93-60720 ..... p 763 N94-13515
CTN-93-60721 ..... p 656 N94-13522
CTN-93-60722 ..... p 600 N94-13488
CTN-93-60723 ..... p 600 N94-13489
CTN-93-60724 ..... p 772 N94-13540
CTN-93-60725 ..... p 791 N94-13490
CTN-93-60726 ..... p 513 N94-13541
CTN-93-60727 ..... p 685 N94-13542
CTN-93-60728 ..... p 511 N94-13543
CTN-93-60729 ..... p 528 N94-13544
CTN-93-60730 ..... p 685 N94-13523
CTN-93-60731 ..... p 632 N94-13474
CTN-93-60732 ..... p 685 N94-13475
CTN-93-60733 ..... p 720 N94-13516
CTN-93-60734 ..... p 502 N94-13369
CTN-93-60735 ..... p 504 N94-14031 #
CTN-93-60736 ..... p 605 N94-14033 #
CTN-93-60737 ..... p 850 N94-14060 #
CTN-93-60738 ..... p 606 N94-14062 #
CTN-93-60739 ..... p 606 N94-14063 #
CTN-93-60740 ..... p 606 N94-14064 #
CTN-93-60744 ..... p 604 N94-13939 #
CTN-93-60745 ..... p 605 N94-13941
CTN-93-60747 ..... p 800 N94-13877 #
CTN-93-60748 ..... p 564 N94-13942
CTN-93-60749 ..... p 603 N94-13829 #
CTN-93-60750 ..... p 715 N94-13830 #
CTN-93-60751 ..... p 777 N94-13831
CTN-93-60752 ..... p 607 N94-14065
CTN-93-60753 ..... p 607 N94-14066
CTN-93-60754 ..... p 752 N94-14051
CTN-93-60755 ..... p 752 N94-14052
CTN-93-60756 ..... p 750 N94-13858
CTN-93-60757 ..... p 750 N94-13944
CTN-93-60758 ..... p 606 N94-14054
CTN-93-60759 ..... p 602 N94-13801
CTN-93-60760 ..... p 602 N94-13802 #
CTN-93-60761 ..... p 526 N94-13859 #
CTN-93-60762 ..... p 516 N94-13898 #
CTN-93-60763 ..... p 557 N94-13866 #
CTN-93-60764 ..... p 675 N94-13945 #
CTN-93-60765 ..... p 675 N94-14035 #
CTN-93-60766 ..... p 603 N94-13832 #
CTN-93-60767 ..... p 733 N94-14141
CTN-93-60769 ..... p 674 N94-13833
CTN-93-60770 ..... p 728 N94-13823
CTN-93-60772 ..... p 603 N94-13818
CTN-93-60773 ..... p 564 N94-13819
CTN-93-60774 ..... p 764 N94-13844
CTN-93-60775 ..... p 623 N94-13834

CTN-93-60776 ..... p 792 N94-13845
CTN-93-60780 ..... p 623 N94-13846 #
CTN-93-60781 ..... p 663 N94-14147 #
CTN-93-60783 ..... p 733 N94-13847 #
CTN-93-60785 ..... p 773 N94-13848 #
CTN-93-60786 ..... p 799 N94-13849 #
CTN-93-60787 ..... p 800 N94-13850 #
CTN-93-60788 ..... p 798 N94-13563 #
CTN-93-60789 ..... p 798 N94-13564 #
CTN-93-60790 ..... p 799 N94-13835 #
CTN-93-60791 ..... p 799 N94-13836 #
CTN-93-60792 ..... p 800 N94-13851 #
CTN-93-60793 ..... p 800 N94-13852 #
CTN-93-60794 ..... p 800 N94-13853 #
CTN-93-60795 ..... p 603 N94-13837 #
CTN-93-60796 ..... p 603 N94-13838 #
CTN-93-60797 ..... p 515 N94-13839
CTN-93-60798 ..... p 777 N94-14360 #
CTN-93-60799 ..... p 571 N94-13840
CTN-93-60800 ..... p 603 N94-13841
CTN-93-60801 ..... p 764 N94-13842
CTN-93-60802 ..... p 603 N94-13843
CTN-93-60803 ..... p 657 N94-14067
CTN-93-60804 ..... p 752 N94-14088
CTN-93-60805 ..... p 515 N94-13867
CTN-93-60806 ..... p 792 N94-13868
CTN-93-60807 ..... p 604 N94-13869
CTN-93-60808 ..... p 604 N94-13870
CTN-93-60809 ..... p 606 N94-14037
CTN-93-60810 ..... p 606 N94-14038
CTN-93-60811 ..... p 751 N94-14014
CTN-93-60812 ..... p 605 N94-14015
CTN-93-60813 ..... p 751 N94-13990
CTN-93-60814 ..... p 751 N94-14016
CTN-93-60815 ..... p 753 N94-14197
CTN-93-60816 ..... p 810 N94-14198 #
CTN-93-60817 ..... p 810 N94-14199 #
CTN-93-60818 ..... p 824 N94-14069 #
CTN-93-60819 ..... p 597 N94-14070 #
CTN-93-60820 ..... p 596 N94-13684 #
CTN-93-60821 ..... p 753 N94-14200 #
CTN-93-60822 ..... p 765 N94-14201 #
CTN-93-60823 ..... p 824 N94-14202 #
CTN-93-60824 ..... p 769 N94-13545 #
CTN-93-60825 ..... p 740 N94-13546 #
CTN-93-60826 ..... p 741 N94-13547 #
CTN-93-60827 ..... p 764 N94-13820 #
CTN-93-60828 ..... p 763 N94-13517 #
CTN-93-60831 ..... p 798 N94-13518 #
CTN-93-60832 ..... p 850 N94-13519 #
CTN-93-60833 ..... p 850 N94-13548 #
CTN-93-60834 ..... p 764 N94-13860 #
CTN-93-60835 ..... p 674 N94-13861 #
CTN-93-60836 ..... p 637 N94-13862 #
CTN-93-60837 ..... p 558 N94-14105
CTN-93-60838 ..... p 751 N94-14017
CTN-93-60839 ..... p 774 N94-13549 #
CTN-93-60840 ..... p 753 N94-14207
CTN-93-60841 ..... p 810 N94-14203
CTN-93-60843 ..... p 607 N94-14204
CTN-93-60847 ..... p 829 N94-13370 #
CTN-93-60848 ..... p 829 N94-13371
CTN-93-60849 ..... p 836 N94-13372
CTN-93-60855 ..... p 569 N94-13367
CTN-93-60856 ..... p 726 N94-14205
CTN-93-60857 ..... p 684 N94-13368
CTN-93-60858 ..... p 801 N94-14206 #
CTN-93-60859 ..... p 663 N94-14195 #
CTN-93-60860 ..... p 824 N94-14196 #
CTN-93-60861 ..... p 671 N94-13565
CTN-93-60862 ..... p 754 N94-14496
CTN-93-60863 ..... p 499 N94-13520 #
CTN-93-60865 ..... p 849 N94-13505 #

CU-1536481 ..... p 512 N94-13238 * #

CUED/A-THERMO/TR.60 ..... p 562 N94-13085 #

CWI-BS-R9222 ..... p 773 N94-13677 #
CWI-BS-R9223 ..... p 765 N94-14018 #
CWI-BS-R9224 ..... p 764 N94-13999 #
CWI-BS-R9225 ..... p 764 N94-14000 #
CWI-BS-R9226 ..... p 765 N94-14001 #
CWI-BS-R9227 ..... p 770 N94-14002 #
CWI-BS-R9228 ..... p 770 N94-14003 #
CWI-BS-R9229 ..... p 751 N94-14004 #
CWI-BS-R9230 ..... p 765 N94-14361 #
CWI-BS-R9231 ..... p 773 N94-14005 #

CWI-CS-R9221 ..... p 768 N94-13496 #
CWI-CS-R9238 ..... p 748 N94-13524 #
CWI-CS-R9239 ..... p 760 N94-13924 #
CWI-CS-R9240 ..... p 740 N94-13525 #
CWI-CS-R9241 ..... p 768 N94-13526 #

D/1993/0238/409 ..... p 505 N94-14153 #

DCN-1-2-ES-44818 ..... p 651 N94-14447 * #

DE92-010562 ..... p 702 N94-13386 #
DE92-016430 ..... p 704 N94-14350 #
DE93-000055 ..... p 701 N94-12914 #
DE93-000091 ..... p 585 N94-14454 #
DE93-000092 ..... p 700 N94-12868 #
DE93-000093 ..... p 701 N94-12902 #
DE93-000138 ..... p 638 N94-14351 #
DE93-000288 ..... p 702 N94-13380 #
DE93-003832 ..... p 761 N94-12859 #
DE93-007581 ..... p 619 N94-12942 #
DE93-007883 ..... p 708 N94-13910 #
DE93-007884 ..... p 709 N94-13911 #
DE93-007887 ..... p 715 N94-13912 #
DE93-007998 ..... p 718 N94-12903 #
DE93-008050 ..... p 655 N94-13387 #
DE93-008849 ..... p 706 N94-12904 #
DE93-009154 ..... p 706 N94-12905 #
DE93-009203 ..... p 800 N94-13913 #
DE93-009287 ..... p 721 N94-13914 #
DE93-009714 ..... p 824 N94-13915 #
DE93-009841 ..... p 743 N94-12991 #
DE93-009843 ..... p 809 N94-14079 #
DE93-009844 ..... p 809 N94-14083 #
DE93-009845 ..... p 809 N94-14108 #
DE93-009940 ..... p 705 N94-12869 #
DE93-009964 ..... p 566 N94-14694 #
DE93-009989 ..... p 712 N94-12906 #
DE93-010006 ..... p 704 N94-14109 #
DE93-010009 ..... p 704 N94-14110 #
DE93-010012 ..... p 851 N94-14455 #
DE93-010021 ..... p 809 N94-14085 #
DE93-010024 ..... p 709 N94-14087 #
DE93-010025 ..... p 584 N94-14089 #
DE93-010026 ..... p 702 N94-13381 #
DE93-010034 ..... p 704 N94-14422 #
DE93-010042 ..... p 704 N94-14423 #
DE93-010126 ..... p 706 N94-13054 #
DE93-010253 ..... p 778 N94-12860 #
DE93-010274 ..... p 651 N94-14046 #
DE93-010319 ..... p 824 N94-14048 #
DE93-010408 ..... p 637 N94-14053 #
DE93-010447 ..... p 746 N94-13382 #
DE93-010667 ..... p 717 N94-14424 #
DE93-010685 ..... p 686 N94-14056 #
DE93-010690 ..... p 676 N94-14456 #
DE93-010712 ..... p 722 N94-14057 #
DE93-010718 ..... p 664 N94-14457 #
DE93-010761 ..... p 825 N94-14458 #
DE93-010791 ..... p 548 N94-12870 #
DE93-010792 ..... p 549 N94-12996 #
DE93-010924 ..... p 664 N94-14565 #
DE93-010999 ..... p 563 N94-13477 #
DE93-011002 ..... p 563 N94-13478 #
DE93-011003 ..... p 779 N94-12997 #
DE93-011072 ..... p 568 N94-12998 #
DE93-011121 ..... p 817 N94-13479 #
DE93-011271 ..... p 748 N94-13480 #
DE93-011555 ..... p 743 N94-12999 #
DE93-011564 ..... p 568 N94-13000 #
DE93-011574 ..... p 804 N94-12813 #
DE93-011581 ..... p 628 N94-12884 #
DE93-011588 ..... p 820 N94-12907 #
DE93-011593 ..... p 670 N94-12908 #
DE93-011602 ..... p 572 N94-14058 #
DE93-011619 ..... p 539 N94-12909 #
DE93-011669 ..... p 561 N94-12841 #
DE93-011673 ..... p 752 N94-14019 #
DE93-011677 ..... p 760 N94-14011 #
DE93-011680 ..... p 759 N94-13043 #
DE93-011685 ..... p 648 N94-13044 #
DE93-011686 ..... p 710 N94-14459 #
DE93-011761 ..... p 624 N94-14012 #
DE93-011791 ..... p 709 N94-14020 #
DE93-011842 ..... p 718 N94-14425 #
DE93-011849 ..... p 571 N94-14021 #
DE93-011871 ..... p 709 N94-14022 #
DE93-011873 ..... p 723 N94-14426 #
DE93-011891 ..... p 581 N94-14432 #
DE93-011894 ..... p 790 N94-12865 #
DE93-011902 ..... p 725 N94-12876 #
DE93-012086 ..... p 800 N94-13908 #
DE93-012146 ..... p 808 N94-13973 #
DE93-012165 ..... p 552 N94-14013 #
DE93-012263 ..... p 818 N94-13216
DE93-012311 ..... p 579 N94-13974 #
DE93-012340 ..... p 561 N94-12910 #
DE93-012347 ..... p 758 N94-12878 #
DE93-012450 ..... p 548 N94-12911 #
DE93-012476 ..... p 561 N94-12881 #
DE93-012479 ..... p 663 N94-13975 #
DE93-012503 ..... p 794 N94-12846 #
DE93-012504 ..... p 742 N94-12883 #
DE93-012522 ..... p 785 N94-14363 #
DE93-012524 ..... p 554 N94-14806 #

DE93-012539 ..... p 759 N94-13470 #
DE93-012540 ..... p 628 N94-12961 #
DE93-012549 ..... p 625 N94-14427 #
DE93-012571 ..... p 656 N94-13481 #
DE93-012575 ..... p 654 N94-12962 #
DE93-012577 ..... p 657 N94-13976 #
DE93-012580 ..... p 658 N94-14175 #
DE93-012581 ..... p 753 N94-14289 #
DE93-012592 ..... p 789 N94-14460 #
DE93-012599 ..... p 654 N94-12963 #
DE93-012605 ..... p 700 N94-14566 #
DE93-012606 ..... p 791 N94-13482 #
DE93-012613 ..... p 573 N94-14364 #
DE93-012631 ..... p 836 N94-13262 #
DE93-012632 ..... p 812 N94-14365 #
DE93-012633 ..... p 570 N94-13512 #
DE93-012639 ..... p 752 N94-14176 #
DE93-012640 ..... p 576 N94-12916 #
DE93-012641 ..... p 798 N94-13513 #
DE93-012642 ..... p 581 N94-14327 #
DE93-012643 ..... p 553 N94-14689 #
DE93-012645 ..... p 760 N94-14177 #
DE93-012646 ..... p 785 N94-14366 #
DE93-012647 ..... p 758 N94-12917 #
DE93-012657 ..... p 787 N94-14804 #
DE93-012658 ..... p 626 N94-14805 #
DE93-012665 ..... p 792 N94-14367 #
DE93-012667 ..... p 772 N94-12919 #
DE93-012671 ..... p 583 N94-12921 #
DE93-012676 ..... p 794 N94-12814 #
DE93-012677 ..... p 773 N94-14178 #
DE93-012681 ..... p 811 N94-14339 #
DE93-012707 ..... p 559 N94-14690 #
DE93-012713 ..... p 580 N94-14179 #
DE93-012715 ..... p 849 N94-14461 #
DE93-012716 ..... p 834 N94-12815 #
DE93-012717 ..... p 846 N94-12816 #
DE93-012718 ..... p 846 N94-12922 #
DE93-012719 ..... p 846 N94-12923 #
DE93-012720 ..... p 846 N94-12924 #
DE93-012721 ..... p 847 N94-12964 #
DE93-012723 ..... p 846 N94-12946 #
DE93-012724 ..... p 846 N94-12947 #
DE93-012731 ..... p 802 N94-14567 #
DE93-012733 ..... p 585 N94-14180 #
DE93-012737 ..... p 779 N94-12949 #
DE93-012738 ..... p 584 N94-13491 #
DE93-012744 ..... p 779 N94-12950 #
DE93-012745 ..... p 782 N94-13492 #
DE93-012750 ..... p 785 N94-14181 #
DE93-012751 ..... p 712 N94-12952 #
DE93-012752 ..... p 581 N94-14340 #
DE93-012754 ..... p 578 N94-13493 #
DE93-012755 ..... p 788 N94-12817 #
DE93-012759 ..... p 804 N94-12818 #
DE93-012765 ..... p 710 N94-14182 #
DE93-012770 ..... p 710 N94-14523 #
DE93-012776 ..... p 795 N94-12953 #
DE93-012779 ..... p 783 N94-13494 #
DE93-012780 ..... p 779 N94-12954 #
DE93-012783 ..... p 775 N94-12955 #
DE93-012836 ..... p 710 N94-14183 #
DE93-012846 ..... p 742 N94-12956 #
DE93-012848 ..... p 561 N94-12819 #
DE93-012852 ..... p 708 N94-13495 #
DE93-012853 ..... p 551 N94-13514 #
DE93-012855 ..... p 576 N94-12912 #
DE93-012856 ..... p 618 N94-12821 #
DE93-012859 ..... p 576 N94-12866 #
DE93-012869 ..... p 572 N94-14184 #
DE93-012872 ..... p 805 N94-13009 #
DE93-012890 ..... p 768 N94-13391 #
DE93-012893 ..... p 707 N94-13383 #
DE93-012901 ..... p 810 N94-14185 #
DE93-012905 ..... p 848 N94-13483 #
DE93-012908 ..... p 756 N94-14844
DE93-012910 ..... p 782 N94-13484 #
DE93-012912 ..... p 811 N94-14304 #
DE93-012915 ..... p 554 N94-14290 #
DE93-012921 ..... p 620 N94-13031 #
DE93-012939 ..... p 555 N94-13248 #
DE93-012942 ..... p 577 N94-13032 #
DE93-012961 ..... p 803 N94-14770
DE93-012963 ..... p 766 N94-14568 #
DE93-012964 ..... p 607 N94-14291 #
DE93-012965 ..... p 795 N94-13033 #
DE93-012967 ..... p 707 N94-13384 #
DE93-012970 ..... p 654 N94-13013 #
DE93-013000 ..... p 512 N94-14292 #
DE93-013016 ..... p 786 N94-14524 #
DE93-013028 ..... p 801 N94-14293 #
DE93-013037 ..... p 580 N94-14311 #
DE93-013038 ..... p 801 N94-14312 #
DE93-013039 ..... p 811 N94-14313 #
DE93-013044 ..... p 773 N94-14314 #
DE93-013045 ..... p 756 N94-14864

DE93-013047 ..... p 760 N94-14315 #
DE93-013048 ..... p 653 N94-14792
DE93-013053 ..... p 573 N94-14316 #
DE93-013084 ..... p 748 N94-13576 #
DE93-013090 ..... p 834 N94-13011 #
DE93-013092 ..... p 742 N94-12864 #
DE93-013093 ..... p 742 N94-12840 #
DE93-013094 ..... p 653 N94-14772
DE93-013100 ..... p 792 N94-14317 #
DE93-013105 ..... p 638 N94-14318 #
DE93-013114 ..... p 578 N94-13118 #
DE93-013118 ..... p 743 N94-13014 #
DE93-013131 ..... p 581 N94-14319 #
DE93-013145 ..... p 791 N94-13015 #
DE93-013148 ..... p 549 N94-13034 #
DE93-013161 ..... p 568 N94-13035 #
DE93-013182 ..... p 773 N94-14320 #
DE93-013184 ..... p 797 N94-13393 #
DE93-013195 ..... p 568 N94-13036 #
DE93-013196 ..... p 705 N94-14510 #
DE93-013198 ..... p 805 N94-13010 #
DE93-013252 ..... p 565 N94-14525 #
DE93-013274 ..... p 798 N94-13577 #
DE93-013278 ..... p 797 N94-13144 #
DE93-013303 ..... p 795 N94-13017 #
DE93-013313 ..... p 619 N94-12994 #
DE93-013345 ..... p 839 N94-14341 #
DE93-013348 ..... p 795 N94-12995 #
DE93-013351 ..... p 801 N94-14342 #
DE93-013372 ..... p 796 N94-13047 #
DE93-013389 ..... p 805 N94-13020 #
DE93-013412 ..... p 786 N94-14526 #
DE93-013414 ..... p 655 N94-13145 #
DE93-013419 ..... p 655 N94-13258 #
DE93-013420 ..... p 655 N94-13259 #
DE93-013421 ..... p 806 N94-13136 #
DE93-013422 ..... p 556 N94-13389 #
DE93-013424 ..... p 631 N94-13249 #
DE93-013425 ..... p 631 N94-13250 #
DE93-013429 ..... p 781 N94-13251 #
DE93-013435 ..... p 781 N94-13241 #
DE93-013450 ..... p 569 N94-13242 #
DE93-013488 ..... p 787 N94-14691 #
DE93-013493 ..... p 781 N94-13348 #
DE93-013506 ..... p 782 N94-13485 #
DE93-013507 ..... p 706 N94-12937 #
DE93-013520 ..... p 707 N94-13486 #
DE93-013522 ..... p 781 N94-13349 #
DE93-013569 ..... p 781 N94-13350 #
DE93-013578 ..... p 581 N94-14343 #
DE93-013598 ..... p 564 N94-13487 #
DE93-013663 ..... p 746 N94-13394 #
DE93-013672 ..... p 550 N94-13351 #
DE93-013688 ..... p 703 N94-13691 #
DE93-013697 ..... p 823 N94-13352 #
DE93-013753 ..... p 582 N94-14511 #
DE93-013755 ..... p 501 N94-13260 #
DE93-013764 ..... p 649 N94-13395 #
DE93-013766 ..... p 812 N94-14344 #
DE93-013767 ..... p 632 N94-13397 #
DE93-013770 ..... p 812 N94-14345 #
DE93-013772 ..... p 655 N94-13261 #
DE93-013773 ..... p 540 N94-13398 #
DE93-013774 ..... p 748 N94-13578 #
DE93-013776 ..... p 814 N94-14695 #
DE93-013788 ..... p 576 N94-12939 #
DE93-013800 ..... p 701 N94-13093 #
DE93-013801 ..... p 703 N94-13693 #
DE93-013814 ..... p 707 N94-13390 #
DE93-013830 ..... p 583 N94-14693 #
DE93-013835 ..... p 786 N94-14569 #
DE93-013839 ..... p 574 N94-14793
DE93-013841 ..... p 653 N94-12898 #
DE93-013842 ..... p 567 N94-12899 #
DE93-013844 ..... p 756 N94-14696 #
DE93-013848 ..... p 569 N94-13137 #
DE93-013850 ..... p 789 N94-13727 #
DE93-013853 ..... p 655 N94-13243 #
DE93-013863 ..... p 779 N94-12940 #
DE93-013864 ..... p 654 N94-13058 #
DE93-013895 ..... p 565 N94-14346 #
DE93-013903 ..... p 631 N94-13244 #
DE93-013904 ..... p 815 N94-14699 #
DE93-013905 ..... p 787 N94-14857 #
DE93-013906 ..... p 780 N94-13018
DE93-013910 ..... p 808 N94-13694 #
DE93-013912 ..... p 776 N94-14584 #
DE93-013913 ..... p 848 N94-13695 #
DE93-013915 ..... p 574 N94-14795
DE93-013930 ..... p 676 N94-14585 #
DE93-013938 ..... p 620 N94-13094 #
DE93-013941 ..... p 849 N94-13019 #
DE93-013947 ..... p 706 N94-13095 #
DE93-013949 ..... p 652 N94-14578 #
DE93-013956 ..... p 568 N94-12977 #
DE93-013958 ..... p 601 N94-13696 #
DE93-013962 ..... p 653 N94-14858 #
DE93-014007 ..... p 834 N94-12980 #
DE93-014008 ..... p 834 N94-13096 #
DE93-014018 ..... p 802 N94-14579 #
DE93-014022 ..... p 780 N94-13097 #
DE93-014025 ..... p 794 N94-12849 #
DE93-014032 ..... p 711 N94-14859 #
DE93-014041 ..... p 566 N94-14586 #
DE93-014043 ..... p 688 N94-14151 #
DE93-014044 ..... p 780 N94-13098 #
DE93-014046 ..... p 548 N94-12981 #
DE93-014053 ..... p 660 N94-12851 #
DE93-014100 ..... p 821 N94-12983 #
DE93-014111 ..... p 584 N94-13099 #
DE93-014118 ..... p 658 N94-14152 #
DE93-014129 ..... p 784 N94-14140 #
DE93-014144 ..... p 797 N94-13100 #
DE93-014147 ..... p 797 N94-13217 #
DE93-014150 ..... p 576 N94-12885 #
DE93-014172 ..... p 755 N94-14581 #
DE93-014192 ..... p 707 N94-13218 #
DE93-014284 ..... p 781 N94-13219 #
DE93-014288 ..... p 789 N94-13220 #
DE93-014306 ..... p 569 N94-13221 #
DE93-014319 ..... p 780 N94-13101 #
DE93-014321 ..... p 787 N94-14580 #
DE93-014325 ..... p 566 N94-14582 #
DE93-014326 ..... p 580 N94-14142 #
DE93-014327 ..... p 805 N94-13102 #
DE93-014334 ..... p 780 N94-13149 #
DE93-014335 ..... p 806 N94-13150 #
DE93-014336 ..... p 552 N94-14111 #
DE93-014344 ..... p 745 N94-13151 #
DE93-014346 ..... p 669 N94-14143 #
DE93-014349 ..... p 785 N94-14466 #
DE93-014350 ..... p 781 N94-13205 #
DE93-014352 ..... p 816 N94-13206 #
DE93-014353 ..... p 785 N94-14144 #
DE93-014354 ..... p 740 N94-13286 #
DE93-014366 ..... p 663 N94-14113 #
DE93-014391 ..... p 788 N94-13103 #
DE93-014395 ..... p 701 N94-12913 #
DE93-014398 ..... p 730 N94-14509 #
DE93-014415 ..... p 658 N94-14114 #
DE93-014418 ..... p 797 N94-13207 #
DE93-014419 ..... p 802 N94-14564 #
DE93-014422 ..... p 788 N94-13208 #
DE93-014423 ..... p 840 N94-14467 #
DE93-014425 ..... p 670 N94-12887 #
DE93-014427 ..... p 766 N94-14737 #
DE93-014438 ..... p 818 N94-14738 #
DE93-014440 ..... p 815 N94-14739 #
DE93-014441 ..... p 781 N94-13283
DE93-014449 ..... p 785 N94-14468 #
DE93-014450 ..... p 702 N94-13402 #
DE93-014452 ..... p 702 N94-13403 #
DE93-014453 ..... p 558 N94-14469 #
DE93-014458 ..... p 789 N94-13209 #
DE93-014473 ..... p 780 N94-13173 #
DE93-014526 ..... p 815 N94-14798
DE93-014553 ..... p 818 N94-14740 #
DE93-014557 ..... p 789 N94-13327 #
DE93-014561 ..... p 717 N94-14328 #
DE93-014565 ..... p 789 N94-13328 #
DE93-014566 ..... p 811 N94-14329 #
DE93-014576 ..... p 815 N94-14773 #
DE93-014577 ..... p 839 N94-14116 #
DE93-014582 ..... p 765 N94-14117 #
DE93-014585 ..... p 558 N94-14119 #
DE93-014586 ..... p 558 N94-14121 #
DE93-014587 ..... p 810 N94-14122 #
DE93-014648 ..... p 562 N94-13001 #
DE93-014655 ..... p 580 N94-14124 #
DE93-014656 ..... p 810 N94-14125 #
DE93-014657 ..... p 808 N94-13881 #
DE93-014677 ..... p 720 N94-13404 #
DE93-014678 ..... p 657 N94-13882 #
DE93-014682 ..... p 807 N94-13405 #
DE93-014683 ..... p 823 N94-13406 #
DE93-014740 ..... p 754 N94-14470 #
DE93-014766-PHASE-1 ..... p 596 N94-13407 #
DE93-014768 ..... p 583 N94-14801
DE93-014774 ..... p 595 N94-13021 #
DE93-014845 ..... p 786 N94-14527 #
DE93-014861 ..... p 785 N94-14471 #
DE93-014904 ..... p 738 N94-14451 #
DE93-014919 ..... p 783 N94-13884 #
DE93-014928 ..... p 651 N94-14452 #
DE93-014959 ..... p 578 N94-13408 #
DE93-014962 ..... p 583 N94-13002 #
DE93-014990 ..... p 817 N94-14453 #
DE93-014996 ..... p 703 N94-13886 #
DE93-014998 ..... p 579 N94-13888 #
DE93-014999 ..... p 782 N94-13409 #
DE93-015001 ..... p 705 N94-14861 #
DE93-015007 ..... p 649 N94-13410 #
DE93-015011 ..... p 596 N94-13889 #
DE93-015019 ..... p 623 N94-13892 #
DE93-015040 ..... p 563 N94-13411 #
DE93-015044 ..... p 573 N94-14474 #
DE93-015066 ..... p 804 N94-13003 #
DE93-015067 ..... p 782 N94-13412 #
DE93-015068 ..... p 563 N94-13413 #
DE93-015074 ..... p 782 N94-13414 #
DE93-015075 ..... p 807 N94-13373 #
DE93-015076 ..... p 730 N94-14802
DE93-015078 ..... p 562 N94-13004 #
DE93-015080 ..... p 717 N94-14294 #
DE93-015082 ..... p 753 N94-14295 #
DE93-015084 ..... p 612 N94-14512 #
DE93-015088 ..... p 581 N94-14337 #
DE93-015093 ..... p 717 N94-14338 #
DE93-015095 ..... p 804 N94-13005 #
DE93-015096 ..... p 839 N94-14330 #
DE93-015099 ..... p 760 N94-14475 #
DE93-015101 ..... p 825 N94-14331 #
DE93-015103 ..... p 811 N94-14332 #
DE93-015104 ..... p 783 N94-13893 #
DE93-015125 ..... p 754 N94-14399 #
DE93-015126 ..... p 539 N94-13006 #
DE93-015133 ..... p 783 N94-13895 #
DE93-015157 ..... p 623 N94-13925 #
DE93-015158 ..... p 784 N94-13896 #
DE93-015177 ..... p 704 N94-14333 #
DE93-015205 ..... p 774 N94-14334 #
DE93-015208 ..... p 654 N94-13022 #
DE93-015210 ..... p 738 N94-14335 #
DE93-015218 ..... p 581 N94-14400 #
DE93-015247 ..... p 761 N94-14476 #
DE93-015258 ..... p 710 N94-14477 #
DE93-015260 ..... p 851 N94-14401 #
DE93-015273 ..... p 825 N94-14433 #
DE93-015277 ..... p 625 N94-14336
DE93-015310 ..... p 744 N94-13024 #
DE93-015357 ..... p 767 N94-13025 #
DE93-015365 ..... p 805 N94-13012 #
DE93-015430 ..... p 813 N94-14478 #
DE93-015460 ..... p 573 N94-14700 #
DE93-015463 ..... p 604 N94-13899 #
DE93-015473 ..... p 800 N94-13900 #
DE93-015474 ..... p 802 N94-14583 #
DE93-015475 ..... p 801 N94-14347 #
DE93-015477 ..... p 802 N94-14570 #
DE93-015500 ..... p 573 N94-14402 #
DE93-015511 ..... p 812 N94-14348 #
DE93-015517 ..... p 573 N94-14537 #
DE93-015550 ..... p 783 N94-13890 #
DE93-015560 ..... p 575 N94-12861 #
DE93-015568 ..... p 704 N94-14355 #
DE93-015582 ..... p 827 N94-14803
DE93-015584 ..... p 784 N94-13927 #
DE93-015595 ..... p 624 N94-13928 #
DE93-015607 ..... p 755 N94-14571 #
DE93-015611 ..... p 794 N94-12862 #
DE93-015622 ..... p 567 N94-12834 #
DE93-015646 ..... p 801 N94-14349 #
DE93-015651 ..... p 755 N94-14528 #
DE93-015691 ..... p 793 N94-14702 #
DE93-015741 ..... p 795 N94-12984 #
DE93-015758 ..... p 562 N94-13045 #
DE93-015787 ..... p 659 N94-14572 #
DE93-015794 ..... p 793 N94-14529 #
DE93-015797 ..... p 812 N94-14362 #
DE93-015803 ..... p 808 N94-13930 #
DE93-015815 ..... p 796 N94-13046 #
DE93-015859 ..... p 851 N94-14587 #
DE93-015885 ..... p 727 N94-12835 #
DE93-015909 ..... p 676 N94-14530 #
DE93-015934 ..... p 784 N94-13952 #
DE93-015935 ..... p 719 N94-13119 #
DE93-015961 ..... p 582 N94-14531 #
DE93-015962 ..... p 660 N94-14863 #
DE93-015970 ..... p 744 N94-13120 #
DE93-015973 ..... p 803 N94-14865 #
DE93-015987 ..... p 822 N94-13121 #
DE93-016018 ..... p 705 N94-14504 #
DE93-016050 ..... p 565 N94-14403 #
DE93-016051 ..... p 811 N94-14296 #
DE93-016065 ..... p 806 N94-13152 #
DE93-016087 ..... p 580 N94-14297 #
DE93-016088 ..... p 757 N94-14866 #
DE93-016090 ..... p 787 N94-14588 #
DE93-016129 ..... p 570 N94-13374 #
DE93-016142 ..... p 567 N94-12836 #
DE93-016201 ..... p 571 N94-13977 #
DE93-016203 ..... p 563 N94-13375 #
DE93-016206 ..... p 706 N94-13079 #
DE93-016256 ..... p 579 N94-13978 #
DE93-016259 ..... p 809 N94-13980 #
DE93-016286 ..... p 809 N94-13981 #
DE93-016289 ..... p 784 N94-13983 #
DE93-016419 ..... p 660 N94-14888 #

DE93-016428 ..... p 639 N94-14434 #
DE93-016434 ..... p 719 N94-13080 #
DE93-016438 ..... p 771 N94-14589 #
DE93-016453 ..... p 754 N94-14435 #
DE93-016454 ..... p 803 N94-14590 #
DE93-016458 ..... p 778 N94-14867 #
DE93-016460 ..... p 676 N94-14591 #
DE93-016483 ..... p 816 N94-14868 #
DE93-016512 ..... p 740 N94-13069 #
DE93-016516 ..... p 582 N94-14436 #
DE93-016521 ..... p 597 N94-14592 #
DE93-016524 ..... p 817 N94-14593 #
DE93-016529 ..... p 658 N94-14437 #
DE93-016531 ..... p 792 N94-14438 #
DE93-016532 ..... p 659 N94-14594 #
DE93-016533 ..... p 658 N94-14442 #
DE93-016535 ..... p 566 N94-14869 #
DE93-016536 ..... p 813 N94-14439 #
DE93-016543 ..... p 659 N94-14595 #
DE93-016548 ..... p 813 N94-14440 #
DE93-016562 ..... p 802 N94-14532 #
DE93-016580 ..... p 625 N94-14533 #
DE93-016581 ..... p 652 N94-14534 #
DE93-016605 ..... p 585 N94-14535 #
DE93-016620 ..... p 774 N94-14441 #
DE93-016624 ..... p 840 N94-14536 #
DE93-016625 ..... p 813 N94-14413 #
DE93-016629 ..... p 786 N94-14514 #
DE93-016640 ..... p 755 N94-14515 #
DE93-016666 ..... p 812 N94-14354 #
DE93-016667 ..... p 577 N94-13070 #
DE93-016698 ..... p 710 N94-14516 #
DE93-016700 ..... p 813 N94-14517 #
DE93-016727 ..... p 718 N94-14518 #
DE93-016729 ..... p 802 N94-14519 #
DE93-016814 ..... p 730 N94-14596 #
DE93-016876 ..... p 814 N94-14597 #
DE93-016972 ..... p 659 N94-14520 #
DE93-016973 ..... p 658 N94-14414 #
DE93-017017 ..... p 780 N94-13071 #
DE93-017056 ..... p 577 N94-13072 #
DE93-017086 ..... p 562 N94-13222 #
DE93-017105 ..... p 755 N94-14521 #
DE93-017106 ..... p 625 N94-14522 #
DE93-017124 ..... p 658 N94-14415 #
DE93-017154 ..... p 790 N94-14893 #
DE93-017161 ..... p 803 N94-14894 #
DE93-017185 ..... p 647 N94-14895 #
DE93-017193 ..... p 651 N94-14416 #
DE93-017201 ..... p 818 N94-14896 #
DE93-017209 ..... p 790 N94-14897 #
DE93-017214 ..... p 627 N94-14870 #
DE93-017223 ..... p 788 N94-14898 #
DE93-017233 ..... p 757 N94-14871 #
DE93-017565 ..... p 788 N94-14872 #
DE93-017903 ..... p 817 N94-14417 #
DE93-018107 ..... p 558 N94-14418 #
DE93-018169 ..... p 785 N94-14419 #
DE93-018171 ..... p 574 N94-14873 #
DE93-018324 ..... p 803 N94-14874
DE93-018819 ..... p 785 N94-14420 #
DE93-500412 ..... p 682 N94-14653 #
DE93-512333 ..... p 582 N94-14513 #
DE93-617529 ..... p 790 N94-14843
DE93-620280 ..... p 585 N94-14829
DE93-620499 ..... p 576 N94-12867
DE93-620574 ..... p 569 N94-13360
DE93-620981 ..... p 797 N94-13240
DE93-621349 ..... p 767 N94-13223 #
DE93-621377 ..... p 836 N94-13361
DE93-621380 ..... p 621 N94-13224 #
DE93-621443 ..... p 782 N94-13362
DE93-621451 ..... p 783 N94-13506
DE93-621606 ..... p 798 N94-13507
DE93-621657 ..... p 794 N94-12853 #
DE93-621665 ..... p 794 N94-12854 #
DE93-621770 ..... p 816 N94-12855
DE93-621785 ..... p 618 N94-12856
DE93-622212 ..... p 804 N94-12893 #
DE93-622698 ..... p 653 N94-12857
DE93-622852 ..... p 767 N94-12895 #
DE93-622853 ..... p 775 N94-13508
DE93-622856 ..... p 632 N94-13509
DE93-622862 ..... p 772 N94-12896 #
DE93-622864 ..... p 775 N94-12843 #
DE93-622865 ..... p 816 N94-12844 #
DE93-622866 ..... p 778 N94-12858
DE93-622896 ..... p 619 N94-12891 #
DE93-622897 ..... p 775 N94-12877 #
DE93-622898 ..... p 778 N94-12879 #
DE93-622899 ..... p 834 N94-12880 #
DE93-622901 ..... p 778 N94-12845 #
DE93-622903 ..... p 769 N94-13536 #
DE93-622956 ..... p 778 N94-12847 #
DE93-622957 ..... p 778 N94-12848 #
DE93-622969 ..... p 779 N94-12882 #
DE93-622971 ..... p 804 N94-12828
DE93-623045 ..... p 781 N94-13225 #
DE93-623049 ..... p 806 N94-13226 #
DE93-623061 ..... p 807 N94-13510
DE93-623190 ..... p 632 N94-13511
DE93-623192 ..... p 569 N94-13227 #
DE93-623203 ..... p 806 N94-13228 #
DE93-623204 ..... p 806 N94-13213 #
DE93-623990 ..... p 788 N94-14875
DE93-624095 ..... p 827 N94-14880
DE93-624144 ..... p 788 N94-14881
DE93-624179 ..... p 617 N94-14883
DE93-625118 ..... p 567 N94-14884
DE93-626409 ..... p 627 N94-14885
DE93-626604 ..... p 772 N94-14886
DE93-626620 ..... p 818 N94-14887
DE93-626621 ..... p 849 N94-14889
DE93-626622 ..... p 772 N94-14890
DE93-626623 ..... p 788 N94-14891
DE93-626637 ..... p 617 N94-14892
DE93-753157 ..... p 795 N94-12944 #
DE93-767969 ..... p 505 N94-14059 #
DE93-767970 ..... p 505 N94-14061 #
DE93-778332 ..... p 718 N94-12837 #
DE93-782887 ..... p 581 N94-14421
DE93-793955 ..... p 700 N94-12822 #
DE93-799057 ..... p 701 N94-13214 #
DE93-799058 ..... p 701 N94-13215 #
DE93-799061 ..... p 705 N94-14679 #

DGLR-92-03-108 ..... p 509 N94-14710 #

DLOR-RN-92-5 ..... p 515 N94-13839
DLOR-RN-92-6 ..... p 515 N94-13867

DLR-FB-92-07 ..... p 700 N94-14428 #
DLR-FB-92-21 ..... p 716 N94-14132 #
DLR-FB-92-23 ..... p 688 N94-14135 #
DLR-FB-92-26 ..... p 639 N94-14443 #
DLR-FB-92-27 ..... p 733 N94-14043 #
DLR-FB-92-30 ..... p 651 N94-14044 #
DLR-FB-92-32 ..... p 637 N94-14045 #
DLR-FB-92-34 ..... p 638 N94-14188 #
DLR-FB-92-37 ..... p 723 N94-14189 #

DLR-MITT-90-15 ..... p 557 N94-13804 #

DM-62 ..... p 632 N94-13535 #

DMS-DR-2476-VOL-1 ..... p 534 N94-12810 * #
DMS-DR-2476-VOL-2 ..... p 536 N94-14047 * #
DMS-DR-2549-VOL-1 ..... p 534 N94-13191 * #
DMS-DR-2549-VOL-2 ..... p 534 N94-12965 * #

DMS-RN-4-92 ..... p 773 N94-13848 #

DNA-TR-92-108 ..... p 769 N94-13731 #

DOE-76-45/28-REV-1 ..... p 823 N94-13352 #

DOE/CE-15974/T4 ..... p 581 N94-14337 #
DOE/CE-23810/11D ..... p 595 N94-13021 #
DOE/CE-23810/6 ..... p 596 N94-13407 #
DOE/CE-23810/8C ..... p 583 N94-14801
DOE/CE-50337/T1 ..... p 701 N94-12913 #

DOE/CH-10093/190 ..... p 701 N94-12914 #
DOE/CH-10093/210 ..... p 701 N94-12902 #

DOE/DP-40092/9 ..... p 796 N94-13047 #

DOE/ER-0586T ..... p 710 N94-14182 #
DOE/ER-10713/T4 ..... p 782 N94-13412 #
DOE/ER-12128/1 ..... p 809 N94-13981 #
DOE/ER-13183/8 ..... p 563 N94-13375 #
DOE/ER-13191/13 ..... p 654 N94-13013 #
DOE/ER-13439/8 ..... p 562 N94-13004 #
DOE/ER-13726/6 ..... p 791 N94-13015 #
DOE/ER-13734/4 ..... p 730 N94-14509 #
DOE/ER-13740/11 ..... p 818 N94-14738 #
DOE/ER-13745/3 ..... p 807 N94-13373 #
DOE/ER-13878/5 ..... p 565 N94-14403 #
DOE/ER-13933/3 ..... p 814 N94-14597 #
DOE/ER-13960/5 ..... p 780 N94-13071 #
DOE/ER-13970/4 ..... p 827 N94-14803
DOE/ER-13971/20 ..... p 779 N94-12940 #
DOE/ER-13978/4 ..... p 717 N94-14338 #
DOE/ER-14056/14 ..... p 654 N94-13022 #
DOE/ER-14181/1 ..... p 575 N94-12861 #
DOE/ER-14187/1 ..... p 562 N94-13001 #
DOE/ER-14193/5 ..... p 571 N94-13977 #
DOE/ER-14205/2 ..... p 784 N94-13983 #
DOE/ER-14214/2 ..... p 785 N94-14419 #
DOE/ER-14275/1 ..... p 806 N94-13152 #
DOE/ER-14280/1 ..... p 573 N94-14402 #
DOE/ER-14281/1 ..... p 567 N94-12834 #
DOE/ER-14306/1 ..... p 562 N94-13222 #
DOE/ER-20050/T1 ..... p 727 N94-12835 #
DOE/ER-25015/T1 ..... p 740 N94-13069 #
DOE/ER-25047/5 ..... p 744 N94-13024 #
DOE/ER-25065/4 ..... p 817 N94-14417 #
DOE/ER-25136/1 ..... p 767 N94-13025 #
DOE/ER-40160/9 ..... p 784 N94-13927 #
DOE/ER-40333/137 ..... p 778 N94-12860 #
DOE/ER-40388/102 ..... p 839 N94-14330 #
DOE/ER-40427/02-N93 ..... p 785 N94-14471 #
DOE/ER-40427/36-N92 ..... p 779 N94-12997 #
DOE/ER-40741/1 ..... p 818 N94-14896 #
DOE/ER-40747/5 ..... p 790 N94-14897 #
DOE/ER-40757/004 ..... p 817 N94-13479 #
DOE/ER-40768/1 ..... p 784 N94-13952 #
DOE/ER-45125/10 ..... p 730 N94-14802
DOE/ER-45133/5 ..... p 804 N94-13005 #
DOE/ER-45141/9 ..... p 812 N94-14354 #
DOE/ER-45147/8 ..... p 781 N94-13283
DOE/ER-45228/65 ..... p 578 N94-13408 #
DOE/ER-45237/7 ..... p 579 N94-13978 #
DOE/ER-45298/9 ..... p 577 N94-13072 #
DOE/ER-45315/17 ..... p 809 N94-13980 #
DOE/ER-45316/T1 ..... p 567 N94-12836 #
DOE/ER-45334/6 ..... p 815 N94-14739 #
DOE/ER-45359/2 ..... p 804 N94-13003 #
DOE/ER-45391/4 ..... p 811 N94-14296 #
DOE/ER-45401/4 ..... p 815 N94-14798
DOE/ER-45415/6 ..... p 563 N94-13477 #
DOE/ER-45415/9 ..... p 563 N94-13478 #
DOE/ER-45418/3 ..... p 558 N94-14418 #
DOE/ER-45431/3 ..... p 570 N94-13374 #
DOE/ER-45438/3 ..... p 577 N94-13070 #
DOE/ER-52147/6 ..... p 654 N94-13058 #
DOE/ER-53098/T9 ..... p 794 N94-12862 #
DOE/ER-53257/6 ..... p 803 N94-14874
DOE/ER-53266/44 ..... p 757 N94-14866 #
DOE/ER-54131/2 ..... p 795 N94-12984 #
DOE/ER-60473/7 ..... p 785 N94-14420 #
DOE/ER-60721/6 ..... p 782 N94-13414 #
DOE/ER-61012/T3 ..... p 719 N94-13080 #
DOE/ER-61014/3 ..... p 706 N94-13079 #
DOE/ER-61034/2 ..... p 730 N94-14596 #
DOE/ER-61474/1 ..... p 719 N94-13119 #
DOE/ER-75582/T1 ..... p 563 N94-13413 #
DOE/ER-75784/1 ..... p 574 N94-14873 #
DOE/ER-75842/1 ..... p 818 N94-13216

DOE/ER/40427-09-N93 ..... p 786 N94-14527 #
DOE/ER/40561-103 ..... p 786 N94-14527 #

DOE/FTR-93010924 ..... p 664 N94-14565 #
DOE/FTR-93012146 ..... p 808 N94-13973 #
DOE/FTR-93013016 ..... p 786 N94-14524 #

DOE/ID-12842/2 ..... p 638 N94-14351 #

DOE/MC-27168/93/C0188 ..... p 701 N94-13093 #
DOE/MC-27168/93/C0189 ..... p 703 N94-13693 #
DOE/MC-28065/3371 ..... p 702 N94-13380 #

DOE/METC-C/93/7068 ..... p 566 N94-14586 #
DOE/METC-C/93/7069 ..... p 688 N94-14151 #
DOE/METC-C/93/7083 ..... p 704 N94-14355 #

DOE/NASA/1087-2 ..... p 519 N94-14448 * #

DOE/PC-92111/T2 ..... p 583 N94-13002 #

DOE/SF-16306/36 ..... p 705 N94-14504 #

DOT-VNTSC-FAA-93-3 ..... p 514 N94-14563

DOT/FAA/AM-93/13 ..... p 732 N94-13193 #
DOT/FAA/AM-93/14 ..... p 738 N94-13972 #
DOT/FAA/AM-93/15 ..... p 738 N94-14023 #
DOT/FAA/AM-93/16 ..... p 736 N94-14854 #
DOT/FAA/AM-93/17 ..... p 735 N94-14846 #

DOT/FAA/CT-TN93/29 ..... p 511 N94-14186 #

DOT/FAA/RD-93/4 ..... p 514 N94-14563

DOT/FRA/NMI-93/02 ..... p 661 N94-13285

DRA-TR-93014 ..... p 528 N94-14876

DREA-CR-90-442-PT-1-PHASE-1 ..... p 558 N94-14105
DREA-CR-90-442-PT-2 ..... p 751 N94-14017

DREA-TM-92-218 ..... p 674 N94-13833

DREO-RN-1118 ..... p 603 N94-13818
DREO-RN-1119 ..... p 606 N94-14064 #
DREO-RN-1122 ..... p 603 N94-13832 #
DREO-RN-1130 ..... p 603 N94-13837 #

DREO-TN-92-10 ..... p 603 N94-13838 #
DREO-TN-92-13 ..... p 603 N94-13829 #
DREO-TN-92-14 ..... p 606 N94-14054
DREO-TN-92-17 ..... p 606 N94-14062 #
DREO-TN-92-3 ..... p 605 N94-14033 #
DREO-TN-92-5 ..... p 606 N94-14063 #
DREO-TN-92-9 ..... p 605 N94-13941

DREO-1166 ..... p 653 N94-14782 #
DREO-17 ..... p 777 N94-13831

DREP-CR-92-47 ..... p 777 N94-14360 #

DREP-LN-91-06 ..... p 715 N94-13830 #

DRES-CR-4-93 ..... p 657 N94-14067

DREV-R-4692-93 ..... p 607 N94-14204

DRIC-BR-318697 ..... p 528 N94-14876

DSIS-92-03763 ..... p 728 N94-13823
DSIS-92-03794 ..... p 674 N94-13833
DSIS-92-03900 ..... p 603 N94-13837 #
DSIS-93-00034 ..... p 603 N94-13818
DSIS-93-00036-VOL-2 ..... p 564 N94-13819
DSIS-93-00071 ..... p 623 N94-13834
DSIS-93-00072 ..... p 764 N94-13844
DSIS-93-00101 ..... p 792 N94-13845
DSIS-93-00137 ..... p 515 N94-13867
DSIS-93-00139 ..... p 773 N94-13848 #
DSIS-93-00151 ..... p 603 N94-13841
DSIS-93-00153 ..... p 764 N94-13842
DSIS-93-00177 ..... p 603 N94-13843
DSIS-93-00179 ..... p 792 N94-13868
DSIS-93-00236 ..... p 623 N94-13846 #
DSIS-93-00237 ..... p 571 N94-13840
DSIS-93-00238 ..... p 752 N94-14088
DSIS-93-00250 ..... p 657 N94-14067
DSIS-93-00258 ..... p 604 N94-13869
DSIS-93-00259 ..... p 604 N94-13870
DSIS-93-00260 ..... p 606 N94-14037
DSIS-93-00261 ..... p 606 N94-14038
DSIS-93-00262 ..... p 751 N94-14014
DSIS-93-00274 ..... p 605 N94-14015
DSIS-93-00275 ..... p 751 N94-13990
DSIS-93-00276 ..... p 751 N94-14016
DSIS-93-00277 ..... p 753 N94-14197
DSIS-93-00282 ..... p 515 N94-13839
DSIS-93-00287 ..... p 777 N94-14360 #
DSIS-93-00308 ..... p 715 N94-13830 #
DSIS-93-00314 ..... p 777 N94-13831
DSIS-93-00345 ..... p 604 N94-13939 #
DSIS-93-00346 ..... p 607 N94-14065
DSIS-93-00347 ..... p 607 N94-14066
DSIS-93-00348 ..... p 752 N94-14051
DSIS-93-00349 ..... p 752 N94-14052
DSIS-93-00350 ..... p 750 N94-13858
DSIS-93-00351 ..... p 750 N94-13944
DSIS-93-00362 ..... p 606 N94-14054
DSIS-93-00382 ..... p 602 N94-13801
DSIS-93-00400 ..... p 603 N94-13829 #
DSIS-93-00477 ..... p 605 N94-13941
DSIS-93-00480 ..... p 564 N94-13942
DSIS-93-00613 ..... p 607 N94-14204
DSIS-93-00649 ..... p 810 N94-14203
DSIS-93-00702 ..... p 753 N94-14207
DSIS-93-00737 ..... p 774 N94-13549 #
DSIS-93-00857-PT-1-PHASE-1 .... p 558 N94-14105
DSIS-93-00858-PT-2 ..... p 751 N94-14017

D658-10313-1 ..... p 575 N94-12792 * #

E-6566 ..... p 509 N94-14780 * #
E-7059 ..... p 548 N94-12807 * #
E-7302 ..... p 538 N94-13918 * #
E-7329 ..... p 620 N94-13110 * #
E-7558 ..... p 665 N94-13056 * #
E-7564 ..... p 537 N94-12809 * #
E-7594 ..... p 552 N94-14102 * #
E-7635 ..... p 538 N94-13111 * #
E-7650 ..... p 648 N94-12874 * #
E-7673 ..... p 510 N94-14847 * #
E-7685 ..... p 622 N94-13786 * #
E-7689 ..... p 554 N94-12871 * #
E-7755 ..... p 629 N94-13027 * #
E-7765 ..... p 631 N94-13385 * #
E-7769 ..... p 541 N94-13917 * #
E-7779 ..... p 628 N94-12968 * #
E-7854-1 ..... p 642 N94-14732 * #
E-7864 ..... p 675 N94-13919 * #
E-7892 ..... p 555 N94-13138 * #
E-7923 ..... p 551 N94-13430 * #
E-7947 ..... p 676 N94-14041 * #
E-7950 ..... p 499 N94-13108 * #
E-7987 ..... p 620 N94-13134 * #
E-7991 ..... p 575 N94-12842 * #
E-7998 ..... p 518 N94-13143 * #
E-8019 ..... p 670 N94-13053 * #
E-8020 ..... p 670 N94-12872 * #
E-8024 ..... p 671 N94-13379 * #
E-8027 ..... p 642 N94-14729 * #
E-8028 ..... p 553 N94-14725 * #
E-8029 ..... p 553 N94-14726 * #
E-8031 ..... p 664 N94-14727 * #
E-8035 ..... p 534 N94-13028 * #
E-8040 ..... p 648 N94-13135 * #
E-8043 ..... p 683 N94-14776 * #
E-8045 ..... p 559 N94-14719 * #
E-8047 ..... p 621 N94-13194 * #
E-8052 ..... p 517 N94-13142 * #
E-8063 ..... p 518 N94-14036 * #
E-8068 ..... p 555 N94-13139 * #
E-8070 ..... p 557 N94-13920 * #
E-8071 ..... p 626 N94-14730 * #
E-8077 ..... p 583 N94-14845 * #
E-8081 ..... p 557 N94-14042 * #
E-8085 ..... p 555 N94-13378 * #
E-8088-VOL-2 ..... p 664 N94-14446 * #
E-8089-VOL-1 ..... p 663 N94-14445 * #
E-8091 ..... p 650 N94-13876 * #
E-8097 ..... p 551 N94-13416 * #
E-8099 ..... p 550 N94-13415 * #
E-8101 ..... p 554 N94-14771 * #
E-8103 ..... p 519 N94-14448 * #
E-8113 ..... p 676 N94-14408 * #
E-8114 ..... p 560 N94-14823 * #
E-8116 ..... p 559 N94-14769 * #
E-8120 ..... p 582 N94-14543 * #
E-8132 ..... p 771 N94-14731 * #
E-8136 ..... p 770 N94-14407 * #
E-8138 ..... p 642 N94-14722 * #
E-8140 ..... p 642 N94-14728 * #
E-8156 ..... p 560 N94-14822 * #
E-8160 ..... p 612 N94-14542 * #
E-8165 ..... p 508 N94-14208 * #

EGG-M-92413 ..... p 550 N94-13351 #
EGG-M-92502 ..... p 548 N94-12870 #
EGG-M-92569 ..... p 549 N94-12996 #
EGG-M-93143 ..... p 746 N94-13394 #

EGG-NE-10391 ..... p 552 N94-14013 #

EGG-10617-1216 ..... p 717 N94-14294 #

EMA-TR-91-1152 ..... p 671 N94-13124 * #

EML-549 ..... p 706 N94-12904 #
EML-93-6-1 ..... p 599 N94-13264 * #

EOC-92-01-0007 ..... p 687 N94-14091 #

EPA/542/R-93/001 ..... p 821 N94-12936 #

ERB-1032 ..... p 740 N94-13546 #
ERB-1033 ..... p 769 N94-13545 #
ERB-1034 ..... p 824 N94-14202 #
ERB-1035 ..... p 741 N94-13547 #
ERB-1036 ..... p 765 N94-14201 #
ERB-1037 ..... p 753 N94-14200 #

ERIM-225300-8-F ..... p 725 N94-13581 #

ERP-1111 ..... p 719 N94-12978 #
ERP-1117 ..... p 834 N94-12971 #

ES/ER/TM-57 ..... p 825 N94-14458 #

ESA-BR-82 ..... p 543 N94-14352 #
ESA-BR-86 ..... p 851 N94-14137 #

ESA-PSS-03-406-ISSUE-1-VOL-1 p 737 N94-13901 #
ESA-PSS-03-406-ISSUE-1-VOL-2 p 738 N94-13902 #
ESA-PSS-05-04-ISSUE-1 ..... p 753 N94-14190 #
ESA-PSS-05-05-ISSUE-1 ..... p 753 N94-14191 #

ESA-SP-1146 ..... p 699 N94-14353 #
ESA-SP-1160 ..... p 733 N94-14860 #

ESA-STM-246 ..... p 731 N94-14862 #

ESA-TT-1260 ..... p 557 N94-13804 #
ESA-TT-1278 ..... p 630 N94-13117 #
ESA-TT-1286 ..... p 776 N94-13692 #

ESC-TR-93-207 ..... p 531 N94-13358

ESM-48 ..... p 806 N94-13226 #

ETDE/JP-MF-93512333 ..... p 582 N94-14513 #
ETDE/JP-MF-93799057 ..... p 701 N94-13214 #
ETDE/JP-MF-93799058 ..... p 701 N94-13215 #
ETDE/JP-MF-93799061 ..... p 705 N94-14679 #

ETN-93-93473 ..... p 625 N94-14096 #
ETN-93-93483 ..... p 760 N94-14187 #
ETN-93-93738 ..... p 716 N94-14132 #
ETN-93-93740 ..... p 688 N94-14135 #
ETN-93-93755 ..... p 684 N94-13123 #
ETN-93-93758 ..... p 687 N94-14127 #
ETN-93-93761 ..... p 729 N94-14128 #
ETN-93-93762 ..... p 729 N94-14129 #
ETN-93-93867 ..... p 824 N94-14072 #
ETN-93-93880 ..... p 686 N94-14073 #
ETN-93-93920 ..... p 722 N94-13985
ETN-93-93921 ..... p 722 N94-13991
ETN-93-93922 ..... p 722 N94-13992
ETN-93-93923 ..... p 722 N94-13993
ETN-93-93929 ..... p 722 N94-13926
ETN-93-93946 ..... p 851 N94-14137 #
ETN-93-93947 ..... p 543 N94-14352 #
ETN-93-93948 ..... p 699 N94-14353 #
ETN-93-93954 ..... p 700 N94-14428 #
ETN-93-93957 ..... p 639 N94-14443 #
ETN-93-93958 ..... p 733 N94-14043 #
ETN-93-93961 ..... p 651 N94-14044 #
ETN-93-93962 ..... p 637 N94-14045 #
ETN-93-93963 ..... p 638 N94-14188 #
ETN-93-93964 ..... p 723 N94-14189 #
ETN-93-93965 ..... p 753 N94-14190 #
ETN-93-93966 ..... p 753 N94-14191 #
ETN-93-93967 ..... p 716 N94-14192 #
ETN-93-93969 ..... p 810 N94-14193 #
ETN-93-93970 ..... p 565 N94-14194 #
ETN-93-93971 ..... p 650 N94-14009 #
ETN-93-93972 ..... p 809 N94-14010 #
ETN-93-93973 ..... p 605 N94-13968 #
ETN-93-93974 ..... p 657 N94-13970 #
ETN-93-93975 ..... p 770 N94-13971 #
ETN-93-93977 ..... p 715 N94-13949 #
ETN-93-93978 ..... p 605 N94-13950 #
ETN-93-93979 ..... p 624 N94-13951 #
ETN-93-93980 ..... p 625 N94-14138 #
ETN-93-94005 ..... p 675 N94-13929 #
ETN-93-94006 ..... p 675 N94-13931 #
ETN-93-94007 ..... p 682 N94-14692 * #
ETN-93-94008 ..... p 675 N94-13933 #
ETN-93-94009 ..... p 675 N94-13986 #
ETN-93-94010 ..... p 775 N94-13987 #
ETN-93-94011 ..... p 542 N94-13988 #
ETN-93-94047 ..... p 597 N94-14808 #
ETN-93-94056 ..... p 819 N94-14449 #
ETN-93-94068 ..... p 519 N94-14450 #
ETN-93-94087 ..... p 819 N94-14809 #
ETN-93-94088 ..... p 818 N94-14462 #
ETN-93-94092 ..... p 700 N94-14544 #
ETN-93-94093 ..... p 700 N94-14810 #
ETN-93-94102 ..... p 774 N94-14545 #
ETN-93-94153 ..... p 773 N94-13677 #
ETN-93-94154 ..... p 765 N94-14018 #
ETN-93-94155 ..... p 764 N94-13999 #
ETN-93-94156 ..... p 764 N94-14000 #
ETN-93-94157 ..... p 765 N94-14001 #
ETN-93-94158 ..... p 770 N94-14002 #
ETN-93-94159 ..... p 770 N94-14003 #
ETN-93-94160 ..... p 751 N94-14004 #
ETN-93-94161 ..... p 765 N94-14361 #
ETN-93-94162 ..... p 773 N94-14005 #
ETN-93-94163 ..... p 768 N94-13496 #
ETN-93-94164 ..... p 748 N94-13524 #
ETN-93-94165 ..... p 760 N94-13924 #
ETN-93-94166 ..... p 740 N94-13525 #
ETN-93-94167 ..... p 768 N94-13526 #
ETN-93-94169 ..... p 723 N94-14546 #
ETN-93-94170 ..... p 723 N94-14707 #
ETN-93-94189 ..... p 642 N94-14708 #
ETN-93-94191 ..... p 724 N94-14709 #
ETN-93-94196 ..... p 509 N94-14710 #
ETN-93-94198 ..... p 751 N94-14006 #
ETN-93-94206 ..... p 579 N94-14007 #
ETN-93-94208 ..... p 511 N94-14008 #
ETN-93-94221 ..... p 833 N94-14811 #
ETN-93-94222 ..... p 686 N94-13994 #
ETN-93-94224 ..... p 627 N94-14812 #
ETN-93-94237 ..... p 751 N94-13995 #
ETN-93-94290 ..... p 770 N94-14150 #
ETN-93-94336 ..... p 650 N94-13527 #
ETN-93-94337 ..... p 503 N94-13528 #
ETN-93-94338 ..... p 763 N94-13529 #
ETN-93-94339 ..... p 503 N94-13530 #
ETN-93-94340 ..... p 503 N94-13531 #
ETN-93-94341 ..... p 570 N94-13532 #
ETN-93-94343 ..... p 632 N94-13533 #
ETN-93-94344 ..... p 570 N94-13497 #
ETN-93-94345 ..... p 528 N94-13498 #
ETN-93-94354 ..... p 756 N94-14813 #
ETN-93-94356 ..... p 574 N94-14814 #

ETN-93-94357 ..... p 560 N94-14815 #
ETN-93-94359 ..... p 814 N94-14697 #
ETN-93-94360 ..... p 626 N94-14698 #
ETN-93-94361 ..... p 626 N94-14711 #
ETN-93-94362 ..... p 756 N94-14712 #
ETN-93-94363 ..... p 626 N94-14713 #
ETN-93-94364 ..... p 756 N94-14714 #
ETN-93-94365 ..... p 761 N94-14716 #
ETN-93-94366 ..... p 616 N94-14717 #
ETN-93-94367 ..... p 768 N94-14718 #
ETN-93-94368 ..... p 815 N94-14720 #
ETN-93-94369 ..... p 787 N94-14721 #
ETN-93-94371 ..... p 768 N94-13499 #
ETN-93-94372 ..... p 725 N94-13500 #
ETN-93-94373 ..... p 721 N94-13686 #
ETN-93-94374 ..... p 722 N94-14071 #
ETN-93-94375 ..... p 671 N94-13501 #
ETN-93-94376 ..... p 844 N94-13502 #
ETN-93-94377 ..... p 837 N94-13503 #
ETN-93-94378 ..... p 837 N94-13504 #
ETN-93-94379 ..... p 720 N94-13587 #
ETN-93-94380 ..... p 528 N94-13588 #
ETN-93-94381 ..... p 510 N94-14800 #
ETN-93-94382 ..... p 651 N94-14149 #
ETN-93-94383 ..... p 711 N94-14723 #
ETN-93-94384 ..... p 720 N94-13589 #
ETN-93-94385 ..... p 771 N94-14807 #
ETN-93-94386 ..... p 657 N94-13996 #
ETN-93-94387 ..... p 703 N94-13997 #
ETN-93-94388 ..... p 624 N94-13998 #
ETN-93-94389 ..... p 839 N94-14075 #
ETN-93-94390 ..... p 616 N94-14724 #
ETN-93-94391 ..... p 774 N94-14703 #
ETN-93-94392 ..... p 807 N94-13590 #
ETN-93-94393 ..... p 793 N94-14704 #
ETN-93-94394 ..... p 815 N94-14705 #
ETN-93-94395 ..... p 647 N94-14816 #
ETN-93-94396 ..... p 617 N94-14817 #
ETN-93-94397 ..... p 793 N94-14856 #
ETN-93-94406 ..... p 737 N94-13901 #
ETN-93-94407 ..... p 738 N94-13902 #
ETN-93-94409 ..... p 733 N94-14860 #
ETN-93-94410 ..... p 731 N94-14862 #
ETN-93-94411 ..... p 622 N94-13552 #
ETN-93-94416 ..... p 511 N94-13534 #
ETN-93-94417 ..... p 515 N94-13687 #
ETN-93-94419 ..... p 673 N94-13726 #
ETN-93-94420 ..... p 673 N94-13787 #
ETN-93-94421 ..... p 499 N94-13904 #
ETN-93-94422 ..... p 674 N94-13905 #
ETN-93-94424 ..... p 527 N94-13906 #
ETN-93-94425 ..... p 674 N94-13803 #
ETN-93-94446 ..... p 505 N94-14152 #
ETN-93-94451 ..... p 752 N94-14039 #
ETN-93-94452 ..... p 637 N94-14040 #
ETN-93-94453 ..... p 708 N94-13821 #
ETN-93-94454 ..... p 542 N94-14107 #
ETN-93-94455 ..... p 650 N94-13665 #
ETN-93-94460 ..... p 570 N94-13666
ETN-93-94461 ..... p 708 N94-13667
ETN-93-94462 ..... p 749 N94-13688
ETN-93-94463 ..... p 824 N94-13879
ETN-93-94464 ..... p 708 N94-13880
ETN-93-94465 ..... p 783 N94-13883
ETN-93-94466 ..... p 777 N94-13885
ETN-93-94481 ..... p 674 N94-13887 #
ETN-93-94483 ..... p 777 N94-14034 #
ETN-93-94485 ..... p 597 N94-14055 #
ETN-93-94487 ..... p 632 N94-13535 #
ETN-93-94488 ..... p 673 N94-13689 #
ETN-93-94489 ..... p 515 N94-13690 #
ETN-93-94496 ..... p 653 N94-14701 #
ETN-93-94497 ..... p 509 N94-14706 #
ETN-93-94498 ..... p 653 N94-14827 #
ETN-93-94500 ..... p 574 N94-14828 #
ETN-93-94501 ..... p 683 N94-14818 #
ETN-93-94504 ..... p 750 N94-13822
ETN-93-94507 ..... p 823 N94-13863
ETN-93-94511 ..... p 750 N94-13805
ETN-93-94512 ..... p 823 N94-13806
ETN-93-94515 ..... p 750 N94-13807
ETN-93-94542 ..... p 662 N94-13808
ETN-93-94579 ..... p 770 N94-13809
ETN-93-94582 ..... p 557 N94-13804 #
ETN-93-94583 ..... p 630 N94-13117 #
ETN-93-94584 ..... p 776 N94-13692 #
ETN-93-94606 ..... p 639 N94-14464
ETN-93-94608 ..... p 617 N94-14819
ETN-93-94609 ..... p 617 N94-14820
ETN-93-94610 ..... p 574 N94-14821

E21-H83 ..... p 650 N94-14029 * #
E21-687 ..... p 650 N94-14029 * #

FE-MIT-92111-2 ..... p 583 N94-13002 #

FFA-TN-1992-18 ..... p 528 N94-13588 #
FFA-TN-1993-03 ..... p 673 N94-13689 #
FFA-TN-1993-05 ..... p 515 N94-13690 #

FFI-92-4005 ..... p 752 N94-14039 #
FFI-92/7012 ..... p 809 N94-14010 #
FFI-92/7047 ..... p 637 N94-14040 #
FFI-93-7007 ..... p 542 N94-14107 #
FFI-93/6001 ..... p 708 N94-13821 #
FFI-93/7008 ..... p 650 N94-13665 #

FFI/RAPPORT-92/7024 ..... p 605 N94-13968 #
FFI/RAPPORT-92/7028 ..... p 657 N94-13970 #
FFI/RAPPORT-92/7029 ..... p 770 N94-13971 #
FFI/RAPPORT-92/7034 ..... p 715 N94-13949 #

FIA-92-20 ..... p 761 N94-12889 * #
FIA-92-29 ..... p 761 N94-12890 * #

FM-9017-482 ..... p 737 N94-13674 * #

FNAL-TM-1838 ..... p 651 N94-14452 #

FNAL/C-92/313-A ..... p 834 N94-13096 #
FNAL/C-92/345-E ..... p 783 N94-13884 #
FNAL/C-93/045/E ..... p 779 N94-12954 #
FNAL/C-93/048/E ..... p 783 N94-13494 #
FNAL/C-93/049-E ..... p 781 N94-13350 #
FNAL/C-93/126 ..... p 783 N94-13895 #
FNAL/C-93/162 ..... p 788 N94-14898 #

FNAL/PUB-93-097-A ..... p 834 N94-12980 #

FOA-B-40416-4.4 ..... p 729 N94-14128 #
FOA-B-40417-4.4 ..... p 729 N94-14129 #

FRCR-435 ..... p 757 N94-14866 #

FSU-1338-592-26 ..... p 718 N94-12839 * #

GA-A-21046 ..... p 801 N94-14293 #
GA-A-21186 ..... p 802 N94-14519 #
GA-A-21257 ..... p 795 N94-12953 #
GA-A-21304 ..... p 802 N94-14570 #
GA-A-21306 ..... p 800 N94-13900 #
GA-A-21308 ..... p 802 N94-14583 #
GA-A-21311 ..... p 801 N94-14347 #
GA-A-21316 ..... p 802 N94-14579 #

GAO/IMTEC-93-2 ..... p 819 N94-13060 #

GKSS/92/E/24 ..... p 617 N94-14819
GKSS/92/E/26 ..... p 617 N94-14820
GKSS/92/E/27 ..... p 574 N94-14821

H-1904 ..... p 520 N94-13255 * #
H-1911 ..... p 520 N94-13254 * #
H-1914 ..... p 516 N94-14106 * #
H-1915 ..... p 517 N94-13791 * #
H-1916 ..... p 516 N94-13256 * #
H-1920 ..... p 519 N94-14855 * #
H-1933 ..... p 537 N94-14853 * #

HD-THEP-92-30 ..... p 778 N94-12847 #

HSV-93-0003 ..... p 793 N94-14548 * #

HUPHY-89-1 ..... p 786 N94-14552 * #

IAEA-CN-56/E-2-4 ..... p 801 N94-14293 #

IAEA-NDS-127(REV-0) ..... p 827 N94-14880

IAR-AN-75 ..... p 504 N94-14031 #
IAR-AN-76 ..... p 526 N94-13859 #

IC-92/317 ..... p 767 N94-12895 #
IC-92/319 ..... p 619 N94-12891 #
IC-92/370 ..... p 775 N94-12877 #
IC-92/409 ..... p 836 N94-13361
IC-93/13 ..... p 769 N94-13536 #
IC-93/14 ..... p 775 N94-13508
IC-93/17 ..... p 632 N94-13511
IC-93/22 ..... p 778 N94-12879 #
IC-93/27 ..... p 834 N94-12880 #
IC-93/31 ..... p 779 N94-12882 #
IC-93/36 ..... p 806 N94-13228 #
IC-93/3 ..... p 632 N94-13509
IC-93/6 ..... p 807 N94-13510
IC-93/7 ..... p 569 N94-13227 #
IC-93/8 ..... p 772 N94-12896 #

ICAF-1866 ..... p 683 N94-14818 #
ICAF-1867 ..... p 574 N94-14828 #

ICAM-91-07-04 ..... p 504 N94-13607 * #

ICASE-93-27 ..... p 499 N94-12852 * #
ICASE-93-28 ..... p 630 N94-13133 * #
ICASE-93-31 ..... p 768 N94-13354 * #
ICASE-93-32 ..... p 630 N94-13114 * #
ICASE-93-33 ..... p 630 N94-13128 * #
ICASE-93-34 ..... p 769 N94-13722 * #
ICASE-93-35 ..... p 767 N94-13202 * #
ICASE-93-38 ..... p 767 N94-13289 * #
ICASE-93-39 ..... p 762 N94-13184 * #
ICASE-93-40 ..... p 769 N94-13725 * #
ICASE-93-41 ..... p 745 N94-13185 * #
ICASE-93-42 ..... p 769 N94-13717 * #
ICASE-93-43 ..... p 636 N94-13817 * #
ICASE-93-44 ..... p 628 N94-12888 * #
ICASE-93-45 ..... p 647 N94-14849 * #
ICASE-93-46 ..... p 636 N94-13785 * #
ICASE-93-47 ..... p 769 N94-13792 * #
ICASE-93-50 ..... p 629 N94-13074 * #
ICASE-93-51 ..... p 636 N94-13718 * #
ICASE-93-52 ..... p 630 N94-13075 * #
ICASE-93-56 ..... p 636 N94-13724 * #
ICASE-93-59 ..... p 749 N94-13721 * #

ICOMP-93-11 ..... p 631 N94-13385 * #
ICOMP-93-27 ..... p 670 N94-12872 * #
ICOMP-93-28 ..... p 642 N94-14729 * #
ICOMP-93-30 ..... p 771 N94-14731 * #
ICOMP-93-31 ..... p 770 N94-14407 * #
ICOMP-93-32 ..... p 642 N94-14722 * #
ICOMP-93-34 ..... p 642 N94-14728 * #

IEPC-93-063 ..... p 534 N94-13028 * #

IFVE-OEF-91-40 ..... p 782 N94-13362

IHEP-OTF-91-137 ..... p 783 N94-13506

IIW-IX-1673-92 ..... p 674 N94-13887 #

ILR-MITT-280(1993) ..... p 510 N94-14800 #

IME-AMT-TR-001 ..... p 663 N94-14195 #

IME-CRE-TR-006 ..... p 637 N94-13862 #

IME-MET-TR-005 ..... p 733 N94-13847 #
IME-MET-TR-006 ..... p 663 N94-14147 #
IME-MET-TR-007 ..... p 764 N94-13860 #
IME-MET-TR-008 ..... p 824 N94-14196 #

IMI-93RT-21200-1436-G ..... p 557 N94-13866 #
IMI-93RT-42400-1476-G ..... p 597 N94-14070 #
IMI-93RT-42400-1477-G ..... p 596 N94-13684 #

INIS-MF-13456 ..... p 569 N94-13360
INIS-MF-13479 ..... p 798 N94-13507
INIS-MF-13494 ..... p 585 N94-14829

INO-92-5102 ..... p 657 N94-14067

INPE-5251-TAE/04 ..... p 818 N94-13427 #
INPE-5271-PRP/159 ..... p 684 N94-13426 #
INPE-5317-PRE/1714 ..... p 688 N94-14131 #
INPE-5345-PUD/048 ..... p 746 N94-13428 #
INPE-5379-TDI/474 ..... p 665 N94-12941 #
INPE-5400-TDI/479 ..... p 719 N94-13175 #
INPE-5424-PRP/172 ..... p 684 N94-13377 #
INPE-5431-PRE/1765 ..... p 720 N94-13429 #
INPE-5444-TDI/490 ..... p 720 N94-13614 #
INPE-5445-TDI/491 ..... p 835 N94-13174 #
INPE-5446-TDI/492 ..... p 837 N94-13449 #
INPE-5448-TDI/494 ..... p 628 N94-12966 #
INPE-5449-TDI/495 ..... p 765 N94-14084 #
INPE-5451-NTC/305 ..... p 685 N94-13610 #
INPE-5454-TDI/496 ..... p 707 N94-13330 #
INPE-5455-TDI/497 ..... p 684 N94-13331 #
INPE-5460-PRE/1768 ..... p 795 N94-12901 #
INPE-5463-PRE/1771 ..... p 801 N94-14024 #
INPE-5465-PRE/1773 ..... p 725 N94-13728 #
INPE-5466-PRE/1774 ..... p 687 N94-14082 #
INPE-5469-TDI/500 ..... p 631 N94-13365 #
INPE-5474-TDI/505 ..... p 829 N94-13245 #
INPE-5475-TDI/506 ..... p 684 N94-13364 #
INPE-5479-PRE/1778 ..... p 686 N94-13789 #
INPE-5480-PRE/1778 ..... p 686 N94-13729 #
INPE-5495-PRE/1786 ..... p 721 N94-13672 #
INPE-5498-TDI/513 ..... p 649 N94-13366 #

IS-M-746 ..... p 568 N94-13000 #

ISAL-91-0012 ..... p 574 N94-14814 #
ISAL-91-0078 ..... p 560 N94-14815 #

ISBN-0-315-51838-3 ..... p 513 N94-13541
ISBN-0-315-52149-X ..... p 791 N94-13490
ISBN-0-315-54370-1 ..... p 600 N94-13488

ISBN-0-315-54373-6 ..... p 600 N94-13489
ISBN-0-315-55435-5 ..... p 656 N94-13522
ISBN-0-315-55623-4 ..... p 720 N94-13516
ISBN-0-315-55958-6 ..... p 511 N94-13543
ISBN-0-315-56062-2 ..... p 661 N94-13521
ISBN-0-315-57172-1 ..... p 685 N94-13542
ISBN-0-315-57212-4 ..... p 772 N94-13540
ISBN-0-315-57755-X ..... p 685 N94-13475
ISBN-0-315-58948-5 ..... p 569 N94-13367
ISBN-0-315-58982-5 ..... p 685 N94-13523
ISBN-0-315-59463-2 ..... p 684 N94-13368
ISBN-0-315-59510-8 ..... p 726 N94-14205
ISBN-0-315-59601-5 ..... p 829 N94-13370 #
ISBN-0-315-60791-2 ..... p 502 N94-13369
ISBN-0-315-61012-3 ..... p 763 N94-13515
ISBN-0-315-61461-7 ..... p 621 N94-13333
ISBN-0-315-61722-5 ..... p 528 N94-13544
ISBN-0-315-61950-3 ..... p 829 N94-13371
ISBN-0-315-62457-4 ..... p 836 N94-13372
ISBN-0-315-63594-0 ..... p 632 N94-13474
ISBN-0-315-72009-3 ..... p 662 N94-13597
ISBN-0-315-72019-0 ..... p 635 N94-13683
ISBN-0-315-72716-0 ..... p 634 N94-13598
ISBN-0-315-73844-8 ..... p 817 N94-13554
ISBN-0-315-73875-8 ..... p 635 N94-13662
ISBN-0-643-05251-8 ..... p 709 N94-14095
ISBN-1-883712-00-9 ..... p 820 N94-12801 #
ISBN-2-921393-11-5 ..... p 499 N94-13520 #
ISBN-9-03-860201-4 ..... p 819 N94-14449 #
ISBN-9-05-411049-X ..... p 819 N94-14809 #
ISBN-9-05-411057-0 ..... p 687 N94-14127 #
ISBN-9-05-411063-5 ..... p 818 N94-14462 #
ISBN-9-05-411066-X ..... p 700 N94-14544 #
ISBN-9-06-275814-2 ..... p 682 N94-14692 * #
ISBN-9-06-814522-3 ..... p 597 N94-14808 #
ISBN-9-26-312485-X ..... p 721 N94-13686 #
ISBN-9-26-312485-X ..... p 722 N94-14071 #
ISBN-9-29-092123-4 ..... p 851 N94-14137 #
ISBN-9-51-384225-8 ..... p 674 N94-13887 #
ISBN-9-51-384234-7 ..... p 597 N94-14055 #
ISBN-9-51-384277-4 ..... p 777 N94-14034 #
ISBN-90-369-2014-0 ..... p 722 N94-13985
ISBN-90-369-2015-9 ..... p 722 N94-13991
ISBN-90-369-2016-7 ..... p 722 N94-13926
ISBN-90-369-2018-3 ..... p 722 N94-13992
ISBN-90-369-2019-1 ..... p 722 N94-13993
ISBN-90-5411-056-2 ..... p 684 N94-13123 #
ISBN-92-9092-021-1 ..... p 699 N94-14353 #
ISBN-92-9092-077-7 ..... p 733 N94-14860 #
ISBN-92-9092-107-2 ..... p 543 N94-14352 #
ISBN-92-9092-208-7 ..... p 731 N94-14862 #
ISBN-951-22-0722-2 ..... p 625 N94-14096 #
ISBN-951-22-0846-6 ..... p 760 N94-14187 #

ISC158-ICN-FR/91-001 ..... p 620 N94-13125 * #

ISVR-TR-212 ..... p 777 N94-14130
ISVR-TR-222 ..... p 663 N94-13874

ITF-92-9 ..... p 788 N94-14875

ITN-93-85188 ..... p 598 N94-13195
ITN-93-85189 ..... p 599 N94-13196
ITN-93-85190 ..... p 600 N94-13537
ITN-93-85191 ..... p 600 N94-13538
ITN-93-85192 ..... p 762 N94-13329
ITN-93-85193 ..... p 748 N94-13539
ITN-93-85194 ..... p 601 N94-13566
ITN-93-85195 ..... p 601 N94-13567
ITN-93-85196 ..... p 763 N94-13568
ITN-93-85197 ..... p 702 N94-13570
ITN-93-85201 ..... p 656 N94-13571
ITN-93-85202 ..... p 719 N94-13188
ITN-93-85203 ..... p 599 N94-13237
ITN-93-85204 ..... p 736 N94-13229
ITN-93-85205 ..... p 630 N94-13197
ITN-93-85206 ..... p 835 N94-13230
ITN-93-85207 ..... p 829 N94-13231
ITN-93-85208 ..... p 847 N94-13232
ITN-93-85209 ..... p 849 N94-14553
ITN-93-85210 ..... p 814 N94-14554
ITN-93-85211 ..... p 826 N94-14555
ITN-93-85212 ..... p 755 N94-14556
ITN-93-85213 ..... p 755 N94-14505
ITN-93-85214 ..... p 771 N94-14506
ITN-93-85215 ..... p 585 N94-14507
ITN-93-85216 ..... p 774 N94-14502
ITN-93-85217 ..... p 815 N94-14825
ITN-93-85218 ..... p 816 N94-14826
ITN-93-85221 ..... p 814 N94-14557
ITN-93-85222 ..... p 566 N94-14558
ITN-93-85223 ..... p 814 N94-14559
ITN-93-85224 ..... p 659 N94-14547
ITN-93-85225 ..... p 639 N94-14503
ITN-93-85226 ..... p 565 N94-14465

IVO-A-10/92 ..... p 682 N94-14653 #

JAERI-M-92-070 ..... p 795 N94-12944 #

JIAA-TR-110 ..... p 501 N94-13266 * #

JINR-D-2-91-499 ..... p 617 N94-14892

JINR-E-14-91-398 ..... p 567 N94-14884
JINR-E-2-92-149 ..... p 818 N94-14887
JINR-E-2-92-322 ..... p 849 N94-14889
JINR-E-5-92-75 ..... p 772 N94-14890

JINR-R-13-91-424 ..... p 627 N94-14885
JINR-R-2-92-47 ..... p 788 N94-14891
JINR-R-5-91-559 ..... p 772 N94-14886

JPL-BIBL-39-32 ..... p 823 N94-13461 * #

JPL-PUBL-80-23-REV-3 ..... p 602 N94-13813 * #
JPL-PUBL-87-4-VOL-15 ..... p 598 N94-13090 * #
JPL-PUBL-91-16 ..... p 549 N94-13055 * #
JPL-PUBL-91-24-VOL-3 ..... p 545 N94-14830 * #
JPL-PUBL-91-44 ..... p 622 N94-13811 * #
JPL-PUBL-91-45 ..... p 602 N94-13810 * #
JPL-PUBL-92-10 ..... p 549 N94-13068 * #
JPL-PUBL-92-15-VOL-1 ..... p 542 N94-14076 * #
JPL-PUBL-92-15-VOL-2 ..... p 542 N94-14077 * #
JPL-PUBL-92-15-VOL-3 ..... p 542 N94-14078 * #
JPL-PUBL-92-1 ..... p 545 N94-13189 * #
JPL-PUBL-92-23 ..... p 749 N94-13784 * #
JPL-PUBL-92-30 ..... p 701 N94-13187 * #
JPL-PUBL-92-32-VOL-1 ..... p 519 N94-14841 * #
JPL-PUBL-92-32-VOL-2 ..... p 519 N94-14842 * #
JPL-PUBL-92-7 ..... p 686 N94-13872 * #
JPL-PUBL-93-02 ..... p 677 N94-14618 * #
JPL-PUBL-93-04 ..... p 727 N94-12793 * #
JPL-PUBL-93-11 ..... p 605 N94-13946 * #
JPL-PUBL-93-12 ..... p 741 N94-13943 * #
JPL-PUBL-93-18 ..... p 532 N94-13796 * #
JPL-PUBL-93-21 ..... p 612 N94-14654 * #
JPL-PUBL-93-22 ..... p 703 N94-13940 * #
JPL-PUBL-93-23 ..... p 657 N94-13812 * #
JPL-PUBL-93-6 ..... p 624 N94-13948 * #
JPL-PUBL-93-7 ..... p 564 N94-13947 * #

JPRS-UEQ-93-006 ..... p 776 N94-14431 #

JPRS-UMS-93-004 ..... p 559 N94-14574 #
JPRS-UMS-93-005 ..... p 559 N94-14575 #
JPRS-UMS-93-006 ..... p 558 N94-14573 #

JPRS-USP-93-003 ..... p 828 N94-13182 #

JTN-93-80426 ..... p 505 N94-14059 #
JTN-93-80427 ..... p 505 N94-14061 #
JTN-93-80452 ..... p 687 N94-14091 #
JTN-93-80453 ..... p 532 N94-14098 #
JTN-93-80454 ..... p 688 N94-14209 #
JTN-93-80459 ..... p 725 N94-13653 #
JTN-93-80461 ..... p 721 N94-13643 #
JTN-93-80462 ..... p 532 N94-13644 #
JTN-93-80463 ..... p 563 N94-13471 #
JTN-93-80464 ..... p 535 N94-13645 #
JTN-93-80465 ..... p 535 N94-13599 #
JTN-93-80466-PT-2 ..... p 737 N94-13472 #
JTN-93-80467 ..... p 536 N94-14099 #
JTN-93-80468 ..... p 842 N94-13655 #
JTN-93-80469-PT-1 ..... p 622 N94-13425 #
JTN-93-80470 ..... p 536 N94-14100 #
JTN-93-80471 ..... p 535 N94-13600 #
JTN-93-80472 ..... p 535 N94-13656 #
JTN-93-80475 ..... p 529 N94-13268 #
JTN-93-80477 ..... p 541 N94-13658 #
JTN-93-80478 ..... p 541 N94-13659 #
JTN-93-80479 ..... p 541 N94-13660 #
JTN-93-80481 ..... p 737 N94-13388 #
JTN-93-80482 ..... p 517 N94-13451 #
JTN-93-80483 ..... p 502 N94-13392 #
JTN-93-80484 ..... p 528 N94-13337 #
JTN-93-80485 ..... p 514 N94-13338 #
JTN-93-80486 ..... p 540 N94-13339 #
JTN-93-80487 ..... p 501 N94-13340 #
JTN-93-80488 ..... p 501 N94-13341 #
JTN-93-80489 ..... p 502 N94-13342 #
JTN-93-80490 ..... p 649 N94-13343 #
JTN-93-80491 ..... p 513 N94-13344 #
JTN-93-80492 ..... p 502 N94-13345 #
JTN-93-80493 ..... p 513 N94-13346 #
JTN-93-80494 ..... p 526 N94-13347 #
JTN-93-80495 ..... p 539 N94-12943 #
JTN-93-80496 ..... p 548 N94-12945 #
JTN-93-80497 ..... p 830 N94-13452 #
JTN-93-80499 ..... p 748 N94-13453 #
JTN-93-80500-PT-3 ..... p 499 N94-12948 #
JTN-93-80501 ..... p 500 N94-12951 #

JTN-93-80502-PT-2 ..... p 502 N94-13454 #
JTN-93-80503 ..... p 551 N94-13455 #
JTN-93-80504 ..... p 649 N94-13456 #
JTN-93-80505 ..... p 513 N94-13457 #
JTN-93-80506 ..... p 563 N94-13458 #
JTN-93-80507 ..... p 514 N94-13459 #
JTN-93-80508 ..... p 570 N94-13460 #

K/ETO-112 ..... p 710 N94-14459 #

KCP-613-4984 ..... p 743 N94-13014 #
KCP-613-4998 ..... p 675 N94-13907 #
KCP-613-5043 ..... p 620 N94-13094 #
KCP-613-5044 ..... p 578 N94-13118 #
KCP-613-5045 ..... p 624 N94-13937 #
KCP-613-5078 ..... p 624 N94-13928 #
KCP-613-5081 ..... p 652 N94-14534 #
KCP-613-5110 ..... p 625 N94-14533 #
KCP-613-5138 ..... p 707 N94-13390 #
KCP-613-5172 ..... p 748 N94-13480 #

KEK-PROC-92-10 ..... p 581 N94-14421

KFK-4759 ..... p 642 N94-14708 #

KFTI-91-10 ..... p 767 N94-13223 #
KFTI-91-11 ..... p 816 N94-12855
KFTI-91-12 ..... p 621 N94-13224 #
KFTI-91-15 ..... p 794 N94-12854 #
KFTI-91-31 ..... p 618 N94-12856
KFTI-91-52 ..... p 797 N94-13240
KFTI-91-9 ..... p 794 N94-12853 #
KFTI-92-35 ..... p 576 N94-12867
KFTI-92-49 ..... p 788 N94-14881
KFTI-92-50 ..... p 617 N94-14883

KIYAI-91-36 ..... p 790 N94-14843

KNMI-PUBL-181 ..... p 722 N94-13926

KNMI-TR-142 ..... p 722 N94-13985
KNMI-TR-143 ..... p 722 N94-13991
KNMI-TR-144 ..... p 722 N94-13992
KNMI-TR-145 ..... p 722 N94-13993

KSC-DL-522-REV-B ..... p 532 N94-14148 * #

KSL-92-38 ..... p 747 N94-13443 * #
KSL-93-35 ..... p 745 N94-13356 * #
KSL-93-60 ..... p 745 N94-13355 * #

L-17188 ..... p 846 N94-12875 * #
L-17200 ..... p 850 N94-13962 * #
L-17203 ..... p 813 N94-14409 * #
L-17219 ..... p 604 N94-13916 * #
L-17227 ..... p 847 N94-13263 * #
L-17231 ..... p 732 N94-13714 * #
L-17238 ..... p 776 N94-14733 * #

LA-SUB-93-168 ..... p 620 N94-13031 #
LA-SUB-93-171 ..... p 554 N94-14290 #

LA-UR-92-3770 ..... p 761 N94-12859 #
LA-UR-93-1142 ..... p 570 N94-13512 #
LA-UR-93-1150 ..... p 812 N94-14365 #
LA-UR-93-1159 ..... p 836 N94-13262 #
LA-UR-93-1212 ..... p 626 N94-14805 #
LA-UR-93-1216 ..... p 787 N94-14804 #
LA-UR-93-1287 ..... p 758 N94-12917 #
LA-UR-93-1292 ..... p 785 N94-14366 #
LA-UR-93-1296 ..... p 760 N94-14177 #
LA-UR-93-1305 ..... p 553 N94-14689 #
LA-UR-93-1306 ..... p 581 N94-14327 #
LA-UR-93-1318 ..... p 798 N94-13513 #
LA-UR-93-1322 ..... p 576 N94-12916 #
LA-UR-93-1338 ..... p 752 N94-14176 #
LA-UR-93-1384 ..... p 811 N94-14339 #
LA-UR-93-1392 ..... p 773 N94-14178 #
LA-UR-93-1393 ..... p 794 N94-12814 #
LA-UR-93-1421 ..... p 583 N94-12921 #
LA-UR-93-1446 ..... p 772 N94-12919 #
LA-UR-93-1449 ..... p 792 N94-14367 #
LA-UR-93-1456 ..... p 581 N94-14340 #
LA-UR-93-1470 ..... p 712 N94-12952 #
LA-UR-93-1471 ..... p 785 N94-14181 #
LA-UR-93-1508 ..... p 782 N94-13492 #
LA-UR-93-1509 ..... p 779 N94-12950 #
LA-UR-93-1527 ..... p 584 N94-13491 #
LA-UR-93-1532 ..... p 779 N94-12949 #
LA-UR-93-1557 ..... p 585 N94-14180 #
LA-UR-93-1564 ..... p 802 N94-14567 #
LA-UR-93-1565 ..... p 766 N94-14737 #
LA-UR-93-1601 ..... p 846 N94-12947 #
LA-UR-93-1602 ..... p 846 N94-12946 #
LA-UR-93-1604 ..... p 847 N94-12964 #
LA-UR-93-1605 ..... p 846 N94-12924 #

LA-UR-93-1606 ..... p 846 N94-12923 #
LA-UR-93-1607 ..... p 846 N94-12922 #
LA-UR-93-1608 ..... p 846 N94-12816 #
LA-UR-93-1609 ..... p 834 N94-12815 #
LA-UR-93-1610 ..... p 849 N94-14461 #
LA-UR-93-1618 ..... p 580 N94-14179 #
LA-UR-93-1657 ..... p 559 N94-14690 #
LA-UR-93-1670 ..... p 670 N94-12887 #
LA-UR-93-1678 ..... p 702 N94-13403 #
LA-UR-93-1686 ..... p 789 N94-13328 #
LA-UR-93-1689 ..... p 702 N94-13402 #
LA-UR-93-1692 ..... p 785 N94-14468 #
LA-UR-93-1705 ..... p 810 N94-14122 #
LA-UR-93-1710 ..... p 558 N94-14121 #
LA-UR-93-1711 ..... p 558 N94-14119 #
LA-UR-93-1717 ..... p 765 N94-14117 #
LA-UR-93-1732 ..... p 839 N94-14116 #
LA-UR-93-1736 ..... p 815 N94-14773 #
LA-UR-93-1785 ..... p 811 N94-14329 #
LA-UR-93-1798 ..... p 717 N94-14328 #
LA-UR-93-1816 ..... p 789 N94-13327 #
LA-UR-93-1824 ..... p 818 N94-14740 #
LA-UR-93-1874 ..... p 780 N94-13173 #
LA-UR-93-1919 ..... p 789 N94-13209 #
LA-UR-93-1927 ..... p 558 N94-14469 #
LA-UR-93-1961 ..... p 740 N94-13286 #
LA-UR-93-1965 ..... p 785 N94-14144 #
LA-UR-93-1968 ..... p 816 N94-13206 #
LA-UR-93-1970 ..... p 781 N94-13205 #
LA-UR-93-1971 ..... p 785 N94-14466 #
LA-UR-93-1980 ..... p 669 N94-14143 #
LA-UR-93-1983 ..... p 745 N94-13151 #
LA-UR-93-2038 ..... p 788 N94-13103 #
LA-UR-93-2066 ..... p 786 N94-14514 #
LA-UR-93-2091 ..... p 813 N94-14413 #
LA-UR-93-2105 ..... p 840 N94-14536 #
LA-UR-93-2132 ..... p 774 N94-14441 #
LA-UR-93-2174 ..... p 585 N94-14535 #
LA-UR-93-2255 ..... p 802 N94-14532 #
LA-UR-93-2323 ..... p 676 N94-14591 #
LA-UR-93-2331 ..... p 778 N94-14867 #
LA-UR-93-2390 ..... p 817 N94-14593 #
LA-UR-93-2415 ..... p 597 N94-14592 #
LA-UR-93-2437 ..... p 582 N94-14436 #
LA-UR-93-791 ..... p 664 N94-14457 #
LA-UR-93-857 ..... p 722 N94-14057 #

LA-12436-MS-VOL-1 ..... p 709 N94-14020 #
LA-12455-MS ..... p 584 N94-13099 #
LA-12482-MS ..... p 794 N94-12849 #
LA-12483-MS ..... p 797 N94-13100 #
LA-12554 ..... p 564 N94-13487 #
LA-12566-MS ..... p 718 N94-14518 #

LAAS-92435 ..... p 751 N94-13995 #
LAAS-92484 ..... p 814 N94-14697 #
LAAS-92492 ..... p 626 N94-14698 #
LAAS-92511 ..... p 626 N94-14711 #
LAAS-92514 ..... p 756 N94-14712 #
LAAS-92515 ..... p 626 N94-14713 #
LAAS-93006 ..... p 756 N94-14714 #
LAAS-93032 ..... p 761 N94-14716 #
LAAS-93042 ..... p 616 N94-14717 #

LAMP-93/1 ..... p 781 N94-13225 #

LBL-PUB-719 ..... p 851 N94-14587 #

LBL-29628 ..... p 625 N94-14336
LBL-31852 ..... p 710 N94-14477 #
LBL-32165-REV-2 ..... p 825 N94-14433 #
LBL-32387 ..... p 851 N94-14401 #
LBL-32529 ..... p 637 N94-14053 #
LBL-32845 ..... p 581 N94-14400 #
LBL-33255 ..... p 658 N94-14414 #
LBL-33257 ..... p 659 N94-14520 #
LBL-33429 ..... p 746 N94-13382 #
LBL-33753 ..... p 574 N94-14795
LBL-33886 ..... p 808 N94-13694 #
LBL-33903 ..... p 848 N94-13695 #
LBL-33937 ..... p 787 N94-14857 #
LBL-33945 ..... p 704 N94-14333 #
LBL-33948 ..... p 776 N94-14584 #
LBL-33971 ..... p 815 N94-14699 #
LBL-33976 ..... p 780 N94-13018
LBL-33995 ..... p 631 N94-13244 #
LBL-34012 ..... p 573 N94-14474 #
LBL-34029 ..... p 816 N94-14868 #
LBL-34131 ..... p 563 N94-13411 #

LIYAF-1644 ..... p 804 N94-12828

LM-AA-003 ..... p 516 N94-13896 #

LPI/TR-93-01 ..... p 842 N94-14298 * #

LR-681 ..... p 675 N94-13929 #
LR-691 ..... p 511 N94-13534 #
LR-693 ..... p 515 N94-13687 #
LR-694 ..... p 675 N94-13931 #
LR-695 ..... p 682 N94-14692 * #
LR-696 ..... p 675 N94-13933 #
LR-697 ..... p 675 N94-13986 #
LR-698 ..... p 775 N94-13987 #
LR-699 ..... p 542 N94-13988 #
LR-701 ..... p 673 N94-13726 #
LR-703 ..... p 673 N94-13787 #
LR-704 ..... p 499 N94-13904 #
LR-705 ..... p 674 N94-13905 #
LR-707 ..... p 527 N94-13906 #
LR-708 ..... p 674 N94-13803 #

LTR-ST-1905 ..... p 675 N94-14035 #
LTR-ST-1909 ..... p 675 N94-13945 #
LTR-ST-1929 ..... p 850 N94-13548 #
LTR-ST-1932 ..... p 674 N94-13861 #
LTR-ST-1934 ..... p 671 N94-13565
LTR-ST-1935 ..... p 754 N94-14496

M-720 ..... p 551 N94-13417 * #
M-723 ..... p 533 N94-14824 * #
M-724-VOL-3 ..... p 844 N94-13146 * #
M-725 ..... p 586 N94-13732 * #
M-730 ..... p 669 N94-12831 * #

MBB-LME-211-S-PUB-507 ..... p 509 N94-14710 #
MBB-LME-251-S-PUB-0492 ..... p 751 N94-14006 #

MCAT-93-13 ..... p 759 N94-13204 * #
MCAT-93-14 ..... p 504 N94-14030 * #
MCAT-93-15 ..... p 520 N94-12799 * #
MCAT-93-16 ..... p 502 N94-13422 * #
MCAT-93-17 ..... p 806 N94-13291 * #
MCAT-93-18 ..... p 527 N94-14322 * #

MDC-92B0034 ..... p 578 N94-13431 * #
MDC-93H0100 ..... p 540 N94-13016 * #
MDC-93H1355 ..... p 550 N94-13147 * #

MHSMP-93-08 ..... p 663 N94-14113 #

MITT-81 ..... p 711 N94-14723 #
MITT-82 ..... p 651 N94-14149 #

MLM-3767 ..... p 573 N94-14316 #

NAL-SP-9315 ..... p 639 N94-14598 #

NAL-TM-646 ..... p 737 N94-13388 #
NAL-TM-649 ..... p 513 N94-13346 #

NAL-TR-1140T ..... p 505 N94-14059 #
NAL-TR-1141T ..... p 505 N94-14061 #
NAL-TR-1144 ..... p 517 N94-13451 #
NAL-TR-1146 ..... p 748 N94-13453 #
NAL-TR-1150 ..... p 502 N94-13392 #
NAL-TR-1161 ..... p 528 N94-13337 #
NAL-TR-1163 ..... p 514 N94-13338 #
NAL-TR-1164 ..... p 526 N94-13347 #
NAL-TR-1166 ..... p 540 N94-13339 #
NAL-TR-1167 ..... p 501 N94-13340 #
NAL-TR-1168-PT-3 ..... p 499 N94-12948 #
NAL-TR-1169 ..... p 501 N94-13341 #
NAL-TR-1170 ..... p 502 N94-13342 #
NAL-TR-1171 ..... p 500 N94-12951 #
NAL-TR-1173 ..... p 649 N94-13343 #
NAL-TR-1175 ..... p 513 N94-13344 #
NAL-TR-1176T ..... p 539 N94-12943 #
NAL-TR-1177 ..... p 548 N94-12945 #
NAL-TR-1178T ..... p 830 N94-13452 #
NAL-TR-1179 ..... p 502 N94-13345 #
NAL-TR-1180T-PT-2 ..... p 502 N94-13454 #
NAL-TR-1181 ..... p 551 N94-13455 #
NAL-TR-1182 ..... p 649 N94-13456 #
NAL-TR-1183 ..... p 513 N94-13457 #
NAL-TR-1184 ..... p 563 N94-13458 #
NAL-TR-1186 ..... p 514 N94-13459 #
NAL-TR-1188 ..... p 570 N94-13460 #

NAMRL-1382 ..... p 734 N94-12975 #
NAMRL-1383 ..... p 735 N94-12982 #

NAS 1.15:102265 ..... p 520 N94-12820 * #
NAS 1.15:102877 ..... p 538 N94-13989 * #
NAS 1.15:103740 ..... p 509 N94-14780 * #
NAS 1.15:103863 ..... p 740 N94-13200 * #
NAS 1.15:103923 ..... p 527 N94-13008 * #
NAS 1.15:103951 ..... p 740 N94-12973 * #
NAS 1.15:103991 ..... p 731 N94-12972 * #
NAS 1.15:104010 ..... p 727 N94-13447 * #
NAS 1.15:104024 ..... p 739 N94-12838 * #
NAS 1.15:104566 ..... p 725 N94-14090 * #
NAS 1.15:104589 ..... p 850 N94-13923 * #
NAS 1.15:104591 ..... p 723 N94-14074 * #
NAS 1.15:104755 ..... p 731 N94-12832 * #
NAS 1.15:104775 ..... p 735 N94-13961 * #
NAS 1.15:104776 ..... p 737 N94-13399 * #
NAS 1.15:104781 ..... p 819 N94-13400 * #
NAS 1.15:105879 ..... p 538 N94-13918 * #
NAS 1.15:106008 ..... p 629 N94-13027 * #
NAS 1.15:106068 ..... p 510 N94-14847 * #
NAS 1.15:106113 ..... p 631 N94-13385 * #
NAS 1.15:106115 ..... p 541 N94-13917 * #
NAS 1.15:106120 ..... p 628 N94-12968 * #
NAS 1.15:106164 ..... p 675 N94-13919 * #
NAS 1.15:106188 ..... p 555 N94-13138 * #
NAS 1.15:106214 ..... p 551 N94-13430 * #
NAS 1.15:106229 ..... p 676 N94-14041 * #
NAS 1.15:106231 ..... p 499 N94-13108 * #
NAS 1.15:106264 ..... p 575 N94-12842 * #
NAS 1.15:106270 ..... p 518 N94-13143 * #
NAS 1.15:106280 ..... p 670 N94-13053 * #
NAS 1.15:106282 ..... p 670 N94-12872 * #
NAS 1.15:106286 ..... p 671 N94-13379 * #
NAS 1.15:106290 ..... p 642 N94-14729 * #
NAS 1.15:106291 ..... p 553 N94-14725 * #
NAS 1.15:106292 ..... p 553 N94-14726 * #
NAS 1.15:106294 ..... p 664 N94-14727 * #
NAS 1.15:106297 ..... p 534 N94-13028 * #
NAS 1.15:106298 ..... p 620 N94-13134 * #
NAS 1.15:106300 ..... p 648 N94-13135 * #
NAS 1.15:106302 ..... p 683 N94-14776 * #
NAS 1.15:106304 ..... p 559 N94-14719 * #
NAS 1.15:106306 ..... p 621 N94-13194 * #
NAS 1.15:106312 ..... p 517 N94-13142 * #
NAS 1.15:106318 ..... p 518 N94-14036 * #
NAS 1.15:106321 ..... p 626 N94-14730 * #
NAS 1.15:106323 ..... p 642 N94-14732 * #
NAS 1.15:106324 ..... p 583 N94-14845 * #
NAS 1.15:106326 ..... p 557 N94-14042 * #
NAS 1.15:106330 ..... p 650 N94-13876 * #
NAS 1.15:106344 ..... p 560 N94-14823 * #
NAS 1.15:106351 ..... p 771 N94-14731 * #
NAS 1.15:106353 ..... p 770 N94-14407 * #
NAS 1.15:106354 ..... p 642 N94-14722 * #
NAS 1.15:106356 ..... p 642 N94-14728 * #
NAS 1.15:106362 ..... p 612 N94-14542 * #
NAS 1.15:106364 ..... p 508 N94-14208 * #
NAS 1.15:107684 ..... p 739 N94-12886 * #
NAS 1.15:107763 ..... p 597 N94-12804 * #
NAS 1.15:108244 ..... p 531 N94-14080 * #
NAS 1.15:108252 ..... p 542 N94-14112 * #
NAS 1.15:108257 ..... p 828 N94-12915 * #
NAS 1.15:108419 ..... p 571 N94-13715 * #
NAS 1.15:108421 ..... p 808 N94-13938 * #
NAS 1.15:108738 ..... p 851 N94-14791 * #
NAS 1.15:108779 ..... p 776 N94-14027 * #
NAS 1.15:108993 ..... p 632 N94-13467 * #
NAS 1.15:109001 ..... p 759 N94-13450 * #
NAS 1.15:109002 ..... p 598 N94-12811 * #
NAS 1.15:109005 ..... p 517 N94-13710 * #
NAS 1.15:109006 ..... p 821 N94-13057 * #
NAS 1.15:109008 ..... p 777 N94-14481 * #
NAS 1.15:109009 ..... p 514 N94-12850 * #
NAS 1.15:109014 ..... p 557 N94-13711 * #
NAS 1.15:109016 ..... p 500 N94-13172 * #
NAS 1.15:109190 ..... p 534 N94-12900 * #
NAS 1.15:109246 ..... p 518 N94-13190 * #
NAS 1.15:109248 ..... p 550 N94-13147 * #
NAS 1.15:109251 ..... p 761 N94-12889 * #
NAS 1.15:109252 ..... p 761 N94-12890 * #
NAS 1.15:109255 ..... p 849 N94-13376 *
NAS 1.15:109265 ..... p 669 N94-13396 * #
NAS 1.15:109268 ..... p 822 N94-13107 * #
NAS 1.15:109272 ..... p 738 N94-13979 * #
NAS 1.15:109276 ..... p 669 N94-14321 * #
NAS 1.15:109280 ..... p 597 N94-14410 * #
NAS 1.15:109327 ..... p 825 N94-14485 * #
NAS 1.15:109328 ..... p 825 N94-14486 * #
NAS 1.15:109329 ..... p 826 N94-14488 * #
NAS 1.15:109330 ..... p 826 N94-14489 * #
NAS 1.15:109331 ..... p 825 N94-14487 * #
NAS 1.15:109413 ..... p 822 N94-13105 * #
NAS 1.15:4452 ..... p 850 N94-13962 * #
NAS 1.15:4491 ..... p 554 N94-12871 * #
NAS 1.15:4493 ..... p 520 N94-13255 * #
NAS 1.15:4503 ..... p 520 N94-13254 * #
NAS 1.15:4504 ..... p 517 N94-13791 * #
NAS 1.15:4505 ..... p 516 N94-13256 * #
NAS 1.15:4511 ..... p 533 N94-14824 * #
NAS 1.15:4517 ..... p 586 N94-13732 * #
NAS 1.15:4518 ..... p 623 N94-13878 * #
NAS 1.15:4525 ..... p 537 N94-14853 * #
NAS 1.15:4531 ..... p 519 N94-14855 * #
NAS 1.15:4533 ..... p 629 N94-13064 * #
NAS 1.15:4536 ..... p 716 N94-13960 * #
NAS 1.21:7011(379) ..... p 733 N94-14412 *
NAS 1.21:7085(05) ..... p 543 N94-14411 *

NAS 1.21:7107 ..... p 823 N94-13401 * #
NAS 1.26:102877 ..... p 538 N94-13201 * #
NAS 1.26:167690 ..... p 534 N94-12810 * #
NAS 1.26:167691 ..... p 536 N94-14047 * #
NAS 1.26:177617 ..... p 510 N94-13247 * #
NAS 1.26:177621 ..... p 512 N94-14744 * #
NAS 1.26:177622 ..... p 538 N94-13257 * #
NAS 1.26:182183 ..... p 620 N94-13106 * #
NAS 1.26:184381 ..... p 683 N94-14484 * #
NAS 1.26:185696 ..... p 534 N94-13191 * #
NAS 1.26:185697 ..... p 534 N94-12965 * #
NAS 1.26:186026 ..... p 516 N94-14106 * #
NAS 1.26:187179 ..... p 674 N94-13873 * #
NAS 1.26:188251 ..... p 827 N94-12800 * #
NAS 1.26:188261 ..... p 543 N94-14483 * #
NAS 1.26:189136 ..... p 557 N94-13920 * #
NAS 1.26:189560 ..... p 527 N94-13127 * #
NAS 1.26:189687 ..... p 578 N94-13431 * #
NAS 1.26:189735 ..... p 596 N94-13141 * #
NAS 1.26:190758 ..... p 537 N94-12809 * #
NAS 1.26:191088 ..... p 828 N94-12931 * #
NAS 1.26:191096 ..... p 622 N94-13786 * #
NAS 1.26:191147 ..... p 555 N94-13139 * #
NAS 1.26:191150 ..... p 676 N94-14408 * #
NAS 1.26:191165 ..... p 559 N94-14769 * #
NAS 1.26:191170 ..... p 555 N94-13378 * #
NAS 1.26:191182 ..... p 664 N94-14446 * #
NAS 1.26:191183 ..... p 663 N94-14445 * #
NAS 1.26:191186 ..... p 551 N94-13416 * #
NAS 1.26:191187 ..... p 550 N94-13415 * #
NAS 1.26:191188 ..... p 554 N94-14771 * #
NAS 1.26:191189 ..... p 519 N94-14448 * #
NAS 1.26:191190 ..... p 582 N94-14543 * #
NAS 1.26:191196 ..... p 560 N94-14822 * #
NAS 1.26:191323 ..... p 562 N94-13115 * #
NAS 1.26:191325 ..... p 604 N94-13909 * #
NAS 1.26:191326 ..... p 736 N94-13132 * #
NAS 1.26:191332 ..... p 540 N94-13140 * #
NAS 1.26:191334 ..... p 759 N94-13177 * #
NAS 1.26:191337 ..... p 671 N94-13124 * #
NAS 1.26:191339 ..... p 762 N94-13131 * #
NAS 1.26:191340 ..... p 648 N94-13176 * #
NAS 1.26:191341 ..... p 620 N94-13125 * #
NAS 1.26:191345 ..... p 661 N94-13129 * #
NAS 1.26:191394 ..... p 745 N94-13130 * #
NAS 1.26:191397 ..... p 822 N94-13116 * #
NAS 1.26:191437 ..... p 516 N94-12829 * #
NAS 1.26:191459 ..... p 575 N94-12792 * #
NAS 1.26:191476 ..... p 499 N94-12852 * #
NAS 1.26:191477 ..... p 630 N94-13133 * #
NAS 1.26:191480 ..... p 768 N94-13354 * #
NAS 1.26:191482 ..... p 630 N94-13114 * #
NAS 1.26:191487 ..... p 630 N94-13128 * #
NAS 1.26:191488 ..... p 769 N94-13722 * #
NAS 1.26:191491 ..... p 767 N94-13202 * #
NAS 1.26:191494 ..... p 767 N94-13289 * #
NAS 1.26:191496 ..... p 762 N94-13184 * #
NAS 1.26:191497 ..... p 769 N94-13725 * #
NAS 1.26:191498 ..... p 745 N94-13185 * #
NAS 1.26:191499 ..... p 555 N94-13267 * #
NAS 1.26:191500 ..... p 769 N94-13717 * #
NAS 1.26:191501 ..... p 636 N94-13817 * #
NAS 1.26:191502 ..... p 628 N94-12888 * #
NAS 1.26:191503 ..... p 647 N94-14849 * #
NAS 1.26:191504 ..... p 636 N94-13785 * #
NAS 1.26:191505 ..... p 554 N94-12833 * #
NAS 1.26:191506 ..... p 769 N94-13792 * #
NAS 1.26:191510 ..... p 629 N94-13074 * #
NAS 1.26:191511 ..... p 636 N94-13718 * #
NAS 1.26:191512 ..... p 630 N94-13075 * #
NAS 1.26:191516 ..... p 636 N94-13724 * #
NAS 1.26:191520 ..... p 749 N94-13721 * #
NAS 1.26:191521 ..... p 539 N94-12976 * #
NAS 1.26:191524 ..... p 540 N94-13016 * #
NAS 1.26:191525 ..... p 654 N94-13091 * #
NAS 1.26:191527 ..... p 595 N94-14026 * #
NAS 1.26:191545 ..... p 622 N94-13797 * #
NAS 1.26:191788 ..... p 822 N94-13126 * #
NAS 1.26:192581 ..... p 718 N94-12957 * #
NAS 1.26:192586 ..... p 660 N94-12791 * #
NAS 1.26:192594 ..... p 830 N94-13448 * #
NAS 1.26:192600 ..... p 652 N94-14497 * #
NAS 1.26:192603 ..... p 669 N94-14101 * #
NAS 1.26:192613 ..... p 648 N94-13326 * #
NAS 1.26:192761 ..... p 754 N94-14368 * #
NAS 1.26:193101 ..... p 535 N94-13934 * #
NAS 1.26:193244 ..... p 829 N94-13178 * #
NAS 1.26:193266 ..... p 842 N94-13855 * #
NAS 1.26:193280 ..... p 848 N94-13476 * #
NAS 1.26:193287 ..... p 823 N94-13461 * #
NAS 1.26:193297 ..... p 829 N94-13181 * #
NAS 1.26:193300 ..... p 838 N94-13781 * #
NAS 1.26:193305 ..... p 671 N94-13179 * #
NAS 1.26:193306 ..... p 500 N94-13180 * #
NAS 1.26:193324 ..... p 829 N94-13287 * #
NAS 1.26:193359 ..... p 849 N94-13965 * #
NAS 1.26:193362 ..... p 602 N94-13720 * #
NAS 1.26:193389 ..... p 617 N94-14743 * #
NAS 1.26:193390 ..... p 508 N94-14326 * #
NAS 1.26:193392 ..... p 630 N94-13078 * #
NAS 1.26:193393 ..... p 638 N94-14086 * #
NAS 1.26:193394 ..... p 541 N94-13955 * #
NAS 1.26:193396 ..... p 599 N94-13264 * #
NAS 1.26:193397 ..... p 833 N94-14358 * #
NAS 1.26:193413 ..... p 649 N94-13464 * #
NAS 1.26:193415 ..... p 822 N94-13062 * #
NAS 1.26:193418 ..... p 828 N94-12970 * #
NAS 1.26:193424 ..... p 835 N94-13233 * #
NAS 1.26:193433 ..... p 792 N94-14473 * #
NAS 1.26:193454 ..... p 713 N94-13335 * #
NAS 1.26:193456 ..... p 712 N94-13334 * #
NAS 1.26:193481 ..... p 562 N94-13048 * #
NAS 1.26:193559 ..... p 803 N94-12796 * #
NAS 1.26:193560 ..... p 727 N94-12795 * #
NAS 1.26:193563 ..... p 718 N94-12839 * #
NAS 1.26:193597 ..... p 628 N94-12959 * #
NAS 1.26:193604 ..... p 664 N94-14848 * #
NAS 1.26:193609 ..... p 830 N94-13462 * #
NAS 1.26:193613 ..... p 577 N94-13089 * #
NAS 1.26:193616 ..... p 503 N94-13463 * #
NAS 1.26:193622 ..... p 731 N94-12960 * #
NAS 1.26:193632 ..... p 844 N94-13234 * #
NAS 1.26:193640 ..... p 836 N94-13446 * #
NAS 1.26:193646 ..... p 512 N94-13238 * #
NAS 1.26:193647 ..... p 575 N94-12789 * #
NAS 1.26:193654 ..... p 835 N94-13171 * #
NAS 1.26:193655 ..... p 835 N94-13239 * #
NAS 1.26:193659 ..... p 520 N94-12799 * #
NAS 1.26:193660 ..... p 790 N94-12797 * #
NAS 1.26:193664 ..... p 711 N94-12788 * #
NAS 1.26:193667 ..... p 821 N94-13030 * #
NAS 1.26:193669 ..... p 713 N94-13465 * #
NAS 1.26:193670 ..... p 835 N94-13203 * #
NAS 1.26:193671 ..... p 712 N94-13293 * #
NAS 1.26:193672 ..... p 706 N94-13170 * #
NAS 1.26:193673 ..... p 501 N94-13292 * #
NAS 1.26:193675 ..... p 619 N94-13026 * #
NAS 1.26:193676 ..... p 540 N94-13109 * #
NAS 1.26:193677 ..... p 629 N94-13007 * #
NAS 1.26:193708 ..... p 839 N94-13864 * #
NAS 1.26:193711 ..... p 539 N94-12790 * #
NAS 1.26:193714 ..... p 839 N94-14404 * #
NAS 1.26:193716 ..... p 832 N94-14146 * #
NAS 1.26:193718 ..... p 572 N94-14133 * #
NAS 1.26:193719 ..... p 599 N94-13236 * #
NAS 1.26:193720 ..... p 759 N94-13204 * #
NAS 1.26:193724 ..... p 540 N94-13112 * #
NAS 1.26:193725 ..... p 600 N94-13466 * #
NAS 1.26:193726 ..... p 598 N94-12920 * #
NAS 1.26:193727 ..... p 619 N94-12897 * #
NAS 1.26:193728 ..... p 744 N94-13113 * #
NAS 1.26:193783 ..... p 833 N94-14359 * #
NAS 1.26:193784 ..... p 833 N94-14405 * #
NAS 1.26:193787 ..... p 717 N94-14306 * #
NAS 1.26:193797 ..... p 558 N94-14050 * #
NAS 1.26:193821 ..... p 842 N94-13199 * #
NAS 1.26:193824 ..... p 621 N94-13186 * #
NAS 1.26:193825 ..... p 543 N94-14120 * #
NAS 1.26:193826 ..... p 564 N94-14025 * #
NAS 1.26:193827 ..... p 804 N94-12934 * #
NAS 1.26:193830 ..... p 533 N94-12806 * #
NAS 1.26:193832 ..... p 553 N94-14682 * #
NAS 1.26:193833 ..... p 561 N94-12830 * #
NAS 1.26:193834 ..... p 807 N94-13444 * #
NAS 1.26:193835 ..... p 804 N94-12873 * #
NAS 1.26:193840 ..... p 660 N94-14904 * #
NAS 1.26:193842 ..... p 793 N94-14903 * #
NAS 1.26:193843 ..... p 788 N94-14905 * #
NAS 1.26:193844 ..... p 647 N94-14906 * #
NAS 1.26:193846 ..... p 554 N94-14907 * #
NAS 1.26:194024 ..... p 712 N94-13092 * #
NAS 1.26:194025 ..... p 832 N94-14305 * #
NAS 1.26:194029 ..... p 715 N94-13956 * #
NAS 1.26:194031 ..... p 770 N94-14429 * #
NAS 1.26:194033 ..... p 833 N94-14406 * #
NAS 1.26:194034 ..... p 841 N94-13088 * #
NAS 1.26:194035 ..... p 625 N94-14325 * #
NAS 1.26:194037 ..... p 513 N94-13957 * #
NAS 1.26:194039 ..... p 567 N94-12825 * #
NAS 1.26:194074 ..... p 526 N94-13469 * #
NAS 1.26:194077 ..... p 841 N94-12823 * #
NAS 1.26:194079 ..... p 842 N94-13561 * #
NAS 1.26:194080 ..... p 845 N94-14492 * #
NAS 1.26:194084 ..... p 844 N94-13671 * #
NAS 1.26:194089 ..... p 740 N94-13363 * #
NAS 1.26:194090 ..... p 791 N94-13353 * #
NAS 1.26:194092 ..... p 737 N94-13712 * #
NAS 1.26:194093 ..... p 847 N94-13288 * #
NAS 1.26:194095 ..... p 545 N94-13189 * #
NAS 1.26:194096 ..... p 612 N94-14654 * #
NAS 1.26:194097 ..... p 701 N94-13187 * #
NAS 1.26:194098 ..... p 598 N94-13090 * #
NAS 1.26:194099 ..... p 549 N94-13068 * #
NAS 1.26:194100 ..... p 549 N94-13055 * #
NAS 1.26:194102 ..... p 545 N94-14830 * #
NAS 1.26:194105 ..... p 727 N94-12793 * #
NAS 1.26:194107 ..... p 732 N94-13782 * #
NAS 1.26:194110 ..... p 686 N94-14081 * #
NAS 1.26:194111 ..... p 836 N94-13423 * #
NAS 1.26:194114 ..... p 635 N94-13676 * #
NAS 1.26:194116 ..... p 535 N94-13935 * #
NAS 1.26:194118 ..... p 833 N94-14493 * #
NAS 1.26:194123 ..... p 729 N94-14097 * #
NAS 1.26:194124 ..... p 727 N94-13210 * #
NAS 1.26:194125 ..... p 502 N94-13422 * #
NAS 1.26:194126 ..... p 806 N94-13291 * #
NAS 1.26:194127 ..... p 847 N94-13211 * #
NAS 1.26:194128 ..... p 841 N94-13083 * #
NAS 1.26:194130 ..... p 728 N94-13562 * #
NAS 1.26:194132 ..... p 768 N94-13421 * #
NAS 1.26:194133 ..... p 656 N94-13420 * #
NAS 1.26:194134 ..... p 789 N94-13419 * #
NAS 1.26:194139 ..... p 571 N94-13891 * #
NAS 1.26:194140 ..... p 762 N94-13253 * #
NAS 1.26:194142 ..... p 713 N94-13418 * #
NAS 1.26:194143 ..... p 637 N94-13827 * #
NAS 1.26:194144 ..... p 808 N94-13875 * #
NAS 1.26:194145 ..... p 663 N94-14134 * #
NAS 1.26:194146 ..... p 516 N94-14104 * #
NAS 1.26:194147 ..... p 579 N94-13964 * #
NAS 1.26:194149 ..... p 766 N94-14444 * #
NAS 1.26:194151 ..... p 747 N94-13443 * #
NAS 1.26:194163 ..... p 625 N94-14324 * #
NAS 1.26:194167 ..... p 512 N94-13082 * #
NAS 1.26:194174 ..... p 500 N94-13076 * #
NAS 1.26:194175 ..... p 714 N94-13816 * #
NAS 1.26:194176 ..... p 728 N94-13865 * #
NAS 1.26:194177 ..... p 739 N94-13086 * #
NAS 1.26:194178 ..... p 847 N94-13087 * #
NAS 1.26:194181 ..... p 752 N94-14139 * #
NAS 1.26:194183 ..... p 621 N94-13336 * #
NAS 1.26:194189 ..... p 737 N94-13674 * #
NAS 1.26:194193 ..... p 643 N94-14741 * #
NAS 1.26:194194 ..... p 627 N94-12803 * #
NAS 1.26:194195 ..... p 545 N94-13953 * #
NAS 1.26:194199 ..... p 750 N94-13828 * #
NAS 1.26:194200 ..... p 745 N94-13356 * #
NAS 1.26:194201 ..... p 745 N94-13355 * #
NAS 1.26:194225 ..... p 673 N94-13673 * #
NAS 1.26:194233 ..... p 638 N94-14356 * #
NAS 1.26:194242 ..... p 786 N94-14549 * #
NAS 1.26:194248 ..... p 660 N94-12802 * #
NAS 1.26:194252 ..... p 511 N94-13424 * #
NAS 1.26:194258 ..... p 733 N94-13824 * #
NAS 1.26:194259 ..... p 504 N94-14030 * #
NAS 1.26:194260 ..... p 527 N94-14322 * #
NAS 1.26:194261 ..... p 586 N94-12805 * #
NAS 1.26:194277 ..... p 742 N94-12808 * #
NAS 1.26:194278 ..... p 758 N94-12938 * #
NAS 1.26:194282 ..... p 716 N94-14049 * #
NAS 1.26:194283 ..... p 796 N94-13084 * #
NAS 1.26:194289 ..... p 760 N94-13921 * #
NAS 1.26:194291 ..... p 763 N94-13603 * #
NAS 1.26:194293 ..... p 770 N94-13922 * #
NAS 1.26:194296 ..... p 504 N94-13607 * #
NAS 1.26:194297 ..... p 748 N94-13586 * #
NAS 1.26:194298 ..... p 743 N94-13023 * #
NAS 1.26:194299 ..... p 823 N94-13192 * #
NAS 1.26:194301 ..... p 831 N94-13681 * #
NAS 1.26:194304 ..... p 831 N94-13679 * #
NAS 1.26:194305 ..... p 714 N94-13707 * #
NAS 1.26:194311 ..... p 848 N94-13708 * #
NAS 1.26:194331 ..... p 754 N94-14472 * #
NAS 1.26:194334 ..... p 750 N94-13932 * #
NAS 1.26:194336 ..... p 714 N94-13825 * #
NAS 1.26:194337 ..... p 800 N94-13854 * #
NAS 1.26:194338 ..... p 714 N94-13709 * #
NAS 1.26:194339 ..... p 715 N94-13826 * #
NAS 1.26:194341 ..... p 836 N94-13332 * #
NAS 1.26:194342 ..... p 721 N94-13675 * #
NAS 1.26:194343 ..... p 838 N94-13716 * #
NAS 1.26:194350 ..... p 572 N94-14123 * #
NAS 1.26:194351 ..... p 662 N94-13800 * #
NAS 1.26:194354 ..... p 709 N94-14103 * #
NAS 1.26:194355 ..... p 539 N94-12827 * #
NAS 1.26:194357 ..... p 846 N94-12826 * #
NAS 1.26:194359 ..... p 527 N94-12824 * #
NAS 1.26:194361 ..... p 545 N94-13067 * #
NAS 1.26:194362 ..... p 828 N94-13104 * #
NAS 1.26:194363 ..... p 578 N94-13246 * #
NAS 1.26:194364 ..... p 792 N94-13719 * #
NAS 1.26:194367 ..... p 783 N94-13856 * #
NAS 1.26:194375 ..... p 796 N94-13081 * #
NAS 1.26:194383 ..... p 712 N94-13212 * #
NAS 1.26:194384 ..... p 791 N94-13682 * #
NAS 1.26:194385 ..... p 532 N94-14148 * #
NAS 1.26:194388 ..... p 607 N94-14369 * #
NAS 1.26:194392 ..... p 715 N94-13954 * #

NAS 1.26:194393 ..... p 536 N94-14323 * #
NAS 1.26:194394 ..... p 832 N94-14357 * #
NAS 1.26:194395 ..... p 832 N94-13894 * #
NAS 1.26:194396 ..... p 532 N94-14068 * #
NAS 1.26:194397 ..... p 650 N94-13814 * #
NAS 1.26:194398 ..... p 650 N94-13815 * #
NAS 1.26:194399 ..... p 844 N94-13958 * #
NAS 1.26:194402 ..... p 729 N94-14494 * #
NAS 1.26:194403 ..... p 637 N94-13959 * #
NAS 1.26:194404 ..... p 716 N94-13967 * #
NAS 1.26:194408 ..... p 638 N94-14308 * #
NAS 1.26:194409 ..... p 515 N94-13618 * #
NAS 1.26:194410 ..... p 832 N94-13966 * #
NAS 1.26:194412 ..... p 565 N94-14480 * #
NAS 1.26:194415 ..... p 514 N94-14495 * #
NAS 1.26:194416 ..... p 714 N94-13793 * #
NAS 1.26:194417 ..... p 842 N94-14298 * #
NAS 1.26:194419 ..... p 793 N94-14548 * #
NAS 1.26:194420 ..... p 501 N94-13266 * #
NAS 1.26:194421 ..... p 705 N94-14430 * #
NAS 1.26:194422 ..... p 661 N94-13445 * #
NAS 1.26:194423 ..... p 728 N94-13473 * #
NAS 1.26:194424 ..... p 651 N94-14447 * #
NAS 1.26:194425 ..... p 716 N94-13969 * #
NAS 1.26:194477 ..... p 845 N94-14479 * #
NAS 1.26:194488 ..... p 770 N94-14307 * #
NAS 1.26:194489 ..... p 840 N94-14482 * #
NAS 1.26:194490 ..... p 741 N94-14136 * #
NAS 1.26:194491 ..... p 612 N94-14501 * #
NAS 1.26:194492 ..... p 721 N94-13723 * #
NAS 1.26:194495 ..... p 683 N94-14500 * #
NAS 1.26:194496 ..... p 519 N94-14841 * #
NAS 1.26:194497 ..... p 519 N94-14842 * #
NAS 1.26:194498 ..... p 542 N94-14076 * #
NAS 1.26:194499 ..... p 542 N94-14077 * #
NAS 1.26:194500 ..... p 542 N94-14078 * #
NAS 1.26:194501 ..... p 602 N94-13813 * #
NAS 1.26:194502 ..... p 602 N94-13810 * #
NAS 1.26:194503 ..... p 622 N94-13811 * #
NAS 1.26:194505 ..... p 749 N94-13784 * #
NAS 1.26:194506 ..... p 657 N94-13812 * #
NAS 1.26:194507 ..... p 703 N94-13940 * #
NAS 1.26:194508 ..... p 532 N94-13796 * #
NAS 1.26:194509 ..... p 741 N94-13943 * #
NAS 1.26:194510 ..... p 605 N94-13946 * #
NAS 1.26:194511 ..... p 564 N94-13947 * #
NAS 1.26:194512 ..... p 624 N94-13948 * #
NAS 1.26:194513 ..... p 665 N94-13148 * #
NAS 1.26:194514 ..... p 665 N94-13153 * #
NAS 1.26:194515 ..... p 677 N94-14618 * #
NAS 1.26:194517 ..... p 602 N94-13799 * #
NAS 1.26:194518 ..... p 650 N94-14029 * #
NAS 1.26:194519 ..... p 543 N94-14683 * #
NAS 1.26:194521 ..... p 582 N94-14539 * #
NAS 1.26:194522 ..... p 508 N94-14541 * #
NAS 1.26:194523 ..... p 508 N94-14538 * #
NAS 1.26:194524 ..... p 559 N94-14715 * #
NAS 1.26:194525 ..... p 652 N94-14684 * #
NAS 1.26:194527 ..... p 659 N94-14576 * #
NAS 1.26:194530 ..... p 533 N94-14540 * #
NAS 1.26:194532 ..... p 845 N94-14577 * #
NAS 1.26:194533 ..... p 536 N94-14310 * #
NAS 1.26:194534 ..... p 552 N94-14309 * #
NAS 1.26:194535 ..... p 741 N94-13788 * #
NAS 1.26:194536 ..... p 840 N94-14688 * #
NAS 1.26:194537 ..... p 840 N94-14685 * #
NAS 1.26:194538 ..... p 818 N94-13984 * #
NAS 1.26:194543 ..... p 686 N94-13872 * #
NAS 1.26:194556 ..... p 643 N94-14745 * #
NAS 1.26:194564 ..... p 682 N94-14692 * #
NAS 1.26:4498 ..... p 648 N94-12874 * #
NAS 1.26:4526 ..... p 670 N94-13063 * #
NAS 1.26:4529 ..... p 844 N94-13146 * #
NAS 1.26:4531 ..... p 629 N94-13073 * #
NAS 1.26:4538 ..... p 776 N94-13897 * #
NAS 1.26:4539 ..... p 744 N94-13065 * #
NAS 1.26:4543 ..... p 629 N94-13066 * #
NAS 1.26:4544 ..... p 596 N94-13798 * #
NAS 1.26:4546 ..... p 532 N94-14851 * #
NAS 1.26:4548 ..... p 574 N94-14850 * #
NAS 1.26:4549 ..... p 729 N94-14028 * #
NAS 1.55:3213 ..... p 551 N94-13417 * #
NAS 1.55:3216 ..... p 841 N94-13183 * #
NAS 1.55:3220 ..... p 521 N94-13294 * #
NAS 1.60:3312 ..... p 846 N94-12875 * #
NAS 1.60:3344 ..... p 620 N94-13110 * #
NAS 1.60:3350 ..... p 847 N94-13263 * #
NAS 1.60:3351 ..... p 732 N94-13714 * #
NAS 1.60:3362 ..... p 604 N94-13916 * #
NAS 1.60:3367 ..... p 776 N94-14733 * #
NAS 1.60:3368 ..... p 813 N94-14409 * #
NAS 1.60:3377 ..... p 665 N94-13056 * #
NAS 1.60:3378 ..... p 552 N94-14102 * #
NAS 1.60:3379 ..... p 538 N94-13111 * #
NAS 1.60:3397 ..... p 596 N94-13790 * #
NAS 1.60:3410 ..... p 669 N94-12831 * #
NAS 1.60:3412 ..... p 729 N94-14032 * #
NAS 1.61:1310 ..... p 548 N94-12807 * #
NAS 1.61:1314 ..... p 550 N94-13265 * #
NAS 1.61:1315 ..... p 545 N94-13713 * #
NAS 1.61:1316 ..... p 844 N94-13963 * #
NAS 1.61:1319 ..... p 623 N94-13871 * #
NAS 1.77:10002 ..... p 552 N94-14463 * #

NASA-CP-3213 ..... p 551 N94-13417 * #
NASA-CP-3216 ..... p 841 N94-13183 * #
NASA-CP-3220 ..... p 521 N94-13294 * #

NASA-CR-167690 ..... p 534 N94-12810 * #
NASA-CR-167691 ..... p 536 N94-14047 * #
NASA-CR-177617 ..... p 510 N94-13247 * #
NASA-CR-177621 ..... p 512 N94-14744 * #
NASA-CR-177622 ..... p 538 N94-13257 * #
NASA-CR-182183 ..... p 620 N94-13106 * #
NASA-CR-184381 ..... p 683 N94-14484 * #
NASA-CR-185696 ..... p 534 N94-13191 * #
NASA-CR-185697 ..... p 534 N94-12965 * #
NASA-CR-186026 ..... p 516 N94-14106 * #
NASA-CR-187179 ..... p 674 N94-13873 * #
NASA-CR-188251 ..... p 827 N94-12800 * #
NASA-CR-188261 ..... p 543 N94-14483 * #
NASA-CR-189136 ..... p 557 N94-13920 * #
NASA-CR-189560 ..... p 527 N94-13127 * #
NASA-CR-189687 ..... p 578 N94-13431 * #
NASA-CR-189735 ..... p 596 N94-13141 * #
NASA-CR-190758 ..... p 537 N94-12809 * #
NASA-CR-191088 ..... p 828 N94-12931 * #
NASA-CR-191096 ..... p 622 N94-13786 * #
NASA-CR-191147 ..... p 555 N94-13139 * #
NASA-CR-191150 ..... p 676 N94-14408 * #
NASA-CR-191165 ..... p 559 N94-14769 * #
NASA-CR-191170 ..... p 555 N94-13378 * #
NASA-CR-191182 ..... p 664 N94-14446 * #
NASA-CR-191183 ..... p 663 N94-14445 * #
NASA-CR-191186 ..... p 551 N94-13416 * #
NASA-CR-191187 ..... p 550 N94-13415 * #
NASA-CR-191188 ..... p 554 N94-14771 * #
NASA-CR-191189 ..... p 519 N94-14448 * #
NASA-CR-191190 ..... p 582 N94-14543 * #
NASA-CR-191196 ..... p 560 N94-14822 * #
NASA-CR-191323 ..... p 562 N94-13115 * #
NASA-CR-191325 ..... p 604 N94-13909 * #
NASA-CR-191326 ..... p 736 N94-13132 * #
NASA-CR-191332 ..... p 540 N94-13140 * #
NASA-CR-191334 ..... p 759 N94-13177 * #
NASA-CR-191337 ..... p 671 N94-13124 * #
NASA-CR-191339 ..... p 762 N94-13131 * #
NASA-CR-191340 ..... p 648 N94-13176 * #
NASA-CR-191341 ..... p 620 N94-13125 * #
NASA-CR-191345 ..... p 661 N94-13129 * #
NASA-CR-191394 ..... p 745 N94-13130 * #
NASA-CR-191397 ..... p 822 N94-13116 * #
NASA-CR-191437 ..... p 516 N94-12829 * #
NASA-CR-191459 ..... p 575 N94-12792 * #
NASA-CR-191476 ..... p 499 N94-12852 * #
NASA-CR-191477 ..... p 630 N94-13133 * #
NASA-CR-191480 ..... p 768 N94-13354 * #
NASA-CR-191482 ..... p 630 N94-13114 * #
NASA-CR-191487 ..... p 630 N94-13128 * #
NASA-CR-191488 ..... p 769 N94-13722 * #
NASA-CR-191491 ..... p 767 N94-13202 * #
NASA-CR-191494 ..... p 767 N94-13289 * #
NASA-CR-191496 ..... p 762 N94-13184 * #
NASA-CR-191497 ..... p 769 N94-13725 * #
NASA-CR-191498 ..... p 745 N94-13185 * #
NASA-CR-191499 ..... p 555 N94-13267 * #
NASA-CR-191500 ..... p 769 N94-13717 * #
NASA-CR-191501 ..... p 636 N94-13817 * #
NASA-CR-191502 ..... p 628 N94-12888 * #
NASA-CR-191503 ..... p 647 N94-14849 * #
NASA-CR-191504 ..... p 636 N94-13785 * #
NASA-CR-191505 ..... p 554 N94-12833 * #
NASA-CR-191506 ..... p 769 N94-13792 * #
NASA-CR-191510 ..... p 629 N94-13074 * #
NASA-CR-191511 ..... p 636 N94-13718 * #
NASA-CR-191512 ..... p 630 N94-13075 * #
NASA-CR-191516 ..... p 636 N94-13724 * #
NASA-CR-191520 ..... p 749 N94-13721 * #
NASA-CR-191521 ..... p 539 N94-12976 * #
NASA-CR-191524 ..... p 540 N94-13016 * #
NASA-CR-191525 ..... p 654 N94-13091 * #
NASA-CR-191527 ..... p 595 N94-14026 * #
NASA-CR-191545 ..... p 622 N94-13797 * #
NASA-CR-191788 ..... p 822 N94-13126 * #
NASA-CR-192581 ..... p 718 N94-12957 * #
NASA-CR-192586 ..... p 660 N94-12791 * #
NASA-CR-192594 ..... p 830 N94-13448 * #
NASA-CR-192600 ..... p 652 N94-14497 * #
NASA-CR-192603 ..... p 669 N94-14101 * #
NASA-CR-192613 ..... p 648 N94-13326 * #
NASA-CR-192761 ..... p 754 N94-14368 * #
NASA-CR-193101 ..... p 535 N94-13934 * #
NASA-CR-193244 ..... p 829 N94-13178 * #
NASA-CR-193266 ..... p 842 N94-13855 * #
NASA-CR-193280 ..... p 848 N94-13476 * #
NASA-CR-193287 ..... p 823 N94-13461 * #
NASA-CR-193297 ..... p 829 N94-13181 * #
NASA-CR-193300 ..... p 838 N94-13781 * #
NASA-CR-193305 ..... p 671 N94-13179 * #
NASA-CR-193306 ..... p 500 N94-13180 * #
NASA-CR-193324 ..... p 829 N94-13287 * #
NASA-CR-193359 ..... p 849 N94-13965 * #
NASA-CR-193362 ..... p 602 N94-13720 * #
NASA-CR-193389 ..... p 617 N94-14743 * #
NASA-CR-193390 ..... p 508 N94-14326 * #
NASA-CR-193392 ..... p 630 N94-13078 * #
NASA-CR-193393 ..... p 638 N94-14086 * #
NASA-CR-193394 ..... p 541 N94-13955 * #
NASA-CR-193396 ..... p 599 N94-13264 * #
NASA-CR-193397 ..... p 833 N94-14358 * #
NASA-CR-193413 ..... p 649 N94-13464 * #
NASA-CR-193415 ..... p 822 N94-13062 * #
NASA-CR-193418 ..... p 828 N94-12970 * #
NASA-CR-193424 ..... p 835 N94-13233 * #
NASA-CR-193433 ..... p 792 N94-14473 * #
NASA-CR-193454 ..... p 713 N94-13335 * #
NASA-CR-193456 ..... p 712 N94-13334 * #
NASA-CR-193481 ..... p 562 N94-13048 * #
NASA-CR-193559 ..... p 803 N94-12796 * #
NASA-CR-193560 ..... p 727 N94-12795 * #
NASA-CR-193563 ..... p 718 N94-12839 * #
NASA-CR-193597 ..... p 628 N94-12959 * #
NASA-CR-193604 ..... p 664 N94-14848 * #
NASA-CR-193609 ..... p 830 N94-13462 * #
NASA-CR-193613 ..... p 577 N94-13089 * #
NASA-CR-193616 ..... p 503 N94-13463 * #
NASA-CR-193622 ..... p 731 N94-12960 * #
NASA-CR-193632 ..... p 844 N94-13234 * #
NASA-CR-193640 ..... p 836 N94-13446 * #
NASA-CR-193646 ..... p 512 N94-13238 * #
NASA-CR-193647 ..... p 575 N94-12789 * #
NASA-CR-193654 ..... p 835 N94-13171 * #
NASA-CR-193655 ..... p 835 N94-13239 * #
NASA-CR-193659 ..... p 520 N94-12799 * #
NASA-CR-193660 ..... p 790 N94-12797 * #
NASA-CR-193664 ..... p 711 N94-12788 * #
NASA-CR-193667 ..... p 821 N94-13030 * #
NASA-CR-193669 ..... p 713 N94-13465 * #
NASA-CR-193670 ..... p 835 N94-13203 * #
NASA-CR-193671 ..... p 712 N94-13293 * #
NASA-CR-193672 ..... p 706 N94-13170 * #
NASA-CR-193673 ..... p 501 N94-13292 * #
NASA-CR-193675 ..... p 619 N94-13026 * #
NASA-CR-193676 ..... p 540 N94-13109 * #
NASA-CR-193677 ..... p 629 N94-13007 * #
NASA-CR-193708 ..... p 839 N94-13864 * #
NASA-CR-193711 ..... p 539 N94-12790 * #
NASA-CR-193714 ..... p 839 N94-14404 * #
NASA-CR-193716 ..... p 832 N94-14146 * #
NASA-CR-193718 ..... p 572 N94-14133 * #
NASA-CR-193719 ..... p 599 N94-13236 * #
NASA-CR-193720 ..... p 759 N94-13204 * #
NASA-CR-193724 ..... p 540 N94-13112 * #
NASA-CR-193725 ..... p 600 N94-13466 * #
NASA-CR-193726 ..... p 598 N94-12920 * #
NASA-CR-193727 ..... p 619 N94-12897 * #
NASA-CR-193728 ..... p 744 N94-13113 * #
NASA-CR-193783 ..... p 833 N94-14359 * #
NASA-CR-193784 ..... p 833 N94-14405 * #
NASA-CR-193787 ..... p 717 N94-14306 * #
NASA-CR-193797 ..... p 558 N94-14050 * #
NASA-CR-193821 ..... p 842 N94-13199 * #
NASA-CR-193824 ..... p 621 N94-13186 * #
NASA-CR-193825 ..... p 543 N94-14120 * #
NASA-CR-193826 ..... p 564 N94-14025 * #
NASA-CR-193827 ..... p 804 N94-12934 * #
NASA-CR-193830 ..... p 533 N94-12806 * #
NASA-CR-193832 ..... p 553 N94-14682 * #
NASA-CR-193833 ..... p 561 N94-12830 * #
NASA-CR-193834 ..... p 807 N94-13444 * #
NASA-CR-193835 ..... p 804 N94-12873 * #
NASA-CR-193840 ..... p 660 N94-14904 * #
NASA-CR-193842 ..... p 793 N94-14903 * #
NASA-CR-193843 ..... p 788 N94-14905 * #
NASA-CR-193844 ..... p 647 N94-14906 * #
NASA-CR-193846 ..... p 554 N94-14907 * #
NASA-CR-194024 ..... p 712 N94-13092 * #
NASA-CR-194025 ..... p 832 N94-14305 * #
NASA-CR-194029 ..... p 715 N94-13956 * #
NASA-CR-194031 ..... p 770 N94-14429 * #
NASA-CR-194033 ..... p 833 N94-14406 * #
NASA-CR-194034 ..... p 841 N94-13088 * #
NASA-CR-194035 ..... p 625 N94-14325 * #
NASA-CR-194037 ..... p 613 N94-13957 * #
NASA-CR-194039 ..... p 567 N94-12825 * #
NASA-CR-194074 ..... p 526 N94-13469 * #
NASA-CR-194077 ..... p 841 N94-12823 * #
NASA-CR-194079 ..... p 842 N94-13561 * #

NASA-CR-194080 ..... p 845 N94-14492 * #
NASA-CR-194084 ..... p 844 N94-13671 * #
NASA-CR-194089 ..... p 740 N94-13363 * #
NASA-CR-194090 ..... p 791 N94-13353 * #
NASA-CR-194092 ..... p 737 N94-13712 * #
NASA-CR-194093 ..... p 847 N94-13288 * #
NASA-CR-194095 ..... p 545 N94-13189 * #
NASA-CR-194096 ..... p 612 N94-14654 * #
NASA-CR-194097 ..... p 701 N94-13187 * #
NASA-CR-194098 ..... p 598 N94-13090 * #
NASA-CR-194099 ..... p 549 N94-13068 * #
NASA-CR-194100 ..... p 549 N94-13055 * #
NASA-CR-194102 ..... p 545 N94-14830 * #
NASA-CR-194105 ..... p 727 N94-12793 * #
NASA-CR-194107 ..... p 732 N94-13782 * #
NASA-CR-194110 ..... p 686 N94-14081 * #
NASA-CR-194111 ..... p 836 N94-13423 * #
NASA-CR-194114 ..... p 635 N94-13676 * #
NASA-CR-194116 ..... p 535 N94-13935 * #
NASA-CR-194118 ..... p 833 N94-14493 * #
NASA-CR-194123 ..... p 729 N94-14097 * #
NASA-CR-194124 ..... p 727 N94-13210 * #
NASA-CR-194125 ..... p 502 N94-13422 * #
NASA-CR-194126 ..... p 806 N94-13291 * #
NASA-CR-194127 ..... p 847 N94-13211 * #
NASA-CR-194128 ..... p 841 N94-13083 * #
NASA-CR-194130 ..... p 728 N94-13562 * #
NASA-CR-194132 ..... p 768 N94-13421 * #
NASA-CR-194133 ..... p 656 N94-13420 * #
NASA-CR-194134 ..... p 789 N94-13419 * #
NASA-CR-194139 ..... p 571 N94-13891 * #
NASA-CR-194140 ..... p 762 N94-13253 * #
NASA-CR-194142 ..... p 713 N94-13418 * #
NASA-CR-194143 ..... p 637 N94-13827 * #
NASA-CR-194144 ..... p 808 N94-13875 * #
NASA-CR-194145 ..... p 663 N94-14134 * #
NASA-CR-194146 ..... p 516 N94-14104 * #
NASA-CR-194147 ..... p 579 N94-13964 * #
NASA-CR-194149 ..... p 766 N94-14444 * #
NASA-CR-194151 ..... p 747 N94-13443 * #
NASA-CR-194163 ..... p 625 N94-14324 * #
NASA-CR-194167 ..... p 512 N94-13082 * #
NASA-CR-194174 ..... p 500 N94-13076 * #
NASA-CR-194175 ..... p 714 N94-13816 * #
NASA-CR-194176 ..... p 728 N94-13865 * #
NASA-CR-194177 ..... p 739 N94-13086 * #
NASA-CR-194178 ..... p 847 N94-13087 * #
NASA-CR-194181 ..... p 752 N94-14139 * #
NASA-CR-194183 ..... p 621 N94-13336 * #
NASA-CR-194189 ..... p 737 N94-13674 * #
NASA-CR-194193 ..... p 643 N94-14741 * #
NASA-CR-194194 ..... p 627 N94-12803 * #
NASA-CR-194195 ..... p 545 N94-13953 * #
NASA-CR-194199 ..... p 750 N94-13828 * #
NASA-CR-194200 ..... p 745 N94-13356 * #
NASA-CR-194201 ..... p 745 N94-13355 * #
NASA-CR-194225 ..... p 673 N94-13673 * #
NASA-CR-194233 ..... p 638 N94-14356 * #
NASA-CR-194242 ..... p 786 N94-14549 * #
NASA-CR-194248 ..... p 660 N94-12802 * #
NASA-CR-194252 ..... p 511 N94-13424 * #
NASA-CR-194258 ..... p 733 N94-13824 * #
NASA-CR-194259 ..... p 504 N94-14030 * #
NASA-CR-194260 ..... p 527 N94-14322 * #
NASA-CR-194261 ..... p 586 N94-12805 * #
NASA-CR-194277 ..... p 742 N94-12808 * #
NASA-CR-194278 ..... p 758 N94-12938 * #
NASA-CR-194282 ..... p 716 N94-14049 * #
NASA-CR-194283 ..... p 796 N94-13084 * #
NASA-CR-194289 ..... p 760 N94-13921 * #
NASA-CR-194291 ..... p 763 N94-13603 * #
NASA-CR-194293 ..... p 770 N94-13922 * #
NASA-CR-194296 ..... p 504 N94-13607 * #
NASA-CR-194297 ..... p 748 N94-13586 * #
NASA-CR-194298 ..... p 743 N94-13023 * #
NASA-CR-194299 ..... p 823 N94-13192 * #
NASA-CR-194301 ..... p 831 N94-13681 * #
NASA-CR-194304 ..... p 831 N94-13679 * #
NASA-CR-194305 ..... p 714 N94-13707 * #
NASA-CR-194311 ..... p 848 N94-13708 * #
NASA-CR-194331 ..... p 754 N94-14472 * #
NASA-CR-194334 ..... p 750 N94-13932 * #
NASA-CR-194336 ..... p 714 N94-13825 * #
NASA-CR-194337 ..... p 800 N94-13854 * #
NASA-CR-194338 ..... p 714 N94-13709 * #
NASA-CR-194339 ..... p 715 N94-13826 * #
NASA-CR-194341 ..... p 836 N94-13332 * #
NASA-CR-194342 ..... p 721 N94-13675 * #
NASA-CR-194343 ..... p 838 N94-13716 * #
NASA-CR-194350 ..... p 572 N94-14123 * #
NASA-CR-194351 ..... p 662 N94-13800 * #
NASA-CR-194354 ..... p 709 N94-14103 * #
NASA-CR-194355 ..... p 539 N94-12827 * #
NASA-CR-194357 ..... p 846 N94-12826 * #
NASA-CR-194359 ..... p 527 N94-12824 * #
NASA-CR-194361 ..... p 545 N94-13067 * #
NASA-CR-194362 ..... p 828 N94-13104 * #
NASA-CR-194363 ..... p 578 N94-13246 * #
NASA-CR-194364 ..... p 792 N94-13719 * #
NASA-CR-194367 ..... p 783 N94-13856 * #
NASA-CR-194375 ..... p 796 N94-13081 * #
NASA-CR-194383 ..... p 712 N94-13212 * #
NASA-CR-194384 ..... p 791 N94-13682 * #
NASA-CR-194385 ..... p 532 N94-14148 * #
NASA-CR-194388 ..... p 607 N94-14369 * #
NASA-CR-194392 ..... p 715 N94-13954 * #
NASA-CR-194393 ..... p 536 N94-14323 * #
NASA-CR-194394 ..... p 832 N94-14357 * #
NASA-CR-194395 ..... p 832 N94-13894 * #
NASA-CR-194396 ..... p 532 N94-14068 * #
NASA-CR-194397 ..... p 650 N94-13814 * #
NASA-CR-194398 ..... p 650 N94-13815 * #
NASA-CR-194399 ..... p 844 N94-13958 * #
NASA-CR-194402 ..... p 729 N94-14494 * #
NASA-CR-194403 ..... p 637 N94-13959 * #
NASA-CR-194404 ..... p 716 N94-13967 * #
NASA-CR-194408 ..... p 638 N94-14308 * #
NASA-CR-194409 ..... p 515 N94-13618 * #
NASA-CR-194410 ..... p 832 N94-13966 * #
NASA-CR-194412 ..... p 565 N94-14480 * #
NASA-CR-194415 ..... p 514 N94-14495 * #
NASA-CR-194416 ..... p 714 N94-13793 * #
NASA-CR-194417 ..... p 842 N94-14298 * #
NASA-CR-194419 ..... p 793 N94-14548 * #
NASA-CR-194420 ..... p 501 N94-13266 * #
NASA-CR-194421 ..... p 705 N94-14430 * #
NASA-CR-194422 ..... p 661 N94-13445 * #
NASA-CR-194423 ..... p 728 N94-13473 * #
NASA-CR-194424 ..... p 651 N94-14447 * #
NASA-CR-194425 ..... p 716 N94-13969 * #
NASA-CR-194477 ..... p 845 N94-14479 * #
NASA-CR-194488 ..... p 770 N94-14307 * #
NASA-CR-194489 ..... p 840 N94-14482 * #
NASA-CR-194490 ..... p 741 N94-14136 * #
NASA-CR-194491 ..... p 612 N94-14501 * #
NASA-CR-194492 ..... p 721 N94-13723 * #
NASA-CR-194495 ..... p 683 N94-14500 * #
NASA-CR-194496 ..... p 519 N94-14841 * #
NASA-CR-194497 ..... p 519 N94-14842 * #
NASA-CR-194498 ..... p 542 N94-14076 * #
NASA-CR-194499 ..... p 542 N94-14077 * #
NASA-CR-194500 ..... p 542 N94-14078 * #
NASA-CR-194501 ..... p 602 N94-13813 * #
NASA-CR-194502 ..... p 602 N94-13810 * #
NASA-CR-194503 ..... p 622 N94-13811 * #
NASA-CR-194505 ..... p 749 N94-13784 * #
NASA-CR-194506 ..... p 657 N94-13812 * #
NASA-CR-194507 ..... p 703 N94-13940 * #
NASA-CR-194508 ..... p 532 N94-13796 * #
NASA-CR-194509 ..... p 741 N94-13943 * #
NASA-CR-194510 ..... p 605 N94-13946 * #
NASA-CR-194511 ..... p 564 N94-13947 * #
NASA-CR-194512 ..... p 624 N94-13948 * #
NASA-CR-194513 ..... p 665 N94-13148 * #
NASA-CR-194514 ..... p 665 N94-13153 * #
NASA-CR-194515 ..... p 677 N94-14618 * #
NASA-CR-194517 ..... p 602 N94-13799 * #
NASA-CR-194518 ..... p 650 N94-14029 * #
NASA-CR-194519 ..... p 543 N94-14683 * #
NASA-CR-194521 ..... p 582 N94-14539 * #
NASA-CR-194522 ..... p 508 N94-14541 * #
NASA-CR-194523 ..... p 508 N94-14538 * #
NASA-CR-194524 ..... p 559 N94-14715 * #
NASA-CR-194525 ..... p 652 N94-14684 * #
NASA-CR-194527 ..... p 659 N94-14576 * #
NASA-CR-194530 ..... p 533 N94-14540 * #
NASA-CR-194532 ..... p 845 N94-14577 * #
NASA-CR-194533 ..... p 536 N94-14310 * #
NASA-CR-194534 ..... p 552 N94-14309 * #
NASA-CR-194535 ..... p 741 N94-13788 * #
NASA-CR-194536 ..... p 840 N94-14688 * #
NASA-CR-194537 ..... p 840 N94-14685 * #
NASA-CR-194538 ..... p 818 N94-13984 * #
NASA-CR-194543 ..... p 686 N94-13872 * #
NASA-CR-194556 ..... p 643 N94-14745 * #
NASA-CR-194564 ..... p 682 N94-14692 * #
NASA-CR-4526 ..... p 670 N94-13063 * #
NASA-CR-4529 ..... p 844 N94-13146 * #
NASA-CR-4531 ..... p 629 N94-13073 * #
NASA-CR-4533 ..... p 629 N94-13064 * #
NASA-CR-4538 ..... p 776 N94-13897 * #
NASA-CR-4539 ..... p 744 N94-13065 * #
NASA-CR-4543 ..... p 629 N94-13066 * #
NASA-CR-4544 ..... p 596 N94-13798 * #
NASA-CR-4546 ..... p 532 N94-14851 * #
NASA-CR-4548 ..... p 574 N94-14850 * #
NASA-CR-4549 ..... p 729 N94-14028 * #

NASA-RP-1310 ..... p 548 N94-12807 * #
NASA-RP-1314 ..... p 550 N94-13265 * #
NASA-RP-1315 ..... p 545 N94-13713 * #
NASA-RP-1316 ..... p 844 N94-13963 * #
NASA-RP-1319 ..... p 623 N94-13871 * #

NASA-SP-7011(379) ..... p 733 N94-14412 *
NASA-SP-7085(05) ..... p 543 N94-14411 *
NASA-SP-7107 ..... p 823 N94-13401 * #

NASA-TM-102265 ..... p 520 N94-12820 * #
NASA-TM-102877 ..... p 538 N94-13201 * #
NASA-TM-102877 ..... p 538 N94-13989 * #
NASA-TM-103740 ..... p 509 N94-14780 * #
NASA-TM-103863 ..... p 740 N94-13200 * #
NASA-TM-103923 ..... p 527 N94-13008 * #
NASA-TM-103951 ..... p 740 N94-12973 * #
NASA-TM-103991 ..... p 731 N94-12972 * #
NASA-TM-104010 ..... p 727 N94-13447 * #
NASA-TM-104024 ..... p 739 N94-12838 * #
NASA-TM-104566 ..... p 725 N94-14090 * #
NASA-TM-104589 ..... p 850 N94-13923 * #
NASA-TM-104591 ..... p 723 N94-14074 * #
NASA-TM-104755 ..... p 731 N94-12832 * #
NASA-TM-104775 ..... p 735 N94-13961 * #
NASA-TM-104776 ..... p 737 N94-13399 * #
NASA-TM-104781 ..... p 819 N94-13400 * #
NASA-TM-105879 ..... p 538 N94-13918 * #
NASA-TM-106008 ..... p 629 N94-13027 * #
NASA-TM-106068 ..... p 510 N94-14847 * #
NASA-TM-106113 ..... p 631 N94-13385 * #
NASA-TM-106115 ..... p 541 N94-13917 * #
NASA-TM-106120 ..... p 628 N94-12968 * #
NASA-TM-106164 ..... p 675 N94-13919 * #
NASA-TM-106188 ..... p 555 N94-13138 * #
NASA-TM-106214 ..... p 551 N94-13430 * #
NASA-TM-106229 ..... p 676 N94-14041 * #
NASA-TM-106231 ..... p 499 N94-13108 * #
NASA-TM-106264 ..... p 575 N94-12842 * #
NASA-TM-106270 ..... p 518 N94-13143 * #
NASA-TM-106280 ..... p 670 N94-13053 * #
NASA-TM-106282 ..... p 670 N94-12872 * #
NASA-TM-106286 ..... p 671 N94-13379 * #
NASA-TM-106290 ..... p 642 N94-14729 * #
NASA-TM-106291 ..... p 553 N94-14725 * #
NASA-TM-106292 ..... p 553 N94-14726 * #
NASA-TM-106294 ..... p 664 N94-14727 * #
NASA-TM-106297 ..... p 534 N94-13028 * #
NASA-TM-106298 ..... p 620 N94-13134 * #
NASA-TM-106300 ..... p 648 N94-13135 * #
NASA-TM-106302 ..... p 683 N94-14776 * #
NASA-TM-106304 ..... p 559 N94-14719 * #
NASA-TM-106306 ..... p 621 N94-13194 * #
NASA-TM-106312 ..... p 517 N94-13142 * #
NASA-TM-106318 ..... p 518 N94-14036 * #
NASA-TM-106321 ..... p 626 N94-14730 * #
NASA-TM-106323 ..... p 642 N94-14732 * #
NASA-TM-106324 ..... p 583 N94-14845 * #
NASA-TM-106326 ..... p 557 N94-14042 * #
NASA-TM-106330 ..... p 650 N94-13876 * #
NASA-TM-106344 ..... p 560 N94-14823 * #
NASA-TM-106351 ..... p 771 N94-14731 * #
NASA-TM-106353 ..... p 770 N94-14407 * #
NASA-TM-106354 ..... p 642 N94-14722 * #
NASA-TM-106356 ..... p 642 N94-14728 * #
NASA-TM-106362 ..... p 612 N94-14542 * #
NASA-TM-106364 ..... p 508 N94-14208 * #
NASA-TM-107684 ..... p 739 N94-12886 * #
NASA-TM-107763 ..... p 597 N94-12804 * #
NASA-TM-108244 ..... p 531 N94-14060 * #
NASA-TM-108252 ..... p 542 N94-14112 * #
NASA-TM-108257 ..... p 828 N94-12915 * #
NASA-TM-108419 ..... p 571 N94-13715 * #
NASA-TM-108421 ..... p 808 N94-13938 * #
NASA-TM-108738 ..... p 851 N94-14791 * #
NASA-TM-108779 ..... p 776 N94-14027 * #
NASA-TM-108993 ..... p 632 N94-13467 * #
NASA-TM-109001 ..... p 759 N94-13450 * #
NASA-TM-109002 ..... p 598 N94-12811 * #
NASA-TM-109005 ..... p 517 N94-13710 * #
NASA-TM-109006 ..... p 821 N94-13057 * #
NASA-TM-109008 ..... p 777 N94-14481 * #
NASA-TM-109009 ..... p 514 N94-12850 * #
NASA-TM-109014 ..... p 557 N94-13711 * #
NASA-TM-109016 ..... p 500 N94-13172 * #
NASA-TM-109190 ..... p 534 N94-12900 * #
NASA-TM-109246 ..... p 518 N94-13190 * #
NASA-TM-109248 ..... p 550 N94-13147 * #
NASA-TM-109251 ..... p 761 N94-12889 * #
NASA-TM-109252 ..... p 761 N94-12890 * #
NASA-TM-109255 ..... p 849 N94-13376 * #
NASA-TM-109265 ..... p 669 N94-13396 * #
NASA-TM-109268 ..... p 822 N94-13107 * #
NASA-TM-109272 ..... p 738 N94-13979 * #
NASA-TM-109276 ..... p 669 N94-14321 * #
NASA-TM-109280 ..... p 597 N94-14410 * #
NASA-TM-109284 ..... p 504 N94-13621 *
NASA-TM-109285 ..... p 518 N94-13623 *
NASA-TM-109286 ..... p 552 N94-13625 *
NASA-TM-109287 ..... p 842 N94-13626 *

NASA-TM-109289 ..... p 540 N94-13628 *
NASA-TM-109290 ..... p 819 N94-13629 *
NASA-TM-109291 ..... p 531 N94-13631 *
NASA-TM-109292 ..... p 504 N94-13632 *
NASA-TM-109293 ..... p 850 N94-13633 *
NASA-TM-109294 ..... p 541 N94-13634 *
NASA-TM-109295 ..... p 749 N94-13636 *
NASA-TM-109296 ..... p 541 N94-13637 *
NASA-TM-109297 ..... p 535 N94-13638 *
NASA-TM-109298 ..... p 531 N94-13640 *
NASA-TM-109299 ..... p 535 N94-13641 *
NASA-TM-109300 ..... p 737 N94-13601 *
NASA-TM-109301 ..... p 708 N94-13602 *
NASA-TM-109302 ..... p 662 N94-13604 *
NASA-TM-109303 ..... p 741 N94-13609 *
NASA-TM-109304 ..... p 737 N94-13611 *
NASA-TM-109305 ..... p 850 N94-13612 *
NASA-TM-109306 ..... p 842 N94-13613 *
NASA-TM-109307 ..... p 737 N94-13615 *
NASA-TM-109308 ..... p 570 N94-13616 *
NASA-TM-109309 ..... p 818 N94-13619 *
NASA-TM-109310 ..... p 552 N94-13617 *
NASA-TM-109311 ..... p 830 N94-13605 *
NASA-TM-109312 ..... p 515 N94-13606 *
NASA-TM-109313 ..... p 518 N94-13608 *
NASA-TM-109314 ..... p 713 N94-13620 *
NASA-TM-109327 ..... p 825 N94-14485 * #
NASA-TM-109328 ..... p 825 N94-14486 * #
NASA-TM-109329 ..... p 826 N94-14488 * #
NASA-TM-109330 ..... p 826 N94-14489 * #
NASA-TM-109331 ..... p 825 N94-14487 * #
NASA-TM-109413 ..... p 822 N94-13105 * #
NASA-TM-109416 ..... p 544 N94-14783 * #
NASA-TM-109468 ..... p 536 N94-14734 *
NASA-TM-109487 ..... p 533 N94-14735 *
NASA-TM-109490 ..... p 537 N94-14736 *
NASA-TM-109491 ..... p 533 N94-14787 *
NASA-TM-109492 ..... p 739 N94-14790 *
NASA-TM-4452 ..... p 850 N94-13962 * #
NASA-TM-4491 ..... p 554 N94-12871 * #
NASA-TM-4493 ..... p 520 N94-13255 * #
NASA-TM-4498 ..... p 648 N94-12874 * #
NASA-TM-4503 ..... p 520 N94-13254 * #
NASA-TM-4504 ..... p 517 N94-13791 * #
NASA-TM-4505 ..... p 516 N94-13256 * #
NASA-TM-4511 ..... p 533 N94-14824 * #
NASA-TM-4517 ..... p 586 N94-13732 * #
NASA-TM-4518 ..... p 623 N94-13878 * #
NASA-TM-4525 ..... p 537 N94-14853 * #
NASA-TM-4531 ..... p 519 N94-14855 * #
NASA-TM-4536 ..... p 716 N94-13960 * #

NASA-TP-3312 ..... p 846 N94-12875 * #
NASA-TP-3344 ..... p 620 N94-13110 * #
NASA-TP-3350 ..... p 847 N94-13263 * #
NASA-TP-3351 ..... p 732 N94-13714 * #
NASA-TP-3362 ..... p 604 N94-13916 * #
NASA-TP-3367 ..... p 776 N94-14733 * #
NASA-TP-3368 ..... p 813 N94-14409 * #
NASA-TP-3377 ..... p 665 N94-13056 * #
NASA-TP-3378 ..... p 552 N94-14102 * #
NASA-TP-3379 ..... p 538 N94-13111 * #
NASA-TP-3397 ..... p 596 N94-13790 * #
NASA-TP-3410 ..... p 669 N94-12831 * #
NASA-TP-3412 ..... p 729 N94-14032 * #

NASA-TT-10002 ..... p 552 N94-14463 * #

NASA-93-01 ..... p 660 N94-14904 * #

NASDA-CM-199-VOL-2 ..... p 688 N94-14209 #
NASDA-CM-199-1 ..... p 532 N94-14098 #

NASDA-CNT-930005-PT-1 ..... p 725 N94-13653 #
NASDA-CNT-930007 ..... p 721 N94-13643 #
NASDA-CNT-930008 ..... p 532 N94-13644 #
NASDA-CNT-930009 ..... p 563 N94-13471 #
NASDA-CNT-930010-PT-A ..... p 535 N94-13645 #
NASDA-CNT-930011 ..... p 535 N94-13599 #
NASDA-CNT-930012-PT-2 ..... p 737 N94-13472 #
NASDA-CNT-930013 ..... p 536 N94-14099 #
NASDA-CNT-930014 ..... p 842 N94-13655 #
NASDA-CNT-930015-PT-1 ..... p 622 N94-13425 #
NASDA-CNT-930016 ..... p 536 N94-14100 #
NASDA-CNT-930017 ..... p 535 N94-13600 #
NASDA-CNT-930018 ..... p 535 N94-13656 #

NASDA-CON-930003 ..... p 529 N94-13268 #

NASDA-TMR-930002 ..... p 541 N94-13658 #
NASDA-TMR-930003-PT-2-3 ..... p 541 N94-13659 #
NASDA-TMR-930004-PT-1-2 ..... p 541 N94-13660 #

NAVY-CASE-73566 ..... p 791 N94-13664
NAVY-CASE-74104 ..... p 556 N94-13663

NCEL-TN-1857 ..... p 683 N94-14902 #

NCR-32157 ..... p 504 N94-14031 #

NDRE-PUBL-93-1001 ..... p 730 N94-14852 #

NIST/SP-850 ..... p 849 N94-13376 *

NISTIR-5001 ..... p 652 N94-14687 #

NLR-TP-91166-U ..... p 650 N94-13527 #
NLR-TP-91291-U ..... p 519 N94-14450 #
NLR-TP-91307-U ..... p 503 N94-13528 #
NLR-TP-91366-U ..... p 763 N94-13529 #
NLR-TP-91387-U ..... p 503 N94-13530 #
NLR-TP-91397-U ..... p 503 N94-13531 #
NLR-TP-91438-U ..... p 570 N94-13532 #
NLR-TP-91477-U ..... p 632 N94-13533 #
NLR-TP-92057-U ..... p 570 N94-13497 #
NLR-TP-92143-U ..... p 528 N94-13498 #

NMRI-92-130 ..... p 733 N94-14879 #

NOAA-TR-NESDIS-70 ..... p 544 N94-13029 #
NOAA-TR-NESDIS-72 ..... p 826 N94-14498 #

NOARL-55 ..... p 725 N94-12990 #

NONP-VT-93-185300 ..... p 504 N94-13621 *
NONP-VT-93-185301 ..... p 518 N94-13623 *
NONP-VT-93-185302 ..... p 552 N94-13625 *
NONP-VT-93-185303 ..... p 842 N94-13626 *
NONP-VT-93-185304 ..... p 540 N94-13628 *
NONP-VT-93-185305 ..... p 819 N94-13629 *
NONP-VT-93-185306 ..... p 531 N94-13631 *
NONP-VT-93-185307 ..... p 504 N94-13632 *
NONP-VT-93-185308 ..... p 850 N94-13633 *
NONP-VT-93-185309 ..... p 541 N94-13634 *
NONP-VT-93-185310 ..... p 749 N94-13636 *
NONP-VT-93-185311 ..... p 541 N94-13637 *
NONP-VT-93-185312 ..... p 535 N94-13638 *
NONP-VT-93-185313 ..... p 531 N94-13640 *
NONP-VT-93-185314 ..... p 535 N94-13641 *
NONP-VT-93-185315 ..... p 737 N94-13601 *
NONP-VT-93-185316 ..... p 708 N94-13602 *
NONP-VT-93-185317 ..... p 662 N94-13604 *
NONP-VT-93-185318 ..... p 830 N94-13605 *
NONP-VT-93-185319 ..... p 515 N94-13606 *
NONP-VT-93-185320 ..... p 518 N94-13608 *
NONP-VT-93-185321 ..... p 741 N94-13609 *
NONP-VT-93-185322 ..... p 737 N94-13611 *
NONP-VT-93-185323 ..... p 850 N94-13612 *
NONP-VT-93-185324 ..... p 842 N94-13613 *
NONP-VT-93-185325 ..... p 737 N94-13615 *
NONP-VT-93-185326 ..... p 570 N94-13616 *
NONP-VT-93-185327 ..... p 552 N94-13617 *
NONP-VT-93-185328 ..... p 818 N94-13619 *
NONP-VT-93-185329 ..... p 713 N94-13620 *
NONP-VT-93-190213 ..... p 544 N94-14783 * #
NONP-VT-93-190265 ..... p 536 N94-14734 *
NONP-VT-93-190284 ..... p 533 N94-14735 *
NONP-VT-93-190287 ..... p 537 N94-14736 *
NONP-VT-93-190288 ..... p 533 N94-14787 *
NONP-VT-93-190289 ..... p 739 N94-14790 *

NPL-DITC-216-93 ..... p 824 N94-13879

NPL-DMM(A)-77 ..... p 570 N94-13666
NPL-DMM(A)-86 ..... p 708 N94-13667
NPL-DMM(A)-90 ..... p 749 N94-13688
NPL-DMM(A)-94 ..... p 662 N94-13808
NPL-DMM(A)-98 ..... p 639 N94-14464

NPL-RSA(EXT)-0039 ..... p 777 N94-13885
NPL-RSA(EXT)-37 ..... p 708 N94-13880
NPL-RSA(EXT)-38 ..... p 783 N94-13883

NRC-31789 ..... p 763 N94-13517 #
NRC-31798 ..... p 769 N94-13545 #
NRC-31827 ..... p 740 N94-13546 #
NRC-31835 ..... p 824 N94-14202 #
NRC-32158 ..... p 526 N94-13859 #
NRC-32815 ..... p 810 N94-14198 #
NRC-33162 ..... p 741 N94-13547 #
NRC-33183 ..... p 765 N94-14201 #
NRC-33188 ..... p 753 N94-14200 #
NRC-33557 ..... p 733 N94-13847 #
NRC-33592 ..... p 663 N94-14195 #
NRC-35347 ..... p 597 N94-14070 #
NRC-36183 ..... p 637 N94-13862 #

NRCC-35853 ..... p 764 N94-13860 #

NREL-TP-451-4853 ..... p 702 N94-13386 #

NREL/SP-420-5439 ..... p 585 N94-14454 #

NREL/TP-410-5335 ..... p 700 N94-12868 #
NREL/TP-411-5013 ..... p 704 N94-14350 #
NREL/TP-411-5453 ..... p 704 N94-14109 #
NREL/TP-411-5456 ..... p 704 N94-14110 #
NREL/TP-411-5457 ..... p 809 N94-14085 #
NREL/TP-421-5150 ..... p 584 N94-14089 #
NREL/TP-422-5259 ..... p 709 N94-14087 #
NREL/TP-442-5623 ..... p 704 N94-14423 #
NREL/TP-451-4961 ..... p 851 N94-14455 #
NREL/TP-463-5428 ..... p 704 N94-14422 #
NREL/TP-471-5536 ..... p 702 N94-13381 #

NRL/FR/7323-92-9412 ..... p 725 N94-12990 #

NRL/MR-6440-92-7170 ..... p 655 N94-13387 #

NRL/MR/7240-93-7026 ..... p 821 N94-13041 #

NSF-ITP-93-42 ..... p 780 N94-13018

NSF-92-16 ..... p 711 N94-12794 #
NSF-92-329 ..... p 819 N94-13982 #
NSF-92-334 ..... p 820 N94-14499 #

NSTS-08281 ..... p 535 N94-13934 * #
NSTS-08282 ..... p 535 N94-13935 * #

NSWCDD/TR-93/91 ..... p 500 N94-12989 #

ONERA-NT-1990-3 ..... p 776 N94-13692 #
ONERA-NT-1991-9 ..... p 630 N94-13117 #
ONERA-NT-1992-10 ..... p 810 N94-14193 #
ONERA-NT-1992-11 ..... p 565 N94-14194 #
ONERA-NT-1992-12 ..... p 650 N94-14009 #

ONERA-P-1992-4 ..... p 716 N94-14192 #

ORA-CP-91-5402-43 ..... p 752 N94-14088

ORAE-DLOR-RN-92-4 ..... p 753 N94-14207

ORAE-PR-614 ..... p 774 N94-13549 #

ORNL/FTR-4283 ..... p 568 N94-12998 #

ORNL/M-2725 ..... p 711 N94-14859 #

ORNL/NPR-92/65 ..... p 569 N94-13242 #

ORNL/TM-12020 ..... p 755 N94-14515 #
ORNL/TM-12170 ..... p 805 N94-13009 #
ORNL/TM-12234 ..... p 756 N94-14696 #
ORNL/TM-12269 ..... p 775 N94-12955 #
ORNL/TM-12287 ..... p 759 N94-13470 #

OZ-92/19 ..... p 778 N94-12845 #
OZ-92/20 ..... p 816 N94-12844 #
OZ-92/27 ..... p 778 N94-12847 #

PB93-154938/GAR ..... p 661 N94-13285
PB93-155166 ..... p 710 N94-14508
PB93-170124 ..... p 820 N94-12801 #
PB93-187136 ..... p 579 N94-13783 #
PB93-196640 ..... p 821 N94-12936 #
PB93-198208 ..... p 626 N94-14686
PB93-198323 ..... p 845 N94-14560
PB93-198331 ..... p 845 N94-14561
PB93-198422 ..... p 849 N94-13376 *
PB93-198851 ..... p 652 N94-14687 #
PB93-199016 ..... p 826 N94-14562
PB93-199693 ..... p 514 N94-14563

PD-AL-9109 ..... p 744 N94-13077 #

PL-TR-92-2293 ..... p 719 N94-12978 #
PL-TR-93-2009 ..... p 834 N94-12971 #

PNL-SA-20914 ..... p 718 N94-12903 #
PNL-SA-21377 ..... p 715 N94-13912 #
PNL-SA-21486 ..... p 709 N94-13911 #
PNL-SA-21491 ..... p 572 N94-14058 #
PNL-SA-21492 ..... p 708 N94-13910 #
PNL-SA-21663 ..... p 572 N94-14184 #
PNL-SA-21677 ..... p 793 N94-14702 #
PNL-SA-22070 ..... p 658 N94-14415 #
PNL-SA-22200 ..... p 782 N94-13485 #
PNL-SA-22257 ..... p 568 N94-13035 #
PNL-SA-22394 ..... p 706 N94-12937 #
PNL-SA-22528 ..... p 580 N94-14297 #

PNL-8478 ..... p 706 N94-12905 #
PNL-8606 ..... p 710 N94-14523 #
PNL-8642 ..... p 755 N94-14571 #

PPL-128 ..... p 800 N94-13853 #
PPL-129 ..... p 800 N94-13852 #

PPL-130 ..... p 800 N94-13851 #
PPL-131 ..... p 799 N94-13836 #
PPL-132 ..... p 799 N94-13835 #
PPL-133 ..... p 798 N94-13564 #
PPL-134 ..... p 798 N94-13563 #
PPL-135 ..... p 800 N94-13850 #
PPL-136 ..... p 799 N94-13849 #
PPL-138 ..... p 602 N94-13802 #
PPL-139 ..... p 800 N94-13877 #
PPL-140 ..... p 801 N94-14206 #

PR-D15-0015 ..... p 830 N94-13448 * #
PR-D15-0018 ..... p 792 N94-14473 * #

PREPRINT-729 ..... p 766 N94-14718 #
PREPRINT-730 ..... p 815 N94-14720 #
PREPRINT-731 ..... p 787 N94-14721 #
PREPRINT-734 ..... p 768 N94-13499 #
PREPRINT-736 ..... p 725 N94-13500 #

PSI-1001/TR-871 ..... p 562 N94-13115 * #
PSI-2090/TR-1140 ..... p 527 N94-13127 * #

PUBL-SER-A-129 ..... p 720 N94-13587 #
PUBL-SER-A-130 ..... p 686 N94-13994 #

PUBL-940151 ..... p 554 N94-14907 * #

RAE-MAT/STR-363 ..... p 574 N94-14828 #

RAE-TM-AERO/PROP-20 ..... p 653 N94-14701 #
RAE-TM-AERO/PROP-21 ..... p 509 N94-14706 #
RAE-TM-AERO/PROP-22 ..... p 653 N94-14827 #

RAE-TM-MAT/STR-1207 ..... p 683 N94-14818 #

RAE-TR-92063 ..... p 574 N94-14828 #

RAL-93-011 ..... p 579 N94-13783 #

REPT-1L161102AH43 ..... p 583 N94-12987 #
REPT-136 ..... p 714 N94-13709 * #
REPT-14/1993 ..... p 578 N94-13468 #
REPT-228 ..... p 700 N94-14810 #
REPT-31-8071(05) ..... p 828 N94-12931 * #
REPT-699-099-359 ..... p 555 N94-13267 * #
REPT-72-92 ..... p 823 N94-13863
REPT-7725 ..... p 758 N94-12930
REPT-83 ..... p 720 N94-13589 #
REPT-86-128 ..... p 543 N94-14483 * #
REPT-92-049 ..... p 750 N94-13822
REPT-92-101 ..... p 770 N94-14150 #
REPT-93-002 ..... p 750 N94-13805
REPT-93-004 ..... p 823 N94-13806
REPT-93-008 ..... p 750 N94-13807
REPT-93-033 ..... p 770 N94-13809
REPT-93B00105 ..... p 723 N94-14074 * #
REPT-93B00106 ..... p 550 N94-13265 * #
REPT-93B00107 ..... p 545 N94-13713 * #
REPT-93B00110 ..... p 844 N94-13963 * #
REPT-93B00111 ..... p 850 N94-13923 * #
REPT-93B00117-VOL-14 ..... p 725 N94-14090 * #
REPT-93D-03-0423-PT-1 ..... p 511 N94-13424 * #
REPT-93E02366 ..... p 623 N94-13871 * #
REPT-93E02367 ..... p 716 N94-13960 * #
REPT-93E02368 ..... p 623 N94-13878 * #
REPT-93 ..... p 724 N94-14709 #
REPT-94044 ..... p 540 N94-13140 * #

RFP-4599 ..... p 565 N94-14346 #

RIACS-TR-91-27 ..... p 748 N94-13586 * #
RIACS-TR-93-02 ..... p 760 N94-13921 * #
RIACS-TR-93-05 ..... p 763 N94-13603 * #
RIACS-TR-93-07 ..... p 770 N94-13922 * #

RL-TR-92-309 ..... p 619 N94-12967 #
RL-TR-93-9 ..... p 758 N94-12930

RSR-C002-93 ..... p 660 N94-12791 * #

RSS-8898 ..... p 533 N94-12806 * #

RTI/4321/Q3-93 ..... p 828 N94-13104 * #
RTI/4968/01F ..... p 619 N94-12967 #

R93-205 ..... p 835 N94-13233 * #
R93-957424-F ..... p 553 N94-14682 * #

S-692 ..... p 731 N94-12832 * #
S-729 ..... p 735 N94-13961 * #
S-730 ..... p 737 N94-13399 * #
S-736 ..... p 729 N94-14028 * #
S-737 ..... p 729 N94-14032 * #
S-741 ..... p 819 N94-13400 * #

SAE-92-1997 ..... p 517 N94-13791 * #

SAND-92-0347 ..... p 539 N94-13006 #
SAND-92-0824C ..... p 809 N94-14079 #
SAND-92-0825C ..... p 809 N94-14108 #
SAND-92-1888C ..... p 501 N94-13260 #
SAND-92-1891C ..... p 748 N94-13578 #
SAND-92-1967 ..... p 612 N94-14512 #
SAND-92-2059C ..... p 742 N94-12956 #
SAND-92-2086C ..... p 686 N94-14056 #
SAND-92-2090C ..... p 540 N94-13398 #
SAND-92-2210C ..... p 655 N94-13261 #
SAND-92-2240C ..... p 676 N94-14456 #
SAND-92-2346C ..... p 628 N94-12884 #
SAND-92-2405C ..... p 743 N94-12999 #
SAND-92-2460C ..... p 539 N94-12909 #
SAND-92-2490C ..... p 814 N94-14695 #
SAND-92-2508C ..... p 812 N94-14344 #
SAND-92-2712C ..... p 649 N94-13395 #
SAND-92-2765 ..... p 754 N94-14399 #
SAND-92-2816 ..... p 652 N94-14578 #
SAND-92-2845C ..... p 670 N94-12908 #
SAND-92-2868C ..... p 705 N94-14861 #
SAND-92-2872C ..... p 703 N94-13886 #
SAND-93-0023C ..... p 561 N94-12841 #
SAND-93-0027 ..... p 568 N94-12977 #
SAND-93-0037C ..... p 619 N94-12942 #
SAND-93-0044C ..... p 752 N94-14019 #
SAND-93-0100C ..... p 582 N94-14511 #
SAND-93-0106C ..... p 561 N94-12819 #
SAND-93-0187 ..... p 800 N94-13908 #
SAND-93-0482C ..... p 782 N94-13409 #
SAND-93-0582C ..... p 576 N94-12866 #
SAND-93-0609C ..... p 809 N94-14083 #
SAND-93-0645 ..... p 653 N94-14858 #
SAND-93-0689C ..... p 743 N94-12991 #
SAND-93-0725C ..... p 632 N94-13397 #
SAND-93-0735 ..... p 601 N94-13696 #
SAND-93-0742C ..... p 759 N94-13043 #
SAND-93-0812C ..... p 648 N94-13044 #
SAND-93-0813C ..... p 804 N94-12813 #
SAND-93-0826C ..... p 576 N94-12912 #
SAND-93-0869C ..... p 820 N94-12907 #
SAND-93-0908C ..... p 760 N94-14011 #
SAND-93-0956C ..... p 758 N94-12878 #
SAND-93-1002C ..... p 596 N94-13889 #
SAND-93-1006C ..... p 618 N94-12821 #
SAND-93-1011 ..... p 753 N94-14295 #
SAND-93-1013C ..... p 812 N94-14345 #
SAND-93-1067C ..... p 551 N94-13514 #
SAND-93-1068C ..... p 579 N94-13888 #
SAND-93-1069C ..... p 561 N94-12910 #
SAND-93-1280C ..... p 623 N94-13892 #
SAND-93-1289C ..... p 801 N94-14349 #
SAND-93-1324C ..... p 817 N94-14453 #
SAND-93-1386C ..... p 755 N94-14528 #
SAND-93-8558C ..... p 710 N94-14183 #

SAO-AXAF-DR-93-039 ..... p 832 N94-14305 * #

SAT-380.02 ..... p 673 N94-13673 * #

SATCOM-93-15 ..... p 612 N94-14501 * #

SDSU-CEP-524067 ..... p 629 N94-13007 * #

SECA-TR-91-8 ..... p 643 N94-14741 * #

SGD-584-PT-1 ..... p 845 N94-14560
SGD-584-PT-2 ..... p 845 N94-14561

SHEP-91/92 ..... p 778 N94-12845 #

SLAC-PUB-5967 ..... p 761 N94-14476 #

SLAC-415 ..... p 805 N94-13020 #

SLAC/SSRL-0009 ..... p 805 N94-13020 #

SM-34 ..... p 665 N94-13042 #

SMC-TR-93-24 ..... p 579 N94-13903 #
SMC-TR-93-26 ..... p 661 N94-13122 #
SMC-TR-93-27 ..... p 659 N94-14681 #

SRA-R93-9083-F-VOL-1 ..... p 647 N94-14906 * #

SSCL-PREPRINT-218 ..... p 755 N94-14581 #
SSCL-PREPRINT-288 ..... p 821 N94-12983 #
SSCL-PREPRINT-409 ..... p 787 N94-14588 #

SSDC-28-REV-1 ..... p 823 N94-13352 #

SSD93D0505 ..... p 536 N94-14323 * #

STK-206-VOL-1 ..... p 531 N94-13358

TDA-PR-42-114 ..... p 607 N94-14389 * #

TEC-0033 ..... p 766 N94-14777 #

TK-ST0213 ..... p 541 N94-13658 #
TK-ST0432 ..... p 541 N94-13659 #
TK-ST0433 ..... p 541 N94-13660 #

TKK-DISS-793 ..... p 760 N94-14187 #
TKK-DISS-794 ..... p 625 N94-14096 #

TKK-MAT-A304 ..... p 760 N94-14187 #

TKK-S-RAD-S194 ..... p 625 N94-14096 #

TM-008-93 ..... p 731 N94-14899 #
TM-93-067 ..... p 595 N94-14026 * #

TN-035 ..... p 638 N94-14356 * #

TR-EE-93-11 ..... p 823 N94-13192 * #
TR-EE-93-1 ..... p 743 N94-13023 * #

TR-HSV-93-0002 ..... p 705 N94-14430 * #

TR-0091(6925-13)-2 ..... p 659 N94-14681 #
TR-1-FSRL-1990 ..... p 539 N94-12790 * #
TR-142 ..... p 779 N94-12894 #
TR-35 ..... p 807 N94-13359
TR-3 ..... p 780 N94-13051 #
TR-468 ..... p 773 N94-13585 #
TR-51 ..... p 577 N94-12986 #
TR-55 ..... p 577 N94-12985 #
TR-92-13 ..... p 824 N94-14072 #
TR-93(3935)-1 ..... p 661 N94-13122 #
TR-93(3935)-4 ..... p 579 N94-13903 #

TRC-CAB-9308 ..... p 602 N94-13799 * #

TVA-BULL-Y-228 ..... p 707 N94-13218 #

TVA/NFERC-92/6 ..... p 707 N94-13218 #

TWR-17674 ..... p 554 N94-14907 * #
TWR-50222 ..... p 652 N94-14497 * #

UAH-5-32734 ..... p 714 N94-13709 * #
UAH-5-32903 ..... p 621 N94-13186 * #
UAH-5 ..... p 683 N94-14484 * #

UCB-PTH-93/14 ..... p 780 N94-13018

UCRL-CR-111879 ..... p 649 N94-13410 #

UCRL-ID-112181 ..... p 706 N94-13095 #
UCRL-ID-112223 ..... p 792 N94-14317 #
UCRL-ID-112576 ..... p 512 N94-14292 #
UCRL-ID-112587 ..... p 619 N94-12994 #
UCRL-ID-112984 ..... p 720 N94-13404 #
UCRL-ID-113019 ..... p 638 N94-14318 #
UCRL-ID-113182 ..... p 657 N94-13882 #
UCRL-ID-113715 ..... p 576 N94-12939 #
UCRL-ID-113834 ..... p 807 N94-13405 #
UCRL-ID-113844 ..... p 823 N94-13406 #
UCRL-ID-113846 ..... p 548 N94-12911 #

UCRL-JC-107852-REV-1 ..... p 725 N94-12876 #
UCRL-JC-107859 ..... p 771 N94-14589 #
UCRL-JC-108982 ..... p 789 N94-14460 #
UCRL-JC-109276 ..... p 656 N94-13481 #
UCRL-JC-109359-REV-1 ..... p 583 N94-14693 #
UCRL-JC-109388 ..... p 653 N94-12898 #
UCRL-JC-109421 ..... p 791 N94-13482 #
UCRL-JC-109651 ..... p 805 N94-13010 #
UCRL-JC-109819 ..... p 723 N94-14426 #
UCRL-JC-109948 ..... p 561 N94-12881 #
UCRL-JC-110000 ..... p 654 N94-12962 #
UCRL-JC-110031 ..... p 625 N94-14427 #
UCRL-JC-110081 ..... p 576 N94-12885 #
UCRL-JC-110084 ..... p 660 N94-14888 #
UCRL-JC-110213 ..... p 654 N94-12963 #
UCRL-JC-110651 ..... p 786 N94-14569 #
UCRL-JC-110675 ..... p 705 N94-14510 #
UCRL-JC-110687 ..... p 567 N94-12899 #
UCRL-JC-110706 ..... p 658 N94-14152 #
UCRL-JC-110922 ..... p 709 N94-14022 #
UCRL-JC-110953 ..... p 802 N94-14564 #
UCRL-JC-110974 ..... p 658 N94-14175 #
UCRL-JC-110982 ..... p 813 N94-14439 #
UCRL-JC-110996 ..... p 580 N94-14311 #
UCRL-JC-111000 ..... p 569 N94-13137 #
UCRL-JC-111025 ..... p 581 N94-14319 #
UCRL-JC-111212 ..... p 753 N94-14289 #
UCRL-JC-111224 ..... p 756 N94-14864
UCRL-JC-111227 ..... p 663 N94-13975 #
UCRL-JC-111233 ..... p 657 N94-13976 #

UCRL-JC-111405 ..... p 797 N94-13217 #
UCRL-JC-111448 ..... p 783 N94-13893 #
UCRL-JC-111458 ..... p 655 N94-13243 #
UCRL-JC-111495 ..... p 653 N94-14772
UCRL-JC-111546 ..... p 797 N94-13393 #
UCRL-JC-111558-REV-1 ..... p 825 N94-14331 #
UCRL-JC-111689 ..... p 834 N94-13011 #
UCRL-JC-111690 ..... p 655 N94-13145 #
UCRL-JC-111717 ..... p 784 N94-14140 #
UCRL-JC-111801 ..... p 655 N94-13258 #
UCRL-JC-111802 ..... p 655 N94-13259 #
UCRL-JC-111816-REV-1 ..... p 760 N94-14475 #
UCRL-JC-111840 ..... p 794 N94-12846 #
UCRL-JC-111844 ..... p 803 N94-14894 #
UCRL-JC-111851 ..... p 808 N94-13881 #
UCRL-JC-111860 ..... p 839 N94-14341 #
UCRL-JC-111868 ..... p 795 N94-12995 #
UCRL-JC-111883 ..... p 760 N94-14315 #
UCRL-JC-111903 ..... p 801 N94-14312 #
UCRL-JC-111904 ..... p 811 N94-14313 #
UCRL-JC-111941 ..... p 811 N94-14332 #
UCRL-JC-111956 ..... p 773 N94-14314 #
UCRL-JC-111969 ..... p 790 N94-12865 #
UCRL-JC-111973 ..... p 568 N94-13036 #
UCRL-JC-112000 ..... p 754 N94-14435 #
UCRL-JC-112060 ..... p 574 N94-14793
UCRL-JC-112067 ..... p 806 N94-13136 #
UCRL-JC-112103 ..... p 700 N94-14566 #
UCRL-JC-112154 ..... p 781 N94-13251 #
UCRL-JC-112165 ..... p 786 N94-14526 #
UCRL-JC-112195 ..... p 748 N94-13576 #
UCRL-JC-112286 ..... p 631 N94-13250 #
UCRL-JC-112287 ..... p 631 N94-13249 #
UCRL-JC-112302 ..... p 801 N94-14342 #
UCRL-JC-112307 ..... p 803 N94-14865 #
UCRL-JC-112341 ..... p 789 N94-13727 #
UCRL-JC-112361 ..... p 803 N94-14590 #
UCRL-JC-112366 ..... p 721 N94-13914 #
UCRL-JC-112408 ..... p 556 N94-13389 #
UCRL-JC-112562 ..... p 647 N94-14895 #
UCRL-JC-112601 ..... p 742 N94-12883 #
UCRL-JC-112602 ..... p 653 N94-14792
UCRL-JC-112624 ..... p 659 N94-14594 #
UCRL-JC-112630 ..... p 658 N94-14114 #
UCRL-JC-112671 ..... p 658 N94-14437 #
UCRL-JC-112678 ..... p 658 N94-14442 #
UCRL-JC-112692 ..... p 566 N94-14869 #
UCRL-JC-112700 ..... p 792 N94-14438 #
UCRL-JC-112829 ..... p 813 N94-14440 #
UCRL-JC-112832 ..... p 581 N94-14432 #
UCRL-JC-112981 ..... p 580 N94-14124 #
UCRL-JC-113093 ..... p 790 N94-14893 #
UCRL-JC-113163 ..... p 797 N94-13207 #
UCRL-JC-113273 ..... p 651 N94-14416 #
UCRL-JC-113290 ..... p 659 N94-14595 #
UCRL-JC-113407 ..... p 810 N94-14125 #
UCRL-JC-113601 ..... p 625 N94-14522 #
UCRL-JC-113606 ..... p 840 N94-14467 #
UCRL-JC-113618 ..... p 627 N94-14870 #
UCRL-JC-113690 ..... p 755 N94-14521 #
UCRL-JC-113710 ..... p 788 N94-13208 #
UCRL-JC-113853 ..... p 639 N94-14434 #

UCRL-LR-105821-92-4 ..... p 795 N94-13017 #

UCRL-MA-108967-REV-1 ..... p 744 N94-13120 #
UCRL-MA-108976-REV-1 ..... p 822 N94-13121 #
UCRL-MA-111145 ..... p 742 N94-12864 #
UCRL-MA-112087 ..... p 742 N94-12840 #

UCRL-52000-93-3 ..... p 849 N94-13019 #

UG-1/93 ..... p 769 N94-13536 #

UILU-ENG-93-4015 ..... p 796 N94-13039 #

UM-P-92/51 ..... p 653 N94-12857
UM-P-92/52 ..... p 778 N94-12845 #
UM-P-92/60 ..... p 775 N94-12843 #
UM-P-92/61 ..... p 816 N94-12844 #
UM-P-92/63 ..... p 778 N94-12847 #
UM-P-92/66 ..... p 778 N94-12848 #
UM-P-92/93 ..... p 778 N94-12858

UM-026952 ..... p 838 N94-13716 * #
UM-522746 ..... p 791 N94-13682 * #

UMA-030601-2-T ..... p 602 N94-13720 * #

UMICH-028918-5-T ..... p 599 N94-13236 * #

URC-80436 ..... p 709 N94-14103 * #

US-PATENT-APPL-SN-004002 ..... p 556 N94-13663
US-PATENT-APPL-SN-031410 ..... p 791 N94-13664

UTTG-28-92 ..... p 836 N94-13361

VKI-LS-1993-03 ..... p 505 N94-14153 #

VTT-PUBS-107 ..... p 674 N94-13887 #
VTT-PUBS-109 ..... p 777 N94-14034 #
VTT-PUBS-116 ..... p 597 N94-14055 #

VYH-PUB-11 ..... p 718 N94-12837 #

W-1/92 ..... p 579 N94-14007 #
W-4G157 ..... p 621 N94-13336 * #
W-9219 ..... p 774 N94-14545 #

WA-9204 ..... p 769 N94-13731 #

WCASP-25 ..... p 718 N94-12918 #

WCDMP-21 ..... p 723 N94-14118 #

WHC-SA-1361 ..... p 573 N94-14364 #

WINCO-11908 ..... p 738 N94-14451 #

WL-TR-92-2125 ..... p 660 N94-12988 #
WL-TR-93-1054 ..... p 513 N94-13703 #
WL-TR-93-2027 ..... p 636 N94-13730 #

WMO-TD-523 ..... p 723 N94-14118 #

WMO-485-VOL-1 ..... p 721 N94-13686 #
WMO-485-VOL-2 ..... p 722 N94-14071 #

WMO/TD-552 ..... p 718 N94-12918 #

WSRC-IM-90-83-9 ..... p 754 N94-14470 #

WSRC-MS-92-485 ..... p 581 N94-14343 #
WSRC-MS-93-222 ..... p 578 N94-13493 #

WSRC-TR-92-438 ..... p 703 N94-13691 #

XC-PL/HANSCOM ..... p 834 N94-12971 #

Y/DZ-990 ..... p 565 N94-14525 #

Y/EN-4612/R1 ..... p 757 N94-14871 #

APPENDIX

NASA SCIENTIFIC AND TECHNICAL INFORMATION PROGRAM PRODUCTS AND SERVICES

The NASA Scientific and Technical Information (STI) Program provides for the collection and announcement of aerospace-related reports and literature obtained worldwide through agreements and exchanges. The result of the collection is the comprehensive NASA STI Database that covers aeronautics, space, and supporting disciplines.

The STI Database, documents generated or obtained by NASA, and products and services derived from or supporting the database are made available to the NASA research community and to the public. Descriptions and sources of these items are presented in the following pages.

Scientific and Technical Aerospace Reports (STAR) is an abstract journal, listing citations with abstracts for aerospace-related reports obtained from worldwide sources. *STAR* is issued on the first of each month, and announces current documents that have been entered into the NASA STI Database during the previous month. The reports are of the following types:

- NASA, NASA contractor, and NASA grantee reports;
- Reports issued by other U.S. Government agencies, domestic and foreign institutions, universities, and private firms;
- Translations in report form;
- NASA-owned patents and patent applications
- Other U.S. Government agency and foreign patents and patent applications
- Domestic and foreign dissertations and theses.

Journal, book, and conference literature, journal translations, and certain foreign dissertations having the same subject scope as *STAR* are announced in a companion journal, *International Aerospace Abstracts (IAA). IAA* is issued on the 1st and 15th of each month and is available from the American Institute of Aeronautics and Astronautics, Technical Information Service, 555 West 57th Street, 12th Floor, New York, NY 10019.

ELIGIBILITY AND REGISTRATION FOR NASA STI PRODUCTS AND SERVICES

Organizations of the type listed below that have registered with NASA can receive products and services.

- NASA offices and installations, contractors, subcontractors, grantees, and consultants;
- Other U.S. Government agencies and their contractors;
- Libraries in the United States that have arrangements with NASA to maintain collections of NASA documents for public reference;
- Other organizations in the United States having a need for NASA documents in work related to aeronautics and space research;
- Organizations abroad that have established reciprocal documents exchange arrangements with NASA.

The central service points—central points of document acquisition and control within qualified organizations—or individuals are eligible to register for NASA STI products and services. Domestic organizations or individuals may be eligible to receive various classes of NASA publications and services and should address their requests for registration or further information to:

ATTN: Registration Services
NASA Center for AeroSpace Information
800 Elkridge Landing Road
Linthicum Heights, MD 21090-2934
301-621-0390

Organizations abroad should direct requests to:

National Aeronautics and Space Administration
Scientific and Technical Information Program (JTT)
International STI Program
Washington, DC 20546-0001
USA
703-271-5640

SUBJECT SCOPE

The subject scope of *STAR* and *IAA* includes all aspects of aeronautics and space research and development, supporting basic and applied research, and applications. Aerospace aspects of Earth resources, energy development, conservation, oceanography, environmental protection, urban transportation, and other topics of high national priority are also covered.

HOW TO USE *STAR* SUBJECT CATEGORIES

Abstracts in *STAR* are categorized by 10 major subject divisions that are divided further into 76 specific subject categories. The subject divisions and categories are listed in the Table of Contents together with a note for each that defines its scope and provides any cross-references. For example:

16 SPACE TRANSPORTATION

Includes passenger and cargo space transportation, e.g., shuttle operations; and space rescue techniques. For related information see also *03 Air Transportation and Safety* and *18 Spacecraft Design, Testing and Performance.* For space suits see *54 Man/System Technology and Life Support.*

CROSS-REFERENCES

Individual *STAR* abstracts are not ordinarily cross-referenced, except for certain conference reports or book translations that have had separate abstracts written for their component papers or chapters. Citations and abstracts of the components follow immediately after those of the parent document. When the subject content of a component differs sufficiently from the general content of the parent, a cross-reference citation also is printed at the end of the category to which it normally would have been assigned if it were independent.

DOCUMENTS ON MICROFICHE

Documents available on microfiche are designated by a pound sign (#) following the accession number.

LIMITED REPRODUCIBILITY

A note of limited reproducibility appears in the citation, if there are factors affecting the reproducibility of more than 20% of the document. These factors include faint or broken type, color photographs, black and white photographs, foldouts, dot matrix print, or some other factor that limits the reproducibility of the document. This notation also appears on the microfiche header.

COLOR COPIES

An increasing number of NASA scientific and technical reports are being produced with color graphs, charts, illustrations, and photographs. An indication that a document has color pages follows the source and pricing (SAP) information in the *STAR* citation.

Registered users of the NASA Scientific and Technical Information Program will receive ordered documents with color at no additional cost, as long as stock copies of the document are available. Otherwise, an additional fee of $2.00 per color page will be charged. The NASA Center for AeroSpace Information staff will contact registered users to determine individual user's needs.

NASA PATENTS AND PATENT APPLICATIONS

Patents and patent applications owned by NASA are announced in *STAR* under appropriate subject categories and are referenced in the *STAR* indexes. In the Report Number Index, patents are indexed by the NASA Case Number, and the U.S. Patent Class. Patent applications are indexed by the NASA Case Number and the U.S. Patent Application Serial Number.

Printed copies of patents (which are not microfiched) are available for purchase from the U.S. Patent and Trademark Office.

When ordering patents, the U.S. Patent Number should be used, and payment must be remitted in advance, by money order or check payable to the Commissioner of Patents and Trademarks. Prepaid purchase coupons for ordering are also available from the U.S. Patent and Trademark Office.

NASA patent application specifications are sold in both paper copy and microfiche by the NASA Center for AeroSpace Information (CASI). The N accession number should be used in ordering either paper copy or microfiche from CASI.

The patents and patent applications announced in *STAR* are owned by NASA and are available for royalty-free licensing. Requests for licensing terms and further information should be addressed to:

National Aeronautics and Space Administration
Associate General Counsel for Intellectual Property
Code GP
Washington, DC 20546-0001

SOURCES FOR DOCUMENTS

One or more sources from which a document announced in *STAR* is available to the public is ordinarily given on the last line of the citation. The most commonly indicated sources and their acronyms or abbreviations are listed below, and their addresses are listed on page A-6. If the publication is available from a source other than those listed, the publisher and his address will be displayed on the availability line or in combination with the corporate source line.

Avail: CASI. Sold by the NASA Center for AeroSpace Information. Prices for hard copy (HC) and microfiche (MF) are indicated by a price code following the letters HC or MF in the *STAR* citation. Current values for the price codes are given in the tables on page A-7.

NOTE ON ORDERING DOCUMENTS: When ordering publications from CASI, use the N accession number or other report number. It is also advisable to cite the title and other bibliographic identification.

Avail: SOD (or GPO). Sold by the Superintendent of Documents, U.S. Government Printing Office, in hard copy.

Avail: BLL (formerly NLL): British Library Lending Division, Boston Spa, Wetherby, Yorkshire, England. Photocopies available from this organization at the price shown. (If none is given, inquiry should be addressed to the BLL.)

Avail: DOE Depository Libraries. Organizations in U.S. cities and abroad that maintain collections of Department of Energy reports, usually in microfiche form, are listed in *Energy Research Abstracts*. Services available from the DOE and its depositories are described in a booklet, *DOE Technical Information Center - Its Functions and Services* (TID-4660), which may be obtained without charge from the DOE Technical Information Center.

Avail: ESDU. Pricing information on specific data, computer programs, and details on Engineering Sciences Data Unit (ESDU) topic categories can be obtained from ESDU International Ltd. Requesters in North America should use the Virginia address while all other requesters should use the London address, both of which are on page A-6.

Avail: Fachinformationszentrum, Karlsruhe. Gesellschaft für wissenschaftlich-technische Information mbH 7514 Eggenstein-Leopoldshafen 2, Germany.

Avail: HMSO. Publications of Her Majesty's Stationery Office are sold in the U.S. by Pendragon House, Inc. (PHI), Redwood City, CA. The U.S. price (including a service and mailing charge) is given, or a conversion table may be obtained from PHI.

Avail: Issuing Activity, or Corporate Author, or no indication of availability. Inquiries as to the availability of these documents should be addressed to the organization shown in the citation as the corporate author of the document.

Avail: NASA Public Document Rooms. Documents so indicated may be examined at or purchased from the National Aeronautics and Space Administration (JBD-4), Public Documents Room (Room 1H23), Washington, DC 20546-0001, or public document rooms located at NASA installations, and the NASA Pasadena Office at the Jet Propulsion Laboratory.

Avail: NTIS. Sold by the National Technical Information Service. Initially distributed microfiche under the NTIS SRIM (Selected Research in Microfiche) are available. For information concerning this service, consult the NTIS Subscription Section, Springfield, VA 22161.

Avail: Univ. Microfilms. Documents so indicated are dissertations selected from *Dissertation Abstracts* and are sold by University Microfilms as xerographic copy (HC) and microfilm. All requests should cite the author and the Order Number as they appear in the citation.

Avail: US Patent and Trademark Office. Sold by Commissioner of Patents and Trademarks, U.S. Patent and Trademark Office, at the standard price of $1.50 each, postage free. (See discussion of NASA patents and patent applications on page A-3.)

Avail: (US Sales Only). These foreign documents are available to users within the United States from the National Technical Information Service (NTIS). They are available to users outside the United States through the International Nuclear Information Service (INIS) representative in their country, or by applying directly to the issuing organization.

Avail: USGS. Originals of many reports from the U.S. Geological Survey, which may contain color illustrations, or otherwise may not have the quality of illustrations preserved in the microfiche or facsimile reproduction, may be examined by the public at the libraries of the USGS field offices whose addresses are listed on page A-6. The libraries may be queried concerning the availability of specific documents and the possible utilization of local copying services, such as color reproduction.

FEDERAL DEPOSITORY LIBRARY PROGRAM

In order to provide the general public with greater access to U.S. Government publications, Congress established the Federal Depository Library Program under the Government Printing Office (GPO), with 53 regional depositories responsible for permanent retention of material, inter-library loan, and reference services. At least one copy of nearly every NASA and NASA-sponsored publication, either in printed or microfiche format, is received and retained by the 53 regional depositories. A list of the regional GPO libraries, arranged alphabetically by state, appears on page A-8. These libraries are *not* sales outlets. A local library can contact a regional depository to help locate specific reports, or direct contact may be made by an individual.

PUBLIC COLLECTION OF NASA DOCUMENTS

An extensive collection of NASA and NASA-sponsored publications is maintained by the British Library Lending Division, Boston Spa, Wetherby, Yorkshire, England for public access. The British Library Lending Division also has available many of the non-NASA publications cited in *STAR*. European requesters may purchase facsimile copy or microfiche of NASA and NASA-sponsored documents, those identified by both the symbols # and * from ESA — Information Retrieval Service European Space Agency, 8-10 rue Mario-Nikis, 75738 CEDEX 15, France.

SUBMITTING DOCUMENTS

All users of this abstract service are urged to forward reports to be considered for announcement in *STAR*. This will aid NASA in its efforts to provide the fullest possible coverage of all scientific and technical publications that might support aeronautics and space research and development. If you have prepared relevant reports (other than those you will transmit to NASA, DOD, or DOE through the usual contract- or grant-reporting channels), please send them for consideration to the NASA Center for AeroSpace Information, 800 Elkridge Landing Road, Linthicum Heights, MD 21090-2934.

Reprints of journal articles, book chapters, and conference papers are also welcome. These will be considered for announcement in *STAR's* companion journal, *IAA*.

You may specify a particular source to be included in a report announcement if you wish; otherwise the report will be placed on a public sale at the NASA Center for AeroSpace Information. Copyrighted publications will be announced but not distributed or sold.

PURCHASE OF *STAR*

STAR is publicly available on annual subscription from the NASA Center for AeroSpace Information (CASI) at $94.00/domestic, $117.00/foreign. Single copy prices: $33.00/domestic, $41.00/foreign.

An annual, cumulative *STAR Index* is also available at $54.00/domestic, $65.00/foreign.

STAR is available to registered users on annual subscription from the NASA Center for AeroSpace Information, ATTN: Registration Services, 800 Elkridge Landing Road, Linthicum Heights, MD 21090-2934.

ADDRESSES OF ORGANIZATIONS

American Institute of Aeonautics
and Astronautics
Technical Information Service
555 West 57th Street, 12th Floor
New York, NY 10019

British Library Lending Division
Boston Spa, Wetherby, Yorkshire
England

Commissioner of Patents and Trademarks
U.S. Patent and Trademark Office
Washington, DC 20231

Department of Energy
Technical Information Center
P.O. Box 62
Oak Ridge, TN 37830

European Space Agency-
Information Retrieval Service ESRIN
Via Galileo Galilei
00044 Frascati (Rome) Italy

Engineering Sciences Data Unit International
P.O. Box 1633
Manassas, VA 22110

Engineering Sciences Data Unit
International, Ltd.
251-259 Regent Street
London, W1R 7AD, England

Fachinformationszentrum Karlsruhe
Gesellschaft für wissenschaftlich-technische
Information mbH
7514 Eggenstein-Leopoldshafen 2, Germany

Her Majesty's Stationery Office
P.O. Box 569, S.E. 1
London, England

NASA Center for AeroSpace Information
800 Elkridge Landing Road
Linthicum Heights, MD 21090-2934

National Aeronautics and Space Administration
Scientific and Technical Information Program
(JTT)
Washington, DC 20546-0001

National Technical Information Service
5285 Port Royal Road
Springfield, VA 22161

Pendragon House, Inc.
899 Broadway Avenue
Redwood City, CA 94063

Superintendent of Documents
U.S. Government Printing Office
Washington, DC 20402

University Microfilms
A Xerox Company
300 North Zeeb Road
Ann Arbor, MI 48106

University Microfilms, Ltd.
Tylers Green
London, England

U.S. Geological Survey Library National Center
MS 950
12201 Sunrise Valley Drive
Reston, VA 22092

U.S. Geological Survey Library
2255 North Gemini Drive
Flagstaff, AZ 86001

U.S. Geological Survey
345 Middlefield Road
Menlo Park, CA 94025

U.S. Geological Survey Library
Box 25046
Denver Federal Center, MS914
Denver, CO 80225

CASI PRICE TABLES

(Effective August 1, 1993)

STANDARD PRICE DOCUMENTS

PRICE CODE	NORTH AMERICAN PRICE	FOREIGN PRICE
A01	$ 9.00	$ 18.00
A02	12.50	25.00
A03	17.50	35.00
A04-A05	19.50	39.00
A06-A09	27.00	54.00
A10-A13	36.50	73.00
A14-A17	44.50	89.00
A18-A21	52.00	104.00
A22-A25	61.00	122.00
A99	Call For Price	Call For Price

MICROFICHE

PRICE CODE	NORTH AMERICAN PRICE	FOREIGN PRICE
A01	$ 9.00	$ 18.00
A02	12.50	25.00
A03	17.50	35.00
A04	19.50	39.00
A06	27.00	54.00
A10	36.50	73.00

IMPORTANT NOTICE

CASI Shipping and Handling Charges
U.S.—ADD $3.00 per TOTAL ORDER
Canada and Mexico—ADD $3.50 per TOTAL ORDER
All Other Countries—ADD $7.50 per TOTAL ORDER
Does NOT apply to orders
requesting CASI RUSH HANDLING.
CASI accepts charges to American Express, Diners Club, MasterCard and VISA.

FEDERAL REGIONAL DEPOSITORY LIBRARIES

ALABAMA

AUBURN UNIV. AT MONTGOMERY LIBRARY
Documents Dept.
7300 University Dr.
Montgomery, AL 36117-3596
(205) 244-3650 Fax: (205) 244-0678

UNIV. OF ALABAMA
Amelia Gayle Gorgas Library
Govt. Documents
Box 870266
Tuscaloosa, AL 35487-0266
(205) 348-6046 Fax: (205) 348-8833

ARIZONA

DEPT. OF LIBRARY, ARCHIVES, AND PUBLIC RECORDS
Federal Documents
Third Floor State Capitol
1700 West Washington
Phoenix, AZ 85007
(602) 542-4121 Fax: (602) 542-4400, 542-4500

ARKANSAS

ARKANSAS STATE LIBRARY
State Library Services
One Capitol Mall
Little Rock, AR 72201
(501) 682-2869

CALIFORNIA

CALIFORNIA STATE LIBRARY
Govt. Publications Section
914 Capitol Mall - P.O. Box 942837
Sacramento, CA 94237-0001
(916) 322-4572 Fax: (916) 324-8120

COLORADO

UNIV. OF COLORADO - BOULDER
Norlin Library
Govt. Publications
Campus Box 184
Boulder, CO 83309-0184
(303) 492-8834 Fax: (303) 492-2185

DENVER PUBLIC LIBRARY
Govt. Publications Dept. BS/GPD
1357 Broadway
Denver, CO 80203
(303) 571-2135

CONNECTICUT

CONNECTICUT STATE LIBRARY
231 Capitol Avenue
Hartford, CT 06106
(203) 566-4971 Fax: (203) 566-3322

FLORIDA

UNIV. OF FLORIDA LIBRARIES
Documents Dept.
Library West
Gainesville, FL 32611-2048
(904) 392-0366 Fax: (904) 392-7251

GEORGIA

UNIV. OF GEORGIA LIBRARIES
Govt. Documents Dept.
Jackson Street
Athens, GA 30602
(404) 542-8949 Fax: (404) 542-8522

HAWAII

UNIV. OF HAWAII
Hamilton Library
Govt. Documents Collection
2550 The Mall
Honolulu, HI 96822
(808) 948-8230 Fax: (808) 956-5968

IDAHO

UNIV. OF IDAHO LIBRARY
Documents Section
Moscow, ID 83843
(208) 885-6344 Fax: (208) 885-6817

ILLINOIS

ILLINOIS STATE LIBRARY
Reference Dept.
300 South Second
Springfield, IL 62701-1796
(217) 782-7596 Fax: (217) 524-0041

INDIANA

INDIANA STATE LIBRARY
Serials/Documents Section
140 North Senate Avenue
Indianapolis, IN 46204
(317) 232-3678 Fax: (317) 232-3728

IOWA

UNIV. OF IOWA LIBRARIES
Govt. Publications Dept.
Washington & Madison Streets
Iowa City, IA 52242
(319) 335-5926 Fax: (319) 335-5830

KANSAS

UNIV. OF KANSAS
Govt. Documents & Map Library
6001 Malatt Hall
Lawrence, KS 66045-2800
(913) 864-4660 Fax: (913) 864-5380

KENTUCKY

UNIV. OF KENTUCKY LIBRARIES
Govt. Publications/Maps Dept.
Lexington, KY 40506-0039
(606) 257-3139 Fax: (606) 257-1563, 257-8379

LOUISIANA

LOUISIANA STATE UNIV.
Middleton Library
Govt. Documents Dept.
Baton Rouge, LA 70803
(504) 388-2570 Fax: (504) 388-6992

LOUISIANA TECHNICAL UNIV.
Prescott Memorial Library
Govt. Documents Dept.
305 Wisteria Street
Ruston, LA 71270-9985
(318) 257-4962 Fax: (318) 257-2447

MAINE

TRI-STATE DOCUMENTS DEPOS.
Raymond H. Fogler Library
Govt. Documents & Microforms Dept.
Univ. of Maine
Orono, ME 04469
(207) 581-1680

MARYLAND

UNIV. OF MARYLAND
Hornbake Library
Govt. Documents/Maps Unit
College Park, MD 20742
(301) 454-3034 Fax: (301) 454-4985

MASSACHUSETTS

BOSTON PUBLIC LIBRARY
Govt. Documents Dept.
666 Boylston Street
Boston, MA 02117
(617) 536-5400 ext. 226
Fax: (617) 267-8273, 267-8248

MICHIGAN

DETROIT PUBLIC LIBRARY
5201 Woodward Avenue
Detroit, MI 48202-4093
(313) 833-1440, 833-1409
Fax: (313) 833-5039

LIBRARY OF MICHIGAN
Govt. Documents Unit
P.O. Box 30007
Lansing, MI 48909
(517) 373-0640 Fax: (517) 373-3381

MINNESOTA

UNIV. OF MINNESOTA
Wilson Library
Govt. Publications Library
309 19th Avenue South
Minneapolis, MN 55455
(612) 624-5073 Fax: (612) 626-9353

MISSISSIPPI

UNIV. OF MISSISSIPPI
J.D. Williams Library
Federal Documents Dept.
106 Old Gym Bldg.
University, MS 38677
(601) 232-5857 Fax: (601) 232-5453

MISSOURI

UNIV. OF MISSOURI - COLUMBIA
Ellis Library
Govt. Documents
Columbia, MO 65201
(314) 882-6733 Fax: (314) 882-8044

MONTANA

UNIV. OF MONTANA
Maureen & Mike Mansfield Library
Documents Div.
Missoula, MT 59812-1195
(406)243-6700 Fax: (406) 243-2060

NEBRASKA

UNIV. OF NEBRASKA - LINCOLN
D.L. Love Memorial Library
Documents Dept.
Lincoln, NE 68588
(402) 472-2562

NEVADA

UNIV. OF NEVADA
Reno Library
Govt. Publications Dept.
Reno, NV 89557
(702) 784-6579 Fax: (702) 784-1751

NEW JERSEY

NEWARK PUBLIC LIBRARY
U.S. Documents Div.
5 Washington Street -
P.O. Box 630
Newark, NJ 07101-0630
(201) 733-7812 Fax: (201) 733-5648

NEW MEXICO

UNIV. OF NEW MEXICO
General Library
Govt. Publications Dept.
Albuquerque, NM 87131-1466
(505) 277-5441 Fax: (505) 277-6019

NEW MEXICO STATE LIBRARY
325 Don Gaspar Avenue
Santa Fe, NM 87503
(505) 827-3826 Fax: (505) 827-3820

NEW YORK

NEW YORK STATE LIBRARY
Documents/Gift & Exchange Section
Federal Depository Program
Cultural Education Center
Albany, NY 12230
(518) 474-5563 Fax: (518) 474-5786

NORTH CAROLINA

UNIV. OF NORTH CAROLINA - CHAPEL HILL
CB#3912, Davis Library
BA/SS Dept. - Documents
Chapel Hill, NC 27599
(919) 962-1151 Fax: (919) 962-0484

NORTH DAKOTA

NORTH DAKOTA STATE UNIV. LIB.
Documents Office
Fargo, ND 58105
(701) 237-8886 Fax: (701) 237-7138
In cooperation with Univ. of North Dakota, Chester Fritz Library
Grand Forks

OHIO

STATE LIBRARY OF OHIO
Documents Dept.
65 South Front Street
Columbus, OH 43266
(614) 644-7051 Fax: (614) 752-9178

OKLAHOMA

OKLAHOMA DEPT. OF LIBRARIES
U.S. Govt. Information Div.
200 NE 18th Street
Oklahoma City, OK 73105-3298
(405) 521-2502, ext. 252, 253
Fax: (405) 525-7804

OKLAHOMA STATE UNIV.
Edmon Low Library
Documents Dept.
Stillwater, OK 74078
(405) 744-6546 Fax: (405) 744-5183

OREGON

PORTLAND STATE UNIV.
Millar Library
934 SW Harrison - P.O. Box 1151
Portland, OR 97207
(503) 725-3673 Fax: (503) 725-4527

PENNSYLVANIA

STATE LIBRARY OF PENN.
Govt. Publications Section
Walnut St. & Commonwealth Ave. -
P.O. Box 1601
Harrisburg, PA 17105
(717) 787-3752

SOUTH CAROLINA

CLEMSON UNIV.
Cooper Library
Public Documents Unit
Clemson, SC 29634-3001
(803) 656-5174 Fax: (803) 656-3025
In cooperation with Univ. of South Carolina, Thomas Cooper Library, Columbia

TENNESSEE

MEMPHIS STATE UNIV. LIBRARIES
Govt. Documents
Memphis, TN 38152
(901) 678-2586 Fax: (901) 678-2511

TEXAS

TEXAS STATE LIBRARY
United States Documents
P.O. Box 12927 - 1201 Brazos
Austin, TX 78711
(512) 463-5455 Fax: (512) 463-5436

TEXAS TECH. UNIV. LIBRARY
Documents Dept.
Lubbock, TX 79409
(806) 742-2268 Fax: (806) 742-1920

UTAH

UTAH STATE UNIV.
Merrill Library & Learning Resources Center, UMC-3000
Documents Dept.
Logan, UT 84322-3000
(801) 750-2684 Fax: (801) 750-2677

VIRGINIA

UNIV. OF VIRGINIA
Aldermman Library
Govt. Documents
Charlottesville, VA 22903-2498
(804) 824-3133 Fax: (804) 924-4337

WASHINGTON

WASHINGTON STATE LIBRARY
Document Section
MS AJ-11
Olympia, WA 98504-0111
(206) 753-4027 Fax: (206) 753-3546

WEST VIRGINIA

WEST VIRGINIA UNIV. LIBRARY
Govt. Documents Section
P.O. Box 6069
Morgantown, WV 26506
(304) 293-3640

WISCONSIN

ST. HIST. SOC. OF WISCONSIN LIBRARY
Govt. Publications Section
816 State Street
Madison, WI 53706
(608) 262-2781 Fax: (608) 262-4711
In cooperation with Univ. of Wisconsin - Madison, Memorial Library

MILWAUKEE PUBLIC LIBRARY
Documents Div.
814 West Wisconsin Avenue
Milwaukee, WI 53233
(414) 278-2167 Fax: (414) 278-2137

*U.S. GOVERNMENT PRINTING OFFICE: 1994-301-249/00001

POSTMASTER
Address Correction Requested
(Sections 137 and 159 Post Manual)

National Aeronautics and
Space Administration
Code JTT
Washington, DC 20546-0001

Official Business
Penalty for Private Use, $300

BULK RATE
POSTAGE & FEES PAID
NASA
PERMIT No. G-27

NASA

POSTMASTER: If Undeliverable (Section 158 Postal Manual) Do Not Return

Please circulate this publication to other colleagues within your organization.

NASA STI PROGRAM
SCIENTIFIC &
TECHNICAL
INFORMATION